International Union of Crystallography

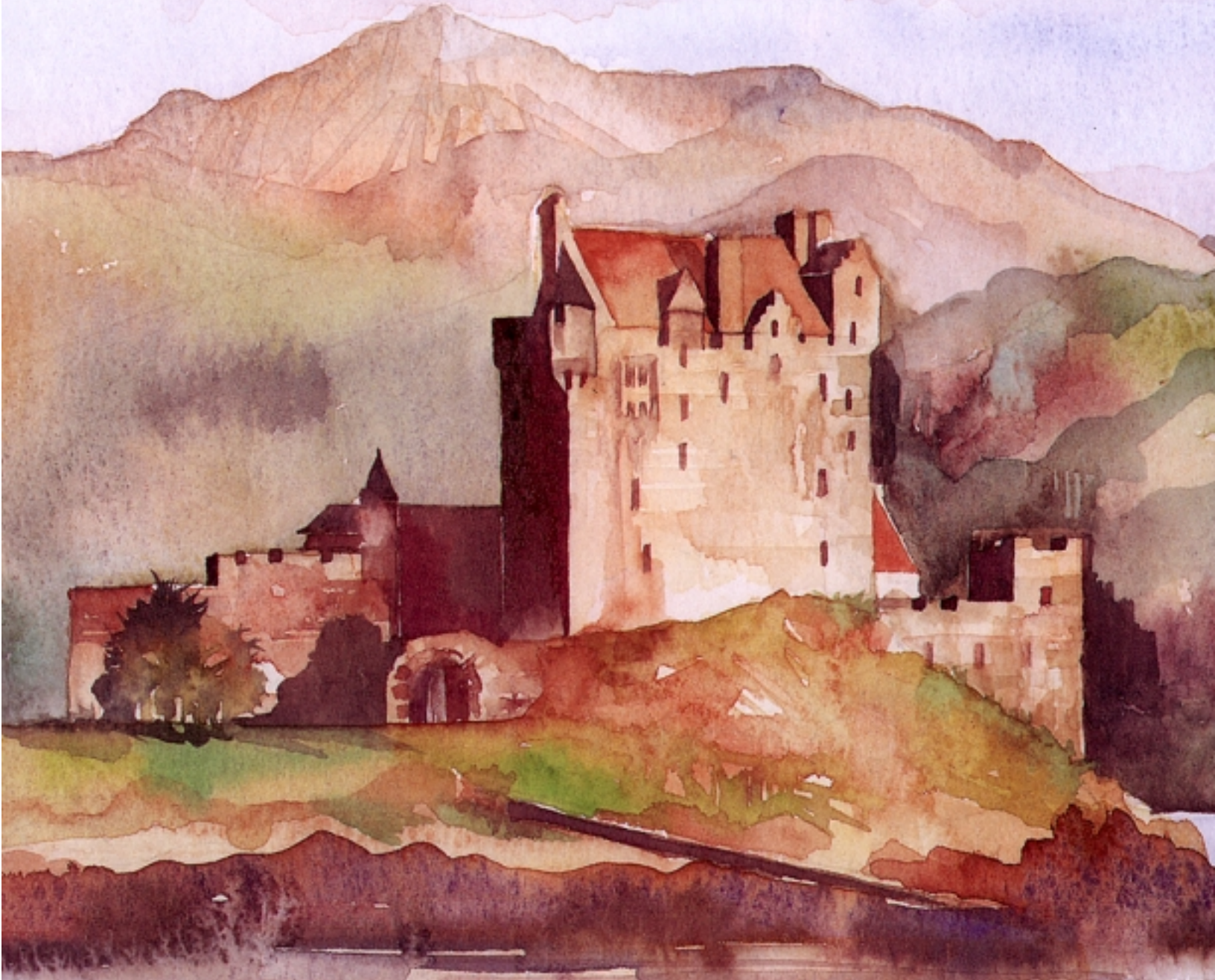

XVIIIth International Congress and General Assembly

Abstracts

TEAMS and COMMITTEES

Programme Team (University of Durham)
Judith Howard, Irene Harries, Ivana Radoslavjevic, Horst Puschmann.

Abstracts Team (Rutherford Appleton Laboratory)
Chick Wilson, Kenneth Shankland, Tony Csoka.

Webmaster Adrian Lapthorn (University of Glasgow)

International Programme Committee

J.A.K. Howard, Chair (UK)
Y. Amemiya (Japan)
E. Antipov (Russia)
P.E. Bourne (USA)
C.P. Brock (USA)
D.L. Dorset (USA)
R. Feidenhans'l (Denmark)
C.J. Gilmore (UK)
A. Katrusiak (Poland)
C. Kruger (Germany)
L.B. McCusker (Switzerland)
K. Lal (India)
G. Oliva (Brazil)
J.L. Smith (USA)
M.A. Spackman (Australia)
J.W. White (Australia)
A. Yonath (Israel)
Ex officio:
W.L. Duax (USA)
M. Kaftory (Israel)
Co-opted:
P.M.D. Fitzgerald (USA)
A.M. Glazer (UK)

Organising Committee

Chris Gilmore, Chair (University of Glasgow)
Frank Allen (CCDC)
Colin Carlile (CLRC, RAL)
Bob Cernik (CLRC, DL)
Bill David (CLRC, RAL)
Andy Freer (University of Glasgow)
Mike Glazer (University of Oxford)
Bob Gould (University of Edinburgh)
Sheila Gould (Beevers Miniature Models)
John Helliwell (University of Manchester)
Judith Howard (University of Durham)
Adrian Lapthorn (University of Glasgow)
Steve Maginn (CCDC)
Ljubica Manojlovic-Muir (University of Glasgow)
Kenneth Muir (University of Glasgow)
Kenneth Shankland (CLRC, RAL)
Norman Shankland (University of Strathclyde)
David Watkin (University of Oxford)
Chick Wilson (CLRC, RAL)
Gill Houston (Northern Networking)

Abstract Book Editors
C.C. Wilson, K. Shankland and T. Csoka

Abstract CD-ROM Production
C.J. Gilmore, S. Mackay and G. Barr

SPONSORS

The Congress acknowledges with gratitude its many sponsors:

Gold Sponsors

3-Dimensional Pharmaceuticals Inc.
Arnold Clark Ltd.
British Crystallographic Association
Bruker AXS GmbH
Cambridge Crystallographic Data Centre
CCP4
CINP Glasgow 1998 Ltd.
Clariant Pigments Technology Research
Compaq
Department of Chemistry, University of Glasgow
Department of Pharmaceutical Sciences, University of Strathclyde
Glasgow City Council
Glasgow Development Agency
Greater Glasgow and Clyde Valley Tourist Board
International Union of Crystallography
Marks and Spencer
Microsource, a Division of Bede
NASA
National Institute of Standards and Technology
Nature
Nature Structural Biology
Nonius BV
Oxford Cryosystems
Philips Analytical
Rigaku
Stoe & Cie GmbH
The Royal Society
Tripos Inc.
Unilever Research
University of Glasgow

Silver Sponsors

AstraZenneca
Charles Supper Company
DuPont Pharmaceuticals Company
Glasgow Museums
International Center for Diffraction Data
Pfizer Central Research
SmithKline Beecham Pharmaceuticals
University of Strathclyde

CONTENTS

The abstracts are numbered by microsymposium and by category. Contributed posters submitted for microsymposia sessions are included with the abstracts for that microsymposium. Other contributed posters are listed under a general category (01-27). Each category has a collection of sub-categories, and while the abstract numbering scheme does not retain these, abstracts on similar topics have been kept together as far as possible, within the constraints of the complexity of the programme and the space limitations in the poster sessions.

KEYNOTE LECTURES

MICROSYMPOSIA

CATEGORIES

KEY TO THE ABSTRACT CODE NUMBERS

The abstract code numbers are constructed as follows:

[1] An initial letter indicating the presentation type:

K = Keynote Lecture
M = Microsymposium Oral Presentation
P = Poster Presentation
C = Open Commission Meeting
JMR = Monteath-Robertson Symposium

[2] Two digits indicating the date in August when the presentation is scheduled.

[3] Two digits equating to a particular session or category.

This code is either the last two digits of the Microsymposium session
OR
The Main Category code.

[4] Three digits indicating the sequence number of:

A talk within a Microsymposium session
OR
A poster within a group of related posters.

For example:

P05.OC.xxx would represent a poster presented on August 5th as part of the Microsymposium 05OC "Physical Properties and Structural Relationships",

while:

P11.05.xxx would represent a poster presented on August 5th in Category 04 "Crystallography of Biological Macromolecules",

and:

M05.DD.xxx would represent a talk delivered on August 5th in the Microsymposium 05DD "Optimisation Methods"

whereas:

C08.JR.xxx would represent a talk delivered on August 8th in the Open Commission Meeting for Journals.

KEYNOTE LECTURES

K05.01.001 CRYSTALLOGRAPHIC ASPECTS OF FERROELECTRIC THIN-FILM MEMORIES. J. F. Scott, School of Physics, University of New South Wales, Sydney 2052, Australia

Ferroelectric thin films are being utilized as capacitors in dynamic random access memories (DRAMs), where their large dielectric permittivities permit a size reduction of x100 compared with silicon dioxide, and as the memory elements themselves in non-volatile RAMs, where the plus and minus polarization states record "1" or "0" in the Boolean algebra of digital computers. This talk reviews subtle aspects of crystal structure in the thin films, and the relationship between electrical performance (leakage current, breakdown fields, switching time) and that structure. Emphasis is placed upon lead zirconate titanate (PZT), barium strontium titanate (BST), and strontium bismuth tantalate-niobate (SBT). Processing of these materials goes through intermediate phases (pyrochlore and defect-fluorite), and EXAFS data from Tsukuba are used to elucidate the latter.

K05.02.001 NUCLEOSOMES. Timothy J. Richmond, ETH Zürich, Institut für Molekularbiologie und Biophysik, ETH-Hönggerberg, CH-8093, Switzerland.

The nucleosome is the universal, repeating element of chromatin and responsible for the two most fundamental levels of DNA organisation within the eukaryotic cell nucleus. The DNA packaging it provides represses gene transcription generally while being intimately involved in gene-specific activation through reversible modification (e.g. acetylation) and major structural alteration (i.e. chromatin remodelling). The nucleosome core particle comprises an octameric protein assembly containing two copies of each of the four core histones, H2A, H2B, H3, and H4, and a roughly equal mass of DNA in 147 bp. Compared to the nucleosome, the core lacks only the relatively short linker DNA connecting nucleosomes and its associated histone H1. The X-ray crystal structure of the nucleosome core particle provides substantial insight into chromatin structure-function relationships, as will be presented. In addition to the protein and DNA components first seen at 2.8 Å resolution1, the atomic structure refined using data to 2.0 Å permits the reliable location of nearly 1,000 water molecules and ions in the electron density map. Comparison of high resolution structures incorporating different DNA sequences reveals the general similarity of DNA conformation imposed by the histone octamer.

1. K. Luger, A. W. Mäder, R. K. Richmond, D. F. Sargent and T. J. Richmond (1997). Crystal Structure of the Nucleosome Core Particle at 2.8 Å Resolution. Nature, 389, 251-260.

K05.03.001 SOLID-STATE REACTIONS. E.V. Boldyreva, Institute of Solid State Chemistry and Mechanochemistry SB RAS, Kutateladze, 18, Novosibirsk, 128, 630128 Russia, email elena@solid.nsk.su.

Several aspects of the interrelations between the structures of crystals and their chemical reactivity are considered and various possibilities of applying crystallography to studying solid-state reactivity are discussed. The main emphasis is made on the following topics:

- solution and solid-state reactions: what is common and what is different;
- the interplay between *intra*- and *inter*molecular interactions in reactions in molecular solids;
- cooperative effects in solid-state reactivity;
- the role of stresses, strain and structural relaxation in solid-state reactions;
- possible applications of variable-temperature and high-pressure crystallography to studying solid-state reactivity;
- inorganic and organic solid-state reactions: what is common and what is different.

K05.04.001 MOLECULAR MECHANISM OF MUSCLE CONTRACTION. K.C. Holmes, Dept. of Biophysics, Max Planck Institute for Medical Research, Jahnstrasse 29, 69120 Heidelberg, Germany

Muscle contains two sets of intedigitating filaments (thick and thin) containing the proteins myosin and actin. The filaments move past each other through the cyclical interaction of the myosin "cross-bridges" with the actin (thin) filaments. Concomitantly, ATP is hydrolyzed. Crystallographic studies have revealed two conformers of the cross bridge, OPEN and CLOSED. Initially, Rayment et al. showed the myosin cross bridge to be pear-shaped, with an elongated head (known as the "motor domain") consisting of a 7-stranded β sheet and a C-terminal neck (or "lever arm"). There is a deep cleft extending from the nucleotide binding site to the actin binding site. The active site, which contains a P-loop and switch 1 and switch 2 regions similar to those found in the G-proteins is relatively OPEN. The C-terminal neck which connects to the thick filament, forms an extended a-helix which binds two calmodulin-like "light chains". The neck is joined onto the motor-domain via a small compact domain called the "converter". EM studies of the actin-myosin complex show that the neck can function as a lever arm. More recent crystallographic studies by Rayment's group using a truncated form of the cross-bridge without the neck but with a number of nucleotide analogues bound in the active site reveal a second conformation of myosin differing in the position of the switch 2 region. This movement closes the active site around the γ-phosphate. It is coupled with a large movement of the converter domain (a 60° rotation). We have also obtained this structure but with ADP.BeF3 in the active site. Carolyn Cohen's group have now shown that this CLOSED conformation can be also be obtained with the neck present. Comparing the two myosin structures shows that the distal end of the neck (as seen from actin in the actin-myosin complex) would move about 11.0nm along the actin filament in response to the opening and closing of the active site. Myosin appears to transport actin by switching between these two states. In the CLOSED form the neck or lever arm is at the beginning of its stroke whereas in the OPEN form it is at the end of the stroke. The transition CLOSED to OPEN enables release of the γ-phsphate which drives the reaction. The preference for OPEN or CLOSED is also controlled actin binding probably via the cleft by a mechanism yet to be discovered.

For references see http://lala.mpimf-heidelberg.mpg.de/~holmes/muscle_refs/

K06.01.001 THE IMPACT OF POWDER DIFFRACTION ON MATERIALS SCIENCE. D. E. Cox, Physics Department, Brookhaven National Laboratory, Upton, NY 11973, USA.

In the past two decades, materials science has evolved into a scientific discipline in its own right, while still retaining a very close interdisciplinary relationship with the more traditional areas of condensed matter physics and chemistry, engineering, metallurgy, ceramics and, more recently, biological and environmental sciences. Typical stages in materials research are synthesis and processing, characterization of structure and

properties, advanced development aimed at optimization of the desired property, and integration into some sort of product or process. Laboratory powder diffraction techniques play a major role during the synthesis stage, providing vital feedback about the phase equilibria and reaction kinetics, and frequently enabling novel phases to be identified, a procedure which nowadays is greatly facilitated by the availability of extensive data bases and powerful search-and-match software. Powder diffraction is also widely used for the characterization of structures and structure-property relationships, and in many cases during the optimization stage. In this context, high-resolution synchrotron x-ray and neutron techniques enable information about structure and microstructure to be obtained at hitherto unattainable levels of detail, and are playing an increasingly important role in materials research.

Powder diffraction has made a very significant impact in a great many areas of materials science, especially in the more basic aspects of this research. The list includes high Tc superconductors, magnetic materials, ferro- and piezoelectrics, electro-optic materials, battery electrodes, hydrogen storage, ceramics, catalysts and molecular sieves, polymers and biominerals, and two recent additions; colossal magnetoresistive materials and novel thermoelectrics. A few examples will be discussed in detail to illustrate the role played by powder diffraction.

Work supported by the U.S. Department of Energy, Division of Materials Sciences, under contract DE-AC02-98CH10886.

K06.02.001 MEMBRANE PROTEIN STRUCTURE, AN EXCITING FRONTIER. Johann Deisenhofer, Howard Hughes Medical Institute, University of Texas Southwestern Medical Center, Dallas, Texas 75235-9050, USA

New three-dimensional structures of integral membrane proteins have appeared at a very low rate, indicating that this class of proteins has remained a major challenge for structural biologists. Obviously, the biological importance of membrane proteins demands that we do better. I will briefly discuss the main technical obstacles and attempts at finding ways to overcome them. I will also give an overview of recent significant progress.

K06.03.001 X-RAY STANDING WAVE TECHNIQUE - STRUCTURE-SENSITIVE SURFACE SPECTROSCOPY. M.V.Kovalchuk, Institute of Crystallography RAS, Leninsky pr. 59, 117333 Moscow, Russia

When X-ray irradiates condensed matters we register either elastic reflected beam (diffraction) or yield of secondary (non-elastic) radiations (photo- and Auger-electrons, characteristics fluorescence, etc.), these data provide spectral surface information (spectroscopy). X-ray diffraction methods possessing unique structural sensitivity, in standard geometry provide information only for rather large volumes of studied sample and do not permit to check structural position of concrete atoms and individual sublattices. Spectroscopy studies which permit to study composition and electron properties of surface and of thin layers due to small escape depth of secondary radiations yield, never provide information on structural position of the atom, secondary radiation of which we measure. X-ray standing wave method combines these two approach advantages. Spectroscopy methods obtain structural sensitivity and X-ray diffraction methods obtain surface sensitivity with spectral selectivity. Report concerns physical basis of X-ray standing wave method: formation and behavior of interference wave fields in various condensed matters for various geometry of scattering and diffraction. Report describes various ways to generate X-ray standing wave field of practically any period (from tenth parts of angstrom up to thousand of microns) are studied, they are based on application of two- and multi beam diffraction, total external reflection, wave-guide structures, multi layered synthetic microstructures. Possibilities of method are demonstrated by experiments made at both standard X-ray sources and with SR application.

K06.04.001 CRYO-ELECTRON MICROSCOPY OF SINGLE PARTICLES: THE STRUCTURE OF THE *E.COLI* RIBOSOME. M. van Heel[1], H. Stark[2], A. Patwardhan[1], R. Matadeen[1], E.V. Orlova[1], T. Pape[1], B. Gowen[1], M. Rodnina[3], R. Brimacombe[4], W. Wintermeyer[3]. [1] Imperial College, Department of Biochemistry, London SW7 2AY, UK. [2] Institut für Molekularbiologie und Tumorforschung, Emil-Mannkopff. Str. 2, D-35037 Marburg, Germany. [3] Institut für Molekularbiologie, Universität Witten, D-58448 Witten, Germany. [4] Max-Planck-Institut für Molekulare Genetik, D-14195 Berlin, Germany.

Electron microscopy of individual non-crystallized macromolecules (single particles) is a very rapid technique for probing the three-dimensional (3D) structure of biological macromolecules. By exploiting the different orientations of the macromolecules in the embedding medium, one may extract 3D information from the data without ever collecting tilt series in the microscope.

The ribosome can be blocked in different phases of the elongation cycle by antibiotic interaction; tRNAs or elongation factors (EF-Tu, EF-G) can be bound to their respective binding sites on the ribosome. Thus many functional states of the ribosome which are only milliseconds apart from each other within the functional time scale can be studied. Recently, the structures of the *E.coli* 70S ribosome in their pre- and post-translocational states have been solved at a level of ~20Å and the positions of the tRNA molecules have been visualised and clearly identified. The structure of the kirromucin-stalled ribosome has also been determined to a resolution of 18Å and has now been refined to 13Å. The analysis of these structures is necessary in order to gain structural insight into protein synthesis, which is of immense importance for the understanding of ribosomal function at the molecular level.

K07.01.001 POLYMORPHISM: THE SAME YET DIFFERENT. Jack D. Dunitz, Organic Chemistry Laboratory, Swiss Federal Institute of Technology, ETH-Zentrum, CH-8092 Zurich, Switzerland.

Polymorphism is the ability of a compound to crystallise in more than one distinct crystal structure. Once regarded as something of a rarity, it is now known to occur extensively, and possibly even ubiquitously. Polymorphs can differ markedly in physical properties — solubility, colour, hardness, etc. — but they differ only slightly in thermodynamic stability. Relative stabilities involve both enthalpic and entropic contributions to the Gibbs free energy and are thus temperature and pressure dependent. For organic crystals, where intermolecular interactions are weak, lattice energy calculations for "virtual" crystal structures of a given compound suggest that many polymorphs may be possible within a narrow energy window. This is one of the factors that makes crystal structure prediction so precarious. Moreover, the crystallization process is not under thermodynamic control, so the polymorph obtained by crystallization from the melt or from solution is not necessarily the most stable one under the given conditions. Transformation to the stable form may occur spontaneously or may be extremely slow, depending on the presence of seeds or crystal defects. The nucleation step is presumably rate limiting but there is at present no general theory of this process.

K07.02.001 X-RAY IMAGING: FROM AMPLITUDE TO PHASE. W. Thomlinson, European Synchrotron Radiation Facility, BP 220, F-38043 Grenoble, France.

Mammography, like all standard medical x-ray imaging technologies, relies primarily on the amplitude properties of x-rays, and does not depend on the phase. This is unchanged since the discovery by Roentgen that the intensity of an x-ray beam, as measured by the exposure on a film, was related to the relative transmission properties of an object. However, various imaging techniques have emerged which depend on the phase of the x-rays as well as the amplitude. Phase becomes important when the beam is coherent and the imaging system is sensitive to interference phenomena. Significant new advances have been made which now promise phase information in medical imaging.

The development of perfect crystal optics and the increasing availability of synchrotron radiation facilities have contributed to a significant increase in the application of phase based imaging in materials and life sciences. Topography has become a significant research and development tool, phase contrast imaging has been applied in both projection and computed tomography modes, and recent applications have been made in the field of medical imaging. A new application to mammography is based on a combination of phase and amplitude information. It has been called Phase Radiography [1] and Diffraction Enhanced Imaging [2]. These applications are significant in the field of medicine because they are applied to highly absorbing systems such as those presented in mammography.

This talk will present a look at the various amplitude and phase dependent imaging techniques, and conclude with a presentation of recent work on Diffraction Enhanced Imaging applied to mammography.

1. V. Ingal, E. Beliaevskaya, et al., Phys. Med. Biol. 43 (1998) 2555.
2. D. Chapman, W. Thomlinson, et al., Phys. Med. Biol. (1997) 2015.

K07.03.001 DIFFUSE SCATTERING. T.R. Welberry, Research School of Chemistry, A.N.U, Canberra, ACT 0200, Australia

Conventional crystal structure analysis of disordered materials using Bragg diffraction data reveals only average one-body structural information, such as atomic positions, thermal ellipsoids and site occupancies. Diffuse scattering, on the other hand, gives two-body information and is thus potentially a rich source of information on how atoms and molecules interact with each other. However, although the presence of diffuse scattering has been known since the earliest days of X-ray crystallography, extracting such information from it is still a far from routine process and quantitative studies are rare. One of the reasons for this has certainly been, until relatively recently, that the intensity levels of diffuse scattering are typically several orders of magnitude lower than for the Bragg peaks, making measurement both difficult and time-consuming. Modern developments in X-ray sources (synchrotrons) and detectors (linear-detectors, area-detectors, image plates) have enormously increased the capability for measuring such weak data and this aspect of the field of study, though still presenting challenges, is no longer the limiting factor.

The greater challenges occur in the interpretation and analysis of diffuse scattering. Traditional approaches, developed largely in the field of alloys and simple oxides, present insurmountable difficulties when systems become more complex or when the magnitudes of atomic displacements become relatively large. More recently, progress has been made in an alternative approach to understanding the local atomic and molecular arrangements in disordered materials, which overcomes some of these difficulties[1]. The method consists of comparing diffraction patterns calculated from a computer model of the disordered structure with measured X-ray diffuse intensities. The advantage of the method is that it can be applied generally to all systems regardless of their complexity or the size of the atomic displacements that might be present. The computer models are generated using real-space Monte Carlo methods which employ near-neighbour effective interactions. The only requirement is the specification of the model in terms of sufficiently few parameters which nevertheless adequately describe the local physics and chemistry.

[1] T.R.Welberry & Th. Proffen (1998), Acta Cryst., A54, 661-674.

K07.04.001 CHAPERONIN ASSISTED PROTEIN FOLDING; THE FINAL STEP IN GENETIC EXPRESSION. Paul B. Sigler, Zhaohui Xu and Lingling Chen HHMI, Yale University, 260 Whitney Ave., MB&B Dept., New Haven, CT 06511

The transmission of information from the gene to its functional protein product involves two template guided polymerization steps followed by a spontaneous folding/assembly process. To achieve the accuracy and rates required to sustain life, the polymerization steps require proofreading and editing mechanisms to mitigate unavoidably high error rates. The energy for these error-correcting steps is supplied by nucleoside triphosphates.

Molecular chaperonins proofread and edit the final step in gene expression, protein folding. The lethality of defective chaperonin mutants indicates that this ATP-driven process is required in all cells as well as in protein synthesizing inclusions (chloroplasts and mitochondria). X-ray crystallographic structure analysis and functional studies of the bacterial chaperonin GroEL/GroES in various stages of its functional cycle have illuminated a remarkable "two-stroke engine" mechanism by which non-native peptides are entrapped, unfolded, refolded in a shielded environment and finally expelled. It is now clear how large allosteric changes within a obligatory double ring structure [seven subunits (eight in archaea and eukaryotes) per ring] execute cycles of peptide binding/folding/release with the quantized consumption of seven ATP molecules per cycle. The mechanism by which such a wide range of misfolded proteins are serviced by GroEL is revealed by recent work that shows oligopeptide segments with different sequences bound firmly with similar conformations to the same GroEL surfaces.

K08.01.001 CRYSTALLOGRAPHY AND THE LITHIUM-ION BATTERY. Josh Thomas, Inorganic Chemistry, Angstrom Laboratory, Uppsala University, Box 538, SE-751 21 Uppsala, SWEDEN.

One of the great technological success stories of recent years has been the Li-ion (and more recently the Li-ion polymer) battery, which is now capturing an ever-increasing fraction of the low-power battery market, especially in the cellular 'phone and lap-top sectors. By the same account, it can be stated that crystallography has indeed played a major role in this development, providing a solid basis for understanding and informed materials engineering in all parts of the battery. This will be illustrated here through a number examples taken from a current standard battery configuration: < graphite anode | polymer electrolyte | transition-metal oxide cathode >. A hallmark of much of the crystallographic work in the development of *electrode materials* has been the incisive use if *in situ* XRD and ND techniques in which the structural changes associated with lithium-ion insertion and extraction processes underlying electrochemical activity have been followed during cell cycling to acquire an intimitate sense of how best to modify structure to optimize cell performance. Such information has been combine with "battery engineering" type data describing the morphology of the composite electrodes (particle-size distribution, choice of

lithium salt, geometrical factors, etc.) to provide a holistic picture of cell function. At a more fundamental level, single-crystal electron density studies have also provided new insights into the subtle mech-anistic detail of redox processes related to lithium-ion insertion/extraction in transition-metal oxide systems. Perhaps somewhat surprisingly, crystallo-graphy has also been shown to play a most valuable - not to say decisive - role in the understanding of lithium-ion transport mechanisms in the *polymer electrolyte* : an impressive series of essentially X-ray "powder" diffraction studies of the system LiX.PEOn [PEO = poly(ethylene oxide)] has provided critical structural information relating to the local environment around the Li-cation and X-anion in a solid polymer electrolyte context. It is clear that the PEO backbone is able to take up a multitude of local conformations to accommodate both free ions and ion-pairs, as are known to occur in the more ionically conducting amorphous LiX.PEOn systems.

K08.02.001 SMALL RIBOZYME STRUCTURE AND MECHANISM. David B. McKay and Joseph E. Wedekind, Department of Structural Biology, Stanford University, Stanford, CA, 94305-5126, USA.

Several small ribozymes (RNA enzymes) which catalyze cleavage of phosphodiester bonds are known. Earlier crystallographic studies on the hammerhead ribozyme revealed a simple tertiary fold for the molecule, but failed to explain the mechanism of catalysis; significant conformational rearrangements of the observed structure must be required to reach the catalytic transition state [1,2]. More recently, we have solved the structure of a “leadzyme”, a Pb^{2+}-dependent ribozyme derived from *in vitro* selection experiments, at 2.7 Å resolution [3]. The crystallographic asymmetric unit accomodates two leadzyme molecules in different conformations, with different metal binding properties. These structures suggest a model for bond cleavage which incorporates both the metal binding properties and the apparent flexibility of the cleavage site of the leadzyme molecule.

1. H.W.Pley, K.M.Flaherty & D.B. McKay (1994). Nature **372**, 68.
2. D.B. McKay (1996) RNA **2**, 395.
3. J.E. Wedekind & D.B. McKay (1999). Nature Struct. Biol., in press.

K08.03.001 WATER STRUCTURES IN ICES AND CLATHRATES: THEME AND PRESSURE VARIATIONS. W.F.Kuhs and F. Gotthardt, MKI Universität Göttingen, Goldschmidstr.1, 37077 Göttingen, Germany, and C.Lobban and J.L.Finney, University College of London, Department of Physics and Astronomy, Gower Street, London WC1E 6BT, UK.

Both water ices and clathrate hydrates consist of three-dimensionally connected assemblies of H-bonded water molecules. Beside two distinct amorphous phases of water, at least thirteen different phases of ice and at least eleven different topologies of clathrate hydrates are known; some of these phases were only very recently identified. The richness of the phase diagram is mainly developed along the pressure axis in p-T-space. Detailed in-situ crystallographic studies on most of these phases have certainly confirmed the theme of tetrahedrality in H-bonded networks of water molecules. This theme, however, is modified in a multitude of variations which very nicely clarify the role of non-H-bonded water-water interactions. The variations of H-bond topologies and (partial) proton ordering indicate that there is a very delicate balance between enthalpic and entropic contributions to the free energy, with the appearance of a number of metastable crystalline phases especially in the pressure range between 0.3 and 1 GPa. Understanding this part of the phase diagram is one of the best possible tests for current models of water-water interactions.

K08.04.001 PROTEIN STRUCTURE MODELING IN THE ERA OF STRUCTURAL GENOMICS. John Moult, CARB, University of Maryland Biotechnology Institute, 9600 Gudelsky Drive, Rockville, MD 20850, USA

The prediction of the tertiary structure of protein molecules from amino sequence information has been a goal of computational biology for more than thirty years. Although we are still not able to compete with experiment, the field has advanced to the point where useful models can be obtained for many proteins. Three large scale, community wide experiments - known as CASP - have now been run to assess what can be done, and what the barriers are to doing more. The results of these experiments will be discussed, focusing on what has been learned about the nature of the problem, what the prospects are for finding universal solutions, and what role structure prediction can play in the era of structural genomics.

K09.01.001 SOLID STATE NMR AS A COMPLEMENTARY TECHNIQUE TO X-RAY DIFFRACTION. Colin A. Fyfe, Department of Chemistry, University of British Columbia, Vancouver, BC, Canada

Solid state NMR and x-ray diffraction have a basic complementary relationship: the former is sensitive to short range effects including ordering while the latter is sensitive to long range orderings and periodicities. In addition, the different time scales of the two experiments means that NMR can provide information on a variety of motions in the solid state not detectable by diffraction experiments giving an additional dimension to the 'structure'. In this lecture, we will review some of the relevant background to solid state NMR and then explore its application firstly to the investigation of various motional processes and subsequently in providing additional information in cases where diffraction studies are incomplete, for example where disorder exists. Lastly, we will describe its use in providing local structural information to aid in the refinement of powder data, including the application of the direct method approach.

K09.02.001 CHARGE DENSITY ANALYSIS AND BOND CHARACTERIZATION OF 3d-TRANSITION METAL COMPLEXES. Yu Wang, Department of Chemistry, National Taiwan University, Taipei, Taiwan ROC

Chemical bond, which makes molecules from independent atoms, is a very important concept in understanding the molecular behavior. Bond characterization is therefore becoming ever needed for predicting the physical and chemical properties of the molecule. The combined quantum mechanical calculation and accurate X-ray crystallography studies are extremely useful for characterizing the chemical bond precisely. Charge density analyses have been applied in terms of deformation density distribution, natural bond orbital analysis and the topological analysis on the total electron density. These analyses provide not only the molecular electron density distribution, but also the information such as bond order, bond type and atom domain in molecule. The complexity of the 3d orbital splitting subjected in the ligand field is well known, this makes the bonding characterization of 3d-transition metal complexes interesting and challenging. Charge density analysis on quite a few such complexes will be discussed systematically. Detail characterization of metal-ligand as well as intra-ligand bond will be described. The valence shell charge concentration (VSCC) of the third quantum shell around the metal ion will be demonstrated by the Laplacian topology, which provides the physical basis for the Lewis model and VSEPR. The great recent advance both in experiment and in theory has made the charge density analysis accessible to even more complicated system, for example, the molecule in its excited or metastable states.

K09.03.001 CRYSTALLOGRAPHY AND NONLINEAR OPTICS. Pamela Thomas, Department of Physics, University of Warwick, Coventry CV4 7AL, UK

Many of the most important materials used in the field of nonlinear optics are single crystals, either organic or inorganic. Therefore, the science of Crystallography has a vital contribution to make to this technologically-valuable field. The emphasis of the talk will be on the important role that an understanding of the crystal structures and physical properties plays in underpinning the device technologies based on these materials.

This talk will focus principally on the crystallography of inorganic crystals used for nonlinear optics. Following a brief review of the basic physics of nonlinear optics and the different types of non-centrosymmetric crystal structure that show significant nonlinear optical properties, the main body of the talk will deal with ferroelectric oxides, such as crystals of the $KTiOPO_4$ (KTP) family and $LiNbO_3$ (LN), which are under extensive research for the production of new optical devices in optics laboratories around the world. A review of many investigations of structure-property relationships in the KTP family, including optical and dielectric properties, structural pseudo-symmetry, twinning and disorder, and high- and low-temperature phase transitions, will be given. The technique of "periodic domain inversion" or "periodic-poling", by which a device architecture is created in a ferroelectric crystal by the introduction of an array of periodic inversion domains into the material, will be introduced and discussed with particular reference to LN and KTP. The role of high-resolution x-ray diffraction and x-ray imaging (including phase-contrast imaging) in characterizing periodically-poled arrays of inversion domains of periods 4-40 μm, will be demonstrated and the useful information concerning domain-wall width, for example, that can be extracted *via* such studies will be discussed. The talk will conclude with a look to the future for both Crystallography and crystals in the field of nonlinear optics.

K09.04.001 ACCURACY IN TRANSLATION: tRNA AND AMINO ACID RECOGNITION BY AMINOACYL-tRNA SYNTHETASES. S. Cusack, EMBL Grenoble Outstation, c/o ILL, 156X, 38042 Grenoble, FRANCE.

Similarities and differences in the modes of recognition of tRNAs and amino acids by their cognate aminoacyl-tRNA synthetases will be discussed with reference to crystal structures of substrate complexes of five Thermus thermophilus class II synthetases: seryl-, lysyl-, prolyl-, histidyl- and asparaginyl-tRNA synthetases.

The native ProRSTT structure has been determined at 2.4Å resolution and with proline bound, at 2.9Å resolution. Preliminary data on the complex of ProRSTT with cognate tRNA have been published at 3.5Å resolution [3]. New results on a ternary complex of ProRSTT with tRNApro and a prolyl-adenylate analogue at 2.85Å resolution will be presented. In addition a new structure of HisRSTT has been determined at 2.4Å resolution without any substrate bound whereas previously the structure was known with histidine and histidyl-adenylate bound [1]. The structure of AsnRS with an analogue of asparginyl-adenylate shows how discrimination between aspartic acid and asparagine is achieved [2].

These structures shed further light on (a) specific amino acid recognition (b) conformational changes associated with amino acid binding (c) the mechanism of amino acid activation (d) the mode of anti-codon recognition by the anti-codon binding domain in class IIa synthetases (e.g. ProRS) compared to class IIb synthetases (e.g. LysRS).

[1] A. Åberg, A. Yaremchuk, M. Tukalo, B. Rasmussen and S. Cusack, Biochemistry. 36, 3084-3094 (1997).
[2] Berthet-Colominas, C., Seignovert, L., Härtlein, M., Grotli, M., Cusack, S. and Leberman, R. EMBO J. 17, 2947-2960 (1998).
[3] Cusack, S., Yaremchuk, A, Krikliviy, I. and Tukalo, M. Structure 6, 101-108 (1998).

K11.01.001 STRUCTURE SOLUTION FROM POWDERS. C. Giacovazzo , A. Altomare, A. Guagliardi, A.G.G. Moliterni and R. Rizzi, Istituto di Ricerca per lo Sviluppo di Metodologie Cristallografiche, CNR, 70125 Bari, Italy, and G. Polidori, Dipartimento di Scienze della Terra, Università di Perugia, 06100 Perugia, Italy.

Crystal structure solution from powders data may play a central role in research and technology because it allows to investigate materials which are not available as a single crystal of adequate size and quality. Owing to the collapse of the three-dimensional lattice onto the 2Θ-axis the ab-initio crystal structure solution is still a challenge. The loss in the experimental information may be overcome by: better design of instruments (e.g., synchrotron radiation, time-of-flight technology at pulsed neutron sources, detectors,) improving the methods for the crystal structure solution (Direct Methods, maximum entropy-likelihood, MonteCarlo, simulated annealing, genetic algorithm, modelling of optimal crystal packing, …). Direct Methods are paying an essential role for enlarging the size of the structures solvable from powder data. The performances of the new version of the package EXPO [1] will be outlined, where use may be made of some prior information.

A. Altomare, M.C. Burla, B. Carrozzini, G. Cascarano, C. Giacovazzo, A. Guagliardi, A.G.G. Moliterni, G. Polidori, & R. Rizzi (1999). *J. Appl. Cryst*., **3**2. In Press.

K11.02.001 STRUCTURAL BASIS OF IMMUNE RECOGNITION. Ian A. Wilson, The Scripps Research Institute, Department of Molecular Biology, La Jolla, CA 92037 U.S.

The immune system combats invading microorganisms, such as viruses and bacteria, by neutralizing them directly or by killing infected cells. Antibodies, in the humoral system, have enormous genetic diversity that can be harnessed for high affinity recognition of a universe of antigens. In the cellular system, T cell receptors (TCR) have similar genetic diversity but bind their antigens with medium to low affinity to allow kinetic control of signaling events. The molecular basis of antigen recognition was initiated over 25 years ago due to the availability of soluble antibodies from multiple myelomas of mouse and human origin. Since then, over 100 structures of antibodies against small haptens, peptides, carbohydrates, and proteins have illustrated how this diversity can be sculpted onto a constant structural framework and has led to an understanding of antibody-antigen interactions, conformational changes in ligand recognition, design of therapeutics, and in the use of antibodies as catalysts. Structural studies of the cellular immune system have been more intractable, however, and only in the past decade or so have the crystal structures of MHC molecules and, more recently, T cell receptors (TCR) become available. Antigens are presented to the TCR as peptide fragments by MHC class I, and class II, or as glycolipids by non-classical MHC molecules, such as CD1. The crystal structures of single peptide-MHC complexes have illustrated how a myriad of peptide antigens can fit into the same MHC binding groove. In the past two years, T cell structure and TCR- MHC-peptide complexes have been made possible through protein engineering in order to express sufficient quantities of soluble material. I shall give an historical perspective on the structural studies of these immune proteins and then focus on our work on antipeptide, antisteroid, antiprotein and catalytic antibodies, various classical and nonclassical MHC molecules,

TCR and TCR-MHC complexes. These immunoprotein systems have contributed a wealth of data to our understanding of ligand-receptor interactions, protein engineering, enzyme catalysis, induced fit, glycoproteins, cell surface receptors and signal transduction.

K11.03.001 CRYSTALLOGRAPHY IN EXTREME CONDITIONS OF PRESSURE AND TEMPERATURE: MYTH OR REALITY? Daniel Häusermann, High Pressure Group, European Synchrotron Radiation Facility, Grenoble, France (now at the Geophysical Laboratory of the Carnegie Institution of Washington)

Considering that 99.9% of the known, non-gaseous, universe is under high pressure and non-ambient temperature, one can wonder why so many crystallographers work at 1 bar… Even in the case of bio-crystallographers, who may argue that 1 bar is the prevalent condition for life, one can advance arguments of pressure sterilization, virus destruction, enzyme deactivation, and maybe even studies of the origin of life using the pressure parameter. So now, can we argue to those convinced, that there is a world of crystallography to explore in conditions of extremes of pressure and temperature ? Looking at the progress made in the last few years, there are plenty of results that show that we are now able to perform complete structural studies of materials in extreme conditions of P and T, and this opens a whole new field of crystallography, and especially of applied crystallography. The availability of intensely bright monochromatic synchrotron radiation and of area detectors now allow the collection of data suitable for structural refinement in conditions fast approaching those prevailing at the center of the Earth. In less extreme conditions, larger samples allow structural studies and characterization of reaction kinetics in materials undergoing chemical synthesis. If to this we also add studies of liquid, and of course of melting, then we see that these new techniques can now be applied to a range of scientific problems spanning most fields of investigation covered today. Finally, one of the main concerns of crystallographers being sample 'quality', we must add that these techniques now also allow the characterization of this quality, as we can measure and even map, stress, strain, texture…

In this lecture we will review the progress which made such measurements possible, give an overview of the recent most exciting results, and demonstrate to the purists that even when we have to relax their 'R-factor' standards to enter the real world, we may still be doing crystallography…

K11.04.001 CRYSTAL STRUCTURE OF A HEPATITIS DELTA VIRUS RIBOZYME: CLUES TO RNA CATALYSIS. A.R. Ferre-D'Amare [1], K. Zhou [2], J.A. Doudna [1,2], [1] Dept. of Molecular Biophysics and Biochemistry, and [2] Howard Hughes Medical Institute, Yale University, New Haven, CT 06520

Hepatitis delta virus (HDV) contains a single-stranded circular RNA genome of 1700 nucleotides, and is coinfectious with Hepatitis B virus. Replication of the HDV genome by a rolling circle mechanism produces linear multimers of both genomic- and anti-genomic RNAs, both of which contain a self-cleaving activity that processes them to unit length. The activity has been mapped to a catalytic RNA, or ribozyme, domain whose function is required for HDV replication in vivo. To understand the catalytic mechanism of the HDV ribozyme, the crystal structure of the genomic sequence was solved at 2.3 Å resolution. The structure revealed a buried active site cleft reminiscent of protein enzymes. Key residues in the vicinity of the labile bond can now be tested for their role in catalysis. The delta ribozyme crystals were obtained by a new approach in which the ribozyme was engineered to bind to the small RNA binding domain of the U1A protein. Preliminary results suggest this may be a generally useful technique for growing high-quality crystals of other RNAs and solving their structures.

K12.01.001 COLOSSAL MAGNETO-RESISTANCE. Paolo G. Radaelli, ISIS Facility, CCLRC, Rutherford Appleton Laboratory, Chilton, Didcot, Oxon, OX11 0QX, UK.

Mn^{+3}/Mn^{+4} mixed-valence oxides (manganites) have been studied for the last fifty years, and represent a cornerstone in our general understanding of transition metal oxides. In the last five years, however, there has been a very significant and rapid surge of interest for these materials, reminiscent of what happened for copper oxides a decade ago. Three main classes of manganites have been intensively studied: the three-dimensional perovskites $A MnO_3$, the layered compounds of the so-called Ruddlesden-Popper series $A_{n+1}Mn_nO_{3n+1}$ and the cubic pyrochlore $Tl_2Mn_2O_7$. This research effort was prompted by the realisation that, in certain temperature ranges, the electrical resistivity of some manganites can be changed by several order of magnitudes in an applied magnetic field, a phenomenon now known as "colossal magneto-resistance" (CMR). CMR is a high-field effect and is therefore widely recognised not to be suitable *per se* for electronics or information-storage applications. Nevertheless, the peculiar electronic structure of CMR manganites can be exploited for devices such as spin valves. In addition to the interest for applications, manganites are studied for their extremely rich physics, which encompasses some of the most interesting phenomena in modern solid-state research: magneto-structural polarons, charge, orbital and magnetic ordering and phase segregation. Crystallographic techniques have given a paramount contribution to manganite research, mainly due to the large electron-lattice coupling. The initial emphasis on correlations between transport and average structural properties (bond lengths, bond angles, etc.) has gradually shifted towards more local structural phenomena, associated with the so-called Jahn-Teller polarons. Charge ordering and some of its more unusual manifestations like "stripes" continue to attract very significant attention. More recently, it has been recognised that the crystal and magnetic structure of some manganites may become intrinsically non-uniform, either dynamically or statically (phase segregation). Consequently, high-resolution diffraction may provide the next breakthrough in our understanding of manganite physics.

K12.02.001 ROLE AND PERSPECTIVES OF *AB-INITIO* MOLECULAR DYNAMICS IN CRYSTALLOGRAPHY. Michele Parrinello, Max-Planck-Institut fur Festkorperforschung, Heisenbergstr. I, D-70569 Stuttgart, Germany

Ab-initio molecular dynamics is a very powerful method for the study of the electronic, structural and dynamical properties of crystals with a very large number of atoms in their unit cell, without the restriction of symmetry or limiting assumptions such as harmonic approximation. If needed, the quantum mechanical behaviour of the nuclei can also be included. The development of ever less expensive and more powerful parallel computers and user-friendly software packages allow mote and more groups to harness the power of this method. We argue that the accuracy and predictive power of *ab-initio* molecular dynamics is such that it can and will be used in the routine refinement of crystal structures. Furthermore, the evolution of a crystal as a function of temperature, pressure and other thermodynamics fields can be investigated. In particular *ab-initio* molecular dynamics has the unique capability of describing the change in chemical bonding that is induced for instance by the application of an external pressure. We will illustrate with a selected number of examples the power of *ab-initio* molecular dynamics, indicate its present limitations and discuss the efforts currently being made to extend its scope.

K12.03.001 THE HIDDEN ORDER OF APERIODIC CRYSTALS. W. Steurer, Laboratory of Crystallography, Swiss Federal Institute of Technology, CH-8092 Zurich, Switzerland.

Aperiodicity and crystalline order - these two terms seem to exclude each other. Ideal translational symmetry is reflected in a reciprocal lattice with peaks (Bragg reflections) at the lattice nodes. Thus, a diffraction pattern with sharp Bragg reflections and no disorder diffuse scattering is characteristic for a perfect crystal such as silicon, for instance. Three reciprocal basis vectors are needed to index its diffraction pattern. Materials with an essentially discrete diffraction pattern which can be indexed with integers with more than three reciprocal basis vectors are called aperiodic crystals. They combine crystalline order in the n-dimensional parameter space with aperiodicity in the 3D physical space.

K12.04.001 STRUCTURAL GENOMICS OF A HYPERTHERMOPHILE: A FEASABILITY TEST. Sung-Hou Kim, Department of Chemistry and Lawrence Berkeley National Laboratory,University of California, Berkeley,CA USA.

Analysis of several genomic sequences indicates that no known biological functions can be assigned to a large fraction of the genes, thus, no assays can be devised to discover or test their functions. Structural biology can play an important role in the search for and the discovery of the functions of these genes. Since the biochemical function of a gene product is tightly coupled to its three-dimensional structure, finding the structure or its folding pattern may provide important insight into the biochemical function of the gene product, which, in turn, may help in understanding its cellular function. Thus, the structural study of genomic products, "structural genomics," may be an important foundation for the understanding of the biochemical and cellular functions of their products, "functional genomics." To test this hypothesis we have been studying the structures of three classes of gene products with unknown structures from a hyperthermophilic Archeon, methanococcus jannaschiia: (1) protein families whose biochemical and cellular functions are known, but their mechanisms are not known; (2) protein families whose cellular functions are known, but their biochemical functions are not known; (3) "hypothetical" protein families for which neither cellular nor biochemical functions are known.

K13.01.001 SUPRAMOLECULAR HYDRATES: HYDROPHILIC *versus* HYDROPHOBIC HYDRATION OF MOLECULES IN THE SOLIDS. Janusz Lipkowski, Institute of Physical Chemistry, Polish Academy of Sciences, Kasprzaka 44, 01 224 Warszawa, Poland

Interaction of water with hydrophobic moieties, and the supramolecular complexes thus formed, are of importance from the point of view of both complexation equilibria and transport properties in aqueous media.

In the crystal structures of supramolecular hydrates two different modes of hydration co-exist. These are: *hydrophilic hydration*, in which water is H-bonded either to, typically, oxygen or nitrogen atoms of the guest species and *hydrophobic hydration* in which water molecules *enclathrate* lipophilic parts of guest moieties.

Structural studies of interaction between water and hydrophobic species have revealed a fascinating variety of the guest-host architecture. Water molecules aggregate to form all possible structure types ranging from small water clusters through one-dimensional chains or two-dimensional layers to extended three-dimensional networks of zeolite or clathrate structural type. The formation of channel structures has also been found. Host component may bear electric charge when containing ionic species replacing water molecules in the host skeleton. The simplest pattern of this sort may be obtained with ionized water (H_3O^+ or OH^-) or halogenide anions substituting some of the water molecules.

The most intriguing factor stabilizing the structures is hydrophobic hydration. It consists of multimolecular combination of weak intermolecular interactions which apparently are the structure determining factor, however difficult to visualize. The guest species play the important role of stabilizing a host framework, thus serving as a *template* in the crystal structure formation.

The illustration part of the paper will consist, in its most part, of recently determined (and partly yet unpublished) crystal structures of hydrates of crown macrocycles and their complexes. By this way both hydrophobic and hydrophilic hydration patterns may easily be demonstrated just by chosing hydration of pure macrocycles, their molecular or acidic complexes. In the last case strong hydrophobic interactions eliminate clathration effects.

K13.02.001 NANOSECOND TIME-RESOLVED CRYSTALLOGRAPHY. Keith Moffat, Department of Biochemistry & Molecular Biology, and CARS, The University of Chicago, Chicago, Illinois, USA.

Mechanism in all chemical and biological reactions involves change in structure, not merely static structure; and these changes can occur very rapidly, from the time scales characteristic of inter-atomic vibrations (femtoseconds) to seconds. Structural reactions can be initiated in the molecules in a single crystal of excellent diffraction quality, for example by illuminating the crystal by a brief laser pulse. The reaction is then followed by the subsequent time-dependence of the intensities of all Laue spots and from them, the X-ray structure amplitudes. That is, the experiments are of the pump-probe variety. The techniques are now in place to conduct such experiments on biological crystals on the nanosecond time scale. Results will be described on heme proteins such as myoglobin and on the simple, bacterial, blue light photoreceptor known as photoactive yellow protein, PYP. PYP has recently been shown to be representative of the so-called PAS/LOV domain proteins which are extremely widely distributed, in numerous biological signalling roles. Thus, it may exemplify a general signalling domain that can respond to light, voltage and chemical signals, either alone or when associated with suitable ligands.

I thank our numerous collaborators, in Chicago, at the ESRF and in Amsterdam. Supported by NIH.

K13.03.001 FRONTIERS IN CHEMICAL CRYSTALLOGRAPHY. H.-B. Bürgi, Laboratory of Crystallography, University of Bern, Freiestr.3, CH-3012 BERN, Switzerland

With the availability of high brilliance radiation sources and fast area detectors, diffraction studies requiring many measurements over a range of temperature, pressure, electric field or photon flux have become quite feasible and provide new information not obtainable from a single measurement.

The temperature evolution of a crystal structure is discussed as an example. Temperature dependence of population parameters can be interpreted in terms of equilibrium constants and changes in enthalpy and entropy for a variety of simple chemical processes, including molecular reorientation, conformational changes, and proton or other atom transfers. The temperature evolution of anisotropic displacement parameters allows to distinguish motion from disorder, but also from systematic error, either in the experiment or in the structural model, and to extract correlations between atomic displacements and associated frequencies of motion. Diffraction experiments over a range of temperature are thus a potentially rich source of information on dynamic processes and disorder phenomena in

crystals. The information is relatively easy to obtain and extends the scope of crystal structure analysis.

K13.04.001 PICOSECOND X-RAY DIFFRACTION.
Justin Wark, Clarendon Laboratory, Department of Physics, University of Oxford, Parks Road, Oxford, OX1 3PU, UK.

The timescale necessary for the recording of X-ray diffraction signals from crystals has reduced spectacularly in recent years: from the several minute continuous exposures towards the beginning of the century, through the first millisecond work in the early 1940's, down to the present day, when we are finally accessing the sub-picosecond regime. Nanosecond and picosecond diffraction sources have been developed using a variety of different methods, including using single bunches of electrons in synchrotrons, X-ray diodes, and emission from laser-produced plasmas. Bright laser-plasma K-α X-ray sources with a few hundred femtoseconds duration have recently been demonstrated, following the development of table-top terawatt laser systems. The ability to record diffraction signals on such short timescales is extremely interesting, as it may allow the observation of electron density during chemical reactions – which has been dubbed "watching molecular movies". Femtosecond timescale X-ray pulses are also being developed utilising synchrotron technology. This talk will review the historical development of these sources, discuss prospects for the future, and outline some of the possible applications of X-ray diffraction on such short timescales.

MICROSYMPOSIA

05OA MACROMOLECULAR MACHINES AND ORGANELLES

M05.OA.001 ROTARY MECHANISM OF ATP SYNTHASE. John Walker, MRC Laboratory of Molecular Biology, Hills Road Cambridge CB2 2QH

ATP synthase is an asymmetrical structure that proceeds through a series of asymmetrical states in its reaction cycle. The high resolution structures of the ground state and of a transition state analogue of the catalytic F1 domain support this view.

M05.OA.002 A DETAILED VIEW OF THE GTPASE ACTIVATING REGION OF THE RIBOSOME: STRUCTURE OF THE L11/RNA COMPLEX. V. Ramakrishnan[1,2], Brian T. Wimberly[1], Rebecca Guymon[1], John P. McCutcheon[1], and Stephen W. White[3], [1]Department of Biochemistry, University of Utah School of Medicine, Salt Lake City, UT 84132, USA, [2]MRC Laboratory of Molecular Biology, Hills Road, Cambridge CB2 2QH, England, and [3]Department of Structural Biology, St. Jude Children's Research Hospital, Memphis, TN 38105 USA.

The ribosome stimulates GTPase activity in the translational elongation factors. The GTPase activating region of the ribosome consists of a highly conserved complex of a 58-nucleotide region of 23S ribosomal RNA and ribosomal protein L11. Here we report the crystal structure of the complex. The RNA folds into a highly compact globular domain consisting of both familiar and novel structural motifs, while protein L11 consists of a C-terminal domain that binds tightly to the RNA and an N-terminal domain that makes only limited contacts with RNA. The structure suggests that the L11 N-terminal domain might function as a switch, by reversibly associating with an adjacent conserved region of RNA. The sites of mutations conferring resistance to the antibiotics thiostrepton and micrococcin are clustered around a narrow cleft between the RNA and a proline-rich helix in the L11 N-terminal domain. The antibiotics are proposed to bind in this cleft, thereby locking the putative switch into a single conformation and altering GTPase activity by elongation factors.

M05.OA.003 A 5Å RESOLUTION X-RAY CRYSTALLOGRAPHIC MAP OF THE LARGE RIBOSOMAL SUBUNIT. Nenad Ban [1,3], Poul Nissen [1], Peter B. Moore [1,2] and Thomas A. Steitz [1,2,3], [1] Department of Molecular Biophysics & Biochemistry, Yale University, New Haven, CT, [2] Department of Chemistry, Yale University, New Haven, CT, [3] Howard Hughes Medical Institute, Yale University, New Haven, CT, USA

The 50S subunit of the ribosome catalyzes the peptidyl-transferase reaction of protein synthesis. We have generated an X-ray crystallographic electron density map of the large ribosomal subunit from *Haloarcula marismortui* at 5 A resolution using data from crystals that diffract to 3 A. Phasing at this resolution relied on data from four heavy atom derivatives improved by density modification procedures. Our map at this resolution shows clearly resolved density for each of the two strands of RNA in those regions that are duplex. There are higher density bumps corresponding to backbone phosphates. Density for numerous proteins can be readily distinguished from that for RNA. Many of the proteins are seen to be crosslinking two or three regions of RNA duplex, perhaps functioning as large molecular staples. Non- duplex regions of rRNA can be identified but are difficult to interpret at this resolution. Extension of phasing to 3 A resolution appears feasible.

M05.OA.004 APPROACHING ATOMIC RESOLUTION IN RIBOSOMAL CRYSTALLOGRAPHY. Ada Yonath, Struc. Biol., Weizmann Inst., Rehovot and Max-Planck Unit for ribosome struc., Hamburg

The translation of the genetic code into polypeptide chains is performed on riboprotein organelles called ribosomes. The ribosomes are built of two subunits which associate upon the initiation of protein biosynthesis. The small subunit (0.85 mD in prokaryotes) provides the sites for mRNA binding, decoding of the genetic information and the initiation of the process. The large subunit (1.45 mD) catalyzes the formation of the peptide bond and provides the progression path of the nascent proteins.

Crystals, diffracting to 3 resolution, were grown from small and large ribosomal subunits of Thermus thermophilus and Haloarcula marismortui, respectively. Data extending to 3.8-7.5 A resolution were collected at cryo temperature with bright synchrotron radiation from native and heavy atom derivatized crystals of both subunits. Each of the resulting MIRAS-phased electron density maps contains regions similar in shape to that observed for the corresponding ribosomal particle by EM reconstructions.

The regions assigned to the ribosomal particles contain the key internal features (e.g. the large subunit tunnel). Details of the map include two main types of density distributions: (a) elongate continuous regions spanning the particles at various directions and showing typical tertiary and secondary- structure features of RNA (single strands and well separated double helices); (b) globular and ellipsoidal regions of lower density, appropriate for the accommodation of ribosomal proteins, some of which show the main-chain folds observed in crystals of isolated ribosomal proteins. Tracing the RNA chains and assignment of the proteins are underway.

For unbiased map interpretation, heavy atom markers are being attached at selected sites on the ribosomal surface either prior or after crystallization. These led to the elucidation of the sites of a specific cysteine and of several surface RNA strands. Examination of the map of the small subunit indicated conformation resembling that observed within the cryo EM reconstructions of the entire ribosome. Consequently, crystals were grown from particles trapped at their activated conformation prior to crystallization, or reactivation was performed while in the crystals.

05OB PRESERVATION AND DECAY AT CRYO TEMPERATURES

M05.OB.001 MACROMOLECULAR CRYSTAL ANNEALING: OVERCOMING THE FEAR OF FLASHING. Gerard J. Bunick*#, Joel M. Harp#, David E. Timm+, and B. Leif Hanson#, *Life Sciences Division, Oak Ridge National Laboratory, Oak Ridge, TN 37831-8080, #The University of Tennessee/Oak Ridge Graduate Program in Genome Science and Technology, and +Department of Biochemistry and Molecular Biology, Indiana University School of Medicine, Indianapolis, IN 46202.

Macromolecular Crystal Annealing was discovered at Oak Ridge National Laboratory and first presented in 1997 at the American Crystallographic Association meeting in St. Louis, Missouri. The flash cooling of macromolecular crystals for x-ray data collection has many benefits as well as the disadvantage of dramatically increased mosaicity for some crystals. Macromolecular crystal annealing has been shown to significantly

reduce the mosaicity of flash-cooled crystals without affecting molecular structure. Improvements in diffraction resolution have been reported for some macromolecular crystals.

The annealing procedure consists of transferring a flash-cooled crystal to a droplet of its original cryoprotectant solution at ambient temperature for approximately three minutes followed by re-flash-cooling to cryogenic temperature. The annealing process has been applied to crystals of many different macromolecules grown from different precipitants and using a variety of cryoprotectants. The method also has been applied to restore diffraction from flash-cooled crystals that were inadvertently partially warmed during transfer to or from cryogenic storage, to crystals that iced during data collection, and to characterize crystal diffraction prior to heavy-atom soak experiments. The favored annealing procedure and several variants will be described. Results will be discussed in relation to crystal mosaicity and radiation damage in flash-cooled macromolecular crystals.

Research sponsored by the Office of Health & Environmental Research, U.S. Department of Energy, under contract No. DE-AC05-960R22464 with Lockheed Martin Energy Research Corp., NIH GM29818, and NASA.

M05.OB.002 CRYO MEASUREMENTS CONDUCTED AT HELIUM TEMPERATURE. P. Kuhn, S.M. Soltis, SSRL, Stanford University, Stanford, CA 94309, USA

The lifetimes of crystals exposed to high intensity x-ray beams from synchrotron sources are finite even when the sample is cryogenically cooled in a nitrogen gas stream. We attempted to perform a systematic study of crystal decay in the x-ray beam depending upon the cooling temperature and cooling rates as well as the incoming x-ray energy. A custom made open flow cryostat was used to cool the sample to temperatures between 45 K and 110 K. The analysis shows that decreased temperatures have only marginal effects on crystal lifetimes. These results are consistent with theoretical results presented earlier (E. Garman, BSR 1998, Argonne, USA). First results will also be presented on new data collection strategies to optimize crystal lifetime and, therefore, data quality.

M05.OB.003 RADIATION DAMAGE AND BEAM HEATING IN PROTEIN CRYSTALS AT CRYO-TEMPERATURES. Colin Nave, SRS Facility, CCLRC Daresbury Laboratory, Daresbury, Warrington WA4 4AD, UK

The wide adoption of cryo-cooling methods has proved to be of tremendous benefit in overcoming the effects of radiation damage during protein crystallography data collection. It is frequently possible to collect a number of high quality data sets from a single crystal without significant errors due to radiation damage. However, smaller crystals are being examined at cryo-temperatures on the most intense X-ray sources and, it is then not always possible to collect a complete data set from a single sample. This was predicted, as primary radiation damage still occurs at cryo-temperatures [1,2]. In addition, it has been found necessary to attenuate or defocus very intense beams, in order to maximise the amount of data that can be collected from a single crystal. This is possibly due to beam heating effects at high intensity.

An overview of the process of radiation damage and beam heating will be covered, together with calculations of these processes under typical conditions. Some suggestions for mitigating the effects will also be given.

1. Henderson, R. (1990). Proc. R. Soc. London Ser. B, 241, 6-8.
2. Gonzalez, A. & Nave, C. (1994). Acta Cryst. D50, 874-877.

M05.OB.004 STRUCTURE OF BOVINE HEART CYTOCHROME c OXIDASE AT CRYOGENIC. T. Tsukihara*, R. Nakashima%, E. Yamashita*, M. Yao*, T. Mizushima*, M. Odoko%, K. Shinzawa-Itoh%, & S. Yoshikawa%, *Institute for Protein Research, Osaka University, Yamada-oka, Suita, Osaka 565-0871, Japan, and %Department of Life Science, Himeji Institute of Technology, Kamigohri, Akoh, Hyogo 678-1201, Japan

Cytochrome c oxidase is the respiratory enzyme complex that is involved in dioxygen reduction coupled with proton pumping. The enzyme complex is consisting of two copies of 13 different subunits, two hemes, two copper centers, Mg, Na, Zn and phospholipids. Out of 13 subunits, 10 are transmembrane proteins, while three are extramembrane proteins.

The enzyme complex was crystallized by the batch method at 277 K from aqueous solution with nonionic detergent, 0.2 % decyl maltoside in 40 mM sodium phosphate buffer, pH 6.8, where the protein concentration was 9.0 % (w/v) and polyethylene glycol 4000 was used as the precipitant. Crystals were soaked in the glycerol solution prior to the cryogenic experiment. A crystal mounted with a fiber loop was frozen by dropping into liquid nitrogen.

X-ray diffraction experiment was carried out at BL41XU of the SPring-8 under the following conditions: temperature, 100 K by using Oxford Cryo-Cooling system; wave length, 0.708 A; crystal-to detector distance, 350 mm; detector, R-axis IV with 300 x 300 mm Imaging plates; oscillation angle, 0.65 degree; and exposure times, 78 or 117 seconds. Total of 429,322 independent reflections in the resolution range from 100.0 to 2.0 A were obtained from 3,685,319 observed reflections. R-merge was 7.7 %, and completeness, 95 %.

Electron density map at 2.0 A resolution showed up not only finer structures but also essential differences in comparison with 2.3 A analysis at room temperature.

M05.OB.005 CHANGES OF CELL DIMENSION DURING DATA COLLECTION OF A SINGLE VIRUS CRYSTAL. Lars Liljas[1,2], John Tate[1], Tianwei Lin[1], J.E. Johnson[1], [1]The Scripps Research Institute, La Jolla, California, USA, and [2]Department of Cell and Molecular Biology, Uppsala University, Uppsala.

A single, frozen crystal was used for data collection of cricket paralysis virus, an insect picorna-like virus. At data processing, it became evident that the data could not be scaled, and an analysis showed that early during the exposure, the crystal underwent a transition, corresponding to change in the c axis of 0.8 %. The crystal structure could be solved using the data collected after the transition. The atomic model built in electron density maps based on the "late" data could be used for phasing of a limited "early" data set to high resolution (2.4Å). Other problems in using cryo-temperatures for virus data collection will be discussed.

05OC PHYSICAL PROPERTIES AND STRUCTURAL RELATIONSHIPS

M05.OC.001 CMR MANGANITES: FROM THE CERAMICS TO THE THIN FILMS, B. Raveau, A. Maignan, C. Martin and M. Hervieu, Lab. CRISMAT (UMR CNRS 6508), ISMRA, 6 Bd du Maréchal Juin, 14050 Caen cedex France.

The manganites $Ln_{1-x}A_xMnO_3$ (A = Ca, Sr), with the perovskite structure form a large series of materials with colossal magnetoresistance (CMR) properties. The investigation of ceramics of these oxides allows two kinds of behaviors to be evidenced, depending on the sign of the carriers. In the hole doped

manganites the CMR effect results form a magnetic field induced transition from a paramagnetic insulating to ferromagnetic metallic state. In the electron doped manganites, the CMR effect originates from a competition between ferromagnetism and antiferromagnetism, in the vicinity of cluster glass region. Several factors are discussed, which govern the magnetotransport properties of these oxides : carrier concentration, average size of the A-site cation $\langle r_A \rangle$, and size mismatch σ^2. In those oxides, the magnetotransport properties are greatly affected by charge-ordering (CO) phenomena . The electron microscopy study of several series of compounds, shows that CO appears in the form of Mn^{3+} and Mn^{4+} stripes, distributed in a commensurate or incommensurate modulated way. The metastability of the CO state may be at the origin of the CMR effect in several materials. The destruction of the CO state and the appearance of CMR can be induced by a magnetic field but also by various radiations, and by Mn-site doping by chromium, cobalt and nickel.

The investigation of the thin film chemistry of the CMR manganites with the composition $La_{0.7}Sr_{0.3}MnO_3$, has allowed several superlattices to be synthesized using sequential laser ablation : X-ray diffraction high resolution electron microscopy studies show a perfect ordering of the layers "$LaMnO_3$" (LMO) and "$SrMnO_3$" (SMO) in the films. The study of the transport properties show that the SMO layers play the role of hole reservoir for the LMO layers. In the latter the holes are delocalized leading to CMR properties, with various characteristics depending on the nature of the superlattice.

M05.OC.002 RELATIONS BETWEEN STRUCTURE AND LITHIUM ELECTROCHEMICAL REACTIVITY IN VANADATES. S. Denis, E. Baudrin, S. Laruelle, M. Touboul and J-M. Tarascon, Laboratoire de Réactivité et de Chimie des Solides, 33 rue Saint-Leu, 80039 AMIENS, FRANCE.

Within the field of energy storage, vanadates have recently generated a new interest as these compounds were shown to be potential candidates for negative electrode material in Li-ion battery. Indeed, it was previously reported that such materials-based electrode display a large Li acceptance/removal at low voltage. For instance, crystallized $LiNiVO_4$, synthesized by the classical high temperature route can react with 7 lithium ions per formula unit when discharged to voltages lower than 0.2 V [1], leading to 800 - 900 mAh/g specific capacities, about twice greater than the actually used graphite electrodes. However, upon the first electrochemical discharge, it was noted that these materials tend to become amorphous. Therefore, our goal was to understand the lithium reaction mechanism within vanadates based on structural investigations.

For this purpose, we prepared different classes of vanadates based on monovalent, divalent and trivalent elements through a "chimie douce" method. Depending on the synthesis conditions, a large panel of compounds having different 3D packing of (VO_4), (VO_6) entities or differing in terms of long vs. local range order were obtained. An electrochemical investigation showed that all these materials, independently of their crystallization state tend to become amorphous upon the first discharge (ie: reduction), but their electrochemical performances are strongly dependent on both the water content and the nature of the counter-cation, which is directly involved in the lithium reaction process [2].

In order to explain the great acceptance of lithium ions within these materials, a structural investigation was undertaken during the first electrochemical cycle, by means of in-situ XRD, Mössbauer and XANES measurements. This study allowed us to propose a Li reaction mechanism different from the classical insertion/deinsertion process.

[1] C. Sigala, D. Guyomard, Y. Piffard and M. Tournoux, *C.R. Acad. Sci. Paris*, t. 320, Série IIb, 523 (1995).
[2] S. Denis, E. Baudrin, M. Touboul and J-M. Tarascon, *J. Electrochem. Soc*., 144 (12), 4099 (1997).

M05.OC.003 STRUCTURE AND ENERGETICS OF Li^+ DIFFUSION IN $Li_{0.5}CoO_2$ BY *AB INITIO* SIMULATIONS. M. Catti, Dipartimento di Scienza dei Materiali, Università di Milano II - Bicocca, via Cozzi 53, 20125 Milano, Italy.

The Li_xCoO_2 ($0 \le x \le 1$) system is well known, from *in situ* X-ray diffraction and electrochemical measurements, to intercalate Li^+ ions reversibly, providing thus a very important cathode material for rechargeable lithium batteries [1]. The structures of these phases are distortions of a FCC sublattice of O atoms, with alternating layers of Co and Li in octahedral holes, and partial occupancy of the Li sites according to the x value. For $x \approx 0.5$ the lattice is monoclinic, but no further structural details are available from the experiment. A theoretical study by *ab initio* quantum-mechanical methods has been undertaken, in order: (i) to predict the equilibrium crystal structure of the intermediate monoclinic $Li_{0.5}CoO_2$ phase; (ii) to determine the energy profile along the Li^+ diffusion path connecting octahedral and tetrahedral holes in the inter-layer region; (iii) to calculate activation energy values for the process of Li^+ transport within the structure. The method used is periodic Hartree-Fock supplemented by an *a posteriori* correction based on DFT (Density-Functional-Theory) estimate of electron correlation energy, such as implemented in the CRYSTAL code [2]. The results would indicate that, at equilibrium, lithium is slightly displaced from the centre of the octahedral hole, and attains a distorted pyramidal coordination consistent with *Pm* rather than *P2/m* symmetry. The computed energy profile of Li^+ along its diffusion path shows a saddle point corresponding to the tetrahedral hole, with a theoretical activation energy of 0.23 eV for oct.→tetr.→oct. hopping. The maximum of the energy curve occurs for direct jumps between adjacent tetrahedral sites, so that the diffusion path oct.→tetr.→tetr.→oct. is less favoured with $E_{act.} = 0.67$ eV.

1. J.N. Reimers & J.R. Dahn (1992). J. Electrochem. Soc., 139, 2091.
2. R. Dovesi *et al* (1998). CRYSTAL98 User's Manual, University of Torino.

M05.OC.004 EXPLORING ELECTROMECHANICAL COUPLING EFFECTS WITH RESONANT ULTRASOUND SPECTROSCOPY. J. Schreuer, E. Haussühl and W. Steurer, Laboratory of Crystallography, ETH Zürich, Sonneggstr. 5, CH-8092 Zürich, Switzerland

Employing the innovative technique of resonant ultrasound spectroscopy (RUS), we studied the elastic behaviour and electro-mechanical coupling phenomena of selected piezoelectric crystals such as $NaBrO_3$, α-quartz, $LiIO_3$ and $LiNbO_3$ between ambient temperature and 1400 K. Due to increasing electric conductivity most of the investigated crystal species show strong attenuation of their low-frequent electroelastic vibrations at elevated temperatures.

Our experimental set-up is based on the RUS-method [1] where the elastic constants are derived from an experimentally measured ultrasonic resonance spectrum of a free vibrating crystal with well defined shape. Advantages of this technique are (i) no medium is required for transducer sample-coupling, (ii) the small sample size and (iii) the short data acquisition time. The elasticity tensor is evaluated by an iterative non-linear least-squares procedure that matches observed and and calculated resonance frequencies by adjusting values for the elastic constants. The crucial step is the correct identification of observed modes. The eigenmodes correspond to stationary solutions of the Lagrangian which can be found by applying variational methods.

In the case of piezoelectric crystals the Lagrangian has to be extended by additional energy terms taking into account electro-mechanical coupling effects [2]. Usually the piezoelectric contribution to resonance frequencies is considerably larger than the experimental error. Thus, the RUS-method offers the unique possibility to study simultaneously the elastic, dielectric and piezoelectric properties of a crystal in a large temperature range.

[1] Ohno, I.: J. Phys. Earth **24** (1976) 355-379.
[2] Ohno, I.: Phys. Chem. Minerals **17** (1990) 371-378.

M05.OC.005 CATION ORDERING IN LAYERED BISMUTH OXIDE FERROELECTRICS. P. Lightfoot, C. Hervoches, School of Chemistry, University of St Andrews, Fife KY16 9ST, UK, A. M. Kusainova, P. Berdonosov and V. A. Dolgikh, Dept. of Chemistry, Moscow State University, Moscow, 119899, Russia and S. Yu. Stefanovich, Karpov Institute of Physical Chemistry, Moscow, 103064, Russia.

We have recently been carrying out a thorough crystallographic study of two families of layered bismuthates which display interesting pyro- and ferro-electric properties. The families concerned are the so-called Sillen and Aurivillius phases. The Aurivillius phases, in particular, are currently very widely studied from the technological point-of-view and, indeed, $Bi_2SrTa_2O_9$ and related phases are now the materials of choice in ferroelectric RAM thin-film technology. Despite this commercial significance, the basic structural chemistry of these materials is very poorly understood. These structures contain fluorite-related cationic metal oxide layers of stoichiometry $[M_2O_2]$ or $[M_3O_4]$, which are sandwiched between anionic halide or perovskite-like blocks, respectively. The occurrence of non-centrosymmetricity and/or ferroelectric properties is found to be critically dependent on the nature of cation ordering within the fluorite or perovskite blocks, as well as the choice of halide. We shall illustrate this with reference to several well-characterised materials including $Bi_4Te_2O_9Br_2$, $BiTe_2O_5Cl$, $Bi_2SrNb_2O_9$ and $Bi_2Sr_2Nb_2TiO_{12}$. We highlight the importance of using a combination of crystallographic techniques *viz*., single crystal X-ray diffraction and variable temperature X-ray and neutron powder diffraction.

P05.OC.001 KINETICS OF DECAY OF A METASTABLE STATE OF ONE-DIMENSIONAL DISORDER SYSTEM. B.V. Petukhov. Institute of Crystallography of Russian Academy of Sciences, Moscow 117333, Russia.

Periodically degenerated energetic relief of the crystal lattice is a fundamental reason for the strong temperature-dependent migration kinetics involving the thermoactivated overcoming of barriers separating adjacent states. The migration of extended objects has some distinctive peculiarities due to the interaction of different degrees of freedom. Some examples are: crystal growth by the steps motion along crystal faces, plastic flow of materials by the dislocation motion along slip plains in the Peierls-Nbarro relief, dynamics of boundaries of two-dimensional phases on crystalline substrates, etc. In all of these cases the interaction of the macroscopically large amount of the different degrees of freedom may be described by one basic model: mass nucleation of kink-soliton pairs and subsequent propagation and merging of kinks and antikinks from neighboring pairs.

A solution of this model for perfect homogeneous systems goes back to the classical Kolmogorov's paper [1] (see also [2]). However, in many real materials there are numerous reasons for uncontrolled disturbances, which drastically modify the ideal Kolmogorov-Johnson-Mehl kinetics. The goal of the present paper is a solution of a generalized model including the influence of a random disturbance of the "white noise" type. An exact solution of the model has been obtained, which shows, in particular, that the rate of the decay of a metastable state of the disorder linear system undergoes a drastic change near a some critical value of the driving force. Below of the critical force the rate of decay becomes essentially slower due to the anomalous nature of the kink motion over random barriers.

1. A.N. Kolmogorov. Bull. Ac. Sci. SSSR. Ser. Mat. No 3, 355 (1937).
2. W. Johnson, R. Mehl. Trans. Amer. Inst. Min. Met. V. 135, 416 (1939).

P05.OC.002 USING OF PV-STATE EQUATIONS AND A CORRELATIVE CRYSTAL THEORY FOR THE INVESTIGATION OF ELASTIC PROPERTIES OF CRYSTALS. N. Pertaya, Solid Physics Department, South Ukraine University of Education, Odessa, Ukraine.

The receipt of PV-equations is the main problem of condensed matter physics. The new approach to the investigation of the elastic properties of crystals, consisting of using of the PV-state equations to determine the analytic connection between the stress tenzor, macrostrain tensor, the change of crystal volume and quantitative characteristics of the between-atom potential was developed in the present work. The PV-state equations were received with the due regard for the crystal anysotropy for the cases of cubic, hexagonal, rhombic and tetragonal symmetry groups.

Also PV-state equations were received in the nought and first approhimations of the correlation theory. The chain of the equations for the correlation functions (density matrixes) was used to calculate the motion of the crystal particles. On the basis of the expressions of first and second order distribution functions the thermal state equation of crystals was obtained in the nought and first approximations of the correlation theory.

The deformation tenzor was determined by X-ray method, the macrostress tenzor was calculated in accordance with the Hook's law for the textured anysotropic solids. The approbation of the present investigation complex was carried out on a-Ti alloys. These results can be the basis of the investigation of macro- and microproperties of real crystals.

P05.OC.003 NEW BISMUTH OXIDES IN THE SILLEN AND AURIVILLIUS FAMILIES. C. Hervoches and P. Lightfoot, School of Chemistry, University of St.Andrews, St.Andrews, Fife KY16 9ST, UK.

We have studied the crystallographic structure of several new phases in the Sillen and Aurivillius families of potential use as ferroelectric materials or ionic conductors.

These materials have a highly flexible chemical composition which affects the details of their crystal structure, which in turn is believed to play a critical role in their important electrical properties.

We have systematically explored the effects of chemical modification on crystal structure and physical properties in order to understand the relationship of composition, structure, and properties [1,2].

X-ray and neutron powder diffraction have been used to characterise several materials including Bi_2AO_4Cl (A = Er, Lu, Y), $Bi_2Sr_2Nb_2TiO_{12}$ and the solid solution $Bi_{2-x}Sr_{2+x}Nb_{2+x}Ti_{1-x}O_{12}$. The latter materials display an unusual cation ordering scheme, hitherto unobserved, which may have important implications for their properties.

[1] V.A. Dolgikh, L.N. Kholodkovskaya, *Russ. J. Inorg. Chem.*, 1992, **37** (5), 488.
[2] S.M. Blake, M.J. Falconer, M. McCreedy and P. Lightfoot, *J. Mater. Chem.*, 1997, **7** (8), 1609.

P05.OC.004 ELECTRON DENSITY IN THE β-$Na_XV_2O_5$ OXYGEN BRONZES AT 9 K. R.P. Ozerov, Mendeleev University of Chemical Technology, Moscow 125047, Russia, B.N. Figgis and A.N. Sobolev, Department of Chemistry, and V.A. Streltsov, Crystallography Centre, The University of Western Australia, Nedlands 6907, WA, Australia, and V.L. Volkov, Institute of Solid State Chemistry, Ekaterinburg 620219, Russia.

Accurate X-ray crystal structure analyses of the β-$Na_xV_2O_5$ single crystal at room temperature and at 9 K have been undertaken in order to investigate the electron density of all metal atoms.

Nonstoichiometric compounds with the chemical formula of $Na_xV_2O_5$, where M is an alkali metal, copper or silver and x = 0.2-0.33, are known as the β-oxygen vanadium bronzes. Reason for such a name is the metallic character of some of their properties. It is generally considered that these properties originate from the special electronic states of the M and V atoms and interatomic interactions in the highly distorted coordination polyhedra.

A single crystal of β-$Na_xV_2O_5$ was grown from a melted mixture of $0.4NaVO_3+0.8V_2O_5$ by the Bridgman method in air. The sodium content (x = 0.31(3)) was determined from the site occupation number at the stage of structure refinement. There are three unique sites of the vanadium atoms in the crystal structure. Two of them (V_1 and V_2) are surrounded by a distorted octahedron of oxygen atoms. The oxygen environment around the third V_3 atom can better be described as pentagonal bipyramid. The deformation electron density (DED) examination revealed no noticeable qualitative distinction in three V atoms, although their charges calculated by Hirshfeld's method show definite difference. A significant DED accumulation near the Na atoms positions is also found. Multipole analysis of the results as well as quantum chemistry calculations are in progress.

The detailed intensity measurement of the 0k0 direction in the reciprocal space doesn't reveal any superstructure reflections with k odd which could be considered as a sign of the b axis doubling.

P05.OC.005 RELATIONSHIP BETWEEN THE CRYSTAL STRUCTURE AND MAGNETISM IN $Gd_5(Si_2Ge_2)$. V.K.Pecharsky[1,2], W.Choe[3], A.O.Pecharsky[1], G.J.Miller[3], and K.A.Gschneidner, Jr.[1,2], Ames Laboratory[1] and Department of Materials Science and Engineering[2], and Department of Chemistry[3], Iowa State University, Ames, IA 50011, USA.

The giant magnetocaloric effect has recently been observed in the ternary $Gd_5(Si_xGe_{1-x})_4$ compounds, where $0 \le x \le 0.5$ [1]. The ferromagnetic ordering temperature is lowered from 276 K at x = 0.5, i.e. $Gd_5(Si_2Ge_2)$ [1] to 240 K at x = 0.45, i.e. $Gd_5(Si_{1.8}Ge_{2.2})$ [1,2]. For the latter composition the magnetic phase transition occurs simultaneously with a crystallographic phase transition [2]. The crystal structure of $Gd_5(Si_2Ge_2)$ was studied at three different temperatures between 163 and 292 K by single crystal x-ray diffraction. All data were collected on a Bruker SMART CCD diffractometer using Mo K_α radiation. The low temperature magnetically ordered form of $Gd_5(Si_2Ge_2)$ crystallizes in the orthorhombic space group Pnma with unit cell parameters a=7.514(1), b=14.792 (2), and c=7.786(1) Å at 163 K; and a=7.513(1), b=14.797(2), and c=7.794(1) Å at 243 K. The high temperature paramagnetic form of $Gd_5(Si_2Ge_2)$ is monoclinic: space group $P2_1/a$ with unit cell parameters a=7.592(2), b=14.825(3), c=7.791(2), Å and γ=93.272(3)^o at 292 K. At room temperature the single crystal is a twin. Tight binding band calculations have been performed on $Gd_5(Si_2Ge_2)$ using the obtained crystal structure parameters to study the Gd-Gd bonding and the ordering of Si and Ge in $Gd_5(Si_2Ge_2)$. The relationship between the crystal structure and magnetism in $Gd_5(Si_xGe_{1-x})_4$ system is discussed.

Support by the Office of Basic Energy Sciences, Materials Science Division of the US DOE (VKP, AOP, and KAG) and by the National Science Foundation, grant No. DMR 9627161 (WC and GJM) is greatly appreciated.

V.K.Pecharsky and K.A.Gschneidner, Jr., Appl.Phys.Lett., **70**, 3299 (1997); V.K.Pecharsky and K.A.Gschneidner, Jr., Phys.Rev.Lett., **78**, 4494 (1997).
L.Morellon, P.A.Algarabel, M.R.Ibarra, J.Blasco, B.García-Landa, Z.Arnold, and F.Albertini, Phys.Rev.B., **58**, 14721 (1998).

P05.OC.006 EVIDENCE FOR DISTINCT POLYMER CHAIN ORIENTATIONS IN KC_{60} AND RbC_{60}. R. Moret, P. Launois, Laboratoire de Physique des Solides, Université Paris-Sud, 91405 Orsay, France, J. Hone and A. Zettl, Department of Physics, University of California at Berkeley and Materials Sciences Division, Lawrence Berkeley National Laboratory, Berkeley, California 94720, USA.

While earlier powder diffraction studies indicated similar structures for KC_{60} and RbC_{60}, we have shown that their relative polymer chain orientations are markedly different [1]. This is probably a key to the understanding of the contrasted electronic properties of these compounds.

The crystals were obtained by insertion of alkali metals into cubic C_{60} crystals at 400°C. Upon cooling to the room temperature polymer phase, orthorhombic variants are formed. In spite of the ensuing complexity we have performed detailed x-ray diffraction and diffuse scattering studies on these crystals. It is shown that the chains are orientationally ordered (no diffuse scattering). Furthermore, we have proved that KC_{60} and RbC_{60} possess different relative chain orientations about their axes, corresponding to the space groups Pmnn and I2/m, respectively. This implies that the intermolecular C_{60}-C_{60} environments are significantly different in the two compounds.

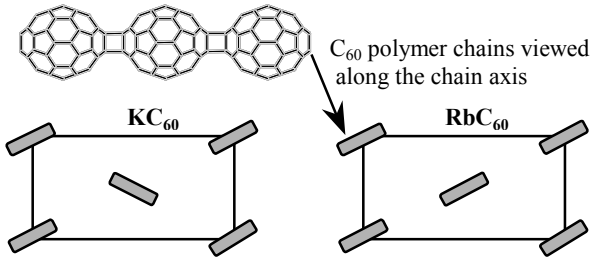

[1] P. Launois, R. Moret, J. Hone, A. Zettl, Phys. Rev. Lett. 81, 4420(1998).

P05.OC.007 GREEN'S FUNCTION APPLIED TO ELASTIC PROPERTIES OF CUBIC CRYSTALS. Yuri Ivanov, Department of Solid physics, South Ukrainian University of Education, Odessa 270020, Ukraine

It's first carried out an analytical expression of equilibrium equation Green's function of cubic single crystal. The effective elastic moduli of some polycrystals in correlation approximation with use of this function have been obtained.

The use of correlation-approximation method for cubic crystals has been studied. The possibility of using this method in the case of any anisotropy of elastic properties has been discussed.

P05.OC.008 POLARONS IN INTERGROWTH TYPE ALKALI METAL TUNGSTEN BRONZES: EVIDENCES BY OPTICAL SPECTROSCOPY. C. H. Rüscher[1], A. Hussain[2] [1]Institut für Mineralogie der Universität Hannover, Welfengarten 1, D-30167 Hannover, Germany [2]Department of Chemistry, Dhaka University, 1000 Dhaka, Bangladesh.

Here we report the first optical spectra of intergrowth tungsten bronzes (ITB) of composition M_xWO_3 with $0.05 < x < 0.15$ and M = K, Rb, Cs. The structure type (e.g. /1/) consist of extended slabs of hexagonal tungsten bronzes (HTB) which are separated by slabs of WO_3 building units. X-ray and TEM pattern show an orthorhombic lattice with one long axis (a ≈ 2-3 nm) and two shorter axis (b ≈ 0.74 nm, c ≈ 0.76 nm), where the c axis is related to the shorter subaxis (c' ≈ 0.38 nm) of the HTB subunit. The optical reflectivity of crystal slices was measured with incident light polarized parallel to their unit cell axis (microscope technique, 600 - 20000 cm^{-1}). The spectra reveal in all cases broad absorption peaks. For E ‖ b highest absorption intensities and the lowest resonance frequency (1000 cm^{-1}) is observed, i.e. a reflectivity of up to 60 % below 4000 cm^{-1} and a minimum in reflectivity at about 8000 cm^{-1}. The E ‖ c component reveal a rather broad feature with slightly increased reflectivity between 1000 and 8000 cm^{-1}. For E ‖ a a resonance structure between 8000 and 16000 cm^{-1} is observed. The absorption is explained by photon assisted hopping of polarons. The electron charge carrier reveal its strongest coupling to phonons parallel to the a direction, and lowest parallel to the b axis. Supported within combined DFG / GTZ - project.

1. A. Hussain, L. Kihlborg Acta Cryst A32 (1976) 551.

P05.OC.009 ATOMIC LEVEL PRESPECTIVE OF THE STRUCTURE OF PHASE DIAGRAMS : Li-Al ALLOYS. J.S. Tse, R. Rousseau, A. Ker and F.X. Lannuzel, Steacie Institute for Molecular Sciences, National Research Council of Canada, Ottawa, Ontario, Canada K1A 0R6.

The relationship between electronic and crystal structure for Li-Al alloys is investigated using electronic structure theory. In particular, we couple *ab initio* density functional calculations and tight binding electronic structure topology analysis *via* a moments decomposition of the density of electronic states. This procedure allows the rationalization of the stability of a crystal structure from the local structure motifs. We will show that the phase diagram for the known phases of Li-Al alloys can be understood by this topolgical analysis. The potential usefulness of the theoretical procedure is demonstrated by combining database mining for the prediction of the structure of a hypothetical metastable Al_3Li_2 alloy phase.

P05.OC.010 VALENCE ORDERING IN THE IODO-BRIDGED ONE-DIMENSIONAL MIXED-VALENCE DIPLATINUM(II,III) COMPLEXES. K. Toriumi, M. Mitsumi, Y. Ozawa, T. Yoshinari, and K. Akashika, Department of Material Science, Himeji Institute of Technology, Harima Science Garden City, Hyogo 678-1297, Japan, and H. Kitagawa, and T. Mitani, Japan Advanced Institute of Science and Technology, Ishikawa 923-1292, Japan.

Halogen-bridged mixed-valence diplatinum complexes $Pt_2(RCS_2)_4I$ (R= CH_3 (**1**), C_2H_5 (**2**), n-C_3H_7 (**3**)) with linear chain structures of repeating units {-I–Pt–Pt–I-} are particular interest because they are possible to take a variety of valence ordering [1]. The crystals of **1** which was first reported by Bellitto et al. [2] exhibit anomalous electrical conducting behavior (T < 300K, semiconductor; 300 K < T < 340 K, metallic) [3]. The variable temperature crystal structure analyses revealed dynamic disorder of the ligands [4].

In order to elucidate the relation between the solid state behavior and the valence ordering of Pt atoms on the linear chain, the compounds **2** and **3** were synthesized and their crystal structure analyses and electrical conducting measurements were carried out [5]. The M-I transition was observed for **2** at about 200 K.

Since the crystal structure analyses provided only the averaged structures, we tried to measure the diffuse scatterings corresponding to low-dimensional valence ordering of Pt atoms. Single crystal X-ray photographs of the compounds **1**-**3** were taken at variable temperatures by using the vacuum type X-ray camera developed by MAC Science Co., Ltd. and us or SPring-8 BL02B1 station. It was revealed that although the diffuse scatterings corresponding to the valence alternation along the linear chain have been observed for **2** above 200 K (metallic state), but changed to the Bragg spots below 100 K (semiconductive state). Similar phenomena were observed for the crystals of **3**.

1. S.A. Borshch, et al. (1998). J. Chem. Phys., 109, 4562.
2. C. Bellitto, et al. (1983). Inorg. Chem., 22, 444.
3. H. Kitagawa, et al. (1997). Synth. Met., 86, 1931.
4. K. Toriumi, et al. (1998). 33rd. ICCC Abstract, 419.
5. M.Mitsumi, et al. (1998). 33rd. ICCC Abstract, 385.

05OD 30 YEARS OF RIETVELD REFINEMENT

M05.OD.001 THE RIETVELD METHOD. H.M. Rietveld.

Thirty years ago the use of powder diffraction was mainly confined to determining spacegroup and/or unit-cell dimensions. Only very simple crystal structures could be solved this way. Single crystal diffraction was the way to determine crystal structures and for most substances large enough crytals could be grown. However, for more and more substances of interest it was impossible to grow these large crystals, especially those required for neutron diffraction.

With the advent of computers, small compared with today's standards, it became feasible to use as data the very large number of step scanned profile intensities in a powder diagram instead of the fewer but severely overlapping integrated intensities.

The method, while originally developed for neutron diffraction, became widely used when it was also adapted to X-ray diffraction. Nowadays the method is used in more than 500 publications per year.

M05.OD.002 NEUTRON POWDER DIFFRACTION – A WORLD OF SUPERCONDUCTORS, GIANT MAGNETO-RESISTANCE ETC. Alan Hewat, Institut Laue-Langevin, BP 156X, Grenoble 38042, FRANCE.

Superconductors, Giant Magneto Resistance, Magnetic Frustration, Zeolite Intercalates, Structural Transitions… these are some of the success stories for Rietveld refinement with neutron powder data The citation index shows that this work had more impact than other neutron scattering experiments in the past 30 years, and in fact was among the most highly cited of all science in some years (eg see http://www.ill.fr/dif/citations/).

The most recent examples concern the mechanism of Giant Magneto-Resistance. A combination of neutron and synchrotron data was used to examine the subtle structural transitions responsible for the GMR effect, the detailed magnetic structure was obtained, and most importantly the 'stripe' structure that has recently generated such excitement, has been shown to be absent in well characterised materials (this meeting).

The most famous examples of the application of Rietveld refinement remain of course in the field of oxide superconductors, and in particular the ideas that lead to the successful search for

new materials. Neutron diffraction had already shown that the highest Tc materials were layer structures, very different from the original Bednorz and Muller material. New experiments at Argonne and Grenoble showed how the hole density in the conducting layer was controlled by 'charge-transfer' from reservoir layers, which then lead to a successful search for new materials with bismuth, thallium and mercury oxide charge reservoirs.

Neutron diffraction has proved to be essential for such work because of the absence of single crystals for very new materials, and because of the greater contrast obtained between oxygen and heavy metal atoms. New diffractometers such as D20 at ILL and GEM at ISIS will extend the application of neutron diffraction to very small samples, and to in-situ chemistry on such samples. The proposed super-D2B and a new machine on the proposed European Spallation Source will also extend applications to problems where very high resolution is needed.

M05.OD.003 APPLICATIONS OF THE RIETVELD METHOD TO INORGANIC MATERIALS. F. Izumi, National Institute for Research in Inorganic Materials, 1-1 Namiki, Tsukuba, Ibaraki 305-0044, Japan.

The past thirty years have seen dramatic developments in the Rietveld method. Further, synchrotron radiation sources and intense neutron sources have enabled us to measure high-resolution powder diffraction data in relatively short times. Imaging plates and position-sensitive detectors have improved counting statistics markedly to permit real-time diffraction experiments and measure intensity data for small amounts of samples. These advances in diffraction techniques have enhanced the utility value of the Rietveld method greatly.

The discovery of a series of high-T_c superconductors has made the Rietveld method much more popular because of its wide applications to their structure refinements. In particular, neutron Rietveld analysis was extensively used for three different types of structural studies:\ (1) determination of new structures, (2) relations between (defect) structures and physical properties, and (3) structural changes in special environments, *e.g.*, under low or high temperature and under high pressure. With Rietveld refinements adopting superspace group approaches, we determined the incommensurately modulated structures of Bi-based superconductors and the composite crystal $Ca_{13.6}Sr_{0.4}Cu_{24+y}O_{41+z}$.

The Rietveld method has been contributing to the development of industrial inorganic materials. One of the most outstanding examples is cathode materials in rechargeable lithium-ion batteries, *i.e.*, $LiNiO_2$, $LiMn_2O_4$, and their related compounds. Further, multi-phase Rietveld analysis is now routinely utilized in the quality control of clinker production in the cement industry, providing reliable mass fractions and structure parameters of alite, belite, $Al_2Ca_3O_6$, $Al_2Ca_4Fe_2O_{10}$, *etc*. owing to fitting of whole powder patterns.

We have recently developed a Rietveld-analysis program, RIETAN-98, with two innovatory features: partial profile relaxation and whole-pattern fitting based on a maximum-entropy method (MEM). Partial profile relaxation means that primary profile parameters of isolated reflections can be locally refined independently of secondary profile parameters. It was united with three split-type profile functions to obtain better fits between observed and calculated patterns, particularly in samples showing anisotropic profile broadening. Further, RIETAN-98 has been combined with a MEED program for the MEM to grow into an integrated software named REMEDY, which makes it possible to carry out MEM analysis and whole-pattern fitting alternately. REMEDY is very effective for modifying incomplete structural models and analyzing highly disordered structures as well as covalent crystals.

M05.OD.004 THE RIETVELD METHOD WITH LABORATORY X-RAYS. D. Louër, Laboratoire de Chimie du Solide et Inorganique Moléculaire, Université de Rennes I, 35042 Rennes, France.

The Rietveld method was applied to powder diffraction data collected with a conventional X-ray source a few years after its advent, using both transmission and reflection optics [1,2]. The delay for its application to X-ray diffraction data was essentially due to the more sophisticated line shape required to describe the observed line profiles. Since then the difficulties have been overcome and the Rietveld method is now familiar to laboratory diffractionists. Among available optics the choice of a diffraction geometry depends on the absorption properties of the material with respect to the wavelength. These practical aspects and the use of monochromatic $K\alpha_1$ radiation or $K\alpha_1$-$K\alpha_2$ doublet will be commented. The precision reached in Rietveld refinements as well as the sensitivity of the method to structural details will be illustrated by examples. However, the most spectacular results in structure analysis arose from the association of the Rietveld method with the other advances occurred in indexing procedures, in pattern decomposition algorithms and in structure solution. The development of *ab initio* structure determination from powder data has completely transformed the chemistry of families of powder materials. Laboratory X-rays are used to characterise the structure of different classes of solids, such as inorganic, coordination, organic and drug compounds. The Rietveld refinement method is applied at the final stage of the studies to demonstrate the relevance of the structure model and to obtain precise atomic coordinates. This will be illustrated from representative examples, including classes of powder materials whose chemistry has been transformed from the use of the Rietveld method. In addition, the impact of the whole profile refinement method, using laboratory X-rays, in the interpretation of structural changes occurring in dynamical studies will be illustrated.

G. Malmros & J.O. Thomas (1977). *J. Appl. Cryst*. 10, 7-11.
R.A. Young, P.E. Mackie & R.B. Von Dreele (1977). *J. Appl. Cryst*. 10, 262-269.

M05.OD.005 SYNCHROTRON RADIATION - PICKING UP THE FLAME AND FANNING THE FIRE. A.N. Fitch, ESRF, BP 220, 38043 Grenoble Cedex, France.

With the arrival of the synchrotron, experienced users of neutrons, and new workers, were attracted towards the use of X-rays and the Rietveld method. Synchrotron radiation has several advantages for powder measurements. The collimation can be exploited to remove aberrations in peak positions that can affect conventional instruments. By working at higher energies with a spinning capillary, absorption and preferred orientation can be minimised. As dedicated instruments became available, the Rietveld method became the preferred way to refine a crystal structure from synchrotron data. However, high resolution data can reveal effects due to a sample's microstructure, and the peak shapes needed to be adapted to contend with anisotropy, strain, particle-size broadening, etc. By carefully tuning the energy, differences in the intensities close to and far from an absorption edge can be analysed to increase the experiment's sensitivity towards a resonantly scattering element. The easiest way to exploit this information was to adopt the Rietveld method to fit concurrently to more than one data set. The natural complementary between X-rays and neutron could also be more efficiently exploited in a joint refinement. The very high intensity at a synchrotron has led to developments in *in-situ* experiments. It is now possible, on a time scale of a few seconds, to collect data that can be refined by the Rietveld method, to reveal the evolution of structure in a sample undergoing rapid physical or chemical change. As the results from Rietveld refinements have been

demonstrated again and again to be reliable, confidence in the powder technique has grown, to the point that structures are now routinely *solved* from powder data, especially using the synchrotron. Whilst the Rietveld method is a method of structure refinement, the basic approach has been exploited to solve structures, by fitting to the diffraction data whilst moving a known fragment or molecule around the unit cell. These techniques are a direct legacy of the original approach, and the current interest in such methods ensures that the basis of the Rietveld technique will endure for years to come. The talk will discuss and illustrate these concepts.

P05.OD.001 AB INITIO STRUCTURE SOLUTION AS PART OF THE RIETVELD REFINEMENT PROCESS. A. Kern and A. Coelho, Bruker-AXS GmbH, Östliche Rheinbrückenstraße 50, D-76187 Karlsruhe

A new Rietveld program system (TOPAS) has been developed with particular emphasis placed on improving stability and convergence. TOPAS is built around a general non-linear least squares system written specifically to integrate various types of X-ray diffraction analyses. This includes the ability to refine laboratory/synchrotron/neutron powder diffraction and single crystal data simultaneously. Input to the program can be either hkl, 2θ and d-spacing intensity peaks, or structural data obtained in a free format. Conversions from ShellXTL, GSAS and FullProf formats are possible.

There are various minimization routines including the Marquardt method of refinement plus line minimization and parameter extrapolation techniques. Sparse matrix methods are used when refining thousands of parameters e.g. for lattice parameter refinement or when extracting integrated intensities.

A remarkable feature of TOPAS is the ability to solve structures by simulated annealing together with user defined penalty functions, rigid bodies and lattice energy minimization techniques including user defined force fields/equations. Rigid bodies take into account space group symmetry. They can be linked and rotated about any axes and hinges.

The numerical speed of TOPAS is an order of magnitude faster than that of existing Rietveld programs. As in addition no more refinement strategy is needed Rietveld refinements can be performed up to 100 times faster! Further key features of TOPAS are:

- Physically meaningful peak shapes can be generated using a new Fundamental Parameters Approach with all parameters refinable.
- Spherical harmonics to describe preferred orientation, anisotropic peak broadening and temperature factors.
- Fits to unequal x-axis steps.

05OE CRYSTALLOGRAPHY AND GEOSCIENCES

M05.OE.001 TOTAL SCATTERING MEASUREMENTS ON DISORDERED CRYSTALLINE SILICATES. Martin T Dove Mineral Physics group, Department of Earth Sciences, University of Cambridge, Downing Street, Cambridge CB2 3EQ

X-ray diffraction has been a pivotal technique in the study of minerals since the earliest days of the technique, and over the past decade or so this has been augmented by neutron powder diffraction. More recently we have been using total neutron scattering measurements to study crystal phases which clearly have considerable disorder on a short length scale. Total scattering involves analysing both the Bragg peaks and the diffuse scattering background, and the Fourier transform of the total scattering pattern gives the pair distribution function. Constrained reverse Monte Carlo methods allow one to construct atomic configurations that are consistent with the diffraction pattern, and these can provide information about the nature of the structural disorder. We illustrate this approach by studies of phase transitions in different silica phases.

M05.OE.002 THERMAL ANOMALIES IN TITANITE AND MALAYAITE. U. Bismayer, Mineralogy, University of Hamburg, Grindelallee 48, D-20146 Hamburg, Germany.

Titanite, $CaTiSiO_5$, and malayaite, $CaSnSiO_5$, exhibit a thermal anomaly near 500 K. Specific heat measurements, synchrotron X-ray diffraction, hard mode spectroscopy and high-resolution transmission electron microscopy [1, 2] were used to study synthetic and natural titanite. At temperatures above the structural transformation *P21/a - A2/a* anisotropic diffuse scattering occur in synthetic titanite and remain visible up to ca. 825 K, where the excess specific heat disappears. In natural crystals the phase transformation near 500 K is suppressed by impurities and defect induced renormalization phenomena alter the critical behaviour.

High-temperature X-ray diffraction and powder IR spectroscopy were used to study the thermal behaviour of malayaite [3]. No diffuse reflections were observed. The crystal structure data show no evidence of a symmetry-breaking phase transition near 500 K. The most obvious change with heating is a tumbling motion of the SnO_6 octahedra and an increase of the thermal displacement ellipsoid of the Ca atom. At this temperature IR spectra show a break in the variation of mode intensities and peak positions. Similarities to the thermal behaviour of the 825 K anomaly in titanite are discussed.

Financial support by BMBF (GUA 05647) and ARC is acknowledged.

1. M. Zhang, E.K.H. Salje, U. Bismayer,H.-G. Unruh , B. Wruck & C. Schmidt (1995). Phys. Chem. Min., **22**, 41.
2. S. Kek, M. Aroyo, U. Bismayer, C. Schmidt, K. Eichhorn & H.G. Krane (1997). Z. Kristallogr., **212**, 9.
3. M. Zhang, H.W. Meyer, L.A. Groat, U. Bismayer, E.K.H. Salje & G. Adiwidjaja (1999). Phys. Chem. Min., in press

M05.OE.003 PROPERTIES OF AL:SI ORDER-DISORDER PHASE TRANSITIONS IN FRAMEWORK SILICATES. T. Malcherek, CNR-CSCC, Dipartimento di Scienze della Terra, Via Ferrata 1, 27100 Pavia, Italy, H. Kroll, Institut für Mineralogie, Westfälische Wilhelms-Universität, 48149 Münster, Germany, E.K.H. Salje, Department of Earth Sciences, University of Cambridge, Cambridge CB2 3EQ, UK.

Using X-ray diffraction, TEM and IR-Spectroscopic methods, equilibrium behaviour and kinetics of cation ordering in the tetrahedral framework of the monoclinic feldspar $BaAl_2Ge_2O_8$ (BAGF) have been studied. Substitution of Ge for Si in natural 2:2 feldspar structures avoids difficulties encountered in direct measurement of Al,Si ordering by X-ray diffraction methods.

A mean field approximation was used to model the observed thermal equilibrium behaviour of the convergent order parameter Q_{od} and a coupled non-convergent order parameter Q_t. Q_{od} discontinuously falls to zero at T_{tr} = 1690K accompanied by a SG symmetry change I2/c↔C2/m. Local fluctuations of Q_{od} near T_{tr} could be observed using TEM DF imaging on quenched samples. The fluctuations indicate the Ising character of the microscopic properties and they agree with short range order observed by Hard Mode Infrared Spectroscopy.

The order parameter fluctuations have important consequences for the ordering kinetics if the feldspar is quenched to lower temperatures. The strong non-uniformity of Q_{od} causes changes in the mechanism by which the equilibrium state is reached. Thus, in comparison to conventional time dependent Ginzburg-Landau behaviour for a uniformly ordered structure, a

significant slowing down of the ordering kinetics is encountered during low temperature annealing.

Possible implications of the observed order-disorder behaviour for Al,Si cation ordering in natural felspar minerals and in other framework silicates such as cordierite are discussed.

M05.OE.004 CRYSTAL MINERALOGY OF SHALES FROM THE GULF OF MEXICO. L.E. Rendón [1], L.de Pablo, M.L. Chavez, R. Monsalvo, G. Miranda [2], [1] Instituto Mexicano de Tecnologia del Agua, Jiutepec, Mor., [2] Geoquimica, Instituto de Geologia UNAM Mexico D.F.

Swelling of active shales is associated with adsorption of chemical species and diagenesis. Active shale, Oligocene-age, containing 50.8% discrete illite, disordered anhydrous, $1H_2O$-, $2H_2O$- and $3H_2O$-layer smectite, and mixed-layer smectite/illite, and having a cation exchange capacity of 83.12 meq/100 g, upon hydration at the in situ temperature of 80°C desorbs 38% of the adsorbed Na^+, some Ca^{2+}, and none K^+ and Mg^{2+} to form predominant discrete illite and disordered $1H_2O$-layer smectite and minor anhydrous and $2H_2O$-layer smectite. Reaction with Na^+, K^+, Ca^{2+}, and Mg^{2+} electrolytes at 22°C reduces adsorbed Na^+ an additional 28% and develops ordered $2H_2O$-layer smectite of finer crystallite size (d(001) 14.59 Å-15.07 Å). At 80°C, 0.0001M electrolytes decrease adsorbed Na+ to 17.59 meq/100 g, K+, Ca2+ and Mg2+ remain constant, and form discrete illite, disordered 1H2O-layer (d(001) 12.21 Å-12.93 Å), $2H_2O$-layer (d(001) 14.34 Å-15.42 Å), and minor anhydrous smectite when the reacting electrolytes are K^+ (d(001) 11.85 Å) or Ca^{2+} (d(001) 10.70 Å). With 0.001M solutions transformation is to $1H_2O$-layer (d(001) 12.34 Å-13.09 Å), $2H_2O$-layer (d(001) 14.25 Å-14.92 Å), and anhydrous smectite when reacting with K^+ (d(001) 11.81 Å). Discrete illite at 22°C reverses readily to smectite and forms at 80°C when the shale reacts with weak electrolytes but not with strong ones which require additional hydration to develop illite. Spacings of the smectite complexes formed at 80°C by 0.0001M electrolyte and hydration are: With Na^+, 12.21 Å, 12.71 Å, and 14.34 Å; with K^+, 11.85 Å, 12.46 Å, and 14.50 Å; with Ca^{2+}, 12.44 Å and 14.42 Å; with Mg^{2+}, 14.48 Å and 15.42 Å. When the electrolyte is 0.001M, Spacings are: With Na^+ 13.08 Å and 14.52 Å; with K^+, 11.81 Å, 12.34 Å, 13.09 Å, and 14.59 Å; with Ca^{2+}, 14.25 Å, 14.92 Å and 12.08 Å; and with Mg^{2+}, 12.49 Å and 12.93 Å. At 80°C Mg^{2+} forms $1H_2O$-layer smectite complexes, Na^+ and K^+ $1H_2O$- and $2H_2O$-layer complexes, and Ca^{2+} only $2H_2O$-layer smectite complexes. The data supports that swelling, variable pore pressure, and instability in active shale are associated with adsorption and cation exchange between the surrounding solution and the smectite surface. Adsorbed cations and hydration leads to different smectite complexes which accommodate differently on the clay surface. Exchange appears to be dependent on activity coefficient gradients between the adsorbed layer and the surrounding solution.

M05.OE.005 NEW DEVELOPMENTS IN CRYSTAL CHEMISTRY OF HIGH-PRESSURE HYDROUS SILICATE PHASES. C.T. Prewitt, H. Yang, J. Konzett, Y. Fei, Geophysical Laboratory and Center for High Pressure Research, Carnegie Institution of Washington, 5251 Broad Branch Road, NW, Washington, D.C. 20015-1305, USA.

High-pressure hydrous silicate phases have attracted much attention for the past 30 years because of their great implications for the presence of water in the Earth's mantle and effects on the Earth's processes. Previous studies on hydrous silicates were focused primarily on the MgO-SiO_2-H_2O system, and a number of phases were identified and labeled as 10Å, 3.65Å, A, B, C, D, E, F, G, and superhydrous B (the "alphabet phases"). However, recent studies showed that phase F is actually superhydrous B, the latter is actually phase C, and phase G possesses the same structure as phase D. Further coordinated work in synthesis and crystallography is apparently needed for a better understanding of crystal chemistry of the high-pressure hydrous phases in the MgO-SiO_2-H_2O system. Also, to provide a wider range of information, we have begun investigating more chemically-complicated hydrous silicate phases synthesized at high pressures and temperatures using the multi-anvil apparatus and have made considerable progress, including synthesis and characterization of the following hydrous phases:

1. ^{M4}K-substituted K-richterite, $K(KCa)Mg_5Si_8O_{22}(OH)_2$ (15 GPa, 1400°C);
2. Clinopyribole, $K_{0.96}Ca_{1.56}Na_{2.51}Mg_{6.01}Al_{1.12}Si_{12}O_{34}(OH)_2$ (10 GPa, 1200°C);
3. Hydrous phase (aenigmatite structure), $Na_2(Mg_{5.30}Al_{0.48})Si_{5.91}O_{18}(OH)_2$ (10 GPa, 1250°C);
4. Na-phase X, $(Na_{1.16}K_{0.01})(Mg_{1.89}Al_{0.14})Si_2O_7H_{0.65}$ (10 GPa, 1250°C);
5. K-phase X, $K_{1.54}Mg_{1.93}Si_{1.89}O_7H_{1.04}$ (16 GPa, 1300°C);
6. Fe-bearing hydrous phase, $Mg_{2.29}Fe^{3+}_{0.60}Si_{1.01}O_6H_{2.15}$ (14 GPa, 1400°C).

Structure refinements/determinations of these phases not only provide us with insights into crystal chemistry of high-pressure hydrous silicates, but also expand our knowledge of deep Earth mineralogy. Our results also suggest that a large number of new structures and relatively exotic phases in the mineral kingdom may be discovered as we further explore the pressure-temperature-composition space.

P05.OE.000 THE CRYSTAL STRUCTURE OF NEW LEAD DODECABORATE $Pb_6B_{12}O_{24}.H_2O$ WITH THE UNIQUE RING $[B_6\ B_6^{\Delta}O_{24}]^{12-}$. T.A.Korchemkina, E.L. Belokoneva, O.V. Dimitrova, Moscow State University, Vorob'evi Gory, Moscow, Russia.

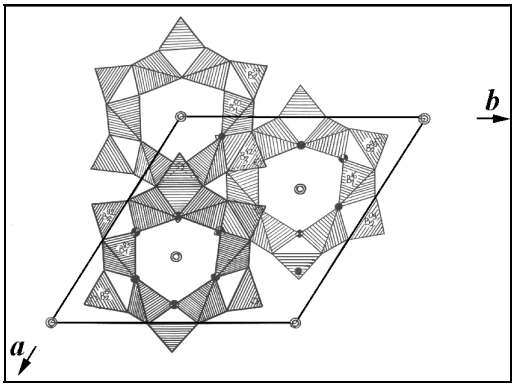

New lead borate has been synthesized during search for new non-linear optical materials in hydrothermal conditions in PbO-B_2O_3-H_2O system. The crystal structure of it was determined using the heavy atom method without knowing the chemical formula. The dodecaborate $Pb_6B_{12}O_{24}.H_2O$ has the unique B-O unit: an independent six-member ring $[B_6B_6O_{24}]^{12-}$ of B-tetrahedra in the structure is surrounded by six B-triangles attached on the external side, sharing the corners. In contrast to many other borates, this unit does not contain OH^- groups, though it is centered by H_2O molecules. Each trigonal cell a=11.432(4), c=17.385(6) contains three rings, repeated by R-translations of R-3m space group. Rings are interleaved by sheets of Pb-polyhedra, parallel to plane ab, located on levels ~0, ~1/3, ~2/3.

The material researched, adds itself to a small group of four lead borates (with and without water), two of which proved to be non-linear optic ones. A newly discovered ring is an important addition to the borates classification.

P05.OE.001 THE HILGARDITE GROUP STRUCTURES AS MEMBERS OF THE OD-FAMILY. E.L. Belokoneva, T.A. Korchemkina, O.V. Dimitrova, S.Yu. Stefanovich, Moscow State University, Vorob'evi Gory, Moscow, Russia.

New centrosymmetric modification of natural hilgardite I $Ca_2[B_5O_9]Cl.H_2O$ - II $Pb_2[B_5O_9](OH).H_2O$ was hydrothermally synthesed. The comparison of two structures led to the conclusion they are built from uniform $[B_{10}O_{21}]^{-12}$ layers as well as synthetic III $Ca_2[B_5O_9]Br$ and may be described within the OD-theory. The symmetry of layer (λ-PO) and the symmetry operation which transfer layer to layer (σ-PO) or two dimentional unit into tree dimentional framework in the structure are described with the grouppoid

$[B_{10}O_{21}]^{-12}{}_{\infty\infty}$ P 1 1 (n) (λ-PO)
[1 1 (1//a//2)] (σ-PO)

For the structure I the transformation of layers is realized by a-glade, for II - by symmetry center 1, for III - by 2-fold axis. The resulting space group of compounds are different: monoclinic Aa and $P2_1/n$ for I and II and orthorhombic Pnn2 for III. All three are typical MDO-polytypes. Triclinic minerals: strontiohilgardite, tyretskite and isostructural syntethic IV $Ca_2[B_5O_9]Cl.H_2O$, as well as parahilgarditeV $Ca_2[B_5O_9]Cl.H_2O$ belong to the same family but with the modification of layer. The building unit of layer is helical chain $[B_5O_{11}]^{-7}$ with the symmetry 1, which undergoes n-glade symmetry operation in first I,II,III structures. It may undergo simple translation t (structure IV) or combination of n and t (n,n,t...) as it is in structure V. So we can write the grouppoid of other rank which describes the transfer of one dimentional unit (chain) into two dimentional (layer)

$[B_5O_{11}]^{-7}{}_{\infty}$ P(1)1 (λ-PO)
[(t//n)1] (σ-PO)

We can predict the structures with sequences 1,a..., or 2,a..., or 1,2..., or 1,2,a... in different variants in accordance with the first grouppoid. More complicate structures may exist until absence of order along the direction of periodicity. n,t...sequence along layer may also vary until disorder along layer. Thus the structures in OD-family are determined by ordering of two- or one-dimentional units (chain or layer). Different minerals of group may coexist in nature. More preferable will be such structures which are more thermodynamically stable and posses lowest entropy as it is typical for polytypes.

P05.OE.002 HIGH-PRESSURE CRYSTAL CHEMISTRY OF Al_2SiO_5 : *AB INITIO* PSEUDO-POTENTIAL CALCULATIONS. Artem R. Oganov, John P. Brodholt, G. David Price, Department of Geological Sciences, University College London, WC1E 6BT, London, UK.

Aluminium is one of the most abundant elements on the Earth, however, a great uncertainty still exists on the form of Al in the largest part of the planet - the lower mantle : some researchers propose $MgSiO_3$-perovskite as a main host of Al in the lower mantle, others propose hollandite-type phase of $(Ca,Mg)Al_2Si_2O_8$ or high-density phase of $MgAl_2O_4$. Recent works [1] showed that a high-pressure form of Al_2SiO_5 with V_3O_5-type structure, found experimentally at high *P-T*-conditions, can be the main host of Al in the lower mantle, comprising up to 5% of its volume. However, more recent experiments [2] have shown that this phase is not formed; instead, kyanite (Al_2SiO_5) transforms into a mixture of corundum (Al_2O_3) + stishovite (SiO_2).

We report results of *ab initio* calculations, based on density functional theory within the framework of generalized gradient approximation (GGA) with plane wave basis set and effective core pseudopotentials. We consider polymorphs of Al_2SiO_5 (kyanite, andalusite, sillimanite and hypothetical V_3O_5-like and pseudobrookite-like phases), SiO_2 (stishovite, quartz) and Al_2O_3 (corundum). A highly converged set of computational parameters was used in order to reproduce small energies of the phase transitions. A good agreement of crystal structures, bulk moduli, atomisation energies and the phase diagram with experiment was found. At the same time, a strong disagreement of calculated lattice parameters and density of V_3O_5-like phase of Al_2SiO_5 with experimental values of [1] is observed, suggesting that the phase synthesised in the latter work cannot be identified as V_3O_5-structured phase of Al_2SiO_5. Also, we found that the most stable high-pressure assembly in Al_2SiO_5 system is corundum+stishovite, and the value of the transition pressure (113 kbar) is in excellent agreement with experimental estimates (99-150 kbar).

1.Ahmed-Zaid I., Madon M.//Nature, 1991, **353**, 426.
2.Schmidt M.W.,Poli S.,Comodi P.,Zanazzi P.F.//Amer.Miner., 1997, **82**, 460.

P05.OE.003 PARTITIONING AND STRUCTURAL BONDING OF FLUORINE IN PHLOGOPITES AND SILICATE MELTS: A SOLID STATE NMR STUDY. M. Fechtelkord, H. Behrens, F. Holtz, Institut für Mineralogie der Universität Hannover, Welfengarten 1, D-30167 Hannover, Germany. and L. A. Groat, Department of Earth and Ocean Sciences, University of British Columbia, 6339 Stores Road, Vancouver, B.C. Canada V6T 1Z4

The micas biotite, phlogopite and muscovite are the preferred phases which incorporate fluorine beside the melts during differentiation of magmas. A detailed study of the fluorine local structure in melt and layer silicates may provide a better understanding of the effect of fluorine enclathration on the chemical and physical properties of the phases and on fluorine partioning.

To study the influence of the OH-/F-ratio and of the Tschermak substitution ($^{[6]}Mg^{2+} + {}^{[4]}Si^{4+} \rightarrow {}^{[4]}Al^{3+} + {}^{[6]}Al^{3+}$) on the local structure of fluorine in phlogopites eight samples with varying OH/F-ratios and compositions of $K(Mg_{3-x}Al_x)[Al_{1+x}Si_{3-x}O_{10}](OH)_{1.5}F_{0.5}$, $0.1 \leq x \leq 0.7$ were hydrothermally synthesized from gels. The phlogopite can be characterized in the ^{29}Si MAS NMR spectrum by three resonances at -83.2 ppm (Q^3(2Al)), -86.9 ppm (Q^3(1Al)) and -90.7 ppm (Q^3(0Al)). Based on the relative intensities of the signals, the calculated Si/Al-ratio can be estimated along the phlogopite-eastonite join [1]. The estimated Si/Al ratio are in good agreement with the initial ratios of the gel. In eastonites with $x \geq 0.5$ the formation of corundum limits the ratio of Si/Al to 2.0 for the phlogopites. The application of $\{^{19}F\}$ ^{29}Si CPMAS NMR shows an increase of the (Q^3(1Al)) and (Q^3(0Al)) signal intensities, which suggests a shorter distance of fluorine located in the cation layers to silicon atoms in the tetrahedral sheets predominantly bonded to other silicon atoms. The ^{19}F MAS NMR spectra show only one signal shifting in dependence on the Al- and F-content.

1. S. Circone, A. Navrotsky, R.J. Kirkpatrick & C.M. Graham (1991). Am. Mineral., **76** 1485-1501.

05OF NANOMATERIALS

M05.OF.001 FROM CLUSTERS VIA NANOSIZED RING-SHAPED AND SPHERICAL (ICOSAHEDRAL) CLUSTERS AND SUPRAMOLECULAR SPECIES TO MATERIALS. Achim Müller, Fakultät für Chemie, Universität Bielefeld, Postfach 100 131, D-33501 Bielefeld, Germany, e-mail: a.mueller@uni-bielefeld.de

In Nature, complex molecular systems like proteins have evolved (natura naturans) which are perfectly suited to their functions. These are produced in a sequence of steps under dissipative conditions – that is, far from quilibrium. The challenge for the chemist is to synthesize correspondingly

complex multi-functional molecules also under non-equilibrium (dissipative) conditions using multi-component one-pot reactions without having to separate and purify each single intermediate product. Relevant model reactions have been discovered in solutions of simple *oxoanions of the transition metals*: Novel types of molecular growth processes with feedback (including a type of induced cascade) are described leading to different *ring-shaped, electron-rich, mixed-valence, giant polyoxomolybdates with nanosized cavities*. These can – due to the generation of defects – be covalently linked together to form *chains* as well as *layered mesoporous compounds* with properties relevant for materials science. They can also start growing again. The largest polyoxometalate cluster obtained on the basis of this growth process to-date has 248 atoms. Remarkably, such giant ring species can also act as *hosts for other clusters forming new types of supramolecular compounds*.

The lecture will be highlighted with a report on the planned synthesis and structure of different *nanosized spherical clusters with icosahedral symmetry* which have similar structures as spherical viruses and *which can be linked in different ways even to layers(!)*. For the first time, discrete molecular species with structures related to some of the Archimedean solids will also be reported.

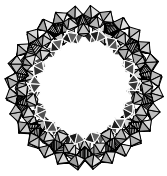

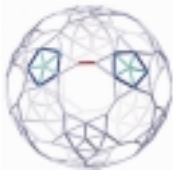

A. Müller, F. Peters, M. T. Pope, D. Gatteschi, „Polyoxometalates: Very Large Clusters – Nanoscale Magnets“, Chem. Rev. 98, 239 (1998)

A. Müller, E. Krickemeyer, H. Bögge, M. Schmidtmann, F. Peters, „Organizational Forms of Matter: An Inorganic Super Fullerene and Keplerate Based on Molybdenum Oxide“, Angew. Chem. Int. Ed. Engl. 37, 3360 (1998)

A. Müller, Syed Q. N. Shah, H. Bögge, M. Schmidtmann, „Molecular growth from a Mo_{176} to a Mo_{248} cluster“, Nature 397, 48 (1999)

M05.OF.002 INORGANIC FULLERENE-LIKE MATERIALS AND NANOTUBES (IF) FROM LAYERED COMPOUNDS. Reshef Tenne, Yshai Feldman, Moshe Homyonfer, Gitti L. Frey, Yaron Rosenfeld Hacohen, Aude Rothschild, Department of Materials and Interfaces, Weizmann Institute, Rehovot 76100, Israel, Jeremy Sloan and John L. Hutchison, Department of Materials, Oxford University, Parks Road OX1 3PH, UK

Using the paradigm of carbon fullerenes, it was shown by Tenne and co-workers[1] that nanoclusters of layered compounds, like MoS_2, are unstable in the planar form and fold into hollow cage structures of various shapes: from spherical and polyhedral to nanotubes of a mm length and cross-section of 10-20 nm diameter (IF). Following this discovery a few methodologies for the systematic synthesis of large amounts of IF-MoS_2 and WS_2, were pursued. Recently, IF structures from various other layered compounds were synthesized. Intercalation of IF-WS_2 rendered these nanostructures as stable suspensions in aprotic solvents and photoelectrochemical cells were subsequently prepared. Recently, the first MoS_2 octahedra having 572 Mo atoms, were reported[2].

The structural, optical, electrochemical, and tribological properties of IF-MoS_2 (WS_2) were investigated in some detail. It was found by Frey et al.[3], that IF-MoS_2 (WS_2) are semiconductors with a tunable bandgap which scales with the size of the nanoparticles. The 2H polytype structure is locally preserved in these nanoparticles. Few extra Raman lines observed in the IF suggest a reduced symmetry compared with the bulk (2H) predecessor. The tribological properties of IF was shown by Rapoport et al.[4] to outperform the ubiquitous solid lubricants 2H-MoS_2 (2H-WS_2). This suggests an eminent range of applications for these nanomaterials. Other applications will be briefly discussed.

1. Tenne, R. et al., Nature 360, 444 (1992); b.Nature, 395, 336 (1998).
2. P.A. Perilla, Nature 397, 114 (1999).
3. Frey, G.L. et al., Phys. Rev. B 57, 6666 (1998).
4. Rapoport, L. et al., Nature 387, 791 (1997).

M05.OF.003 MAGNETIC (NANO) COLLOIDS. A. P. Philipse, Department of Chemistry, Utrecht University, Netherlands.

Preparation and properties will be discussed of magnetic colloids (iron, cobalt, ironoxide) in the nanometer size range, dispersed in a liquid phase. The particles are coated with a non-magnetic polymer or inorganic layer. The magnetic (dipolar) interactions between the (permanently magnetized) particles strongly depend on the particle radius and the thickness of the coating. This dependence gives rise to a rich variety in size and morphology of particle structures formed in presence or absence of a magnetic field. Experiments (and some ideas) on this structure formation will be presented.

M05.OF.004 STRUCTURE AND QUANTIZED CONDUCTANCE OF NANOWIRES STUDIED BY A COMBINED STM AND ELECTRON MICROSCOPE. K.Takayanagi [1], Y.Kondo, H.Ohnishi [2], Y.Ohshima [1]. [1] Department of Materials Sciences and Engineering, Tokyo Institute of Technology, Nagatuta, Yokohama, Japan. [2] ERATO project, Japan Science and Technology, Tachikawa, Tokyo, Japan

Metal nanowires were formed by the technique of scanning electron microscope (STM), and their structures were studied by ultra-high vacuum (UHV) electron microscopy. A miniaturized STM was built in an UHV electron microscope to investigate the electronic conductances the nanowires, simultaneously with their structures. Gold nanowires were found to be consisted of atom strands. Each of the strands conssisted of a linear chain of gold atoms. The structure of the gold nanowires were found to change as their diameter decreases, because of symmetry breaking. The linear chain of gold atoms, or a single strand of gold atoms, was formed finally between the two electrodes, being suspended in vacuum. The strand had anomalously long spacings between the gold atoms, compared with the nearest neighbour distance in the face centered cubic crystal.

Details on the structures and their conductance quantization are presented, in addition to the experimental details.

M05.OF.005 ABSTRACT NOT AVAILABLE. M. Moeller

P05.OF.001 MELTING OF Sn NANOCRYSTALS INVESTIGATED BY SURFACE BRILLOUIN SCATTERING AND X-RAY DIFFRACTION. C.E.Bottani[1], A. LiBassi[1,2], B.K.Tanner[2], A.Stella[3], P.Tognini[3], P.Cheyssac[4] and R.Kofman[4]. 1: INFM-Dipartimento di Ingegneria Nucleare, Politecnico di Milano, Via Ponzio 34/3, 20133 Milano (Italy) 2: Department of Physics, University of Durham, South Road, Durham DH1 3LE (UK) 3: INFM-Dipartimento di Fisica "A.Volta", Universita' degli Studi di Pavia, Via A.Bassi 6, 27100 Pavia (Italy) 4: Laboratoire de Physique de la Matière Condensée, URA 190, Université de Nice-Sophie Antipolis, 06108 Nice Cedex (France)

Brillouin scattering of light off surface acoustic phonons and synchrotron (Daresbury and ESRF) X-ray diffraction have been used together for the first time to study the size-dependent melting transition of tin nanocrystals embedded in a silica film on a Si(100) substrate. A jump in the spectral shift of the surface phonon peaks was detected across the melting temperature and the nature of the transition was confirmed by the vanishing of the tin-related Bragg diffraction peaks in the same temperature range. The observed melting temperature was found to depend on the nanocrystals size and to be different from the bulk tin melting temperature. A simple effective medium tretament of the elastic constants of the film containing solid-liquid inclusions explains the observed behaviour in the Brillouin spectra. A strong central peak, possibly related to entropy fluctuations, was also observed just before melting.

P05.OF.002 X-RAY DIFFRACTION STUDY OF NANOCRYSTALLINE ZrO_2 - Y_2O_3 POWDERS. D.G. Lamas and N.E. Walsöe de Reca, PRINSO (Programa de Investigaciones en Sólidos) CITEFA-CONICET-UNSAM, Zufriategui 4380 (1603) Villa Martelli, Pcia. de Buenos Aires, Argentina.

Zirconia-based ceramics have been widely investigated due to their excellent mechanical and electrical properties, which strongly depend on the crystal structures and phase changes. One of the most notable characteristics of some zirconia-based solid solutions is the existence of three tetragonal forms, all belonging to the $P4_2/nmc$ space group. The stable tetragonal form is called the t-form, which is restricted to the solubility limit predicted by the equilibrium phase diagram. There is also a t'-form with a wider solubility, but unstable in comparison with the mixture of the t-form and cubic phase. Finally, the t"-form has an axial ratio c/a of unity, but with the oxygen atoms displaced along the c axis from their ideal sites of the cubic phase (8c sites of the Fm3m space group). The t'/t" and t"/c boundaries have been investigated in several systems, including ZrO_2-Y_2O_3. However, only arc-melting ZrO_2-Y_2O_3 powders have been carefully studied.

In this work, the tetragonal forms presented in nanocrystalline ZrO_2 - X mol% Y_2O_3 (X = 2.8, 4, 5, 6, 7, 8, 9, 10, 11, and 12) powders synthesised by a combustion route have been studied by X-ray diffraction applying the Rietveld method. Crystallite sizes were about 10nm. It was found that the axial ratio c/a decreased with an increase of Y_2O_3 content and became unity at 9% Y_2O_3. The oxygen displacement from the ideal fluorite site was about 0.24Å for all compositions. Powders in the composition range of ZrO_2 - 9 to 12 mol% Y_2O_3 were calcined at 1000°C and 1400°C in order to investigate the influence of the crystallite size. All of them presented the t"-form, but with smaller oxygen displacement, which was about 0.15Å for powders calcined at 1000°C and 0.12Å for powders treated at 1400°C. Although these results must be confirmed by neutron diffraction, this work shows that the oxygen displacement strongly depends on the crystallite size, resulting in the enlargement of the t" region in comparison with arc-melting powders, which presented the t"/c boundary at 11% Y_2O_3.

P05.OF.003 MECHANICALLY INDUCED DISORDER IN INVERSE SPINEL FERRITES. V. Sepelak, Institute of Geotechnics, Slovak Academy of Sciences, 04353 Kosice, Slovakia, and K.D. Becker, Institute of Physical and Theoretical Chemistry, TU Braunschweig, 38106 Braunschweig, Germany.

The structural and magnetic evolution in nickel ferrite ($NiFe_2O_4$) and magnesium ferrite ($MgFe_2O_4$) caused by the high-energy milling has been investigated by X-ray diffraction, Mössbauer spectroscopy and electron microscopy. With the prolongation of the mechanical activation time, $NiFe_2O_4$ and $MgFe_2O_4$ are transformed into a metastable nanocrystalline state that is characterised by the mechanically induced cation redistribution between tetrahedral (*A*) and octahedral [*B*] sites. The reduced concentration of iron ions at (*A*) sites in the mechanically treated samples, leading to the variation in the number of magnetic and nonmagnetic (*A*)-site ions as nearest neighbours of the Fe^{3+}[*B*] ions, results in a broad distribution of magnetic hyperfine fields at the octahedral sites. The probabilities of the different [*B*]-site surroundings and the Mössbauer subspectral areas are used to calculate the cation inversion parameter in the mechanically activated ferrites. Good agreement between the degree of inversion obtained from both independent procedures is found to allow us to isolate from the [*B*]-site magnetic field distribution profile the contribution due to the varying number of magnetic and nonmagnetic (*A*)-site neighbours. The broadly distributed hyperfine magnetic fields at the Fe^{3+}[*B*] nuclei are attributed to the competing exchange interactions of the Fe^{3+}[*B*]-O^{2-}-Fe^{3+}[*B*] type with deformed bond angles. The mechanically induced cation redistribution leads to a reduction of the average magnetic field at [*B*] site. Taking into account the nanoscale nature of the mechanically treated samples, a superparamagnetic relaxation effect explains a collapse of the magnetic hyperfine fields far bellow the Curie temperature in strongly activated ferrites.

The authors would like to express their gratitude to the Alexander von Humboldt Foundation for support of V. S.

05AA MOTOR PROTEINS AND MUSCLES

M05.AA.001 STRUCTURAL STUDIES OF MYOSIN. Ivan Rayment, Cary B. Bauer, Andrew M. Gulick, Robert Smith, Matthew Schroeder, James B. Thoden, and Gary Wesenberg. Institute for Enzyme Research and Department of Biochemistry, University of Wisconsin, Madison, Wisconsin, USA.

Directed movement is one of the hallmarks of life and is accomplished by enzymes that convert the energy from the hydrolysis of MgATP into mechanical work. Understanding how this is achieved at the molecular level represents a major intellectual challenge. At this time it would appear that a very limited number of strategies have evolved to carry out this task. Three major classes of molecular motors have been identified, myosin, dynein and kinesin which play different roles in cellular movement. Of these, myosin is the most abundant and has been studied more extensively than any others. The last decade has seen a dramatic improvement in our understanding of the molecular basis of motility. Even so there is still much more to be learned. For example, although the first crystal structures of actin and myosin provided a wealth of information, in reality, they represented only a partial view of one point in the contractile cycle. To overcome this problem a series of structures of a genetically truncated and modified myosin heads complexed with an extensive series of substrate analogs, several non-nucleotide substrates and ATP itself have been determined. As discussed here these structures have provide considerable insight into how ATP hydrolysis is coupled to movement.

M05.AA.002 SCALLOP MYOSIN HAS AT LEAST THREE CONFORMATIONAL STATES. A. Houdusse [1], A.G. Szent-Gyorgyi [2], C. Cohen [3], [1] CNRS EP2075, Faculte de Pharmacie, Paris, France, [2] Biology Department, Brandeis University, Waltham, MA, USA, [3] Rosenstiel Research Center, Brandeis University, Waltham, MA, USA

Three conformational states of a proteolytic subfragment (S1) from scallop striated muscle myosin have been determined by X-ray crystallography. The most unusual one has been visualized from the crystal structure of scallop S1 complexed with MgADP, which has been solved at 2.5 Å resolution, and reveals a new conformation of the myosin head. In this structure, the converter and the lever arm are in very different positions from those in either transition or "near-rigor" state structures; moreover, - for the first time - the SH1 helix is seen to be unwound. Biochemical studies indicate that this conformational state corresponds to a weak actin-binding state (Nitao and Reisler, 1998, Biochemistry 37, 16704-10). We thus believe that this new structure represents one of the pre-hydrolysis ("ATP") states of the contractile cycle, in which the myosin heads stay detached from actin. The other two crystal forms, albeit diffracting to lower resolution (4Å), show that scallop S1 adopts a conformation in the absence of nucleotide similar to that seen in chicken skeletal myosin (Rayment et al. 1993 Science 261, 50-8) and a conformation in the presence of ADP.VO4 which is similar to that of transition state structures (Fisher et al. 1995 Biochemistry 34, 8960-72; Dominguez et al. 1998 Cell 94,559-71). Comparison of the overall organization of the myosin head in the three states show how the conformation of three flexible "joints" produces rearrangements of the four major subdomains in the myosin head with different bound nucleotides.

M05.AA.003 THE NCD DIMER CRYSTAL STRUCTURE REVEALS UNIQUE FEATURES 0F MINUS END DIRECTED KINESIN MOTORS. E. Sablin, R. Case, S. Dai, C. Hart, A. Ruby, R. Vale and R. Fletterick, University of California, San Francisco, CA 94143, USA.

Motors of the kinesin superfamily move either to the plus or minus end of microtubules. Crystal structures of the catalytic motor cores of conventional kinesin (a plus end motor involved in organelle transport) and NCD (a minus end motor involved in chromosome segregation) are nearly identical; therefore, the structural basis for their opposite polarity of movement is unresolved. Here, we show that the NCD “neck”, 13 class-specific residues adjacent to the superfamily-conserved catalytic core, is essential for minus end motility, since mutagenesis of the neck residues reverses the direction of NCD motion. By solving the 2.5 Å structure of a functional NCD dimer[1], we show that the NCD neck (a coiled coil) differs from the corresponding region in the kinesin neck (interrupted β strand) , although both necks interact with similar elements in the catalytic cores. The distinct neck architectures confer different symmetries to the NCD and kinesin dimers and position these motors with appropriate directional bias on the microtubule.

1 Sablin E. P., et al. Direction determination in the minus end directed kinesin motor NCD. Nature **395**, 813-816 (1998).

M05.AA.004 THE FASCINATING STRUCTURE OF AN ACTIN CROSSLINKING PROTEIN. Steven C. Almo, Elena Fedorov, Alexander Fedorov Dept. of Biochemistry, Albert Einstein College of Medicine

Actin crosslinking proteins assemble individual actin filaments (F-actin) into higher order aggregates, such as bundles and networks, that are involved in a wide range of functions including cell motility, cytokinesis and the establishment and maintenance of cell morphology. Crosslinking proteins generally contain two F-actin binding site, and it is this bivalency that allows for crosslinking. Fascin is a 58kD actin crosslinking protein first identified in sea urchin eggs. Homologs have subsequently been found throughout the coelomocytes, and in Drosophila, amphibians and mammals. Fascin localizes to a number of different F-actin based structures including microvilli and acrosomal processes in sea urchins and starfish, and the lamellopodia, filopodia and stress fibers in mammalian cells. The crystal structure of human fascin reveals four tandemly repeated 120 amino acid modules that display the beta-trefoil fold observed in interleukin- 1beta and fibroblast growth factor. The four domains are arranged to form a bi-lobed structure that displays near two-fold symmetry. The organization of this protein is discussed with respect to its crosslinking function.

M05.AA.005 STRUCTURE OF THE BACTERIAL TUBULIN HOMOLOG FtsZ IN 2D- AND 3D-CRYSTALS. Jan Löwe and Linda A. Amos MRC Lab. of Molecular Biology Hills Road Cambridge CB2 2QH UK

The three-dimensional structure of FtsZ has been determined by X-ray crystallography in the monomeric state and by three-dimensional electron microscopy in the polymerized state. During septation, the essential bacterial cell-division protein FtsZ forms a filamentous ring which divides the two daughter cells. FtsZ from the hyperthermophilic methanogen *Methanococcus jannaschii* has been cloned, expressed in *E. coli*, and the X-ray crystal structure of the 372 residues containing protein has been solved at 2.8Å resolution. FtsZ is a two-domain protein with a Rossmann-fold related GTPase domain and a second domain of unknown function. The three-dimensional structure of FtsZ is closely related to eukaryotic tubulin. Using sheets of polymerized FtsZ the low-resolution 3D structure of FtsZ protofilaments has been determined and shows dimers of FtsZ forming a double-protofilament. FtsZ protofilaments resemble tubulin protofilaments very closely. Taking everything together, FtsZ can be regarded as a true tubulin homologue with implications for the origin of the cytoskeleton.

M05.AA.006 NUCLEOTIDE-DEPENDENT CONFORMATIONAL CHANGES OF THE MYOSIN MOTOR DOMAIN AND ITS MONOMERIC ACTIN COMPLEX IN SOLUTION. K. Wakabayashi, Y. Sugimoto, S. Kimura, Y. Takezawa and T. Arata, Division of Biophysical Engineering, Graduate School of Engineering Science, and Department of Biology, Graduate School of Science, Osaka University, Toyonaka, Osaka 560-8531, Japan.

Nucleotide-dependent conformational changes of the myosin motor domain (subfragment-1, S1) have extensively investigated by synchrotron X-ray solution scattering. In the presence of MgATP, the radius of gyration (Rg) of S1 decreased to ~4.5 nm from ~4.8 nm of the nucleotide-free S1. Thus an S1 molecule becomes compact in the intermediate state having ADP and Pi during hydrolysis of ATP. This was confirmed by the fact that S1s bound ADP and phosphate analogs such as AlF_3, BeF_x and VO_4 had similar Rg values to that in ATP solution. Modelling studies using atomic data [1] have indicated that the compaction of the S1.ADP.Pi was caused by a large movement of a light chain-binding region, corresponding to an about 5-nm displacement at its tip. When an S1 bound ADP which mimicks a release of Pi had a Rg value between those of the S1.ADP.Pi and a nucleotide-free S1 and the magnitude of a movement of a light chain-binding region was half that in the S1.ADP.Pi model.

We succeeded in making the complex of a non-polymerizable G-actin and S1, and the solution structure of it was determined by X-ray solution scattering analysis. The Rg and the maximum chord length (Dmax) were ~4.9 nm and ~16.8 nm,

respectively. The best-fit model of the complex was obtained by putting the actin subunit on the tip of the catalytic domain of S1 where the N-terminal domain of G-actin attached to the region between upper and lower 50 kD domains in S1. In this model, S1 orientated with its long axis more perpendicular to the actin axis than in an acto-S1 model of the decorated actin filament. When MgADP bound to S1 in this complex, the Rg and Dmax decreased by about 0.3 nm and 2 nm, respectively. The best-fit model of the complex with ADP was obtained by rotating the two molecules each other through nearly 90^{o} around the long axis of S1 with retaining their binding sites.

[1] Sugimoto et al., submitted for publication.
[2] Arata et al., Adv. Exp. Med. Biol. 400 (1998). In press.

P05.AA.001 X-RAY CRYSTALLOGRAPHY AND ELECTRON CRYOMICROSCOPY OF A MICROTUBULE MOTOR: THE NCD DIMER. F. Kozielski, S. De Bonis [1], W.P. Burmeister [2], C. Cohen-Addad, R.H. Wade [1]. [1] Institut de Biologie Structurale, 41 avenue des Martyrs, 38027 Grenoble Cedex 01, France, [2] European Synchrotron Radiation Facility, 38043 Grenoble Cedex 01, France

Drosophila ncd is a member of the kinesin superfamily of microtubule motor proteins. It is involved in chromosome segregation, moves towards the minus end of microtubules and has the motor domain at the C-terminus of its heavy chain. We expressed, purified and crystallized the functional homodimer (amino acids 295 - 700) in the presence of MgATP. The crystals, space group $C222_1$, two dimers per asymmetric unit, have unit cell dimensions a=116.2 Å, b=148.8 Å and c=261.5 Å. Using data collected at the ESRF, the ncd dimer structure was solved to 2.9 A by molecular replacement using the recently published perfectly 2-fold symmetric ncd dimer structure (Sablin et al., 1998, Nature, 395, 813 - 816) as a search model. This previous ncd structure was obtained from a different crystal form (P6(1)22) that has a single monomer per asymmetric unit. We compare the two ncd dimer structures and discuss their similarities and differences. We will show the results of docking our new atomic resolution structure into the three-dimensional reconstruction of the microtubule-ncd complex obtained by electron cryomicroscopy in the presence of ADP. Finally, we will compare these new results to those previously obtained for the conventional kinesin heavy chain dimer (Kozielski et al., 1997, Cell, 91, 985 - 994; Kozielski et al., 1998, Current Biology, 8, 191 - 198). This has the motor domain on the N-terminus and is a plus-end-directed motor involved in organelle transport.

P05.AA.002 THE TIME-RESOLVED DIFFRACTION STUDIES OF MUSCLE USING SYNCHROTRON RADIATION. A.A.Vazina, P.M.Sergienko [1], Rapp G., Kunst N. [2], A.M.Gadzhiev [3], M.A.Sheromov [4], [1] Institute of Theoretical and Experimental Biophysics of RAS, Pushchino, Moscow Region, 142292, Russia, [2] EMBL c/o DESY, Hamburg, D-22603, Germany, [3] Institute of Physiology of Az. AS, Baku, 370100, Azerbaijan, [4] Budker Institute of Nuclear Physics, SD of RAS, Novosibirsk, 630090, Russia

The ability of striated muscle to potentiate their twitch response after preliminary stimulation and/or fatigue has been studied. The changes of kinetic rates in the time courses of tension response and intensities of diffraction reflections at short-term stimulus history were investigated. Two different protocols were used for the collection of the data: a)frog sartorius muscle was stimulated by double pulse interval 30-300 ms; b)effect of potentiation by fatigue was examined. Experiments with time resolution of 1-10 ms have been carried out using SR of VEPP-3 (Novosibirsk) and DORIS (Hamburg). The time course of the intensity changes of equatorial reflections (1,0) and (1,1), the background underneath them, meridional reflections at spacing 44.0, 21.4, 14.3 nm and the time course of tension response P(t) have been studied. The model calculations of diffraction patterns at various radial or/and angle position of myosin cross-bridges are presented. The marked increase of tension response added by second pulse is accompanied by intensity flash of meridional reflection 14.3 nm. The monotonous character of another reflections time course is not disrupted.

We suppose in the active muscle the myosin cross-bridges of 3 thick filaments produce in the vicinity of every thin filament the short-living mesophase with 14.3 nm axial spacing (life time about 40 ms). The active myosin cross-bridges are not incorporated into helix range of thin filament. Thus the force generation of muscle proceeds upon interaction of the myosin thick and actin thin filaments in the incommensurate structural framework. We assume principle of dynamic correspondence of symmetries is crucial in biological motion [1].

1. A.A.Vazina. (1987), Nucl.Instr.Meth.in Phys.Res., v.261, 200.

05BB THE PHASE PROBLEM IN ELECTRON CRYSTALLOGRAPHY

M05.BB.001 PHASE DETERMINATION BY MAXIMUM ENTROPY AND LIKELIHOOD IN ELECTRON CRYSTALLOGRAPHY. C.J. Gilmore and A.A.Stewart, Department of Chemistry, University of Glasgow, Glasgow G12, 8QQ, Scotland UK, I.G. Voigt-Martin, Institüt für Physikalische Chemie der Universität Mainz, D-55099 Mainz, Germany and D.L. Dorset, Hauptman-Woodward Institute, 73 High Street, Buffalo, NY 14203-1196,USA.

Phase determination in electron crystallography is not easy. The data often suffer from systematic errors in the intensities arising from dynamical scattering; the sampling of reciprocal space is generally incomplete and the effective data resolution much less than the 1.1-1.3Å expected by direct methods. The maximum entropy (ME) method combined with likelihood evaluation first formulated by Bricogne [1] is capable of overcoming some of these problems, and, indeed, is often most effective with data at 2Å resolution or less.

In this formalism the data are normalised, and sets of phased reflections are generated by the use of origin fixing reflections combined with intensities in which the associated phases are permuted These phased data act as constraints in a constrained entropy maximisation to give an ME map, $q^{ME}(\underline{x})$. Each phase combination is subjected to likelihood estimation which assess how well the hitherto unphased reflection amplitudes are predicted from the FT of $q^{ME}(\underline{x})$.

We present here results on both small and macromolecules. Some of these are non-linear optical materials [2,3]; some taken from Dorset [4] and some are macromolecules [5].

CJG acknowledges support from Eastman Kodak, Rochester.

[1] G.Bricogne (1984) Acta Cryst. A40, 410-445.
[2] I.G. Voigt-Martin, Z.X. Zhang, U.Kolbe & C.Gilmore (1997) Ultramicroscopy 43-59.
[3] I.G. Voigt-Martin, Gao Li, U. Kolbe, H. Kothe, A.V. Yakimanski, A.V. Tenkovisev & C.J.Gilmore (1999) Phys. Rev. 59, in press.
[4] D.L. Dorset 'Structural Electron Crystallography', Plenum Press, 1995
[5] D.L.Dorset & C.J.Gilmore (1999) Acta Cryst. A55, in press.

M05.BB.002 CRYSTALLOGRAPHIC PHASE DETERMINATION IN ELECTRON CRYSTALLOGRAPHY. Douglas L. Dorset, Electron Diffraction Department, Hauptman-Woodward Medical Research Institute, 73 High Street, Buffalo, NY14203-1196 USA

Because multiple beam scattering is strongly expressed in electron diffraction, it has been often stated that true ab initio structure analyses would be virtually impossible, except for cases where the weak phase object would be satisfied (i. e. thin crystals of light atom materials). Recent experience with a variety of materials has modified this viewpoint somewhat. Actually, the only requirements for a successful determination of kinematical phases are two-fold: that reflections from the most significant parts of the unit cell transform can be measured and that the experimental Patterson function is well-correlated to the autocorrelation function of the actual crystal structure. These structures explain why, for example, a large 3D data set from triphenylene, giving a good fit to the known crystal structure, are not assigned accurate phase terms by direct methods; diffraction intensities from the most important unit cell projections are still missing from the sampled data. On the other hand, nearly complete electron diffraction data from an alloy are easily assigned phases by the tangent formula. Nevertheless, dynamical effects are still very pronounced in the latter case and much weaker in the former case. In general, the refinement step is where multiple beam perturbations impose the greatest challenge to structure improvement (but here dynamical effects can also be used as a refineable variable) even though they do not necessarily restrict the derivation of the initial phase model. Atomic resolution is also not required in some cases. Significant progress has been made in the direct phase determination of protein structures - for example, starting with a low-resolution basis set from the Fourier transform of an image and extending to the resolution of the diffraction pattern. More recently, filling in 'missing cone' information has been shown to give acceptable results, even though the amplitudes are not so well estimated as are the phases. True ab initio determinations have been possible for proteins which are well simulated by globular substructures, e. g. projections of α-helices. In this case, the problem is reduced to rescaling the data to simulate the pseudo-atomistic distribution of mass, as suggested originally by D. Harker. Supported by NSF CHE-9730317 and NIH GM-46733

M05.BB.003 THE PRECESSION TECHNIQUE IN ELECTRON CRYSTALLOGRAPHY. APPLICATIONS TO STRUCTURE DETERMINATION. J. Gjønnes, V. Hansen, E. Sørbrøden, P. Runde and K. Gjønnes, Centre for Materials Science, University of Oslo, Gaustadalleen 21, N-0371 Oslo, Norway.

Electron diffraction patterns from crystals are usually taken with a stationary beam (and crystal), in contrast to X-ray work where the crystal is rotated to produce integrated intensities. With the electron beam entered along a zone axis, dynamical scattering effects are exacerbated.

The recently invented precession technique [1] is a different approach to quantitative electron diffraction: Off-axis beam configurations are used, integrated intensities are obtained, dynamical effects are reduced, more reflections and three-dimensional data can be collected [2]. A 'guided beam' system [3] implemented on a Jeol 2000FX microscope in Oslo will be described. Principles for intensity calculations, relating to precession, and applications to structure determination of alloy phases will be presented.

1. R. Vincent and P.M. Midgley (1994) Ultramicroscopy 53, 271-292.
2. J. Gjønnes, V. Hansen, B.S. Berg, P. Runde, Y.F. Cheng, K. Gjønnes, D.L. Dorset and C.J. Gilmore (1998) Acta Cryst. A54, 306-319.
3. E. Sørbrøden, P. Runde and A. Olsen (1998) Electron Microscopy 1998, Proc. ICEM 14, Cancun Mexico 1998 Vol. 1, 425-426.

M05.BB.004 INVERSION OF ELECTRON ROCKING CURVES DIFFRACTED FROM STRAINED CRYSTALS. R. Vincent, H. H. Wills Physics Laboratory, University of Bristol, Bristol BS8 1TL, UK.

Presently, quantitative analysis of the Bragg-diffracted intensities within convergent beam electron diffraction (CBED) patterns has been focused on the measurement of structure factors for perfect crystals. However, many crystals contain inhomogeneous strains within the illuminated column which are encoded into diffracted intensities in the rocking curves. The two-beam equations for calculating kinematic and dynamical rocking curves from a strained crystal are well known, but it is less obvious that the inverse problem can be easily solved when only the diffracted intensities are measured. Considering first the kinematic equation, the diffracted amplitude in standard notation is given by

$$A_g(s) = \int_{-\infty}^{\infty} U_g(z)\ \exp(-2\pi i g R(z))\ \exp(-2\pi i s z)\ \mathrm{d}z,$$

where $gR(z)$ is the component parallel to $\boldsymbol{g}$ of the displacement vector $\boldsymbol{R}$, measured in units of the planar spacing. The integral is taken between $\pm\infty$, but is non-zero only for $z \in [0, t]$, where t is the crystal thickness measured along z, the beam direction. This equation is rewritten as the Fourier transform pair $A(s) \Leftrightarrow U(z)\ \exp(-2\pi i g R(z))$, where subscripts have been omitted. For a crystal with constant U_g along z, the rocking curve becomes equivalent to the Fourier transform of a pure phase object with compact support of width t. There exists a unique solution for the phase function, which is recovered by an iterative method known as the Gerchberg-Saxton algorithm. Experimental results are described in [1]. For dynamical diffraction, the equations are non-linear, and a pattern-matching approach is required based upon a Fourier expansion of $R(z)$. An algorithm using global optimization methods was used to minimise the difference between observed and calculated intensities in dynamical two-beam rocking curves.

1. R. Vincent and T. D. Walsh (1999), Ultramicroscopy (in the press).

P05.BB.001 MAXIMUM ENTROPY METHODS FOR PHASE EXTRAPOLATION: PREDICTING THE MISSING CONE IN ELECTRON DIFFRACTION. Andrew Stewart and C.J. Gilmore Department of Chemistry, University of Glasgow, Glasgow G12, 8QQ, Scotland UK.

The missing cone problem arises in electron diffraction from experimental limitations on sample tilt, and the difficulties in getting suitably oriented specimens in data collection. This missing data can make the process of structure solution and refinement more difficult, but once a model has been derived maximum entropy methods can be used to predict both the phases and amplitudes of the missing reflections and so generate more accurate models.

To do this, the data are normalised, and a basis set is defined in which all the measured reflections with model-derived phases and experimental amplitudes are included. These data act as constraints in a constrained entropy maximisation to give a map, $q^{ME}(\underline{x})$ whose Fourier transform generates phase and amplitude information for non-basis set reflections which includes those in the missing cone as well as data outside the resolution limit.

We present here results on both small and macromolecules (with the former taken from Dorset, 'Structural Electron Crystallography', Plenum Press, 1995):

Basic Copper Chloride

Poly(1,4-trans-cyclohexanediyl Dimethylene Succinate) (Poly-t-CDS)

Poly(1-butene), Form III

Rubredoxin using ideal data

Rubredoxin using experimental data to 6Σ.

In all cases, the quality of extrapolation was good, no scaling of predicted intensities was needed and mean phase errors were often below 30^o.

The method has obvious potential for phase extension in protein crystallography, and we are currently exploring this. It is possible to use phase permutation methods to assist in this process by using trial phases for key unphased reflections.

We acknowledge support from Eastman Kodak, Rochester.

P05.BB.002 DIRECT MEASUREMENT OF PHASE-INVARIANTS AND STRUCTURE AMPLITUDES FROM 3 BEAM CBED PATTERNS. J. Etheridge, A. F. Moodie and C. J. Humphreys, Dept of Materials Science and Metallurgy, University of Cambridge, Pembroke St, Cambridge, CB2 3QZ, UK.

It has been shown theoretically that, for centrosymmetric crystals, the three-phase invariant and the magnitudes of three structure amplitudes are determined directly by the coordinates of two unique points identifiable in a three beam convergent beam electron diffraction pattern [1]. The experimental application of this result will be described and, in particular, it will be shown that the phase-invariant is readily determined, in some cases by inspection. Estimates of the magnitudes of the structure amplitudes can be made to sufficient accuracy for the determination of the crystal structure but not for the measurement of bonding. The conditions that optimise the accuracy in the measurement of a given three structure amplitudes will be described. Examples from a range of compounds will be presented.

1. A. F. Moodie, J. Etheridge & C. J. Humphreys, Acta Cryst. (1996). A52, 596-605.

P05.BB.003 GEOMETRY OF THREE BEAM PHASE DETERMINATION. A. F. Moodie, J. Etheridge and C. J. Humphreys, Dept of Materials Science and Metallurgy, University of Cambridge, Pembroke St, Cambridge, CB2 3QZ, UK.

For centrosymmetric crystals the locus of two beam intensity distribution in the convergent beam disc of a three beam pattern is a degenerate hyperbola, and the sign of the phase invariant is determined by the sheet on which the centre of the distributions lie. When the symmetry of inversion that leads to the degeneracy is relaxed by the smooth increase of the antisymmetric component of the structure amplitudes, a hyperbola of increasing gap is generated and the distribution of intensity increasingly departs from two beam form. The sign of the phase invariants is still determined by the sheet on which the "quasi two beam centres" lie but the magnitude depends on gap and position. Possible structural applications will be discussed.

P05.BB.004 THE VALIDITY OF QUASI-KINEMATIC THEORY IN ELECTRON CRYSTALLOGRAPHY. H. J. Whitfield and A. F. Moodie, Dept of Applied Physics, Royal Melbourne Institute of Technology, GPO Box 2476V, Melbourne, 3001, Australia and J. Etheridge and C. J. Humphreys, Dept of Materials Science and Metallurgy, University of Cambridge, Pembroke St, Cambridge, CB2 3QZ, UK.

It is dynamical interaction which leads to a direct and unique solution of the phase problem, albeit so far only within the three beam approximation [1]. For the last quarter of a century, however, many structures have been determined using a combination of high resolution electron microscopy and electron diffraction (preferably convergent beam) employing indirect iterative procedures which are necessarily non-unique. While, in general, the comparison of observed and calculated intensity distributions in both direct and reciprocal space necessarily involves n-beam dynamical computation, some classes of structures lend themselves to quasi-kinematical analysis. The conditions under which such treatments have some validity will be discussed. In the determination of atomic positions the procedures involved frequently absorb dynamical scattering effects into the atomic scattering factors, which then no longer describe the atomic potential. Even in the most favourable cases, refinement of the potential distribution, and hence, ultimately also of the atomic positions, will necessitate the comparison of full dynamical calculations with low temperature data.

1. A. F. Moodie, J. Etheridge & C. J. Humphreys, Acta Cryst. (1996). A52, 596-605.

05CC REAL TIME 'IN SITU' REACTION CHEMISTRY

M05.CC.001 THE DEVELOPING FIELD OF PHOTO-CRYSTALLOGRAPHY: TIME-RESOLVED STUDY OF LIGHT-INDUCED TRANSIENT SPECIES. P. Coppens, Department of Chemistry, SUNY at Buffalo, Buffalo, NY 14260-3000, USA.

X-ray analysis traditionally serves to elucidate the ground state structure of solids. This limitation can now be challenged. Following our analysis of novel low-temperature stable light-induced linkage isomers of transition metal nitrosyl complexes [1], we are developing methods for time resolved studies of transient species using synchrotron radiation [2]. A very fast shutter has been constructed [3], which is to be used in conjunction with a 5-10KHz pulsed Nd-YAG laser. To reduce the laser power requirements, the heat to be dissipated in the crystal, as well as exciton-exciton annihilation, crystals are engineered such that the photo-active molecules are diluted by inert species [4]. Candidates for time-resolved studies will be discussed and preliminary spectroscopic and crystallographic results will be presented.

Support of this work by the National Science Foundation (CHE9615586, CHE9522232) and the U.S. Department of Energy (DE-FG02-86ER45231) is gratefully acknowledged.

1. P. Coppens, D.V. Fomitchev, M.D. Carducci & K. Culp (1998). *J. Chem. Soc., Dalton Trans.,* **6**, 865.
2. Y. Ozawa, M. R. Pressprich and P. Coppens (1998). *J. Appl. Cryst.,* **31**, 128.
3. W.K. Fullagar, C.D. Kim, G. Sagerman & P. Coppens, to be published.
4. Y. Zhang, G. Wu, B.R. Wenner, F.V. Bright & P. Coppens (1999). *Crystal Eng*., in press.

M05.CC.002 DIASTEREOSELECTIVE PHOTOCYCL-IZATION OF 2,4,6-TRIISOPROPYLBENZOPHENONE DERIVATIVES. S. Ohba, Department of Chemistry, Keio University, Hiyoshi 3, Kohoku-ku Yokohama 223-8522, Japan, and Y. Ito, Department of Synthetic Chemistry and Biological Chemistry, Kyoto University, Kyoto 606-8501, Japan.

Crystal-to-crystal photoreaction has potentialities to get information of the process of topochemical reaction by X-ray diffraction. However, the problem was the crystal cracking during the reaction in most cases. This problem could be technically

overcome by tuning the wavelength of light. On the other hand, the asymmetric synthesis utilizing crystalline environment is one of the promising fruits in solid-state reaction.

2,4,6-Triisopropylbenzophenones photocyclize efficiently into the corresponding benzocyclobutenols not only in solution but also in the solid state. The crystal structures of 3'- or 4'-substituted derivatives were reported along with some relationships between the crystal structures and photoreactivities [1]. An optically active substituent, (S)-methylphenyl-alanine, has been introduced to yield the non-centrosymmetric crystal structure. Asymmetric synthesis using the powder sample proceeded with a diastereomer excess (d.e.) of 87%. However, the recrystallization of the photoproduct gave only very thin needle crystals. By irradiation of light from 250 W ultrahigh pressure Hg lamp for 7 hrs through long-pass filter UV36 (T=15% at 350 nm), photoreaction in a single-crystal completed 100% without loss of crystallinity. The crystal structure after photocyclization indicates that the nearer methine H was predominantly abstracted by the carbonyl O atom in the reaction [2].

1. S.Fukushima, Y. Ito, H.Hosomi & S. Ohba (1998). Acta Cryst. B54, 895.
2. H.Hosomi, Y.Ito & S. Ohba (1998). Acta Cryst. B54, 907.

M05.CC.003 USE OF SYNCHROTRON RADIATION FOR "IN SITU" INVESTIGATION OF THE SOLID STATE REACTIONS. N.Z.Lykhov, A.V.Bessergenev, B.B.Bokhanov, Yu.A.Gaponov, V.P.Isupov, M.A.Korchagin, M.R.Sharafutdinov, B.P.Tolochko [1], S.G.Nikitenko [2], [1] Institute of Solid State Chemistry and Mechanochemistry, Novosibirsk, Kutateladze 18, 620128, Russia, [2] Institute of Catalysis, Novosibirsk, Lavrentev 5, 620090, Russia

The characteristics of chemical reactions in solids: (1) local process,(2) high velocity, (3) nuclei formation in the crystal volume - makes special methods of investigation necessary. Kinetics of solid state reactions were obtained for follow systems using X-ray diffraction of synchrotron radiation and XAFS: ceramic synthesis (WO_3+NiO); ceramic synthesis with phase transitions during reaction (MoO_3+NiO); polyphase systems synthesis ($YBa_2Cu_3O_6$); selfpropagating high temperature synthesis (Ni+Al, BaO_2+TiO + Ti); nucleation and growth of Ni particles 50 A size in $Al(OH)_3$ matrix; mechanochemical synthesis of quasicrystalls and theirs phase transformations; reactions of exothermic systems BaO_2+W. Investigations of the mentioned reactions shows, that combination of synchrotron radiation diffraction and XAFS are a powerful methods to research the dynamics of the phase forming in complex systems.

1. N.Lyakhov, Yu.Gaponov, B.P.Tolochko. Solid State Ionics, (1997), v. 101-103, 1251-1256.
2. S.G.Nikitenko, A.N.Aleshaev, G.N.Kulipanov, S.I.Mishnev, B.P.Tolochko. J. DE PHYSIQUE IV, (Supplement au Journal de Physique III, 4), (1997), Vol. 7, C2, 549-552.
3. S.V. Chernov, S.G.Nikitenko, B.P.Tolochko. Ibidem, 961-964.

M05.CC.004 PHOTOINDUCED METASTABLE STRUCTURES IN SEVERAL ORGANIC CRYSTALS. Y. Ohashi, H. Uekusa, A. Sekine, T. Ohhara, M. Kawano, J. Harada, Department of Chemistry, Tokyo Institute of Technology, O-okayama, Meguro-ku, Tokyo 152-8551, Japan

The process of chemical reaction in a crystal can be observed by the stepwise X-ray crystal structure analyses if the crystallinity is kept during the reaction. We have found a variety of photoisomerizations of cobaloxime complexes in which the reactions proceed with retention of the single crystal form. Recently the technique was applied to observe the metastable structures in organic and metal complex crystals.

The first example is the 3-1 photoisomerization of the cyanopropyl group bonded to the cobalt atom in cobaloxime complexes. When the crystals were irradiated with a xenon lamp, the 3-cyanoproyl group was isomerized to the 2-cyanopropyl group and then was transformed to the 1-cyanopropyl group. Such a two-step reaction was clearly analyzed by X-ray and neutron structure analyses of the cobaloxime crystals. The second example is the metastable structure of the ruthenium complex with the NO group as an axial ligand. When the complex crystal was exposed to the light (<450 nm), about 8% of the NO group was upside down. The inverted ON group was clearly analyzed by X-rays at 103 K. And when the crystal was irradiated with the light (>600 nm), it was restored to the original one.

The third example is the metastable state of the photochromic crystal. When the crystal of salicylideneaniline was irradiated with the light (<370 nm), its color turned from pale yellow to dark red. The dark red color turned back by irradiation with another light (>530 nm). The metastable structure of the dark red color species was analyzed by X-rays. The result revealed that the photochromism of salicylideneaniline is caused by an interconversion between the enol and trans-keto forms.

The fourth example is the structure of a metastable radical pair of the hexaarylbiimidazolyl derivative. The C-N bond connecting the two triaryl-imidazolyl rings was cleaved by the irradiation to form a radical pair composed of two planar molecules. The CW-ESR experiments at 77 K clearly indicated a triplet-state signal of the radical pair. The crystal structure analyzed at 103 K showed the structure of the radical pair produced by the irradiation. The radical pair converted to the original form thermally, which was ascertained by X-ray analysis.

M05.CC.005 TOPOCHEMICALLY VERSUS NON-TOPOCHEMICALLY CONTROLLED SOLID-STATE METHYL REARRANGEMENT. M. Kaftory, E. Handelsman-Benory, M. Botoshansky, V. Shteiman, and M. Greenberg, Department of Chemistry, Technion Israel Institute of Technology, Haifa, 32000, Israel.

The combination of supramolecular architecture in solids together with the ability of molecules to react intermolecularly makes such systems valuable for the study of cooperate bulk phenomena. Recently we have studied the solid-state intermolecular methyl transfer in cyanurates and thiocyanurates. It was found that 1, 2, and 3 undergo topochemically controlled solid-state methyl rearrangements. The rearrangement product in each of the solid-state reaction is topochemically controlled and is dependent of the supramolecular architecture.

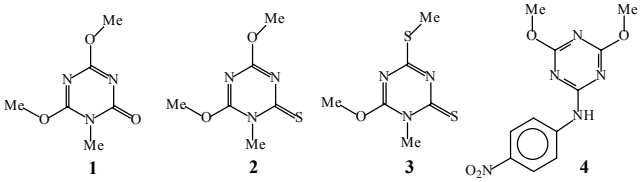

The product obtained from 1 was a result of O to N methyl migration, while those obtained from 2, and 3 resulted from O to S methyl migration. Compound 4, on the other hand, undergoes solid-state methyl rearrangement revealing at least four different products. It will be shown that this is a result of non-topochemically controlled solid-state reaction.

The structures - product relationships and the mechanism of the solid-state methyl rearrangement will be discussed.

05DD OPTIMISATION METHODS (sponsored by Tripos Inc.)

M05.DD.001 STOCHASTIC OPTIMISATION: SIMULATED ANNEALING AND THE GENETIC ALGORITHM. C. Jennison, Department of Mathematical Sciences, University of Bath, Bath BA2 7AY, UK.

Many practical problems of optimising high-dimensional functions with multiple local optima fall outside the domain of standard numerical algorithms. Recent years have seen considerable interest in two stochastic optimisation techniques, simulated annealing and the genetic algorithm, which use different forms of random search to solve such problems. In the following, we suppose it is desired to find the value of x which maximises an objective function f(x).

Simulated annealing starts with a random walk algorithm that one could use to draw a random value of x with probability proportional to f(x). However, as this random walk continues it is modified so as to sample from successively more peaked functions, accentuating the high values of f(x) and

diminishing the low values. Ultimately, the hope is that the process will become trapped in smaller and smaller regions surrounding the global maximum of f(x) and the global solution, or at least a near-optimal x, will be found. The genetic algorithm operates by creating a population of possible solutions, x, and letting these develop in a manner similar to natural evolution. Population members with higher values of the objective function f(x) are given a higher probability of selection as parents for the next generation. Offspring inherit components of x from both parents with occasional chance mutations. The aim is that solutions will 'evolve' towards the optimum and a good, or even an optimal,solution will eventually be generated.

I shall discuss theoretical foundations of both methods and note their messages for practical implementation. Examples will be used to illustrate qualitative points about each method and to make controlled comparisons.

1. Jennison, C., Franconi, L. & Sheehan, N. A. (1995) Stochastic optimisation: simulated annealing and the genetic algorithm. In Complex Stochastic Systems and Engineering, (ed. D. M. Titterington), Oxford: Clarendon Press, 209-213.
2. Jennison, C. & Sheehan, N. A. (1995) Theoretical and empirical properties of the genetic algorithm as a numerical optimizer. Journal of Computationaland Graphical Statistics, 4, 296-318.
3. Franconi, L. & Jennison, C. (1997) A comparison of genetic algorithms and simulated annealing in an application to statistical image reconstruction. Statistics and Computing, 7, 193-207.

M05.DD.002 APPLICATION OF THE DIFFUSION EQUATION METHOD TO GLOBAL OPTIMIZATION. H.A. Scheraga, Baker Laboratory of Chemistry and Chemical Biology, Cornell University, Ithaca, NY 14853-1301, USA

The Diffusion Equation Method (DEM) was originally designed to surmount the multiple-minima problem in the conformational analysis of molecules, by deforming the potential energy hypersurface by the DEM [1]. It has been applied to argon clusters [2], oligopeptides [3], and the predic- tion of crystal structures [4,5]. In recent applications [4-6], the unsmoothing (reversing) part of the DEM algorithm has been modified to include multiple trajectories, with perturbation at each stage of the reversing procedure, thereby improving the performance of the procedure.

The revised procedure has now been applied to the conformational analysis of very long polyalanine chains and of protein A [6], and also to the phase problem in crystallography.

1. L.Piela, J.Kostrowicki & H.A.Scheraga (1989). J. Phys. Chem.,93,3339.
2. J.Kostrowicki, L.Piela, B.J.Cherayil & H.A.Scheraga (1991). J. Phys.Chem.,95,4113.
3. J.Kostrowicki & H.A.Scheraga (1992). J. Phys. Chem.,96,7442.
4. R.J.Wawak, K.D.Gibson, A.Liwo & H.A.Scheraga (1996). Proc. Natl. Acad.Sci., USA,93,1743.
5. R.J.Wawak, J.Pillardy, A.Liwo, K.D.Gibson & H.A.Scheraga (1998). J.Phys. Chem.,102,2904.
6. J.Pillardy, A. Liwo, M. Groth & H.A. Scheraga (1999) J. Phys. Chem, submitted.

M05.DD.003 GENETIC ALGORITHMS FOR MOLECULAR RECOGNITION. G. Jones [1], R.C. Glen [2], A.R. Leach [3], R. Taylor [4], P. Willet [5], [1] Arena Pharmaceuticals, 6166 Nancy Ridge Drive, San Diego CA 92121, USA, [2] Tripos Inc, 1699 South Hanley Road, St Louis MO 63144, USA, [3] Glaxo Wellcome Medicines Research Centre, Gunnels Wood Road, Stevenage SG1 2NY, UK, [4] Cambridge Crystallographic Data Centre, 12 Union Road, Cambridge CB2 1EZ, UK, [5] Department of Information Studies, University of Sheffield, Western Bank, Sheffield S10 2TN, UK

Genetic algorithms (GAs) are novel optimization algorithms which emulate the process of Darwinian evolution to solve complex search problems. Guided by the mechanics of evolution, successive generations of populations of artificial creatures called chromosomes search the fitness landscape of a problem to determine optimal solutions. The aplication of GAs to problems in computational chemistry and biology is the subject of much investigation.

Computational problems in molecular recognition are extremely demanding. Not only are powerful search engines capable of solving multiple minima problems required, but also an appreciation of the process of molecular recognition is required to generate suitable target functions. We have developed a GA for ligand docking that explores the full range of ligand flexibility and available binding modes. In validation studies involving 134 protein/ligand complexes a 72% success rate was achieved. Using similar techniques a related program was able to elucidate pharmacophores from a series of active compounds, while accounting for the conformational variance of the actives.

1. G. Jones, P. Willett, R.C. Glen, A.R. Leach & R. Taylor (1997) J. Mol. Biol. 267, 727.
2. G. Jones, P. Willett & R.C. Glen (1995). J. Comput. Aid. Mol. Des. 9, 532
3. G. Jones, P. Willett & R.C. Glen (1995). J. Mol. Biol. 254, 43.

M05.DD.004 SIMULATED ANNEALING AS A TOOL FOR STRUCTURE DETERMINATION FROM POWDER DIFFRACTION DATA. W.I.F. David, K. Shankland and T Csoka, ISIS Facility, Rutherford Appleton Laboratory, Chilton, Didcot, Oxon. OX11 0QX, UK.

Over the past decade, there have been many attempts at structure determination from powder diffraction data. The algorithms used fall into two main types: traditional techniques such as Patterson and Direct Methods and, more recently, global optimisation methods based around techniques such as simulated annealing and genetic algorithms. This talk will focus on simulated annealing techniques with particular emphasis on algorithm development and its specific implementation in the area of structure solution from powder diffraction data [1]. Efficient algorithms will be described for both the search methods employed and the evaluation of candidate solutions. These algorithms will be illustrated with the structure solutions of drug structures ranging from polymorph pairs to multiple salt forms. The current limits of the technique will be discussed with a resume of remarkable successes and failures. The importance of

the inclusion of additional chemical information will be highlighted.

David, W.I.F., Shankland, K. and Shankland, N., *Chem Commun*, 1998, 931.

M05.DD.005 PHASING BY *AB INITIO* MODELLING: CONDITIONAL DYNAMICS, A NOVEL N-PARTICLE OPTIMIZATION METHOD. Piet Gros, Dept. of Crystal and Structural Chemistry, Bijvoet Center for Biomolecular Research, Utrecht University, Padualaan 8, 3584 CH Utrecht, The Netherlands.

For a direct phase determination method in protein crystallography we are developing an *ab initio* modelling (AIM) procedure. To enable optimization of randomly distributed loose atoms with respect to protein geometries we have developed a N-particle optimization method coined “Conditional Optimization” or “Conditional Dynamics”.

Direct phasing of protein-diffraction data sets at resolutions of 2 to 3 Å remains an elusive goal. Critical for a general solution to the phase problem will be the efficient use of available sources of information. In our procedure, we optimize randomly distributed loose atoms against observed crystallographic data and against prior structural data, i.e. known protein geometries. We developed a N-particle method that allows a rigorous treatment of geometrical restraints without the need of assigning fixed atom types or a fixed topology. Moreover, this procedure allows the incorporation of chiral restraints enforcing right-handedness of the model. This method of Conditional Optimization is being incorporated into an optimization protocol using maximum-likelihood based simulated annealing and multiple independent trials. The method of Conditional Optimization and examples on test calculations will be presented.

05EE MICROSTRUCTURE AND TEXTURE OF REAL MATERIALS

M05.EE.001 STRUCTURE - MICROSTRUCTURE RELATIONSHIPS IN CERAMIC OXIDES. V. Massarotti, D. Capsoni and M. Bini, Dipartimento di Chimica Fisica e CSTE-CNR, Universita’ di Pavia, Viale Taramelli 16, 27100 Pavia (Italy)

Solid solutions and ceramic oxides are widely used for applications in different fields: catalysis, design of devices, sensors and doped multilayer capacitors with peculiar electric properties, electrode materials in electrochemistry, semiconductors devices and homogeneous glass-ceramic superconductors. In all these cases and in many others the most recent research shows that microstructure has a definite influence on some peculiar properties. The precise determination of microstructural parameters is of great interest for the understanding of the correlations existing among grain and crystallite size, defects, composition and other properties of the materials.

A number of cases will be reported in which the microstructural aspects are remarkably important for the characterization of samples prepared in a very wide range of annealing conditions and for which is suitable to take into account the strain and size effects, to obtain the best interpretation of the observed peak profile broadening (1). In other cases, the explanation for the anisotropic peak broadening, observable in the diffraction patterns, are given in terms of line defects. On the basis of a recently proposed model, the effects of some kind of dislocations can be taken into account to fit the experimental peak-width (2). Using such a model, the microstructural features of cubic $LiMn_2O_4$ spinel, that can affect its electrochemical behaviour, can be investigated by line profile analysis of X-ray diffraction patterns.

1. V.Massarotti, D.Capsoni, M.Bini, A.Altomare & A.G.G.Moliterni (1998). Mat. Sci. Forum, 278-281, 873.
2. V.Massarotti, D.Capsoni, M.Bini, P.Scardi, M.Leoni & T.Ungar (1999). Mat. Sci. Forum, in the press.

M05.EE.002 SHORT AND INTERMEDIATE RANGE ORDER IN MATERIALS USING THE ATOMIC PAIR DISTRIBUTION FUNCTION METHOD. Simon J. L. Billinge, Th. Proffen, Department of Physics and Astronomy and Center for Fundamental Materials Research Michigan State University

Many of the most interesting recently discovered new materials are significantly structurally disordered. Furthermore, the disorder often plays an important in role in the interesting properties. It is clear that techniques which can characterize the short-range order in such materials will become increasingly useful. We have been developing the atomic pair distribution function (PDF) technique for analyzing x-ray and neutron powder diffraction data. This is a real-space approach which {\it yields the structure as a function of length-scale} on nanometer length-scale. Thus, if a material has locally ordered domains with some characteristic correlation length, the local structure can be found from the low-r region of the PDF. Also, in favourable circumstances, the domain size and inter-domain order can be determined.

I will describe the technique showing examples of how length-scale dependent structures can be obtained. I will discuss recent advances in data collection and modelling, and show the application to oxide materials which exhibit a microscopic electronic phase separation phenomenon.

We acknowledge funding from NSF 97-00966 and DOE DE-FG02-97ER45651

M05.EE.003 MATERIALS SCIENCE APPLICATIONS OF HIGH ENERGY SYNCHROTRON RADIATION. H.F. Poulsen, D. Juul Jensen and T. Lorentzen, Materials Research Department, Risø National Laboratory, DK-4000 Roskilde. U. Lienert and Å. Kvick, ESRF, BP 220, F-38043 Grenoble Cedex

High energy X-rays from synchrotrons are the basis of a new diffraction tool, combining high flux and large penetration power. Local micron-scale studies can be performed on materials science properties such as grain orientations, strain and phase identification within the *bulk* of millimetre thick specimens. The properties of the individual grains can be investigated along with mappings of the grain boundary topology. Likewise, embedded volumes and interfaces become accessible. Moreover, hard x-rays are well suited for *in-situ* studies of samples in complicated environments.

The prospect of the technique will be illustrated by a series of examples, ranging from local strain and texture measurements in gradient and composite type of samples to *in-situ* characterisation of the phase transformation and texturing mechanisms in high Tc superconducting tapes. Emphasis will be put on a series of recrystallisation experiments where the nucleation and grain growth of the individual grains is followed during an annealing.

In the end, 3DXRD, a new experimental station at ESRF will be presented. The station is dedicated to three-dimensional mappings of the microstructure. It operates in the energy range of 40-100 keV with a spatial resolution of 5x5x50 μm or better. The set-up utilises micro-focusing optics, high-resolution 2D detectors, and new techniques for improving the depth resolution: tracking and focusing analyser optics.

M05.EE.004 THE APEX STRUCTURE OF CO-PRODUCED CARBON AND BORON NITRIDE CONES. L.N. Bourgeois, Y. Bando, K. Kurashima and T. Sato, National Institute for Research in Inorganic Materials, Namiki 1-1, Tsukuba 305-0044, Japan.

Conical whiskers of layered compounds such as graphite and hexagonal boron nitride (h-BN) are interesting materials because their conical morphology results from the introduction of a local topological defect at the cone apex. In the honeycomb array characteristic of graphite and h-BN basal planes, such topological defect is thought to be a non-hexagonal ring (e.g. a pentagon or a square). These defects are known to form the basis of curved nanostructures like fullerenes and buckytubes. Therefore a comparison of their occurrence in two systems known to harbour nanostructures is worthy of study.

In this work, the defect structure at the apex of co-produced carbon and BN whiskers [1] is investigated by high-resolution transmission electron microscopy and electron diffraction. Analysis of high-resolution images shows that the cones are helical with helical pitch equal to one, and in some rare cases, two. This strongly supports a nucleation scenario involving the formation of a single ring defect as the cone nucleus. In addition, a careful measure of the cone apex angle for many cones, using electron diffraction patterns, indicates that the great majority of BN cones have apex angles corresponding to a square-like ring-defect. In contrast, pentagon-like defects are by far the most common type in carbon cones. This confirms theoretical studies [2] which showed that even-membered rings, and in particular squares, should be the most stable ring-defect in BN.

T. Sato (1996). in NIRIM Research Report, edited by NIRIM, Tsukuba, Ch. 3, Vol. 89, p.12.
X. Blase, A. De Vita, J.-C. Charlier and R. Car (1998). Phys. Rev. Letts., **80**, 1666.

M05.EE.005 SINGLE GRAIN ANALYSIS OF STORED ENERGY IN COLD-ROLLED STEEL BY X-RAY MICRODIFFRACTION. M. Drakopoulos, I. Snigireva, A. Snigirev [1], O. Castelnau, T. Chauveau, B. Bacroix [2], C. Schroer [3], T. Ungar [4], [1] ESRF, 38043 Grenoble, France, [2] LPMTM-CNRS, University Paris-Nord, 93230 Villetaneuse, France, [3] II. Physikalisches Institut, RWTH, Aachen, Germany, [4] Eötvös University Budapest, 1445 Budapest, Hungary

Single grain properties like orientation, size, dislocation density, and internal strain may vary extremely even between neighbour grains, and therefor the material under research has to be regarded as heterogeneous in the micrometer scale. One process of great industrial and scientific interest which is dominated by these properties is recrystallisation. Plastic deformation or annealing lead to an heterogeneous strain- and dislocation field in the material and store energy which also is deposited heterogeneously in the volume. The progression of the following recrystallisation then strongly depends on the distribution of the stored energy inside the material. The dislocation- and strain-field can be experimentally observed with x-ray diffraction and quantitatively determined by line profile analysis of the diffracted beam [1].In this work the local strain- and dislocation state of single grains in a polycrystalline material was examined. The samples have been cold-rolled steels before recrystallisation. After taking an orientation map with Back Scattered Electron Diffraction (EBSD) the sample was further analysed with x-ray micro-diffraction. A 4-circle diffractometer with a xyz-stage for the sample was used. The incoming beam was focused with an Compound Refractive Lens [2]. The line-profiles have been recorded using a 2-dimensional gas-filled detector. For alignment of beam, grain-positions and diffractometer centre a alignment system based on a direct calibration with x-rays has been developed.For 20 different grains 6 orthogonal reflections per grain have been recorded. The average grain size was around 20 micrometer. The line profiles from different reflections result in a 3-dimensional information of the dislocation- and strain-state of single grains.

P05.EE.002 ANISOTROPY OF DIFFRACTION LINE PROFILE PARAMETERS AND REAL STRUCTURE OF MATERIALS. R. Kuzel, Faculty of Mathematics and Physics, Charles University, Ke Karlovu 5, CZ-121 16, Prague, Czech Republic

Powder diffraction line profiles often show significant anisotropy of certain parameters - positions (cubic lattice parameters), broadening, intensities (static Debye-Waller factors). This can be not only parasitic effect which should be avoided or corrected in structure refinement but it can also be a source of valuable information on real structure of materials - their micro- or nanostructure and/or lattice defect types. A short review of the problem is given and examples are presented with different explanation of the observed anisotropies.

The anisotropy of dislocation-induced line broadening indicates prevailing dislocation types as it has been shown for several hexagonal and cubic materials both theoretically and experimentally. Different line broadening anisotropies are characteristic of other lattice defects such as stacking faults, precipitates, dislocation loops. In fine powders, the anisotropy of line broadening can help to determine the shape of particles. Strong anisotropies of cubic lattice parameters observed on protective coatings were explained by significant sample inhomogeneity when differently oriented grains (texture components) had different microstructures and by the oriented microstresses. Severe anisotropy of static Debye-Waller factors (diffuse scattering - quasilines) observed in aged Cu-Be samples with precipitates could only be explained considering preferred orientation of the precipitates with respect to the surface.

P05.EE.003 DOMAIN TEXTURE OF Cu_3Au FILMS IMAGED BY COHERENT X-RAY DIFFRACTION. I. K. Robinson, J. A. Pitney, I. A. Vartaniants, R. Appleton and C. P. Flynn, Department of Physics, University of Illinois, Urbana, IL 61801, USA

X-ray diffraction with a coherent beam will preserve the crystallographic phase of the entire object under illumination. The interference between domains in a textured material is encoded as intensity modulations in the diffraction pattern which can be recorded with a high-resolution detector. In principle, this can be inverted to an *image* of the texture. We have recorded such diffraction patterns using the (100) and (110) diffraction peaks of a crystalline thin film of Cu_3Au with (111) orientation. Undulator radiation of 8.5keV from the Advanced Photon Source was required for the coherence. The texture in this sample is due to antiphase domains which are around 1000A in size. The diffraction patterns have been inverted using the Gerchberg-Saxton and hybrid-input-output algorithms to produce images of the domain texture. In this paper we will report our progress towards understanding the convergence of the algorithm and the uniqueness of the texture images we have obtained.

P05.EE.004 CRYSTAL STRUCTURE OF γ_1' MARTENSITE IN Cu-Al-Ni ALLOY. A.E. Skourikhin and A.T. Kosilov, Voronezh State Technical University, Physics of metals department, Moskovski prospekt 14, 394026 Voronezh, Russia, and A.Yu Vasilenko, Voronezh State Technology Academy, Physics department, prospekt Revoluci 19, 394000 Voronezh, Russia.

The thermoelastic γ_1' martensite formed upon cooling and room temperature aging in single crystal and polycrystal Cu-Al-Ni

alloy has been studied by means of X-ray diffraction. The main features are the appearance of (001) reflection and lowering of differences between intensities of (200) and (002) reflections for polycrystals. Specimens, appearance of (321) and (323) reflections and great decrease of intensities for (400) and (402) reflections in diffraction pattern of rotating single crystal, gradual changing of intensities for some reflection during aging.

Such a behavior allows to propose a modified 2H structure of γ_1' martensite. Namely, in the orthorhombic coordinate the each second layer parallel to the basal plane is shifted to the position (a/2-x,0,c/2) from the normal (a/3,0,c/2) with $a/8<x<a/6$ and a=4.382 Å, b=5.356 Å, c=4.222 Å. Some shuffling of (100) planes or individual atoms in [001] direction is believed. The last proposition follow from appearance of (001) reflection, relative intensities of (200) and (002) reflections and decreasing of (002) reflection intensity during aging.

The new stacking position of the each second layer parallel to the basal plane and shuffling in [001] direction are confirmed by a hard sphere model of atoms including relative dimensions of Cu and Al atoms and computer simulation of structure using the Morse potential and minimum energy condition.

05FF FERROIC STRCUTURES

M05.FF.001 STUDIES OF FERROIC CRYSTALS BY OPTICAL METHODS. A.M. Glazer Department of Physics, University of Oxford, UK.

Ferroic crystals are characterised by a variety of, in principle, switchable properties, which in turn means that they tend to exhibit within a single crystal several domain states. Optical properties, which are very dependent on small changes in the crystal structure, can be used to study these domain states. In particular, measurements of the linear birefringence are a particularly sensitive probe for this, and so techniques for making such experiments will be briefly reviewed. Originally, birefringence was measured by traditional compensator techniques, but with the advent of high-speed computing, high-resolution graphic boards and CCD cameras, it is now possible to make very precise and more informative birefringence measurements. One of the latest ways of doing this is to combine birefringence studies with modern techniques of image analysis, so that one can obtain information throughout the whole of the specimen simultaneously rather than a simple spot measurement. This will be illustrated by a microscope system that enables the optical retardation to be separated from orientation and absorption effects for any image. New techniques also for measuring optical rotation in crystals will also be discussed briefly.

M05.FF.002 FERROELECTRIC AND ANTIFERRO-ELECTRIC TRANSITIONS IN MIXED PEROVSKITES D. Pandey, Materials Science and Technology, Banaras Hindu University, Varanasi-221005, India.

This talk presents an overview of recent results on the structural phase transitions in (Sr,Ca)TiO3 [SCT], Pb(Zr,Ti)O3 [PZT] and (Pb,Ba)ZrO3 [PBZ]. (i) A combined x-ray, electron and neutron diffraction study on SCT has revealed a series of tilt transitions which play a crucial role in the stabilisation of ferroelectric (FE), glassy and antiferroelectric (AFE) phases. (ii) In PZT ceramics a combined high temperature x-ray and piezoelectric measurements has shown that the coexistence of the rhombohedral phase with tetragonal for the MPB compositions is not responsible for the maximum electromechanical response as hitherto believed for decades. (iii) In the PBZ system high temperature XRD and dielectric results have explained as to why it becomes relaxor for more than 25% Ba using Landau theory considerations.

M05.FF.003 RELAXOR FERROELECTRICS. R. Blinc, J. Stefan Institute, Jamova 39, 1000 Ljubljana, Slovenia.

Relaxor phases are typically found [1] in structurally disordered perovskites of the $A_yA'_{(1-y)}B_xB'_{(1-x)}O_3$ type. They are believed to provide a conceptual link between ferroelectrics and dipolar glasses and besides have found use in numerous applications in view of their outstanding electromechanical properties. The nature of the diffuse phase transition in the relaxors has remained the subject of some controversy. No macroscopic symmetry change has been observed down to the lowest temperatures in zero electric field. The low temperature state is characterized by a broad frequency dispersion in the complex dielectric constant, a logarithmic polarization decay, and a slowing dynamics. Randomly oriented pinned nanodomains induced by compositional fluctuations coexist with reorientable polar clusters. The basic open question is whether the relaxor phase represents (i) a ferroelectric state broken up into nanodomains under the constraint of quenched random fields or (ii) a dipolar glass state.

Measurements of the local polarization distribution function and of the Edwards-Anderson glass order parameter in $PbMg_{1/3}Nb_{2/3}O_3$ and $Pb(Sc_{0.5}Ta_{0.5})O_3$ via 2D NMR have shown that the results are very different from the ones previously obtained for dipolar or quadrupolar glasses but quantitatively agree with a newly proposed spherical random bond-random field model (SRBRF) of relaxor ferroelectrics. This model can in addition to other glassy features also quantitatively describe the anomaly in the temperature dependence of the third order dielectric nonlinearity which cannot be explained by a para- to ferroelectric transition in random fields. The SRBRF model also predicts that the peak in the nonlinear dielectric susceptibility disappears in the presence of a non-zero electric field as indeed observed, and that a ferroelectric long range ordered state appears for $E > E_c$.

L. E. Cross (1994), Ferroelectrics, **151**, 305.

M05.FF.004 THEORY OF MORPHOTROPIC PHASE BOUNDARIES. Yoshihiro Ishibashi, Department of Applied Physics, School of Engineering, Nagoya University, Chikusa-ku, Nagoya 464-8603, Japan

Solid solutions based on the perovskite ferroelectric crystals show excellent physical properties as sensors and actuators, especially when the composition lies close to the morphotropic phase boundary. This is due to the situations that, in the vicinity of the morphotropic phase boundary, the transversal electric susceptibilities tend to diverge, some components of elastic stiffness constants become extremely small and, as the result, the electromechanical coupling constant approaches unity. These phenomena can be easily explained by the Landau theory with the free energy function written in terms of the polarization components which are the bases of the T1u irreducible representation of the point group m3m[1]. At the morphotropic phase boundary, the free energy function is found to become almost isotropic in the space spanned by three polarization components. The results can be also applied to the family of the rare-earth Fe2 compounds, which are ferromagnetic (ferrimagnetic).

1. Y. Ishibashi and M. Iwata: Jpn. J. Appl. Phys. 37, Pt.2 (1998) L985.

M05.FF.005 ELECTRON LEVEL STRUCTURES AND PHYSICAL PROPERTIES. M.Sakata, Department of Applied Physics, Nagoya University, Nagoya 464-8601, Japan,

In most structure analyses by X-ray diffraction for understanding physical properties and structural relationships, main interests are bond lengths. They can be easily calculated from the atomic coordinates, which are refined structural parameters in the least squares refinement. This type of work may be called atomic level structure analyses, because it concerns only the central positions of atoms. Huge amount of knowledge concerning bond lengths has been accumulated in the past years, which is very helpful to understand physical properties and structural relationships. Nonetheless it does not deny the importance of studying electron level structures, because many physical properties are closely related to the behavior of electrons in solid. Such a situation is the same in the case of ferroic structures, too. In particular, it is very important to study both atomic and electronic level structures of ferroic structures involving hydrogen atoms, because both structures may be very different due to deformation of electron clouds which belong to hydrogen atoms.

So far, such electron level structure analyses have been done by multi-pole analyses or difference Fourier transformations. Recently, a new sophisticated method to study electron level structures has been developed, that is, the Maximum Entropy Method (MEM). By MEM, electron level structures of quite a few crystalline materials have been so far obtained. These works seems to be proving that even from a X-ray powder data set where the number of structure factors determined is rather limited, MEM can yield a physically meaningful total electron density distribution, which agree with the observed structure factors within experimental errors as a whole.

To have better understanding of physical properties and structural relationships of ferroic substances, the recent results of electron level structures for 1) ferroic substances involving hydrogen atoms such as KDP and ADP, 2) non-hydrogen ferroic substances like $SrTiO_3$ and 3) some other topics will be discussed in the talk.

06OA MEMBRANE PROTEINS AND TRANSMEMBRANE SIGNALLING

M06.OA.001 STRUCTURE AND ACTIVATION BY DIMERISATION OF THE INTEGRAL MEMBRANE ENZYME OMPLA, OUTER MEMBRANE PHOSPHOLIPASE A. Bauke W. Dijkstra and Arjan Snijder, Laboratory of Biophysical Chemistry, Groningen University, Nijenborgh 4, 9747 AG Groningen, the Netherlands

Outer membrane phospholipase A (OMPLA) is an integral membrane enzyme located in the outer membrane of Gram-negative bacteria. Its structure has been determined by X-ray crystallography. Monomeric OMPLA consists of a 12-stranded anti-parallel β-barrel with a convex and a flat side and with approximate dimensions of 16x30x45 $Å^3$. The 12 amphipathic β-strands traverse the membrane in an up-and-down fashion forming a hydrophobic outer surface.

The active site contains Ser144 and His142, as established from chemical modification and site-directed mutagenesis experiments. It is located on the exterior of the β-barrel, positioned just outside the outer leaflet ring of aromatic residues. Besides the serine and histidine, the active site contains an asparagine residue (Asn156). Its carboxamide side chain is at hydrogen bonding distance from the Nδ1 atom of His142, probably fixing the orientation of the His142 side chain.

The activity of the enzyme is regulated by reversible dimerisation with the dimer being the active form. Covalent inhibition of OMPLA results in increased dimer stability which allowed for the crystallisation of the dimer. The monomers associate in a parallel fashion to form a homo-dimer such that the two active sites are located at the outer leaflet side of the membrane. Surprisingly little structural rearrangements occur (r.m.s. difference between monomer and dimer is 0.4 Å for 257 Cα atoms). The key interaction stabilising the dimer seems to be a double hydrogen bond formed between the side chains of glutamine 94 from one monomer and its counterpart in the other monomer, nearly in the middle of the membrane-embedded part.

Dimerisation results in productive active sites, with two substrate binding pockets created at the interface between the two monomers.

M06.OA.002 CRYSTAL STRUCTURE OF THE OUTER MEMBRANE ACTIVE TRANSPORTER FEPA FROM E. COLI. S.K. Buchanan[1], B.S. Smith[1], L. Venkatramani[2], D. Xia[1], L. Esser[1], M. Palnitkar[1], R. Chakraborty[2], D. van der Helm[2] and J. Deisenhofer[2]. [1]Howard Hughes Medical Institute and Department of Biochemistry, UT Southwestern Medical Center, 5323 Harry Hines Blvd., Dallas, TX 75235-9050, USA. [2]Department of Chemistry and Biochemistry, The University of Oklahoma, 620 Parrington Oval, Norman, OK 73019-0370, USA.

Ferric enterobactin receptor (FepA) is an 80 kD integral outer membrane protein from *E. coli* which binds ferric enterobactin (719 daltons) and transports it into the periplasm; it also serves as the receptor for colicins B and D. FepA belongs to the family of high affinity, active transport receptors which specifically transport iron chelates and vitamin B_{12} across the outer membrane, against a concentration gradient. FepA recognises and binds ferric enterobactin in the absence of other factors, but ligand transport requires energy derived from the proton motive force across the inner membrane. This is accomplished through physical interaction with an integral inner membrane protein complex, TonB-ExbB-ExbD, a part of which is believed to span the periplasm.

The structure of FepA has been solved at 2.4Å resolution by multiwavelength anomalous diffraction (MAD) on selenomethionine-containing crystals at 170ºC. Two distinct functional domains are revealed: (1) a 22-stranded β-barrel spans the outer membrane and contains large extracellular loops which appear to function in ligand binding, and (2) a globular N-terminal domain folds into the barrel pore, inhibiting access to the periplasm and contributing two additional loops for potential ligand binding. We postulate that these loops provide a signalling pathway between the coupled processes of ligand recognition and TonB-mediated transport. The blockage of the pore suggests that the N-terminal domain must undergo a conformational rearrangement to allow ligand transport into the periplasm.

M06.OA.003 TWO CONFORMATIONAL STATES OF THE LIGAND-GATED ALLOSTERIC MEMBRANE RECEPTOR FHUA. Dino Moras, Bernard Rees, André Mitschler, Luc Moulinier [1], Kaspar P. Locher, Ralf Koebnik, Jurg P. Rosenbusch [2], [1] Laboratory of Structural Biology (CNRS), IGBMC, 1 rue L. Fries, BP 163, Illkirch Cedex/France, [2] Department of Microbiology, Biozentrum, University of Basel, Klingelbergstr. 70, CH-4056 Basel/Switzerland

FhuA protein facilitates ligand-gated transport of ferrichrome-bound iron across Escherichia coli outer membranes. Its crystal structure, in the presence and absence of ferrichrome reveals two distinct conformations. The monomeric protein consists of a hollow, 22-stranded, antiparallel b-barrel (residues 160-714), which is obstructed by a plug (residues 19-159). The binding site of ferrichrome, an aromatic pocket near the cell surface, undergoes minor changes upon association with ligand. These are propagated across the plug, eventually resulting in substantially different protein conformations at the periplasmic

face. Our findings reveal the mechanism of signal transmission and suggest how the energy-transducing TonB complex senses ligand binding.

M06.OA.004 TRANSMEMBRANE SIGNALLING ACROSS THE OUTER MEMBRANE OF *E. COLI*: CRYSTAL STRUCTURE OF FHUA WITH BOUND LIPOPOLYSACCHARIDE. Kay Diederichs, Andrew D. Ferguson, Eckhard Hofmann and Wolfram Welte, Fakultät für Biologie, Universität Konstanz, M656, Konstanz D-78457, Germany, and James W. Coulton, Department of Microbiology and Immunology, McGill University, 3775 University Street, Montreal H3A 2B4, Canada.

Transport across the outer membrane of Gram-negative bacteria is mediated by distinct classes of transport mechanisms, including passive diffusion through non-specific porins, facilitated diffusion via substrate-specific porins, and active transport by energy dependent high-affinity receptors. FhuA, receptor for ferrichrome in *E. coli*, is a member of a family of integral outer membrane proteins, which, together with the energy transducing protein TonB, mediate active transport of ferric siderophores across the outer membrane. In addition to binding ferrichrome, FhuA also functions as the primary receptor for the structurally related antibiotic albomycin, for several bacteriophages, for the peptide antibiotic microcin 25, and for the bacterial toxin colicin M. Here we present the three-dimensional structure of FhuA in two conformations, with and without ferrichrome at 2.7 Å and 2.5 Å resolution, respectively [1]. The structure was solved by multiple anomalous dispersion phasing using data collected from a single selenomethionyl crystal at 100 K. FhuA is a β-barrel composed of 22 antiparallel β-strands. In contrast to the typical trimeric arrangement found with porins, FhuA is monomeric. Located within the β-barrel is a structurally-distinct domain, the 'cork', consisting mainly of a mixed four stranded β-sheet multiple short α-helices. Upon binding of ferrichrome-iron, conformational changes are transduced to the periplasmic pocket of FhuA, signalling the ligand-loaded status of the receptor. Sequence homologies and mutagenesis data are used to propose a structural mechanism for TonB-dependent siderophore-mediated transport across the outer membrane. Structural implications for energy transduction, bacteriophage binding and the use of siderophore-antibiotic conjugates are discussed. In addition, a single *E. coli* K-12 lipopolysaccharide molecule has been identified noncovalently bound to the membrane-embedded region of FhuA. The crystal structure of lipopolysaccharide, description of the interactions with outer barrel wall of the protein and a proposed binding motif for lipolysaccharide binding proteins is presented.

[1] A.D. Ferguson, E. Hofmann, J.W. Coulton, K. Diederichs, W. Welte (1998) *Science* 282, 2215-2220.

M06.OA.005 STRUCTURE OF BACTERIORHODOPSIN AT 1.55 Å RESOLUTION. Hartmut Luecke, Brigitte Schobert, Hans-Thomas Richter, Jean-Philippe Cartailler and Janos K. Lanyi, University of California, Irvine, CA 92697-3900, U.S.A.

The atomic structure of the light-driven ion pump bacteriorhodopsin and the surrounding lipid matrix was determined by x-ray diffraction of crystals grown in cubic lipid phase. At 1.55 Å resolution, features not seen before become evident. In the extracellular region an extensive 3-dimensional hydrogen-bonded network of protein residues and seven water molecules leads from the buried retinal Schiff base and the proton acceptor Asp^{85} to the membrane surface. Near Lys^{216} where the retinal binds, transmembrane helix G contains a π-bulge that causes a non-proline kink. The bulge is stabilized by hydrogen-bonding of the main-chain carbonyl groups of Ala^{215} and Lys^{216} with two buried water molecules located between the Schiff base and the proton donor Asp^{96} in the cytoplasmic region. The results indicate extensive involvement of bound water molecules in both the structure and the function of this seven-helical membrane protein. A bilayer of 18 tightly bound lipid chains forms an annulus around the protein in the crystal. Contacts between the trimers in the membrane plane are mediated almost exclusively by lipids.

M06.OA.006 ABSTRACT NOT AVAILABLE. R.M. Stroud

M06.OA.007 STRUCTURE ANALYSIS AND LIGAND-BINDING SITE OF THE BOVINE BRAIN PHOSPHATIDYLETHANOLAMINE-BINDING PROTEIN. L. Serre, B. Vallée, N. Bureaud, F. Schoentgen and C. Zelwer. Centre de biophysique moléculaire. C.N.R.S. Rue Charles Sadron, 45071 Orléans Cedex 2, France.

PEBP is a basic protein isolated from bovine brain, which binds *in vitro*, phosphatidylethanolamine as well as GTP. Although its precise biological role is still unknown, PEBP is present in mammalian cells exhibiting morphogenesis activity. Besides, sequence alignments showed that the mammal PEBP belongs to a protein family which also includes CEN, a protein involved in inflorescence architecture control, TSF1 a suppressor of cdc25 mutation in yeast, i.e. proteins which seem to be related to developmental processes.

To get new insights on PEBP function, we solved the X-ray structures of the bovine brain PEBP and of the PEBP complexed to the polar head of phosphatidylethanolamine. These structures show that PEBP and its family constitute a structural protein family that the phospholipid binding site is a small cavity located close to the protein surface. In a conserved region, the PEBP structure displays also two cis-peptide bonds that correspond to interesting natural mutations of *Arabidopsis* and Tomato plants.

Although these structures do not yet give clues on the precise *in vivo* function of PEBP, they show that PEBP exhibits some similarities with the C-terminal domain of a Rho GDP-dissociation inhibitor which negatively regulates Rho-family GTPases and the calcium/phospholipid binding-domains of synaptotagmin I, a synaptic vesicle membrane protein, and some phospholipases (cytosolic PLA2 and PLCδ1). We believe that PEBP may have a similar function and be a membrane binding protein as well, which would interact with other proteins and perhaps would modulate their catalytic activities.

M06.OA.008 CRYSTAL STRUCTURE OF SENSOR DOMAIN OF HEME-BASED OXYGEN SENSOR FIXL FROM RHIZOBIUM MELILOTI. H. Miyatake, S. Adachi, H. Nakamura, K. Tamura, T. Iizuka, Y. Shiro [1], M. Kanai [2], T. Tsuchiya [3], [1] The Institute of Physical and Chemical Research (RIKEN), RIKEN Harima Institute, 323-3 Mikazuki-cho, Mihara, Sayo, Hyogo 679-5143, Japan, [2] Faculty of Science, Kanagawa University 2946 Tsuchiya, Hiratsuka-shi, Kanagawa 259-1293, Japan, [3] Department of Molecular Genetics Medical Research Institute Tokyo Medical and Dental University, 1-5-45, Yushima, Bunkyo-ku, Tokyo 113-8510, Japan

FixL is a transmitter protein in the two-component system which acts as an oxygen-sensor and regulates histidine kinase activity when the symbiotic rhizobia resides in root nodules of host plants. The oxygen sensor domain of Rhizobium meliloti FixL (FixLN) was purified by His-tag and isoelectronic-focusing chromatographies. Dynamic light scattering measurement of FixLN thus obtained showed that the oxygen sensor domain of R. meliloti FixL is present as a homo-dimer in solution. A crystal of R. meliloti FixLN in the met (Fe3+) form was grown in 100mM

acetic acid/NaOH buffer at pH 4.6 in the presence of 200mM ammonium acetate using 40 %(w/v) PEG 4000 as a precipitant. A crystal of the ferrous CO form of FixLN was also prepared by reduction of the met crystal with dithionite under an atmosphere of CO. The crystals (0.2mm x 0.05mm x 0.01mm) belong to the monoclinic system (C2) with cell dimensions of a=60.94Å, b=37.44Å, c=54.14Å and beta=115.29°, and give X-ray diffractions with 1.7 Å resolution at station BL44B2 of SPring-8, Japan. The solvent content of the crystal was only 23 %, which was abnormaly low for protein crystals. Because all of soaking trials were failed, we carried out MAD experiment making use of the heme iron as an anomalous scatterer. Bijvoet difference Patterson maps show a clear peak corresponding to the heme iron in FixLN. The MAD electron density map calculated by program SOLVE was enough interpretable to build the initial model, with knowledge that FixLN belongs to PAS domain superfamily. PAS-containing proteins are likely to mediate macromolecular interactions along signalling pathways with their N-terminal regions. Interestingly, it was revealed that the FixLN formed a homo-dimer with the "N-terminal cap". The dimeric interaction was dominantly made by "leucin zipper-like" hydorphobic forces, supplemented with some salt bridges. This is the first crystallographic evidence which shows PAS-containing proteins make a homo-dimer with their N-terminal regions.

We will also discuss about how FixLN senses oxygen based upon structural comparison between met- and CO-FixLN, which is an oxygen mimic adduct. "Oxygen sensing mechanism by heme-doming" is proposed for B.japonicum FixLN by Gilles-Gonzalez et al. B.japonicum FixLN, however, presents as a monomer in crystal maybe because it lacks N-terminal cap. We will focus on this point that the heme-doming mechanism is also appliable to our R. meliloti FixLN, because there may be intrinsic difference in their assembly states.

M06.OA.009 STRUCTURE OF THE FIRST 3 DOMAINS OF THE TYPE 1 IGF RECEPTOR. T.P.J. Garrett[1], N.M. McKern[2], M. Lou[1], M.J. Frenkel[2], J.D. Bentley[2], G.O. Lovrecz[2], T.C. Elleman[2], L.J. Cosgrove[2,3] and C.W. Ward[2]. Biomolecular Research Institute[1] and CSIRO Division of Molecular Science[2], 343 Royal Parade, Parkville, Victoria, 3052, Australia. [3]Current Address: CRC for Tissue Growth and Repair, Adelaide, SA

The type 1 insulin-like growth factor receptor (IGF-1R) belongs to a family of vertebrate cell surface receptors which also include insulin receptor. However homologues have also been found in many invertebrates, including some of the simplest multicellular animals. The ligands for this family are protein hormones which induce a variety of metabolic and mitogenic responses. IGF-I and IGF-II are primarily produced as a consequence of growth hormone signalling and are essential for normal growth and development. They also seem necessary in malignant transformation of some cells. Insulin is a major mediator in glucose homeostasis and induces lipid, protein and glucose metabolism in a variety of tissues. Although many other cell-surface receptors dimerize upon binding their ligands the mature IGF-1R pre-exists as a disulfide-linked homodimer. Thus binding of the hormone to the extracellular portion is believed to induce a structural change in the receptor which is transmitted across the membrane to allow transphosphorylation of the tyrosine kinase domains.

We have determined the structure of the first three domains of the type 1 insulin-like growth factor receptor (L1-cys rich-L2 domains) to 2.6 Å resolution by X-ray diffraction. This corresponds to the first half of the extracellular portion and it contains two regions which have been implicated in ligand specificity. L1 and L2 are homologous and adopt the a fold which represent a new type of structural domain. The cys-rich region also shows unique structural features, being composed of small disulfide-bonded modules associated in a novel manner. At the centre of the molecule is a space of sufficient size to accommodate a hormone ligand. Two regions of the receptor which are involved in hormone-binding map to this site. Thus this structure gives a first view of how members of the insulin receptor family might interact with their ligands.

P06.OA.001 A NOVEL ELECTRON TRANSFER MECHANISM SUGGESTED BY CRYSTALLOGRAPHIC STUDIES OF CYTOCHROME *bc1* COMPLEX. Di Xia[1,2], Hoeon Kim[1], Chang-An Yu[2], Johann Deisenhofer[1], [1]HHMI and Department of Biochemistry, UT Southwestern Medical Center, Dallas, [2]Laboratory of Cell Biology, DBS/NCI/NIH, [3]Department of Biochemistry, Oklahoma State University.

The crystal structure of bovine mitochondrial cytochrome *bc1* complex, an integral membrane protein complex of 11 different subunits with a total molecular weight of 242 kDa, demonstrated a tightly associated dimer consisting of three major regions: a matrix region primarily made of subunits core1, core2, 6 and 9; a trans-membrane-helix region of 26 helices in the dimer contributed by cytochrome *b*, cytochrome *c1*, the Rieske iron-sulfur protein (ISP), subunits 7, 10 and 11; and an inter-membrane-space region composed of extra-membrane domains of ISP, cytochrome *c1* and subunit 8. The structure also revealed the positions of and distances between irons of prosthetic groups, and two symmetry related cavities in the trans-membrane-helix region upon dimerization of the *bc1* complex. Extensive crystallographic studies on crystals of *bc1* complexed with inhibitors of electron transfer (ET) identified binding pockets for both Qo and Qi site inhibitors. Discrete binding sites for subtypes of Qo site inhibitors have been mapped onto the Qo binding pocket, and bindings of different subtypes of Qo site inhibitors are capable of inducing dramatic conformational changes in the extra-membrane domain of ISP. A novel ET mechanism for the *bc1* complex consistent with crystallographic observations will be discussed.

P06.OA.002 CRYSTALLIZATION OF THE REACTION CENTER OF PHOTOSYSTEM II AND OF ISOLATED REACTION CENTER COMPONENTS. Noam Adir, Rina Anati, Valeria Cheredman, Yelena Dobrovetzki and Natalia Lerner Department of Chemistry, Technion, Technion City, Haifa 32000 Israel

Photosynthesis is the process by which plants transform the energy of the sun into useful chemical energy. The primary reactions occur between a variety of cofactor molecules bound to large membrane protein complexes called reaction centers. Of the different reaction center types, one of the most complex is that of Photosystem II, found in all higher plants, green algae and cyanobacteria. It is the site of the initiation of linear electron flow, proton gradient formation and oxygen evolution. Reaction center II (RCII) contains 9 proteins, 7 different cofactor types and has a molecular weight of about 280,000. RCII, isolated from either spinach or pea photosynthetic membranes, have been crystallized [1]. The crystals were grown from RCII monomers in the presence of mixtures of detergents at a higher detergent/protein ratio than previously reported for other membrane proteins. The crystals grew as hexagonal rods with dimensions of up to 1 x 0.3 x 0.3 mm. The crystals diffracted to a maximum resolution of about 6.5Å, and belong to a hexagonal space group with unit cell dimensions of a = 495Å, b = 495Å, c = 115Å, $\alpha = \beta = 90^{o}$, $\gamma = 120^{o}$. Thermoluminescence measurements of RCII from solubilized crystals showed that the crystallized RCII was competent in electron transfer to exogenous electron acceptors. These and other measurements detected heterogeneities in the crystallized RCII, which may be the reason for crystal disorder.

Because of the large size and complexity of RCII, we are also trying to isolate various protein components and determine their structure separately: *i*. Oxygen evolution in RCII is

dependent on the presence of a tetramanganese cluster, protected by a membrane-associated protein called the 33kDa OEC protein. We have successfully isolated this protein, purified to homogeneity and crystals have been obtained. *ii*. RCII is connected to the main antenna, LHCII by a number of intermediate membrane bound antenna molecules. One of them, CP29, has been isolated and crystals have been obtained. *iii*. Within the core of all RCII complexes is a unique dipeptide 15kDa transmembrane b-type cytochrome called cytochrome b_{559}. Overexpression of a unique fused gene product, reconstitution and crystallization trials will be described.

[1] Adir, N. (1999) *Acta Crys.* D. *in press*

P06.OA.003 NEUTRON CRYSTALLOGRAPHY OF LH2 AT LOW RESOLUTION: THE LOCATION OF DETERGENT & AMPHIPHILE VOLUMES. S.M. Prince, T.D. Howard, R.J.Cogdell & N.W. Isaacs; University of Glasgow, Glasgow, G12 8QQ UK. D.A.A. Myles & C. Wilkinson; EMBL, B.P.156, 38042 Grenoble Cedex 9, France. M.Z.Papiz; Daresbury Laboratory, Warrington, WA4 4AD UK.

The peripheral light-harvesting complex (LH2)[1] from the purple bacteria *Rps. acidophila* strain 10050 is an integral trans-membrane protein complex. These LH2 complexes are constructed from nonomeric oligomers of a unit comprising two polypeptides with associated non-covalently bound pigment molecules. During isolation and when crystallised the hydrophobic trans-membrane portion of these molecules is enclosed in a detergent micelle[2]. This micelle is disordered at the atomic level and is not observed in the X-ray structure. Low resolution crystallographic experiments using the diffraction properties of neutrons and D_2O/H_2O contrast variation allow the location of volumes having systematic proton densities [3]. We will assign all of the discrete volumes in the LH2 crystals namely protein, solvent, detergent, phospholipid and amphiphile.

The information gained in this experiment will allow us to discover the influence of the detergent on crystalline packing and the location of any systematic lipid content in the crystal. We will also be able to precisely determine the trans-membrane portions of this molecule, and the interaction of the protein complex with the micelle.

McDermott *et al.* 1995 Nature **374**, 517-521.
Garavito *et al.* 1986 J. Cryst. Growth **76**, 25-30.
Pebay-Payroula *et al.* 1995 Structure **3**. 1051-1059

P06.OA.004 CRYSTALLOGRAPHIC STUDIES OF A LOW-LIGHT LIGHT-HARVESTING COMPLEX A.M. Lawless, N. Hartigan, H.A. Tharia and M.Z. Papiz, CLRC Daresbury Laboratory, Daresbury, Warrington, WA4 4AD, UK

In photosynthetic purple bacteria, solar energy can be directly trapped by the carotenoids and bacteriochlorophylls of the light-harvesting system. Considerable impetus has been given to this field of research by the structure determinations of the Reaction Centre (RC) and Light Harvesting Complexes I and II (LH1, LH2). The relative numbers of LH2's expressed per RC:LH1 is determined by environmental factors such as temperature and light. Carotenoids fill the gap in the visible part of the spectrum where Bchl's do not absorb and protect against oxidation. B850 pigments stabilise and prepare the energy for transfer by linking together to form an energy storage ring. B800 pigments give additional light-energy capturing power and may add variability to the system allowing the complex to be tailored for specific environmental conditions.

The low-light LH2 complex from *Rhodopseudomonas palustris* has been characterised by HPLC. Sequence analysis of LH2 from cells grown at 300 lux was found to be a mixture of high- and low-light peptides. Crystals of this complex prepared in dodecylmaltoside were monoclinic (P2 or P21) a=99.4, b=133.4, c=180.4 Å and b=100.5^o and diffracted to 12 Å resolution. Crystal quality was found to be related to the ability to grow the cells below 90lux, thus reducing the heterogeneity of the complex. Cells grown at 50 lux produced LH2 >95% pure in terms of contamination from high-light peptides. Diffraction from these crystals has been consistent to around 5.2Å, although this is along one direction in reciprocal space. Data have been collected to 7.0 Å resolution and self rotation functions indicate an axis of NCS 50^o from the unique axis.

We hope to report further progress on this unusual LH2 complex which, in addition, has special spectroscopic characteristics and is markedly different to the other two LH2 complexes for which the structure is known.

P06.OA.005 CRYSTALLISATION & CRYOCOOLING OF COLOURED CRYSTALS - MORE ADVENTURES WITH LIGHT HARVESTING PROTEINS. Tina D. Howard [1], Steve M. Prince [2], Richard J. Cogdell [1], Neil Isaacs [2], [1] Division of Biochemistry, Davidson Building, IBLS, University of Glasgow, Glasgow, G12 8QQ, UK, [2] Protein Crystallography, Joseph Black Building, University of Glasgow, Glasgow, G12 8QQ, UK.

We have developed a method of slowly introducing a cryoprotectant into crystals of the integral membrane protein Rps. acidophila 10050 LH2. As a result of this new procedure the resolution of the structure has been increased from 2.5Å1 to 2.0Å. This method is currently being extended to a new tetragonal crystal form of the protein which we have recently obtained (current resolution 3.7 Å).

Crystals of similar proteins involved in light harvesting in different species of purple photosynthetic bacteria (wild type and mutant strains) have also been produced. Alongside optimising these conditions to improve the diffraction of these crystals, crystallisation experiments are being extended to the "core complex" and "LH1" proteins involved in the later steps of the photosynthetic process in purple photosynthetic bacteria.

1. McDermott et al. Nature 374, 517 (1995).

06OB STRUCTURAL ENZYMOLOGY AND UNUSUAL CHEMISTRY

M06.OB.001 NiFe AND Fe-ONLY HYDROGENASES DISPLAY UNUSUAL COORDINATION TO ACTIVE SITE Fe. Juan C. Fontecilla-Camps IBS/LCCP, CEA-CNRS, Grenoble 38027, France

Many microorganisms are capable of either produce hydrogen, as a way to get rid of low potentiel electrons, or oxidize it to get reducing power. Often hydrogen-producers are found is association with hydrogen-consumers, forming ecosystems that have been proposed as a possible origin for eukaryotic cells (1). Hydrogen metabolism is, for the most part, carried out by two types of metalloenzymes: the NiFe and Fe-only hydrogenases. We have extensively studied these two classes of proteins from sulfate-reducing organisms using X-ray crystallography. A combination of crystallographic and IR spectroscopic analyses have established that the active site of the NiFe-hydrogenases is made out of a NiFe binuclear center displaying extensive cysteine thiolate and (Fe) CO and CN coordination (2-3). More recently, we have shown that a somewhat similar active site is present in the Fe-only hydrogenase from Desulfovibrio desulfuricans (4). The presence of triple-bonded molecules as ligands of Fe centers in the two evolutionary unrelated enzymes rises the question of the function of a low-spin, possibly low redox, Fe center in hydrogen catalysis. In addition to this similarity, NiFe and Fe-only hydrogenases share comparable electron transfer pathways made

out of cubane-type [4Fe4S] clusters and hydrophobic channels that appear to serve as privileged gas access paths to the active site (4-5).

(1) Martin, W. & Müller Miklos (1998) Nature, 392, 35
(2) Happe et al. & Bagley, K.A. (1997) Nature, 385,126
(3) Volbeda, A., Garcin, E., Piras, C., de Lacey, A., Fernandez, V.M., Hatchikian, E.C., Frey, M. and Fontecilla-Camps, J.C. (1996) J. Am. Chem. Soc. 118, 12989-96
(4) Nicolet, Y., Piras, C., Legrand, P., Hatchikian, E.C. and Fontecilla-Camps, J.C. (1999) Structure 7, 13-23
(5) Montet, Y., Amara, P., Volbeda, A.,Vernede, X., Hatchikian, E.C., Field, M.J., Frey, M and Fontecilla-Camps, J.C. (1997).Nature structural biology 4, 523- 526

M06.OB.002 A MOVIE OF CATALYSIS IN THE COPPER-CONTAINING QUINOENZYME AMINE OXIDASE. Carrie M. Wilmot[1], Janos Hajdu[2], Colin G. Saysell[1], Michael J. McPherson[1], Peter F. Knowles[1] & Simon E.V. Phillips[1]. [1]School of Biochemistry and Molecular Biology, University of Leeds, Leeds LS2 9JT, U.K. [2]Department of Biochemistry, Uppsala University, S-751 23 Uppsala, Sweden.

A series of structures has been obtained from the flash freezing of crystals of *E. coli* amine oxidase (ECAO) exposed to substrate, using the technique of X-ray crystallography. This, in essence, has provided a "movie" of catalysis composed of "snapshots" from the catalytic cycle of this ubiquitous enzyme. ECAO belongs to a family of copper-containing enzymes, which contain the organic cofactor 2,4,5-trihydroxyphenylalanine quinone (TPQ). Copper amine oxidases catalyse the oxidation of primary amine substrates to their corresponding aldehydes, with the subsequent release of ammonia and hydrogen peroxide.

Recently we have used a single crystal micro-spectrophotometer to examine the timecourse of the reaction in the crystal, as a function of rich spectral changes that occur upon the addition of substrate. We have flash frozen crystals at different time points during the reaction to maximise the amounts of spectrally distinct intermediates. These have been supplemented by anaerobic substrate-reduced flash frozen crystals, some of which are in complex with oxygen mimics. The structures (1.9-2.3Å resolution) reveal dramatic movements of the quinone cofactor. They also show the first known crystallographic observation of dioxygen bound to a mononuclear copper enzyme. The product aldehyde is seen to play a hitherto unexpected role in the reaction. Suggested roles for conserved residues within the active site are evident, as well as proton transfer pathways.

This work was supported by an EMBO short term fellowship awarded to C.M.W, and the BBSRC. These data were collected at the ESRF and Daresbury SRS.

M06.OB.003 STRUCTURE OF METHYL-COENZYME M REDUCTASE: IMPLICATIONS FOR THE CATALYTIC MECHANISM. U. Ermler and W. Grabarse, Max-Planck-Institut für Biophysik, Heinrich-Hoffmann-Straße 7, 60528 Frankfurt, Germany and S. Shima, M. Goubeaud and R.K. Thauer, Max-Planck-Institut für terrestrische Mikrobiologie and Laboratorium für Mikrobiologie der Philipps-Universität, Karl-von-Frisch-Straße, 35043 Marburg, Germany.

Methyl-coenzyme M reductase - the key enzyme of biological methane formation - catalyzes the reduction of methyl-coenzyme M to methane by oxidizing coenzyme M and coenzyme B to the corresponding heterodisulfide under participation of coenyzme F_{430}, an unusual Ni-porphinoid (1). This highly complicated biochemical reaction is embedded into a large protein complex of nearly 300 kDa arranged as a heterohexamer $(\alpha,\beta,\gamma)_2$ (2). The active site is buried in a hydrophobic segment of a 30 Å long narrow channel which is locked after substrate binding. Five post-translationally modified amino acids were observed at or close to the active site region. Crystal structures of methyl-coenzyme M reductase were determined from several catalytically inactive enyzme states that allow conclusions for different intermediates of the reaction cycle. Based on these studies and also based on spectroscopic and chemical data an enzymatic mechanism was proposed that involves radical intermediates and a Ni-methyl compound.

1. R.K. Thauer (1998). *Microbiology* **144**, 2377-2406.
2. U. Ermler, W. Grabarse, S. Shima, M. Gaubeaud and R.K. Thauer (1997). *Science* **278**, 1457-1462.

M06.OB.004 MULTISTEP CATALYSIS IN THE ZINC METALLOPROTEIN 3-DEHYDROQUINATE SYNTHASE. K.A. Brown and E.P. Carpenter, Dept. Of Biochemistry, Imperial College, London SW7 2AY,UK, and J.W. Frost, Dept. of Chemistry, Michigan State University, East Lansing, Michigan 48824-1322, USA, and A.R. Hawkins, Dept. of Biochemistry and Genetics, University of Newcastle upon Tyne, NE2 4HH, UK.

3-Dehydroquinate synthase (DHQS) is an NAD^+-dependent metalloenzyme which converts 3-deoxy-D-*arabino*-heptulosinate 7-phosphate (DAHP) to 3-dehydroquinate. It is a member of the shikimate pathway which is required for the synthesis of aromatic amino acids and other ring-containing compounds. The pathway is present in plants, bacteria, microbial eukaryotes and, most recently discovered, apicomplexan parasites including *Plasmodium falciparum* - the cause of malaria (1). Mutation of the *aroB* gene encoding DHQS results in attenuation of pathogen virulence (2). The absence of this pathway in mammals and its requirement for virulence has thus identified DHQS as a potential target for the development of new drugs with anti-microbial/anti-parasitic activity.

A long-standing interest in the catalytic function of DHQS exists because of its unusual ability to perform a number of chemical reactions in its active site, namely: alcohol oxidation, phosphate β-elimination, carbonyl reduction, ring opening, and an intramolecular aldol condensation. An important step towards understanding the complex mechanism of this enzyme is our recent determination of the crystal structure of DHQS from *Aspergillus nidulans* (3). This structure reveals an active site which possesses wide variety of interactions between metal, dinucleotide, substrate analogue and protein suggesting that this mechanism involves a complex interplay between all of these elements.

1. Roberts, F., *et al*., *Nature*, 1998, **393**, 801-805.
2. Gunel-Ozcan, A., Brown, K.A., Allen, A.G. and Maskell, D.J., *Microbial Pathogen*., 1997, **17**, 169-174.
3. Carpenter, E.P., Hawkins, A.R., Frost, J.W. and Brown, K.A., *Natur*e, 1998, **394**, 299-302.

M06.OB.005 ABSTRACT NOT AVAILABLE. P. Babbit

P06.OB.001 ORBITAL STEERING & ENTROPY: A BIMOLECULAR PHOSPHORYL TRANSFER TRANSITION STATE AT 1.3Å RESOLUTION. Michael S. Chapman, Genfa Zhou, James L. Gattis, Pamela S. Pruett, Thayumanasamy. Somasundaram, W. Ross Ellington. Institute of Molecular Biophysics, Florida State University, Tallahassee, FL32306.

The structure of Arginine Kinase, a homologue of the ATP-buffering creatine kinase, has been determined as a complex with MgADP, nitrate, and arginine at 1.86Å resolution (Zhou *et al* 1998). The current refinement at approximately 1.25Å resolution will be presented with kinetic analysis of active site mutants. In

this transition state analogue complex, the γ-phosphoryl of ATP (which is transferred through a planar transition state) is replaced by a nitrate ion. In the stable complex the substrates ***are not*** constrained covalently. To our knowledge this is the first high resolution structure of an active bimolecular enzyme as a transition state analogue complex.

Structural and kinetic analysis of this system offers a unique opportunity to compare the fundamentals of mechanism in bimolecular reactions to the unimolecular reactions (hydrolases, isomerases, etc.) predominately studied in the past. As in unimolecular systems there is evidence of acid-base catalysis, strain, and charge bias enhancing activity. The structure also shows very precise alignment of substrates with angles of approach within a few degrees of ideal for in-line transfer of the ATP γ-phosphoryl. These observations are consistent with the proposals of Jencks & Koshland (*ca* 1970) that entropy reduction and/or the steering of orbitals along trajectories for nucleophilic attack may be the predominant means of catalysis in multimolecular reactions.

Zhou, G., Somasundaram, T., Blanc, E., Parthasarathy, G., Ellington, W.R., Chapman, M.S.. "Transition state structure of arginine kinase: Implications for catalysis of bimolecular reactions." PNAS. **95**: 8449-8454. 1998.

P06.OB.002 RNASES: DOMAIN SWAPPING AND A TIME-RESOLVED STUDY OF CATALYSIS. Ingrid Zegers, Joeri Deswarte, Remi Loris, Jan Steyaert, Lode Wyns, Department of Ultrastructure, Vrije Universiteit Brussel – VIB.

The structure of a trimeric domain swapped form of barnase was determined by X-ray crystallography at a resolution of 2.2 Å from crystals of space group R32. Residues 1-36 of one molecule associate with residues 41-110 from another molecule related through three-fold symmetry. The resulting cyclic trimer contains three protein folds that are very similar to monomeric barnase. Both swapped domains contain a nucleation site for folding, and domain swapping is consistent with the description of the folding process of monomeric barnase as the formation and subsequent association of two foldons. The formation of swapped multimers can explain the observation that barnase forms oligomers in acidic denaturing conditions. As the catalytic site of the swapped barnase is constituted by domains of different molecules, two different inactive mutants may regain activity through heterologous domain swapping. This is a new approach to the functional complementation of enzyme activity, and may be of use in a variety of domains. Domain swapping, the misassembly of proteins and alternate folded conformations have recently received much interest, as they are thought to be linked to diseases like Alzheimer's and prion-transmissible encephalopathies. The swapped form of barnase could serve as a model system for the study of these phenomena. Fortunately, the monomeric form of the protein, including its folding process, is extremely well characterized. The use of a substrate that is hydrolysed over a period of days has made it possible to analyse the reaction catalysed by RNase T1 by X-ray crystallography.RNase T1 was co-crystallised with exo guanosine 2',3' cyclic phosphorothioate (exo cGPS), and structures of the complex were determined at times ranging from 1 day to three months. The structures show the hydrolysis of exo cGPS to 3'-GMP over a period of a week, and a subsequent conformational change in the 3'-GMP product. It is shown that RNases catalyse the forward and reverse reactions of the equilibrium between a phsophodiester (or 3'-GMP) and a cyclic nucleotide via an inverse mechanism. In addition, the structures provide an explanation for the differential behavior of RNase T1 towards exo- and endo-cyclic thiophosphates.

P06.OB.003 STRUCTURE OF ASPARTATE β-SEMIALDEHYDE DEHYDROGENASE. A.T. Hadfield, Dept. Biochemistry, Bristol University, University Walk, Bristol BS8 1TD; G. Kryger[+], G.A. Petsko, Brandeis University, Waltham, MA 02254; J. Ouyang, R.E. Viola, University of Akron, Ohio. ([+]Curr. add: Weizmann Institute, Israel)

Aspartate β-semialdehyde dehydrogenase (ASADH) lies at a branch point in the biosynthetic pathway through which bacteria, fungi and the higher plants synthesize diaminopimelate and lysine from aspartate. Blocks in this biosynthetic pathway are lethal, making ASADH an attractive target for anti-bacterial, fungicidal, or herbicidal agents. The enzyme, which is active in *E. coli* as a dimer, catalyses the NADPH-mediated reductive phosphorylation of β-aspartyl phosphate, with a mechanism similar to glyceraldehyde-3-phosphate dehydrogenase. The structure of the apo-enzyme from *E. coli* has been solved using a combination of single isomorphous replacement and non-crystallographic symmetry, and used to solve, by molecular replacement, the structure of a ternary complex with NADP, phosphate and the substrate-mimicking inhibitor S-methyl cysteine sulfoxide.

Each monomer has two distinct domains. The N-terminal domain forms an approximate Rossmann fold, binding NADP. An α-helix, cradled by a six stranded β-sheet, is central to the second domain. This β-sheet forms the dimerisation interface. A two-helix bundle forms a third subdomain, which has the appearance of an arm lying across the top of the opposite monomer. Comparison of the apo and holo crystal structures indicates there is a closure of the two domains upon binding of the co-factor NADP. The active site contains residues from both domains, including a loop and an α-helix which are only ordered in the holo structure. The inhibitor forms a covalent bond with the active site cysteine, Cys 135, analagous to a long-lived covalent intermediate that has been characterised. The structures give insight into the mechanism of action of this enzyme both in terms of global structural changes and the contribution of individual amino acids to substrate binding and catalysis at the active site.

P06.OB.005 CRYSTALLOGRAPHIC STUDIES OF PLANT GLUTATHIONE TRANSFERASES. R. Thom and A. Lapthorn, Protein Crystallography, Dept. Chemistry, Glasgow University, University Avenue, Glasgow, G12 8QQ, UK

Gluthathione Transferases (GSTs) are ubiquitous enzymes which catalyse the nucleophilic addition of glutathione (GSH) to a chemically diverse series of substrates containing an electrophilic centre. In plants, in addition to conferring tolerance to commercially important herbicides, GSTs also bind auxin, act in the anthocyanin pigmentation pathway and provide cellular protection from oxidative stress.

In maize GSTs are the most abundant non photosynthetic enzyme in the plant cell comprising as much as 1% of the soluble leaf protein, existing as isoenzymes with distinct substrate specificities. A number of plant GST X-ray structures have now been elucidated allowing a more detailed understanding of the relationship between the enzyme structure and catalytic activity [1].

We report here the elucidation of the apo enzyme GST I from maize, in comparison with the ligand-bound structure indicating the mechanism for theta class GST isoenzymes.

Together with other GST structures this explains herbicide resistance and selectivity in maize as well as other crop plants.

1. Prade, L., Huber, R. & Bieseler, B. (1998). Structure **6**: 1445 - 1452

P06.OB.006 STRUCTURAL EVIDENCE FOR A HYDRIDE TRANSFERRING MECHANISM IN QUINOPROTEIN GLUCOSE DEHYDROGENASE. A. Oubrie, H.J. Rozeboom, K.H. Kalk, B.W. Dijkstra Department of Biophysical Chemistry, University of Groningen, Groningen, The Netherlands

The soluble quinoprotein glucose dehydrogenase (s-GDH) from Acinetobacter calcoaceticus requires the cofactor pyrroloquinoline quinone (PQQ) to oxidise a wide range of mono- and disaccharides to their corresponding lactones [1]. Despite considerable effort [2,3], the reaction mechanism of s-GDH and other PQQ-dependent enzymes has not been resolved. We have elucidated the three-dimensional structure of the holo-enzyme, which folds into a beta-propeller structure consisting of six four-stranded beta-sheets. PQQ binds near the top of the barrel. A ternary complex of the enzyme with the inhibitor methylhydrazine (MH) revealed the presence of one covalent PQQ-MH complex, identifying the reactive part of the orthoquinone group. Moreover, a glucose binding study affords the first view of a quinoprotein-substrate complex. The interactions between glucose and s-GDH explain the enzyme's broad substrate specificity. On the basis of the position of glucose with respect to PQQ and the putative catalytic base His144 we have been able to formulate a reaction mechanism involving proton abstraction by His144 in concert with hydride transfer from glucose to the cofactor and subsequent tautomerisation to PQQH2.

1. A.J.J. Olsthoorn & J.A. Duine (1996). Arch. Biochem. Biophys. 336, 42-48.
2. A.J.J. Olsthoorn, T. Otsuki & J.A. Duine (1998). Eur. J. Biochem. 255, 255-261.
3. A.J.J. Olsthoorn & J.A. Duine (1998). Biochemistry, 37, 13854-13861.

P06.OB.007 ACYL-TRANSFER BY N-MYRISTOYLTRANSFERASE INVOLVES C-TERMINAL CARBOXYLATE AS A GENERAL BASE CATALYST. K. Fütterer[1], R.S. Bhatnagar[2], T.A. Farazi[2], J.I. Gordon[2], G. Waksman[1], Departments of [1]Biochemistry and Molecular Biophysics, and [2]Molecular Biology and Pharmacology, Washington University School of Medicine, Box 8231, St. Louis MO 63110, USA.

MyristoylCoA:protein N-myristoyltransferase (Nmt) attaches the 14-carbon fatty acid myristate to the N-terminal glycine of many eukaryotic and viral proteins. Pathogenic fungi, including *Candida albicans* and *Cryptococcus neoformans*, require Nmt for growth and replication making Nmt an important anti-fungal drug target. Nmt is specific for the rare lipid myristate as mandated for the proper function of its substrate proteins.

We have solved the x-ray crystal structure of *Saccharomyces cerevisiae* Nmt1p, to 2.9 Å resolution, bound to two ligands representing the lipid donor and acceptor substrates. The Nmt-fold possesses an internal pseudo-two-fold symmetry in which each half of the molecule is structurally homologous to the GCN5-related N-acetyltransferase superfamily, despite a lack of detectable sequence homology. The N-terminus of the peptide substrate analog is juxtaposed to the backbone carboxylate of the protein and in proximity to the "reactive" carbonyl of the myristoylCoA analog. This carbonyl faces two main chain amide nitrogens, which form an apparent oxyanion hole.We have developed a model for the catalytic mechanism based on the ternary complex structure: (I) the backbone carboxylate, acting as a general base, deprotonates the N-terminal ammonium of the substrate peptide; (II) direct nucleophilic attack by the peptide on myristoylCoA with acyl transfer proceeding through a single tetrehedral intermediate; (III) stabilization of the tetrahedral intermediate by the oxyanion hole.

The involvement of the enzyme's backbone carboxylate as a general base catalyst is unique. In order to test the proposed mechanism of catalysis we have started structure refinements of complexes involving natural substrates. We have shown through mutagenesis of nucleophilic side chains in the active site that acyl transfer does not involve an acyl-enzyme intermediate. Further mutagenesis studies involving the backbone carboxylate and residues forming the oxyanion hole have been initiated.

P06.OB.008 STRUCTURE AND ACTION OF 3-DEOXY-D-*ARABINO*-HEPTULOSONATE-7-PHOSPHATE SYNTHASE. R. H. Kretsinger, R. H. Bauerle and I. A. Shumilin, Department of Biology, University of Virginia, Charlottesville, VA 22903, USA.

In microorganisms and plants, the first step in the biosynthesis of aromatic compounds is the condensation of phospho*enol*pyruvate (PEP) and D-erythrose-4-phosphate (E4P) giving 3-deoxy-D-*arabino*-heptulosonate-7-phosphate (DAHP). This reaction is catalyzed by DAHP synthase (DAHPS). In *E. coli* there are three DAHPS isoforms, each specifically inhibited by Phe or Trp or Tyr.

The crystal structure of the Phe inhibited form of DAHPS complexed with PEP and Pb^{2+} was determined by MAD phasing. Data (C2 a = 210.7 b=51.1, c=147.7 Å, β=116.2°; tetramer per asymmetric unit) were measured at BNL, beamline X4A, to 2.6Å. The final R is 20.9%; Rfree is 26.7%.

The tetramer consists of two tight dimers whose monomers are joined by a pair of shared, three stranded β-sheets. The monomer, 350 residues, is a $(\beta/\alpha)_8$ barrel with several additional β-strands and α-helices. The PEP and Pb^{2+} are at the C-end of the β-strands of the barrel, as is a SO_4^{2-} inferred to occupy the position of the phosphate of E4P. The coordination of the Pb^{2+}, at the essential divalent cation site, is hemidirectional and involves, on one part, side chains of Cys61, His268, Glu302, and Asp326 as well as a water bridging to Lys97. The plane of PEP is 3.7 Å from the Pb^{2+} ion on the other side from the protein ligands. PEP is further coordinated by side chains of Arg's 92 165 & 234, Lys's 97 & 186, and His268. Numerous mutations that affect catalytic activity are distributed around the C-end of the β-barrel. Other mutations that reduce feedback inhibition cluster about a cavity near the two fold axis of the tight dimer and ~20 Å from the active site. The cooperativity of inhibitor binding is consistent with the proximity of the inhibitor binding sites to this dimer axis. The few residues responsible for tetramerization of two tight dimers in DAHPS(Phe) are highlighted by their differences in dimeric DAHPS(Trp) and DAHPS(Tyr).

P06.OB.009 STRUCTURE AND MECHANISM OF A CARBON-CARBON BOND HYDROLASE. D.E. Timm, H.A. Mueller, P. Bhanumoorthy [1], J.M. Harp, G.J. Bunick [2], [1] Indiana University School of Medicine, Indianapolis, Indiana, 46202, USA, [2] Life Sciences Division, Oak Ridge National Laboratory, Oak Ridge, Tennessee, 37831, USA

Fumarylacetoacetate hydrolase catalyzes the final step of tyrosine and phenylalanine catabolism, and its deficiency causes the fatal metabolic disease hereditary tyrosinemia type I. This enzyme catalyzes a novel biochemical reaction involving the hydrolytic cleavage of a carbon-carbon bond in fumarylacetoacetate to form fumarate and acetoacetate. Fumarylacetoacetate hydrolase (FAH) has no known sequence homologs and functions by an unknown enzymatic mechanism. The crystal structure of this enzyme determined by automated analysis of multiwavelength anomalous diffraction data represents the first structure of a hydrolase that acts specifically on carbon-carbon bonds.

This structure also defines a new class of metalloenzymes characterized by a unique alpha/beta fold. The structure of FAH complexed with its physiologic products suggests a variation of

the Asp-His-Ser catalytic triad mechanism, involving a His base hydrogen bonded to a Glu carboxyl group. The nucleophilic Ser side chain is replaced in FAH by a water molecule bound to a carboxylate ligand of a Ca2+. The octahedrally coordinated Ca2+ participates in catalysis by binding substrate, activating the water molecule and stabilizing a carbanion intermediate. Thus, the fumarylacetoacetate hydrolase structure represents a new class of metalloenzymes, suggests a unique variation of a common biochemical mechanism and reveals the molecular basis for mutations causing the hereditary tyrosinemia type I.

P06.OB.010 UNUSUAL FOLDED CONFORMATIONS OF NAD+. CRYSTAL STRUCTURES AND MOLECULAR DYNAMICS SIMULATIONS. J.J. Tanner [1], P.E. Smith [2], S.-C. Tu and K.L. Krause [3], [1] Department of Chemistry, University of Misouri-Columbia, Columbia MO 65211, USA, [2] Department of Biochemistry, Kansas State University, Manhattan, KS 66506, USA, [3] Department Department of Biology and Biochemistry, University of Houston, Houston, TX 77204, USA

Nicotinamide adenine dinucleotide (NAD+) is a ubiquitous biological small molecule and it is a major electron acceptor in the oxidation of fuel molecules. NAD+ adopts extended conformations when bound to enzymes, however, its solution structure is thought to be much more compact or folded. We report the 2.1 Å crystal structure of the enzyme flavin reductase P with NAD+ bound in the active site. NAD+ adopts an unusual, folded conformation in which the adenine and nicotinamide rings stack in parallel, with an inter-ring distance of 3.6 Å. The folded NAD+ binds with its pyrophosphate next to the cofactor FMN isoalloxazine and its nicotinamide C4 atom 10 Å from the putative site of hydride transfer on the isoalloxazine. Our structure offers the first crystallographic evidence of a folded NAD+, and it suggests that the folded state of NAD+ might be important for release of product from the enzyme. We analyzed the structure and dynamics of this folded NAD+ model using explicit solvent molecular dynamics simulations on the nanosecond time scale. These calculations reveal folding and unfolding transitions, and demonstrate that folded conformations are stable in solution.

P06.OB.011 LIPOXYGENASE REVISITED. Diana R. Tomchick[1], Krzysztof Lewinski[1], Anatoly Kiyatkin[1], Ted Holman[2], Janusz Steczko[3], Bernard Axelrod[3], Wladek Minor[1], [1]Department of Molecular Physiology and Biological Physics, University of Virginia, Charlottesville, VA 22906, USA, [2]Department of Chemistry and Biochemistry, University of California-Santa Cruz, USA, [3]Department of Biochemistry, Purdue University, USA.

Lipoxygenases are non-heme, non-sulfur iron dioxygenases that catalyze the hydroperoxidation of polyunsaturated fatty acids that contain one or more (Z,Z)-1,4-pentadiene moieties. The commonly accepted enzymatic mechanism involves hydrogen atom abstraction to form a pentadienyl radical, which reacts with oxygen. A large kinetic isotope effect, which implies hydrogen atom tunnelling, has been observed for both plant and human enzymes. Arachidonic acid is the predominant mammalian substrate, which yields products that are precursors of highly potent physiological effectors involved in such processes as carcinogenesis, asthma, vasoconstriction, inflammation and formation of atherosclerotic plaques. Development of lipoxygenase inhibitors as therapeutic agents is an extremely active research field, which would be aided by a better understanding of the structural basis of the reaction mechanism.

The paradigm for lipoxygenase kinetic, spectroscopic and other biophysical studies is the soybean L-1 isozyme, which crystallizes in a very high-resolution form (1.4 Å). A recent structure of an inhibited mammalian 15-lipoxygenase at medium resolution (2.4 Å) reveals a similar overall fold to the soybean enzyme, despite a much smaller size (ca. 670 vs. 840 residues). Certain aspects of the active site are not conserved between the two enzymes, including iron ligands and residues in the specificity pocket. We have analyzed the structures of numerous active site mutants of the soybean L-1 enzyme, and shall relate our structural, kinetic and spectroscopic results to the current mechanistic and structural models for wild type lipoxygenase specificity. Progress on complex structures of the soybean enzyme with several inhibitors and on the human 15-lipoxygenase will also be presented.

06OC CHEMICAL INSIGHTS FROM CHARGE DENSITY STUDIES (Sponsored by Dept. Chemistry, University of Glasgow)

M06.OC.001 UNUSUAL BONDS AND MOLECULAR PROPERTIES: FACTUAL OR FICTITIOUS? R. Destro, Department of Physical Chemistry and Centro CNR, University of Milan, I-20133 Milano, Italy.

Experimental electron densities in molecular crystals, as obtained from low-temperature X-ray diffraction data interpreted with an aspherical-atom formalism [1], almost routinely undergo topological analysis according to Bader's quantum theory of atoms in molecules (QTAM) [2]. It has been pointed out [3] that "such studies ... constitute probably the most active area of current research on experimental electron densities". The usual outcome is a corroboration of well-established chemical notions, with a full, quantitative characterization of all interatomic interactions.

However, in some instances expected critical points are not found, or unanticipated features of the charge density are revealed by the topological analysis [4]. Similarly, unusual values are sometimes obtained for molecular properties (*e.g.* dipole moments) derived from a multipole refinement of X-ray data. It appears that it is not always easy to distinguish between genuine features, hence new chemical insights, and artifacts due to limitations of the model adopted.

Examples of both kinds will be presented and discussed.

1. R. F. Stewart (1976). Acta Cryst. **A32**, 565.
2. R. F. W. Bader (1990). Atoms in molecules: a quantum theory. International series of monographs on chemistry, Vol. 22. Oxford University Press.
3. M. A. Spackman (1998). Annu. Rep. Prog. Chem., Sect. C, Phys. Chem., **94**, 177.
4. R. Destro & F. Merati (1995). Acta Cryst. **B51**, 559.

M06.OC.002 NEW INSIGHTS INTO THE EVALUATION OF ELECTROSTATIC MOLECULAR PROPERTIES FROM X-RAY DIFFRACTION DATA. Yuriy A. Abramov, Department of Chemistry, SUNY at Buffalo, Buffalo, NY 14260-3000 USA; chem9989@acsu.buffalo.edu

Different aspects of the evaluation of the electrostatic molecular properties, such as electrostatic moments and electrostatic interaction energy, will be considered starting from the X-ray refinement strategy. A multipole refinement of X-ray diffraction data is known as the most straightforward way of deriving these properties [1,2]. However, due to the lack of intrinsic physical (quantum mechanical) constraints in the unrestricted multipole refinement of observed structure factors, the static molecular multipole charge density is not guaranteed to be physically meaningful. This effect can introduce a pronounced *experimental basis set superposition error* in the evaluation of the electrostatic molecular properties. This error can be greatly reduced by a restricted multipole charge density model [3] in which atomic charges are constrained at κ–refinement values [1].

An application of the restricted multipole model to the evaluation of molecular dipole moments and intermolecular interaction energies in a number of α-amino acids and in 4-amino-4'-nitrobiphenyl will be presented. Experimental results will be compared with results of CHARMM force-field and quantum-mechanical calculations.

P. Coppens, *X-ray Charge Densities and Chemical Bonding,* Oxford University Press, New York, 1997.
P. Coppens, Yu.A. Abramov, M. Carducci, B. Korjov, I. Novozhilova, C. Alhambra & M.R. Pressprich (1999). *J. Am. Chem. Soc.*, in press.
Yu.A. Abramov, A.V. Volkov & P. Coppens (1999), to be published.

M06.OC.003 INSIGHT INTO INTRA- AND INTERMOLECULAR INTERACTIONS FROM TOPOLOGICAL ANALYSIS OF CRYSTAL CHARGE DENSITIES. Sine Larsen, Claus Flensburg, Hanne S. Bengaard and Henning O. Sørensen, Centre for Crystallographic Studies, Universitetsparken 5, 2100 Copenhagen, Denmark.

The topological analysis introduced by R.F. Bader for the analysis of theoretical charge densities [1] has also proven applicable for the analysis of experimental charge densities. Methods have also been developed for computation of the zero flux surfaces defining the atomic basins in the experimental charge densities [2], which enables calculation of the properties for atoms in crystals. These computational methods have been used to analyse the crystal charge densities for compounds that show unique intra- and intermolecular interactions.

It is not usual to find carbon as a ligand to Co(III), as we do in the classical Werner coordination compound $[Co(NH_3)_5 CH_3]\ S_2O_6$ [3]. Judged from the molecular geometry the four equatorial NH_3 ligands are distinctly different from the one that is trans to the coordinating CH_3^- anion. From the analysis of the experimental charge density it was possible to make a classification of the Co- ligand interactions and of the intermolecular interactions between the ions. Properties for the different fragments in the structure provided additional chemical insight.

Hydrogen bonds seem to be the most significant intermolecular interaction in molecular crystals and little attention is given to other weaker interactions in the crystal. The topological analysis is very useful to characterise the different hydrogen bonds. A detailed analysis of the theoretical and experimental crystal charge density of optically active para-fluoromandelic acid revealed bond critical points that correspond to much weaker interactions, that was not apparent from the geometrical analysis.

R.F. Bader, Atoms in Molecules: A Quantum Theory (1990), Clarendon Press, Oxford Science Publications: Oxford.
C. Flensburg & D. Madsen (1999) submitted for publication.
P. Kofod, P. Harris & S. Larsen (1997) Inorganic Chemistry, 36, 2258.

M06.OC.004 TOPOLOGICAL PROPERTIES OF VARIOUS AMINO ACIDS: A COMPARATIVE STUDY. P. Luger and R. Flaig, Institut für Kristallographie, Freie Universität Berlin, Takustr. 6,14195 Berlin, Germany, and T. Koritsanszky, Department of Chemistry, University of the Witwatersrand. Private Bag 3, WITS 2050, Johannesburg, South Africa.

It could be shown recently [1] that the combination of synchrotron radiation at a short wavelength of $\lambda \approx 0.5$ Å with a CCD area detector allows the collection of high resolution diffraction data, in a few days or even hours, which are well suited to obtain accurate charge densities. This short acquisition time makes the method applicable to larger molecules or to perform comparative studies of a class of chemically related compounds. Taking advantage of these experimental developments we have investigated the charge densities of seven amino acids. Thus, including those studied previously, data of about half of the 20 naturally occuring amino acids are available for comparison.

We report on a number of chemically important properties of these molecules, such as the electrostatic potentials, electric moments and topological figures of the densities derived in terms of the aspherical-atom formalism using the same refinement model and strategy. The agreement is found exceptionally good for the density values at critical points $[(r)\backslash vec]_b$ of chemically equivalent bonds and it is satisfactory for other topological parameters characterizing atomic interactions ($\nabla^2\ \rho([(r)\backslash vec]_b)$, bond ellipticity). Such a comparison can be considered as the first step towards experimental verification of Bader's concept on topological segmentation of molecules [2]. Further inportant aspect of these studies is the mapping and characterization of weak intermolecular interactions, that are of interest for biological recognition processes. Here the experimental Laplacian and the electrostatic potential play a significant role.

1. T. Koritsanszky, R. Flaig, D. Zobel, H.-G. Krane, W. Morgenroth, P. Luger, Science 279 (1998), 356-358.
2. P.L.A. Popelier, R.F.W. Bader, J. Phys. Chem. 98, (1994), 4473.
We thank the BMBF (project 05 SM8 KEA 0) and the Fonds der Chemischen Industrie for financial support.

M06.OC.005 CHARGE DENSITY AND ELECTROSTATIC PROPERTIES OF NATURAL AND INDUSTRIAL ALUMINO-SILICATES: SUCCESS AND PROBLEMS. M. Souhassou, N.E. Ghermani, F. Porcher, S. Kuntzinger, Y. Dusausoy and C. Lecomte, LCM^{3}B, UPRESA CNRS 7036, Université Henri Poincaré, Nancy I, Faculté des Sciences, BP 239, 54506 Vandoeuvre-lès-Nancy Cedex.

Charge density analysis of natural and industrial zeolites as well as other alumino silicate minerals[1-7] will be described. Special care will be given to the determination of the net charges, moments and electrostatic potential, quantities very important for understanding the industrial potentiality of these materials.

Electrostatic features of coesite[2], natrolite[3], scolecite[4], spodumene[5], zeolite A[6] and X[7] will be compared and discussed. It will be shown that even if charge density is precisely obtained from accurate conventional or synchrotron data, calculation of some properties like net charges is still a matter of discussion.

1. F.E. Hill, G.V. Gibbs, M.B. Boisen (1997). J. Phys. Chem. Minerals, 24, 164-178 and 582-592.
2. J.W. Downs (1995). J. Phys. Chem., 99, 6849-6856.
3. N.E. Ghermani, C. Lecomte, Y. Dusausoy (1996). Phys. Rev. B53, 9, 5231-5239.
4. S. Kuntzinger, N.E. Ghermani, Y. Dusausoy, C. Lecomte (1998). Acta Cryst. B54, 819-833.
5. S. Kuntzinger, N.E. Ghermani (1999). Acta Cryst. B55, 000.
6. F. Porcher, M. Souhassou, Y. Dusausoy, C. Lecomte (1998). C.R. Acad. Sci. Paris IIC, 701-708.
7. F. Porcher, M. Souhassou, Y. Dusausoy, C. Lecomte (1999). Eur. J. Miner., 000.

P06.OC.001 CHEMICAL BONDING AND SUPERPOSITION EFFECTS ON THE ELECTRON DENSITY. Ivar Olovsson, Inorganic Chemistry, Ångström Laboratory, Box 538, S-751 21 Uppsala, Sweden, Halina Ptasiewicz-Bak, Institute of Nuclear Chemistry and Technology, Dorodna 16, 03-195 Warszawa, Poland and Garry J. McIntyre, Institut Laue-Langevin, 156X, F-380 42 Grenoble, France.

There appears to be conflicting experimental evidence on the redistribution of the charge density in the lone-pair and other regions of a molecule due to the interaction with its nearest neighbours. In some experimental as well as theoretical deformation density maps a decrease in the lone-pair density has

been reported, whereas in other cases an increase has been found. It appears that two major counteracting factors are responsible for these differences: an increase in the lone-pair density is expected due to the polarising influence of the neighbours, whereas simple superposition of the isolated monomer densities will lead to an apparent decrease due to the overlap with the negative contours of the neighbouring atom. Depending on which of these factors is the dominant one, an increase or decrease may thus be found.

In Uppsala a series of hydrates of transition metal hydrates have been systematically studied: $Na_2Ni(CN)_4 \cdot 3H_2O$, $Ni(NO_3)_2 \cdot 6H_2O$, $NiSO_4 \cdot 6H_2O$, $NiSO_4 \cdot 7H_2O$, $NiCl_2 \cdot 4H_2O$, $CoSO_4 \cdot 6H_2O$ and $CrCl_3 \cdot 6H_2O$. The object was in the first place to determine the electron density around the transition metal ion, but was also of special interest to study whether it would be possible to obtain good densities of the water molecules in the presence of such a heavy scatterer as a 3d metal ion.

The charge density has been determined at RT and 25-30K by multipole refinement against single crystal X-ray intensity data. The charge density based on the fitted deformation functions of all atoms in the structure is compared with the individual densities calculated from deformation functions of only the metal ion or the separate water molecules. In this way the effect of simple superposition of the individual densities has been studied. Polarisation of the lone-pair densities, reflecting the different co-ordination of the water molecules, is clearly evident.

P06.OC.002 TOPOLOGICAL ANALYSIS OF THE CHARGE DENSITY IN SHORT HYDROGEN BONDS. Jacob Overgaard, Georg K. H. Madsen, Bo B. Iversen, Finn K. Larsen, Department of Chemistry, University of Aarhus, Dk-8000 Århus C, Denmark, Garry I. McIntyre, Institut Laue-Langevin, BP 156, 38042 Grenoble CEDEX 9, France and Arthur J. Schultz, Intense Pulsed Neutron Source, Argonne National Laboratory, Argonne, IL 60439, USA.

Some short O-H--O and N-H--O hydrogen bonds (HB) have been characterized by combined analysis of X-ray and neutron diffraction data. The intramolecular keto-enol HB in benzoylacetone[1] with an O--O distance of 2.502(4)Å proved to be an asymmetric (1.25(1),1.33(1)Å) Low Barrier HB. The zero point vibrational energy of the proton exceeds the barrier of transfer allowing the proton to move between the oxygen atoms with a mean square displacement (m.s.d.) of 0.106 $Å^2$ at 20 K. Nitromalonamide is another compound with an intramolecular keto-enol HB. It has a shorter O--O distance (2.391(3) Å) yet a more asymmetric (1.14(1), 1.31(1) Å) single well HB. The proton has a m.s.d. of 0.031 $Å^2$ at 20 K as determined by neutron diffraction at the ILL high flux reactor. The topology of the charge density (CD) in these short O-H--O HB's are compared.

Short N-H--O HB's in the complex of betaine, imidazole and picric acid was studied similarly, based on diffraction data collected at 28 K, - synchrotron X-ray data by imaging plate detection at beamline X3A1, NSLS Brookhaven, and neutron diffraction data by white beam time-of-flight technique at IPNS, Argonne. The complex serves as a model for the active site of serine protease, the catalytic triad, and the system is attractive since it contains three different short N-H--O contacts (<2.7 Å) in the same crystal. Analysis of the CD shows that all three short HB's have hydrogen localized at the nitrogens and that none are LBHB. The H--O interactions are all predominantly electrostatic interactions ($\nabla^2\rho>0$ at the bond critical points) between closed shell atoms. Results of ab initio calculations for the systems are compared with the experimental results.

[1] G. K. H. Madsen, B. B. Iversen, F. K. Larsen, M. Kapon, G. M. Reisner and F. H. Herbstein, *J. Am. Chem. Soc*. **1998**, *120*, 10040-10045.

P06.OC.003 POLYHEDRAL REPRESENTATION OF ATOMS IN CRYSTAL STRUCTURES. T. Balic-Zunic, Geological Institute, University of Copenhagen, DK-1350 Copenhagen K, Denmark

The atomic domains in molecules or crystals are bounded by surfaces of zero flux in the gradient vector field of the charge density [1]. In electron density maps they can be recognized as surfaces of low electron density which separate neighbouring atoms, and define their domains. The atomic domains in crystal structures closely resemble polyhedra with faces perpendicular to interatomic vectors. Therefore, the most appropriate representation of an atom in a crystal is the atomic domain polyhedron. In topological analyses, e.g. in defining atomic coordinations or structural relations, the use of element-specific atomic models in the form of polyhedra with defined shape-size variations is superior to the traditional model of spheres with defined radii. In most inorganic crystal structures a satisfactory partition in atomic domains can be achieved also without accurately determined charge densities. The procedure is similar to the determination of Voronoi-polyhedra, supplemented by expected domain sizes. In the course of crystal structure partitioning the planes are put perpendicular to interatomic vectors at positions of the expected minima of electron density calculated from predetermined parameters. The closest polyhedron closed this way around an atom represents its domain. To determine the parameters for the calculation of plane positions an IAM-based procedure can give satisfactory results. For each element pair sums of the spherically averaged electron densities of overlapping atoms are calculated and the positions of minima determined over a range of interatomic distances. Over the range of bonding distances the position of minimum usually varies linearly with the interatomic distance, and can be defined by two parameters. The partition parameters, domain determinations, and some applications will be presented.

1. R.F.W. Bader (1991). Chem.Rev., 91, 893-928.

06OD CHALLENGING RIETVELD REFINEMENTS

M06.OD.001 QUANTITATIVE PHASE ANALYSIS OF PORTLAND CEMENT BY RIETVELD REFINEMENT. I.C. Madsen and N.V.Y. Scarlett, CSIRO Minerals, Box 312, Clayton South, Victoria 3169, Australia

The quantitative analysis of Portland cement by Rietveld refinement may well strike fear into the heart of even the hardiest crystallographer. This is due to the presence of a myriad of crystallographically ill-defined phases whose reflections exhibit a high degree of overlap in the powder pattern.

Non-XRD methods of quantitative phase analysis of Portland cement such as optical microscopy and the Bogue method have severe limitations. Optical microscopy presents a significant sampling challenge and the Bogue method, based upon the breakdown of XRF analyses into component phases, is dependent upon dubious assumptions. Single peak XRD methods are also fraught with danger due to the difficulty in finding free-standing peaks of sufficient strength to provide a reliable estimate of intensity.

Traditional Rietveld refinement requires detailed knowledge of the crystal structures of each of the component phases in the material. This is not possible in the case of Portland cement where the component phases do not always match the published structures due to (i) different levels of impurity substitution and (ii) variable degrees of hydration in the sulphate phases. Rietveld refinement of synthetic cement mixtures has shown the technique able to cope with the overlap problem when the crystal structures are known.

This paper describes the use of a modified Rietveld approach where the intensities of the diffraction peaks can be estimated by observation of patterns of the materials of interest. The main advantage of this approach lies in the ability to manually alter the individual peak intensities in the reflection intensity files to better match the observed peak heights in the pattern. The only requirement is that each of the I_{obs} be indexed and the unit cell dimensions known, thus allowing adjustment of the peak positions through refinement of the unit cell parameters (if necessary).

M06.OD.002 RIETVELD REFINEMENTS OF INCOMMENSURATE MODULATIONS IN COMPLEX OXIDES. D. Grebille and O. Pérez, CRISMAT, ISMRA, 14050 Caen Cedex, France, and G. Baldinozzi, Lab. CPS, Ecole Centrale de Paris, 92295 Châtenay-Malabry Cedex, France, and J.F. Bérar, Lab. de cristallographie, CNRS BP 166, 38042 Grenoble Cedex, France.

Incommensurate modulations are frequently encountered in the refinement of crystal structures. Their symmetry and structure can be properly described using the superspace formalism, which is now commonly implemented in refinement programs using single crystal diffraction data.

Unfortunately, single crystal data are not always available, or can be biased in the case of polydomain samples. In these cases, powder diffraction is very easy to use and Rietveld refinements have proved their efficiency in solving complex structures. In particular, in the case of incommensurate phases, the metric refinement is generally more accurate using a well resolved powder diffraction pattern, and the continuous measurement of the whole background allows to fix all the weak intensities of higher order satellite reflections for example.

The Rietveld refinement program XND [1] can now take advantage of the superspace symmetry description for the refinement of incommensurately modulated structures. Several examples are given concerning complex oxide structures:

- occupation and displacement modulation in the tunnel structure $Ba_2Ca_2In_6O_{12}$;
- modulated structure of the complex perovskite Pb_2CoWO_6 and comparison with an equivalent refinement using single crystal data;
- modulated structure of the ferrite $Bi_2Sr_3Fe_2O_9$ using neutron powder diffraction data and X ray single crystal data.

J.F. Bérar & G. Baldinozzi, (1998) I.U.Cr-C.P.D. Newsletter 20, 3.

M06.OD.003 COMBINED RIETVELD AND STEREOCHEMICAL RESTRAINT REFINEMENT OF PROTEIN CRYSTAL STRUCTURES. R.B. Von Dreele, Lujan Center, Los Alamos National Laboratory, Los Alamos, NM 87545, USA

By combining high resolution x-ray powder diffraction data and stereochemical restraints, Rietveld refinement of protein crystal structures has been shown to be feasible. This talk will outline the procedures used for these refinements and show the quality of the resulting protein structure by comparison with known single crystal results and evaluation of protein stereochemical parameters.

Supported by US DOE/BES.

M06.OD.004 RIETVELD REFINEMENT OF THE ZEOLITE UTD-1, A 117 ATOM PROBLEM. Ch. Baerlocher, T. Wessels, L.B. McCusker, Laboratory of Crystallography, ETH, Zürich, Switzerland.

The zeolite UTD-1 has been shown to have a 1-dimensional channel system with 14-ring pore openings, but its structure, at least in the calcined form, has been reported to be an intergrowth of at least two polymorphs [1]. All of the polymorphs proposed have orthorhombic symmetry.

A new synthesis procedure using the fluoride method yielded a highly crystalline sample of UTD-1, so high-resolution synchrotron powder diffraction data were collected on the as-synthesized form at the SNBL in Grenoble (λ = 0.6480 Å, 1.8 - 37 $^\circ 2\theta$). The pattern could only be indexed on a monoclinic cell (a = 14.963, b = 8.4704, c = 30.010 Å, β = 102.7°) and the most likely space group appeared to be $P2_1/c$. By applying our new texture approach to structure determination from powder data, the crystal structure could be solved directly. The framework topology proved to be that of polymorph C of reference [1], but in the space group $P2_1/c$ it has 16 Si and 32 O atoms in the asymmetric unit. In order to verify that the new material is in fact fully ordered (i.e. a pure end-member), a Rietveld refinement was undertaken.

The location and orientation of the template cation (bis(pentamethyl-cyclopentadienyl)cobalt(III)) could be established easily from the difference Fourier map. However, because of short contacts between symmetry related molecules, its occupancy had to be restricted to 1/2. Furthermore, significant intensity differences for certain reflections were observed. A symmetry reduction to Pc solved both problems, but required a refinement with 117 non-hydrogen atoms (32 Si, 64 O, 1 Co and 20 C atoms) or a total of 349 positional parameters. Using 444 geometric restraints with a common weight factor of 1, the refinement converged with R_F = 0.043 and R_{wp} = 0.132 (R_{exp} = 0.101). This proves (1) that a true end-member for UTD-1 exists, and (2) that it is possible to refine complex structures with ca 350 structural parameters using the Rietveld method, if high quality synchrotron powder data are available.

R.F. Lobo, M. Tsapatsis, C.C. Freyhardt, S. Khodabandeh, P. Wagner, C.Y. Chen, K.J. Balkus, S.I. Zones and M.E. Davis, *J. Am. Chem. Soc.*, **119**, 8474 (1997).

M06.OD.005 SITING OF TITANIUM ATOMS IN THE TITANOSILICALITE CATALYST TS-1. J. Eckert, C. J. Hijar, K. C. Ott, Los Alamos National Laboratory, Los Alamos, NM 87545, USA, and R. Jacubinas, Engelhard Corporation, Iselin, NJ 08830-0770, USA.

The titanosilicalite TS-1 has proven to be one of the most important catalysts discovered in the last decade because it catalyzes the epoxidation of olefins with acqueous hydrogen peroxide under mild conditions. Its activity has been ascribed to Ti atoms inserted into the silicalite framework in place of Si. Despite the widespread use of this catalyst, however, very little is know about the actual siting of the Ti atoms. The principal reason for this is that there relative amount of Ti is very small (no more than one per 30 Si) and that these may be disordered over the 12 inequivalent tetrahedral (T) sites in the MFI structure. A number of theoretical studies did indeed predict random siting for the Ti atoms among the 12 T-sites. We describe the results of a series of neutron powder diffraction studies which clearly demonstrate that Ti siting in TS-1 is not random and discuss the implications thereof for the activity of these catalysts.

This work was supported by the United States Department of Energy under contract number W-7405-ENG-36 with the University of California. The work has benefitted from the use of facilities at the Manuel Lujan Jr. Neutron Scattering Center, a national user facility funded by the United States Department of Energy, Office of Basic Energy Sciences.

M06.OD.006 RIETVELD REFINEMENT OF REHYDRATED $AlPO_4$-34, A TRICLINIC NIGHTMARE. A. Meden, Faculty of Chemistry, University of Ljubljana, Slovenia, L.B. McCusker and Ch. Baerlocher, Laboratory of Crystallography, ETH, Zurich, Switzerland.

In its as-synthesized form, the molecular sieve $AlPO_4$-34, with a chabazite-like framework topology (**CHA**), is triclinic. This distortion from the ideal rhombohedral symmetry is caused by the presence of ordered Al-F-Al bridges. Upon calcination, the F-bridges are removed and the material adopts the higher symmetry. However, rehydration of the calcined material produces another well-crystallized, triclinic phase, which transforms to yet another triclinic phase at 23 ^{o}C. NMR spectra show that both 5- and 6-coordinate Al are present in both of these phases. The high crystallinity, the triclinic deformation, and the NMR results are indicative of an ordered arrangement of water molecules in the low-temperature structure. To elucidate this arrangement, and to clarify the reason for the change of symmetry upon hydration, a Rietveld refinement, using synchrotron powder diffraction data collected at 15 ^{o}C (SNBL at ESRF), was undertaken.

Refinement was initiated with a triclinically distorted chabazite-like framework structure, and the positions of the water molecules were located in a series of Fourier maps. Four models (in $P\bar{1}$ and $P1$, each with interchanged Al and P atoms) were investigated. Anisotropic peak broadening and peak asymmetry had to be fitted in the final refinement.

The low-temperature triclinic phase of hydrated $AlPO_4$-34 proved to be non-centrosymmetric with a total of 48 atoms in the asymmetric unit (including 12 fully occupied water postions). Five water molecules coordinate to Al atoms of the framework, producing two octahedral and one 5-coordinate Al. One water molecule is situated within the double six-ring and the rest are located in the central cage. The octahedral Al atoms are ordered along one of the *pseudo*-rhombohedral axes as in the case of the fluoride-containing triclinic precursor. The TG and NMR (1D and 2D) results are fully consistent with the refined structure.

06OE NEUTRON STUDIES OF STRESS/STRAIN

M06.OE.001 INSIGHTS ON POLYCRYSTALLINE DEFORMATION USING NEUTRON DIFFRACTION. M.A.M. Bourke. LANSCE, Los Alamos National Laboratory, Los Alamos, New Mexico, 87545, USA

By collecting neutron diffraction data during in situ uniaxial compression or tension tests - the origins of bulk deformation behavior can be studied at the microstructural level. Measurements at LANL have provided insights on disparate processes including; codeformation in multiphase systems, creep, twinning, stress induced phase transformations. Also a large effort has addressed the validation of micromechanical models (both self consistent and finite element) that attempt to describe the effects of anisotropic elastic and plastic behavior of specific grain orientations in a polycrystalline aggregate.

This talk will discuss the constraints and current limitations on these types of measurements at a pulsed neutron source. Interpretations from texture and strain evolution will be discussed for three examples; 1) micromechanical model validation in beryllium 2) twinning in a Uranium alloy and 3) stress induced phase transformations in NiTi and NiTi-TiC. Plans for a load frame furnace suite with a 250 KN 1500°C capability that will operate on a new neutron spectrometer, SMARTS, will also be outlined.

M06.OE.002 NEUTRON STRESS ANALYSIS IN ENGINEERING COMPONENTS. A.Pyzalla, Strukturforschung, Hahn-Meitner-Institut, Glienicker Straße 100, D-14109 Berlin, Germany

The significance of residual stresses with respect to the mechanical and technological properties of components, especially their strength and fatigue limit, has been acknowledged for almost one and a half century now. There are a number of applications that require the determination of the residual stress state within the whole component or at least within large parts of the component.

Whereas X-ray residual stress analysis is confined to near surface layers, absolute residual stress values in the bulk of components can be determined non-destructively by neutron diffraction. In case of multiphase materials phase specific residual stress values can be obtained. Thus, neutron residual stress analysis now is an important and in wide parts of the industry accepted tool with respect to the optimisation of multiphase materials and technical single crystals alloys, manufacturing processes and component's design but also for a verification of numerical calculations of the residual stress state.

Examples for engineering materials and components, which were characterised and optimised using neutron residual stress analyses are e.g. metal and ceramic matrix composites as well as single crystal turbine blades, turbine disks, impellers, extruded, shot peened and deep-rolled as well as brazed or welded components.

M06.OE.003 EXPLOITING SYNCHROTRON RADIATION FOR ENGINEERING STRESS MEASUREMENTS. P.J. Withers, *P.J. Webster, **A.M. Korsunsky, Manchester Materials Science Centre, Grosvenor St., Manchester, M1 7HS, *Telford Institute, Civil Engineering, Salford University, **Dept. of Mech., Manufacturing & Materials, University of Newcastle, UK

The arrival of third generation synchrotron sources has provided the engineer with very intense penetrating X-ray beams for residual stress analysis. Energies in the range 25-300keV are available, giving rise to penetrations of many centimetres in aluminium and significant distances even in steel and nickel. In this paper we introduce the basic principles and methods. Current methods are sub-divided into three distinct groups, white beam, monochromatic $\theta/2\theta$ and whole Debye Scheerer ring analysis methods are described. In each case the principal advantages and limitations will be discussed largely with reference to practical examples.

The white beam method provides a large portion of the diffraction profile making it well suited to the study of multiple phase materials and those with complex crystal structures. In addition, it is ideal for kinetic studies for which it is necessary to follow the evolution of a number of peaks. The energy resolution of current detectors tends to limit the maximum strain resolution achievable. The method will be introduced with reference to a recent study on stresses in thermal barrier coatings comprising a top-coat, bond coat and substrate.

Theta/two theta studies can provide excellent strain resolution, fast measurement times and reasonable spatial resolution (~100x100x800μm). This has meant that the technique is ideal for two and three dimensional mapping of residual strain distributions in a range of components. We will include examples of laser shock peening,TIG welding and stir welding. The insensitivity of the approach to near surface aberrations will also be discussed.

Debye Scheerer ring analysis using high energy beams provides a wealth of information about the in-plane stress state with very high lateral spatial resolution. It is best suited to plate and sheet type problems. The strengths and limitations of the method will be demonstrated with reference to stresses in Ti/SiC composites and in welded plates. Special attention will be

focused on ways of increasing the longitudinal definition of the gauge volume and the analysis of full diffraction ring data acquired using a CCD detector.

M06.OE.004 RESIDUAL STRESSES AND MICROSTRAIN INVESTIGATION IN FATIGUED TESTED SPECIMEN. M. Ceretti [1], K. Hirschi [1],B. Marini [2], J.M. Sprauel [3], J.P. Lauriat [4]; [1] Laboratoire Léon Brillouin, CEA Saclay, F-91191 Gif sur Yvette (France), [2] SRMA, CEA Saclay, F-91191 Gif sur Yvette (France), [3] Laboratoire MecaSurf, ENSAM, F-13617 Aix en Provence (France), [4] LURE, Université Paris XI, Orsay (France).

Neutron diffraction has been used to estimate plastic strains along the line of the crack of a fatigue test specimen made of commercial austenitic steel AISI 316. Some microstructural parameters, such as an average size of coherently diffracting blocks, mean-square microstrain and dislocation density have been deduced from the broadening of diffraction profiles using Keijser's approach. Three dimensional measurements were performed on three compact tension specimen with different load ratios. The dimension of the plastic zone close to the crack tip was estimated and the elastic lattice strains have been determined. The results are in agreement with finite element calculations. Complementary measurements were made by using synchrotron radiation at the sample surface. Plastic strains were determined using a recently developed model taking into account the contribution of elastic strain heterogeneity (ESH) on the profiles broadening. The obtained values of separated size, strain and ESH contribution are in a good agreement with those published elsewhere for this kind of steel characterised by a strong dependency on the type of the hkl reflection.

M06.OE.005 ENGIN-X: A NEW INSTRUMENT DESIGN FOR ENGINEERING STRAIN MEASUREMENTS. M W Johnson, M R Daymond, ISIS Facility, Rutherford Appleton Laboratory, Chilton, Didcot, Oxon. OX11 0QX.

Neutron strain scanning is a non-destructive technique that provides important insights into stress distributions deep within engineering components and structures. As such it has become an increasingly important tool within engineering, leading to improved manufacturing processes to reduce stress and distortion. It has also helped to define structural integrity lifing procedures more precisely.

We outline a new design for a neutron strain scanner, ENGIN-X, which will bring an order of magnitude increase in performance over current neutron strain-scanning instrumentation. The gain in performance has been achieved by establishing quantitative methods for defining the instrument's efficiency, and then maximising them in the design. The method of achieving the order of magnitude improvement will be described, and the possible applications of the improved instrument discussed.

A ten fold increase in performance over currently available technology will enable innovative research of direct relevance to the engineering industry in at least four particular areas: area strain mapping, deep measurements, high spatial resolution and real time studies.

06OF ADVANCES IN LIQUID STRUCTURE DETERMINATION

M06.OF.001 TOOLS FOR THE ANALYSIS OF LIQUIDS DIFFRACTION DATA. A K Soper ISIS Facility, Rutherford Appleton Laboratory, Chilton, Didcot, Oxon, OX11 0QX

The last ten years or so have witnessed the development of new methods for the interpretation of liquids diffraction data which are analogous to those already used by crystallographers for some 30 years. In essence all these new techniques attempt to build a 3-dimensional model structure of the system under investigation based on available diffraction data and other constraints on the structure that are known. The reconstruction of the structure of a liquid or disordered material is both easier and more difficult than the equivalent crystallographic problem: on the one hand there are relatively few, and only diffuse, peaks in the diffraction pattern to refine. Against this formally such a reconstruction from diffraction data alone is not possible, and the lack of crystallographic symmetry and long range order on which to build a model structure leads to serious ambiguities. In fact there is no single structure to be found, but instead an ensemble of structures, and it is the reconstruction of this ensemble that is at the heart of any disordered material structure refinement. To achieve this with any degree of reliability it is essential to include as much additional (e.g. chemical) information into the problem as is available. The talk will outline recent progress in this field, with examples from true liquids, amorphous materials, and materials with some crystalline character.

M06.OF.002 COMPLEMENTARY NEUTRON AND X-RAY DIFFRACTION FROM LIQUIDS. David L. Price, Marie-Louise Saboungi, Yaspal S. Badyal, Dean R. Haeffner and Sarvjit D. Shastri Argonne National Laboratory Argonne, IL 60439, USA

The high-energy x-rays available from synchrotron sources extend the range of liquids that can be readily studied with x-ray diffraction, especially liquids that are corrosive or have high melting points. Since the partial structure factors have generally different weights in the total structure factors measured by neutrons and by x-rays, the ability to measure both provides information at the partial level. In addition, a detailed comparison can provide information about the distribution of the electrons relative to the nuclei and about magnetic properties. These ideas will be illustrated by three examples of recent work at the Advanced Photon Source: molten iron chloride, liquid potassium-lead, and water.

Work supported by the U.S. Department of Energy, Office of Basic Energy Sciences, Division of Materials Sciences, under Contract W-31-109-ENG-38.

M06.OF.003 SINKING THE ICEBERG: STRUCTURES OF AQUEOUS SOLUTIONS OF HYDROPHOBIC MOLECULES. J.L. Finney, Dept of Physics and Astronomy, University College London, Gower Street, London WC1E 6BT, UK, D.T. Bowron, European Synchrotron Radiation Facility, B.P. 220, 38043 Grenoble Cedex, France, and A.K. Soper, ISIS Facility, Rutherford Appleton Laboratory, Chilton, Didcot, Oxon OX11 0QX, UK.

The hydrophobic interaction is central to much of chemistry and biology. However, the molecular mechanisms underlying it are poorly understood. The conventional rationale of Frank and Evans argues that the source of the entropic driving force is a structural ordering of the water molecules in the hydration shell of the non-polar group, resulting in an entropic gain as the hydration water is expelled to the bulk when two non-polar groups come together in solution.

Recent developments in both neutron and x-ray sources and instrumentation, coupled with new procedures to assist interpretation of the experimental data from relatively complex multi-component solution systems, have allowed us to determine in unprecedented detail the structures of molecules in solution. Not only can we see directly for the first time the hydration structure of a non-polar group in solution, but we can also see

how solute molecules associate in solution, as temperature, concentration, or other solution conditions are changed. Using recent results from ISIS and ESRF, the standard molecular interpretation of the hydrophobic interaction is seen to be incomplete. Further development of these procedures promises to give us the ability to effectively perform crystallography in the liquid state. Moreover, state-of-the-art procedures to model the experimental results promise a revolution in liquid structural studies similar to that brought about for powder crystallography through Rietveld refinement techniques.

M06.OF.004 THE STRUCTURE OF FLUIDS IN LAYERED MATERIALS. G.D.Williams, N.T.Skipper*, M.V.Smalley, J.K.Walters, A.K.Soper, Department of Physics and Astronomy, University College London, & ISIS, Rutherford Appleton Laboratory.

The presentation will discuss time-of-flight neutron diffraction studies of the structure of fluids intercalated into clays and graphite. The main focus will be on the determination of liquid density profiles normal to the solid surfaces, using oriented samples and isotopic labelling. Results for aqueous solutions in colloidal clay minerals show that two layers of partially oriented water form at each clay surface. The structure in this region is dominated by hydrogen bonding of water to the negatively charged clay platelets. In graphite-potassium-ammonia systems, a 2-dimensional liquid monolayer is formed, in which neither potassium nor ammonia is registered to the underlying graphite structure.

M06.OF.005 WHAT DO WE KNOW ABOUT HYDRATION WATER AND WHAT IS STILL THERE TO KNOW. Fabio Bruni, Dipartimento di Fisica, Universita di Roma III, via della Vasca Navale 84, ROMA I-00146, Italy

In the evolution of life systems, water has been a component of transcendent importance. Water is in fact one of the essential components of life, and its functions are manifold. At the microscopic level, discrete H_2O molecules or small clusters are implicated in the maintenace of biologically active conformations of nucleotides, proteins, and carbohydrates. Macrostructures, such as membranes, are stabilized and sustained by the presence of critical numbers of bound water molecules. In metabolism and synthesis, H_2O is the universal reagent in any process that involves hydrolysis, condensation, reduction, or oxidation, and that includes most biochemical reactions.

The physical properties of water close, or confined, to intracellular solid interfaces, such as the surface of proteins or membranes, still represent an open problem, and it is certainly true that for the extent with which its experimentally determined properties differ from its behavior when in bulk aqueous solutions, water is without peer. Moreover the modifications to its bulk behavior when water is in confined geometry is important for technological applications such as mining and corrosion inhibition as well.. Structural and dynamical properties of water may be affected by both purely geometrical confinement and/or interaction forces at the interface; reliable and realistic model systems have therefore to be studied in order to discriminate between the two cases. Recent results, obtained by mean of experiments and molecular dynamics simulations, on confined water will be presented and compared.

P06.OF.001 THE UBBELOHDE EFFECT IN ROOM TEMPERATURE LIQUIDS. C. J. Benmore, ISIS Facility CLRC Rutherford Appleton Laboratory, Chilton, Didcot, Oxon OX11 OQX, U.K. B. L. Tomberli and P. A. Egelstaff, Dept. of Physics, University of Guelph, Guelph, Ontario, CANADA, N1G 2W1, and J. Neuefeind, HASYLAB, Notkestr. 85, 22603 Hamburg, GERMANY.

The Ubbelohde or H/D isotope effect has been measured by a direct method for hydrogenated and deuterated molecular liquids at room temperature under their normal vapour pressures using 101.2 keV X-ray diffraction. The effect in both intra- and inter-molecular terms is revealed by small but observable differences between the electronic structure factors of the two liquids at the same temperature. After Fourier transforming, the data are analysed in terms of the changes in their electron density correlation functions. A brief description of the X-ray technique used to measure the Ubbelohde effect in liquids is presented and the results are discussed with regard to how the isotopic substitution influences both the intra- and inter-molecular structure of the liquid.

06AA STRUCTURAL MOTIFS AND MULTIDOMAIN PROTEINS

M06.AA.001 STRUCTURAL CLASSIFICATION OF PROTEINS: A GUIDE TO THE PROTEIN WORLD. Alexey G. Murzin, Centre for Protein Engineering, MRC Centre, Cambridge CB2 2QH, UK

Large protein structures can be divided into domains formed by separate folded segments of the protein chains. However, for the majority of known structures, the domain division is not unambiguous. There are several different definitions of protein domain that usually correlate but sometimes conflict with each other.

Structural classification of proteins, SCOP, suggests a consensus definition of the protein domain as its basic classification unit. SCOP, having embodied the known theories of protein structure and evolution, organizes all known protein domains hierarchically according their structural similarity and near and far evolutionary relationships.

In my review of known relationships amongst proteins of known structure, I will focus on several recurrent structural domains from multidomain proteins, in particular, those involved in the biosynthesis of nucleotides and nucleic acids. Selected examples will demonstrate various pathways from a simple to a more complex protein structure. They also will illustrate the origins of many different specialized functions from a small set of primordial structural and functional modules.

M06.AA.002 CARBAMOYL PHOSPHATE SYNTHETASE: A LONG JOURNEY HOME. Hazel M. Holden*, Frank M. Raushel§, and James B. Thoden*, *Department of Biochemistry, University of Wisconsin , Madison Wisconsin, 53705 §Department of Chemistry, Texas A&M University, College Station, Texas, 77843

Carbamoyl phosphate synthetase, hereafter referred to as CPS, catalyzes perhaps one of the most remarkable biological reactions ever described whereby carbamoyl phosphate is assembled from one molecule of bicarbonate, two molecules of Mg^{2+}ATP, and one molecule of glutamine. The carbamoyl phosphate so produced is subsequently employed in the biosynthesis of both arginine and pyrimidine nucleotides. Due in part to its important metabolic role and to the large number of substrates, products, and effector molecules that bind to it, CPS has been the focus of intense investigation for more than thirty

years Prior to the successful structural determination of the *Escherichia coli* CPS $(\alpha,\beta)_4$-tetramer in 1997, it was unclear how this enzyme was able to orchestrate the synthesis and stabilization of three separate reaction intermediates: carboxyphosphate, ammonia, and carbamate. From research in this laboratory, it is now known that glutamine and nucleotide binding sites are separated by more than 90 Å and, in accordance with most biochemical data, it has now been suggested that some type of substrate channeling occurs within the α,β-heterodimer. The structures of various CPS complexes will be discussed in light of this putative channeling. This work was supported in part by grants from the NIH (GM55513 to H. M. H. and DK30343 to F. M. R.).

M06.AA.003 STRUCTURE AND FUNCTION OF BOTULINUM NEUROTOXIN TYPE A. Raymond C. Stevens Department of Chemistry, University of California at Berkeley, Berkeley, CA 94720, USA.

Botulinum neurotoxin (BoNT), a food-borne pathogen produced by Clostridium botulinum, is a 150 kD protein with three ~50 kD functional domains: binding, translocation, and catalytic[1]. It acts by binding a receptor on pre-synaptic nerve endings and undergoing receptor-mediated endocytosis. The acidity of the endosome triggers the translocation domain to form a pore, allowing for the transfer of the catalytic domain across the membrane into the cytosol. The catalytic domain is a zinc metalloprotease specific for one of three proteins involved in synaptic vesicle membrane fusion. Substrate cleavage results in inhibition of neurotransmitter release and, ultimately, causes the paralysis seen in botulism. The crystal structure of BoNT serotype A has been determined to 3.2 Å resolution[2]. The binding domain shares structural homology with the tetanus neurotoxin binding domain[3]. The translocation domain structure reveals a striking pair of 105 Å long a-helices and a ~50 residue 'belt' which wraps completely around the perimeter of the catalytic domain, occluding access to the active site zinc. The unusual fold implies that the mechanism of pore formation and translocation for BoNT/A is radically different from that thought to occur in other bacterial toxins. The catalytic domain structure of BoNT/A reveals a buried, negative active site that imposes structural restrictions on the cleavage of its SNAP-25 substrate. The toxin appears as a hybrid of varied structural motifs and suggests a modular assembly of functional subunits to yield pathogenesis.

1. Montecucco, C. & Schiavo, G. Structure and function of tetanus and botulinum neurotoxins. Quarterly Rev. Biophys. 28, 423-472 (1995).
2. Lacy, D. B., Tepp, W., Cohen A. C., DasGupta, B. R., Stevens, R. C. Crystal structure of botulinum neurotoxin type A and implications for toxicity. Nature Struct. Biol. 4, 898-902 (1998).
3. Umland, T. C. et al. Structure of the receptor binding fragment Hc of tetanus neurotoxin. Nature Struct. Biol. 4, 788-792 (1997).

M06.AA.004 STRUCTURAL BASIS FOR THE RECOGNITION OF ANGIOGENIN BY PLACENTAL RIBONUCLEASE INHIBITOR, A LRR PROTEIN. A.C.Papageorgiou and K.R.Acharya, Dept. of Biology and Biochemistry, University of Bath, Bath BA2 7AY, UK, and R. Shapiro, Center for Biophysical and Biochemical Sciences and Medicine, and Dept of Pathology, Harvard Medical School, Boston, MA02115, USA

Human placental ribonuclease inhibitor (hRI) is a leucine-rich repeat protein (LRR) that binds to human Angiogenin (Ang), a blood-vessel inducing protein and member of the pancreatic RNase superfamily, with very high affinity (K_i<1fM [1]). The hRI-Ang complex has been successfully crystallised and the structure was determined to 2.0 Å resolution [2]. The hRI-Ang binding interface is large and encompasses 26 residues from hRI on 13 different repeat units and 24 from Ang on seven segments of Ang, resulting to 124 contacts in total. This structure, in combination with extensive functional data on the complex available from previous studies [3] now provides a detailed view of how Ang is recognised by hRI. A structural comparison with the porcine RI-pancreatic RNase [4] has been carried out in order to understand the association of the inhibitor with members of the RNase superfamily. Although the overall docking is similar in both complexes, it appears that the inhibitor is able to recognise distinctive features unique to each member of the family. A detailed analysis will be presented. The structural information derived from the hRI-Ang tight complex could provide a lead to design small, active hRI derivatives or mimics suitable for therapeutic use.

[1] Lee, F.S., Shapiro, R. & Vallee, B.L. (1989) *Biochemistry* **27**, 225-230.
[2] Papageorgiou, A.C., Shapiro, R. & Acharya, K.R. (1997) *EMBO J.* **16**, 5162-5177.
[3] Chen, C.Z. & Shapiro, R. (1997) *PNAS* **94**, 1761-1766.
[4] Kobe, B. & Deisenhofer, J. (1995) *Nature* **374**, 183-186.

M06.AA.005 TROA, A ZINC-BINDING COMPONENT OF A T. PALLIDUM ABC TRANSPORT SYSTEM WITH NOVEL TOPOLOGY; C.A. Hasemann, Y-H. Lee [1], R.K. Deka, M.V. Norgard, J.D. Radolf [2], [1] Departments of Internal Medicine and Biochemistry, UT Southwestern Med. Ctr., Dallas, Texas 75235-8884, [2] Department of Microbiology, UT Southwestern Med. Ctr., Dallas, Texas 75235

The crystal structure of TroA, a zinc-binding protein component of an ABC transport system in Treponema pallidum, was determined at a resolution of 1.8 Å. The organization of the protein is largely similar to other periplasmic ligand-binding proteins (PLBP), in that two independent globular domains interact with each other to create a zinc-binding cleft between them. The structure has one bound zinc pentavalently coordinated to residues from both domains. Unlike previous PLBP structures that have an interdomain hinge composed of beta strands, the N- and C- domain of TroA are linked by a single long backbone helix. This helix interacts with both the N- and C-domains, constituting a firmer hinge than the beta strand hinge used in other PLBPs. This unique backbone helix was possibly adopted in evolution to limit the hinge motion associated with the exchange of zinc. TroA is a member of a large family of cation binding proteins from diverse bacterial species. Therefore, the structure of TroA represents a new structural family of ABC transporter metal binding proteins, distinct from the classical PLBP family.

P06.AA.001 STRUCTURE OF COAGULATION FACTOR X-BINDING PROTEIN COMPLEXED WITH GLA DOMAIN. H.Mizuno and Z.Fujimoto, National Institute of Agrobiological Resources, Tsukuba, Japan, and H.Atoda and T.Morita, Meiji Pharmaceutical University, Kiyose, Japan

Coagulation factor binding proteins from snake venom are heterodimers consisting of two homologous subunits. Each subunit has sequence homology to the carbohydrate-recognition domain of C-type lectin. These proteins have no lectin activity, but bind to their cognate Gla domains(GD). We have solved the structure of factor IX and factor X-binding protein(IX/X-bp) at 2.5 Å resolution.[1] The structure showed that a central loop projects into the adjoining subunit and contributes to an intertwinned dimer formation in a manner similar to domain swapping. This forces a large conformational change on the hinge region classically concerned in carbohydrate-binding, and may result in the disruption of the lectin active site. The next step is to

know the GD-binding site and to investigate the atomic details of the interaction with it.

Recently we have solved and refined the structure of factor X-binding protein(X-bp) complexed with factor X GD peptide 1-44 at 2.3 Å resolution with the crystallographic R factor of 0.20. The folding of X-bp is very similar to that of IX/X-bp. The GD-binding site is on a concave surface surrounded by the two subunits as expected from the structure of IX/X-bp. The structure of the GD is similar to that of Ca bound GD of prothrombin fragment I. Seven bound calcium ions are observed, one of which is involved in the interaction with X-bp. The detailed binding mode between X-bp and GD will be presented.

[1] Mizuno, H., *et al*. (1997) *Nature Structural Biology* **4**, 438-441

P06.AA.002 HIGH-RESOLUTION CRYSTAL STRUCTURES OF COMMON DOMAINS OCCURRING IN NUCLEIC ACID-BINDING PROTEINS. U. Heinemann, A.M. Babu, K. Decanniere, H. Delbrück and U. Mueller, Forschungsgruppe Kristallographie, Max-Delbrück-Centrum für Molekulare Medizin, Robert-Rössle-Str. 10, D-13125 Berlin, Germany.

Nucleic acid-binding proteins are commonly made of ubiquitous domains occurring in proteins of diverse function. Recently, we have analysed a set of common domains at high resolution finding surprising effects of mutations on protein stability, a known domain fold with an unlikely function and remarkably structural homology across a wide evolutionary divide.

Following our earlier work on bacterial cold shock proteins [1,2] we have now determined the crystal structure of the homolog from the thermophilic *Bacillus caldolyticus* at 1.17 Å resolution. A comparison with the structures of cold shock proteins with very similar sequence from mesophilic bacteria and the analysis of single-site mutants sheds light on the determinants of protein thermal stability.

The C-terminal domain of the transcription factor KorB from RP4-infected *Escherichia coli*, KorB-C, has a fold closely resembling the SH3 fold first seen in eukaryotic signal transduction proteins. The 1.7-Å crystal structure of KorB-C shows a unique dimer arrangement which is of functional importance.

The histones HMfA and HMfB from the hyperthermophilic archaeon *Methanothermus fervidus* [3] have been analysed at resolutions down to 1.48 Å. The proteins are surprisingly similar to the eukaryal histones as present in the nucleosome core particle. A closely similar mode of non-specific DNA binding is expected.

1. H. Schindelin, M.A. Marahiel, U. Heinemann (1993). Nature **364**, 164.
2. H. Schindelin, W. Jiang, M. Inouye, U. Heinemann (1994). Proc. Natl. Acad. Sci. USA **91**, 5119.
3. K. Decanniere, K. Sandman, J.N. Reeve, U. Heinemann (1996). Proteins: Struct. Funct. Genet. **24**, 269.

06BB STRUCTURE FROM PICTURES: DIRECT MACROMOLECULAR STRUCTURE DETERMINATION BY ELECTRON MICROSCOPY

M06.BB.001 STRUCTURE OF ROTAVIRUS AND FUNCTIONAL CORRELATIONS USING THREE-DIMENSIONAL ELECTRON MICROSCOPY. B. V. Venkataram Prasad[1], J. A. Lawton[1], and M. K. Estes[2] [1]Department of Biochemistry, and [2] Division of Molecular Virology, Baylor College of Medicine, Houston, TX 77030.

Rotaviruses are complex, relatively large (1000 Å) nonenveloped icosahedral viruses. They are the major causative agents of severe diarrhea in children and animals. Rotaviruses are double-stranded RNA (dsRNA) viruses belonging to the family *Reoviridae*. Of the eleven proteins encoded by the genomic RNA, six are structural and five are non-structural. Three-dimensional electron cryomicroscopy (cryoEM) has been used to study the virus structure not only in its native state but also in various functional states to establish structure-function relationship.

The mature rotaviruses are triple-layered particles (TLPs). During the process of cell entry the outer-most layer consisting of VP7 and the spike protein VP4 is lost and the resulting double layered particles (DLPs) become transcriptionally active. CryoEM of actively transcribing DLPs has shown that the nascent mRNA molecules are synthesized inside the intact DLPs, and are extruded through the channels at the icosahedral vertices. Difference imaging of the native and recombinant particles has shown that VP1 and VP3 which posses the enzymatic activities for transcription are anchored to the inner surface of VP2 at the icosahedral vertices. A significant portion of the genomic RNA is icosahedrally ordered and forms a dodecahedral structure surrounding these enzyme complexes. In recent studies the question of why the mature particles (TLPs) are transcriptionally inactive, and what is the interdependence of the various stages of transcription such as initiation, elongation, and translocation, has been addressed using anti-VP6 monoclonal antibodies which affect the transcriptional process in rotavirus. CryoEM studies of the DLPs complexed with these antibodies have shown that it is possible to gate the release of transcripts and affect transcriptional efficiency. We acknowledge support from NIH grants AI 36040 (BVVP), DK 30144 (MKE), and a training fellowship to JAL (GM-08280).

M06.BB.002 ALLOSTERIC MOVEMENTS IN THE CHAPERONIN ATPASE CYCLE. Helen Saibil, Alan Roseman*, Neil Ranson, Shaoxia Chen, Guy Schoehn, Department of Crystallography, Birkbeck College, Malet St, London WC1E 7HX, UK, and Brent Gowen, Department of Biochemistry, Imperial College, London SW7 2AY, UK *present address: MRC Laboratory of Molecular Biology, Cambridge CB2 2QH, UK

Chaperonin-assisted protein folding proceeds through cycles of ATPase action by the large chaperonin GroEL or its homologues, and involves concerted, rigid body movements of the 3 domains in each subunit. Transient binding of the small chaperonin GroES forms an enclosed chamber about 70 Å across, in which folding of a protein subunit takes place. Access to the chamber is regulated by the nucleotide cycle, which controls the binding and release of GroES. In addition, the domain movements cause an alternation between low and high affinity binding for non-native protein substrates, by changing the accessibility of the hydrophobic binding sites. Binding, encapsulation and release states alternate between the two back-to-back 7-membered rings of GroEL, with the movements communicated by subtle alterations of the inter-ring interface.

Using cryo EM we have obtained 3D reconstructions of chaperonin complexes in several different nucleotide states, revealing the very large hinge rotations that accompany the functional cycle. We have recently extended the resolution of our single particle analysis to 10 Å, and are currently trapping ATP-bound states by vitrifying cryo EM samples with a stopped-flow mixer/rapid freezing device. Reaction mixtures are trapped in less than 1 second, well within the 15 second half time for ATP hydrolysis. We are now characterizing GroEL-ATP and GroEL-GroES-ATP complexes, which are folding-active states. Combining the cryo EM maps with the atomic structures of the domains provides a detailed structural basis for understanding the allosteric mechanism of chaperonins and control of their interactions with folding protein substrates.

M06.BB.003 FINDING THE SMALL DIFFERENCE: ELECTRON CRYOMICROSCOPY OF A DECA-PEPTIDE BOUND TO HEPATITIS B CORE PROTEIN. B. Böttcher Institut für Physikalische Chemie, Universität Freiburg, Albertstraße 23a, 79104 Freiburg, Germany M.R. Dyson Peptide Therapeutics, 321 Cambridge Science Park, Milton Road, Cambridge CB4 4WG, UK (present address) K. Murray Institute of Cell and Molecular Biology, University of Edinburgh, Edinburgh EH9 3JR, UK R.A. Crowther Medical Research Council, Laboratory of Molecular Biology, Hills Road, Cambridge CB22QH, UK

It was recently shown that it was possible to determine the fold of the peptide chain in an icosahedrally organised particle without the necessity of having crystals [1]. The availability of field emission gun microscopes equipped with stable cryo stages was one major prerequisite for the collection of data of sufficient quality. Combination of thousands of particles from micrographs at different levels of defocus was needed in the subsequent image processing. We describe here how these methods were employed to locate a ten amino-acid peptide bound to the hepatitis B core protein [2]. The peptide had been selected to bind to the core protein and was then shown to block interaction of core with the long viral surface antigen [3]. Hepatitis B core protein can be expressed in E. coli where it assembles into icosahedral shells of two sizes containing either 180 (T=3) or 240 (T=4) subunits. For electron cryomicroscopy these shells were either frozen directly or mixed with the peptide (GSLLGRMKGA) prior to freezing.

Independent maps of all four types of shells (T=3 with and without peptide and T=4 with and without peptide) were calculated to a resolution of 8.3 Å. Because the expected differences in density were small, standard deviation maps were calculated, first for the native shells then for the native shells plus peptide and finally for the native and native plus peptide data combined. In the standard deviation maps for the combined data a set of strong peaks was seen at the tips of the spikes which was absent in the standard deviation maps from the single data sets. Difference maps between corresponding maps with and without peptide were then computed. These maps indicated that the peptide was bound at the tips of the spikes on the local 2-fold axes. From these results it is clear that electron cryomicroscopy and image processing of single icosahedrally organised particles is a powerful method to detect differences as small as a deca-peptide directly, without the necessity of extra labelling such as heavy atom clusters.

1. B. Böttcher et al., Nature, 386 (1997) 88.
2. B. Böttcher et al., EMBO J., 17 (1998) 6839.
3. M.R. Dyson and K. Murray, Proc. Natl. Acad. Sci.USA, 92 (1995) 2194.

M06.BB.004 STRUCTURE OF GAP-JUNCTION INTERCELLULAR CHANNELS - FROM MAPS TO MODELS. V.M. Unger [1][3], N.M. Kumar, N.B. Gilula [1], M. Yeager [1][2], [1] The Scripps Research Institute, Dept. of Cell Biology, La Jolla, CA 92037, USA, [2] Scripps Clinic, Division of Cardiovascular Diseases, La Jolla, CA 92037, USA, [3] Max-Planck-Institute for Biophysics, Dept. of Structural Biology, 60528 Frankfurt/Main, Germany

Gap junction intercellular channels mediate electrical and metabolical coupling between adjacent cells. Our previous electron-crystallographic analysis of a recombinant gap junction channel revealed the arrangement of all the transmembrane alpha-helices in the twelve connexin subunits that form the channel. Furthermore, the density map at 7.5 Angstrom resolution suggested that the connexin polypeptide chains do not adopt an alpha-helical conformation within the extracellular space where two hemi-channels dock to form a cell-to-cell conduit. An extension of our data to an in-plane resolution of 6 Angstrom, reveals significant detail within the extracellular domain of the channel. Using this improvement, and by taking into account the clues obtained from multiple sequence alignments and biochemical data, we now propose an assignment of the predicted transmembrane alpha-helices in the sequence to the resolved transmembrane domains in the density map. Furthermore, we propose the likely molecular boundary of the connexin subunit. In our current model, residues on transmembrane helices 1 and 3 have direct access to the aqueous pore, while helices 2 and 4 are assigned to the two transmembrane domains in the structure that are in direct contact with the lipid bilayer. We have used this assignment to correlate the sequence of the four connexin transmembrane helices with individual cross-sections in the density map. The resulting model provides potential explanations for the disruptive effects of naturally occurring mutations associated with X-linked Charcot-Marie-Tooth disease and, for the first time, provides detailed predictions for the likely interaction between connexin subunits within the lipid bilayer.

M06.BB.005 MICROTUBULE STRUCTURE AND DYNAMICS. Eva Nogales [1][2], Kenneth H. Downing [2], [1] Department of Molecular and Cell Biology, UC Berkeley, CA 94720, US, [2] Life Science Division, Lawrence Berkeley Natl. Lab., CA 94720

Microtubules are built by the self-association of ab-tubulin dimers. The polymerization process involves the head-to-tail binding of dimers that results in the protofilament, and lateral interactions between parallel protofilaments to form the microtubule wall. We obtained the structure of the tubulin dimer by electron crystallography of zinc-induced tubulin sheets. Each tubulin monomer contains an N-terminal, nucleotide-binding domain, a smaller second domain, and a predominantly helical C-terminal region. A high resolution model of the microtubule has been generated by docking the crystal structure of tubulin into a 20-Å map of the microtubule . The excellent fit defines the orientation of the tubulin structural features within the microtubule, and provides a structural basis for the GTP-related dynamic behaviour of microtubules. The exchangeable nucleotide is exposed on the plus end, while the proposed catalytic residue in a-tubulin is exposed at the minus end. Longitudinal contacts between tubulin subunits bring the catalytic domain in one dimer in contact with the nucleotide of the next, linking, at the molecular level, the processes of polymerization and GTP hydrolysis Lateral contacts between protofilaments are dominated by the interaction of a g-phosophate-sensitive helix with the "M-loop", a loop with hinge elements that in b-tubulin contributes to the binding site of taxol.

Nogales et al., (1998) Nature 391, 199-203
Nogales et al., (1999) Cell 96, 79-88
Nogales et al., (1998) Nature Struct. Biol. 5, 451-458

P06.BB.001 A MODEL FOR *OCTOPUS* HEMOCYANIN DERIVED FROM ELECTRON CRYOMICROSCOPY AND X-RAY CRYSTALLOGRAPHY. M. E. Cuff, B. Gowen, K. I. Miller*, E. V. Orlova, A. Patwardhan, M. van Heel. Department of Biochemistry, Imperial College, London SW7 2AY, UK. *Department of Biochemistry and Biophysics, Oregon State University, Corvallis OR 97331, USA.

Octopus hemocyanin is a hollow cylinder with D_5 point group symmetry and a molecular mass of 3.4 MDa. Each 340kDa subunit has seven oxygen-binding units that are more protease-resistant than the intervening linker regions which occur serially along the polypeptide chain. Among all molluscan hemocyanins, these 'functional units' possess between 40-70% primary sequence identity and each contains one binuclear copper center that reversibly binds oxygen.

We have assembled a high resolution model for *Octopus* hemocyanin by docking the non-crystallographic dimer of functional unit Odg [1] into a 24Å map obtained by electron cryomicroscopy and angular reconstitution. Furthermore, this dimer appears to fit well into the density identified as the 'morphological unit' of the 15Å reconstruction of another molluscan hemocyanin, the type 1 from keyhole limpet [2]. Whereas the protomers in the crystallographic dimer are related by a near perfect 2-fold, this is not the case for the morphological unit where most are heterodimers. Also, it is likely that the precise angular relationship within and between these dimers varies with the cooperative state of the molecule. Nonetheless, our observations lead us to propose this structural dimer to be a building block for all molluscan hemocyanins. Employing the complete primary sequence for the *Octopus* hemocyanin subunit, we propose a path for the polypeptide chain within the decamer and possible divalent cation-binding sites.

1 M. E, Cuff, K. I. Miller, K. E. van Holde, W. A. Hendrickson (1998) JMB. 278:855-870.
2 E. V. Orlova, P. Dube, J. R. Harris, E. Beckman, F. Zemlin, J. Markl, M. van Heel. (1997) JMB 271:417-437.

06CC X-RAY AND NEUTRON COMPLEMENTARITY

M06.CC.001 OVERVIEW OF COMPLEMENTARITY BETWEEN NEUTRONS AND X-RAYS WITH TYPICAL EXAMPLES. C. Vettier, European Synchrotron Radiation Facility, France

The advent of third generation synchrotron sources has rendered more acute the debate on the complementarity between neutrons and x-rays. The unprecedented progresses made in the x-ray source brilliance have not been matched by parallel developments on the neutron side. As a consequence, the studies that were impossible with x-rays due to vanishing scattering cross sections or due to the need of extremely high resolution, are now feasible and potential results compare favourably with neutron results.

Two categories of research fields can be distinguished: studies for which the one or the other probe has a leading advantage in terms of cross section (scattering and absorption) and/or source properties (energy range, brilliance), and those for which the enhanced source characteristics have put performances of both probes at the same level. Progress made in instrumentation will be discussed. When considering various fields such as soft and hard materials science research, magnetism and biological studies, it is clear that both scattering probes are needed in condensed matter research. During this review, experimental results will be presented to illustrate the complementarity of neutrons and x-ray synchrotron radiation in many areas. It will be stressed that scientists must be aware of the capabilities of both probes and have easy access to them.

M06.CC.002 $PrBa_2CU_3O_{6+X}$; A CASE STUDY IN THE COMPLEMENTARITY OF X-RAY AND NEUTRON MAGNETIC SCATTERING. J.P. Hill [1], A.T. Boothroyd [2], D.F. McMorrow, N.H. Andersen [3], A. Stunault, C. Vettier [4], Th Wolf [5], [1] Dept. of Physics, Brookhaven National Laboratory, Upton NY 11973, USA, [2] Clarendon Laboratory, Oxford University, Oxford, OX1 3PU, UK, [3] Condensed Matter Physics and Chemistry Department, Riso National Laboratory, DK-4000 Roskilde, Denmark, [4] European Synchrotron Radiation Facility, BP 220, 38043 Grenoble Cedex, France, [5] Forschungszentrum Karlsruhe, ITP D-76021 Karlsruhem, Germany.

X-ray scattering as a probe of magnetism offers a useful complement to that of neutron scattering. Particular strengths include element specificity, high reciprocal space resolution and the ability to study very small volume samples. We illustrate the utility of this complementarity with a case study; an investigation of the magnetism of PrBa_2Cu_3O_{6+x}. This material is of great interest as an anomalous (non-superconducting) member of the (RE)Ba_2Cu_3O_{6+x} series, where RE=Y or a rare-earth. The element specificity of resonant x-ray magnetic scattering is exploited to study the magnetism of the Pr and the Cu in a model independent manner, and we unambiguously demonstrate that the Pr does order, resolving a debate in the literature. X-rays also offer extremely high reciprocal space resolution and this led to the discovery of a previously unknown incommensurate modulation. A strength of neutron magnetic scattering is the ability to perform energy resolved measurements and we utilize this to demonstrate that the modulation is static. Finally, high resolution x-ray measurements of the copper structure at higher temperatures reveal that it is commensurate, ruling out one model for the suppression of superconductivity in this material. These latter results represent the first observation of x-ray magnetic scattering from copper moments in a high-Tc compound.

M06.CC.003 SPHERICAL NEUTRON POLARIMETRY AND COMPLEMENTARITY WITH X-RAYS. E. Lelièvre-Berna and F. Tasset, Institut Laue Langevin, Av. des Martyrs, BP 156, 38042 Grenoble Cedex 9, France.

Spherical neutron polarimetry (SNP) is the only technique which can give access in (Q,ω) space to 16 measured quantities related to the 16 independent correlation functions involved in the most general mixed nuclear/magnetic neutron scattering process.

Among the interesting topics which can be investigated with this novel polarimetric technique, there are non-trivial magnetic structures and precise antiferromagnetic form factor determinations as well as magnetic excitations.

Compared to X-ray techniques, SNP gives a direct way of investigating spin/lattice correlation functions and is a powerful technique for determining antiferromagnetic configurations.

M06.CC.004 NEUTRON PROTEIN CRYSTALLOGRAPHY BY THE USE OF A NEUTRON IMAGING PLATE. N.Niimura, Advanced Science Research Center, Japan Atomic Energy Research Institute, Tokai-mura, Naka-gun, Ibaraki-ken, 319-1195, Japan

In the latter half of 20th century, X-ray single crystal structure analysis has been used to determine the three dimensional structures of biological macromolecules such as

proteins and DNA, to bring many of the mysteries of life sciences to light. This structural information contributes to the understanding of the physiological function of proteins and DNA. This field is called structural biology. Structural biology is one of the most important fields in the life sciences that will interest human beings in the 21st century. There is already clear evidence that hydrogen atoms and water molecules around proteins and DNA play a very important role in many physiological functions. However, since it is very hard for X-rays to determine the positions of hydrogen atoms in protein molecules, detailed discussion of protonation and hydration can be only speculative in many cases.

On the other hand, neutron diffraction provides an experimental method of directly locating hydrogen atoms. To date, there are relatively few examples of neutron crystallography in biology since it takes considerable time to collect a sufficient number of Bragg reflections due, in past, to the low flux of neutrons illuminating the sample. To use a large area detector is one way of the faster data collectin.

We have developed a neutron imaging plate (NIP), where the neutron converters, ^{6}Li or Gd were mixed with photostimulated luminescence materials on a flexible plastic support. [1] The dynamic range and spatial resolution of our NIP were obtained as 1:10^5 and less than 0.2 mm, respectively and the neutron detection efficiency of some NIP reached about 80 % at neutron wavelength 1Å.These distinctive features are applicable for neutron diffraction experiments from bio-macromolecules.

In this paper two examples of the application of NIP for neutron diffraction from a lysozyme single crystal were given. One is used for the Laue diffractometer (LADI) installed at ILL in Grenoble [2] and the other is for the diffractometer of monochromatic beam (BIX) installed at JAERI [3].

1. N.Niimura et al., Nucl. Instrum. & Methods. A349, 521-525 (1994)
2. N.Niimura et al., Nature Struct. Bio. 4, 909-917 (1997)
3. I.Tanaka et al., J. Phys. & Chem. Solids (1999) (in preparation)

M06.CC.005 SMALL-ANGLE NEUTRON AND X-RAY SCATTERING STUDIES OF BLOCK COPOLYMER MICELLES: ISOTOPE EFFECT. Jan Skov Pedersen, Condensed Matter Physics and Chemistry Department, FYS-108, Risø National Laboratory, DK-4000 Roskilde, Denmark.

Block copolymers are constituted of two chemically distinct polymer blocks covalently bonded together. When dissolved in a solvent which is a selective solvent for one blocks, micelles are formed with a core of the non-soluble parts and a diffuse corona of the soluble chains. The small-angle scattering data from such systems can be analysed to quite high resolution by a recently calculated analytical form factor for a model with a homogeneous core surrounded by chains obeying Gaussian statistics [1]. In order to obtain as much information as possible on the structure, neutron contrast variation measurements can be performed on polymers with one of the blocks per-deuterated. By using deuterated and hydrogenated solvent, the core and the corona can be measured separately, whereas mixtures provides additional information on the interference term. We have studied micelles of *d*-polystyrene-polyisoprene of relatively high molecular weight (40000-40000 and 40000-80000) in decane. The micellar structure in the deuterated and hydrogenated solvent was also measured by X-ray scattering and unexpected isotope effects were found. The aggregation number of the micelles depend on the isotope form of the solvent unless the samples are extremely carefully prepared. In a related study we have found isotope effects for the aggregation state of *d*-poly(ethylene oxide)-poly(propylene oxide)-*d*-poly(ethylene oxide) in water. However in this case, the difference is evident already from the neutron data as variation of the length of the rod-like micelles is observed.

1. J.S. Pedersen & M.C. Gerstenberg (1996). Macromolecules **29**, 1363.

P06.CC.001 EFFECTS OF HYDROGEN BONDING ON COVALENT GEOMETRIES AS OBSERVED BY NEUTRON DIFFRACTION. Steiner, T., Institut für Kristallographie, Freie Universität Berlin, Takustr. 6, 14195 Berlin, Germany

Hydrogen bonds X–H···A affect the geometries of both involved groups. These effects are most pronounced for the bonds involving the H-atom, that are the X–H bond, the R–X–H angle and also R–Y–X–H torsion angles. To describe the effects, the position of the H-atom must be known with good precision, so that only structural data based on neutron diffraction experiments can be used.

Best known is the lengthening of the covalent X–H bond, which has been described for the homonuclear hydrogen bonds O–H···O and N–H···N by several groups of authors. For heteronuclear hydrogen bonds of various types, this effect has been characterized only very recently [(1) and references therein]. New experimental data are shown here, in particular on inter-anion hydrogen bonds which are treated controversially in the literature.

Much less is known on how hydrogen bonding affects covalent bond angles (1, 2) and torsion angles. Neutron diffraction data showing these effects are presented. In particular, the rotation of methyl groups bonded to C(sp3) by C–H···O hydrogen bonding, which has been subject of some dispute, is discussed.

Steiner, T. (1998). *J. Phys. Chem. A*, 102, 7041.
Steiner, T. (1998). *Acta Cryst.* B54, 464.

06DD INDUSTRIAL ON-LINE X-RAY ANALYSIS

M06.DD.001 ORIENTATION MEASUREMENT OF AERO-ENGINE SINGLE CRYSTAL COMPONENTS. C.J.Small, C.C. Baxter, Rolls-Royce plc, P.O.Box 31, Derby, DE24 8BJ, UK.

The improvements in the operating efficiency of the modern gas turbine has driven the need for new materials with improved properties at elevated temperatures, particularly in materials for high-pressure turbine blade applications. This in turn has required the development of specialised single crystal casting technology. However the performance of such cast materials is critically dependent of the relative orientation of the crystal axes to the component geometry. As the process has an inherent variability there is a urgent need for an inspection techniques that can give an accurate determination of the crystal axes relative to the component geometry. The inspection technique must also be suited to the production environment, where high component numbers and lack of highly specialised NDE personnel call for a fast, expert system, which gives an unambiguous “pass or fail” decision. Rolls-Royce investigations into a wide range of inspection techniques has resulted in the development of S.C.O.R.P.I.O (Single Crystal Rapid Processing and Interpretation Operation), an integrated NDE system which satisfies all the above mentioned requirements. S.C.O.R.P.I.O is a development of the back-reflection Laué X-ray diffraction technique, which is extensively used in laboratories around the world. Traditionally the main drawbacks of the Laué technique as a production inspection method has been the costs and time involved in exposing and processing the film on which the diffraction patterns are recorded, and the time and level of expertise required to interpret the patterns. S.C.O.R.P.I.O overcomes the problems associated with film by using a Real-Time X-ray detector, the output of which is fed directly into a PC based analysis system.

This presentation will describe the design and application of the Rolls Royce S.C.O.R.P.I.O system and show how it is integrated into the turbine blade production process.

M06.DD.002 ROUTINE MEASUREMENTS OF HETERO-EPITAXIAL LAYERS. Mary Halliwell, Philips Analytical, Almelo, The Netherlands.

There are two approaches to making routine measurements using rocking curve analysis.

In the first a simple double crystal diffractometer is used with the sample laid on a horizontal table which incorporates X and Y translations. This offers a fast and convenient way to map variations in the layer, particularly the lattice parameter variations in heteroepitaxial layers. This method is favoured where the instrument can be dedicated to measuring layers which are all grown on substrates of the same material with approximately the same orientation and relatively simple analysis is required.

The second approach uses diffractometers where the achievable resolution is adjustable by using different combinations of monochromator crystals, and the intensity can be boosted by the use of multilayer mirrors. With these more versatile instruments a wide range of materials can be studied and the increased dynamic range allows for much more detailed analysis of layer structures.

Rocking curve simulation using the Takagi-Taupin theory is the universal tool for interpreting the x-ray data from the complex layer structures grown for modern devices. Recent advances in automatic fitting of simulations will be discussed.

M06.DD.003 ON LINE MONITORING OF THE FISCHER TROPSCH REACTION. B. Rebours, O. Ducreux, J. Lynch and M. Roy-Auberger, Institut Français du Pétrole, 1 & 4 Avenue de Bois Préau, F-92852 Rueil Malmaison

Interest in Fischer-Tropsch reaction, which transform syngas ($CO + H_2$) into long-chain hydrocarbons of high purity, is increasing as environmental regulations on fuels are becoming more severe. The activity of cobalt catalysts in Fischer-Tropsch synthesis is usually attributed to the active sites located on the surface of cobalt metal particles formed after reduction. The activation and reaction process of such catalysts have been studied by *in situ* X-ray powder diffraction.

The sample holder of an XRK Anton Paar reaction cell allows reactant gas flow through a thick powdered sample of the catalyst and simulate a fixed bed reactor. The gas handling system of the reactor cell has been designed to mimic testing conditions of cobalt Fischer-Tropsch catalysts. Reactants and gas products are analysed at the exit by gas chromatography, and liquid products are condensed after the cell. Conversion rate and selectivity are followed as a function of the time. An associated microreactor working in the same conditions as the X-ray diffraction cell allows transfer of the tested catalyst to vacuum characterisation techniques such as XPS or TEM without any contact with air. These methods, with FTIR of adsorbed CO, contribute to interpretation of the results.

After activation of catalysts under hydrogen at atmospheric pressure, the XRD diagram of the cobalt metal phase, although containing some lines of both f.c.c and h.c.p cobalt metal forms, cannot be interpreted as a simple mixture of the two forms. The shape of the signal was simulated using DiFFax, and a model of unique metal phase with cubic/hexagonal stacking disorder was assumed.

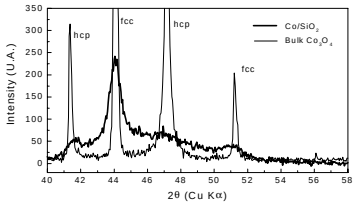

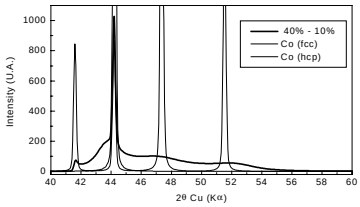

Under Fischer-Tropsch conditions (503K, 3 bar, H_2:CO=9:1) XRD analysis shows the formation of a cobalt carbide and decrease of the metal phase over the period 80 to 300 hours on stream. The cobalt metal phase can be regenerated under hydrogen, with some structural modifications. The role of the carbide in the deactivation of the catalysts and in the selectivity toward long chain paraffins will be discussed.

M06.DD.004 ON-LINE PRODUCTION CONTOL IN THE CEMENT, PLASTER AND MINING INDUSTRIES. M. Bellotto, CTG Italcementi Group, Rue des Technodes, 78931 Guerville Cedex, France. keywords: on-line quantitative phase analysis, cement industry, plaster industry, mining industry.

The strive towards a better process control to limit production costs is pushing towards on-line analysis even those industries, like the cement, mining and gypsum ones, which are traditionally considered as « low tech ». Common features of such industries is the fact they process large volumes of solids, and that mineralogical control of the production is necessary. Thus X-ray diffraction is used, or is going to be used, as a sensor to monitor the processes, in very much the same way as a pH-meter or a thermocouple. The added difficulty comes from the sampling which, one way or another, is always needed before the analyses. During wall board manufacturing operations, gypsum is dehydrated in heated kettles to bassanite. Overburning the material to anhydrite results in excessive energy consumption and subsequent monetary losses, as well as in a quality degradation of the product. From a process control perspective an on-line mineral monitor of the gypsum content in the bassanite product from the kettles can be used to optimize burner control settings. The analysis can be accomplished by diverting a stream of bassanite from the kettles directly to the analyzer via a conveyor belt, with no sample preparation.

In the mining industry, phase quantification is used to control the flotation process and to dose the chemical additives. In such a way better economics and a regular production quality can be achieved.

In the cement industry on-line X-ray diffraction is used to measure the amount of unreacted « free » lime in the fired material (clinker) at the kiln outlet. The complete on-line clinker mineralogical analysis is possible, even if it is complicated by the complex phase assemblage typically observed, and by the polymorphism exhibited by the major phases. The use on-line of Rietveld quantitative analysis, currently performed in the central research laboratories, can be a solution to the difficulties encountered so far.

M06.DD.005 HIGH-RESOLUTION X-RAY DIFFRACTION AND QUALITY COTROL OF INP-BASED FIBER-OPTIC COMMUNICATION LASERS. Joka M. Vandenberg, Lightwave Devices Research,Lucent Technologies, Bell Laboratories,Murray Hill, New Jersey 07974-0636, USA

High-resolution x-ray diffraction(HRXRD) is emerging as the leading non-destructive characterization tool for the crystal growth of quantum well lasers. Over the years HRXRD has evolved from a sophisticated research technique into a wide range of industrial applications. In this talk I will discuss how HRXRD becomes an integral part in the development of improved device performance, process and quality control, and product yield. Within this framework, trends in x-ray diagnostics and characteristic x-ray features as well as dynamical simulations of InP-based multi- quantum well lasers and electroabsorption modulators will be presented, including some aspects of the selective area growth of lasers.

P06.DD.001 XRPD QUANTITATIVE PHASE ANALYSIS PERFORMED *IN SITU* AT HIGH TEMPERATURE. E. Mazzucato, A.F. Gualtieri, P. Venturelli and A. Viani, Dipartimento di Scienze della Terra, Università di Modena e Reggio Emilia, Modena 41100, Italy.

To our knowledge this is the first time quantitative phase analysis (QPA) is performed in non environmental conditions. The aim of this work is overcome the difficulties rising from strong peak overlap. The technique is applied to NiO based black ceramic pigments. In this system NiO, potential carcinogenic agent, combines with other phases to crystallise new spinel-like phases. Accurate quantitative determination of residual free NiO is essential because of its hazardous effects even at low concentrations. Unfortunately there are no widely accepted methods for such determination in ceramics so far, the main reason being experimental difficulties. In fact, QPA by X-ray powder diffraction (XRPD) may fail because all diffraction peaks of NiO overlap to those of spinel since the latter has a space group $Fd\ \bar{3}m$ with a≈8.4 Å and NiO has a space group $Fm\ \bar{3}m$ with a≈4.18 Å. To overcome this problem, in this work QPA has been performed *in situ* at high temperature to resolve the peak overlap of NiO and spinel by taking advantage of differential thermal expansion of the two phases (Fig.1).

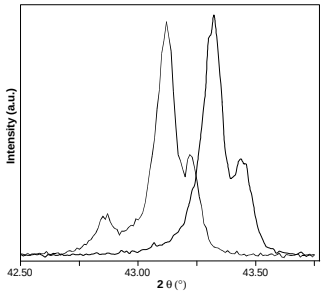

Fig.1. A sample containing 2 wt% NiO collected at room temperature (thin line) and high temperature (600 °C, thick line). The more intense peak [spinel (400)] hides the (200) peak of NiO at room temperature while at 600 °C these two peaks become well resolved.

06EE INTERFACES, THIN FILMS AND MULTILAYERS

M06.EE.001 ANALYSIS OF SEMICONDUCTOR QUANTUM-DOT SYSTEMS BY GRAZING INCIDENCE X-RAY SCATTERING TECHNIQUES. T. H. Metzger, I.Kegel, M. Rauscher, Z. Kovats, and J. Peisl, Center for NanoScience (CeNS) at Sektion Physik, Ludwig-Maximilians-Universität, D-80539 München and R. Paniago, Departamento de Física, Universidade Federal de Minas Gerais, Caixa Postal 702, 30123-970, Belo Horizonte, Brazil and V. Holy, Masaryk University, 61137 Brno, Czech Republic.

The growth of lattice mismatched semiconductor heterostructures often results in strain-driven, self-organised formation of islands with nanometer dimensions. The opto-electronic properties of such quantum dots are dominated by dot size and strain. We have developed x-ray scattering techniques at grazing incidence to analyse shape, strain and ordering of the dots. New results on three different semiconductor systems will be presented, demonstrating the versatility of the methods which can be applied to free-standing and buried dots:

In case of Ge islands grown on boron terminated Si(111) we applied grazing incidence small angle x-ray scattering (GISAXS) to assess their shape and size distribution. We find nearly perfect triangular pyramids, incoherently connected to the substrate. They are limited by three {113} facets and show a high degree of orientation alignment.

For the system InAs on GaAs (001) we find dome-like coherent InAs dots. An "iso-strain-scattering" technique has been developed to determine the lattice parameter distribution in the dots, which ranges between the lattice parameter of GaAs at the foot and InAs at the top of the dots. A linear interdependence of dot radius and strain is found. A similar analysis has been applied to ring shaped objects ("quantum donuts").

For Ge dots embedded in SiGe (001) superlattices, self-assembling processes yield vertical and lateral dot ordering. This ordering is quantified by applying a random walk argument to analyse grazing incidence diffraction measurements. The Ge dots on the sample surface form a disordered lateral square lattice. The vertical stack ordering of the Ge dots increases with decreasing Si spacer layer thickness.

M06.EE.002 THE STRUCTURE OF EPITAXIAL THIN FILMS. R.A.Cowley, Oxford Physics, Clarendon Laboratory, Parks Road, Oxford, OX1 3PU.

The structure of (110) Nb films grown on sapphire and (100) GaSb films grown on GaAs have been studied by high-resolution x-ray scattering techniques. In both cases there is a lattice mismatch between the film and the substrate and the structure of the film has been studied as the thickness increases from about 80Å to 5000Å. The films were grown in Oxford by MBE techniques for the Nb films and by MOVPE techniques for the GaSb films and the experiments performed with triple crystal diffractometers in Oxford, on the X-MAS beam line at the ESRF, and the X22A beam line at the NSLS. The results are qualitatively similar for both materials. Rocking curve scans through Bragg reflections from planes perpendicular to the growth direction show two components. A narrow component that shows the planes are on average flat over 50000Å and a broad component which has an approximately Lorentzian squared profile. For the GaSb films there are also incommensurate peaks with wave vectors corresponding to the separation of the mis-fit dislocations. As the thickness of the films increases the mean square fluctuation about the average position of the atomic planes increases and the correlation length of these fluctuations which is much longer than the separation of the mis-fit dislocations increases. The consequences of these results for the growth of seed layers and a comparison of the results with possible theoretical models will be discussed.

I am grateful to my many collaborators: A. Babkevich, J.P. Hill, N.J. Mason, A. Stunnalt, R.C.C. Ward, M.R. Wells and A.R. Wildes. Financial support was provided by the EPSRC.

M06.EE.003 X-RAY REFLECTIVITY AND DIFFUSE SCATTERING STUDIES OF PERIODIC MULTILAYERS. M.K.Sanyal, J. K. Basu, S.Banerjee, A.Datta and S. Hazra Saha Institute of Nuclear Physics, Calcutta - 700 064, INDIA

Specular reflectivity and off-specular diffuse scattering measurements of x-ray beams enables us to gather important

structural information regarding the top surface and buried interfaces of a periodic multilayer systems [1]. The merit of these x-ray scattering techniques will be illustrated using a MOCVD grown semiconductor multilayer and an metal-organic multilayer grown by Langmuir Blodgett (LB) technique. We shall present here an iterative inversion scheme [2] to extract electron density profile of a multilayer structure as a function of depth from the specular reflectivity data. In epitaxial semiconductor multilayers, understanding of interfacial roughness and inter diffusion is very important to develop proper devices. We shall demonstrate here the possibility of separating out these two contributions in the electron density profiles of interfaces by utilizing information obtained from the analysis of diffuse scattering data. The extracted compositional profile may be used [2] to calculate structural details of the film around (00l) diffraction peaks. Here we shall also present results [3] of reflectivity and diffuse scattering studies of cadmium arachidate LB films and formation of nanometer sized CdS particles in the interfaces of these films exposed to hydrogen sulphide environment.It was found that CdS particles remain confined at each multilayer interfaces. Logarithmic in-plane correlation, characteristic of capillary waves on liquid surfaces, was observed in both exposed and unexposed LB films.

[1] M.K. Sanyal, Radiat.Phys.Chem 51,487, 1998.
[2] M.K. Sanyal, S.Hazra, J.K. Basu and A. Datta, Phys. Rev. B58, R4258, 1998.
[3] J.K.Basu and M.K. Sanyal, Phys. Rev. Lett. 79, 4617, 1997.

M06.EE.004 RECONSTRUCTION OF SURFACE MORPHOLOGY FROM COHERENT X-RAY SCATTERING. I.A. Vartanyants, I.K. Robinson, J.A. Pitney, J.L. Libbert Department of Physics, University of Illinois, Urbana, IL 61801, US

Coherent X-ray Diffraction (CXD) is a new experimental technique that has emerged from the development of brilliant synchrotron-radiation sources of X-rays. While incoherent X-ray reflectivity from a rough surface would give rise to a superposition of pure specular and diffuse components, the equivalent CXD experiment yields an interference pattern that intermixes both of these components. CXD experiment performed in the specular reflectivity geometry after phase retrieval procedure could give a real image of the crystal surface (in analogy with the phase contrast imaging). In this work we will discuss the origin of these interference patterns seen in different CXD experiments and demonstrate a phase retrieval algorithm which can be used to invert it and reconstruct to one-dimensional height images. Convergence properties of this inversion algorithm will be analysed. Examples of phase reconstruction of the surface morphology of Si samples as a function of time will be demonstrated.

M06.EE.005 INTERFACIAL STRUCTURES OF BONDED SI WAFERS. R. Feidenhans'1, M. Nielsen, P.B. Howes [1], S. Weichert, F. Grey [2], J. Vedde [3], [1] Risø National Laboratory, DK-4000 Roskilde, Denmark, [2] Microelektronik Centret, Technical University of Denmark, DK-2800 Lyngby, Denmark, [3] TOPSIL Semiconductor Materials A/S, DK-3600 Frederikssund, Denmark.

Direct bonding of Si wafers is a process where two wafers are pressed together at high temperature to obtain covalent bonding between the wafers. This is a process increasingly used in micro technology devices. In order to investigate the atomic structure in the interface between the two wafers, we have performed synchrotron x-ray diffraction on a variety of different samples. The bonding is obtained in a two-stage process. First the two wafers with mirror flat hydrogen terminated (001) surfaces, are pressed together under clean room conditions. This yield a weak van der Waal type bonding. Secondly the wafers are heat treated at 1000 °C under a nitrogen atmosphere resulting in a much stronger covalent bonding.

The interface may be looked upon as a model grain boundary with zero tilt but with a predetermined twist angle (mutual rotation around [001]) given by the relative orientation of the two crystals. In the interface region the bonding produce a periodic displacement field determined by the rotational misfit, and this in turn give rise to satellite reflection in x-ray diffraction. By measuring the scattering from the satellites as function of the in-plane and the out of plane momentum transfer we get detailed information about the atomic structure of the interface. Measurements were done on samples with twist angles between 0.4° and 7.5°. We find that parallel to the interface the periodic displacement have a very long range order, presumably given by the bulk Si crystal. In direction perpendicular to the interface the range of the displacements, i.e. the interface thickness, is inversely proportional to the twist angle. The results are compared to calculated structure factors applying a model with a periodic net of screw dislocations.

Measurement have also been performed on samples with the same twist angle, but annealed to different temperature, which shows that the covalent bonding form around 800 °C.

P06.EE.001 GRAZING INCIDENCE X-RAY DIFFRACTION STUDIES OF (100) AND (111) ORIENTED FE/AU MULTILAYERS. B.D.Fulthorpe, J.Clarke, B.K.Tanner, Department of Physics, University of Durham, South Road, Durham, DH1 3LE, UK., P.A.Ryan, B.J.Hickey, Department of Physics, University of Leeds, Leeds LS2 9JT UK.

A series of Fe/Au multilayers grown by molecular beam epitaxy on either a MgO substrate with an Fe seed layer or a sapphire substrate with a Nb buffer have been studied using Grazing Incidence X-ray Diffraction at the XMaS beamline, ESRF Grenoble. In this surface diffraction scattering geometry the scattering planes are perpendicular to the plane of the film and measurements are sensitive to in-plane strain and atomic disorder.

Well defined 4- and 6- fold symmetries show the Au layer to be deposited with good (100) and (111) epitaxy in the MgO and sapphire systems respectively. The sharp, high intensity peaks indicate little in-plane crystalline disorder. In contrast, scans performed at the Fe 002 reflection show the crystalline quality of the deposited layers in both systems to be poor and of comparable perfection in each case. Alignment of the Fe 001 and Au 110 reflections in the Fe/Au grown on sapphire corresponds to lattice matching in this direction. Analysis of allowed reflections shows that a mixture of fcc and bcc Fe was present in the multilayers grown on sapphire.

The in-plane lattice parameter for Fe and Au was determined, from coupled $\theta/2\theta$ scans in the horizontal plane, to be in close agreement with standard bulk values with any deviation attributed to a small degree of in-plane strain. A strong Nb signal was detected in the sapphire system even though the Nb layer is well beyond the depth sensitivity of the incident beam. The Nb symmetry indicates (111) oriented epitaxial growth, similar to the Au layers, in contrast to RHEED measurements which suggest the Nb is deposited with a (110) epitaxy.This suggests the presence of Nb within the top 30Å of the multilayer stack which may suggest a surfactant growth mechanism.

P06.EE.002 LATERAL AND VERTICAL ORDERING OF SELF-ASSEMBLED GE/SI QUANTUM DOTS IN SUPERLATTICES. I. Kegel, T.H. Metzger, CeNS at Sektion Physik, Ludwig-Maximilians-Universität München, D-80539 München, J. Stangl, G. BauerInstitut für Halbleiterphysik, Johannes Kepler Universität, A-4040 Linz, Austria

We present a comprehensive ordering analysis of self-assembled quantum dots in a Ge/Si superlattice. The analysis of

both lateral and vertical correlations employs the *strain modulation* in the Si-spacer layers rather than the geometric contrast of the dots themselves. The small angle intensity modulation around different surface Bragg reflections is modeled with a one-dimensional approximation of lattice lines, yielding a nearest neighbor disorder parameter and a correlation length for different directions in the surface plane. In addition, the symmetry of the local ordering together with size and orientation of the pyramidal dots can be inferred from the experimental results. Lateral ordering is induced by the columnar stacking of the dots within the superlattice. The deviation of the dots' position from a perfectly aligned stack is analyzed in terms of a lateral random walk from layer to layer. The analytical expression for the scattering intensity in the vicinity of the surface Bragg peak shows that the quantum dots induce Bragg sheets, whose half widths along the growth direction q_z increase quadratically with lateral momentum transfer $q_{||}$. At large $q_{||}$, the half width levels off asymptotically to the value of an oscillation induced by a single bilayer. This behavior is confirmed by the experimentally determined functional dependencies. From the half widths, we are able to make quantitative estimates for the generic model parameter, describing the lateral shift in position of consecutive dots in a column. For the present case of dots with a square base, a geometrical stacking fault was derived.

P06.EE.003 TOTAL REFLECTION X-RAY AND FLUORESCENCE FOR SMALL D-SPACE MULTILAYER CHARACTERISATION. S.I. Zheludeva, N.N. Novikova, E.Yu. Tereschenko [1], N.N. Salaschenko [2], [1] Shubnikov Institute of Crystallography, Moscow, Russia, [2] Institute of Physics of Microstructure, N. Novgorod, Russia

Small d-space (0.8 - 20 nm) multilayers play an important role in X-ray optics, mainly as optical elements of normal incidence for "water window" range. The main problem of their characterisation in the process of adjusting deposition conditions is their low Bragg reflectivity due to drastic influence of interface perfection to multilayer parameters. The aim of the paper is to reveal the possibilities of multilayer characterisation using only X-ray total reflection (TR) angular range. The problem of obtaining information about multilayers (thickness and density of the layers, concentration gradients, interface interdiffusion and roughness) using besides X-ray reflectivity spectral selective angular dependence of X- ray fluorescence from definite layers is analysed. Special construction of the specimen containing multilayer is proposed. Theoretical aspects of secondary radiation yield from such systems (including the analysis of X-ray wave fields), experimental results and calculations for different small d-space structures at TR region are presented.

This work was supported by the Russian Foundation of Fundamental Research, project no. 98-02-16704.

P06.EE.004 THE EFFECT OF INTERFACE AND CRYSTAL PERFECTION ON MAGNETOTRANSPORT IN EPITAXIAL AU/FE MULTILAYERS. B.K.Tanner, T.P.A.Hase, B.D.Fulthorpe, S.B.Wilkins, Dept. of Physics, University of Durham, South Road, Durham, DH1 3LE, U.K. and P.A.Ryan, D.J.Dekadjevi and B.J.Hickey, Dept. of Physics & Astronomy, University of Leeds, Leeds, LS2 9JT, U.K.

X-ray reflectivity, diffuse scatter, fluorescence and surface diffraction, all at grazing incidence, have been used to study the relation between structure and magnetotransport properties of epitaxial Au/Fe multilayers grown by MBE on sapphire and MgO respectively. Despite the multilayers grown on MgO having rougher interfaces, the antiferromagnetic coupling and associated giant magnetoresistance are higher than for equivalent thickness layers grown on sapphire. High resolution high angle X-ray diffraction shows the (001) MgO substrates result in (001) oriented Au layers and the *a* plane sapphire and its (110) Nb buffer give (111) orientation Au layers. Both multilayers have crystallographically abrupt interfaces with little interdiffusion, the MgO system showing parabolic dependence of the rocking curve width with satellite order, as predicted for a rough inteface by the model of Holý *et al*. Under prolonged exposure to the focussed beam at the XMaS beamline at the ESRF, high order satellites disappeared from a multilayer on sapphire, indicating that substantial interface diffusion was occurring. Grazing incidence diffraction data show good in-plane order and little strain in the Au layers grown on either substrate. The quality of the Fe layers is relatively poor and similar in the two cases. Alignment of the [100] direction in the Fe with the [110] in the Au was observed in the system on sapphire. A six-fold symmetric diffraction pattern of sharp peaks, which could not be attributed to either the Au or the Fe lattice and corresponded to a lattice spacing of 2.33Å, was also observed in this system. Grazing incidence fluorescence measurements as a function of angle show unequivocally that Nb exists in the Au/Fe multilayer above the buffer layer. Simulation of the angular dependence of the fluorescence data shows that this is not simply a surface layer.

P06.EE.005 QUANTIFICATION OF ORDERED DOMAINS IN III-V COMPOUND HETEROSTRUCTURES. M.S. Goorsky, R.R. Hess, C.D. Moore, R.L. Forrest, and T. Neilsen, Department of Materials Science and Engineering, UCLA, Los Angeles, CA 90095-1595

We determined the degree of ordering in single layer $In_xGa_{1-x}P$ on GaAs and $In_yGa_{1-y}As$ on InP epitaxial heterostructures and in GaAs-based solar cells using double axis and triple axis x-ray diffraction. Although ordering in III-V heterostructures has been observed using x-ray diffraction techniques, little information about the degree of ordering or the crystalline perfection of the ordered domains has been reported. In this study, the ½ (115) ½ (113) reflections were employed to detect the presence of CuPt-type ordering. The ½ (115) reflections were investigated in both glancing and skew geometries to determine the parameters of the ordered regions and the presence of different ordered variants along different crystallographic directions. Reciprocal space mapping provided information about the origins of peak broadening in the ordered domains; unlike earlier studies which only employed double axis measurements, we determined that the broadening originates from a combination of tilts and finite domain size. Comparison of the superlattice and fundamental zincblende reflections (½ (115) and (224) have comparable footprints) provided for a means to quantify the extent of ordering; these values were confirmed with transmission electron microscopy and photoluminescence measurements.

06FF MOLECULAR MAGNETS

M06.FF.001 CLUSTERS AND EXTENDED ARRAYS WITH PARAMAGNETIC METAL IONS AND NITROGEN DONOR LIGANDS. Kim R. Dunbar,* Cristian Campos, Rodolphe Clerác, Jennifer A. Smith and Paul Szalay, Department of Chemistry, Texas A&M University, College Station, Texas, 77840.

The use of polypyridine-type ligands in closed-shell supramolecular chemistry is well-documented, but their use in open-shell metal systems has been much less explored. We are using both convergent and divergent synthetic methodologies to assemble paramagnetic metal ions with bis- and tris-chelating ligands based on bipyridine, terpyridine, and bipyrimidine functionalities. Depending on the choice of co-ligands and the topology of the nitrogen donors, one can design clusters with square, rectangular and trigonal-based geometries. Ligands such

as bis-pyridylphenazine (bptz), tetra-pyridylpyrazine (tppz), and hexaazatriphenylene (hat) are among some of the bridging ligands being employed in these studies. Other molecular assemblies under investigation employ octahedral metal ions in the synthesis of paramagnetic squares and cubes with cyano or metal-dicyano linking groups. The choice of capping ligands are two *cis*-directing bidentate chelates for the squares and *fac*-coordinating tris(pyrazolylborate) "caps" for the cubes. The magnetic properties of the various clusters under investigation are being explored in hopes of gaining further insight into the influence of size, shape, single ion anisotropy and magnitude of ground state S values on the magnetic properties of large paramagnetic clusters.

M06.FF.002 DESIGN OF CRYSTAL AND MAGNETIC STRUCTURES OF TRANSITION METAL COMPLEXES WITH ORGANIC FREE RADICALS. H. Iwamura, N. Koga, and K. Inoue National Institution for Academic Degrees, Nagatsuta, Midori, Yokohama 226-0026, Faculty of Pharmaceutical Sciences, Kyushu University, Maidashi, Higashi, Fukuoka 812-8582, and Institute for Molecular Science, Okazaki, Aichi 444-8585, Japan

Bis- and tris(aminoxyl) radicals and di(4-pyridyl)diazomethane form with M(hfac)2 {M = Mn(II) or Cu(II), and hfac = hexafluoroacetyl-acetonate} crystalline complexes having linear, cyclic, and network structures. Organic 2p and metal 3d spins in these complexes order at 3.4-46 K depending on the dimension of the extended structures and the magnitude of the exchange coupling between the adjacent spins. In the crystals of one-dimensional systems, the polymeric chains are isotactic in that free radicals or hexacoordinated metal centers have severally the same sign of chirality along any given chain. When the chains are syndiotactic, they form rings or cross-link to form two-dimensional honeycomb or three-dimensional parallel-crosses networks.

M06.FF.003 MULTIFUNCTIONAL COORDINATION COMPOUNDS: DESIGN AND PROPERTIES. Silvio Decurtins, Department of Chemistry and Biochemistry, University of Bern, Freiestrasse 3, CH-3012 Bern

Our laboratory has reported on the synthesis and structure determination of coordination solids which typically behave as host/guest compounds with different lattice dimensionalities. Thereby, the idea of a reasonable strategy looks straightforward: mix metal ions with a preference for a particular coordination geometry with bridging ligand systems - and it is important to control both the kinetics and thermodynamics of the assembly process - then, a crystalline network will nucleate and grow. As a consequence, a whole class of a new material with a specific chemical composition but with a wide variety with respect to the incorporated metal ions from the transition-metal series and the lanthanide series has been synthesized and structurally well defined. The benefits are twofold: First, a valuable know-how in the synthesis and crystal engineering of extended molecular network compounds has now been established which clearly will be of great value for the synthetic development of further supramolecular materials. Second, a broad range of physical techniques, like magnetization studies, photophysical studies and neutron scattering experiments, has been applied for the investigation of the whole spectrum of the inherent physical properties.

H.W. Schmalle, R. Pellaux, S. Decurtins, Z. für Kristallographie 1996, 211, 533.

M06.FF.004 EXTENDED STRUCTURES OF METAL DICYANAMIDES AND THEIR MAGNETIC ORDERING. K.S. Murray, S.R. Batten, G.D. Fallon, P.Jensen, B. Moubaraki, D.J. Price and E.H-K Tan, Chemistry Department, Monash University, Clayton, Victoria 3168, Australia.

In 1997/98 a series of known transition-metal dicyanamide complexes [1] of type α-$M(N(CN)_2)_2$ were found to adopt a single 3D-network rutile-like structure in which the octahedral M(II) ions are connected by three-connecting $N(CN)_2^-$ ligands. Detailed structural and magnetochemical studies on this isostructural family of compounds made by ourselves [2] and two other groups [3,4] revealed a fascinating and diverse array of types of long range magnetic order. Thus, the Cu(II) complex is a paramagnet, Co(II) and Ni(II) complexes are ferromagnets and Mn(II) and Fe(II) complexes are spin-canted antiferromagnets (weak ferromagnets), with ordering temperature of less than 20K. Structural and electronic reasons for these differences in magnetism will be presented.

A large series of 2D-linked compounds of type $M(N(CN)_2)_2(L)$, where M = Mn, Fe, Co, Ni, Cu and L = pyrazine and 4,4'-bipyridine, will be described, some of which display interpenetrating double-net structures. To date, most of these compounds display weak coupling without long range orders. Anionic complexes of type $[M(N(CN)_2)_3]^-$ also display beautiful sheet-like extended structures.

M06.FF.005 POLYNUCLEAR HOMO- AND HETERO-METALLIC CLUSTERS AND CHAINS - STRUCTURE AND MAGNETISM. L.K. Thompson, C.J. Matthews, S.R. Parsons, L. Zhao and D.O. Miller, Department of Chemistry, Memorial University, St. John's, Newfoundland, A1B 3X7, Canada, and C. Wilson and J.A.K. Howard, Department of Chemistry, University of Durham, Durham DH1 3LE, UK.

Polyfunctional, donor rich diazine ligands, with both N-N and O bridging groups, react with a variety of transition metal cations in a self assembly process to produce a series of homo-metallic and hetero-metallic spin coupled clusters. Tetranuclear clusters with square M_4O_4 cores (M=Mn(II), Co(II), Ni(II), Cu(II)) and rectangular mixed bridge $M_4(N\text{-}N)_2O_2$ cores (M=Co(II), Cu(II)) are formed by direct reaction of the ligands with metal salts. Mixed metal, rectangular and square clusters ($Fe(III)_2Co(II)_2(N\text{-}N)_2O_2$, $Fe(III)_2\ Ni(II)_2O_4$) form in an unusual self assembly process starting with a mononuclear Fe(III) complex and reacting with the other metal salt. Pentanuclear, homoleptic Mn(II) and Co(II) clusters are formed in an unprecedented self assembly process where the trigonal bi-pyramidal cores involve just alkoxide bridges between metal centres, and there is an exact match between the coordination algorithm of the metals and the donor groupings of the six coordinated ligands. A strategy for cluster growth by building upon a Cu_4O_4 core with a ligand which has additional exterior coordination capacity will be illustrated with an unusual 4+1 pentanuclear complex, and by a tactic in which two identical spin-coupled dinuclear Cu(II) fragments are tied together with a strapping ligand to form a tetranuclear Cu(II) cluster. The structural and magnetic properties of key examples of these novel classes of clusters will be discussed and the magnetic properties explained in terms of the bridging interactions.

The structures and magnetic properties of some trinuclear and tetranuclear Ni(II) and Cu(II) complexes of a group of extended, flexible diazine ligands will also be described, including a novel tetrahedral Ni(II) cluster, and a linear, spiral trinuclear Ni(II) derivative.

M06.FF.006 MAGNETIC PHASE DIAGRAMS FOR MOLECULE-BASED FERROMAGNETS. Olivier Kahn, Laboratoire des Sciences Moléculaires, Institut de Chimie de la Matière Condensée de Bordeaux, UPR CNRS No 9048, 33608 Pessac, France.

The goal of our lecture is to introduce the dimension « magnetic anisotropy » in the field of molecule-based magnets. For that, we will focus on three cyano-bridged $Mn^{II}Mo^{III}$ compounds synthesized from the $[Mo^{III}(CN)_7]^{4-}$ precursor. Two of the compounds have a three-dimensional structure. Their formulas are $Mn_2(H_2O)_5Mo(CN)_7 \bullet nH_2O$, with n = 4 for the α phase, and n = 4.75 for the β phase. One of the compounds, of formula $K_2Mn_3(H_2O)_6[Mo(CN)_7]_2 \bullet 6H_2O$, has a two-dimensional structure, with K^+ cations and water molecules located between double-sheet layers. The compounds crystallize in the monoclinic system, and the lattice symmetries are very low. For the three compounds, we succeeded to grow well-shaped single crystals suitable for magnetic anisotropy measurements. These measurements have revealed the existence of several magnetically ordered phases for the three-dimensional compounds, and of field-induced spin reorientations for the three compounds. For the very first time in the field of molecular magnetism, we were able to determine the magnetic phase diagram for each compound. We obtained additional information from magnetic data recorded in the ac mode, with both zero and non-zero static fields. Finally, we found that when the non-coordinated water molecules are released, the long-range magnetic ordering temperatures are shifted toward higher temperatures. Irrespective of the structural details, the Mo^{III}-C-N-Mn^{II} interaction was found to be ferromagnetic. We will discuss this unexpected result, and propose a mechanism accounting for this. We will also discuss the factors governing the magnetic anisotropy of the compounds.

P06.FF.001 TEMPERATURE AND PRESSURE DEPENDENCE OF THE CRYSTAL STRUCTURES OF SPIN CROSSOVER FE(II) COMPOUNDS. P. Guionneau, J.F. Létard, Y. Barrans, J. Gaultier, D. Chasseau, O. Kahn, Laboratoire des Sciences Moléculaires, Institut de Chimie de la Matière condensée de Bordeaux, UPR 9048, Pessac, France, J.A.K. Howard, Durham Crystallography Group, Chemistry Department, Science site, Durham DH1 3LE, U.K.

The electronic transition called spin crossover is commonly encountered among metal complexes. This phenomenon derives from the existence of two different configurations for the metallic ion characterized by different spin states. In general, such a transition can be induced by thermal changes, pressure effects or exposure to electromagnetic rays and be smooth or abrupt, accompanied, or not, with a hysteresis phenomenon. The series of the $Fe(PM\text{-}L)_2(NCS)_2$ spin crossover complexes, provided us the occasion to study similar molecules with very different features of temperature or pressure induced transitions. The crystal structures of four complexes were determined in the high spin state (high temperature) and in the low spin state (low temperature) allowing us to link the topology of the intermolecular interactions to the features of the transitions. For instance, the strong combination of intersheet and intrasheet intermolecular contacts between phenyl rings seems to be the relevant parameter which govern the abruptness of the transition. In the same way, the increase of the hysteresis effect is related to the presence of strong intermolecular contacts associated with an irregular iron network in the high spin state. The pressure strongly affects, in a reversible or irreversible mode, the temperature of transition and the width of the hysteresis.

P06.FF.002 MOLECULAR DISTORTION IN A NICKEL COMPLEX COUPLED TO A REVERSIBLE PHASE TRANSITION WITH SUPRAMOLECULAR AGGREGATION. Fernando Palacio,[§] Larry R. Falvello,[†] Michael A. Hitchman,[‡] Isabel Pascual,[†] Arthur J. Schultz[¶], Horst Stratemeier,[‡] Milagros Tomás,[†] Esteban P. Urriolabeitia,[†] and Dianna M. Young[¶], [†]University of Zaragoza - C.S.I.C., Department of Inorganic Chemistry, Plaza San Francisco s/n, E-50009 Zaragoza, Spain. [‡]University of Tasmania, Department of Chemistry, Box 252-75, Hobart, Tasmania 7001, Australia. [§]C.S.I.C.-University of Zaragoza, Department of Condensed Matter Physics, Plaza San Francisco s/n, E-50009 Zaragoza, Spain. [¶]Intense Pulsed Neutron Source, Argonne National Laboratory, Argonne, IL 60439-4814, USA.

The six-coordinate coordination complex trans-[Ni(cyan-*N*)$_2$(NH$_3$)$_4$] has been characterized in the solid state by x-ray and neutron diffraction at temperatures ranging from 11 K to 298 K, by electronic spectroscopy over the temperature range 14-297 K, and by magnetic susceptibility measurements from 1.8-300 K. At room temperature the solid has the space group Fmmm, and the nickel center lies on a site of mmm symmetry. At lower temperatures, the space group changes to Cmcm without appreciable change in the unit cell parameters, and the molecule lies at a site of m2m symmetry. The shape of the molecule changes smoothly with temperature variations from room temperature down to about 140 K, in a behavior characteristic of second-order phase transformations. The molecular shape varies, but by lesser amounts, below 140 K. Possible causes of this phenomenon are discussed. The increase in intensity on cooling of some of the bands observed in the polarized crystal spectrum of the complex is consistent with the change in structure of the complex. Bonding parameters derived from the transition energies indicate that the cyanurate produces a very weak ligand field, which is consistent with the long metal-ligand bond length to this ligand. The magnetic properties of the solid display Curie-Weiss behavior through the temperature range of the most pronounced molecular shape changes, but antiferromagnetic interactions become significant below 50 K, with antiferromagnetic ordering at 2.61 K. The propagation pathways for the magnetic interactions are inferred.

P06.FF.003 ELECTRON DENSITY DISTRIBUTIONS OF Cu(II) AND Co(II) COMPLEXES SHOWING MAGNETIC INTERACTIONS. M. Yasui, N. Akiyama, R, Takayama, T. Ishikawa, D. Hashizume and F. Iwasaki, Dept. of Applied Phys. and Chem. The Univ. of Electro-Communications, Chofu, Tokyo 182-8585, Japan.

Recently some transition metal complexes showing magnetic interactions were investigated [1]. We have carried out the structure analyses of Cu(II)-pyrimidine and Co(II)-pyrimidine complexes which show magnetic interactions. In these complexes, metal atoms are bridged by a pyrimidine to form a one-dimensional chain and a three-dimensional network for Cu and Co complexes, respectively. Such a polymeric structure is considered to be essential for magnetic interactions. In order to elucidate the correlation between magnetic properties and interactions of bridging ligands with 3d electrons, the electron density distributions of $[Cu(II)(NO_3)_2(pm)_3]$ (**1**) (ferromagnetic interactions), $[Cu(II)(NO_3)_2(pm)_2(H_2O)_2]$ (**2**) (antiferromagnetic interactions) and $[Co(II)Cl_2(pm)_4]$ (**3**) (antiferromagnetic interactions) were investigated with a multipole refinement technique using X-ray intensity data at a low temperature. The Cu atom in **1** is coordinated square pyramidally by two O atoms and three N atoms. Additionally, two weak interactions between O and Cu are observed. In **2**, the Cu atom is coordinated octahedrally by four O and two N atoms. The Co atom is coordinated octahedrally by two Cl and four N atoms in **3**. The deformation density maps of **2** show six peaks around the Cu

atom, which are located to avoid the ligands. These peaks can be assigned as 3d electrons. Electron densities for lone-pairs of ligands are also clearly observed. In the case of **1**, the Cu atom has a pseudo seven-coordination so that the interpretation of electron densities around the Cu atom gives some difficulties. The multipole refinement on **3** is in progress.

1. T. Ishida, K. Nakayama, M. Nakagawa, W. Sato, Y. Ishikawa, M. Yasui, F. Iwasaki, and T. Nogami (1997). Synthetic Metals, **85**, 1655-1658.

07OA PROBLEMATICS IN MACROMOLECULAR STRUCTURES: (I) PHASING (sponsored by Rigaku)

M07.OA.001 DETECTING AND EXPLOITING NON CRYSTALLOGRAPHIC SYMMETRY IN MOLECULAR REPLACEMENT

. Jorge Navaza, CNRS, France.

Crystal structures containing many independent molecules in the asymmetric unit are in general may be difficult problems to solve by MR. The reason of the difficulties cannot be ascribed solely to the inherent limitation of the usual formulation of the method, i.e. rotation searches performed independently of the translation ones. Indeed, very often the best values of rather robust criteria correspond to wrong one-body positions. Therefore, it is the overall strategy of the method, based on locating one body after the other that fails if the first bodies are not correctly placed.

The symmetry elements detected by the self rotation and the Patterson functions, associated to strong correlations between the positions of the molecules in the asymmetric unit, may be used to reduce the effective number of independent bodies to be located by MR. A distinction is made between 'frustrated' crystallographic symmetries, i.e. those that are almost crystallographic ones, and 'standard' non-crystallographic symmetries, which are taken into account by specific techniques. These have been successfully applied to many body macromolecular crystal structures, with important save in time and computational effort [1].

[1] Navaza, J., Panepucci, E. H. and Martin, C. (1998). Acta Cryst. **D54**, 817-821.

M07.OA.002 PUSHING THE BOUNDARIES OF MOLECULAR REPLACEMENT WITH MAXIMUM LIKELIHOOD.

Randy J. Read, Department of Haematology, University of Cambridge, Cambridge Institute for Medical Research, Wellcome Trust/MRC Building, Hills Road, Cambridge CB2 2XY, UK.

As the database of known macromolecular structures grows exponentially, the molecular replacement method can solve ever more crystal structures. Nonetheless, it sometimes fails, perhaps because of the use of heuristic target functions. The great success of maximum likelihood in structure refinement suggests that likelihood-based targets may have a similar impact on molecular replacement.

The use of likelihood for molecular replacement was first suggested by Bricogne (CCP4 Proceedings, 1992), who provided some approximations that could be computed quickly, and an interpretation of the likelihood function in terms of current molecular replacement targets.

The likelihood target used in structure refinement is appropriate for the translation problem in molecular replacement, or even for simultaneous rotation and translation. In contrast, in a rotation search the positions of the symmetry-related molecules, and thus the relative phase of their contributions, are still unknown. The likelihood target must be built on probability distributions that take account of this extra level of ambiguity. Such distributions have been derived using techniques developed by Shmueli and coworkers (Shmueli & Weiss, Introduction to Crystallographic Statistics, IUCr Monograph 6, 1995) in the context of intensity distributions to which the central limit theorem cannot be applied.

Both likelihood functions require values for a σ_A curve as a function of resolution, which are normally estimated once one has a complete atomic model. Fortunately, reasonable values can be estimated in advance by exploiting correlations between sequence identity and coordinate deviation.

Initial tests are extremely promising. Likelihood-based molecular replacement has much better signal to noise and significantly greater accuracy, so that previously insoluble problems can be overcome.

M07.OA.003 MULTIPLE SAMPLINGS OF THE RECIPROCAL LATTICE AND MAP AVERAGING AS A SOURCE OF PHASE INFORMATION.

Kevin Cowtan, University of York

Multiple-crystal averaging has been applied with great success to the problem of phase improvement, and multiple crystal forms hold potential as a source of ab-initio phase information. In theory, if the magnitudes of the continuous molecular transform are available, then direct phasing is trivial either in real or reciprocal space. In practice, the molecular transform is obfuscated by both symmetry and coarse sampling, thus in general techniques are currently limited to phase improvement. However phasing a small molecule has been demonstrated from a single atomic position using 6 copies of the molecule across 3 crystal forms. In practice the use of frozen crystals is now a common source of slightly non-isomorphous crystal forms, which are in some cases useful as a source of phase information. Trials with simulated data demonstrate the usefulness of this approach and the limits arising from noise in the data and non-isomorphism in the crystals.

M07.OA.004 STRUCTURE DETERMINATION OF E. COLI CLPP USING 14-FOLD NON-CRYSTALLOGRAPHIC SYMMETRY AVERAGING.

Jimin Wang Department of Molecular Biophysics and Biochemistry, Yale University, New Haven, CT 06520-8114, U.S.A.

We have determined the crystal structure of E. coli ClpP at 2.2 angstroms resolution using a de novo non-crystallographic symmetry (NCS) averaging procedure. ClpP is one of five known large ATP-dependent proteolytic complexes, which regulate many cellular processes through rapid protein degradation. ClpP is a homo-tetradecameric oligomer as revealed by ultracentrifugation analysis; it has a hollow cylinderic structure with a height of 75 angstroms and inner and outer diameters of 35 and 100 angstroms as derived from small-angle x-ray scattering studies; and it has two back-to-back stacked rings of heptamers as determined by electron microscopy. Combined with these biophysical data, we were able to solve the phase problem from x-ray diffraction intensity data alone in the determination of the crystal structure. The hollow cylinderic structure was placed in the unit cell by a packing search program within 5 angstroms of accuracy, and the noncrystallographic symmetry matrices were directly derived from self-rotation function. The initial structure provided initial phases for reflections between 80 and 20 angstroms, and allowed us to extend the phases to the 2.2 angstroms resolution limit by iterative NCS averaging with matrix refinement and mask redetermination. This method should have a general application to the phasing problem in the structure determination of many biological oligomers.

M07.OA.005 TRIPLET-PHASE DATA COLLECTION WITH AN OSCILLATING CRYSTAL TECHNIQUE IN REFERENCE-BEAM GEOMETRY. Qun Shen[1], Stefan Kycia[1], and Ivan Dobrianov[2], [1]Cornell High Energy Synchrotron Source (CHESS) and [2]Department of Applied Engineering Physics, Cornell University, Ithaca, New York 14853, USA

It has been known that 3-beam x-ray diffraction can be used to measure triplet-phases of the structure factors directly from a diffraction experiment, typically using an azimuthal scan or ψ-scan technique. One serious limitation of this conventional ψ-scan technique is that 3-beam interference profiles are measured one at a time. Therefore the whole experimental procedure is rather tedious and time-consuming when many 3-beam profiles are to be measured, as usually needed in the case of macromolecular structures. To solve this problem, recently we have developed a new reference-beam diffraction method [Phys. Rev. Lett. 80, 3268 (1998)] to collect 3-beam interference data, using an oscillation camera in a Bragg-inclined geometry and an area detector such as a CCD. This technique has been shown applicable to both small molecule com-pounds and larger structures such as a protein. In addition to being able to collect a complete set of 3-beam interference data in a short time period, the reference-beam geometry offers other advantages such as a simplified polarization dependence and a single dynamical phase that is common to all 3-beam profiles collected in a data set. Once fully developed and automated, this technique may become a powerful tool for phasing crystal structures in conjunction with the direct methods. This work is supported by NSF grant DMR 97-13424 through CHESS.

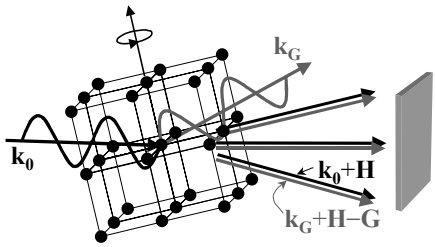

07OB ENGINEERING MACROMOLECULES FOR CRYSTALLISATION

M07.OB.001 USE OF MODULES FOR RNA CRYSTALLIZATION Adrian R. Ferre-D'Amare & Jennifer A. Doudna, Department of Molecular Biophysics and Biochemistry, Yale University, New Haven CT 06520-8114, USA

The rate-limiting step in the determination of the structure of complex RNAs is often the growth of crystals. Even when crystals are successfully grown, these commonly do not diffract X-rays to high enough resolution. This could be because the molecular surface of folded RNAs is dominated by a regular array of phosphates, leading to neighboring molecules packing out of register in the crystal. In order to overcome this problem, we have developed two classes of crystallization modules, molecular moieties that are inserted into the sequences of the target molecules to provide differentiated surfaces which can make crystal contacts. The modules are placed in such a way that they do not affect the structure and function of the RNA segment of interest. The first class of modules employs the components of a long-range intramolecular RNA interaction, which are recruited to make instead a directional and stereospecific crystal contact [1]. In the second class of module, we introduce a cognate site for a sequence-specific RNA binding protein into the target RNA molecule. The complex formed between the engineered RNA and a strongly basic RNA-binding protein has not only a patch of positive charge, but also the large variety of surface functional groups of the protein available for making crystal contacts. Using this approach, we obtained crystals of an engineered hepatitis delta virus ribozyme bound to the RNA-binding domain of the U1A protein. The rhombohedral crystals diffracted X-rays to beyond 2.2 Å resolution. We prepared selenomethionyl U1A protein and co-crystallized it with the RNA to solve the structure of the complex by the MAD method [2]. Use of the crystallization modules is being extended to a variety of RNA molecules.

1. A.R. Ferre-D'Amare, K. Zhou & J.A. Doudna (1998). J.Mol.Biol., 279, 621.
2. A.R. Ferre-D'Amare, K. Zhou & J.A. Doudna (1998). Nature, 395, 567.

M07.OB.002 ENGINEERING IMPROVEMENTS IN CRYSTALS- EXPERIENCES OF RNP DOMAIN CONTAINING PROTEINS S. R. Price [1], C. Oubridge, K. Nagai [2], [1] Dept. Biochemistry and Molecular Biophysics, Columbia University, New York USA, [2] MRC Laboratory of Molecular Biology, Hills Road, Cambridge, UK

There is no substitute for good data in the solution of crystal structures. The utilisation of molecular biology techniques to overcome technical difficulties in the preparation of diffraction quality crystals has proven extremely powerful. I shall describe our experiences in the solution of two protein-RNA complex structures and how Protein- and RNA-engineering allowed the solution of these structures. RNA sequence changes proved critical to the generation of useful crystals. In addition, problems caused during heavy atom derivitisation were overcome by the judicious use of protein-engineering combined with a biochemical assay. It is highly unlikely that these structures would have been solved if these techniques had not been employed.

M07.OB.003 COVALENT TRAPPING OF A CATALYTIC HIV-1 REVERSE TRANSCRIPTASE/ SUBSTRATE COMPLEX. H. Huang and G. L. Verdine, Department of Chemistry and Chemical Biology, Harvard University, Cambridge, MA 02138, USA. R. Chopra and S. C. Harrison, Howard Hughes Medical Institute and Department of Molecular and Cellular Biology, Harvard University, Cambridge, MA 02138, USA.

A combinatorial disulfide crosslinking strategy was used to trap a complex of human immunodeficiency virus-type 1 (HIV-1) reverse transcriptase with a DNA template:primer and a deoxynucleoside triphosphate (dNTP), thereby enabling the growth of co-crystals suitable for high-resolution structural analysis. The crystals contain a fully assembled active site poised for catalysis. The crosslink itself appears to be conformationally mobile, and the surrounding region is undistorted, suggesting the crosslink is a structurally passive device that merely acts to prevent dissociation of the catalytic complex. Conformational changes that accompany formation of the catalytic complex produce distinct clusters of the residues that are altered in viruses resistant to nucleoside analog drugs. The positioning of these residues in the neighborhood of the dNTP helps to resolve some long-standing puzzles about molecular basis of resistance. The covalent trapping strategy described here may be useful with other protein-DNA complexes that have been refractory to structural analysis.

M07.OB.004 CRYSTALLOGRAPHIC STUDIES OF E. COLI RNA POLYMERASE SUBUNITS. Gongyi Zhang, Seth A. Darst, The Rockefeller University, New York, NY 10021 USA.

E.coli RNA polymerase (RNAP) contains an essential catalytic core of two alpha subunits (each 36.5 kDa), one Beta(150.6 kDa), and one beta'(155.2) subunit, each having

sequence hololog from bacteria to man. The alpha subunit, which plays a critical role by serving as the initiator for RNAP assembly, contains protein-protein interaction determinants for alpha dimerization, for the interaction of beta to form a2b subassembly, and for the interaction with beta' to form core RNAP. Limited proteolysis has shown that the alpha subunit comprises at least two domains, an N-terminal domain(NTD), which is fully competent for RNAP assembly and basal transcription in vitro, and a C-terminal domain(CTD), which is dispensable for basic assembly and transcription but interacts with the UP-element of certain promoters and is required in vivo to interact with a wide array of transcription activators. Due to crystallization problems, the alpha structure was unknown. By creating dozens of truncation and point mutations of alpha NTD, we eventually obtained one mutation that yielded good crystals for structure determination. Encouraged by these results, we made the same mutaion in the context of full length alpha. This version of alpha crystallized and the crystals diffract to 2.5 angstrom. We have applied this approach successfully to other proteins as well.

M07.OB.005 STRUCTURE OF HTLV-1 GP21 ECTODOMAIN CRYSTALLIZED AS AN ENGINEERED MALTOSE-BINDING PROTEIN CHIMERA. B. Kobe, R.J. Center, B.E. Kemp and P. Poumbourios, St. Vincent's Institute of Medical Research, 41 Victoria Parade, Fitzroy, Victoria 3065, Australia.

Human T cell leukemia virus type 1 (HTLV-1) is a retrovirus associated with adult T-cell leukaemia and tropical spastic paraparesis/HTLV-1-associated myelopathy. Envelope glycoproteins (Env) mediate the attachment and subsequent membrane fusion of virions and infected cells with target cells. The native HTLV-1 Env consists of a receptor-binding subunit (SU) gp46, and a non-covalently associated transmembrane subunit (TM) gp21, formed by a proteolytic cleavage of a polyprotein precursor gp62. Receptor binding triggers conformational changes in retroviral SU-TM complexes that result in TM-mediated fusion. While the cellular receptors for HIV-1 SU gp120, CD4 and the chemokine receptors have been extensively studied, the HTLV-1 gp46 receptor(s) are unknown.

We report the crystal structure of the HTLV-1 gp21 ectodomain (residues 338-425, gp62 numbering) at 2.5 Å resolution. We used a novel strategy for crystallisation and structure determination whereby the gp21 segment was linked to maltose-binding protein (MBP) as a crystallisation tag of known three-dimensional structure. Guided by the available biochemical data and structure predictions, the linker between MBP and gp21 was engineered to reduce flexibility, and C-terminal truncations were made to improve the quality of the crystals. The MBP domain was used to obtain the initial phases by the method of molecular replacement. The method employing MBP-chimeras may have a general application in crystallisation and structure determination.

The structure of gp21 shows an N-terminal trimeric coiled coil, a disulfide-bonded loop that stabilises a chain reversal, and a C-terminal sequence that packs against the coil in an extended anti-parallel fashion. Comparison of the gp21 structure with the structures of other retroviral TMs contrasts the conserved nature of the coiled coil-forming region and adjacent disulphide-bonded loop with the variable nature of the C-terminal ectodomain segment. The structure points to these features having evolved to enable the dual roles of retroviral TMs: conserved fusion function and an ability to anchor diverse SU structures to the virion envelope and infected cell surface. The observed structure of gp21 most likely represents the post-fusion conformation, and jointly with the experimental evidence accumulated through cell biological, biochemical, biophysical and structural studies prompts a revised model for retroviral TM-mediated membrane fusion.

07OC PHASE TRANSITIONS

M07.OC.001 DENSITY FUNCTIONAL STUDIES OF PHASE TRANSITIONS: THE FCC-BCC TRANSITION IN METALS. Karlheinz Schwarz, Institute of Physical and Theoretical Chemistry, Technische Universität Wien, A-1060 Vienna, Getreidemarkt 9/158, Austria

The importance of Density Functional Theory (DFT) is steadily increasing in chemistry and physics especially for ground state properties of large systems including transition elements. DFT provides an efficient way to approximately treat exchange and correlation effects. In the early version of DFT within the local density approximation (LDA) deviations from experimental data were found, e.g. overbinding. The use of the generalized gradient approximation (GGA) has led to a significant improvement with nearly chemical accuracy so that structural optimizations or thermo-chemical studies are often well described within DFT/GGA. These aspects rely on the total energy of the systems involved and are based on integral quantities. The Linearized-Augmented-Plane-Wave (LAPW) method as embodied in the WIEN97 code [1] is one among the most accurate schemes to solve the Kohn-Sham equations, the basis of DFT. A fcc-bcc phase transition can be modeled by a displacive transition following the Bain path [2]. A body centered tetragonal unit cell changes from fcc to bcc if the c/a ratio varies form sqrt(2) to 1. LAPW calculations provide the energy hypersurface E(V,c/a) as function of volume and c/a. Finite temperature effects can be accounted for by allowing fluctuations in both of these two variables, V and c/a. The combination of quantum mechanical DFT calculations with statistical thermodynamics (using a Ginzburg-Landau approach) provides an efficient scheme for treating phase displacive transitions.

K.Schwarz and P.Blaha, Lec.Notes in Chem. 67, 139 (1996)
V.Sliwko et al J, Phys.Cond.Matter 8, 799 (1996)

M07.OC.002 COMPOSITIONALLY AND/OR DISPLACIVELY FLEXIBLE PHASES AND THEIR ASSOCIATED PHASE TRANSFORMATIONS. R.L.Withers, J.G.Thompson and S.Schmid Research School of Chemistry, Australian National University, Canberra, A.C.T, 0200, Australia.

The conventional concept of crystalline phases as translationally periodic objects characterized by well-defined stoichiometries, unit cells and space group symmetries (in three dimensions), and with structures which represent a unique free energy minimum in local parameter space, is a deeply entrenched idea in solid state chemistry. There have, nonetheless, always existed a significant range of compositionally and/or displacively flexible systems whose chemistry and “crystallinity” are not best expressed in this form [1-3]. The very flexibity of such systems suggests a delicate balance of forces which can be “tipped” one way or the other via slight changes in external conditions or composition. It is important not just to “solve” for the structures of any such phases in isolation but also to relate the various phases within such systems.

Structure refinement of flexible phases often necessitates a modulated structure approach [1-2]. Even when this is apparently not the case, *e.g* in the case of long period superstructures, a modulation wave approach still has distinct advantages as it enables a unified description of superficially distinct but clearly related variant phases as well as of the phase transformations that such flexible phases often undergo as a function of temperature, composition *etc*. Examples to be discussed include wide range, non-stoichiometric solid solutions [1] and displacively flexible tetrahedral framework structures [2].

1. R.L.Withers, S.Schmid & J.G.Thompson (1998). Prog. Solid St. Chem., 26, 1.
2. J.G.Thompson, R.L.Withers, S.Palethorpe & A.Melnitchenko (1998). J. Solid State Chem. 141, 29.
3. R.L.Withers &J.G.Thompson (1997). In *In situ Microscopy in Materials Research* (Ed.P.Gai), Kluwer, 301.

M07.OC.003 FERROELASTIC PHASE TRANSITIONS. E.K.H. Salje Department of Earth Sciences Cambridge University, Downing Street Cambrdge CB2 3EQ, UK.

Ferroelastic phase transitions often generate characteristic domain pattern. Such patterns consist of twin boundaries, their junctions and complex structures which contain twin boundaries as basic elements (e.g. combs, zig-zag patterns, stripe patterns, needle and trumpet domains etc). The thicknesses of twin walls are determined by X-ray diffraction methods using dedicated 7-circle diffractometers. Typical wall thicknesses were found to be between 1nm and 7 nm (Salje 1993). It is shown that the interaction between domain walls and crystal surfaces lead to the formation of lattice instabilities including the formation of elastic 'funnels' which enable diffusion through the surface into the twin wall. Enhanced oxygen and sodium diffusion is shown in WO3 and related structures.

E.K.H.Salje (1993) Phase Transitions in Ferroelastic and Co-elastic crystals,Student edition, Cambridge University Press, Cambridge, UK
J. Novak and E.K.H.Salje(1998) Simulated mesoscopic structures of a domain wall in ferroelastic lattices Eur. Phys. J. B4,279-284

M07.OC.004 STRUCTURAL STUDY OF THE MODULATED PHASES OF BETAINE CALCIUM CHLORIDE DIHYDRATE (BCCD). O. Hernandez, LDS2M, U.F.R. de Physique, U.S.T.L., 59655 Villeneuve d'Ascq, France, M. Quilichini, J.-M. Kiat and A. Cousson, L.L.B., C.E.A. / Saclay, 91191 Gif-Sur-Yvette, France, J. M. Pérez-Mato and G. Madariaga, D.F.M.C., U.P.V., 48080 Bilbao, Spain, J. M. Ezpeleta, D.F.A. II, U.P.V., 01080 Vitoria-Gasteiz, Spain, L. G. Vieira and J. L. Ribeiro, Departamento De Física, Universidade Do Minho, 4709 Braga, Portugal, M. R. Chaves and A. Almeida, Departamento De Física, Universidade Do Porto, 4150 Porto, Portugal, P. Thuery, S.C.M., C.E.A. / Saclay, 91191 Gif-Sur-Yvette, France, and A. Klöpperpieper, Fachbereich Physik, Universität Des Saarlandes, 66041 Saarbrücken, Germany

We present a structural study of the one-dimensional displacively modulated compound BCCD. The structures of two low temperature commensurate phases of the Devil's staircase-type phase diagram of BCCD, the four-fold and five-fold phases, have been determined by single-crystal neutron diffraction. In both phases, the atomic modulation functions are highly anharmonic with an almost one-third contribution of the third-order harmonic with respect to the first-order one. On the basis of four-dimensional symmetry arguments, we interpret the anharmonicity of the modulation as a soliton regime with respect to the lowest-temperature non-modulated ferroelectric phase. The physical consequences of this low temperature structural anharmonicity are discussed. The previous X-ray four-circle data of the four-fold phase, that had led to a single-harmonic model, have been re-analysed. The discrepancy with the neutron structural model that persists is explained by an irradiation effect at constant temperature : X-rays induce an unusual time-decay of the intensity of high-order satellite peaks (up to ≅ -80 % after 86 hours for third-order ones). Structural conclusions concerning the ``T_s-anomaly'' from an analysis of X-ray area-detector diffractometer data in the four-fold phase of 2 % brominated BCCD are presented.

M07.OC.005 HIGH-PRESSURE INCOMMENSURATE TO NORMAL TRANSITION IN ÅKERMANITE, $Ca_2MgSi_2O_7$. R.J. Angel, J.D.C. McConnell, C.A. McCammon, F. Seifert, Bayerisches Geoinstitut, Universität Bayreuth, D95440 Bayreuth, Germany

Insights into the structural changes accompanying the Incommensurate-Normal (IC-N) phase transition in åkermanite ($Ca_2MgSi_2O_7$) have been obtained through a combination of symmetry analysis, *in-situ* single-crystal high-pressure diffraction and *in-situ* high-pressure Mössbauer spectroscopy.

Åkermanite is tetragonal, space group $P\text{-}42_1m$ and theoretical considerations show [1] that the incommensurate modulated structure stable at room conditions is based upon the irreducible representations A_2 and B_1 of point group -42m. The IC structure is therefore two-dimensional in nature, and consists of the two structural components P-4 and $P2_12_12$. The presence of these two structural components within the crystal structure has been confirmed by *in-situ* high-pressure Mössbauer spectroscopy of Fe-doped åkermanite. The spectra consist of two distinct and sharp doublets corresponding to the two different environments for the Fe/Mg sites in the two component structures. These two absorption doublets merge to a single doublet in the high-pressure N-phase at pressures in excess of 1.8 GPa.

In-situ lattice parameter measurements at high pressure show that the N to IC transition occurs at 1.718(6) GPa. It is accompanied by a large expansion of the c-axis ($e_{33} = 1.6x10^{-3}$ at room P). Smaller spontaneous strains in the (001) plane ($e_{11} = e_{22} \sim -1.0x10^{-4}$) are attributable to the development of the orthorhombic $P2_12_12$ component structure in the IC phase. The pressure evolution of e_{33} shows that the transition is continuous with an effective critical exponent of 0.20(3), indicating that the fourth-order terms in the free energy expansion of the IC phase cancel, as required by symmetry criteria.

[1] J.D.C. McConnell (1999). Zeit. für Kristallogr., in press.

P07.OC.001 PHASE TRANSITIONS AND STRUCTURES BETWEEN 10 AND 293 K OF $M(I)M(III)(NH_3)_6(ClO_4)_2X_2$. A.N. Sobolev and B.N. Figgis, Department of Chemistry, University of Western Australia, Nedlands, W.A. 6907, Australia, and R.W.Henning and A.J.Schultz, IPNS, Argonne National Laboratory, IL 60439, USA, and P.A. Reynolds, Research School of Chemistry, Australian National University Canberra, ACT 0200, Australia.

Eighteen crystal structures of ten hexaammine-M(III) double salts of the title formula have been determined by X-ray diffraction where M(I), M(III) and X are NH_4, Co, Cl **(1)**; Cs, Co, Cl **(2)**; NH_4, Ru, Cl **(3)**; K, Ru, Cl **(4)**; Rb, Ru, Cl **(5)**; Cs, Ru, Cl **(6)**; Cs, Cr, Cl **(7)**; Cs, Cr, Br **(8)**; K, Cr, Cl **(9)**; K, Os, Cl **(10)**. The structures of all except **(9)** were determined at 293 K ; **(1), (4), (5)** and **(6)** have also been determined at 92 K; and those of **(5), (7), (8), (9)** and **(10)** at 10 K. At 293 K all are isomorphous, trigonal *R*-3*m*, *Z* = 3, of extremely simple and symmetrical structure. At lower temperatures most crystals undergo a subtle reversible phase change to an equally simple twinned, but atomically ordered, R-3 phase. In these twinned salts, the hexaammine-M(III) and perchlorate ions are rotated from 3 to 11 degrees about the threefold axis to remove the former mirror plane in the *R*-3*m* crystal. Thermal parameters, unit cells, transition temperatures (T_C) (determined by Differential Scanning Calorimetry) and structures vary systematically with M(I) ionic radii and M(III)-N distances. The K^+ members remain R-3m, while the larger M(I) and longer M(III)-N members undergo the greatest rotations with the highest transition temperatures. One of the latter, Cs, Co, Cl **(2)**, has been examined by neutron diffraction at 10, T_C-10, T_C+10 and 290 K. The observed twin populations, orientational order parameter and deuterium disordering indicate that a simple model involving differing

ranges of ionic orientational correlations is appropriate for all these crystals at all temperatures.

P07.OC.002 THE PHASES OF MERCURIC IODIDE. M. Hostettler, H. Birkedal, K. J. Schenk, H. P. Weber and D. Schwarzenbach, Institut de Cristallographie, Université de Lausanne, BSP Dorigny, CH-1015 Lausanne, Switzerland.

At room temperature, HgI_2 crystallizes from 2-chloro-ethanol in either or all of three modifications: the red one (α), thermodynamically stable, the yellow one, related to the high temperature phase (β), and the orange modification, metastable at all temperatures or at least in the range: 100-400K. Owing to the importance of the α-phase as an electronic material, some parts of the HgI_2 P-T phase diagram have been intensively studied in the past [1]. There are no less than 5 different phases at moderate temperatures (T < 600K) and pressures (P < 1.5GPa) [2]. The general features of the phase diagram seem to be well known, but several of the phases are only partially characterized.

Orthoscopic optical studies of the α to β transition, at 400K, are presented. There is a large hysteresis, the yellow crystal has been observed to persist upon cooling in some cases down to 360K. Different nucleation behaviours have been observed when passing through the transition in opposite directions. This indicates a reconstructive mechanism. A model describing the transition from a layered compound (α) to a molecular crystal (β) has been derived from X-ray powder diffraction patterns. The tetrahedral HgI_4 structural motif of the α-phase transforms into a HgI_2 motif with a strongly deformed octahedral Hg-coordination.

We are currently undertaking high pressure powder diffraction measurements of the barotropic α to γ phase transition. The determination of the structure of the γ-phase may shed more light on the transition mechanisms in this system.

1. E. D. Tonkow, N. A. Tikhomirova (1971). Sov. Phys. Cryst., **15**, 945.
2. C. Guminski (1997). Journal of Phase Equilibria, **18**, 206.

P07.OC.003 THE PHASE TRANSFORMATION $Co_2Ge(h) \rightarrow Co_2Ge(l)$. N. Audebrand, M. Ellner and E. J. Mittemeijer. Max-Planck-Institüt für Metallforschung, Seestr. 92, D-70174 Stuttgart, Germany.

The phase transformation $Co_2Ge(h) \rightarrow Co_2Ge(l)$ could not be possible according to the published binary phase diagram Co-Ge [1]. In the present investigation, this transformation has been clearly observed by means of X-ray diffraction, metallographical and differential scanning calorimetry measurements. The (high-temperature) berthollidic phase $Co_2Ge(h)$, according to the published phase diagram stable in the composition range $0.33<x_{Ge}<0.43$, shows a defect Ni_2In structure [Pearson-Parthé symbol *hP*(6-*n*), space group $P6_3/mmc$]. Microscopical analysis, using polarized light, of the slowly cooled bulk alloy $Co_{66}Ge_{34}$ revealed multiple twinning in all grains. Such twinning can be a consequence of shape accommodation due to a polymorphic phase transformation. The Guinier pattern ($CoK\alpha_1$ radiation) of the alloy $Co_{66.6}Ge_{33.3}$ heat treated at 775 K for 5 days yielded diffraction lines of the phase $Co_2Ge(l)$: Co_2P type structure (*oP*12, *Pnma*). The refined lattice parameters of this (low temperature) phase are: a_o = 5.0504(4) Å, b_o = 3.8378(3) Å and c_o = 7.2960(5) Å [M_{20} = 109, F_{26} = 98(0.0078, 34)]. The Guinier pattern of the liquid quenched, splat-cooled, alloy $Co_{66.6}Ge_{33.3}$ showed diffraction lines of only the high-temperature phase $Co_2Ge(h)$ yielding the following refined lattice parameters: a_h = 3.9639(4) Å, c_h = 5.022(1) Å, c_h/a_h = 1,2669>√(3/2) [M_{20} = 139, F_{10} = 63(0.0047, 34)]. The ideal relationship between an orthorhombic and a hexagonal unit cells is: $a_o = c_h$; $b_o = a_h + b_h$; $c_o = -a_h + b_h$ with $c_o/b_o = \sqrt{3}$. The polymorphic phase transformation $Co_2Ge(h) \rightarrow Co_2Ge(l)$ is associated with a strong lattice distortion in the plane $(100)_o$ because c_o/b_o = 1.9011 (but the distortion a_o/c_h = 1.006 is near to the ideal value: 1). Consequently, the change of the average atomic volume $\Delta\overline{V}$ associated with the phase transformation is important, *i.e.*, 0.39 Å^3. Differential scanning calorimetric measurement showed that the phase transformation occurs at about 960 K upon heating.

1. T.B. Massalski, H. Okamoto, P.R. Subramanian & L. Kacprzak (1990). Binary Alloy Phase Diagrams, Second Edition, Vol. 2. ASM International, The Materials Information Society, 1189.

P07.OC.004 ORDER PARAMETER COUPLING AND CRITICAL BEHAVIOUR OF DEBYE-WALLER FACTOR IN PEROVSKITES. H. Boysen, H. Lehnert and F. Frey, Institut für Kristallographie der Universität München, 80333 München, Germany, and P. Radaelli and Th. Hansen, ILL, 38042 Grenoble, France.

The critical behaviour of various perovskite-like compounds, $LaAlO_3$, $PbTiO_3$ and $LiNbO_3/LiTaO_3$, has been investigated by neutron powder diffraction around their phase transitions *via* detailed structure refinements including anharmonic Debye-Waller factors. The results were analysed in frame of Landau theory using the fluctuation-dissipation theorem to relate the susceptibility to the atomic displacement parameters (ADP's).

In the purely displacive case of $LaAlO_3$ ($Pm3m \leftrightarrow R\bar{3}c$) the rotations of O_6-octahedra, the spontaneous strain and $\boldsymbol{U}_{11}$(O) show the expected critical behaviour. There is, however, no exact linear-quadratic coupling between order parameter and strain: the metric becomes cubic roughly 30 K below the proper T_c. This is related to spontaneous creation of domains imposing the average cubic symmetry *via* internal stresses. In $PbTiO_3$ ($Pm3m \leftrightarrow P4mm$) there are four structural degrees of freedom (*z*-shifts of the various atoms). In the low temperature polar space group the origin is not fixed by symmetry. Analyses of the ADP's show that all $\boldsymbol{U}_{33}$'s except $\boldsymbol{U}_{33}$(Ti) are critical. Therefore, *z*(Ti) is not critical and the natural parameter to be kept fixed. Again deviations from the expected Landau behaviour are found for the spontaneous strain indicating the occurrence of stress which is further confirmed by specific peak broadenings. Anharmonic ADP's reveal a certain disorder of Pb, i.e. there is an additional order-disorder component which is also found in $LiNbO_3$ and $LiTaO_3$ ($R\bar{3}c \leftrightarrow R3c$). While this is only a secondary effect in $LiTaO_3$, there is a strong competition of both ordering mechanisms, a „superionic" and a „ferroelectric" one, in $LiNbO_3$ causing a more complex critical behaviour. This difference can be related to the actual geometries of the structures. ADP's define the centre of the O_6-octahedra as (non-critical) origins in this case. Deviations from Landau behaviour are again found in the strain indicating spontaneous re-polarisations below T_c.

P07.OC.005 PRETRANSITIONAL PHENOMENA ON THE PHASE TRANSITION OF ABO_4-TYPE FERROELASTIC COMPOUNDS. Y. Kuroiwa, S. Aoyagi and A. Sawada, Department of Physics, Okayama University, Tsushima, Okayama 700-8530, Japan, and T. Shobu, Department of Physics, Chiba University, Yayoi, Chiba 263-8522, Japan, and Y. Noda, RISM, Tohoku University, Katahira, Sendai 980-8577, Japan and S. Tsunekawa, IMR, Tohoku University, Katahira, Sendai 980-8577, Japan.

Precursor phenomena on the first-order phase transition are found in some materials. It is important to study the precursor phenomena since the phenomena are considered to be a key to solve the origin of the first-order phase transition. We have investigated precursor phenomena in ferroelastic compounds, and

found new-type precursor phenomena on the first-order phase transition of $LaNbO_4$ and $NdNbO_4$ [1, 2].

X-ray diffraction studies were performed at the home laboratory and the synchrotron radiation facility, SPring-8 (BL02B1). $LaNbO_4$ and $NdNbO_4$, which have a scheelite structure ($I4_1/a$) in the high temperature phase, transformed to a slightly distorted pseudo-scheelite structure (I2/a) at 768K and 930K, respectively. The lattice parameters changed discontinuously at the phase-transition temperature. Anomalous temperature-dependence of the profiles of Bragg reflections was observed on the phase transition. The intensities decreased remarkably and the profiles broadened such as diffuse scattering, as the phase-transition temperature was approached. In addition, anisotropic diffuse scattering was observed around the Bragg reflections. Similar phenomena on such Bragg Broadening are observed in a ferroelastic compound Na_2CO_3. In the present work, the precursor phenomena observed in $LaNbO_4$ and $NdNbO_4$ are discussed by comparison with the critical phenomena on the second-order phase transition of $BiVO_4$.

Y. Kuroiwa, H. Muramoto, T. Shobu, H. Tokumichi, Y. Noda & Y. Yamada (1995). J. Phys. Soc. Jpn. 64, 3798.
Y. Kuroiwa, K. Nozawa, J. Ikegami, T. Shobu, Y. Noda & S. Tsunekawa (1998). J. Korean Phys. Soc. 32, S84.

P07.OC.006 HYDROGEN ORDERING AND ELECTRON DISTRIBUTION ON THE PHASE TRANSITION OF SQUARIC ACID. Y. Noda, Research Institute for Scientific Measurements, Tohoku University, 2-1-1 Katahira, Aobaku, Sendai, 980-8577 Japan, and H. Kimura, Department of Physics, Chiba University, Yayoi, Chiba 263-8522, Japan.

Squaric acid (3,4-dihydroxy-3-cyclobutene-1,2-dione; $C_4H_2O_4$), that is abbreviated as H2SQ, undergoes antiferroelectric phase transition at 370K for H-compound and at 516K for D-compound[1]. The crystal structure was already determined by X-ray [2] and neutron diffraction[3]. The space group changes from I4/m (H-compound, Z=2, a=c=6.1340Å, b=5.3415Å, 395K) to $P2_1/m$ (Z=2, a=6.1325Å, b=5.2749Å, c=6.1431Å, β=89.96°, 300K).

We have performed precise X-ray structural analyses at 300K, 322K, 342K and 363K in the low temperature phase, and 374K, 395K in the high temperature phase to study the phase transition phenomena of this compound. From the differential Fourier analysis, we found electron distribution of hydrogen atoms in the hydrogen-bond region. Not only the hydrogen atoms, but also bonding electrons along C-C bond and C-O bond were clearly observed.

Equivalent C-C bond length in the high symmetry phase splits to a double bond C=C and a single bond C-C in the low symmetry phase. We have measured the C-C bond length as a function of temperature. By using the differential Fourier synthesis, we determined the order parameter of a hydrogen atom whose position changes from double minima to single minimum. The behaviour of the order parameter of a hydrogen atom is similar to the strain that is calculated from the temperature dependence of the monoclinic angle. The hydrogen-bond length was also measured as a function of temperature, and the lattice distortion (axis length) is entirely explained by the change of the hydrogen-bond length. These results suggest the coupling nature and the transition mechanism of H2SQ.

D. Semmingsen and J. Feder (1974). Solid State Comm. **15**, 1369.
D. Semmingsen (1973). Acta Chem. Scand. **27**, 3961
D. Semmingsen *et al* . (1977). J. Chem. Phys. **66**, 4405

P07.OC.007 PHASE TRANSITIONS IN HMTA. M. Gardon, K. J. Schenk, and G. Chapuis, Institut deCristallographie, Université de Lausanne, BSP Dorigny, CH-1015Lausanne, Switzerland.

Hexamethylenetetramine azelate (HMTA) is a fascinating member of the $C_6H_{12}N_4$-$HOOC(CH_2)_nCOOH$ family (with n=7). The structures of the different phases of HMTA were investigated anddetermined by XRD techniques. HMTA undergoes three thermotropic phasetransitions at ambiant pressure. The four phases were labelled I, II,III and IV from high to low temperature. All transitions are of firstorder and reversible, except transition II→I. PhaseII is disordered while phase III and IV are ordered. The cell-doublingII→III transition has a ferroelastic character andcorresponds to a reorganisation of the COOH terminals responsible of thedisorder in phase II. Transition III→IV is ofnon-ferroelastic nature and is also associated to a doubling of theprevious cell. Optical studies of phase I at high temperature werenecessary to elucidate its nature. Orthoscopy has revealed that the II→I transition is preceded by a gradual wrinkling (over 30°C) of the (0 1 0) surface which iscleansed during the phase transformation leaving behind a neat crystalsurface. Analogy between optical and calorimetric results has beendemonstrated. We aim to emphasize at a first stage the questions whichappear when considering only the limited structural approach provided by XRD experiments. We explain how to go beyondthese frontiers and what kind of response can be given byconsidering other techniques like NMR and IRspectroscopy. Finally, results from other members of this family(n=4,...,14) are combined with the ones from HMTA in order toelaborate general features governing the thermal behavior of thesecompounds.

P07.OC.008 CHARGE, ORBITAL AND MAGNETIC ORDERING IN $Ln_{0.5}A_{0.5}MnO_3$ AND $Ca_{1-X}Bi_XMnO_3$. P.M. Woodward, J. Goldberger [1], T. Vogt, D.E. Cox [2] and K.Z. Baba-Kishi [3], [1] Department of Chemistry, Ohio State University, Columbus, OH 43210-1185, USA, [2] Physics Department, Brookhaven National Laboratory, Upton, NY 11973, USA, [3] Department of Applied Physics, The Hong Kong Polytechnic University, Hong Kong, China

Phase transitions, driven by various combinations of charge, orbital and magnetic ordering, in the systems, $Ln_{0.5}A_{0.5}MnO_3$ (Ln = La, Pr, Nd, Gd, Sm, Y; A = Ca, Sr) and $Ca_{1-x}Bi_xMnO_3$ ($0 < x < 0.3$), have been studied using high-resolution synchrotron x-ray and neutron powder diffraction techniques. The information obtained in the powder diffraction studies is supplemented with TEM and magnetic susceptibility measurements.

Despite prolonged high-temperature heat treatments (~1500° C) the $Ln_{0.5}Sr_{0.5}MnO_3$ compounds containing larger rare-earth ions (La^{3+} and Pr^{3+}) show a persistent polytypism at room temperature in the charge-delocalized state. The two structural modifications observed adopt different octahedral tilt systems, $a^0a^0c^-$ (space group *I4/mcm*) and $a^-b^0a^-$ (space group *Imma*). Variable temperature X-ray and neutron diffraction studies show that at low temperatures the tetragonal *I4/mcm* structure undergoes orbital and antiferromagnetic ordering, but no evidence for charge ordering is observed. In contrast, the orthorhombic *Imma* structure transforms to the charge-ordered, antiferromagnetic CE-type structure at low temperature. As the size of the lanthanide ion is decreased eventually *Pnma* symmetry (tilt system $a^-b^+a^-$) is observed at room temperature. The appearance Pnma symmetry corresponds to the disappearance of the charge-ordered CE-type structure at low temperature. This suggests a strong correlation between octahedral tilting and the low temperature magnetic structure.

Two distinctly different orbitally ordered states are observed at low temperature in the $Ca_{1-x}Bi_xMnO_3$ system. Structural studies show that when $x \sim 0.3$ the filled e_g orbitals are located in the *ac* plane, arranged in a zig-zag pattern similar to that observed for $LaMnO_3$ or $La_{0.5}Ca_{0.5}MnO_3$. Whereas, when $x \sim 0.2$ the occupied e_g orbitals appear to all align in the same direction. Structural refinement results for each of these ordered structures will be presented.

P07.OC.009 X-RAY STUDY OF STRUCTURE AND PHASE TRANSITIONS IN $Cs_3Sb_2I_9$ CRYSTAL. Novikova M.S. and Makarova I.P, Institute of Crystallography RAS, Leninski pr. 59, Moscow, 117333 Russia and Bagautdinov B.Sh,. Institute of Solid State Physics RAS, Chernogolovka, 142432 Russia and Blomberg M.K. University of Helsinki, FIN-00014, Finland, and Chapuis G, Universite de Lausanne, Institut de christallographie, 1015 Lausanne-Dorigny, Switzerland.

$Cs_3Sb_2I_9$ crystal belongs to a wide family of ferroelectrics $A_3B_2X_9$. Recently it was found in [1] that this compound undergoes two low temperature phase transitions (PT) at 86 and 74 K. X-ray structural study revealed that this compound crystallizes in two different modifications: hexagonal ($P6_3/mmc$, Z=2) [2],and trigonal [3] ($P\ \bar{3}m1$, Z=1). The samples that undergo PT were carefully studied on the four-circle diffractometer «Enraf-Nonius»-4F and the refinement showed that the symmetry is trigonal. The experiment was carried out in the whole sphere of the reciprocal space. Program complex JANA94 was used for refinement. The absorption correction was made by numerical integration using the shape of the crystal. Two-circle diffractometer «Siemence»-D500 and four circle diffractometer «Huber»-5042 were used for helium studies. Three modulated PT were found with the help of x-ray method. PT at 86 K is characterized by the appearance of the superstructural reflections $q_1 = 1/2c^*$ and does not change the geometry of the reciprocal space. According to x-ray data the trigonal symmetry is preserved. Below 78 K new superstructural reflections were observed with $q_2 = 1/2c^* +(1/2 +\delta)a^*$. At 72 K δ vanishes. This last PT is found to be of the first order.

The work is supported by Swiss National Science Foundation Grant N7SUPJ48718

[1] Aleksandrova , I.P., Sukovsky, A.A., Melnikova, S.V. et al. Phys Solid State,39,1977,846.
[2] Chabat, B & Parté, E. Acta Cryst. B34,1978,645.
[3] Kun, S.V., Lasarev V.B., Peresh E. Yu. et al. Neorganic Materials, 1993, 29, N3, 410.

P07.OC.010 EFFECT OF LASER HEATING ON STRUCTURAL STATE OF IRON-NICKEL ALLOYS. V.E. Danilchenko, B. Polchuk, Institute for Metal Physics, Academy of Sciences of Ukraine, 36 Vernadsky Blvd., 252680 Kiev, Ukraine

After laser heating of metals the specific structural state of surface layer is caused by high level of internal stresses, dispersion of phase components, by possible redistribution of alloying elements and by realisation of phase transformation in nonequilibrum conditions. In formation of complex of physical and mechanical properties of surface layer essential role is played by phase transitions, fulfilling with volume effect and supplying the distinctions in physical properties of phases.

Present work investigates the influence of laser treatment on martensitic transformation characteristics and crystalline structure of gamma- and alpha-phases in Fe-Ni alloys. Laser melting of surface of metastable austenitic Fe-Ni alloys led to the change of martensitic transformation completeness during subsequent cooling in liquid nitrogen: in binary (Fe-30%Ni) and carbonrich (Fe-24.5%Ni-0.55%C) alloys the austenite stabilisation was supervised owing to which the martensitic transformation proceeded more slowly. In alloy Fe-29%Ni-1.9%Ti-2%Al the martensitic transformation completeness was substantially increased. The austenite stabilisation in binary alloy was connected with structural factors and with increase of carbon content in gamma-solid solution at the expense of dissolution of graphite globulars during laser melting. Martensite transformation activization in Fe-Ni alloy with Ti and Al was defined by change of level of internal stresses forming during cooling of melting layer.

P07.OC.011 PHASE TRANSITIONS, ELASTIC CONSTANTS AND ELECTRON DISTRIBUTION IN KDP-FAMILY. M.T. Medetbekov[1,2], Hassel Ledbetter[3], Sudook Kim[3], Boris N. Kodess[1,2], L.A. Butman[2] , Z.K. Gubaydulin[1,2], [1]Department of Crystal Metrology, VNIIMS, 119361 Moscow, Russia, [2] ICS&E, Aurora, CO 80012, USA, [3] Materials Reliability Division NIST, Boulder, CO 80303, USA

Using single and powder X-ray diffraction at temperatures of 295, 250, 220, 210, 200, 100, and 90 K, electron paramagnetic resonance, EPR, and acoustic-resonance spectroscopy we studied $K(H_2-D_2)PO_4$-family that show order-disorder phase transformations. In solid solutions one sees unusually high "isotopic effect" for all characteristics including 90 degrees increase of T_c when 90% of Deuterium is substituted by Hydrogen. This leads to a far from equilibrium state of the system with bifurcated hydrogen bonds. The high sensitivity of such a "precritical" system to factors such as high pressure, plastic deformation and deformation fields arising due to vacancies, doped elements, irradiation and others was established. Difference Fourier synthesis and elastic-stiffness tensor C_{ij} constants at ambient temperature give evidence that KDP differs from DKDP both for electron structure and dynamic-lattice-parameters. The first 38 measured resonance frequencies are plotted versus the predicted frequencies based on two analyses: an elastic analysis and a piezoelectric analysis. For DKDP, agreement between measurement and prediction is better for the nonpiezoelectric analysis, against many literature reports for the KDP (KH_2PO_4).

The reversible phenomena was established after irradiation for both poly- and monocrystals. Relaxation of the EPR spectrum associated with birth and dissolution of color centers and changes of structural parameters after perturbation actions were more noticeable for DKDP. The data is reviewed from the point of view of "before T_c" nucleation of tetragonal phase and the fact that mobility of domain walls is significantly higher for DKDP.

P07.OC.012 PHASE TRANSITON AND SECOND HARMONIC GENERATION OF A CYCLODEXTRIN COMPLEX WITH A NONLINEAR OPTICAL CHROMOPHORE. Ali N. Rashid, R. Shoemaker, K. Kirschbaum*, J. J. Stezowski, Department of Chemistry University of Toledo, Toledo OH, Department of Chemistry University of Nebraska-Lincoln, NE 68588.

Organic molecular crystals are of great interest due to their large nonlinear optical properties and their large damage threshold. Nonlinear optics is the study of the interactions of materials with electromagnetic fields to produce new fields, which are different in phase, frequency or modulation. One manifestation of which is second harmonic generation. However, most aromatic molecular crystals pack in a centrosymetric fashion, which forbids second harmonic generation (SHG). One way to assure that crystals will be non-centrosymmetric is to introduce naturally chiral components. This study uses β-cyclodextrin (β-CD), for this purpose and reports a study of a supramolecular inclusion complex that is formally a 3:2 guest-host complex with p-nitroanaline as the guest. Crystals of the complex, prepared by slow evaporation of an aqueous solution, display C2 space group symmetry at room temperature and $P2_1$ space group symmetry at 20K. The respective lattice parameters are: {a=19.5082, b=24.4657, c=15.9775 β=109.026 for C2 and a=15.733, b=23.845, c=19.496, β=109.362 for $P2_1$}. Efforts are underway to determine the temperature and character of the phase transition. Crystal structure determinations are in progress for the complex at room temperature and at 20K. Current R-values are R1 = 0.0694 for 6110 contributing data and R1 = 0.1170 for 14272 contributing data. There is considerable disorder in the guest molecules. Current interpretation of the structural models indicates some differences in the orientation of the guest

molecules at the two temperatures. In addition to further improvement in the crystallographic models, applications of other methods such as differential scanning calorimetry, solid state NMR spectroscopy and theoretical calculations are being pursued to further characterize the system.

P07.OC.013 THE PHASE TRANSITIONS IN THE FAMILY OF A-TYPE $A_3B_2X_9$ COMPOUNDS. P.E. Tomaszewski and A. Pietraszko, Institute of Low Temperature and Structure Research, Polish Acad. Sci., POB 1410, 50-950 Wroclaw, Poland, and A.M. Yaremko, Institute of Semiconductor Physics, Ukr. Acad. Sci., 252028 Kiev, Ukraine

The anionic sublattice of more than 200 known crystals with the formula $A_3B_2X_9$ are built up of at least 3 different networks. $Rb_3Bi_2Br_9$ and $Rb_3Sb_2Br_9$ belong to the rather rare type ***A***. The structure motif composed by 6-membered $(B_2X_9^{-3})_n$ layers is realised in different space groups from trigonal prototype structure with P-3m1 symmetry even to monoclinic Pc.

Our X-ray experiments were performed using KM-4 four-circle automatic diffractometer (CCD version) of *KUMA Diffraction* to reveal the possible changes of the structure when passes through the high temperature phase transitions suggested by the existence of the domain structure observed in polarised light. DSC studies revealed transitions at 378 K for $Rb_3Sb_2Br_9$ and at 319, 325 and 456 K for $Rb_3Bi_2Br_9$. Consecutive high-temperature X-ray studies showed the disappearance of diffraction peak splitting. The disappearance of domain structure indicates on the change of crystal system at the phase transition, thus, for the ferroelastic character of the transition. The crystal structure were solved in both, high- and room-temperature, phases. For $Rb_3Sb_2Br_9$: $P2_1$ with 13.683(1), 7.778(1), 19.264(2) Å, $\beta=90.335(9)^o$ at 290 K, P-3m1 with 7.889(4), 9.667(10) Å at 440 K; for $Rb_3Bi_2Br_9$: $P2_1/c$ with 13.6059(8), 7.9222(4), 19.4169(10) Å, $\beta=90.615(4)^o$ at 290 K. The prototype structures correspond well to that of $Cs_3Bi_2Br_9$. The characteristic feature is rather high thermal motion of the terminal bromines leading even to the atom splitting in the low-temperature phases. The phase transitions in our crystals are mainly due to the rotation of the BX_3 groups leading to the deformation of 6-membered rings and inclination of pseudo-trigonal axis b. This new mechanism was not observed in the compounds with organic A where the freezing of A-ions was responsible for phase transitions. The establishing of correct symmetry (different from that of literature) open a new regard to the family of $A_3B_2X_9$ crystals with a prototype P-3m1 phase.

07OD 'IN SITU' STUDIES USING POWDER DIFFRACTION

M07.OD.001 IN-SITU STUDIES USING POWDER DIFFRACTION. P. Norby, Department of Chemistry, University of Aarhus, DK-8000 Århus C, Denmark

The need for understanding, improving and controlling the properties of advanced materials has led to an increased interest in in-situ studies, i.e. characterization of materials under real working conditions or during formation. Time resolved in-situ powder diffraction has become a very valuable and versatile tool for studying synthesis, chemical reactions and phase transitions. Examples include studies of catalytical materials at real working conditions or synthesis of microporous materials under hydrothermal conditions. Information obtainable from this type of experiments include kinetics, real time observation of structural changes and detection and identification of intermediate or precursor phases.

The talk will present results from a number of time resolved in-situ studies using synchrotron and neutron powder diffraction. Special emphasis will be put on in-situ studies of hydrothermal synthesis of microporous and layered materials, intercalation reactions and thermal transformation and decomposition of inorganic materials. Results from a combined powder diffraction and MAS NMR study of dehydration and phase transitions of a cadmium-glycine complex will be given.

The recent implementation of a facility for time resolved in-situ synchrotron X-ray powder diffraction at the European Synchrotron Radiation Facility, ESRF, will be described. The facility is situated at the Italian beamline, GILDA, and consists of a capillary based microreaction cell, a hot air heater and a Translating Imaging Plate, TIP, system for collection of time resolved powder diffraction data. Results from the first experiments will be presented.

M07.OD.002 IN SITU X-RAY ENERGY DISPERSIVE STUDIES OF INTERCALATED COMPOUNDS. Christopher Hall, Schlumberger Cambridge Research, High Cross, Madingley Road, Cambridge CB3 0EL, UK.

Synchrotron energy-dispersive X-ray diffraction is an effective means of observing mineralogical changes in dense suspensions and pastes under hydrothermal conditions. In the context of oilfield materials engineering, we have studied in detail the behaviour of swelling clays stabilised with a variety of polymers of low molecular mass. These clay/polymer complexes are well defined intercalates and their formation can be observed through changes in basal spacing. Of particular interest is the thermal stability of such complexes. We have also exploited a tomographic form of the diffraction experiment to observe thin clay membranes exposed to solutions of varying composition. This work illustrates the way in which highly penetrating synchrotron X-rays can be used to monitor processes in bulk materials in complex sample cells.

M07.OD.003 ORDER-DISORDER REACTIONS IN MINERALS FROM NEUTRON POWDER DIFFRACTION. Alessandro Pavese, Dipartimento Scienze della Terra, Universita degli Studi di Milano, Via Botticelli 23, 20133-Milano, Italy.

Most mineral families undergo cation order-disorder (OD) reactions activated by temperature/pressure (Artioli et al, 1995; Pavese et al, 1999; Redfern et al, 1997); this subject has aroused an increasing interest in research, given that determining the cation partitioning as a function of *P* and/or *T* is key to get insight into the environmental conditions experienced at formation. OD-transformations can cause space group changes (convergent cation ordering, after Carpenter et al, 1994), or leave it unaffected (non-convergent cation ordering). Neutrons have reveled an appropriate radiation to investigate cation partitioning in crystalline matter, in especial because OD-reactions oftentimes involve quasi-isoelectronic atoms, hard to be reliably distinguished by X-ray. Furthermore, being the neutron scattering lengths independent on the θ-angle allows one to combine classic Rietveld refinement techniques (providing ''effective site scattering lengths'') with advanced minimization methods, for attaining the atomic distribution. Here a set of results encompassing micas/omphacites/spinels are presented, to provide an overview about how neutron powder diffraction is a flexible technique to cope with a variety of aspects pertaining to cation partitioning in natural/synthetic minerals, at non-ambient conditions.

In case of phengitic micas (sheet minerals), OD-reactions thermally activated lead to convergent ($3T \Leftrightarrow 2M_1$, *i.e.* polytype to polytype transformation promoted by particular *P/T* ratio conditions) and to non-converget cation ordering ($3T \Leftrightarrow 3T$, $2M_1 \Leftrightarrow 2M_1$), both due to the Mg/Al and Al/Si partitioning over the octahedral (M2, M3) and tetrahedral (T1, T2) sites, respectively (Pavese et al, 1997).

Omphacites (chain minerals) undergo convergent thermally activated OD-transformations (P2/n⇔C2/c) stemming from the Mg/Al/Fe and Ca/Na readjustment over the sixfold (M1, M11) and eightfold (M2, M21) coordination sites, respectively. A two steps process underlies this OD-reactions (Pavese et al, 1999).

Spinels (AB_2O_4) have been long investigated for their non-convergent OD-transfomations that originate from mixing over the tetrahedral and octahedral sites of A and B chemical species, as a consequence both of heating and of pressure (Pavese et al, 1999).

Artioli G, Rinaldi R, Wilson CC, Zanazzi PF (1995) Am. Miner. 80: 197-200.
Carpenter MA and Salje EKH (1994) Am. Mineral., 79, 1068-1083.
Pavese A, Artioli G, Hull S (1999) Am. Mineral. in press.
Pavese A, Bocchio R, Hull S (1999) Am. Mineral. in preparation.
Pavese A, Ferraris G, Prencipe M, Ibberson R (1997) Eur. J. Mineral., 9, 1183-1190
Redfern SA, Henderson CM, Knight KS and Wood BJ (1997) Eur J Min 9: 287-300.

M07.OD.004 IN-SITU KINETIC STUDY OF PORTLAND CEMENT HYDRATION. M. Bellotto, L. Bonafous, X. Launay, CTG Italcementi Group, Rue des Technodes, 78931 Guerville Cedex, France; S. L. Colston, A.C. Jupe, S.D.M. Jacques and P. Barnes, Industrial Materials Group, Department of Crystallography, Birkbeck College, Malet Street, London WC1E 7HX, UK. keywords: in-situ cement hydration, energy dispersive diffraction, synchrotron radiation powder diffraction.

The properties of a cement slurry result from a complex interplay of chemical and physical processes. With an ideal "well-behaved" paste its flow properties are maintained for a sufficient working period prior to rapid hardening to achieve the desired mechanical strength. To control such a behaviour additives are currently added to the mix of clinker and gypsum which constitutes normal Portland cement. Such additives, both mineral and polymeric, have several applications: to control the particle size distribution, to modify the liquid-phase composition and to modify the surface state of the mineral phases. A single additive, however, induces multiple effects and therefore its exact mechanism of action is difficult to elucidate. Thus, in order to develop less empirical formulation strategies, reliable kinetic data need to be acquired.

The hydration kinetics of several Portland cements (both laboratory-synthesized and industrial forms) have been monitored using velocity-imposed rheometric measurements and by synchrotron-based energy dispersive powder diffraction. In particular the effect of addition of poly-electrolytes on the nucleation and growth of the hydrates has been assessed together with the macroscopic effect on the flow characteristics. The reactions at the onset of hydration are critically dependent on the composition of the solution, both as mineral and polymeric ions. In particular the formation of ettringite from the solid tri-calcium aluminate and aqueous sulfate ions is modified by the presence of poly-electrolytes. Such a study has been made possible by use of (synchrotron) energy dispersive diffraction which is capable of collecting, in-situ, well resolved patterns from the complex multiphase pastes during hydration with time resolutions of the order of tens of seconds.

M07.OD.005 TOWARDS TIME RESOLVED NEUTRON DIFFRACTION: D20, A HIGH INTENSITY NEUTRON POWDER DIFFRACTOMETER. T. Hansen and P. Convert, Institut Laue-Langevin, BP 156, 38042 Grenoble Cédex 9, France.

The monochromatic beam of D20 has a high flux of up to $7.5 \cdot 10^7$ n·cm^{-2}·s^{-1}. Two vertically focussing monochromators give wavelengths of $\lambda = 0.9$, 1.3 or 2.4 Å. Soller collimators allow to adjust the divergence of the incident polychromatic beam. The Position Sensitive Detector (PSD) has a radius of 1.5 m and an aperture of 160° with 10 cells per degree (2θ) with *microstrip* detection electrodes. The 1600 cells are connected to 1600 amplifiers, followed by 1600 anti-coincidence logics and a fast Data Acquisition System (DAS) with parallel input, allowing counting rates up to $5 \cdot 10^4$ s^{-1} per cell.

The large stationary PSD, the high flux at sample, the choice of wavelength and resolution makes D20 a versatile instrument. It provides scientifically and experimentally a broad range of applications from numerous successive short acquisitions to follow the evolution of a sample up to long acquisitions to obtain a very high precision in intensity. Several representative experiments show these various fields: thermodiffractometry (phase transitions - crystallisation of amorphous Y-Fe-alloys, amorphisation of crystalline precursors), magnetism (magnetic structures of intermetallic $R_2T_3X_9$ and of Ag_2RuO_4), kinetics (dynamic studies of cement transformations and of battery charging), stroboscopy (orientation of flat or rod-shaped particles in moving suspensions under shear gradient - dynamic study at start and stop of flow), texture (quantitative texture analysis of composite materials), small samples (magnetic order on 3 mg sample in cryostat; preferred orientation in 1 mm slice of rat femur, 6 mg), absorbing samples (distances in natural Eu-hydrides), disordered systems (variation of mercury structure factor with density), physisorption (2D-ordered alcane monolayers on graphite).

The time-resolution of only seconds opens new opportunities for *in situ* neutron diffraction studies of solid state reactions. Therefore, tools, which will be suggested, are needed to analyse the huge amount of sequential powder diffractograms reliably and fast, and to extract the contained information completely.

P07.OD.001 IN-SITU X-RAY DIFFRACTION IMAGING OF POLYCRYSTALLINE MATERIALS. T. Wroblewski, Hamburger Synchrotronstrahlungslabor HASYLAB, Deutsches Elektronen-Synchrotron DESY, D-22603 Hamburg, Germany.

A novel method allows imaging using the radiation diffracted by polycrystalline samples [1] (and/or their fluorescence). It applies a micro-channel plate (MCP) as collimator in front of a position sensitive detector (CCD-camera) such allowing the position resolved detection of radiation from a sample area of more than 1 cm^2. The spatial resolution is proportional to the sample to detector distance (currently 12 μm for 12 *mm* distance).

The times to obtain an image displaying the radiation diffracted by a polycrystalline specimen into the direction of the MCP reach from few minutes down to less than a second allowing the observation of dynamic processes.

One example is the recrystallization of cold rolled copper during annealing [2]. The fact that the entire sample is probed simultaneously throughout the whole process enables the observation of early stages of the nucleation and growth processes without prior knowledge of where such processes occur.

It was shown that, after a certain growth period, the size of the individual crystallites remains constant. No correlation between the time of nucleation and the final size of the crystallites could be observed but the whole process can be described by the model of self organized criticality also applicable to 1/f-noise [3].

Further investigations in the field of materials process characterization like that of an electric light bulb during operation or of polymers during deformation will be presented.

1 T. Wroblewski et al., X-ray Imaging of Polycrystalline Materials, Rev. Sci. Instrum., **66** (1995) 3560
2 T. Wroblewski, E. Woldt, Non-ambient μ-diffraction, to be published in Advances in X-ray Analysis **42**
3 P. Bak, Ch. Tang & K. Wiesenfeld, Phys. Rev. Lett **59** (1987) 381

P07.OD.002 *IN SITU* POWDER DIFFRACTION STUDIES OF HYDROTHERMAL SYNTHESIS OF LAYERED TITANIUM PHOSPHATES. A. M. Krogh Andersen, Department of Chemistry, Odense University, DK-5230 Odense M, Denmark and P. Norby, Department of Chemistry, University of Aarhus, DK-8000 Aarhus C, Denmark.

We have studied hydrothermal synthesis of α-$Ti(HPO_4)_2 \cdot H_2O$, using *in situ* time-resolved synchrotron powder diffraction. The starting materials for the synthesis were amorphous titanium phosphate and phosphoric acid (85 %). The samples were contained in sealed quartz capillaries. When synthesis above 100°C was performed an external pressure was applied to obtain hydrothermal conditions. A position sensitive detector was used, enabling fast data collection. Full powder patterns were obtained in 30-60 seconds. The syntheses were performed at temperatures from 50 to 200°C.

Preliminary results show that the crystallisation of α-$Ti(HPO_4)_2 \cdot H_2O$ starts at approximately 50°C and the crystallisation kinetics was followed up to 130°C. The amount of crystalline material was estimated from integrated intensities of selected reflections in the diffraction pattern. The crystallisation curves were fitted using a first order rate expression. At higher temperatures transformation of α-$Ti(HPO_4)_2 \cdot H_2O$ to β-$Ti(PO_4)(H_2PO_4)$ was observed.

P07.OD.004 In-Situ POWDER DIFFRACTION STUDIES OF DISORDER TRANSFORMATIONS IN BROWNMILLERITES. S.A. Speakman and S.T. Misture, NYS College of Ceramics at Alfred University, 2 Pine St., Alfred, NY 14802, USA

In-situ powder diffraction is used to investigate the order-disorder transformations in modified Brownmillerite materials. The affect of cation selection and doping on the anion order-disorder transformation temperature is examined using high temperature x-ray diffraction. In addition to simply determining phase transformation temperatures, in-situ XRD using position-sensitive detectors allows quantification of the reactions with time. The extent of disordering that occurs is measured in an attempt to determine if the systems fully disorder or only partially disorder. The structural changes observed using in-situ XRD are correlated to changes in the ionic conductivity of the materials.

In-situ diffraction results on barium indate and several iron-based brownmillerites demonstrate that the 'disordered' materials are not straightforward random cubic structures, even several hundred degrees above the disordering temperatures.

The diffraction study is aided by computer simulation to further understand the defect structure and stability of potentially important materials. Successful calculation of stable crystal structures of In and Fe-based Brownmillerite ceramics and subsequent experimental investigations are presented. The computational methods employed rely on ionic potentials, namely the Buckingham potential and core-shell pairs for polarizable ions. Lattice parameters and ion coordinates agree with experiment. In addition, a defect analysis using the Mott-Littleton approach has shown that Schottky pairs are expected to form, and their association energies have been calculated.

P07.OD.005 A NEW HEATING DEVICE FOR X-RAY POWDER DIFFRACTION STUDIES UNDER WATER VAPOUR PRESSURES UP TO 1000 MBAR. M. Oetzel, F.-D. Scherberich, G. Heger, *AiXtal* Institute for Crystallography, RWTH Aachen, D-52066 Aachen, Germany

Hydration and dehydration procedures in science as well as in industry are very sensitive not only on time and temperature but also on environmental water vapour pressure. Hence, in situ diffraction studies under controlled temperature and defined water vapour pressure conditions can be very helpful to study such processes.

To satisfy the diverse demands a new heating cell for a Siemens D 500 powder diffractometer has been constructed [1]. With this device it is possible to examine powder specimens under water vapour pressures up to 1000 mbar in a sample temperature range from 20°C to 1000°C. Because the environment of the sample is heated separately, examinations under constant water vapour pressures as well as under constant relative humidities can be done up to an environment temperature up to 200°C.

The presented HT unit consists of a moulded Pt or Cu block with a resistance heating. The encapsulated thermocouple is mounted between the heating and the surface of the block to ensure the best possible controlling of sample temperature. The half circle shaped cover is also resistance heated and has a double layered window made out of capton foil. The space between the foils can be floated with hot dry air to prevent water condensation at higher water vapour pressures. Humidity and air temperature in the chamber are sensor controlled.

With the above described heating device, which has already proven its performance in an application for the gypsum industry [2], a combination of time-resolved, temperature- and humidity-controlled X-ray diffraction is now applicable.

We gratefully thank the SICOWA Verfahrenstechnik für Baustoffe GmbH & Co. KG , Aachen, Germany for financial support.

[1] Oetzel, M. et al., Powd. Diffr. (to be published)
[2] Oetzel, M. et al., ZKG International (to be published)

P07.OD.006 TIME-RESOLVED STUDIES USING SR:INTERMETALLIC SYNTHESIS. Å.Kvick, C.Curfs, G.Vaughan [1], M.A.Rodrigues, I.G.Cano [2], X.Turillas [3], [1] ESRF,BP 220,38043 Grenoble Cedex, France, [2] Inst. de Ceramica y Vidrio,Arganda del Rey, Madrid, Spain, [3] Inst Eduardo Torroja,Madrid,Spain

The Materials Science beamline (ID11) at the ESRF has been instrumented to follow reactions in-situ on a time-scale down to ~4 millisecs using a high- speed CCD camera coupled to an image-intensifier X-ray sensitive detector with 1000*1000 pixel frames. The pixel resolution is 100 microns. This set-up has been used to follow self-propagating high-temperature syntheses (SHS) in the quarternary system Al-Ni-Ti-C in order to obtain inter-metallic ceramic composites. These products have properties that make them highly attractive for many industrial applications.They have low density,excellent oxidation resistance and high melting points (~1900K). Unfortunately poly- crystalline AlNi has poor ductility and low wear resistance due to poor creep resistance at high temperatures. These problems may be overcome by reinforcement by aluminum oxide fibres or ceramic powders. These reactions have been studied by time-resolved powder diffraction on very short time-scales. The initial powder mixtures were pressed to cylinder specimens and the reaction were started by a spark at one end of the cylinders. A highly collimated X-ray beam at high energy has been used to record diffraction patterns from a specific region of the starting pressed powder cylinders in transmission. As the reaction proceeds along the cylinder the powder patterns from the initial sample, the pre-heated region, the reaction front ,post-heated region and the final product have been recorded. The phases occurring during the processes have been identified and information on the reaction mechanisms and nucleation kinetics have been obtained.

07OE AMORPHOUS MATERIALS: SMALL ANGLE SCATTERING

M07.OE.001 X-RAY AND NEUTRON SMALL ANGLE SCATTERING WITH AMORPHOUS Si-C-N CERAMICS. P. Lamparter, S. Schempp, J. Bill and F. Aldinger, Max-Planck-Institut für Metallforschung, D-70174 Stuttgart, FRG.

Precursor-derived ceramics present a novel type of materials for high temperature applications. Amorphous Si-C-N ceramics were produced by pyrolysis of different polymers at 1050 °C. Small angle scattering revealed an inhomogeneous structure on a length scale of some ten Å. From the contrast between X-ray and neutron scattering it could be deduced that the inhomogeneities are amorphous Si_3N_4 precipitates embedded in a carbon-enriched Si-C-N matrix. A theoretical model is presented on the base of a polydisperse system of positionally correlated hard spheres which is able to describe the experimental scattering curves. Further heat treatments of the ceramics up to 1450 °C cause a coarsening of the inhomogeneous structure where the volume fraction of the Si_3N_4 precipitates does not change. The kinetics of this process is described by a Gibbs-Evett-Leake model.

M07.OE.002 STRUCTURAL TRANSFORMATIONS IN NANOSTRUCTURED MATERIALS. A.F. Craievich, Instituto de Física, CP 66318,05315-970, USP, São Paulo, SP, Brasil.

SAXS combined with the use of i) a powerful X-ray incoming beam produced by electron storage rings and ii) a cell for temperature control of the sample, offers interesting possibilities for studying *in situ* structural transformations occurring in materials which are heterogeneous at a nanometric scale. This type of study aims at the characterisation of i) the different structures formed during the transformations and ii) the kinetical aspects of the processes. This last information provides an insight into the physical and/or chemical mechanisms involved in the structural transformations. Different mechanisms are active in the several stages of the sol-gel process for material preparation, such as aggregation in liquid phase, gelation, drying and sintering. The precursors may be solutions of organic alkoxides and the final systems powdered or monolithic and nearly homogeneous materials. Since all intermediate structures along the process are heterogeneous at a nanometric scale, the whole transformation can be monitored using only SAXS. The different composite materials may be structurally very simple, e. g. nearly single-mode spherical particles, embedded in a homogeneous matrix. Alternatively, they may be very disordered and exhibit fractal structures, as is the case of a number of gels and aerogels. Several investigations on nanostructured materials, including semiconductor (PbTe, CdSe, CdSTe) and metallic (Ag) nanocrystals embedded in a glass matrix, different silica based precursor sols, gels produced by monomer aggregation and xerogels which result from drying of wet gels, will be reported. Recently published results on organic-inorganic nanostructured hybrid materials will be presented. An example in which it is shown how ASAXS provides useful information on complex systems consisting of a nanoporous matrix containing semiconductor nanocrystals will be described. The recent SAXS experiments reported in this communication were performed at the synchrotron facility of LNLS, Campinas, Brazil, and the others at LURE, Orsay, France.

M07.OE.003 MAGNETIC MICROSTRUCTURE OF NANOSTRUCTURED METALS STUDIED BY SMALL-ANGLE NEUTRON SCATTERING. J.F. Löffler, California Institute of Technology, W. M. Keck Laboratory, Pasadena, CA 91125, USA. and H.B. Braun and W. Wagner, Paul Scherrer Institut, CH-5232 Villigen PSI, Switzerland. and A. Wiedenmann, Hahn-Meitner-Institut, D-14109 Berlin, Germany. and G. Kostorz, ETH Zürich, Institut für Angewandte Physik, CH-8093 Zürich, Switzerland.

In consolidated nanostructured materials, i.e. in bulk materials with grain sizes in the nanometer range, the grain size is comparable to or even smaller than the width of a domain wall. Thus, the resulting macroscopic magnetic properties are largely determined by the grain size and the exchange interactions between adjacent grains. In Fe, for example, we find a maximum of the coercive field at a size of around 35 nm with a steep decrease towards smaller grain sizes.

In order to understand in more detail the connection between microscopic structure and macroscopic behavior, we performed magnetic small-angle neutron scattering experiments on nanostructured Fe, Co and Ni. The experiments reveal spontaneous (zero-field) magnetic correlations across the interfaces, which extend over many individual grains. The correlation length strongly depends on grain size and exhibits a minimum, which for Fe lies in the range of 35 nm. For grain sizes below this minimum length scale the correlation length sharply increases.

We explain our results on the basis of a random-anisotropy model. This model takes into account that the effective anisotropy constant results from a statistical average of the anisotropies of the magnetically coupled grains. Based on a detailed quantitative discussion of the interplay between grain size and pinning, we find that the random-anisotropy model breaks down at a length scale $\pi\delta$ with δ the bulk domain-wall width. This is in excellent agreement with our experimental results on Fe, Co and Ni.

We further investigated in detail the response of the intergranular magnetic correlations to external fields. We find that the magnetization relaxation occurs via rotation of entire domains, which confine several grains. This behavior can be explained by a modified Stoner-Wohlfarth model.

M07.OE.004 SMALL ANGLE SCATTERING STUDIES ON A PRESSURE INDUCED PHASE TRANSITION IN A TERNARY MICROEMULSION. H. Seto, D. Okuhara, Y. Kawabata, and T. Takeda, Faculty of Integrated Arts and Sciences, Hiroshima University, 1-7-1 Kagamiyama, Higashihiroshima 739-8521, Japan, and M. Nagao, Neutron Scattering Laboratory, Institute for Solid State Physics, The University of Tokyo, 106-1 Shirakata, Tokai 319-1106, Japan .

A pressure induced phase transition from droplet to lamellar / bicontinuous structure in a ternary microemulsion was investigated by means of small angle neutron scattering (SANS), X-ray scattering (SAXS) and neutron spin echo (NSE).

A mixture of surfactant AOT (dioctyl sulfosuccinate sodium salt), water and n-decane is known to form microemulsion, whose characteristic repeat distance is about 100 Å. At room temperature and ambient pressure, its structure is known to be a water-in-oil droplet in wide range of volume fractions of three ingredients. Recently, Nagao and Seto observed a pressure induced phase transition to a coexistence phase of lamellar and bicontinuous structures for some mixtures with the same water to oil ratio [1]. Although the mean repeat distance d at ambient pressure depends on a surfactant concentration, d of the lamellar was the same for all the samples observed, and the disorder parameter d/ξ, of the bicontinuous structure could be scaled with $P\text{-}P_s$, where ξ a correlation length and P_s a transition start pressure.

When a molar ratio of water to AOT is kept at 40.8, the radius of each droplet is determined to be about 50 Å, and only the droplet volume fraction ϕ is increased with decreasing decane volume fraction. In this study, a pressure dependence of the structure of the microemulsion system was investigated for various droplet concentrations $0.35 < \phi < 0.7$. Static features were clarified by means of SANS and SAXS, and dynamic features by means of NSE.

1. M. Nagao & H. Seto (1999), Phys. Rev. E **59**, No. 3 (1999).

M07.OE.005 INDUCED STRUCTURAL CHANGES AT PARAFFIN-GRAPHITE INTERFACES. E.P. Gilbert, P.A. Reynolds and J.W. White, Research School of Chemistry, Australian National University, Canberra, ACT 0200, Australia.

Small-angle X-ray Scattering has been used to investigate the structures and phase behaviour of normal paraffins, with carbon number, *n*, between 10 and 20, when adsorbed on and inside the gallery structures present in exfoliated graphite. Ordering of the hydrocarbon molecules occurs at the interface and this surface crystalline structure persists at least thirty degrees above the melting temperature of the bulk crystalline phase. The surface-adsorbed structure is a lamellar arrangement different from the bulk phase. Below the bulk melting point, T_m, and for alkanes with even *n*, two distinct diffraction peaks are observed in the small-angle region, one associated with the bulk phase and the other with the surface structure. For alkanes with odd *n*, only one peak is observed below T_m; above T_m a significant reduction in peak intensity is found, indicating melting of the bulk, but a peak remains. The peak intensity at $T = T_m$ increases with *n*, indicating increasing surface stabilisation with increasing chain length. The separation between T_m and the temperature at which the diffracted intensity is greatest decreases as *n* increases and the values of the former agree well with values associated with a metastable phase transition observed previously.

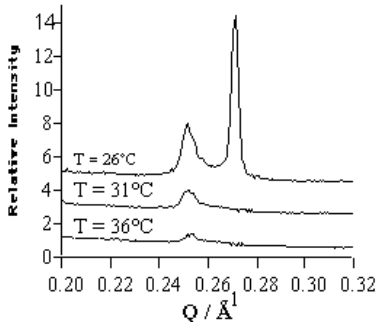

SAXS patterns for *n*-octadecane adsorbed on graphite at 26, 31 and 36°C.

P07.OE.001 PHASE BEHAVIOUR OF BLENDS OF LINEAR AND BRANCHED POLYETHYLENES VIA ULTRA-SMALL-ANGLE NEUTRON SCATTERING. M. Agamalian and G.D. Wignall, Oak Ridge National Laboratory*, Oak Ridge, TN 37830-6393, USA, R.G. Alamo, Florida Agricultural and Mechanical University and Florida State University College of Engineering, Tallahassee, FL 32310, USA, L. Mandelkern, Institute of Molecular Bio-physics, Florida State University, Tallahassee, FL 32306, USA.

Small-Angle Neutron Scattering (SANS) experiments have indicated that mixture of linear (high density) and long chain branched (low density) polyethylenes (HDPE/LDPE) from a one-phase mixture in the melt [1]. However, the maximum spatial resolution of pinhole SANS camera is ~ 10^3 Å and it has been suggested [2] that such experiments do not provide unambiguous evidence for a homogenous melt. Thus the SANS data might also be interpreted as arising from a bi-phasic melt with a very large particle size (~ 3 μm), because most of the scattering from the different phases would not be resolved. We have addressed this hypothesis by means of Ultra-Small-Angle Neutron Scattering (USANS) experiments, using a newly developed Bonse-Hart USANS facility [3], which can resolve particle dimensions up to 30 μm. The experiments confirm that HDPE/LDPE blends are homogenous in the melt on the length scales probed by pinhole SANS and by USANS. Blends of linear and short-chain branched polyethylenes phase separate when the branch content is sufficiently high [4]. It is shown that USANS resolves both the size of the dispersed phase (~ 4 μm), and the forward cross-section [$d\Sigma/d\Omega(0) \sim 10^8$ cm^{-1}], which is six orders of magnitude higher than for homogenous blends.

*Managed by Lockheed Martin Energy Research Corp. under contract DE-AC05-84OR2140 for the U.S. Department of Energy.

1. R.G. Alamo et al (1994) Macromolecules, 27, 411.
2. C. Schipp et al (1996) Polymer, 37, 2291.
3. M. Agamalian et al (1997) J. Appl. Crystallogr., 30, 345.
4. R.G. Alamo et al (1997) Macromolecules, 30, 561.

07OF CATALYSTS AND SURFACES

M07.OF.001 FIRST-PRINCIPLES CALCULATION OF THE STRUCTURE OF OXIDE SURFACES. S.P. Bates, Department of Chemistry, Trinity College, University of Dublin, Ireland

The capability of first-principles simulation methods to predict the surface structure of oxides is demonstrated, with the examples of the low index surfaces of TiO2 and SnO2. The computational technique is based on density functional theory and the pseudopotential approximation and utilises a parallel code that can be run efficiently on multi-processor PC's, as well as large supercomputers. Particular attention is focussed on the choice of suitable calculation variables and their effect on the predicted surface structures. These accurate theoretical descriptions of the surface form the starting points of simulation of simple reactions and processes.

M07.OF.002 MELTING OF N-ALCOHOL MONOLAYERS ON GRAPHITE: EFFECT OF MOLECULAR LENGTH. K.Morishige, Department of Chemistry, Okayama University of Science, Okayama 700-0005, Japan

The structures and melting of n-alcohols(methanol to nonanol) adsorbed on graphite have been studied by x-ray diffraction.

All the monolayers of n-alcohols studied here consist of rows of molecules in a head-to-head arrangement with OH groups close to each other and zigzag chains of hydrogen bonds occur along the short axis of the unit cell. Melting behavior shows odd-even effect of carbon atom number in the range of carbon number of 2-7[1]. Two-dimensional smectic liquid crystals are formed in melting processes of the complete monolayers of odd alcohols while those of even alcohols melt directly into liquids. Octanol and nonanol show different behavior of melting, suggesting a different mechanism of melting.

1. K.Morishige & Y.Sakamoto(1995). J.Chem.Phys.,103,2354.

M07.OF.003 INTERFACE INDUCED STRUCTURE IN CONCENTRATED SURFACTANT SOLUTIONS. S.A. Holt and J.W. White, Research School of Chemistry, Australian National University, ACT 0200, Australia.

We have demonstrated that grazing incidence diffraction studies of mesoporous films self-assembled at the air/liquid interface can be carried out in very short periods of time with image plates at synchrotron sources [1]. The structure of concentrated surfactant solutions at the air/liquid interface is also amenable to study by this method. The high flux available at third generation sources means that data can be collected over a wide range of reciprocal space in less than one minute. We have applied this method, in conjunction with specular reflectivity, to the study of concentrated solutions of cetyl trimethylammonium chloride solutions as a function of temperature and concentration. Not only are we able to observe that the surface ordering decreases with concentration (25 – 6 wt%) but that for a given concentration there exists surface phase transitions as a function of temperature.

S.A. Holt, G.J. Foran & J.W. White. L*angmuir*. Accepted for Publication (1999).

M07.OF.004 ELUCIDATING METAL SURFACE COMPOUNDS: PUTTING CRYSTAL STRUCTURAL INFORMATION TO WORK. S. G. Harris, R. O. Gould, D. A. Nation, S. Parsons, P. A. Tasker and R. E. P. Winpenny, Department of Chemistry, The University of Edinburgh, Edinburgh EH9 3JJ, UK.

It goes without saying that metals and their alloys play a huge role in our society. It is an obvious concern then that all metals, with the exception of gold, are thermodynamically unstable with respect to oxygen in acid solution, which means that the writing is on the wall for all our metallic artefacts. Although all metals exposed to the atmosphere suffer eventual degradation, the kinetics of corrosion are often slowed by passivation, such as the formation of a stable oxide layer on aluminium.

Metals can be further stabilised by application of specific organic additives, which are thought to form impervious, insoluble films. However, hampering the science of corrosion protection is the lack of information about structural compositions of such films, even after attempts to probe with surface physical experiment.

We are striving to contribute structural information to this field using molecular modelling techniques. It is known that surface films are coordination complexes and so must have analogous structural features to 'small molecule' complexes. This allows us to parallel any surface simulations with comprehensive search & analysis of relevant structural data available both locally and in the CSD [1]. In this way we have been able to shed light on surface films formed by various organic 'actives' on iron [2], copper and aluminium. A case study will be presented.

[1] F. H. Allen and O. Kennard, *Chemical Design Automation News*, 1993, **8(1)**, 1 & 31-37.

[2] M. Frey, S. G. Harris, J. M. Holmes, D. A. Nation, S. Parsons, P. A. Tasker, S. J. Teat and R. E. P. Winpenny, *Angew. Chem. Int. Ed.*, 1998, **37(23)**, 3245-3248.

M07.OF.005 SPONTANEOUS CHIRAL SEPARATION IN LANGMUIR MONOLAYER FILMS AND CHIRAL DISORDER. I. Kuzmenko, M. Lahav and L. Leiserowitz, Department of Materials and Interfaces, the Weizmann Institute of Science, Rehovot 76100, Israel, K.Kjær, Condensed Matter Physics and Chemistry Department, Risø National Laboratory, DK-4000 Roskilde, Denmark, Jens Als-Nielsen, Niels Bohr Institute, H.C.Ørsted Laboratory, Copenhagen, Denmark

Spontaneous separation of enantiomers, discovered by Pasteur some 150 years ago, is driven by the same thermodynamic and kinetic factors both in two- and three-dimensional crystals. However, amphiphilic crystalline monolayers at an interface cannot possess a center of inversion, the most common symmetry element in bulk crystals. This fact should in principle lead to better chances for spontaneous separation in the Langmuir or Langmuir-Blodgett monomolecular films. On the other hand, the monolayers of most amphiphiles studied to date incorporate long aliphatic chains that have an intrinsic tendency to pack in a herring-bone motif requiring glide plane symmetry, thus creating a bias towards racemate formation. Moreover, 2D crystals supposedly have much higher degree of molecular and therefore enantiomeric disorder compared to bulk crystals. All these factors necessitate a careful choice of molecules to guarantee enantiomeric separation in two-dimensions.

We made use of acid-base interactions between two different chiral amphiphilic molecules (p-pentadecylmandelic acid and p-tetradecylphenylethylamine) to achieve spontaneous chiral segregation from a racemic mixture at the air-water interface, as shown by grazing incidence X-ray diffraction. The extent of possible chiral disorder for the two acid and base components is examined. We show that even in apparently crystalline monolayers the oblique lattice symmetry is insufficient evidence for spontaneous segregation of chiral molecules in two dimensions due to possible chiral disorder.

P07.OF.001 STRUCTURE, COORDINATION, AND VIBRATIONAL FREQUENCIES OF DI- AND MONOMETHYL ALUMINUM, ZINC, AND BORON DERIVATIVES ON A CHEMICALLY MODIFIED SiO_2 SURFACE. S.K. Ignatov and A.G. Razuvaev, Department of Chemistry, University of Nizhny Novgorod, pr. Gagarina 23, Nizhny Novgorod 603600, Russia, and A.A. Bagatur'yants and M.V. Alfimov, Photochemistry Center, Russian Academy of Sciences, ul. Novatorov 7a, Moscow 117421, Russia, and O. Gropen, Department of Chemistry, Faculty of Science, University of Tromsø, 9037 Tromsø, Norway

The geometrical and electronic structure of di- and monomethyl aluminum, zinc, and boron surface groups bonded to a SiO2 surface have been studied using *ab initio* clusters calculations at the HF/6-31G(d), MP2/6-31G(d), and B3LYP/6-31G(d) levels. The effects of boundary conditions and the effects of the cluster size have been examined using various cluster models. Minimal clusters $(H_3SiO)_3Si–O–Al(CH_3)_2$, $(H_3SiO)_3Si–O–ZnCH_3$, and $(H_3SiO)_3Si–O–B(CH_3)_2$ correctly describe the geometry and the main physical properties of the corresponding surface groups. Various coordination modes of the organometallic surface groups under consideration have been examined. The vibrational frequencies and IR intensities of di- and monoalkyl surface derivatives have been calculated at the B3LYP/6-31(d) level for various surface models. Experimental IR bands of silica with chemisorbed trimethylaluminum have been interpreted based on the calculated results. The observed IR bands of trimethylaluminum deposited on a preannealed SiO_2 surface at low temperatures in regions of 2800-3000, 1400-1450, and 600-950 cm^{-1} have been assigned to vibrations of monoalkyl surface species and physisorbed trimethylaluminum. The evolution of the IR spectra of the modified silica surface on heating from 300 to 1273 K are assigned to monoalkylaluminum surface derivatives. The observed IR band at 868 cm^{-1} can be assigned to the vibrations of Si-O-Al cyclic structures.

07AA PROTEIN-NUCLEIC ACID INTERACTIONS

M07.AA.001 EUKARYOTIC GENE EXPRESSION: A STRUCTURALIST'S VIEW. S. K. Burley, The Rockefeller University & Howard Hughes Medical Institute

Gene expression in eukaryotes is regulated in response to a host of developmental and environmental signals, which direct individual cells and tissues to synthesize specific subsets of proteins required for homeostasis. Over the past three decades, biochemists and molecular geneticists have made enormous contributions to our knowledge of the diverse mechanisms by which gene expression is controlled during transcription, RNA splicing, and translation. At each of these three major synthetic steps en route to the gene product, highly-complex phylogenetically-conserved macromolecular assemblies are responsible for both chemical catalysis and regulation. With recent advances in synchrotron radiation, high-speed computing, and crystalline sample preparation/preservation, structural biologists are studying large macromolecular assemblies at the level of atomic detail. These structures are having a very considerable intellectual impact. They provide elegant mechanistic explanations for much of what we know, and are changing our experimental approach to molecular biology.

M07.AA.002 HUMAN TOPOISOMERASES I: STRUCTURE, ACTION, INHIBITION AND CANCER. W.G.J. Hol [1][2], M.R. Redinbo [1], L. Stewart [1], J.J. Champoux [3], [1] Department of Biological Structure, University of Washington, Seattle, WA 98195, [2] Howard Hughes Medical Institute, Box 357370, Seattle, WA 98195, [3] Department of Microbiology, University of Washington, Seattle, WA 98195.

Human topoisomerases I are co-responsible for maintaining the proper topology of DNA in cells. DNA is involved in numerous complicated processes and as a result does frequently become overwound or underwound. This has serious repercussions for the interactions of proteins with DNA - and hence it is essential that the proper topology of DNA is maintained all the time. Topoisomerases I are able to relax DNA by transiently breaking one strand, making a covalent link with one end of the break point, allowing the DNA to relax and resealing the broken strand. A much happier DNA is the result of this careful "controlled rotation" process and topoisomerases may therefore be considered as major psychotherapists in living cells, striving for optimal happiness of a complicated and elongated patient.

The crystal structures of several complexes of human topoisomerase I with DNA could be elucidated after inspecting over a thousand crystals on six different synchrotrons. The resultant structures provide deep insight into the functioning of this sophisticated enzyme. However, the mode of action of camptothecin and other so-called "topo poisons", two of which are in use for treatment of cancer, remains an intriguing puzzle so far.

M.R. Redinbo, L. Stewart, P. Kuhn, J.J. Champoux, and W.G.J. Hol 1998 Crystal Structures of Human Topoisomerase I in Covalent and Noncovalent Complexes with DNA. Science, 279:1504-1513.
L. Stewart, M.R. Redinbo, X. Qiu, W.G.J. Hol and J.J. Champoux 1998 A Model for the Mechanism of Human Topoisomerase I. Science, 279:1534-1541.
M.R. Redinbo, J.J. Champoux, W.G.J. Hol 1999 Structural insights into the function of type IB topoisomerases. Curr. Opin. Struct. Biol. 9:29-36.

M07.AA.003 MISMATCH RECOGNITION AND REPAIR BY THE *E.COLI* G:U/T MISMATCH GLYCOSYLASE. Laurence Pearl[1], Tracey Barrett[1], Orlando Schärer[2], Renos Savva[3], Tom Barlow[4], Tom Brown[4], George Panayotou[5], Jo Jiricny[6], Gregory Verdine[2], [1]Centre for Structural Biology, Chester Beatty Laboratories, Institute of Cancer Research; [2]Dept. of Chemistry and Chemical Biology, Harvard University; [3]Dept. of Crystallography, Birkbeck College; [4]Dept. of Chemistry , University of Southampton; [5]Ludwig Institute for Cancer Research, University College London; [6]Inst. for Medical Radiobiology, Zürich.

The mismatch specific MUG/TDG family of DNA glycosylases are able to initiate the base-excision repair of G:U, G:T and G:ethenoC mismatched base-pairs in DNA. Structural and biochemical studies of the E.coli MUG enzyme have revealed the structural basis for their specificity, which depends on recognition of the widowed guanine rather than the scissile pyrimidine 'flipped-out' into the active site. Structures of the free enzyme, and complexes with abasic products and trapped substrate DNA molecules, reveals the intricate conformational changes that accompany the base-excision reaction.

M07.AA.004 B-DNA AT ATOMIC RESOLUTION: HELIX END-CAPPING AND GROOVE INTERACTION BY NI-PORPHYRIN. M. Bennett, A. Krah, M.R. Sanderson [1], E. Garman [2], R. Mckenna, S. Neidle [3]. [1] The Randall Institute. Dept. of Biomedical Sciences. King's College, 26-29 Drury Lane, London WC2B 5RL, UK. [2] Dept of Molecular Biophysics, The Rex Richards Building , South Parks Road, Oxford OX1 3QU, UK. [3] CRC Biolmolecular Sciences Unit, The Institue of Cancer Research, Sutton, Surrey, Surrey SM2 5NG, UK.

The crystal structure of a hexameric B-DNA type duplex complexed with a metalloporphyrin has been solved by a MAD experiment and refined to an R-factor of 10.5% against 0.9Å data. Special aspects of this structure include its crystal packing arrangement, disordering of the sugar-phosphate backbone, weak vertical hydrogen bonds, hydration network, end-capping of DNA helices by porphyrin, end-to-end dimerisation of DNA helices, interaction of porphyrin meso-substituents in the minor DNA helical groove and buckling of the porphyrin ring.

The structure was solved by MAD data collection of crystals grown with the bromo-derivitised DNA sequence dCCTAGG. Phases to 1.6Å with a mean figure of merit of 0.86 were calculated, the electron density map was of a high quality with atomic centres clearly present. High resolution data has also been collected and the structure refined, the use of local non-crystallogrphic symmetry restraints proved critical. The structure exhibits bond lengths with rmsd of 0.02Å with other nucleotide structures.

M07.AA.005 INTERACTIONS OF THE *TRP* RNA-BINDING ATTENUATION PROTEIN WITH COGNATE SINGLE STRANDED RNA. A.A. Antson, E.J. Dodson, G.G. Dodson, York Structural Biology Laboratory, University of York, York Y01 5DD, UK and X.-P. Chen, P. Gollnick, Department of Biological Sciences, Cooke Hall State University of New York at Buffalo, Buffalo, NY 14260, USA.

X-ray structure of *trp* RNA-binding attenuation protein (TRAP) from *B.stearothermophilus* in complex with 53-base RNA molecule provides the structural basis for the transcription regulation of *trp* (*trpEDCFBA*) operon.

In several *Bacilli* transcription of the *trp* operon is regulated by TRAP, in response to changes in the intracellular concentration of L-tryptophan [1]. The TRAP molecule is an assembly of 11 identical subunits related by rotational symmetry

[2]. During transcription, when TRAP is activated by L-tryptophan, it binds specifically to a leader region of the *trp* operon RNA transcript. The cognate RNA region is organised as eleven GAG or UAG triplets separated by two or three nucleotide spacers [3]. By binding and arresting the RNA region, TRAP disrupts the formation of an "antiterminator" hairpin structure and allows formation of an alternative, transcription termination hairpin.

We have determined the structure of TRAP in complex with $(GAGAU)_{10}GAG$ 53-base RNA at 1.9Å resolution. In the structure, each GAG triplet is bound in a pocket formed by β-strands. The circular arrangement of TRAP subunits generates a belt of 11 GAG binding sites with a diameter of about 80Å. Each RNA triplet is bound specifically with almost no direct interactions formed between the sugar-phosphate backbone and the protein. Now crystals are also available for complexes of TRAP with several different RNA sequences. These structures will help to address the specificity of TRAP/RNA interactions.

1. P.Gollnick (1994). *Molecular Microbiology* 11, 991-997.
2. A.A.Antson, J.Otridge, A.M.Brzozowski, E.J.Dodson, G.G.Dodson, K.S.Wilson , T.M.Smith, M.Yang, T.Kurecki, P.Gollnick (1995). *Nature*, 374, 693-700.
3. P.Babitzke, J.T.Stults, S.J.Shire, C.Yanofsky (1994). *J.Biol.Chem.*, 269, 16597-16604.

P07.AA.001 T4 ENDONUCLEASE VII, A DNA JUNCTION RESOLVASE WITH A NEW FOLD AND AN UNUSUAL DOMAIN-SWAPPED DIMER. Hans Raaijmakers, Imre Törö, Dietrich Suck [1], Olivier Vix [2], Stephan Golz, Börries Kemper [3], [1] European Molecular Biology Laboratory, Meyerhofstrasse 1, 69117 Heidelberg, Germany, [2] Synthelabo Biomoleculaire, 16 Rue d'Ankara, F67080 Strasbourg, [3] Dept. of Genetics, Univ. of Cologne, Zülpicherstr. 47, 50674 Köln, Germany.

Phage T4 endonuclease VII (Endo VII) was the first enzyme shown to resolve Holliday junctions. Unlike other resolvases, e.g. yeast CCE1 or E.coli RuvC, Endo VII recognizes a broad range of branched DNA substrates ranging from cruciform DNA to single-base mismatches.The 2x18 kDa Endo VII shows little sequence homology with other resolvases and, as a unique feature, contains one zinc ion per monomer tetrahedrally coordinated by four cysteines, which is essential for stabilizing the fold.

We have determined the crystal structures of the Ca2+ -bound wild-type and the inactive N62D mutant enzymes at 2.5Å and 2.1Å, respectively. The Endo VII monomers, which do not have a stable fold on their own, form an elongated, highly intertwined molecular dimer exhibiting extreme domain-swapping. The major dimerization element are two pairs of antiparallel helices forming a novel '4-helix cross' motif. The two other domains are each made up of the 55 N-terminal of one and 50 C-terminal aminoacids of the other monomer. The unique fold, almost completely lacking ß-sheet structure and containing a zinc ion, does not resemble any of the known junction-resolving enzymes. The S-shaped dimer has two 'binding-bays' separated by about 24Å which are lined by positively charged residues and contain near their base residues known to be essential for activity. These include Asp40 and Asn62, which both function as ligands for the bound calcium ions. A pronounced bipolar charge distribution suggests that branched DNA substrates bind to the positively charged face with the scissile phosphates interacting with the divalent cations. A model for the complex with a 4-way junction consistant with the available biochemical data will be presented.

While the overall protein architecture is the same in both wild-type and N62D mutant structures, there is a significant change in the orientation of the rigid (N- and C)-terminal domains relative to the central dimerization domain. The position of two NCS related helices in the '4-helix cross' are each shifted roughly half a helical turn relative to each other without however disrupting the hydrophobic core of the dimerization interface.

We are currently refining the mutant structure to 1.3Å resolution and are crystallizing EndoVII - DNA complexes.

P07.AA.002 STRUCTURAL BASIS OF FIDELITY BY DNA POLYMERASE I ENZYMES. G. Waksman, Y. Li, S.V. Korolev, and V. Mitaxov, Department of Biochemistry and Molecular Biophysics, Washington University School of Medicine, Saint Louis, MO63110, USA.

Eleven distinct crystal structures of the large fragment of *Thermus aquaticus* DNA polymerase I (Klentaq1) have been determined. For example, the crystal structures of two ternary complexes of Klentaq1 with a primer/template DNA and dideoxycytidine triphosphate and that of a binary complex of the same enzyme with a primer/template DNA were solved to a resolution of 2.3, 2.3 and 2.5 Å, respectively (EMBO Journal, vol 17, pp7514-7525 (1998)). One ternary complex structure differed markedly from the two other structures by a large reorientation of the tip of the fingers domain. This structure, designated "closed", represented the ternary polymerase complex caught in the act of incorporating a nucleotide. In the two other structures, the tip of the fingers domain was rotated outward by 46^{o} ("open") and this orientation of the fingers domain was similar to that of the apo form of Klentaq1 (PNAS, vol. 92, pp9264-9268 (1995)). These structures provided the first direct evidence in DNA polymerase I enzymes for a large conformational change responsible for assembling an active ternary complex. More recently, the structures of three additional ternary closed complexes with primer/template DNA and incoming dideoxyadenosine triphosphate, dideoxyguanosine triphosphate, and dideoxythymidine triphosphate have also been determined to 2.3 Å each. Together with the previous ternary closed complex structure, these structures show a snug fit of the protein around the incoming nucleotide, thereby demonstrating that the protein displays remarkable plasticity within the active site. Only in one ternary complex, that of the primer/template/ddGTP/Klentaq1 complex, a large change in side chain conformation resulting in additional hydrogen bonding interactions with the incoming base was observed. These rearrangements may constitute a structural basis for the higher rate of ddGTP incorporation compared to other dideoxynucleoside triphosphates by Klentaq1.

P07.AA.003 THE STRUCTURE OF THE WILD TYPE DTXR-DNA COMPLEX REVEALS A METAL BINDING THIRD DOMAIN. Ehmke Pohl, Dept. of Biological Structure, University of Washington, Seattle, USA, Randall K. Holmes, Dept. of Microbiology, University of Colorado, Denver, USA and Wim G.J. Hol. Dept. of Biological Structure and Biochemistry, Howard Hughes Medical Institute, University of Washington, Seattle, USA.

The diphtheria toxin repressor (DtxR) is the best characterised member of a family of iron-dependent regulator proteins also designated IdeR in gram-positive bacteria. These regulators are activated by Fe(II) and bind DNA as a homo dimer to prevent the transcription of the following genes. In Corynebacterium diphtheriae DtxR controls the expression of several proteins involved in the iron-uptake as well as its major pathogenic factor Diphtheria Toxin [1].

Here, we report the crystal structure of wild type DtxR activated by Co(II) in complex with a synthetic 21mer duplex DNA at 3.2Å resolution [2]. The structure shows two DtxR dimers on nearly opposite sides of the DNA oligonucleotide without any dimer-dimer contacts. The activation mechanism appears to involve both metal binding sites and a hinge motion of the N-terminal DNA-binding domain with respect to the dimerization domain.

Furthermore, our crystal structure reveals crucial parts of the SH3-like C-terminal domain (residues 121-226) that has been absent in previous structures [3]. In all four crystallographically independent DtxR monomers this domain contributes to metal binding at site 1 with two conserved residues. This interaction for the first time suggest an essential role of the SH3-like domain in the activation mechanism of DtxR.

[1] J.H. Lee, K. Ault, J. Liu, M.P. Schmitt and R.K. Holmes (1997). Infect. Immun. 65 4273-4280.
[2] E. Pohl, R.K. Holmes and W.G.J. Hol (1999) submitted for publication.
[3] A. White, X. Ding, J. van der Spek, J.R. Murphy and D. Ringe (1998). Nature 394 502-507.

P07.AA.004 STRUCTURES OF A NOVEL COMPLEX OF NUCLEIC ACID AND A CATALYTIC FRAGMENT OF REVERSE TRANSCRIPTASE. Millie M. Georgiadis, Shabir Najmudin, and Dunming Sun, Waksman Institute, Dept. of Chemistry, Rutgers University, Piscataway, NJ

We have obtained a novel complex of a catalytic fragment of Moloney murine leukemia virus reverse transcriptase (MMLV RT) with nucleic acid and determined two crystal structures at 2.3Å resolution. Reverse transcriptase, an essential retroviral enzyme, uses RNA- and DNA-directed DNA polymerase activities and an RNaseH activity to produce a double-stranded DNA copy from the single-stranded RNA genome of the retrovirus. The catalytic fragment is comprised of the fingers and palm domains of RT and retains polymerase activity. Both crystal forms include two catalytic fragment molecules and a single symmetric 8/8-mer DNA molecule in the asymmetric unit. Each catalytic fragment molecule provides a binding site for the oligonucleotide. The protein-DNA interactions include primarily hydrogen-bonding interactions with sugar atoms and base atoms in the minor groove of the DNA. These interactions should be possible for any sequence of DNA or RNA. Two conserved residues in the fingers domain of the catalytic fragment are important for DNA binding, Asp 114 and Arg 116, which form an ion-pair in the complex. We now refer to this binding site as the DXR site. Six of the hydrogen bonds found in each binding site are the same, and four of these involve the side chain atoms of Arg 116.

In order to determine the functional significance of the DXR binding site, we have substituted Ala for Asp 114 or Arg 116 in the full-length MMLV RT and characterized the enzymes. The specific activities of the enzymes were similar, but the products generated in polymerase assays were significantly shorter for the substituted enzymes. The substitutions affect processivity of the enzymes, the ability to incorporate many nucleotides prior to product dissociation, indicating that the newly identified DXR site plays a role in translocation of nucleic acid during polymerization. Our crystal structures provide the first models of a proposed intermediate step important in the mechanism of translocation.

P07.AA.005 CRYSTAL STRUCTURE OF THE REPLICATION INITIATOR PROTEIN RepE54 OF MINI-F PLASMID COMPLEXED WITH AN ITERON DNA AT 2.6Å RESOLUTION. H. Komori*, F. Matsunaga**, Y. Higuchi*, M. Ishiai**, C. Wada** and K. Miki*. *Department of Chemistry, Graduate School of Science, Kyoto University, Sakyo-ku, Kyoto 606-8502, Japan. **Institute for Virus Research, Kyoto University, Sakyo-ku, Kyoto 606-8501, Japan.

DNA replication is provoked by the binding of initiator proteins to the region of DNA replication origin. Regulation of DNA replication by initiator protein binding is one of the most important issues for ordered cell proliferation. The RepE, replication initiator protein of mini-F plasmid in Escherichia coli, exhibits two major functions. RepE exists mostly as dimer and binds to operator of *RepE* as an autogenous repressor, which is so stable that chaperones are required to facilitate their monomerization and initiate replication. One mutant, RepE54, is stable in the monomeric form without aggregations, while the wild-type protein tends to form aggregations easily making crystallization difficult. We have successfully crystallized RepE54 complexed with DNA. Here, we report for the first time the crystal structure of the prokaryotic initiator protein (RepE54) complexed with DNA. The structure was solved by the multiple isomorphous replacement method and refined to R = 21.3% at 2.6Å resolution. The crystal structure of the RepE54-DNA complex showed a new type of the DNA-binding modes. RepE54 is composed of two distinct N- and C-terminal domains which are structurally similar to each other and related by a non-crystallographic dyad, although no such similarity has been expected from its amino acid sequence. The helix-turn-helix motifs of both domains bind to the major groove of DNA with different binding affinities. The recognition helix of the C-terminal domain makes multiple specific contacts with the DNA bases, while that of the N-terminal domain has nonspecific interactions with the DNA backbones. It is also found from hypothetical model of RepE dimer bound to the operator that the N-terminal domains of dimer face with each other and then are responsible for dimerization. The structure suggests that the C-terminal domain plays the leading role in DNA binding, while the N-terminal domain has the additional role in dimerization. This functional difference of both domains is essential for the differential binding to the origin and the operator.

07BB BIOINFORMATION AND DATABASES (sponsored by NIST)

M07.BB.001 IDENTIFICATION OF STRUCTURAL NEIGHBORS AND HOMOLOGOUS CORE STRUCTURES. S. Bryant. NCBI, NIH, Bethesda, MD 20894, USA.

NCBI's 3D structure database now contains roughly 30,000 protein domain structures and 3,000,000 structure-structure alignments (1). This information is accessible at http:/www.ncbi.nlm.nih.gov/Entrez/Structure, using a WWW browser and molecular graphics viewer (2). Structure "neighbours" are detected and aligned by the VAST algorithm (Vector Alignment Search Tool) (3). VAST identifies structural similarities that are surprising in a statistical sense, those where the number of secondary structure elements that may be superimposed is greater than one would expect to see by chance. VAST also computes the most surprising atomic superposition, by comparing the RMS and length of alternative alignments to the background distribution expected by chance. These statistical definitions are useful in a search and retrieval system, where one does not wish to bias results according to subjective judgements or classifications. It may nonetheless be difficult to interpret structural similarity, since this can alternatively indicate descent from a common ancestral gene or convergence to a stable folding architecture. To assist in this interpretation we define the HCS (Homologous Core Structure) of protein families and show that a test for the presence of the HCS is effective in discrimination of homologs and "analogs" among structure neighbours. In the talk I will describe VAST, the statistical similarity thresholds it employs, and recent research in definition of homologous core structures.

1. Marchler-Bauer A, Addess KJ, Chappey C, Geer L, Madej T, Matsuo Y, Wang Y, Bryant SH:MMDB: Entrez's 3D Structure Database. Nucleic Acids Research 1999, 27:240-243.
2. Hogue CWV, Ohkawa H, Bryant, SH: A dynamic look at structures: WWW- Entrez and the molecular modeling database. Trends Biochem. Sci. 1996, 21:226-229.
3 Gibrat J-F, Madej T, Bryant SH: Surprising similarities in structure comparison. Current Opinion in Structural Biology. 1996, 6:377-385.

M07.BB.002 ReLiBase - A DATABASE FOR ANALYSING RECEPTOR-LIGAND INTERACTIONS. Manfred Hendlich, Institute for Pharmaceutical Chemistry University of Marburg, Germany.

The dramatic increase of publicly available high resolution protein structures has resulted in an enormous amount of information about protein-ligand interactions. ReLiBase is the first database system which provides a selective and efficient access to structures of protein-ligand complexes. It has been designed to allow a wide range of queries relevant for structure based drug design. Ligands with certain topological properties and complexes with specific interactions between proteins and ligands can be identified within seconds to minutes. To enable a detailed characterisation of protein-ligand interactions a complete chemical description of protein ligands including bond orders and atom types has been added.

Recently, several new modules have been added to the ReLiBase core. This includes methods for detecting local similarities in binding sites of non-related proteins, tools for analysing and comparing water structures in binding sites and methods for analysing ligand induced conformational adaptations.

A custom-written database engine and a graphical user interfaces provide an efficient environment for the formulation of complex queries. ReLiBase is currently available to the academic community on the World Wide Web at the Protein Databank and the European Bioinformatics Institute.

M07.BB.003 CATH STRUCTURAL FAMILIES: INSIGHTS INTO PROTEIN EVOLUTION AND FUNCTION. Orengo, C.A, Bray, J., Todd, A. Pearl, F. & Thornton, J.M., Biomolecular Structure and Modelling Unit, University College, London

The rapid progress of the international genome projects has resulted in a wealth of sequence information for protein families. There are nearly 400,000 sequences known which can be grouped into ~20,000 families. Although the structural data has lagged behind the sequences, analysis suggests that with the advent of structural genomics initiatives we may soon have structural representatives for many evolutionary protein families. Since structure can provide crucial information on a protein's biological role, the next step is to accumulate and analyse functional data within these families.

At UCL, we have clustered all the well-resolved protein structures, in the PDB, into structural families. Proteins are first divided into separate domains and both sequence and structure alignment methods used to identify relationships. Data on families is stored within the CATH database (**C**lass, **A**rchitecture, **T**opology or fold and **H**omologous superfamily). To date, there are ~18,000 domains within CATH, which cluster into ~1100 homologous superfamilies and ~650 fold families.

Techniques are now being developed for assigning structural families to genome sequences. For example, we can identify probable families for >30% of proteins in Mycoplasma Genitalium (Salamov et al. 1999). Tools are also being developed for analysing available functional data within each homologous superfamily. Protein ligand interactions are identified and displayed (DOMPLOT, Todd et al. 1998) and correlations between sequence and structure motifs are captured using a new analysis program (CORA, Orengo, 1999).

M07.BB.004 IDENTIFICATION OF BIOISOSTERIC MOLECULES USING FIELD-BASED SIMILARITY SEARCHING. Peter Willett, University of Sheffield.

This paper discusses techniques for similarity searching in databases of three-dimensional chemical structures represented by steric, electrostatic and hydrophobic fields. Searches of several files of bioactive molecules demonstrate that field-based searching provides an effective way of identifying structural resemblances between molecules even in the absence of any obvious skeletal similarities. Such searches hence provide a method of database access that is complementary to existing, fragment-based methods for chemical similarity searching.

M07.BB.005 IDENTIFYING STRUCTURAL DOMAINS IN PROTEINS: IS THERE A UNIQUE SOLUTION? Shoshana J. Wodak [1,2], and Lorenz Wernisch[2], [1] Unte de Conformation de Macromolecules Biologiques, Universite Libre de Bruxelles, CP160-16, Ave. F. Roosevelt, 1050 Brusselles, Belgium. [2] EMBL Outstation, European Bioinformatics Institute, Wellcome Trust Genome Campus, Hinxton, Cambridge, CB10 1SD, UK.

The issue of subdividing protein molecules into structural and functional units has come up repeatedly over the last 25 years. In the early days the main emphasis was on identifying structural units capable of folding independently and of being stable on their own. Some attempts were made to link such units to exon/intron boundaries, and thereby with evolutionary processes. In recent years, with the number of known protein structures reaching over 10,000, the major incentive has been to devise automatic methods for identifying domains that can form the basis for a consistent protein classification.

Currently, there are over a dozen different methods for automatically assigning domains limits from the protein atomic coordinates. In general, the assignments by the different methods show only partial agreement. This has been interpreted as resulting primarily from the inherently difficulty in coping with the natural complexity of proteins, and dealt with by using consensus assignments by several methods.

We will discuss the concepts underlying the definitions of structural and functional domains, review the different types of approaches used to derive domain assignments and illustrate their application to protein structure classification protein folding and enzyme function.

P07.BB.001 THE GEOMETRY OF METAL-LIGAND INTERACTIONS RELEVANT TO PROTEINS. Marjorie M Harding, Institute of Cell and Molecular Biology, University of Edinburgh, Michael Swann Building, Edinburgh EH9 3JR, Scotland.

For a selection of metals (Ca, Mg, Mn, Fe, Cu, Zn at present) and ligands (water, carboxylate, imidazole, thiolate etc) which commonly occur in proteins geometrical data have been extracted from the Cambridge Structural Database, CSD [1] (*ca* 4500 observations, all with $R < 0.065$). Mean metal-donor atom distances are tabulated, together with sample standard deviation and range of observed values, for each metal-ligand combination. Where practicable subsets with different coordination numbers and/or oxidation state are given. Also included are interbond angles at the ligand donor atom, the orientation of carboxylate and imidazole groups and some other aspects of ligand geometry.

One objective of this work is to make the information conveniently available to protein crystallographers[2] – for use in interpretation of electron density maps, or as target distances in restrained refinement, when medium resolution diffraction data (2-3 A) must be used, also for the checking or validation of results of protein structure determination. Further, this analysis of preferred geometry and range of allowed geometry may contribute to the basic understanding of the function of different metals in metalloproteins .

Further work, in close collaboration with the Cambridge Crystallographic Data Centre, will analyse the geometry found in metalloprotein structures in the Protein Data Bank, selecting those which are more accurately determined. A pilot project[3] showed

that the mean of 146 Zn-$N_{imidazole}$ distances in 46 proteins, 2.07(11)A was not greatly different from that in 'small molecules', 2.00(2)A, although the 'spread ' of values was, as expected, much greater in the protein results.

[1] Allen, FH & Kennard, O (1993) Chem Design and Automation News, 8,1 & 31.
[2] Harding, M M (1999) Acta Cryst. D, *in preparation*.
[3] Gruneau,A (1998) University of Edinburgh.

P07.BB.003 OUR VISION FOR THE NEW PROTEIN DATA BANK. Helen M. Berman, John Westbrook, Kyle Burkhardt, Zukang Feng, Shri Jain, Rachel Kramer, Bohdan Schneider, Christine Zardecki [1], Peter Arzberger, Phil Bourne, John Badger, Helge Weissig [2], Gary Gilliland, Phoebe Fagan, Hillary Gilson, Diane Hancock, Narmada Thanki, Greg Vasquez [3], The Research Collaboratory for Structural Bioinformatics, [1] Rutgers University, Piscataway, NJ, USA, [2] San Diego Supercomputer Center, University of California, San Diego, USA, [3] National Institute of Standards and Technology, Gaithersburg, MD, USA

On October 1, 1998, the Research Collaboratory for Structural Bioinformatics (RCSB) became responsible for the management of the PDB. The RCSB members are Rutgers, the State University of New Jersey, the San Diego Supercomputer Center of the University of California, San Diego, and the National Institute of Standards and Technology.

The vision of the RCSB (http://www.rcsb.org/) is to enable new science by providing accurate, consistent, and well-annotated structure data via the application and development of modern information technology.

Data is deposited and processed by the RCSB using an integrated data processing system called ADIT (the AutoDep Input Tool). ADIT provides rapid and reliable data processing, and is also being used to revisit all existing structures in the PDB to create a more uniform archive.

The RCSB has also developed a query and reporting interface to search across the PDB archive. Searches and reports can be generated for single or multiple structures. As the quality of the data improves, the reliability of the query results will improve.

These systems and plans for extending the capabilities of the new PDB will be described.

This project is funded by the National Science Foundation, the Department of Energy, and two units of the National Institutes Of Health: the National Institute Of General Medical Sciences and the National Library Of Medicine.

07CC SHORT RANGE ORDER AND DIFFUSE SCATTERING

M07.CC.001 DIFFERENT APPROACHES TO THE PROBLEM OF DIFFUSE SCATTERING. R.I.Barabash, Metal Physics Department, National Technical University of Ukraine, apt.25, str. Proreznaya 4, Kiev, 252003, Ukraine.

The presence of point defects or precipitates in the crystals results in the appearance of intensive diffuse scattering around matrix reciprocal lattice points. The shape of isodiffuse surface depends on the symmetry of of displacement field caused by defects. For point defects with cubic symmetry of displacement field the shape of isodiffuse surface is always double-drop. The change of such symmetry to tetragonal one results in apple or single drop shape of isodiffuse surface. Matrix anisotropy results in the distortion of isodiffuse surface of scattering but the type of it is retained.

Symmetric part of the diffuse scattering coincides with classic Huang scattering while asymmetric part is first of all connected with the difference in structure amplitudes between host (A) and impurity (C) atoms. When matrix consists of two or more host atoms (for example A and B) additional weak peaks occur due two the difference between their structure amplitudes. Impurity atoms in such matrix result in the formation of diffuse scattering around all (both weak and strong) initial peaks. The formation of clusters increases asymmetry of diffuse scattering intensity distribution. With the increase of precipitate size the character of isodiffuse surface may be changed essentially. In case of small defect concentration phenomenological description of scattering is correct, for high concentration of defects it is necessary to use microscopical analysis. The characteristics of diffuse scattering intensity distribution are related to the defect concentration and the type of displacement field around them. It gives possibility to solve the inverse task of scattering and determine the parameters of real structure for solid solutions and precipitation related crystals.

M07.CC.002 DETERMINATION OF LOCAL DISORDER IN SiO_2 AT HIGH TEMPERATURE USING TOTAL SCATTERING. David A. Keen, ISIS Facility, Rutherford Appleton Laboratory, Chilton, Didcot, Oxon OX11 0QX U.K.

At high temperatures many crystalline materials display significant structural disorder which may not be straightforward to characterise in terms of an average structure. In contrast, the Fourier transform of the total scattering is a direct measure of the instantaneous local structure. In this talk I shall describe how, using a combination of Rietveld analysis and modelling of total scattering data, a more complete picture of high temperature structural disorder can emerge.

I shall illustrate this approach with examples from the high-temperature polymorphs of silica (quartz, tridymite and cristobalite) and compare their instantaneous local structures to the structure of quenched silica glass.

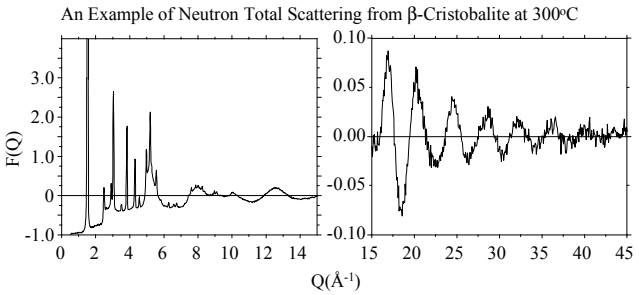

M07.CC.003 DIFFUSE SCATTERING AND MICROSTRUCTURE IN CRISTOBALITE AND TRYDIMITE TYPE STRUCTURES. H. Lemmens, G. Van Tendeloo, S. Amelinckx, EMAT, University of Antwerp, Groenenborgerlaan 171, B-2020 Antwerp, Belgium.

Electron diffraction techniques, dark field imaging and high resolution electron microscopy are used to study the origin of diffuse scattering in the high temperature cristobalite phase of silica $(Si_{0.9}Ge_{0.1})O_2$. The metastable phase at lower temperatures undergoes a structural phase transition near 530 K. The low temperature α-cristobalite has $P4_12_12$ symmetry, the high temperature β-cristobalite has space group Fd3m. This high temperature symmetry however is an idealized structure and Hatch and Ghose [1] proposed this form to be a dynamic average of α-type phases. The domain structure in the β-phase is studied by electron diffraction and dark field imaging. The microstructure of the α-phase is studied by high resolution electron microscopy and different local structures are characterized such as a mixed trydimite/cristobalite layering.

Trydimite type structures like $BaAl_2O_4$ and $BaGa_2O_4$ are shown to undergo a paraelectric to ferroelectric phase transition with the formation of translation and orientation variants. These domains and their interfaces are studied by high resolution electron microscopy. Dark field imaging in diffuse spots shows curved anti phase boundaries, some of them forming closed loops. Under electron beam heating a breathing type motion of these anti phase boundaries is observed, similar to the ones observed before in anorthite by Van Tendeloo et al.[2].

D.M. Hatch and S. Ghose (1991), Phys. Chem. Minerals, 17, 554.
G. Van Tendeloo, S. Ghose and S. Amelinckx (1989), Phys. Chem. Minerals, 16, 311.

M07.CC.005 DIFFUSE SCATTERING IN DECAGONAL $AL_{70}NI_{15}CO_{15}$. E. Weidner, LMU Muenchen, K. Hradil, Univ. Wuerzburg, F. Frey, T. Scholpp, LMU, Muenchen, M. De Boissieu, A. Letoublon, LTPM, St. Martin d'Heres,M. Capitan, ESRF, Grenoble, W. Morgenroth, DESY, Hamburg

Decagonal quasicrystals exhibit longrange aperiodic order in 2 dimensions and periodicity in the third, perpendicular direction. The diffraction patterns of $Al_{70}Co_{15}Ni_{15}$ show diffuse scattering of significant intensity as well as sharp Bragg peaks, indicating superorder and disorder: (1) satellite reflections, (2) diffuse *streaks*, (3) modulated diffuse layers perpendicular to the periodic direction (4) diffuse scattering near the Bragg peaks (5) diffuse maxima arranged in the shape of a pentagon (6) diffuse scattering in the center of a pentagon. For a review of various models explaining these phenomena, see [1]. High resolution measurements confirmed [2] for this phase the that the centers of the satellite pairs do not coincide with the position of the Bragg peak, but are shifted slightly, as predicted by a linear phason strain model. The average structure remains quasiperiodic as indicated by Bragg peaks at positions corresponding to an unstrainded qc. *Random phason fluctuations* cause diffuse scattering near the Bragg peaks, the integral diffuse intensity increases with the internal component of the reflection. The diffuse pentagon has been interpreted as a type II superstructure [3], this model is based on the proposition that the diffuse maxima form a regular pentagon. High-resolution measurements show that the positions agree with those predicted by the *phason strain*-model. Measurements at the ESRF have detected scattering in the center of a pentagon, at the position of a strong S1 reflection [4].

Funded by the DFG under nr. FR747/13

[1] W. Steurer and F. Frey. Phase Transitions **67** (1998), 319-361
[2] M. Kalning, Ph. D. Thesis, 1996, Christian-Albrechts-Univ. Kiel
[3] S. Ritsch, Phil. Mag. A **71** (1995), No. 3, 671-685
[4] K. Edagawa, M. Ichihara, K. Suzuki, S. Takeuchi. Phil. Mag. Lett. **66**(1992), No.1, 19-25

P07.CC.001 THE ORDER - DISORDER TRANSFORMATION IN $Al_{70}Ni_{15}Co_{15}$ QUASICRYSTAL. H. Abe, National Defense Academy, Yokosuka 239-8686, Japan, and T. Tamura and J. Bai, Oak Ridge National Laboratory, Tennessee 37831, USA, and D. Le Bolloc'h and S.C. Moss, University of Houston, Texas 77204, USA.

$Al_{70}Ni_{15}Co_{15}$ (ANC) alloys are well known to contain a decagonal phase. Recently many studies of ANC have been carried out in relation to an order-disorder transformation at high temperature. It is suggested that local atomic rearrangements, caused by phason softening, contribute to diffuse scattering around Bragg reflection [1]. Here we study the precise atomic short-range order (SRO) relating to this transformation. Our measurements are on a single quasicrystal of ANC at X14A in the National Synchrotron Light Source. Anomalous-x-ray scattering was used to clarify the atomic arrangements between Ni and Co, since the atomic number difference is only one. Three incident energies were selected to be 7.686, 8.098 and 8.304 keV (3λ method). We observed a large contrast difference in the diffuse scattering intensity with this method. SRO diffuse intensity are proportional to $|f_{Ni} - f_{Co}|^2$, reflecting the clear existence of SRO between Ni and Co atoms.

Y. Ishii, Phys. Rev. B**45**, 5228 (1992).

P07.CC.002 THE ANALYSIS OF DIFFUSE SCATTERING AND SHORT RANGE ORDER USING THE ATOMIC PAIR DISTRIBUTION FUNCTION. Th. Proffen and S.J.L. Billinge, Department of Physics and Astronomy, Michigan State University, East Lansing, MI 48824-1116, USA.

The analysis of diffuse scattering and the determination of the local atomic arrangements holds the key to a deeper understanding of the properties of modern materials. Since conventional structure refinement based on Bragg reflections can only reveal information about the **average** structure, the interest in methods to analyse diffuse scattering is increasing.

A convenient method to study these local arrangements is the analysis of the atomic pair distribution function (PDF) [1,2] which is obtained via Fourier Transform from powder diffraction data. The obtained PDFs are analysed via the full profile refinement based on a structural model having a size of only one or a few unit cells. The results are then compared to the long-range average values obtained via normal Rietveld [3] refinement. The potential of the PDF refinement technique will be illustrated on systems ranging from simple Ni and $In_{1-x}Ga_xAs$ to the more complex system of $La_{1-x}Ca_xMnO_3$.

The program PDFFIT used for the refinements is part of the diffuse scattering software package DISCUS [4] and is available free of charge from the authors.

[1] T. Egami, in "Local Structure from Diffraction" edited by S.J.L. Billinge and M.F. Thorpe, Plenum Press, 1998, page 1
[2] S.J.L. Billinge & T. Egami, *Phys. Rev. B*, **47**, 14386 (1993)
[3] H.M. Rietveld, *J. Appl. Cryst.* **2**, 65 (1969)
[4] Th. Proffen & R.B. Neder, *J. Appl. Cryst.* **30**, 171 (1997)

P07.CC.003 ORDER, DISORDER AND SHORT RANGE ORDER IN ZIRCONIUM OXYNITRIDES. I. Kaiser, H. Boysen and F. Frey, Institut für Kristallographie, LMU, 80333 München, Germany, M. Lerch, Silicatchemie, 97070 Würzburg, Germany, T. Hansen and P. Convert, ILL, 38042 Grenoble, France, and D. Hohlwein, HMI, 14109 Berlin, Germany.

Zirconia, ZrO_2, doped with cations of lower valency is a technologically important material, e.g. with respect to its high ionic conductivity. A new alternative to create the necessary vacancies on the oxygen lattice is the doping with higher valency anions like nitrogen. Especially co-doped ternary probes have interesting properties. While for cation doped material the conductivity is affected by short range order (cluster), the N-doped samples also exhibit different long range vacancy ordering depending on the N content, and some N/O-order. Both disappear at high temperatures.

To analyse these order phenomena neutron experiments were performed at MAN1 and MAN2/FRM1, D20/ILL, and E2/HMI. The Bragg intensities were refined using the Rietveld program including anharmonic contributions to the Debye-Waller factor to determine the diffusion pathways of the anions. The modulated diffuse background, analysed with a Warren-Cowley formalism, gives information about the short range order.

All investigated phases are modifications of the fluorite structure type, with different ordering of the vacancies and concomitant relaxations of the surrounding atoms. Some anion positions show a preference of N occupation partly at variance with MAPLE calculations. The calculated diffusion pathways are similar in all systems at high temperatures, but the number of

diffusing ions is varies. The refinement of the diffuse background is based on a defect-cluster including a vacancy connected with a Zr atom, where the oxygens shift towards the vacancy and the cations away from it. The gradual disappearance of the short range order at high temperatures causes the ionic conductivity.

This work is supported by funds of the DFG under FR747/12-2.

P07.CC.004 DIFFUSE SCATTERING INTENSITIES FROM SELECTED CRYSTALLINE SAMPLES RECORDED WITH NEUTRON IMAGING PLATES. Ulrich C. Wildgruber, Physics Department, Brookhaven National Laboratory

Neutron sensitive Imaging Plates (NIP's) make it possible to collect diffracted neutrons with high spatial resolution and efficiency over large areas simultaneously. The usefulness of NIP's to map reciprocal space will be demonstrated with crystalline samples of C60, Pr2NiO4.215 and Zr0.8Nb0.2. We will show that there is a significant potential to collect diffuse intensity distributions up to q = 12.6 rec.Å.

The objective of this study is to collect diffuse intensities with NIP's at room temperature from an aged sample of Zr0.8Nb0.2 before and after heat treatment at 1273K and quenching to room temperature. The Zr-Nb system forms alloys with a bcc high temperature phase (β phase) and a hexagonal or trigonal lowtemperature phase (ω phase). The athermal ω phase is formed diffusionless by displacing atom rows parallel to [111]. The ideal heaxagonal ω phase however is formed only for small (< 2 wt %) Niobium concentrations. For Niobium concentrations in the range of 17 to 30 wt % diffuse scattering appears in the vicinity of the theoretical Bragg positions [Hall, B.A., Roberts J. A. Acta Met. **8** 575 (1960)]. The diffuse intensity increases with the amount of Niobium until the transition β -> ω is suppressed for concentrations greater than 30 wt %. The spatial distribution of the diffuse signal is basically the same in a wide temperature range from 6K to 1273K although it is sharper and significantly stronger at low temperatures [Keating, D.T. LaPlaca, S.J. J. Phys. Chem. Solids **35** 879 (1974)]. We will compare the data of this study with older neutron data collected with a single detector. The extended q-volume accessible in the case of NIP detection demands new strategies for data reduction and model refinement.

P07.CC.005 DIFFUSE SCATTERING BY RANDOM SOLID SOLUTIONS. R.I.Barabash [1], M. F.Thorpe [2], J. S. Chung [3], [1] Metal Physics Department, National Technical University of Ukraine, apt.25, str.Proreznaya 4, Kiev, 252003, Ukraine, [2] Physics & Astronomy Department, Michigan State University, East Lansing, MI 48824-1116, USA, [3] Department of Physics, Chungbuk National University, Gaeshin-dong,Cheongju-shi, 361-763, Republic of Korea

Modern simulation techniques on lattices allow the individual atomic displacements to be found and hence the associated diffuse X-ray or neutron scattering to be calculated directly. In this paper we use both the direct lattice simulations based on a lattice model of the crystalline alloy and the method of fluctuation waves in the continuum limit, to analyze the diffuse scattering by random solid solutions of a semiconductor alloy A1-xBxC. We consider both a single impurity atom in the crystal and also the case of a concentrated solid solution (with different concentrations of impurities x = 0.5; x = 0.3; x = 0.7 etc). The displacement field caused by a single impurity atom was analyzed for the alloy Ga1- xInxAs and compared with the case of a defect in an elastically isotropic medium. In the continuum limit, the substitution of the host atom by an impurity atom is accompanied by hydrostatic pressure across the surface of the impurity atom due to the size mismatch between the host and impurity. This results in the appearance of an inverse square displacement field in the matrix. The actual displacement field in Ga1-xInxAs is slightly more complicated and contains small tangential components as well as radial components. A crystalline alloy has a mean long-range order that leads to Bragg peaks and the associated diffuse scattering is divergent very close to these Bragg peaks. The shape of the diffuse scattering intensity distribution in different sections of reciprocal space is computed for the lattice, is compared with the continuum approximation. For the limiting case of a single defect in the crystal, the continuum approach agrees well with the results of direct lattice simulations. For concentrated random solid solutions where the angular and central spring constants are equal everywhere, the diffuse scattering intensity is proportional to the intensity for one defect case and scales with concentration as x (1-x). * Work supported in part by the US National Science Foundation and Department of Energy.

07DD THICK COATINGS

M07.DD.001 THE STUDY OF FILMS AND COATINGS USING GLANCING ANGLE X-RAY DIFFRACTION R J Cernik, Synchrotron Radiation Departmant, CLRC Daresbury Laboratory, Warrington WA4 4AD

Synchrotron radiation is an ideal probe for studying the structure of surfaces. Evidence for this can be found in the large number very successful studies of the structure of perfect surfaces using glancing angle X-rays. These are usually carried out in vacuum with cleaved surfaces or in-situ growth of epi layers. These are not usually suitable for industrial surfaces which have to work under realistic circumstances. For these materials deposited in thick or thin coatings two techniques have proved very valuable. These are glancing angle X-ray diffraction and reflectivity. The latter has combined specular and diffuse scattering to gain information on the lateral correlation length and surface roughness. Fringe spacing can be used to measure layered structures and diffraction is a very sensitive probe of structure as a function of depth. This presentation will cover the way in which these techniques are implimented on station 2.3 at Daresbury Laboratory for the study of a variety of coatings.

M07.DD.002 GLANCING ANGLE XRD MEASUREMENTS ON METALLURGICAL COATINGS. D. Rafaja, R. Kuzel and V. Valvoda, Faculty of Mathematics and Physics, Charles University, Ke Karlovu 5, CZ-121 16, Prague, Czech Republic.

The glancing angle X-ray diffraction (GAXRD) techniques are used to study a wide range of materials, but the application of the GAXRD in the analysis of metallurgical coatings is still dominant. The main advantage of the GAXRD is that the penetration depth of X-rays can easily be tuned up by changing the inclination of the sample with respect to the primary and diffracted beams. In particular, the penetration depth depends strongly on the angle of incidence of the primary beam, while the dependence of the penetration depth on the diffraction angle is rather weak. Thus, the GAXRD is applied to perform "layer-by-layer" measurements at constant penetration depths by keeping the angle of incidence constant in individual detector scans.

On the other hand, such a scanning of the reciprocal space is much more complex than in the symmetrical mode, as the direction of the diffraction vector changes during the measurement. Thus, the analysis of the diffraction patterns becomes more complicated, which holds especially for diffracted intensities if the coatings contain preferred oriented crystallites. Besides, intensity corrections for instrumental effects differ strongly from the intensity corrections used for symmetrical measurements.

In the contribution, the main attention will be paid to the GAXRD using the quasi-parallel beam optics. The experimental

results will illustrate the use of this technique in the depth-resolved X-ray diffraction, in the residual stress measurements and in the investigation of the anisotropic crystal deformation in cubic materials. The subjects of the experimental study are the PVD and CVD metallurgical coatings, ion-implanted CVD metallurgical coatings and thick metallurgical coatings prepared by reactive diffusion.

M07.DD.003 PROBLEMS RELATED TO THE DEPTH RESOLVED RESIDUAL STRESS ANALYSIS IN STRONGLY TEXTURED PVD-COATINGS. Ch. Genzel, Hahn-Meitner-Institut Berlin, Glienicker Str. 100, 14109 Berlin, Germany.

Hard coatings deposited by physical vapour deposition methods are widely used today to improve the mechanical properties of technical parts, for example the resistance to abrasive wear. In many cases, high compressive stresses up to some GPa develop during the coating process within the films, which contribute to the mechanical behaviour in a positive manner. In order to combine favourable mechanical properties like high hardness on the top of the coatings with a sufficient adhesiveness at its interface, efforts are made to adjust defined internal stress gradients with respect to the film thickness.

Therefore, the knowledge of both, the amount and the distribution of the residual stresses within the coatings, is of great practical interest. However, due to the small diffracting volume as well as texture, X-ray diffraction at polycrystalline coatings often leads to line profiles of rather weak intensity, and therefore, stress analysis involves a series of difficulties.

Starting from a general overview of the problems related to X-ray film stress analysis, several methods are compared concerning their suitability for the detection of non- uniform residual stress fields $\sigma(z)$. It will be shown that the choice of the appropriate method depends strongly on the material to be investigated. If the layers are strongly textured and their thickness is small compared with the penetration depth τ of the X-rays, the scattering vector method [1] offers some advantages, because the lattice strain depth profiles $\varepsilon_{\varphi\psi}(hkl,\tau)$ are obtained even for fixed positions of the scattering vector with respect to the sample reference system. Based on this measuring principle, a self consistent method will be presented, which yields the stress depth profiles $\sigma_{ij}(\tau)$ (i, j = 1, 2, 3) as well as the strain-free lattice spacing $d_0(hkl)$ even without some reference material [2].

[1] Genzel, Ch. (1994). *phys. stat. sol. (a)* 146, 629 - 637.
[2] Genzel, Ch. submitted to J. Appl. Cryst.

M07.DD.004 MICROSTRUCTURE AND RESIDUAL STRESS IN PLASMA SPRAYED TBCS. M. Leoni, P. Scardi, Università di Trento, Facoltà di Ingegneria, Dipartimento di Ingegneria dei Materiali, via Mesiano, 77 - 38050 Trento, Italy.

Plasma sprayed Thermal Barrier Coatings (TBCs) find a growing number of applications for the protection of hot parts in combustion engines. Their performance and life is strongly related to the microstructure of the material and to the residual stresses generated by the deposition process, and their variation due to service (cycling).

Diffraction techniques are particularly suited to the study of two important features of these systems: phase composition and residual stress. The former is particularly relevant for zirconia TBCs, where three polymorphs (monoclinic, tetragonal and cubic) can be present in the coatings or develop after service. The knowledge (and control) of phase composition is extremely important as it strictly relates to the structural stability of the coatings. The Rietveld method, that can be used on both X-ray and neutron diffraction data, turns out as a very effective tool as it permits a non-destructive phase analysis without standards, and can also be used for routine quality control.

The measurement of residual stresses in thick ceramic coatings is one of the major steps towards the improvement of the durability of coated components. Traditional X-ray stress measurements based on the reflection geometry are not sufficient to give information on the variation of the residual stress through the coating thickness, because of the high absorption of zirconia with respect to the film thickness (millimetre range). Nevertheless, by combining these techniques with data coming from a mechanical modelling of the coating-substrate system, or some destructive stress analysis, the in-depth stress profile can be determined.

This kind of analysis, not involving a direct measurement of the inner coating region, will be shown to be consistent with true through-thickness measurements conducted by neutron diffraction, confirming the great potentiality of combining multiple measurement techniques for the analysis of complex stress states.

M07.DD.005 ABSTRACT NOT AVAILABLE. J.-L. Lebrun

07EE POLYMORPHISM IN INDUSTRY (sponsored by Dept. Pharmaceutical Sciences, Strathclyde University)

M07.EE.001 THE IMPACT OF POLYMORPHISM ON DRUG DEVELOPMENT: A REGULATOR'S VIEWPOINT. Wilson H. DeCamp, Division of New Drug Chemistry III, Food and Drug Administration

A general overview will be presented of the typical interactions between a drug company and the FDA during the development of a drug. The physical chemistry of the solid state bulk drug, especially its potential for crystallizing in multiple solid state forms, can significantly influence the development of both the synthetic process and the analytical chemistry of the drug. The drug is marketed and used as a finished drug product, which must be controlled to assure consistent quality. When the drug substance is known to be polymorphic, it can present special analytical concerns for the product. These topics will be discussed from two points of view: the type of information that should be acquired during drug development and how this information relates to issues of drug quality.

M07.EE.002 POLYMORPH CHARACTERISATION BY SOLID-STATE NMR. Robin K. Harris, Department of Chemistry, University of Durham, South Road, Durham, DH1 3LE, UK

Polymorphism is ubiquitous in many chemical industries (pharmaceutical,polymer, dyestuffs, ceramics etc.) so that techniques for distinguishing and characterising the different forms are essential for R&D, scale-up, manufacture, patent establishment and patent protection. Whilst single-crystal diffraction methods give detailed information in many cases, they fail or are inadequate in others. In recent years magic-angle spinning NMR has come to be the method of choice for many purposes. Its advantages will be stressed and examples given from several different industries. Crystallographic data, including asymmetric unit information and non-bonded interatomic distances, can be obtained. Questions of intermolecular interactions, structural disorder, molecular-level mobility and domain structure in heterogeneous systems will be emphasized. The combination of solid-state NMR information with powder diffraction data for complete structure determination is a growth

area. The future challenge is the simulation of intermolecular effects on chemical shifts a prelude to reversing this process. Naturally, solvates present similar problems and opportunities.

M07.EE.003 POLYMORPHISM IN PROTEIN CRYSTALS. Martin McMillan, 3-Dimensional Pharmaceuticals, Inc., Eagleview Corporate Center, 665 Stockton Drive, Exton, Pennsylvania 19341, USA

Because proteins are labile and polyvalent, the effects of pH, temperature, and additives - among many possible influences - on solubility minima are quite evident from the observation that protein molecules regularly crystallize in several polymorphic forms. In this general presentation, we will highlight a few interesting protein polymorphs and examine their packing motifs. To end, we will consider some practical aspects of polymorphism in a drug discovery setting.

M07.EE.004 SOLID STATE POLYMORPHIC TRANSFORMATIONS INDUCED BY VARIATIONS IN TEMPERATURE AND PRESSURE. K.S. Knight and K Shankland, ISIS Facility, Rutherford Appleton Laboratory, Chilton, Didcot, Oxon. OX11 0QX, UK., and N Shankland, Department of Pharmaceutical Sciences, University of Strathclyde, Strathclyde, G1 1XW, UK.

Polymorphism in industry is particularly problematic where problems arise in the advanced stages of product development. Recent problems with the HIV protease inhibitor ritonavir [1] once again underline the need for a comprehensive polymorph screen, including a search for phase transformations in the solid state. It is the surveying capability of powder diffraction which we wish to highlight here, using pyrene as an example.

We have utilised the advantages of neutron-time-of-flight techniques, namely fixed instrument geometry and total pattern integration, to rapidly determine the phase diagram of perdeuterated pyrene as a function of both temperature and pressure, Figures 1 and 2, below.

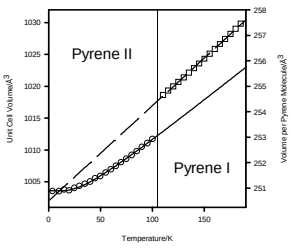

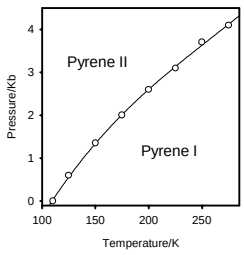

As a result of this work, we have been able to *(a)* resolve the order of the phase transition *(b)* refine the low-temperature and high-pressure structures, proving their equivalence *(c)* determine the equations of state of pyrene I at 225K and pyrene II at 95K and *(d)* evaluate the temperature dependence of the thermal expansion tensors in both polymorphs.

Recent data, currently under analysis, show the viability of cold neutrons for determining the rate of the solid-state transformation as a function of both pressure and temperature.

[1] SCRIP No. 2370, September 16th, page 13, PJB Publications Ltd, 1998.

M07.EE.005 CRYSTAL STRUCTURE PREDICTION USING ATOM CONTACT DISTRIBUTIONS FROM THE CAMBRIDGE STRUCTURAL DATABASE. Sam Motherwell Cambridge Crystallographic Data Centre, 12 Union Rd, Cambridge CB2 1EZ, UK.

It is now well established that most molecules exhibit a range of many close-packed calculated structures all within about 2 kcal/mole of the global minimum, and thus are possible polymorphs [1]. To predict which polymorphs are more likely to be observed, one can attempt to compare the structures with the Cambridge Structural Database (CSD) which contains mostly those easily crystallisable polymorphs under normal laboratory conditions. A methodology has been developed for calculation of probable crystal structures based on the intermolecular atom-atom distances in the CSD. GA methods [2] have been used to find calculated crystal structures using rigid molecular models in common space groups. A fitness function is calculated which is a minimum when the calculated distance frequency distribution agrees best with the CSD for each atom-type in the molecule. All contacts are counted to each atom, giving a frequency distribution for a normalised distance $D = R_{ij} - R_v$, where R_{ij} is the distance between atoms i and j, and R_v is the sum of the van der Waals radii. The method makes no assumptions about energy, but seeks to reproduce the CSD frequencies characteristic of a selected set of similar molecules in the CSD. Extra fitting information can be given for patterns of close contact $D < R_v$, where a sample of chemically similar CSD molecules shows a good probability of occurrence, H-bonds being a typical example. These expectation values can be set even though we have no theoretical explanation of such patterns, and may often have kinetic reasons for formation [3].

1. S.L.Price & K.S.Wibley, J. Phys. Chem. A (1997) 101, 2198-2206.
2. W.D.S.Motherwell, Nova Acta Leopoldina, (1999) NF79, 89-98.
3. A.Gavezzotti, Acc. Chem. Res. (1994) 27, 309-314.

07FF ORGANOMETALLIC AND CO-ORDINATION CHEMISTRY (sponsored by Dept. Chemistry, University of Glasgow)

M07.FF.001 COORDINATION COMPOUNDS ARE NOT ALWAYS SOLIDS. David W. H. Rankin, Paul T. Brain, Carole A. Morrison and Heather E. Robertson, Department of Chemistry, University of Edinburgh, West Mains Road, Edinburgh, EH9 3JJ, UK.

Gas-phase structures are often dramatically different from those of the same compounds in the crystalline phase - and if it can possibly be done, we should always determine both. It is the structure of the free molecule which is still obtained in most theoretical computations, and it is of crucial importance for understanding gas-phase reactions.

Coordination (and organometallic) compounds are often volatile enough to allow electron diffraction data to be collected, but the molecules are usually large and complex. However, we have developed a method in which we make use of both theoretical and experimental data. Parameters which are not well defined by the experimental data are flexibly restrained, making use of series of calculations with increasing size of basis set and increasing level of theory. The refinement optimises the fit to both sets of data, giving structures which make the best of both worlds.

The method will be illustrated by recent examples, chosen (a) to show the complexity of molecules which can now be studied in the gas phase, (b) to demonstrate the changes in structure which can occur on vaporisation / crystallisation, and (c) to explain the relevance of the gas-phase structures of some compounds to their chemistry.

M07.FF.002 THE CONTRIBUTION OF POWDER DIFFRACTION METHODS TO STRUCTURAL COORDINATION CHEMISTRY. A. Sironi Dipartimento di Chimica Strutturale e Stereochimica Inorganica Università di Milano, via Venezian 21, I 20133 Milano (Italy) and N. Masciocchi Dipartimento di Scienze Chimiche, Fisiche e Matematiche, Università dell'Insubria, sede di Como, Via Lucini 3, I 22100 Como (Italy)

In the last seven years, we have been active in the field of structural Powder Diffraction (PD) with the goal of developing a general procedure for the characterisation of moderately complex coordination and organometallic compounds using unsophisticated, widely available (but well conditioned) laboratory equipment [1].

Given that *only the lack of suitable single crystals makes PD structural studies worthwhile*, we may attempt to circumscribe the meaningful use of X-ray PD as a structural tool to *i)* insoluble, thermally unstable compounds which cannot be (re)crystallised from solution or from the melt; *ii)* metastable phases destroyed or modified upon manipulation; *iii)* twins, when the presence of double or multiple diffraction spots makes the 'single crystal' way of sampling the reciprocal lattice inefficient; *iv)* very small crystals or crystal aggregates; *v)* gas/solid, liquid/solid and solid state reactions fragmenting and misorienting the coherent domains of the starting crystals but conserving the (poly)crystalline nature of the sample.

The structural use of X-ray PD spans the whole periodic table but here we will discuss its growing importance in coordination chemistry by taking examples from our current studies on rhenium hydrido carbonyl clusters where complementarity between single crystal and PD analyses emerges.

1. N. Masciocchi and A. Sironi (1997) J. Chem. Soc. Dalton Trans. 4651

M07.FF.003 COMBINED THEORETICAL AND STRUCTURAL DATABASE STUDIES OF BINUCLEAR TRANSITION METAL COMPLEXES. Santiago Alvarez, Departament de Química Inorgànica and Centre de Química Teòrica, Universitat de Barcelona; Diagonal 647, 08028 Barcelona, Spain.

The combination of quantum chemical calculations on model compounds and structural database analyses has allowed us to establish some trends on the structural chemistry and dynamic behavior of binuclear transition metal compounds. Calculations in which a bonding parameter is frozen and the rest of a model molecular structure is optimized mimics the effects of chemical substitutions, solvation molecules or packing forces in a crystal, thus allowing to reproduce known structural correlations or predict new ones. Furthermore, from a well planned set of calculations one should be able to identify the electronic, geometric or steric origin of such structural correlations. The cases to be discussed include (a) the conformational choice within three families of doubly bridged binuclear complexes of square planar d^8 metal ions, (b) the effect of the *umbrella* motion of the ligands on the metal-metal bond diatance in a variety of M_2L_{2n} complexes, (c) the correlation between the geometry of the coordination sphere around Cu atoms and the cleavage of the oxygen-oxygen bond in synthetic analogues of oxyhemocyanin, and (d) the continuous structural variation along the reaction path that takes from weakly associated Cu(I) linear complexes CuXL to rhombic $Cu_2X_2L_2$ dimers.

M07.FF.004 UNDERSTANDING ORGANOMETALLIC REACTIONS ON THE BASIS OF CRYSTAL STRUCTURES. K. Angermund, M. Kessler and V. R. Jensen. Max-Planck-Institut für Kohlenforschung, Kaiser-Wilhelm-Platz 1, D-45470 Mülheim an der Ruhr, Germany.

Many organometallic reactions, especially those which are of commercial interest, are very fast and highly selective catalytic processes. Crystal structure analysis on the other hand, operates on a considerably larger time scale, and usually describes the structure of catalytically inactive species, adopting conformations which are stable in the crystal field at a certain temperature. Yet, much of the necessary information for the understanding of catalytic reactions may still be contained in crystal structures of the reaction educts and products. Several methods for extracting such information will be presented during the lecture. Their degree of complexity will vary from simple "distortions" of structures [1], for which almost no energy calculations are necessary, to the concept of "accessible molecular surface" (*ams*) [2], which in some respect can be regarded as an extension of Tolman's cone angle [3], and to more complex models for true transition state structures based on theoretically (pre)calculated molecular fragments [4]. The chemical examples will cover the area of hydrovinylation, hydrogenation of CO_2 and olefin polymerisation.

[1] K. Angermund, A. Eckerle, F. Lutz (1995). Z. Naturforsch. B, 50, 488.
[2] K. Angermund, W. Baumann, E. Dinjus, R. Fornika, H. Görls, M. Kessler, C. Krüger, W. Leitner, F. Lutz (1997). Chem. Eur. J., 3, 55.
[3] C. A. Tolman (1977), Chem. Rev., 77, 313.
[4] K. Angermund, G. Fink, R. Kleinschmidt, V. R. Jensen (1999). in preparation; K. J. Børve, Ø. Espelid, V. R. Jensen, J. A. Støvneng, O. Swang (1998). Kjemi 10:22.

M07.FF.005 NOVEL COORDINATION CHEMISTRY OF C_2^{2-} AND RELATED ANIONS. Thomas C. W. Mak and Guo-Cong Guo, Department of Chemistry, The Chinese University of Hong Kong, Shatin, New Territories, Hong Kong, China.

The literature contains scant information on the ligand behaviour of C_2^{2-} (acetylide dianion, acetylenediide), in contrast to the rich coordination chemistry of its isoelectronic analogues N_2, CO, NO^+ and CN^-. Although silver acetylide (Ag_2C_2, also known as silver carbide) was first prepared as an impure yellowish powder by Berthelot in 1866, there is as yet no single crystal X-ray structure information owing to its sensitivity to mechanical shock and low solubility in common solvents. Recently we initiated a research project to synthesize and elucidate the X-ray crystal structures of novel compounds containing silver acetylide as a component, so as to shed some light on the nature of the interaction between the acetylide dianion and silver(I) ions.

We report here the synthesis and crystal structure of the following double salts:

- $Ag_2C_2 \cdot 8AgF$, in which an acetylide dianion is completely enclosed within a Ag_9 cage of a chandelier-like assembly of ten silver atoms.[1]
- $Ag_2C_2 \cdot 2AgClO_4 \cdot 2H_2O$, in which the C_2^{2-} species acts in a μ_6-$\eta^1,\eta^1 : \eta^2,\eta^2 : \eta^2,\eta^2$ bonding mode that binds the silver cations into an unprecedented two-dimensional planar array.[2]
- $Ag_2C_2 \cdot AgNO_3$, $Ag_2C_2 \cdot 5AgNO_3$ and $Ag_2C_2 \cdot 5.5AgNO_3$, in which the C_2^{2-} dianions are fully encapsulated in the cavities of an octahedron, a monocapped trigonal prism and a monocapped octahedron, respectively.[3]

Our recent structural studies on novel coordination modes of the cyanide,[4] azide,[5] and thiocyanate[3] anions in related double salts of silver(I) will also be presented.

1. G.-C. Guo, G.-D. Zhou, Q.-G. Wang, T. C. W. Mak, *Angew. Chem. Int. Ed. Engl*. **1998**, *37*, 630.
2. G.-C. Guo, Q.-G. Wang, G.-D. Zhou, T. C. W. Mak, *Chem. Commun*. **1998**, 339.
3. G.-C. Guo and T. C. W. Mak, to be published.
4. G.-C. Guo, T. C. W. Mak, *Angew. Chem. Int. Ed. Engl*. **1998**, *37*, 3183.
5. G.-C. Guo, T. C. W. Mak, *Angew. Chem. Int. Ed. Engl*. **1998**, *37*, 3268.

P07.FF.001 STRUCTURAL CHARACTERIZATION OF A SERIES OF NOVEL MONOOXOVANADIUM(V) COMPLEXES. S.-X. Liu, Dept. of Chem., Fuzhou University, Fuzhou 350002, China.

The relationships among structure, spectroscopy, and reactivity must be elucidated in order to understand fully the role of vanadium in biological systems. Thirty one novel monovanadium(v) complexes were synthesized and characterized by X-ray diffraction at room or low temperature, IR, Raman, UV, ^{1}H NMR spectra and cyclic voltammetry measurements.

There are a distorted octahedral configuration with [VO(ONO)(OO)] [1-3], [VO(ONO)(ON)] or [VO(ONO)(O)(O)] [2] type and a distorted square pyramidal configuration with [VO(ONO)(O)] or [VO(ONS)(O) type in the vanadium atoms of these monooxovanadium(V) complexes. However, most of vanadium atoms in the known vanadium hydrazone complexes have a square pyramidal [VO(ONO)(O)] coordination., only three complexes have octahedral [VO(ONO)(O)(O)] or [VO(ONO)(ON)] coordination. Some complexes reported by us represent the first structural characterization of any vanadium hydrazone complex with VO(ONO)(OO) coordination. The complex $VO(C_{15}H_{12}N_2O_3)(C_3H_7O)(H_2O)$ is the first example of a VO^{3+} complex with V-O(H_2O) bond. The order of the V-O and V-N coordination bond distances and the coordination effects of the different ligands are discussed. There are some hydrogen bonds in some of these monooxovanadium complexes, forming an infinite chain in the crystals. Therefore, some of these complexes are supermolecular complexes.

The author thanks the financial support of the Natural Science Foundation of Fujian Province of China. The author thanks the financial support from University of Durham, UK for our crystal structure determination of some complexes at low temperature.

1. S.-X. Liu & S. Gao (1998), Inorg. Chim. Acta, 282, 149.
2. S. Gao, Z.-Q. Weng, & S.-X. Liu (1998) Polyhedron, 17, 3595.
3. S.-X. Liu, S. Gao, J.W. Yao & J.A.K. Howard (1998), BCA Spring Meeting Abstracts, CP12.

P07.FF.002 LITHIUM PHOSPHAVINYLIDENE CARBENOIDS. M. Nieger, T. Baumgartner, O. Schmidt and E. Niecke, Institut für Anorganische Chemie, Universität Bonn, D-53121 Bonn, Germany.

Carbenoids have attracted a great deal of interest because of their potential as synthetic building blocks in organic chemistry [1]. The presence of both an electronegative element and a metal at one carbon atom leads to a unique bonding situation with a 'chameleon like' ambident character of this carbon atom [2]. The carbenoide centre of phosphavinylidenes is significantly stabilized by incorporation into π-systems.

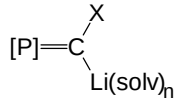

(X = F, Cl, Br)

Here, the structures of lithium phosphanylidene (X = Cl) [3] and phosphoranylidene carbenoids (X = F, Cl, Br) [4], as well as a lithiated bis-(ylene) phosphorane (X = H) [5] are presented, highlighting the first stable fluoro-lithio and the *E/Z* isomers of the chloro-lithio phosphoranyl-idene carbenoids. The structural parameters are investigated in detail. The connection between structural features and bonding in phosphavinylidene carbenoids will be discussed.

1. Review: G. Köbrich (1967). Angew. Chem. Int. Ed. Engl., 6, 41-53.
2. W.W. Schoeller (1995). Chem. Phys. Lett., 241, 21-25.
3. E. Niecke, M. Nieger, O. Schmidt, D. Gudat & W.W. Schoeller (1999). J. Am. Chem. Soc., in press.
4. E. Niecke, P. Becker, M. Nieger, D. Stalke & W.W. Schoeller (1995). Angew. Chem. Int. Ed. Engl., 34, 1849-1851. T. Baumgartner, D. Gudat, E. Niecke & T.J. Schiffer (1999). submitted.
5. T. Baumgartner, B. Schinkels, D. Gudat, M. Nieger & E. Niecke (1997). J. Am. Chem. Soc., 119, 12410-12411.

P07.FF.003 DIRECT OBSERVATION OF A SOFT MOLECULAR DEGREE OF FREEDOM IN THE SOLID STATE. U. Englert, G.E.Herberich, and J. RosenplŠnter, Institute for Inorganic Chemistry, RWTH Aachen, Prof.-Pirlet-Str. 1, 52074 Aachen, Germany.

In the boratabenzene complex $InMe(C_5H_5BMe)_2$ two six-membered rings are coordinated to In. Due to the electropositive effect of the boron its carbon neighbors in the adjacent ring positions represent preferred coordination partners for the metal center. NMR results show that the compound is dynamical in solution with effective lateral symmetry for the boratabenzene ligands, presumably due to a fast degenerate exchange of the indium coordination between the above mentioned positions of the ring. In the crystal the space group is $P2_1$ with eight molecules per unit cell, i. e. four independent molecules. Due to the presence of two heterocyclic ligands per molecule eight different metal-ligand bonding geometries may be investigated in the same solid state structure. They show a remarkable variability in terms of the shortest In-C-distances ranging from 2.395(8) to 2.523(9)Å [1]. A synopsis of all eight projections of the metal atoms on the least squares plane through an idealized ring ligand helps to understand the bonding situation: each metal projection corresponds to a snapshot of the molecule in an energetically favourable conformation. The overall picture shows that the soft structural parameter in the solid state reflects the dynamical situation in solution. Lattice energy calculations [2,3] are used to compare the experimentally established structure to hypothetical alternatives with a smaller number of independent molecular constituents per asymmetric unit.

[1] Englert, U.; Herberich, G. E.; RosenplŠnter, J.*Z. anorg. allg. Chem., 623* (1997) 1098.
[2] Williams, D. E. "PCK83, a crystal molecular packing analysis program" Quantum Chemistry Programs Exchange, 1983.
[3] Schmidt, M. U.; Englert, U. *J. Chem. Soc. Dalton Trans.* (1996)2077.

P07.FF.004 BOND-VALENCE MODEL OF THE SEMICOORDINATION IN COPPER-OXYGEN AND COPPER-NITROGEN COMPLEXES F. Valach, Department of Chemical Physics, Faculty of Chemical Technology, Slovak University of Technology, SK-812 37 Bratislava, Slovak Republic.

The basic assumption of the bond valence model [1] is that each bond between atom *i* and *j* can be assigned a bond valence s_{ij} fulfilling the rule: $V_i = \sum_j s_{ij}$ (1) V_i is the valence of atom *i*. For

the localised bonds with the orbital interaction between neighbouring atoms the bond valence as the function of inter-nuclear distance *r* was derived in the form:

$$s = \sum_{v=1}^{\infty} \frac{\alpha_v}{r^v} \quad (2)$$

α_v are constants dependent on the nature of the bonded atoms. Existence of discontinued transition from chemical bonding to the nonbonding state in the direction of alongated bond of CuO_6 and CuO_5 chromophores limits the index v to the highest value 5 for Cu-O bond. Such supreme manifestation of coordination sphere plasticity [2] is estimated as semicoordination. The parameters α_v ($v = 1-5$) were fitted using formulae (1) and (2) for structures with Cu-O and Cu-N bonds. Mutual dependence between the bond length in copper coordination sphere with chromophores, CuO_6, CuO_5, CuN_6, and CuN_4O_2 has been derived and compared with the experimental structural correlations. Within the copper atom coordination with CuO_5 chromophore the apical Cu(II)-O bond lengths of binuclear carboxylic complexes were predicted.

1. I. D. Brown, in *Structure and Bonding in Crystals*, Vol. 2., eds. M..O'Keefe and A. Navrotsky. Academic Press, New York, 1981, pp. 1-30.
2. J. Gažo et al., *Coord. Chem. Rev.* **19**, 253 (1976).

P07.FF.005 THE DEVELOPMENT OF AN INDUSTRIAL CATALYST THROUGH THE USE OF CRYSTALLOGRAPHY. David J. Ager, Amihai Eisenstadt, and Scott A. Laneman, NSC Technologies, 601 East Kensington Road, Mount Prospect, IL 60056, USA, and Albert S. C. Chan, Monsanto Corporate Research, 800 Lindbergh Avenue, St. Louis, MO 63167 USA, Frank Fronczek, Louisiana State University, Boca Raton, LA 70803 USA, and Cynthia X. Day, Crystalytics Co., P.O. Box 82286, Lincoln, NE 68501 USA.

Crystallography has played an important role in the development of development of the Monsanto ruthenium-BINAP catalysts that are used for the production of intermediate for the pharmaceutical industry. The most important member of this class of catalyst is a polymer $[Ru(BINAP)Cl_2]n$ that cannot be characterised in the solid state as it is a mixture of compounds [1]. However, the discovery of this compound was found due to omission of sodium acetate in an attempt to prepare $[Ru(BINAP)(OAc)_2]$; crystallography showed that the major product was a novel ruthenium-phosphine oxide complex [2]. Other members of the catalyst class contain the $[Ru(BINAP)(acac)_2]$ moiety. Structural elucidation of these catalysts has provided insight into the factors that govern stereochemical control during asymmetric hydrogenations. Finally, during a new preparation of the BINAP ligand [3], the intermediate organometallic species was obtained as a solid and whose structure was found by crystallography. The presence of this compound showed that a different mechanism was operating for the formation of the carbon–phosphorus bond than for previous approaches.

1. A.S.C. Chan & S.A. Laneman (1993), US Patent, 5,198,561.
2. A.S.C. Chan & S.A. Laneman (1994), Inorg. Chim. Acta, 165.
3. D.J. Ager, M.B. East, A. Eisenstadt & S.A. Laneman (1997), J. Chem. Soc., Chem. Commun., 2359.

P07.FF.006 NEUTRON DIFFRACTION STUDIES ON $(\eta^6\text{-}C_7H_8)(OH)(H)Fe\text{-}\{Sn[CH(SiMe_3)_2]_2\}_2$: A COMPOUND SUSPECTED OF HAVING A Fe-H-Sn AGOSTIC INTERACTION. Robert Bau, Jörg J. Schneider and Sax A. Mason, Department of Chemistry, University of Southern California, Los Angeles, CA 90089, U.S.A., Institut für Anorganische Chemie, Universität Essen, Essen 45117, Germany, and the Institut Laue-Langevin, Grenoble 38042, France.

The reaction of bis(toluene)iron with $Sn[CH(SiMe_3)_2]_2$ followed by hydrolysis yields the title compound, the hydroxo hydrido complex $(\eta^6\text{-}C_7H_8)(OH)(H)Fe\{Sn[CH(SiMe_3)_2]_2\}_2$ (1). Originally, ^{1}H-NMR analysis of (1) suggested the presence of a three-center "agostic"

Fe-H-Sn interaction, based on a significantly large ^2J(Sn,H,Fe) proton NMR coupling constant of 286.6 Hz. A single-crystal neutron diffraction analysis of (1), however, shows its structure to be classical, with a normal terminal Fe-H single bond [1.575(8)Å]. The Sn…H distances of 2.482(9) and 2.499(9) Å found in (1) were judged to be too long to correspond to any significant Sn…H bonding interaction. Final R factor = 7.6% for 4960 reflections collected at 20K.

P07.FF.007 CRYSTAL ENGINEERING OF MICROPOROUS 3-D METAL COORDINATION POLYMERS. Stephen S-Y. Chui, Ian D. Williams, Alvin Siu and Samuel M-F. Lo, Department of Chemistry, Hong Kong University of Science and Technology, Clear Water Bay, Hong Kong, China, A. Guy Orpen and Jonathan P.H. Charmant, School of Chemistry, University of Bristol, Cantock's Close, Bristol, BS8 1TS UK.

The engineering of new crystalline open-framework materials, which are complementary to zeolites, is of both scientific interest and considerable commercial value. Metal coordination polymers offer many attractive features in this regard due to the relative ease with which they may be chemically modified. The main issues which need to be addressed for producing potentially useful materials are a) control of framework dimensionality b) pore size engineering c) prevention of network interpenetration d) control of framework stability and e) chemical functionalization of the framework.

Using recent examples from our work we will demonstrate how framework dimensionality can be controlled through ligand multifunctionality, coordination number and minimization of ancillary ligation; pore sizes can be modified using larger polyfunctional ligands, ancillary ligand modification or use/self-assembly of cluster-type building blocks; network interpenetration can be circumvented by creating voids <50% ; and how stability can be improved though control of coordination options or through formation of ceramic hydroxide cores.

A thermally stable cubic polymer $[Cu_3(TMA)_2(H_2O)_3]n\ xH_2O$ exemplifying many of these desirable features has been prepared in excellent yield and purity by both solvothermal and RT methods. (1) It has interpentrating pores of 1nm dimension, yet is stable to removal of both the channel and ligated aqua groups and can be chemically functionalized using ligands such as pyridine. Preliminary results of the sorption properties of this and its chemical derivatives will be reported.

(1) Chui, S.S-Y., Lo, S.M-F., Charmant, J.P.H., Orpen, A.G., Williams, I.D. Science Feb. (1999).

P07.FF.009 CRYSTALLOGRAPHIC AND SPECTROSCOPIC STUDIES OF PLATINUM(II) COMPLEXES WITH PYRIDINE DERIVATIVES. C. Tessier and F. D. Rochon. Departement de chimie, Universite du Quebec a Montreal, P.O. Box 8888, Succ. Centre-Ville, Montreal, Quebec, Canada, H3C 3P8.

The antitumor properties of *cis*-Pt-amine complexes have been known for a few decades. More recently, *trans*-$Pt(pyridine)_2Cl_2$ has shown comparable cytotoxicity with *cisplatin* towards Leukemia L1210 cells. The mixed-ligand *cis*-$Pt(NH_3)$(2-Mepyridine)Cl_2 species is a very active compound which is currently in clinical trials. We have recently started a very detailed study of complexes of the types *cis*- and *trans*-$Pt(Ypy)_2X_2$ (where Ypy =pyridine derivative and X = I, Cl, NO_3). The chloro and

iodo compounds of pyridine have been known for a long time but the nature of the Pt-pyridine bond is still unknown. Pyridine derivatives have empty π* orbitals, which can accept back-donation from the metal. The results of our study have shown how the use of crystallography, multinuclear (^{195}Pt, ^{1}H and ^{13}C) NMR and IR spectrocopy can bring interesting new information on the nature of the Pt(II)-ligand bonds especially with pyridine ligands. Six different pyridine derivatives were used and the 36 complexes were synthesized by slight variations of published methods. Thirteen compounds were studied by X-ray diffraction methods. Most structures have shown the *anti* conformation of the two pyridine ligands, while one contained the two ligands in a *syn* conformation. The relative *trans* influence of the ligands used in this project will be discussed.

08OA CRYSTALLOGRAPHY AND NMR OF RNA

M08.OA.001 ABSTRACT NOT AVAILABLE. T. Steitz

M08.OA.002 ABSTRACT NOT AVAILABLE. J.D. Puglisi

M08.OA.003 NMR STUDIES OF RNA-PROTEIN COMPLEXES AND MULTIMOLECULAR ASSEMBLIES DURING GENE EXPRESSION. Gabriele Varani - MRC Laboratory of Molecular Biology Hills Road - Cambridge CB2 2QH - UK

RNA-protein complexes play a central role in every aspect of the post-transcriptional regulation of gene expression. Our work aims at understanding the structural principles underlying RNA-protein recognition and the mechanism by which gene expression occurs and is regulated. One extreme example in RNA recognition is provided by human U1A, a protein that recognizes partially single stranded RNA in a highly specific faction. A very different example of RNA recognition is provided by is the structure of the Staufen dsRBD domain in complex with double stranded RNA, a non-sequence specific complex. The comparison with X-ray studies of related protein-RNA complexes provides an opportunity to describe the convergence and complementarity of information provided by the two techniques. At a more complex structural and biochemical level, biological regulation can be achieved not only by modulating RNA recognition, but also through RNA-dependent protein-protein interactions in the multimolecular assemblies that constitute structural and functional units during gene expression. As a paradigm to understand these processes, we are studying the 40 kDa ternary complex between two human U1A proteins and the U1A polyadenylation regulatory element RNA. Recent advances in the NMR method makes structures of this size and larger a challenging but entirely feasible goal. The ternary complex regulates expression of the U1A protein itself by interfering with the formation of the poly(A) tail in the cell nucleus. Interaction with RNA induces a conformational change in the protein that allows two U1A molecules to bind cooperatively and to interact with Poly(A)-polymerase enzyme. Thus, apparently distinct molecular recognition events are triggered by an RNA-dependent conformational change to ensure exquisite specificity in the regulation of Poly(A) polymerase activity.

M08.OA.004 FRET ANALYSIS OF U1A PRE-mRNA 3'-UTR GLOBAL STRUCTURE. David M.J. Lilley, Richard J. Grainger and David G. Norman, CRC Nucleic Acid Structure Research Group, Department of Biochemistry, University of Dundee, Dundee DD1 4HN, United Kingdom.

FRET is a valuable method for obtaining long-distance information in nucleic acids. U1A pre-mRNA contains a U1A binding element in its 3' untranslated region (UTR), comprising two asymmetric loops separated by a four basepair duplex. Using FRET we have measured the bending angle of a single UTR loop, obtaining an included bend angle of 100°. The FRET data for the complete 3'-UTR element suggest a dihedral angle between the outer helical segments of 35°. We can observe binding of U1A protein to the 3'-UTR element by a change in the fluorescence anisotropy of Cy3 attached to one of the helical ends. In parallel with the binding we observe a marked increase in FRET efficiency between fluorophores attached at the two 5' termini, indicating a significant change in global conformation induced by the binding of the protein.

R.J. Grainger, D.G. Norman and D.M.J. Lilley (1999) Binding of U1A protein to the 3' untranslated region of its pre-mRNA *J. Molec. Biol.* 288, 585-594.

M08.OA.005 STRUCTURE OF THE MATURED FORM OF THE DIMERIZATION INITIATION SITE OF HIV-1(Mal) GENOMIC RNA. P. Dumas, E. Ennifar, M. Yusupov, P. Walter, R. Marquet, B. Ehresmann, C. Ehresmann, IBMC-CNRS, 15 rue Descartes F67084 STRASBOURG

An important step of the replication cycle of retroviruses is the dimerization of its RNA genome prior to encapsidation. The Dimerization Initiation Site (DIS) is made of a hairpin closed by a loop with a self-complementary sequence of 6 nt [1]. This allows the formation of a transient 'kissing-loop complex' (Fig.1) which is thought to be matured *in vivo* by the basic viral nucleocapsid protein (NCP) into an elongated duplex [2]. We have crystallized a 23nt fragment corresponding to the DIS hairpin [3]. In some occasions, either perfectly or partially twinned crystals were obtained (space group $P3_121$). The structure was solved by the MIR method by use of bromo and iodo-uridine, as well as $Ru(NH_3)_6$, and subsequently refined at 2.3Å resolution (Rfree=21.5%). The structure obtained is a 22 bp symmetrical duplex corresponding to the matured form. It shows two non-canonical Watson-Crick-like G-A bp adjacent to two bulged adenine residues (Fig.2). The latter, lying almost on top of each other, form a striking base grip which could be a recognition signal, either *in trans* for one protein (possibly the NCP), or *in cis* for some site within the viral RNA. A network of 8 magnesium cations is clearly visible, with one being unusually chelated across the major groove by the 3'-phosphates of each bulge.

Figure 1

Figure.2

1. Skripkin, E. *et al.*, Proc. Natl. Acad. Sci. USA, **91** (1994) 4945-4949.
2. Muriaux, D. *et al.*, J. Biol. Chem. **271** (1996) 33686-33692.
3. Yusupov, M. *et al.*, Acta Cryst. **D55 (**1999) 281-284.

08OB LARGE UNIT CELLS: SOURCES, DETECTORS AND DATA

M08.OB.001 DESIGN OF BEAMLINES FOR MACRO-MOLECULAR CRYSTALLOGRAPHY AT 3RD GENERATION SOURCES. Gerd Rosenbaum, Argonne National Lab, Argonne, IL 60439, USA

The high flux emitted into a very narrow cone by undulators at 3rd generation storage rings makes them an ideal source for crystallography on macromolecular crystals with large unit cells. The purpose of the beamline optics is to transform the characteristics of the beam emitted by the undulator into those which are optimal for the crystallographic experiment. Generally, the optimum is a match between the sizes of the image of the source, the size of the sample and the size and spatial resolution of the detector used for recording the diffraction peaks. Strategies for beamline layout, with emphasis on suitability for small crystals with large unit cells, will be presented in general and in detail for systems using high resolution area detectors.

M08.OB.002 DATA COLLECTION FROM LARGE UNIT CELL CRYSTALS USING CCD AND LARGE IP DETECTORS ON ID14 AT THE ESRF. S. Wakatsuki, ESRF, B.P.220, 38043 Grenoble, France

The high brilliance protein crystallography beamlines at the ESRF, ID2PX and ID14/EH1-4 have made hitherto unfeasible diffraction experiments possible. These include data collection from extremely large structures (thus weakly diffracting) and very small crystals. Key factors for the success of such experiments are high brilliance, low divergence, stable optics, and large and fast detectors. X-ray beams from undulator sources on third generation synchrotron sources satisfy the first two conditions, while modern beam line design provides reliable optics which can withstand the heat load of high brilliance X-ray beam. The low divergence of the X-ray beams on ID14, on the order of 10 microradians, enables separation of diffraction spots corresponding to d-spacing of a few thousands of Ångstroms.

The choice of detectors is also of critical importance. We chose two types of detectors: fiber optics coupled CCD and image plate (IP) detectors. The point spread function of the detectors must be comparable to the physical dimensions of diffraction spots from crystals of 50 to 200 microns in size. The overall dimension, thus the number of pixels, needs to be sufficiently large in order to collect a large number of diffraction orders. For example, the 2k by 2k CCD detector on ID14/EH4 can record 500-550 diffraction orders with a duty cycle of 10 frames per minute.

Another solution for capturing as many diffraction orders as possible is to use image plates since larger active areas can be achieved more readily. We have developed a Weissenberg camera with an active area of 800 mm by 800mm for one of the experimental stations, EH3. Two image plates, 40 cm by 80 cm, are placed on a flat wall by a robot from an IP storage/erasure device standing next to the robot. The image plates are read out using an off-line IP drum scanner with 100 micron pixel size.

Recent examples of medium- to high- resolution data collection from crystals with large unit cell dimensions will be presented.

M08.OB.003 DATA PROCESSING USING DPS. C.G. van Beek and M.G. Rossmann, Department of Biological Sciences, Purdue University, W-Lafayette, IN 47907, USA.

A new set of programs is being developed for the processing of X-ray diffraction data collected on oscillating single crystals. These programs are based on extensive experience by us [1][2] and others [3], but also take into account the opportunities provided by frozen crystals and 2-D detectors such as CCD devices.

Data collected on frozen crystals of proteins, nucleic acids and other biological macromolecules often have relatively large mosaic spreads. As the mosaic spread approaches the useful oscillation range, special care has to be taken not to rely upon methods of data processing that are based on the availability of full recorded reflections.

With this in mind several programs have been developed as part of the Data Processing Suite (DPS). The auto-indexing [4] program and scaling [5] program are now in daily use; an integration program is to follow. Recent additions to the scaling program include statistics for assessing the quality of the anomalous signal of anomalous dispersion data.

These programs are freely available, for more information see: www-structure.bio.purdue.edu/~viruswww/Rossmann_home/dps/index.shtml

[1] M.G. Rossmann (1979). J. Appl. Cryst., 12, 225
[2] M.G. Rossmann, A.G.W. Leslie, S.S. Abdel-Meguid, T. Tsukihara (1979). J. Appl. Cryst., 12, 570
[3] Collaborative Computational Project, Number 4 (1994), Acta Cryst., D50, 760
[4] I. Steller, R. Bolotovsky and M. G. Rossmann (1997). J. Appl. Cryst., 30, 1036
[5] R. Bolotovsky, I. Steller and M.G. Rossmann (1998). J. Appl. Cryst., 31, 708

M08.OB.004 STRUCTURE OF REOVIRUS CORES. Stephen C. Harrison and Karin Reinisch, Howard Hughes Medical Institute and Harvard University, Cambridge MA, and Max Nibert, University of Wisconsin, Madison, WI

The structure of the core of reovirus has been determined, using crystals in space group F432, a=1249 Å, which diffract to about 3.5 Å. There are over 300 kDa in the icosahedral asymmetric unit and over 1.5 MDa in the crystallographic asymmetric unit. Data were collected using tandem image plates at the F1 beamline at CHESS. Initial phases were determined using a 28 Å resolution cryoEM reconstruction (from T. Baker, Purdue University), and phases were extended to 3.8 Å using fivefold averaging. There are two copies of the lambda1 protein in the icosahedral asymmetric unit: they have somewhat different conformations and largely non-equivalent contacts. Their packing and fold are related to VP3 of orbivirus cores (Stuart and co-workers). The lambda2 protein forms chimney-like protrusions around the fivefold axes. Each subunit appears to contain three of the enzymatic active sites required for RNA capping: one guanylyl transferase and two methylases. There are two copies of the sigma2 protein in the icosahedral asymmetric unit, plus a third copy on the icosahedral dyad (and hence present in two orientations, statistically). Sigma2 appears to serve as an adaptor for the outer layer of proteins in the complete virus particle. Further comparisons with cryoEM images of virions and infectious subviral particles yield information about rearrangements during the process of infection and about mechanisms of mRNA extrusion.

M08.OB.005 CRYSTALLOGRAPHIC STUDIES OF A T=7, dsDNA VIRUS CAPSID WITH A DIAMETER OF 650Å. J. E. Johnson[1], W. R. Wikoff[1], L. Liljas[1,3], R. L. Duda[2], and R. W. Hendrix[2] [1]Dept. Mol. Biol. The Scripps Research Institute, La Jolla, CA, 92037, USA [2]Dept. of Biol Sci., University of Pittsburgh, Pittsburgh, PA, 15260, USA [3]Biomedical Center, Department of Molecular Biology, University of Uppsala, Uppsala, Sweden

Empty capsids of the dsDNA bacteriophage HK97, a lambda-like phage, were prepared by co-expressing the capsid protein gene and a virally encoded protease in an E. coli system.

420 copies of the 42kD subunits spontaneously assemble into a capsid with a diameter of 450Å which contains about 50 copies of the protease [1]. Assembly activates proteolytic cleavage of the subunit removing 102 residues from the amino terminus and auto digestion of the protease. Maturation expansion to a 650Å diameter particle (head II) results from DNA packaging and initiates an auto catalytic cross linking between side chains of ASN356 and LYS169 and this results in an extraordinary chain linking of the hexamer and pentamer morphological units making the particles impervious to SDS treatment [2]. Here we report the 3.5Å structure of head II, which explains expansion, cross-linking and chain-mail. The particles crystallize in space group $P2_1$ a=580Å, b=625Å, c= 790Å, β=90.0° [3]. The structure was solved by phase extension with a cryoEM reconstruction serving as an initial phasing model at 30Å resolution [4]. Low resolution (200-15Å) data that allowed overlap with the resolution of the cryoEM model were collected on beam line 4-2 at SSRL [5], 5Å data were collected on beam line F1 at CHESS and data to 3.5Å resolution were collected on beam line 14BM-C at APS.

1. Hendrix, R. & Duda, R. Advances in Virus Research 50, 235-288 (1998).
2. Duda, R. Cell 94, 55-60 (1998).
3. Wikoff, W., Duda, R., Hendrix, R. & Johnson, J. Virology 243, 113-118 (1998).
4. Conway, J., Duda, R., Cheng, N., Hendrix, R. & Steven, A. J. of Mol. Biol. 253, 86-99 (1995).
5. Tsuruta, H., Reddy, V., Wikoff, W. & Johnson, J. J. Mol. Biol. 284, 1439-1452 (1998).

P08.OB.001 A LOOOOONG C AXIS; NOT A VIRUS, THOUGH. Yves Bourne[1], Wim P. Burmeister[2], & Pascale Marchot[3] [1]CNRS UPR 9039 Architecture et Fonction des Macromolécules Biologiques, Institut de Biologie et Microbiologie Structurale, Marseille, France. [2]Experiments Division, European Synchrotron Radiation Facility, Grenoble, France. [3]CNRS UMR 6560 Ingénierie des Protéines, IFR Jean Roche, Faculté de Médecine Nord, Marseille, France.

Crystals of mouse acetylcholinesterase, an α/β hydrolase, in complex with the peptidic inhibitor fasciculin (Fas2-mAChE complex) belong to space group $P6_522$ with cell dimension c ≥ 500 Å whether $AmSO_4$ or PEG is used as a precipitant [1, 2]. Separation of the resulting overlapping spots usually requires a very large crystal-detector distance, but the maximal resolution achieved is not sufficient to permit detailed intrepretation of the structures. High quality X-ray data were collected at the ESRF beamline ID14-EH3 equipped with i) a combination of a 2k x 2k CCD detector on a 2θ arm for fast screening of crystals and determination of the orientation matrix, ii) a Weissenberg camera with a very large active area using image plates (up to 80 x 80 cm), iii) an industrial robot for automatic exchange of the image plates, iv) an off-line image plate scanner [3]. With this set-up, we collected complete data with resolution up to 2.5 Å with a total oscillation of 36° and a 3° oscillation range, with the long c axis of the crystal being roughly aligned to the spindle axis; the crystal-to-detector distance was 590 mm. In this particular case, data collection required a single manual intervention. Five complete data sets were collected: a « native » Fas2-mAChE complex, and four ternary Fas2-mAChE-2nd inhibitor complexes obtained either by co-crystallization of the three partners or by soaking of the Fas2-mAChE crystals with the 2nd inhibitor. Details on the large image plate device, the data, and the refined structures will be presented.

[1] Marchot P, Ravelli RBG, Raves ML, Bourne Y, Vellom DC, Kanter J, Camp S, Sussman JL, & Taylor P (1996) Soluble monomeric acetylcholinesterase from mouse: expression, purification, and crystallization in complex with fasciculin. *Protein Sci.* 5, 672-679
[2] Bourne Y, Taylor P, & Marchot P (1995) Acetylcholinesterase inhibition by fasciculin: crystal structure of the complex. *Cell* 83, 503-512
[3] ESRF Newsletter apr. 1997, vol. 28, pp. 30-32 (http://www.esrf.fr/exp_facilities/ID14EH3/user_guide.html)

P08.OB.003 FIRST RESULTS FROM A NOVEL MICROFOCUS X-RAY GENERATOR FOR X-RAY CRYSTALLOGRAPHY. Ewa Ciszak[1], Mikhail Gubarev[1], Marshall Joy[1] and Walter Gibson[2] [1]NASA/G. Marshall Space Flight Center, Huntsville, AL 35812, USA, [2]State University of New York at Albany, NY 12222, USA.

The success of the Synchrotron radiation laboratories has not reduced the need for laboratory based x-ray diffraction systems. Indeed, the success of synchrotron laboratories in study of smaller and more complex crystals has pointed out the importance of high brightness x-ray sources in close proximity to crystal growth activity, ideally located in the same laboratory.

We present here the initial performance results from a microfocus x-ray generator combined with a polycapillary concentrator, which is being developed for crystallography. The 40-Watt, 35-micron FWHM x-ray source has been optimised for use with short focal length polycapillary optics to maximise the solid angle of collection of the emitted x-rays. We present measurements of the x-ray photon flux from the microfocus source/optics combination for 0.5mm and 1mm diameter beams, the spectral characteristics of the emergent beam and compare these results with measurements taken from standard rotating anode/optics systems.

08OC HIGH PRESSURE STRUCTURES AND PHASE TRANSITIONS

M08.OC.001 HIGH PRESSURE - HIGH TEMPERATURE POWDER DIFFRACTION STUDIES OF BINARY HALIDES. S. Hull, The ISIS Facility, C.L.R.C. Rutherford Appleton Laboratory, Chilton, Didcot, Oxfordshire, OX11 0QX, United Kingdom.

The high pressure structural behaviour of the 'simple' binary halides of stoichiometry AX and AX_2 (X=F, Cl, Br and I) has long been a popular topic for both experimental and ab-initio theoretical study. The results of recent high pressure neutron and X-ray diffraction studies of these materials will be presented and compared with calculations of their structural behaviour. Particular emphasis will be placed on the following two systems.

i) The silver and copper mono-halides are interesting compounds because their bonding character is intermediate between ionic and covalent. CuCl, CuBr, CuI and AgI adopt the tetrahedrally co-ordinated zincblende structure under ambient conditions whilst AgF, AgCl and AgBr are octahedrally co-ordinated with the rocksalt arrangement. In general, the expected phase transition sequence zincblende→rocksalt→CsCl-type occurs, though many intermediate phases of lower symmetry are observed. However, in AgCl and AgBr the continuous rhombohedral transformation from zincblende to rocksalt predicted by electronic structure calculations [1] does not occur.

ii) The high temperature behaviour of di-halides with the cubic fluorite crystal structure has been widely investigated owing to the superionic behaviour associated with extensive thermally-induced dynamic anion disorder. Under pressure, many of these compounds transform to the orthorhombic cottunite structure and there has been debate within the literature concerning possible superionic behaviour within this denser arrangement. High pressure - high temperature neutron diffraction studies have been

performed to resolve this issue and shed light on the relative importance of crystal structure in promoting superionic behaviour.

[1] G.S.Nunes, P.B.Allen and J.L.Martins, Phys. Rev. B, **57**, 5098 (1998).

M08.OC.002 STRUCTURAL SYSTEMATICS OF HEAVY ALKALINE METALS AT HIGH PRESSURES. U. Schwarz, MPI fuer Chemische Physik fester Stoffe, Pirnaer Landstr. 176, D-01257 Dresden, K. Syassen and O. Jepsen, MPI fuer Festkoerperforschung, Heisenbergstr. 1, D-70569 Stuttgart, M. Hanfland, ESRF, BP 220, F-38043 Grenoble, and K. Takemura, National Institute for Research in Inorganic Materials, Tsukuba, Japan

We investigated crystal structures and bonding properties of the heavy alkaline metals at high pressures. Recently, the orthorhombic crystal structure of the high-pressure modification Cs-V (P>11 GPa) has been determined by means of angle dispersive x-ray powder diffraction at the ESRF [1]. The characteristic feature of this Cmca-structure, which can be viewed as a distorted fcc packing, are layers of corner-sharing octahedra. Within the equatorial plane of the octahedra each atom has a fifth contact to an atom in a neighboring polyhedron which is the shortest nearest-neighbor-distance in the crystal structure. Subsequent investigations revealed that the high-pressure phases Si-VI (38 GPa < P < 50 GPa) [2] and Rb-VI (P > 48 GPa) crystallize in the same space group and show similar axial ratios and free positional parameters.

The chemical bonding of Cs-V and Si-VI was studied within the local density functional approach by means of the TB-LMTO-ASA bandstructure method. For Cs-V the calculations reveal regions of high electron density and attractors of high ELF values in the centres of the octahedra which exhibit strong similarities to a framework of condensed octahedral clusters with two electrons per polyhedron [3]. For silicon we observe Si_2-dumbbells in every second layer of the crystal structure and in the alternating layers four-bonded silicon atoms form puckered nets.

Currently, the high pressure modifications K-III and Rb-IV are under investigation. Progress regarding phase stability and crystal structure will be reported.

[1] U. Schwarz et al., Phys. Rev. Lett., 81 (1998) 2711.
[2] M. Hanfland et al., Rev. Lett., in press.
[3] A. Savin, et al., Angew. Chem. Int. Ed. 36, 1808 (1997).

M08.OC.003 PHASE TRANSITION IN AX_4 TYPE MOLECULAR CRYSTALS UNDER PRESSURE. Nozomu Hamaya and Kyoko Sato, Graduate School of Humanities and Sciences, Ochanomizu University, Tokyo 112, Japan

Crystals consisting of tetrahedral molecules AX_4 (A: group IV atoms, X: halogens) exhibit a variety of structures at high pressure. Stannic iodide SnI_4 represents AX_4 type molecular crystals and undergoes successive pressure-induced phase transition from an insulator crystalline phase, to a metallic crystalline phase at 7 GPa, to an amorphous state at about 15 GPa and to a non-molecular crystalline phase at 61 GPa at room temperature. Our recent x-ray diffraction study showed that a new crystalline phase became stable at 500K and 7 GPa. Crystal structure of the non-molecular phase at 63 GPa was studied using the anomalous x-ray dispersion below the K absorption edge of Sn. Measured photon-energy dependence of the intensity of diffraction peaks suggests a formation of the disordered alloy in which both Sn and I ions are randomly located at the fcc lattice sites.

Phase transition in GeI_4 and $SnBr_4$ were also studied at high pressure. In GeI_4, the amorphous phase appeared at about 30 GPa and persisted to the maximum pressure of our study, 100 GPa, which is much higher than the recrystallization pressure of 61 GPa in SnI_4 into a non-molecular structure. This indicates that the difference in size or electronic structure of cation plays an important role in dissociation of tetrahedral molecules. A high-pressure phase of $SnBr_4$ was newly observed at 3 GPa and found to have the same crystal structure as that SnI_4 and GeI_4 exhibited at 1 atm. Structural disordering proceeded gradually above 10 GPa, but several, broad diffraction peaks still remained at 30 GPa. On the basis of those results, we will discuss structural systematics of the AX_4 type molecular crystal at high pressure.

M08.OC.004 HIGH PRESSURE PHASE TRANSITIONS IN CARBON DIOXIDE. Choong-Shik Yoo, Lawrence Livermore National Laboratory, Livermore, California 94550

Application of high-pressure strongly perturbs chemical bonds, electronic and crystal structures, thermal and mechanical properties, and reactivities of solids. These perturbations provide opportunities for synthesizing novel materials and metastable phases. At high pressures, the electron kinetic energy increases, and the intermolecular potential becomes highly repulsive in nature. Therefore, a fundamental principle of high-pressure phase transition is to soften the repulsive potential by electrons delocalizing and forming extended bonds amongst neighboring molecules. The mechanisms which often occur in molecular solids at high pressures are (i) ionization, (ii) polymerization, (iii) metallization. In this paper, we present the experimental evidences for high-pressure transitions to ionic and polymeric phases of molecular carbon dioxide occurring prior to the metallization, based on our micro-Raman and x-ray investigations.

Work performed under the auspices of the U.S. DOE by the LLNL under contract number W-7405-ENG-48. This work has been done in collaborations with V. Iota, H. Cynn, K. Visbeck, M. Nicol, D. Hauserman, S. Carlson.

M08.OC.005 THEORETICALLY SERACHING FOR NEW MATERIALS UNDER HIGH PRESSURE. Shinji Tsuneyuki, Institute for Solid State Physics, University of Tokyo, Roppongi, Tokyo 106-8666, JAPAN.

Thanks to the recent development of computational science approaches, it is often not so difficult to predict stable structures and electronic properties of unknown materials theoretically, if we could know or assume rough arrangement of the constituent atoms in the materials. One of the most useful and reliable methods for that purpose is the first-principles molecular dynamics (FPMD) method or Car-Parrinello method, in which atoms are moved according to the interatomic forces calculated at each MD step based on the density functional theory. Combined with the constant-pressure formalism in the traditional MD, it can be a powerful tool for high-pressure physicists who search for new materials or phase transitions.[1]

We report two applications of FPMD in high-pressure physics. The apparently fcc phase of SnI_4 observed very recently above 61 GPa by an X-ray measurement [2] is identified as substitutional solid solution of tin and atomic iodine. We also predict that some graphite intercalation compounds could transform into novel crystalline phases under high pressure.

1. Y. Tateyama, T. Ogitsu, K. Kusakabe and S. Tsuneyuki, Phys. Rev. B54, 14994(1996); Phys. Rev. B55, R10161(1997) and references therein.
2. N. Hamaya, K. Sato, K. Usui-Watanabe, K. Fuchizaki, Y. Fujii and Y. Ohishi, Phys. Rev. Lett. 79, 4597(1997).

M08.OC.006 SOME REMAINING ISSUES WITH THE PHASES OF IRON SULFIDE. J. B. Parise, CHiPR[§] and Geosciences, SUNY, StonyBrook, NY 11794-2100, USA, W. G. Marshall, ISIS Facility, Rutherford Appleton Laboratory, Didcot, UK, and M. I. McMahon, R. J. Nelmes, D. R. Allan, S. A. Belmonte and C. Vanpeteghem, Department of Physics and Astronomy, University of Edinburgh, Mayfield Road, Edinburgh, EH9 3JZ, UK [§] Center for High Pressure Research, an NSF funded Science and Technology Center

The sulfides containing iron are amongst the more important high-pressure planetary accessory minerals. They have also received renewed interest of late as possible platforms for the formation of amide bonds, a significant reaction in studies of the origin of life (Wächtershäuser 1988). There are conflicting details reported of the phases forming in the Fe-S binary at high-pressures and high-temperatures however (see for example Fei et al., 1995; Kusaba et al., 1998). Some of the issues raised in these reports include:

1) The existence and nature of the high temperature phase formed upon transition from troilite; 2) the thermodynamic stability of the MnP-related phase formed at pressures intermediate between those where troilite and "FeS-III" are stable; 3) the role of composition on the behavior of FeS and 4) the electronic and magnetic properties of phases in the FeS-binary and other ternary-sulfides containing iron. The low temperatures involved in many of these transitions, and resultant sluggish reaction kinetics, might explain some of the conflicts in the literature. The differences between the in situ techniques used to study these materials may also be relevant. The largest contributor, however, is probably small differences in composition and sample homogeneity. In this presentation, the results of recent in situ X-ray and neutron powder diffraction experiments addressing these issues will be discussed. The small differences in the diffraction patterns of the phases involved make the use of high-resolution powder diffraction techniques, along with combined nuclear and magnetic scattering, advisable.

Fei et al. (1998) Science, 268:1892-1894
Kusaba et al. (1998) J. Phys. Chem. Solids, 59: 945-950
Wächtershäuser G. (1988) System Appl. Microbiol. 10:207-210

P08.OC.001 POLYMERIZED STRUCTURES OF C_{60} AND C_{70} SUPERHARD PHASES. N.R. Serebryanaya, V.D. Blank and G.A. Dubitsky, S.G. Buga, Technological Institute for Superhard & New Carbon Materials, 142092 Troitsk Moscow Reg. Russia, and L.A. Chernozatonsky, Institute of Chemical Physics of RAS, 117334 Moscow, Russia, and S.N. Sulyanov, Institute of Crystallography of RAS, 117333 Moscow, Russia.

Superhard phases of C_{60} and C_{70} (their hardness is equal to the diamond one) have been found after high pressure (13 GPa)- high temperature (2100 K) treatment with use of a diffractometer Kard-6 with a flat proportional chamber on the fast delay lines [1]. C_{60}-crystal structure has been determined as a three-dimensional polymerized one with 24 single covalent bonds. It is a cubic closest-packed structure of C_{60} cages and the other fullerite-like clusters are in the octahedral cavities. C_{60} cages are deformed and the real symmetry is orthorhombic one. C_{70} crystal structure is the same but more distorted. Atom coordinates have been obtained by molecular mechanics methods. Good fit to the C_{60} profile was obtained by the Rietvild analysis program DBWS9411. The densities calculated from X-ray diffraction data accord with experimental densities measured by the flotation method.

Crystalline states remain up to 900-1000 K, then fullerite cages collapse producting different 3D-polymerized disordered structures. The cross-linked layered disordered structure is observed in the both fullerites up to 9.5 GPa and above 900 K. At P≥12.5 GPa the second type of disordered structure is observed. This structure is transient to diamond states and the diffraction pattern has one wide halo at 2.18-2.16 Å. It is the hardest phase found only for C_{60}. The P-T phase diagram of C_{60} and C_{70} is plotted with use of X-ray diffraction data.

1. V.D. Blank, N.R. Serebryanaya et al (1998). Phys.Lett. A, **248**, 415.

P08.OC.002 STRUCTURAL STUDIES OF SEMICONDUCTORS AT HIGH PRESSURE AND HIGH TEMPERATURE. C. Vanpeteghem, S.A. Belmonte, M.I. McMahon, D.R. Allan and R.J. Nelmes Department of Physics and Astronomy, The University of Edinburgh, Edinburgh EH9 3JZ, UK

Our research on the high-pressure phases of III-V and II-VI semiconductors has shown that most phases are site-ordered [1], but that there are some exceptions to this such as the Imma phase of GaSb [2]. We have also identified many misinterpreted phases and one of our most surprising discoveries is the complete absence of the diatomic beta-tin structure [3], despite numerous previous reports of its existence. Rather, it appears that all systems transform into complex lower-symmetry structures, which have variable atomic coordinates that are often strongly pressure dependent. This makes the high-pressure study of semiconductors more complex, and thus more interesting, than previously thought.

The absence of the diatomic beta-tin structure is very unexpected since theoretical calculations on GaAs and GaP [4] have reported that this structure has an energy lower than that of Cmcm, the orthorombic phase actually found. Until now no site-ordered tetragonal structure, with the exception of HgO-II, has been observed in any of the III-V or II-VI systems.

We are currently developing combined high-pressure high-temperature (HP/HT) diffraction techniques to make more detailed studies of atomic ordering in these systems. Experiments on GaSb under such conditions have found a transition from the Imma structure, which is a slight orthorhombic distortion of site-disordered beta-tin, to a true tetragonal beta-tin structure. Further HP/HT studies will not only allow us to clarify the complex matter of site-ordering but will also allow us to investigate the full P-T dependence of the structural systematics of semiconductors - an area which is relatively unexplored. The most recent results of all this work will be presented.

[1] R.J.Nelmes and M.I. McMahon, Semiconductors and Semimetals, Vol. 54, 145 (1998).
[2] M.I.McMahon et al., Phys. Rev. B 50, 13047 (1994).
[3] R.J.Nelmes et al., Phys. Rev. Lett. 79, 3668 (1997).
[4] A.Mujica and R.J. Needs, Phys. Rev. B55, 9659 (1997).

P08.OC.003 EFFECT OF HIGH PRESSURE AND CHEMICAL SUBSTITUTION ON STRUCTURE OF TETRAVALENT METALS. V.F. Degtyareva, Institute of Solid State Physics, Russian Academy of Sciences, Chernogolovka, Moscow district, 142432 Russia, W.B. Holzapfel, FB Physik, Universität-Paderborn, 33095 Paderborn, Germany.

Pressure action and chemical substitution lead very often to similar trends with respect to structural changes. While the light group IV elements Si and Ge have a common peculiar high-pressure form with *simple hexagonal* (*hP*1) structure, this structure does not occur for Sn. However, the *hP*1 phase can be produced in Sn at normal pressure by alloying with ~10 at.% Hg or ~20 at.% In. This observation raises the question, which structural sequence will be obtained in these alloys under pressure.

High-pressure structural studies using diamond anvil cells and energy dispersive X-ray diffraction with synchrotron radiation revealed for $Sn_{.9}Hg_{.1}$ the transformation from *hP*1 to a *body-centered tetragonal* phase, *tI*2, as for pure Sn, with nearly the same axial ratio $c/a \approx 0.92$. However, for $Sn_{.8}In_{.2}$ different structural sequence *hP*1→*intermediate*→*hP*2 was found under

pressure with more similarities to pure Si. The intermediate low symmetry phase of Sn_8In_2 seems to be closely related to an orthorhombic distortion of *hP*2, different to the complex structure of Si-IV. These results demonstrate the strong dependence of the high-pressure structural sequences in Sn alloys on the special chemical substitution.

Effects of pressure on the structural behavior for metals and alloys with nearly 4 valence electrons are discussed with respect to other recent high pressure studies with observation of *hP*1 in the Al-Ge [1], Cd-Sb and Zn-Sb [2] binary alloys and of *tI*2 in the III-V compound InBi [3].

1. V. F. Degtyareva, F. Porsch, E. G. Ponyatovskii, W. B. Holzapfel, Phys. Rev. B **53**, 8337 (1996)
2. V. F. Degtyareva, I. Bdikin, S. S. Khasanov, Fiz. Tverd. Tela **39**, 1509 (1997) [Phys. Solid State **39**, 1341 (1997)]
3. V. F. Degtyareva, M. Winzenick, and W. B. Holzapfel, Phys. Rev. B **57**, 4975 (1998)

P08.OC.004 PHASE DIAGRAM OF $KNbO_3$ UP TO 30 GPa AND FROM 700 K DOWN TO 10 K. D. Gourdain, J.C. Chervin, B. Canny, Ph. Pruzan, Physique des Milieux Condensés UMR 7602, Université P & M Curie B77 75252 PARIS Cedex 05, France, M. Hanfland, ESRF, BP220, 38043 Grenoble Cedex, France.

Investigations of the phase diagram of $KNbO_3$ using x-rays diffraction and Raman scattering are reported. Experiments were performed in the diamond anvil cell up to ~ 30 GPa and from the atmospheric Curie temperature (700 K) down to 10 K.

At room pressure this compound is well known to undergo the phase transition sequence: cubic → tetragonal → orthorhombic → rhombohedral. The cubic solid is paraelectric, the other being ferroelectric. As pressure increases a lowering of the various transition temperatures was expected, and observed for $BaTiO_3$,[1,2] however the phase diagram of this type of compound is hardly known. At room temperature the vanishing of the ferroelectricity in $KNbO_3$ was observed at ~ 10 GPa using Raman scattering.[3]

Above and below ambient temperature, high pressure analysis were performed along isothermal or isobaric paths with micro Raman scattering and angular dispersive x-ray diffraction. Data were obtained on the p-T locations of the various transitions, the vibrational dynamics and the equation of state. Our preliminary results show that the different ferroelectric states are close domains in the p-T diagram: the various transition temperatures decrease linearly at low pressure, these drops become more rapid, and consequently non-linear, on further compression. The modifications of the Raman spectrum, on increasing pressure, will be presented and the values of the parameters of the equations of state will be discussed.

1. G.A. Samara (1987), Ferroelectrics 73, 145.
2. T. Ishidate, S. Abe, H. Takahashi, and N. Mori (1997), Phys. Rev. Lett. 78, 2397
3. D. Gourdain, E. Moya, J.C. Chervin, B. Canny, and Ph. Pruzan (1995), Phys. Rev. B 52, 3108.

P08.OC.005 NEUTRON DIFFRACTION STUDIES OF THE HYDROGEN BOND UNDER HIGH PRESSURE. M. Guthrie, J. S. Loveday, R. J. Nelmes, Dept. of Physics and Astronomy, The University of Edinburgh , Mayfield Rd, EDINBURGH, EH9 3JZ, UK

The hydrogen bond is an important interaction to a wide range of science from the physics of the interiors of giant planets to the behaviour and function of biological molecules. The behaviour of hydrogen bonded materials under high pressure probes the density dependence of the O-H and H...O interactions and hence provides fundamental and widely applicable insight into the nature of the bond itself. The ability to observe the changes in structure induced by pressure is a crucial part of this understanding. For example, our early neutron diffraction study of ice VIII [Nelmes et al, Phys. Rev. Lett. **71, (**1993), 1192] provided the first accurate information on the structural pressure dependence of H-bond dimensions over a 10GPa range. This showed that the previously-held assumptions used to interpret the vibrational spectroscopy of H-bonded solids at high pressure were significantly incorrect in this case, and consequently are suspect in others.

We have now extended our studies of H-bonded materials at high pressure using the Paris-Edinburgh cell at the ISIS pulsed neutron source to explore two new aspects. It has emerged from work at ambient pressures that the H-bonds in hydroxides are significantly different from those in molecular solids. In addition, there has been a suggestion that H...H repulsive interactions may play a far more significant role in high-pressure behaviour than has been generally recognised. We will present studies of the alkali hydroxides which provide new insight into these inter-bond effects as well as new information on the O-H and H...O interactions. Successful experiments have already been performed on KOD. The results appear to question the assumed minimum H...H separation and suggest that proton repulsion is not the mechanism for the observed high-pressure phase transition in this case.

P08.OC.006 STRUCTURAL EVOLUTION OF RUTILE-TYPE AND $CaCl_2$-TYPE GERMANIUM DIOXIDE AT HIGH PRESSURE. J. Haines, J. M. Léger and C. Chateau, Laboratoire de Physico-Chimie des Matériaux, C.N.R.S., 1, place Aristide Briand 92195 Meudon cedex, France and A. S. Pereira, Instituto de Fisica and Escola de Engenharia, UFRGS, 91501-970 Porto Alegre, Brazil.

Germanium dioxide undergoes a transition from the tetragonal, rutile-type to the orthorhombic, $CaCl_2$-type phase at 26.7 GPa. The detailed structural evolution of both phases at high pressure in a diamond anvil cell has been investigated by Rietveld refinement using angle-dispersive, x-ray powder diffraction data. These data were obtained on a laboratory source equipped with x-ray capillary optics and an imaging plate. Nitrogen and 16:3:1 methanol:ethanol: H_2O were used as pressure-transmitting media and laser annealing was performed to avoid deviatoric stress. The square of the spontaneous strain $(a-b)/(a+b)$ in the orthorhombic phase was found to be a linear function of pressure and no discontinuities in the cell constants and volume were observed indicating that the transition is second-order and proper ferroelastic. Compression of the GeO_6 octahedra was found to be anisotropic with the axial Ge-O distances decreasing to a greater extent than the equatorial distances. Above the phase transition, the columns of edge-sharing octahedra tilt about their 2-fold axes parallel to **c**. The present work has enabled systematic relationships in the homologous series, SiO_2, GeO_2, SnO_2, to be identified.

P08.OC.007 STRUCTURE OF THE HIGH-PRESSURE PHASE OF Fe_2O_3. G. Kh. Rozenberg, O. Naaman, M. P. Pasternak, School of Physics and Astronomy, Tel Aviv University, 69978, Tel Aviv, Israel, D. Hausermann, T. Lebian, ESRF, BP220, F-38043 Grenoble Cedex, France

The high-pressure form of Fe_2O_3 has been the subject of extensive investigation because of its significance in earth sciences. Early shock-wave and subsequent static compression experiments have shown that at 50 GPa hematite undergoes a structural phase transformation to a considerably denser structure (the HP phase), which could be assigned either to a "distorted corundum" (Rh_2O_3 II-type) or to an orthorhombic perovskite structure. Supported by the high-pressure Mössbauer studies it

was suggested that HP phase is characterised by two kinds of iron ions of different charge [1]. This incited the authors to choose the perovskite option to the HP phase with formula ABO_3 where A and B stand for different iron charge states and which could accommodate six-fold coordination number.

To elucidate the nature of the HP phase we performed XRD studies in the angle-dispersive mode, using the TAU miniature DAC and up to 80 GPa, at the ESRF ID30 beam-line. The diffraction peaks corresponding to the HP phase are first observed at ~ 45 GPa. The diffraction patterns of the pure HP phase recorded above 70 GPa could be exactly indexed to the distorted corundum structure (Rh_2O_3-II-type) with space group *Pbna*. This structure with formula A_2O_3 can be assigned only in case of a single cation position. This is in full agreement with recent Mössbauer studies revealing a single HP Fe^{3+} spectral component at P>72 GPa [2].

The present studies ascertain that at ~50 GPa hematite undergoes a transition from a corundum α-Fe_2O_3 to a distorted corundum Rh_2O_3-II structure.

1. T. Suzuki, T. Yagi, A. Akimoto et al., in Solid State Physics under Pressure, p. 149, KTK Scient. Publ., Tokyo (1985).
2. M. P. Pasternak, G. Kh. Rozenberg, G. Yu. Machavariani, O. Naaman, R. D. Taylor, and R. Jeanloz, to be published.

P08.OC.008 PHASE TRANSITIONS AND CRYSTAL STRUCTURES OF TWO IONIC CONDUCTORS AT HIGH PRESSURE. S. Werner[1], H. Schulz[1], B. Maximov[2], M. Sirota[2], [1]Institut für Kristallographie und Angewandte Mineralogie, Universität München, Theresienstr. 41, D-80333 München, Germany; [2]Institute of Crystallography, Academy of Science of Russia, Leninsky pr. 59, 117333 Moscow, Russia

Phase transitions and crystal structures of the two ionic conductors $Na_4TiO(PO_4)_2$ (NTP) and $Na_{4.5}Fe(O,F)(PO_4)_2$ (NFP) were investigated at pressures up to 12 GPa utilizing diamond anvil cells and single crystal diffraction techniques.

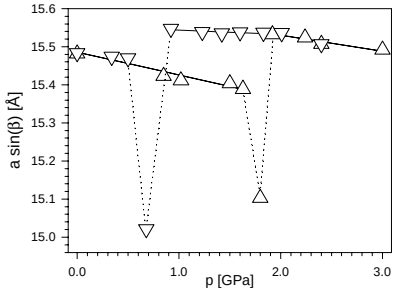

Fig.: NTP - a·sin(β) *vs.* pressure, triangles pointing up/down denote increasing/decreasing pressure.

For NTP, a phase transition is observed at a pressure of 1.8(1) GPa. At this pressure, the volume of the unit cell decreases by 2.4%. The back transformation at decreasing pressure is observed at 0.6(3)GPa, the phase transformation is characterized by a large hysteresis of 1.2 GPa. Furthermore, a marked instability of the unit cell parameters a·sin(β) and b is observed in conjunction with the phase transition (Fig.). Above 3 GPa, single crystals are destroyed, probably due to a second phase transition.

For NFP, up to 12 GPa, three phase transitions are obvious from sudden changes in the unit cell parameters a, b and c at 1.39(8), 4.5(3) and 6.0(2) GPa. No hysteresis could be detected within pressure cycles. The first and third phase transiton are also indicated by colour changes of the crystals from dark orange to pink and to violet. At six different pressures, reflection intensities were measured utilizing synchrotron radiation at HASYLAB to determine the structures of the high pressure phases.

P08.OC.009 PRESSURE DEPENDENCE OF STRUCTURE AND COMPOSITION IN THE XENON HYDRATE SYSTEM. J.L. Finney [1], C. Lobban, A. Klapproth, W.F. Kuhs [2], [1] Dept of Physics and Astronomy, University College London, Gower Street, London WC1E 6BT, UK, [2] MKI, Universität Göttingen, Goldschmidtstrasse 1, 37077 Göttingen, Germany

Clathrate hydrates are solid water structures which form a lattice of cages capable of enclosing guest molecules. These cages remain stable only through the inclusion of the guest, and would otherwise collapse. Most current research on these systems is motivated by the natural gas clathrates as a possible energy resource. In industry, clathrate formation has been a persistent and expensive annoyance in the transportation of hydrocarbons, with natural gas clathrate causing blockages in pipelines.

The actual amount of gas held within these clathrate structures in situ is uncertain, although it is thought likely that the cages are not fully occupied. It is generally assumed that the filling of the cages follows a Langmuir isotherm with increasing fugacity of the guest. Such a model is possible only by making certain assumptions (J.H. van der Waals and J.C. Platteeuw, Adv. Chem. Phys, 2, (1959), 1). First, the free energy of the water lattice should be independent of guest occupation. This is inconsistent with NMR work (J.A. Ripmeester, C.I. Ratcliffe, and J.S. Tse, J. Chem. Soc. Farad. Trans. I, 84, (1988), 3731) which indicates considerable guest-host interactions for xenon clathrate. Secondly, guest-host interactions are assumed negligible, which seems at least questionable at higher pressures and lower temperatures.

Using neutron scattering measurements on powder samples, we have refined the structures and guest occupancies for the xenon clathrate at 273K at guest pressures of 5, 7, 15, 25, and 50 bar. At all pressures investigated, the large cage is fully occupied. The occupation of the small cage varies with pressure, increasing to 92±2% at 25 bar. As pressure increases further, the small cage occupancy decreases, clearly violating Langmuir behaviour quite markedly. In addition to the guest occupancy behaviour, the detailed structures as a function of guest pressure are presented.

P08.OC.010 HIGH PRESSURE PHASE DIAGRAMS OF BINARY LANTHANIDE ALLOYS BETWEEN La, Ce, AND Pr. O. Degtyareva and W.B. Holzapfel, FB 6 Physik, Universität-Paderborn, 33095 Paderborn, Germany.

Due to the irregular behaviour of Ce under pressure in comparison with the other "regular" lanthanide metals [1], irregularities are also expected for Ce alloys under pressure. Due to the fact that La under pressure reveals a reentrant behaviour with respect to the *fcc* (*cF*4) → *distorted fcc* (*hR*8?) → *fcc* (*cF*4) transition [2] and Pr shows a special transition to an α-U (*oC*4) phase with *f* electron delocalization [3], alloys of these two elements with each other and with their neighbouring element Ce were of special interest.

In all three cases, 5 alloys with atomic ratios $0.1 \le x \le 0.9$ have been studied under pressures up to 32 GPa in diamond anvil cells (DACs) with energy dispersive X-ray diffraction (EDXD) using synchrotron radiation in HASYLAB (DESY, Hamburg).

As expected, the Ce rich alloys $Ce_{1-x}Ln_x$ with $x \le 0.2$ show the same structural sequence under pressure as pure Ce, however, the occurrence of the *oC*4 structure is suppressed with respect to the occurrence of only the (metastable?) monoclonic (*mC*4) phase up to the pressure where the transition to the ultimate *bct* (*tI* 2) phase occurs. The transitions to *tI* 2 are shifted to higher pressures with increasing of Ln content compared to the pure Ce case. In the Pr rich alloys with La transitions to the *oC*4 structure are also shifted to higher pressures. *hR*8 phase seems to persist in all the $La_{1-x}Pr_x$ alloys with $x < 0.8$ to the maximum pressure of the present experiments.

Systematics in the variations of the axial ratios with pressure and alloy concentration for different structures are discussed.

1. K.A. Gschneider, Jr, L.R. Eyring *Handbook on the physics and chemistry of Rare Earth*, North-Holland, Amsterdam (1978) Vol.1
2. M. Seipel, F. Porsch, and W.B. Holzapfel (1997) High Press. Res. 15, 321
3. Y.C. Zhao, F. Porsch, and W.B. Holzapfel (1995) Phys. Rev. B 52, 134

P08.OC.011 PRESSURE DEPENDENCE OF OCTAHEDRAL REGULARITY ON $Ca(OH)_2$, $Mg(OH)_2$ AND $Co(OH)_2$. T. Nagai, T. Yamanaka Department of Earth and Space Science, Graduate School of Science, Osaka University, Toyonaka, Osaka 560-0043, Japan

We have performed a synchrotron x-ray powder diffraction study of $Ca(OH)_2$, $Mg(OH)_2$ and $Co(OH)_2$ under room temperature pressurization to 10.4 GPa, to 16.0 GPa and to 15.0 GPa, respectively. We used the diamond anvil cells technique and the data were collected with an imaging plate detector at BL-18C in Photon Factory at KEK, Japan.

$Ca(OH)_2$, $Mg(OH)_2$ and $Co(OH)_2$ are isostructural with CdI_2 type and the structure has a strong anisotropy. The c-axis is much softer than the a-axis and, thus, the c/a ratio decreases with pressure. There is no remarkable discontinuity in the compression curves. The bulk modulus of $Ca(OH)_2$, $Mg(OH)_2$ and $Co(OH)_2$ were determined as 34.6 GPa, 55.5 GPa and 56.0 GPa, respectively.

Ca, Mg and Mg atoms are sitting at the special position (0, 0, 0). The atomic position of O atoms, (1/3, 2/3, z), has been successfully refined using Rietveld analysis of x-ray powder diffraction patterns. It has been reported that H disorder occurs at around 5 GPa in $Mg(OH)_2$ and this study clearly suggests that the H disorder has great influence on the compression behavior. We can discuss octahedral regularity on the basis of O-cation-O angles obtained from the structure refinements. The results indicate that CaO_6, MgO_6 and CoO_6 octahedron approach to the regular configuration with pressure and it is interesting that CaO_6 in portlandite seems to become a regular octahedron at a little below the amorphization pressure.

P08.OC.012 THE HIGH-PRESSURE CRYSTAL STRUCTURES OF THE FUNDAMENTAL ALCOHOLS AND CARBOXYLIC ACIDS. D.R. Allan [1], S.J. Clark [2], [1] Department of Physics and Astronomy, University of Edinburgh, Edinburgh, UK, [2] Department of Physics, University of Durham, Durham, UK

The structure and dynamics of molecular solids are intimately related to the interactions of the molecules, which in turn are connected to their molecular form and symmetry. In order to develop an understanding of the structural systematics of polar molecule systems it is vital that a homologous series of chemically similar compounds is studied. The monoalcohols H(CH2)nOH and the monocarboxylic acids H(CH2)nCOOH are both important, and prototypic, series of compounds which form a rich variety of crystal-structure types at low temperature. Until recently, however, relatively little was known about the high-pressure behaviour of these fundamental systems.

We have embarked on a series of studies to establish the high-pressure crystallography of the monoalcohols and monocarboxylic acids (among other systems) and we have found a surprising wealth of structures which, in each case, differ distinctly from their low-temperature forms. The results of our studies on the monoalcohols methanol and ethanol, and the monocarboxylic acids formic acid, acetic acid and propionic acid, will be presented.

P08.OC.014 HIGH-PRESSURE PHASE TRANSITION IN LEAD PHOSPHATE, $Pb_3(PO_4)_2$. R.J. Angel, Bayerisches Geoinstitut, Universität Bayreuth, D95440 Bayreuth, Germany, and U. Bismayer, Mineralogische-Petrographisches Institut, Universität Hamburg, Grindelallee 48, D20146 Hamburg, Germany.

We have studied the high-pressure behaviour of lead phosphate, $Pb_3(PO_4)_2$, at high pressures and room temperature by single-crystal X-ray diffraction. $Pb_3(PO_4)_2$ is an improper ferroelastic material that is a prototype for a large class of ferroelastics. At room conditions it displays C2/c symmetry, and at 453K transforms to a phase with global R-3m symmetry. The transition mechanism is related to a shift of the Pb atoms away from the triad of the hexagonal phase, together with a correlated tilt of the PO_4 tetrahedra. The transition is complicated by the persistence of short-range order above the transition temperature leading to domains with mobile walls in material of high chemical purity [1].

Unit-cell parameters were determined from two crystals at a number of pressures up to a maximum of 4 GPa. At pressures in excess of 1.8 GPa the unit-cell parameters become hexagonal within the experimental uncertainties, confirming an earlier report [2]. The symmetry-breaking spontaneous strains in the low-pressure monoclinic phase below 1.7 GPa vary linearly with pressure, indicating that the transition is second-order in character with a transition pressure of 1.78(1) GPa. This behaviour is in agreement with theoretical predictions and clearly shows the variation of the third order term of the free energy expansion (with its near-tricritical behaviour at high-temperatures, [3]) and is similar to the second-order behaviour observed under conditions of uniaxial stress [1].

[1] Bismayer et al. (1982): *J. Physique* **43**, 1379-1388.
[2] Decker et al. (1979): *Phys. Rev. B* **19**, 3552-3555.
[3] Salje et al. (1993): *Acta Cryst.* **B49**, 387-392.

P08.OC.015 THEORETICAL STUDIES OF THE STRUCTURES AND PROPERTIES OF HIGH PRESSURE FORMS OF PON. D.D. Klug, J.S. Tse, Steacie Institute for Molecular Sciences, National Research Council of Canada, Ottawa, Ontario, Canada K1A 0R6 and J. Haines, Laboratoire de Physico-Chemie des Matériaux, CNRS, 1 Place Aristide Briand, 92195, Meudon Cédex, France

Phosphorous Oxynitride, PON, that is isoelectronic with SiO_2 has been studied using density functional plane-wave methods in order to determine the structures and properties of possible high pressure phases. The phase transition pressures to several possible high-pressure phases are predicted. The bulk modulus and elastic constants of high-pressure phases are calculated in order to determine if these materials may be candidates for superhard solids. The physical basis for the different pressure behavior of the α-quartz and β-cristobalite structures and their physical properties is investigated.

P08.OC.016 NEW HIGH PRESSURE PHASE OF PbS. V.B.Begoulev, Yu.A.Timofeev, B.V.Vinogradov, High Pressure Physics Institute RAS, Troitsk, Moscow region, 142092, Russia

PbS is a narrow gap semiconductor crystallizing in the NaCl-type crystal structure (PbS I). Under pressure PbS undergoes transitions to orthorombic phase PbS II (TlI-tipe structure) at 2.2 GPa (T=300 K) and to cubic CsCl-tipe structure phase PbS III at about 21.5 GPa (T=300 K). It was known also that PbS III phase is superconductor.

In the present work we report the detection of a phase transition to a new high pressure phase PbS IV at 36 GPa (T=300 K). For these studies we used a high pressure cell with diamond

anvils. One of the anvils was made from synthetic polycrystalline diamond («carbonado») and had a flat working surface. The second anvil was produced from natural diamond and had a conical top trancated by a spherical surface radius of 1 mm. We used a powder of PbS (size of grain was 1-5 mkm). A thikness of a powder layers was 10-20 mkm.

New method for the detection of phase transitions and construction of P-T phase diagrams of substances has been applied to this investigation. The method is based on use of micronic ruby gauges for the measurements of pressure distribution curves. When the phase transition takes place, a «shoulder-like» feature arises on a pressure distribution curve. The observation of a change of a feature position with temperature makes it possible to construct P-T diagram of a substance investigated.

Fig.1 shows the results of pressure distribution measurements in PbS under different loads at T=300 K.

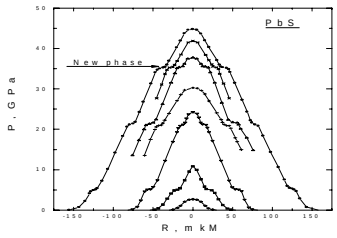

Fig.1. Pressure distribution curves in PbS under different loads at T=300 K.

When the maximum pressure in a sample of PbS was more than 4.8 GPa, a «shoulder-like» feature occured on a pressure distribution curve that corresponded to PbS I – PbS II transition. The second feature at P=21 GPa corresponds PbS II – PbS III transition. At 36 GPa a new «shoulder-like» feature occurs on a pressure distribution curve that corresponds to PbS III – PbS IV transition. We suppose that new high pressure phase PbS IV is superconductor.

P08.OC.019 HIGH-PRESSURE STRUCTURAL AND ELECTRONIC TRANSITIONS OF TRANSITION METAL OXIDES. R.J. Hemley, Q.Z. Guo, J.F. Shu, J. Badro, V.V. Struzhkin, S. Shieh, J. Z. Hu, R. E. Cohen, S. Gramsch, H.K. Mao, Geophysical Lab., Carnegie Institution, 5251 Broad Branch Rd. NW, Washington, DC 20015, USA; and C.C. Kao, NSLS, Brookhaven National Lab., Upton, NY 11973, USA.

Transition metal monoxides, MnO, FeO, CoO, and NiO in NaCl (B1) structure, have been studied in diamond cells to 150 GPa at ambient temperature. Radial diffraction employing synchrotron x-radiation is used for determination of elasticity and crystal structure. High-resolution x-ray fluorescence spectroscopy is used for identification of high-low spin states. All samples show softening in shear elastic tensor element with increasing pressure that leads to second-order, displacive phase transitions below 100 GPa. The cubic B1 symmetry is reduced to rhombohedral or lower symmetries at the transitions. The predicted high-pressure magnetic collapses based on calculations of B1 structure are shifted to higher pressures in the lower symmetry phases.

P08.OC.020 MULTIMEGABAR COMBINATORIAL STUDIES OF EQUATIONS OF STATE AND PRESSURE SCALE. H.K. Mao, J.F. Shu, J. Badro, S. Merkel, R.J. Hemley [1], G. Shen [2], C.S. Zha [3], T. LeBihan, D. Hausermann [4], [1] Geophysical Lab., Carnegie Institution, Washington, DC 20015, USA, [2] APS, Argonne National Lab., Argonne, IL 60439, USA, [3] CHESS, Cornell University, Ithaca, NY 14853, USA, [4] ESRF, BP-220, F-38043 Grenoble Cedex, FRANCE

We studied the covariance of ruby fluorescence shift and lattice parameters of 18 polycrystalline materials, V, Fe, Co, Ni, Cu, Ag. Pd, Mo, Nb, Ta, Re, Ir, Pt, Au, Pb, MgO, NaCl, and KCl, under multimegabar compressions. Each sample of 1-2 micron thick and 5-10 micron diameter were arranged in a grid in a diamond cell chamber which was filled with helium pressure medium to ensure uniform hydrostatic pressure. Each sample was probed independently with monochromatic x-ray beam of 5 X 5 micron size at ESRF ID30 Beamline. High resolution x-ray diffraction patterns were collected with FastScan image plates. A new primary pressure scale is obtained from the combination of Brillouin scattering and x-ray diffraction date of MgO. The study includes all commonly used pressure standards and yields a comprehensive, accurate, new pressure scale. In addition, it provides direct correlation of equations of state for these benchmark materials.

P08.OC.021 X-RAY STUDIES OF DISORDERED SYSTEMS AT HP-HT USING THE P-E PRESS AND A MULTICHANNEL COLLIMATOR. M. Mezouar, ESRF, B.P. 220, 38000 Grenoble, France

The determination by X-ray diffraction of the evolution at high pressure and high temperature of inter-atomic distances, and number of first neighbours of disordered systems (liquids, amorphous materials), is of great importance in various domains such as materials science or geophysics. However, many experimental problems (high background signal, chemical reactivity of liquid phases, etc.) limits this kind of study. This poster is dedicated to the recent progress realised at beamline ID30, ESRF. In particular, the development of a multichannel collimator (Sollers slits system) interfaced to a detector based on image-plates has lead to a substantial improvement of the signal to noise ratio, and allows the study of disordered systems under extreme conditions of pressure and temperature. Several examples will be presented, including the behaviour under high pressure of liquid metals of columns V and VI in the periodic table.

08OD APPLICATIONS OF LINE-BROADENING

M08.OD.001 ANALYSIS OF X - RAY DIFFRACTION LINE BROADENING IN STRUCTURALLY INHOMOGENEOUS POLYCRYSTALLINE MATERIALS. P. Klimanek, Freiberg University of Mining and Technology, Institute of Physical Metallurgy, D-09596 Freiberg/Sa., Germany

Real polycrystals (i.e. powders, coatings, or bulk materials interesting in materials science and technology) consist, in many cases, of crystallites with significantly different degree of structural perfection defining a lattice-disorder statistics. The macroscopically observable X - ray (or neutron) diffraction peaks of such structurally inhomogeneous materials are diffraction multiplets formed by superposition of the partial reflections due to the volume fractions of the lattice disorder statistics [1-4], and the reflection characteristics have the meaning of com-plicated microstructure averages depending on

- the type of the lattice-disorder statistics,
- the grain size distribution and/or the texture of the various crystallite fractions, and
- the spatial arrangement of the structurally different crystallites.

In the present paper some basic aspects of the analysis and interpretation of diffraction multi-plet profiles are discussed and illustrated by experimental results obtained with model specimens. (powders) and real bulk materials. Separation of partial reflections of diffraction multi- plets, which is particularly important in the examination of diffraction line broadening due to lattice disorder of the 2nd kind (e.g. dislocation structures, stacking

faults and micro-twins, stress-active precipitates etc., [5,6]), becomes possibly in certain limits if the lattice disorder statistics

- has only two crystallite fractions with clearly different defect structures (e.g. in partially re- crystallised materials),
- can be related to preferred spatial arrangement of the crystallites (e.g. in materials with microstructure gradients), or
- is in close connection with preferred orientations (texture components) of the grains (e.g. in plastically deformed metals and alloys)

The case of texture- related analysis of X-ray diffraction line broadening is treated in some detail for cold-rolled Cu and α-Fe [7]. The results demonstrate that analysis of X-ray (or neutron) diffraction-line broadening is a suitable tool for detailed integrated substructure characterisation even in bulk materials with complicated sample architecture.

[1] Klimanek, P. : Freiberger Forschungsheft B 265, 74 - 93. Dt. Verlag für Grundstoffindustrie, Leipzig 1988

[2] Klimanek, P. in: X-Ray and Neutron Structure Analysis in Materials Science (Ed. J. Hasek), Plenum Press, New York 1989, 125-137.

[3] Klimanek,P. : Proc. EPDIC 1, Mat.Sci.Forum 79-82 (1991) Part 1, 73-84

[4] Klimanek, P.: Proc. ICOTOM 10, Mater.Sci.Forum 157-162 (1994) 1119

[5] Krivoglaz, M.A.: Theory of X-ray and thermal neutron scattering by real crystals (In Russian). Nauka, Moscow 1967

[6] Krivoglaz, M.A.: Theory of X-ray and neutron diffraction by non-ideal crystals (In Russian). Naukova Dumka, Kiev 1983

[7] Weidner, A.: Thesis, Freiberg University of Mining and Technology 1998

M08.OD.002 DIFFRACTION-LINE BROADENING BY LATTICE IMPERFECTIONS; ANALYSIS THROUGH LINE-PROFILE SYNTHESIS. E.J.Mittemeijer[1,2], R.Delhez[2], Th.H.de Keijser[2], T.C.Bor[2] and L.Velterop[2], 1: Max Planck Institute for Metals Research, Seestraße 92, 70174 Stuttgart, Germany, 2: Laboratory of Materials Science, Delft University of Technology, Rotterdamseweg 137, 2628AL Delft, The Netherlands.

Lattice imperfections as dislocations and misfitting precipitates and smallness of the diffracting crystallites cause broadening of diffraction lines. The traditional methods of line-broadening analysis decompose the observed line profiles in parts of which the broadenings are dependent on ("strain broadened" part) and independent of ("size broadened" part) the order of reflection. This line-profile decomposition is subject to severe assumptions made for in particular the "strain broadened" part. As a result large errors can occur if the assumptions do not apply to the specimen concerned (*e.g.* van Berkum et al., Acta Cryst.A52, 1996, 730-747). Furthermore, the "size" and "strain" parameters obtained by such methods are often difficult to interpret. An alternative procedure is possible: line-profile synthesis on the basis of a model *appropriate for the specimen concerned*. From the comparison of calculated line profiles and the measured one the model parameters are found and thereby the characteristics of the lattice imperfections considered. Of course, this approach only works if a correct model can be constructed. The line-profile synthesis route is adopted here for two cases.

Firstly, the effect of stacking and growth faults is analysed. It follows by application of the line-profile synthesis route that some of the approximations formerly used in the derivation of analytical relations between line-profile parameters (*e.g.* profile-maximum position) and fault densities are unjustified. In certain not extreme cases even the sign of the shift of the profile maximum is predicted wrongly !

Secondly, the effect of misfitting inclusions on matrix reflections is analysed. Also in this case irregularities are found. For example the relation between the width of the strain broadened profile and the root mean square strain in the specimen is not necessarily linear, as traditionally assumed.

M08.OD.003 CRYSTALLITE SIZE DISTRIBUTIONS AND X-RAY DIFFRACTION LINE BROADENING. J.Ian.Langford, School of Physics and Astronomy, University of Birmingham, Birmingham B15 2TT, UK, and Daniel Louër, Laboratoire de Chimie du Solide et Inorganique Moléculaire (URA CNRS 1495), Université de Rennes I, 35042 Rennes cedex, France.

When the mean size of crystallites is obtained from X-ray diffraction data, it is normally assumed that diffracting domains have the same size and shape. While a Williamon-Hall plot often indicates that the latter is a reasonable assumption, on average, there is always a distribution of size. This causes the mean size obtained from integral breadths or the Warren-Averbach method to be over-estimated by an amount which depends on the nature and width of the distribution[1]. Additionally, the shape of line profiles, notably the form of their tails, is also affected profoundly. Their shape can be characterised by the parameter ϕ = FWHM/integral breadth and reflections can have any form, from approximately Gaussian (ϕ=0.939) for a narrow normal distribution of size, through Lorentzian (ϕ=0.637), to significantly super-Lorentzian (ϕ=0.5 or less) for a lognormal distribution with a large standard deviation.

From curves of the variation of ϕ with standard deviation or variance for different distributions and simulated line profiles, the corresponding quantity can be estimated for experimental reflections. This and the approximate mean size obtained in the usual way can be used as starting values for calculating line profiles for a given morphology and an assumed distribution. These parameters can then be refined by comparing the calculated and experimental diffraction patterns until the best 'fit' is obtained, to give estimates of the true mean and the standard deviation of the distribution. This procedure is demonstrated by means of data for a nanocrystalline sample of CeO_2, for which the crystallites are approximately spherical. In addition to obtaining crystallite-size distributions, the procedure automatically models line profiles meaningfully in cases where microstrain is negligible. Its implementation could thus be used to advantage in the Rietveld method for structure refinement from powder data.

1. Rao, S. & Houska, C.R. (1986). *Acta Cryst.* **A62**, 6-13.

M08.OD.004 THE DISLOCATION MODEL OF STRAIN ANISOTROPY. T. Ungar, Department of General Physics, Eotvos University Budapest, Pazmany Peter setany 1/A, H-1518, P.O.B 32, Budapest, Hungary

Line broadening means broadening of a Bragg reflection in the vicinity of a fundamental reciprocal lattice point. Due to reciprocity of real and reciprocal space this implies that the strain fields of defects causing this kind of broadening must have a long range character. Dislocations are the only lattice defects satisfying this criterion. On the other hand they exibit a strong contrast anisotropy as it is well known in transmission electron microscopy (TEM). In a TEM experiment the contrast of a dislocation disappears when $\boldsymbol{bg}=0$, where $\boldsymbol{b}$ is the Burgers vector of the dislocation and $\boldsymbol{g}$ is the diffraction vector. The strain part of line broadening is related to the mean square strain which, in terms of dislocations is: $\langle\varepsilon_{g,L}^2\rangle \cong \rho^* ln(R_e/L)/(2\pi^2 g^2)$, where ρ^* and R_e are the *formal* density and the effective outer cut off radius of dislocations and L is the Fourier length. The *formal* and the true dislocation densities are coupled by the contrast factors C of dislocations: $\rho^*=\rho(\pi g^2 b^2 C)/2$, which depend on the relative directions of $\boldsymbol{g}$, $\boldsymbol{b}$ and $\boldsymbol{l}$, ($\boldsymbol{l}$ being the line vector of dislocations): $C=C(\boldsymbol{g},\boldsymbol{b},\boldsymbol{l})$. The values of C can be evaluated numerically for different crystal and dislocation systems. For different dislocation systems or in a polycrystal C can be averaged and is denoted: $\overline{C}$. It has been shown recently that in cubic crystals: $\overline{C}=\overline{C}_{h00}(1-qH^2)$, where $\overline{C}_{h00}$ corresponds to $h00$, $H^2=(h^2k^2+h^2l^2+k^2l^2)/(h^2+$

$k^2 + l^2)^2$ and q is a parameter depending on the elastic constants of the crystal and can be evaluated numerically. Based on the above relations it has also been shown that the Williamson-Hall plot and the Warren-Averbach method can be rationalised for strain anisotropy by replacing g or g^2 by $gC^{1/2}$ or g^2C. The so *modified* Williamson-Hall plot and *modified* Warren-Averbach method provide reliable values for crystallite size and for strain, latter in terms of dislocation densities. Combining the *modified* plots with the scheme of the contrast factors provides a comprehensive tool to describe the microstructure of real crystals. The procedure is also apt for including it into a Rietveld refinement procedure.

M08.OD.005 DEALING WITH ANISOTROPIC PEAK BROADENING IN RIETVELD REFINEMENTS. Peter W. Stephens, Department of Physics & Astronomy, State University of New York, Stony Brook, NY 11794-3800 USA.

The use of high-resolution powder diffraction, especially at synchrotron radiation and pulsed neutron sources, places strict demands on the ability of the experimenter to correctly model the diffraction line shape. The widely used Rietveld technique treats the diffraction line width as a smooth function of *d*-spacing, whereas, for many samples of interest, the peak width depends on the diffraction indices (*hkl*) in a more complicated fashion. In this talk, I will discuss two sources of irregular dependence of peak widths on *d*-spacing.

The first is anisotropic strain broadening, which can be generally modeled as a distribution of lattice parameters within the sample [1]. I will present several applications of a recently-developed algorithm for treating this effect in whole-profile fitting techniques [2]. Examples include Na-para-hydroxy benzoate [3], $Co(N(CN)_2)_2$, $Mn(N(CN)_2)_2$, and K_4C_{60}.

The second is short-range orientational disorder of molecules within an extended crystal lattice, such as is observed in the low-temperature $P2_13$ phase of $C(Si(CH_3)_3)_4$ [4]. I will show that the Rietveld analysis of that data actually relates the observable peak width to the *phase* of the diffraction peak, a rather unusual circumstance.

This work, performed at the NSLS, is based on collaborations with and contributions from G.M. Bendele, D.E. Cox, R.E. Dinnebier, R. Von Dreele, and other authors of the works cited below.

P. Thompson *et al*., *J. Less-Common Met.* **129**, 105 (1987);
J. Rodriguez-Carvajal *et al.*, *J. Phys. Condens. Matter* **3**, 3215 (1991);
N.C. Popa, *J. Appl. Cryst*., **31**, 176 (1998).
P.W. Stephens, *J. Appl. Cryst.*, in press (1999).
R.E. Dinnebier *et al.*, submitted to *J. Appl. Cryst.*
R.E. Dinnebier *et al.*, submitted to *Acta Cryst. B*.

P08.OD.001 DISLOCATIONS IN $LaNi_{(5-x)}M_x$ (M=Co, Mn, Al, Sn) STUDIED BY X-RAY DIFFRACTION LINE BROADENING. R. Černý, Laboratoire de Cristallographie, Université de Genève, 24, quai Ernest-Ansermet, CH-1211 Genève 4, Switzerland, and J.-M. Joubert, Laboratoire de Chimie Métallurgique des Terres Rares, CNRS - UPR 209, 2-8, rue Henri Dunant, F-94320 Thiais Cedex, France.

Real structure of $LaNi_{(5-x)}M_x$ (M = Co, Mn, Al, Sn) before and after several hydrogen absorption-desorption cycles was studied from the line broadening in powder diffraction patterns measured at the Swiss Norwegian Beam Line (BM1) at the ESRF (Grenoble). The theory of Krivoglaz and his co-workers [1] was used, and the whole line broadening and its anisotropy were explained as due to dislocations in the $LaNi_{(5-x)}M_x$ crystals. The orientation factors χ for reflections in the hexagonal crystal system and for different dislocations types were expressed analytically by Klimanek & Kuzel jr. in [2]. The effect of different substituting elements M was studied in mono- and multi-substituted alloys. The prismatic slip system (slip plane $\{0\bar{1}10\}$) with dislocations having Burgers vector $\boldsymbol{a}/3 < \bar{2}110 >$ was found to be dominating in the cycled non-substituted and Co-substituted alloys in accord with [3 and 4]. Dislocations with Burgers vector $\boldsymbol{c}$ <0001> were found in the cycled alloys substituted with Mn, Al and Sn as it was observed for non-substituted alloys in [5]. The observed dislocation densities in cycled alloys were in the order of 10^{10} cm^{-2} having low values for Al- and Sn-substituted alloys and high values for non-substituted and Co- and Mn-substituted alloys.

[1] Krivoglaz, M.A. (1969) Theory of X-ray and Thermal Neutron Scattering by Real Crystals. New York: Plenum.
[2] Klimanek P. & Kuzel R. jr. (1988) *J. Appl. Cryst.* **21**, 59-66.
[3] Wu E., Kisi E.H. & Gray E.Mac.A. (1998) *J. Appl. Cryst.* **31**, 363-368.
[4] Kim G.H., Lee S.G., Lee K.Y., Chun Ch.H. & Lee J.Y. (1995) *Acta Metall. Mater*. **43**, 2233-2240.
[5] Inui H., Yamamoto T., Zhang Di. & Yamaguchi M. (1998) *Journal Alloys Comp.* **269**, 294-296.

P08.OD.002 X-RAY LINE PROFILE ANALYSIS OF NANOCRYSTALLINE SILICON NITRIDE. J. Gubicza, T. Ungár [1], I. Mohai, J. Szépvölgyi [2], [1] Department of General Physics, Eötvös University, H-1518 Budapest P.O.B. 32, Hungary, [2] Research Laboratory of Materials and Environmental Chemistry, Chemical Research Center, Hungarian Academy of Sciences, H-1025 Budapest, Pusztaszeri ut 59-67. Hungary

Nanostructured silicon nitride powder has been produced in a thermal plasma reactor by vapor phase reaction of silicon tetrachloride and ammonia [1] and annealed at different temperatures between 1250 and 1500°C. The effect of heat-treatment on particle-size, size distribution and lattice distortion in the crystalline fraction of the powder was studied by high-resolution X-ray diffractometry. The X-ray line profiles were evaluated for particle-size and lattice distortion by the newly developed methods of the modified Williamson-Hall plot and the modified Warren-Averbach analysis [2]. It was found that the particle-size increased with increasing annealing temperature. The particle-size distribution was obtained by a recently developed numerical procedure using the size parameters provided by the modified Williamson-Hall plots of the FWHM and the integral widths and the modified Warren-Averbach method [3]. The experimental values of the average particle-size determined either by X-rays or by transmission and scanning electron microscopy or calculated from the specific surface area (obtained by the BET method) of the powder are compared with each other. The particle-size values provided by the different methods are discussed in terms of the volume fraction of the amorphous phase and agglomeration.

1. J.Szépvölgyi, F.L.Riley, I.Mohai, I.Bertóti & E.Gilbart (1996). J. Mater. Chem., 6, 1175.
2. T.Ungár & A.Borbély (1996). Appl. Phys. Letters, 69, 3173.
3. T.Ungár, A.Borbély, G.R.Goren-Muginstein, S.Berger & A.R.Rosen, Nanostructured Mater., submitted for publication.

P08.OD.003 PRECIPITATE-RELATED STRAIN IN REACTOR-PRESSURE-VESSEL STEELS. Davor Balzar, Materials Science and Engineering Laboratory, National Institute of Standards and Technology and Department of Physics, University of Colorado, Boulder, Colorado, 80303, U. S. A. and Hassel Ledbetter, Materials Science and Engineering Laboratory, National Institute of Standards and Technology, Boulder, Colorado, 80303, U. S. A.

Diffraction-line-broadening analysis (DLBA) and small-angle neutron scattering (SANS) were used to characterize the

embrittlement of ferritic steels used in nuclear-reactor pressure vessels. It is believed that the embrittlement is caused by formation of small (1-2 nm) copper-rich precipitates (CRPs). Because the CRPs are so small, it is difficult to monitor the kinetics of their formation and growth directly. However, small CRPs are coherent with the *bcc* matrix, which causes local matrix strain and interaction with the dislocation strain fields, thus impeding dislocation mobility. As CRPs grow, at some critical size the bulk crystal structure of copper (*fcc*) is achieved, the CRPs are no longer coherent with the matrix, and the matrix strain is relieved.

We prepared a series of surrogate low-alloy ferritic-steel specimens with 1.1 mass % copper. The specimens were annealed for different times at 450 °C, which resulted in a different state of precipitation. SANS measurements showed that the precipitate size distribution broadens and shifts toward larger sizes as a function of annealing time. Mechanical hardness showed an increase with annealing time, followed by a decrease, which can be associated with the onset of the precipitates' incoherence. DLBA showed that the strain-related broadening dominated and correlated with mechanical hardness and precipitate volume fraction, as determined from the SANS measurements. A model of strain broadening will be presented to explain these results.

P08.OD.004 A NEW FUNDAMENTAL PARAMETERS APPROACH. A. Coelho and A. Kern, Bruker-AXS GmbH, Östliche Rheinbrückenstraße 50, D-76187 Karlsruhe

A new general convolution based approach to describing X-ray powder diffraction line profiles has been developed [1]. The shapes of line profiles are governed by the emission profile, instrument, and specimen aberrations. Accurate descriptions of the emission profile and instrument aberrations are a necessary prerequisite to determining the specimen aberrations. The specimen aberrations are dependent upon the geometry of the experimental conditions and the deviation of the phase(s) from ideal polycrystalline crystals. The present work aims to accurately describe the specimen aberrations arising from the geometry of the experimental conditions using single line fitting up to Rietveld methods. This includes i) the description of peak shifts and peak shapes as a function of the linear absorption coefficient of the specimen and the specimen thickness and ii) the change in peak shapes of individual phases due to differing axial divergence effects arising from preferred orientation.

An accurate description of the specimen aberrations due to the geometry of the experimental conditions, together with an accurate description of the emission profile and instrument aberrations opens the path for investigating the structurally based specimen aberrations.

1. R.W. Cheary & A.A. Coelho (1992). J Appl. Cryst., 25, 109 - 121.

P08.OD.005 STRUCTURE AND MECHANICAL PROPERTIES Ti-Al. L.A. Kommel[1], V.K Ovcharov[3], B.N. Kodess[2,3], G.P.Teterin[4], N.G. Kisel[3] , M.I. Ermolova[3]. [1] TTU, Tallin Estonia [2] ICS&E Aurora, CO, USA [3] VNIIMS Moscow, Russia; [4] MSOU, Moscow, Russia

The bimetallic valves were produced using new IFFM technique. IFFM technique is a combination of the two known methods (forging and casting) from which a new quality emerges. As a result of rapid solidification of Ti-36Al-4Nb melt, ordered TiAl and Ti_3Al phases are formed in the valve disk. Microstructure, microhardness and composition profiles across the joint demonstrate that the diffusion process reliably connects two types of alloys. The combination of pressure and rapid solidification of the melt results in materials with fine-grained structure and improved mechanical properties being produced. The diffraction pattern was determined by XRD techniques using CuK-α radiation in X-ray diffractometers. Bragg angles and the half-width of Bragg-intensity profiles of reflections of high and low order for the two intermetallic phases were measured. Hardness measurements were undertaken using 15-g, 50-g and 100-g loads using Micromet-2001 and PMT-3 testers. Analysis of X-ray pictures of valve heads exposes two major sets of Bragg reflections. Each set corresponds to γ-phase (TiAl) and α_2-phase (Ti_3Al) respectively. α_2-phase presence is in the range of 8-15% of the total content, according to the intensity analysis. The fact of presence of α_2-phase indicates that rapid solidification occurs at temperatures exceeding 1200^{o}C. The ratio of the width of γ–(004/002) and α_2-(400/200) reflections is within the limits 1.30-1.38. This reflects the fact that broadening of Bragg reflections is a result of the microscopic stresses caused by pressure and solid-state phase transformations. Note, that the calculated intensity of summarized stresses for the inlet and exhaust valves reaches the maximum magnitude on the external surface of the valve head and is equal to 169-263 MPa for steel valves. In case of the bimetallic valve (TiAl head and Ti-based alloy stem), the stress is 388 MPa.

08OE DIFFICULT STRUCTURES

M08.OE.001 STRUCTURES FROM (VERY) LOW MELTING COMPOUNDS AND THOSE WHICH FORM PLASTIC OR GLASSY PHASES. Roland Boese,* Hans-Christoph Weiss, Jordi Benet-Buchholz and Venkat R. Thalladi, Institut für Anorganische Chemie, Universität-GH Essen, Universitätsstraße 5-7, D-45117 Essen, Germany.

For a systematic investigation of the series of *n*-alkanes [1] and their α,ω-disubstituted derivatives which exhibit the so-called even/odd alternation of their melting points, we faced several problems to grow single crystals in their ordered low-temperature phases.

The *in situ* method with an automated CO_2 laser crystallization device developed in our laboratories, was applied to crystallize the *n*-alkanes from propane to *n*-nonane. The melting point of propane is 83 K and its crystal growth has been accomplished by applying liquid helium as an open gas stream cooler. This necessitated the modification of our standard low-temperature device which uses liquid nitrogen. Higher *n*-alkanes, such as *n*-nonane, crystallize in a rotatory disordered phase and the crystals shatter by further cooling into the low-temperature phase. In order to circumvent the high temperature phase, crystal growth has been performed from a solution of *n*-nonane in *n*-pentane such that the saturation point is at a temperature below the phase transition. This yielded the crystals of the ordered low-temperature phase.

Ethyleneglycol, the first member in the series of α,ω-alkane diols, solidifies in a glassy state. Attempts to induce nucleation by various techniques including ultrasonic shock waves or adding some impurities have not been fruitful. However, when we attempted to cocrystallize it with another proton acceptor, phenazine, we could grow a single crystal and determine the solid state structure.

R. Boese, H.-C. Weiss, D. Bläser (1999). Angew. Chem. Int. Ed. Engl. **38**, in press.

M08.OE.002 DIFFICULT STRUCTURES: IMPROVING YOUR CHANCES WITH SYNCHROTRON RADIATION. William Clegg, Department of Chemistry, University of Newcastle upon Tyne NE1 7RU, UK and CLRC Daresbury Laboratory, Warrington WA4 4AD, UK.

Some crystal structures are difficult to solve or refine because the data are of inferior quality. Sometimes this is just a problem with the overall level of intensity scattered by very small crystals. On other occasions (or in addition to this), there may be

intrinsic structural problems, such as twinning, pseudo-symmetry, or various forms of disorder, which are reflected (not always obviously) in the quality of the diffraction data. The use of synchrotron radiation instead of a conventional laboratory X-ray source can often provide a straightforward solution to the problem of low intensity, turning difficult problems into something resembling routine studies. Furthermore, the greater intensity and higher degree of collimation of the synchrotron beam can help to resolve questions of pseudo-symmetry (such as space group ambiguities and supercells), reveal twinning evidence in the data, and provide better quality data for unravelling disorder, especially if the data are collected at reduced temperature. Unstable materials can be more readily studied with the opportunity for high-speed data collection using a modern area detector with synchrotron radiation. The wavelength tunability of synchrotron radiation adds a further tool for tackling difficult structures, particularly in the use of anomalous dispersion effects in distinguishing between some atom types.

On the other hand, synchrotron single-crystal studies may uncover problems which are not suspected from conventional X-ray data!

Examples will be given of problems solved at Daresbury Laboratory, using the new SRS single-crystal diffraction station 9.8, together with a discussion of approaches to the development and exploitation of synchrotron radiation facilities in chemical and materials crystallography.

M08.OE.003 CRUNCH: GETTING THE MAXIMUM OUT OF DETERMINANTS. R. de Gelder [1], R.A.G. de Graaff [2], [1] NSR Centre for Molecular Structure, Design and Synthesis, University of Nijmegen, Toernooiveld, 6525 ED Nijmegen, The Netherlands, [2] Leiden Institute of Chemistry, Gorlaeus Laboratories, University of Leiden, PO Box 9502, 2300 RA Leiden, The Netherlands

CRUNCH [1,2] is a system of programs aimed at solving ab initio small and medium sized structures. The program was developed to deal with cases where the usual methods fail, due to bad data, large number of atoms, etc. Phase determination is done by a unique procedure based on the concurrent maximization of Karle-Hauptman determinants. The most important steps determining the success of the method are:the use of a matrix-construction method based on considerations from graph theory the combination of interdependent matrices via the common minor strategy the application of a fast and stable phase-refinement procedur -the location of suspect phases via the analysis of symmetry relation -the extension of trial models to the complete structure by a Fourier recycling metho based on the R2-function

The overall strategy of the system will be commented upon and a brief survey will be given of the methods available to the users of CRUNCH [3].

A well known example of the succes of CRUNCH is the solution of a structure which was put on the internet by Dr. Huffman (140 non-hydrogen atoms, P1) [4]. A number of other examples for which the CRUNCH procedure proved to be very succesful will also be given.

1. R. de Gelder, R.A.G. de Graaff and H. Schenk (1993). Acta Cryst., A49, 287-293.
2. R.A.G. de Graaff and R. de Gelder (1996). Acta Cryst., A46, C-53.
3. CRUNCH is available at http://chemb0b.leidenuniv.nl:80/~rag/
4. IUCr Newsletter Vol. 3 No. 1, page 8. http://www.iucr.ac.uk/cww-top/int.news.exm2.html

M08.OE.004 EXPANSION OF GLOBAL VALIDATION CRITERIA TO 3-D: THE *R*-TENSOR. Sean Parkin, Biochemistry Department, Duke University Medical Centre, Durham, N.C., 27710, USA.

In difficult crystal structure determinations, objective tools to analyse and diagnose problems can be essential to the process of steering a refinement to completion. A simple, general method for expansion of common global quality criteria to include spatial information is described.

Aside from information derived from the (partial) structure itself, much of the quantitative information used in the course of a difficult refinement is in the form of global validation statistics such as various R-values, goodness-of-fit etc. Although helpful, the utility of such scalar quantities to describe the behaviour of a three-dimensional entity is obviously limited. Side-by-side comparison of observed and calculated structure factors is often a powerful way to resolve structural problems, but it is inherently subjective.

A simple method to quantify variations in a given validation statistic over the three dimensions of reciprocal space can be constructed. In it, a (3x3) matrix, the R-tensor, is constructed which allows an effective value for the statistic in question to be calculated for different points or regions of reciprocal space. A wealth of additional information over traditional scalar statistics is obtained which can help to steer refinement strategy and to assess the final product.

Details of the algorithm and some results are given. A FORTRAN77 program 'RT' is also available from the author at the e-mail address: sean@xray.duke.edu.

M08.OE.005 DIFFICULT STRUCTURES – MAKING THEM FIT FOR THE CHEMIST. Anthony Linden, Institute of Organic Chemistry, University of Zürich, Winterthurerstrasse 190, CH-8057 Zürich, Switzerland.

Difficult structures involving small molecules may be classified into two broad categories: those with difficulties that can be minimised with care, and those with inherent unavoidable properties which make the successful completion of the structural analysis a complicated process. The potential causes of difficulties encountered in each of these categories will be discussed briefly, together with suggestions on how to minimise them, make the best of unavoidably poor data, and extract the most out of an awkward refinement.

Difficult structures in the first category can frequently be overcome by carefully planning and monitoring the experiment. The key is to ensure that the best and most complete data possible has been recorded using the best crystal that can reasonably be obtained. Crystal growth sometimes requires huge doses of patience and perseverance, and poor data can often be traced to curtailed attempts in this area. Other considerations that can assist with this category include the resolution of space group or Laue symmetry ambiguities, detection of spurious intensities, recognition of twinning, and the appropriate application of absorption corrections.

The second category of difficult structures generally involves problems with structure solution or refinement. If the structure will not solve, has the full range of structure solution options been exhausted? The power of fragment orientation routines should not be underestimated. Subtle changes in program defaults can enhance the chances of solving structures from weak data. Complicated or unsatisfactory refinements usually result from disorder, twinning, pseudo-symmetry, missed symmetry, included solvent, insufficient, weak or poor data, over-refinement, or systematic errors in the data. Refinement restraints and constraints are powerful tools for controlling ill-behaved models, but their excessive use can also lead to incorrect models or conclusions. Severely disordered solvent molecules can sometimes be treated by attempting to eliminate their contribution to the reflection data.

Once the best possible result has been obtained, how much information can be extracted from the structure analysis? The chemist needs to know how to avoid over-interpreting or misinterpreting the results. How can the results best be presented

and utilised? Above all, report clearly and concisely any non-routine procedures used to treat the difficulties.

P08.OE.001 EMPTY ORBITAL AND HYDROGEN ATOM LOCATION WITH XTALVIEW - CORRELATION WITH DENSITY FUNCTIONAL THEORY. C.J. Cardin, D.J. Cardin, P.M. Rodger and A.K. Todd, Chemistry Department, The University of Reading, Whiteknights, Reading, RG4 6AD

The use of neutral atom scattering factors for Ni in the crystal structure determination of the first acyclic metal fullerene derivative [1] produced an unexpected feature when using a difference electron density map calculated using the program XtalView to locate the single H atom on the fullerene surface. Despite a routine room temperature image plate data collection, clear negative electron density for the empty d orbitals on both nickel atoms was visible using standard software. The orientation of this LUMO was subsequently confirmed by density functional theory calculations. In another example, the structure of tetrakis(2,4,6-tri*iso*propylohenyl)diphosphine, map examination showed the presence of an unusual disorder which could otherwise not have been interpreted. Electron density maps are rarely examined by chemical crystallographers these days, but the information content of the data collected by the rotation method on area detectors is greater than statistics suggest. 'Map quality' is not readily quantified.

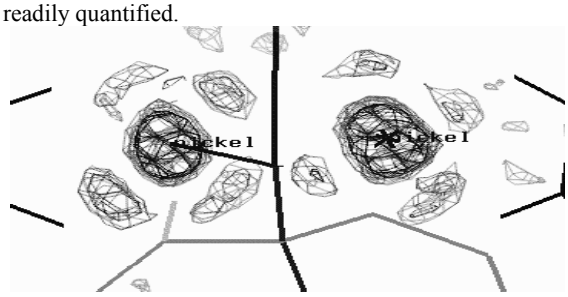

The synthesis of dicobalt and dinickel complexes of trimethylsilylethynyl-1,2-dihydrofullerene; Characterisation by nmr and structure of the first acyclic metal fullerene derivative: Molecular structure of [η^2-Ni-2(η-C_5H_5)$_2$- fullerene] by F. Banim, C.J. Cardin, D.J. Cardin, M. Pistocchi, A.K. Todd, *Journal of Physics and Chemistry of Solids* **1997**, *58*, 1919-1923.

P08.OE.002 MODULAR APPROACH IN MODELING THE CRYSTAL STRUCTURE OF SOME MINERALS. G. Ferraris and Belluso E., DSMP Univ. Torino, Italy, and S.V. Soboleva, IGEM – RAS Moscow, Russia, and E.V. Sokolova, Moscow State Univ., Moscow, Russia

Typically, a group of compounds forms a polysomatic series [1] P_pQ_q if the structure of each member can be described as a linear combination of *P* and *Q* modules with composition C_p and C_q. In most cases the two building modules are slices with thickness t_p and t_q and very close periodicity in the two directions (*e.g.*, **a** and **b**) which define the contact surface; the third periodicity **c** corresponds to the stacking of the slices. Composition (*C*) and metric of the members linearly vary with the modules *P* and *Q* and a member P_pQ_q shall show: *(i)* $c \sim pt_p + qt_q$, $b \sim b_p \sim b_q$ and $a \sim a_p \sim a_q$; *(ii)* $C = pC_p + qC_q$. Actually, the modules can show substitutions and minor modifications; non planar modules can be necessary. In some cases, the above relationships can just be an inspiring starting point. The application of the modular approach in modeling a crystal structure [1] is particularly efficient when the structure of several related compounds is known; it can be necessary when other methods cannot be applied, *e.g.*, for lack of single crystal data. The procedure shall be described for the following compounds for which only TEM and powder diffraction data were available:

- nafertisite, $(Na,K,\ )_4(Fe^{2+},Fe^{3+},\ )_{10}[Ti_2O_3Si_{12}O_{34}](O,OH)_6$, related to astrophyllite, $(K,Na)_3(Fe,Mn)_7[Ti_2O_3Si_8O_{24}](O,OH)_4$, and bafertisite, $Ba_2(Fe,Mn)_4[Ti_4O_4Si_4O_{14}](O,OH)_2$;
- kalifersite, $(K,Na)_5(Fe^{3+})_7[Si_{20}O_{50}(OH)_6]\bullet 12H_2O$, related to palygorskite, $Mg_5[Si_8O_{20}(OH)_2]\bullet 8H_2O$, and sepiolite, $Mg_8[Si_{12}O_{30}(OH)_4]\bullet 2H_2O$;
- polymorph of nacaphite, $Na_2Ca[PO_4]F$, based on modules of nacaphite and arctite, $(Na_5Ca)Ca_6Ba(PO_4)_6F_3$;
- seidite-(Ce), $Na_4(Sr,Ce)_2Ti[Si_8O_{22}]F\bullet 5H_2O$, modeled by comparison with miserite, $(Ca,K,\ )_{0.5}KCa_5(RE)[Si_8O_{22}](OH)F\bullet 0.5H_2O$.

1. Ferraris, G. (1997). *Modular aspects of minerals.* S. Merlino (ed.) – Budapest, Eötvös Univ., 275-295.

08OF ADVANCED BATTERY AND FUEL CELL MATERIALS

M08.OF.001 CRYSTAL CHEMISTRY OF HYDROTHERMALLY SYNTHESIZED INTERCALATION ELECTRODES. M. Stanley Whittingham and Peter Y. Zavalij Institute for Materials Research and Chemistry Dept, State University of New York at Binghamton, Binghamton, NY 13902-6016, USA

The unique layered structures of manganese and vanadium oxides and their derivatives are of particular interest because of their capacity to intercalate lithium and other cations between their layers that makes them promising candidates for cathode materials in secondary lithium batteries.

We have made a systematic study of the structural changes occurring when vanadium oxides are synthesized hydrothermally from aqueous media containing organic species over a wide range of pH. The coordination of the oxygen around the vanadium is found to increase from four under neutral pH conditions through square pyramidal to six in distorted octahedra at low pH values. A new vanadium dioxide phase and those containing double sheets of vanadium oxide octahedra are found to be the most electrochemically active. In contrast tetrahedral vanadium is found to be less active because of the resistance of V(IV) to take up tetrahedral coordination.

Layered manganese oxides with crystal chemistry similar to the well-known layered titanium disulfides have also been formed. Their crystal chemistry will be described, and the changes occurring on redox reaction will be outlined.

This work is being supported by the National Science Foundation (vanadium oxides) and the US Department of Energy (manganese oxides).

M08.OF.002 SYNTHESIS, NEUTRON DIFFRACTION AND MAGNETIC PROPERTIES OF CATHODE MATERIALS FOR LITHIUM BATTERIES. R. Kanno[a], R.K.B. Gover[a], A. Hirano[a], T. Kamiyama [b], and B. J. Mitchell[c], Department of Chemistry, Faculty of Science, Kobe University, Institute of Materials Science, University of Tsukuba, Intense Pulsed Neutron Source, Argonne National Laboratory.

In recent years, one particular area in Li ion battery research that has received a great deal of attention has been the layered phases $LiCoO_2$ and $LiNiO_2$. Both systems have a layered rocksalt structure, where alternating layers of Li and *M* (Ni or Co) occupy the octahedral sites of a cubic close packed oxygen array. Stoichiometric $LiNiO_2$ is difficult to prepare, due to the high temperature preparation conditions. Non-stoichiometry is associated with Li deficiency and the presence of Ni in the Li layer sites. It is thought that the Ni ions act as local pinning centres, which restricts the motion of the Li ions within the layers. In this study, the nonstoichiometry of $Li(Ni_{1-x}\text{-}Co_x)O_2$ (x=0.0, 0.2) has been controlled by varying starting material, composition and preparation temperature. X-ray and neutron Rietveld analysis has

been used to determine the composition of the materials prepared, and the electrochemical properties have been examined.

In $LiNiO_2$, the non-stoichiometry leads to a significant degradation in the charge/discharge properties, and its mechanism depends on the non-stoichiometry. Magnetic property is an another indication of the non-stoichiometry. The stoichiometric composition, y=0.00 in $Li_{1-y}Ni_{1+y}O_2$ showed a spin glass transition at 8K. The transition temperature increased with y from 0.00 to 0.05, and cluster glass behaviour was observed for the compositions, x>0.05. The behaviour is consistent with the compositions determined by X-ray and neutron Rietveld analysis.

In an attempt to improve the electrochemical properties of $LiNiO_2$, Co doped system has been widely studied. The composition y in $Li_{1-y}(Ni_{0.8}\text{-}Co_{0.2})_{1+y}O_2$ varied with the synthesis conditions, and the best samples prepared with useable capacities of the order of ~190 mAh/g have been found to be highly stoichiometric in nature by neutron diffraction. The spin glass behaviour in $Li_{1-y}(Ni_{0.8}Co_{0.2})_{1+y}O_2$ is also very sensitive to the composition changes. Relationships between the synthesis conditions, structures, charge/ discharge mechanism, and magnetic properties will be discussed.

M08.OF.003 STRUCTURE AND PROPERTIES OF LAYERED $LiNi_{1-y}M_yO_2$ PHASES. C. Delmas, Institut de Chimie de la Matière Condensée de Bordeaux-CNRS, and Ecole Nationale Supérieure de Chimie et Physique de Bordeaux, Av. Dr Schweitzer, 33608 Pessac Cedex (France).

Since $LiCoO_2$ was proposed as positive electrode material in Lithium-Ion batteries, a very strong interest has been devoted to lithium nickel oxide, which is considerably cheaper than the homologous cobalt phase. Unfortunately, the difficulty for obtaining lithium nickel oxide with a composition close to the ideal stoichiometry has inhibited for years the development of lithium-ion batteries with this positive electrode material. In fact, its true chemical formula is $Li_{1-z}Ni_{1+z}O_2$; the extra-nickel ions situated within the lithium sites play a dramatic role on the electrochemical behaviour. Recently, the preparation problems have been overcome ; nevertheless, the materials must be optimised in order to meet the requirements imposed by the applications. A considerable research activity has been devoted to studying the effects of cationic substitution for nickel. In our laboratory, the effect of cobalt, iron, aluminium and magnesium has been considered. Structural and physical characterisations will be discussed in relation with the electrochemical behaviour in lithium batteries. Special attention will be devoted to the characterisation of these materials by X- ray diffraction and also by methods which provide information at the local scale like EXAFS, NMR and Mössbauer spectroscopies.

The author wishes to thank I. Saadoune, A. Rougier, J.P. Pérès, G. Prado, C. Louchet, A. Demourgues, L. Croguennec, M. Grune, P. Gravereau, F. Weill, L. Fournés and M. Ménétrier for their contribution and CNES, SAFT, CEE (contract CT 95-0064) and Région Aquitaine for financial support.

M08.OF.004 NEUTRON DIFFRACTION STUDIES LANTHANUM GALLATE SOLID ELECTROLYTES AT HIGH TEMPERATURES. J.T.S. Irvine, University of St. Andrews, School of Chemistry, St Andrews, Fife, Scotland, UK KY16 9ST, P.R. Slater, Department of Chemistry, School of Physical Sciences, University of Surrey, Guildford, Surrey GU2 5XH and T. Ishihara and Y. Takita, Oita University, Department of Applied Chemistry, Dannoharu 700, Oita 870-11, Japan

$LaGaO_3$ doped with Sr and Mg has recently been shown to exhibit high oxide ion conductivity in both oxidising and reducing conditions and is currently being investigated as an alternative electrolyte material for use in solid oxide fuel cells. Ionic conductivity in this perovskite increases with doping, indicating that defect aggregation is not a major problem in this material.

In this study, we have investigated the structures of $LaGaO_3$ and $La_{0.9}Sr_{0.1}Ga_{0.8}Mg_{0.2}O_{3-\delta}$ by high-resolution neutron diffraction over the temperature range 25-1000°C, using the HRPD facility at the Rutherford Appleton Laboratory. On initial examination, both samples showed similar behaviour with a transition from orthorhombic (Pbnm) to rhombohedral (R3c) symmetry on heating. On more detailed examination it was observed that the doped samples were actually monoclinic (I2/a) over much of the temperature range. At the lowest temperatures the structure was pseudo-orthorhombic, changing to pseudo-rhombohedral between 250 and 500°C. Between 500 and 750°C, the monclinic distortion disappeared and the structure became rhombohedral. Significant changes are also seen in the $Ga\text{-}O_6$ octahedra on doping $LaGaO_3$ with much more distortion in the doped phase. Fundamental structural parameters such as O-O jump distance change dramatically with temperature, so it is inappropriate to consider a single activation energy for conduction in this system.

M08.OF.005 PARTIAL DISORDER IN $(Sc_yYb_{1-y})_2Ti_2O_7$ PYROCHLORE : IN-SITU NEUTRON DIFFRACTION STUDY OF A POSSIBLE OXYGEN CONDUCTOR. K. Eberman, Max-Planck-Institut für Festkörperforschung, Heisenbergstraße 1, 70569 Stuttgart, Germany; B. J. Wuensch, Massachusetts Institute of Technology, Boston, MA, 02139, USA; and J. D. Jorgensen, Materials Science Division, Argonne National Laboratory, Argonne, IL, 60439, USA.

A stability region for pyrochlores of the type $A^{3+}_2B^{4+}_2O_7$ has previously been found to include compositions having a cation radius-ratio $R_A{}^{+3}$:$R_B{}^{+4}$ between 1.54 and 1.80 for titanates [1] and between 1.40 to 1.71 for stannates [2]. In solid solutions where a larger Zr^{4+} ion is substituted on the B-site, progressive disorder has been observed near the perimeter of this stability regime for pyrochlores such as $Y_2(Zr_yTi_{1-y})_2O_7$ [3], $Y_2(Zr_ySn_{1-y})_2O_7$, and $Gd_2(Zr_yTi_{1-y})_2O_7$ [4]. This partial disordering is primarily among the anion array, which amounts to an increase in charge-carrier concentration [$V_o^{\bullet\bullet}$], and thus to an increase in ionic conductivity of up to two orders of magnitude. We are aware of only one study, other than the present, of disorder induced by substitution of a small ion on the A-site [5].

We present the analysis of neutron diffraction data taken continuously up to high-temperature (1400°C) for the entire solid solution series $(Sc_yYb_{1-y})_2Ti_2O_7$ (y = 0.00, 0.09, 0.20, 0.30, 0.40, and 0.52) together with the analysis for $Lu_2Ti_2O_7$. Preliminary results indicate that partial disorder is induced by both the chemical substitution and by increased temperature. For up to y = 0.30 the powders crystallized as single-phase pyrochlores, beyond which a second phase appears. The short hopping distances for oxygen anions among these pyrochlores of diminutive lattice parameter, together with the partial disorder among the anion array should allow for a direct interrogation of the transport mechanism in the Fourier synthesis maps.

1 O. Knop, F. Brisse, and L. Castelliz, Can. J. Chem., 47, 971-990 (1969).
2 F. Brisse and O. Knop, Can. J. Chem., 46, 869-873 (1968).
3 C. Heremans, B. J. Wuensch, J. K. Stalick, and E. Prince, J. Sol. State. S. Chem., 117, 108-121 (1995).
4 P. K. Moon and H. L. Tuller, in Sol. State. Ionics, MRS Symp. Proc. Vol. 135, eds. G. Nazri, R. A. Huggins, and D. F. Shriver, Pittsburgh, 149-155 (1989).
5 J. E. Greedan, Mat. Res. Bull., 14, n.1, 13-19, (1979).

P08.OF.001 LITHIUM LOCATION BY NEUTRON DIFFRACTION IN NASICON-TYPE α- AND α'-$LiZr_2(PO_4)_3$. M. Catti and S. Stramare, Dipartimento di Scienza dei Materiali, Università di Milano II - Bicocca, via Cozzi 53, 20126 Milano, Italy.

Within the NASICON family of ionic conductors, Li-containing compounds have not been thoroughly investigated so far from the structural point of view, mainly because lithium is a poor X-ray scatterer. On the other hand, a full knowledge of the Li^+ atomic environment is essential to understand the mechanisms of ionic mobility in these materials. With this aim, we studied $LiZr_2(PO_4)_3$ synthesized by solid state reaction at 1200 °C, which is reported to be rhombohedral $R\bar{3}c$ above 50 °C (α phase) and monoclinic C2/c at room temperature (α' phase), on the basis of conventional X-ray diffractometry [1]. Data were collected for the α and α' modifications at 150 and 25 °C, respectively, on the time-of-flight High Resolution Powder Diffractometer (HRPD) at the ISIS facility of the Rutherford Appleton Laboratory, Chilton, U.K., in the d_{hkl} range 0.7 to 2.5 Å. The α' phase turned out to be actually triclinic, consistent with recent X-ray results [2], and its Rietveld refinement converged in space group $C\bar{1}$ for 4226 data and 105 variables, with final agreement factors R_p=0.0672, wR_p=0.0929, $R(F^2)$=0.0617. A monoclinic pseudo-symmetry - x,y,1/2-z is observed for all atoms but lithium, which is disordered over two sites Li1 and Li2 with occupancies 0.71(3) and 0.29(3). Both Li1 and Li2 are in distorted tetrahedral coordinations, with <Li-O>=2.09 and 2.18 Å, respectively. Pairs of centrosymmetrical Li1 sites are located within half of the available M' holes of the NASICON structure, which are split into two independent sets by triclinic breaking of symmetry. The α structure was refined in space group $R\bar{3}c$ to R_p=0.0355, wR_p=0.0439, $R(F^2)$=0.1308, and here again Li is split into two sites Li1 and Li2 with tetrahedral surroundings. However, in this case the disorder is much higher, because all possible M' holes contain Li1 atoms with fractional occupancy, so that the larger conductivity of the α with respect to α' phase is fully accounted for.

1. D. Petit et al. (1986). Mat. Res. Bull., 21, 365.
2. J. E. Iglesias & C. Pecharromán (1998). Solid State Ionics, 112, 309.

P08.OF.002 MODELLING CONDUCTION PATHWAYS FOR SOLID ELECTROLYTES. St. Adams, MKI, Univ. Göttingen (Germany) and J. Swenson, Dep. of Appl. Physics, Chalmers Univ. of Technology, Göteborg (Sweden).

Conduction pathways for a variety of crystalline and amorphous Ag^+ ion conducting systems, including AgI-AgM_xO_y (M = B, Mo, P, V), AgI polymorphs and MAg_xI_y (M=Rb, Hg), are modelled as isosurfaces of minimum Ag bond-valence mismatch. The resulting pathway models are discussed in the light of experimental observations to elucidate relevance and limitations of the bond-valence approach. Beyond a description of the pathway topology the bond-valence pseudopotentials yield estimates of migration enthalpies and jump probabilities related to impedance and spectroscopic data.

The variation of the valence mismatch around regular silver sites closely mimics the experimental Ag probability density distribution. Bond-valence models moreover provide information on interstitial sites, for which the low occupancy precludes experimental investigations of atomic displacement parameters. In systems with complex anion disorder, structural determinations yield only an averaged picture. Thus bond-valence calculations for such systems were based on typical local co-ordinations for the mobile ions derived from complementary molecular dynamics simulations.

The simplicity of the bond-valence sum approach permits a modelling of comparatively large model systems and hence also of glassy ion conductors. Structural models of the molecular glass $(AgI)_{0.75}$ -$(Ag_2MoO_4)_{0.25}$, the network glass $(AgI)_{0.6}$-$(Ag_2O$-$2B_2O_3)_{0.4}$ and undoped borate glasses have been determined by reverse Monte Carlo (RMC) modelling based on neutron and x-ray diffraction data employing bond-valence constraints to reduce the number of unphysical Ag^+ co-ordinations. Due to the complexity of the pathways in glass systems and the snapshot character of RMC models, representative results (e.g. on the fraction of mobile ions, their local mobility, the involvement of differently co-ordinated Ag^+ in the long range ion transport, the spatial extension of pathways etc.) are derived from statistical evaluations of the percolation of Ag^+ along bond-valence sum isosurfaces.

08AA PREDICTION, DOCKING AND PATTERN RECOGNITION

M08.AA.001 ABSTRACT NOT AVAILABLE. J. Janin

M08.AA.002 ABSTRACT NOT AVAILABLE. I. Kuntz

M08.AA.003 ABSTRACT NOT AVAILABLE. D. Jones

M08.AA.004 THREADING WITH EXPLICIT MODELS FOR EVOLUTIONARY CONSERVATION OF STRUCTURE AND SEQUENCE. S.H. Bryant, A. Panchenko, A. Marchler-Bauer National Center for Biotechnology Information, National Institutes of Health, Building 38A, Room 8N805, 8600 Rockville Pike,Bethesda, MD 20894, USA

We have attempted to predict the three-dimensional structures of 19 proteins for the CASP3 experiment, each showing less than 25% sequence identity with known structures. Predictions were based on a threading method that aligns the target sequence with the conserved cores of structural templates, as identified from structure-structure alignments of the template with homologous neighbors. Alternative alignments were scored using contact potentials and a position-specific score matrix derived from sequence neighbors of the template. We find that this method identified the correct structural family for 11 of the 19 targets and predicted the remaining 8 targets to be similar to "NONE" of the templates, avoiding false positives. Threading alignments were relatively accurate for 10 of the 11 targets, including alignments for 6 of 7 identified at CASP3 as fold-recognition targets, sharing no sequence motifs with proteins of known structure. These predictions were ranked "first place" by the CASP3 assessor, and it appears that threading with family-specific models for structure and sequence conservation has improved threading prediction accuracy. A retrospective analysis of these and other CASP3 predictions clearly shows the limitations of current theading methods, however. To be detectable by threading, structural similarity must be extensive, such that 60% or more of residues may be superimposed to 2.5 Angstroms or less.

P08.AA.001 EXPLANATIONS FOR α-HELIX AND β-SHEET PROPENSITIES BASED ON CONFORMATIONAL FEATURES. P. Chakrabarti and D. Pal, Department of Biochemistry, Bose Institute, P-1/12 CIT Scheme VIIM, Calcutta 700054, India.

Since the elucidation of propensity values for amino acid residues to occur in different secondary structures by Chou and

Fasman [1], experiments have been designed to measure these. Although there is a broad agreement between different sets of values there is no universal explanation for the differences in propensity values. Extending our work on the features of the main-chain and side-chain conformations, (ϕ, ψ and χ_1) using the Brookhaven Protein Data Bank [2] we find that the α-helical propensity for a residue depends on the overall similarity in the distribution of its main-chain conformation with that of Ala, such that a stretch of residues having a high overall similarity to Ala can cooperatively form a helix. Similarly, the volume in the (ϕ, ψ, χ_1)-space occupied by a residue correlates with its β-sheet propensity. These explanations provide new insight into the folding of secondary structures, and the parameters calculated can be used for the prediction of secondary structures in proteins.

1. P.Y. Chou & G.D. Fasman (1978). Adv. Enzymol. 47, 45-148.
2. P. Chakrabarti & D. Pal (1998) Protein Engng. 11, 631-647.

P08.AA.002 A BRUTE FORCE PATTERN RECOGNITION ALGORITHM. R.J. Morris and V.S. Lamzin, EMBL Outstation Hamburg c/o DESY, Notkestrasse 85, Geb.25A, D-22603 Hamburg, Germany, and A. Perrakis, EMBL Outstation Grenoble c/o ILL, BP 156, Avenue des Martyrs 156X, 38042 Grenoble Cedex, France.

We present a new algorithm for tracing protein/DNA chains in crystallographic electron density maps. We formulate the task of finding the best chain (or set of chains) as a linear programming problem with integer decision values. The objective function is the vector product of the binary decision variables (connection - no connection) with a connection score vector. The scores are based on known stereochemical information. For proteins the 3D distribution of C_α valence and dihedral angles - an extension to the distribution used for validation in [1] - has proven to be particularly useful. In this way we *force* the algorithm to find only well-geometrised fragments. Although this formulation belongs to the so called NP-hard class problems we have developed algorithms that deliver good results in a very efficient manner thus making the problem tractable.

The results of the automatic map interpretation are used in the form of stereochemical restraints for the ARPwARP [2,3] refinement procedure. The incorporation of iterative pattern recognition routines into ARPwARP not only resulted in a significant improvement regarding CPU time but was also in many cases vital for the refinement to proceed.

[1] Kleywegt, G. J. (1997), Validation of Protein Models from C^α Coordinates Alone, *J. Mol. Biol.*, **273**, 371-376
[2] Lamzin, V. S. and Wilson, K. S. (1997), Automated refinement for protein crystallography, *Methods in Enzymology*, **277**, 269-305
[3] Perrakis, A. and Sixma, T. K. and Wilson, K.S. and Lamzin, V. S. (1997), wARP: Improvement and extension of crystallographic phases by weighted averaging of multiple refined dummy atomic models, *Acta Cryst.*, **D53**, 448-455

P08.AA.003 ELECTROSTATICS IN PROTEIN-PROTEIN DOCKING. M. Eisenstein, A. Heifetz, and E. Katchalski-Katzir. Departments of Chemical Services and Chemical Biology, The Weizmann Institute of Science, Rehovot 76100, Israel.

Previously we have presented an algorithm for protein-protein and protein-ligand docking, based on geometrical surface complementarity, and demonstrated its usefulness for predicting the structures of binary complexes and of supra-molecular aggregates [1-3]. Another prominent characteristic of proteins, which plays an important role in molecular recognition, is electrostatics. Yet, attempts to introduce electrostatics in our algorithm by us and by others only marginally improved the docking results [4].

The computed electrostatic interaction energies appear to be very sensitive to the exact relative position of the interacting molecules. Thus, a relative rotation of only 2 degrees may strongly affect the resultant electrostatic energy. This is a severe disadvantage in a stepwise scanning procedure as ours, which may miss the exact relative orientation of the docked molecules by a few degrees. It might be critical in docking attempts where structures of the uncomplexed proteins or model structures are used. Therefore, we looked for an alternative representation of the electrostatic characteristics of protein surfaces, which is less sensitive to the exact structural details and which can be efficiently incorporated in our docking algorithm.

Currently, we are developing a simplified "patches" representation of the electrostatic features of the docked molecules, which can be combined with an efficient scanning procedure that requires essentially the same amount of computation time as our geometrical docking. Initial results indicate that with the new representation the contribution of electrostatics to the overall surface matching score is considerably less sensitive to small orientational mis-matches and that it significantly increases the score of the correct structure and lowers the scores of many false positive solutions.

1. E. Katchalski-Katzir, I. Shariv, M. Eisenstein, A.A. Friesem, C. Aflalo and I.A. Vakser (1992). *Proc. Natl. Acad. Sci.* USA, **89**, 2195-2199.
2. M. Eisenstein, I. Shariv, G. Koren, A.A. Friesem and E.Katchalski-Katzir (1997). *J. Molec. Biol*., **266**, 135-143.
3. M. Eisenstein and E. Katchalski-Katzir (1998). *Lett. in Pept. Sci.*, **5**, 1-5.
4. H.A. Gabb, R.M. Jackson and M.J. Sternberg (1997). *J. Molec Biol.*, **120**, 106-120.

08BB PROBLEMATICS IN MACROMOLECULAR STRUCTURE (II): FITTING AND REFINEMENT (sponsored by CCP4)

M08.BB.001 ERRORS AND REPRODUCIBILITY IN ELECTRON DENSITY MAP INTERPRETATION. Sherry L. Mowbray, T. Alwyn Jones, Charlotte Helgstrand, Jill A. Sigrell, Alexander D. Cameron, Department of Molecular Biology, Swedish University of Agricultural Sciences and Uppsala University, Biomedical Centre, Box 590, S-751 24 Uppsala, Sweden.

Three investigators, with varying levels of experience, independently built the structure of *E. coli* ribokinase into an MIR map at 2.6 Å resolution, and then refined it. The refinement/rebuilding processes converged to give similar structures, although each "final" model had its own particular pattern of errors that remained. The subsequent refinement of the same structure at 1.8 Å resolution allowed an overall quality check of each of the lower-resolution models, and an analysis of which graphics-based tools were most efficient in locating these errors in general. Criteria that are useful in the application of Ramachandran, pepflip, rotamer side chain and real-space fit analyses are presented.

M08.BB.002 THROUGH PROTEIN MODEL SPACE WITH THE SPEED OF ARP/WARP. V.S. Lamzin, R.J. Morris and A. Perrakis. European Molecular Biology Laboratory, Outstations in Hamburg (Germany) and Grenoble (France).

An exponentially growing amount of challenging biological questions seeks answers through the structure determination of more and more proteins and their complexes. The number of new structural entries deposited in Protein Data Bank has been increasing over the last years and reached about 1,400 structures in 1997 alone. This puts much emphasis on the

availability of fast, reliable, objective and easy-to-use procedures for solution, building and refinement of these structural models.

We present the 'warpNtrace' method to automatically and without user intervention build and refine a protein model, starting from diffraction data extending to a resolution of higher than 2.3 Å and reasonable estimates of crystallographic phases. The method is an integral part of the ARP/wARP suite and is based on an iterative procedure describing the current electron density map as sets of unconnected atoms and then searching for protein-like patterns. The autotracing is combined with the reciprocal space refinement so that an almost complete protein model can be obtained in a fully automated way. The procedure can be applied starting from any source of phase information, experimental, computational or a combination of these. The time required for building a protein structure can be shortened from several man-days or even man-months to a few CPU hours on inexpensive workstations.

Several dozens of protein structures have already been reported to have been built and refined using 'warpNtrace'. The applications include the *Leishmania* surface protein (Leishmanolysin); a mercury derivative of 20 kDa xylanase which was solved at 2.0 Å resolution essentially *ab initio*, using SAD signal only; β-mannanase where sequence guesses from the autotraced fragments were used to design oligonucleotide primers to clone the gene; cyanase - a very large structure comprising ten monomers where the decamer is formed by a pentamer of dimers in an unusual way; GroEL apical domain where the whole procedure from the start of diffraction data collection to the completely autotraced protein structure took only 3 days.

M08.BB.003 EIGENVALUES ARE THE ANSWER, WHAT IS THE QUESTION? L.F. Ten Eyck, San Diego Supercomputer Center, University of California at San Diego, 9500 Gilman Drive, La Jolla 92093-0505, USA.

Atomic resolution protein structures have shown that essentially the same type of model describes both macromolecular and small molecule crystal structures. Incorporation of anisotropic thermal parameters, explicit hydrogen atoms, and static disorder models give similar levels of improvement in fit of the model to the observations in both cases. Adequately modelling this electron density distribution with fewer parameters is necessary at less than atomic resolution, but unfortunately is still an unsolved problem. The eigenvalue spectrum of the normal matrix for either least squares or maximum likelihood refinement is a precise and comprehensive tool for evaluating alternative parameterisations of the model. The eigenvalues and eigenvectors show the precision of parameter determination, the full multivariate correlation among all parameters and the effects of both constraints and restraints on the refined solution.

M08.BB.004 *AB INITIO* SOLUTION AND REFINEMENT OF AN 11 KDA PSEUDO-PROTEIN AGAINST MEROHEDRALLY TWINNED DATA. T.R. Schneider, J. Kärcher, E. Pohl, P. Lubini, and G.M. Sheldrick, Institute for Inorganic Chemistry, University of Göttingen, Tammanstr. 4, 37077 Göttingen, Germany

Merohedral twinning is a frequently observed (and frequently undetected but nevertheless existing) complication in both small molecule and protein crystallography. Here we describe the *ab initio* structure solution and refinement of mersacidin, a lantibiotic effective against gram-positive bacteria, based on data from a twinned crystal.

A single molecule of mersacidin contains 20 amino acids, about half of which are post-translationally modified. The compound crystallizes in the space-group $P3_2$ pretending to be $P3_221$ as a result of merohedral twinning. The asymmetric unit contains six molecules resulting in a crystallographic problem equivalent to a protein of 120 residues. At cryogenic temperatures crystals diffracted to 1.1Å on BW7B at EMBL Hamburg (100% complete, $R_m = 4.9\%$).

After very crude deconvolution of the data into contributions from the different twin domains, the program SHELXD[1] succeeded in solving the structure *ab initio*. Three quarters of the atoms were automatically located in the first electron density map. Starting from this model, refinement was performed against the original twinned data using the program SHELXL[2] employing a mixture of small molecule and protein techniques. Key steps were the introduction of tight restraints on the non-standard amino acids exploiting the local non-crystallographic symmetry and substantial phase improvement by automatic placement of dummy atoms in a way similar to ARP[3].

The current crystallographic R-value is 13.6%. The atomic model reveals an extremely tight packing including a non-crystallographic two-fold axis and a set of cleavage planes that provide a possible physical explanation for the merohedral twinning.

[1] Sheldrick GM, Gould RO: Structure Solution by iterative peaklist optimization and tangent expansion in space group P1, *Acta Cryst*. **B:423-431** (1995).
[2] Sheldrick GM, Schneider TR: SHELXL: High Resolution Refinement, Methods in Enzymology, 277:319-343 (1997).
[3] Lamzin VS, Wilson KS: Automated Refinement of Protein Models, Acta Cryst D49:129-147 (1993).

M08.BB.005 EFFECTS OF TLS THERMAL PARAMETERS IN MACROMOLECULAR REFINEMENT. Winn, M.D.[1], Mikhael Isupov[2] and Murshudov, G.N. [1,3], [1]CLRC Daresbury Laboratory, Warrington, WA4 4AD, UK [2]Dept of Chemistry and Biological sciences, University of Exeter, Exeter, UK [3]Chemistry Department, University of York, York, YO1 5DD, UK

Because of limited resolution, the description of the atomic model in terms of a sufficiently small number of parameters is one of the most important steps in macromolecular refinement. Translation libration screw (TLS), using only 20 parameters per rigid body, is one possibility for reducing the number of thermal parameters required. Computationally, the necessary derivatives with respect to the TLS parameters are calculated in terms of the gradients and second derivatives for individual anisotropic U values. For the latter, the FFT routine is used. This means that the procedure is fast and can be used routinely. Refinement of TLS parameters has been implemented in the program REFMAC available from CCP4 [1].

Examples of this use of TLS will be given. For a 2.0Å example with 5881 atoms, after refinement of 80 TLS parameters the free-R value dropped by 3.5%. For a 1.7Å case with 835 atoms, addition of only one set of TLS parameters improved the free-R value by 2.5%.

Refinement of these parameters in parallel with individidual positional, isotropic and anisotropic thermal parameters will also be presented. In addition, since different molecules in the unit cell might well have different overall thermal parameters, removing the TLS contribution from the individual atomic thermal parameters is expected to improve and extend the application of NCS restraints in the refinement.

[1] CCP4 Acta Cryst **D50** (1994) 760-763

P08.BB.001 IMPROVED METHODS FOR CRYSTALLOGRAPHIC ENERGY MINIMIZATION. John Badger [1] Dan Berard [2] and Sandor Szalma [2 1] , San Diego Supercomputer Center, PO Box 85608, San Diego, CA 92186, [2] Molecular Simulations Inc., 9685 Scranton Road, San Diego, CA 92121

It has generally been assumed that crystallographic refinement protocols based on simulated annealing with torsion angle dynamics have a much larger radius of convergence than protocols based on gradient-based energy minimization. We have developed a multi-stage energy minimization protocol that combines (i) the maximum likelihood targets (Pannu & Read, Acta Cryst. A52, 659, 1996), (ii) the Babinet bulk solvent scattering correction, (iii) the adopted basis Newton-Raphson (ABNR) energy minimization algorithm incorporating second derivative information.

Each of these factors improves the quality of the refinement and appears to have a larger impact on the results obtained by energy minimization than results obtained by simulated annealing. In tests (10 trials for each method) with a model containing an rms backbone error of 1.6Å; the energy minimization protocol was as effective as torsion angle dynamics for refining the model. This model appears to be on the limits of refinability since no method was able to improve the structure when the coordinate errors were increased to 2.0Å;. Analyzing the results of the multiple trials with these methods we found that there is a smaller variation in the quality of results with the energy minimization protocol than with the torsion angle dynamics protocol.

For this reason, energy minimization may be the most reliable approach for many refinements. In addition, we found that the ABNR energy minimization method refinesmodels to a lower energy than the Powell energy minimization method, avoiding numerical problems that lead to abandonment of the line search. However, for a very narrow range of difficult refinement problems (rms backbone error 1.8Å;) the more stochastic dynamics based approach was able to produce 2/10 good solutions (as well as some very poor solutions) while the solutions obtained from the energy minimization protocol were less well converged.

This refinement methodology is available in X-PLOR 98.1 from Molecular Simulations Inc.

P08.BB.002 MAXIMUM LIKELIHOOD REFINEMENT OF ADENOVIRUS TYPE 5 HEXON WITH TNT. John J. Rux and Roger M. Burnett, The Wistar Institute, 3601 Spruce Street, Philadelphia, PA 19104, USA.

Solving the adenovirus type 5 hexon (Ad5) structure was initially thought to be a straight-forward molecular replacement problem. Ad5 is the major protein component of the icosahedral adenovirus capsid. The very long chain (951 aa) forms two 8-stranded "viral" jelly-rolls at the subunit base. The trimer has highly convoluted loops making three towers visible by EM as "bumps" on the outer surface of the virus capsid. As the Ad5 sequence is closely related to that of the known Ad2 [1] (86 % aa identity), and both crystallize isomorphously, the structure solution appeared trivial.

The sequence heterogeneity between Ad2 and Ad5 occurs mainly in the loop structures. Initially, these were removed and the highly conserved base (690 aa, or 73% of structure) was used as a starting model. Various refinement and fitting attempts stalled, yielding models with Rfree values of 35-40 %. The successful approach began with a starting model containing the base plus poly-Ala loops. Refinement with TNT against a maximum likelihood (ML) target has yielded a 2.5 Å structure with R = 17.6 %, Rfree = 23.1 %, 0.004 Å RMSD bonds, and 1.444 ° RMSD angles.

The new structure reveals substantial differences from the starting model: a reverse tracing of a 65 aa loop; an up to 41 aa shift in the sequence registry for 130 aa at the N-terminus; small register shifts of 1-2 aa in other portions of the structure; and increased secondary structure. These findings explain some previously puzzling structural and experimental observations: a "missing" N-terminus; a long stretch of "buried" acidic residues; and a hypervariable sequence with conserved secondary structure.

The success of the Ad5 structure solution illustrates that current techniques such as Rfree analysis and ML refinement when applied to previously accepted models may yield much higher quality structures — and some surprises.

1. F.K.Athappilly, R.Murali, J.J.Rux, Z.Cai, R.M.Burnett (1994). J.Mol.Biol., 242, 430-455.

08CC STRUCTURES AND TECHNIQUES AT EXTREME PRESSURES AND TEMPERATURES

M08.CC.001 PHASE TRANSITIONS IN GEOPHYSICS. Raymond Jeanloz, Depts. Geology & Geophysics and Astronomy, University of California, Berkeley, CA 94720-4767, USA

Phase transitions play a key role in geophysics, both in helping to interpet the observed structure of the Earth and in order to understand the dynamics of the planet's deep interior. Crystal-structural transitions are relatively well characterized at the conditions of the mantle, and are found to exert a surprising influence on convection and large-scale heat transfer of the interior. More recent ultrahigh-pressure studies of coupled electronic and structural transitions in transition-metal oxides begin to provide an understanding of intense chemical and physical interactions between the Earth's metallic core and rocky mantle. High-pressure experiments and theory have helped lead the geophysical observations, thus revealing new insights about the long-term evolution of our planet.

M08.CC.002 SINGLE-CRYSTAL X-RAY DIFFRACTION AND SPECTROSCOPY AT MEGABAR PRESSURES. H.K. Mao, L.W. Finger, R. J. Hemley Geophysical Lab. and Center for High Pressure Research, Carnegie Institution of Washington, 5251 Broad Branch Rd. NW, Washington, DC 20015-1305, USA.

Detailed crystal structure refinement at pressures above 20 GPa has been previously obtained only with polycrystalline diffraction methods. High-pressure single-crystal x-ray diffraction, which provides far more comprehensive and accurate information on crystallography, has been limited to lower pressures and a small reciprocal space within a 90° cone of the diamond-cell axis. We have developed a special diamond cell to extend high-pressure single-crystal x-ray diffraction far beyond the previous limit. X-ray transparent gasket allows access to the full reciprocal space of the single crystal sample. Structure refinement can be performed with either monochromatic or polychromatic x-radiation. The technique also opens new areas of high-pressure single-crystal x-ray spectroscopic studies including electron and phonon dispersions and Compton scattering.

M08.CC.003 THE SHEAR STRENGTH AND ELASTIC MODULI FROM THE LATTICE-STRAINS MEASURED UNDER NON-HYDROSTATIC COMPRESSION. A. K. Singh, Materials Science Division, National Aerospace Laboratories, Bangalore 560017, India.

The stress state of the sample compressed in a diamond anvil cell (DAC) tends to be non-hydrostatic, particularly in the megabar

range. Successful attempts have been made to model the non-hydrostatic stress state of the sample and develop a theory to compute the lattice strains produced by such stresses [1-3]. A recently developed technique [4,5] permits the measurement of the lattice strains along different directions with respect to the load axis of a DAC. The analysis of these data, obtained under non-hydrostatic compression, gives the shear strength and single-crystal elastic moduli of the specimen material [6-9]. These data can be also analyzed using the present theory to derive the equation of state (pressure-volume relation) that corresponds to hydrostatic compression. The present analysis provides the only method of estimating the shear strength and elastic moduli to a few hundred gigapascals. The results of such analysis of iron data have been used recently to discuss the anomaly in the seismic wave-velocity through the earth's inner core [10].

[1] A. K. Singh, J. Appl. Phys. **73**, 4278 (1993); **74**, 5920 (1993)
[2] A. K. Singh and C. Balasingh, J. Appl. Phys. **75**, 4956 (1994)
[3] T. Uchida, N. Funamori, and T. Yagi, J. Appl. Phys. **80**, 739 (1996)
[4] H. K. Mao and R. J. Hemley, High Press. Res. **14**, 257 (1996)
[5] H. K. Mao et al, Phys. Earth Planet. Inter. **96**, 135 (1996)
[6] A. K. Singh et al, Phys. Rev. Lett. **80**, 2157 (1998);
[7] A. K. Singh et al, J. Appl. Phys. **83**, 7567 (1998)
[8] T. S. Duffy et al, Phys. Rev. (communicated)
[9] T. S. Duffy et al, J. Appl. Phys. (communicated)
[10] H. K. Mao et al, Nature, **396**, 741 (1998).

M08.CC.004 THE AB INITIO CALCULATION OF THE STRUCTURE AND STABILITY OF IRON. G. David Price, L. Vocadlo, D. Alfe, J. Brodholt and M. J. Gillan, Departments of Geological Sciences, and Physics, University College London, Gower Street, London WC1E 6BT.

The Earth's inner core is predominantly made of metallic iron crystallizing out of the outer core which consists mainly of liquid iron with some lighter alloying element. The temperature at the outer core/inner core boundary (ICB) is unknown, but even some knowledge of the structure and melting temperature of pure iron under these conditions would provide an invaluable constraint on the ICB temperature; however, current estimates of the melting temperature of pure iron under core conditions vary by several thousand degrees. To help resolve these uncertainties, we are performing ab initio computer calculations on both the solid and liquid phase of iron under core conditions in order to determine the Gibbs free energy and temperature of the melt transition. The calculations are being performed using the projector augmented-wave method (PAW) which is a generalization of the linear augmented-plane-wave method (LAPW) and the pseudopotential method. The vibrational free energy of the solid phase are calculated using the frozen phonon technique to obtain the harmonic vibrational spectrum; an anharmonic contribution to the free energy can be obtained from ab initio molecular dynamics by thermodynamic integration from the harmonic reference system using a coupling constant method. Similarly, the free energy of the liquid can be calculated from ab initio molecular dynamics simulations by thermodynamic integration from an appropriate model reference system. We will first present our calculated results and review future developments.

M08.CC.005 STRUCTURAL STUDY OF MAGNESITE AND DIAMOND UNDER HIGH PRESSURE. G. Fiquet Laboratoire de Sciences de la Terre, UMR CNRS 8515, ENS Lyon, 46 Allée d'Italie, 69364 Lyon cedex 07, France, gfiquet@geologie.ens-lyon.fr

We report here two series of X-ray diffraction experiments that have been carried out to determine the compression properties of (1) a natural magnesite compound and (2) synthetic diamond samples of different isotopic constitutions (^{12}C and ^{13}C). Angle dispersive X-ray diffraction experiments were carried out at the high-pressure beamlines ID30 and ID09 of the ESRF (Grenoble, France). X-ray beam at wavelengths from 0.3 to 0.45 Å were used in association with imaging plates to collect data over a 2-theta interval from 4 to 25°, suitable for structural refinements.

X-ray diffraction pattern were recorded to 113 GPa on a mixture of magnesite and platinum powders, loaded in a diamond-anvil cell and annealed with an infrared YAG laser. Rietveld structural refinements show that the principal structural change with increasing pressure is a very large compression of the MgO_6 octahedra on the cost of a slight expansion of the CO_3 groups. Above 60 GPa however, MgO_6 octahedra almost stop compressing and the overall compression is in turn accomodated by a compression of the CO_3 groups.

Several runs were carried out in a diamond-anvil cell on synthetic diamond powders of different isotopic compositions (^{12}C and ^{13}C). A mixture of methanol-ethanol-water 16 :4 :1 in volume was used up to 15 GPa to provide hydrostatic pressures around the samples , whereas nitrogen or argon were used to 20 GPa. Le Bail profile refinements were applied to the diffraction patterns, in order to obtain reliable high-pressure cell parameters for diamond as well for the pressure transmitting media. Preliminary results indicate very similar compression properties for both compounds, in disagreement with ultrasonics and Brillouin scattering experiments which reported up to 17% increase in the bulk modulus of ^{13}C diamond with respect to ^{12}C diamond.

Hurley et al., *J. Appl. Phys*., 76, 12, 1994 ; Ramdas et al., *Phys. Rev. Lett*., 71, 1, 1993

M08.CC.006 CHEMISTRY OF LIGHT MOLECULES AT HIGH PRESSURE AND TEMPERATURE. Guido L. Chiarotti, International School for advanced Studies, Via Beirut 2, I-34100, Trieste, Italy

The combined effect of high Pressure (P) and Temperature (T) may alter significantly the chemical properties of molecular systems because high-P reduces the molecular dissociation barriers and high-T helps in overcoming them. In this talk I shall review our recent works on the study of chemical reactions at high PT, using first principles computer simulations. In particular I shall discuss the high PT induced methane dissociation [1], the superionic and metallic behaviour of water and ammonia at high PT [2], the transformation of molecular carbon dioxide (CO_2) into nonmolecular carbonate phases similar to alpha-quartz SiO_2. The simulation predicts this transformation to occur above 40 GPa, with a more facile transformation for T higher than 1800 K [3].

[1] F. Ancilotto, G.L. Chiarotti, S. Scandolo, E. Tosatti, Science 275, 1288 (1997).
[2] C. Cavazzoni, G.L. Chiarotti, S. Scandolo, E. Tosatti, M. Bernasconi, and M. Parrinello, Science 283, 44 (1999).
[3] S. Serra, C. Cavazzoni, G.L. Chiarotti, S. Scandolo, E. Tosatti, Science, to appear (1999).

P08.CC.001 THE "ETH DIAMOND-ANVIL CELL" DESIGN FOR SINGLE-CRYSTAL XRD AT NON-AMBIENT PT CONDITIONS. R. Miletich, H. Reifler, and M. Kunz, Laboratory for Crystallography, ETH Zentrum, CH-8092 Zürich, Switzerland

Diamond anvil cells (DAC's) provide the capability of generating large stable pressures. Angle-dispersive diffraction on single crystals aiming for high-precision diffraction data requires modifications to the DAC design in order to optimize application on a four-circle diffractometer.

Our new design is based on the BGI-type DAC [1]. It is a modular DAC system which allows a room-temperature (RT) high-pressure (HP) module to be replaced by a high-temperature (HT) part. The principle design based on (1) the mechanism for adjusting the parallelism of the opposing diamond culets, (2) the

stability as achieved by four guide pins, and two pairs of left- and righthanded bolts, and (3) the large opening angle of 90° has been transfered to the new ETH-DAC, which in overall gains from both less weight and smaller size relative to the original BGI design.

Modification of the exchangeable RTHP module include a spring-loaded mounting system of the diamond anvils on the beryllium seats, which allows a quick replacing of the anvils. The anvil shape has been modified to achieve both larger table sizes and a smaller anvil height. The HPHT module, which is based on single-crystal diamond backing plates instead of the Be seats, allows external heating by a resistance furnace in an Ar-H_2 atmosphere. The design of the new cell and first results of application will be presented.

1. D.R.Allan, R.Miletich, R.J.Angel (1996) Rev. Sci. Instrum. 67, 840-2

P08.CC.002 IRON AT EARTH'S CORE CONDITIONS: AN AB-INITIO SIMULATION STUDY. G.L. Chiarotti, A. Laio, S. Scandolo [1], S. Bernard [2], E. Tosatti [1,3], [1] International School for Advanced Studies, Via Beirut 4, I-34014 Trieste, Italy, [2] Commissariat a l'Energie Atomique, DRIF ,BP 12, F-91680 Bruyeres le Chatel, France, [3] International Centre for Theoretical Physics, I-34014 Trieste, Italy

We present a theoretical description of iron at earth's core pressure and temperature conditions as obtained by a combination of first-principles and classical molecular dynamics simulations.We calculate the melting temperature, the density, and the elastic properties of solid and liquid iron at inner-core boundary conditions. Geophysical implications on the structure of the earth's core are discussed.

P08.CC.003 LATTICE STRAINS UNDER NON-HYDROSTATIC COMPRESSION: A DISCUSSION OF THE ASSUMPTIONS IN THE THEORY. A. K. Singh, Materials Science Division, National Aerospace Laboratories, Bangalore 560 017, India.

The recently derived general equations for the lattice strains [1-3] produced by non-hydrostatic compression in an opposed-anvil setup explain quantitatively the orientation dependence of the lattice strains measured by a newly developed technique [4,5]. The analyses using these equations of the lattice-strain data under non-hydrostatic compression give the shear strength, single-crystal elastic moduli, and the equation of state corresponding to a hydrostatic compression [6-9]. While deriving these equations, the following assumptions regarding the experimental conditions are made. (1) The anvils are assumed to be perfectly rigid and parallel. (2) The incident beam and the line-of-sight of the energy dispersive detector are assumed to pass through the geometric center of the sample. (3) The sample is assumed to be an aggregate of randomly oriented crystallites. (4) The yield stress of the crystallites in a polycrystalline sample is assumed to be independent of the crystallite-orientation with respect to the load direction. In practice, departures from these assumptions are expected. The changes in the lattice-strain equations arising from these departures are considered in this presentation.

[1] A. K. Singh, J. Appl. Phys. **73**, 4278 (1993); **74**, 5920 (1993);
[2] A. K. Singh and C. Balasingh, J. Appl. Phys. **75**, 4956 (1994);
[3] T. Uchida, N. Funamori, and T. Yagi, J. Appl. Phys. **80**, 739 (1996);
[4] H. K. Mao and R. J. Hemley, High Press. Res. **14**, 257 (1996);
[5] H. K. Mao et al, Phys. Earth Planet. Inter. **96**, 135 (1996);
[6] A. K. Singh et al, Phys. Rev. Lett. **80**, 2157 (1998);
[7] A. K. Singh et al, J. Appl. Phys. **83**, 7567 (1998);
[8] T. S. Duffy et al, Phys. Rev. (communicated);
[9] T. S. Duffy et al, J. Appl. Phys. (communicated).

P08.CC.004 X-RAY IN SITU STUDIES OF SOME REFRACTORY OXIDES, CARBIDES, METALS AND ALLOYS AT HIGH P-T CONDITIONS. N.A.Dubrovinskaia, L.S.Dubrovinsky, S.K.Saxena Department of Earth Sciences, Uppsala University

Despite the importance of refractory ceramics, metals and alloys for industrial applications (for example, the Co-Ti-C, Co-W-C and Fe-Al-C systems), basic knowledge of the individual phases, phase relationships, and their thermodynamic properties is still incomplete. Thermal expansion and compressibility data are rather sparse.

Very reliable data can be obtained by in situ X-ray experiments. We obtain powder X-ray diffraction data with a Siemens X-ray system consisting of a Smart CCD Area Detector and a direct-drive rotating anode as X-ray generator. With the capillary optic (X-ray optical stage, model CS-SRA/P-HP) installed, a high- intensity focus of X-rays is produced at the sample position, and its width is controlled by the choice of field aperture.

For the compressibility study we use the DXR-GMW diamond anvil cell (DAC) (Diacell Products, UK). In this cell a high pressure is applied to a sample by forcing two diamond anvils together along a common axis by means of a metal membrane assembly driven by a gas pressure. To increase pressure, one needs not therefore to remove the cell from the stage during an experiment. It means that additional alignment procedures are not required, and accurate data can be obtained. Both diamond anvils are mounted on beryllium plates, which are transparent for X-rays. In thermal expansion studies we heat a sample internally.

Using our in-house facilities we obtained new X-ray in situ data on thermal expansion of refractory metals (Cr, Ta) and thermal expansion, phase relations and compressibility of alloys and compounds in Fe-Al-C, Co-Ti-C , and Co-W-C systems.

For example, we found a rapid increase of thermal expansion for chromium Cr at temperatures higher than 1200 K, which confirmed a theoretically calculated large increase of entropy due to a contribution from magnetic fluctuations (Smag). From a direct in situ measurement of volume dependence of pressure for Co6W6C, its isothermal bulk modulus (K300,0) was found to be higher than that of diamond (444(3) GPa). A phase transition from cubic to rhombohedral structure was observed for TiC at pressure higher than 20 GPa. First time the isothermal bulk modulus was found from direct measurements for both phases.

P08.CC.005 STRUCTURAL STUDIES OF OXYGEN AT HIGH PRESSURE BY THE SINGLE-CRYSTAL TECHNIQUE. G.Weck, Service de Physique de la matière condensée, CEA/DIF/DPTA, 91680, Bruyeres-le Chatel, France

We have performed energy dispersive X-ray diffraction experiments on a oxygen single-crystal in helium up to 115 GPa. From 22.5 GPa to 96 GPa the diffraction line (7 different classes) are well indexed in the A2/m monoclinic lattice proposed by Johnson et al for the ε-phase. Between 96 and 110 GPa, a displacive phase transition (discontinuous change in angle and energy of diffraction) is observed that keep the single crystal. At 110 GPa the resting line do no more fit with the monoclinic cell and a triclinic cell is proposed for the metallic phase. The d-spacing variation with pressure for two experiments is presented in the figure below. Particularly, the separation between the (02-2) and (022) d-values at 110 GPa confirm a triclinic deformation.

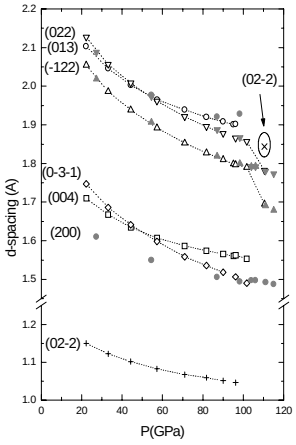

Fig 1: Pressure dependence of d-spacing. Symbols with dotted lines represents the first experimental data, the full symbols are for the second experiment.

P08.CC.006 COMPARATIVE CRYSTAL CHEMISTRY OF SOME SILICATES AT VERY HIGH PRESSURES. L. Zhang, Institute of Mineralogy, University of Marburg, 35032 Marburg, Germany

The fact that divalent iron (Fe) and magnesium (Mg) can form complete solid solutions in many silicates is attributed to their similar bonding properties. Indeed, bulk moduli (K) for Fe and Mg endmember were very close. Although bulk moduli of Fe endmember seem systematically larger than their Mg counterparts, it was impossible from experimental data available to decipher their high pressure behaviour. From KV = constant [1,2] a higher compressibility of Fe endmember at high pressures would be predicted.

Recent refinements on intensity and lattice parameter data from single crystal diffraction on silicate minerals ($Mg_3Al_2(SiO_4)_3$, $Fe_3Al_2(SiO_4)_3$, $Mn_3Al_2(SiO_4)_3$, $Ca_3Al_2(SiO_4)_3$, $Ca_3Fe_2(SiO_4)_3$, (Mg_2SiO_4, Fe_2SiO_4, Mn_2SiO_4, Co_2SiO_4, $CaMgSi_2O_6$, $CaFeSi_2O_6$) at pressures up to 33 GPa [3,4,5] provide new insights into the role of bonding properties of individual cation in the polyhedral compression. Precise measurements of the lattice parameters by multi-loading the crystals in one pressure cell allow direct determination of the differential compressibility $\Delta\beta = \beta_a - \beta_b$ between two crystals at high pressures. The results show that Mg endmembers are systematically more compressible than its Fe counterparts. This is manifested uniquely in the different compressibilities of Mg and Fe polyhedra that is clearly related with their different bonding properties, whereas the polyhedral coordination and crystal structure type appear to be of marginal significance.

The above results demonstrate that the assumption of similar chemical bonding of Fe and Mg for silicates is inappropriate. The new results helps to understand the compression mechanism and indicate that the bulk modulus of Fe endmember in a solid solution is higher than that of the Mg endmember.

[1] Anderson DL, Anderson OL (1970) J Geophys Res 75:3494-3500.
[2] Hazen RM, Finger LW (1979) J. Geophy Res 84:6723-6728.
[3] Zhang Li, Ahsbahs H, Kutoglu A, Hafner SS (1997) Amer Mineral 82:245-258.
[4] Zhang Li, Ahsbahs, H, A. Kutoglu (1998) Phys Chem Minerals 25:301-307.
[5] Zhang, Li (1998) Phys Chem Minerals 25:308-312.

P08.CC.007 IN SITU X-RAY DIFFRACTION STUDY OF DIAMOND SYNTHESIS USING CATALYSTS UNDER HIGH PRESSURES. W.Utsumi, T.Mizutani, O.Shimomura [1], T.Taniguchi, S.Nakano [2], N.Nishiyama [3], K.Funakoshi [4]. [1] Kansai Research Establishment, Japan Atomic Energy Research Institute, Mihara, Mikazuki-cho, Hyogo 679-5143, Japan. [2] National Institute for Research in Inorganic Materials, Namiki, Tsukuba,Ibaraki 305-0044, Japan. [3] Department of Earth Sciences,Ehime University, Matsuyama 790-8577, Japan. [4] Japan Synchrotron Radiation Research Institute, Mihara, Mikazuki-cho, Hyogo 679-5198, Japan

In situ x-ray diffraction experiments were carried out to observe graphite to diamond transition under high pressures and high temperatures. Experiments were carried out under the P-T conditions up to 13GPa and 2100°C using a large volume press installed on BL04 beamline at the SPring-8. Three different materials, Ni, $K_2Mg(CO_3)_2$, and $MgCO_3$ were used as diamond formation catalysts and results were compared.

When Ni was used as a catalyst, diamond was always formed just at its melting temperature. On the other hand, using $K_2Mg(CO_3)_2$ as a catalyst, diamond did not appear at the temperature where catalyst started to melt. In order to synthesize diamond using this catalyst, higher temperature than its melting point was needed. Pressure dependence of two important temperatures, melting temperature of catalysts and diamond formation temperature, were obtained. For $MgCO_3$ experiment, this catalyst did not melt until 2100°C at 9.3GPa. However, at around 1800°C, which was far below the melting temperature, clear cubic diamond peaks appeared. This data indicates that graphite- diamond transition occurred without melting of the catalyst and that solid $MgCO_3$ can play a role of diamond formation catalysts.

P08.CC.008 SOME ASPECTS HOW TO PREPARE AND TO CARRY OUT A HIGH TEMPERATURE MEASUREMENT. M.Ermrich, X-ray Laboratory Dr. Ermrich, Westring 80, D-64354 Reinheim, Germany

High temperature X-ray diffraction investigations have got a significant place in every ‘up-to-date’ laboratory. The basic conditions to get diagrams with high resolution over the whole angle region in a short time are delivered by various types of high temperature attachments, which are adaptable to use the advantages of the different geometries of the goniometers, and the availability of linear and area detectors. But it is necessary to consider some aspects to prepare and to carry out a successful experiment.

Geometry: Powders, foils, compact materials and / or thin films require different geometries, e.g. capillary, transmission or reflection mode with all their advantages and disadvantages. The well-known difficulties of diffraction, preferred orientation, absorption effects, small amounts, penetration depth ... get especially critical.

Calibration: Finding out optimal calibration substances for the wanted temperature region (using their transition temperatures, melting points and / or thermal expansion coefficients), a well defined gas flow, an optimized temperature measurement, known temperature gradients - facts, which are indispensable for the experiment.

Heating element: It has to satisfy different requirements like no reaction with the sample or the inert gas, homogeneous heating ‘without’ temperature gradients, sample adapted sizes or movements, easy and stable adjustment.

These main points of view will be discussed together with both the present possibilities and experiences. Some examples will be given.

08DD NON-STRUCTURAL APPLICATIONS OF RIETVELD ANALYSIS

M08.DD.001 RIETVELD QUANTITATIVE PHASE ANALYSIS (RQPA). Julius Schneider, Institute of Crystallography and Applied Mineralogy, Universität München, Theresienstraβe 41, D-80333 München, Germany

Powder diffraction is one of the few techniques which is truly phase sensitive. It has proved to be an ideal tool for quantitative phase analysis (QPA) in such diverse fields as mineralogy, geology, solid state chemistry, materials science, pharmacy , archeology etc. Based on the pioneering work of Rietveld (1969) on precise quantitative analysis of whole powder patterns, Hill & Howard (1987) derived a simple relation between the weight fractions of individual components in multiphase mixtures and their corresponding scale factors in the Rietveld refinement. This offers a standardless method of QPA, as the role of the experimentally determined phase pure standards is taken over by the known atomic structure models of the phases. The ready availability of computer programs and of structure model data bases (ICSD, CDB) greatly eases the practical use of RQPA. It's great flexibility relies on the variability of structural as well as instrumental parameters allowing ready adaptation of the generated powder patterns to the number of phases, to changes in chemical composition, in unit cell dimensions,in profile shape or profile widths, to instrumental conditions etc. Generating "ideal" multiphase powder patterns, the detection and computational correction of systematic errors like preferred orientation, etc. is greatly facilitated. Modified methods allow inclusion of non-diffraction methods or on-line operations in plants. Examples include phase transitions at elevated temperatures.

Rietveld H. M. (1969), J. Appl. Cryst. 2, 65-71
Hill R. J. & Howard C. J. (1987), J. Appl. Cryst. 20, 467-474

M08.DD.002 APPLICATION OF NEW WEIGHT FUNCTION TO THE WHOLE-PATTERN L.S. FITTING FOR QUANTITATIVE PHASE ANALYSIS. S. Hayashi and H. Toraya, Ceramics Research Laboratory, Nagoya Institute of Technology, Tajimi 507-0071, Japan

In the quantitative phase analysis (QPA), whole-powder-pattern fitting (WPPF) techniques such as for Rietveld refinement or whole-powder-pattern decomposition (WPPD) have some advantages over single-line methods: 1) feasibility of analyzing complex powder pattern and 2) averaging effects for random and systematic errors and resultant improvement in accuracy and precision. The strong peaks, which can be largely shifted by preferred orientation and/or particle statistics, in the low angle region are, however, very influential on the accuracy in the QPA. Therefore, in our previous study [1], these strong peaks must be excluded from the least-squares refinement of scale factors by shortening the 2qs-range for WPPF. However, such a handling of the intensity data is sample-dependent and less general. Recently, the new weigh function with a form $w=1/Y^e$ (e>1) was introduced into the minimization function in Rietveld refinement [2]. It gives heavier weights on weak peaks and lessens the influence of strong peaks, and the uniform distribution of weighted errors thus obtained resulted in the improvement of the accuracy in structural parameters. The new weight function was expected to resolve the problem of strong peaks in the QPA using WPPF. In the present study, it was tested in the QPA using Rietveld refinement and the WPPD method. The accuracy in the QPA was significantly improved by the new weight function, even if the strong peaks were included in the least-squares refinement.

1. S. Hayashi and H. Toraya (1999). J. Ceram. Soc. Japan **107** (in press).
2. H. Toraya (1998). J. Appl. Cryst. **31**, 333.

M08.DD.003 PROFILE MODELLING IN THE RIETVELD METHOD BASED ON THE LATTICE DEFECT STRUCTURE. P. Scardi, M. Leoni, Università di Trento, Facoltà di Ingegneria, Dipartimento di Ingegneria dei Materiali, via Mesiano, 77 - 38050 Trento, Italy.

Recent developments in the Rietveld method give a growing importance to the refinement of materials microstructure together with their structure. The reason is twofold: a proper modelling of microstructure-related features in the diffraction pattern usually results in a better fitting of the experimental data, which means a better quality of the refined structural data; on the other hand, a valuable information, typically of interest for materials science studies, can be obtained. So far, advancements were mostly addressed to the first point (better structure data), while the use of the Rietveld method for the study of microstructure is still an active research topic, and the potentialities of this approach are still to be revealed. This is particularly true for what concerns profile modelling, where conventional algorithms have a more or less phenomenological basis. The purpose of the present work is to show how a modelling of the line and plane defect structure can be introduced in the Rietveld method, and more generally within a whole pattern fitting procedure [1].

This new approach has considerable advantages over conventional methods of line profile analysis, as it permits a simultaneous modelling of lattice defects and scattering domain structure using the whole information (or a large portion) of the diffraction pattern. Different types of defect can be considered together, in terms of average domain size, dislocation density and cut-off radius, as well as stacking fault and twinning probabilities.

The model, which is based on the Fourier modelling of line profiles, was developed for fcc materials, but can be extended to other symmetries with suitable changes. A further point of interest to materials science is the relation that can be established between line profile parameters and elastic properties of the studied phases: when dislocations play an important role, the line broadening anisotropy can be directly related to the elastic anisotropy of the materials.

1. P. Scardi and M. Leoni, J. Appl. Cryst. (1999). Submitted

M08.DD.004 DETERMINATION OF MACROSCOPIC ELASTIC AND PLASTIC STRAIN BY RIETVELD ANALYSIS OF DIFFRACTION SPECTRA. M.R. Daymond, ISIS Facility, CLRC Rutherford Appleton Lab., OX11 0QX, UK, M.A.M. Bourke & R.B. Von Dreele, Los Alamos National Lab., NM 87545, USA, A.M. Korsunsky, Dept. of Mechanical Engineering, Uni. of Newcastle, NE1 7RU, UK.

The variation of macrostrain deep within engineering components is frequently determined using neutron diffraction. It is often desirable to minimise the sampling volume in order to maximise the spatial resolution, though this increases the required measurement time. At reactors, macrostrain behaviour is inferred from a single lattice reflection (deemed to be representative of the bulk response). At a pulsed source, a complete diffraction pattern is recorded and accordingly it is natural to fit the entire diffraction spectra using a Rietveld refinement, maximising use of the available information. This means that an idealised crystal structure is fit to the measured distorted crystal structure, which includes deviation of the measured lattice reflections from the ideal due to hkl dependent elasto-plastic strain anisotropy.

Elastic macrostrains calculated from lattice parameter changes in Rietveld refinements (without accounting for hkl dependent anisotropy) are comparable to the bulk elastic response

and also to the response obtained from a single lattice reflection typically used by practitioners at a steady state source.

By incorporating a description of the *elastic* strain anisotropy expected into the Rietveld code, an empirical but quantitative evaluation of *plastic* strain history is possible. Examples of this approach in cubic and hexagonal metals and in composite materials will be given.

M08.DD.005 EFFECT OF DATA QUALITY ON QUANTITATIVE PHASE ANALYSIS (QPA) USING THE RIETVELD METHOD. N.V.Y. Scarlett, I.C. Madsen and T. Lwin, CSIRO Minerals, Box 312, Clayton South, Victoria 3169, Australia

Quantitative phase analysis using the Rietveld method has become a valuable tool in modern X-ray diffraction. XRD is a recognised research tool and has been successfully employed in the developmental stages of many industrial processes but is now becoming increasingly important as a means of process control either in quality control laboratories or on-line in a plant.

In on-line applications, the optimisation of data collection regimes is of critical importance if rapid turn-around, and hence timely process control, is to be achieved. This paper examines the effect of data quality on the quantification of phases in well characterised suites of minerals.

A range of data collection regimes has been systematically investigated with a view to determining the minimum data required for acceptable quantitative phase analysis. Data has been collected with ranges in (i) step width from 0.01 to 0.3º 2θ, (ii) step counting times from 0.0125 to 4 sec/step and (iii) upper scan limits from 33 to 148º 2θ.

The data has been analysed using Rietveld based methods with two distinctly different analytical approaches (i) refinement of only pattern background and individual scale factors for each phase, and (ii) refinement of unit cell dimensions, overall thermal parameters, peak width and shape in addition to the background and scale factors.

Results to date indicate that, for structurally well-defined materials requiring minimal parameter refinement (i.e. the first set of analysis conditions), phase quantification via the Rietveld method is remarkably robust. In fact, the analysis for the major phases remains stable under all data collection conditions. Evidence of refinement instability is only apparent in the quantification of minor phases (approx 1wt%) with diminishing data quality.

P08.DD.001 QUANTITATIVE PHASE ANALYSIS USING THE REFERENCE INTENSITIES OR THE WHOLE XRD PATTERN. B. Grzeta, Rudjer Boskovic Institute, POB 1016, 10001 Zagreb, Croatia.

A new procedure for quantitative X-ray diffraction phase analysis based on the matrix-flushing principle [1] is proposed. The method involves preparation of (*i*) a mixture of examined multicomponent system and corundum at the one-to-one weight ratio, and (*ii*) a mixture of a pure component, the weight fraction of which is to be determined - say *X*, and corundum at the one-to-one weight ratio. There follow two approaches of X-ray diffraction analysis procedure. In the first one the intensities of the strongest diffraction line of the component *X* and of corundum are to be measured for both mixtures (*i*) and (*ii*). The weight fraction of the component *X* is related to the ratios of integrated intensities of the strongest lines of that component and corundum for the mixture (*i*) and mixture (*ii*). The second approach uses the whole XRD powder patterns of the mixtures (*i*) and (*ii*), and involves the whole-powder-pattern decomposition of these patterns. The weight fraction of the component *X* is then related to the ratios of the sum of all diffracted intensities for the component *X* and the sum of all diffracted intensities for corundum, in both mixtures (*i*) and (*ii*) respectively. Examples were worked out using the fitting programs *PROFIT* and *WPPF* [2]. For quick result the first analysis approach gives satisfactory accuracy, but for more accurate result the latter one is better.The author expresses gratitude to Professor H. Toraya for kindly providing his computer programs.

1. F. H. Chung (1974). J. Appl. Cryst., 7, 519-525.
2. H. Toraya (1986). J. Appl. Cryst., 19, 440-447.

P08.DD.002 FINAL OUTCOMES OF THE IUCR CPD ROUND ROBIN ON QUANTITATIVE PHASE ANALYSIS. I.C. Madsen, CSIRO Minerals, Box 312, Clayton South, Victoria 3169, Australia

Since 1997 the IUCr Commission on Powder Diffraction has been sponsoring a round robin on quantitative phase analysis (QPA). The round robin focuses on the analysis of powder diffraction data specifically for the derivation of phase abundances.

The general goals of the round robin include (i) the documentation of methods & strategies used in QPA, (ii) assessment of levels of accuracy & precision achievable in QPA, (iii) identification of specific problems in QPA and the development of recommended analytical procedures and (iv) the creation of a set of standard samples for future reference.

The samples used the study consist of mixtures of major and minor components covering a wide range of analytical complexity. Initial samples are synthetic mixtures of crystallographically 'simple' materials and should present little problem to the analyst. Additional samples introduce problems such as preferred orientation, microabsorption and amorphous content to assess the degree to which these problems affect QPA. Several very complex materials have also been included in the sample suite including a natural granodiorite, synthetic bauxite and a mixture of pharmaceutical phases. These last three samples represent a significant analytical challenge as they exhibit preferred orientation, microabsorption and grain size effects in addition to severe peak overlap.

This presentation will include summaries of statistical analysis of participant returns for all samples in the study along with the identification of some of the problems encountered by participants.

08EE INTERFACIAL STRUCTURES

M08.EE.001 CHARACTERIZATION OF BIOMIMETIC BILAYER MEMBRANES USING NEUTRON REFLECTIVITY. S. Krueger and C.F. Majkrzak, NIST Center for Neutron Research, NIST, Gaithersburg, MD 20899, and C.W. Meuse and A.L. Plant, Biotechnology Division, NIST, Gaithersburg, MD 20899.

Neutron reflectivity is being used to characterize the structure of novel synthetic alkanethiol and phospholipid biomimetic systems, or hybrid bilayer membranes (HBMs), which are formed on gold-coated single crystal silicon substrates, and which are in contact with aqueous solution. The biomimetic characteristics of the HBMs make them not only an important tool for understanding and characterizing membrane protein structure and function but also commercially significant for a number of applications including biosensors, tissue engineering, and bioelectronics and biocatalysis. Parameters of interest in the neutron reflectivity experiments include thickness of the bilayer and its individual components, hydration of the head groups, and depth of penetration of peptides into the bilayer. Structural changes in the bilayer due to the presence of peptides are also being investigated.

Measurements have been made on HBMs consisting of a monolayer of octadecanethiol and a monolayer of d_{54}-DMPC, and on HBMs with a monolayer of thiahexaethyleneoxide octadecane, which contains a hydrophilic ethyleneoxide "spacer" moiety that replaces the octadecanethiol layer. Data were obtained at 28^{o}C, where the DMPC layer is in the fluid phase, both in the absence and in the presence of the membrane-active peptide, melittin, in the solution. Neutron scattering length density (SLD) profiles of the lipid structure perpendicular to the plane of the bilayer have been obtained from the reflectivity measurements. The reflectivity data and resultant SLD profiles will be discussed in terms of structural models for the HBMs and the location of melittin in the bilayer. A progress report on measurements of new HBM matrices designed to accommodate transmembrane proteins will also be presented.

M08.EE.002 STRUCTURAL CONFORMATION OF GLOBULAR PROTEINS ADSORBED AT DIFFERENT INTERFACES. [1] J.R. Lu, T.J. Su [2], R.K. Thomas [3], J. Penfold [1], Department of Chemistry, University of Surrey, Guildford GU2 5XH, UK, [2] Department of Physical & Theoretical Chemistry, South Parks Road, Oxford OX1 3QZ, UK, [3] ISIS Neutron Facilities, Rutherford Appleton Laboratory, Chilton, Didcot, OX11 0QX, UK

We have studied the adsorption of a number of model globular proteins at the air-solution and solid-solution interfaces using specular neutron reflection. The high depth resolution of neutron reflection together with the use of deuterium labelling to the solvent and to the solid surface makes the technique sensitive to the distribution of the in situ protein layers along the surface normal direction. The accurate determination of the protein layer distribution together with the known dimension of globular proteins allows us to infer the preferred conformation of the adsorbed protein molecules at different interfaces. We have investigated the effect of solution pH and ionic strength on the adsorpion of poteins at several different interfaces and found that for all the interfaces studied the level of adsorption is dominated by the extent of electrostatic repulsion within the adsorbed protein layers and is little affected by the interaction between the protein and the substrate surface. At a given surface the preferred structural conformation of globular proteins is also dictated by the lateral repulsion. The effect of surface hydrophobicity on the adsorption of globular proteins was also investigated and the surface hydrophobicity was varied by chemically grafting a monolayer of long chain alkane with different functional groups on the outer surface. It was found that the least adsorption occurs at the intermediate surface hydrophobicity. The nature of the surface properties on the extent of denaturation of the protein molecules will also be discussed.

M08.EE.003 POLYMER BRUSHES AT THE AIR-LIQUID INTERFACE STUDIED BY NEUTRON REFLECTION AND SURFACE TENSION MEASUREMENTS. M.S. Kent, Sandia National Laboratories, Albuquerque, NM., J. Majewski, G. S. Smith, Los Alamos National Laboratories, Los Alamos, NM., L. T. Lee, Lab. Leon Brillouin, CEN-Saclay, 91191 Gif-sur-Yvette Cedex, France, S. Satija, NIST Center For Neutron Research, National Institute of Standards and Technology, Gaithersburg, MD., F. Rondelez, Laboratoire P.S.I. Institut Curie-Section de Physique et Chimie, 11 rue Pierre et Marie Curie, 75005 Paris, France

Polymer brushes are layers of polymer chains in which only one end of each long chain molecule is anchored to the surface. Such tethered chain structures have been investigated for their potential to deliver unique properties to surfaces, because they occur in various microphases of block copolymers, and because they provide an interesting system to examine the balance of ethalpic and entropic contributions to free energy. In this work, Langmuir monolayers of PDMS-PS diblock copolymers on organic liquids are used as a model polymer brush system. The PDMS block adsorbs at the air surface while the PS block dangles into the subphase liquid. With this model system the air surface can be made either repulsive, neutral, or attractive for the tethered chain segments by choosing a subphase liquid which has a surface tension which is lower, equal to, or greater than that of PS, respectively. The segmental profile of the dangling PS block is determined by neutron reflection as a function of the molecular characteristics of the copolymers and the solution conditions. We emphasize quantitative comparisons with analytical profile forms and scaling predictions. Simultaneous with the study of the profile form, the free energy of the chains is examined through the surface tension.

M08.EE.004 NEUTRON REFLECTIVITY MEASUREMENTS OF POLYMER INTERDIFFUSION IN REAL TIME. D.G. Bucknall, ISIS Facility, RAL, Oxon, OX11 0QX and S.A. Butler and J.S. Higgins, Dept of Chem Eng, Imperial College, London, SW7 2BY

Neutron reflection (NR) studies of diffusion in thin solid polymer films has until recently only generally been applied to high molecular weight amorphous polymer systems. Measurements are usually taken at room temperature well below the Tg's of the polymers so that the interfacial structure is frozen in. However there is also much interest in small molecule diffusion into high molecular weight polymers. In this case the normal approach to NR measurements may not be applicable since small molecule diffusion may still occur at room temperature on time scales less than the typical NR measurement times of a few hours.

Using the SURF reflectometer at the ISIS Facility of the Rutherford Appleton Laboratory and specially designed reflectivity sample cells it is possible to study the interdiffusion between polymers and small molecules such as oligomers in real time. To demonstrate the technique the real-time diffusion between hydrogenated and deuterated polystyrene (PS) has been measured at 115C taking reflectivity profiles every 6 minutes in a limited window of reciprocal space. The interfacial width obtained from such data shows a change in time dependence as predicted from theory and a diffusion coefficient has been calculated. The interdiffusion between oligomers and high molecular polymers have also been studied using NR, again in real time with reflectivity profiles taken every 20-60 seconds. Even with the limited data sets the interfacial width and profile has been determined as a function of time. This has shown the interface to be highly asymmetric with an interface position which moves with time. These data have been compared to theoretical predictions for non-Fickian diffusion.

M08.EE.005 ON THE STRUCTURE OF THIN WETTING FILMS. A. Doerr, W. Press, M. Tolan, J.P. Schlomka, T. Seydel, W. Prange, Institut für Experimentelle und Angewandte Physik der Universität Kiel, D-24098 Kiel, Germany

Properties of thin wetting films have been studied by X-ray reflection techniques and grazing incidence diffraction. Films of several organic liquids had thicknesses ranging between 2 nm and 25 nm. Reflection measurements reveal, that the densities vary considerably near the substrate (Si/SiO2). The actual values depend on the packing properties [2] of the molecules: the density is enhanced for the more globular cyclohexane molecule and lowered for the more elongated perfluorohexane and hexane [2,3]. In the analysis, inversion techniques, which themselves are an interesting object of study [2,4], have been used. The profile at the interface liquid-gas, on the other hand, is determined by thermally

activated capillary waves [5,6]. A direct prove results from the diffuse scattering.

Also, first depth-profiled measurements of the liquid structure factor and thus of the local structure on an atomic scale are presented. A very direct access to the competition between surface tension (more generally: interaction within the liquid) and substrate-liquid interaction is provided by the scattering from wetting films on gratings with a shallow lateral structures.

[1] M. Plischke and D. Henderson; J.Chem. Phys. 84, 2846 (1986)
[2] A.K. Doerr; PhD-Thesis, Kiel 1999
[3] A.K. Doerr, M. Tolan, T. Seydel, W. Press; Physica B 248, 263 (1998), M.K. Sanyal et al.; submitted
[4] R. Lipperheide, G. Reiss, H. Fiedeldey, S.A. Sofianos, H. Leeb;Phys. Rev. B 51, 11032 (1995)
[5] S.K. Sinha, E.B. Sirota, S. Garoff, H.B. Stanley; Phys.Rev. B 38, 2297 (1988)
[6] J.M. Tidswell, T.A. Rabedeau, P.S. Pershan, S.D. Kosowski; Phys. Rev. Lett. 66, 2108 /1991)

08FF STRUCTURE-PROPERTY RELATION-SHIPS IN CHIRAL COMPOUNDS

M08.FF.001 ABSOLUTE STRUCTURE AND ABSOLUTE CONFIGURATION. H. D. Flack and G. Bernardinelli, Laboratoire de Cristallographie, University of Geneva, Switzerland

Fundamental notions concerning absolute structure and absolute configuration, and their determination from single-crystal diffraction measurements, are presented and reviewed. A compendium of terms with definitions useful in this field is provided. For absolute structure and its determination, the separate but interacting influences of the structure, the macroscopic reorientation ambiguities of the crystal (crystal polarity) and the inversion-distinguishing power of an X-ray diffraction experiment with dispersive scatterers are examined. Important experimental and algorithmic details of the current methods used for absolute-structure determination are provided. Characterisation of the crystals for absolute-structure determination and the molecules for absolute configuration determination are treated. Attention is given to the analysis of absolute structure and absolute configuration in twinned crystals. Formal proofs of the invariance properties of crystal polarity and of the analysis of absolute structure in twinned crystals are provided.

M08.FF.002 CHIRALITY RECOGNITION IN SOLID AND SOLUTION STATES. R. Kuroda, Department of Life Sciences, Graduate School of Arts and Sciences, The University of Tokyo, Komaba, Meguro, Tokyo 153–8902, Japan.

Three cases will be described where chiral – achiral molecular interactions are involved in chirality induction and/or recognition. First, a racemic solution of the chiral compound 7 bromo–1,4,8–triphenyl–2,3–benzo[3,3,0] octa2,4,7–trien–6–one (1) produces an inclusion compound with various achiral solvents. Depending on the type of solvent, the inclusion compound contains either one of the enantiomers or both of the host compound 1 [1]. For example, α-picoline, toluene and CBr_4 optically resolve the host compound to produce crystals of a 1:1 adduct with one of the enantiomers, whereas their respective analogues γ-picoline,benzene and $CHBr_4$ produce an adduct with racemic host. To understand the chiral discriminations, crystal structures of several racemates and conglomerates have been determined and compared. The racemic crystal of 1 on its own (without any guest) exhibits polymorphism. Interestingly, when one type of crystal is placed under picoline vapour, molecules in the crystal rearrange themselves to form microcrystals of another crystal structure[2]. Thus, crystals obtained from solution and those under vapour have different structures.

In the second case, for the first time 1,2–chloroethane was trapped and observed in a chiral near–eclipsed form [3] and 1–chloropropane in the truly eclipsed form [4] at room temperature in a 1:1 inclusion complex with an optically active host molecule. Finally, induced chirality in a prochiral compound in the solid–state was successfully employed in an enantio selective photoreaction[5], where solid–state CD provided valuable information [5,6].

1. F. Toda & K. Tanaka (1990). Tetrahedron Asymmetry, 1, 359.Ü
2. R. Kuroda (1998). Xth ISMRI abstracts, L–15. Í
3. F. Toda, K. Tanaka & R.Kuroda (1997) J. Chem. Soc., Chem. Comm 1227.
4. R. Kuroda, H. Fujiwara & F. Toda, to be submitted.
5. F. Toda, H. Miyamoto, S. Kikuchi, R. Kuroda & F. Nagami, J. Am. Chem. Soc. 118,11315 (1996).
6. R. Kuroda, T. Homma, to be submitted.

M08.FF.003 INTERACTIONS IN OPTICALLY NONLINEAR CHIRAL CRYSTALS AS SEEN BY IR AND RAMAN SPECTROSCOPY. M.M. Szostak, Institute of Physical and Theoretical Chemistry, Wroclaw University of Technology, 50-370 Wroclaw, Poland.

Monoclinic sucrose crystals reveal second harmonic generation [1] which origin seems to be connected with pronounced anharmonicity of CH_2 and OH stretching vibrations, especially of those with transition moment directions perpendicular to optical axis a^*. The most anharmonic OH oscillator participate in the strongest hydrogen bonding which forms and infinite chain with spiral arrangement[2,3]. In optically nonlinear crystal of 4-isopropylphenol (4-IP) it is a hydrogen bonded helix which constitutes the unique channel for intermolecular charge transfer [4].

As the cooperativity in a certain type of bent H...O hydrogen bondings leads to a charge separation [5], it is possible that the Zerbi model of vibrational contribution to optical nonlinearity [6] applies also to the sucrose and 4-IP crystals.On the basis of IR and Raman relative intensities of bands a hypothesis is proposed that in chiral crystals a proton transfer between two positions in a bent hydrogen bond corresponds to the bond alteration in the two-state model of Zerbi.

[1]. M.J. Rosker and C.L. Tang (1984), IEEE J.Quantum Electron. 20, 334.
[2]. M.M. Szostak and J. Giermańska (1990), J. Mol. Struct. 219, 95.
[3]. J.Giermańska and M.M. Szostak (1991), J. Raman Spectrosc. 22, 107.
[4] M.M. Szostak, T. Misiaszek, S. Roszak, J.G. Rankin and R.S. Czernuszewicz (1995), J.Phys.Chem, 99, 14992.
[5]. V.-C. Tse and M.D. Newton (1977), J.Amer.Chem.Soc. 99, 611.
[6]. C. Castiglioni, M. Del Zoppo and G. Zerbi (1996), Phys. Rev.B 53, 13319.

M08.FF.004 INVESTIGATING THE STRUCTURAL GROUNDS OF CHIRAL RESOLUTION THROUGH CO-CRYSTALLISATION. Zs. Böcskei, K. Simon, Z. Kovári, T. Gérczei, P. Huszthy, A. Mravik, D. Kozma, E. Fogassy, Chinoin Pharmaceuticals Eötvös University and The Technical University of Budapest, Hungary

Diastereomeric salt formation is the most widely applied technique for chiral resolution. In the past few years several new methods were elaborated[1-5] at the Technical University of Budapest which generalise the basic principle of the classic method. Metal co-ordination mediated optical resolutions were successfully applied to separate racemic acids[2,4], esters[1] and alcohols[3] using different salts of the cheap resolving agent O,O'-dibenzoyl-tartaric acid (DBTA). The crystal structures of these

compounds assisted in the better understanding of the structural principles governing the resolution processes. In other instances the resolution of alcohols was achievable through molecular complex formation with DBTA without the metal mediator[5]. The crystal structures revealed a large number of isostructural molecular complexes with a constant framework of DBTA layers connected by the guest hydroxyls. The structures were used in the interpretation of the different degrees of resolution achieved by the method. In one case we also studied the most elegant, although perhaps the most expensive method for chiral resolution: the application of a tailor-made chiral crown host.

Finally, the structure of a solid solution type diastereomeric salt of an isoquinoline derivative will be presented to illustrate the limitations of the method of diastereomeric salt formation. We explain the failure of the resolution on the basis of the structure.

1 A. Mravik, Zs. Böcskei, Z. Katona, I. Markovits, Gy. Pokol, D.K. Menyhárd, E. Fogassy *Chem. Comm*. (1996). 1983-1984.
2 A. Mravik, Zs. Böcskei, Z. Katona, I. Markovits, E. Fogassy *Angew. Chem*. (Intnl. Ed. Engl.) (1997). **36,** 1534-1536.
3 A. Mravik, Zs. Böcskei, K. Simon, F. Elekes, Z. Izsáki *Chemistry - A European Journal* (1998).1621-1627.
4 F. Elekes, Z. Kovári, A. Mravik, Zs. Böcskei, E. Fogassy *Tetrahedron: Asymmetry* (1998). **9,** 2895-2900.
5 D. Kozma, Zs. Böcskei, Cs. Kassai, K. Simon, E. Fogassy *Chem. Comm.* (1996). 753-754.

M08.FF.005 FROM ACHIRAL BUILDING BLOCKS TO CHIRAL ARCHITECTURES. Mike Zaworotko, Kumar S. Biradha and Konstantin V. Domasevitch, Department of Chemistry, The University of Winnipeg, 515 Portage Avenue, Winnipeg, Manitoba, R3B 2E9, Canada

That solid state architecture profoundly influences bulk physical properties and therefore function of solids has provided impetus for recent activity in the field of *crystal engineering*. The nature of crystal engineering means that chemists can design new crystal structures without the need to develop new molecular structures. This presentation will focus upon the development of new classes of chiral solid that are built from the simplest of achiral building blocks. We shall present two basic classes of compound which are chiral for very different reasons: (i) helical supramolecular structures which are built from either centrosymmetric or non-centrosymmetric building blocks and are sustained by either hydrogen bonds (cf. urea) or metal-ligand bonds[1]; (ii) chiral supramolecular adducts which induce chirality where it would otherwise not occur e.g. in centrosymmetric host frameworks (chiral adducts of benzene guest molecules are illustrated alongside). We shall discuss a number of metal-organic structures that represent (i) and (ii). Particular emphasis will be placed upon interpretation of the results in the broader context of crystal engineering.

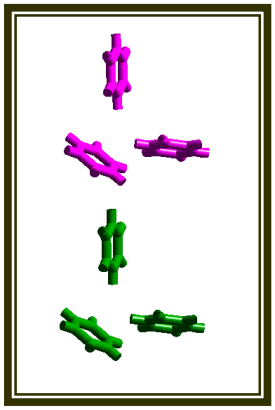

Biradha, K.; Seward, C.; Zaworotko, M.J. "Helical Coordination Polymers with Large Chiral Cavities", *Angew. Chem., Int. Ed. Engl*., in press.

P08.FF.001 LYSINE REPLACING HISTIDINE IN THE ACID-BASE CATALYSIS OF D-LACTATE DEHYDROGENASE. A. Razeto and V. L. Lamzin, EMBL c/o DESY Notkestrasse 85 D-22603 Hamburg, K. S. Wilson, Dept. of Chemistry, York University Heslington YO1 5DD UK, S. Kochhar, Nestle` Research Centre, Vers-chez-les-Blanc, P.O. Box 44, CH-100 Lausanne 26, Switzerland.

NAD-dependent D-Ldh and L-Ldh catalyse the same chemical reaction, differing only in the chirality of the product (or substrate), D- and L-lactate respectively. Even though the two enzymes belong to structurally different families, site-directed mutagenesis, kinetic and structural studies indicate that the same residues are involved in substrate binding and catalysis: His-296, Glu-264, Arg-235 (numbering according to the D-Ldh L. bulgaricus sequence) [1, 2]. His-296 has for a long time been considered as the acid-base group playing a key role in the catalysis. However recent studies have shown that mutation of this histidine to lysine does not result in a significant change in k_{cat} and K_m. This thus suggested that either the histidine is not indispensable in catalysis or its function in the mechanism can well be performed with lysine. In order to better understand the reasons underlying this phenomenon, crystallographic studies have been carried out. Diffraction data for the crystal of the H296K mutant of *L. bulgaricus* D-Ldh have been collected on X11 beamline (EMBL/DESY) to 1.9 Å resolution. Two D-Ldh dimers are present in the asymmetric unit. The structure has been solved by molecular replacement and is currently being refined. The electron density maps have already confirmed replacement of histidine by lysine in the enzyme active site. Full analysis will be presented after refinement of the structure is complete.

1. Kochhar, S., Hunziker, P. E., Leong-Morgenthaler, P. L., Hottinger, H. (1992), *J. Biol. Chem.*, **4**, 8499-8513.
2. Stoll, S., V., Kimber, M., S., Pai, E. F. (1996), *Structure*, **4**, 437-447.

P08.FF.002 STRUCTURAL RATIONALE FOR THE SPONTANEOUS RESOLUTION OF DL-ALLO-ISOLEUCINE. Bjørn Dalhus and Carl Henrik Görbitz, Department of Chemistry, University of Oslo, PO Box 1033 Blindern, N-0315 Oslo, Norway.

The spontaneous resolution of the racemate DL-allo-isoleucine is rationalized on the basis of an analysis of interatomic distances in the crystal structures of DL-isoleucine and the DL-isoleucine:DL-allo-isoleucine 1:1 mixture.

There is a systematic distribution of the four stereoisomers in the DL-isoleucine:DL-allo-isoleucine crystal. A detailed analysis of interatomic distances between alternative positions for the disordered side-chain atoms unveil two different molecular chains in the crystal. Each such chain accommodates a single diastereomeric pair (L-isoleucine:D-allo-isolecine or D-isoleucine:L-allo-isoleucine) only. The crystal is built up by a stacking of such chains in two dimensions, and three different packing modes for the two types of chains are discussed.

P08.FF.003 RESOLUTION OF RACEMIC ALCOHOLS VIA DIASTEREOMERIC SALT FORMATION. Heidi A. Ernst, Sine Larsen, Centre for Crystallographic Studies, University of Copenhagen, Denmark.

Diastereomeric salt formation and subsequent fractional crystallisation is a classical method widely used for separation of racemic acids with optically active bases and vice versa. To make use of this method for resolution of racemic alcohols the alcohol must be converted into a derivative capable of salt formation. A common approach is reaction of the racemic alcohol with phthalic acid anhydride or succinic acid anhydride forming the racemic

mono esters. The efficiency of the following resolution depends strongly on the difference in solubility of the diastereomeric salts. Information about intermolecular interactions of importance for this chiral discrimination can be obtained by crystal structure analysis of diastereomeric salts.

We have prepared the phthalic acid mono esters of racemic 2-butanol, 2-pentanol and 2-hexanol. The subsequent resolution was carried out using the alkaloid brucine as resolving agent. At present the less soluble salts have been isolated in pure form. The crystal structures of brucinium-2-pentyl-phthalic-acid-mono-ester-ethyl-acetate-solvate and brucinium-2-hexyl-phthalic-acid-mono-ester-acetone-solvate and in addition those of the racemic 2-butyl-phthalic-acid-mono-ester and 2-pentyl-phthalic-acid-mono-ester have been determined. These structures are analysed in terms of packing mode and specific intermolecular interactions between the chiral molecules to elucidate the structural basis for chiral discrimination in the process of resolution via diastereomeric salt formation.

09OA ENDOCYTOSIS AND EXOCYTOSIS

M09.OA.001 ABSTRACT NOT AVAILABLE. W.I. Weis

M09.OA.002 X-RAY CRYSTAL STRUCTURE OF THE SNARE COMPLEX AND THE CRYSTAL STRUCTURE OF SYNAPTOTAGMIN C2AB. R. Bryan Sutton and Axel T. Brunger, Howard Hughes Medical Institute and Department of Molecular Biophysics and Biochemistry, Yale University, New Haven, CT 06518, phone: 203-432-5595, FAX: 203-432-6946.

The fusion of neurotransmitter filled vesicle with their target membranes in neuronal cells is mediated by a class of membrane fusion proteins known as SNAREs. Assembly of the synaptic fusion SNARE complex leads to membrane fusion. We have solved the X-ray crystal structure of the core of the synaptic fusion complex composed of cytoplasmic fragments of the vesicle associated protein synaptobrevin II, and the target membrane associated proteins, syntaxin-1A and SNAP-25B. At the center of the SNARE complex is a highly conserved ionic layer. This layer may serve a crucial role in the assembly or disassembly of the synaptic fusion complex. The fusion activity of the synaptic fusion complex is regulated by transient Ca2+ concentrations on the pre-synaptic membrane. The receptor of these Ca2+ signals may be the synaptic vesicle associated protein, synaptotagmin. Synaptotagmin is a 50 kDa protein with a short intravesicular amino-terminus, a transmembrane domain, two tandem domains and a short carboxy terminal region. We have solved the crystal structure of the cytosolic portion of synaptotagmin III including the C2A, C2B-domains and the carboxy-terminal tail.

R.B. Sutton, D. Fasshauer, R. Jahn, and A.T. Brunger. Crystal structure of a SNARE complex involved in synaptic exocytosis at 2.4 Å resolution. *Nature* **395**, 347-353 (1998).

M09.OA.003 THE STRUCTURE OF CLATHRIN. E. ter Haar, T.L. Kirchhausen, Dept. of Cell Biology and Center for Blood Research, Harvard Medical School, Boston MA 02115, USA and S.C. Harrison, Howard Hughes Medical Institute and Children's Hospital Laboratory of Molecular Medicine, Boston MA 02115

Clathrin triskelions form the lattice that organizes recruitment of proteins to coated pits and helps drive vesiculation of the lipid bilayer. Clathrin is recruited to the plasma membrane by adapter molecules bound to cytoplasmic domains of trans-membrane receptors. Clathrin binds the adapter molecules with the N-terminal domain of the clathrin heavy chain. The N-terminal domain of clathrin is a seven blade β–propeller, well adapted to interact with multiple partners, such as AP-1, AP-2 sorting adapter complexes and the nonvisual arrestins. We have determined the 2.9Å structure of the clathrin terminal domain in complex with the clathrin-binding domain of arrestin-3. The arrestin-binding site is a groove between blade 1 and 2 and facilitates binding of arrestin via hydrophobic and β-sheet-like interactions.

M09.OA.004 THE CLATHRIN FILAMENTOUS LEG IS A REPEATING SUPERHELIX WITH HELIX FACES FOR MEDIATING SELF-ASSEMBLY. Peter K. Hwang, Joel A. Ybe, Frances M. Brodsky and Robert J. Fletterick, Department of Biochemistry & Biophysics, G. W. Hooper Foundation, Department of Microbiology & Immunology, University of California San Francisco, San Francisco, CA 94143 USA

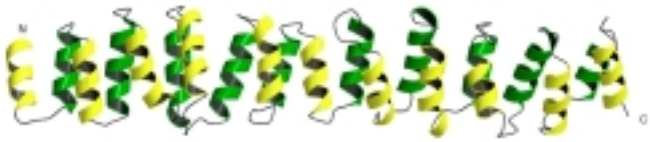

Clathrin self-assembly is required for the formation of coated vesicles that mediate protein sorting during endocytosis and intracellular organelle biogenesis. The clathrin triskelion is a trimer of three heavy chain subunits, each folding into a filamentous leg and capable of binding a single light chain subunit. We have determined the crystal structure, to 2.6A resolution, of a leg segment vital in controlling assembly. The structure reveals an elongated right-handed superhelix coil of α-helices, generated from 29-residue structural units of paired antiparallel helices. Structural and sequence alignments indicate these units are organized into a longer 145-residue motif that repeats seven times to produce the entire filamentous portion of the triskelion leg. Sequence analysis predicts that the clathrin motif appears in other proteins, most of which are involved in vacuolar protein sorting. A resulting model of the triskelion leg proposes continuous, flat surfaces of packed helices as the basis for clathrin heavy chain self-assembly, light chain binding, and trimerization.

M09.OA.005 PROTEIN-PROTEIN RECOGNITION IN CLATHRIN-MEDIATED ENDOCYTOSIS. P. R. Evans, D. J. Owen and H.T.McMahon, MRC Laboratory of Molecular Biology, Hills Road, Cambridge, CB2 2QH, UK

Clathrin mediated endocytosis is the main mechanism by which proteins and lipids are internalised from the cell surface. Clathrin coated vesicles are formed when a patch of membrane containing the components to be internalised becomes invaginated due to the binding of a protein coat, made of clathrin and its adaptor (AP2) complex, on its cytoplasmic side. The vesicle is finally 'pinched' off the membrane through the action of dynamin (reviewed in [1]).

The role of AP2 is pivotal. It recognises short sequence motifs on the proteins which marks them for internalisation mainly via the μ2 subunit and provides a mechanical link to the clathrin scaffold of the coat. In addition it recruits a number of proteins with a variety of regulatory roles in coated vesicle genesis via the α subunit. We have determined the crystal structures of several domains of the AP2 heterotetramer, including the ear domain of α-adaptin and part of μ2-adaptin, as well as the SH3 domain of amphiphysin [2], and combined the structural information with *in vitro* and *in vivo* assays to understand the nature of many of these protein / protein interactions.

The 2.7Å resolution crystal structure of the internalisation signal binding domain of μ2-adaptin was solved complexed with peptides corresponding to the internalisation signals of a number of proteins [3]. The protein is an all β-sheet, banana-shaped

structure. The signal peptides adopt an extended conformation forming an extra strand on the edge of one of the sheets. Specificity is conferred by hydrophobic pockets which bind the tyrosine and the leucine in the peptide. In the crystal the protein forms dimers which could increase the strength and specificity of binding to dimeric receptors. The surface of μ2 possesses a very positive electrostatic potential indicating that it may interact with the negatively charged headgroups of the phospholipid membrane.

1. S. L.Schmidt (1997) Ann. Rev. Biochem, **66**, 511-548
2. D.J. Owen, P.Wigge, Y.Vallis, J.D.A.Moore, P.R.Evans & H.T.McMahon (1998), EMBO J. **17**, 5273-5285
3 D.J.Owen & P.R.Evans, (1998) Science, **282**, 1327-1332

M09.OA.006 CRYSTAL STRUCTURE OF THE ECTO-DOMAIN OF HUMAN TRANSFERRIN RECEPTOR. C. Martin Lawrence, Stephen Harrison, Laboratory of Molecular Medicine Howard Hughes Medical Institute 320 Longwood Avenue Boston, MA 02115, USA

The transferrin receptor (TfR) undergoes multiple rounds of clathrin-mediated endocytosis and re-emergence at the cell surface, importing iron-loaded transferrin (Tf) and recycling apotransferrin after discharge of iron in the endosome. We have determined the structure of the dimeric ecto-domain of the human TfR at 3.2 Angstroms resolution. The first domain of the three domain monomer closely resembles carboxy- and aminopeptidases. The sequence of nearly the entire TfR ectodomain is similar to that of membrane glutamate carboxy-peptidase II (mGCP), a dipeptidase that cleaves the neurotransmitter NAAG, but TfR does not itself have protease activity. The other two domains appear to regulate ligand binding and mediate dimerization. We propose models for the interactions of TfR with Tf and with HFE, a protein thought to modulate affinity for Tf.

P09.OA.001 THE STRUCTURAL BASIS OF PROTEIN RECOGNITION BY S100 EF-HAND PROTEINS. A. Lewit-Bentley and S. Réty, LURE, BP34, 91898 Orsay, France, V. Gerke, Institute for Medical Biochemistry, ZMBE, University of Münster, von-Esmarch-Straße 56, 48149 Münster, Germany and F. Russo-Marie, INSERM U332, ICGM, 22 rue Méchain, 75015 Paris, France

S100 proteins are a family of small EF-hand calcium-binding proteins probably involved in cytoskeleton dynamics. Among their cellular targets described to date are several annexins, another family of calcium, but also phospholipid, binding proteins. Annexins may be involved in processes such as exo- and endocytosis, especially when complexed to S100 proteins. We have solved the structure of a complex between two members of the S100 protein family, p11 and S100C, and their cognate peptides, the N-termini of annexin II [1], and annexin I.

The basic unit for the S100 protein is a tight, non-covalent dimer. With two EF-hand motifs per monomer, the dimer is a four EF-hand entity like calmodulin. Unlike calmodulin, though, the S100 complexes bind two, rather than one, peptides per S100 dimer. While calmodulin folds to enclose its target peptide, in the S100 complexes the peptides are periferal. Each annexin peptide forms hydrophobic interactions with both S100 monomers, as well as a small number of specific hydrogen bonds. The two complex structures are extremely close, in spite of significant sequence differences.

While S100C binds Ca^{2+} ions in both its EF-hands, p11 has modified EF-hands that are incapable of metal binding. The close similarity of the two structures shows that p11 has adopted a fold that makes it ready to bind target molecules in the absence of any metal. Using our results we can now propose models for the entire annexin/S100 complexes.

The S100 proteins are, in both cases, cross-linked by S-S bridges, within the dimer for S100C and between two dimers for p11. We speculate that these proteins may be under subtle redox control in situations where they participate in the maintenance of cellular structures.

1. Réty S., Sopkova J. Renouard M., Osterloh D., Gerke V., Tabaries, S., Russo-Marie F. & Lewit-Bentley, A. (1999). Nature Struct. Biol. **6**, 89-95.

09OB NEW FRONTIERS IN MACROMOLECULAR CRYSTALLISATION (sponsored by NASA)

M09.OB.001 THE USE OF DYNAMIC LIGHT SCATTERING AS A PREDICTIVE TOOL FOR PROTEIN CRYSTALLIZATION: HOW GOOD IS IT?. T. Bergfors, Department of Cell and Molecular Biology, Biomedical Center, Box 596, > SE-751 24 Uppsala Sweden.

Dynamic light scattering (DLS), like size exclusion chromatography and native polyacrylamide gel electrophoresis (PAGE), are methods for determining the size homogeneity of macromolecules. Numerous studies report a correlation between the DLS profile of a protein and whether it can crystallize or not. In the study presented here, 35 proteins were characterized by both DLS and native PAGE to determine which of the two methods was most predictive of the subsequent crystallization behavior. 81% of the proteins crystallized had DLS profiles with a homogeneous size distribution. By contrast, only 61% of the proteins which stained as single bands on native PAGE produced crystals. The diffraction quality of the crystals was also compared to the DLS profiles of the proteins. Proteins which did not crystallize usually had polydisperse DLS profiles and multiple bands on PAGE. Interestingly some polydisperse proteins did produce highly diffracting crystals while some monodisperse proteins completely failed to crystallize. These exceptions and their implications for the usefulness of DLS as a predictive tool will be discussed. Finally, practical recommendations for performing the DLS experiments will be presented.

M09.OB.002 MICROGRAVITY PROTEIN CRYSTAL GROWTH. Lawrence J. DeLucas, Karen Moore, Marianna Long, Terry Bray, Mike Harrington, Johanna Lewis, William McDonald, William Crysel, Lance Weiss and Craig Smith, Center for Macromolecular Crystallography, University of Alabama at Birmingham

Since 1985, the Center for Macromolecular Crystallography (CMC) has performed microgravity protein crystal growth experiments on thirty-seven U.S. space shuttle missions. The candidate proteins flown on these missions were selected based on scientific evaluation by a protein selection committee consisting of researchers from academia, industry and NASA. Microgravity-grown crystals were analyzed by the associated principal investigators and compared to crystals obtained from ground-control experiments, as well as the best data available from any protein batch or crystallization method. In addition to supporting microgravity crystallization, NASA has also supported a wide range of laboratory studies to elucidate the fundamental mechanisms/variables that affect the crystallization process, in an effort to develop enhanced 1g and microgravity crystallization methods. Results from our microgravity program clearly indicate that crystals of enhanced quality and, in some cases, superior size can be obtained from the microgravity environment. The development of sophisticated "dynamically-controlled" laboratory crystallization systems have allowed us to control the approach to nucleation and post-nucleation growth phase, thereby optimizing 1g and microgravity crystallization

conditions. More recently, the CMC, in conjunction with industry partners, has developed a robotically-controlled X-ray Crystallization Facility for the International Space Station.

M09.OB.003 OPTIMIZING CRYSTALLIZATION CONDITIONS USING THE ANALYTICAL ULTRACENTRIFUGE. J. Behlke and O. Ristau,Department of Protein-Interactions, Max Delbrück Center for Molecular Medicine, D-13092 Berlin, Germany.

Although methods for protein crystallization have been studied intensively in the past the crystallization of biological material remains a limiting step in the determination of the three-dimensional structure using X-ray diffraction. Protein crystallization can be considered as a complex molecular assembly process. A basic problem is finding optimal solution conditions that induce protein-protein interactions that are suitable for crystallization. Usually optimal solution conditions are derived from screening methods considering various parameters. To reduce this number we have developed a method of analytical ultracentrifugation that allow to determine the second virial coefficient (B_2) of a protein solution that is sensitive to protein-protein and protein-solvent interactions. The contributions to this parameter are complex in interpretation for aggregates but more simple for monomers. Our method allows to accurately determine B_2 (error < 5 %)[1]. This enables us to differentiate between the excluded volume and Donnan effect. The high contribution of electrostatic repulsion to B_2 induced by the net charge of the protein can be reduced by addition of neutral salts. The remaining part should be comparable to the excluded volume part of B_2 to induce the aggregation or nucleation events which lead to the formation of crystals and can be demonstrated too.

1. J. Behlke & O. Ristau (1999). J. Biophys. Chem. 76, 13-23.

M09.OB.004 PROTEIN CRYSTAL GROWTH USING ORDERED SELF ASSEMBLED MONOLAYERS. Christine M. Arnold, Ramon Villazana, Michael Graupe, T. Randall Lee and Jonathan M. Friedman, Department of Chemistry, University of Houston - CHEM 5641, 4800 Calhoun, Houston, TX 77004, USA

Four types of chemically unique, transparent self-assembled monolayers (SAMs) were prepared on glass coverslips typically used for protein crystallization. The SAM-functionalized surfaces appeared to exhibit a much higher degree of order and chemical uniformity than silanized glass, as judged by contact angle measurements with hexadecane. These characteristics led to a reproducible increase in the range of solution conditions under which large crystals of proteins were observed to form. The results are rationalized in terms of a marked reduction in the rate of non-productive nucleation relative to the rate of crystal growth.

M09.OB.005 DETERMINING THE MOLECULAR GROWTH MECHANISMS OF PROTEIN CRYSTAL FACES BY ATOMIC FORCE MICROSCOPY. Arunan Nadarajah,[1] Huayu Li,[1] and Marc L. Pusey,[2] [1]Department of Chemical and Environmental Engineering, University of Toledo, Toledo, OH 43606 and [2]Biophysics Branch ES76, NASA/Marshall Space Flight Center, Huntsville, AL 35812.

A high resolution atomic force microscopy (AFM) study had shown that the molecular packing on the tetragonal lysozyme (110) face corresponded to only one of two possible packing arrangements, suggesting that growth layers on this face were of bimolecular height. Analysis of the packing also indicated that growth of this face should proceed by the addition of growth units of at least tetramer size corresponding to the 4_3 helices in the crystal. In this study an AFM linescan technique was devised to measure the dimensions of individual growth units on protein crystal faces as they were being incorporated into the lattice. Images of individual growth events on the (110) face of tetragonal lysozyme crystals were observed, shown by jump discontinuities in the growth step in the linescan images as shown in the figure. The growth unit dimension in the scanned direction was obtained from these images. A large number of scans in two directions on the (110) face were performed and the distribution of lysozyme growth unit sizes were obtained. A variety of unit sizes corresponding to 4_3 helices, were shown to participate in the growth process, with the 4_3 tetramer being the minimum observed size. This technique represents a new application for AFM, allowing time resolved studies of molecular process to be carried out.

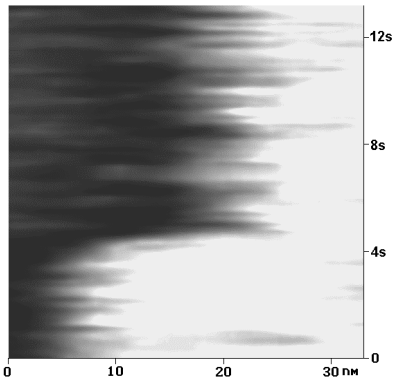

M09.OB.006 POST-CRYSTALLIZATION SOAKING IMPROVES THE DIFFRACTION QUALITY OF MTCP-1 CRYSTAL. Zheng-Qing Fu [1][2], Garrett C. Du Bois [1], Sherry P. Song [1], Robert W.Harrison [1], and Irene T. Weber [1]. [1] Kimmel Cancer Center, Thomas Jefferson University, Philadelphia, PA19107, USA. [2] Bruker AXS, Inc., Madison, WI 53719, USA.

Significant improvement of X-ray diffraction quality of MTCP-1 protein crystals was observed on post-crystallization soaking. The MTCP-1 crystals, grown from 1.5M ammonium sulfate in Tris buffer pH7.8, diffracted to 3.0 angstrom with streaky spots and diffuse scattering, which suggested defects in the crystals. Some crystals showed possible twinning. After soaking in an artificial solution with 2.0M ammonium sulfate, the crystals had much stronger diffraction up to 1.9 angstrom, and all spots were clearly formed without streaking. Selenomethionine-enriched MTCP-1 crystals demonstrated similar effects after soaking. Data sets from the soaked crystals have been used to solve the structure by MAD phasing. This very simple technique has not yet been reported for crystallization of other proteins. So, it is not clear whether this phenomenon is generally useful, nor what happens during the soaking. In general, the diffraction quality and resolution of crystals are determined by the molecular packing or correlation between the molecules, as well as the molecular building blocks. For protein crystals, the loose packing (due to the flexible surface residues) and the large volume of disordered solvent generally results in weak diffraction with high diffuse scattering. Mutation of residues on the protein surface can produce a different lattice type and altered packing. Also, dehydration of some protein crystals can improve the diffraction (private communication with B.C. Wang, W. Furey, A. McPherson). The crystal lattice usually shrinks on dehydration. However, no significant lattice shrinking was observed on MTCP-1 crystals after soaking, and, most importantly, the streaking and diffuse scattering due to disorder was eliminated or significantly reduced after soaking. The lattice shrinking alone is unlikely to give a satisfying explanation. So, we propose another mechanism. The remarkable difference of the diffraction quality may arise from rearrangement of the surface residues during soaking, similar to the annealing of small molecular crystals. During

crystallization, some surface residues may not pack optimally, or may form inappropriate interactions. In other words, the system may be trapped in a local energy minimum. Soaking in a different solution introduces certain disturb to the system. When the disturb is strong enough to overcome the potential barrier, the surface residues and thus the contacts among them may be rearranged in favor of the energy, which corrects the packing error and leads to the improvement of diffraction.

Fu et al., PNAS USA 95, 3413-3418, 1998.
Jelsch et al, Proteins 31, 320-333, 1998

M09.OB.007 NASA'S BIOLOGICAL CRYSTAL GROWTH PROGRAM ON THE INTERNATIONAL SPACE STATION. C.E. Kundrot NASA/MSFC, Mail Code ES76, MSFC, AL 35812, USA.

NASA's Biological Crystal Growth Program (BCG) on the International Space Station (ISS) will consist of two phases. The first phase is during assembly of the ISS and will accomodate payloads that currently fly in the orbiter middeck. The second phase begins after assembly of the ISS is complete and BCG payloads will occupy part of the Biotechnology Facility aboard the ISS. During both phases of the program, there will be two types of BCG payloads. One will emphasize the production of crystals for structure determination back on Earth. These types of payloads will allow hundreds of crystallization conditions to be tested. The second type of payload will be designed to study the crystallization process with the primary aim of developing new methods to further optimize the use of the microgravity environment. Access to these facilities is through the NASA BCG Guest Investigators program. Details of the crystallization hardware, the Guest Investigator program, and the operational aspects of the program will be described.

P09.OB.001 RESOLUTION IMPROVEMENT TO 0.9 Å IN CRYSTALS OF HUMAN ALDOSE REDUCTASE. E. Howard, V. Lamour, A. Mitschler, P. Barth, D. Moras and A. Podjarny. UPR 9004 de Biologie Structurale, IGBMC, 67404 Illkirch, France

As the action of human aldose reductase (hAR) is thought to be linked to the pathogenesis of diabetic complications, analysis of the catalytic mechanism and development of specific inhibitors has attracted many efforts. We report here the overexpression in E. coli of the recombinant hAR using a T7 based expression system and its purification using metal affinity column. The peptidic sequence of recombinant hAR has been completly verified and its catalytic constants determined (Km = 6mM and kcat = 0.5 sec-1). In addition, the native and SeMet hAR were crystallized with the cofactor NADP+ at 4°C in presence of the precipitating agent PEG 6000 using the vapor diffusion method. The crystals diffract to high resolution (1.1 Å) and belong to the P21 space group with unit cell parameters a= 49.97 Å b= 67.14 Å c= 48.02 Å b= 92.2° with one molecule per asymmetric unit. These crystals were further improved by changing the crystallisation temperature to 24° and applying micro-seeding techniques. The last tests at the LURE synchrotron source indicated a resolution limit of 0.9 Å. The analysis of these crystals should allow the analysis of the protonation state of the residues involved in catalysis.

P09.OB.002 QUANTITATIVE MODELING OF MOLECULAR FEATURES OBSERVED ON THE (110) FACE OF TETRAGONAL LYSOZYME. Mary Ann Perozzo[1], Huayu Li[2], John Konnert[1], Arunan Nadaradjah[2] and Marc L. Pusey[3]. [1]Laboratory for the Structure of Matter, Naval Research Laboratory, Washington, DC 20375, USA, [2]Department of Chemical and Environmental Engineering, University of Toledo, Toledo, OH 43606, USA, [3]Biophysics Branch ES76, NASA/Marshall Space Flight Center, Huntsville, Alabama 35812, USA.

The molecular features observed on the (110) face of lysozyme with the atomic force microscope (AFM) have been simulated with a model, the parameters of which are atomic coordinates, van der Waals radii and assumed tip shape. The model parameters are adjusted to maximize the correlation coefficient between the experimental and simulated images.

The figure displays the model image inserted into the experimental image. The correlation coefficient between the two images is 0.91. To obtain this degree of correlation, the molecules were displaced over 6 Å from their positions within the bulk of the crystal. Molecular dynamics and energy minimization have been carried out with XPLOR to check the plausibility of the model surface. That the intermolecular interactions at the surface are different from those within the crystal may have implications concerning the growth mechanism(s) of the crystals.

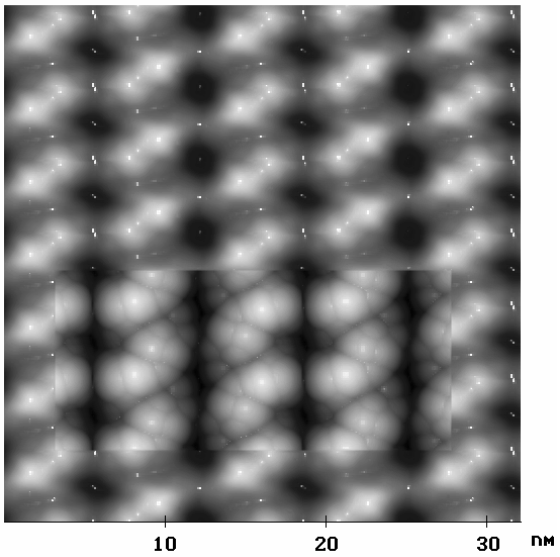

This research was supported by the U. S. National Aeronautics and Space Administration and the Office of Naval Research.

P09.OB.003 CRYSTAL QUALITY ANALYSES BY X-RAY DIFFRACTION OF PROTEINS GROWN BY NEW AND CLASSICAL TECHNIQUES. M. Soriano-García [1], V. M. Bolaños-García [2], J. Mas-Oliva and A. Moreno [3]. [1] Dept. Bioestructura. Instituto de Química, UNAM. Mexico, D.F. 04510. MEXICO. [2] Dept. Bioquímica. Instituto de Fisiología Celular, UNAM.Mexico, D.F. 04510 MEXICO, [3] Dept. Bioquímica. Instituto de Química, UNAM. México, D.F. 04510 MEXICO.

Protein crystallization has been the crucial step in the three-dimensional structural analysis for X-ray crystallography. There are several approaches to overcome this task, nowadays the most popular is crystal screening I and II from Hampton Research Co. These useful kits have well established statistical conditions in order to search for the best crystallization conditions, but do not explain what is really happening or what the important crystal growth parameters are from the qualitative point of view to be considered all over crystal growth phenomena. In addition, there is a lack of knowledge about the kinetic crystallization parameters

that are important in protein nucleation control in order to have high quality crystals for 3D X-ray characterization. Thus, using the implementation of the gel acupuncture technique, which permits the crystallization in capillary tubes, our goal in this work will be focused on monitoring the quality of crystals from model proteins such as thaumatin, lysozyme, concanavalin *A* by X-ray analyses. This crystal quality could be controlled by the porous network of the silica gel, which is used as a membrane in the aforementioned implementation of the gel acupuncture technique based on either the nucleation or transport phenomena investigations. The quality of crystals grown by classical techniques are compared with crystals grown in capillary tubes. Additionally, the annealing techniques for increasing the quality of protein crystals is explained from the basis of the supersaturation control.

Grant from DGAPA-UNAM project IN 218597.

P09.OB.004 FLUORESCENCE STUDIES OF PROTEIN CRYSTAL NUCLEATION. Marc L. Pusey Biophysics ES76, NASA/MSFC, Huntsville, AL 35812

Fluorescence can be used to study protein crystal nucleation through methods such as anisotropy, quenching, and resonance energy transfer (FRET), to follow pH and ionic strength changes, and follow events occurring at the growth interface. We have postulated, based upon a range of experimental evidence that the growth unit of tetragonal hen egg white lysozyme is an octamer. Several fluorescent derivatives of chicken egg white lysozyme have been prepared. The fluorescent probes lucifer yellow (LY), cascade blue, and 5-((2-aminoethyl)aminonapthalene-1-sulfonic acid (EDANS), have been covalently attached to ASP 101. All crystallize in the characteristic tetragonal form, indicating that the bound probes are likely laying within the active site cleft. Crystals of the LY and EDANS derivatives have been found to diffract to at least 1.7 Å. A second group of derivatives is to the N-terminal amine group, and these do not crystallize as this site is part of the contact region between the adjacent 43 helix chains. However derivatives at these sites would not interfere with formation of the 43 helices in solution. Preliminary FRET studies have been carried out using N-terminal bound pyrene acetic acid (Ex 340 nm, Em 376 nm) lysozyme as a donor and LY (Ex ~425 nm, Em 525 nm) labeled lysozyme as an acceptor. FRET data have been obtained at pH 4.6, 0.1M NaAc buffer, at 5 and 7 % NaCl, 4°C. The corresponding Csat values are 0.471 and 0.362 mg/ml (~3.3 and ~2.5 x 10-5 M respectively). The data at both salt concentrations show a consistent trend of decreasing fluorescence intensity of the donor species (PAA) with increasing total protein concentration. This decrease is more pronounced at 7% NaCl, consistent with the expected increased intermolecular interactions at higher salt concentrations reflected in the lower solubility. The calculated average distance between any two protein molecules at 5x10-6 M is ~70nm, well beyond the range where any FRET can be expected. Results from these and ongoing studies will be presented.

P09.OB.005 IDENTIFICATION OF ANIONS AND CATIONS IN PROTEINS USING A SCANNING PROTON MICROPROBE (SPM) Elspeth Garman, Laboratory of Molecular Biophysics, Department of Biochemistry, University of Oxford, Oxford, OX1 3QU, U.K.

The identification of anions and cations in protein structure electron density is often inferred from the temperature factor of the ion and from its coordination distances to surrounding amino acids. In many cases unambiguous identification is not possible without the use of additional techniques.

The application of a scanning proton microprobe to the identification of anions and cations in protein samples is described. Using this technique, all elements heavier than neon (atomic number 10) can be detected at a sensitivity of 1 part in a million of the dry weight. The incident proton beam induces X-ray emission from the atoms in the sample, and the X-ray spectrum is detected in a lithium drifted silicon detector which has good energy resolution. Each element has a unique X-ray emission spectrum and the different elements can thus be identified. If the protein sequence is known, quantitative information on the number of cations and/or anions per protein molecule can be obtained by using the sulphur concentration from methionines and cysteines as an internal calibration.

Results from more than ten different proteins have been obtained using the Oxford SPM (1), which can routinely produce a 1 micron by 1 micron beam size. The technique allowed unambiguous identification of various elements in all the protein samples, and quantitative measurements have been made in five cases. The method of sample preparation and the advantages and limitations of the technique will be presented. The technique has been used both on protein solutions as a diagnostic tool following protein purification and also on protein crystals for identification of putative ions in solved structures. Although the method has not previously been fully described, results of measurements have already been reported in the literature on a range of proteins including HIV1 reverse transcriptase with an oligonucleotide bound (2), an EGF-like domain of Factor IX (3), a viral neuraminidase (4), and protein phosphatase 1 (5).

The technique should prove a useful addition to the analytical tools available to the structural biologist.

1. Grime G.W., Dawson, M., Marsh, M., McArthur, I.C. and Watt, F. (1991) Nucl Instr and Methods in Phys Res. B54: 52-63.
2. Jones, E.Y., Stuart, D.I., Garman, E.F., Griest, R., Phillips, D.C., Taylor, G.L., Matsumoto, O., Darby, G., Larder, B., Lowe, D., Powell, K., Purifoy, D., Ross, C.K., Somers, D., Tisdale, M. and Stammers, D.K. (1993) Journal of Crystal Growth 126: 261-269.
3. Rao, Z., Handford, P., Mayhew, M., Knott, V., Brownlee, G.G. and Stuart, D. (1995) Cell 82: 131-141.
4. Taylor, G., Garman, E., Webster, R., Saito T. and Laver, G. J.Mol.Biol. (1993) 230: 345-348.
5. Egloff, M.-P., Cohen, P.W.T., Reinemer, P. and Barford, D. (1995) J.M.B. 254: 942-959.

P09.OB.006 CRYSTALLISATION AND X-RAY STRUCTURAL STUDIES ON THE CAROTENO ASTAXANTHIN PROTEINS. N E Chayen[1], P F Zagalsky[2], J B C Findlay, A C T North [3], E J Gordon[4], P J Rizkallah [5], T J Boggon, J Raftery, J R Helliwell [6]. [1] Blackett Laboratory, Imperial College of Science, Technology and Medicine, Prince Consort Road, London SW7 2 BZ, UK. [2] Biochemistry Department, Royal Holloway, University of London, Egham, Surrey, TW20 0EX, UK. [3] Department of Biochemistry and Molecular Biology, University of Leeds, UK. [4] IBS, Grenoble, France. [5] SRS, Daresbury Laboratory, WA4 4AD, UK. [6] Chemistry Department, University of Manchester, Manchester, M13 9PL, UK.

Carotenoproteins provide the varied colouration of many invertebrate species. Examples include the multimacromolecular complex crustacyanin of the lobster carapace and also the astaxanthin proteins V620 and V600 of the surface-living oceanic chondrophore Velella velella. The function of these proteins is probably cryptic colouration, and whereby the oligomerisation to the multimacromolecular complex affects the wavelength response of the carotenoid. Crystallisation of various proteins in this related family has now been successfully achieved [1-6]. Isomorphous heavy atom derivatives have been difficult to obtain and xenon binding studies indicate only weak binding upto 25 bar pressure for apo C1 [7]. MAD experiments on a (non-isomorphous) heavy atom derivative and of a seleno- methionine variant of the lobster

apo C1 crustacyanin subunit are planned as well as xenon pressure experiments on apo A1.

[1] Wright, C E et al 1992,J Mol Biol 224 283-284,Lobster ApoC2.
[2] Chayen, N E et al 1996,Acta Cryst D52 156-159,Lobster ApoC1.
[3] Chayen, N E et al 1996,Acta Cryst D52 409-410,Lobster beta 2.
[4] Chayen, N E et al 1999,Acta Cryst D55 266-268,Vellella C1.
[5] Chayen, N E, Helliwell, J R, Rizkallah, P J and Zagalsky, P F Acta Cryst D in prep Lobster,apo A1.
[6] Chayen, N E and Helliwell, J R Physics World May 1998 inc apoC1 and the special oil method.
[7] Boggon, T J 1998 PhD Thesis University of Manchester.

P09.OB.007 THE EFFECT OF IMPURITIES ON PROTEIN CRYSTAL GROWTH: CASE STUDIES ON EARTH AND IN MICROGRAVITY. R.A. Judge, AMMSA, NASA/MSFC, Huntsville, AL 35812, USA, M.G. Sportiello, Chemical Engineering Department, ECCH 111, University of Colorado-Boulder, Boulder, CO 80309, USA, and E. H. Snell, Biophysics ES 76, NASA/MSFC, Huntsville, AL 35812, USA.

The presence of protein impurities is reported to be one of the major impediments in obtaining crystals of appropriate size and quality for x-ray structure analysis. In ground based research, studies on the impact of impurities on two crystallization systems, ovalbumin[1] and lysozyme[2], revealed that impurities consisting of proteins structurally different from the target protein are unlikely to have a negative impact upon crystal growth rates or solubility and are not incorporated in to the crystals. Impurities that adversely effect crystallization, appear to be impurities that have a structural similarity to the target protein and that are incorporated into the crystal. In light of this, one theory offered for the reported improvements in crystal size and crystal quality in microgravity, is that in the microgravity environment, impurity incorporation into the growing crystal may be reduced [3]. Results from recent crystallization experiments on STS-95, will be presented to show the effect of microgravity, in comparison to ground based studies, for the incorporation of impurities for two crystallization systems, lysozyme and glucose isomerase. The effect of microgravity on the reduction of incorporated impurities, and the resulting effects on crystal size and crystal quality will be discussed. Crystal quality measurements were performed for these two systems at the Stanford Synchrotron source.

Judge, R.A., Johns, M.R., & White, E.T. (1995). Protein purification by bulk crystallization: The recovery of ovalbumin. *Biotechnol. Bioeng*. **48,** 316-323.
Judge, R.A., Forsythe, E.L., & Pusey, M.L. (1998). The effect of protein impurities on lysozyme crystal growth. *Biotechnol. Bioeng*. **59,** 776-785.
Carter, D.C., Lim, K., Ho, J.X., Wright, B.S., Twigg, P.D., Miller, T.Y., Chapman, J., Keeling, K., Ruble, J., Vekilov, P.G., Thomas, B.R., Rosenberger, F., Chernov, A.A. (1999). Lower dimer impurity incorporation may result in higher perfection of HEWL crystals grown in microgravity: A case study. *J. Crystal Growth.* **196**, 623-637.

P09.OB.009 DYNAMICALLY CONTROLLED PROTEIN CRYSTAL GROWTH: NEW HARDWARE AND RECENT RESULTS. T.L. Bray, D.L. Powell, R.J. Gray, A. Arabshahi, and L.J. DeLucas, University of AL at Birmingham, Center for Macromolecular Crystallography, 1716 University Blvd., Birmingham, AL 35294, USA, and W.W. Wilson, Dept. of Chemistry, Mississippi State University, Starkville, MS 39762, USA.

Our laboratory has been working for several years to develop systems capable of controlling the concentration and/or supersaturation of protein solutions as a means of gaining control of the kinetics of protein aggregation, nucleation, and crystal growth. Efforts have focused on two methods, vapor diffusion and temperature, to achieve these goals. In addition, humidity, temperature, and static light scattering sensors are used to monitor the protein solutions and to allow real-time modification of the experiments in response to solution events. This approach allows virtually any desired evaporation or temperature profile to be investigated and for optimization of crystallization results.

The vapor diffusion systems utilize a controlled flow of dry gas to vary the evaporation rate of solvent from the growth solution, affecting the kinetics of protein aggregation, nucleation, and crystal growth. We have developed new, modular hardware components that have allowed us to create large capacity systems and to collect data on many different proteins. The results continue to demonstrate that control of the evaporation rate directly affects the crystal populations and sizes in a systematic fashion, with slower evaporation profiles generally producing smaller populations of larger crystals than faster evaporation profiles.

The temperature systems utilize the variable solubility versus temperature dependence exhibited by some proteins as the means to control the supersaturation of the protein solution. Execution of temperature ramps has been used to produce systematic variation in crystallization results. Temperature control is achieved using thermoelectric devices, which allow the temperature of a given protein solution (and hence the superasaturation) to be varied as precisely and rapidly as the user desires.

P09.OB.010 THE ROLE OF Mg++ IONS IN THE CRYSTALLIZATION OF AN OLIGONUCLEOTIDE. Stephen P. Cape, Moha Shah, and Paul Todd, Department of Chemical Engineering, University of Colorado, Boulder, Colorado, 80309.

Nearly all solutions made for the study of DNA, RNA, nucleoside phosphates, and oligonucleotides contain divalent magnesium ions. It is thought that in vivo and in vitro a stable cation-anion complex is formed, and that this complex is the physiological and chemical reacting unit in aqueous solutions. Additionally, Mg++ is one of the solutes that is manipulated in the crystallization of oligonucleotides, and most published mother liquors specify a Mg++ concentration. While investigating the possibility of replacing methypentane diol (MPD) with poly(ethylene glycol) (PEG) we found that a critical equilibrium exists that depends on Mg++ concentration. The solubility, crystallization and aggregation of a specific RNA dodecamer ("UU-dodecamer") were investigated. This oligomer exists as a duplex with Watson-Crick hydrogen bonds except in the case of 2 U's complementing 2 U's. Using MPD and PEG as precipitants, and manipulating ionic strength with monovalent ions, molecular interaction studies were performed as a systematic function of Mg++ concentration. These consisted of crystallization, determination of osmotic second virial coefficient by static light scattering, solubility equilibria, and aggregate growth measured by dynamic light scattering. The manipulation of Mg++ concentration is at least as important as controlling the concentration of the traditional precipitants MPD and PEG, leading to the notion that, at suitable concentrations Mg++ serves as "precipitant", and its control plays a significant role in the growth of high-quality crystals for diffraction study.

Research supported by NASA Grant NAG8-1165.

P09.OB.011 THE EFFECT OF pH ON THE GROWTH RATES OF TETRAGONAL LYSOZYME CRYSTALS. Elizabeth L. Forsythe,[1] Arunan Nadarajah,[2] and Marc L. Pusey,[3] [1]Universities Space Research Association, 4950 Corporate Drive, Suite 100, Huntsville, AL 35805, [2]Dept. of Chemical and Environmental Engineering, University of Toledo, Toledo, OH 436006, and [3]Biophysics SD48, NASA/MSFC, Huntsville, AL 35812.

Although the growth rates of protein crystals continues to be well studied, most investigations have focused on the effect of protein concentration and temperature, as measured by the supersaturation, on the growth rates. In this study a comprehensive investigation of the effect of pH on tetragonal lysozyme crystal growth rates was undertaken. The measurements were made with an automated growth rate apparatus capable of simultaneously measuring the growth rates of several crystals in a single run. Growth rates of the (110) face of tetragonal lysozyme crystals were measured dro pH values ranging from 4.0 to 5.4 at different salt and protein concentrations and temperatures. Lowering the ph increases the net positive charge of the protein, which might be expected to decrease the growth rates due to enhanced electrostatic repulsion. However, the growth rates were found to increase sharply with decreasing pH. These effects prevailed at all temperatures and protein and salt concentrations. The strong dependence on pH suggests the importance of electrostatic interactions to protein crystal growth, but its inverse relationship also suggests that this effect is a complex one.

09OC PHYSICAL PROPERTIES AND NOVEL MATERIALS UNDER HIGH PRESSURE

M09.OC.001 SUPERCONDUCTIVITY AND MAGNETISM IN THE SPIN LADDER COMPOUND (Sr, Ca)$_{14}$Cu$_{24}$O$_{41}$. Jun Akimitsu, Aoyama-Gakuin University, Setagaya, Tokyo, 157-8572, JAPAN

In recent years, much attention has been focused for the spin ladder compound, which is composed of two legs and CuO_2 chains. The ground state of a spin ladder compound is given by spin singlet in so-called "rungs" which interact with each other along the chains. Most interesting point of this system is an expectation of the superconductivity in the doped spin ladder system. Two years ago, we found the superconductivity in the doped spin ladder compound $Sr_{0.4}Ca_{11.6}Cu_{24}O_{41}$ under high pressure. We report in the conference the present experimental situation of the superconducting and magnetic properties of the $(Sr,Ca)_{14}Cu_{24}O_{41}$ single crystal. In particular, special attention has been focused on the superconducting properties under pressure. The superconducting transition under high pressure is accompanied by the metallic resistivity across the ladders.This strongly suggests that pressure brings about the dimensional crossover from one-to two-dimension and the superconductivity in this system is a consequence of insulator to superconductor transition in the anisotropic two-dimensional system. We also observed the coexistence between antiferromagnetism and spin gap state at ambient pressure which will be also discussed in the conference.

M09.OC.002 HIGH PRESSURE MÖSSBAUER STUDIES ON HEAVY FERMION SYSTEMS. M.M. Abd-Elmeguid II. Physikalisches Institut, University of Cologne, 50937 Cologne, Germany.

The purpose of this talk is to demonstrate how recent experimental results obtained from 170Yb high pressure Mössbauer studies on selected Yb heavy fermion systems provide valuable information on the nature of the ground state of this class of materials.

M09.OC.003 SEARCH FOR SUPERCONDUCTIVITY AT Mbar REGION. K.Amaya and K.Shimizu, Graduate School of Engineering Science, Osaka University,1-3 Machikaneyama, Toyonaka, Osaka, Japan.

Search for superconductivity at Mbar region performed by the use of DAC and dilution refrigerator is shortly reviewed.

Observed materials are simple systems such as I,Br,S and O (1) as well as organic iodanil and ionic CsI (2). Electric and magnetic measurements employed are also discussed.

(1) K.Shimizu et al.,Nature,393(1998)767.
(2) M.I.Eremets et al.,Science,281(1998)1333.

M09.OC.004 HIGH-PRESSURE NEUTRON-DIFFRACTION STUDY OF NEW MAGNETIC PHASES IN MIXED-VALENCE *f*-ELECTRON COMPOUNDS. J.-M. Mignot, LLB, CEA-CNRS, CEA/Saclay, 91191 Gif sur Yvette, France, I.N. Goncharenko, RRC "Kurchatov Institute", Moscow 123182, Russia, P. Link, LLB, CEA-CNRS, CEA/Saclay, 91191 Gif sur Yvette, France T. Matsumura and T. Suzuki, Department of Physics, Tohoku University, Sendai, 980-77, Japan.

Advanced high-pressure neutron-diffraction techniques based on sapphire- and diamond-anvil cells now provide access to the 0-10 GPa range for measurements on single-crystals at liquid-helium temperature. This offers a unique opportunity to gain an insight into the physical properties of materials in which the magnetism depends sensitively on interatomic distances. In mixed-valence rare-earth compounds, such a situation occurs because two different 4*f*-electron configurations with markedly different ionic radii are nearly degenerate in energy. Furthermore, fluctuations between these two valence states deeply affect the magnetic properties of the material at low temperatures.

We present novel results obtained on the thulium monochalcogenide series Tm*X* (*X*= S, Se, Te). These systems behave quite differently from usual mixed-valence compounds in which magnetic fluctuations are known to destabilize the 4*f* magnetic moments. Here, on the contrary, a variety of magnetically ordered phases exists at low temperature, and transport measurements have revealed pronounced changes when pressure is applied, including several transitions between semiconducting and metallic states.

The magnetic structures of the new high-pressure phases have been determined in TmTe (ferromagnetic above 2 GPa) and in TmS (lock-in antiferromagnetic at P= 5.7 GPa). In the former compound, the observed pressure dependence of the Curie temperature and of the thulium magnetic moment might correspond to the proximity of a quantum critical point.

M09.OC.005 ABNORMAL PROPERTIES OF SINGLE WALL CARBON NANOTUBES UNDER PRESSURE. D.E. Sklovsky, V.A. Nalimova, Department of Chemistry & Physics of High Pressures, Moscow State University, Moscow 119899, Russia, V.L. Kuznetsov, Boreskov Institute of Catalysis, Lavrientieva 5, 630090, Novosibirsk, Russia J.E. Fischer Department of Materials Science and Engineering and Laboratory for Research on the Structure of Matter, University of Pennsylvania, Philadelphia PA 19104 USA.

Single wall carbon nanotubes (SWNT) produced by double laser ablation of metal-doped graphite targets* were studied under the high quasi hydrostatic pressures up to 90 kbar in different types of anvil apparatus.

Piston-cylinder volumetric studies have shown the remarkably high and reversible volume compressibility of SWNT material up to 30 kbar, a factor 3-5 greater than the theoretically calculated values. The model of deformations at high pressures, based on crushing or flattening of SWNT cross-section from circular to elliptical is presented.

At 90 kbar pressure and room temperature the tubular structure of nanotube was shown to undergo phase transition to planar graphene planes - to graphite. The mechanism of such phase transition is proposed.

* The authors wish to thank A. Thess, A.G. Rinzler and R.E. Smalley of Rice University, Houston, USA for provision of purified SWNT material.

M09.OC.006 STRUCTURAL PRINCIPLES OF SIMPLE ELEMENTS AND INTERMETALLIC ALLOYS AT HIGH PRESSURE. J.S. Tse, Z.Q.Li, R. Rousseau, K. Uehara and D.D. Klug, Steacie Institute for Molecular Sciences, National Research Council of Canada, Ottawa, Ontario, Canada K1A 0R6 and J. Xie, Theoretical Division, Los Alamos National Laboratory, Los Alamos, NM 87548, U.S.A.

The effect of pressure on simple element such as diamond, gallium, and cesium and intermetallic alloys such as the K-Ag system have been examined by theoretical electronic structure and phonon calculations. Selected results will be reported on the following investigations including the observation of a negative thermal expansion coefficient in diamond at high pressure and low temperature; the phonon spectra associated with the iso-structural phase transition in Cs II – Cs III; and an interpretation for the unusual electronic structure of Cs IV. We will also discuss the validity of the Zintl's concept and the application of Miedema's rules in the electronic structure of intermetallic alloys at high pressure.

P09.OC.001 HIGH-PRESSURE AND HIGH TEMPERATURE EQUATION OF STATE OF PERICLASE. A. Dewaele and G. Fiquet, École Normale Supérieure de Lyon, 69364 Lyon Cedex 07, France, D. Andrault, IPGP, 75252 Paris Cedex 05, France and D. Hausermann, ESRF, 38042 Grenoble Cedex, France.

We present here an experimental determination of the Equation of State (EoS) of periclase at high pressure and high temperature. Motivations of this study are: (1) MgO is probably the second most abundant material in the Earth's lower mantle; its EoS is thus needed to constrain chemical models of the Earth; (2) lots of theoretical methods have been used to calculate the EoS of MgO and must be tested; (3) thanks to its large pressure and temperature stability domain, MgO can be used as a pressure calibrant in high pressure experiments.

We have carried out volume measurements on MgO, in a CO_2-laser heated diamond-anvil cell, up to 55 GPa and 2400 K, using monochromatic X-Ray diffraction at the ESRF (France). Temperature has been deduced from the thermal emission spectrum of the sample, and pressure by the use of a pressure calibrant (Platinum) mixed with the sample. Thermal pressure was taken into account in this way. Two-dimensional powder diffraction patterns were used to determine the MgO and Pt lattice unit cell parameters by LeBail refinement.

Inversion of the P-V-T data of MgO leads to the values of K_T (incompressibility), α (the thermal expansion coefficient) and their first pressure and temperature derivatives. The values of these parameters are: at ambient temperature, K_0 = 161 GPa, K'_0 = 3.95 (with a third-order Birch-Murnaghan equation of state); under high temperature: $\alpha(P = 0,T) = (3.0+0.0012\ T)\ K^{-1}$; $(\partial K_T / \partial T)_P$ = -0.022(3) GPa/K. The harmonic Debye model seems to correctly describe the temperature dependence of the volume under high pressure; with γ_0 = 1.54, (Grüneisen parameter under ambient conditions), a value of q (parameter that describes volume dependence of γ) of 1 ±0.3 is obtained.

P09.OC.002 PRESSURE EFFECT ON PHASE TRANSITION IN NaV_2O_5. K.Ohwada, H. Nakao, N. Takesue, M. Isobe, Y. Ueda and Y. Fujii, Institute for Solid State Physics, The University of Tokyo, 7-22-1 Roppongi, Minato-ku, Tokyo 106-8666 Japan, and Y. Wakabayashi and Y. Murakami, Photon Factory, Institute of Material Science, High Energy Accelerator Research Organization(KEK), Tukuba, Ibaraki 305-0801, Japan.

Very recently we have successfully observed two types of phase transitions in NaV_2O_5, i.e. spin-gap formation driven by charge order and lattice dimerization at low temperature (T_c=35K at 1atm.) and pressure induced structural phase transition at room temperature. Na atoms in its orthorhombic structure are located between V_2O_5-layers composed of two-dimensionally connected VO_5-pyramids and play a role of an electron donor to create a magnetically active V^{4+}(S=1/2). Pressure dependence of the lattice dimerization behavior of NaV_2O_5 has been studied at low temperatures for the first time. We measured the temperature dependence of the superlattice intensity from a single crystal up to 1.2GPa. The phase transition is significantly suppressed as $dT_c/dP \sim -13(1)$(K/GPa)), and the negative slope is consistent with the anomalous volume expansion below T_c through Ehrenfest's relation. Anomalous lattice properties and structural phase transition of NaV_2O_5 have also been studied under hydrostatic high pressure at room temperature using powder x-ray diffraction techniques. The c-axis along the stacking direction of V_2O_5-layers contracts rapidly and the b-axis along the one-dimensional magnetic chain direction expands, while the a-axis contracts up to about 4GPa and then begins to expand. Structural analysis of NaV_2O_5 and the previous data of V_2O_5 indicate that the Na atoms between the V_2O_5-layers govern these lattice properties. A structural phase transition is found to take place around 13GPa. A detailed structure analyzed by the Rietveld method reveals that the approach of the apical oxygen of VO_5-pyramid of under layer to the V atom in VO_5-pyramid plays an important role in the phase transition.

P09.OC.003 SINGLE WALL CARBON NANOTUBES AT PRESSURES UP TO 9.0 GPa. D.E. Sklovsky, V.A. Nalimova, Department of Chemistry & Physics of High Pressures, Moscow State University, Moscow 119899, Russia, A.D. Bozhko, Department of Low Temperature Physics, Moscow State University Moscow 119899 Russia; G.N. Bondarenko, Topchiev Institute of Petrochemical Synthesis, Russian Academy of Sciences, Leninsky pr., 29, Moscow, Russia, E.D. Obraztsova, Natural Sciences Center, General Physics Institute RAS, 38 Vavilov street, 117942, Moscow, Russia, V.L. Kuznetsov, Boreskov Institute of Catalysis, Lavrientieva 5, 630090, Novosibirsk, Russia, J.E. Fischer Department of Materials Science and Engineering and Laboratory for Research on the Structure of Matter, University of Pennsylvania, Philadelphia PA 19104 USA.

This poster presentation is supposed to complement to the talk on abnormal properties of single wall carbon nanotubes (SWNT) under pressure, describing the variety of methods, applied for this investigation. The precise volumetric technique along with XRD, HRTEM, Raman- and IR-spectroscopies enabled to elaborate the model of SWNT deformation under pressure, describing the unusually high and reversible volume compressibility of this material up to 30 kbar - crushing or flattening of SWNT cross-section from circular to elliptical.

In situ resistivity *vs.* pressure investigations in different types of anvil apparatus up to 9 GPa pressure showed the different mechanisms of local defect formation in nanotube material in different pressure ranges and proved the higher stiffness of alkali metal doped SWNT material.

XRD and HRTEM studies of SWNT samples quenched at different pressures evidenced the phase transition from SWNT ropes to planar graphite even at room temperature.

P09.OC.004 PRESSURE-INDUCED TRANSITION FROM Eu (4f) TO Co (3d) MAGNETISM IN $EuCo_2P_2$. M.M Abd-Elmeguid, M. Chefki, H. Micklitz, C. Huhnt, W. Schlabitz [1], M. Reehuis, W. Jeitschko [2], [1] II. Physikalisches Institut, Universität zu Köln, Zülpicher Strasse 77, D-50937 Köln, Germany, [2] Anorg.-Chemisches Institut, Westf. Wilhelms-Universität Münster, Wilhelm-Klemm-Strasse 8, D-48149 Münster, Germany

Magnetically ordered $EuCo_2P_2$ (Eu(2+); TN=66.5 K) undergoes a pressure-induced isostructural phase transition at p(c) = 3.1 GPa. 151Eu high-pressure Mössbauer experiments (0 <= p <= 5 GPa) reveal a valence transition of Eu from Eu(2+) to nonmagnetic Eu(3+) (7F0) at p > p(c) with the consequence that the disappearance of the Eu(4f) sublattice magnetism is accompanied by a simultaneous appearance of Co(3d) sublattice magnetism (TN= 260K). The latter is explained by the filling of the 3d states.

P09.OC.005 STRUCTURAL AND MAGNETIC PHASE TRANSITIONS UNDER HIGH PRESSURE IN THE AMNF4 (A=CS,RB,K) SERIES. M.C. Moron and F. Palacio [1], M. Ishizuka, S. Henmi, S. Endo [2], [1] Instituto de Ciencia de Materiales de Aragón, CSIC-Universidad de Zaragoza, E-50009 Zaragoza (Spain), [2] CREST (JST) and Research Center for Materials Science at Extreme Conditions, Osaka University, Toyonaka, Osaka 560 (Japan)

The $AMnF_4$ (A=Cs,Rb,K) series of layered-perovskites consist of two- dimensional network of layers of Jahn-Teller distorted MnF_6 octahedra, separated by the alkali ions. A reduction on the size of the alkali ion when going from CsMnF4 through $RbMnF_4$ to $KMnF_4$ (chemical pressure), shows a reduction of the unit cell volume and crystal symmetry.(1) The size of the alkali ion also has a dramatical effect on the magnetic behavior of these compounds. Neutron powder diffraction experiments evidence that $CsMnF_4$ orders as a ferromagnet below 18.9K, while the other members of the series exhibit antiferromagnetic ordering at lower temperatures. Synchrotron x-ray powder diffraction experiments, performed on the members of the series under high pressure up to 18GPa, have shown the equivalence between chemical and hydrostatic pressure along this series. Thus, the crystal structure of $CsMnF_4$ (tetragonal) changes at 1.4GPa and 6.3GPa to, respectively, the crystal symmetry of $RbMnF_4$ (orthorhombic) and $KMnF_4$ (monoclinic).(2) Changes in magnetism, in particular from ferro- to antiferromagnetic ordering, may be expected to occur when increasing pressure on $CsMnF_4$. We have investigated the magnetic behavior of this compound under pressure following the evolution of the magnetization with temperature up to pressures of 4GPa by using a diamond-anvil cell cooled down to 1.5K and a SQUID vibrating magnetometer. Our results indicate that there is also a close correlation between chemical and hydrostatic pressure effects on the magnetic structure of the $AMnF_4$ series. The relationships of these magnetic in character results with the structural properties of this series are discussed.

1. Moron, Palacio and Rodriguez-Carvajal. J. Phys.: Condens. Matter, 5(1993) 4909.
2. Moron, Palacio and Clark. Phys. Rev. B, 54 (1996) 7052

P09.OC.006 X-RAY CRYSTAL STRUCTURES OF MOLECULAR CONDUCTORS AT LOW TEMPERATURE AND UNDER HIGH PRESSURE . D. Chasseau, D. Le Pevelen, Y. Barrans, G. Bravic, J. Gaultier, P. Guionneau. Laboratoire des Sciences Moléculaires, Institut de Chimie de la Matière Condensée de Bordeaux, UPR CNRS 9048, Avenue du Dr A. Schweitzer, F-33608 Pessac Cedex.

Electrical and magnetic properties of molecular conductors have been intensively studied for the last twenty years as a function of temperature and pressure. For a better understanding of these properties, it is necessary to know the evolution of the structural properties in the same conditions. For this reason, our research group has developed for the last ten years a specific X-Ray diffraction technique which allows to visualize the reciprocal space and to determine the crystal structure of molecular compounds from 400 K to 7 K (ambient pressure) and from 1 bar to 15 kbar (room temperature). Very recently, two new results were obtained on molecular conductors under high pressure and at low temperature (6 kbar at 7 K). Thus, it is now possible, from a structural point of view, to have access to the (P, T) phase diagram of this kind of compounds.

The molecular salt $(TSeT)_2Cl$ presents a very high conductivity at ambient conditions. Its resistivity indicates the occurrence of a first order transition at 5kbar between two metallic states. The X-ray analysis performed at 5 kbar (300K) shows a change in the crystal symmetry which leads to a reorganisation of the Cl^- anions and of the (TSeT) network. This crystal structure, at 5 kbar, remains the same when the temperature is lowered to 7 K.

$(TMTSF)_2ClO_4$, was the first molecular salt to become superconducting at ambient pressure. Previous results, obtained by X-ray diffuse scattering, have shown the existence of superstructure reflections (wave vector 0 1/2 0) at 24 K. The crystal structure has been refined at 7 K (ambient pressure) in the (a, 2b, c) unit cell and shows clearly the ordering of the ClO_4 anion. On the contrary, the X-ray measurements, at 5 kbar (7 K), have not shown the existence of these superstructure reflections; the ClO_4 anion, in the (a, b, c) unit cell remains disordered. In both cases, dimerization of the TMTSF stacking is reduced.

09OD SYNCHROTRONS AND CHARGE DENSITY ANALYSIS

M09.OD.001 CHARGE DENSITY ANALYSIS AT THE SUNY X3 BEAMLINE AT THE NATIONAL SYNCHROTRON LIGHT SOURCE. P. Coppens, G. Wu and A. Volkov, Department of Chemistry, SUNY at Buffalo, Buffalo, NY 14260-3000, USA.

Because of its brightness, high intensity and energy, synchrotron radiation is eminently suitable for charge density analysis. Nevertheless, full realization of its potential has been quite a slow process. The reasons are manyfold and include beam instabilities which may not significantly affect other experiments and may therefore be ignored by those responsible for operation of the facility, sample instabilities and incomplete absorption of the beam by the area detector phosphor when hard radiation is used. This talk will discuss lessons learned in the last three years, successful examples of very low temperature synchrotron charge density studies, with both imaging plates and CCD detectors, and the interpretation of the results.

Support of this work by the National Science Foundation (CHE9615586, CHE9522232) and the U.S. Department of Energy (DE-FG02-86ER45231) is gratefully acknowledged.

M09.OD.002 ON THE QUALITY OF EXPERIMENTAL DENSITIES FROM SYNCHROTRON-CCD DATA T. Koritsanszky, Department of Chemistry, University of the Witwatersrand, Private Bag 3, WITS 2050, Johannesburg, South Africa.

The experimental determination of the electron density (ED) in the crystalline state relays on the precision and the resolution of X-ray diffraction data and on the adequacy of the refinement model applied to interpret them. Both of these aspects of the method are being revolutionized; the technical procedure

involved is due to the application of synchrotron (SYN) radiation combined with CCD intensity detection, the interpretation is due to sophisticated computer packages to reduce the data, to monitore the refinement and to analyse the ED extracted. Recent successes [1] suggest routine applications with increasing demand for extending such studies to large systems of biological relevance but the basic dilemma remains; to what extent a good fit of the data implies accuracy. The question can be approached - although cannot be answered - by comparative studies of different types. Here we report on comparing fine details of EDs obtained by using the same refinement model in the interpretation of different data either of the same crystal or of different crystals of chemically analog systems. These includes comparisons of EDs of: a. serine (conventional and CCD, SYN and MoKα) b. an antithrombotic farmacon (CCD, SYN and MoKα), c. two penicillines (CCD and SYN). The multipole refinements were performed with the program package XD [2] and the comparisons are based on the topological properties [3] of the static EDs. The results show that the SYN-CCD technique can lead to relative accurate and consistent densities suggesting the importance of high data resolution and redundancy reachable.

1. T. Koritsánszky, R. Flaig, D. Zobel, H.-G. Krane, W. Morgenroth, P. Luger, Science 279, 356 (1998)
2. T. Koritsánszky, S. Howard, R.P. Mallinson, Z.W. Su, T. Richter, N.K. Hansen: XD, A Computer Program Package for Multipole Refinement and Analysis of Charge Densities from X-ray Diffraction Data. Freie Universität Berlin. User Manual (1995).
3. R.F.W. Bader, ``Atoms in Molecules", Monograph, Clarendon Press, Oxford, (1990).

M09.OD.003 SYNCHROTRON CHARGE DENSITIES IN ACTION. Bo Brummerstedt Iversen, Department of Chemistry, University of Aarhus, DK-8000 Århus C, Denmark.

It is well known that synchrotron radiation potentially can improve the accuracy of experimental charge densities (CD) due to reduction of systematic errors. CD's of a quality comparable to the best conventional densities now can be measured regularly.[1] This allows a shift of focus away from methodological aspects, and in the talk recent applications of CD analysis in enzyme catalysis and intramolecular electron transfer processes will be discussed.

The cleavage of peptide bonds is an important reaction in nature, which involves the catalytic triad of residues (Ser--His--Asp) in the active site of the serine proteases class of enzymes. It has been suggested that a low-barrier hydrogen bond is involved in the reaction mechanism as a partial proton transfer between His^{57} and Asp^{102}. In order to investigate short N-H--O bonds, we have carried out combined very low temperature (28 K) X-ray and neutron diffraction studies of the cocrystal between betaine, imidazole and picric acid. The complex serves as a model for the catalytic triad, and the system is attractive *a priori* since it contains three different short N-H--O contacts (< 2.7Å) in the same crystal.

Polynuclear transition metal complexes occur widely in nature and their study spans fields reaching from biology to photo-physics. In bio-inorganic chemistry oxy-bridged polymetal systems have received enormous attention. In the case of intra-molecular electron transfer processes much work has been devoted to the classical basic carboxylates. We are undertaking a project involving systematic CD studies of a number of such compounds. In the talk results on a mixed valence compound, $Fe_3O(COOC(CH_3)_3)_6(C_5H_5N)_3$ will be presented. Since the system allows great flexibility in the variation of either the metals, the bridging ligands or the terminal ligands, it is hoped that comparative studies will give an increased understanding and control of the electronic structure of the central M_3O core.

[1] B. B. Iversen, F. K. Larsen, A. A. Pinkerton, A. Martin, A. Darovsky, P. A. Reynolds, *Inorg. Chem*. 1998, 37, 4559-4566; *Acta Crystallogr. Sect B.* 1999, in press.

M09.OD.004 ROOM TEMPERATURE ELECTRON DENSITY DISTRIBUTION IN SODIUM-NITROSYL-PRUSSIDE. A. Kirfel[1], H.-G. Krane[1] and W. H. Morgenroth[2]; [1]Mineral.-Petrol. Institut, Universität Bonn, [2]Mineral.-Petrogr. Institut, Universität Hamburg, Germany.

Due to the excitability of metastable electronic states at low temperatures resulting in a potential use as optical storage medium, $Na_2[Fe(CN)_5NO]2H_2O$ (space group Pnnm) has attracted much interest, and several structure analyses both by neutron and X-ray diffraction including electron density studies have been performed at low temperatures, e.g. [1]. In order to study i) the electron density distribution of the ground state, and ii) the quality of CCD-data in comparison to data conventionally recorded with a scintillation detector (SC), diffraction measurements were carried out on a 0.42 mm diameter sphere using synchrotron radiation at λ = 0.56Å (beam line D3, HASYLAB, Hamburg). For s_{max} = 0.92$Å^{-1}$, the raw data consisted of 13119 (SC, 7 days exposure) and 66075 (CCD, 3.5 days) reflections yielding 3684 and 3786 unique reflections, respectively $(R(F^2)_{int}$ = 0.015 and 0.037). Final agreement indices for conventional IAM refinements were R(F) = 0.0213 (SC) and 0.0296 (CCD).

Identical multipole structure refinements using VALRAY [2] converged at R(F) = 0.0103 (SC) and 0.0197 (CCD), again indicating a somewhat lower, but still sufficient quality of the latter data. This is also supported by ensuing calculations of static deformation density maps whose features are in good mutual agreement. Agreement is also found with theoretical calculations, except for the NO-group situated on the mirror plane m. In both analyses, the oxygen atom of this group is found to exhibit a chemically anomalous deformation pattern, i.e. extraordinary high $\Delta\rho$-peaks of several el/A^3 approximately 0.20 A above and below the mirror plane. Since various refinements with lowered symmetry, split oxygen positions, and anharmonic vibrations for the oxygen atom failed to produce conclusive results, radiation induced changes of the NO-bonding may be suspected.

[1] M.D. Carducci, M.R. Pressprich, P. Coppens (1997), J. Am. Chem. Soc., **119**, 2669.
[2] R.F. Stewart, M.A. Spackman (1983), VALRAY USERS MANUAL, Dept. Of Chem., Carnegie-Mellon University, Pittsburgh PA, USA.

M09.OD.005 DIRECT OBSERVATION OF ORBITAL ORDER IN $NdSr_2Mn_2O_7$ BY MEM CHARGE DENSITY STUDY. M.Takata, Dept. of Material Science, Shimane University, Mtasue 690-8504, Japan, and E.Nishibori, K.Kato and M.Sakata, Dept. of Applied Physics, Nagoya University, Nagoya 464-8601, Japan, and Y.Moritomo, Center for Integrated Research in Science and Engineering, Nagoya University, Nagoya 464-8601 and PRESTO, JST, Japan.

Recent extensive experimental and theoretical investigations on the doped manganites of perovskite-like structure, which shows colossal magnetoresistive (CMR) properties, begins to reveal a crucial role of the orbital degree of freedom on the magnetic as well as the electronic properties. Among such substances, $NdSr_2Mn_2O_7$ is well known as the layered manganite, which is of tetragonal (I4/mmm) and shows a definite antiferromagnetic transition at T_N =150K. The origin of the antiferromagneticity has been thought to be due to spontaneous ordering of the Mn $\boldsymbol{dx^2\text{-}y^2}$ orbital as for the itinerant $\boldsymbol{e_g}$-electrons. An accurate X-ray charge density study must allows us to reveal a bonding electron localized between the Mn and O atoms associated with Mn($\boldsymbol{3d}$)-O($\boldsymbol{2p\sigma}$) hybridization. Supposing that the orbital ordering really exist in MnO_2 plane in an

antiferromagnetic state, an anisotropy of Mn-O bonding feature in MnO_6 octahedron must be found in the charge density distribution at $T < T_N$. Here, we report the results of direct observation of orbital ordered state of $NdSr_2Mn_2O_7$ in the form of real space charge densities obtained by Maximum Entropy Method(MEM)/Rietveld method[1] using synchrotron radiation powder data. The results very clearly show, for the first time, an electronic layer structure ascribed to the layered antiferromgnetic structure of $NdSr_2Mn_2O_7$.

1. M.Takata, *et al.*(1995) *Nature,* **377**, 46.

M09.OD.006 EXTINCTION-FREE SINGLE-CRYSTAL SR DIFFRACTION EXPERIMENTS USING SMALL CRYSTALS. N.Ishizawa, Materials and Structures Laboratory, Tokyo Institute of Technology, 4256 Nagatsuta, Midori-ku, Yokohama 226, Japan

Three-dimensional synchrotron X-ray diffraction data obtained for a small single crystal approximately 10 μm in size were found to be scarcely affected by extinction and provide unambiguous information of charge density in crystals.

Diffraction data were collected at beam line 14A, Photon Factory, KEK, which is equipped with a horizontal-type four-circle diffractometer [1] utilising focused X-rays. The APD detector [2], comprising of four avalanche photodiodes stacked along the beam path, was employed in part of this study. Neither attenuator nor dead time corrections were necessary as all the diffracted intensities were within the dynamic range 10^{-2} - 10^{8} cps of the detector. Case studies for inorganic crystals, including a 10 μm $(Ca,Y)AlO_4$ crystal and a 8 μm $LiNbO_3$ crystal revealed accurate charge densities of the compounds. The maximum peak intensity reached over 10^6 cps. A subtle, though significant, composition deviation from the stoichiometry was confirmed in both compounds. Two close atomic positions occupied respectively by the host and replacing atoms in solid solution were resolved in $(Ca,Y)AlO_4$. An example is shown where the conventional extinction correction included in the least-squares procedure can invoke artifacts if it is applied over a certain limit, leading to misunderstanding of the true nature of charge densities.

1. Satow, Y. & Iitaka, Y. (1989). Rev. Sci. Instrum. **60** [7], 2390-93.
2. Kishimoto, S., Ishizawa, N. & Vaalsta, T. P. (1998). Rev. Sci. Instrum., **69**[2] 384-391

M09.OD.007 X-RAY ANALYSIS OF CHARGE DENSITY UNDER MAGNETIC FIELDS. V.A. Streltsov and D.du Boulay, Crystallography Centre, The University of Western Australia, Australia. and R.P. Ozerov, Mendeleev University of Chemical Technology, Russia.

Remarkable changes to the electron distribution in haematite, α-Fe_2O_3 and magnetostrictive Laves, RFe_2 (R=Tb and Sm) have been observed from synchrotron (Photon Factory BL14-A) X-ray diffraction measurements at room T with applied magnetic fields of order 0.07 T at the sample position.

Haematite is a weak ferromagnet at room T. Although its structural symmetry is rhombohedral, the magnetic symmetry is monoclinic. Under magnetic fields in the single domain state, the lattice is expected to deform matching the magnetic symmetry. However, no statistically significant displacement of the Fe atom from its rhombohedral position were found. But, strong distortion of the charge density, especially in the plane perpendicular to the field direction was observed. Superlattice monoclinic reflections of marginal significance were detected. These reflections were considered in [1] as those originating in X-ray photon-spin interactions. Alternatively, they might be explained by the scattering of X-ray photons by part of the charge density distorted due to spin's magnetic interactions.

In an applied field, $TbFe_2$ and $SmFe_2$ undergo large strains along a cubic body diagonal, resulting in rhombohedral distortions. The current atomic model of anisotropic magnetostriction and its variation from positive to negative in $TbFe_2$ and $SmFe_2$, respectively, is based on the proposed asymmetry of the 4*f* electron densities of rare earths [2]. Analysis of the experimental data revealed strong reorganisation of the difference electron density challenging this model.

Brunel, M. & de Bergevin, F. (1981). *Acta Cryst.* A**37**, 324-331.
Cullen, J. R. & Clark, A. E. (1977). *Phys. Rev.* B**15**, 4510-4515.

P09.OD.001 SYNCHROTRON RADIATION CHARGE DENSITY STUDY OF UREA USING A SIX-CIRCLE DIFFRACTOMETER. H. Birkedal, P. Pattison, D. Schwarzenbach and H.-P. Weber, Institut de Cristallographie, Université de Lausanne, BSP Dorigny, 1015 Lausanne, Switzerland, and K. Knudsen, SNBL, ESRF, BP 220, 38043 Grenoble Cedex, France, and R. Mathiesen, Institutt for fysikk, NTNU, 7043 Trondheim, Norway, and D. Madsen, ESRF, BP 220, 38043 Grenoble Cedex, France.

We present a new charge density study of urea obtained using synchrotron radiation at the Swiss Norwegian Beam Line at the ESRF. The beam line is equipped with a six-circle kappa-diffractometer and a point detector. Data of very high quality were collected at 120K. The data are of unprecedented resolution for urea with $\sin(\theta)/\lambda_{max} = 1.442 Å^{-1}$. A total of 3958 reflections were measured, which average to 1826 unique reflections with R_{int}(all) = 1.29% . Of the unique reflections, 1346 have $F_o^2 > 3\sigma(F_o^2)$. The data are compared with earlier laboratory data [1]. The charge density is modeled by refinements with VALRAY [2], the agreements factors being $R(F^2) = 1.31\%$ and $wR(F^2) = 1.76\%$. We discuss the complete topology of the charge density of urea and atomic properties obtained by integration over the atomic volumes. The results are compared with periodic restricted Hartree-Fock ab initio calculations [3].

1. S. Swaminathan *et al.* (1984), Acta Cryst., **B40**, 398.
2. R. F. Stewart, M. A. Spackman, C. Flensburg (1998) VALRAY Reference Manual.
3. C. Gatti *et al.* (1994), J. Chem. Phys., **101**, 10686.

09OE MICROPOROUS MATERIALS

M09.OE.001 COMPUTER SIMULATION OF ZEOLITE CRYSTAL STRUCTURES. Robert G. Bell, Davy Faraday Research Laboratory, Royal Institution of Great Britain, 21 Albemarle Street, London W1X 4BS, UK

With the advances in computing power seen over the last decade, the atomistic modelling of zeolite framework structures using potential-based energy minimisation methods has become an almost routine procedure. In our laboratory, these types of simulation, in conjunction with experimental techniques, have been used to notable effect in detailed structural studies of a number of microporous materials[1,2]. Using Monte Carlo methods it is additionally possible to predict the siting of adsorbed molecules within the crystalline host framework[3]. This presentation will review progress in the field to date, including the study of MCM-41 type mesoporous materials[4], and will further discuss the relationship between framework topology and lattice energy, and its implications for the synthesis of new framework materials.

1. G. Sankar, R.G. Bell, J.M. Thomas, M.W. Anderson, P.A. Wright & J. Rocha, *J. Phys. Chem*., **100**, 449 (1996).
2. R.G. Bell & G.D. Price, in *Computer Modelling in Inorganic Crystallography* C.R.A. Catlow ed., Academic Press, London (1997) and references therein.
3. Z.A. Kaszkur, R.H. Jones, R.G. Bell, C.R.A. Catlow & J.M. Thomas, *Mol. Phys.*,**89**, 1345 (1996)**.**
4. R.G. Bell, in *Proceedings of the 12th International Zeolite Conference*, MRS, Warrendale, USA (1999).

M09.OE.002 HOST-GUEST INTERACTIONS IN ZEOLITES AS STUDIED BY SOLID-STATE NMR AND X-RAY TECHNIQUES. Andrew R. Lewis,[1] Anix C. Diaz,[2] and Colin A. Fyfe, Chemistry Department, University of British Columbia, Vancouver, B.C. V6T 1Z1, Canada. [1] Present address: Laboratoire de Matériaux Minéraux, ENSCMu, Université de Haute-Alsace, 3 rue Alfred Werner, 68093 Mulhose Cedex, France. [2] Present address: Intevep S.A. Departamento de Análisis y Evaluación, Centro de Investigación y Apoyo Technológico Filial de Petróles de Venezuela, Apdo. 76343 Caracas 1070 A Venezuela.

We report solid-state NMR methods developed for locating guest species within the channels and cages of inorganic microporous materials. The ultimate aim of these experiments is the determination of the 3-dimensional structures of the host-guest complexes formed by zeolites and sorbed organic molecules or other guests. Such techniques are important because relatively little is known about the exact location of guest species within these framework structures; single crystal X-ray structure determinations are often precluded by the lack of suitable crystals, and Rietveld refinement of powder data may not always provide reliable guest locations.

Using Magic Angle Spinning combined with Cross Polarization from nuclei in the guest species to ^{29}Si nuclei in the framework of siliceous microporous materials, we have been able to demonstrate the feasibility of measuring accurate host-guest distances. In addition, we have successfully determined the location and orientation of *p*-xylene molecules within the channels of ZSM-5. The NMR-determined distances and structures are in agreement with the corresponding information obtained from single crystal X-ray diffraction refinements. These NMR techniques can be extended to other systems, and the structures obtained serve as a useful check of the validity of structures predicted from molecular modeling calculations.

M09.OE.003 DYNAMICS OF MOLECULES IN POROUS MATERIALS INVESTIGATED BY NEUTRON SPECTROSCOPY. B. Asmussen[1)], I. Krasnov[1)], C. Gutt[1], W. Press[1)], W. Langel[2)], R. Kahn[3)], M. Ferrand[4)],1) Institut fuer Experimentelle und Angewandte Physik, Univ. Kiel, Germany, 2) Univ. Greifswald, Germany, 3) LLB, Saclay, France, 4) ILL, Grenoble, France.

Structure and dynamics of condensates in porous media are strongly influenced by the presence of pore walls. The presentation will focus on the (rotational and translational) dynamics of methane molecules in various mesoporous host materials (silicagels, Controlled Pore Glasses, MCM-41, porous TiO_2) with pore diameters d covering a wide range 20 Å ≤ d ≤ 350 Å. Basing on extensive measurements of sorption isotherms, different degrees of filling could be realized: (1) pores completely filled with methane and (2) walls of the host material covered by a multilayer film.

High-resolution inelastic incoherent neutron scattering with time-of-flight techniques is a powerful tool for the investigation of dynamical processes of hydrogen containing molecules due to the large scattering cross section of the proton. The rotational spectra of methane condensates at low temperatures (T ~ 5 K, i.e. in the regime of quantum rotations) can be used as very sensitive probes for strength and symmetry of local potentials. They allow us to distinguish between a core of unperturbed solid CH_4 in its low-temperature phase II in the center of the pores and an orientationally disordered layer on the pore walls.

Quasielastic neutron measurements have covered the region of the melting-transition of the methane condensates (70 K ≤ T ≤ 95 K). The onset of translational motions of the condensate molecules at the melting point leads to a corresponding decrease in the elastic intensity in the neutron spectra. For the multilayer coverages, this decrease is smeared out over a broad temperature range ΔT = 20 K. The melting was found to be much more abrupt for the filled pores, but here the melting point shifts (depending on the pore diameter) to lower temperatures, compared to the bulk value. The results from the dynamical experiments are supported by strucutral investigations with x-ray diffraction and neutron small-angle scattering.

D. Balszunat, B. Asmussen, G. Coddens, M. Ferrand:*Dynamics of methane guest molecules in porous media*,Physica B **226** 184 (1996)
C. Gutt, B. Asmussen, I. Krasnov, W. Press, W. Langel, R. Kahn:*Dynamics of Methane Molecules in the Mesopores of Controlled-Pore Glass at Low Temperatures*,accepted for publication in Phys. Rev. B

M09.OE.004 NEGATIVE THERMAL EXPANSION IN ZEOLITES. D. A. Woodcock, P. Lightfoot and P. A. Wright, School of Chemistry, University of St. Andrews, Purdie Building, North Haugh, St. Andrews, Fife, UK, KY16 9ST, M.A. Camblor, L.A. Villaescusa, M.J. Díaz-Cabañas, Insituto de Technologia Química, Avda. Los Naranjos s/n, 46071 Valencia, Spain and D. Engberg, ISIS Facility, CLRC Rutherford Appleton Laboratory, Chilton, Didcot, Oxon. OX11 0QX

Negative thermal expansion has been found to be present in numerous zeolite and microporous framework structures such as the pure silica polymorphs ITQ-1, ITQ-3, SSZ-23[1] and faujasite[2], AlPO-17[3] and ZSM-5[4]. AlPO-17 is of particular interest as it is the most contracting material known.

Our in house X-ray diffraction experiments on ITQ-1, ITQ-3 and SSZ-23 revealed that all three materials showed a contraction as a function of temperature on each axis, but that the contraction did not appear to be due to any obvious structural characteristics. For example, ITQ-1 is a layer structure, the layers lying perpendicular to the c axis. It might be expected that the strongest contraction would be between the layers and that α_c would be more pronounced than either α_a or α_b. This proved not to be the case and it was concluded that a detailed structural study would be necessary in order to understand fully the subtle causes of these dramatic effects.

We present here the results of neutron powder diffraction experiments from the OSIRIS instrument at the ISIS facility, introducing both some new materials and some suggestions on a possible mechanism.

1 D.A. Woodcock, P. Lightfoot, P.A. Wright, L.A. Villaescusa, M.J. Díaz-Cabañas, M.A. Camblor (1999), J. Mater. Chem, in press
2 M.P. Attfield, A.W. Sleight, (1998), Chem. Commun, 601
3 M.P. Attfield, A.W. Sleight, (1998), Chem. Mater, **10**, 2013
4 S. H. Park, R.W. Große Kunstleve, H. Graetsch, H. Gies, (1997), Studies in Surface Science and Catalysis, **105**, 1989

M09.OE.005 FIRST DETERMINATION OF ELECTROSTATIC PROPERTIES OF SYNTHETIC ZEOLITES FROM HIGH RESOLUTION X RAY DIFFRACTION. F. Porcher, M. Souhassou, Y Dusausoy, C. Lecomte N.-E. Ghermani, LCM^{3}B, CNRS UPRESA 7036, Université Henri Poincaré, Nancy 1, BP 239, Vandoeuvre lès Nancy cédex and H. Graafsma, European Synchrotron Radiation Facility, B.P. 220, 38043 Grenoble cédex

The peculiar physico-chemical properties of zeolites are based on the existence of large cavities in their structure that can lodge neutral or charged hosts molecules. The sorption properties are related to the structure of the flexible alumino-silicated framework and to the distribution of the exchangeable charge compensating cations inside the pores. Despite numerous studies, the later influence is still not well understood, mainly because the cation distributions are highly disordered and very uncertain, particularly for aluminum-rich zeolites.

As a first approximation, the interaction between cations and sorbed molecules is limited to the long range electrostatic interactions, the dispersion term being negligible for cation-sorbant distances of few angstroems. It is therefore possible to evaluate the sorption energies from the electrostatic potential of empty dehydrated zeolites. This later can be derived from the electron density distribution of the material.

Since this system is too large (~700 atoms per unit cell) for accurate ab initio calculations[1] and since molecular dynamic calculations requires empirical atomic charges, high resolution X ray diffraction is a necessary tool for the estimation of electron density and electrostatic properties that govern the sorption mechanisms in the zeolite.

In this goal, we have measured high resolution X ray diffraction data sets on dehydrated NaX[3], LiX and CaX zeolites using synchrotron radiation (λ = 0.248Å, ESRF) and a rotating anode (Mo(Kα), LCM3B): Structural, electron density and electrostatic properties derived from these experiments will be discussed.

[1] Angyan *et al*., Czechoslovak Chem. Commun., 1988, **53**, 2308
[2] Preuss *et al*., J. Phys. Chem., 1985, **89**, 2955
[3] Porcher *et al*., European Journal of Mineralogy, 1999, **00**

P09.OE.002 NEW INORGANIC-ORGANIC OPEN FRAMEWORKS. Z. A. D. Lethbridge and P. Lightfoot, School of Chemistry, University of St Andrews, Purdie Building, North Haugh, St Andrews, Fife, KY16 9ST, UK.

Inorganic open frameworks such as zeolites and aluminophosphates are well known. Non-tetrahedral metal structures have also been synthesised, for example the iron phosphate $[H_3N(CH_2)_3NH_3]_2[Fe_4(OH)_3(HPO_4)_2(PO_4)_3]$ [1]. Metal organic frameworks are another expanding family of materials, containing metal atoms bridged by organic ligands. These are usually rigid oxygen or nitrogen donors, as in the material reported by Yaghi et. al. $Co(C_6H_3(COO)_3)(NC_5H_5)_2.2/3NC_5H_5$ [2].

Here, we report results of our work, which aims to synthesise frameworks containing both inorganic and organic anions. It is hoped that these hybrid materials will combine the thermal stability of inorganic frameworks with the wide structural diversity of organic materials. We have made use of phosphate anions, and organics such as dicarboxylic acids, bipyridyl and pyrazine.

K.-H. Lii & Y.-F. Huang (1997), J. Chem. Soc. Chem. Commun., 839-840.
O. M. Yaghi, G. Li & H. Li (1995) Nature, **378**, 703-706.

P09.OE.003 STABLE CRYSTALLINE MICROPOROUS SOLIDS FROM LINKED METAL BORATE CLUSTER ASSEMBLIES. Ian D. Williams, Herman H-Y. Sung, Alvin Siu and Mingmei Wu, Dept of Chemistry, Hong Kong University of Science and Technology, Clear Water Bay, Hong Kong, China.

The development of hydrothermal and molten boric acid flux syntheses of metalloborates, especially vanadoborate clusters [1] has now been extended to heterometallic borate compounds yielding novel stable microporous compounds.

The mixed-valence cluster $[V_{12}B_{18}O_{60}H_6]^{10-}$ can be formed hydrothermally from V_2O_5, borax and ethylenediamine (en), as its water soluble Na salt, which allows for cation exchange. From this, the formation of neutral expanded 'super clusters' $[V_{12}B_{18}O_{60}H_6\{M(en)_2\}_6]$ is possible for M = Zn, Ni, and Co. Modified hydrothermal synthesis with $Zn(OAc)_2$ also allows preparation of the green tetragonal phase (a = 17.147(3), c =20.329(4)Å) This has an open 2-D polymer network containing $[Zn_4V_{10}B_{28}]$ cluster units. These incorporate Zn atoms within the cluster skeleton which assist formation of 10-membered vanadyl rings. The clusters are connected through additional $Zn(en)_2$ bridges which ligate via cluster V=O groups.

By contrast addition of $Cd(OAc)_2$ to the hydrothermal reaction mixture can result in formation of stable microporous compounds with 3-D interpenetrating channels. A body centred cubic phase $[V_{12}B_{18}O_{60}H_6\{Cd(en)(H_2O)\}_3]$ with 6Å channels has been characterized (space group Ia-3d, a = 31.972(3)Å). In this the Cd atoms form cross-links between clusters by chelate attachment to cluster O-B-O groups. A second cubic phase of space group Pn-3 (no previous examples in CSD) and a = 19.100(3)Å has been prepared in good yield and purity. This is isomeric to the body-centered compound and also has a similar open network of 3-D intersecting channels. It has been studied by high T single crystal diffractometry and shown to retain its crystallinity even after water loss and heating up to 300°C. Further results on the surface area studies, sorption and magnetic properties of these novel linked cluster materials will be presented.

[1] I.D.Williams, H.H-Y.Sung, M.Wu, X.X.Zhang and J.Yu, Chem. Commun., (1998) 2463.

09OF POLYMORPHISM AND ISOMORPHISM (sponsored by Bruker AXS)

M09.OF.001 POLYMORPHISM AND ITS RELATION TO ISOSTRUCTURALITY. Alajos Kálmán and László Fábián, Institute of Chemistry, Chemical Research Center, Hungarian Academy of Sciences, Budapest, P.O.Box 17., H-1525, Hungary

Since the structure determinations of the *reappearing* low melting (358K) dimorph of 1,2,3,5-tetra-*O*-acetyl-β-D-ribofuranose [1], the anhydrous form of sulfaguanidine [2] and the recognition of isostructurality shown by digirezigenin [3] and several digitoxigenin derivatives [4] along with the plethora of related papers in the literature, we have become more and more convinced that similar molecules can have dissimilar crystal structures and that dissimilar molecules can have similar structures. A connection between *polymorphism* and the less common crystal *isostructurality* was exemplified first by a group of paradisubstituted benzylideneanilines [4,5].

Further examples: (*A*) While 5-methoxysulfadiazine exhibits a wide range of polymorphism its clathrates built up with (a) dioxane, (b) tetrahydrofuran and (c) chloroform are isostructural [6]. (*B*) Novel inclusion compounds formed by a Pietfort-type host compound 2,4,6-tris-(3,5-di-*t*-butylphenoxy)-1,3,5-triazine were found recently [7] to exhibit isostructurality, polymorphism and pseudopolymorphism, as well. Details of these investigations compared with others are discussed.

Sponsor: The Hungarian Research Fund, Grant No. OTKA T023212.

1. M. Czugler, A. Kálmán, J. Kovács & I. Pintér (1981). *Acta Cryst.* B**37,** 172- 177.
2. A. Kálmán, M. Czugler & Gy. Argay (1981). *Acta Cryst.* B**37,** :868-877.
3. A. Kálmán, Gy. Argay, B. Ribár, S. Vladimirov & D. Zivanov-Stakic (1984). *Croat. Chem. Acta,* **57**, 519-528.
4. A. Kálmán, L. Párkányi & Gy. Argay (1993). *Acta Cryst.* B**49,** 1039-1049.
5. I. Bar & J. Bernstein (1987). *Tetrahedron,* **43**, 1299-1305.

6. M. R. Caira & R. Mohamed (1993). *Supramolec. Chem.* **2**, 201-207.
7. L. Fábián, P. Bombicz, M. Czugler, A. Kálmán, E. Weber & M. Hecker (1999). *Chem. Eur. J.* in preparation.

M09.OF.002 POLYMORPHISM AND DISORDER. T.R. Welberry, Research School of Chemistry, A.N.U, Canberra, ACT 0200, Australia

The energy difference between different polymorphs for organic crystals is estimated to be of the same order of magnitude as the energy for torsional conformation parameters in many organic molecules, so that it is often found that molecules with torsional degrees of freedom may adopt different conformations in different polymorphs. Similarly, many examples of disordered crystals occur in which, to a first approximation, a given (rigid) molecule exists in either of two different orientations within a particular molecular site, and the energy difference between these possibilities is also of a comparable magnitude. In order to understand the relationship between disorder, molecular conformation and polymorphism a very detailed analysis of the crystal structure is required.

Analysis of disordered systems by conventional crystal structure determination using Bragg reflections may reveal the average molecular site in sufficient detail that the two different molecular orientations can be distinguished. However, even if this is the case, this is an incomplete picture of what is going on in the crystal, and in order to make predictions about the relative stability of different polymorphs, a detailed local structural picture is paramount. Such information cannot be obtained from the Bragg experiment but it is obtainable from diffuse scattering experiments [1]. In this paper we outline the methods that may be used to obtain this information.

The methodology is illustrated with reference to the systems p-chloro-N-(p-methylbenzylidine)aniline, $C_{14}H_{12}ClN$ (MeCl), and p-methyl-N-(p-chloro-benzylidine)aniline, $C_{14}H_{12}ClN$ (ClMe). These compounds are just two examples from a number of parasubstituted benzylidene anilines that have been of interest to theoretical chemists studying the way in which shape and conformation influences the crystal structure of a compound [2].

[1] T.R.Welberry & B.D. Butler (1994), J. Appl. Cryst., 27, 205-231.
[2] I.Bar & J.Bernstein (1983), Acta. Cryst., B39, 266-272.

M09.OF.003 POLYMORPHS OF BENZFURAZAN-1-OXIDES AND THEIR ISOMORPHISM (SOMETIMES) WITH PHTHALIC ANHYDRIDES. Doyle Britton, W. E. Noland, M. Pinnow [1], C. R. Ojala [2], W. H. Ojala [3], J. Z. Gougoutas [4], [1] Department of Chemistry, University on Minnesota, Minneapolis, MN 55405, [2] Department of Chemistry, Normandale Community College, Bloomington, MN 55431, [3] Department of Chemistry, University of St. Thomas, St. Paul, MN 55105, [4] The Bristol-Myers Squibb Pharmaceutical Research Institute, P.O. Box 4000, Princeton, NJ 08543

5,6-Dichlorobenzfurazan-1-oxide (CBF) forms three polymorphs at ordinary temperatures. All three involve disorder across a two-fold or pseudo-two-fold axis. 4,5-Dichlorophthalic anhydride (CPA) is isosteric with the disordered CBF and forms crystals that are isomorphous to CBF polymorph A. Polymorph C contains two-dimensional layers that are similar to those in A but that stack differently. 4,5-dibromophthalic anhydride is not isomorphous with CPA but again contains two-dimensional layers that are similar to those in CPA but that stack differently. 5-Chlorobenzfurazan-1-oxide is actually a disordered mixture of the 5- and 6-chloro isomers at all accessible temperatures. The analogous 5-bromobenzfurazan-1-oxide is isomorphous with the same disorder at room temperature but forms an ordered polymorph a low temperature. In spite of the molecular isomerization during the transformation, a single crystal of one form transforms to a single crystal of the other.

M09.OF.004 COLOR POLYMORPHISM. J.-O. Henck, Universität Innsbruck, Institut für Pharmakognosie, Josef-Moeller-Haus, Innrain 52, A-6020 Innsbruck, Austria**,** J. Bernstein and A. Ellern, Ben-Gurion University of the Negev, Department of Chemistry, P.O.Box 653, Beer-Sheva 84105, Israel

What are the major scientific questions facing researchers in polymorphism? First, although the appearance of a new polymorphic structure in any particular system is no longer a surprise, the *a priori* prediction of the existence of polymorphism or any particular crystal structure is still essentially beyond our ability. Secondly, even assuming that a specific system might be predicted to be polymorphic, there are no prescriptions for preparing those polymorphic structures that could be expected. Third, even supposing that we know how to prepare predicted polymorphic forms there is almost no way of predicting the properties they would have.

Polymorphism means variety in structure, and since variety in structure implies variety in properties, those whose research deals with polymorphism are practitioners in a wide variety of techniques and disciplines. The ability to characterize and obtain a particular preferred polymorph can determine the success or failure of a product. Such considerations are an increasingly important factor in industrial development and production of new materials, from e.g. pigments to pharmaceuticals. One of the latest published dramatic examples is the case of Norvir (the protease inhibitor ritonavir) [1].

The color and properties of solid pigments and dyes also depend on their crystal structure. Different polymorphs of such materials can have different colors [2]; thus they are excellent systems for investigating structure-property relationships. In 1910 Hantzsch [3] described a series of mono-, di- and trinitroaniline derivatives showing color polymorphism ("Chromoisomerie"). In this contribution we will present the thermodynamic and structural relationships among the phases of a number of compounds exhibiting color polymorphism.

1. http://www.iapac.org/norvir/description.html
2. J. Bernstein, R. Davey and J.-O. Henck, Angew. Chem., (accepted)
3. A. Hantzsch, Ber. Deutsch. Chem. Ges. 43, 1665 (1910).

M09.OF.005 POLYMORPHISM IN 2,6-DIHYDROXYBENZOIC ACID : OSTWALD'S RULE, SOLVENT EFFECTS AND MOLECULAR SELF ASSEMBLY. R. J. Davey, H. Alison, N. Blagden, and S. Fuller, Colloids, Crystals and Interfaces Group, Department of Chemical Engineering, UMIST, Manchester M60 1QD, UK.

The impact of the solvent on the polymorphic outcome of crystallisation from solution is well known[1] but poorly understood. At the same time the process of crystallisation from solution is a key experimental feature of many aspects of crystal engineering as practised both academically and industrially in the pharmaceutical and specialty chemicals sectors.

The work reported here focuses on a particular material, 2,6-dihydroxybenzoic acid, which is known to be polymorphic with forms 1 and 2 having been grown for crystallographic studies from toluene and chloroform respectively[2,3]. Structurally the two polymorphs exhibit different hydrogen bonding networks: in form 1 molecules pack as H-bonded dimers while in the non-centric form 2 they form infinite H-bonded chains. One of the objectives of this study has been to understand the role of the solvent in determining the polymorphic outcome of different crystallisation strategies. Firstly thermodynamic data concerning the thermochemistry and solubility of the two polymorphs will be

presented. This is complemented by spectroscopic data and MOPAC calculations aimed at exploring possible modes of molecular self assembly in solution. Finally crystallographic data is used to assess the likely impact of the solvent on the competing processes of nucleation and crystal growth from the two solvents. Overall the study demonstrates the importance of combining crystallographic data with other sources of information in order to understand a process as complex as crystallisation in a polymorphic system.

M09.OF.006 SOME INTERESTING POLYMORPHS I HAVE KNOWN. Walter C. McCrone, McCrone Research Institute, Chicago, IL USA

I will select several unusual polymorph systems from pharaceutical companies who look for thermodynamically unstable crystal forms to achieve higher solubility and from those who produce and use explosives who want the most stable forms to be assured of a safe high density product.

P09.OF.001 DISAPPEARING POLYMORPHS AND THE ROLE OF IMPURITIES AND REACTION BY-PRODUCTS. N. Blagden, R.J. Davey, Colloids, Crystals and Interfaces Group, Department of Chemical Engineering, UMIST, PO Box 88, Manchester M60 1QD, UK.

The phenomenon of polymorphism, whereby a molecule can adopt more than one crystal structure is well known in crystal chemistry In terms of developing a robust process for isolating polymorphic materials a purely structural approach is limited since it neglects the role of kinetics in determining the appearance of polymorphic structures. This was recognised by Ostwald (1899) in his famous Rule of Stages. This situation is highlighted by the issue of so called 'disappearing polymorphs' i.e. the sudden appearance of a new structure or the unexplained disappearance of an existing one. The role of additives and reaction by-products in controlling polymorph appearance in this context will be discussed. A combined modelling and experimental strategy has been applied to the problem of impurity and reaction by-product influence on the appearance of polymorphs from solution. Two examples will be discussed. **Case (I)**, from a pure aqueous solution of sulphathiazole after 24 hrs at 25 ^{o}C the most stable phase, form IV of sulphathiazole was isolated. This work shows for the first time that a reaction by-product, ethamidosulphathiazole, from the final hydrolysis stage at concentrations as low as 1 mol % stabilises the metastable modification, form I. The role of the impurity was accounted for from an analysis of the respective hydrogen bond networks and crystal morphologies of each phase. **Case (II),** trimesic acid at 1 mol % is capable of stabilising the meta stable form of glutamic acid from solution for one week, thermostated at 40 ^{O}C. This contrast with a pure aqueous suspension which transform in under half an hour. The trimesic acid was shown to mimic the conformation of glutamic acid in the stable β form and thus disrupts the transformation from the metastable α from, this was accounted for through growth inhibition of the fastest growing faces of the stable β form.

P09.OF.002 PHASE TRANSITION BY GRINDING OF SALICYLIDENEBENZYLAMINES. REMARK-ABLE CHANGE IN THE CHROMIC BEHAVIOR. Shiori Yoshida, Koki Takasawa, Toshikatsu Fujiwara and Keiichiro Ogawa, Department of Chemistry, Graduate School of Arts and Sciences, The University of Tokyo, Komaba, Meguro-ku, Tokyo, 153-8902 Japan

Salicylideneanilines belong to a class of the most popular compounds indicating thermo- or photochromism. These phenomena, which are ascribed to tautomerism, are known to be mutually exclusive. However, some derivatives of *N*-salicylidenebenzylamine, which has a methylene group inserted between C=N and the phenyl group, are known to be both thermo- and photochromic. *N*-(2-hydroxy-4-methoxybenzylidene)benzyl-amine (**1**) is one of such compounds reported by Hadjoudis *et al* [1]. We report here a remarkable difference in chromic behavior and the phase transition between polymorphic forms of **1**.

The crystalline film which was prepared from the melt (form I) showed thermochromism and photochromism. The crystals that recrystallized from ether solution (form II) did not show either thermo- or photochromism. The X-ray powder patterns of the both forms were, however, identical. The facts indicate that a phase transition from the form I to II takes place on grinding.

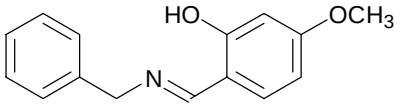

1

1. E. Lambi, D. Gegiou & E. Hadjoudis (1994). J. Photochem. Photobiol. A: Chem., 86, 241-246.

09AA WHY LOW RESOLUTION? METHODS AND OUTCOMES

M09.AA.001 LOW RESOLUTION PHASING. ACHIEVEMENTS AND PERSPECTIVES. V.Y.Lunin, Institute of Mathematical Problems of Biology RAS, Pushchino, Moscow region, 142292 Russia, and A.G.Urzhumtsev, LCM^{3}B, Faculté des Sciences, Université Henri Poincaré, Nancy I, 54506, Vandoeuvre-lès-Nancy, France and A.D.Podjarny, UPR de Biologie Structurale, IGBMC, BP 163, 67404 Illkirch CEDEX, CU de Strasbourg, France.

Until the last decade, the low resolution (LR) reflections were traditionally neglected due to experimental and modeling problems. However, phasing the LR data is important for a number of cases, especially when the LR image has valuable information in itself (e.g., the ribosome); crystals do not diffract to high resolution; a LR cut-off causes large image distortions; molecules are a mixture of ordered and disordered regions *etc*. Furthermore, the knowledge of LR phases or a molecular envelope may be useful (and sometimes necessary) to enhance the possibility of direct methods. The traditional experimental approaches to phasing macromolecular data may be applied to LR reflections to some extent only, making it necessary to develop direct LR phasing methods. When phases of middle and/or high resolution reflections are available, those of LR reflections (and partially, magnitudes) may be estimated from these data. In the other case *ab-initio* phasing procedures must be applied.

The main problem in LR *ab-initio* phasing is that all suggested figures of merit FOM) for LR phase sets have the same features, unfavorable for phasing:

- the best value of FOM may be coupled with a wrong phase set;
- the FOM corresponding to the true phases may be relatively low;
- the local phase refinement may result in high FOMs without any phase improvement.

The cluster analysis methods and several suggested procedures of best cluster choice, adapted to this problem, allow to overcome the problem to some extent.

M09.AA.002 *AB INITIO* PHASING OF LOW RESOLUTION DATA. David A. Langs, Hauptman-Woodward Medical Research Institute, Inc., 73 High Street, Buffalo, NY, 14203, U.S.A.

There are a number of necessary conditions to be met in devising a plan to phase low resolution data by *ab initio* direct methods. Firstly, one must find reliable real & reciprocal space figures of merit that are optimal for the correct phases and significantly worse for all other values of the phases. This implies the true values of the phases would be stable toward further optimization of the FOM's. It would also be desirable that these properties would hold if the data set were reduced to a smaller fraction which included just the largest structure factor amplitudes. This might make the sampling of plausible random phase trials more efficient. Secondly, one would have to devise a strategy by which the phases can be reliably refined to optimize the FOM values in an efficient manner. Finally it would necessary to show that low resolution solutions can be obtained from some of the random phase starting sets if we are persistent.

Perhaps it may be possible to achieve all these things without consciously thinking of such things as structural models, solvent flatting, histogram fitting, phase invariants, density modification, entropy and likelihood.

Research support from NIH grant GM-46733 is gratefully acknowledged.

M09.AA.003 SOLVENT MODELLING AT LOW RESOLUION. A.G.Urzhumtsev, LCM3B, UPRESA 7036 CNRS, Université Henri Poincaré – Nancy 1, B.P. 239, 54506 Vandoeuvre-les-Nancy.

The voids between macromolecules in a crystal are filled by smaller molecules, many of those placed differently in different unit cells. This disorder in space as well as in time gives en effect of the "disordered solvent": a specific contribution to the diffraction intensities, important at the resolution of about 5-6Å and lower, which should be modelled together with the macromolecule itself. Even more, this solvent modelling should be done *before* the construction of an atomic model, as early as the envelope is known, to reduce the errors in the electron density maps.

The first idea to model the bulk solvent contribution is to calculate structure factors from the *flat solvent region* and to choose the optimal scale factors for them to minimise the discrepancy between experimental amplitudes and the ones calculated from an available atomic model plus solvent [1]. This approach was further developed and modified by several researchers. An alternative approach is to model the solvent density distribution as a function of the distance $\boldsymbol{D}$ to the molecular envelope [2].

The points, equidistant to the envelope can be, nevertheless, in quite different conditions, in cavities or at convexities, which can be distinguished when the envelope is calculated at different resolutions. Typical 2D histograms of the couples {ρ-value, $\boldsymbol{D}$}, corresponding to the *set of envelopes* calculated at different resolutions, can be *used together* to estimate the density value at a given point. A more direct modelling of the bulk solvent needs to simulate the space disorder among *different cells*. It can be replaced by the generation of *many* models identical in all cells and by averaging structure factors over *all generated models*. This can bring an alternative information to model the solvent contribution.

1. S.E.V. Philips (1980) *J.Mol.Biol*., **142**, 531-554.
2. B.P. Schoenborn (1988) *J.Mol.Biol*., **201**, 741-749.

M09.AA.004 PSEUDOATOM GLOBS AND DIRECT PHASE DETERMINATION - RUBREDOXIN AT 6 Å RESOLUTION. Mary P. McCourt, Douglas L. Dorset, Electron Diffraction Department, Hautpman-Woodward Medical Research Institute, 73 High Street, Buffalo, NY 14203-1196 USA.

The re-scaled pseudoatom scattering factor approximation to the Fourier transform of globular density units has been very useful for the low- resolution direct phase analysis of integral membrane proteins with high alpha-helix content (using electron diffraction amplitudes). For a 3-D application, the crystal structure of rubredoxin was determined from experimental x-ray data by direct methods at 6 Å resolution. The Sayre equation expanded a relatively small basis set and screening criteria, such as density flatness and the Patterson correlation coefficient, selected the best of several possible solutions. In the two-dimensional determination, principal peak positions were located in the maps, giving a mean phase error of 58 deg. for all 17 hk0 reflections after two cycles of Fourier refinement. In the three-dimensional determination, the initial phase set could be compared to the original x-ray model as a mean deviation of 85 deg for all 127 hkl reflections but only 54 deg. for the 23 most intense maxima. Refinement improved the overall fit (mean error: 77 deg. but only 62 deg. for the 23 most intense reflections). Because the phase value of the strongest reflection was greatly improved, the electron density map was closer to that of the actual structure. However, assumption of globular substructure causes the 3-D density map to become discontinuous. The success of this phasing attempt is quite surprising for an example where the solvent space contains a high concentration of ammonium sulfate, where the contrast at low resolution should be reversed. On the other hand, simulations of 'missing cone' problems with this protein model revealed the same accuracy for predicting missing phase information, irrespective of whether the observed or calculated x-ray amplitudes were used for expanding the basis set.

Supported by NIH GM-46733.

M09.AA.005 VERY LOW RESOLUTION PHASING OF RIBOSOMAL PARTICLES USING MOLECULAR REPLACEMENT WITH MODELS FROM EM. I. Agmon, Weizmann Institute, Rehovot, Israel; A. Tocilj and A. Yonath, Weizmann Institute, Rehovot, Israel and MPG, Hamburg, Germany

The ribosome is the universal cell organelle which plays an essential role in protein biosynthesis; it catalyzes the translation of genetic information encoded in mRNA into proteins. The elucidation of the ribosome structure, which is a prerequisite for understanding the molecular mechanism of protein biosynthesis, is therefore of great interest.

The packing schemes of the whole 70S ribosome and the large subunit (50S) from Thermus Thermophilus were determined at very low resolution using molecular replacement, with 3D cryo EM reconstructions serving as models. The applicability of such a procedure for correctly placing particles lacking internal symmetry in their crystallographic cells, was shown by Urzhumtzev & Podjarny [1].

The MR searches gave a single well contrasted solution for each of the particles, which permitted the determination of their position and orientation in the unit cells, followed by the assembling of very low resolution maps.

Several types of verification tests were performed, all found to support the MR results. These include: 1. packing examination; 2. scaling Fc from the suggested structures to Fobs; 3. using calculated phases to locate heavy atom sites (T50S); 4. comparing a projection of the suggested packing to that observed previously in electron micrographs of thin sections of crystals (T70S).

1. Urzhumtzev, A., Podjarny, A. (1995) Acta Cryst. D51, 888-895.

P09.AA.001 THE CONNECTIVITY-BASED CHOICE IN MACROMOLECULAR LOW RESOLUTION AB-INITIO PHASING. N.L.Lunina and V.Y.Lunin, Institute of Mathematical Problems of Biology RAS, Pushchino, Moscow region, 142292 Russia and A.G.Urzhumtsev, LCM^{3}B, Faculté des Sciences, Université Henri Poincaré, Nancy I, 54506, Vandoeuvre-lès-Nancy, France.

The known figures of merit (FOM) do not allow usually, to make unambiguous choice of the best phase set when applied in a restricted low-resolution (LR) zone. Nevertheless, when coupled with cluster analysis methods they allow to reduce the phase problem to the problem of the choice among a relatively small number of alternative phase sets [1]. The connectivity features may be used as an additional criterion to perform this choice. The idea to use the number of connected components in the region of high electron density values as a FOM was suggested first [2] for middle and high resolution syntheses. It is expected at these resolutions to have the minimal possible number of connected components for well phased syntheses and multiple "drops" for the badly-phased ones. On contrary, LR poorly phased syntheses show rather merged molecular images than multiple drops and the region of high density at a good LR synthesis usually contains as many equal connected images as the number of molecules in the unit cell is. The minimal possible cut-off level in a Fourier synthesis, still resulting in the desired number of connected components, may be used as a selection criterion in LR ab-initio phasing. A special modification of LR syntheses can be applied in some cases to make them more suitable for the application of this criterion [3].

1. V.Y.Lunin, N.L.Lunina, T.E.Petrova, A.G.Urzhumtsev & A.D.Podjarny (1998). Acta Cryst., D**54**, 726-734.
2. D.Baker, A.E.Krukowski & D.A.Agard (1993). Acta Cryst. D**49**, 186-192.
3. V.Y.Lunin, N.L.Lunina & A.G.Urzhumtsev (1998). Acta Cryst. A, submitted.

P09.AA.002 AB INITIO PHASING USING MOLECULAR ENVELOPE FROM X-RAY SOLUTION SCATTERING. Q. Hao, De Montfort University, Leicester, LE1 9BH, UK, F. E. Dodd, J. G. Grossmann and S.S. Hasnain, CLRC Daresbury Laboratory, Warrington, WA4 4AD, UK.

A method for macromolecular structure determination is presented which utilizes the low resolution molecular shape obtained from solution X-ray scattering data. The molecular shape of a protein is an important structural property and can be determined directly by the small angle scattering technique. The idea of locating this molecular shape in the crystallographic unit cell has been tested with experimental diffraction data from nitrite reductase (NiR) [1]. The conventional Patterson search [2] proved to be unsuccessful as the intra-envelope vectors are uniformly distributed and do not match those of intra-molecular (atom to atom) vectors. A direct real space search for orientation and translation was then performed. A self rotation function using 2.8Å crystallographic data yielded polar angles of the non-crystallographic three-fold axis. The knowledge of the orientation of this axis has reduced the potential 6-dimensional search to 4 (Eulerian angle γ and three translational parameters). The direct 4-dimensional search within the unit cell has produced a clear solution. The electron density map based on this solution agrees well with the known structure and the phase error calculated from the map was 61 degrees within 20Å resolution. It is anticipated that the low resolution envelope can be used as a starting model for phase extension by the maximum entropy and density modification method.

1. Q. Hao, F. E. Dodd, J. G. Grossmann & S. S. Hasnain (1999), *Acta Cryst*. **D55**, 243-246.
2. Collaborative Computing Project, Number 4 (1994), *Acta Cryst*. D50, 760-763.

09BB MOLECULAR BASIS OF DISEASE AND TOXICITY

M09.BB.001 STRUCTURAL STUDIES ON HIV-1 CORE PROTEINS. Christopher P. Hill, Biochemistry Department, University of Utah School of Medicine, 50 N. Medical Drive, Salt Lake City, UT 84132, USA.

Retroviruses, such as HIV-1, assemble into virions comprised primarily of the Gag protein. Cleavage of Gag into its constituent domains of matrix (MA), capsid (CA), and nucleocapsid (NC) proteins, is performed by the viral protease, and serves to signal for a dramatic rearrangement of the viral core that is known as maturation.

The viral MA protein serves as the membrane-binding domain of Gag and remains associated with the membrane following maturation. We have determined the X-ray crystal structure of HIV-1 MA. This reveals a trimeric association that is conserved in three different crystal forms and in the crystal structure of the protein from SIV. Mutagenic data suggest that the crystallographic trimer is biologically relevant and indicates the likely membrane-binding surface.

The HIV-1 CA protein forms an essential interaction with the cellular protein cyclophilin A (CypA). We have determined the crystal structure of a complex between the CA N-terminal domain and CypA. This result suggests that CypA may function as a sequence specific binding protein, although the basis of HIV-1's requirement for CypA remains unclear. We have also determined the crystal structure of the CA C-terminal domain, which is the dimerization domain of full-length CA. This structure reveals the dimerization interface and provides a model for the full-length protein. A combination of the high-resolution crystal structures with cryo electron microscopic analysis of capsid assemblies provides a model for the cone-shaped core of mature infectious virions.

M09.BB.002 CRYSTALLOGRAPHIC STUDIES OF THE ANTHRAX LETHAL TOXIN. Robert Liddington, Biochemistry Department, University of Leicester, U.K. New address from 10/99: The Burnham Institute, 10901 North Torrey Pines Rd., La Jolla, CA 02037 USA.

Anthrax is probably best known as an agent of biological warfare, but the toxin produced by anthrax is also being developed for medical use as a protein delivery system that could deliver useful proteins into cells. Anthrax Toxin comprises two distinct proteins: the so-called Protective Antigen (M.W. 83 kDa), named for its use in vaccines; and the Lethal Factor (M.W. 87 kDa), a metalloprotease whose target is currently under investigation [1]. The two proteins are harmless by themselves, but in combination they kill their host by invading macrophages and overstimulating the immune response, leading to death by toxic shock. We have recently determined the crystal structure of the 735-residue Protective Antigen in its monomeric form as well as the membrane-inserting heptamer (M.W. 440 kDa) that is produced following activation on the host cell surface [2]. We have recently made substantial progress in the structure determination of Lethal Factor, and this will be presented. Heptameric PA binds tightly to Lethal Factor; the complex is endocytosed, and acidification of the endosome triggers membrane insertion and translocation of the Lethal Factor into the cytosol. The structural information is now being used in the design of experiments that will elucidate how these steps are achieved at the atomic level [3].

1. Duesbery, N.S. et al., & Vande Woude, G.F.“ Proteolytic inactivation of MAP-kinase-konase by anthrax lehtal factor” Science 280: 734-737 (1998)
2. Petosa, C, Collier RJ, Klimpel KR, Leppla SH, Liddington RC. “Crystal structure of the anthrax toxin protective antigen” *Nature* 385, 833-838 (1997).
3. Benson, EL, Huynh PD, Finkelstein A, Collier RJ. Identification of residues lining the anthrax protective antigen channel. *Biochemistry* 37, 3941-3948 (1998).

M09.BB.003 STRUCTURE OF A THIOL-ACTIVATED CYTOLYSIN AND A MODEL OF ITS MEMBRANE FORM. J. Rossjohn, S.C. Feil, W.J. McKinstry, R.K. Tweten & M.W. Parker. The Ian Potter Foundation Protein Crystallography Laboratory, St. Vincent’s Institute of Medical Research, 41 Victoria Parade, Fitzroy, Victoria 3065, Australia. Dept. of Microbiology and Immunology, The University of Oklahoma Health Sciences Center, Oklahoma City, Oklahoma 73190, USA.

The mechanism of protein insertion into membranes has generated biological interest. The thiol-activated cytolysins (TACs) are pore-forming toxins that are secreted by taxanomically diverse species of gram-positive bacteria which in turn are responsible for life-threatening infections. To date, more than 20 members have been characterized, including perfringolysin O (PFO) from *Clostridium perfringens*, pneumolysin from *Streptococcus pneumoniae* and listeriolysin O from *Listeria monocytogenes*. Each toxin consists of a single polypeptide chain with molecular weights ranging from 50kDa to 80kDa. The sequence identity amongst the family is high (40 to 70%) suggesting they will all have very similar three-dimensional structures. There is nothing in the primary structures of the TACs to explain how the toxins can insert into membranes to form pores. The longest stretch of sequence identity between the toxins is a C-terminal conserved tryptophan rich sequence (the Trp-rich motif) 458 ECTGLAWEWWR) 468 (PFO numbering). This Trp-rich motif is implicated in binding to the receptor, cholesterol. The toxins share a common mode of action in killing eukaryotic cells: they interact with the target cells via the receptor, cholesterol, which is followed by oligomerization and membrane insertion. This integration into the membrane results in the formation of large oligomeric pores, with diameters exceeding 150Å, causing cell lysis. The structure of PFO was solved by the MIR method. Here I present the 2.2Å crystal structure of PFO, an unusually elongated rod-shaped molecule of dimensions 115Å x 55Å x 30Å, rich in β-sheet. The data presented reveals how the toxin changes from a completely water-soluble protein to a membrane pore.

M09.BB.004 A KEY ENZYME IN INFLAMMATION WITH A BIFUNCTIONAL ACTIVE SITE: LEUKOTRIENE A_4 HYDROLASE AT 1.95 Å RESOLUTION. Marjolein Thunnissen[1], Pär Nordlund[1] & Jesper Haeggström[2]. [1]Department of Biochemistry, University of Stockholm, Arrhenius laboratories A4, S -106 91Stockholm, Sweden: [2]Department of Medical Biochemistry & Biophysics, Karolinska Institute, S-171 77 Stockholm, Sweden.

The eicosanoids (prostaglandins, thromboxanes and leukotrienes) have been shown to play a role in many processes such as inflammation, hypersensitivity and allergic reactions, in diseases such as asthma and arthritis. The potent chemotactic leukotriene B_4 is formed from arachidonic acid via the sequential action of two enzymes: 5-lipoxygenase catalyzes the formation of the epoxide intermediate LTA_4 which is in turn converted into LTB_4 by the enzyme LTA4 hydrolase. In addition to its epoxide hydrolase activity, LTA_4 hydrolase also possesses peptidase/amidase activity towards synthetic substrates. Site directed mutagenesis studies have shown that His295, His299 and Glu318 are Zn binding ligands and that Glu296 is the catalytic amino-acid for the peptidase activity, for which a general base mechanism has been proposed. Much less is known about the epoxide hydrolase activity, although mutations at positions 296 and 383 showed that these residues are not essential. Combined with the fact that the Zn^{2+} ion is essential for both reactions, it appears that the active sites are not identical but rather overlapping. In view of the potential importance of LTA_4 hydrolase as a target for the treatment of inflammatory diseases, novel selective inhibitors have been developed based on substrate mediated inactivation of the enzyme. With the help of structural information, these compounds might be used as lead compounds and ultimately be developed into novel anti-inflammatory drugs.

We have recently solved the crystal structure of human LTA_4 hydrolase complexed with the transition analogue bestatin at 1.95Å resolution. The structure of the 69 KDa protein was determined by MAD methods and is currently being refined. The protein is folded into three domains: N-terminal, catalytic and a C-terminal domain which together form a flat triangular arrangement. Between the domains a deep cleft is formed in which the Zn^{2+} binding site is located. The N-terminal domain has structural homology with bacteriochlorophyll *a,* while the catalytic domain has surprising structural similarity to thermolysin, although sequence identity is minimal. The structure provides the basis for understanding substrate binding, the molecular mechanisms of catalysis, the manner in which the two catalytic functions are organised and the basis for suicide inactivation. Based on the structure we can propose a putative LTA_4 binding site and reaction mechanisms for both the epoxide reaction as well as for the peptidase activity.

M09.BB.005 THE ADENOVIRUS FIBRE SHAFT FOLD, A TRIPLE BETA-SPIRAL. M.J. van Raaij, N. Cohet, S. Cusack [1], G. Lavigne, A. Mitraki [2], [1] EMBL Grenoble outstation, 9 rue Jules Horowitz, 38000 Grenoble, France, [2] Institut de Biologie Structurale, Grenoble, France

Adenovirus binds to its host cells via its trimeric fibre protein. The serotype 2 fibre protein contains three domains: a small N-terminal viral anchor sequence, a long thin shaft containing a 21-fold repeating sequence and a C-terminal cell attachment domain, of which the structure is known. It is of prime interest for gene therapy. We have now solved the atomic structure of the of four of the 21 repeats at 2.4 Å resolution. The shaft repeats contain a striking hitherto unknown fold composed of beta- strands, which allows us to explain its extra-ordinary stability. This fold may have homology in the bacteriophage T4 tail fibre and certain insect silks.

M09.BB.006 CONFORMATIONAL DISEASE : SERPINS AS A MODEL FOR PRION AND OTHER DEMENTIAS. R.W. Carrell, P.E. Stein and D.A. Lomas, Structural Medicine, Dept. of Haematology, University of Cambridge, Cambridge Institute for Medical Research, Hills Road, Cambridge CB2 2XY, UK.

The serpins provide a model for other protein families that have similar inherent ability to change fold. Such transitions however involve risks, as their aberrant occurrence can result in intermolecular linkages with consequent tissue deposition and disease. There is now great interest in such conformational diseases which include the perplexing neurodegenerative disorders; Alzheimer’s dementia and the prion encephalopathies. A series of crystallographic studies of the serpins illustrates the structural diversity of the molecular associations potentially involved : from dimerisation and polymerisation to fully ordered amyloid-fibril formation. The exposed reactive centre loop of serpins readily takes up a ß-pleated structure to allow its insertion as an extra middle strand in the 5-stranded A ß-sheet of the molecule. Pathologically intermolecular linkage can occur from

what is in effect a domain swap, with the reactive loop of one molecule aberrantly inserting into the middle of the A-sheet of the next, to give loop-sheet polymers. But linkage can also occur by external strand addition or displacement. This latter mechanism in the serpin antithrombin demonstrates in precise structural detail the sequential changes occurring at the onset of a conformational disease, with particular relevance to current proposals for the conformational infectivity of the prion encephalopathies. The initial change in antithrombin is a monomeric transition to the inactive 6-stranded latent form, followed by a propagation of conformational change to a normal active molecule with linkage of the two and with glycoform selectivity followed by stabilisation of the complex by heparin-type GAGs. The model is validated with respect to the dementias by recent findings by colleagues (A. Shrimpton, R. Davis, P. Holohan; Syracuse New York) of mutations, in a neurone-specific serpin, present in families with inclusion-body dementias. The mutations provide a striking confirmation of proposals for a conformation-based mechanism for late-onset dementias.

P09.BB.001 THE STRUCTURE OF CLOSTRIDIUM PERFRINGENS ALPHA-TOXIN: A GANGRENEOUS TALE. C. E. Naylor, J. T. Eaton, N. Justin, D. Moss and A. K. Basak, Dept of Crystallography, Birkbeck College, Malet Street, England, WC1E 7HX and A. Howells and R. Titball, CBD, Porton Down, Salisbury, SP4 0QJ, England.

C. perfringens α-toxin is the key virulence determinant in gas-gangrene disease, and has also been implicated in a number of other diseases of man and animals. The toxin is a 370 amino acid zinc metalloenzyme which has phospholipase C, sphingomylinase and haemolytic activities. In the presence of calcium ions, α-toxin can cleave membrane packed phospholipid. Here, we present the structure of the *C. perfringens* α-toxin. It is a 2 domain structure. The N-terminal, catalytic domain (residues 1-246) shows an anticipated structural homology to the non-toxic *B. cereus* phospholipase C. Both proteins contain 3 bound zinc ions: the residues that ligate the metal ions are completely conserved between the two proteins. There are a number of structural differences between the two enzymes, however, and these will be described. The C-terminal domain (residues 255-370) is essential for membrane binding, and is associated with toxicity. This domain has a strong, structural analogy to the eukaryotic C2 domain fold. The C2 domain is normally found acting as a phospholipid and/or calcium-binding domain in intracellular second messenger proteins. This homology has been useful in defining a possible model for membrane binding, which, when compared with other, analogous, but non-toxic, phospholipases, has implicated structural features important for toxicity.

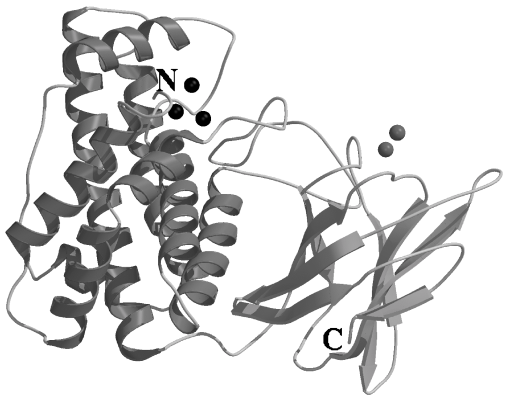

Secondary Structure Cartoon of α-toxin. Zinc ions are shown as black spheres, possible calcium binding sites are highlighted as grey spheres.

P09.BB.002 INSIGHT INTO THE CARDIOLIPIN BINDING BY HUMAN β2-GLYCOPROTEIN I, A KEY STEP IN "ANTI-PHOSPHOLIPID-SYNDROME". B.Bouma [1], J.M.H. van den Elsen [1], R-B. G. Ravelli [2], A. Schouten [1], D.A. Horbach [3], Ph.G. de Groot [3], J. Kroon [1] and P. Gros [1]. [1] Bijvoet Center for Biomolecular Research, Crystal and Structural Chemistry, Utrecht University, Padualaan 8, 3584 CH Utrecht, The Netherlands, [2] EMBL Grenoble outstation, Jean Marie BOIS, BP 156, 38042 Grenoble CEDEX 9, France, [3] Department of Haematology, University Hospital Utrecht, P.O. box 85500, 3508 GA Utrecht, The Netherlands.

The crystal structure of β2-Glycoprotein I (β2GPI), the antigen for anti-β2GPI autoantibodies, provides putative insight into the mechanism of its binding to cardiolipin, an event preceding the autoimmune response in patients with "Anti-Phospholipid-Syndrome" (APS).

The structure of the 45 kDa β2GPI has been determined by the MIR method at 2.7 Å resolution. The orthorhombic crystals contain an extremely high solvent content of 83%, and the asymmetric unit contains one protein molecule. The structure was first built at 3.75 Å using the NMR structure of Vaccinia Virus Complement Control Protein to search for the Sushi domain folding pattern. The final model consists of a.a. residues 1-309, 319-326 and sugar residues attached to four Asn residues. The protein is built up by an elongated chain of four Sushi domains and a fifth modified Sushi domain. The β2GPI-cardiolipin interaction region is located in the fifth domain and consists of a recognition loop with the motif KNKEKK, as deduced by peptide binding studies. The position of this loop and the location of other residues gives structural detail about β2GPI interaction with negatively charged phospholipids. The putative model for β2GPI in the removal of apoptotic cells is supported by this structural insight. The packing arrangement in the crystal gives information about possible β2GPI dimerization interfaces and putative antibody binding sites. The structure-function relationship with respect to APS is currently being evaluated.

P09.BB.004 STRUCTURE OF BACILLUS THURINGIENSIS D-ENDOTOXIN CRY1AC AND LOCATION OF ITS RECEPTOR BINDING SITES. J.Li, D.J.Derbyshire [1], D.J. Ellar [2]. [1] MRC Laboratory of Molacular Biology, Hills Road, Cambridge CB2 2QH, UK, [2] Biochemistry Department, Cambridge University, 80 Tennis Court Road, Cambridge CB2 1GA, UK

Cry1Ac is a pore-forming toxin specifically active against lepidopteran insects. A membrane receptor from the susceptible insects has been identified as aminopeptidase N (APN). N-acetylgalactosamine (GalNAc) was shown to be part of APN, and it competitively inhibits the binding of Cry1Ac to this receptor. We have crystallised trypsin-activated Cry1Ac from B.t. ssp. HD-73 in space group P1, with 4 molecules in a unit cell of dimensions a = 51.78Å, b = 113.23Å, c = 123.41Å, α = 113.10°, β = 91.50° and γ = 91.49°. The structure has been determined at 2.36 Å resolution by molecular replacement from Cry1Aa (PDB code 1CIY) followed by 4-fold averaging. The atomic model, comprising 4 copies of a continuous polypeptide chain between residues 33 and 611 and 591 solvent molecules, has been refined to an R-factor of 21.6% (R-free = 27.3%), with 90% of the residues in the most favoured regions of the Ramachandran plot.

In domain I (helix bundle) responsible for the pore formation, Cry1Ac is highly similar to Cry1Aa with an rms Ca distance of 0.36Å. In domain II (b-prism) they are similar over the sheets (rms Ca distance = 0.61Å), but at the apex loops 2 and 3 have distinct conformations. These localised differences correlate well with sequence exchange and mutagenesis data which implicate residues in these two loops in the initial binding to the receptor. In domain III (b-sandwich), however, striking structural differences between the two toxins are found. In

particular, Cry1Ac shows an insertion relative to Cry1Aa of six residues which form a protruding loop. The inserted sequence is unique to Cry1Ac among the Cry toxins. Exchange of a short sequence which contained the insertion loop, and mutations within this loop, have been found to reduce the specific toxicity of Cry1Ac and abolish GalNAc-dependent receptor binding. Therefore Cry1Ac possesses a second receptor binding site in the region of the domain III insertion, distant from the previously known binding site at the apex of domain II. Furthermore, the outer sheet of domain III in Cry1Ac shows a relative rotation by about 8° and a very different twist when compared with Cry1Aa. Contrasting this difference with the general conservation of domain III structure between the Lepidoptera-specific Cry1Aa and Coleoptera-specific Cry3A suggests that the additional binding site in domain III may be unique to Cry1Ac, which may account for its greater potency among the Cry toxins.

09CC HIGH PRESSURE DATA ACQUISITION AND ANALYSIS

M09.CC.001 NEW METHODS FOR INDEXING IN HIGH-PRESSURE POWDER DIFFRACTION. Scott A. Belmonte and Richard J. Nelmes, Department of Physics and Astronomy, The University of Edinburgh, Mayfield Road, Edinburgh, EH9 3JZ, U.K.

When determining structures from powders, indexing the powder pattern is the crucial first step. If a pattern cannot be indexed no further progress can be made on structure solving. Many materials are being found to have remarkably complex structures at high pressure, with quite large unit cells and many independent atomic coordinates. This complexity combined with the limited quality of the data available in high-pressure experiments make indexing many powder patterns far from trivial. In fact, in these cases, indexing is often the limiting step in the structure determination process.

With this in mind, a new, general, approach for indexing powder patterns based on whole-pattern fitting and genetic-algorithm optimisation of lattice parameters will be presented in detail. The advantages of such a method for indexing powder patterns from materials at high pressure will be discussed together with the possible limitations of the approach. Examples of the successful application of this method will be given.

A second novel technique that exploits information from a textured powder sample to aid indexing will also be described briefly [1]. It will be shown how variations in intensity around powder rings due to preferred orientation can contain information about the lattice parameters.

[1] "TEXTURE AS AN AID TO INDEXING AND STRUCTURE SOLUTION IN POWDER DIFFRACTION", same authors, this Congress.

M09.CC.002 IN SITU X-RAY STUDY IN ELECTRICALLY HEATED DAC – FORM CRYSTAL STRUCTURES TO STRUCTURE OF THE EARTH. L. Dubrovinsky, S. Saxena, S. Rekhi, Department of Earth Sciences, Uppsala University

Since their discovery in 1895, X-rays have proven to be a vital tool of science, making it possible to examine previously hidden worlds ranging from the tiniest of atoms to the most distant galaxies in space. Experimental studies of geophysically important materials at high pressures require in situ x-ray diffraction. It is practically the only method which provides direct information on phase relations and structures. We developed electrical heating assemblage for DAC which allows us to collect diffraction patterns in multimegabar pressure range at temperature to 1200 C using synchrotron or in-house X-ray facilities.

External electrical heating assemblage employs flexible graphite foils of thickness around 1.5 mm. In such a design, both the diamonds and gasket can be heated homogeneously to over a temperature of about 1200ºC. Two rectangular slabs (25*10mm^2) were amputated from a flexible graphite foil of thickness 1mm. Small pieces (10*10mm^2) of the graphite foil of thickness 0.5 mm were glued at the edges of these slabs along their lengths using high temperature graphite glue. These small pieces at the edge of the slabs make the assemblage stable on the cell and "concentrate" the heat on the sample and diamonds. The slabs were indented simultaneously and the Re-gasket was placed in between them. Two molybdenum electrodes (thickness 4mm) were carefully inserted between the two slabs of graphite foils and finally glued using a high temperature ceramic glue. The sample was heated using a DC power supply, with an operating range up to 200A/50V. The maximum current needed for heating a sample at 200 GPa to 1000 C was around 150 A. For measuring the temperature, a Pt/Pt13%Rh precision thin microthermocouple with a junction diameter less than 25 m was used. The junction of thermocouple was carefully inserted between the two parts of the graphite heater foils as shown in figure, such that it can touch the gasket sitting between them.

We used electrically heated DAC to study thermal expansion and phase transition of iron, $MgSiO_3$ perovskite and silica at high pressure and used results for analysis composition and the structure of the Earth.

M09.CC.003 HIGH P-T NEUTRON DIFFRACTION EXPERIMENTS AT LANSCE. Yusheng Zhao, Robert V. Von Dreele, LANSCE, Los Alamos National Laboratory, Los Alamos, NM 87545, U.S.A.

In-situ high P-T neutron diffraction experiments provide unique opportunities to study texture, hydrogen bonding, magnetic moments, structural and thermal parameters of light elements (eg. H, Li, C) and heavy elements (eg. Ta, U, Pu,), which are virtually impossible to determine by x-ray diffraction techniques. For example, we can derive thermoelasticities and Debye-Waller factors as function of pressure and temperature using in-situ high P-T neutron diffraction techniques. These applications can also be extended to a much broader spectrum of scientific problems. For instance, puzzles in Earth science such as the carbon cycle and the role of hydrous minerals for water exchange between lithosphere and biosphere can be directly addressed. Moreover, by introducing in-situ shear, texture of metals and minerals accompanied with phase transitions at high P-T conditions can also be studied by high P-T neutron diffraction experiments.

We have successfully conducted high P-T neutron diffraction experiments at LANSCE and achieved simultaneous high pressures and temperatures of 10 GPa and 1500 K. With an average 5-6 hours of data collection, the diffraction data is of sufficient high quality for the determination of structural parameters and thermal vibrations. We have collected the diffraction patterns of an amorphous material (carbon black), a hydrous mineral (MgOD), and some metals (Mo and Ta). The aim of our research is to accurately map bond lengths, bond angles, and neighboring atomic environments in P-T space. Studies on high-pressure crystal chemistry and thermoelastic equations of state are also ongoing. We are conducting further development of high P-T technology with respect to the press, anvil and furnace design, thermal and electric insulation, selection of gasket materials and re-enforcement rings, protection of electric and thermocouple leads, etc. We expect to ultimately achieve pressures of 30 GPa and temperatures of 2000 K with our new press TAP-98 and new beam-line HIPPO at LANSCE.

M09.CC.004 KINETIC STUDIES AT HIGH PRESSURE AND HIGH TEMPERATURE-DATA ANALYSIS. M. Mezouar and A. P. Hammersley, ESRF, Grenoble, France

A new set-up for collecting high quality data suitable for structural refinements at high pressures and high temperatures has been developed on the beam-line ID30 at the European Synchrotron Radiation Facility (ESRF). The possibility to use high X-ray energies, high brilliance of third generation source, new fast imaging plate detector interfaced to the Paris-Edinburgh large volume press has lead to a significant reduction of acquisition time and improvement of the quality of the data. The rapid acquisition of high quality 2D images allows time resolved experiment in one-minute range and gives access to the kinetics of phase formation and chemical reaction. However, these kind of experiments generate enormous quantities of data, and automatic analysis of this data is highly desirable. In FIT2D the "FILES SERIES" option "INTEGRATE" has been developed to allow the combination of interactive data analysis and subsequent automated analysis. Raw data may optionally be corrected for detector distortions, and integrated to 1-D 2-theta scans with user defined making. After successful integration of the first image the integration is repeated automatically for subsequent images. This allows efficient analysis of enormous quantities of data (Gbytes). Several examples will be presented including:

- The formation processes of the high Tc superconducting compounds $HgBa_2CuO_{4+d}$ and $HgBa_2Ca_2Cu_3O_{8+d}$ [1] from the complex mixing precursors: $BaCuO_2$, Ca_2CuO_3 and HgO at high pressure (2 to 4 GPa) and high temperature (up to 1200°C).
- The in situ study of the C_{60} polymerization at HP and HT.

[1] S. Le Floch, P. Bordet, P. Toulemonde, A. Prat, R. Argoud, J. J. Capponi, M. Mezouar (1998). First in-situ X-ray Characterisation of High Tc Superconductor Synthesis at High Pressure and High Temperature, In Preparation.

[2] L. Marques, M. Mezouar, J-L. Hodeau, M. Nunez-Regueiro, N. R. Serebryanaya, V. A. Ivdenko, V.D. Blank, G. A. Dubitsky (1998).'Debye-Scherrer Ellipses' from 3-D Fullerene Polymers: a pressure anisotropy memory signature.

M09.CC.005 APPLICATION OF MAXIMUM ENTROPY TO HIGH-PRESSURE X-RAY POWDER DATA: CAN IT HELP TO FIND THE PROTONS? R.J. Papoular, LLB, CEA-Saclay, 91191 Gif-sur-Yvette, France.

This paper will focus on the the joint use of powder diffraction data analysis and Maximum Entropy to help track down protons in solids from X-ray data. A Lebail-like analysis will first be introduced to produce error bars on extracted Lebail-intensities. In a second step the use of a non-uniform electron density prior within the framework of Maximum Entropy electron density reconstructions will be advocated to push down the threshold of detectability of weak scatterers. As an example, the data analysis of synchrotron x-ray data pertaining to $Ca(OH)_2$ data under high pressure and the validity of the related results will be discussed. Limitations on the stand-alone application of ME will be stressed, and the use of complementary data processing techniques advocated.

P09.CC.001 SINGLE CRYSTAL DIFFRACTOMETRY AT HIGH PRESSURES. L.W. Finger, Geophysical Laboratory, Carnegie Institution of Washington, 5251 Broad Branch Rd., NW, Washington DC 20015, USA, and R.J. Angel, Bayerisches Geoinstitut, Universität Bayreuth, D95440 Bayreuth, Germany.

Over the past decade we have been developing both hardware and software for the purpose of obtaining more precise measurements of lattice parameter variations with pressure through single-crystal diffraction.

The program SINGLE has been developed to control four-circle diffractometers and to perform both lattice parameter measurements and intensity data collections. Elements of the software essential for obtaining precise lattice parameters include full peak-profiling, the use of Hamilton's method of eight-position centring [1], and vector-least-squares fitting of the UB matrix to the diffractometer setting angles of reflections [2]. The consequences of ignoring these procedures will be illustrated in the poster.

The software is written to be mostly machine- and platform-independent; the computer-diffractometer interface is an entirely separated part of the software and can be rewritten for new installations. SINGLE is currently being used to drive four-circle diffractometers in laboratories in the Geophysical Laboratory, the Bayerisches Geoinstitut, ETH Zürich, and University College London. A comparative study of data collected at these installations is currently under way and will be presented. In particular, the influence of the choice of peak profile function for various diffractometer configurations and the implications for diffractometer design will be discussed.

[1] King, H., and L.W. Finger: *J. Appl. Crystallogr., 12*, 374-378, 1979.

[2] Ralph, R.L., and L.W. Finger: *J. Appl. Crystallogr., 15*, 537-539, 1982.

P09.CC.002 COMBINED CCD/IMAGING PLATE DETECTION SYSTEM FOR MONOCHROMATIC XRD STUDIES AT HIGH PRESSURES AND TEMPERATURES AT THE X-17 BEAMLINE, NSLS. J. Chen, M. T. Vaughan, D. J. Weidner, C. C. Koleda, K. J. Baldwin, W. Huebsch and J. B. Parise, CHiPR§ and Geosciences, SUNY, StonyBrook, NY 11794-2100, USA. § Center for High Pressure Research, an NSF funded Science and Technology Center

The Translating Imaging Plate (TIP) detection system has largely fulfilled its original potential for the acquisition of high quality monochromatic powder diffraction data, allowing the study of time resolved phenomena at high pressure (Chen et al., 1998; Parise *et al.,* 1998). This has allowed not only the elucidation of phase transitions, but also refinement of crystal structure based upon these data (Chen et al., 1998), thereby allowing the transition to be followed on an atomistic level.

Unfortunately, some of the advantages of polychromatic studies, chiefly the excellent collimation, which excludes parasitic scattering from the high pressure vessel, and the quasi-real-time feed back of the diffraction data, are lost in the monochromatic IP experiment. The former problem can be solved using software techniques (Chen *et al*, 1998) but the later can be problematic. For example, a TIP has a limited translation range and requires real-time feedback to provide a trigger to activate the plate at a time appropriate to capture the transition. Ideally this would be done without resorting to guesswork, or to several loadings of the high pressure device. Coupling a CCD detector with the TIP can provide this feedback. Such a device has been installed on the large volume DIA apparatus (SAM-85) at the X-17 beamline at the National Synchrotron Light Source. The device has been tested and used in several classes of experiments. These include rheological studies of olivine, determination of phase transitions in Fe_2SiO_4 and FeS and other applications requiring the resolution, ready quantification and texture analysis afforded by monochromatic powder diffraction with area detectors.

Chen *et al*. (1998) Rev. High Press. Sci. Technol., 7, 272
Parise et al. (1998) Ann. Rev. in Mat. Sci. 28, 349-420

P09.CC.003 FIRST COUPLING OF LOW TEMPERATURE AND HIGH PRESSURE TECHNIQUES FOR MOLECULAR CRYSTAL X-RAY STRUCTURES. Y. Barrans, J. Gaultier, D. LePevelen, D. Chasseau, Laboratoire des Sciences Moléculaires, Institut de Chimie de la Matière Condensée de Bordeaux, 87 avenue du Dr. A. Schweitzer, UPR CNRS 9048 F-33608, Pessac, France.

Since 15 years, two apparatus have been developped by J.G. to study organic single crystal structures either down to 10K or up to 3GPa, and now crystals under pressure can be analyzed by X-Rays down to 7K. Both of them use a vertical He closed cycle APD Displex 202 cryostat. The crystal on a brass rod is linked to the cold finger and surrounded by two Be walled containers. The inner one is filled with He. Between both of them is a heat shield and high vacuum is established.

(i) the special normal beam diffractometer Huber-Gaultier is equipped with the 6.5K cryostat. A specific program is used to collect up to 90% of the diffracted intensities in the whole space with MoKα radiation and a scintillation detector. New containers allow now measurements with the pressure cell (4x4 cm cylinder, diamond anvils, crystal in the hole of a Be gasket filled with a liquid). For the first time in the world, diffracted intensities of molecular compounds have been collected with the coupled techniques low temperature + high pressure and the solved crystal structures show very interesting results (thesis, D.LP, 1999).

(ii) a specially designed camera permits to get Bragg, Weissenberg and Laue patterns from room temperature to 10K with the 10K cryostat. It is used to study the behaviour of crystals, especially the phase transitions, and can be followed by structure determination with the diffractometer measurements It has been modified to receive the pressure cell.

09DD OPTO-ELECTRONIC MATERIALS

M09.DD.001 FERROELECTRIC OXIDES FOR OPTOELECTRONIC APPLICATIONS. Ch. Buchal, Forschungszentrum Juelich GmbH, Institut fuer Schicht-und Ionentechnik ISI-2, D 52425 Juelich, Germany

We discuss the physics and structure- properties- relations of the optical perovskites and related materials and their applications for optoelectronic devices and functions, especially: - optical waveguides - modulators - non-linear devices as frequency converters - amplifiers and lasers - photorefractive components - holographic storage. The following processing issues will be addressed: Ion implantation for doping and damage engineering, waveguide fabrication, epitaxy and thin film growth and patterning.

M09.DD.002 BLUE LIGHT GENERATION BY FREQUENCY DOUBLING AND SUM-FREQUENCY MIXING OF LASER DIODES IN $KnbO_3$. D. Fluck and P. Günter Nonlinear Optics Laboratory, Swiss Federal Institute of Technology ETH-Hönggerberg HPF E7, 8093 Zürich, Switzerland.

Potential applications of compact blue lasers include data storage, colour printing, displays, biofluoresence, photolithography, remote sensing, chemical and biological species detection, high resolution spectroscopy, underwater monitoring and communication. Direct second-harmonic and sum-frequency generation (SHG, SFG) with near infrared semiconductor laser diodes (LDs) offers the possibility of robust, compact and reliable blue lasers.

$KNbO_3$ crystals are very attractive for frequency conversion of near infrared LDs into the blue spectral range due to its high nonlinear optical coefficients, its numerous phase-matching (PM) configurations, and the absence of optical damage and gray tracking effects. Efficient blue light generation at 430 nm and 490 nm by noncritical PM SHG with LDs in $KNbO_3$ has been demonstrated for single-pass, resonant and waveguide configurations. Other wavelengths in the 415 to 475 nm spectral range can be efficiently generated by making use of $KNbO_3$ for SFG with commercially available single-mode AlGaInP, AlGaAs and InGaAs laser diodes.

We will review recent results on compact and efficient blue lasers based on noncritical PM SHG and SFG in $KNbO_3$ and discuss the advantages and disadvantages of different approaches including novel configurations.

M09.DD.003 MATERIALS AND DEVICES FOR Si-BASED OPTOELECTRONICS. S. Coffa, S. Libertino, G. Franzò and A. La Magna, CNR-IMETEM, Catania, Italy

Ion implantation can be successfully used to engineer the optical properties of crystalline Si and to obtain efficient light emission from this semiconductor. A detailed analysis of Er incorporation in Si and the role of codoping with O and F will be presented. Furthermore the mechanisms of excitation (by electron-hole recombination or impact excitation) and Auger-de-excitation of rare-earth ions in Si have been elucidate using photo- and electroluminescence, deep level transient spectroscopy and conductivity measurements. The detailed knowledge of the physical properties of the Er:Si system allowed us to fabricate Si LEDs operating at 1.54 μm with a quantum efficiency of 0.1% at room temperature and allowing direct modulation of the light output at frequencies of 10-100 MHz. These devices have been integrated with Si on insulators rib waveguides fabricated using standard lithography and reactive ion etching and exhibiting losses below 1 dB/cm at $\lambda > 1.2$ μm. These novel device structures have been used to design and fabricate electrically pumped optical amplifiers and lasers whose performances will be presented. Finally, in the talk the state-of-the art performances and perspectives of ion implanted Si light emitters using implantation of rare earths (Er, Tm), isoelectronic impurities (such as C) and Fe (forming small β-$FeSi_2$ precipitates) will be compared and their compatibility with ULSI Si technology assessed.

M09.DD.004 EPITAXIAL GROWTH OF ZnSe- AND GaN-BASED STRUCTURES FOR SHORT WAVELENGTH EMITTERS. Detlef Hommel Universität Bremen, Institut für Festkörperphysik, Kufsteiner Str., D-28334 Bremen

Both ZnSe and GaN are promising materials for short wavelength LEDs and laser diodes (LDs). Whereas GaN-based structures cover the spectral range from ultraviolet to (nearly) red in electroluminescence (LED) LDs emitting between 360 – 450 nm have been realized. Nevertheless, long lifetime stimulated emission has been obtained only around 400 nm (violet). For shorter wavelength a higher Al-content in the cladding layers is needed which increases the probability of cracks in the structure. Longer wavelengths require a higher In-content which is hampered by the miscibility gap between InN and GaN. Therefore, ZnSe-based LDs are the only possibility for the green spectral region where the human eye has its highest sensitivity.

The similarities and basic differences in the growth of GaN- and ZnSe-based structures will be presented and molecular beam epitaxy (MBE) and metal organic chemical vapor phase epitaxy (MOVPE) as growth methods compared. Both materials differ in the defect density they can withstand without disturbing their functionality. Typical etch pit densities (EPDs) for ZnSe LDs must be well below 10^4 cm^{-3} whereas GaN-LDs are still operating when the defect density is at least 3 orders of magnitude higher. The reasons for that will be discussed. In the case of ZnSe the heteroepitaxial approach on (110) GaAs will be compared to the homoepitacial one on conducting ZnSe substrates. Epitaxial

lateral overgrowth (ELOG) and other methods reducing the defect density will be presented in the case of GaN devices. Whereas large GaN crystals as substrate materials are still not available the hydride vapor phase epitaxy (HVPE) as well as thick MOVPE buffer layers offer the possibility of a quasi-homoepitaxial growth.

In an outlook the future of both material systems will be discussed from the crystal growth point of view.

M09.DD.005 FILM DEFECTS AND GROWTH DYNAMICS IN WIDE BANDGAP EPITAXY. F. A. Ponce, Department of Physics and Astronomy, Arizona State University, Tempe, AZ 85287-1504, U.S.A.

The III-V nitride semiconductors have achieved a high degree of notoriety in the last few years due to their unique properties and optoelectronic applications [1]. Light emitting devices based on double heterostructure InGaN/GaN films have been produced with light emission efficiencies exceeding incandescent lighting. Blue diode lasers with continuous operation for more than 10,000 hours have been reported and their commercial availability has recently been announced. The high optoelectronic performance of these materials follow a crystallographic nature that is very different from other semiconductors. Large dislocation densities are observed ($\sim 10^{10}$ cm^{-2}) and are associated with a columnar array of defect-free crystallites. The microstructure strongly depends on the initial stages of growth which rely on low temperature *nucleation* layers needed to overcome the natural tendency of three-dimensional island growth. The resulting defect structure plays a key role in the relaxation of thermal stresses, allowing the local growth of high quality heterostructures under otherwise highly unfavorable conditions. The nature of the substrate/thin film interfaces will be discussed, as well as the role of the buffer layer. Details of the dislocation arrangement and structure and correlation with light emitting properties will be presented for GaN thin films as well as for InGaN quantum well structures.

[1] F. A. Ponce and D. P. Bour, Nature Vol. 386, 351 (1997).

P09.DD.001 POWDER OR SINGLE CRYSTAL STRUCTURE - EXEMPLIFIED BY β_{co}-(BEDT-TTF)$_2$I$_3$. D. Madsen [1,2], M. Burghammer [1], S. Fiedler [1] and H. Müller [1]. [1] ESRF, BP220, F-38043 Grenoble Cedex, France. [2] Centre for Crystallographic Studies, University of Copenhagen, Universitetsparken 5, DK-2100 Copenhagen, Denmark.

The organic superconductor β-(BEDT-TTF)$_2$I$_3$ is a well-known system [1]. Former studies on electrochemically produced crystals have shown that the crystals contain a mixture of phases and that the T_c is 1.4K. Furthermore, a structural phase transition is observed at 175K [2]. Using a novel preparation method, a powder has been obtained containing a pure phase of β_{co}-(BEDT-TTF)$_2$I$_3$ with a T_c of 7.1-7.9K [3]. A powder study of the phase pure crystals was performed at 293K, but the refinement showed unrevealed structural features related to the superconducting properties of the compound. At ID13 at the ESRF, we have therefore performed a single-crystal study on several crystals with dimensions about 10×10×2μm. Full data collections were carried out to a resolution of about 0.7Å at 293(2)K, 200(2)K, 130(2)K, and 100(2)K with an LN2 cryostream, and a dataset at 35(5)K with an LHe cryostream constructed at the EMBL Grenoble Outstation. A structural phase-transition was observed between 200K and 130K of the phase pure single-crystals as was previously observed in the electrochemically produced crystals [2]. Full structure refinements have been carried out for the datasets at 293(2)K and 200(2)K while the datasets at 130(2)K, 100(2)K and 35(5)K still are under quantitative evaluation (Jan. 99).

1. H. Endres, H.J. Keller, R. Swietlik, D. Schweizer, K. Angermund and C. Krüger, *Z. Naturforsch.* **41 a** (1986), 1319-1324.
2. A. Nogami, S. Kagoshima, T. Sugano and G. Saito, *Synthetic Metals*, **16** (1986), 367-377.
3. H. Müller, S.O. Svensson, A.N. Fitch, M. Lorenzen and D.G. Xenikos, *Advanced Materials*, **9** (1997), 11, 896-900.

P09.DD.002 EVOLUTION TOWARDS CENTROSYMMETRY OF THE NLO MATERIAL RbTiOPO$_4$ IN THE TEMPERATURE RANGE 293 - 973 K. P. Delarue and C. Lecomte, Laboratoire de Cristallographie et Modélisation des Matériaux Minéraux et Biologiques, LCM3B UPRESA 7036, Université Henri Poincaré, Nancy I, Faculté des sciences, BP 239, 54506 Vandoeuvre Lès Nancy Cédex, France. M. Jannin and G. Marnier, Laboratoire de Physique de l'Université de Bourgogne, LPUB UPRESA 5027, Faculté des sciences Mirande, BP 400, 21011 Dijon Cédex, France.

The crystal structure of rubidium titanyl phosphate, RbTiOPO$_4$ (space group Pna2$_1$), has been refined at room temperature, and at 473, 673, 873 and 973 K, by using single-crystal x-ray diffraction techniques. The data show a large anharmonic motion of the rubidium ions increasing with temperature. A model, which splits the Rb sites, describes the large and gradual Rb ions displacement versus temperature until the phase transition temperature (centrosymmetric space group Pnan). It permits to show the influence of these Rb ions displacements on the framework and principally on the shortest and largest bonds of the titanyl group. The study of the deviation to the centrosymmetric structure correlates directly the change towards centrosymmetry of the titanyl groups with the observed variation of the second harmonic generating (SHG) intensity.

09EE DYNAMIC ASPECTS OF MOLECULAR CRYSTALS

M09.EE.001 MULTI-TEMPERATURE ADP'S: INSIGHT INTO THE DYNAMICS OF CRYSTAL STRUCTURES. S.C.Capelli, H.B.Bürgi Laboratorium für Kristallographie der Universität Bern, Schweiz.

The observation that diffraction intensities decrease with temperature[1] proved that crystals are not dead objects but that atoms in crystals move around their equilibrium positions. Anisotropic displacement parameters (ADP), determined by x-ray or neutron diffraction, quantify this observation; they describe the time and space average distribution of atoms around their mean position in crystals.

Many components contribute to these parameters: the mean square atomic displacements from all possible motions (libration, translation, internal vibrations), from disorder (static or dynamic) and from systematic errors (either in the data or in the refinement model).

An analysis of ADP's aimed at uncovering non-trivial details of the dynamics of molecules in crystals must separate the different contributions and provide information on the correlation of atomic motions. Although in a single temperature diffraction experiment this information is lost, it can be retrieved from the temperature dependence of ADP's.

An algorithm capable of achieving these goals has been developed and implemented in a computer programm[2]. Accurate multi-temperature ADP's have been analyzed for a number of molecules. In each case an improved description of the crystal structure and of the molecular dynamics were obtained. The information would not have been accessible from ADP's measured at a single temperature.

[1] P.Debye, *Verh.Dtsch.Phys.Ges.*, 1913, 15, 738.
[2] M.Foertsch, Ph.D Thesis, University of Bern, 1997.

M09.EE.002 STRUCTURAL CHANGE FOR THERMOCHROMY OF SALICYLIDENEANILINES. THE FIRST OBSERVATION BY X-RAY ANALYSIS. Keiichiro Ogawa, Yoshiro Kasahara, Yohko Ohtani and Jun Harada, Department of Chemistry, Graduate School of Arts and Sciences, The University of Tokyo, Komaba, Meguro-ku, Tokyo, 153-8902 Japan.

Reversible change in color of substances with variation of the temperature is known as thermochromism and has attracted much interest from chemists for a long time. *N*-Salicylideneanilines belong to a class of the most popular thermochromic compounds. For example, the crystals of *N*-(5-chloro-2-hydroxybenzylidene)aniline (**1**) are orange-red at room temperature and pale yellow at 77 K, and their color changes reversibly with variation of temperature. Extensive studies have revealed that the thermochromism of *N*-salicylideneanilines originates from the tautomerism between the OH and NH forms. A change in the crystal structure for their thermochromy has, however, never been observed, although an attempt to do so was reported for **1** by Bregman et al. We wish to report the first observation of a crystal structure change for the thermochromy of ***N***-salicylideneanilines, using variable temperature X-ray analysis of *N*-(5-chloro-2-hydroxybenzylidene)-4-hydroxyaniline (**2**) [1].

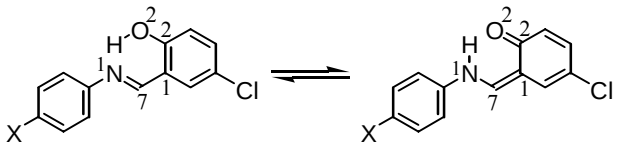

OH form **NH form**

1 : X = H **2** : X = OH

[1] K.Ogawa, Y. Kasahara, Y. Ohtani & J. Harada (1998). J. Am. Chem. Soc., 120, 7107.

M09.EE.003 A UNIFIED APPROACH TO NUCLEAR DENSITY: NEUTRON DIFFRACTION, INELASTIC SCATTERING AND SIMULATION. G. J. Kearley, B. Nicolai, and M. R. Johnson, Institut Laue Langevin, BP156, 38042, Grenoble, Cedex 09, France, P. Schiebel, Institut fur Kristallographie, Universitat Tubingen, 72070, Tubingen, Germany.

Time-averaged nuclear density is conveniently fitted within the harmonic approximation, but a physical justification for this, and the true nature of the underlying dynamics are not necessarily considered. Maximum entropy and reverse Monte Carlo methods make no such assumption, but their success depends critically on the quality of the data, and again the dynamics can only be inferred. The dynamics of the nuclei is measured directly by inelastic neutron scattering and it is now relatively simple to analyse these data by molecular dynamics, which normally includes all aspects of classical motion, or molecular mechanics when quantum motion is dominant. This analysis leads back to the time-averaged nuclear density.

We will present examples where consistency between neutron diffraction, spectroscopy and numerical simulation has been achieved so that nuclear density distributions can be understood rather than just "fitted".

M09.EE.004 PHYSICS FROM CHEMISTRY? ORGANIC STRUCTURES AT MORE TEMPERATURES BY A MULTIPLE SINGLE CRYSTAL METHOD. C. C. Wilson, ISIS Facility, CLRC Rutherford Appleton Laboratory, Chilton, Didcot, Oxon OX11 0QX, UK.

A novel multiple crystal data collection method has recently been developed on the single crystal diffractometer SXD at the ISIS pulsed neutron source. The method allows neutron diffraction data to be obtained simultaneously from several randomly oriented crystals of even low-symmetry molecular materials. The method exploits the ability of time-of-flight neutron Laue diffraction to resolve the overlapping diffraction patterns from a multiple crystal sample. This opens up the possibilities of collecting data sets more rapidly (for example in variable temperature structure scanning), under more extreme sample environment conditions and from smaller single crystal samples.

The presentation will describe the method and highlight its application in one area: that of studying organic crystal structures at many temperatures. The use of such variable temperature methods can lead to new insights into the physics underlying chemical structures, and often more structure determinations at more temperatures are required in order to distinguish between subtly different physical models.

Since the method has been applied to neutron diffraction data, the focus has been on examining hydrogen atom parameters, particularly the anisotropic displacement parameters, and there is often much of interest happening even in apparently innocuous ("normal") crystal structures. Examples will be presented of "anomalous" behaviour of hydrogen atoms revealed by multiple temperature data collection, and the modelling enabled by increasing the number of data sets available.

M09.EE.005 STRUCTURE AND DYNAMICS OF *T*-BUTYLCALIX[4]ARENE-TOLUENE INCLUSION COMPOUND. G. D. Enright, E. B. Brouwer, C. I. Ratcliffe and J. A. Ripmeester, Steacie Institute for Molecular Sciences, NRC, Ottawa, Canada, K1A 0R6.

By using a combination of solid state NMR (^{1}H and ^{13}C CP/MAS) and X-ray diffraction we have shown that *t*-butylcalix[4]arene-toluene is a fluxional guest-host system at room temperature. As the temperature is lowered the NMR measurements indicate that the guest motion changes from 90° to 180° jumps about the 4-fold axis, thus freezing in the guest-induced elliptical distortions of the host lattice. At even lower temperatures the 180° reorientations cease and the local symmetry is further reduced. Our initial diffraction studies (Cu Kα) indicated that even at the lowest temperatures space-averaging results in a high lattice symmetry (tetragonal, space group P4/n) unchanged from that observed at room temperature. At low temperatures weak, transient diffraction peaks were noted at half-integral values of h,k, indicating possible correlations in the alignment of guests in adjacent calixarene sites. We have recently collected low-temperature diffraction data with Mo K_α radiation. Surprisingly the half-integral peaks were persistent and not as weak. The structure could be solved in P4 revealing layers of ordered, elliptically-distorted calixarene cavities (at 2-fold sites) alternating with layers of fully disordered elliptical cavities (at 4-fold sites).

M09.EE.006 STOCHASTIC THERMAL MOTION ANALYSIS AND THE RADON-NIKODYM PROPERTY. Carroll K. Johnson, Chemical and Analytical Sciences Division, Oak Ridge National Laboratory*, Oak Ridge, TN 37831-6197, USA.

Atom positions a_1, a_2, scaled anisotropic temperature factor matrices B_1, B_2, and Radon-Nikodym density (RND) $\omega_{2,1}$, (derivative of Gaussian density μ_2 with respect to μ_1 assuming absolute continuity), provide a stochastic estimate of correlated thermal motion. Let $C = B_2^{-1/2}$ (a symmetric matrix), $b = C(a_2\text{-}a_1)$, $c(x) = C(x\text{-}a_1)$, and $D_{2,1} = C(B_1\text{-}B_2)C$. The symmetric Hilbert-Schmidt matrix $D_{2,1}$ yields eigenvalues λ_k and eigenvectors e_k, k=1,2,3. The Gaussian RND equation [1] is

$$\omega_{2,1} = \frac{d\mu_2}{d\mu_1}(x) =$$

$$\exp\left(-\frac{1}{2}\left(\sum_{n=1}^{3} \left(e_k^t c(x)\right)^2 \frac{\lambda_k}{(1+\lambda_k)} - \ln(1+\lambda_k) \right) + c^t(x)b - \frac{b^t b}{2} \right)$$

Since RND is always ≤ 1 there is a separatrix (partition) surface at $\omega_{2,1}(x) = 1$ (which is also $\omega_{1,2}(x) = 1$), on which $\mu_1(x) = \mu_2(x)$. Additional atom pairs and chain differentiation $\frac{d\mu_2}{d\mu_3} = \frac{d\mu_2}{d\mu_1}\frac{d\mu_1}{d\mu_3}$ provides a dented body partition [2] surrounding each Gaussian centroid. Contoured dented body drawings can be made by ORTEP type calculations at increasing probability density levels, with plotting of ellipsoid pair intersections (closed 4th-order curves).

Critical net [3] peak, pass, pale, and pit points occur at atom centroid, kissing point for two ellipsoids, intersection point of three (or more) ellipsoids, and dented body corners, respectively. Dented body face areas (integrated ω density) and face curvature provide motion correlation and convex set chemical grouping information, respectively. Experimental testing of this RND approach is underway.

*Operated by Lockheed Martin Energy Res. Corp. for the U.S. Dept. of Energy under Contract No. DE-AC05-96OR22464. C.D.,

[1] I.I. Gihman and A.V. Skorohod, The Theory of Stochastic Processes I, Springer, 1974, pp 496.
[2] R.D. Bourgin, Geometric Apects of Convex Sets with the Radon-Nikodym Property, Lect. Notes in Math. 993 Springer, 1983.
[3] C. K. Johnson, M.N. Burnett, and W.D. Dunbar, Crystallographic Computing 7, Eds., P.E. Bourne and K. Watenpaugh (in press).

M09.EE.007 THE FIRST *IN SITU* DIRECT OBSERVATION OF LIGHT-INDUCED RADICAL PAIR FROM HABI DERIVATIVE BY X-RAY CRYSTALLOGRAPHY. M. Kawano and Y. Ohashi, CREST, Japan Science and Technology Corporation, and Department of Chemistry, Tokyo Institute of Technology, Tokyo 152-8551 Japan, and T. Sano and J. Abe, Department of Photo-Optical Engineering, Tokyo Institute of Polytechnics, Kanagawa 243-0297 Japan.

A radical species plays an important role as a reactive intermediate in chemical reactions and biological system. While a number of radicals in solid state have been extensively investigated by spectroscopic methods, crystallographic approach is relatively less common for unstable radicals, and has been applied to stable radicals, *viz.* radical ion pairs, stabilized radicals, and so on, which can be crystallized. To our knowledge, the crystallographic investigation on energetically unstable reactive radical pairs (RPs) has never been reported. We report the unprecedented example of the *in situ* direct observation of RP of a photo/thermochromic compound, hexaarylbiimidazolyl derivative (*o*-Cl-HABI), cryotrapped in a single crystal by X-ray diffraction. There are two crystallographically independent *o*-Cl-HABI molecules, A and B, in a unit cell before irradiation. The C-N bond connecting two triaryimidazolyl rings of not A but only B molecule is cleaved by irradiation to produce two planar radicals (RP). The irradiated crystal thermally converts into the initial dimer structure, which can be crystallographically confirmed. The CW-ESR experiments of the single crystal were carried out in the temperature range from 77 K to room temperature. Irradiation on the single crystal at 77 K produced a triplet-state signal of RP accompanied with Δm_S = 2 transition. The geometries of the initial dimer and RP are in good agreement with the theoretical results calculated by DFT Beck3LYP/6-31G*.

P09.EE.001 ANOMALOUS CH3 ROTATIONAL DYNAMICS AND CRYSTAL STRUCTURE OF MANGANESE ACETATE. Beatrice Nicolai [1], Gordon J. Kearley [1], Alain Cousson [2], Werner Paulus [2] [3], Francois Fillaux [4], [1] Institut Laue Langevin, BP156, 38042 Grenoble, FRANCE, [2] Laboratoire Leon Brillouin, CE Saclay, 91161Gif sur Yvette Cedex, France, [3] Universite de Rennes 1, Laboratoire de Chimie du solide et Inorganique Moleculaire, LCSIM/UMR6511, Campus de Beaulieu, Avenue du general Leclerc, 35042 Rennes Cedex, France, [4] LADIR-CNRS, 2 rue Henry Dunant, 94320 Thiais, France

Manganese acetate contains three crystallographically distinct CH_3 groups all of which undergo quantum-rotational tunnelling at low temperatures, but curiously, show no measurable librational (or torsional) transitions. To investigate this problem we have determined the low-temperature structure of manganese acetate by single crystal neutron diffraction and have measured the librational ground-state splitting by single crystal neutron scattering. This allows us to assign tunnelling transitions to each of the three distinct CH_3 rotors and thus to calculate the rotational potential for each of them from the known crystal structure. However, the measured tunnel splittings are very different from those calculated via the rotational potential from the crystal structure. Nevertheless, a classical molecular dynamics simulation reveals highly anisotropic proton density, particularly for one of the CH_3 groups, which compares well with the thermal parameters from the diffraction study, and reveals that classical, thermally activated rotation, in this crystal does not occur about a simple fixed axis. This explains the apparent disagreement between the tunnelling spectrum and the crystal structure and may explain the absence of librational transitions.

09FF GROWTH OF MESOSCOPIC CRYSTALS

M09.FF.001 BETWEEN CRYSTAL GROWTH AND PHASE TRANSFORMATION KINETICS IN NANO-CRYSTALLINE TITANIA. J.F. Banfield and H. Zhang [1], R. Lee Penn [2], [1] Dept. Geology and Geophysics, University of Wisconsin-Madison, WI 53706, USA, [2] Dept of Earth and Planetary Sciences, Johns Hopkins University, Baltimore, MD 21218, USA

Crystal growth and phase transformation kinetics of nanocrystals are strongly interconnected. The activation energy for crystal growth is low, ~ 70 kJ/mol, and growth in porous aggregates occurs rapidly. Until particles grow to greater than ~ 14 nm, the phase transformation is prohibited because anatase is more thermodynamically stable than rutile. Anatase-to-rutile transformation kinetics depend on temperature and aggregate structure. With higher packing densities and lower temperature, the transformation of nano-anatase to rutile occurs predominantly via interface nucleation.

Interface nucleation was studied using low-temperature hydrothermal experiments. Growth occurs largely by oriented attachment: contacting crystals rotate to achieve interfacial coherence, followed by elimination of the joining surface. Interfacial coherence can be achieved with the second particle in two possible orientations, leading either to single or twinned crystals. The phase transformation is initiated in twin surfaces, which share structural elements with rutile, and proceeds via a mechanism that combines bond bending and atomic displacements. Particle rotation is inhibited in dry powders, but smaller structural units common to rutile are apparently achieved (Ea ~ = 170 kJ/mol). When packing is less dense and/or the temperatures are higher, transformation occurs primarily via surface nucleation (Ea ~ = 465 kJ/mol) over longer reaction times. Particle growth and phase transformation in dry powders can be markedly retarded by partially separating the 6 nm or 8 nm

diameter anatase particles with 6 nm diameter nano-alumina. Both initial crystal size and packing densities affect the extent of retardation. We infer that higher retardation of crystal growth and phase transformation will occur in more densely packed aggregates, where interface nucleation is important.

M09.FF.002 QUANTUM EFFECTS IN ULTRATHIN METAL OVERLAYER EPITAXY. Zhenyu Zhang, Solid State Division, Oak Ridge National Laboratory, Oak Ridge, TN 37831-6032, USA and Department of Physics, University of Tennessee, Knoxville, TN 37996, USA

This talk presents the main results from recent studies of metal overlayer growth on semiconductor substrates [1]. It will be shown that a variety of novel phenomena can exist in such systems, resulting from several competing interactions. The confined motion of the conduction electrons within the metal overlayer can mediate a surprisingly long-range repulsive force between the metal-semiconductor interface and the growth front, acting to stabilize the overlayer. Electron transfer from the overlayer to the substrate leads to an attractive force between the two interfaces, acting to destabilize the overlayer. Interface-induced Friedel oscillations in electron density can further impose an oscillatory modulation onto the two previous interactions. These three competing factors, all of electronic nature, can make a flat metal overlayer critically, marginally, or magically stable, or totally unstable against roughening. We further show that, for many systems, these electronic effects can easily win over the effect of stress. First-principles studies of a few representative systems support the main features of the present "electronic growth" concept [2]. We also present experimental support of the concept [3].

Work done with the collaborators listed. Supported by US Department of Energy and US National Science Foundation.

[1] Z. Y. Zhang, Q. Niu, and C.-K. Shih, Phys. Rev. Lett. 80, 5381 (1998).; Z. G. Suo and Z. Y. Zhang, Phys. Rev. B 58, 5116 (1998).
[2] J.-H. Cho, Q. Niu, and Z. Y. Zhang, Phys. Rev. Lett. 80, 3582 (1998).
[3] L. Gavioli, K. R. kimberlin, M. C. Tringides, J. F. Wendelken, and Z. Y. Zhang, Phys. Rev. Lett. 82, 129 (1999).

M09.FF.003 IRRADIATION INDUCED GRAIN GROWTH, PHASE TRANSFORMATION AND DEFECT EVOLUTION IN NANOCRYSTALLINE MATERIALS. M.Rose, H.Hahn and A.G.Balogh, Department of Materials Science, Darmstadt University of Technology, Darmstadt, Germany

Microstructural defect evolution and grain growth in nanocrystalline Pd and ZrO_2 samples during energetic particle irradiation was studied. Nanocrystalline samples with different initial grain sizes, ranging from 10 to 300 nm prepared by the inert gas condensation (IGC) technique, were irradiated using 1 MeV electrons and 0.2 – 4 MeV Kr^+ ions with fluences from $1*10^{15}$ to $2*10^{16}$ ions/cm^2. Irradiation experiments were performed partially in-situ at the 1 MV high voltage transmission electron microscope of the Max-Planck-Institute, Stuttgart and at the heavy ion accelerator – transmission electron microscope set-up of the Argonne National Laboratory, Argonne.

The irradiation induced grain growth and the defect density were studied by X-ray diffraction and by transmission electron microscopy (TEM). A strong correlation between grain size and defect density was found, showing drastic reduction of defect clusters in small grains below 50 nm. This correlation was linear for the smaller grains, reaching a saturation value of about $3*10^{-3}$ defect cluster / nm^2 in ZrO_2 and about $1.5*10^{-2}$ defect cluster / nm^2 in Pd for grains larger than 100-120 nm. The irradiation induced defects annihilated completely at the nanocrystalline grain boundaries for grains, smaller than a critical grain size of about 25 nm. Using the temperature dependence of the defect free regions, diffusion coefficients in both nanomaterials have been determined and temperature ranges for thermal diffusion and radiation enhanced diffusion (RED) were separated.

In the irradiated nanocrystalline ZrO_2 samples a phase transformation was found. The tetragonal phase, which is normally stable above 1200 °C first, was observed by X-ray diffraction measurements at room temperature above an irradiation fluence of $2*10^{16}$ ions/cm^2.

The reduced defect density of the nanocrystalline samples, interpreted as enhanced radiation resistance, could give emphasis to applications for irradiation environments and space research.

M09.FF.004 CRYSTALLITE AGGREGATION CONTROLLED BY SUCCESSIVE NUCLEATION. Mu Wang*, Da-Wei Li, Xiao-Bo Yin, Wen-Jun Liu and Nai-Ben Ming, Division of Optical and Scanning Probe Microscopy, National Laboratory of Solid State Micro-structures, Nanjing University, Nanjing, China

In nonequilibrium situations the growth morphology is very often ramified and fractal-like, especially in the early stage of 2D growth [1]. In many cases the aggregate consists of crystallites of limited size [2]. Sometimes the crystallographic orientations of these crystallites are strongly correlated [3]. The mechanism of these aggregation behaviors seems still not completely understood. Our recent experi-ments demonstrated that the crystallographic anisotropy and surface kinetics play important parts in the aggregation process, which may be responsible for the periodic roughening transitions occurring to the crystallites surface [4], and also for the anisotropic successive nucleation which leads to a remarkable correlation on the crystallographic orientations of crystallites in fractal aggregation [3]. We suggest that these observations provide in-depth insights to the aggregation mechanism when the crystallite size is below a certain value.

[1] Z. Zhang and M. G. Lagally, Science, 276, 377 (1997)
[2] N.-B. Ming, M. Wang, and R.-W. Peng, Phys. Rev. E, 48, 621 (1993)
[3] M. Wang, et al., Phys. Rev. Lett., **80**, 3089 (1998)
[4] M. Wang, et al., Europhys. Lett., **41**, 61 (1998)

M09.FF.005 ABSTRACT NOT AVAILABLE. Y. Arakawa

M09.FF.006 DEVELOPING A STRUCTURALLY BASED MODEL FOR NUCLEATION: FROM MOLECULAR AGGREGATION TO PRODUCT CONTROL. M.J. Quayle [1], R.J. Davey [1], G.J. Tiddy [1], J. Garside [1], H.G. Alison [1], G. Jones [2] and D.T. Clarke [2]. [1] Colloids, Crystals and Interfaces Group, Department of Chemical Engineering, UMIST, P.O. Box 88, Manchester. M60 1QD. UK. [2] Synchrotron Radiation Department, CCLRC Daresbury Laboratory, Warrington. WA4 4AD. UK.

The process of primary nucleation is currently being investigated, *in situ*, using synchrotron radiation. The clasical description of primary nucleation is derived from Ostwald's Law of stages [1] and Volmer's kinetic formalism [2]. Though the thermodynamics of liquid – solid phase transformations have been comprehensively described [3], the kinetic aspects have, however, been limited by the size and timescales at which available experimental techniques can probe a transforming system.

A stopped flow reactor is employed to carry out batch crystallisations which result from rapid reaction or 'drown out', through the mixing of two liquid components. Simultaneous small

and wide angle X-ray diffraction experiments are performed on these nucleating systems in real time with detectors that have a time resolution of 10 milliseconds. Thus it is possible to track the development of long and short range order together with the size scale of any emerging or transforming phase.

Systems that have been studied include copper phthalocyanine, 4-methoxy-*E*-cinammic acid, histidine·HCl·H_2O and 2,6-dibromo-4-nitroaniline by mixing of concentrated solutions with water; the cocrystallisation of 1,4-diiodobenzene / 1,4-dinitrobenzene and tetracyanoethene / tetracyanquinodimethane systems and the precipitation of copper carbonate from copper nitrate and sodium carbonate solutions.

[1] W. Ostwald, *Z. Phys. Chemie (Liepzig)*, 1897, 22, 289.
[2] M. Volmer, *Kinetic den Phasenbildung,* Steinkopf, 1939, Leipzig.
[3] see for example P.W. Atkins, Physical Chemistry, 1990, OUP, Oxford.

M09.FF.007 ABSTRACT NOT AVAILABLE. C.M. Arnold

11OA THE IMMUNE SYSTEM AND DESIGNED ENZYMES

M11.OA.001 THE STRUCTURE OF THE HUMAN HIGH-AFFINITY IgE RECEPTOR FROM 5 CRYSTAL FORMS. Scott C. Garman, Jean-Pierre Kinet#, and Theodore S. Jardetzky. Department of Biochemistry, Molecular Biology, and Cell Biology, Northwestern University, 2153 Sheridan Road, Evanston, IL 60208, USA, and #Laboratory of Molecular Allergy and Immunology, Harvard Medical School, Boston, MA 02215, USA.

Antibody Fc receptors couple the diversity of soluble antibodies to the variety of responses available to differentiated immune cells. Allergic responses result from signaling through the IgE Fc receptor on the surface of mast cells. We have solved the structure of the antibody-binding portion (α) of the receptor FcεRI found on the surface of mast cells. Allergens binding to IgE antibodies cause signaling through FcεRIα and result in release of the powerful immune mediators from the cells.

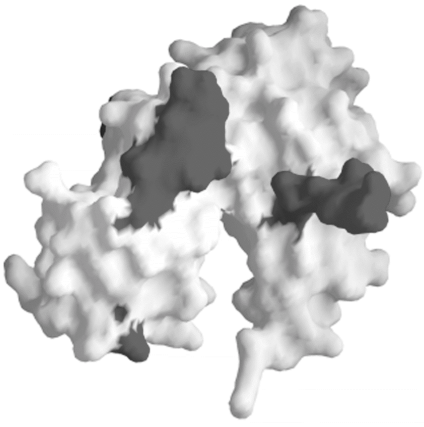

We have solved the structure of FcεRIα in five space groups using different cell lines and constructs. We used MIRAS methods for the best-diffracting crystal form (2.4Å) and MR methods for the others (3.8-3.1Å). The seven N-linked carbohydrates (shown as dark patches) show changes among the different crystal forms. The FcεRIα molecule contains two Ig domains bent over to reveal a patch of four exposed tryptophans at the top of the molecule, away from the membrane-spanning region.

M11.OA.002 CYTOKINE RECEPTOR COMPLEXES VERSES CELL ADHESION INTERACTIONS - UPPING THE AFFINITY. Y. Jones, University of Oxford, UK.

Abstract not available.

M11.OA.003 THE STRUCTURAL EVOLUTION OF A CATALYTIC ANTIBODY. E.C. Mundorff[1], M.H. Hanson[1], P.G. Schultz [1], R.C. Stevens[1] [1]Materials Science Division, Lawrence Berkeley National Laboratory and Department of Chemistry, University of California, Berkeley, Berkeley, CA 94720.

Through the use of catalytic antibodies we are able to explore the relationship between binding energy and catalysis in protein structure. In this study we examined the affinity maturation of the antibody AZ-28 which catalyses the oxy-Cope rearrangement, a pericyclic reaction which is common in organic synthesis but for which there is no known enzyme. Although the six mutations produced during affinity maturation of AZ-28 increases the binding affinity to the hapten, one somatic mutation, Ser(L34)Asn, causes a dramatic decrease in the catalytic rate. The germline antibody possesses a catalytic rate that is close to that of chorismate mutase, an enzyme which also catalyzes a pericyclic reaction, and through affinity maturation this rate decreases to a more modest rate for the mature antibody with a k_{cat}/k_{uncat} of 169,000 and 5300 respectively for the germline and mature antibodies. A structural analysis of this system was pursued to gain an understanding of the interplay between binding energy and catalysis. The x-ray crystal structures of the germline analogue of AZ-28 with and without hapten have each been solved to 2.0Å resolution and are compared with the previously solved structure of AZ-28 with hapten[1]. In the structure of the mature AZ-28 with hapten, it appears that while bound more tightly the hapten is restricted into a catalytically unfavorable conformation through multiple binding interactions. The three structures show only small variations in the active site. However, subtle differences at L34 substantially alter catalysis. In the mature AZ-28 there is a hydrogen bond between L34 and H100a effectively tying together the CDRL1 and CDRH3 loops. In the germline plus hapten structure this hydrogen bond is lengthened to a water-bridged hydrogen bond. This appears to give the CDRH3 loop increased flexibility in the germline structure and also may release some restrictive interactions between the CDRH3 and the hapten. The high catalytic rate of the germline therefore may be facilitated by a higher degree of breathing within the active site. Thus, this system provides unique insight into the evolution of binding energy and its effect on biological catalysis.

1. Ulrich, H., E. Mundorff, B. Santarsiero, E. Driggers, R. Stevens, P. Schultz, Nature 389 (1997) 271-5.

M11.OA.004 STRUCTURE OF A HETEROPHILIC ADHESION COMPLEX BETWEEN HUMAN CD2 AND CD58 (LFA-3). Jia-huai Wang [1], Alex Smolyar [1], Kemin Tan [1], Jin-huan Liu [1], Mikyung Kim [1], Zhen-yu J. Sun[2], Gerhard Wagner[2],Ellis Reinherz[1], [1] Immunobiology Division, Dana-Farber Cancer Institute, Harvard Medical School, Boston, MA. 02115, USA, [2] Department of Biological Chemistry and Molecular Parmacology, Harvard Medical School, Boston, MA. 02115, USA.

Interaction between CD2 and its counter-receptor, CD58 (LFA-3), on opposing cells optimizes immune recognition, facilitating contacts between helper T lymphocytes and antigen presenting cells as well as between cytolytic effectors and target cells. Here we report the crystal structure of the heterophilic adhesion complex between the amino terminal domains of human

CD2 and CD58. A strikingly asymmetric, orthogonal, face-to-face interaction involving the major b-sheets of respective immunoglobulin (Ig)-like domains with poor shape complementarity is revealed. In the virtual absence of hydrophobic forces, interdigitating charged amino acid side chains form hydrogen bond and salt link network at the interface. These charged interactions not only ensure high specificity, but also provide binding energy for this low affinity adhesion. These features explain CD2-CD58 dynamic binding, which is best suited to permit the T cell to broadly sample the surface of an opposing cell in search of the correct antigenic pepetide/MHC complex and co-stimulatory ligands. We have also inferred from sequence comparison that there is a subfamily within the Ig superfamily (IgSF) that utilizes the same interaction mode for cell adhesion, but the physico-chemical character of the subset of residues involved in interface determines the relative binding affinity to meet the different biological requirement.

M11.OA.005 STRUCTURE OF THE INHIBITORY NATURAL KILLER CELL RECEPTORS. Peter D. Sun, Jeffrey C. Boyington, Greg Snyder, Aisha N. Riaz, Apisit Patamawenu, John E. Coligan, Andrew G. Brooks. Structural Biology, NIAID, National Institutes of Health, 12441 Parklawn Drive, Rockville, MD 20852, USA.

The cytolytic activity of natural killer (NK) cells are modulated by several families of extracellular receptors which recognize surface antigens such as class I major histocompatability complex (MHC) molecules on the surface target cells. These receptors are generally members of either the Ig superfamily or the superfamily of C-type lectin. KIR2DL2 is a natural killer cell inhibitory receptor with two Ig domains and has been shown to interact with allotype HLA-Cw3 where as CD94/NKG2s are members of C-type lectin receptors that have been shown to interact with the nonclassical MHC class I molecule HLA-E. Here we report the 2.9 Å resolution crystal structure of the KIR2DL2 ectodomain and the 2.6 Å resolution crystal structure of the C-type lectin domain of CD94. The hinge angle of KIR2DL2 is approximately 80º, 14º larger than that observed in KIR2DL1 and 5º different from that of a second crystal form of 2DL2, suggesting that the interdomain hinge angle is not fixed. The putative ligand binding site is formed by residues from several variable loops with charge distribution apparently complementary to that of HLA-C. The packing of the receptors in the orthorhombic crystal form offers an intriguing model for receptor aggregation on the cell surface. The structure of CD94 reveals a novel variation to the C-lectin fold with one major α-helix being absent and the lack of the canonical calcium binding site. CD94 forms a unique dimer where the missing α-helix, replaced by a loop, becomes part of the dimer interface. The hydrophobic nature of the interface residues appears to be preserved among the sequences of CD94 and NKG2. We suggest a putative HLA_E binding region based on the structure and sequence variations.

P11.OA.001 PEPTIDE BINDING AND T CELL RECOGNITION OF CLASS I MHC MOLECULES. Edward J. Collins, Rui Zhao, Jennifer Kuhns and Timothy Kirksey, Department of Microbiology and Immunology, University of North Carolina, Chapel Hill, NC USA 27510

Designing peptides with enhanced binding to class I MHC to modulate immune responses requires a full understanding of the interactions of peptide and class I MHC. In order to understand these interactions, we have studied a variety of class I MHC/peptide systems. The structures of two class I MHC/peptide complexes derived from human and mouse that are both recognized by the same T cell receptor show that the T cell receptor does not recognize similar surfaces in charge or shape between the two molecules. Structures of an ignored and antagonistic ligands to this same T cell show interesting structural permutations which have more to do with peptide binding and plasticity of the MHC than with T cell recognition. Examination of structures of potential candidates for HIV therapy show the reasons for increased affinity and potential reasons for altered recognition by the immune system. The structure of a poor binding ligand to HLA-A2 shows that the peptide makes no apparent stabilizing contacts within the center of the peptide. The effects on immunogenicity with relation to flexibility of well binding ligands are different. APL based on the structure of the poor binder show increased binding affinity and different immunological properties.

P11.OA.003 CRYSTALLOGRAPHIC ANALYSIS OF THE SYN ELIMINATION ABZYME 1D4. N.A. Larsen, A. Heine, B.F. Cravatt, R.A. Lerner, and I.A. Wilson. Department of Molecular Biology, BCC 206, The Scripps Research Institute, 10550 N. Torrey Pines Rd., La Jolla, CA 92037, USA.

The catalytic antibody 1D4 selectively catalyzes a highly disfavored syn-elimination reaction. 1D4 significantly accelerates the sterically-hindered transformation over its background reaction. We seek to understand the structural basis for this reactivity. Four high-resolution x-ray diffraction data sets were collected: unliganded 1D4, 1D4 co-crystallized with two stereoisomeric substrate analogs, and 1D4 co-crystallized with a rigid bicyclic transition state analog. Crystals of the unliganded 1D4 and crystals of the substrate analog and transition state analog complexes diffracted to 1.80 Å, 1.90 Å, 2.05 Å, and 1.75 Å, respectively. The structures were determined by molecular replacement using AMoRe, and our current models were refined using CNS and SHELXL. Electron density maps unambiguously show the transition state analog nestled between the hypervariable loops, which form the active site. The molecular surface representation shows that this active site forms a deep binding pocket. The transition state analog fits snugly into this binding pocket, forming close contacts mainly with the second and third hypervariable loops of the heavy chain (H2 and H3). Further comparison of the structures reveals significant conformational differences in the H2 loop. Structural differences in the active site, in particular H2, may have important mechanistic implications. We report here the x-ray crystal structures of 1D4, as well as a proposed mechanism for catalysis of the syn-elimination reaction.

11OB METALLOPROTEINS, ELECTRON TRANSPORT AND EXAFS

M11.OB.001 CRYSTAL STRUCTURES OF REACTION INTERMEDIATES OF CYTOCHROME P450$_{CAM}$. Ilme Schlichting, Max Planck Institute, Dortmund, Germany; Joel Berendzen, Kelvin Chu, Biophysics Group Los Alamos National Laboratory; Robert M. Sweet, Biology Department, Brookhaven National Laboratory; Dagmar Ringe, Gregory A. Petsko, Rosenstiel Center, Brandeis University; Steven Sligar, Department of Biochemistry & Beckman Inst. for Advanced Science and Technology, University of Illinois

Cytochrome P450 enzymes form a family of ubiquitous heme proteins named after an absorption band at 450 nm when complexed to carbon monoxide (CO). P450 enzymes are mixed-function mono-oxygenases. They play a critical role in the synthesis and degradation of many physiologically important compounds and xenobiotics. This makes cytochrome P450s an attractive target for pharmaceutical or environmental industries. The biochemical relevance of the P450-mono-oxygenases in general is their unique ability to catalyze the hydroxylation of non-activated aliphatic or aromatic hydrocarbons. The biochemically and structurally best characterized P450 is P450$_{cam}$

from *Pseudomonas putida*, which catalyzes the stereospecific 5-exo-hydroxylation of camphor. Although many structures of different $P450_{cam}$ complexes have been determined by Poulos and coworkers, the structure of the biochemically important oxygen complex of $P450_{cam}$ has not been determined yet as it is unstable (halflife ca. 3 min at 4C) due to autooxidation. This requires to collect the diffraction data of the short-lived complex either fast (e.g. by the Laue method) or to prolong its life time. Only the latter approach worked in our hands: we use cryocrystallography to determine the crystal structures of unstable intermediates occuring along the reaction pathway of $P450_{cam}$: We chemically reduce ferric P450.camphor crystals to generate the ferrous complex. The ternary P450.camphor.O2 complex is generated by diffusion of oxygen. X-ray radiolysis can be used to trigger the mono-oxygenase reaction in frozen crystals. The intermediate(s) generated can be transformed to the product 5-hydroxy-camphor by rapid thawing and refreezing of the crystals. The methods used, and the structures obtained will be discussed.

M11.OB.002 SPECIFICITY AND MECHANISM OF THE HYDROXYLATING DIOXYGENASE – NAPHTHALENE DIOXYGENASE. S. Ramaswamy, A. Karlsson, E. Carredano, D. Choudhury, H. Eklund [1], R.E. Parales, J. Parales, D.T. Gibson [2], [1]Department of Molecular Biology, Swedish University of Agricultural Sciences, Box 590, Biomedical Center, Uppsala 75124, Sweden, [2]Department of Microbiology, University of Iowa, Iowa City, Iowa 52242, USA.

The initial reaction in the degradation of many aromatic compounds is catalysed by multicomponenet ring hydroxylating dioxygenase systems which add both atoms of dioxygen to the aromatic ring. The first structure of this class of enzymes - that of naphthalene dioxygenase has been determined [1]. Naphthalene dioxygenase catalyses the dihyroxylation of naphthalene to cis-naphthalene dihyrodiol.

The structure revealed that the enzyme is a hexamer of the (alpha)3 beta(3) type. The Rieske center of one subunit is close to the mono-iron active site of its neighbour - the histidine ligand of one is connected the histidine ligand of the other through a single aspartic acid (asp 205) residue.

In order to understand the mechanism of action of this enzyme we have determined structures of the enzyme complexed with substrates/inhibitors with the Fe in both the oxidised and reduced states. We also have determined the structure of the enzyme with an intermediate in the dioxygenation of indole in the active site. Present efforts are focussed on trying to produced a dioxygen/NO bound form of the enzyme in crystals. We hope to put together all these and combine them with mutational studies to work out the possible mechanism of action of naphthalene dioxygenase.

1. B. Kauppi, K. Lee, E. Carredano, R.E. Parales, D.T. Gibson, H. Eklund, and S. Ramaswamy. (1998) STRUCTURE 6 (5), 571-587.

M11.OB.003 POLARIZED EXAFS MEASUREMENTS ON ORIENTED SINGLE CRYSTALS OF CARBONMONOXY-MYOGLOBIN. H.C. Freeman, P.J. Ellis and D. Shi, School of Chemistry, University of Sydney, N.S.W. 2006, Australia, and J.E. Penner-Hahn, Department of Chemistry, University of Michigan, Ann Arbor, MI 48109-1055, USA, and J.A. Ibers and C. Slebodnick, Department of Chemistry, Northwestern University, Evanston, IL 60201, USA.

The geometry of the heme-Fe-C-O site in carbonmonoxymyoglobin (MbCO) is of chemical and biological interest, but has been notoriously difficult to determine [1]. Despite extensive studies by X-ray diffraction, neutron diffraction and vibrational spectroscopy, accurate values for the Fe-C-O angle as well as the tilt of the Fe-C bond with respect to the porphyrin plane have remained elusive. X-ray absorption measurements on MbCO in frozen solution have so far not been helpful, since the EXAFS is dominated by the contributions of the porphyrin atoms.

The problem of resolving the EXAFS contributions of the axial C and O atoms from those of the porphyrin atoms can, in principle, be overcome by taking advantage of the symmetry properties of sperm-whale MbCO crystals. We have recorded polarized Fe *K*-edge X-ray absorption spectra of single crystals of sperm-whale MbCO in six orientations, and have fitted a 3-dimensional model of the heme-Fe-C-O site simultaneously to the six sets of EXAFS data. In the refined model, the Fe-C bond is tilted by 6±1° from the normal to the porphyrin plane, the Fe-C-O angle is 170±3°, and the orientation of the C-O bond is approximately normal to the porphyrin plane. The N(porphyrin)-Fe-C-O torsion angle is not determined uniquely. The robustness of the model has been tested and will be discussed. The value of the Fe-C-O angle is supported by a novel analysis of pre-edge features in the XANES of frozen MbCO solutions and a series of model compounds.

[1] T.G. Spiro & P.M. Kozlowski (1997) J. Biol. Inorg. Chem, 2, 516-520; C. Slebodnick & J.A. Ibers, ibid., 521-525; T. Vangberg, D.G. Bocian & A Ghosh, ibid., 526-530; M. Lim, T.A. Jackson & P.A. Anfinrud, ibid., 531-536; J.T. Sage, ibid., 537-543; J.S. Olson & G.N. Phillips Jr., ibid., 544-552.

M11.OB.004 X-RAY ABSORPTION SPECTROSCOPY OF MOLYBDENUM AND TUNGSTEN ENZYMES. Graham N. George, Stanford Synchrotron Radiation Laboratory, P.O. Box 4349, MS 69, Stanford, California 94309, U.S.A.

Molybdenum and tungsten are the only second and third period transition metals with well defined biological functions. In most cases these metals function in metalloenzymes in the catalysis of two electron oxidation-reduction reactions involving the transfer of an oxygen from the metal to the substrate, or the reverse reaction. Both metals possesses highly flexible chemistries which allows them to adopt a variety of configurations in the enzyme systems. Recent X-ray absorption spectroscopic results on several molybdenum and tungsten enzymes will be presented, and the structural information reviewed and compared with the information available from protein crystallography. In many cases these are at odds and possible reasons for this will be discussed.

M11.OB.005 XAFS AND CRYSTALLOGRAPHIC STUDIES OF COPPER PROTEINS. S Samar Hasnain, Synchrotron Radiation Department, CCLRC Daresbury Laboratory, Warrington WA4, Cheshire, UK Email: S.Hasnain@dl.ac.uk

Crystallographic, XAFS and site directed mutagenesis studies of three copper proteins, namely Rusticyanin, Cu-Zn bovine superoxide dismutase and Cu1-Cu2 nitrite reductase would be presented to emphasise the interplay between the two X-ray techniques. Results from a combined study of high to atomic crystallographic structures [Rusticyanin (1.27Å), superoxide dismutase (1.6Å) and nitrite reductase (2.1Å)] and ultra-high resolution XAFS [~0.2Å at the metal centres] will be presented to demonstrate the importance of this approach in providing the structural basis for the biochemisty of these proteins. The example of Cu-Zn bovine superoxide dismutase illustrates the importance of on-line monitoring of the redox states of metalloproteins crystals by XANES.

P11.OB.001 THE INVESTIGATION OF THE STRUCTURE AND FUCTION OF DENITRIFYING ENZYMES. A. Jafferji, [1] V. Fulop, [2] S. Ferguson, [3], [1] Laboratory of Molecular Biophysics, University of Oxford, [2] Department of Biological Sciences, University of Warwick, [3] Department of Biochemistry, University of Oxford.

The bacterial denitrifying pathway conists of four distinct steps, the conversion of nitrate to nitrite, catalysed by nitrate reductase, nitrite to nitric oxide, catalysed by nitrite reductase, nitric oxide to nitrous oxide, catalysed by nitric oxide reductase and nitrous oxide to nitrogen gas, catalysed by nitrous oxide reductase.

The structure of nitrite reductase has been determined (Fulop et al., 1995), however further studies need to be carried out to determine the relationship between the structure and function of this enzyme and the interaction of this enyzme with the physiological electron donors, cytochrome c550 and pseudoazurin. The structures of the other enzymes are unknown.

Work has been carried out to determine the structure of nitrous oxide reductase and understand the mechanism of action of nitrite reductase and will be presented.

P11.OB.002 THE X-RAY STRUCTURE OF ``PRISMANE'' PROTEIN CONTAINING TWO NOVEL 4FE CLUSTERS. S.J.Cooper[1,2], S.Bailey[1], D.Garner[2], W.R.Hagen[3], P.F.Lindley[4], [1] Daresbury Lab, CCLRC, Warrington WA4 4AD, Cheshire, England, [2] Univ Manchester, Dept Chem, Manchester M13 9PL, England, [3] Agr Univ Wageningen, Dept Biochem, Wageningen, Netherlands, [4] ESRF, BP 220, F-38043 Grenoble, France.

In 1989 an unknown protein was discovered that co-purified with the soluble hydrogenase of a sulphate reducing anaerobic bacterium *Desulfovibrio vulgaris*. On the basic of EPR spectroscopic analysis it was proposed that the iron sulphur prosthetic group of this protein was unprecedented in its structure and redox chemistry: [6Fe-6S] prismane core with four stable oxidation states within a relatively narrow redox-potential window of *ca* 0.5V [1]. The crystal structure of this so called `prismane protein' has now been determined to 1.6Å [2] and does *not* contain a 6Fe cluster. The protein consists of two 4Fe clusters situated 12Å apart close to the interface formed by three domains. Cluster 1, a conventional [4Fe-4S] cubane, is bound near the N-terminus by an unusual sequential arrangement of four cysteine residues. This differs significantly from typical linkage in high-potential iron proteins, aconitase and bacterial ferredoxins. This cluster is bound near the N-terminus of the molecule close to the exterior of the protein and may participate in electron transfer. Cluster 2 appears to be unique among the iron sulphur containing protein whose structures have so far been elucidated. The cluster comprises both O and S bridges between the 4 iron atoms. Two iron atoms (Fe5, Fe6) have what could be described a tetrahedral local environment whilst the other two (Fe7,Fe8) are trigonal bipyramidal. Between Fe7 and Fe5 is unidentified electron density which appears to be partially occupied by a mono or dinuclear species and may represent a substrate binding site.

[1] Hagen W.R. *et al* (1989) J Chem Soc Faraday Trans I 85:4083-4090
[2] Arendsen A. F. *et al* (1998) JBIC 3:81-95

P11.OB.003 THE STRUCTURE OF AURACYANIN, A 'BLUE' COPPER PROTEIN FROM *CHLOROFLEXUS AURANTIACUS*. C.S.Bond, H.C.Freeman, J.M.Guss, M.Maher, M.C.J.Wilce, K.Willingham, Department of Biochemistry, University of Sydney, NSW 2006, Australia, R.E.Blankenship and F.Selvaraj, Department of Chemistry and Biochemistry, Arizona State University, Tempe, Arizona.

Auracyanin is a 'blue' single-Cu protein (cupredoxin) produced by the green, filamentous, thermophilic, phototropic bacterium *Chloroflexus aurantiacus*. *Chloroflexus* occupies an important position in current hypotheses concerning the evolution/origin of photosynthesis. Two auracyanin genes are present in *C. aurantiacus* (auracyanins A and B). The structure presented here is that of auracyanin B

Hexagonal crystals of dimensions 0.3 mm x 0.3 mm x 0.6 mm ($P6_422$, a=115.7, c=54.6) grow at pH 7.5 (50 mM Hepes buffer, 2 M Li_2SO_4). The Crystals can be cryo-cooled for data collection by quick washing in a solution of 20% MPD in artificial mother liquor. Data extending to 2.4Å at four wavelengths around the Cu *K* edge (~1.38Å) were used to solve the structure, and a further 1.55Å data set was collected for refinement (BioCARS beamline BM-14D, Advanced Photon Source).

The structure has one auracyanin molecule per asymmetric unit (139 amino acid residues and one Cu atom) along with 248 water molecules, 2 sulfate ions and a chloride ion. The final residuals (REFMAC) are $R = 0.205$ and $R_{free} = 0.234$.

This structure sheds light on the position auracyanin occupies in the family of cupredoxins. Structurally, auracyanin lies between plastocyanin and azurin. While the overall fold is very similar to azurin, the structure of the loops surrounding the Cu site and the geometry of the Cu site itself contain aspects common to both.

P11.OB.004 HIGH RESOLUTION STRUCTURES OF MANGANESE SUPEROXIDE DISMUTASE. Ross A. Edwards and Geoffrey B. Jameson, Institute of Fundamental Sciences, Massey University, Palmerston North, New Zealand, Mei Whittaker and James W. Whittaker, Department of Biochemistry and Molecular Biology, Oregon Graduate Institute of Science and Technology, Portland, OR 97291-1000, USA, and Edward N. Baker, School of Biological Sciences, University of Auckland, Auckland, New Zealand.

The structures of site-directed mutants of manganese superoxide dismutase from Escherichia coli are complementing functional studies that address the mechanism of action of this key enzyme. In addition to the native enyme1 and iron-substituted derivative,2 structures of active-site mutants Y34F, Q146L and Q146H, and of gateway mutants H30A and Y174F are being determined to 2.1 Å resolution or better. In the case of the Y174F mutant, synchrotron data (DESY, Hamburg) have been obtained for the functionally active reduced (Mn(II)) and oxidised (Mn(III)) forms of the enzyme to 0.9 Å resolution, and for the azide data to 1.25 Å were collected. Key data processing statistics are summarised in the table for the high resolution pass of the data collection:

	Mn(II)	Mn(III)	Mn(II)-azide
Resolution range, Å	1.8 - 0.90	2.4 - 0.9	2.5 - 1.25
Completeness (final shell), %	91 (81)	96 (67)	95 (94)
Rmerge (final shell)	0.057 (0.41)	0.045 (0.37)	0.053 (0.33)
I/((I)(final shell)	22 (2.4)	22 (2.4)	19 (3.6)

For the Mn(II) and Mn(III) structures we hope to gain insight into proton movements in the active site. The azide derative models putative interactions of the superoxide substrate with the active site.

[1] Edwards RA, Baker HM, Whittaker M, Whittaker JW, Jameson GB and Baker EN. 1998. J. Biol. Inorg. Chem. 3: 161-171.
[2] Edwards RA, Whittaker M., Whittaker JW, Jameson GB and Baker, EN. 1998. J. Am. Chem. Soc. 120: 9684-9685.

P11.OB.005 COMPLETION OF THE PLANT PEROXIDASE REACTION CYCLE. A. Henriksen and M. Gajhede, Protein Structure Group, Dept. of Chem., Univ. of Copenhagen, Universitetsparken 5, DK-2100 København Ø, Denmark and A.T. Smith, School of Biol. Sci., Univ. of Sussex, Brighton BN1 9QG, U.K.

The distal arginine is highly conserved in plant peroxidases and it has been considered to play a minor role in O-O bond cleavage and ligand binding including H_2O_2 binding. Its major, but not very well defined role has been considered to be assisting substrate oxidation. We have solved the X-ray structure of the binary HRPC*-ferulic acid complex and the ternary HRPC*-CN-ferulic acid complex to 2.0 and 1.45 Å respectively. Ferulic acid is a natural occurring phenolic compound found in the plant cell wall and it is an *in vivo* substrate for plant peroxidases. The X-ray structures demonstrates the flexibility of the aromatic donor binding site in plant peroxidases and highlight the role of the distal arginine in substrate oxidation and ligand binding. Cyanide or ferulic acid binding does not affect the position of the distal arginine in the distal heme cavity. Distal arginine contributes significantly to stabilization of the HRPC*-CN complex by supplying a short hydrogen bond of 3.0 Å, demonstrating that distal arginine will also be able to contribute with a similar interaction to O-O bond cleavage. In addition, the arginine has a short hydrogen bond of 3.0 Å to the phenolic oxygen, which has another short hydrogen bond of 2.6 Å to a structurally conserved water molecule in the distal cavity. This structurally conserved water molecule is further linked with a hydrogen bond of 2.9 Å to backbone oxygen of P139, a conserved residue within the superfamily of plant peroxidases, and to the distal histidine with a hydrogen bond of 3.5 Å.

A general mechanism of peroxidase substrate oxidation (Compound I → Compound II and Compound II → resting state) is proposed.

11OC HIGH PRESSURE STUDIES OF BIOLOGICAL AND OTHER SOFT MATTER

M11.OC.001 PRESSURE DEPENDENCE OF THE PHASE BEHAVIOUR OF POLYMER BLENDS AND DIBLOCK COPOLYMERS. Kell Mortensen, Henrich Frielinghaus, Risø National Laboratory, Dietmar Schwahn, Forschungszentrum Jülich, Germany.

Studies of the phase behaviour of polymer systems have proven that the sensitivity to fluctuations is much more distinct than originally anticipated based on theoretical arguments. In blends of both homo- and diblock co-polymers, studies have revealed that fluctuations give rise to significant re-normalised critical behaviour. In block copolymers fluctuations have even more pronounced effects, as it changes the second order critical point at $f = 0.5$ to first order, and additional complex phases are stabilised. It has been argued that the free volume causes an entropic contribution to the Flory-Huggins interaction parameter, χ, and is thereby responsible for the re-normalised behaviour. These properties can experimentally be studied through measurements of the structure factor $S(q)$, obtained as a function of temperature and pressure. Most results on homo-polymer blends are in agreement with the argument that free volume will cause additional entropic contributions to the free energy. Studies on block copolymer systems shows, however, more diverging results, with no generalised rule for the effect on T_c versus pressure. In systems including the polymer PDMS, both homo-polymer blends and diblock copolymers show unique character in the phase diagram. For the diblock copolymer of PEP and PDMS, for example, this manifests itself as first a melting of the ordered mesophase, and subsequently a re-entrant ordered structure. An unexpected singularity in the conformational compressibility, as identified from the peak-position, q*, is moreover observed.

M11.OC.002 POLYMER STRUCTURES AT ELEVATED PRESSURE. H. E. King, Jr., Exxon Research and Engineering Co., Annandale, NJ 08801, USA

Polymers, e.g. synthetic macromolecules having an amorphous or partially crystalline nature, exhibit structures at several length scales. Elevated-pressure studies have aided our understanding of the origin of these structures, and I will discuss several examples to give both a historical perspective and to highlight areas of current interest. For crystalline polymers, the role of high pressure is best exemplified by the extensive studies of linear polyethylene which have shown that for P>330 MPa, chain folding in the crystals is suppressed and "extended-chain crystals" dominate. As is well known, this change closely parallels the appearance of a hexagonal phase in the P-T phase diagram. The importance of this phase to the crystallization behavior as well as its relation to the rotator phases of the alkane molecules are two areas of continuing discussion. For amorphous polymers, the relevant structure is a modified random walk, with details of the monomer-monomer correlation function reflecting interactions between monomers and their surroundings. Therefore, studies of the chain dimensions via neutron or light scattering give information on the thermodynamics of solubility. In polymer blends, use of small angle neutron scattering along with the random phase approximation of de Gennes allows one to directly obtain the polymer-polymer interaction energy. This energy has been measured for polyolefin mixtures as functions of both T and P. Much of the data can be collapsed to a single function of density, presumably due to the dominance of van der Waals interactions. Polymer dimensions for isolated chains in solvents have also been measured as a function of P. There it is found that the chain dimensions of non-ionic water-soluble polymers are influenced by high pressures. One can understand this through appeal to pressure and temperature dependence of hydrogen-bond strength and hydrophobicity. A thermodynamic model for this has been developed and is found to well describe the data.

M11.OC.003 PATTERNS IN THE PHASE AND STRUCTURAL BEHAVIOUR OF LYOTROPIC LIQUID CRYSTALLINE SYSTEMS AT HIGH PRESSURE. R. H. Templer, The Department of Chemistry, Imperial College, London SW7 2AY

Lyotropic liquid crystalline phases form when amphiphilic molecules are mixed with water. The amphiphiles assemble into interfaces where the polar headgroup moities screen the apolar hydrocarbon chains from aqueous contact. These flexible, fluid interfaces form a diverse range of liquid crystalline structures, from periodic stackings of lamellar bilayers, through the warped bilayers of the bicontinuous phases and the hexagonal packings of cylindrical monolayers to the complex cubic packings of spherical micelles.

Conventionally researchers have explored the phase and structural behaviour of these systems with small angle X-ray diffraction, in response to variations in the water composition and temperature. In the last decade a number of groups have extended these studies to include the effects of applied hydrostatic pressure. The experimental complexities of such measurements are of course greater than the more conventional studies, but the great advantage of pressure studies is that it provides a further, independent thermodynamic parameter with which to probe our current understanding of the behaviour of these materials. In this talk, recent work on the phase and structural behaviour of lyotropic liquid crystalline phases as a function of pressure and temperature will be discussed in terms of the general patterns

which can be observed. At the qualitative level we believe that the observations can be rationalised in terms of the effect that pressure has in reducing the desire for interfacial curvature and increasing the energetic cost of hydrocarbon chain extension.

M11.OC.004 PROTEINS UNDER PRESSURE: A MOLECULAR MECHANISM OF PRESSURE-INDUCED UNFOLDING. G. Hummer, Theoretical Biology and Biophysics Group T-10, Los Alamos National Laboratory, Los Alamos, New Mexico 87545, U.S.A.

Proteins unfold under pressures of a few kilobar. However, a molecular mechanism of pressure-induced denaturation remained elusive. Aggravating this lack of a molecular understanding of pressure effects on proteins is that pressure denaturation appears to contradict the standard model of protein stability. Proteins are believed to be stabilized by a hydrophobic core of non-polar amino acids. Upon unfolding, these interior residues become solvent exposed. According to the standard model, proteins should become more stable at pressures above a few kilobar, where the solubility of non-polar molecules in water decreases. This apparent contradiction can be resolved by inverting the standard model of protein unfolding [1]. We focus on the transfer of water into the protein interior rather than the transfer of interior amino acids into water. Indeed, pressure reduces the stability of hydrophobic aggregates in water by insertion of water molecules. We propose a 'swelling mechanism' of pressure-induced unfolding of proteins. Implications on the structural characteristics of the unfolded ensemble, folding and unfolding kinetics, and combined temperature and pressure effects will be discussed.

G. Hummer, S. Garde, A. E. García, M. E. Paulaitis & L. R. Pratt (1998) Proc. Natl. Acad. Sci. U.S.A., **95**, 1552.

M11.OC.005 HIGH PRESSURE X-RAY CRYSTALLOGRAPHIC STRUCTURE OF MYOGLOBIN. P. Urayama, S.M. Gruner [1], G.N. Phillips, Jr. [2], [1] Department of Physics, Cornell University, Ithaca, New York 14853-2501, USA, [2] Department of Biochemistry and Cell Biology, Rice University, Houston, Texas 77005-1892, USA.

Pressure is a significant parameter in biological systems, as pressures in the kilobar range affect reaction kinetics, rigidify membranes, disrupt quaternary associations, and unfold proteins. Of the various high pressure biological techniques, macromolecular crystallography is the least utilized. The only high pressure structure is of hen egg-white lysozyme at 1 kbar, in which Kundrot and Richards find an anisotropic compressibility, no domain hinge movement, and an average decrease in the temperature factor [1]. Now, we present a second high pressure protein structure -- sperm whale myoglobin at 1.5 kbar. We will also describe current high pressure techniques, and a possible alternative for facilitating the collection of high pressure data.

1. C.E. Kundrot and F.M. Richards (1987). J. Mol. Biol., 193, 157.

M11.OC.006 PRESSURE EFFECTS ON PROTEIN STABILITY AND FOLDING KINETICS. C. A. Royer, Centre de Biochimie Structurale, INSERM U414, Faculte de Pharmacie, 15 ave. Charles Flahault 34060 Montpellier France

The factors controlling the process of protein folding remain in large part to be characterized. We have employed pressure perturbation techniques in the study of protein folding and unfolding transitions, as a complement to more traditional approaches employing temperature or chemical perturbations. Mutational studies on the pressure unfolding of staphylococcal nuclease indicate that solvent excluded voids and cavities contribute significantly to the value of the volume changes observed.

The effect of pressure on unfolding and folding rate constants yields the values of the volumes of activation for these processes. The changes in system volume for these transitions provides information about the nature of the transition state and the role of solvation in the rate-limiting step of protein folding and unfolding. Temperature studies have revealed the basis for the shape of the P-T phase diagram of proteins. Comparison of a number of different protein systems has allowed correlation of volume effects with structural and topological constraints imposed by the sequence.

P11.OC.001 THE EFFECT OF HIGH PRESSURE ON THE PHASE SEPARATION AND GELATION OF AGAROSE IN WATER. D.W.N. Edington, J. Crain and W.C.K. Poon, Department of Physics and Astronomy, The University of Edinburgh, Mayfield Road, Edinburgh EH9 3JZ, Scotland, UK

Systems which possess both a gel transition and undergo spinodal decomposition are of great interest. If developing spatial inhomogeneities due to phase separation are arrested by gelation, a complex morphology results which can be controlled by altering the system composition, or as we show here, by altering the pressure at which gelation occurs.

Recent work at Edinburgh showed that a hydrostatic pressure of 1 kbar has a dramatic effect on the spinodal decomposition of gelatin in a 30/70% mixture of methanol and water, but has little effect on the gelation temperature. We extend the study to look at aqueous agarose - another example of a system in which both gelation and spinodal decomposition occur. Preliminary results of spectroscopic (Raman and Brillouin) measurements at higher pressure will also be presented.

P11.OC.002 EFFECT OF PRESSURE ON THE STABILITY AND PHASE BEHAVIOUR OF LYOTROPIC LIPID MESOPHASES AND MODEL MEMBRANE SYSTEMS. R Winter, A. Gabke, and J. Woenckhaus, University of Dortmund, Physical Chemistry I, Otto-Hahn-Straße 6, D-44227 Dortmund, Germany

Lipids, which provide valuable model systems for membranes, display a variety of polymorphic phases, depending on their molecular structure and environmental conditions. By use of x-ray and neutron diffraction, infrared spectroscopy and calorimetry, the temperature and pressure dependent structure and phase behaviour of lipid systems, differing in chain configuration and headgroup structure have been studied. Besides lamellar phases also non-lamellar phases have been investigated. Hydrostatic pressure has been used as a physical parameter for studying the stability and energetics of lyotropic mesophases, but also because high pressure is an important feature of certain natural membrane environments (e.g., marine biotopes) and because the high pressure phase behaviour of biomolecules is of biotechnological interest. Neutron scattering in combination with the H/D contrast variation technique has been used to the study of lateral organization of phase-separated binary lipid mixtures. By using the pressure-jump relaxation technique in combination with time-resolved synchrotron x-ray diffraction, the kinetics of different lipid phase transformations was also investigated. The time constants for completion of the transitions depend on the direction of the transition, the symmetry and topology of the structures involved, and also on the pressure-jump amplitude.

P11.OC.003 DOES HIGH PRESSURE STABILISE LYOTROPIC INVERSE BICONTINUOUS CUBIC PHASES? R. H. Templer , O. Ces and J. M. Seddon, The Department of Chemistry, Imperial College, London SW7 2AY

In studies of homologous series of amphiphile / water mixtures which form inverse lyotropic liquid crystalline phases it has been observed that a reduction in chain length stabilises the inverse bicontinuous cubic phases with respect to the inverse hexagonal phase. We believe that this arises because the shorter chain lengths give rise to a reduced desire for interfacial curvature and are unable to accomodate the variation in chain extension required to pack into the inverse hexagonal phase. We therefore hypothesised that increasing hydrostatic pressure would have a similar effect, since it should also reduce the desire for interfacial curvature and stiffen chains to extension. We will present the results of small angle X-ray studies at high pressure on a homologous series of ether linked phosphatidylethanolamines in water. The evidence indicates that at high pressures there is indeed a triple point from which a region of stability for the inverse bicontinuous cubic phases unfolds.

11OD CRYSTAL ENGINEERING

M11.OD.001 ENGINEERING OF MOLECULES, ASSEMBLIES, CRYSTALS. Jerry L. Atwood, Department of Chemistry, University of Missouri-Columbia, Columbia, MO 65211, USA

One of the important early roles of crystallography was the deduction of molecular structure. Only very recently have the principles of crystallography been seen as an avenue toward the design of the solid state. In this presentation, the use of synthons to prepare complex, useful assemblies and solids will be described. The general principles by which polygons (synthons) are arranged to form assemblies in solution or crystals in the solid state will be presented. It is anticipated that the golden age of crystal engineering is upon us, and that crystallography will play a leading role in these exciting developments.

M11.OD.002 CRYSTAL ENGINEERING USING CONCERTED PHENYL EMBRACE MOTIFS. Ian Dance, School of Chemistry, University of New South Wales, Sydney 2052, Australia.

Inorganic and organometallic molecules commonly have peripheral aryl and heteroaromatic substituents: for instance, the ligands PPh_3, bipyridyl, and terpyridyl and relatives are widespread, and Ph_4P^+ is known by synthetic chemists as an excellent cation for the crystallisation of anions of all types. This occurs because multiple phenyl embraces are dominant crystal supramolecular motifs. These motifs use concerted edge-to-face and offset-face-to-face local interactions between aryl substituents. The common sixfold phenyl embrace (6PE) between two Ph_4P^+ ions is frequently elaborated into one–, two– and three-dimensional networks. The hexagonal array of 6PE is a significant three-dimensional crystal supramolecular motif, which has allowed the crystal engineering of unusual anions.

This lecture will describe the variety and scope of multiple phenyl embrace motifs in crystal structures, as well as calculations of their supramolecular energies, and their applications in crystal engineering.

M11.OD.003 CONTROL AND MEMORY OF CHIRALITY IN HELICAL COORDINATION POLYMERS FROM ACHIRAL COMPONENTS. Y. Aoyama, Institute for Fundamental Research of Organic Chemistry, Kyushu University, Hakozaki, Higashi-ku, Fukuoka 812-8581, Japan, and CREST, Japan Science and Technology Corporation (JST)

An achiral anthracene-pyrimidine derivative **1** (5-(9-anthracenyl)pyrimidine) forms adduct **1**•$Cd(NO_3)_2$•H_2O•EtOH (**2**) in a chiral space group $P2_1$. The metal ion is hexa-coordinated with two pyrimidine ligands (equatorial cis), water and ethanol (equatorial cis), and two nitrate ions (axial trans). The chirality arises from a pyrimidine-Cd^{2+} helical array and is preserved not only in each crystal via homochiral interstrand water-nitrate hydrogen bonding but also in all the crystals in the same chirality as a result of single-colony homochiral crystal growth. Compound **1** also forms achiral (*Pbca*) trihydrate adduct **1**•$Cd(NO_3)_2$•$3H_2O$ (**3**) having nonhelical pyrimidine-Cd^{2+} zigzag chains. Achiral zigzag polymer **2** and chiral helical polymer **3** are interconvertible with each other in the solid states upon exchange of volatile ligands (ethanol and water). The helix winding associated with the conversion of adduct **3** to **2** can be made homochiral by seeding.

M11.OD.004 REACTIVE MOLECULAR CRYSTALS: DESIGN, DISCOVERY AND UNDERSTANDING. Bruce M. Foxman, Department of Chemistry, Brandeis University, Waltham, MA 02454-9110 USA

How can we use our knowledge of molecular solid-state chemistry, crystal packing, and chemical reactivity to *engineer* new reactive materials? In recent years, we have designed several solid-state reactions by using structural analogies derived from the Cambridge Structural Database (examples from organic and inorganic chemistry will be discussed). Following the initial design work, we developed two new series of metal salts and complexes with unique reactivity properties. Solid metal alkynoates and alkenoates undergo oligomerization and polymerization reactions when exposed to ^{60}Co γ-rays. For example, irradiation of solid sodium *trans*-2-butenoate leads to a linear trimer, *one of eight* possible diastereomers, in high yield. Studies of crystalline metal complexes containing such unsaturated ligands provide new insight into solid-state reactivity. In addition to the use of hydrogen bonding and bilayer interactions as agents for the production of reactive phases, changes in metal ion within an isomorphous set of structures may have profound effects on reactivity. We will present recent results which serve to (a) demonstrate the influence of the metal on crystal and molecular structure (including bilayer formation) as well as solid-state reactivity; (b) provide evidence for the unprecedented formation of isotactic polymer via ^{60}Co irradiation of metal salts; (c) deepen our understanding of principles related to the topochemical postulate (is a given solid-state reaction WYSIWYG {what you see is what you get}?).

M11.OD.005 WEAK BUT PERSISTENT: C-H...Y BONDS IN ANION-CATION RECOGNITION IN NUCLEOSIDE SALTS. M.Jaskolski, Deptartment of Crystallography, A.Mickiewicz University and Center for Biocrystallographic Research, Institute of Bioorganic Chemistry, Polish Academy of Sciences, Poznan, Poland.

Molecular recognition requires precise tuning of the interacting recognition points. Yet, it is surprisingly often that favored supramolecular patterns are retained or reproduced, even in altered chemical contexts, through the phenomenon of molecular mimicry. An excellent example is provided by interactions in which classic hydrogen bonds are replaced by C-H...Y bonds. In the crystal structures of N3-protonated cytidinium and 2'-deoxycytidinium salts with composite XY_n anions, such as

$H_2PO_4^-$, NO_3^-, SO_4^{2-}, SiF_6^{2-}, ClO_4^- and BF_4^-, that are capable of accepting hydrogen bonds through their Y atoms, the dominating motif of cytosinium...anion interactions consists of a pair of hydrogen bonds donated from the $N3^+$-H protonation site and from the exoamino N4-H41 group *cis* to N3, and accepted by two Y centers of one anion. This multipoint recognition pattern is stable and robust and thus can be classified as a supramolecular synthon. In the broader class of N3-protonated, N1-substituted cytosinium salts with composite anions it occurs with high frequency. The biologically inactive C5 side of the cytosine system mimics the $N3^+$-H type synthon and shows a propensity to form an analogous motif involving the N4-H42 exo-amino group. In this secondary motif a C5-H5...Y hydrogen bond replaces the strong $N3^+$-H...Y interaction. Since the C-H...Y bond is weaker, the secondary motif shows higher deformability and is less frequent in a survey of the Cambridge Structural Database.

M11.OD.006 VERY SHORT C-H···X AND X-H…C INTERACTIONS IN SOME ORGANIC PHOSPHONIUM AND IMIDAZOLIUM SALTS. M.G. Davidson, J.A. Cowan, A.E. Goeta, J.A.K. Howard, P. Küpper, S. Lamb, M.A. Leech, Department of Chemistry, Science Site, South Road, Durham DH1 3LE, UK; S.A. Mason, Institut Laue-Langevin, BP 156, 38042 Grenoble Cedex 9, France; and J. Clyburne, Department of Chemistry, Acadia University, Wolfville, NS, Canada B0P 1X0.

The existence and structural importance of C-H···X hydrogen bonds between relatively acidic C-H groups and electronegative atoms or electron rich π-systems is well recognized. [1] In order to study such interactions in the absence of stronger intermolecular forces, we have synthesized (by deprotonation of organic acids with phosphorus ylides) and structurally characterized (by low-temperature X-ray and neutron diffraction) a number of phosphonium aryloxides, amides and phosphides. In the solid state, these salts all contain extensive C-H…X interactions (where X = O, N, or P). [2] We have identified common structural motifs within these salts and have thereby been able to rationalize more complex supramolecular structures, for example those of inorganic 'onium' salts and organic salts containing multifunctional anions. By analogy with the synthesis of phosphonium salts from phosphorus ylides, we have recently extended our work by using N-heterocyclic carbenes to deprotonate organic acids to give 'organic' imidazolium salts. Where the organic acid is a phenol, imidazolium aryloxides result which contain very short C-H…O interactions. Of more significance, however, is our recent isolation and X-ray characterization (at 30 K) of a carbene: amine adduct which, because deprotonation of the amine does not occur, contains an N-H…C hydrogen bond. This is, to our knowledge, the first definitive example of an X-H…C hydrogen bond (where X = N or O) to be characterized in the solid state.

[1] G.R. Desiraju, Angew. Chem., Int. Ed. Engl, 1995, 34, 2328 and references therein.

[2] M.G. Davidson, *J. Chem. Soc. Chem. Commun.,* **1995**, 919; M. G. Davidson and S. Lamb, *Polyhedron*, **1997**, *16*, 4393; M. G. Davidson, K. B. Dillon, J. A. K. Howard, S. Lamb and M. D. Roden, *J. Organomet. Chem*, **1998**, *550*, 481.

P11.OD.001 BEYOND THE FIRST DIMENSION: ORGANIC/ INORGANIC HYBRID MATERIALS ASSEMBLED *VIA* HYDROGEN BONDS. Alicia M. Beatty and Christer B. Aakeröy, Department of Chemistry, Kansas State University, Manhattan, Kansas, 66506 (U.S.A.)

Higher-dimensional supramolecular assemblies are desirable because of their stability (strength) and versatility (materials!). In pursuit of such systems, crystal engineers typically assemble organic networks *via* directional intermolecular forces (esp. hydrogen bonds) *or* metal-containing networks using coordinate-covalent interactions. Our recent contributions merge these approaches: we use *hydrogen bonds* to assemble *metal-containing* networks. Thus we have the advantages of both worlds: flexible hydrogen-bonded networks (to accommodate an assortment of guests), and a variety of coordination geometries (e.g. square planar, octahedral) that are not available in organic systems. While we began with the test-case of silver, which (due to its tendency to adopt linear coordination geometries) readily forms low-dimensional networks, we will demonstrate the utility of this approach for the assembly of 1-D, 2-D and 3-D networks, using a variety of metal ions. The aim is to assemble metal complexes to form materials for a variety of applications, such as host/guest materials for separations and catalysis, molecular wires, and magnetic materials.

P11.OD.002 OPEN FRAMEWORK ENGINEERING IN NIOBIUM OXOCHLORIDE CLUSTER CHEMISTRY. Ekaterina V. Anokhina, Michael W. Essig, Cynthia S. Day, and Abdessadek Lachgar, Department of Chemistry, Wake Forest University, Winston-Salem, NC 27109 USA

The “mixed ligand approach” has been shown to be a successful strategy to modify structural and physical properties of materials in a controlled way. We used a combination of oxide and chloride ligands in octahedral clusters $[Nb_6L_{18}]^{n-}$ to synthesise a new family of open framework cluster compounds with 1D, 2D, and 3D networks. Single crystal x-ray diffraction analysis showed that their structural features are unprecedented in the crystal chemistry of compounds based on octahedral clusters. Comparative analyses of these structures show strong correlations between the arrangement of the oxide and chloride ligands in the cluster unit and the cluster framework topology. We will demonstrate that the complex and novel cluster connectivity corresponds to the packing of chloride and oxide ligands that minimises their electrostatic repulsions. The presence of cavities and redox-active clusters in these compounds could lead to their application in heterogeneous catalysis and intercalation chemistry.

P11.OD.003 TOWARDS A PICTORIAL GLOSSARY OF INTER-MOLECULAR INTERACTIONS. M.A. Spackman, J.J. McKinnon & A.S. Mitchell, Division of Chemistry, University of New England, Armidale NSW 2351, AUSTRALIA.

We have recently described a remarkable new way of exploring molecular crystals using a novel partitioning of crystal space [1-3]. These molecular Hirshfeld surfaces, so named because they derive from Hirshfeld’s stockholder partitioning [4], divide the crystal into regions where the contribution from the electron distribution of a sum of spherical atoms for the molecule (the promolecule) exceeds the contribution from the corresponding sum over the crystal (the procrystal). They reflect intermolecular interactions in a novel visual manner, offering a hitherto unseen picture of molecular shape in a crystalline environment. Surface features characteristic of different types of intermolecular interactions can be identified, and Hirshfeld surfaces are remarkably different for different polymorphic forms of the same material.

Specific surface features can be revealed by colour coding distance from the surface to the nearest atom in a neighbouring molecule. Close contacts are coloured red (hot spots!), others range through yellow and green to blue for the most distant contacts (cold spots!). This simple device provides a remarkable and immediate visual fingerprint of the types of interactions present, and even reflects their relative strengths from molecule to molecule. For example, the surface for triphenylene reveals two distinct regions: numerous red dimples at one end, characteristic of C–H…π interactions, and a flat green/blue region at the other end, characteristic of π - π stacking.

Compilation of a pictorial glossary is underway, using identifiable patterns of interaction between small molecules to rationalize the often complex mix of interactions displayed by large molecules. Applications of this new tool to a wide variety of interaction types common in molecular crystals will be presented.

[1] M.A. Spackman & P.G. Byrom, *Chem. Phys. Lett.*, **267**, *215* (1997).
[2] J.J. McKinnon, A.S. Mitchell & M.A. Spackman, *Chem. Eur. J.*, **4**, *2136* (1998).
[3] J.J. McKinnon, A.S. Mitchell & M.A. Spackman, *Chem. Commun.*, *2071* (1998).
[4] F.L. Hirshfeld, *Theor. Chim. Acta*, **44**, *129* (1977).

P11.OD.004 USING HIRSHFELD SURFACES TO VISUALIZE INTERMOLECULAR INTERACTIONS IN POLYMORPHIC SYSTEMS. J.J. McKinnon, A.S. Mitchell & M.A. Spackman, Division of Chemistry, University of New England, Armidale NSW 2351, AUSTRALIA, and S.L. Price, Centre for Theoretical and Computational Chemistry, University College London, 20 Gordon St, London WC1H 0AJ, UK.

The existence of more than one stable crystal packing arrangement for a particular molecule hints at a very general, and rather subtle, balance between the various types of intermolecular interaction in the formation of molecular crystals. In recent work we have been investigating a remarkable new way of exploring molecular crystals using a novel partitioning of crystal space [1-3]. These molecular Hirshfeld surfaces reflect intermolecular interactions in a striking visual manner, offering a hitherto unseen picture of molecular shape in a crystalline environment.

Colour coding distance from the surface to the nearest atom in a neighbouring molecule reveals specific surface features: close contacts are coloured red (hot spots!), others range through yellow and green to blue for the most distant contacts (cold spots!). Hirshfeld surfaces can be surprisingly similar (e.g. *p*-dichlorobenzene) or dramatically different (e.g. oxalic acid) for different polymorphs, and the colour coding of distances in this fashion can reveal the underlying interactions responsible, and the ways in which their exploitation differs between polymorphs. Because it can summarize information on all close intermolecular interactions simultaneously, we have been using this simple application of Hirshfeld surfaces as a visual tool in the exploration of a number of polymorphic systems.

To date, we have applied this analysis to molecular systems such as acridine, benzene, *p*-dichlorobenzene, fumaric acid, indigo, oxalic acid and terephthalic acid. Detailed examples of colour-coded Hirshfeld surfaces for these systems will be presented, along with more quantitative information derived from the surfaces and tentative conclusions arising from this study.

[1] M.A. Spackman & P.G. Byrom, *Chem. Phys. Lett.*, **267**, *215* (1997).
[2] J.J. McKinnon, A.S. Mitchell & M.A. Spackman, *Chem. Eur. J.*, **4**, *2136* (1998).
[3] J.J. McKinnon, A.S. Mitchell & M.A. Spackman, *Chem. Commun.*, *2071* (1998).

P11.OD.005 APPLICATION OF CRYSTAL-ENGINEERED TETRAPYRIDYLPORPHYRIN COMPLEXES TO HYDROGEN-BONDED SUPRAMOLECULAR ASSEMBLY ON A GOLD SURFACE. Robin D. Rogers, Grant A. Broker, C. V. Krishnamohan Sharma, Brian T. Pyevich, Jason A. Swenson, and Gregory J. Szulczewski, Department of Chemistry, The University of Alabama, Tuscaloosa, AL 35487, USA.

Tetrapyridylporphyrin (TPyP) has been used to construct porous 1D and 2D networks using coordinating metal halides (MX_2; M = Hg, Cd, Pb). For example, the 1:2 complexes of TPyP and HgX_2, (X=I, Br), form porous 1D coordination polymers. The shape and mode of aggregation of 1D polymers leads to the formation of 2D layers with a second type of cavity. Both the cavities in these complexes are capped by solvent molecules and form a bilayer architecture.

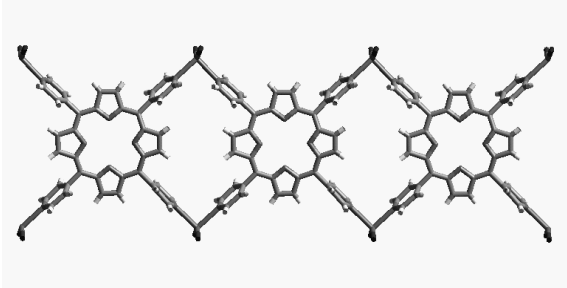

The design strategies realized with the synthesis of crystalline solids, have now been applied to organization of porphyrinic chromophores on a surface through hydrogen-bonds, providing a powerful means for the design of novel complexes with useful functional properties. Acid-terminated self assembled monolayers where constructed by immersion of thin gold surfaces in methanolic mercaptyl acid solutions and then immersion in chloroformic solutions. The acid terminated surfaces readily hydrogen-bond with tetrapyridylporphyrin. This presentation will discuss the characterization of these self-assembled, hydrogen-bonded layers of porphyrins through the use of XPS, ellipsometry, and reflection IR. Model crystal structures of hydrogen bonded TPyP complexes will also be presented.

P11.OD.006 CRYSTALS BY DESIGN: IN-SITU ATOMIC FORCE MICROSCOPY INVESTIGATION OF SURFACE GROWTH MORPHOLOGY AND KINETICS. T.A. Land (a), M.T. McBride (b), M. Luo (b), G.T.R. Palmore (b), J.J. DeYoreo (a) a) Lawrence Livermore National Laboratory, Livermore, California, 94550 b) University of California Davis, Department of Chemistry, Davis, CA, 95616

We have used In-situ atomic force microscopy (AFM) to elucidate how changes in molecular structure are manifested in the evolution of surface morphology and step dynamics during growth. The premise of this work is to be able to control the arrangement of molecules in crystalline solids by exploiting the strength, directionality and selectivity of hydrogen bonds. In these experiments, in-situ AFM has been used to investigate the growth of a series of increasingly complex derivatives of 2,5-diketopiperazine (DKP) crystals in order to understand what factors control how molecules assemble into a solid. DKPs are a family of molecules known to form both strong and weak hydrogen bonds with adjacent molecules. Results of in-situ AFM experiments show that growth of GLYDKP occurs on monomolecular steps generated by complex screw dislocations. The step velocity is highly anisotropic with rapid growth occurring in the direction of the strong hydrogen bonds (i.e. N-H--O) and slow growth occurring in the direction of the weak hydrogen bonds (i.e. C-H--O). This anisotropy results in very elongated elliptical shaped hillocks with two very different types of step edges being formed. Very straight steps are observed in the weak hydrogen bonding direction and very ragged steps are observed in the strong hydrogen bonding direction. Due to the symmetry of the crystal, a phenomenon of step interlacing is observed as step velocities alternate between fast and slow with each successive layer. The alternate production of fast and slow type steps results in single steps bunching to form double steps as observed by AFM. Fundamental material parameters have been determined: by measuring the step velocities as a function of supersaturation the kinetic coefficient has been determined, and from measurements of the critical length for step advancement the step edge free energies have been determined. These results will be discussed in the context of how changes in the molecular structure influence the morphology and the kinetics of crystal growth.

This work was performed under the auspices of the U.S. Department of Energy by Lawrence Livermore National Laboratory under contract No. W-7405-ENG-48.

P11.OD.007 INTERACTIONS INVOLVING C≡C–H GROUPS IN CRYSTALLINE SOLIDS. B.M. Kariuki, J.M.A. Robinson, K.D.M. Harris, D. Philp, School of Chemistry, University of Birmingham, Edgbaston, Birmingham B15 2TT, U.K.

As part of our interest in understanding "weak" hydrogen-bonding type interactions in solids, we have recently investigated interactions involving C–H hydrogen bond donor groups, with particular focus on ethynyl (C≡C–H) groups. Results from these studies will be described, including the following.
(1) Investigations of the competitive formation of different types of C≡C–H···π interactions in materials for which different π systems are available for accepting the C≡C–H···π interaction.
(2) Investigations of C≡C–H···O interactions, including the discovery and characterization of an exceptionally strong C–H···O interaction.
(3) Investigations on the interchangeability of halogen and C≡C–H substituents in the crystal structures of di-substituted and tri-substituted benzenes.

P11.OD.008 NEUTRON AND X-RAY STUDIES OF N-H--O/ N--H-O HYDROGEN BOND TAUTOMERISM IN BIPYRIDINIUM PYROMELLITATES. Ian D. Williams, Samuel M-F. Lo, Alvin Siu and Toby Mak, Dept of Chemistry, Hong Kong University of Science and Technology, Clear Water Bay, Hong Kong, China, Judith A.K. Howard and John Cowan, Chemistry Department, University of Durham, Durham, DH1 3LE, UK and Sax A. Mason, Institut Laue Langevin, BP156, 38042, Grenoble, Cedex9, France.

As part of a program to engineer new molecular ferroelectrics involving N-H--O/ N--H-O tautomerism, a series of organic molecular salts have been prepared using hydrothermal crystallization through reaction of 4,4'-bipyridine (4,4'-bipy) and pyromellitic acid (benzene-1,2,4,5-tetracarboxylic acid or 1245-H_4). Three different phases of 2:1, 1:1 and 1:2 stoichiometry have been isolated as crystals >2mm dimension. The 1:1 phase was examined using neutron diffraction at 215K and the distribution of the acidic hydrogens determined. The structure was shown to be [4,4'-bipy-H_2][1245-H_2]H_2O in space group P-1 with Z =1, with two of the acidic H on bipyridinium ions and two involved in ordered intramolecular H-bonds within the dihydrogen pyromellitate dianion.

By x-ray diffraction, the 1:2 phase [4,4'-bipy-H_2] [1245-H_3]$_2$ gave an answer in C2/c in which all non-hydrogen atoms could be located, but the final R-value was only 12% and thermal parameters of several oxygens were unreasonable. The pseudo-symmetry was resolved using neutron data at 20K on D19 (ILL) lambda = 1.3108(1)Å. From this, refinement in C2/c blows up, but in Cc gives R1 0.0238 (wR2 = 0 .0663) The carboxylates in two separate pyromellitates are shown to possess different twist angles. The study also allows definitive assignment of hydrogens to doubly protonated bipyridinium ions and N-H--O tautomerism.

Finally the 2:1 phase has been shown by x-ray diffraction to be 2[bipy-H][1245-H_2] and to contain ordered N-H--O and O-H--N contacts. The two tautomeric states are clearly close enough in energy that coulombic effects dictate the formation of the mono-protonated bipyridine rather than bipyridinium ion in this case.

P11.OD.009 APPROXIMATE SYMMETRY IN CRYSTAL ENGINEERING: PACKING ENERGIES OF RACEMATES AND QUASIRACEMATES. R.E. Davis and N.-L. Chang, Department of Chemistry and Biochemistry, The University of Texas at Austin, Austin, TX 78712-1167, USA and K.A. Wheeler, Department of Chemistry, Delaware State University, Dover, DE 19901, USA

We are interested in designing pairs of molecules that can form quasiracemic crystals. A quasiracemate can be described as a molecular crystal related to a true racemate by a not-too-extensive change in the structure of one of two enantiomeric components, e.g., (*R*)-X and (*S*)-X', where X and X' are sterically similar molecules. This similarity can be achieved by substitution of groups that are sterically similar, though they may be electronically quite different. The resulting quasiracemate crystal, though approximately centrosymmetric in its steric features, is strictly noncentrosymmetric in other aspects, including electronic and optical properties -- a possible advantage for some crystal engineering applications.

We compare hydrogen-bond patterns, packing arrangements and calculated crystal packing energies of proposed or known quasiracemates with those of related racemates (*R,S)*-X and (*R,S)*-X' of known structure. The goal of these studies is a better understanding of factors that favor formation of this special type of cocrystal and the identification of experimentally plausible quasiracemic systems for synthesis and further study.

Supported in part by the Robert A. Welch Foundation, Grant F-233 and in part by the United States Air Force Office of Scientific Research, Grant F49620-97-1-0263.

P11.OD.010 APPROXIMATE SYMMETRY AS A TOOL TO GENERATE MOLECULAR MOTIFS. K.A. Wheeler, M. Hendi, and S. Fomulu, Department of Chemistry, Delaware State University, Dover, DE 19901, USA and R.E. Davis, Department of Chemistry and Biochemistry, The University of Texas at Austin, Austin, TX 78712-1167, USA.

This research is aimed at controlling noncentrosymmetric arrangements of molecules in crystalline solids by exploiting the structural preference for centrosymmetric molecular patterns. Studies of crystal structure data have revealed the tendency for organic molecules to form centrosymmetric patterns. This preference is 10:1 for crystals of achiral, nonpolar organic molecules, and about 4:1 for all structures.

Our efforts center on exploiting this statistical preference for centrosymmetry as a reliable tool towards crystal engineering by:

- Designing and synthesizing quasiracemic crystals. A quasiracemate is described as a molecular crystal composed of (*R*)-X and (*S*)-X', where X and X' are sterically similar molecules.
- Determining and comparing a complete family of related crystal structures [i.e., (*R,S*)-X, (*R,S*)-X', (*R*)-X, (*S*)-X') and quasiracemate (*R*)-X/(*S*)-X'].
- The objective of these studies is to better understand the role of centrosymmetric patterns as a dominant reliable packing motif for crystal engineering studies.

Supported by the Robert A. Welch Foundation (Grant F-233), the Air Force Office of Scientific Research (Grant F49620-97-1-0263), and the National Science Foundation (Grant DMR-9414042).

P11.OD.011 GRAIN BOUNDARIES AND THEIR REGULAR STACKS FOR HIGH TEMPERATURE SUPERCONDUCTING MICROELECTRONICS. E.A. Stepantsov, Institute of Crystallography RAS, Leninski prospect 59, RU-117333 Moscow, Russia, and M.A.Tarasov, Institute of Radio Engineering and Electronics RAS, Mokhovaya 11, RU-103907 Moscow, Russia, and V.Strbik, Institute of Electrical Engineering SAS, SK-84239 Bratislava, Slovakia, and Z.G.Ivanov and T.Claeson, Physics Department, Chalmers University of Technology, S-41296 Gothenburg, Sweden.

Method of multi crystal composite fabrication by means of solid state crystal intergrowth has been developed and optimized for creation of artificial grain boundary (bicrystal) and regular stack of several parallel such boundaries (multi crystal). Such boundaries demonstrate high structural perfection and geometric flatness, and their crystallographic characteristics are monitored with accuracy of a few angular minutes. Composites of Y-ZrO_2 crystals have been used as substrates for epitaxial growth of high critical temperature superconducting (HTS) films. The artificial grain boundary epitaxially grows from the substrate into the HTS film. Such boundary in HTS film form a high quality Josephson junction. Using such a complex with five parallel grain boundaries of symmetrical type and misorientation angle of 24^o separated by a distance of 20 μm in YBaCuO films, we have fabricated series and parallel arrays of Josephson junctions. Such arrays have been used in integrated circuits of two topological types. The first type was a square array of 5x5 junctions forming three Josephson transmission lines with superconducting control lines. The second type comprises one dimensional array of 5 junctions, integrated with a planar log-periodic antenna. Fabricated structures demonstrated parameters consistent with those of individual Josephson junctions, oscillating dependencies of the critical current on magnetic field produced by control lines, and multiple Shapiro steps under submillimeter-wave radiation.

P11.OD.012 LANTHANIDE IONS AS PART OF THE CRYSTAL ENGINEER'S TOOL BOX. Lillian M. Rogers, Grant A. Broker, C. V. Krishnamohan Sharma, and Robin D. Rogers, Department of Chemistry, The University of Alabama, Tuscaloosa, AL 35487, USA.

Much of the current activity in crystal engineering of coordination polymers has focused on utilizing octahedral metal ions (for the available right angles) and linear or angular pyridine-like spacer ligands (e.g., 4,4'-bipyridine, pyrazine, pyrimidine). We are currently exploring larger, more oxophilic metal ions such as the lanthanides which allow an expansion of the coordination sphere from 6 to as high as 12. Using lanthanides, one can easily induce dissymmetry at metal centers simply by coordination with suitable ligand(s) which may thus result in controllable 1D, 2D, or 3D chiral networks with the aid of complementary hydrogen bonding functional groups.

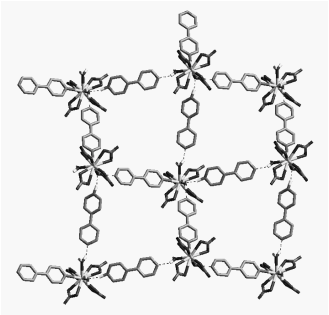

Lanthanum nitrates readily react with bifunctional ligands such as 1,2-bis(4-pyridyl)ethane (bpe), or 4,4'-bipyridyl (bipy) to form chiral open hydrogen bonded complexes under suitable experimental conditions. The crystal structure of [bpeH][$La(NO_3)_4(OH_2)$(bpe)] reveals complementary divergent hydrogen bonding sites located on the back bone of an anionic 1D coordination polymer resulting in a 2D pleated-sheet structure with unusual cavities. Each of these cavities is threaded by two 1D hydrogen bonded linear chains of monoprotonated $bpeH^+$ ligands forming an unprecedented polypseudorotaxane, or "molecular Chinese blinds" structure. The existence of this superb interlocking system offers yet another example of nature's clever ability to solve the void space problem in solids with impeccable self-organization.

P11.OD.013 THE INTERACTION OF N-HETROCYCLIC CARBENES WITH ORGANIC ACIDS. J.A.Cowan, M.G.Davidson, J.A.K.Howard, P.Kuepper, M.A.Leech, Chemistry Department, University of Durham, South Road, Durham, DH1 3LE.

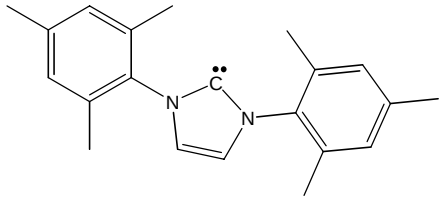

1,3-dimesitylimidazol-2-ylidene.

Carbenes are generally unstable. However, in the C_3N_2 ring, derived from imidazolium, it becomes more stable. The crystal structures of a variety of compounds in combination with the above molecule were investigated. We have found that uniquely, in certain conditions, the carbon atom's lone pair of electrons may act as an acceptor for a X-H..C hydrogen bond. In other situations the carbon becomes protonated, and the hydrogen bond is effectively reversed. This has resulted in an extremely short hydrogen bond. The structures formed by the ligand and metal centres have also produced some very interesting complexes.

Data were collected using a BRUKER SMART area detector, at temperatures down to 100K. The most interesting structures will be repeated at 30K, and further related structures will be investigated.

P11.OD.014 HYDROGEN BONDS BETWEEN OXIME AND CARBOXYL GROUPS — USEFUL TOOL FOR CRYSTAL ENGINEERING. Jan K. Maurin[a,b] and Beata Paluchowska[b], [a]Drug Institute, Chełmska 30/34, 00-725 Warsaw, [b]Institute of Atomic Energy, 05-400 Świerk-Otwock, Poland.

Ten of eleven structures of organic compounds containing both oxime and carboxyl group suggest that oxime group can recognize carboxyl group selectively forming seven-member hydrogen bonded ring. This hydrogen bonded arrangement resembles very much situation observed in both oximes and carboxylic acids hydrogen bonded dimers where six- and eight-member rings are formed, respectively. The preference for oxime-carboxyl interaction was proved also by cocrystalization of oximes with carboxylic acids. Relatively high stability of systems with "multiple hydrogen bonds" is well-known and utilized by crystal engineering.

The *ab initio* quantum chemical modeling was performed for the hypothetical systems containing acid-acid and oxime-oxime dimers and then compared with the results obtained for the system consisted of acid-oxime complexes. This results shows, that oxime-carboxylic acid co-crystals should be favored for 1:1 mixtures of oximes and acids although the energy gain comparing to the usual dimeric systems isn't very high.

Similar calculations have been performed for the systems where oxime and carboxyl groups are placed in one molecule. The

results obtained support and explain the experimental observations for this class of compounds.

Selective recognition of the oxime group by the carboxyl group (and vice versa) makes it possible to utilize this phenomena in crystal engineering for obtaining hydrogen bonded polar chains of molecules and hence polar structures. Although the oxime group could form "multiple hydrogen bonds" with other donor-acceptor groups, such bondings are not so selective as reported here.

11OE QUANTITATIVE ELECTRON DIFFRACTION AND MICROSCOPY

M11.OE.001 BULK STRUCTURES USING DYNAMICAL DIRECT METHODS. L. D. Marks and W. Sinkler, Department of Materials Science and Engineering, Northwestern University, Evanston, IL 60208, USA.

A standard method of determining structures is (kinematical) x-ray diffraction and Direct Methods. This works well if a reasonable size single crystal is available, but it can be difficult and expensive in both time and money to grow such a crystal. An alternative method of obtaining diffraction data is to use transmission electron diffraction. It is simple to obtain information from areas as small as 10nm in a few seconds, making it a very attractive approach.

Unfortunately transmission electron diffraction is rarely, if ever kinematical. Instead it is strongly dynamical which appears to make Direct Methods unworkable. However, if one uses a generalization of Direct Methods using a Feasible Set approach [1], this is not the case. Handled correctly one is obtaining a pseudo-inversion of the diffraction data which gives initial estimates of the atomic positions for subsequent refinement (using either dynamical diffraction models or powder diffraction data).

We have recently been able to employ this approach to solve two previously unknown oxide structures [2]. As a consequence of the dynamical effects [3], it turns out that light atoms (e.g. oxygen) are easier to find at realistic thicknesses. These results will be described as well as extensions to more general cases and the possibility of general pseudo-inversion of dynamical diffraction data from defects.

1. L. D. Marks, W. Sinkler and E. Landree, Acta Cryst A, in press.
2. W. Sinkler, L. D. Marks, D. D. Edwards, T. O. Mason, K. R. Poeppelmeier, Z. Hu and J. D. Jorgenson, Journal of Solid State Chemistry (1998) **136**, 145.
3. W. Sinkler, E. Bengu and L. D. Marks, Acta Cryst (1998) **A54**, 591.

M11.OE.002 THE PRECESSION TECHNIQUE IN ELECTRON CRYSTALLOGRAPHY. APPLICATIONS TO STRUCTURE DETERMINATION. J. Gjønnes, V. Hansen, E. Sørbrøden, P. Runde and K. Gjønnes, Centre for Materials Science, University of Oslo, Gaustadalleen 21, N-0371 Oslo, Norway.

Electron diffraction patterns from crystals are usually taken with a stationary beam (and crystal), in contrast to X-ray work where the crystal is rotated to produce integrated intensities. With the electron beam entered along a zone axis, dynamical scattering effects are exacerbated.

The recently invented precession technique [1] is a different approach to quantitative electron diffraction: Off-axis beam configurations are used, integrated intensities are obtained, dynamical effects are reduced, more reflections and three-dimensional data can be collected [2]. A 'guided beam' system [3] implemented on a Jeol 2000FX microscope in Oslo will be described. Principles for intensity calculations relating to precession, and applications to structure determination of alloy phases will be presented.

1. R. Vincent and P.M. Midgley (1994) Ultramicroscopy 53, 271-292.
2. J. Gjønnes, V. Hansen, B.S. Berg, P. Runde, Y.F. Cheng, K. Gjønnes, D.L. Dorset and C.J. Gilmore (1998) Acta Cryst. A54, 306-319.
3. E. Sørbrøden, P. Runde and A. Olsen (1998) Electron Microscopy 1998, Proc. ICEM 14, Cancun Mexico 1998 Vol. 1, 425-426.

M11.OE.003 USE OF QUANTITATIVE CBED IN MATERIALS SCIENCE. R. Holmestad, C.R. Birkeland, K. Marthinsen, and R. Høier, Dept. of Physics, Norwegian University of Technology and Science (NTNU) N-7034 Trondheim, Norway and J.M. Zuo, Dept. of Physics and Astronomy, Arizona state University, Tempe, AZ, 85287-1504, USA.

The small probe used in Convergent Beam Electron Diffraction (CBED) can give information from minuscule regions beyond the reach of other diffraction methods [1]. By matching experimental CBED patterns with simulations it is possible to determine structure parameters with high accuracy.

The quantitative method is based on pixel-by-pixel comparisons of experimental and theoretical (using Bloch wave theory) intensities. Over the last few years, energy filtering, new digital recording systems, recent development in theory and tremendous advances in computer power have made significant progress in quantitative analysis of CBED.

We will present examples of quantitative CBED used in materials science. Lattice parameters are determined in SiC 4H [2] utilising HOLZ lines in CBED centre disks. Low order structure factors are refined in TiAl intermetallics [3] and CaF_2 from systematic row CBED patterns, to obtain information on bonding charge-density distributions. Three-phase invariants are found in the non-centrosymmetric crystal InP.

Spence JCH and Zuo JM (1992) Electron Microdiffraction, Plenum.
Zuo JM, Kim M and Holmestad R (1998) J. Elec. Micr. 47, 121.
Holmestad R and Birkeland CR (1998) Phil.Mag A, 77, 1231.

M11.OE.004 STRUCTURE REFINEMENT FROM ELECTRON DIFFRACTION DATA TAKING FULL ADVANTAGE OF THE PROPERTIES OF THE SCATTERING. J.Jansen, H.W.Zandbergen, National Centre for HREM, Laboratory of Materials Science, Delft University of Technology, Rotterdamseweg 137, 2628 AL Delft, The Netherlands.

Due to the strong interaction between electrons and crystals, in most cases the kinematical diffraction theory is not a reasonable approximation. Therefore we developed a least-squares procedure to refine crystal structures which incorporates a full dynamical calculation (MSLS). The resulting R-factors obtained with MSLS are comparable in magnitude with the ones one get in single crystal X-ray diffraction. When trying to fit HREM images to dynamically calculated pictures, a similar good match is never achieved. One of the reasons may be scattering contributions. To verify this, we took diffraction patterns with and without energy filtering and diffraction patterns formed by electrons in the plasmon peak of the energy spectrum. Our studies indicate that a substantial amount of electrons is inelastically scattered. On the other hand it appeared that the energy filtering does not have a significant effect on the refined structure and the R-factor. The reason for this is 2-fold 1) since we use integrated intensities, the incoherency between zero-loss and plasmon electrons is of no importance. 2) inelastic scattered electrons with large scattering angles contribute only to the background of diffraction patterns; proper handling of the background eliminates this. Part of our research concerns the applicability of MSLS for structures from relatively thick crystals (>400Å). At those thicknesses the program gets, as expected, very sensitive to the crystal tilt used in the calculations. Another effect observed is that lighter atoms next to heavy atoms tend to move from their correct position. Since we

did those experiments with inorganic materials charge distributions may be a cause for this error. Another explanation may be the present limitations of the multislice method used in the calculations.

M11.OE.005 QUANTITATIVE HREM: VIEWPOINTS ON RESOLUTION, PRECISION AND EXPERIMENTAL DESIGN. A.J. den Dekker, J. Sijbers, and D. Van Dyck Department of Physics, University of Antwerp (RUCA), Groenenborgerlaan 171, B-2020 Antwerp, Belgium.

In principle, quantitative electron microscopy allows the extraction of structural detail beyond the point resolution and even beyond the information limit of the microscope. Essentially, this is achieved as follows. It is assumed that one has a model for the object and the imaging process, including electron object interaction, imaging and recording. This model contains parameters, such as the atom positions (or the positions of projected columns) which are unknown beforehand and have to be determined by the experiment. This is done by fitting the model to the experimental images (or diffraction patterns) with respect to the model parameters, using a proper criterion of goodness of fit (preferably maximum likelihood). In the absence of noise, this would result in a perfect fit, so that exact values for the model parameters would be obtained. The atom positions could then be determined with unlimited precision, independent of the particular setting of the microscope. Notice, that this would also mean that two atoms could always be resolved, no matter how closely spaced, so that there would be no limit to resolution. In reality, however, the precision with which the model parameters can be determined, will always be dose limited. This is due to the inevitable presence of counting noise. Resolution is then reduced to the precision with which atom positions can be determined. From parameter estimation theory [1], one can calculate the lowest possible error bar (standard deviation) on the position of an atom (column) as a function of the controllable experimental parameters for a given electron dose. The experimental parameters corresponding to the lowest error bar (i.e., the highest precision) then suggest the optimal experimental design. For more details we refer to [2].

A. Van den Bos, Chapter 8 in: Handbook of Measurement Science, Vol. 1, P.H. Sydenham (ed.), 331-377 (1982).
A.J. den Dekker, J. Sijbers, and D. Van Dyck, paper accepted for publication in Journal of Microscopy (1999).

P11.OE.001 ELECTRON DIFFRACTION FROM MICRO- AND NANOPARTICLES. E. I.Suvorova, Ph. A. Buffat. Centre Interdépartmental de Microscopie Électronique, EPFL, Lausanne CH-1015, Switzerland

On the basis of X-ray and electron diffraction patterns from large regions materials can be called "amorphous" if they give diffuse ring patterns. For diffraction from small crystals the extension of the scattering power around the reciprocal lattice points becomes appreciable in direction perpendicular to the incident beam. The diffraction spots are no longer sharp but are spread out into patches [1]. Assembly of imperfect small crystals with various orientations relatively to the electron beam will provide broadening diffuse rings.

During the study of the crystal growth mechanism of hydroxyapatite which has a large hexagonal unit cell consisting 42 atoms where the Ca atoms are the most heavy it was found that different growth conditions (temperature, supersaturation, concentrations) resulted in formation of crystals with different sizes from a few nm to 1-2 microns. For clarifying the nucleation mechanism it was very important to know the state of hydroxyapatite at the first stage of precipitation from the aqueous solutions. The dry specimens were powders consisting of crystal agglomerates. Selected-area electron diffraction patterns obtained from assemblies of nanocrystals were broad diffuse rings while the polycrystalline and single diffraction patterns were observed from microcrystals. The average size of the individual nanoparticles was 20 nm, microcrystals could reach 1-2 microns. Using electron micro-probes of 3.5-10 nm size gave a possibility to determine the crystalline structure of nanoparticles when the incident beam illuminates only a small area of the specimen and only this area contributs to the diffraction pattern. The size of the microdiffraction depends on the demagnification of the probe-forming lenses, on the electron source size, and on the focus setting, aperture size, and spherical abberation constant of the probe-forming lens. Field emission tip W/ZrO applied in this work had 1micron in size with the crossover diameter of 15 nm (accelerating voltage 300 kV, diameters of the C1aperture 2mm and C2 - 30 microns), convergence angles 2-3 mrad, the spherical aberration constant was 0.65 mm. Hydroxyapatite nanoparticles had a fine grain structure that gave sharp spotty rings. By HRTEM and image calculations with the EMS software [2] the grain sizes and a set of their orientations were determined for individual nano- and microparticles.

1. J.M.Cowley (1988). Elastic scattering of electrons by crystals, in High- Resolution Transmission Electron Microscopy and Associated Techniques. Ed. P.R.Buseck, J.M.Cowley, L.Eyring, pp.58-128.
2. P.A.Stadelmann (1987). Ultramicroscopy 21, p.131.

P11.OE.002 AN ANALYTIC EXPRESSION IN CLOSED FORM FOR THE ELECTRON EXIT WAVE. P. Geuens, J. H. Chen, A. J. den Dekker, D. Van Dyck, EMAT, University of Antwerp (RUCA), Groenenborgerlaan 171, B-2020 Antwerp, Belgium.

Recently important progress has been made in quantitative structure refinement starting from high resolution electron images and diffraction patterns. The most tedious part in the refinement is the repetitive calculation of the exit wave. A simple expression for the exit wave would allow speeding up both quantitative refinement and image calculations drastically compared to standard multislice or Blochwave calculations.

In this work a simple analytic expression is obtained for the exit wave, of high energy diffracted electrons, for a zone axis plane wave illumination, by parameterisation of the numerical dataset of the normalised and scaled 1S-state presented by Van Dyck and Chen [1].

The electrons are trapped in the electrostatic potential of the atom columns parallel to the electron beam. Hence it is possible to describe the wave function of the diffracted electrons, in terms of the eigenstates of the two-dimensional projected electrostatic potential of the atom columns. It has been shown that this potential has only one important bound eigenstate, which by analogy is called the 1S-state [2].

The Levenberg-Marquardt procedure [3] was used for parameterisation. One normalised gaussian is found to be a sufficient fit. Hardly any improvement is obtained by using two gaussians or one gaussian and an exponential function. The intensities of various diffracted beams in Cu[100] as a function of thickness, calculated both with the presented method and with the standard multislice method, were found in good agreement. The difference between the results is only marginal and smaller than the experimental accuracy.

1. D. Van Dyck and J.H. Chen (1998) , Acta Cryst. A, in press.
2. D. Van Dyck and M. Op de Beeck (1996), Ultramicroscopy, 64, 99.
3. D. W. Marquardt (1963), J. Soc. Ind. Appl. Math., 11, 431.

P11.OE.003 COMPARISON OF ACCURATE X-RAY AND ELECTRON DIFFRACTION DETERMINED STRUCTURE FACTORS FOR α-Al_2O_3. P.N.H. Nakashima and V.A. Streltsov, Department of Physics and A.W.S. Johnson, Centre for Microscopy, UWA, Nedlands 6907, Australia.

To accurately measure the low order structure factors of α-Al_2O_3, two-dimensional convergent beam electron diffraction data from parallel sided platelets (~0.5 μm) have been matched using the Bloch-wave refinement program of Zuo and Spence [1]. In order to further test the precision of the method, as demonstrated in [2], room temperature data sets were collected at 200 and 300 kV, using various crystal thicknesses and orientations. A Philips EM 430 TEM, a Gatan Image Filter™ and a CCD with YAG scintillator were used.

Synchrotron X-ray diffraction data from two small crystals (~10-30 μm) were collected with 0.71 [2] and 0.75 Å wavelengths respectively, using the Photon Factory BL14A diffractometer with a high-speed avalanche photodiode (APD) detector.

The low order Fourier coefficients of the crystal potential determined by electron diffraction were converted to dimensionless X-ray structure factors. The ratios between these structure factors are used to determine the extent of extinction in the synchrotron data.

J.M. Zuo, Acta Cryst. (1993). A**49**, 429.
M. Saunders et al., Ultramicroscopy **60** (1995), 311-323
E.N. Maslen et al., Acta Cryst. (1993). B**49**, 973.

P11.OE.004 HREM STUDY AND STRUCTURE MODELING OF THE η' PHASE IN AGE-HARDENING Al-Zn-Mg ALLOYS. X.Z. Li, V. Hansen and J. Gjønnes, Centre for Materials Science, University of Oslo, Gaustadalléen 21, N-0317 Oslo, Norway and L.R. Wallenberg, National Center for HREM, Inorganic Chemistry 2, Chemical Center, Lund University, Box 124, S-22100 Lund Sweden.

It is known that the age-hardening effect of commercial Al-Zn-Mg alloys is due to the formation of fine precipitates. One of the most important hardening precipitates is the metastable η' phase [1]. The lattice of the η' phase has a hexagonal lattice with a=0.496 and c=1.402 nm. Knowledge of the η' structure is considered as an essential key to improved understanding of the precipitation process. Several studies relating to the structure of this phase were reported in the literature, however, a definite crystal structure has not been established yet.

In the present work [2], the structure of the η' phase has been studied at atomic level by means of high-resolution electron microscopy (HREM). The individual precipitates were examined in high-resolution images. The HREM images provide valuable structure characteristics of the η' phase. Defects in the structures of individual precipitates have also been observed.

Since the existing models cannot account for the observed images, a new model of the η' phase has been proposed on the basis of the observed images and the structure of the η-$MgZn_2$ phase. Image simulation of the new model shows a good agreement between calculated images and experimental ones Structural features in the present model have been illustrated in comparison with the model proposed by Auld and Cousland [3]. The formation of defects in the structure of the η' phase has also been discussed.

1. J. Lendvai (1996). Materials Science Forum, **217-222**, 43.
2. X.Z. Li, V. Hansen, J. Gjønnes and L.R. Wallenberg (1999). Acta mater., submitted.
3. H. Auld and S. McK. Cousland (1974). J. Aust. Inst. Met., **19**, 194.

P11.OE.005 HIGH-RESOLUTION ANALYTICAL ELECTRON MICROSCOPY OF FULLERENES AND NANOTUBES IN BORON NITRIDE. D. Golberg, Y. Bando, W. Han, K. Kurashima, and T. Sato, National Institute for Research in Inorganic Materials, Tsukuba, Ibaraki 305-0044, JAPAN, and O. Stéphan, Université Paris-Sud, Orsay 91405, FRANCE, and C. Goringe, University of Sydney, NSW 2006, AUSTRALIA.

Here we report on the precise structural investigation of boron nitride (BN) fullerenes and nanotubes as compared to their carbon (C) counterparts by means of high-resolution transmission electron microscopy (HRTEM), electron energy loss spectroscopy, and nanodiffraction.

Single- and multi-shelled BN fullerenes were synthesized *in situ* from graphitic BN in a JEM-3000F field emission electron microscope by applying intense electron irradiation. Multi-walled BN nanotubes were prepared by laser heating of cubic and hexagonal BN under superhigh nitrogen pressure (up to 15 GPa), or through general substitution chemical reaction from carbon nanotubes.

In contrast to C fullerenes, whose HRTEM images look quasi-spherical (icosahedral symmetry), BN fullerenes displayed rectangle/square-like HRTEM images when viewed in specific projections. The experimentally observed images perfectly matched computer simulated ones for the octahedral structural model. Appearance of four-member ring defects (squares) in the graphene-like BN sheet at the expense of five-member ring defects (pentagons) typical for C was accounted for by the octahedral symmetry of the BN fullerenes. It is thought that a square defect leading to a B-N-B-N atomic chain is favoured in BN due to the higher stability of B-N chemical bonds compared to B-B and N-N bonds.

In contrast to C nanotubes, which show a wide range of helicities, multi-walled BN nanotubes typically displayed remarkable ordering of the tubular shells in a non-helical "zig-zag" form with B-N bond parallel to the tube axis. This is considered to be due to the existense of selection criteria for lip-lip interactions between tube shells in BN nanotubes compared to C ones. BN nanotube tip-ends were found to be blunt in accordance with the stability of even-member ring defects (squares and/or octagons) in contrast to the conical tip-ends caused by pentagonal ring defects in C nanotubes.

P11.OE.006 QUANTITATIVE HIGH RESOLUTION ELECTRON DIFFRACTION FOR DETERMINATION OF THE ELECTROSTATIC POTENTIAL. Avilov A., Kuligin A., and Lepeshov G., Institute of Crystallography RAS, Moscow, Russia 117333, Pietsch U., Potsdam University, Germany, Spence J., Arizona State University, Tempe, AZ, Tsirelson V., Mendeleev University, Moscow, Russia

The structure analysis by with the high resolution electron diffraction (HRED) is based on the use of high energy electron diffraction to reconstruct the electrostatic potential (ESP) and its analysis to extract the structure information. Since ESP is connected with all fundamental physical properties of crystal, its precise determination presents an important problem. To solve this problem this work is devoted to the development of the precise HRED, to quantitative determination of the distribution of ESP in the binary ionic crystals and to the working out of methods of direct calculation of properties of crystals from the electron diffraction data.

The development of quantitative HRED demands solving a number of problems: the precise measurement of intensity of diffraction patterns (DP); calculation of the primary extinction effects (as soon as secondary extinction is absent); and accounting for the inelastic scattered electrons.

The modified scanning of DP system with the statistical accuracy of measurement about 1% was developed. The methods

of the accounting for the effects of primary extinction for partly oriented polycrystalline films, which are normally used in HRED were worked out. The precise HRED investigations of binary ionic crystals MgO, LiF and NaF have been made. The distributions of ESP in this substances were reconstructed with high accuracy both with the aid of Fourier synthesis and by with the analytical models. Some physical properties were calculated (as diamagnetic susceptibility and static electron polarizability). The known in precise X-rays structure analysis κ-model was used for the analysis of the nature of chemical bonding for the first time in HRED. Received results correlate well with precise X-rays data and the results of the calculations by Hartree-Fock method.

Work is supported by CRDF grant No. RP1-208, RFBR grant No. 98-03-32654 and DFG grant No. Pi 217/13-1.

P11.OE.007 ELECTRON DIFFRACTION INTENSITIES FROM PARTICLES AND ZONES IN A MATRIX. GP-ZONES IN AN AlMgZn ALLOY. V. Hansen, L.K. Berg, X.Z. Li and J. Gjønnes, Centre for Materials Science, University of Oslo, N-0317, Norway, M. Knutson-Wedel, Chalmers University of Technology, S-412 96 Gøteborg, Sweden, G. Waterloo, Hydro Raufoss Automotive Research Centre, 2830 Raufoss, Norway

Precipitation hardening alloys are characterised by a dispersion of metastable particles or zones in the nm size-range. Electron crystallographic techniques are the most efficient techniques for obtaining structure information from such systems, which call for quantitative measurement of different intensities from coherent particles, embedded in a metal matrix.

The structures of coherent zones and precipitates in an Al-(Mg, Zn) alloy that occur along the transformation path during a two-step ageing treatment at 100°C and 150°C have been investigated by HREM and electron diffraction. Electron diffraction intensities were measured from photographic films and image plates, taken in a JEOL 200CX and a LEO 412 energy-filtering microscope. Dynamical diffraction effects involving matrix reflections must be included in the interpretation - or reduced by selection of open aluminium projections. Three-dimensional intensity distributions have been constructed and interpreted in terms of two types of zones (GP(I) and GP(II)) and the metastable hardening phase η'. A new structure model for ordering within the GP(I)-zones is presented. The structures are discussed in relation to the transformation sequence from GP-zones via the metastable phase n' to the stable phase η-$MgZn_2$.

P11.OE.009 REFINEMENT OF CRYSTAL STRUCTURAL PARAMETERS BY CONVERGENT-BEAM ELECTRON DIFFRACTION. K.Tsuda, M.Tanaka Research Institute for Scientific Measurements, Tohoku University, Sendai 980-8577, Japan

A new method to refine crystal structural parameters using convergent-beam electron diffraction (CBED), which is applicable to nm-size crystal structure analysis, is presented. This method is based on the fitting between theoretical calculations and experimental intensities of energy-filtered two-dimensional CBED patterns containing higher-order Laue zone (HOLZ) reflections. The two-dimensional CBED data provide much more structural information than zero- and one-dimensional data. The use of HOLZ reflections is essential for method because small displacements of atoms can be sensitively detected using HOLZ reflections with large reciprocal vectors. For this purpose, a new Omega-filter transmission microscope (JEM-2010FEF) which can take energy-filtered CBED patterns up to a high angle with a small distortion, and a new analysis program to refine structural parameters which is based on many-beam Bloch wave calculations and non-linear least squares fitting have been developed. Structural parameters of the intermediate phase of hexagonal $BaTiO_3$ have been refined by the new method. Hexagonal $BaTiO_3$ undergoes a second order phase transformation at 222K from the high-temperature phase of the space group $P6_3/mmc$ to the intermediate phase of the space group $C222_1$.

P11.OE.010 QUASICRYSTAL APPROXIMANTS IN THE Ga-Mn SYSTEM STUDIED BY ELECTRON CRYSTALLOGRAPHY. S. Hovmöller, M. Boström, K. Sun, X.D. Zou, Structural Chemistry, Stockholm University, S-106 91 Stockholm, Sweden.

Several new quasicrystal approximants are found in the Ga-Mn system [1]. Structure models for three of them were derived by the tiling method [2]. This method requires as a starting model a known crystal structure with close structural relationships with the approximant. HREM images of the approximant are compared with those of the known structure. Common tiles are found and the structural model of the unknown approximant is generated using the atomic arrangement in the tiles of the known structure.

It was not possible to derive a structure model for a tetragonal approximant (T-phase, a = 1.25 nm and c = 2.50 nm), since no known structures, related to this T-phase, were found. Instead we try solve the crystal structure from high resolution electron microscopy (HREM) images and refine the atomic coordinates against electron diffraction intensities [3], in short by electron crystallography.

HREM images and selected area electron diffraction patterns of the T-phase are taken along several different zone axes. Only very thin regions of the crystals, where dynamic scattering is minimal, are used. Amplitudes and phases of the structure factors are extracted from the Fourier transforms of each HREM image. Amplitudes are also obtained from electron diffraction patterns. Crystallographic symmetry constraints are imposed on the amplitudes and phases. Projected potential maps are obtained from each zone axis by inverse Fourier transformation of the amplitudes and phases.

We are now trying to construct an atomic structure model in 3D of the T-phase by combining all the projections into one 3D potential map.

J.S. Wu & K.H. Kuo. (1997). Metall. Mater. Trans. A, 28, 729
J.S. Wu, X.Z. Li & K.H. Kuo. (1998). Phil. Mag. Lett., 77, 359; J.S. Wu, S.P. Ge, & K.H. Kuo. Phil. Mag. A. in press.
T.E. Weirich, *et al*. (1996). Nature (London), 382, 144.

11OF PEROVSKITE MATERIALS

M11.OF.001 THE UNUSUAL DIELECTRIC PROPERTIES OF PEROVSKITES: FROM NONVOLATILE MEMORIES TO MEDICAL IMAGING. N. Setter, Ceramics Laboratory, EPFL - Swiss Federal Institute of Technology, 1015 Lausanne, Switzerland

Recent advances in dielectric materials with perovskite and perovskite-based layer structures show great potential for meeting the demands for higher sensitivities, operation at higher frequencies and higher temperatures, smaller power consumption and further miniaturisation of next generation electronic and sensorial components:

Bismuth containing ferroelectric perovskite-based layer structure materials with suppressed ferroelectric fatigue have been developed [1]. This is a key feature towards the commercialisation of ferroelectric non-volatile memories.

Suppression of piezoelectric hysteresis has been demonstrated in other bismuth-based layer structure ferroelectrics [2], making them useful for high temperature piezoelectric sensors.

The control of the temperature coefficient of the resonance frequency of high permittivity dielectrics, critical for high

performance of microwave resonators for wireless communication, was shown [3] to be possible using structural arguments.

Positional disorder in lead-based complex perovskites is known since some time to be responsible for the so-called relaxor behaviour, giving rise to useful properties such as very high permittivity and electrostriction. Certain relaxor-ferroelectrics single crystals have been shown recently to possess giant piezoelectricity [4], potentially very useful for improved resolution of ultrasonic medical imaging.

These and other unusual dielectric, piezoelectric, pyroelectric and ferroelectric properties of perovskite ceramics will be reviewed with emphasise on the role of crystalline structure in achieving excellent functionality.

1. C.A.Paz de Araujo, J.D.Cuchiaro, L.D.McMillan, M.C.Scott. and J.F.Scott, Nature (London) 374, 627 (1995)
2. I. M. Reaney and D. Damjanovic, J. Appl. Phys. 80, 4223 (1996)
3. E. L. Colla, I. M. Reaney, and N. Setter, J. Appl. Phys 74, 3414, (1993) 4. T. S. Shrout and J. E. Park

M11.OF.002 ORDERING, MIXED-VALENCE AND METALLIC CHARACTER ALONG THE REDOX RANGE IN $LnBaM_2O_{5+w}$ (M = Fe and Co). Pavel Karen, Department of Chemistry, University of Oslo, Box 1033 Blindern, N-0315 Oslo, Norway.

A full replacement of the perovskite coordination-octahedra with ordered square pyramids leads to doubling of the unit-cell according to formula $AA'M_2O_5$. Suitably sized trivalent lanthanides (Ln) as A atoms and Ba as the A' atom are able to stabilize this arrangement for transition metals M like Mn, Fe and Co. The implied non-integer average valence $M^{2.5+}$ and an entire vacant oxygen site are the main ingredients for a multitude of structural, electronic, magnetic and electric properties changing along a wide solid-state redox-stability range. $LnBaM_2O_{5+w}$ phases with selected combinations of Ln = Nd, Sm, Gd, Y and M = Fe, Co are studied on quenched samples with *w* varied between 0.00 and 0.80. Structural consequences are investigated by powder neutron and synchrotron x-ray diffraction and involve distortions of the tetragonal (S.G. *P4/mmm*) prototype and/or further ordering schemes for significant compositions in terms of *w*. Valence and spin states of M are studied by ^{57}Fe Mössbauer spectroscopy (for M = Co, 1% of it is replaced by ^{57}Fe). A mixed-valence AF state $Fe^{2.5+}$ is observed at room temperature for the prototype composition and fades away with increasing *w*. Upon cooling below the transition temperature of around 200 K, the $Fe^{2.5+}$ state separates into a high-spin Fe^{3+} state and Fe^{2+} with unusually low internal magnetic field. The transition is associated with a small change in magnetic susceptibility and a weak thermal effect, implying a charge ordering into an electron localized state. Samples with the most reduced M = Fe and the most oxidized M = Co have a silver luster appearance at room temperature, and optical reflectivity spectra as well as electrical conductivity measurements illustrate changes in the occurrence of the metallic character as a function of *w* and temperature. The $Fe^{2.5+}$ valence state mixing coincides with the metallic state and is therefore closely reminiscent of the Verwey transition in magnetite, Fe_3O_4, one of the earliest examples of charge ordering in a transition metal oxide.

M11.OF.003 ORDERED AND DISORDERED STRUCTURAL CONTROL OF PEROVSKITE PROPERTIES. J. P. Attfield, Department of Chemistry and IRC in Superconductivity, University of Cambridge, Cambridge CB2 1EW, UK.

Many transition metal oxide perovskites and related materials show remarkable conducting properties such as colossal magneto-resistances at the metal-insulator transition in $Ln_{1-x}M_xMnO_3$ and superconductivity in $Ln_{2-x}M_xCuO_4$. Changes in electronic behaviour with hole doping level x have been extensively studied, but there are also variations in property when different Ln^{3+} (lanthanide) or M^{2+} (Ca, Sr, Ba) cations are used. We have shown that these cation effects may be described by two quantities, the mean radius of the Ln/M cations (equivalent to the well known perovskite tolerance factor) and the disparity in their radii, parameterised by the statistical variance in the radius distribution. Experiments reveal that both the metal-insulator transition temperature in $Ln_{1-x}M_xMnO_3$ perovskites [1] and the critical temperature of $La_{2-x}M_xCuO_4$ superconductors [2] are very sensitive to changes in either of these quantities. The results enable simple quadratic relationships for the size and disorder effects to be derived [3]. Powder neutron diffraction has been used to determine how both ordered and disordered structure change with cation size and variance giving insight into the structure-property relations.

1. L.M. Rodriguez-Martinez & J.P. Attfield (1996). Phys. Rev. B, 54, R15622.
2. J. P. Attfield, A. L. Kharlanov & J. A. McAllister (1998). Nature, 394, 157.
3. J. P. Attfield (1998). Chem. Mater., 10, 3239.

M11.OF.004 NEW SUPERCONDUCTING BISMUTH-ATES IN PEROVSKITE RELATED SYSTEMS. C. Bougerol-Chaillout and P. Bordet, Laboratoire de Cristallographie CNRS, BP166, 38042 Grenoble cedex 9, France; S.M. Kazakov, J. Pshirkov, S.N. Putilin, and E.V. Antipov, Chemistry Department, Moscow State University, Moscow 119899, Russia and M. Hanfland, ESRF, BP220, 38043 Grenoble cedex France.

Following the discovery of $BaPb_{1-x}Bi_xO_3$ (T_c~12K) in 1975 by Sleight et al. [1] and that of $Ba_{1-x}K_xBiO_3$ (T_c~40K) by Mattheiss et al. [2], we have been able to synthesize a new bismuth-based oxide, $SrBiO_3$, and to induce superconductivity by K or Rb doping [3] performed under high pressure. T_c maximum is about 12K when the K-substitution is larger than 45%, the solubility limit being around 60%. These new compounds have a distorted perovskite-based structure. Powder synchrotron and neutron diffraction have shown that, as a function of K doping, the symmetry changes from monoclinic (space group $P2_1/n$) to tetragonal (space group I 4/mcm) and remains the same down to 4K. Above room temperature, $SrBiO_3$ keeps the same structure until decomposition around 700°C, whereas the K-doped phases decompose around 300°C. An increase of T_c was observed when resistivity was measured as a function of pressure. On a structural point of view, powder synchrotron studies carried out at room temperature indicate that pressure induces an increase of the tetragonal distortion. In the case of $SrBiO_3$, no noticeable change was observed. By increasing the Sr/Bi ratio above 1, it has been possible to obtain a new cubic perovskite phase having a double lattice parameter.

Recently, we focussed on the search for Rudelsden Popper type compounds containing bismuth. $(Sr,A)_3Bi_2O_7$ compounds with A=K, or Rb have been obtained. The average structure was refined in the tetragonal I4/mmm space group, however, superstructure reflections observed by electron microscopy indicate that the real structure has a larger unit cell.

1. A.W. Sleight et al., Solid State Comm. (1975) 17, 27-28
2. L.R. Mattheiss,et al., Phys. Rev. B (1988) 37, 3745-3746
3. S.M. Kazakov et al., Nature (1997) 390, 148

M11.OF.005 ANION- AND CATION-DEFICIENT HEXAGONAL PEROVSKITES. R.V. Shpanchenko, Department of Chemistry, Moscow State University, 119899 Moscow, Russia.

Mixed anion- and cation-deficient hexagonal oxides with perovskite-like structures have been synthesised and studied by X-ray diffraction and high resolution electron microscopy. Anion and cation vacancies in such compounds are localised in a structural block containing two or three face shared octahedra.

Anion-deficient perovskites $AnBnO_{3n-d}$ (A = Ba, Sr; B= rare earth, Zr, Al) were obtained for different rare earth elements. Their structures consist of alternating BaO_3 and BaO_2 layers. The presence of Al atoms with a stable tetrahedral co-ordination provides a possibility for anion ordering with a formation of Al_2O_7 groups.

Cation deficient hexagonal perovskites $AnB_{n-d}O_{3n}$ (A= Ba, Sr, La; B = Ta, Zr, Ti, Ni) were obtained in the $Ba_5Ta_4O_{15}$ - ABO_3 systems. An electrostatic interaction between B-cations located in the neighbouring octahedra is an important parameter influencing a type of close-packing and cation ordering. A presence of two cations with different charges in the B-framework results in their ordering among different positions. Inter-growth structures ($Ba_5Ta_4O_{15}$ ´ n(Ba,Sr)ZrO_3) are obtained only with Zr. In this case compounds with general formula $(Ba,Sr)_{5+n}Ta_5Zr_nO_{15+3n}$ (n=1,2) form. However, a replacement of Zr^{4+} by Ti^{4+} results in a formation of new structures: $Ba_{10}Ta_{7.04}Ti_{1.2}O_{30}$ (10H) and $Ba_8Ta_4Ti_3O_{24}$ (8H), where only pairs of face shared octahedra are present instead of columns of three face shared octahedra. In the latter structures, the B-cations and vacancies are located in the (10H) and (8H) compounds in a disordered and ordered manner, respectively. The further ordering in the B-sublattice takes place upon replacement of Ti^{4+} by Ni^{2+} in the $Ba_8Ta_6NiO_{24}$ structure due to the larger charge difference.

M11.OF.006 STRUCTURAL AND MAGNETIC PHASES TRANSITIONS IN THE NEW PEROVSKITE $HoBaCo_2O_5$. E.Suard, Institut Laue Langevin, Av. des Martyrs, F-38042 Grenoble, F.Fauth, Swiss Light Source (SLS), Paul Scherrer Institute, CH-5232 Villigen PSI, V.Caignaert, Laboratoire CRISMAT-ISMRA, Bd du M^{al} JUIN, F-14050 CAEN, I.Mirebeau, Laboratoire Léon Brillouin, CE-Saclay, F-91191 Gif sur Yvette.

In the new ordered oxygen deficient perovskite $HoBaCo_2O_5$, we have observed by neutron powder diffraction two structural phase transitions at 350K and 210K, corresponding to the occurrence of magnetism and charge ordering, respectively. In the paramagnetic domain ($T_N \approx 350K$), the crystal structure is tetragonal with P4/mmm space group and derives from the perovskite structure. Cell parameters are $a=b\approx a_p$, $c\approx 2a_p$ where a_p is the cell parameter of the cubic perovskite. The structure is described with an alternate stacking of holmium and barium layers along *c* direction, and rows of CoO_5 pyramids as in $YBaCuFeO_5$ structure [1]. When cooling down, a magnetic moment appears on the Co sites resulting in an AF structure with a propagation vector k=(½ ½ 0). The Co spins point along a crystallographic direction in the *ab* plane and therefore induce an orthorhombic distortion of the nuclear structure. In the temperature range $210K<T<350K$, the space group is Pmmm. For $T<210K$, we have observed a doubling of the cell in the b direction and solved the nuclear structure in the Pmmb space group, leading to the existence of two different sites for the Co atoms. It is interpreted by a charge ordering of the Co^{2+}/Co^{3+} cations over these two sites, which also induces a perturbation in the magnetic ordering due to the existence of two magnetic sublattices with Co^{2+} HS and Co^{3+} HS. Both transitions have been confirmed by DSC and resistivity measurements.

L.Er-Rakho et al, J. Solid State Chem. 73, 531 (1988)
V.Caignaert et al, J. Solid State Chem. 114, 24 (1995)

P11.OF.001 *IN-SITU* NEUTRON DIFFRACTION STUDY OF PZN-PT PIEZOELECTRIC SINGLE CRYSTAL UNDER AN APPLIED VOLTAGE. J. S. Forrester and E. H. Kisi, The University of Newcastle, Callaghan, NSW, 2308, Australia, and R. Piltz, Australian Nuclear Science Technology Organisation, PMB 1, Menai, NSW, 2234, Australia.

A new class of piezoelectric ceramics known as PZN-PT have recently been discovered. Unlike typical piezoelectric ceramics (*e.g.* lead zirconate titanate (PZT)) which can show strains of only 0.17% in a strong electric field (1), the new single crystal, $Pb(Zn_{1/3}Nb_{2/3})O_3$-$PbTiO_3$ can exhibit strains of up to 1.7% in an electric field of 120 $kVcm^{-1}$ (2). The underlying cause for this phenomenon is poorly understood, but is likely to be related to a field induced crystal structure transformation. Recent studies of the piezoelectric and dielectric properties (3) have suggested that the initially rhombohedral symmetry becomes tetragonal during application of the field.

The current work aims to determine details of the crystal structure, and using *in-situ* neutron diffraction experiments in an electric field, to examine structural changes and phase transformations. Diffraction data is being collected while the crystal is subjected to increasing applied voltage in the range 0-120 $kVcm^{-1}$ and the results will be discussed in detail.

(1) R. F. Service, Science, **275**, p. 1878 (1997).
(2) S-E. Park and T. R. Shrout, Materials Research Innovations, **1** (1), p. 20 (1997).
(3) D. S. Paik, S-E. Park, S. Wada, S. F. Liu and T. R. Shrout, J. Appl. Phys. **85** (2), p. 1080 (1999).

P11.OF.002 POINT DEFECTS AND EXTENDED DEFECTS IN THE PEROVSKITE-STRUCTURED TITANATES. R. Waser, Institut für Werkstoffe der Elektrotechnik II, RWTH Aachen University of Technology, D-52056 Aachen, and Institut für Festkörperforschung, Forschungszentrum Jülich, D-52425 Jülich, Germany

A large variety of dielectric and ferroelectric ceramic components today is build upon alkaline earth and lead titanates and solid solution derivatives. A key to understand, to tune, and to tailor the electronic properties of the components is the control of the defect structure of the crystal lattice. This control has to cover the bulk of the ceramic grains as well as the region in the vicinity of interfaces such as grain boundaries and surfaces.

Recent research results have shown that point defect models in combination with the Poisson relation and the continuity equation permit to describe the grain boundary impedances in titanate ceramics in all details. At the surface, additional phase separation processes may occur which seem to be accompanied by the formation of extended defects.

The present understanding of the interrelationship of the extended defects and the point defects in titanates as well as their impact on the electrical properties will be discussed.

P11.OF.003 SYNTHESIS, STRUCTURE AND ELECTRON DENSITY DISTRIBUTION OF $SrFeO_{3-x}$ AND (Sr-Ba)TiO_3 B.N. Kodess[1,5], V.K. Ovcharov[1], A. Bush[2], V.G. Smotrakov[3], V.A.Sarin[4], A.M. Balagurov[6], L.A Butman[5], A.Y. Boyko[5] [1] Department of Crystal Metrology, VNIIMS, 119361 Moscow, Russia, [2] MIREA, 119 382 Moscow, Russia, [3] RSU, Rostov/Don, Russia [4] INR, 117312 Moscow, V-312, [5] ICS&E, Aurora, CO 80015, USA, [6] JINR, Dubna, Russia,

Strontium titanate ($SrTiO_3$) shows a displacive phase transition of cubic to tetragonal phase transitions at 110 K. T_c for system of $Sr_xBa_{1-x}TiO_3$ single crystals with x=0.025 is ~ 28 K. Oxygen-deficient perovskite of Sr exist in tetragonal symmetry at temperatures above 270 K.

Synthesis of stochio- and non-stochiometric monocrystalls of solid solutions of perovskite with variable composition and oxygen has been conducted. Verneuil methods has been used for titanate strontium and barium and zone melting with radiant heating for ferrate strontium. Determination of structural parameters of these and Standard References Materials has been conducted using accurate x-ray measurements in full sphere on four-circle CAD-4 and KM-4 diffractometers as well as time-of-flight neutron diffraction on High-Resolution Fourier Diffractometer on the IBR-2 reactor. Lattice parameters of ferrate strontium a=в=3.8535(3) and c=3.8781(3) Å correspond to $SrFeO_{2.79}$ composition. Their value is non-dependent from order of reflection; this is evident from stacking fault. Similar distortion of the cubic system were observed for $SrTiO_{2.7}$ with a=b=3.918, c=3.881. Substitution of Sr with Ba produces extra space around ions of Sr and increases lattice parameters from 3.905(1) to 3.920(1) for values of x = 0.25.

Deformation density maps and atomic displacements in pure perovskite and solid solutions were studied by high-precision X-ray diffraction analysis of single crystals. Also analysis of main features of electron distribution was performed. Electron density maps show distinct aspherity of charge both near transition-metals atoms as well as near strontium and barium atoms.

P11.OF.004 EXPERIMENTAL STUDIES OF OCTAHEDRAL TILTING IN PEROVSKITES. C.J. Howard, Australian Nuclear Science and Technology Organisation, Private Mail Bag 1, Menai, NSW 2234, Australia, and B.J. Kennedy, School of Chemistry, The University of Sydney, Sydney, NSW 2006, Australia and B.C. Chakoumakos, Solid State Division, Oak Ridge National Laboratory, Oak Ridge, TN 37831, USA.

Following a recent group theoretical study of octahedral tilting in perovskite [1], a number of related experimental studies have been completed, and the results are reported here. The interest in this work has been to examine the rotation and/or distortion of the oxygen atom octahedra in metal oxides having perovskite type structures. Neutron diffraction was used to determine the oxygen positions from which the octahedral rotations and distortions were derived.

Results are given for a number of compounds, including $SrZrO_3$, $SrHfO_3$, $CaTiO_3$, $NaTaO_3$ and $LaGaO_3$. In each case, the crystal structures have been followed to high temperatures, and intermediate phases between the room temperature orthorombic and high temperature cubic phase identified.

Close attention has been paid to temperature regimes in which only a simple octahedral tilt (tilt around a single symmetry axis) pertains. Each of the first four compounds transforms to cubic from a tetragonal phase (with octahedral tilt around the fourfold axis), and in each case, as far as can be determined from our measurements, the tilt angle in the tetragonal phase decreases continuously towards zero as the temperature is raised. There are interesting differences, however, in the functional form of this variation, suggesting the transition may be second order in some cases and of tricritical type in others. The $LaGaO_3$ transforms at modest temperature to a rhombohedral phase, but though the tilt angle in this phase decreased slowly with increasing temperature, the sample reacted with the sample can before the supposed transformation to cubic.

1. C.J. Howard & H.T. Stokes (1998). Acta Cryst. B**54**, 782.

11AA DRUG DISCOVERY AND DESIGN (sponsored by 3-Dimensional Pharmaceuticals)

M11.AA.001 WHY ARE β-LACTAMS SO SPECIAL? - STABLE AND UNSTABLE ACYL-ENZYME COMPLEXES OF SERINE PROTEASES. R.C. Wilmouth, I.J. Clifton, N.J. Westwood, S. Kassamally, C.V. Robinson and C.J. Schofield, The Oxford Centre for Molecular Sciences and The Dyson Perrins Laboratory, University of Oxford, South Parks Road, Oxford OX1 3QY, UK.

Comparison of the crystal structures of the acyl-enzyme complexes formed between a serine protease, porcine pancreatic elastase (PPE), and peptidic or lactam-derived inhibitors demonstrates why certain complexes may be resistant to hydrolysis and gives insights into the success of β-lactams as enzyme inhibitors.

Mass spectrometric screening revealed that a natural heptapeptide, human β-casomorphin-7 (BCM7), reacted with PPE to form an unusually stable acyl-enzyme complex. The X-ray structure[1] of this complex showed that the ester carbonyl was located in the oxyanion hole and, above it, in an optimal position for attack a well defined 'hydrolytic' water molecule was identified.

β-Lactam containing antibiotics remain amongst the most important therapeutic agents in clinical use and, more recently, β-lactams have been developed as inhibitors of serine proteases. The structure of the stable complex formed between PPE and a monocyclic β-lactam[2] showed that, in comparison to the PPE:BCM7 complex, the ester carbonyl had rotated out of the oxyanion hole with concomitant displacement of the hydrolytic water. A series of γ-lactam inhibitors based upon the monocyclic β-lactam were synthesised to investigate further the 'special' nature of the β-lactam ring. In the crystal structure of the acyl-enzyme complex formed between PPE and one of these monocyclic γ-lactams, displacement of the hydrolytic water was again observed but without rotation of the ester carbonyl. The combined knowledge of these structures suggests ways in which these γ-lactams and similar inhibitors might be modified to improve their inhibitory properties.

(1) Wilmouth, R.C. *et al. Nature Structural Biology* **4**, 456-62 (1997).
(2) Wilmouth, R.C. *et al. Biochemistry* **37**, 17506-13 (1998).

M11.AA.002 DISCOVERY & X RAY STRUCTURE DETERMINATION OF NOVEL CYCLOPHILIN LIGANDS. G. Kontopidis, P. Taylor, and M. Walkinshaw. Structural Biochemistry Group, ICMB, University of Edinburgh, Edinburgh EH9 3JR

We have used cyclophilin A as a template for the design and discovering of novel small molecule ligands. Putative ligands were selected by two different methods; by structure similarity and using the docking program LIDAEUS. Twenty nine small molecules were selected from a small molecule database and were tested with a fluorescence assay and PPIase assay for binding activity. Six new ligands have been discovered which bind to Cyp-A. The X-ray structures of a number of the ligands including 3-acetyl-1 methyl piperidine, ethyl-piperidine glyoxylate, dimethyl sulfoxide, tetramethylene sulfoxide and cyclopentanone have been solved and refined.

The structural analysis of the native and ligand structures revealed a hydrophobic pocket surrounded by residues Asn 102, Met 61, Arg 55 and His 122, a hydrogen bond donor site of the main chain nitrogen Asn 102, and another hydrogen bond donor site of the guanidinium of Arg 55. Some significant side chain movements are observed on binding of some of the ligands. The ligands can be classified into 2 different families of compounds.

The piperidine family shares structural similarities with natural dipeptide substrates of Cyp-A. Dimethyl sulfoxide (DMSO), tetramethylene sulfoxide and cyclopentanone form the DMSO family.

M11.AA.003 IRREVERSIBLE HIV-1 PROTEASE INHIBITOR: STRUCTURE, DESIGN AND KINETICS OF CYCLIC UREA EPOXIDES. Chong-Hwan Chang, Indawati De Lucca, Ronald Klabe, Jodie Duke, Edward Huston, Nicolas Hodge, Paul Aldrich, David Nugiel, George DeLucca, James Meek, DuPont Pharmaceuticals Company, Experimental Station, Wilmington, DE 19880

The human immunodeficiency virus (HIV) encodes an aspartic protease (PR) that cleaves the *gag* and *gag-pol* viral proteases into replicative enzymes and structural proteins. We have previously described the design and synthesis of cyclic ureas (CUs) as a novel, potent, non-peptide inhibitors of HIV PR. The CU with its seven-membered ring heterocycle is a very efficient chemical scaffold for many varieties of substituents at the S1, S2, S1', S2' binding sites of protease. To overcome difficulties of a necessity of a large molecule to fit the all the binding sites for a potent inhibitor, of a plasma protein binding, and of a drug resistant mutation, a irreversible inhibitor has been designed while keeping the CU-scaffold.

The designed cyclic urea epoxides should react with the aspartic acid in the active site to form a covalent bond. Kinetic studies indicate that the second order rate constant (k_{inact}/K_I) ranges from $1.4x10^3$ to $3.3x10^6$ M^{-1} min^{-1}.

The three-dimensional structure of HIV PR complexed with a irreversible CU has been determined with 1.8 Å diffraction data. The inhibitor binds covalently with the catalytic aspartate. While forming the bond, the aspartate residue shifts toward the center of the active site. The largest shift, 1.7 Å, occurs at the side chain of aspartate while the shifts of CU is considerably small.

The details of the binding mode and kinetics data will be discussed.

M11.AA.004 NOVEL MODES OF ANTIBIOTIC INTERACTIONS WITH ELONGATION FACTOR Tu. F. Jurnak, S.E. Heffron, S. Mui, K. Abel, A. Auroa, S. Watkins Department of Physiology and Biophysics, University of California, Irvine, CA 92697

The laboratory has solved the three-dimensional structures of two EF-Tu-antibiotic complexes and several additional complexes are in progress. All structures have been solved by molecular replacement methods. The first structure is that of a trypsin-modified EF-Tu-GDP-tetracycline complex. The complex crystallizes in space group P21, with a = 69.7 Å, b = 156.1 Å, c = 134.8 Å, b = 95.4° and six molecules per asymmetric unit. The structure has been refined to a crystallographic R factor of 18.7% at a resolution of 2.7 Å. The structural analysis reveals that the active phenylidiketone moiety of tetracycline binds to the GTPase center of EF-Tu. The results suggest a novel, but overlooked, mechanism of tetracycline inhibition of protein synthesis. The second structure is that of an EF-Tu-GDP-GE2270A complex. GE2270A is a member of the cyclic thiazolyl peptide antibiotic class. The antibiotic inhibits bacterial protein synthesis by binding to EF-Tu, with such a strong affinity that the protein must be denatured to release the antibiotic. The complex crystallizes in C2, with a = 133.47 Å, b = 45.17 Å, c = 144.00 Å, b = 94.64° and two molecules per asymmetric unit. The structure has been refined to a crystallographic R factor of 20.0% at a resolution of 2.3 Å. The structural analysis reveals that the GE2270A binds to the second domain of EF-Tu, primarily through hydrophobic interactions. The extraordinary high affinity of the antibiotic for the protein is due to the formation of a protein salt bridge formed over the antibiotic. A comparative analysis of all conformations of EF-Tu suggests that GE2270A inhibits protein synthesis by preventing the conformational change associated with the GTP state as well as sterically competing with the binding site of the aminoacyl group of charged tRNA. If completed, the results of other EF-Tu-antibiotic structures will also be presented.

M11.AA.005 POTENT, BIOAVAILABLE THROMBIN INHIBITORS: DRUG CANDIDATES FROM STRUCTURE BASED DRUG DESIGN, COMBINATORIAL CHEMISTRY AND CHEMI-INFORMATICS. John C. Spurlino, F. Raymond Salemme, Martin McMillan, Roger Bone, Richard M. Soll, Bruce Tomczuk, Tianbao Lu, Carl R.Illig, Larry Murphy, Anna Radzicka, Troy Randle, Stephen Eisennagel, and Frank Lewandowski. 3-Dimensional Pharmaceuticals, Inc., Eagleview Corporate Center, 665 Stockton Drive, Exton, Pennsylvania 19341, USA.

Efficient drug discovery is facilitated greatly by the knowledge of three dimensional molecular structures of protein-inhibitor complexes gained from crystallographic methods. Structure-activity relationships (SAR) need not be inferred in a limited fashion simply from the regiochemistry of an inhibitor and pharmokinetic data when direct structural information is available. Crystallography is an essential technique of modern drug discovery but to be most effective it needs to be coupled in an iterative, high throughput loop with the parallel synthetic methods of combinatorial chemistry, and high throughput screening assays. The huge amounts of information generated in this loop need to be assessed and then used to guide the drug design through the next cycle. The realm of chemi-informatics gives tools to correlate individual pieces of physicochemical properties or observations and categorize trends in similarity or diversity among a vast number of compounds.

Here we present some results of successful efforts to design potent, bioavailable thrombin inhibitors based heavily on SAR from the x-ray crystallographic studies of dozens of thrombin-inhibitor complexes. This information was coupled intimately with parallel high throughput analysis, synthesis, screening, and further structural elucidation to give an efficient, shortened drug discovery process.

P11.AA.001 DISPLACEMENT OF WATER IN THE DNA MAJOR GROOVE BY A DNA INTERCALATOR AT ATOMIC RESOLUTION. A.K.Todd[a], J.H.Thorpe[a], A.Adams[b], W.A.Denny[c], and C.J.Cardin[a], [a]Chemistry Department, University of Reading, Whiteknights, Reading RG6 6AD, U.K., [b]Biochemistry Department, University of Sydney, Sydney 2006, Australia. [c]Faculty of Medicine and Health Sciences, University of Auckland, N.Z.

The X-ray structure of compound *N*-[2-(dimethylamino)ethyl-9-amino-5-bromo-4-carboxamide (**1**), was determined by MAD methodologies. It is a derivative of the antitumour agent *N*-[2-(dimethylamino)ethyl]-4-carboxamide (**2**) which is currently undergoing clinical trials in the UK. Compound (**1**), although slightly less potent than (**2**) displays similar biological activity and like (**2**) is known to be a mixed topoisomerase type I and II poison. The acridine chromophore intercalates preferentially between CpG bases with the side chain; $(CO)NCH_2CH_2NH^+(CH_3)_2$, which appears to be a critical structural feature in the activity of this class of compounds, protruding into the major groove and forming a hydrogen bond between the dimethylamino terminus of the side chain and the O6 of an adjacent guanine group. The roughly symmetrical intercalation site allows binding of the drug in two orientation, this results in orientational disorder in the crystal. The disorder of the bound drug is translated via water H-bonded interactions to

produce disorder of the nearby 5-bromouridine group, illustrating the side chain's ability to disrupt the highly conserved major groove hydration.

P11.AA.002 CRYSTAL STRUCTURES OF HUMAN SQUALENE SYNTHASE ENZYME:INHIBITOR COMPLEXES. J.Pandit, D.E. Danley, G.K. Schulte, S.M. Mazzalupo, T.A. Pauly, F.M. DiCapua, C.M. Hayward, E.S. Hamanaka, J.F. Thompson and H.J. Harwood Jr. Pfizer Central Research, Groton, CT 06340, USA.

We have determined the crystal structure of recombinant human squalene synthase (rhSQS) to assist in the discovery of selective, potent inhibitors of SQS which could be developed as potential anti-hypocholesterolemic drugs.

Squalene synthase catalyzes the biosynthesis of squalene, a key cholesterol precursor, through a reductive dimerization of two C_{15} farnesyl diphosphate (FPP) molecules. Since FPP is located at the final branchpoint in the isoprenoid biosynthesis pathway, its conversion to squalene through the action of SQS represents the first committed step in the formation of cholesterol.

The structures of rhSQS complexed with different inhibitors, in combination with biochemical and mutagenesis data have also provided insights into critical features underlying the unique two-step reaction mechanism of this enzyme. The first half-reaction is a prenyl transfer reaction, leading to the formation of a stable intermediate, presqualene diphosphate (PSPP). In the second half reaction, PSPP loses inorganic pyrophosphate, incorporates a hydrogen from NADPH and rearranges to form squalene.

The protein is folded as a single domain, with a large cleft in the middle of one face. One end of this cleft is exposed to solvent, and lined by conserved aspartate and arginine residues, which are known from mutagenesis experiments to be involved in binding FPP. The other end of the channel leads to a completely enclosed pocket surrounded by conserved tyrosines and phenylalanines. These observations, along with mutagenesis data identifying residues that affect substrate binding and activity, suggest that two molecules of FPP bind at one end of the channel, where the active center of the first half-reaction is located, then the stable reaction intermediate moves into the deep pocket, where it is sequestered from solvent and the second half-reaction occurs.

Examination of the co-crystal structures has allowed, for the first time, for a detailed examination of the binding mode of SQS inhibitors at both active centers, and should aid in the design of more potent and specific inhibitors.

P11.AA.003 STRUCTURE OF SHV-1 β–LACTAMASE AND ITS COMPLEX WITH TAZOBACTAM. J.R. Knox, A.P. Kuzin, M. Nukaga, Y. Nukaga, A.M. Hujer†, and R.A. Bonomo†. Department of Molecular Biology, University of Connecticut, Storrs, CT 06269; †Department of Veterans Affairs, Cleveland, OH 44106.

The SHV-1 β-lactamase is prevalent in clinical strains of *Klebsiella* resistant to penicillin and cephalosporin antibiotics. SHV-1 is the prototype of 11 natural mutants that have arisen in the last 10 years in response to the heavy use of new cephalosporins. The x-ray structure of SHV-1 has been determined to 1.97 Å resolution. The 28.8 kDa enzyme crystallizes from PEG6000 at pH 7 in $P2_12_12_1$ with cell dimensions a = 49.6, b = 55.6, c = 87.0 Å. A molecule of the Cymal-6 detergent required for crystallization is clearly seen linking enzyme molecules in the crystal lattice. The structure was solved by MR and has been refined with XPLOR to an R factor of 0.18 (R_{free} = 0.25) for all non-zero data from 8.0 to 1.97 Å. Deviations of bonds and angles from ideal values are 0.018 Å and 1.8°, resp. Overlay of all 263 Cα atoms in the SHV-1 and TEM-1 β-lactamase results in a deviation of 1.4 Å (rms). Largest deviations occur in the H10 helix (218-224) and in the loops between strands in the β-sheet. All atoms in residues 70, 73, 130, 132, 166, and 234 in the catalytic site of SHV-1deviate only 0.23 Å from atoms in TEM-1. However, the width of the substrate-binding cavity in SHV-1, as measured from the 104-105 and 130-132 loops on one side to the 235-238 β-strand on the other side, is 0.7 to 1.2 Å wider than in TEM-1. A structural analysis of the highly different affinity of SHV-1 and TEM-1 for the β-lactamase-inhibitory protein BLIP focuses on interactions at position 104 (Asp or Glu). An intermediate in the reaction of SHV-1 with the suicide inhibitor tazobactam has been mapped at 100°K and is being refined with 2 Å data.

Work supported by U.S Department of Veterans Affairs and NIH AG-00634.

P11.AA.004 THE STRUCTURE OF THE CATALYTIC SUBUNIT OF CDC25B AT 1.9 RESOLUTION. R.A. Reynolds, Physics Dept. Grand Valley State Univ., Allendale, MI 49401 USA, A.W. Yem, C.L. Wolfe, M.R. Diebel and K.D. Watenpaugh, 7255-209-102, Pharmacia and Upjohn, 301 Henrietta St., Kalamazoo, MI 49001 USA.

Cdc25 dual-specific phosphatases are responsible for the dephosphorylation and activation of cyclin-dependent protein kinases resulting in cell cycle progression. Blockage of this progression is a strategy being pursued for the design of novel anit-cancer drug templates. A domain of cdc25b containing the catalytic subunit has been crystallized and the structure solved using MIR techniques. This recombinant human subunit incorporates residues 356-556 and was determined to be stable for crystallization at 4°C using dynamic light scattering techniques. Mercury and Tungstate derivatives were used to determine initial phases. Data collected at 100K were over 95% complete to 1.92 with the resulting structure having an R_F = 13.8% (R_{free} =18.6%) for data greater than $2\sigma_F$. The protein consists of six α-helical regions, three strands of parallel β-sheet, and a considerable amount of less well defined structure. The signature motif (HCX_5R) of the catalytic site was observed with both sulfate and tungstate bound. A second sulfate binding site encompasses residues which are highly conserved in the cdc25 family. In addition to binding two sulfates, two cysteine residues are observed as beeing modified by β-mercaptoethanol and an additional strong electron density peak in a charged pocket is consistent with the binding of a chlorine ion. Although this construct has disorder at both ends, the C-terminal end forms a helical region which lays against the rest of the subunit forming a groove which was not observed in the cdc25a structure

Fauman *et al.,* Cell **93**, 617-625, 1998

P11.AA.005 CRYSTALLOGRAPHIC AND COMPUTATIONAL COMPARISON OF ISOMERIC ANTI-MYCOBACTERIAL AMIDRAZONES. C. H. Schwalbe, C. Gallagher, P. R. Lowe, D. C. Billington, D. L. Rathbone & K. J. Tims, Pharmaceutical Sciences Institute, Aston University, Aston Triangle, Birmingham B4 7ET, U.K.

Crystal structures [1] of four 2-heteroarylcarboxamidrazones consistently revealed intramolecular N...H-N-H...N hydrogen bonds from each amino group, and small twists along the chain (torsion angles T1 to T5) which incline the planes of R1 and R2 at ca. 10°.

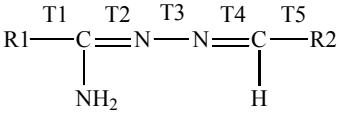

We report here two structures bearing a common R2 = *p*-benzyloxy-*m*-methoxyphenyl but with R1 attached differently: R1

= 2-pyridyl in **I**, 4-pyridyl in **II**. Paradoxically, some 2-pyridyl and 4-pyridyl isomers (e.g. when R2 = *p-t*-butylphenyl) are equi-active against *Mycobacterium fortuitum*, but **I** is nearly as active as isoniazid while **II** is inactive. Replacement of N...H-N-H hydrogen bonding in **I** by C-H...H-N-H clash in **II** alters T1 but still leaves H atoms only 2.22(3) Å apart. T3 in both **I** and **II** disagrees with the averaged absolute values from [1]. T1-T5 in degrees are tabulated below:

Source	T1	T2	T3	T4	T5
<|1|>	175.5	178.3	173.3	176.6	5.6
I	-168.7	176.5	157.6	177.6	3.8
II	154.6	172.4	147.9	173.4	-13.4
3-21G	153.6	178.8	178.3	179.9	0.2
AM1	131.7	178.3	175.4	179.1	19.0

Ab initio 3-21G molecular orbital optimisation of **II** with R2 simplified to phenyl corroborated the short H...H contact and the T1 twist. It removed the anomaly in T3, which may be due to packing requirements of R2. The semi-empirical AM1 method widened the H...H contact via greater T1 twisting and a partially pyramidal amino group, a trend exaggerated by PM3 and MNDO.

1. C. H. Schwalbe, P. R. Lowe, B. Gordon, D. L. Rathbone & D. C. Billington, J. Pharm. Pharmacol. (1998), **50** (Supplement), 245.

11BB MACROMOLECULES AT HIGH RESOLUTION: REFINEMENT AND VALIDATION

M11.BB.001 THE RELATIONSHIP BETWEEN R_{free} AND R IN A CORRECTLY REFINED PROTEIN STRUCTURE. Ian J Tickle, Roman A Laskowski and David S Moss, Department of Crystallography, Birkbeck College, Malet Street, London WC1E 7HX, UK.

The last five years have seen a large increase in the use of cross-validation in the refinement of macromolecular structures from X-ray data. In this technique, a test set of reflections is set aside and used to calculate a free R-factor. Although this R-factor is frequently quoted in presenting experimental results and is expected to be higher than the R-factor from the working set, no theory has existed to say how much higher it should be. We have derived the statistically expected values of the ratio of the free R-factor to the R-factor calculated from the working set for a structure where weights correctly account for experimental and model errors. These estimates have been compared with the observed ratios from 725 macromolecular structures in the Protein Data Bank and the results have been related to resolution and the number of reflections per atom.

Tickle, I J, Laskowski, R A and Moss D S, R_{free} and the R_{free} ratio. Part I: Derivation of expected values of cross-validation residuals used in macromolecular refinement, Acta Cryst., (1998), D54, 547-557.

M11.BB.002 SUBTILISIN AT ATOMIC RESOLUTION. R. Bott, G. Ganshaw, Genencor International, Palo Alto CA 94304, Mark Knapp, LLNL Livermore CA 94550, Peter Kuhn and Mike Soltis, SSRL, Menlo Park CA 94025

Subtilisin a serine protease of the "subtilase" class is one of the most extensively studied enzymes and a target for protein engineering. The three-dimensional structure has been determined by both X-ray crystallography and NMR. Subtilisin has a very ordered structure in NMR experiments[1]. There are numerous non exchanging hydrogen atoms. X-ray cryo-crystallographic data can be collected well beyond 1.0 Å.

We have previously reported determination of the structure of Bacillus lentus subtilisin at 0.78 Å from a crystal grown at pH 5.9 [2]. At pH 5.9, the enzymes displays approximately 10% of its optimal activity while at pH 8.6 the enzyme is fully active. We have collected data from crystals at pH 8.6 to a resolution of 0.85Å. While the overall structure is unchanged we can detect subtle changes in difference maps that are attributed to the specific ionization of a carboxylate group. These results, along with a comparison of the refine coordinates, currently in progress, will be presented .

Martin et al. (1997) Structure 5, 521-532.
Kuhn et al. (1998) Biochemistry 37, 13446-13452.

M11.BB.003 ANISOTROPIC REFINEMENT AND OTHER ADVANCES OF USING FFT PROCEDURES. Murshudov, G.N.[1,2,*], Lebedev, A.[3], Vagin, A.A.[1] and Dodson, E.J.[1], [1]Chemistry Department, University of York, [2]CLRC, Daresbury Laboratory, [3]MPG-ASMB c/o DESY, Hamburg, [*]e-mail: garib@yorvic.york.ac.uk

Refinement of individual atomic anisotropic atomic displacement parameters (ADP) using FFT has already been proven to be fast [1]. For example for 5 000(x9 = 45 000 parameters) atoms with 450 000 reflections (at 0.89Å resolution) one cycle of refinement using an O_2 SGI takes approximately 30 minutes of CPU time. Various tests of anisotropic refinement implemented in the program REFMAC [2] (available from CCP4 [3]) will be discussed. The merits of mixed refinement where some parts of structure have isotropic and some anisotropic ADPs will also be presented.

Usually individual atomic anisotropic refinement is performed at high resolution. In these cases anomolous pairs should be considered as separate observations, and although they represent dependent random variables the dependence is not linear. Maximum likelihood equations which use FFT and take this into account have been derived. It is expected that this technique will increase the power of the refinement even at relatively low resolutions, especially in the presence of strong anomolous scatterers.

[1] Murshudov, G.N., Vagin, A.A., Lebedev, A., Wilson, K.S. & Dodson, E.J. Acta Cryst. **D55** (1999) 247-255
[2] Murshudov, G.N., Vagin, A.A. & Dodson, E.J. Acta Cryst **D53** (1997) 240-255
[3] CCP4 Acta Cryst **D50** (1994) 760-763

M11.BB.004 ULTRA HIGH RESOLUTION STRUCTURE OF CRAMBIN: FIRST CHARGE DENSITY ANALYSIS OF A PROTEIN. Christian Jelsch §, Martha M. Teeter *, Virginie Pichon-Pesme §, Robert H. Blessing # & Claude Lecomte §. § Laboratoire de Cristallographie et Modelisation des Materiaux Mineraux et Biologiques LCM3B-UHP-CNRS BP 239. 54506 Vandoeuvre-lès-Nancy Cedex FRANCE, * Department of Chemistry, Boston College, Chestnut Hill, MA 02167, USA, # Hauptman-Woodward Medical Research Institute, Buffalo, NY USA

Diffraction data of crambin crystals have been collected at ultra high resolution (0.54 Å) using synchrotron radiation at the EMBL Outstation in Hamburg. After a first refinement using SHELXL-97 [1], the structure has been refined with an adapted version of MOLLY, a program [2] which uses a charged non-spherical atom model describing the electron distribution on the molecule.

First, the charges and electron density multipoles of the protein atoms were taken from our database [3] of transferable average parameters obtained from several small peptides and amino acid charge density analyses.

Then, the average charge density parameters of the polypeptide mainchain atoms have been refined. The average peptide unit deformation electron density, which reveals the effect of bonding aspherical electron density, is comparable but slightly weaker to the one obtained from parameters transfer and compares very well with that obtained by ab initio calculation on a small peptide.

The high diffraction power of the crambin crystals is due to the low thermal displacement parameters of the protein atoms [4]. This study on the protein crambin shows that biological macromolecules start now to be accessible to charge density experiments.

Dr. Lamzin, Dauter & Wilson are gratefully acknowledged for their contribution in the diffraction data collection.

[1] Sheldrick G.M. and Schneider, T. *Methods in Enzymology*, 277, pp 319-343, Academic Press. (1997).
[2] Hansen N.K. & Coppens P. *Acta Crystallogr*., A34, 909-921 (1978).
[3] Pichon-Pesme, V., Lecomte, C. & Lachekar, H. *J. Phys. Chem*., 99, 6242-6250 (1995)
[4] Jelsch C., Pichon-Pesme V., Lecomte C. & Aubry A. *Acta Crystallogr*. D54, 1306-1318 (1998).

P11.BB.001 ATOMIC RESOLUTION STRUCTURES OF ADH. R. Meijers and V. S. Lamzin, EMBL c/o DESY Notkestraße 85 D-22603 Hamburg, FRG, E.S. Cedergren-Zeppezauer, Biokemi, Kemicentrum, Box 124, 22100 Lund, Sweden, H.W. Adolph, Fachrichtung 12.4, Biochemie, Postfach 151150, Universität des Saarlandes, D-66041 Saarbrücken, FRG, Z. Dauter, Brookhaven Nat. Lab., Bldg. 725A-X9, Upton, NY 11973, USA, K. S. Wilson, Dept. of Chemistry, York University, Heslington YO1 5DD, UK.

The atomic resolution structures of ADH give new and intriguing insights into the mechanism of hydride tranfer. Alcohol dehydrogenase (ADH) is a NAD+-dependent oxidoreductase acting on electron donors containing a CHOH-group such as primary and secondary alcohols. The catalytic dehydrogenation proceeds by a mechanism of hydride ion transfer from substrate to NAD+ combined with proton transfer from substrate to solution. The horse liver ADH is a 80kDA dimer [1] containing 4 zinc ions which can be substituted by cadmium. 4Cd-ADH is a useful enzyme probe when measuring ligand binding to Cd in the active site with perturbed angular correlation of gamma rays (PAC) [2]. A crystalline abortive complex of 4Cd-ADH with NADH and methyl pentane diol MPD was prepared to check the feasibility of the replacement of zinc by cadmium. Cryo data extending to 1.1 Å were collected for complexes with cadmium and zinc respectively. A glutamate near the active site extends partly towards the metal in the cadmium complex but not in the zinc complex. The nicotinamide ring of NADH that is involved in hydride transfer is severely distorted in both complexes.

1. Eklund, H., Samama, J-P., Wallen, L., Brändén, C-I., Å, Å. and Jones, T. A. (1981), *J.Mol.Biol.* **146**, 561-587
2. Hemmingsen, L., Bauer, R., Bjerrum, M. J., Zeppezauer, M., Adolph, H. W., Formicka, G. and Cedergren-Zeppezauer, E.S. (1995), *Biochemistry* **34**, 7145-7153

P11.BB.003 PATTERNS IN WATER-PROTEIN DISORDER SUBSTATES & PEPTIDE GEOMETRY IN CRAMBIN CRYSTALS AT 0.54 Å RESOLUTION. M. M. Teeter, Dept. of Chemistry, Merkert Chemistry Building, Boston College, Chestnut Hill, MA 02167.

Refinement of X-ray data, collected to 0.54 Å and 100 K at the EMBL Hamburg Outstation of the DESY synchrotron, reveals crambin substates not only of side chains but also for the backbone. Further, disordered protein positions are correlated in space with water substates, for this mixed sequence form of crambin. The interrelations of modelled water substates to each other are analysed and origins of the disorder are discussed.

Comparison of disorder in this crystal structure is made with the pure sequence forms of crambin (Yamano and Teeter, 1994; Yamano, *et al.*, 1997.) Surprisingly, although protein substates are reduced by half in the pure form crystals, considerable water substate disorder remains. A hypothesis for this residual water disorder is advanced. The implication of crambin's water and protein disorder for crystal structures at lower resolution is discussed. A template for modelling such water and a strategy for refinement is being developed.

Complete disorder modelling improves protein geometry statistics and suggests improved values for target peptide geometry in proteins.

Acknowledgements: Dr. Christian Jelsch contributed to refinement of the 0.54 Å data. Dr. Victor Lamzin provided invaluable help in data collection.

1. Yamano, A. and Teeter, M.M. (1994). Correlated disorder of the pure Pro22/Leu25 form of crambin at 150 K refined to 1.05 Å resolution. J. Biol. Chem. 19, 13956-13965.
2. Yamano, A., Heo, N.H. and Teeter, M.M. (1997). Crambin crystal structure of the Ser22/Ile25 form confirms solvent, side chain substate correlations. J. Biol. Chem. 272, 9597-9600.

P11.BB.004 MULTI-PURPOSE EXTERNAL REFERENCE FILE FOR MACROMOLECULES. Vagin, A.A.[1,*], Greaves, R.[1], Dodson, E.J.[1], Wilson, K.S.[1] and Murshudov, G.N.[1,2], [1]Structural Biology laboratory, University of York, [2]CLRC, Daresbury Laboratory, [*]e-mail: alexei@yorvic.york.ac.uk

The external reference file (ERF) for the chemical description of the structural units of the macromolecules (proteins, DNA/RNA, sugars etc) as well as small inorganic and organic molecules and the programs to manage it will be presented. This ERF can be used for several purposes: refinement, graphics, validation. The extended mmCIF dictionary format makes the ERF self-explanatary, simple to correct and add new information.

An automated procedure to create list of restraints corresponding to the input coordinates in the PDB or mmCIF formats using the ERF has been implemented in the program MAKECIF. The LIBCHECK program has also been developed to manage and check the content of the ERF. It can create new ERF entries from different sources: PDB, CDS, CIF, SMILE.

Its application for refinement will be discussed.

P11.BB.005 ON BUILDING A DATA BANK OF TRANSFERABLE EXPERIMENTAL ELECTRON DENSITY PARAMETERS: APPLICATION TO VERY HIGH RESOLUTION PROTEIN STRUCTURES. C. Lecomte, C. Jelsch and V. Pichon-Pesme, LCM^{3}B, UPRESA CNRS 7036, Université Henri Poincaré, Nancy I, Faculté des Sciences, BP 239, 54506 Vandoeuvre-lès-Nancy Cedex.

Very precise electron distribution obtained from very high resolution X-ray diffraction on small peptides is used to calculate new scattering factors which contains aspherical features due to chemical bonding[1-4] like covalent bonds, d electrons or lone pairs. It will be shown that these scattering factors can be transferred to refine high resolution oligopeptide and protein structures[5].

Application to small proteins and the limits of applicability in terms of resolution, B factors, disorder[6] will be given. Some applications in the future in like deriving partial atomic charges, electrostatic potential or d electron population in the case of metallo proteins will be discussed.

1. C. Lecomte (1995). Advances in Molecular Structure Research, Vol. I, JAI Press Inc., I et M Hargittai Eds, 261-302.
2. V. Pichon-Pesme, C. Lecomte, R. Wiest, M. Bénard (1992). J. Amer. Chem. Soc., 114, 2713-1715.
3. V. Pichon-Pesme, C. Lecomte, H. Lachekar (1995). J. Phys. Chem., 99, 6242-6250.
4. P. Coppens (1998) Acta Cryst. A54, 779-788.
5. C. Jelsch, M. Teeter, V. Pichon-Pesme, V. Lamzin, R.H. Blessing, C. Lecomte (1999). In preparation.
6. C. Jelsch, V. Pichon-Pesme, C. Lecomte, A. Aubry (1998). Acta Cryst. D54, 1306-1318.

11CC NEW FRONTIERS IN HIGH PRESSURE CRYSTALLOGRAPHY

M11.CC.001 NEW SINGLE-CRYSTAL DIFFRACTION TECHNIQUES AT HIGH PRESSURE. M.I. McMahon. Department of Physics and Astronomy, The University of Edinburgh, Edinburgh EH9 3JZ, UK.

Recent advances in 2-dimensional detectors have enabled great progress to be made in refining high-pressure crystal structures from powdered samples. However, considerably more detailed structural information on high-pressure phases could be obtained if single-crystal samples were utilised. Unfortunately, the strongly first-order nature of the phase transitions experienced by many materials at high-pressure means that single-crystal samples rarely survive intact into the high-pressure phase.

While single-crystal samples of high-pressure phases can be obtained by annealing at high temperature or by slow cooling from the melt, we have recently found that systems such as InSb, Ce and Ba have high-pressure phases that recrystallise spontaneously at room temperature. Although such samples are not normally mono-crystalline, but contain many crystallites, some of these are sufficiently large to enable (in principle) single-crystal data sets to be collected. The problem then becomes one of identifying which of the many observed reflections in a spotty powder pattern come from the same sample crystallite.

Methods for overcoming this problem, and allowing reflections from a single-crystallite to be identified, will be presented. The merits of CCD-based area detectors over conventional 4-circle diffractometers will be discussed, and results will be given for test single-crystal studies with multi-crystallite samples. Work is also in progress to grow single-crystal samples under pressure at high temperature and the latest results will be shown.

M11.CC.002 MAGNETIC NEUTRON DIFFRACTION IN THE 50 GPA PRESSURE RANGE. Goncharenko I.N. [1], Mirebeau I. [2], Ochiai A. [3], [1] Laboratoire Leon Brillouin, CEA Saclay, 91191; Gif-sur-Yvette, France and Russian Research Center "Kurchatov Institute", 123182 Moscow, Russia, [2] Laboratoire Leon Brillouin, CEA Saclay, 91191 Gif-sur-Yvette, France, [3] Niigata University, Ikarashi-Ninocho 8050, Niigata-shi, Niigata-ken 950-2181, Japan

Magnetic neutron diffraction is the most powerful method to study magnetic order in solids. Therefore, progress in high pressure magnetic crystallography is closely related with developments in high pressure neutron techniques. We report here recent results on neutron diffraction studies of magnetic structures and magnetic phase transitions in the 50 Gpa pressure range.

The experiments have been performed in the Laboratoire Leon Brillouin, in collaboration with the RRC "Kurchatov Institute". We developed a specialized high pressure powder diffractometer for magnetic studies. We use sapphire or diamond anvil cells, adapted for neutron measurements. We discuss the current stage of the project and the future developments, bringing neutron studies to the same pressure range as for X-ray crystallography. The progress in the neutron instrumentation and pressure techniques allowed us to study various magnetically ordered materials in the wide range of pressures (50 GPa) and temperatures (down to 1.5 K). The talk includes several examples of high pressure neutron diffraction studies, like studies of magnetic order in the "model Heisenberg magnets" EuX and GdX (X =chalcogen or pnictogen). The drastic increase of the available pressure range changed crucially knowledge about magnetic interactions in the "model" semiconductors under pressure. We observe new pressure induced magnetic phases and abnormal enhancement of the ferromagnetic interactions with pressure.

M11.CC.003 PRESSURE DEPENDENCE OF DISORDER: COMPUTER SIMULATION OF RECONSTRUCTED DENSITIES. Karsten Knorr, Institut für Geowissenschaften, Mineralogie / Kristallographie, Universität Kiel, Olshausenstr. 40, D 24098 Kiel, Germany and Fritz Mädler, Hahn-Meitner-Institut Berlin GmbH, Glienicker Str. 100, D 14109 Berlin, Germany.

Recently, the structure of KPF_6 at ambient conditions and the pressure dependence of the electron-density distribution of the disordered PF_6^- ion in the cubic phase have been studied experimentally by X-ray single crystal diffraction [1]. We analysed the density distribution resulting from a maximum entropy reconstruction by using a flexible evolutionary algorithm which imitates mechanisms of the biological evolution in order to optimise a suitable cost function [2]: To fit the rigid PF_6^- anion to the density maxima, its orientation angles (θ, ϕ, ψ) were mutated at random. In order to evaluate possible re-orientation paths of the fragment we allowed congruent mappings of the PF_6^- octahedron within the space available in the structure. Thus, we found two different pathways for the reorientation which together fully explain the shape of the electron density found experimentally [1].

For a ``virtual pressure experiment'' we simulated the steric hindrance experienced by the octahedra during reorientation by confinement of the available space. The change in the shape of the density distribution under increasing pressure can be explained by ordering and a superposition of the differently oriented PF_6^- octahedra, in excellent agreement with the experimental findings [1].

1. Sowa, H., Knorr, K., Mädler, F., Ahsbahs, H. & Kutoglu, A.: The high-pressure behaviour of the cubic phase of KPF_6: An X-ray single crystal and entropy maximization study (1999) subm. to Z. Kristallogr.
2. Knorr, K. & Mädler, F.: Application of evolution strategies to disordered structures. (1998) J.Appl.Cryst. subm.

M11.CC.004 STREAM-LINING DATA ANALYSIS AND GOING FURTHER. A P Hammersley, T Günzel, A Fitch, European Synchrotron Radiation Facility, BP 220, 38043 Grenoble Cedex, France

The enormous increase in cheaply available computing power means:

i. Existing analysis methods can be applied quickly

ii. Much larger problems can be tackled

iii. New forms of analysis can be undertaken and new problems tackled

To realise the full potential of the computing power new and more flexible software is needed.

Examples of software developments will be presented in the field of High Pressure powder diffraction. FIT2D allows integration of 2-D images to 1-D ``2-theta'' scans. This is now used routinely with huge images, and automation has been added which allows routine treatment of hundreds of images. FIT2D is useful for time-resolved in-situ studies (e.g. mineralogy), and with weakly scattering samples of intermediate crystallinity (e.g. fullerenes). The program ``CINDEX'' has been developed to faciliate interactive indexing of 2-theta scans. This provides a

stream-lined interface to a number of standard indexing algorithms. On recent PC's the whole process is fast enough make the analysis interactive; the fast feed-back simplifying the analysis process.

The challenge is to develop software to tackle more difficult problems automatically. Indexing of mixed phase samples is such an area. Algorithms will be enhanced with more powerful search techniques. Similar techniques may be useful for mixed phase single crystal indexing, whilst the availability of cheap 3-D graphics may provide alternative interactive techniques.

M11.CC.005 NUCLEAR RESONANT SCATTERING OF SYNCHROTRON RADIATION - A NEW TOOL FOR HIGH PRESSURE RESEARCH. H.F.Grünsteudel, A.Barla, R.Rüffer, A.I.Chumakov, J.Metge, O.Leupold* and K.Quast. European Synchrotron Radiation Facility, BP 220, F-38043 Grenoble Cedex *on leave from II. Institut f. Experimentalphysik, Univ.Hamburg, Luruper Chaussee 149, D-22761 Hamburg

The central idea to excite nuclear levels using synchrotron radiation is to combine its advantages like high brilliance, pulsed time structure and high degree of linear polarization with the high energy resolution of the Mössbauer effect (e. g. $\approx 10^{-13}$ in the case of ^{57}Fe). In the nuclear decay following the pulsed excitation, intensity modulations (``quantum beats'') can be observed in a simple transmission geometry (Nuclear Forward Scattering). Quantum beats originate from nuclear level splitting due to electric and/or magnetic hyperfine interactions, the beat frequencies being characteristic for the splitting. Background radiation originating from scattering by the electronic system of the sample (instantaneous) is separated from the (delayed) nuclear scattering and is discriminated by means of a fast detector system and fast electronics, leading to an excellent signal to noise ratio. The well established diamond anvil cell technique is therefore especially suited, as scattering by the diamond anvils does not spoil the signal. Further techniques are on the horizon to explore high pressures and high temperatures simultaneously.

We present the method and discuss major achievements compared to traditional energy resolved Mössbauer spectroscopy. Recent experiments will be discussed and latest developments for the resonance energies of ^{57}Fe, ^{151}Eu and ^{119}Sn will be shown.

M11.CC.006 INELASTIC X-RAY SCATTERING UNDER HIGH PRESSURE. K. Hämäläinen, Department of Physics, POB 9, FIN-00014 University of Helsinki, Finland

Inelastic scattering at high momentum transfer, usually referred as Compton scattering, is a unique tool to probe directly the electron ground state properties. For example, the measured Compton profile gives the momentum density of the scattering electrons, which is directly related to the charge density, band structure and the wavefunctions. The advent of synchrotron radiation has recently made it possible to use crystal analyzers to significantly improve the momentum resolution. This has opened up new possibilities to study fine structures related to the Fermi surface topology. Recently, several studies have been done on novel materials varying the sample environment (temperature, magnetic field) or crystal direction or doping. We will report Compton scattering studies on sodium under high pressure accomplished at beamline ID15 at ESRF using both large volume and diamond anvil cell.

Sodium 3s electrons form within very good approximation a free electron gas. Several fundamental properties of solids can be understood surprisingly well by treating the system as a non-interacting electron gas. However, in many solid state systems the electron-electron correlation effects can play a crucial role in determining the system behavior. Separating these effects from the other overlapping solid state contributions experimentally via a direct measurement is not that simple task. The Compton scattering can in principle be utilized to directly produce the quasiparticle renormalization constant Z_F that is given by the jump of momentum density at the Fermi break. The correlation effects depend on the free electron density and the various theories predict significantly different density dependencies. Only few experiments have been done to access different electron densities using different elements (typically Li, Be and Na). However, in this way it is very difficult to separate the band structure effects, for example, from the correlation effects. Therefore, we have studied sodium at different pressures to directly modify the free electron density without a major change of the atomic structure.

P11.CC.001 INSTRUMENTATION FOR NUCLEAR RESONANT SCATTERING IN HIGH PRESSURE RESEARCH. H.F.Grünsteudel, A.Barla, L.E.Schröder, M.Mezouar, K.Quast, J.Metge, R.Rüffer, A.I.Chumakov, O.Leupold* and H.Grünsteudel**. European Synchrotron Radiation Facility, BP 220, F-38043 Grenoble Cedex, *on leave from II. Institut f. Experimentalphysik,Univ. Hamburg, Luruper Chaussee 149, D-22761 Hamburg, **on leave from Kemisk Institut, Odense Universitet, Campusvej 55, DK-5230 Odense

In Nuclear Resonant Scattering low-energy nuclear transitions are excited by synchrotron radiation pulses. Specially adapted X-ray optics, fast detectors, various machine timing modes and demanding sample environment are necessary. The natural linewidth of such transitions is of the order of $\approx 10^{-9}$eV while an undulator has typically a bandwidth of the order of $\approx 10^{2}$eV. The incident radiation (energy $\approx 10^{4}$eV) can be monochromatised to the meV range by high resolution monochromators based on perfect silicon crystals. We present several designs for the resonance energies of ^{57}Fe (14413eV) and ^{151}Eu (21542eV).

For high pressure experiments focussing techniques are employed to match the small sample sizes of typically 100x100 μm^2 or smaller. We present our recent developments to achieve variable focal spot size at several distances from the source for the resonance energies mentioned above.

Further on we present new installations and developments for high pressure experiments at low temperature ($\approx$ 2K) in external magnetic fields up to 6T. First high pressure high temperature experiments have been carried out and will be discussed.

P11.CC.002 NUCLEAR RESONANT SCATTERING OF SYNCHROTRON RADIATION BY ^{119}Sn. A.Barla[1], H.F.Grünsteudel[1], R.Rüffer[1], A.I.Chumakov[1], J.Plessel[2], M.M.Abd-Elmeguid[2], (1) European Synchrotron Radiation Facility, BP 220, F-38043 Grenoble Cedex, (2) II. Physikalisches Institut, Universität zu Köln, Zülpicherstrasse 77, D-50937 Köln

Nuclear Resonant Scattering became a new tool in high pressure for the investigation of electronic and magnetic properties of a wide variety of systems using Nuclear Forward Scattering (NFS) as well as the dynamics using Nuclear Inelastic Scattering (NIS). So far most of the work has been performed on iron containing samples. We report here on the development of this technique for tin compounds. Our NFS measurements on β-Sn and SnO_2 at room temperature (RT) allowed an accurate determination of hyperfine parameters and Lamb-Mössbauer factor. A first application to high pressure has been carried out on UNiSn. This system shows a triple transition at $T_N \approx 45$K from semiconducting, paramagnetic and cubic (for $T > T_N$) to a metallic, antiferromagnetic and tetragonal phase. High pressure is an important tool to understand the relationship between the disappearance of the semiconducting gap and the onset of antiferromagnetism. We present our first high pressure test NFS measurements on UNiSn.

Finally, NIS is valuable for the investigation of dynamical properties especially of phase transitions. It measures the phonon density of states (DOS) as well as the Lamb-Mössbauer factor. The thermodynamic properties of Sn have recently drawn considerable interest due to its ambivalent behaviour at the borderline between covalent and metallic bonding [1]. Here we present our NIS measurements at RT and at T ≈ 100K on β-Sn, together with the DOS obtained at the lower temperature.

[1] R. Ravelo et al., Phys. Rev. Lett. 79, 2482 (1997)

P11.CC.003 ANHARMONIC EFFECTIVE PAIR POTENTIAL OF α-AgI TYPE CuBr DETERMINED BY EXAFS UNDER PRESSURE. Maki Okube, Akira Yoshiasa, Osamu Ohtaka, Tomokazu Ito, Graduate school of Science, Osaka University, Toyonaka, Japan, Osamu Kamisima, Research Institute for Scientific Mesurements, Tohoku University, Sendai,Japan, Yosimori Katayama, SPring-8, Akoh, Hyogo, Japan.

The anharmonic effective pair potentials

$$V(u) = [(\alpha u^2)/ 2!]+[(\beta u^3)/ 3!]+[(\gamma u^4)/ 4!]$$

for Br-Cu bond in α-AgI type CuBr have been investigated by the EXAFS technique. The EXAFS spectra near the Br K-edge were measured at 773, 873 and 973 K under the pressure of 7 GPa using synchrotoron radiation from SPring-8. In the parameter fiting, we have directly carried out the numerical integration of EXAFS function and evaluated the precise anharmonic effective pair potentials [1,2]. The Grüneisen parameters γ_G are calculated from the obtain values of α and β. The statistical distribution of Cu in α-AgI type CuBr and superionic conduction mechanisum have been discussed based on the effective pair potential and distribution of Br-Cu distances. The time spent on a lattice site is greater than the time spent between the potential-energy minima. However, the probability of finding mobile ions at saddle-point position can be regard as siginificant and is several per cent in the superionic conducting phase.

[1] A.Yoshiasa and H.Maeda, Solid State Ionics, accepted
[2] A.Yoshiasa et al, J.Synchrotron Rad., in press

P11.CC.004 NEUTRON SCATTERING STUDY OF STRUCTURE AND DYNAMICS OF AMMONIUM HALIDES UNDER HIGH PRESSURE. D.P.Kozlenko, A.M.Balagurov and B.N.Savenko, Frank Laboratory of Neutron Physics, Joint Institute for Nuclear Research, 141980 Dubna Moscow Reg., Russia, and V.P.Glazkov and V.A.Somenkov, RRC "Kurchatov Institute", 123182 Moscow, Russia and S.Hull, ISIS Facility, CLRC Rutherford Appleton Laboratory, Chilton, Didcot, Oxon OX11 0QX, UK.

Structural changes in ammonium halides ND_4Cl, ND_4Br and ND_4F at pressures up to 40 kbar and ND_4I at pressures up to 86 kbar have been studied by means of neutron diffraction at room temperature. The pressure dependencies of the lattice parameter *a* and the deuterium position parameter *u* were obtained. It was found that the order - disorder II-IV phase transition in ND_4Br and ND_4Cl occurs at equal critical values of *u*, u_{cr}=0.152(2). For ND_4F, *u* is initially higher than u_{cr} and only the ordered CsCl type phase III (analogous to the phase IV of the other ammonium halides) exists at high pressure. For ND_4I, no II-IV phase transition was observed. A phase transition into the recently discovered high pressure phase V was detected in ND_4I at $80 < P < 86$ kbar. The structure of ND_4I(V) was found to be the same as the structure of the low temperature phase ND_4I(III) - tetragonal one with antiparallel ordering of ammonium ions, space group *P4/nmm*. The critical value of *u* for the II-V phase transition in ND_4I, *u*=0.148(2) is close to the u_{cr} for the II-IV transition in ND_4Cl and ND_4Br. Under pressure N-D bond length remains nearly constant for all the investigated compounds.

Vibrational spectra of NH_4I and NH_4F have been studied by means of incoherent inelastic neutron scattering at pressures up to 40 kbar. Libration and transverse optical (TO) modes frequencies as functions of pressure were obtained. Both frequencies increase under pressure. For NH_4F, libration frequency was found to be considerably larger in comparison with the one for the other ammonium halides.

P11.CC.005 MODELLING HIGH PRESSURE STRUCTURES USING THE BOND VALENCE (IONIC) MODEL I.D.Brown, Brockhouse Institute for Materials Research, McMaster University, Hamilton, Ontario, Canada L8S 4M1.

In the ionic model, the cohesive force supplied by the electrostatic attraction between charged ions provides an internal pressure which is opposed by the repulsive contact forces that prevent the solid from collapsing to a point. The internal pressure is of the order of 10 GPa. The behaviour of a crystal under hydrostatic pressure can therefore be simulated by increasing the ionic charges in order to increase the internal pressure. Changing these charges changes the bond flux or bond valence allowing the length of the compressed bonds to be calculated from the bond valence - bond length correlation. This leads to a simple formula for the bond compressibility.

The model also predicts that for the NaCl type structures the product of the bond force constant and the bond compressibility is equal to B - R/2, where B is the bond valence paramter (generally taken as 0.37Å) and R is the bond length, a relationship that is obeyed within the accuracy of available results.

The model is being tested on a number of compounds. Preliminary results of comparisons with experiment will be presented.

P11.CC.006 P-V EQUATION OF STATE OF MINERALS BY BRILLOUIN SCATTERING:GH PRESSURE MINERALOGY. Jay D. Bass, Stanislav V. Sinogeikin [1] and Jennifer M. Jackson [2], [1] Department of Geology, University of Illinois, 1301 W. Green St., Urbana, IL 61801 USA, [2] Department of Civil Engineering and Geology, University of Notre Dame, Notre Dame, Indiana

High pressure crystallography and acoustic measurements provide highly complimentary information. Both provide the bulk modulus (K) and its pressure derivatives, which are necessary to model the composition of planetary interiors. Brillouin scattering is a type of vibrational spectroscopy in which sound speeds are obtained from the frequency shift of light scattered by acoustic phonons. Only small (tens of microns) samples are required, so it can be performed at high-P using diamond cells and the pressure derivatives of moduli and velocities can be measured. This allows the P-V EOS to be accurately calculated without actual volume measurements. Our Brillouin scattering studies on minerals include MgO, garnets, pyroxenes, and the spinel-structured high-P gamma-phase of olivine. For $MgSiO_3$ orthoenstatite, XRD observations of a change in the atomistic at 4 GPa are found to have no effect on the EOS parameters as determined by Brillouin. High-P Brillouin experiments on garnet and gamma-phase utilizing a diamond cell suggest that the variation in bulk modulus and sound speeds with P are significantly less than those in the transition zone of the Earth (410-660 km depth). The seismologically determined properties of the transition zone are therefore likely due to phase transitions in minerals within this depth range.

11DD STRUCTURE SOLUTION FROM POWDER DATA – MOLECULAR COMPOUNDS (sponsored by Clariant GmbH)

M11.DD.001 CRYSTAL STRUCTURES OF PHARMACEUTICALS SOLVED FROM POWDER DATA BY GLOBAL OPTIMISATION METHODS K. Shankland and W.I.F. David, ISIS Facility, Rutherford Appleton Laboratory, Chilton, Didcot, Oxon. OX11 0QX, UK.

Powder diffraction has, in recent years, been increasingly and more ambitiously applied to the study of pharmaceutical compounds. While several years ago, a pharmaceutical company would use powder diffraction as a simple signature for polymorph recognition, there is now the real potential of complete structure determination for moderately complicated molecular structures. However, pharmaceuticals represent a challenging class of compounds for the application of traditional techniques of structure solution such as direct methods to powder diffraction data. This is because there are normally a large number of atoms to be located and seldom any atoms heavier than chlorine to assist with the phasing process.

Recent developments in global optimisation methods of structure solution [1] exchange these old issues and traditional methods for a new set of problems and algorithms which though difficult are proving more tractable. Complications in these new global optimisation methods arise because pharmaceuticals generally exhibit a significant amount of torsional flexibility and are often marketed as salt forms. These factors combine to increase the number of variables that need to be optimised in any search procedure that seeks to locate the entire molecule within the crystallographic unit cell *via* a stochastic optimisation process.

Efficient algorithms have been implemented for both the search methods employed and the evaluation of candidate solutions. These algorithms will be illustrated with the structure solutions of pharmaceuticals ranging from polymorph pairs to multiple salt forms.

David, W.I.F., Shankland, K. and Shankland, N., *Chem Commun*, 1998, 931.

M11.DD.002 DIRECT METHODS AND SYSTEMATIC OVERLAP J.Rius, Institut de Ciència de Materials de Barcelona, CSIC. Campus de la UAB. E-08193 Bellaterra, Spain

Besides accidental overlap, systematic overlap constitutes one of the principal limitations for the solution of crystal structures from powder diffraction data. Unlike accidental overlap which affects all type of structures, systematic overlap is restricted to high-symmetry ones (e.g. 65% of the space groups compatible with a hexagonal lattice). It will be shown how the direct methods sum function can be adapted to cope with data extracted from patterns containing systematic overlap. Preliminary results indicate that at least for moderate sized inorganic structures, systematic overlap should not represent a serious drawback for the direct methods application. In contrast to the usual two-stages procedures employed for solving structures with accidental overlap, here both multiplet decomposition and phase refinement are carried out simultaneously. This procedure will be discussed with two examples.

M11.DD.003 ROUTINE STRUCTURE SOLUTION OF MOLECULAR SOLIDS USING POWDER DIFFRACTION: THE MALARIA PIGMENT. S. Pagola and P. W. Stephens, Dept. of Physics and Astronomy, SUNY at Stony Brook, Stony Brook, NY 11794, USA; D. S. Bohle and S. K. Madsen, Dept. of Chemistry, Univ. of Wyoming, Laramie, WY 82071-3838, USA.

The crystal structure solution of molecular solids of moderate complexity is currently achieved using synchrotron X-ray powder diffraction as a routine procedure. The high resolution and high ratio signal to noise allow the easier determination of the unit cell, systematic absences and space groups. Based in the knowledge of the molecular geometry and cell contents is possible to postulate different trial solutions in the direct space. The agreement between the calculated and observed integrated intensities is used as a cost function to minimise in the simulated annealing method. Using this procedure it was possible to solve the crystal structure of several organic small molecules [1].

Malaria pigment (beta-Hematin) is a solid material formed from the degradation of hemoglobin in red cells by the plasmodium parasite that causes malaria. It was thought it was a biopolymer of heme units linked by iron-carboxylate bonds [2]. New chemical methods of synthesis of beta-Hematin allowed its preparation as a powder of enough crystallinity to determine the unit cell (triclinic symmetry, Z=2), to corroborate the equivalence with the pigment obtained from infected red cells [3], and now to solve the crystal structure using simulated annealing. The structure shows Fe-O interheme bonds giving rise to heme dimers. The remaining carboxylate of each heme is involved in hydrogen bonds with neighbor dimers in the crystal. Since the action of antimalarial drugs is not completely understood, this unanticipated structure is a significant result in the understanding and design of antimalarial compounds.

[1] Y.G. Andreev et al, J. Chem. Soc., Dalton Trans., (1998) 4071. S. Pagola et al, unpublished.
[2] A.F.G. Slater et al, Proc. Natl. Acad. Sci. USA, **88** (1991) 325.
[3] D.S. Bohle et al, J. Biol. Chem. **272** (1997) 713.

M11.DD.004 SOLUTION OF FLEXIBLE MOLECULAR STRUCTURES FROM POWDER DIFFRACTION DATA USING SIMULATED ANNEALING. Y. G. Andreev and P. G. Bruce, School of Chemistry, University of St. Andrews, St. Andrews, Fife KY16 9ST, Scotland.

Structure solution is one of the most challenging and fashionable topics in powder diffraction at present. Recently developed direct-space methods of simulated annealing and genetic algorithms mark a breakthrough in *ab initio* solution of molecular structures using powder data. Simple molecular structures represented by a single rigid or semi-rigid molecule in the asymmetric unit can be routinely solved in a matter of hours. Difficult structures containing several flexible molecular moieties in the asymmetric unit require much more effort.

We present a method of simulated annealing for structure solution from powders using full-profile fit of powder patterns. The issue of what type of structure should be considered as difficult-to-solve, with regards to number of atoms in the asymmetric unit, molecular flexibility and the number of independent moieties, is addressed. The method is illustrated by examples of *ab initio* solution of previously unknown molecular structures containing highly flexible molecules. Among the examples is the structure of the polymer/salt complex $(CH_2CH_2O)_6$:$LiAsF_6$ the solution of which involved 79 variable parameters including 23 bond lengths, 25 bond lengths and 15 torsion angles.

M11.DD.005 DO MICROCRYSTAL DIFFRACTION FACILITIES MAKE STRUCTURE SOLUTION FROM POWDER DIFFRACTION DATA OBSOLETE? C.S. Frampton, Roche Discovery Welwyn, Broadwater Road, Welwyn Garden City, Hertfordshire AL7 3AY, UK.

A major step in the development of any pharmaceutical material is the study and quantification of its polymorphic behaviour. The methods of choice for the structural characterisation of the various polymorphic forms, including

solvates and hydrates, are the combined techniques of single crystal X-ray diffraction and powder X-ray diffraction.

In many cases however, it is extremely difficult to produce single crystals that are of a suitable quality with which to obtain a full single crystal X-ray structural analysis. It is for these samples that the prospect of obtaining a full structure from *ab-initio* methods using the X-ray powder diffraction pattern alone is particularly exciting. One drawback of this methodology at the present time is that its application is restricted to relatively simple systems. With the advent of CCD detectors for small molecule crystallography and their subsequent installation on synchrotron beamlines, *e.g.* Station 9.8 at Daresbury SRS, the ability to obtain structures from microcrystalline samples has become feasible with no real limits on structural complexity.

This presentation will focus on the structural characterisation of several polymorphic forms of an α-TNF Converting enzyme inhibitor using both *ab-initio* structure solution from powder diffraction data methods and microcrystal X-ray diffraction techniques.

P11.DD.001 MOLECULAR CRYSTAL STRUCTURES FROM LABORATORY POWDER DIFFRACTION DATA: RELIABILITY AND REPRODUCIBILITY OF THE RESULTS. V.V. Chernyshev, A.V. Yatsenko and L.A. Aslanov, Moscow State University, Department of Chemistry, 119899 Moscow, Russia, E.J. Sonneveld and H. Schenk, University of Amsterdam, Laboratory of Crystallography, Nieuwe Achtergracht 166, Amsterdam 1018 WV, The Netherlands

On the basis of dozen unknown molecular crystal structures of C-nitro heterocycles and anthracene-derived dyes, successfully solved from laboratory X-ray powder diffraction data, the practical aspects of structure determination are discussed. The abundance of degrees of freedom, pre-assumptions and applied corrections in crystal structure determination from low-resolution powder data generate the problem of reliability and reproducibility of the obtained results. The comparison of the crystal structures solved from laboratory powder diffraction data with those obtained from synchrotron and neutron data, clearly show the real and reliable possibility of molecular crystal structure solution from laboratory X-ray data with sufficient accuracy in a case of only one rigid fragment in the asymmetric unit. As a consequence of the crystal structure solution the correct molecular structures of some of the investigated compounds were obtained distinguishing between several isomers which were indistinguishable by spectroscopic and quantum chemical methods. As follows from our results the most effective way in crystal structure solving of a series of small molecule organic compounds is to use mainly an X-ray laboratory diffractometer, in transmission mode preferably, and to use synchrotron and neutron facilities in any 'non-standard' cases.

P11.DD.002 USING STRUCTURE ENVELOPES AS MASKS IN STRUCTURE SOLUTION FROM POWDER DATA. S. Brenner, L.B. McCusker, Ch. Baerlocher, Laboratory of Crystallography, ETH, Zurich, Switzerland

A structure envelope, which effectively describes the coarse features of a crystal structure, can be used to advantage as a mask in direct-space methods of structure determination from powder data. It is generated from just a few (1-9) of the strongest, low-index reflections (i.e. precisely those reflections that are generally well-separated in a powder diffraction pattern).

However, to generate the structure envelope, the phases of these reflections must first be determined. To do this, a combination of the Sayre equation, the pseudoatom method and phase permutation has been developed. A pseudoatom is used to describe a prevelant building unit in the structure (e.g. $SiO_{4/2}$ in a zeolite), so *pseudo* atomic resolution can be achieved (e.g. at 3.0 Å). All reflections up to this resolution are involved in the process. Phase sets are generated by permutation (the Golay code is used to improve efficiency) and then extended with the Sayre equation. The resulting phase sets are ranked according to several criteria. For zeolite structures, the FOM from the Sayre equation is generally sufficient to phase the 1-5 reflections needed, but for organic structures, where more reflections are usually necessary, additional criteria (e.g. sign statistics, appearance of the Fourier map) must also be taken into consideration.

The use of a structure envelope as a mask in the FOCUS approach to zeolite structure determination from powder data proved to be beneficial, so it was then combined with a simulated annealing approach for application to organic structures. This combination allowed the structure of a tripeptide ($C_{32}N_3O_6H_{53}$, $P2_12_12_1$, a = 61.03, b = 11.18, c = 5.08 Å) to be solved. The phases of nine reflections were estimated for a centrosymmetric projection along [001] and a 2-dimensional envelope generated. This was used to find favorable starting positions and configurations for simulated annealing runs. Eight torsion angles were varied without restriction and three more were allowed to move within a range of 40°. The peptide linkages and the phenyl ring were kept planar, and the rotation and translation of the whole molecule was subjected to a penalty function calculated from the fit of the molecule to the envelope.

P11.DD.003 STRUCTURE DETERMINATION FROM POWDER DATA. Gerhard Engel, Steffen Wilke, Olaf König, Frank Leusen, Molecular Simulations Ltd., 230/250 The Quorum, Barnwell Road, Cambridge CB5 8RE, UK.

Increasingly powerful methods have been developed recently to facilitate the crystal structure determination from powder data. Based on earlier work at Molecular Simulations [1], we have developed a fast and efficient indirect structure solution package, called POWDER SOLVE, which is fully integrated into MSI's modelling environment.

Positions and orientations of structural fragments within the unit cell are modified to obtain optimal agreement between experimental and simulated powder patterns. An efficient global optimization algorithm allows the method to be applied to organic and inorganic systems. Validation work shows that the method can be applied successfully to systems with up to 18 degrees of freedom with moderate computational effort. At the same time, the package can also be used as a stable and powerful tool for rigid-body Rietveld refinement.

As for related techniques [2,3], the experimental powder pattern (not necessarily from a synchrotron source) must be successfully indexed prior to the simulation, and peak shapes and background parameters must be determined. For this purpose, we have implemented a modification to the Pawley method [4], which avoids the instabilities inherent to the original algorithm.

[1] C.M. Freeman, J.M. Newsam, S.M. Levine, and C.R.A. Catlow, *J. Mater. Chem.* **3**, 531 (1993).
[2] K.D.M. Harris, M. Tremayne, P. Lightfoot, and P.G. Bruce, *J. Am. Chem. Soc.* **116**, 3543 (1994).
[3] K. Shankland, W.I.F. David, and T. Csoka, *Zeitschr. fuer Kristallographie* **212**, 1 (1997).
[4] G. S. Pawley, J. Appl. Crystallogr. **14**, 357 (1981).

P11.DD.004 STRUCTURE DETERMINATION OF TWO LITHIUM 4-HALOGENOMETHYLBENZOATES FROM POWDER DIFFRACTION DATA. H. Ehrenberg[1,2], O. Herzberg, B. Hasse, M. Epple[3], [1] Darmstadt University of Technology, Materials Science, Petersenstr. 23, D-64287 Darmstadt, Germany, [2] Hamburger Synchrotron Radiation Laboratory (HASYLAB) at Deutsches Elektronen-Synchrotron (DESY), Notkestrasse 85, D-22603 Hamburg, Germany, [3] Institute of Inorganic and Applied Chemistry, University of Hamburg, Martin-Luther-King-Platz 6, D-20146 Hamburg, Germany

Poly(hydroxymethylbenzoic acid), an aromatic polyester, can be prepared by heating alkali salts of the corresponding chloromethylbenzoic acid above 100°C. An alkali halide is eliminated, and the organic remainder of the molecule polymerizes. The reaction takes place in the solid state. After this reaction, a composite of polymer and salt remains, out of which the salt can be removed by washing with water, leaving behind a highly porous polymer with pores in the sub-micrometer range. The reaction takes place in a number of combinations of alkali metal and halogen. Notable exceptions are the lithium salts of 4-chloro- and 4-bromomethylbenzoic acid that do not polymerize but only decompose.

A structural interpretation of this reaction is only possible with knowledge of the molecular packing in the starting compounds. Unfortunately, suitable single crystals of these compounds could not be obtained. Therefore, we have solved the structures of the two lithium compounds ab initio from synchrotron powder diffraction data. Both compounds are isostructural and crystallize in the monoclinic space group P21/c. The molecules are packed in parallel layers with the halogen atoms of every two layers pointing to each other. Layers of lithium cations are coordinated by oxygen atoms from carboxylic groups. The structure does not support a topochemical polymerization mechanism and therefore well explains the results of the chemical reactivity studies.

P11.DD.005 CRYSTAL STRUCTURES FROM X-RAY POWDER DATA. W. Lasocha, A.Rafalska-Lasocha, M.Michalec. Faculty of Chemistry Jagiellonian University,30-060 Krakow, ul. Ingardena 3, Poland, S.Boryczka. Silesian Medicine Academy, 41-200 Sosnowiec, Jagiellonska 4, Poland. H Schenk, Lab. v. Kristallografie, University Amsterdam, Nieuve Achtergracht 166, 1018WV Amsterdam, The Netherlands

Crystal structures of several compounds have been solved from a powder diffraction data using combination of different techniques. The complexity of the investigated compounds range from 12 to 27 atoms in the asymmetric unit. The samples represent: pure organic compound ($C_{25}O_2H_{18}$, Space Group P 2_1/c, 27 atoms in asymmetric unit), organic compounds with heavy atoms ($C_3H_6NS.ClO_4$, SG: $P2_1$/c, 20 atoms in asymm. unit, $C_3H_6NS.Br$, SG: $P4_22_12$, 12 atoms in asymm.unit) and organometallic compound ($VO_5C_{12}Cl_2.H_2O$, SG: C c, 21 atoms in asymm. unit). In most cases the pattern decomposition was performed by LSQPROF program, while the phase problem was solved using SHELXS, SIRPOW95, PATSEE or SIMPEL programs. The crystal structures were completed and refined by the Rietveld method using XRS-82 program. Most of the structures were solved from laboratory data. Obtained by different methods results will be compared. Important and useful observations will be pointed out and discussed.Support of Polish Committee of Scientific Research (KBN Grant No. 0312/TO9/98/15) is kindly acknowledged.

P11.DD.006 SOLVING MOLECULAR CRYSTAL STRUCTURES FROM POWDER DIFFRACTION DATA USING GENETIC ALGORITHMS. K.D.M. Harris, B.M. Kariuki and R.L. Johnston, School of Chemistry, University of Birmingham, Birmingham B15 2TT, U.K.

Many solids can be prepared only as microcrystalline powders and are not suitable for structural characterization by conventional single-crystal diffraction methods. For such materials, it is necessary to tackle structure determination using powder diffraction data. Although there are many examples in which traditional techniques for structure solution from powder diffraction data have been applied successfully, organic molecular crystals represent a particularly challenging case. For these reasons, we have focused in recent years [1–4] on the development and implementation of new methods for structure solution from powder diffraction data, with emphasis on addressing the specific challenges encountered for molecular crystal structures. Our methods are based on a direct-space strategy in which a hypersurface defined by the profile R-factor (R_{wp}) is searched using Monte Carlo [1,2] or Genetic Algorithm [3,4] techniques. As part of our recent research in this field, we have carried out systematic explorations to find the optimum ways of implementing the different operations (such as mating, mutation and natural selection) within the Genetic Algorithm technique. These studies have provided important information on the strategies for implementing Genetic Algorithms in structure solution, and have yielded important insights concerning the character of the hypersurfaces being explored. In this research, we have applied our methods to solve the crystal structures of complex molecular materials defined by a significant number of variable torsion angles.

The presentation will describe new developments in our understanding of fundamentals of the Genetic Algorithm technique and the optimum strategies for its implementation in powder structure solution. Recent results obtained from the application of this method to solve structures of molecular crystals will be presented.

[1] K.D.M. Harris, M. Tremayne, *Chem. Mater.*, **8**, 2554 (1996)
[2] M. Tremayne, B.M. Kariuki, K.D.M. Harris, *Angew. Chemie Int. Ed. Engl.*, **36**, 770 (1997)
[3] K.D.M. Harris, R.L. Johnston, B.M. Kariuki, *Acta Cryst.*, **A54**, 632 (1998)
[4] B.M. Kariuki, P. Calcagno, K.D.M. Harris, D. Philp, R.L. Johnston, *Angew. Chemie Int. Ed. Engl.*, in press [publication date: March 1999]

P11.DD.007 CRYSTAL STRUCTURES OF FLEXIBLE ORGANIC MOLECULES DETERMINED FROM POWDER DATA. Martin U. Schmidt, Clariant GmbH, Pigments Technology Research, G 834, D-65926 Frankfurt a.M., Germany and Robert E. Dinnebier, Lehrstuhl für Kristallographie der Universität Bayreuth, D-95440 Bayreuth, Germany

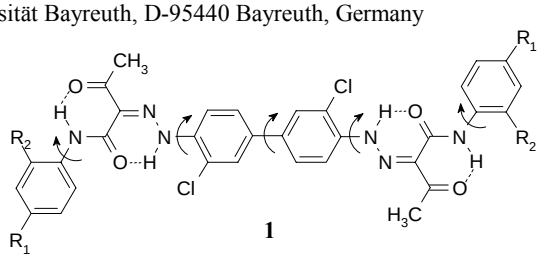

1

a)R_1=R_2=H, $P2_1$/c, Z=4.

b) R_1=R_2=CH_3, c) R_1=H, R_2=CH_3, both $P\bar{1}$, Z=1

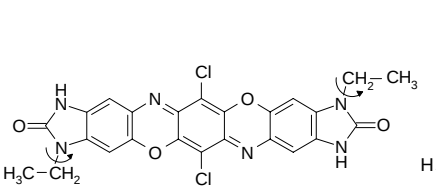

2: $P\bar{1}$, Z=1

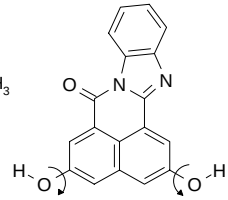

3: $Pna2_1$, Z=4

The crystal structures of five industrial organic pigments were solved by energy minimization techniques. The intramolecular degrees of freedom indicated by arrows were optimized together with the arrangement of the molecules. Subsequently the structures were refined by rigid body Rietveld methods, using synchrotron powder data. In cases 1a-c it was also possible to refine all non-hydrogen atoms individually without applying any constraints or restraints (44 independent atoms for 1a).

1. M. U. Schmidt, R. E. Dinnebier, *J. Appl. Cryst.,* 1999, in press.

P11.DD.008 DIRECT SPACE STRATEGIES FOR STRUCTURE SOLUTION. M. Tremayne and C. Glidewell, School of Chemistry, The Purdie Building, University of St. Andrews, St. Andrews, Fife, KY16 9ST, UK.

The crystal structure determination of molecular materials from X-ray powder diffraction data is a rapidly expanding field and has grown substantially in the last few years mainly due to the development and application of direct space based techniques of structure solution [1-4].

In this paper we present results in which the performance of a direct space method (here based on the Monte Carlo approach) is enhanced by the use of good structure solution strategy for the system under consideration. Application of these techniques to powder data significantly affected by preferred orientation will be discussed. Structure solution strategies that combine reciprocal space with direct space methods, and X-ray powder diffraction with crystal structure prediction will also be demonstrated.

These methods will be illustrated by systems that exhibit polymorphism, and materials in which the primary interest is in the intermolecular aggregation, particularly the hydrogen bonding schemes. Examples such as cocrystals will also be presented in which the structure solution process is complicated by the presence of more than one molecule in the asymmetric unit.

1 M.Tremayne, B.M.Kariuki & K.D.M.Harris (1997), *Angew. Chemie*, 36, 770
2 W.I.F.David, K.Shankland & N.Shankland (1998), *Chem. Comm*., 931
3 B.M.Kariuki, H.Serrano-Gonzalez, R.L.Johnston & K.D.M.Harris (1997), *Chem. Phys. Lett*., 280, 189
4 Y.G.Andreev, P.Lightfoot & P.G.Bruce (1997), *J.Appl.Cryst*., 30, 294

11EE MAGNETIC AND INELASTIC SCATTERING

M11.EE.001 DETERMINATION OF MAGNETIC STRUCTURES USING NEUTRON SPHERICAL POLARISATION ANALYSIS. P.J. Brown, Institut Laue Langevin, Avenue des Martyrs, PO Box 156, 38042 Grenoble Cedex, FRANCE

Determination of magnetic structure from measurement of the intensities of neutrons (or X-rays) scattered by magnetic Bragg reflections is in some ways a more difficult problem than determination of the crystal structure. This is because the magnetic structure factor is a vector quantity so that directional as well as phase information is lost in measuring just the intensity. Spherical polarimetry provides a way of recovering some of this lost information. Magnetic neutron scattering is due to a magnetic dipole interaction between the neutron's magnetic moment and the fourier components of the magnetic induction in the crystal. This interaction gives rise to changes in direction of the neutron dipole moment (polarisation) which are highly dependent on their relative orientations. Spherical polarimetry consists in determining the direction of scattered neutron polarisation for any chosen incident polarisation direction. It has been implemented at ILL by developing a CRYogenic Polarisation Analysis Device which is now the second generation CRYOPAD II [1]. Spherical polarisation analysis using CRYOPAD has been able to solve a number of magnetic structure problems which were intractable by other means. For instance it has enabled the absolute orientation of the magnetic moments in magneto-electrics, relative to applied electric and magnetic fields, to be determined for the first time [2]. It is particularly valuable in the study of non-collinear magnetic structures where it has already shown that certain previously determined structures were incorrect [3,4]. Additionally it provides a means for precision determination of antiferromagnetic form factors.

1. Brown P J, Forsyth J B and Tasset F, (147) **Proc. Roy. Soc. Lond.** 442. 1993
2. Brown P J, Forsyth J B and Tasset F, (663) **J.Phys. Condens. Matter** 10. 1998
3. Brown P J Crangle, J, Neumann K-U, Smith J J and Ziebeck K R A, (4729) **J.Phys. Condens. Matter** 9. 1997
4. Brown P J and Chattopadhyay T, (9167) **J.Phys. Condens. Matter** 9. 1997

M11.EE.002 MAGNETISM OF HIGHLY CORRELATED MULTILAYERS BASED ON CERIUM AND IRON. W. Felsch, M. Arend and M. Muenzenberg, I. Phys. Institut, Universitaet Goettingen, Germany, and G. Krill, LURE, Université Paris-Sud, 91405 Orsay, France.

The 4f-electron states of the rare-earth element Ce are at the borderline between localization and itinerancy. Both cases can be realized, depending on the degree of hybridization between the 4f- and conduction-electron states, either in the γ or α phase of the pure metal or in compounds with transition metals. Dramatic differences in the physical properties result, reflected in a magnetic and nonmagnetic ground state in the γ- and α-phase-like electronic Ce configurations, respectively. For Ce/Fe multilayers, experiments of X-ray absorption (XA) and X-ray magnetic circular dichroism (XMCD) signal strong electronic correlations at the interfaces, involving the Ce-4f and 5d, and the Fe-3d states. The result is an α-phase-like Ce configuration (4f states delocalized) with ordered 4f and 5d magnetic moments even at room temperature. While the 4f polarization is limited to the direct interface, the 5d polarization extends deeply into the Ce layers. Remarkably, magnetic order on the 5d states can exist without a polarization of the 4f states. There is evidence that the 5d states in these structures are very close to a ferromagnetic instability.

The introduction of hydrogen into Ce in these multilayers, resulting in structures $CeH_{2-\delta}$/Fe, leads to a relocalization of the 4f states, i.e. a γ-phase-like electronic configuration of Ce. A profound modification of the bulk magnetic properties results, like a reorientation of the magnetic easy axis from in plane to out of plane as the temperature is decreased [1]. Angle- and temperature-dependent XMCD experiments permit to trace down the microscopic mechanism of this transition to a perpendicular orientation of the Ce-4f magnetic moment at the interfaces, due to a crystal-field induced single-ion anisotropy. By a complex interplay of hybridization and exchange effects this orientation is transferred to the Fe-3d states via the Ce-5d states.

[1] O. Schulte, F. Klose, and W. Felsch, Phys. Rev. B **52**, 6480 (1995).

M11.EE.003 R_2BaNiO_5 COMPOUNDS: HALDANE SPIN CHAINS IN STAGGERED MAGNETIC FIELDS. Andrey Zheludev, Physics Department, Brookhaven National Laboratory, Upton, NY11973-5000, USA.

The quantum-disordered ground state and the famous Haldane gap in the magnetic excitation spectrum have kept S=1 one-dimensional Heisenberg antiferromagnets at the center of attention of condensed matter physicists for the last 15 years. Of particular interest is the behavior of such systems in staggered magnetic fields. In the past this problem was not given much attention in literature, as the required conditions were thought to be almost impossible to realize in an experiment. One clever trick to obtain a field oscillating on the microscopic scale is to make use of an intrinsic magnetic modulation in a material that, in addition to integer-spin Heisenberg chains, has other magnetic ions. Should the latter become ordered magnetically with an appropriate propagation vector, they will project an effective staggered exchange field on the Haldane spin chains. A neat

realization of this mechanism was recently found in a class of linear-chain rare earth nickelates with a general formula R_2BaNiO_5. Extensive neutron diffraction and inelastic neutron scattering studies of several compounds of this type allowed us for the first time to experimentally investigate the influence of a strong staggered field on the properties of S=1 quantum spin chains and particularly on the triplet Haldane-gap excitations.

M11.EE.004 SPIN DENSITIES IN FERROMAGNETS. J.A. Duffy, Department of Physics, University of Warwick, Coventry, CV4 7AL, UK.

Direct measurements of the spin density of a ferromagnet can reveal useful information about the distribution of spin moments, and about the electronic structure. These momentum space spin densities are obtained via synchrotron based Compton scattering experiments. Several examples of the recent work of the Warwick group are presented. Firstly, in the Gd-Y system, where magnetic ordering is believed to be driven by the polarisation of the Y electrons, the magnetic Compton profile revealed that there is an induced spin moment on the Y electrons. More recently, the spin densities in two magnetoresistive materials have been investigated. In $SmMn_2Ge_2$, a giant magnetoresistive material, negative polarisation of the Sm spin moment has been observed for the first time. The spin density of the colossal magnetoresistive perovskite, $La_{0.7}Sr_{0.3}MnO_3$, is also discussed. Finally, possible future applications of the technique are described.

M11.EE.005 DIRECT OBSERVATION OF ORBITAL ORDERING BY RESONANT X-RAY SCATTERING. Youichi Murakami, Photon Factory, Institute of Materials Structure Science, High Energy Accelerator Research Organization, Tsukuba, 305-0801, Japan

Over the last few years, magnetic-field-induced phenomena in perovskite-type manganites have attracted a great deal of attention. In the study of these materials, it has been recognized that the charge, spin and orbital degrees of freedom each play important roles in the electric and magnetic properties. Synchrotron X-ray diffraction is very powerful tool to observe such charge and orbital ordering. Here the direct observation of orbital ordering by resonant x-ray scattering will be presented.

Dipole resonant x-ray scattering from ordered Mn 3d orbitals has been observed near the Mn K-absorption edge in a layered, bi-layered, and three-dimensional perovskite-type manganites. The polarization of the scattered photons is perfectly rotated and the azimuthal angle dependence shows a characteristic twofold symmetry. A theory of the resonant scattering mechanism has been developed by considering the splitting of the Mn 4p levels due to the Mn 3d orbital ordering. The stability of the orbital ordering in these compounds will be discussed when the hole is doped or the external field are applied.

P11.EE.001 ANTIFERROMAGNETIC ORDERING OF THE RARE EARTH IONS R^{3+} IN $R_2Ba_4Cu_7O_{15-\delta}$ (R=Er, Dy). G. Böttger, Laboratorium für Kristallographie, ETH Zürich, 8092 Zürich, Switzerland, and P. Fischer, J. Mesot, B. Roessli, P. Allenspach and A. Furrer, Laboratorium für Neutronenstreuung, ETH Zürich & Paul Scherrer Institut, 5232 Villigen PSI, Switzerland, and A. Dönni, Department of Physics, Niigata University, Ikarashi-Ninomachi 8050, Niigata 950-21, Japan, and Y. Aoki and H. Sato, Department of Physics, Faculty of Science, Tokyo Metropolitan University, Hachioji-shi 192-03, Japan.

The structure and the magnetic properties of the high-temperature superconductor $R_2Ba_4Cu_7O_{15-\delta}$ (R=Er, Dy; $0.05 \le \delta \le 0.7$) have been studied by elastic and inelastic neutron scattering, specific heat and magnetic susceptibility measurements. The polycrystalline samples have been prepared by a sol-gel-technique at ambient pressure. The high transition temperatures to superconductivity T_c=89 K for $Er_2Ba_4Cu_7O_{14.92}$ and T_c=91 K for $Dy_2Ba_4Cu_7O_{14.95}$ indicate a good sample quality. Specific heat measurements show a magnetic phase transition for each of the investigated samples. The Néel temperature T_N is about 1 K for $Dy_2Ba_4Cu_7O_{15-\delta}$ and $0.50 \le T_N \le 0.54$ K for $Er_2Ba_4Cu_7O_{15-\delta}$. Except for the case of $Er_2Ba_4Cu_7O_{14.3}$ the specific heat data of the $R_2Ba_4Cu_7O_{15-\delta}$ samples can be interpreted with an anisotropic 2D-Ising model. The specific heat data for $Er_2Ba_4Cu_7O_{14.3}$ can only be understood by assuming two different types of magnetic clusters to be present in this sample. Such an interpretation is supported by the results of neutron crystal-field spectroscopy demonstrating the presence of at least two distinctly different surroundings of the rare-earth ions. Additionally, we have investigated the temperature dependence of the relaxation rate of the crystal-field transitions in $Er_2Ba_4Cu_7O_{14.92}$ and $HoBa_2Cu_4O_8$ by inelastic neutron scattering. These measurements give evidence for the opening of an electronic gap (pseudogap) in the normal state at about 200 K. The main observed features can be best reproduced by considering a strongly anisotropic gap function. The magnetic ordering of the rare-earth ions in $R_2Ba_4Cu_7O_{15-\delta}$ ($\delta \approx 0$) has been determined by neutron diffraction for R=Er, Dy. For the first a long-range antiferromagnetic order in $Er_2Ba_4Cu_7O_{14.92}$ has been observed time in a $R_2Ba_4Cu_7O_{15-\delta}$ compound. The magnetic Er moments are oriented parallel to the *b*-axis. They are coupled antiferromagnetically along the *a*- and *c*-axis and ferromagnetically along the *b*-axis. Finally, the results of a recent neutron diffraction experiment on the magnetic ordering in $Dy_2Ba_4Cu_7O_{14.95}$ will be presented.

11FF INTERMOLECULAR INTERACTIONS

M11.FF.001 PINPOINTING MOLECULAR INTERACTIONS VIA CRYSTALLINE THIN FILMS. Leslie Leiserowitz, Dept. of Materials and Interfaces, The Weizmann Institute of Science, Rehovot, Israel

Molecular Interactions may be elucidated from the structural properties of thin crystalline molecular films at the air-solution interface. We take advantage of the fact that it is now possible to establish, in favourable cases, the structures of such films to near atomic resolution with the use of grazing incidence X-ray diffraction using synchrotron radiation. The topics we shall cover include:

(1) Induced nucleation of ice using monolayers of long-chain alcohols from which we may glean information on the role played by the orientation of alcohol OH groups for promoting ice nucleation by epitaxy [1].

(2) The role played by N-H...O hydrogen bonds and molecular conformation in the spontaneous separation of racemic mixtures of amphiphiles on water into onolayer crystallites of opposite handedness [2,3].

(3) The effect on polymorphic behaviour of inter- and intra-layer forces involving long chain alkanes in thin crystalline films [4]

(4) The interplay between acid-base interactions, molecular conformation and chirality, in determining the formation of interdigitated bilayers at the air-solution interface [5]

[1] (a) Gavish, M.; Popovitz-Biro, R.; Lahav, M., Leiserowitz, L. Science 1990, 250, 973. (b) Popovitz-Biro, R.; Wang, J. L.; Majewski, J.; Shavit, E.; Leiserowitz, L., Lahav, M. J. Am.Chem.Soc. 1994, 116, 1179. (c) Wang, J. L.; Leveiller, F.; Jacquemain, D.; Kjaer, K.; Als-Nielsen, J.; Lahav, M., Leiserowitz,

L. J. Am. Chem. Soc. 1994, 116, 1192. (d) Majewski, J.; Popovitz-Biro, R.; Bouwman, W. G.; Kjaer, K.; Als-Nielsen, J.; Lahav, M., Leiserowitz, L. Chem.Eur.J. 1995, 1, 304. (e)Majewski, J.; Popovitz-Biro, R.; Edgar, R.; Arbel-Haddad, M.; Kjaer, K.; Bouwman, W.; Als-Nielsen, J.; Lahav, M., Leiserowitz, L. J. Phys. Chem. B 1997, 101, 8874.

[2] (a) Weissbuch, I.; Berfeld, M.; Bouwman, W.; Kjaer, K.; Als-Nielsen, J.; Lahav, M., Leiserowitz, L. J. Am. Chem. Soc. 1997, 119, 933. (b) Kuzmenko, I.; Kjaer, K.; Als-Nielsen, J.; Lahav, M., Leiserowitz, L. J. Am. Chem. Soc. 1999, In Press.

[3] Weinbach, S. P.; Weissbuch, I.; Kjaer, K.; Bouwman, W. G.;Als-Nielsen, J.; Lahav, M., Leiserowitz, L. Adv. Mater. 1995, 7, 857.

[4] Kuzmenko, I.; Buller, R.; Bouwman, W. G.; Kjaer, K.; Als-Nielsen,J.; Lahav, M., Leiserowitz, L. Science 1996, 274, 2046.

M11.FF.002 HALOGEN SUBSTITUENTS AS SUPRAMO-LECULAR SYNTHONS. I. Csöregh, Structural Chemistry, Arrhenius Laboratory, Stockholm University, Sweden; T. H. Brehmer, and E. Weber, Organische Chemie, TU Bergakademie Freiberg, Germany; and F. H. Cano, Instituto Química-Física, Rocasolano (CSIC), Madrid, Spain.

Intermolecular interactions involving halogen substituents, particularly chlorines, have been proved to enhance crystal formation, thus providing a tool for crystal engineering of both homomolecular and heteromolecular solids. In order to study the effect of various halogens on the crystalline architecture, the *cis*-9,10-diphenyl-9,10-dihydroanthracene-diols **1-4,** differing only in the *p*-phenyl substituents **R** (*cf.* scheme), have been synthesised, crystallised and investigated using X-ray diffraction.

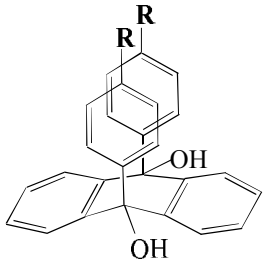

Host (R)	Solvent/ Guest	Stoichio-metry	V_{cell}/Å^3	Space group	
2 (Cl)	Toluene		4153(1)	P-1	0.051
2 (Cl)	DMSO	(2 : 3)	5472(1)	I2/a	.057
2 (Br)	toluene		4217.0(15)	P-1	.048
2 (Br)	toluene/trace of $CHCl_3$		4198.6(1)	C/c	.065
2 (Br)	chloroform	(1 : 1)	5080.1(4)	Pbcn	.075
2 (Br)	DMSO	(2 : 3)	5463.4(4)	I2/a	.087
3 (I)	toluene		1096.7(2)	P-1	.018
3 (I)	ethanol	(1 : 2)	2638(2)	$P2_1$	
4 (CH_3)	toluene		2023.5(5)	$P2_1/c$	.036
4 (CH_3)	THF	(1 : 1)	2551.0(9)	$P2_1/c$	.066

*refinement is in progress.

The crystals of **1-4** were grown from a variety of solvents, yielding crystalline compounds with or without inclusion of guest molecules, hence indicating also the influence of the solvents on the realised packing motif. Structural details with emphasis on the effects of various halogens on the balance of intermolecular interactions will be discussed.

M11.FF.003 SOLID STATE REACTIVITY IN POLYMORPHS OF *ORTHO*-ETHOXY-*TRANS*-CINNAMIC ACID. Demetrius C. Levendis and Manuel A. Fernandes, Centre for Molecular Design, Department of Chemistry, University of the Witwatersrand, Private Bag 3, PO Wits, 2050, South Africa.

The crystal structures of three polymorphs of *ortho*-ethoxy-*trans*-cinnamic acid have been established for the first time. In this paper we report how weak intermolecular interactions determine which polymorph crystallizes and also determine the products and probable mechanisms of the [2,2] solid state photodimerization.

In the crystals, hydrogen bonded dimers of cinnamic acid form layers that are held together in the lattice by weak C-H...O=C interactions, very similar to those found in *p*-toluic acid[1]. In the case of the alpha polymorph, neighbouring ethylene groups are not ideally aligned for [2,2] photodimerization. A shift of one molecule along the C=C direction would be required. During irradiation, the crystal shears along the <-101> direction. This cracking gives vital clues to the mechanism of the solid state reaction.

The beta 'polymorph' is actually a solvated crystal where channels in the crystal with 3-fold symmetry are occupied by benzene molecules. Weak interactions between the benzene and the cinnamic acid molecules stabilise this form. Crystals of Ortho-EtO-cinnamic acid (thiophene) are isomorphous to the beta polymorph and appear to be thermodynamically and photochemically more stable than the benzene form.

Bernstein, J., Etter, M. C. & Leiserowitz, L (1994). In *Structure Correlation*, edited by H. B. Burgi & J. D. Dunitz, pp. 436-463. Weinheim (Federal Republic of Germany): VCH.

M11.FF.004 CRYSTALLINE POLYMERS OF METALLOPORPHYRINS TAILORED BY SPECIFIC INTERACTIONS. Israel Goldberg, School of Chemistry, Tel Aviv University, 69978 Tel Aviv, Israel.

In light of the tremendous versatility of porphyrins and metalloporphyrins in mediating electron and energy transfer, their utility as redox catalysts, and their dynamic photophysical properties, there has been a widespread interest in the design and synthesis of multiporphyrin architectures. In this context, the ability to control the supramolecular organization of such molecular entities by noncovalent interactions is a crucial step on the road to formulation of new materials for specific applications.

Recent investigations have shown that predictable architectures of oligomers and polymers from metallomacrocyclic building blocks can be rationally designed by selection of the coordination geometry of metals, suitable functionalization of the porphyrin framework, and the structure of multitopic ligands involved in the supramolecular synthesis. Relevant examples of successful attempts to assemble crystalline multiporphyrin (often porous) domains will be discussed. They include: (i) the generation of polymeric patterns sustained by external metal centers or multidentate bridging ligands, (ii) the formation of large arrays by utilizing hydrogen-bonding forces (e.g., β-molecular networks with hollow architectures), (iii) the construction of homogeneous as well as heterogeneous coordination polymers of varying dimensionality and crystalline porosity, propagated by metal-to-ligand interactions. [1,2]

Current efforts are directed at the construction (by combination of the different modules of supramolecular design in the same material) of more structurally robust porous molecular crystals, and assessment of potential utility of such structures as molecular sensors and solid state catalysts.

R. Krishna Kumar, S. Balasubramanian, I. Goldberg, *Chem. Commun.* **1998**, 1435-1436.
R. Krishna Kumar, I. Goldberg, *Angew. Chem. Int. Ed.* **1998**, *37*, 3027-3030; *Angew. Chem.* **1998**, *110*, 3176-3180.

M11.FF.005 SUPRAMOLECULAR CHEMISTRY OF BENZENE POLYCARBOXYLATES. Mark R.J. Elsegood, William Clegg, Simon J. Richards, Matthew J. Hemmings, Katy E. Holmes and Colette Harvey. Department of Chemistry, Bedson Building, The University of Newcastle-upon-Tyne, Newcastle-upon-Tyne, NE1 7RU, UK.

Benzene polycarboxylates are excellent candidates for the study of intermolecular interactions and use in crystal engineering applications since their solid state structures exhibit both extensive hydrogen bonding and π-stacking between layers. The rigid shapes of the acids and their predisposition to form intermolecular hydrogen bonding motifs with regular geometries additionally leads to the formation of cavities within the structures, reminiscent of zeolites. Such cavities may be filled with host solvent or other molecules, or may act as templates for shape specific reactions.

We are currently investigating a number of aspects of this chemistry: (a) Alkali metal complexes of 1,3,5-benzenetricarboxylic acid and 1,2,4,5-benzenetetracarboxylic acid for which we have obtained structural results for the monosodium salt of the former and the disodium salt of the latter. (b) Organic salts of the 1,3,5 acid and guanidinium, which both have 3-fold molecular symmetry. These have extended structures with several cations and anions in the asymmetric unit. (c) We have structural data on a number of alcohol clathrate compounds, some with related hydrogen bond motifs and layering. (d) Transition metal complexes exhibiting both molecular and framework structures. Data sets were measured at low temperature using a Bruker SMART CCD area detector diffractometer.

Leading up to the Congress we hope to obtain structural results obtained with a newly installed Bede Scientific Microsource X-ray generator, and conduct some exploratory high resolution studies investigating the detailed electron density distributions in some of these compounds using the SMART diffractometer. Any results obtained by then will be presented in preliminary form.

P11.FF.001 UNCONVENTIONAL N-H···H-Os HYDROGEN BOND IN AN IMINO TRIOSMIUM COMPLEX. D. Viterbo, S. Aime, R. Gobetto, M. Ferritz, M. Milanesio, E. Valls - Dip. di Chimica IFM, Università di Torino, and Dip. di Scienze e Tecnologie Avanzate, Università del Piemonte Orientale (Alessandria), Italy

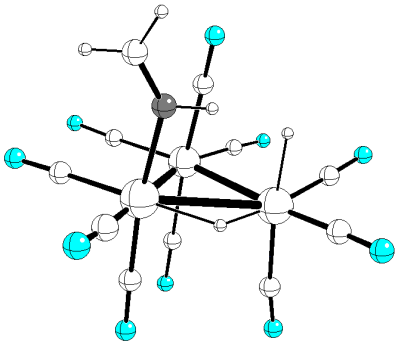

Imino metal complexes are often obtained by modification of a previously coordinated ligand such as nitriles, oximes, amines, etc. In trinuclear derivatives this reactivity leads to systems in which the organic ligand occupies a bridging position. Until now, there has been no example of terminal imino ligands in polynuclear systems. Here we show that the stabilization of a coordinated imine may be obtained on the surface of a triosmium cluster possibly stabilized by the formation of an unconventional intramolecular hydrogen bonding interaction between the N-H moiety and a terminal hydride ligand [1]. The crystal structure of the $H(\mu\text{-}H)Os_3(CO)_{10}(HN{=}CPh_2)$ complex is shown in the figure (Ph groups substituted by H). Because of the rather severe absorption effects the hydrogen atoms can not be located with certainty in the difference maps, but they can be reasonably located by geometrical considerations. Indeed in the Os-H···H-N system the H···H distance (≈2.0Å) is much shorter than the normal 2.4Å vdW contact. This result is in keeping with the NMR analysis, based on longitudinal relaxation time measurements, which also indicate a short H···H contact (≈2.1Å). In order to obtain a more accurate localization of the H atoms and to gain some insight of the nature of this new type of hydrogen bond we are currently performing some *ab-initio* theoretical calculations on this complex.

1. R. Crabtree, Science, **282** (1998), 2000

P11.FF.002 ESTIMATION OF EFFECTS OF SUBSTITUENTS ON CRYSTAL PACKING BY FORMING MIXED CRYSTALS. D. Hashizume, N. Takashima, R. Miki, M. Yasui and F. Iwasaki Department of Applied Physics and Chemistry, The University of Electro-Communications, Chofu, Tokyo 182-8585, Japan

4-(4-X-Phenylmethyleneamino)-TEMPO radicals (TEMPO; 2,2′-tetramethylpiperidyl-1-oxyl) have been studied as organic magnets. In the course of the studies, we found that Me, Cl and Br derivatives are crystallized into different crystal forms although the size or character of the substituents are similar. In order to elucidate effects of these substituents on the packing of the crystals, we prepared mixed crystals composing of Me and Cl derivatives, and Cl and Br derivatives.

By mixing the both components in methanol, mixed crystals were obtained from the resultant solutions in any mixing ratio. Crystal structures of the mixed crystals are isomorphous to those of either components, and the both crystal forms of components were observed at the intermediate component ratio. The molecules are disordered only at the substituents but the other moieties are ordered.

We focus on the changes of the contacts between the substituents as the component ratio in the mixed crystals, and will discuss the effects of these substituents on the crystal formation.

P11.FF.003 STRUCTURE, FORMATION AND INTERACTION OF COILED-COILS: FROM LEUCINE ZIPPERS TO INTERMEDIATE FILAMENTS. P. Burkhard[1], R. Kammerer[1], M. Steinemtz[1], S. Strelkov[1], H. Herrmann[2], and U. Aebi. [1]M.E. Müller Institut, Biozentrum der Universität Basel, 4056 Basel, Switzerland, [2]German Cancer Research Center, Heidelberg, 69120, Deutschland.

Subunit oligomerization of many proteins is mediated by coiled-coil domains. Although the basic features contributing to the thermodynamic stability of coiled coils are well understood, their assembly kinetics have not yet been dissected. Here we report a 13-residue sequence pattern - xxLExchxcxccx - which occurs with limited sequence variation in many parallel 2-stranded coiled coils (cf. kinesin, myosin, tropomyosin, plectin), and which is a prerequisite for the assembly of the Dictyostelium actin-bundling protein cortexillin I and the yeast transcriptional activator GCN4. In contrast to arbitrarily chosen heptad repeats, coiled-coil "trigger" sequences form relatively stable monomer helices and thus represent autonomous folding units mediating coiled-coil formation. Last but not least, trigger sequences will be useful in *de novo* protein design.

We have also crystallized the entire 18 heptad-repeat long dimer rod (termed Ir) of cortexillin I and solved its atomic structure. Strickingly, the structure of the trigger sequence can be distinguished from the rest of the Ir dimer rod by its unique intrahelical ion pairing pattern. In pursuit to understand intermediate filament (IF) structure and assembly at atomic detail, we are exploring the different modes of dimer-dimer interactions implicated in IF assembly by X-ray crystallography of "mini-constructs" engineered from IF proteins, so that each mini-construct harbors the central IF dimer rod segment(s) specifying a particular homo- or hetero-typic dimer-dimer association mode.

1. R. A. Kammerer et al., (1998).An autonomous folding unit mediates the assembly of two-stranded coiled coils. *PNAS.* 95, 13419-13424
2. M. O. Steinmetz et al., (1998).A distinct 14 residue site triggers coiled-coil formation in cortexillin I. *EMBO J.* 17, 1883-1891

P11.FF.004 THE HYDROGEN BOND STRENGTH IN TERMS OF THE TOPOLOGICAL PROPERTIES OF THE ELECTRON DENSITY DISTRIBUTION. E. Molins[1] E. Espinosa[1,2] and C. Lecomte[2]. [1]Institut de Ciència de Materials de Barcelona (CSIC). Campus de la UAB, 08193 Cerdanyola (Barcelona), Spain. [2]Laboratoire de Cristallographie et Modélisation des Matériaux Minéreaux et Biologiques, UPRESA CNRS 7036, Université Henri Poincaré, Nancy 1, BP 239, 54506 Vandoeuvre-lès-Nancy CEDEX, France.

Interatomic interactions such as hydrogen bonds (HB's) can be adequately described and classified by the topological properties of the electron density $\rho(r)$ at the (3,-1) critical points r_{CP}, where the gradients of $\rho(r)$ vanish [1]. We have analysed [2] the topological properties of $\rho(r)$ at the intermolecular critical points of 83 experimentally observed HB's [X-H...O (X= C, N, O)] on a large set of compounds, obtained from accurate X-ray diffraction experiments. In spite of different models, methods and experimental conditions employed to obtain the topological properties of $\rho(r)$, we show that, for closed-shell interactions, the kinetic energy density $G(r_{CP})$ and the potential energy density $V(r_{CP})$ at the critical point, depend exponentially on the H...O distance. We point out the positive correlation found between the $V(r_{CP})$ and the HB energy when their functionalities against the H...O distance are compared. Recently [3], we have also observed that the positive and the negative curvatures of $\rho(r)$ at the H...O critical point exhibit linear relationships against, respectively, $G(r_{CP})$ and $V(r_{CP})$. The proportional behaviors found between those quantities show that the strength of the hydrogen bond interaction can be indistinctly interpreted in terms of any of them.

1. R.F.W. Bader *Atoms in Molecules: a Quantum Theory* (Clarendon Press, Oxford, 1990).
2. E. Espinosa, E. Molins, C. Lecomte. Chem. Phys. Lett. (1998), 285, 170.
3. E. Espinosa, C. Lecomte, E. Molins. Chem. Phys. Lett. (1999), 000, 000.

P11.FF.005 MOLECULAR COMPLEXES FOR THE STUDY OF ENANTIODISCRIMINATIVE PROCESSES. F. Bachechi [1], M. Flieger [2], M. Sinibaldi [3], [1] Istituto di Strutturistica Chimica Area della Ricerca di Roma, C.N.R., C.P. 10, 00016 Monterotondo St. (Roma), Italy, [2] Institute of Microbiology, Academy of Scieces of the Czech Republic, 142 20 Prague 4-Krc, Czech Republic, [3] Istituto di Cromatografia, Area della Ricerca di Roma, C.N.R., C.P. 10, 00016 Monterotondo St. (Roma) Italy

The resolution of optical isomers by liquid chromatography requires a chiral selector able to form reversible interactions with the enantiomers and labile diastereoisomeric complexes with different degrees of stability. Since the stability difference between the complexes affects the degree of chiral discrimination and the efficiency of the chiral selector, studies of the mechanism of chiral recognition are particularly relevant, as they provide the basis for the development of new chiral stationary phases.

Recently a chiral selector, based on the ergot alkaloid terguride, (+)1-(3-allylpropyl)-(5R,8S,10R)-terguride, have been developed to resolve optically active isomers. This new chiral stationary phase is successfully used for the separation of several classes of carboxylic acids racemates as dansyl derivatives of amino acids, halogen-substituted 2-aryloxypropionic acids (herbicides), 2-arylpropionic acids and the structurally similar flobufen (anti-inflammatory drugs).

Crystals from molecular complexes, that the selector forms with the more retained enantiomer of a racemic mixture, are not easily obtained, but their crystal structures allow a clear insight into the enantiodiscriminative mechanism. Here the crystal structure of the complex between (+)1-(3-allylpropyl)-(5R,8S,10R)-terguride and (R)-N-dansylserine will be discussed together with analogous complexes, that the selector forms with other analytes to illustrate the interactions at the basis of the chiral recognition.

11GG BULK CRYSTAL GROWTH AND SURFACE PHENOMENA

M11.GG.001 RAPID CRYSTAL GROWTH FROM SOLUTIONS: MECHANISMS OF GROWTH AND DEFECT FORMATION. N.Zaitseva, I.Smolsky, L.Carman, R.Ryon, Lawrence Livermore National Laboratory, University of California, P.O.Box 808, Livermore, CA 94550, USA. E-mail: zaitseva1@llnl.gov

The technique of rapid crystal growth [1] gave a base for the successful development of the technology for production of large KDP and DKDP crystals (more than 50 cm in size) for the National Ignition Facility (NIF) laser being built at Lawrence Livermore National Laboratory.

High growth rates, 1-2 orders of magnitude faster than in conventional methods, became possible due to increased solution stability and the shift of the growth process into the region of high supersaturations. This condition emphasized new mechanisms of growth which have not been observed on the large scale or have not been explained previously.

One of such mechanisms is growth on steps generated by the corners and edges of a growing crystal. In faceted crystals this works as a correction mechanism for preserving the crystallographic shape of the faces and edges deviated from the singular directions by the existence of vicinal hillocks. It also explains the phenomena of fast regeneration of the seed from any shape to the right crystallographic habit of minimum surface energy.

Another mechanism is connected with the observation of large crystal facets which grow in the absence of dislocations at a normal growth rate of about one order of magnitude less than growth on dislocation sources under the same conditions. This phenomena is more pronounced in crystals with a low number of dislocations growing at high temperature. Two-dimensional nucleation, when quasi-molecular units attach to the growing surface directly, is a possible explanation of this phenomena.

The growth mechanisms, together with the other factors, such as impurities, hydrodynamics and crystal size, influence the growing surface structure, which at the end determines the optical quality of the crystals. The connection between the defect formation process and the surface structure will be presented.

N.P.Zaitseva, J.J.DeYoreo, M.R.Dehaven, R.L.Vital, K.E.Montgomery, M.Richardson, L.J.Atherton, J.Cryst.Growth 180 (1997) 255.

M11.GG.002 SOLUTION GROWTH OF MIXED ALUM CRYSTALS AND STUDY OF THEIR OPTICAL INHOMOGENEITIES. A.G.Shtukenberg and Yu.O.Punin, Crystal Genesis Laboratory, Geological Faculty, 199034 St.Petersburg State University, St.Petersburg, Russia, E-mail: sasha@as3607.spb.edu; H.Klapper and E.Haegele, Mineralogisch-Petrologisches Institut, University of Bonn, D-53115 Bonn, Germany.

We have carried out detailed investigations of optical anomalies in mixed crystals of alums ($(K,NH_4)Al(SO_4)_2 \cdot 12H_2O$ and $K(Al,Cr)(SO_4)_2 \cdot 12H_2O$) using *in-situ* observation of crystal growth at controlled conditions as well as *ex-situ* optical and X-ray topographic methods. The large mixed crystals (up to 10 cm diameter) were grown from aqueous solutions by lowering the temperature under strong stirring with reversal of rotation. The crystals display a pattern of strong optical inhomogeneities. The

aim of this work is to clarify the origin of these inhomogeneities. Optical anomalies in mixed crystals arise by three causes: 1. Mismatch strains due to compositional inhomogeneities; 2. Strain caused by dislocations; 3. Kinetic ordering of atoms (growth dissymmetrization). It was shown that all three sources of optical anomalies occur in alum mixed crystals, forming the observed complex optical pattern. Even stationary growth conditions lead to optical inhomogeneities in the shape of growth sector-zoning (induced by growth dissymmetrization) and of optical anomalies along dislocation bunches (induced by elastic strain). Non-stationary growth conditions lead to some additional optical effects: zoning and sub-sector zoning. Three interrelated factors determine these additional effects: (1) Compositional inhomogeneities lead to significant inhomogeneous mismatch strain and (2) to different degree of ordering of the mixing atoms; (3) Different directions, heights and velocities of growth steps induce different degrees of ordering of mixing atoms. All kinds of inhomogeneities are discussed in detail in connection with growth conditions. The results obtained can be used for other mixed crystals with optical anomalies.

This work is supported by Russian RFBR grant # 98-05-64151 and German DAAD grant # A/97/53466.

M11.GG.003 GROWTH AND CHARACTERISATION OF NEARLY PERFECT BISMUTH GERMANATE CRYSTALS. Krishan Lal[a], R.V.Anantha Murthy[a], M.Ravikumar[a], A.Choubey[a], G. Bhagavannarayana[a], Lyudmila Kharachenko[b], V. Shleguel[b], V. Guerasimov[b] and Yu. Shubin[b], [a]National Physical Laboratory, Dr. K. S. Krishnan Road, New Delhi 110012, India, [b]Institute of Inorganic Chemistry, SB RAS, Novosibirsk, Russia.

Bismuth Germanium Oxide (BGO) $Bi_3Ge_4O_{12}$ are grown from melt to meet the stringent requirements as scintillators for X-rays and γ-rays. Till recently, Bridgman method had been employed to grow BGO crystals with good degree of perfection. Recent efforts have shown that nearly perfect BGO single crystals can be grown by Low Thermal Gradient (LTG) Czochralski method with Automatic Weight Control Process [Murthy et al, J. Crystal Growth 1999]. For structural characterization, high-resolution X-ray diffractometry and topography methods were employed. Point defects and their clusters have been investigated by diffuse X-ray scattering measurements. The crystal growth system has been developed at IIC, Novosibirsk and the multi-crystal X-ray diffractometers employed in this study were developed at NPL. The crucible weighing system has an accuracy of 10 mg in 1 kg range and 50 mg in 25 kg range. The diameter control is effected through crucible weight control. The temperature gradient above the crystal – melt interface is negligible in a zone of ~4 cm. Platinum crucible was used to melt the charge, which was heated at a rate of 250^o C/h. Nearly perfect crystals were grown under following growth conditions: pulling rate - 2.5 mm/h, seed rotation rate - 38 rpm, growth rate - 30 g/h and post growth cooling rate - 150^o C/h. Crystal dimensions were ~ 80 mm long and ~ 40 mm in diameter [weighing ~ 800g]. Diffraction curves were quite sharp with typical half width values of ~9 arc sec in the central region. Some regions at the periphery had *very* low angle grain boundaries with angular tilts of only ~33 arc sec. Thermal annealing at elevated temperatures reduced the tilt angles and improvements in crystalline perfection were observed. Diffuse X-ray scattering measurements showed significant differences in defect structure with direction of growth. Variations in trace impurities in starting materials, which apparently led to different tinges, did not produce appreciable effect on the point defect clusters.

M11.GG.004 ATOMIC FORCE MICROSCOPY OF ORGANIC CRYSTALS. M. Plomp, F.F.A. Hollander, K. Waizumi, P.J.C.M. van Hoof and W.J.P. van Enckevort, RIM Laboratory of Solid State Chemistry, University of Nijmegen, Toernooiveld 1, 6525 ED, Nijmegen, the Netherlands.

Atomic Force Microscopy (AFM) is a powerful method for imaging crystal surfaces from a microscopic to a molecular scale, which has been applied to metal, semiconductor, ionic, and, as in this presentation, organic crystals. We investigated both *in situ* and *ex situ* growth patterns on the surfaces of fat, protein and paraffin crystals. All crystals showed monomolecular step patterns on their faces.

Different polymorphs of tripalmitate fat crystals were examined. On a microscopic scale very anisotropic growth spirals (see figure) and stacking faults were discriminated. On a smaller scale molecular resolution images could be made.

Insulin protein crystals showed growth both via screw dislocations and 2D nucleation.

On n-$C_{23}H_{48}$ paraffin crystals growth and etching took place during *ex situ* imaging. This was caused by tip-induced local melting of the surface. Measurements on n-$C_{40}H_{82}$ crystals showed the occurrence of crossing steps. This phenomenon was caused by post-growth stress in the crystals, leading to slip movement of screw dislocations.

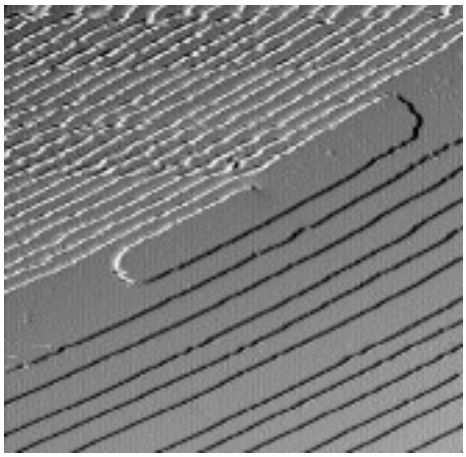

Growth spiral as observed on the (001) face of a tripalmitate crystal.

All these investigations provide insight into the growth of organic crystals. This is important for various industries and for X-ray structure determination.

M11.GG.005 ATOMIC FORCE MICROSCOPY INVESTIGATION OF TRENDS IN SURFACE DYNAMICS DURING GROWTH FROM SOLUTIONS. J.J. De Yoreo, T.A. Land, C.A. Orme [1], H.H. Teng, P.M. Dove [2], M.T. Mc Bride, T.L. Martin, G.T.R. Palmore [3], [1] Department of Chemistry and Materials Science, Lawrence Livermore National Laboratory, Livermore, CA 94550, [2] School of Earth and Atmospheric Sciences, Georgia Institute of Technology, Atlanta Georgia 94550, [3] Department of Chemistry, University of California at Davis, Davis, CA 94671.

Using force microscopy to image crystal surfaces during growth from solutions, we investigated the dependence of growth mechanism, surface morphology, step kinetics and impurity effects on supersaturation in a variety of systems including simple ionic solids (KH_2PO_4, $CaCO_3$ and Ca_3PO_2), hydrogen bonded organic compounds (2,5-diketopiperazines), and Van der Waals bonded macromolecules (proteins). From the dependence of critical step length and step speed on supersaturation, we determined the step edge free energy, kinetic coefficient of elementary steps, and free energy barrier to 1D nucleation at step edges. The wide variety of molecular sizes and bonding allowed us to examine differences in the behaviour of systems for which the step edge energy and the

kinetic coefficient vary by over three orders of magnitude. Here we present a comparative analysis in terms of standard thermodynamic models. We find that the supersaturation at which two-dimensional nucleation occurs is well correlated with the magnitude of the step edge energy and that there is a systematic trend in step kinetics with increasing complexity of growth units. We also show that the magnitude of step edge roughness and step fluctuations varies dramatically among these systems, and that the near-equilibrium step kinetics is often dominated by impurity effects. We then examine the interaction of Fe^{3+}, Al^{3+} and Cr^{3+} impurities with steps on the {100} face of KDP as it enters and emerges from the "dead zone. Within the "dead zone", the surface consists of an intertwined array of immobile elementary steps and macrosteps. As the supersaturation increases, contrary to what is expected from standard models, the surface emerges from the dead zone by propagation of macrosteps which are unhindered by the impurities while the elementary steps remain immobile. As the supersaturation is increased further, the elementary steps begin to advance, but at a slower speed than the macrosteps. At sufficiently high supersaturations, both step types are highly mobile, but the effect of impurities on step motion results in a progressive doubling of steps heights with distance from the step source until macrosteps containing many hundreds of elementary steps dominate the surface.

M11.GG.006 IN SITU ATOMIC FORCE MICROSCOPY STUDIES OF MACROMOLECULAR CRYSTAL GROWTH. A. Malkin, Yu.G. Kuznetsov, A. McPherson [1] Department of Molecular Biology and Biochemistry, University of California, Irvine, CA 92697-3900, USA.

Crystal growth, defects structure and cessation of growth. The growth of twelve protein and virus crystals was investigated in situ using AFM. It was revealed that all the classical growth mechanisms such as growth on dislocations, growth by two- and three-dimensional nucleation and normal growth mechanism operate in macromolecular crystals. Supersaturation dependencies of tangential, normal growth rates and rates of two-dimensional nucleation were measured and several fundamental crystallization parameters were determined. Point defects, dislocations, stacking faults and inclusions were observed and mechanisms of their formation were revealed. The defect density in several different macromolecular crystals was calculated and these data were correlated with the ultimate resolution to which a crystal diffracts. We have observed how the crystals stopped to grow due to the formation of adsorption layer of impurities on the crystalline surface.

Molecular resolution imaging. AFM images at the molecular level have been obtained and structure of the surface layer was resolved for a number of macromolecular crystals. For several crystals molecular structures of the growth step edge and its advancement due to formation of one-dimensional nuclei on the step edge were revealed. High-resolution images of the surface layer of turnip yellow mosaic virus (TYMV) crystals allowed the first direct visualization of the capsomere structure of a virus by AFM. Hexameric and pentameric capsomers of the T=3 capsides are readily discriminated from one another and are clearly visible. Adsorption of individual virus particles and formation of clusters of virus particles on the crystalline surface were visualized. Surface transitions on the (101) face of TYMV crystals were revealed. Three entirely different lattice structures of the surface layer were observed and these patterns transformed sequentially from one to another under specific supersaturation conditions

M11.GG.007 KDP PRISM FACE GROWTH AT LOW STEP VELOCITIES L.N.Rashkovich, O.A.Shustin, T.G.Chernevich, Physics Department, Moscow State University, Moscow 119899, Russia

Research of crystallization processes when velocity of elementary growth layers is under 100 A/s, i.e. close to the non-investigated dead zone of supersaturations, is now possible only with application of atomic force microscope. Up to now this work was never done although being important for understanding of interaction mechanism between steps and impurities adsorbed at the surface or other defects, as well as for crystal growth technology.

Crystallization was conducted in moist media. Method is based on inverse proportionality of solubility to the thickness of solution film on crystal surface. Solution moistens measuring tip of the nanoscope, and therefore solution layer under the tip is thicker. For this reason growth proceeds only in the area of surface scanning and close to this area.

The work describes morphological modifications of preliminarily rough surface in process of generation of singular face and dislocational hillocks.

It was shown for complicated dislocational sources forming multi-thread spirals, that with changes of supersaturation the distance between threads of neighboring spirals is changing, being able to cause development of macrosteps.

Two mechanisms of encapturing obstacles by growing layer are discussed: formation of "sack" (in case of a big obstacle) and encapturing of impurity atoms during kinks movement. In the first case it is easy to determine size of critical nuclei.

Dependence of step velocity on supersaturation and dependence of inter- thread distance on the radius of critical nucleus were obtained through independent measurement of step velocity and rotation period of dislocational spiral.

Drastic surface morphology change with addition of aluminum ions to solution is discussed. These experiments were done in solution flow washing the surface.

12OA VIRUSES AND VIRAL PROTEINS

M12.OA.001 CRYSTAL STRUCTURE OF HUMAN HEPATITIS B CAPSID. A. G. W. Leslie, S. A. Wynne and R. A. Crowther, MRC Laboratory of Molecular Biology, Hills Road, Cambridge CB2 2QH, U.K.

The crystal structure of human hepatitis B capsid with T = 4 icosahedral symmetry has been determined at 3.3Å resolution, using heterologous expression in *Escherichia coli* of capsid protein with the basic C-terminal region (aa 150-185) deleted. The structure was solved using phases derived from a 7.4Å resolution map determined by electron cryomicroscopy (Böttcher *et al*., 1997). Icosahedral averaging and solvent flattening were used to extend the phases to 3.3Å resolution. The capsid protein fold is largely helical, as predicted by spectroscopic measurements, and is in excellent agreement with the fold derived by electron cryomicroscopy. The monomer fold is stabilised by an extensive hydrophobic core formed by residues which are highly conserved amongst human variants. The capsid protein forms very stable dimers by the association of two amphipathic α-helical hairpins, producing a four helix bundle which corresponds morphologically to the spikes on the capsid surface. The dimer-dimer interactions which result in capsid formation involve residues located towards the C-terminus of the truncated protein, which helps to explain the observed dependence of shell formation on the exact length of the construct. The hepatitis B capsid is highly antigenic, and is very effective as a carrier for foreign epitopes. The major immunodominant region (aa 78 - 83) lies at the tips of the spikes. There is a cluster of conserved residues in the same location, which may play a role in specific interactions with the surface antigen during envelopment of the capsid.

Böttcher, B., Wynne, S.A. and Crowther, R.A. (1997) Nature, 386, 88-91.

M12.OA.002 PROBING THE INTERIOR OF THE BLUETONGUE VIRUS CORE PARTICLE. J. M. Diprose, P. Gouet, J. M. Grimes, R. Malby and D. I. Stuart, Laboratory of Molecular Biophysics, Oxford University, Oxford OX1 3QU, UK, and S. Zientara, C.N.E.V.A. Alfort, Laboratoire Central de Recherches Veterinaires, BP67, 94703 Maisons Alfort Cedex, France, and J. N. Burroughs and P. P. C. Mertens, Institute for Animal Health, Pirbright Laboratory, Pirbright, Woking GU24 0NF, UK.

The bluetongue virus core particle is the active transcriptional unit of the virus, consisting of an icosahedral capsid surrounding the enzymatic components and segmented dsRNA genome. The structure of the core was recently solved [1], revealing much about the high-symmetry capsid components but less about the low-symmetry minor proteins and RNA.

An analysis of the structural restraints imposed by the capsid allows us to estimate the concentration of RNA within the core at 410 mg/ml, indicating the genome may be organised as a liquid crystal. Further evidence for this comes from the observation of powder rings of correct spacing in the diffraction patterns collected. Cross-averaging between the structure of serotype 1 (space group $P2_12_12$) and serotype 10 (space group $P4_12_12$) has allowed the identification of structure internal to the capsid conserved between serotypes. Layers of electron density are seen, consistent with the suggested organisation of the genome segments. Density located on the 5-fold icosahedral axis just inside the capsid has been putatively assigned to the polymerase/transcriptase and capping enzymes. Solvent contrast variation experiments reinforce this picture of the internal arrangement of the core particle.

1. J. M. Grimes et al (1998), Nature **395** 470-478

M12.OA.003 ABSTRACT NOT AVAILABLE. W.A. Hendrickson

M12.OA.004 THE CRYSTAL STRUCTURE OF ADENOVIRUS KNOB BOUND TO ITS CELLULAR RECEPTOR CAR. M.C.Bewley, P. Freimuth, K. Springer and J.M. Flanagan. Biology Department, Brookhaven National Laboratory, Upton, New York, 11973, USA.

Understanding the mechanism of adenovirus entry onto host cells is key to designing viable Adeno-based gene therapy vectors. The first step in this pathway is the attachment of the fibre knob domain to its cellular receptor. We have solved the crystal structure of Ad12 knob in complex with domain 1 of its cellular receptor CAR (Coxsackie and Adenorirus Receptor) to 2.6Å resolution. The knob-CAR interface buries a large surface area, but there are few specific contacts between the two proteins, resulting in the formation of a 170$Å^3$ cavity. There are many features of the interface that are similar to that of HIV gp120 in complex with its receptor CD4. CAR is also the cellular receptor for subgroup B of Coxsackie virus. The two viruses compete for binding on CAR, indicating that at least part of the site is shared

The structure of the knob-CAR complex will be presented and compared to that of HIV gp120-CD4. Mutagenesis data, which provides supporting evidence of the validity of the complex, will also be presented. In addition, we will present an explanation for the inability of certain adenovirus serotypes to bind to CAR and we will discuss the implications of our structure on the Canyon hypothesis, presenting possible binding sites for Coxsackie B.

M12.OA.005 WHEN BIG THINGS REFUSE TO CRYSTALLIZE: COMBINING EM AND X-RAY CRYSTALLOGRAPHIC DATA. Jordi Bella, Yizhi Tao and Michael G. Rossmann, Department of Biological Sciences, Purdue University, West Lafayette, IN 47907, USA

In spite of the spectacular successes of virus crystallography, both past and present, a considerable number of interesting problems in virology still elude tackling by crystallographic techniques. Hard-to-crystallize examples include non-icosahedral viruses, antibody-virus, or receptor-virus complexes. Cryo-electron microscopy (cryo-EM) techniques may prove invaluable in such cases, and the combination with data obtained from X-ray diffraction experiments can provide models at near-atomic resolution.

The interaction between the major group of Human Rhinoviruses (HRVs) and their cellular receptor, Intercellular Adhesion Molecule-1 (ICAM-1), has been studied by this combined approach [1]. Cryo-EM reconstructions of complexes between HRV and fragments of ICAM-1 have been interpreted by fitting coordinates obtained from crystal structures of the individual components. This fit has been optimized by rigid-body refinement against structure factors from the cryo-EM map. Fragments of ICAM-1 used in the reconstruction have different degrees of glycosylation. Whereas glycosylation sites show conformational disorder, they can still be identified in the cryo-EM reconstructions, and thus help to refine the orientation of the ICAM-1 fragment model.

The study of the assembly pathway of ϕ29, a dsDNA tailed bacteriophage, provides another example of synergism between cryo-EM and X-ray data [2]. The cryo-EM reconstruction of the prolate head of ϕ29, with only 5-fold symmetry, has allowed for the visualization in situ of the head-tail connector, the central component of the DNA packaging machinery. Crystallographic data indicates that this connector has 12-fold symmetry, thus incommensurate with that of the head. This mismatch may be required to rotate the connector during DNA packaging.

[1] In collaboration with P.Kolatkar, N.H.Olson and T.S.Baker at Purdue University, as well as N.Verdaguer and I.Fita at CID, Barcelona, Spain.
[2] In collaboration with P.Leiman, N.H.Olson and T.S.Baker at Purdue University, and D.L.Anderson at University of Minnesota

P12.OA.001 STRUCTURE OF THE 2A CYSTEINE PROTEINASE FROM HUMAN RHINOVIRUS 2. J.F.W. Petersen [1], M.M. Cherney [1], H.-D. Liebig [2] T. Skern [2], E. Kuechler [2] and M.N.G. James[2], [1] Department of Biochemistry, U. of Alberta, Edmonton, Alberta, T6G 2H7, Canada, [2] Institute of Biochemistry, U. of Vienna, A-1030 Vienna, Austria.

The crystal structure of the 2A proteinase from human rhinovirus serotype 2 (HRV2-2A) has been solved to 1.95 Å resolution by MAD phasing over the absorption edge of zinc. HRV2-2A is involved in the first cleavage of the viral polyprotein which is an intramolecular (cis) cleavage between the N-terminus of HRV2-2A and the C-terminus of the structural protein VP1. In addition HRV2-2A causes the shut-off of the host cell's protein synthesis by cleaving the eukaryotic initiation factor eIF4G. The structure has an unusual, although chymotrypsin-related, fold comprising a unique four-stranded β-sheet as the N-terminal domain and a six stranded β-barrel as the C-terminal domain. A tightly bound zinc ion essential for the stability of HRV2-2A is tetrahedrally co-ordinated by three cysteine sulphurs and one histidine nitrogen located at the junction of the N- and C-terminal domains. The active site consists of a catalytic triad formed by His18, Asp35 and Cys106 and is stabilised by an extensive hydrogen bonding network involving Asp35. Modelling studies reveal that productive substrate binding requires an induced fit in

a cleft formed by a flexible β-hairpin loop containing two tyrosine residues. This model of substrate binding explains furthermore the specificity of the subsites S4, S2, S1 and S1' as well as the cleavage of the host protein eukaryotic initiation factor eIF4G leading to the inability of the infected cell to translate its own capped mRNA. The structure of HRV2-2A suggests that self-processing of the picornaviral polyprotein occurs intramolecularly.

12OB PROTEIN-CARBOHYDRATE INTERACTIONS AND CELL ADHESION

M12.OB.001 MULTIVALENCY AND PROTEIN-CARBOHDYDRATE INTERACTIONS. James M. Rini[1], John R. Walker[1], Yuri D. Lobsanov[1], Bhushan Nagar[1], Jung-Kay Chiu[1], Martin Young[2], and Chi-Hung Siu[3]. [1]Departments of Molecular & Medical Genetics & Microbiology and Biochemistry, University of Toronto, Toronto, Ontario, M5S 1A8, Canada, and [2]Institute for Biological Sciences, NRC, Ottawa, Ontario, K1A OR6, Canada, and the [3]Banting and Best Department of Medical Research and Biochemistry, University of Toronto, Toronto, Ontario, M5S 1A8, Canada.

Both structural and biochemical analysis has shown that many, if not all, lectin types use multivalency to define the affinity and specificity for their carbohydrate ligands. Included among these are lectins responsible for mediating cell-cell and cell-matrix interactions, as well as molecular recognition processes.

The x-ray crystal structures of two new highly multivalent lectins - a decameric C-type lectin from Western diamondback rattlesnake venom (RSL) and discoidin from *Dictyostelium discoideum* - will be presented. RSL is a potent platelet activator and is found to be composed of two 5-fold symmetric pentamers related by a crystallographic 2-fold rotation axis. The ten carbohydrate-binding sites are solvent exposed and located on the "edge" of the decamer. Discoidin is developmentally regulated and important in mediating *D. discoideum* cell-streaming. The structure reveals a stalk-like trimer presenting 9 galactose binding sites. An array of three carbohdyrate-binding sites at each end of the trimer results in what appears to be a bifunctional cross-linker well suited to interacting with glycoconjugate containing surfaces.

In both cases the relative disposition of their carbohydrate-binding sites suggest structure-function relationships which will be discussed in light of that seen in other lectin structures.

M12.OB.002 STRUCTURAL BASIS OF A PEPTIDE MIMICKING THE OLIGOSACCHARIDE ANTIGEN OF AN ANTIBODY (SYA/J6). N.K. Vyas[a], M.N. Vyas[a], B.M. Pinto[b], J.K.Scott[b], S.L. Harris[b], M.A. Johnson[b], M.K. Chevernak[c], D.R. Bundle[c] and F.A. Quiocho[a,d], ([a])Dept.of Biochemistry, Baylor College of Medicine, One Baylor Plaza, Houston, TX 77030, USA, ([b])Department of Chemistry, Simon Fraser University, Burnaby, B.C., Canada, V5A 1S6, ([c])Department of Chemistry, University of Alberta, Edmonton, Alta, Canada, T6G 2G2, ([d])Howard Hughes Medical Institute, Baylor College of Medicine, One Baylor Plaza, Houston, TX 77030, USA

Understanding the molecular basis of peptide mimicry of oligosaccharide will be useful in rational drug design, vaccine development and places where substitution for natural ligand is desired. The monoclonal antibody (mAb) specific for oligosaccharide when screened against phage displayed peptide libraries, revealed an important fact that interacting peptides contain consensus sequence specific for the mAb and compete with the original antigen[1]. At present structural data for such polyspecificity is not well established. The crystallographic studies presented here are for a Fab segment of mAb (SYA/J6)[2], directed against the cell surface O-polysacchride of Gram negative bacteria, Shigella flexneri, in complex with two oligosaccharide epitopes (natural and synthetic) and the octa-peptide with very similar affinity for the SYA/J6 Fab, along with the unliganded Fab. All four structures were determined by the molecular replacement method. The final resolution of these structures ranges from 1.8 to 3 Å. All the data sets were collected at Synchrotron centers. The refinement using the CNS suites of programs (Axel Brunger, Yale University) gives crystallographic R factor for these structures below 0.25 (free R below 0.30). Analyses of results show, probably for the first time, that the peptide is bound in the combining site of the Fab where oligosaccharide, the natural epitope, binds. Peptide interacts with the CDRs of both heavy and light chains, but interacts with different regions of the CDRs. This suggests that peptido-mimetics is not a structural or stereo-mime but imparts its own specificity mimicking the biological role of oligosaccharide. The functional compatibility of peptide and oligosaccharide makes peptide a mime but not an inhibitor.

(1) S.L. Harris et al, Proc. Natl. Acad. Sci. USA(1997), 94,2454-2459
(2) M.N. Vyas et al, J. Mol. Biol. (1993) 231, 133-136

M12.OB.003 SUBSTRATE RECOGNITION BY ENDO-β-N-ACETYLGLUCOSAMINIDASES. Patrick Van Roey, Christopher A. Waddling, Anthony L. Tarentino and Thomas H. Plummer Jr. Wadsworth Center, New York State Dept. of Health, Albany, NY 12201-0509 USA.

Flavobacterium meningosepticum secretes three endoglycosidases, Endo F_1, F_2 and F_3. The three enzymes release asparagine-linked oligo- saccharides from glycoproteins by cleaving the β(1-4)-glycosidic link between the core N-acetylglucosamines. The three enzymes differ greatly in their substrate specificities. Endo F_1 only cleaves high-mannose oligosaccharides. Endo F_2 shows preference for biantennary complex glycans and Endo F_3 cleaves triantennary and α(1-6)-fucosylated biantennary oligosaccharides. We have determined the crystal structures of Endo F_1 and Endo F_3. The enzymes have an $(\beta/\alpha)_8$-barrel fold in which the catalytic glutamic acid residue is located at the end of β-strand 4. The geometries of the two enzymes differ greatly in the area of the loops of β/loop/α-units 2 and 3. In Endo F_1, the main feature in this area is a β-hairpin formed by loop 2. In Endo F_3, this hairpin is replaced by two short α-helices, one each from loops 2 and 3. The structure of Endo F_3 in complex with the biantennary octasaccharide, (Gal-GlcNAc-Man)$_2$-Man-GlcNAc, reveals unambiguously that this area functions as the primary recognition site by tightly binding the α(1-6)-mannose branch. Protein-carbohydrate interactions are similar to those seen in carbohydrate-lectin complexes. The α(1-3)-mannose branch lies over the surface of the protein in the areas of loops 1 and 8 and makes less specific interactions. O1 of the reducing end N-acetylglucosamine forms a bifurcated hydrogen bond with the carboxylate group of the catalytic residue, Glu128. Asp126 is within hydrogen-binding distance from the amine group of the N-acetyl- glucosamine and in position to stabilize the intermediate in a substrate assisted reaction mechanism. Research supported in part by NIH grants GM-50431 (PVR) and GM-34071 (ALT and THP).

M12.OB.004 STRUCTURES OF CHITOTRIOSIDASE AND HC gp39: A LEAD IN THE UNDERSTANDING OF HUMAN CHITINASES. Fabrizia Fusetti, Henriëtte J. Rozeboom, Tjaard Pijning, Annemarie S. de Haan*, Ebo S. Bos* and Bauke W. Dijkstra, University of Groningen, Department of Chemistry, Nijenborgh 4, 9747 AG Groningen,NL (*) NV Organon , Department of Analytical Chemistry , PO Box 20, 5340 BH Oss, NL

Chitinases are glycosyl hydrolases that are found in all organisms in which chitin is a structural component. Surprisingly, proteins highly homologous to chitinases have also been identified

in human. Among these the 39 kDa cartilage glycoprotein (HC gp39) and the enzyme chitotriosidase are particularly intriguing. Their precise physiological role is still unknown. They might be involved in defence mechanisms against pathogens, in tissue remodelling, and in cellular differentiation and high levels of both proteins have been associated with pathological conditions. Chitotriosidase is enzymatically active towards natural chitin but the physiological substrate has not been identified so far. This enzyme is a very reliable marker for the diagnosis of Gaucher disease, a genetic lysosomal storage disorder affecting glucocerebroside metabolism and resulting in mental retardation. In contrast, HC gp39 does not display any chitinolytic activity although it has maintained the ability to bind chitin. Overexpression of HC gp39 has been detected during inflammatory processes of the joints suggesting its potential use as a marker for rheumatoid arthritis.

To address the many questions on the function and the ligand binding properties of human chitinases, we have determined the crystal structures of HC gp39 and of the enzyme chitotriosidase. Both structures show an overall fold similar to that of other chitinases belonging to the glycosyl hydrolase family 18. They display a two domain structure consisting of a main $(\beta\alpha)_8$ barrel domain in which an $\alpha+\beta$ folded domain is inserted. The structure of a complex with a bound chitin fragment shows that HC gp39 holds the sugar chains in the groove present at the C-terminal side of the barrel, in a manner similar to bacterial and plant chitinases, confirming a close evolutionary relationship. These structures are a useful template to explain biochemical results and to discuss the suggested hypotheses on the role of human chitinases.

M12.OB.005 CRYSTAL STRUCTURE OF A MAMMALIAN GALACTOSYLTRANSFERASE Louis N. Gastinel, Christian Cambillau and Yves Bourne AFMB, CNRS-UPR 9039, 31 Chemin Joseph Aiguier 13402 cédex 20 Marseille, France

β1,4Galactosyltransferase, β4Gal-T1, catalyzes the transfer of galactose from UDP-Gal to terminal β-N-acetylglucosamine (GlcNAc) residues forming the poly-N-acetyllactosamine core structures present in glycoproteins and glycosphingolipids. In mammals, β4Gal-T1 associates with α-lactalbumin, a protein expressed exclusively in lactating mammary epithelial cells, to synthesize lactose. β4Gal-T1 is a member of a large family of homologous β4GalT where individual members appear to use different types of glycoproteins and glycolipids as substrates[1,2]. The 2.4 Å resolution crystal structure of the catalytic domain of bovine β4Gal-T1 (residues 133 to 402) consists of a single domain, composed of eleven β-strands, six α-helices and two short 3_{10} helices. The central part of the structure resembles the typical α/β Rossman fold found in a large number of nucleotide-binding protein structures. One face of the molecule contains a deep pocket of 13 Å in diameter. The bottom of the pocket contains the Arg228 side chain (F226NRA) and the signature sequences specific to the β4GalT family[3], Asp252 of DVD, Glu317 and Asp318 of WGWGG(R)EDD. UDP-Gal binds with the uracil moiety deeply buried between Phe226 and Arg191 side chains of the new motif PF(H)RXR, the phosphate groups are located near the DVD motif and the galactose moiety close to the EDDD motif and the Tyr286 side chain. The side chain of Trp314 located close to the EDDD motif, could be a good candidate for interaction with GlcNAc or other sugar acceptors. The only free cysteine Cys342, not conserved among β4GalT family, has is side chain buried and is unlikely to play a direct role in catalysis. A single patch of residues found at the surface and conserved only in β4Gal-T1 and β4Gal-T2 proteins is located in the α6 α-helix and involves residues Gln358, Arg362, His365, Thr369 and Met370. These residues are close to Trp314, suggesting that Trp314 may be involved in the GlcNAc binding site which may be used by glucose upon α-lactalbumin binding.

1) Shaper, N.L. et al. The Chicken genome contains two functional non allelic β1,4galactosyltransferase genes. *J. Biol. Chem*. **272**, 31389-31399 (1997).
2) Almeida, R. et al. A family of human β4galactosyltransferases. *J. Biol. Chem*. **272**, 31979-31991 (1997).
3) Van die, I., Bakker, H. & Van den Eijnden, D.H. Identification of conserved amino acid motifs in members of the β1,4-galactosyltransferase gene family. *Glycobiology*, **7**, V-IX (1997).

P12.OB.001 SUGAR BINDING, PLANT HORMONE BINDING AND NOVEL QUATERNARY STRUCTURE OF TWO LEGUME LECTINS. Thomas W. Hamelryck[1], Remy Loris[1], Julie Bouckaert[1], Minh-Hoa Dao Thi[1], Gerard Strecker[2], Anne Imberty[3], Elias Fernandez[4], Lode Wyns[1], Marilynn E. Etzler[4], [1]Laboratorium voor Ultrastructuur, Vlaams Interuniversitair Instituur voor Biotechnologie,Vrije Universiteit Brussel, Paardenstraat 65, B-1640 Sint-Genesius-Rode, Belgium, [2]Université des Sciences et Technologies de Lille, Bâtiment C9, 59655, Villeneuve D'Ascq CEDEX, France, [3]CERMAV-CNRS (affiliated to the University Joseph Fourier), BP 53, F-38041 Grenoble Cedex 9, France, [4]Section of Molecular and Cellular Biology, University of California, Davis, CA 95616, USA

The tetrameric *Dolichos biflorus* seed lectin (DBL) has an interesting specificity among the legume lectins because it binds GalNAc readily while it binds Gal very weakly. In addition, DBL is an adenine/cytokinin plant hormone binding legume lectin. DBL was crystallized with the blood group A trisaccharide GalNAc(α1-3)[Fuc(α1-2)]Gal (2.8 Å resolution), the high affinity ligand GalNAc(α1-3)GalNAc (Forssman disaccharide) (2.6 Å resolution) and adenine (2.65 Å resolution). The structure of DBL in complex with adenine shows that some legume lectins possess a hydrophobic binding site which depends on their quaternary structure. DB58, a dimeric vegetative lectin from the same plant, adopts a novel quaternary structure in which this site is strictly conserved. A sandwiched α-helix mediates quaternary structure and is part of the adenine/cytokinin plant hormone binding site in both DBL and DB58.

The DBL sugar complexes illustrate that specific binding of an *N*-acetylated sugar is achieved through a give-and-take mechanism: a lack of aromatic stacking against the sugar ring is compensated by a favorable interaction of the *N*-acetyl group with the lectin. The latter interaction not only depends on the presence of a specific subsite, but also on the correct positioning of the sugar ring by the specificity loop. High affinity binding of the Forssman disaccharide is solely mediated via the formation of a small, solvent shielded hydrophobic cavity and does not involve any additional hydrogen bonds.

P12.OB.002 THE COMPLEXES OF BOTH PARTS OF THE TRIMANNOSIDE MAN A1-3(MAN A1-6)MAN A1-OME WITH CON A. J. Bouckaert, R. Loris, L. Wyns, Ultrastructure, Vrije Universiteit Brussel, Paardenstraat 65, B-1640 Sint-Genesius-Rode, Belgium.

Man a1-6Man a1-OMe and Man a1-3Man a1-OMe, the two dimannoside parts of the highly specific epitope Man a1-3(Man a1-6)Man a1-OMe of concanavalin A, were crystallized in complex with this lectin. The structures were refined to a resolution of 2.0 Å and 2.9 Å respectively. The interactions between the sugar and the lectin as we observe them in the crystal structures largely explain the thermodynamic differences in enthalpy and entropy for the binding of the two dimannosides. In both structures, the first sugar unit binds in the monosaccharide (mannose or glucose) binding site. Man a1-6Man a1-OMe binds essentially the same way as is observed in the concanavalin A-trimannoside complex (1,2). The first mannoside binds in the

monosaccharide binding site. The second mannoside makes only one extra hydrogen bond and few van der Waals contacts compared to the monosaccharide. It occupies approximately the place of the core mannoside in the Man a1-3(Man a1-6)Man a1-OMe complex but its O2 hydroxyl makes no interactions in contrast to the trimannoside complex. Man a1-6Man a1-OMe binds with an almost equal affinity as Me- a-D-Man while Man a1-3Man a1-OMe and Man a1-3(Man a1- 6)Man a1-OMe bind respectively 4 and 60 times better. Man a1-6Man a1-OMe binding is accompanied by a slightly higher enthalpy change and a compensating entropy cost than binding of the monosaccharide Me- a-D-Man, however the same affinity as for Me- a-D-Man is maintained. The quasi absence of extra protein-carbohydrate interactions of Man a1- 6Man a1-OMe compared to Me- a-D-Man suggests that desolvation and the conformational restriction of the a1-6 glycosidic linkage may be the most important contributors to these differences. The first mannoside of Man a1-3Man a1-OMe binds in the monosaccharide binding site, in contrast to what is observed for the trimannoside complex, where it binds into a subsite formed by Pro13, Thr15 and Asp16. The second mannoside of Man a1-3Man a1- OMe makes strong van der Waals contacts with the protein along the side of the binding groove with Tyr12, Tyr100 and Leu99. Its large (negative) heat capacity change, enthalpy change and entropy cost probably reflect the importance of the expulsion of solvent during binding along this subsite build up of aromatic side chains.

1. Naismith, J.H. & Fields, R.A. J.Biol.Chem. 271, 972-976 (1996).
2. Bouckaert, J., Maes, D., Poortmans, F., Wyns, L. & Loris, R. J.Biol.Chem. 271, 30614-30618 (1996).

P12.OB.003 DUAL AFFINITY LABELING OF THE ACTIVE SITE OF HUMAN LYSOZYME WITH AN N–ACETYL LACTOSAMINE DERIVATIVE. M. Muraki and K. Harata, National Institute of Bioscience and Human–Technology, Tsukuba, Ibaraki 305–8566, Japan, and N. Sugita and K.I. Sato, Kanagawa University, Yokohama, Kanagawa 221–0802, Japan.

The 2',3'–epoxypropyl β-glycoside of N–acetyllactosamine (Gal-β1,4–GlcNAc–Epo) doubly labelled human lysozyme (HL). This presented the first observation of dual binding of ligand to lysozyme. The labelled HL was crystallised (space group $P2_12_12_1$with unit cell dimensions a=56.45A, b=62.30A, c=32.98A) and the X–ray structure was determined at 2.3 A resolution, which identified the two Gal-β1,4-GlcNAc-Epo moieties inside the catalytic cleft of HL [1].

The attachment sites were the side–chain carboxylate groups of the catalytic residues Glu35 and Asp53 in HL. The first Gal-β1,4-GlcNAc-Epo moiety located virtually the same way as observed in the HL labelled with Gal-β1,4-GlcNAc-Epo molecule [2]. The second Gal-β1,4-GlcNAcEpo moiety was recognised via the carbohydrate–carbohydrate interaction with the first Gal-β1,4-GlcNAc-Epo moiety in addition to the protein–carbohydrate interaction with the catalytic cleft of HL through a number of hydrogen bonds as well as many van der Waals contacts. The two N–acetylglucosamine residues stacked with each other, while the two rings of galactose residues approximately shared the same plane.

The results demonstrated that the HL labelled with single Gal-β1,4-GlcNAc-Epo worked as a novel N–acetyllactosamine–binding protein, and the second labelling was performed by way of the first–ligand assisted recognition of the second ligand.

[1] M. Muraki, K. Harata, N. Sugita and K.–I. Sato (1999) Biochemistry, 38, 540–548
[2] M. Muraki, K. Harata, N. Sugita and K.–I. Sato (1996) Biochemistry, 35, 13562–13567.

P12.OB.004 STRUCTURE OF ARTOCARPIN. M. Vijayan, K.Sekar*, P. Geetha Rani, A. Surolia and J.V. Pratap, Molecular Biophysics Unit and *Bioinformatics Centre, Indian Institute of Science, Bangalore, India.

Artocarpin, a homotetrameric, 66 kD *moraceae* lectin isolated from the seeds of jackfruit (*Artocarpus Integrifolia*), is specific to mannose. Among other things, it mediates the T-cell dependent B-cell maturation. The primary structure of artocarpin shows considerable similarity to jacalin, another lectin from the same source whose structure has been solved in this laboratory [1],although jacalin is specific to galactose. Moreover the jacalin monomer is made of two chains, while artocarpin is a single polypeptide chain. Two crystal forms, both belonging to space group $P2_1$, with one and two tetramers in the asymmetric unit respectively were obtained and intensity data were collected. The structures were solved by molecular replacement calculations using the jacalin tetramer as the search model and that with one tetramer in the asymmetric unit has been refined to an R value of 19.0%. The overall fold is similar to jacalin.

The carbohydrate binding region exhibits considerable differences compared to jacalin. The N-terminal glycine of the α chain of jacalin is now part of a linker region that connects the α and β chains of the jacalin monomer. Tyr A78, which stacks against galactose in jacalin, is replaced by Thr in artocarpin. Asp A125 is conserved, albeit with a different side chain conformation,as suggested by Rosa *et al.,*[2], although this difference does not appear to be a consequence of steric hindrance with the linker peptide. Modelling of galactose into the binding site does not show any substantial difference from the hydrogen bonding pattern observed in the crystal structure of jacalin. The loss of the stacking interaction provided by Tyr A78 in jacalin, might however be significant. A complete elucidation of the geometrical basis of the carbohydrate specificity of artocarpin should await the X-ray analysis of a complex of the lectin with a mannose derivative, which is in progress.

[1] R. Sankaranarayanan *et al.,* (1996). Nat. Struct. Biol. **3**, 596-603.
[2] J.C. Rosa *et al.,* (1999). Protein Science **8** (1), 13-24.

P12.OB.005 STRUCTURAL BASIS OF CARBOHYDRATE SPECIFICITY IN HUMAN GALECTIN-10 (CHARCOT-LEYDEN CRYSTAL PROTEIN). G.J. Swaminathan and D.D.Leonidas, Dept. of Biology and Biochem., University of Bath, Bath BA2 7AY, UK, and S.J. Ackerman, Dept. of Biochem. and Molecular Biology, University of Illinois at Chicago, Chicago, Illinois 60612, USA, and K.R.Acharya, Dept. of Biology and Biochem., University of Bath, Bath BA2 7AY, UK.

The autocrystallising Charcot-Leyden crystal (CLC) protein, a small hydrophobic protein exhibiting weak lysophospholipase activity, is a major constituent of human eosinophil and basophil granules [1]. The presence of typical CLC crystals in a variety of body tissues is considered to be a signature of eosinophil-associated inflammation. However, CLC shows no sequence similarities to any known lipolytic enzymes, and its role in eosinophil and basophil function remains speculative. The crystal structure of CLC determined at 1.8Å resolution showed striking similarities in overall structural fold with that of galectins [2], possessing a carbohydrate recognition domain (CRD) with 7 of 12 conserved residues among galectins, and 6 of 8 residues known to be directly involved in sugar binding. The carbohydrate-specificity of CLC is under study in our laboratory by crystallographic studies of CLC-sugar complexes using a wide variety of sugars. Our results indicate that although CLC has similarities with galectins in overall structural fold and a partially conserved CRD, it demonstrates affinity towards mannoside sugars unlike other galectins. The results of

our structural studies will be discussed in light of the possible function for CLC in the eosinophil granule.

1. S.J. Ackerman,(1993). in *Eosinophils: Biological and Clinical Aspects* (Makino, S. & Fukuda, T., Eds.) pp 33-74, CRC, Michigan, USA.
2. D.D. Leonidas, B.L. Elbert, Z. Zhou, H. Leffler, S.J. Ackerman and K.R. Acharya (1995). *Structure* 3, 1379-1393.

P12.OB.006 3D STRUCTURE OF PLANT ASPARTIC PROTEINASE, A GLYCOSYLATED NATIVE CARDOSIN A. M. A. Carrondo, C. Frazão, I. Bento, J. Costa, C. M. Soares, I.T.Q.B. Apartado 127, 2780-Oeiras, Portugal and P. Veríssimo, C. Faro, E. Pires Dept. de Bioquímica, Univ. de Coimbra, 3000-Coimbra, Portugal.

Plant aspartic proteinases (AP) have been detected, extracted and characterized from seeds, leaves and flowers of a broad variety of plant species, and are involved in specific physiological roles [1]. Most of them contain in their cDNAs an insertion coding for a polypeptide segment of about 100 residues, known as PSI (plant specific insert). Cardosins are AP from the flowers of *Cynara cardunculus* L. [2] and their milk clotting activity have been exploited in Portugal since the Roman Era in the manufacture of traditional cheeses. Preliminary crystallographic data on cardosin A was published in [3]. The refined cardosin A crystallographic structure to 1.72 Å resolution includes two glycosylated molecules, built up by two (30 and 15 kD) peptide chains, in a total of 649 amino-acids. The base of the active site cleft is made of β-strands forming the typical, two abutting φ-like structures which contain the two catalytic aspartates (Asp 32 and Asp 215), with side chains held coplanar and within hydrogen bonding distances to involving main chain and conserved side chain groups. A water molecule is bound to both aspartate carboxyls by hydrogen bonds. The glycosyl content in cardosin A is described by 19 sugar rings attached to Asn 67 and Asn 257, localised on the molecular surface in two glycosylation sites, in each of the molecules, *i.e.* one site *per* polypeptide chain. An hydrogen bond between Gln 126 (Oε1) of the parent protein and Manβ4 (O2) renders the monosaccharide oxygen sterically unaccessible to accept a xylosyl residue, transferred by xylosyltransferase, as usually the case in glycans of the plant complex type.

This crystal structure [4] suggests a possible mechanism by which cardosin A might be orientated at the cell surface so that its RGD sequence could be recognised by the receptor from pollen.

1- Kervinen, *et al.* Adv. Exp. Med. Biol. (1999) 362, 241-254.
2- Veríssimo, P., *et al. Biotech. Letters* (1995) 17, 614-645
3- Bento, I. *et. al. Acta Cryst.*, (1998) D54, 991-993.
4- Frazao, C. *et al*. (1999) submitted.

12OC APERIODIC AND INCOMMENSURATE STRUCTURES (I)

M12.OC.001 QUASICRYSTAL OR RANDOM TILING? IN SITU SYNCHROTRON MEASUREMENTS OF DECAGONAL AL-CO-NI AT HIGH TEMPERATURE. T. Haibach, A. Cervellino and W. Steurer, Laboratory of Crystallography, Swiss Federal Institute of Technology, ETH Zurich, CH-8092 Zurich, Switzerland.

Stable $Al_{70}Co_{12}Ni_{18}$ represents a commensurate superstructure [1,2] of decagonal $Al_{72.5}Co_{17.5}Ni_{10}$. Both structures exhibit sharp Bragg peaks in X-ray diffraction experiments. Whether these two structures are exactly quasiperiodic or belong to the class of random tilings [3] is still not clarified.

We performed *in situ* high temperature X-ray measurements at the synchrotron source Hasylab. At various temperatures high-resolution one- and two-dimensional peak profiles of selected reflections were collected. Two-dimensional profile scans show that there is no phase transition to twinned approximants or nanodomain structures in the investigated temperature range. The analysis of the integral intensities, however, reveals a linear dependence with temperature whose coefficient is the perpendicular space norm of the main reflections. The results give evidence that the phasonic Debye-Waller factor of the basic structure is proportional to the temperature. The high temperature phase is proposed to belong to the class of random tilings.

1. K. Edagawa, H. Sawa & S. Takeuchi (1994). Phil. Mag. Lett., **69**, 227
2. T. Haibach, A. Cervellino, M.A. Estermann & W. Steurer (1999). Phil. Mag. A, in press.
3. C.L. Henley (1991), in: Quasicrystals: The State of the Art. (ed. by D.P. Di Vicenzo & P.J. Steinhardt) Singapore: World Scientific, 429

M12.OC.002 REFINEMENT OF QUASICRYSTAL STRUCTURES. Akiji Yamamoto, Nat. Inst. Res. Inorg. Mat., Namiki 1, Tsukuba, 305 Japan.

A nontrivial problem in quasicrystal analyses is how to describe accurate quasicrystal structures or how to introduce structural parameters. One successful attempt for this problem is the use of cluster models in higher dimensional space. This model enables us to introduce more than 50 reasonable parameters for icosahedral quasicrystals and 100 for decagonal ones, which allow us to determine the detailed positions of atoms in the cluster and their thermal and occupational parameters. The first successful result was obtained in the analysis of the icosahedral Al-Pd-Mn quasicrystal. The cluster model assumes large clusters situated at the vertices of 3-dimensional Penrose pattern with an edge length of about 20Å. The clusters include more than 100 atoms. This model has 15 positional, 7 thermal and 28 occupational parameters and gave an R_w-factor of 0.106 for 1137 independent reflections [1]. Such a large cluster was shown to exist in the 2/1 approximant [2]. Recently, a decagonal Al-Mn-Pd quasicrystal was successfully analyzed with a noncentrosymmetric space group [3]. It consists of large columnar clusters with about 20Å diameter. The cluster model used includes 207 parameters and gave R_w=0.119 for 1428 independent reflections. The success of the analyses of typical quasicrystals implies that it is possible to analyze quasicrystal structures in detail with more than 1000 reflections when high quality single domain quasicrystals are used.

1. Yamamoto et al. (1994). Aperiodic '94, p393 (World Scientific, Singapore)
2. K. Sugiyama et al. (1997). Z. Krist. 213, 90.
3. S. Weber and A. Yamamoto (1998). Acta Cryst. A54, 997.

M12.OC.003 THE LOW TEMPERATURE SUPER-STRUCTURE OF NaV_2O_5. J. Lüdecke, A. Jobst, S. van Smaalen, Laboratory of Crystallography, University of Bayreuth, D-95440 Bayreuth, Germany, E. Morre, C. Geibel, MPI for Solid State Chemistry, D-01187 Dresden, Germany, H.-G. Krane, Hasylab, DESY, D-22603 Hamburg, Germany.

NaV_2O_5 displays magnetic ordering at temperatures below 35 K as shown by susceptibility measurements [1]. The magnetic ground state is connected with a commensurate distortion of the lattice leading to a ($2a\times2b\times4c$) supercell. Consequently it has been assumed that the phase transition is of spin-Peierls character [2]. Here a full determination of the modulated low temperature structure will be presented. The phase transition to the superstructure leads to a loss of the inversion symmetry. The displacements of all atoms could be determined. In agreement with magnetic ordering, the major displacements occur on the V

atoms. In contrast to the spin-Peierls compound $CuGeO_3$ the distortion pattern appears to be transverse to the one dimensional magnetic chains. The data cannot be understood in terms of a pure spin-Peierls transition, but additional charge ordering has to be assumed to explain the magnetic ordering. A complete understanding of the observed structure of the ground state of NaV_2O_5 has not been achieved yet but the proposed structure is in agreement with other experimental results.

1. M. Isobe and Y. Ueda, J. Phys. Soc. Jpn. **65**, 1178 (1996)
2. Y. Fujii et al., J. Phys. Soc. Jpn. **66**, 326 (1997)

M12.OC.004 INTERPRETATION OF MODULATED AND COMPOSITE STRUCTURES. M. Dusek and V. Petricek, Institute of Physics, Acad. Sci. of the Czech Republic, Na Slovance 2, 182 21 Prague, Czech Republic**.**

Contemporary structure analysis of modulated and composite crystals involves more and more complicated structures. The necessity of visualising crystal structures, usually described in the superspace, is obvious not only for presentation and interpretation of results but also for the solution during the structure analysis. The usage of standard crystallographic programs for this purpose is usually laborious and limited.

Here we present three topics: calculation of distances, visualisation of multidimensional electron density maps and plotting of modulated and composite structures. All of them are implemented in computing system JANA98[1] as programs CONTOUR and PICTUR and tested on examples of some hexagonal perovskites, hexamethylenetetramine sebacate and quininium (R)-mandelate. The distances calculation of modulated and composite crystals is based on the general theory as summarised in [2].

The plotting program PICTUR uses three dimensional cell expansion with calculation of translation-dependent positional, occupational and temperature modulation changes and successive calculation of distances. It works automatically also for sawtooth positional modulation and set of orthogonalized harmonic waves. The program has special mode for plotting structure fragments together with t-sections by electron density map and for making "animated" plots as a function of varying t coordinate. Program CONTOUR plots sections by multidimensional electron density maps and visualises modulation functions.

1. V. Petricek & M. Dusek (1998). Crystallographic computing system JANA98, Inst. of Physics, Acad. Sci. of the Czech Republic.
2. S. van Smaalen (1991), Phys.Rew.B, **43**, 11330-11341.

M12.OC.005 AN INTERPRETATION ON THE DIFFUSE SCATTERING IN $Cd_5(PO_4)_3Br_{1-x}$. Sven Lidin, Marat Moustiakimov and Peter Henning. FOOS kemi, Arrhenius Laboratory, Stockholm University, 106 91 Stockholm, Sweden

Single crystals of cadmium phosphate bromide grown from a cadmium bromide melt exhibit highly structured diffuse scattering in addition to the Bragg scattering from the basic apatite structure. This additional scattering occurs in layers perpendicular to **c***, and takes the shape of hexagonal honeycomb nets. It shows pronounced, Bragg-like, maxima at the positions *h+1/3 k+1/3 l* and *h+2/3 k+2/3 l* where *l* is close to 0.78 **c***, and may therefore to a first approximation be treated as an incommensurate modulation with a modulation wave vector **q**=1/3 1/3 0.78. This implies that the 3D space group of bromapatite, $P6_3/m$, should be replaced by the 4D superspace group R:$P\bar{3}$:-11. The remaining, rational, part of the modulation wave vector is then $\mathbf{q}^i$ = 0 0 0.78.

This behaviour can also be studied in the corresponding vanadate bromide and iodide, but here the Bragg-like ordering is weaker, and the diffuse nature of the scattering is more pronounced.

The scattering from a single crystal specimen was measure on a STOE imaging plate system, and the data obtained was refinable down to an R-value of 5% for main reflections and 12% for satellites using a saw-toot type displacive modulation for Br. The halogenide is simply to large for the cavity in which it resides, and spills over into the regime that should be occupied by the next Br which is displaced away from its ideal position, pushing the next Br even further away. This displacement accumulates until the accompanying strain becomes to great and a Br vacancy results.

The average structure agrees well with earlier reports, but the local Br ordering is intriguing; while the ordering in the individual Br channels is easy to understand simply from a steric point of view, the additional rhombohedral ordering between the channels is unexpected. The atoms surrounding the Br channels seem unaffected by the modulation, and the ordering may be attributed to an electrostatic effect. The diffuse streaks that join up the Bragg-like spots that are treated in this analysis may be attributed to imperfections in this electrostatic ordering. There is no reason to believe that the intra channel ordering is altered, since all diffuse scattering resides in the same plane perpendicular to **c***, but the rhombohedral ordering is weak, and several other ordering modes will yield electrostatically neutral solutions, as in monoclinic ClAp and OHAp.

P12.OC.001 STUDIES ON VARIATION OF CLUSTER DISTRIBUTION IN INCOMMENSURATE Co-ÅKERMANITE BY A SIMULATION. M. Ohmasa, K. Kusaka, K. Hagiya and N. Haga, Department of Life Science, Himeji Institute of Technology, Hyogo 678-1297, Japan, and K. Iishi, Department of Mineralogical Science and Geology, Yamaguchi University, Yamaguchi 753-8512, Japan.

The variation of the wave length or the component *q* of the modulation wave due to temperature change has been described in studies on åkermanite since Seifert et al. found the phenomena [1]. To know a change of the modulated structure with such variation of *q* or temperature, we usually need new data collection and refinement processes, although the new structure is essentially similar to the old one. A new simulation method was thus developed to get structure information without such processes and to look successive changes of the structure caused by the change of *q* or temperature. The displacement u_{ij}^T (i=1, 2, 3 corresponding to *x*, *y*, *z*) of jth atom at temperature *T* can be approximately expressed as

$$u_{ij}^T = \sqrt{I^T / I^{R.T.}} \sum_k A_{ijk}^{R.T.} trig(s,t),$$

where $I^T / I^{R.T.}$ is the ratio of intensity at *T* to intensity at *R.T.* (room temperature), $A_{ijk}^{R.T.}$ *k*th amplitude of the modulation wave and $trig(s,t)$ a trigonometric term with phases *s* and *t* at *T*. The atomic positions at *T* can be then calculated with the above formula.

The method was applied to study variation of the incommensurate structure of Co-åkermanite. The structure is characterized by clusters formed with four coordination polyhedra of the six-coordinated Ca together with a Co-tetrahedron and by the octagonal arrangement (an octagon) of the clusters [2]. The simulation with different *q*'s displayed that distribution of the octagons changes with q-values sensitively and ordered distributions of the octagons are formed for rational *q*'s (*e.g.* q = 2/7). The number of the octagons in a unit area also changes with *q*'s. The histogram of the numbers of the octagons versus *q*'s indicate a maximum at q = 0.294.

1 F. Seifert *et al*. (1987) Phys. Chem. Minerals **14**, 26.
2 K. Kusaka *et al*. (1998) Mineral. J. **20**, 47.

12OD STRUCTURE SOLUTION FROM POWDER DATA – INORGANIC MATERIALS

M12.OD.001 OVERVIEW OF COMPUTER PROGRAMS FOR STRUCTURE SOLUTION FROM POWDER DATA AND THEIR APPLICATION TO INORGANIC MATERIALS. Xavier Solans. Departament de Crista·lografia, Universitat de Barcelona. Spain.

In the issue of the November 1998 of *Scientific Computing World*, David Bradley (pages 16-17) states that standard methods for crystal structure determination from powder diffraction data are error prone and often produce incorrect structural predictions and he concludes his manuscript indicating that the crystal structure determination from powder data is not at present routine.

All computer programs for crystal structure determination have well-defined methodology and strategy. The successful use of a computer program depends on the crystal structure of the sample, the pattern measured and the user's strategy, which must agree with those defined in the computer program.

An overview of the computer programs used for structure solution from powder data will be carried out, where the experimental conditions of intensity collection will be emphasised.

M12.OD.002 SOLUTION OF FRAMEWORK CRYSTAL STRUCTURES FROM POWDER DIFFRACTION DATA BY MONTE CARLO METHODS. Michael W. Deem and Marco Falcioni, Chemical Engineering Department University of California Los Angeles, CA 90095-1592 USA.

We describe a new, biased Monte Carlo scheme to determine the crystal structures of zeolites from powder diffraction data [1]. We test the method on all publicly known zeolite materials, with success in all cases. We show that the method of parallel tempering is a powerful supplement to the biased Monte Carlo.

[1] Marco Falcioni and Michael W. Deem, ``A Biased Monte Carlo Scheme for Zeolite Structure Solution," J. Chem. Phys. 110 (1999) 1754-1766.

M12.OD.003 ZEOLITE STRUCTURE DETERMINATION FROM POWDER DATA USING THE "FOCUS" METHOD. R.W. Grosse-Kunstleve [1], L.B. McCusker & Ch. Baerlocher [2], [1] Yale University, New Haven, Connecticut 06520-8114, U.S.A., [2] Laboratory of Crystallography, ETH Zentrum, CH-8092 Zurich, Switzerland.

The technologically and industrially important zeolites are often synthesized and used in polycrystalline form. However, the determination of a zeolite structure from powder diffraction data is generally a non-trivial matter, because these materials tend to crystallize with relatively high symmetries and large unit cells. This automatically leads to a high degree of reflection overlap. Furthermore, the only structural information known *a priori* for zeolites are typical bond lengths and bond angles, and the fact that they can be described as having 3-dimensional, 4-connected framework structures.

To address the problem posed by zeolite structures, the program FOCUS, which integrates both the crystal chemical information and powder diffraction data into the structure determination process, was developed. FOCUS combines automatic Fourier recycling with a topology search specific to zeolites. Experience shows that this approach of using chemical and geometrical knowledge can compensate for some of the information that is lost as a result of the overlap problem.

Four examples of the application of FOCUS serve to illustrate its potential and its limitations. The solutions of the structures of two aluminophosphate molecular sieves, YUL-89 (AWO topology) and YUL-90 (ZON topology), demonstrate routine applications of the procedure. The high silica zeolite ZSM-5 (MFI topology), which has 12 Si-atoms (38 framework atoms) in the asymmetric unit, and the gallophosphate Cloverite (-CLO topology), whose framework is not fully 4-connected, provide examples of extremly difficult cases, which challenge the limits of the FOCUS algorithm.

M12.OD.004 STRUCTURE SOLUTION FROM POWDER USING PARETO-OPTIMIZATION OF PATTERN DIFFERENCE AND POTENTIAL ENERGY. H. Putz, German National Research Center for Information Technology (GMD), Scientific Computation and Algorithms Institute (SCAI), Schloss Birlinghoven, D-53754 Sankt Augustin, Germany and J.C. Schön, Inst. f. Anorg. Chemie d. Uni Bonn, Gerhard-Domagk-Str. 1, D-53121 Bonn, Germany.

Most of the "classical" methods for "ab initio" solution of crystal structures from powder diffraction diagrams depend on the knowledge of the intensity for each reflection I(hkl), in analogy to single crystal methods. Unfortunately, in many cases a severe overlap of different reflections makes it difficult to determine these values with sufficient accuracy [1, 2].

For this reason, the so called "direct space methods" propose a structural model independent of the powder diffraction diagram. Beginning with some arbitrarily chosen atomic starting configuration, the difference between the calculated and the measured diffraction pattern (costfunction) is minimized through repeated change of the atomic arrangement.

In practice for most crystalline solids this prescription results in the system quickly getting trapped in some minimum that does not correspond to a physically reasonable atomic arrangement. The reason for this lies in the landscape of the costfunction which includes numerous deep local minima.

Our concept implies a combined optimization of the difference between the calculated and the measured diffraction pattern and of the potential energy of the system ("Pareto-optimization"). Merging both hypersurfaces blurs the minima that belong to only one of the two surfaces, and strengthens those which belong to both of them. Thus, conventional global optimization methods (e.g. Simulated Annealing) can be used. This concept was tested successfully on a large variety of ionic, metallic and molecular compounds.

[1] K.D.M. Harris, M. Tremayne, Chem. Mater. **8**, 2554 (1996)
[2] D. Louër, Acta Cryst. A**54**, 922 (1998)

M12.OD.005 USING TEXTURE TO FACILITATE STRUCTURE SOLUTION. T. Wessels, C. Baerlocher and L.B. McCusker, Lab. f. Kristallographie, ETH-Zentrum,CH-8092 Zürich, Switzerland

The limiting factor for *ab initio* crystal structure solution from powder data arises from the collapse of three-dimensional single-crystal data onto the single dimension of a powder diffraction pattern, and the resulting peak overlap in 2-theta.

This problem can be reduced significantly if textured rather than random powder samples are used. A sample with pronounced preferred orientation can be regarded as being something between a completely randomly oriented powder and a single crystal with a corresponding increase in the information contained in the diffraction data. Using a textured sample and exploiting the high intensity and parallel nature of synchrotron radiation, a single-crystal-like set of intensities can be extracted,

and crystal structures as complex as those routinely solved by single-crystal methods can be determined.

To test the viability of the method, a measurement on a textured sample of ZSM-5 was performed. The extracted pseudo single crystal data set was input to a direct methods program, and all 12 of the Si and 19 of the 26 O positions were found in the top 40 peaks of the E-map. In a second test, measurements on a textured sample of the aluminophosphate Mu-9 with unknown crystal structure were performed. Intensity extraction followed by the application of direct methods revealed a rather unusual aluminophosphate structure (framework formula $Al_{66}P_{72}O_{288}$ per unit cell). All P atoms are tetrahedrally coordinated and 4-connected (i.e. form oxygen bridges to four Al atoms), whereas the Al atoms are 4- and 6-connected to P atoms of the framework. Finally, the method was applied to a sample of the as synthesized form of UTD-1, prepared using a modification of the published synthesis procedure. The structure was solved in the space group $P2_1/c$ (for Rietveld refinement the symmetry had to be lowered to Pc). In the initial E-map all 16 Si atoms and 17 of the bridging oxygens could be found. Subsequent electron density maps allowed the remaining 15 oxygens and the Co to be located.

P12.OD.002 STRUCTURE DETERMINATION OF GUEST-HOST SYSTEMS USING POWDER REFINEMENTS AND COMPUTER SIMULATIONS. G.Nalini, S.Yashonath and T.N.Guru Row, Solid State and Structural Chemistry Unit, Indian Institute of Science, Bangalore-560012.

The use of Rietveld technique for the determination of structures where the starting models are available is extensively used with accurate powder diffraction data. In guest-host systems, the model of the host molecule is generally available based on earlier crystallographic studies. The guest molecule is constrained within the matrix generated by the host with weak interactions which render the guest molecule to be in more than one configuration at a given temperature. The basic idea is to locate the guest molecule using molecular dynamic simulations at the given temperature and identify the resulting electron density distribution on a difference Fourier map generated based on the powder diffraction data. Examples involving Zeolite NaY as the host and rare gases like Argon and Xenon as guests provide valuable insight into these features. The data sets have been generated on a STOE-STADI/P diffractometer using an Oxford Cryo- system to enable data collection at required temperatures. The simulations have been performed using a locally developed CBMC methodology.

P12.OD.003 CRYSTALLOGRAPHIC THERMAL PARAMETERS FROM POWDER NEUTRON DATA: A STUDY OF ISOTOPICALLY SUBSTITUTED CuO. Paul F. Henry, Mark T. Weller, Chemistry Department, Southampton University, Highfield, Southampton, Hampshire, SO17 1BJ, UK, Chick C. Wilson, ISIS Facility, CLRC Rutherford Appleton Laboratory, Chilton, Didcot, Oxon., OX11 0QX, UK.

The evolution of the anisotropic thermal parameters in copper (II) oxide with temperature has been studied in detail both theoretically and experimentally using x-rays. However, extraction of similar quality information from powder diffraction data has proved problematical. In this work we have employed powder neutron diffraction, using isotopically substituted CuO, to extract detailed crystallographic information from powdered samples. The contrast in neutron scattering lengths between ^{63}Cu (6.43 fm) and ^{65}Cu (10.61 fm) allows collection of multiple data sets which can then be refined using a single crystallographic model to obtain extra structural information.

A major problem with structure refinements using powder diffraction data is the estimation of background and thus extraction of accurate peak intensities. For time-of-flight neutron sources and instruments, such as POLARIS, this is a particular problem due to relatively high backgrounds, non-linear backgrounds and, at short time-of-flights/low d-spacing, total overlap of peak profiles completely eliminating true background values. This generally produces strong correlation between refined thermal parameters and the choice of background. One way of overcoming this problem is to study chemically identical materials (thus with identical thermal parameters and producing identical backgrounds) but with different isotopes, yielding different intensity reflections. Simultaneous refinement of these data sets allows a much more accurate deconvolution of background (constant) and peak intensity (dependent on isotope) and thus thermal parameters. Comparison of the anisotropic thermal parameters with those from single crystal x-ray studies and theoretical measurements are presented.

P12.OD.005 DO PARAELECTRIC CRYSTALS NECESSARILY HAVE A NON-POLAR SYMMETRY GROUP? Xavier Solans, Jorge Mata, M.Teresa Calvet and Mercè Font-Bardia, Departament de Cristal-lografia, Universitat de Barcelona. Spain.

The crystal structures of $LiNH_4SO_4$ at 298, 423, 483, 523 and 571 K have been solved. The three ferroelectric structures (at 298, 423 and 483 K) and the two paraelectric structures at 523 and 571 K show the same group $P2_1nb$, which is polar. According to Neumann's principle the value of a physical parameter should remain invariant if it is subjected to a symmetry operation of its point group. From this, a ferroelectric crystal, which shows spontaneous polarization, requires a polar group for this crystal-type. All crystals with a non-polar space group are paraelectric; but does this imply that all paraelectric crystal must have a non-polar point group?. The experimental results presented here, together with the computation of the spontaneous polarization in each solved structure, using an ionic model, which vanishes at 523 and 571K, show that the non-polar space-group, although it is sufficient condition, is not a necessary condition for paraelectric crystals.

12OE X-RAY OPTICS (sponsored by Microsource, a division of Bede)

M12.OE.001 HIGH ENERGY X-RAY MICROOPTICS FOR DIFFRACTION, IMAGING AND SPECTROSCOPY A. Snigirev, ESRF, BP 220, 38043 Grenoble, France

The last several years have seen a tremendous breakthrough in the development of microoptics for high energy X-rays. Micro- and submicro-meter beams can be generated with Bragg-Fresnel Optics [1], Fresnel Zone Plates and Compound Refractive Lenses [2] in the energy range from 5 to 100 keV. Use of this optics along with high brilliance and spatial coherence of the X-ray beam provided by the third generation synchrotron radiation sources such as ESRF makes possible to realize high energy X-ray microscopy techniques. X-ray micro- diffraction [3], fluorescence [4] and imaging [5,6] are very powerful techniques for the nondestructive studies in material science and biology. The micro- fluorescence, imaging and diffraction beamline (micro-FID) has been successfully commissioned at the ESRF and various microscopy applications to study samples from biology, geology and material science have been performed.

1. I. Snigireva, A. Souvorov, A. Snigirev, "X-ray Microscopy and Spectroscopy" Eds.: J. Thieme, G. Schmahl, D. Rudolph, E. Umbach, Springer-Verlag, Berlin Heidelberg, 1998, IV37 - IV44.
2. A. Snigirev, V. Kohn, I. Snigireva, B. Lengeler, Nature, vol. 384, 49-51, 1996.

3. H. Biermann, B. Grossmann, S. Mechsner, H. Mughrabi, T. Ungar, A. Snigirev, I. Snigireva, A. Souvorov, M. Kocsis, C. Raven, Scripta Materiala, vol. 37, No. 9, 1309-1314, 1997.
4. F. Adams, K. Janssens, A. Snigirev, Journal of Analytical Atomic Spectrometry, vol. 13, 319-331, 1998.
5. Z. H. Hu, P. A. Thomas, A. Snigirev, I. Snigireva, A. Souvorov, P. G. R. Smith, G. W. Ross, S. Teat, Nature, vol. 392, 690-693, 1998.
6. A. Koch, C. Raven, A. Snigirev, P. Spanne, J. Opt. Soc. Am. A, vol. 15, No. 7, 1940-1951, July 1998.

M12.OE.002 PHASE-CONTRAST IMAGING AND PHASE RETRIEVAL USING X-RAYS. S.W. Wilkins[a], D. Gao[a], T.E. Gureyev[b], A. Pogany[a], and A.W. Stevenson[a] , [a]CSIRO, Manufacturing Science & Technology, PB33 Clayton Sth MDC, Clayton, Vic 3169 Australia [b] CSIRO, Forestry & Forest Products, PB10 Clayton Sth MDC, Clayton, Vic 3169 Australia.

Conventional X-ray radiography which has prevailed for the past 100 years relies on differential absorption in a sample to produce contrast. Recently a variety of methods for producing X-ray contrast via refractive (i.e. phase) effects have been proposed, see [1] and [2] and references therein. Our emphasis is on *in-line imaging* using high spatial coherence sources both in the laboratory [3] and at SR facilities [4]. Discussion of some of the key theoretical aspects of this work will be presented, including:i) non-interferometric methods for phase/amplitude retrieval [5-7], ii) the effects of *partial coherence* [6], and iii) factors affecting *contrast and resolution* [6]. Experimental results will also be presented demonstrating the very significant levels of new information that can be gained by these techniques, pointing to exciting new imaging applications for X-rays in science, medicine, and industry.

1. U. Bonse & M. Hart. *Appld. Phys. Letts.* 6, (1965) 155-6; *Z. Phys.* 188, (1965) 154-64; *Acta Cryst.* A 24, (1968) 240-5.
2. T.J. Davis, D. Gao, T.E. Gureyev, A.W. Stevenson, and S.W. Wilkins, *Nature* 373, (1995) 595-8.
3 S.W. Wilkins, T.E. Gureyev, D. Gao, A. Pogany, and A. Stevenson, *Nature* 384, (1996) 335-8.
4. A. Snigirev, I. Snigireva, M. Suvorov, M. Kocsis,., & V. Kohn, *Rev. Sci. Instrum*. 66, (1995) 5486-92.
5. K.A. Nugent, T.E. Gureyev, D. Cookson,, D.Paganin, & Z.,Barnea, *Phys. Rev. Letts.* 77, (1996) 2961-4.
6. A. Pogany, D. Gao, & S.W. Wilkins,. *Rev. Sci Instrums* 68, .(1997) 2774;
7. Gureyev T.E. and Wilkins S.W., *J.Opt.Soc.Am. A* 15, (1998) 579-85. *Optics Comm.* 147, (1998) 229-32.

M12.OE.003 X-RAY WAVEGUIDES: A NOVEL OPTICS FOR NANO-DIFFRACTION. S. Lagomarsino and A. Cedola, Istituto Elettronica Stato Solido (IESS) - CNR, 00156 Roma, Italy and S. Di Fonzo and W. Jark, Sincrotrone Trieste - 34012 Basovizza - Trieste, Italy and C. Giannini and L. De Caro, CNRSM, 72100 Brindisi, Italy

Sub-micrometric X-ray beams can be produced by waveguides for medium-high energy x-rays (13-30 KeV). The waveguides consist in a multilayer structure constituted of: an ultra-flat substrate; a metal layer few tens of nm thick; a layer of low-density material (for ex. C) having a thickness of the order of 100 nm; a thin (few nm) metal film. A collimated x-ray beam impinging at grazing incidence on such a structure is subjected, at given incidence angles, to a resonance effect which can enhance the e.m. intensity inside the C film of tens or hundreds times with respect to the incident intensity[1]. When the resonance condition is met, the beam can travel along the film and come out at its end. The beam is highly coherent and in the first resonance has a divergence of about 1 mrad. In a vertical section it can be well approximated to a Gaussian beam originated by a point source[2]. With this beam we obtained phase contrast images with record resolution of 140 nm.[3] Here we will concentrate on the diffraction application. We demonstrate the possibility to measure Reciprocal Space Maps with a spatial resolution down to 100 nm or less. We applied this technique to the evaluation of local strain generated on the Si substrate by the edges of oxide stripes of different widths. A discussion on the potentialities of this novel technique will be given.

[1] S. Lagomarsino, W. Jark, S. Di Fonzo, A. Cedola, B. Mueller, P. Engstrom, and C. Riekel, J. Appl. Phys. **79**, 4471 (1996)
[2] W. Jark, S. Di Fonzo, S. Lagomarsino, A. Cedola, E. Di Fabrizio, A. Brahm, and C. Riekel, J. Appl. Phys. **80**, 4831 (1996)
[3] S. Lagomarsino, A. Cedola, P. Cloetens, S. Di Fonzo, W. Jark, G. Soullié and C. Riekel, Appl. Phys. Lett., 71, 2557 (1997)

M12.OE.004 MULTILAYER MIRRORS. James H. Underwood, Center for X-ray Optics, Lawrence Berkeley National Laboratory, University of California, Berkeley, CA USA 94720

Using modern vacuum deposition technology, structures consisting of alternating layers of high- and low-Z materials, with individual layers having thicknesses of the order of nm, can be fabricated on suitable substrates. These structures act as multilayer interference reflectors for x-rays, soft x-rays and extreme ultraviolet (EUV) light. Their high reflectivity and moderate energy bandwidth ($10 < E/\Delta E < 100$) make them a valuable addition to the range of optical components available to construct instrumentation for x-rays with photon energies from a few keV to tens of keV. They are particularly useful in synchrotron radiation beamlines as mirrors and dispersive elements. They may be used to for produce focal spots with micrometer scale sizes, for applications such as fluorescent microprobing, microdiffraction and microcrystallography. Multilayer reflectors also have a wide range of applications at lower photon energies, in particular in the EUV region, where normal incidence multilayer reflectors allow the construction of space telescopes and optics for EUV lithography. This paper outlines the principles of the design of multilayer reflectors, in particular the choice of materials and the limitations imposed on performance by substrate and layer roughness. A representative variety of applications is discussed.

M12.OE.005 TUNABLE X-RAY POLARIZATION FILTER WITH PERFECT CRYSTALS. Y. Amemiya and Y. Hasegawa, Engineering Research Institute, University of Tokyo, Yayoi, Bunkyo, Tokyo 113, Japan, Y. Ueji, The Graduate University for Advanced Studies, Oho, Tsukuba, Ibaraki 305, Japan, K. Okitsu, National Research Laboratory of Metrology, Umezono, Tsukuba, Ibaraki 305, Japan, J. M. Ablett and D. P. Siddons, NSLS, Brookhaven National Laboratory, Upton, NY 11973, USA.

Conventionally, x-ray linear polarizers have been based on near-45 degree Bragg-case reflections from highly perfect crystals. Typically, they have been realized as multiple-reflection channel-cut devices. Even though such instruments perform well, they suffer from the disadvantage that the polarized beam is non-stationary as the energy is scanned.

The possibility of a transmission-type x-ray linear polarizer is investigated using a thin Bragg reflector as a polarizing filter. In this device, the transmitted beam (rather than the Bragg-reflected beam) is the useful output of the device. Consequently, the position and the direction of the transmitted beam are unchanged as the energy is changed, or even when the polarization direction to be filtered out is changed. Theoretical considerations as well as preliminary transmissivity measurements are presented. We examine the cases in which perfect crystals of silicon and diamond are used. A polarization ratio, defined as IH/IV, higher than 105 was observed in experiments to measure the performance characteristics of the proposed x-ray polarizing

reflector. The transmission-type x-ray linear polarizer is well suited for spectroscopic measurements with polarized x-rays. Future applicaitons of this polarization filter are presented.

Present address1: Department of Applied Physics, University of Tokyo, Hongo, Bunkyo, Tokyo 113-8656, JAPAN
Present address2: Engineering Research Institute, University of Tokyo, Yayoi, Bunkyo, Tokyo 113-8656, JAPAN

M12.OE.006 X-RAY DIFFRACTION IN FINITE PERFECT CRYSTALS. G. Thorkildsen, Department of Mathematics and Natural Science, Stavanger College, Ullandhaug, 4004 Stavanger, Norway.

The boundary-value Green function technique has been used along with the Takagi-Taupin equations [1] to investigate diffraction phenomena in finite perfect crystals subject to an incoming plane wave. This includes extinction, absorption and rocking curve calculations [2]. Starting from Maxwells equations in a periodic dielectric medium, the differences and similarities between the present approach and the fundamental theory of dynamical scattering [3] are discussed. The geometrical region structures associated with point sources [4], the surface integrations necessary to calculate diffracted power and the concept of extended volumes [5] are explored. The displacement fields are handled either by series expansions or in the case of straight line boundaries by analytical functions provided by Uragami [6]. Anomalous scattering are included using a complex expansion parameter. Scattering planes with circular, rectangular and triangular shapes are studied. Examples of numerical results are related to silicon and germanium.

1. Takagi, S.(1969) *J. Phys. Soc. Jpn,* **26**, 1239-1253.
2. Thorkildsen, G. & Larsen, H.B. (1998) *Acta Cryst.* A**54**, 172-185, 186-190, 416-429.
3. Pinsker, Z. G. (1978) *Dynamical Scattering of X-rays in Crystals*. Berlin: Springer-Verlag.
4. Saka, T., Katagawa, T. & Kato, N. (1972) *Acta Cryst.* A**28**, 102-113, 113-120.
5. Becker, P. (1977) *Acta Cryst.* A**33**, 667-671.
6. Uragami, T. S.(1971) *J. Phys. Soc. Jpn,* **31**, 1141-1161.

P12.OE.001 THE STANDING WAVE FORMED BY GRAZING-INCIDENCE X-RAYS IN A MULTILAYER WITH PLANES NORMAL TO SURFACE. P.A. Bezirganyan (Jr.), Dep. of Computer Science, State Engineering University of Armenia, #6, Korjune St., Yerevan 375009, Armenia, and A.P. Bezirganyan and S.E.Bezirganyan, Dep. of Physics, Yerevan State University, #1, A. Manoogian St., Yerevan 375025, Armenia, and H.A. Bezirganyan (Jr.), Dep. of Informatics and Applied Mathematics, Yerevan State University, #1, A.Manoogian St., Yerevan 375025, Armenia.

X-ray standing waves (XSW) in multilayers have been observed (see the pioneer papers [1-3]) by fluorescence measurements similar to those using natural crystals. In the grazing angle incidence x-ray dif-fraction (GID) geometry the XSW technique uses the dynamical x-ray standing wave fields formed very close to sample entrance surface by the lattice planes perpendicular or nearly perpendicular to this surface. Above the sample surface the entire wave field intensity is periodical and is modulated along this surface (e.g. see [4]).

We consider X-ray GID by a periodical multilayer with layers' interface planes normal to vacuum-multilayer entrance surface, and assume that two types of amorphous layers have enough optical contrast to give a strong diffraction. The XSW technique in the GID case makes it possible to study atomic arrangement (correlation) and interfaces of multilayers very close to entrance surface. The mathematical model corresponding to the investigated amorphous multilayer is constructed. The description of the standing wave formation is based on the method of construction of eigenvalues and eigenfunctions for this model.

1. J.H. Underwood & T.W. Barbee (1981). Appl.Opt., 20, 3027.
2. T.W. Barbee & W.K. Warburton (1984). Mater.Lett., 3, 17.
3. J.B. Kortright & A.Fischer-Colbrie (1987). J.Appl.Phys, 61 (3), 1130.
4 A.P. Bezirganyan & P.A. Bezirganyan (1988). Phys.Stat.Sol.(a), 105, 345.

P12.OE.002 OPTICAL COMPONENTS FOR POLARIZATION ANALYSIS OF SOFT X-RAY RADIATION. H. Grimmer, M. Horisberger, S. Tixier, O. Zaharko, Paul Scherrer Institute, CH-5232 Villigen PSI, Switzerland, H.-Ch. Mertins and F. Schäfers, BESSY, D-14195 Berlin, Germany.

An instrument for measuring polarization typically consists of a phase shifter and a linear polarizer. Up to 600 eV, periodic structures can be used consisting of alternating layers of two materials, one of which has an absorption edge in the photon energy region of interest [1]. The phase shift of the transmitted beam and the intensity of the reflected beam show maxima at energies just below the edge. By means of DC magnetron sputtering, phase shifters have been deposited on 100 nm thick Si_3N_4 films and linear polarizers on Si wafers. The latter were designed to work at the Brewster angle, where only s-polarized radiation is reflected. The corresponding multilayer period decreases from 8.5 nm at 100 eV to 1.4 nm at 600 eV. A reflectance of 6.8% was obtained at 512 eV for 150(V/Ni). It was shown that an Al coating reduces the oxidation of Ti/Ni multilayers.

In order to extend polarization measurements into the 1 keV region, the use of magnetic effects like magnetic circular dichroism (MCD) is being explored. This effect has been measured in 100(Fe/C) transmission multilayers close to the Fe L edge (700-750 eV). It is expected to be largest if the magnetic moments are aligned ferromagnetically and parallel or antiparallel to the beam direction, i.e. perpendicular to the layer surface. This can be realized at room temperature in periodic multilayers with 1 nm thick FeCoV layers separated by nonmagnetic layers, as shown for FeCoV/Ce by Moessbauer spectroscopy [2]. Presently, thin films of transition metal/rare earth metal alloys are being produced and investigated, in which perpendicular spin orientation at room temperature is also expected.

1. H.-Ch. Mertins et al., Synchrotron Radiation News 11 (1998) 42-46.
2. S. Tixier et al., Physica B 234-236 (1997) 473-474.

P12.OE.003 RAY-TRACING STUDY OF A PARALLEL-BEAM TWO-AXIS DIFFRACTOMETR FOR POWDER AND THIN-FILM DIFFRACTION. H. Toraya, H. Hibino and T. Ohnish, Ceramics Research Laboratory, Nagoya Institute of Technology, Tajimi 507-0071, Japan

A two-axis diffractometer was built for versatile uses in powder and thin-film diffraction in x-ray laboratory. Its design is based on a parallel-beam optics using flat-specimen reflection geometry and capillary-specimen transmission geometry. The diffractometer consists of two rotary tables (Huber 410 and 420) for the θ and 2θ axes and an encoder (Heidenhein, ROD 800) for reading the 2θ angle. Optical elements on the incident beam side were a parabolic multi-layer mirror, channel-cut crystal monochromators and slit systems. Horizontal parallel-slits or a flat analyzer crystal can be equipped on a detector arm together with a scintillation counter with a maximum count rate of 3M cps (Rigaku, SC300). These elements can be selectively combined in order to fit with experimental purposes, requiring narrow and strictly monochromatic beam or less parallel beam but with more flux. Ray-tracing was first conducted for analyzing the performance of each optical component. Its results were further

examined by comparing them with theoretical models, when they are available, and observed profiles. Results of the present study provide useful information for simulating instrumental alignment, interpreting the shapes of observed diffraction profiles, evaluating the precision of the diffractometer, and optimizing the optics.

P12.OE.004 HIGH ENERGY X-RAY MICROSCOPY WITH COMPOUND REFRACTIVE LENSES. I. Snigireva, M. Drakopoulos, A. Snigirev [1], B. Lengeler, C. Schroer, M. Richwin, J. Tummler, B. Benner [2], [1] ESRF, B.P. 220, 38043 Grenoble, France, [2] Physicalisches Institut, RTWH Aachen, 52062 Aachen, Germany

Recently compound refractive lenses made from low-Z materials have been proposed and already applied for focusing high energy X-rays [1-3]. In the present paper, we describe refractive lenses with a parabolic profile and rotational symmetry around the optical axis. They are genuine imaging devices, similar to glass lenses for visible light. The lenses focus in two directions. Due to their parabolic shape they show practically no spherical aberration. They can withstand the full radiation ("white beam") of an ESRF undulator source and might therefore be suited to be used together with future free electron laser sources.

Based on these lenses a high energy X-ray microscope for microdiffraction, microimaging and microfluorescence was proposed and tested at the ESRF ID22 beamline. A focal spot size in the order of micrometer was achieved in energy range from 12 keV to 40 keV. First applications for stress analysis in deformed steels and microspectroscopy (microEXAFS and microXANES) were realized and results will be presented in the paper. In the imaging mode it was demonstrated that an area 300 mm in diameter with resolution of about 0.3 microns can be imaged with 15 - 30 keV X-rays [4]. Implementation of refractive lenses with parabolic profile opens up an interesting perspective for high-resolution diffraction and imaging techniques.

1. A. Snigirev, V. Kohn, I. Snigireva, B. Lengeler, Nature,vol. 384, 49-51, 1996.
2. A. Snigirev, V. Kohn, I. Snigireva, A. Souvorov, B. Lengeler, Applied Optics, vol. 37, No. 4, 653-662, February 1998.
3. B. Lengeler,. Tummler, A. Snigirev, I. Snigireva, C. Raven, Journal of Applied Physics, vol. 84, No. 11, 5855-5861, 1998.
4. B. Lengeler, M. Richwin, C. Schroer, J. Tummler, M. Drakopoulos, I. Snigireva, A. Snigirev to be published.

P12.OE.005 A COMPARISON OF OPTICS SYSTEMS FOR MACROMOLECULAR CRYSTALLOGRAPHY, Joseph D. Ferrara, Cheng Yang, Adam Courville, Molecular Structure Corporation, The Woodlands, TX, 77380, USA.

We have done a complete and detailed evaluation of different multilayer optics systems (Osmic Cross-coupled MaxFlux Optics and Osmic Confocal MaxFlux Optics) as compared to MSC/Yale Total Reflection Mirrors. We have studied the usable flux, spectral purity, divergence, beam profile and data quality. The most striking results have been obtained using the Osmic #4 and Osmic #7 Confocal MaxFlux Optics, which were designed for 0.1 mm and 0.2 mm focal spots, respectively, in conjunction with a 0.3 mm focal spot. These optics configurations provide a 5.8-fold increase in flux and an 8.2-fold increase in flux through a 0.2 mm diameter area as compared to the MSC/Yale Mirrors. The balance of flux and divergence in the context of the single crystal x-ray diffraction experiment will be discussed in light of these results.

P12.OE.006 EVALUATION OF PARALLEL BEAM OPTICS FOR POWDER DIFFRACTOMETERS. S.T. Misture, New York State College of Ceramics at Alfred University, Alfred, NY 14802, USA

The use of multilayer and capillary optics on powder diffractometers for powder diffraction, thin film diffraction, and reflectivity will be presented. Evaluations were based on instrumental resolution, accuracy of lattice parameters, peak-to-background ratios, absolute intensities, and Rietveld results. Advantages and disadvantages of various instrumental configurations will be discussed.

Several powder specimens with a broad range of absorption coefficients were measured with internal standards, as well as several thin films and commercial thin film coatings.

Using an incident-beam graded multilayer optic for parallel beam measurements increased the absolute intensities by 3 to 6 times and increased the peak-to-background ratios by 2 to 6 times, compared to 'parallel' beam measurements using Soller collimators. In addition, the instrumental resolution and x-ray profile shape is improved significantly when the optic is used, because of the parallel nature of the incident beam.

Adding a second multilayer optic to the receiving side improves the resolution and peak-to-background further, and provides ample collimation to perform 'parallel-beam' x-ray reflectivity. Reflectivity data indicate that order-of-magnitude improvements in dynamic range may be obtained with resolution similar to that possible with parafocusing instruments.

P12.OE.007 TECHNIQUES AND LABORATORY APPLICATIONS FOR FOCUSED BEAM X-RAY DIFFRACTION. N. Loxley, D.K. Bowen, G. Fraser, M. Taylor and J. Wall, Bede Scientific Instruments Ltd, Durham, UK and L. Pina, A. Inneman, R. Hudec, Reflex sro, Prague CZ

The production and use of "microfocused" X-ray beams for materials diffraction and fluorescence was initiated in synchrotron radiation sources in the early 1980s. Recently, focused beams with high intensities have been achieved in the laboratory. The technology of these beams will be reviewed. Synchrotron radiation sources have clear advantages when sub-micron beams are required but in the range from approximately 5 μm to 1 mm, microfocus X-ray sources are highly effective. It is essential to tailor the size, divergence and intensity of these "minibeams" to the measurement, and we shall review the range of applications in relation to the available source/optics combinations. Two applications resulting from our recent X-ray optics research are discussed in more detail. The first is the in-process evaluation of semiconductor wafers by diffraction from an area no larger than a single die, typically 0.5 × 0.5 mm. This extends the application of on-line XRD in the semiconductor fabrication industry from the examination of whole wafers or "witness" samples to a much later stage in the process. The "monitor die" is masked off from the etching processes, but is exposed to all the deposition processes (epitaxial or thin film). Hence it can be used to monitor parameters such as composition and thickness of the layers even at advanced stages of the process, at a loss of only 10^{-5} of the potential yield.

The second is the identification of "library" compounds generated in the relatively new field of combinatorial chemistry. This method mimics the methods of the human immune system for selecting effective antibodies from a library of some 10^{12} antibodies. Combinatorial chemistry has been used for over a decade in drug generation and organic chemistry synthesis and is now moving into the field of materials science. In this application, hundreds or thousands of compounds are synthesized in parallel on a wafer. This is effected by deposition of combinations of thin films of source materials through a set of masks so that each cell (also typically 0.5 mm square) contains a different combination. The wafers are then reacted to form the compounds, and tested for

the desired properties. The technique has so far been very successful in identifying new magnetic materials with high GMR, high-temperature superconductors and luminescent materials. However, with previous X-ray technology, bulk samples had to be grown separately to characterize the structures. This is a slow process and, moreover, important structural characteristics of the film might be lost. The ability to take rapid, high-quality XRD data from sub-mm areas and analyze them with a search/match program that can be configured for the combinatorial problem, such as the Bede ZDS program, will provide higher and more accurate throughput in this important field.

12OF GIANT MAGNETO RESISTANCE MATERIALS

M12.OF.001 CHARGE ORDERING IN MANGANITES: IS THE Mn(III)-Mn(IV) PICTURE APPROPRIATE?. Juan Rodríguez-Carvajal, Laboratoire Léon Brillouin (CEA-CNRS), CEA/Saclay, 91191 Gif sur Yvette Cedex, FRANCE.

Charge ordering (CO) in manganites, of composition close to that of the CMR materials, is supposed to be the consequence of a spatially periodic charge localisation giving rise to well defined Mn(III) and Mn(IV) ionic species. The basic driving force is the Coulomb repulsion between electrons eventually associated with electron-lattice couplings as the Jahn-Teller effect. We discuss the results obtained from neutron diffraction experiments demonstrating that the Mn(III)-Mn(IV) picture *is not appropriate* to describe CO in Mn-perovskites. We shall compare the Mn-O distances, polyhedra distortions and valence-bond calculations on the low temperature crystal structure of the spinel $LiMn_2O_4$ [1] with those obtained for perovskites. The comparison shows that the ionic picture is well supported in the case of $LiMn_2O_4$ but not in perovskites as $R_{1/2}D_{1/2}MnO_3$ (R=La, Pr; D=Sr, Ca). The average Mn-O distances for the different crystallographic Mn-sites in $LiMn_2O_4$ are distributed in two groups consistent with the presence of Mn(III) (d=2.01 Å) and Mn(IV) (d=1.91 Å) species. In Mn-perovskites there is no evidence of such a strong difference between different Mn-sites in the published data. Recent results obtained from single crystal neutron diffraction experiments on Mn-perovskites do not provide any crystallographic evidence of well defined Mn(III)-Mn(IV) ordering. The best simple description of the CO phenomenon in perovskites should be constructed in terms of fractional orbital occupation on both Mn d-orbitals and oxygen p-orbitals.

1. J. Rodríguez-Carvajal *et al*, Phys. Rev. Lett. 81, 4660 (1998).

M12.OF.002 THE CHARGE ORDERING AND MAGNETIC TRANSITIONS IN Mn^{3+}/Mn^{4+} PEROVSKITES, Z. Jirak, Institute of Physics, Prague, Czech Republic.

Recent data on the low-temperature structures and antiferromagnetic arrangements in the $Ln_{1-x}A_xMnO_3$ perovskites give new insight into the nature of charge and/or orbital ordered states and their temperature evolution. It appears that manganites in the compositional region of so-called T' (pseudotetragonally elongated) structure (0.85>x>0.75) and some compounds of the $I4_1/mcm$ parent symmetry in the T (pseudotetragonally compressed) region (0.75≥x>0.3) show an orbital ordering (polarization) with no charge order. In that case the e_g electrons are homogeneously distributed over all manganese sites. They occupy orbitals which are aligned into rows or planes and the magnetic structures are of the C and A type, respectively. On the other hand, the phases of the Pnma or Imma parent symmetry in the T region exhibit the concomitant charge and orbital ordering. To our knowledge, it occurs exclusively for ideal Mn^{3+}/Mn^{4+} ratios of 1:1, 1:2 and 1:3 (x=0.5, 0.67 and 0.75). The magnetic structures are of the CE type or analogous. A departure from the ideal Mn^{3+}/Mn^{4+} ratios results in an electronic phase separation and a phase with delocalized e_g electrons may be formed as found both for x<0.5 and x>0.5 . This second phase is distinguished by the metrics of the perovskite lattice which is rather pseudocubic and by the ferromagnetic coupling between the (antiferromagnetic) CE-like planes. It should be noted to the above mentioned charge ordered structures that, even if the valence distribution is regular, there is often certain orbital disorder on the Mn^{3+} sites known as discommensurations. The array of these discommensurations changes with decreasing temperature, supposedly by a dislocation process, and the structure tends to an ideal (commensurate) order.

M12.OF.003 EFFECT OF OXYGEN ISOTOPE SUBSTITUTION ON MAGNETIC STRUCTURE OF $(LA0.25PR0.75)0.7CA0.3MNO3$ V. Yu. Pomjakushin, A. M. Balagurov, D. V. Sheptyakov [1], P. Fischer [2], N. A. Babushkina [3]. [1] Joint Institute for Nuclear Research, 141980, Dubna, Moscow region, Russia, [2] Paul Scherrer Institute (PSI), CH-5232 Villigen PSI, Switzerland, [3] RSC ``Kurchatov Institute", Kurchatov sq.1, 123182, Moscow, Russia

The oxygen isotope effect on the magnetic structure and charge ordering in $(La_{0.25}Pr_{0.75})_{0.7}Ca_{0.3}MnO_3$ was studied by neutron powder diffraction. At first it was found that two investigated samples, one of those contained the natural mixture of isotopes (99.7% ^{16}O, metallic at T<=100K), and the other one enriched by ^{18}O in 75% (insulating in all temperature range) are structurally identical at room temperature. At the temperature lowering the sample with ^{16}O undergoes subsequent antiferromagnetic T(AFM)=150K) and ferromagnetic (T(FM)=110K) transitions, resulting in the non-collinear FM structure, while in the sample with ^{18}O the pure AFM ordering (T(AFM)=150K) is revealed. No indications of phase segregation at low temperature were found.

M12.OF.004 SPIN-CHARGE-LATTICE COUPLING IN REDUCED DIMENSIONS IN THE CMR OXIDE $La_{2-2x}Sr_{1+2x}Mn_2O_7$, x=0.3-0.5 Dimitri N. Argyriou [1], John F. Mitchell [1], Jason Gardner [2], Paolo G. Radaelli [3], David E. Cox [4], Heloisa N. Bordallo [1] and James D. Jorgensen. [1.] Argonne National Laboratory, Argonne, IL 60439, USA, [2] Los Alamos National Laboratory, Los Alamos, NM, 87545, [3] ISIS Facility, Rutherford Appleton Laboratory, Chilton. OX11 0QX, UK, [4] Brookhaven National Laboratory, Upton, NY, 11973

Spin-charge-lattice degrees of freedom in the layered CMR manganites $La_{2-2x}Sr_{1+2x}Mn_2O_7$ result in a rich structural and magnetic phase diagram over a relative small compositional range (0.3<x<0.5). We find that the electronic doping (x) plays a critical role in varying the degree and direction of the spin-charge-lattice coupling. Using neutron diffraction measurements we have measured the structural properties of these materials as a function of temperature and pressure through the coincident insulator-metal and magnetic transitions at T_{IM}. We find that charge is transferred predominately to Mn $d_{x^2-y^2}$ orbitals below T_{IM} for compositions x<0.36 and to $d_{3z^2-r^2}$ orbitals for 0.36<x<0.4. Accompanying these variations in orbital occupancy of the Mn ion, are pronounced changes in the spin arrangement below T_{IM}. For x=0.3 we find an antiferromagnetic structure along the *c*-axis that exhibits antiferromagnetic inter-bilayer coupling while the intra bilayer coupling remains ferromagnetic. For 0.32<x<0.36 we find a ferromagnetic structure with the easy axis along *c*, while for 0.36<x<0.4 the easy axis is in the *ab*-plane. For x=0.5, equal amounts of Mn^{3+} and Mn^{4+} ions order below T_{CO}~200K. Unlike similar phenomena observed in the manganite perovskites this charge ordered state is only stable between ~200-100 K.

M12.OF.005 ORBITAL ORDERING AND ANISOTROPIC BEHAVIOR IN $Nd_{1-x}Sr_xMnO_3$. H. Kawano, Solid State Division, Oak Ridge National Laboratory, Oak Ridge, Tennessee 37831, R. Kajimoto and H. Yoshizawa, Neutron Scattering Laboratory, I. S. S. P., University of Tokyo, Tokai, Ibaraki, 319-1106, Japan, H. Kuwahara*, Joint Research Center for Atom Technology (JRCAT), Tsukuba, Ibaraki 305-8562, Japan, Y. Tokura, JRCAT, Tsukuba, Ibaraki 305-8562, Japan and Department of Applied Physics, University of Tokyo, Bunkyo-ku, Tokyo 113-8656, Japan, K. Ohoyama and M. Ohashi**, Institute for Materials Research, Tohoku University, Sendai 980-8577, Japan *PRESENT ADDRESS : Faculty of Science and Technology, Sophia University, Chiyoda-ku, Tokyo 102-8554, Japan. **PRESENT ADDRESS :Faculty of Engineering, Yamagata University, Yonezawa, Yamagata 990-8510, Japan.

We have performed neutron diffraction measurements on melt-grown polycrystalline samples of $Nd_{1-x}Sr_xMnO_3$ system with $0.49 < x < 0.75$[1]. As a function of x, the system shows a systematic variation of the magnetic and crystal structures. We found that this variation is accompanied by a change of the character of the Mn e_g orbitals. The MnO_6 octahedra are apically compressed in the CE-type and A-type antiferromagnetic (AFM) states due to the $d(3x^2-r^2)/d(3y^2-r^2)$ or $d(x^2-y^2)$ orbital orderings, respectively, whereas in the C-type AFM state, they are apically elongated by the rod-type $d(3z^2-r^2)$ orbital ordering. In addition, we have performed inelastic neutron scattering experiments on the spin dynamics in the Ferromagnetic [2] and the A-type AFM[3] states of $Nd_{1-x}Sr_xMnO_3$. Spin wave spectra in both states shows a distinct two-dimensional character. We will discuss that these results can be consistently interpreted from a viewpoint of the underlying orbital orderings.

[1] R. Kajimoto et al., (unpublished)
[2] H. Kawano et al., cond-mat/9808286
[3] H. Yoshizawa et al., Phys. Rev. B **58**, R571 (1998).

P12.OF.001 THE EFFECT OF CONFORMAL ROUGHNESS ON SPIN-VALVES. J. Clarke and B.K. Tanner Department of Physics, University of Durham, South Road, Durham. DH1 3LE U.K. and C.H. Marrows, F.E. Stanley and B.J. Hickey, Department of Physics and Astronomy, University of Leeds, Leeds. LS2 9JT U.K. and R.J.T. Bunyan, Defence Evaluation and Research Agency (DERA), Electronics Sector, St. Andrews Road, Malvern, Worcestershire. WR14 3PS U.K.

Equivalent spin-valves grown on silicon oxide substrates produced either by thermal oxidation of Si (100) wafers or low pressure chemical vapour deposition of the oxide have been studied by x-ray scattering, atomic force microscopy and magnetotransport measurements. Grazing incidence x-ray scattering measurements have also been made on the bare substrates. The x-ray measurements, supported by atomic force microscopy images, show a large difference not only between the roughness of the two substrate types but also that of the spin-valves deposited on them. A high degree of conformality is observed in the roughness of the spin-valves. Magnetoresistance measurements made on the spin-valves show that the switching point of the sample grown on the low pressure chemical vapour deposited substrate is shifted away from the ideal zero point due to increased coupling and both the giant magnetoresistance and exchange field are seen to fall with increasing roughness.

P12.OF.002 PECULIARITIES OF ATOMIC AND MAGNETIC STRUCTURES OF $(La_{1-y}Pr_y)_{0.7}Ca_{0.3}MnO_3$ ($0.50 \le y \le 0.75$). D.V. Sheptyakov, A.M. Balagurov, V.Yu. Pomjakushin and V.L. Aksenov, Frank Laboratory of Neutron Physics, JINR, Dubna, Russia, and N.A. Babushkina and L.M. Belova, RRC Kurchatov Institute, Moscow, Russia, and O.Yu. Gorbenko and A.R. Kaul, Chemistry Department, Moscow State University, Moscow, Russia, and P. Fischer, M. Gutmann and L. Keller, PSI, Villigen, Switzerland.

Evolution of structural and magnetic properties of the CMR-compound $(La_{1-y}Pr_y)_{0.7}Ca_{0.3}MnO_3$ has been studied by neutron diffraction in the temperature range from 10 to 293 K for several compositions ($0.50 \le y \le 0.75$). It is shown that changes in transport and magnetic properties are directly connected with rearrangement of the atomic structure. Phase transition to the metallic state arises at the same time with ferromagnetic ordering of manganese moments. The dramatic oxygen isotope effect on the magnetic structure and charge ordering is found for $(La_{0.25}Pr_{0.75})_{0.7}Ca_{0.3}MnO_3$. At the temperature lowering the sample with ^{16}O undergoes subsequent antiferromagnetic and ferromagnetic transitions, resulting in the non-collinear FM structure, while in the sample with ^{18}O the pure AFM ordering is found. The temperature dependencies of the diffraction peak intensities associated with charge ordering are also quite different in the samples with ^{16}O and ^{18}O and correlate with the behavior of the electrical resistivity and the magnetic structure. The temperature dependencies of the unit cell parameters demonstrate several distinctive features: non-linear dependencies close to T_{CO} charge ordering temperature, sharp jump at the temperature of FM ordering, which is also well visible in $V_c(T)$ dependence.

P12.OF.003 MAGNON DAMPING BY MAGNON-PHONON COUPLING IN CMR MANGANITES N. Furukawa Department of Physics, Aoyama Gakuin University, Setagaya, Tokyo 157-8572, JAPAN

We study the magnon damping effect caused by strong magnon-phonon coupling in CMR manganites. Recent neutron scattering experiments show anomalous increase in magnon linewidth as the magnon branch crosses an longitudinal optical phonon branch. Assuming a strong magnon-phonon coupling due to Jahn-Teller interaction in manganites, we theoretically calculate the magnon linewidth as a function of magnon frequency. The result is consistent with the experiment. We also discuss some crucial tests to verify the above dumping mechanism.

12AA CELLULAR AND MOLECULAR REGULATION

M12.AA.001 ERYTHROPOIETIN RECEPTOR ACTIVATION AND SIGNALLING. I.A. Wilson, O. Livnah, and E.A. Stura, The Scripps Research Institute, Department of Molecular Biology, La Jolla, CA 92037 U.S.A., and D.L. Johnson, S.A. Middleton, and L.K. Jolliffe, R.W. Johnson Pharmaceutical Research Institute, Raritan, NJ 08869-0602 U.S.A.

A surprising development in the cytokine receptor field was the discovery of a short 20-residue peptide agonist that mimics the biological activity of the erythropoietin (EPO) natural hormone [1]. The crystal structure of the EPO receptor with an agonist peptide EMP1 showed that the peptide itself dimerizes and induces a symmetric dimerization of the receptor [2] that differs from the asymmetric dimerization of the EPO-EPOR complex [3].

Our recent work has focused on the difference between agonist and antagonist peptides and their effect on receptor dimerization and signal transduction. The antagonist peptide EMP33 can still dimerize the receptor, yet does not cause cell

proliferation [4]. Hence, the nature of the oligomeric assembly seems to play a role in the biological potency of the ligands and in subsequent intracellular phosphorylation events [1, 3, 4]. We have also undertaken x-ray structural studies of the EPO receptor in the absence of bound ligand. The unliganded receptor surprisingly forms a dimer that is substantially different from any peptide or EPO receptor complex. Our data suggest that preformed EPOR dimers occur on the cell surface and that ligand induces a conformational change in the receptor association [5]. Importantly, this model has now been tested on living cells by a protein fragment complementation assay that shows distinct dimer assemblies exist on the cell surface for unliganded and liganded EPOR [6].

1. N. C. Wrighton, et al., Science (1996), 273:458-463.
2. O. Livnah, et al., Science (1996), 273:464-471.
3. R. S. Syed, et al., Nature (1998), 395:511-516.
4. O. Livnah, et al., Nat. Struct. Biol. (1998), 5:993-1004.
5. O. Livnah, et al., Science (1999), 283:in press.
6. I. Remy, et al., Science (1999), 283:in press.

M12.AA.002 STRUCTURAL BASIS OF THE ALLERGIC RESPONSE : STUDIES OF THE HUMAN HIGH AFFINTITY IGE RECEPTOR. T.S. Jardetzky & S.C. Garman, Department of Biochemistry, Molecular Biology and Cell Biology, Northwestern University, Evanston, IL 60208, and J.P. Kinet, Laboratory of Molecular Allergy and Immunology, Harvard Medical School, Boston, MA 02215

The high affinity IgE Fc-receptor (FcεRI) triggers the activation of effector cells, leading to the release of specific mediators of the immune response that initiate allergic reactions, anaphylactic shock and the killing of parasites. Human FcεRI exists in two forms, as an $\alpha\beta\gamma 2$ tetramer or an $\alpha\gamma 2$ trimer. The α subunit is involved in IgE binding and the β and γ subunits are the signal transduction modules. FcεRI belongs to a family of antibody Fc-receptors (FcRs) that play an important role in the immune response by coupling the specificity of secreted antibodies to a variety of cells of the immune system. Fc-receptors that bind IgG (FcγRI, FcγRII, and FcγRIII) mediate a variety of inflammatory reactions, regulate B-cell activation, and also trigger anti-parasitic reactions through phagocytes and potentially Natural Killer cells. Recent experiments with transgenic mice have demonstrated that the FcRs control key steps in the immune response previously thought to be carried out by the complement system.

We have solved the crystal structure of the IgE-binding domains of the FcεRI α-subunit by multiple isomorphous replacement methods [1]. A receptor α-subunit fragment expressed in insect cells yields crystals that diffract X-rays to a resolution of 2.4 Å using a high energy synchrotron source. The receptor is formed of two truncated Ig domains that fold into a bent two-domain structure that is different from other tandem Ig domain structures (figure 1). Carbohydrate moieties are observed at three of the seven N-linked attachment sites. The IgE-binding site has been identified in the second domain of the receptor and includes a prominent loop that projects from the receptor surface. The crystal structure implicates nearby residues in the first domain that may be involved in antibody binding and suggests models for the formation of a complex with the IgE-Fc region. Our structural studies provide a foundation for understanding the specificity and function of this important class of immune-system receptors.

[1] S.C. Garman, J.P. Kinet & T.S. Jardetzky (1998) Crystal structure of the human high-affinity IgE receptor, **Cell**, 95, 951-961

M12.AA.003 ACTIVATION AND INHIBITION OF MAP KINASES. E. J. Goldsmith, B. Canagarajah, Z. Wang, A. Khokhlatchev and M. H. Cobb, Department of Biochemistry, UT Soutwestern Medical Center at Dallas, Dallas, TX 75235-9050.

The MAP kinases transduce of extracellular signals, and phosphorylate and activate transcription factors leading to tranformation, proliferation and other changes in the cellular program. Multiple parallel MAP kinase pathways are differentially responsive to growth factors and environmental stresses. MAP kinases are activated by phosphorylation at two sites. The structure of the active form of the MAP kinase ERK2 shows that phosphorylation forms the active site and P+1 specificity pocket. (B. Canagarajah, A. Khokhlatchev, M. H. Cobb and E. J. Goldsmith (1997). *Cell* **90**, 859-869.) Phosphorylation also promotes dimerization at a site close to the phosphorylation sites in ERK2. Dimerization leads to nuclear retention, and structurally masks a nuclear export signal. (A. V. Khokhlatchev, B. Canagarajah, J. Wilsbacher, M. Robinson, M. Atkinson, E. J. Goldsmith and M. H. Cobb (1998). *Cell* **93**, 605-615.) The dimerization also permits MAP kinases to interact with dimeric transcription factor substrates.

P38, is a MAP kinase acitvated in response to cytokines, and is the protein target of SB203580, an antiinflammitory agent synthesized by Smith Kline Beecham. P38 shares 40% sequence identity with ERK2. Crystallographic analysis of the SKB inhibitors bound to both p38 and ERK2 reveal the origin of specificity of the inhibitors for p38 to be attributable specific amino acid replacements in the active site, and differences in the size and shape of the active site derived from distal amino acid replacements. These data provide insight into how to make specific protein kinase inhibitors. (Z. Wang, B.J. Canagarajah, J. C. Boehm, S. Kassis, M. H. Cobb, P. R. Young, S. Abdel-Meguid, J. L. Adams, and E. J. Goldsmith (1998). *Structure* **6**, 1117-1128.)

M12.AA.004 RECOGNITION AND REGULATION IN TYROSINE KINASE SIGNALLING CASCADES Michael J. Eck, Department of Biological Chemistry and Molecular Pharmacology, Harvard Medical School, and the Dana-Farber Cancer Institute, 44 Binney Street, Boston MA 02115

Activation of growth factor or immune receptors on the cell surface initiates a cascade of tyrosine phosphorylation events that induces recruitment and activation of down-stream signalling proteins. Faithful execution of the appropriate signalling program requires tight control of the activity of these cytoplasmic signalling enzymes, which include non-receptor tyrosine kinases, phosphatases, and phospholipases. How are such enzymes activated in a manner that is tightly coupled to their appropriate sub-cellular localization? Crystal structures of the Src tyrosine kinase, SHP-2 phosphatase, and the adaptor protein c-Cbl will be discussed to show how modular domains such as SH2 and SH3 domains have evolved dual roles as both “recognition” and “regulatory” modules, and how they have divergently evolved to coordinate recognition with catalytic activation. The Cbl structure suggest that these signalling domains may in turn be regulated by other cellular inputs.

M12.AA.005 POWERING THE ABC TRANSPORTER: THE STRUCTURE OF THE ATP-BINDING CASSETTE, RBSA at 1.6Å RESOLUTION. Cynthia Stauffacher[1], Shelly Armstrong[1], Huide Zhang[2], Lydia Tabernero[1], and Mark Hermodson[2], [1]Department of Biological Sciences, [2]Department of Biochemistry, Purdue University, Lilly Hall, State Street, West Lafayette, IN

The structural family of ABC transporters are involved in the unidirectional transport of a wide variety of molecules across

membranes. Multiple different ABC transporters have been found in the genomes of species from bacteria and archeabacteria to mammals, and include a number of transporters involved in human disease. These molecules all contain a minimum of two copies of an integral membrane domain and two copies of an ATPase domain, called the ABC, or ATP-binding cassette. Although the sequence identity of these transporters is not high, three signature regions in the ATP-binding domain of the transporter define the class. We have undertaken the X-ray crystallographic study of the ATP-binding cassette of the ABC transporter, RbsA/C, and have solved the 1.6Å structure of the N-terminal RbsA ABC with bound MgADP. The RbsA ABC revealed is a three-layered mixed alpha/beta structure with a barrel-like domain containing the nucleotide binding site. The overall structure of the molecule bears little resemblance to other ATPases, although the nucleotide binding site does show local similarity, particularly in the region of the Walker A and B motif structures. The MgADP is bound in a relatively open pocket with a clearly defined site for the gamma phosphate, and a set of tightly bound water molecules, one of which appears to be held in a position suitable for participation in catalysis. The ABC transporter signature motif does not appear to be part of the active site of RbsA, but is located on a separate helical domain, which we propose is involved in interdomain interactions important for transport function. Homology modeling based on the RbsA ATP-binding cassette has now been used for the analysis of other members of the ABC transporter family, such as the multidrug resistance P-glycoprotein and the CFTR channel protein.

P12.AA.001 STRUCTURE OF MAMMALIAN IMPORTIN α REVEALS AUTOINHIBITION BY A PSEUDO-NUCLEAR LOCALIZATION SIGNAL. T. Teh and B. Kobe, Structural Biology Laboratory, St. Vincent's Institute of Medical Research, 41 Victoria Parade, Fitzroy, Victoria 3065, Australia.

Nuclear proteins are synthesised in the cytoplasm and need to be imported into the nucleus through the nuclear pore complexes. Such import is directed by special signals, the best characterised being the classical nuclear localisation sequence (NLS), consisting of one or two clusters of basic residues. The receptor that recognises NLSs is the importin heterodimer. Importin α contains the NLS binding site, and importin β is responsible for the actual translocation through the pore. The nuclear import is proposed to be driven by the asymmetric distribution of GDP- and GTP-bound forms of Ran. The current models predict a high-affinity form (for NLS binding) of the nuclear import receptor in the cytoplasm, and a low-affinity form in the nucleus where the receptor must release its cargo and return to the cytoplasm without it. Importin β plays a key role in the conversion between the two forms, because Ran-GTP binding to importin β in the nucleus causes its dissociation from importin α and the release of the cargo protein.

We determined the crystal structure of the full-length mouse importin α at 2.5 Å resolution (R = 18.9%, Rfree = 24.0%). The structure shows a large elongated C-terminal superhelical domain containing tandemly arranged armadillo repeats, and a less structured N-terminal importin β-binding domain containing an internal pseudo-NLS bound to the NLS-binding site. This observation provides the structural basis for the regulatory switch between the cytoplasmic, high-affinity form, and the nuclear, low-affinity form for NLS binding of the nuclear import receptor. Importin β conceivably converts the low- to high-affinity form by binding to a site overlapping the autoinhibitory sequence in a process resembling intrasteric regulation of protein kinases.

The structure also illuminates the determinants for the binding of diverse NLS sequences. The binding is achieved through a complex combination of interactions that include polar interactions orienting the NLS backbone, hydrophobic interactions with the non-polar portions of large side chains conferring the affinity, and complementary electrostatic interactions with the positively charged NLS side chains providing the specificity. The arm repeats provide a structural framework with a long shallow groove where strategically positioned side chains can sculpt the appropriate surface details. The nature of the interactions bears similarities with the similarly promiscuous but high affinity peptide recognition by MHC complexes. Analyses suggest that HEAT repeats constituting importin β may have a structure similar to armadillo repeats.

P12.AA.002 CRYSTAL STRUCTURE OF ERA: A GTPase-DEPENDENT CELL CYCLE REGULATOR CONTAINING AN RNA-BINDING MOTIF. Xinhua Ji, Xin Chen and Donald L. Court, ABL-Basic Research Program, National Cancer Institute – Frederick Cancer Research and Development Center, Frederick, Maryland 21702, USA.

ERA forms a unique family of GTPase that is widely conserved and essential in bacteria. ERA functions in cell cycle control by coupling cell division with growth rate. ERA homologues are also found in eukaryotes. We have determined the crystal structure of ERA from *Escherichia coli* at 2.4-Å resolution using a combination of MIR and MAD phasing. The structure reveals a two-domain arrangement of the molecule: an N-terminal domain that resembles p21 Ras and a C-terminal domain that is unique. Structure-based topological search of the C-domain fails to reveal any meaningful match, although sequence studies suggest that it may contain a KH-domain. KH-domains are RNA-binding motifs that usually occur in tandem repeats and exhibit low sequence similarity except for a conserved segment VIGxxGxxIK. We have identified a βααβ fold that is shared by the C-domain of ERA and the KH-domain and contains the VIGxxGxxIK sequence. We propose that the βααβ fold is the RNA-binding motif, the minimum structural requirement for RNA-binding. ERA is observed as dimers in crystal. The dimer formation involves a significantly distorted switch II region, which may shed light on how ERA protein regulates downstream events.

P12.AA.003 CONTROL OF CELL DIFFER-ENTIATION: SPO0A AND PHOSPHATE RELAY IN SPORULATING BACTERIA A.J. Wilkinson, R.J. Lewis, J.A. Brannigan [1], K. Muchova, I. Barak [2], G. Leonard [3], [1] Department of Chemistry, University of York, York, YO1 5DD, UK, [2] Institute of Molecular Biology, Slovak Academy of Sciences, Dubravska cesta 21, 842 51 Bratislava, Slavak Republic, [3] ESRF. Avenue des Martyrs, Grenoble, France

The formation of a resistant spore is the ultimate survival strategy and sporulation in B. subtilis is perhaps the simplest and best understood example of cellular differentiation. Involving as it does, the activation of numerous genes and the expenditure of a large amount of energy, sporulation is under stringent control. The master control element in the decision to sporulate is Spo0A, a gene-activator/repressor protein whose activity is regulated by phosphorylation. Spo0A-phosphate is formed via a multi-component 'phosphorelay'system fed by sensor kinases and drained by protein phosphatases. We have very recently solved the structure of the phosphoacceptor domain of Spo0A by MAD phasing of SeMet derivative data, revealing an unexpected quaternary organisation with important implications for signal transduction. Together with the structures of two other phosphorelay components, Spo0F and Spo0B [1,2], the structure provides (i) a basis for interpreting the effects of numerous '0A' mutations (ii) a framework for understanding phosphate transfer between proteins and (iii) an opportunity to understand how an extended system of proteins exerts biological control.

1. Madhusudan, Zapf, J., Whiteley, J. M., Hoch, J. A., Xuong, N. H. & Varughese, K. I. (1996) Structure 4, 679-690
2. Varughese, K.I., Madhusudan, Zhou, X.Z., Whiteley, J.M. & Hoch, J.A. (1998) Molecular Cell 2, 485-493.

12BB AB INITIO AND MOLECULAR REPLACEMENT PHASING METHODS

M12.BB.001 TOWARDS AN AB INITIO METHOD FOR THE DETERMINATION OF MACROMOLECULAR CRYSTAL STRUCTURES. Peter Main, Department of Physics, University of York, York YO1 5DD,England

A method for the complete ab initio determination of macromolecular crystal structures using X-ray diffraction data from a single crystal is being developed at York. A Monte Carlo procedure is used to set up trial electron density maps consistent with the observed diffraction pattern and the predicted electron density histogram, taking into account the resolution and solvent content. Cluster analysis based on that carried out by Lunin et al.[1] is then used to provide a map, typically at about 10-15 , which shows the molecular envelope. A method to extend these low resolution phases using wavelet analysis is now under development. The problem is one of adding the right amount of detail to the right place in a map. It has been found that wavelet analysis, which effectively decomposes an image into different levels of detail, gives precise control over this (Main et al., [2]). The amount of detail is given by the statistics (histograms) of the wavelet coefficients which can be predicted for increased resolution with the positions of new features guided by the diffraction pattern. At present, 10A starting phases can be extended to about 7A with acceptable phase errors but with the addition of further information it is hoped that they can be extended to the resolution at which existing density modification tecniques can be used. The program DM ([2]), now part of the CCP4 protein crystallography program library, is normally used on MIR, MAD or molecular replacement maps, but also forms an important part in the ab initio method. DM can take an electron density map in which the tertiary structure of the molecule is resolved and increase its resolution to that of the X-ray data prior to interpretation.

[1] Lunin, V.Yu., Urzhumtsev, A.G. and Skovoroda, T.P. (1993) Acta Cryst., A46, 540-544.
[2] Main, P. and Wilson, J. In preparation.
[3] Cowtan,K. and Main,P. Acta Cryst., D49, 148-157 (1993).

M12.BB.002 STRENGTHS AND WEAKNESSES OF MOLECULAR REPLACEMENT. Dodson, E.J., Chemistry Department, University of York

Molecular replacement as a technique has come of age, and it is timely to review the class of problems it can solve. The first applications were to search for non crystallographic symmetry with the aim to improve phasing. As more related proteins were studied the emphasis moved to fitting known models into new crystal forms. This technique is now fairly straightforward; it is fair to claim that a) if the Xray data is complete, and b) if model domains have an rms deviation in CAs from the unknown structure of less than 1.0, then a solution will be obtained, even when there are several segments in the asymmetric unit of the unknown structure.

Contributions from other areas are helping. More and more macromolecular structures can be grouped into families, where there are similarities in the folds. These can be used in somewhat the same way as NMR models by analysing the structures for domains and overlapping multiple copies.

The challenge of determining NCS or cross-crystal operators before an atomic model is available has not been fully met. Averaging , both within and between crystal forms is a powerful way to improve and refine the phases of structure amplitudes, but this can only be used when there is a transformation matrix to map the molecules onto each other. Examples will be discussed where satisfactory matrices have been obtained by using uninterpretable electron density derived from poor phases as a search model.

New target functions are coming available. The traditional method has depended on Patterson overlap, which allow the exploitation of FFTs. As computors become faster, this may not be so important, and full 6 dimensional searches to other targets can be envisaged.

M12.BB.003 AB-INITIO CALCULATION OF ENVELOPES FOR MACROMOLECULES BY MAXIMISATION OF LIKELIHOOD. Petrova T.E., Lunin V.Y., IMPB RAS, 142292 Pushchino, Moscow Region, Russia and Podjarny A.D. UPR de Biologie Structurale, IGBMC, BP 163, 67404 Illkirch CEDEX CU de Strasbourg, France.

Generally, the first stage in the low-resolution phasing of proteins is obtaining the envelope. The goal of this work is to determine whether the generalised likelihood (GL) [2] can be used as a criterion for the choice of the best one from a set of possible envelopes, which either fulfill real space constraints or are calculated from proposed phase sets. For every envelope, the value of GL, which is an analogue of statistical likelihood, can be calculated by means a Monte-Carlo type computation. A great number of pseudo-atomic models are randomly generated inside the envelope. The GL value is estimated as the frequency of appearance of models with magnitude correlation greater than some fixed level.

A family of possible envelopes, which were obtained by permuting the phases of a group of strong low-resolution reflections and calculating the mask of a fixed volume for every phase set, were considered. The tests with the neutron diffraction data for the $tRNA^{Asp}$-Asp RS complex showed that ranking the envelopes according to the GL value allows the choice of a few ones, including that corresponding to the correct phase set. The phase extension procedure, which is analogous to the building of the phasing tree [1], allows the determination of the correct envelope and phase set. The results obtained were compared with the results of the choice of the best envelope from the family of spherical envelopes [3] using the same GL criterion.

1. Bricogne, G., Gilmore, C.J. (1990). Acta Cryst., A**46**, 284-297.
2. Lunin, V.Y., Lunina, N.L., Petrova, T.E., Urzhumtsev, A.G., Podjarny, A.D. (1998) Acta Cryst., D54, 726-734.
3. Petrova, T.E., Lunin, V.Y., Podjarny, A.D. Acta Cryst. A, is accepted to be published

M12.BB.004 USE OF THE FAST TRANSLATION SEARCH FOR LOCATION OF HEAVY ATOM SITES FOR MAD/MIR/SIR PHASING. P.D. Adams, R.W. Grosse-Kunstleve, A.T. Brunger, HHMI/Yale University, Dept. of MB&B, New Haven, Connecticut 06511, U.S.A.

The Fast Fourier Transform translation function [1] has been implemented in the program Crystallography & NMR System [2]. This CPU efficient translation function is used in two different areas of phase determination: molecular replacement, and the automatic location of heavy atom sites for MAD/MIR/SIR phasing. We have developed a new and highly automated heavy-atom search procedure which combines the fast translation function, Patterson superposition functions and Patterson-Correlation refinement. An empirical dead-end elimination procedure is used to dramatically reduce computing time. The search procedure can be applied to both native and difference Patterson maps. Differences can be anomalous, dispersive or isomorphous. The weighted average of several different Patterson

maps can be used. The procedure was successfully tested with experimental data for a number of structures at low (3.2 Angstroms) to high (1.8 Angstroms) resolution with up to 30 heavy atom sites in the asymmetric unit. Even for a large number of heavy atoms, the correct sites can be found in less than one day on a high-speed workstation, usually in a matter of minutes for cases with a good signal.

[1] Navaza, J., Vernoslova, E. (1995) Acta Cryst., A51, 445-449.
[2] Brunger, A.T., Adams, P.D., Clore, G.M., DeLano, W.L., Gros, P., Grosse-Kunstleve, R.W., Jiang, J.-S., Kuszewski, J., Nilges, M., Pannu, N.S., Read, R.J., Rice, L.M., Simonson, T., Warren, G.L. (1998) Acta Cryst., D54, 905-921.

M12.BB.005 FINDING SELENIUMS WITH SnB. Charles M. Weeks[1], P. Lynne Howell[2], Ashley M. Deacon[3], Robert H. Blessing[1], G. David Smith[1,4], Russ Miller[1], Steven E. Ealick[3] and Herbert A. Hauptman[1], [1]Hauptman-Woodward Inst., 73 High St., Buffalo, NY 14203-1196, USA, [2]Structural Biol. and Biochem., Res. Inst., The Hospital for Sick Children, 555 University Ave., Toronto, M5G 1X8, Canada, [3]Dept. of Biochem., Molecular and Cell Biol., Cornell University, Ithaca, NY 14853, USA, [4]Roswell Park Cancer Inst., Elm & Carlton Sts., Buffalo, NY 14263, USA.

SnB version 2.0 [Weeks, C.M. & Miller, R. (1999), J. Appl. Cryst. 32, in press] is a computer program that implements the dual-space (Shake-and-Bake) approach to ab initio direct phase determination. It has successfully solved conventional problems involving as many as 1200 unique non-H atoms as well as large substructures such as the SeMet derivative of an epimerase which has 70 selenium sites. Substructure applications require only the 2.5-3.0Å data normally included in MAD measurements, and data sets truncated even to 5Å have led to solutions. It is important, however, to include accurate low-resolution data. So far, the best results have been obtained from consideration of single-wavelength, peak anomalous difference data alone, possibly because this approach avoids the introduction of any errors resulting from incorrect scaling between two data sets. Independent SnB analysis of data measured at different wavelengths, on the other hand, can provide valuable confirmation for questionable sites.

The key to successful use of difference data is careful data processing and computation of normalized difference magnitudes. It is essential that all erroneously large magnitudes be excluded prior to phasing. The SnB v2.0 program package accomplishes this by providing a convenient interface to the DREAR data-processing programs [Blessing, R.H. (1997) J. Appl. Cryst. 30, 421-426] which allow for fine control of the data-screening process. Default values, based on empirical study of known structures, are provided for all parameters in the main SnB phasing program. Thus, phasing can be performed automatically if desired. For further information concerning SnB, please refer to http://www.hwi.buffalo.edu/SnB/.

Research supported by GM-46733 (NIH) & ACI-9721373 (NSF).

M12.BB.006 EXAMPLES OF MACROMOLECULAR *AB INITIO* WITH HIGH RESOLUTION DATA. I. Usón and G.M. Sheldrick, Institut für Anorganische Chemie, Universität Göttingen, Tammannstr. 4, 37077 Gööttingen, Germany

High resolution ab initio macromolecular structure solution based on real/reciprocal space iteration with the 'half-baked' method[1,2] (inspired by Shake & Bake[3], but different in detail) will be illustrated by the solution of sulphur- or chlorine containing structures which were not amenable to conventional direct methods despite exhaustive solution attempts. Ways to improve the starting random phases using the Patterson function that lead to an improved success rate of the method will be discussed. The method relies not on the solution of the Patterson to locate the sites of the heavier atoms, but rather employs a probabilistic Patterson sampling, to screen random starting phases for consistency with the Patterson function.

The method will be illustrated with some examples including hirustasin, a 55 amino acid serine protease inhibitor containing 5 disulphide bridges, which can be solved by SHELXD with either 1.2 A low temperature data, or with 1.4 A room temperature data [4].

[1] Sheldrick G.M.: SHELX applications to macromolecules, in Direct methods for solving macromolecular structures. Proceedings of the NATO advanced study institute on direct methods for solving macromolecular structure. Kluwer Academic Publishers. Ed. S. Fortier 401-411 (1998).
[2] Sheldrick G.M. & Gould R.O.: Structure solution by iterative peaklist optimization and tangent expansion in space group P1, Acta Cryst. B51:423-431 (1995).
[3] Miller R., DeTitta, G.T., Jones, R., Langs, D.A., Weeks, C.M. & Hauptman, H.A.: On the application of the minimal principle to solve unknown structures. Science. 259:1430-1433 (1993).
[4] Usón, I. Sheldrick G.M., de La Fortelle, E., Bricogne, G., Di Marco, S., Priestle, J.P., Grütter, M.G., & Mittl, P.R.E. The 1.2 A structure of hirustasin reveals the intrinsic flexibility of a family of highly disulphide-bridged serine proteases, Structure. 7: 55-63 (1999).

P12.BB.001 AN ALGORITHM FOR AB INITIO ELECTRON DENSITY RECONSTRUCTION IN MACROMOLECULAR CRYSTALLOGRAPHY. J. L. van der Plas, R. P. Millane, Whistler Center for Carbohydrate, Research Computational Science and Engineering Program

A new electron density modification (EDM) algorithm has been developed and applied to ab initio phasing in macromolecular crystallography. EDM is generally used to improve experimental phases and/or extend phases to higher resolution, but we find that the new algorithm can converge to the correct electron density without any initial experimental phases when conventional EDM fails to do so. The new algorithm is based on the hybrid-input-output algorithm (HIO), which was originally developed for 2D image processing in astronomy. The new algorithm appears to be less affected by local minima than conventional EDM. Instead of simply applying constraints to the electron density, the HIO algorithm computes a driving function, that is modified at each cycle depending on how well the constraints are satisfied. Our algorithm consists of using HIO and conventional EDM in each phase extension step.

To investigate the effectiveness of the new algorithm compared to conventional EDM, both were tested on a set of synthesized structure factors calculated from a 340 A unit cell containing one Cowpea Mosaic Virus (CPMV) particle, a virus with 60-fold icosahedral symmetry, where the 5-fold axis was noncrystallographic. The synthesized diffraction data were modified by adding 10% noise and removing reflections with a resolution less than 100 A, to better represent actual experimental data. Starting with random phases, both algorithms were used to attempt to refine the phases between 100 and 20 A resolution. The phases obtained were then used to extend to 6 A resolution in five more steps. The new algorithm proved far more effective in finding the correct phases than did conventional EDM. The new algorithm therefore promises to be a useful tool for ab initio structure determination in macromolecular crystallography.

P12.BB.002 REAL-SPACE DIRECT METHODS FOR PROTEINS. M.M. Woolfson, J. Foadi, Physics Department and E. Dodson, K.S. Wilson and Yao Jia-xing, Chemistry Department, University of York, York YO10 5DD, U.K.

It has been shown to be possible to solve moderate size proteins starting with a fragment that may or may not be part of the structure under investigation. For a P1 structure the fragment, which can be as small as 1% of the structure, does not need to be

oriented or positioned but favourable orientations may be found by Patterson methods. A modified Patterson superposition map, using the sum function, has been found to be advantageous in improving the starting set of phases from the fragment.

Usual phasing procedures using phase relationships are weak and not very useful for large structures. However, the Sayre equation and non-negativity criteria apply as well to large structures as to small. Successive refinement from the starting phases is carried out in real space, firstly applying the Sayre equation (L.S. Refaat, C. Tate, & M.M. Woolfson, 1995, *Acta Cryst*. **D51**, 1036-1040) followed by density modification in the form of an improved version of low-density elimination (M. Shiono & M.M. Woolfson, 1992, *Acta Cryst.* A**48**, 451-456). The method is a multi-solution one and an effective figure of merit, based on the correlation coefficient between estimated and actual values of structure amplitudes of non-phased reflections, enables the progress of phase refinement to be followed and correct solutions to be unambiguously identified.

A P1 structure with 1 428 atoms, including 10 sulphur atoms and 286 water atoms, was solved starting with small fragments containing 10 atoms taken from another, and unrelated, structure. For the best solutions, phases found for the 16,761 reflections with |E| >1 had mean phase error (unweighted) down to 20.4°. Experiments have shown that much larger structures might also be soluble by this kind of approach, although the optimum way of obtaining the initial fragment has still to be determined.

P12.BB.003 EXPERIMENTALLY DETERMINED TRIPLET PHASES USED FOR STRUCTURE SOLUTION ON LYSOZYME. Kerstin Hölzer[a,b], Edgar Weckert[b], Klaus Schroer[a,b], and Kurt Hümmer[b], [a]Biology Department, Brookhaven National Laboratory, Upton, New York 11973, USA, [b]Institut für Kristallographie, Universität Karlsruhe (TH), D-76128 Karlsruhe, Germany

Advances in the experimental triplet phase determination using three-beam diffraction allowed the measurement of a large set of triplet phases on protein crystals [1]. For the evaluation of a structure solution based on measured triplet phases, tetragonal HEW Lysozyme was chosen as a test structure [2]. At the ESRF bending magnet BM1 (SW/NOR CRG) it was possible to determine about 100 triplet phases per day on a good-quality lysozyme crystal. From the total of 850 measured triplet phases one derive 750 structure-factor phases. The resolution of the reflections involved in the three-beam cases extends from 35 to 2.5 Å, with the maximum of the distribution at 4 Å. The mean difference of the structure-factor phases to the PDB entry 193L [3] is 16°. The quality of the resulting e-density map allows a straightforward and nearly complete interpretation, and the starting model was refined to an R-value of 17.4 %. Afterwards the influence of the experimentally phased reflections to the quality of the e-density map was investigated by applying criteria based on resolution and intensity. Thus, the number needed for an interpretable e-density map was reduced to 550 phased reflections by using the reflections with the highest intensities and a resolution > 3.6 Å.

Now the equipment necessary for the three-beam interference experiment is being installed also at the NSLS (X26C) and will be available soon as an additional tool for structure-solution methods.

[1] Weckert, E., Hümmer, K., Acta Cryst.(1997),A**53**, 108-143
[2] Hölzer, K., PhD-Thesis (1998), Universtität Karlsruhe (TH), Germany
[3] Vaney, M. C., Maignan S., Riès-Kautt M., Ducruix A., Acta Cryst. (1996), D**52**, 505-517

P12.BB.004 OPTIMAL SELECTION OF MEASURED TRIPLET PHASES: MAXIMUM-ENTROPY AND DENSITY MODIFICATION METHODS. E. Weckert, R. Müller, Institut für Kristallographie, Universität Karlsruhe, D-76128 Karlsruhe, Germany and K. Hölzer, Biology Department, BNL, Upton, NY 11973, USA.

It has been shown that a sufficient number of triplet phases can be measured by the three-beam interference method [1,2] in order to calculate an interpretable map from the derived single phases. The difficult task of combining triplet to single phases can be accomplished by a maximum entropy based technique [3]. The aim of the presented investigation is to reduce the number of required measured triplet phases. Promising results could be obtained by the following procedure: (i) The use of Maximum Entropy and Likelihood methods to derive the most probably base-phase set from measured triplet phases and extrapolation of the phases of non-base reflections with proper weights. (ii) Further improvements of the phases by density modification techniques [4]. (iii) Application of an automatic refinement protocol [5] to this density. For the case of tetr. lysozyme a set of 850 triplet phases and a 1.5 Å intensity data set this procedure will give a map with a correlation coefficient higher than 90% compared to the F_{obs} map. The procedure is still working if the number of triplet phases is reduced to about 500. The results of these calculations as well as first applications to an unknown protein crystal structure will be presented.

1. E. Weckert, K. Hümmer (1997) Acta Cryst. A53, 108-143.
2. K. Hölzer (1998) PhD Thesis, Universität Karlsruhe.
3. G. Bricogne (1984) *Acta Cryst.* A**40**, 410-445.
4. K. Cowtan (1994) Joint CCP4 and ESF-EACBM Newsletter on Protein Crystallography, **31**, 34-38.
5. A. Perrakis, T.K. Sixma, K.S. Wilson, V.S. Lamzin (1997) *Acta Cryst.* D**53**, 448-455.

P12.BB.006 A NEW CLASS OF HEME PROTEINS. STRUCTURE OF PLANT HEMOGLOBIN FROM RICE : A SIMPLE PROTEIN WITH A COMPLICATED SOLUTION. Boguslaw Stec, *Mark S. Hargrove, #Eric A. Brucker, John S. Olson, George N. Phillips Jr. Dept. of Biochemistry and Cell Biol., Rice University, 6100 Main St., Houston TX 77005, * 4128 Molecular Biology Building, Department of Biochemistry, Biophysics, and Molecular Biology, Iowa State University,Ames , IA 50010, Baxter Healthcare Corp., 2545 Central Ave., Suite FD-1, Boulder, CO 80301

We have solved and refined a representative of a new class of heme containing proteins: nonsymbiotic hemoglobin from rice (nsHb). The protein crystallized in the trigonal $P3_121$ space group. The initial attempts to solve the structure with molecular replacement failed. It was finally solved by a combination of MIR and Single Atom Anomalous Dispersion methods. The structure solution was complicated by a partial superposition of Patterson peaks and symmetry ambiguities. It was later refined in X-plor to R=21.2% with excellent stereochemistry. The final structure contains two molecules in an asymmetric unit which corresponds well with the results from solution studies which suggested a dimeric organization for this protein. The dimer present in the asymmetric unit is different from previously observed ternary arrangements seen in other hemoglobins. It seems to have a weak interface which raises some mechanistic question. The individual subunits exhibit a classical globin fold but different enough so that molecular replacement failed. Each subunit contains an unusual heme environment in which the iron atom is bonded to both proximal and distal histidine residues. A similar arrangement was previously seen in the cytochrome b family. The significant kinetic difference is that the oxygen binding kinetics are very fast, compared to the cytochromes. The structural details of this simple protein, as well as the complicated history of attempts to solve the structure will be provided in the presentation.

Acknowledgments: NIH - AR40252 (G.N.P.), USPHS - GM35649 and Robert A. Welch Foundation - C-612 (J.S.O.)

P12.BB.007 THE PAIR-FUNCTIONAL: A NEW DIRECT METHOD. A.D. McLachlan, MRC Laboratory of Molecular Biology, Hills Road, Cambridge, CB2 2QH, UK

The "Pair-Functional Principle" of classical statistical mechanics [1] states that there is a unique many-atom statistical ensemble which can be made to reproduce the unphased observed X-ray intensity data from any physically feasible atomic crystal structure. The ensemble has the maximum entropy consistent with the data. It is equivalent to the many-body Boltzmann distribution of N identical atoms in thermal equilibrium under a set of fictitious pairwise interaction potentials. These potentials, derived from the direct correlation function of the observed originless Patterson function, are specific and unique for any given set of observations. The paired-atom ensemble is like a dense fluid of atoms in the unit cell, with long-range periodic interactions that depend on relative distance and orientation. Each atom feels the total pairing field from all the others, and at low temperatures the fluid condenses into the correct X-ray solution. The search for the molecular structure is guided by the "Perfect Pairing Postulate": the correct solution will usually be an N-atom configuration within the ensemble that has the maximum statistical potential consistent with the observed intensities. Pairing searches have successfully solved Sheldrick's test structures of 100-200 atoms, and larger real molecules, including Anderson, Prive and Eisenberg's alpha1 helical peptide of 400 atoms. The solution method uses a temperature-dependent self- consistent field generated by the pair potentials, where each atomic peak is positioned and generated by triangulation in the combined fields of all the others in the cell. A simpler method, tested recently, is called "Pair and Square". It uses alternate cycles of best paired peak picking followed by the tangent formula.

1. A.D. McLachlan & R.A. Harris (1961). J. Chem. Phys. 34,1451-2.

12CC PSEUDO-SYMMETRY AND TWINNING

M12.CC.001 LOW OBLIQUITY IN PSEUDO-SYMMETRY OF LATTICES AND STRUCTURES, AND IN TWINNING BY PSEUDO-MEROHEDRY. Y. Le Page, ICPET, National Research Council of Canada, Ottawa, Canada K1A 0R6.

A new life starts for the old concept of obliquity, the angle between a lattice row and the perpendicular to a lattice plane. Lattice symmetry, space-group symmetry, as well as twinning by merohedry involve *exact perpendicularity* between lattice rows and lattice planes. In the same way, near-perpendicularity *ie low values of obliquity,* is a central concept in the prediction, analysis and interpretation of metric pseudo-symmetry of lattices, of pseudo-symmetry of structures and of twinning by pseudo-merohedry or by reticular pseudo-merohedry. So far, only passive use seems to have been made of this quantitative criterion. We show here that low obliquity can now be used actively as a means of prediction.

The problem of finding low-obliquity directions in lattices with known cell parameters boils down to finding, for each set (*hkl*) of Miller indices for lattice planes, all lattice vectors shorter than an upper limit calculable from the *d*-spacing and the maximum obliquity, and with integer indices [*uvw*] which solve the linear Diophantine equation:

$hu+kv+lw=n$ [eqn 1] , where n is a given integer.

It can be shown that the cases of pseudo-symmetry of lattices and structures, as well as the case of twinning by pseudo-merohedry do not involve values of n other than 1, 2 or 3 if the lattice is referred to a primitive reference system. If that system is Buerger-reduced, values of h, k, l, u, v, w other than 0, ± 1 or ± 2 cannot be involved in the solution. The case of twinning by reticular pseudo-merohedry involves maximum values of n and of indices which are multiplied by the twin index.

A novel straightforward solution method for the short lattice vectors which satisfy [1] for general values of h,k,l and n will be presented. Its application to detection of metric pseudo-symmetry of lattices, to detection of pseudo-symmetry of structure models and to prediction of twin laws will be explained. A corresponding software program capable of finding *all* solutions of [1] very fast within a given obliquity, for even large values (like 10^5) of h, k, l and n, and of tackling in this way the above applications, will be installed for Internet interrogation at URL http://ylp.icpet.nrc.ca/oblique/ at the time of the meeting.

M12.CC.002 TWINNING OF CRYSTALS: TWIN LAW, LATTICE RELATIONS, LIMITING CASES. Th. Hahn, Institut für Kristallographie, RWTH Aachen, D-52056 Aachen, Germany, and H. Klapper, Mineralogisches Institut, Universität Bonn, D-53115 Bonn, Germany, and V. Janovec, Institute of Physics, Academy of Sciences, CZ-18040 Prague 8, Czech Republic.

A twin is characterized by a *twin law*, which traditionally is described by a single, morphologically prominent twin operation. All twin operations relate the lattices of two twin partners in such a way that they have either a lattice row (minimal condition), or a lattice plane, or the entire lattice in common: *crystallographic orientation relation*. There exist seven types of binary (order two) twin operations for the general case.

The notion of twin law can be generalized: The *eigensymmetry H* of the crystal is extended by a twin operation to the *composite symmetry K* (supergroup of index 2). The resulting *coset* contains all twin operations which define the same orientation relation between the two twin partners (*alternative twin operations*). Hence, the full coset is a more adequate description of the twin law. A different way of expressing the twin law is the anti-symmetry symbol of the composite symmetry *K*. More complicated relations exist for multiple (*e.g*. cyclic) twins.

Special attention is devoted to the *minimal condition* of twinning, *i.e*. the limiting cases between twinning and arbitrary intergrowth. Two types of twin, both discovered already in the 19th century, belong to this category:

(i) the so-called *Kantennormalengesetz* of micas (Tschermak, 1904) in which an irrational twofold twin axis is normal to a rational lattice row common to both partners (one-dimensional coincidence);

(ii) the so-called *median law* of pseudo-hexagonal gibbsite, $Al(OH)_3$ (Brögger, 1892). It consists of an irrational twofold twin axis which relates as bisector (median) two non-equivalent but strongly pseudo-equivalent lattice rows (pseudo one-dimensional coincidence).

Both intergrowths are doubted as twins by some authors. We accept the Kantennormalengesetz as the 'minimal twin', whereas there is conflicting evidence for the median law as a twin law: only approximate coincidence of two lattice rows *vs*. frequent and reproducible occurrence of the 'twin'.

M12.CC.003 PROTEIN STRUCTURES AND TWINNING. Geoffrey B. Jameson, Institute of Fundamental Sciences, and Bryan F. Anderson, Institute of Molecular BioSciences, Massey University, Palmerston North, New Zealand.

Low symmetry crystal classes of trigonal/hexagonal (3, 6) and tetragonal systems (4) predispose protein crystals to merohedral twinning, leading to X-ray diffraction data acquiring higher symmetry (32, 6; 622; 422) than that from the underlying

true lattice. A simple and robust test for detecting twinning is the ratio $T = \langle F^2 \rangle / \langle F^2 \rangle$ examined over ~5 resolution shells. For no twinning or pseudo-centering, theoretical values of T are 0.785 (acentric) and 0.637 (centric); for perfect twinning (two equal twin components), values are 0.886 (acentric) and 0.785 (centric). Unrecognised twinning in a macro-molecular structure, where usually the data:parameter ratio is poor, may lead to misfortune in refinement. Twinning may also lead to apparently valid but overlapped solutions using molecular replacement methods. An internally consistent solution for a single twin domain may be retrieved by examination of the correlation coefficient as a function of twin fraction.[1]

SHELXL offers exceptionally convenient structure refinement, using the data as measured. Following refinement, observed data are de-twinned in order to provide observed and calculated |F| (with calculated phase angle) for calculation of Fourier maps, via an ancillary program SHELXPRO. The half-molecule R121D mutant of human lactoferrin crystallises in space group P32, but due to twinning (hkl and -h-kl perfectly overlapped; twin fraction = 0.44) data to 3.0 Å have pseudo-hexagonal symmetry and apparent space group $P6_2$. Four domains corresponding to two molecules in the asymmetric unit were located by MR, and the structure refined using SHELXL. The omitted C-terminal portion of the molecule was identified, as well as a number of differences in main-chain and side-chain conformations relative to the search molecule. Currently, R = 0.16 and $R_f = 0.20$.

[1] Breyer WA, Kingston RL, Anderson BF and Baker EN. 1999. Acta Cryst. D55, 129-138.

M12.CC.004 WHAT THE CSD CAN TELL US ABOUT PSEUDO-SYMMETRY. Anthony L. Spek, Bijvoet Centre for Biomolecular research, Utrecht University, Utrecht 3584 CH, NL

The asymmetric part of a molecular crystal structure contains in general only one molecule. This situation is described as Z' = 1. Z' may be less than 1 when the molecule possesses a symmetry element that happens to coincide with a corresponding symmetry element in the crystal.

Molecular structures with Z' > 2 or higher are not uncommon. Steroids as an example often crystallize in pairs in space group $P2_1$ or $P2_12_12_1$. The interesting observation in such cases is that one can often discern pseudo symmetry relations between such 'dimers'. This local symmetry however doesn't appear to be (fully) compatible with the lattice symmetry.

This paper reports on our findings on this issue based on the data in the Cambridge Structural Database using the ADDSYM tool in PLATON. ADDSYM is an extended version of the powerful MISSYM algorithm (Y. Le Page) for detecting missed (real) symmetry. ADDSYM, though designed to point at 'Marshable' structure reports, turns out to be also useful as a tool to point at interesting cases of pseudo-symmetry.

The complete CSD (about 200000 entries) has been run through PLATON/ADDSYM providing a list of more than 3000 cases of missed or pseudo-symmetry. A few examples of pseudo-symmetry thus found will be discussed in some detail (e.g. a structure in $P2_1$ with Z' = 2, beta near to 90 degrees and pseudo $P2_12_12_1$).

M12.CC.005 PSEUDOSYMMETRY (OR NOT) IN STRUCTURES HAVING Z'>1. Carolyn Pratt Brock and Brian O. Patrick, Department of Chemistry, University of Kentucky, Lexington, KY 40506-0055, USA.

Many structures having Z'>1 are pseudosymmetric, but some are not. The latter group includes those crystals in which an important set of intermolecular interactions is incompatible with crystallographic symmetry. Examples of such structures include those of some monoalcohols C_nH_mOH and *vicinal*-dialcohols $C_nH_m(OH)_2$. Molecules that fill space poorly (*e.g.*, simple biphenyl derivatives) also seem to be more likely than most to crystallize with Z'>1.

Pseudosymmetric structures having Z'>1 may result from crystal cooling. Any solid-solid phase transition encountered during cooling will almost certainly reduce crystal symmetry. Such transitions are more likely if there is a large-amplitude thermal vibration at the temperature of crystal growth. The decrease in vibrational amplitudes with with decrease in temperature often leads to unfavorable intermolecular contacts that can be resolved by small, symmetry-breaking displacements. Examples of such structures include those of the linear polyphenyls.

Enantiomerically pure materials quite often pack so that two independent molecules are related by an approximate inversion center.

Other structures with Z'>1 are highly pseudosymmetric for no obvious reason. Crystals studied at room temperature may, of course, have been grown by precipitation during cooling of a hot solution. This explanation, however, does not explain all the structures in this class.

Several structures of this last type will be discussed. In some cases the structures are so pseudosymmetric that they can be refined in a higher symmetry cell with a subset of the intensity data to R < 0.10. The displacement ellipsoids resulting from such refinements then show quite clearly how the independent molecules actually differ. Possible reasons for the symmetry breaking will be discussed.

M12.CC.006 TWINNING AND POLYMORPHISM IN *o*-NITROANILINE. M.Nieuwenhuyzen, School of Chemistry, The Queen's University of Belfast, Belfast BT9 5AG, Northern Ireland.

The polymorphic nature of *o*-nitroaniline has long been known, although to date only one form has been characterised crystallographically, in 1978 Dhaneshwar *et al* determined the structure of the γ form[1]. As part of an extensive examination of amino-nitro substituted systems and their tendency to be polymorphic[2-3], this structure was re-determined as well as the structure of a second polymorph. This presentation compares and contrasts the hydrogen bonding motifs in these materials and examines the nature of the twinning in these two polymorphs. Data collected using station 9.8, a Bruker SMART system and the Siemens P4 are compared and contrasted.

N.N.Dhaneshwar, S.S.Tavale, L.M.Pant Acta Crystallogr.,Sect.B, **34**, 2507,1978
C. B. Aakeröy, A. M. Beatty, M. Nieuwenhuyzen, M. Zou, J. Mat.Chem., 1385-1389, 1998.
C. B. Aakeröy, S. L. Price, M. Nieuwenhuyzen, J. Am. Chem. Soc., **120**, 35, 8986 – 8993, 1998.

M12.CC.007 CRYSTAL STRUCTURE OF $La_{0.8}MnO_{3-\delta}$ C.M.R. THIN FILM BEFORE AND AFTER ANNEALING ; X.R.D., T.E.M., X.A.N.E.S. STUDIES. H. Vincent, M. Audier, S. Pignard, G. Dezanneau, J.P. Senateur, LMGP (CNRS UMR 5628), ENS de Physique de Grenoble, BP 46, 38402 St Martin d'Heres, France.

Thin films of $La_{1-x}MnO_{3-\delta}$ composition have been deposited by a new patented process, called Injection-MOCVD [1]. Films deposited on MgO are epitaxial. For x=0.2, the as-deposited film has a semiconducting-metal and para-ferromagnetic transition at about 220 K ; after annealing under air during 3 h at 700°C, this transition temperature is about 310 K. Annealed film presents at room temperature and under low magnetic film one of the best known magnetoresistive sensitivity (30% per Tesla in [0,

1 T] range) [2]. In order to understand this performance improvement, we studied the crystal structure of this film, before and after annealing. For the first time to our knownledge, X.R. data collections have been recorded from an 1 mm^2 thin film piece, using a classical 4-Circle-diffractometer designed for single crystals. About 5000 reflections have been measured in each case from two pieces of the same film, one as deposited, the other one after annealing. Both films have apparent cubic symmetry and their cell parameter is twice the classical perovskite one. In fact, the true crystal structure is monoclinic and microdomain twinned. Space groups are nevertheless different I2/b and $P2_1/a$. Atomic positions of all the atoms have been determined using SHELXL-93 and MXD [3] refinement programs ; R and wR factors calculated on F^2 (730 independant reflections with $I / \sigma(I) \geq 2$) are about 6%. The as-deposited film is found lacunar on oxygen sites too ; annealing under air reduces the vacancy rate and increases the Mn^{4+} / Mn^{3+} ratio. XANES study confirms these results and estimates at 23% the increasing of this ratio. T.E.M. observations performed on both films agree completely with previous conclusions. Moreover they show that some MgO substrate areas close to the film are constrained and distorded after annealing ; their lattice becomes cubic F with a cell parameter twice the MgO usual one [4].

1. J.P. Senateur, F. Weiss, R. Madar, French Patent PCT FR9400858 (1993)
2. S. Pignard, H. Vincent, J.P. senateur, J. Pierre, J. Appl. Phys., **82**, 999, (1997)
3. P. Wolfers, J. Appl. Cryst, **23**, 554 (1990)
4. H. Vincent, M. Audier, S. Pignard, G. Dezanneau, Phys Rev. B (submit.)

P12.CC.001 STRUCTURE REFINEMENT OF Cu_8GeS_6 II USING X-RAY DIFFRACTION DATA FROM A MULTIPLE- TWINNED CRYSTAL. M. Onoda, X.-a. Chen, K. Kato, A. Sato & H. Wada, National Institute for Researches in Inorganic Materials, Namiki 1-1, Tsukuba, Ibaraki, 305-0044, Japan.

The structure of the orthorhombic room-temperature phase Cu_8GeS_6 II has been refined on the basis of X-ray diffraction data from a 12-fold twinned crystal applying a six-dimensional twin refinement technique. For 1804 unique reflections measured using MoKα radiation, R_F was 0.083 with 77 structure parameters and 12 scale factors. The symmetry operations and the unit cell are (0,0,0; 1/2,1/2,0)+ x,y,z; y,x,z; 1/4-x,3/4-y,1/2+z; 3/4-y,1/4-x,1/2+z; a=b=9.9073(3)Å, c=9.8703(4)Å, α=β=90°, γ=90.642(4)°. The standard setting of the space group and the reduced unit cell are $Pmn2_1$; A=7.0445(3), B=6.9661(3), C=9.8699(5)Å.

Fig. 1 The major twin domains 1-6. The minor twin domains 7-12 are related to the domains 1-6 by a two-fold rotation on [111] respectively.

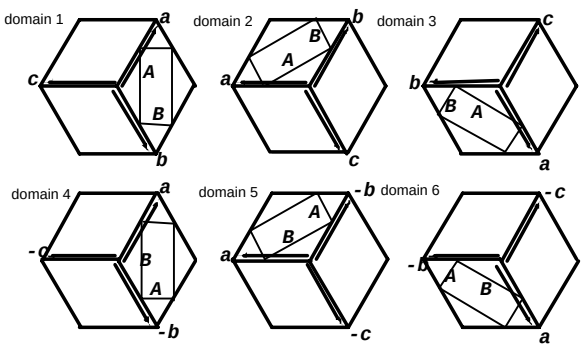

P12.CC.003 NON-MEROHEDRAL TWINNING AND THE CCD AREA DETECTOR Victor G. Young, Jr. [1] and Robert A. Sparks [2], [1] Department of Chemistry, University of Minnesota, Minneapolis, MN 55455, USA, [2] Bruker-AXS, Inc., 6300 Enterprise Lane, Madison, WI 53719, USA

Non-merohedral twinning is a better understood problem since the arrival of CCD area-detector diffractometers in our laboratories. These have not only increased the throughput for straightforward structure determinations, but have also provided a superior tool to assist in the unravelling of tangled reciprocal lattices brought about by non-merohedral twinning. This presentation will include discussion of strategies for indexing, data collection, integration of intensities, and least-squares refinement. Strategies for handling the partial overlap of reflections will be discussed. Examples of all common non-merohedral twinning motifs will be examined.

P12.CC.004 TURKISH ORNAMENTS ARE TWINS OF CRYSTALS. H.Necefoglu, Department of Chemistry, Faculty of Arts and Sciences, Kafkas University, Kars, TURKEY

In this report crystallographic aspects of ancient, medieval and modern Turkish ornaments are deal with. Crystallographic Patterns (CPs) are considerably different from other patterns. In the process of the construction of CPs, symmetry appears as a result of combination, but not as a means of its formation as is characteristic of other ornaments. Their symmetries are analogous with symmetries of natural objects. The atoms and molecules dispose themselves in crystals just as elements arrange themselves in CPs. In other words, CPs are constructed according to the same principle of crystal formation, i. e. the principle of tight packing.

The following are characteristic of CPs: The edge of ornament elements draw the edge of the figure; Maximal compactness of the ornament elements; Lack of background or transformation of background to ornament elements; Minimisation of the variety of ornament elements; Symmetry is not used for form creation, and it appears as a result.

The similarity (isomorphism) of crystals and ornaments enables us to describe the ornaments with structural analysis terms, and the similarity between ornaments and crystal structures can also be used in chemistry education. This will bring an aesthetical aspect to education. An invisible part of nature can be studied as ornament creation.

Each newly created CP is the structural scheme of a number of possible compounds. The familiarity with such ornaments and the ability to create them are important in solving compound structures.

12DD COMBINED POWDER DIFFRACTION, EXAFS AND DAFS

M12.DD.001 CHARACTERISING SEMICONDUCTOR NANO-PARTICLES WITH IN SITU EXAFS, XRD AND SAXS. GN Greaves* and G Sankar† *Department of Physics, University of Wales, Aberystwyth, SY23 3BZ, UK †The Royal Institution, 21 Albemarle Street, London, WX1 4BS, UK

Both EXAFS and X-ray Powder Diffraction (XRD) have been combined with Small Angle X-ray Scattering (SAXS) to characterise the nucleation of semiconductor nano-particles in cadmium exchanged sodium zeolite Y (Cd/Na:Y). X-ray experiments have been performed at the Synchrotron Radiation Source (SRS) using a specially developed miniature muffle furnace with large scattering windows. After ion exchange Cd/Na:Y was treated with sodium hydroxide, which is known to promote the precipitation of semiconductor particles. Following heating to 500(C, these were identified from cadmium EXAFS as cadmium oxide crystallites. With a size, estimated from the

cadmium shell coordination number, of 15Å+/-10Å, the nanoparticles were not evident in XRD. Instead XRD recorded the crystallography of the host through dehydration to eventual collapse to an amorphised high density phase at temperatures in excess of ~650°C. Exploring 0.0015<q<0.7Å-1, SAXS revealed a change from bulk fractal scattering to Porod scattering, identified as resulting from the semiconductor nanophase - the crossover yielding a characteristic particle size of ~20+/-5Å. Moreover the dimesionallity of the semiconductor microstructure was found to change with rising temperature, eventually becoming 3 dimensional above 450°C. In a parallel study, cadmium oxide was synthesised from a cadmium hydroxide gel utilising the same temperature schedule as for Cd/Na:Y. The kinetics of the transformation from Cd(OH)2 to CdO were determined from XRD - the linewidths pointing to particle sizes developing from 140Å to 270Å by 560°C. Interestingly, the SAXS invariant and the onset of Porod scattering were found to progress in an analogous fashion to the synthesis of cadmium oxide incarcerated in zeolite Y. In particular the development of particle volume and nanocrystalline dimensionallity point to dendritic growth, with the exception that particle sizes are significantly larger for unconstrained growth.

M12.DD.002 COMBINED XRD, XAFS AND PL FOR HIGH PRESSURE STUDIES. A.V. Sapelkin and S. Bayliss Department of Chemistry and Physics, School of Applied Sciences, De Montfort University, The Gateway, Leicester, LE1 9BH, UK

A new facility for simultaneous EXAFS, XRD and Photoluminescence (PL) measurements under high pressures is being developed for use on station 9.3 at Daresbury Laboratory. The rig includes translational and rotational stages for positioning the sample mounted inside a diamond anvil high pressure cell. Translations are necessary to align the sample in the x-ray beam and rotations are required to minimize influence of diamond glitches in the EXAFS spectrum. PL spectroscopy is carried out using a He-Cd (325 nm and 442 nm wavelengths) laser and spectrometer. Data acquisition facilitates motor control and a video camera and monitor is used for remote sample alignment. Pressure calibration is carried out with the above optical system using the fluorescence from ruby chips mounted with the sample inside the diamond anvil cell. The idea of the development of the high pressure facility (code named HI-PREXX) is to enable users to make multi-technique high pressure experiments at any suitable station at a synchrotron source. Furthermore full remote operation of the rig allows simultaneous collection of optical and structural data whilst varying the pressure. The set-up is very flexible and can be tailored for a particular experiment, such as time or temperature-dependent measurements. The Hi-PREXX system will be described, and results presented from initial experiments conducted on the 1-BM-A beamline at the APS and on Station 9.3 at Daresbury Laboratory. Analysis of data from high pressure experiments on amorphous and crystalline GaSb and crystalline and nanocrystalline GaN will be given. Particular attention will be paid to comparing the use of Energy Dispersive EXAFS (EDE) and Quick Scanning EXAFS (QUEXAFS) techniques under pressure in conjunction with XRD. Finally, points associated with the equipment development and beamline properties for future experiments will be discussed.

M12.DD.003 MEASURING XRD/XAFS FROM HIGH TEMPERATURE OXIDES AND LIQUIDS. C. Landron, Centre de Recherches sur les Materiaux a Haute Temperature, CNRS, 45071 Orleans cedex 2, France.

In-situ characterisation has been performed on various oxides at very high temperature by using a laser heating system and aerodynamic levitation. A containerless investigation by synchrotron radiation has been used on the basis of the combination of X-ray Absorption Spectrometry in fluorescence mode and X-ray Diffraction on millimetre sized spheres of refractory oxides. For this, an analysis cell, operating under various gas conditions from room temperature up to 2800°C, has been developed.

Experiments have been carried out at LURE (Orsay, France), at ESRF [1] (Grenoble, France) and at SRS (Daresbury, UK) [2]. We have studied the long-range order and the local structure in YAG, zirconia, iron oxides and rare-earth oxides. We have shown that the X-ray absorption and X-ray diffraction data, calculated from in-situ synchrotron radiation experiments, contain valuable information on the different types of disorder in solid oxides. This technique proposes also an opportunity to gain a complete insight into the local structure in liquids. The information is directly derived from the temperature dependence of the spectra with the characteristic parameters of the structure described by the pair correlation function. The synchrotron radiation data obtained by this contactless technique present implications for the understanding of the solidification process in liquid oxides by crystallisation or vitrification.

1 C. Landron, L. Hennet, J.P. Coutures, M. Gailhanou, M. Gramond, and J.F. Berar (1998). Europhys. Letts., 44, 429.
2 L Hennet, C Landron, P Berthet, J-P Coutures, T.E Jenkins, C Aletru and G.N. Greaves (1999), accepted in Jpn. J. Appl. Phys.

M12.DD.004 COMBINED EXAFS-XRD APPLIED TO ORGANIC SOLID STATE REACTIONS. M. Epple. Institute of Inorganic and Applied Chemistry, University of Hamburg, Martin-Luther-King-Platz 6, D-20146 Hamburg, Germany

X-ray absorption spectroscopy (EXAFS) and X-ray diffraction (XRD) represent complementary methods for the study of solid compounds. While diffraction techniques yield specific information on the long-range order, EXAFS gives information on the Ångstrom scale around specific elements. Contrary to diffraction, EXAFS does not require long-range order, therefore liquid and amorphous phases can be detected as well. The combination of both techniques is especially powerful if they are applied in-situ, i.e. during a solid-state reaction. Detection of both short- and long-range order can uncover intermediate phases and identify final products. Quantitative evaluation of both methods is possible, and the reaction extent can be computed for all phases present.

Reactions involving molecular crystals ("organic solid state reactions") are of importance, e.g., in materials science and in pharmaceutical technology. Unfortunately, the most common elements in organic compounds (hydrogen, carbon, oxygen, nitrogen) are not available for EXAFS analysis, therefore heavier elements (like, Cl, Br) must be present if the method is to be applied. Examples for successful applications of the combined EXAFS-XRD technique that gave through insight into solid-state reaction mechanisms will be reported.

M12.DD.005 RECENT DEVELOPMENTS IN D.A.F.S. J.L. Hodeau, H. Renevier, S. Bos, V. Favre-Nicolin, P. Wolfers, Laboratoire de Cristallographie - CNRS, BP 166, 38042 Grenoble 9, France

The Diffraction Anomalous Fine Structure (DAFS) spectroscopy provides in the same experiment information regarding the local atomic environment through X-ray absorption processes and long-range order information through diffraction processes. Anomalous scattering and DAFS can provide site selective and chemical selective structural information.

After an introduction to the DAFS spectroscopy, we will show the experimental requirements for such studies. Efforts are being made at different Synchrotron Radiation Facilities to

develop the data acquisition with different experimental set-up: a) the energy-scanned one which uses classical monochromatic optics (J.O. Cross et al. J. Synchrotron Rad. 5, 911 (1998)) and b) the Dispersive Diffraction one that uses dispersive optics and a 2D position sensitive detector (N. Sugioka et al. J. Synchrotron Rad. 5, 908 (1998), V. Favre-Nicolin et al. J. Appl. Cryst submitted). We will briefly present these two set-ups and discuss their strengths and limitations. We will also present the analysis of the EDAFS oscillations (Extended DAFS) and point out the interest of using the DAFS spectra to recover quantitative information about the crystallographic structure and particularly the positions and Debye Waller factors of the anomalous atoms.

At last we will report different applications of the DAFS spectroscopy: (i) the study of strained III-V semiconductor thin films by using both a single first shell analysis and a multishell analysis; (ii) the use of DAFS site selectivity in superlattices to obtain information about their interfaces; (iii) DAFS site specification to separate overlapping X-ray absorption edges;

(iv) the use of DAFS spatial selectivity in powdered catalytic samples containing diluted particles; (v) valence difference studies on manganese oxide powders; (vi) DAFS on superlattice or forbidden reflections in oxides to extract the precise positions of the anomalous atoms.

12EE PEROVSKITE AND RELATED MATERIALS

M12.EE.001 LOW TEMPERATURE CRYSTALLOGRAPHIC STUDY OF THE $HgBa_2CuO_{4+\delta}$ HIGH Tc SUPERCONDUCTOR. Pierre Bordet and Fabienne Duc, Laboratoire de Cristallographie CNRS, BP166, 38042, Grenoble Cedex 9, France

Recent theoretical as well as experimental works have focused on the importance of the charge inhomogeneities in the CuO_2 planes for the mechanism of superconductivity in the High-Tc cuprates. For most of these compounds, such weak effects are in competition with lattice distortions due to bond mismatch, which can lead to strong structural changes with temperature (phase transitions, superstructures). The High-Tc mercury cuprates are free of such bond mismatch, because of the quasi-absence of in-plane bonds in the reservoir layers. Hg-1201 is the best candidate for precise structural studies, due to its simplicity, and the absence of stacking faults.

In order to investigate the existence of structural distortions in the Hg-1201 compound, we have undertaken a detailed low temperature structural study by means of single crystal x-ray and synchrotron diffraction, powder neutron diffraction and EXAFS.

Static disorder in the HgO_δ layers reveals the tendency toward formation of weak Hg-O bonds in the presence of extra oxygens. The observation of diffuse scattering could be related to short range ordering of such bonds or to charge inhomogeneities in the CuO_2 planes. Strong anharmonic displacements of the cations as well as anisotropy of the thermal parameters indicate a marked difference between the average and local structures. This is confirmed by coupled EXAFS and neutron data which reveal an anomalous behavior of the Cu-O and Cu-Ba displacement correlations above Tc.

M12.EE.002 COMPUTER MODELING, GROUP THEORETICAL ANALYSIS AND STRUCTURE PREDICTION OF DISTORTED PEROVSKITES P.M. Woodward, P.N. Santhosh [1], H.T. Stokes [2] and J.L. Fiallega [3]: [1] Department of Chemistry, Ohio State University, Columbus, OH 43210-1185, [2] Department of Physics and Astronomy, Brigham Young University, Provo, UT 84602-4675, [3] FDP Corporation, 2140 S. Dixie Highway, Miami, FL 33133

Perovksite and perovskite related materials make up one of the most prevalent and important structure families in all of materials science. The aristotype perovskite structure is very simple. However, the vast majority of perovskite materials are distorted from the ideal structure. We have examined the structural features which result when octahedral tilting distortions are combined with (a) 1:1 cation ordering in $A_2MM'X_6$ compounds, (b) 2:1 cation ordering in $A_3M_2M'X_9$ compounds, (c) layered cation ordering in $AA'M_2X_6$ and $AA'MM'X_6$ compounds and (d) Jahn-Teller distortions of the MX_6 octahedra. Using the principles of group theory and symmetry, complete crystallographic descriptions (space groups, lattice parameters, atomic positions) of the structures, which result from the combined action of octahedral tilting and (a) – (d) above, have been determined.

Analyzing the combined effect of octahedral tilting with cation ordering and/or Jahn-Teller distortions on the A-site coordination sphere, allows us to identify those combinations which lead to the most stable structures. The stability of $A_2MM'X_6$ structures, where M' is a Jahn-Teller ion (i.e. Mn^{3+}) and M has regular octahedral coordination (i.e. Mn^{4+}), has implications for structural studies involving charge ordering in the $Ln_{1-x}A_xMnO_3$ perovskites.

As a result of this work the software program SPuDS has been developed to calculate crystal structures of distorted perovskites using only the composition as input. The accuracy, availability and potential uses associated with this software package will be discussed.

M12.EE.003 CHARGE SEGREGATION IN $RNiO_3$ PEROVSKITES: SIMULTANEOUS METAL-INSULATOR AND STRUCTURAL TRANSITION. M.T. Fernández-Díaz, Institut Laue-Langevin, B.P. 156X, F-38042 Grenoble Cedex, France, J.A. Alonso, M.J. Martínez-Lope, M.T. Casais, Instituto de Ciencia de Materiales de Madrid, C.S.I.C., Cantoblanco, E-28049 Madrid, Spain, J.L. García-Muñoz, Institut de Ciència de Materials de Barcelona, C.S.I.C., Campus UAB, Bellaterra, E-08193 Barcelona, Spain and M.A.G. Aranda, Departamento de Química Inorgánica, Cristalografía y Mineralogía, Facultad de Ciencias, Universidad de Málaga, E-29071 Málaga, Spain.

$RNiO_3$ perovskites (R = 4f rare earth) are one of the few families of undoped oxides showing a metal to insulator transition as a function of temperature. The origin this first-order transition has been one of the long-standing questions associated with these compounds.

Our neutron and synchrotron diffraction data of small-rare-earth members of the series provide the first observation of changes in the crystal symmetry at the metal-insulator (MI) transition in $RNiO_3$ perovskites. At high temperatures, $RNiO_3$ are orthorhombic and metallic and below T_{MI} they change to a monoclinic insulator. This fact unambiguously shows the tight electron-lattice coupling. The structural reorganization at T_{MI} gives rise to two crystallographically independent Ni positions and the insulating phase consist of alternating expanded ($Ni1O_6$) and contracted ($Ni2O_6$) octahedra along the three directions of the crystal cell. This finding indicates a mutual self-doping process occurs, in which there is an accumulation of extra charge at Ni1 sites at expenses of inducing charge defects at the adjacent Ni2 sites. This charge modulation phenomenon of wave vector $\mathbf{k}_{cubic}$ = (1/2,1/2,1/2) in the pseudocubic basis is the driving force for the orthorhombic to monoclinic transition concurrent with the metal to insulator transition.

From the magnetic point of view, the antiferromagnetic structure of the Ni sublattice is the same to the one previously reported for less distorted $RNiO_3$ compounds, with a magnetic propagation vector $\mathbf{k}_{mag}$ = (1/2,0,1/2).

M12.EE.004 OXYGEN VACANCY STRUCTURES: A NEW ROUTE TO METASTABLE CMR RUDDLESDEN-POPPER PHASES J. F. Mitchell, J.E. Millburn, M. Medarde, A. Berger, D.N. Argyriou, Materials Science Division, Argonne National Laboratory, Argonne, IL 60439 USA

By use of intermediates containing large numbers of oxygen vacancies, we have extended the phase diagram of the Ruddlesden-Popper (R-P) series $La_{1-2x}Sr_{1+2x}Mn_2O_7$ beyond the normally accessible range $0.3 \leq x \leq 0.5$ and into the Mn^{4+}-rich regime. Colossal magnetoresistive (CMR) manganites display a fantastic range of structural, magnetic, and electronic phases as a function of hole concentration, temperature, magnetic field, etc. Although the bulk of research has concentrated on the 3-D perovskite manganites, the ability to study anisotropic magnetic and electronic interactions made available in reduced dimensions has prompted growing interest in the R-P phases of the manganite class. By using high temperature techniques to synthesize oxygen deficient inter-mediates, we have succeeded in making metastable phases with $0.5 \leq x \leq 1.0$. The intermediate compounds are unusual among oxygen vacancy structures in the R-P class, as the vacancies lie in the nominally MnO_2 conduction planes rather than between them. We will describe the synthesis, crystal and magnetic structure, and properties of these phases and explore the broader picture of the electronic and magnetic phase diagrams of these layered materials. We will also discuss the existence of ordered oxygen vacancy structures and highlight the extreme sensitivity of these structures to cation stoichiometry.

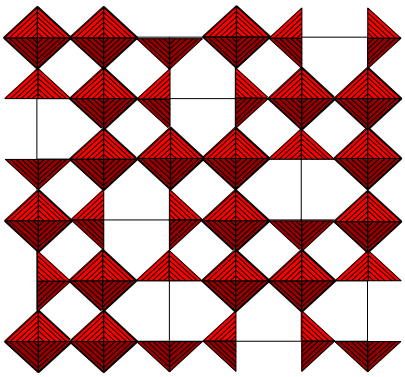

M12.EE.005 ORDER DISORDER IN $LnBaMn_2O_{6-x}$ PEROVSKITES. V. Caignaert, F. Millange, B. Domenges and B. Raveau, CRISMAT-ISMRa, Bd du M[al] Juin, F-14050 Caen, and E. Suard, Institut Laue Langevin, Av. des Martyrs, F-38042 Grenoble

Cation ordering in perovskite structures may induce physical properties that differ from those of disordered allotypes. Only few studies evidence this phenomenon owing to the difficulty to obtain the disordered and ordered forms. The disordered cubic perovskites $LnBaMn_2O_6$ (*Ln= La*, *Pr*, *Nd*) have been synthesized by solid state reaction and compared to the ordered perovskites, obtained by topotactic oxidation of $LnBaMn_2O_5$ oxygen-deficient perovskites.

The $LnBaMn_2O_5$ compounds (*Ln= La-Ho*, *Y*), synthesized under inert atmosphere, crystallized with the tetragonal space group P4/nmm ($a \approx \sqrt{2}a_p$, $c \approx 2a_p$ where a_p is the cell parameter of the cubic perovskite). The structure, allotype of $YBaCuFeO_5$, is described with an alternate stacking of rare earth and barium layers along the *c* axis. In addition the Mn^{+2} and Mn^{+3} cations adopt a rock-salt arrangement. The two magnetic sublattices are connected by an antiferromagnetic interaction, which lead to a ferrimagnetic behavior. The sign and the intensity of superexchange interaction in the (ab) plane are related to the value of the Mn^{+2}-O-Mn^{+3} angle.

The structure and the magnetic properties of the ordered $LnBaMn_2O_6$ depend of the rare-earth ionic radius. The Lanthanum compound is tetragonal (space group: P4/mmm; $a \approx a_p$, $c \approx 2a_p$) and ferromagnetic (F) while the Neodymium is orthorhombic (space group: Cmma; $a \approx b \approx c \approx 2a_p$) and antiferromagnetic (AF). Two magnetic transitions are observed in $PrBaMn_2O_6$. The comparison between the ordered and disordered compounds reveals strong differences in the physical properties.

By topotactic reduction of $LnBaMn_2O_6$, new oxygen-deficient perovskites $LnBaMn_2O_{5.5}$ (*Ln= La-Ho*, *Y*), are synthesized (space group: Ammm; $a \approx a_p$, $b \approx 2a_p$, $c \approx 4a_p$).

P12.EE.001 IN-SITU NEUTRON DIFFRACTION STUDY OF MIXED CONDUCTIVITY $SrFeCo_{0.5}O_Y$ MATERIAL, B.J. Mitchell and J.W. Richardson Jr., IPNS, Argonne National Laboratory, 60439, IL, USA, B. Ma and U. Balachandran, ET, Argonne National Laboratory, J.P. Hodges and J.D. Jorgensen, MSD, Argonne National Laboratory.

$SrFe_{1-x}Co_xO_y$ mixed ionic and electronic conductors possessing high oxygen permeability have created considerable interest for use as oxygen separation membranes. $SrFeCo_{0.5}O_y$ (SFC2) was shown to have the best properties in this series [1]. SFC2 is actually a complex assembly of phases; the composition and weight fractions dependent upon temperature and oxygen partial pressure. In-situ and ex-situ diffraction studies have identified $SrFe_{1.5-a}Co_aO_y$ (236), $SrFe_{1-b}Co_bO_{3-\delta}$ (perovskite), $(Co_{1-c}Fe_c)_3O_3$ (rocksalt) and $(Co_{1-c}Fe_c)_3O_4$ (spinel) to be present under certain conditions. We shall demonstrate that the 236 perovskite-rocksalt intergrowth crystal structure as described in the literature [2] is incorrect, and describe the variable nature of the cobalt and oxygen contents of individual phases under synthesis conditions and at oxygen partial pressures believed to be present across operational ceramic membranes.

B. Ma, U. Balachandran, B.J. Mitchell, J.W. Richardson Jr., J.P. Hodges, J.D. Jorgensen, "Oxygen Transport in the $Sr_2Fe_{3-x}Co_xO_y$ System", MRS Fall Meeting Boston, December 1998.
A. Yoshiasa, K. Ueno, F. Kanamaru and H. Horiuchi, *Mat. Res. Bull.*, **21**, 175-181, 1986.

P12.EE.002 SUPERCONDUCTING CUPRATES: FROM LAYERS THROUGH LADDERS TO CHAINS. T.I. Ivanova, O.V. Frank-Kamenetskaya and I.V. Rozhdestvenskaya, Department of Crystallography, Saint-Petersburg State University, 199034 Saint-Petersburg, Russia.

In the past few years the attention was being gradually shifted towards the degradation of dimensionality of the Cu-O modules in the structures of the superconducting (SC) cuprates seeking for the one which is intrinsically related to the appearance of SC state. It turned from *two-dimensional* infinite CuO_2-planes in various perovskite-like phases through *quasi-one-dimensional* Cu_2O_3-planes containing two-legged ladders in $(Sr,Ca)_{14}Cu_{24}O_{41+y}$ (T_c = 12-9 K at a pressure of 3-4.5 GPa) [1] to *one-dimensional* infinite CuO_2-chains in the ladder compound and in the newly synthesised $Ba_2Cu_{3-x}O_{6-y}$ crystals (T_c = 5-13 K) [2]. All the modules consist of similar CuO_4-squares but have different mode of their linkage. The squares share either corners to form CuO_2-planes or edges to form CuO_2-chains. Ladders represent the case where corner- and edge-sharing squares alternate. The coincidence of the temperatures of SC transitions in $Ba_2Cu_{3-x}O_{6-y}$ and in the ladder compound with the temperature (10 K) of the sharp magnetic transition in another infinite-chain compound $Sr_{0.73}CuO_2$ [3] seems to be intriguing.

Reported is the $Ba_2Cu_{2.89}O_{6-y}$ crystal structure (sp.gr. ***Pccm***, ***a*** = 13.065, ***b*** = 20.654 and ***c*** = 11.431 Å [4]). It contains parallel CuO_2-chains assembled into sheets which are separated by the layers of Ba atoms. The primary difference between the structures of all known infinite-chain compounds appears to be in the mode of stacking of Cu-O sheets along *c*-axis. They are shifted in [100] direction by ½ of Cu-Cu distance in $Sr_{0.73}CuO_2$ and in the CuO_2-substructure of ladder compound but are rotated by 115.4° in $Ba_2Cu_{2.89}O_{6-y}$. This defines the differences in the symmetry of their crystal structures but suggests the similarity of the translations normal to the layers.

The work was supported by INTAS and by Russian Council of Ministers.

1. S. Maekawa, *Science* **273** (1996) 1515.
2. S.V. Moshkin et al., *Tech. Phys. Lett.* **23** (1997) 954.
3. J. Karpinski et al., *Physica C* **274** (1997) 99.
4. I.V. Rozhdestvenskaya et al., *Physica C* **311** (1998) (in press).

P12.EE.003 CRYSTAL STRUCTURE DETERMINATION AND RIETVELD REFINEMENT OF NB-DOPED $PB(ZR_{0.97}TI_{0.03})O_3$ CERAMIC MATERIAL. Hongchao Liu and Hideo Toraya, Ceramics Research Laboratory, Nagoya Institute of Technology, Asahigaoka, Tajimi 507-0071, Japan

ab initio crystal structure analysis and Rietveld refinement were employed to investigate the crystal structures of $Pb(Zr_{1-x}Ti_x)O_3$ [PZT (1-x/x)] series ceramic materials. In this work, the crystal structure of a orthorhombic phase of Nb-doped $Pb(Zr_{0.97}Ti_{0.03})O_3$ ceramic material was reported. For complex distortion in the crystal structure, the powder diffraction data were collected with high-resolution synchrotron radiation source. The orthorhombic symmetry was confirmed by the indexing procedure. However, the Rietveld refinement showed that the diffraction pattern of this ceramic material could not be fitted well with published structural models of space group Pbam and Pba2. The whole pattern profile fitting and crystal structural analysis based on the powder diffraction data showed the most appropriate space group for this material is Pnnm, rather than the widely accepted Pbam or Pba2. The structure was then solved with space group Pnnm by the direct methods. The obtained structural parameters confirm that Zr atoms participate in the displacement along *z-axis*. They also support that local disorder appears in the oxygen substructure as observed by Glazer et al [1] in single crystal study, since the obtained amount of oxygen atoms is larger than the chemical formula shows. The origin of disorder was attributed to the existence of micro-domain smaller than x-ray coherence length in the studied ceramic material.

[1] Glazer, A. M., Roleder K. & Dec J., *Acta Cryst.*, 1993, **B49**, 846

P12.EE.005 IN-SITU SYNCHROTRON DIFFRACTION STUDY OF THE HP-HT SYNTHESIS OF HIGH Tc MERCURY CUPRATES. P.Bordet, S. LeFloch, A. Prat, Laboratoire de Cristallographie CNRS, BP166, 38042, Grenoble Cedex 9, France, M. Mezouar, ESRF, BP220, 38043 Grenoble France

High-pressure high temperature synthesis techniques have been extensively used in the past few years for the discovery of new oxide materials, particularly high Tc superconducting oxides. However, the complexity in tuning the many synthesis parameters (starting material composition and oxidation state, pressure, temperature, gradients, etc.), as well as the impossibility to control the reaction mechanisms (but only by analysing the reaction products), has hindered the development of this powerful synthesis technique. This was particularly true in the case of the $HgBa_2Ca_{n-1}Cu_nO_{2n+2+\delta}$ series of high Tc cuprates, where the member obtained depends on precise oxidation state of the precursor material, and temperature range chosen. In order to get better insight into the reaction mechanism of these materials and to optimise their synthesis conditions, we have undertaken an in-situ synchrotron diffraction study at the ID30 beamline of the ESRF, using the Paris-Edinburgh large volume pressure cell. The combination of a high energy of 77 keV and fast 2D detector allowed us to obtained good quality diffraction spectra on the time scale of a minute up to ≈ 1200°C and 4GPa. The synthesis conditions used in the laboratory belt type apparatus for the synthesis of the Hg-1201 and Hg-1223 mercury cuprates were carefully reproduced (gold capsule, starting compositions, pressure and temperature). We could then determine the pressure and temperature stability ranges of the various phases involved in the reaction process, as well as the kinetics of reactions. For example, in the case of the Hg-1223 compound synthesis at 3GPa, the mixture of HgO and prereacted oxide precursor first form the $CaHgO_2$ compound which partly transforms on heating into a new $Ca_4Hg_6O_{10}$ high-pressure phase. These phases react at higher temperatures to form mercury cuprates of increasing n value at increasing temperature. Single phase Hg-1223 is then obtained at T=1000°C.

P12.EE.006 CRYSTAL STRUCTURE OF A FERROMAGNETIC SUPERCONDUCTOR. A. C. McLaughlin and J. P. Attfield, Department of Chemistry and IRC in Superconductivity, University of Cambridge, Cambridge CB2 1EW, UK, and A. N. Fitch, ESRF, BP 220, F-38420 Grenoble, France, and J. L. Tallon, Industrial Research Ltd., P.O. Box 13130, Lower Hutt, New Zealand.

A remarkable new ruthenocuprate has been prepared in which ferromagnetism and superconductivity co-exist at low temperatures [1]. The structure of this material has been refined using highly-resolved powder X-ray diffraction data collected on ESRF instrument BM16. Room temperature and 4 K data have been analysed, giving information about the twists and tilts of the metal oxide polyhedra within this layered structure.

1. J.L. Tallon, C. Bernard, M.E. Bowden, T.M. Stoto, B. Walker, P.W. Gilberd, G.V.M. Williams, D.M. Pooke, M.R. Presland, J.P. Attfield, A.C. McLaughlin and A.N. Fitch. Nature (to be published).

P12.EE.007 SYNTHESIS OF FUNCTIONAL PEROVSKITE OXIDES WITH LANTHANUM IN A-SITE FROM AQUEOUS SOLUTIONS. T. Yao, Y. Uchimoto, T. Sugiyama and Y. Nagai, Department of Fundamental Energy Science, Graduate School of Energy Science, Kyoto University, Yoshida, Sakyo-ku, Kyoto, 606-8501, JAPAN

Functional perovskite oxides with lanthanum in A-site: $LaMeO_3$ (Me=Cr, Mn, Fe, Co or Ga) have interesting properties and now are paid a great attention as candidates for electrode, cathode, anode or interconnecting materials for solid oxide fuel cells and high-temperature steam electrolyzers. Thin films, either dense or porous, are desirable because of the high surface area, the reduction of both the ion-diffusion path length and electrical resistance, light and compact system construction and so on. Chemical vapor deposition, sputtering and sol-gel methods are used for preparing thin films, however, these methods have some disadvantages in actual use. For chemical vapor deposition and sputtering, expensive vacuum equipment is required and the film area is restricted. For sol-gel method, the film geometry is limited, and moreover, heat-treatment, which is injurious because of the possibility of a change in the shape and/or size of the film and crack formation, is inevitable to form crystalline states. A method for forming films from an aqueous solution is expected to be advantageous because no vacuum, no high temperature and no expensive apparatus will be required and substrates even with wide areas and/or complicated shapes are available. For the above reason, we have been studying about the synthesis of functional ceramic materials from aqueous solutions and we have presented the methods for synthesizing ZrO_2 and $LaCrO_3$, $LaMnO_3$, $LaFeO_3$ and $LaCoO_3$ from aqueous solutions[1,2,3], previously. Recently, we have developed the method and have made it possible to synthesize $LaGaO_3$ from aqueous solution.

Powder of $LaMeO_3$ perovskite was dissolved in hydrofluoric acid and a solution of fluoro-complex ions was obtained. Boric acid was added to the solution, the fluoride ions were consumed by the formation of BF_4-, and then the fluoro-complex ions were hydrolyzed to $LaMeO_3$ in order to increase the

amount of fluoride ions. X-ray diffraction peaks attributed to the respective perovskite oxides were observed on the soaked substrates. The peaks were sharp and strong enough to confirm the high crystallinity. A number of synthesized particles of $LaMeO_3$ were observed on the substrates in scanning electron microscope images.

[1] T.Yao, T.Inui and A.Ariyoshi, J.Am.Ceram.Soc., 79, 3329 (1996)
[2] T.Yao, A.Ariyoshi and T.Inui, J.Am.Ceram.Soc., 80, 2441 (1997)
[3] T.Yao, J.Mater.Res.,13, 1091 (1998)

P12.EE.008 ANOMALOUS MANGANESE-OXYGEN BOND COMPRESSIBILITY IN LAYERED MANGANITES. K. V. Kamenev, M. R. Lees, G. Balakrishnan and D. M^{c}K. Paul, Department of Physics, University of Warwick, Coventry CV4 7AL, UK.

We present the results of neutron diffraction study of $(La_{0.6}Nd_{0.4})_{1.2}Sr_{1.8}Mn_2O_7$ oxide by time-of-flight technique under pressures of up to 18 kbar. This material belongs to the class of double-layer manganites which became a subject of intense interest after a large magnetoresistance effect was found in $La_{1.2}Sr_{1.8}Mn_2O_7$ [1].

In the layered $(La_{0.6}Nd_{0.4})_{1.2}Sr_{1.8}Mn_2O_7$ the tetragonal lattice is composed of double MnO_2 sheets separated by $[(La_{0.6}Nd_{0.4})_{0.4}Sr_{0.6}]_2O_2$ NaCl-type block layers. Each manganese ion participates in three types of interatomic links: i) within the MnO_2 sheet; ii) between the adjacent MnO_2 sheets forming a double-layer; and iii) between the adjacent double-layers. We have found that in paramagnetic phase the manganese-oxygen covalent bond involved in the inter-double-layer link expands under applied pressure, while the other two types of bonds contract. We explain such an anomalous extension of the apical manganese-oxygen bond under pressure in terms of the electronegativity equalization principle.

The results of neutron diffraction are combined with high-pressure resistivity and magnetic ac susceptibility data to discuss the effect of structural changes on transport and magnetic properties of the layered manganites.

[1] Y. Moritomo *et al.*, Nature **380**, 141 (1996)

12FF TEACHING CRYSTALLOGRA|HY

M12.FF.001 EXPERIENCES IN TEACHING NEW TECHNIQUES TO THE CRYSTALLOGRAPHIC COMMUNITY. Bi-Cheng Wang, Department of Biochemistry and Molecular Biology, University of Georgia, Athens, GA 30602 U.S.A

In the last decade, we have witnessed a revolution in crystallographic methodology and the expansion of crystallography into many new scientific disciplines.

To provide students with necessary crystallographic knowledge to meet todayís challenges, we at the University of Georgia (UGA) have emphasized both the basics of crystallography and the application of the latest crystallographic techniques. Students at UGA are offered a number of crystallography courses including: a one-semester graduate course in crystallography as well as numerous lectures on crystallography in several other graduate and undergraduate courses.

Since 1997, UGA has hosted the American Crystallographic Association (ACA) Summer Course in Crystallography. This is an intensive 12-day course with lectures in mornings and evenings, and hands-on laboratory sessions in afternoons. The first eight days of the Course are devoted to fundamental crystallography as applied to small molecule crystallography. The last four days of the Course are on the application of crystallography to macromolecular structures. For 1999 Summer Course information see www.uga.edu/~biocryst/ACA99.html.

The data collection facilities on the UGA campus, include Nonius and Bruker single crystal diffractometers, Rigaku and MarResearch image plate detectors and a Bruker CCD detector as well as Silicon Graphics workstations in the UGAís Molecular Graphics Laboratory have been used in lectures, hands-on experiments, and demonstration in the Summer Course.

In the past two years, UGA has also hosted the Bruker and R-Axis Users Group Meetings. These meetings provide the crystallographic community an opportunity to learn from experienced users about data collection hardware and techniques, data processing programs, structure determination packages, and the use of second and third generation synchrotron sources.

Aspects of the ACA Summer Course and the Bruker and R-Axis Users Meetings will be discussed.

M12.FF.002 TEACHING CRYSTALLOGRAPHY ON THE INTERNET. David S Moss, Clare E Sansom, Jeremy K Cockcroft, Ian J Tickle and Huub P C Driessen. Department of Crystallography, Birkbeck College, Malet St., London WC1E 7HX, UK.

The Department of Crystallography at Birkbeck College has been a pioneer in delivering formal courses at advanced University level using the medium of the Internet. Our Advanced Certificate Courses in Principles of Protein Structure (PPS) and Protein Crystallography (PX) are accredited, one-year, part-time courses that lead to the award of an Advanced Certificate from London University. Principles of Protein Structure has run as an accredited course every year since 1996, and over 150 students have completed it. The protein crystallography course was offered for the first time in the 1997-8 academic year. Four PPS graduates have taken, or are currently taking, this course. Many students on both courses work in the pharmaceutical industry. Others take one of our courses as part of their graduate studies programme; some of these come from emerging economic areas. Forty students from central and eastern Europe have taken the PPS course with bursaries from the Open Society Institute.

Course material is distributed via the World Wide Web, with a new section released every few weeks. The material is developed in-house but makes extensive use of many excellent Internet resources for structural biology: pre-eminently, of course, the Protein Data Bank. Interaction between students and tutors takes place via email discussion lists and tutorials using the “BioMOO” virtual reality conference system. In these tutorials, students can question their tutors about any aspect of the course in “real time”. Formal assessment consists of an examination, for which students need to attend in person at one of a number of local centres, and project work. A new course, the Advanced Certificate in Powder Diffraction, will be starting in October 1999 and we hope to be able to offer Internet-based M.Sc. degrees in structural biology from 2000.

M12.FF.003 CRYSTALLOGRAPHY FOR MATERIALS SCIENTISTS - THE MATTER SOFTWARE CONSORTIUM. Peter J Goodhew, Ann Fretwell, Andrew Green, MATTER Project, Materials Science & Engineering, University of Liverpool, L69 3GH, UK

The MATTER project is supported by a consortium of 19 Universities and its aim is to produce and support software for use in the teaching of materials science. 20 modules have been produced so far, covering a large range of subject matter. Protocols have been developed for the production and evaluation of each module and this typically involves collaboration between one or two academics and members of the development team.

Undergraduate crystallography teaching is supported by a new software module in the MATTER series. This is described

here as an illustration of the approach. The module exploits the interactive and graphical capabilities of the computer in presenting concepts which are of key importance to students of materials science. These include symmetry operations, point and space groups, indexing of planes and directions and the building of common structures using space-filling spherical atoms.

The approach adopted in the module is to start from two dimensional lattices, which provide a less extensive set of rules and examples which are easier for the student to master. Three dimensional lattices are then developed in a fairly conventional way. The use of interactive exercises ensures that understanding is developed as the student proceeds. Graphical interactions are used where they are most effective. First-year classes have been taught using this module and assessed using a companion software package. Student and staff response has been very positive, particularly to the computer-based assessment.

A further module on introductory diffraction follows a similar style. Extracts from both modules will be used to illustrate the presentation. Further details of these and other modules produced by the MATTER team can be found at www.liv.ac.uk/~matter/home.html.

M12.FF.004 TEACHING POWDER DIFFRACTION FOR MATERIALS SCIENCE. Karimat El-Sayed, Physics Department, Ain Shams University, Cairo, Egypt

The plan of the topics was designed according to the need of other courses given to the M.Sc materials science students. The contents of the powder diffraction course were perfectly selected from lectures given by International lecturers (experts in powder diffraction) at schools held in Egypt. Their lectures as well as their practical sessions and lectures materials were the sources of the development of the powder diffraction course presented in this paper. In the I U Cr XVII Congress (1996) at Seattle, USA, a short talk was given about teaching crystallography in general for physics students in Egypt in which we mentioned that powder diffraction and electron microscopy techniques are the main contents of the M.Sc post graduate course. In this paper an overview will be given on the main contents of the powder diffraction course.

The course contents are: Powder diffraction instrumentation - Data collection strategies and Cautions - Amorphous and polycrystalline diffraction patterns - Indexing of powder diffraction patterns - Analytical functions used in powder diffraction line profile - Profile fitting procedures - Phase identifications using the powder diffraction file - Phase diagrams and phase transformations - Structural characterization and crystal structure refinements (using Rietveld and the two stage methods) - Solid/solid reaction - Lattice strain and stress analysis - Microstructural analysis for materials having either intrinsic or extrinsic properties - Quantitative analysis of phases - Degree of disordering in disordered materials - Lattice and super lattice detection - Preferred orientation and expitaxial growth.

M12.FF.005 TEACHING DIFFRACTION WITH THE AID OF COMPUTER SIMULATIONS R.B. Neder, Institut für Mineralogie, Am Hubland, 97074 Würzburg, Germany and Th. Proffen, Department of Physics and Astronomy, Michigan State University, East Lansing, MI 48824-1116, USA

Computer simulations are a versatile tool to enhance teaching diffraction physics and related crystallographic questions. Students attain a very high degree of motivation and very effective learning is achieved. Computer simulations allow students to visualize a crystal structure and its Fourier transform. No physical limitations apply to the structure and a systematic approach can be taught by simulation individual atoms, small clusters of molecules, and any extended structure. These simulations can be used to enhance standard illustrations. The most efficient use is made, though, if the students perform their own computer experiments. They will rapidly acquire a rich experience on the correlation between structure and diffraction pattern by modifying given simulations and ultimately by experimenting with own simulations.

In this talk we present a course that guides students from the diffraction by a single atom to diffraction by complex disordered materials. The material includes simulations of: diffraction by individual atoms and small clusters, the geometry of real versus reciprocal space, the effect of structural modifications on the Fourier transform, the crystallographic phase problem, inverse- and difference-Fourier transforms, anomalous scattering, powder diffraction, and diffuse scattering.

A separate section deals with examples related to structure solution via direct methods. These examples illustrate intensity statistics, determination of origin, and phase relationships.

Neder, R.B. & Proffen, Th.: J. Appl. Cryst. **29** (1996) 727.

P12.FF.003 THE STORY ABOUT ONE CRYSTALLOGRAPHIC COLLECTION. T.K.Ivanova Earth Science Museum at Lovonosov Moscow State University, University,Square,1, 119899 Moscow, Russia, and G.I.Dorokhova ,Department of Geology, Mocow State University, Sguare,1, 119899, Moscow, Russia, and E.N. Belova, Institution of Cristallography of the Russian Academy Science, Moscow, Russia

The invaluable contribution to the study of mineral, working out their crystal chemical systematization (that of silicates,in particular) have been made by the founder of the British and Russian crystal chemical school-the father and son W.G.Bragg and W.L.Bragg and the academician N.V.Belov. In 1970 the morld scientific community celebrated the 80-th birthday of William Laurance Bragg-the patriarch of crystallography, author of the first definitions of crystall structures based on the usage of X-ray structural analysis.In connection with the anniversary date the International symposium had been held in London; there were invited the scientists from Russia -the academicians N.V.Belov and B.K.Vainshtein (the director of the Institute of Crystallography of the USSR Academy of Sciences).

The Russian crystallographers wanted to express their special respect to the outstanding scientist. Within the precincts of the Institute of Crystallography the splendid idea had arised: as the present for W.L.Bragg, to create the collection of structure models of minerals using the polyhedra method of structure depiction, which had been developed by Linus Pauling, the american scientist and Nobel prize laureate twice, and improved by N.V.Belov. Yrii Semakin, the expect modeller from the Institute of Crystallography, the two similar collection were made One collection was solemnly given as present to the hero of the anniversary W.L.Bragg, the other -left in the Institute of Crystallography for the memory of that non-ordinary event.

Howdays the main part of the “Bragg‘s” collection is kept in Shubnikov Institute of Crystallography of the the Russian Academy of Sciences-N.V.Belov’s Museum.(Moscow). In 1989 Belov’s daughter Elena Belova made the present -she gave some of the models to the Earth Science Museum at Lomonosov Moscow State University for the text illustration of the poster-memorial “Structural Mineralogy of N.V.Belov”.

P12.FF.005 INNOVATIVE TECHNOLOGIES FOR BI-LINGUAL EDUCATIONAL DICTIONARY AND KNOW-LEDGE BASE FOR CRYSTALLOGRAPHY. A.Y. Boyko[2], B.N. Kodess[1,2], Z. Sidikov [2], [1]VNIIMS, Moscow, 119361, Russia, [2] ICS&E, Aurora, CO 80015, USA

Understanding of new approaches to application of materials gained its reflection in the system of integrated

education. Material science and crystallography education in the US, Great Britain, Russia as well as at the centers of materials science in many countries of Europe and Japan, is based on the integration of knowledge about various properties of crystals and methods of their growing**.** Methodology and a product of efforts in compilation of the new Russian-English-Russian dictionary and knowledge base for purposes of education, translation and support of complete and current databases are described.

Elements of artificial intelligence are used for the purposes of the information retrieval, classification and presentation. Generic and crystallography-related knowledge and expertise are presented in form of an expert system, constructed from factual, procedural and other types of knowledge. The system exploits such methods of knowledge manipulation as backward and forward chaining, fuzzy logic and neural nets. Among other uses, this approach provides capability of computer-assisted context analysis for translation of text in the area of materials science and crystallography. Content of the knowledge base itself reflects a shift in the system of key concepts and terms of crystallography towards the field of dynamic systems and modeling at various levels of the concept of open systems.

The implemented approach embraces development of the content of basic concepts in materials science, which are new as well as traditional to the field. The concepts are product of research of new phenomenon in materials, advances in applications of materials, and introduction of new technologies.

The concise version of the dictionary is for reference, standardization and educational purposes mostly. It contains about 9000 terms related to the crystallography and other general concept of physics and chemistry of materials science. Extended version of the dictionary includes a hierarchical system of related words originating from intersecting thesauruses. For example, 60 terms related to defects in the thematic index of the concise version are extended into a system of more than 2500 related words etc. The polysemy of words and the introduction of more than 30000 interrelated words and collocations support the interdisciplinary nature of the content. Another basic principle of compiling this dictionary version was to provide a reader the ability to read any abstracts from publications such as Physics Abstracts (Solid State section), "Metadex"(Metals Abstracts), "Ceramical Abstract" and corresponding "VINITI " abstract etc, without addressing any other technical dictionary.

P12.FF.006 ON THE ROCKS... CRYSTAL GROWTH FOR HIGH SCHOOLS. C. Teixeira, Centro de Química Estrutural, Instituto Superior Técnico, Av. Rovisco Pais 1049-001 Lisboa, Portugal

In spite of all the importance crystals have in our daily life and modern technology, the subject of crystal growth is either completely absent, or reduced to a trivial purification technique, in most part of General Chemistry textbooks. The magnificent beauty of single large crystals has not yet been exploited for teaching purposes. This beauty can be largely enhanced, if giant crystals of well known inorganic compounds are allowed to grow from supersaturated aqueous solutions on rough surfaces like those of rocks and shells. With a right choice of the substances, using non expensive glassware at schools, universities, or even at home, one can easily obtain a large collection of spectacular samples, covering the chemistry of most common elements of the Periodic Table and their compounds. Some examples of this rich diversity are: isomorphous metallic salts, like alums and schönites, forming solid solutions with a large variety of colours; occlusion of dyes into the crystals of transparent substances; habit modifiers purposely added to the solutions, or contained in the rock or shell composition; reactions between the solutes and the components of the rocks and shells, etc. Since 1994, 180 high school teachers were trained by our research group in this field, sponsored by Ministry of Education (FOCO Program) and Ministry of Science and Technology, (Ciência Viva Program). Many of these teachers were able to perform these experiments with their students, included in their regular laboratory programs of Chemistry, Physics, Geology, Arts or at their "Science Clubs" in schools.

C. Teixeira (1998) "On the Rocks... Crystallization on Rough Surfaces" (video+text) Instituto Superior Técnico.
C. Teixeira, A. Santana, C. Mesquita (1994) "Química", Boletim da Sociedade Portuguesa de Química, 53, 50.
C. Teixeira, A. Sousa, I. Trigueiros (1997) ibid, 66, 25.

13OA HOT MACROMOLECULAR STRUCTURES (I)

M13.OA.001 AN ORIGINAL SYSTEM OF IRON ACQUISITION FROM HEME: STRUCTURAL STUDY OF THE EXTRACELLULAR COMPONENT. P. Arnoux , M. Czjzek [1], R. Haser [2], N. Izadi, A. Lecroisey [3], C. Wandersman [4], [1] AFMB, IBSM, CNRS, 13402 Marseille, France, [2] IBCP, CNRS, 69367 Lyon , France, [3] Laboratoire de RMN, Institut Pasteur, 75724 Paris,France, [4] Laboratoire de Physiologie Cellulaire, Institut Pasteur, 75724 Paris, France

Iron is involved in many essential reactions such as photosynthesis, respiration and nitrogen fixation showing its importance in biological processes. Bacteria have different way to use the extracellular available iron. A major change occurs during the host infection where bacteria have to face drastic iron limitation. They have developed various ways in using the host's iron from iron containing proteins. Serratia marcescens can use the iron from hemoglobin through the secretion of a hemophore called HasA (1) which takes up the heme from hemoglobin and shuttles it to the outer membrane receptor HasR, which in turn, releases heme into the bacterium. The mechanism by which HasA is secreted in the extracellular medium appeals to an ABC transport system.

We have determined the crystal structure of the heme/HasA complex at 1.9Å. The architecture and topology of the complex reveals a new type of fold. The 178 residues are structured in a highly curved six stranded β-sheet again which are packed, on one side, the four α-helices. The fourteen last residues, which were known to be important in the secretion mechanism, are present but are not seen in the e/density. This argues in favor of an unstructured sequence which places the four last hydrophobic residues accessible to the solvent and potentially interacting with the membrane and/or membrane proteins. The heme is located at the interface between the a and b part of the molecule and is held by two exposed loops containing the two iron ligands His32 and Tyr75. This type of iron coordination, together with the high surface complementarity between the heme and the protein, lead to a low dissociative constant since it is less than 10nM (2). The -550mV redox potential of the heme can be explained by the coordination type and the high solvent exposure of the heme. The heme binding site structure showed that the His83 Nd is hydrogen bonded to the Tyr75 OH ligand. This novel arrangement of the residues around the heme group suggests a mechanism for the processes involved in both heme uptake and release.

(1) Létoffé, S. et al. Proc. Natl. Acad. Sci. USA 91, 9876-9880 (1994).
(2) Izadi, N. et al. Biochemistry 36, 7050-7057 (1997).

M13.OA.002 THE CRYSTAL STRUCTURE OF C-TERMINAL MEROZOITE SURFACE PROTEIN 1, A HIGHLY PROTECTIVE MALARIA VACCINE CANDIDATE. Graham A. Bentley, Véronique Chitarra and Inge Holm, Unité d'Immunologie Structurale, Institut Pasteur, 25 rue du Dr. Roux, 75724 Paris, France; Stephane Pêtres, Laboratoire de Technologie Cellulaire, Institut Pasteur, Paris France; Shirley Longacre, Unité de Parasitologie Expérimentale, Institut Pasteur, Paris, France.

The GPI-bound surface protein MSP1 from the Plasmodium merozoite is synthesised as a precursor ranging from 180 to 250 kDa, which matures to the final C-terminal product of 90 - 100 resides, depending on species. Correct maturation of MSP1 is essential for successful erythrocyte invasion by the parasite since antibodies specific for the protein, or the addition of protease inhibitors which prevent cleavage of the polypeptide, can block this process. Nonetheless, the precise role of MSP1 has not been characterised. We have determined the crystal structure of a soluble baculovirus recombinant form of C-terminal MSP1 from P. cynomolgi at 1.8 Å resolution by isomorphous replacement. The structure comprises two EGF-like domains, and sequence comparisons strongly suggest that the same conformation is present in all species of Plasmodium, including P. falciparum and P. vivax which are pathogenic in man. In particular, conserved inter-domain contacts between the two EGF modules should preserve the unusually compact form of the molecule in all species. Recombinant C-terminal MSP1 is a promising malaria vaccine candidate since it confers excellent protective efficacy in primate vaccination trials. Antisera obtained from vaccinated monkeys, or from animals with natural immunity acquired through infection by the parasite, recognise the recombinant protein in its native form but not in the disulphide-reduced state, showing that the epitopes are conformational. Expression systems or refolding protocols for recombinant C-terminal MSP1 that are capable of reproducing the native pairing of cystine links are therefore an essential requirement for vaccine production. A model of C-terminal MSP1 from P. falciparum based on the P. cynomolgi crystal structure shows that the dimorphic residues in this species are sufficiently spaced to form non-overlapping B-cell epitopes. The heterogeneity of the antibody response should therefore be insensitive to dimorphic permutations, and consequently two recombinant constructs carrying, respectively, the alternate residues at these sites should suffice to induce antiserum responding to all common polymorphs of C-terminal MSP1.

M13.OA.003 PROTEIN PROSTHETICS: X-RAY STRUCTURE OF THE *E. COLI* FIMC-FIMH CHAPERONE-ADHESIN COMPLEX. Stefan Knight and Devapriya Choudhury, Department of Molecular Biology, Uppsala Biomedical Center, Swedish University of Agricultural Sciences, Box 590, S-753 24 Uppsala, Sweden., Andrew Thompson, EMBL Grenoble Outstation, C/o Avenue des Martyrs, BP 156X, 38042 Grenoble, France, Vivian Stojanoff, ESRF, Avenue des Martyrs, 38400 Grenoble, France, Solomon Langermann, MedImmune, Inc., Gaithersburg, Maryland 20878, Jerome Pinkner and Scott J. Hultgren, Department of Molecular Microbiology, Washington University School of Medicine, St Louis, Missouri 63110, U.S.A.

The X-ray structure of the bacterial adhesin that mediates colonization of uropathogenic *E. coli* to the bladder epithelium, FimH, in a complex with its chaperone, FimC, was solved to 2.5 Å resolution. FimH consists of an NH_2-terminal mannose-binding domain and a COOH-terminal pilin domain used for incorporation of the adhesin into the pilus. The pilin domain of FimH has the same immunoglobulin-like topology as the NH_2-terminal domain of PapD-like chaperones, except that the seventh strand is missing. This creates a deep scar on the surface of the domain, leaving part of the hydrophobic core exposed. A donor strand complementation mechanism was revealed in which the chaperone donates a strand to the pilin domain. We propose that an extension at the NH_2-terminus of pilins participate in a donor strand exchange mechanism in pilus assembly. The donor strand complementation mechanism provides the first example of a class of proteins for which the primary sequence does not contain all of the steric information needed for correct folding.

M13.OA.004 STRUCTURE OF A HETEROPHILIC ADHESION COMPLEX BETWEEN HUMAN CD2 AND CD58 (LFA-3). Jia-huai Wang [1], Alex Smolyar [1], Kemin Tan [1], Jin-huan Liu [1], Mikyung Kim [1], Zhen-yu J. Sun[2], Gerhard Wagner[2],Ellis Reinherz[1], [1] Immunobiology Division, Dana-Farber Cancer Institute, Harvard Medical School, Boston, MA. 02115, USA, [2] Department of Biological Chemistry and Molecular Parmacology, Harvard Medical School, Boston, MA. 02115, USA.

Interaction between CD2 and its counter-receptor, CD58 (LFA-3), on opposing cells optimizes immune recognition, facilitating contacts between helper T lymphocytes and antigen presenting cells as well as between cytolytic effectors and target cells. Here we report the crystal structure of the heterophilic adhesion complex between the amino terminal domains of human CD2 and CD58. A strikingly asymmetric, orthogonal, face-to-face interaction involving the major b-sheets of respective immunoglobulin (Ig)-like domains with poor shape complementarity is revealed. In the virtual absence of hydrophobic forces, interdigitating charged amino acid side chains form hydrogen bond and salt link network at the interface. These charged interactions not only ensure high specificity, but also provide binding energy for this low affinity adhesion. These features explain CD2-CD58 dynamic binding, which is best suited to permit the T cell to broadly sample the surface of an opposing cell in search of the correct antigenic pepetide/MHC complex and co-stimulatory ligands. We have also inferred from sequence comparison that there is a subfamily within the Ig superfamily (IgSF) that utilizes the same interaction mode for cell adhesion, but the physico-chemical character of the subset of residues involved in interface determines the relative binding affinity to meet the different biological requirement.

M13.OA.005 THE CRYSTAL STRUCTURE OF LEECH ANTI-PLATELET PROTEIN, AN INHIBITOR OF HAEMOSTASIS. E.G. Huizinga[1,2], A. Schouten[1], T.M. Connolly[3], J. Kroon[1], J.J. Sixma[2] & P. Gros[1]. (1) Department of Crystal and Structural Chemistry, Bijvoet Center for Biomolecular Research, Utrecht University. (2) Department of Haematology, University Hospital Utrecht. (3) Department of Biological Chemistry, Merck Sharp & Dohme Research Laboratories, West Point, Pennsylvania.

Leech anti-platelet protein (LAPP) is a collagen binding protein from the leech *Haementeria officinalis*. It interferes with the adhesion of blood platelets to collagen by blocking the binding of von Willebrand factor and integrin $\alpha_2\beta_1$ We have determined the crystal structure of recombinant LAPP using single isomorphous replacement with anomalous scattering combined with solvent flattening and three-fold molecular averaging. The model of LAPP has been refined at 2.2 Å resolution (R-factor 21.5%; Rfree 23.7%). LAPP contains two distinct domains. The 89 residue C-terminal domain consists of a 6-stranded anti-parallel β-sheet. On one side the β-sheet is flanked by an α-helix, on the other side by two extended loops. Despite the absence of detectable sequence homology the fold of LAPP resembles closely that of the N-domain of hepatocyte growth-factor. The r.m.s. fit for 69 aligned Cα positions is 2.0 Å . The best conserved part with an r.m.s fit of 1.4 Å for 36 aligned Cα positions is the central β-sheet and the α-helix that packs against it. The central β-sheet in LAPP contains one additional strand contributed by the N-terminal region of the domain. The conserved features also include two disulfide bonds that link the α-helix to the core of the protein, indicating that these bonds may form an important stabilizing element in this type of fold. The 36-residue N-terminal domain of LAPP is rich in glycines, lacks hydrophobic residues and is not visible in the electron density map. Although LAPP has been shown to exist as a monomer in solution at neutral pH, the crystal packing suggested that LAPP may form tightly interacting

dimers. Dynamic light scattering experiments confirm that LAPP undergoes dimerization at pH 4.5, the pH used for crystallization.

M13.OA.006 CRYSTAL STRUCTURE OF ALLERGENIC DOMAIN OF THE MAJOR GRASS POLLEN ALLERGEN, PHL P5B. K.R. Rajashankar[1], A. Bufe[2], W. Weber[1] and Ch. Betzel[1], [1]Institute of Physiological Chemistry, UKE, c/o DESY, Building 22a, Notkestrasse 85, 22603 Hamburg, Germany; [2]Forschungzentrum Borstel, Klinische Allergology, Parkallee 22, 23845 Borstel, Germany.

Phl p 5b is a major allergen from timothy grass pollen which induces allergic rhinitis and bronchial asthma in millions of allergic patients world-wide. Until today there are no structural reports on this group of allergens. As an important step towards understanding the interactions between pollen allergen and components of the human immune system, we have determined the three-dimensional structure of the allergenic domain of Phl p 5b.

The protein adopts a compact four-helical bundle structure which dimerises by involvement of one intermolecular disulphide bridge. A repeating sequence motif observed in this protein seems to be typical for all group V and VI grass pollen allergens and this motif assumes helix-turn-helix topology. It is not clear whether the nuclease activity found for this protein is essentially connected to the allergenic property.

Native X-ray intensity data up to 1.98 Å were collected at 120 K using synchrotron radiation at the beam line BW6 (HASYLAB, DESY, Hamburg). Crystals belong to space group $C222_1$ with unit cell parameters a = 38.97, b = 50.36, c = 107.80Å and Z=4. Derivative (Mercury) data up to 3.0Å were collected using Cu K_α radiation. The CCP4 suite of programs were used for most of the phasing calculations. Application of anomalous data complemented the phasing procedure. Backbone of the protein model was traced using a density modified SIRAS map calculated with the phases from a six site heavy atom model. Phase extension and phase combination methods were used to build the complete model. The model was refined using the torsion-angle molecular dynamics slow-cooling refinement protocol of X-PLOR. The final model has 102 amino acid residues and 97 solvent molecules with agreement factors of R = 19.7% and R-free = 24.1%. The structural features of this pharmaceutically important protein, Phl P5b, will be discussed with clinical and biological implications.

P13.OA.001 THE CRYSTAL STRUCTURE OF AN INVERTEBRATE PENTRAXIN-LECTIN WITH A NOVEL MOLECULAR ASSEMBLY. Annette K. Shrive, Jamie R. Cartwright, Alison M. Metcalfe and Trevor J. Greenhough, School of Life Sciences, Keele University, Staffs ST5 5BG, UK.

C-reactive protein (CRP) and serum amyloid P component (SAP) are members of the pentraxin family of oligomeric serum proteins which has been conserved through evolution, although an invertebrate SAP-like pentraxin has not previously been identified and it has been postulated that CRP and SAP are products of gene duplication within vertebrate, even mammalian evolution. The known pentraxin structures human CRP [1], human SAP [2] and rat CRP [3] are all mammalian and all exhibit cyclic pentameric symmetry.

We have isolated SAP from the haemolymph of the phylogenetically ancient invertebrate horseshoe crab *Limulus polyphemus* and determined the three dimensional structure by x-ray crystallography. The structure of the previously undiscovered *Limulus* SAP, the first invertebrate lectin structure to be determined, reveals the pentraxin fold and a novel doubly-stacked octameric ring. Pairs of protomers, one from each octameric ring, form continuous, twisted β-sheet structures across the hexadecamer. Comparison of known *Limulus* pentraxin sequences with the human and *Limulus* SAP structures, particularly in the region of the ligand-binding site, provides convincing evidence that the observed pentraxin sequence heterogeneity in *Limulus* may be due to the presence of multiple CRP-like pentraxins with distinct ligand-binding properties. A complex and diverse pattern of competitive ligand binding, involving not only PC and PE but also carbohydrate moieties, may be a general feature of *Limulus* pentraxins. The crystal structure and the discovery of both prototypic pentraxins in *Limulus* raise the possibility that both were present in the common ancestors of arthropods and chordates over 500 million years ago.

[1] Shrive *et al*. (1996). Nature Structural Biology **3**, 346-354
[2] Emsley *et al*. (1994). Nature **367**, 338-345
[3] Greenhough *et al*. (1996). Unpublished results.

P13.OA.002 YEAST RNA POLYMERASE II STRUCTURE AT 5 Å RESOLUTION. J. Fu, P. David, D. Bushnell, A. Gnatt and R. Kornberg. Department of Structural Biology, Stanford University School of Medicine, Stanford, CA 94305, USA.

RNA polymerase II (pol II) forms the core of the giant eukaryotic transcription machine responsible for all mRNA synthesis. Pol II assembles with general transcription factors onto a promoter, forming a pre-initiation complex. It then initiates mRNA synthesis and clears the promoter to enter a phase of highly processive RNA chain elongation. The formation of the pre-initiation complex, promoter clearance and transcription elongation are all under intricate regulation in response to developmental needs and environmental changes. Knowledge of the three-dimensional structure of pol II is required in order to fully understand the regulatory mechanisms and functional roles of the many protein-protein and protein-nucleic acid interactions involved in transcription.

Pol II presents a formidable challenge to the method of heavy-atom isomorphous replacement, due to its enormous size. Pol II is composed of 15 polypeptides of 12 different types, with a total mass of 550 kDa. We have grown yeast pol II crystals diffracting to 3.1 Å resolution, obtained multiple isomorphous derivatives with heavy-metal clusters and resolved the phases to 5 Å. The resulting MIRAS map shows well connected density features, many of them rod-shaped and indicative of α-helices. The molecular outline in the current X-ray map agrees well with the molecular envelope previously determined at 16 Å by electron crystallography [1], validating the current phase solution. In one region, a small domain, packed against the majority of the molecule in the electron-microscope (EM) structure, pivots away from the majority of the molecule by nearly 40°. As a result of this conformational change, a narrow channel previously noted in the EM structure is transformed into a groove which runs into the presumed DNA binding channel [1,2]. The key to success in phasing the pol II diffraction lay in the modeling of the scattering factor for an 18-tungsten cluster bound to pol II at a single site. Techniques and procedures used in the crystallization screen, flash-freezing and treatment of the heavy-metal cluster data will be discussed.

1. Darst, *et al*. (1991). *Cell*, **66**, 121-128.
2. Leuther, *et al*. (1996). *Cell*, **85**, 773-779.

P13.OA.003 A NOVEL PROTEIN RADICAL SITE IN THE CRYSTAL STRUCTURE OF AN ANAEROBIC RIBONUCLEOTIDE REDUCTASE. Derek T. Logan[1], Jessica Andersson[2], Britt-Mare Sjöberg[2] & Pär Nordlund[1], Depts. Of Biochemistry[1] and Molecular Biology[2], Stockholm University, S-106 91 Stockholm, Sweden.

Ribonucleotide reductases (RNRs) occupy a pivotal role in the life of cells, as they are the only enzymes to catalyse the first dedicated step of DNA synthesis, i.e. the reduction of

ribonucleotides to deoxyribonucleotides. Despite the apparent simplicity of the reaction, free radical chemistry must be employed. RNRs can be divided into three classes based on the mechanisms they employ for radical generation, which are amazingly varied.

We have solved the crystal structure of a class III RNR [1]. This type of RNR is expressed by facultative or obligate anaerobes under anaerobic conditions. They generate a stable glycyl radical, in contrast to the structurally characterised class I enzymes, which use tyrosyl radicals. Our work provides the first structural evidence that the three classes of RNR have a common evolutionary ancestor, in spite of statistically insignificant sequence homology. In addition, it reveals the structure of a novel protein glycyl radical site. This lies in close proximity to the active site, again in contrast to class I, where the radical is probably transferred over a long hydrogen-bonded path before being made available for catalysis. However, the structure shows that one of three conserved cysteine residues in the active site, essential in class I and II RNRs, is not conserved in class III, which obliges us to reconsider the proposed reaction mechanism.

The class III RNR structure suggests that a growing family of anaerobic glycyl radical enzymes, including pyruvate formate lyase, may also be structurally related to RNRs and provides an appealing evolutionary scenario where enzymes involved in primary metabolism became the first to be able to catalyse the difficult reduction of ribonucleotides. Preliminary data on the structural basis for allosteric regulation of class III RNRs will also be presented.

[1] D.T. Logan, J. Andersson, B.-M. Sjöberg & P. Nordlund (1999) *Science,* in press.

P13.OA.004 COLICIN E3 AND ITS IMMUNITY PROTEIN: AN ENZYMATIC CYTOTOXIN AND ITS INHIBITOR. M. Shoham, S. Soelaiman and C. Li, Case Western Reserve University, School of Medicine, Department of Biochemistry, 10900 Euclid Ave, Cleveland, Ohio 44106-4935, USA. E-mail: shoham@biochemistry.cwru.edu

Colicin E3 is a multifunctional elongated protein cytotoxin that kills cells by inactivation of their ribosomes. The 68kDa *E. coli* protein is composed of three domains responsible for receptor binding on the outer membrane, translocation across the plasma membrane and killing the infected cell inside the cytoplasm, respectively. The C-terminal domain acts as an RNase that nicks 16S rRNA at a specific site, thereby blocking protein biosynthesis in the ribosomes. The immunity protein acts as a specific inhibitor of this RNase function by forming a specific 1:1 complex with colicin E3. Interactions between colicins and immunity proteins are extremely tight with subfemtomolar affinity.

The crystal structure of free immunity protein has been determined to a resolution of 1.8Å by MIR phasing. The secondary structure consists of a four-stranded antiparallel β-sheet flanked by three α-helices, all located on one side of the sheet. The two molecules in the asymmetric unit are covalently linked by a putative zinc ion that is coordinated to the single cysteine of each subunit.

Cocrystals of colicin E3 and the immunity protein diffract to 2.8Å resolution. They belong to the monoclinic space group $P2_1$ with unit cell dimensions a =66.6, b = 193.6, c = 84.3Å and β = 113.2°. There are four binary complex molecules per asymmetric unit. Several suitable heavy-atom derivatives have been found, and the structure determination is in progress by MIR phasing and non-crystallographic symmetry averaging.

P13.OA.006 THE STRUCTURE OF E. COLI ADP RIBOSE HYDROLASE: A PARADIGM FOR NUDIX HYDROLASES? S.B. Gabelli[1], M.A. Bianchet [1], M.J. Bessman [2], L.M. Amzel[1], [1]Department of Biophysics and Biophysical Chemistry.School of Medicine. Johns Hopkins University. [2]Department of Biology. Johns Hopkins University.

Nudix hydrolases1, previously known as MutT proteins catalyze the hydrolysis of diverse nucleoside diphosphates . The family is characterized by the consensus sequence GX5EX7REAXEEX2L. This sequence appears to be a versatile nucleoside and catalytic site present in more than two hundred enzymes found throughout nature from archae and prokaryotes to eukaryotes. The common feature of the substrates of nudix enzymes is the diphosphate linkage which is hydrolyzed by the enzymes. We have determined the first crystal structure of a nudix hydrolase: the ADP ribose hydrolase, product of the ORF209 E.Coli gene. It hydrolases ADP-ribose to AMP and ribose 5-P. Crystals were grown by vapor diffusion at 18o C using polyethylene glycol as precipitant. Crystals belong to space group $P2_12_12_1$, cell constants a=66.9 , b=67.9 , c=98Å. , and diffract to 1.9Å using a synchrotron source. The Crystal contains two molecules in the asymmetric unit related by a local two fold axis. The structure was solved by MIRAS techniques using the program SOLVE2. Initial phases were further improved and extended by density modification and histogram matching using the program DM3. The refinement of the structure is in progress.

1 Bessman, M.J., Frick, D.N., O'Handley, S.F. The MutT Proteins or "Nudix" Hydrolases, a family of versatile, widely distributed, housecleaning enzymes. JBC, 271:25059-25062, 1996.
2 Terwilliger, T. C. and Berendzen J.(1996) Correlated phasing of multiple isomorphous replacement data. Acta Cryst. D52,749-757.
3 Cowtan K. D. (1994), Joint CCP4 and ESF-EACBM Newsletter on Protein Crystallography, 31, p34-38. 'dm': An automated procedure for phase improvement by density modification.

P13.OA.007 THE CRYSTAL STRUCTURE OF FOLYLPOLY-GLUTAMATE SYNTHETASE TO 2.4Å RESOLUTION. C.A. Smith, X. Sun and E.N. Baker, School of Biological Sciences, University of Auckland, Auckland, New Zealand and A.L. Bognar, Department of Medical Genetics and Microbiology, University of Toronto, Toronto ON Canada M5S 1A8

Folylpolyglutamate synthetase (FPGS), responsible for the addition of a polyglutamate tail to folate and folate derivatives, is an ATP-dependent enzyme isolated from eukaryotic and bacterial sources. The enzyme plays a key role in the metabolism of dietary folates and the retention the intracellular folate pool [1]. The enzyme is also able to polyglutamylate a range of antifolate anticancer drugs, making these compounds better substrates for their target enzymes. We have determined the 2.4Å resolution crystal structure of the MgATP complex of the enzyme from *Lactobacillus casei* [2]. The structural analysis reveals that FPGS is a modular protein consisting of two domains, one with a typical mononucleotide-binding fold, and the other strikingly similar to the folate-binding enzyme dihydrofolate reductase. We have located the active site of the enzyme in a large interdomain cleft, adjacent to an ATP-binding P-loop motif. Opposite this site, in the C-domain, a cavity likely to be the folate binding site has been identified and inspection of this cavity and the surrounding protein structure suggests that the glutamate tail of the substrate may project into the active site. A further feature of the structure is a well-defined Ω-loop which contributes both to the active site and to interdomain interactions. The determination of the structure of this enzyme represents the first step toward the elucidation of the molecular mechanism of polyglutamylation of folates and antifolates.

1. Shane B (1989). *Vitam. Horm.* **45**, 263-335.
2. Sun X, Bognar AL, Baker EN & Smith CA (1998). *Proc Natl Acad Sci* **95**, 6647-6652.

P13.OA.008 CRYSTAL STRUCTURE DETERMINATION OF THE SMALL GTPASE SAR1, A REGULATOR FOR ENDOPLASMIC RETICULUM (ER) BUDDING. Mingdong Huang, Cheng-Qian Wang, William E. Balch, Ian A. Wilson Departments of Molecular Biology and Cell Biology The Scripps Research Institute 10550 N. Torrey Pines Rd. La Jolla, CA 92037

Movement of protein from the endoplasmic reticulum (ER) to the Golgi involves vesicle carriers that bud from specific sites on the ER membrane. Cargo exiting the ER includes both endogenous transport components that must be recycled from post-ER compartments, and newly synthesized proteins that are delivered to downstream subcellular destinations and the cell surface. Cargo is sorted from resident ER proteins and selected for export by interacting with COPII coat components. Sar1 is the pivotal GTPase that regulates cargo selection and vesicle formation, and is essential for cell growth and development. Sar1 function is unrelated to other GTPases belonging to the Ras superfamily of GTPases such as ARF1 involved in budding from the Golgi and Rab proteins involved in vesicle fusion. We have successfully crystallized the Sar1 protein and its selenomethionine derivative in PEG conditions using a sitting drop setup, and collected a native data set to 2.5Å. The current data set is 98.8% complete with an Rmerge of 17.8%. The crystal belongs to $P2_1$ space group with cell parameters of a=53.4Å, b=61.7Å, c=71.1Å, ß=107.5°. There are two Sar1 molecules in the asymmetric unit as estimated from Matthews coefficient. The structure determination and refinement is currently underway.

13OB TIME-RESOLVED DIFFRACTION AND PROTEIN DYNAMICS

M13.OB.001 INTRODUCTION TO THE MICROSYMPOSIUM. Ilme Schlichting, Max Planck Institute for Molecular Physiology, Dortmund, Germany;

In the general excitement of a time when new protein structures are published every week, it is often forgotten that a structure in itself does not tell one how the molecule works. For that, one needs to know a great deal about mechanism, intermediates and dynamics; a structure is only a beginning, although an important one. Due to the large gap between the time scales of protein motions or enzymatic reactions on the one hand and the crystallization and data aquisition on the other hand crystallographic determination of structures of reaction intermediates is usually not straightforward. It can be made feasable by either slowing or trapping the reaction (e.g. by cooling, or/and using poor substrates, suboptimal pH, and slow mutants) or by decreasing the data acquisition time (e.g by using the Weissenberg or Laue geometry). Both approaches require that the intermediate of interest can be generated fast and efficiently in the crystal. In addition, physico-chemical analysis methods need to be established to follow the reaction as it proceeds in the crystal. Reactions can be triggered by changes in thermodynamic parameters such as temperature or pressure, by concentration changes, by light or other radiation.

The tools for doing time-resolved crystallographic studies have developed rapidly; only a couple of years have passed since the first application of the Laue method to solve a protein structure [1] or to follow an enzymatic reaction after photolysis of a caged substrate [2]. Recently, studies with nanosecond time-resolution of reversible light-triggered reactions have become feasable at third generation synchrotrons [3].

[1] Hajdu, J. et al (1987) Nature 329:178-181.
[2] Schlichting, I. et al. (1990) Nature 345:309-315.
[3] Srajer, V. et al. (1996) Science 274:1726-1729.

M13.OB.002 KINETIC CRYSTALLOGRAPHY OF PHOSPHORYL TRANSFER CATALYZED BY GLUTATHIONE SYNTHETASE. Hiroaki Kato*, Masaharu Endo*, Amane Aoyagi*, Dominique Bourgeois†, Ilme Schlichting¶, Soichi Wakatsuki†, Toru Nakatsu*, Jun Hiratake* & Jun'ichi Oda*§. *Institute for Chemical Research, Kyoto University, Uji, Kyoto 611-0011, Japan; ¶Max Planck Institut für Molekulare Physiologie, Abteilung Physikalische Biochemie, Rheinlanddamm 201, 44139 Dortmund, Germany; †ESRF, BP-220, Grenoble, Cedex, France; §Fukui Prefectural University, 4-1-1 Kenjojima, Matsuoka, Fukui 910-1195, Japan.

Glutathione synthetase (GSHase) catalyzes the synthesis of gluta-thione from MgATP, γ-L-glutamyl-L-cysteine (γ-Glu-Cys) and glycine. The reaction is thought to proceed through the formation of an acyl-phosphate intermediate, γ-Glu-Cys phosphate, followed by nucleophilic attack of glycine to yield glutathione. In the light of the proposed reaction mechanism, we synthesized a transition state analogue (TSA), in which the C-terminal carboxyl group is replaced with a tetrahedral phosphinyl group with 2-carboxyethyl moiety mimicking the incoming glycine[1]. The compound is slowly- and tightly- bound (K_i = 21nM) to GSHase in the presence of MgATP. X-Ray diffraction analysis has shown that the tight-binding species is a phosphorylated TSA produced in the enzyme active site. The slow catalytic rate (the half life is 4 min in the crystalline state) renders the system suitable for analysis by kinetic crystallography. To start the reaction synchronously, we thus crystallized the enzyme complexed with TSA and caged ATP. This system makes it possible to release ATP upon photolysis to initiate the phosphorylation of TSA within the enzyme active site. Flash photolysis was achieved with a Xe flash lamp developed by Gert Rapp, EMBL, Hamburg. Photolytic efficiency was determined by HPLC from the contents of the caged and released nucleotides in the crystals. After reaction initiation several snapshots of the reaction were obtained at intervals of several seconds with millisecond time resolution using the Laue technique. A high-resolution structure at the beginning of the reaction was also captured by rapid freezing technique with liquid nitrogen. Beamline ID9 at the ESRF has been used for the data collection of Laue diffraction, and ID14/EH3 for that of monochromatic one. The methods used, and the structures obtained will be described.

1 Hiratake, J., *et al.* (1994) *J. Am. Chem. Soc.* **116**, 12059–12060.

M13.OB.003 TIME-RESOLVED ENZYME CRYSTALLOGRAPHY. Gregory A. Petsko, Departments of Biochemistry and Chemistry and Rosenstiel Basic Medical Sciences Research Center, Brandeis University, Waltham, MA 02254

The structures of enzymes determined by X-ray crystallography are a dual average over the time required to collect the diffraction data and all of the unit cells in the crystal lattice. Since most enzymatic reactions are finished in less than a second, the temporal averaging process makes it impossible to visualize an enzyme-substrate directly by X-ray crystallography under normal conditions. The spatial averaging also imposes the requirement that every molecule in the lattice be at the same stage of the reaction during data collection. It is clearly important to be able to look at productive complexes, but it is also very difficult to do so for most crystalline enzymes. The advent of Laue diffraction techniques (Amoros et al., 1975) using synchrotron radiation has made it possible to collect protein crystal data sets on a

millisecond time-scale (Hajdu and Johnson, 1990). To carry out time-resolved studies of enzyme reactions at atomic resolution, the most significant problem is the problem of synchronization: it is necessary that all of the molecules in the crystal be at the same stage of the reaction at the same time (Ringe et al., 1992). Four techniques have been developed to achieve this, and some success has been obtained with each one. Photo- activation has the widest applicability, and has been used to obtain time- resolved structures of the human oncogene protein H-ras p21 in both its active (GTP-bound) and inactive (GDP-bound) states (Schlichting et al.,1990). Although these results are encouraging, several serious problems remain: First, the requirement of the Laue technique for a very well-ordered crystal is a major obstacle to many studies. Efforts to ease this problem are needed. Second, the fundamental issues in time-resolved crystallography are now chemical rather than crystallographic. Methods for the rapid initiation of other reactions must be developed (for a clever approach, see Stoddard et al., 1991). Third, it is imperative that the kinetics of the process in question be studied in the crystal before any diffraction experiments are done. We need better ways to make those solid state kinetic measurements. Fourth, we should make use of combined methods, such as cryoenzymology plus Laue diffraction or site-directed mutagenesis plus Laue diffraction, to bring many processes into the time regime in which we currently can work. Fifth, we have to be able to deconvolute diffraction data that come from a mixture of two or three discrete species. Sixth, we need better methods of obtaining good electron density maps from partial data sets (Campbell et al., 1990). Finally, it seems to me that some of the most important events in any enzymatic reaction are not going to be accessible: consider the formation and decomposition of a transition state as an example. I will close my talk by discussing the role of computational biochemistry in filling in those frames of our enzymatic movie that we cannot observe directly by time-resolved X-ray crystallography.

M13.OB.004 DYNAMICAL MODELS OF PEANUT LECTIN DISACCHARIDE COMPLEXES G M Bradbrook[1,2], J V Pratap[1], J Raftery[2], B P Reddy[1], A Surolia[1], M Vijayan[1] and J R Helliwell[2], [1] Molecular Biophysics Unit, Indian Institute of Science, Bangalore, India, [2] Department of Chemistry, Univeristy of Manchester, Manchester, M13 9PL, UK.

Peanut lectin, a 110 kD tetrameric lectin, from Aracheas Hypogea, is specific to galactose and has a high affinity for the T-antigenic disaccharide, Gal(1-3) GalNac. From calorimetric data, T-antigen has a 20 fold higher affinity than lactose (Gal (1-4) Glc). Nanosecond MD simulations have been performed at different temperatures for both the complexes. The free sugars in an unbound, hydrated state were also subjected to nanosecond MD simulations.

The dynamical models of the protein-saccharide interactions derived from this study have been used to estimate the difference in binding enthalpy between the two complexes. A reasonable agreement between the dynamical models and calorimetric data was obtained. Similarly, the H-bonding patterns observed in the dynamical models are in agreement with those seen in the crystal structure.

Further, the models indicate some alternate binding motifs also for the protein-disaccharide complexes, offering some explanations for the mutant studies done on this protein. These rare and energetically less favourable states could play an important role in preventing dissociation of the complex and thereby yielding a higher association constant. From this, it is suggested that approaches to ligand design may include the promotion of a series of bound states.

M13.OB.005 TIME-RESOLVED MACROMOLECULAR CRYSTALLOGRAPHY AND PROTEIN MOLECULAR DYNAMICS . J R Helliwell, Department of Chemistry, University of Manchester, Manchester, M13 9PL, UK.

High intensity sources have opened up time-resolved monochromatic and Laue diffraction structural studies via reactions initiated in protein crystals. SR source, detector (CCDs) and Laue data processing software have radically improved in the last few years. Ultrafast (sub-nanosecond) reversible 'pump probe' experiments have become possible at ESRF. Irreversible processes pose a variation of the data acquisition challenge for which pixel detectors look promising. Cryo-crystallography opens up freeze trapping approaches, guided by spectral signals and/or Laue data and electron density map time slices. Cryo-protection of the protein crystal sample also allows ultra-high resolution data collection ie with high X-ray data to parameter ratio in model refinement; anisotropic displacement parameters (ADPs) then indicate directional dynamics and/or disorder effects. Protein molecular dynamics trajectories yield another estimate of atomic movements, larger than from ADPs, but this might be reconciled with the crystallographic model refinement since X-ray diffraction patterns often show diffuse scattering in addition to the Bragg scattering. In another aspect neutron Laue diffraction has opened up a wider range of protein structure studies with neutrons than hitherto, which makes feasible larger unit cells and/or smaller protein crystals for H/D exchange structural information and placement of bound water deuterium atom positions. The integration of this broad range of static and time-resolved dynamics information offers then a considerable insight into macromolecular structure and interactions. Examples will be given from studies on hydroxymethylbilane synthase (HMBS) and concanavalin A (without and with saccharides).

Acknowledgements: I am very grateful to all the persons listed in these publications for many happy collaborations. This work is based on protein crystallographic data measured over many years at the Daresbury SRS, ESRF and Cornell synchrotron X-ray sources and more recently at the Institut Laue Langevin neutron source. The intensive crystallographic and molecular dynamics computations that these studies involved were done on the Manchester Structural Chemistry SG Workstations and SG Challenge. I am also very grateful for research grant support over the years from The Wellcome Trust, SERC, EPSRC, BBSRC, EU and The British Council.

J R Helliwell 1992 Macromolecular Crystallography with Synchrotron Radiation CUP;
J R Helliwell and P M Rentzepis Eds 1997 Time-Resolved Diffraction, OUP;
J R Helliwell et al. 1998 Faraday Trans 94, 2615-2622;
A Haedener et al. 1999 Acta Cryst D55 in press;
A Deacon et al. 1997 Faraday Trans 94, 4305-4312;
J Habash et al. Faraday Trans 94, 4313-4317;
G Bradbrook et al. 1998 94, 1603-1611. See also relevant references therein.

P13.OB.001 STRUCTURE AND FUNCTION STUDIES OF HYDROXYMETHYLBILANE SYNTHASE. J.R. Helliwell, J.Raftery, J.Habash, P Faulder (1), F.Schotte, M.Wulff (2), A.Haedener (3), (1) Department of Chemistry, University of Manchester, (2) ESRF, Grenoble (3) Department of Chemistry, University of Basle

Hydroxymethylbilane synthase (EC 4.3.1.8, HMBS), also known as porphobilinogen deaminase, is the third enzyme in the biosynthetic pathway of the tetrapyrroles which include haem, chlorophyll, vitamin B12 and similar pigments. HMBS catalyses the polymerisation of four molecules of porphobilinogen to form hydroxymethylbilane. A dipyrromethane cofactor is present in the HMBS holoenzyme and is covalently attached to a cysteine side-chain (Cys242). There are four covalent enzyme-substrate

intermediate complexes existing in the catalytic pathway, i.e. ES1, ES2, ES3, ES4. Previously, a reduced, active selenomethionine form of the holoenzyme has been solved to 2.4A using the MAD method principally at SRS station 9.5 and subsequently also at ESRF BM14 [1]. Time-resolved Laue diffraction has since been employed at ESRF to study the enzyme structure (K59Q mutant) during catalysis [2,3]. The experimental Laue difference maps revealed an elongated peak near the active site, most prominent at 2 hours, commencing at the position of ring 2 of the oxidised cofactor (the putative binding site for substrate) and directly above the critical Asp84 carboxyl side chain implicated in the first ring coupling step. The density then extended past residues that are known from protein engineering to affect later stages of the catalysis, and out into open solvent. In order to improve the 'static' protein structure, and to establish freeze trapping conditions, since the time-evolution of this irreversible (i.e. in terms of the colourless to red colour change) reaction in the crystal has now been established from the Laue diffraction, cryo temperature data has been collected on the reduced, active wild-type HMBS holoenzyme to 1.65A at ESRF (ID09). Moreover two other cryo data sets were measured for the wild type HMBS crystals on ID09 involving freezing after two hours soaking of a crystal in substrate solution and also an inhibitor soaked crystal. Difference Fourier map evaluation and model refinement is underway. The missing loop of residues 49 to 57 in all current HMBS structures undertaken at ambient temperature is of keen interest in these cryo studies. Progress with the structural studies will be reported.

[1] A Haedener, PK Matzinger, AR Battersby, S McSweeney, A W Thompson, AP Hammersley, S J Harrop, A Cassetta, A Deacon, W N Hunter, Y P Nieh, J Raftery, N Hunter and J R Helliwell Acta Cryst D in press.

[2] J R Helliwell, Y P Nieh, A Cassetta, J Raftery, A Haedener, A CNiemann, A R Battersby, P D Carr, M Wulff, T Ursby, J P Moy and A W Thompson, chapter 8 in J R Helliwell and P M Rentzepis Eds "Time-resolved Diffraction" OUP.

[3] J R Helliwell, Y P Nieh, J Raftery, A Cassetta, J Habash, P D Carr, T Ursby, M Wulff, A W Thompson, A C Niemann and A Haedener Faraday Trans 1998, 94, (2615-2622).

P13.OB.002 LAUE-DIFFRACTION AT ID09: TIME-RESOLVED STUDIES ON PHOTOACTIVE PROTEIN CRYSTALS AT PHYSIOLOGICAL TEMPERATURES. R. Kort [1], F. Schotte [1], K.J. Hellingwerf [2], E.M. Landau [3], K. Moffat [4] and M. Wulff [1]. [1] European Synchrotron Radiation Facility, Grenoble, France, [2] Laboratory for Microbiology, University of Amsterdam, The Netherlands, [3] Biozentrum, University of Basel, Switzerland and [4] Department of Biochemistry and Molecular Biology, University of Chicago, USA.

The beamline for structural kinetics at the ESRF is the white beam station ID09. The time structure of synchrotron radiation in single-bunch or hybrid mode in combination with a 900 Hz chopper allow the isolation of 100-ps X-ray pulses. After reaction initiation by a laser pulse, these polychromatic X-ray pulses can probe crystal structures, with a delay chosen by the user, ranging from the sub-nanosecond to millisecond time scale (Wulff *et al*., 1997). The use of protein crystals that display a reversible reaction triggered by light, enables stroboscopic data collection for the accumulation of sufficient intensity for a Laue diffraction experiment. Crystallizable proteins with intrinsic photoactivity, inducing physiologically relevant conformational changes in a cyclic chain of reactions, are excellent model systems for the type of experiment discussed here: X-rays at IDO9 probed an early intermediate of the bacterial photosensor photoactive yellow protein at 1 nanosecond after reaction initiation, showing how this protein (i) accommodates rapid chromophore isomerization without collisions and (ii) can store energy by this restricted movement for larger structural changes required for signal transduction (Perman *et al*., 1998). In addition, the use of this technique on crystals of the retinal-containing proton pump bacteriorhodopsin (BR) may catch essential structural changes for the pumping mechanism. Future plans will be revealed.

Perman, B., Srajer, V., Ren, Z., Teng, T., Pradervand, C., Ursby, T., Bourgeois, D., Schotte, F., Wulff, M., Kort, R., Hellingwerf, K. and Moffat, K. (1998) Energy transduction on the nanosecond time scale: early structural events in a xanthopsin photocycle. *Science*, **279**, 1946-50.

Wulff, M., Schotte, F., Naylor, J., Bourgeois, D., Moffat, K. and Mourou, G. (1997) Time-resolved structures of macromolecules at the ESRF: Single-pulse Laue diffraction, stroboscobic data collection and femtosecond flash photolysis. *Nuclear Instruments and Methods in Physics Research A*, **398**, 69-84

P13.OB.003 ELECTRON DIFFRACTION OF TRAPPED BACTERIORHODOPSIN INTERMEDIATES. Richard Henderson and Sriram Subramaniam, MRC Laboratory of Molecular Biology

We have studied the photocycle of the light-driven proton pump bacteriorhodopsin, using time-resolved plunge-freezing of naturally occurring two-dimensional crystals to trap particular intermediate states, followed by electron diffraction structure analysis to determine their atomic structure. We have investigated specific intermediates that occur in the later stages of the wild type bacteriorhodopsin photocycle as well as a variety of mutant proteins with kinetic defects in the photocycle. The timescale of the flash and trap experiments range from 0.5 milliseconds to several seconds.

Our experiments demonstrate that in wild-type bacteriorhodopsin, a large conformational change occurs within 1 msec after illumination. This large structural change occurs in the M intermediate and with only small differences also in the N and O intermediates. However, a considerably larger variation in structure is observed when the same intermediates are trapped in different mutants. In one spectacularly clear case, the D96G/F171C/F219L triple mutant, the full extent of the conformational change is already present in the dark with minimal additional light-induced changes. Our observations thus support a simplified view of the wild type photocycle in which the structures of the initial state and the early intermediates are (K, L and M1) well-described by one protein conformation while the structure of the later intermediates (M2, N and O) are well-approximated by the other protein conformation. In wild type bacteriorhodopsin and most mutants, this conformational change between the M1 and M2 states is likely to be a major factor in efficiently switching accessibility of the retinal Shiff base from one side of the membrane to the other.

13OC APERIODIC AND INCOMMENSURATE STRUCTRES (II)

M13.OC.001 RANDOM TILING MODELS OF QUASICRYSTALS AND INCOMMENSURATE PHASES. Michael Widom, Department of Physics, Carnegie Mellon University, Pittsburgh PA, 15213, USA.

Aperiodic tilings of space model incommensurate and quasicrystalline materials. While certain tilings may *force* a quasiperiodic structure, similar structure arises spontaneously in *random* tilings. Random tilings may be appropriate models for entropically stabilised quasicrystals that are thermodynamically stable equilibrium states at high temperatures only. Successes of the theory of random tilings include exact solutions, prediction of crystal-incommensurate and incommensurate-quasicrystal phase transitions, and the prediction of phason elasticity which implies specific observable patterns of diffuse scattering. The outlook for

the future includes the derivation of random tiling models from atomistic models of quasicrystals via ab-initio total energy calculations, and modelling defect structures such as grain boundaries and dislocations and their interactions.

M13.OC.002 COLOR SYMMETRY IN QUASI-PERIODIC STRUCTURES. Ron Lifshitz Condensed Matter Physics, California Institute of Technology, Pasadena, CA 91125, U.S.A.

Color symmetry groups are powerful abstract tools which can be used for the classification of properties such as alloy ordering and magnetic phases in solids. The development of a theory of color symmetry for quasiperiodic crystals [1] is therefore a natural step in the evolution of modern crystallography.

I shall give an outline of this theory, starting from a brief introduction (for the non specialist) of the notion of symmetry in quasicrystals, which will then be generalized to the case of colored quasicrystals. I shall describe the color space group classification scheme which emerges, and give applications, ranging from colored quasiperiodic tilings to the super-lattice ordering observed in certain decagonal and icosahedral quasicrystals.

1. R. Lifshitz, Reviews of Modern Physics, 69, (1997) 1181.

M13.OC.003 IN SITU STUDY OF THE SUPERLATTICE ORDERING OF THE ICOSAHEDRAL ALPDMN PHASE. M. de Boissieu (1), A. Letoublon (1), T. Ishimasa (2), M. Boudard (1), M. Audier (3), 1 LTPCM, INPG, UMR CNRS 5614, BP 75 38402 St Martin d'Heres Cedex (France), 2 Department of Nuclear Engineering, School of Engineering, Nagoya University, Nagoya 464-01 Japan, 3 LMGP, UMR CNRS 5628, St Martin d'Heres, France.

The reversible transition between the i-AlPdMn phase and the F2M phase has been studied by in-situ X-ray and neutron diffraction and transmission electron microscopy. The transition takes place around 720°C, the i-phase being stable only at high temperature. The F2M low temperature phase is multidomains, with crystallographic orientational relationship between domains imparting an overall icosahedral symmetry. Each domain presents a diffraction pattern with a cubic symmetry and S1 superstructure reflections. The mechanism of the phase transition was followed by in situ-X-ray diffraction. In the initial stage of the transformation streaks of diffuse scattering appear, which then condense into superstructure reflections. There is a correlation between the intensity of the diffuse scattering and the phason component of the wavevector, which indicates that the transition is phason driven. The F2 phase, previously identified by T. Ishimasa, is a transient state towards the F2M phase.

M13.OC.004 NON-PERIODIC POINT SETS AND THEIR GENERALIZED SYMMETRIES Michael Baake [1] and Dieter Joseph [2], [1] Institut fuer Theoretische Physik, Universitaet Tuebingen,Auf der Morgenstelle 14, D-72076 Tuebingen, Germany, [2] Max Planck Institute for Physics of Complex Systems, Noethnitzer Str. 38, D-01187 Dresden, Germany

While the symmetries of crystals are well understood, this is not so for the hierarchy of ordered states between crystalline and amorphous, of which quasicrystals form only one example. In particular, classification attempts based upon direct or upon reciprocal space techniques will lead to different results -- quite in contrast to the crystallographic situation. This talk introduces appropriate direct space equivalence concepts such as local indistinguishability or local equivalence and discusses their relation with standard concepts.

M13.OC.005 MATHEMATICAL QUASICRYSTALS WITH TORIC INTERNAL SPACES AND DIFFRACTION. Jean-Louis Verger-Gaugry, Institut Fourier, UJF Grenoble, Mathematics Department - BP 74 - Domaine Universitaire, 38402 - Saint Martin d'Hères, France.

Aperiodic Crystals viewed as Delaunay sets of points, $\Lambda \subset IR$, on the real line, having an average lattice, are studied in the context of mathematical quasicrystals with toric internal space and cut-and-congruence schemes. The windows exhibit variable Hausdorff dimensions and the fractal rates of occupancy, at infinity, of the lattices associated with the Delaunay sets are shown to be simply related to the scaling exponents of the Fourier transform of the autocorrelation of Λ in the diffraction process, with Hausdorff 0-dimensional windows. We show that scaling exponents of the intensity can be defined without limit for the autocorrelation, allowing the study of the singular continuous component of the spectral measure. The case of the Meyer set formed by the Thue-Morse sequence is explicitly developed to exemplify and justify this approach.

P13.OC.001 STRUCTURAL STATE OF BETA(CSCL)-SOLID SOLUTION IN QUENCHED QUASICRYSTAL-FORMING ALLOYS ALCUFE. E.V.Shalaeva [1], A.F.Prekul [2], [1] Institute of Solid State of Chemistry, Ural Div., Russ. Academy of Sci., Ekaterinburg 620219, Russia, [2] Institute of Metall Physics, Ural Div., Russ. Academy of Sci., Ekaterinburg 620219, Russia

With the discovery of stable quasi-crystalline (i-) phases, the components of which are elements with good metallic properties, a tide of interest has been at its height in studying the structural transformations that are accompanied with stabilization of the system due to the gain in electron energy. Of particular interest is the experimental investigation of structural state of cubic phases that undergo transformation into i-phase, in looking for signs of instability in the crystal lattice with regard to such phase transformation that is theoretically described as a reconstructive transition of displacement type.

With the goal of searching for such signs, the structural characteristics were studied for the quenched beta(CsCl)-solid solution in the system of AlCuFe. Within the composition range of Cu-Fe between 26-12 and 28-14 at.%, a biphasic state (i+beta-solution) is observed that is characterized with a great content of beta-solution which can be heat treated into a nearly uniform i-phase.

The electron microscopy revealed that in the quenched quasicrystal-forming alloys $Al_{62.5-x}Cu_{25-y}Fe_{12.5-z}$, near the concentration region of the ordered tau-phases the structure of beta-solution is characterized with a combined short-range order, showing both the concentration and atomic displacement wave features. The displacement-type order is of the nature of the incommensurable waves of displacement that are typical for the disordered state of alloys with a bcc-lattice that show instability in terms of the bcc --> omega-phase transition. Possible sequences were analyzed for the phase transition of beta (CsCl) solid solution into i-phase with the involvement of the short-range order of omega-type displacement.

P13.OC.003 APPROXIMATE SYMMETRY OF THE QUASICRYSTALS. I.N.Mochtchenko, A.I.Aizenberg, I.K.Mochtchenko, North Caucasus Scientific Center, Pushkinskaia 140, Rostov-on-Don, 344006, Russia.

Using the theory of the almost periodicity function we showed that the quasicrystals is characterised by the approximate symmetry. The elements of such symmetry are the elements of the group of the motion of the Euclidean space, which transform quasicrystal into itself with some error. The group of approximate

symmetry is generated by the subgroup of the exact point symmetry and the subgroup of the almost periods. Such group determines all symmetry and quasiperiodicity properties of the quasicrystal. The condition of the equality of approximate symmetry for several objects is obtained: the moduluses induced by the spectrums of the objects must be equal. The models having real approximate symmetry, but sample structures are presented. For example, the model of decagonal quasicrystals is the quasilattice, which consist from fife periodic lattices formed by the 5-fold axis from one. Such models allow to investigate symmetry and many macroscopic physical properties such as selected rule, the topology of the phase diagrams etc.

The theory of the representations of approximate groups is developed. Such representations are the homomorphic matrix groups of approximate symmetry. They connect with the representations of superspace group, but do not equal them and distinguish by the translation elements and the core of homomorphism. The last is isomorphic to some approximate subgroup. The condition of this is next: the modulus induced by the real spectrum must be included to modulus induced by the spectrum of the core of homomorphism. It is also obtained that the invariants of the representations of the superspace groups are the almost invariants of the approximate groups. The obtained results allow to investigate the quasicrystals using the method elaborated for crystals (Landau theory of phase transitions etc.)

This work was supported by RFBR, grant N 97-02-17024.

P13.OC.004 DIFFRACTION PATTERNS OF DD-Ta-Te QUASICRYSTALS WITH FRACTAL OCCUPATION DOMAINS. Akiji Yamamoto Nat. Inst. Res. Inorg. Mat. Namiki 1, Tsukuba, 305 Japan.

A recently found Ta-Te quasicrystal is the first stable phase with dodecagonal (DD) symmetry.[1] It shows square-triangle tiling of 20Å atom clusters similar to the Stampfli tiling [2] but the latter includes many skinny rhombus. There are two clusters with the 6-hold rotation symmetry but with different orientations. One is related to the other by [$\bar{1}$2]. In order to remove the skinny rhombus, we need to use fractal occupation domains. This leads to 5-dimensional cluster models with fractal occupation domains for realistic models of the DD phase.

Recently two 5-dimensional models of the DD Ta-Te quasicrystals with 'pinwheel-shaped' occupation domains are proposed.[3] They have the 5D space group $P[\bar{1}2]m2(12^5mm)$ and both lead to an existing tetragonal approximant structures with a = 37.58, c = 20.66 Å by the introduction of a linear phason strain. These two models have same in the cluster arrangement but different in their orientation. In this paper, the detectability of the fractal occupation domains by diffraction experiments is examined.

The diffraction patterns of the two models indicate that the both models show characteristic intensity distribution in the DD Ta-Te but they are indistinguishable from each other in practice or from the third model with random cluster orientations because of a small difference in diffraction intensity. This suggests that we can not prove whether a quasicrystal has fractal occupation domains or not by means of usual X-ray experiments.

1. F. Krumeich, M. Conrad, and B. Harbrecht (1994) ICEM 13-Paris 751.
2. .P. Stampfli (1986). Helv. Phys. Acta, 59, 1260
3. .A. Yamamoto (1999). submitted to Phys. Rev. Lett.

13OD STRUCTURE SOLUTION FROM POWDERS USING ELECTRON AND POWDER DIFFRACTION TECHNIQUES

M13.OD.001 SOLVING STRUCTURES OF MICROCRYSTALS BY HIGH RESOLUTION ELECTRON MICROSCOPY AND CRYSTALLOGRAPHIC IMAGE PROCESSING. X.D. Zou, Structural Chemistry, Stockholm University, S-106 91 Stockholm, Sweden

High resolution electron microscopy (HREM) can be used for structure determination of micro/nano-crystals too small for single crystal X-ray diffraction [1]. One of the most important advantages of using HREM is that the crystallographic structure factor phase information is present in the images. The phases, as well as the amplitudes, can be extracted from the Fourier transform of the HREM images by crystallographic image processing.

HREM images are very sensitive to the electron optical conditions of the microscope, such as electron beam tilt, spherical aberration, defocus and astigmatism of the objective lens. They are also distorted by crystal misalignment. Furthermore, the strong interaction between the crystal and electrons gives rise to dynamic effects which makes the relation between HREM images and the structure complicated. In general, phases extracted directly from the HREM images are not exactly the same as the crystallographic structure factor phases.

Most of these distortions can be compensated by crystallographic image processing. The effects of dynamic scattering are difficult to compensate for before we know something about the crystal structure. However, in most cases it is possible to find so thin crystals (< 10nm) that most scattered electrons are kinematical. Here we will demonstrate how the amplitudes and phases extracted from the image are related to the structure factors of the crystal and how a crystal structure is solved from HREM images. The accuracy of atomic positions obtained from images is usually better than 0.2Å. The structure model can be further refined against electron or X-ray powder diffraction data. This method will be demonstrated on several compounds including oxides, metal-rich clusters and silicate minerals.

1. T.E. Weirich *et al.* (1996) Nature 382 144.

M13.OD.002 STRUCTURAL STUDY OF ZEOLITE RELATED MATERIALS BY ELECTRON CRYSTALLOGRAPHY. O. Terasaki, A. Carlsson, M. Kaneda, Y. Sakamoto, T. Ohsuna, S. Ritsch, K. Hiraga [1], P. Wagner [2], [1] Department of Physics, CREST-JST and Institute for Materials Research, Tohoku University, Sendai, Japan, [2] Division of Chemistry & Chemical Engineering, CALTEC, Pasadena, USA.

Micro- and mesoporous materials are of importance for making containers of quantum confined materials as well as for catalysts in chemical industries. More than a hundred different materials have been reported and new interesting materials are frequently synthesised. Knowledge of the structure of these materials is the key for understanding their properties. They are synthesised in micrometer size that is too small for single crystal X-ray analysis and they sometime contain faults, and therefore it is rather difficult to solve new structures from powder X-ray diffraction profile without having some structural clues. Electron crystallography is a very powerful method for solving/characterising the structures of these materials. Since the density of the materials is low, it is expected that dynamical scattering effect will be less serious than for other inorganic materials. The framework connectivity and the wall geometry are the most essential point to know for the structures of microporous and mesoporous materials, respectively. There are two methods for phase recovery among various reflections, from HREM images and by the direct method which has been developed for X-ray analysis. The amplitudes for the reflections are obtained either from the image or from electron diffraction patterns. The resolution is, of course, higher for the latter. We have succeeded

in characterising mesoporous material by the former and in solving a new structure of microporous material by the latter.

M13.OD.003 ELECTRON DIFFRACTION STRUCTURE ANALYSIS – AN OPTION WHEN THE POWDER METHOD FAILS TO SOLVE THE STRUCTURE. Thomas E. Weirich, Darmstadt University of Technology, Materials Science - Div. Structural Research, Petersenstrasse 23, 64287 Darmstadt, Germany

Exploiting X-ray powder data for structure determination consists of three parts (a) the determination of the correct unit cell parameters and space group (b) finding a rough structure model close enough to the true structure (c) completing and refining the structure model. While the latter is nearly routine work utilising the Rietveld technique, it turns out in practice that the first two steps are often extremely difficult to overcome. The indexing of powder patterns is often ambiguous due to the accidental or systematic overlap of diffraction peaks and the subsequent extraction of reliable intensities - which is an indispensable precondition for solving the structure - is still a non-trivial problem.

Electron diffraction structure analysis of micro-crystallites is an option to by-pass many obstacles in the early stages of a structure determination from powder data. The electron diffraction (ED) patterns from small single crystals consist of well separated spots which enable straightforward indexing and a readily determined unit cell. Structural modulations can easily be recognised. Systematic absences for space group determination are much more reliably obtained from ED than from X-ray powder data. In the case of polyphasic samples, ED is superior since it allows the separate investigation and characterisation of the different crystallites. Recent it was shown that crystal structures can be solved by direct methods using ED data from crystallites containing only non-light elements.

The combination of structure analysis by ED and X-ray powder diffraction is a powerful tool for structure investigations on many materials which are beyond the capabilities of the powder method. In particular, many structural problems which suffer from pronounced preferred orientation of the crystallites or by poor crystallinity of the sample can be tackled with the proposed approach.

M13.OD.004 POWDER XRD AND ELECTRON MICROSCOPY APPLIED TO THE LOW TEMPERATURE OXIDATION OF ANOSOVITE TO ANATASE. I.E. Grey, CSIRO Minerals, Clayton, Australia 3168, L.M.D. Cranswick, CLRC Daresbury Laboratory, Warrington, WA4 4AD, UK, R. Stranger, Dept. of Chemistry, ANU, Canberra, ACT 0200, Australia and T.J. White, Nanyang Technological Institute, Singapore 639798.

Decreasing peak resolution of powder X-ray diffraction patterns (PXRD), for example due to line broadening or peak overlap, results in increasing ambiguity in the structural model used to fit the data. Poorly resolved patterns can be equally well fitted by a number of different structure models. In these situations, other techniques are needed in combination with the powder diffraction analysis to reduce the ambiguity. A particularly suitable complementary technique is transmission electron microscopy. The electron diffraction (ED) patterns can be used to establish correct unit cell parameters and possible space groups, and orientation relationships between coexisting phases, while high resolution TEM images can provide starting models of atomic arrangements for the powder refinements, as well as providing information on local ordering in disordered structures.

We have used TEM methods to assist in the PXRD refinements of the structures of phases formed during the low temperature oxidation of trivalent titanium in anosovite, (Mg, Mn, Fe, Ti)$(Ti^{3+}, Ti^{4+}, Al)_2O_5$. When finely ground anosovite is heated for extended periods at ~100°C, it transforms to a new C-centred monoclinic phase having $a_m \sim a_{anos}$=9.9Å, $b_m \sim b_{anos}$=3.75Å, $c_m \sim 2xc_{anos}$=21.1Å, β=93.1°. Further heating at a higher temperature of ~400°C results in a transformation to a disordered form of anatase. ED patterns show that the anatase crystallites are oriented relative to the anosovite such that $(101)_{anat}$ // $(001)_{anos}$ and $[010]_{anat}$ // $[010]_{anos}$. The application of the TEM/ED data to generating models of the intermediate monoclinic superstructure phase for PXRD refinement will be described.

M13.OD.005 STRUCTURE DETERMINATION OF ϕ-$Bi_8Pb_5O_{17}$ BY ELECTRON AND POWDER X-RAY DIFFRACTION. M. Gemmi, INFM, Università di Bologna, Viale Berti Pichat 6, 40127 Bologna, Italy; A.Migliori, CNR-LAMEL, Area della Ricerca di Bologna, Via Gobetti 101, 40129 Bologna, Italy; D. Belletti, G. Calestani, L. Righi, Dip. di Chimica Generale ed Inorganica and CNR-CSSD, Università di Parma, Viale delle Scienze, 43100 Parma, Italy; M. Santarosa, M. Bettinelli, A. Speghini, Dip. Scientifico e Tecnologico, Università di Verona, Ca' Vignal, Strada Le Grazie, 37134 Verona, Italy.

By heating tetragonal β_2-$Bi_8Pb_5O_{17}$ above 450°C, a new fast ionic conducting material (ϕ), that transforms above 590°C in the cubic β phase, is obtained [1]. Attempts to determine the ϕ structure by XRD failed in the past, because of the impossibility to grow single crystals and of the extreme complexity of the powder diffraction spectra. The structure has now been determined by sinergic use of electron and X-ray powder crystallography. 33 ED patterns were recorded in SAED mode using a Slow Scan CCD camera in 22 different zone axes. The QED package [2] was used for cell determination, 3-D indexing and intensity extraction. ϕ-$Bi_8Pb_5O_{17}$ is triclinic, s.g. P-1, a=7.4550(2), b=14.1677(3), c=7.2053(1)Å, α=97.185(1), β=118.464(1), γ=80.684(2)° and the cell contains 19 independent atoms. The rough position of the eight heavy atoms was found by direct methods (SIR97) [3] on merged 3-D ED data and the model was refined by Rietveld technique (GSAS) [4] on powder XRD data by fixing the stoichiometric Bi and Pb occupancy on each site. The oxygen atoms were located in successive steps in ΔF maps obtained with electron and XRD data by using the previously Rietveld refined model. Final residuals were R_{wp}=7.32% R_p=5.12%.

[1] J. C. Boivin & G. Mairesse, Chem. Mater. (1998) **10,** 2870.
[2] D. Belletti, G. Calestani, M. Gemmi & A. Migliori (1999) subm. to Utramicroscopy.
[3] A. Altomare et al. (1998) J. Appl. Cryst., in press.
[4] A.C. Larson & R.B. von Dreele (1988)LAUR86-748 LANL New Mexico

P13.OD.001 TEREPTHALATE SALTS. SALTS OF MONOPOSITIVE CATIONS. James A. Kaduk, BP Amoco PLC, Naperville IL 60566

The crystal structures of dilithium, disodium, and diammonium terephthalate have been solved *ab initio* using Monte Carlo simulated annealing techniques, and refined using synchrotron powder data. The use of synchrotron data was critical to obtaining the correct unit cells. Both reciprocal space and real space minimizations were necessary in the structure solutions. The structure of dipotassium terephthalate has been refined using standard single crystal techniques. Although over 8×10^9 pounds of terephthalic acid is produced each year, very little is known about the nature of terephthalate complexes.

$Li_2C_8H_4O_4$ crystallizes in the monoclinic space group $P2_1/c$, with a = 8.35921(5), b = 5.13208(2), c = 8.48490(5) Å, β = 93.1552(4)°, V = 363.451(3) Å^3, and Z = 2. The Li are tetrahedrally-coordinated, and the packing of the terephthalate anions is reminiscent of the γ packing of aromatic hydrocarbons.

$Na_2C_8H_4O_4$ crystallizes in the orthorhombic space group $Pbc2_1$, with a = 3.54804(5), b = 10.81604(16), c = 18.99430(20) Å, V = 728.92(2) Å^3, and Z = 4. The coordination of the two independent Na is trigonal prismatic, and the TA packing resembles the β packing of hydrocarbons. Each carboxylate group of the TA is chelated to one Na, and is bonded to four other Na above and below the ring plane. The carboxylates are rotated approximately 20° out of the ring plane. $(NH_4)_2C_8H_4O_4$ also crystallizes in $Pbc2_1$, with a = 4.0053(5), b = 11.8136(21), c = 20.1857(24) Å, V = 955.1(2) Å^3, and Z = 4. The cations and planar anions are linked by hydrogen bonds, and the TA packing is a looser version of the β packing. $K_2C_8H_4O_2$ crystallizes in $P2_1/c$, with a = 10.561(4), b = 3.9440(12), c = 11.535(5) Å, β = 113.08(3)°, V = 442.0(3) Å^3, and Z = 2. The K is trigonal prismatic, and the TA packing is also β. These structures form enough of a data base to begin to understand the energetics of the packing of terephthalate anions, and to use this information in determining the solid state structures of process-related terephthalate salts.

P13.OD.002 ELECTRON CRYSTALLOGRAPHY ON NLO-ACTIVE COMPOUNDS. U. Kolb , A. Yakimanski and I.G. Voigt-Martin Institut für Physikalische Chemie, Johannes Gutenberg-Universität Mainz, Welder Weg 11, 55099 Mainz

Microcrystalline compounds can be investigated by selected area electron diffraction, giving structural information which cannot be gained by x-ray methods. In addition structures can be visualised in real space directly using high resolution technique (HRTEM). In diffraction mode three dimensional data sets can be measured by tilting the sample around suitable axes (max. tilt angle ±60°). Determination of the unit cell and the space group is usually possible with enough projections and can be refined using a combination of x-ray powder diffraction and packing energy calculations. From the NLO-active compounds 4-nitrophenyl-hexyl-urethan (NPHU) and 3-para nitrophenyl-propan-1-ol (NPP), with a non-linear optical activity up to 80 times urea, ≈100-200 Å thick crystals were grown from ethanol. For structure analysis using simulation methods [1] cell dimensions, space group, an initial model of the molecule obtained from semiempirical, quantum mechanical calculations [2] and structure factor amplitudes were used. Packing energy minimisation and simulation of diffraction patterns are performed alternatingly gaining a good R-factor. Based on the obtained atomic coordinates, hyperpolarizability tensors were calculated using quantum mechanical methods and related to the crystal by appropriate co-ordinate transformation [3]. Separately, a 3D-data set was buildt up and statistical ab initio methods such as "Maximum Entropy" [4] were used.

[1] I.G. Voigt-Martin, U. Kolb, International School of Crystallography, 26th course: Elektroncrystallography, Erice (1997).
[2] J.J.P. Stewart, MOPAC6.0 *A General Purpose Molecular Orbital Package*, QCPE.
[3] A.V. Yakimanski, I.G. Voigt-Martin, U. Kolb, G.N. Matveeva, A.V. Tenkovtsev Acta Cryst. A53, 603-614 (1997).
[4] I.G. Voigt-Martin, Z.X. Zhang, U. Kolb, C. Gilmore Ultramicroscopy 68, 43 (1997).

P13.OD.003 CRYSTAL STRUCTURE DETERMINATION OF ζ-AgZn. A. Olsen, P. E. Runde and O. B. Karlsen, Centre for Materials Science, University of Oslo, Gaustadalléen 21, 0371 Oslo, Norway.

The crystal structure of Ag_2Ga was recently [1] determined by single crystal X-ray diffraction to be hexagonal (space group $P\bar{6}2m$), and not trigonal ($P\bar{3}$) as earlier reported. This leaves the low temperature ζ phase, sometimes referred to as the ζ' phase, in the silver-zinc system as the only phase in the literature to have the trigonal AgZn-type of structure. ζ-AgZn was determined by Edmunds and Qurashi by X-ray powder diffraction data, [2]. It was reported to have trigonal symmetry with space group $P\bar{3}$, nine atoms in the unit cell and cell dimensions a = *0.76360 nm* and c = *0.28197 nm*. Because of the new structure determination of Ag_2Ga and the fact that it was reported to be isostructural to ζ-AgZn, we have reinvestigated the structure of the ζ phase using transmission electron microscopy (TEM) and X-ray powder diffraction.

Results from selected area electron diffraction (SAED) suggested the hexagonal Bravais lattice and cell dimensions as above. No general or special reflection conditions were found. Convergent beam electron diffraction (CBED) experiments show symmetry consistent with the $P\bar{6}2m$ space group and not with $P\bar{3}$. Rietveld refinement of X-ray data based on the trigonal model [2] did not result in convergence. A starting model for Rietveld refinement based on space group $P\bar{6}2m$ and the Ag_2Ga structure with complete disorder was then tried. The refinement converged with R_p = 0.063 and cell dimensions a = *0.76379 nm*, c = *0.28188 nm*. The Zn atoms fully occupy *1a* and *2d* positions. The remaining zinc and all Ag atoms share the *3f* and *3g* positions.

1. A. E. Gunnæs, A. Olsen, P. T. Zagierski, B. Klewe, O. B. Karlsen A. Aasen. (1998). Z. Kristallogr. **213,** 639-644.
2. I. G. Edmunds and M. M Qurashi (1951). Acta Cryst. **4**, 417-425.

P13.OD.005 TRICE - A PROGRAM FOR RECONSTRUCTING 3D RECIPROCAL SPACE AND DETERMINING UNIT CELL PARAMETERS X.D. Zou, Structural Chemistry, Stockholm University, S-106 91 Stockholm, Sweden and A. Hovmöller, Rudbeck School, S-192 51, Sollentuna, Sweden

Determination of crystal unit cell is the first and an important step of *ab initio* structure determination. This is often a very difficult step of structure determination by X-ray powder diffraction, especially when the sample contains several different phases. It is possible to obtain electron diffraction patterns of individual micro/nano sized crystals in transmission electron microscopes. Due to the very short electron wavelength (~ 0.02 Å), an electron diffraction pattern is an undistorted representation of a two dimensional section of the three dimensional reciprocal lattice. The 3D reciprocal lattice can be obtained by tilting the crystal in the microscope and collecting a series of diffraction patterns from the same crystal.

In practice, it is not easy to reconstruct the 3D reciprocal lattice and determine the unit cell dimensions manually from the diffraction pattern series. We have developed a program system - Trice for this purpose. Electron diffraction patterns are digitised into a PC. The position and intensity of each diffraction spot from each diffraction pattern in the tilt series are determined and refined by the program system ELD [1]. These data plus the direction of the tilt axis and angle of tilt are used as input for Trice.

Trice combines the electron diffraction patterns of different orientations and reconstructs a part of the 3D reciprocal lattice. The 3D reciprocal lattice can be rotated and visualised from any direction. The unit cell parameters are determined directly by Trice. Normally diffraction patterns from three different orientations are enough for determining the unit cell. The lattice type and symmetry can be also determined from the 3D reciprocal lattice. Trice runs under Windows95, 98 and NT. The unit cell parameters can be further refined against X-ray powder diffraction data to higher accuracy.

1. X.D. Zou, Y. Sukharev & S. Hovmöller (1993) Ultramicroscopy 52, 436.

13OE ABSORPTION CORRECTIONS

M13.OE.001 COMPARISON OF ABSORPTION CORRECTIONS FOR CRYSTALS IN THE INTERMEDIATE ABSORPTION RANGE. Larry R. Falvello, University of Zaragoza-C.S.I.C., Department of Inorganic Chemistry, Plaza San Francisco s/n, E-50009 Zaragoza, Spain.

Comparisons are made between the results of single crystal structure determinations in which different absorption correction techniques have been used, for samples with linear absorption coefficients μ in the range of 10 – 50 mm^{-1} (near and beyond the upper end of the range typically found, for example, for organometallic complexes of the third series of transition metals). Measured absorption corrections using traditional ψ-scans, three-dimensional ψ-scans, and Laue-equivalent data are considered, along with *a posteriori* calculated corrections. Uncorrected data are also included in the comparisons. The effects on both the structural results, including anisotropic displacement parameters and the data themselves will be described.

M13.OE.002 EMPIRICAL CORRECTION FOR ANISOTROPIC ABSORPTION AND "ABSORPTION-LIKE" EFFECTS. Robert H. Blessing, Hauptman-Woodward Medical Research Institute, 73 High Street, Buffalo, New York 14203, USA. blessing@hwi.buffalo.edu

An absorption anisotropy (or anisotropic scaling) correction calculated from differences among multiply measured data equivalent by symmetry and/or azimuth rotation is implemented in the program SORTAV (Blessing, 1995). The principles, practice, and calibration of the correction calculation will be reviewed, and recent improvements in the program implementation will be described. Among the improvements are down-weighting or rejection of outlier measurements (Blessing, 1997) and use of the eigenvalue filtering technique (Watkin, 1994) in the least-squares fit of correction parameters that might be effectively perfectly correlated or indeterminate from the available data in an unfiltered fit.

Research support from USDHHS PHS NIH grant no. GM46733 is gratefully acknowledged

Blessing, R.H. (1995). An Empirical Correction for Absorption Anisotropy. *Acta Cryst.*, A**51**, 33-38.
Blessing, R.H. (1997). Outlier Treatment in Data Merging. *J. Appl. Cryst.*, **30**, 421-426.
Watkin, D. (1994). Control of Difficult Refinements. *Acta Cryst.*

M13.OE.003 SADABS: A PROGRAM FOR EXPLOITING THE REDUNDANCY OF AREA-DETECTOR X-RAY DATA. Ludger Häming[1] George M. Sheldrick[2], [1]Bruker Analytical X-ray Systems GmbH, Karlsruhe, Germany, [2]Institut für Anorganische Chemie, University of Göttingen, Germany

The use of area-detectors with nearly or literally no readout time, like CCD detectors or multi-wire proportional counters, opened the possibility of a much improved data collection strategy. Instead of restricting the experiment just onto the asymmetric part of reciprocal space these detectors are able to scan the complete reciprocal sphere. The standard data collection protocol for the SMART system will already give redundant data. Depending on the Laue-group symmetry of the sample and the expected absorption effects, a small modification of such a strategy will lead to sufficient redundancy. These redundant intensity measurements do not only contain symmetry related reflections but also multiple observations of Bragg reflections under slightly different geometrically conditions.

SADABS exploits this data redundancy to reduce various systematic errors in the measured intensities and puts the esds on a more absolute scale. For instance effects like crystal or beam decay can be treated by a smoothed scale factor for each X-ray diffraction frame. This treatment does also correct against effects which are due to changes in the sample volume irradiated (e.g. needle shaped crystals). X-ray absorption appears not only within the crystal but also within its support. SADABS uses spherical harmonic functions to model the overall absorption effects of the experimental setup. The individual measured Bragg intensities are fitted to the mean of their equivalent observations. In addition a correction for the lamba/2 contribution can be applied.

Blessing, R.H., Acta Cryst. (1995), A51, 33
Kirschbaum, K., Martin, A., Pinkerton, A.A., J.Appl.Cryst. (1997), 30, 514

M13.OE.004 DIFABS REVISITED. D.J.Watkin, Chemical Crystallography Laboratory, 9 Parks Road, OXFORD, OX1 3PD, UK. & A.N. Chernega, Institute of Organic Chemistry, National Academy of Sciences of Ukraine, Ul. Murmanskaya, 5, Kiev-94, 253600, UKRAINE.

Since its appearance in 1983, DIFABS and DIFABS-like programs have divided the crystallographic community more deeply than almost any other controversy. The pro- and anti-DIFABS lobbies are drawn up like opposing armies. This is a fruitless confrontation, since a useful compromise almost certainly exists. The original implementation of DIFABS was an excellent first attempt at utilising a concept, but it suffered from various problems which have clouded the differentiation between concept and implementation. Amongst the problems are:

1 The name. The process actually adjusts the model (or data) for *any* systematic residual between Fo and Fc as a function of diffraction geometry.

2 In the original code, Fo was modified (*as with most other absorption corrections*). There is no reason why corresponding changes cannot be made to Fc as part of the modelling process.

3 In 1983, most data were collected on serial (conventional) diffractometers, giving little redundancy in the data. The use of DIFABS with area detector data is closely related to a constrained multi-scan correction.

The value of DIFABS cannot easily be assessed unless a broad body of experience is available. The growing use of crystallography as a first-line analytical method, the growing use of area detector diffractometers for routine data collection, and the growing use of the oil-drop crystal mounting technique means it is time to look closely at DIFABS once again.

M13.OE.005 CRYSTAL SHAPE MEASUREMENT FOR ABSORPTION CORRECTION BY USE OF CCD CAMERA. Akihito Yamano, Katsunari Sasaki, Tsuneyuki Higashi, X-ray Research Laboratory, Rigaku Corporation, 3-9-12, Matsubara-cho, Akishima-shi, Tokyo 196-8666, Japan

It is well known that the absorption correction based on the crystal shape is the most precise and reliable among various correction methods. Accordingly, the Notes for Authors of Acta Crystallographica Section C says that analytical or numerical corrections are strongly recommended when the absorption effect of a sample crystal is judged to be significant. The traditional method of obtaining the crystal shape is to use a four-circle or kappa goniometer and a telescope, bit it requires certain knowledge of crystallography and some experiences.We have developed an easy method to obtain the crystal shape by the use of a CCD camera. The procedure of the method is as follows. Photographs of a crystal are taken at various goniometer settings. Crystal boundary in each photography is manually defined on a

screen using graphical tools. The boundaries are then analyzed to make a set of Cartesian planes. We have also written a Gaussian absorption correction program which accepts Cartesian planes as a crystal shape. All the programs written in C run currently on an SGI and are being transported to a PC on Windows95/98 OS. A next step is to add a function identifying a crystal boundary in a semi-automatic manner.

13OF STRONG CLOSED SHELL INTERACTIONS IN CRYSTALS

M13.OF.001 WEAK INTERACTIONS IN CRYSTALS OF GOLD(I) COMPOUNDS. L.G. Kuz'mina, Institute of General and Inorganic Chemistry, Russian Academy of Sciences, Leninskii pr. 31, Moscow 117907, Russia, and A.A. Bagatur'yants, Photochemistry Center, Russian Academy of Sciences, ul. Novatorov 7a, Moscow 117421, Russia, J.A.K. Howard, Chemistry Department, University of Durham, Durham DH1 3LE, UK.

Unusual structures of mono and polynuclear (including small clusters) Au(I) compounds are considered. These structures are characterized by a manifestation of strong closed-shell Au...Au aurophilic interactions and Au...heteroatom and Au...π–system secondary bonding. The pronounced tendency to form closed-shell aurophilic bonds often gives unpredictable results when weak organic acids undergo simple auration with $[O(AuPPh_3)_3]BF_4$. Either small clusters or dimeric compounds rather than mononuclear gold(I) complexes form in this case (via Au...Au interaction). An example when simple auration results in the cleavage of a C-N bond is also known. Structural nonrigidity of some Au(I) compounds is discussed within the concept of secondary bonds and suggested as a way of modeling some dynamic processes. Differences in structural manifestations of formally isolobal AuL^+, HgR^+, and H^+ are discussed.

We thank the Russian Foundation for Basic Research for funding this work (projects 98-03-33142 and 99-03-33180).

M13.OF.002 THEORETICAL STUDIES OF CLOSED-SHELL INTERACTIONS. N. Runeberg, Department of Chemistry, University of Helsinki, POB 55, 00014 Helsinki, Finland.

The attraction between systems with fully occupied shells has recently gained a lot of attention in inorganic chemistry, covering both its experimental and theoretical aspects (for a review see ref.[1]). One common type of closed-shell attractions is the *metallophilic* attraction, typically found between d^{10} coinage-metal centers. The attraction between closed-shell cationic gold(I) centers represents the strongest, and most thoroughly studied class of this metallophilic interaction. Although the strength of this interaction is comparable with strong hydrogen bonds or weak covalent bonds, it cannot be satisfactorily explained by classical theory, such as hybridization. Theoretical studies indicate that the aurophilic attraction is an electron-correlation effect, strengthened by relativity. Extensive ab initio studies shows that the attraction at large distances is dominated by a dispersion contribution, described as interactions between instantaneous dipoles. When approaching equilibrium distances the dispersion contribution is accompanied by a newly identified ionic contribution, represented by instantaneous charge-transfers between the gold-centers.[2]

[1] P.Pyykkö. *Chem. Rev.*, **97**, 597-636, (1997).
[2] N.Runeberg, M.Schütz and H.-J. Werner. *J. Chem. Phys.*, Accepted, (1999).

M13.OF.003 ELECTRON-DENSITY VIEW ON THE CLOSED-SHELL INTERACTIONS. V. G. Tsirelson, Quantum Chemistry Division, D.I. Mendeleev University of Chemical Technology, Moscow 125047, Russia.

This presentation considers the closed-shell atomic and molecular interactions in crystals from the electron-density view. These interactions are characterised within Bader's topological theory by the negative value of Laplacian of the electron density (ED) in the (3,-1) critical point on the interaction line. The value of the ED at this point deviates from 0.01 e·E in compounds of the inert gases till 0.3 e·E in the perovskites. Corresponding-ly, the strength of the closed-shell interactions is different. The deformation ED and Laplacian of the ED as well as a full pattern of the critical points in the ED was determined in the inert gas compounds, rock- salt and molecular crystals, perovskites and silicates. The analytical models were used in order to reconstruct the accurate quasi-static parameters of the electron density (ED) from both experimental and Hartree-Fock X-ray structure amplitudes determined with accuracy of 1-2%. Electrostatic potential (EP) also reflecting the nature of the interatomic interactions was considered additionally. It was found that interrelated analysis of the topological features of the ED and EP allows to better understand the limits of the close-packing concept of crystals as well as a nature of distortion of the ideal atomic close-packing. An origin of the one-dimensional EP maximum on the anion-anion line in rock-salt type crystals was investigated and connected with mutual sizes of cations and anions. The important role of regions of the electron deconcentration in the atomic valence shells in the formation of the closed-shell interactions is stressed.

The support of this study by the Russian Foundation for Basic Researches (grants 96-03-00071G and 98-03-32654) and the Deutsche Forschungs-gemeinschaft (grant 435 RUS 113/128/0) is gratefully acknowledged.

M13.OF.004 CATION AGGREGATES IN IONIC SOLIDS: THEIR RELATION TO THE PARENT METALS. A. Vegas. Instituto de Química Física "Rocasolano", CSIC, Serrano 119, E-28006 Madrid, Spain.

An inspection to the cation arrays of ionic solids reveals [1,2 and references therein] that cations are not the "isolated entities" predicted by the ionic model. In many ionic compounds, cations are forming aggregates which reproduce both, topology and distances of the parent metals structures, as if some kind of interaction would exist between them. Thus, the (100) planes of the Ti-subarray in the rutile (TiO_2) structure are identical to the (100) planes of *hcp*-Ti, the Mg atoms in olivine (Mg_2SiO_4) form aggregates which are fragments of the structure of *hcp*-Mg, in the bixbyite-type structure of In_2O_3, the In atoms form a structure which is a distortion of the lattice of elemental In, and in spinel ($MgAl_2O_4$), the Al-subarray is just one half of the *fcc* structure of Al metal. Although we give here only some significant examples, a systematic study of all the crystal structures contained in ICSD reveals that, for a given metal, the distribution of the cation-cation distances is not uniform but present maxima which coincide with the values of the shortest M-M distances in the pure metals. In some cases, maxima coincident with the second-nearest neighbours are also present.

These features occur not only with cations which adopt a noble gas configuration (Mg^{2+}, Al^{3+}, Sc^{3+}, Ti^{4+}) but also with atoms which have not a closed-shell, as they are the cations of the Rare Earths [2]. They are difficult to justify with the ionic model and it could be explained if we assume an inclomplete redox process between cations and anions and that part of the non-transfered electrons could be used in the formation of M-M interactions.

The impression is that metallic nets do not need necessarily to be broken down in atoms to form a compound. They are only transformed, modified or broken in fragments by the inclusion of the anions, but maintaining the topology and distances of the parent metals.

1. R. Isea, A. Vegas & A. Ramos-Gallardo (1998). *Acta Cryst.* **B54**, 35-40.
2. A. Vegas & R. Isea (1998). *Acta Cryst.* **B54**, 732-740.

M13.OF.005 CLOSED-SHELL BONDING IN IONIC CRYSTALS FROM THE PERSPECTIVE OF THE ATOMS IN MOLECULES THEORY. V. Luaña, A. Martín Pendás, A. Costales, P. Mori-Sánchez, and M. A. Blanco Departamento de Química Física y Analítica, Universidad de Oviedo, 33007-Oviedo, Spain.

The quantum mechanical laws of motion are, in general, not applicable to arbitrary regions within a molecular or crystalline system. It is only when regions are bounded by surfaces with zero flux of the gradient of the electron density ($[(\nabla)\vec{\rho}\cdot[(n)\vec{\rho}] = 0$) that all quantum mechanical laws hold and all observables are locally well defined. Upon this single requirement a rigorous, well defined, and unique theory of chemical bonding has been developed: the Atoms in Molecules (AIM) theory of R. F. W. Bader and collaborators [1].

We have used the AIM theory to analyze the electron density in a large variety of compounds and several crystalline families [2,3,4,5]. Some of the main results emerging from our work will be presented in this talk. Of particular importance is the coherence of the bonding properties in crystals and molecules once the interatomic distance is properly accounted for. Many ionic crystals have been found to exhibit secondary bonding, i.e. bonding between second and further neighbors, this behavior being mainly controlled by the particular crystalline structure and ionic size.

[1] R. F. W. Bader, *Atoms in Molecules - A Quantum Theory*, (Oxford U.P., Oxford, 1990).
[2] A. Martín Pendás, A. Costales, and V. Luaña, Phys. Rev. B **55** (1997) 4275-4284.
[3] V. Luaña, A. Costales, and A. Martín Pendás, Phys. Rev. B **55** (1997) 4285-4297.
[4] A. Martín Pendás, A. Costales, and V. Luaña, J. Phys. Chem. B **102** (1998) 6937-6948.
[5] V. Luaña, A. Costales, P. Mori-Sánchez, and A. Martín Pendás, J. Phys. Chem. B (in press).

P13.OF.001 RECOGNIZING FRAGMENTS OF THE NOBLE GASES STRUCTURES IN THEIR COMPOUNDS. A. Vegas. Instituto de Química Física "Rocasolano", CSIC, Serrano 119, E-28006 Madrid, Spain.

The compounds of the Noble Gases, in the solid state, tend to reproduce part of the elemental crystal structures of the gases. This feature, which has been found to be a general trend in metal oxides [1], is also observed in the noble gases compounds, indicating that elements, in spite of being coordinated by other atoms, tend to preserve their structure when forming compounds.

In the tetragonal structure of KrF_2, the molecules are parallel to the (002) planes, producing an slight expansion of the elemental *fcc* structure of Kr in the *ab* plane but maintaining the **c** axis (5.83 Å) almost identical to the **a** parameter of elemental Kr (5.72 Å). However, in XeF_2, the linear molecules are parallel to the **c** axis of the tetragonal net, and the exfoliation takes place along the **c** axis, but maintaining almost unaltered the (002) planes of *fcc*-Xe (Xe-Xe distances of 4.31 and 4.38 Å, respectively). In the monoclinic phase of XeF_4, the distortion is greater, The Xe atoms, at (0,0,0) and (1/2, 1/2, 1/2) form an I monoclinic net which is a distortion of the tetragonal I cell contained in *fcc*-Xe, but where the **c** axis (6.20 Å) correspond almost to the **b** axis in the monoclinic cell (5.92 Å) and where the shortest Xe-Xe distances are only 0.2 Å longer than in the element. In the mixed crystal $XeF_2 \bullet XeF_4$, the Xe atoms form linear chains, separated at 4.50 Å (4.38 Å in the element).

The most striking structure is XeF_6. Although the Xe atoms are coordinated by six F atoms, they form tetrahedral and octahedral clusters in which the Xe-Xe distances (4.22 and 4.40 Å respectively) are close to the value in elemental Xe. Thus, the structure can be regarded as the elemental structure of Xe, broken in fragments (octahedra and tetrahedra), by the inclusion of the F atoms. It is also surprising that Xe atoms of different tetrahedra form squares (l = 6.24 Å) which are identical to the (100) faces of elemental Xe (a = 6.20 Å), This makes that *fcc*-Xe could also be reconstructed by forming unit cells with an octahedron and two parallel squares.

1. R. Isea, A. Vegas & A. Ramos-Gallardo (1998). *Acta Cryst*. **B54**, 35-40.

13AA HOT MACROMOLECULAR STRUCTURES (II)

M13.AA.001 CRYSTAL STRUCTURE OF THE ATP-BINDING SUBUNIT OF AN ABC TRANSPORTER. L.-W. Hung, E.O. Lawrence Berkeley National Laboratory, I. X. Wang, K. Nikaido, P.-Q. Liu and G. F.-L. Ames, Department of Molecular and Cell Biology, University of California, Berkeley, and S.-H. Kim, E.O. Lawrence Berkeley National Laboratory and Department of Chemistry, University of California, Berkeley, Berkeley CA 94720

We report the crystal structure at 1.5 Å resolution of HisP, the ATP-binding subunit of the histidine permease, an ABC transporter from *Salmonella typhimurium*. Members of the ABC transporter superfamily are widely found in prokaryotes and eukaryotes. Among the eukaryotic members, several are medically important proteins, such as the cystic fibrosis transmembrane conductance regulator (CFTR), the P-glycoprotein (MDR: muti-drug resistance protein), and the transporter associated with antigen processing (Tap1/Tap2). ABC transporters have two highly conserved ATP-binding domains and two transmembrane domains. We correlate the crystal structure of HisP with the biochemical, genetic, and biophysical properties of the wild type and of numerous mutant HisP proteins as well as with the properties of mutant CFTR and MDR proteins.

The overall shape of the crystal structure of the HisP monomer is that of an "L" with two thick arms; the ATP-binding pocket is near the end of one of the arms. A six-stranded β-sheet spans both arms of the "L" with a domain of α + β type on one side and a domain of mostly α-helices on the other side of the sheet. The overall fold of the structure is different from that of any known protein. However, the topology of the ATP binding pocket is close to that of RecA and of the α- and β-subunits of bovine F1 ATPase. In agreement with the notion that HisP forms a dimer in vivo, a dimer consisting of two monomers related by a two-fold axis is also found in the crystal structure of HisP. All available biochemical data about HisP in the HisQMP2 complex are compatible with the characteristics of HisP in the crystal structure. The structure of HisP provides a basis for understanding properties of ABC transporters and those of defective CFTR proteins.

M13.AA.002 CRYSTALLOGRAPHIC STUDIES OF THE MIP PROTEIN FROM LEGIONELLA PNEUMOPHILA. A. Riboldi-Tunnicliffe, R. Hilgenfeld. IMB, Department of Structural Biology and Crystallography, Beutenberg Str 11, Jena D-07745, Germany

Macrophage infectivity potentiator protein (MIP) is located on the outer membrane of L.pneumophila, the causative agent of Legionnaires' disease. This protein has been shown to be one of the major virulence factors of this organism (Fischer et al., 1992). MIP belongs to the protein class of peptidyl prolyl cis/trans isomerases (PPIases) which catalyse the cis/trans isomerisation of the peptide bond at the N-terminal side of the amino acid proline. MIP belongs to the family of FK506 binding proteins; these bind and are inhibited by the macrolides FK506 and rapamycin, both are important as suppressors of T-cell activation (Hacker et al., 1993). Sequence analysis suggested the presence of 2 domains (Ludwig et al., 1994). Initial attempts to solve the structure by molecular replacement using human FKBP12 as a model proved impossible with little or no density extending beyond the model. However, this model did reveal the presence of a tightly bound zinc ion within the structure. With this information we were able to perform a MAD experiment on the zinc edge, and solve the structure to 2.4A. The structure of the MIP dimer is highly unusual. the N-terminal domain is a small helical dimerisation module which we belive to be a novel fold, comprising residues 10-50. This is followed by a very long isolated alpha-helix the C-terminal of which carries the FKBP domain. The two FKBP domains of the dimer are approx. 21A apart. This unusual structure suggests modes of interaction with a receptor and new ideas for the design of drugs directed against Legionella and Chlamydiae.

1) Fischer, G., Bang, H., Ludwig, B., Mann, K. and Hacker, J. (1992) Molecular Microbiology 6, 1375-1383
2) Hacker. J., Ott, M., Wintermeyer, E., Ludwig, B. and Fischer, G. (1993) Int. J. Med. Microbiol. Virol. Parasitol. Infect. Dis. 278, 348-358
3) Ludwig, B., Rahfeld, J., Schmidt, B., Mann, K., Wintermeyer, E., Fischer, G. and Hacker, J. (1994) FEMS Microbiology letters 118, 23-30

M13.AA.003 THREE-DIMENSIONAL STRUCTURE OF A NOVEL ADENYLYLTRANSFERASE IN THE CO-ENZYME A BIOSYNTHETIC PATHWAY. Tina Izard & Arie Geerlof, Department of Biochemistry, University of Leicester, LE1 7RH, UK

Coenzyme A (CoA), the principal acyl carrier in all living cells, is required for numerous synthetic and degradative reactions and is also involved in the control of intermediary metabolism. It is invariably synthesised from pantothenate (vitamin B5), cysteine and ATP in five steps.

Phosphopantetheine adenylyltransferase (PPAT) is an essential enzyme in bacteria that catalyses a rate limiting step in coenzyme A (CoA) biosynthesis, by transferring an adenylyl group from ATP to 4'-phosphopantetheine, yielding dephospho-CoA (dPCoA). Its structure is of interest in gaining a new knowledge base that broadens our understanding of the metabolic origins of an important co-factor for human metabolism.

PPAT from Escherichia coli has been overexpressed, purified and crystallised. The PPAT-dPCoA co-crystals belong to the space group I23 with unit cell dimensions a = 135 Å. Here we present the three-dimensional structure of PPAT and some insights into its mechanism of reaction.

M13.AA.004 TRANSCRIPTIONAL REGULATION OF PURINE BIOSYNTHESIS IN *B. SUBTILIS*. S.Sinha[1], B.S.Shin[2], S.Lange[1], P.Rappu[3], J.M.Krahn[1], D.R.Tomchick, P. Mäntsälä[3], H.Zalkin[2] and J.L.Smith[1]. [1]Dept. of Biological Sciences and [2]Dept. of Biochemistry, Purdue University, West Lafayette, IN 47907,USA; [3]Dept. of Biochemistry and Food Chemistry, Turku University, Turku, Finland.

Proteins encoded by the *purR* operon in *B. subtilis* are responsible for transcriptional regulation of genes of *de novo* purine biosynthesis from the precursor PRPP. Two translationally coupled genes from the *purR* operon, *purR* and *orf2*, encode a 285-residue, transcription initiation repressor, PurR, and a 125-residue protein, Orf2, respectively[1]. A PurR homodimer binds to unknown specificity elements in a long segment of control-site DNA of the *pur*, *purA* and *purR* operons[2]. PRPP induces these operons by inhibiting DNA binding of PurR. Orf2 modulates PurR function *in vivo* by an unknown mechanism. Structures of the two proteins have provided information important to elucidating their functions.

Structures of both proteins have been solved using MAD techniques; PurR to 2.3Å by SeMet MAD (space group *P*1, a=65.4 Å, b=72.5 Å, c=83.4 Å, α=84.7°, β=84.6°, γ=67.5°, z=4 monomers) and Orf2 to 1.7 Å by Hg MAD (space group $P6_5$, a=b=53.5 Å, c=204.9 Å, z=18 monomers).

PurR belongs to the Type I phosphoribosyltransferase (PRTase) structural family. Unlike the catalytic PRTases, PurR uses the PRTase fold to bind PRPP as an effector molecule. A highly basic N-terminal helix-turn-helix (HTH) domain may be responsible for DNA binding. However, the mode of DNA binding may differ in PurR and other dimeric HTH DNA binding proteins, as an extensive hydrophobic interface between the PurR HTH domains appears to fix the DNA recognition helices in an unusual orientation.

Orf2 is the first structural representative of a widely distributed protein family of unknown function. The extensive subunit interface of Orf2 indicates that it is a biological trimer. Its electrostatic surface potential suggests Orf2 and DNA do not interact directly. Residues conserved in various Orf2 homologs map to a single, solvent-accessible pocket, suggestive of a ligand or substrate binding site.

Supported by NIH grant DK-42303 from the USPHS to JLS

1. Weng *et al.* (1995) Proc. Nat. Acad. Sci. 92: 7455-7459.
2. Shin *et al.* (1997) J. Bacteriol. 179: 7394-7402.

M13.AA.005 CRYSTAL STRUCTURE OF HUMAN HMG-COA REDUCTASE. Eva S. Istvan[1], Maya Palnitkar[2], and Johann Deisenhofer[1,2]. [1]Dep. of Biochemistry, University of Texas Southwestern Medical Center, Dallas, TX, USA. [2]Howard Hughes Medical Institute, Dallas, TX, USA.

3-hydroxy-3-methylglutaryl-coenzyme A (HMG-CoA) reductase catalyzes the committed step in the biosynthesis of sterols such as cholesterol and isoprenoid compounds such as farnesyl-PP. Although cholesterol is required for eukaryotic membrane structure, and protein farnesylation is essential for cell growth, overaccumulation of products of the mevalonate pathway can be toxic and lead to hypercholesterolemia. Inhibitors of HMG-CoA reductase are widely used in therapy as cholesterol-lowering drugs.

We solved the structure of the 50kDa catalytic domain of human HMG-CoA reductase in the presence of substrate at 2.6 Å resolution. The protein crystallizes in space group $P2_1$ as a dimer of dimers with four molecules in the asymmetric unit. Human HMG-CoA reductase shares 20% sequence identity with *Pseudomonas mevalonii* reductase, which has been solved at 3.0Å[1]. Although the overall fold is similar, the structure of the human enzyme is significantly different from the *P.mevalonii* structure, and Patterson searches with the structure of the bacterial enzyme failed. Multiple isomorphous replacement techniques were also unsuccessful because of severe non-isomorphicity problems. The structure was finally solved by MAD using the seleno-methionine variant. 42 of the 68 seleno-methionines present in the asymmetric unit could be located by direct methods using the package *Shake-and-Bake* (v2.0)[2]. Additional 16 sites were identified using anomalous difference fourier techniques. The structure refinement to 2.1Å is now in progress.

1 C.M. Lawrence et al. (1995) *Science* 268, 1758-1762.
2 www.hwi.buffalo.edu/SnB.

M13.AA.006 THE STRUCTURE OF A REGULATORY COMPLEX CONTAINING A UNIQUE RNA BINDING PROTEIN FROM THE AMIDASE OPERON OF *PSEUDOMONAS AERUGINOSA*. B.P. O'Hara, R. Norman, T. Barrett, S.M. Roe, P.T.C. Wan, R. Drew and L.H. Pearl. Dept. of Biochemistry and Molecular Biology, University College London, Gower Street, London WC1E 6BT, UK.

Pseudomonas aeruginosa is an opportunistic Gram-negative bacterium responsible for chronic lung infections in cystic fibrosis and immunologically suppressed conditions. Signal transduction in bacteria occurs via two component regulatory systems, with a histidine protein kinase sensor and a response regulator. In effect, a molecular switch regulated by a phosphorylation cycle. However, expression of the amidase operon of *Pseudomonas aeruginosa* is regulated by a novel signal transduction pathway, which, while using a two component system, is controlled by a steric hindrance mechanism.

In this system AmiC is the ligand sensor and AmiR the response regulator, a transcription anti-termination factor. Under inducing (acetamide) growth conditions AmiR binds to the operon RNA leader transcript to prevent formation of transcription terminator and allow operon expression. In the presence of the co-repressor butyramide, AmiC and AmiR form a non-active complex. Acetamide causes dissociation of the regulatory complex and represents a unique molecular switch, regulating operon expression.

We have isolated, purified and crystallised a stable soluble AmiC/AmiR complex in the presence of the non-inducing ligand butyramide. The crystals, which diffracted to 2.2Å, belong to the monoclinic spacegroup C2, with two molecules of AmiR and two molecules of AmiC in the asymmetric unit. AmiR is a dimer, with each monomer interacting with one AmiC molecule. The AmiR N-terminal domain is structurally similar to the classic response regulator receiver domain (CheY-fold). The C-terminal domain consists of a long helix with a final helix-turn-helix, which, from mutational studies, contains the sequence specific RNA binding motif.

13BB THE MAD METHOD

M13.BB.001 SOLVE - AUTOMATED MIR AND MAD STRUCTURE DETERMINATION. Thomas C. Terwilliger, Joel Berendzen, Structural Biology Group, Los Alamos National Laboratory, Los Alamos, NM 87545 Biophysics Group, Los Alamos National Laboratory, Los Alamos, NM 87545.

We have developed a fully automated procedure for determination of heavy atom sites and calculation of native phases in a MAD experiment or in all derivatives in an MIR experiment. The only input required consists of the space group and cell constants, resolution limits, the type of heavy atoms present, and the scaled data. The output consists of ranked sets of refined heavy atom parameters and native electron density maps. The most important new feature of the procedure is the scoring of potential solutions. Four criteria are used in scoring. The first corresponds to peak heights at expected positions in the Patterson function. The second is peak heights at heavy atom positions in "omit" heavy atom difference Fouriers. The third is the figure of merit of the phasing obtained. The fourth is the non-randomness of the native Fourier obtained. Each of these criteria are evaluated based on the Z-score obtained from a comparison of the solution being tested and the mean over many solutions. The procedure uses a Patterson search procedure (a modified version of HASSP) to obtain plausible starting solutions. The solutions are scored and ranked. One at a time, solutions are considered as test starting solutions for generation of new solutions by addition or deletion of individual sites. After calculation of native phases from a test solution, difference Fourier maps (and cross-difference Fourier maps for the MIR case) are used to identify possible additional sites. New solutions are scored and included in the ranked list of solutions. The procedure is iterated until no additions or deletions to existing highly-ranked solutions yield an improvement in score. SOLVE is now installed at several synchrotron sources (including the ESRF, NSLS beamlines X-4A, X-8c, and X-12C; SSRL beamlines 7-1 and 9-1, CHESS, the ALS, and the APS) so that crystallographers can solve structures immediately after data is collected. MAD structures with as many as 52 selenium sites in the asymmetric unit have been solved with our procedure, and a number of structures have been solved within hours of data collection. We are now exploring the application of density analysis and modification techniques to the maps output by SOLVE. The presence of distinct regions of protein and solvent in macromolecular crystals has been widely used to improve crystallographic phases through solvent flattening techniques. The same characteristics can be used to evaluate phase quality in direct methods and to rank heavy-atom solutions in the MAD and MIR approaches. The presence of solvent and protein regions can be evaluated either in real-space and in reciprocal-space. The reciprocal-space calculations can be formulated in a series in which only a small number of terms need to be evaluated. Possible applications of measures of macromolecular map quality will be discussed

M13.BB.002 CRYSTAL STRUCTURES OF THE SYNAPTIC FUSION MACHINERY SOLVED BY MAD PHASING. Axel T. Brunger, R. Bryan Sutton, C. Ostermeier, L. M. Rice, and R. Yu, Howard Hughes Medical Institute and Department of Molecular Biophysics and Biochemistry, Yale University, New Haven, CT 06518

Our primary focus is to understand the molecular mechanism of synaptic neurotransmission, and how this process is controlled and regulated by a set of dynamically interacting proteins. Vesicle fusion occurs in several stages: tethering, docking, priming, and Ca2+-dependent fusion. We are investigating the proteins involved at each of these stages by X-ray crystallography, nuclear magnetic resonance, and other spectroscopic methods. We have recently solved the structures of a core of the synaptic fusion complex, the D2 domain of the SNARE complex dissociating chaperon NSF, and the Rab3A-rabphilin-3A complex by MAD phasing. Structure solution of the synaptic fusion used a combinatorial labeling strategy. Each component of the complex was labeled individually or in combination with other components. MAD experiments were carried out on each of the labeled complexes. Phase combination of the resulting probability distributions produced more accurate phases than could be obtained from any of the individual MAD experiments. In addition, solution of the heavy atom site positions was simplified for the MAD experiments involving subsets of the total number of methionines in the complex. This multi-MAD technique was essential for structure solution of this complex and other vesicle-fusion related structures since the crystals were highly mosaic, diffracted weakly, and were highly variable.

1) R.B. Sutton, D. Fasshauer, R. Jahn, and A.T. Brunger, Crystal structure of a SNARE complex involved in synaptic exocytosis at 2.4 Å resolution. *Nature* **395**, 347-353 (1998).
2) R.C. Yu, P.I. Hanson, R. Jahn, and A.T. Brunger, Structure of the ATP-dependent oligomerization domain of N-ethylmaleimide sensitive factor complexed with ATP, *Nature Structural Biology* **5**, 803-811 (1998).
3) C. Ostermeier and A.T. Brunger, Structural basis of Rab effector specificity: crystal structure of the small G protein Rab3A complexed with the effector domain of rabphilin-3A, *Cell* **96**, in press (1999).

M13.BB.003 PROTEIN PROSTHETICS: X-RAY STRUCTURE OF THE *E. COLI* FIMC-FIMH CHAPERONE-ADHESIN COMPLEX. Stefan Knight and Devapriya Choudhury, Department of Molecular Biology, Uppsala Biomedical Center, Swedish University of Agricultural Sciences, Box 590, S-753 24 Uppsala, Sweden., Andrew Thompson, EMBL Grenoble Outstation, C/o Avenue des Martyrs, BP 156X, 38042 Grenoble, France, Vivian Stojanoff, ESRF, Avenue des Martyrs, 38400 Grenoble, France, Solomon Langermann, MedImmune, Inc., Gaithersburg, Maryland 20878, Jerome Pinkner and Scott J. Hultgren ,Department of Molecular Microbiology, Washington University School of Medicine, St Louis, Missouri 63110, U.S.A.

The X-ray structure of the bacterial adhesin that mediates colonization of uropathogenic *E. coli* to the bladder epithelium, FimH, in a complex with its chaperone, FimC, was solved to 2.5 Å resolution. FimH consists of an NH_2-terminal mannose-binding domain and a COOH-terminal pilin domain used for incorporation of the adhesin into the pilus. The pilin domain of FimH has the same immunoglobulin-like topology as the NH_2-terminal domain of PapD-like chaperones, except that the seventh strand is missing. This creates a deep scar on the surface of the domain, leaving part of the hydrophobic core exposed. A donor strand complementation mechanism was revealed in which the chaperone donates a strand to the pilin domain. We propose that an extension at the NH_2-terminus of pilins participate in a donor strand exchange mechanism in pilus assembly. The donor strand complementation mechanism provides the first example of a class of proteins for which the primary sequence does not contain all of the steric information needed for correct folding.

M13.BB.004 MAD STRUCTURE DETERMINATION AT THE CORNELL HIGH ENERGY SYNCHROTRON SOURCE. Steven E. Ealick, Department of Chemistry and Chemical Biology, Cornell University, Ithaca, NY 14853

Station F-2 at the Cornell High Energy Synchrotron Source (CHESS) is routinely used for MAD structure determination. Station F-2 provides rapidly tunable, doubly focused optics consisting of a Si(111) double crystal monochromator with a fixed offset and a vertically focusing mirror. The second monochromator crystal is saggitally focused. The station is equipped with an oscillation camera, a Quantum-4 CCD X-ray detector, a low temperature apparatus, computers for data collection and data analysis and hardware for monitoring and calibrating the station energy. The station has been used to solve dozens of MAD structures, primarily utilizing the Se absorption edge. However, structures have also been solved using the absorption edges of Br, Cu, Fe, Hg, Ho, Pt, Tb and others. As MAD structure determination has become more and more routine, structures of greater and greater complexity are being solved. During the past few years much of our research and development effort has focused on solving MAD structures with weak anomalous signals or structures containing large numbers of anomalous scattering atoms. The former requires accurate data, free from systematic errors, while the latter is limited by the ability to locate the positions of the anomalous scattering atoms. Accurate data is facilitated by combining synchrotron radiation, CCD detectors and cryocrystallography. Location of large numbers of anomalous scattering atoms is made possible through direct methods. The CHESS facilities will be described and several recent examples of MAD structures will be presented. These include the structure determination of the 1:3 interferon-gamma/receptor complex, which contains six ordered Se atoms in 120 kDa of protein and the structure determination of ADP-L-glycero-D-mannoheptose 6-epimerase, which contains 70 Se atoms in an asymmetric of 370 kDa. In the case of the receptor complex, the Se atoms positions were located by molecular replacement by positioning the known structure of interferon-gamma in the unit cell. In the case of the epimerase, 66 Se atom positions were located using the Shake-and-Bake method based on Hauptman's minimal function.

M13.BB.005 THE STRUCTURAL BIOLOGY CENTER'S 19ID UNDULATOR BEAMLINE AT APS: MAD PHASING. R. Sanishvili, R. Alkire, N. Duke, G. Evans †, S. Ginell, L. Keefe*, G. Rosenbaum, F. Rotella, M. Walsh‡, R. Zhang, and A. Joachimiak. Structural Biology Center, Argonne National Laboratory, Argonne, IL 60439, USA. †Currently at MRC-LMB, Cambridge, UK. ‡Currently at IRBM, Rome, Italy. * Currently at IMCA, Chicago, USA.

Multiple wavelength anomalous dispersion (MAD) is rapidly becoming the method of choice for initial phasing in macromolecular crystallography. The major reasons for this are the growing availability of synchrotron radiation sources and improvements in the experimental and theoretical techniques. Undulators, producing high flux, high brilliance X-ray beams at third generation synchrotrons, have not been extensively tested for MAD phasing. Hence, the success of this method was one of the major criterion for commissioning of 19ID undulator beamline of Structural Biology Center (SBC) at the Advanced Photon Source (APS).

To date, a wide variety of elements have been successfully used as anomalous scatterer, with K and LIII absorption edges in the energy range from 7.1 to 17.16 keV utilizing the undulator's 1st (fundamental) and 3rd harmonic radiation.

Typically, fluorescence scans are taken from macromolecular crystal changing (increasing) the monochromator energy in small steps. The choice of wavelengths can be made directly from the scans. Alternatively, f' and f" values can be calculated based on these scans using Kronig-Kramers transformations and plotted against energy. Then 3-4 wavelength MAD data is usually collected from a fresh crystal.

Thus far, about 10 successful MAD experiments have been carried out by members of the SBC staff and more than 20 by user groups participating in the commissioning of the beamline. Various experimental configurations have been used, such as mirror plane and inverse beam geometries, collecting data in small rotational wedges or in one continuous scan for each wavelength etc.

Crystallographic statistics of these MAD experiments, along with the details of most representative examples, will be presented.

P13.BB.001 ATOMIC RESOLUTION MAD PHASING. A. González, R. Morris, V. Lamzin, P. Alzari*, EMBL, Hamburg Outstation, Notkestrasse 85, 22603 Hamburg, Germany. *Unite de Biochimie Structurale, Institut Pasteur, 25 rue du Dr. Roux, F-75724 Paris.

One of the greatest advantages of using anomalous dispersion methods for phasing protein structures is the achievement of unbiased accurate phases to as high resolution as the crystals diffract. Collecting MAD data to very high resolution has several advantages:

High resolution maps are easier to interpret. It becomes possible to build up automatically a large part or all of the structure with modern electron density interpretation techniques.

Totally model-independent phases can be used for evaluation of the solvent structure, structure validation purposes and to study the structural changes induced by binding of heavy atom compounds.

We have collected a three wavelength MAD data set from a mercury derivative of Endoglucanase A (CELA) to 1 Å resolution on the EMBL Hamburg beamline BW7A. From these data, we were able to obtain high quality phases and maps at atomic resolution. The analysis of the model built in the MAD

map and the comparison between this model and the refined native structure will be presented.

P13.BB.002 TRICHROMATIC CONCEPT FOR MAD METHOD AT SPring-8 RIKEN BEAMLINE I. M. Yamamoto and T. Kumasaka, The Institute of Physical and Chemical Research (RIKEN), Mihara, Mikazuki-cho, Sayo-gun, Hyogo 679-5143, Japan, E. Yamashita, Institute for Protein Reseach, Osaka University, Yamadaoka, Suita, Osaka 565-0871, Japan, H. Moriyama and T, Ueki, Japan Synchrotron Radiation Research Institute (JASRI), Mihara Mikazuki-cho, Sayo-gun, Hyogo 679-5198, Japan

At SPring-8, RIKEN beamline I (BL45XU) is designed and developed to accumulate a number of three-dimensional structures with multi-wavelength anomalous diffraction (MAD) method. We have proposed the trichromatic concept as a new solution for MAD phase determination. This concept is that MAD data sets at three different wavelengths are easily taken for the same protein crystal without changing any beamline setting by use of a tandem vertical undulator and a trichromator. The MAD method has the big advantages for accuracy and convenience in phase evaluations. The essential requirement for the MAD method is the tunability of the wavelength. High flux and high energy resolution are also important for the MAD. These requirements are satisfied by the features of third generation synchrotron radiation facility. However, the development of the MAD method as a routine macromolecular crystallography is not so straight forward because of the contribution of the anomalous diffraction is minimal. To insure the accuracy in the MAD experiment, it is essential to minimize systematic error so that actual signals in Bijvoet and dispersive differences are precisely measured as possible. In the MAD experiment, at least three sets of diffraction data have to be collected with three different wavelengths. The wavelengths also have to be tuned as quickly possible with good reproducibility.

Trichromator consists of three pairs of transparent diamond double crystal monochromators and collinearly introduces three monochromatized wavelengths on the identical beam direction. To choose the any combination of each three monochromatic beams, a beam chopper is installed. A cylindrical bend mirror determines the final beam direction and focus. We have finished the initial construction of the beamline and trichromatic undulator beams have been utilized for the MAD data collections. The current experimental station consists of a 4-circle offset goniometer and imaging plate detector R-AXIS IV. We have collected MAD data sets including several anomalous compounds (zinc, mercury, selenium, etc.) and successfully determined MAD phases. The present status and some results of RIKEN beamline I will be presented.

P13.BB.003 MULTIWAVELENGTH ANOMALOUS DISPERSION: DATA COLLECTION STRATEGY. V. Stojanoff, European Synchrotron Radiation Facility, G. Sainz, EMBL Grenoble Outstation and ESRF, G. Leonard, European Synchrotron Radiation Facility, A. Teplitsky, Hebrew University of Jerusalem, S. McSweeney, EMBL Grenoble Outstation and ESRF, G. Shoham, Hebrew University of Jerusalem, Y. Shoham, Technion-IIT and A. Thompson, EMBL Grenoble Outstation and ESRF.

Macromolecular structure determination by the multi-wavelength anomalous dispersion (MAD) method has been increasingly used in recent years. Several data collection strategies have been employed, but the most frequently used is the one originally established by Hendrickson and co-workers [1]. This method is based on minimising systematic errors in data collection by collecting Bijvoet and dispersive differences as close in time as possible. This can be achieved either by positioning the crystal to record Bijvoet pairs on the same frame or by using ïnverse beam" geometry. Data is collected in either case by dispersive differences in small angular wedges at different wavelengths with rapid wavelength cycling. However, good results have also been obtained at the ESRF from completely random crystal orientations by collecting highly redundant data sets or from the collection of complete data sets for each wavelength. This strategy allows to maintain the wavelength constant for long periods of time thus making the MAD method accessible to non-rapidly tunable beam lines.

We present a comparison of data collected with several commonly used strategies for the same crystal, beam line and detector : a) Sample aligned to give Bijvoet pairs on the same image; b) inverse beam geometry, random geometry but data collected by measuring Friedel pairs at ϕ and (ϕ+ 180^o); c) Random geometry; d) Data collected in angular wedges with the wavelength corrected between each wedge, inverse beam geometry.

Results showing the quality of the final maps as well as the relative ease of structure determination will be presented for each method, and discussed in the light of recent results obtained on ESRF beam lines.

1. W.A. Hendrickson, A. Pahler, J.L. Smith, Y. Satow, E. A. Merritt & R. A. Phizackerley (1989) PNAS, **86**, 2190-4.

P13.BB.004 MAD PHASING 370KDA FROM 70 SELENIUM ATOMS: THE STRUCTURE OF ADP-L-GLYCERO-D-MANNOHEPTOSE 6-EPIMERASE. Ashley M. Deacon [1], Yisheng Ni, William G. Coleman, Jr. [2], Steven E. Ealick [1], [1] Department of Chemistry and Chemical Biology, Cornell University, Ithaca, NY 14853, [2] Laboratory of Biochemistry and Genetics, National Institute of Diabetesand Digestive and Kidney Diseases, NIH, Bethesda, MD 20892

ADP-L-glycero-D-mannoheptose 6-epimerase catalyzes the NADP dependent interconversion of ADP-D-glycero-D-mannoheptose and ADP-L-glycero-D-mannoheptose. The latter is a key intermediate in the biosynthesis of the lipopolysaccharide inner core in several genera of pathogenic and non-pathogenic gram-negative bacteria.

ADP-L-glycero-D-mannoheptose 6-epimerase from E. Coli crystallises in the presence of the catalytic inhibitor ADP-glucose, with two pentamers in the crystallographic asymmetric unit. The crystal structure has been determined by MAD phasing using the selenomethionyl protein. The computer program SnB (Shake and Bake) was used to locate 65 out of the 70 selenium atoms found in the asymmetric unit. A model, comprising 10 molecules of the enzyme, each with tightly bound NADP and less tightly bound ADP-glucose has been refined to 2.0A resolution.

The monomer subunit is arranged in two domains, a large N-terminal domain consisting of a seven-stranded Rossmann fold, associated with NADP binding and a smaller alpha/beta C-terminal domain involved in substrate binding. The overall fold is very similar to UDP-galactose epimerase and GDP-4-keto-6-deoxy-D-mannose epimerase/reductase, although both these enzymes are observed as dimers.

Details of the structure determination and of the catalytically important NADP and substrate binding sites will be presented.

P13.BB.005 WAVELET DENOISING OF POWDER DIFFRACTION PATTERNS. V. Jorík and M. Ďurík, Ľ. Smrčok, Department of Inorganic Chemistry STU, SK-812 37 Bratislava, Slovak Republic and Institute of Inorganic Chemistry SAS, SK-842 36 Bratislava, Slovak Republic

X-ray powder diffraction patterns taken under very different experimental conditions were denoised by the method

called thresholding of wavelet coefficients. The patterns were first transformed by discrete wavelet transform (DWT, Coiflet4 wavelet) [1,2] and then the level-dependent soft-thresholding method (MAD) was applied [3]. The example given below shows denoising of a pattern of a coke with two sharp peaks from a Ni-holder (N-number of points, I in counts). It was found that wavelet denoising in contrast to polynomial filters neither shifted nor distorted the diffraction profiles [4].

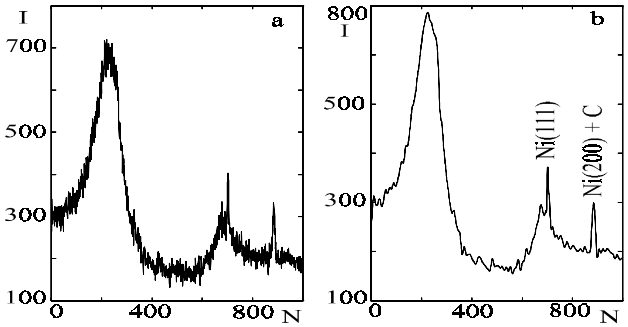

[1] Chui, Ch.K. Wavelets : a Mathematical Tool for Signal Analysis. SIAM, 1997.
[2] Barclay,V.J., Bonner, R.F., Hamilton, I.P. Anal. Chem. 69 (1997) 78-90.
[3] Donoho, D.L., Johnstone, I.M. Biometrika 73 (1986) 625-633.
[4] Smrčok, Ľ., Ďurík,M., Jorík,V. Powder Diffraction (1998) Submitted.

13CC SYMMETRY

M13.CC.001 SYMMETRY APPROACHES TO APERIODIC CRYSTAL STRUCTURES. Janssen T., Institute of Theoretical Physics, University of Nijmegen, The Netherlands

The symmetry of well ordered but aperiodic crystal structures can be described in several ways. One can mention representation theory, colour symmetry, superspace and the Fourier space approach. A summery and comparison of the various methods will be given and a number of examples, of compounds and structures, will be discussed.

Because the various approaches are, to a large extent, equivalent it is worthwhile to consider ways of translation of the notations used for these different approaches.

M13.CC.002 MAGNETIC FRIEZE, ROD, AND LAYER GROUPS. Daniel B. Litvin, Department of Physics, The Pennsylvania State University, Penn State Berks Campus, P.O. Box 7009, Reading, PA 19610-6009, U.S.A.

The magnetic subperiodic groups, i.e. the 31 types of magnetic frieze groups, 394 types of magnetic rod groups, and 528 types of magnetic layer groups have been re-derived and symbols defined in analogy to the Opechowski-Guccione symbols for magnetic space groups. For one group of each type of magnetic subperiodic group, information is given of the group's diagrams of symmetry elements and of the general positions/spins, asymmetric unit, symmetry operations, generators selected, positions, with site symmetry, coordinates, and spins, and symmetry of special projections.

M13.CC.003 STRUCTURE OF A QUASICRYSTAL WITHOUT ATOMIC CLUSTERS. Eiji Abe and An Pang Tsai, National Research Institute for Metals, 1-2-1 Sengen, Tsukuba 305, Japan

It is now believed that the quasicrystals could all be explained by some atomic clusters having the same point symmetry of the corresponding quasicrystalline phase. Here we report the first quasicrystal structure without these atomic clusters.

High-resolution transmission electron microscopy (HRTEM) has been applied to study the real atomic structure of the decagonal (*d*-) quasicrystal in the Zn-Mg-rare-earth (RE) system, which is the first *d*-phase based on Frank-Kasper phase. The phase revealed a high-structural perfection comparable to that of the *d*-AlNiCo which is known as the best *d*-quasicrystalline phase (the tenfold symmetry diffraction patterns of these phases are analogous [1]). We have found that the *d*-ZnMgRE phase has a novel structure in which the atomic arrangement in the tenfold symmetry plane can simply be interpreted as the Penrose tiling decorated by individual atoms - the simplest realization of the Penrose tiling as a real atomic structure. This is supported by the fact that a similar local atomic configuration exists in the Zn_7Mg_4 crystal structure. This simple structural model is in sharp contrast to the idea of atomic clusters, which has been successfully used to describe the structure of quasicrystals till now. It is suggested strongly that the symmetric atomic clusters are not an essential factor for quasicrystal formation.

Instead of the atomic clusters, a new idea of *quasi-unit-cell* and its *covering* [2] is applied for structural description. We discuss the structural similarity between the *d*-ZnMgRE and the *d*-AlNiCo based on their corresponding crystal structures of the Zn_7Mg_4 and the $Al_{13}Fe_4$ compounds. In order to confirm further a validity of the *quasi-unit-cell* description for the *d*-AlNiCo, we employ a through-focus imaging of HRTEM with atomic resolution to judge whether the symmetry breaking fashion [2] is due to chemical disordering of the atomic cluster [3] or not.

We thank Prof. P. J. Steinhardt for valuable advice regarding the overlap tiling. Stimulating discussions with Drs. T. J. Sato, H. Takakura, K. Saitoh are greatly acknowledged. This work is partly supported by CREST, Japan Science and Technology Corporation.

[1] E. Abe, T.J. Sato and A.P. Tsai, Philos. Mag. Lett., **77**, 205 (1998).
[2] P.J. Steinhardt, H.-C. Jeong, K. Saitoh, M. Tanaka, E. Abe and A.P.Tsai, Nature **396**, 55 (1998).
[3] Y. Yan, S.J. Pennycook, A.P. Tsai, Phys. Rev. Lett., **81**, 5145 (1998).

M13.CC.004 CLUSTER COVERING OF OCTAGONAL MnSiAl QUASICRYSTALS. S.I. Ben-Abraham, Department of Physics, Ben-Gurion University, IL-84105 Beer-Sheba, Israel and F. Gähler, Institute for Theoretical and Applied Physics, Stuttgart University, D-70550 Stuttgart, Germany.

A likely mechanism for the formation of quasicrystals is by maximally covering space with overlapping stable atomic clusters, thus minimizing the energy and producing long-range correlations and order [1]. The geometric counterpart was put forward by Gummelt [2] who constructed the Penrose tiling by covering the plane with overlapping copies of a single decagonal patch. Octagonal quasicrystalline phases closely related to the β-Mn structure have been observed in the CrNiSi, VNiSi, MoCrNi and MnSiAl systems [3,4]. Jiang, Hovmöller and Zou [5] have experimentally determined the structure of $Mn_{80}Si_{15}Al_5$: octagonal layers *A* alternating with tetragonal layers *B'* and *B"* (mutually rotated by 45°) with an 8_4 screw axis. The layers can be described as decorations of the arrowed octagonal Ammann-Beenker tiling (ABT↑) [6-8]. We represent the decoration abstractly by a novel two-color version of ABT↑. The covering cluster of the quasicrystal corresponds to an octagonal patch of the colored tiling. The patch appears in two variants with complementary colors. The complete 3D quasicrystal has a centered octagonal translation module (the generalization of the lattice concept). The space group is $I8_4/mcm$.

[1] H.C. Jeong and P.J. Steinhardt (1994): Phys. Rev. Lett. **73**, 1943.
[2] P. Gummelt (1996): Geometriae Dedicata **62**, 1.
[3] N. Wang, H. Chen and K.H. Kuo (1987): Phys. Rev. Lett. **59**, 1010.
[4] N. Wang, K.K. Fung and K.H. Kuo (1988): Appl. Phys. Lett. **52**, 2120.

[5] J.C. Jiang, S. Hovmöller and X.D. Zou (1995): Phil. Mag. Lett. **71**, 123.
[6] F.P.M. Beenker (1982): report 82-WSK-04 (TH Eindhoven).
[7] R. Ammann, B. Grünbaum and G.C. Shephard (1992): Discrete Comp.Geom. **8**, 1.
[8] F. Gähler (1998): *Quasicrystals 6*, S. Takeuchi and T. Fujiwara, eds., (World Scientific, Singapore), p. 95.

M13.CC.005 ALLOTWINNING AND ITS IDENTIFICATION IN MICAS THROUGH THE MINIMAL RHOMBUS APPROACH. M. Nespolo (Natl. Inst. Res. Inorg. Mat., Tsukuba, Ibaraki 305-0044 Japan) T. Kogure (Tokyo Univ., Grad. Sch. Sci., Mineral. Inst., Tokyo 113-0033 Japan) H. Takeda (Chiba Inst. Techn., Res. Inst., Tsudanuma, Chiba 275-0016, Japan) G. Ferraris (Torino Univ., Dept. Sci. Mineral. Petrol, 10125 Torino, Italy)

The oriented association of two polytypes of the same compound is called *allotwin*[1]. While twin operations are point group operations not belonging to the crystal symmetry, allotwin operations can be symmetry or pseudo-symmetry operations belonging to the crystal symmetry as well[1].

The presence of twins in micas can be anakyzed from their diffraction pattern by means of the *minimal rhombus*[2,3]. This is an asymmetric unit containing nine geometrically independent reciprocal lattice rows parallel to *c**. Reflections along the single-layer repeat ($0.1Å^{-1}$) on each of the geometrically independent rows depend on the number and relative orientation of twinned individuals. The number and position of the reflections identify the twin laws. In an oxybiotite sample from Ruiz Peak, New Mexico, two examples of allotwins involving $1M$ and $2M_1$ crystals (120º and 60º rotations respectively) have been discovered by means of single crystal X-ray diffraction method with a precession camera[3]. The 60º rotation is relatively rare in micas.

The polytype stacking sequence identification by means of the analysis of the periodic distribution of the intensities can be hindered by the presence of allotwinning involving two polytypes with the same number of layers and the same crystal lattice. The two lattices coincide and the measured periodicity results from the composition of intensity distribution of the allotwinned crystals. The allotwin may be mistaken for a single crystal and a wrong stacking sequence may be deduced. This problem, here illustrated for micas, can be present in any type of compounds showing polytypes and twins.

1. Nespolo, M., Kogure, H. & Ferraris, G. (1999). *Z. Krist*. **214**, 5-8.
2. Nespolo, M., Takeda, H. Ferraris, G. & Kogure. T. (1997). *Mineral. J*. **19**, 173-186.
3. Nespolo, M. (1998). Doctoral dissertation, Univ. Tokyo.

P13.CC.001 BOND-VALENCE DISTRIBUTIONS AND THE SYMMETRY OF CHEMICAL GRAPHS. J. S. Rutherford, Department of Applied Chemistry, National University of Science & Technology, Bulawayo, Zimbabwe.

The automorphism group of a chemical graph is isomorphic with some permutation group. This allows the classification of elements of the graph, such as the vertex set or the edge set, in terms of reducible representations of this permutation group, and the creation of vertex space or edge space vectors which transform as the irreducible representations of that group.

Using this approach, solutions to the bond-valence network problem may be expressed as a sum over symmetry-adapted basis vectors of the edge-space of the graph. This sum takes the form

$$\mathbf{s} = \sum_{i=1}^{\dim(U)} K(\Gamma_i)\,\mathbf{u_i} + \sum_{j=1}^{\dim(Z)} x(\Gamma_j)\,\mathbf{z_j}$$

that is a fixed sum of terms over the symmetrised cut-space, U(G), of the graph, and a variable sum of terms over the corresponding cycle-space, Z(G). The cut-space basis vectors, $\mathbf{u}_i$, are given by

$$\mathbf{u_i} = \frac{1}{\sqrt{\lambda(\Gamma_i)}}\mathbf{B}^t\,\mathbf{v}(\Gamma_i)$$

$\mathbf{B}^t$ being the transpose of the incidence matrix, $\mathbf{B}$, $\lambda(\Gamma_i)$ a non-zero eigenvalue of the singular square matrix $\mathbf{BB}^t$, and $\mathbf{v}(\boldsymbol{\Gamma_i})$ a corresponding eigenvector. The coefficient $x(\Gamma_j)$ is an arbitrary scalar, restricted only by the requirement that the bond-valences cannot be negative, while

$$K(\Gamma_i) = \frac{\mathbf{v}(\Gamma_i)\cdot\mathbf{f}}{\sqrt{\lambda(\Gamma_i)}}$$

f being a vector of the atom-valences.

P13.CC.002 GROUP-THEORETICAL METHODS FOR NONLINEAR DYNAMICS IN CRYSTALS. H.T. Stokes, A.D. Smith, and D.M. Hatch, Brigham Young University, Provo, Utah 84602, USA, and G.M. Chechin, V.P. Sakhnenko, and M.Yu. Zehtser, Rostov State University, Rostov-on-Don, Russia.

Nonlinear forces in crystals cause large numbers of normal modes to be coupled, resulting in a large set of coupled equations of motion. Group-theoretical methods can be used to effectively decouple (in some sense) small numbers of these equations from the rest, resulting in smaller, more manageable problems to solve. These isolated groups of dynamic variables are called “bushes” of modes. An excitation in a given bush will remain in that bush and not spread to any other modes in the crystal. This result is rigorous and does not depend on the strength of the nonlinearity nor the strength of the coupling between modes. Furthermore, the bushes can be put into universality classes, based on the form of the potential energy governing the dynamics of the modes in the bush. We found the universality classes of bushes with small number of modes for all possible crystals.

P13.CC.003 INTERPRETING A STRUCTURE OF REAL CRYSTALLINE MATERIALS. B.S.Semukhin, A.N.Sergeev, S.V.Rudnev Department Physics of Strength, Institute of Strength Physics and Material Science Siberian Branch of Russian Academy of Sciences,Tomsk,Russia, [2]Tomsk State Politechnical University, [3] Tomsk State Politechnical University

In the article method of crystalline structure description is proposed, based on organisations of space of crystal by means of the elliptical Riemannian space .It has been shown that kinematics approximation, by means of the small modification, correctly describes integral intensities X-ray diffraction reflexes and in this drawing near, however an invariant structured element has to be necessarily chosen as a scattering volume.

13DD AB INITIO STRUCTURE PREDICTION

M13.DD.001 MOLECULAR SIMULATION TECHNIQUES AND STRUCTURE PREDICTION. Clive M. Freeman, Alan M. Gorman, Steve M. Levine, Frank J.J. Leusen [1], Michael W. Deem, Marco Falcioni [2], John M. Newsam [1]; [1] Molecular Simulations Inc, 9685 Scranton Road, San Diego CA 92121, USA; [2] Chemical Engineering Department, University of California, Los Angeles, CA 90095, USA

Techniques for predicting and solving crystal structures based on powder diffraction data and simple descriptions of

interatomic interactions been employed for many years. Advancing computational capabilities combined with recent algorithmic developments have, however, resulted in greatly increased opportunities for structure solution in challenging crystallographic circumstances. Such procedures exploit standard techniques of computer simulation in combination with hybrid potential energy functions to yield structures that are sterically and experimentally plausible. These methods have been especially useful in the investigation of microcrystalline framework structured materials for which powder diffraction may be the primary experimental route to structural information. In contrast to traditional refinement procedures, which use rapidly convergent but locally biased least squares methods, analogy with physical simulations has prompted the use of simulated annealing and tempering as optimization methods in several recent studies. Metropolis Monte Carlo or Molecular Dynamics based annealing procedures provide the 'searching' characteristics that underlie the required global minimization of structure solution. Applications to framework structured solids, condensed metal oxides and molecular crystal structures will be described.

Acknowledgement: The MSI Catalysis and Sorption and Pharmaceutical Development Consortium Projects are supported by industrial, academic and government institutions.

M13.DD.002 STRUCTURE PREDICTION OF SOLIDS VIA INVESTIGATION OF POTENTIAL ENERGY SURFACES. J. Christian Schön, M. Jansen Max-Planck-Institut für Festkörperforschung, Heisenbergstr. 1, D-70569 Stuttgart, Germany

Predicting the existence and structure of hypothetical compounds, and suggesting routes to their synthesis, is a major goal in the field of solid state chemistry. Already the first step, the prediction of compounds capable of existence, is highly complex, since a multitude of atomic arrangements are possible that corresponds to local minima of the (free) energy at some temperature. The approach presented here concentrates on the investigation of potential energy surfaces, identifying local minima, which are surrounded by high enough energy barriers and carry enough entropic weight, to give them sufficient kinetic and thermodynamic stability.

We will show applications of this approach both to ionic systems and compounds consisting, in addition to single atoms/ions, of fixed building units, such as molecules and complex ions. Using such units allows the introduction of charge carrying molecules on the one hand, and on the other hand avoids the optimisation moves that are needed otherwise for the creation of these building units.

M13.DD.003 THE PREDICTION OF INORGANIC CRYSTAL STRUCTURES USING A GENETIC ALGORITHM AND ENERGY MINIMISATION. S.M. Woodley and C.R.A. Catlow, Davy-Faraday Research Laboratory, The Royal Institution of Great Britain, 21 Albemarle Street, London W1X 4BS, P.D. Battle, Inorganic Chemistry Laboratory, University of Oxford, South Parks Road, Oxford OX1 3QR and J.D. Gale, Department of Chemistry, Imperial College, South Kensington SW7 2AY.

We successfully 'predict' the structures of a wide range of known binary oxides and various known ternary oxides, including perovskites, pyrochlores and spinels. The method, which is capable of reproducing different phases of a compound, is based upon that developed by Bush *et al* [1] who successfully predicted the previously unknown structure of Li_3RuO_4.

Initially a genetic algorithm is used to generate plausible structures from a knowledge of only the dimensions and constituents of the unit cell. The quality of the structures is assessed using a cost function which is based on the Bond Valence Model and the Coulombic interaction energy. Our cost function is a robust measure of geometry violation but at the same time it is cheap to compute; both necessary qualities for any genetic algorithm. The lattice energy, based on the Born model of a solid, for the more plausible candidate structures is then minimised using a local optimiser in order to increase the accuracy of the atomic co-ordinates predicted for the crystal structure. The method has been implemented within the General Utility Lattice Program (GULP) [2,3], thus facilitating the calculation of the physical properties (for example, elastic constants) of the phase.

[1] Evolutionary programming techniques for predicting inorganic crystal structures, T.S. Bush, C.R.A. Catlow and P.D. Battle, J. Mat. Chem. 5 1269-1272 1995.
[2] Empirical potential derivation for ionic materials, J.D. Gale, Phil. Mag. B73 3-19 1996.
[3] GULP: A computer program for the symmetry-adapted simulation of solids, J.D. Gale, J. Chem. Soc., Faraday Trans. 93 629-637 1997.

M13.DD.004 DIRECT USE OF DATABASE INFORMATION FOR CRYSTAL STRUCTURE PREDICTION. J.P.M. Lommerse W.D.S. Motherwell Cambridge Crystallographic Data Centre, 12 Union Road, Cambridge CB2 1EZ, United Kingdom.

Currently, in organic chemistry most crystal structure prediction methods are based on the calculation of a (static) lattice enthalpy, assuming that the lowest energy structure coincides with the experimental crystal structure. Effects of pressure and entropy are usually neglected. But probably more importantly, the whole process of crystal growth is not accounted for. One approach to tackle this latter problem could be the use of Molecular Dynamics simulations, but there is still a long way to go before the actual simulation of crystal growth can be realised. Another approach might be the use of experimental data as stored in the Cambridge Structural Database[1]. Using these data one may implicitly account for kinetics as well as for other "hidden" factors determining the formation of the actual crystal structures. Here, we use data representing interactions between functional groups within the crystal structures. For each functional group a field that surrounds the molecule of interest can be set up and combined in order to predict the most likely orientations and contacts between molecules. Due to the amount of statistical data available, the accuracy of this method in terms of prediction of cell dimensions, position and orientation of the molecules in the cell is limited. In order to overcome this problem the method allows for "refinement" by empirical potential energy functions [2].

1. F.H. Allen, J.E. Galloy, O.J. Johnson, et al. (1991). J. Chem. Inf. Comput. Sci. 31, 187-204.
2. A. Gavezzotti (1994). Acc. Chem. Res. 27,309-314.

M13.DD.005 PREDICTING THE CRYSTAL STRUCTURES OF ORGANIC MOLECULES BY LATTICE ENERGY MINIMISATION. S.L. Price, Department of Chemistry, University College London, 20 Gordon Street, London WC1H 0AJ.

Many methods have been proposed for predicting possible crystal structures of organic molecules, using only the molecular structure, based on the assumption that the observed crystal structure will be that which has the most favourable lattice energy. We have been testing the validity of this approach by using particularly accurate models for the intermolecular forces to evaluate the lattice energy. The electrostatic contribution is evaluated from the atomic multipoles obtained from an ab initio wavefunction of the molecule. Using such a model potentials and the MOLPAK search procedure [1], we have found the low energy minima in the lattice energy for a wide variety of organic

molecules, such as uracil [2], alloxan [3], carboxylic acids, including polymorphic systems such as indigo [4]. This approach has been successful in making blind predictions, as in the case of 5-azauracil [5]. However, although the known structures are found at or near the global minimum, in many cases there are unknown structures within the energy range of possible polymorphs.

By combining the results of many lattice energy minimisation methods on a wide range of molecules, it is clear that having a lattice energy at or near the global minimum is a necessary, but often not sufficient condition, for the structure to be observed. This raises many questions as to the factors that control crystallization and polymorphism, and how these can be represented for more reliable predictive methods.

1. Holden, J. R.; Du, Z. Y.; Ammon, H. L. J. Comput. Chem. 1993, 14, 422.
2. Price, S. L.; Wibley, K. S. J. Phys. Chem. A 1997, 101, 2198.
3. Coombes, D. S.; Nagi, G. K.; Price, S.L. Chem Phys Letts 1997, 265, 532.
4. Price, S. L.; Beyer, T. Trans. Amer. Cryst. Assocn 1999, in press.
5. Potter, B. S.; Palmer, R. A.; Withnall, R.; Chowdhry, B. Z.; Price, S. L. J. Molec. Struc. 1999, in press

M13.DD.006 COMPUTER MODELLING OF COMPLEX MOLECULAR IONIC MATERIALS. R.A. Jackson and K.A. Mort, Chemistry Department, School of Chemistry and Physics, Keele University, Keele, Staffs ST5 5BG, UK.

Molecular ionic materials present a considerable challenge in computer modelling because any potential model employed must accommodate both ionic and covalent forces. Moreover, many such materials exist in a number of phases, making further demands on the potential.

This paper will describe how energy minimisation and molecular dynamics techniques have been used to model a series of these materials. Potentials have been obtained by empirical fitting to structures and properties of representative materials, and in the case of materials containing both molecular anions and molecular cations, potentials for each ion are obtained separately and then combined. This procedure is illustrated for the case of ammonium nitrate, where ammonium halides and alkali metal nitrates are modelled first, and the molecular ion potentials transferred.

Results will be presented of calculations of structural and lattice properties of metal phosphates, perchlorates, chlorates and nitrates, and of ammonium halides. Attention will then be focused on ammonium nitrate, where a potential was fitted to the low temperature phase, and molecular dynamics used to simulate the higher temperature phases. It will be shown that such complex materials can be reliably simulated by relative simple potential models, provided both ionic and covalent interactions, and the balance between them, are correctly represented.

P13.DD.001 THEORETICAL STUDIES OF THE STRUCTURE AND CATALYTIC PROPERTIES OF PLATINUM-GOLD CLUSTER COMPOUNDS. A.A. Bagatur'yants and S.S. Konyukhov, Photochemistry Center, Russian Academy of Sciences, ul. Novatorov 7a, Moscow, 117421 Russia, and O. Gropen, Faculty of Science, University of Tromsoe, 9037 Tromsoe, Norway, and L.H. Pignolet, Department of Chemistry, University of Minnesota, Minneapolis, MN 55455, USA

The electronic and geometrical structure of platinum–gold clusters of composition $[PtAu_6(PH_3)_7]^{2+}$ (I), $[Pt(CO)Au_6(PH_3)_7]^{2+}$ (II), $[Pt(H)Au_7(PH_3)_8]^{2+}$ (III), $[PtAu_8(PH_3)_8]^{2+}$ (IV), and $[Pt(CO)Au_8(PH_3)_8]^{2+}$ (V) and the frequencies of CO vibrations in II and V have been calculated using the density functional theory (DFT) within the LDA approximation. The structural and spectroscopic results have been compared with experimental data for related complexes. Potential energy surfaces for the reaction of oxidative addition of H_2 to I and IV have been investigated. Intermediate molecular complexes ($I...H_2$ and $IV...H_2$) and the final dihydride structures (H-I-H and H-IV-IV) have been located on the calculated potential energy surfaces. The experimental catalytic activity of $[PtAu_6(PR_3)_7]^{2+}$ and $[PtAu_8(PR_3)_8]^{2+}$ is analyzed on the basis of obtained results. The possible sites of the location of the hydride ligand in III have been determined on the basis of DFT calculations.

P13.DD.002 *AB INITIO* STUDY OF THE STRUCTURE OF A PURE (0001) SURFACE OF β-SILICON NITRIDE AND SURFACE GROUPS CHEMISORBED ON THIS SURFACE UNDER CONDITIONS OF CVD FROM DICHLOROSILANE AND AMMONIA. A.A. Safonov and A.A. Bagatur'yants, Photochemistry Center, Russian Academy of Sciences, ul. Novatorov 7a, Moscow, 117421 Russia; AOZT Soft-Tec, Nakhimovskii prosp. 34, Moscow, 117218 Russia, and A.A. Korkin, Predictive Engineering Laboratory, Semiconductor Products Sector, Motorola, Inc. 2200 W. Broadway Rd., Mesa, AZ 85202

The structure of a (0001) surface of β-Si_3N_4 has been investigated theoretically based on *ab initio* calculations within a cluster approach. It is shown that the dangling bonds on the surface are relaxed to form diatomic >Si=N– surface groups. The calculated Si=N bond length 1.62 A is considerably shorter than typical lengths of crystalline Si–N bonds (1.74–1.76 A), and the surface atoms of these diatomic groups are significantly displaced from their bulk crystalline positions. The >Si=N– surface groups are combined by threes through a central N atom to form a pattern of isolated quasi-planar seven-atomic islands at the surface. Examining the sequential hydrogenation of separate >Si=N– groups in such an island has indicated that each group can be considered as an independent surface site. Clusters modeling the silicon nitride surface covered by various chemically bonded groups (–H, –Cl, $–NH_2$, $–SiH_2Cl$, $–SiHCl_2$, >Si, –SiH, –SiCl) have been calculated. The mechanism of film growth in the chemical vapor deposition (CVD) of β-Si_3N_4 from NH_3 and SiH_2Cl_2 has been analyzed in detail. It has been found that the film growth is controlled by the following reaction steps: (1) H_2 or HCl abstraction from chemisorbed chlorosilyl ($–SiH_2Cl$ or $–SiHCl_2$) groups to form silylene (–SiH or –SiCl) surface groups, (2) coupling reactions between NH_3 and chemisorbed chlorosilyl groups or between SiH_2Cl_2 and chemisorbed $–NH_2$ groups with HCl elimination, and (3) similar coupling reactions between chemisorbed chlorosilyl and $–NH_2$ groups.

P13.DD.003 PREDICTIONS OF CRYSTAL PACKING FOR CARBOXYLIC ACIDS USING ACCURATE INTERMOLECULAR POTENTIALS. Theresa Beyer, Sarah L. Price, Centre for Theoretical and Computational Chemistry, University College London, 20 Gordon Street, London WC1H OAJ, U.K.

Carboxylic acids show a variety of packing motifs [1], based on chains and dimers and some are polymorphic. As current potentials have difficulty in reproducing the experimental crystal structures for this group of molecules, they represent an insufficient basis for crystal structure prediction [2] and understanding which motifs are found. We use an accurate model for the intermolecular forces based on a Distributed Multipole expansion (DMA) of an ab initio charge distribution for the dominant electrostatic contribution and an empirical atom-atom repulsion-dispersion potential. This potential reproduces the crystal structures and the available heats of sublimation of several carboxylic acid structures. Using this theoretically developed potential, we performed a systematic search [3] for minima in the

lattice energies for a variety of carboxylic acids and investigated the low energy structures in terms of their hydrogen bonding motifs. This both tests the structure prediction methodology and shows for which molecules the chain and dimer motifs are competitive in energy.

1. Leiserowitz, L., Acta Cryst., 1975, B 32, 775.
2. Mooij, W.T.M., et al., J. Comput. Chem., 1998, 19, 4, 459
3. Holden, J.R., Du, Z., and Ammon, H.L., J. Comput. Chem., 1993, 14, 422.

13EE DATA ACCURACY AND DETECTORS (sponsored by Stoe)

M13.EE.001 THE ACCURATE MEASUREMENT OF ANOMALOUS SIGNAL. A Thompson, EMBL Grenoble Outstation

One of the reasons that the technique of MAD (see for example, Hendrickson, Science 254, 51 - 58, 1991) has become such a successful method of solving the phase problem for macromolecular crystal structures is the huge improvements recently made in both X-ray area detection and processing software. The requirements for successfully measuring a small anomalous signal will be discussed in the light of recent data collected on ESRF BM14 using both image plate and CCD detectors. The limit of measuring very small anomalous signals under typical beamline conditions will be discussed, and some future possibilities in data collection suggested.

M13.EE.002 USE OF ONE WAVELENGTH ANOMALOUS DATA. Z. Dauter and M. Dauter, NCI Frederick and Brookhaven National Lab., Bldg. 725A-X9, Upton, NY 11973, USA.

The classic MIR method of solving macromolecular structures relies on isomorphous substitution of heavy atoms, where phasing is based on changes of reflection amplitudes for different derivatives with respect to the native data. The anomalous signal of heavy atoms, if measured, can be used in addition. MAD technique requires the presence of anomalous scatterers and utilises both dispersive differences between different wavelengths and anomalous differences within one wavelength data.

It is possible to obtain meaningful phases based purely on the anomalous signal contained in only one data set measured at a single wavelength. The anomalous signal may come from the scatterers inherently present in the native structure (metals or sulfur) or from the atoms introduced as derivatives or occupying ordered solvent sites.

The successful application of single wavelength dispersion (SAD) requires very high accuracy of the data, since the anomalous differences are usually small compared to the reflection amplitudes. The Bijvoet differences from ten sulfur and eight chlorine atoms present in the structure of tetragonal lysozyme amount on average to 1.5% of the reflection amplitudes, nevertheless they are sufficient to obtain the experimental Fourier map of very high quality. The six bromide solvent atoms in lysozyme give anomalous signal of about 5% of normal diffraction, which is enough to produce interpretable electron density to a resolution as low as 3 Å.

The anomalous scatterers partial structure usually has to be solved by direct methods. Recent advances in this field makes it possible to find positions of many, up to 100, anomalous scatterers. The subsequent phasing of protein amplitudes can be done with the direct methods or the maximum likelihood approach, combined with the electron density modification.

In the light of significant improvements in detector and software technology leading to a rapid acquisition of accurate X-ray diffraction data, the SAD technique may provide an attractive alternative for macromolecular phasing, since it requires less data collection time than other approaches.

M13.EE.003 REVIEW OF PRESENT AND FUTURE DETECTOR TECHNOLOGY FOR MACROMOLECU LAR CRYSTALLOGRAPHY. Edwin M Westbrook, Argonne National Laboratory.

The demands on detectors for macromolecular crystallography come from two directions: data collection at home and data collection at synchrotron sources. Each set of demands have unique features. For home facilities, pressure is to keep coats down, convenience and reliability up, and to be highly efficient recording weak diffraction. At synchrotrons beamlines, the demand is for high performance and the most important metrics of performance are to maximize the size of the sensitive area, and to minimize the time necessary to record “good” data. This latter demand incorporates the needs for high efficiency and for fast electronics.

This discussion will review existing detector technology (multiwire proportional counters; imaging phosphor plates; CCD systems) and systems now under development (counting and integrating semiconductor pixel arrays; amorphous Silicon TFT arrays), focusing attention on how attributes of each technology present solutions for home and synchrotron facilities.

M13.EE.004 CALIBRATION OF THE CCD DETEC-TOR. Zbyszek Otwinowski[1], Wiadek Minor[2], [1]DUT Southwestern Medical Center at Dallas, Dallas TX 75235, [2]Department of Molecular Physiology and Biological Physics, University of Virginia, Chariottedville, VA 22906, USA.

CCD detector characteristics can be incorporated into data reduction software by one of two mechanisms:

- diffraction image transformation into data that would result from a distortion-free, uniform-response detector;
- implementation of detector response function into date analysis software, and the applying the response function during autoindexing refinement and Bragg’s peak integration stages

The first approach is inferior, in performance, accuracy and precision. For basic reasons, geometric distortion corrections applied to pixel data cannot preserve the shape of the Bragg peaks. The misalignment of pixels before and after geometric corrections makes data from a group of raw data pixels contribute to a single corrected pixel. This introduces two artifacts: peaks are broadened and the random variations get averaged out, resulting in lower precision of the profile fitting procedure. if spots are very close, broadening of reflections increases impact of reflection tails on measurement of nearby reflections, resulting in loss of accuracy. However, there is very little impact on measurement of strong, well separated reflections. The information loss due to the geometric correction is similar in magnitude to information loss when 4 pixels are binned into one pixel.

The HKL.-2000 can apply detector spatial distortion and non-uniform response functions. The measured data are used to estimate the DC-offset and the readout noise from non-light sensitive part of the CCD.

M13.EE.005 ON THE USE OF CCD DETECTORS FOR VERY HIGH RESOLUTION X RAY DIFFRACTION AND CHARGE DENSITY ANALYSIS. Claude Lecomte[a], Sandrine Kuntzinger[a], Slimane Dahaoui[b], Nour Eddine Ghermani[a] [a]LCM3B,Upresa CNRS 7036, Univ Henri Poincaré , Nancy, F54506 Vandoeuvre-les Nancy cedex , France [b]Crystallography group, Dept of Chemistry, University of Durham, England.

Since three or four years, diffractometers equipped with two dimensional detectors, mainly CCD, are used for charge density analysis. Some results are reported using synchrotron sources (1,2) some others were obtained from laboratory machines, Nonius or Siemens-Brucker (3-6).

The crystals studied are minerals (1,6), organic (2,3,5) or organometallic (4) compounds using molybdenum or silver radiation for conventional sources or very short wavelengths in synchrotron experiments. All analyses revealed realistic electron density maps and electrostatic properties, but some of them are of slighthly less quality than those obtained from conventional 1D sealed tube diffratometers.Therefore, in this talk, the CCD results will be analyzed with a special emphasis on data reduction and on estimation of standard incertainties for intensity measurements. Strategy for data collection/reduction and results will be presented in the case of crystal with large unit cell parameters (7).

One important conclusion, to reach excellent quality results is that researchers in the charge density field and in any other very accurate domain, should have the possibility to study, to read, and to modify the data reduction routines (integration, scaling, corrections , sigma square calculations…etc) according to their specific problems.

1 Graafsma, H., Souhassou, M., Puig-Molina, A., Harkema, S., Kvick, A., and Lecomte,C. (1998). *Acta Crystallogr*. **B54** , 193-195

2 Koritsansky, T. , Flaig, R., Zobel, D., Krane, H. D., Morgenroth, W., and Luger,P (1998). *Science*, **279**, 356-358

3 Martin, A., Pinkerton, A. A. (1998). *Acta Crystallogr*.**B54**, 471-477

4 a) Macchi, P., Prosperio, D. M., Sironi, A. (1998). *J.Am.Chem.Soc*. **120**, 1447-1455; b) Macchi, P., Prosperio, D. M., Sironi, A., Soave, R., and Destro, R. (1998). *J.Appl. Crystallogr*. **31**, 583-588

5 Dahaoui, S., Jelsch, C., Howard, J. A. K., and Lecomte, C. (1999) *Acta Crystallogr*. *B55* ,000-000; Kuntzinger, S., Dahaoui, S., Ghermani, N. E., Lecomte, C., and Howard, J. A. K. (1999). submitted to *Acta Crystallogr*. **B**.; Dahaoui, S., Pichon-Pesme, V., Howard, J. A. K and Lecomte, C. (1999), submitted to *J. Phys. Chem*. **A**.

P13.EE.001 DATA COLLECTION STRATEGIES WITH A CCD-DIFFRACTOMETER. Michael Bolte and Stephan Rühl, Institut für Organische Chemie, J.-W.-Goethe-Universität, Marie-Curie-Str. 11, D-60439 Frankfurt, Germany.

Diffractometers with position sensitive counters have sped up drastically the collection of X-ray reflections – but the question arises how to obtain an optimal data set in spite of a shorter data collection time. This was our motivation to test various data collection strategies using a CCD detector and evaluate the influence of the variable parameters.

All investigations were carried out on small organic molecules, common in routine structure determination. In the course of our experiments the impact of the following parameters was evaluated:

- time for measuring a single image,
- scan angle,
- size of the collimator,
- crystal to detector distance,
- resolution of the detector,
- scan mode (φ-scans or ω-scans),
- redundancy of the data,
- crystal size.

All these parameters were systematically varied in order to find optimal values for the crystal in question. Although using the default values recommended by the manufacturer leads to good results, adjusting the data collection parameters according to the actual problem can improve substantially the quality of the data without loss of precision.

The achievable improvement of the data quality is shown with four different compounds by comparison of several figures of merit, e.g. R(int), R(σ), R1 and wR2. The different data sets collected with a CCD detector were also compared with the data collected on a four-circle diffractometer using the same crystals.

P13.EE.002 DECONVOLUTION OF THE PSF OF AREA DETECTORS USING THE MAXIMUM ENTROPY METHOD. H. Graafsma and A. Puig-Molina, European Synchrotron Radiation Facility, BP 220, 38043 Grenoble, France and R.Y. de Vries, Chemical Physics Laboratory, University of Twente, PO Box 217, 7500 AE Enschede, The Netherlands.

One of the (many) design parameters of area detectors is the point-spread-function (PSF). One generally tries to either minimise the PSF to maximise the spatial resolution, or to match the PSF to other experimental conditions. However, a reduction of the PSF generally means a reduction of the conversion screen thickness and with that an undesired reduction of the detector sensitivity. A program has been written to apply the maximum entropy method (MEM) for deconvolution of the two-dimensional point-spread-function (PSF) of two-dimensional X-ray detectors. The goal is to increase the spatial resolution of existing area detectors, and therefore, improving the detector performance, without sacrificing sensitivity. The method is robust, model and image independent and only depends on the correct description of the two-dimensional point-spread-function and gain factor of the detector.

A significant enhancement of both the spatial resolution and the contrast ratio has been obtained for the phase contrast images recorded with an ultra high resolution X-ray imaging detector. The method has also been applied to Laue and monochromatic diffraction images of protein crystals, showing an important improvement in both peak separation of overlapping peaks and signal to noise ratio of medium and weak peaks.

The principle of the method will be presented and examples from both imaging and diffraction will be presented.

P13.EE.003 PROBLEMS WITH SIMPLE STRUCTURES CAUSED BY λ/2 CONTAMINATION. Horst Borrmann, Max-Planck-Institut für Chemische Physik fester Stoffe, Pirnaer Landstr. 176, D-01257 Dresden, Germany.

Characteristic radiation employed in a typical X-ray diffraction experiment with laboratory sources contains contribution from harmonics of λ, mostly λ/2. This contamination may be removed by energy discrimination when a scintillation counter is used to detect the scattered intensities. For area detectors based on CCDs or image plates, this effect becomes a potential source of errors. However, such errors were found negligible for routine single crystal data sets [1].

We found λ/2 contributions quite problematic in course of reinvestigating the structures of $LiOsF_6$ and $LiAuF_4$ from single crystal data. For $LiOsF_6$ doubling of all three axes was indicated by area detector data. The problem to determine the correct structure is enhanced by the fact that three rather closely related structure types are known for ABF_6 type compounds. An even more interesting case was found with $LiAuF_4$. The special structural arrangement together with λ/2 contamination results in severe difficulties with evaluation of the proper unit cell but also with space group assignment. Unexpected distortions within the published structure [2] are obvious artefacts from choosing too low symmetry. Although this consequence is frequently emphasized by R.E. Marsh and others, the particular case of $LiAuF_4$ is unusual as no centre of symmetry is added.

We found $LiAuF_4$ a very helpful test case throughout the evaluation process of an area detector system.

1. K. Kirschbaum, A. Martin & A.A. Pinkerton (1997). *J. Appl. Crystallogr*., **30**, 514.
2. U. Engelmann and B.G. Müller (1991). *Z. Anorg. Allg. Chem.,* **598**, 103.

P13.EE.004 STANDARD REFERENCE MATERIALS FOR STRUCTURAL INVESTIGATIONS FOR SINGLE AND POWDER DIFRACTOMETERS. V.K.Ovcharov[1)] , B.N. Kodess[1,2)] , L.A. Butman[2)], I.L.Kommel[1)] , A. M. Balagurov[3)], V.A. Sarin[3)] , I. S. Smirnov[(1)], [1] Department of Crystal Metrology, VNIIMS, 46 Ozernaya St., 119361 Moscow, Russia, [2] ICS&E, Aurora, CO 80015, USA, [3] JINR, Dubna, Russia.

An interlaboratory experiment has been conducted on measurement of interplane distances, lattice parameters and intensity ratio for a set of pure elements (Si, Ge), low-quartz (SiO_2), Al_2O_3, silicide vanadium and yttrium cuprates. The data has been collected from a number of set-ups (more than 20 diffractometers) using X-ray and neutron radiation. The unit-cell parameters of single crystals quartz temperature a = 4.9130 (1) , c= 5.4050 (1) where cell parameters are in angstroms. Similar data for standard for internal pressure in diamond-anvil cells have been determined by single-crystal diffraction at ambient temperature a=4.91300 (11), c=5.40482 (17) A. [1].

Data for silicon was compared with such from PTB and NIST (neutron method). Moreover, similar interlaboratory (12-16 laboratories) experiment has been conducted for powder samples of Si-V and Y-Ba-Cu-O systems to determine their composition (mass ratios of major components and impurities) using various physical and chemical methods. Based on results of metrological certification, a number of batches of Si, SiV_3 gained the status of Standard Reference Materials.

Electron-difference-density maps of alpha-SiO_2 were calculated using custom-designed software. The maps feature notable similarities in the areas of Si-O-Si bonding and low variability in the interatomic areas. This data gives us also optimistic outlook on usage of samples of this type in the project of round-robin for measurement of electron density distribution.

[1] Angel, R.J.; Allan, D.R.; Miletich, R.; Finger, L.W. , Journal of Applied Crystallography, 1 Aug. 1997, vol.30, pt.4:461-6.

P13.EE.005 ON THE USE OF EQUIVALENT REFLECTIONS. T. Gustafsson, Inorganic Chemistry, Ångström Laboratory, Box 538, SE-751 21 Uppsala, Sweden.

Different strategies can be used for the collection of single-crystal diffraction data. It is common practise that only a unique data set is collected to reduce measuring time. If two or more sets of unique reflections are measured using reduced measuring times the total number of photons collected during the experiment can be kept constant with only a marginal increase in experiment time. Such a strategy will help detect random errors during the experiment such as multiple scattering or equipment malfunction. It will also produce a data set, which contains not one but several unique data sets. The subsequent treatment of such a data set can follow several different routes. That recommended when the resulting structure is intended for publication in *Acta Cryst.* is to merge the data into one unique set. The main reason for merging the data is to ensure that the equivalent reflections should not be treated as a set of independent observations in the least squares refinement. A second approach is then simply to use the unmerged data set in the least squares refinement. The main reason for doing this is that the extinction correction is generally not identical for all reflections within a set of equivalents.

It is difficult to find fully convincing arguments to favour the use of the one or the other of these two approaches. Both have therefore been followed for a data set collected on sodium nitrite. The respective differences in R-values, standard errors on refined parameters and $\delta\rho$- maps will be discussed.

13FF TOPOGRAPHY

M13.FF.001 IMAGING WITH THIRD GENERATION SYNCHROTRON X-RAYS. Jürgen Härtwig, Peter Cloetens, José Baruchel, E.S.R.F., BP220, F-38043 Grenoble cedex, France.

Imaging is based on the spatial variations, across a specimen, of (1) the absorption, and/or (2) the scattering, and/or (3) the optical phase of the beam.

The first third-generation synchrotron radiation facility in operation, the ESRF, includes beam-lines dedicated largely or totally to imaging, fed by insertion devices tailored and/or adjustable for the experiment, and supported by technical development in instrumentation, e.g. for operation at controlled temperature, or in detector systems. Beyond this essential practical novelty, features of third generation synchrotron radiation sources that are significant in relation with imaging applications are

a) the higher intensity of the X-ray beams in comparison with previous sources, with a larger fraction of photons with high energies (10-100 keV)

b) the fact that the source is small and far from the specimen.

The latter point, equivalent to the statement that the X-ray beams have low angular divergence as seen from any point in the specimen, or large spatial coherence, is qualitatively the most influential. In particular, it makes phase radiography, and its 3D companion phase tomography, instrumentally very simple, and lead to novel possibilities for diffraction topography.

The various new experiments correspond to a combination of (1,2,3) with (a,b). We will give more emphasis to examples performed using:

(1a)Absorption microtomography

(2a) X-ray Bragg-diffraction imaging (topography): real-time experiments, highly absorbing specimens (single crystals or quasicrystals)

(2b)High sensitivity determination of strain differences, e.g. in magnetically driven mechanical resonance effects

(3b) Phase radiography and phase tomography through simple propagation

(2,3b) Combination of phase radiography with Bragg-diffraction imaging, and the phase effects in Bragg diffraction images (in particular the direct determination of structure factor phase from twinned regions).

M13.FF.002 THE TOPOGRAPHIC SUITE : A TOOL FOR X-RAY TOPOGRAPHY STUDY OF MATERIALS. Yves Epelboin, A. Soyer LMCP, UMR 7590 CNRS, Universités P.M. Curie and D. Diderot, case 115, 75252 Paris Cedex 05, France and V. Mocella ESRF, BP 220, 38043 Grenoble Cedex, France

Third generation synchrotron have renewed the possibilities to use topographic settings for the study of materials, hence the necessity of versatile simulation programs to characterize their intrinsic quality.

A new generation of programs, based on the integration of Takagi-Taupin equations, has been designed on the principles of TRANSQ[1]: the computation of the deformation is made in a separate program allowing to easily change the model without modifying the simulation program. The optical characteristics of the source are correctly taken into consideration, assuming either an incident coherent plane wave or a distribution of incoherent point sources along the surface of the crystal in the case of white beam topographs[2].

The suite is made of TRANSQ (white beam topography in the Laue case), TOPLANE (plane wave Laue topography), TOPRC (computation of rocking curves in the Laue case), REFPLANE (plane wave Bragg topography), REFRC (computation of rocking curves in the Bragg case). This later has been especially designed to study epitaxial thin layers taking into

consideration both the deformation between the epilayer and the substrate and the differences in the structure factors of both parts.

Examples of applications will be shown: stroboscopic images of piezoelectric materials, 3 D defects in quasicrystals, influence of the heat load at ESRF and of the curvature of the sample on the rocking curve profile

1. Y. Epelboin (1996) J. Appl. Cryst., **29**, 331-340
2. V. Mocella, Y. Epelboin, J-P. Guigay (1999) submitted to Acta. Cryst.

M13.FF.003 TOPOGRAPHIC RETICULOGRAPHY, MICRORADIOGRAPHY AND X-RAY INTERFERENCE EXPERIMENTS ON LINE 7 AT THE SRS, DARESBURY. A. R. Lang and A. P. W. Makepeace, H. H. Wills Physics Laboratory, University of Bristol, Tyndall Avenue, Bristol BS8 1TL, UK.

The long beamline (80 m) at Topography Station 7.6 plus the small source vertical FWHM of 0.23 mm together facilitate novel techniques and observations. For crystal perfection assessments involving detection and measurement of lattice misorientations, reticulography yields quantitative data at arcsecond resolution more directly and speedily than double-crystal topography. In reticulography a fine-scale X-ray absorbing mesh is placed between a Laue-diffracting crystal specimen and the topograph-recording photographic plate. The mesh splits the diffracted beam into an array of individually identifiable microbeams. Direction differences between microbeams, which give the orientation differences between the crystal elements reflecting them, are measured from their relative shifts within the array when mesh-to-plate distance is changed [1]. Synchrotron X-ray microradiographic imaging is an essential prerequisite for the collection of diffraction data from a particular individual small crystallite embedded within a mat containing thousands of similarly small-sized crystallites, and is proving fruitful in studies of CVD diamond films [2]. At Station 7.6 the transverse coherence length is great enough in the vertical plane for informative X-ray interference experiments to be performed there. Biprism interference patterns have been successfully recorded at several wavelengths using an X-ray biprism formed from two similar polished rectangular-section diamond bars meeting edge-to-edge [3].

[1] A. R. Lang & A. P. W. Makepeace (1996). J. Synchrotron Rad. **3**, 313-315.
[2] A. R. Lang, A. P. W. Makepeace & J. E. Butler (1998). Diamond Relat. Mat. **7**, 1698-1708.
[3] A. R. Lang & A. P. W. Makepeace (1999). J. Synchrotron Rad. **6**, Part 2, in press.

M13.FF.004 SYNCHROTRON WHITE BEAM X-RAY TOPO-GRAPHIC STUDIES OF SUPERSCREW DISLOCATIONS IN SILICON CARBIDE SINGLE CRYSTALS. Michael Dudley and Xianrong Huang, Department of Materials Science and Engineering, State University of New York at Stony Brook, Stony Brook NY 11794-2275, USA.

The use of Synchrotron White Beam X-ray Topography (SWBXT) to study superscrew dislocations in 4H- and 6H-SiC single crystals, commercially grown using the Physical Vapor Transport technique, is reviewed. Superscrew dislocations in SiC are shown to be growth dislocations, aligned parallel to the *c*-axis, with very large Burgers vectors of magnitude equal to n*c*, where n is an integer and *c* is the lattice parameter. Superscrew dislocations with b≥3*c* for 4H, and b≥2*c* for 6H are found to have hollow-cores (often referred to as "micropipes"). For hollow-core superscrew dislocations (micropipes) in both 4H and 6H, Frank's thermodynamically based, theoretical relationship between Burgers vector and core radius (F.C. Frank, Acta Cryst., 4, 497, (1951)) has been tested and found to approximately hold, confirming the screw dislocation nature of micropipes. The very large Burgers vector magnitude of superscrew dislocations provides an ideal system wherein X-ray topographic contrast formation mechanisms can be examined at a magnified level. This has enabled the development of a modified approach to dislocation image contrast formation under low absorption conditions. The contrast observed from superscrew dislocations on SWBXT images recorded in transmission, grazing-incidence reflection, and back-reflection geometry has been successfully simulated using this modified approach, providing further confirmation of the screw dislocation nature of micropipes. Possible origins of superscrew dislocations are also discussed.

M13.FF.005 DOUBLE CRYSTAL X-RAY TOPOGRAPHY: D-VALUE MAPPING OF CRYSTAL GROWTH DEFECTS. A.E.Voloshin, I.L.Smolsky, Shubnikov Institute of Crystallography of RAS, Moscow, Russia, N.P.Zaitseva, Lawrence Livermore National Laboratory, Livermore, CA, USA, A.G.Shtukenberg, St.Petersburg State University, St.Petersburg, Russia.

Quantitative characterization of point-to-point lattice parameter changes in crystals based on computer processing of plane wave X-ray topographs provides new possibilities in material science. Evaluation of crystal homogeneity is based on a relationship between the variations of point defect concentration and the deformation value near the sample surface. The near-surface distortions estimated as a result of calculations over the series of topographs provide data either for correct quantitative comparison with numerically simulated strain field, or for direct d-value mapping. This technique provides an observation of areas up to 10 cm^2, locality 3-10 μm and rather high sensitivity to crystal lattice distortions ($\Delta d/d$ up to 10^{-7}-10^{-8}).

The technique described was applied to the analysis of KDP group crystals grown from aqueous solution under different conditions. The problems investigated are: correct measurement and comparison of inhomogeneities in growth bands in traditionally and rapidly grown crystals, lattice distortions inside the vicinal sectors on dipyramidal and prismatic faces of rapidly grown KDP crystals, lattice mismatch between pyramidal and prismatic growth zones and it dependence on the growth temperature and growth rate. Moreover, the combined measurements of the lattice parameters and the deuterium concentration in different parts of rapidly grown DKDP crystal demonstrate that the most of possible reason of inhomogeneity in these crystals is hydrogen-deuterium non-stoichiometry.

Also the mixed crystals $(K,NH_4)Al(SO_4)_2 \cdot 12H_2O$ have been investigated. A composition of these crystals depends on growth conditions and determines the crystal internal stresses and some optical anomalies formation.

M13.FF.006 HIGH RESOLUTION X-RAY DIFFRACTION STUDY OF GaAs COILED MEMBRANES PRODUCED BY MICROMACHINING. Krishan Lal and Niranjana Goswami, National Physical Laboratory, New Delhi – 110 012, India, and J. Miao and H. L. Hartnagel, Institut fuer Hochfrequenztechnik, Technische Hochschule Darmstadt, D-64283 Darmstadt, Federal Republic of Germany.

Free standing GaAs coiled membranes produced for force sensor applications were characterized regarding real structure to evaluate their long term stability and quality of performance. Their fabrication involves photolithography, implantation by 2 MeV N^{++} ions followed by selective etching of (100) GaAs wafers which produced the membrane and a cavity beneath it. The membranes were 70 μm wide, ~ 5.3 mm long and ~2μm thick. Different segments of coil were separated by a gap of ~ 30 μm. A five crystal X-ray diffractometer developed at NPL was used in (+, –,

+) configuration with Mo $K\alpha_1$ exploring beam. High resolution X-ray diffractometry and topography experiments were performed in Bragg geometry with (4 0 0) (symmetric) and (5 $\bar{1}$ $\bar{1}$) (asymmetric) diffracting planes. For diffractometry, exploring beam dimensions were reduced to 1.2mm (height) x 10 μm (width) in order to selectively illuminate different sensor segments. However, due to geometrical considerations, at any linear position of the specimen, more than one segment of the membrane was irradiated. Therefore, the diffraction curves showed two or more peaks. From a set of thirteen different diffraction curves, peaks due to individual segments were identified. Their half widths varied in the range: 58 – 166 arc sec. Diffraction curve halfwidths for bulk crystals were ~ 26 arc sec. This shows that there is considerable broadening due to processing steps. Also, there were substantial angular tilts between sensor segments, which were determined through the analysis of diffraction curves. In a typical case, the tilt angles were in the range: 15 – 325 arc sec, which is quite significant. The high resolution diffraction topographs confirmed these tilts and at a time only two segments with tilt angle of 15 arc sec could be observed. Also, the topographs revealed that the walls of the of the cavity created by etching are tapered and its bottom was found to be uneven. A thin strip of the wafer is found to be freely hanging around the cavity.

01. INSTRUMENTATION AND EXPERIMENTAL TECHNIQUES

P06.01.001 PROTEIN - MEMBRANE - FIBRE CRYSTALLOGRAPHY WITH SPALLATION NEUTRONS: Benno P. Schoenborn and Paul Langan, Life Sciences Division, Los Alamos National Laboratory, Los Alamos N.M. 87545, USA

Suitable instruments on spallation neutron sources are ideal for diffraction studies of protein crystals and oriented molecular complexes (1). With spallation neutrons and their time dependent wavelength structure, diffraction data may be readily selected electronically with an optimal wavelength bandwidth and cover the whole Laue spectrum as time (wavelength) resolved spectra. This optimizes data quantity and quality with best peak to background ratios and provides adequate spatial and energy resolution to eliminate diffraction peak overlaps.

To maximize flux within this energy range a partially decoupled moderator will be used (2). Such a diffraction station is now being built at the upgraded Los Alamos Spallation Neutron Source that will run at 800 MeV with a current of 200 micro amperes. The Station will use a kappa geometry goniometer with a large (2900 cm^2) position sensitive cylindrical He detector with a resolution of 1.3 mm and a counting rate exceeding 1 million neutrons/second.

The current status of the station development can be obtained from the Web site at: http://lsdo.lanl.gov/nsb/

This work is supported by OBER of the Department of Energy

1) Benno P. Schoenborn and Eric Pitcher; Neutron Diffractometers for Structural Biology at Spallation Neutron Sources. In Neutron in Biology Plenum Press New York and London 1996.
2) Benno P. Schoenborn, John D. Court, Allen C. Larson and Phil Ferguson;Moderator Decoupling Options for Structural Biology at Spallation Neutron Sources. J. Neutron Res. 7/2 1999.

P06.01.002 HIPPO, THE HIGH-PRESSURE PREFERRED ORIENTATION DIFFRACTOMETER AT LANSCE. R. B. Von Dreele [1], K. Bennett [2], H.-R. Wenk [3], [1] Lujan Center, Los Alamos National Laboratory, Los Alamos, NM 87545 USA, [2] Lujan Center, Los Alamos National Laboratory, Los Alamos, NM 87545 USA, [3] Department of Geology and Geophysics, University of California, Berkeley, CA 94720 USA

A consortium of University of California faculty and National Laboratory researchers is building a new time-of-flight neutron diffractometer, HIPPO, for materials studies at the Los Alamos Neutron Science Center (LANSCE) under the auspices of the Department of Energy. The instrument, which will become available in fall 2000, has the extremely high count-rates necessary to study materials under a wide variety of environmental conditions (10-2000K, 0-20GPa, 12T magnet) in small (1mm3) and large samples (2cm diameter). The 3D arrangement of detectors covering 4.6m2 area allows direct measurements of crystal orientation distributions in polycrystalline materials. The analysis of TOF diffraction patterns with versatile Rietveld codes provides simultaneous information on crystal structure, texture, microstructure and phase proportions. Some applications include kinetics of reactions, structure of glasses and melts, high-pressure investigations of complex systems, evolution of texture and anisotropy during deformation and recrystallization. The project is aimed at creating an instrument with high data throughput and easy access to researchers and students. While the HIPPO instrument will be part of the national user facility operated by LANSCE, the scientific program will be guided by the UCMRD consortium with the goal of satisfying national priorities and establishing an environment of scientific excellence.

P06.01.003 AN IMAGE-PLATE THERMAL-NEUTRON LAUE DIFFRACTOMETER FOR PHYSICS AND CHEMISTRY. G.J. McIntyre and C. Wilkinson, Institut Laue-Langevin, BP 156, 38042 Grenoble Cedex 9, France, D. Myles, EMBL Outstation Grenoble, BP 156, 38042 Grenoble Cedex 9, France, and J. Cowan, Chemistry Department, University of Durham, Durham DH1 3LE, UK.

The use of large-area neutron image plates and quasi-Laue diffraction with cold neutrons has been demonstrated, with the LAue DIffractometer (LADI) at the ILL, to offer a considerable speed advantage over conventional monochromatic-wavelength diffractometers for data collection from biological samples [1,2]. Trials with LADI on a thermal-neutron beam show that such an instrument also has a very promising future in small unit-cell crystallography, allowing very rapid data collection, typically a few minutes to one hour for single exposures that are frequently sufficient for full structure refinement to precision approaching that of conventional monochromatic data.

Following these trials, a modification of LADI, better suited to the demands of physicists and chemists, has been proposed. Like LADI, it will consist of a cylindrical image-plate detector, first held stationary while the crystal which lies on the axis of the cylinder is irradiated by the white beam, and then spun around its axis for on-line read-out by a laser. Unlike LADI, the axis of the cylinder will be vertical to facilitate access by heavy cryostats and pressure cells, and the irradiated surface of the image plates will be read directly to give a 2-3-fold gain in efficiency.

Thermal LADI will complement the more-precise traditional single-crystal diffractometers, offering the possibilities of extensive reciprocal-space surveys, particularly for detection of incommensurate nuclear or magnetic modulations, complete data collections through phase transitions, study of very small samples, and fast initial characterisation of topical new materials.

1. F. Cipriani, J.-C. Castagna, C. Wilkinson, P. Oleinek and M.S. Lehmann, J. Neutron Research, **4** (1996) 79-85.
2. N.Niimura, Y. Minezaki, T. Nonaka, J.-C. Castagna, F. Cipriani, P. Høghøj, M.S. Lehmann and C. Wilkinson, Nature Structural Biology.**4** (1997) 909-914.

P06.01.004 HIGH-RESOLUTION NEUTRON FOURIER DIFFRACTION FOR POWDERS AND SINGLE CRYSTALS. A.M.Balagurov, V. Yu. Pomjakushin, V.G.Simkin [1] [1] Joint Institute for Nuclear Research, 141980, Dubna, Moscow region, Russia.

New ideas and novel electronics have renewed interest to neutron scattering correlation technique which has become again popular after a long period of disregard. In this paper, application of the correlation Fourier technique for diffraction experiments at long pulse neutron sources and the experience of operating the HRFD instrument, the first neutron high resolution Fourier diffractometer at the LPS-type source, the IBR-2 pulsed reactor in Dubna, are discussed. The relative full width of the resolution function of HRFD depends on the maximum modulation frequency of the incident neutron beam and now can be as small as 0.0009. At present HRFD is used for structure refinements of powders, for experiments with single crystals if it's a very high d-spacing resolution is needed, and for residual stress investigations in bulk samples. The recent results of high-resolution powder studies of Hg-based HTSC structures, investigation of phase separation phenomenon in La2CuO4+y, and semiconductor - metal phase transition in CMR compounds performed with HRFD are given in the paper.

P06.01.005 LIGHT STORAGE MATERIAL Sr [Fe(CN)5NO] 4·H2O. J. Schefer, PSI Villigen, Switzerland Th. Woike and M. Imlau, University at Cologn, Germany

Strontium nitroprusside tetra-hydrate is one of the candidates for understanding the mechanism of the metastable states produced by illuminating specific materials with visible light. We are presently investigating the ground state in the temperature range between 10 and 300K in order to clarify all phase transitions.

Sr $[Fe(CN)_5NO]$ $4H_2O$ (Strontium nitroprusside tetra-hydrate) yields metastable states if illuminated at low temperatures [1]. As the structure is very sensitive to the bonding of water (weak hydrogen bonds are present as shown in [2], we carefully checked for structural changes in the temperature range needed for future single crystal diffraction measurements.

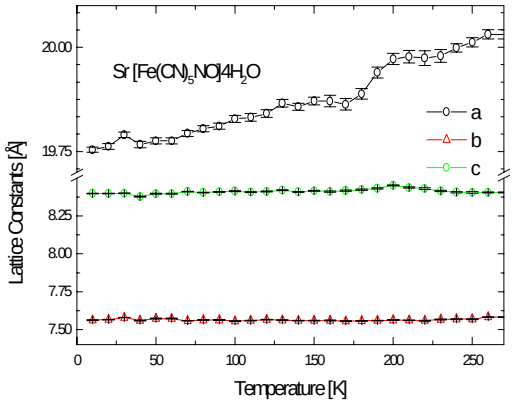

Due to the big unit cell (C2/m, a=20.08, b=7.51 and c=8.42Å, β=98.4°, [3]), a detailed structure analysis is not possible with the DMC-diffractometer at SINQ due to the long wavelength (λ=2.559 Å) and medium resolution: We have to wait here for HRPT and TriCS. However, the DMC is excellent for the determination of phase transitions, lattice expansions and superstructures, which will be of importance in the interpretation of the structure of the metastable states. The results show, that no structural phase transitions are present down to 50 K. This is in contradiction to the DTA datain [4], which give hints for additional phases from di- and mono-hydrates. The absence in our sample could be due to our preparation method, as we made polycrystalline material by grinding single crystals, probably the best method in order to make very pure samples.

[1] H. Zöllner, W. Krasser, Th. Woike, S. Haussuehl, Chem Phys. Lett. **161**, 497 (1989)
[2] A. Navaz and O. Piro, J. of Solid State Chem. **120**,1 (1995)
[3] E.E. Castellano, O.E. Piro and B.E. Rivero, Acta Cryst. **B33**, 1725 (1977)
[4] G. Chevrier, A. Navaz and J.M. Kiat, Mat. Science Forum **278-281**, 648 (1998)

P06.01.006 EVOLUTION OF COHERENT γ′ PRECIPITATES IN A NI-12 AT. % AL ALLOY WITH A BIMODAL PARTICLE SIZE DISTRIBUTION. H. A. Calderon[1], J. Cruz[1] and J. Skov Pedersen[2], [1]Instituto Politécnico Nacional, México D. F., 07738, [2]RisØ National Laboratory, DK-4000, Roskilde, Denmark.

The evolution of coherent γ′ precipitates in a Ni-12 at. % Al alloy with a bimodal particle size distribution has been studied by means of small angle neutron scattering (SANS) and transmission electron microscopy (TEM). Oriented single crystals parallel to (100) and (110) have been used for TEM and SANS, respectively. Specimens have been aged at two different temperatures in order to form a bimodal particle size distribution. A first aging was carried out at 1113 K for 5 h to create large precipitates and a second aging was performed at 923 K for different times to create smaller precipitates. SANS patterns originating from the smaller particles show scattering anisotropy with strong correlation peaks in <001> directions. Such anisotropy increases with the aging time evidencing particle alignment and shape changes during the coarsening process. The experimental data have been used to obtain particle size distributions (PSD´s) of the smaller precipitates. The fitting routine uses a modified paracrystal cluster model in the local monodisperse approximation. This model reproduces the scattering intensity in different directions. During fitting the particle shape can be varied by adjusting the degree of faceting of spheres used for describing the particles. A smooth and positive size distribution is obtained by the fitting algorithm as well as quantities such as specific surface and volume fraction. TEM has been used to obtain PDS´s from direct measurements and also to determine the kinetics of the coarsening. The two sets of results are compared in the size range where both techniques are applicable.

P07.01.001 DOES CONVENTIONAL POWDER DIFFRACTION BEAT A SYNCHROTRON ? A. Le Bail, Laboratoire des Fluorures, Université du Maine, Avenue O. Messiaen, 72085 Le Mans, Cedex 9, France.

At a given complexity level, one expects Rietveld refinements from synchrotron data being less challenging than from conventional X-ray. *Ab initio* structure determinations are expected also to be easier by synchrotron powder diffractometry. A few years ago, it was said possible to make Rietveld refinements on much bigger structures than could be determined solely from powder data. Because of recent advances in methods for locating previously known molecules in crystalline cells, this statement was recently modified in "we can now determine structures biggest than we could refine without interatomic distance constraints".

The belief in synchrotron data superiority is unconditional. However, some studies are realized by selecting low-wavelength (down to 0.7Å) and small angular ranges (1-60°2θ). Such choices may correspond to lowest resolution than conventional equipment would provide with CuKα radiation. A modern in-laboratory powder diffractometer may give full width at half maximum as low as 0.04°2θ. This is mathematically as good as 0.02° at a synchrotron facility when choosing λ = 0.72 Å. A good example is that of sample 2 (tetracycline hydrochloride) of the **Structure Determination by Powder Diffractometry Round Robin** [1] for which one participant preferred to solve the structure by using the conventional rather than the synchrotron data (both were provided).

Of course the synchrotron superiority is quite real due to highest resolution, intensity and tunability. Anyway, superb conventional X-ray powder patterns will be shown at this congress, supporting the comparison with 'bad' synchrotron data, apart from the time for obtaining them (3 to 6 days).

1. http://www.cristal.org/SDPDRR/

P07.01.002 SUBTHRESHOLD STRUCTURAL DEFECT FORMATION OF CRYSTALS USING SYNCHROTRON RADIATION. H.N.Yeritsyan, A.A.Sahakyan, S.K.Nickogossyan, A.S.Hovhannisyan; Yerevan Physics Institute, 2 Alikhanian Brothers St., Yerevan, Armenia

The structural defect formation usually takes place in solids under superthreshold process if the external energy transfer (E) to the material atom is greater than energy (E_d) for an atom displacement and vacancy – interstitial pair production.

Under certain conditions (for example, at high level excitation of electron subsystem) the subthreshold defect production might have large probability .One of the most famous

in this respect is estimated an impurity –ionization mechanism (IIM) proposed by Klinger [1]. The IIM may be efficient when the Energy of Coloumb interaction E_c between the host atom and impurity atom ions exceeds Ed. In this case the Auger ionization of an host atom inner shell seemed to be high enough. The estimations showed high probability of this effect when using synchrotron radiation (SR): high intensity, sufficient time of positive charge localization of ionized host atom, required energy for inner shell ionization of host material atom, Synchrotron Radiation is suggested with related high sensitivity structural experiment to study the SR damage process in solids, i. e. to investigate the defect structure formation mechanism in-situ. Some previous results of experimental attempts with semiconductor crystals are optimistic.

1. M.I.Klinger Soviet Phys.Semiconductor. 13, p.925 (1979).

P07.01.003 LIGHT INDUCED MAGNETIZATION OF $K_xCo_y[Fe(CN)_6]$ STUDIED BY SYNCHROTRON RADIATION. Hwo-Shuenn Sheu, Jyh-Fu Lee, Yuch-Cheng Jean and Ting-Wei Kang, Synchrotron Radiation Research Center, Hsinchu 30077, Taiwan

The aim of designing a molecular-based magnet is to increase the critical temperature and the tunability by applying external fields. Both T_c and field-induced properties have made big breakthrough in the development of Prussian Blue family compounds recently. The magnetism of $K_{0.2}Co_{1.4}[Fe(CN)_6]$ can be switched by shining blue (450nm) and red (650nm) light at the temperature below 20K. A proposed mechanism is via one e-jump between Co and Fe during light irradiation. X-ray absorption spectroscopy was employed to study the Co and Fe valence change as well as the spin sates during the light irradiation. XRD revealed that the space group is Fm3m with cell parameter ~10.41Ă. The thermochromism of this compound between room temperature and 90ºC have also studied by X-ray absorption spectroscopy.

P07.01.004 HIGH ENERGY, LOW TEMPERATURE RESONANT X-RAY DIFFRACTION STUDY OF CAESIUM IODIDE. A.M.T. Bell and J.P. Attfield, University Chemical Laboratory, Lensfield Road, Cambridge, CB2 1EW, UK.

The high X-ray energies available at the European Synchrotron Radiation Facility have been used to discover whether large resonant X-ray scattering effects, comparable to the normal scattering, can be observed at the K edges of heavy elements. High resolution powder diffraction data have been collected on a sample of CsI at ambient temperature and at 4 K on beamline BM16.

Synchrotron X-ray wavelengths were set at the Cs K-edge (0.3453 Å), I K-edge (0.3741 Å), and off the absorption edges (0.3900 Å). The 4 K data enable reflections to be observed to very high $\sin(\theta/\lambda) = 1.9$ Å^{-1}. Resonant scattering is evident from the enhanced intensities of the odd (h+k+l) peaks. The refined I f' from the 4K data is -6.2(2) electrons/atom. In comparison, the non-resonant scattering factor at the maximum $\sin(\theta/\lambda)$ is f = 8.8 electrons/atom, showing that resonant effects can be comparable to the normal scattering under such conditions.

P07.01.005 DANES AND ANOMALOUS STUDIES OF SPIN-LADDER COMPOUNDS BY USING MONOCHROMATIC AND DISPERSIVE DIFFRACTION. S. Bos, S. Pachot, V. Favre-Nicolin, P. Bordet, J.E. Lorenzo, H. Renevier, J.L. Hodeau, Lab. de Cristallographie-CNRS, BP 166, 38042 Grenoble Cedex 9 France, G. Dhalenne, A. Revcolevski, Lab. Chimie des Solides B‰t 414, 91405 Orsay France, O. Mathon, R. Tucoulou, ESRF BP 220, 38043 Grenoble France.

DAFS (Diffraction Anomalous Fine Structure) technique probes the energy-dependent intensity variations of a diffraction peak as the energy is tuned near an absorption edge of an atom of the sample: the long-range structural information contained in the diffraction peak is combined with the chemical and local structure selectivity of x-ray absorption spectroscopy. The intensities of reflections are sensitive to the relative contributions of the various anomalous sites and, in particular to the different valence states of the anomalous atom. Such an information can be obtained by studying the near edge region of the spectra (DANES).

This method is of particular interest for the study of transition metal oxides. We have used this technique to investigate the distribution of copper valence states in the spin-ladder compound $Sr_{14-x}Ca_xCu_{24}O_{41}$ (x=12) that contains both CuO_2 chains and Cu_2O_3 planes with two-leg ladders.

One set of experiment has been performed with monochromatic optics on D2AM beamline at the ESRF. As intensity variations of several Bragg reflections are collected versus energy, the data collection using classical monochromatic optics is quite long. For this reason, we have developed an experimental mode (Dispersive Diffraction) that allows simultaneous intensity collection over the whole energy range of interest. A Dispersive Diffraction experiment has been carried out on BM5 beamline at the ESRF. We will here present the results obtained using the two experimental strategies and discuss the data analysis developed for such methods.

P07.01.006 CCD-STUDIES OF DIFFUSE SCATTERING AT BEAMLINE F1 (HASYLAB/DESY). C. Paulmann, W. Morgenroth, D. Mathes and U. Bismayer, Mineralogisch-Petrographisches Institut, Universität Hamburg, Grindelallee 48, D-20146 Hamburg, Germany

The Kappa-diffractometer at HASYLAB/DESY (beamline F1) is equiped with a commercial CCD-detector system since summer 1997. The system includes software for diffractometer controlling, data collection and data processing. Besides standard data collections, the combination of a powerful radiation source with a fast area detector system recommends the beamline especially for studies of weak diffraction phenomena and time-resolved studies. CCD-studies were performed on several disordered minerals, covering a wide range of different types and distributions of diffuse scattering:

1) Incorporation of radiogenic elements in natural titanites gives rise to significant structural damages (Frenkel defects, quasi-amorphous regions) due to alpha-recoil collision cascades. This causes broad Bragg reflections (FWHM > 1.5°). Annealing of these samples (> 673 K) leads to a recrystallization of the damaged regions and to a progressive sharpening and an increasing integral intensity of the reflections. Below 673 K only Frenkel defects and associated lattice relaxations are annealed.

2) Sr-doped lead phosphate was studied below and above the ferroelastic transition point. At room temperature splitted Bragg reflections caused by the ferroelastic domain structure can be observed . Weak scattering between these reflections is induced by the domain wall volume. Above T_c the splitting disappears and the high-symmetry is adopted.

3) Detailed measurements of diffuse scattering in mullite show a broad and structured distribution of diffuse scattering which can be attributed to short-range ordering of anion-defects.

Special data processing routines were developed to handle problems which are difficult to solve by using the standard software (e.g. special background corrections, corrections for fluctuating primary beam intensity, data reduction routines, data conversion to different target formats, numerical values of rocking curve data). Further details about the studies and software will be presented.

P07.01.007 X-RAY DIFFRACTION AT SUB-MICRON SPATIAL RESOLUTION FOR MEASUREMENT OF THIN FILM STRESS. H. A. Padmore, R. Celestre, A. MacDowell and J. R. Patel, Lawrence Berkeley National Laboratory, MS 2-400, Berkeley CA 94720, USA, B. Batterman, Department of Applied and Engineering Physics, Cornell University, Ithaca, New York 14853, T. Marieb, Intel Corporation, 3065 Bowers Ave, Santa Clara, CA 95052

The advent of high brightness 3rd generation synchrotron radiation x-ray sources, together with recent advances in x-ray optics are for the first time allowing the application of x-ray diffraction techniques on the microscale. We have developed a system at the Advanced Light Source (ALS) in Berkeley based on a bending magnet source of synchrotron radiation, together with a 4 crystal monochromator, and elliptically bent grazing incidence mirrors. The 4 crystal monochromator is arranged in a + - - + configuration, and can be removed from the beam by simple rotation. It is therefore possible to produce monochromatic or white light co-linearly. Light is then focused by a pair of elliptical cylinders arranged in a crossed configuation, and a focus size of 0.8 microns has been achieved. Our initial studies have been of stress in thin films of Al-Cu and Cu under hydrostatic and electromigration induced stress. The measurements are carried out on thin film wires encapsulated in a passivation layer as used in interconnect structures in modern integrated circuits. Measurement of stress distributions in the individual grains in a polycrystalline wire is important in understanding failure mechanisms such as void formation during current flow. Grain orientation is derived directly from the Laue diffraction pattern, and stress is determined by measurement of the energy of several reflections. The complete strain tensor of each grain can then be deduced. This new method should have widespread application in materials science.

1 Grain orientation mapping of passivated Aluminum interconnect lines with x-ray micro-diffraction, A. A. MacDowell, C. H. Chang, H. A. Padmore, J. R. Patel and A. C. Thompson, Materials Research Society, **524** (1998) 55-58, San Francisco, April 1998

P07.01.008 STATUS OF TIME-RESOLVED SMALL-ANGLE X-RAY DIFFRACTION TECHNIQUE AT SIBERIAN AND MOSCOW SR CENTRES. P.M.Sergienko, V.S.Gerasimov, A.A.Vazina [1], V.N.Korneev [2], G.N.Kulipanov, V.M.Aulchenko [3], V.G.Stankevich [4], [1] Institute of Theoretical and Experimental Biophysics of RAS, Pushchino, Moscow Region 142292, Russia, [2] Institute of Cell Biophysics of RAS, Pushchino, Moscow Region 142292, Russia, [3] Budker Institute of Nuclear Physics, SD of RAS, Novosibirsk 630090, Russia, [4] Research Scientific Center "Kurchatov Institute", Moscow 123182, Russia

The improved version of small-angle diffractometer is described. It makes the focusing collimation of the SR beam: monochromator is situated in front of polysectional mirror [1]. The angle resolution is 0.2 mrad, the range of spacing of the measured reflections is 1.0-100.0 nm. The specimen cell lets to keep the muscle in living state, temperature range is 2-10°C. It is realised the isometric and isotonic contraction. The frog sartorius muscle can be stimulated by double pulse interval of 1-500 ms.

Optical and X-ray small-angle diffractometers were physically combined in the new version of set-up. The SR and laser beams were coaxially coincided on the same point of the muscle using the special semitransparent mirror, which reflected the laser beam and passed the X-ray beam. For registration of optical diffraction patterns the 2-channel principle was realised [2].

The new generation of fast, high efficient, parallax-free, one-coordinate, proportional detector OD-3 with counting rate up to 10 MHz at spatial resolution of 160 mkm and short time frame (1 mks) is used [3]. It is opened the absolutely new possibility for registration of short-living states in living systems.

1. A.A.Vazina et al. (1979), Biofizika, v.24, 495 (in Russian).
2. A.M.Gadzhiev et al. (1989), NIM in Phys.Res, v.A289, 728
3. V.M.Aulchenko et al.(1998), NIM in Phys.Res., v.A405, 269.

P07.01.009 COHERENCE PROPERTIES OF THE ESRF MAGNETIC SCATTERING BEAMLINE: OBSERVING MAGNETIC SPECKLE PATTERNS. F. Yakhou[1], F.Livet[2], A. Letoublon[2], M. de Boissieu[2], F. Bley[2], C. Vettier[1], [1]ESRF, BP 220 F38043 Grenoble Cedex, France, [2]LTPCM-ENSEEG, BP 75 F38402 St Martin d'Hères, France

The coherence properties of a high brilliance beam from two phased undulators were analyzed at both 7.6 keV and 3.73 keV (uranium Miv absorption edge) on the ID20 magnetic scattering beamline. A coherent beam was obtained by properly collimating the 1.4 10^{-4} spectral bandwidth beam from a double Si (111) monochromator. The transverse coherence length could be matched to the collimating pinhole apertures by controlling the aperture d_s of a secondary set of slits placed after the optics. The high quality focusing optics of this ultra high vacuum beamline with two Be windows only provided a 350x80 μm^2 (HxV) spot size at the pinhole position, that resulted in a ~10^9 ph/s and 7.8 10^7 integrated coherent flux through ϕ10 and ϕ20 mm pinholes with a 60x60 μm^2 secondary source size, at 200 mA ring current, at 7.6 and 3.73 keV respectively. The coherence properties of the beam were retrieved from the statistical analysis [1] of the static speckle patterns produced by a silica aerogel that were recorded with a 384x576 pixel CCD camera. The degree of coherence β as given by the contrast of the speckle pattern was found to be around 50% at both energies, which is by far the highest and best coherent fluxes achieved up to now.
This high coherent flux enabled us to record a magnetic speckle pattern at 100 K arising from the disorder inherent to domain formation in the type-I antiferromagnetic system UAs, taking advantage of the huge enhancement of the magnetic scattering amplitude when the energy is tuned to the M-edges of Uranium.Such coherent scattering experiments on magnetic systems should give a unique insight on the physics of magnetic domains

1. F. Livet et al., J. Synchrotron Rad. 5 (1998) and references therein.

P07.01.010 X-RAY NATURAL OPTICAL ACTIVITY AT THE Ni *K*-EDGE MEASURED BY USING AN X-RAY POLARIMETER WITH PHASE RETARDERS. Y. Ueji, The Graduate University for Advanced Studies, 1-1 Oho, Tsukuba, 305-0801 Japan, K. Okitsu, K. Sato and Y. Amemiya, University of Tokyo, 7-3-1 Hongo, Bunkyo, 113-8656 Japan.

We have successfully measured the x-ray natural optical activity of a single crystal of $NiSO_4 \cdot 6H_20$ at Ni *K*-edge by using a x-ray polarimeter[1] which consists of x-ray polarizer, phase retarder, and analyzer. In this experiments[2], x-ray natural circular birefringence (XNCB) and x-ray natural circular dichroism (XNCD) have been simultaneously measured by

analyzing the polarization state of the x-ray beam transmitted with the sample. The space group of the sample crystal belongs to one or the other of the enantimorphic pair $P4_12_12$ or $P4_32_12$ and it was known that this sample shows NCD in infrared, visible and ultraviolet regions[3].

The sample was a (001) plate of about 0.2 mm in thickness and the c-axis (optic axis) of the sample was set to be parallel with the x-ray beam axis so that the effects of the linear birefringence and linear dichroism were minimized. A small peak of 0.5 mrad was found at a pre *K*-edge, and a large peak of as much as 5 mrad was observed at the *K*-edge in the spectrum of polarization rotation, *i.e*., in the XNCB spectrum. In the spectrum of the polarization ellipticity , *i.e*., in the XNCD spectrum, the maximum ellipticity reached 0.004. It was found that the Kramers-Kronig relation holds between XNCB and XNCD spectra.

The XNCD spectrum of the same sample was also measured with a circular polarized x-ray beam whose helicity was switched alternately by using double phase retarders which compensate the spherical aberration[4]. The XNCD spectra didn't change against the rotation and the inversion of the c-axis of the sample with respect to the x-ray beam axis, ensuring that the effect of the linear birefringence and linear dichroism is negligible. The XNCD spectrum measured with circular polarized x-rays coincided with those measured by using the x-ray polarimeter.

1. Okitsu, K. *et al*. (1998). J. Synchrotron Rad. **5**, 995-997.
2. Ueji, Y. *et al*. to be submitted.
3. Ingersoll, N. *et al*. (1940). Phys. Rev. **57**, 1145-1153.
4. Okitsu, K. *et al*. poster presentation in IUCr99, Glasgow.

P07.01.011 CCD DETECTORS FOR NON-CRYSTALLINE DIFFRACTION. J.C. Phillips, Bruker AXS, Inc., Madison, WI USA, L.Häming, Bruker AXS, Karlsruhe, Germany

CCD detectors have been successfully used in all types of crystallography in large numbers for some time. There is now a growing use of these detectors for other applications, often linked with synchrotron radiation as the X-ray source. These applications include powder diffraction, time-resolved diffraction and microdiffraction. Examples of such uses will be presented.

P07.01.012 DEVELOPMENT OF MICRO-AREA DIFFRACTION SYSTEM WITH MICRO-PINHOLES USING MONOCHRO-MATIC SR. K. Hagiya, M. Ohmasa and N. Haga, Dept. of Life Science, Himeji Inst. of Tech.,Hyogo 678-1297, Japan, K. Ohsumi, Inst. of Materials Structure Science, High Energy Accelerator Research Organization, Tsukuba 305-0801, Japan, Y. Kohmura, Harima Research Establishment, Inst. of Physical and Chemical Research, Hyogo 679-5143, Japan, K. Kusaka, K. Murakami and S. Noguchi, Dept. of Life Science, Himeji Inst. of Tech., Hyogo 678-1297, Japan and S. Arai, Dept. of Earth Science, Kanazawa Univ., Kanazawa 920-1192, Japan

Studies on inhomogeneity of rock forming minerals are important to elucidate growing and/or cooling process recorded in the minerals. Examinations of the phenomena are usually investigated by EPMA and/or optical microscopy. Most rock samples are mounted on slides and thinned to 30μm in thickness. Since the form of the samples is not convenient for diffraction studies, no diffraction study except Laue method has so far been carried out. As absorption of incident X-ray through slides was too large, Laue method (back-reflection type) has so far been employed [1,2] although indexing of Laue patterns of unknown sample is extremely difficult. Thus micro-area diffraction system has been developed to measure diffraction of the fine crystallites and/or domains in thin sections with high brilliance and high energy monochromatic X-ray beam.

The experiments were carried out on the R&D beamline BL47XU at SPring-8. The wave length of the incident beam from the undulator was adjusted to 0.7Å with Si double-crystal monochrometer. Pinholes with various sizes were prepared for the experiments. The diameters of the micro-beams through the pinholes were measured at three positions by scanning a slit before an ion chamber. The effective diameters of the pinholes and the divergence of the micro-beams were estimated from them. Two pinholes with diameters of 4.7μm and 3.2μm full width at half maximum are available. The divergence was 19μrad and 29μrad respectively. They were applied to measure diffraction patterns of a thin section (thickness: 30μm) of Cr-spinel crystals segregated from olivine host crystals in dunite from Iwanai-dake, Hokkaido, Japan. The distance between the pinhole and the sample was 10mm and the camera length was 79mm. Oscillation photographs of these minerals were successfully recorded on a flat imaging plate (Fuji Co. LTD.) and will be shown together with crystallographic analyses.

1 K. Ohsumi *et al*. (1996) Acta Cryst., **A52**, C-23.
2 M. Ohmasa *et al*. (1996) Photon Factory Activity Reports, **13**, 49.

P07.01.013 HARD X-RAY PHASE-CONTRAST IMAGING WITH A MICROFOCUS SOURCE. A.W. Stevenson[a], D. Gao[a], T.E. Gureyev[b], A. Pogany[a] and S.W. Wilkins[a], [a]CSIRO Manufacturing Science & Technology, Private Bag 33, Clayton South MDC, Victoria 3169, Australia, [b]CSIRO Forestry & Forest Products, Private Bag 10, Clayton South MDC, Victoria 3169, Australia.

Since Röntgen's discovery of X-rays in 1895 the vast majority of radiographs have been collected and interpreted on the basis of absorption contrast and geometrical (ray) optics. In recent years the possibility of utilising phase-contrast effects has received considerable attention, much of this activity stemming from the possibility of producing X-ray beams of suitably high coherence at synchrotron sources (see [1] for example). A description of a phase-contrast imaging technique which utilises a laboratory-based microfocus X-ray source to achieve the required spatial coherence, and does not rely on there being a high degree of chromatic coherence, will be described [2]. The method employs a relatively large object-to-image distance to allow wave interference (Fresnel diffraction) to occur and manifest itself as contrast formation in the intensity distribution recorded at the image plane.

Various examples of phase-contrast images and a theoretical description of image structure in terms of the Kirchhoff formulation will be used to elucidate important features of the technique. These include the ability to provide improved information from weakly-absorbing features of an object such as soft tissue, including edge enhancement; inherent magnification; improved signal-to-noise.

1. A. Snigirev, I. Snigireva, V. Kohn, S. Kuznetsov & I. Schelokov, Rev. Sci. Instrum. 66, (1995), 5486-5492.
2. S.W. Wilkins, T.E. Gureyev, D. Gao, A. Pogany & A.W. Stevenson, Nature. 384, (1996), 335-338: S.W. Wilkins, Aust. Pat. PN 2112/95 (28 March, 1995).

P07.01.014 HIGH SPATIAL RESOLUTION X-RAY IMAGING SYSTEM WITH A CCD DETECTOR COUPLED WITH AN X-RAY MAGNIFIER. K. Sato, Y. Hasegawa, K. Kondo, K. Miyazaki, and Y. Amemiya, Department of Applied Physics, University of Tokyo, 7-3-1 Hongo, Bunkyo, Tokyo 113-8656, Japan.

Recently, Faraday rotation as well as linear birefringence in an x-ray regime were measured by using an x-ray polarimeter. In order to investigate the polarization effect in microscopic scale, the x-ray polarization microscopy is expected to be a promising

strategy. The development of a high resolution x-ray imaging system is essential for this microscopy.

We decided to use the CCD-detector. The CCD detector consists of (1) phosphor (Gd_2O_2S:Tb, 10•m thick on glass plate), (2) magnifying optical lens (×2.5, ×5, ×10), and (3) CCD camera cooled down to –50°. The CCD camera has an imaging area of 1024×1280 pixels of 6.7•m×6.7•m.

The experiments to evaluate the performance characteristics of the high resolution x-ray imaging system were performed at BL-15C, Photon Factory (KEK). The energy of the incident beam was tuned at 7.709 keV by Si (111) pre-monochromator. The knife-edge technique was applied for the evaluation of the spatial resolution. The spatial resolution of the detector of 7.9•m was obtained in terms of full width at half-maximum (FWHM) of line spread function (LSF). We intended an x-ray magnification for higher resolution with the use of asymmetric Si (111) Bragg reflection. The crystals with the magnification factors 1.0, 3.3, 6.3, and 12.8 were used. The spatial resolution of this imaging system was improved up to 1.2•m.

This 2D x-ray imaging system will be applied to the polarization microscopy.

P07.01.015 ATOM RESOLVING X-RAY HOLOGRAPHY: RECENT PROGRESS IN THEORY AND EXPERIMENT. D.V.Novikov [1], F.N.Chukhovskii, B.Adams, T.Hiort, E.Kossel, G.Materlik, Hamburger Synchrotron-strahlungslabor HASYLAB at Deutsches Elektronen-Synchrotron DESY, Notkestr. 85, D-22607 Hamburg, Germany [1]also H.C.Orsted Lab. Universitetsparken 5, DK2100 Copenhagen Denmark.

Atom resolving X-ray holography is a novel method for direct imaging of atoms in solids. We discuss the basic ideas of direct fluorescent (XFH) and multiple energy (MEXH) X-ray holography and the latest theoretical and experimental progress in this field. A rigorous theory of X-ray holography based on classical electrodynamics is developed. The equations obtained take into account second-order X-ray scattering effects and can be applied for restoration of the electron charge density from holographic data. The influence of wave coherence properties, absorption and sample dimensions as well as atom position determination from incomplete data sets are considered . Experimental holograms of Cu_3Au and Fe in XFH, MEXH and modified MEXH schemes are presented, together with reconstructed images, obtained by a simple Fourier transform based reconstruction algorithm. The dependence of the accuracy and precision of the images on the experimental conditions, problems of artefact suppression and possible application fields of the method are discussed.

1. M.Tegze, G.Feigel, Nature **380**, 49 (1996)
2. T.Gog, P.M. Len, G. Materlik, D. Bahr, C.S. Fadley, and C. Sanchez-Hanke), Phys. Rev. Lett. **76**, 3132 (1996)
3. D.V.Novikov, B.Adams, T.Hiort, E.Kossel, G.Materlik, R.Menk, A.Walenta, **5**, 315 (1998)
4. B.Adams, D.V.Novikov, T.Hiort, E.Kossel, G.Materlik, Phys.Rev.B , **57**, 7526 (1998)

P07.01.016 A TOPOGRAPHIC METHOD FOR DETERMINATION OF THE RESONATORS VIBRATION AMPLITUDE USING THE RS AT ESRF B. Capelle, J. Detaint, Y. Epelboin LMCP, CNRS, case 115, Universités P.M. Curie and D. Diderot, 75252 Paris Cedex 05, France

X-ray topography is one of the most powerful techniques to assess the vibration modes of the piezoelectric devices. We have previously demonstrated that stroboscopic topographies of vibrating thickness shear resonators made using the time structure of the synchrotron radiation contain contrasts which can be used to determine very accurately the vibration amplitude mode when the amplitude of the vibration is sufficiently small. In this communication, we present a new method that allows the direct determination of the vibration amplitude of devices used in most of their applications ranging from some µW up to several mW. This method is based upon the use of a white beam with an extremely small divergence. The distortion of the lattice planes due to the vibration is by several order of magnitude larger than the width of the intrinsic rocking curve so that each region with a different deformation diffracts a radiation with a different wave length. It means that the diffracted rays are deflected with different angles according to the local Bragg angle. For an incident beam delimited by a very thin slit (of the order of 20 mm) in the symmetric arrangement, the width of the diffraction image obtained on a film is thus a function of the local rotation of the lattice plane. So, we obtain a direct recording of the vibration amplitude along the slit.To obtain further details on the vibration modes, the stroboscopic technique was employed. On the whole, this new method which makes use of the very improved characteristics of the beam delivered by the third generation synchrotron at ESRF, allows to directly determine the vibration amplitude of the piezoelectric devices with a very high precision in the case of thickness shear modes.

P08.01.001 ULTRA LOW TEMPERATURE CRYST-ALLOGRAPHY USING AN OXFORD-CRYOSYSTEMS HELIX OPEN-FLOW HELIUM CRYOSTAT. M.A. Leech, J.A.K. Howard and A.E. Goeta, Department of Chemistry, University of Durham, South Road, Durham, DH1 3LE, UK.

The measurement of X-ray diffraction data at temperatures lower than 80 K, has until recently been limited to the use of closed-cycle helium refrigerators. Although this has become a well established technique [1] for temperatures down to 10 K, it has its drawbacks: the equipment is expensive and needs considerable maintenance; the crystal must be enclosed within two or three evacuated shrouds, resulting in high X-ray backgrounds and difficulties in centring the crystal; the crystal must be cooled slowly, making it difficult to handle sensitive samples. Using the HELIX cryostat, temperatures down to 30 K can be obtained in an open flow of He gas. The open-flow nature of the device gives it a number of advantages: crystals can be flash cooled, enabling air or moisture sensitive samples to be handled easily; Crystals can quickly screened for quality; the crystal is visible, so can be centred easily and if necessary, can be exposed to a number of external influences, such as a light source.

The work presented in this poster includes the commission and calibration of the HELIX device on the laboratories Bruker SMART-CCD diffractometer, together with a number of examples of its use.

[1] Larsen, F. K. (1995). *Acta Cryst*. **B51**, 468-482.

P08.01.002 LOW TEMPERATURE X-RAY STRUCTURE DETERMINATION USING COMPRESSED AIR INSTEAD OF LIQUID NITROGEN. Jamie F. Bickley, Gavin T. Lawson, Frederic Rivals and Alexander Steiner, Department of Chemistry, University of Liverpool, Crown Street, Liverpool L69 7ZD, UK

It has become standard that X-ray structure analysis is carried out at low temperature. In general crystallography laboratories rely upon applying a cold nitrogen gas stream to cool crystals. The gas is usually supplied from a storage vessel containing liquid nitrogen. However, using liquid nitrogen is a rather expensive method, which can lead to large bills somewhere in the region of several K$ per diffractometer per year. In addition, the storage container has to be refilled regularly which cost precious working hours.

We present a low-temperature device that avoids the usage of liquid nitrogen, but instead uses pre-dried compressed air. This system can provide temperatures from +100°C down to -80°C, which is sufficient for routine structure determination of air and moisture sensitive materials. The cooling unit consists of the XR Sample Cooler supplied by FTS Kinetics {for a detailed view see http://www.ftssystems.com}. It only requires a compressed air supply, which is available in most research laboratories.

This device is built onto an image plate diffractometer (STOE-IPDS) and is in constant use. The system is virtually maintenance free and highly cost efficient, due to the low purchase price, which is a fraction of the price of a liquid nitrogen based cryosystem. On our poster we will present the set-up described above in more detail, accompanied by some interesting structures which have been determined using this system.

P08.01.003 A PORTABLE CRYOSTREAM TO TRANSFER CRYSTALS. F. Wien, T. Rutherford, M. Bennett, and M.R. Sanderson. Division of Biomedical Sciences, Randall Institute, King's College London. WC2B 5RL UK.

A portable cryostream, the King's Cryogun, has been developed in our laboratory for the transfer of crystals at cryogenic temperatures. The cryogun provides a constant stream of nitrogen vapour at a temperature of 130K. The King's cryogun has been tested on a variety of macromolecular crystals and used succesfully to transfer crystals between goniometer and storage cryovials. Experiments with protein and DNA crystals have revealed no significant deterioration of diffraction quality or increase in mosaicity after repeated transfer steps. The use of the King's cryogun has become essential for our synchroton experiments: crystals are tested in-house for diffraction quality, the best crystals are transferred to cryostorage and remounted at the synchroton using the cryogun (1,2). This retrieval technique has proved to be time-saving and reliable.

1. M.S. Bennett, F. Wien, J.N. Champness, T. Batuwangala, T. Rutherford, W.C. Summers, H. Sun, G. Wright and M.R. Sanderson. (1999). FEBS Lett. 443, 121-125.
2. B-DNA at atomic resolution: Helix end-capping and groove interaction with a Ni-porphyrin M.S. Bennett et al. Submitted to PNAS.

P08.01.004 DEVELOPMENT OF A COOLING SYSTEM FOR SINGLE CRYSTAL MEASUREMENTS AT 4 K. Ch. Mensing, M. Wörle, P. Corrodi and R. Nesper, Inorganic Chemistry Laboratory, ETH Zürich, CH.

We developed a cooling system based on commercially available helium cryostats [1] which allows us to perform single crystal and powder measurements at temperatures of 4.3 K and ambient pressure, and below 4 K with reduced pressure. The cooling system is mounted on a standard image plate diffraction system [2]. The temperature can be stabilized and controlled very accurately. The cryostat can easily be removed to allow standard measurements as well. The working principle and first results are presented.

1. Stoe IPDS; Fa. Stoe & Cie, Darmstadt, D
2. Janis Research Company, Inc., Wilmington, MA, USA

P12.01.001 WAVELENGTH SCANNING DIFFRACTOMETRY WITH A QUADRUPLE MONOCHROMATOR. M. Hashihayata, K. Munakata, S. Kuwajima, A. Okazaki and Y. Soejima, Department of Physics, Kyushu University, Fukuoka 812-8581, Japan

In order to make high-resolution measurements of X-ray resonant scattering such as XANES, EXAFS and DAFS, the wavelength-scanning type of diffractometry has been developed. For getting high quality incident X-ray beams, a germanium quadruple monochromator made by Philips (PW1754) is used: two channel-cut monochromators are rotated by stepping motors at the minimum step of 1.2 μrad. At the wavelength $\lambda \sim 0.15$ nm, the resolution $\Delta\lambda/\lambda=2\times10^{-5}$, and the angular divergence 2.4 μrad are attained. The software for controlling the wavelength scanning is combined with that for controlling the four-circle goniometer. Therefore, the intensity measurement as a function of incident wavelength can automatically be made for absorption, scattering and diffraction experiments. By using the X-ray generator with an Au rotating-anode operated at 50 kV- 40 mA, the wavelength of incident X-ray is covered in a range 0.06 - 0.20 nm with the 440 diffraction of the monochromator; the intensity is 500 cps for the beam size 0.3×3 mm^2 at the position of the specimen. In the present paper, examples of the application to high-resolution EXAFS measurements will be demonstrated; the details of the system will also be discussed. Because the incident intensity is not sufficient for the experiments, the system will be more effective if coupled with synchrotron X-ray source.

P12.01.002 INSTRUMENTAL EFFECTS UPON THE GLANCING ANGLE XRD MEASUREMENTS. D. Rafaja, R. Kuzel and V. Valvoda, Faculty of Mathematics and Physics, Charles University, Ke Karlovu 5, CZ-121 16, Prague, Czech Republic and G. Cappuccio, INFN-LNF-Lab. Dafne Luce, Via E. Fermi 40, P.O. Box 13, I-00044 Frascati, Italy.

Diffraction techniques employing the glancing angle X-ray diffraction (GAXRD) are very popular in the last time, as they offer many features to study coatings and thin films. The main advantage of the GAXRD is that the thickness of the material being analysed can easily be changed varying the angle of incidence. Another benefit of the GAXRD is a very low sensitivity of the peak shift to the potential sample displacement. However, the instrumental effects are not completely summarised and explained yet. This fact, of course, causes problems if the splitting of the physical and instrumental effects in the diffraction pattern should be done with a very high precision.

The poster shows a systematic study of the instrumental effects such as line broadening or changes in the line shape and in the registered intensities. These effects, which are caused by the finite divergence of the primary beam and by the limited acceptance of a long Soller collimator placed in the diffracted beam, were investigated by using various “standard” samples. An explanation of the observed phenomena is offered, which is based on a “ray-tracing” calculation.

Besides, an application of this approach is illustrated. As an example, we have measured diamond coatings deposited on TiC substrates at glancing angles to estimate their thickness. The measured intensities must first be corrected for a limited sample size, for a finite divergence of the primary beam and for the real acceptance of the Soller collimator to arrive at the true diffracted intensities, which are modified just by the absorption (and the thickness) of the coating.

P12.01.003 X-RAY ROTATION-TILT METHOD (XRTM) - A NEW X-RAY DIFFRACTION TECHNIQUE. J. Bauch, H.-J. Ullrich and J. Brechbühl, Dresden University of Technology, Institute of Materials Science, Mommsenstr. 13, D-01062 Dresden, Germany.

A new X-ray diffraction technique, marked by the authors as X-ray Rotation-Tilt Method (XRTM) and based on an idea of our own from 1977, has been developed within the scope of a project of the Deutsche Forschungsgemeinschaft. The principle is briefly presented in the following: XRTM is a method where local X-ray interferences are produced by directing an X-ray or synchrotron beam from an external source with default

monochromatic radiation of high intensity and a small diameter (e.g. application of capillary optics) on a crystalline region of a sample. Thereby for each diffracting net plane set a cone can be indicated with the half-opening angle equal to ($90°-\Theta_{hkl}$) for which the Bragg equation is satisfied. Each time the incidenting monochromatic X-ray beam coincides with a shell line of the interference cone on the diametrically opposite side of the shell of the cone, a small spot is produced by the "reflected" beam. By means of a special movement of the sample it is possible to accumulate such cones spot-by-spot on a detector system (e.g. film, image plate or CCD-area-detector) located on the back. These reflexes imaged on the detector form the so-called XRTM lines. For the complete spot-by- spot accumulation of such lines on a detector system a scientific device has been developed, at which sample and detector are coupled at a defined distance and which are jointly and simultaneously rotated and tilted around the sample point investigated such that the normal vectors belonging to all net plane sets run through all directions in the half space successively. The XRTM technique has certain advantages compared to other X-ray diffraction methods (e.g. Kossel technique) with regard to informational content and high accuracy. It can thus be considered a global novelty. This method can be optimally used for an unlimited range of substances due to the free choice of wavelength and the fact that it requires no vacuum. The intensity-to-background ratio is extremely high in comparison to the Kossel technique. A further advantage is the possibility of selective "adjustment" of reflexes at high Bragg angles. Therefore, this technique can be applied for a wide range of problems in materials diagnostics, e.g.: high-accuracy determination of crystallographic orientations (for example small grain boundary angles of rotation and tilt angles ≥0.02°), dislocation density determination, determination of decrease in symmetry, high-accuracy determination of lattice constants ($\Delta a/a \leq 10^{-5}$), precision determination of interplanar spacings (local stresses/strains ($\Delta d/d \leq 10^{-5}$) and phase identification in microregions.

P12.01.004 X-RAY OPTICS FOR LABORATORY SOURCES. M. Kunz, H. Reifler, G. Böttger, R. Miletich, A. Friedrich, Labor für Kristallographie, ETH Zentrum, CH-8092 Zürich and P. Pattison, Institut de Cristallographie, Université de Lausanne, CH-1015 Lausanne.

The quality of lab-source X-ray beams can be improved without loss of intensity by the use of some simple X-ray optics. We present the combination of a Si(111)-Fankuchen monochromator with a pair of mirrors mounted on a sealed-tube 4-circle diffractometer.

A horizontally bouncing Si(111) monochromator selects only a narrow segment of the highly divergent X-rays generated by a Mo-tube, thus creating a highly parallel and monochromatic beam. Together with a small Darwin width of 4'', the virtual absence of mosaic spread of such a monochromator–causes an intensity loss of about 80% on a 0.1 mm sample compared to a standard pyrolitic graphite (002) monochromator. An additional intensity loss is created by the need to use only Kα1 radiation due to the horizontal monochromator- and diffraction-geometry. This loss can be compensated by a surface mis-cut of 4° with respect to the diffraction planes. Such a 'Fankuchen monochromator' causes a compression of the beam and thus an intensity gain in the diffraction plane.

In order to obtain additional intensity on the sample, a pair of horizontally tapered mirrors will replace the standard 0.3mm collimator. Using a Cr coating as reflecting surface and a taper of 3 mrad causes an optimal intensity gain of a factor of 5 on a 0.1 mm diameter sample when compared to a 0.3 mm collimator.

With this combination of Fankuchen monochromator and X-ray mirrors we are thus able to decrease divergence and improve monochromaticity of a Mo sealed tube X-ray source. This will further improve the accuracy of measurements of equation of states as a function of pressure and temperature as well as the quality of diffracted intensities.

P12.01.005 REMOTE CONTROL FOR SINGLE CRYSTAL DIFFRACTION IN MICROGRAVITY. James F. Fait, IMCA-CAT, Illinois Institute of Technology, 3300 South Federal St, Chicago, IL 60616 USA.

A single crystal diffraction system has been designed for use in the microgravity environment of the International Space Station. Control of the diffraction experiment by earth based scientists is a necessary requirement of the instrument. A protocol and software for remote control of a commercial CCD area detector and the associated goniometer and generator has been developed. Health and Status for the entire system is maintained and sent in a heartbeat message, and detailed status is mirrored both on the data collection computer and at the ground station. Details of the diffraction experiment are relayed to a local control system to be forwarded to the ground station, and the frame data is forwarded to the Ground Science Station for display. Local control of the system via a Crew Interface Port is available, as well.

The design criteria and the implementation of the control system will be explained, as well as examples of more conventional uses for this control system.

P12.01.006 NIST RUBY SPHERES AS SRM FOR DIFFRACTOMETER ALIGNMENT. T. Siegrist, Bell Laboratories, Murray Hill, NJ 07974 USA, and Inorganic Chemistry, Lund University, Sweden; W. Wong-Ng, M. Levenson, J. Armstrong, L.P. Cook, NIST Gaithersburg , MD 20899 USA; E.J. Gabe and G. Enright, SIMS, NRC, Ottawa, Canada, K1A 0R6; L. Finger, Geophysical Laboratory, Washington DC 20015, USA; H. Evans, US Geological Survey, Reston, VA 22092, USA; G. DeTitta, Hauptman-Woodward Medical Research Institute, Buffalo, NY 14203, USA, and C.R. Hubbard, Oak Ridge National Laboratory, Oak Ridge, TN 37831, USA.

X-ray structural determinations using automatic data collection and structure solution schemes require accurate initial cell parameter data. A lattice parameter reference standard is critical for alignment of single crystal diffractometers. Small ruby spheres have proven to be an excellent reference material. The high hardness of ruby allows the grinding of 150μm diameter spheres, which produce strong reflections at high angles for copper as well as for molybdenum radiation. From centred reflections at high angles, high precision lattice parameters can be obtained.

A series of 42 rubies were measured on three Enraf-Nonius CAD-4 and a Picker diffractometer. The data were corrected for thermal expansion and for refraction. The average unit cell parameters obtained are $a = 4.76080 \pm 0.00029$ Å (expanded uncertainties), and $c = 12.99568 \pm 0.00087$ Å. Five different samples of powdered rubies were also measured on a Guinier camera, giving good agreement with the values obtained from the single crystal spheres, $a = 4.76093 \pm 0.00031$ Å, and $c = 12.9959 \pm 0.0023$ Å.

P12.01.007 MICROFOCUS X-RAY TUBE AND INTER-CHANGEABLE FOCUSING OPTICS: ACHIEVEMENTS NOW AND FUTURE PROMISE: U.W.Arndt and A.C.Bloomer, MRC Laboratory of Molecular Biology, Hills Rd, Cambridge CB2 2QH, UK

Data will be presented from the novel MicroSOURCE X-ray generator [1] installed in our laboratory with ellipsoidal specularly reflecting mirrors. We have studied the performance

of both the tube [2] and the mirrors [3]. Results are compared with those expected theoretically.

Diffraction data from proteins show the power of this device, especially for smaller crystals. Suitable choice of mirror enables the size and divergence of the X-ray beam to be altered readily to match the different requirements of successive samples. Present performance is limited by imperfections in the mirrors; improved mirrors are now in production. Other types of mirrors, such as multi-layer optics, and mirror arrangements, are under consideration. Higher output from the tube is confidently expected with clear developments which are already in progress. The modular nature of this system enables simple incorporation of such changes on-site in a laboratory setting.

For crystals of sizes 300 micron or less, needing a small well collimated beam with low divergence, the output from this X ray tube running at 24 watts (i.e. 48kV and 0.5mA) the flux is similar to that available from much larger and more complex rotating anode generators. The relative performance of the microfocus tube and mirror system becomes increasingly advantageous with the study of ever smaller crystals.

[1] Generator and mirrors supplied by Bede Scientific Instruments Ltd, Durham, UK.
[2] U.W.Arndt, J.V.P.Long, and P.Duncumb, (1998). A micro-focus X-ray tube with focusing collimators. , J. Appl. Cryst. 31, (6), pp.936-944.
[3] U.W.Arndt, P.Duncumb, J.V.P.Long, L.Pina, and A.Inneman, (1998). *Focusing mirrors for use with microfocus X-ray tubes.* ,J. Appl. Cryst. 31, (5), pp.733-741.

P12.01.008 BEAMLINE ID14 EH2 FOR MACRO-MOLECULAR CRYSTALLOGRAPHY AT THE ESRF. E. P. Mitchell, H. Belrhali, W. P. Burmeister and S. Wakatsuki, European Synchrotron Radiation Facility, BP-220, F-38043 Grenoble Cedex, France and S. McSweeney, European Molecular Biology Laboratory, Grenoble Outstation c/o ILL, BP-156X, F-38042 Grenoble Cedex, France.

Beamline ID14 [1] at the ESRF is a dedicated resource for protein crystallography. There are a total of four stations planned on the high-b undulator section, one of which is ID14 EH2. The radiation sources for the beamline are presently a 23mm undulator, peak output at 13300keV, and a tunable 42mm period undulator. X-ray beams for the side stations are produced using the (111) reflections from three thin transparent monochromator diamond crystals positioned in the white beam and the straight through beam provides X-rays for the final station.

Station EH2 is a fixed energy beamline (0.932Å), using either Laue or Bragg synthetic diamond crystals and a planar Ge (220) crystal to bring the beam back parallel with the straight through beam. The beam is focused onto the sample position with a 35cm long rhodium coated fixed radii toroidal mirror.

The experimental hutch is equipped with a CCD detector (X-Ray Research 160mm, 3.5 second read out for 2048 x 2048 pixels) and a single axis phi spindle goniometer. The goniometer has motorised crystal alignment axes to allow automatic and remote positioning of samples.

The station is presently (December 1998) undergoing commissioning and limited user operation is expected in Spring 1999. To date satisfactory data has been collected from tetragonal lysozyme crystals in unfocused mode on an image plate system.

1. S. Wakatsuki, H. Belrhali, E. P. Mitchell, W. Burmeister, S. M. McSweeney, R. Kahn, D. Bourgeois, M. Yao, T. Tomizaki and P. Theveneau (1998). J. Synchrotron Radiation 5, 215-221.

P12.01.009 THE SOFT X-RAY SIX-CIRCLE DIFFRACTOMETER FOR SCATTERING / DIFFRACTION. C. K. Chen , C. H. Chung, C. H. Shu, Y. R. Lee, and S. L. Chang, Department of Physics, National Tsing Hua University, Hsinchu, Taiwan 300, R. O. C. Y. C. Jean and K. Y. Liu, Synchrotron Radiation Research Center, Hsinchu, Taiwan 300, R.O.C.

A six-circle soft x-ray diffractometer with κ-φ geometry has been constructed and commissioned with 1-9 Kev DCM (Double Crystal Monochromater) beam line at Synchrotron Radiation Research Center. The Fifty degree inclined κ-axis provides more degree of freedom and momentum coverage in reciprocal lattice space, as specially designed. The diffractometer is usually operated in high vacuum chamber, because soft x-ray is strongly absorbed by atmosphere. Both sphere errors and angular positional errors have been verified within the values of specification. Four experiments, including powder diffraction, θ-2θ scan, reflectivity of multi-layer thin films, and multiple diffraction, will be discussed. All experiments have been done at the vacuum of 10^{-6} torr. The quartz standard powder, zeolites, Ti_2O_5 / SiO_2 /Zerdur multi-layer thin films, and Si(111) single crystal are investigated. The excellent capability of the diffractometer in characterizing both mesoscopic and microscopic materials structure analysis is shown.

W. Jark and J. Stohr, Nucl. Instrum. Methods Phys. Res. **A266**, 654-658, (1988)
Y. Fujii, K. Yoshida, T. Nakamura, and K. Yoshida, Rev. Sci. Instrum. **68**, 1975-1979, (1997)
C. Kao, J. B. Hastings, E. D. Johnson, D. P. Siddons and G.C. Smith, Phys. Rev. Lett. **65**, 373, (1990)

P12.01.010 SYNCHROTRON DIFFRACTION WITH VARIABLE WAVE LENGTH FOR INVESTIGATIONS OF SEMICONDUCTOR HETEROSYSTEMS R.M.Amirzhanov, A.V. Kolesnikov, M.A.Revenko,E.M. Trukhanov [1], S.G. Nikitenko [2], [1] Institute of Semiconductors Physics, 630090, Novosibirsk, Russia, [2] Institute of Catalysis, 630090, Novosibirsk, Russia.

The results of diffraction investigations of semiconductor heterosystem structure using the variable wave length of the incident synchrotron beam are presented. For such kind X-ray investigations, the wave length becomes constant, but the angle between the incident beam and the sample surface is changed. As a rule, the rocking curves obtained from semiconductor layer systems contain two or more peaks, and the angular distances between the peaks permit us to analyse the heterosystem structure state. This state can be pseudomorphic or plastically relaxed depending on the density of misfit dislocations. The advantageous in measuring of crystal lattice distortions and superlattice structure parameters associated with using the synchrotron radiation are demonstrated. The proposed method is potentially suitable for in situ diffractometry registrations during the molecular beam epitaxial growth due to the angle of beam incidence is constant and the sample remains immobile. The formulas for determination of tetrahedral and rhombohedral distortions of an epitaxial heterosystem from data of spectral rocking curves are presented. The nature of rhombohedral distortions are discussed for the first time. The main structural parameters of superlattices are also determined from the mentioned spectral data. The experimental results are obtained for semiconductor systems GaAlAs/GaAs grown by molecular beam epitaxy.

P12.01.011 ROTATED-INCLINED FOCUSING MONOCHROMATOR FOR PROTEIN CRYSTALLOGRAPHY. Nobuhisa Watanabe[1], Mamoru Suzuki[1], Yasuo Higashi[2] and Noriyoshi Sakabe[3,] [1]Photon Factory, Inst. of Materials Structure Science, High Energy Accelerator Research Org., Tsukuba, Japan, [2]Mechanical Engineering Center,High Energy Accelerator Research Org., Tsukuba, Japan, and [3]Tsukuba Advanced Research Alliance, Univ. of Tsukuba, and Foundation for Advancement of International Sciences,Tsukuba, Japan.

A new single-crystal focusing monochromator for protein crystallography has been developed. In order to achieve simultaneous tuning of the beam demagnification rate and the radius of curvature for focusing over a wide wavelength range, the surface of an inclined monochromator was cylindrically bent.The monochromator is able to tune these two parameters simultaneouslywith a single rotation of the crystal about the azimuthal axis. A new monochromator incorporating this idea has been developed for beamline BL6B at the Photon Factory. The monochromator was designed for use in the wavelength range 0.87 to 1.90 Å and beam focusing was tested at wavelengths of 1.04, 1.38 and 1.74 Å. A well compressed and focused beam was obtained at all three wavelength by rotation about the azimuthal axis only. Horizontal intensity profile of the focused beam with the azimuthal axis rotation at 1.38 Å is shown in the figure.The monochromator could focus the X-ray beam to less than 0.8 mm FWHM in the horizontal direction.

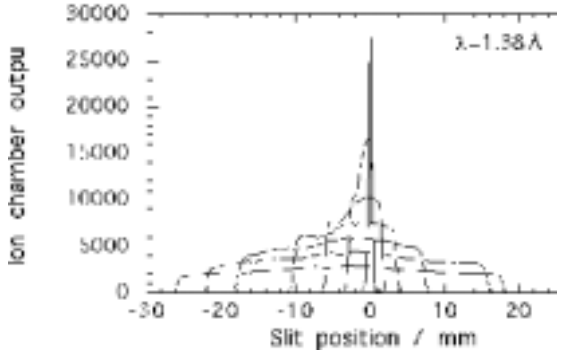

P12.01.012 PROGRESS TOWARDS COLLABORATORY SOFTWARE FOR MACROMOLECULAR CRYSTALLOGRAPHY AT A SYNCHROTRON BEAMLINE. R.M. Sweet and J.M. Skinner, Biology Department, Brookhaven National Laboratory, Upton, NY 11973, sweet@bnl.gov

Development of software tools to allow collaboration by remote scientists will help to drive this golden age for synchrotron macromolecular crystallography (PX). The development of MAD phasing and crystal freezing, new area-sensitive detectors, flexible diffractometers, and good software are responsible for an unprecedented wave of productivity. A collaboration between the Biology Department and the National Synchrotron Light Source aims to provide hardware, software tools, methods, and personnel to provide new resources for PX at Brookhaven.

Several possible uses for collaboratory software are to allow the professor at home to help his students at the beamline to make tactical decisions about data collection, to allow workers at home to carry some of the burden for data reduction and monitoring of data collection, to assist local beamline scientists in monitoring and tutoring student operators, and possibly to allow complete data collection from a remote site with a technician mounting specimens at the synchrotron.

The principal collaboratory software tool is a Java-based browser program. The current status of the experiment is displayed, including the sweep of data chosen, the status of the x-ray ring and beamline alignment, and details about the most recent image taken. Controls exist that allow rudimentary control of the beamline and data-collection apparatus from the Java applet.

A VRML/Java tool has been constructed that can be used either to simulate the data that would be collected with a particular data sweep, or to display the data being measured at a moment in time at the beamline. Primitive data are shown in one color; those generated by space-group symmetry appear in another.

The Biology/NSLS collaboration at Brookhaven is funded by the OBER and OBES of the US Dept. of Energy, and by grants from the NIH and NSF.

P12.01.014 NEW SYNCHROTRON RADIATION BEAMLINE AT CHESS. D.H. Bilderback[1,2], H.D. Abruna[3], J.D. Brock[2], B.H. Cooper[4], K.D. Finkelstein[1], E.F. Fontes, Jr. [1], S.M. Gruner[1,4], R.L. Headrick[1], S. W. Kycia[1], C.K. Ober[5], Q. Shen[1,5], K.W. Smolenski[1]. [1]CHESS, [2]School of Applied & Engr. Physics, [3]Dept. of Chemistry and Chemical Biology, [4]Dept. of Physics, [5]Dept. of Materials Science & Engr., Cornell University, Ithaca, New York, 14853.

A new wiggler beamline is to be constructed at the CHESS laboratory over the course of the next 2 years. The ultra-high flux x-ray beamline, called G-line, will serve both Cornell faculty and general CHESS users. The new facilities will be contained in a one floor, 3000 ft^2 (300^2 m) partially underground building. Three stations in tandem (two of which can operate simultaneously) will use the x-rays to study dynamically evolving materials, including thin film growth, patterned surfaces, electrochemical interfaces, polymers, liquid crystals, biomaterials, and systems with novel electronic properties. A new 49-pole wiggler will feed both the G-line (from positrons) and the present CHESS A-line (from electrons) which will undergo further upgrade as well. The wiggler will have a 15 keV critical energy during 5.3 GeV, 500 ma/beam operation of CESR. The design, construction, and operation of the new G-line will occur with the help of Cornell faculty members, CHESS, and the Cornell Center for Materials Research. A completion date of 2001 is anticipated.

We also describe very preliminary plans for a possible dedicated CHESS II ring in the context of a larger long-range plan to build a new dual-bore collider for B-meson physics with 3 A circulating currents in the same tunnel as the present CESR machine. CESR would then become dedicated to producing synchrotron radiation.

P12.01.015 THE CANADIAN LIGHT SOURCE. J. Wilson Quail[1], Louis T.J. Delbaere[2], Emil L. Hallin[3], Barry Hawkins[4], Ronald G. Cavell[5] & Dennis M. Skopik[3]. [1]Dept. of Chemistry, University of Saskatchewan, Saskatoon, S7N 5C9 Canada, [2]Dept. of Biochemistry, University of Saskatchewan, Saskatoon, S7N 5E5 Canada, [3]Saskatchewan Accelerator Laboratory, University of Saskatchewan, Saskatoon, S7N 5C6 Canada, [4]UMA Projects, Saskatoon, S7H 0V1 Canada, [5]Dept. of Chemistry, University of Alberta, Edmonton, T6G 2G2 Canada

For over eight years the Canadian Institute for Synchrotron Radiation (CISR) has been working to establish a synchrotron radiation facility in Canada. In 1996, after site visits by an international evaluation team to consider two proposals for a Canadian Light Source (CLS), the CISR endorsed the recommendation of the evaluation committee that the CLS be constructed at the University of Saskatchewan in Saskatoon. Funding for the CLS will be finalised by April, 1999 and construction will begin in the summer of 1999, with completion within 5 years. The CLS will be a 2.9 Gev 3rd generation storage ring using an existing 300 Mev linear accelerator at the Saskatchewan Accelerator Laboratory as an injector. Twelve beam lines will be part of the initial construction, including two beamlines for protein crystallography. There will be capacity for over 60 beamlines in the facility. A website has been created (http://cls.usask.ca/) to provide information about the Canadian

Light Source. Details of the design of the synchrotron and the beamlines will be described in the poster.

P12.01.016 SAMPLE ENVIRONMENTS FOR THE CURVED IMAGE-PLATE DETECTOR ON STATION 9.1 AT THE SRS DARESBURY. M.A. Roberts, E.J. MacLean and G. Bushnell-Wye, CLRC Daresbury Laboratory, Daresbury, Warrington, Cheshire WA4 4AD, UK, M. Ellerby, W.A. Steer and J.L. Finney, Department of Physics and Astronomy, University College London, Gower Street, London WC1E 6BT, UK.

The development of the curved image-plate technique for X-ray diffraction that we [1, 2] and others [3, 4] have undertaken has enabled data to be collected in minutes opposed to hours, since a complete diffraction image is collected in a single exposure. Integration around a significant fraction of the Debye-Scherrer cones means even further reductions in data collection times and enhanced visibility of weak features. This rapidity also broadens the scope for time-resolved experiments involving, for example, structural changes associated with thermal treatment of materials.

We have designed both a high temperature furnace (1125K) and a closed cycle helium cryostat (15K) that will allow data to be collected from a rotating capillary sample. A number of materials have been investigated as a means of characterising these environmental chambers and will be presented here.

1. G. Bushnell-Wye, J.L. Finney & J.D. Wicks (1995). Rev. Sci. Instrum. **97**, 557.
2. M.A. Roberts, J.L. Finney & G. Bushnell-Wye (1998). Mat. Sci. Forum **278-281**, 318.
3. F. Rizzo, S. Doyle & T. Wroblewski (1995). Rev. Sci. Instrum. **97**, 479.
4. B. Kennedy & J.Foran (1995). J.Appl. Cryst.

P12.01.017 THE FUTURE POWDER DIFFRACTION STATION AT THE SWISS SYNCHROTRON FACILITY (SLS). F. Fauth, B. Patterson, C. Brönnimann, Swiss Light Source, Paul Scherrer Institut, CH-5232 Villigen-PSI, Switzerland; P. Pattison, Université de Lausanne, CH-1015 Lausanne, Switzerland.

The Swiss Light Source (SLS) is a 2.4 GeV synchrotron radiation facility presently under construction in Switzerland [1]. The powder diffraction (PD) station is one part of the materials science beamline, which is also dedicated to computer microtomography and glancing-incidence X-ray techniques. The beamline insertion device is a 65-pole minigap wiggler (2 m long, magnetic gap=7.5 mm, B_{max} = 2T), implying E_{crit}=7.5 keV and K=9.2. The operating energy range extends from 5 to 40 keV. The beamline optics consist of a vertically collimating mirror, a sagitally double monochromator and a vertically focusing mirror. The focal lengths of the monochromator and second mirror can be adjusted to the position of the different experimental stations. The PD station is located at the 1:1 demagnification position (37m) of the beamline optics. Here, the initial vertical collimation and focusing yields a high energy resolution (0.014%) with a vertical FWHM-divergence of 0.23 mrad. The expected flux at 15 keV is 4.6 x 10^{14} photons/sec/($d\lambda/\lambda=10^{-3}$) into a focus of 0.5 x 0.5 mm^2. A high precision 2-circle θ-2θ diffractometer will allow high resolution powder-diffraction measurements using capillary and flat-sample holders. Texture and strain measurements will be possible by further using an Eulerian cradle. In parallel to a moveable scintillation detector (with and without analyzer crystal option), we wish to include a position-sensitive Si-microstrip detector covering a 60° angular range with high resolution (0.01°). Such a detector is under evaluation, and preliminary tests on a prototype have been performed under real experimental conditions at the Swiss-Norwegian Beamline of the ESRF. Results are presented here.The main challenges for this type of detector are signal-to-noise ratio at low photon energy and the electronic read-out of up to 20000 strips on time scale of milliseconds. First operation of the SLS is forseen in the summer of 2001.

1. see `http//www1.psi.ch/www_sls_hn` for further details

P12.01.018 X-RAY INSTRUMENTATION FOR BEAMLINES AT KURCHATOV SR SOURCE IN MOSCOW. M.V.Kovalchuk, S.I.Zheludeva, Yu.N.Shilin, V.V.Lider, O.P.Aleshko- Ozhevsky, D.M.Kheiker, E.M.Pashaev. I.G.Arutunian. A.V.Shubnikov Institute of Crystallography RAS, Leninsky pr., 59, 117333 Moscow, Russia.

We present six X- ray experimental stations that will be installed by the Institute of Crystallography at Kurchatov SR source in Moscow.

Station *"Protein Crystallography*" is designed for studies of atomic structures of macromolecular single crystals, namely, proteins, etc.

Station X- ray *"Structure Analysis*" is intended for studies of atomic structures and electron density of single crystals of organic and inorganic compounds.

Station "*High- precision X- ray Optics*" is designed for implementing modern high- resolving X- ray diffraction methods of investigation of real crystals and crystalline objects: triple-crystal diffractometry, X- ray standing wave method with recording fluorescence and secondary photoelectrons, surface diffraction, multibeam diffractometry. The station can be used in studies of different practically important objects, including semiconductor single crystals and heterostructures, multilayer structures, Langmuir- Blodgette films.

Station *"X- ray Crystallography and Material Science*" is aimed on high- precision structural studies of crystalline matter by X- ray multi- crystal topography and diffractometry: determination of dislocation and microdefect concentration and arrangement, mosaic structure parameters, deformation fields; investigation of diffuse scattering; characterization of heterostructures, superlattices, multilayers.

Station *"X- ray topography*" is designed for *in situ* ivestigations of real crystal structures using TV- system or photographic plate. Construction of the station permits to use various attachments for subjecting sample to high (low) temperature treatments, magnetic and electric fields, mechanical stresses, etc.

Station *"Photoelectron X- ray Standing Wave*" is intended to study structural perfection of crystal surface- bound layers using XRSW method with the detection of photo- and Auger electrons.

P12.01.019 THE DIFFRACTION EXPERIMENT: FROM PICOSECOND EXPOSURE TIME TO PICO-SECOND TIME RESOLUTION. B.P.Tolochko, O.V.Evdokov [1], A.N.Aleshaev, M.V.Fedotov, V.A.Kiselev, G.N.Kulipanov, P.V.Logachev, N.A.Mezentcev, S.I.Mishnev, I.Y.Protopopov, M.A.Sheromov [2], [1] Institute of Solid State Chemistry and Mechanochemistry, Kuteteladze 18, Novosibirsk, 630128, Russia, [2] Budker Institute of Nuclear Physics, Novosibirsk, 630090, Russia

For implementation of experiments with a nanosecond time resolution we use fast displacement of a electron beam in the storage ring by electromagnetic field impact [1]. The fast change of orbit of electrons results in displacement of a beam of synchrotron radiation. The parallel displacement of synchrotron radiation beam happens with a speed near 200 km/sec. It allows to conduct scanning a synchrotron radiation beam on a sample (or an angle). By establishing after a sample a positional sensitive X-ray detectors we received diffraction patterns with a time resolution equal to time between electrons bunches (250 nsec on VEPP-3

and 5 nsec on VEPP-4 and exposition time 1 nsec and 100 psec respectively). The described scheme used for research with a nanosecond time resolution the behaviour a crystal structure under fast external influence. We made theoretical estimations which shown a practical capability, of the
scheme at VEPP-4, which will allow to realise a beam scanning of synchrotron radiation with speed near 10000 km/s that will allow to receive a 10 picosecond time resolution (period between frames) and the same exposure time.

1. S.G.Nikitenko, B.P.Tolochko, A.N.Aleshaev, G.N.Kulipanov, S.I.Mishnev. J. DE PHYSIQUE IV, (Supplement au Journal de PhysiqueIII, 4), (1997),Vol. 7, C2, 549-552.

P12.01.020 BEAMLINE 14: THE NEW MULTIPOLE WIGGLER BEAMLINE FOR PROTEIN CRYSTALLOGRAPHY ON THE SRS. E. Duke, M. Wardell, M. Bailey, S. Buffey, S. Kinder, A. Grant, M. MacDonald, C. Nave. CLRC Daresbury Laboratory, Warrington, Cheshire. WA4 4AD. U.K.

Beamline 14 is a new multipole wiggler beamline on the SRS at Daresbury Laboratory. The insertion device, a 2.0T multipole wiggler magnet will provide radiation for two stations dedicated to protein crystallography. A description of the station components will be given. Preliminary results from the beamline commissioning will be presented.

P12.01.021 SEARCHING FOR THE BEST PROTEIN CRYSTALS: SYNCHROTRON-BASED MEASUREMENTS OF CRYSTAL QUALITY. Gloria Borgstahl [1], Eddie Snell [2], Henry Bellamy [3], Walter Pangborn [4], Chris Nielson [5], Andy Arvai [5], Jeff Ohren, [1] Matt Pokross [1], [1] Department of Chemistry, University of Toledo, Toledo, OH 43606-3390, [2] Marshall Space Flight Center, Huntsville, AL 35812, [3] Stanford Synchrotron Radiation Laboratory, CA, [4] Hauptmann-Woodward Institute, Buffalo, NY, [5] ADSC, Poway CA

We are developing X-ray diffraction methods to quantitatively evaluate the quality of protein crystals. The ultimate use for these crystal quality assessments will be to optimize crystal growth and freezing conditions to obtain the best diffraction data. We have combined super-fine phi slicing with highly monochromatic, low divergence synchrotron radiation and the ADSC Quantum 4 CCD detector at the Stanford Synchrotron Radiation Laboratory beamline 1-5 to accurately measure crystal mosaicity. Comparisons of microgravity- versus earth-grown insulin crystals using these methods will be presented.

P12.01.022 THE STRUCTURAL BIOLOGY CENTER AT THE ADVANCED PHOTON SOURCE. Gerd Rosenbaum, Randy Alkire, Norma C. Duke, Stephan L. Ginell, Frank Rotella, Ruslan Sanishvili, Rong-guang Zhang, and Andrzej Joachimiak, Center for Mechanistic Biology and Biotechnology, Argonne National Laboratory, Argonne, IL 60439 USA.

The Structural Biology Center (SBC) is a Collaborative Access Team funded by the U.S. Department of Energy that operates a national user facility for macromolecular crystallographic research at the Advanced Photon Source at Argonne National Laboratory. The SBC operates an insertion-device beamline, 19ID, and a bending-magnet beamline, 19BM. Each beamline is equipped with a fully tunable monochromator, collimator slits, high-precision sample and detector positioning systems, and high-resolution x-ray optics designed to deliver a stable, intense, highly focused x-ray beam with low angular divergence onto crystal samples. The intensity of x-rays on the crystal is monitored with a beam-intensity monitor. The monochromator is designed to reach most absorption edge energies used in macromolecular crystallography. For MAD experiments the absorption spectra are monitored with a fluorescence detector. Crystals are mounted on a miniaturized Kappa goniostat, aligned using dual video cameras, and maintained at 100K with a liquid nitrogen cryosystem. Diffraction images are collected at high speed with a 3x3 mosaic (3072 x 3072 pixels) CCD area detector that has been optimized for short exposures. Data are collected and processed efficiently with either HKL2000 or d*TREK which take advantage of high-throughput computing environment. Highlights of recent data collection will be presented and the general user program will be introduced.

This work was supported by the U.S. Department of Energy, Office of Biological and Environmental Research, Under Contract W-313-109-ENG-38.

P12.01.023 THE BIO-CRYSTALLOGRAPHY BEAMLINE (BL41XU) AT SPRING-8 N. Kamiya [1], M. Kawamoto [2], Y. Kawano [1], and S. Park [1], [1] RIKEN Harima Institute, The Institute of Physical and Chemical Research (RIKEN), Mikazuki-cho, Mihara, Sayo, Hyogo 679-5143, Japan, [2] Japan Synchrotron Radiation Institute, Mikazuki-cho, Mihara, Sayo, Hyogo 679-5143, Japan.

The Bio-Crystallography beamline1) dedicated for macromolecular crystallography (BL41XU) was opened at SPring-8 on October in 1997 for public users from domestic and overseas countries. The X-ray source is an invacuum-type standard undulator at SPring-8, from which highly brilliant X-rays is available as the fundamental and third-harmonics emissions in a wide energy range of 7-38 keV. One of the most serious problems for beamline commissioning was high heat-load over 10 kW from the undulator, and the problem was overcome by using a standard monochromator system at SPring-8, a rotated-inclined double crystal monochromator (RIDCM) with a pin-post water cooling mechanism. The RIDCM works as the first cooling optics on which the high heat-load is deposited. The monochromatized beam from the RIDCM is focused by two X-ray mirrors independently in horizontal (H) and vertical (V) directions. The focal spot size was about 200 (H) x 300 (V) micrometer at a storage ring current of 70 mA. On this condition, the photon flux was measured to be 2 x 10^12 at an X-ray energy of 12.4 keV. The highly brilliant X-rays around 12.4 keV were very useful for accurate data collections from small crystals less than 100 micrometer with relatively large unit cells over 200 A. After the beamline commissioning for automatic change of X-ray energy, the multiple isomorphous replacement technique with optimized anomalous scattering (MIROAS) has just been available for new structure determinations, which is an objective for this beamline construction. Because some imperfection remains in the silicon crystal of RIDCM at fabrication of the pin-post structure, unfortunately, the energy resolution of BL41XU is at present about 5 x 10^-4 and not optimized yet. Another remarkable feature of BL41XU is an availability of high-energy X-rays up to 38 keV. As well known, barium is a main component of imaging plate (IP) phosphor. Data collections on barium K-edge, 37.6 keV, and those around Xenon K-edge, 34.6 keV, are tested using IP detectors.

1) N. Kamiya et al., Rev. Sci. Instrum. 66, 1703 (1995).

P12.01.024 STRUCTURE REFINEMENT BASED ON INTENSITIES OF LAUE SPOTS OBTAINED BY POLYCHROMATIC SYNCHROTRON RAD. K.Ohsumi [1] T.Osaka [2] K.Hagiya and M.Ohmasa [3] [1] Inst. of Materials Structure Science, 1-1 Oho, Tsukuba, Ibaraki, Japan [2] Faculty of Science, Unv. Tokyo [3] Faculty of Science, Himeji Institute of Technology, Kamigoori, Akou, Hyougo, Japan

Intensities of Laue spot obtained by polychromatic synchrotron radiation(SR) are represented by the equation below. Those of each Bragg reflection are modified not only by Lp factor, absorption (A(l)) and extinction(E(l)) effects but also a spectrum of incident SR (Io(l)) and quantum efficiencies of a detector with respect to wavelengths (P(l)).

A product of the last two factors at the sample position could be expressed as an Gaussian function indicated below, which is confirmed by modifying the spectrum of SR of the radiation point at the bending magnet with absorption due to Be windows and vacuum path.

Io(l)a1(J(l)) =exp(-a (l-lm)2)(J(l))

In the process of a structure refinement, the IoP(l) is optimized simultaneously together with the structural parameters, that is the structural parameters are determined based on the IoP(l). But their parameters, as, al and lm, are optimized in different values for each refinement.

We have examined whether errors in measurement of diffracted intensities much affect the parameters of structure or those of IoP(l) using five Laue intensities, free from absorption effect, of molybdenum(Mo) sphere with a diameter of 8 mm. As the result, the errors change the parameters of IoP(l) but do not alter those of structure significantly, taking into account of their standard deviations.

K.Ohsumi, K.Hagiya and M.Ohmasa: J. Appl. Cryst.,(1991).24, 340-348.

P12.01.025 CRYSTALLOGRAPHY ON DIAMOND. A PROPOSED 3RD GENERATION SYNCHROTRON RADIATION SOURCE IN THE UK. C. Nave, S.L. Bennett, S.P. Collins, SRS Facility, CCLRC Daresbury Laboratory, Daresbury, Warrington WA4 4AD, UK

DIAMOND is a proposed new synchrotron radiation source to be built in the United Kingdom. The machine could be equipped with a variety of insertion devices including multipole wigglers, undulators and wavelength shifters. These will provide X-rays covering a wide energy range, suitable for crystallographic investigations in the field of biology, chemistry, physics, material science and surface science. A description of the machine will be given, together with examples showing the type of x-ray beamlines which could be constructed to cover crystallographic requirements in these areas of science.

P12.01.026 AUTOMATIC IP DATA COLLECTION SYSTEM FOR TIME-RESOLVED PROTEIN CRYSTALLOGRAPHY USING MONOCHROMATIC SR XRAYS. N.Sakabe[1,5,6], K.Sakabe[1,2,6], Y.Miyamoto[1,6], K.Sasaki[2,6], T.Higashi[3,6], J.Miyahara[4], N.Igarashi[5,6], M.Suzuki[5,6], N.Watanabe[5,6]. [1]FAIS,305-005,Japan, [2]Nagoya Univ.,464-8601,Japan, [3]Rigaku corp., 186-8603,Japan, [5]KEK,PF,305-0801,Japan, [6]Guest researchers of TARA Sakabe project in TARA, Tsukuba Univ.,305-8577,Japan.

We construct a new type of on-line data collection system for installation at BL6C at the PF. This system consists of a Weissenberg type camera with a rotation mechanism to change the recording frames of a cylindrical IP cassette having a radius of 400mm,an image reader equipped with five reading heads, an eraser, a cassette transportation mechanism, a control console, computers and a data server.In order to collect a full data set continuously, two IP cassettes are employed. While the images recorded on one cassette are being read, diffraction images are recorded on the other cassette automatically. A large IP is stuck onto the inside of the IP cassette. The cassette has 36 small rectangular holes at equal intervals along the circumference to allow the primary beam to pass(Sakabe et al. J. Synchrotron Rad.(1997)4,136-146).The exposure area (frame) on the IP can be selected by upper and lower adjustable screens. The frame exchange time is only 1sec and reading time is 8 min. Normal exposure time is 1 min using 1A X-ray at the PF. Thus, a full set of the data (18 frames)at 2.9A resolution can be recorded within 19 min. However the exposure time reduces 1 sec using very brilliant SR X-ray such as Spring8 BL41XU. Thus we will be able to record the full set of data within40sec.In this condition this system can be applied to time-resolved protein crystallography Some applications will be presented. This work was supported by JSPS-RFTF96R14501.

P12.01.027 DESIGN OF A HIGH-PRECISION, MONOCHROMATIC BEAM POSITION MONITOR FOR 5-25KEV SYNCHROTRON RADIATION. R.W.Alkire, Gerold Rosenbaum [1], G. Evans [2], [1] Center for Mechanistic Biology and Biotechnology, Argonne National Laboratory, Argonne, IL, 60439, USA, [2], MRC Laboratory of Molecular Biology, Hills Road, Cambridge, CB2 2QH, England.

To take full advantage of the highly intense undulator radiation and very low source emittance available at the Advanced Photon Source, a novel monochromatic beam position monitor with 1-2micron sensitivity has been developed. Design consists of four PIN diodes positioned upstream of a 0.5micron thick metal foil placed in the X-ray beam. X-rays absorbed by the metal foil generate fluorescence radiation, which is then detected by the diode array. Using conventional difference over the sum techniques for vertical and horizontal diode pairs, two-dimensional position information is obtained. The device is compact, inexpensive to construct, operates in vacuum and has a working range of 8mm x 10mm that can be expanded with design modifications. Although optimized for use in the 5-25keV energy range, the upper limit can be extended by changing metals and/or adjusting foil thickness. This device is currently in use at the Structural Biology Center, beamline 19ID, at the Advanced Photon Source.

P12.01.028 ON THE ADVANTAGES USING AN AREA DETECTOR FOR THE MEASUREMENT OF TRIPLET PHASES FROM PROTEIN CRYSTALS. R. Müller, E. Weckert, J. Zellner, Institut für Kristallographie, Universität Karlsruhe (TH), D-76128 Karlsruhe, Germany and M. Drakopoulos, ESRF, F-38043 Grenoble, France.

It has been shown [1] that in principle a protein structure of 15kDa can be solved by using measured triplet phases [2]. About 850 triplet phases were determined experimentally.

Because of radiation damage at maximum 150 triplet phases can be measured from one crystal. At the current state of experiment about 5 triplet phases per hour can be determined (synchrotron radiation). Therefore a sufficient number of low mosaicity crystals is needed.

A new method of measuring many triplet phases simultaneously using an area detector was suggested and, therefore, the rate of measured triplet phases was supposed to be increased drastically [3].

In this method the interference profiles of several primary reflections with one centered secondary reflection are collected simultaneously. Up to now only experiments in one GaAs crystal have been published. Our goal was to test the efficiency of this method on protein crystals.

The interference profiles might be affected by: (i) neighbouring three-beam cases, (ii) scaling problems, (iii) mosaicity.

The method has been simulated by using a scintillation detector. The lack of angular resolution of an area detector, which integrates the rocking curves of the primary reflections, would cause the even low mosaicity to influence the interference profiles seriously so that many profiles become uninterpretable.

[1] Weckert, E., Hölzer, K., Schroer, K., Zellner, J., Hümmer, K. *Acta Cryst.* (1999), D, submitted. [2] Weckert, E., Hümmer, K. *Acta Cryst.* (1997), A**53**, 108-143. [3] Shen, Q. *Phys. Rev. Lett.* (1998) **80**, 3268-3271.

P12.01.029 PROPOSED CRYSTALLOGRAPHIC BINARY FILE AND IMAGE-SUPPORTING CIF WITH API AND DICTIONARY. H. J. Bernstein [1], P. J. Ellis [2], A. P. Hammersley [3], A. J. Howard [4], J. W. Pflugrath [5], R. M. Sweet [6], J. D. Westbrook [7], [1] Bernstein + Sons, Bellport, NY, USA, [2] Stanford Synchrotron Radiation Laboratory, SLAC, Stanford, CA, USA, [3] European Synchrotron Radiation Facility, Grenoble, CEDEX, FR, [4] Center for Synchrotron Radiation Research and Instrumentation, IIT, Chicago, IL, USA, [5] Molecular Structure Corporation, The Woodlands, TX, USA, [6] Biology Dept., Brookhaven National Laboratory, Upton, NY, USA, [7] Dept. of Chemistry, Rutgers, The State University of New Jersey, Piscataway, NJ, USA

The Crystallographic Binary File (CBF) format is a complementary format to the Crystallographic Information File (CIF), supporting efficient storage of large quantities of experimental data in a self-describing binary format. The Image-supporting Crystallographic Information File (imgCIF) format is a proposed pure-ASCII extension to CIF to assist in ASCII debugging and archiving of CBF files. It also will allow for convenient and standardized inclusion of binary images such as maps, diagrams, and molecular drawings into publication CIFs. It is our expectation that, for large images, the raw binary CBF format will be used both within laboratories and for interchange among collaborating groups. For smaller chunks of binary data either format should be suitable, with the ASCII imgCIF format being more appropriate for interchange and archiving. The initial aim is to support efficient storage of raw experimental data from area-detectors (images) with no loss of information compared to existing formats. A DDL2-based dictionary of extensions to the mmCIF dictionary defining imgCIF/CBF has been developed. The dictionary includes tags to define the structure of arrays of image data and the relationship between the images and the parameters of a data collection. A software library to support imgCIF/CBF has been developed. CBFlib is a library of ANSI-C functions providing a simple mechanism for accessing Crystallographic Binary Files (CBF files) and Image-supporting CIF (imgCIF) files. The CBFlib API is loosely based on the CIFPARSE API for mmCIF files.

P12.01.030 USE OF A MICROSOURCE X-RAY TUBE AND GENERATOR WITH A FOUR-CIRCLE DIFFRACTOMETER. Paul Champkin and William Clegg, Chemistry Department, Bedson Building, University of Newcastle-Upon-Tyne, Newcastle-Upon-Tyne, NE1 7RU, U.K.

A four circle Stoe diffractometer is being fitted with a new type of X-ray generator and tube manufactured by the microsource division of Bede Scientific Instruments Ltd. This hardware will replace an existing generator and brings with it many new advantages.

The new compact, low power, high brightness X-ray generator and tube with focussing optics(1) uses X-ray radiation from a copper target with intensity comparable to that of a rotating anode source. With a power consumption of only tens of watts (compared to around 2-3kW for a normal generator) this generator uses a microfocus of the electron beam onto the target along with ellipsoidal mirrors for collection and concentration of the generated X-rays to bring about this outstanding efficiency.

Once in operation this setup will allow for the study of small, weakly diffracting samples that before may have called for synchrotron radiation. The customisation work involved in fitting the new equipment along with some preliminary results will be reported. The potential use of the new generator with other single crystal diffraction equipment will also be discussed.

(1) U.W. Arndt, J.V.P. Long and P. Duncumb, J.Appl.Cryst. (1998), 31, 936-944.

P12.01.031 MACROMOLECULAR CRYSTALLOGRAPHY WITH A 7.5 T WIGGLER ON A 1 GEV SOURCE. T. Rabedeau[1], P. Kuhn[1], G.-A.Voss[2], E. Weihreter[3], & H. Winick[1] [1]SSRL Stanford, USA [2]DESY Hamburg, Germany, [3]BESSY Berlin, Germany

The majority of macromolecular crystallography (PX) experiments can be conducted effectively on low to medium energy storage rings equipped with high-field wigglers. For a typical protein crystal with 0.1-0.3mm transverse dimensions and 0.2° or greater mosaicity, the relevant measure of source performance is flux into the ~$(0.5\text{mm-mrad})^2$ sample acceptance phase space. Since this acceptance phase space is significantly larger than the ~0.05mm-mrad x 0.001mm-mrad source phase space of a typical undulator on a high energy, third generation storage ring, the sample does not require nor fully utilize the undulator brightness.

Consider a 13 pole, 7.5T wiggler on a 1GeV upgrade of BESSY-I (termed BESSY-Ia). Such a wiggler produces 1.1e13 photons/sec*0.1%bp in the sample acceptance phase space at 12keV for the ring parameters noted below. This compares reasonably to the performance of PX sources on many higher energy rings: 6.1e13 for the BW6 wiggler at HASYLAB, 7.1e12 for the BL9 wiggler at SSRL (1.7e14 with the SPEAR3 upgrade), and 5.4e12 for an NSLS bend magnet. The corresponding figure for an APS undulator A is 4.8e14.

This high useful flux from a low energy ring is achieved by using a super-conducting wiggler (Ec=5keV) on a high current ring designed to produce small beam dimensions at the source point. We have conducted a study of such a source, based on the BESSY-I 0.8 GeV storage ring. This ring will be closed at the end of 1999 due to BESSY-II being fully operational. We propose a modification of this ring to achieve the following parameters: 1.0 GeV, 0.7 A stored current, horizontal/vertical emittance 50/1.5 nm-radians, horizontal/vertical source dimensions and divergence's (1 sigma) at the wiggler location of 0.45/0.028 mm and 0.11/0.05 mrad. The lifetime is expected to be about 4 hr and can be extended by increasing the bunch length and/or the vertical beam size.

P12.01.032 THE SWISS LIGHT SOURCE PROTEIN CRYSTALLOGRAPHY BEAMLINE. C. Schulze-Briese, C. Broennimann, G. Heidenreich, H. Auderset, Q. Chen, G. Ingold, M. Janousch, M. Lange, C. Pradervand, M. Shi [1], U. Lienert, A.K. Freund [2], [1] Swiss Light Source at PSI, CH-5232 Villigen PSI, Switzerland, [2] European Synchrotron Radiation Facility, BP 220, F-38043 Grenoble Cedex, France

The SLS protein crystallography beamline is designed for the measurement of X-ray diffraction data from biological crystals with large unit cell dimensions as well as protein micro-crystals. It is fully MAD compatible and will be well suited for atomic resolution protein crystallography. Design and test of the main components - in-vacuum minigap undulator, decoupled, dynamically focussing optics and large area, fast read-out pixel detector - will be described in detail. SLS will be the first synchrotron which makes explicit use of the high harmonics from in-vacuum minigap undulators. The proposed undulator realisation and expected performance will be reported. The contradicting requirements of micro-focussing and high beam parallelism are overcome by the use of two dedicated diffractometers at 8:1 and 2.5:1 demagnification position. The flexibility of the optics allows the beam to be focussed at these

positions or to focus on the detector. The prototype components yielded a focal spot size of 15 µm x 25 µm and dynamical focussing was demonstrated. The energy range of 5 to 17.5 keV covers all relevant K- and LIII-absorption edges and the energy resolution or 0.02% compatible with the requirements of the MAD technique. The dedicated pixel detector is based on a silicon pixel sensor connected to an Application Specific Integrated Circuits (ASIC) read-out chip is under development in collaboration with the PSI High Energy Physics Group. It will combine fast frame rates and high dynamic range (*15 bit counter) on a large area. The analog and digital part of the pixel architecture as well as the bump-bonding were successfully tested. First photons on sample are expected in the fall of 2001.

P12.01.033 CHARACTERIZATION OF A LOW POWER X-RAY SOURCE FOR USE IN CRYSTALLOGRAPHIC DATA COLLECTION. Lance Weise [1], John Wall [2], Neil Loxley [2], Mark Taylor [2], Craig Smith [1], [1] Center for Macromolecular Crystallography, University of Alabama at Birmingham, Birmingham, Alabama, 35294-0005 USA, [2] Bede Scientific Ltd., Bowburn South Industrial Estate, Bowburn, Durham, DH6 5AD, United Kingdom

A microfocus X-ray source based on the work of Uli Arndt et al, and developed by Bede Scientific Ltd. was characterized in terms of intensity, divergence, spectral purity, and beam profile. The Bede Microsource was run at 25 to 30 Watts of power and utilized the unique Reflex ellipsoidal shaped mirror optic. A comparison was made to conventional rotating anode systems using a standard graphite monochromater, double focusing mirror systems, and a multilayer focusing system. X-ray diffraction data were collected from a number of protein crystals using a Bruker CCD area detector. The data were processed and reduced with the program SAINT. The results indicate the X-ray system and CCD detector combination gives results comparable to that which can be collected using conventional laboratory X-ray sources running at 4-5 kilowatts of power.

P12.01.035 BIOLOGICAL CRYSTALLOGRAPHY AT THE ADVANCED LIGHT SOURCE Gerry McDermott[1], Carl Cork[1], Li-Wei Hung[1], Keith Henderson[1], Natasha Khlebtsova[1], Trey Simmons[1], Howard Padmore [2], and Thomas Earnest [1], [1] Macromolecular Crystallography Facility at the Advanced Light Source, Physical Biosciences Division, Lawrence Berkeley National Laboratory, Berkeley, CA 94720, [2] Advanced Light Source Division, Lawrence Berkeley National Laboratory, Berkeley, CA 94720

The Macromolecular Crystallography Facility at the Advanced Light Source has been operational as a national user facility for biological crystallography since November, 1997, when the initial beamline was commissioned. This beamline was optimized as a high-throughput beamline for multiwavelength anomalous diffraction experiments. The MAD experiments benefit greatly from the low emittance and positional stability of the ALS which promote high energy resolution and lack of energy drift even between storage ring refills. To date over 200 users from more than 50 research groups have used this beamline. Two monochromatic beamlines are under construction, one of which will be built as a high-throughput, robotics-based beamline for Novartis Institute for Functional Genomics [Stevens, Schultz, Santarsiero]. Furthermore three more MAD beamlines are under development based on superconducting bending magnets as sources. We are also collaborating with LBNL and UCSD scientists and engineers to develop a massively-parallel pixel-array detector with high dynamic range and photon-counting capabilities. A scientific program concentrating on the structural biophysics of signal transduction and large biomolecular complexes takes full advantage of this technology and gives further scientific motivation to the development of instrumentation.

The Macromolecular Crystallography Facility at the Advanced Light Source is principally funded by the Office of Biological and Environmental Research of the Department of Energy with other funding from Amgen, Roche Biosciences, University of California at Berkeley, Lawrence Livermore National Laboratory, and the Genetics Institute.

P13.01.001 BACKGROUND REDUCTION BY A VACUUMCHAMBER FOR AREA DETECTORS. H.-G. Krane[1], A. Kirfel[1] and W. H. Morgenroth[2]; [1]Mineral.-Petrol. Institut, Universität Bonn, [2]Mineral.-Petrogr. Institut, Universität Hamburg, Germany.

Area detectors combined with intense X-ray sources suffer from a relatively high background due to their large aperture. Close to the primary beam, this background is further enhanced by air scattering. In order to avoid this unwanted effect, the sample can be mounted and investigated in a vacuumchamber [1]. An improved version was constructed and built for the HUBER 512 Eulerian cradle at HASYLAB beamline D3. The X-ray beam (≤ 1mm in diameter) enters the chamber through a collimator tube sealed into it. The scattering produced by the 75 µm Kapton foil entrance window is shielded by a 2 mm pinhole ending about 13 mm in front of the sample. The diffracted radiation leaves the chamber through a secondary 75 µm Kapton foil detector window of effectively 75 mm diameter. The beamstop catches the beam inside the chamber. For high temperature applications, the chamber can be equipped with a removable graphite furnace up to 1300 K at the sample position. A special vacuum seal provides free sample rotation about the Φ-axis. For $\omega = 2\Theta = 0^{\circ}$, also the χ-circle can be freely rotated. With the shortest sample-detector distance of 50 mm, it is possible to record reflections with scattering angles up to $2\Theta = 30^{\circ}$. Using $\lambda = 0.40$ Å, a (usually sufficient) data resolution of 0.65 $Å^{-1}$ can be achieved. Even for samples of low symmetry (e.g. monoclinic), all independent reflections can be recorded with one revolution of Φ at $\chi = 0^{\circ}$.The vacuumchamber was tested using a SMART-CCD-detector. The background is generally reduced and air scattering in the vicinity of the primary beam disappears after evacuation. The equipment is useful for the investigation of weak scattering phenomena such as diffuse scattering, superlattice reflections and structure determination of small samples, both at room and elevated temperatures.

[1] R. B. Neder et.al.: Z. Kristallogr. **211** (1996), 591.

P13.01.002 RAPID X-RAY DIFFRACTION MEASUREMENT AND STRUCTURE ANALYSIS USING MICRO STRIP GAS CHAMBER. H. Uekusa, Y. Ohashi, A. Ochi, T. Tanimori, Faculty of Science, Tokyo Institute of Technology, Tokyo 152, JAPAN.

Rapid X-ray diffraction measurement is an essential technique to realize the time-resolved observation of crystalline-state reactions. By using an accumulating type two-dimensional detector (IP or CCD), total measurement time can be cut down to a few hours or less in the laboratory system. However, to achieve a shorter time resolution of seconds or sub seconds, the use of a photon counting type two-dimensional detector is required.

Recently, MSGC (Micro Strip Gas Chamber) was developed for the rapid X-ray data collection. MSGC is a gaseous detector like MWPC, so it has both photon counting and two-dimensional imaging properties. The features of the detector are a large detective area of 10 x 10cm, a fine positional resolution of 100 micrometer and an excellent capability for high counting rate up to 10^7 cps by utilizing the fast data acquisition system. Thus

both positional and timing information can be stored for later image reconstruction and analysis.

X-ray diffraction measurement system consists of a MSGC detector, one axis goniometer and a laboratory X-ray generator was constructed in order to examine the ability of MSGC in X-ray crystallography. As the preliminary experiments showed the satisfactory accuracy and fast data acquisition speed, the diffraction data of the organic crystal were collected rotating the crystal continuously. The reciprocal space was constructed from the stored positional and counting data, and recognized reciprocal lattice points were easily indexed and integrated. The structure analysis using this intensity data gave the satisfactory results.

P13.01.003 AUTOMATED IMAGING PLATE DATA ACQUISITION FOR SMALL MOLECULAR CRYSTALLOGRAPHY. Tsuneyuki Higashi, Katsunari Sasaki, X-ray Research Laboratory, Rigaku Corporation, 3-9-12, Matsubara-cho, Akishima-shi, Tokyo 196-8666, Japan

Data collection on a four-circle diffractometer is highly automated. Together with the development of an easy-to-use structure analysis package, the technique of x-ray crystal structure analysis has been widely spread over many non-crystallographers but are interested in structures of small molecule compounds. However, imaging plate diffractometers are far from the automation.Even in the well-used data prcocessing package, users have to select functions in pull-down menus.We have developed an automated data-acquisition system for a Rigaku-Rapid Imaging Plate diffractometer. In the system, machine manupulation software and data processing software are combined. A series of functions are successively carried out; standard flows are indexing of intial images, refinement of the setting matrix, spot size estimation, integration, merging of individual intensity files, scaling, Laue symmetry determination, post refinement, and output of reflection data. The Weissenberg method in data collection and symmetry-related absorption corrections are options. Under the Weissenberg mode, suited crystallographic axes are selected and a sample crystal will be automatically aligned. The system works without any problem if crystal quality is good. A current goal of the automation is to have similar functionalities with a four-circle diffractometer.

P13.01.004 ONE AND TWO-COORDINATE DETECTORS FOR SSRC. V.M.Aulchenko, S.E.Baru, L.I.Shekhtman, V.M.Titov [1], B.P.Tolochko [2], [1] Budker Institute of Nuclear Physics, Lavrentev st. 11, Novosibirsk, 630090, Russia, [2] Institute of Solid State Chemistry, Novosibirsk, 630128, Russia

For last five years work has been in progress in BINP on the construction of one- and two-coordinate X-ray detectors: OD-3.1, OD-3.2, DED-5 and MSIC-detector for Siberian Synchrotron Radiation Centre [1].OD-3.1, (OD-3.2) - position sensitive parallax-free detectors, based on Multi Wire Proportional Chamber with focal distance 35 cm (150 cm) was developed for powder diffraction and SAXS experiments. DED-5 - area detector is intended for Laue diffraction, SAXS, protein crystallography (DED-5-P - parallax-free modification). MSIC - position sensitive parallax-free detector based on Micro-Strip Ionisation Chamber is under construction at this moment and test of the prototype.D-160 - position sensitive parallax-free detector, based on Multi Wire Proportional Chamber with focal distance 135 cm are developing for powder diffraction experiment. At this moment we finished the test of the prototype. The detectors are working with time resolution 1 microsecond in frame-by-frame mode. Detectors parameters (*-in scanning mode)

Detector	Aperture (mm)	FWHM (mm)	Number of channels	Count rate (MHz)
OD-3.1	200x10	0.18	3328	10
OD-3.2	200x25	0.15	3328	10
DED-5	384x384	1.5 x 1.5	65536	5
MSIC	100x10	0.1	1024	no limits
D-160	2760x5	1.2 (* 0.12)	6600	3300

1. V.M.Aulchenko et al, J. Synchrotron Rad. (1998).5, 263-267.

P13.01.005 MORE THAN ONE STRUCTURE FROM A SINGLE DATA COLLECTION? Christer Svensson, Inorganic Chemistry 2, Lund University, PO Box 124, S-221 00 Lund, Sweden.

In studies of small-molecule single crystals with area detector X-ray diffractometers, the detector is normally used very inefficiently in terms of the number of reflections sampled per frame and unit area. The largest part of each frame is an exposure of background only!

To increase the information density of an experiment with the present design of area detectors, data could be collected for several crystals simultaneously. A multi crystal method could be useful for example to increase the accuracy in comparative studies, where several samples are taken through the same cycles of temperature and/or pressure variations. It is probably also the cheapest solution towards a higher throughput for service crystallography facilities.

The Lund single-crystal diffractometer control program has been extended to handle frames from the Bruker SMART CCD-type detector: the location of spots, their indexing and integration, including the handling of twinned and modulated samples.

To investigate the feasibility of multi crystal experiments, and to test some of the functionality of the program, an aggregate crystal was prepared and mounted on a glass fibre by glueing three different single crystals together in arbitrary orientations. A hemisphere data set was collected using the SMART program and the narrow-frame method with "standard" settings of data collection parameters. Our local program was then used for evaluation of the frame data. In this first test of the method, the three crystals were rather large, with displacements of the order of 0.1 to 0.2 mm of their centres of gravity from the instrument centre. These displacements, which were refined by the program, identified which crystal gave rise to which diffraction pattern. After integration of the complete data set, which is in progress, output data files can be written which include either intensities from only non overlapped spots of one crystal (for structure solution) or a combination of non overlapped and overlapped spots from different crystals (for structure refinements).

For the multi crystal method to be successful, some further modifications are required in eg. absorption correction and structure refinement programs.

Progress on the data reduction and structure solution/refinement using the above and forthcoming multi crystal experiments will be reported.

P13.01.006 LATEST CRYSTALLOGRAPHIC RESULTS ON BIOLOGICAL SAMPLES WITH LARGE SINGLE CCD DETECTORS. E.R. Hovestreydt, Bruker-axs GmbH, Karlsruhe, Germany, M.R. Pressprich, S.I. Foundling and R.D. Durst, Bruker-axs Inc, Madison, Wisconsin.

After a very successful start of CCD technology in the Chemical (typically called small-molecule) Crystallography market, chip technology has advanced such that for some time CCD detectors have become available with very interesting specifications for Biological (formerly called protein) Crystallography.

Contrary to common belief, modern CCD detectors with their high resolution and ever larger size come very close to the orders of diffraction obtained with common imaging plate systems. Readout times that are almost an order of magnitude shorter will enable most efficient use of precious synchrotron or rotating anode measuring time.

The SMART 6000 CCD combines a large format 4K CCD chip with a 1.5:1 fiberoptic taper, optimised specifically for high sensitivity.

This new detector has a 135 mm diameter fiberoptics taper bonded to the largest available scientific grade 4K CCD (6.1 cm x 6.1 cm).

Combined with its large imaging area, the system will be of superior advantage in the collection of X-ray data using a copper target from micro crystals of biological macromolecules or organic compounds, and using a molybdenum target for charge density analysis or general chemical, mineral and materials structures.

Results of measurements done with this novel detector will be presented.

P13.01.007 DATA COLLECTION WITH A DELTA-CIRCLE- IMAGEPLATE DIFFRACTOMETER. Thomas Huber and Hans Burzlaff, Lehrstuhl für Kristallographie und Strukturphysik, Universität Erlangen-Nürnberg, Bissmarckstr. 10, 91054 Erlangen, Germany

The description of the instrument was already presented on the Seattle Congress 1996. The construction of the instrument allows data collection at high angle regions up to 2-theta = 110 degrees since the imageplate detector is moved by the 2-theta axis. In the meantime several sets of data for crystal structures of different complexity have been collected. They are compared with four-circle diffractometer data conventionally measured. Special investigations refer to the accuracy of the imageplate data and its suitability for electron density determination. The properties of the data and the instrument will be discussed. As a practical example for electron density investigations a small molecule structure will be presented.

Following the present experiences with the system it is very probable that the instrument can also be used for data collection of big molecule structures like proteins.

1. Huber, Th., Lange, J., Burzlaff, H., Acta Cryst A52 Suppl., Pp.C-27 (1996)
2. Thomas Huber, Andreas Kinne, Joachim Lange, Michael Thoms, Hans Burzlaff, Zeitschrift für Kristallographie, Suppl. Issue No. 15, S.205 (1998)

P13.01.008 CCD DETECTOR SYSTEMS FOR SINGLE-CRYSTAL STUDIES: BENEFITS OF SCANNING FOUR AXES CONCURRENTLY. Leo H. Straver, Anita Coetzee, Rob W. W. Hooft, Frank van Meurs, Nonius B.V., Application Laboratory, PO Box 811, 2600 AV Delft, The Netherlands

The integration of 4-circle goniometer and a CCD detector offers unique features that optimise and extend the experiments possible on such a system; more efficient data collections using preferred crystal orientations. At a smaller crystal-to-detector distance, this strategy will avoid overlaps, thus enhancing the data collection efficiency. Aligned exposures around any vector. A preview of the lattice allows observation of lattice effects before starting data collection. In addition, it is an ideal tool to study time and temperature dependent crystal lattice changes. Visualisation of rocking curves and indexing using virtual axes scans (Phi-Chi Scans). Determination of profile centres and shapes from pairs of virtual axes scans. Powder emulation exposures. A super fast spinning combination of three concurrently scanning axes. Allows for quick confirmation of sample identity. All experiments were done on a KappaCCD system.

P13.01.009 MEASURING WITH Cu-RADIATION ON A SMALL CCD SYSTEM; FICTION OR PRACTICE? Frank van Meurs, Anita Coetzee, Rob W.W. Hooft, Leo H. Straver, Bram J. Schierbeek, Nonius BV, Application Laboratory, PO Box 811, 2600 AV Delft, The Netherlands.

Single-crystal diffraction systems equipped with small CCD detectors are generally considered being ideal for employing Mo-radiation. It should be noted however that, when equipped with the proper “phosphor” and a four-circle goniometer, these systems are equally good with Cu-radiation. Some implications of the choice of the radiation on the efficiency of data collection, completeness of the data set and quality of the data obtained shall be discussed. A comparison with serial diffractometer data shall be given.

P13.01.010 DEVELOPMENT OF ARRAYED CCD X-RAY DETECTORS WITH A 100% DUTY-CYCLE RATE FOR AUTOMATED PROTEIN CRYSTALLOGRAPHY. K. Ito and N. Sakabe, Institute of Applied Biochemistry, University of Tsukuba, Tsukuba, 305-8572 Japan, Y. Amemiya, Department of Applied Physics, School of Engineering, The University of Tokyo, 7-3-1 Hongo, Bunkyo, Tokyo, 113-8656 Japan

A 2 x 2 module (153.5 x 76.8 mm^2 active area size) arrayed CCD X-ray detector has been developed for automated protein crystallography with use of the synchrotron radiation at Photon Factory, Japan. One module of the arrayed CCD X-ray detector consists of a phosphor (Gd_2O_2S:Tb, 15 mg/cm^2) which is deposited on an aluminized sheet, fiber optic-taper (FOT) and a CCD as an image sensor. This FOT has a demagnification ratio of 3.2:1 and high X-ray resistant. The CCD has an imaging area of 25 mm x 25 mm with 1024 x 1024 pixels of 24 μm x 24 μm. Only the upper half area (1024 x 512 pixel) of each CCD is used as an active image area, whereas the bottom half is used as a data storage area. Image data recorded in the active area are transferred to the data storage area with a time of 1.6 ms. The next image data are recorded in the image area while the previous image data are transferred to a frame grabber in a computer with a time of 2 s. This scheme enables us to detect successive X-ray diffraction patterns with a 100% duty-cycle rate; Neither the interruption of the rotation of the sample crystal nor the X-ray shutter for intermitted exposures are required during the data acquisition. The CCD are cooled to -30 degree with Peltier devices.

Results of the evaluation of the performance characteristics of the detector will be shown as well as experimental results with actual protein crystal.

A 3 x 6 modules (230.4 x 230.4 mm^2 active area size) arrayed CCD X-ray detector is under construction based on the technique accumulated with the 2 x 2 module CCD X-ray detector.

P13.01.011 KM4RED – THE DATA REDUCTION PROGRAM OF THE KM4CCD SYSTEM. M. Meyer[*†], W. A. Paciorek[*§], G. Chapuis[*] and D. Kucharczyk[‡] *Institute of Crystallography, University of Lausanne, BSP-Dorigny, CH-1015 Lausanne; [†]Kuma Diffraction Instruments GmbH, PSE-Ecole Polytechnique Federal Lausanne, CH-1015 Lausanne; [‡]Kuma Diffraction Ltd., Al. Akacjowa 15b PL-53 122 Wroclaw; [§]Global Phasing Ltd., Sheraton House, Castle Park, Cambridge CB3 0AX, England

The KM4CCD system, a Kappa 4-circle goniometer with CCD area detector, originated in a collaboration project between the University of Lausanne and Kuma Diffraction Ltd. The

Institute of Crystallography is responsible for the software development of this instrument. With the KM4CCD system we follow an open software strategy, contrasting to most commercial systems. Interested users receive source codes and may extend the system capabilities for special applications (incommensurate crystals, quasi-crystals, high-pressure attachments and alike). These extensions may then be shared among the user community.

The framework of the development project we investigated in several works the instrument calibration of modern imaging diffractometers, especially the instrument description[1)] and distortion correction of tapered CCD detectors[2)].

The program KM4RED implements these achievements. The poster presents the program features. Besides the KM4CCD format the program also supports the MAR research image formats (image plate and CCD) and thus may be an interesting alternative for Denzo and XDS for the field of "problematic samples".

W. A. Paciorek, M. Meyer & G. Chapuis (1998): "On the Geometry of Modern Imaging Diffractometers". Accepted to Acta Cryst. A.
W. A. Paciorek, M. Meyer & G. Chapuis (1998): "Geometric distortion corrections for fiber optic tapers in X-ray CCD detectors". Accepted to J. Appl. Cryst.

P13.01.012 AREA DETECTORS ON BEAMLINES – ABSTRACT INCORPORATING LARGE AREA DETECTORS INTO SYNCHROTRON BEAMLINES: THE CHESS EXPERIENCE. D. Szebenyi, M. Cook, A. Deacon, S. Ealick, C. Heaton, I. Kriksunov, J. LaIuppa, W. Miller, and D. Thiel; MacCHESS, Cornell University, Ithaca, NY 14853, USA

CHESS, the Cornell High Energy Synchrotron Source, has been, and continues to be, a leader in the use of innovative x-ray area detectors at its beamlines. We describe here the process of meshing a new detector with other beamline components to create a reliable and efficient system for collecting high-quality diffraction data. Important items include:

Customization of detector hardware and software - mounting detector on beamline, porting control software to local computer, establishing communication between detector control software and beamline hardware, special requirements for data collection at this particular beamline.

Safety - e.g. protection of detector from direct x-ray beam.

Data handling considerations - sufficient storage space, backup devices, and network bandwidth for raw data produced by the detector.

Data reduction software - available at the beamline for initial indexing and strategy calculations, and subsequent complete processing, and also available to users' home labs for later processing.

Training - thorough grounding of beamline staff in capabilities and operation of system, provision of manuals and other instruction for users.

Testing of entire system - collection and processing of multiple data sets by both expert and novice users, and resulting improvements in system's reliability, accuracy, and ease of use.

Continuing evaluation and improvement - modifications based on user comments, other hardware and software upgrades as they become available.

Having gone through all of the above, the three macromolecular beamlines at CHESS are now equipped with well-tested 2x2 mosaic CCD detectors from Area Detector Systems, and are producing excellent, biologically important, data. Future plans include continued incorporation of new detectors, as they become available.

P13.01.013 THE OPTIMAL GAIN AND DYNAMIC RANGE OF CCD DETECTORS FOR X-RAY DIFFRACTION. R. D. Durst*, P. Mueller†, C. Campana*, S. Foundling*, Z. Jin*, J. Phillips*, M. Pressprich*, *Bruker AXS, Inc, 6300 Enterprise Ln., Madison, WI 53719 USA †Universitaet Goettingen, Institut fuer Anorganische Chemie, Tammannstr. 4, D-37073 Goettingen, Germany.

Conventional CCD-based detectors for x-ray diffraction require large fiber-optic demagnification ratios in order to achieve useful active areas. Thus, these detectors exhibit modest single-photon signal-to-noise ratios (of order 1) which limits their ability to accurately characterize weak reflections. The application of large format CCDs has allowed newer generations of detectors to achieve higher sensitivity with a commensurate improvement in low-level data quality. Recently, by combining a wafer-scale CCD with an advanced x-ray phosphor true single-photon sensitivity has been achieved (that is, a signal-to-noise ratio sufficiently high so as to unambiguously distinguish a single x-ray photon from the detector noise background).

However, for an integrating detector such as a CCD the total charge storage per exposure is fixed and finite and thus an increase in gain implies a decrease in the dynamic range. This tradeoff between dynamic range and sensitivity is studied both theoretically and experimentally. The impact of the system gain, detector noise, scattered x-ray background, spatial resolution, binning ratio and rocking curve on sensitivity and dynamic range is derived.

The design of a prototype CCD detector with single photon detectivity is described and its experimental sensitivity and dynamic range are compared to these theoretical models.

P13.01.014 *AUTOMAR*: DATA REDUCTION SOFTWARE FOR MAR DETECTORS. Klaus S. Bartels and Claudio Klein, x-ray research GmbH, Segeberger Chaussee 34, D-22850 Norderstedt, Germany

In the last couple of years, considerable progress has been made to automate data reduction of area detector data. Traditionally, the most severe obstacle for getting the data processed has been the indexing step. Available programs differ mostly in the likelihood of obtaining the relevant crystal parameters required for integration. We concentrated our efforts mainly on this task and developed an entirely new data processing package called *autoMAR*. The program suite includes: Spot finding and autoindexing: Based on refinement of zone-axes the autoindexing features new algorithms for fully automatic determination of cell parameters and lattice types as well as crystal orientation and mosaicity. The method is extremely reliable and has very high success rates for indexing anything from ruby (5 Ang. cell axes) to virus patterns. Spot prediction and integration with various degrees of sophistication including site-dependent experimental and Bayesian profile fitting Summation of partials, post-refinement and scaling of intensities Calculation of data collection strategies for optimizing data collection time and/or completeness. Graphical user interface based on X-Windows/Motif with intuitive look & feel. Visual feedback from all stages of data processing and graphical output of results. The processing results of a number of data sets from both Image Plate and CCD-detectors will be presented.

P13.01.016 THE MULTIPLE-DETECTOR SYSTEM FOR THE POWDER DIFFRACTOMETER AT BEAMLINE B2 (HASYLAB). W.-H.Kaps, J.Ihringer, W.Prandl, M.Schilling, Institut für Kristallographie der Universität Tübingen, Charlottenstr.33, 72070 Tübingen, Germany

We have designed and manufactured a multiple-detector system with four flat Si (111) crystal analysers and four scintillation counters. Using the small divergence of the incident

beam the Bragg reflection angles (2theta) are measured with highest angular resolution and independent of the sample position.

A single stepping motor simultaneously adjusts all crystal analysers. In addition the relative positions of the angles are set by individual drives. Due to the identical design and the simultaneous control of the four analyser diffractometers data corrections are not needed. Simultaneous profile refinement of the four data sets is done by program SIMREF [1] which has been particularly designed for powder data from different sources.

The multiple-detector system is intended for a wavelength range of $0.4<\lambda<1.7$Å. Cross talk between the entrance and the exit of the analysers at short wavelengths is eliminated by adjustable lead shields. Special analyser shielding houses adapted to the beam path enhance the typical peak / background ratio to 300 to 1.

An important application are experiments with different wavelengths to use the anomalous scattering of X-rays for phase determination and to differentiate different groups of atoms.

We acknowledge financial support by the BMBF (05SM8VTA3).

[1] H.Ritter, http://www.uni-tuebingen.de/uni/pki/simref/simref.html, (1998)

02. METHODS FOR STRUCTURE DETERMINATION

P05.02.001 A NOVEL RIETVELD REFINEMENT CODE FOR MOLECULAR MATERIALS. M.J. Jones and R.B. Hammond, Centre for Molecular and Interface Engineering, Department of Mechanical and Chemical Engineering, Heriot-Watt University, Edinburgh EH14 4AS.

Rietveld refinement[1] is an established method in powder diffraction. Presently several computer programs[2] for full profile refinement of powder diffraction data exist, none of which are designed specifically for organic, molecular crystalline materials. The main drawback of these existing programs is their lack of ability to define and maintain the *molecular* geometry in the course of structure refinement. Commonly, rigid body, and/or bond length (and thus, indirectly, bond angle) constraints are applied to molecules or molecular fragments. In many cases, however, these methods are not suitable, or indeed insufficient, for constraining the refinable atomic parameters to sensible or known molecular geometries.

We present here a new program for Rietveld refinement of powder diffraction data. The most important innovation of this program is the incorporation of molecular mechanics techniques to compute the total (lattice and molecular) energy for each refinement cycle. The calculated energy is used in a penalty function, thus avoiding unrealistic molecular geometries. The relative merits of employing systematic restraints based upon molecular mechanics 'observations' compared with formal constraints operating on atomic positions is under examination. In addition, the use of internal coordinates to define both atomic parameters and bond length and angle constraints is investigated.

The design and philosophy of the program are discussed.

1. H.M. Rietveld, *Acta Cryst.*, **22**, 151, 1967
2. R.A. Young, in *The Rietveld Method*, pp. 1, Oxford University Press, Oxford, 1995.

P05.02.002 RIETVELD ANALYSIS ON THE HIGH RESOLUTION FOURIER DIFFRACTOMETER. V.B. Zlokazov, A.M.Balagurov, FLNP JINR, 141980 Dubna, Moscow region, Russia.

MRIA - a program for a full profile analysis of multiphase powder neutron diffraction was originally designed as the only peak shape independent and fast fit routine which made it indispensible for treating the time-of-flight RTOF (reversed time-of-flight) spectra on the Dubna High Resolution Fourier Diffractometer [1]. However, the area of applications of RTOF methods being growing gradually new features were added to MRIA which widely extended the class of problems being solved by this program. 1. The mode for the analysis of neutron diffraction spectra obtained from the conventional neutron diffractometers (λ = *const*) was implemented. 2. Techniques for taking into account the texture effects in the Rietveld analysis were added. 3. The treatment of magnetic diffraction for collinear structures was included. 4. The automatic three-dimensional peak search in Fourier synthesis has been developed [2]. The report goes over these new features in more detail.

Zlokazov V.B., Chernyshev V.V. Jour.of Appl.Cryst. (1992) 25,447-451.
Zlokazov V.B. Jour.of Appl.Cryst.(1997). 30, p.996-1001.

P05.02.003 RIETVELD REFINEMENT OF INTER-MEDIATE PHASES IN THE Mo-Re SYSTEM OF ALLOYS. J.L. Garin and R.L. Mannheim, Department of Metallurgical Engineering, Universidad de Santiago de Chile, Casilla 10233, Santiago, Chile.

The existence of σ and χ phases in binary molybdenum-rhenium alloys has received much attention because of the important effects that the formation of these phases has on the properties of the industrial alloys [1].

In order to update earlier crystallographic data [2] and at the same time investigate the evolution of the σ/χ ratio upon non-equilibrium cooling of the alloy, a Rietveld analysis of X-ray powder patterns was conducted on the material.

The samples were synthesised by sintering mixtures of Mo and Re powders in the composition range of 80 - 87% Re, at elevated temperatures under controlled Ar-H_2 atmosphere.

The room temperature X-ray analysis was carried out over the range of 10 - 105° (2θ), with 4750 step intensities, assuming Pseudo-Voigt profiles for all reflections. A total of 16 groups of atomic co-ordinates and isotropic thermal parameters were refined, together with other operational parameters such as scale factors, preferred orientation coefficients, surface roughness, background polynomial coefficients and so on. There are five kinds of crystallographically equivalent positions for the 30 available atoms in the unit cell of σ and four positions for the 58 atoms in the cell of χ. Consequently both σ phase ($MoRe_2$, $D8_5$) and χ phase ($Mo_{13}Re_{45}$, A12) are structurally characterised by a disordered arrangement of Mo and Re atoms in space groups P42/mnm and I-43m respectively; owing to these facts the occupation factors were also varied to determine the right stoichiometry of each phase.

The study finally revealed that the σ/χ ratio for a given composition of the alloy increased with cooling rate during the sintering process.

1. J.C. Carlen and B.D. Bryskin (1994), J. Mat. Eng. Perf., 3(2), 282-291.
2. C.G. Wilson (1963), Acta Crystallogr. 16, 724-730.

P05.02.004 X-RAY DIFFRACTION STUDY OF THE QUATENARY INTERMETALLIC COMPOUND $YAl_8(Co,Cr)_{3.6}$. R.G.Zakharov, S.A.Petrova, V.L.Zyazev, and N.A.Vatolin, Institute of Metallurgy, Urals' Division, Russian Academy of Science, Ekatherinburg, 620 016, Russia.

X-ray structural investigation of the $YAl_8(Co,Cr)_{3.6}$ alloy was carried out with the use of an automated diffractometer DRON-UM1 ($Cu_{K\alpha}$-radiation, pyrographite monochromator on the diffracted beam). A crystal system determined by the TREOR autodetecting program [1] occurs to be a tetragonal one with lattice parameters a = 8.909(1)E, c = 5.097(1)E (F30=80 (.010, 39)). The intermetallic compound is isostructural to the RT_4Al_8 and RT_6Al_6 compounds (R – rare-earth metal, T – 3d-metal) with $ThMn_{12}$ structural type, I4/mmm space group (PSC: tI26) [2].

For the whole-profile-pattern crystal structure refinement with the Rietveld method DBWS-9411 program version [3] was used. The starting values for atomic occupation and position type were estimated with a 'heavy atom' method. From the calculations (R_{wp}=13.1%, R_p=10.8%, R_b=8.7%) it was established that atoms of yttrium are arranged the 2(a) sites, the 8(i) and 8(j) positions are occupied by atoms of aluminium, and 3d-metal atoms are situated at the 8(f) sites.

This work is supported by the Russian Foundation for Fundamental Research (grant N 98-03-32655).

Werner P.-E.(1984). TREOR, Univ.of Stockholm, Sweden, 1984.
Felner I.(1980). J.Less-Common Metals, 72, 1980
Young R.A., Sakthivel A., Moss T.S., and Paiva-Santos C.O.(1995). Program DBWS-9411, Atlanta, U.S.A, 1995

P05.02.005 NEUTRON POWDER DIFFRACTION STUDY OF NdOF BETWEEN 1.5 AND 300 K. M. Lastusaari and J. Hölsä, Department of Chemistry, University of Turku, FIN-20014 Turku, FINLAND, and J. Rodriguez-Carvajal, Laboratoire Leon Brillouin, (CEA-CNRS), Centre d'Etudes de Saclay, F-91191 Gif sur Yvette Cedex, FRANCE and L. Beaury and J. Derouet, Laboratoire de Chimie Appliquée de l'Etat Solide, UMR 7574 CNRS, ENSCP, F-75231 Paris Cedex 05, FRANCE.

A preliminary X-ray powder diffraction study carried out to explain the anomalous behaviour of the paramagnetic susceptibility of polycrystalline hexagonal neodymium oxyfluoride, NdOF, as a function of temperature revealed anomalous behaviour of the lattice parameters as well [1]. Since no structural details were obtained from the X-ray powder diffraction study a neutron powder diffraction investigation was found necessary.

The structure of NdOF was consequently studied at 1.5, 25, 55, 100, 200 and 300 K by neutron powder diffraction, Rietveld analyses and bond valence calculations. The Rietveld refinements yielded a good fit to the hexagonal space group R3m (No. 166). The unit cell volume and parameters *a* and *c* decrease with decreasing temperature, but the *a* parameter value reaches its minimum at 55 K, and thereafter starts to increase. The *c* parameter value decreases smoothly to 25 K but then drops sharply to 1.5 K to compensate for the change in the *a* value. The unit cell volume remains practically constant below 55 K. It is possible that the behaviour of the unit cell parameters is due to a small distortion from the centrosymmetric structure, but the possible distortions are too small to be observed from the powder diffraction data.

The bond valence calculations indicated that the maximum stability of the hexagonal structure is achieved at 1.5 K. The bond valence calculations give no explanation for the anomalous evolution of the cell parameters, however.

1. Beaury, L., Calvarin, G., Derouet, J., Hölsä, J., and Säilynoja, E., *J. Alloys Comp.* **275-277** (1998) 646.

P05.02.006 POWDER DIFFRACTION EXPERIMENTS IN CAPILLARY GEOMETRY USING MULTIPLE-DETECTORS AT PHOTON FACTORY. S. Yamazaki and H. Toraya, Ceramic Research Laboratory, Nagoya Institute of Technology, Tajimi 507-0071, Japan

A synchrotron radiation powder diffractometer with a multiple-detector-system at the Photon Factory was originally designed for the use in a flat specimen reflection geometry (FSRG) using an asymmetic 2θ-scan mode at a fixed incident angle. In last year, an equipment became available for recording intensities from a capillary specimen in transmission geometry (CSTG). Profile intensities were measured using monochromatized beam with the wave length of 0.7Å and Ge(111) crystal analyzers. Angular resolution, preferred orientation, particle statistics and the accuracy of refined structural parameters were examined in a comparison with the data obtained in FSRG. Samples used for testing were coarse grained α-SiO_2, $CaCO_3$ and Mg_2SiO_4. FWHM's obtained in CSTG [$CaCO_3$, an inner diameter of capillary (ϕ) = 0.5 mm, 2θ = 10 ~ 70°] were generally smaller by 20 ~ 30% than those in FSRG. The minimum FWHM's were 0.009 and 0.016° for 112 reflections from the α-SiO_2 powders in capillaries with ϕ = 0.1 and 1.0 mm, respectively. In CSTG, the number of reflections, of which intensities were shifted by more than 5% by preferred orientation, was only 10% in a total of 181 reflections from $CaCO_3$, whereas they were 67% in FSRG. In re-packing tests using the coarse grained α-SiO_2, intensity variations of individual reflections, which would arise from particle statistics, were much smaller in CSTG (ϕ = 0.5 mm) than those in FSRG. The accuracy of structural parameters obtained in the Rietveld refinements of $CaCO_3$ and Mg_2SiO_4 using FSRG was, however, than in CSTG, and it will be ascribed to a better counting statistics in FSRG.

P05.02.007 OVERCOME THE LIMITATION OF RIETVELD METHOD USING ELECTRON DENSITY PLOT. A. A. Ramadan, S. Selman, A. T. Matter and S. T. Nasser, Physics department, Helwan University, Helwan, Cairo, Egypt.

The great limitation of Rietveld method is faced up due to the correlation between some crystallographic parameters such as displacement (temperature) factor and site occupancy. This may lead to a false minimum with reasonable reliability factors and final acceptable Rietveld plot. In order to avoid such limitation, means of single crystal structure determination, such as the Fourier electron density map, can be applied as a complementary approach. Therefore, instead of one step in the usual Rietveld method, three steps are required:

i) Full-pattern fitting by Rietveld method, and estimating of the values of F_{clc} and α_{clc} from the refined model,

ii) Estimation of the values of ?F_{obs} from profile matching method of LeBail which is not biased by the model, and

iii) Construct electron density plots (ρ_{obs}, ρ_{clc} and $\Delta\rho = \rho_{obs} - \rho_{clc}$) in one dimension. From these plots one can judge whether the obtained minimum is true or false. Any discrepancy in the refined values of displacement factor, or fractional coordinates or site occupancy can be identified.

Simulated diffraction patterns of spinel structures, with small and large differences in the atomic number of the constituent elements using Fe- and Mo-Kα radiation, were considered as the observed data. GSAS software and FullProf program were used. The sharpening or broadening of the peak in the Fourier plots and their shift as well as the positive and negative values in Δρ are the good indicators. Therefore, this proposed three-step procedure could be considered as a λ.

P05.02.008 TAKE CARE OF FOURIER-FILTERING TECHNIQUE FOR BACKGROUND REFINEMENT IN RIETVELD METHOD. M. El-Shabiny and I. S. Ahmed, Physics Dept., NRC, Cairo, and A. A. Ramadan, Physics Dept., Helwan University, Helwan, Cairo, Egypt.

In powder diffraction patterns fitting by Rietveld method, the total observed scattering is reliably modeled by convoluting calculated Bragg intensities with a instrumental resolution function and adding a background contribution. Poor estimates of the background lead to badly wrong and physically unreasonable values of thermal parameters and site occupancies. Background refinement is commonly accomplished through the use of empirical phenomenological functions such as polynomials. In case of non-monotonically varying background shown as broad oscillations, a particular interesting approach that is the Fourier-filtering technique is implemented recently in Rietveld programs such as FullProf program. What are the consequences to the Rietveld refinement?; a question given and answered by Richardson [1]. Another answer is discussed in this work. A simulated diffraction pattern of provoskite structure was considered as the observed data and FullProf program is used. A wrong model was then considered for the calculated diffraction patterns with crystallographic parameters far from the true values. It is known that the refinement of the step in the turn-on sequence of the refined parameters. Refinement of the background was accomplished by three-order polynomial while the other (wrong) parameters were kept fixed as the starting step in the refinement. Very clear difference in the Rietveld plot was observed with high value of R_{wp}. When the Fourier-filtering technique was used with FWINDOW parameter of 5 to 20 and also the other parameters were kept fixed, a perfect fitting in the Rietveld plot was observed with very law value of R_{wp}; which is, of course, a false minimum. Now, leaving the fixed parameters free, no change towards the

correct values was achieved and values of R_{wp} still law. Therefore, if this technique has to be applied, it should be used with very great care; it may give a good but misleading shape of Rietveld plot and law reliability factor but false minimum with completely wrong crystallographic parameters.

J. W. Richardson, Jr.(1993)."The Rietveld Method", Edt. R. A. Young, IUCr, Oxford Univ. Press, p. 102.

P05.02.009 SIMULATION OF X-RAY DIFFRACTION PATTERN OF $CuIn_xGa_{1-x}Se_2$ THIN FILMS BY RIETVELD METHOD. H. Pal, M. De and A. K. Pal, Department of Materials Science, Indian Association for the Cultivation of science, Jadavpur, Calcutta- 700 032, India

$CuIn_x Ga_{1-x}Se_2$ solar cell thin films have been prepared by vacuum evaporation technique. The main diffraction peaks observed correspond to the (112), (220) and (312) which confirm the tetragonal chalcopyrite structure of our films. There is a preferential orientation in the direction of the (112). We have simulated X-ray diffraction pattern of the films considering scattering factors of ionized atoms (Cu^{+1}, In^{+3}, Ga^{+3} and Se^{-2}). The intensity of the X-ray profile is corrected due to preferred orientation, crystallite sizes and microstrains. The simulated pattern contains extra lines compared to the experimental pattern. Secondly, we have simulated the pattern considering scattering factors of neutral atoms (Cu, In, Ga and Se) and on correcting the intensity due to the preferred orientation, crystallite sizes and microstrains, the pattern is found to fit well with the experimental pattern. It is expected that the experimental X-ray pattern should fit well with the first simulated pattern. But our observation is different. Attempts are being made to explain such anomalous observation.

P05.02.010 APPLICATION OF RIETVELD METHOD FOR STUDYING THE STRUCTURAL CHARACTERISTICS OF SUBSTITUTED COPPER FERRITE COMPOUND. S.M. Hammad*, I.S. Ahmed Farag*, M.A. Ahmed**, A.M. Moustafa*, * Physics Department National Research Centre, Dokky, Cairo, Egypt, ** Physics Department, Faculty of Science, Cairo University.

A series of ferrite samples of the chemical composition $Cu_{0.7}$ $(Zn_{0.3-x}Mg_x)Al_{0.3}Fe_{1.7}O4$ [x=0.05, 0.1, 0.15 and 0.2], prepared by ceramic technique at 1000°C, are found to have cubic spinel structure. On the basis of the Rietveld analysis and applying the full pattern fitting of Rietveld method using FullProf program, the exact coordinates of atoms, the unit cell dimensions, the oxygen parameter, the atom occupation factors, isotropic temperature factors, the profile shape parameters as well as the interatomic distances have been determined.

It was found that the lattice parameter decreases with increasing the Mg content this may be attributed to the influence of the difference between the ionic radius of Mg and Zn cations. Also the variations of the cation distribution has been discussed on the basis of site preferrence, size and valence of the substituting cations.

The residual isotropic microstrain in the samples may be attributed to the inversion behavior and the relative values of cation ionic radius in the tetrahedral and octahedral sites.

P05.02.011 BAYESIAN FOURIER MAPS FROM POWDER DIFFRACTION DATA. W.I.F. David and D S Sivia, ISIS Facility, Rutherford Appleton Laboratory, Chilton, Didcot, Oxon. OX11 0QX, UK.

Fourier maps from powder diffraction data are usually constructed using traditional Fourier transform techniques where the observed structure factors are obtained by the method originally proposed by Rietveld (1969). In this method, the observed structure factor magnitudes at a particular point in the diffraction pattern are apportioned according to the associated calculated structure factor magnitudes. This is an elegant approximation to the correct values but clearly biased towards the calculated structural model. Additionally no account is taken of observed structure factor uncertainties including the correlation between overlapping reflections. In this poster, a Bayesian method is proposed that uses an entropic prior with calculated structure factors from a Rietveld refinement and a likelihood constructed from the observed Bragg peak intensities and their correlation obtained from a simultaneous Pawley profile refinement. Examples from inorganic and molecular crystal structures will be shown.

Rietveld, H.M. (1969) *J. Appl. Cryst*. **2** 65-71.

P05.02.012 MAXIMUM ENTROPY IN LAUE. Yong Xie, Quan Hao Department of Chemistry, De Montfort University, Leicester LE1 9BH

1. In a Laue diffraction pattern, 10-20% of the spots result from the exact superposition of two or more reflections that are 'harmonics'; a high proportion of these are low-resolution reflections. For the solution of large or difficult structural problems, the intensities of the remaining 80-90% of the reflections may not be sufficient, thus the evaluation of the intensities of the components of the multiple spots is important.We developed a new method based on maximizing the entropy of the Patterson function subject to the constraint imposed by the observed intensities of overlapping reflection. This method does not need data redundancy and therefore is of particular interest for time-resolved studies on a short time scale. A new computer program (ME) was developed and tested with Laue diffraction data. It showed this new method gives good results.

2. In protein crystallography, low-resolution reflections are especially important in defining the molecular mask and polypeptide backbone. However, in Laue data collection, the loss of low-resolution reflection data can be as high as 40-50%. For evaluation the unobserved reflections, a new method is presented based on maximizing the entropy of the Patterson function subject to the constraint imposed by the observed and deconvoluted intensities. A new computer program (MES) was developed and tested with Laue diffraction data. It showed inclusion of unobserved reflections in low resolution significantly improved the connectivity of electron density map.

P05.02.013 MAXIMUM ENTROPY METHOD IN PROBLEMS OF X–RAY DIFFRACTION ANALYSIS. B. Z. Belashev, Institute of Geology, Karelian Research Centre RAS, Petrozavodsk, 185610, Russia, A. N.Yakovlev, Petrozavodsk State University, Petrozavodsk, 185640, Russia.

Burg's maximum entropy method (MEM) is commonly used along with Frieden's version of MEM designed to solve Rayleigh's inverse problem: reduction of observation data to a perfect instrument by eliminating the known apparatus function. The signal sought for is estimated by solving a variation problem, maximizing signal estimation entropy, the linear relation of the signal sought for being retained along with the blur and noise function. The working capacity of this version of MEM was demonstrated by recognizing singlets, doublets, and complex multiplets from blurred bands, using various blur functions and various Poisson and additive white noise levels.

Our modification of Frieden's MEM, which is connected with selection of approximated data blur functions, can be used to increase resolution and to determine the most probable structure of the blurred bands of spectra. The algorithm was used for short-

range identification of amorphous materials and liquids from available X-ray diffraction data. Ordered ice-like-structured clusters were found to exist in liquid water. Short-range identification of amorphous materials is possible, using an X–ray diffraction pattern and its autocorrelation function.

The use of MEM in the problem of determining the parameters of an elementary cell in the crystalline lattice of materials lowers noise level, allows to find out whether the peak of the X–ray pattern studied is structurally simple or complex, and to more precisely determine the position of peak constituents. In this case, the error in the parameters of an elementary cell in the crystalline lattice of materials proves to be much smaller than the one in the conventional method. MEM was used to determine the parameters of an elementary cell in a standard quartz sample.

P06.02.001 PROTONS IN PROTEINS: NEW HORIZONS IN NEUTRON CRYSTALLOGRAPHY. D.A.A. Myles and F.Dauvergne, EMBL-Oustation, Av. des Martyrs, F38042 Grenoble, France. and C. Wilkinson and P. Timmins, ILL, Av. des Martyrs, F38042 Grenoble, France.

A new protein crystallography instrument (LADI), dedicated to cold neutron Laue diffraction, is able to reveal key details of the hydrogen structure in large biological macromolecules, even at medium resolutions (>1.5Å) [1]. This is an important advantage since hydrogen atoms, which account for 50% of the atoms in a biological structure and mediate much of biological activity, cannot be seen at all at the medium resolution limits (>1.5Å) typical of most X-ray protein structure determinations. Moreover, as the scattered neutrons from hydrogen and deuterium have different phase, neutrons are uniquely able to distinguish between hydrogen (negative density) and deuterium (positive density) exchanged positions in the crystal. Analysis of the pattern and extent of H/D exchange can therefore provide a direct and elegant probe of group accessibility, mobility and of exchange dynamics

The great advantage and potential of the new LADI instrument is the speed with which data may be collected. The combination of a broad bandpass quasi-Laue geometry and a novel 2π, neutron sensitive image plate detector [2], provides order of magnitude gains in efficiency compared with conventional diffractometers. This makes feasible studies of larger biological complexes and/or smaller crystals than have previously been possible. The instrument is optimized for data collection to >1.5Å resolution from medium size proteins (~30kDa), sufficient to locate individual hydrogen atoms of special interest, water structures or other small molecules that can be marked with deuterium to be particularly visible. Current studies aim to answer specific questions concerning enzymatic mechanism, solvent effects, structure dynamics and their implications. Instrument performance and application will be illustrated by some recent results.

[1] N.Nimura, Y.Minezaki, T.Nonaka, J.C.Castagna, F.Cipriani, P.Hoghoj, M.S.Lehmann & C.Wilkinson. (1997), *Nature Struct. Biol*., **4**, 909-917.

[2] F. Cipriani, J.C. Castagna, M. S. Lehmann & C. Wilkinson, *Physica B* **, 213,** 975**,** (1995)

P06.02.002 STRUCTURE OF CONCANAVALIN A EXHAUSTIVELY EXCHANGED IN D_2O BY NEUTRON LAUE DIFFRACTION AT 2.4A RESOLUTION. Jarjis Habash, James Raftery, Rachel Nuttall, Helen J Price, John R Helliwell [1], Clive Wilkinson [2], Mogens S. Lehmann [3], A. Joseph Kalb (Gilboa) [4], [1] Deparment of Chemistry, University of Manchester, Manchester M13 9PL,UK, [2] EMBL, F38042, Grenoble Cedex, France, [3] ILL, F38042, Grenoble Cedex, France, [4] The Weizmann Institute of Science, Rehovot, Israel

Structural studies by neutron diffraction permit quantitative evaluation of H/D exchange and direct observation of hydrogen (deuterium), which can yield vital information on biochemical processes at the most intimate atomic level. Such an approach exploits the difference in neutron scattering lengths between hydrogen and deuterium, which is not feasible via X-ray diffraction. Hydrogen atoms can be found from protein crystallography via ultra-high resolution data collection involving synchrotron radiation, cryoprotection of the sample and fast CCD-based electronic detectors. Recently we have shown that both neutron and ultra-high resolution structural studies of the 25kDa protein concanavalin A are feasible. The neutron data collection involved Laue geometry, which harnesses a broader band of neutron wavelengths than a monochromatic neutron beam, and a very large IP detector thus allowing data collection in a reasonable period. In the most recent experiment we have studied a more fully H2O/D2O exchanged concanavalin A crystal, soaked in D2O over a period of 2 months, rather than vapour exchange over a period of 21 days used earlier. A deuterated concanavalin A crystal (space group I222, unit cell parameters a=88.7, b=86.5 & c=62.5A) was used to collect neutron Laue data at the Institut Laue Langevin in Grenoble with a neutron wavelength range of 2.49-3.5A. Also an X-ray based refinement to 1.8A of a deuterated crystal, prepared under the identical conditions to the one used in the neutron experiment, was used as the starting model for the neutron refinement to 2.4A resolution. The neutron refined model fits the neutron density maps well, as seen previously. All peptide NH's were investigated via a number of models for exchange. The best refinement residuals were for partial H/D exchange, which for such extensive beta sheet is not unexpected. The carboxyl proton on Asp 28 referred to previously appears now however to have exchanged for deuterium indicating that the method of deuterium exchange has indeed been effective in that respect. Most noticeably there is now much more positive density visible in the bound solvent region as expected for complete D2O solvent exchange as opposed to H2O cancellation effects, at these resolutions, for the solvent in the partially exchanged crystal of our previous study. The current experiment afforded the chance then to study the bound water deuterium atoms. Using the 148 water oxygen positions from the 1.8A X-ray model, deuterium atoms were afixed to them automatically by XPLOR. The positions of these deuteriums were then refined against the neutron data and they generally moved into density from positions initially often pointing out of neutron density. In particular the bound waters at the Mn site were investigated further whereby they were omitted from the model, model refinement continued and which then showed up clearly in the omit maps. These were not seen in the previous study. This is then an example of contrast variation and firmly shows the identity of these ligands as waters as well as orienting their deuterium atoms. This study is part of a programme of work involving the detailed elucidation of protein saccharide interactions at the molecular level.

Funding from The Wellcome Trust, BBSRC and EPSRC to JRH is gratefully acknowledged. The LADI diffractometer is at the Institut Laue Langevin in Grenoble, France.

A Deacon et al 1997 Faraday Trans 94, 4305-4312; J Habash et al Faraday Trans
94, 4313-4317; G Bradbrook et al 1998 Faraday Trans 94, 1603-1611; Harrop SJ
1996 Acta Cryst D52, 143-155. See also relevant references therein.

P06.02.003 SUPERSTRUCTURES OF $M_2P_2O_7$ (TI, ZR) FROM COMBINED X-RAY AND NEUTRON POWDER DIFFRACTION DATA. Miguel A. G. Aranda, Sebastián Bruque and Enrique R. Losilla, Departamento de Química Inorgánica, Universidad de Málaga, 29071 Málaga, Spain, and Jesús Sanz, ICMM, CSIC, Cantoblanco, 28049 Madrid, Spain

MP_2O_7 (M=Si, Ge, Sn, Ti, Zr, Hf, …) compounds crystallize in a cubic substructure (s.g. P a $\bar{3}$, a ~ 8 Å) but they display a complex (3×3×3) superstructure. The interest of these materials is due to the low thermal expansion coefficients they present, that in some cases are negatives as for ZrV_2O_7. The cubic (3×3×3) structure is very complex with 50 atoms in the asymmetric part of the unit cell. To get precise and accurate structural parameters we have carried out joint Rietveld refinements of neutron and laboratory X-ray diffraction data at several temperatures. Although, the crystal structure of Ti^{4+} and Zr^{4+} compounds are usually quite similar, we will show that these superstructures are not very similar and that their thermal evolutions are quite different. This structural study will be related to the ^{31}P MAS NMR data of these samples. The superstructure is developed to relax many linear P-O-P groups (in the substructure) which yields 6 independent pyro groups due to 11 crystallographically different phosphorus atoms. Thermal expansion data and the relation between crystal structures and ^{31}P NMR spectra will be discussed.

P08.02.002 DISORDER IN CRYSTALLOGRAPHY. Alok Kumar Mukherjee, Department of Physics, Jadavpur University, Calcutta 700 032, India.

Disorder is usually an unmitigated nuisance in X-ray structural crystallography and often associated with poor quality of diffraction data leading to apparently high final R factor. But certain types of disorder are both esthetically appealing and potentially informative about the bonding and chemistry of the compounds in which they occur. The following examples taken from our recent crystallographic investigations of metaloorganic compounds reveal different types of structural disorder and possible strategies to tackle them.

(1) Solvent Disorder: In the Oxo-Peroxo molybdenum (VI) compound $[MoO(O_2)\ (QO_2\ )\ ]\ 0.5\ CH_2CL_2$ (QOH = quinoline-8-ol), space group P $\bar{1}$, Z=2, the dichloromethane (CH_2CL_2) solvent molecules are disordered statistically within interstitial holes between the ordered $[MoO(O_2)\ (QO_2)]$ molecules.

(2) Orientational disorder: In the dinuclear tungsten-sulfur complex, $[(W_2S_{12})\ (C_8H_{20}\ N)_2\ ]$, space group I $\bar{4}$ c 2, Z=8, the $(W_2S_{12})^{2-}$ anions are located at crystallographic two-fold sites. The terminal bidentate S_4 - ligands of the anion are disordered over two orientations with occupancy factors 0.61(1) and 0.39(1), respectively.

(3) Symmetry imposed disorder: The heterobinuclear sulfido complex, $[PPh_4\ ]_2\ [\ S_2WS_2Hg(C \equiv CH)_2\ ]$, crystallizes in space group P $\bar{1}$ with Z=1 . Since the anion, $[S_2WS_2Hg\ (C \equiv CH)_2]^{2-}$ containing dissimilar metals (Hg,W) and different terminal ligands (S,CCH) has no center of symmetry, the centrosymmetric space group P $\bar{1}$ has been accommodated by introducing a two fold disorder. The structure has been solved and refined using Hg/W and S/C atoms disordered over the same positions and having identical thermal parameters.

P08.02.003 CONSTRAINED REFINEMENT OF COMMENSURATELY MODULATED DIMETHYLTIN DICHLORIDE DIBENZYL SULFOXIDE, A.D. Rae, Research School of Chemistry, Australian National University, Canberra, ACT 0200, Australia, Seik Weng Ng, Institute of Postgraduate Studies and Research, University of Malaysia, 50603 Kuala Lumpur, Malaysia, M.W. Gluth, LG International Gmbh, 60528 Frankfurt, Germany.

The $P2_12_12_1$ average structure of Dimethyltin dichloride dibenzyl sulfoxide has been reported (S.W. Ng & A.L. Rheingold, *J. Organomet. Chem*., **378**, (1989), 339-345). We now report the superstructure, also in space group $P2_12_12_1$ but with the *a* axis increased 7 fold. This is a commensurate case of the 3+1 dimensional superspace group, $P2_12_12_1(\alpha 00)$, with α = 8/7 and a coherent overlap of satellite reflections with structure factors $F(\mathbf{g} + m\mathbf{q})$ and $F(\mathbf{g}' - (7-m)\mathbf{q})$. The asymmetric unit contains 7 pseudo translationally related molecules and the structural parameters of an asymmetric unit are given by

$$\Delta p_j(\mathbf{1},\mathbf{t}_m) = a_{j0} + \Sigma_{n=1,3}\,[a_{jn}\cos(n\omega(\mathbf{t}_m)) + b_{jn}\sin(n\omega(\mathbf{t}_m))],$$

where $\omega(\mathbf{t}_m) = 2\pi\,\mathbf{q}.\mathbf{t}_m$, $\mathbf{q}$ = 8/7 $\mathbf{a}_o^*$ and $\mathbf{t}_m = m\mathbf{a}_o$, m = 0 to 6. $\Delta p_j(\mathbf{1},\mathbf{t}_m)$ is the change from the parent structure value of the jth molecule based parameter describing the molecule defined by the parent structure translation operation $(\mathbf{1},\mathbf{t}_m)$ acting on the reference molecule. Sets of 7 modulation wave parameters, a_{jn} and b_{jn}, offer an alternative description to sets of 7 parameters $\Delta p_j(\mathbf{1},\mathbf{t}_m)$ and permit a hierarchical approach to structure determination and refinement. The program *RAELS96* was used for the refinement. Standard parameters, including those defining local axes used to define refinable local co-ordinates, are defineable in terms of extra parameters, in this case the modulation wave parameters. For an incommensurately modulated structure, parameters $a_{jn}+ib_{jn}$ can be changed by a global phase Φ to $\exp(in\Phi)\ (a_{jn}+ib_{jn}) = (a'_{jn}+ib'_{jn})$ changing structure factors $F(\mathbf{g} + m\mathbf{q})$ to $\exp(im\Phi)\ F(\mathbf{g} + m\mathbf{q})$. For our commensurate structure, this allowed comparative refinement to demonstrate the correctness of our model for $F(\mathbf{g} + m\mathbf{q}) + F(\mathbf{g}' - (7-m)\mathbf{q})$. The modulation appears to involve transverse waves allowing a more dense packing of molecules by shortening the *a* axis repeat and allowing the phenyl rings to have better contact.

P08.02.004 THE R2-CRITERION AS A FIGURE OF MERIT IN PATTERSON APPLICATIONS. Paul T. Beurskens, Gezina Beurskens, Randy Israel and René de Gelder, University of Nijmegen, 6525 ED Nijmegen, The Netherlands.

After 65 years of Patterson methods, Patterson applications play a major role in most crystal-structure investigations of small- or macromolecular, periodic or aperiodic, single- or polycrystalline materials.

In the DIRDIF-program system for the crystal structure analysis of inorganic, and small and medium-sized (metallo-)organic molecules two distinctly different types of Patterson methods are used.

I.For heavy-atom structures (ranging from an organic molecule with one sulphur atom to a coordination complex with 13 gold atoms) the heavy atom position(s) is (are) extracted from the Patterson synthesis. In those cases where more than one set of atomic positions are found to be compatible with the Patterson, the R_2 criterion can be used to select the most probable set.

II.For molecular structures where the approximate geometry of part of the molecule is known (or a limited number of configurations can be predicted) the vector-search strategy is used to find the orientation of the input molecular model, and its position relative to the symmetry elements. In many cases more than one possible solution is found, and the most probable solution (atomic coordinates of the model in the unit cell) can be selected using the R_2 criterion.

The conventional, unweighted R_2 value is

$$R_2 = \Sigma\,(F_o^2 - F_p^2)^2 / \Sigma\,F_o^4$$

where Σ is the sum over all reflections and F_p is the structure amplitude calculated for the trial partial structure (heavy atoms or molecular fragment). For the use of R_2 as a reliable criterion [1], F in this definition is substituted by F/g where g is the normalizing factor for F_o ($E_o = F_o/g$).

The use of R_2 as a figure of merit greatly enhances the applicability of Patterson methods in automated structure-solution procedures.

1. W.K.L. van Havere & A.T.H. Lenstra (1983). Acta Cryst. A39, 920-924.

P08.02.005 PSEUDOSYMMETRY AND STRUCTURES WITH MORE THAN ONE MOLECULE IN THE ASYMMETRIC UNIT. Rita G. Hazell, Department of Chemistry, Aarhus University, DK 8000, Århus C, Denmark

Lately we have come across several structures with more than one molecule in the asymmetric unit, and with pseudosymmetry, and as it was pointed out by Carolyn Pratt Brock [1], this means that refinement is only stable if constraints are applied; in some cases some or all the restrictions can be lifted in the final stages, though. The programs we use for this are based on the principles outlined by G.S. Pawley [2] and will be described, and the use illustrated by examples.

The structures investigated fall into different categories, and we look for possible reasons for the behavior: in one type of optically active compound it seems to be the rule, that they crystallize in a non-centro- symmetric space group but in a nearly centrosymmetric arrangement, except that the chiral part destroys this symmetry. Another crystal grew from a racemic mixture under partial resolution, again in a pseudo-symmetric arrangement; in this case the hydrogen bond scheme favoured the non-centrosymmetric arrangement, but the packing was loose enough for mistakes to occur, so a disordered structure resulted, causing even more trouble for the refinement.

1. Carolyn Pratt Brock, Acta Cryst. A52, 1996, C-43,
2. G.S.Pawley, Adv. in Structure Research by Diffraction Methods 4, 1971, 1.

P08.02.007 REFINEMENT OF TWO TWINNED SINGLE CRYSTALS. Jürgen Kopf, Ulrich Behrens, Institut für Anorganische und Angewandte Chemie der Universität Hamburg, Martin-Luther-King-Platz 6, D-20146 Hamburg, Deutschland und Otto Jarchow, Mineralogisch-Petrographisches Institut der Universität Hamburg, Grindelallee 48, D-20146 Hamburg, Deutschland.

The existence of twinning has often prevented investigators from successfully measuring, phasing and completing the refinement of such structures, even though the X-ray intensity data were of very high quality. Two twinned structures, one example from organic the other from organometallic chemistry, with Z' = 3 were refined with SHELXL97 [1] and will be presented. The two solved structures belong to twin class IV [2]. In this class some reflections completely overlap and some behave as single crystal data. The common orthorhombic super-lattice of the twin individuals can be constructed from the monoclinic sub-lattice of the overlapped reflections. In our cases the single individuals belong to space group $P2_1/a$ and form a three-fold primitive (0,0,0; 1/3,0,1/3; 2/3,0,2/3) unit cell. We will describe how the twinning was recognized, measured and solved and how the twin matrix was derived. Different refinement strategies with the SHELXL97 program will be discussed.

[1] Sheldrick, G. M. (1997). *SHELXL97. Program for the Refinement of Crystal Structures* . University of Göttingen, Germany.
[2] Jarchow, O. (1998). *Überstrukturen und Verzwilligungen. Vorlesungs- skript* . University of Hamburg, Germany.

P08.02.008 ABSORPTION CORRECTION OF CCD-DATA FROM WB (LIN.ABS.COEFF.=1370 cm^{-1}). M. Ruf, L. Häming, E. Hovestreydt Application Laboratory, Bruker-Analytical X-Ray Systems, Karlsruhe, Germany

A successful crystal structure determination depends upon the accurate analysis of the X-ray diffraction pattern of the single-crystal specimen. The measured intensities may often be affected by other factors, such as absorption of X-rays by the crystal being analyzed.

Appropriate corrections must be applied to the experimental data to account for such effects if accurate, publication-quality results are to be obtained.

The SMART 1000 CCD System has been used to carry out a structure determination of WB with a linear absorption coefficient of 1370 cm^{-1}.

For a specimen with well defined faces the SMART crystal face indexing routine has bee used, which allows the faces of the specimen to be indexed and measured through the standard video microscope. These crystal face indices have been used to apply a numerical Gaussian absorption correction.

The high redundancy of the data and calculated direction cosines for every reflection together with the Laue class were used to apply an empirical absorption correction using SADABS. The program performs absorption correction for incident and diffracted beam.

Both methods provide easy to use tools for appropriate absorption correction. The data from both, numerical and empirical, absorption corrections yield publication quality results whereas it is not possible to refine the structure against uncorrected data.

P08.02.009 DISORDER AND TWINNING OF THE REACTION PRODUCTS OF MELAMINE AND PCL_5. F. Belaj, Institute of Inorganic Chemistry, Karl-Franzens-University of Graz, A-8010 Graz, Austria.

By reaction of melamine with PCl_5 in $C_2H_4Cl_2$ a triclinic (**T1**) and a monoclinic (**M**) modification of 2,4,6-tris(trichlorophosphazeno)-1,3,5-triazine containing solvent molecules and PCl_6^- anions (and Cl^- anions in **M**) were obtained. Due to disorder of the solvent molecules the R-indices R1 were larger than 0.1 and the position of the positive charge could not be localized [1] although the single crystal data were collected at 95K. Recrystallization from $C_2H_2Cl_4$ resulted in another triclinic phase (**T2**) but did not solve the problem. Only when the disorder of the solvent molecules (and partly of $NPCl_3$ groups directed to solvent molecules) was resolved, the hydrogen atoms attached to a nitrogen atom of the triazine ring could be localized and the three compounds unambiguously identified as $H[C_3N_3(NPCl)_3]_2^+ PCl_6^- \cdot C_2H_4Cl_2$ (**T1**), $[HC_3N_3(NPCl_3)_3]_2^+ Cl^- PCl_6^- \cdot 3C_2H_4Cl_2$ (**M**), and $[HC_3N_3(NPCl_3)_3]^+ Cl^- \cdot C_2H_2Cl_4$ (**T2**).

From these ionic compounds the solvent-free molecular compound $C_3N_3(NPCl_3)_3$ could be synthesized by sublimation. The intensity-weighted reciprocal lattice shows 6/m symmetry but refinements in several hexagonal and trigonal space-groups resulted in R-indices R1 not smaller than 0.22. Finally the structure could be solved and a twinned model be refined to R1 = 0.0492 (7938 significant unique reflections, 381 parameters) without any constraints (except fixing the origin) in the space group P 3_1. The examination of the arrangement of the molecules in the unit-cell shows that there are good reasons for twinning of this compound. Whereas both molecules of the asymmetric unit of this trigonal compound show the most symmetric conformation, all the five independent cations determined in the three asymmetric units of **T1**, **M**, and **T2** show almost planar but asymmetric conformations with the H atoms always bonded to those N atoms of the triazine rings from which two $NPCl_3$ groups are turned away.

[1] F. Belaj, Phosphorus, Sulfur, and Silicon, **109-110**, 71-74 (1996).

P08.02.010 STRUCTURAL CHARACTERIZATION OF THE FAULTED PHI-TYPE ZEOLITE LZ-276. Richard M. Kirchner [1] and Robert W. Broach [2], [1] Manhattan College, Chemistry Department, Bronx, NY 10471, USA, [2] UOP Research & Development, 50 E. Algonquin Road, Des Plaines, IL 60017 USA

Structural characerization of the faulted phi-type zeolite LZ-276 was successfully accomplished using diffraction pattern simulations and statistical analyses. Powder x-ray diffraction patterns (PXRD) for LZ-276 display both sharp and broad peaks suggesting disorder. TEM selected area diffraction patterns show twin spots and considerable streaking parallel to {00l} indicating faulting along c. Attempts to model the disorder using Rietveld techniques were unsatisfactory. However, the PXRD pattern of LZ-276 was successfully simulated using the DIFFaX technique [1]. An all-silica model was presumed using idealized atom positions and cell coordinates taken from the structure of chabazite. Cell parameter a was determined from indexing the sharp peaks in the PXRD pattern, while c is an average value for similar chabazite-type (CHA) structures. Idealized atomic coordinates from a distance least-squares (DLS) refinement were used in the DIFFaX program to simulate the powder pattern. The simulated pattern agrees well with the experimental pattern and indicates a faulting probability of 0.10 (10% random faulting). The generation and distribution of new and different sized cages formed by faulting, and how these may affect physical properties such as sorption, will be described.

1. MacDIFFAX, version 1.801, M. M. J. Treacy, J. M. Newsam and J. W. Deem, Proc. R. Soc. Lond., 1991, 433, 499.

P09.02.002 LOW RESOLUTION PHASING OF SUPER OXIDE DISMUTASE (SOD) USING THE PROGRAM FSEARCH. D. Ockwell, M Hough and Q. Hao, De Montfort University, Leicester, LE1 9BH, UK, and S.S. Hasnain, CLRC Daresbury Laboratory, Warrington, WA4 4AD, U.K.

Solution of the phase problem is of primary importance in crystallographic structure determination and often the most difficult and time-consuming. Isomorphous and molecular replacement methods require the availability of an isomorphous heavy-atom derivative or the structure of a homologous protein, respectively, before the problem can be addressed. An alternative method utilising the low-resolution molecular shape determined from solution X-ray scattering data using the program FSEARCH had located the molecular shape of the three-fold axis molecule nitrite reductase (AxNiR) from Alcaligenes xylosoxidans within the crystallographic unit cell [1]. The heart of the method involves locating the molecule within the crystallographic unit cell by first using the program ALMN in the CCP4 suit [2] to ascertain the polar angles of the non-crystallographic axis followed by a four dimensional search (Eulerian angle γ and three translational parameters). In light of the success of this technique, the program FSEARCH is being developed and modified further to handle general structures from all space groups. As a test for the veracity of this method, work is under way locating the orientation of the two-fold axis molecule super oxide dismutase (SOD) within the unit cell. Systematic data absences in the experimental data would cause FSEARCH to fail in its search for the correct orientation solution. However, given a complete dataset FSEARCH produced the lowest R factors for *a priori* correct solution and high R factors for random incorrect orientation.

1. Q. Hao, F. E. Dodd, J. G. Grossmann & S. S. Hasnain (1999), *Acta Cryst*. **D55**, 243-246.
2. Collaborative Computing Project, Number 4 (1994), *Acta Cryst*. D50, 760-763.

P09.02.003 AB INITIO PHASING OF A PROTEIN, PSEUDOAZURIN AT 1.55Å RESOLUTION BY DIRECT METHOD. Monika Mukherjee, Department of Solid State Physics, Indian Association for the Cultivation of Science, Calcutta 700032, India.

The direct method program MULTAN/SAYTAN has been successfully applied to solve three small known proteins, aPP (302 protein atoms, space group C2), rubredoxin (397 protein atoms, space group $P2_1$) and Rnap1 (808 protein atoms, space group $P2_1$) ab-initio with atomic resolution data (<1.2Å resolution). To explore the possibility of this methodology to lower resolution data and crystal having higher symmetry, the present study of ab-initio phasing of a known protein, pseudoazurin (space group $P6_5$,cell parameters a=b=50.0(1), c=98.5(3)Å; 917 protein atoms + Cu + 93 solvent water in the asymmetric unit and data to 1.55Å) was undertaken by direct method.

By making several 1000 trials at 1.55Å resolution with sets of initially random phases MULTAN88 yielded ab-initio phases for 1000 reflections with lowest mean phase error of 68.2^o (79.4^o for the enantiomorph pair). Using top 1000 peaks as input from the E-map, the unstrained least-squares refinements using the conjugate gradient algorithm (CGLS) were carried out by changing the range of resolutions. After the first 10 cycles of refinement the R value was 0.233 (for 6-2.5Å resolution). The corresponding values for the subsequent cycles with increased resolution ranges were R=0.226, 0.280, 0.303 for 9-2.5Å, 9-2.0Å, 9-1.55Å respectively. Interpretation of the Fourier map at this stage showed a distorted tetrahedral geometry around the copper site. Building of the protein model was however not successful due to poor connectivity of the map. Efforts are on to improve the quality of the maps by solvent flattening / density modification before any further least-squares refinement is contemplated.

P09.02.004 A TRANSLATION-PACKING FUNCTION FOR POSITIONING A PROTEIN MOLECULE USING VERY LOW ORDER REFLECTIONS. K. M. Andersson and S. Hovmöller, Dept. of Structural Chemistry, Arrhenius Laboratory, Stockholm University, S-106 91 Stockholm, Sweden.

A method for predicting the position of protein molecules in the unit cell based on the very low order reflections and packing considerations is presented. At very low resolution, the electron density is very blurred, such that a protein molecule may well be approximated as a sphere [1]. A sphere with the same volume as the unknown protein [2] was translated in small (2-3 Å) steps in the unit cell until maximum overlap between the amplitudes calculated from the sphere and the true protein was found.

A molecular packing using spheres can be calculated to restrain the allowable regions. This makes the positioning of the protein molecule even more reliable. Structure factors of the 10 or so lowest order reflections were calculated with a sphere at the best position. These structure factors agreed closely to those of the true structure [3]. The combined translation and packing algorithm has been successfully tested for 16 proteins. For 12 out of 16 proteins tested, the position of the center of the molecule was correctly predicted to within 5 Å. The phase error for these reflections are less than 40°.

Furthermore, a qualitative deduction of deviations from the spherical model can be gained by comparing structure factors from the spherical model and the true protein. This may be used to modify the initial spherical model to a non-spherical envelope. The very low resolution phasing obtained by this method may be used as powerful starting set for phase extension methods like maximum entropy [4].

1. K.M. Andersson & S. Hovmöller (1996). Acta Cryst., **D52**, 1174.
2. K.M. Andersson & S. Hovmöller (1998). Z. Kristallogr., **213**, 369.
3. K.M. Andersson (1999). submitted to J. Appl.Cryst. 4. K.M. Andersson & C.G.J. Gilmore (1999). to be submitted.

P09.02.006 TOWARDS MACROMOLECULAR ENVELOPE DETERMINATION USING ANOMALOUS DISPERSION AND CONTRAST VARIATION. W. Shepard†, M. Ramin†, R. Kahn§, J. Vivat§, E. Girard§ & R. Fourme† † LURE, Bât. 209d, Université Paris-Sud, 91898 Orsay, France, § IBS, 41 Avenue des Martyrs, 38027 Grenoble, France

Contrast variation can be generated by diffusing an anomalous scatterer into the solvent regions of a macromolecular crystal and then tuning the X-ray wavelength in the vicinity of an appropriate absorption edge [1]. This method has been implemented as a low resolution variant of MAD known as MASC [2], an acronym for Multiple-wavelength Anomalous Solvent Contrast, where the anomalous partial structure is no longer punctual and ordered, but instead an extended density confined to the solvent region of the crystal. As such, the MASC method directly provides the structure factor moduli of the solvent regions in the crystal, an important step in determining the macromolecular envelope.

Test case studies [3] on proteins of varying size (molecular weights from 14kDa to 174kDa) and soaked in a variety of anomalous scatterers show good agreement with the expected anomalous signal: very strong in the lowest resolution shells and rapidly diminishing with increasing resolution. In virtually all of the cases studied, the anomalous effects also reveal the presence of the anomalous scatterer bound in ordered sites combining MAD and MASC signals.

Methods of general applicability for phasing the normal structure factors of the anomalous structure in the MASC case (equivalent to the $^{\circ}F_A$ in the MAD case) are being investigated. We shall report results obtained using different approaches, in particular with spherical harmonics, for reconstituting the macromolecular envelope from MASC data.

1. Bricogne, G. (1993) *Acta Cryst.*, **D49**, 37-60.
2. Fourme, R., Shepard, W., Kahn, R., l'Hermite, G. & Li de la Sierra, I. (1995) *J.Synchr. Rad.* **2**, 36-48.
3. Ramin, M., Shepard, W., Fourme, R. & Kahn, R. (1999) *Acta Cryst.*, **D55**, 157-167.

P11.02.001 CRYSTAL STRUCTURE DETERMINATION OF PHARMACEUTICALS FROM POWDER X-RAY DIFFRACTION. S.A. Murphy and R.B. Hammond, Centre for Molecular and Interface Engineering, Department of Mechanical and Chemical Engineering, Heriot-Watt University, Edinburgh, EH14 4AS, and R. Roberts, Zeneca Pharmaceuticals Ltd, Hurdsfield Estate, Macclesfield, Cheshire, SK10 2NA.

One long term goal of the scientific community is to be able to predict crystal structures ab initio from knowledge of the molecular structure (1). However, in the shorter term, development of a routine methodology to allow solution of crystal structures of molecular, organic materials by combining powder X-ray diffraction with molecular modelling seems more tractable. To achieve structure solution from powders, a major task is the generation of reliable trial structures to refine. A computer program carrying out a systematic search for packing arrangements in the unit cell has been developed, treating the molecule as either a rigid body or as a flexible entity with up to two internal rotations. Calculated lattice energies and the match of the theoretical and experimental powder patterns are employed to rank the trial structures. Structures already studied as rigid bodies include indigo, 6,13-dichlorotriphendioxazine, phenanthrene, and the pharmaceutical materials primidone and paracetamol. Two torsions describing the orientation of the phenyl moieties, have been treated explicitly in the case of benzophenone (2). Further studies have been undertaken for primidone in which the internal degrees of freedom are treated within the systematic search. Results will be presented for primidone which contrast the use of the systematic searches for trial structures in a fixed unit cell with a Monte Carlo, simulated annealing method, based on calculated lattice energies, which has also been developed.

Maddox, J., Nature, 335 15 (1988) 201. :
Gavezzotti, A., Acc. Chem. Res., 27 (1994) 309-314.
Hammond, R. B., Roberts, K. J., Docherty, R., Edmondson, M., J. Phys. Chem., B101 (1997) 6532-6536.

P11.02.002 STRUCTURE DETERMINATION FROM POWDER X-RAY DIFFRACTION DATA: APPLICATION TO HYDROGEN-BONDED SYSTEMS. E.D.L. Smith, R.B. Hammond, and K.J. Roberts, Centre for Molecular and Interface Engineering, Department of Mechanical and Chemical Engineering, Heriot-Watt University, Edinburgh EH14 4AS, U.K and R. Docherty, Zeneca Specialties Research Centre, Hexagon House, Blackley, Manchester M9 8ZS, U.K.

When determining crystal structures of organic molecular materials from high-resolution powder diffraction data the key step is the generation of reliable trial structures for final refinement. Recent advances have been made with respect to this and there are presently several approaches: Metropolis Monte Carlo; genetic algorithms; systematic grid search. The systematic approach uses a grid based search of rotations and translations to assess **all** the possible packing arrangements within a given unit cell. Calculated lattice energies in conjunction with a quantitative comparison of the calculated and experimental diffraction pattern are used to rank the trial structures. The application of two independent ranking methods provides a more robust basis upon which to select trial structures. The strategy is applied to anhydrous theophylline, which contains both oxygen and nitrogen as possible hydrogen bonded atoms. A systematic search found two packing arrangements within the same unit cell, exhibiting clearly distinct hydrogen bonding motifs. These were 'indistinguishable' in terms of their calculated lattice energy or a comparison of their respective, calculated powder X-ray diffraction patterns. Subsequent to commencing this work, one of these structures was independently verified by single crystal techniques. However, in the literature there is evidence to suggest that there exists another polymorph. The research presented here seeks to determine whether this is the case. In addition, the methodology described above was applied to previously determined structures (with similar functional groups), in order to test the feasibility of alternative hydrogen bonding motifs for a given molecule without substantial change of the unit cell.

P11.02.003 AB-INITIO POWDER STRUCTURE ANALYSIS OF TWO POLYMORPHS OF DIHYDROXYSILICON PHTHALOCYANINE. Y.Kojima, Y.T.Osano, T.Ohashi, Yokohama Research Center, Mitsubishi Chemical Corporation, Yokohama 227-8502, JAPAN

We report ab-initio X-ray powder structure determination of two polymorphs of [$Si(OH)_2Pc$], where Pc=phtalocyaninato. We found that one of the polymorphs(Phase II) shows high sensitivity for an electrophotographic photoreceptor but the other(Phase I) doesn't have the photosensitivity. The difference in the sensitivity depends on only the crystal structures. This material has not been able to be grown to single crystal with enough size for single crystal X-ray analysis but it is very important to determine the crystal structures of the two polymorphs to understand mechanism of performance of the electrophotographic photoreceptor. In this work we carried out ab-initio X-ray powder structure analysis. The compound crystallizes in space group P-1

(Phase I), Z=1 with unit-cell parameters a=12.992(1)Å, b=7.2830(8)Å, c=6.861(1)Å, α=104.413(7)º, β=101.575(8)º, γ=96.973(6)º and in space group $P2_1/n$ (Phase II), Z=2 with unit-cell parameters a=12.749(5)Å, b=14.578(6)Å, c=6.7727(3)Å, β=94.353(2)º. Both phases have symmetry center in the molecules (on Si atom) and intermolecular hydrogen bonds (O-H...N). These hydrogen bonds modes of Phase I and Phase II are the same. The main difference packings was revealed between the crystals, Phase II crystal has the herringbone structure, on the other hand in Phase I all molecules form the parallel stack columns.

P11.02.004 CRYSTAL STRUCTURES OF REMACEMIDE BASE, NITRATE AND ACETATE FROM X-RAY POWDER DIFFRACTION DATA. L.McBride[1], K.Shankland[2], W.I.F. David[2], G. Steele[3]. 1. Pharmaceutical Sciences, University of Strathclyde, UK. 2. ISIS Facility, Rutherford Appleton Laboratory, UK. 3. Astra Charnwood, UK.

Powder X-ray diffraction data were collected for the Astra Charnwood compound remacemide base and its nitrate and acetate salts. The data were collected at 130K on BM16 of the European Synchrotron Radiation Facility (λ=0.85075Å). High quality simulated annealing solutions were obtained with ease for all three structures. Crystallographic data for the 3 compounds are given in the table.

The remacemide molecule adopts similar conformations in the nitrate and acetate salts, and a markedly different conformation as the free base.

	Remacemide base	Remacemide nitrate	Remacemide acetate
Space grp	$P2_1/c$	$P2_1/a$	$P2_1/c$
a /Å	8.92452	11.72513	15.39513
b / Å	16.53619	8.93186	6.76487
c / Å	9.84803	15.87040	17.34326
β / °	93.806	95.955	93.134

P11.02.005 TRANSITION METAL COMPLEXES CONTAINING NEW PYRAZINE DERIVED LIGANDS: STRUCTURE DETERMINATION FROM LAB X-RAY POWDER DATA. A. Neels, T. Assoumatine and H. Stoeckli-Evans, Institut de Chimie, Université de Neuchâtel, 2000 Neuchâtel, Switzerland.

Pyrazine and its derivatives have been used in the formation of fascinating 1D, 2D or 3D polymeric structures. These compounds are studied for their interesting macroscopic behaviour such as molecular magnetism or photochemical properties.

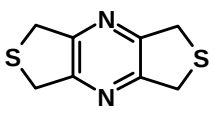

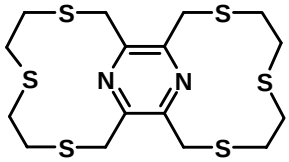

Some new sulphur containing pyrazine derivatives have been designed and studied in complexation reactions with various transition metal ions. The ligand ***L1*** forms easily polymeric compounds with copper(I), silver(I) or gold(I). Since the gold complex could only be obtained in micro-crystalline form, its structure was solved by X-ray powder methods and then Rietveld refined. The diversity of the coordination possibilities of the ligand ***L1*** is documented by a structure comparison.

The new bis-macrocyclic ligand ***L2*** has been synthesised and used in the formation of some first row transition metal complexes. The reaction of ***L2*** with nickel(II) nitrate resulted in the formation of an insoluble micro-crystalline product, which was used in a X-ray powder diffraction experiment. The structure of this binuclear nickel(II) complex containing 21 atoms per asymmetric unit was determined from these laboratory X-ray powder data.

P11.02.006 CRYSTAL STRUCTURE OF 3,5-DI-*ISO*-PROPYL-4-NITRO-PYRAZOLE FROM X-RAY POWDER DIFFRACTION DATA. L.E. Ochando and J.M. Amigó, Departamento de Geología, Universidad de Valencia, Campus de Burjassot, Spain , J. Rius, Institut de Ciència de Materials de Barcelona, CSIC, Catalunya, Spain, and D. Louër, LCSIM - UMR 6511, Université de Rennes I, 35042 Rennes, France.

The crystal structure of the titled compound has been solved from laboratory X-ray powder diffraction data by Patterson Search methods [1]. Crystal data : monoclinic symmetry with the unit cell parameters a = 28.800(5) Å , b = 6.485(1) Å and c = 17.944(3) Å, β = 138.17(1)° , *C2/c* space group, $C_9H_{15}N_3O_2$, Z = 8 , 293 K. This new pyrazole derivative has not been studied before by diffraction methods. Because of difficulties in preparing single-crystals which were suitable for a classical single-crystal analysis, diffraction measurements in a limited scattering range were carried out on untreated powder sample. This study is a continuation in structural characterisation of pyrazole compounds as described previously [2]. Indexation of the powder diffraction data gave a high figures of merit: M_{20} = 20.3 and F_{30} = 35.1(0.0067, 127). Eighty-five unambiguously indexed and thirty-seven systematically overlapped integrated intensities were extracted by means of the whole pattern fitting program AJUST [3]. The search model was oriented in the monoclinic unit cell by the program ROTS96 [4]. The subsequent rigid-body Rietveld refinement will be performed with the program RIBOLS [5] and will be presented and discussed.

[1] Rius, J.; Miravitlles, C. (1987). *J. Appl. Cryst.* **20** , 261-264.
[2] Ochando, L.E. *et al.* (1997). *Acta Cryst.* **B53** , 939-944
[3] Rius, J. et al. (1996). Anales de Química Int. Ed. **92**, 223 - 227.
[4] Rius, J.; Ochando, L.E. (1996). ROTS96, a program system for solving molecular structures by Patterson search methods. ICMAB-CSIC, Catalunya, Spain
[5] Rius, J. (1989). RIBOLS : A rigid-body least squares program for powder data. ICMAB-CSIC, Catalunya, Spain

P11.02.008 *IN-SITU* STUDY OF THE SOLID STRUCTURE OF HCFCS AND HFCS BY X-RAY POWDER DIFFRACTION. M. Brunelli, European Synchrotron Radiation Facility, B.P. 220, F38043 Grenoble Cedex, France A. N. Fitch, European Synchrotron Radiation Facility, B.P. 220, F38043 Grenoble Cedex, Department of Chemistry, Keele University, Staffordshire, ST5 5BG, UK

The hydrochlorofluorocarbons (HCFCs) and the hydrofluorocarbons (HFCs) are the replacement refrigerant of the ozone-depleting chlorofluorocarbons (CFCs) which are being phased out as a result of the Montreal Protocol (1988). The advantage of these compounds is that they are more reactive chemically and break down at lower altitudes before they reach the ozone layer. Powder diffraction is a suitable technique because it is far easier to handle the fluids as powders. We studied the low temperature crystal structure of 1-Chloro-1,1-difluoroethane (142b, CF_2ClCH_3), 1,1-difluoroethane (152a, CH_3CHF_2) and 1,1,1,2-Tetrafluoroethane (134a, FCH_2CF_3) using high resolution synchrotron powder diffraction on beam-line BM16 at ESRF, Grenoble.

On BM16 we have built an *in-situ* gas-handling system that allows volatile compounds to be condensed directly in a thin-walled glass capillary mounted on the axis of the diffractometer. Following the condensation, the capillary can be disconnected from the gas line, and spun normally for powder diffraction studies. The *in-situ* experimental set-up will be presented. Powder

diffraction patterns of the solids phases have been measured down to 80 K using the Cryostream cold-nitrogen-cooler.

P11.02.009 SPACE GROUP DETERMINATION FROM A SAMPLE OF POWDER DIFFRACTION INTENSITIES USING A BAYESIAN METHOD. A.J. Markvardsen, W.I.F. David and D.S.Sivia, ISIS Facility, Rutherford Appleton Laboratory, Chilton, Didcot, Oxon. OX11 0QX, UK.

Space-group determination from powder diffraction data is often hampered by difficulties in reliably determining systematic reflection absences. This arises because powder diffraction patterns contain, almost without exception, Bragg peak overlap resulting from the projection of three dimensions of diffraction data on to the one dimension of the diffraction pattern.

We present a Bayesian method for reliably determining the probability distribution of different space groups from a least-squares integrated-intensity (Pawley) refinement of the powder diffraction data. The method involves the Monte Carlo integration technique to calculate the probabilities of different space group choices given a set of powder diffraction intensities, and the results indicate that it is possible to extract the space group reliably and quickly from powder diffraction data.

P12.02.000 DIRECT DETECTION OF BIJVOET DIFFERENCES FOR CU Kα RADIATION IN A LIGHT-ATOM MOLECULE. Shoichi Sato, X-ray Research Laboratory, Rigaku Corporation, Matsubaracho 3-9-12, Akishima, Tokyo 196-8666, Japan

Detection of Bijvoet differences of a light-atom molecule by means of common laboratory X-ray source is usually very difficult. In the present investigation on α-cytidine, however, the differences could be successfully detected by an application of routine method of structure analysis by four-circle diffractometry with a spherically shaped crystal. Inspection of the diffraction data collected on an AFC5 with Cu Kα radiation showed that many reflections had large intensity deviations from those of other Bijvoet pairs, especially as intensity enhancements of the weaker ones. Such intensity deviation of a particular reflection was similarly observed for its Friedel mate. This trend strongly suggested that the deviation came from not some accidental instability of the instrument but multiple reflection and that the angular settings of the crystal were very good in the course of data collection. After reflections with deviations of eight times its own esd from the mean value of the equivalents were removed, the rest was averaged to a set of Bijvoet pairs and used for the structure refinement. From 30 Bijvoet differences with large ΔF/esd, the absolute configuration of the molecule could be determined without ambiguity so that the observed and calculated differences had the same senses. The absolute configuration thus deduced was consistent with that already reported by Subramanian & Hunt [1] on a chloride crystal. The R values were R=0.0232, Rw=0.0312, S=1.60 and Flack parameter was 0.03(3) for the correct configuration; whereas those for the inverse structure were slightly large as R=0.0235, Rw=0.0319 and S=1.60. All the results showed no contradiction on the configuration of the molecule. [α-Cytidine: C9H13N3O5, orthorhombic, $P2_12_12_1$, Z=4; a=13.985(1), b=14.765(1) and c=5.117(1)Å; V=1056.6(2)Å^3.]

1. E.Sabramanian & D.J.Hunt. (1970). Acta Cryst. B26, 303.

P12.02.001 DIRECT PHASE DETERMINATION FOR MACROMOLECULAR CRYSTALS BY STEREOSCOPIC MULTI-BEAM IMAGING. S.L. Chang, C.H. Chao, Y.S. Huang, F.J. Liang, Yu.P. Stetsko, H.C. Chien, and C.K.Chen, Department of Physics, National Tsing Hua University, Hsinchu, Taiwan, Y.C.Jean and H.S.Sheu, Synchrotron Radiation Research Center, Hsinchu, Taiwan, R.O.C. and H.S.Yuan, Institute of Molecular Biology, Academia Sinica, Taipei, Taiwan, R.O.C.

Phase information necessary for determining single-crystal structure is lost in the intensity measurement of x-ray reflection. For macromolecular crystals, anomalous dispersion (AD) and heavy atom derivatives are usually employed in phase determination. Here, without invoking AD and derivatives, we demonstrate the direct phase determination of a large number of reflections collected in a short time from macromolecular crystals using a stereoscopic oscillation-crystal imaging technique in a multi-beam diffraction geometry, where two crystallographic axes in opposite directions are employed as the rotation axes. The intensity contrast of the diffraction spots and of the diffraction profile (distribution) versus the varying tilt Bragg angle of the rotation axis in the stereoscopically-related two images yields qualitative and quantitative phase information, respectively. More than 1000 multiple diffraction profiles of tetragonal lysozyme are obtained at the rate of 100 profiles per 30 minutes and more than 500 phases are determined. This technique thus provides a new practical way for direct phase determination of macromolecular crystals.

P12.02.002 COMBINED DIRECT METHODS WITH ISOMORPHOUS REPLACEMENT AND ANOMALOUS SCATTERING TECHNIQUES. S.Banumathi and D.Velmurugan Department of Crystallography and Biophysics, Univesity of Madras, Guindy Campus, Chennai-600 025, INDIA.

In the past fifteen years, the role of anomalous scattering (AS) or isomorphous replacement (IR) technique when combined with traditional direct methods had been widely studied. Applications of these new formulae on error free data of macromolecules seem promising. Attempts are here made in combining both anomalous scattering and isomorphous data with traditional direct methods so as to strengthen the direct method formalism to macromolecular phasing. The joint and conditional probabilitiy distributions are derived for the triplet, quartet and sextet invariants using their first neighborhood for the above situation. Details of the mathematical derivation will be presented. Attempts are being made to apply these formuale with error free data of macromolecules.

P12.02.003 AUTOMATIC PATTERSON METHODS. FROM INORGANIC COMPOUNDS TO PROTEINS. F. Pavelcik, Department of Inorganic Chemistry, Faculty of Natural Sciences, Comenius University, 842 15 Bratislava, Slovak Republic.

The problem of crystal structure determination, usually formulated as the phase problem, can be reformulated as the problem of global optimisation

$$M(\{\mathbf{r}_i\}) = \Sigma_H [F_O^2 - \Sigma_k \Sigma_l f_k f_l \exp(2\pi \mathbf{H}(\mathbf{r}_k - \mathbf{r}_l))]^2, \qquad k, l=1,2,...,N.$$

The reasonable estimates of vector differences, $\mathbf{r}_k - \mathbf{r}_l$, can be obtained from the Patterson function.

Automatic Paterson methods have been developed for heavy atom (inorganic) structures [1] and later extended for organic structures [2]. Recently we have been successful in solving small proteins measured at atomic resolution by these methods.

The structure determination consists of three steps: (a) selection of one or more pivot atoms. Pivot atoms are

systematically generated by symmetry minimum or vector symmetry minimum functions. (b) Atomic minimum superposition function based on these pivot atoms. (c) Automatic Fourier recycling starting from peaks of the superposition map. Fourier recycling is combined with procedures for elimination of false peaks (e.g. holographic refinement). The three steps are repeated until the structure is solved. The best solution is completed by repeated least squares refinement and $2F_o$-F_c or F_o-F_c syntheses. Few examples are given here (2FDN - Ferredoxin, 1AB1 - crambin, 1AA5 - vancomycin, VITD2 - vitamin D_2, Aa - Amino acid residue):

BL238	P-1	$C_{44}H_{60}N_8Na_4O_4$	Z=4	R=0.12
VITD2	$P2_1$	$C_{28}H_{44}O$	Z=8	R=0.17
2PEN	$P2_1$	$C_{65}H_{91}N_{18}O_{25}S_4$	Z=2	R=0.17
1AA5	$P4_32_12$	$C_{134}H_{254}N_{18}O_{96}Cl_8$	Z=8	R=0.22
1AB1	$P2_1$	46Aa	Z=2	R=0.18
2FDN	$P4_32_12$	55Aa, $2(Fe_4S_4)$	Z=8	R=0.16

F. Pavelcik (1994). Acta Cryst. **A50**, 467-474.
F. Pavelcik (1998). J. Appl. Cryst. **31**, 960-962.

P12.02.004 APPLICATION OF THE 'DIRECT METHODS' DIFFERENCE SUM FUNCTION TO THE SOLUTION OF RECONSTRUCTED SURFACE. X. Torrelles, J. Rius, C. Miravitlles [1], S. Ferrer [2], [1] Institut De Ciencia De Materials De Barcelona (C.S.I.C.), [2] E.S.R.F., Bp.-220, F-38043 Grenoble Cedex (France)

The determination of reconstructed surfaces from diffraction data is normally performed in two stages: i) the (x,y) projection of the reconstruction is determined by direct interpretation of the two dimensional partial Patterson map computed with the intensities of the reconstruction in-plane reflections only, and ii) this projection is subsequently expanded to three dimensions by fitting the full data set (in-plane plus out-of-plane data). Unfortunately, interpretation of two dimensional Patterson maps is not a trivial task for reconstructions with large unit cells. Here, an alternative procedure based on the application of the 'direct methods' difference sum function is presented which reduces the two steps to a single highly automated one. This is achieved by simulating an extra periodicity normal to the surface which takes into account all atoms of the reconstruction. In this way a set of reconstruction reflections is generated which can be processed with the same methodology as for superstructure reflections in bulk superstructures. Two known reconstructed surfaces have been selected as test examples: Ge(001) c(4x2) and GaAs(001) p(2x4) [1].

[1] Torrelles, Rius, Miravitlles and Ferrer, Surface Science, (1999), (in press).

P12.02.005 HALF-INTEGRAL STRUCTURE FACTORS AND THE PHASE PROBLEM. A.Mishnev, Latvian Institute of Organic Synthesis, 21 Aizkraukles St., LV 1006, Riga, Latvia

X-Ray diffraction by a crystal can be described by means of different sets of parameters. Conventional approach employs the formulation in terms of standard index (SI) structure factor (SF) magnitudes and phases. In the present work unknown parameters describing the structure are half-integral (HI) (having half-integral Miller indices) SF's, which are related to the SI SF *via* the discrete Hilbert transforms (DHT) [1-2]:

$$F(n_1,n_2,n_3) = -(i/\pi^3)\sum_{h,k,l} F(h+1/2, k+1/2, l+1/2) \times [(n_1-h-1/2)(n_2-k-1/2)(n_3-l-1/2)]^{-1}. \quad (1)$$

The phase problem is formulated as finding HI SF or HI intensities instead of the phases of SI SF. For this purpose the electron density (2) and the Sayre's equation (3) have been expressed in terms of HI SF:

$$\rho(x,y,z) = (1/7V)\sum\sum\sum F(h/2, k/2, l/2)\exp[-i\pi(hx+ky+lz)] \quad (2)$$

$$\begin{aligned} F(n_1,n_2,n_3) = (\theta/7V)\sum\sum\sum \{&F(h+1/2, k, l)F(n_1-h-1/2, n_2-k, n_3-l) \\ &+ F(h, k+1/2, l)F(n_1-h, n_2-k-1/2, n_3-l) \\ &+ F(h, k, l+1/2)F(n_1-h, n_2-k, n_3-l-1/2) \\ &+ F(h+1/2, k+1/2, l)F(n_1-h-1/2, n_2-k-1/2, n_3-l) \\ &+ F(h, k+1/2, l+1/2)F(n_1-h, n_2-k-1/2, n_3-l-1/2) \\ &+ F(h+1/2, k, l+1/2)F(n_1-h-1/2, n_2-k, n_3-l-1/2) \\ &+ F(h+1/2, k+1/2, l+1/2)F(n_1-h-1/2, n_2-k-1/2, n_3-l-1/2)\} \end{aligned} \quad (3)$$

All experimental SI SF magnitudes and small amount of phased SI SF are used as constraints for HI SF magnitude and phase determination. The HI SF are recovered by minimizing the least squares residuals for DHT (1), HI Sayre's equation (3) and prior phase information by a gradient method.

1. A.F.Mishnev (1993). *Acta Cryst.* A49,159-161.
2. A.F.Mishnev (1996). *Acta Cryst*. A52, 629-633.

P12.02.006 UPGRADING THE TWIN VARIABLES ALGORITHM FOR LARGE STRUCTURES. G.Tsoucaris, Laboratoire de Physique, Tour B, Centre Pharmaceutique, Université Paris Sud, 92290 Châtenay-Malabry, FR, P. Tzamalis, K.Bethanis, A.Hountas, Physics and Meteorology Laboratory, Agricultural Univ. of Athens, 75 Iera Odos, 118-55, GR, A.F.Mishnev, Institute of Organic Synthesis, Latvian Academy of Sciences,1006Riga, LV.

Two novelties particularly relevant in the context of Direct Methods, have been applicated in Twin Variables method (Hountas, Tsoucaris,1995)[1].

- The use from the very beginning of a very large set of additional variables defined on reciprocal lattice vectors which can be located beyond the limiting resolution of the observed structure factors. Despite the *extreme dilution* of a very limited initial phase information into this large set of auxiliary variables, the algorithm allows phase refinement and phase extension both within the observed reciprocal sphere and the so called *super-resolution* shell.

- the use of the *crystallographic symmetry as a new figure of merit (FOM) and as a reliable test* for the correctness of the phase extension process.

Tests on real data of protein structures with up to 1000 independent non hydrogen atoms have been performed and considerable refinement and extension in resolution of the phased structure factors from initial 3.5Å to final 1.2Å has been attained.

Preliminary results have been given in two communications (2).

The project is granted by N.A.T.O L.G. 951447

Hountas and G. Tsoucaris. "Twin variables and Determinants in Direct Methods". Acta Cryst. (1995). **A51**, 754-763.

a) G. Tsoucaris, A. Mishnev and A. Hountas. "New developments of the twin variables approach to the crystal structure determination". Abstract PS02.03.15, IUCr Meeting, Seatle, WA (USA), 1996.

b) K. Bethanis, P. Tzamalis, A. Hountas, A. Mishnev and G. Tsoucaris. "Phase extension by the twin variable algorithm". Poster communication in ASI summerschool in Ettore Majorana Centre, Erice, Sicily, Italy. May 22 - June 2, 1997.

P12.02.007 SAYRE'S EQUATION FOR PHASE DETERMINATION AND ANHARMONIC TEMPERATURE VIBRATION OF ATOMS. Sabita Das and G.B. Mitra ,CSS Department , Indian Association for the Cultivation of Science, Calcutta- 700032, India.

Sayre's equation for phase determination tacitly assumes that all the atoms ,constituting the crystal under study , have the same types of atoms throughout the crystal so that the temperature factors of the atoms will additionally be the same in all directions. In actual cases, there is often atomic heterogeneity and anisotropy and anharmonicity of the temperature factors. The squared atoms assumed in deriving the Sayre's equation can be shown to be due to the averaging process of the products of terms in the crystal structure factors. The average terms will depend to a great extent on the anisotropy and anharmonicity of the atomic scattering factors . Mathematical expression derived shows that the extent of anisotropy and anharmonicity of the vibration of the electrons in the atoms constituting the crystal studies leaves a great stamp on the Sayre's constant studies.

P12.02.008 SIR99, A STEP TOWARDS SIR2001: A TOOL FOR AB INITIO CRYSTAL STRUCTURE SOLUTION OF PROTEINS. M.C. Burla and G. Polidori, Dipartimento di Scienze della Terra, Università di Perugia, 06100 Perugia, Italy, and B. Carrozzini and C. Giacovazzo, Dipartimento Geomineralogico, Università di Bari, 70125 Bari , Italy, and M. Camalli and R. Spagna, Istituto di Strutturistica Chimica "G. Giacomello", CNR, C.P. 10 - Monterotondo Stazione - 00016 Roma, Italy.

Shake-and-Bake [1] and more recently Half-Bake [2] have immoderately enlarged the size of crystal structures solvable by direct methods. These programs repeatedly cycle both in real and in reciprocal space, and structure (or phase) refinement is performed in each space.
A more traditional point of view is at the basis of SIR99. It will be shown how and why traditional programs like SIR97 [3] can evolve to SIR99, a package able to solve macromolecular structures, without repeatedly switching from direct to reciprocal space and viceversa. At the end of the procedure a satisfactory structural model with reasonable bond lengths and angles, and sufficiently low values of the crystallographic residual R are obtained, without any user intervention.
The SIR99 has been successfully applied to several large crystal structures among which we notice the following proteins: Crambin, Rubredoxin, Toxin II, Vancomicin and Gramicidin.

C.M. Weeks, G.T. De Titta, R. Miller & H.A. Hauptman (1993). *Acta Cryst*., D**49**, 179-181
G.M. Sheldrick (1998). In: *Direct Methods for Solving Macromolecular Structures*. Ed. By S. Fortier. Kluwer Academic Publishers, Dordrecht, pp. 401-411
A. Altomare, M.C. Burla, M. Camalli, G. Cascarano, C. Giacovazzo, A. Guagliardi, A.G.G. Moliterni, G. Polidori, & R. Spagna (1999). *J. Appl. Cryst*., **3**2. In Press.

P12.02.009 EXPONENTIAL SHAKE-AND-BAKE: CAN SUCCESS BE GUARANTEED? Hongliang Xu, Herbert A. Hauptman, Charles M. Weeks, and Russ Miller, Hauptman-Woodward Medical Research Institute, Inc., 73 High Street, Buffalo, NY 14203-1196, USA.

Shake-and-Bake is a multitrial direct-methods procedure that automatically and repetitively shuttles trial structures between real and reciprocal space (initial coordinates are chosen at random). Phase refinement depends on using a parameter-shift technique to reduce the value of the cosine minimal function (COS). In recent studies, the cosine minimal function has been replaced by one of exponential type(EXP) [1], resulting in a significantly improved success rate. Applications to three large P1 structures (alpha-1 peptide [471 non-H atoms, 1Cl], vancomycin [547 non-H atoms, 12Cl] and lysozyme [1295 non-H atoms, 10S]) have shown that incompleteness of data is typically a more serious problem than measurement errors. By extending error-free data to sufficiently high resolution, 100% success (convergence of trial structures to solution) could be achieved in all three cases by use of the exponential minimal function under appropriate conditions. In general, parameter shift angles of 120-140° gave the best results

This research was supported by NIH grant GM-46733

[1] Xu et al. (1998). Abstract P160, ACA Annual Meeting, Arlington, VA

P12.02.010 COMPARATIVE RESULTS OF ESTIMATES IN COMBINED DIRECT METHODS FOR HIGHER INVARIANTS OR NEIGHBORHOODS. Subhasshini Parthasarthy and D.Velmurugan, Department of Crystallography and Biophysics, University of Madras, Guindy Campus, Chennai-600 025, INDIA.

Results are available in literature on the working of (DMAS) and (DMIR)in the case of Triplets and Quartets. While the results are available for Triplets in their first neighborhood both in the case of DMAS and DMIR, new formulae are derived for second neighborhood for the above mentioned cases. The comparative results on the role of neighborhoods in the relative accuracy on the estimation of the invariants will be presented. The applications are made with the error free data of cytochrome c550. Results for Quartets (in DMAS) and Quintets (in DMIR) in their second neighborhood will help us in arriving at the relative advantages or otherwise of higher invariants and higher neighborhoods.

P12.02.011 REAL SPACE AB INITIO PHASING OF PROTEIN CRYSTALS WITH HIGH RESOLUTION DATA. N. Matsugaki & M. Shiono, Faculty of Science, Kyushu University, Fukuoka, Japan.

A simple density modification, low density elimination (LDE) [1,2], has been developed and implemented as a computer program for solving macromolecular crystals *ab initio* with multi-solution strategy. The remarkable feature of the program is that the phase determination is completely carried out in real space. *Ab initio* phase determination was demonstrated for various known protein structures (molecular weight of 4K - 14K Dalton) which give atomic resolution data. In addition, test trials were made using synthetic data at 1.18Å of a known metalloprotein crystal, which consists of about 4600 independent atoms with 4 cobalt atoms (the space group is $P2_1$ and $Z = 4$): we carefully introduced realistic errors into the data. The initial phases were calculated from a structure containing only one atom in an asymmetric unit, whose coordinate was obtained from a peak in the Patterson-Harker section. After multiple trials out of the highest 20 peaks in descending order, one solution was obtained. The data collection of the crystal is in progress.

[1] Shiono, M. & Woolfson, M. M. (1992). *Acta Cryst.* **A48**, 451-456
[2] Refaat, L. S. & Woolfson, M. M. (1993). *Acta Cryst.* **D49**, 367-371

P12.02.012 COMBINING SHAKE-AND-BAKE WITH MULTIPLE BEAM DIFFRACTION DATA: A SIMULATION. Herbert A. Hauptman1, Charles M. Weeks1, Hongliang Xu1, and Qun Shen2. 1Hauptman-Woodward Medical Research Institute, Inc., 73 High St., Buffalo, NY 14203-1196 USA and 2Cornell High Energy Synchrotron Source (CHESS), 283 Wilson Laboratory, Cornell University, Ithaca, NY 14853 USA.

The minimal principle formulates the phase problem as one in constrained global minimization. The function to be minimized (the objective function) is a measure of the mean-square difference between the triplet cosine invariant and its expected value. One anticipates that, by replacing the objective function by one which measures the mean square difference

between the triplet sine and cosine invariants and their experimentally measured values (rather than their expected values), the power of Shake-and-Bake will be increased. Simulations in which average errors in estimated values of the triplet invariants as large as 50° are permitted show that the expected improvement is in fact realized even at resolutions of 1.5Å or lower. Since the multiple beam diffraction experiment yields estimates of the triplets having average errors of 25° or less, it is expected that the ability to combine Shake-and-Bake with multiple beam diffraction will increase the power of the direct methods. This research was supported by NIH grant GM-46733.

P12.02.013 STRUCTURE DETERMINATION OF A MANNANASE USING THE SAD SIGNAL AT 1.65 Å RESOLUTION. E. Sabini[1], H. Schubert[1], G. Murshudov[1], Matti Siika-Aho[2], Merja Penttila[2] & K.S. Wilson[1] [1]Structural Biology Laboratory, Department of Chemistry, University of York, York, UK. [2]VTT Biotechnology and Food Research, P.O. Box 1501, FIN-02044 VTT Espoo, Finland.

The native structure of a family 5 mannanase from *Tricoderma reesei* has been solved at 1.5 Å resolution using an innovative method based on the Single Anomalous Dispersion signal (SAD) to the resolution of the derivative data, 1.65Å. The success of the procedure used is of especial interest because of the molecular weight of the protein (40kDa).

Glycoside hydrolase family 5 contains many enzymes the majority of which are cellulases whose sequence are only distantly related to the *T. reesei* mannanase. Structures for a number of cellulases from this family are known but none were successful as molecular replacement search models for the *T. reesei* mannanase.

Moreover, since inadequate isomorphous phase information was available, the quality and strength of the anomalous phase information of a non-isomorphous platinum derivative was investigated. The co-ordinates of the two platinum sites were refined using MLPHARE and useful phases were produced using only the anomalous scattering information (SAD).

An atomic model was built in an automated cyclic procedure containing two alternating steps: (1) unrestrained maximum-likelihood refinement in reciprocal space to match properly calculated and observed structure-factor amplitudes and (2) substantial modification of the current atomic model in real space. The procedure produced excellent electron density maps that allowed straightforward building of an essentially complete atomic model.

[1] Sabini, E., Brzozowski, A. M., Dauter, M., Davies, G.J., Wilson, K.S., Paloheimo, M., Suominem, P., Siika-Aho, M., and Penttilä, M. (1998). Acta D Crystallographica. In press.

P12.02.014 DIFFRACTION ANOMALOUS FINE STRUCTURE ON FORBIDDEN AND SUPERLATTICE REFLECTIONS OF $PbZrO_3$, Y.Soejima, T. Toda, T. Nogami and Y. Yamasaki, Department of Physics, Kyushu University, Fukuoka 812-8581, Japan

The characteristics of diffraction anomalous fine structure (DAFS) on forbidden and superlattice reflections have theoretically been discussed on the basis of the symmetry operation in the superstructure of $PbZrO_3$ (ref.). For the forbidden reflections, the site-selectivity of DAFS is well explained in terms of Patterson symmetry of the space group Pbam: since all the Zr atoms occupy 8i site, the environment around the atom is unique. Moreover, all the interatomic vectors connected to Zr atoms are related by mirror symmetry. This results in the fact that the DAFS oscillation vanishes when the polarization of incident X-ray is parallel or normal to the vectors. In contrast, Pb atoms occupy 4g and 4h sites; this means that there are two kinds of circumstances around the Pb atoms. It is found that the DAFS oscillation around the Pb edge vanishes only when the polarization of incident X-rays is parallel or normal to the a- or b-glide plane. For the superlattice reflections, the pattern of DFAS oscillation is affected by the contributions of Pb and Zr atoms to the construction of the superstructure; the detail will be discussed at the presentation. We will also discuss a use of the DAFS for the superstructure determination.

T. Toda, T. Nogami, K. Yamasaki and Y. Soejima, J. Appl. Cryst. (1998) **31**, 423-429.

P12.02.015 DIFFRACTION ANOMALOUS FINE STRUCTURE ON SATELLITE REFLECTION IN Rb_2ZnCl_4. S. Nagao, S. Kuwajima and Y. Soejima, Department of Physics, Kyushu University, Fukuoka 812-8581, Japan

To investigate the local structure of the incommensurate phase of Rb_2ZnCl_4, the diffraction anomalous fine structure (DAFS) on satellite reflections around the Zn K absorption edge has been measured in both the incommensurate and commensurate phases. It is found that the structure factor observed is not affected by anomalous dispersion, in the energy region below the absorption edge; this is consistent with the fact that the modulation mainly consists of that of Cl anions. In the energy region above the absorption edge, intensity oscillation due to DAFS has clearly been observed. That is, the DAFS oscillation pattern on satellite reflections remarkably differs from that on fundamental reflections, in particular in the energy region about 150 eV above the absorption edge; for the region with higher energies the difference is not significant. The difference of the DAFS pattern between the incommensurate and commensurate phases gives us detailed information on the local atomic circumstances around the Zn atoms in the modulated structure. The DAFS oscillation observed at Rb K absorption edge will also be discussed at the presentation.

P12.02.016 PHASE DETERMINATION BY THE WAVELENGTH-MODULATED DIFFRACTION METHOD. H. Iwasaki, N. Nakamura, Y. Yoshimura, A. Ishikawa and T. Koganezawa Faculty of Science and Engineering, Ritsumeikan University, Kusatsu, Shiga 525-8577, Japan

Based on a newly developed method of phase determination [1], X-ray diffraction patterns of single crystals of ferrocene derivatives were taken with synchrotron radiation with continually changing wavelength in the vicinity of the K-absorption edge of the Fe atom. Bragg reflections appeared as elongated spots in the patterns and an intensity gradient derived from their intensity profile has yielded, if the positions of the Fe atoms are properly assumed, the phase of the structure factor for the centrosymmetric case. For non-centrosymmetric crystals, the intensity gradients measured at two wavelength regions or the intensity gradients measured for the Bijvoet pair of reflections yield the phase by solving two simultaneous linear equations. The wavelength-modulated diffraction method is free from the problem of intensity scaling often encountered in other methods of phase determination.

1. H. Iwasaki, T. Yurugi & Y. Yoshimura (1998). Acta Cryst. A, submitted.

P12.02.017 THE STRUCTURE OF $IIA^{MANNITOL}$: ON THE CUTTING EDGE OF MAD. R.L.M. van Montfort, Department of Crystallography, Birkbeck College, London WC1E 7HX, UK, T. Pijning, K.H. Kalk, G.T. Robillard and B.W. Dijkstra, BIOSON Research Institute, University of Groningen, 9747AG Groningen, The Netherlands

The bacterial phosphoenolpyruvate-dependent phosphotransferase system (PTS) catalyses the cellular uptake and subsequent phosphorylation of carbohydrates, and plays a crucial role in the regulation of various metabolic pathways. Its carbohydrate-specific enzymes II (E_{II}s) are usually composed of two cytoplasmic domains, IIA and IIB, and a transmembrane domain IIC. The IIA domains catalyse the transfer of a phosphoryl group from the phosphocarrier protein HPr to IIB, which phosphorylates the transported carbohydrate. We have determined the structure of the *Escherichia coli* mannitol-specific IIA domain, IIA^{mtl}, by a three-wavelength MAD experiment on a selenomethionine variant of IIA^{mtl}. The 16.3 kDa seleno-substituted IIA^{mtl} contained only one selenium atom per molecule. Nevertheless, the four selenium sites in the asymmetric unit could easily be located in both the anomalous and dispersive Patterson maps. An interpretable electron density map was obtained after fourfold averaging. The structure was refined at 1.8 Å resolution to an R-factor of 19.0% (R_{free} 24.2%). The fold of IIA^{mtl} consists of a single five-stranded mixed β-sheet, flanked by helices on both sides. The phosphorylation site of IIA^{mtl} is located in shallow crevice lined with hydrophobic residues. Two residues flanking the phosphorylation site adopt two different conformations in the different IIA^{mtl} molecules. These conformations might represent different states of the active site, required for the different phosphoryl transfer reactions in which IIA^{mtl} is involved.

P12.02.018 DATA TO MAPS: AUTOMATED MAP GENERATION FOR HEAVY ATOM STRUCTURE DETERMINATION. P. Emsley and Neil W. Isaacs, Dept. of Chemistry, University of Glasgow, Glasgow, G12 8QQ, UK.

CHART is a wrapper for SHELXS[1] and the CCP4 Program Suite[2,3,4] that creates (density modified) MIR(AS) or MAD maps suitable for density fitting. The starting point is MIR(AS) data sets. CHART terminates with what it considers to be an optimal density modified map. CHART has a minimalist GUI, which should be suitable for novice crystallographers and hopefully can be easily integrated with the CCP4 GUI. CHART incorporates a ``divide and conquer'' procedure which can optimize many parameters, such as number of molecules in asymmetric unit, resolution limits or best solvent content.

CHART is released under the GNU GPL and can be obtained from http://www.chem.gla.ac.uk/~paule/chart.

1. Sheldrick, G.M., (1990). *Acta. Crystallographica* **A**, 467 - 473.
2. Collaborative Computing Project No. 4, (1994). *Acta Crystallographica. D* **50**, 760 - 766.
3. Otwinowski, Z., (1991), In Wolf, W., Evans, P. R., & Leslie, A. G. W., editors, *Proceedings of the CCP4 Study Weekend 25-26 January 1991*, pages 80 - 85, Daresbury Laboratory, Warrington, UK. Science and Engineering Research Council.
4. K. Cowtan (1994), Joint CCP4 and ESF-EACBM Newsletter on Protein Crystallography, 31, p34-38.

P12.02.019 MASC METHOD IN PROTEIN CRYST-ALLOGRAPHY : SEARCH FOR SUITABLE CONTRAST AGENTS. E.Girard, R.Kahn and J.Vicat, Institut de Biologie Structurale, 38027 Grenoble, France.

In MASC experiments a physical contrast variation is obtained by tuning the x-ray wavelength in the absorption edge of an anomalous scatterer present at high concentration and dispersed through the solvent channels of protein crystals. These anomalous scatterers, introduced into the crystal either by soaking or by co-crystallisation, should not bind to the protein.
The ideal compound should (i) contain atom(s) with large anomalous features (white lines), (ii) be neutral to avoid binding to charged regions of the protein and (iii) be water soluble at high concentrations.

Experiments with a brominated non-detergent sulfobetaine, a neutral zwitterion are reported. Hen egg white lysozyme crystals containing up to 0.72M of this compound have been obtained and no binding to the protein was observed.

Experiments with neutral compounds containing stronger anomalous scatterers, such as platinum and rare earth atoms are in progress and will be reported.

L.Vuillard *et al*, *J. Crystal Growth*, (1996), **168**, 150-154
Ramin *et al*, *Acta Cryst*. (1999), D55, 157-167

P12.02.020 USE OF SIR/SAS DATA TO SOLVE A SE-ATOM SUBSTRUCTURE. C. Lemke and P.L. Howell Structural Biology and Biochemistry, Hospital for Sick Children, Toronto, M5G 1X8 and Department of Biochemistry, University of Toronto, Toronto, M5S 1A8.

Argininosuccinate synthetase (AS) catalyzes the reversible ATP dependent ligation of citrulline and aspartate to produce argininosuccinate, AMP and inorganic pyrophosphate. The primary role of AS is in the urea cycle, which is involved in the arginine biosynthesis of all organisms and in the detoxification of ammonia of ureotelic organisms. AS is rate limiting in this cycle, and also the arginine-citrulline cycle. When activated, the arginine-citrulline cycle provides the cell with a ready supply of arginine for the overproduction of nitric oxide (NO) by iNOS. While overproduction of NO plays a beneficial role in host defense, it is also responsible for the hypotension associated with septic and cytokine induced circularory shock.

The structure of *E. Coli* AS, has been determined to 1.6Å resolution. The selenium atom substructure was determined using both SIR and SAS data and the direct methods program SnBv2. Data were collected on a selenomethionyl AS crystal (Cu Kα radiation) and were used in conjunction with a 1.6Å native (S-Met) data set to calculate isomorphous diffE magnitudes using the DREAR program package. SnBv2 subsequently found 13 of the 16 Se atom positions. These positions were confirmed and the three remaining Se positions located using anomalous diffE magnitudes calculated from the peak data of a 3-wavelength MAD experiment. All 16 Se positions were used to solve the structure by treating the MAD data as a special case of MIR. The structure of the protein, its comparison with other members of the pyrophosphate subfamily (e.g. GMP and NAD+ synthetase) to which AS belongs and the SIR/SAS methods for Se-substructure determination will be presented. Funded by a grant from the Medical Research Council of Canada.

P12.02.022 MAD PHASING WITH TWO DIFFERENT TYPES OF ANOMALOUS SCATERERS. G. Bourenkov and H. D. Bartunik, Max-Planck Research Unit for Structural Molecular Biology, Protein Dynamics group, MPG-ASMB c/o DESY, Notkestrasse 85, 22603 Hamburg, Germany.

The usage of the MAD method in the phasing of protein structures can be considerably extended to applications involving two different types of anomalous scatterers in the same structure. Such MAD experiments, which have not yet become common practice, offer a high potential. Simple statistical considerations prove that even in a two-energy case the phasing power will be approximately twice as high for two types of anomalous scatterers (two different absorption edges) as compared to the case of a single type of scatterer with the same total number of sites. Full advantage of the presence of two types of scatterers can be taken by performing measurements at five energies. Further gain is achieved due to the relative simplicity of locating the reference scatterers and determining the correct enathiomorph.

Recent experience with structure determination by MAD using two types of anomalous scatterers will be summarized. These include structures of a Zn-proteinase incorporating Se-Met [1], heavy-metal derivatives of metalloproteins, and proteins

containing two different metals in their native state. The possibility to use such MAD techniques for the phasing of large molecular weight structures will be discussed.

1. F.-X. Gomis-Ruth, K. Maskos, M. Betz, A. Bergner, R. Huber, K. Suzuki, N Yoshidam H. Nagase, K. Brew, G. P. Bourenkov, H.D. Bartunik and W. Bode, (1997) *Nature*, **398**, 77-81

P12.02.023 DIRECT DETERMINATION OF CRYSTAL STRUCTURE OF HUMAN FERRO-CHELATASE USING [2Fe-2S] ANOMALOUS SCATTERING SIGNAL FROM IN-HOUSE DATA AND SOLVENT FLATTENING. Chia-Kuei Wu[1,2], Amy Burden[1], John P. Rose[1], Joe Ferrara[3], Harry A. Dailey[1], and Bi-Cheng Wang[1], [1]Department of Biochemistry and Molecular Biology, University of Georgia, Athens, GA30602, [2]Department of Crystallography, University of Pittsburgh, Pittsburgh, PA 15260 and [3]Molecular Structure Corporation, 3200 Research Forest Dr., The Woodlands, TX 77381,

The structure of human ferrochelatase has been solved using Fe-SAD (single wavelength anomalous diffraction) data collected in-house on a Cu rotating anode. To the best of our knowledge, this is the first example of a protein structure of this size (86 kDa per asymmetric unit) being solved using only single-wavelength Fe anomalous scattering data collected in-house.

The protein phases were obtained using the ISAS procedure (Wang, *J. Enzymol*. 115: 90, 1985). The sulphur atoms coordinated to the Fe atoms were determined from the Fe-phased Bijvoet difference Fourier and added to the phasing process. The resulting electron density map showed good connectivity, side chain density, the 2Fe-2S cluster, numerous helices and a long beta sheet. In addition, the majority residual peaks in the initial Fe-phased Bijvoet difference Fourier were found to correspond to the sulphur atoms of methionine and cysteine residues and aided in fitting the sequence to the electron density. The structure is now under refinement.

Ferrochelatase is the terminal enzyme in heme biosynthesis and catalyzes the insertion of ferrous iron into protoporphyrin IX to form protoheme IX. The mammalian enzyme is associated with the mitochondrial membrane and contains an 2Fe-2S cluster. The human enzyme has been overexpressed in *E. coli* and crystallized. The crystals, which diffract to 2Å resolution, belong to space group $P2_12_12_1$ with cell constants of a = 93.2 Å, b = 87.6 Å, c = 110.1 Å, and contain two molecules per asymmetric unit.

The initial Bijvoet difference Patterson maps showed a strong signal for the iron atoms and an experiment was then designed to maximize the anomalous signal to investigate if the Fe signal alone is sufficient to solve the structure. Details of the structure determination process will be presented.

P12.02.024 AN EFFICIENT PROBABILISTIC APPROACH FOR MAD PHASING. A. Lebedev, G. P. Bourenkov and H. D. Bartunik, Max-Planck Research Unit for Structural Molecular Biology, MPG-ASMB c/o DESY, Notkestrasse 85, 22603 Hamburg, Germany; G. N. Murshudov, CLRC, Daresbury & Structural Biology Laboratory, University of York, U.K.

A probabilistic model of an X-ray phasing experiment has been built following a Bayesian approach. The model accounts for the main features of the experiment; uncertainties in all parameters of the model are considered during calculation of the moments of structure factors. Due to the specific form of the probability distribution function, it has been possible to develop a fast algorithm for its maximisation. In the theoretical consideration, observable random variables refer to channels of a detector (to the pixels of a 2D-detector), which means that the algorithm could be extended to include the processing of a raw data, scaling and merging of equivalents along with the refinement of reference atom parameters. Experimental data are expressed in the form of the conditional probability distribution function of the observable random variables, given the crystal structure factors. In the algorithm the quadratic approximation of the logarithm of this function is used (which corresponds to the "normal distribution of the experimental intensities"). The consistent treatment of experimental data and model uncertainties and the development of an appropriate algorithm are especially important in MAD experiments, which are characterised by low signal to noise ratio.

P12.02.025 STRUCTURE OF THE UREA+ SUBERIC ACID INCLUSION COMPOUND AT ROOM TEMPERATURE AND BELOW 205K. I. Peral, G. Madariaga, T. Breczewski, Departamentos de Física de la Materia Condensada y Física Aplicada II, Facultad de Ciencias, Universidad del País Vasco, Apdo. 644,48080 Bilbao, Spain.

In urea inclusion compounds guest molecules are located in a structure of linear and parallel tunnels formed by an extensively hydrogen-bonded arrangement of urea molecules (host substructure). Structural compatibility between host and guest components is fundamental to most inclusion phenomena. As a consequence, appropriate guest molecule must be based on a sufficiently long alkane chain with only a limited degree of substitution of this chain allowed [1].

The urea+suberic acid inclusion compound undergoes a structural phase transition at 205K. Our work on this compound has been focused on the resolution of the structure of both phases.

Oscillation photographs show that the c^*_g and c^*_h axis of both subsystems are parallel but mutually incommensurate ($\rho=c^*_g/c^*_h=0.908(1)$). The rotational symmetry and the detected systematic absences of the diffracted intensities allow to assign the superspace group $X3_112(00\rho)$ (a=b=14.163(5) Å, c=10.979(4) Å, $\alpha=\beta=90^o$ $\gamma=120^o$). The superspace group is fairly enough to establish the guest packing in the urea tunnels. Suberic acid molecules are located along the tunnels, with an orientational disorder generated by the 3 fold axis. There exists a correlation of $^1/_3c_g$ between the relative positions along the urea tunnels of guest molecules belonging to adjacent tunnels. Nevertheless, the weakness of the interaction host-guest prevents an accurate determination of the guest molecules positional parameters. X-ray diffraction experiments in the low temperature phase are in progress.

1. Hollingsworth M. D. and Harris K. D. M. *Comprehensive Supramolecular Chemistry*, ed. D. D. MacNicol, F. Toda and R. Bishop Perga- mon Press, Oxford, **6**, (1996) 177.

P12.02.026 THREE DIMENSIONAL EXAFS OF PROTEINS USING CRYSTALLOGRAPHIC DATA. Richard W. Strange, Kan C. Cheung & S. Samar Hasnain, Synchrotron Radiation Department, CCLRC Daresbury Laboratory, Warrington, Cheshire WA4 4AD, UK.

We describe a new approach to EXAFS data analysis which uses high resolution crystallographic information combined with full inter-ligand multiple scattering theory. This approach can yield 3D EXAFS information at atomic resolution at metal centres in proteins and the method can be extended to provide a similar model of the metal centre where no crystallographic data is yet available. We illustrate this by application to the type-1 and type-2 Cu centres of the nitrite reductase from *Alcaligenes xylosoxidans* for which crystallographic data at 2.1Å resolution is available.

P12.02.027 THE D.A.F.S. SPECTROSCOPY : TECHNIQUES AND APPLICATIONS. J.L. Hodeau, H. Renevier, M.G. Proietti*, J. Garcia*, J.F. Berar, S. Bos, V. Favre-Nicolin, P. Wolfers, Lab. de Cristallographie-CNRS, BP 166, 38042 Grenoble 9, France, (*) ICMA-CSIC, Univ de Zaragoza, 50009 Zaragoza, Spain

The DAFS (Diffraction Anomalous Fine Structure) spectroscopy is an atomic and site selective probe which gives XAFS-like information on the electronic structure and the local atomic environment as well as on the long range ordered crystallographic structure. A DAFS experiment consists in measuring the Bragg peak intensities as a function of the energy of the incoming X-ray beam. Much efforts are being made at the French CRG (Collaborative Research Group) beamline BM2-D2AM at the ESRF (European Synchrotron Radiation Facility) to develop the data acquisition and the data analysis.

After an introduction to the DAFS spectroscopy, we will show the experimental requirements for such studies. We will present the analysis of the EDAFS oscillations (Extended DAFS) and point out the interest of using the DAFS spectra to recover quantitative information about the crystallographic structure and particularly to the positions and Debye Waller factors of the anomalous atoms.

Several applications will illustrate the spatial and site selectivity of the DAFS spectroscopy. For the study of powdered catalytic samples containing diluted particles, we can separate the absorption spectra of the particles from those of the support. On superlattices we can extract the EDAFS information of the interface layers, corresponding to 6% of the multilayer. On thin films such as strained III-V semiconductors, we could obtain quantitative information by using both a single first shell analysis and a multishell analysis on the raw data using theoretical phase shifts and amplitudes [1], and we found that Ga-P and GaAs bond distances in the Ga(As1-xPx) single epilayer remain very close to their respective bulk values, independent of the residual strain. In conclusion we will discuss the strengths and limitations of DAFS method.

1. M.G. Proietti, H. Renevier, J.L. Hodeau, J. Garcia, J.F. Berar, P. Wolfers, Phys. Rev B59 (fev. 1999)

P12.02.028 XANES-SPECTRA AND THE CONDUCTION BAND OF SEMICONDUCTORS $AgGaS_2$, $CdGa_2S_4$, and $InPS_4$. A.A.Lavrenryev, B.V.Gabrelian, I.Ya.Nikiforov, V.A.Dubeyko, Don State Technical University, 344007, Rostov-on-Don, Gagarin sq.1, Russia.

The semiconductor compounds $AgGaS_2$, $CdGa_2S_4$, and $InPS_4$ are of interest because their crystal structures form the row: chalcopyrite - defective chalcopyrite - twice defective chalcopyrite. In this row the atom of sulphur in $AgGaS_2$ has 4, in $CdGa_2S_4$ - 3, and in $InPS_4$ - 2 the nearest neighbours. For all these compounds the XANES K-spectrum of sulphur and K-absorption spectrum of phosphorus in $InPS_4$ with the X-ray spectrograph DRS-2 have been obtained with the resolution about 0.2 eV. Using FEFF7 code [1] in the approximation of the multiple scattering theory of high order the K-absorption spectra of S and P in the compounds investigated have been calculated. The obtained theoretical curves reflect satisfactorily all the particularities of the experimental spectra. The local partial density of states of all components in these compounds have been calculated in the frame of the full multiple scattering theory in the approximation of the local coherent potential [2]. The same crystal potential calculated according to FEFF7 code, has been applied. In this case the curves of DOS show all features of the fine structure of the experimental spectra. It was found, that the transition from "pure" chalcopyrite to the defective and twice defective one results in the change of the fine structure of XANES-spectra. The investigation of the influence of the core vacancy on the partial unoccupied p-DOS has been carried out. This influence is shown to be rather strong for p-states of phosphorus, and it can not be neglected when one calculates the form of XANES of K-spectra of P in the sulphides.

1. S.I.Zabinsky, J.J.Rehr, A.Ankudinov, R.C.Albers, M.J.Eller (1995). Phys. Rev. B**52**, *4*, 2995.
2. B.L.Gyorffy (1972) Phys. Rev. B**5**, *6*, 2382.

P12.02.029 THE FEATURES OF THE CONDUCTION BAND OF SEMICONDUCTORS GaN and BN IN DIFFERENT CRYSTALLOGRAPHIC MODIFICATIONS. B.V.Gabrelian, A.A.Lavrentyev, I.Ya.Nikiforov, T.P.Zhdanova, Don State Technical University, 344007, Rostov-on-Don, Gagarin sq.1, Russia.

The compounds GaN and BN are the wide-gap semiconductors. Being of high hardness BN is applied as superhard material as well as light-emitting diod in different optoelectronic devices. Using the FEFF7 code [1] the XANES K-absorption stectra of Ga, N, and B in semiconductors GaN and BN have been calculated. The calculations have been carried out for the cubic (zinc-blend) and hexagonal (wurtzit) modifications of GaN and BN. For BN the graphite modification has been also investigated. The satisfactory agreement between the calculated and experimental XANES K-spectra has been achieved. Using the same crystal potential the local partial densities of electron states of B, N, and Ga have been calculated in the approximation of the local coherent potential (full multiple scattering). The distributions of the partial densities of electron states of the compounds investigated have the rich fine structure that depends on the type of the crystallographic modification. It can be seen at the experimental X-ray spectra too.

1. S.I.Zabinsky, J.J.Rehr, A.Ankudinov, R.C.Albers, M.J.Eller (1995) Phys. Rev. B**52**, *4*, 2995.

P12.02.031 USE OF POWDER X-RAY DIFFRACTION IN DETERMINATION OF TUNNEL STRUCTURE TYPE ION EXCHANGERS. A. Clearfield, X. Ouyang, D.M. Poojary, Department of Chemistry, Texas A&M University, College Station, Texas 77842-3012 USA

A group of inorganic ion exchangers has recently been synthesized and their structures determined “ab initio” from in house powder X-ray data. These compounds have framework structures enclosing tunnels or cavities in which are sited exchangeable cations. The phase changes and structures of these compounds brought about by exchange of protons, alkali and alkaline earth cations will be described. Powder neutron diffraction was utilized to locate acid H atoms (in collaboration with Santiago Garcia-Granda, University of Oviedo). This structural information revealed details of the exchange mechanism.

P12.02.032 CRYSTAL STRUCTURE OF A NEW BINARY RHENIUM-OXIDE. T. Hartmann, G. Miehe, G. Wltschek, H. Fuess, Materials Science, Darmstadt University of Technology, Petersenstr. 23, D-64287 Darmstadt, Germany, H. Ehrenberg, Interdisciplinary Research Centre in Superconductivity, University of Cambridge, Madingley Road, Cambridge, CB3 0HE, United Kingdom, T. Buhrmester, Institute for Physical Chemistry, Darmstadt University of Technology, Petersenstr. 20, D-64287 Darmstadt, Germany, J. Galy, CEMES/CNRS, 29 Rue J. Marvig, F-31055 Toulouse Cedex 4, France

The crystal structures of ReO_2 [1,2], ReO_3 [3] and Re_2O_7 [4] have already been reported, but, except for attempted indexing in a tetragonal [5] and a monoclinic [6] setting, the structure solution

of Re_2O_5 is still missing. Therefore a pellet containing ReO_2 and ReO_3 in ratio 1:1, which gave the theoretical composition Re_2O_5, was heated in an arc melting furnace under argon atmosphere. The very hygroscopic, royal blue product has been investigated by X-Ray powder diffraction using a STOE STADI-P with germanium-monochromatized Cu-Kα-radiation and a position-sensitive detector with 6° aperture in transmission mode. The diffraction pattern could be indexed on the basis of a tetragonal cell, the structure solution from powder data revealed space group $I\bar{4}$ m2. The structure refinement by the Rietveld method lead to a = 5.1716(4) Å and c = 13.356(2) Å with Re(1)-atoms on the 4f-site (0, ½, 0.0199(3)) and Re(2)-atoms on the 2d-site (0, ½, ¾). Oxygen-atoms with O(1) on the 8g- (0.25, 0.25, 0) and O(2) on the 4f-site (0, ½, -0.85(4)) forming layers of tetragonal pyramides with shared corners give a five-fold coordination of the Re(1)-atoms. The Re(2)-atoms should be coordi-nated by four oxygen-atoms either on the 8i- or half occupying the 16j-site forming isolated tetrahedra, but because of very high isotropic temperature factors, the oxygen-positions could not be determined precisely. This structure model yields to the stoichiometry Re_3O_{10} for the studied compound.

[1] Magneli, A., Acta Chem. Scand. **11** (1957) 28-33.
[2] Rogers, D.R., Shannon, R.D., Sleight, A.W., Gilson, J.l., Inorg. Chem. **8** (1969) 841-49.
[3] Meisel, K., Z. anorg. Allgem. Chem. **207** (1932) 121-28.
[4] Krebs, B., Angew. Chem. **7** (1968) 291.
[5] Tribalat, S., Delafos, D., Piolet, C., Comp. Rend. **261**(4) (1965) 1008-11.
[6] Colaitis, D., Lebas, D., Lecaille, C., Mater. Res. Bul. **8**(6) (1973) 627-34.

P12.02.033 STRUCTURE DETERMINATION OF Nd_2CuO_4 FROM ELECTRON DIFFRACTION DATA. C. Bougerol-Chaillout, D. Tranqui, Laboratoire de Cristallographie CNRS, BP166, 38042 Grenoble cedex 9, France; M. Gemmi, A. Migliori, CNR-LAMEL, Via Gobetti, 101, I-40129 Bologna, Italy; G. Calestani, Dip. Chimica Generale ed Inorganica, Universitˆ di Parma, Viale delle Scienze, I-43100 Parma, Italy.

Nd_2CuO_4 is tetragonal (I4/mmm, a = 3.945(2) Å, c= 12.176(4) Å, space group I 4/mcm) and remains the same down to 4K. Above room temperature, $SrBiO_3$ keeps the same structure until decomposition around 700°C, whereas the K-doped phases decompose around 300°C. Electron diffraction data corresponding to the [100], [110], [210], [111], and [311] zone axes were recorded on crystallites of a powder sample. Two different procedures were used : the microdiffraction mode with a condensor aperture of 15µm and a spot size of 7nm, and the SAED mode over an area of 300nm in diameter. In the former case, data were recorded on photographic films, which were digitised using a CCD Kodak Megaplus camera; the IDL software was used for integration; in the latter case data were directly recorded on a Gatan Slow Scan CCD camera and intensities were extracted using the QED v1.0 package [1]. Two approaches were used to solve the structure. From a Patterson type analysis, which was successfully used previously in the case of a complex oxide [2], two sets of Nd-Nd and Nd-Cu vectors on the Patterson projection map along [110] were identified and thus Nd and Cu atoms were located. By direct methods, tested using SIR97 [3] with a 3-D data set of intensities obtained by merging (R=0.28) the ED patterns using common rows of reflections, the Nd, Cu and one O atoms could be identified in the E-map of the first solution. The remainder of the structure was completed by difference-Fourier technique and by symmetry considerations and refined using electron data. In spite of a high final R-factor, obviously due to dynamical effects, the refinement gave reasonable isotropic temperature factor and led to a model in close agreement with neutron data.

[1] D. Belletti, G. Calestani, M. Gemmi, A. Migliori (1999) QED v1.0: A package for quantitative ED data treatment, sub. to Utramicroscopy.
[2] C. Chaillout, E. Gautier, D. Tranqui, Proc. 14th International Congress on Electron Microscopy, Cancun Mexique (1998)[3] A. Altomare et al., (1998) J. App. Cryst., in press

P12.02.034 Ta_2P, A CASE STUDY OF COMBINING THE ADVANTAGES OF ELECTRON DIFFRACTION AND X-RAY POWDER DIFFRACTION. M. Boström, Stockholm University, Structural Chemistry, 106 91 Stockholm, Sweden, magnusb@struc.su.se and Th. E. Weirich, Darmstadt University of Technology, Materials Science, Petersenstrasse 23, 64287 Darmstadt, Germany, weirich@hrzpub.tu-darmstadt.de

The feasibility of solving inorganic heavy atom crystal structures by direct methods with electron diffraction intensity data was investigated in a recent study with Ta_2P as an example [1]. All the 24 Ta positions in the unit cell could be located from the ED data using the direct methods program SIR97 [2]. However, none of the phosphorus atoms in the cell could be detected in that study. In the present study we show the powerful possibilities given by combining electron crystallography with x-ray powder methods for solving inorganic crystal structures from powders. X-ray powder diffraction data was collected on a STOE diffractometer. A Rietveld refinement was done with the Ta positions determined from the ED data as a starting model. After refining the Ta positions with the X-ray powder data the 12 P atoms in the unit cell could be located by difference Fourier synthesis. Also is shown that the heavy atom structure could be solved directly by image processing of high resolution electron micrographs.

1. T. Weirich , (1998) *Crystallography Reports*, **43**, 956
2. G. Cascarano *et al*., (1996) *Acta Cryst.,* **A52**, C-79

P12.02.035 STRUCTURAL INVESTIGATIONS OF CLUSTER COMPOUNDS IN THE SYSTEM $BA_4NB_2O_9$ - NB/NB_2O_5 - TIO_2. G. Nilsson, Dept. of Inorganic Chemistry, and G. Svensson, Dept. of Structural Chemistry, Arrhenius Laboratory, Stockholm University ,S-106 91 Stockholm

Several syntheses were made in the system $Ba_4Nb_2O_9$ - Nb/Nb_2O_5 - TiO_2 , varying the Nb/Nb_2O_5 ratio in order to obtain different oxidation states of Nb (+2 → +4). The samples prepared were not found to be single phase, but several yielded single crystals. Single crystals, all identified as new phases, were taken from three different samples and single crystal *X*-ray diffraction data was collected for each on a STOE image plate system. Three types of compounds where found with different degrees of cluster condensation. One structure, isostructural with the compound $Ba_4Nb_{14}O_{23}$, containing triple chains of corner sharing Nb_6 octahedra, was refined, showing partial or replacement of Nb by Ti at specific Nb positions. The composition of the compound was found to be approximately $Ba_4Nb_{13}TiO_{23}$, as determined by the structural refinement, which is in good agreement with findings in electron dispersive spectroscopy (EDS) investigation. A second phase, with two dimensional condensed Nb_6O_{12} clusters, is believed to be related to the compound $Ba_2Nb_5O_9$, with partial replacement of Nb for Ti. The third, new phase, was structurally solved (R_w=2.68%, R_{obs}=2.68%) and found to be monoclinic with the space group Cm and the cell parameters *a*=8.9373, *b*=15.4798, *c*=9.4145 Å and γ=90°. It is a close packed pseudohexagonal structure with merohedral multiple twinning, containing three different types of metal clusters, Nb_6O_{12}, Ti_3O_{13} and Ti_3O_{10}. More over, high resolution transmission electron investigations and electron diffraction showed the occurence of defects and disorder. The composition was refined to $BaNb_{5.915}Ti_{4.185}O_{16}$ which is in good agreement with what was found in EDS analysis. This compound will be further discussed.

P12.02.036 CRYSTAL STRUCTURE OF $Nd_5W_{11}O_{39}$. C. Grenthe[1], M. Sundberg[1], A. Guagliardi[2] and P.-E. Werner[1], [1]Department of Inorganic and Structural Chemistry, Arrhenius laboratory, Stockholm University, S-106 91 Stockholm, Sweden, and [2]C.N.R.-IRMEC c/o Dip. Geomineralogico Campus Universitario, Via Orabona, 4, 70125 Bari, Italy.

The crystal structure of $Nd_5W_{11}O_{39}$ has been determined by a combination of X-ray powder diffraction, high-resolution transmission electron microscopy (HRTEM) and electron crystallography methods. The unit cell dimensions are *a*= 3.862, *b*=35.951 *c*=21.897 Å, space group *Pbcm* (No.57).

HRTEM images (JEOL 3010, 300kV) taken along the *a*-axis showed all the projected neodymium and tungsten positions. EDS-analysis of individual crystals indicated an Nd-content of about 30-33 at%.

The direct method program system EXPO (1) was used to determine the three dimensional distribution of the cations. All metal atom positions were found in approximately two planes perpendicular to *a*. The oxygen atoms were then introduced into the model by consideration of interatomic (W-O), (Nd-O) and (O-O) distances. The final R_F value obtained by Rietveld refinement was 12.9%.

The structure is built up of pentagonal columns (PC - a WO_7 pentagonal bipyramid sharing its equatorial edges with five WO_6 octahedra, stacked by cornersharing) connected to ReO_3-type fragments consisting of three octahedra. These units form ´pillars´ along *c*. These ´pillars´ are joined by pairs of tilted octahedra (W_2O_{11} groups) to form corrugated layers perpendicular to *b*. The Nd atoms (7- or 8-coordinated) are located in the space between these layers, and form the only link between them. $Nd_5W_{11}O_{39}$ thus represents an entirely new type of PC structure.

The unit cell parameters of $Nd_5W_{11}O_{39}$ are similar to those previously reported for $Nd_{10}W_{22}O_{81}$ (2). No structure model of the latter compound has been published, however.

1. A. Altomare, M.C. Burla, M. Camalli, B. Carrozzini, G.L. Cascarano, C. Giacovazzo, A. Guagliardi, A.G.G. Moliterni, G. Polidori and R.Rizzi, *J. Appl. Cryst.* **32**(1999)339.
2. M. Yoshimura, H. Morikawa and M. Miyake, *Mat. Res. Bull* 10,(1975)1221.

P13.02.001 NANOSECOND TIME-RESOLVED X-RAY CRYSTALLOGRAPHY: EARLY STRUCTURAL EVENTS IN THE PHOTOCYCLE OF A XANT. Perman, Ben [1], Srajer, Vukica [2], Ren, Zhong [2], Teng, Tsu-yi [2], Anderson, Spencer [1], Pradervand, Claude [2], Ursby, Thomas [3], Bourgeois, Dominique [4], Schotte , Friederich [4], Wulff, Michael [4], Kort, Remco [5], Hellingwerf, Klaas [5], Moffat, Keith [2], [1] Department of Biochemistry and Molecular Biology, and the [2] Consortium for Advanced Radiation Sources, University of Chicago, Chicago IL 60637, USA; [3] Molecular Biophysics, Chemical Center, Lund University, P.O.B 124, S-221 00 Lund, Sweden; [4] European Synchrotron Radiation Facility, 38043 Grenoble Cedex, France; 5Laboratory for Microbiology, E.C. Slater Institute, 1018 WS Amsterdam, The Netherlands

Photoactive yellow protein (PYP) is a member of the xanthopsin family of eubacterial blue light photoreceptors. On absorption of light, PYP enters a photocycle that ultimately transduces the energy contained in a light signal into an biological response. Time-resolved X-ray crystallography was used to analyze a series of thermal intermediates in the relaxation of the protein after photoelectronic excitation of the chromophore. Laue data with nanosecond time resolution was collected at white beam station ID-9 at the ESRF at several time points between 1ns and 10ms. Trends in the data were interpreted through |F1ns| - |Fdark| difference Fourier maps. One intermediate structure has been refined against differences in the observed structure factors. This structure reveals regions of flexibility that comprise the chromophore binding pocket. Specific regions of flexibility lower the activation energy barrier between the dark state, denoted pG, and [pR], and help initiate entrance into the photocycle. The combination of new H-bonds and steric hinderance serve to explain why the chromophore does not simply undergo immediate thermal relaxation to the pG state and why PYP has a high quantum yield of entrance into the photocycle. This study provides direct structural results on the initial processes of transduction of light energy and evidence for the rapid evolution of an important physiological signal.

P13.02.002 TIME-RESOLVED PROTEIN CRYSTALLOGRAPHY BASED ON LIMITED-BANDWIDTH LAUE DATA COLLECTION WITH A CCD. H. D. Bartunik, G. Bourenkov, D. Kosciesca, Max-Planck Research Unit for Structural Molecular Biology, Protein Dynamics group, MPG-ASMB c/o DESY, Notkestrasse 85, 22603 Hamburg, Germany, A. N. Popov, European Molecular Biology Laboratory (EMBL) Hamburg Outstation, Notkestrasse 85, 22603 Hamburg, Germany.

The use of the limited-bandwidth Laue diffraction technique and a CCD detector with rapid readout permits measurements of a complete set of structure factors to high resolution within at total of about 100 sec. This is demonstrated by a number of applications using bandwidth $\Delta E/E \approx 5\text{-}10$ % on the wiggler beamline BW6 at DORIS and a MAR CCD detector system. The bandwidth has been defined by a graphite double-crystal monochromator and by a multilayer monochromator, respectively. The readout time of the MAR CCD detector was about 5 sec. Highly complete sets of structure factors have been obtained from series of still exposures at different angles of crystal rotation. The quality of the data proved to be comparable to the case of the conventional monochromatic rotation method. The new diffraction method offer a number of potential advantages over fine-angular interval white-beam Laue methods [1]. These include a) a higher signal-to-noise ratio, b) the absence of harmonic overlaps, c) strongly reduced effects of radiation damage, d) the possibility to use crystals of much higher mosaicity.

The method is also of interest for Laue diffraction experiments using (tapered) undulator radiaton with similar bandwidth. The limited-bandwidth Laue diffraction technique may be applied on even shorter time scales when pixel detectors [2] or other area detectors with extremely short read-out times become available.

X. Yang, Z. Ren and K. Moffat, *Acta Cryst.* (1998). D**54**, 367-377
Ng. H. Xuong, P. Datte, E. Beuville, T. Earnest, H. Padmore, J. Millaud, D. Nyrgent (1996). I.U.Cr. Abstracts, S0083

P13.02.003 A WAVE FIELD OF PROBABILITY AND THE FORM OF CRYSTALS. G.P. Shpenkov, Institute of Mathematics and Physics, Technical University, 85-796 Bydgoszcz, Poland, and L.G. Kreidik, Department of Physics, Technical University, 220027 Minsk, Belarus.

The relation between the form and contents is vital to the understanding of the structure and geometry of crystal substances. The roentgenographic method has greatly enhanced the understanding of this relation. At the same time, in some degree, the study of the structure has diverted attention from the investigation of crystal forms. However, an analysis of the characteristic angles of crystals, determining their form, was and still is an important scientific problem.

We offer such an analysis for the first time on the basis of the abstract wave theory of probabilistic processes. The notion of the density of phase probability Ψ is introduced.

Discrete elements of the wave probabilistic field are considered as "atoms" of such an abstract discrete-wave field. The correspondence of the mass numbers of the abstract atoms of the probabilistic wave field with the atoms of real physical space is demonstrated here.

The application of a theory of the wave phase probability for material spaces in the solid state is presented. The material realization of the superposition of elementary solutions, obtained from the equation for the wave field of probability, is shown in concrete examples of the crystal structure of natural minerals. The characteristic angles of the minerals are compared with the corresponding angles of the polar function of the wave phase probability.

The theoretical data presented confirm that the directions of the chemical bonds are determined by the superposition of elementary solutions of the equations for the wave field of probability. These results can be used for the prediction of the molecular and crystalline structures.

P13.02.004 PREDICTION OF CRYSTAL STRUCTURES OF TWO RARE SUGARS - INFLUENCE OF ATOMIC CHARGE TYPES. Ďurík, M., Smrčok, L, Tunega, D., Institute of Inorganic Chemistry, Slovak Academy of Sciences, SK-842 36 Bratislava, Slovak Republic.

Crystal structures of two sugars RKSA1 ($P2_1$) and RKSA5 ($P6_2$) (40 atoms per molecule) were predicted by potential energy minimization method. Two types of atomic charges - Mulliken (M) and those derived from molecular electrostatic potential (E) were used in calculations together with Williams force field. For each type of atomic charges 20 trial crystal structures were generated either with cell parameters optimized (O) or fixed (F). Each generated crystal structure was compared to the corresponding experimental powder pattern collected on STOE diffractometer by means of Rietveld refinement. A scale factor, zero-point, *W* and *Q* were the only refined parameters.The numbers of correct crystal structures were as follows:

RKSA1: 2 (M/F), 3 (E/F), 1 (M/O), 1 (E/O);

RKSA5: 1 (M/F), 1 (E/F), 0 (M/O), 0 (E/O).

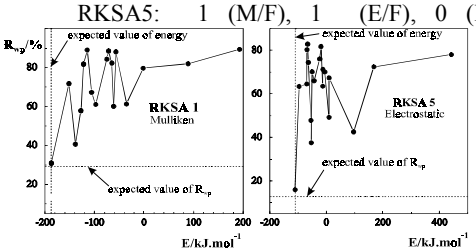

All successful predicted structures corresponded to the expected minimum of potential energy.

Conclusion: the force field we used was not very sensitive to the choice of atomic charges, though they differed a lot for some atoms within the molecules.

P13.02.005 INTERATOMIC POTENTIAL FITTING FOR STRUCTURE MODELING OF ALKALINE EARTH CUPRATES. N.N.Eremin, L.I.Leonyuk, V.S.Urusov, Geological Faculty of Moscow State University, Moscow, Russia.

The main aim of this study was to carry out pair potential model, which was able to predict and describe satisfactorily the crystal structure and some physical properties of alkaline-earth cuprates. All calculations were performed using GULP [1] program package. As it was found, the conventional procedure of Cu-O pair potential parameters fitting failed to find an optimal set, available to reproduce crystal structure of any alkaline-earth cuprate. That is why the purely ionic pair potential model was modified in the following way: Firstly, for the correct modeling of CuO_4 group planar geometry the O-Cu-O three body harmonic potential was taken into account. Secondly, it was found that some Morse potential contribution to the simple Buckingham Cu-O potential enables to improve essentially the cuprates crystal structure modeling.

The developed pair potential set seems to be well transferable for different cuprates, in spite of the variety in CuO_4 groups linking. This pair potential model was applied in this work for Ca_2CuO_3, $CaCuO_2$, $SrCuO_3$ and $(Sr_{1.19}Ca_{0.73})Cu_2O_4$ crystal structure modeling. It was shown, that for all tested compounds the differences between experimental [2-4] and calculated unit cell parameters are no more then 2%, and the largest atomic shifts are less then 0.012 fractional units. Some physical (elastic) and energetic properties of compounds were predicted. A few further recommendations for structure modeling of related compounds were given.

1. J.D.Gale. GULP, London: Royal Institution and Imperial College, 1992-94.
2. A.Arakcheeva, V.Schamrai, L.Leonyuk, G.Lubman. Kristallographia (in Russian), V39 (1994), 928-931.
3. V.C.L.Teske und H.Muller-Buschbaum. Z. fur anorg. und allgem. Chemie B.370, (1970), p. 234-241.
4. L.Leonyuk, G.-J. Babonas, V.Rybakov, E.Sokolova, R.Szymczak, V.Maltsev, L.Shvanskaya // J.Phys.Chem.Solids, V.59, N9, (1998), pp. 1591-1595.

P13.02.006 COMPUTER SIMULATION TO PREDICT STEROID POLYMORPHS. Paul Verwer, CAOS/CAMM Center

The completeness of polymorph predictions, as well as the expected accuracy of the calculated lattice energies was investigated, by comparing the results of crystal packing predictions on steroids with the polymorphs known from the CSD [1], and by comparing the calculated energies of pairs (or triples) of steroid polymorphs that are experimentally known to exist. In all calculations, the Cerius2 [2] software was used, in combination with the Dreiding-2.21 force field [3]. Steroids were used in these calculations because they represent a class of molecules which are not too small, not very flexible but neither fully rigid, of moderate polarity and also of industrial relevance.

It was found that calculated energy differences between experimentally observed polymorphs are usually less than 4 kcal/mol, indicating that this is a reasonable energy window to use in polymorph predictions. Due to the Monte Carlo based search algorithm, the set of predicted polymorphs will differ between runs. Because all structures in the 4 kcal/mol energy window are not always found, repeating the prediction runs is necessary not to miss any structures.

Finally an automated procedure has been tested to find crystal structures of stereoids containing hydroxyl groups, irrespective of the initial orientation of those groups, which can be a problem if the energy barrier between the rotamers is high. This eliminates the need to carry out separate prediction runs for every single rotamer.

[1] F.H. Allen and O. Kennard, Chem. Design Autom. News, 8, 31 (1993)
[2] Cerius2 User Guide, March 1997, Molecular Simulations Inc., 9685 Scranton Road, San Diego, CA, USA.
[3] S.L. Mayo, B.D. Olafson, and W.A. Goddard III, J. Phys. Chem., 94, 8897 (1990).

P13.02.007 EXPO: THE LAST ADVANCES. A.G.G. Moliterni, C. Giacovazzo, A. Altomare, A. Guagliardi, and R. Rizzi, Istituto di Ricerca per lo Sviluppo di Metodologie Cristallografiche, CNR, 70125 Bari, Italy, and G. Polidori, Dipartimento di Scienze della Terra, Universita', 06100 Perugia, Italy

The package EXPO [1] is devoted to solve crystal structures from powder data. The program first estimates the intensity values of each reflection *via* a pattern decomposition, then finds a structural model *via* Direct Methods. The main features of EXPO including the new ones, are the following: Automatic peak-search and preliminary FWHM refinement; Automatic integrated intensities extraction;Automatic structure solution by Direct Methods; Optimisation of extraction process by exploiting several kinds of prior information; Preliminary automatic Rietveld refinement ; A powerful graphic interface both for profile analysis and structure interpretation; A combined use of neutron and X-ray data, or electron and X-ray data to improve the quality of the structural model. By courtesy of Prof. P. E. Werner , we have integrated the program TREOR [2], in the version of EXPO under development. Several modifications into TREOR are in progress to increase the effectiveness of the indexing process; a friendly graphical interface has also been added.

1. A. Altomare, M.C. Burla, M. Camalli, B. Carrozzini, G. L. Cascarano, C. Giacovazzo, A. Guagliardi, A.G.G. Moliterni, G. Polidori & R. Rizzi (1999). J. Appl. Cryst., 32. In Press.
2. P. E. Werner et al., (1985). J. Appl. Cryst., **18,** 367-370

P13.02.008 CRYSTAL STRUCTURE DETERMINATION WITH THE PIMM FORCE FIELD. H. J. Lindner and T. Goerdten Institute of Organic Chemistry, Technical University of Darmstadt, 64287 Darmstadt, Germany

As our PIMM force field programme shows to be a promising tool to model crystal packings of organic compounds[1], a basic new feature has been added to simplify the determination of crystal structures of organic compounds starting from powder data alone. The global optimization of energy-based fitness values hase proven to be applicable for this purpose, but the success of this method is bound to the quality of the used potential functions and shows to be a time-consuming method. In addition, in the case of compounds whose crystal structures depend highly on electrostatic interactions even more complicated model functions than now implemented in the PIMM force field have to be used to locate local minima properly. A more effective way for the practical need of obtaining an unknown crystal structure is to directly optimize crystallographic figures of merit as the goodness-of-fit χ^2 or the residual value *R* with the implemented simulated annealing based algorithm. The possibility to check out a large amount of trial structures eases the treatment of high dimensional problems such as the calculation of flexible molecules.

T. Goerdten, H. J. Lindner, ECM-18, Eighteenth European Crystallographic Meeting, Book of Abstracts C6-P1, Praha 1998

P13.02.010 THE CATION-ORDERED SUPERSTRUCTURE OF NA_6 SODIUM SODALITE BY POWDER DIFFRACTION AND COMPUTER SIMULATION. *Branton J. Campbell, †‡Bo B. Iversen, *Jose M. Delgado, †Nick P. Blake, †Scott R. Shannon, †Susan Latturner, *†Galen D. Stucky and *†Anthony K. Cheetham. *UCSB Materials Research Lab, Santa Barbara, CA 93106, US, †UCSB Dept. of Chemistry, Santa Barbara, CA 93106, US, ‡Presently at the U. of Aarhus Dept. of Chemistry, DK-8000 Aarhus C, Denmark.

The combination of computer simulation and powder diffraction methods can greatly facilitate the characterization of complex structures when powder diffraction data alone is inadequate. We have investigated the structure of $Na_6Al_6Si_6O_{24}$ sodalite below its phase transition near 500 K, using both variable temperature synchrotron X-ray powder diffraction and lattice-energy minimization calculations. The low-temperature pseudo-tetragonal supercell was indexed using both the superlattice reflection positions and the splittings of the ordinary reflections. The average cation location was then determined, by constrained Rietveld refinement, to be near the center of the six-ring window. Possible cation configurations within the supercell were first enumerated, and then evaluated by employing both classical force-field energy and density functional theory calculations, and by comparing calculated and experimental diffraction data. Particular attention was paid to the structural features and Bragg reflections associated with the formation of the superstructure. We finally obtained a cation-ordered superstructure that both minimizes the lattice energy and adequately models the diffraction data.

P13.02.011 DEVELOPMENTS IN POWDER INDEXING: FROM CRYS2RUN TO THE INDEXER'S WORKBENCH. R.Shirley, School of Human Sciences, University of Surrey, Guildford, Surrey GU2 5XH, UK.

"The powder-indexing problem is history - just use a synchrotron..."

Data quality is certainly crucial for indexing a powder diffraction pattern when the unit cell is unknown, but indexing's solution space tends to be hostile, and limitations of specimen quality often mean that even synchrotron data cannot assure success, especially for the products of phase transitions and other specimens with poor texture and doubtful purity. With the growth in Rietveld method studies, the need for reliable indexing has never been greater, but the three classic programs in general use (ITO, TREOR and DICVOL) are each at least 20 years old, and again an IUCr Congress has come round which seems to lack any clear programme category for powder-indexing software.

The "Indexer's WorkBench" is a proposed co-operative project to integrate 32-bit versions of the available mature indexing programs into a single system running from a common graphical front end, to be implemented in parallel versions for 32-bit Windows and for LINUX. The implementers will form a virtual project team communicating over the internet. Apart from the classic programs, it is hoped that newer methods such genetic algorithms will be included, and both line-position and profile data supported. Those interested in taking part are invited to contact the author at R.Shirley@surrey.ac.uk.

CRYS2RUN will also be demonstrated. This is a simple script-based system for non-specialists that runs under MSDOS and calls the major indexing programs using CRYS as a front end, feeding data automatically to the indexing programs via the format-translator QDAT. CRYS is now at v9.28. Through CRYS2RUN, it supports ITO v12, TREOR90 and DICVOL91, and also now LZON and LOSHFZRF (new PC versions of the combined Shirley, Louër & Visser zone-finding/heuristic/dichotomy programs). CRYS2RUN, CRYS, QDAT, etc., are available free for non-commercial use via the CCP14 web site (see http://www.ccp14.ac.uk/tutorial/crys/index.html).

03. COMPUTERS IN ANALYSIS, MOLECULAR MODELLING AND MOLECULAR DESIGN

P07.03.001 SIMULATION OF DIAMOND (100) AND (110) SURFACE STRUCTURE AND SURFACE ENERGY. Chongmu Lee, Department of Metallurgical Engineering, Inha University, 253 Yonghyeon-dong, Inchon 402-751, Korea

The structures and energies of diamond (100) and (110) surfaces have been calculated by the computer simulation employing the lattice statics technique based on Tersoff potential. The simulation results suggest that the reconstruction patterns of the (100) and (110) surfaces are (1×1) and (2×1) respectively and that the surface energies of the two surfaces are 6,671.3 and 4,032.0 erg/cm2, respectively. According to the simulation results the surface reconstruction of the (100) surface mainly consists of the reduction of the interlayer spacing between the first and second atomic layers, whereas that of the (110) surface consists of the contraction of the interplanar spacing between the neighboring atoms in the first atomic layer as well as the contraction of the interlayer spacing between the first and second atomic layers. Besides them the stress components of the first four atomic layers of the surfaces were obtained and their effects on the surface adsorption were discussed.

P07.03.002 HIGH FASHION IN EDINBURGH: USING CSD DATA TO MODEL METAL OXIDE SURFACE INTERACTIONS. Andrew Parkin, Steven Harris, David Henderson, Simon Parsons and Peter Tasker, Edinburgh Centre for Surface Coordination Chemistry, Department of Chemistry, University of Edinburgh.

Our approach to modelling the interactions of metal surfaces with various donor groups involves the use of predetermined crystal data, in particular from the CSD and the ICSD. As most metals are lightly oxidised in air we use known crystal structures of the appropriate metal oxide or hydroxide to identify the most prominent growth faces, taking into account classical morphological theory. Then, by studying single-crystal forms of ligands both free and bound to various metal clusters or single metal atoms, we can use a pattern-matching approach to constructing a model for the interaction of a ligand with the correct surface of our metal oxide.

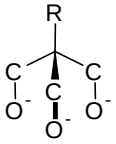

Most of the work to date has been performed on aluminium oxide and the theories developed from the above approach have been tested using surface adsorption studies. Our initial aim is to try to explain how a surface-active ligand binds and we hope to develop this remit towards ligand design. The modelling has also been used to predict likely interactions of carboxylate, phosphate, and the so-called “tripodal ligands” (shown in the diagram) with aluminium, and to explain the successes (and failures!) of our attempts to make these complexes.

P08.03.001 A COMPARATIVE STUDY OF SOME ABSORPTION CORRECTION PROGRAMS. J. F. Van der Maelen Uría, M. Pérez-Priede, and S. García-Granda, Dpto. Química Física y Analítica, Facultad de Química, Universidad de Oviedo, E-33006 Oviedo, SPAIN.

A comparative study of different empirical and semiempirical absorption correction methods widely used for structure determination in single-crystal X-ray diffraction procedures is made in order to shed some light on the controversy about their utility and the meaning of the parameters used by them. A new version of the local data reduction program called REFLEX [1] has been used to accomplish this work. This version of the program performs the calculation of the direction cosines for the data by using two different but equivalent algorithms, which allows us the use of such empirical absorption correction methods as SHELXA and the new version of DIFABS running over F^2 included in the EUCLID program package. Both these methods, together with the empirical XABS2 method and the semiempirical EMPABS method, are used to make a comparative study of the absorption correction for some mono-, bi-, and trinuclear Ru compounds as well as other organometallic compounds containing W [2].

Calculations show that both SHELXA and DIFABS give quite the same results for every compound studied, whereas XABS2 has to be used in conjunction with EMPABS in order to take into account the dependence of the absorption correction in other variables apart from θ. On the whole, the preferred method for applying absorption correction (when an accurate description of the sample shape and size is very difficult, if not impossible, to obtain) has found to be the semiempirical EMPABS method (given a ψ-scan properly made) followed by the empirical XABS2 method.

[1] S. García-Granda, A. Aguirre-Pérez, A. Gutiérrez-Rodríguez, E. García-Rodríguez, J. F. Van der Maelen Uría, and M. Pérez-Priede (1998). *REFLEX*, University of Oviedo.

[2] J. Barluenga, M. Tomás, E. Rubio, J. A. López-Pelegrin, S. García-Granda, and M. Pérez-Priede (1999). J. Am. Chem. Soc., **121**, xxx-xxx (in the press).

P08.03.002 POWDERX - A WINDOWS95-BASED PROGRAM FOR POWDER X-RAY DIFFRACTION DATA PROCESSING. Cheng Dong, National Laboratory for Superconductivity, Center for Condensed Matter Physics & Institute of Physics, Chinese Academy of Science, P. O. Box 603, Beijing 100080, China.

A Windows95-based program (PowderX) has been written for powder x-ray data processing and analysis. PowderX takes full advantage of the graphical interfaces of the Windows95. It uses pull-down menus and mouse to control the program executions. PowderX provides the convenient tools for processing powder x-ray diffraction data. It can be used for plotting x-ray patterns, data smoothing, background subtraction, α2 elimination, peak search, indexing and correcting zero-angle errors. PowderX has many useful features:

A new and accurate Cu $K\alpha_2$ elimination algorithm is used.

Zero-angle shift can be corrected automatically after peak search and no internal standard material is required.

Read data in more than 10 different format, including data obtained by diffractometer from several well-known makers (Mac Science, Philips, Rigaku, Siemens, etc.).

PowderX can also be used for data format conversions and prepared data for ab-initio crystal structure determination, whole-pattern fitting and Rietveld refinement programs such as DBWS, EXPO, FULLPROF, GSAS, RIETAN, SIMPRO and XFIT.

It is very easy to use. It can produce the input file for Treor90 after peak search automatically too. Only minor editing is needed.

It can perform both automatic and manual peak search and background subtraction.

Index of crystal plane can be automatically labeled in the plot if you know the lattice parameters.

It is freely available for academic and non-commercial use. The present version of PowderX can be obtained by mailing the author, Cheng Dong at chengdon@aphy.iphy.ac.cn.

P08.03.003 DIRECT-SEARCHER AUTOMATIC SYSTEM (Ver. 4) FOR SOME ORGANIC COMPOUNDS RUNNING ON PCs. K. Okada, Ricoh Research and Development Center, Yokohama, Japan, and S. Okada, Science University of Tokyo, Tokyo, Japan.

The DIRECT-SEARCHER system version 4 (DS*SYSTEM4) has been developed and consists of more than twenty main programs and subroutine libraries. The main new features are: (1) development of a new phase solver ShakePSD (Shake Patterson, Search and Direct methods), (2) update of a least-squares program LSBF for refining on $|F_o(h)|$ or $F_o(h)^2$ considering anomalous dispersion terms, (3) adaptation of the interface to/from other program systems (DIRDIF, *Shake and Bake*, Shelex, PLATON/PLUTON, Cerius2 and CSD), and (4) preparation of Postscript and HP-GL files with CRT display for graphical output on MS-Windows 95/98 and NT 3.x/4.0/5.0 operating systems.

ShakePSD becomes an automatic phase solver being able to handle both heavy-atom methods (Patterson function and search for all remaining atoms) and direct methods (tangent formula and/or minimal function[1]) within one program. The input data are cell constants, space group, number of atoms with atomic kinds and observed structure factors $|F_o(h)|$. The outputs are 2D-projection diagrams of the molecules in a unit cell. The ShakePSD program succeeds over previous capabilities[2], adopts the minimal function for power up of the traditional direct methods, and determines with certainty molecule fragments.

The revised LSBF program refines atomic parameters by the least-squares method with the block-diagonal or the full-matrix approximations which treats anomalous dispersions, refining on $|F_o(h)|$ and $F_o(h)^2$.

[1] Hauptman, H. A. A Minimal Principle in the Phase Problem; Moras, D., Podjarny, A. D. and Thierry, J. C. Eds.; *Crystalloraphic Computing 5. From Chemistry to Biology*; Oxford University Press; Walton Street, Oxford, 1991; pp 325-332.

[2] Okada, K. and Okada, S. A DIRECT-SEARCHER Automatic System (Version 3) for Some Organic Compounds Running on Personal Computers. *J. Chem. Inf. Comput. Sci.* 1997, *37(3)*, 522-528.

P08.03.004 ANISOTROPIC CRYSTAL STRUCTURE VALIDATION STATISTICS: THE *R*-TENSOR. Sean Parkin, Biochemistry Department, Duke University Medical Centre, Durham, N.C., 27710, USA. sean@xray.duke.edu

An expansion of global validation statistics to include important spatial information is presented.

Assessment of quality at various stages of crystal structure determination invariably entails comparison of a variety of global indicators. At the data reduction stage, quality is assessed using R_{merge} and $I/\sigma(I)$. Later, progress in structure solution and refinement is checked by the goodness-of-fit, variants of the *R*-index, R_{cryst}, and its cross-validation counterpart, R_{free}. While such statistics are important and provide a convenient means of comparison, as scalar quantities they are quite inadequate. Any truly representative validation statistic should at the very least reflect the three-dimensional nature of the diffraction pattern and molecular model. The need for better measures of crystal structure quality has been stressed in recent years [1].

The proposed method obtains the elements of a (3x3) matrix, the *R*-tensor, via a least-squares scheme. An effective value of the particular statistic in question can then be obtained for any point or region of reciprocal space. Variation amongst effective *R*-indices (for example) for different classes of reflection can provide a wealth of additional information that can help to steer refinement strategy and to assess the final product.

Details of the algorithm and some results are given. A FORTRAN77 program 'RT' is also available from the author at the e-mail address above.

1. E.Dodson, G.J.Kleywegt & K.Wilson. (1996). *Acta Cryst*. D**52**, 228-234.

P08.03.005 SQUIDGY ELECTRONS, SHAKING THE ATOMS AND DUST IN THE STRUCTURE. D.J.Watkin, R.Cooper, Chemical Crystallography Laboratory, 9, Parks Road, OXFORD OX1 3PD L.Schroeder, A. Cousson, Laboratoire Leon Brillouin (CEA a CNRS), CE Saclay, Batiment 563, 91191 GIF-SUR-YVETTE Cedex (France), W.Paulus, RWTH Aachen, Institut fur Kristallographie, Jõgerstrasse 17-19, 52056 AACHEN (Allemagne)

Development of the CRYSTALS program continues in two major directions - the provision of a safe environment for routine work (see CRYSTALLOGRAPHIC TOOLS FOR CHEMISTS, ms 12FF), and the incorporation of useful facilities previously only found in stand-alone programs. Amongst recent introductions are:

1 Modified distributions to permit the modelling of electron density distributed uniformly along a line or over an annulus or spherical shell. These can be mixed with conventional thermal parameters to produce 'peaky' distributions.

2 Controlled perturbation of structures. Sophisticated refinement of difficult structures can lead to false minima. The stability of the solutions can be probed by perturbing and re-refining the structure.

3 Voids and loose packing in a structure have been modelled by filling the voids with dust-like pseudo-atoms. These can be operated on just like normal atoms, providing a useful tool for the understanding of packing.

4 Groups of atoms (or molecules) can be replaced by the enveloping ellipsoid of inertia, and these ellipsoids used to represent the molecules in packing diagrams. The ellipsoids can be mixed with conventional atoms to high light packing features.

P08.03.006 NEW FEATURES OF THE PROGRAM FULLPROF. J. Rodríguez-Carvajal, T. Roisnel, A. Daoud-Aladine and A. Bouvet, Laboratoire Léon Brillouin (CEA-CNRS), CEA/Saclay, 91191 Gif sur Yvette Cedex, FRANCE.

We present an analysis of the new features included in the last beta-version of the program FullProf. Extensive changes have been made in the source code of the program in order to increase its capabilities and to conform to the new Fortran standard. The program is written in a subset of Fortran 90 and can be compiled with ELF90 [1]. The new features include:

Multi-pattern capabilities. Three executable versions of the program exist: single pattern, fixed multi-pattern, and multi-pattern with dynamic memory allocation: the number of patterns to be treated is fixed at run time by a setting file. The user may combine different X-ray and neutron (CW and/or TOF) diffraction patterns in order to refine crystal and magnetic structures with a total control of their relative weight.

Refinement of incommensurate crystal structures. Incommensurate structures can now be refined either from a powder profile or from single crystal data. This part of the program is still being testing. The formulation is based on Fourier components of atomic displacements in 3D space. The symmetry constraints between Fourier components should be provided by the user and may be obtained from group representation theory.

The Windows 9x/NT version of FullProf can be run through the program WinPLOTR [2] that is a complete graphic interface to FullProf.

The complexity of the input control file (of extension "pcr" and called PCR-file) for non-experienced users may be overcome by using the new Java interface that allows the full preparation of this file. The interface is independent of the platform and contains full graphics features.

[1] D.L. Shirer, Computers in Physics **12**(2), 166 (1998).
[2] J. Rodríguez-Carvajal and T. Roisnel. CPD Newsletter **20**, Summer 1998.
See also http://www-llb.cea.fr/fullweb/version.htm.

P08.03.007 PEAK PROFILE FUNCTION FOR POWDER DIFFRACTOMETRY WITH BRAGG-BRENTANO GEOMETRY. T. Ida and K. Kimura, Department of Material Science, Faculty of Science, Himeji Institute of Technology, Kamigori-cho, Hyogo 678-1297, JAPAN.

Experimental diffraction peaks in powder diffractometry with Bragg-Brentano geometry are generally shifted and become asymmetric due to the effects of (1) vertical (axial) divergence of the incident and diffracted beams, (2) flat-specimen, and (3) sample transparency. The above effects are mathematically treated as convolutions with asymmetric window functions. Recently, we have found analytical formulas for the vertical divergence in Bragg-Brentano geometry [1], and also an efficient method for numerical calculation of the convolution [2].

In this study, we have constructed an advanced model for the peak profile by triple convolution of the pseudo-Voigt function with the above three effects, the shape of which is determined by well-defined instrumental parameters and the linear absorption coefficient and thickness of the specimen. The validity of the model is examined by least-squares fitting to the experimental diffraction peak profiles of diluted lanthanum hexaboride (LaB_6) samples, the transparency of which are varied by mixing with different amount of starch. It has been found that the model function fairly well reproduces the experimental profiles (typically less than several % in R-factor) only by adjusting the parameters for the location and intensity of the peak, even in the case of heavily distorted profiles of the highly transparent sample with the linear absorption coefficient of 1 mm^{-1}.

1. T. Ida (1998), Rev. Sci. Instrum. 69, 2268.
2. T. Ida (1998), Rev. Sci. Instrum. 69, 3837.

P08.03.008 A NEW IDEA ON THE MOLECULAR REPLACEMENT METHOD FOR PROTEIN CRYSTALLOGRAPHY Nobuo Tanaka [1], Masami Kusunoki [2], [1] Faculty of Bioscience and Biotechnology, Tokyo Institute of Technology, [2] Institute for Protein research, Osaka University

The recent development of the computer has made it possible to search vectors from all atoms of the model quite cheaply. The present idea is to fix copies of molecules in the unit cell by calculating the observed Patterson function and the vector map calculated from the model with varied orientations. The fitting between the observed Patterson map and calculated vector map of the model which is rotated by the Euler angles is calculated quickly with the fast Fourier transform. The biggest FIT for each is collected to construct the map from which the prominent peaks are picked up as the plausible orientations. The obtained Euler angles are dedicated to the rotation of the model for the successive conventional translation search. The degree of the overlap among molecules is estimated from the volume occupied by all molecules. The unit volume is calculated to put one molecule arbitrarily in the unit cell. The present research has been undertaken as one of research and development applying advanced computational science and technology.

P08.03.009 A FORTRAN PROGRAM FOR CHOOSING REFLECTION-SETS IN AN OPTIMUM WAY FOR CROSS-VALIDATION CALCULATION. S. Parthasarathy and A. Abdul Ajees, Department of Crystallography and Biophysics, University of Madras, Guindy Campus, Chennai – 600 025, India, and H. Schenk, Laboratory for Crystallography, University of Amsterdam, Nieuwe Achtergracht 166, 1018 WV Amsterdam, The Netherlands.

Validation and cross-validation are methods of assessing the predictive ability of a statistical model and choosing between alternative models. They are based on the idea that models should be judged by their ability to predict new data, rather than the degree to which they fit the data from which their parameters were estimated. Cross-validation is an extension of validation and it aims to use the data more efficiently. Cross-validation method for choosing between two models consists of the following steps : (i) Dividing the data into k subsets (S_i , i = 1 to k, say) whose sizes are as nearly equal as possible, (ii) estimating the model parameters of one model by the validation method by using one of the subsets as the test set and calculating the free R-value for the reflections of the work set constituted by the union of the remaining k-1 subsets, (iii) repeating step(ii) k times, each time using a different subset as the work set and the union of the remaining k-1 subsets as the corresponding test set, (iv) finding the mean value of the k free R-values thus obtained, (v) repeating steps (ii) - (iv) for the other model, and (vi) selecting the model for which the mean free R-value is smaller.

An optimum way of partitioning the given set of reflections taking into account the probability distribution law of the intensities is proposed. The algorithm of the method is implemented in a Fortran porgram called CROSSVAL.

P08.03.010 TOWARDS IMPROVED REFINEMENT WITH AN ENSEMBLE-AVERAGED POTENTIAL. Rob Grothe, Molecular Biology Institute, University of California at Los Angeles

A refinement program must address two issues: selecting a quantity to maximize and deciding how to find its maximum over possible protein structure models. There is a consensus that probability is the right quantity to maximize. Maximizing a model's probability (or likelihood) density is equivalent to minimizing its energy. When Bayes' Law is used to construct the probability density of a model given observed data, the energy function is the sum of a prior energy, based upon interatomic interactions, and a data likelihood energy. These terms are often denoted by E_chem and E_xray. The formulation of E_xray has received much attention. This work focuses upon improving E_chem, the assignment of energy to a model, prior to consideration of diffraction data. A crystallographic model of a protein is an ensemble of states specified by a centroid state, which gives the average position for each atom, and atomic displacement parameter values. Until now, the prior energy assigned to a model has been the energy of the model's centroid state, neglecting the variations about the centroid. The energy of the centroid state only approximates the desired quantity: the average energy over an ensemble of states consistent with the model. This ensemble is a special case of the canonical ensemble of statistical mechanics, in which the most frequently occurring states have low energy. Since we are only interested in those states consistent with a given model, the most likely states also lie close to the model's centroid relative to its atomic displacement parameter values. Rapid, accurate estimates of this ensemble-average energy and its gradient are computed by sampling neighborhood-average energies. The ensemble-average energy has much less curvature than the conventional (static centroid) energy function. It is believed that the limited radius of convergence of conventional refinement programs results from

inappropriately sharp priors which fail to consider the uncertainty or variation in atom positions.

P08.03.011 QUANTITATIVE ANALYSIS OF ANOMALOUS ATOMIC THERMAL MOTION IN AN ORGANIC NON-LINEAR OPTICAL MATERIAL. J. M. Cole, School of Physical Sciences, University of Kent, Canterbury, Kent, CT2 7NR, UK, C. C. Wilson, ISIS Facility, CLRC Rutherford Appleton Laboratory, Chilton, Didcot, Oxon, OX11 0QX, UK, and J. A. K. Howard, Chemistry Department, University of Durham, South Road, Durham, DH1 3LE, UK.

A single-crystal neutron and X-ray diffraction study of the organic non-linear optical material, 3-(1,1-dicyanoethenyl)-1-phenyl-4,5-dihydro-1H-pyrazole (hereafter DCNP) is presented. The study was conducted in order to relate the structural characteristics of the compound to its physical properties [1-3]. The neutron study shows that some unusual atomic thermal motion is present in part of the molecule. Subsequent variable-temperature (90K, 100K, 200K, 290K) single-crystal X-ray diffraction experiments on DCNP were carried out in order elucidate the cause of the atypical thermal motion and to rule out the possibility of disorder, a looming phase-transition or some subtle form of twinning. These results show that libration is the cause of this anomalous motion. Three regions of the molecule appear to librate in an independent but concerted manner: predominantly in the molecular plane about the phenyl group, secondly in the nitrile group branch and slightly in the pyrazole group. The libration is fully characterized using THMA11 algorithms [4]. As a result, suitable corrections to the bond geometry and anisotropic displacement parameters of DCNP are made. The libration is also shown to enhance the non-linear optical effect.

A. Miniewicz, K. Palewska, J. Lipinski, R. Kowal & B. Swedek (1994). Mol. Cryst. Liq. Cryst., 253, 41-50.
S. Allen, T. D. McLean, P. F. Gordon, B. D. Bothwell, M. B. Hursthouse & S. A. Karaulov (1988). J. Appl. Phys., 64, 2583-2590.
S. N. Black, R. J. Davey, P. R. Morley, P. Halfpenny, E. E. A. Shepherd & J. N. Sherwood (1993). J. Mater. Chem., 3, 129-132.
K. N. Trueblood (1990). THMA11. Program for Thermal Motion Analysis. University of California, Los Angeles, U.S.A.

P08.03.012 STRUCTURE DETERMINATION FROM POWDER DIFFRACTION DATA BY USE OF A SWARM ALGORITHM. T. Csoka and W.I.F. David, ISIS Facility, Rutherford Appleton Laboratory, Chilton, Didcot, Oxon. OX11 0QX, UK.

Recent years have shown an increase in the use and success of global optimisation search methods, specifically Genetic Algorithms [1,2] and Simulated Annealing [3], in structure determination from powder diffraction data. The Swarm algorithm [4] can be used as a viable alternative to both these methods. As in a GA, the Swarm algorithm uses a population of solution vectors, which change over time, mimicking the behaviour of a swarm of insects or a flock of birds. Accordingly, the Swarm uses co-operative adaptation techniques rather than the competitive techniques employed by GAs.

The algorithm will be illustrated with the crystal structure solutions of a range of drug substances, including salt forms.

1. Shankland, K., David, W.I.F., Csoka, T. Z. Krist, 1997, 212
2. K.D.M. Harris, R.L. Johnston, B.M. Kariuki, Acta Cryst., A54, 632 (1998)
3. David, W.I.F., Shankland, K., Shankland, N., Chem Commun, 1998, 931
4. Huber, T., van Gunsteren, W.F., J Phys Chem, 1998, 102

P08.03.013 A PARALLEL COMPUTER FOR A GENETIC ALGORITHM BASED CRYSTAL STRUCTURE SOLUTION PROGRAM. K. Shankland and T. Csoka, Rutherford Appleton Laboratory, Chilton, Didcot, Oxon. OX11 0QX, U.K.

Genetic algorithm based programs typically possess intrinsic coarse grained parallelism. This is certainly the case for 'the GAP', a program designed to solve crystal structures from powder diffraction data [1].

Within 'the GAP', hundreds of potential structure solutions are evaluated for a particular generation, each evaluation consisting of generating trial diffraction data and comparing it with measured diffraction data via the method of correlated integrated intensities. As each evaluation is independent of the others, the system lends itself to a parallel implementation, particularly if an 'island model' is used.

One straightforward design for a parallel computer is based on the 'pile of PCs' concept. We constructed a cluster of four diskless dual Pentium Pro 166Mhz PCs using commodity components, and enabled communications via a matrix of 100Mb ethernet connections. A parallel version of 'the GAP', written in C and using the MPICH library, was implemented on the cluster under the control of the Linux operating system.

The benefits and difficulties encountered whilst implementing this parallel version of 'the GAP' will be fully discussed.

[1] K. Shankland, W.I.F. David and T. Csoka, *Z. Krist*, 212, 550-552 (1997)

P08.03.014 GRAPHICAL REPRESENTATION OF ALTERNATE CONFORMERS. F. C. Bernstein, H. J. Bernstein : Bernstein + Sons, Bellport, NY 11713, USA

It is challenging to display alternate conformers, microheterogeneity and multiple NMR models in ways which convey a clear understanding of correlated and uncorrelated conformations. Assigning a color to each conformer and massing the bulk of the molecule under a background color works for broad-scale representations of molecular surfaces and secondary structure, but can become confusing when atom-by-atom representations are used with stick bonds, especially when each element is also to be assigned a distinct color. We suggest a banded-bond/dotted-atom representation, with illustrations from a new version of RasMol able to accept mmCIF and PDB data for macromolecules and core CIF data for small molecules. The impact of similar changes and CIF adaptation for other popular graphics programs are discussed.

P08.03.015 SOFTWARE FOR ANALYSIS AND MANIPULATION OF CRYSTAL STRUCTURES. David J. Duchamp, Kalamazoo, MI 49009-9159

CrystMol, a personal computer software package, provides for display, analysis, and manipulation of crystal and molecular structures of varying complexity, ranging from one-atom structures to macromolecules. CrystMol was designed as both a teaching and research tool with crystallography and crystal structures as the focus. The current released version provides interactive rotation, translation, zooming, and clipping of structures drawn in a variety of display styles including: line, stick, ball, ball & stick, thermal ellipsoid, space filling, and various combinations of these. Space group symmetry is built in, and symmetry-related units may be easily added and deleted, facilitating the study of symmetry and crystal packing. Other facilities include an electronic notebook, user libraries of structures, support for disordered structures, and three-dimensional building and editing of structures. Standard metrics

with standard deviations are available, including: bond distances, bond angles, torsion angles, non-bonded distances, hydrogen bonds, and best planes. CrystMol supports structure input by several means, including both small molecule and macromolecular versions of the Crystallographic Information File (CIF), Cambridge Data Base files, and Protein Data Bank (PDB) format files. The current released version requires a PowerPC Macintosh computer, but porting to Windows 98 is contemplated.

The next version of CrystMol is under active development, and ideas and suggestions are being solicited. The current version and current plans have been influenced significantly by discussions at the 1998 ACA Meeting and feedback from those who tested the initial version. Along with numerous other features, the next version will provide for interactive linking to background calculation applications, and a background molecular mechanics application is currently under development. One of the main challenges in design of CrystMol has been the handling of disorder (microheterogeneity) in structures, both small molecule and macromolecular. The current version makes a try at this, but new ideas from the crystallographic community would be very welcome. The author would welcome any and all suggestions on how to make CrystMol more useful in research and teaching.

To facilitate such discussions, the status of the current and development versions of CrystMol will be discussed, along with current plans. The author will be available to demonstrate CrystMol on a laptop Macintosh if suitable arrangements can be made.

P08.03.016 A MODELING SYSTEM OF MOLECULAR USED ON MICROCOMPUTER. T. Shao Fan Lin, Yomng Bing Peng Ron Chen, Lian Hu Wei, W. D. Zhang [1], Yu.Hua.Xu [2], [1] Central Laboratory, Nankai University, Tianjin 300071, P.R.China, [2] Guangdong Part Time University of Science and Technology Guangzhou 510090 P.R.China

A modeling system of molecular and crystal structure used on IBM/586 is reported in this paper. The programming language is C++ and it can be run in WINDOWS-95 or WINDOWS-98. The modeling of the molecular and the crystal structures can be completed conveniently using those 3D-dimension coordinates of atoms and the parameters of unite cell. It is very useful for crystallographers. The system has following functions: 1. Model building: The system provides powerful and convenient functions to building the 2D or 3D structural formula of an organic compound on screen: A. Drawing on screen using mouse-pointing. B. Choosing the fragments from fragment library then modify them C. Linking between sub-structures and fragments. D. Above functions can be done in 2D or 3D dimension. Then program stores those structural messages into computer 2. Modeling of molecular structure. Three kinds of molecule models can be displayed, which are stick, stick-ball and full space. Those models can be enlarged, reduced, moved and rotated. 3. Modeling of unite-cell crystal structure including the edges, atoms and bonds between atoms in the unit-cell. The model of unit-cell can be enlarged, reduced, moved and rotated too. 4. The 3D-dimension coordinate of any atom, the distance between any two atoms, the angel between the three atoms, and the angel of two planes, which are fixed by four atoms and the length of the sides of unit-cell can be measured on the screen. The system can be connected with PCPDFWIN database of ICDD and single crystal databank of Cambridge, read the data of organic compound in the databanks and display it.

P08.03.017 DINO, A VISUALIZATION SYSTEM FOR STRUCTURAL DATA. A. Philippsen Biozentrum, University of Basel, Basel 4055, Switzerland

DINO allows the visualization of different structural data types obtained by X-ray crystallography, NMR, electron microscopy, AFM and theoretical calculations, namely structures, surfaces, trajectories, scalar fields (such as electron densities or electrostatic potentials), height-grids and geometric primitives.

Using realtime 3D graphics through the OpenGL (TM) library, DINO offers both schematic and high quality graphics, transparency, depthcueing and perspective corrected stereo (crystal eye stereo on equipped machines), ready for direct output in TIFF, RGB, PostScript or Raster3D format.

At the time of writing supported formats include: PDB (coordinates), XPLOR/CNS (coordinates and maps), CCP4(maps), UHBD (potentials), MSMS (molecular surfaces), CHARMM (coordinates and trajectories) and TIFF (greyscale height-grids).

Supported architectures: SGI, DEC, Linux

DINO is freely available on the WWW: http://www.bioz.unibas.ch/~xray/dino

P08.03.020 COMPARISON OF MOLECULAR STRUCTURES DETERMINED BY X-RAY METHODS WITH THE RESULTS QUANTUM CHEMICAL CALCULATIONS. G. Raabe, Institut für Organische Chemie, Rheinisch-Westfälische Technische Hochschule Aachen, Prof.-Pirlet Straße 1, D-52056 Aachen, Germany.

Interactions between molecules in the solid state might stabilize molecular structures which would be considered unusual for the isolated molecule in the gas phase.

Such crystal- or lattice effects can be detected and explained using the solid state structure of a molecule as starting geometry in quantum chemical geometry optimizations for the free molecule. Most of the available computational methods either belong to the group of the strongly parameterized semiempirical procedures, the non-empirical *ab initio* methods, or to those schemes derived from density functional theory. Due to the size of most of the molecules under consideration, semiempirical methods are still frequently used in this field. However, some of these procedures might fail if the molecule contains structural elements which were not considered in the set of compounds used to derive the set of the underlying semiempirical parameters. Usually *ab initio* methods yield correct results in such cases. These non-empirical computational methods, however, might also lead to misinterpretations of the experimentally observed structure if, for example, the geometry optimizations are carried out at the *Hartree-Fock* level and thus correlation effects are omitted from the calculation of the gradients.

In general, knowledge of the limitations of the computational methods mentioned above is not only of utmost importance if one attempts to detect and to interpret lattice effects but also if it is the point to generate molecular structures to be used in the modelling of crystal lattices.

In this paper the author reports on possible pitfalls in the application of some quantum chemical methods in order to detect lattice effects and to obtain molecular geometries to be used in calculations carried out in order to predict hitherto unknown crystal structures.

P08.03.021 ANALYSIS OF WEIGHTING SCHEMES. R. Spagna and M. Camalli, Istituto di Strutturistica Chimica CNR, C.P.10, 00016 Monterotondo Stazione, Roma, Italy.

16 weighting schemes, taken from the more common used in literature, and a wrong and an unrealistic scheme for comparison were implemented in the program CAOS. We run refinements using data of 13 known structures of medium size complexity. The starting model was composed by the atomic coordinates refined with unitary weights and isotropic thermal parameters. Then the full-matrix refinement (on $|F|$) was repeated using each of the 18 weighting schemes until convergence was reached with anisotropic thermal parameters for

non-hydrogen atoms. After convergence, some additional cycles were added with two procedures of weight-modification designed to lessen the effects of outliers.

For each weighting scheme, we calculated the distribution of $<\Delta^2>$, $<1/w>$ and $<w\Delta^2>$ against $\sin\theta/\lambda$ and $|F|$. To compare the results, we calculated the mean value, M, and the standard deviation , $\sigma(M)$, from the distribution of $<w\Delta^2>$ and we took into account the value of $\sigma(M)$ to evaluate how much the distribution of $<w\Delta^2>$ was constant.

In order to understand by how much the refined versions differ for each structure, we calculated three indices

$IND1 = 100.0* [R\%_{(highest)}-R\%_{(lowest)}]/ R\%_{(lowest)}$

$IND2_j = <\Delta x/u_x+\Delta y/u_y +\Delta z/u_z >$

$IND3_j = (<\Delta r^2>)^{½} = (<\Delta x^2>+<\Delta y^2>+<\Delta z^2>)^{½}$

where Δx, Δy, Δz were the coordinate differences between the atoms of the version having the lowest R% and the atoms of the *j*th version, and the u_x, u_y and u_z were the e.s.u.'s of the atomic coordinate.

To try to answer the question, which is the best weighting scheme, we calculated indices of confidence obtained by calculating the averages for each weighting scheme:

$index_j=\sum_{i=1,13}(R_{lowest,i}/R_{j,i})/13$

where $R_{i,j}$ is the R factor of *i*th structure using the *j*th weighting scheme and $R_{lowest,i}$ is the lowest R obtained for the *i*th structure.

P11.03.001 A MODEL THAT CORRELATES SIDE-CHAIN CONFORMATIONS OF FF-MAS RELATED COMPOUNDS AND THEIR ACTIVITIES. D.R. Boer, H. Kooijman and J. Kroon, Department of Crystal and Structural Chemistry, Bijvoet Center for Biomolecular Research, Utrecht University, The Netherlands.

A recent discovery has shown that the final stage of the development of a human egg cell (called meiosis) is triggered by an intermediate in the post-squalene biosynthesis of cholesterol. The compound was found in the follicle fluid, where the egg cell is maturing before ovulation, and was subsequently called follicle fluid-meiosis activating sterol (FF-MAS). It is evident that the hypothetical receptor mediating this trigger could be an interesting target for development of contraceptive and fertility-increasing drugs. We are currently trying to derive structure-activity relationships for FF-MAS and related compounds.

The structure of FF-MAS resembles that of cholesterol: it consists of a rigid steroid skeleton framework of 4 fused rings, with a stretched side-chain attached to it. By varying the side-chain structure, while retaining the skeleton of FF-MAS, the influence of side-chain conformation on activity can be assessed. This poster describes the correlation between activities and side-chain conformations that are present in the crystal structures of a number of FF-MAS derived compounds.

The conformational space of the side-chain was searched using crystal structure data from the Cambridge Structural Database (CSD). Principle Component Analysis (PCA) was applied to analyse the data. The conformations found were clustered in 3 areas. To correlate conformation with activity, the PCA results were applied to the appropriate parameters found in five crystal structures of the FF-MAS related compounds, the activities of which had been determined. Conformations of side-chains of active compounds were found to occur within one cluster, whereas side-chain conformations of inactive molecules were occurring in a different one. The PCA results can therefore be used as a pharmacophore model for the side-chain moieties of the FF-MAS related compound series.

P11.03.002 AN EFFICIENT FLEXIBLE SEARCH METHOD TO DISCOVER NEW LIGANDS FROM 3D DATABASE BASED ON AUTOMATIC DOCKING. M. Y. Mizutani and A. Itai, Institute of Medicinal Molecular Design (Key Molecular Inc.), 5-24-5 Hongo, Bunkyo-ku, Tokyo 113-0033, JAPAN.

On a target macromolecule, easily finding novel lead compounds with various core structures will greatly contribute to rational drug design. We have developed an efficient method for finding ligand candidates from among a number of flexible compounds included in 3D database when the receptor structure is known. The method, named ADAM&EVE, makes use of our automatic docking method ADAM [1], and is able to select ligand candidates based on the stability of interaction energy of the most stable docking structure of each small compound and receptor. As same as ADAM method, ADAM&EVE can fully explore the conformational space for each compound to construct the stable docking models.

Our method has been applied to several test cases, and all the cases were successful. In the case of acetylcholinesterase (AChE), 25 hit compounds that have different core structures to known ligands were found to have moderate potent activities ($IC50 = 10^{-6} \sim 10^{-7}$ M). Also in other test cases, new active compounds were discovered by our method.

M. Y. Mizutani, N. Tomioka & A. Itai (1994). J. Mol. Biol., 243, 310-326.

P11.03.003 STRUCTURAL INFORMATION DATA-BASE AND MODEL BUILDING USING KINK PARA-METERS OF NUCLEIC ACID STRUCTURES. S. Fujii, School of Pharmaceutical Sciences, University of Shizuoka, 52-1 Yada, Shizuoka-Shi 422-8526, Japan

The conformational flexibility of torsion angles in nucleic acid is very diverse and the number of torsional angle combination would be virtually infinity. The current structural description is the helicoidal parameters of the base moiety aspect to helical axis. However, for curved or kink fragments, the definition of helix axis is much more complicated. The kink parameters would provide the tolerant aspect for irregular structure. The program BIOCON calculates the kink parameters using the coordinates in PDB format. The algorithm of the normalized base calculation and the kink parameter definition accord to Lavery and Sklenar method. The calculated kink parameters are written in mmCIF format using data description language. The model building program, HLX5 has been also developed. In stead of torsion angle, the helical and/or kink parameters are elected as the input information to generate the starting global structure. The building performance is threefold. (i) Generation of structure and coarse connectivity check: Input terms are basic geometrical information such as base pairing scheme and also helical and/or kink parameters, such as tip, inclination and twist angles, and displacements. The glycosyl torsion angle and sugar puckering mode also are treated as independent values. The structural generation is accomplished in accordance with allowed helical parameters. The resulting O3'-C4' distance, of which O3' and C4' atoms are belonged to 3'-link and 5'-link moieties, respectively, is used as selection determinant. (ii) Fine connectivity check: The further conformer space search is carried with fine step among the above selected domain of variable values. Besides the same distance indicator O3'-C4', the short contacts not only between strands but also between the adjacent linked nucleotides are checked. Algorithm Metropolis is constructed to reduce computer time in this procedure. (iii) Energy minimization: Program package X-PLOR affords the convenient calculation to manipulate the structure maturation.

P11.03.004 STRUCTURE OF APO *T.cruzi* GLYCERALDEHYDE-3-PHOSPHATE DEHYDROGENASE: IMPLICATIONS FOR DRUG DESIGN. Oliva, B.G. Guimaraes, L.F. Delboni, M.C. Nonato, M.T. Pupo, Instituto de Física de São Carlos, USP, Cx.P.369, 13560, São Carlos, SP, Brazil, F. Pavao, Instituto de Química de São Carlos, USP, J. Mafezolli, P.C. Vieira, Departamento de Química, Universidade Federal de São Carlos

Aiming at the design of specific inhibitors of the enzyme GAPDH from the parasite *Trypanosoma cruzi*, causative agent of Chagas' disease, the crystallization and structure determination of this enzyme was undertaken. We report here the structures of the apo-form of the enzyme. Crystals were obtained in microgravity at 22ºC (VDA2) by vapor diffusion, with protein solution at 8 mg/ml, 5 mM of chalepin (coumarin derivative), 0.1 M sodium cacodilate at pH 7.1, 0.1 M calcium acetate and 16% PEG 8000. The crystals have grown to a size of 0.2x0.3x0.5 mm after the 9 days, and belong to the space group $P2_1$ with unit cell dimensions a=82.2 Å, b=85.1 Å, c=105.4 Å, β=96.4º and one tetramer per asymmetric unit. Diffraction intensities were collected at 100 K to 1.95 Å resolution and 78% completeness with an R_{merge} of 10.7%. The structure was determined by molecular replacement with a search model of *T. cruzi* glycosomal holo-GAPDH cryo-crystal structure refined in our laboratory at 2.15 Å. Initial refinement aimed at the possible identification of the binding of the inhibitor chalepin was conducted without NCS symmetry using REFMAC to final R=20.5% and R_{free}=30.0%, with a model containing 359 aminoacids per monomer and 848 water molecules in the asymmetric unit. The apo enzyme shows extensive conformational changes when compared with the NAD bound structure. The catalytic domain remains essentially unchanged whereas the NAD binding domain shows a global rotation of 2.8°, followed by internal changes that lead to an opened NAD binding site, with modifications at the hydrophobic pocket adjacent to the adenine moeity originally observed in the holo-form.

Acknowledgements: HHMI, WHO (TDR grant 940854), PADCT/SBIO, CNPq, FAPESP and PRONEX/MCT.

P11.03.005 ENZYME SPECIFICITY AS MODELLED BY A SERIES OF SIX METHYLASES IN THE VITAMIN B_{12} BIOSYNTHETIC PATHWAY. K.S. Wilson and H.L. Schubert Protein Structure Group, Department of Chemistry University of York, Heslington, York, England YO10 5DD and E. Raux, J. Roper and M.J. Warren Department of molecular Genetics, Institute of Ophthalmology, University College London, London EC1V 9EL

Many aspects of rational drug design and enzyme engineering rely of a limited set of information regarding the way and enzyme dictates its specificity for its particular substrate. These aspects are not well understood, though individual cases have been investigated using enzyme mutagenesis and extensive drug screening. Mutagenesis can probe the aspects of a structure that are essential for substrate binding or for maintaining the overall structure, while extensive drug screens test the flexibility of an active site to accommodate a range of compounds. Rarely does nature present a series of enzymes within a genome that possess a similar three dimensional structures and similar though distinct substrates.

Over thirty enzymatic steps are required to synthesise vitamin B_{12} including 8 single-carbon methylations carried out by six independent methylases. The structure of one such methylase from *Bacillus megaterium* was recently solved to 2.4 Å resolution[1]. Based on this structure the other five methylases encoded in the *B. megaterium* pathway have been modelled and their substrate binding sites compared to identify residues that may impart particular aspects of substrate specificity, while retaining the same overall structure and relative catalytic activity.

1 Schubert, H.L., Wilson, K.S., Raux, E., Woodcock, S. & Warren, M.J, (1998) *Nature Struc. Bio.* **5(7)**, 585-592.

P11.03.006 MODEL OF MACROPHAGE STIMULATING PROTEIN β CHAIN, A DOMAIN RESPONSIBLE FOR RECEPTOR BINDING. Maria Miller[1], Alla Danilkovitch[2] and Edward J. Leonard[2]. [1] Macromolecular Structure Laboratory, ABL-BRP, and [2]Laboratory of Immunobiology, NCI-Frederick Cancer Research and Development Center; Frederick, MD 21702, USA

Macrophage stimulating protein (MSP) activates the RON receptor protein-tyrosine kinase. MSP and its close homologue, hepatocyte growth factor (HGF) form a distinct family of growth factors that evolved from plasminogen. They are produced as single chain precursors and are converted to their mature form by cleavage to disulfide-linked α,β-chain heterodimers. Their β-chain serine protease-like domains are devoid of enzymatic activity due to mutations in the catalytic triad. Despite structural similarities, the high affinity receptor binding regions are different α chain for HGF [1] and β chain for MSP [2]. We carried out modeling and site-directed mutagenesis studies of the MSP β chain serine protease domain and showed that the region corresponding to the S1 specificity pocket is critical for the receptor binding ability of MSP. MSP is able to bind RON with high affinity only after proteolytic cleavage, which in zymogens causes conformational changes leading to formation of a mature binding site. The residues critical for zymogen activation are conserved in MSP and HGF, suggesting that the structural basis for conversion to the biologically active growth factors is the same as for zymogen activation. Based on the comparison with HGF we proposed that both HGF and MSP have two receptor binding sites of different affinity, one on the α chain and one on the β chain, and a monomeric ligand induces receptor dimerization.

Research sponsored in part by the National Cancer Institute, DHHS, under contract with ABL.

1. Lokker, N.A. et al.; (1992) EMBO. 11, 2503-2510.
2. Wang, M.H. et al.; (1997) J.Biol.Chem. 272, 16999-17004.

P11.03.007 ROLES OF THE SHORT-RANGE AND LONG-RANGE INTERACTIONS ON PROTEIN LOOP CONFORMATION. Yuzhen Han, Zhijie Liu, Weizhong Li, Luhua Lai, Institute of Physical Chemistry & College of Chemistry, Peking University, Beijing 100871, China

Short peptides in proteins can be classified into two groups according to whether they will always take a conserved conformation: conserved peptides are those that will always take the same conformation independent of protein environment; variable peptides are those that will change conformation under different protein environment. Structurally conserved peptides may act as nucleation site in protein folding.

P12.03.002 *AB INITIO* CRYSTAL SOLUTION OF A PROTEIN WITH 132 AMINO-ACID RESIDUES BY LDE METHOD. M. Shiono and N. Matsugaki, Faculty of Science, Kyushu University, Fukuoka, Japan, and G. Kurisu, Institute for Protein Research, Osaka University, Osaka, Japan and S. Harada, Graduate School of Pharmaceutical Sciences, The University of Tokyo, Tokyo, Japan and Y. Kai, Faculty of Engineering, Osaka University, Osaka, Japan.

The X-ray crystal structure of the zinc endoprotease produced by *Streptomyces caespitosus* (ScNP)[1] has been solved *ab initio* at 1.05 Å resolution by Low Density Elimination (LDE) method[2],[3] refining completely random phase sets. The protein consists of 132 amino-acid residues and the molecular weight is approximately 14 KDa. Multi-solution strategy is employed and 6 solutions out of 10 trials were obtained. An initial structural model with 677 atoms out of 1017 belonging to the protein was built by analysing the resultant map. The complete structure was obtained by least squares refinement and Fourier analysis. Although the crystal structure of ScNP was already solved at 1.6 Å resolution, the analysis was carried out by Kyushu University group who did not know any information for the protein structure except the amino-acids sequence.

G. Kurisu, T. Kinoshita, A. Sugimoto, A. Nagara, Y. Kai, N. Kasai & S. Harada (1997). *J. Biochem.* **121**, 304-308
L. S. Refaat & M. M. Woolfson (1993). *Acta Cryst*. **D49**, 367-371.
M. Shiono & M. M. Woolfson (1992). *Acta Cryst*. **A48**, 451-456

P12.03.003 AUTOMATIC MAP INTERPRETATION. Thomas J Oldfield, Molecular Simulations Inc., Department of Chemistry University of York Heslington York YO10 5DD UK

Recent developments in recombinant DNA techniques, crystallisation protocols, X-ray data collection techniques and devices, and computing have led to a substantial increase in the speed and number of protein structure determinations in modern crystallographic laboratories. However, there still remains a number of key stages in the crystallographic process which limit the rate of structure determination. One of these is fitting electron density maps, either in the initial stages of tracing a chain to a new map, or in the manual rebuilding during refinement. This is a particularly onerous task, requiring many days and often weeks of working at a graphics terminal with maps and model. The presentation will show how methods developed within the program QUANTA can be used to automate the interpretation of electron density maps of proteins, both in the denovo tracing stage and in the model building stage. The level of automation provided by the presented methods is defined by the quality of the data, but this is significant even where the resolution is moderate (3Å) and initial phase error is high (75 degrees). At higher resolution the map tracing and model building is almost entirely carried out by the software. Examples of the use of the application using real data will show that a 10-100 fold reduction in the interpretation time is possible regardless of the data quality where data is useful. The electron density applications available within of QUANTA represent novel and effective tools for speeding up all aspects of map interpretation. The various modules (X-AUTOFIT, X-LIGAND, X-SOLVATE, X-BUILD and X-POWERFIT) have been developed in close collaboration with the large number of crystallographers working on projects in the Protein Group at York. These tools provide the crystallographer with map skeletonisation, map masks, CA-tracing, fuzzy logic sequence assignment, real space torsion angle refinement using grid/gradient/Monte Carlo protcols, interactive regularisation, model building recording, validation, ligand conformational searching and water fitting all in a single application.

04. CRYSTALLOGRAPHY OF BIOLOGICAL MACROMOLECULES

P05.04.001 THE ACTIN-BINDING REGION OF UTROPHIN CRYSTALLISES AS A HEAD-TO-TAIL DIMER. Nicholas H. Keep [1], Andrew Sutherland-Smith[2], Carolyn A. Moores[2], Fiona L.M. Norwood[2], Steven J. Winder[3] and John Kendrick-Jones[2], [1]. Department of Crystallography, Birkbeck College, University of London, Malet St London WC1E 7HX [2]. MRC Laboratory of Molecular Biology, Hills Road, Cambridge CB2 2QH [3]. Institute of Cell and Molecular Biology, University of Edinburgh, Mayfield Road, Edinburgh EH9 3JR

The structure of the actin-binding region from the dystrophin homologue, utrophin has been solved at 3.0 Å. This region belongs to a superfamily of actin-binding proteins that includes spectrin, α-actinin and fimbrin. All these actin-binding regions consist of two calponin homology domains, CH1 and CH2. The individual domains are similar to other structures of calponin homology domains. They are about 100 amino acids long. The structure is all α-helical with four main helices, three roughly parallel and the fourth roughly perpendicular to these.

In the utrophin structure there are two actin-binding regions in the asymmetric unit such that CH1 of one region makes extensive contacts with CH2 of the second region and so makes a head-to-tail dimer. This is in contrast to the structure of the equivalent region of fimbrin, where the two CH domains come from the same protein chain. The possible implications for models of the actin binding in this family of proteins are discussed.

P05.04.002 DISSECTING THE OVERALL STRUCTURE OF THE GIANT MUSCLE PROTEIN TITIN INTO ITS DOMAINS BY X-RAY CRYSTALLOGRAPHY. Olga Mayans, Jochen Wuerges and Matthias Wilmanns, EMBL c/o DESY, Notkestrasse 85, D-22603 Hamburg, Germany and Mathias Gautel, EMBL Heidelberg, Meyerhofstrasse 1, 69117 Heidelberg, Germany.

Two domains of the giant muscle protein titin have been determined by X-ray crystallography, this allowing modelling of numerous related domains from the same protein. Because of its size and its flexibility the three-dimensional structure of titin cannot be determined by diffraction methods. Therefore, we are aiming to assemble an atomic picture of this giant protein by solving X-ray structures of various domains or segments and fit them into low resolution EM images of titin.

The giant muscle protein titin forms the third filament system in striated muscles of vertebrates. It has a molecular weight of about 3 MDa (26926 aas) and a length of about 1 μm, spanning half of the sarcomeric unit from the Z disk to the M line. During development, titin contributes to the muscle ultrastructure by acting as a template for the assembly of sarcomeric proteins whilst in mature muscle it is responsible for elasticity and resting tension. The sequence of titin reveals a modular architecture, with 248 copies of immunoglobulin-like (IG) domains and fibronectin type-III domains arranged in a specific pattern. One single catalytic domain is comprised in the molecule, a serine kinase, referred to as titin kinase (TK) near the C-terminus of the titin molecule.

We have started our investigations by determining the high resolution X-ray structure of TK in its auto-inhibited form [1]. The structure demonstrated that the active site is blocked by a tyrosine from the P+1 loop. Subsequent studies revealed an unprecedented activation mechanism of this kinase by binding of calcium/calmodulin and tyrosine phosphorylation by a so far unknown up-stream kinase. More recently, we have solved a crystal structure of the first IG-like domain in the I band, called I1, using another IG-like structure, the telokin domain from myosin light chain kinase [2], as structural template. The I1 structure serves as a template to model numerous other immunoglobulin-like domains in titin and will provide insight into the molecular basis of titin elasticity.

(1) Mayans *et al*., Nature 395:863-869 (1998)
(2) Holden *et al*., J Mol Biol 227:840-851 (1992)

P05.04.004 STRUCTURAL STUDIES OF THE MOTILE PROTEIN IN NEMATODE SPERM, THE MAJOR SPERM PROTEIN (MSP). A. M. E. Baker and A. J. McCoy, MRC Laboratory of Molecular Biology, Hills Road, Cambridge, CB2 2QH, UK, H. E. Smith and S. D. Ward, Department of Molecular and Cell Biology, University of Arizona, Tucson, AZ 85721, USA, T. M. Roberts, Department of Biological Science, Florida State University, Tallahassee, FL 32306, USA, and M. Stewart, MRC Laboratory of Molecular Biology, Hills Road, Cambridge, CB2 2QH, UK.

The simplicity and specialisation of nematode sperm cells makes them an ideal system for investigating the fundamental mechanism of amoeboid cell motility. Locomotion in nematode sperm is generated by vectorial assembly and bundling of filaments of the major sperm protein (MSP). The structure of the MSP filaments and bundles is central to understanding these processes at the molecular level. To investigate this we have generated a number of different crystal types in which the MSP chains are arranged in helical assemblies. *Ascaris* MSP forms both tetragonal and orthorhombic crystals whereas *C. elegans* MSP-142 generates a different tetragonal form. X-ray crystallography has shown that in tetragonal *Ascaris* crystals the helices have 16 chains arranged as dimers in 5 turns [1], and similar helices were found in the tetragonal *C. elegans* crystals. The helices are apolar and therefore it is unlikely that motor proteins play a significant role in generating the protrusive force in nematode sperm motility. In each of the tetragonal crystal structures, we have found 2 types of interface involved in subfilament formation, and have identified the residues at each interface. The fact that the tetragonal structures are different and yet the packing interactions are preserved suggests that these interactions are important in filament formation and bundling. Supported in part by the MRC, NIH, USDA and the Royal Society.

T. L. Bullock, A. J. McCoy, H. M. Kent, T. M. Roberts and M. Stewart (1998), Nat. Struct. Biol. 5, 184-189.

P05.04.006 ANCHORING ACTIN - THE STRUCTURE OF THE ACTIN BINDING DOMAIN OF ALPHA-ACTININ. F. Ekström [1], G. Stier [2], U.H. Sauer [1], [1] Umeå Center for Molecular Pathogenesis, Umeå University, S901 87 Umeå, Sweden, [2] EMBL-Heidelberg, Meyerhofstr. 1, D-69012 Heidelberg, Germany

We will present the structure of the Actin-Binding-Domain (ABD) of α-Actinin, the first example of a Calponin-Homology (CH) domain involved in muscle architecture.

α-Actinin anchors Actin and the giant protein Titin within the Z-disc of striated muscle. The ABD is located at the N-terminus of α-Actinin and comprises two CH domains in tandem. The C-terminus of the protein interacts with Titin via Calmodulin like EF hands.

The structure of the N-terminal 268 residues containing two CH domains is under determination. The model will be refined against synchrotron data extending to 1.8 Å resolution. Ananlysis of the features of the α-Actinin ABD will be with respect to related proteins such as β-Spectrin [1,2], Fimbrin [3] and Utrophin [4].

[1] K.Djinovic Carugo, S.Banuelos, M.Saraste (1997) Nat. Struct. Biol., 4, 175
[2] S.Banuelos, M.Saraste, K.Djinovic Carugo (1998) Structure, 6, 1419
[3] S.C. Goldsmith, et al. (1997) Nat. Struct. Biol., 4, 708
[4] N.H.Keep et al. (1999) J. Mol. Biol., 285, 1257

P05.04.007 RABBIT MUSCLE CREATINE KINASE - CRYSTAL STRUCTURE AND ITS IMPLICATIONS. J. K. Mohana Rao and Alexander Wlodawer, Macromolecular Structure Laboratory, NCI-FCRDC, ABL - Basic Research Program, P. O. Box B, Frederick, MD 21702, USA.

The crystal structure of homodimeric rabbit muscle creatine kinase (rMCK) was solved to a resolution of 2.35 A recently [Rao, Bujacz and Wlodawer: FEBS Letters (1998) 439, 133-137]. This structure was compared to those of the octameric chicken mitochondrial (Mt) CK and the related monomeric arginine kinase (AK). The sulfates in rMCK (crystals of which were grown from ammonium sulfate) occupy the phosphate positions of ATP or ADP in MtCK and AK. The dimer interfacein CK is stabilized by a small number of hydrogen bonds that remain invariant in the muscle (M), brain (B) and Mt enzymes. These interactions are not facilitated in AK because of the substitution of Asp54 by Leu, of Arg148 by Ala and of Asp210 by Tyr. This may be the reason why only monomers occur in AK. Since the residues involved in these interactions are identical in the M and B enzymes, MB heterodimers can and do occur. There is a distinct difference in the active site region depending upon whether ATP or ADP is present. Models of the BB and MB dimers are also being developed based on the present structural data. These and other structural results will be presented.

Research sponsored by the National Cancer Institute, DHHS, under contract with ABL.

P05.04.009 TRPRS: THREE-STATE BEHAVIOR, INDUCED FIT, CONFORMATIONAL COUPLING, AND FREE-ENERGY TRANSDUCTION, C. W. Carter, Jr., V. A. Ilyin, X. Huang, Y. Yin, P. Retailleau, P. Vachette[¶], A. Longo, and M. Hu, Biochemistry and Biophysics, Univ North Carolina, Chapel Hill, NC. [¶]LURE, Orsay, France

Tryptophanyl-tRNA synthetase (TrpRS) appears to assume three distinct conformations during tryptophan activation. Ca coordinates for ground-state, activated pre-transition state, and product complexes differ by at least five times the r.m.s. deviation within each family. The following new aspects of this three-state behavior obtained from crystal structures, in parallel with solution X-ray scattering, suggest that conformational forces are poised to favor transfer of the a-phosphoryl high-energy bond from pyrophosphate to the amino acid and then from the activated amino acid to the cognate tRNA:

The ATP binding site is structurally fragmented in ligand-free TrpRS.

An open, ternary AMP:tryptophan:TrpRS complex isomorphous with ligand-free TrpRS implies that either an intact nucleoside triphosphate or an aminoacyl-adenylate analog is necessary to induce active site-closure.

Solution scattering and a TrpRS:$[ATP]_2$ complex isomorphous to the closed, pre-transition state show that ATP binding is sufficient to close the active site, driving the first step of the "induced-fit" catalytic cycle.

A product-analog:pyrophosphate:TrpRS complex mimics the Michaelis complex for the pyrophosphate-exchange reaction, the reverse of aminoacylation. Adding pyrophosphate to the product complex does not reverse the second conformational change if the adenosyl-tryptophan bond is stabilized. Thus, transfer of the high-energy AMP-PPi bond to the tryptophan carboxylate stabilizes the product-complex conformation, which binds the activated amino acid before its transfer to cognate tRNA.

A high-quality nonpolar core linking the helical domain and its $tRNA^{Trp}$ anticodon binding determinants to the highly conserved isoleucine in the active-site T**I**GN signature couples active-site chemistry to tRNA binding.

The TrpRS structures confirm in detail conclusions from pre-steady state kinetics of TyrRS active-site mutants. Specifically, residues interacting with the nucleotide ribose are separated in the ligand-free enzyme, consistent with the observation that mutations exert their effect only in the transition state. By implication, other and perhaps all class I aminoacyl-tRNA synthetases may have similar conformational states. The "three-state" cycle: triphosphate => phosphorolysis-products => unliganded => triphospate strongly resembles the conformational cycles of energy-transducing and signaling enzymes like myosin and F1 ATPase,. (Supported by NIH GM48519-02)

P05.04.010 IMPROVING THE RESOLUTION BY REVERSIBLE FREEZING COMBINED WITH SOLVENT CONCENTRATION SCREENING. A.N. Popov and V.S. Lamzin, EMBL Hamburg Outstation, c/o DESY, Notkestasse 85, Hamburg 22603, Germany, and V.R. Samygina, The Institute of Crystallography, Russian Academy of Sciences, Leninsky pr. 59, Moscow 117333, Russia.

A new method of improving the diffraction limit for macromolecular crystals is proposed. The method is based on reversible multiple refreezing combined with searching for the solvent concentration providing the best crystal ordering. Using this method for E.Coli inorganic pyrophosphatase complexed with calcium and with calcium and pyrophosphate allowed us to improve resolution limit and collect data sets up to atomic resolution.

The pyrophosphatase crystals grown from 1.8M sodium chloride and 200mM sodium acetate pH 5.0 diffracted to 1.8 Å. The crystal was first flash frozen from a cryosolution containing the mother liquor and 27% glycerol. Then the crystal was transferred back to cryosolution with increased by 0.05M concentration of sodium chloride. The procedure was repeated several times. On every cycle the diffraction was checked. The highest resolution (1.2 Å) was attained when the concentration of sodium chloride reached 2.2M. The effect was reproducible. The same results have been obtained using other crystals of phyrophosphatase. This simple technique may be useful to improve the diffraction quality of protein crystals generally.

P05.04.011 AN OPEN FLOW HELIUM CRYOSTAT FOR MACROMOLECULES. B. Leif Hanson*, Anthony Martin#, Joel M. Harp*, Damon A. Parrish#, Christopher G. Bunick+, Kristin Kirschbaum#, A. Alan Pinkerton#, and Gerard J. Bunick*+; *University of Tennessee/Oak Ridge Graduate Program in Genome Sciences and Technology, #Chemistry Department, University of Toledo, Toledo, OH, 43606, and +Life Sciences Division, Oak Ridge National Laboratory, Oak Ridge, TN 37831-8080

A helium cryostat developed at the University of Toledo was recently described in the *Journal of Applied Crystallography*. The liquid He consumption of the device is sufficiently low to allow the acquisition of complete diffraction data from a protein crystal on a single 250 L tank of liquid He. This helium cooling system has been tested on macromolecules, using crystals of chicken egg lysozyme, sperm whale myoglobin, concanavalin A, and the nucleosome core particle. Phase changes in terbium vanadate crystals indicate that temperatures delivered by the cryostat were < 33 K at the crystal position. The observed unit cell dimensions in the macromolecular crystals were consistent with temperatures < 77K.

Large crystals approaching suitability for neutron diffraction studies were successfully flash-cooled and a large crystal of lysozyme was rescued for data collection after undergoing a cycle of macromolecular crystal annealing (MCA) following poor flash-cooling. The results of these studies show that this device might be an especially useful adjunct both for neutron diffraction studies and at high intensity synchrotron X-ray sources, in addition to its use in the standard macromolecular repertoire.

Research supported by the Office of Health & Environmental Research, U.S. Department of Energy, under contract No. DE-AC05-960R22464 with Lockheed Martin Energy Research Corp., NIH GM29818, NASA, and through OBOR and the Office of Naval Research (contract N00014-95-1-0013).

P05.04.012 STUDIES OF THE LIGANDS OF C-ABL SH3 DOMAIN. A. Douangamath[*], G. Superti-Furga[f], M. Wilmanns[*].[*] EMBL-Hamburg, c/o DESY, Notkerstraße 85, 22603 Hamburg, Germany. [f] EMBL-Heidelberg, Meyerhofstraße 1, 69012 Heidelberg, Germany

C-Abl, a non-receptor tyrosine kinase located in the nucleus and in the cytoplasm, is the cellular homolog of v-Abl, an oncogene of the transforming retrovirus A-MuLV (Abelson Murine Leukemia Virus). This protein of 150 kDa contains a SH2 and a SH3 domain, known to mediate protein-protein interactions with specific tyrosine phosphorylated sequences and proline-rich motifs, respectively. Some evidences from the last few years show the involvement of c-Abl in the cell growth regulation, in the response to DNA damage and in the cytoskeleton regulation [1]. In the cells, the activity of c-Abl is negatively and tightly regulated by the association of the SH3 domain with extracellular factors [2] In order to understand the regulation mechanism of c-Abl involving the SH3 domain, we would like to get the crystal structure of the complex SH3 domain and its partner. Among the possible ligands of c-Abl, we chose Pag, the product of the Proliferation Association Gene [3]. It is an antioxidant protein of 22 kDa localised also in the nucleus and in the cytoplasm. Although the binding of Pag to the SH3 domain still remains to be clarified, the role of Pag in the inhibition of c-Abl tyrosine kinase activity has been defined to be SH3-domain-dependant. We have established the protocols for the expression and the purification of Pag and the optimisation of the crystallisation conditions is in progress.

Wang J. Y. J. 1993. Curr. Op. in Gen. and Dev. **3**: 35-43
Jackson P. and Baltimore D. 1989. EMBO J. **8**:449-456
Wen S. T. and Van Etten R. 1997. Genes & Development **11**:2456-2467

P05.04.013 DRUG ACTION ON CALMODULIN - COMPLEXES WITH ANTAGONISTS OF DIFFERENT TYPES. V. Harmat, G. Bunkóczy, J. Debreceni, Zs. Böcskei, G. Náray-Szabó [1], B. G. Vértessy, J. Ovádi [2], [1] Dept. of Theoretical Chemistry, Eötvös Loránd Univeristy, H-1518 Budapest 112. POB 32, Hungary, [2] Institut of Enzymology, Biological Research Center of the HAS, H-1518 Budapest POB 7, Hungary.

Calmodulin (CaM), being one of the most important intracellular mediators of Ca(2+)-dependent signalling in eucariotic cells, plays an important role in the modulation of several biochemical processes. Upon Ca(2+) binding CaM changes its conformation facilitating its binding to its target proteins and influencing their action. Modulation of CaM activity is achieved by several antagonists which differ in both chemical structure and mechanism of action. Structural details of antagonist binding are known only for a phenotiazine drug (trifluoperazine [1,2,3]), and an arylalkylamine type molecule [4], two competitive antagonists which occupy the very same binding pockets as the side chains of the CaM recognising peptides of several target enzymes.

Preliminary experiments suggest that the above arylalkylamine type molecule binds in a different way in complexes of different CaM-ligand ratios. Crystallization of an 1:1 Ca-CaM - arylalkylamine is in progress. Biochemical tests indicated that vinblastine derivatives have different binding sites and can also bind to apo-CaM. Crystallisation trials are in progress with quaterner complexes Ca-CaM, target peptides and noncompetitive antagonists. Crystals with vinblastine type compounds have been produced both in presence and in absence of Ca(2+). The analysis of the complex structures can help to better understand the mechanism of CaM antagonism of these molecules.

1. Cook,W.L. et al (1994) Biochemistry 33,15259-15265
2. Vandonselaar, M. et al (1994) Nat. Struct. Biol.1, 795-801
3. G. Vertessy, B. et al. (1998) Biochemistry 37, 15300-15310
4. V. Harmat et al. J. Biol. Chem. to be submitted

P05.04.014 SEX AT THE MOLECULAR LEVEL: THE CRYSTAL STRUCTURE OF A FERTILISATION PROTEIN. N. Kresge and C. D. Stout, The Scripps Research Institute, 10550 N. Torrey Pines Rd., La Jolla, California 92037, and V. D. Vacquier, The Scripps Institution of Oceanography, University of California, San Diego, La Jolla, Calilfornia 92093.

The structures of a gamete recognition protein (lysin) from two species of abalone have been determined, which has lead to insights on how lysin interacts with an egg receptor protein and the role it plays in acting as a barrier to cross-species fertilisation.

At the molecular level, fertilisation begins with the penetration of the egg's outer coat by the sperm. Abalone sperm accomplish this task by releasing a 16kDa protein (lysin) onto the surface of the egg's Vitelline Envelope (VE). Lysin then binds to the Vitelline Envelope Receptor for Lysin (VERL) and creates a hole in the VE by a non-enzymatic mechanism. Percent identity of lysins from different species ranges from 63% to 90%, and lysins exhibit species specificity - they will not easily bind to or dissolve VEs from other abalone species.

As part of an effort to understand, at atomic resolution, lysin's interaction with VERL and its role in species-specificity, we have solved the crystal structures of lysin from Haliotis rufescens (red abalone) and Haliotis fulgens (green abalone) to 1.35Å and 1.7Å respectively. Both molecules consist of an amphipathic 5 helix bundle with two tracks of basic residues running the length of one side, and a solvent-exposed hydrophobic patch on the other side. Neither lysin has obvious binding pockets or active sites suggesting the whole surface of lysin is its "active site". The overall folds of the two proteins are remarkably similar with a c-alpha rms deviation of 1.0Å, indicating that its species-specificity lies in the locations of non-conserved residues and in subtle side-chain rearrangements.

P05.04.016 STRUCTURE OF THE PH DOMAIN FROM BRUTON'S TYROSINE KINASE IN COMPLEX WITH IP4 K. Djinovic Carugo, E. Baraldi [1], M. Hyvönen [2], P. Lo Surdo [1], A. M. Riley, B.V.L. Potter [3], R. O'Brien, J. E. Ladbury [4], M. Saraste [1], [1] European Molecular Biology Laboratory, Meyerhofstrasse 1, D-69012, Heidelberg, Germany, [2] Department of Biochemistry, University of Cambridge, 80 Tennis Court Road, CB2 1GA Cambridge, UK, [3] Wolfson Laboratory of Medicinal Chemistry, Department of Pharmacy and Pharmacology, University of Bath, Claverton Down, Bath, BA2 7AY, UK, [4] Department of Biochemistry and Molecular Biology, University College London, Gower Street, London WC1E 6BT, UK

The activity of Bruton's tyrosine kinase (Btk) is important for the maturation of B cells. A variety of point mutations in this enzyme results in a severe human immunodeficiency known as X-linked agammaglobulinemia (XLA). Btk contains a PH domain which specifically binds phosphatidylinositol 3,4,5-trisphosphate and hence responds to signalling via phosphatidylinositol 3-kinase. Point mutations in the PH domain may abolish membrane binding, preventing signalling via Btk.

We have determined crystal structures of the wild type PH domain and a gain-of-function mutant E41K in complex with inositol 1,3,4,5-tetra-kisphosphate. It binds to a site that is similar to the Ins(1,4,5)P3 binding site in the PH domain of phospholipase C-delta. A second Ins(1,3,4,5)P4 molecule is associated with the domain of the E41K mutant, suggesting a mechanism for its constitutive interaction with membrane.

Our data provide an explanation for the specificity and high affinity of the interaction with PtdIns(3,4,5)P3 and lead to a classification of the XLA mutations that reside in the Btk PH domain. Missense mutations which do not simply destabilize the PH fold either directly affect the interaction with the phosphates of the lipid head group or change electrostatic properties of the lipid binding site. One point mutation (Q127H) cannot be explained by these facts, suggesting that the PH domain of Btk carries an additional function such as interaction with a G-alpha protein.

P05.04.017 STRUCTURAL AND BIOCHEMICAL STUDIES ON RCC1 THE GUANINE EXCHANGE FACTOR FOR THE SMALL GTP-BINDING PROTEIN RAN. L. Renault[#], Y. Azuma[+], J.A. Garcia-Ranea*, A. Valencia*, T. Nishimoto[+] and A. Wittinghofer[#], [#]Max-Planck-Institut für molekulare Physiologie, Rheinlanddamm 201, 44139 Dortmund, Germany, [+]Department of molecular Biology, Graduate School of Medical Science, Kyushu University, Maidashi, Fukuoka 812, Japan, *Protein Design Group, CNB-CSIC, Campus U. Autonoma, Cantoblanco, Madrid M-28049, Spain.

The protein RCC1, for Regulator of Chromosome Condensation, has been originally identified as a control element of the cell cycle [1]. Biochemically, RCC1 is the guanine nucleotide exchange factor (GEF) of the small regulatory GTP-binding protein Ran (Ras-like nuclear GTP-binding protein). This GEF activity makes RCC1 an essential element in the GTPase cycle of Ran as it controls the timing of molecular processes that are regulated by the transition of Ran to the GTP-bound form. The molecular switch Ran regulates two important biological pathways: nucleo-cytoplasmic transport and cell cycle progression [1].

The structure of human RCC1, solved to 1.7 Å resolution by X-ray crystallography, reveals a seven-bladed β-propeller, formed by internal repeats of 51-68 residues per blade [2]. These repeats are also found in more than 20 different proteins, not related to RCC1. The structure is very similar to the seven-bladed β-propellers found in the β-subunit of heterotrimeric G proteins, and explains the consequences of a wide range of known mutations, which affect the radial arrangement of the repeated units. Based on site-directed mutagenesis [3], one face of the β-propeller has been proposed as the interacting face with the GTPase Ran, whereas the opposite face is thought to be involved in chromatin interaction. A model of the Ran-RCC1 interaction using biochemical and structural docking experiments has been obtained recently and it allows us to gain further insight into the guanine exchange release mechanism induced by RCC1 on Ran [4].

[1]. T. Seki, N. Hayashi & T. Nishimoto (1996). J. Biochem. 120, 207-214.
[2]. L. Renault, N. Nassar, I. Vetter, J. Becker, C. Klebe, M. Roth & A. Wittinghofer (1998). Nature 392, 97-101.
[3]. Y. Azuma, H. seino, T. Seki, S. Uzawa, C. Klebe, T. Ohba, A. Wittinghofer & T. Nishimoto (1996). J. Biochem. 120, 82-91.
[4]. Y. Azuma, L. Renault, J.A. Garcia-Ranea, A. Valencia, T. Nishimoto & A. Wittinghofer (submitted for publication).

P05.04.019 CRYSTAL STRUCTURE OF THE CALMODULINS IN COMPLEX WITH ANTIPSYCHOTIC PHENOTHIAZINE-TYPE DRUGS. M. Senda, T. Senda, Department of BioEngineering, Nagaoka University of Technology, Nagaoka, Niigata 940-2188, JAPAN. H. Kasai, Tokyo Metropolitan University of Health Siences Arakawa-ku, Tokyo 116, JAPAN, and Y. Mitsui, Department of BioEngineering, Nagaoka University of Technology, Nagaoka, Niigata 940-2188, JAPAN.

Calmodulin (CaM) is a ubiquitous Ca^{2+}-binding protein of 148 amino acid residues present in all eukaryotic cells. It has been known that the CaM molecule can bind such small compounds as trifluoperazine (TFP) and chlorpromazine (CHL) as well as a variety of target peptides (or proteins). To date two groups have reported on the crystal structures of CaM in complex with TFP. These analyses showed that CaM in complex with TFP assumed a the compact shape, which is similar to that of CaM complex with a target peptide. However, the number of the TFP molecule bound to CaM, and the location of bound TFP molecules vary in each crystallographic analysis. To gain a precise insight into the three-dimensional structure of CaM in complex with small compounds such as TFP and CHL, we undertook reexamination of the crystal structure analyses on CaM in complex with the small compounds.

Crystal structure of CaM in complex with TFP was solved using a multiple isomorphous replacement procedure. Using this structure as a search model, the crystal structure of the CaM-CHL complex was then solved by a molecular replacement method. The overall structures of CaM were almost identical to each other and to that found in the previously reported CaM-TFP complex structure. In the present TFP complex, one TFP bound to the hydrophobic pocket of the N-terminal domain of CaM, the other TFP binding to the C-terminal domain. In the CHL complex, the C-terminal binding site was equivalent while the other binding site appeared unique.

P05.04.021 CRYSTAL STRUCTURE OF HUMAN RHOA^{V14} COMPLEXED WITH GDP. Kentaro Ihara, Toshiyuki Shimizu, Shinya Kuroda, Kozo Kaibuchi, and Toshio Hakoshima, Faculty of Bioscience, Nara Institute of Science and Technology, 8916-5 Takayama, Ikoma, Nara 630-0101, Japan.

The crystal structure of RhoA^{V14} complexed with a GDP and a Mg^{2+} ion was determined at 2.2 ≈ resolution by the molecular replacement technique. Compared with RhoA^{N25}-GDP (1), the switch I (27-46) region shows significantly large structural displacements that are also dissimilar to those of RhoA^{V14}-GTPγS (2). In the switch I, some residues displaced more than 20 ≈ from the corresponding main-chain C_α carbon atoms of RhoA^{N25}-GDP. It seems to be unlikely that these structural changes due to the difference in the mutated residues. In RhoA^{V14}-GDP, the switch II can be traced with no interruption, although three residues are missing in RhoA^{N25}-GDP. This stabilization of the switch II in RhoA^{V14}-GDP seems to be due to the contacts with the side-chain of Val14. In spite of the large displacements, the conformational changes between the GDP- and GTP-bound forms were occurred only in the switch regions. It is known that the switch II regions of the Ras family members display various conformations especially in the GDP-bound form (3). These results may suggest the existence of multiple quasi-stable states in the switch regions of RhoA bound to GDP. Similar observations are reported in the

solution strucutres of H-Ras (4), although they are in the GTP-bound forms.

(1) Wei, Y., Zhang, Y., Derewenda, U., Liu, X., Minor, W., Nakamoto, R. K., Somlyo, A. V., Somlyo, A. P., and Derewenda, Z. S. (1997). *Nat. Struct. Biol.* **4**, 699-703.
(2) Ihara, K., Muraguchi, S., Kato, M., Shimizu, T., Shirakawa, M., Kuroda, S., Kaibuchi, K., and Hakoshima, T. (1998). *J. Biol. Chem.* **273**, 9656-9666.
(3) Cherfils, J., Menetrey, J., Le Bras, G., Le Bras, G., Janoueix-Lerosey, I., de Gunzburg, J., Garel, J.-R., and Auzat, I. (1997). *EMBO J.* **16**, 5582-5591.
(4) Ito, Y., Yamasaki, K., Iwahara, J., Terada, T., Kamiya, A., Shirouzu, M., Muto, Y., Kawai, G., Yokoyama, S., Laue, E. D., W‰lchli, M., Shibata, T., Nishimura, S., and Miyazawa, T. (1997). *Biochemistry* **36**, 9109-9119.

P05.04.022 STRUCTURAL STUDIES OF NEUROTROPHINS AND THEIR RECEPTORS. M.J. Butte, Graduate Group in Biophysics, University of California San Francisco, Box 0448, 513 Parnassus, San Francisco, CA 94143 USA; W.C. Mobley, Department of Neurology, Stanford University, Stanford CA 94305 USA; and R.J. Fletterick, Dept. of Biochemistry and Biophysics, University of California San Francisco, San Francisco CA 94143 USA.

The neurotrophins are cystine-knot growth factors that control the survival, proliferation, differentiation, and programmed cell death of developing neurons and are potential therapeutics for neurodegenerative diseases. Two classes of cell-surface receptors have been found for these secreted proteins: the Trk family, which are receptor tyrosine kinases that show selectivity for each neurotrophin and are essential for neuronal development; and $p75^{NTR}$, a member of the tumor necrosis factor receptor (TNFR) superfamily that binds all the neurotrophins with equal affinity and plays a role in neuronal apoptosis. To clarify the open issues of the structural basis of receptor specificity and the mixed roles of the Trk receptors and p75 in neurotrophin signaling, we have undertaken biochemical and x-ray crystallographic studies of the neurotrophins and their receptors. So far, we have solved the structure of human neurotrophin-3 (NT-3) homodimer, which reveals structural clues to NT-3 specificity with TrkC. Co-crystallization studies of the neurotrophin BDNF with its partner TrkB are underway to expand our structural understanding of neurotrophin/Trk interaction. Using limited proteolysis, mass spectrometry, and surface plasmon resonance interaction analysis, we are determining the domains of p75 that are most important for neurotrophin binding. Co-crystallographic analysis of these fragments is underway. We will report on our progress to date on these structural and biochemical experiments, including the structure of NT-3.

P05.04.023 THE CRYSTAL STRUCTURE OF D-GLUCARATE DEHYDRATASE, A MEMBER OF THE ENOLASE SUPERFAMILY Andrew M. Gulick [1], David R. J. Palmer [2], Brian Hubbard [2], John A. Gerlt [2], and Ivan Rayment [1]. [1] The Institute for Enzyme Research and Department of Biochemistry, University of Wisconsin, Madison, USA. [2] Department of Biochemistry, University of Illinois, Urbana, USA

The Enolase superfamily of enzymes represents several enzymes with limited sequence homology that exhibit a conserved structural fold and catalyze similar chemistry. The enzymes contain an N-terminal domain composed of helices and sheets, followed by a C-terminal barrel domain. The barrel consists of alternating helices and strands in which the 8 parallel strands form a closed sheet in the form of a barrel. The active site of these enzymes is located at the cavity formed at the C-terminus of the strands in the barrel. This architecture allows residues from all of the barrel strands to interact with the substrate.

Glucarate dehydratase (GlucD) catalyzes the elimination of water from (D)-glucarate to form 5-keto-4-deoxy-(D)-glucarate. We have determined the structure of this enzyme from two sources, E. coli and P. putida. The E. coli GlucD structure was determined in the absence of any bound substrate, in the presence of the product, and also two inhibitors, 4-deoxy-(D)-glucarate and the hydroxamate of glucarate. The structures demonstrate the conservation of important residues for specific catalytic roles, as well as the recruitment of additional residues involved in the binding of the substrate. Specifically, a large loop from the N-terminal domain, which is disordered in the unliganded form, and an extended C-terminal domain form important interactions with the product and inhibitor molecules.

P06.04.001 THE STRUCTURAL MECHANISM FOR HALF-THE-SITES REACTIVITY IN THYMIDYLATE SYNTHASE. Amy C. Anderson, Robert H. O'Neil and Robert M. Stroud. Department of Biochemistry and Biophysics, University of California at San Francisco, San Francisco, CA 94143-0448.

We have determined the first structural mechanism for the basis of half-the-sites reactivity, an extreme form of negative cooperativity, in an enzyme. The co-crystal structure of thymidylate synthase from *Pneumocystis carinii* (PcTS) with its substrate, dUMP, and a cofactor mimic, CB3717, at 2.6 Å resolution shows an asymmetric dimer with two molecules of substrate bound, yet only one molecule of the cofactor analog bound. The structural evidence reveals the mechanism by which binding of the cofactor or an antifolate inhibitor to one monomer renders the opposite monomer catalytically inactive and incapable of binding a second molecule of cofactor.

A structural analysis program was used to create a three-dimensional movie of the conformational changes. This structural comparison shows that covalent bond formation between the catalytic cysteine and dUMP in one monomer is accompanied by conformational changes that translate to residues across the molecular two-fold axis at the dimer interface, generating the asymmetry seen between the two active sites. The asymmetry prevents a covalent bond, and hence, catalysis, in the second active site. Additionally, the conformational changes break hydrogen bonds between a key asparagine residue and dUMP in the second monomer, allowing a misorientation of the substrate and a rise in the K_M for cofactor since the orientation of the cofactor is directly dependent on the orientation of the pyrimidine base.

P06.04.002 STRUCTURAL STUDIES INVESTIGATING THE CATALYTIC INTERMEDIATES OF GALACTOSE OXIDASE. Susan J. Firbank, Elinor Vinecombe, Carrie M. Wilmot, Michael J. McPherson, Peter F. Knowles & Simon E.V. Phillips. School of Biochemistry and Molecular Biology, University of Leeds, Leeds LS2 9JT, U.K.

Galactose oxidase is the simplest known copper containing oxidase. It is an extracellular enzyme produced by *Fusarium spp.* which catalyses the stereo-selective oxidation of specific primary alcohols ranging from small molecules to polysaccharides. The two electron redox reaction follows the general scheme:

$$RCH_2OH + O_2 \rightarrow RCHO + H_2O_2$$

The crystal structure has been determined to 1.7Å revealing a novel thioether bond between tyrosine 272 and cysteine 228, with tryptophan 290 stacking over this thioether bond. Insight into the reaction mechanism has been gained using spectroscopic, kinetic and mutagenesis studies in conjunction with the structure.

Recently a different crystal form has been identified which allows the catalytic turnover of D-galactose. We are hoping to use this crystal form to investigate the spectrally distinct intermediate structures of galactose oxidase produced during the reaction, by monitoring the timecourse of the reaction using a microspectrophotometer, and flash freezing the crystals at the various stages. This technique has recently been used to characterise intermediates in the catalytic cycle of *E. coli* amine oxidase.

P06.04.003 MUTANTS OF ASPARTATE SEMIALDEHYDE DEHYDROGENASE: ESSENTIAL BACTERIAL BIOSYNTHETIC ENZYME. C.N.Y.A. Shammas, J. Axcell, A.T. Hadfield, Dept. Biochemistry, Bristol University, University Walk, Bristol BS8 1TD; C. James, R.E. Viola, University of Akron, Ohio.

Aspartate β-semialdehyde dehydrogenase lies at a branch point in the biosynthetic pathway through which bacteria, fungi and the higher plants synthesize diaminopimelate and lysine from aspartate. Blocks in this biosynthetic pathway are lethal, making ASADH an attractive target for anti-bacterial, fungicidal, or herbicidal agents. The enzyme, which is active in *E. coli* as a dimer, catalyses the reductive phosphorylation of β-aspartyl phosphate, with a mechanism similar to glyceraldehyde-3-phosphate dehydrogenase. The structure of the apo-enzyme and of a ternary complex with NADP, phosphate and the substrate-mimicking inhibitor S-methyl cysteine sulfoxide has been solved [1].

The crystal structures above suggest a role in the mechanism of the enzyme for a conserved histidine. Mutation of this histidine results in greatly reduced activity. We currently have crystals of the enzyme in complex with NADP alone and also that of site directed mutants including His274Gln.

[1] A.T. Hadfield, *et al.* 1999 IUCr abstracts (0235).

P06.04.004 UNRAVELLING THE RIBONUCLEOLYTIC MECHANISM OF ANGIOGENIN : AN ATYPICAL RIBONUCLEASE IMPLICATED IN NEOVASCULARIZATION. G.V. Subbarao and D.D. Leonidas, University of Bath, UK and R. Shapiro, Harvard Medical School, Boston, USA, and K.R. Acharya, University of Bath, UK.

Angiogenin (Ang), a member of the RNase superfamily having a 33.1% sequence homology is a 14.1 kDa protein (123 AA), is implicated in the onset of vasculature, both in human health and disease. Although Ang has approximately 10^5-10^6 times lower ribonucleolytic activity than RNase A, it is observed that this diminished ribonucleolytic activity is an obligatory prelude to its angiogenic potency. The structure of human Met(-1) Ang demonstrated that Gln-117 hinders active site acess, partly accounting for it's diminished ribonucleolytic. It has been suggested that the residues from the C-terminus also contribute to the impediment of the active site.

The focus of our work is to gain structural insights into the ribonucleolytic activity of Ang by characterisation of the C-terminus and the active site. Subsequently, high-resolution X-ray crystallographic structures of Ang variants D116H, Des121-123, H13A and I119A-F120A Ang were determined. Ang differs from RNase A in substrate specificity and appears to be modulated by the 'B_1' subsite, having a strong (12- to 20- fold) preference for cytosine vs. uracil nucleotides. In order to understand the structural role of the 'B_1' subsite, variants T44D and T80A Ang have been overexpressed and purified. The structure of a variant from a peripheral subsite of Ang, H8A Ang has also been determined. A detailed analysis of the structure-function relationships of all the mentioned variants and their implications for inhibitor design will also be presented.

P06.04.005 A TRANSITION STATE ANALOG COMPLEX OF *ESCHERICHIA COLI* PHOSPHOENOLPYRUVATE CARBOXYKINASE-AlF_3-ADP-Mg^{2+}. Athena M. Sudom, J. Wilson Quail, Hughes Goldie and Louis T. J. Delbaere, Departments of Chemistry, Biochemistry and Microbiology, 107 Wiggins Road, University of Saskatchewan, Saskatoon, Saskatchewan, S7N 5E5 Canada.

The mechanism of reversible transfer of the γ-phosphate of ATP by phosphoenolpyruvate carboxykinase (PCK) onto its substrate is of great interest. It is known that metallofluorides are accurate analogs of the transition state in the context of kinase mechanisms, and so AlF_3 and ADP were crystallized in complex with PCK. AlF_3 forms a trigonal bipyramid that mimics the transition state of phosphoryl transfer, allowing investigation into the catalytic mechanism of this kinase. PCK is indispensable in gluconeogenesis for its role in decarboxylation and phosphorylation of oxaloacetate to form phosphoenolpyruvate, ADP, and CO_2.

Initially, crystals of *E. coli* PCK were grown in complex with AlF_3, magnesium and ADP via hanging drop vapour diffusion at 21°C. The components of the hanging drop protein solution were as follows: 6 mg ml^{-1} PCK, 0.8 mM $Al(NO_3)_3$, 4 mM NaF, 5 mM $MgCl_2$, 2 mM ADP, 0.1 mM EDTA, 200 mM ammonium acetate, 100 mM sodium acetate buffer (pH 5.0), 0.1 mM dithiothreitol (DTT) and 12% polyethylene glycol 4000 (PEG). The reservoir solution contained 30% PEG 4000, 100 mM sodium acetate buffer (pH 5.0) and 200 mM ammonium acetate.

Diffraction data were collected to the maximum resolution of 2.0 Å at the Photon Factory in Tsukuba, Japan. The monoclinic unit cell dimensions were a = 126.0, b = 95.8, c = 46.6Å, β = 95.6° with space group C2. The initial round of refinement gave an R factor of 25.5%. Further analysis is ensuing.

This research is funded by the Medical Research Council of Canada.

P06.04.006 CRYSTAL STRUCTURE OF PHOSPHOGLUCOSE ISOMERASE / AUTOCRINE MOTILITY FACTOR / NEUROLEUKIN. Yuh-Ju Sun, Chia-Cheng Chou and Chwan-Deng Hsiao, Institute of Molecular Biology, Academia Sinica, Taipei, Taiwan 11529, ROC, Wei-Shone Chen, Veterans General Hospital, Taipei, Taiwan, 11217, ROC, Rong-Tsun Wu, Graduate Institute of Biopharmaceutical Science, National Yang-Ming University, Taipei, Taiwan, ROC and Menghsiao Meng, Graduate Institute of Agricultural Biotechnology, National Chung Hsing University, Taichung, Taiwan 40227, ROC.

Phosphoglucose isomerase (PGI), a glycolytic enzyme, was recently described to exhibit the equivalent function as neuroleukin (NLK) as well as autocrine motility factor (AMF) of tumor cells. Here we present the first complete crystal structure of phosphoglucose isomerase cell from *Bacillus stearothermophilus* at 2.3 Å resolution. The structure of PGI is a open twist α/β structure. The functional form of PGI is a dimer, each subunit consists of two globular domains and two protruding loops. The subunits associate in an arm-to-arm hug fashion. The proposed substrate binding-site is in both the domain interface and the subunit interface. A mechanism for enzymatic specificity and activity is postulated. We also demonstrate that PGI exhibits cell motility-stimulating activity on CT-26 mouse colon cancer similar to that of endogenous AMF, and that PGI enhances neurite outgrowth in terms of length and density on neuronal progenitor cells observed in NLK.

P06.04.007 CRYSTAL STRUCTURE OF A BIOSYNTHETIC THIOLASE IN COMPLEX WITH ACETOACETYL-COA. Y. Modis, European Molecular Biology Laboratory, Postfach 10.2201, D-69012, Heidelberg, Germany and R.K. Wierenga, Department of Biochemistry, University of Oulu, FIN-90570, Oulu, Finland.

The crystal structure of biosynthetic thiolase from the bacterium Zoogloea ramigera in complex with its substrate, acetoacetyl-CoA, was solved at 2.35 Å resolution.

Thiolases can function either degradatively in the β-oxidation pathway of fatty acids, or biosynthetically in the synthesis of various fuel molecules, cholesterol and steroid hormones.

The tetrameric biosynthetic thiolase from Zoogloea ramigera [1] has the same subunit structure as the dimeric yeast degradative thiolase whose structure was solved previously [2], but the biosynthetic thiolase contains a striking and novel cage-like tetramerisation motif. A molecule of acetoacetyl-CoA, which is a thiolase substrate, is visible in two of the four active sites in the tetramer. The mode of binding of the substrate shows in molecular detail how the substrate is activated for nucleophilic attack by the catalytic cysteine residue, Cys89, leading to the formation of a covalent substrate-enzyme reaction intermediate. Finally, the shape of the active site pocket of biosynthetic thiolase reveals the basis for the short-chain substrate specificity of the enzyme [3].

[1] S. Thompson, F. Mayer, O.P. Peoples, S. Masamune, A.J. Sinskey & C.T. Walsh, Biochemistry **28**, 5735 (1989)
[2] M. Mathieu, Y. Modis, J.Ph. Zeelen, C.K. Engel, R.A. Abagyan, A. Ahlberg, B. Rasmussen, V.S. Lamzin, W.-H. Kunau & R.K. Wierenga, J. Mol. Biol. **273**, 714 (1997)
[3] Y. Modis & R.K. Wierenga, submitted for publication (1999)

P06.04.008 PRELIMINARY X-RAY STUDIES OF 12S FORM OF PHOSPHOFRUCTOKINASE 1 FROM SACCHAROMYCES CEREVISIAE. I. Mechin[a], G. Kopperschläger[b], W. R. Rypniewski[a] at [a]European Molecular Biology Laboratory (EMBL) c/o DESY, Germany, [b]Institute of Biochemistry, Medical Faculty, University of Leipzig, Germany.

Extensive crystallographic studies have been carried out on bacterial phosphofructokinase1 but until now no eukaryotic PFK1 has been crystallised in a form suitable for X-ray analysis. PFK1 catalyses the conversion of fructose 6-phosphate into fructose 1,6-bisphosphate in the presence of MgATP. It is an allosteric key enzyme in glycolysis, with various effectors, both activators and inhibitors. In baker's yeast PFK1 is a hetero-octamer ($\alpha_4\beta_4$) of molecular weight approximately 800 kDa (21S). As a result of an early gene duplication each eukaryotic subunit consists of two homologous parts, each repeat similar to one prokaryotic subunit. One of them is thought to have lost catalytic function and acquired a regulatory role. In yeast a second gene duplication event is supposed, forming two different types of subunits called α and β. Yeast PFK1 octamer consists of 16 prokaryotic like units with heterogeneous terminal regions responsible for subunit association.

The 12S form of yeast PFK1 is obtained by limited proteolytic cleavage of the native enzyme by chymotrypsin in the presence of ATP, leading to the truncation of C- and N- terminal parts. As a consequence the 21S octamer dissociates to form two 12S tetramers of identical size composed of partially degraded α" and β' subunits. This truncated form is catalytically active, possesses similar kinetic properties to the native enzyme and shows no micro-heterogeneity.

The size of yeast PFK1 makes the crystallography a challenge but structure solution feasible. The 12S PFK1 enzyme was crystallised under a variety of conditions. The crystals have been characterised. Diffraction data have been collected to 2.9Å under cryogenic conditions, on the EMBL beamline at the DORIS storage ring in Hamburg. Work is in progress to solve the structure by molecular replacement using the bacterial subunit as the research model. Preliminary results will be presented.

P06.04.009 ATP BINDING TO THE N-TERMINAL DOMAIN OF HUMAN HEXOKINASE TYPE I REVEALED BY X-RAY CRYSTALLOGRAPHY. C. Rosano, M. Bolognesi [1], E. Sabini [2], M. Bianchi, G. Serafini, E. Bartolucci M. Magnani [3], [1] Advanced Biotechnology Center-IST and Dept. of Physics, University of Genova, Largo R. Benzi 10 16132 Genova (I), [2] Department of Chemistry, University of York, Heslington, York (UK), [3] Institute of Biological Chemistry, University of Urbino, Via Saffi 2, 61029 Urbino (I)

Human Hexokinase type I (HKI) is the enzyme starting glucolysis in the brain through the ATP-based glucose → glucose-6-phosphate (G6P) phosphorylation reaction.

HKI, which plays a key role in normal but also in malignant cancer cells, can be found bound to the mitochondrial membrane as well as in a cytoplasmic soluble form.

The enzyme associated with the membrane is dimeric or tetrameric; release from the membrane is favoured by nucleotides such as ATP, GDP, UDP.

Crystals of HKI belong to the monoclinic space group P21 with unit cell constants a=82.42 Å, b=174.35 Å, c=86.28 Å, beta=90.54º. Diffraction data were collected at 100 K at the EMBL/DESY synchrotron radiation facility in Hamburgh (D), beamline X11.

A total of 68,573 unique reflections up to 2.67 Å resolution were measured for a completeness of 87%, Rmerge=4.8%.

The structure of HKI was solved by molecular replacement methods using a previously determined human hexokinase model (PDB code 1HKB).

The HKI structure was refined through cycles of simulated annealing/slowcooling first, followed by maximum likelihood refinement with conjugate gradients. The final R factor is 0.208.

The electron density is continuos all over the dimeric protein, clearly showing the binding of glucose and G6P at both domains of each subunit.

Remarkably, an unexpected AMP-PNP molecule is found in a surface cleft next to the N-terminal part of the protein.

Based on their strategic location next to the membrane anchoris segments, it is proposed that the two nucleotide binding sites are involved in the control of HKI membrane association-dissociation processes.

P06.04.010 X-RAY STUDIES OF TWO GLYCOLYTIC ENZYMES FROM THE ARCHAEON SULFOLOBUS SOLFATARICUS. Crowhurst, G., Isupov, M. N. and Littlechild, J. A., Schools of Chemistry and Biological Sciences, University of Exeter, Exeter, UK.

Two glycolytic enzymes phosphoglycerate kinase (PGK) and glyceraldehyde-3-phosphate dehydrogenase (GAPDH) from the thermostable archaeon *Sulfolobus solfataricus* (which grows optimally at pH 3.5 and at 87°C) have been cloned into a pET expression system and overexpressed in *Escherichia coli*. Crystals of GAPDH were grown in space group $P42_12_12$ with unit cell dimensions a=b=102.3Å, c=181.6Å in PIPES pH 6.5, in the presence of cofactors NAD^+ and $NADP^+$ using 33% ammonium sulfate as the precipitant. The X-ray structure of apo GAPDH has been solved using isomorphous replacement method. The overall fold of this archaeal GAPDH is similar to that of eukaryotic and prokaryotic counterparts with which the enzyme shares low sequence identity (under 22 %), although there are additional, mainly α-helical, secondary structure elements. The long additional α-helix and following additional β-strand of catalytic domain β-sheet at the C-terminus of the enzyme create an

additional link between the catalytic and NADP+ binding domains. A conserved Asp at the end of the second β strand is replaced by Lys as the enzyme has a preference for $NADP^+$. Although the enzyme was originally reported to catalyse the reaction on glyceraldehyde the sulphate ions bound at the inorganic phosphate and the substrate phosphate binding sites suggest a preference for glyceraldehyde-3-phosphate. Although this archaeal GAPDH active site resembles that of the prokaryotic enzymes the residues of the catalytic domain are all shifted one β-strand across its β-sheet. Several ion pair clusters of up to 15 charged residues and a disulfide bond rarely found in intracellular proteins contribute to the marked enzyme thermostability (an activity half life of 17h at 80°C).

Small needle crystals of *S. solfataricus* PGK have been obtained from polyethylene glycol at a concentration of 24% w/v and 0.1M Tris-HCl buffer pH 8.5, using the hanging drop method.

P06.04.011 CRYSTALLOGRAPHIC STUDIES ON TRANSITION STATE MIMIC COMPLEXES IN THE XYLANASE/CELLULASE CEX. Valerie Notenboom and David Rose, Department of Medical Biophysics, University of Toronto, Toronto M5G 2M9, Canada, and Stephen G. Withers, Department of Chemistry, University of British Columbia, Vancouver V6T 1Z1, Canada.

The reaction mechanism employed by retaining β-1,4-glycanases has long thought to be a double displacement mechanism involving a covalent reaction intermediate. Significant evidence has been accumulating over the years supporting the existence of such an intermediate. Recently, crystallographic studies have shown the direct observation of the covalent reaction intermediate in the family 10 glycosidase Cex from using mechanism based 2-fluoro inhibitors [Notenboom *et al.,*1998, *Biochemistry* **37**:4751; White *et al.*, 1996, *Nat. Struct. Biol.* **3**:149], as well as trapping the intermediate in a mutated enzyme [Notenboom *et al.*,1998, *Nat. Struct. Biol.* **5**:812] . Details of the reaction driving forces are not well understood, in particular the enzyme-substrate interactions stabilizing the transition states that are flanking the covalent reaction intermediate are as yet unclear. Several residues surrounding the disaccharide during catalysis have been implicated in the reaction mechanism, as well as a possibly significant stabilizing force involving the 2'-hydroxy group of the proximal saccharide itself. As one approach to deconvolute these interactions present during different stages of catalysis we are looking at the crystal structures of several enzyme substrate complexes in which the substrate is a mimic of the proposed transition states. The main characteristics of these transition states are a partial positive charge carried by the cyclic oxygen and the C-1 carbon, and a planar conformation around this anomeric carbon. The compounds xylobiosyl imidazole and xylobiosyl lactam oxime exhibit these characteristics and have been shown to be good inhibitors of Cex (K_i 150 nM and 370 nM respectively). The crystal structures of Cex in complex with these compounds will be presented.

P06.04.012 CRYSTAL STRUCTURE OF DEOXYCYTIDYLATE HYDROXYMETHYLASE FROM BACTERIOPHAGE T4. S. W. Suh, H. K. Song, and S. H. Sohn, Department of Chemistry, College of Natural Sciences, Seoul National University, Seoul 151-742, Korea.

Bacteriophage T4 deoxycytidylate hydroxymethylase (EC 2.1.2.8), a homodimer of 246-residue subunits, catalyzes hydroxymethylation of the cytosine base in deoxycytidylate (dCMP) to produce 5-hydroxymethyl-dCMP. It forms part of a phage DNA protection system and appears to function *in vivo* as a component of a multienzyme complex called deoxyribonucleoside triphosphate (dNTP) synthetase. We have determined its crystal structure in the presence of the substrate dCMP at 1.6 Å resolution. The structure reveals a subunit fold and a dimerization pattern in common with thymidylate synthases despite low (~20 %) sequence identity. Among the residues that form the dCMP binding site, those interacting with the sugar and phosphate are arranged in a similar configuration as in the deoxyuridylate binding site of thymidylate synthases. However, the residues interacting directly or indirectly with the cytosine base show a more divergent structure and the presumed folate cofactor binding site is more open. Our structure reveals a water molecule properly positioned near C-6 of cytosine to add to C-7 methylene intermediate during the last step of hydroxymethylation. On the basis of sequence comparison and crystal packing analysis, a hypothetical model for the interaction between T4 deoxycytidylate hydroxymethylase and T4 thymidylate synthase in the dNTP-synthesizing complex has been built.

P06.04.013 X-RAY STUDIES OF TRYPTOPHANASE. M. N. Isupov[1], A.A. Lebedev[2], E.H. Harutyunyan[2], F.A. Antson[3], K.S. Wilson[3], G.G. Dodson[3], L.N. Zakomirdina[4], J. A. Littlechild[1] and I.S. Dementieva[4], 1 Schools of Chemistry and Biological Sciences, University of Exeter, Exeter, UK. 2 Institute of Crystallography, Leninsky pr. 59, Moscow, Russia 3 Department of Chemistry, University of York, York, UK 4 Institute of Molecular Biology, Vavilov Street 32, Moscow, Russia.

Tryptophanase is a bacterial PLP-dependent enzyme that catalyses *in vivo* degradation of L-tryptophan to yield indole, pyruvate and ammonia. Indole produced by enteric bacteria is metabolised into the neurological poison oxindole during the course of acute hepatic failure while the indole formation from tryptophan, catalysed by tryptophanase is a limiting step in oxindole synthesis. Tryptophanase is also a possible virulence determinant in meningitis, otitis and a number of other severe diseases caused by *Haemophilus influenzae*[1]. There is therefore a possible medical interest for structure-based development of tryptohanase inhibitors. The structure of the holotryptophanase from *Proteus vulgaris* [2] have been determined by molecular replacement using the related PLP-dependent enzyme tyrosine phenol lyase model [3]. A structure of *E.coli* tryptophanase which is over 80 % identical to *H. influenzae* tryptophanase is currently being refined at 2.7 Å, as is a 3.0 Å complex of *P.vuglaris* tryptophanase with a competitive inhibitor oxindolyl-L-alanine which traps the tryptophanase reaction at a quinonoid intermediate stage.

1. Martin, K., Morlin, G., Smith, A., Nordyke, A., Eisenstark, A. & Golomb, M. (1998). *J. Bacteriol*. 180, 107-118.
2. Isupov, M.N., Antson, A.A., Dodson, E.J., Dodson, G.G., Dementieva, I.S., Zakomirdina, L.N., Wilson K.S., Dauter, Z., Lebedev A.A. & Harutyunyan, E.H. (1998). *J. Mol. Biol*. 276, 603-623.
3. Antson, A.A., Demidkina, T.V., Gollnick, P., Dauter, Z., Von Tersch, R.L., Long, J., Berezhnoy, S.N., Phillips, R.S., Harutyunyan, E.H. & Wilson, K.S. (1993). *Biochemistry*, 32, 4195-4206.

P06.04.014 CRYSTALLOGRAPHIC STUDIES OF E.COLI MHPC. F. Mohammed, G. Dunn, J.B. Cooper, D. Thompson S.P. Wood [1], T.D.H. Bugg, T.Robertson [2], [1] School of Biological Sciences, University of Southampton, Southampton SO16 7PX, UK, [2] Department of Chemistry, University of Southampton, Highfield, Southampton SO17 1BJ, UK

The E.coli MhpC (2-hydroxy-6-keto-nona-2,4 diene-1,9-dioic acid-5,6-hydrolase) is a C-C hydrolase (Mr 29000) involved in the catabolic pathway for the degradation of the aromatic compound, phenylpropionic acid. MhpC catalyses the hydrolytic cleavage of a C-C bond from 2,3 dihydroxyphenylpropionic acid to give succinic acid and 2-hydroxy-penta-2,4-dienoic acid.

The cleavage reaction occurs via an enzyme activated nucleophile which could be an activated water molecule or an amino acid side chain. By determining the three dimensional structure of the native enzyme we will gain further understanding of the catalytic mechanism.

The MhpC crystals were grown using the hanging drop vapour diffusion method. This enzyme crystallizes in the orthorhombic space group P21212 with cell dimensions a=144.60Å b=144.15Å c=62.23Å. A 2.9Å native data set has been collected with in-house equipment under cryogenic conditions.

Phase determination by isomorphous replacement is in progress.

P06.04.015 HIGH RESOLUTION COMPLEXES OF TYPE II DEHYDROQUINASES. A. W. Roszak, J. R. Coggins and A. J. Lapthorn, Dept's of Chemistry and Biochemistry, University of Glasgow, Glasgow, G12 8QQ, Scotland, U.K.

Dehydroquinate dehydratase [dehydroquinase or DHQase, EC 4.2.1.10] catalyses the dehydration of 3-dehydroquinate [DHQ] to 3-dehydroshikimate, a reaction common to two metabolic pathways, (i) the biosynthetic shikimate pathway [present in microorganisms and plants but absent in animals] and (ii) the catabolic quinate pathway in fungi (1). DHQase has been found to fall into two unrelated classes of enzyme, type I and type II (2). The existence of two distinct types of DHQase in microorganisms [e.g., *Escherichia coli* has a type I enzyme whereas *Streptomyces coelicolor, Helicobacter pylori* and *Mycobacterium tuberculosis* possess type II enzymes] offers a unique opportunity to inhibit selectively pathogenic microorganisms using the type II enzyme as a drug target.

Structures of several inhibitor complexes of the enzyme from *Streptomyces coelicolor* and *Mycobacterium tuberculosis* have been determined to better than 1.8Å resolution. We can compare these complexes with 1.6Å structure of a mutant DHQase (R23A) complexed with the reaction product, 3-dehydroshikimate. These structures provide a detailed picture of the enzyme active site [14 residues have been identified lining the active site] and have allowed us to develop a model of the enzyme mechanism. The proposed reaction mechanism requires abstraction of an axial proton from C2 of the substrate by a tyrosine residue. Site-directed mutagenesis of this key residue and other residues are now underway in order to confirm the model and to aid in assigning the relative contributions of residues to substrate binding and catalysis.

(1) Hawkins, *et al.,* (1993) *J. Gen. Microbiol.* **139**, 2891-2899.
(2) Kleanthous, *et al.,* (1992) *Biochem. J.* **282**, 687-695.

P06.04.016 THE S2 SUBSITE OF CYSTEINE PROTEASES: TWO CRYSTAL STRUCTURES OF PAPAIN WITH BOUND DIAZOMETHYLKETONE INHIBITORS. M.Kozak, R. Janowski, Dept of Crystallography, A.Mickiewicz Univ, Poznan, Poland, E.Jankowska, Z.Grzonka, Faculty of Chemistry, Univ of Gdansk, Poland, M.Jaskólski,Center for Biocrystallographic Res, Pol Acad Sci, Poznan, Poland.

Papain from the latex of Carica papaya is the best studied representative of a superfamily of cysteine proteases. Cysteine proteases are a major component of lysosomal proteolytic systems and play a significant role in intracellular proteolysis. In abnormal cases, uncontrolled activity of cysteine proteases may lead to serious tissue-degenerative disorders, such as muscular dystrophy, osteoporosis, pulmonary emphysema, and tumors. Our previous crystallographic studies of papain inhibited by chemically reacting the enzyme's thiol nucleophile with an oxirane ring attached to a peptidic fragment (ZRLVψ[CH_2-NH]-CO-) showed that the inhibitor's P2 site (Val) does not occupy the S2 pocket of the enzyme, in contrast to earlier conclusions that P2-S2 complementarity is essential for productive inhibition and for enzyme specificity. Our observation has been confirmed by careful analysis of other complexes based on the same chemical principle (reactive oxirane function) in which no significant P2-S2 association could be found. In the next step, we have synthesized another inhibitor, with similar amino acid sequence, ZRLVG-, but with a different, diazomethyl (DAM), reactive group attached. A covalent complex between papain and this inhibitor has been formed and crystallized. The structure has been solved by molecular replacement and refined to R=0.168 for X-ray data extending to 1.78 Å resolution. The structure demonstrates again no specific association between the S2 pocket and the inhibitor's P2 site. This persistent lack of P2-S2 interactions in our ZRLV-type inhibitors is in contrast to the early findings by Drenth that covalent, methylketone- type, inhibitors containing the peptidic sequence -FX-CH_2- had invariably the side chain of the phenylalanine P2 subsite located in the enzyme's S2 pocket. As a step towards understanding these differences we have synthesized a new inhibitor, ZLFG-DAM, containing phenylalanine at the P2 site, and reacted it with the active site of papain. Single crystals of the complex have been grown and diffraction data to 2.0 Å resolution have been collected. The structure of the complex has been solved by molecular replacement and refined to R=0.170. It unambiguously reveals that the P2 phenylalanine side chain is located in the S2 pocket of the enzyme. We therefore conclude that in covalent complexes, hydrophobicity of the P2 residue is not sufficient for productive binding of the inhibitor in the S2 pocket of papain and that the bulkiness of this residue is equally important. This does not preclude, however, that even smaller residues, like Val, may be effective during recognition and docking prior to the formation of the covalent link

Research supported by grant 279/P04/97/13 from KBN (Poland).

P06.04.017 CRYSTAL STRUCTURE OF A HETERODIMERIC PLA_2 COMPLEX FROM TWAIWAN VIPER: STRUCTURAL ANALOGUE OF VIPOXIN. Ch. Betzel[1], N. Genov[2], Inn-Ho Tsai[3] and K.R. Rajashankar[1] [1]Institute of Physiological Chemistry, UKE, c/o DESY, Building 22a, Notkestrasse 85, 22603, Hamburg, Germany [2]Institute of Organic Chemistry, Bulgarian Academy of Sciences, Sofia 1113, Bulgaria, [3]Institute of Biological Chemistry, Academia Sinica, P.O. Box 23-106, Taipei, Taiwan, R.O.C

The heterodimeric complex from Taiwan viper (*Vipera russelli formosensis*) (F4/F7 complex), a 28 kDa molecule, is composed of a neurotoxic Phospholipase A_2 (designated F4) and a non-toxic PLA_2 like component (F7). Despite a high sequence identity of 65%, the biological and pharmacological activities of F4 and F7 are contrasting. While F4 shows PLA_2 enzymatic activity, F7 is very weak in this. F4 is neurotoxic while F7 is not. Interestingly, F7 potentiates the lethal potency and neurotoxicity of F4. F4/F7 complex can be considered as the first structural analogue of Vipoxin. - a heterodimeric complex of a highly toxic PLA_2 (Vp) and a catalytically inactive PLA_2 like natural inhibitor (Inh) - found in Bulgarian viper (*Vipera ammodytes meridionalis*). The primary structure of F4 and F7 are 92% identical to those of Vp and Inh, respectively. Despite this similarity, there are marked difference in the biochemical and pharmacological properties of F4/F7 complex and Vipoxin. Hence F4/F7 complex appears like a natural mutant of Vipoxin complex with altered biochemical and pharmacological properties. The 3-D structure of F4/F7 complex will provide structural basis for these differences and augment the knowledge on modulation of PLA_2 activity and toxicity.

F4/F7 complex was crystallized using hanging-drop vapour diffusion and macroseeding techniques. The space group is monoclinic $P2_1$ (a=74.92, b=85.13, c=78.16 Å and β=95.12º) with four molecules of F4/F7 complex in the asymmetric unit. The structure was determined using molecular replacement method. We will present a comparative analysis of the structural features of

the complexes F4/F7 and Vipoxin. Both structures were analysed with synchrotron radiation to 2.0 Å resolution and are so far the only known heterodimeric PLA_2 complexes.

P06.04.018 THREE POLYMORPHIC FORMS OF E. COLI ASPARAGINASE II D90E MUTANT. D.Borek, M.Kozak, Dept of Crystallography, A.Mickiewicz Univ, Poznan, Poland, M.Jaskólski, Center for Biocrystallographic Res, Pol Acad Sci, Poznan, Poland.

Asparaginases convert asparagine to aspartic acid and ammonia. There is a group of these enzymes, found in the periplasm of some bacteria, which have high asparaginase affinity ($K_m \sim 10^{-5}$ M) and variable degree of glutaminase activity. Some of them, from *E. coli* (EcAII) and from *Erwinia chrysanthemi* (ErA), are valuable drugs in the treatment of certain kinds of leukemia. The crystal structure of EcAII revealed a triad of catalytic residues (T89-K162-D90) in the active center and the oligomeric nature of the enzyme. All known bacterial asparaginases are 222-(pseudo)symmetric ABCD homotetramers with four active sites created within pairs of monomers (AC and BD). In order to elucidate the role of the catalytic residues in the enzymatic process and substrate specificity, we have characterized crystallographically a D90E mutant of EcAII (kindly provided by Prof. K.Röhm, Philipps Univ., Marburg) in which the catalytic-triad aspartic acid has been replaced by a similar but bigger Glu residue. The mutant protein has been obtained in three different crystal forms. One of them (I), grown from a solution containing 2M sodium citrate and Hepes, pH 7.5, is trigonal ($P3_121$) and contains the active-site-competent AC dimer in the asymmetric unit. Forms II ($P2_12_12$) and III ($P2_12_12_1$, $P2_12_12$ or $P222_1$) are orthorhombic, but have different contents of the asymmetric unit. Form II (grown at pH 9.0 using PEG-MME 500 as precipitant) has one complete tetramer plus the AC dimer in the asymmetric unit. Form III (grown analogously to form I) has one tetramer in the asymmetric unit. Complete diffraction data have been collected for forms I (2.6 A) and II (2.3 A). For form III, which is very unstable in the X-ray beam, only incomplete (60%) data are available (2.3 A). The crystal structures of forms I and II have been solved and refined to the crystallographic R factor of 0.21 and 0.24, respectively. Electron density maps unambiguously confirm the mutation and illustrate the reduction of the size of the active site cavity upon D90 $\rightarrow$ E90 substitution. In spite of the different crystallisation conditions (pH) for forms I and II, none of the eight independent active sites seems to be occupied, in contrast to the EcAII structures reported earlier which invariably have the reaction product, aspartate, bound in the active site.

P06.04.019 STRUCTURES IN THE VITAMIN B_{12} BIOSYNTHETIC PATHWAY. H.L. Schubert and K.S. Wilson Protein Structure Group, Department of Chemistry University of York, Heslington, York, England YO10 5DD E. Raux, J. Roper, M.J. Warren Department of molecular Genetics, Institute of Ophthalmology, University College London, London EC1V 9EL.

Vitamin B_{12} is an essential mammalian dietary factor synthesised by various microorganisms. The thirty enzymes are required for its synthesis that can utilize up to 1% of a bacterial proteome. In addition to a lengthy and intricate biosynthesis, alternate aerobic and anaerobic synthetic routes exist, and encompass such diverse chemistry as single-carbon methylation, ring contraction, side chain amidation, and metal ion chelation. The X-ray structures of two individual enzymes have recently been solved, the precorrin-4 methylase from *Bacillus megaterium*, CbiF, and the anaerobic cobalt chelatase from *Salmonella typhymurium*, CbiK.

Though the initial steps in tetrapyrrole cofactor biosynthesis are identical, beyond the intermediate uroporphobilinogen III the pathways diverge and share no common enzymatic steps other than metal ion insertion. Two general classes of chelatases can been identified. The heterotrimeric, ATP dependent chelatases encompass the aerobic cobalamin biosynthetic pathway, the magnesium chelatase from chlorophyll biosynthesis and the nickel chelatase involved in F_{430} production. Monomeric ATP-independent chelation occurs in anaerobic cobalamin, haem and sirohaem production. The structure of two monomeric chelatases have now been solved, protoporphyrin IX ferrochelatase and the anaerobic cobalt chelatase. Though these two enzymes were though to be non-homologous, the structures have turned out to be remarkably similar and aspects of both reactions can be understood more clearly through a comparison of the two structures.

P06.04.020 X-RAY CRYSTAL STRUCTURE ANALYSIS OF A MUSHROOM RIBONUCLEASE FROM LENTINUS EDODES. Y.Kitagawa, A.Komaki, K.T.Nakamura [1], H.Kobayashi, N.Inokuchi, T.Koyama [2], K.Ohgi, M.Irie [3], [1] School of Pharmaceutical Sciences, Showa University, Tokyo 142-8555, Japan, [2] College of Pharmacy, Nihon University, Chiba 274-8555, Japan, [3] Hoshi College of Pharmacy, Tokyo 142-8501, Japan

A T2 type ribonuclease was isolated and purified from an edible mushroom, lentinus edodes (RNase LE2). It does not have strict base specificity but is preferable in the order of A>G>C>U. The RNase LE2 consists of 239 amino acid residues and shows approximately 30% sequence identity to the other T2 type ribonucleases (such as T2 and Rh).

We obtained two types of crystal. One is from the solution with the precipitant of PEG8000 (Form I) and the other is with ammonium sulfate (Form II). Both crystals belonged to the same space group $P2_12_12_1$, with unit cell dimensions of a=71.38, b=87.28, c=33.46 Å for the Form I crystal, and of a=71.23, b=90.88, c=31.43 Å for the Form II crystal. The crystal structure of RNase LE2 was solved by the molecular replacement methods using the AMoRe program package, with the structure of ribonuclease Rh as the search model (1).

The structure has been refined with an overall R factor of 23% and a free R factor of 29% up to 2.34 Å resolution. Water molecules have not included in the refinement yet. The further refinement is under way. The basic structure is composed of 4 β-strands and 6 α-helices. The detailed structure of RNase LE2 and its implications to the catalytic mechanism of ribonucleases will be discussed.

(1) K.T.Nakamura et. al. J.Mol.Biol, 255, 310-320, 1996

P06.04.021 CRYSTAL STRUCTURES OF RIBONUCLEASE LE COMPLEXED WITH RNA FRAGMENT SHOW THE ADDITIVITY OF SUBSTRATE FRAGMENT. N. Tanaka, J. Arai and K.T. Nakamura, School of Pharmaceutical Sciences, Showa University, Tokyo 142-8555, Japan, and N. Inokuchi and T. Koyama, College of Pharmacy, Nihon University, Funabashi 274-0063, Japan, and K. Ohgi and M. Irie, Hoshi College of Pharmacy, Tokyo 142-8501, Japan.

Ribonuclease LE (RNase LE) from cultured tomato (*Lycopersicon esculentum*) cell is a member of the RNase T_2 family showing broad base specificity. RNase LE consists of 205 amino acid residues and has a molecular mass of 22,666 Da. As basis for further studies on the chemistry and molecular biology of T_2 family ribonucleases, here we report on the first example of three-dimensional structure of a plant ribonuclease, RNase LE.

Crystals of RNase LE belong to an orthorhombic space group $P2_12_12_1$with cell dimensions of a = 74.02 Å, b = 78.79 Å and c = 32.93 Å. There is one molecule per asymmetric unit. The structure has been solved by the multiple isomorphous

replacement method using five derivatives and refined to an R value of 0.205 (free R value of 0.283) at 1.65 Å resolution.

The structure consists of seven α-helices and seven β-strands, belonging to α+β type structure. Comparison of the structure of RNase LE with that of RNase Rh, a microbial RNase belonging to the RNase T_2 family, shows that, while the overall folding topology are similar to each other, insertion and deletion are found at the N-terminal regions.

The substrate-fragment complex crystals were obtained by transferreing the native crystals into a series of substrate-fragment solutions containing guanosine 2'-monophosphate (2'-GMP: inhibitor), guanosine 3'-monophosphate (3'-GMP: substrate fragment), guanosine 5'-monophosphate (5'-GMP: substrate fragment), or deoxyguanylyl-3,5-deoxyguanosine (d(GpG): substrate analogue). The structures of these four complexes have been solved by the difference Fourier method and refined to R values below 0.20 at 1.8 Å resolution.

These complexes reveal interesting features: the substrate fragments and substrate analogue bound in the productive binding mode while inhibitor bounds non-productive binding mode; and the binding mode of 3'-GMP at B_1 subsite and that of 5'-GMP at B_2 subsite are similar to that of d(GpG) bound at both B_1 and B_2 subsite. These observations show that the binding of substrate fragments may conform to the principles of additivity.

P06.04.022 STRUCTURE OF THE CHITINASE FROM JACK BEAN M. Hahn [(1)], M. Hennig [(2)], B. Schlesier [(3)] and W. Höhne [(1)], (1) Institut für Biochemie der Charité, Humboldt-Universität, Monbijoustr.2, 10117 Berlin, Germany. (2) F. Hoffmann-LaRoche AG Pharma Research 65/308 CH-4070 Basel, Switzerland. (3) IPK Gatersleben, Corrensstr. 3, 06466 Gatersleben, Germany

Chitinases hydrolyze the β-1,4-glycosidic bond between N-Acetylglucosamins in chitin, one of the most abundant biomolecules. Chitinases in plants function as defense proteins against fungi. The structure of barley chitinase was solved previously [1,2]. It is a α-helical protein with three disulfide bridges and a putative substrate-binding groove along the molecule. The chitinase from jack bean was purified from seeds and crystallized in space group $P6_1$. The monomeric enzyme consists of 243 amino acids and is 66% identical in sequence to the chitinase from barley. It could be solved with molecular replacement using the barley enzyme as a search model. The refined structure has a R-factor of 18.7% (R_{free}= 22.2%) at a resolution of 1.8 Å. R.m.s. deviations from standard bond lengths/bond angles are 0.008 Å/1.43°, respectively. The overall fold and the secondary structures are the same as in the barley enzyme. The superposition of all C_α-positions of the two enzymes gives a r.m.s. deviation of 0.98 Å. The conserved amino acids are located in the interior of the protein and in the binding groove, whereas mutated positions are mostly found on the protein surface. A cleavage mechanism with inversion of configuration at the anomeric carbon was proposed for the barley chitinase [3]. In our structure a water molecule was found, that binds to the proposed residues in the active site. It could act as the nucleophil in substrate cleavage and supports the idea of a single rather than a two-step mechanism for this type of enzyme.

1. H.K. Song & S.W. Suh (1996). Acta Cryst. D52, 289-298.
2. P.J. Hart, H.D. Pfluger, A. T. Monzingo, T. Hollis & J.D. Robertus (1995) J. Mol. Biol. 248, 402-413.
3. K.A. Brameld & W.A. Goddard III (1998). P.N.A.S. 95, 4276-4281.

P06.04.023 BENZYLALCOHOL DEHYDROGENASE - A HIGH-PERFORMANCE ADH FOR SPECIALISED SUBSTRATES. Jeremy Beauchamp[†], David Gillooly[‡], Charles Fewson[‡] and Adrian Lapthorn[†], [†]Dept. of Chemistry & [‡]IBLS, University of Glasgow, Glasgow G12 8QQ. UK.

The structure of benzyl alcohol dehydrogenase (BADH) from *Acinetobacter calcoaceticus* has been determined at 2.2Å resolution. The enzyme is an anomalously efficient member of the zinc-dependant type II alcohol dehydrogenase family that enables *A. calcoaceticus* to use benzyl alcohol and similar molecules as its sole energy source.

Crystals were grown using an initial sparse-matrix screen followed by refinement of the most promising conditions. Careful control of the reducing environment, precipitant concentration and additives were critical for the production of high quality crystals. Despite this, the crystals were short-lived and diffracted poorly after more than a week in the mother liquor. Data were collected, however, at Daresbury SRS (9.5) and the structure was solved by molecular replacement using AMoRe with subsequent refinement using Refmac.

The structure implies an enzyme mechanism that is extremely well characterised in the horse-liver alcohol dehydrogenase system. However, there are highly significant adaptations for the substrates peculiar to BADH. The implications for enzyme engineering, molecular evolution and the reaction mechanisms of the alcohol dehydrogenase family will be discussed.

P06.04.024 CRYSTAL STRUCTURE OF CYTOSOLIC CREATINE KINASE: PROPOSED CATALYTIC MECHANISM. Dominic Tisi[1],Ben Bax[2] and Andreas Loew[3], Biophysics Section, Blackett Laboratory, Imperial College, Prince Consort Road, London SW7 2BZ, Uk, Department of Crystallography, Birkbeck College, Malet Street, London WC1E 7HX, UK and University of Illinois at Chicago, Department of Biochemistry and Molecular Biology, College of Medicine West, 1819 West Polk Street, Chicago, USA

Creatine kinase (E.C.2.7.3.2) (CK) belongs to the family of ATP:guanidino phosphotransferases and plays an essential role in energy metabolism. CK catalyses the reversible transfer of the phosphate moiety from phosphocreatine (PCr) to ADP, generating creatine and ATP.

Here we report the crystal structure of a cytosolic isoform of CK derived from bovine photoreceptor cells. The structure of bovine retinal brain type creatine kinase (brB-CK) homo dimer has been solved initially to 2.7Å and then further to a resolution of 2.3Å with one monomer in the asymmetric unit. The brB-CK monomer consists of a small helical domain consisting of 6 helices and a large domain comprising of an 8 stranded anti-parallel § sheet surrounded by 7 helices. The proposed nucleotide and creatine binding sites are located in a cleft between the two domains. The overall fold of brB-CK is similar to that of Mi_b-CK, a CK isoform located in the mitochondrial inter membrane space. Further to this, through comparative studies of the transition state complex of horseshoe crab arginine kinase, a close homologue of creatine kinase, those regions of brB-CK involved in substrate binding and catalysis have been identified.

P06.04.025 HISTIDINE DECARBOXLASE COOPERATIVITY IS CONTROLLED BY A pH DEPENDENT α-HELIX CONFORMATIONAL CHANGE. Jon D. Robertus, Arthur F. Monzingo, Elisabeth Schelp, Scott Worley and Stephen Ernst, Institute of Cellular and Molecular Biology, Department of Chemistry and Biochemistry, University of Texas, Austin TX, 78712.

Histidine decarboxylase (HDC) from *Lactobacillus* catalyzes the conversion of histidine to histamine and CO_2. A histidine/histamine shuttle system generates energy for the cell and also neutralizes the cytoplasmic pH in the lactic acid producing bacteria. HDC is activated by low pH and inhibited at neutral pH; its cooperative kinetics suggests interconversion of the

trimeric enzyme between a high Km T state and a low Km R state. The putative R state of HDC, pH 4.5, was solved by others nearly 15 years ago. This molecule revealed that active sites are formed at the interfaces of HDC trimers. It also revealed a close interaction of aspartate side chains, including D53, across the intermolecular interface. This interaction may be part of a trap that binds protons at low pH, stabilizing the R state; at high pH the protons are pulled out and charge repulsion triggers a structural change. We have now solved the pH 8 structure of HDC at 3 Å resolution to analyze the T state. We also created a site directed mutant involving D53; this mutant has T state kinetics and suggests it is also in the T quaternary structure. Both T form crystals reveal that an active site helix, anchored by D53 is disrupted and that the histidine binding site is altered by the conformational change. We also solved the structure of the mutant HDC with a covalent inhibitor, HME, in the active site. This substrate analog forces the active site into the R state reforming the active site α-helix. This shows that substrate as well as protons, can stabilize the R state.

P06.04.026 CRYSTRAL STRUCTURE ANALYSES OF THE ENZYMES INVOLVED IN THE DEGRADATION OF POLYCHLORINATED BIPHENYLS. T. Senda, K. Sugimoto, E. Masai, M. Fukuda and Y. Mitsui, Department of BioEngineering, Nagaoka University of Technology, Nagaoka, Niigata 940-2188, JAPAN.

Polychlorinated biphenyls (PCBs) are widely distributed, toxic and carcinogenic, environmental pollutants. PCBs are significantly recalcitrant to biodegradation due to their chemical stability. The total amount of PCBs released into the biosphere is *ca.* 750,000 tons. PCBs have accumulated and concentrated in the tissues of fish, birds and other wildlife. The accumulation of PCBs has even been observed in human bodies. A few of the toxic symptoms caused by PCBs involve headache, pain of joints and hypertension. Since 1973, a number of microorganisms that could degrade PCBs have been isolated and characterized. In addition some field attempts at PCB biodegradation have been carried out.

To date the major biodegradation pathway of PCBs has been established. Thus, four specific enzymes, biphenyl dioxygenase (BphA), dihydrodiol dehydrogenase (BphB), 2,3-dihydroxybiphenyl dioxygenase (BphC) and 2-hydroxyl-6-oxo-6-phenylhexa-2,4-dienoic acid hydrolase (BphD) are sequentially involved in the oxidative degradation of PCBs into chlorobenzoates and 2-hydroxypenta-2,4-dienoate. Three-dimensional structural information of these enzymes is required for a rational improvement of the degradation pathway to utilize these enzymes for bioremediation. Thus we have carried out the crystallographic analyses of these enzymes derived from microbes that can degrade PCBs and related aromatic compounds. To date we have determined the crystal structures of an electron transfer component of BphA (BphA4), BphB, BphC, and BphD. In addition, analyses of structure-function relationships have been carried out using a variety of mutant proteins. These structure-based studies on the whole degradation pathway will provide a novel insight into the function and mechanism of the degradation pathway of PCBs, which must be useful for the rational improvement of the degradation pathway.

P06.04.027 CRYSTAL STRUCTURE AND PROPOSED MECHANISM FOR METHIONINE γ-LYASE FROM *TRICHOMONAS VAGINALIS*. G. Goodall, Protein Crystallography, Dept. of Chemistry, University of Glasgow, Glasgow. G12 8QQ, UK. G.H. Coombs, Biochemical Parasitology, Division of Infection and Immunity, University of Glasgow, Glasgow, G12 8QQ, UK; A. Lapthorn, Protein Crystallography, Dept. of Chemistry, University of Glasgow, Glasgow. G12 8QQ, UK.

Methionine γ-lyase (MGL) (E.C. 4.4.1.11) is a pyridoxal 5'-phosphate (PLP) dependent enzyme able to catalyse αγ- and αβ-elimination as well as γ and β replacement reactions on the sulphur containing amino acids L-methionine and L-cysteine and their analogues. The enzyme has only been detected in anaerobic micro-organisms at this time and is thought to be absent from yeast and mammals where multiple PLP dependent enzymes carry out similar reactions. The human parasite *T. vaginalis* is the causative agent of trichomoniasis the most prevalent non-viral sexually transmitted disease in the world. The parasite has an exceptionally high level of activity of MGL and two genes have recently been cloned from the parasite which encode for isoforms of the enzyme [1]. The exact role of the enzyme for the parasite is still under investigation but there is evidence that the enzyme is responsible for the activation of pro-drugs *in vivo*.

We have overexpressed and purified both forms of the enzyme and successfully crystallised the first of these, MGL1. The crystals are trigonal, space group $P3_112$ with a=b=88.53Åand c=217.85Å. The crystals were shown to diffract to 1.6Å at Daresbury SRS station 9.5 where a complete 2.2Å dataset was collected. The structure was solved by molecular replacement using AMoRe [2]. The structure of native and an inhibitor complex of MGL1 have now been obtained and with data from site directed mutagenesis experiments we are able to propose a model for the enzyme mechanism. Studies are now under way to design specific inhibitors of the enzyme for possible use *in vivo*.

[1] Mckie,A.E., Edlind,T., Walker,J., Mottram,J.C. and Coombs,G.H. (1998) J.Biol.Chem .**273**, 5549-5556.
[2] Navaza, J. (1994) *Acta Crystallogr.*, **A50**, 157-163.

P06.04.028 X-RAY CRYSTAL STRUCTURE AT 2.4 Å RESOLUTION OF HUMAN GLUCOSAMINE-6-FOSFATE DEAMINASE (GLCN6PDH). R. Arreola, [1], L. I. Álvarez-Añorve [2], L. Morante, E. Hojales [1], [1] Departamento de Reconocimento Molecular y Bioestructura, Instituto de Biotecnología, Universidad Nacional Autónoma de México, Cuernavaca, Morelos, México, [2] Departamento de Bioquímica, Facultad de Medicina,Universidad Nacional Autónoma de México, México city, D.F.México.

GlcN6PDH catalyses the transformation of D-Glucosamine-6-fosfate to fructose-6-fosfate and ammonia (E.C.5.3.1.10) (Calcagno,M.et.al.personal communication). The enzyme is hexameric whith identical sub-units 289 residues each. Biochemical function is conserved with regard to E.coli deaminase (Altamirano, M.et.al.1995) (primary sequence has 52% of identity). Desaminase enzyme has wide distribution in evolutive scale (eubacteria, protoctista, invertebrates, insects and mammals). The enzyme is present in humans and hamsters, in many cells types, which shares high energy requirements. In particular it has been found in spermatozoids, in isolated fractions that produce calcium oscillations in ovocite cells (Parrinton,P.et.al.1996). The structure of GlcN6PDH has been determinated and refined to 2.4 Å resolution, using molecular replacement. Spatial group is p212121 with cell parameters 113.38Å, 115.93Å, 181.43Å, 90°,90°,90°. The structure is complexed whit allosteric activator N-acetyl-glucosamine-6-phosphate and the competitive inhibitor 2-deoxy-2-amino-glucitol- 6-phosphate. Comparative superposition of E. coli and human monomers showed an r.m.s. 0.452. The active site residues are notably conserved as compared with the E.coli conformations in state R. An exception is 43 residue (change from Gly to Ser in GlcN6PDH) that produce a new hydrogen bond with Arg 172 side chain. The C-terminal helix 8 of GlcN6PDH is very different to E. coli GlcN6PD probably related with experimentally observed different allosteric properties. Helix 8 forms a cavity surrounding more closely the allosteric site building a hydrophobic pocket that lodge the N-Acetyl group. A new hydrogen bond joints the activator with His 262 confirming the biochemical data about high

affinity of allosteric activator. This project was supported by DGAPA-UNAM IN23598. R.A. received a grant from CONACyT. We acknowledge Sonia Rojas for technical support for crystallisation.

P06.04.029 STRUCTURAL ANALYSIS OF STREPTOMYCES OLIVACEOVIRIDIS β-XYLANASE BY MOLECULAR REPLACEMENT METHOD. Z. Fujimoto and H. Mizuno, National Institute of Agrobiological Resources, Tsukuba, Japan, and A. Kuno, S. Yoshida and I. Kusakabe, University of Tsukuba, Tsukuba, Japan, and H. Kobayashi, National Food Research Institute, Tsukuba, Japan

Xylanases (EC 3.2.1.8) or endo-1,4-β-D-xylanases hydrolyze the β-1,4-glycosidic bonds within the xylan backbone and belong to either family F/10 or G/11, on the basis of the amino acid sequence similarities of their catalytic domains. Family F/10 xylanase consists of catalytic domain comprising a $(\beta/\alpha)_8$-barrel, C-terminal substrate-binding domain, and a linker region connecting two domains. By now, five family F/10 xylanase structures have been determined, however, they are only of their catalytic domains. Recently we succeeded in crystallizaion of intact *Streptomyces olivaceoviridis* E-86 β-xylanase (FXYN). To understand the substrate-recognition or binding mechanism of this enzyme, we have analyzed the structure of FXYN.

The crystals belong to orthorhombic space group $P2_12_12_1$, with cell dimensions of a =79.6Å, b =95.2Å, and c=140.3Å, including two molecules per asymmetric unit. Diffraction experiment on the native crystal was carried out at the Photon Factory in Tsukuba to 1.9Å resolution, resulting a completeness of 94.2% and an R_{merge} of 0.055.

Structural analysis was performed firstly by the molecular replacement method. As a search model, a structural model of the catalytic-domain of FXYN (residues 1-300) was build with the program MODELER in QUANTA program package using two catalytic-domain structures; xylanases from *Streptomyces lividans* (1xas) and *Cellulomonas fimi* (2exo). This model was subjected to molecular replacement using the 8-3.5 Å resolution data with the program AMoRe in CCP4 suite, finally resulting the correlation of 52.1 and *R*-value of 46.6. The quality of the electron density map was sufficient to identify amino acids in the catalytic domain. The structure was refined with the program XPLOR to 2.5Å resolution, and resulted in a *R*-factor of 32.4. The resultant Fo-Fc map gave electron density corresponding to the substrate-binding domains, and the 3Fo-2Fc map allowed us to identify some Trp residues. Amino acid residues were added into the model one by one on the renewed map. This process was repeated, and finally all of 123 residues in this domain were assigned. Subsequent refinements were carried out to a resolution of 1.9 Å and R/R_{free}-factors were lowered to 21.0/25.3.

P06.04.030 STRUCTURE OF D-GLYCERALDEHYDE-3-PHOSPHATE DEHYDROGENASE FROM PALINURUS VERSICOLOR Shi-ying Song, Yue-quan Shen, Zheng-jiong Lin, National Laboratory of Biomacromolecules, Institute of Biophysics, Academia Sinica, Beijing 100101, China

D-Glyceraldehyde-3-phosphate dehydrogenase (GAPDH) is an important enzyme in both glycolysis and glyconeogenesis. A series of crystal structures of GAPDH from Palinurus versicolor (PV), South China sea Lobster, were determined. The structure of PV native enzyme has been published (Song, et al. 1998). The isomorphous structures of carboxymethylaed GAPDH and apo-GAPDH have also been refined at high resolution to a reasonable stereochemistry and final R-factor of 17.4% (1.88Å) and 17.1% (2Å) respectively. The whole tetramer of apo-GAPDH exhibits good 222 molecular symmetry. The conformational change induced by coenzyme binding is similar to but less than that found in Bacillus stearothermophilus GAPDH. The differences between these two species during apo-holo transition are attributed to the sequence differences. In the structure of active-site carboxymethylated GAPDH connected to Cys149 is stabilized by a hydrogen bond between its OZ1 and Cys149N, the modification of Cys149 induced conformational changes in the active-site, in particular, the site of sulphate ion Pi and segment 208-218 nearby. It is proposed that the carboxymethyl group takes the place of the acyl group of the reaction intermediate and the catalytic mechanism of this enzyme is discussed in the light of a comparison of the structures of the native and the carboxymethylaed GAPDH.

[1] Song, S.-y., Li, J. and Lin, Z.-j. (1998), Acta Cryst. D54, 558-569.

P06.04.031 CRYSTAL STRUCTURE OF THE *VMA1*-DERIVED ENDONUCLEASE BEARING AN N-TERMINAL PROPEPTIDE. R. Mizutani and Y. Satow, Graduate School of Pharmaceutical Sciences, Y. Ohya, Graduate School of Science, University of Tokyo, Tokyo 113-0033, Japan, M. Kawasaki, The Tokyo Metropolitan Institute of Medical Science, Tokyo 113-8613, Japan, Y. Anraku, Teikyo University of Science and Technology, Yamanashi 409-0193, Japan.

The 120-kDa nascent product the *VMA1* gene of *Saccharomyces cerevisiae* auto-catalytically excises out the 50-kDa endonuclease VDE (*VMA1*-derived endonuclease) and splices the two external polypeptides to form the 70-kDa subunit of the vacuolar H^+-ATPase. Only six proximal and four distal amino acids are required for auto-catalytic processing of folding-dependent *in vitro* protein splicing. Another recombinant named XA-VDE is similar in construction but is a splicing-negative polypeptide in which cysteines 284 and 738 at the splicing junctions are replaced with alanines. In order to obtain structural insight of the protein splicing reaction, we have carried out a 2.0 Å resolution crystallographic study on the XA-VDE protein.

The XA-VDE protein was crystallized using polyethylene glycol as a precipitant. The structure was determined by the molecular replacement method using the mature VDE structure as a search model, and has been refined to an *R* factor of 0.204. Gly 282 and Val 283 in the N-terminal region are clearly observed in electron densities, and are located in the vicinity of the side chain of His 362 which is requisite for the splicing reaction. As the C-terminal region from Ala 738 to Arg 741 has no convincing densities, the XA-VDE protein was subjected to high resolution mass spectrometry. The observed mass of 51,569 Da is in close agreement with a predicted mass for a polypeptide lacking the C-terminal region (51,577 Da). The structures of the XA-VDE and mature VDE proteins give an rms positional difference of 0.5 Å for alpha carbons, indicating the external peptide has little effect on the overall XA-VDE structure. We propose that the mechanism of the cleavage at the C-terminal region involves succinimide formation at the downstream splicing junction, which results in the cleavage as in the later step in protein splicing reaction.

P06.04.032 K187T MUTANT CYCLOPHILIN B FROM *E. COLI* COMPLEXED WITH TETRAPEPTIDE. M. Konno, Y. Sano, Y. Kawaguchi, and Y. Yamagishi, Department of Chemistry, Ochanomizu University, Otsuka, Bunkyo-ku, Tokyo 112-8610 Japan and S. Fushinobu and H. Matuzawa, Department of Biotechnology, University of Tokyo, 1-1-1 Yayoi, Bunkyo-ku, Toyko 113-8657 Japan.

Cyclophilins are ubiquitous and abundant proteins for which a natural role has not been found. Cyclophilin A (CyPA) is present in the cytosol and cyclophilin B (CyPB) binds to the membrane with the signal sequence in N-terminal. Crystals of CyPB of the wild type from *E. coli* never were obtained. In

consideration of two conditions 1) mutants decrease no PPIase activity 2) residues hydrated to disturb interactions between molecules should be replaced by more hydrophobic residues, compared with *E. coli* CyPA, two kinds of mutants of K187T and H110F were prepared. Crystals of these mutants have been grown. Crystals of the complex of K187T mutant protein and tetrapeptide (Acetyl-Ala-Ala-Pro-Ala-7-amido-4-methyl-cumarine) belong to *trigonal,* space group *P*32, *a*=*b*=78.96 Å, *c*=56.17 Å, *Z*=6. Two protein molecules and one tetrapeptide are included in asymmeric unit. The intensity data were collected at synchrotron radiation in the Photon Factory KEK Japan. The structure has been resolved by molecular replacement methods using the structure of *E. coli* CyPA as a search model. The refinement gave *R*=0.223 at 2.0 Å resolution.

Two molecules I and II in *E. coli* CyPB have the β-barrel structure consisting eight-antiparallel β-strands with two α-helices at the top and the bottom, as *E. coli* CyPA, yeast CyPA, human CyPA and CyPB have. The hydrophobic cleft is formed by side chains of Phe77, Met78, Phe128, Phe136, Lue137 and Tyr146 over upper β-sheet. A tetrapeptide including *cis*-proline is inserted into this cleft of one molecule II. The cumarine ring lies parallel into the benzene ring of Phe136. Another molecule I has no tetrapeptide. The side chains of Lue184, Ser185, Thr187 on β8 and Lue32, Thr34 on β1 of molecule I form hydrophobic interactions with those of the adjacent molecule II.

P06.04.033 THE X-RAY CRYSTAL STRUCTURE OF A TN5 TRANSPOSASE-RELATED PROTEIN DETERMINED TO 2.9 Å RESOLUTION. D.R. Davies, I. Rayment [1], L.A.M. Braam, W.S. Reznikoff [2], [1] Institute for Enzyme Research and Department of Biochemistry, University of Wisconsin, Madison, Wisconsin, USA, [2] Department of Biochemistry, University of Wisconsin, Madison, Wisconsin, USA.

We report the three-dimensional structure of the Tn5 transposase inhibitor protein, a slightly truncated version of the full length transposase enzyme. The inhibitor protein prevents transposition through a self-regulatory mechanism unique to transposon Tn5. The inhibitor protein differs from the full length transposase only by the absence of the first 55 N-terminal amino acid residues. It is 421 amino acid residues in size, and contains the active site of the transposase and a C-terminal domain involved in protein-protein interactions. A portion of the protein fold of the catalytic core domain is similar to the folds of HIV-1 integrase, Avian Sarcoma Virus integrase, and bacteriophage Mu transposase. The Tn5 inhibitor contains an insertion in this conserved catalytic core that extends the central beta sheet from five to nine strands. All three of the conserved acidic residues that make up the "DDE" motif of the active site are visible in the structure. An arginine residue that is strictly conserved among the IS4 family of bacterial transposases is present at the center of the active site, suggesting a catalytic motif of "DDRE." A novel C-terminal domain forms a dimer interface across a crystallographic twofold axis. Although this dimer represents the structure of the inhibited complex it provides insight into the structure of the synaptic complex.

P06.04.034 CRYSTAL STRUCTURE OF A FAMILY G XYLANASE FROM *ASPERGILLUS NIGER* AT 2.4 Å RESOLUTION. U. Krengel, Center for Structural Biology, Chalmers University of Technology and Göteborg University, Department of Biochemistry and Biophysics, P.O. Box 462, 403 50 Göteborg, Sweden, and B. W. Dijkstra, BIOSON Research Institute, University of Groningen, Department of Biophysical Chemistry, Nijenborgh 4, 9747 AG Groningen, The Netherlands.

Xylanases belong to the glucanase enzyme family and are characterized by their ability to break down various xylans to produce short-chain xylo-oligosaccharides. Since the enzyme plays a crucial role in the breakdown of plant cell walls and cell wall constituents, it is of major importance for a large number of industrial applications ranging from the clearing of fruit juices to benefits in paper industry. In food industry, xylanase-supplemented food plays an important role in effective feeding and reduction of animal excrements. Especially fungal xylanases, which generally have lower pH-optima, are ideally suited to release important nutrients in such acidic environments as the animal stomach.

One of the xylanases, the endo-1,4-β-xylanase I (EC 3.2.1.8) from *Aspergillus niger*, is produced at industrial scale by the company Gist-Brocades in Delft (The Netherlands). It has a pH-optimum of 3.5, consists of 184 amino acids and has a molecular mass of 20 kD. Various crystal forms of the enzyme could be obtained with the hanging drop method, using inorganic salts as precipitants. The X-ray structure of the *A. niger* xylanase has been solved by molecular replacement, using the coordinates of a xylanase from *Trichoderma harzianum* (D. Rose, personal communication) as a model. Like all the other members of the family G xylanases of which the structure has been solved to date, the *A. niger* xylanase has an extensive β-sheet structure and contains only one α-helix at the outside of the molecule. Two mostly antiparallel β-sheets are stacked against each other and are twisted around a deep, long cleft which is lined with many aromatic amino acids and which is big enough to accommodate several xylose residues. The two conserved glutamic acid residues Glu-79 and Glu-170, which habe been shown to be involved in catalysis in other members of the xylanase G family, are reaching into this cleft from opposite sides. A mechanism is proposed which explains the unusually low pH-optimum of this xylanase.

P06.04.035 STRUCTURE OF THE FLAVOENZYMES: MORPHINONE REDUCTASE AND PETN REDUCTASE Peter C.E. Moody, Daniel H Craig, Terez M Barna and Nigel S Scrutton, Department of Biochemistry, University of Leicester, Leicester LE1 7RH, U.K. & Neil C Bruce Institute of Biotechnology, University of Cambridge, Cambridge CB2 1QT UK

We have determined the structures of both morphinone reductase (to 2.0Å) and pentaerythritol tetranitrate (PETN) reductase (to 1.5Å). These enzymes are members of the Old Yellow Enzyme family of flavoenzymes and catalyse the reduction of morphinone to hydromorphone using NADH and the reduction of PETN, TNT or glycerol trinitrate using NADPH respectively. They have enormous potential in the production of analgesics and the bioremediation of explosive contaminated land. The structures will be presented in complex with various substrates and inhibitors, and compared to OYE. The nature of the reactions catalysed by these enzymes and their specificities will be discussed in the context of these similar structures.

P06.04.036 CRYSTAL STRUCTURE OF A NIFS-LIKE PROTEIN FROM *ESCHERICHIA COLI*. T. Fujii, M. Maeda, H. Mihara, T. Kurihara, N. Esaki and Y. Hata, Institute for Chemical Research, Kyoto University, Uji, Kyoto 611-0011, Japan.

CsdB, the *csdB* gene product from *Escherichia coli*, is a pyridoxal 5'-phosphate(PLP)-dependent protein, which decomposes L selenocysteine, L-cysteine sulfinic acid and L-cysteine, into selenium, sulfur dioxide and sulfur, respectively, and L-alanine. This enzyme shares 23% sequence identity with the NifS protein, that catalyzes the decomposition of L cysteine and functions in the nitrogen fixation system of *Azotobacter vinelandii* by supplying sulfur to stabilize or repair the iron-sulfur cluster of the nitrogenase component protein. In order to clarify structure-function relationships of a family of NIFS-like proteins,

we have determined the three-dimensional structure of CsdB by X-ray crystallographic analysis.

The crystals of CsdB were grown by a hanging drop vapor diffusion method using sodium acetate as a precipitant. They belong to space group $P4_32_12$ with unit cell dimensions of $a = b = 128.1$ Å and $c = 137.0$ Å. Two heavy-atom derivatives were prepared using phenyl mercury acetate and potassium tetracyanoplatinate. Diffraction data for the native and two derivative crystals were collected on an R-AXIS IIc imaging plate detector system. The structure was solved by the multiple isomorphous replacement method with anomalous scattering and density modification techniques. The structure was refined to an *R*-factor of 0.187 at 2.8 Å resolution.

CsdB is a homo-dimer with the subunit composed of 406 amino-acid residues and one PLP. The overall fold of the subunit is similar to those of the α-family of PLP-dependent enzymes, represented by an aspartic acid aminotransferase. The subunit consists of three parts: the large domain of an α/β fold containing a seven-stranded β-sheet flanked by helices, the small domain containing a four-stranded β-sheet with three α-helices, and the N-terminal segment. However, CsdB has several structural features which are different from those of other families of enzymes. A β-hairpin loop protruding from one subunit of the dimer interacts with an α-helix in the lobe extending from the small domain to the large domain of the other subunit. These two portions of β-hairpin loop and the lobe form one side of a limb of an active site in the enzyme. The most striking structural feature of CsdB is that the side chain of Cys364, a putative catalytic residue, which lies on the extended lobe, is close enough to interact with γ-atom of the substrate.

P06.04.037 X-RAY CRYSTALLOGRAPHIC ANALYSIS OF THE CATALYTIC MECHANISM OF L-2-HALOACID DEHALOGENASE. Y. Hata, Y.-F. Li, T. Fujii, T. Kurihara and N. Esaki, Institute for Chemical Research, Kyoto University, Kyoto 611-0011, Japan.

L-2-Haloacid dehalogenase from Pseudomonas sp. YL is a dimeric enzyme that catalyzes the hydrolytic dehalogenation of L-2-haloalkanoic acid to yield the corresponding D-2-hydroxyalkanoic acid. The enzyme subunit consists of 232 amino acid residues with molecular weight of 26,179. Our mass-spectroscopic studies revealed that the enzymatic reaction proceeds by the two-step mechanism via ester intermediate. In order to elucidate the catalytic mechanism of the enzyme based on structural changes in process of the reaction, crystal structures of the enzyme have been determined in the forms of the native, the ester intermediate and the enzyme-product complex. The subunit is composed of two structurally distinct domains; the core domain for catalysis and the subdomain for dimerization. The core domain has an a/b-structure formed by a six-stranded parallel b-sheet flanked with five a-helices, and the subdomain has a four-helix-bundle structure. The catalytically important rsidues of Asp10, Thr14, Arg41, Ser118, Lys151, Tyr157, Asn177 and Asp180 are located in the active site cleft between both domains. The negatively charged substrate is probably taken into the enzyme by the electrostatic interaction with Arg41 at the active site entrance. In the active site, the carboxyl group of the substrate is fixed by the hydrogen bonds to the side chain of Ser118, and the alkyl group of the substrate is stabilized in the hydrophobic pocket, which is primarily composed of Lys151, Asn177 and Trp179 and may play an important role in determining the stereospecificity of the enzyme. The halogen atom is abstracted from the substrate C2 atom by the guanido group of Arg41, and concurrently Asp10 in the opposite side makes an nucleophilic attack on the C2 atom to form the ester intermediate. In this process, the Walden's inversion occurs at the C2 atom of the substrate, and consequently the substrate moiety adopts a D-configuration. In the intermediate formation, the regions of Asp10-Ser20 and Leu117-Arg135 move into the active site, the side chain of Asp10 rotates largely, and a new water molecule occurs in the vicinities of Asp10, Ser175, Asn177 and Asp180. The water molecule is probably activated by the deprotonated carboxyle group of Asp180 and serves as the nucleophile for hydrolysis of the ester intermediate. After the hydrolysis, the carboxyl group of Asp10 rotaes so as to be hydrogen-bonded to that of Asp180. Finally the product is released, and the enzyme is restored to the original state.

P06.04.038 STRUCTURAL STUDY OF CobA: AN ADENOSYL TRANSFERASE INVOLVED IN THE VITAMIN B_{12} BIOSYNTHETIC PATHWAY. Cary B. Bauer[1], Maris Fonseca[2], Jorge Escalante-Semerena[2], and Ivan Rayment[1], Departments of Biochemistry[1] and Bacteriology[2], University of Wisconsin, Madison, WI 53705, USA.

Vitamin B_{12}, an essential human nutrient, represents one of the most complex organic cofactors to be employed in living systems. The successful three-dimensional structural determination of a coenzyme form of this vitamin, namely 5'-deoxyadenosylcobalamin, represented a landmark in X-ray crystallography. The biosynthesis of this complex molecule requires numerous steps including an adenosyl transfer from ATP to the cobalt atom of cobyric acid. The enzyme responsible for this step in *S. typhimurium* is CobA. This 196 amino acid protein is capable of binding a variety of cobalamin compounds which are substituted at the upper ligand including cyano-, hydroxy-, and the previously mentioned adenosylcobalamin. We have very recently determined the crystal structure of CobA in the absence of any substrate. This form of CobA crystallizes in $P6_522$ with unit cell dimensions of a=b=49.38, c=250.10 and was solved utilizing MAD phasing on data collected on a selenomethionine substituted protein. The structure reveals a molecular dimer which contains a mixed helix/sheet topology. We currently have obtained diffraction quality crystals in which CobA was co-crystallized in the presence of both hydroxycobalamin and adenosylcobalamin. We expect to be able to present the structures of these substrate bound forms in addition to the apo form. The combination of these structural results will hopefully shed light on the mechanism involved in this step of the synthetic pathway.

P06.04.039 OPEN STRUCTURE OF PIG MUSCLE 3-PHOSPHOGLYCERATE KINASE (PGK) WITH BOUND MG-ADP AND 3-PHOSPHOGLYCERATE (3PG). M. Vs Kazinczy, & A. N. Szilgyi, Institute of Enzymology, BRC, Hung. Acad. Sci., Budapest, Hungary & M. Ghosh, Laboratory of Molecular Biophysics, Department of Biochemistry, University of Oxford, UK

The mechanism of relative domain movements and its role in the catalysed phospho-transfer is investigated on PGK, a typical two-domain kinase, which catalyses the phospho-transfer from 1,3-bisphosphoglycerate to MgADP to form 3-phosphoglycerate and MgATP. Crystals of pig muscle PGK were grown in the presence of MgADP and 3-PG in 2.5 M phosphate, pH 8.0, i.e. under the conditions which has resulted in crystals of the closed, catalytically competent conformation of Trypanosoma brucei PGK (1). The crystal structure of the ternary complex has been determined at 1.8Å resolution with R=20.8% and Rfree=24.1%. This structure interestingly shows that the enzyme is in an open conformation, in contrast to that of T. brucei PGK, despite the fact the crystals were grown under similar conditions.

The mode of interaction of the phosphates of the nucleotide with PGK is remarkably different in the two structures. In the pig muscle PGK structure, the β-phosphate of MgADP does not interact with helix 13 which is a key element in the interdomain region. Systematic comparison of all the available PGK ternary complex structures with different domain positions has revealed

the importance of this contact with the nucleotide, and delineated at atomic level, a very probable mechanism of the domain closure. In addition to the previously observed C- and N-hinge points, the importance of the interdomain helices 13 and 14 as well as the connecting β-sheet L is now demonstrated and a third hinge point is proposed.

1. B.E. Bernstein, P.A.M. Michels & W.G.J. Hol, (1997),*Nature*, **385**, 275-278.

P06.04.040 STRUCT ANALYSIS OF CALF SPLEEN PURINE NUCLEOSIDE PHOSPHORYLASE COMPLEXES WITH TRANS-STATE INHIBITORS. A.A.Fedorov, G.A.Kicska, E.V.Fedorov, W.Shi [1], P.C.Tyler, R.H.Furneaux [2], V.L.Schramm, S.C.Almo [1], [1] Albert Einstein College of Medicine, Bronx,NY,10461,USA, [2] Carbohydrate Chemistry Team,Industrial Research Limited, Lower Hutt,New Zealand

Purine nucleoside phosphorylase (PNP) catalyzes the reversible phosphorolysis of ribonucleosides and 2'-deoxypurine ribonucleosides to the free bases and the corresponding ribose 1-phosphates. PNP is a key enzyme in the purine salvage pathway. Absence of PNP activity in humans is associated with specific T-cell immune suppression. Its key role in these two processes has made PNP an important drug design target. The structures of the calf spleen PNP bound to the transition state inhibitors immucillin-H (Ki* = 23 pM) and immucillin-G (Ki* = 72 pM) have been determined and refined at 1.5 and 2.0 A resolution respectively. The PNP complexes were obtained by co-crystallization with the inhibitors at 1:1.1 (PNP monomer: inhibitor) molar ratio. The refined structures of PNP complexes have good geometry with R factors 18.4 and 16.4%; free R-factors 23.2 and 24.6% respectively. The structures of PNP-immucillin complexes were compared with known PNP-substrate and PNP-product complexes and all conformational changes have been characterized. Ligand dependent loop 241-265 moves closer to the active site when compared to the corresponding substrate analog and product complexes; bound phosphate ion is closer to the ribose ring than in PNP-substrate analog complex; hydrogen bonds are shorter than observed in substrate analog and product complexes. Bound immucillins show that positive charge of the transition state oxocarbenium ion is stabilized by phosphate and ribose O5'; negative charge of the transition state purine ring is stabilized by hydrogen bonds donation from Asn 243 ND2 and from a water molecule to ribose O6.

P06.04.041 STRUCTURAL STUDIES OF PHOSPHONO-ACETATE HYDROLASE: A PHOSPHORUS-CARBON BOND CLEAVAGE ENZYME. M.M. Benning [1], A. Kim [2], D. Dunaway-Mariano [2] and H.M. Holden [1]. [1] Department of Biochemistry, University of Wisconsin, Madison, Wisconsin 53705. [2] Department of Chemistry, University of New Mexico, Albuquerque, New Mexico 87131.

Phosphonates are naturally occurring organophosphorus compounds that are similar to phosphate esters but contain a direct phosphorus-carbon linkage. The P-C bond is resistant to acid- and base-catalyzed hydrolysis as well as to enzymes that hydrolyze phosphate esters The phosphonoacetate hydrolase catalyzes the production of acetate and inorganic phosphate from phosphonacetate via a metal ion assisted hydrolytic cleavage of the P-C bond. The native enzyme was isolated from Pseudomonas fluorescens and crystallizes in the monoclinic space group $P2_1$ with cell constants of a=57 Å, b=128 Å, c=138 Å, b=95o. We have also crystallised the enzyme in the presence of an inhibitor, phosphonoformate. These crystals belong to the orthorhombic space group $P2_12_12_1$ with cell constants of a=115 Å, b=128 Å, c=138 Å. The crystal structure of the hydrolase will be presented.

P06.04.042 FUNCTION OF DIHYDROOROTATE DEHYDROGENASES (DHOD). S.Norager and S.Larsen, Centre for Crystallographic Studies, Department of Chemistry, University of Copenhagen, Universitetsparken 5, DK-2100 Copenhagen O, Denmark. O.Bjornberg and K.F.Jensen, Center for Enzyme Research, Institute of Molecular Biology, University of Copenhagen, Solvgade 83H, DK-1307 Copenhagen K, Denmark.

The DHODís catalyse the oxidation of (S)-dihydroorotate to orotate through reduction of their prosthetic FMN group. This is the only redox-reaction in the *de novo* biosynthesis of pyrimidine nucleotides. From the known sequences the DHODís can be split into two main families. The family 1 enzymes are located in the cytosol, while the family 2 enzymes are membrane associated. The family 1 enzymes can be further divided into two subgroups A and B. The crystal structures have been determined for the two DHODís from *Lactococcus lactis* that are representative of group A[1] and B[2]. The A type enzyme exists as a homodimer and has the same FMN associated binding site for the substrate and the e-acceptor. The B type enzyme is a heterotetramer. Substrate binding takes place at the two FMN containing subunits, that resemble the DHODA structure. This dimer interacts with the other two subunits that each contain a FAD and a [2Fe-2S] cluster. The presence of FAD in these latter subunits enables the enzyme to use NAD^+ as e-acceptor.

The structure of the DHODA enzyme complexed with the product orotate[3] showed that orotate stacks above the FMN isoalloxazine ring system and is attached by hydrogen bonds to the surrounding residues. Several DHODA mutants have been prepared and characterised kinetically to elucidate the reaction mechanism, and for two of these, N67A and P56A, the crystallographic studies are currently in progress. Asn67 forms a hydrogen bond to the orotate pyrimidine ring, and influences the orientation of the orotate in the binding site. Pro56 is part of a flexible loop, which covers the orotate binding cavity. The P56A mutant has a much lower K_M for the binding of orotate than the wild type enzyme.

1. P.Rowland, F.S.Nielsen, K.F.Jensen & S.Larsen (1997) Structure 5:239-252.
2. P.Rowland, F.S.Nielsen, K.F.Jensen & S.Larsen (in preparation).
3. P.Rowland, O.Bj¯rnberg, F.S.Nielsen, K.F.Jensen & S.Larsen (1998) Protein Science 7:1269-1279.

P06.04.043 CRYSTAL STRUCTURE OF BRASSICA THIOREDOXIN. K.K. Kim, S. C. Ha, Y. O. Hong and S. Y. Lee. Plant Molecular Biology and Biotechnology Research Center, Gyeongsang National University, Chinju 660-741, Korea

Thioredoxin is a ubiquitous protein and has a large number of known functions. Generally, it acts as a hydrogen donor for several essential reductase via thiol-redox mechanism. Several crystal structures of thioredoxin from different species, including *E. coli,* human, cyanobacteria and green alga, were determined. Although they show different functions and substrate specificities, the overall structure of thioredoxin is well conserved among species. Plant has many isoforms of thioredoxin and those may be required for modulating their substrate specificities.

Cytosolic thioredoxin h from the plant *Brassica campestris* (btrxh) has been studied for understanding the substrate specificity in plant thiol-redox reaction. The crystal structure of oxidized btrxh was solved by molecular replacement starting from the crystal structure of human thioredoxin. Current model has been refined to a crystallographic R-factor of 23 % (R-free = 27 %) at 2.3 A resolution. It has a typical thioredoxin fold which consists of a five-stranded β-sheet core surrounded by four α helices. The active site is well conserved either in sequence (46-WCGPC-50) and in structure with other thioredoxins. Interestingly, the first β strand in symmetry equivalent molecule

makes a tight contact to the groove close to the active site. That is the mimic of thioredoxin-substrate interaction which was observed in human thioredoxin-NFκB complex. Therefore, it is postulated that a btrxh-substrate interaction is similar to the human thioredoxin-substrate interaction, and these interactions could be shared in thioredoxin families.

P06.04.044 THREE-DIMENSIONAL STRUCTURE OF THE ENZYME DIAMINOPIMELATE EPIMERASE FROM *HEMOPHILUS INFLUENZAE*. Maurizio Cirilli*^, Renjian Zheng^, Giovanna Scapin~, John S. Blanchard^, *Istituto Strutturistica Chimica, CNR-Roma, 00016 Monterotondo St. (Roma), Italy, ^Department of Biochemistry, Albert Einstein College of Medicine, 1300 Morris Park Avenue, Bronx, New York 10461, ~Merck Research Laboratories, RY50-105, P.O. Box 2000, Rahaway, New Jersey 07065.

The crystallographic structure of Diaminopimelate epimerase (E.C. 5.1.1.7) from the bacteria *Hemophilus Influenzae* has been solved at 2.7 Å resolution by Multiple Isomorphous Replacement . The enzyme crystallizes in the C2221 space group with cell parameters a=102.1 Å, b=115.4 Å, c=66.3 Å and one molecule in the asymmetric unit. The refined model had a conventional R factor of 19.0% and a R_{free} factor of 24.2%. The 274 amino acid residues enzyme consists of two structurally homologous domains each containing eight β-strands and two α-helices. This arrangement of secondary structure elements give rise to a completely new fold as resulted by searching for possible matches in PDB database by DALI server. The two domains are highly homologous and are related by a pseudo two-fold symmetry axis. The superimposed domains have an rms deviation of 1.7 Å.

P06.04.045 CRYSTALLOGRAPHIC STUDIES ON SHIKIMATE DEHYDROGENASE. J. K. F. Maclean, A. J. Lapthorn, Dept. of Chemistry and Biochemistry, University of Glasgow, Glasgow, G12 8QQ, UK. and J. R. Coggins, IBLS, University of Glasgow, Glasgow, G12 8QQ, UK.

Shikimate Dehydrogenase (SDH) is the fourth enzyme of the shikimate pathway, and catalyses the NADPH-linked reduction of 3-dehydroshikimate to shikimic acid. We are engaged in an effort to determine the structures of several shikimate pathway enzymes, both to increase our understanding of the enzyme mechanisms, and to achieve a better understanding of the process of molecular recognition. SDH is one of only two such enzymes whose structures are still unresolved. We hope that the structure of SDH will provide the starting point for a programme of rational inhibitor design.

SDH crystals grow in space group C2, with a=110.0Å, b=139.5Å, c=102.6Å, β=122.24°. The packing density is $2.8Å^3Da^{-1}$, which corresponds to four molecules per assymetric unit. These crystals diffract to 2.2Å and exhibit interesting pseudosymmetry. While the true lattice is C-centred monoclinic, it is indistinguishable from a larger F-centred orthorhombic lattice at low resolution. We have used this observation to derive matrices which describe the 222 non-crystallographic symmetry within these crystals. These, in conjunction with phase information from several heavy atom soaks, have been used to generate promising initial averaged electron density maps. We will present the recent progress in our attempt to determine the three-dimensional structure of SDH.

P06.04.046 STRUCTURE/FUNCTION STUDIES ON SHIKIMATE KINASE. A. J. Lapthorn, J. K. F. Maclean, Dept. of Chemistry and Biochemistry, University of Glasgow, Glasgow, G12 8QQ, UK. and D. J. Boam and J. R. Coggins, IBLS, University of Glasgow, Glasgow, G12 8QQ, UK.

Shikimate kinase catalyses the fifth reaction on the shikimate pathway, in which shikimic acid is phosphorylated to produce shikimate 3-phosphate, using ATP as a co-substrate. The shikimate pathway is essential for the biosynthesis of aromatic compounds in plants, microorganisms and apicomplexan parasites. However it is absent from animals and is therefore an attractive target for the design of novel antibiotics and herbicides.

We have previously determined structures of shikimate kinase from the plant pathogen *Erwinia chrysanthemi* complexed with ADP and shikimic acid [1]. From these structures we have designed and generated a series of active site mutants to probe the contribution of various amino acid residues to substrate recognition and catalysis. Several of these mutants, which have significantly reduced catalytic activity of the enzyme, have been crystallised to date.

The structure of the p-loop mutant K15M has been solved and refined at 2.5Å resolution. The enzyme crystallises in space group $C222_1$, a=43.0Å, b=75.1Å, c=106.1Å, with a single molecule in the assymmetric unit, corresponding to a solvent content of 37%. This structure is of particular interest as the mutation results in an unexpected change in the overall conformation of the p-loop. To our knowledge, this is the first structure of a kinase p-loop mutant.

1. T. Krell, J. R. Coggins & A. J. Lapthorn (1998). J. Mol. Biol., 278, 983-997

P06.04.047 CRYSTALLIZATION AND STRUCTURE DETERMINATION OF ECTI, A SERINE PROTEASE INHIBITOR FROM ENTEROLOBIUM. R.C. Garratt, M.C. Nonato, M. Bonfadini, and L.M. Beltramini [1], and I.F.C. Batista, M.U. Sampaio and C.A.M. Sampaio [2], [1]Instituto de Física de São Carlos, Universidade de São Paulo, São Carlos 13560-250, SP, Brazil, [2] Depto. Bioquímica, Universidade Federal de São Paulo, UNIFESP/EPM, São Paulo, SP, Brazil

Protein enzyme inhibitors are distributed in a large range of biological materials. They have been studied in detail in part because of their use as tools in the study of enzyme mechanisms. Seed serine protease inhibitors are divided according to sequence/structural properties into six superfamilies : Kunitz, Bowman-Birk, Potato I and II, Squash and Cereal inhibitors. The Enterolobium contortisiliquum trypsin inhibitor (EcTI) belongs to the plant Kunitz inhibitor family, and consists of 174 amino acid residues and contains two disulphide bridges. It is homologous to other trypsin inhibitors from the same family, such as STI (Soybean trypsin inhibitor) and ETI (Erithryna caffra trypsin inhibitor).

EcTI was purified to the homogeneity by acetone precipitation, ion-exchange and gel filtration chromatographs. Crystals of EcTI were obtained at 19 ºC, by the vapour diffusion technique with 15%PEG 8000 / 0.5M Lithium sulfate as precipitating agent.

The crystals obtained with EcTI belong to the space group $P2_1$ and diffract up to 2.4Å resolution on capillary mounting using a rotating anode source. The structure determination by molecular replacement using 1TIE (Erythrina Trypsin Inhibitor - Kunitz De-3) as a model indicates the presence of one monomer in the asymmetric unit. The structure of EcTI presents the expected b-trefoil motif.

Partially supported by UNIFESP, CNPq and FAPESP

P06.04.048 CRYSTAL STRUCTURE OF *E. COLI* CYANASE AT 1.65 Å DETERMINED USING MAD PHASING. A. Joachimiak[1], M.A. Walsh[1], A. Perrakis[2] & P.M. Anderson[3], [1]Center for Mechanistic Biology and Biotechnology, Argonne National Laboratory, Argonne IL 60439, USA, [2]European Molecular Biology Laboratory, Grenoble, France, [3]Dept. Biochemistry, University of Minnesota-Duluth, Duluth, MN 55812, USA

Cyanase, a homo-decamer of 17-kDa subunits, is an inducible enzyme in *Escherichia coli* that catalyzes the reaction of cyanate with bicarbonate to produce ammonia and carbon dioxide. The enzyme crystallizes in the triclinic space group P1 with unit cell dimensions of a = 76.34 Å, b = 81.03 Å, c = 82.30 Å, α = 70.3°, β = 72.23° and γ = 66.43° and contains one 170-kDa decamer in the AU and 40 potential selenium sites. A four-wavelength MAD experiment was collected to 2.25 Å resolution at 100 K at the Argonne National Laboratory Structural Biology Center's undulator beamline at the Advanced Photon Source. The positions of the selenium atoms were found automatically (CNS & CCP4) and maps of high quality were produced. The solvent-flattened map (DM) was used as input to the wARP procedure, which extended and improved phases and produced an initial protein model. The model was refined (REFMAC) against data collected to 1.65 Å resolution (R=15.2%, R_{free}=19.0%). Structures of the enzyme complexed with chloride (cyanate analogue) and oxalate (proposed transition state analogue), were also determined. The structures show that active site of cyanase is formed by the side chains of four adjacent subunits of the homo-decamer. The combination of an x-ray source with high brilliance, a large mosaic CCD area detector with a rapid read-out time, and recent developments in crystallographic software have provided a platform for accelerated crystal structure determination and refinement.

This work was supported by the U.S. Department of Energy, Office of Biological and Environmental Research, Under Contract W-313-109-ENG-38.

P.06.04.049 CRYSTAL STRUCTURE OF HYALURONIDASE, A MAJOR ALLERGEN FROM BEE VENOM. Z. Markovič-Housley, T. Schirmer, L.N. Soldatova, U. R. Müller. Biocenter, Basel & Ziegler Spital, Bern, Switzerland; FDA, Rockville, Maryland, USA.

Hyaluronidase from bee venom (Hya) is a hydrolase that specifically cleaves the β-1,4-glycosidic bond of hyaluronic acid, the most abundant glycosaminoglycan of vertebrate extracellular spaces, thereby facilitating the penetration of venom constituents into the skin. Hya is a major allergen of bee venom which can induce serious systemic IgE-mediated anaphylactic reactions in humans. The atomic structure of Hya is the first step towards identifying epitope residues responsible for the IgE-mediated potency of hyaluronidase and thereafter, the development of allergen-specific forms of therapy. The crystal structure of recombinant (*Baculovirus*) bee venom Hya has been determined at a resolution of 2.0 Å by the method of multiple isomorphous replacement and represents the first structure of any member of the glycosidase family 56. The overall fold resembles an $(\beta/\alpha)_8$ barrel, common among many hydrolases, with the exception that only seven strands form the barrel, and thus, the barrel appears open on one side. The active site residues Asp110 and Glu112 are located at the C-terminal end of β-strand 4, in a large groove on the protein surface. These residues are conserved amongst hyaluronidases of bee and hornet (56 % sequence identity) and the related PH-20 proteins from mammalian testis and plasma (20% sequence identity). In most glycosidases, two carboxylates are required for acid/base catalysis and the hyaluronidases are no exception: mutation of Asp111 and Glu113 of human sperm PH-20 protein (equivalent to Asp110 and Glu112 in Hya) leads to an inactive protein. A number of aromatic residues line both sides of the active site groove to form a hydrophobic surface that is well positioned to participate in the binding of sugars through nonpolar interactions. The groove (about 30Å x 9Å) appears to be large enough to accommodate a hexasaccharide of hyaluronic acid, which is the smallest substrate.

P06.04.050 X-RAY CRYSTALLLOGRAPHY OF MAJOR NITROREDUCTASE FROM *ESCHERICHIA COLI* (NfsA). Toshiro Kobori, Woo Cheol Lee, Takako Akagi, Departments of Applied Biological Chemistry and Biotechnology, Graduate School of Agricultural and Life Sciences, University of Tokyo, Tokyo 113-8657, Japan, Hiroshi Sasaki, Biotechnology Research Centre, University of Tokyo, Tokyo 113-8657, Japan, Shuhei Zenno, Kaoru Saigo, Department of Biophysics and Biochemistry, Graduate School of Science, University of Tokyo, Tokyo 113-0033, Japan, and Masaru Tanokura, Departments of Applied Biological Chemistry and Biotechnology, Graduate School of Agricultural and Life Sciences, University of Tokyo, Tokyo 113-8657, Japan.

NfsA is the major oxygen-insensitive NAPDH:nitrocompound oxidoreductase (nitroreductase) from *Escherichia coli*. Oxygen-insensitive niroreductases catalyze the reduction by two electron transfer mechanism and are not inhibited by oxygen. Biochemical studies have suggested that NfsA is an FMN-containing flavoprotein with a molecular mass of approximately 26kDa and can use only NADPH as an electron donor, in contrast to NfsB, which is another nitroreductase in *E. coli* and can use either NADH or NAPDH as an electron donor. We have overexpressed NfsA protein in *E. coli* and crystallized NfsA in the presence of FMN by the vapor diffusion method using polyethylene glycol 6000 as a precipitant at 5°C. The obtained crystals had a plate-like shape. The crystals belonged to the triclinic space group *P*1 with cell dimensions, *a* = 52.2 Å, *b*=52.7Å, *c*=53.3Å, α = 75.1°, β = 60.1°, γ = 60.5°. Assuming that there are two molecules per unit cell, the crystal volume per unit molecular mass (*V*m) and the solvent content are 1.98Å^3/Da and 37.9% respectively. Because biochemical experiments have suggested that NfsA acts as a dimer in the solution, the crystals should contain one dimer in a unit cell. The crystals diffracted X-rays to at least 2.3Å resolution, by using the Weissenberg camera for macromolecular crystallography with a synchrotron radiation in the Photon Factory at High Energy Accelerator Research Organization, Tsukuba, Japan. Structural analysis is in progress by the molecular replacement method.

P06.04.051 X-RAY STRUCTURE ANALYSIS OF PYRUVATE FORMATE-LYASE AT 5 Å RESOLUTION. Andreas Becker, Klaus Scheffzek and Wolfgang Kabsch, Max-Planck-Institut für medizinische Forschung, Abteilung Biophysik, Jahnstraße 29, D-69120 Heidelberg, FRG, and A.F.Volker Wagner, Sabine Schulz and Joachim Knappe, Institut für Biologische Chemie/ Biochemie Zentrum Heidelberg, Universität Heidelberg, Im Neuenheimer Feld 501, D-69120 Heidelberg, FRG.

Pyruvate formatelyase (PFL, a_2, 170kDa), a key enzyme of energy-metabolism in anaerobic E.coli cells, synthesizes Acetyl-CoA (and formate as coproduct) from pyruvate and CoA. It catalyzes the cleaveage of the C1-C2-carbon bond of pyruvate via a reversible radical mechanism. A crucial catalytic element of the enzyme is a free and stable organic radical located at Gly734 [1].

So far only two structures of a radical enzymes are known; ribonucleotide reductase class Ia from *E.coli* [2] and class Ib from *Salmonella typhimurium* [3] contain a tyrosyl-radical in R2-subunit, which is Fe(III) stabilized. In contrast the glycyl-radical in PFL is only stabilized by the 3D-structure of the protein.

Large PFL crystals were obtained by the dialysis method using PEG as precipitant. They belong to the tetragonal space

group $P4_32_12$ or its enantiomorph (a=b=160Å, c=161Å) with one PFL homodimer per asymmetric unit.

Using synchrotron radiation (EMBL c/o DESY, BW7B) crystals diffract to 2.6Å. In our laboratory using rotating anode radiation we have collected a complete native dataset to 3.4Å resolution and a number of heavy atom derivative datasets.

We prepared heavy atom datasets from crystals of mutant proteins, where cysteins at positions 122, 159 and 524 are replaced by serine. All of the heavy atom derivatives heve been solved at 6Å resolution, which led to unique identification in the primary sequence of each heavy atom sites. The two polypeptide chains of the dimer are related by a pure two-fold rotation (without screw component). At present the structure has been solved at 5Å resolution showing a number of distinctive a-helices and b-sheets.

The identification of the heavy atom labelled cysteins in the map are expected to simplify the construction of the atomic model.

[1] A.F.V. Wagner, M. Frey , F.A. Neugebauer, W. Schäfer & J. Knappe. (1992). Proc.Natl.Acad.Sci.U.S.A. **89**, 996
[2] P. Nordlund, B.-M. Sjoeberg & H. Eklund (1990). Nature **345**, 593; U. Uhlin & H. Eklund (1994). Nature **370**, 502
[3] M. Eriksson , A. Jordan & H. Eklund (1998). Biochemistry **37**, 13359.

P06.04.052 INHIBITION OF HEXOKINASE ACTIVITY BY DECAVANADATE: CRYSTALLOGRAPHIC AND KINETIC STUDIES. Agnete la Cour, Oren P. Anderson, Debbie C. Crans, and Boyan Zhang, Department of Chemistry, Colorado State University, Fort Collins, Colorado 80523, USA.

Hexokinase has been suggested to play a role in facilitating the diabetic state given its physiological function of phosphorylating glucose. We have undertaken kinetic studies in solution of a series of vanadium-containing oxometalate ions and identified these as competitive inhibitors of yeast hexokinase B, with a surprising selectivity based on charge and shape. Activity studies of yeast hexokinase B crystals suggested that the enzyme is also active in the solid state. Inhibition studies of hexokinase crystals soaked in a decavanadate solution suggested that decavanadate inhibits the enzyme in the solid state, thus indicating that decavanadate may be found in the active site of the enzyme in the crystals. We have undertaken crystallographic studies with the goal of determining the molecular interactions of species such as decavanadate with the enzyme. Yeast hexokinase B crystallizes in the orthorhombic space group $P2_12_12_1$, however with two different unit cells. We have collected low temperature data to a resolution of 1.8 Å for a prismatic crystal form (a = 58.571(6), b = 57.584(6), c = 163.263(20) Å); this form is the same as that in the previous 2.1 Å structural study [C. M. Anderson, R. E. Stenkamp, & T. A. Steitz (1978). *J. Mol. Biol*., 123, 15]. We have also collected low temperature data to 2.5 Å for a crystal of a plate-like crystal form (a = 57.90(4), b = 92.97(10), c = 213.84(6) Å) that had been soaked in a decavanadate solution. In the earlier structure determination the identities of 17% of the amino acids were not assignable. We will present a 1.8 Å structure of hexokinase B with all amino acids assigned from the known protein sequence. The data from the decavanadate-soaked crystals had not yielded a structure at the time of submission of this abstract. However, we expect to document the existence of decavanadate in the active site of the enzyme and to make a first estimation of the nature of the interactions between the decavanadate ion and the enzyme.

P06.04.053 *E. coli* ASPARTYL-tRNA SYNTHETASE - $tRNA^{Asp}$ COMPLEX: SECOND STEP OF THE AMINOACYLATION REACTION. S. Eiler, A.C. Bregeon, L. Moulinier, J.-C. Thierry and D. Moras. Laboratoire de Biologie Structurale, Institut de Génétique et de Biologie Moléculaire et Cellulaire, CNRS/INSERM/ULP, 1 rue Laurent Fries, BP 163, 67404 Illkirch Cédex, C.U. de Strasbourg, France.

The 2.4 Å resolution crystal structure of the *E. coli* aspartyl-tRNA synthetase - $tRNA^{Asp}$ with aspartyl-adenylate shows all substrates ready for the transfer of the aspartic acid moiety from the activated aspartyl-adenylate to the 3'-hydroxyl of the terminal adenosine of $tRNA^{Asp}$. Amino acid residues and water molecules involved in the specific recognition of the substrates in the enzymatic mechanism, have been identified. Most of the residues involved in the catalysis and amino acid substrate recognition are strictly conserved in all AspRSs, a few of them are only conserved within eucaryotes, archaea or eubacteria. A mechanism governing the two steps of the enzymatic aspartylation reaction common to all AspRSs but different for the role of one amino acid is proposed. The eucaryotic or archaeal serine, essential for the stabilisation of intermediate states in the two steps of the aspartylation reaction, is replaced in eubacteria by a glutamine from a different position in the catalytic site.

P06.04.054 STRUCTURAL COMPARISONS OF TYPE I 3-DEHYDRO-QUINASES. D.A.Porter, I.McNae, D.Alexeev, L.Sawyer, ICMB, The University of Edinburgh, Swann Building, Mayfield Road, Edinburgh EH9 3JR, UK and A.K.Shrive, Department of Physics, Keele University, Staffordshire ST5 5BG and I.Polikarpov, LNLS, CP 6192, 13083-970 Campinas, Brazil and J.R.Coggins, Division of Biochemistry and Molecular Biology, The University, Glasgow, G12 8QQ and A.R.Hawkins, Department of Biochemistry & Genetics, University of Newcastle, Newcastle NE2 4HH, UK

The enzyme 3-dehydroquinase (DHQase, EC 4.2.1.10) catalyses the dehydration of 3-dehydroquinate to form 3-dehydroshikimate and so introduce the first double bond in the biosynthesis of the aromatic nucleus. The mechanism proceeds by a *syn*- or *cis*-elimination for the Type I enzyme and involves an imine (Schiff base) intermediate, in contrast to the Type II enzyme that uses an entirely different mechanism. As the shikimate pathway is absent from mammals, studies of the inhibition of the constituent enzymes may provide suitable lead compounds for herbicide and antibiotic development. We have solved the crystal structure of the native Type I enzyme from *Salmonella typhi* and describe the modification to the structure that occurs upon substrate binding. This provides a basis that is used in conjunction with various solution studies to propose a detailed molecular mechanism. Further, the better studied enzyme from *Escherichia coli* has also been solved at 2.8Å resolution and we compare the two structures, particularly their active sites and subunit contacts.

We are grateful to the BBSRC for financial support.

P06.04.055 STRUCTURAL INVESTIGATION OF CYTOCHROME C'. L. Ramirez[1], P. Trieu[1], R. McNulty[1], B. Schick[1], H. Axelrod[2], K. Kantardjieff[1]. [1]Department of Chemistry & Biochemistry and W.M. Keck Foundation Center for Molecular Structure California State University, Fullerton, CA 92634. [2]Department of Physics. University of California, San Diego. La Jolla CA 92093-0319.

Cytochrome C' is a bacterial protein found in photosynthetic bacteria. The protein is a 28kDa dimer of four helix bundles. Each monomer contains four antiparallel helices, which bind a heme prosthetic group. Cytochrome C' is found in various photosynthetic bacteria and has been shown to increase in

concentration during photosynthesis. The protein has a low redox potential, which suggests that if it is involved in the electron transfer process, it is not a terminal oxidase. The heme prosthetic group is pentacoordinate and in a high spin state, further supporting its role in electron transfer. The three dimensional structure of cytochrome c' has been determined in *Rhodopseudomonas palustris* (N. Shibata *et al.* In press.), *Chromatium vinosum* (Z. Ren *et al.* In press.), *Alcaligenes denitrificans* (A.J. Dobbs *et al.* In press.), *Alicaligenes sphaeroides* (A.J. Dobbs *et al.* In press.), *Rhodobacter capsulatus* (T.H. Tahirov *et al.* J. Mol. Biol. 1996.), and *Rhodocyclus gelatinosus* (M. Archer *et al.* J. Biol. Inorg. Chem. 1997.) (inexhaustive search). A comparison of the three dimensional structures of Cyt C' displays a high similarity in tertiary structure but a low sequence homology (M. Archer *et al.* J. Biol. Inorg. Chem. 1997.). Highly conserved sequences are at the heme binding sites. Cyt C' binds small ligands such as CO and CN^-. In the case of *Chromatium vinosum,* ligand binding causes dimer dissociation (R.J. Kassner. Biochim. Biophys. Acta, 1991.). Structure elucidation will give some insight into 1.) the role of Cyt C' in electron transfer processes during photosynthesis, 2.) amino acid sequence relation to protein folding, and 3.) ligand induced dissociation.

P06.04.056 CRYSTAL STRUCTURES OF NATIVE AND E202Q MUTANT HUMAN ACETYLCHOLIN-ESTERASE COMPLEXED WITH FASCICULIN-II. G. Kryger [1], K. Giles [1,2], L. Toker [2], B. Velan [3], A. Lazar [3], C. Kronman [3], D. Barak [3], N. Ariel [3], A. Shafferman [3], I. Silman [2] and J.L. Sussman [1, 4]. [1] Department of Structural Biology, Weizmann Institute of Science, Rehovot 76100, Israel. [2] Department of Neurobiology, Weizmann Institute of Science, Rehovot 76100, Israel. [3] Israel Institute of Biological Research, Ness Ziona 70450, Israel. [4] Biology Department, Brookhaven National Laboratory, Upton, NY 11973, USA.

Knowledge of the 3D structure of human acetylcholinesterase (AChE) is of importance for drug design, in particular of anti-Alzheimer drugs, and for design of safer and more effective insecticides. A construct of recombinant human AChE (rHuAChE) was made in which the C-terminus had been truncated. This was done to facilitate crystallization by partly alleviating the problem of polymorphism, i.e. the co-expression of monomers, dimers and tetramers. Both WT rHuAChE and the E202Q mutant were expressed in HEK 293 cells, and co-crystallized as a stoichiometric complex with the polypeptide toxin, fasciculin-II (FAS-II), purified from the venom of the green mamba. Synchrotron data were collected from single cryo-cooled crystals. The WT rHuAChE/FAS-II and E202Q structures refined to 19%/25.5% and 19%/24% R/Rfree, at 2.8Å and 2.9Å resolution, respectively, using the *Torpedo californica* AChE (*Tc*AChE)/FAS-II structure as a starting model. Both structures contain ~400 solvent molecules. The WT structure shows three sugar rings at one of the three known glycosylation sites, N350. The E202Q structure shows the same three sugar rings on N350, an additional ring on N265, and residues 493-496, which are disordered in the WT structure. rHuAChE/FAS-II shows high degree of structural similarity with the two other, already published, complexes of AChE with FAS-II, viz. of *Tc*AChE and of mouse AChE, especially in the active-site region and within the aromatic gorge. Small variations can be found in some loops and in the insertion/deletion regions. Our results thus open the way to a study of subtle differences in structure which may account for species-dependent differences in specificity for substrates and inhibitors.

P06.04.057 THREE DIMENSIONAL STRUCTURE OF A DEHYDROGENASE AT 2.8Å RESOLUTION. Alpana Seal C&MB Division,S.I.N.P.,1/AF Bidhan Nagore, Calcutta 700064 India

The metabolic breakdown of long chain fatty acids, in most organisms, proceeds through beta oxidation pathway. L-3 hydroxyacyl CoA dehydrogenase is one of the four enzymes involved in mitochondrial beta-oxidation cycle which utilizes NAD as a cofactor and L-3-hydroxy- acyl CoA as substrate.

Polyalanine model from a orthorhombic form C222(1) of this dimeric 70KD protein with 5.25Å data using MIR techniques showed distinct bilobal appearance, NAD molecule being bound to the larger of the two lobes near the interface with the small lobe(1).

One 2.8 Å data set consisting of Hg (three major, three minor sites), Pt and a pseudo heavy atom derivative (NAD) were used to get MIR phases. Solvent flattened map was used to get the initial skeleton. Density modification was done using non crystallographic symmetry. Subsequent model building is underway to best fit the maps. NAD enzyme interaction and possible mode of interactions between fatty acid and the enzyme will be described.

(1) 1983 J.B.C,258,2383-2389

P06.04.058 CRYSTAL STRUCTURE OF BACILLUS CEREUS β-AMYLASE AND ITS COMPLEXES WITH SUBSTRATE ANALOGS. T. Oyama, Y. Kishimoto, and Y. Nitta, College of Agriculture, University of Osaka Prefecture, Sakai, Osaka 599-8531, Japan, and Y. Takasaki, Faculty of Engineering, Miyazaki University, Miyazaki 889-2155, Japan, and M. Kusunoki, Institute for Protein research, Osaka University, Suita, Osaka 565-0871, Japan.

The crystal structure of β-amylase from *Bacillus cereus* var *mycoides* was determined by multiple isomorphous replacement and was refined to a final *R*-factor of 0.186 for 102,807 reflections with $F/\sigma(F) \sim 2.0$ at 2.2Å resolution with r.m.s. deviations from ideality in bond lengths and bond angles of 0.014 Å and 3.0°, respectively. The β-amylase molecule folds into three domains of A, B, and C. Domain B consists of a $(\beta/\alpha)_8$ barrel structure. Domain C has a similar fold to raw starch binding domains of cyclodextrin glycosyltransferase and glucoamylase. One calcium ion is bound in domain A and is not involved in catalysis.

To understand substrate binding mode, we determined crystal structures of complexes of the β-amylase with three kinds of substrate analogs of maltose, Glc-Glc-Xyl, and α-cyclodextrin, and the complexes showed different binding modes and conformational chugs of the enzyme. Maltose molecules bound to subsites 1 and 2 in the catalytic cleft and site B on domain B distant from the catalytic cleft. In the maltose complex, a flexible loop of residues 93-97 moved 10 Å into a closed form, shielding the catalytic site from the solvent.

To clarify the role of the catalytic residues of Glu172 and Glu367, we determined crystal structures of complexes of the β-amylase with two kinds of specific inhibitors of 2',3'-epoxypropyl-α-D-glucopyranoside and 3',4'-epoxybutyl-α-D-glucopyranoside, leading to the conclusion that Glu172 and Glu367 are in the non-dissociated and dissociated form, respectively.

P06.04.059 THE REACTION AND INHIBITION MECHANISM OF *DROSOPHILA* ADH BY X-RAY CRYSTALLOGRAPHY. NAD-KETONE ADDUCT AT 1.4Å. J. Benach and R. Ladenstein, Center for Structural Biochemistry, NOVUM, Karolinska Institutet, S-141 57 Huddinge, Sweden, S. Atrian and R. Gonzàlez-Duarte, Dept. of Genetics, University of Barcelona, E-08028 Barcelona, Spain.

Drosophila alcohol dehydrogenase (DADH) is an NAD^+ dependent enzyme that catalyzes the oxidation of alcohols to aldehydes/ketones. DADH is the member of the short-chain dehydrogenases/reductases family (SDR) for which the largest amount of biochemical data has been gathered during the last three decades. The crystal structures of one binary form (NAD^+) and three ternary complexes with NAD^+·acetone, NAD^+·3-pentanone and NAD^+·cyclohexanone were solved at 2.4 Å, 2.2 Å, 1.4 Å and 1.6 Å resolution , respectively. From the molecular interactions observed, the reaction mechanism could be inferred. The structure of DADH undergoes a conformational change in order to bind the coenzyme. Furthermore, upon binding of the ketone, a region that was disordered in the apo form (186-191) [1] gets stabilized and closes the active site cavity by creating either a small helix (NAD^+·acetone, NAD^+·3-pentanone) or an ordered loop (NAD^+·cyclohexanone). The active site pocket comprises a hydrophobic bifurcated cavity which explains why the enzyme is more efficient in oxidizing secondary aliphatic alcohols (preferably R form) than primary ones. Difference Fourier maps showed that the ketone inhibitor molecule has undergone a covalent reaction with the coenzyme in all three ternary complexes. Due to the presence of the positively charged ring of the coenzyme (NAD^+) and the residue Lys^{155}, the amino acid Tyr^{151} is in its deprotonated (tyrosinate) state at physiological pH. Tyr^{151} can subtract a proton from the enolic form of the ketone and catalyze a nucleophilic attack of the C_α atom to the C4 position of the coenzyme creating an NAD-ketone adduct. The binding of these NAD-ketone adducts to DADH accounts for the inactivation of the enzyme. The catalytic reaction proceeds in a similar way, involving the same aminoacids as in the formation of the NAD-ketone adduct. The pKa value of 9-9.5 obtained by kinetic measurements on apo DADH can be assigned to a protonated Tyr^{151} which is converted to an unprotonated tyrosinate (pKa 7.6) by the influence of the positively charged nicotinamide ring in the binary enzyme-NAD^+ form. pH independence during the release of NADH from the binary complex enzyme-NADH can be explained by either a lack of electrostatic interaction between the coenzyme and Tyr^{151} or an apparent pKa value for this residue higher than 10.0. Finally, from the available crystallographic and biochemical data, Ser^{138} -also conserved in the SDR family- might assist the proper positioning of the hydroxyl or carbonyl group of the substrate.

[1] Benach, J., Atrian, S., Gonzàlez-Duarte, R. & Ladenstein, R. (1998*J. Mol. Biol.* 282, 383-399.

P06.04.060 ASV INTEGRASE: STRUCTURAL SECRETS OF ITS CATALYTIC DOMAIN. J. Lubkowski, F. Yang, Z. Dauter, J. Alexandratos, and A. Wlodawer, NCI-FCRDC, ABL-Basic Research Program, Frederick, MD 21702, USA, M. Andrake, G. Merkel, and A. M. Skalka, Institute for Cancer Research, Fox Chase Cancer Center, Philadelphia, PA 19111, USA

We are reporting atomic resolution crystal structures of the core domain of integrase (IN) from avian sarcoma virus (ASV) and its mutant Asp64→Asn, as well as high resolution structures of three other active site mutants, →Asn, Asp121→Cys, and Glu157→Gln. Altogether, the new structural information presented here is based on refinement of nearly 15 structures, using synchrotron quality x-ray data. The resolution of these structures varies between 1.0 Å and 1.8 Å. These unparalleled x-ray data for ASV IN deliver new structural information about the flexible, active site loop of the enzyme and clear some inconsistences in the description of this fragment previously reported. The very high resolution and quality of these structures allows a complete description of the water structure around the catalytic core domain of ASV IN, the dynamic properties of this enzyme, the multiple conformations of disordered residues, and non-solvent molecules bound to the enzyme. The detailed dynamic description of the flexible active site region, in particular the loop formed by residues 144-154, suggests the conformational changes which may be associated with substrate binding. The pH dependence of active site loop mobility provides a new, more complete interpretation of the pH vs. activity profile observed for ASV IN. Structures of the active site mutants clearly show the factors responsible for loss of their catalytic activity. The chemical substitution of few atoms, followed by structural changes of substituted residues for Asp64→Asn, was found to suppress completely capability of these mutants to bind divalent metal (Mn, Mg) cations, necessary for catalysis.

Because these are the highest resolution structures reported for the core domain of ASV IN so far and because of the very careful refinement protocol applied, the structures reported here should be considered as the reference for future studies of this enzyme.

P06.04.061 CONFORMATIONAL FLEXIBILITY IN A NEW CRYSTAL FORM OF BILE SALT ACTIVATED LIPASE. Julian C.-H. Chen, Larry J.W. Miercke, Jolanta Krucinski, Robert M. Stroud. Graduate Group in Biophysics and Department of Biochemistry and Biophysics, Box 0448, UCSF, San Francisco, CA 94143-0448

The conformational changes associated with activation of lipases has been studied extensively, however, only a couple of lipases have been studied in both the inactive and activated forms.

We have obtained a new crystal form of bovine pancreatic bile salt activated lipase. The asymmetric unit is composed of three monomers, all in different conformations. Taken together with two structures of the protein solved earlier, we observe multiple conformations of the bile salt binding loop. This suggests that lipases may not necessarily have one particular closed state, but that the activation process stabilizes the open, substrate-accessible conformation. These structures also show a ~1.0 A rmsd between them, implying that domain movements may be also be involved during activation of cholesterol esterase, as opposed to localized changes found in other lipases.

P06.04.062 FARNESYL PROTEIN TRANSFERASE COMPLEXED WITH A CAAX PEPTIDE AND FPP ANALOGUE. C. Strickland, W. Windsor, R. Syto, L. Wang, R. Bond, Z. Wu, J. Schwartz, L. Beese, H. Le, P. Weber, Department of Structural Chemistry, Schering-Plough Research Institute, 2015 Galloping Hill Rd, Kenilworth NJ, 07033

The crystallographic structure of Acetyl-Cys-Val-Ile-selenoMet-COOH and alpha-hydroxyfarnesylphosphonic acid (HFP) complexed with rat farnesyl protein transferase (FPT) is reported. In the ternary complex, the bound substrates are within van der Waals contact of each other and the FPT enzyme. HFP binds in an extended conformation in the active site cavity where positively-charged sidechains and solvent molecules interact with the phosphate moiety and aromatic sidechains pack adjacent to the isoprenoid chain. The backbone of the bound CaaX peptide adopts an extended conformation and the sidechains interact with both FPT and aHFP. The cysteine sulfur of the bound peptide coordinates to the active site zinc. Overall, peptide binding and recognition appear to be dominated by sidechain interactions. Comparison of the structures of the ternary complex and

unliganded FPT shows that major rearrangements of several active site side-chains occur upon substrate binding.

P06.04.063 THE THREE-DIMENSIONAL STRUCTURE OF R-PHYCOERYTHRIN FROM *Gracilaria chilensis* AT 2.2 Å RESOLUTION. M. C. Bunster B., J.. A. Martínez-Oyanedel, C. Contreras-Martel and J.C.Fontecilla-Camps. Laboratorio de Biofísica Molecular, Facultad de Ciencias Biológicas, Universidad de Concepción, Casilla 160-C Concepción, Chile , and Laboratoire de Cristallographie et Cristallogenese des Proteines, Institut de Biologie Structurale J. P. Ebel, CEA/CNRS, Grenoble, France.

The three dimensional structure at 2.2 Å resolution, of R-phycoerythrin from *Gracilaria chilensis* one of the components of phycobilisomes, has been solved by X-ray diffraction methods. This is the first crystallographic report produced by our group in Chile, with the collaboration of the group in Grenoble for the data adquisition.

The protein was crystallized by vapor diffusion using sitting drops insets, with HEPES buffer at pH 7.0 and ammonium sulfate as precipitant. Red crystals grew after three weeks; they were used for macroseeding under the same conditions. The crystal diffracted to 2.2 Å resolution using synchrotron radiation at beamline BM14 of the European Synchrotron Radiation Facility at Grenoble.

The data were collected under cryogenic conditions(100ºK)with a completness of 98.6%. The crystals are rhombohedral, space group R3, with unit cell parameters a = b= 187 Å , c = 59.1 Å, $\alpha = \beta = 90º$ y $\gamma = 120º$ .The structure of R-phycoerythrin from *Polysiphonia urceolata* were used for molecular replacement to obtain the phases. The non-crystallographic symmetries were used in the refinement of the model.

The electron density maps show a high predominance of helical regions in the α and β subunits, and the chromophores are clearly defined. At this moment we have refined to a R factor of 34% and a R_{free} of 35% .

We will present the complete structure of the $\alpha\beta$ heterodimer and a model for the functional unit.

This work was supported by Dirección de Investigación, Universidad de Concepción 973172-1 and the collaboration Program Chile-France ECOS -CONICYT PC96B02.

P06.04.064 ALLOSTERIC MECHANISM OF THE MOLECULAR CHAPERONIN GroEL. Jianpeng Ma[1], Zhaohui Xu[2], Paul B. Sigler[2], and Martin Karplus[1] [1]Department of Chemistry and Chemical Biology, Harvard University, 12 Oxford St., Cambridge, MA02138. [2]Department of Molecular Biophysics and Biochemistry, Howard Hughes Medical Institute, Yale University, New Haven. CT06510

The chaperonin GroEL/GroES assisted protein folding cycle appears to involve large allosterically coordinated domain movements. To supplement the data available from the structures of stable intermediates, normal mode and targeted molecular dynamics simulations have been used to study the internal motions of GroEL.

Normal mode analyses of individual subunits and a multisubunit construct demonstrate that the observed displacements of the domains (hinge bending, twisting) arise from the intrinsic flexibility of the subunits. Simulations of the transition from the "closed" (ligand-free) to the "open" (GroES-bound in one ring) crystal structure show the transients that occur and provide stereo-chemical insights into biochemical and mutagenesis studies of the allosteric behavior of the GroEL assembly.

P06.04.065 CRYSTALLOGRAPHIC STUDIES ON THE COMPLEX CHEY-CHEA124-257. P. Gouet, N. Chinardet, M. Welch, L. Mourey, V. Guillet and J.P. Samama, Groupe de Cristallographie Bologique, IPBS-CNRS, 205 route de Narbonne, 31077 Toulouse Cedex, France

The histidine kinase, CheA, and the response regulator, CheY, are members of the two-component systems, which mediate signal transduction in prokaryotes and a few eukaryotes. These two proteins are part of the chemotaxis pathway. CheY regulates the rotation of the flagella and therefore the motion of the bacteria.

The protein CheA from *E. coli*, 71 kDa in molecular weight, is made of several functional domains connected by flexible linkers. The second domain, residues 124-257, also termed P2, is responsible for the molecular recognition of CheY. This response regulator, 14 kDa in molecular weight, consists of a single domain containing an essential aspartate residue, Asp57, whose phosphorylation by CheA leads to the activation of the protein.

Structural information on histidine kinases is limited, and the structure of the CheY-P2 complex was the first report of a protein complex in the two-component systems [1]. We have recently solved the structure of this complex to 2.1 Å in a space group of higher symmetry, $P2_12_12_1$. Cell parameters are a=53.8 Å b=76.6 Å c=157.6 Å and the asymmetric unit contains 2 molecules of complex. Water molecules have been positioned, revealing a specific pattern in the active site of CheY. Further experiments showed, that this pattern can change upon phosphorylation.

1. M. Welch, N. Chinardet, L. Mourey, C. Birck & J.P. Samama (1998). Nature Struct. Biol., **5**, 25-28.

P06.04.066 X-RAY CRYSTAL STRUCTURE OF A DECAMERIC C-TYPE LECTIN FROM RATTLESNAKE VENOM. John R. Walker[1], Bhushan Nagar[1], N. Martin Young[2] and James M. Rini.[1] [1]Departments of Molecular & Medical Genetics & Microbiology and Biochemistry, University of Toronto, Toronto, Ontario, M5S 1A8, Canada, and [2]Institute for Biological Sciences, National Research Council, Ottawa, Ontario, K1A 0R6, Canada.

The C-type lectin domain is found in proteins mediating a number of biological recognition processes including immune surveillance, lymphocyte homing, and receptor mediated endocytosis. Like other carbohydrate binding proteins, the C-type lectins use multivalency to increase the affinity and selectivity for their oligosaccharide ligands. In many snake venoms, C-type lectins appear to assist in the disruption of hemostasis. Western diamondback rattlesnake (*Crotalus atrox*) venom, for example, contains an oligomeric galactose-binding C-type lectin (RSL) which is a potent platelet activator.

We have solved the structure of RSL in two different $C222_1$ crystal forms by a combination of heavy atom methods and molecular replacement. The first form is a thiodigalactoside co-crystal (a=110Å, b= 151Å, c=95Å, resolution=2.4Å), while the second form is a lactose co-crystal (a=63Å, b=179Å, c=138Å, resolution=2.2Å). In both cases, the lectin is found to be a decamer composed of two 5-fold symmetric pentamers related by a crystallographic 2-fold rotation axis. Each monomer of the decamer possesses the canonical C-type lectin fold. The two pentameric disks (each 32Å thick, 104Å in diameter) are held together by five C86-C86 disulfide crosslinks connecting monomers on opposing pentamers. A considerable cavity, lined by acidic residues, is formed in the interface between the disulfide linked pentamers. With the exception of that arising from the bridging disulfides, no surface area is buried between opposing pentamers. In contrast, approximately ~1200 $Å^2$ of surface area on each monomer is buried by protein-protein contacts within the

pentamer. The ten carbohydrate-binding sites located on the rim of the decamer suggest a role for multivalent interactions.

P06.04.067 CRYSTALLIZATION OF REACTION CENTER WITH LIGHT-HARVESTING PROTEINS 1 FROM RHODOPSEDOMONAS VIRIDIS. Takayuki Odahara, Kazuaki Harata Biomolecular Department, National Institute of Bioscience and Human-Technology, 1-1 Higashi, Tsukuba, Ibaraki, 305-8566 Japan

To fully understand the functions of proteins, it is essential to determine their tertiary structures. Integral membrane proteins, embedded in lipid bilayer of biomembranes in well organized manner, fulfill fundamental biological functions such as energy conversion, chemical sensing, and ion transport. Most of crystals of integral membrane proteins have been obtained by the empirical search of the crystallization condition based on a try and error method. In order to break through such a situation and to get a rational guideline for the crystallization, it is necessary to derive useful common features of the crystallization conditions previously succeeded. So far we have systematically determined solubility diagrams for several integral membrane proteins in different detergents, precipitants and temperatures. It was shown that the prediction of the solubility of amorphous precipitate, which provides useful information for the choice of crystallization conditions, is possible.

There are still open questions concerning the initial energy transfer from the light-harvesting protein 1 to reaction center in the first step of the photosynthetic reaction in purple bacteria. We applied our guideline to the crystallization of the complex of those integral membrane proteins and ten different crystallization conditions of the protein were obtained. We are characterizing those crystals by the X-ray diffraction.

P06.04.068 CRYSTALLOGRAPHIC STUDIES OF THE INTERMEDIATE FILAMENT PROTEIN VIMENTIN. S.V. Strelkov, P. Burkhard, P.M. Steinert[1], N. Geisler[2], H. Herrmann[3], and U. Aebi, M.E. Müller Institut, Biozentrum der Universität Basel, 4056 Basel, Switzerland,[1]NIH, Bethesda, [2]Max Planck Institute for Biophysical Chemistry, Göttingen, [3]German Cancer Research Center, Heidelberg.

We report on the progress with the structure determination of vimentin, the first intermediate filament (IF) protein [1,2] to be studied by X-ray crystallography. Until now, the IF proteins resisted a successful crystallisation because of (*i*) their intrinsic ability to self-assemble into filaments and also (*ii*) their rod-like shape with the length of about 500 Å. We overcome these obstacles by examining a series of overlapping vimentin fragments, with the ultimate goal of resolving the complete molecule. This information is crucial for establishing the process of the IF assembly.

The predominant central part of vimentin is predicted to be a double-stranded α-helical coiled coil. Our experience suggests that coiled coils up to about 100 Å in length can often be crystallised while longer ones have a tendency for nonspecific aggregation [3]. Z2B is a soluble fusion protein containing 31 residues of the GCN4 leucine zipper [4] followed by residues 385 to 412 of human vimentin. We have obtained crystals of Z2B and collected diffraction data to 1.9 Å resolution. Molecular replacement with the known structure of the GCN4 zipper yielded three solutions corresponding to the same noncrystallographic dimer but differing by 7-residue register shifts. The final model (crystallographic R=0.20, R_{free}=0.24) contains a continuous coiled coil starting at the N-terminus and ending with residue 405 of vimentin. A number of other soluble vimentin fragments, including those representing the central coiled coil region as well as the N- and C-terminal globular domains, is currently being subjected to crystallisation and preliminary X-ray analysis.

1. H. Herrmann, & U. Aebi (1998) *Curr. Opin. Struct. Biol.* **8**, 177.
2. H. Herrmann, *et al.* (1996) *J. Mol. Biol.* **264**, 933.
3. S.V. Strelkov, *et al.* (1998) *Acta Cryst.* D**54**, 805.
4. E.K. O'Shea, J.D. Klemm, P.S. Kim, & T. Alber (1991) *Science* **254**, 539.

P06.04.069 STRUCTURE OF PHOSPHPLIPIDS IN A MEMBRANE PROTEIN COMPLEX, BOVINE HEART CYTOCHROME C OXIDASE. T.Mizushima*, M.Yao*, N.Inoue*, H.Aoyama*, E.Yamashita*, H.Yamaguchi*, T.Tsukihara*, R.Nakashima[#], K.Shinzawa-Itoh[#], R.Yaono[#], S.Yoshikawa[#], * Institute for Protein Research, Osaka University, 3-2 Yamada-oka, Suita 565-0871, Japan. [#] Department of Life Science, Himeji Institute of Technology, Kamigohri Akoh, Hyogo 678-1297, Japan.

Cytochrome *c* oxidase is a membrane protein complex, existing in the mitochondrial inner membrane. This enzyme is composed of two monomers, each containing thirteen different subunits. Purified cytochrome *c* oxidase usually contains several phospholipids. They are cardiolipin (CL), phosphatidylcholine (PC), phosphatidylethanolamine (PE), and phosphatidylglycerol (PG). Cardiolipins are essential for maximal activity of the enzyme complex and can not be replaced by other phospholipids without loosing the activity. However the binding sites and functions of the phospholipids are still unknown.

The crystal structure of bovine heart cytochrome c oxidase at 2.8Å resolution has located eight phospholipids in the enzyme molecule. Then X-ray analysis at the higher resolution of 2.3 Å elucidated 14 phospholipids, three CL, one PC, three PE and seven PG, were in the monomer. All phospholipids were found in the transmembrane region, five of them were at intermembrane side, and the other nine were at matrix side. One CL, two PE, and one PG were placed in the intermonomer space. Especially the CL played assistant role to make the dimeric structure. One PE and two PG were located in the large cleft of subunit III. This cleft seemed a pool of oxygen molecule. Dioxygen molecules could approach to the dioxygen reduction site from the pool in the subunit III which was likely to keep the hydrophobic dioxygen molecules. These phospholipids were bound to the protein by salt bridges or hydrogen bonds between the polar head groups and amino acid, and also by the hydrophobic interaction between the fatty acids and the hydrophobic amino acid residues in the transmembrane region. Each phospholipid joined protein subunits together to form the enzyme complex.

P06.04.070 STRUCTURAL EXAMINATION OF THE LAST METAL-ION COORDINATING RESIDUE IN A PARVALBUMIN EF-HAND SITE. M. Susan Cates [1], Emai L. Ho [2], Michael B. Berry [3], Qi Li [4], James D. Potter [5], George N.Phillips, Jr. [6], [1] Dept. of Biochemistry and Cell Biology, Rice University, Houston, TX, 77005-1892, [2] Dept. of Biochemistry and Cell Biology, Rice University, Houston, TX, 77005-1892, [3] Dept. of Biochemistry and Cell Biology, Rice University, Houston, TX, 77005-1892, [4] Dept. of Molecular & Cellular Pharmacology, University of Miami School of Medicine, Miami, FL, 33136, [5] Dept. of Molecular & Cellular Pharmacology, University of Miami School of Medicine, Miami, FL, 33136, [6] Dept. of Biochemistry and Cell Biology, Rice University, Houston, TX, 77005-1892

Parvalbumin mutants have been created to examine the effect of individual EF-hand domain residues on Ca2+-binding. The PVEF parent mutant contains a conservative F102W mutation, plus a D51A mutation which inactivates one of the protein's two Ca2+-binding sites at physiological levels of Ca2+. Structural comparison to the wild type EF site shows that the

D51A mutation does not effect Ca2+ coordination by the active EF site. Ca2+-binding parameters for the active site of PVEF also show wild type behavior.

The PVEF-E101D mutant has the PVEF mutations plus an E101D mutation in the functional EF-hand. Residue 101 is the last coordinating residue in the second EF-hand binding site. Crystal structures have been obtained of both PVEF-E101D bound to Ca2+ and PVEF-E101D bound to Mg2+. The conformation of the mutated EF-hand in Mg2+/PVEF-E101D is typical of a Mg2+/EF-hand, with the exception of some F helix rearrangement to accommodate the shorter ASP. The Ca2+/PVEF-E101D structure shows that the ASP residue is unable to bind Ca2+ in the bidentate mode adopted by the wild type GLU. The resulting 6-fold Ca2+ coordination in the mutant is usually characteristic of Mg2+. Moreover, PVEF-E101D shows only a 10-fold greater preference for Ca2+ over Mg2+, while wild type has a 10,000-fold preference for Ca2+-binding.

Supported by the Robert A. Welch Foundation, NLM, NIH, and the Keck Center forComputational Biology

P06.04.071 CRYSTAL STRUCTURE OF 40KDA CALCIUM-BINDING PROTEIN (CBP40) SPECIFIC TO PLASMODIA OF P. POLYCEPHALUM. W. Iwasaki [1], H. Sasaki [2], A. Nakamura, K. Kohama [3], M. Tanokura [1], [1] Department of Applied Biological Chemistry, Graduate School of Agricultural and Life Sciences, University of Tokyo, Yayoi 1-1-1, Bunkyo-ku, Tokyo 113-8657, Japan, [2] Biotechnology Research Centre, University of Tokyo, Yayoi 1-1-1, Bunkyo-ku, Tokyo 113-8657, Japan, [3] Department of Pharmacology, Gunma University, School of Medicine, Maebashi, Gunma 371, Japan.

A calcium binding protein with the molecular mass of 40kDa (CBP40) was purified from the lower eukaryote Physarum polycephalum by Kohama et al. The cDNA of CBP40 was identical with cDNA named LAV1 which had been cloned from a plasmodial-specific mRNA of P. polycephalum by Pallotta et al. CBP40 consists of 355 amino acids and contains four EF-hand domains in its C-terminal half region. The function of CBP40 remains unknown. In order to know the function of CBP40, we determined the crystal structure at 3.0Å resolution. Recombinant CBP40 expressed in E.coli was purified and crystallized in the presence of EDTA. The crystals belonged to the trigonal space group $P322_1$ with a=b=64.39Å and c=207.22Å. The crystals diffracted X-rays to resolution of 3.0Å at room temperature and 2.7Å at 100K. The crystals of calcium-binding form were obtained by soaking into a CaCl2 solution, which gave diffraction data of similar quality. The structure was determined by multiple isomorphous replacement method using two heavy atom derivatives of Hg and Sm. The refined model at 3.0Å resolution has an R-value 22.6%. The final model at higher resolution (2.7Å) will be obtained by the molecular replacement method using the model of 3.0Å. The structure is very rich in a-helices and its topology shows the notable feature, which provides insights about function of CBP40 and evolution of the EF-hand family.

P06.04.072 STRUCTURE OF AN XRCC1 BRCT DOMAIN: A NEW PROTEIN PROTEIN INTERACTION MODULE. Xiaodong Zhang†, Solange Moréra†, Paul A. Bates^, Philip C. Whitehead§, Arnold I. Coffer§, Karl Hainbucher†, Rachel A. Nash‖, Michael J. E. Sternberg^,Tomas Lindahl‖ and Paul S. Freemont† Molecular Structure and Function, ^Biomolecular Modelling, §Protein Isolation and Cloning and ‖Mutagenesis Laboratories, Imperial Cancer Research Fund 44 Lincoln's Inn Fields London WC2A 3PX, UK ‖ICRF Clare Hall Laboratories South Mimms Herts EN6 3LD, UK

The BRCT domain (BRCA1 C-Terminus), first identified in the breast cancer suppressor protein BRCA1, is an evolutionarily conserved protein-protein interaction region of about 95 amino acids found in a large number of proteins involved in DNA repair, recombination, and cell cycle control. We report the first three-dimensional structure and fold of a BRCT domain determined by X-ray crystallography at 3.2Å resolution. The structure has been obtained from the C-terminal region of the human DNA repair protein XRCC1. It comprises a four-stranded parallel β–sheet surrounded by three α-helices, which form an autonomously folded domain. The compact XRCC1 structure explains the observed sequence homology between different BRCT motifs and provides a framework for modelling other BRCT domains. Furthermore, the established structure of an XRCC1 BRCT homodimer suggests potential protein-protein interaction sites for the complementary BRCT domain in DNA ligase III, since these two domains form a stable heterodimeric complex. Based on the XRCC1 BRCT structure, we have constructed a model for the C-terminal BRCT domain of BRCA1, which is frequently mutated in familial breast and ovarian cancer. The model allows insights into the effects of such mutations on the fold of the BRCT domain.

1. Xiaodong Zhang, Solange Moréra, Paul A. Bates, Philip C. Whitehead, Arnold I. Coffer, Karl Hainbucher, Rachel A. Nash, Michael J. E. Sternberg,Tomas Lindahl and Paul S. Freemont. (1998). *The EMBO Journal*, Vol. 17 No. 21 pp. 6404-6411.

P06.04.073 THE ARCHITECTURE OF FLAVO-ENZYMES ON THE BASIS OF THE TERTIARY STRUCTURE OF YEAST LIPOAMIDE DEHYDROG-ENASE. T. Toyoda† and A. Takenaka, Faculty of Bioscience and Biotechnology, Tokyo Institute of Technology, Yokohama, Japan; † Present institution: Institute of Medical Science, University of Tokyo, Tokyo, Japan; and T. Sekiguchi, Faculty of Science and Engineering, Iwaki Meisei University, Fukushima, Japan.

Lipoamide dehydrogenase (E3), which is the common component in 2-oxo acid dehydrogenase complexes, is classified as a member of the pyridine nucleotide-disulfide oxidoreductase family. The x-ray structure of yeast E3 has been solved at 2.7Å resolution (R=20.2%, Rfree=26.2%) and compared with those of the other four proteins, trypanothione reductase, glutathione reductase, NADH peroxydase, and thioredoxin reductase, in the same family. E3 is a homo dimeric enzyme similar to the former three proteins, so that the subunits consist of four domains (FAD, NADH, central, and interface domains). The FAD and the NADH domains are composed of a similar topology of their secondary structures containing a Rossmann fold essential for the catalytic reactions. Although the amino acid sequence identities are rather lower among them, the central and the interface domains are also similar in the secondary structural topology. Differences occur only near the substrate binding pockets. In thioredoxin reductase, however, the latter two domains are missing. These facts suggest that proteins in the family are evolved from the common ancestor to catalyze the similar reaction, oxidation/reduction of a disulfide bond with electron transfer through NAD(P)H and FAD. The p64k protein in the family has an additional domain. Therefore it is noted at the present that there are at least three subclasses in the architectures of this family depending on the number of domains.

P06.04.074 VARIATIONS ON THE JELLY-ROLL THEME. I.J Clifton, L-C Hsueh, Z-H Zhang, C.J Schofield, Oxford Centre for Molecular Sciences, Dyson Perrins Laboratory, Oxford OX1 3QY, UK, and K. Harlos, Laboratory of Molecular Biophysics, Rex Richards Building, Oxford OX1 3QU, UK.

The crystal structures of several 2-oxoglutarate dependent oxygenases have now been determined. The structures of

isopenicillin *N* synthase [1] and deacetoxycephalosporin *C* synthase [2] have already been published. The new structures of two further representatives of this family, proline 3-hydroxylase (type II) and clavulanic acid synthase, are described and compared to those earlier structures.

All these non-haem iron-containing enzymes share a common architecture based on a central jelly-roll barrel. This eight-stranded β barrel with simple winding topology is found in many protein structures, however this family of proteins seems to use the jelly-roll barrel in an unusual way, as a housing for an iron atom. The iron is held on one interior surface of the barrel, like a pearl in an oyster. Ligands from the enclosing surfaces form the binding sites for the substrates. The range of structures we now have allow us to speculate about the biochemical repertoire of this simple and versatile jelly-roll-iron architecture. They also have implications for the evolution of the family of 2-oxoglutarate dependent oxygenases and allow detailed mechanisms to be proposed.

1. P.L. Roach, I.J. Clifton, C.M.H. Hensgens, N. Shibata, C.J Schofield, J. Hajdu, J.E. Baldwin (1997). Nature, **387**, 827-830.
2. K. Valegard, A.C.T van Scheltinga, M.D. Lloyd, T. Hara, S Ramaswamy, A. Perrakis, A. Thompson, H.J. Lee, J.E. Baldwin, C.J. Schofield, J. Hajdu, I. Andersson (1998). Nature, **394**, 805-809

P06.04.075 STRUCTURE OF LEFT-HANDED β-HELICAL ACETYLTRANSFERASES. Naveen Chandra (1), Jaruwaree Snidwongse (2), Iain A. Murray (2) and Peter C. E. Moody (1), 1) Department of Biochemistry, University of Leicester, Leicester LE1 7RH, UK, 2) Department of Molecular Biology and Biotechnology, University of Sheffield S10 2TN UK

XAT (Xenobiotic Acetyltransferase) from Agrobacterium SAT (Serine Acetyl transferase from E.coli and Nodl from Rizobium leguminosarum are members of the recently discovered family of trimeric left-handed parallel β-helical CoA O-acetyl transferases. Although they share a common core and acetyl donor, there is a wide variety of acceptor substrates. We are studying the structures of these enzymes with the aim of discovering the way in which the common structural core can accommodate such a diversity of specificities.

We have refined the structure of apo-XAT to 1.5Å and the acetyl-CoA derivative to 2.0Å. We will describe these structures and the crystallographic evidence that SAT and Nodl also belong to this family will be shown. Progress in the determination of the structures of SAT and Nodl will be reported.

P06.04.076 THREE-DIMENSIONAL STRUCTURE OF 2-DEHYDRO-3-DEOXYGLUCARATE (DDG) ALDOLASE FROM ESCHERICHIA COLI. Tina Izard, Nic Blackwell & Ron A Cooper, Department of Biochemistry, University of Leicester, LE1 7RH, UK

2-dehydro-3-deoxyglucarate (DDG) aldolase (EC 4.1.2.20) catalyses the reversible aldol cleavage of 2-dehydro-3-deoxy galactarate or 2-dehydro-3-deoxy glucarate to pyruvate and tartronic semialdehyde. The aldol condensation is an important reaction in synthetic chemistry, although the more complicated the desired product, the less efficient the reaction due to poor control over stereochemistry. Aldolases carry out specific condensations with exquisite control on the stereochemistry. In addition, because aldolases can be regulated depending on the concentrations of reactants and products, these enzymes are attractive as catalysts for synthetic chemistry. Aldolases catalyse a variety of aldol condensation or cleavage reactions and are mechanistically divided into two classes. The class I aldolases use an active-site lysine residue in Schiff base formation with substrate whilst the class II enzymes require a metal cofactor. DDG aldolase belongs to class II enzymes. DDG aldolase from Escherichia coli has been overexpressed, purified and crystallised. The DDG aldolase crystals belong to the space group R32 with unit cell dimensions a = b = 125 , c = 175 Å, γ = 120°. Here we present the three-dimensional structure of DDG aldolase and some insights into its mechanism of reaction.

P06.04.078 STRUCTURE OF RABBIT HAEMOPEXIN AT 2.1Å. B.F.Anderson, Institute of Molecular Biosciences, Massey University, Palmerston North, New Zealand. H.M.Baker and E.N.Baker, Laboratory for Structural Biology, University of Auckland, Auckland, New Zealand. M.Paoli, Department of Biochemistry, University of Cambridge, Cambridge, England.

Haemopexin is a mamalian, serum glycoprotein that sequesters free haem with high affinity from the bloodstream and only releases it upon interaction with a specific receptor on the surface of liver cells where it is internalised(1,2). The molecule is thus a haem scavenger and so acts to protect the organism from free-haem oxidative damage as well as conserving and recycling this important prosthetic molecule. The deglycosylated protein has been solved at lower resolution and shown to contain two 4 bladed propellor domains(3). Native, fully glycosylated, rabbit haemopexin complexed with haem crystallises in spacegroup P4, a=b=139.39, c=51.13Å.The crystals diffract to 2.1Å and contain two molecules in the asymmetric unit. The structure was solved by molecular replacement using as a search model the N an C domains taken from the lower resolution deglycosylated structure solved previously(3). AmoRe gave no useable results in spacegroup P4 but four of the expected 8 domains were located in a low resolution data set processed as monoclinic. The remaining domains were positioned by modelling. L.S refinement gives current working and free Rfactors of 0.31 and 0.35 respectively for all P4, 30.0-2.1Å data. Each molecule comprises two structurally homologous, 4 bladed propellor domains with the haem bound, through histidine residues, between them. An unusual feature is that the haem is bound with the propionates partially buried while the opposing methyl and alkyl groups point toward the solvent.

1. Mueller_Eberhard, U., Methods in Enzymology 163, 536-565 (1988).
2. Wu, M.I., and Morgan, W.T., Proteins 20, 185-190 (1994).
3. Paoli, M., Personal communication.

P06.04.079 CRYSTALLOGRAPHIC STUDIES OF THE NADP-DEPENDENT β-KETO ACP REDUCTASE FROM *ESCHERICHIA COLI*. Martin Fisher,[1] Wayne Martindale,[2] Antoni R. Slabas,[2] David W. Rice[1] and John B. Rafferty[1]. [1]Krebs Institute for Biomolecular Research, Department of Molecular Biology and Biotechnology, The University of Sheffield, Sheffield, S10 2TN, UK, and [2]Lipid Molecular Biology Group, Department of Biological Sciences, The University of Durham, Durham, DH1 3LE, UK.

Fatty acid biosynthesis is a critical metabolic function which provides both cellular building materials and energy storage reserves. It is catalysed by a complex enzyme pathway, the fatty acid synthetase system (FAS). This can be classified into two types based upon whether the enzymes which catalyse the individual steps in the pathway reside as catalytic sub-domains on one or two multifunctional polypeptides (Type I) or are located on separate polypeptide chains (Type II). A Type II FAS is found in plants and many bacteria, including *E.coli*, where there are six successive steps in the elongation of the fatty acid chain. Each step involves carboxylation, transacylation, condensation, reduction, dehydration and a further reduction of the incoming substrate with the resultant incorporation of a two-carbon unit into the growing chain. The first reductive step is catalysed by an NAD(P)- dependent β-keto acyl carrier protein reductase (BKR)

which reduces the keto group of a β-keto acyl ACP substrate to its hydroxy product.

The *E.coli* BKR has been crystallized by the hanging-drop method of vapour diffusion using polyethylene glycol of average molecular weight 1450 Da. The crystal belongs to the hexagonal space group $P6_122$ with unit-cell dimensions of a=b=68 and c=359 Å. Crystal packing analysis confirms that the asymmetric unit contains a dimer, where each monomer has a molecular weight of 28kDa. Crystals were mounted in capillary tubes and a data set was collected by the rotation method with 2° rotations per frame at an X-ray wavelength of 0.872Å on station 9.6 at the Synchrotron Radiation Source (SRS), Daresbury Laboratory, using a large MAR image plate. The crystals have been shown to diffract to better than 2.5Å resolution. Molecular replacement studies, coupled with isomorphous replacement data from a cysteine mutant and a selenomethionine incorporated protein, have given us an interpretable 2.5 Å map showing the orientation of the protein within the unit cell and by using the least-squares molecular refinement program, TNT, a model of BKR has successfully been built and refined. The structure is reminiscent of a typical Rossmann fold and as predicted resembles that of enoyl ACP reductase, the enzyme which catalyses the other reductive step in the FAS cycle.

We have recently obtained a crystal which contains the NADPH cofactor within the nucleotide-binding site of BKR and data have been collected to 2.5Å resolution on station 9.6 at the SRS. Refinement of the data is currently in progress.

P06.04.080 SEQUENCE DEPENDENCE OF CONFORMATION AND SUPERMOLECULAR STRUCTURE IN COLLAGEN-LIKE PEPTIDES. Rachel Z. Kramer[1], Jordi Bella[1,2], Luigi Vitagliano[3], Manju Venugopal[4], Patricia Mayville[1], Barbara Brodsky[4] and Helen M. Berman[1]. [1]Department of Chemistry, Rutgers University, Piscataway NJ 08855, [2]Present address: Department of Biological Sciences, Purdue University, West Lafayette IN 47907, [3]Centro di Studio di Biocristallografia, CNR and Dipartimento di Chimica, Universita' di Napoli, 80134 Napoli Italy, [4]Department of Biochemistry, University of Medicine and Dentistry of New Jersey, Piscataway NJ 08855.

We have determined the structures of three homotrimeric collagen-like peptides. These studies demonstrate a strong synergy among sequence, hydration, and supermolecular structure and provide the first visualization of how the sequence of collagen defines local variations in triple-helical conformation. The crystal structure of $(PPG)_{10}$ [1] demonstrates that the involvement of hydroxyproline in an extended hydration network is critical for the lateral assembly and supermolecular structure of collagen. The structure of $(POG)_4EKG(POG)_5$ [2] displays an axial staggering among molecules, reminiscent of that observed in D-periodic collagen fibrils and demonstrates the sequence dependence of axial packing. $(POG)_3ITGARGLAGPOG(POG)_3$ was designed to model the region of human type III collagen C-terminal to the collagenase cleavage site. The structure of this peptide [3] displays variable triple-helical symmetry along the molecule, demonstrating the sequence dependence of molecular conformation.

Research supported by NIH grants GM21589, AR19626 and a Molecular Biophysics Training Grant.

[1] Kramer, et al. (1998) J. Mol. Biol. 280, 623-638.
[2] O is used as the standard one-letter code for hydroxyproline.
[3] Kramer, et al. (in press) Nature Structural Biology.

P06.04.081 A TRIMER-OF-HAIRPINS AS A DOMINANT MOTIF IN VIRAL MEMBRANE-FUSION PROTEINS. V.N. Malashkevich and P.S. Kim, Whitehead Institute, Howard Hughes Medical Institute, Department of Biology, MIT, Nine Cambridge Center, Cambridge, MA 02142, USA

High-resolution crystal structures of cores of the transmembrane subunits (TM) from the envelope glycoproteins of human and simian immunodefficiency viruses (HIV-1 and SIV), Visna and Ebola viruses, reveal a trimer of α–helical hairpins as a common motif. Each polypeptide chain in the trimer folds into a helical-hairpin conformation, in which two antiparallel helices are connected by a loop region. The N-terminal helices from each monomer form a central, three-stranded coiled coil that is positioned to support the hydrophobic "fusion-peptide" region of the protein. C-terminal helices pack in an antiparallel manner into hydrophobic grooves on the surface of this coiled-coil core. The abundance and structural conservation of this trimer-of-hairpins motif within the families of retroviruses, filoviruses, paramyxoviruses, and orthomyxoviruses, lacking any sequence homology within their envelope glycoprotein domains, suggests that this motif is critical for the fusion between viral and host cell membranes. This structural motif presumably corresponds to the fusion-active state, distinct from the native (non-fusogenic) state. In each case the N-terminal region of the protein, which contains the fusion peptide, is brought close to the C-terminal region, which connects to the transmembrane helix of the protein. Thus, given that the fusion peptide inserts into the cell membrane and the transmembrane helix is anchored in the viral membrane, the likely role of the hairpin structure is to facilitate the apposition of the viral and cellular membranes. These structures may assist in the discovery of a new class of agents that prevent viral infection. Indeed, synthetic peptides corresponding to the C-terminal helices of the trimer-of-hairpin structures in HIV-1 or in paramyxoviruses are inhibitors of entry by those viruses.

P06.04.082 THE REFINED CRYSTAL STRUCTURE OF THE AUGMENTER OF LIVER REGENERATION. John P. Rose[1], Chia-Kuei Wu[1,2], Tamara A. Dailey[1], Harry A. Dailey[1], and Bi-Cheng Wang[1], Department of Biochemistry and Molecular Biology University of Georgia, Athens GA 30602, U.S.A. and [2]Department of Crystallography, University of Pittsburgh, Pittsburgh PA 15260 U.S.A

The extraordinary regenerative capacity of the mammalian liver known since mythological times has been the focus of study for more than a century. The structure of a cytosolic factor first described by MoJunkin and Breuhaus in 1931 now termed augmenter of liver regeneration (ALR) has been determined at 2.5 Å resolution. ALR is associated with increased hepatocyte replication in the liver of weanling rats and in the regenerating adult liver remnant after partial hepatectomy. This factor has recently been shown to significantly enhance the success rate of fetal pancreatic islet transplantation in rodents and may prove to be useful for other purposes.

Sequence analysis shows that ALR has a unique sequence but shares a 50% homology with the product of the dual-function gene ERV1 of *Saccharomyces cerevisiae*. The ALR sequence predicts an all-alpha structure with little beta sheet. An incomplete Zn-finger like binding motif is also suggested.

Biochemical studies show that ALR contains bound Zn and FAD. This is intriguing since the ALR sequence showed no recognizable dinucleotide-binding motif. Thus, ALR may exhibit a new mode of dinucleotide binding.

The crystal structure revealed that ALR is an all-alpha cone shaped four-helix bundle. The flavin ring of the bound FAD sits in the mouth of the cone while its adenosine tail lies in a grove between the N-terminal and C-terminal helices. Details of the structure and structure analysis will be presented.

Work supported by the Georgia Research Alliance and The University of Georgia.

P06.04.083 CRYSTALLOGRAPHIC STUDIES ON β-LACTOGLOBULIN L.Sawyer, S.-Y.Wu and G.Kontopidis, Structural Biochemistry Group, ICMB, The University of Edinburgh, Swann Building, Mayfield Road, Edinburgh EH9 3JR, UK and D.M.Pérez & P.Puyol, Food Technology, Veterinary Faculty, University of Zaragoza, 50013 Zaragoza, Spain.

The milk whey protein β-lactoglobulin (BLG) from ruminants is a dimer of M_r 36,000 with two polypeptide chains of 162 residues. There are 2 cystines and a cysteine. Genetic variants exist and the protein, which is an archetypal lipocalin, is present in many, but not all, mammalian species.

The behaviour of BLG has been shown to be important to the processing properties of milk and in particular the pH and temperature dependence of the aggregation that occurs above 60°C appears to involve a disulphide interchange mechanism. The effects of heat treatment are modified by the presence of ligands both attached to the free –SH group and also bound to an internal cavity. The structures of 3 crystal forms of the free protein and the protein with bound ligands have been determined both in Edinburgh and elsewhere. These structural results together with the latest ligand-binding data will be discussed in the light of the large amount of solution data that have accumulated over the past 60 years.

We are grateful to an EU Concerted Action (MADGELAS) and the BBSRC for financial support.

P06.04.084 PECTIN METHYLESTERASE IS A PARALLEL β-HELIX PROTEIN WITH TWO CATALYTIC ASPARTATES. John Jenkins[1], Drummond Smith[1], Kathryn Worboys[1], Olga Mayans[2] and Richard Pickersgill[1], [1]Institute of Food Research, Whiteknights Road, Reading RG6 6BZ, UK, [2] EMBL, Notkestrasse 85, D-22603, Hamburg, Germany

Pectin methylesterase is one of the four types of enzyme involved in degrading the homogalacturanon backbone of pectin together with pectate lyase, pectin lyase and polygalacturonase and has an important role in plant growth, fruit ripening and in microbial pathogenesis. The sequences of pectin methylesterases are not obviously homologous to any protein with a known 3-dimensional structure.

Pectin methylesterase from *Erwinia chrysanthemi* has been expressed, purified and crystallized from 2 M ammonium sulfate at pH 6.8 with two 342 amino acid molecules in the asymmetric unit of the $P2_1$ unit cell. Addition of 25% glycerol allows data to be collected at 100 K. Three heavy atom datasets were used for phasing with an overall figure of merit of 0.48. The phases were improved and extended to 2.4Å resolution using the program DM.

The averaged map revealed a right handed parallel β-helix architecture which suggested distant homology with the pectic lyases and polygalacturonase and allows the nomenclature of PB1, T1, PB2, T2, PB3 and T3 to be used. The active site (by homology and sequence conservation) lies on PB1 in a cleft formed by N-terminal T3 and C-terminal T1 loops. Two aspartates, D178 and D199, are on neighbouring coils of the parallel β-helix. They are surrounded by many aromatic residues suggesting an analogy to the active site of pectin lyase although none are conserved. The two aspartates suggest a similar mechanism to that of the aspartyl proteases. Thus pectin methylesterase shows striking examples of both convergent and divergent evolution. The current model has a free R value of 24.78% and a working R value of 20.19% with 402 water molecules.

P06.04.085 STRUCTURAL ANALYSIS OF ALLERGENS: CRYSTAL STRUCTURE OF HEV B 6.02 (HEVEIN) AT 1.5 Å RESOLUTION. A. Rodríguez-Romero, P. Llinas, A. Hernandez-Santoyo, Instituto de Química, Universidad Nacional Autónoma de México, Circuito Exterior, Ciudad Universitaria, Coyoacán 04510. Mexico, D:F.

Hypersensitivity reactions to natural rubber latex (NRL) proteins have been increasingly recognized during the past two decades. It is well documented that a high percentage of health care workers and patients who have undergone multiple operations are allergic to NRL and manufactured NRL products such as gloves, catheters, condoms, etc. Different studies have revealed various antigenic proteins with Mr from 5 to 200 KDa in latex preparations, and some of them have already been identified. Prohevein (Hev B 6.01) and hevein (Hev b 6.02) have been shown to be major IgE-binding allergens and in the former the principal epitopes have been located in its N-terminal hevein domain. Recently, substantial progress has been made in the purification and molecular characterization of several NRL allergens that has facilitated the assessment of their significance and given grounds for proper comparison of results obtained by different researchers. However, information on the tertiary structure of allergens is limited; just a few structures of airborne allergens and one contact allergen have been reported1. The knowledge of the structure of these proteins will make it simpler to identify and change surface epitopes, thus improving immunotherapy.

We report here the structure of Hev B 6.02 (hevein) at 1.5 Å resolution. The protein was crystallized from MPD in space group $P2_12_12$ with cell parameters a=31.81 Å, b=58.93 Å and c= 22.51 Å. Complete data set was collected at SSRL beamline 7-1 with an overall R-merge of 5.0 %. The structure was solved using molecular replacement with AmoRe (Navaza, 1994) and refined using CNS (Brunger, 1998). Details of the structure and a comparison with other allergens will be presented. Finally, we have found that hevein binds to neutrophiles.

This work was supported by DGAPA, UNAM grant IN-201997.

[1] Rodriguez-Romero, A., et al., (1991) FEBS Lett. 291, 307-309.

P06.04.086 X-RAY STRUCTURE ANALYSES OF MUTANT REACTION CENTRES AFFECTING PROTON TRANSFER AND QUINONE BINDING. A. Kuglstatter, G. Fritzsch, H. Michel [1], L. Baciou [2], [1] MPI fuer Biophysik, Abt. Molekulare Membranbiologie, 60528 Frankfurt/M, Germany, [2] Centre de Genetique Moleculaire, CNRS, 91198 Gif-sur-Yvette, France

The structures of three mutant reaction centres from the photosynthetic purple bacterium Rb. sphaeroides have been determined by X-ray crystallography to 2.6-2.8 Å resolution. The mutants have been constructed to interrupt a chain of tightly bound water molecules that is assumed to be involved in proton transfer from the cytoplasm to the secondary quinone (QB) [1,2]. The mutations Pro L209 -> Tyr and Pro L209 -> Phe do not disturb the chain. Instead, these residues take up a conformation in which three surrounding side chains are displaced. The position of QB is shifted compared to the wild-type protein. In the Pro L209 -> Glu mutant the introduced residue is located within the water chain and the binding site of QB is unchanged.

1. L. Baciou & H. Michel (1995), Biochemistry 34, 7967-7972
2. J. Tandori et al. (1999) in Photosynthesis: Mechanisms and Effects (G. Garab, ed.), Kluwer Academic Publishers, Dordrecht (in press)

P06.04.087 NEUTRON PROTEIN CRYSTALLOGRAPHY REVEALS HYDROGEN BONDING AND BOUND WATER STRUCTURE Y. Minezaki, N. Niimura, Advanced Science Research Center, Japan Atomic Energy Research Institute, Tokai-mura, Ibaraki, 319-1195, JAPAN

X-ray protein crystallography is a powerful tool for structural biology and it has helped to shed light on many important processes in life. But many fundamental principles are still poorly understood because of the lack of structural information on hydrogen, which constitutes half of the atoms in protein molecules. In principle, it is very difficult to get information of hydrogen positions by X-rays. In contrast, neutron protein crystallography has a great potential for investigating the complete structure of a protein, including the positions of the hydrogen atoms. However, only a few experiments have been reported to date since it takes an enormous amount of experimetal time to collect data, eg. about several months. Recently we have shown that the whole data set of hen egg-white lysozyme could be collected in only 10 experimental days by using neutron imaging plates coupled with the neutron quasi-Laue method. All of the 960 hydrogen atoms in the lysozyme molecule and in 157 bound water molecules could be identified. We have proceeded further with this analysis and have focused on the hydrogen bonding patterns and the water structure in more detail.

We have investigated the nature of intramolecular backbone hydrogen bonds of "N-H…O" type, which play an important role in the stabilization of the secondary structure of proteins. The distance distribution of H bonds can be divided into two categories, one of which is assigned to the alpha-helix and beta-strand regions, and another of which is assigned to loop region.

We have found that other types of hydrogen bonds exist besides the normal single (X-H…Y) hydrogen bond. They are the bifurcated (double) and trifurcated (triple) hydrogen bonds. Since many acceptors and donors exist close each other in a globular protein, the possibility of forming bifurcated and trifurcated hydrogen bonds is higher than usual. Our statistical analysis supports this conclusion. Even in the alpha-helix and beta-sheet regions, many bifurcated hydrogen bonds were found. We have categorized these types of bonds into several groups.

Another unusual hydrogen bond we have found is the aromatic hydrogen bond, which involves an interaction between the pi-electron cloud of an aromatic ring and a hydrogen-bond donor. One water molecule was found associated with the indole pi-ring of Try62, while another one was found near that of Try123.

The authors are grateful to prof. R. Bau for critical discussion.

P06.04.088 SYNCHROTRON SAXS STUDY OF THE STRUCTURAL CHANGES CAUSED BY SOLVENTS IN POLY-URETHANE MEMBRANES. H.Grigoriew[1], A.Wolińska-Grabczyk[2], A.G.Chmielewski[1], J.Domagała[3] [1]Institute of Nuclear Chemistry and Technology, Dorodna 16. 03195 Warsaw, Pl, [2]Institute of Coal Chemistry PAS, Sowińskiego 5, 44102 Gliwice, Pl, [3]Institute of Physics PAS Al.Lotników 32/46, 02668 Warsaw, Pl

When poly-urethanes composed of hard and soft segments of various length were swelled by solvents, we found: i. for shorter soft segments - ordering of hard domains which size depends on the hard segment length, ii. for longer soft segments - no ordering but only more dispersed structure.

Segmented polyurethanes are regarded as multiblock copolymers of $(AB)_n$ type in which A and B are the hard- and the soft-segment repeat units. The polyurethanes studied are composed of poly(tetramethylene oxide)-based soft segments and hard segments composed of 2,4-tolylene diisocyanate (TDI) chain extended with 4,4-diphenylmetane diamine (PP). The structural variations of composition within the series studied come from the different molar masses of the soft-segments (2000 or 1000) and/or different length of the hard-segments (TDI PP or 3(TDI PP) sequences).

SAXS experiment was performed on A2 beamline at HASYLAB-DESY using time-resolved mode, with raising temperature from room to 70^{o}C and then cooling. The dry membranes and membranes saturated with benzene and with ethanol were measured. The following changes were obtained on SAXS curves for subsequent materials: i. TDI PP/1000 -an intense, broad maximum of 17nm, which decreases with raising of temperature, ii. 3(TDI PP)/1000 -position of the maximum is 22nm, iii. TDI PP/2000 -no maximum, R_g decreases from 15nm for dry to 9nm for swelled membrane.

The effects are similar for both solvents but more intense for benzene.

1. H.Grigoriew, A.G.Chmielewski, J.Membr.Sci., 142 (1998), 87-95.
2. J.Muszyński, A.Wolińska-Grabczyk, P.Penczak, J. Appl. Polym. Sci., 1999, in press.

P06.04.089 DO WATER-PROTEIN HYDROGEN BONDS COMPENSATE FOR INTERACTIONS IN THE STREPTAVIDIN-BIOTIN COMPLEX? R.E. Stenkamp [1,2], S. Freitag [2,3], I. Le Trong [1,2], L.A. Klumb [3], V.Chu [3], D. Hyre [3], J.E. Penzotti [3], R. To [3], T.P. Lybrand [3] and P.S.Stayton [3]; [1] Dept. of Biological Structure, Univ. of Washington, Seattle, WA 98195, [2] Biomolecular Structure Center, Univ. of Washington, Seattle, WA 98195 [3] Dept. of Bioengineering, Univ. of Washington, Seattle, WA 98195

The hydrogen bonds between water and unliganded streptavidin differ significantly from those formed in the protein/biotin complex. Both the pattern and structure of the hydrogen bonds change when biotin binds to the protein. This might explain the large enthalpic contribution to the high free energy of binding. Comparison of several high resolution ligand-free crystal structures improves our model of the number and location of water molecules in the biotin binding site. Preliminary examination of the superposed structures show that water molecules do not simply replace the hydrogen-bond acceptor and donor atoms in the biotin complex. The polar ureido oxygen atom of biotin accepts three hydrogen-bonds in its interactions with streptavidin. A water molecule can accept two hydrogen- bonds and thus can not completely substitute for the ureido oxygen. Also, the covalent structure of biotin, particularly the ureido group, sterically restrains the locations of its hydrogen-bond donors and acceptors. Van der Waals contacts between individual water molecules preclude their occupation of the same positions as the ureido oxygen and nitrogen atoms. The superposed water molecules cluster near the positions of the ureido nitrogen atoms, but slightly displaced from them. This leads to a spatial difference in the hydrogen-bonds in the unliganded and liganded structures which can account for part of the binding free energy. A recent atomic resolution structure of one of the mutants shows that MPD from the crystallization solution binds loosely to the biotin binding site. The possible effect of this on our models for the unliganded structures will be discussed. This work is supported by NIH grant DK-49655.

P06.04.090 CRYSTAL STRUCTURE ANALYSIS OF CONGER EEL GALECTINS. T. Shirai, C. Mitsuyama, Y. Niwa, Y. Matsui, H. Hotta, T. Yamane, T. Ogawa and K. Muramoto, Department of Biotechnology and Biomaterial Chemistry, Graduate School of Engineering, Nagoya University, Nagoya 464-8603, Japan, and Department of Biological Resource Science, Graduate School of Agricultural Science, Tohoku University, Sendai 981-8555, Japan.

Congerins are members of galectin family, animal β-galactoside-binding S-type lectins, from conger eel (*Conger myriaster*). Congerin is a homodimer of 14 kDa subunit. Having one carbohydrate-binding site on one subunit, the dimer has two carbohydrate-binding sites that enable the dimer to cross link molecules or cells that have bl-galactoside-moieties. Congerins show the activity in aggregating murine bacteria implying a biological defense function of the protein. We have crystallized congerin I in ligand-free and lactose-liganded forms. The both crystals are isomorphic each other, and belong to orthorhombic space group $P2_12_12$. The asymmetric unit contains one monomer, two fold axis of the dimer overlaps to the crystallographic two fold axis. Full data sets to resolution of 1.5 A and 1.6 A for lactose-liganded and ligand-free form crystals, respectively, were collected using the synchrotrons X-ray source from Photon Factory, National Laboratory for High Energy Physics. The crystal structures were determined using molecular replacement method. Bovine galectin was used as a search model.

A comparison of the carbohydrate-binding sites in both forms shows that the structures around the sites are nearly identical. Exceptionally, a loop that conforms a part of the binding-site moves 0.5-0.9 A between the free and liganded forms. The lactose in the binding site forms eleven hydrogen-bonds directly with protein atoms. In the ligand-free form, nine of the eleven hydrogen-bonds are formed between water molecules and the protein atoms. The water molecules in the free-binding site occupy the space for oxygen atoms of lactose in liganded-form. This observation implies carbohydrate-binding of congerin is entropy-driven process.

P06.04.091 STRUCTURE DETERMINATION OF APOE3 IN THREE SPACEGROUPS BY MAD OR MOLECULAR REPLACEMENT TECHNIQUES. Michael Forstner [1], Brent Segelke [1], Bernhard Rupp [1] Yvonne Newhouse [2], Karl Weisgraber [2], [1] Biomolecular Crystallography Facility, Lawrence Livermore National Laboratory, Livermore, CA 94551, USA, [2] Gladstone Institute for Cardiovascular Disease, University of California San Francisco, San Francisco, CA 94141, USA

Apolipoprotein E (ApoE) plays a key role in cholesterol metabolism serving as a ligand for members of the low-density lipoprotein (LDL) receptor family. Genetic variants of ApoE are associated with both atherosclerosis and Alzheimer's disease, two of the most prominent causes of death in Western society. Our lab has pursued the structure determination of biologically relevant fragments of ApoE3 as well as complexes and the fragments of several isoforms or mutants, in order to probe the structural determinates of its biological and pharmacological function. Initial efforts to determine these structures by molecular replacement were surprisingly difficult suggesting either that there was considerable variability in the structure from crystal to crystal or that the initial model was not a suitable molecular replacement probe. To resolve these problems, the structure of the 22kD fragment of ApoE3 was determined anew, to high resolution, by multiple anomalous dispersion (MAD) techniques in each of two new crystal forms and by molecular replacement (MR) in yet a third crystal form. Given these three structures we are now able to examine the variability of the structure as well as the effects of crystal packing on local conformations within the molecule. This is a useful means of demonstrating the magnitude of errors or conformational variability, residue by residue, not otherwise demonstrable by x-ray crystallographic techniques. This is particularly useful in the study of ApoE as a considerable portion of the molecule is described by weak density in all crystal forms. We are also able to compare the benefit of several crystallographic techniques such as de novo MAD phasing versus MR, or "automated structure" determination with ARPP and their effect on the ultimate coordinate error or map quality.

P06.04.092 NON-PROLINE *CIS* PEPTIDE BONDS IN PROTEINS. R. Hilgenfeld, A. Jabs, and M.S. Weiss, Institute of Molecular Biotechnology, Department of Structural Biology & Crystallography, Beutenbergstr. 11, 07745 Jena, Germany.

In a non-redundant set of 571 proteins from the Brookhaven PDB, a total of 43 non-proline *cis* peptide bonds were identified. Average geometrical parameters of the well-defined *cis* peptide bonds in proteins determined at high resolution show that some parameters, most notably the bond angle at the amide bond nitrogen, deviate significantly from the corresponding one in the *trans* conformation. Since the same feature was observed in *cis* amide bonds in small molecule structures found in the Cambridge Structural Data Base, a new set of parameters for the refinement of protein structures containing non-Pro *cis* peptide bonds is proposed.

A striking preference was observed for main-chain dihedral angles of the residues involved in *cis* peptide bonds. All residues N-terminal and most residues C-terminal to a non-Pro *cis* peptide bond (except Gly) are located in the β-region of a φ/ψ plot. Also, all of the few C-terminal residues (except Gly) located in the α-region of the φ/ψ plot constitute the start of an α-helix in the respective structure.

In the majority of cases, an intimate side-chain/side-chain interaction was observed between then flanking residues, often involving aromatic side-chains. Interestingly, most of the cases found occur in functionally important regions such as close to the active site of proteins. It is intriguing that many of the proteins containing non-proline *cis* peptide bonds are carbohydrate-binding or processing proteins.

The occurrence of these unusual peptide bonds is significantly more frequent in structures determined at high resolution than in structures determined at medium and low resolution, suggesting that these bonds may be more abundant than previously thought. We developed an algorithm for the identification of possibly overlooked *cis* peptide bonds that exploits the deviations of geometrical parameters from ideality. A few likely candidates based on our algorithm have been identified and are discussed.

P06.04.094 THE STRUCTURE OF MISTLETOE LECTIN I. H.Niwa, R.A.Palmer. Department of Crystallography, Birkbeck College, Malet street, London, WC1E 7HX, UK.

The structure of mistletoe lectin I (MLI) at 3Å resolution is presented. Mistletoe lectins from *Viscum album* are type-II ribosome inactivating proteins (RIPs), comprising a toxic A-chain and a carbohydrate binding lectin B-chain, linked by a disulphide bond. Other members of this family include the plant toxins ricin and abrin whose structures are known, and modeccin. Mistletoe lectin is of interest as a component of mistletoe extract used in an alternative medicine for cancer treatment in northern Europe. Three isolectins MLI, MLII and MLIII occur in the mistletoe plant. Although they share a similar primary structure, they differ in carbohydrate affinity and cytotoxic effects on target cells. In addition, while MLII and MLIII are monomers, MLI, the most abundant of the three, forms non-covalent bound dimers.

The structure of MLI was solved using hexagonal crystals [1] by molecular replacement using ricin as a search model and the possible dimer structure was proposed [2]. The structure has been refined to 3Å. Although MLI has structural homology with ricin and abrin, there are significant differences in some loop regions. The lectin-parts of RIPs form β-trefoil folding. MLI exists as an $[AB]_2$ dimer with internal crystallographic two-fold symmetry. Domain 1 of the B-chains are non-covalently associated by the interaction of a hairpin triplet from each molecule, forming a double trefoil structure. The disulphide bond of domain 1 of MLB at Cys20-Cys39 of the B-chain (α) is not conserved, an evolutionary mutation with respect to ricin having replaced Cys39 with serine. This mutation appears to allow the (α)

hairpin the flexibility required to take up its place at the dimer interface, and also suggests a rationale for why ricin does not form dimers.

1. Sweeney, E. C., Palmer, R. A. and Pfueller, U. (1993). J. Mol. Biol., **234**, 1279-1281
2. Sweeney, E. C., Tonevitsky, A. G., Palmer, R. A., Niwa, H, Pfueller, U., Eck, J., Lentzen, H., Agapov, I. I. and Kirpichnikov, M. P. (1998) FEBS Letters, **431**, 367-370

P06.04.095 CRYSTAL STRUCTURE OF THE CELLULAR HYDROGEN PEROXIDE REGULATORS. H.-J. Choi, D.-H. Shin [1], S. W. Kang, S. G. Rhee [2], S.-E. Ryu [1], [1] Center for Cellular Switch Prottein Structure, Korea Research Institute of Bioscience and Biotechnology, Taejon 305-600, South Korea, [2] Lab of Cell Signaling, NHLBI, NIH, Maryland 20892, USA

Hydrogen peroxide (H_2O_2) has been recognized recently as an intracellular messenger that is involved in the growth factor signaling, transcription regulation and apoptosis. A family of novel peroxidases, named peroxiredoxins (Prx), regulate the intracellular concentration of H_2O_2 by reducing it in the presence of an appropriate electron donor. They regulate the activity of NF-¥êB, enhance natural killer cytotoxicity and protect cells from apoptosis. To understand the structural mechanism of the Prx enzymes, we determined the crystal structure of hORF6, a human 1-Cys Prx. The crystal structure of hORF6, which is the first to be determined among members of the Prx family, reveals a dimer of a protein containing two discrete domains where the N-terminal domain has a thioredoxin fold and the C-terminal domain is used in an arm exchange for dimerization. The active site cysteine (Cys 47), which exists as cysteine-sulfenic acid in the crystal, is located at the bottom of a relatively narrow pocket. The positively charged environment surrounding Cys 47 accounts for the peroxidase activity of the enzyme, which contains no redox cofactors. Since Cys-SOH in the ROS target proteins must be stable for a certain period of time to exert its signaling effect, the Cys-SOH stabilizing environment of the hORF6 active site pocket can be a model for the redox center of the ROS target proteins.

P06.04.096 CRYSTAL STRUCTURE OF HUMAN NUCLEOSIDE DIPHOSPHATE KINASE A. Kyeongsik Min, Sun Young Kim*, Kong-Joo Lee*, and Se Won Suh, Department of Chemistry, College of Natural Sciences, Seoul National University, Seoul 151-742, Korea, *College of Pharmacy, Ewha Womans University, Seoul 120-750, Korea.

Nucleoside diphosphate (NDP) kinases provide precursors for DNA and RNA synthesis and are involved in a variety of cellular functions. In human, several NDP kinases play important roles in proliferation, tumour metastasis, and transcriptional regulation. Human NDP kinase A, product of the *nm23-H1* gene, is a metastasis suppressor, while human NDP kinase B, product of the *nm23-H2*, is a transcription factor of the *c-myc* oncogene in addition to their enzymatic activity. NDP kinase A is a hexameric enzyme consisting of identical 17.1 kDa subunits. Although the two proteins are closely related in sequence (88% identity), they serve different cellular functions.

Crystal structure of human NDP kinase A has been solved by molecular replacement using human NDP kinase B (1) as a starting model. The model has been refined to a crystallographic R-factor of 20.7 % using 6.0–2.2 Å data. The root mean square deviations from ideal stereochemistry are 0.009 Å for bond lengths and 0.99° for bond angles.

Human NDP kinase A hexamer has D3 symmetry and can be viewed as a dimer of trimers. The six subunits are nearly identical in their structures and they fold into a compact α/β domain of 132 residues followed by a 17 residue extension at the C-terminus. The tertiary and quaternary structures are highly similar to those of other NDP kinases whose structures have been reported (2,3). A comparison of the two human NDP kinase structures provides insight into their functional differences.

1. Morera, S. *et al.* (1995) Structure 3, 1307-1314.
2. Dumas, C. *et al.* (1992) EMBO J. 11, 3203-3208.
3. Chiadmi, M. *et al.* (1993) Structure 1, 283-293.

P07.04.001 STRUCTURE OF PHOSPHOLIPASE A_2 FROM *DABOIA RUSSELLI PULCHELLA* AT 2.5Å RESOLUTION. Vikas Chandra, Punit Kaur and T.P.Singh, Department of Biophysics, All India Institute of Medical Sciences, New Delhi 110 029, India.

Phospholipase A_2 enzymes hydrolyze phospholipids at the sn-2 position of the glycerol backbone. The Russell's viper was classified into two classes. The class 1 contains *Viper russelli russelli, Viper russelli siamensis* and *Viper russelli formosensis* whereas class 2 has *Daboia russelli pulchella*. The sequence identity between the PLA_2's from these two classes is 47%. One of the typical differences between the sequences of the two classes is that the sequence of the class 1 contains Asn at the N-terminus, while class 2 has Ser. The novel PLA_2 from *Daboia russelli pulchella* has been crystallized in the space group $C222_1$ with unit cell dimensions a=77.01, b=92.29, c=76.90Å and contains two molecules in the asymmetric unit. The intensity data were collected to 2.5Å resolution with a completeness of 99%. The structure was solved by molecular replacement using the structure of PLA_2 from *Crotalus atrox* as a model. It has been refined to an R-factor of 0.21. The structure has revealed an entirely new form of interactions between the two molecules of the homodimer, an interesting intermix of hydrogen bonds and hydrophobic interactions. These are significantly different than those found in other homodimers and even in heterodimers involving phospholipase A_2 .

P07.04.002 STRUCTURAL CHARACTERIZATION OF THREE ARCHAEL ADENYLATE KINASES OF VARYING THERMOSTABILITY. A. R. Turner, T. Fulmer, J. Konisky, G. N. Phillips, Jr., Department of Biochemistry and Cell Biology, Rice University, Houston, TX.

We are studying the structural differences between three highly related adenylate kinases (ADKs) from three members of the *Methanococcus* genus of the Archae: the mesophile *M. voltae*, the thermophile *M. thermolithotrophicus*, and the hyperthermophile *M. jannaschii*. We have performed analytical ultracentrifugation experiments with *M. thermolithotrophicus* ADK and observed a predicted molecular weight of 100 kDa, suggesting a hexamer. Consistent with these results, dynamic light scattering (DLS) experiments predict the molecular weight to be 110 kDa. DLS data for the remaining ADKs predict similar molecular weights. Additionally, we have identified conditions under which each of these enzymes crystallize. *M. voltae* native data was collected for cubic crystals (0.2 x 0.5 mm) to 2.5 Å at BIOCARS beamline at the Advanced Photon Source. This data indexed to space group I23 with unit cell dimensions a=b=c=200.5 Å. Molecular replacement methods are currently underway using the recently solved 2.6 Å structure of the trimeric archael adenylate kinase from *Sulfolobus acidocaldarius* [1].

Supported by U.S. Department of Energy, Office of Biological & Environmental Research (J.K.), the Robert A. Welch Foundation (G.N.P.), W. M. Keck Center for Computational Biology, and National Institutes of Health Training Grant (A.R.T.).

1. C. Vonrhein, H. Bonisch, G. Schafer and G. E. Schulz (1998). JMB, **282**, 167-79.

P07.04.003 STRUCTURAL STUDIES ON ACROSIN, A SERINE PROTEASE FOUND IN MAMMALIAN SPERMATOZOA. Rebecca Tranter[1], Roy Jones[2] and Leo Brady[1]. [1]University of Bristol, U.K. and [2]Babraham Institute, Cambridge, U.K.

Acrosin is a trypsin-like serine protease found in all mammalian spermatozoa where it plays a major role in fertilization. The protein is formed by autoactivation events at both the N and C termini of its inactive zymogen precursor, proacrosin, to yield the active heterodimer. Acrosin is thought to have two major roles in fertilization, firstly in forming specific binding interactions with receptor molecules on the surface of the ovum and secondly, in using its proteolytic activity to help sperm penetrate the extracellular matrix of the ovum. It has previously been shown that inhibition of proacrosin prevents fertilization from occurring, and this leads to interest in the protein as a target for novel contraceptive drugs. Suramin is a compound which competes with molecules on the ovum surface for binding to proacrosin and inhibits fertilization. The drug is highly toxic to humans, but has potential as a lead compound for the design of low toxicity contraceptive agents. We aim to crystallize acrosin and determine its structure by X-ray crystallography followed by structures of the protein complexed to suramin. It is envisaged that this information will aid the design of mimetics of suramin which have a lower toxicity while retaining the inhibitory effects of the drug.

P07.04.004 CRYSTALLOGRAPHIC STUDIES OF A BROAD SPECIFICITY DEHYDROGENASE. B.Dhaliwal, M.Banfield, R.L.Brady and J.J Holbrook. Department of Biochemistry, University of Bristol, Bristol BS8 1TD U.K.

2-hydroxyacid dehydrogenases are the group of enzymes that catalyse the reversible reduction of NAD^+ by 2-hydroxyacids to yield NADH and 2- keto acids in a stereospecific manner. D-hydroxyisocaproate dehydrogenase (D-HicDH) is a member of the D-2- hydroxyacid dehydrogenase family. It was discovered when a genomic library from *Lactobacillus delbrueckii* subsp. *bulgaricus* was used to complement an *E.coli* strain lacking lactate dehydrogenase and pyruvate formate lyase grown in anaerobic conditions. It is a broad specificity D-hydroxyacid dehydrogenase of commercial importance. In order to assign functions to specific amino acid residues mutants had been constructed ; most of these had reduced catalytic efficiency when compared to the wild type enzyme. Surprisingly however, a H205Q mutant was shown to have increased k_{cat} , K_M and K_i values. These properties make H205Q D-HicDH a potentially effective catalyst for use in the pharmaceutical industry where chirally pure 2-hydroxyacid derivatives are needed in the production of antihypertensives. The structure - function relationships of the wild type and H205Q mutant D-HicDH are being investigated using x-ray crystallography.

P07.04.005 CRYSTAL STRUCTURE OF Thi1, A PROTEIN INVOLVED IN DNA REPAIR AND THIAMINE BIOSYNTHESIS. P.H.C. Godoi and G. Oliva, Instituto de Química e Instituto Física de São Carlos, Universidade de São Paulo, 13560-970, CP369, São Carlos-SP, Brazil; D.D. Luche and C.F.M. Menck, Instituto de Ciências Biomédicas, Universidade de São Paulo, 05508-900, São Paulo, Brazil.

It is widely known that many diseases such as cancer, abnormal ageing processes and other genetically inherited diseases are related to DNA damage in the cell. In this project we intend to solve the structure of a recently identified protein, possibly related to DNA repair in *A. thaliana* [1].

The thi1 deleted gene, lacking the bases coding for a transit peptide into chloroplasts, was subcloned into a pET-28 plasmid vector after a 6xHis tag. This procedure allowed large-scale expression and purification of the recombinant protein on an immobilized metal chelate affinity column.

Plate crystals were obtained in two different conditions at 277K, in 800mM $(NH_4)_2SO_4$, 100mM Bicine pH8.8, and in 20% PEG6k, 100mM Bicine pH9.0. The best crystals grew after 14 days in ammonium sulfate, with maximum size of 1.5 x 1.5 x 0.05mm however attempts made in order to improve its crystal size and habit did not lead to any significant change.

Diffraction experiments intended to characterise these crystals were performed at the Brazilian Synchrotron Laboratory (LNLS) but because of its size and specially its habit, such crystals could not be mounted into capillary tubes and systematically cracked during the process. Collecting data by cryocrystallography seemed to be the best alternative but at that time the beam line has not provided cryo-cooling facilities.

In spite of it, small glass spatulas [2] have recently been used at cryogenic temperatures, since crystals hardly could be transferred to cryoloops. New trials are still in progress.

Machado, C.R. *et al.* (1996) Thi1, a thiamine biosynthetic gene in *Arabidopsis thaliana*, complements bacterial defects in DNA repair. Plant Mol. Biol. 31, 585-593
Håkon Hope, personal communication.

P07.04.006 CRYSTAL STRUCTURE OF THE COMPLEX OF CONCANAVA-LIN A AND TRIPEPTIDE YPY. Zhen Zhang, Minxie Qian, Qichen Huang and Youqi Tang, Department of Chemistry, Peking University, Beijing 100871, P. R. China; and Keyi Wang, Dafu Cui and Moyi Li, Shanghai Institute of Biochemistry, Academia Scinica, Shanghai 200031, P. R. China

Concanavalin A(ConA) is the best known plant lectin, with a specific saccharide-binding site, which has been determined by crystallographic method, and a hydrophobic binding site, which is known by indirect proof but keeps mystery in crystallography. The crystals of the complex of ConA with tripeptide YPY was acquired by soaking the crystals of ConA with two kinds of the solution of YPY, separately. The data with 2.4Å resolution was collected and the structure of the complex was refined by X-PLOR and TURBO-FRODO program to crystallographic R-factor value of 0.175 and 0.186 and free-R-factor value of 0.237 and 0.266. The space group was I222 and the asymmetric unit contains one molecule. The tripeptide binds at a site which is different from the saccharide-binding site. This site lies in the surface of ConA and was surrounded by three symmetry related molecules. It departs from Mn and Ca with the distance ca.15Å. YPY forms four or five H-bonds with ConA, depending on the solution condition, and a intramolecular H-bond. In addition, There are many hydrophobic residues near this site and the hydrophobic side chain of YPY can interact with them, which benefit the stable of YPY greatly. The site for YPY departs from saccharide site with a distance 13Å. These two binding sites neighbored each other through the residue 14N(H-Bond with saccharide) and 15T(H-bond with YPY). This relation between them may be used to explain why the binding of ConA with phage bearing hexapeptide including YPY motif can be inhibited by MeαMan[1].

1. Jamie K. Scott, Duraikkannu Loganathan, R.Blaine Easley, Xiaofen Gong, and Irwin J. Goldstein. Proc. Natl. Acad. Sci. USA Vol.89, pp, 5398-5402, June 1992

P07.04.007 CRYSTALLOGRAPHIC STUDY OF DNA POLYMERASE FROM HYPERTHERMOPHILIC ARCHAEON *PYROCOCCUS KODAKARAENSIS*. H. Hashimoto†, S. Takeuchi†, T. Matsumoto†, T. Inoue†, Y. Kai†, T. Yuasa§, M. Nishioka§, S. Fujiwara§, M. Takagi§, T. Imanaka‡ Dept. of †Materials Chemistry and §Biotechnology, Osaka University, Suita, Osaka 565-0871, JAPAN ‡Dept. of Synthetic Bioligical Chemistry, Kyoto University, Yoshidahonmachi, Sakyo-ku, Kyoto 606-8501, JAPAN.

DNA polymerases are a group of enzymes that use single-stranded DNA as a template for the synthesis of the complementary DNA strand. These enzymes play an essential role in nucleic acid metabolism, including the process of DNA replication, repair and recombination. DNA polymerases can be classified into four major groups: family A, family B, family C and family X. In this study, we report crystallization and preliminary X-ray diffraction analysis of family B DNA polymerase from hyperthermophilic archaeon *Pyrococcus kodakaraensis* KOD1 (KOD DNA polymerase). KOD DNA polymerase is an enzyme that is of very considerable biological, technological, and economic importance. It is widely used in carrying out polymerase chain reaction (PCR) experiments.

KOD DNA polymerase was crystallized by the hanging-drop vapor diffusion method. All the X-ray diffraction measurements were carried out with $\lambda = 1.00$ Å synchrotron X-ray in KEK-PF, Japan. The diffraction pattern of the crystal extends to 3.0 Å resolution and a full set of diffraction data from native crystal was successfully collected at 290 K. The crystal belongs to the space group $P2_12_12_1$ and unit-cell dimensions were a =112.8, b = 115.4 and c = 75.4 Å. The presence of one molecule per asymmetric unit gives a crystal volume per protein mass (V_m) of 2.74 $Å^3Da^{-1}$ and a solvent content of 54.8% by volume. A heavy-atom derivative search is now in progress.

P07.04.008 ANALYSIS OF LIGAND BINDING TO OPPA PROTEIN BY TITRATION CALORIMETRY AND X-RAY CRYSTALLOGRAPHY. L.M.Wright, T.G.Davies, J.Woodford, J.R.Tame and R.E.Hubbard, Structural Biology Laboratory, Department of Chemistry, University of York, York, YO1 5DD, U.K.

We have examined ligand binding to the periplasmic oligopeptide binding protein OppA using isothermal calorimetry and X-ray crystallography. OppA is in several ways an ideal system for study by calorimetry since it is a highly soluble, non-aggregating protein which will bind to a variety of peptides with a fixed stoichiometry of 1:1. The affinity of peptide ligands for OppA falls within the experimental window of the technique, roughly 10^{-4}M to 10^{-8}M. The enthalpy and affinity of binding may therefore be measured and compared to the X-ray crystal structures of the protein-peptide complexes. These show that the binding pocket remains essentially constant regardless of the peptide sequence bound and all peptides are bound in the same way. From these results we hope to build a scoring function, breaking down the free energy contributions of individual groups to the overall observed free energy of binding. The structure of OppA complexed to 35 different peptides of the type Lys-X-Lys (where X is any amino acid, natural or not) show that internal water molecules play a significant role in ligand binding. The structure of the apo protein has also been determined by X-ray crystallography. Together these structures show a clear clustering of equivalent water molecules within the ligand binding site. Comparison of the structures of the different complexes and the thermodynamics of binding allow us to attempt to determine the key interactions driving binding. The use of non-natural amino acids allows us to vary the ligand very slightly and generate series of related peptides. These show that the enthalpy and entropy changes on binding vary considerably even for minor changes to the peptide and the complex. The protein exploits entropy-enthalpy compensation to accommodate a variety of chemical groups within the binding site.

P07.04.009 SRP PROTEIN TRANSLOCATION PATHWAY. T. Gariani[1],T. Samuelsson[2] & E. Sauer-Eriksson[1] ([1]UCMP, University of Umeå, [2]Department of Medical Biochemistry, Göteborg University).

Every cell must communicate with its surrounding. This is done by the help of secreted proteins. This translocation process can be achieved through two means: Signal Recognition Particle (SRP) dependent or SRP independent pathway. Translocation using the SRP dependent pathway is dependent on two control events, exerted at the SRP mediated targeting stage, and during the insertion/translocation step of the nascent protein into a proteinaceous channel on the membrane. Although most of the translocation process in bacteria is done in a SRP independent manner, the SRP subunits 4,5S RNA, Ffh and their receptor FtsY are essential for viability[(1, 2)] and their depletion results in defective protein secretion of proteins important for cell physiology (e.g FtsE/X) [(2)]. GTP is required for the functioning of FtsY[(3)]. The GTP was found to influence the protease sensitivity of FtsY indicative of a conformational change. This feature is likely to modulate the FtsY interaction with SRP. As a consequence, the SRP-mediated translocation of secretory proteins in E.Coli may be affected by the conformational state of FtsY. A mycoplasma homolog (47 kDa) to the α unit of the mammalian and E.Coli SRP receptor (FtsY) has been identified. This Mm-FtsY has a weak intrinsic GTPase activity (Kd = 3.5 μM) however a noticeable increase of this activity is recorded when the MmFtsY is combined with the N/G domain of MmFfh [(4)]. Expression and purification tests on various constructs of the MmFTSY have been conducted. Crystals of a truncated MmFTSY construct have been obtained. Data collection yielded a data set to 2.0 Å resolution and indexing showed a $P2_12_12$ space group. Expression, purification and diffraction of a Seleno-methionine derivative were as well performed in order to be able to determine the protein structure.

(1) Luirink *et al.*, EMBO J., 13, 2289-2296, (1994).
(2) Ulbrandt *et al.*, Cell, 88, 187-196, (1997).
(3) Kusters *et al.*, FEBS Letters, 372, 253-258, (1995).
(4) Macao *et al.*, *Mol Microbiol.* 24, 523, (1997).
(5) Montoya *et al.*, *Nature*, 385, 365-367, (1997).

P07.04.010 CRYSTALLOGRAPHIC STUDIES OF HUMAN SORBITOL DEHYDROGENASE. O. El-Kabbani, R. P.-T. Chung, L.G. Sparrow, T. Iwata and D.A. Carper, Department of Medicinal Chemistry, Monash University, Parkville, Vic 3052, Australia, CSIRO, Division of Molecular Science, Parkville, Vic 3052, Australia and National Eye Institute, NIH, Bethesda, MD 20892, U.S.A.

Sorbitol dehydrogenase catalyzes the conversion of sorbitol to fructose with NAD^+ as coenzyme. Sorbitol dehydrogenase (the second enzyme) and aldose reductase (the first enzyme) comprise the polyol pathway of glucose metabolism. This pathway is believed to be involved in the development of diabetic complications. Sorbitol dehydrogenase is homologous to the long chain alcohol dehydrogenases (around 350 residues). While the tertiary structure of sorbitol dehydrogenase is yet to be determined, a model for sheep sorbitol dehydrogenase was constructed using the high resolution structure of horse alcohol dehydrogenase[1]. With only 25% overall residue identity between the two enzymes, modeling studies indicate extensive structural differences between the predicted model and the tertiary structure of sorbitol dehydrogenase, particularly in the active site region[2]. Kinetic studies of sorbitol dehydrogenase indicate that

conformational changes occur at some stage in the course of the sorbitol dehydrogenase reaction[1]. Additionally, conformational changes are of great importance in the functioning of the structurally related alcohol dehydrogenase[1]. Hence, important structural details are expected from the crystal structure determination of sorbitol dehydrogenase holoenzyme, which will be used to elucidate its catalytic mechanism. Crystals of human sorbitol dehydrogenase holoenzyme were grown from buffered ammonium sulfate solution at pH 8.5 using the hanging drop vapor diffusion method. Progress in the structure determination of human sorbitol dehydrogenase/NAD^+ complex will be presented.

1. J. Jeffrey and H. Jornvall. Adv. Enzymol. Molec. Biol. 1988; 61:47.
2. C. Karlsson, H. Jornvall and J. O. Hoog. Adv. Exp. Med. Biol. 1995; 372:397.

P07.04.011 STRUCTURAL STUDIES ON THE A1 DOMAIN OF VON WILLEBRAND FACTOR AND A GAIN-OF-FUNCTION MUTANT. Kottayil I. Varughese, Reha Celikel And Zaverio Ruggeri. Department of Molecular and Experimental Medicine, The Scripps Research Institute, La Jolla, CA 92037.

Bleeding from damaged blood vessel is stopped by platelet adhesion and thrombus formation at the site of injury. Platelet adhesion starts when the subendothelial matrix is exposed to the blood stream and this process requires the binding of the platelet glycoprotein Ib-IX-V receptor complex to the A1 domain of von Willebrand Factor(vWF). As a part of our efforts to gain definitive information on the mechanism and regulation of this key process in hemostasis and thrombosis, we have solved the three dimensional structure of A1 domain in complex with a function blocking antibody two years ago. An intriguing pathophysiological property of the A1 domain results from the occurrence of 'gain-of-function' mutants, responsible for type IIB von Willebrand disease that enhance plasma vWF binding to GP Ibα interfering with platelet adhesion to immobilized vWF. The mechanism responsible for this effect is unknown. We have hypothesized that out of a total of 10 such mutations, three mutations alter the conformation of the A1 domain giving rise to this altered property. We have determined the crystal structure of one such mutant, I546V and interestingly there are significant conformational changes at the proposed GP-Ibα binding site. The structure of this mutant was also solved as a complex with the function blocking antibody NMC-4. The data were collected at the Stanford Synchrotron Radiation Laboratory at 90°K to a resolution of 2.0 Å.

P07.04.012 THE STRUCTURE OF A FATTY ACID CONDENSING ENZYME IN COMPLEX WITH DIFFERENT SUBSTRATES Johan Gotthardt Olsen[*], Anders Kadziola[*], Mads Siggaard-Andersen[f], Penny von Wettstein-Knowles[f], and Sine Larsen[*], [*]Centre for Crystallographic Studies, University of Copenhagen, Universitetsparken 5, 2100 Copenhagen Ø, Denmark [f]Institute of Molecular Biology, Department of Protein Chemistry, University of Copenhagen, Øster Farimagsgade 2A, 1353 Copenhagen K, Denmark

β-Ketoacyl-[Acyl Carrier Protein] I (KAS I) from *Escherichia coli* catalyses the two carbon unit elongation of fatty acids in a three step process: 1) Transfer of a fatty acyl residue from a fatty acyl-acyl carrier protein thioester (acyl-ACP) to an active site cysteine, 2) recognition of malonyl-ACP and decarboxylation of malonyl to give an acetyl-ACP carbanion, 3) carbanion attack on the carboxyl carbon of the enzyme bound fatty acid. The cysteine Sγ then acts as a leaving group and the product of the reaction is β-ketoacyl-ACP.

The crystal structure of KAS I has been determined to 2.3 Å resolution by molecular replacement using the crystal structure of KAS II [1] as a search model (38% amino acid sequence identity). Recently, diffraction data were collected from crystals of an active Cys163→Ser mutant which was demonstrated to bind the fatty acid substrate more tightly than the wild type. At the MAX Lab synchrotron in Sweden, we succeeded in getting diffraction data extending to between 2.0 and 1.85 Å resolution on several fatty acyl-enzyme thioesters. These data enable us to define a substrate binding pocket which reveals clues to substrate specificity characteritics which distinguish the KAS'es and also to suggest a model for the three step enzymatic Claisen condensation catalysed by condensing enzymes from the fatty acid biosynthetic pathways.

[1] Huang, W., Jia, J., Edwards, P., Dehesh, K., Schneider, G., and Lindqvist, Y. (1998) **EMBO J.** 17/5 (1183 - 1191)

P07.04.013 YERSINIA ADHESIN YADA. H. Nummelin, A. Goldman [1]. Y. El Tahir, P. Ollikka, M. Skurnik [2]. [1] Department of Biochemistry and Food Technology, University of Turku, FIN-20014 Turku, Finland and Turku Centre for Biotechnology, University of Turku and Åbo Akademi University, P.O. Box 123, FIN-20521 Turku, Finland, [2] Department of Medical Biochemistry, University of Turku, FIN-20014 Turku, Finland

YadA is trimeric fibrillar outer membrane protein encoded by the Yersinia virulence plasmid [1]. YadA is largely responsible for the adhesion of Y. enterocolitica and Y. pseudotuberculosis to the intestinal tissues in vitro, through binding to the collagen, laminin and fibrinonectin in the extra cellular matrix on the surface of the host cells [1]. The structure of the binding site for collagen in most collagen-binding proteins is still unknown, because only one crystal structure in known so far [2]. We have produced and purified YadA to crystallize it and to determine its crystal structure and binding site to collagen. For the production of YadA, 78 amino acid carboxy-terminal deletion mutant of yadA of Y. enterocolitica, which encodes for monomeric protein without a membrane anchor, was constructed, cloned into pQE30 and transformed into E. coli M15. The N-terminal His-tagged protein was collected from cytoplasm by sonication and centrifugation and purified from supernatant using metal chelating affinity column and imidazole gradient. After dialysis of imidazole the protein is concentrated in dialysis bag against polyethylene glycol to 16 mg/ml. 20 mM Na-phosphate buffer, pH 7.5, 300 mM NaCl and 5 % glycerol has been used for crystallization. Initial crystal screenings have yielded small crystals.

[1] S.C. Straley, E. Skrzypek, G.V. Plano & A.B. Bliska (1993). Infect. Immun., 61, 3105-3110.
[2] J. Symersky, J.M. Patti, M. Carson, K. House-Pompeo, M. Teale, D. Moore, L. Jin, A. Scneider, L.J. DeLucas, M. Höök & S.V.L. Narayana (1997). Natrure Struct. Biol. 4, 833-838.

P07.04.015 UNUSUAL STRUCTURAL FEATURES IN DOMAIN A AND E OF THE RIBOSOMAL 5S RNA FROM THE BACTERIUM THERMUS FLAVUS. M. Perbandt, S. Lorenz, M. Vallazza and V.A. Erdmann, Freie Universität Berlin, Inst. für Biochemie, Thielallee 63, 14195 Berlin, Germany and Ch. Betzel, Universität Hamburg, Inst für Phys. Chemie, UKE, c/o DESY, Notkestr.85, 22603 Hamburg, Germany

The ribosomal 5S RNA is approximately 120 nucleotides long and is an integral part of the large ribosomal subunit. Several parts of the 5S rRNA interact specifically with several ribosomal proteins [1-3]. Nevertheless its precise role in protein synthesis remains unclear. It is clear that reconstituted 50S ribosomal subunits, lacking the 5S rRNA, are inactive in proteinbiosynthesis. Structural studies will support a more detailed understanding of the 5S rRNA function. Our extensive attempts to crystallise ribosomal 5S RNA have led to crystals, which diffract to about 7.5Å. For the investigation of some special features like GU basepairs and hairpin-loops in the ribosomal 5S RNA from Thermus flavus we have divided the 5S rRNA into five domains (A to E) and have solved three crystal structures: Helix I of domain A has been determined at 2.4Å. Helix V of domain E without the terminal hairpin-loop has been determined at 1.6Å and Helix V of domain E including the terminal hairpin-loop has been determined at 3.0Å. Furthermore it was possible to observe a general mode of intermolecular interaction, which occur only in RNA structures and it was possible to demonstrate the structural importance of water molecules for the stability of RNA-molecules.

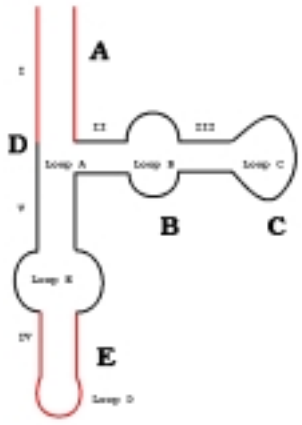

P07.04.016 SEQUENCE SPECIFIC EFFECTS IN Z - DNA. N. Gautham, C. Sadasivan, P. Karthe, P Satheesh Kumar, Department of Crystallography and Biophysics, University of Madras, Guindy Campus, Chennai 600 025, India and S. Krishnaswamy School of Biotechnology, Madurai-Kamaraj University, Madurai 625 012, India

Single crystal X-ray analyses of oligonucleotides have shown that the uniform right-handed A and B type double-helical structures of DNA proposed by Watson and Crick are modulated by a sequence-dependent microheterogeneity. We have investigated the occurrence of similar sequence effects in the structure of the left-handed Z helix, which was first seen in crystals of the hexamer $d(CGCGCG)_2$ [1]. We have grown crystals of the following sequences and have obtained their structures: $d(CCCGGG)_2$, d(TGCGCG).d(CGCGCA), d(CACGCG).d(CGCGTG) and d(CGTGCG).d(CGCACG). All four hexamers crystallise as hexagonal close-packed columns of Z-DNA duplexes. However, subtle differences in the packing interactions lead to different unit cells – the first and third are orthorhombic $P2_12_12_1$, and the second and the last are monoclinic C2 and $P2_1$ respectively. Refinement of the structures lead to the following conclusions. a) The regular model of Z-DNA with a strict dinucleotide repeat, which is based on the structure of $d(CGCGCG)_2$ [2], can exist even in the presence of A.T base pairs, but for stability requires a minimum of four continuous C.G base-pairs in alternation. b) Left-handed DNA can exist even in the absence of long stretches of alternating pyrimidine-purine sequences. c) Left-handed DNA helices, like the right-handed duplexes, show polymorphism and sequence-dependent microheterogeneity.

Wang, A.H.-J, Quigley, G.J., Kolpak, F.J., Crawford, J.L., van Boom, J.H., van der Marel, G. & Rich. A. (1979), Nature, 282, 295-310.
Wang, A.H.-J, Quigley, G.J., Kolpak, F.J., van der Marel, G., van Boom, J.H., & Rich. A. (1981) Science, 211,171-176.

P07.04.017 CRYSTALLIZATION AND PRELIMINARY X-RAY STUDIES OF SHORT SINGLE-STRANDED DNA FRAGMENT, D(GCGAAGC). J. Vévodová and J. Marek, Laboratory of Biomolecular Structure and Dynamics, Masaryk University Brno, Czech Republic

Studied oligonucleotide having a sequence d(GCGAAGC) has been described as an extraordinary stable hairpin structure in solution [1]. Melting point of the structure consisting of the two hydrogen bonding G-C base pairs and of the GAA loop is as high as 76.5°C, the highly stacked structure shows strong resistance against nucleases contained in *E. coli* extracts as well [1].

Crystallization trials were conducted using the Hampton Nucleic Acid Mini Screen [2]. The diffracting crystals were obtained at 4°C by the hanging drop vapor-diffusion technique from 10% MPD, 20 mM Cobalt Hexamine,12 mM NaCl, 80 mM KCl in 40 mM Sodium Cacodylate-HCl pH 5.5 solution with 35% v/v MPD as the dehydratant.

The crystals diffracting at BL711 station in MAXII synchrotron in Lund to resolution below 2 Å (at 100 K) belong to tetragonal space group $P4_32_12$ (or $P4_12_12$) with unit cell parameters a=48.28, c=63.36 Å. Structure determination is curently in progress.

The work was supported by grant No VS96095 of the Dept. of Education of the Czech Republic and by travelling grant (JM) of Svenska Institutet.

1. I. Hirao, G. Kawai, S. Yoshizawa, Y. Nishimura, Y. Ishido, K. Watanabe & K. Miura (1994), Nucleic Acids Research, 22, 576-582.
2. I. Berger, Ch. Kang, N. Sinha, M. Wolters & A. Rich (1996), Acta Cryst., D52, 465-468.

P07.04.018 ATOMIC RESOLUTION STRUCTURE OF d(GCGAATTCG). M. Soler[1], L. Malinina[1,2] and J.A. Subirana[1]. [1]Departament d'Enginyeria Química, Universitat Politècnica de Catalunya, Diagonal 647, E-08028 Barcelona, Spain. [2]Engelhardt Institute of Molecular Biology RAS, Vavilova 32, 117984 Moscow, Russia.

We present here the highest resolution B-DNA duplex obtained so far, a nonamer at 0.89Å resolution. Our results confirm the observation of Van Meervelt et al [*(1995) Nature 374, 742-744)*] that the crystal contains (CG)*G triplets as a fragment of a triple helix. The atomic resolution data set has allowed us to determine the structure of the nonamer and associated molecules and ions in great detail. We have found four fully hydrated Magnesium ions located in the major groove interacting with nucleic acid bases. The spine of hydration appears to be partially occupied by Sodium ions, with a fully hydrated Magnesium ion at one end. We have modelled some disordered phosphate groups with two possible conformations. Besides, it provides a view of a partially ordered peptide chain located on the major groove. The previous nonamer structure was determined to around 2.05Å with 2,800 unique reflections. Our structure was determined in the same space group ($P2_12_12_1$) with over 32,500 reflections.

P07.04.019 A NOVEL STRUCTURAL FORM OF A Co(II)-DNA COMPLEX. Shaunivan L. Labiuk, Lata Prasad, J. Wilson Quail, Louis T. J. Delbaere and Jeremy S. Lee. Departments of Biochemistry and Chemistry, University of Saskatchewan, 107 Wiggins Road, Saskatoon, Saskatchewan, S7N 5E5, Canada.

Zn^{2+}, Ni^{2+} and Co^{2+} (but not Mg^{2+} or Ca^{2+}) ions bind to duplex DNA at pHs above 8 and cause a conformational change which does not bind ethidium bromide. This structure has been named M-DNA ('metal'-deoxyribonucleic acid) It has been proposed that M-DNA might contain *intercalated* metal ions. So

far, the actual site of metal ion binding has remained enigmatic. A pH titration experiment showed that during M-DNA formation, protons were released. Thus it has been proposed that the metal ions in M-DNA coordinate with the imino protons of thymine and guanine bases in duplex DNA, causing a release of the corresponding protons. This conclusion, however, is speculative and it is important that a crystal structure be obtained. For this reason, a synthetic hexanucleotide was chosen and crystallization experiments were performed under conditions which promote the formation of M-DNA.

Crystals of a cobalt complex with DNA were grown at 21° C via the hanging drop equilibration technique. The hanging drops contained 0.8 mM of the synthetic self-complimentary hexanucleotide d(GGCGCC), 50 mM Tris-HCl buffer (pH 8.1) and 10 mM $CoCl_2$. The reservoir solution contained 25 % to 30 % 2-methyl-2,4-pentanediol (MPD), 50 mM Tris-HCl buffer and 10 mM $CoCl_2$.

Diffraction data were collected at the Photon Factory in Tsukuba, Japan to a maximum resolution of 2.7 Å. The tetragonal unit cell dimensions were a = b = 69.72 Å, c = 54.35 Å and $\alpha = \beta = \gamma = 90.0°$. The space group was found to be $P4_22_12$. The structural analysis is currently in progress.

This research is funded by the Medical Research Council of Canada.

P07.04.020 d(CGTACG)$_2$ WITH THE BOUND DRUGS 9-AMINO-DACA AND 9-AMINO-6BROMO-DACA AT 1.6Å AND 1.3 Å RESPECTIVELY. J.H.Thorpe, A.K.Todd, W.A.Denny, A.Adams and C.J.Cardin, Chemistry Department, University of Reading, Whiteknights, Reading, RG6 6AD, U.K. Biochemistry Department, University of Sydney, Sydney 2006, Australia, and 'Faculty of Medicine and Health Science' University of Auckland, N.Z.

DACA is an anti-tumour agent currently undergoing clinical trials in the UK, which is known to inhibit both topoisomerases I and II.

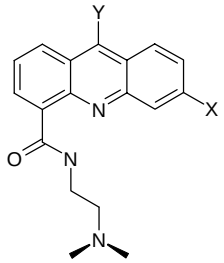

Derivatives

1 : DACA X = H, Y = H
2 : 9NH$_2$ X = H, Y = NH$_2$
3 : 6Br, 9NH$_2$ X = Br, Y = NH$_2$

The structural analyses carried out here are of the 9-amino derivatives to resolutions of 1.3 Å for the 6-bromo and 1.6 Å for the native drugs using the DNA duplex sequence d(CG(5-BrU)ACG)$_2$ and d(CGTACG)$_2$ respectively. We have shown that the 4-carboxamide side chain is located in the major groove with the precise H-bonding pattern differing for each drug examined. The 9-amino group has been shown to be the only part of the drug to extend in to the minor groove forming a rather interesting inter duplex H-bonding interaction. The existence of a spacer molecule has also been shown binding between each stacking helix exhibiting changes in the 4-carboxamide orientations of each derivative which appears to be dependent upon the pK$_a$ of the bound drug. A complete analysis of the water structure has also been achieved showing some interesting interactions, both with the DNA and the bound drug molecule.

P07.04.021 MOLECULAR DYNAMICS OF UNUSUAL NUCLEIC ACID STRUCTURES: i-DNA, G-DNA, AND ZIPPER-LIKE STRUCTURES. Jiří Šponer, J. Heyrovský Institute of Physical Chemistry, Academy of Sciences of the Czech Republic, Dolejškova 3, 182 23 Prague 8, Czech Republic, Naďa Špačková, Institute of Biophysics, Academy of Sciences of the Czech Republic, Královopolska 135, 612 65 Brno, Czech Republic and Imre Berger, Institute for Molecular Biology and Biophysics, ETH-Hönggerberg, CH-8093 Zurich, Switzerland.

We have carried out a set of nanosecond-scale molecular dynamics simulations of various unusual nucleic acid structures: four-stranded i-DNA molecules, four-stranded parallel and anti-parallel G-DNA molecules, and zipper-like duplex structures. Total length of all simulations exceeded 60 ns and the study thus belongs to the most extensive MD projects carried out on nucleic acids so far. Starting structures have been taken from high-resolution oligonucleotide crystal data and NMR studies. The calculations provided a new insight into the role of base stacking interactions in these molecules. Also the behaviour of loop regions of G-DNA molecules and the influence of cations on their stabilisation has been characterised. In most cases an excellent agreement has been found between theoretical and experimental structures. All simulations were carried out using the AMBER95 force field and the particle mesh Ewald method for long-range interactions. The simulations were supplemented with high-level ab initio calculations to estimate the accuracy of the force field and to evaluate electronic effects not included in the pair-additive force field.

1. N. Špačková, I. Berger, M. Egli, J. Šponer (1998). J. Am. Chem. Soc., **120**, 6147.
2. N. Špačková, I. Berger, J. Šponer (1999). Submitted to J. Am. Chem. Soc.
3. J. Šponer, H.A. Gabb, J. Leszczynski, P. Hobza (1997). Biophys. J., **73**, 76.

P07.04.022 THE INCREDIBLE SHRINKING CRYSTAL: FORMATION OF A THREE-DIMENSIONAL DNA POLYMER, AND IMPLICATIONS FOR DNA CONDENSATION. George R. Clark and Christopher J. Squire, Chemistry Department, University of Auckland, Auckland, New Zealand, Roger F. Martin, Peter MacCallum Cancer Research Institute, Melbourne, Australia and Jonathan White, Chemistry Department, University of Melbourne, Melbourne, Australia.

During an investigation of the stereochemical basis for single-strand cleavage of DNA by iodinated Hoechst derivatives, we determined the crystal structure of the complex between the minor groove binding ligand *meta*-iodo *para*-methoxy Hoechst 33258 and the DNA dodecamer d(CGCGAATTCGCG)$_2$. It was subsequently discovered, by a series of serendipitous events, that controlled dehydration caused the crystals to shrink to approximately 75% of their initial volume, become remarkably stable, and show a dramatic improvement in the resolution of the X-ray diffraction data (from 2.4 to 1.6 Å). Crystal structures have been determined for the "normal" (solvent content 40%) and "fully shrunken" (solvent content 20%) crystals, and for a number of intermediate "partially shrunken" states. The Hoechst ligand is located in two binding sites, with opposite orientations, in the minor groove of the "normal" structure, but detaches from the DNA and re-locates into just one site in a single orientation as the crystal shrinks. The "fully shrunken" crystal exists as an infinite polymeric network, in which the dodecamer duplexes are crosslinked by coordinate bonds through magnesium cations. We have deduced a mechanism for the structural and conformational changes that occur as the crystal dehydrates and the network polymer forms. The Mg-DNA network contains 2DNA-Mg and 3DNA-Mg bridges, which provide a model for *in vivo* Mg-facilitated DNA-DNA tertiary interactions such as self-association, condensation, supercoiling and genome packaging,

and for Mg-activation of enzymes involved in nucleic acid biochemistry.

P07.04.023 STRUCTURE OF A DOUBLE-STRANDED DNA CONTAINING A CISPLATIN INTERSTRAND CROSS-LINK: CONFORMATION AND HYDRATION. Ch. Zelwer, F. Coste, L. Serre, M. Leng and J.M. Malinge, Centre de Biophysique Moléculaire, C.N.R.S., rue Charles Sadron, 45071 Orléans Cedex 2, FR, and W. Shepard, Laboratoire pour l'Utilisation du Rayonnement Electromagnétique, Université de Paris 11, 91405 Orsay Cedex, FR, and M. Roth, Institut de Biologie Structurale, 41 rue des Martyrs, 38027 Grenoble Cedex, FR.

We solved at 1.6 Å resolution the crystal structure at 100K of a double-stranded DNA decamer containing a single cisplatin interstrand cross-link, *using the anomalous scattering (MAD) of platinum as a unique source of phase information.* Cisplatin is a powerful antitumor drug whose target is cellular DNA. In the reaction between DNA and cisplatin, covalent intrastrand and interstrand cross-links are formed. Two structures of a double-stranded decamer with an interstrand cross-link (ICL) combining NMR with different conformational data from electrophoretic experiments, have been published recently[1,2]. In both models the double-helix is bent and unwound but with significantly different angle values. The crystallographic model exhibits significant differences with both solution structures, for the overall distortion parameters and the local structure of the adduct as well. The platinum coordination is plane and nearly square. The platinum residue is embedded into a cage of 9 water molecules linked to the cross-linked guanines, to the two ammine groups, and, to the phosphodiester backbone through other water molecules. This water molecule organisation is discussed in relation to the chemical stability of the interstrand cross-link, the formation of the interstrand adduct and its recognition by repair enzymes. 92 water molecules were identified after refinement based on Fobs (R= 17%) and 174 after use of the MAD phases obtained from SHARP in a REFMAC refinement based on Maximum Likelihood optimisation (R= 15%).

(1) Huang H., Zhu L., Reid B.R., Drobny G.P. & Hopkins P.B. (1995) *Science*, 270, 1842-1845. (2) Paquet F., Pérez C., Leng M. (1996) *J. Biomol. Struct. Dynam.*, 14, 67-77.

P07.04.024 PEPTIDE NUCLEIC ACID (PNA). -X-RAY STRUCTURAL STUDIES. H. B. Rasmussen, Biochemistry, Health Care Discovery, Novo Nordisk A/S, DK-2880 Bagsvaerd, Denmark and J.S. Kastrup, Dept. of Medicinal Chemistry, Royal Danish School of Pharmacy, DK-2100 Copenhagen, Denmark

PNA (Peptide Nucleic Acid) is an oligonucleotide analogue in which the entire backbone has been replaced by a backbone composed of N(2-aminethyl)glycine units [1]. PNA hybridises with both DNA and RNA and possess many of the properties desired of an antisense/antigene drug candidate, including stability towards nucleases, proteases, peptidases and human serum.

X-ray structural determination at 1.7 Å resolution of a PNA-PNA duplex [2] verified that a double helical structure can occur without the presence of either DNA or RNA. Furthermore the structure revealed a unique helix (P-form) among known Watson-Crick base paired helices.

	Twist	Rise	Base tilt	Displacement	Bases per turn
PNA P-form	19.8	3.2Å	1.0	8.3 Å	18
DNA B-form	36.0	3.4Å	0.0	-0.1 Å	10

In order to elucidate the dependence of the helical form on the bases and the backbone, we have crystallised and solved the structure of different analogues with modifications in either base or backbone. Furthermore to provide information on the inducement of helical handedness by chiral amoino acids, we have solved the structure of a complex where a chiral center have been introduced. Latest we have crystallised a PNA dodecamer (2.7Å resolution) a non complementary PNA decamer (2.2Å resolution).

Egholm, M. Buchardt, O. Christensen, L., Behrens, C., Freier, S. M., Driver, D.A., Berg, R.H., Kim, S.K., Norden, B. & Nielsen, P.E. (1993) Nature 365, 565.
Rasmussen, H., Kastrup, J.S., Nielsen, J.N., Nielsen, J.M., Nielsen, P.E. (1997) Nature Struct. Biology vol.4, 98.

P07.04.025 STRUCTURE AND RECOGNITION OF TANDEM G.A BASE PAIRS ASSOCIATED WITH HUMAN CENTROMERE SEQUENCE. Y.-G. Gao, H. Robinson, A. H.-J. Wang, University of Illinois at U/C, Urbana, IL 61801 USA and R. Sanishvili, A. Joachimiak, Argonne National Lab, Argonne IL 60439 USA

G.A mismatched base pairs are frequently found in nucleic acids. Centromere DNA sequences contain unusual repeating motifs, e.g., (GAATG)n.(CATTC)n found in human chromosome. The purine-rich strand of this repeating pentamer sequence forms duplex and hairpin structures with unusual stability. The high stability of those structures is contributed by the "sheared" G.A base pairs and such base pairs present a novel recognition surface for ligands and proteins. We have solved the crystal structure, by the multiple wavelength anomalous (MAD) method, of a DNA decamer in which the centromere core sequence motif GAATG is embedded. Three crystal forms were refined to near-atomic resolution. The structures reveal the detailed conformation of tandem G.A base pairs and their unique hydrogen bonding surface has interesting interactions with bases, cobalt(III) hexaammine, hydrated magnesium ion and water molecules. The results are relevant in the understanding of the structure associated with human centromere sequence in particular and G.A base pairs in nucleic acids in general.

Supported by NSF (MCB 98-0829) and NIH (GM 41612)

P07.04.027 CRYSTALLOGRAPHIC STUDIES ON DNA DAMAGE AND MUTATION. T. Chatake[1], A. Ono[2], Y. Ueno[3], A. Matsuda[3] and A. Takénaka[1] [1]Faculty of Bioscience and Biotechnology, Tokyo Institute of Technology, Nagatsuda, Midori-ku, Yokohama 226-8501, Japan, [2]Graduate School of Science, Tokyo Metropolitan University, Hachioji, Tokyo, 192-0364, Japan, and [3]Graduate School of Pharmaceutical Sciences, Hokkaido University, Nishi 6, Kita 12, Kita-ku, Sapporo 060-0812, Japan

DNA replication in biological systems always requires the highest accuracy. Some mutagens cause several mutations including cancer, which may be ascribed to the mis-matching in the Watson-Crick base pairing. Extensive studies showed that oxyamine such as hydroxyamine and methoxyamine attacks amino groups of DNA bases. When an adenosine residue on the template DNA is methoxylated, not only thymidine but also cytidine residues are incorporated into the opposite strand of newly synthesiz-ing DNA. In order to elucidate the reason why DNA polymerase allows such a transition between pyrimidines, two DNA dodecamers with the nucleotide sequence of d(CGCGXATYCGCG), where X is commonly deoxy-N^6-methoxyadenosine and Y is deoxythymidine or deoxycytidine, have been synthesized and their crystal structures determined.

Both the two dodecamers have no significant conformational changes from the original B-form dodecamer (Shui *et al*., *Biochem*. 37, 8341-8355, 1998). The adenosine residues form a typical Watson-Crick type base pair with the

thymidine residues even methoxylated. On the other hand, the electron density map clearly indicates that the methoxyadenosine residue forms a pair with the cytidine residue through the two hydrogen bonds, N6(ade)...N4(cyt) and N1(ade)...N3(cyt). This paring is identical to the canonical Watson-Crick base pairing. For these hydrogen bonds, methoxyadenosine should take an imino form through tautomerization allowed by methoxylation. The imino form has donor-acceptor sites for hydrogen bonding similar to those of guanine base. Therefore, it is concluded that methoxylation makes adenosine possible to mimic guanosine and so cytidine residue is mis-incorporated by DNA polymerase into the opposite strand.

P07.04.028 ULTRA HIGH RESOLUTION DNA STRUCTURES. H. Robinson, Y.-G. Gao, A. H.-J. Wang, University of Illinois at U/C, Urbana, IL 61801 USA and R. Sanishvili, A. Joachimiak, Argonne National Lab, Argonne IL 60439 USA

Recent advances in X-ray crystallography have allowed the study of a variety of DNA structures at resolution beyond 1.0 Å. We have examined structures in several different types of conformations, e.g., B-DNA, A-DNA, Z-DNA, DNA with unusual base pairing and DNA/drug complexes. From these studies we are able to provide improved parameterization for structures that must be examined at lower resolution. This improved characterization of DNA structures is especially useful in handling disordered segments of the DNA backbone. At low resolution, disordered segments often are incompletely resolved and thus are modeled as a single model intermediate between two more stable conformations. With these improved characterizations of structures at ultra high resolution, the low resolution disordered regions of DNA structures can be recognized and modeled more effectively. Examples of several ultra high resolution DNA structures will be presented.

Supported by NSF (MCB 98-08298) and NIH (GM41612)

P07.04.029 STRUCTURE OF A PSORALEN CROSS-LINKED DNA DUPLEX P. Shing Ho, Brandt Eichman, Blaine Mooers [1], Marie Alberti, John Hearst [2], [1] Department of Biochemistry and Biophysics, Oregon State University, Corvallis, OR 97331, USA, [2] Lawrence Berkeley Lab, 1 Cyclotron Road, Berkeley, CA 94720, USA

Psoralen is class of photochemotheraputic agents that cross-link the two-strands of a DNA double-helix. The structure of a psoralen-DNA adduct was first determined in solution by NMR (1). The highly bent conformation of the DNA observed in this structure, however, was not consistent with gel mobility studies which showed that the DNA remains unbent in the adduct (2, 3). We have crystallized the psoralen adduct of the self-complementary sequence d(CGCGTACGCG), where the two thymine bases of the duplex are covalently cross-linked by the drug. The crystals diffract to 2.2 Å resolution, and are in the monoclinic space group C2, with unit cell parameters of a = 70.2 Å, b = 23.4 Å, c = 37.1 Å, and beta = 112.2°. The DNA in the crystal is linear B-DNA, consistent with the solution studies (2, 3), with an average helical rise of 3.36 Å. The central T-A base pairs are unwound by 32° by the intercalated drug. This structure, therefore, shows the details of the distortions induced by the intercalation and covalent cross-link formed with the drug, as well as the solvent rearrangements resulting from these distortions.

1. M. T. Tomic, D. E. Wemmer, and S.-H. Kim (1987) Science, v238: 1722-1725.
2. R. R. Sinden and P. J. Hagerman (1984) Biochemistry, v23: 6299-6303.
3. T. E. Haran and D. M. Crothers (1988) Biochemistry, v27: 6967-6971.

P07.04.031 A METJ VARIANT INTERACTS WITH NON-PALINDROMIC DNA SEQUENCES. H.C. Dawkes and S.E.V. Phillips, School of Biochemistry and Molecular Biology, University of Leeds, Leeds LS2 9JT,UK, and S. Elworthy and P. G. Stockley, School of Biology, University of Leeds, Leeds, LS2 9JT, UK .

MetJ is the methionine repressor responsible for the methionine biosynthesis in *Escherichia coli*. In the presence of its co-repressor S-adenosyl methionine (SAM), MetJ dimers bind to arrays of palindromic 8-base pair DNA consensus sequences of the type AGACGTCT, termed the met box [1]

Specific recognition of two base pairs in the DNA operator occurs via hydrogen bonds from Lys23 and Thr25 of MetJ to base edges in the major groove. A long side chain is thought to be required at position 23 and a short side chain required at position 25 [2]. Substitutions were made at these positions producing the variant K23S/T25R. SELEX experiments revealed a reduced affinity for the palindromic met box, instead displaying a preference for non-palindromic sequences.

Previous crystallographic studies of wild-type MetJ reveals the dimer binds to the met box contacting equivalent phosphate residues at two distinct sites in the palindromic DNA sequence. Since K23S/T25R recognises a non-palindromic sequence, its interaction with DNA should be unique and unsymmetrical.

MetJ K23S/T25R crystals diffract to 2.8Å and co-crystallisation with non-palindromic DNA sequences should reveal details of both protein dimer-dimer interactions and protein-DNA interactions.

S.E.V. Phillips, I. Manfield I. Parsons, B.E. Davidson, J.B Rafferty, W.S. Somers, D. Margarita, G.N. Cohen, I. Saint-Girons, P.G. Stockley, Nature, 341, 1989
M. Suzuki Protein Engineering, 8, 1995.

P07.04.032 THE STRUCTURE OF AHRC, THE ARGININE REPRESSOR/ACTIVATOR PROTEIN FROM BACILLUS SUBTILIS. Caitríona Dennis, Mark Parsons and Simon Phillips, School of Biochemistry and Molecular Biology, University of Leeds, Leeds, U.K., and Nicholas Glykos, IMBB, PO BOX 1527, 71110 Heraklion, Crete, Greece.

The structure of AhrC, the site-specific DNA-binding protein from *B. Subtilis* which controls the concentration of the amino acid arginine, has been solved to 2.7 Å using combined phases from molecular replacement and a heavy atom derivative. AhrC functions in response to elevated concentration of L-arginine. It both represses the transcription of arginine biosynthetic genes and activates transcription of arginine catabolic genes. Unusually for a DNA-binding protein, AhrC is a hexamer and is proposed to interact with one, two or three DNA recognition sequences within the control regions of arginine biosynthetic and catabolic genes.

Crystals of AhrC are orthorhombic and contain 1 hexamer in the asymmetric unit. The hexamer is made of 6 monomers containing 2 domains - an oligomerisation domain and a DNA-binding domain. A molecular replacement solution was obtained using the hexameric core structure (oligomerisation domains) from ArgR, a homologous protein from *E.coli* as a trial model. Phase information from a Niobium Cluster derivative was used to help find the DNA-binding domains.

Refinement of this structure is currently underway, 6 fold averaging and the maximum likelihood option of CNS is being incorporated. The structure looks symmetrical only within the core domains. The DNA-binding domains adopts slightly different orientations around this core hexamer with little interactions between their corresponding oligomerisation domain and with other DNA-binding domains.

P07.04.033 1.0Å AND ENZYME-DNA COMPLEX STRUCTURES OF ENDONUCLEASE IV REVEAL SPECIFICITY FOR DAMAGE RECOGNITION AND CATALYSIS. D.J. Hosfield, Y. Guan, and J.A. Tainer, Dept. of Molecular Biology and the Skaggs Institute for Chemical Biology, The Scripps Research Institute, La Jolla, CA 92037, USA, and B.J. Haas, and R.P. Cunningham, Dept. of Biological Sciences, Center for Biochemistry and Biophysics, State University of New York-Albany, Albany, NY 12222, USA.

The long term viability and propagation of all living cells depend upon a number of ubiquitous DNA repair pathways. A major DNA damage intermediate in these pathways, resulting from oxidative, enzymatic, and spontaneous processes, is an abasic site, which can be detected and processed by Endonuclease IV (Endo IV). This evolutionarily conserved, Zn-dependent metallo-endonuclease specifically recognizes abasic sites and catalyzes the first step of their release from duplex DNA.

The structure of *Escherichia coli* Endo IV was determined using MAD techniques with data collected from four wavelengths near the Zn absorption edge, and refined against high resolution data that extends to 1.0Å resolution. Anisotropic B-factor refinement, using the program Shelx-97, gave a final model with excellent stereochemistry and R=12.6% (R_{free}=15.0%). This structure provides accurate measures of bond lengths and bond angles, and provides, to the best of our knowledge, the highest resolution description of a tri-nuclear Zn cluster yet obtained by X-ray crystallography. The mechanism of abasic site binding and chemical catalysis was elucidated by analysis of both a wild-type and site directed mutant complex of Endo IV bound to duplex DNA containing a centrally located abasic site analogue. In the mutant structure the scissile P-O3' bond remains intact while in the wild-type complex this bond is broken. These two structures characterize substrate and product complexes and in combination with the 1.0Å enzyme structure resolve key issues and provide a detailed mechanism regarding the chemical events and subtle structural changes underlying DNA damage recognition and chemical catalysis.

P07.04.034 CRYSTALLISATION AND PRELIMINARY X-RAY CRYSTALLOGRAPHIC ANALYSIS OF BACTERIOPHAGE T7 ENDONUCLEASE I: A HOLLIDAY JUNCTION RESOLVING ENZYME. J.M. Hadden, M.A. Convery and S.E.V. Phillips, Department of Biochemistry and Molecular Biology, University of Leeds, Leeds, LS2 9JT, UK. N. Ito, Biomolecular Engineering Research Institute (BERI), 6-2-3 Furuedai, Suita, Osaka 565, JAPAN. A. Declais and D.M.J. Lilley, CRC Nucleic Acid Structure Group, Department of Biochemistry, University of Dundee, DD1 4HN, UK.

Genetic recombination is a fundamental process in the evolution of all living organisms. This process results in the exchange of sequences between DNA segments and plays a fundamental role in the production of new genetic variants. The four-way DNA (Holliday) junction is an important intermediate in the recombination process.

Bacteriophage T7 encodes a 149 amino acid residue protein, endonuclease I, which has been shown to bind and cleave four-way DNA junctions *in vitro*. A number of mutants of T7 endonuclease I have been isolated that bind, but do not cleave DNA junctions. These mutants are particularly useful for studying the binding process.

We have crystallised one such mutant both unbound and in complex with a synthetic Holliday junction.

Crystals of the isolated protein belong to the space group $P2_12_12$ and have cell dimensions of a=123.2Å, b=134.8Å and c=61.2Å. These crystals were found to diffract beyond 2Å at the ESRF. Our best quality data set has been processed to 2.8Å and has the following statistics; R_{merge} 4.5%, 99.4% complete with a multiplicity of 3.8 and I/σI of 6.4. Crystals of the protein in complex with DNA belong to the space group $P4_22_12$ and have cell dimensions of a=77.3Å, b=77.3Å, c=151.3Å. A data set has been processed to 3.5Å and has the following statistics; R_{merge} 10.5%, 98.2% complete with a multiplicity of 5.6 and I/σI of 1.8.

We are currently in the process of screening for heavy atom derivatives for both crystal types. We have also introduced several methionine residues into the protein and are in the process of substituting these with selinomethionine.

P07.04.035 TYPE II RESTRICTION ENDO-NUCLEASES: STRUCTURE, FUNCTION AND ENGINEERING OF NOVEL PROPERTIES. A.K. Roidis and M. Kokkinidis, University of Crete, Dept. of Biology, PO Box 2208, GR-71409 Heraklion, Crete, Greece and Institute of Molecular Biology and Biotechnology (IMBB), PO Box 1527, GR-71110, Heraklion, Crete, Greece.

Type II restriction endonucleases provide a rich source of information about protein-DNA interactions. They have gained an enormous importance in Molecular Biology due to their applications in recombinant DNA technologies, genome mapping, manipulation of chromosomes and health care. Recent crystallographic studies have revealed novel DNA-binding motifs and new modes of DNA recognition. To understand the precise mechanisms underlying sequence specific DNA recognition we have initiated crystallographic studies of wild type and mutated restriction endonucleases *Eag*I and *Pvu*II [1] in the apoenzyme form and as complexes with DNA. The aim of these studies is to develop novel specificities by protein engineering and to examine systematically the roles of individual residues and bases involved in specific and non-specific binding.

1. A. Athanasiadis, M. Vlassi, D. Kotsifaki, P. Tucker, K.S. Wilson & M. Kokkinidis (1994), Nature, Struct. Biology 1, 469-475.

P07.04.036 STRUCTURAL DATA OF THE TRANSCRIPTION COFACTOR PC4. Sjors H.W. Scheres, Jeroen Brandsen, Jean M.H. van den Elsen, Jan Kroon, Piet Gros; Dept. of Crystal and Structural Chemistry, Bijvoet Center for Biomolecular Research, Utrecht University; Padualaan 8, 3584 CH Utrecht, The Netherlands

PC4 (human positive cofactor 4) is a transcription cofactor that can both coactivate and repress activator dependent class II gene transcription. The structure of the C-terminal domain (residues 63-127) has been solved by X-ray diffraction in our lab [1]. This structure shows a new structural motif reminiscent of the single stranded (ss)DNA-binding motif in human replication protein A. The orientation of the binding grooves on the dimer suggests that two ssDNA strands running in opposite directions can be bound to the protein. This agrees with the biochemical findings that heteroduplex DNA can be bound to the protein with high affinity. This binding mode is most likely involved in the repressing mode of PC4 [2].

For its role as coactivator the N-terminal domain plays a more prominent role. Recent biochemical studies have shown that in the absence of transcription factor IIH (TFIIH) the activator function of PC4 is lost and transcription is strongly repressed by PC4 [3]. In the same study it has been shown that PC4 can be phosphorylated by TFIIH and TFIID. Most likely, phosphorylation is to take place on the serine-rich N-terminal domain of PC4. To understand more of the coactivator function new crystals were grown of PC4. Up till now however the structure of this construct could not be solved because of twinning in the crystals.

Here we present structural data of PC4 in the context of its combined role of both coactivator and repressor and the twinning of the new crystals is discussed.

[1] J. Brandsen *et al.* Nature Struc. Biol. **4**, 900-903 (1997)
[2] S. Werten *et al.* EMBO J. **17**, 5103-5111 (1998)
[3] S. Malik *et al.* Proc. Natl. Acad. Sci USA **95**, 2192-2197 (1998)

P07.04.037 THE STRUCTURE OF THE OCTAMERIC RUVA-HOLLIDAY JUNCTION COMPLEX. S.M. Roe, M. Oram, A. Keeley, I. Tsaneva and L.H. Pearl, Dept. of Biochemistry and Molecular Biology, University College London, Gower Street, London WC1E 6BT, UK, and T. Barlow and T. Brown, Dept. of Chemistry, University of Southampton, Highfield, Southampton, SO17 1BJ, UK.

Holliday junctions, created by exchange of strands between homologous DNA molecules, occur as intermediates in homologous recombination and double strand DNA break repair. The main pathway for processing the junctions in bacteria involves the RuvABC proteins.

RuvA binds specifically to the Holliday junction and isomerises the DNA from a stacked-X structure to a square-planar structure. RuvB is a DNA-dependant ATPase. It forms hexameric rings around the DNA and provides the motor of branch migration, but has no specificity for Holliday junctions without RuvA. RuvA and RuvB have been shown to form a complex which promotes ATP-dependant branch migration. RuvC is a junction-specific endonuclease, which resolves the junction to reform separate duplex DNA molecules.

Previous crystallographic studies of *E. coli* RuvA have shown the creation of a square-planar tetrameric complex, and have suggested a model for the interaction with DNA. We have determined the structure of *M. leprae* RuvA complexed with a synthetic Holliday junction, to 3.0Å. This clearly shows the RuvA to be an octameric shell with four tunnels through which the DNA can slide. The octamer is stabilised by the presence of a conserved tetramer-tetramer interface and we believe it to be the probable in vivo structure for the branch migration complex.

Although the Holliday junction itself suffers from statistical disorder, we are able to define key residues involved in DNA binding and suggest a mechanism for strand separation by RuvA. Labelling of the DNA is being carried out to determine the extent of the disorder.

P07.04.038 STRUCTURE-FUNCTION STUDIES ON RESIDUES OF PURR INVOLVED IN COREPRESSOR BINDING AND ALLOSTERISM. Joy L. Huffman and Richard G. Brennan, Department of Biochemistry, Oregon Health Sciences University, Portland, OR, U.S.A.

The crystal structures of corepressor-bound and free *E. coli* Purine Repressor (PurR) have implicated several residues in corepressor binding and specificity and intramolecular signal transduction (allosterism). Residue W147 is key for the allosteric response, but in most members of the LacI/GalR family, position 147 is an arginine. Three substitutions at residue 147 have been characterized *in vivo* and *in vitro*. PurR (W147F) displays a decreased affinity for both operator and corepressor. PurR (W147A) and (W147R), on the other hand, act as super repressors *in vivo*. Each of the mutant PurR holo complexes has crystallized isomorphously to wild-type. Interestingly, only the W147F apo complex has crystallized but is isomorphous to wild-type. Structures of these mutants have been solved beyond 2.7 Å using molecular substitution. Since the corepressor binding site is over 40 Å from the DNA binding domain, structural studies on these mutants should further our understanding of the allosteric regulation of DNA binding proteins.

Additional mutations have been made within the corepressor binding pocket to augment our thermodynamic and structural understanding of ligand specificity. Under study are residues R190, which is the corepressor identity determinant of the *E. coli* PurR, and T192 which contacts the N7 and C8 atoms of the corepressor. The effects of a smaller basic residue at position 190, which is observed in the *H. influenza* PurR, and the loss of a hydrogen bond and van der Waals contact on corepressor binding and affinity will be discussed and their structures presented.

P07.04.039 THE STRUCTURAL BASIS OF DUAL-FUNCTION TRANSCRIPTIONAL CONTROL IN THE LYSR FAMILY PROTEIN, CYSB. K.H.G. Verschueren, C. Addy, G.N. Murshudov, E.J. Dodson, A.J. Wilkinson. Structural Biology Laboratory, University of York, York YO1 5DD, UK.

The LysR-type transcriptional regulators (LTTRs) form a large family of bacterial gene activator proteins which control the expression of genes associated with a multitude of highly diverse cellular processes. They act either as tetramers or dimers of identical polypeptides, 270-330 amino acid residues in length and share stretches of sequence similarity over ~270 residues of which the strongest conservation lies in their N-terminal DNA binding domain.

We are investigating the mechanism of transcriptional regulation by CysB, an LTTR involved in cysteine biosynthesis in Gram-negative bacteria. The proteins involved in the process are highly regulated and this regulation is dependent on the activity of CysB, a tetrameric protein of identical 36 kDa subunits (324 residues). Like most LysR family proteins, CysB has a dual regulatory function, acting as transcriptional activator at one or several *loci* whilst negatively regulating transcription of its own gene. The interactions of CysB with *cys* promoters have been shown to be extremely complex.

The 1.8Å crystal structure of a dimeric chymotryptic fragment of CysB from *Klebsiella aerogenes*, residues 88-324, containing the cofactor-binding domain has been elucidated using a combination of MIR techniques and multi-crystal averaging. The core of the structure consists of two α/β domains connected by a short two-stranded hinge region. A deep cavity formed between the two domains represents the inducer binding site and is occupied by a sulphate anion. The inducer binding domain of the monomer closely resembles those of the IPTG and hypoxanthine binding domains of *lac* repressor and PurR respectively. However the subunit organisation of the two molecules in the CysB(88-324) dimer is quite different to that in *lac* repressor and PurR. Whereas in the latter the two-fold axis of symmetry relating monomers in the dimer is parallel to the long axis of the cofactor binding domain, in CysB(88-324) it is perpendicular to this axis. This is expected to position the N-terminal DNA binding domains at opposite ends of the molecule perhaps accounting for the unusually large DNA footprints produced by CysB. Recently we have obtained well-diffracting crystals of the intact CysB(1-324). We hope to present the structure of the full-length CysB at the meeting.

P07.04.040 THE STRUCTURE OF PLASMID-ENCODED TRANSCRIPTIONAL REPRESSOR CopG, UNLIGANDED AND BOUND TO ITS OPERATOR. M. Coll, F.X. Gomis-Rüth, M. Solà, A. Párraga, A. Guasch, Institut de Biologia Molecular de Barcelona, CSIC, Jordi Girona 18, 08034 Barcelona, Spain, P. Acebo, M. Espinosa, G. del Solar, Centro de Investigaciones Biológicas, CSIC, Velázquez, 144, 28006 Madrid, Spain, R. Eritja, EMBL, Meyerhofstraße 1, 69117 Heidelberg, Germany and A. González, EMBL, c/o DESY, Notkestraße 85, 22603 Hamburg, Germany.

The structure of the transcriptional repressor CopG has been solved unliganded and bound to its target operator DNA. The protein, encoded by the promiscuous streptococcal plasmid pMV158, is involved in the control of plasmid copy number. The structure of this repressor, which is the shortest reported to date and the first isolated from a plasmid, has a homodimeric ribbon-

helix-helix arrangement. CopG cooperatively associates, completely protecting several turns on one face of the double helix in both directions from a 13-bp pseudosymmetric primary DNA recognition element. In the complex structure, one protein tetramer binds at one face of a 19-bp oligonucleotide containing the operator, with two β-ribbons inserted into the major groove. The DNA is bent 60^{o} by compression of both major and minor grooves. The protein dimer displays topological similarity with Arc and MetJ repressors. Nevertheless, the functional tetramer has a unique structure with the two vicinal recognition ribbon elements at a short distance, thus inducing strong DNA bend. Further structural resemblance is found with helix-turn-helix regions of unrelated DNA-binding proteins. In contrast to these, however, in CopG the bihelical region has a role in oligomerization instead of DNA recognition.

P07.04.041 CRYSTAL STRUCTURE OF A HUMAN TFIIB-TBP-DNA COMPLEX AT 2.65 A RESOLUTION F.T.F. Tsai [1], and P.B. Sigler [1,2], [1] Department of Molecular Biophysics and Biochemistry, [2] Howard Hughes Medical Institute

The TATA-box binding protein (TBP) and transcription factor IIB (TFIIB) belong to a set of general transcription factors (GTFs) that is a key component of the RNA Polymerase II pre-initiation complex. The latter assembles on a promoter and is required for the transcription of all protein encoding genes in eukaryotes and archaea. The crystal structure of several GTF-DNA complexes, including that of a eukaryotic and archaeal TBP-TFIIB-DNA complex, respectively, have been solved. However, despite of the overall structural similarities, the two structures differ with respect to the relative orientation of the TBP bound to the promoter. It is believed that the determinant for this polarity may lie in the sequence immediately upstream of the TATA-box, the so-called IIB recognition element (BRE), which was absent in both previously solved crystal structures.

Here we present the crystal structure of a human ternary TFIIBc-TBPc-DNA complex at 2.65 A resolution, containing one version of the selection-optimised BRE. The crystals belong to the monoclinic space group, P21, with unit cell dimensions: a=118.5 A, b=122.3 A, c=140.2 A, and beta=113.1 degrees. The structure was determined essentially by molecular replacement and revealed the presence of five ternary complexes per asymmetric unit, which together have a molecular weight of nearly 300 kDa. The five ternary complexes were found to stack head-to-tail and were held in helical register by the G:C base pairs of the 5' overhang. We are currently refining this structure using simulated annealing and improper NCS.

P07.04.042 CRYSTAL STRUCTURES OF THE 64M-2 ANTIBODY FAB FRAGMENT AND ITS COMPLEXES WITH DNA (6-4) PHOTOPRODUCTS. H. Yokoyama, R. Mizutani, and Y. Satow, Graduate School of Pharmaceutical Sciences, University of Tokyo, Tokyo 113-0033, Japan, Y. Komatsu and E. Ohtsuka, Graduate School of Pharmaceutical Sciences, Hokkaido University, Sapporo 060-0812, Japan, O. Nikaido, Faculty of Pharmaceutical Sciences, Kanazawa University, Kanazawa 920-0934, Japan.

The 64M-2 murine antibody recognizes ultraviolet-induced (6-4) DNA photoproducts. In order to elucidate the structure of the (6-4) photoproducts as well as recognition mechanisms by the antibody, we determined the crystal structures of the 64M-2 Fab fragment and of its complexes with the (6-4) photoproducts of dT(6-4)T (d2mer) and dTT(6-4)TT (d4mer) by the molecular replacement method.

The native Fab structure was refined to an *R* factor 0.163, the d2mer complexed one to 0.199, and the d4mer complexed one to 0.209. In these complexes obtained at 2.4 Å resolution, the side-chains of Trp 33H, His 35H, Arg 95H, and Tyr 100iH interact with the bases of the T(6-4)T moiety through hydrogen bonds and van der Waals contacts. One of the planes of the bases is nearly perpendicular to the other. This is ascribable to the conformational restraints on the covalent (6-4) bond from the base moiety. The 5'- and 3'-side bases are in the *anti* and *high-anti* conformation relative to each deoxyribose ring, respectively. The torsion angles ζ and α for the phosphodiester bonds, O3'-P and P-O5' of the T(6-4)T moiety, are in the *gauche*$^{-}$ and *gauche*$^{-}$ range, respectively. The torsion angle γ about C5'-C4' bond is in the *gauche*$^{+}$ range. Tyr 32L, Leu 93L, and Ser 58H are situated near the sugar-phosphate backbone of the T(6-4)T moiety. In the d4mer complex, 5'- and 3'-side phosphate groups adjacent to the T(6-4)T moiety form hydrogen bonds with the side-chains of Asn 28L and Ser 58H, respectively. The thymine base at the 5'-terminal is in interaction with Tyr 32L, Lys 50L, and Tyr 100iH, whereas the thymine base at the 3'-terminal is not in contacts with the Fab.

P07.04.043 THE BIPARTITE DNA BINDING DOMAIN OF C. ELEGANS TC3 TRANSPOSASE BOUND TO TRANSPOSON DNA. Titia K. Sixma, Gertie van Pouderoyen, René F. Ketting*, George Verlaan*, Ronald H.A. Plasterk*, Divisions of Molecular Carcinogenesis and *Molecular Biology, Netherlands Cancer Institute, Plesmanlaan 121,1066 CX Amsterdam, Sixma@nki.nl.

Transposons are regions of DNA that 'jump' in the genome. They encode specific proteins to make this possible. In the Tc1/mariner class of transposons this is accomplished by a single transposase protein, which excises the transposon DNA and inserts it elsewhere. To understand the recognition of the Tc3 transposase for the transposon DNA we are studying crystal structures of the binding domains of C. elegans Tc3A complexed to the recognition region of the DNA.

The bipartite DNA binding domain of Tc3A has been crystallized in complex with the recognition region on the Tc3 transposon. Crystals were successfully designed to retain the packing found with the N-terminal protein domain and a smaller oligomer [1], by extension with precisely one half turn of DNA. The N-terminal domain structure [1] was used to solve the structure of the bipartite domain to 2.6 Å using molecular replacement.

The second DNA binding domain binds in the major groove. The linker extends through the minor groove. It is not yet clear whether the second domain in the second molecule in the asymmetric unit also binds DNA. Further refinement and a heavy atom derivative search are in progress.

[1] van Pouderoyen, G., Ketting, R., Perrakis, A., Plasterk, R., Sixma, T.K., EMBO J. 16 (1997) 6044-6054.

P07.04.044 CRYSTAL STRUCTURE OF A SYNAPTIC CRE RECOMBINASE - *LOX*P COMPLEX. D. Suck, J.E.W. Meyer, F. Buchholz, H. Dreher, F. Stewart, EMBL, Meyerhofstr.1, D-69117 Heidelberg, Germany.

The structure of a synaptic Cre recombinase - DNA complex has been determined at 3.2Å resolution from orthorhombic crystals containing four Cre monomers bound to two synapsed wild-type *lox*P sites in the asymmetric unit. The structure suggests that a Cre-induced kink in the spacer region initiates first-strand cleavage during site-specific recombination.

The 38.5 kD Cre protein from phage P1 belongs to the λ integrase family of site-specific recombinases which proceed through the formation of a Holliday junction and a covalent phosphotyrosine protein-DNA intermediate. Cre recognizes a 34bp target site ("*lox*P site") consisting of two 13bp repeats separated by an non-symmetric 8bp spacer.

Data were collected under cryo conditions at the BW7B beamline at the EMBL outstation in Hamburg and the structure was solved by molecular replacement (AMoRe) using the coordinates of a complex containing Cre bound to a symmetrized *lox*-site formed from a 16mer and 19mer oligonucleotide [1]. Applying tight geometric and B-factor restraints, and adding independent phase information from an EMTS derivative (SHARP), the Cre-*lox*P structure was refined to an R-factor of 21.8% (R_{free} = 27.0%) using the program Refmac.

The tetrameric Cre-*lox*P complex shows local 2-fold symmetry with an arrangement of subunits closely resembling that seen in the structure solved by van Duyne and coworkers [1]. There are however slight, but significant changes in quaternary structure involving rigid body movements of domains and furthermore, while two of the subunits are closely similar in structure to the Cre-*lox*A [1] complex, the other two show distinct differences, particularly around the active site and the linker region between N- and C-terminal domains.

A striking feature of the synaptic Cre-*lox*P structure is a kink in the spacer region of the DNA adjacent to the first strand cleavage site associated with a 45 degree major groove-directed roll and complete unstacking of bases at this step. This finding may provide an explanation for the observed order of strand exchange in Cre-induced recombination.

1. F. Guo, D.N. Gopaul & G.D. Van Duyne (1997). Nature, **389**, 40-46.

P07.04.045 CRYSTAL STRUCTURE OF IRF-2 COMPLEXED WITH DNA CONTAINING A TANDEM REPEAT OF CORE SEQUENCES. T.Shimizu, Y.Fujii, M.Kusumoto, T.Hakoshima [1], Y.Kyogoku[2], T.Taniguchi[3], [1] Department of Molecular Biology, Nara Institute of Science and Technology, Takayama Ikoma Nara, Japan. [2] Institute for Protein Research, Osaka University, Yamadaoka Suita Osaka, Japan. [3] Department of Immunology, Graduate School of Medicine, University of Tokyo, Hongo Bunkyoku Tokyo, Japan

The family of interferon regulatory factor(IRF) transcription factors is important in the regulation of interferons(IFNs) in response to infection by virus and in the regulation of interferon-inducible genes. IRF-2 was originally identified as a competitor of IRF-1, a transcriptional activator of the interferon system. In addition, IRF-2 and IRF-1 are also involved in several regulatory processes and immune systems.

The family shows extensive homology among their DNA-binding domains in the N-terminal regions. IRF members are believed to bind to similar DNA sequences with tandem repeats of GAAA with mostly two inserted bases.

The crystal structure of IRF-1 bound to DNA at 3Å resolution(1) gave a structural view of the binding to a single GAAA core. However, the structural basis for the diverse binding properties of the IRF family members is largely uncharacterized.

Here, we have crystallized(2) and determined the crystal structure of a DNA binding domain of IRF-2 complexed with DNA whose sequence is designed to form a tandem repeat of the core sequence. The current model was refined to R-factor/Rfree 20.4% and 24.3%, respectively. The structure at higher resolution(2.2Å) established the detailed framework of DNA recognition, especially water-mediated interactions. Moreover, we found that AANNGAAA is the sequence physically recognized by IRF-2. The facts well explain the diverse binding properties of the IRF family members, which bind to both single and tandemly-repeated sequences. Our analysis also reveals DNA structural deformations, indicating a cooperative binding of IRFs to tandem repeats of the core sequence.

1. C.R.Escalante, J.Yie, D.Thanos and A.K.Aggarwal(1998) Nature 391, 103-106
2. M.Kusumoto, Y.Fujii, Y.Tsukuda, T.Ohira, Y.Kyougoku, T.Taniguchi, T.Hakoshima(1998) J.Struct.Biol. 121, 363-366

P07.04.046 STRUCTURAL ANALYSIS OF NUCLEIC ACID COMPLEXES WITH A CATALYTIC FRAGMENT OF REVERSE TRANSCRIPTASE. Shabir Najmudin, Dunming Sun, Marie Cote, and Millie Georgiadis, Waksman Institute, Dept. of Chem., Rutgers University, Piscataway, NJ

Reverse transcriptase is an essential retroviral enzyme that makes a double-stranded DNA copy from the single-stranded RNA genome of the retrovirus using RNA- and DNA-directed DNA polymerase activities and an RNaseH activity. We have determined high resolution structures of Moloney murine leukemia virus reverse transcriptase (MMLV RT) complexed with nucleic acid in three distinct crystal lattices. The catalytic fragment is comprised of the fingers and palm domains of RT and retains polymerase activity. Although retroviral RTs all perform similar functions, the architectures of the enzymes are quite different. MMLV RT is monomeric as isolated but has been proposed to form homodimers in the presence of nucleic acid, based on gel retardation results. HIV-1 RT and ASV RT, representing the other two observed architectures, are both heterodimeric with the second smaller subunit resulting from proteolytic processing of the larger subunit. Based on our crystallographic analysis, we have analyzed dimer formation and assessed its functional significance in MMLV RT.

Two crystal forms (Forms I and II) are monoclinic and include two catalytic fragment molecules and a single symmetric 8/8-mer DNA molecule in the asymmetric unit. The third crystal form is orthorhombic and has one catalytic fragment molecule and one DNA molecule (6/10-mer) in the asymmetric unit. The protein-DNA interactions are similar in each crystal. But, the crystal packing and protein-protein interactions differ significantly. In Form I crystals, the two molecules in the asymmetric unit have few protein-protein interactions. More significant protein interactions are found between two dimers in the crystal. In Form II crystals, the two molecules in the asymmetric unit form a homodimer. Interactions involve 16 residues from the A molecule and 15 residues from the B molecule burying 1,500 $Å^2$ of surface area. In a preliminary analysis of crystal packing interactions in the third crystal form, we have found significant and interesting differences.

P07.04.047 RESTRICTION ENDONUCLEASES BGL II VS. BAM HI: WHAT A DIFFERENCE A BASE MAKES. Christine M. Lukacs [1], Rebecca Kucera, Ira Schildkraut [2], Aneel K. Aggarwal [1], 1. Mount Sinai School of Medicine, Department of Physiology and Biophysics/Structural Biology, New York, NY, 2. New England Biolabs, Inc., Beverly, MA.

Extensive high-resolution crystallographic studies in our laboratories have delineated the atomic contacts made between the restriction endonuclease Bam HI and its target DNA site, and have shown its mechanism of action. [1-3] However, there is nothing obviously remarkable about these contacts, as compared to other DNA binding proteins, to rationalize the incredible specificity of restriction endonucleases for their target sites. In order to help further our understanding of this phenomenon, we have undertaken the structure determination of Bgl II, a restriction endonuclease of similar size to Bam HI, also functionally dimeric, whose symmetric recognition sequence differs from that of Bam HI by only one base pair – A|GATCT vs. G|GATCC – yet has a completely unrelated primary sequence. Bgl II complexed with a symmetric DNA 16-mer forms crystals in space group $P2_12_12_1$ which diffract beyond 2.0 Å resolution. Selenomethionine substituted protein and brominated oligonucleotide have provided good crystals for use in MAD experiments. Details of the

structure determination and a structural analysis of the complex will be presented.

1. M. Newman, T. Strzelecka, L.F. Dorner, I. Schildkraut, A.K. Aggarwal (1994) Nature 368, 660-664.
2. M. Newman, T. Strzelecka, L.F. Dorner, I. Schildkraut, A.K. Aggarwal (1995) Science 269, 656-663.
3. H. Viadiu, A.K. Aggarwal (1998) Nat. Struct. Biol. 10, 910-916.

P07.04.048 THE RUNT DOMAIN, A NOVEL DNA BINDING FOLD S. Bäckström, S.H. Huang [1], M. Wolf-Watz [2], U.H. Sauer [1], [1] Umeå Centre for Molecular Pathogenesis, Umeå University, S-901 87 Umeå, Sweden, [2] Dept. of Biotechnology, Royal Institute of Technology, Novum, S-141 57 Huddinge

The acute myeloid leukemia related protein AML1 or its hetero-dimerization partner CBFb are the most common cause for acute human leukemias. The evolutionary conserved Runt Homology Domain (RUNT domain) comprises the N-terminal 190 residues of AML1 which harbours both the DNA binding and hetero-dimerization activities. Recently is was shown, that dephosphorylation of AML1 by the Ca2+/Calmodulin dependent phosphatase Calcineurin (CN) activates AML1 by improving both its binding to CFBb and DNA [1].

The Runt domain might represent a new class of DNA binding protein folds as there is no sequence similarity to any structurally described DNA binding fold. Preliminary studies by NMR and secondary structure predictions suggests that the runt domain comprises six b-strands, two a-helices and a nucleotide binding motif [2].

We have collected synchrotron data to 1.7 Å resolution and will present structure of the RUNT domain in the presence of its cognate DNA.

[1] Holm, M., Xie, X-Q., Wolf-Watz, M. and Grundström T. (1997) Calcineurin activation of AML1 and PEBP2aA. (submitted for publication)
[2] Wolf-Watz, M, Xie, X-Q., Holm, M., Grundström, T. and Härd, T (1998) Solution properties of the free and DNA-bound runt domain of AML1 (manuscript in preparation)

P07.04.049 LOW SALT CRYSTAL STRUCTURES OF T7 RNA POLYMERASE AND ITS TRANSCRIPTION BUBBLE. C.-J. Chen[1,2], F. Schubot[1], Z.-J. Liu[1], J. P. Rose[1], and B.-C. Wang[1], [1]Department of Biochemistry and Molecular Biology, University of Georgia, Athens, GA 30602, U.S.A. [2]Department of Crystallography, University of Pittsburgh, Pittsburgh, PA 15260, U.S.A.

The flow of genetic information from DNA to protein is a two-step process, with RNA as an intermediate. DNA-dependent RNA polymerase is the key enzyme responsible for the biosynthesis of RNA, a process known as transcription. This process, which decodes the genetic information from DNA, with RNA as an intermediate, is one of the most significant events in a biological system.

Bacteriophage T7 RNA polymerase, a single peptide chain polymerase with a molecular weight of about 99kDa, was previously crystallized under high-salt conditions[1], however, these crystals were not suitable for the formation of DNA-RNA and RNAP complexes as the presence of salts reduces the binding affinity of DNA to RNAP. A search for low salt crystallization conditions has yielded a new low-salt crystal form of T7 RNA polymerase in a space group P3121, which also lead us to produce the crystals of T7 RNAP-DNA-RNA bubble complex in the same space group with the larger unit cell. The Electron density maps clearly show density of the appropriate dimensions of the DNA-RNA bubble duplex complexed with T7 RNAP. We report here the three-dimensional structure of T7 RNAP at 2.7 Å resolution and T7 RNAP DNA-RNA bubble complex at 4.0 Å resolution.

1. Sousa, R., Chung, Y.-J., Rose, J. P. and Wang, B.-C. (1993) The crystal Structure of Bacteriophage T7 RNA Polymerase at 3.3 Å resolution. Nature, 364, 593.

P07.04.050 PRELIMINARY CRYSTALLOGRAPHIC STUDIES OF THE YEAST MITOCHONDRIAL TRANSCRIPTION FACTOR, MTF1P. F. D. Schubot, C.-J. Chen, J.P. Rose, and B.-C. Wang, Department of Biochemistry and Molecular Biology, University of Georgia, Athens, Ga 30602, U.S.A.

Transcription in the mitochondria of Saccharomyces cerevisiae is carried out by a two subunit RNA polymerase[1]. The core enzyme, RPO41p, is a 153 kDa protein that shows strong homology with bacteriophage RNA polymerases. However, while these phage RNA polymerases do not require a co-factor for promoter recognition and initiation of transcription, RPO41p only recognizes its promoter in the presence of the s-like factor MTF1p (43kDa). The current model suggest that MTF1p, similar to s-factors such as s70 in E.coli., after association with the core enzyme binds to the promoter and targets the core enzyme to the initiation site[2].

Single crystals have been obtained for the mitochondrial transcription factor MTF1p. In low-temperature X-ray crystallographic studies these crystals diffracted beyond 3.0 Å. The protein crystallized in the monoclinic space group C2. The cell constants are a= 90.0 Å; b= 44.5 Å; c= 98.8 Å; There is one molecule in the asymmetric unit. The Rmerge is 5.5%.

[1] A. H. Schinkel, M. J. A. Groot Koerkamp, and H. F. Tabak (1988) EMBO Journal, 7, 3255.
[2] D. A. Mangus, S.-H. Jang, and J. A. Jaehning (1994) J. Biol. Chem., 269, 26568.

P07.04.051 CRYSTAL STRUCTURE OF MOLECULAR CHAPERONE HSP40. Bingdong SHA, Department of Cell Biology, Univ. of Alabama at Birmingham, Birmingham, AL 35294-0005, USA

Heat-shock protein 70(Hsp70), one of the major molecular chaperones, has been shown to play a central role in many cellular processes. Heat-shock protein 40(Hsp40) works as a co-chaperone for Hsp70. Hsp40, bound by substrate, can interact directly with Hsp70 to stimulate the ATPase activity of Hsp70. Hsp40 can also bind to unfolded polypeptide and prevent them from aggregation *in vitro* as an independent molecular chaperone.Hsp40/Hsp70 system is highly involved in many cellular functions such as protein biosynthesis and degradation, protein trafficking, steroid signal transduction. *S. cerevisiae* Hsp40 Sis1 C-terminal peptide-binding domain has been determined by X-ray crystallography.

P07.04.052 THE THREE-DIMENSIONAL STRUCTURE OF THE RNA-BINDING DOMAIN OF RIBOSOMAL PROTEIN L2. Isao Tanaka, Atsushi Nakagawa, Masae Taniguchi and Harumi Hosaka. Division of Biological Sciences, Graduate School of Science, Hokkaido University, Sapporo 060-0810, Japan. Takashi Nakashima, and Makoto Kimura. Laboratory of Biochemistry, Faculty of Agriculture, Kyushu University, Fukuoka 812-8512, Japan

In all living cells, protein synthesis is carried out in cellular organelles called ribosomes. These large ribonucleoprotein complexes are generally organized in two subunits of unequal size. In prokaryotic *Escherichia coli* ribosomes, the large (50S) subunit consists of 34 proteins and 5S

and 23S rRNAs, while the small (30S) subunit is a complex of 21 proteins and 16S rRNA. Ribosomal protein L2 is the largest protein component in the ribosome. It is located at or near the peptidyl transferase center and has been a prime candidate for the peptidyl transferase activity. It binds directly to 23S rRNA and plays a crucial role in its assembly. The three dimensional structure of the RNA-binding domain of L2 from *Bacillus stearothermophilus* has been determined at 2.3Å resolution by X-ray crystallography using the Se-Met MAD method. The RNA-binding domain of L2 consists of two recurring motifs of about 70 residues each. The N-terminal half domain (pos. 60 - 130) is homologous to the OB-fold and the C-terminal half (pos. 131 - 201) is homologous to the SH3-like barrel. Both structure motifs are often found in RNA- or DNA-binding proteins, and their RNA-binding sites have been predicted to be regions constructed by the loops protruding outward from the barrel axis. The residues Arg86 and Arg155, which have been identified by mutation experiments to be involved in the 23S rRNA binding, are located on the protruding loops at the gate of the interface region between the two domains. *Bst*L2-RBD appears to bind the target RNA on the cleft formed by the N- and C-terminal domains, which probably confers on protein L2 a specific recognition for the target RNA. The molecular architecture suggests how this important protein has evolved from the ancient nucleic acid binding proteins to create a 23S rRNA-binding domain in the very remote past.

P07.04.053 CRYSTALLIZATION OF rRNA APTAMER BINDING WITH THE RIBOSOMAL PROTEIN S8. N. Davydova and A. Liljas, Molecular Biophysics, Lund University, POB 124, S-221 00 Lund, Sweden, H. Moine, B. Ehresmann and Ch. Ehresmann, UPR 9002, Institute for Molecular and Cellular Biology, 67084 Strasbourg, France, and Maria Garber, Institute of Protein Research, 142292 Pushchino, Moscow Region, Russia.

Ribosomal protein S8 plays a key role in 30S ribosomal subunit assembly through interaction with 16S rRNA. Its binding site consists of two base paired helical regions that flank a phylogenetically conserved core element containing 9-13 nucleotides. Recently the solution structure of S8 binding rRNA fragment from *Escherichia coli* has been defined using NMR spectroscopy (1), and the crystal structures of S8 protein from *Bacillus stearothermophilus* (2) and *Thermus thermophilus* (3) have been determined. Some conclusions about the importance of different RNA residues for S8-RNA binding were presented in these publications. However there are still many questions which could be solved by crystal structure of the RNA fragment itself and in complex with the protein.

In Selex experiments S8 binding RNA aptamers from *T. thermophilus* with different changes in core region were obtained (4). After search for crystallization conditions for RNA aptamers, one of them was crystallized in the present work. The attempts to crystallize wild type rRNA fragment were unsuccessful.

The native data set was collected at beamline BL711 at MAXII synchrotron in Lund. Crystals diffract to 2.9 Å resolution. The space group of observed crystals was found to be P1, with cell dimensions a=30.17 Å, b=45.65 Å, c=100.82 Å, α=93.47°, β=95.04°, γ=102.71° and four molecules in the asymmetric unit. These values correspond to V_m (volume of asymmetric unit/molecular weight) of 2.39 Å^3/Da, which is in the range usually found for RNA crystals. Heavy atom derivatives search is in progress.

1. Kalurachchi, K. and Nikonowicz, P. (1998). *J. Mol. Biol.* **280**, 639-654.
2. Davies, C. et al. (1996). *Structure* **4**, 1093-1104.
3. Nevskaya, N. et al. (1998). *J. Mol. Biol.* **279**, 233-244.
4. Moine, H. et al. (1997). *RNA* **3**, 255-268.

P07.04.054 TOWARDS A NEW CRYSTAL FORM OF BACTERIOPHAGE MS2 COAT PROTEIN. W.T. Horn, M.A. Convery, N.J. Stonehouse, P.G. Stockley and S.E.V. Phillips, Faculty of Biological Sciences, University of Leeds, Leeds, LS2 9JT, UK.

MS2 is a T=3 icosahedral bacteriophage with a single stranded RNA genome that infects *E. coli. In vivo* an RNA stem loop binds to a phage protein coat dimer, acting both to initiate phage self assembly and to inhibit viral replicase gene translation. Structures of the MS2 phage particle and both wild type[1] and aptamer[2] stem loops bound to MS2 capsids have been determined.

It has been demonstrated that the MS2 coat protein can be used as a supramolecular scaffold to anchor small RNA motifs covalently bound to the stem loop sequences, thus allowing their structural determination. Using this system it is no longer necessary to search for individual crystallisation conditions for each RNA.

In vivo, RNA is stabilised by interactions with metal ions and therefore their presence is important to ensure the RNA structure determined is of biological relevance. However, current crystallisation conditions for MS2 utilise a sodium phosphate buffer which leads to precipitate formation on addition of metal ions.

One possible solution is to carry out MS2 crystallisation under different conditions. Trials are currently being undertaken and several of the crystal types obtained are being characterised.

1) Valegård, K., Murray, J.B., Stockley, P.G., Stonehouse, N.J. & Liljas, L. Crystal structure of an RNA bacteriophage coat protein-operator complex. *Nature,* **371,** 623-626 (1994).
2) Rowsell, S., Stonehouse, N.J., Convery, M.A., Adams, C.J., Ellington, A.D., Hirao, I., Peabody, D.S., Stockley, P.G. & Phillips, S.E.V. Crystal structures of a series of RNA aptamers complexed to the same protein target. *Nature Structural Biology,* vol 5 no. 11, 970-975 (Nov 1998).

P07.04.055 STRUCTURE AND FUNCTION STUDIES OF POLY(A) POLYMERASE FROM S. CEREVISIAE. N.C. Picken[1], W. Keller[2], J. Jäger[1]. [1]School of Biochemistry and Molecular Biology, University of Leeds, Leeds, UK, LS2 9JT. [2]Dept. Cell Biology, Biozentrum, University of Basel, Basel Switzerland.

Poly(A) polymerase (PAP) is involved in the maturation of pre-mRNAs. Poly(A) tails are found on essentially all mRNAs and have a variety of different functions such as control of mRNA turnover and translation efficiency. In order to gain an understanding of this enzyme it is desirable to determine its crystal structure.

Yeast PAP has been chosen for structural studies. This has a shorter amino acid sequence and is assumed to be a more compact enzyme and therefore more suitable for crystallisation experiments. With 58% overall sequence homology to its mammalian counterparts the structure of Yeast PAP could also provide information about these enzymes.

Light scattering experiments have been carried out using PAP from *S. cerevisiae* and *S. pombe*. Both His-tagged and untagged samples were used and the results showed that PAP is monomeric and is monodisperse and would therefore appear suitable for crystallisation experiments.

Previous crystallisation experiments have resulted in initial conditions which gave rise to small rod shape crystals. However these diffracted poorly, to around 8Å under cryo-conditions, and further crystallisation experiments are being carried out to produce better diffracting crystals.

P07.04.056 3D STRUCTURE OF THE TATA-BOX BINDING PROTEIN FROM A THERMOPHILI-CARCHAEBACTERIUM, *SULFOLOBUS ACIDOCALDARIUS*. Hideaki Koike[1], Norio Kudo[1,2], Yoshie Kawashima[1], Masaru Tateno[1], Kazuhiko Yamasaki[1] and Masashi Suzuki[1,2] ([1]AIST-NIBHT CREST Centre of Structural Biology, [2]Graduate School of Human and Environmental Sciences, University of Tokyo)

The 3D structure of the TATA-box binding protein (TBP) from a thermophilic archaebacterium, *Sulfolobus acidocaldarius*, has been determined in the resolution of 2.7Å with the R-factor being 26.6%. Crystals of the TBP were obtained by the vapour diffusion method using sulfate salts as precipitants. The crystal was identified to be of the orthorhombic space group, P21212, and thus is different from any other reported crsytals of TBPs. Two independent molecules were identified positioning in the asymmetric unit of 64.0x81.2x88.1 Å. A 3D model was constructed by replacing amino acid side-chains in the crystal structure of TBP of another species (1PCZ), and modified by energy minimization. In order to produce best agreement with the crystallographic data, the inter-domainal connection in the model was changed systematically while keeping the domainal structures intact, and then the co-ordinates of each atom in the domains were changed. The process was repeated until the best R-factor and freeR values were recorded. In the final structure the overall combination of the secondary structures was found essentially kept the same, but differences in position and conformation were observed in the residues in distal region from the centre of the molecules and loops connecting the region and the central β-strand. On the basis of the determined TBP structure and known TBP structures of other species, and of the amino acid sequences of TBPs of archabacterial species that possess different optimal growth temperature values, the domainal thermostability and the inter-domainal thermal flexibility are being studied. The TBP of a hypr-thermophilic archaebacterium, *Pyrococcus* sp. OT3 (Opt. T., close to 100°C) is, in general, more stable than TBPs of two thermophilic archaebacterial species, *Sulfolobus acidocaldarius* (Opt. T., 75°C), and *Thermoplasma volcanium* (Opt. T., 60°C). The TBP from *Thermoplasma* showed higher thermal stability upon decreasing the KCl concentration, while the other two TBPs, in contrast, upon increasing the KCl concentration. Specific amino acid residues and more global factors that determine the thermostability and its salt dependence are being investigated. An amino acid position that is possibly important for the thermal flexibility has been identified on the inter-domainal surface, which is occupied by a large aromatic residue, Phe, in the TBP from *Pyrococcus*, and a small residue, Ala, in that from *Thermoplasma* and *Sulfolobus*, while the smallest residue, Gly, in those of the eukaryotic origin.

P07.04.057 CRYSTALLOGRAPHIC STUDIES OF HISTONE-LIKE SUBUNITS OF TFIID. S. Werten, C. Romier, C. Birck, O.Poch, M. Ruff, G. Mengus, A.C. Lavigne, I. Davison, D. Moras IGBMC, Illkirch, France.

Transcription initiation in eukaryotes by RNA polymerase II requires the assembly of a macromolecular complex at the core promoter of a gene. The multi-subunit factor TFIID plays a key role in the formation of this complex, as it recognizes the core promoter DNA and is the interaction target for many transcriptional activators. TFIID is composed of the TATA-binding protein (TBP) and a number of TBP-associated factors (TAFIIs). Recently, some of the TAFIIs have also been found in other macromolecular complexes (hTFTC, ySAGA and hPCAF) that are involved in transcription. Three of the TAFIIs - hTAFII80, hTAFII31 and hTAFII20 - display strong similarity, both in sequence and structure, to histones H4, H3 and H2B, respectively. Consequently, TFIID has been proposed to contain a nucleosome-like core, consisting of two H2A/H2B-like homodimers of hTAFII20 and a H3/H4-like heterotetramer of hTAFII80 and hTAFII31. A similar core structure could exist in hTFTC, ySAGA and hPCAF. However, this model does not address the role of the additional TAFIIs that are found in TFIID. We have therefore started the structural study of other subcomplexes within TFIID. This work has recently led to the determination of the structure of the complex formed by hTAFII18 and hTAFII28. Although the full-length proteins were used for crystallization, crystals contained truncated polypeptides due to proteolysis within the crystallization droplet. The crystals belong to space group $P2_12_12_1$ with a=45.4, b=48.4 and c=77.6 Å. The structure was solved by using exclusively anomalous data from crystals soaked with pCMBS that showed a decrease of 7 Å in the c-axis compared to the native crystals. The mercury-bound structure was refined at a resolution of 2.6 Å and was then used to solve the native structure by molecular replacement. This latter structure was refined at 3 Å and showed no real difference with the mercury-bound one. Unexpectedly, the two proteins were found to interact through histone folds, which cannot be classified within the four canonical families (H2A/B, H3, H4). Sequence analysis revealed that the protein SPT3, found in the TFTC, SAGA and PCAF complexes, contains at its N- and C-termini two histone fold motifs which are strongly homologous to the histone fold motifs of hTAFII18 and hTAFII28, respectively. Since both hTAFII18 and hTAFII28 are absent from TFTC, SAGA and PCAF, SPT3 may be the structural equivalent in these complexes of the two TAFIIs in TFIID.

P07.04.058 MACROMOLECULAR CRYSTALS : A QUESTION OF INTERACTION POTENTIALS. F. Bonneté, A. Le Verge, S. Finet and A. Tardieu, LMCP, CNRS - Universités Paris VI et Paris VII, 4 Place Jussieu, 75252 Paris Cedex 05, France; L. Belloni, SCM, DRECAM, CE Saclay, 91191 Gif sur Yvette Cedex, France.

Biological macromolecules in solution interact with each other through medium range (from a few Å to a few nm) interaction potentials. These potentials control the macromolecular distribution in solution, the macromolecular phase diagram and the crystallization process. We have shown previously that Small Angle X-ray Scattering (SAXS) is a convenient tool to characterize the resulting potential, either attractive or repulsive, and to follow the changes induced by the crystallizing agents (1). The approach, applied to lysozyme crystallization, demonstrated that protein interactions are involved and not agregation, and that particle are in the attractive regime (2). In the present study, simulation methods derived from statistical mechanics were coupled to SAXS to find out the best fit potentials able to account for the experimental lysozyme SAXS data.

The currently used models in the colloidal field are derived from the DLVO (Derjaguin, Landau, Verwey, Overbek) potential where three types of interactions play a major role : hard sphere, electrostatic, van der Waals. In a series of X-ray experiments, the best fit parameters to determine from the shape of the scattering curves are the hard core diameter and the depth and range for both the repulsive and the attractive contribution to the resulting potential. The attractive potential at the isoelectric point was found to be short range (i.e. between zero and 6 Å) as already found for gamma-crystallins (3), and equivalent to an adhesive sphere potential. Decreasing the pH at low ionic strength introduces a repulsive coulombic component which can be screened by salt. To account for the anion specificity on lysozyme crystallization, following the reverse order of the Hofmeister series, some modifications of these potentials are, however, required.

The whole of the data demonstrate that the colloidal approach may be applied with success to lysozyme crystallization.

1 Bonneté F., Vidal O., Robert M.C. and Tardieu A. 1996, *J. Crystal Growth* **168**, 185
2 Ducruix A., Guilloteau J.P., Ries-Kautt M. and Tardieu A. 1996, *J. Crystal Growth* **168**, 28
3 Malfois M.,Bonneté F.,Belloni L. and A. Tardieu 1996, *J. Chem. Phys.* **105 B,** 3290

P07.04.059 A NEW CRYSTAL STRUCTURE FOR THE DNA SEQUENCE d(CGCGAATTCGCG). GN Parkinson, EM Johansson and S Neidle, The CRC Biomolecular Structure Unit, The Institute of Cancer Research, Sutton, Surrey SM2 5NG, UK

The DNA sequence d(CGCGAATTCGCG) has been the subject of intensive study following on from its original crystallographic analysis by Dickerson and Drew. In particular, the features of sequence-dependent structure and minor-groove hydration first described in the original structure have been taken as the paradigm for DNA flexibility and hydration. However there continues to be controversy surrounding the role played by crystal packing forces in producing these effects.

We have solved the crystal structure of d(CGCGAATTCGCG) in the hitherto unreported space group $P3_212$, with cell dimensions a = b = 26.39 Å and c = 98.78 Å. Crystals were obtained in the presence of Ba^{2+}, and diffraction data has been collected to 1.8 Å on beam line 9.5 at the Daresbury Synchrotron source. The structure has been solved by molecular replacement, using a decamer as the search fragment, and refined by X-PLOR. Uniquely for a native DNA dodecamer, the duplex formed has crystallographic 2-fold symmetry, and the asymmetric unit is a single strand of d(CGCGAATTCGCG). The sequence-dependent and hydration features of this structure will be presented in detail.

P07.04.060 FIRST HIGH RESOLUTION STRUCTURE OF AN RNA FRAGMENT FROM MAMMALIAN SRP RNA. Klemens Wild, Oliver Weichenrieder & Stephen Cusack: EMBL Grenoble Outstation, France.

The mammalian Signal Recognition Particle (SRP) is an 11S cytoplasmic ribonucleoprotein complex consisting of the SRP RNA (300 nt) and six proteins. SRP mediates the cotranslational targeting of secretory proteins to the translocation apparatus in the endoplasmatic reticulum membrane.

We have crystallized and solved the structure at 2.0 Å resolution of an RNA fragment comprising 29 nt of helix 6 of mammalian SRP, the principal binding site of SRP19. The structure was solved by the MAD method using the anomalous signal from Br-U which was incorporated into the RNA via an *in vitro* transcription. Clean RNA 3' ends were generated by ribozyme technology. Due to the intolerance of the ribozyme active site for Br-U, the maximum occupancy of Br-U in the molecule had to limited to 50%.

Instead of forming a monomeric hairpin structure with a GGAG tetraloop, in the crystal the RNA forms 28-mer duplexes with distorted A-RNA geometry and the overhanging base being flipped out. Duplex formation is a general problem in the crystallization of RNA hairpins. Aligning parallel to the crystallographic 3-fold axis, the duplexes give rise to infinite helices thus forcing the previously formed hairpin to open up. Despite the dimerization, 24 out of the 28 base pairs represent the presumed native structure with only the tetraloop forming an artificial 5'-GGAG-3'/3'-GGAG-5' purin bulge containing an internal GA tandem mismatch. The irregularities of the native part of the structure include a 5'-AC-3'/3'-CA-5' tandem mismatch with protonated and non-protonated adenine bases and GU wobble base pairs. Moreover, the crystal packing creates a 5'-GU-3'/3'-GU-5' tandem wobble base pair forming a cross strand purin stack. The high resolution allows a detailed analysis of the model including magnesium and water moelcules. The native structure containing the SRP RNA specific GNAR tetraloop is modeled using the well-known GNRA hairpin fold.

P07.04.061 CRYSTAL STRUCTURE OF A COMPLEX BETWEEN THE SEQUENCE d(CGCGAATTCGCG) AND A NOVEL MINOR-GROOVE DRUG. EM Johansson, GN Parkinson, J Mann[1] and S Neidle, The CRC Biomolecular Structure Unit, The Institute of Cancer Research, Sutton, Surrey SM2 5NG, UK and [1]Dept of Chemistry, University of Reading, Berkshire RG6 6AH, UK

The crystal structures of over 25 complexes between minor groove drugs and DNA oligonucleotide sequences have now been solved in this laboratory. We have recently embarked on the design of novel minor-groove ligands, exploiting this knowledge-base, with special reference to the roles played by hydrogen-bonding and van der Waals forces in defining sequence-specificity. One such series is based on a head-to-head arrangement for two bis-benzimidazole rings (Neidle et al, Chem. Comm, 1999, in press).

We now report the crystal-structure analysis of a complex between the sequence d(CGCGAATTCGCG) and a symmetric head-to-head bis-benzimidazole with substituent propyl-dimethylamino side-chains. The structure crystallises in the space group $P2_12_12_1$, with cell dimensions a = 25.145, b = 39.924 and c = 65.648 Å. Intensity data were collected on a flash-frozen crystal at 100 K to a resolution of 2.0 Å. The structure is isomorphous with other dodecamer complexes; it has been refined by XPLOR and SHELX-97. The current R and R_{free} values are 0.20 and 0.28 respectively, with > 100 water molecules and a hydrated magnesium ion having been located.

The drug is symmetrically bound in the minor groove, with the benzimidazole groups hydrogen bonding to A:T base pairs. The side-chains are not hydrogen-bonded, but are held more loosely in the wider G:C minor groove regions.

P07.04.062 STRUCTURE OF MUTANT TEF1W OF THE SRC SH2 DOMAIN COMPLEXED WITH PHOSPHOTYROSINE CONTAINING PEPTIDES. Joseph Nachman, Matthew Kimber, Annie Cunningham, and Emil Pai, Ontario Cancer Institute and Department of Biochemistry, University of Toronto, Toronto, Ontario M5S 1A8, Canada; Gerald Gish and Antony Pawson, Samuel Lunenfenld Research Institute, Mount Sinai Hospital, Toronto, Ontario M5G 1X5, Canada.

A common device through which receptor tyrosine kinases access their intracellular targets involves receptor autophosphorylation at Tyr sites, which consequently bind the Src homology 2 (SH2) domains of cytoplasmic signaling proteins. The affinities with which SH2 domains bind to phosphorylated peptide motifs generally depends on the sequence of amino acids immediately C-terminal to the phosphotyrosine. It has previously been shown that changing a single amino acid at the EF1 position of the Src SH2 domain from Thr to Trp converts its binding specificity to resemble that of the Grb2 SH2 domain, and that this mutant Src SH2 domain functions *in vivo* during *C. elegans* development in place of the Grb2 (SEM-5) SH2 domain. We have solved the X-ray crystal structure of the mutant TEF1W Src SH2 domain in complex with phosphopeptides (pYEEI and pYVNV) that normally bind preferentially to Src or Grb2 domains, respectively. The presence of Trp at the EF1 position blocks the normal path of pYEEI peptide bound to the mutant Src SH2 domain, but readily accommodates a pYVNV peptide. The conformations of the pYVNV peptide bound to the mutant Src SH2 domain and the Grb2 SH2 domain are virtually identical. Our results strikingly illustrate how SH2 domains distinguish between different phosphorylated sites, and suggest a mechanism through which simple substitutions could allow for rapid evolution of SH2

domain specificity, and thus for increased complexity in pTyr signaling.

P08.04.001 SERINE PROTEASES INTERACTIONS WITH ECOTIN: A GENERAL SERINE PROTEASE INHIBITOR FROM E. COLI. Stephanie Wang [1], Sarah Gillmor [2], Charles Craik [3], Robert Fletterick [4], [1,3] Department of Pharmaceutical Chemistry, [2] Program in Biophysics, [3,4] Department of Biochemistry and Biophysics, University of California at San Francisco, CA 94143, U.S.A.

Protease activities are found to be associated with various biological processes. Many small or macromolecular inhibitor have found in nature. Understanding the interactions between proteases and their macromolecular inhibitors provides many insights for elucidating the mechanism of protease actions as well as for designing new inhibitors which may be of therapeutic significance. Ecotin, a macromolecular inhibitor discovered from E. Coli. periplasm, has the unusual property of inhibiting a variety of serine proteases regardless of their substrate specificity. Crystal structures of complexes of ecotin-rat trypsin and ecotin-crab collagenase revealed novel tetrameric complexes formation. Each complex contains two ecotin and two protease molecules. Each ecotin molecule contacts two protease molecules at two different binding sites. How does ecotin interact with its cognate proteases at the different binding sites? Can we engineer ecotin to alter its inhibitory profile against various cognate proteases or to create novel inhibitory activities against non-cognate proteases?

To elucidate the details of interactions between ecotin and its cognate serine proteases, we are solving the structures of complexes between rat trypsin and ecotin variants with different mutations at the protease binding sites. Structures of complexes between rat trypsin and four different ecotin variants have been determined by X-ray crystallography. Diffraction data have been collected for a fifth complex. The structure is currently being solved. Crystallisation experiments are being carried for several other complexes between rat trypsin and ecotin mutants. Extensive comparison studies of the structures of these complexes will help us to understand the interactions between ecotin and rat trypsin, one of its cognate serine proteases.

Wild type ecotin fails to inhibit thrombin, a serine protease which shares high sequence and structural homology with rat trypsin. However, a single mutation in ecotin turns it into a moderate inhibitor against thrombin. We are investigating possible structural changes which allow this drastic change of inhibitory profile by determining the crystal structure of the complex between thrombin and the ecotin mutant. Initial studies have resulted in crystals which diffracted to 3Å. Crystallisation conditions are being optimized for better quality crystals which will give higher resolution data.

The interactions between ecotin and different serine proteases provide knowledge for understanding basic protein-protein interactions. Such knowledge we gain here will also serve as basis for designing novel inhibitors against targets such as viral proteases.

P08.04.002 THE LOSS OF HYDROPHOBIC CORE PACKING INTERACTIONS IS STRONGLY CORRELATED TO THE LOSS OF PROTEIN STABILITY. M. Vlassi, NCSR "Demokritos, Ag. Paraskevi, GR-15130 Athens, Greece, G. Cesareni, Dipartimento Di Biologia, Tor Vergata, Il Universita degli Studi di Roma, Rome, Italy and M. Kokkinidis, Department of Biology, University of Crete, & Institute of Molecular Biology and Biotechnology, GR-71110 Heraklion, Crete, Greece.

Globular proteins are characterized by well-packed hydrophobic cores which play important roles in protein folding and stability. The small homodimeric ROP protein follows the 4-α-helical bundle structural motif and its folding and stability are largely determined by a regular pattern of hydrophobic core interactions [1]. In order to examine structural and thermodynamic responses to core mutations in proteins, the crystal structures of two large-to-small (Leu→Val/Ala) substitutions of the core residue Leu41 of the ROP protein have been determined.

Both substitutions are destabilizing [2] and lead to formation of cavities. The main responses to mutations are the collapse of the central part of the alpha-helix containing the site of mutation, shifts of internal water molecules, and in L41A, the trapping of a water molecule in the cavity created by the mutation. These effects counteract the increase in cavity size, so that the actual cavities are much smaller than what would be expected in the absence of the above effects.

A new parameter (Δn_h) is introduced as a measure of the number of Van der Waals contacts lost. For ROP, barnase and T4 lysozyme mutants there is a good correlation between Δn_h and the free energy of unfolding $\Delta\Delta G$ relative to wild-type protein. The Δn_h turns out to be more suitable for analysing structural and energetic responses to mutation than other parameters, such as cavity volumes and packing densities.

M. Vlassi, D. Tsernoglou, Z. Dauter and M. Kokkinidis (1994) Nature, Struct. Biol. 1, 706-714.
C. Steif, H-J. Hinz and G. Cesareni, (1995) Proteins Struct. Funct. Genet. 23, 83-96.

P08.04.003 STRUCTURAL STUDIES OF UBIQUINONE BINDING SITES IN BACTERIAL PHOTOSYNTHETIC REACTION CENTRES. P.K. Fyfe*, J.P. Ridge and M.R. Jones* Department of Molecular Biology and Biotechnology, Krebbs Institute, Firth Court, University of Sheffield, Western Bank, Sheffield, S10 2UH. U.K. and K.E. McAuley-Hecht, R.J. Cogdell Department of Biochemistry and N.W. Isaacs, Department of Chemistry, University of Glasgow, University Avenue, Glasgow, G12 8QQ. U.K. *Current Address: Department of Biochemistry, School of Medical Sciences, University of Bristol, University Walk, Bristol, BS8 1TD. U.K.

Several crystal structures of the bacterial photosynthetic reaction centre from *Rhodopseudomonas viridis* and *Rhodobacter sphaeroides* are now available [1,2]. The availability of these structures has greatly enhanced our understanding of how these integral membrane pigment:protein complexes function, and has allowed the rational design of site-directed mutants to probe structure/function relationships within the complex. X-ray crystallography is now also being applied to the mutant complexes themselves, with several crystal models revealing hitherto unexpected structural arrangements. This presentation will discuss the results of studies of several complexes bearing mutations in one of the two ubiquinone binding sites, and in particular a 2.1Å model of a Q_A minus mutant complex (AM260W) which showed very high occupancy of the Q_B binding site. There has recently been much debate in the field as to the position assumed by the Q_B cofactor in the native complex, with early crystal models showing only very poor occupancy of this site. More recently two groups have made use of reconstitution with quinones and/or chemical analogues to attempt to overcome this problem [1,2]. The AM260W crystal structure gives the first well resolved model of the site in a complex which has not been chemically treated to obtain the high occupancy.

1 C.R.D. Lancaster & H. Michel (1997). Structure, 5, 1339-1359.
2 M.H.B. Stowell, T.M. McPhillips, D.C. Rees, S.M. Soltis, E. Abresch & G. Feher (1998). Science, 276, 812-816.

P08.04.004 SPECIFIC BINDING OF CARDIOLIPIN TO AN INTEGRAL MEMBRANE PROTEIN. K.E. McAuley, K. McKendrick, R.J. Cogdell, Department of Biochemistry and N.W. Isaacs, Department of Chemistry, University of Glasgow, Glasgow G12 8QQ, UK and P.K. Fyfe*, J.P Ridge and M.R. Jones*, Department of Molecular Biology and Biotechnology, Krebbs Institute, Firth Court, University of Sheffield, Western Bank, Sheffield, S10 2UH. U.K.

*Current Address: Department of Biochemistry, School of Medical Sciences, University of Bristol, University Walk, Bristol, BS8 1TD

Cardiolipins are an important class of anionic phospholipid. Cardiolipin has been shown to have a regulatory role in the activity of a number of integral membrane proteins [1-3] e.g. cytochrome *c* oxidase which has an absolute requirement for cardiolipin for function [4]. Despite the fact that extensive study has been made of the role of anionic lipids in biomembrane function, relatively little is known about the molecular details of the interactions between these lipids and the proteins to which they bind. Recently, we determined the structure of a mutant photosynthetic reaction centre with a bound cardiolipin molecule. The lipid binds to the surface of the protein, with interactions between the phosphate headgroup of the lipid and arginine/histidine residues of the protein. There are also extensive van der Waals interactions between the acyl chains of the lipid and grooves on the protein surface. Based on the analysis of this structure, several mutant complexes have been made to study the effect of cardiolipin on the function of this membrane protein.

1 P.V. Ioannou & B.T. Golding (1979) Prog. Lipid Res. 17, 279-318
2 F.L. Hoch (1992) Biochim. Biophys. Acta 1113, 71-133
3 W. Dowhan (1997) Annu. Rev. Biochem. 66, 199-232
4 Y.C. Awasthi, T.F. Chuang, T.W. Keenan, F.L. Crane (1971) Biochim. Biophys. Acta 226, 42-52

P08.04.005 CRYSTAL STRUCTURE OF THE MUTANT F99S/M153T/V163A OF THE GREEN FLUORESCENT PROTEIN. R.Battistutta, A. Negro and G. Zanotti, Dipartimento di Chimica Organica, Centro Studi sui Biopolimeri and Dipartimento di Chimica Biologica, Università degli Studi di Padova, 35131 Padova, Italy.

The Green Fluorescent Protein from the jellyfish *Aequorea victoria* is a single domain protein of 238 aminoacids, that converts blue radiation into green light. GFP is characterized by the presence of a chromophore that originates from a post-translational autocatalitic cyclization of the tripeptide segment -S65-Y66-G67-, with successive dehydrogenation of the α-β bond of the tyrosine. In the mature protein the chromophore exhibits two characteristic absorption bands, at 395 nm and at 475 nm, and emits green light with an emission maximum around 508 nm. Due to its intrinsic fluorescence properties, GFP is widely used as fluorescent probe in several biotechnological applications. In the last three years, structures of wild-type GFP and of several mutants have been solved. By DNA shuffling techniques, the mutant F99S/M153T/V163A (GFP-sta) was found to be around 42-fold more fluorescent *in vivo* than the wt-GFP [1]. GFP-sta was crystallised in the tetragonal space group $P2_12_12_1$, and the structure was solved with the molecular replacement method. While the topology and the overall structure of the GFP-sta is similar to the other Green Fluorescent Proteins, nevertheless same interesting and peculiar features are present in our mutant. The two dimers in the asymmetric unit are not identical, particularly as far as the environment of the chromophore is concerned. In two chains the conformation of the side chain of Thr203 allows an hydrogen bond between the OH of this residue and that of the chromophore in absence of any water molecule. On the ground of the results presented here, we propose that the increase in the cell content of mature fluorescent protein is due to a more efficient folding process *in vivo* of the GFP-sta mutant.

1. A. Crameri, E.A. Whitehorn, E. Tate & W.P.C. Stemmer (1996) Nature Biotechnology, 14, 315-319.

P08.04.006 STUDY ON CARBOXYL-TERMINAL MODIFIED THERMOSTABLE 3-ISOPROPYLMALATE DEHYDROGENASE STRUCTURE. Z. Nurachman, S. Akanuma,[1] T. Oshima,[2] and N. Tanaka; Dept. Life Sci., TITech., Yokohama 226, Japan; [1]) RIKEN, Wako 351, Japan; [2]) Dept. Molec. Biol., Tokyo Univ. of Pharm. and Life Sci., Hachioji 192, Japan.

To understand the role of amino acid sequences at carboxyl terminus in maintaining thermostability, mutant structure of 3-Isopropylmalate dehydrogenase (IPMDH) of *Thermus thermophilus* has been solved. Advanced study on the improvement of thermostability for IPMDH was performed by creating mutants such as tandem sequence duplication mutants at C-terminus region , named HD177, HD708, and HD711 (Fig. 1.) (1). The α-helix at C-terminus of HD177 and HD708 is short. However, it is conserved in HD711. The thermostability of the mutants is lower than that of A172L. However, the protein is more thermostable, more elongated. The molecular model evidence shows that the side chains of A342 and F343 position of HD711 are located on unfavorable ionic region and the side chain of E341 is situated on adverse hydrophobic pocket. These interactions loose a tightness of structures at C-terminal region and reduce its thermostability. In addition, the hydrophobic extended sequences at C-terminus, which is exposed to solvent region, contribute weakening the structure. These phenomena imply that the interactions stabilizing the α-helix at C-terminus might have important role in regulation of thermophilic property. The function of these interactions has analogy with screw function in scissors. If they tighten or loosen, it could regulate the enzyme thermostability up or down without changing a significant catalytic constant.

```
A172L   333 TEAFTATVLRHLA 345
HD177   333 --------GMGI 344
HD708   333 ---------TATVGI 346
HD711   333 -------EAFTATVGI 349
```

Fig.1. Aligned amino acid sequences of IPMDH A172L and the mutants at the carboxyl terminus region. Conserved amino acid residues are represented by a hyphen and tandem sequence duplications are underlined. The italic character of A172L sequences indicate the α-helix structure.

[1] Akanuma, S. (1998), Doctoral Thesis, Dept. of Life Sci., Tokyo Inst. of Tech., Tokyo, Japan.

P08.04.007 RELATIONSHIPS BETWEEN STRUCTURE AND STABILITY IN MUTANT HUMAN LYSOZYMES. Yuriko Yamagata, Graduate School of Pharmaceutical Sciences, Osaka University, Suita 565-0871, Japan and Jun Funahashi, Kazufumi Takano and Katsuhide Yutani, Institute for Protein Research, Osaka University, Suita 565-0871, Japan

Today we are in the era of structural genomics. When almost all protein folds are known, information about protein stabilization mechanisms will be useful for fold assignment and comparative protein structure modeling. To elucidate correlative relationships between structural change and thermodynamic stability in proteins, we have constructed about 100 mutant human lysozymes and determined their thermodynamic parameters of denaturation and crystal structures using differential scanning calorimetry and X-ray crystallography, respectively. Analyzing data base of stability/structure for mutant human lysozymes, we

have found that changes in stability due to amino acid substitutions are interpreted as the sum of changes in overall hydrophobic effect, side-chain conformational entropy, hydrogen bonds, the number of buried water molecules, cavity volume, secondary structure propensity and other effects (1, 2 and Funahashi et al. and Takano et al., submitted). The magnitudes of the contribution of these factors to protein stability have been estimated as the function of structural parameters using data of about 55 mutants with negligible other effects. For example, the change of hydrophobic effect is evaluated as the sum of 0.178ΔΔASA(non-polar) and –0.013ΔΔASA(polar), where ΔΔASA(non-polar) and ΔΔASA(polar) represent the difference in ΔASA of non-polar and polar atoms of all residues in a protein, respectively, upon denaturation between the wild-type and mutant proteins. These relationships between structure and stability can be used as monitors for the validity of fold assignment and comparative protein structure modeling.

Takano, K., Yamagata, Y. & Yutani, K. (1998) J. Mol. Biol., 280, 749.
Yamagata, Y. et al., & Yutani, K., (1998) Biochemistry, 37, 9355.

P08.04.008 STABILITY OF A JELLYROLL FOLD: CRYSTAL STRUCTURE OF THE *BACILLUS* HYBRID ENZYME GLUXYN-1. J. Aÿ [(1)], F. Götz [(2)], R. Borriss [(2)] and U. Heinemann [(3)], (1) Institut für Biochemie der Charité, Humboldt-Universität, Monbijoustr.2, 10117 Berlin, Germany. (2) Institut für Biologie, Humboldt-Universität, Chausseestr.117, 10115 Berlin, Germany. (3) Forschungsgruppe Kristallographie, Max-Delbrück-Centrum für Molekulare Medizin, Robert-Rössle-Str.10, 13122 Berlin, Germany

Protein folding is a very interesting feature to understand more about the biological role of proteins in a cell. Former crystal structures of circularly permuted 1,3-1,4-β-glucanases [1,2] showed, that the jellyroll fold is a highly stable structure motif. As a consequence of our work about the stability of the jellyroll fold we designed the bifunctional *Bacillus* hybrid enzyme GluXyn-1. To construct GluXyn-1 two jellyroll proteins, the 1,3-1,4-β-glucanase of *Bacillus macerans* and the 1,4-β-xylanase of *B. subtilis* were joined by insertion of the entire domain XYN into the cpMAC-59, the circularly permuted variant of the wtGLU. The insertion protein generated by protein engineering folds into a stable protein and shows a comparable activity to the parental proteins [3]. The crystal structure of the two domain protein was determined at 2.1 Å resolution and refined to a R = 17.7 % and R(free) = 22.4 %. The structure is comparable to the crystal structure of the parental enzymes. The jellyroll fold of both domains survive and tolerate the insertion of an autonomous folding domain. There is a significant hinge bending between the domains. Both active sites are independent to each other, thus explaining the observed enzymatic activity. The results show that the protein folding for a jellyroll protein depends on long ranging intramolecular contacts in the sequence. Additionally there is a new way to build stable end-to-end fusion proteins.

1. M. Hahn, K. Piotukh, R. Borriss & U. Heinemann (1994) P.N.A.S. 91, 10417-21
2. J. Aÿ, M. Hahn, K. Decanniere, K. Piotukh, R. Borriss & U. Heinemann (1998) Proteins Struct. Funct. Genet. 30, 155-167
3. J. Aÿ, F. Götz, R. Borriss & U. Heinemann (1998) P.N.A.S. 95, 6613-18

P08.04.009 STRUCTURAL STUDIES OF A PHOTOSYNTHETIC REACTION CENTRE HYDROGEN BONDING MUTANT. K.A. McKendrick, K.E. McAuley-Hecht, R.J. Cogdell, Department of Biochemistry and N.W. Isaacs, Department of Chemistry, University of Glasgow, University Avenue, Glasgow, G12 8QQ UK and P.K. Fyfe*, D. Spiedel and M.R. Jones* Department of Molecular Biology and Biotechnology, Krebbs Institute, Firth Court, University of Sheffield, Western Bank, Sheffield, S10 2UH UK *Current address: Department of Biochemistry, School of Medical Sciences, University of Bristol, University Walk, Bristol, BS8 1TD.

Structural and functional studies on site-directed mutants of the photosynthetic reaction centre (RC) from *Rhodobacter sphaeroides* have been important in increasing our understanding of how this integral membrane protein-cofactor complex functions. This presentation will discuss one of several complexes in which the hydrogen bonding state of the primary donor (P) a bacteriochlorophyll dimer, has been altered. In the wild-type complex P has one hydrogen bond [1,2]. The mutant HL168F was designed to break this H-bond and spectroscopic evidence indicates that this is the case[3]. The FT-Raman spectrum of wild type RC contains a band at 1620cm^{-1}, assigned to this H-bond. This is completely absent in the mutant. The optical spectrum of the mutant is similar to that of the wild type complex with the exception that the P* (reduced P) absorption band is blue-shifted [1,2]. This has previously been suggested to be due to out of plane rotation of the P_L C2-acetyl . Diffraction data on this mutant was collected to 2.6 Å and is currently under refinement. The results of the crystallographic study will be discussed in this presentation.

1 T.A. Mattioli, J.C. Williams, J.P. Allen & B. Robert, (1994). Biochemistry 33, 1636-1643.
2 J.P. Allen, & J.C. Williams, (1995). Journal of Bioenergetics and Biomembranes 27, 275-283.
3 T.A. Mattioli, X. Lin, J.P. Allen, & J.C. Williams, (1995). Biochemistry 34, 6142-6152.

P08.04.010 BURIED CHARGE IN PROTEINS: HYDROPHOBIC MUTATIONS IN MUCONATE LACTONIZING ENZYME. T. Kajander, L. Lehtio, S. Helin, and A. Goldman [1], D.M. Cohen and P.C. Kahn [2], U. Schell [3], [1]Centre for Biotechnology, University of Turku and Abo Akademi University, Turku, Finland, [2]Department of Biochemistry and Microbiology, University of Rutgers, New Brunswick, USA, [3] Institute for Microbiology, University of Stuttgart, Stuttgart, Germany

It is a well known fact that the hydrophobic effect is the main stabilising force in protein folding. On the other hand the per centage of charged accessible surface buried in proteins increases as the size of the protein increases. Therefore buried charge for enzymes may be a way to destabilise the structure as the size of the hydrophobic core increases. This can be necessary to i ntroduce strain or flexibility required for e.g. catalytic activity. Also, charged residues can have specific structural roles, sometimes even on the expense of stability, in any case providing a partial explanation for the marginal stability of proteins, regardless of their size [1]. We have further studied the effect of hydrophobic mutations on such buried charges in muconate lacto nizing enzyme (MLE) [2], which has a particularly hydrophilic hydrophobic core [2]. We have established unfolding conditions for MLE (an octamer of multidomain monomers of 40 kDa) with a single thermal transition in 0.4 M GndHCl and measured unfolding as a func tion of temperature by fluorescence emission at a maximum of 337 nm with a Tm of 50 C for the wild type. For one of the varia nts, D178N Tm=54 C. The structure of D178N variant at 2.5 A shows that the main cause for increase in Tm is the removal of charge, as the isosteric asparagine replaces D178 without any distortion of the protein.

1 G.I. Makahatdze, P.L. Privalov (1995) Adv. Prot. Chem. 47, 307-425
2. S.Helin, P.C. Kahn, B.L. Guha, D.G. Mallows, and A. Goldman (1995). J. Mol Biol.254, 918-941

P08.04.011 HARVESTING NATURES DIVERSITY TO IMPROVE PROTEIN STABILITY. A. Shaw, A.G. Day, C. Mitchinson, Bott R. Genencor International Inc 925 Page Mill Rd. Palo Alto CA94304 USA.

Currently, industrial scale starch liquefaction is constrained to operating at pH6.0 and above, with resulting economic disadvantages. More economically advantageous low pH liquefaction is prevented because the enzyme used in the process, Bacillus licheniformis a-amylase (BLA) becomes unstable at lower pH, at the high temperature used. The aim of this study was to engineer a BLA variant that can be used at low pH and high temperature. The results have led to the development of a very simple, yet rational method for identifying stabilizing variants, based on natures existing diversity. The implications of these results are that there is sufficient sequence diversity in nature to realize protein engineering goals. The key is to understand how to harness this diversity for success. As the biological information explosion continues, utilizing natures diversity will play a increasingly prominent role in development of rational protein engineering methods.

P08.04.012 STRUCTURE-BASED ASSIGNMENT OF BIOCHEMICAL FUNCTION OF A HYPOTHETICAL PROTEIN: A TEST CASE OF STRUCTURAL GENOMICS. Thomas I. Zarembinski[*‡], Li-Wei Hung[*‡], Hans-Joachim Mueller-Dieckmann[*‡], Kyeong-Kyu Kim[*‡], Hisao Yokota[*], Rosalind Kim[*], and Sung-Hou Kim[*‡]. [*]Physical Biosciences Division of Lawrence Berkeley National Laboratory, [‡]Department of Chemistry, University of California, Berkeley, CA 94720

As a test of structure-based functional assignment of proteins of unknown function, we report the crystal structure of one such protein, MJ0577, from a hyperthermophile, *Methanococcus jannaschii*, at 1.7-Å resolution. The structure contains a bound ATP, suggesting MJ0577 is either an ATPase or an ATP-mediated molecular switch which we confirm by biochemical experiments. Furthermore, the structure reveals different ATP binding motifs that are shared among many homologous hypothetical proteins in this family. This result indicates that structure-based assignment of molecular function is a viable approach for the large-scale biochemical assignment of proteins and for discovering new motifs, a basic premise of structural genomics.

P08.04.013 PROTEOMICS AND THE SHOTGUN APPROACH TO STRUCTURE. Thomas S. Peat, Janet Newman, Geoff Waldo & Thomas C. Terwilliger Los Alamos National Laboratory, NM, USA

Sequence information from the human genome, as well as other genomes, is entering public databases at an astonishing rate. The sequences of at least 20 microbes have been completed and the entire sequences of two eukaryotes are now known (S. cerevisiae and C. elegans). Many more microbial genomes are being sequenced and the entire human genome should be known within the next three years. This genetic information codes for a wide variety of proteins and RNA, many of which were previously unknown. This large number of novel molecules needs to be examined biochemically and structurally. The initial results of a Pilot Investigation into Genomic Structures (PIGS) is reported here. 42 open reading frames (ORFs) were chosen from the recently sequenced hyperthermophile Pyrobaculum aerophilum for PCR amplification from genomic DNA. 36 of these expressed protein when put into an expression vector and 20 of these were soluble at least to some level. Six of these proteins expressed well and were highly soluble. These six were purified and set up in crystallization screens and of these, two crystallized. Both structures are presented as well as the details of this pilot investigation.

P09.04.001 CRYSTALLIZATION OF HIV-1 PROTEASE IN THE COMPLEX WITH PEPTIDOMIMETIC INHIBITORS. H. Jerabkova, J. Hasek, Institute of Macromolecular Chemistry AS CR, Heyrovskeho nam. 2, 162 06 Praha 6, CR, J. Brynda, Institute of Molecular Genetics AS CR, Flemingovo nam. 2, 166 37 Praha 6, CR, M. Hradilek, Institute of Organic Chemistry and Biochemistry AS CR, Flemingovo nam. 2, 166 37 Praha 6, CR

Inhibitors of HIV-1 protease are promising therapeutic agents studied in the treatment of AIDS. Determining of precise interactions between inhibitors and protease by crystallographic techniques can be helpful in explaining the basis of effective inhibition and lead to design of new drugs [1]. Most tight-binding inhibitors of HIV-1 protease are believed to contain isosteric hydroxyl group that forms a hydrogen bond with the active-site aspartates. However the inhibitor without isosteric hydroxyl group showed in our tests stronger inhibition than most of the structures with hydroxyl group [2].

Complexes of HIV-1 protease with inhibitors of hydroxyethylamine type - Boc-Phe[$CH(OH)CH_2NH$]Phe-Gln-Phe-NH_2 (K_i = 14 nM) and ethylamine type Boc-Phe[CH_2CH_2NH]Phe-Glu-Phe-NH_2 (K_i = 0.05 nM) have been subjected to the crystallization screening. Ammonium sulphate, ammonium phosphate, PEG-4000 and NaCl were used as precipitants at pH 4-5. Best results were obtained by vapour diffusion technique at 6-8 °C.

Wlodaver A. & Erickson J. W. (1993): Annu. Rev. Biochem. 62, 543
Konvalinka et al. (1997): Eur. J. Biochem. 250, 559

P09.04.002 *IN-SITU* STUDY OF DEHYDRATION-INDUCED RELAXATION AND DISORDER IN PROTEIN CRYSTALS. I. Dobrianov, C. Kimmer, C. L. Caylor, S. G. Lemay, K. D. Finkelstein, and R. E. Thorne, Cornell University, Ithaca, NY 14850 USA.

Controlled crystal dehydration provides a simple model for the effects of post-growth crystal treatments such as heavy atom compound binding, ligand binding, and cryoprotectant soaks. These treatments all involve molecular diffusion through the crystal, can cause changes in lattice constant, molecular hydration and conformation, and these in turn can cause lattice strains, cracking, mosaic broadening and changes in diffraction resolution. Dehydration studies using lysozyme show that the unit cell shrinks and that the molecules shift, rotate, and undergo small conformational changes as water loss increases. Below 90% r.h., the diffraction resolution degrades dramatically.

We have used X-ray topographs, mosaic and θ-2θ scans, and diffraction patterns collected *in situ* during dehydration of tetragonal lysozyme crystals to study how lattice constants, lattice strains, defects, and diffraction resolution evolve in time. X-ray images reveal characteristic patterns of disorder that are suggestive of a crystal drying out. For dehydrations to 83-87% r.h., the image contrast completes its evolution in 2-3 hours, and lattice constants reach steady-state values in a comparable time. However, the time for degradation of the diffraction resolution varies from an hour to several days much longer than the time for equilibration of the crystal water content with the largest variations occurring for relative humidities above 86%. This suggests that lysozyme molecules can remain in an ordered metastable configuration for extended periods before undergoing the motions and conformation changes that degrade the diffraction resolution. Consequently, for more general post-growth treatments, the development of methods for maintaining the lattice in a metastable configuration may allow high-quality data to be obtained when a given treatment introduces substantial equilibrium disorder.

We have used X-ray topography and other diffraction measurements to characterize the response of tetragonal lysozyme crystals to dehydration. Topographs show characteristic patterns of disorder including cracks and dislocations that are suggestive of a crystal drying out.

P09.04.003 THE CRYSTALLIZATION AND CRYSTAL STRUCTURE OF A BOWMAN-BIRK INHIBITOR FROM VIGNA UNGUICULATA. K. N. Rao, C. G. Suresh [1], R. Lewis [2], [1] Division of Biochemical Sciences, National Chemical Laboratory, Pune-411008, India, [2] Department of Chemistry, University of York, York YO1 5DD, U.K.

The seeds of leguminous plants are a good source of protein inhibitors of proteases. The occurrence of several iso-inhibitors in these plants makes the purification and characterisation of a single inhibitor difficult. Bowman-Birk type inhibitors (BBI's) are low molecular weight proteins and the presence of several disulphide bridges in them imparts a compact structure to the protein. The Vigna unguiculata seeds contained many double-headed (trypsin / chymotrypsin) Bowman-Birk type iso-inhibitors. We have isolated and purified a single iso-inhibitor from these seeds.

The inhibitor crystals were obtained using hanging drop vapour diffusion method at pH 4.0 and 30% saturated ammonium sulphate from a 50 mg / ml protein solution. The crystals were in monoclinic space group P21 with cell dimensions a = 32.4, b = 61.8, c = 32.9 Angstroms, beta = 114.5 degrees. The X-ray data were collected under cryo (120 K) conditions. The crystals were small and diffracted to 2.5 Angstrom resolution only. The structure was solved using molecular replacement method with tracy bean BBI co-ordinates (PDB entry 1PI2) as model. The asymmetric unit was a dimer of closely interacting monomers. The Matthew's number calculated from MW 15,500 Da for the dimer was 1.95 Angstroms 3/D, and the corresponding solvent content was 37%.

P09.04.004 HOW DO MACROMOLECULAR IMPURITIES CREATE DISORDER IN PROTEIN CRYSTALS? C. L. Caylor, I. Dobrianov, S. G. Lemay, C. Kimmer, S. Kriminski, and R. E. Thorne, Laboratory of Atomic and Solid State Physics, Cornell University, Ithaca, NY 14853 USA; K.D. Finkelstein, Cornell High-Energy Synchrotron Source (CHESS), Ithaca, NY 14853 USA; W. Zipfel, Department of Applied and Engineering Physics, Cornell University, Ithaca, NY 14853 USA; B. R. Thomas and A. A. Chernov, Center for Microgravity and Materials Research, University of Alabama in Huntsville, Huntsville, AL 35899, USA.

At times responsible for dislocation and crack formation, generation of twins and polycrystalline and amorphous aggregates, and degradation of crystal mosaicity and diffraction resolution, macromolecular impurities present in growth solutions are among the most important factors affecting protein crystal growth and quality. The mechanisms by which macromolecular impurities degrade crystal diffraction properties have been investigated using X-ray topography, high-resolution diffraction line shape measurements, crystallographic data collection, chemical analysis, and two-photon excitation fluorescence microscopy. Hen egg-white lysozyme crystals grown from solutions containing either a structurally unrelated protein (ovotransferrin) or a related protein (turkey egg-white lysozyme) can exhibit significantly broadened mosaicity due to formation of cracks and dislocations but have overall B factors and diffraction resolutions comparable to those of crystals grown from uncontaminated lysozyme. Direct fluorescence imaging of the three-dimensional impurity distribution shows that impurities incorporate with different densities in sectors formed by growth on different crystal faces and that impurity densities in the crystal core and along boundaries between growth sectors can be much larger than in other parts of the crystal. These nonuniformities create stresses that drive formation of the defects responsible for the mosaic broadening. Our results provide a rationale for the use of seeding to obtain high-quality crystals from heavily contaminated solutions and have implications for the use of crystallisation for protein purification.

P09.04.005 PURIFICATION AND CRYSTALLISATION OF RECOMBINANT HAMSTER DIHYDROOROTASE. M. J. Maher, D. T. C. Huang. C. A. Collyer and R. I. Christopherson, Department of Biochemistry, University of Sydney, NSW 2006, Australia.

Infection with malarial parasites is one of the major infectious causes of mortality worldwide. The evolution of drug resistant organisms increasingly compromises our ability to treat this disease. Consequently, it is necessary to identify new exploitable therapeutic targets and discover potential inhibitors for these targets. Dihydroorotase catalyses the third reaction in the pathway for *de novo* biosynthesis of pyrimidine nucleotides, which leads to the synthesis of RNA and DNA. The malarial parasite *Plasmodium falciparum*, in contrast to humans, is unable to scavenge uridine as a precursor of pyrimidine nucleotides. Therefore blockage of its dihydroorotase activity is toxic and eventually fatal to the organism.

Hamster dihydroorotase has been purified from the soluble extract of *Escherichia coli* using ammonium sulfate fractionation, affinity and anion exchange chromatographies [1]. The final anion exchange step is crucial to obtaining highly pure, crystallisable protein. The protein as isolated is a dimer, with one Zn atom per subunit and a specific activity of 2.5-3.0 units/mg. After testing a wide range of crystallisation conditions, we have obtained crystals of dihydroorotase under three different conditions: sodium formate as precipitant at pH 6.0-6.6 (rod-shaped crystals of maximum dimensions 0.2 x 0.02 x 0.02 mm); sodium formate as precipitant at pH 7.5 (lens-shaped, plate-like crystals of maximum dimensions 0.3 x 0.1 x 0.02 mm, weak diffraction to an approximate resolution of 8 Å has been recorded) and ammonium sulfate as precipitant, pH 6.5 (bipyramidal crystals of 0.05 mm in their maximum dimension).

[1] Williams N. K., Peide Y., Seymour K. K., Ralston G. B. and Christopherson R. I. (1993) *Protein Engineering*, 6, 333-340.

P09.04.006 CRYSTALLIZATION AND CRYSTALLOGRAPHIC STUDIES OF PHOSPHOENOLPYRUVATE CARBOXYLASE FROM MAIZE. H. Matsumura[1], M. Terada[1], S. Shirakata[1], T. Inoue[1], Y. Kai[1], T. Yoshinaga[2], Y. Ueno[3] and K. Izui[3], [1]Department of Materials Chemistry, Graduate School of Engineering, Osaka University, Suita, Osaka, 565-0871, [2]Department of Public Health, Graduate School of Medicine, and [3]Division of Applied Biosciences, Graduate School of Agriculture, Kyoto University, Sakyo-ku, Kyoto, 606-8501, Japan.

Phosphoenolpyruvate carboxylase (EC 4.1.1.31) is a key enzyme in the fixation of atmospheric CO_2 in C_4 and crassulacean acid metabolism (CAM) plants. PEP carboxylase catalyses the irreversible carboxylation of PEP to form oxaloacetate and inorganic phosphate, the first committed step in the fixation of external CO_2 in these plants. The enzyme from maize is activated by glucose 6-phosphate and glycine, while it is inhibited by malate. Its sensitivity to malate is significantly reduced by phosphorylation at Ser-15 in the light. PEP carboxylase from maize is a homotetrameric enzyme with a molecular mass of approximately 440 kDa. It is important to determine the three-dimensinal structure of PEP carboxyalse from maize and to

elucidate the light-induced regulation of PEP carboxylase in plants.

PEP carboxylase was purified from the leaves of maize plants in the light period, and crystallized by the hanging-drop vapor diffusion method at 293 K. The typical size of these crystals was 0.5 x 0.3 x 0.05 mm. The X-ray diffraction data for native crystals were collected at the synchrotron radiation source of the Photon Factory (Tsukuba, Japan). The diffraction pattern of the crystal extends to 3.0Å resolution. The PEP carboxylase crystals belong to an orthogonal space group $C222_1$ with lattice constants of a = 160.2, b = 175.6, and c = 255.5 Å. Presently we are trying to solve the structure by the molecular replacement method, in parallel with the isomorphous replacement technique.

P09.04.007 THE IMPORTANCE OF THE ISO-ELECTRIC POINT IN PROTEIN CRYSTALLIZATION. Abel Moreno [1], Víctor Martín Bolaños-García, Jaime Mas-Oliva [2], [1] Departamento de Bioquímica, Instituto de Química, UNAM. México D.F. CP04510 Deleg. Coyoacan. MEXICO. [2] Departamento de Bioquímica, Instituto de Fisiología Celular, UNAM. México D.F. CP04510 Deleg. Coyoacan. MEXICO.

It is well known that the availability of crystals has been the bottle neck for many years. This is because little has been explored on the physical and chemical properties of the protein solutions to study in detail the crystallization phenomena [1, 2]. In this work, the influence upon aggregation behavior of the temperature as well as the pH over model proteins, such as hen egg white lysozyme and thaumatin I from Taumatococcus daniellii, is reported. Additionally, it is shown a new device, based on the gel acupuncture implementation [3], used for studying the influence of the isoelectric point upon protein crystallization. It is also presented and discussed how by using this new device it is possible to explain the crystal growth phenomena and the aggregation behavior throughout the crystallization experiments. A photographic recording of the crystal growth of lysozyme and thaumatin was obtained as a function of the pH as well as for the temperature.

[1] Víctor M. Bolaños-García, Jaime Mas-Oliva, Manuel Soriano-García and Abel Moreno. (1998) J. Molecular Structure 440, 1-8.
[2] Abel Moreno,Víctor Martín Bolaños-García and Manuel Soriano-García. (1998) J. Biomol.Techniques 1, 005 (Electronic Journal. http://www.abrf.org/JBT/JBT.html)
[3] García-Ruiz Juan Manuel, Moreno Abel, Viedma C., & Coll Miguel. (1993) Mat. Res. Bull. 28, 541.

P09.04.008 THE USE OF MERGED PROTEIN CRYSTALLIZATION TECHNIQUES FOR THE STUDY OF PROTEIN NUCLEATION PHENOMENA. Víctor Martín Bolaños-García, Jaime Mas-Oliva [1], Abel Moreno [2], [1] Departamento de Bioquímica, Instituto de Fisiología Celular, UNAM. México D.F. CP04510 Deleg. Coyoacan. MEXICO, [2] Departamento de Bioquímica, Instituto de Química, UNAM. México D.F. CP04510 Deleg. Coyoacan. MEXICO.

There is a growing interest to develop new practical techniques for increasing the quality of protein crystals as well as crystal growth techniques for X-ray investigations. If well many advances have been obtained on the crystallization of proteins, most of the time it is necessary to growth the crystal up for 3D structural studies. The aim of this work is to solve the problem of growing crystals up to maximum size with high optical and structural qualities for X-ray analysis, merging several crystal growth techniques. In order to have comparable results, three model proteins have been evaluated focused on their crystal growth: lysozyme, thaumatin and concanavalin A. We have taken into account the new trends in crystal growth and it was developed the first set-up of a new crystal growth design for protein crystallization. This new design was based on the gel acupuncture technique [1] and the crystallization of proteins using oils as it has been published by Naomi Chayen et al., [2]. Our proposal combines the transport properties using gels as a dialysis membrane and the oil as a new hypothetical membrane. Finally, we show how using these (oil/gel) barriers it is possible to control the nucleation process and the rate of reaching supersaturation.

[1] García-Ruiz J. M., Moreno A., Viedma C., & Coll M. (1993) Mat. Res. Bull. 28, 541.
[2] Chayen, N. E. et al. (1996) Quat. Rev. Biophys. 29, 227.

P09.04.009 ROLE OF PURITY OF RESTRICTION ENDONUCLEASE *Eco*RII IN THE CRYSTALLIZATION PROCESS OF THIS ENZYME. Elisaveta A. Karpova, Biophysics ES 76, NASA/MSFC, Huntsville, USA 35812

The effect of protein purity on the crystallization process and resulting quality of crystals grown are broadly discussed. We have obtained crystals of restriction endonuclease *Eco*RII (*Eco*RII), space group I23 and cell parameters a = b = c = 160 Å, $\alpha = \beta = \gamma = 90^o$, and have studied the influence of the purity of this enzyme on the crystal growth process. *Eco*RII endonuclese belongs to type II restriction-modification enzymes (subclass IIe). *Eco*RII catalyzes the specific cleavage of double strand DNA at specific site 5'-↓CCA/TGG-3' (the cleavage position is indicated by the arrow (↓)).

This enzyme was purified by 4 and 5 steps purification procedures using ion-exchange and affinity chromatography. Two samples with different purity were characterized by SDS-gel electrophoresis and by specific activity test. We will present the crystallization data of these two different samples and influence of their purity on the crystallization process and quality of grown crystals.

This work is supported by National Research Council Research Associated Programs at MSFC, USA

P09.04.010 PURIFICATION AND CRYSTALLI-ZATION OF MYELIN BASIC PROTEIN. Andy Freer, Tanweer Ahmed, Ruijun Pan, Department of Chemistry, University of Glasgow, Glasgow G12 8QQ & Ian Griffiths, Veterinary School, Garscube Estate, University of Glasgow, Glasgow G61 1QK, UK.

Compact myelin, the insulating material of axons, contains a high proportion of lipid and several proteins which are highly enriched in, or specific to myelin. The highly hydrophobic transmembrane proteolipd protein, PLP and the extrinsic, hydrophilic myelin basic protein, MBP are the major myelin proteins of the central nervous system (CNS) accounting for 50% and 30% respectively of total protein. Myelin, is essential for the salutatory conduction of impulses and its loss or malformation leads to devastating consequences as demonstrated in multiple sclerosis (MS), acute disseminating encephalomyelitis and myelinosis which are primarily associated with MBP and several fatal genetic disorders associated with mutations in PLP. Presently, there is little structural information as to the role of these membrane proteins in myelination and hence our understanding of the architecture of the compact myelin sheath and the molecular pathology of diseased myelin is limited.

In this paper we describe a novel procedure for the isolation and purification of MBP under non-denaturing conditions which preserves secondary structure. Essentially, we treat MBP as a true membrane protein and extract using the mild detergent LDAO. The MBP isoforms were separated by conventional cation exchange chromatography using CM52. By employing these milder conditions purification is effected in the absence of lipid. This lipid free protein (LF-MBP) is different from that extracted by conventional acid/methanol routes, but may be similar to the lipid bound protein (LB-MBP) as extracted by

Riccio *et al*. The striking similarity here is that both are CD active, indicating secondary structure, whereas classical methods denature the protein. We also clearly identified the presence of a dimer and monomer form of MBP (applicable to several of the isoforms) and showed that only the dimer was CD active, with secondary structure which approximated to that predicted from the amino acid sequence.

Having obtained the major isoform of MBP as a pure dimer, crystallization trials were set up using conventional screening procedures. Crystals were obtained from several of the screening conditions indicating PEG as the precipitant. We have collected data on crystals from three of these conditions to a resolution of 2.8 Å with our in house Nonius DIP system. From the best condition we have 98% completion with unit cell dimension: a = 36.037 , b = 42.791, c = 96.009 Å, β = 95.02 ° in the space group $P2_1$ which gives (from a Matthews value of 2.1) one dimer per asymmetric unit. A partial platinum derivative has just been collected.

Riccio, P., Rosenbusch, J.P. & Qualgliariello, E. (1984) FEBS Lett. 177, 236-244.

P09.04.011 INTERNAL CARRIER PROTEINS FOR THE IMPROVEMENT OF THE CRYSTALLIZATION POTENTIAL OF MEMBRANE PROTEINS. C.K. Engel, L. Chen [1], H.R. Kaback [2], G.G. Privé [1], [1] Ontario Cancer Institute, 610 University Av., Toronto, CA, [2] HHMI, University of California Los Angeles, USA

Two of the main problems in the crystallization of membrane proteins are the difficulty to produce large amounts of stable protein, and the small polar surface area for crystal contact formations. We try to overcome these problems simultaneously by creating internal fusion proteins, where soluble carrier proteins are fused into loop regions of the membrane protein. The carrier protein increases the polar surface area of the fusion protein and therefore the stability in solution and the area available for crystal contact formation. In addition, carriers can be used to introduce convenient spectral or enzymatic properties, making the fusion protein easier to handle than the native molecule [ref. 1]. As model system we use the lactose (lac) permease, a secondary transporter from Escherichia coli. It has been shown [ref. 2], that cytochrome b562 (cyt. b562) can be fused into the central internal loop at the intracellular side of lac permease. The construct was successfully expressed and purified. It showed similar lactose transport activity as the wild type lac permease and essentially identical absorption spectra as native cyt. b562. Absorption in the visible range by the cyt. b562 carrier gives the fusion protein a red color ('red permease') and makes it easy to monitor expression, purification and concentration of the construct. The fusion construct can be expressed in high quantities and purified to homogeneity. In respect to crystallization, larger carrier proteins with a larger polar surface area are expected to have improved properties. We are therefore investigating other soluble proteins as carriers. We have introduced, for example, the 20 kD FAD-dependend flavodoxin from Escherichia coli into the central loop of lac permease. Although this carrier is considerably larger than cyt. b562, both fusion constructs show the same activity in respect to lactose transport. We are currently optimizing the expression and purification procedure for this construct. All constructs will be tested for their crystallization potential. Our ultimate goal is the crystallization and successful structure determination of lac permease.

[1] Privé, G.G. & Kaback, H.R. (1996) J. Bioenergetics and Biomembranes, 28, 29-34
[2] Privé, G.G. et al. (1994) Acta Cryst. D50, 375-3792

P09.04.012 CRYSTALLISATION OF TRANSTHYRETIN LOCKED IN AMYLOID FOLD. A. Hörnberg[1], A. Olofsson[2], E. Lundgren[2], and E. Sauer-Eriksson[1]. ([1]Umeå Center for Molecular Pathogenesis and [2]Department of Cell and Molecular Biology, Umeå University, S-901 87 Umeå, Sweden.)

Transthyretin (TTR) is a human plasma protein composed of four identical subunits (127 residues each). The protein is predominantly synthesised in the liver with the main function in transporting the thyroid hormone, but it also plays a major role in the transport of the hydrophobic vitamin A. TTR is normally a stable and soluble protein, however under certain conditions the protein can alter its conformation and form insoluble amyloid fibers. The accumulation of TTR fibers cause two different human diseases, senile systemic amyloidosis (SSA) and familial amyloidosis with polyneuropathy (FAP I).

In order to understand the nature of the structural changes required for generation of amyloid new TTR-mutants with high potential to form amyloid have been constructed [1]. Against these mutants monoclonal antibodies have been generated [2]. These antibodies also display activity against amyloid fibres, but not to wildtype TTR or mutants exhibiting the wildtype fold. We have initiated a crystallographic project with the aim to determine the structure of such a mutant/antibody complex. Crystallisation trials are in progress.

1. G. Goldsteins, et al., Biochemistry 1997, 5346-5352.
2. G. Goldsteins, et al.,PNAS, in press.

P09.04.013 TWO CRYSTAL FORMS OF 20S PROTEASOME FROM BOVINE LIVER. M.Unno[#1], Y.Tomisugi[#2], T.Mizushima[#1], Y.Morimoto[#2], N.Yasuoka[#2], K.Tanaka[#3] and T.Tsukihara[#1], #1. Institute for Protein Research, Osaka University, 3-2 Yamada-oka, Suita, Osaka 565-0871, JAPAN, #2.Department of Life Science, Himeji Institute of Technology, Kamigohri Akoh, Hyogo 678-1297, JAPAN, #3. The Tokyo Metropolitan Institute of Medical Science, 3-18-22 Honkomagome, Bunkyo-ku, Tokyo 113-0021, JAPAN

Proteasomes are large, non-lysosomal, multicatalytic proteinase. It is responsible for the degradation of intracellular proteins, a process important for regulation of metabolism and cell division and, in higher animals, for immunological responses. The crystal structures of 20S proteasomes from the archaebacterium and from the yeast have been reported by R.Huber *et al*. However, that of mammalian has been not reported. So we are trying to determine the 3D structure of 20S proteasome from bovine liver.

We prepared and crystallized 20S proteasome from bovine liver. Some crystals diffracted x-rays up to 2.5A when using synchrotron radiation. These crystals belonged to $P2_12_12_1$ with cell dimensions a=122Å, b=193Å, c=319Å. However, the crystals were quickly deteriorated and couldn't collect the full data set from one crystal. So We have purified and crystallized repeatedly. Crystals were obtained in almost same conditions, but the concentration of buffer or salt was a little different. When we collected x-ray diffraction data of another crystal, we found the second crystal form. The second type of crystals belong to $P2_12_12_1$ with cell dimensions a=203Å b=319Å c=360Å.

We determined the preliminary phase of the first crystal by molecular replacement method. And we calculated self rotation function of the second crystal and found non-crystallographic 3-fold and 2-fold axes.

P09.04.014 CHARACTERIZATION AND CRYSTALLIZATION OF A NOVEL *SARCOCYSTIS MURIS* LECTIN. J. J. Müller[1], E.-Ch. Müller[2], A. Feske[1], H. Klein[3], Th. Montag[3], U. Heinemann[1] and A. Otto[2], [1]Forschungsgruppe Kristallographie, Max-Delbrück-Centrum für Molekulare Medizin, Robert-Rössle-Str. 10, D-13092 Berlin, Germany, [2]Forschungsgruppe Proteinchemie, Max-Delbrück-Centrum für Molekulare Medizin, Robert-Rössle-Str. 10, D-13092 Berlin, Germany, [3]Paul-Ehrlich-Institut, Federal Agency for Sera and Vaccines, FG Parasitologie/ Diagnostika, Paul-Ehrlich-Straße 51-59, D-63225 Langen, Germany.

A novel *Sarcocystis muris* major microneme antigen from cyst merozoites has been detected and analysed by Edman degradation and mass spectrometry whereby it was possible to find a new gene. This protein plays a role during host cell recognition by invading parasites. The protein consists of 138 amino acids with 72.5 % and 65.2% identity with the GEN2 and GEN4 products of the *Sarcocystis muris* genome establishing a new family. Significant homology exists with *Toxoplasma gondii* expressed sequence tags. All of the twelve cysteinyl residues build up disulphide bridges, two of those are attributed by mass spectrometry to motifs as found in diverse parasitic proteins, growth factors, and the apple domains of kallikrein and blood coaggulation factor XI [1]. Crystals of *Sarcocystis muris* lectin have been grown by vapor diffusion. The crystals belong to the primitive orthorhombic space group $P2_12_12_1$ with cell parameters A=53.57 Å, B=128.76 Å, C=158.18 Å. There are four molecules in the asymmetric unit. The crystals diffract to 2.1 Å resolution at 100°K at the EMBL BW7A beamline at the DORIS storage ring , DESY, Hamburg.

[1] Klein, H., Mehlhorn, H. and Rüger, W. (1996) Parasitol. Res. **82**, 230-237.

P09.04.015 EFFECTS OF AN EXTERNAL ELECTRIC FIELD ON THE PROTEINS CRYSTALLIZATON C. Didierjean, M. Taleb, C. Jelsch, J. P. Mangeot, A. Aubry, Groupe Biocristallographie, Laboratoire de Cristallographie et Modélisation des Matériaux Minéraux et Biologiques UPRESA CNRS 7036, B. P. 239, 54506 Vandoeuvre-lès-Nancy, France, B. Capelle, Laboratoire de Minéralogie et Cristallographie UMR CNRS 7590, case 115, 4 place Jussieu, 75252 Paris, France.

Protein molecules contain different ionic and polar groups. As a result, they inherently have a quite significant charge depending on the pH of the solution. The environment of the molecules and of their aggregates in the crystallization medium can be changed when applying an external electric field. The interaction of charged molecules with an external electric field might alter their distribution inside the solution and lead to local nucleation. From these considerations, it is possible to imagine that the external electric field can influence the crystallization of proteins and possibly promote the formation of crystals with good quality and size. The purpose of the present poster is to show the effects of an external electric field on the crystallization of biological macromolecules.

Very pure lysozyme protein at pH 4.5, with sodium chloride as crystallizing agent, has been crystallized. Two experimental devices have been developed. The first one has allowed observing a slight effect of the electric field on the crystallization by reducing the mosaic spread of the crystals. In order to increase the strength of the electric field in the crystallization solution, a second device has been developed in which many dielectric media were eliminated. An undeniable effect of the electric field has been observed in this case especially on the number and size of crystals. The electric field affects strongly the nucleation rate of lysozyme. In addition the behavior of the protein in solution under an electric field has been studied. Results concerning the concentration variation of the lysozyme into the solution and solubility diagrams will be presented.

P09.04.016 CRYSTALLIZATION OF A PUTATIVE TRANSCRIPTION FACTOR, ASNC AND 3-METHYL ADENINE GLYCOSYLASE FROM A HYPERTHERMOPHILIC ARCHAEBACTERIUM, *PYROCOCCUS* sp. OT3. Norio Kudo[1,2], Mark, D. Allen [2], Hideaki Koike[2], and Masashi Suzuki[1,2] ([1] Graduate School of Human and Environmental Sciences, University of Tokyo, [2] AIST-NIBHT, CREST Centre of Structural Biology)

We report crystallization of 3-methyl adenine glycosylase and a putative transcription factor, AsnC, from a hyperthermophilic archaebacterium, *Pyrococcus* sp. OT3.

The proteins were expressed by *E. coli* systems and purified. Crystals were grown by the sitting drop vapour diffusion method at 5°C, using PEG 6000 and LiCl as precipitant for the glycosylase and AsnC, respectively. The crystal of the glycosylase was shown to diffract X-ray upto 3.0Å. The space group was identified to be rhombic, R32. Three independent molecules were identified positioning in the asymmetric unit of 168.0x 168.0x 117.0Å. The crystal of AsnC was shown to diffract X-ray upto 2.3Å. The space group was identified to the hexagonal. Four independent molecules were identified positioning in the asymmetric unit of 97.0x 97.0x 98.3Å.

Archaebacteria are different from eukaryotes or eubacteria, and constitute the life's third domain. While analyzing archaebacterial genomic DNA sequences we noticed that the transcription and replication systems were chimera of eukaryotic and eubacterial ones. The AsnC protein and the 3-methyl adenine glycosylase are eubacterial representatives involve in the archaebacterial systems, and thus determination of their 3D structures is expected to contribute to the understanding of the origin and evolution of living organisms.

P09.04.017 CRYSTAL STRUCTURE OF HEN EGG-WHITE LYSOZYME WITHIN HIGH MAGNETIC-FIELD ENVIRONMENT T.Sato, Department of Life Science, Faculty of Bioscience and Biotechnology, Tokyo Institute of Technology, Yokohama, Japan, and G.Sazaki, Institute for Materials research, Tohoku University, Sendai, Japan and Y.Katsuya, Hyogo Prefecture Industrial Technology Center, Kobe, Japan and Y.Matsuura, Institute for Protein research, Osaka University, Suita, Japan

Crystals of tetragonal hen egg-white lysozyme were grown with the high magnetic apparatus of High Field Laboratory for Superconducting Materials, and without a magnetic field, respectively. Both crystals were grown in 2.5% NaCl as a crystallizing agent at pH 4.5. The X-ray diffraction patterns of the best diffracting crystals were recorded using R-AxisIIc and an imaging plate system. The crystals grown with and without a magnetic field showed the similar maximum resolution upto 2Å. In the presence of a magnetic field, the number of formed crystals decreased because of the low nucleation rate. The *a* and *b* axes of the unit cell expanded by 0.2%, or *c* axis also increased by 0.1%. In general, the crystals of a variety of diamagnetic proteins, e.g. lysozyme, may be perfectly aligned by an intense static external magnetic field due to the slight anisotropy in the magnetic susceptibility of the protein caused by the three structural elements ; alpha-helix, beta-sheet and the aromatic rings of amino acid residues. Structure refinement of the crystals have been carried out with the program X-PLOR. The two structures are nearly identical with the root-mean-square deviation on all protein atoms. The changes in the ordered water molecules and the expansibility of all of the solvent in the crystal will be reported here. Two ions consist of one chloride ion and one sodium ion at the interface between adjacent lysozyme molecules. These ions may stabilize a

crystal packing. We may have obtained highly ordered arrays of diamagnetic protein by the effect of a magnetic field, which permitted us to gain larger crystals. When lysozyme is placed in a direct current magnetic field of 10 Tesla strength the protein molecules become highly ordered, aligning their long axis perpendicular to the field direction. Clearly then, the protein crystals can be aligned by the field and must thus have their crystal susceptibility along the field direction, corresponding to crystallographic *c* axis. It was then evident that we can suppress formation of the crystallising nuclei owing to increase solubility of the protein with this magnetic arrangement. It is sugested that the application of a magnetic field may be allowed to improve protein crystal growth from microcrystals.

P09.04.018 A RATIONAL APPROACH TO GROW AND TREAT CRYSTALS OF HCMV PROTEASE AND ITS INHIBITOR COMPLEX. Chungeng Qian [1], Lisette Lagacé [2], Marie-Josée Massariol [2], Catherine Chabot [2], Christiane Yoakim [2], Robert Déziel [2], Liang Tong [1]. [1]Boehringer Ingelheim Pharmaceuticals, Inc.,900 Ridgebury Road/P. O. Box 368, Ridgefield, CT 06877, U.S.A. [2]Boehringer Ingelheim(Canada) Ltd., Bio-Méga Research Division, 2100 rue Cunard, Laval, Québec, Canada H7S 2G5.

Protein crystallization is generally regarded as a field of art rather science. Here we demonstrate that one could do better if exploring scientific approach during crystallization trials, the way in which we have crystallized both hCMV protease and its inhibitor complex. For free enzyme crystals, we put tremendous effort to improve the diffraction limit by optimizing crystallization conditions, raising precipitant concentration in reservoir and soaking crystals in artificial mother liquors containing six components. Crystals diffracting to 2.0Å resolution were finally obtained, leading to the elucidation of the three dimensional structure of the enzyme using MAD method. For inhibitor complex crystals, initial attempts with co-crystallization and soaking experiments at pH 6.0 did not produce conclusive results. We therefore choose to co-crystallize the complex at pH 8.0, optimal for the enzyme and the inhibitor activity. Using 20 to 50 mM spermine in the crystallization buffer, crystals of two peptidomimetic inhibitor complexes were obtained at pH 7.5 and 8.0 respectively. Spermine was required for the inhibitor complexes to be crystallized at pH 8.0, possibly neutralizing net negative charges of hCMV protease due to its acidic pI 5.5. A 2.7Å data set was collected from one of the inhibitor complex and the structure determined using molecular replacement method.

P09.04.020 INVESTIGATION OF RAT BRAIN L-3-HYDROXYACYL-CoA DEHYDROGENASE AND IT'S ROLE IN ALZHEIMER'S DISEASE. Ailsa Powell[*], Frank Gunn-Moore[+], Leo Brady[*], [*]University of Bristol, UK, [+]University of Edinburgh, UK.

The human brain L-3-hydroxyacyl-CoA dehydrogenase (LHCDH) has been found to have an identical primary sequence to endoplasmic reticulum amyloid β-peptide binding protein (ERAB)[1].

LHCDH is an intracellular enzyme that catalyses the following reaction, which is the third step of the fatty acid β-oxidation pathway: L-3-hydroxyacyl-CoA + $NAD^+ \leftrightarrow$ NADH + H^+.

In Alzheimer's disease, amyloid β-peptide binds ERAB and causes it to redistribute to the plasma membrane. The neuronal dysfunction and death found in Alzheimer's disease has been linked to the presence of extracellular amyloid β-peptide in the brain. ERAB is overexpressed in Alzheimer's disease, but by blocking ERAB it is possible to prevent the toxic effect of amyloid β[2].

The rat brain ERAB gene has been cloned into a pET-15b vector and has been expressed as a his-tagged protein. By crystallising and solving the structure of rat brain LHCDH, it may be possible to gain a better understanding of amyloid β toxicity in Alzheimer's disease. It is also hoped to identify inhibitors of this enzyme and see if they affect the binding of amyloid β-peptide.

1. He X.Y., Schulz H. & Yang S.Y. (1998) *J. Biol. Chem.* 273, 10741-10746
2. Yan S.D., Fu J., Soto C., Chen X., Zhu H., Al-Mohanna F., Collison K., Zhu A., Stern E., Saido T., Tohyama M., Ogawa S., Roher A. & Stern D. (1997) *Nature* 389, 689-695

P09.04.021 THE CRYSTAL STRUCTURE OF SUPERANTIGEN STREPTOCOCCAL PYROGENIC EXOTOXIN A1 WITH ZINC AT 2.8 Å RESOLUTION. M.D. Baker, A.C. Papageorgiou and K.R. Acharya, Department of Biology and Biochemistry, University of Bath, Claverton Down, Bath, BA2 7AY, UK, and C.M. Collins, Department of Microbiology and Immunology, University of Miami, FL 33101, USA.

Superantigens are toxins produced by several strains of *Staphylococcus aureus* and *Streptococcus pyogenes* with the unique ability to induce profound T-cell proliferation by cross-linking MHC class II molecules with T-cell receptors. These toxins act at nanomolar concentrations and unlike conventional antigen are not processed internally by the antigen presenting cells. Each superantigen activates a subset of the total T-cell repertoire bearing specific Vβ chains. Thus, superantigens are able to stimulate a much larger proportion of the T-cells than conventional peptide antigens. Crystallographic and biochemical [1] studies have suggested that superantigens have evolved a number of different ways to interact with MHC class II molecules and T-cell receptors despite their common overall architecture [3].

Streptococcal pyrogenic exotoxin A1 (SpeA1) is produced by *Streptococcus pyogenes* and has been associated with severe infections such as scarlet fever and Streptococcal Toxic Shock Syndrome (STSS) [2]. The crystal structure of SpeA1 has been determined at 2.6 Å resolution [3] and is similar to that of other superantigens , having the greatest similarity with staphylococcal enterotoxin C. A putative zinc binding site was identified, although no zinc ion was found to be present. Direct evidence for the binding of zinc to SpeA1 was obtained by soaking SpeA1 crystals in 2.5 mM zinc solution. Data to 2.8 Å resolution was collected at 100°K. The implications of zinc binding to SpeA1 for MHC class II recognition will be discussed.

1. A.C. Papageorgiou and K. R Acharya(1997) Structure **5** 991-996
2. J.B. Kline and C.M. Collins (1996) Infection & Immunity **64**(3) 861-869.
3. A.C. Papageorgiou *et al* (1999) EMBO **18**(1) 9-21

P09.04.022 STRUCTURAL STUDIES ON THE TOXIC EFFECTS OF ORGANOCHLORINE PESTICIDES. M. Suwalsky and F. Villena, University of Concepcion, Casilla 160-C, Concepcion, Chile, and C.P. Sotomayor, Catholic University of Valparaiso, Valparaiso, Chile.

Organochlorine pesticides are ubiquitous in the environment because of their widespread use and persistence in soil. In general, the molecular mechanisms of pesticide toxicity are poorly understood. However, the lipophilicity of most compounds makes lipid-rich membranes a plausible target of their interaction with living organisms. Thus, alterations in the organization of their lipid bilayers are likely to constitute a mechanism for modulation of membrane protein functions. In the course of in vitro system search for the toxicity screening of chemicals, different cellular models have been applied to examine the adverse

effects of pesticides. We will describe the interaction of several organochlorine pesticides with cell membranes of human erythrocytes and molecular models. The latter consisted of bilayers built-up of dimyristoylphospatidylcholine (DMPC) and dimyristoyl-phosphatidylethanolamine (DMPE), representative of phospholipid classes located in the outer and inner monolayers of the human erythrocyte membrane, respectively. Considering the lipophilic nature of the pesticides and the amphiphilic character of phospholipids, their interactions were assayed in hydrophobic and aqueous media in a wide range of concentrations. The capacity of the pesticides to perturb the bilayer structure of DMPC and DMPE was determined by X-ray diffraction. Human erythrocytes incubated with the same compounds were observed by scanning electron microscopy to detect shape changes induced by the pesticides. Additional techniques such as fluorescence spectroscopy on large unilamellar vesicles and electrophysiological measurements of frog nerve-skin preparations incubated with the pesticides were also used. The experimental results allowed to conclude that organochlorine pesticides alter the molecular structure of lipid bilayers thereby modifying biophysical and physiological properties of cell membranes.

This work is supported by grants from FONDECYT (1960680) and DIUC 95.24.09-1).

P09.04.023 3D STRUCTURES OF DROSOPHILA ACETYLCHOLINESTERASE: IMPLICATIONS FOR INSECTICIDE DESIGN. M. Harel, G. Kryger, J.L. Sussman [1], I. Silman [2], T.L. Rosenberry, W.D. Mallender [3], T. Lewis, R.J. Fletcher [4], M. Guss [5], [1] Department of Structural Biology, Weizmann Institute of Science, Rehovot 76100, Israel, [2] Department of Neurobiology, Weizmann Institute of Science, Rehovot 76100, Israel, [3] Pharmacology Department, Mayo Clinic, Jacksonville, FL 32224, USA, [4] Zeneca Agrochemicals, Jealott's Hill Station, Bracknell, Berkshire, UK, [5] Department of Biochemistry, University of Sydney, Sydney, NSW 2006, Australia

The 3D structures of Drosophila melanogaster acetylcholinesterase (DmAChE), and of its complex with an iodine-containing putative insecticide, were solved by a combination of SIR and molecular replacement, starting from the 2.7 A structure of Torpedo californica AChE (TcAChE), with which it has 36% sequence identity. The SIR phases were obtained by freeze-trapping of xenon atoms. The structures were refined to R=26.1% (R-free=30.5%) for the native structure, and R=23.0% (R-free=26.8%) for the complex. The structure of DmAChE shows the same overall fold and deep and narrow active-site gorge as TcAChE, human and mouse AChEs. It displays a Ca rms deviation of 0.78 A, using the 342 best fitting residues out of 586. However, there are large deviations (up to 8 A) in the positions of some loops, and the C-terminal helix is shifted by 3 A relative to TcAChE. The substitutions in 10 (out of 30) sidechains facing into the active- site gorge in DmAChE, relative to TcAChE, cluster mostly near the top of the gorge, near the peripheral binding site. Upon binding of the inhibitor, which resembles the anti-Alzheimer drug, tacrine, the aromatic rings of both the flexible mid-gorge residue, Y370(F330) [parentheses indicate TcAChe numbering], and of the choline-binding residue, W83(W84), change their conformation so as to stack against two aromatic groups of the inhibitor. The marked structural differences between the active-site gorges of the insect and vertebrate AChEs reveal several features which might provide the basis for more selective insecticides. The structure of DmAChE shows the same overall fold and deep and narrow active-site gorge as TcAChE, human and mouse AChEs.

P09.04.024 STRUCTURE OF HUMAN TRANSTHYRETIN COMPLEXED WITH ENVIRONMENTAL POLLUTANTS: A NEW MODE OF BINDING. Minakshi Ghosh, Atlanta Cook and Louise Johnson, Laboratory of Molecular Biophysics, University of Oxford, Rex Richards Building, South Parks Road, Oxford OX1 3QU, United Kingdom.

Transthyretin (TTR) is one of three serum proteins responsible for the transport of the hormone thyroxine. It has been found in recent years that some polyhalogenated aromatic hydrocarbons present in the environment interact with transthyretin in competition with thyroxine, its natural ligand. Evidences suggest that these compounds have a potentially adverse effect on the endocrine system of laboratory animals and may therefore harm both humans and wildlife (1). Pentabromophenol, which is used as a fire retardant, and 2,4,6-tribromophenol are two such compounds. They have shown high affinity for TTR. Pentabromophenol, in particular has a relative potency ~ 15 times that of thyroxine in vitro experiments.

Our current work has revealed some unusual and interesting features in the binding of bromophenol ligands with TTR. The crystal structures of human serum TTR, complexed with Pentabromophenol and 2,4,6-tribromophenol, have been solved and refined for 20-1.8Å resolution data.

Firstly, the ligands bind exclusively in the so-called “reverse mode”, with the phenolic group pointing towards the mouth of the binding cavity. This is in contrast with most other TTR-ligand structures where the phenolic group points towards the centre of the binding cavity. Secondly, for pentabromophenol, it is observed that the bindings of the ligand are different at two binding sites of the protein, in spite of the fact these sites are related by a non-crystallographic symmtery. This agrees with chemical data showing that there is a 100 fold difference in the binding affinities for the first and second thyroxine. In all the structural studies done prior to this current work, the ligands and the surrounding residues of the protein have shown to have identical conformations at the two binding sites.

1. A. Brouwer, D.C. Morse, M.C. Lans, A.G. Schuur, A.J. Murk, E. Klasson-Wheeler, A. Bergman and T.J. Visser, (1998), *Toxicology and Industrial Health*, **14**, No 1/2, 59-84.

P09.04.025 LOW RESOLUTION PROJECTION MAPS OF SCRAPIE PRION PROTEIN CRYSTALS FROM REVERSE MICELLAR SOLUTIONS. Holger Wille [1], Vincent Guenebaut, Robert M. Stroud, David A. Agard [2], Stanley B. Prusiner [1,2] [1] Institute for Neurodegenerative Diseases, Department of Neurology, University of California, San Francisco, CA 94143-0815, U.S.A. [2] Department of Biochemistry and Biophysics, University of California, San Francisco, CA 94143, U.S.A.

The N-terminally truncated scrapie isoform of the prion protein (PrP 27-30) is highly insoluble. Solubilization into monomers and dimers was only achieved through the use of reverse micellar systems. Three separate combinations of organic solvents and detergents were particularly successful in solubilizing PrP 27-30 (Wille and Prusiner, 1999, Biophys. J., in press). Divalent uranyl ions induced the solubilized prion protein to form small two- and three-dimensional crystals. Other multivalent metal ions did not induce PrP 27-30 to form crystals. Different reverse micellar solutions resulted in distinct crystalline lattices as judged by electron microscopy and electron diffraction. Image processing allowed us to analyze conventional electron micrographs to see if these crystals would give ultrastructural information on the scrapie isoform of the prion protein. We used correlation mapping and averaging on the crystal lattices to improve the signal to noise ratio. The limit of resolution in the power spectra was at ~2.5 nm with occasional spots out to ~1.2 nm. The latter images showed some intramolecular details that

could be interpreted as secondary structure elements. Other crystals appeared to contain prion protein dimers, and showed two separate uranyl-complexing densities per protein molecule, allowing speculations on the sites of glycosylation. The limitation to low resolution data stems from the type of instrument used and the practice of high dose imaging. Future efforts will focus on gathering high resolution data by use of low dose cryo-electron microscopy and attempt to improve the crystalline order.

P09.04.026 TETANUS TOXIN GANGLIOSIDE BINDING DOMAIN, 1.57Å NATIVE AND DERIVATIVE STRUCTURES. Mark Knapp, Brent Segelke, Bernhard Rupp. Macromolecular Crystallography Group, Lawrence Livermore National Laboratory, 7000 East Avenue, Mail Stop L-452, Livermore, CA 94550 USA.

The disease known as Tetanus is caused by a neurotoxin produced by the anaerobic bacterium *Clostridium Tenati.* It acts upon the presynaptic membranes of both central and peripheral nervous systems; its effect is to block the release of neurotransmitters causing paralysis. Tetanus toxin is a 150kDa protein made up of two major parts: a 50-kDa light chain and 100-kDa heavy chain. The light chain is the enzymatic portion of the protein responsible for its toxicity. The heavy chain is made up of a translocation domain and a 51-kDa component (the C Fragment) which binds to the gangliosides of the neuron cell membrane and determines neuron specificity.

The crystal structure of the C Fragment has been determined to 1.57Å resolution. Both native protein and heavy atom derivative structures are reported. Data for the native protein and two heavy atom derivatives (Hg, Au) were collected in-house to 2.5Å resolution. MIR phases were used for the initial electron density map with which the Cα backbone was traced. A MAD experiment using the Au derivative was done at SSRL, producing data > 97% complete for all four wavelengths. The model was partially built using the MAD phasing. Through the combination of the MAD and MIR phases a map (without model bias) of outstanding quality was created, greatly superior to either of the MIR or MAD maps alone. 90% of the sequence was assigned with this map. Use of phase extension and the wARP technique have produced a complete model at 1.57Å. Current work is directed to determining the protein/ganglioside complex structure.

This work was performed under the auspices of the U.S. Department of Energy by Lawrence Livermore National Laboratory under contract no. W-7405-ENG-48

P09.04.027 METAL TRANSPORT IN PNEUMOCOCCAL VIRULENCE. Michael C. Lawrence, Patricia A. Pilling, V. Chandana Epa, Bettina L. Ferguson and Jeffrey J. Gorman, Biomolecular Research Institute, 343 Royal Parade, Parkville, Victoria 3052, Australia, and James C.Paton, Women's and Children's Hospital, North Adelaide, South Australia 5006, Australia.

The pneumococcal surface protein PsaA plays a role in the transport of zinc and/or manganese across the cell membrane in *Streptococcus pneumoniae*. The protein has been shown to be critical to the virulence of the organism: psaA$^-$ mutants are completely avirulent in mouse models [1]. We have recently determined the structure of PsaA via X-ray crystallography using multiple isomorphous replacement [2]. Details of the PsaA structure will be presented. The protein consists of two pseudo-symmetric α/β domains linked by a single "backbone" helix, and represents the first structure of an ABC-type receptor from a Gram-positive bacterium, and the first structure of a zinc/manganese transporter. A metal binding site is located between the protein domains and is formed by the side chains of two histidines, an aspartate and a glutamate. The site is occupied in the crystal, most likely by Zn^{2+}. The unexpected presence of the metal ion in this structure and the buried nature of its binding site suggests that the site is likely one of high affinity. Release of the metal ion will most likely therefore require a structural transition. We are currently seeking to determine the nature and structure of the metal-free form of the protein; details of progress towards this goal will also be presented.

1. Berry, A. M. & Paton, J.C. (1996). *Infect. Immun*., **64**, 5255-5262.
2. Lawrence, M.C., Pilling, P.A., Epa, V.C., Berry, A.M., Ogunniyi, A.D. & Paton, J.C. (1998). *Structure*, **6**, 1553-1561.

P09.04.028 CRYSTAL STRUCTURE OF RAT TRANSTHYRETIN COMPLEX WITH TETRAIODOTHYROACETIC ACID AT 1.8A RESOLUTION. Andrzej Wojtczak, Tadeusz Muziol [1], Vivian Cody, Joseph R. Luft, Walt Pangborn [2], [1] N. Copernicus University, Gagarina 7, 87-100 Torun, Poland, [2] Hauptman-Woodward Medical Research Institute, Buffalo, NY 14203

Transthyretin is a tetrameric serum protein responsible for transporting about 20% of the circulating thyroxine (T4) in man, while in lower vertebrates, it is the only carrier. Structure activity data show that hormone metabolites have different binding affinities for TTR depending on their substitution pattern. Thus, the metabolite, tetraiodothyroacetic acid (T4Ac) is the strongest binder to TTR with T4 only 39%. Ligand binding is known to stabilize TTR tetramer formation, an important property in amyloid fibril formation, the cause of familial polyneuropathy, a fatal genetic disease characterized by single point mutations of TTR. Rat TTR is 85% homologous to the human protein and crystallizes in a tetragonal space group with a complete tetramer in the asymmetric unit. Human TTR crystallizes in an orthorhombic lattice and has a unique dimer in the asymmetric unit of the lattice. In order to understand the binding selectivity of thyroid metabolites and to understand the effect of point mutations on amyloid fibril formation, we carried out structural studies on rTTR and its hormone complexes. We report the crystal structure of rTTR complexed with T4Ac and compare these results with those of its hTTR complex. The current refinement of synchrotron low temperature data collected at CHESS for rTTR-T4Ac using XPLOR, is R=23.5%, Rfree = 30.0%, at 2.7A resolution and reveals disorder in the binding orientation of the ligand in the A/C binding domain, and a single population in the B/D domain. This model places the phenolic ring iodine atoms in the P3/P2' pockets on the opposite sides of the channel, while the diiodobenzyl iodines bind in the P1/P1' pockets, similar to that of rTTR-T4. The acetic acid carboxylate group forms a salt bridge to Lys-15 near the channel entrance. These data are similar to those observed in the hTTR-T4Ac complex which indicated multiple modes of binding for T4Ac in both binding domains. There was also indication of a second binding population with the metabolite bound deeper in the channel with a skewed diphenyl ether conformation rather than the expected twist-skewed conformation. Analysis of these data indicate that multiple modes of ligand binding are possible and provide insight into ligand binding selectivity and how sequence differences relate to amyloid formation.

Supported in part by Polish KBN 6/P04A/032/11 (AW) and TW00225 (VC).

P09.04.029 TETANUS TOXIN HC AND COGNATE CARBOHYDRATES. C.Fotinou [1], P.Emsley [1], N.Fairweather [2], C.Watts [3] and N.W.Isaacs [1], [1] Department of Chemistry, University of Glasgow, Glasgow, G12 8QQ, UK, [2] Department of Biochemistry Imperial College of Science, Technology & Medicine, South Kensington, London SW7 2AZ, [3]Department of Biochemistry, University of Dundee,MSI/WTB Complex, Dow Street, Dundee, DD1 5EH

Tetanus Toxin (TeNT) is produced by the bacteria *Closdridium tetani* in an attempt to kill its host by paralysis and suffocation.

TeNT is synthesised as a single polypeptide chain which undergoes cleavage to produce a mature toxin consisting of the N-terminal 50kD fragment linked via a disulphide bond to the 100kD C-terminal fragment (the H chain). The 50kD fragment of the C-terminal portion of the H chain (known as Hc or fragment-C) is responsible for ganglioside binding, which is essential for binding to neuronal cells.

TeNT undergoes trans-synaptic migration and targets the neuronal cells of the spinal cord. The mechanism consists of 4 stages: cell binding, vesicular internalisation, cytoplasmic translocation and cleavage of the substrate by the toxin L-chain. It is in order to start to understand these mechanisms that we have solved the structure of tetanus toxin Hc.

The structure consists of 2 domains, the N-terminal domain, which is a β sandwich and the C-terminal domain, which is a β-trefoil. The trefoil contains the putative ganglioside binding sites. It has been found that the gangliosides GT1b and GD1b have the highest binding affinity.

The determination of the Hc-ganglioside or Hc-cognate complexes will provide information about the type of interactions which occur during TeNT binding.

Small crystals of the Hc-GT1b complex have been grown. Data have been collected on crystals of Hc soaked in carbohydrates which are subunits of the ganglioside molecule.

P09.04.030 STRUCTURAL STUDIES OF THE HIGHLY AMYLOIDOGENIC TRANSTHYRETIN MUTANT G53S/E54D/L55S. Therese Eneqvist and Elisabeth Sauer Eriksson, Umea Center for Molecular Pathogenesis, Anders Olofsson and Erik Lundgren, Department of Cell and Molecular Biology, Umea University, S-901 87 Umea, Sweden

Transthyretin (TTR) is a homotetrameric plasma protein responsible for transport of the thyroid hormone thyroxine and retinol binding protein in complex with vitamin A. Mutations in TTR causes familial amyloidotic neuropathy (FAP), a lethal disease associated with motor- and sensor dysfunction. FAP is a form of amyloidosis, a group of diseases caused by structurally altered proteins that accumulate into insoluble fibrils and disrupt organ functions. There are at least 16 human proteins capable of forming amyloid, all different in structure and function. However, all amyloid fibrils contain cross-β structure and are associated with certain molecular components suggesting a more universal amyloidogenic fold. So far only the native conformations of amyloid proteins are known.

There are several structures of both native and mutant TTR and all show the native conformation. In order to detect the structural changes that lead to amyloid formation we are studying a group of highly amyloidogenic mutants of human TTR. These mutants spontaneously form aggregates in solution exposing epitopes that are recognized by amyloid-specific antibodies.

The crystal structure of the highly amyloidogenic G53S/E54D/L55S mutant is currently being refined at 2.3Å resolution. This mutant shows a new crystal form for transthyretin, the trigonal space group $p3_221$, with unit cell dimensions a = b = 58.31Å and c = 228.95Å.

P11.04.001 X-RAY CRYSTALLOGRAPHIC STUDY OF HUMAN HEMATOPOIETIC PROSTAGLANDIN D_2 SYNTHASE T. Inoue†, N. Okazaki†, Y. Kai†, D. Irikura§, O. Hayaishi§, M. Yamamoto‡, T. Kumasaka‡, Y. Urade§ †Dept. of Materials Chemistry, Osaka University, Suita, Osaka 565-0871, JAPAN §Dept. of Molecular Behavioural Biology, Osaka Bioscience Inst., Osaka 565-0874, JAPAN ‡Harima Inst., The Inst. of Physical and Chemical Research (RIKEN), Hyogo 679-5143, JAPAN.

Prostaglandins (PGs) are a widely distributed group of eicosanoids that are involved in the control of various defence and homeostatic mechanisms in the body. Hematopoietic prostaglandin (PG) D synthase is the key enzyme for production of the D and J series of prostanoids in the immune system and must cells. The crystal structure analysis of human PGD_2 synthase has been performed with MAD method by using the data for one Hg-derivative. Diffraction intensity data were collected at three wavelengths monochromatized by diamond trichromator with synchrotron radiation (BL45-XU beamline, SPring-8, Japan). The image data were recorded on RAXIS-IV imaging-plate system (Rigaku), and processed and scaled with *DENZO* and *SCALEPACK*. The program *MLPHARE* in the *CCP4* suite was used for refinement of atomic parameters and phase calculation. Phases were calculated up to 2.5 Å, and the overall figure of merit was 0.331 for 28,957 reflections. A density modification and NCS-averaging was carried out for phase improvement with the program *DM*. The electron density obtained after solvent density modification was of good quality and the chain could be traced. The atomic model was built using the program *O* and *TURBO*. Simulated annealing with *X-PLOR* 3.0 was carried out for the refinement. The present crystallographic *R*-factor at 2.3 Å resolution is 0.199 for 25,168 reflections between 10-2.3 Å with 201 water molecules. The free *R*-factor for the remaining 5% of the expected data within this resolution range was 0.212. The refinement at higher resolution is under progress.

P11.04.002 THE GROWTH AND ANALYSIS OF HUMAN THYROID PEROXIDASE CRYSTALS. E. Hendry and G. Taylor School Biomedical Sciences, University of St. Andrews, St. Andrews, Fife KY16 9TS, UK, and F. Grennan Jones, K. Ziemnicka, J. Furmaniak and B. Rees Smith, FIRS Laboratories, RSR Limited, Parc Ty Glas, Cardiff CF4 5DU, UK.

Thyroid peroxidase (TPO) catalyses the iodination and coupling reactions in thyroid hormone synthesis. It is also a major autoantigen in autoimmune thyroid disease and an important marker of thyroid disorders. Crystals of human TPO have been grown in order to determine the 3-D structure of the enzyme. The structure will help in the understanding of the enzyme mechanism, the nature of the interactions with autoantibodies, and the role of TPO in thyroid disease.

Recombinant immunoreactive TPO has been expressed to a high level in the High Five insect cell line [1]. The protein was purified by ion exchange chromatography and gel filtration. Crystals were grown in 12% PEG 4K at pH 6.75 with a TPO concentration of 18 mg/ml in a buffer of NaCl, PO_4 and KI.

Diffraction data were collected to 6 Å resolution processed using DENZO and SCALEPACK. The crystals belong to the 32 crystal class with unit cell dimensions of a=b=99.1 Å, c=216.0 Å and α=β=90°, γ=120°. A tentative molecular replacement solution has been found using myeloperoxidase as a phasing model, and an electron density map has been calculated to 7 Å resolution.

TPO is has a carbohydrate content of at least 12 kDa and the presence of multiple glycoforms or mobile carbohydrates chains may prevent high resolution diffraction. Work is underway to deglycosylate TPO, and, in addition, co-crystallisation with human monoclonal autoantibodies is being investigated.

1. F. Grennan Jones *et al*. J. Mol. Endocrin. 17, 165-174.

P11.04.003 CRYSTAL STRUCTURE OF CHONDROITINASE B FROM *F. HEPARINUM* WITH A DERMATAN SULPHATE DISACCHARIDE PRODUCT
Miroslaw Cygler[1,2], Weijun Huang[1], Allan Matte[1], Yeong Shik Kim[3], Robert J. Linhardt[4] and Hongsheng Su[5] [1]Biotechnology Research Institute, 6100 Royalmount Ave., Montréal QC, H4P 2R2 Canada; [2]Montréal Joint Centre for Structural Biology, Montréal QC Canada; [3]Nat. Prod. Res. Inst., SNU, Seoul 110-460, Korea; [4]Med. Nat. Prod. Chem., University of Iowa, PHAR-S328, Iowa City 52242, USA and [5]IBEX Technologies Inc., 5485 Paré St., Montréal QC, H4P 1P7 Canada

The crystal structure of chondroitinase B from *Flavobacterium heparinum*, complexed with a dermatan sulphate disaccharide product, has been determined and refined (R_{work}=0.181, R_{free}=0.217) at 1.7Å resolution. This is the first structure of a product or substrate molecule bound to a polysaccharide lyase. The dermatan sulphate product consists of an unsaturated uronic acid, with the double bond between C4 and C5, linked β-(1→3) to N-acetylgalactosamine. The complex was obtained by soaking a native crystal of chondroitinase B in 30 mM disaccharide in cryoprotectant for 18h, followed by freezing directly in the nitrogen cold stream. Electron density corresponding to the disaccharide product was clearly visible in the initial difference map calculated at 1.7Å. The location of the disaccharide binding site is within the cleft formed by loops protruding from the β–helix, similar to that suggested for several polysaccharide degrading enzymes having the β–helix fold. Both direct and water mediated interactions contribute to product binding. A sulphate group at C-4 of N-acetylgalactosamine interacts directly with Arg364, and via a water molecule with Arg318. Arg318 and Arg363 interact with the carboxyl group of the uronic acid, and Arg271 stabilizes the galactosamine ring by interacting with the ring O atom and the C1 hydroxyl group. Comparison of the native and complex structures reveals no significant structural changes in the protein upon disaccharide binding. Further studies are in progress to elucidate the catalytic mechanism and substrate specificity of this enzyme.

P11.04.004 X-RAY STRUCTURE OF AN INHIBITOR PROTEIN AND LOCATION OF ITS SECOND REACTIVE SITE.
J.K.Dattagupta, A.Podder, C.Chakrabarti, U.Sen, S.Ravichandran and D. Mukhopadhyay, Crystallography & Molecular Biology Division, Saha Institute of Nuclear Physics, 1/AF Bidhannagar, Calcutta 700 064, India.

The crystal structure of an α-chymotrypsin inhibitor protein of Kunitz (STI) family isolated from winged bean (*Psophocarpus tetragonolobus*) seeds, will be reported. This is a single polypeptide chain having a molecular weight of 20,244 Da with 183 amino acid residues. The structure of the protein has twelve antiparallel β-strands with connecting loops arranged in a β-trefoil fold common to other homologous serine protease inhibitors in this family, like soybean trypsin inhibitor, *Erythrina caffra* trypsin inhibitor, proteinase K inhibitor from wheat germ and also winged bean albumin belonging to the same family, as well as to some non-homologous functionally unrelated proteins like Interleukin-1α, Interleukin-1β, Human fibroblast growth factor, Abrin-a sugar complex, Interleukin-1 receptor antagonist and Amaranthin. This inhibitor protein was found to have the unique property of inhibiting bovine α-chymotrypsin in the molar ratio 1:2 at higher concentrations of the enzyme indicating that the inhibitor has two reactive sites. The conformation of the first reactive site loop in the structure is found to be stabilized through hydrogen bonds mainly formed by the side-chain of Asn 14, which intrudes inside the cavity of the reactive site loop, with the side-chain and main-chain atoms of some residues in the loop region. Analysis of the crystal structure of the protein led to the location of the second reactive site, about which no prior biochemical information was available. This site was identified mainly on the basis of a best fit structural study of the available canonical conformation of the serine protease inhibitor reactive sites. The structural results have also been used to understand the mechanism of inhibition against chymotrypsin at the molecular level. X-ray structures of the recombinant and two mutant forms of the inhibitor protein are also being determined in our laboratory.

P11.04.005 X-RAY STRUCTURAL STUDIES WITH HUMAN THIOREDOXIN PEROXIDASE.
E. Schröder, M. I. Isupov and J. A. Littlechild, Departments of Chemistry and Biological Sciences, University of Exeter, Exeter, EX4 4QD, UK.

Thioredoxin Peroxidase-1 (TDX1), previously known as Natural Killer Enhancing Factor-B, is an intracellular member of the peroxiredoxins, an emerging family of antioxidant enzymes with monomeric masses of 20-29kDa. Their biological interest lies in their ability to combat oxidative stress by degrading hydrogen peroxide and organic hydroperoxides to water or to the corresponding alcohol. Over the last few years, peroxiredoxins have been shown to play roles in tyrosine kinase signalling and in apoptosis. The ability of TDX1 to prevent the attachment of monocytes to endothelial cells in response to oxidised lipoproteins suggests that this enzyme may help combat the effects of atherosclerosis. In common with other peroxiredoxins, TDX1 readily forms disulphide-linked dimers under oxidising conditions and oligomers under reducing conditions with an approximate molecular mass of 350kDa. A cysteine located close to the N-terminus is completely conserved among all PRX enzymes and is essential for catalysis, although most peroxiredoxins also contain a conserved cysteine located towards the C-terminus, which is a requirement for their regulation by thioredoxin. Non-recombinant human TDX1 has been purified to homogeneity from red blood cells and two crystal forms have been grown by vapour diffusion: monoclinic $P2_1$ crystals (a = 88.9 Å, b = 107.0 Å and c = 119.5 Å, and β = 110.9) and orthorhombic $P2_12_12_1$ crystals (a = 57.2 Å, b = 185.3 Å and c = 226.5 Å). The asymmetric unit in both crystal forms is likely to be oligomeric, containing 6-14 molecules (assuming a solvent content of 30-75%), which is consistent with the tendency of TDX1 to form discrete oligomers in solution. The diffraction from both crystal forms extends to beyond 2.0 Å resolution using synchrotron radiation. Complete native data sets have been collected on the X11 Hamburg beam-line under cryogenic conditions to 1.8 Å and 2.7 Å resolution from monoclinic and orthorhombic crystals respectively. A search for heavy atom derivatives is currently in progress.

P11.04.006 PROBING THE STRUCTURAL BASIS OF PROTEIN THERMOSTABILITY.
H. Walden and G.L. Taylor School Biomedical Sciences, University of St. Andrews, St. Andrews, Fife KY16 9TS, UK, and R. Hensel Dept. Microbiology, FB9, Universität-GH Essen,, Universitätsstrasse 5, 45117 Essen, Germany, and G.S.Bell, D.W. Hough and M.J. Danson, School Biological Sciences, University of Bath, Claverton Down, BA2 7AY,, UK.

Triosephosphate isomerase (TIM) is a glycolytic enzyme which catalyses the interconversion of glyceraldehyde-3-phosphate and dihydroxyacetone phosphate. All the bacterial and eukaryal TIM sequences published to date are homomeric dimers and each subunit consists of an eight stranded αβ-barrel domain. However, the TIM sequence of the hyperthermophilic Archaeon *Pyrococcus woesei*, which grows at an optimu temperature of 100°C, is a homotetramer [1]. Another difference is the length of the deduced protein sequence - bacterial and eukaryal TIMs are 240-260 residues in length, while the *P. woesei* TIM comprise only 224 residues.

Preliminary crystallographic studies of native *P. woesei* TIM have been carried out [2], and to date, molecular replacement

has been unsuccessful. Attempts are currently being made at heavy atom isomorphous replacement.

There are several TIM crystal structures available from bacterial and eukaryal sources, enabling a comparative study of mesophilic and thermophilic TIMs, which should provide some insight into the nature of protein thermostability.

1. Kohlhoff, M.K., Dahm, A & Hensel, R. (1996) *FEBS Lett.* **383** 245-250.
2. Bell, G.S., Russell, R.J.M., Kohlhoff, M., Hensel, R., Danson, M.J., Hough, D.W. & Taylor, G.L. (1998) *Acta Cryst.* D**54** 1419-1421.

P11.04.007 CRYSTAL STRUCTURE AND PRIMARY SEQUENCE OF *THERMOASCUS AURANTIACUS* XYLANASE: BASIS OF THERMOSTABILITY. R. Natesh, P. Bhanumoorthy, P.J. Vithayathil, K. Sekar, S. Ramakumar, M.A. Viswamitra, Department of Physics / Bioinformatics Centre, Indian Institute of Science, Bangalore-560012, India.

Thermoascus aurantiacus xylanase is a thermostable enzyme which hydrolyses xylan, a major hemicellulose component in the biosphere. Earlier biochemical studies on the protein extracted from a local strain of the fungus reveal that the enzyme retains its activity even at 70°C and hence is likely to be industrially relevant. More than 10 salt bridges which together with a disulfide bond between Cys 255 and Cys 261 might be contributing to the thermostability of the protein. To our knowledge we observe for the first time in F/10 family xylanase structures, a proline in the middle of a helix. In addition we also observe a unique salt bridge between Arg 124 and Glu 232 which links sequencially separated segments of the protein and might be contributing to thermostability. Our study suggests that in addition to the number of interactions their location is also an important factor for thermostability.

Intensity data were collected from crystals that belong to space group $P2_1$ with a = 41.7, b = 68.1, c = 51.4 Å and β = 113.6°, Z = 2. The structure was solved by molecular replacement using the ***Streptomyces lividans*** xylanase as a search model. The amino acid sequence was determined from electron density maps aided by multiple alignment of related xylanase sequences. The sequence thus obtained provides a correction to the sequence reported earlier based on biochemical methods. The final 1.8 Å resolution refined protein model with 301 residues and 266 water molecules has a R of 16.0 % and R_{free} of 21.1 % with good stereochemistry. The single polypeptide chain assumes $(\alpha/\beta)_8$ TIM-barrel fold and belongs to F/10 family of glycoside hydrolases. The active site consists of two glutamates located at the C-terminus end of β-barrel conforming to the double displacement mechanism for the enzyme action.

P11.04.008 MECHANISM OF PHOSPHORYL HYDROLYSIS; WHAT MAKES AN ENZYME A GOOD CATALYST? P.Heikinheimo[α], V.Tuominen[α], R.Lahti[β], B.S.Cooperman[γ] & A.Goldman[α,β] [α]Turku Centre for Biotechnology, P.O. Box 123, FIN-20521 Turku, Finland, [β]Department of Biochemistry, University of Turku, FIN-20014 University of Turku, Finland, [γ]Department of Chemistry, University of Pennsylvania, Philadelphia, PA 19104, USA

The detailed mechanism and quantum mechanical basis for enzymatic catalysis remains incompletely understood[1]. What makes enzymes good catalysts for a reaction? Is it 'orbital steering' and bringing the reactants together in the right orientation or do enzymes also provide e.g. short, high energy hydrogen bonds. Are there other explanations?

Inorganic pyrophosphatases (PPases) provide a good working model to study the mechanism of phosphoryl hydrolysis. They catalyse the hydrolysis of inorganic pyrophosphate (PP_i) to two phosphate molecules by extensive use of metal ions[2]. The kinetics and the pH dependence of the reaction are thoroughly studied[3,4] and in addition to the resting state and mutant structures[2,5], a refined structure of the substrate/product equilibrium around the transition state is available at 1.1 Å resolution. This structure allows us to address issues of H-bond length and orbital steering directly. We have evidence for ultra-short H-bonding between the proposed general base (D117) and the nucleophile (Wat1), explaining their matching pK_a's, but our structures show that 'orbital steering' or transition state stabilisation are *not* part of the catalytic mechanism. We also see specific binding of the product, which suggests that lowering the substrate restoring forces increases the probability of each transition state producing product. This, in conjunction with subtle product release mechanisms, affords diffusion controlled catalysis in this class of phosphoryl hydrolysing enzymes, and we propose a standard model for the mechanism of biocatalysis.

1. Cannon, W. R., *et al.* & Benkovic, S. J. *Nature Structural Biology* **3**, 821 (1996).
2. Heikinheimo, P. *et al.* & Goldman, A. *Structure* **4**, 1491-1508 (1996).
3. Pohjanjoki, P., *et al.* & Cooperman, B.S. *Biochemistry* **37**, 1754-1761 (1998).
4. Baykov, A. *et al.* & Cooperman, B.S. *Biochemistry* **35**, 4655-4661 (1996).
5. Tuominen, V. *et al.* & Goldman, A. *J. Mol. Biol*. **284**, 1565-1580 (1998).

P11.04.009 A NEW CLASS OF INORGANIC PYROPHOSPHATASE. A.J. Milner, T.W. Young, S.A. White, School of Biochemistry, University of Birmingham, Edgbaston, Birmingham, West Midlands, B15 2TT.

Inorganic pyrophosphatase (PPase, E.C.3.6.1.1) is a ubiquitous enzyme which plays an important role in overall cell metabolism (Chen et al, 1990). It has recently been reported that the PPase from Bacillus subtilis has been purified and that its amino-acid sequence (Young et al, 1998), subunit molecular mass and requirement for manganese ions make it different from the PPases isolated from other organisms (Kuhn and Ward, 1998). Subsequent work has resulted in the proposition that this protein belongs to a new class of PPase (class C). This classification is based on sequence and activity differences between the B. subtilis PPase and the PPases that have been characterised from other prokaryotes (class A) and eukaryotes (class B). Crystals, grown by hanging drop vapour diffusion, reach a maximum size of 0.2mm in the largest dimension. A preliminary data set has been collected, analysis suggests an orthorhombic unit cell (a=81.4 Å, b=133.3 Å, c=155.2 Å, α=β=γ=90°) with c222 symmetry. The latest results will be presented.

1. Chen, J., Brevet, A., Fromant, M., Leveque, F., Schmitter, J.M., Blanquet, S. & Plateau, P. (1990). Pyrophosphatase is essential for growth of Escherichia coli. J. Bacteriol, 172, 5686-5689.
2. Kuhn, N.J. & Ward, S. (1998). Purification, properties and multiple forms of a manganese-activated inorganic pyrophosphatase from Bacillus subtilis. Archives of Biochemistry and Biophysics, 354, 47-56.
3. Young, T.W., Kuhn, N.J., Wadeson, A., Ward, S., Burges, D. & Cooke, G.D. (1998). Open reading frame yybQ of Bacillus subtilis encodes a soluble inorganic pyrophosphatase with distinctive properties: The first of a new class of pyrophosphatases? Microbiology, in press

P11.04.010 ADC ESTERS, AUTOCLEAVAGE AND CATALYSIS: WHAT THE STRUCTURES SAY. F.von Delft[1], A.Albert[1], V.Dhanaraj[1], U.Genschel[2], M.K.Rajmee[2], M.Witty[2], R.Pulido[3], T.L.Blundell[1], A.G.Smith[2], C.Abell[3]. (**1**) Biochemistry, Cambridge University, CB2 1GA, UK (**2**) Plant Sciences, Cambridge University, CB2 3EA, UK (**3**) Chemical Laboratory, Cambridge University, CB2 1EW, UK.

The 2.2 Å crystal structure[1] of *E. coli* Aspartate Decarboxylase has, for the first time, revealed the structure of an ester intermediate, produced during the enzyme's auto-cleavage. Self-catalyzed backbone N- to O/S-acyl shifts, resulting in a (thio-)ester intermediate, are the first step in the maturation of several diverse self-cleaving biological systems. In ADC, this leads to formation of a catalytic pyruvoyl co-factor. The structure is homo-tetrameric: three subunits appear fully processed while the fourth contains the uncleaved chain containing the ester. This intermediate is a trapped species, since residues necessary for ester cleavage (T57/Y58) seem too far removed for effective catalysis in the uncleaved subunit. We propose that self-cleavage occurs cyclically around the tetramer, as a sequential and negatively co-operative process: successive subunits cleave more slowly.

Two crystal structures of ADC with bound substrate analogues (α-methylaspartate at 1.7 Å and β-alanine at 1.9 Å resolution) confirm the initial model of substrate binding and catalysis. The binding cavity is located between two subunits, and the substrate binds as a Schiff base to a pyruvoyl group in the *trans* conformation. R54 and W47 from the adjacent subunit form, respectively, a salt bridge and an aromatic stacking interaction with the substrate's β-carboxylate group. This positions the negatively charged departing α-carboxylate group in a hydrophobic pocket formed by Y58, I60 and the pyruvoyl methyl group, thus driving α-decarboxylation. The resulting α-carbanion is stabilised by π-bond delocalisation across the Shiff base-pyruvoyl system, and is most likely protonated by a bound water, connected to the solvent *via* the H-bonding network of G24 and Y57, and K9 and H11 from the adjacent subunit.

[1] Albert *et al.* (1998) Nature Structural Biology **5(4)**, pp. 289-293.

P11.04.011 FERROCHELATASE IN COMPLEX WITH AN INHIBITOR, N-METHYL MESOPORPHYRIN. D. Lecerof, M. Fodje and S. Al-Karadaghi [1] M. Hansson, A. Hansson [2] [1] Dept. of Molecular Biophysics, Lund University, Box 124, 221 00 Lund, Sweden [2] Dept of Biochemistry, Lund University, Box 124, 221 00 Lund, Sweden.

Ferrochelatase is the terminal enzyme in the haem synthesis pathway. It catalyses the insertion of a ferrous ion into protoporphyrin IX forming haem b. In humans, the autosomal dominant disease protoporphyria is due to the reduced activity of ferrochelatase. Here we present the structure of ferrochelatase from Bacillus Subtilis in complex with N-methyl mesoporphyrin (N-MMP) refined to 2.1 Å, thereby providing the basis for a deeper understanding of the mechanisms of enzyme catalysed metal chelating.

The active site of ferrochelatase consists of a deep cleft in which N-MMP is bound with its carboxyl groups reaching out to the surface. Compared with the native structure [1], the loops which interact with the incoming inhibitor in the active site have moved by about 2-3 Å, in order to make room for the inhibitor. The methylated imidiazol ring of N-MMP is tilted by about 40 degrees with the methyl group close to His183, suggested earlier to be involved in catalysis. Besides this pronounced tilting, the rest of the N-MMP is not plane, indicating a strained conformation of the molecule. As previous studies of antibodies elicited to N-MMP showed catalytic activity at rates up to 10 % of ferrochelatase rate [2], these results suggest that the bound conformation indeed is that of a transition state analogue. The structures of the complexes of Co2+, Cu2+ and Zn2+ with the apo-enzyme and the enzyme:N-MMP complex have also been studied. The results show 3 different metal binding sites in ferrochelatase. The implications of these findings to the mechanism of porphyrin metallation will be discussed.

[1] Al-Karadaghi, S., Hansson, M., Nikonov, S., Jönsson, B. & Hederstedt, L. (1997) Structure, 5, 1501-1510.
[2] Cochran, A.G. & Schultz, P.G. (1990) Science, 249, 781-783.

P11.04.012 CRYSTAL STRUCTURE OF AROMATIC AMINO ACID AMINOTRANSFERASE FROM *Pyrococcus horikoshii*. K. Harata, W.-D. Schubert,* E. Matsui, K. Ishikawa, and I. Matsui, National Institute of Bioscience and Human-Technology, Tsukuba, Ibaraki 305-8566, Japan. *Present address: Institut für Kristallographie, Freie Universität, Takustr. 6, 14195 Berlin, Germany

Amino acid aminotransferase, which has pyridoxal-5'-phosphase (PLP) as a co-enzyme, is an enzyme to transfer the amino group from an amino acid to an ap-keto acid. We have obtained the enzyme (ArAT) specific for aromatic amino acids from *Pyrococcus horikoshii*, a hyperthermophile which grows at near 100º C. ArAT with the optimum temperature of *ca*. 90º.C consists of 389 amino acids. Crystals were obtained from 3M 1,6-hexane-di-ol solution with pH 7.5 containing 10mM $MgCl_2$. Cell dimensions were a=64.01, b=124.87, and c=128.78 Å, and the space group was $P2_12_12_1$ with Z=8 (V_m=2.93 Å^3/Da). X-ray diffraction data were collected to 2.1 Å resolution on an Nonius FAST diffractometer equipped with FR571 rotating anode generator. The structure was solved at 3 Å resolution by the MIR method using four heavy atom derivatives and refined at 2.1 Å resolution to the R-value of 0.185 (R_{free}=0.253).

Two molecules in the asymmetric unit are related with a local twofold axis and the active site consists of amino acid residues from the two molecules. The main chain folding is similar to the structure of aspartate aminotransferase from *E. coli* and some of amino acid residues in the active site are conserved in spite of low sequence similarity. The PLP molecule is bonded to Lys232 and the pyridine ring is in the face-to-face contact with the phenyl group of Phe121.

P11.04.013 CRYSTALLOGRAPHIC STUDYES OF ASPARTATE AMINOTRANSFERASE FROM A THERMOPHILIC *CYANOBACTERIUM*. K. Hamada[1], K. Nozawa[1], Y. Sawa[2], Y. Mezaki[3], Y. Katsuya[3], T. Kumasak[4] and M. Yamamoto4, [1]Interdisciplinary Faculty of Science and Engineering, Shimane University, Matsue 690-8504, Japan, [2]Faculty of Life and Environmental Science, Shimane University, Matsue 690-6504, Japan, [3]Hyogo Prefectural Institute of Industrial Research, SR-laboratory, Kamigori, Hyogo 678-1201, Japan, [4]RIKEN, Harima Institute, Mikazuki, Hyogo 679-5143, Japan.

Aspartate aminotransferase (AspAT) is a pyridoxal 5'-phosphate (PLP)-dependent enzyme and catalyzes the reversible transfer of the amino group of aspartate to 2-oxogulutarate by the ping-pong Bi Bi mechanism. AspAT from a thermophilic cyanobacterium, *Phormidium lapideum* (*Pl*AspAT) is a thermophilic and thermostable enzyme which retains its structure and reaches maximal activity at 80 °C. AspAT from *P. lapideum* shares with mesophilic eukaryotic and bacterial counterparts a large number of catalytically significant feature. However, the sequence homology of *Pl*AspAT is not exceeding 20% against mesophilic eukaryotic and bacterial enzymes, and that is 40% level against thermophilic bacterial enzymes. The differences observed, which reflect the evolutionary distance between Archaea, Eukarya, Bacteria, may be able to account for the enzyme adaptation to high temperatures. *Pl*AspAT expressed in *E. coli.* containing the plasmid of *Pl*AspAT was purified, and crystallised with the essential cofactor of PLP by the hanging drop technique using ammonium sulfate as precipitant. Of three different crystal forms of monoclinic, tetragonal, and rhombic observed, the monoclinic crystals were most suitable for X-ray structure analysis. The crystals belong the monoclinic space group C2 with unit cell dimensions of a = 122.1 , b = 110.8, c = 87.8 Å and b = 97.1°. A V_m value of 3.30 Å^3/Da indicated that a dimmer was contained in the asymmetric unit. Native data set to 2.5 Å resolution was collected using synchrotron radiation at the Photon

Factory, KEK, and SPring-8. The structure analysis by molecular replacement method is now in progress.

P11.04.014 ENTROPIC ALLOSTERIC EFFECT FOUND TROUGHT THE X-RAY STRUCTURE OF THE GLUCOSAMINE 6-PHOSPHATE DEAMINASE FROM *E. coli*., E. Horjales, S. Morales and E. Rudiño-Piñera, Molecular Recognition and Biostructure Department, Biotechnology Institute, National Autonomous University of Mexico (UNAM), Av. Universidad No. 2001, Col. Chamilpa, CP. 62210, Cuernavaca, Morelos, MEXICO. E-mail: horjales@ibt.unam.mx

The allosteric transition between the R and T forms in allosteric enzymes can be explained through conformational changes between both conformers, but the use of high resolution diffraction data (which validate the use of temperature factors B) shows in our case the different vibrational components between the R and T forms centred in particular in the active site lid (residues 158-185). In the present case the protein Glucosamine 6-phosphate deaminase (which catalyses the reversible reaction between glucosamine 6-phosphate and fructose 6-phosphate and ammonium) structure was solved in presence of trace amounts of its allosteric activator (N-acetyl glucosamine 6-phosphate (NAG6P)) , giving a final R=0.214 (R_{free}=0.264) at 2.8 Å resolution. This native R form presents the NAG6P only in the allosteric site, and b values below 70 with a continuous electron density map at 1.0 σ in the lid.

In other hand, the protein crystallographic structures solved from the T and R mutants Y254F (which kinetically shows its importance as two-way switch mechanism in the allosteric transition (1)) present the same structure as its respective native molecule, in the case of the Y254F R form a NAG6P is ligated only in the allosteric site (with a free active site). The mutants Y254F R and T forms were solved at 2.15 Å and 1.94 Å resolution, with R=0.216 (R_{free}=0.261) and R=0.212 (R_{free}=0.228) respectively. Our results prove that the lid is clearly less mobile in R conformer. The Y254F mutant also shows that the kinetical differences with the native form are only explained with an entropic component in the allosteric transition.

Acknowledgements: We wish to thank Dr. Mario Calcagno for supplying the purified protein, Sonia Rojas-Trejo for technical assistance, the SSRL for data collection time. This study has been supported by DGAPA-UNAM (Grant IN-201295). S. Morales and E. Rudiño are supported by CONACyT.

(1) G. M. Montero-Moran, et al, Biochemistry (1998), vol. 37, 7844-7849.

P11.04.015 CRYSTAL STRUCTURE OF AN E96A MUTANT OF GLUCOSE DEHYDROGENASE FROM *BACILLUS MEGATERIUM* Keizo Yamamoto[1], Masami Kusunoki[2], Genji Kurisu[2], Itaru Urabe[3], and Shiro Tabata[1], [1]Department of Chemistry, Nara Medical University, Kashihara, Nara 634-0813, [2]Institute for Protein Research, Osaka University, Suita, Osaka 565-0871, [3]Department of Biotechnology, Graduate School of Engineering, Osaka University, Suita, Osaka 565-0871, Japan

Glucose dehydrogenase from *B.megaterium* is a tetrameric enzyme with four identical subunits. The enzyme is inactivated at pH 9.0 due to the dissociation of the tetramer into inactive monomers, and the monomers reassociate at pH 6.5 into the fully active tetramer. The E96A mutant is in the tetrameric state even at pH 9.0 and the activity is 85% of that kept at pH 6.5. In order to elucidate the mechanism of increasing stability of the intersubunit interaction and/or tertiary structure of the protomer, we have been carring out the X-ray studies of the E96A mutant.

The enzyme was crystallized by the hanging-drop vapor diffusion method with PEG2000 as a precipitant, followed by a microseeding technique. The crystals belongs to the monoclinic space group C2 with cell dimensions of a=121.96 Å, b=66.64 Å, c=120.06 Å and β=93.44°, contains four subunits per asymmetric unit. Diffraction data were collected on Weissenberg camera with synchrotron radiation at the BL18B in Photon Factory, KEK, Japan. Molecular replacement was used to determine an initial phase set. Refinement is in progress using X-PLOR and the current R-factor is 0.24 for data to 2.5 Å resolution.

P11.04.016 CRYSTALLIZATION OF OROTIDINE 5'-MONOPHOSPHATE DECARBOXYLASE P.Harris, J.-C.N.Poulsen, S.Larsen, Centre for Crystallographic Studies, University of Copenhagen, Denmark and K.F.Jensen, Center for Enzyme Research, University of Copenhagen, Denmark.

Orotidine 5'-monophosphate decarboxylase (ODCase) catalyses the decarboxylation of orotidine 5'-monophosphate (OMP) to uridine 5'-monophosphate (UMP), the sixth and last step in the *de novo* biosynthesis of UMP (a precursor of other pyrimidine mononucleotides). At physiological temperatures ODCase enhances the rate of reaction by a factor of 10^{17}, thus it is the most proficient enzyme known [1]. Despite the extensive enzymological studies of ODCase [2] no information is available on the three dimensional structure of this enzyme, so important in pyrimidine biosynthesis.

Trigonal crystals are obtained using Na-formate as precipitant. Cryocooled, these crystals diffracted to 2.8 Å at the BW7B beamline at the EMBL, Hamburg. The space group is $P3_1$ and the cell dimensions are $a = b = 142.52$ Å and $c = 105.12$ Å which indicates 4, 6 or 8 molecules in the asymmetric unit, corresponding to 75, 62 or 50 % solvent content, respectively.

A new crystal form, where an inhibitor is bound, has been obtained using PEG4000 as precipitant. At the BL711 beamline at MAXII in Lund, Sweden, these crystals diffracted to at least 2.2 Å. The cell dimensions are $a = 61.85$ Å, $b = 96.77$ Å and $c = 148.33$ Å and the space group is identified as $P2_12_12_1$ indicating two molecules in the asymmetric unit for a solvent content of 69%.

Progress of the structure solution will be presented.

1. A. Radzicka, R. Wolfenden (1995). *Science* **267**, 90.
2. J.K.Lee, K.N.Houk (1997). *Science* **276**, 942.

P11.04.017 STRUCTURE OF AN EXOGLUCANASE COMPLEXED WITH CONDURITOL B EPOXIDE FROM A 50μ CRYSTAL USING MONOCAPPILARY OPTICS. JN Varghese, A van Donkelaar, Biomolecular Research Institute, 343 Royal Parade, Parkville, Victoria 3052 Australia, M.Hrmova, GA Fincher , Dept. of Plant Science, Waite Institute, University of Adelaide, Urrbrae, South Australia 5064, and DX Baliac, Z Barnia, Dept. of Physics, University of Melbourne, Parkville, Victoria 3052, Australia.

The 3-D structure of β-D-exohydrolase from Barley seed has been determined previously by X-ray crystallography (Varghese et al. 1999). The native structure was found to have a glucose moiety bound in a deep pocket formed by an intimate association of two domains of the protein. The structure presented in this abstract confirms the location of the active site of the molecule, by showing that conduritol B epoxide displaces the bound glucose and forms a covalent bond with one of the proposed catalytic acids (E491). This reaction is consistent with hydrolytic mechanism of this glucose hydrolase.

The X-ray data were collected from a frozen 50μ crystal mounted on a MAR180 imaging plate detector, using an Elliot GX20 running at 33kV and 20mA using a 100μ cup, and an ellipsoidal glass monocapillary (Baliac et al. 1996) with a 100μ focus at the crystal. This system delivers an intensity 28 times that

of an equivalent unfocussed beam at the specimen, allowing micro-protein X-ray data to be collected using laboratory sources.

Varghese JN, Hrmova M, Fincher GA, The 3D structure of Barley β-D-exohydrolase: a family 3 glucosyl hydrolase (1999) Structure (in press)
Balaic DX, Barnea Z, Nugent KA, Garrett RF, Varghese JN, Wilkins SW, Protein crystal diffraction patterns using a capillary-focused synchrotron x-ray beam (1996) J. Synch.Rad. 3,289-295.

P11.04.018 THE CRYSTAL STRUCTURE OF 1-AMINOCYCLOPROPANE-1-CARBOXYLIC ACID DEAMINASE FROM YEAST. M. Yao, H. Sugimoto, T. Ose, A. Horiuchi, A. Nakagawa and I. Tanaka, Graduate School of Science, Hokkaido University, Sapporo, Japan, D.Yokoi, T.Murakami and M. Honma, Graduate School of Agriculture, Hokkaido University, Sapporo, Japan, S. Wakatsuki, ESRF, Grenoble, France.

1-Aminocyclopropane-1-carboxylic acid (ACC) deaminase, a pyridoxal phosphate(PLP)-dependent enzyme found in microorganisms, catalyzes a reaction of cleavage ACC to α-ketobutyrate and ammonia by cyclopropane ring-opening. ACC is a key intermediate in the biosynthesis of a plant hormone ethylene which affects diverse growing and fruit ripening. Interestingly, introduction of ACC deaminase gene in plants was reported to reduce the production of ethylene and delay ripening progression of fruits, although ACC deaminase has never been found in higher plants with the exception of transgenic plants. The three dimensional structure of ACC deaminase from yeast *Hansenula saturnus* (yACCD) was determined by MAD method using mercury atoms as anomalous scatterer.

The two crystal forms were obtained for mercury derivative of yACCD by co-crystallization. The 2.0Å native data and 2.8Å MAD data of the orthorhombic form and 2.5 Å MAD data of the trigonal form were collected using synchrotron radiation at the ESRF of France and Photon Factory of Japan, respectively. Initial phasing was done independently for the two forms. The model was built based on 2.8Å electron density map after improvement by non-crystallographic symmetry averaging of multiple crystal forms. The molecular dynamic refinement is currently underway at 2.0Å resolution using native data.

The structure of yACCD can be divided into two different size domains (small domain and PLP-binding domain). Both domains have open twisted α/β−sheet structures. The PLP co-enzyme is positioned close to the big internal gap between the two domains and covalently bound to Lys54.

P11.04.019 HUMAN AND BACTERIAL GLUCOSE 6-PHOSPHATE DEHYDROGENASE: IMPLICATIONS OF SPECIFIC STRUCTURAL CHANGES. Shannon W.N. Au, Veronica M.S. Lam, Department of Biochemistry, University of Hong Kong, H. Richard Levy, Department of. Biology, Syracuse University, Syracuse, NY 12344, USA, Sheila Gover & Margaret J. Adams, Laboratory of Molecular Biophysics, Department of. Biochemistry, University of Oxford, OX1 3QU, UK.

G6PD catalyses the first committed step of the pentose phosphate pathway, oxidising glucose 6-phosphate to its δ-lactone. In the human erythrocyte, the reduced coenzyme NADPH generated by this step protects against oxidative stress. In bacteria such as *Leuconostoc mesenteroides,* the enzyme is also required for catabolism for which it utilises NAD^+. Our 2Å structure of the dual-specific *L. mesenteroides* apo-enzyme dimer showed how residues conserved in all known G6PD sequences could play a crucial role in binding coenzyme and substrate. Kinetic studies of site directed mutants have confirmed our predictions and complement our structural studies of different binary and ternary complexes aimed at defining the molecular basis of the two modes of enzyme action.

Human G6PD deficiency is an extremely common enzymopathy; more than 100 point mutations have been identified, some giving rise to severe clinical symptoms. Dimers and tetramers of the erythrocyte enzyme are in a functional equilibrium. We have a 3Å structure of the commonest Chinese deficient variant, Canton (R459L), and a 2.6Å structure of an active, more thermally stable, mutant constructed by deletion from the normal human enzyme of the 25 N-terminal residues absent in bacteria. Both form tetramers which are "dimers of dimers", but there are significant local changes of conformation between the two, and from the bacterial structure. Plasmids have been constructed in which the point mutations for the Canton and Kaiping (R463H) variants have been combined with the N-terminal deletion. By extending to higher resolution and using crystals of these mutants, we aim to understand the structural bases of deficiency.

P11.04.020 CRYSTALS OF MALTOSE TRANSACETYLASE. L. Lo Leggio and S. Larsen, Centre for Crystallographic Studies, Copenhagen University, Universitetsparken 5, 2100 Copenhagen Ø, Denmark and K. W. Harlow and G. J. Abel, Danisco Biotechnology, Langebrogade 1, Box 17, 1001 Copenhagen K, Denmark

Maltose transacetylase (Mac) is an *E. coli* enzyme which transfers an acetyl group from acetyl-CoA to several sugar substrates. The primary sequence of Mac has an imperfect tandem-repeated hexapeptide motif [1] which strongly suggests that the protein will have the left-handed parallel β-helix architecture already observed in three acyl-transferases and a carbonic anhydrase. Two crystal forms have been characterized by collecting data at BL711 at the MAX II synchrotron in Lund, Sweden. Other crystallization conditions are being optimized.

Hexagonal needles with apparent P622 symmetry are grown reproducibly using ammonium sulphate as precipitant. The cell edges were a=b= 97.8 Å and c=90.3 Å and a 1.53 Å data set was collected at 100 K. However there is some indication of merohedral twinning for these crystals, so that P622 may not be the real space group.

A second crystal form has been grown using PEG as precipitant with MPD as an additive. We were able to collect data to 3.1 Å (100 K) at MAX II. The crystals belong to space group R3 with cell edges a=b= 156.0 Å and c= 142.4 Å (in hexagonal setting). Four to ten monomers of Mac in the asymmetric unit produce values of V_m within the range commonly observed for proteins. The progress in the structure solution of Mac will be described.

1. Vuorio, R, Härkönen, T, Tolvanen, M, Vaara, M (1994). *FEBS Letters* **337**, 289

P11.04.021 THE CRITICAL ROLE OF SOLVENT MOLECULES IN THE INDUCED FIT-MECHANISM OF THE ANTIBIOTIC TARGET MUR-A. S. Eschenburg, Max-Planck Institute for Medical Research, Department of Biophysics, 69120 Heidelberg, Germany, and E. Schönbrunn, Colorado State University, Department of Biochemistry and Molecular Biology, Ft. Collins Co80523, USA, and N. Amrhein, Swiss Federal Institute of Technology, Institute of Plant Sciences, 8092 Zurich, Switzerland.

MurA (UDP-N-acetylglucosamine enolpyruvyltransferase, EC 2.5.1.7) initiates the biosynthesis of the heteropolymer murein, the major structural element of the bacterial cell wall. It catalyzes the transfer of the intact enolpyruvyl moiety of phosphoenolpyruvate (PEP) to the 3-hydroxyl of UDP-N-acetylglucosamine (UDP-GlcNAc). This mechanistically unusual reaction is associated with substantial conformational changes in the enzyme.

The two-domain protein MurA is built up by the six-fold repetition of a folding unit consisting of two parallel α-helices and a four-stranded β-sheet [1]. The catalytically essential residue Cys115 is located in a flexible loop, which, in the course of the enzymatic reaction, moves about 20 Å towards the inter-domain section [2]. The large conformational changes upon binding of substrates and/or the naturally occuring inhibitor fosfomycin are predominantly mediated by UDP-GlcNAc [3].

We characterized the dynamics of a number of single-site mutants of MurA by various techniques. The high resolution X-ray crystallographic analysis of wild-type MurA (d_{min} 1.55 Å) and mutants with altered dynamic properties (d_{min} 1.70 Å to 1.90 Å) revealed that the arrangement of solvent molecules in the cleft between the two globular domains is critical for the motility of the enzyme and its induced fit mechanism.

[1] E. Schönbrunn, S. Sack, S.Eschenburg, A. Perrakis, F. Krekel,N. Amrhein, and E. Mandelkow. *Structure* 4, 1065 (1996).
[2] T. Skarzynski, A. Mistry, A. Wonacott, S.E. Hutchinson, V.A. Kelly, and K. Duncan. *Structure* 4, 1465 (1996).
[3] E. Schönbrunn, D.I. Svergun, N. Amrhein, and M.H.J. Koch. *Eur. J. Biochem*. 253, 406 (1998).

P11.04.022 CRYSTAL STRUCTURE OF LUCIOLA CRUCIATA FIREFLY LUCIFERASE COMPLEXED WITH MgATP. T. Nakatsu and H. Kato, Institute for Chemical Research, Kyoto University, Uji, Kyoto 611-0011, Japan and K. Hirokawa, N. Kajiyama and E. Nakano, Research & Development Division, Kikkoman Corporation. Noda, Chiba 278-8601, Japan

The crystal structure of Luciola cruciata firefly luciferase complexed with MgATP was determined by molecular replacement using unliganded luciferase from Photinus pyralis (sequence similarity is 67 %) as a search model. The overall structure consists of two domains. Each domain is similar that of Photinus pyralis luciferase, but a conformational change by a domain rotation with about 90 degree was caused by MgATP binding.

Firefly luciferase catalyzes the luminescence reaction through the oxidation of d-luciferin in the presence of MgATP, and molecular oxygen. In the first step, d-luciferin is reacted with MgATP to form an enzyme-bound luciferyl adenylate and pyrophosphate. Then the luciferyl adenylate intermediate is oxidized by molecular oxygen, and produce AMP, CO2 and an electronically excited state of oxyluciferin, which subsequently returns to the ground state with concomitant emission of visible yellow-green light. The enzyme efficiently converts chemical energy into light with a quantum yield of 0.88.

The luciferase from Luciola cruciata is functional as a monomer of molecular weight of about 60K with 548 amino acids. The T217I mutant enzyme was crystallized by hanging drop vapor diffusion method using PEG4000. The crystals belong to the space group $P\,2_12_12_1$ with cell constant a = 58.1 Å, b = 181.7 Å and c = 54.2 Å,. The intensity data of crystals were collected on a RIGAKU R-AXIS IIc to 2.3 Å resolution. The crystal structure was solved by molecular replacement using AMORE. The initial model was rebuilt by fitting correct sequence into the $2F_o$- F_c electron density map. The refinement of the model was carried out with REFMAC and X-PLOR 3.851. Current molecule includes 531 residues and the R and R_{free} values are 0.23 and 0.29 respectively at 12.0 - 2.5 Å resolution. The further refinement is in progress.

P11.04.023 STRUCTURAL STUDIES ON CARBAMOYL PHOSPHATE SYNTHETASE. James B. Thoden and Hazel M. Holden, Department of Biochemistry, University of Wisconsin, Madison, WI, 53705, USA, and Frank M. Raushel, Department of Chemistry, Texas A&M University, College Station, TX, 77843, USA

Carbamoyl phosphate synthetase (CPS) from *Escherichia coli* catalyzes the formation of carbamoyl phosphate from glutamine, bicarbonate, and two molecules of MgATP. Carbamoyl phosphate is used in the first steps of two biosynthetic pathways. In one it is coupled with aspartate in a reaction catalyzed by aspartate transcarbamoylase and is eventually incorporated into pyrimidine nucleotides. In the other it reacts with ornithine and is used to produce arginine and/or urea.CPS is a heterodimeric enzyme composed of a small (40K) glutaminase subunit and a large (120K) synthetase subunit. Glutamine is hydrolyzed in the small subunit to produce ammonia. The ammonia is then used by the large subunit to produce carbamoyl phosphate by a set of reactions at two active sites. The ammonia is first converted to carbamate by reaction with carboxyphosphate produced by one molecule of MgATP and one molecule of bicarbonate. At the next active site the carbamate is phosphorylated by a second molecule of MgATP to give the final product. The generation of these highly reactive intermediates (ammonia, carboxyphosphate, and carbamate) has necessitated that the enzyme develop a way to channel them through its interior, thus keeping them away from bulk solvent where they would rapidly decompose. The enzyme is under the allosteric control of various effector molecules including potassium, ornithine, and UMP. Under most conditions CPS is active as an $\alpha_4\beta_4$-heterotetrameric species. Despite the large size of the tetrameric enzyme (640K) the crystals diffract to at least 2 Å with synchrotron radiation, allowing for detailed structural analyses of the interactions between these effector molecules and the enzyme.

P11.04.024 δ CRYSTALLIN: A MODEL FOR STUDYING THE ENZYMATIC MECHANISM OF ARGININOSUCCINATE LYASE. Liliana M. Sampaleanu, Francois Vallée, Anita Chakraborty and P. Lynne Howell. Structural Biology and Biochemistry, The Hospital for Sick Children, Toronto, Ontario, and Dept. of Biochemistry, University of Toronto, Toronto, Ontario, Canada

Structural and functional analysis of wild type, chimera and site-directed mutants of duck δ-1 and δ-2 crystallin have been used to probe the enzymatic mechanism of argininosuccinate lyase (ASL), the urea cycle enzyme that catalyses the reversible breakdown of argininosuccinate to arginine and fumarate. The major soluble component of avian eye lenses, δ-crystallin, is directly related to ASL. In duck lenses there are two δ crystallin isoforms, δ-1 and δ-2. The two proteins are 94% identical in amino acid sequence and while δ-2 is the duck orthologue of ASL, δ-1 is enzymatically inactive. Domain swapping experiments have been used to assess the role of each structural domain of the δ-crystallin monomer. The kinetic and thermodynamic analysis of the chimeras revealed that only the N-terminal domain is crucial for recovery of ASL activity in δ-1 crystallin. The residues implicated in the catalytic mechanism of δ-2/ASL are conserved in δ-1. This suggests that the lack of catalytic activity in δ-1 crystallin is due to the conformational changes observed in the structural comparisons of δ-2 crystallin mutants (H91N and H162N with bound substrate) and turkey δ-1 crystallin. These structural studies have also revealed which residues interact with the substrate and that a conformational change occurs in the N-terminal domain on substrate binding. Site directed mutagenesis studies of δ-2 crystallin have confirmed the importance of a number of residues in substrate binding and catalysis. Our current understanding of the structure and function of ASL/δ-crystallin will be presented.

Funded by a grant from the Medical Research Council of Canada.

P11.04.025 STRUCTURE OF T AND R CONFORMERS FROM A MUTANT (K160E) OF GLCN6P DEAMINASE WITH MICHAELIS-TYPE KINETICS., E. Rudiño-Piñera and E. Horjales, Molecular Recognition and Biostructure Department, Biotechnology Institute, National Autonomous University of Mexico (UNAM), Av. Universidad No. 2001, Col. Chamilpa, CP. 62210, Cuernavaca, Morelos, MEXICO. E-mail: rudino@ibt.unam.mx

The glucosamine 6-phosphate deaminase (GlcN6P deaminase) is an allosteric enzyme which catalyses the reversible reaction between glucosamine 6-phosphate and fructose 6-phosphate and ammonium. In the allosteric site of the protein (which is activated with N-acetyl-glucosamine-6-phosphate (NAG6P)) the residue K160 is part of the interactions that bind the NAG6P, the mutation K160E changes the electrostatic balance in the allosteric site and produce a michaellian kinetics (1). In the present work we solved the x-ray crystallographic structure of the T conformer of GlcN6P deaminase K160E at 2.1Å giving a final R=0.219 (Rfree=0.233). The R conformer ligated with the competitive inhibitor 2 desoxy-2-amino-D-glucitol-6-phosphate was crystallised. The present state of the refinement shows an R=0.269 (Rfree=0.325) at 2.3 Å resolution. The conformations are the same as in the native forms, but exist differences in the temperature factors (B) distribution of the active site lid (residues 158-185).

The explanation of the crystallographic facts in relation with the kinetical studies is still in progress.

Acknowledgements: We wish to thank Dr. Mario Calcagno and Samuel Lara for supplying the purified mutant protein and for helpful discussions, Sonia Rojas-Trejo for technical assistance, the SSRL for data collection time. This study has been supported by DGAPA-UNAM (Grant IN-201295). E. Rudiño-Piñera is supported by CONACyT .

(1) S. Lara and M. L. Calcagno, Personal communication, 1999

P11.04.026 X-RAY STRUCTURE OF MN^{2+}-BOUND PHOSPHOENOLPYRUVATE CARBOXYLASE FROM *E. COLI*. Y. Kai[1], H. Matsumura[1], M. Terada[1], S. Shirakata[1], T. Inoue[1], T. Yoshinaga[2], and K. Izui[3], [1]Department of Materials Chemistry, Graduate School of Engineering, Osaka University, Suita, Osaka, 565-0871, [2]Department of Public Health, Graduate School of Medicine, and [3]Division of Applied Biosciences, Graduate School of Agriculture, Kyoto University, Sakyo-ku, Kyoto, 606-8501, Japan.

Phosphoenolpyruvate carboxylase (EC 4.1.1.31) catalyses the irreversible carboxylation of PEP to form oxaloacetate and inorganic phosphate. A divalent metal ion such as Mn^{2+} or Mg^{2+} is required for activity of the enzyme. The enzyme is widespread in higher plants, algae and many kinds of bacteria, and plays an anaplerotic role by replenishing C_4-dicarboxylic acid to the tricarboxylic acid cycle. PEP carboxylase from *E. coli* is an allosteric enzyme which is activated by CoASc or fructose 1,6-bisphosphate and inhibited by L-aspartate. Although we have determined the crystal structure of *E. coli* PEP carboxylase complexed with L-aspartate, the reaction mechanism for PEP carboxylase was not determined clearly, because neither substrate analogue or metal is bound to the enzyme. At present we are trying to crystallize *E. coli* PEP carboxylase complexed with substrate analogue and metal. The previous studies suggested that Mn^{2+} or Mg^{2+} can bind to the active site of PEP carboxylase even in the absence of PEP. It is improtant to determine the metal binding site in the enzyme, which would provide the molecular mechanism for catalysis. We crystallized Mn^{2+}-bound PEP carboxylase from *E. coli* and determined the location of Mn^{2+} binding to the active site. The structure of the Mn^{2+}-bound enzyme was refined to a crystallographic *R* factor of 22% (R_{free} = 26%) at 2.6 ≈ resolution. These results will provide insight into the mechanism of substrate binding.

P11.04.027 MOUSE ORNITHINE DC: SUICIDE INHIBITOR COMPLEX WITH DFMO AND STEREOCHEMCIAL IMPLICATIONS. Marvin L. Hackert, Andrew Kern, Marcos Oliveira, Jeff Almrud, Don Carroll, Steve Ernst and Phil Coffino[1], Dept. of Chemistry and Biochemistry, Univ. of Texas at Austin, Austin, TX 78712, and [1]Dept. of Microbiology and Medicine, UCSF, San Francisco, CA 94143.

Ornithine decarboxylases (ODCs) are PLP-dependent enzymes which initiate the first and rate-limiting step in the biosynthesis of polyamines. Polyamine metabolism is a target for the design of new anticancer and antiparasitical compounds. Sequence comparisons reveal four Groups of PLP-dependent decarboxylases, but there appear to be only two structural motifs. Decarboxylases of Groups I, II, and III possess a PLP-binding domain that resembles that found in the AAT's as seen in the structure of the bacterial ODC from *Lactobacillus* 30a. The eukaryotic ODCs belong to the Group IV decarboxylases which also includes biosynthetic ArgDC and diaminopimelate DC.

The crystal structure of mouse ODC (mODC') has been determined to 1.6Å resolution by multiple isomorphous replacement and the structure of a suicide inhibitor complex with DFMO is being refined to 2.5Å resolution. ODC is active as a 100Kda dimer formed through a head-to-tail interaction between monomers. Each monomer contains two domains: an α/β-barrel domain which binds the cofactor, and a second domain consisting mostly of β-structure. Only the dimer is catalytically active, since its two active sites are constructed of residues from both monomers. The suicide inhibitor DFMO is found covalently linked to K69 but not C360 as expected. The analysis of the mODC'/DFMO complex, together with modelling studies of the external aldimine intermediate, provide insight into the stereochemical characteristics of PLP-dependent decarboxylation and reveals unexpected stereochemical differences with other PLP-dependent enzymes and with the bacterial ODCs.

Supported in part by grants NIHGM 30105 and the Foundation for Research.

P11.04.028 CRYSTALLIZATION AND PRELIMINARY X-RAY STRUCTURE ANALYSIS OF A CISTEINE PROTEASE FROM THE PILEUS MEXICANUS LATEX: MEXICAIN. Ma. Carmen Oliver-Salvador [1], Abel Moreno-Carcamo [2], Richard Laursen, Zhirui Lian [3], Manuel Soriano-Garcia [2], [1] Unidad Profesional Interdisciplinaria de Biotecnologia, IPN and Departamento de Bioestructura, Instituto de Quimica, UNAM, [2] Departamento de Bioestructura, Instituto de Quimica, UNAM, [3] Department of Chemistry, Boston University, Boston, MA, USA

The cysteine proteases from plants (Caricaceaes and Bromelaceas) are a group of enzymes used industrially, and their application in food and beer industry has a great commercial value (25% of enzyme trade). In addition, these enzymes are used for pharmaceutical purposes. The archetypal papain from Carica papaya latex has considerable uses such as: beer and tanning industries, meat tenderization, etc. Mexicain is also a cysteine peptidase, isolated from Pileus mexicanus (Caricaceae). The mexicain, is one of the most abundant enzyme in the latex. This plant is related to papaya (C. papaya). Mexicain hydrolyze casein with or without cysteine. Besides benzoyl-L-arginine ethyl ester (BAEE) & N-Benzoyl-DL-arginine -4-nitroanilide (BAPNA). Mexicain has 214 amino acid residues (Mr=23,718 Da) and possesses 62.8% (identity) in amino acid sequence with chymopapain (IYAL) and 81.3 % (homology). Mexicain PIv E-64 has been crystallized at 18C by the hanging-drop vapor diffusion method. The reservoir solution contained 10% (w/v) PEG 6000, 0.1M citric acid pH 4.0. Equal volumes of the reservoir solution and 10 mg/ml protein solution in distillated water were mixed to give 6 ml drops. Small rod- shaped crystals were grew within three months. The crystals are orthorhombic and diffract X-ray up

to 2.8 resolution. The optimization of the crystal size and the data collection method using synchrotron radiation is under way.

Ma. Carmen Oliver-Salvador thanks COFFA-IPN

P11.04.029 STRUCTURAL BASIS FOR STEREOSPECIFIC OXIDOREDUCTION: CRYSTAL STRUCTURES OF TWO TROPINONE REDUCTASES. A. Yamashita,[1,4] K. Nakajima,[2] H. Kato,[1] H. Akama,[2] T. Nakatsu,[1] S. Wakatsuki,[3] T. Tomizaki,[3] T. Hashimoto,[2] Y. Yamada,[2] and J. Oda[1,5], [1]Institute for Chemical Research, Kyoto University, Uji, Kyoto 611-0011, Japan, [2]Graduate School of Biological Sciences, Nara Institute of Science and Technology, 8916-5, Takayama, Ikoma, Nara 630-0101, Japan, [3]ESRF, BP-220, Grenoble, Cedex 09, France, [4]RIKEN Harima Institute, 323-3, Mihara, Mikazuki, Hyogo 679-5143, Japan, [5]Fukui Prefectural University, 4-1-1 Kenjojima, Matsuoka, Fukui 910-1195, Japan.

A pair of tropinone reductases (TR) has the opposite stereospecificity on the 3-carbonyl group reduction of tropinone: TR-I forms tropine with the 3α- hydroxyl group, while TR-II forms pseudotropine with the 3β- hydroxyl group. In spite of this different specificity for tropinone reduction, two enzymes have same stereospecificity for NADPH and share 64 % identical residues in their amino acid sequences. We report here the crystal structure of both TR-I and TR-II, and the structural basis of their enzymatic catalysis, especially how these enzymes control their strict stereospecificities.

The crystal structures of both TRs have been determined independently at 2.4 Å (for TR-I) and 2.3 Å (for TR-II) resolution using MIR [1]. The overall structures of the two enzymes were strikingly similar. Further determination of the crystal structure of TR-II complexed with $NADP^+$ and pseudotropine at 1.9 Å resolution revealed the detailed structure of the active site. The NADP(H) binding mode and the positions of catalytic residues were similar between TR-I and TR-II. The substrate binding site of TR-II showed the good complementarity to the bound substrate (pseudotropine). In addition, electrostatic interaction between the substrate and the binding site seems to fix the binding position and orientation of the substrate. On the other hand, the corresponding area in TR-I which is presumed to be the binding site provides different van der Waals surfaces and electrostatic natures from that in TR-II. These differences likely contribute to differentiating the substrate binding mode of TR-I from that of TR-II; TR-I binds the substrate in " upside-down" orientation compared to TR-II. These results suggest that the active site structures of the both enzymes control their substrate binding modes and determine their reaction stereospecificities.

1. Nakajima *et al.* (1998) *Proc. Natl. Acad. Sci. USA*, **95**, 4876-4881.

P11.04.030 ALLOSTERIC REGULATION OF 5-PHOSPHORIBOSYL-1-PYROPHOSPHATE SYNTHASE. Frank Nygaard and Sine Larsen. Centre for Crystallographic Studies, Universitetsparken 5, University of Copenhagen, DK-2100 Copenhagen, DENMARK

PRPP synthase (PRS) which synthesizes 5-phosphoribysyl-1-pyrophosphate (PRPP), is one of the important enzymes in the pyrimidine and purine *de novo* biosynthesis and salvage pathway. It is a highly regulated enzyme justified by its position between several biological pathways. Inorganic phosphate and ADP serve as allosteric activator and inhibitor respectively. The three-dimensional structure of PRS from *Bacillus subtilis* (*b.s.*), which share ~50% sequence identity with the human PRS, has recently been determined in complexes with the allosteric inhibitor, ADP, and the activator, SO_4^{2-} (mimicking a PO_4^{2-} ion) (1). A sequence alignment of the more than 40 known PRS sequences, together with the *b.s.* structure, shows that many residues which are important for catalysis and its regulation are conserved.

Infantile or childhood onset of hyperuricemia and gout accompanied by neurodevelopmental disorders in humans has been ascribed to mutations in the *prs* gene causing a superactive PRS with decreased phosphate requirement and increased ADP inhibitor-resistance. Six such mutants, of which all are point mutations, have to date been identified (2). In order to further investigate the allosteric regulation of the PRS, six *b.s.* mutants containing the equivalent human mutations causing superactive PRS'es have been constructed. These mutants are being used for both structural as well as kinetic studies of the allosteric regulation of the PRPP synthase.

1. Eriksen TA, Kadziola A, Bentsen AK, Harlow K, Larsen S. *Submitted*
2. M.A.Becker, P.R.Smith, W.Taylor, R.Mustafi, R.L.Switzer (1995) *J.Clin.Invest.***96**:2133-41

P11.04.031 THE CRYSTAL STRUCTURES OF THE COMPLEXES BETWEEN BOVINE BETA-TRYPSIN AND TEN P1 VARIANTS OF BPTI. A.O. Smalås, R. Helland and O. Sundheim [1], J. Otlewski [2], M. Dadlez [3]. [1] Department of Chemistry, University of Tromsø, 9037 Tromsø, Norway. [2] Institute of Biochemistry and Molecular Biology, University of Wroclaw,Tamka 2, 50-137 Wroclaw, Poland. [3] Institute of Biochemistry and Biophysics, Polish Academy of Sciences, Pawinskiego 5a, Warsaw, Poland.

The X-ray structures have been determined for ten complexes formed between bovine beta-trypsin and P1 variants (Gly, Asp, Glu, Gln, Thr, Met, Lys, His, Phe, Trp) of bovine pancreatic trypsin inhibitor (BPTI). All complexes were crystallised from the same conditions. The structures of the P1 variants Asp, Glu, Gln and Thr, are reported here for the first time in complex with any serine proteinase. The resolution of the structures ranged from 1.75 to 2.05 Å and the R-factors were about 19-20 %. The association constants of the mutants ranged from 1.5x104 to 1.7x1013 M-1. All structures could be fitted into well defined electron density, and had very similar global conformations. All P1 mutant side chains could be accomodated at the primary binding site, but relative to the P1 Lys, with small local changes within P1-S1 interaction site. These comprised: (1) changes in the number and dynamics of water molecules inside the pocket, (2) multiple conformations and non-optimal dihedral angles for some of the P1 side chains, Ser190 and Gln192, and (3) changes in temperature factors of the pocket walls as well as the introduced P1 side chain. Binding of the cognate P1 Lys is characterised by almost optimal dihedral angles, hydrogen bonding distances and angles, in addition to considerably lower temperature factors. Thus, the trypsin S1 pocket seems to be designed particularly for lysine binding.

P11.04.032 STRUCTURE OF HUMAN MITOCHONDRIAL ALDEHYDE DEHYDROGENASE AT 1.9Å. Monica. Niederhut and Thomas D. Hurley. Department of Biochemistry and Molecular Biology. Indiana University School of Medicine, Indianapolis, IN 46202

The mitochondrial form of aldehyde dehydrogenase is encoded by the ALDH2 gene and is one of nine known human genes for aldehyde dehydrogenase. The mitochondrial form is a tetramer of identical 55 kD subunits and is known to be the primary enzyme responsible for the oxidation of acetaldehyde to acetate during ethanol metabolism. We previously reported the structure of the ALDH2 isoenzyme from beef liver at 2.65Å which shares 95% sequence identity with the human enzyme. Here we report the crystallization and structure determination of the recombinant human ALDH2 enzyme expressed and purified from *E. coli*. The data could be indexed in the space group $P2_1$ with the

following cell dimensions a=101.4Å, b=176.1Å, c=101.5Å, β=95.0º. The crystals exhibit diffraction to >1.8Å and a 97% complete data set to 1.92Å was collected at the X12C beam line at the National Synchrotron Light Source. The model was initially refined using X-PLOR 3.8 and is now being refined with REFMAC. Currently the model contains residues 7-500 in each subunit, a bound cofactor molecule with an associated Mn^{2+} ion in each subunit, and a total of 1700 water molecules in both tetramers within the asymmetric unit. At this point in the refinement the R-free value is 28.5% and the R-work is 22.6% for all data between 35 and 1.92Å, using a bulk solvent correction. NCS-restraints have been imposed to this point in the refinement. However, clear differences can be seen in the structure and future rounds of refinement will not utilize ncs-restraints. The electron density for the bound cofactor also appears to vary in its overall intensity when compared between subunits. These subtle differences in subunit structure may be related to the enzyme's ½ sites reactivity, in which only two of the four identical active sites in the enzyme appear to function at any given instant. Supported by AA11982.

P11.04.033 CRYSTALLOGRAPHIC STRUCTURE OF THYMIDYLATE SYNTHASE FROM BACILLUS SUBTILIS. Kristin M. Fox, Department of Chemistry, Union College, Schenectady, NY 12308, Frank Maley, and Patrick Van Roey, Division of Molecular Medicine, Wadsworth Center, New York State Department of Health, PO Box 509, Albany, NY 12201-0509, USA

Thymidylate synthase (TS) converts dUMP to dTMP by transferring a methyl group from 5,10-methylene tetrahydrofolate to dUMP. This reaction is crucial for DNA synthesis, as it is the sole *de novo* source of dTMP. In addition, the uniqueness of the reductive methylation reaction has lead to study of the reaction mechanism by many different methods. Clarification of this mechanism has been provided by the determination of the structures of TS from several organisms, especially that from *Escherichia coli*. *B. subtilis* contains two genes for TS, ThyA and ThyB. The sequence of the *B. subtilis* ThyA enzyme is quite different from other TS's, and has a 2.5 fold greater k_{cat} than *E. coli* TS. Sequence analysis of residues in the active site area of *E. coli* TS showed that a histidine implicated in the hydrogen bonding network important for catalytic activity is replaced by valine in *B. subtilis* TS. The structure of the ThyA *B. subtilis* TS in a ternary complex with 5-fluoro-dUMP and 5,10-methylene tetrahydrofolate has been determined to 2.5 Å resolution. Overall, the structure is similar to that of the *E. coli* enzyme. However, there are significant differences in the structures of two loops, the dimer interface and the details of the active site. The effects of the histidine to valine substitution, but also of a serine to glutamine substitution, and the addition of a loop over the active site area may account for the differences in k_{cat} found between the two enzymes.

P11.04.034 STRUCTURE OF APS KINASE: AN ENZYME INVOLVED IN SULFUR ASSIMILATION. Ian J. MacRae[1], Irwin H. Segel[1], and Andrew J. Fisher[1,2]. [1]Section of Molecular and Cellular Biology and [2]Department of Chemistry, University of California, Davis CA 95616

Sulfur is the sixth most abundant element found in biological molecules. However, the most prevalent form of inorganic sulfur found under our oxygen atmosphere is the unreactive form sulfate (SO_4^{2-}). This fully oxidized form of sulfur is far too stable to be used directly as a substrate for incorporation into biological molecules under normal cellular conditions. To circumvent this problem, and use sulfate as a sulfur source, assimilatory organisms have evolved an enzymatic sulfate activation pathway. The first step in this sulfate fixation process is catalyzed by ATP sulfurylase which transfers the adenylyl group of ATP onto sulfate to produce adenosine-5'-phosphosulfate (APS). APS is then phosphorylated by the enzyme APS kinase to form 3'-phospho-adenosine-5'-phosphosulfate (PAPS). PAPS, the product of APS kinase, is used as "activated sulfate" in cells. It can serve as a substrate for making sulfate esters or be reduced to sulfite which is ultimately used in cysteine biosynthesis.

A cDNA clone of APS kinase from the assimilatory fungus *Penicillium chrysogenum* has been expressed in *E. coli*. The soluble enzyme was purified to homogeneity and crystallized in the orthorhombic space group $C222_1$ with unit cell parameters of a =79.4 A, b = 83.9 A, and c = 142.4 ⊕. Initial phases were calculated from two derivatives using MIR methods. The APS kinase structure is currently in the final stages of refinement at 1.9 Å resolution. Consistent with previous biochemical studies (J. Biol. Chem. **260**: 1535 - 1544, 1985), the enzyme crystallized as a homodimer. Each subunit is composed of a parallel β sheet sandwiched between two α-helical bundles. The Walker A motif (residues 32-39, GLSAGKS in this enzyme) forms a typical ATP - binding P-loop. Serine-107, shown not to be a phosphoryl acceptor, but suggested to reside in the substrate binding pocket (J. Biol. Chem. **273:** 28583 - 28589, 1998), lies adjacent to the P-loop. These features point to the vicinity of the active site. The overall conformation establishes APS kinase as a member of the super family of mononucleotide binding proteins with particular structural homology to adenylate kinase, 6-phosphofructo-2-kinase, and the catalytic core of p21-Ras.

P11.04.035 STRUCTURE OF THE HUMAN N^5,N^{10}-METHYLENTETRAHYDRO-FOLATE DEHYDROGEN-ASE/ CYCLOHYDROLASE BOUND TO THE INHIBITOR N^5,N^{10}-CARBONYL-TETRAHYDRO-FOLATE. Andrea Schmidt, Yunge Li, Marc Allaire and Miroslaw Cygler, Biotechnology Research Institute, NRC, Canada; Robert E. MacKenzie, Dept. Biochem., McGill University, Montreal, Canada.

The enzyme N^5,N^{10}-methylen[H4]folate dehydrogenase/ cyclohydrolase DC301 consists of two domains, catalyzing sequential reactions with a shared substrate binding site. The dehydrogenase reaction is NADP dependent, and the cofactor was present in the native structure [Allaire *et al. Structure* 6, 173 (1998)]. We have now determined the structure of the enzyme cocrystallized with the substrate-like inhibitor N^5,N^{10}-carbonyl-[H4]folate in the presence of NADP. DC301 forms dimers in solution and the crystal contains one dimer per asymmetric unit, the two molecules differing in the hinge angle between the two domains. The inhibitor was found only bound to molecule A, which has a narrower substrate binding cleft. The position and orientation of the inhibitor molecule is well defined although the glutamate sidechain and the outermost part of the pteridine ring are rather poorly defined in the electron density map. The inhibitor interacts with the protein via H-bonds to Asp125, Lys56 and the backbone O and NH of amino acids 101, 273 and 276, and stacking interaction with Tyr52. NADP is located opposite to the tyrosine, with its nicotine ring located beneath the imidazone ring of the inhibitor. Tyr52 and Lys56 are part of the Tyr-X_3-Lys motif encountered in the SCAD protein family and had been proposed to take part in the cyclohydrolase step. Lys56 is in a position to interact with both the carbonyl group of the imidazone and the hydroxy group in position 4, possibly also N5, and therefore appears to play an essential role in binding and catalysis. The observed location of Tyr56 positions its OH group too far from the substrate's reactive part. Therefore, this sidechain may be important for the proper positioning of the substrate, but likely plays no direct role in the enzymatic reaction. This is consistent with mutagenesis studies.

We would like to thank Drs. J. Toth, V. Chen, Mr. J. Ray and Eli Lilly and Company for providing the inhibitor and for financial support.

P11.04.036 CRYSTAL STRUCTURE ANALYSIS OF FERREDOXIN AND FERREDOXIN-NADP$^+$ REDUCTASE FROM MAIZE ROOT. G.Kurisu, R.Igarashi, S.Suzuki, M.Kusunoki and T.Hase, Institute for Protein Research, Osaka University, Suita, Osaka 565-0871, Japan.

In the electron transfer system of photosynthesis, Ferredoxin (Fd) works as an electron carrier to Ferredoxin-NADP$^+$ reductase (FNR). Specifically Fd is reduced by Photosystem I (PSI) in the chloroplast. Then FNR receives the electron from the reduced Fd. Finally it catalyzes the reduction of NADP$^+$ to NADPH. Recently it was found that the non-photosynthetic tissues such as fruits or roots have Fd and FNR isomers distinct from photosynthetic ones. These second types of Fd and FNR are involved in an electron transfer process to some Fd-dependent enzymes from NADPH supplied via the oxidative pentose phosphate cycle. In order to understand this electron transfer pathway and how it differs from a photosynthetic one, we started the crystallographic analysis of the isomers.

Non-photosynthetic Fd and FNR from maize root were expressed in *E.coli*. and purified to sufficient quality for crystallization. Crystals of Fd were prepared using the ammonium sulfate as a precipitant ($P2_12_12_1$, a=79.8, b=104.51, c=66.43 Å). A crystal structure of the Fd was solved at 2.5 Å resolution by MR method. Main chain structures are quite similar to those of other plant type Fds. On the other hand, crystals of FNR were obtained using the sodium citrate ($P3_121$, a=59.44, b=59.55, c=187.09 Å). We have collected the X-ray diffraction data up to 1.65 Å resolution from one crystal at the Photon Factory. The molecular structure was solved by MR method using AMORE. Refinement of this structure is in progress.

P11.04.037 CRYSTAL STRUCTURE OF MAMMALIAN PURPLE ACID PHOSPHATASE TO 1.55 Å RESOLUTION. L.W. Guddat[1], A. S. McAlpine[1], D. Hume[1], S. Hamilton[1], J. De Jersey[1], J. L. Martin[2]. Department of Biochemistry[1] and Centre for Drug Design and Development[2], The University of Queensland, St. Lucia, Qld, Australia 4072.

Purple acid phosphatases are a group of non-specific phosphomonoesterases that are widespread in nature. Mammalian purple acid phosphatases were first identified in pig uterine secretions and in bovine spleen. High concentrations of the enzyme have also been found in osteoclasts and macrophages. The physiological role and enzymatic specificity of the protein are unknown. Its abundance in pig allantoic fluid, suggests a role in iron transport between the mother and fetus. Experiments with transgenic mice indicate that purple acid phosphatases play an important role in bone homeostasis[1]. Purple acid phosphatases are characterised by a redox active, binuclear metal centre. In mammals, the metal centre is spin coupled Fe(III)-Fe(II). The distinctive purple colour results from a charge transfer transition between a tyrosinate and the Fe(III) at 560nm.

To date the only reported structure of a purple acid phosphatase is that of the red kidney bean enzyme[2,3]. Despite very low sequence homology, a tentative model for the structure of mammalian purple acid phosphatase has been proposed based on a sequence alignment and secondary structure prediction[4]. Here, we report the high resolution structure (1.55 Å) of the phosphate-bound enzyme, purified from pig allantoic fluid. The structure was solved using the MIR method. For the first time, the critical hydroxo bridge is shown providing additional insight into the catalytic mechanism and active site structure of this class of enzyme. Comparison of the structures of the mammalian and plant purple acid phosphatases show that their binuclear metal sites are almost identical but significant differences nearby may be important for substrate specificity. Internal two-fold pseudo symmetry suggests that the binuclear metal ion centre may have evolved from a combination of mononuclear domains. The structural elucidation of the mammalian enzyme is a significant step towards rational drug design that could lead to treatments for bone diseases.

[1] Hayman et al. (1996) Development 122:3151.
[2] Strater et al. (1995) Science 268:1489.
[3] Klabunde et al. (1996) J Mol Biol 259:737.
[4] Klabunde et al. (1995) FEBS Lett 267:56.

P11.04.038 MOLECULAR MECHANISM OF SUBSTRATE ANALOG RECOGNITION BY FLAVIN REDUCTASE, FRase I, FROM BIOLUMINESCENT BACTERIUM. Masaru Tanokura, Toshiro Kobori, Departments of Applied Biological Chemistry and Biotechnology, Graduate School of Agricultural and Life Sciences, University of Tokyo, Tokyo 113-8657, Japan, Hideaki Koike, Hiroshi Sasaki, Biotechnology Research Centre, University of Tokyo, Tokyo 113-8657, Japan, and Shuhei Zenno, Kaoru Saigo, Department of Biophysics and Biochemistry, Graduate School of Science, University of Tokyo, Tokyo 113-0033, Japan.

FRase I from the bioluminescent bacterium *Photobacterium* (*Vibrio*) *fischeri* is a flavin reductase and is considered to play an essential role to the luminescence by supplying the reduced form of flavin mononucleotide ($FMNH_2$) to luciferase. The crystallographic and biochemical studies have indicated that the enzyme acts as a homodimer in solutions and holds tightly one FMN molecule per subunit. We report the crystal structures of the complexes of the enzyme with coumarin derivatives to elucidate the molecular mechanism of substrate recognition by the enzyme.

Based on the enzyme kinetics, coumarin derivatives, including *o*-coumaric acid, 4-hydroxycoumarin, warfarin, and dicoumarol, were indicated to act as competitive inhibitors, while coumarin itself did not inhibit the enzyme at all. Thus the coumarin derivatives occupy the same binding site of the enzyme as substrates. The crystals of FRaseI-inhibitor complexes were obtained by soaking inhibitors to FRaseI crystals. The crystals diffracted X-rays to around 2.0 Å resolution, by using the Weissenberg camera for macromolecular crystallography with a synchrotron radiation in Tsukuba, Japan. In the crystal structures of the enzyme-inhibitor complexes, coumarin derivatives were sandwiched with the FMN cofactor and side chain of phenylalanine-124 at an active site of the enzyme. In addition, each of the inhibitors hydrogen-bonded to the main chain amide nitrogen of isoleucine-43 of the other subunit at its hydroxyl group. Comparison of the structure with that of FRP, another flavin reductase, has shown that phenylalanine-124 is important for the recognition of the inhibitors by FRase I.

P11.04.039 THE CRYSTAL STRUCTURE OF GABA-AMINOTRANSFERASE, A TARGET FOR ANTIEPILEPTIC DRUG THERAPY. Storici, P., Capitani, G.,. De Biase, R.A. John, J.N. Jansonius and T. Schirmer, Division of Structural Biology , Biozentrum, University of Basel, CH-4056 Basel, Switzerland; Deptartment of Biochemical Sciences, University La Sapienza, I-00185 Rome, Italy; School of Molecular and Medical Biosciences, University of Wales, CF1 3US Cardiff, UK.

γ-aminobutyrate aminotransferase (GABA-AT; EC 2.6.1.19) is a pyridoxal 5'-phosphate (PLP) dependent enzyme which belongs to the subgroup of aminotransferases acting on ω-amino acids, i.e. amino acids containing the removable amino

group in a position distal to the carboxyl group. This α_2-dimeric enzyme is involved in the breakdown of the inhibitory neurotransmitter GABA in that it converts, by a ping pong bi bi type reaction mechanism, GABA and 2-oxoglutarate into succinic semialdehyde and L-glutamate, respectively.

GABA-AT is presently regarded as one of the most interesting targets for antiepileptic drugs because its selective inhibition raises GABA concentrations in the brain.

The crystal structure of pig liver GABA-AT was solved by molecular replacement using the model of human ornithine aminotransferase (OAT) with which it shares 23% sequence identity. Due to the low similarity with the search model and the presence of two dimers per asymmetric unit, the cross-rotation function was not readily interpretable. The problem was solved by using the resulting list of 50 rigid body-fitted solutions for an exhaustive two-dimer search. Subsequent four-fold molecular averaging and phase extension to 3 Å yielded well-defined unbiased electron density. The success of this approach is remarkable, since the dimeric search model comprised only 24 % of the atoms of the two dimers contained in the asymmetric unit. Structural superposition of the final refined GABA-AT monomer with OAT shows a relatively large r.m.s. deviation of 2.1 Å for 390 Cα positions.

GABA-AT has the same fold as OAT, with some local differences which can explain the origin of the different substrate specificities. The antiepileptic drug vinyl-GABA is modeled into the active site and an explanation is offered for the efficacy of this mechanism-based inactivator.

P11.04.040 PRELIMINARY CRYSTALLOGRAPHIC STUDIES OF A PHOSPHOENOLPYRUVATE (PEP) SYNTHETASE FROM *PRYOCOCCUS FURIOSUS*. Zhi-Jie Liu[1], Andrea M. Hutchins[1], M. Gary Newton[2], John P. Rose[1], Michael W. Adams[1], Bi-Cheng Wang[1]; [1]Department of Biochemistry & Molecular Biology, University of Georgia, Athens, GA 30602, USA; [2] Department of Chemistry, University of Georgia, Athens, GA 30602, USA

Phosphoenolpyruvate (PEP) synthetase catalyses the ATP-dependent conversion of pyruvate to phosphoenolpyruvate. The 98 kDa PEP synthetase from *Pyrococcus furiosus* has been isolated, purified to homogeneity and crystallized. The crystals were obtained by hanging-drop vapor-diffusion. Preliminary X-ray diffraction analysis indicates that the crystals belong to tetragonal space group $P4_12_12$ or $P4_32_12$ with unit-cell dimensions of a = b = 100.76 Å, c = 220.23 Å. The presence of one PEP synthetase molecule in the asymmetric unit gives a Matthews coefficient (Vm) of 2.85 $Å^3$ Da^{-1} and a calculated solvent content of 57% by volume. Native data to 2.0 Å has been collected at beamline ID-17 (IMCA-CAT) Advanced Photon Source, Argonne National Laboratory. The search for heavy atom derivatives is in progress.

P11.04.041 STRUCTURE AND CATALYTIC MECHANISM OF THE RHODANESE FROM *Azotobacter vinelandii*. D.Bordo, D.Deriu, and M.Bolognesi, Advanced Biotechnology Center ñ IST and Department of Physics-INFM, University of Genova, Italy.

Rhodanese is a thiosulfate:cyanide sulfurtransferase enzyme which is widely distributed among the mayor phyla. The best known catalyzed reaction is the transfer of a sulfane sulfur from thiosulfate to cyanide. The protein has been identified, cloned, overexpressed, purified and crystallized with the method of the hanging drop. Crystals belonging to the orthorombic space group $P2_12_12$ were obtained after a period of several months using the hanging drop setup and in presence of magnesium sulfate as precipitant.

The multiple isomorphous replacement technique was successfully used to obtain initial phase information. Several techniques, including maximum likelihood, solvent flattening, and phase extension were applied to the initial phases, and the final 1.8A map resulted of excellent quality. Most part of the main and side chains could be located with automated procedures, and the protein model of the complete amino acid chain (271 amino acids) could be refined to an R value of 17.4% (free-R factor, 21.9%).

In spite of a folding similar to that of the bovine rhodanese, to which the primary sequence of A.vinelandii rhodanese is 28% identical, the residues surrounding the active site cysteine display remarkable differences. Studies on the catalytic mechanism indicate that Arg235 undergoes wide side chain rearrangements and play a relevant role in the interaction with the substrates.

P11.04.042 PYRUVATE FORMATE LYASE LARGE DOMAIN: THE SECOND MEMBER OF THE RIBONUCLEOTIDE REDUCTASE FAMILY. V.-M. Leppänen[αβ], M. Merckel[β], D.L. Ollis[βγ], K. Wong[δ], J. Kozarich[δ] and A. Goldman[βα] [α]Centre for Biotechnology, University of Turku and Åbo Akademi University, POB 123, Turku, Finland, [β]Department of Biochemistry, University of Turku, Finland, [γ]Research School of Chemistry, Australian National University, ACT, 2614, Australia, [δ]Merck Research Laboratories, POB 2000, Rahway, NJ, USA

Pyruvate formate lyase (EC 2.3.1.54; PFL) catalyzes a key step in anaerobic glycolysis in *E. coli* by converting pyruvate and CoA to formate and acetylCoA. The enzymatic reaction has been proposed to proceed by an unusual radical cleavage of pyruvate, involving an essential Cα-radical of Gly 734 and two cysteines, Cys418 and Cys419 that may form thiyl radicals required for catalysis (reviewed by Wong and Kozarich)[1].

We have solved the first structure of a proteolytic fragment (1-624) of this class of enzymes at 2.8 Å resolution. We see a novel right-hand like two-domain structure, and a β-finger inserted into a part-barrel structure that exposes both Cys418 and Cys419 in a turn between two strands. The PFL structure also localizes several residues near the active site cysteines that may play a role in defining the catalytic mechanism.

The structure reveals a striking structural homology to the aerobic ribonucleotide reductase (RNR Type I)[2] as the catalytic domain of PFL can be superimposed on the aerobic RNR R1 protein, including 8 of the 10 strands in the unusual RNR a/b barrel. The relationship is undetectable at the sequence level. There is now a clear but very distant evolutionary relationship between PFL and aerobic RNR. Given the limited sequence and striking mechanistic homology between anaerobic RNR and PFL, we propose that enzymes with relatively stable amino-acid free radicals have a common fold, including at least PFL, aerobic RNR and anaerobic RNR.

1. Wong, K.K. and Kozarich, J.W. (1994). In H. Sigel (Eds.), *Metal Ions in Biological Systems Vol. 30: Metalloenzymes Involving Amino-Acid Residues and Related Radicals*. Marcel Dekker, Inc., New York. (pp. 279-313).
2. Uhlin, U. and Eklund, H. (1994) Nature, 370, 533-539

P11.04.043 CRYSTAL STRUCTURES OF PURINE NUCLEOSIDE PHOSPHORYLASES FROM MICRO-ORGANISMS Koellner, G., Tebbe, J., Saenger, W. Institut für Kristallographie, Takustr. 6, 14195 Berlin, Germany, Bzowska, A., Wielgus-Kutrowska, B., Shugar, D. Departrment of Biophysics, University of Warsaw, Zwirki i Wigury 93, 02-089 Warsaw, Poland, and Luic, M. Rudjer-Boskovic Institute Bijenicka 54 10000 Zagreb Croatia.

Crystal structures of the enyzme Purine Nucleoside Phosphorylase (PNP) from *E.coli* in complex with Formycin A and Formycin B and *Cellulomonas sp.* in complex with phosphate and 8-iodoguanine are presented.

PNP is an ubiquitous enzyme, which catalyzes the reversible phosphorolysis of naturally occuring purine nucleosides and many analogues. Considerable attention is currently devoted to development of potent specific inhibitors of phosphorylases from various sources, because of their potential pharmaco-logical applications (e.g. as immunosuppressive or antiparasitic agents).

PNP from *E.coli* belong to the second class of PNPs which are also called high-molecular-weight or adenosine phosphorylases and appear as hexamers. PNP from *cellulomoas sp*. are trimeric, which usually is typical for mammalian PNPs. Both enzymes have very little sequence idenity to each other and to mammalian PNPs, but all three PNPs (mammlian, *E.coli* and *cellulomonas sp*.) have structural homologies: the core of each monomer consists of a nine-stranded mixed β-sheet surrounded by α-helices.

Koellner, G., Luic, M., Shugar, D., Saenger, W. & Bzowska, A. (1997). *J. Mol. Biol.* **265**, 202-216.
Bzowska, A., Tebbe, J., Luic, M., Wielgus-Kutrowska, B., Schröder, W., Shugar, D., Saenger, W. & Koellner, G. (1998) *Acta Crystallogr.,* **D54,** 1061-1063.
Koellner, G., Luic, M., Shugar D., Saenger, W. & Bzowska, A. (1998) *J. Mol. Biol.* **280**, 153-166.

P11.04.044 CRYSTAL STRUCTURE OF REPETITIVE B-DOMAIN OF THE COLLAGEN BINDING SURFACE PROTEIN OF *STAPH. AUREUS*. Champion CS Deivanayagam, Rebecca L. Rich, Sita Danthuluri, Rick T. Owens, Joseph M. Patti, Magnus Hook, Lawrence, J. DeLucas and Sthanam, V.L . Narayana. *Center for Macromolecular Crystallography, 286 BHSB, 1918 University Boulevard, University of Alabama at Birmingham, AL 35294-0005, USA and #Center for Extracellular Matrix Biology, Albert K.Alkek Institute of Biosciences and Technology, Texas A&M University, 2121 Holcombe Boulevard, Houston, TX 77030-3303, USA.

A 135kDa protein (*cna*) from the newman strain of *Staphylococcus aureus* has been identified as a collagen binding MSCRAMM (microbial surface components recognizing matrix molecules)[1]. Molecular characterization of the gene revealed the presence of a non-repetitive A-domain and a repetitive B-domain. For analyzing the structure function relationship of this collagen adhesin, we determined the crystal structure of CBD19, which represents the smallest sub-fragment of the A-domain with measurable collagen binding activity [2]. In this report we present our structural studies of B_1 and B_1B_2 fragments of ***cna***.

Crystals of B_1 and B_1B_2 were grown using hanging drop vapor diffusion method[3]. Crystal structure of B_1 was solved by MIR method and the crystal structure of B_1B_2 was determined by molecular replacement using B_1 as the initial model. The overall structure of B_1 has two immunogloblulin like domains placed side by side. B_1 exhibits a different fold, although the overall structure is similar to the IgSF structures. It also carries an ëLDVí motif on the C-D loop region, which is strikingly similar to that observed in I-CAM2 and V-CAM1 structures [4,5], and are known to bind integrins. Although the function for B-domains is not clear, these repeat domains could project the A-domain over the bacterial cell wall aiding the binding to collagen [6], and may also bind to integrins. The crystal structure of B_1B_2 exhibits interesting domain duplication and swapping features.

1. Patti, J.*M et.al., Ann. Rev. Microbiol*, **48**, 585-617.
2. Symersky, J., *et.al.,* (1997) *Nature Struct. Biol.* **4,** 833-838.
3. Deivanayagam, C.C.S *et.al.,* (1999) *Acta crystallogr.* **D55**, 554-556.
4. Casanovas, J.M*., et.al*., (1997) *Nature*, **287**, 312-315.
5. Jones, E.Y., *et.al.,* (1995) *Nature* **373**, 539-544.
6. Rich. R.L., *et.al.,* . (1998) *Biochemsitry* **37**, 15423-15433.

P11.04.045 A NEW STRUCTURE-BASED REACTION MECHANISM FOR UREASE: WHY UREA HYDROLYSIS COSTS TWO NICKELS. S. Benini and W. R. Rypniewski, EMBL c/o DESY Notkestraße 85 D-22603 Hamburg, K. S. Wilson, Dept. of Chemistry, York University Heslington YO1 5DD UK, S. Ciurli, Inst. of Agricultural Chemistry, Bologna University, Viale Berti Pichat 10 I-40127, S. Mangani Dept. of Chemistry Siena University, Pian dei Mantellini 44 I-53100.

Urease catalyses the hydrolysis of urea in plants, algae, fungi, bacteria, to yield ammonia and CO_2. Urease is involved in pathologies (including cancer) induced by gastroduodenal infections by *H. pylorii*. The search of urease inhibitors has so far relied upon extended screen tests, while a structure-based drug design approach would give more direct results. The elucidation of the structure of the active sites of enzymes and the reaction and inhibition mechanism are fundamental for this approach. The highly conserved amino acid sequences of all known ureases and the constant presence of two Ni ions and of their ligands in the active sites imply a common catalytic pathway. The structure of urease from *B. pasteurii* has been studied extensively. Good quality data have been collected for native (2.00 Å) and acetohydroxamic (1.55 Å), β-mercaptoethanol (1.65 Å), diamidophosphate (2.00 Å) and mercaptoethanolamine (1.90 Å) inhibited enzyme. The comparison between native and inhibited urease suggested a new reaction mechanism that overcomes the problems encountered by the mechanism proposed for *K. aerogenes* urease. The new reaction mechanism and an overview of all structures is presented.

Benini, S., Rypniewski W. R. R., Wilson K. S., Ciurli S. and Mangani S. *J. of Bio-inorg. Chem*, **3**, 268 (1998)
Benini, S., Rypniewski W. R. R., Wilson K. S., Ciurli S. and Mangani S. *Structure*, *in press* (1999)
Karplus P. A., Pearson M. A., and Hausinger R. *Acc. Chem. Res.* **30**, 330 (1997)

P11.04.046 CRYSTALLOGRAPHIC STUDIES OF JACK BEAN UREASE IN COMPLEX WITH AN ANTIBODY FRAGMENT. L. Smith, C. M. Wilmot and S. E. V. Phillips, School of Biochemistry and Molecular Biology, University of Leeds, Leeds, LS2 9JT, UK, K. Cromie, and P. van der Logt, Biorecognitions unit, Unilever Research, Colworth House, Sharnbrook, Bedford, MK44 1LQ, UK.

Urease allows an organism to use external and internally generated urea as a nitrogen source. It catalyses the hydrolysis of urea to form ammonia and carbon dioxide. Urease probably participates also in the systematic nitrogen transport pathways and possibly acts as a toxic defence protein. Jack bean urease (JBU) was the first known nickel metalloenzyme(1) and was first crystallised in 1926, by J. B. Sumner.(2) It is a large protein, in solution it normally exists as trimers and hexamers of identical 96 kDa subunits.

Although there have been crystals for over 70 years, the structure has not yet been determined. The crystals diffract to a resolution of 3.5 Å,(3) and belong to the space group $F4_132$ with a = 364 Å. The large unit cell, high symmetry and relatively weak diffraction have made this structure sifficult to solve.

We have managed to produce an Fv, a 24 kDa antibody fragment, that has a high affinity to JBU, using a Pichia pastoris expression system, and purified using a his-tag. One Fv binds to

one monomer of JBU, forming a 120 kDa complex, although the complex can still form oligomers. Whilst in this complex, the urease activity is not affected.

We report here the structure of JBU in the space group R32, a = b =229.7 Å, c = 131.5 Å.

N.E. Dixon, C. Gazzola, R.L. Blakely, B. Zerner (1975) J. Amer. Chem. Soc. 97, 4131
J.B. Sumner (1926) J. Biol. Chem. 69, 435
E. Jabri, M.H. Lee, R.P. Hausinger, P.A. Karplus (1992) J. Mol. Biol. 227, 934

P11.04.047 STRUCTURAL STUDIES ON HUMAN AND BOVINE XANTHINE OXIDASE. A. Pearson, G. Taylor, School of Biomedical Sciences, The University of St. Andrews, UK, and R. Harrison, School of Biology and Biochemistry, The University of Bath, UK.

Xanthine oxidase (XO) is a dimeric (2 x 150 kDa) metalloprotein that catalyses the last step in purine catabolism. It is also able to act as an NADH oxidase and has been implicated in the production of reactive oxygen species in ischaemic injury [1]. Each monomer contains one molybdopterin, one FAD and two iron sulphur clusters [2]. We have so far obtained micro-needles and micro-plates of folate affinity-purified bovine milk XO and micro-needles of human milk XO. The difficulty encountered in obtaining diffraction quality crystals may be due to microheterogeneities in the 'pure' enzyme, as various inactive forms (lacking one or more co-factors) have been shown to exist [3]. We are currently investigating methods of further purifying XO by separating the various active and inactive forms.

To this end we are developing the use of SEM X-ray microanalysis and ICPS as tools for determining quantitatively the amounts of iron, molybdenum and phosphorous in XO preparations.

XO domain models have been constructed based on the aldehyde oxidoreductase structure (high sequence homology to the molybdopterin and FeS domains) [4] and the MurB (structural similarity to carbon monoxide dehydrogenase, a XO related enzyme [Dobbek, personal communication]) structure [5]. It is hoped these models will be useful as phasing models in molecular replacement.

We are also sequencing the human milk enzyme in order to investigate whether the XO activity in enzyme preparations from different sources (human milk-low, human liver-high, bovine milk-high) is sequence related.

[1] McCord. (1985) New Engl. J. Med. 312 159-163.
[2] Nishino et al. (1997) Biochem. Soc. Trans. 25 783-786.
[3] Gardlik et al. (1987) Arch. Biochem. Biophys. 259 363-371.
[4] Romao et al. (1995) Science 270 1170-1176.
[5] Benson et al. (1996) Structure 4 47-54

P11.04.048 STRUCTURE OF DIOL DEHYDRATASE REVEALS A NEW B_{12}-BINDING MODE AND A ROLE OF ESSENTIAL POTASSIUM ION. N. Shibata and J. Masuda, Department of Life Science, Himeji Institute of Technology, 1475-2 Kanaji, Kamigori, Ako, Hyogo 678-1297, Japan, and T. Tobimatsu and T. Toraya, Department of Bioscience and Biotechnology, Faculty of Engineering, Okayama University, Tsushima-Naka, Okayama 700-6082, Japan, and K. Suto, Y. Morimoto and N. Yasuoka, Department of Life Science, Himeji Institute of Technology, 1475-2 Kanaji, Kamigori, Ako, Hyogo 678-1297, Japan.

We report on a crystal structure of a novel vitamin B_{12} enzyme and a B_{12}-dependant radical reaction mechanism. The structure reveals that an essential potassium ion deeply buried in protein interior participates in substrate-binding and the reaction. Diol dehydratase catalyzes the conversions of 1,2-diols to the corresponding deoxy aldehydes, which requires adenosylcobalamin and monovalent cation as a cofactor. Apoenzyme is composed of three polypeptide chains with molecular weights of 60k (α), 24k (β), and 19k (γ). Crystal structures of other B_{12}-enzymes reveal that a Co-dimethylbenzimidazole (Co-DBI) bond is broken and a histidine coordinates to Co instead of DBI. On the contrary, diol dehydratase has been reported that it conserves the intrinsic Co-DBI bond.

Crystals of diol dehydratase-cyanocobalamin complex were grown by vapor diffusion. Native data were collected at SPring-8 and the structure was determined by MIRAS. Diol dehydratase is dimer of $\alpha\beta\gamma$ unit and α subunit has the TIM barrel motif. Cyanocobalamin is located between a C-terminal face of the TIM barrel and β subunit. DBI was found in β subunit side and the enzyme keeps the Co-DBI bond. An active site is on the upper side of the cobalamin. A deep cavity found in the TIM barrel forms the active site. The K^+ ion is found at the center of the TIM barrel and it holds a 1,2-propanediol molecule. A C1 atom of the propanediol is about 8 Å above Co atom. An adenosyl group should occupy the cavity between the corrin ring and the propanediol molecule. An activation of Co-adenosyl bond yields an adenosyl radical, reacting with 1,2-diol compound. The K^+ ion may assist migration of hydroxyl group.

P11.04.049 STRUCTURES OF CUZN SUPEROXIDE DISMUTASE IN TWO CRYSTAL FORMS: SUGGESTIONS OF A FUNCTIONAL ASYMMETRY IN THIS ENZYME. M.A. Hough and S.S. Hasnain, CLRC Daresbury Laboratory, Warrington, Cheshire, WA4 4AD, UK.

Copper, zinc superoxide dismutase (CuZnSOD) scavenges the superoxide radical O_2^- to form O_2 and H_2O_2 and forms part of the defence mechanism of cells against free radical oxidative damage. The enzyme is present in all eukaryotic organisms and in some prokaryotes. The active site structure of the enzyme in the oxidised, Cu^{II}-SOD form has been well established by protein crystallography [1]. Two crystal structures of Cu^{I}-SOD have yielded conflicting results each of which support a different proposed enzymatic mechanism. We present a crystal structure of bovine CuZnSOD (BSOD) at 1.65Å resolution in which each subunit of the dimer adopts a different copper site coordination consistent with one subunit containing Cu^{II} and the other Cu^{I}. The structure provides clear support for a proposed enzymatic mechanism involving the protonation of the bridging His61 and it's dissociation from copper. A medium resolution crystal structure of Cu^{II}-BSOD in a different space group is also presented in which one subunit exhibits much higher temperature factors than the other. This behaviour is shown to be the result of differing crystalline environments for the two subunits. These structures provide some credence to the suggestion that there may be a functional asymmetry between the subunits of the dimer.

[1] Tainer, J. A., Getzoff, E.D., Beem, K.M, Richardson, J.S. & Richardson, J.C. (1982) J. Mol. Biol. 160, 181-217.

P11.04.050 CRYSTAL STRUCTURE OF Ni-Fe HYDROGENASE IN REDUCED FORM AT 1.4Å RESOLUTION. H. Ogata, K. Miki, Division of Chemistry, Graduate School of Science, Kyoto University, Sakyo-ku, Kyoto 606-8502 Japan, N. Yasuoka, Department of Life Science, Faculty of Science, Himeji Institute of Technology, Kamigori, Hyogo 678-1297 Japan, T. Yagi, Shizuoka University, Oya, Shizuoka 422-8529, Japan, Y. Higuchi, Division of Chemistry, Graduate School of Science, Kyoto University, Sakyo-ku, Kyoto 606-8502 Japan.

Hydrogenases are fundamental metalloenzymes for bacterial hydrogen metabolism. These enzymes are able to regulate the proton gradient between inside and outside of the

periplasmic membrane and to catalyze the reversible oxidoreduction of molecular hydrogen, in conjunction with a specific electron acceptor, cytochrome c_3. The active site of Ni-Fe hydrogenase in the oxidezed form is suggested to be a binuclear Ni-Fe complex having three non-protein diatomic ligands to the Fe atom and three bridging ligands between the Fe and Ni atoms. Here, we report the crystal structure of Ni-Fe hydrogenase in the reduced form of *Desulfovibrio vulgaris* Miyazaki F revealed by X-ray crystallography at 1.4 Å resolution. The folding pattern in the reduced form is very similar to that in the oxidized form. The electron density map shows that the monatomic bridging ligand reported as sulfur species at the Ni-Fe active site disappeared upon reduction with molecular hydrogen in the presence of its electron carrier. In addition, we found that the reduced enzyme released H_2S under the atmosphere of the hydrogen gas in the presence of electoron carriers. Therefore, we suggest that the monatomic sulfur bridge at the Ni-Fe site has to be removed for the enzyme to be activated.

P11.04.051 CRYSTALLOGRAPHIC AND ELECTRON DONATION STUDIES OF NITRITE REDUCTASE. Fraser E. Dodd, Loretta M. Murphy, S. Samar Hasnain [1], Robert R. Eady, Barry E. Smith [2], [1] CCLRC Daresbury Laboratory, Warrington, WA4 4AD, U.K., [2] Nitrogen Fixation Laboratory, John Innes Centre, Colney, Norwich, NR4 7UH, U.K.

Denitrification is one of the main steps of the global nitrogen cycle that is sustained by prokaryotic organisms [1]. Denitrifying bacteria use two entirely different enzymes in this process, one based on haem *cd1* prosthetic groups and the other on type 1 - type 2 Cu centres. Copper containing nitrite reductases (NiRs) are sub-divided into blue and green NiRs which are respectively thought to be redox partners of azurins and pseudoazurins. Crystallographic structures of the blue nitrite reductase from *Alcaligenes xylosoxidans* (*Ax*NiR) in the oxidised and the substrate bound form respectively to 2.1Å and 2.8Å resolution have been published [2]. The 2.1Å resolution of the hexagonal form of *Ax*NiR is presented here allowing a comparison with the crystallographic structures of the green NiRs [3]. There is a striking difference in the overall surface charge distribution between the two sub-groups, providing a structural explanation for their different reactivities to pseudoazurin or azurin and supporting the view that electron transfer proceeds via complex formation.

To investigate the specificity of protein-protein interaction between copper containing NiRs and type 1 copper proteins we have cross reacted proteins from a number of different bacterial species under turnover conditions. Blue NiRs, from *Pseudomonas aureofaciens* and *Ax*NiR, and a green NiR *Alcaligenes faecalis* S-6 NiR were each reacted with cupredoxins from *Alcaligenes xylosoxidan, Alcaligenes denitrificans, Pseudomonasaeruginosa* and *Alcaligenes faecalis* S-6. Progress curve data were collected for each NiR/type 1 copper protein pair in order to compare the efficiency with which reoxidation of the type 1 copper protein occurred.

[1] Payne, W.J. Denitrification in the Nitrogen Cycle (Plenum, 1985).
[2] Dodd, F.E., Hasnain, S.S., Abraham, Z.H.L., Eady, R.R. & Smith, B.E. (1997) *Acta Cryst.* D53, 406-418 .
[3] Dodd, F.E., Van Beeumen, J., Eady, R.R. & Hasnain, S.S. (1998) *J. Mol. Biol* 282, 369-382.

P11.04.052 THE STRUCTURE OF DI-MANGANESE CATALASE FROM *THERMUS THERMOPHILUS* AT 1.0 Å RESOLUTION. S.V. Antonyuk and W.R. Melik-Adamyan, The Institute of Crystallography, Russian Academy of Sciences, Leninsky pr.59, Moscow 117333, Russia, and A.V.Popov and V.S. Lamzin, EMBL Hamburg Outstation , c/o Desy, Notkestrasse 85, 22603, Germany, and P.M. Harrison and P.J. Artymiuk and V.V. Barynin**,** The Krebs Institute for Biomolecular Research, Department of Molecular Biology and Biotechnology, The University of Sheffield, Sheffield S10 2TN, UK.

Atomic resolution structures have revealed accurate geometries for the active sites of native manganese catalase at pH 8.5, and that of the enzyme inhibited by chloride at pH 5.5. The two data sets were from the cubic crystal form of the enzyme (a=b=c=132 Å, space group $P2_13$, 2 subunits per a. u.) and were collected at 100K to 1.05 and 0.98 Å resolution respectively. The structures of the native di-manganese catalase and of the chloride complex have been refined to an R-factor of 11.2% and 11.5% respectively. The initial model used was that of Mn catalase at room temperature (1.6 Å resolution, R-factor 15.5%) [1].

Di-manganese catalase carries out the disproportionation of hydrogen peroxide. A natural di-manganese active site plays the role of heme of the unrelated heme-containing catalases. It is thought that di-manganese catalase cycles between (Mn^{2+},Mn^{2+}) and (Mn^{3+},Mn^{3+}) states in the catalase reaction [2]. We propose a detailed mechanism for the peroxide disproportionation reaction, based on comparing details of the active centres in the native and inhibited di-manganese catalase structures, which are in the different oxidation states and show important conformational differences.

1. V.V.Barynin, P.D.Hempstead, A.A.Vagin, S.V.Antonyuk, W.R.Melik-Adamyan, V.S.Lamzin, P.M.Harrison & P.J.Artymiuk, (1997) J.Inorganic Biochem. 67, 196. **2**. S.V.Khangulov, V.V.Barynin & S.V.Antonyuk, (1990) Biochim. Biophys. Acta, 1020, 25-33.

P11.04.053 CRYSTAL STRUCTURE OF MAMMALIAN CYTOCHROME P450. P.A.Williams, V. Sridhar, J. Cose, E.F. Johnson, D.E. McRee. Dept of Molecular Biology and Department of Experimental Medicine, The Scripps Research Institute, 10550 North Torrey Pines Road, La Jolla, CA 92037, USA

The eukaryotic cytochromes P450 form a broad class of membrane-associated enzymes that catalyse a wide range of monooxygenase reactions. Cytochromes P450 are 50-55kDa haem proteins that play a central role in many synthetic and degradative oxidation reactions with substrates that include fatty acids, prostaglandins, exotins and steroid hormones. P450s are ubiquitous across eukaryotes and prokaryotes. Each P450 is optimised to catalyse a particular monooxygenation reaction, although many exhibit broad substrate specificity. An essential difference between the microsomal and bacterial P450s is the membrane-bound nature of the microsomal P450 as opposed to the soluble nature of the bacterial P450s. It has widely been thought that microsomal cytochromes P450 may receive their substrates from the lipid bilayer as opposed to the cytosol, due to the lipophilic nature of P450 substrates.

We have determined the structure of an engineered microsomal P450 to 3.0Å by the MAD technique using the signal from the single haem iron, supplemented by MIR phases. In addition, data have been collected from several other variants that exhibit a wide range of catalytic activities. The structure of microsomal P450 reveals that while the structure has a conserved core that is very similar to the bacterial structures, there are large differences in structure apparently due to the membrane-association of the microsomal P450. An analysis of the crystal packing contacts suggests an engineering rationale that may be

applied to facilitate the crystallisation of other members of the mammalian cytochrome P450 family.

P11.04.054 CRYSTALLOGRAPHIC STUDIES ON XANTHINE OXIDASE PURIFIED FROM RAT LIVER. A. L. Carvalho, J. M. Dias and S. Teixeira, Departamento de Química, FCT, UNL, 2825-114 Caparica, Portugal and G. Bourenkov, H. Bartunik, Max-Planck Research Unit for Structural Molecular Biology, MPG-ASMB c/o DESY and R. Huber, Max-Planck Institut für Biochemie, 82152 Martinsried, Germany and L. Maia and L. Mira, Faculdade de Ciências, UL, Lisboa, Portugal and M. J. Romão, Departamento de Química, FCT, UNL, 2825-114 Caparica, Portugal.

Xanthine Oxidase from rat liver (a homodimer enzyme of ca 300kDa) has been obtained and attempts to solve the structure are being made. Each of the monomers contains one flavin adenide dinucleotide (FAD), two different kinds of [2Fe-2S] centres and one molybdopterin co-factor. Limited proteolysis has allowed the crystallisation. Two different crystalline forms of the protein were obtained: a cubic-shaped morphology and a star-shaped morphology grown in different crystallisation conditions. Two complete data sets were collected at BW6 beamline of DESY synchrotron (Hamburg, Germany) from the shock-frozen crystals. The cubic-shaped crystals diffracted to 2.6Å resolution and belong to the cubic space group P23 with cell constants a=b=c=156Å. 38122 unique reflections were recorded between 20.0 and 2.6Å with Rmerge=6.9% (26.8% in the outer shell) and a completeness of 97.5% (76.9% in the outer shell). The overall I/sigI was 22.8 while in the outer shell it was 4.8. The star-shaped crystals diffracted to 2.7Å resolution belonging to space group C2 with cell constants a=173.4Å, b=124.1Å and c=109.3Å, with beta=128.4º. 43576 unique reflections were collected between 39.6 and 2.75Å with Rmerge=9.9% (29.5% in the outer shell) and a completeness of 92.6% (77.2% in the outer shell). The overall I/sigI was 15.1 while in the outer shell it was 3.3. Attempts are being made to solve the structure by Molecular Replacement methods using the xanthine oxidase-related aldehyde oxido-reductase (MOP) of Desulfovibrio gigas [1] and the CO-dehydrogenase of Oligotropha carboxidovorans [2].

1. Romão, M. J., Archer, M., Moura, I., Moura, J. J. G., LeGall, J., Engh, R., Schneider, M., Hof, P., Huber, R. (1995) Science, 270, 1170-1176.
2. Dobbek, H., Gremer, L., Meyer, O., Huber, R., Science, submitted.

P11.04.055 REFINEMENT OF THE ALDEHYDE OXIDO-REDUCTASE FROM *DESULFOVIBRIO GIGAS* (MOP) AT 1.28 Å. J.M. Rebelo, J.M. Dias, M.J. Romão, Departamento de Química, Universidade Nova de Lisboa, 2825-114 Monte da Caparica, Portugal, Gleb P. Bourenkov, Hans D. Bartunick, MPG-ASMB, DESY, Hamburg, Germany, and R. Huber, Max-Planck-Institute für Biochemie, Am Klopferspitz, D-82152 Martinsried, Germany.

The aldehyde oxido-reductase from the sulfate reducing bacterium *Desulfovibrio gigas* (MOP) is a member of the xanthine oxidase family of enzymes (1). MOP has 907 residues on a single polypeptide chain, a MCD cofactor and two [2Fe-2S] centers. Data from improved crystals were collected, and the crystal structure was anisotropically refined at 1.28 Å resolution for 226751 unique reflections. Refinement started with rigid body refinement from a previous 1.8 Å model (2-3). Accurate geometric parameters for the two [2Fe-2S] clusters and for the Molybdopterin Cytosine Dinucleotide – MCD, are now available. The final model contains 12223 atoms and refined to a final R factor of 16.5 and a Rfree of 20.8 for a resolution range (24.4 – 1.28Å). Overall rms bond distances and angles are 0.005 Å and 1.083 Å. Overall comparison of the model quality to the previous one was made. The previous presence of an isopropanol inhibitor molecule near the active site was verified which validates the earlier proposed mechanism. Several Cl^- and Mg^{2+} ions from the crystallization solution and 1246 water molecules were identified.

M.J. Romão, J. Knäblein, R. Huber and J.J.G. Moura (1997) *Prog. Biophys. Molec. Biol.* **68**, 121-144.
M.J. Romão, M. Archer, I. Moura, J.J.G. Moura, J. LeGall, R. Engh, M. Schneider, P. Hof, R. Huber (1995) *Science* **270**, 1170-1176.
R. Huber, P. Hof, R.O. Duarte, J.J.G. Moura, I. Moura, M Liu, J. LeGall, R. Hille, M. Archer, M.J. Romão (1996*) Proc. Natl. Acad. Sci. USA* **93**, 8846-8851.

P11.04.056 X-RAY STUDIES OF A NITRITE REDUCTASE: PRELIMINARY RESULTS. C.A. Cunha, J.M. Dias, G. Almeida, C. Costa, J.J.G. Moura, I. Moura and M.J. Romão, Departamento de Química, Universidade Nova de Lisboa, 2825-114 Monte da Caparica, Portugal, and A. Thompson, European Synchrotron Radiation Facility, BP 220, F-38043 Grenoble Cedex, France

The nitrite reductase (NIR) from *Desulfovibrio desulfuricans* ATCC 27774 performs the dissimilatory reduction of nitrite to ammonia involving a 6 electron reduction (1,2). NIR is a membrane bound enzyme which is induced by growing the bacteria with nitrate rather than sulfate. It has two subunits of molecular masses 63 kDa and 19 kDa as determined by electrospray mass spectrometry as well as is observed by SDS-PAGE. It is thought that each subunit contains five heme groups, one of which is a high-spin ferric heme which is probably the substrate binding site. The oxidized form of this enzyme was crystallised by vapour diffusion, at 20ºC. The crystallization conditions contain PEG as precipitant, $CaCl_2$, HEPES as buffer and zwittergent 3-10. Two crystal forms are obtained. One of them was characterized and belongs to the space group $P2_1$, with unit cell dimensions a=79.0 Å, b=142.5 Å and c=104.3 Å, β=91.26º. MAD data was collected in the iron absorption edge using synchrotron radiation at ESRF. Three data-sets have been collected at the wavelengths 0.9537 Å, 1.7396 Å and 1.7388 Å with a resolution up to 2.8 Å. The overall $I/\sigma(I)$ was 13.8, 9.2 and 9.5 and the overall R_{merge} was 5.3, 7.2 and 7.4, respectively, for each of the data-sets. The structure is being solved using the programs SOLVE and SHARP, and the current state of the analysis will be presented.

1. C.Costa, J.J.G.Moura, I.Moura, Y. Wang & B.H.Huynh (1996) *J. Biol. Chem.*, **271** 23191-23196
2. I.Moura, S.Bursakov, C.Costa & J.J.G.Moura (1997) *Anaerobe*, **3** 279-290

P11.04.057 COMBINING CALCIUM-DEPENDENT REGULATION WITH PROTEASE ACTIVITY - CRYSTAL STRUCTURE OF CALPAIN. Christopher M. Hosfield, John S. Elce and Zongchao Jia. Department of Biochemistry, Queen's University, Kingston, ON, K7L 3N6, CANADA.

Calpains are structurally unique enzymes in that they possess cysteine-protease activity that is completely dependent on calcium binding to their two EF-hand domains. Binding of calcium is believed to produce a substantial conformational change, generating an active calpain with the ability to cleave a number of substrates.

Ubiquitous in mammalian tissue, calpains appear to be involved in the cleavage of substrates concerned with cytoskeletal remodeling and signal transduction in response to fluctuations in the intracellular concentration of calcium. Some potential physiological substrates include protein kinase C, p53, spectrin and fodrin.

The crystal structure of this heterodimeric enzyme was determined using MAD with selenium as the anomalous scatterer. In order to facilitate structure determination through multi-crystal

averaging, MAD data were collected on monoclinic and triclinic crystal forms. Electron density maps resulting from a four wavelength experiment on the $P2_1$ crystal, and a two wavelength experiment on the $P1$ crystal were interpretable.

Currently, the fold of the enzyme is visible while most of the backbone and many side chains have been fit into the maps. The structure reveals that the dimerization interface between the catalytic large (80 kDa) subunit and the small (21 kDa) regulatory subunit exists primarily through interactions between the two homologous calcium-binding domains. A linker of approximately 20 residues joins the calcium-binding domain to the remainder of the large subunit, which includes the residues of the catalytic triad at the active site. This linker may act as a trigger for amplification of a calcium-induced conformational change in the large subunit. Structural refinement is in progress, and biological implications will be discussed.

P11.04.058 CRYSTALLOGRAPHIC STUDIES OF D.GIGAS FORMATE DEHYDROGENASE. S. Teixeira, J.M.Dias, A.L. Carvalho, M.J. Almendra, I. Moura, J. Moura and M.J. Romão, Dept. Química, F.C.T., U.N.L., 2825-114 Caparica, Portugal, and G. Bourenkov and H. Bartunik, Max-Planck Research Unit for Structural Molecular Biology, MPG-ASMB c/o DESY, 22603 Hamburg, Germany.

Formate dehydrogenase (FDH) isolated from *Desulfovibrio gigas* catalyses the oxidation of formate to CO_2 , a reaction which involves the release of two electrons. FDH is a periplasmic enzyme constituted of two subunits of 88KDa and 29KDa (SDS-PAGE). It contains two [4FE-4S] clusters and a molybdopterin cofactor composed of two MGD (molybdopterin guanine dinucleotide) units coordinated to a tungsten atom. This is the first example of a tungsten-containing formate dehydrogenase.

The vapour diffusing method was used to obtain the crystals in sitting drops under optimised conditions. Red needle-shaped crystals grew in 1-2 days at 4ºC. Cryo conditions were established and Synchrotron X-Ray data were collected at 100K in the BW6 beamline of the MPG-ASMB in DESY. 163901 unique reflections were collected between 22.59 and 2.03 Å resolution. Data were processed with Denzo and Scalepack in spacegroup $P2_1$ with cell dimensions a = 73.8Å, b = 111.3Å, c = 156.6Å and β =93.7º. An overall $I/\sigma(I)$ of 11.9 was obtained, with an R_{merge} of 7,1% (27% in the outer shell) and a completeness of 99.2% (99.6% in the outer shell). Spectroscopic data suggest that FDH's largest subunit (88KDa) may be homologous to the periplasmic nitrate reductase (NAP, 77KDa), for which the structure has already been solved [1]. Work is currently being done in trying to use NAP to model the FDH's large subunit by molecular replacement.

[1] J.M. Dias, M.E. Than, A. Humm, R. Huber, G. P. Bourenkov, H.D. Bartunik, S. Bursakov, J. Calvete, J. Caldeira, C. Carneiro, J.J.G. Moura, I. Moura, M.J. Romão, (1999), Structure 7, 65-79.

P11.04.059 CRYSTAL STRUCTURES OF FERRIC-NO COMPLEXES OF FUNGAL NITRIC OXIDE REDUCTASE AND ITS SER286 MUTANTS. S.-Y.Park, S-I.Adachi, E.Obayashi, N.Kamiya, T.Iizuka, Y.Shiro [1], H.Shimizu [2], H.Shoun [3], [1] The Institute of Physical and Chemical Research (RIKEN), RIKEN Harima Institute, Mikazuki-cho, Sayo, Hyogo 679-5143, Japan. [2] Gakushuin University, Mejiro, Toshima-ku, Tokyo 170, Japan. [3] Institute of Applied Biochemistry, University of Tsukuba, Tsukuba, Ibaraki 305, Japan.

Fungal nitric oxide reductase (NOR) is a heam-enzyme catalyzing reduction of NO to N2O through its ferric-NO complex as a first intermediate. Crystal structures of the ferric-NO complex of its wild type, Ser286-->Val and Ser286-->Thr mutant enzymes were determined with 1.7Å resolution at cryogenic temperature (100K).

These are first reports of the ferric-NO complex of heamprotein, showing a linear but slightly tilt NO binding to the heam iron, in sharp contrast to the bent NO coordination in ferrous heamproteins. Replacement of Ser286 with valine or threonine hardly alters the NO coordination structure, but significantly influences positions of water molecules in the active site. Consequently, the hydrogen bond network in the active site is disturbed, in consistency with dramatic loss of the NO reduction reactivity of the enzyme upon the mutations.

We have conclusively defined the water molecule just adjacent to the iron-bound NO as a proton donor to the Fe-NO moiety, and the specific hydrogen bond network including Ser286 as an a proton delivery machinery in the NO reduction reaction by the fungal NOR.

P11.04.060 A PROLINE-SPECIFIC AMINOPEPTIDASE WITH A DINUCLEAR MANGANESE CENTRE. J.M. Guss[1], C.S. Bond[1], N.E. Dixon[2], H.C. Freeman[3], P.W. Lilley[3], J.A. Wilce[1], M.C.J. Wilce[1] and K. Willingham[1], [1]Department of Biochemistry and [3]School of Chemistry, University of Sydney, NSW 2006, Australia, [2]Research School of Chemistry, Australian National University, ACT 0200, Australia.

Proline-specific aminopeptidases cleave the N-terminal residue from oligopeptides in which the penultimate residue is proline. The structure of the *E. coli* enzyme (AMPP) has been solved and refined in two crystal forms using isomorphous and molecular replacement methods [1]. Structures have also been solved for enzyme/inhibitor complexes. AMPP forms tetramers, which persist in both crystal forms. Each monomer has two domains. The active site is entirely located in the C-terminal domain but its surrounds are provided by three of the four subunits.

The heart of the active site is a dinuclear Mn(II) cluster, in which the Mn atoms are separated by 3.3 Å. The metal atoms are bridged by carboxyl groups of protein side chains and a solvent identified from the pH and by analogy with arginase as hydroxide. The structure of the complex with the product-like inhibitor Pro-Leu supports the hypothesis that the bridging hydroxide acts as the nucleophile in the catalytic reaction.

The catalytic domain of AMPP is very similar to the single domain of methionine aminopeptidase (a cobalt enzyme) and the catalytic domain of creatinase (not a metalloenzyme), as predicted from sequence homology [2]. More surprisingly the N-terminal domains of AMPP and creatinase are also similar despite lack of sequence similarity. AMPP also shares a high degree of sequence similarity with both bacterial and mammalian prolidases - proline-aminopeptidases specific for dipeptide substrates.

[1] Wilce et al. (1998). Proc. Natl. Acad. Sci. U.S.A. **95**, 3472-3477.
[2] Bazan et al. (1994). Proc. Natl. Acad. Sci. U.S.A. **91**, 2473-2477.

P11.04.061 STUDIES IN FRUSTRATION : THE STRUCTURE OF BOVINE PORPHOBILINOGEN SYNTHASE. H.L. Carrell, Amy K Katz, Carol E. Afshar, Liat Shimoni-Livny, Trixie Wagner, E.K.Jaffe and Jenny P. Glusker. The Institute for Cancer Research, The Fox Chase Cancer Center, Philadelphia, PA 19111, USA.

The metalloenzyme porphobilinogen synthase (5-aminolevulinate dehydratase) catalyzes the condensation of two molecules of 5-aminolevulinic acid to give porphobilinogen which is the monopyrrole precursor of all biological tetrapyrroles, the porphyrins, corrins, chlorins and other cofactors. The inhibition of PBGS by Pb(II) is known to contribute to neurotoxicity in children. Bovine PBGS is an octameric 280 kD protein consisting of eight subunits (35 kD) with four active sites. Each dimeric

active site binds two functionally distinct types of Zn(II) as well as aminolevulinic acid molecules which have different chemical fates. Bovine PBGS crystallizes from ammonium sulfate at p*H* 6.1 as square parallelopipeds and are tetragonal in space group *I*422 with *a*=125 Å and *c*=200 Å and 4 octameric molecules/cell. Thus there are 2 subunits or 1 dimer in the asymmetric unit. The crystal structures for two modifications of the PBGS have been carried out by molecular replacement using the reported structure of the enzyme from *Saccharomyces cerevisiae*(1). The structure of PBGS with 5-chlorolevulinate covalently bound to four of the eight subunits has been solved to 2.7 Å resolution. The second structure is that of a lead(Pb^{II}) modified enzyme, the crystals of which were discovered to contain no metal ions at all, and thus are apo-PBGS. The structure for this form of the protein has been determined to 2.3 Å resolution. The structural details and a comparison of the structure with the previously reported structures will be presented and discussed. "Where have all the metals gone?" is a question to be pondered and perhaps answered.

Acknowledgment. This work was carried out under grant CA-10925 from the National Institutes of Health.

1. P.T.Erskine, N.Senior, S.Awan, R.Lambert, G.Lewis, I.J.Tickle, M.Sarwar, P.Spencer, P.Thomas, M.J.Warren, P.M.Shoolingin-Jordan, S.P.Wood, J.B.Cooper Nat.Struct.Biol. Vol 4, 1025 (1997)

P11.04.062 WHICH FUNCTIONAL GROUPS DOES A DIVALENT METAL ION MOST LIKE TO BIND TO: STRUCTURE AND ENERGETICS. Jenny P. Glusker, Amy K. Katz, H. L. Carrell, Liat Shimoni-Livny, Trixie Wagner, Carol E. Afshar, Philip George [1], Charles W. Bock [2], [1] The Institute for Cancer Research, The Fox Chase Cancer Center, Philadelphia, PA 19111, USA, [2] The Philadelphia College of Textiles and Science, Philadelphia, PA 19144, USA

The roles of divalent metal ions in biological systems form the basis of this study. Their coordination chemistry has been investigated by analyses involving the Cambridge Structural Database, the Protein Data Bank and ab initio molecular orbital calculations. The metal ions described here include magnesium, calcium, manganese, zinc, copper, and lead. Each divalent ion shows a specific preference for binding directly to oxygen, nitrogen and/or sulfur in liganding groups in proteins. Methods for analyzing and representing this are introduced, together with the resulting data obtained for the ions listed above.

The roles of divalent metal ions in biological systems form the basis of this study. Their coordination chemistry has been investigated by analyses involving the Cambridge Structural Database, the Protein Data Bank and ab initio molecular orbital calculations. The metal ions described here include magnesium, calcium, manganese, zinc, copper, and lead. Each divalent ion shows a specific preference for binding directly to oxygen, nitrogen and/or sulfur in liganding groups in proteins. Methods for analyzing and representing this are introduced, together with the resulting data obtained for the ions listed above.

The extent to which the coordination number in the innermost coordination shell around a divalent metal ion can be changed as a ligand, such as a water molecule, moves between its inner and second coordination shell has been investigated; this is relevant to many biochemical reactions that occurs at the metal site in an enzyme. The energetic consequences were determined by molecular orbital calculations. These energy changes are low for zinc and calcium, but are high for magnesium and divalent manganese. These findings have implications for the roles of the metal ions in biochemical reactions and have been further investigated by analyses of proposed metalloenzyme mechanisms and their crystal structures listed in the Protein Data Bank.

Any effect of the metal ion on the ligand, such as polarization, is also relevant to the catalytic mechanisms of metalloenzymes. First the ability of the divalent metal ion to ionize water has been investigated by ab initio molecular orbital calculations. This gives a relative scale of the polarizing abilities of the various metal ions. Then the extent to which the polarizing ability of the metal ion is a function of its immediate ligands in the first coordination sphere has been analyzed. For example, the replacement of a water molecule in the inner coordination sphere by a carboxylate group reduces the ability of the metal ion to polarize water. Finally the propensity of certain metal ions to take part in specific structural motifs on binding to an enzyme, and the utility of such motifs to the action of the enzyme, are described.

This work was supported by a grant CA-10925 from the National Institutes of Health, US Public Health Service.

P11.04.063 THE ROLE OF IRON BINDING DEDUCED FROM CRYSTAL STRUCTURES OF PHENYLALANINE HYDROXYLASE. T. Gleichmann, I.G. Jennings, R.G.H. Cotton, B. E. Kemp and B. Kobe, Structural Biology Laboratory, St. Vincent's Institute of Medical Research, 41 Victoria Parade, Fitzroy, Victoria 3065, Australia.

The mononuclear non-heme iron dependent enzyme phenylalanine hydroxylase (PheOH, phenylalanine 4-monooxygenase) catalyses the hydroxylation of phenylalanine to tyrosine in the presence of 6(R)-L-*erythro*-tetrahydrobiopterin (BH_4) and dioxygen. This is the rate limiting step in phenylalanine catabolism and neurotransmitter biosynthesis. Phenylalanine is both an essential amino acid and toxic at pathophysiological levels. Consequently, defects in PheOH cause hyperphenylalaninemias (HPA) including phenylketonuria (PKU), a common metabolic disorder that can result in severe mental retardation. Likewise, the enzyme is tightly regulated by phenylalanine activation, phosphorylation, BH_4 inhibition and at the transcriptional level. PheOH is a member of the family of aromatic amino acid hydroxylases that also include tyrosine hydroxylase and tryptophan hydroxylase. They all consist of a regulatory, a catalytic and tetramerization domain; in solution PheOH exists as a mixture of dimeric and tetrameric forms.

To assess the structural determinants of iron-binding we have determined structures of phosphorylated, C-terminally truncated, dimeric PheOH (PheOH-24) in apo-, Fe- and In-bound states. The iron incorporated in the expressed protein can be extracted with 1,10-phenanthroline from the Fe-PheOH-24 crystals yielding apo-PheOH-24 crystals and subsequently replaced by In^{3+} using the soaking technique to yield In-bound crystals. All three crystal forms are isomorphous and have the symmetry of spacegroup $P4_322$. Both the metal-free apo- and In-bound structures represent catalytically inactive forms of PheOH.

The iron is bound at the floor of a deep pocket in the catalytic domain, octahedrally coordinated by His285, His290, Glu330 and three water molecules. The coordination geometry for In^{3+} in In-PheOH and a similarly located water molecule in apo-PAH are comparable to iron in the native form, with shorter distances to In^{3+} and longer distances to the water molecule as compared to the native PheOH. The Glu330 changes the ligation mode: bidendate for In-PheOH, monodendate for apo-PheOH and a mixture of both for the native PheOH.

The metal ion forms a hypothetical high valent iron-oxo intermediate, which is postulated to react with phenylalanine in the hydroxylation process. In contrast, In is unable to substitute for Fe during the reaction.

P11.04.064 COMPARISON OF ZINC LIGAND COORDINATION OF MATRIX METALLOPROTEASES AND INHIBITOR COMPLEXES Karl D. Hardman, DuPont Pharmaceuticals Company, Experimental Station E353/148H, Wilmington, DE 19880-80353, USA

The coordination geometries of high resolution crystal structures (better than 1.7 Ang.) of the catalytic zinc sites for a number of Matrix-Metalloprotease (MMP)/ inhibitor complexes have been compared with other zinc proteases and small molecule

zinc complexes. The purpose was to establish if different inhibitors with the same coordination ligands but different interactions with the protein imposed any significant alteration of the coordination geometry of the zinc.

In addition, positions of neighboring side chains which are not zinc ligands were compared to estimate their contributions to catalysis and/or electronic stability of the active site. For example, the conserved methionine of the metzincin (thimet) classes of zinc proteases plays an unknown role in the structure and catalysis. Previous considerations of the catalytic mechanism of these proteases have not addressed possible effects of this thioether group. However, mutation of this side chain to serine has resulted in approximately a 100-fold loss in activity against a peptide substrate in MMP3 (stromelysin-1).

P11.04.065 CRYSTAL STRUCTURE OF HUMAN PHENYLALANINE HYDROXYLASE IN NATIVE AND INHIBITOR BOUND FORMS. H. Erlandsen and R. C. Stevens, Department of Chemistry, University of California, Berkeley, CA. 94720, USA, T. Flatmark, Department of Biochemistry and Molecular Biology, University of Bergen, Årstadveien 19, N-5009 Bergen, Norway, and E. Hough, Protein Crystallography Group, Chemistry Department, University of Tromsø, N-9037 Tromsø, Norway.

The non-heme, iron dependent metalloenzyme, mammalian phenylalanine hydroxylase (EC 1.14.16.1, phenylalanine 4-monooxygenase, PheOH) catalyzes the hydroxylation of l-phenylalanine to l-tyrosine in the prescence of 6(*R*)-L-erythro-5,6,7,8-tetrahydrobiopterin and dioxygen, the initial and rate-limiting step in the catabolism of this amino acid [1]. Phenylketonuria (PKU) is an autosomal recessive disease caused by mutations in the PheOH gene, which results in considerable heterogeneity both in terms of clinical, metabolic and enzymatic phenotypes. More than 280 different PKU mutations have been reported so far. The mechanism with which the hydroxylation occurs is not yet fully understood, but the enzyme is believed to proceed through an ordered binding of tetrahydrobiopterin, molecular oxygen and phenylalanine substrate. ^{18}O kinetic isotope effect measurements [2] suggest a one-electron transfer from the tetrahydrobiopterin to oxygen to form a superoxide anion as the first reactive. This radical pair would then couple to form a 4a-peroxytetrahydrobiopterin intermediate. The crystal structure of a truncated form of hPheOH (containing the catalytic domain) has been solved to 2.0Å resolution in its native, iron containing state and also in catecholamine (dopamine, noradrenaline and adrenaline) inhibitor bound states. Crystallographic studies of this enzyme and its binding of inhibitors, substrate and co-factor, will help elucidate the molecular basis of their binding to the active site, as well as give a structural rationale for the PKU mutations.

1 S. Kaufman (1995) *Adv. Enzymol.* 70, 103-220.
2 Francisco *et al.* (1998) *J. Am. Chem. Soc.* 120, 4057-4062.

P11.04.066 CRYSTAL STRUCTURE OF A DIOXYGENASE LIGAB WHICH IS A PROTOCATECHUATE 4,5-DIOXYGENASE. K. Sugimoto, T. Senda, H. Aoshima, E. Masai, M. Fukuda and Y. Mitsui, Department of BioEngineering, Nagaoka University of Technology, Nagaoka, Niigata 940-2188, JAPAN

Sphingomonas paucimobilis SYK-6 utilizes an extradiol type catecholic dioxygenase, LigAB (a protocatechuate 4,5-dioxygenase), to oxidize protocatechuate (PCA). The enzyme belongs to the family of class III extradiol type (catecholic) dioxygenase catalyzing the ring opening reaction of protocatechuate and related compounds. Primary structure of LigAB has suggested that the enzyme has no evolutionary relationship with the family of class II extradiol type dioxygenase for which the crystal structures have been determined for several member enzymes. Both the class II and class III enzymes utilize non-heme ferrous center to catalyze the addition of dioxygen to its substrate. Through elucidating the crystal structure of LigAB, we aim at providing a structural basis for discussing the function of the class III enzymes in general and comparing structures and functions between the class II and class III enzymes.

The crystal structure of LigAB was determined using an MIR method. Subsequently the crystal structure of LigAB in complex with a substrate, PCA, was determined. The three-dimensional structure of LigAB is completely different from that of the class II extradiol type dioxygenases. This implies that, as implicated by primary structure comparison, no evolutionary relationship exists between the classes II and III enzymes. The iron coordination sphere of LigAB in complex with its substrate, however, shares many geometrical characteristics to that of class II enzymes. Moreover the disposition of the putative catalytic base relative to the coordination sphere is very similar between the two kinds of enzymes. These results strongly suggest that the classes II and III enzymes share a common catalytic mechanism despite the completely different three-dimensional structures. Thus the present case appears to be another clear example of convergent evolution of two proteins having no overall sequence and structural similarity to each other.

P11.04.067 THE STRUCTURES OF 5-AMINOLAEVULINATE DEHYDRATASE FROM *E. COLI* AND YEAST. P.T. Erskine, E.Norton, P.M. Shoolingin-Jordan, S.P. Wood and J.B. Cooper. School of Biological Sciences, University of Southampton, Southampton, SO16 7PX, UK, and R. Newbold and M.J. Warren. Institute of Ophthalmology, London, EC1V 9EL, UK.

5-aminolaevulinate dehydratase (ALAD, porphobilinogen synthase) is a key early enzyme of the porphyrin and corrin biosynthetic pathways which catalyses the condensation of two 5-aminolaevulinic acid (ALA) molecules to form the pyrrole porphobilinogen (PBG). The yeast ALAD structure (solved at 2.3 Å by MAD at ESRF, Grenoble with Dr A. Thompson [1]) was used to solve the *E. coli* enzyme at 2.0 Å by molecular replacement [2]. Both ALADs form large homo-octameric structures with 422 symmetry in which each subunit adopts the TIM-barrel fold with a 20-30 residue N-terminal arm forming extensive inter-subunit interactions. Pairs of monomers associate with their arms wrapped around each other to form compact dimers. Four dimers interact principally via their arm regions to form the octamer which has all eight active sites exposed on the surface. At the base of each active site are two lysine residues (195 and 247 in *E. coli* numbering), one of which, Lys 247, forms a Schiff base link to the substrate ALA. Close by is the catalytic zinc binding site formed by three cysteines (Cys 120, 122 and 130) and a solvent molecule. The *E. coli* enzyme possesses another well defined zinc binding site in which the metal ion is coordinated by Glu 232 and five solvent molecules buried at a subunit interface. This octahedrally coordinated metal binding site and its proximity to the active site may account for the activating properties which magnesium ions have on the enzyme. The structure of the inhibitor laevulinic acid bound to both ALADs [2, 3] reveals that a large loop covering the active site (residues 197-220) undergoes a substantial ordering on binding the inhibitor.

1. Erskine, P., *et al*., Nat. Str. Biol. (1997) **4**, 1025. 2. Erskine, P., *et al*., Biochem. (1999) in press. 3. Erskine, P. *et al*., Prot. Sci. (1999) submitted.

P11.04.068 THE STRUCTURE OF A CLASS II ALDOLASE COMPLEXED WITH PGH REVEALS DETAILS OF MECHANISM AND SPECIFICITY. William N. Hunter, David R. Hall, Department of Biochemistry, University of Dundee, Dundee, DD1 5EH, United Kingdom, Gordon A. Leonard, Joint Structural Biology Group, ESRF, BP 220, F38043 Grenoble CEDEX, France, Christopher D. Reed, C. Ian Watt, Department of Chemistry, University of Manchester, Oxford Road, Manchester, M13 9PL, United Kingdom, and Alan Berry, School of Biochemistry and Molecular Biology, University of Leeds, Leeds, LS2 9JT, United Kingdom.

The structure of a Class II fructose-1,6-bisphosphate aldolase in complex with the substrate analogue and inhibitor phosphoglycolohydroxamate (PGH) has been determined using X-ray diffraction terms to a resolution of 2.0Å. PGH resembles the ene-diolate transition state of the physiological substrate dihydroxyacetone phosphate. It is well ordered and bound in a deep polar cavity at the C-terminal end of the $(\alpha/\beta)_8$ barrel where it chelates the catalytic zinc ion using hydroxyl and enolate oxygens. Trigonal bipyramidal coordination of the zinc is completed by three histidines. A complex network of hydrogen bonds occurs at the catalytic centre and are required to organise the position of key functional groups and metal ion ligands. A well defined monovalent cation binding site is observed following significant re-organisation of loop structures. This assists the formation of a phosphate binding site on one side of the barrel that tethers PGH in the catalytic site. The positions of functional groups of substrate and putative interactions with key amino acids are identified. Knowledge of the complex structure complements spectroscopic and site-directed mutagenesis studies and contributes to the understanding of the mechanism and substrate specificity of this family of enzymes. A reaction mechanism distinct from that of other Class II aldolases is proposed. The results suggest that the Class II aldolases should be sub-divided into two groups on the basis of both distinct folds and mechanism.

P11.04.069 THE STRUCTURE OF DI-MANGANESE CATALASE FROM *LACTOBACILLUS PLANTARUM* AT 1.8 Å RESOLUTION. V.V. Barynin and P.M. Harrison and P.J. Artymiuk , The Krebs Institute for Biomolecular Research, Department of Molecular Biology and Biotechnology, The University of Sheffield, Sheffield S10 2TN, UK, and S.V. Antonyuk, The Institute of Crystallography, Russian Academy of Sciences, Leninsky pr.59, Moscow 117333, Russia, and V.S. Lamzin, EMBL Hamburg Outstation , c/o Desy, Notkestrasse 85, 22603, Germany, and M.M. Whittaker and J.W. Whittaker, Dept. of Biochemistry and Mol. Biology, Oregon Graduate Institute, Portland, OR 97291-1000, USA

The *L. plantarum* catalase structure has confirmed the hexameric nature of this enzyme with a novel arrangement of di-Mn catalase domains in the monomer. The first coordination sphere of the di-Mn cluster in the active site is composed of three Glu and two His ligands. Only the His ligands and a (Mn,Mn) bridging Glu have the same geometry as the equivalent *T.thermophilus* manganese catalase residues. The positions of the Mn-monodentate Glu's of the active site are different. There are also three solvent ligands to Mn's. Both the Mn ions of the *L. plantarum* catalase active site are six-coordinate. The data set was obtained from the monoclinic crystal form of the native enzyme (a=75.5, b=97.6, c=108.0 Å, α=90.0, β=107.2, γ=90.0, space group $P2_1$, 6 subunits per a. u.) and was collected at 293K to 1.84 Å resolution. The structure has been solved by molecular replacement. The initial model used was that of a core of the *T.thermophilus* manganese catalase hexamer structure [1]. The structure of the *L. plantarum* catalase has been refined to an R-factor of 14.8% (free R of 20.3%). Comparison of the *L. plantarum* and *T.thermophilus* catalase structures has revealed that there are two distinct but related subfamilies of catalase in the manganese catalase family with different design of the hexamers and the active sites.

1. V.V.Barynin, P.D.Hempstead, A.A.Vagin, S.V.Antonyuk, W.R.Melik-Adamyan, V.S.Lamzin, P.M.Harrison & P.J.Artymiuk, (1997) J.Inorganic Biochem. 67, 196.

P11.04.070 CRYSTAL STRUCTURES OF FRAGMENTS TR_1C AND TR_2C FROM CALMODULIN L-L. Olsson and L. Sjölin, Dept. of Inorganic Chemistry and the Centre for Structural Biology, University of Göteborg, SE-412 96 Göteborg, Sweden

Calmodulin is a relatively small calcium binding protein, involved in the regulation of several biochemical processes in various organisms. The 148 amino acids are folded into two globular domains connected by a long solvent exposed alpha-helix. Each domain has a large hydrophobic cleft and two EF-hands, the characteristic helix-loop-helix motifs in calcium binding proteins, and each EF-hand binds one Ca^{2+} ion.

The fragments, which were expressed in E. coli, consist of amino acids 1 to 75 (tr_1c) and amino acids 76 to 148 (tr_2c). Tr_1c crystallizes in the space group $C222_1$ with unit cell dimensions a=34.5 Å, b=67.7 Å and c=60.0 Å, and data were collected to 1.8 Å resolution. Tr_2c crystallizes in the space groups $P4_32_12$ and $P4_3$ and also in yet another tetragonal space group with a=b=61.5 Å and c=73.2 Å. This crystal diffracts to 1.5 Å resolution. These structures were solved using rotation/translation functions, with the two calmodulin domains as models.

Comparisons between the X-ray structures of the whole calmodulin molecule and tr_1c and tr_2c, respectively, show that the structure of one single domain is not largely dependent on the second domain. This is advantageous since, for example, dynamic studies with NMR are more convenient with smaller molecules. The globular fragments contain two Ca^{2+}-binding EF-hands each, and the hydrophobic clefts observed in calmodulin are also found in these fragments.

The structures of tr_1c and tr_2c will be presented, and compared with the parent calmodulin structure.

P11.04.071 METALLO-β-LACTAMASE FROM B. CEREUS 569/H: MONO- OR BI-NUCLEAR ENZYME? Stella Maris Fabiane, M. K. Sohi, B. J. Sutton, Molecular Biology and Biophysics Group, The Randall Institute, King's College London, 26-29 Drury Lane, London WC2B 5RL, UK.

Elucidation of the mechanism of metallo-β-lactamases is an important step in the production of drugs to counteract bacterial resistance to β-lactam antibiotics. Following the structure determination of the metallo-β-lactamase from *B. cereus* 569/H/9 at 1.9Å [1], its active site structure has now been probed by changing the pH of the crystals.

At pH 5.2, there are two Zn^{2+} ions in the active site. The first of these, Zn1, has a high affinity to the protein (1μM) and the second, Zn2, has a low affinity (24mM). When the pH of the crystal is raised to 6.0, the structures solved in two different space groups at 1.7Å (crystal grown from ammonium sulphate, space group $P3_121$, R_{cryst}=20%) and 1.9Å (crystal grown from PEG 8000, space group C2, R_{cryst}=24.2%) show that Zn2 has moved out of the active site and the previously co-ordinating cysteine (Cys168) residue is oxidised to the sulfinic form, SO_2. The same is true for crystals transferred to pH 7.5 (2.0Å, space group $P3_121$, R_{cryst}=18.1%). There is also considerable movement of another of the ligands to Zn2, His210. These data indicate that there are substantial conformational and chemical changes in the active site depending upon pH, throughout the pH range over which the enzyme is active.

All structures, whether mono- or bi-zinc, reveal a water molecule tightly bound to Zn1, which is the probable nucleophile for β-lactam ring hydrolysis. A catalytic mechanism is proposed.

[1] Fabiane *et al.* (1998). Biochemistry, **37**, 12404-12411.

P11.04.072 1.27Å CRYSTAL STRUCTURE OF RUSTICYANIN AND POINT MUTATIONS OF SER86 AND MET148. Ian Harvey [1], John Hall [2], Lalji Kanbi [1,2], S. Samar Hasnain [1,2], [1] Syncrotron Radiation Department, CLRC Daresbury Laboratory, Warrington, WA4 4AD, UK, [2] Faculty of Applied Sciences, De Montfort University, Leicester, LE1 9BH, UK

Rusticyanin is the highest redox potential single blue copper protein, from the acidophilic chemolithotroph Thiobacillus ferrooxidans. Its crystal structure has been determined and refined to 1.27Å resolution using SHELX with anisotropic temperature factors. Errors have been determined by full matrix inversion. This is the only single blue copper protein which has been determined to this resolution and is refined in this way. A number of mutants have been expressed in E.coli, including mutations at Met 148 and Ser86 (Asp, Asn,Gln, Leu). This residue is adjacent to the copper ligand His85 and is a conserved Asn in other blue proteins. The oxidised form of all four Ser mutants are less acid stable than the wild-type protein, although the mechanism of lability varies. These mutations modulated the redox potential by more than 110 mV. The characteristics of these mutants support the idea that this residue is in part responsible for the acid stability and redox potential.

Similarly, the Met 148 ligand has been mutated to Leu, Lys, Glu & Gln showing remarkable variation in clour & redox potential. The effect of these mutations would be discussed in the light of our 1.27Å resolution crystallographic structure of Rusticyanin.

P11.04.073 CRYSTAL STRUCTURE OF *PORPHYRA YEZOENSIS* CYTOCHROME c_6. Tomokazu Sasaki, Akira Uchida and Isao Oonishi, Department of Biomolecular Science and Fuminori Yoshizaki, Department of Biology, Faculty of Science, Toho University, Miyama, Funabashi 274-8510, Japan

Cytochrome c_6 transfers electrons from the cytochrome b_6f complex to the cytochrome *P700* in photosynthesis. The protein is a small type cytochrome *c*. Plastocyanin is also known to have the same function as cytochrome c_6, but no structural similarities are recognized between them. Cytochrome c_6 contains a heme prosthetic group which is mainly composed of alpha helices, while plastocyanin, a copper containing protein, is largely made up of beta sheets. Some algae have the ability to synthesize both cytochrome c_6 and plastocyanin; cytochrome c_6 replaces plastocyanin when copper is deficient, while other algal species synthesize either cytochrome c_6 or plastocyanin solely. The red alga *Porphyra yezoensis* has only cytochrome c_6 of 85 amino acid residues with a redox potential of 342 mV.

Two crystal forms with good quality for X-ray diffraction have been obtained. The crystals belong to the space group $P2_12_12_1$ with cell dimensions a=46.7, b=49.5 and c=37.1≈ (orthorhombic form) and the space group $P4_32_12$ with cell dimensions a=48.2 and c=83.0 ≈ (tetragonal form). Each crystal form has one molecule in an asymmetric unit. The structure of cytochrome c_6 in each crystal form was solved by molecular replacement and refined by simulated annealing.

The cytochrome c_6 in each form has almost the same structure, being very similar to those of other algal species; two long alpha helices at both ends of the chain cross at nearly right angles to each other and the heme is covalently linked to the two cysteine residues. Dimerization about the heme crevice is found in tetragonal crystal form, whereas no such dimerization is present in orthorhombic form.

P11.04.074 IRON SUPEROXIDE DISMUTASE FROM THE HYPERTHERMOPHILE SULFOLOBUS SOLFATARICUS. T. Ursby, LCCP, IBS, 41 avenue des Martyrs, F-38027 Grenoble Cedex 1, France and S. Al-Karadaghi, Molecular Biophysics, Center for Chemistry and Chemical Engineering, Lund University, P.O.Box 124, S-22100 Lund, Sweden and B.S. Adinolfi, E. De Vendittis and V. Bocchini, Dipartimento di Biochimica e Biotecnologie Mediche Università di Napoli Federico II, Via S. Pansini 5, I-80131 Naples, Italy.

We have determined the structure of superoxide dismutase (SOD) from the hyperthermophile *Sulfolobus solfataricus* to 2.3 Å resolution by molecular replacement (R_{cryst} 16.8%, R_{free} 19.8%) [1]. There are two identical monomers in the asymmetric unit (space group C2; a=76.3 Å, b=124.3 Å, c=60.3 Å, β = 128.8º). The monomer has a molecular weight of 24 kDa and consists of 210 amino acid residues of which 205 are visible in the electron density map. The overall fold of the monomer of *S. solfataricus* SOD is similar to that of other known Fe or Mn-SODs. *S. solfataricus* SOD forms a very compact tetramer of a type similar to that of SOD from the hyperthermophile *Aquifex pyrophilus* [2]. Both structures show an elevated number of inter-subunit ion-pairs compared with the mesophilic SOD from *Mycobacterium tuberculosis* and the thermophilic SOD from *Thermus thermophilus*. However, in contrast to the *A. pyrophilus* SOD structure, the number of intra-subunit ion-pairs and inter-subunit hydrogen bonds is not higher than in the compared mesophilic and thermophilic SOD structures. The electron density also revealed an unexpected and unusual covalent modification of a conserved tyrosine in the active site. The modification was shown to lower enzyme activity.

T. Ursby, B.S. Adinolfi, S. Al-Karadaghi, E. De Vendittis & V. Bocchini (1999) J. Mol. Biol. **286**, 391-407.
J.H. Lim, Y.G. Yu, Y.S. Han, S. Cho, B.Y. Ahn, S.H. Kim & Y. Chu (1997) J. Mol. Biol. **270**, 259-274.

P11.04.075 TOWARD IMPROVED BIODEGRADATION OF PCBS: STRUCTURES OF COMPONENTS OF BIPHENYL DIOXYGENASE. Christopher L. Colbert, Mathew Chakko, Giuseppe Terracina, and Jeffrey T. Bolin Dept. of Biological Sciences, Purdue University, West Lafayette, IN 47907-1392, USA

The first step in the aerobic microbial degradation of biphenyl and polychlorinated biphenyls (PCBs) utilizes a short electron transfer chain to facilitate dioxygenase-catalyzed formation of a *cis*-dihydrodiol from the aromatic substrate. The electron transfer chain includes a ferredoxin reductase (BphG), a Rieske-type ferredoxin (BphF), and the ring-hydroxylating dioxygenase ($BphA_1A_2$). We determined the structures of the ferredoxin from *Burkholderia cepacia* to 1.6Å resolution and the biphenyl dioxygenase from *Comomonas testosteroni* to 2.2Å resolution in the absence of O_2. Intrinsic Fe atoms provided MAD phasing information in both cases.

The structure of BphF is the first for a dioxygenase ferredoxin (Fd) and affords an opportunity for comparisons with Rieske subunits from other systems. For the refined model, R_{work}=20.6% and R_{free}=22.7%. The redox properties of dioxygenase Fds differ significantly from those of the Rieske proteins of the bc_1 (mitochondria) and the b_6f (chloroplasts) complexes: the midpoint potentials of the former are ~450mV lower and are relatively independent of ionic strength and pH. Others proposed that differences in the accessibility of the clusters are the cause of these variations, and that the Fe_2S_2 cluster of the dioxygenase Fd was likely to be sequestered. Despite low

sequence identity and variations in key segments of the cluster binding domain, BphF clearly shows a remarkable overall similarity to the bc_1 and b_6f structures, and the Fe_2S_2 cluster has equivalent solvent accessibility. Therefore, the differences in redox properties must arise from other factors. The BphF system allows for a detailed study of the subtleties of protein control of redox potential using mutagenesis coupled to biochemical, structural, and computational studies.

Biphenyl dioxygenase is an $\alpha_3\beta_3$ heterohexamer. Each α subunit binds one Rieske Fe_2S_2 cluster and catalyzes ring-hydroxylation at a mononuclear, non-heme Fe(II) active site. Comparison of the biphenyl and naphthalene dioxygenases provides insight into key aspects of structure and catalysis. Moreover, the structure of biphenyl dioxygenase can be used in conjunction with that of BphF to identify features involved in protein-protein association and electron transfer.

Support from NIH grant R01-GM52831 is gratefully acknowledged.

P11.04.076 STRUCTURE AND REACTION MECHANISM OF GLYOXALASE II Alex D. Cameron[‡], Marianne Ridderström[§], Birgit Olin[§], Bengt Mannervik[§] and T. Alwyn Jones[¶], [‡]Dept. of Chemistry, University of York YORK, YO10 5DD; Departments of Molecular Biology[¶] and Biochemistry[§], Uppsala University, Biomedical Center, Box 590, S-751 24, Uppsala, Sweden.

Glyoxalase II is the second of two enzymes in what has been termed the glyoxalase system. The physiological role of this system appears to be to detoxify methylglyoxal which is produced as a byproduct of glycolysis. With the use of glutathione as coenzyme the methylglyoxal is converted to D-lactic acid. Glyoxalase II, a thiolesterase, catalyses the conversion of D-lactoylglutathione which is produced by glyoxalase I to form D-lactic acid and glutathione. Recently it has been reported that glyoxalase II is a member of a family that includes the metallo-β-lactamases (MBLs), of which the structure is known. The MBLs contain either a mono or a binuclear zinc binding site. Conservation amongst the family, of the residues involved in binding the zinc in the MBLs, suggested that glyoxalase II may be a metalloenzyme.

We have solved the structure of human glyoxalase II by SIRAS. The enzyme consists of two domains. The N-terminal domain is built up of a 4 layered β-sandwich. It is this domain which is similar to the MBLs. This includes the bi-nuclear metal binding site which was apparent in the associated electron density maps at one edge of the β-sandwich. The C-terminal domain, not found in the MBLs, is built mainly of α-helices. The active site is situated at the domain interface. We have succeeded in soaking a substrate analogue into the active site. The position of the analogue next to the metal centre suggests a mechanism for hydrolysis in which a water molecule shared between the two metal ions acts as a nucleophile in the reaction. Such a proposal was also made for the the MBLs but without the crystallographic evidence of a substrate analogue in the active site.

P11.04.077 HIGH RESOLUTION STRUCTURE OF THE ACTIVE SITE OF THE HEMOPROTEIN FROM SULFITE REDUCTASE. M. E. Stroupe, B. R. Crane, and E. D. Getzoff, The Scripps Research Institute, La Jolla, CA 92037, USA.

The chemical properties of metalloenzymes are related to the detailed structure of the metallic cofactors used in catalysis. Sulfite Reductase (SiR) catalyses the six electron reduction of sulfite to sulfide by coupling the reducing power of two flavin molecules to a redox-active Fe_4S_4 cluster and an iron-containing siroheme (of the bacteriochlorin class). Each of eight 66-kDa flavoproteins that make up the holoenzyme contain one FAD and one FMN [1]. The four 64-kDa hemoproteins complete the holoenzyme and couple the Fe_4S_4 cluster to the siroheme through an endogenous cysteine ligand [2]. The 1.6 Å resolution structure of the hemoprotein suggests that structural perturbations in the Fe_4S_4 cluster and the siroheme may play a role in driving the reduction of sulfite by facilitating cofactor coupling [3]. Using high-intensity synchrotron radiation and frozen crystals, a higher resolution structure is attainable. The non-canonical geometry of its metal cofactors reveals how the SiR protein environment contorts the inorganic compounds to efficiently perform a complex chemical process.

M. Eschenbrenner, J. Coves, and M. Fontecave (**1995**). *FEBS Letters* , 374, 82.
B. R. Crane, L. M. Siegel, and E. D. Getzoff (**1997**). *Biochemistry*, 36, 12101.
B. R. Crane, L. M. Siegel, and E. D. Getzoff (**1995**). *Science*, 270, 59.

P11.04.078 CRYSTAL STRUCTURE OF CATECHOL 2,3-DIOXYGENASE (METAPYROCATE CHASE) FROM PSEUDOMONAS PUTIDA MT-2. A. Kita*, S. Kita**, I. Fujisawa*, K. Inaka**, T. Ishida***, K. Horiike***, M. Nozaki***, K. Miki*, *Department of Chemistry, Graduate School of Science, Kyoto University, Sakyo-ku, Kyoto 606-8502, Japan, **Research Laboratory of Resources Utilization, Tokyo Institute of Technology, Nagatsuta, Midori-ku, Yokohama 226-8503, Japan, ***Department of Biochemistry, Shiga University of Medical Science, Seta, Ohtsu, Shiga 520-2192, Japan

Catechol dioxygenases have a key role in the degradation of aromatic moelcules in the environment by soild bacteria. Catechol 2,3-dioxygenases catalyze the incorporation of dioxygen into catechol and the extradiol ring cleavage to form 2-hydroxymuconate semialdehyde. Catechol 2,3-dioxygenase (metapyrocatechase, MPC) from Pseudomonas putida mt-2 was the first extradiol dioxygenase to be obtained in a pure form and has been studied extensively. MPC is a tetramer of identical subunits, each with a single non-heme ferrous ion and 307 amino acids; the enzyme is designated as (a-Fe2+)4. Crystals of MPC enough for X-ray work were obtained from sodium citrate solution by vapur-diffusion procedure with direction-restricted stepwise seeding method at 4°C [1]. The three-dimensional structure of MPC has been determined at 2.8Å resolution by the multiple isomorphous replacement method [2]. The crystallographic R and free R (5% subset) factors for the reflections between 10 to 2.8Å resolution are 0.200 and 0.280, respectively. The structure shows that the four subunit molecules are related by a noncrystallographic 222 symmetry. The monomer comproses N-terminal and C-terminal domains, which are structurally similar to each other and related by a local twofold axis. The structure of the MPC subunit resembles that of 2,3-dihydroxybiphenyl dioxygenase, although there is low amino acid sequence identity between these enzymes. The active site structure reveals a distorted tetrahedral Fe(II) site with three endogenous ligands (His153, His214, and Glu265) and an additional molecule that is most probably acetone. The present MPC structure shows that the putative acetone molecule is directly ligated to the iron atom to block the Fe(II) binding sites.

1. A. Kita, S. Kita, K. Inaka, T. Ishida, K. Horiike, M. Nozaki & K. Miki (1997). J. Biochem., 122, 201.
2. A. Kita, S. Kita, I. Fujisawa, K. Inaka, T. Ishida, K. Horiike, M. Nozaki & K. Miki (1999). Structure, 7, 25.

P11.04.079 STRUCTURES OF SUBUNITS IIIA AND IV ILLUMINATE COOPERATIVE OXYGEN BINDING BY LIMULUS HEMOCYANIN. Karen A. Magnus [1], Shenping Liu [2], [1] Department of Biochemistry, Case Western Reserve University School of Medicine, Cleveland, OH 44106, USA, [2] Department of Biochemistry, Case Western Reserve University School of Medicine, Cleveland, OH 44106, USA - present address: Department of Chemistry, Cornell University

The structures of subunits IIIa and IV of Limulus polyphemus (horseshoe crab) hemocyanin were determined by molecular replacement using the backbone structure of subunit II (1OXY) as the test molecule. Because both crystal forms have large unit cells, data were collected at the Cornell High Energy Synchrotron Source. Phases for the oxygenated hemocyanin subunit IV were improved by averaging, solvent flattening and histogram matching. The resultant electron density map was of sufficient quality that the identities of many amino acids could be seen. The dicopper active site of subunit IV is the same as in subunit II. Interestingly, subunit IV hemocyanin also has density at the same position postulated to be an allosteric effector in subunit II, suggesting the possibility of a general cooperative mechanism for all arthro- pod hemocyanins. Hemocyanin subunit IIIa is the only Limulus subunit capable of catalyzing the decomposition of hydrogen peroxide. This subunit does not have the key "oxygen sensor" phenylalanine at its position 49, thus conferring special properties on its active site.

Supported by NSF MCB9305250 and MCB9817090.

P11.04.080 CRYSTALLIZATION AND PRELIMINARY CRYSTALLOGRAPHIC ANALYSIS OF ACONITASE FROM THERMUS THERMOPHILUS HB8. Hiroshi Aoyama, Shin-ichi Kawaguchi, Yorinao Inoue [1], Minori Kuraishi, Seiki Kuramitsu [2]. [1] SPring-8, The Institute of Physical and Chemical Research (RIKEN), 323-3 MIkazuki-cho, Mihara Sayo, Hyogo 679-5143, Japan, [2] Graduate School of Science, Osaka University, 1-1 Machikaneyama-cho, Toyonaka, Osaka 560-0043, Japan

Aconitase [citrate(isocitrate) hydrolyase, EC 4.2.1.3] catalyzes the stereospecific conversion of citrate to isocitrate via cis-aconitate in the tricarboxylic acid cycle. The enzyme contains iron-sulfer cluster, which functions as not redox reaction but hydratases.

We crystallized aconitase by a hanging-drop vapor diffusion method. Crystals were grown in 100 mM Hepes buffer at pH 7.0, using ammonium sulfate as a precipitant. They belong to the orthorhombic system, with unit cell dimensions of a=95.4, b=170.3, c=185.5Å.

X-ray data collection were carried out at beamline BL45XU of SPring-8. The crystal diffracts beyond 2.8Å. The structure analysis is in progress.

This work is a part of the "Structurome Project" that aims at structure determination of all the proteome components of T. thermophilus HB8 at SPring-8, Harima Institute of RIKEN.

P11.04.081 CRYSTAL STRUCTURE OF HYDROXYLAMINE OXYDOREDUCTASE IN AN ORTHORHOMBIC FORM. N. Igarashi, Institute of Materials Structure Science, High Energy Accelerator Research Organization, Tsukuba, 305-0801, Japan, K. Hiraishi and N. Tanaka, Faculty of Bioscience and Biotechnology, Tokyo Institute of Technology, Yokohama, 226-8501, Japan

We have solved the X-ray crystal structure of hydoxylamine oxidoreductase (HAO) from an autotrophic bacterium *Nitrosomonas europaea* obtains [1]. HAO catalyzes the oxidation of hydroxylamine to nitrite. The enzyme has a molecular mass of 200 kDa with 24 hemes which participate in catalytic function and electron transport. The crystal structure revealed the peculiar heme assembly and the “dielectron transfer” mechanism. However, the complete molecular structure still remains unsolved because of the crystal packing. In order to determine the entire three-dimensional structure of HAO, we have carried out the X-ray studies on this enzyme in another crystal form.

In our previous paper [1], obtained crystals were hexagonal space group $P6_3$ with unit cell dimensions of a=b=96.2Å, c=265.6Å and with two subunits per asymmetric unit. After screening for crystallization, new crystals suitable for the X-ray diffraction experiment were acquired by equilibration of HAO solution (20 mg/ml) against 17% (w/v) PEG4000 in 50mM potassium phosphate buffer (pH6.5). HAO crystallized in the orthorhombic space group $P2_12_12_1$ with unit cell dimensions of a=126.4Å, b=171.7Å, c=100.5Å and with one trimer molecule per asymmetric unit. Intensity data were collected up to 3.5Å resolution at BL6A in the Photon Factory.

Molecular replacement using the coordinates of HAO subunit has been successful and the current R-factor is 22%. The overall molecular assembly is the same as the one in the hexagonal crystal form. Further refinement is in progress. Structural details and comparison between the different crystal forms of HAO will be presented.

1. N. Igarashi, H. Moriyama, T. Fujiwara, Y. Fukumori & N. Tanaka (1997). *Nature Struct. Biol.*, **4**, 276-284.

P11.04.082 THREE-DIMENSIONAL STRUCTURE OF THE REDUCED FORM OF A NINE HAEM CYTOCHROME C AT PH 7.5 AND PH 9.5 I. Bento, P. M. Matias, R. Coelho and M. A. Carrondo, ITQB-UNL, P. O. Box 127, P-2780 Oeiras, Portugal

The nine haem cytochrome c has been isolated form Desulfovibrio desulfuricans ATCC 27774 cells grown under both nitrate and sulfate respiring-conditions [1]. Its physiological function is not yet known, but it is believed to be part of the periplasmic assembly of proteins involved in recycling the molecular hydrogen release by the cells as a result of the lactate metabolisation [2]. Nine haem cytochrome c is a monomer of 37.8 kDa, with 292 residues and nine heam groups colvalently bound to the polypeptidic chain [2,3]. Reduced crystals were obtained by adding sodium dithionite to the oxidized crystals, grown as described by Matias et. al. (1999), after transfering them to a set of new crystallization drops at different pH values. Two data sets, from two crystals reduced at different pH values (7.5 and 9.5) were collected at ESRF (BM-14 and EH-3) in Grenoble. The first data set showed a resolution of 2.0Å and the second a resolution of 1.8Å. Both crystals belong to the monoclinic space group with two molecules in the asymmetric unit. In this presentation we report the results of the structure refinement of the two reduced forms at pH 7.5 and 9.5. Also, the differences found will be discussed.

1. Liu et. al.(1988), J. Bacteriol. 170, 5545-5551.
2. Matias et. al. (1999), Structure, in press.
3. Varela et. al. (1996), Acta Cryst. D52, 1202-1208.

P11.04.083 STRUCTURE - FUNCTION RELATIONSHIPS IN BOTULINUM NEUROTOXIN TYPE B. S. Swaminathan, S. Eswaramoorthy, & J. Hartling, Biology Department, Brookhaven National Laboratory, Upton, NY 11973, USA

Clostridial neurotoxins belong to the class of AB toxins with separate domains for activity and binding. Botulinum and tetanus neurotoxins cause neuroparalytic syndromes of botulism and tetanus, which are characterized by serious neurological disorders. These toxins are among the most poisonous, with their

LD_{50} in humans in the range of 0.1 - 1 ng per kg. Of the seven serotypes, A to G (BoNT, EC 3.4.24.69), produced by *Clostridia botulinum,* only BoNT/A, B and E have been implicated in cases of botulism in humans. These toxins produced as a single chain of 150 kDa are cleaved by an endo protease before being released into a heavy chain of 100 kDa and a light chain of 50 kDa held together by a single disulfide bond. Except for BoNT/E, other botulinum neurotoxins are released as di-chains which are multifold more poisonous than single-chain toxins. BoNTs block the release of acetylcholine at the neuromuscular junction causing flaccid paralysis. The presence of a conserved zinc binding motif HEXXH in the middle of the light chain has led to the discovery that these toxins are zinc endopeptidases acting specifically on protein components of the same neuroexocytosis apparatus present in cytosol.

BoNT/B has been crystallized in the space group $P2_1$ with unit cell dimensions a = 78.16, b = 125.56, c = 94.26 Å and β = 112.46° with two molecules per unit cell. These crystals diffract at least to 2.0 Å resolution. Native and derivative data have been collected at the National Synchrotron Light Source, Brookhaven National Laboratory. The crystal structure has been determined by a combination of MIR and MAD methods. Results from the structural analysis and the functional relationships of the three distinct domains observed in the crystal structure will be discussed.

Research supported by the Office of Non-proliferation and National Security of the U.S. Department of Energy under prime contract No. DE-AC02-98CH10886 with Brookhaven National Laboratory.

P11.04.084 TOWARDS THE CRYSTAL STRUCTURE DETERMINATION OF GLYCEROL DEHYDROGENASE FROM THERMOTOGA MARITIMA. Vasundara Srinivasan, Kesen Ma, J. P. Rose, Michael W. W. Adams and B.-C. Wang, Department of Biochemistry and Molecular Biology, University of Georgia, Athens, GA 30602, U.S.A.

Glycerol dehydrogenases catalyze the reversible reaction of glycerol to glyceraldehyde. This enzyme has been isolated from several organisms. One of the most thermostable is from Thermotoga Maritima, which is an anaerobic, hyperthermophilic organism growing optimally at 80°C.

Glycerol dehydrogenase from Thermotoga is a tetramer with a subunit molecular weight of 45 kDa. The isolated enzyme contains both 'Fe' and 'Zn' and is NAD dependent. This enzyme has been crystallized by hanging drop vapor diffusion method using 2-Methyl -2,4-pentane diol as the precipitant. The crystals diffracted to a resolution of 1.4Å at the EMBL Hamburg Synchrotron source and belong to the space group I422 with cell dimensions of a =105.2 Å, c = 134.4 Å. Heavy atom derivative data using Pt has also been collected to a resolution of 2.3 Å and the structure solution is in progress.

Elucidation of the structure will give an insight into the thermostability and metal binding characteristics of the enzyme. It will also enable comparisons to be made with other classes of enzymes.

P11.04.085 CRYSTALLOGRAPHIC STUDY OF HEMOGLOBIN FROM THE GREEN ALGA *C.EUGAMETOS*. Pesce, A. Advanced Biotechnology Center and Department of Physics-INFM, University of Genova, Italy, and Couture, M. and Guertin, M., Department of Biochemistry, Laval University, Quebec-Canada, and Ascenzi, P., Department of Biology, Third University of Roma, Italy, and Bolognesi, M. Advanced Biotechnology Center and Department of Physics-INFM, University of Genova, Italy.

Besides the universal occurrence of hemoglobin (Hb) in vertebrates, heme-based oxygen carriers are widespread also in invertebrates, plants, fungi, protozoa and bacteria. This discovery has brought about unexpected views on the functional properties and structural organization in this protein homology family.

Here we present our current work and results on the crystallographic analysis of hemoglobin from the unicellular green alga *C.eugametos*. In this alga, a Hb (Chlamy_Hb) is expressed in response to visible light: this constitutes the first evidence for the presence of Hb in chloroplasts. Chlamy_Hb was expressed as the H19 mutant (121 amino acid residues), bearing shortened N-terminal helix. Very thin and small crystals have been grown in a week and a native data set has been collected at ESRF in Grenoble, at 1.53 Å resolution. The crystals belog to space group $P2_12_12_1$ (unit cell: a = 34.6 Å, b = 53.1 Å, c = 67.2 Å, one molecule per asymmetric unit).

Due to low sequence homology with known Hb structures, it was not possible to solve the structure via Molecular Replacement.

Up to now, we have found phase information with the MIR method, using an uranyl-acetate and a potassium-tetrachloroplatinate derivative (data sets collected in house, 16-3.1 Å resolution). Two sites were found for uranium and one for platinum. Heavy atom refinement and phase extraction was performed by Phases, to 3.1 Å resolution. Map quality was improved using Sharp, and at this stage the map is good enough to build part of the model, using O.

P11.04.086 STRUCTURAL STUDIES OF DERIVATIVES OF COPPER-CONTAINING AMINE OXIDASE FROM ARTHROBACTER GLOBIFORMIS. Hiroshi Yamaguchi, Misa Kim, Takeshi Hiromoto, Takeshi Narita and Megumi Yoshimura, School of Science, Kwansei Gakuin University, Nishinomiya, Hyogo 662-8501, Japan, Hideyuki Matsunami and Katsuyuki Tanizawa, Institute of Scientific and Industrial Research, Ibaraki, Osaka 567-0047, Japan

Copper-containing amine oxidase (EC 1.4.3.6) catalyzes the oxidative deamination of various biogenic primary amines to the corresponding aldehydes, ammonia and hydrogen peroxide. The enzyme also contains a covalently bound organic cofactor, 2,4,5-trihydroxyphenylalanyl (topa) quinone, which is formed by the post translation of tyrosine residue in the presence of Cu^{2+} and oxygen molecule. To elucidate the mechanism of the topa quinone formation, we are studying structures of various derivatives of phenylethylamine oxidase from Arthrobacter globiformis (AGAO). Each subunit of the dimeric enzyme has a molecular size of about 70kDa and consists of 638 amino acid residues.

Wild-type and several mutants of AGAO were purified in the copper/topa quinone-less precursor form (apoenzyme), which contains the precursor tyrosine residue in an unmodified state. Crystals of apoenzyme bound with Ni^{2+} and with Co^{2+} at the copper site were obtained by both of the cocrystallization and soaking methods using the corresponding metal ions. Crystals of several mutant enzymes were also obtained. All crystals are isomorphous and belong to the space group C2 with cell dimensions about a=158Å, b=64Å, c=93Å and β=112°. Diffraction data of these crystals were collected on imaging plate diffractometers installed in rotating anode X-ray generator in house and at the station BL44B2 of SPring8, and on a large Weissenberg camera at the station BL18b of the Photon Factory. Structures of these crystals were refined by using a program XPLOR. These structures will be reported and the mechanism of post-translational formation of the topa quinone cofactor in AGAO will be discussed on the bases of those structures.

P11.04.087 CRYSTAL STRUCTURE OF THE VANADIUM DEPENDENT HALOPEROXIDASE FROM C. OFFICINALIS. M.N.Isupov, A.R.Dalby, A.A.Brindley, J.A.Littlechild Departments of Chemistry and Biological Sciences, University of Exeter, Stocker Road, Exeter, EX4 4QD, UK.

The crystal structure of the Corallina officinalis vanadium bromoperoxidase has been determined by single isomorphous replacement and refined at 2.3Å resolution to an R-factor of 18% (R-free 23%). The enzyme consists of 598 amino-acid residues folded into a single a -helical domain. The centre of this domain is formed by a four helix bundle, at the end of which the active site is located. Two bromoperoxidase subunits interact to form a tight dimer. The arrangement of subunits in the dodecamer has 23 point symmetry. At the centre of the dodecamer is a spherical cavity made up of the N-terminal helix from each of the twelve subunits.

A comparison of the three-dimensional structures of the Cor. officinalis bromoperoxidase and the chloroperoxidase from the fungus Curvularia inaequalis reveals similarities in their active sites. A monomer of the fungal enzyme can be structurally aligned with a dimer of the algal enzyme. This would suggest that the two enzymes share a common ancestor. The differing halogen specificity between the two enzymes appears to be controlled by the electrostatics within the vanadium-binding active site.

Brindley, A.A., Dalby, A.R., Isupov, M.N. and Littlechild, J.A. (1998) Acta Cryst. D54 p454-457.

P11.04.088 MOLECULAR EVOLUTIONARY ASPECTS OF PLASTOCYANINS BASED ON CRYSTAL STRUCTURES N. Okazaki†, T. Inoue†, N. Shibata†, H. Sugawara†, M. Gotowda†, S. Hamanaka†, T. Kohzuma§, F. Yoshizaki‡, and Y. Kai† †Dept. of Materials Chemistry, Osaka University, Osaka 565-0871, JAPAN, §Dept. of Chemistry, Faculty of Science, Ibaraki University, Ibaraki 310-0000, JAPAN, ‡Dept. of Biology, Faculty of Science, Toho University, Chiba 274-8510, JAPAN.

Plastocyanin is a small (91-105 amino acids) copper-binding protein, which functions as an electron transfer shuttle from cytochrome *f* of the b_6/f complex to $P700^+$ of Photosystem I in chloroplasts of algae and higher plants, and also in many cyanobacteria. We have determined the structures of plastocyanins from higher plant *silene*, green alga, *Ulva pertusa*, fern *Dryopteris crassirhizoma*, and cyanobacterium *Synechococcus* sp. PCC7942 at high resolution. Plastocyanins have a half-turn helix between two β-sheets at position 52 to 55 in eucaryotic plastocyanins. However, the conserved residue of Gly49 is changed to Ala49 in the fern plastocyanin, in which a three-turn helix is formed. The copper structures as well as the backbone structures of four plastocyanins are quite similar with that of poplar plastocyanin in spite of the sequence divergence among plastocyanins from cyanobacteria, algae and higher plants. However, the surface structures are strikingly different with each other. The negative charged acidic patch around Tyr83, which is thought to be important for docking with physiological redox partners, located on the east side of the molecule. The cyanobacteria and fern plastocyanins have only two acidic residues around Tyr83, and those are neutralized by basic residues. However, the latter plastocyanin possesses two acidic clusters at position 59-61 and 65-67. On the other hand, in all plastocyanins from higher plant the acidic clusters locate at position 42-44 and 59 to 61, while in all plastocyanins from green algae residues 58 and 59 are deleted. As the result, the charge distribution is quite different with each other, and these findings may provide new insights into the molecular evolutionary aspects of plastocyanins.

P11.04.089 CRYSTALS OF FAB+hCG COMPLEX AND FABS. M.A. Dingwall and N. W. Isaacs. Department of Chemistry, Joseph Black Building, University of Glasgow, G12 8QQ, U. K.

hCG, M_W ~40kDa, is a member of the family of Glycoprotein Hormones which includes Luteinizing Hormone, Follicle Stimulating Hormone, and Thyroid Stimulating Hormone. All are glycosylated and have cystine knot growth factor fold. The holo-hormone consists of α and β subunits which are species specific. The 92 residue α-subunit is identical but the β-subunit varies in size and sequence according to the hormone. The β-subunit defines biological specificity. The holo-hormone is required for function. hCG is the only placental member of the Glycoprotein Hormone family, and is essential for maintainence of early pregnancy.

Monoclonal antibodies(mabs), M_W ~150kDa, against hCG are used in the early detection of pregnancy, design of antifertility vaccines, in the detection of certain cancers, and investigations of receptor binding. Fragment antibodies (Fab) have been prepared by papain digestion.

Crystals of hCG+FabB111 and hCG+A113 complexes show weak diffraction. FabB111 and FabINN-hCG-53 (Fab53) crystals have been grown. Antibody B111 is directed against the C-terminal region of the β-subunit. Diffraction data has been collected to 2.8Å for the FabB111 on a MAC Science 2020 Image Plate at room temperature. The structure has been solved by molecular replacement using AMoRe [1], and refinement is in progress. Antibody INN-hCG-53 is directed against c1/c2 epitope that involves residues from both subunits of the hormone. A crystal of Fab53 has shown diffraction to 2.8Å at the synchrotron radiation source, Station 9.6, Daresbury, at room temperature.

(1) Narvaza. J. 1994. Acta Cryst. A50, 157-163.

P11.04.090 CAMELID SINGLE-DOMAIN ANTIBODIES: MORE NEW FEATURES. Decanniere, K., Desmyter, A., Lauwereys, M., Muyldermans, S. & Wyns, L. Vlaams Instituut voor Biotechnologie, Vrije Universiteit Brussel, Paardenstraat 65, B-1640 St. Genesius Rode.

In addition to normal antibodies, the serum of camelidae contains antibodies consisting of heavy chains only. These antibodies bind with high affinity and high specificity, and they are a fully functional part of the immune system. A substantial part of single-chain antibodies have competitive enzyme inhibiting capacity. The structure of the variable domain (VHH) cAb-Lys3 in complex with its antigen lysozyme shows how this can be achieved: part of the 24 amino acid long CDR3-loop of cAb-Lys3 inserts into the active site cleft of lysozyme, blocking it for the substrate. The remaining residues of the CDR3-loop are used to cover the VL-interface.

Recently, the structure of the VHH cAb-RN05 with its antigen RNase A showed high-affinity binding of an antibody using only two CDR-loops. A considerable number of the interactions involve main chain atoms from either the antibody or the antigen. Although cAb-RN05 has a “short” 11 amino acid CDR3-loop, it also folds back over the VL-side, making the protein less hydrophobic.

The analysis of the cAb-RN05 structure also confirmed an observation made for cAb-Lys3: the H1 and the H2-loop of both antibodies deviate from the known canonical structures. We therefore question the general validity of the canonical structures.

Currently, the structure of cAb-CA05 with specificity for carbonic anhydrase is under analysis. This antibody could be crystallized both as free antibody and in complex with the antigen. Preliminary results show yet another mode of binding, involving only the CDR3-loop.

The wide variety of binding modes revealed by only 3 structures make the VHH-domains of single-chain antibodies an interesting model system for protein-protein interactions.

P11.04.091 CRYSTAL STRUCTURE OF THE HUMAN P58 KILLER CELL INHIBITORY RECEPTOR (KIR2DL3, NKAT2). Katsumi Maenaka , Nathan Zaccai, Taeko Maenaka, David I. Stuart, and E. Yvonne Jones, Laboratory of Molecular Biophysics, Rex Richards Building, South Parks Road, Oxford OX1 3QU U.K. and Takeo Juji, Japanese Red Cross Central Blood Centre, Hiro-o, Shibuya-ku, Tokyo 120 Japan.

Human killer cell inhibitory receptors (KIRs), which belong to the immunoglobulin (Ig) superfamily, inhibit or activate the cytotoxic activity of natural killer (NK) cells by specific binding to MHC class I molecules on the target cell.

The extracellular region of the human p58 KIR specific for HLA-Cw3 related MHC class I (KIR2DL3, NKAT2) was produced and crystallised in 9-10% PEG8000, 50mM HEPES, 8% ethylene glycol, 0.5% octyl-β-glucoside, pH7.5, at 294K [1]. The crystal structure of KIR2DL3 has been solved at 3Å resolution. The structure shows the predicted topology of two tandem Ig-like domains but comparison with the previously reported structure of KIR2DL1 specific for HLA-Cw4 [2] reveals an unexpected change of 23° in the relative orientation of these domains. The altered orientation maintains the unusually acute inter-domain elbow angle, which therefore appears to be a distinctive feature of the KIRs. The putative MHC class I binding site which is located on the outer surface of the elbow, spanning both domains, can be modulated by differences in the relative domain orientations. This observation has implications for the general mechanism of KIR/MHC Class I complex formation.

1. K. Maenaka, T. Juji, K. Tadokoro, K. Harlos, D.I. Stuart, & E.Y. Jones (1998). Acta Cryst. **D54**, 433-435.
2. Q.R. Fan, L. Mosyak, C.C. Winter, N. Wagtmann, E.O. Long, & D.C.Wiley (1997). Nature **389**, 96-100.

P11.04.092 CRYSTAL STRUCTURE OF CD2-BINDING DOMAIN OF CD58. Shinji Ikemizu, Karl Harlos, David I. Stuart, E. Yvonne Jones, Laboratory of Molecular Biophysics, Rex Richards Building, South Parks Road, Oxford OX1 3QU UK and Simon J. Davis, Molecular Sciences Division, Nuffield Department of Clinical Medicine, John Radcliffe Hospital, Oxford, OX3 9DU, U.K.

The crystal structure of a CD2-binding chimeric form of CD58, solved to 1.8Å resolution [1], reveals that the ligand binding domain of CD58 has the expected IgSF V-set topology and shares several of the hitherto unique structural features of CD2, underlining their close evolutionary relationship. The chimeric protein

The chimeric protein was expressed in CHO cells and deglycosylated with endo H. Crystals grew in the presence of 1.1-1.5M ammonium sulphate, 50 mM Tris pH 8. Diffraction data were collected in-house at 297K and on BM14 of the ESRF at 100K to resolution of 3.0Å and 1.8Å respectively. The structure was determined by molecular replacement using the program AmoRe with the rat CD2 [2] as a search model. Initially, an unambiguous solution was found and a model was built using those diffraction data to 3.0Å. Subsequently, the model was refined and the phases extended to 1.8Å using data collected at ESRF. The current R and Rfree are 0.202 and 0.243, respectively. The refined atomic model comprises residues 1 to 171 of the chimera, 3 N-linked GlcNAc carbohydrates and 197 ordered water molecules.

Ikemizu, S., et al.(1998) PNAS in press.
Jones, E.Y., et al.(1992) Nature 360, 232-239.

P11.04.093 THE STRUCTURE OF CALCIUM-DEPLETED HUMAN C-REACTIVE PROTEIN FROM PERFECTLY TWINNED CRYSTALS. Mohamed A.M. Ramadan, Annette K. Shrive and Trevor J. Greenhough, School of Life Sciences, Keele University, Staffs ST5 5BG, UK, and John E. Volanakis and Larry J. DeLucas, University of Alabama at Birmingham, Birmingham, Alabama 35294 USA.

Human C-reactive protein (CRP) is the classical acute-phase reactant produced in response to tissue damage and inflammation, and is used almost universally as a clinical indicator of infection and inflammation. CRP and serum amyloid P component (SAP) are members of the pentraxin family of oligomeric serum proteins which has been conserved through evolution, homologues having been found in every species in which they have been sought.

While the Ca-dependent ligand-binding specificity of CRP for phosphocholine moieties has long been recognised, the ligand-binding and functional properties of Ca-depleted CRP remain the subject of some debate. In order to clarify the conformational changes which accompany calcium binding, the structure of Ca-depleted human CRP has been determined by X-ray crystallography.

Crystals of calcium-depleted human CRP are invariably twinned and those suitable for analysis are merohedral type II twins of point group 4 single crystals. Although R_{symm} values clearly indicate point group 422, the 50/50 twinning is revealed by the intensity statistics. The structure has been solved by molecular replacement using the Ca-bound human CRP structure [1], revealing two independent pentamers which form a face to face decamer across the twinning 422 2-fold axis. Cycles of intensity deconvolution, density modification (10-fold ncs) and model building (*O*), eventually including refinement (*X-PLOR*), give a final R-factor of 0.19 (R-free = 0.20). The structural changes which accompany calcium binding, and their implications for ligand, C1q and receptor-binding, will be discussed.

[1] Shrive *et al*. (1996). Nature Structural Biology **3**, 346-354

P11.04.094 STRUCTURE OF A SCAVENGER RECEPTOR CYSTEINE-RICH DOMAIN SHEDS LIGHT ON AN ANCIENT SUPERFAMILY. E. Hohenester, T. Sasaki and R. Timpl, Biophysics Section, Blackett Laboratory, Imperial College, Prince Consort Road, London SW7 2BZ, UK, and Max-Planck-Institut für Biochemie, D-82152 Martinsried, Germany.

Scavenger receptor cysteine-rich (SR) domains are found widely in cell surface molecules and some secreted molecules of the immune system, with about 3% of all known leukocyte receptor molecules containing SR domains [1]. The SR domain is evolutionarily ancient: SR domains in marine sponges and sea urchins are ≈30% identical to human homologues. The biological functions of SR domains are generally not well understood, but in some proteins they have been shown to mediate protein-protein interactions and ligand binding. We have determined the 2.0 Å crystal structure of the single SR domain (≈110 residues) of human Mac-2 binding protein, a tumour-associated antigen and extracellular matrix protein. The first structure of an SR domain reveals a novel fold composed of a six-stranded β-sheet cradling an α-helix. Sequence alignment demonstrates that the structure is a valid template for the entire SR superfamily. This allows a structural interpretation of previous mutagenesis data on ligand binding by the lymphocyte receptor CD6. The SR domain structure also reveals a curious close structural similarity to certain toxins. The pattern of disulfide bridges is completely unrelated, however, arguing against an evolutionary relationship.

[1] D. Resnick, A. Pearson and M. Krieger (1994). The SRCR superfamily: a family reminiscent of the Ig superfamily. TIBS 19, 5-8.

P11.04.095 THE CRYSTAL STRUCTURE OF MRP8, A MEMBER OF S100 CALCIUM-BINDING PROTEIN FAMILY, AT 1.9 Å RESOLUTION. A.Nakagawa, K.Ishikawa and I.Tanaka, Division of Biological Sciences, Graduate School of Science, Hokkaido University, Sapporo 060-0810, Japan, and J.Nishihira, Central Research Institute, Hokkaido University, Sapporo 060-8638, Japan.

MRP8 (macrophage migration inhibitory factor-related protein 8) is a calcium-binding protein belonging to the family of S100 proteins, which is mostly expressed in myeloid cells and monocytes in events of acute and chronic inflammation. This protein was identified together with MRP14 in the synovial fluid of rheumatoid arthritis; MRP8 and MRP14 are reported to be involved in various biological events such as cytoskeltal-membrane interactions, regulation of cellular differentiation and cell-cycle progression beyond inflammatory reaction. MRP8 possesses two calcium-binding EF-hands shown by biochemical studies; however, its three dimensional structure has not been reported. In this study, we attempted to solve the three dimensional structure of MRP8 in a complex with Ca^{2+} by X-ray crystallography.

The structure of human MRP8 in a complex with Ca^{2+} was determined at 1.9 Å resolution by X-ray crystallography. The structure was initially solved by MAD phasing of ytterbium(Yb)-substituted crystal. MRP8 monomer consists of two helix-loop-helix (EF-hand) motifs that are joined by a 8-residues linker, and each EF-hand binds one Ca^{2+}. The MRP8 dimer is formed by non-covalent interactions between large hydrophobic patches of the two monomers that are related by a non-crystallographic two-fold symmetry.

In the Yb-substituted structure, Ca^{2+} bound to the C-terminal EF-hand was substituted Yb^{3+}, whereas the N-terminal EF-hand was not. The differential affinity of these two EF-hands to Ca^{2+} may affect the protein conformation of MRP8, which may induce variable forms of the complex with MRP8 homodimer or heterodimer with MRP14.

P11.04.096 CRYSTAL STRUCTURE OF HUMAN D-DOPACHROME TAUTOMERASE AT 1.54Å RESOLUTION. Hiroshi Sugimoto, Masae Taniguchi, Atsushi Nakagawa, Isao Tanaka, Division of Biological Sciences, Graduate School of Science, Hokkaido University, Sapporo 060-0810, Japan, and Masaki Suzuki and Jun Nishihira, Central Research Institute, School of Medicine, Hokkaido University, Sapporo 060-0815, Japan

D-dopachrome tautomerase (DDT) shows a low sequence homology (33%) with the macrophage migration inhibitory factor (MIF) and possesses similar tautomerase activity as well. Recent studies have identified MIF as pituitary hormone and immunoregulator. Therefore, interest in the structure-function relationship between DDT and MIF has increased as regards inflammation and immune responses. The diffraction data of human DDT were collected at the Photon Factory and the initial model was obtained by molecular replacement method. We refined the model, yielding an *R* factor of 0.164 and a free *R* factor of 0.192 in the resolution range of 20-1.54Å. The crystal structure shows cylindrical homotrimeric formation that has extensive contact between subunits by inter-subunit β-sheets. Its overall topology and trimeric formations are similar to human MIF. The Pro1 is located at the bottom of a positively charged pocket in which the conformations of Lys32 and Ser63 are highly conserved. A detailed comparison with human MIF, bacterial CHMI, and 4-OT structures revealed significant differences in the active site, the inter-subunit contacts and charge distribution on the molecular surface. It can be concluded that these features are related to the physiological role and tautomerase activity of MIF and DDT.

P11.04.097 CRYSTAL STRUCTURE OF THE SM3 ANTIBODY AGAINST POLYMORPHIC EPITHELIAL MUCIN MUC1 J.M. Lally[1], P. Dokurno[1], J. Taylor-Papadimitriou[2] and P.S. Freemont[1] [1] Molecular Structure and Function Laboratory, [2] Epithelial Cell Biology Laboratory, ICRF, PO Box 123, London, WC2A 3PX

The MUC1 epithelial mucin is a transmembrane glycoprotein with the extracellular domain made up largely of exact tandem repeats of 20 amino acids, each of which contains five potential glycosylation sites. Attention has been focused on this mucin as a tumour antigen because not only is it over-expressed in breast and other carcinomas, but it is aberrantly glycosylated making it antigenically distinct from the normally processed mucin. In breast tumours, the O-glycans which are added are shorter, resulting in the exposure of epitopes on the core protein which are normally masked. Several monoclonal antibodies recognising the core of the MUC1 repeat unit have been reported [1]. We have solved the structure of one of these antibodies, namely SM3 in complex with a 13-residue fragment of the MUC1 repeat [2]. We have also collected diffraction data from the SM3 antibody in complex with the 13-residue peptide containing the β-D-N-acetylgalactosamine (GalNAc) bound to the central threonine residue of the MUC1 core.The electron density map shows density consistent with the presence of a sugar residue attached to the central threonine. Such a modified peptide would be more akin to the natural state of the mucin on the carcinoma cell surface.

[1] M.R. Price, et al.,*Tumor Biol.*, **19** (Suppl. 1) 1 (1998).
[2] P. Dokurno, P.A. Bates, H.A. Band, L. M.D. Stewart, J.M. Lally, J. Taylor-Papadimitriou, D. Snary, M.J.E. Sternberg, P.S. Freemont, *J. Mol. Biol.*, **284**, 713 (1998).

P11.04.098 GLYCOSYLATION AND FUNCTION? STRUCTURAL AND BIOLOGICAL CHARACTERISATION OF NONGLYCOSYLATED AND GLYCOSYLATED HBP. L.F. Iversen[1], P.B. Rasmussen[1], I.K. Larsen[2], H.J. Flodgaard[1] and J.S. Kastrup[2], [1]Novo Nordisk A/S, Novo Allé, DK-2880 Bagsvaerd, Denmark, [2]Dept. of Medicinal Chemistry, Royal Danish School of Pharmacy, Universitetsparken 2, DK-2100 Copenhagen, Denmark.

Previously, we have determined the structure of glycosylated heparin binding protein (HBP) [1] and elucidated the biological functions of HBP by the use of glycosylated protein (as it is found in vivo) [2]. HBP is strongly involved in host defence against infections. HBP is a chemoattractant for monocytes [3]. The three N-glycosylation sites of human HBP have been mutated to produce a nonglycosylated HBP (ng-HBP) mutant. ng-HBP has been crystallised and tested for biological activity. Complete X-ray data have been collected to 2.1 Å and the structure has been fully refined to an R-factor of 18.4%. The ng-HBP structure reveals that neither the secondary nor the tertiary structure have changed due to the removal of the glycosylation, compared to the glycosylated HBP structure. Although N-linked glycosylation occurs concomitant with polypeptide synthesis and therefore possesses the ability to influence early events in protein folding, we see no evidence of glycosylation influencing the structure of the protein. Also, the overall stability of ng-HBP seems to be unaffected as compared to glycosylated HBP as judged by the B-factors derived from the two X-ray structures. The flexibility of a glycosylation site might be determined by the local polypeptide sequence and structure rather than the specific glycosylation attached to a certain site The biological assay data indicate that ng-HBP has reduced potency as compared to its glycosylated counterpart, in that ng-HBP in combination with lipopolysaccharide (LPS), is less capable of stimulating monocytes cytokine release. The ability of ng-HBP to function as a LPS presenting protein towards the monocytes seems grately

affected by the removal of glycosylation. Protein fold, structure and stability are apparently similar for nonglycosylated and glycosylated HBP molecules, however the biological activity seems to be critically influenced by glycosylation.

1. Iversen L.F. et al., 1997. *Nature Struc.Biol.* 4:265-268.
2. Rasmussen P.B. et al.,1996. *FEBS letters* 390:109-112.
3. Flodgaard H.J. et al., 1991. *Eur.J Biochem.* 197:535-547.

P11.04.099 HUMAN HEPARIN BINDING PROTEIN: STRUCTURE AND FUNCTION OF TWO MUTANTS. A.K. Pedersen[1,2], L.F. Iversen[2], B.B. Stoffer[1], I.K. Larsen[1] and J.S. Kastrup[1]. [1]Department of Medicinal Chemistry, Royal Danish School of Pharmacy, Universitetsparken 2, 2100 Copenhagen, Denmark. [2]Novo Nordisk A/S, Novo Alle, 2880 Bagsværd, Denmark.

Heparin binding protein (HBP), also known as CAP37 or azurocidin, is a multifunctional protein with diverse and far reaching implications in host defence and inflammation. The antibiotic activity of HBP, directed against Gram-negative bacteria, was one of the first functions of HBP to be elucidated . HBP binds strongly to the lipid A component of endotoxin, and it has been suggested that the bactericidal effect of HBP is due to binding of lipid A [1].

HBP is an inactive serine protease homologue, and the inactivity is caused by selective mutations in the active-site triad (H41S and S175G). The human HBP exhibits 44 % sequence identity with human neutrophile elastase [2]. Despite the inactivity of HBP, the serine protease inhibitor BPTI (bovine pancreatic trypsin inhibitor) is still capable of binding to HBP [3].

HBP consists of 225 amino acid residues, possesses three putative N-glycosylation sites, and is highly glycosylated. Human HBP has been expressed in the baculovirus system as a 28 kDa protein, resulting in a glycosylation degree of 13 % [4]. The structure of native glycosylated HBP has been determined at 2.3 Å resolution at room temperature [1] and at 1.1 Å resolution at 120 K [5].

In order to identify amino acid residues of importance for lipid A and BPTI binding, respectively, two different mutants have been designed ([R23S,F25E]hHBP and [G175Q]hHBP). X-ray data have been collected to 2.5 Å and 1.9 Å, respectively, of the mutants. Structure determinations and refinements are in progress.

[1] L.F. Iversen, J.S. Kastrup, S.E. Bjørn, P.B. Rasmussen, F.C. Wiberg, H.J. Flodgaard, and I.K. Larsen, Nature Struct. Biology B 4, 265 (1997)
[2] H. Flodgaard, E. Østergaard, S. Bayne, A. Svendsen, J. Thomsen, M. Engels, and A. Wollmer, Eur. J. Biochem B 197, 535 (1991)
[3] L.C. Petersen, J.J. Birktoft, and H. Flodgaard, Eur. J. Biochem.. B 214, 271 (1993)
[4] P.B. Rasmussen, S. Bjørn, S. Hastrup, K. Norris, L. Thim, F.C. Wiberg, and H. Flodgaard, FEBS Lett. B 390, 109 (1996).
[5] S. Karlsen, L.F. Iversen, I.K. Larsen, H.J. Flodgaard, and J.S. Kastrup, Acta Cryst. D54, 598 (1998)

P11.04.100 STRUCTURAL STUDIES ON A N-TERMINALLY TRUNCATED C3d,g FRAGMENT OF THE COMPLEMENT SYSTEM. G. Zanotti, A. Bassetto, Dept. of Organic Chemistry and Biopolymer Research Center, U. of Padova, Padova, Italy, and M. Stoppini, Dept. of Biochemistry, U. of Pavia, Pavia, Italy and C. Folli, and R. Berni, Inst. of Biochemical Sciences, U. of Parma, Parma, Italy

The complement system is the primary humoral mediator of antigen-antibody reactions. It consists of at least 20 chemically and immunologically distinct plasma proteins capable of interacting with one another, with antibody, and with cell membranes. Following activation of the system, these interactions lead to the generation of biological activity which ranges from lysis of a spectrum of different kinds of cells, bacteria, and viruses to direct mediation of inflammatory processes.

Serum complement protein C3 plays a central role in both classical and alternative pathways of complement activation. The C3dg fragment, an activation product of C3, is involved in the amplification of antigen signal to B lymphocytes through the interaction with the B cell complement receptor CR2.

The C3dg fragment has been purified from rat plasma. A N-terminally truncated form of this fragment has been crystallised by vapour diffusion and diffraction data have been collected under cryogenic conditions by using the ELETTRA synchrotron source. Two crystal forms have been found: a) a tetragonal space group $P4_32_12$, with one molecule in the asymmetric unit and a resolution limit of 1.4 Å; b) an orthorhombic space group $P2_12_12_1$, with four molecules in the asymmetric unit and a resolution limit of 1.9 Å. The structure has been solved for both crystal forms, using the molecular replacement method, and refined. In both cases the C3d,g fragment presents a fold very similar to the C3d fragment [1] and a dimeric arrangement in the crystal.

[1] Nagar, B., Jones, R. G., Diefenbach, R. J.., Isenman, D. E. and Rini, J. M. Science 1998, 280, 1277-1281

P11.04.101 CRYSTAL STRUCTURE OF MHC CLASS II ASSOCIATED INVARIANT CHAIN FRAGMENT IN COMPLEX WITH CATHEPSIN L Gregor Guncar, Galina Pungercic, Ivica Klemencic, Vito Turk, Dusan Turk @ Department of Biochemistry and Molecular Biology, Josef Stefan Institute, Jamova 39, 1000 Ljubljana, Slovenia

Lysosomal cysteine proteases cathepsins S and L play crucial roles in degradation of invariant chain during maturation of MHC class II molecules and antigen processing. p41 form of invariant chain includes a fragment, which specifically inhibits cathepsin L but not S. The crystal structure of p41 fragment, a sequence homologue of the thyroglobulin type-1 domains, has been determined at 2.0 Å resolution in complex with cathepsin L. Structure of the p41 fragment has revealed a novel fold of cysteine protease inhibitors. It consists of two subdomains, each stabilized by disulfide bridges. The first subdomain is an α-helix - β-strand motif, whereas a β-strand arrangement is the predominant feature of the second subdomain. The wedge shape and three-loop arrangement of p41 fragment bound to the active site cleft of cathepsin L is reminiscent of the inhibitory edge of cystatins, and is the first observed example of convergent evolution in cysteine protease inhibitors. However, the different fold of the p41 fragment enables additional contacts with the top of the R-domain of the enzymes, which defines the specificity determining S2 and S1' substrate binding sites. This enables inhibitors based on the thyroglobulin type-1 domain fold, in contrast to the rather nonselective cystatins, to exhibit specificity for their target enzymes.

P11.04.102 STRUCTURAL BASIS FOR THE BINDING OF AN ANTI-CYTOCHROME C ANTIBODY TO ITS ANTIGEN. Shankari E. Mylvaganam [1,2], Yvonne Paterson [3] and Elizabeth D. Getzoff [1]. [1] The Scripps Research Institute, Dept. of Molecular Biology MB4, 10550 N. Torrey Pines Rd., La Jolla, CA 92037 USA, [2] Structural Bioinformatics, Inc., Dept. of Structural Sciences, 10929 Technology Place, San Diego, CA 92127 USA and [3] University of Pennsylvania, Dept. of Microbiology, PA 19104, USA.

The structural mechanism involved in the binding of the IgG_1 monoclonal antibody E8 to its highly charged protein antigen horse cytochrome *c* (cyt *c*) is revealed by the crystal structures of the antigen-binding fragment (Fab) of E8 bound to cyt *c* (FabE8-cyt*c*), determined to 1.8Å resolution, and of the uncomplexed Fab E8 (FabE8), determined to 2.26Å resolution. The antigen binds to the pre-formed V_L `hill' and $V_H$ `valley' shape of the grooved E8

paratope. The E8-cyt*c* association covers a buried surface area (1084Å^2) similar to that of other protein-antigen antibody interfaces, but is unique in that the E8 antibody uses V_L and V_H equally to bind its antigen. All six complementarity determining regions of E8 contact the antigen, covering three major discontiguous segements (33 to 39; 56 to 66; 96 to 104) and two minor sites on cyt *c*. This crystallographic definition of the E8 epitope complements and extends biochemical mapping and two-dimensional nuclear magnetic resonance with hydrogen-deuterium exchange studies. Local changes in atomic positions in both the cyt-*c* (of up to 9Å) and E8 (4Å) and 48 bound water molecules at the FabE8-cyt*c* interface facilitate antibody-antigen interactions. The antibody-antigen interactions include 13 hydrogen bonds, five ion pairs and 67 van der Waals contacts. Our comparative studies of FabE8-cyt*c* x-ray structure with the 1.8Å resolution x-ray structure of D1.3Fv-hen-egg-white lysozyme (HEL) complex reveal how the nearly identical V_L sequences of E8 and D1.3 antibodies bind to their respective antigens. Details of the antibody/antigen complementarity, conformational change, interactions and solvation will be presented.

P11.04.103 HIGH RESOLUTION CRYSTAL STRUCTURE OF FREE ANTIBODY HYHEL-63 AND COMPLEX WITH ITS ANTIGEN HEN EGG-WHITE LYSOZYME Hongmin Li[1], Yili Li[2], Sandra J. Smith-Gill[2] and Roy A. Mariuzza[1], [1]Center for Advanced Research in Biotechnology, University of Maryland Biotechnology Institute, 9600 Gudelsky Drive, Rockville, MD 20850 USA; [2]National Cancer Institute, National Institute of Health, Frederick, MD 21702-1201 USA

A detailed knowledge of the molecular basis of protein-protein recognition is an essential element in understanding protein function. Monoclonal antibodies specific to hen egg-white lysozyme have been studied extensively by X-ray crystallographic techniques, providing valuable information on the molecular architecture of protein-protein interactions. Here we report the high resolution crystal structure of the antigen binding fragment (Fab) of the monoclonal antibody HyHel-63, both free and bound to its protein antigen. HyHel-63 is an IgG2a(κ) antibody specific for hen egg-white lysozyme. The sequence of HyHel-63 is about 90% homologous to that of HyHel-10, a well characterized antibody specific for the same antigen. The affinity of HyHel-63 is lower than that of HyHel-10. Both the free Fab fragment and Fab complexed with lysozyme were crystallized in two crystal forms and four sets of X-ray diffraction data were collected to high resolution under cryo-conditions (for free Fab: space group C2: 2.0A; P1: 1.9Å; for the complex: space group $P4_22_12$: 2.0A; $P4_12_12$: 2.8Å). The epitope on hen egg-white lysozyme recognized by HyHel-63 is similar to that recognized by HyHel-10; however, some differences were observed between the two structures. A more detailed comparison of free and complexed Fab and of different crystal forms will be described.

P11.04.104 STRUCTURE OF THE SINGLE-CHAIN FV MFE-23: INTERMOLECULAR CONTACTS PROVIDE A MODEL FOR ANTIBODY-ANTIGEN INTERACTIONS M. K. Boehm[1,2], A. L. Corper[3], T. Wan[3], M. K. Sohi[3], B. J. Sutton[3], J. D. Thornton[2], P. A. Keep[2], K. A. Chester[2], R. H. J. Begent[2], S.J. Perkins[1] [1] Dept. Biochemistry and [2] Dept. Oncology, Royal Free Campus, Royal Free and UC Medical School, UCL, Rowland Hill St., London NW3 2PF, UK. [3] Randall Institute, King's College London, 26-29 Drury Lane, London WC2B 5RL, UK.

MFE-23 is an important murine filamentous phage-derived single-chain Fv antibody molecule which targets colorectal cancer through its specificity for carcinoembryonic antigen (CEA), a cell-surface member of the immunoglobulin superfamily. MFE-23 used in this study contains an N-terminal V_H domain joined by a $(Gly_4Ser)_3$ linker to a V_L domain (κ chain) with an 11-residue C-terminal myc-tag. The crystal structure was determined at 2.4 Å resolution by molecular replacement with an R_{cryst} of 19.0%. In the crystal lattice, two MFE-23 molecules were associated back-to-back, related by a crystallographic two-fold axis. Five of the six antigen-binding loops (*L1, L2, L3, H1, H2*) conformed to known canonical structures. The sixth loop *H3* was fitted to well-ordered electron density, and its structure was atypical of those previously described for H3 loops, being defined by a buried Thr-H100 residue. The antigen binding site displayed a large acidic region mainly located within *H2* and a large hydrophobic region within *H3*. A striking feature of the intermolecular packing within the crystal was a large region of contact and surface complementarity between the *H1*, *H2* and *H3* loops and the DEBA β-sheet of an adjacent molecule. These interactions involved salt bridges and hydrogen bonds, and the intermolecular contacts coincided with residues in *H1*, *H2* and *H3* that were predicted to be important for antigen contacts. A previously-described mutation that significantly perturbed MFE-23 binding to CEA corresponded to a *H3* residue that participates in these lattice contacts. It is concluded that these contacts may provide a model for antigen binding.

P11.04.105 LARGE PEPTIDE AND GLYCOPEPTIDE ANTIGEN PRESENTATION BY MHC CLASS I MOLECULES. Jeffrey A. Speir[1], James Stevens[2], Ussama M. Abdel Motal[3], Etienne Joly[2], Mikael Jondal[3], Kristen Fischer Lindahl[4], Geoff W. Butcher[2], and Ian A. Wilson[1], [1]The Scripps Research Institute, La Jolla CA USA, [2]The Babraham Institute, Babraham Cambridge UK, [3]Karolinska Institutet, Stockholm Sweden, [4]University of Texas Southwestern Medical Center, Dallas TX USA

Post-translationally modified peptides and peptides bulged from the MHC class I binding groove have the potential to alter T cell reactivity through hapten interactions with the TCR and altered exposed peptide conformations, respectively. We have determined the crystal structures of two representative MHC complexes having the largest and longest single peptides observed in MHC class I molecules. H-2Kb restricted glycopeptide RGY8-6h-Gal2 generates CTL expressing both a/b TCR, specific for glycopeptide, and g/d TCR, specific for the disaccharide. The 2.2A resolution crystal structure of Kb/RGY8-6h-Gal2 demonstrates the central region of the TCR footprint is dominated by the highly exposed carbohydrate and thus explains the generation of carbohydrate-specific T cell responses. Rat MHC class I RT1.Aa is believed to be the maternally-transmitted factor responsible for tissue graft rejection between rats expressing polymorphic forms of mitochondrial ATPase 6. Indeed, RT1.Aa complexed with a 13 residue peptide from ATPase 6 elicits full CTL activity in vitro and is the first rat CTL epitope and minor histocompatibility antigen identified at the molecular level. The preliminary crystal structure of RT1.Aa/13N3E reveals the N and C-termini of 13N3E are both anchored in the RT1.Aa binding groove and a distinct peptide conformation for each of the two molecules occupying the asymmetric unit. One conformation, free of crystal contacts, is bulged near the C-terminus highly exposing four of the peptide residues. The other conformation, influenced by crystal packing contacts, is in a completely different conformation in order to adapt to its new environment. Interestingly, the polymorphic residue of 13N3E remains highly exposed in either conformation. Together these complexes represent highly exposed MHC class I antigens that can readily change structure and therefore significantly alter the nature of the TCR-MHC interaction.

P11.04.106 THE CRYSTAL STRUCTURE OF HORSESHOE SHAPED HEMOLIN MONOMER: A NOVEL MECHANISM FOR HOMOPHILIC ADHESION? Xiao-Dong Su[1], Louis N. Gastinel[2], Pamela J. Bjorkman[3], [1]Department of Molecular Biophysics, Center for Chemistry and Chemical Engineering, P.O. Box 124, Lund University, S-221 00 Lund, Sweden, [2]AFMB, CNRS UPR 9039, 31 Chemin Joseph Aiguier, 13402 Marseille Cedex 20, France, [3]Division of Biology 156-29, and Howard Hughes Medical Institute, California Institute of Technology, Pasadena CA

Hemolin, an insect immunoglobulin superfamily member, is a lipopolysaccharide-binding immune protein induced during bacterial infection. The 3.1 Å crystal structure reveals a bound phosphate and patches of positive charge that may represent the lipopolysaccharide binding site, and a new and unexpected arrangement of four immunoglobulin-like domains forming a horseshoe. Sequence analysis and analytical ultracentrifugation suggest that the domain arrangement is a feature of the L1 family of neural cell adhesion molecules related to hemolin. These results are relevant to interpretation of human L1 mutations in neurological diseases, and suggest a domain swapping model for how L1 family proteins mediate homophilic adhesion.

P11.04.107 1.9Å STRUCTURE OF THERAPEUTIC ANTIBODY CAMPATH-1H Fab IN COMPLEX WITH A SYNTHETIC PEPTIDE ANTIGEN: A.C.Bloomer and L.C.James, MRC Laboratory of Molecular Biology, Hills Road, Cambridge CB2 2QH, UK and G.Hale & H.Waldmann, Sir William Dunn School of Pathology, South Parks Road, Oxford, OX1 3RE, UK

CAMPATH-1 antibodies have a long and successful history in the treatment of leukaemia, autoimmune disease and transplant rejection. The first antibody to undergo 'humanisation', CAMPATH-1H permits treatment with limited patient anti-globulin response. It recognises the CD52 antigen which is a small glycosylphosphatidylinositol(GPI)-anchored protein expressed on lymphocytes and it mediates cell depletion. We present the 1.9Å structure of Fab from CAMPATH-1H complexed with a peptide analogue of the antigenic determinant of CD52.

Analysis of the CAMPATH-1H binding site reveals features of the CDRs that contrast with most other known antibodies:
L3 plays a dominant role in antigen binding. H3 participates in only two main-chain interactions in CAMPATH-1H, although this loop is usually essential for effective antigen recognition.

The CAMPATH-1H binding site is highly basic; ionic interaction with the ethanolamine phosphate in the GPI anchor of CD52 has long been thought to be important in antigen binding. The structure reveals a number of important specific ionic interactions, including Lys53H but not Lys52bH as previously suggested. Prolonged treatment with CAMPATH-1H can lead to patient anti-idiotype responses which may be exacerbated by the unusually high number of basic residues in the antibody. This suggests that a strategy where redundant basic residues are replaced with neutral counterparts may be effective in further reducing the immunogenicity of this versatile and widely used antibody.

This CAMPATH-1H structure is guiding current antibody engineering in three important ways:

- rational design of a higher-affinity antibody
- removal of potentially immunogenic residues not affecting antigen-binding
- facilitating the design of non-binding mutants for use as tolerogens.

P11.04.108 THE STRUCTURE OF THE SUPERANTIGEN STAPHYLOCOCCAL ENTEROTOXIN H DETERMINED TO 1.7 Å RESOLUTION. M. Håkansson, K. Petersson, L. A. Svensson, Molecular Biophysics, Lund University, Box 124, 221 00 Lund, H. Nilsson, G. Forsberg, P. Björk, P. Antonsson, Active Biotech Research AB, Box 724, 220 07 Lund

Staphylococcal enterotoxin H (SEH) has been determined to 1.7 Å resolution using data from the crystallographic beamline, BL711, at the MAX-laboratory. It has the conventional superantigen fold; a β-grasp domain and a smaller β-barrel domain. Superantigens are molecules of biological interest, since they trigger the immunosystem by cross-linking T cell receptors (TcR) and MHC class II molecules in a more non-specific way than a normal antigen. SEH has a pI of 5.7 and exhibits a markedly negatively charged surface in a probable MHC class II binding region. The large deviations in both MHC and TcR binding regions implies substantial differences in receptor interactions compared to related superantigens. SEH was solved by molecular replacement technique making use of the SEA structure (Schad *et al*, 1995) as a model. SEA and SEH share 37 % sequence identity and the root mean square deviation of Cα between the structures are 2Å. At present the SEH model contains 210 amino acids, 100 water and four sulphate molecules. The R- and R_{free}-factors are 0.204 and 0.235, respectively.

Schad EM, Zaitseva I, Zaitsev VN, Dohlsten M, Kalland T, Schlievert PM, Ohlendorf DH, Svensson LA. 1995. Crystal structure of the superantigen staphylococcal enterotoxin type A. EMBO J 14: 3292-3301.

P11.04.109 THE 2.16 Å REFINED STRUCTURE OF 38-KDA PROTEIN ANTIGEN B (PAB) FROM *MYCOBACTERIUM TUBERCULOSIS*. Nand K. Vyas, Meenakshi N. vyas, Abha Choudhary and Florante A. Quiocho. Department of Biochemistry and Howard Husghes Medical Institute, Baylor College of Medicine, Houston, Tx-77030, USA

The World Health Organization (WHO) estimates that about one third of the world population is infected by mycobacteria of *M. tuberculosis complex*. Tuberculosis kills about 2 to 3 million people each year. The efficacy of BCG vaccine varies from 0 to 80% when tested in different population of the world. The multi-drug-resistant tuberculosis and the high susceptibility of tuberculosis in HIV/AIDS infected population are the major public health concerns according to the WHO. For rational design of diagnostic reagents and subunit vaccines, high resolution structures of several species-specific antigens are needed. Among well characterized secreted protein antigens, the 38 kDa protein antigen b (Pab) from *M. tuberculosis* is a species-specific immunodominant antigen. We have determined the X-ray structure of this antigen to understand its biological and immunological functions. We have previously demonstrated unequivocally that Pab is phosphate-binding protein, that, like its couterpart in gram-negative bacteria, is involved in active transport.

To determine the three-dimensional structure of Pab, a recombinant protein prepared in our laboratory, was used to obtain single crystals by vapour diffusion method. X-ray diffraction data from a orthorhombic single crystal (space group P2(1)2(1)2 and cell dimensions: a=125.38 Å, b= 71.27Å and c=73.43 Å) were collected to 2.16 Å resolution. An Initial Pab structure, two molecules (A and B) in the asymmetric unit, was determined by docking of the structure of *E. coli* phosphate-binding protein (PBP) in the 4.0 Å MIR electron density map. Refinement of the Pab structure at 2.5 Å resolution showed that the electron density for molecule B was weaker than the molecule A. At this stage R-factor was 0.27 and R-free was 0.37, which indicated a possible positional disorder in molecule B. We have

now determined two postions for molecule B in the asymmetric unit of cell and free-R is 0.27 and regular R-factor is 0.24 for the 2.16 Å resolution data. The refined structure has allowed us to determine antigen-phosphate interactions and mapping of the known B and T cell epitopes.

P11.04.110 STRUCTURE, FUNCTION AND EVOLUTION OF SERUM PENTRAXINS FROM INVERTEBRATES TO HUMANS. Trevor J. Greenhough, Annette K. Shrive, Mohamed A. Ramadan, Alison M. Metcalfe, Jamie R. Cartwright and Margaret Hopkins, School of Life Sciences, Keele University, Keele, Staffs ST5 5BG, UK

The serum pentraxins C-reactive protein (CRP) and amyloid P-component (SAP) are members of a conserved family of cyclic oligomeric Ca-binding proteins, homologues of which have been found in mammals, fish, amphibians and the phylogenetically ancient horseshoe crab *Limulus polyphemus*. In humans, CRP plays a pivotal and complex role in the immune response and is the classical acute-phase reactant produced in response to tissue damage and inflammation. SAP-like pentraxin homologues are circulating lectins. Humoral components, such as the pentraxins, which are directly implicated in non-specific host defence and innate immunity and which have been preserved over long evolutionary periods, provide an ideal basis for the study of the evolution of the immune system and of molecular phylogeny and protein evolution.

The sequence homology and conservation of the pentraxins, and of their ligand-binding specificities has long since been recognised and evidence from electron micrographs has suggested that the cyclic nature of protomer aggregation across species is generally conserved. A more detailed view of these structures at the x-ray level shows that while the protomer fold and a cyclic mode of aggregation are conserved, the number of protomers and their relative orientations within the cyclic, biologically functional oligomer show remarkable variations between species.

The crystal structures of pentraxins from four species ranging from an invertebrate to humans will be presented. The conservation and evolution of the pentraxins and their ligand-binding specificities, their relationship to lectins, and the resulting implications for the evolution of innate immunity, will be discussed in the light of this new structural evidence.

P11.04.111 CHLOROQUINE BINDS TO L-LACTATE DEHYDROGENASE IN THE MALARIAL PARASITE (*PLASMODIUM FALCIPARUM*. Jonathan A. Read, Kay W. Wilkinson, Rebecca Tranter, Richard B. Sessions & R.Leo Brady, Department of Biochemistry and Centre for Molecular Recognition, University of Bristol, Bristol BS8 1TD.

Although the molecular mechanism by which chloroquine exerts its effects on the malarial parasite *Plasmodium falciparum* remains unclear, the drug has previously been found to interact specifically with the glycolytic enzyme lactate dehydrogenase from the parasite. In this study we have determined the crystal structure of the complex between chloroquine and *Plasmodium falciparum* lactate dehydrogenase. The bound chloroquine is clearly seen within the NADH binding pocket of the enzyme, occupying a similar position to the adenyl ring of the cofactor. Chloroquine hence competes with NADH for binding to the enzyme, acting as a competitive inhibitor for this critical glycolytic enzyme. Specific interactions between the drug and amino acids unique to the malarial form of the enzyme suggest this binding is selective. Inhibition studies confirm that chloroquine acts as a weak inhibitor of lactate dehydrogenase, with mild selectivity for the parasite enzyme. As chloroquine has been shown to accumulate to millimolar concentrations within the food vacuole in the gut of the parasite, even low levels of chloroquine within the host blood may contribute to the biological efficacy of the drug and explain how specificity problems are not encountered. The structure of this enzyme-inhibitor complex provides a template from which the quinoline moiety might be modified to develop more efficient inhibitors of the enzyme.

P11.04.112 SINGLE POINT-MUTATION YIELDS 30-FOLD INCREASE IN BINDING AFFINITY OF A CARBOHYDRATE-SPECIFIC SCFV. Sonia I. Patenaude [1], Roula Thomas [1], C. Roger MacKenzie [2], N. Martin Young [2], Stephen V. Evans [1], [1] Department of Biochemistry, University of Ottawa, Ottawa K1H 8M5, Ontario, Canada, [2] Institute for Bioclogical Sciences, National Research Council of Canada, Ottawa K1A 0R6, Canada

The interactions between carbohydrate-specific antibodies and their antigens are typically of low affinity. Part of this weak binding lies in the fact that carbohydrate antigens are generally T-cell independant and cannot induce affinity maturation. Generation of mutant monoclonal antibodies with higher affinity for their carbohydrate antigens while maintaining the specificity of the wild-type antibody has proven challenging. We have used the three-dimensional crystal structure of an antibody scFv specific for the blood group A oligosaccharide antigen to design a number of site-directed mutants which show improved affinity while maintaining specificity. The higher affinities can be directly correlated with trends in amino acid mutations such as polarity, surface complementarity and side chain aliphatic character.

P11.04.113 INCOMPLETE MIMICRY OF THE RODENT BY A HUMANIZED FORM OF AN ANTI-γ-INTERFERON ANTIBODY. P.A. Ramsland, Z.-C. Fan, L.W. Guddat[†] and A.B. Edmundson. Oklahoma Medical Research Foundation, 825 NE 13th Street, Oklahoma City, OK 73104, USA. [†]Present address: Centre for Drug Design and Development, University of Queensland, St Lucia, Qld 4072, Australia.

The three-dimensional structures of "humanized" and mouse-human chimeric antigen-binding fragments (Fabs) of a murine anti-γ-interferon antibody have been determined by X-ray analyses at 2.9 Å resolution (Fan *et al*., J. Mol. Recognit. **12**:19-32). Comparison of these structures revealed that three of the four domains are nearly identical: V_L and C_L of the light (L) chains and C_H1 of the heavy (H) chains. However, the complementarity determining regions (CDRs) of the V_H domains do not resemble each other to the degree expected of loops with identical sequences. The substitution of serine for proline at position 7 allowed the N-terminal segment (designated 4-1) of the humanized V_H to be closely juxtaposed with the adjacent β strand (4-2). This tightening resulted in a decrease in space available for the last portion of the H chain framework region 1 (HFR1) and the first part of HCDR1, and led to the formation of an α-helix involving residues 25-32. In the humanized Fab, HCDR1, which is sandwiched between HCDR2 and HCDR3, modified the structures of both regions. HCDR2 was forced into a bent and twisted orientation both at the crown (around proline H52a) and the base of the loop. HCDR3 was also adjusted in shape and topography. In summary, the structural effects of humanization were (1) to increase the order of the HCDRs; (2) to confine the HCDRs into a smaller space; and (3) to change the directionality, accessibility and relative positions of side chains likely to serve as contacts in the binding of the γ–interferon antigen. Similarities in binding affinities of the two molecules can be rationalized by limited induced fit adjustments in their structures on antigen binding.

We thank, for supplying the antibodies, Protein Design Labs, Inc., Mountain View, CA 94043, USA.

P11.04.114 THE STRUCTURE AND MECHANISM OF THE BIOTIN BIOSYNTHETIC ENZYMES. D.Alexeev and L.Sawyer, Structural Biochemistry, ICMB, The University of Edinburgh, Michael Swann Building, King's Buildings, Mayfield Road, Edinburgh EH9 3JR, UK, and D.J.Campopiano, M.Alexeeva, S.P.Webster and R.L.Baxter, Edinburgh Centre for Protein Technology, The University of Edinburgh, Joseph Black Chemistry Building, West Mains Road, Edinburgh EH9 3JJ, UK.

Biotin is a vitamin synthesised only by bacteria and plants. They cannot use external biotin and have to rely on their own. We receive biotin from eating plants, and this makes the biotin biosynthetic pathway attractive for engineering the herbicides harmless to humans. Biotin is synthesised in four steps by four major enzymes: the products of the genes *bioF*, *bioA*, *bioD* and *bioB*. We have cloned, expressed and purified all four of them. Three enzymes have been crystallised: 8-amino-7-oxonanoate synthase (AONS, the product of the gene *bioF*), 7,8-diaminonanoate synthase (DANS from the gene *bioA*) and dethiobiotin synthetase (DTBS from *bioD*). We have solved the structures of AONS and DTBS and present the detailed study of their reaction mechanisms here.

DTBS is a unique ATP-dependent carboxylase that catalyses the insertion of CO, derived from carbon dioxide, in between the vicinal amino groups of the substrate, eventually resulting in formation of the *ureido* ring of dethiobiotin, the immediate precursor of biotin. We have examined by crystallography various trapped complexes of DTBS with substrates, products, reaction intermediates and their mimics. This information has been combined with kinetic measurements and site directed mutagenesis from which we propose the reaction mechanism and present a design for an inhibitor which targets the adenine binding site.

AONS belongs to the α-family of pyridoxal-5'-phosphate dependent enzymes. We present the structure of AONS in both the apo- and holo- forms, the structure of a reaction intermediate and the inhibited form of the enzyme. By analogy with related PLP-enzymes and using our spectroscopic, structural and mutational data, we have modelled the mechanism of AONS.

P11.04.116 NEW CRYSTAL FORM AND HIGH-RESOLUTION ANALYSIS OF PHOTO-REACTIVE NITRILE HYDRATASE IN THE ACTIVE FORM. Y. Kawano, N. Kamiya [1], N. Odaka, M. Yohda, I. Endo [2], [1] Division of Protein X-ray Crystal Analysis, RIKEN Harima Institute, The Institute of Physical and Chemical Research (RIKEN), Mikazuki-cho, Sayo-gun, Hyogo, 323-3, Japan. [2] Biochemical Systems Laboratory, The Institute of Physical and Chemical Research (RIKEN), Wako, Saitama 351-01, Japan.

Nitrile Hydratase (NHase) catalyzes the hydration of nitrile compounds to their corresponding amides and is used for the industrial production of acrylamide. NHase produced from Rhodococcus sp. N-771 consists of a- and b- subunits each with molecular weights of about 23k Da. The enzyme has a catalytic center of non-heme iron surrounded by a sequence of C109-X-L-C112-S-C114 in the a-subunit, which is highly consensus around NHases already known. The iron center is associated with an endogeneous nitric oxide (NO) in the inactive form, and the dissociation of NO molecule by irradiation of visible light leads the enzyme to the active form. The crystal structure of the inactive NHase has been analyzed at 1.7Å resolution by our group (Nature Struc. Biol. 5, 347-351 (1998)). This work clearly shows the NO molecule as a sixth ligand of the iron center. The NO molecule is stabilized by an unusual claw setting composed of three oxygen atoms of C112-sulfinic acids, hydroxyl group of S113 and C114-sulfenic acid. The two of three cystein residues in the consensus sequence of claw setting are post-translationally modified. The crystal structure of active NHase has also been analyzed by the other group (Structure 5, 691-699 (1997)). Unfortunately, however, the structure is only at a resolution of 2.6Å, which is insufficient for clarifying the claw setting structure in the active form. In order to realize much higher resolution analysis for the active NHase, we have searched a new crystal form. The new crystal obtained belongs to monoclinic system, space group C2 with cell dimensions of a=113.8Å, b=60.2Å, c=81.6Å, b=125.1º, and diffracts up to 1.5Å resolution. The high-resolution analysis of active enzyme will reveal conformational changes of the claw setting structure between the inactive and active NHases.

P11.04.117 STRUCTURAL ALLERGOLOGY: MAPPING B-CELL EPITOPES FROM CRYSTALLOGRAPHIC DATA. M. Gajhede, O. Mirza and A. Henriksen, Protein Structure Group, Department of Chemistry, Copenhagen University, Universitetsparken 5, DK-2100 Copenhagen, Denmark and H. Ipsen and M. D. Spangfort, Biochemical Allergy Research, ALK-Abelló, Bøge Alle 6-8, DK-2970 Hørsholm, Denmark.

The prevalence of allergic disorders has steadily increased in the Western world during the last decade and atopic individuals often show allergic reactions in response to protein allergens derived from pollens of trees and grasses, house dust and storage mites, animal dander and moulds. There are signs indicating that this increase is related to the general changes in the environment that has occurred during the later decades. Since allergy can have very severe symptoms or even be lethal, improved therapeutic tools (vaccines) is one of the large challenges of the next decade. One of the possible targets of a vaccine are the B-cell epitopes that can be identified using a combination of sequence alignments of related allergens and structure determination.

We have previously studied the conserved surface patches on the major allergen from birch pollen Bet v 1[1]. Here three patches on Bet v 1 was identified as common for the known major tree pollen allergens based on sequence alignment. Thus, any IgE recognizing these patches on Bet v 1 are prospective dominant epitopes and will be able to cross-react and bind to other Fagales major pollen allergens and give rise to allergic symptoms.

In order to confirm these results the two participants have done the crystal structure of a complex between Bet v 1 and the Fab fragment of a murine monoclonal antibody raised against Bet v 1 (BV16 Fab) (Mirza et al. submitted). The structure of the Bet v 1-BV16 Fab complex showed that the interaction surface was identical to one of the 3 predicted epitopes.

Recently we have done the structure of Ves v 5, a major allergen from the wasp venom (Henriksen et al. in preparation). Since there was not significant sequence similarity to any protein with known structure, the structure was solved by the MIR method to 1.9 Å resolution. An analysis of the structure and the B-cell epitopes will be presented.

1. Gajhede M, Osmark P, Poulsen FM, Ipsen H, Larsen JN, Joost vNR, Schou C, Lowenstein H, Spangfort MD: X-ray and NMR structure of Bet v 1, the origin of birch pollen allergy. Nat.Struct.Biol. 3:1040, 1996

P11.04.118 CRYSTAL STRUCTURE ANALYSIS OF FV FRAGMENT OF ANTIBODY (HYHEL10) COMPLEXED WITH HEN EGG LYSOZYME. H. Kondo, Bioscience and Chemistry Division, Hokkaido National Industrial Research Institute, Tsukisamu-Higashi 2-17, Toyohira, Sapporo 062-8517, Japan, K. Tsumoto, M. Shiroishi, Department of Biomolecular Engineering, Graduate School of Engineering, Tohoku University, Sendai 980-8579, Japan, M. Matsushima, Rational Drug Design Laboratories, Fukushima 960-1242, Japan, and I. Kumagai, Department of Biomolecular Engineering, Graduate School of Engineering, Tohoku University, Sendai 980-8579, Japan

In order to elucidate roles of non-covalent forces involved in antigen-antibody interactions in the structural aspects, we determined three-dimensional structure of Fv fragment of wild-type anti-hen egg white lysozyme (HEL) monoclonal antibody HyHEL10 complexed with HEL at 2.3Å resolution limit by molecular replacement method using HyHEL10 Fab fragment-HEL structure (Padlan *et al*., PDB code:3HFM) as a search model. In Fv-HEL complex, a salt bridge, which has not been observed in Fab-HEL complex, are found. In addition, some water molecules are found to locate in Fv-HEL interface, forming water-mediated hydrogen bonds between antigen and antibody. Furthermore, the area of the interface increases in about 10%. These structural changes are considered to compensate for unfavorable effect which is occurred by deletion of the constant regions of Fab, leading to the minimum decreased affinity of the antibody Fv fragment toward its antigen.

P11.04.119 CRYSTAL STRUCTURE OF S. CEREVISIAE UBC1 - CONFORMATIONAL FREEDOM IN A UBIQUITIN CONJUGATING ENZYME. R.S. Williams, R. Green, G. Garen, M.J. Ellison and J.N.M. Glover, Department of Biochemistry, University of Alberta, Edmonton, Alberta, T6G 2H7, Canada

The crystal structure of the core catalytic domain (aa 1-150) of Saccharomyces cerevisiae ubiquitin conjugating enzyme 1 has been determined at 1.9Å resolution. Ubc1(1-150) crystallized as a dimer and comparison of the two molecules in the monoclinic (p21) asymmetric unit reveal that Ubc1(1-150) can exist in distinct open and closed conformations. Regions conferring domain motion have been delineated through analysis of RMS phi-psi differences and alpha-carbon displacements of least-squared aligned coordinates for the two monomers. Comparisons with nuclear magnetic resonance dynamics data for human Ubc9 [1] indicate common regions of flexibility in Ubc core domains.

1. Q. Liu, Y-C. Yuan, B. Shen, D.J. Chen, and Y. Chen (1999). Biochemistry, 38, 1415-1425.

P11.04.120 CRYSTAL STRUCTURE OF A MAMMALIAN PURPLE ACID PHOSPHATASE WITH A μ-(HYDR)OXO BRIDGED DI-IRON CENTER. Eva H. Johansson[1] , Ylva Lindqvist[1], Helena Kaija[2], Pirkko Vihko[2] and Gunter Schneider[1], [1]Department of Medical Biochemistry and Biophysics, Karolinska Institutet, S-171 77 Stockholm, Sweden and [2]Biocenter Oulu and WHO Collaborating Centre for Research on Reproductive Health, University of Oulu, FIN-90220 Oulu, Finland

The crystal structure of purple acid phosphatase (PAP) from rat bone has been determined by molecular replacement and the structure has been refined to 2.2 Å resolution to an R-factor of 21.3 % (R-free 26.5 %). The core of the enzyme consists of two seven-stranded mixed β-sheets, with each sheet flanked by solvent-exposed α-helices on one side. The two sheets pack towards each other forming a β-sandwich. The di-iron center, located at the bottom of the active site pocket at one edge of the β-sandwich, contains a μ-hydroxo or μ-oxo bridge and both metal ions are observed in an almost perfect octahedral coordination geometry. The electron density map indicates that a μ-(hydr)oxo bridge is found in the metal center and that at least one solvent molecule is in the first coordination sphere of one of the metal ions.

The crystallographic study of rat PAP reveals that the mammalian enzymes are very similar in the overall structure to the plant enzymes in spite of 18 % overall sequence identity. In particular, coordination and geometry of the iron cluster is preserved in both enzymes and comparison of the active sites suggests a common mechanism for the mammalian and plant enzymes. However, significant differences are found in the architecture of the substrate binding pocket.

P12.04.001 HEMAGGLUTININ-NEURAMINIDASE FROM NEWCASTLE DISEASE VIRUS - THE CONTINUING SAGA. S.J. Crennell, A. Portner,[†] T. Takimoto,[†] and G.L.Taylor[‡]. School of Biology and Biochemistry, University of Bath, BA1 7RH, U.K.[†]St Judes Childrens Research Hospital, Memphis, TN, U.S.A. [‡]School of Biomedical Sciences, University of St. Andrews, KY16 9TS, U.K.

Hemagglutinin-Neuraminidase, (HN), one of the two surface proteins of paramyxoviruses, mediates the attachment of the virus to host cells and as such is a candidate for drug design not only against Newcastle disease (NDV), but also mumps and parainfluenza[1] whose HN share 33 and 25% sequence identity respectively with NDV HN.

HN was crystallised from 0.2M$(NH_4)_2SO_4$, 25%PEG4K and 0.1M acetate buffer pH4.6 in space group $P2_12_12_1$ with cell a≈73,b≈78 c≈200 Å. Native X-ray data have been collected to 1.98Å resolution on beamline X11 of the DESY synchrotron, Hamburg. HN has a predicted[2] structural similarity to influenza neuraminidase which shares 17% sequence identity but molecular replacement using the structures of influenza neuraminidases, bacterial neuraminidases or models based on these has been unsuccessful.

The crystals are very flexible, surviving abrupt changes of 3 pH points with severe lack of isomorphism being a major problem. 40 different native data sets and 165 derivative data sets at a variety of pH have cell dimensions varying by up to 16Å and have not yielded an isomorphous derivative. Multi-wavelength anomalous dispersion data collected on ESRF beamline BM14 from a Di-μ-iodobis(ethylene diamine)diplatinum(II) nitrate (PIP)-soaked crystal were processed with PHASES to give an overall figure of merit of 0.498 to 3.2Å. Phase extension has not yet given an interpretable map even when combined with in-house phased data sets in multi-crystal averaging.

1. T. Bousse, T. Takimoto, A. Portner, *Virology*, **209**, 654, (1995).
2. P.M.Colman, P.A.Hoyne, M.C.Lawrence, *J. Virology*, **67**, 2972, (1993).

P12.04.002 EXPRESSION AND PURIFICATION OF RECOMBINANT EBOLA VIRUS NUCLEOPROTEIN FOR CRYSTALLOGRAPHIC STUDIES. J.A. Potter and G. L. Taylor, University of Bath, Claverton Down, Bath, BA2 7AY, UK, and A. Fooks, CAMR, Porton Down, Salisbury, Wiltshire, SP4 OJG, UK.

The Ebola virus is an extremely virulent African haemorrhagic fever virus belonging to the *Filoviridae* family. The virions are composed of a central core formed by a ribonucleocapsid complex (RNP) which is surrounded by a lipid envelope derived from the host cell plasma membrane. The major structural RNP protein is the 83.3 kDa nucleoprotein (NP). The N-terminal 400 amino acids of NP show a high degree of homology within the filovirus family (1). This region, in common with other nonsegmented, negative strand RNA viruses, is hydrophobic. The less-conserved hydrophilic C-terminal half is highly acidic and may facilitate virion assembly by interacting with the matrix proteins or the putative second nucleoprotein, VP30.

Recombinant NP (cloned from Zaire subtype of Ebola virus) has been expressed as a histidine-tagged fusion protein in S*podoptera frugiperda* (Sf9) cells using the baculovirus expression system. The protein has an observed molecular weight of 104 kDa as determined by SDS PAGE and Western blots using both guinea-pig sera and anti-histidine monoclonal antibody. The

histidine-tagged protein will be purified by chromatography using resins charged with nickel ions. The purified sample will be used for crystallisation trials with the ultimate aim of deriving the atomic structure of NP using x-ray crystallography.

1. A. Sanchez, M.P. Kiley, B.P. Holloway, J.B. McCormick, and D.D. Auperin (1989). Virology 170, 81-91.

P12.04.003 TOWARDS THE STRUCTURE OF THE HERPES SIMPLEX VIRUS 1 SINGLE STRANDED DNA BINDING PROTEIN. Marina Mapelli, Hans van der Zandt and Paul Tucker, European Molecular Biology Laboratory, 69112 Heidelberg, DE.

ICP8 is the Herpes Simplex Virus 1 (HSV 1) single-stranded DNA-binding protein. It is a 128KDa nuclear zinc metalloprotein and participates in all the processes related to DNA replication, recombination and repair. It also has a function in the regulation of late gene expression. ICP8 binds ssDNA sequence non-specifically and cooperatively. The stoichiometry of binding falls in the range of 12 to 22 nucleotides, with a K_d of 0.2 mM and a cooperativity parameter ω of 38.

ICP8 is expressed in insect cells infected with a recombinant baculovirus. Purification is achieved by affinity and size exclusion chromatography. Despite the tendency to aggregation, it is possible to obtain a soluble and monomeric sample suitable for crystallization trials. The first ICP8 crystals grew by vapour diffusion in hanging drops as very thin plates. They exhibited poor (d_{min} = 7Å) and anisotropic diffraction.

Investigations were started in order to reduce the sources of structural or conformational microheterogeneities within the protein or between domains.

Limited proteolysis experiments in the presence and absence of ssDNA, suggested the existence of a 300 residue N-terminal domain not directly involved in DNA binding. The deletion mutant was produced but was found to be insoluble, probably indicating that a hydrophobic surface exists between domains. Genetic evidence supported by sequence analysis suggested that a 28 residue C-terminal tail, containing the nuclear localization signal, is likely to be unstructured and exposed. Therefore a mutant lacking 60 residues at the C-terminus was designed (ICP8ΔC). This mutant is soluble and monomeric and crystallizes under several conditions. Crystals are thicker, but retain a platy morphology. Nevertheless the diffraction pattern is greatly improved leading to a maximum resolution of 3.5Å. Recently two cysteines mapped on the N-terminal part of the protein, were identified as responsible for the cooperative nature of the binding [1], in agreement with the previous findings that cooperativity involves intermolecular contacts between free sulphidryl groups. We therefore decided to mutate the two cysteines to serines, to improve the protein stability and hopefully favour crystal growth. The new crystals look promising but their characterization is still at a preliminary stage.

1. Dudas, K.D. and Ruyechan, W.T. (1998) J. Virol. *72*, 257-265.

P12.04.004 STRUCTURAL MODEL FOR THE RNA IN SATELLITE TOBACCO MOSAIC VIRUS. A. McPherson, S. B Larson, J. Day, A. Greenwood, and Yu. G. Kuznetsov. University of California, Irvine, Molecular Biology & Biochemistry, Irvine, CA 92697-3900.

The 1.8 Å structure of satellite tobacco mosaic virus (STMV) reveals approximately 50% of the genomic RNA organised as helical segments centred at icosahedral twofold axes, plus additional "free nucleotides". Proteolysis of 17 nm virions was shown by QELS to result in stable particles of 11 nm diameter which corresponds to the diameter of the RNA core. Amino terminal strands of protein subunits, the last twelve residues of which bear seven positive charges, appear to be included in the nucleic acid cores. Using QELS, it was shown that RNA cores remained condensed particles to about 75º C. Preparations of STMV, when examined by AFM, also showed some helicoid bodies of about 40-50 nm. which apparently reflect the structure of the RNA molecules when released from the virion. Low resolution difference Fourier analyses allowed us to delineate the paths of amino terminal strands which wrap tightly around the helical segments of RNA. An idealised model was constructed of the entire encapsidated RNA molecule based on the most efficient path of thirty helical stem–loop elements, connected by single stranded linkers, passing from dyad to dyad. The model consumes virtually all of the 1058 available nucleotides. Analysis of RNA base sequence in terms of secondary structure shows it is compatible with the model in that thirty stem–loop elements could indeed be expected to appear along the RNA. The predicted stems, based on Watson–Crick base pairing, vary in the number of base pairs, and have loops of variable sizes. Nonetheless, the array of stem–loop elements is a realistic variation on the idealized model, and is consistent with the RNA distribution observed by X-ray analysis.

P12.04.005 THE ROLE OF CAPSID PROTEIN INTERACTIONS IN THE DETERMINATION OF PARVOVIRAL TROPISM AND PATHOGENICITY. Mavis Agbandje-McKenna[1], Antonio Llamas-Saiz[2], Concepción Foces-Foces[2], Eva Hernando[3], Jose M. Almendral[3], Maria Kontou[1], Ian Portman[1], Robert McKenna[1]. [1]Department of Biological Sciences, University of Warwick, Coventry, CV4 7AL, UK; [2]Departmento de Cristografía, Instituto de Química-Física "Rocasolano", CSIC, Serrano 119, 28006 Madrid, Spain; [3]Centro de Biología Molecular "Severo Ochoa" (UAM-CSIC), Universidad Autónoma de Madrid, Cantoblanco, 28049 Madrid, Spain.

The successful infection of a host cell by a virion involves a series of macromolecular interactions. For the ssDNA parvoviruses, including minute virus of mice (MVM), canine parvovirus (CPV), feline parvovirus, porcine parvovirus and Aleutian mink disease parvovirus , the capsid protein has been shown to play a crucial role in host cell tissue tropism *in vitro* and pathogenicity *in vivo*. Two allotropic variants of MVM, MVMp (prototype fibrotropic strain) and MVMi (immunosuppressive strain), can serve as ideal models for defining tropism and pathogenicity-specific capsid interactions for the *Parvoviridae*, as a result of their pronounced differences in tissue tropism and pathogenicity, despite their 97% identity at the nucleotide level, with only 14 amino acids differing between the sequence of their major capsid protein, VP2.

The high resolution structure of infectious virions and empty capsids of MVMi has been determined by X-ray crystallography. Analysis of the MVMi capsid structure indicated that amino acids which differ between MVMi and MVMp, and have been identified, by molecular genetics, as being important for host tropism are clustered on the capsid surface, most likely forming a surface feature used for receptor recognition. The residues are involved in both intra- and inter-subunit interactions. This analysis also suggested that capsid stabilising interactions in MVMi involving allotropic amino acids were less likely to exist in MVMp, offering a possible explanation for their observed tropism differences since the block in restricted infections appears to be due to the inability of this capsid region to interact with differentiation specific host cell factors. The structure of the MVMp capsid has been determined to 3.25Å resolution. The analysis of the MVMp capsid structure, its comparison to the available MVMi capsid structure and the functional implications of their capsid protein interactions, particularly with respect to *in vitro* tissue tropism and *in vivo* pathogenicity, will be presented.

P12.04.006 CRYSTAL STRUCTURE OF TOBACCO NECROSIS VIRUS AT 2.25 Å RESOLUTION. K. Fukuyama, Y. Oda, K. Saeki, Department of Biology, Osaka University, Toyonaka, Osaka 560-0043, Japan, T. Maeda, Research Institute for Bioresouces, Okayama University, Kurashiki, Okayama 710-0046, Japan and H. Naitow, T. Tsukihara, Institute for Protein Research, Osaka University, Suita, Osaka 565-0871, Japan

Tobacco necrosis virus (TNV) is a spherical virus and is often associated with its satellite virus, satellite tobacco necrosis virus. TNV contains ss-RNA as a genome which is about 3.8 kb long. The virus shell consists of 180 subunits of a single protein (ca. 30 kDa), which are arranged in a T=3 icosahedral surface lattice. The amino acid sequence of the coat protein of TNV used in this study was determined by protein and c-DNA analyses. TNV was crystallized in the space group $P4_232$ with a=b=c=336.4 Å and two particles are in the unit cell [1,2]. The asymmetric unit contains 15 subunits (5 subunits for each A, B, and C subunits).

X-ray diffraction data were collected at room temperature with oscillation method ($\Delta\omega$=0.5°) using synchrotron radiation (λ=1.00 Å) of BL6A at PF, Tsukuba, Japan. 298,768 unique data to 2.25 Å resolution were obtained with R_{merge}=7.9 % and completeness=99 %. Starting from the ($2F_o$-F_c) map at 5 Å resolution [3], the resolution of the map was extended by solvent flattening and 5-fold averaging of the electron density. Most amino acid residues could be unambiguously identified in the final electron density map. 86 residues at the amino-termini of the A and B subunits and 56 residues of the C subunit were disordered. Refinement by X-PLOR yielded R=25.3 % and R_{free}=27.3 % for the 2.25 Å resolution data. The subunit proteins have Jelly roll barrel structure. Five Ca ions per icosahedral asymmetric unit are located at the interface of the subunits. Detailed structure of TNV and structural comparison with other viruses will be presented.

1. K. Fukuyama et al. (1987). J. Mol. Biol. 196, 961-962.
2. T. Tsukihara et al. (1990). Acta Cryst. B46, 855-860.
3. M. Bando et al. (1994). Acta Cryst. D50, 878-883.

P12.04.007 STRUCTURE CHARACTERISTICS OF HIV-1 MUTANT INHIBITORS OF HYDROXYETHYLAMINE TYPE. J.Hasek, J.Duskova, J.Dohnalek, H.Jerabkova, E.Buchtelova. Institute of Macromolec.Chemistry, Academy of Sciences of the Czech Republic, Heyrovskeho nam.2, 162 06 Praha 6.

The structures studied in our group include HIV-1 protease BRU-1 and its mutants V82A, G48V/L91M and A71V/V82T/I85V complexed with subnanomolar (K_i range 0.02-200 nMol) inhibitors Boc- Phe- Ψ[(R/S)CHX CH_2 NH] - Phe - Glu/Gln/Ile - Phe - NH_2 /1/. The measurement under liquid nitrogen temperatures allowed us to localize up to several hundreds of solvent water molecules. In some cases, the glycerol molecules used as cryo-protectant for flash-freezing of the crystal were found adsorbed at the surface of protease. The bonding between HIV PR and inhibitor was defined uniquely in all cases /2,3,4/.

The efficiency of hydroethylamine inhibitors of HIV PR was attributed, at least in former works from early ninetieths, mainly to placement of the hydroxyl group between asp(25) and asp(125), i.e. to the site, where activated water forming the transition state of substrate is theoreticaly supposed. However, the hydroxyl groups in several complexes of N-protected tetrapeptide hydroxyethylamine inhibitors are bonded differently and do not fit the former supposition. It confirms that the main role of hydroxyl group is to protect splitting and that its bonding between aspartates 25, 125 is not of principal importance for inhibitor bonding. The supposed OH hydrogen bonding in the "active site" is replaced by hydrogen bonds formed by other groups of the inhibitor in some cases.

The principal project is supported by GACR 203/98/PO31, GAAV A4050811 and the experimental equipment was supported by 203/98/K023.

J.Konvalinka et al. (1997). Eur.J.Biochem. 250, 559-566.
J.Hasek et al. (1998). Materials Structure in CBPT, 5, 437.
J.Dohnalek et al. (1998). Materials Structure in CBPT, 5, 105.
J.Mesters et al. (1998). Materials Structure in CBPT, 5, 104.

P12.04.009 HOW ADENOVIRUS BINDS SINGLE-STRANDED DNA. Jörg Hendle, Panagiotis N. Kanellopoulos, Bas van Breukelen[#], Peter C. van der Vliet[#] & Paul A. Tucker. European Molecular Biology Laboratory – Hamburg Outstation, Notkestr. 85, 22603 Hamburg, Germany and [#]Department of Physiological Chemistry, Utrecht University, 3508 TA Utrecht, The Netherlands

The adenovirus DNA binding protein from adenovirus type 5 binds to single-stranded DNA cooperatively, and non-sequence specifically. The protein is involved in DNA replication, regulation of mRNA formation and selection of host-range specificity. The two zinc ions required for activity do not bind DNA directly but stabilize structural motifs involved in the binding of DNA.

The 17 residues of the C-terminus are in an extended conformation and form a hook-like structure that tightly interacts with the next molecule thereby forming a chain of proteins crucial for the cooperative binding of single-stranded DNA. Asn512 is the hinge residue connecting the globular core of the protein with the C-terminal hook (1, 2). Thus Asn512 may provide the flexibility essential for the different types of protein-protein and protein-DNA interaction allowing the DNA binding protein a wide range of substrates in terms of DNA conformation and sequence.

The crystal structure of the Asn512Pro mutant determined at 2.3 Å resolution shows a better defined and more rigid molecule relative to the wild type structure. The distribution of temperature factors and the quality of the electron density map of the model allow us to suggest a number of corrections to the wild type structure. The biochemical data on hinge region mutants including results from DNA unwinding assays and *in vitro* replication assays will be presented.

1. Tucker *et al.* (1994), EMBO Journal **13**, 2994-3002.
2. Kanellopoulos *et al.* (1996), Journal of Molecular Biology **257**, 1-8.

P12.04.010 THE STRUCTURE OF HUMAN HEXOKINASE I MONOMER MADE POSSIBLE DUE TO MUTATIONS IN DIMER INTERFACE: A NEW INSIGHT ON REGULATION OF ATP AFFINITY. A.E. Aleshin, X. Liu, H.J. Fromm, R.B. Honzatko Department of Biochemistry and Biophysics, Iowa State University, Ames, IA 50011, USA; G.P. Bourenkov, H.D. Bartunik, MPG-ASMB, c/o DESY, Notkestrasse 85, 22603 Hamburg, Germany .

Hexokinase is the first enzyme of the glycolytic pathway. Hexokinase I and two other mammalian isozymes share a specific structure, which arises putatively from the duplication and fusion of a primordial gene for 50 kDa hexokinase. Hexokinase I, expressed in brain and red blood cells, is inhibited by its product glucose-6-phosphate (G6P) and relieved of that inhibition by inorganic phosphate (Pi). At low concentrations hexokinase I is a monomer, but it dimerizes at concentrations above 1 mg/ml.

Recent crystallographic structures of recombinant human hexokinase I are of a dimer, the relationship of which to the kinetically characterized monomer is unclear. Here we present the structures of a hexokinase I monomer made possible by mutations which disrupt the dimer interface. The monomer, complexed with G6P and glucose, has a rod-like conformation almost identical to

that of a subunite of the dimer. Another structure of monomeric hexokinase I was obtained by soaking the crystals with ADP. It provides for the first time a reliable information about the location of the ATP binding site in hexokinases. The comparison of conformations of G6P and ADP bound structures suggests how the N-terminal half of the enzyme could regulate ATP affinity.

An additional ADP molecule binds to hexokinase I near its N-terminal helix, which is known to anchor the enzyme to the mitochondrial membrane. This additional binding site may be involved in transport of ADP to mitochondrial matrix.

P12.04.011 Cd^{2+}-SUBSTITUTED CARBOXYPEPTIDASE A: NEW INSIGHT INTO THE CATALYTIC MECHANISM. Anette Frost Jensen, Jens Thostrup Bukrinsky, and Sine Larsen, Centre for Crystallographic Studies, Department of Chemistry, University of Copenhagen, Universitetsparken 5, DK-2100 Copenhagen, Denmark, and Morten J. Bjerrum, Chemistry Department, The Royal Veterinary and Agricultural University, Thorvaldsensvej 40, DK-1871 Frederiksberg C, Denmark.

Carboxypeptidase A from bovine pancreas is a zinc enzyme. The enzyme catalyses the hydrolysis of peptide bonds from the C-terminal, with a preference for substrates which have an aromatic residue at the n-1 position.When Zn^{2+} is replaced by Cd^{2+}, the enzyme retains 30% of the native activity with optimum around pH 7.5. Chloride ions are known to affect the reaction. Since Zn^{2+} is spectroscopically silent, the chemically similar Cd^{2+} has been substituted in the enzyme as a probe in NMR and PAC (perturbed angular correlation of γ-rays spectroscopy) investigations of the Cd^{2+}-ligand interactions.

We have collected data from Cd^{2+}-substituted crystals produced at three different conditions, CdCPA(7.5): pH 7.5, low (2 mM) chloride concentration, CdCPA(7.5, Cl): pH 7.5, high (250 mM) chloride concentration, CdCPA(5.5): pH 5.5, low chloride concentration. The resolution varies from 1.72 Å to 2.00 Å with 90-95 % complete data in the outer resolution shell. All three structures show identical coordination environment of the Cd^{2+} which is six-coordinated. Three protein ligands, two histidines and one glutamic acid coordinate as well as two water molecules. The native Zn^{2+} has the same protein ligands but has only one water coordinating. No specific binding sites for the chloride ions have been found.

The coordination geometry of the Cd^{2+} enzyme is a good model for the enzyme-substrate binding in the native enzyme and it reveals new aspects of the reaction mechanism. Previously, the Cd^{2+} enzyme was considered to be five-coordinated as the native enzyme. This assumption was based on an unrefined structure. New interpretation of the spectroscopic results are thus required. This work shows that accurate determination of protein structures are important to fully understand mechanistic features studied by other techniques.

This work was supported by the Danish National Research Foundation.

P12.04.012 CRYSTAL STRUCTURE OF THE E. COLI NITROREDUCTASE PROTEIN. GN Parkinson, JV Skelly, DA Suter and S Neidle The CRC Biomolecular Structure Unit, Institute of Cancer Research, Sutton, Surrey SM2 5NG, UK

E. Coli nitroreductase catalyses the reduction of nitro groups to the corresponding hydroxylamines, which can then be further activated to form cytotoxic DNA cross-linking agents. The enzyme has been used in several prodrug approaches (ADEPT, GDEPT and VDEPT) for the tumour-selective activation of cytotoxic alkylating drugs, notably the aziridinyl prodrug CB1954.

We have determined the three-dimensional structure of this enzyme, in order to gain insight into the mechanism of activation, and to provide a basis for the rational design of more effective prodrugs.

The recombinant 24kD enzyme was crystallised in the tetragonal space group $P4_32_12$, with unit cell dimensions of a=b=57.74 Å and c=275.51 Å and two molecules in the asymmetric unit. Diffraction data to 2.14 Å was collected on a laboratory R-AXISII image-plate. The crystal structure has been solved by molecular replacement methods, using X-PLOR, and employing the recently-determined structure of the nitroreductase Frase I (PDB code IVFR), as a starting model. There is 31.3% sequence homology between the two enzymes. The structure is currently being refined using X-PLOR. Details of the structure, in particular the active site geometry, will be presented.

P12.04.013 CRYSTALLOGRAPHIC INSIGHTS INTO THE HYDRIDE TRANSFER MECHANISM OF NADPH-CYTOCHROME P450 REDUCTASE. Paul A. Hubbard, Rosemary Paschke, *Anna Shen, *Charles B. Kasper, and Jung-Ja P. Kim. Dept. Of Biochemistry, Medical College of Wisconsin, Milwaukee, WI 53226 and *McArdle Labortaory for Cancer Reseach, University of Wisconsin - Madison, WI 53706, USA.

NADPH-cytochrome P450 oxidoreductase (CPR) is a monomeric enzyme bound to the outer face of the endoplasmic reticulum of all mammalian cells. Its primary function is that of electron transfer from the two electron donor of NADPH to the one electron heme acceptor, cytochrome P450 via the FAD and FMN redox centers. The structure from expressed rat protein was previously solved in our lab, and shown to contain two structurally homologous regions; a flavodoxin like FMN domain and a ferredoxin-$NADP^+$ reductase like fold which binds cofactors NADPH and FAD in two separate domains. Between the two flavin cofactors is a linking domain with no sequence homology to any other known protein. The indole ring of W677, the penultimate residue, is seen to stack against the *re*-face of the FAD, presumably stabilizing an inactive conformation by preventing direct hydride transfer between NADPH and the flavin.

The cloned rat gene was mutated to remove the two C-terminal residues W677 and S678, and the purified protein was shown to retain stoichiometric amounts of FMN and FAD. Crystals were grown at 19.5^{o}C under similar conditions to that of the wild type in the presence of $NADP^+$. Diffraction data were collected and processed with Denzo to 2.7A resolution using an R-AXIS II image plate at 4 ^{o}C. The structure was solved with CNS by using the difference Fourier method, using phases calculated from the refined native structure. Results are in agreement with previous proposals, and clearly show the A-face of the nicotinamide moiety stacking against the *re*-face of the isoalloxazine ring of FAD. The pyrophosphate linkage of the cofactor has undergone significant rotation in order to achieve an almost perpendicular orientation to that found in the crystal structure of the wild type. This adds further evidence to the direct hydride transfer mechanism previously proposed.

P12.04.014 UNDERSTANDING THE ACTIVE SITE OF AN ENZYME : CRYSTAL STRUCTURES OF ESCHERICHIA COLI NAD-SYNTHETASE Rosario Recacha[1], Caroline Ozment [1], Joseph Barchue [1], Dharmalingam Prahadeeswaran [1], Lawrence J. DeLucas [1] & D. Chattopadhyay [1,2], [1] Center for Macromolecular Crystallography, University of Alabama at Birmingham, Birmingham, AL 35294, USA, [2] Division of Geographic Medicine, School of Medicine

NAD and NADP are essential coenzymes for all living organisms. NAD can be synthesized either de novo or through salvage pathway. These two pathways converge at the level of nicotinic acid mononucleotide and the two final steps on the biosynthetic pathway are in common. The enzyme NAD-

synthetase [EC 6.3.5.1], which belongs to the amidotransferase family, catalyzes the final step in the Priess-Handler pathway for NAD synthesis. This reaction involves transfer of an amino group from ammonia (or glutamine) to nicotinic acid adenine dinucleotide (NAAD) in the presence of ATP and magnesium. Bacterial enzymes use ammonia in preference to glutamine. The reaction consists of two steps. In the first step, ATP hydrolysis occurs and adenylated-NAD is formed. In the second step, NAD is formed via nucleophilic addition of ammonia. We have determined the crystal structure of E. coli NAD-synthetase in the free enzyme form, in complex with NAAD and ATP, and in complex with NAAD and a non-hydrolyzable ATP-analogue. All structures are refined to at least 2.0 Å resolution. The overall structure of the enzyme is very similar to the only known structure of NAD-synthetase enzyme (from Bacillus subtilis). These structures reveal the substrates and divalent cation binding sites. The NAAD and ATP complex structure determined at 1.8 A resolution shows the active site accommodating an adenylated reaction intermediate.

P12.04.015 STRUCTURAL BASIS FOR THE SUBSTRATE SPECIFICITY OF PROTEIN TYROSINE PHOSPHATASES J. Yang, Z. Cheng, T. Niu, X. Liang, G.W. Zhou [1], Z.J. Zhao [2], [1] Program in Molecular Medicine, University of Massachusetts Medical School, Worcester, Massachusetts 01605, USA, [2] Department of Medicine, Vanderbilt University, Nashville, Tennessee 37232, USA

Protein tyrosine phosphatases (PTPs) are a group of structurally and functionally diversified enzymes. Precise regulation of their physiological functions depends largely on their substrate specificity. SHP-1, a SH2 domain containing PTP, is an important negative regulator in the B cell antigen receptor, T cell antigen receptor, c-Kit and cytokine signal transduction pathways. Deficiency of SHP-1 will result in severe abnormalities in the immune system. We have determined the crystal structures of the catalytic domain of SHP-1 complexed with two phosphotyrosyl decapeptides, pY469 and pY495, originated from its physiological substrate SIRP. The structures have been refined to crystallographic R values of 19.9% and 20.5%, respectively. Both peptides bound to the catalytic domain of SHP-1 in extended conformations. From the complex structures, we identified six well-defined substrate binding sub-pockets. This is the first time that the substrate binding sub-pockets of a PTP are identified. The substrate specificity of SHP-1 is determined by the residues at P-4 and even further minus positions in the phosphotyrosyl substrates, and the recognition sites for these residues are the beta5-loop-beta6 motif and loop beta6/beta7 in the enzyme. We also observed a novel residue shift at the hydrophobic P-2 sub-pocket. The P-2 sub-pocket bound the P-2 Leu residue in the pY469 complex structure and the P-3 Phe residue in the pY495 complex structure. Since the hydrophobic P-2 sub-pocket is highly conserved in PTPs, the residue shift may be a common phenomenon for PTPs. This novel residue shift has provided a new guideline for identifying substrates for PTPs. We also compared other native PTPs structures with our complex structures. We concluded that the substrate specificity of PTPs may be determined by two regions: the P-4 and further minus sites, and the P+4 and even further plus sites, in the phosphotyrosyl substrates. The recognition of these two regions comes from the hyper-variable beta5-loop-beta6 and the alpha5-loop-alpha6 motifs in PTPs.

P12.04.016 MOLECULAR STRUCTURE OF IMP DEHYDROGENASE FROM *STREPTOCOCCUS PYOGENES*. Rong-guang Zhang, Gwyndaf Evans, Eliezer Huberman, Andrzej Joachimiak, Frank Rotella, Edwin M. Westbrook, and Frank R. Collart, Argonne National Laboratory, Argonne, IL 60439 USA.

IMP dehydrogenase (IMPDH) is an essential enzyme that catalyzes the first step unique to GTP synthesis. To provide a basis for the evaluation of IMPDH inhibitors as antimicrobial agents, we have expressed and characterized IMPDH from the pathogenic bacterium, Streptococcus pyogenes. Our results show that the biochemical and kinetic characteristics of S. pyogenes IMPDH are similar to other bacterial IMPDH enzymes. However, the lack of sensitivity to mycophenolic acid and the Km for NAD (1180 μM) exemplify some of the differences between the bacterial and mammalian IMPDH enzymes, making it an attractive target for antimicrobial agents. To evaluate the basis for these differences, we determined the crystal structure of the bacterial enzyme at 1.9 Å with substrate bound in the catalytic site. The structure was determined using selenomethionine-substituted protein and multi-wavelength anomalous (MAD) analysis of data obtained with synchrotron radiation from the undulator beamline (19ID) of the Structural Biology Center at Argonne's Advanced Photon Source. S. pyogenes IMPDH is a tetramer with its four subunits related by a crystallographic fourfold axis. The protein is composed of two domains: a TIM barrel domain that embodies the catalytic framework and a cystathione (-synthase (CBS) dimer domain of so far unknown function. Using information provided by sequence alignments and the crystal structure, we prepared several site-specific mutants to examine the role of various active site regions in catalysis. These variants implicate the active site flap as an essential catalytic element and indicate there are significant differences in the catalytic environment of bacterial and mammalian IMPDH enzymes. Comparison of the structure of bacterial IMPDH with the known partial structures from eukaryotic organisms will provide an explanation of their distinct properties and contribute to the design of specific bacterial IMPDH inhibitors. This work was supported by the US Department of Energy, Office of Biological and Environmental Research, under Contract W-31-109-ENG-38.

P12.04.017 CHARACTERIZATION OF HUMAN BONE ALKALINE PHOSPHATASE IN *PICHIA PASTORIS*. Christine C. Malone, Eva Ciszak and Laurel J. Karr, USRA, Huntsville, Alabama 35810 and SD48, NASA/MSFC, Huntsville, Alabama 35812.

A soluble form of human bone alkaline phosphatase has been expressed in a recombinant strain of the methylotrophic yeast *Pichia pastoris*. We constructed a plasmid containing cDNA encoding for human bone alkaline phosphatase, with the hydrophobic carboxyl terminal portion deleted. Alkaline phosphatase was secreted into the medium to a level of 32mg/L when cultured in shake flasks, and enzyme activity was 12U/mg, as measured by a spectrophotometric assay. By conversion to a fermentation system, a yield of 880mg/L has been achieved with an enzyme activity of 968U/mg. By gel electrophoresis analysis, it appears that greater than 50% of the total protein in the fermentation media is alkaline phosphatase.

Although purification procedures are not yet completely optimized, they are expected to include filtration, ion exchange and affinity chromatography. Our presentation will focus on the purification and crystallization results up to the time of the conference. Structural data should provide additional information on the role of alkaline phosphatase in normal bone mineralization and in certain bone mineralization anomalies.

P12.04.114 STRUCTURE-ACTIVITY CORRELATIONS AMONG A SERIES OF HYBRID TMQ-PTX ANALOGUES COMPLEXED WITH HUMAN DHFR. Vivian Cody, Nikolai Galitsky, Joe Luft, Walt Pangborn Aleem Gangjee Molecular Biophysics Department, Hauptman-Woodward Medical Res. Inst, Buffalo, NY,14203 USA. Division of Medicinal Chemistry, Duquesne University, Pittsburgh, PA 15282

Pneumonia caused by opportunistic infectious agents is a major cause of mortality among patients with AIDS. Antifolates have been shown effective adainst the dihydrofolate reductase (DHFR) from Pneumocystis carinii (pc) which is a target for drug design studies. The lipophilic quinazoline trimetrexate (TMQ) and the pyridopyrimidine piritrexim (PTX) are potent inhibitors of human DHFR with moderate potency for pcDHFR. To further optimize pcDHFR selectivity, a series of hybrid analogues combining the pyridopyrimidine of PTX with the trimethoxy anilino group of TMQ were made, including those with reversed C9-N10 bridge modifications. Inhibition data against rat liver (rl) and pcDHFR were enhanced by N-methylation. To understand these structure-activity relationships we report crystal data for nine hDHFR complexes with TMQ and two of its hybrid analogues, including the first structural data for a reversed bridge antifolate. One complex crystallizes in a tetragonal space group and the others are rhombehedral; however, two crystallize in an independent R3 lattice. Of these, only one is a ternary complex with NADPH, even though all were co-crystallized in the presence of cofactor. Differences in the packing of hDHFR in the alternate R3 lattice result in better definition of flexible outer loop regions compared to the predominate R3 lattice. All inhibitor conformations are similar to each other and to methotrexate (MTX), including the reversed bridge analogues. When these inhibitors were modeled in the active site of pcDHFR, all hydrophobic contacts were weaker than in hDHFR, consistent with their decreased potency against pcDHFR. Although the bridge conformations were similar, the orientation of the N10-methyl in the most potent and selective of this series differs and makes tighter contacts to Leu-22 than MTX. PcDHFR selectivity (rl/pc ratio) is increased 10-fold for all N-methyl analogues, while reversed bridge analogues lower potency, but not selectivity. The presence of a 5-methyl substituent also enhances potency and selectivity. Compared to TMQ, the N8 of these hybrides interact with the conserved water that forms a hydrogen bond network with Glu-30 and Trp-24 in hDHFR. Supported in part by GM-51670 (VC) and AI-30900 (AG).

P12.04.115 RATIONAL DESIGN OF FLAVONOIDS AS POTENTIAL ALDOSE AND ALDEHYDE REDUCTASE INHIBITORS. Elisabeth V. Fletcher, Roland P.-T. Chung, Mark von Itzstein and Ossama El-Kabbani, Department of Medicinal Chemistry, Victorian College of Pharmacy, Monash University, Parkville, VIC 3052 Australia

It has been shown that aldose reductase (ALR2) is implicated in the development of diabetic complications. Thus ALR2 inhibitors seem to offer the possibility of preventing or arresting the progression of the complications. The search for effective ALR2 inhibitors has been underway for 25 years but as yet have not proven to be unequivocally effective.

Naturally occurring flavonic compounds (2-phenyl-4H-1-benzopyran-4-one derivatives) are known to exert several pharmacological activities. In particular they are antioxidants and are able to inhibit ALR2 and the related aldehyde reductase (ALR1).

Several flavonoids, known to exhibit ALR2 inhibition, have been modelled in the active sites of the recent structures of ALR1 and ALR2.[1] Based on the corresponding binding energies we have designed several novel molecules, incorporating a carboxylate (a functional group present in ALR1 and ALR2 inhibitors[1]) into the flavonoid molecule. The carboxylate is hydrogen bonded to the active site residues Tyr 48, His 110 and Trp111, whilst π-stacking is also observed between Trp 219 and the hydrophobic ring of the flavonoid molecule.

A crystal structure determination of ALR1 in complex with coenzyme and flavonoid is currently underway. Data obtained from the structure will be used in further refinement of inhibitors.

1. O. El-Kabbani, D. K. Wilson, J.M. Petrash and F. A. Quiocho. Molecular Vision 1998; 4:19 <http://www.molvis.org/molvis/v4/p19>

P12.04.116 STRUCTURAL ANALYSIS OF PNEUMOCYSTIS CARINII DHFR TERNARY COMPLEX WITH A NOVEL PYRROLO ANTIFOLATE. Nikolai Galitsky, Vivian Cody, Dawn Rak, Walt Pangborn, Aleem Gangjee. Department of Molecular Biophysics, Hauptman-Woodward Medical Research Institute, Buffalo, NY. School of Pharmacy, Duquesne University, Pittsburgh, PA

Pyrrolo[2,3-d]pyrimidine based antifolates are a new class of inhibitors that have a 6-5 ring system instead of the conventional bicyclic 6-6 fused ring system of pteridine, quinazoline or pyrido[2,3-d]pyrimidine. These antifolates have been shown effective anticancer agents against a number tumor cell lines and as shown by the pyrrolopyrimidine, LY231514, which has a 4-oxo substituent, is a multitarget antifolate. Although the parent of LY231514 was designed as an inhibitor of thymidylate synthase, it inhibits at least five enzymes in the folate pathway, including dihydrofolate reductase (DHFR). Data from a series of pyrrolopyrimidine derivatives of the antibacterial trimethoprim in which the 4-amino group was cyclised, showed that a 6-methyl derivative had equivalent activity to trimethoprim. Structural data for the E. coli DHFR complex showed that these rigid analogues bind with the same orientation as trimethoprim. To further define the structure activity correlations among pyrrolopyrimidine antifolates, a 4-methyl derivative of the novel pyrrolo[2,3-d]pyrimidine classical antifolate was synthesized and shown as active as methotrexate against hDHFR. We report the first crystal structure of Pneumocystis carinii DHFR ternary complex with NADP+ and N-[4-[2-(2-amino-3,4-dihydro-4-methyl-7H-pyrrolo[2,3-d]pyrimidin-5-yl)ethyl]benzoyl]-L-glutamic acid, collected to 2.1A resolution on an RaxisIV at room temperature. Analysis of these data, currently refined to 2.4A resolution, show that the pyrrolopyrimidine ring is oriented such that the pyrrolo N hydrogen bonds to a conserved water that is between Glu-32 and Trp-27, similiar to that of the novel furopyrimidine classical antifolate reported previously. This orientation places the 4-methyl group in a hydrophilic pocket normally occupied by the 4-amino group of antifolates, and differs from that of the trimethoprim pyrrolopyrimidine derivative. These data suggest that the antifolate shifts its position in the active site such that the 4-methyl contacts are greater than those for the 4-amino of the furopyrimidine structure, thereby relieving the strain of these contacts. When this structure is compared to the hDHFR furopyrimidine complex, it is noted that the 4-amino contacts are weaker in hDHFR than in pcDHFR. Supported in part by GM-51670 (VC) and AI-41473 (AG).

P12.04.117 PLASMEPSIN II, A HEMOGLOBIN-DEGRADING ENZYME FROM *P. FALCIPARUM,* IN COMPLEX WITH NON-PEPTIDIC INHIBITORS. Abelardo. M. Silva, R. Randad, D. Medjahed, S. V. Gulnik, B.Yu, J. W. Erickson, T.S. Haque[1], J. Ellman[1], Structural Biochemistry Program, National Cancer Institute/SAIC, Frederick, Maryland 21702, USA. (1) Department of Chemistry, University of California, Berkeley, CA 94720, USA.

Malaria, a disease caused by parasites of the genus *Plasmodium*, is among the most widespread infectious diseases in the world, afflicting several hundred million and killing nearly two million people per year, mainly children. *P. falciparum*, invades erythrocytes and consumes nearly all of its host's hemoglobin as a source of nutrients during growth and development. The parasite encodes two homologous aspartic proteases - plasmepsins I and II - which are essential components of its hemoglobin degradation pathway and are novel targets for

antimalarial drug development. We described earlier the crystal structure of plasmepsin II in complex with pepstatin A, which was the first report of a protein structure from *P. falciparum*. We present now the structures of plasmepsin II in complex with potent non-peptidic inhibitors of the enzyme, which also inhibit the growth of *P. falciparum* in culture. Inhibitors were designed on the basis of our first structure, and also derived from combinatorial libraries. Two new crystal forms were found. One of them corresponds to the space group P2, with one molecule in the asymmetric unit. Monomers interdigitate around a crystallographic two-fold axis burying an area exceeding 2000 $Å^2$. The second form corresponds to space group I222 with one molecule in the asymmetric unit. The monomers also extensively interact around a crystallographic two-fold axis, and while the surfaces in contact are the same observed in monoclinic and trigonal crystals, the relative orientation of the monomers is different. Interactions mediated by a second two-fold axis, although less extensive than the first one, are also observed. All these structures show the high variability in dimeric interactions; an unusual flexibility of the binding cavity; and, open the question about the state of aggregation of the functional enzyme, which directly affects the structure of the binding cavity itself.

P12.04.118 CRYSTAL STRUCTURE OF THE BIFUNCTIONAL N-ACETYLGLUCOSAMINE 1-PHOSPHATE URIDYLTRANSFERASE (GLMU). Kieron Brown [1], Suzanne Dixon [1], Frederique Pompeo [2], Dominique Mengin-Lecreulx [2], Christian Cambillau [1], Yves Bourne [1]. [1] AFMB-CNRS, 31 ch. J. Aiguier, 13402 Marseille, France. [2] CNRS, Universite Paris-Sud, 91405 Orsay cedex, France.

N-acetylglucosamine 1-phosphate uridyltransferase (GlmU) is a unique cytoplasmic bifunctional enzyme involved in the biosynthesis of the nucleotide activated UDP-GlcNAc which is the most important precursor for the biosynthetic pathways of peptidoglycan and lipopolysaccharide in bacteria. The crystal structure of a truncated form of GlmU has been solved at 2.25A resolution using multiwavelength anomalous dispersion techniques.

The structure is composed of two separate domains connected by a long alpha-helical arm, an N-terminal domain is consistent with the dinucleotide-binding Rossmann fold, and a C-terminal domain which adopts a left-handed parallel beta-helix structure found in homologous bacterial acetyltransferases. The structure reveals the binding site of the product UDP-GlcNAc, and exemplifies a prototypic structure for other members of the large family of XDP-sugar bacterial pyrophosphorylase enzymes which share sequence homology with the N-terminal domain of GlmU.

P12.04.119 1.9Å STRUCTURE OF HSV THYMIDINE KINASE: LIGAND BINDING TO NATIVE AND MUTANT ENZYMES. M.R. Sanderson, M.S. Bennett, F.Wien and J.N. Champness, Division of Biomedical Sciences, Randall Institute, King's College, 26-29 Drury Lane, London, WC2B 5RL, UK, and W.C. Summers, Department of Therapeutic Radiology, Yale University School of Medicine, 333 Cedar Street, New Haven, CT 06520-8040, USA, and Hongmao Sun and George Wright, Department of Pharmacology, University of Massachusetts Medical School, Worcester, MA 01655, USA, and M.E. Black, Division of Biology and Biomedical Sciences, Washington University, 660 S. Euclid Avenue, St. Louis, MO 63110-1093, USA.

Viral thymidine kinase provides the first step in the activation of anti-herpes drugs such as aciclovir (Zovirax). Highest resolution structures to date (1.9Å) of ligand/enzyme complexes have revealed significant details of interactions of drug molecules with the enzyme active site, and these studies, as well as studies of ligand binding to mutant enzyme, will be presented. The results are of value in the development of more effective chemotherapy, not only for herpes infections, but also, potentially, in gene-therapy of brain tumours which have been made to express the enzyme by transfection.

P12.04.120 STRUCTURE OF DIHYDROFOLATE REDUCTASE OF M. TUBERCULOSIS: NEW TB-SPECIFIC DRUG POSSIBILITIES REVEALED. Rongbao Li[a,b], Worachart Sirawaraporn[c] and Wim G. J. Hol[a,b,d], [a]Department of Biological Structure, [b]Howard Hughes Medical Institute and Biomolecular Structure Center, University of Washington, Seattle, WA 98195, USA; [c]Department of Biochemistry, Mahidol University, Bangkok 10400 Thailand; [d]Department of Biochemistry, University of Washington, Seattle, WA 98195, USA

Dihydrofolate reductase catalyzes the NADPH-dependent reduction of dihydrofolate to tetrahydrofolate and is essential for the synthesis of thymidylate, and therefore of DNA. Inhibition of the enzyme activity leads to the halt of DNA synthesis and cell death, thus the enzyme has been studied extensively as a drug target for several diseases, including bacterial, protozoal and fungal infections, neoplastic diseases and autoimmune diseases. Dihydrofolate reductase from Mycobacterium tuberculosis, a human pathogen responsible for the death of millions every year, has been co-crystallized with its co-factor NADPH and methotrexate and trimethoprim, two inhibitors being employed as antitumor and antimicrobial therapeutic agents. The crystals have one molecule in the asymmetric unit and are in space group P41. The crystal structures of two ternary complexes containing NADPH and methotrexate or trimethoprim, and of one binary complex containing NADPH have been determined to 1.7 Å resolution by single isomorphous replacement plus anomalous scattering followed by phase improvement with solvent flattening procedures. Structural comparison of these complexes with human dihydrofolate reductase indicates that the protein fold is similar but the environments of both NADPH and the inhibitors contain interesting differences, which can be exploited for designing selective inhibitors to tubercular dihydrofolate reductase. Therefore, dihydrofolate reductase of M. tuberculosis provides a potential TB drug target.

P12.04.121 DISCOVERY OF THE MODES OF ACTION OF INHIBITORS OF EUKARIOTIC TOPOISOMERASE I. Paulene M. Quigley[a], Matthew R. Redinbo[b], James J. Champoux[c], Wim G. J. Hol[a,b,d], [a]Department of Chemistry, University of Washington, WA 98195 USA; [b]Biomolecular Structure Center, University of Washington, Seattle, WA 98195, USA; [c]Department of Microbiology, University of Washington, Seattle, WA 98195, USA; [d]Howard Hughes Medical Institute, University of Washington, Seattle WA, 98195 USA.

Topoisomerase I functions in eukariotic cells to relax the superhelicale tension generated by essential processes such as DNA replication. Cancer cells show particular sensitivity to disruption of thes processes due to their high rate of proliferation. In fact drugs like camptothecin serve as an effective anti cancer treatments through their targeting of the Topoisomerase I-DNA complex. Despite the great variety of Topoisomerase I inhibitors that exist, their specific modes of action remains unclear. Hence, through the crystallization of Topoisomerase I-DNA complex with known inhibitors, we hope to elucidate the structural basis of inhibition and thereby lead to more potent treatments.

Structures of human topoisomerase I have revealed how the enzyme clamps around the DNA duplex to form a transient covalent complex between Tyr 723 and the 3'-hydroxyl of the

scissile strand. Camptothecin, a recently approved cancer drug, promotes the lifetime of this 'cleavage complex', thereby forming obstacles on the DNA highway, leading to cell death. Numerous other classes of topoisomerase poisons have been described, although their precise mode of action remains unclear. We hope to gain insight into the modes of action of Topoisomerase I inhibitors by crystallographic investigation.

1 M. R. Redindo et al., Science 279, 1504 (1998)
2. L. Stewart et al., Science 279, 1534 (1998).

P12.04.122 COMPARISON OF THE UNINHIBITED HUMAN FACTOR XA STRUCTURE AND THE TAP INHIBITED BOVINE FACTOR XA STRUCTURE. Anzhi Wei, Richard S. Alexander, Chong-Hwan Chang, DuPont Pharmaceuticals Company, Experimental Station, Wilmington, DE 19880, USA

The function of factor Xa is to convert prothrombin into thrombin which in turn converts fibrinogen into fibrin. The location of factor Xa at the intersection of the intrinsic and extrinsic paths of the coagulation cascade makes it an attractive antithrombotic drug target .

The crystal of apo human factor Xa was crystallized by using polyethylene glycol as a precipitant. The crystal belongs to space group $P4_12_12$ with unit cell dimensions of a=b=94 Å and c=119 Å, and diffracts to 2.0 Å resolution, which is higher than previously reported (2.5Å).

The bovine factor Xa was crystallized in complexed form with recombinant tick anticoagulant peptide (rTAP) with PEG 8000. The crystals were obtained in two different crystal forms : Form I belongs to space group $P4_22_12$ with unit cell dimensions of a=b=133.1 Å and c=68.8 Å and diffracts to 3.0 Å. Form II belongs to $P4_12_12$ (or $P4_32_12$) with dimensions of a=b=126.5 Å and c=146.7 Å; it contains two complexes per asymmetric unit and diffracts to 2.5 Å.

The sequence of bovine factor Xa shares a high sequence identity with the human factor Xa: light chain exhibits 70% and the heavy chain shows 84% identity. The sequence identity is noticeably higher around the calcium-binding and the catalytic regions. This homology reflects the functional importance of these two regions of factor Xa. Between the complexed bovine factor Xa and apo human factor Xa, the overall rms. deviation around Ca atoms is 1.03 Å and 0.92Å at the catalytic regions. The high homology between two species also reflects the general agreement of the results on the reaction between rTAP and bovine or human factor Xa.

The structures of apo human factor Xa and complexed rTAP_bovine factor Xa provide a key to understanding its novel mode of binding, the existence of a multi-step pathway for the inhibition of fXa by rTAP, and a possible use for designing new selective inhibitors of fXa. The details of the structural comparison between human and bovine fXa, will be presented.

P12.04.123 A COMBINATORIAL APPROACH TO THE CRYSTAL STRUCTURE OF TOPOISOMERASE I COMPLEXED WITH ANTICANCER DRUGS. Lance J. Stewart[1], Hidong Kim[1], Alex Burgin Jr.[2], David Zembower[3], Philippe Pourquier[4] and Yves Pommier[4]. [1]Emerald BioStructures, Inc., 7869 NE Day Rd. W, Bainbridge Island, WA 98110, USA; [2]San Diego State University, 5500 Campanile Dr., San Diego, CA 92182, USA; [3]MediChem Research, Inc., 12305 So. New Avenue, Lemont, IL 60439, USA; [4]National Cancer Institute, Laboratory of Molecular Pharmacology, Bethesda, MD 20892, USA

Human topoisomerase I (topo I) is the sole intracellular target of camptothecin (CPT) and other "topo I poisons," some of which are among the most promising anticancer drugs ever identified. Emerald BioStructures, Inc. is actively engaged in a phase I Small Business Innovative Research study that seeks to elucidate the X-ray crystal structure(s) of human topo I in ternary complex with DNA and topo I poisons which include CPT, derivatives thereof, and several other non-CPT anticancer compounds which target topo I. We have developed several new "combinatorial" crystallization research tools that have allowed us to rapidly identify crystal forms of human topo I whose growth depend on the presence of all three components: topo I, DNA, and poison. This combinatorial approach is generally applicable to any structure-based drug design project. The progress towards the X-ray structure determination of our topo I crystals will be presented.

P12.04.124 STRUCTURAL STUDIES OF LIGANDS BOUND TO THE IMMUNOSUPPRESION TARGET LCK. X. Zhu, P. Rose, D. R. Stover, H. Zhao, L. Toledo & K. A. Morgenstern, Kinetix Pharmaceuticals, Inc., 200 Boston Ave. Medford, MA 02155, USA

The tyrosine kinase lck is predominantly expressed in T cells and appears to be the first kinase activated upon the TCR/MHC engagement. As an attractive immunosuppression target, lck has been crystallized in our laboratory. We have determined the structures of this enzyme to high resolution with several specific and non-specific ATP-competitive inhibitors. These novel lck and inhibitor complexes display subtle but distinct protein conformations around the bound ligands. Correlated with our structural activity data, we show that the non-specific lck inhibitors interact with the residues well conserved in the kinase family. The lck-specific inhibitors, on the other hand, adopt the ATP bound conformation of the protein, and interact with several residues specific to lck. A comparison of the lck structures to other protein kinases bound with their specific inhibitors is also discussed. Finally, our complex structure of lck and an ATP analog reveals that the gamma phosphate is not in the proper conformation for phospho-transfer. Instead, it represents an intermediate step of the conformational transition from the apo form to the ternary complex of lck/ATP/substrate.

P12.04.125 CRYSTAL STRUCTURE OF MISTELTOE LECTIN I FROM VISCUM ALBUM. R. Krauspenhaar, S. Eschenburg, M. Perbandt (1), V. v. Kornilov (2), S. Stoeva, W. Voelter (3), N. V. Konareva, I. V. Mikailov, A. Mikhailov (4), C. Betzel (1), (1) Inst. of Physiol. Chemistry, Uni. Hamburg, Hamburg, Germany, (2) Inst. Cell Biophys. Russian Academy of Sciences, Pushino, Russian Federation (3) Inst. Physiol. Chem. Uni. Tübingen, Tübingen Germany, (4) Inst. Crystall. Russian Academy of Sciences, Russian Federation,

The crystal structure of the ribosome inactivating protein (RIP) misteltoe lectin I (ML-I) from Viscum album has been solved by M.R..

The structure has been refined to a crystallographic R-factor 24 % SR data up to 2.7 Angstrom resolution. The heterodimeric 63 kDa protein consists of a toxic A subunit which exhibits RNA-glycosidase activityand a galactose specific lectin B subunit. The overall protein fold is similar to that of ricin from Ricinus communis. Unlike ricin ML-I is already medically applied as a component of a commercially available misteltoe extract with immunostimulating potency for the treatment of human cancer. The 3D structure revealed structural details of this pharmaceitically important protein and will give more insights into the structure-function-relationship for further protein engeneering towards drug design studies. the relative high sequence homology and the conserved secondary structure enabled a structural accurate comparison to ricin and revealed differences in the vicinity o the active site, in the high galatose binding side as well as in the interface regions between A and B chain, which might account for the altered cytotoxitiy of ML-I.

Structural studies will be presented and compared to other known ribosome inactivating proteins.

P12.04.126 CRYSTAL STRUCTURE OF TETRA-DIMERIC C-TYPE LECTIN PROTEIN FLAVOCETIN-A FROM HABU VENOM. K. Fukuda [1], H. Mizuno, Z. Fujimoto [2], H. Atoda, T. Morita [3], [1] University of Tsukuba, Tsukuba Science City, Ibaraki 305-8572, Japan. [2] National Institute of Agrobiological Resources, Tsukuba Science City, Ibaraki 305-8602, Japan. [3] Meiji Pharmaceutical University, Kiyose, Tokyo 204-8588, Japan.

Flavocetin-A (FL-A) is a member of C-type lectin superfamily. FL-A was isolated and purified from the venom of habu snake Trimeresurus flavoviridis. Unlike other family members, it is a high molecular mass protein (149 kDa) composed of alpha-subunits of 16.5 kDa, 135 residues, and beta-subunits of 13.7 kDa, 125 residues. This protein binds specifically to glycoprotein (GP) Ib alpha-subunit in the platelet membrane GPIb-IX-V complex and functions as a competitive blocker of von Willebrand factor-binding in platelet agglutination under conditions of high shear stress. We have determined the X-ray crystal structure of FL-A as a first step in understanding the molecular basis for the GPIb-binding specificity.

The structure of FL-A was solved by molecular replacement using the structure of coagulation factors IX/X-binding protein (IX/X-bp) [1], a heterodimer of C-type lectin-like domains, as a search model (55% identity with the sequence of heterodimer subunit in FL-A). The current model has a crystallographic R-factor of 21.9% (free-R=30.5%) at 2.5 Å resolution. Expected from the structure of IX/X-bp, each subunit of FL-A showed an intertwined heterodimer fold made of disulfide-linked alpha- and beta-subunits. These subunits are related by a crystallographic fourfold symmetry parallel to the c-axis and connected by an additional disulfide-bond between C-terminal region in the alpha-subunit and N-terminal region in the beta-subunit. Thus, the overall structure of FL-A revealed a cyclic tetradimer $(alpha/beta)_4$ connected by alternate disulfide-linkages. It also displayed a large solvent channel inside the tetradimer molecule, and this is consistent with a relatively large solvent content of 67% in the crystal. Details of the structure of FL-A and comparison with IX/X-bp will be discussed.

1. H. Mizuno, Z. Fujimoto, M. Koizumi, H. Kano, H. Atoda, & T. Morita. (1997). Nature Struct. Biol., 4, 438-441.

P12.04.127 MOLECULAR REPLACEMENT STUDIES OF TRICHOSANTHES KIRILOWII LECTIN. M.Li, Y.-P.Wang, J.-J.Chai, R.-C.Bi [1], K.-Y.Wang [2], [1] Institute of Biophysics, Chinese Academy of Sciences, Beijing 100101, China, [2] Institute of Biochemistry,Chinese Academy of Sciences, Shanghai 200031, China

Trichosanthes Kirilowii lectin (TKL) was isolated and purified from the same plant tissue as trichosanthin [1], a type ¢ñ ribosome-inactivating protein(RIP) consisting of a single peptide chain. Like ricin [2], a type ¢ò RIP, it contains two peptide chains A and B each having a molecular weight of about 30kDa. TKL has some properties similar to those of trichosanthin or ricin, but it has not been found so far that TKL has the ribosome-inactivating activity.

TKL has been crystallized in space group $P2_12_12_1$ with cell dimensions a=44.7A, b=69.5A, c=180.9Å, and the diffraction data were collected to 2.7A resolution. The molecular replacement method was applied to solve this structure. In consideration of the unknown sequence of TKL, several known structures of type RIP and A and B-chains of type RIP were used respectively as the search model. The correct solution was found and verified by the method of Romit profile analysis [3]. It was found that this method is quite powerful for verification of the molecular replacement solution even in the case where the sequence of the structure to be solved is unknown and only the general laws of homology are available. The structure model, which was obtained with A- and B-chain of abrin-a [4], a type ¢ò RIP, as separate search models, shows the same spatial arrangement of the two subunits as in the abrin-a. So TKL structure possesses the features of RIP peptide folding. A refinement of the structure is in progress.

[1] Pan, K. et al. (1986). Scientia Sin. 29, 26.
[2] Rutenber, R. et al. (1991). Proteins: Struct. Func. Genet. 10, 240.
[3] Tsuchiya, D. & Takenaka, A. (1998). Acta Cryst. D54, 151.
[4] Tahirov, T. H. et al. (1995). J. Mol. Biol. 250. 354.

P12.04.128 IMMUNOGLOBULIN DOMAINS I-II OF NEURAL CELL ADHESION MOLECULE (NCAM). Christina Kasper, [1] Hanne Rasmussen, Jette S. Kastrup and Ingrid Kjøller Larsen, Royal Danish School of Pharmacy, Dept. of Medicinal Chemistry, DK-2100 Copenhagen, [1] Novo Nordisk A/S, DK-2880 Bagsværd

The neural cell adhesion molecule (NCAM) is a multifunctional, cell surface glycoprotein belonging to the immunoglobulin superfamily. NCAM is involved in recognition and adhesion between cells from many tissue origins, mediated via a homophilic binding mechanism. The adhesive properties of NCAM have been investigated on a putative involvement of NCAM in cancer, and the results indicate that expression of NCAM leads to a reduced cell migration and metastatic potential [1]. NCAM is also known to be involved in various morphoregulatory processes and in intracellular signal transduction underlying e.g. neurite outgrowth [2,3].

Three major isoforms are expressed in brain. Two are transmembrane, while the third is attached to the membrane via a lipid-anchor. The extracellular part of NCAM is identical in all isoforms and consists of five N-terminal immunoglobulin (Ig) domains and two membrane proximal fibronectin type three (F3) domains [2,4]. Even though it has been a well known fact for almost 20 years that NCAM binds to NCAM, the sequence(s) involved in the interaction have not yet been localized. Many different hypotheses have been put forward, ranging from single domain to multidomain interactions.

Through crystallization and structure determination of various NCAM domains we wish to increase the knowledge on NCAM structure and on the homophilic binding leading to intercellular adhesion.

NCAM IgI-II has been crystallized in space group P21, with 4 molecules/a.u. Native data have been collected at BM14 (ESRF, Grenoble) to 1.85 A.

It has not been possible to solve the structure by molecular replacement. Thus we have turned towards a HA-solution of the structure. Many HA-derivative crystals have been tested, but with consistent non-isomorphy problems. Therefore, a full MAD data set was collected to 2.8 A at BM14 (ESRF, Grenoble). The structure has been solved and refinements are in progress.

1. Edvarsen K, Pedersen P-H, Bjerkvig R, Hermann G.G, Zeuthen J, Laerum O., Walsh F.S and Bock E. Int. J. Cancer, 58, 116-122, 1994
2. Goridis C and Brunet J-F. Semin.Cell Biol., 3, 189-197, 1992
3. Baldwin T.J, Fazeli M.S, Doherty P and Walsh F.S. J. Cell. Biochem.,61, 502-513, 1996
4. Chothia C. and Jones E.Y. Annu. Rev. Biochem., 66, 823-862, 1997

P12.04.129 STRUCTURE OF THE FMN-BINDING DOMAIN OF HUMAN CYTOCHROME P450 REDUCTASE. HPC Driessen[1], J Clapperton[1], Q Zhao[1], S Modi[4], G Smith[3], M Paine[3], PD McDonagh[4], CR Wolf[3], L-Y Lian[4], GCK Roberts[4], D Tew[2]. [1]ICRF Unit of Structural Molecular Biology, Department of Crystallography, Birkbeck College, Malet Street, London WC1E 7HX, UK; [2]Smith Kline Beecham Research, The Frythe, Welwyn, Hertfordshire AR6 9AR, UK; [3]ICRF Molecular Pharmacology Unit, Biomedical Research Centre, Ninewells Hospital and Medical School, University of Dundee, Dundee DD1 9SY, UK; [4] Centre for Mechanisms of Human Toxicity, Department of Biochemistry and Biological NMR Centre, University of Leicester, P.O. Box 138, Lancaster Road, Leicester LE1 9HN, UK.

NADPH-cytochrome P450 reductase is a key component in the cytochrome P450 monooxygenase system. The FMN-binding domain transfers electrons from the NADPH/FAD domain to cytochrome P450, which plays a pivotal role in drug and xenobiotic metabolism. The human domains have been individually expressed, and can be reconstituted to form a complex with catalytic activity in the reduction of cytochrome c and in donating electrons for cytochrome P450-dependent monooxygenase reactions. The crystal structure of the FMN-binding domain has been determined and shows high similarity to that of the bacterial flavodoxins. The residues important for FMN binding have been identified, indicating a striking conservation of the FMN binding site. The protein has an unusual surface charge distribution leading to a very strong dipole, which may be involved in docking substrates into place for electron transfer. Within the general negative surroundings of the FMN, several acidic residues have been identified by mutagenesis experiments to be important for electron transfer to cytochrome P450 2D6 and/or cytochrome c, indicating which part of the surface is likely to be involved in substrate binding.

P12.04.130 PRELIMINARY CRYSTALLOGRAPHIC STUDIES ON A PENTAFUNCTIONAL ENZYME, *AROM*. B. Lohkamp, T. Krell and J.R. Coggins, Institute of Biomedical and Life Science, University of Glasgow, Glasgow G12 8QQ, UK, J.K.F. Maclean and A.J. Lapthorn, Department of Chemistry, University of Glasgow, Glasgow G12 8QQ, UK.

In microorganisms and plants essential aromatic compounds such as folic acid and aromatic amino acids are synthesised from the precursor chorismate. Chorismate is synthesised in seven steps by the enzymes of the shikimate pathway [1]. In bacteria there are seven monofunctional enzymes, whereas in plants there are 6 enzymes with steps 3-4 catalysed by a bifunctional enzyme. In fungi the situation is very different with the central steps (2-6) of the pathway catalysed by *AROM*, a pentafunctional enzyme. This multi-enzyme is a homodimer, each chain contains ~1,600 amino acids separated into 5 domains. These domains share a high degree of sequence homology with the corresponding monofunctional enzymes present in bacteria.

We have overexpressed and purified *AROM* from several species of fungi [2], and have determined several different crystallisation conditions using sparse matrix screening. Small crystals grow after 6-10 weeks and are about 50 μm in the largest dimension. To date structures homologous to 4 of the 5 domains of *AROM* have been solved by ourselves and other groups. We hope to use these as search models to solve the structure of *AROM* by molecular replacement. The crystal structure of *AROM* will help us to understand both the functional and structural advantages of arranging enzymes together as a multi-enzyme. In addition the structure will provide a basis for the rational design of antifungal drugs.

J.R. Coggins *et al.* (1987) Meth. Enzymol., **142**, 325-341
L.D. Graham, F.M. Gillies & J.R. Coggins (1993) Biochim. Biophys. Acta, **1216**, 417-424

P12.04.131 CRYSTALLOGRAPHIC ANALYSIS OF DRUG INTERACTIONS WITH HUMAN SERUM ALBUMIN. A.Bhattacharya, T.Grune, N.P.Franks and S.Curry, Biophysics Section, Blackett Laboratory, Imperial College, London SW7 2BZ, UK

Human serum albumin (HSA), the most abundant protein in the circulatory system, binds an incredible array of ligands [1]. Though its principal function is the transport of fatty acids, it is also known to sequester toxic lipophilic metabolites such as bilirubin and to limit the free plasma concentration of many drugs to less than 10% of the administered dose. Despite the affinity of HSA for this diverse array of compounds, it is known that only a small number of distinct binding locations exist. We have recently determined the crystal structure of HSA complexed with a fatty acid (myristate) [2]. We now wish to investigate the nature of drug binding sites on the protein and have solved the structures of HSA-myristate complexed with a variety of physiologically important ligands, including the anticoagulant Warfarin and Thyroxine, a hormone produced by the Thyroid gland.

For both of these ligands, the free concentration in the blood may be severely affected by binding to HSA and this can give rise to clinical complications.

Our studies reveal interplay between fatty acid and drug binding to the protein. Elucidation of the precise nature of drug interactions with HSA and HSA-fatty acid complexes will help to define important structural characteristics of protein-drug binding sites and may suggest ways to allow better control of the pharmacokinetics of drugs which bind to albumin

1. T.Peters, All about albumin (1995). Academic Press, San Diego.
2. S.Curry, H.Mandelkow, P.Brick and N.Franks (1998). Nature Structural Biology, 5, 827-835.

P12.04.132 CRYSTAL STRUCTURE AND PROPOSED AMINO ACID SEQUENCE OF A THERMOPHILIC XYLANASE FROM THE FUNGUS *PAECILOMYCES VARIOTI* BAINIER AT 1.59Å P. Rajesh Kumar, S. Eswaramoorthy, P. J. Vithayathil and M. A. Viswamitra* Department of Physics, Indian Institute of Science, Bangalore 560 012. INDIA.

We report here the amino acid sequence and the 1.59Å crystal structure of a thermophilic xylanase (PVX) from the fungus, *Paecilomyces varioti* Bainier (PvB). The enzyme has potential applications in the paper industry as an effective substitute for the toxic chlorine based chemicals. It also joins hands with the cellulase enzymes to be called as a potent air-borne and skin allergen, causing dermatitis and allergic rhinitis. The fungus also deserves special attention due to its pathogenicity on patients who possessed major post-surgical complications. It would be worthy to understand this opportunistic infection in terms of the enzymes it expresses and PVX is one such extra-cellular enzyme secreted by this organism. Of special mention is that PVX is the first enzyme from this organism whose three dimensional structure has been determined so far. The crystals belong to the orthorhombic space group, $P2_12_12_1$, with cell dimensions, a=38.7, b=54.1 & c=90.1Å, and the X-ray diffraction data was collected on an image plate with a rotating anode, at the MBU, IISc, India. The structure was solved using molecular replacement methods. Only about 10% of the amino acid sequence was available through biochemical means. The rest of the sequence was arrived using a combination of sequence and structural alignments and a good quality electron density up to 1.59Å. Sequence and structural comparisons between this enzyme and its mesophilic relatives confirm the presence of a

disulphide linkage in the structure of PVX as an obvious cause for increased thermostability. We have analysed several other physical properties and sequence related properties to figure out the reasons for increased thermostability of this class of xylanases. Details of the structure solution, analysis and the interpretation of the reasons for increased thermostability will be presented. The sequence and the structure are deposited with the SWISS-PROT and the PDB.

We thank DBT, JNCASR and INSA, India, for support, and one of us, P.R.K. thanks the CSIR, India, for a Senior Research Fellowship.

P12.04.133 THE ATOMIC RESOLUTION (1.15Å) STRUCTURE OF A NOVEL BACTERIAL ESTERASE. P.C.Bourne, M.N.Isupov and J.A.Littlechild. Departments of Chemistry and Biological Sciences, University of Exeter, Stocker Road, Exeter, EX4 4QD, UK.

The crystal structure of a novel bacterial esterase has been determined by X-ray diffraction to 1.15Å resolution. The enzyme exists as a homodimer belonging to the α/β hydrolase fold family of proteins, with a central core of eight mostly parallel β-strands surrounded by 13 α-helices. The structure was solved using Multiple Isomorphous Replacement (MIR) and averaging of diffraction data from crystals of two different morphologies. The structure has been refined isotropically with an overall R factor of 16.8% and a free R-factor of 18.6%. Refinement of anisotropic temperature factors is proceeding.

Esterase enzymes have found use in a wide variety of biotransformation reactions, catalysing the hydrolysis and transesterification reactions of a broad range of natural and unnatural substrates. This structure represents the largest hydrolase solved to atomic resolution at the present time.

P12.04.134 STRUCTURAL STUDIES ON BOVINE α-LACTALBU-MIN. E.D. Chrysina[1], K. Brew[2] and K.R. Acharya[1], [1]Department of Biology and Biochemistry, University of Bath, Claverton Down, Bath, BA2 7AY, UK, [2]University of Miami School of Medicine, USA.

The biosynthesis of lactose in the lactating mammary gland, is controlled by the activity of the lactose synthase complex. This enzyme consists of two proteins: Galactosyltransferase (GT), the catalytic protein and α-Lactalbumin (LA) the regulatory component [1]. LA is a calcium binding protein. Functional analysis using protein engineering and X-ray crystallographic techniques is in progress with the aim to investigate regions of LA that are implicated in the interaction of GT and in modulating glucose binding, the role of the highly flexible regions of LA in the interaction with GT and the functional significance of metal ion binding to LA. The gene for bovine LA has been cloned and expressed in Prof. K. Brew laboratory.

Recent site-directed mutagenesis experiments on bovine LA have probed two substructures and identified certain residues involved in LA's function [2]. Kinetic analysis of selected single site mutants show that changes in these regions have significant effects on LA's function. In the absence of a 3D structure for GT, only tentative conclusions can be made about the role of particular residues from kinetic results on these mutants. Thus, it is important to follow a 'structure-based' approach. This should enable information and conclusions to be made about the altered functional properties of a particular mutant. With this aim, a series of LA variants at regions proposed to be directly involved in LA action in LS complex were produced. The structure of LA variants along with an Apo-form of bovine LA will be presented during this meeting.

1. K. Brew & J.A. Grobler (1992). In Advanced Dairy Chemistry, Fox, P., ed., vol. 1, Elsevier Press, London, 191.
2. V.A. Malinovskii, J. Tian & J.A. Grobler (1996). Biochemistry, 35, 9710.

P12.04.135 2.6A STRUCTURE OF PREFERENTIALLY ACTIVE ISOFORM OF HUMAN ANTITHROMBIN. X.Y. Pei [1], R. Skinner [2], J.P. Abrahams [3], R.W. Carrell [1], [1] Structural Medicine Division, Department of Haematoloty, Cambridge Institute for Medical Research, University of Cambridge, Cambridge CB2 2XY, UK, [2] Uniniver, UK, [3] Biophysical Structural Chemistry, Leiden Institute of Chemistry, Gorlaeus Laboratories, Leiden University; Einsteinweg 55 / P.O. Box 9502 2300RA, Leiden, The Netherlands.

Here we present the crystal structure of a dimer of beta-antithrombin at 2.6A, one molecule being in the active inhibitory form (I-form) with linkage through its reactive center loop (RCL) to a second molecule in the latent conformation (L-form). Both the I- and L- forms of beta-antithrombin show clear but different changes at Asn135 when compared to alpha-antithrombin. In particular the internal orientation, with well-defined it bonding, of Asn135 in the L-form provides an explanation for the constant fraction of unglycosylation antithrombin (beta-antithrombin) present an synthesis, indicating it is a structural consequence and not an index of an inadequate glycosylation system. The only change indicating a direct reason for the higher heparin affinity of beta-antithrombin is a shift of one of the primer binding residues, Arg129, to an optional orientation. The likely reason for the overall increase in affinity is the greater flexibility of the hD-s2A loop containing Asn135) that undergoes conformational rearrangement on the binding of heparin. The result allowed us to study the physiology of beta-antithrombin in the blood circulation and to design phamecoutic drug for the thromboembolic disease.

1. C.B.Peterson & M.N.Blackburn (1985). J. Biol. Chem. 260, pp610-615.
2. I.V.Turko, B.Fan and P.G.W>Getins (1993). FEBS, Vol335, No1, pp9-12.

P12.04.136 ATOMIC STRUCTURES OF INORGANIC PYROPHOSPHATASE COMPLEXED WITH CALCIUM AND CALCIUM-PYROPHOSPHATE. V.R. Samygina[1], A.N. Popov[2], V.S. Lamzin[2], N.N. Vorobeva [3], S.A. Kurilova [3], T.I. Nazarova [3], S.M. Avaeva [3], [1]Institute of Crystallography, Russian Academy of Sciences, Leninsky pr. 59, Moscow 117333, Russia, [2]Europen Molecular Biology Laboratory (EMBL), c/o DESY, Notkestrasse 85, 22603 Hamburg, Germany, [3]Belozersky Institute of Physico-Chemical Biology, Moscow State University , Moscow 119899, Russia.

The refined atomic resolution structures of E.coli inorganic pyrophosphatase (PPase) complexed with calcium and calcium-pyrophosphate (CaPPi) permit us to suggest a possible inhibiting and functioning enzyme mechanism. PPase catalyzes the cleavage of the phosphoanhydride bond in molecule of inorganic pyrophosphate, which is product of many biosynthetic reactions. Thus PPase controls the level of pyrophosphate in the cell. Divalent metal ions , where magnesium ions are most effective, are required for the activity of PPase. Four Mg^{2+} ions take part in hydrolysis : two of them are bound to the enzyme with different affinity before pyrophosphate binding, and the other two are bound in the presence of substrate. Calcium acts as an inhibitor.

The new conditions under which E.coli PPase crystallises have been determined. Using special cryogenic technique and synchrotron radiation diffraction data sets were collected up to 1.2 Å for complexes with Ca^{2+} ions and CaPPi, whereas all previous structures of E.coli PPase have been determined at resolution not higher than 1.9 Å .The crystals of complex with Ca^{2+} have been

obtained using the co-crystallisation, the CaPPi complex have been obtained by co-crystallisation together with additional soaking. The binding sites for substrate molecule and metal ions have been identified on the difference electron density map. The changing of positions of several functional groups and some parts of a polypeptide chain were observed after Ca^{2+} and substrate binding. It explains well known inhibiting effect of Ca^{2+} binding and allows to elucidate some details of catalysis mechanism.

P12.04.137 STRUCTURE REFINEMENT OF FMN-BINDING PROTEIN AT ULTRA-HIGH RESOLUTION. K. Suto, N. Shibata, Y. Morimoto, N. Yasuoka. Department of Life Science, Faculty of Science, Himeji Institute of Technology, 1475-2, Kanadechi, Kamigori, Ako-gun, Hyogo 678-1297, Japan

Crystal of FMN-binding protein (FMN-bp) diffract up to 0.84 Å resolution at 100K, and diffract up to 1.10 Å at room temperature. The data were collected at SPring-8, Japan. Assignments of the atom species have been easily carried out, judging from the peak height on electron density, for example, in the case of the O, N, C atoms at side chain of aspartic acid and / or threonine. Double conformers were found and located in the main chain atoms of five residues as well as the side chains of 9 residues. Some peaks in the difference Fourier map could be assigned for hydrogen atoms including in hydrogen bonding.

FMN-bp from *Desulfovibrio vulgaris* Miyazaki F is the smallest flavoprotein and has 122 residues and one FMN cofactor in a monomer [1]. The purified sample was crystallized by the hanging-drop vapor diffusion method. Addition of 20% glycerol or 30% MPD to crystallization condition dramatically improved quality of the crystals. Initial phases were determined by the MIR method. FMN-bp exists as a dimer in an asymmetric unit, and two FMNs are held in cleft between two monomers. The high resolution data were measured using a Rigaku R-AXIS IV at BL44B2, SPring-8 (wavelength 0.700 Å). The refinement was carried out using XPLOR for preliminary stage, and then using SHELX-97. *R*work and *R*free with isotropic refinement were decreased to 0.152 and 0.181 for 8.0 - 1.20 Å. Structure refinement with anisotropic temperature factors with higher resolution data is now underway, and the result will be reported.

1. Kitamura, M., *et al.*, (1994). *J. Biol. Chem*. **269**, 5566-5573.

P12.04.138 A 1.1A CRYSTAL STRUCTURE OF THE MOLYBDATE BOUND PERIPLASMIC BINDING PROTEIN MODA2. Lalji Kanbi [1], David Lawson, Clare Williams, Richard Pau [2], Samar Hasnain [1], [1] CLRC Daresbury Laboratory, Warrington WA4 4AD, UK & Biomolecular Science, De Montfort University, Leicester LE1 9BH, [2] Nitrogen Fixation Laboratory, John Innes Centre, Norwich, NR4 7UH, UK

Azotobacter vinelandii is the only bacterium known so far which possesses two periplasmic molybdate binding proteins which are denoted ModA1 and ModA2. Both are components of high affinity transporters, with a binding pocket highly specific for the larger oxydianions molybdate and tungstate. The molybdenum is primarily utilised in the cofactors of oxidoreductases (eg. nitrogenase and dimethyl sulfoxide reductase). Recently, we have reported the structure of ModA2 in its tungstate bound form (Lawson et al. 1998), where the primary sequence was determined directly from electron density maps. Here we report an independent ab initio [italics] structure determination using isomorphous data from the molybdate and the tungstate bound forms extending to resolutions of 1.2 A and 1.1 A respectively. Maps calculated from Single Isomorphous Replacement Anomalous Scattering phases are of high quality. The resultant crystal structure will provide an independent determination of the primary structure. Anisotropic refinement with SHELX at 1.1 A resolution is currently in progress.

The results of this work will be presented.

Lawson, D.M., et al(1998). Ligand size is a major determinant of specificity in periplasmic oxyanion-binding proteins: the 1.2 A resolution crystal structure of Azotobacter vinelandii ModA.Structure,6;1529-1539

P12.04.139 MULTIPLE CONFORMATIONS OF CATALYTIC SER AND HIS IN ACETYLXYLAN ESTERASE AT 0.90A AND 85K. Debashis Ghosh[1,2], Mark Sawicki[2], Mary Erman[1], Daniel R Weeks[1], Puloma Lala[2], Walter Pangborn[1], Daniel J Thiel[3], Hans Jörnvall[4], Jaime Eyzaguirre[5] and Naiyin Li[1]. [1]Hauptman-Woodward Institute, Buffalo, New York. [2]Roswell-Park Cancer Institute, Buffalo, New York. [3]Cornell High Energy Synchrotron Source, Ithaca, New York. [4]Karolinska Institutet, Stockholm, Sweden. [5]Pontificia Universidad Catolica de Chile, Santiago, Chile.

Acetylxylan esterase (AXE II; 207 amino acids) from *Penicillium pupurogenum* has substrate specificities towards acetyl esters of β-D-xylopyranoside residues in a xylan chain and belongs to a new class of α/β hydrolases. The crystal structure of AXE II has been determined by isomorphous difference and anomalous scattering from iodine atoms introduced by iodination of the crystal. The structure of the iodinated complex of the enzyme at 1.80A resolution reveals the formation of iodotyrosines at two locations of the polypeptide. The native structure has been refined to 0.90A and 1.10A resolutions with the data collected at the Cornell High Energy Synchrotron Source at 85K and 295K, respectively. The tertiary structure consists of a doubly-wound α/β sandwich, having a central six-stranded parallel β-sheet flanked by two parallel α-helices on each side. The catalytic residues Ser 90-His 187-Asp 175 are located at the C-terminal end of the sheet, a highly exposed region of the molecule. The serine and histidine sidechains in the 295K structure shows the frequently observed conformation in which Ser 90 sidechain is *trans* and the hydroxyl group is in the plane of the imidazole ring of His 187. However, the structure at 85K displays an additional conformation in which Ser 90 sidechain is *cis*, away from the imidazole plane of the histidine residue. The His 187 sidechain forms a hydrogen bond with a sulfate ion and adopts an altered conformation to accommodate it. The only other known hydrolase that has a similar tertiary structure is *Fusarium solani* cutinase. The exposed nature of the catalytic triad suggests that AXE II is a pure esterase.

P12.04.140 STUDIES ON THE THREE-DIMENSIONAL STRUCTURES OF PHYCOBILI-PROTEINS. J.P. Zhang, T. Jiang, W.R. Chang, J.Y. Liu, D.C. Liang, National Laboratory of Biomacromolecules, Institute of Biophysics, Academia Sinica, Beijing 100101, China

The phycobiliproteins in algae can be divided into three main classes: phycoerythrins (PE), phycocyanins (PC) and allophycocyanins (APC) according to their visible light absorption properties. Energy transfer proceeds successively in the direction of PE→PC→APC→chlorophyll with an overall efficiency of almost 100%.

The structure of R-Phycoerythrin (R-PE) from *Polysiphonia urceolata* was determined by MIR method and refined at 1.9Å resolution. The crystals belong to space group R3 with unit cell dimensions of a=b=189.8Å, c=60.1Å. The subunit composition of R-PE is $(\alpha_2\beta_2)_3\gamma$. The interactions between chromophores and protein are observed in high resolution. The four phycoerythrobilin chromophores α84, α140a, β84 and β155 in an (αβ) unit are each covalently bound to a cysteine residue through ring A. The phycourobilin chromophore is bound to a cysteine β50 by ring A and bound to cysteine β61 by ring D. The ring A and ring D of phycourobilin deviate from the conjugate plane formed by ring B and ring C and the four rings form a boat-

shaped structure. R-PE contains a 34K Da γ subunit that is assumed to lie in the central channel of the molecular disc $(\alpha_2\beta_2)_3$. The energy transfer and the interactions between protein residues and chromophores are discussed.

R-phycocyanin (R-PC) from *Polysiphonia urceolata* has been isolated and crystallized. Diffraction data were collected up to 2.4Å resolution. The structure determination by molecular replacement method is in progress.

Allophycocyanin (APC) from red alga *Porphyra yezoensis* has been crystallized in three crystal forms. The space group of form 3 is R32 with cell dimensions a=b=105.3, c=189.4Å and one αβ unit in the asymmetric unit. Low-resolution structure of APC was solved by molecular replacement method and the structure refinement at 2.2Å resolution is in progress.

P12.04.141 PROTEIN CARBOHYDRATE INTERACTIONS AT ATOMIC RESOLUTION. James H. Naismith, Davina N. Moothoo, David A.R. Sanders [1], Andy Howard [2], Paul Faulder, Rachel B Nuttall, James R. Raftery, John R. Helliwell [3], 1. Biomolecular Sciences, St Andews University, Scotland, 2. Advanced Photon Source, Argonne, Illinois, USA, 3. Chemistry Dept, University of Manchester, M13 9PL, UK

We have been seeking to probe carbohydrate interaction by structural methods to provide a molecular rationale for binding affinities observed by calorimetery. This is vitally important if modelling approaches for protein carbohydrate interactions are to progress. Currently even the most sophisticated of these approaches fails to predict either the orientation or affinity of carbohydrate binding. We have chosen to study the lectin concanavalin A. It is an ideal model system. Its protein carbohydrate interactions are well characterised by calorimetery, it is readily available and we are able to obtain complexes with many different carbohydrates. As part of this program we have now collected data at cryotemperature at the APS IMCA undulator beamline, and with a CCD detector, to 1.20 Å resolution from crystals of the concanavalin A Man alpha 1-2 Man complex. The structure shows in atomic detail the concanavalin A disaccharide interaction unequaled to our knowledge by any other protein carbohydrate complex.

P12.04.142 THE STRUCTURE OF CASPASE 8 AT ATOMIC RESOLUTION. William Watt, Keith D. Watenpaugh Alfredo G. Tomasselli, Kenneth A. Koeplinger, Ana M. Mildner, Robert L. Heinrikson Structural, Analytical and Medicinal Chemistry, Pharmacia and Upjohn, Kalamazoo, Michigan Protein Science, Pharmacia and Upjohn, Kalamazoo, Michigan

Caspase 8 is a cysteine proteinase that is considered to be a prime initiator in a cascade of events leading to proteolytic activation of caspase 3, the executioner of programmed cell death, or apoptosis. We have cloned and expressed an inactive, precursor form of human caspase 8 that was produced in high yield as inclusion bodies in Escherichia coli. The protein was solubilized and refolded to give an inactive, single-chain precursor which, upon concentration, auto activated to yield authentic and highly active caspase 8. The recovery of pure enzyme was 10 mg/liter of bacterial culture. The structure of the caspase 8 covalently linked to Ac-IETD-aldehyde has been solved by x-ray crystallography and refined using a 1.2 Å dataset (a=b=62.4Å, c=129.25Å, space group $P3_121$, RF=0.15 for the refined structure). The asymmetric unit consists of a heterodimer with a crystallographic dyad generating the biologically active tetramer. While the basic protein fold is very similar to that of caspase 1 and caspase 3, the substrate binding region has significant differences which explain the specificity of caspase 8. The Ac-IETD-aldehyde is bound covalently to the catalytic cysteine with the aspartic acid buried in the protein. The structure forms the basis of an active structure-based drug design project.

P12.04.143 NEUTRON-LAUE & ATOMIC RESOLUTION X-RAY ANALYSIS OF ENDOTHIAPEPSIN. J.B. Cooper and P.T. Erskine. School of Biological Sciences, University of Southampton, Southampton, SO16 7PX, UK, and D.A.A. Myles. Institut Laue-Langevin and EMBL, Grenoble, France.

Aspartic proteinases are a family of enzymes involved in a number of important physiological and pathological processes. Until now, no aspartic proteinase has been subjected to a successful neutron diffraction analysis due to the limited size of the crystals. However, the recent development of the neutron-Laue technique at ILL (Grenoble), has allowed us to collect neutron data to 2.2 Å on a complex of endothiapepsin with a transition state analogue. Current proposals for the catalytic mechanism of aspartic proteinases are largely based on X-ray structures of inhibitor complexes but these proposed mechanisms differ in the assignment of protonation states to the catalytic groups and intermediates during the reaction. Our objective is to define the positions of the protons at the active site by exhaustive refinement using the neutron data. In line with work on serine proteinases where neutron diffraction has provided some of the most definitive data on the catalytic mechanism, we expect that our work will have a greater significance for studies of the aspartic proteinase enzymes where mechanistic studies by other techniques have been largely inconclusive.

The co-crystals of endothiapepsin with the inhibitor H-261 are monoclinic ($P2_1$) and have unit cell dimensions of a = 43.1 Å, b = 76.1 Å, c = 43.0 Å, β = 97.0°. A large deuterated crystal was mounted on the LADI instrument at ILL and has so far yielded neutron data to 2.2 Å. The data have an R-merge of 13.7 %, a completeness of 81% and mean multiplicity of 2.0. In parallel we have obtained X-ray data to 1.1 Å resolution from a frozen crystal of the same complex at beam line BW7B at DESY (Hamburg). These data have an R-merge of 12.5 %, a completeness of 99.8 % and a mean multiplicity of 3.7. Least-squares refinement of the structure with these datasets is in progress using SHELX-97 (G.M. Sheldrick).

P12.04.144 CRYSTAL STRUCTURE OF THE CATALYTIC DOMAIN OF CHITINASE A1 FROM *BACILLUS CIRCULANS* WL-12. T. Matsumoto, T. Nonaka, Y. Mitsui, Department of BioEngineering, Nagaoka University of Technology, Kamitomioka, Nagaoka, Niigata 940-2188, Japan, H. Katohda, M. Hashimoto, T. Watanabe, Department of Agricultural Chemistry, Faculty of Agriculture, Niigata University, Ikarashi-2, Niigata, Niigata 950-2181, Japan

Chitinases are enzymes for the hydrolysis of the chitin, which is the homopolymer of *N*-acetylglucosamine. *Bacillus circulans* WL-12 secretes at least six kinds of chitinases into the culture medium. Chitinase A1, the main chitinase of this bacterium, consists of three kinds of domains (a catalytic domain, two type III homology units of fibronectin, and C-terminal short segment). The catalytic domain of chitinase A1 is composed of 419 amino acid residues (Mr. 45489). It was crystallized at 20°C by vapor diffusion method using polyethylene glycol as a precipitant. Structural analysis was attempted by a molecular replacement method. A molecular model of the catalytic domain of chitinase A1 based on the three dimensional structure of chitinase A from *Serratia marcescens* was constructed by homology modeling technique. It was possible to determine the orientation of the catalytic domain of chitinase A1 from a series of rotation search. However, there were many areas where it was difficult even to interpret the electron density distribution for the main chain, and accordingly the refinement of the crystal structure failed. However, interpretation of the electron density map became possible after the phases were expanded and improved using the X-ray diffraction data up to 1.5Å resolution. Currently we are refining the three dimensional structure, adding the anisotropic

displacement parameters to the calculation, using the diffraction data up to 1.13Å resolution. As a result of the refinement at an atomic resolution, it became possible to identify the orientation of the imidazole ring of the histidine residues and to distinguish the nitrogen atom from the oxygen atom in the side chain of the asparagine and glutamine residues.

P12.04.145 THE HISTONE OCTAMER OF THE NUCLEOSOME CORE PARTICLE IN KCL/PHOSPHATE: STRUCTURE TO 2.15Å RESOLUTION IN SPACE GROUP $P6_5$. J.P. Baldwin, S.J. Lambert, A.J. Reid, and M.J. Donovan, Beckman Laboratory, School of Biomolecular Sciences, Liverpool John Moores University, Byrom St., Liverpool L3 3AF, UK, and J.M. Nicholson, Daresbury Laboratory, Warrington, Cheshire WA4 4AD, UK, and L. Chantalat, Laboratoire de Crystallographie Macromoleculaire, Institut de Biologie Structurale, 41 Avenue des Martyrs, 38027 Grenoble 1, Cedex, France.

Intact histone-core octamers of the nucleosome crystallise in space group $P6_5$ using 2M KCl and 1.35M phosphate [1, 2]. The octamers pack, one per unit cell, in a left-handed helical arrangement with six octamers per turn in a c-axes repeat of 102.6Å, providing a useful model for nucleosome packing in chromatin higher-order structure. The $P6_5$-octamer structure has been refined to 2.15Å resolution and 70% of the total amino acids are conserved with a mean positional difference of 0.5Å compared with the octamer in the nucleosome core particle at 2.8Å resolution [3], with a near-identical distribution of temperature factors, between 20 and 60Å^2. A further 6% of the total amino acids are assigned in the $P6_5$ structure and are positioned differently from those in the nucleosome core particle with temprature factors between 20 and 100Å^2. N-terminal basic domains accounting for the remaining 24% of the total amino acids, are disordered as are 20% of those in the nucleosome core particle. 540 highly-ordered water molecules are clearly assigned with many H_2O - H_2O hydrogen bonds. They form sheet-like structures over regions of the surface of the octamer, the highly basic cage at the centre of the octamer and in channels leading from the central cage to the surface of the octamer. Several phosphate groups from the crystallisation buffer have been assigned on the outside of the octamer. The role of the two C-terminal α helices of histones H2B in binding DNA in the condensed chromatin higher-order structure and the possible role in the movement of octamers around RNA polymerase in transcription is discussed.

R.J. Carter, S.J. Lambert, L. Chantalat, F.C.F. Körber, J.M. Nicholson & J.P. Baldwin (1996). Acta Cryst., **D52**: 569-570.
S.J. Lambert, J.M. Nicholson, L. Chantalat, A.J. Reid, M.J. Donovan & J.P. Baldwin (1999). Acta Cryst. **D**. (in press)
K. Luger, A.W. Mader, R.K. Richmond, D.F. Sargent & R.J. Richmond (1997). Nature **389**: 251-260.

P12.04.146 0.9Å STRUCTURE OF A KUNITZ DOMAIN FROM THE A-3 CHAIN OF HUMAN TYPE VI COLLAGEN B. Arnoux, M.C. Vaney, A. Ducruix [1], K. Norris, F. Norris [2], [1] Laboratoire d'Enzymologie et Biochimie Structurales, CNRS, 91198 Gif sur Yvette, France, [2] Health Care Discovery, Novo Nordisk A/S, DK-2820 Gentofte, Denmark

The C-terminal Kunitz-type domain from the alpha-3 chain of human type VI collagen (C5), a single 58 amino acid residue chain with three disulfide bridges, was cloned, expressed and crystallized in a monoclinic form, space group P21, with a=25.2Å, b=37.7Å, c=28.5Å and b=109.3°. A previous refinement was done at 1.2 Å at room temperature (R=13.6%, between 7 and 1.2 Å) with anisotropic temperature factors [1] and the model subjected to normal mode calculation. The results indicate fluctuations with a large anisotropy since the total fluctuations are close to the largest component of the principal axes of fluctuations. The anisotropy in the crystal fluctuations are less marked. However a good correlation between the theoretical fluctuations and the X-ray profiles are observed. Besides this crystal structure at room temperature, two NMR structures of C5, also at room temperature were published [2,3]. To decouple static and dynamic disorder, a new data set at low temperature was collected at the EMBL Hamburg outstation. The anisotropic refinement of the protein-water-ion model at 0.9Å resolution using the program SHELXL-97 is in progress. Ultrahigh resolution data provides a solid base for getting a better insights into the hydration shells of proteins. The comparison of this low-temperature model with the previous ones (room temperature, NMR) will lead to a complete description of the molecule, including domain movements and relative flexibility of surface loops using normal mode analysis. The localization of ion and water molecules will also be discussed in term of folding.

1. K. Mérigeau, B. Arnoux, D. Perahia, K. Norris, F. Norris & A. Ducruix (1998). Acta Cryst. D54, 306-312.
2. M. Zweckstetter, M. Czisch, U. Mayer, ML Chu, W. Zinth, R. Timpl & T. A. Holak (1996). Structure, 4, 195-209.
3. M.D. Sørensen, S. Bjørn, K. Norris, O. Olsen, L. Petersen, T.L. James & J.J. Led (1997). Biochemistry, 36, 10439-10450.

P12.04.148 ATOMIC RESOLUTION STRUCTURES OF HEME PROTEINS AT 100 K. G.S. Kachalova and H.D. Bartunik, Max-Planck Research Unit for Structural Molecular Biology, MPG-ASMB c/o DESY, Notkestr. 85, 22603 Hamburg, Germany, A.N. Popov, EMBL-Outstation Notkestr. 85, 22603 Hamburg, Germany, V. Samygina and E. Harutyunian, Russian Academy of Sciences, Institute of Crystallography, Moscow, 117333 Russia.

The low-temperature (100K) crystal structures of myoglobin and leg hemoglobin in the deoxy, met and CO liganded states have been refined at atomic resolution (0.9 – 1.1Å). Comparison to the corresponding room temperature structures shows significant differences in the conformations due to the cooling. Taking the example of CO myoglobin, substantial changes are observed in the overall conformation and in the interactions between the bound ligand and its immediate environment. The cooling in particular changes the Fe-C-O binding geometry, the distance of the heme iron from the plane defined by four pyrrol nitrogens, and the distances between the CO oxygen and distal residues. Furthemore, the bondlength between the Fe and proximal histidine, and the conformation of the porphyrin are affected. On the other hand, the number of sites of the distal histidine is not affected by cooling, neither in deoxy nor in CO myoglobin. Despite the cryo-induced conformational changes, the low-temperature structures provide information on the interaction between the heme group and the protein matrix, which is relevant for an interpretation of the structure-function relationships in heme proteins under physiological conditions.

P12.04.149 THE 0.97 Å RESOLUTION STRUCTURE OF CYTOCHROME C-553 FROM *BACILLUS PASTEURII*. STRUCTURAL AND FUNCTIONAL ANALYSIS. W. R. Rypniewski[@], S. Benini[@], A. Gonzalez[@], K. S. Wilson[£], S. Ciurli[$]. [@]EMBL c/o DESY Notkestraße 85 D-22603 Hamburg, Germany [£]Dept. of Chemistry, York University Heslington YO1 5DD, UK, [$]Inst. di Chimica Agraria, Bologna University, Viale Berti Pichat 10 I-40127.

The gram-positive, highly ureolytic *B.pasteurii* is an obligate aerobe and facultative alkaliphile that grows optimally at pH 9.2 in the presence of high amounts of NH_4^+ salts or urea. The cytochromes from alkaliphilic bacteria are characterised by distinctly low reduction potentials, a feature that has been proposed to facilitate electron transfer to the membrane bound oxidase in the presence of the large negative membrane potential

associated with the alkaline growth medium. Cytochrome c-553 from *B. pasteurii* has been extensively studied using ^{1}H NMR and direct cyclic voltammetry [1]. The NMR spectra indicate a His-Met axial coordination of the low spin (S=1/2) heme iron. The pH dependence of the NMR signals display a ionisation step with pK_o=5.7. The pH dependence of the reduction potential determined by cyclic voltammetry indicates potentials for the protonated and deprotonated forms of +71 mV and +58 mV, respectively. The thermodynamic and spectroscopic data indicate a large solvent-derived entropic effect as the main cause for the low reduction potential. The protein has been crystallised and data have been collected to 0.97 Å [2]. The ultra high resolution allowed us to solve the structure by a completely automated procedure using ARP and REFMAC. Refinement using SHELXL gave a final R_{factor}=11.5%. Cytochrome c-553 is a small heme protein (71 residues) with a very exposed heme. The high resolution provided the most accurate analysis of a heme containing protein to date. Comparison of different cytochromes belonging to the c class has been used to analyse the relationship between the folding, accessibility of the heme to the solvent and the reduction parameters [3].

[1] Benini, S., Borsari, M., Ciurli, S., Dikiy, A., Lamborghini, M. (1998) *J. Bioinorg. Chem.* 3 371-382
[2] Benini, S., Ciurli, S., Rypniewski, W.R., Wilson, K.S. (1997) *Proteins: Struc. Func. Genetics*. 28 580-585
[3] Benini, S., Rypniewski,W.R., Gonzalez, A., Wilson, K.S. Ciurli, S. *Proteins: Struc. Func. Genetics*. Submitted

P12.04.150 CRYSTAL STRUCTURE OF *E.Coli* MurD/UMA/ AMPPCP COMPLEX AT 1.5 Å RESOLUTION. N.Y. Chirgadze, G. M. Birch, L. C. Blaszczak, S.L.Briggs, D.K. Clawson, N. G. Halligan, J. E. Mcgee, S. Sigmund, M. C. Smith, R.W. Schevitz. Lilly Research Laboratories, Eli Lilly & Company, Indianapolis, IN 46285, USA.

The crystal structure of His-tagged *E.coli* UDP-N-acetylmuramoyl-L-alanine-glutamate:D-glutamate (MurD) in a complex with UDP-MurNAc-L-Ala (UMA) and adenosine 5'-[β,γ-methylene] triphosphate (AMPPCP), a non-hydrolyzable ATP analog, has been determined at 1.5 Å resolution using X-ray crystallography to aid in the design of MurD inhibitors. MurD, essential to cell wall containing bacteria, is an attractive target for drug development. Crystals of the complex were obtained from 20% MME PEG5000, 0.2M LiCl, and 0.1M MES buffer at pH=6.1, under nitrogen, by the vapor diffusion technique at 20°C. $MgCl_2$, UMA, and AMPPCP were present at 1.5 eq. Crystals belong to the orthorhombic space group, $P2_12_12_1$, with unit cell parameters *a*=49.0 Å, *b*=84.9 Å, *c*=115.3 Å, with one molecule per asymmetric unit. Diffraction data were collected on a synchrotron beam line ID-17 at the Advanced Photon Source at 100K. The phase problem was solved by molecular replacement using the 1UAG[1] structure as a search model. The current crystallographic R-value is 21.6% (R_{free}=24.3%). Two loops, 221-225 and 241-244 not resolved in 1UAG structure, are well defined in our electron density. In contrast to 1UAG, no oxidation of Cys208, Cys227 or carbamylation of Lys198 was observed. Both UMA and AMPPCP are well resolved in the electron density. The UMA uridine moiety has a different conformation in our structure from 1UAG, as a result of a small shift of the N-terminal domain. AMPPCP binds between the middle and C-terminal domains causing the latter to move with a maximum displacement in C_α atoms of 5 Å. The C-terminal domain moves as a rigid body pivoting around residue Gly298 and closing the ATP binding cleft. AMPPCP binding is characterized mostly by electrostatic (Lys115, Arg302 and Lys319) and hydrogen bond interactions, both directly with protein and through structural water molecules. In addition, the crystal structure of a complex with a transition state analog-like inhibitor was determined at 2.6 Å resolution. The binding mode of the inhibitor mimics in part the position of phosphate and MurNAc portion of UMA, and reveals the glutamic acid binding site.

1. Bertrand J.A. *et al*. **1997** The EMBO J., vol.16 No.12 pp. 3416-3425

P13.04.001 STRUCTURE OF FORMYLTETRA-HYDROFOLATE SYNTHETASE FROM *CLOSTRIDIUM THERMOACETICUM* DETERMINED BY MAD. Lukasz Lebioda, Ramin Radfar, Ronald Shin, J. D. Odom, and R. Bruce Dunlap, Department of Chemistry and Biochemistry, University of South Carolina, Columbia, SC 29208,USA, Charles R. Lovell, Department of Biological Sciences, University of South Carolina, USA, Wladek Minor, Department of Molecular Pharmacology and Biophysics, University of Virginia, USA, and George M. Sheldrick, Institut fur Anorganische Chemie, Universitat Gottingen, Germany

The tetrahydrofolate (THF)-mediated transfer of one-carbon units is crucial to purine and pyrimidine biosynthesis. One of the key THF mediated reactions is the ATP-dependent activation of formate by formyltetrahydrofolate synthetase (FTHFS) (EC 6.3.4.3). In *Clostridium thermoaceticum,* FTHFS exist as a homotetramer of 240 kDa and is activated by monovalent cations (ammonium or potassium).

A plasmid coding for FTHFS was incorporated into the methionine auxotroph *E. coli* strain DL-41 and overexpressed in media containing selenomethionine. The selenomethionyl FTHFS exhibited similar kinetic behavior to the wild type enzyme, however, it did differ from the wild type in that the enzyme retained 100% of its activity when Ca^{2+} was substituted for Mg^{2+}, as opposed to 70% for the wild type.

X-ray diffraction data were collected at –160 ºC at the Structural Biology Center beamline at the Argonne synchrotron source using four wavelengths. The positions of 28 sites of Se atoms were established using the SHELX-M software. Experimental phases were obtained using the MLPHARE software and optimized using solvent flattening and histogram matching with the DM program from the CCP4 system.

The subunit is built of two domains, each of them belonging to the αβ class. The enzyme has an unusual quaternary structure with the four subunits being approximately in one plane, forming an arrangement with the shape of the letter "X". There are numerous intersubunit contacts at each of the "four corners". The site of monovalent cation binding was established by exchange of ammonium sulfate with cesium sulfate.

P13.04.002 TRAPPING THE CO^{3+}-INSULIN STATE BY SEMI-TIME-RESOLVED CRYO-CRYSTALLO-GRAPHY. L.C. Perkins and F.C.F. Körber, School of Biomolecular Sciences, Liverpool John Moores University, Byrom Street, Liverpool L3 3AF, UK, and J.M. Nicholson, PX-Facility Group, SR Department, CCLRC-Daresbury Laboratory, Daresbury, Warrington WA4 4AD, UK.

Thomas and Wollmer [1] have shown spectroscopically that hexameric insulin which is co-ordinated to cobalt ions instead of zinc can undergo a variety of structural transitions. We have been able to initiate one of these transitions, triggered by the oxidation of Co^{2+} to Co^{3+} in the crystal through the addition of hydrogen peroxide. Although there is a definite colour change in crystals subjected to this treatment, X-ray crystallographic structure determinations of the end-states at room temperature indicate that the metal ions are predominantly octahedrally co-ordinated and the structures are virtually identical [2]. As it is obvious that in the mother liquor the hydrogen peroxide is rapidly decomposed, we concluded that the metal ion in the end state had reverted to Co(II).

In order to capture the Co(III)-insulin state, crystals mounted on hairloops were flash-frozen at various times after initiating the transition, and almost complete diffraction data sets were recorded to a resolution of 2.4 Å. Currently, the intermediate structures are being refined and compared with a 1.2 Å cryo-cooled Co(II)-insulin structure [3]. Present results indicate that, after being subjected to hydrogen peroxide for 5 minutes, the Co is tetrahedrally co-ordinated. His B10 and the adjacent section of the insulin B-chain seem to have undergone a small shift. Very high B-values for the Co-ion suggest that the Co may be involved in the decomposition of the peroxide.

1. B. Thomas and A. Wollmer (1989). Biol.Chem. Hoppe-Seyler, Vol. 370, p.1235-1244.
2. P. McMichael, PhD thesis (1997). Liverpool John Moores University.
3. J.M. Nicholson and F.C.F. Körber, "The Structure of Co(II)-insulin at 1.2 Å Resolution", manuscript in preparation.

P13.04.003 PHOTOLYSIS AND GEMINATE REBINDING OF CO HEMOGLOBIN STUDIED BY SINGLE-BUNCH LAUE DIFFRACTION. S. Adachi, S.-Y. Park, T. Iizuka [1], H. Morimoto [2], T. Ursby [3], D. Bourgeois, M. Wulff [4], V. Srajer, T.-Y. Teng, Z. Ren, C. Pradervand, W. Schildkamp, K. Moffat [5], [1] The Institute of Physical and Chemical Research (RIKEN), Harima Institute, Sayo, Hyogo, Japan, [2] Department of Biophysical Engineering, Osaka University, Toyonaka, Osaka, Japan, [3] Department of Molecular Biophysics, Lund University, Lund, Sweden, [4] European Synchrotron Radiation Facility (ESRF), Grenoble Cedex, France, [5] Department of Biochemistry and Molecular Biology and the Consortium for Advanced Radiation Sources, The University of Chicago, Chicago, IL, USA

The crystal of T-state HbACO (Mg-Fe hybrid HbACO) was photolyzed by nanosecond YAG-laser-pumped dye laser, and 150 ps x-ray pulses emitted by a single electron bunch of ESRF storage ring [1,2] were used to obtain Laue diffraction data with nanosecond time resolution during subsequent CO rebinding process at ESRF BL3/ID9. The Laue diffraction dataset at time delay of 2 ns between laser and x-ray was refined by X-PLOR and a possible docking site of CO in the heme pocket of b2 subunit of HbA was found in the 2Fo-Fc map. The site was similar to the docking site which was found in myoglobin. These time-resolved experiments reveal the structures of hemoglobin photoproducts, provide a structural foundation to spectroscopic results and molecular dynamics calculations.

1. D. Bourgeois et al. (1996) J. Synchrotron Rad., 3, 65-74.
2. V. Srajer et al. (1996) Science, 274, 1726-1729.

P13.04.004 HUMAN CERULOPLASMIN: CRYSTALLOGRAPHIC STUDY OF THE SUBSTRATE AND INHIBITOR BINDING SITES V.Zaitsev [1], I.Zaitseva [1], M.Papiz [1] and P.Lindley [2] [1] CCLRC Daresbury Laboratory, Warrington, Cheshire, WA4 4AD, UK [2] ESRF, BP-220, F-38043 Grenoble Cedex, France

Ceruloplasmin is a multi-copper oxidase,which contains over 60% of the copper present in plasma. It is an acute phase reactant that exhibits a 2- to 3-fold increase over the normal concentration of 300 µg/ml in adult plasma. However, the precise physiological role(s) of ceruloplasmin has been the subject of intensive debate and it is likely that the enzyme has a multi-functional role including iron oxidase activity and the oxidation of biogenic amines [1,2]. The three-dimensional X-ray structure of the human enzyme shows that the molecule is comprised of 6 cupredoxin-type domains arranged in a triangular array [2]. There are 6 integral copper atoms per molecule (mononuclear sites in domains 2,4 and 6 and a trinuclear site between domains 1 and 6) and two labile sites with roughly 50% occupancy . Further structural studies on binding of metal cations by the enzyme indicated a putative mechanism for ferroxidase activity [3]. Medium-resolution X-ray studies (3.0-3.5 Å) have recently been undertaken, which located the binding sites for an inhibitor (azide) and various substrates (aromatic diamines, biogenic amines and d-lysergic acid ethylamide, LSD). The binding site of the azide moiety is topologically equvalent to one of the sites reported for ascorbate oxidase [4]. However, there are two distinct binding sites for amine substrates; aromatic diamines bind on the bottom of domain 4 remote from the mononuclear copper site, whereas the biogenic amines typified by serotonin, epinephrine, norepinephrine and dopa bind in close vicinity to that utilized by cations in domain 6 and close to the mononuclear copper. These binding sites are discussed in terms of possible oxidative mechanisms [5].

[1] Saenko, E.L., et al.(1994) J.Trace Elem.Expt.Med.,7: 69-88
[2] Zaitseva, I., et al.(1996) J.Biol.Inorg.Chem., 1:15-23
[3] Lindley, P, et al. (1997) J.Biol.Inorg.Chem., 2:454-463
[4] Messerschmidt, A., et al (1993), J.Mol.Biol. 230:997-1014
[5] Zaitsev, V. et al (1999) J.Biol.Inorg.Chem., submitted.

P13.04.006 CRYSTAL STRUCTURE OF CCDB, A TOPOISOMAERASE POISON FROM E. COLI. R. Loris, M.-H. Dao-Thi, L. Wyns, Vrije Universiteit Brussel, Paardenstraat 65, B-1640 Sint-Genesius-Rode, Belgium.

The crystal structure of CcdB, a protein that poisons E. coli gyrase, was determined in three crystal forms. The protein consists of a 5-stranded anti-parallel (-pleated sheet followed by a C-terminal (-helix. In one of the loops of the sheet, a second small 3-stranded anti-parallel (-sheet is inserted that sticks out of the molecule as a wing. This wing contains the LysC proteolytic cleavage site that is protected by CcdA and therefore forms a likely CcdA recognition site. A dimer is formed by sheet extension and by extensive hydrophobic contacts involving three of the five methionines and the C-terminus of the (-helix. The surface of the dimer on the side of the (-helix is overall negatively charged, while the opposite side as well as the wing sheet is dominated by positive charges. We propose that the CcdB dimer binds into the central hole of the 59 kD N-terminal fragment of GyrA, after disruption of the head dimer interface of GyrA.

P13.04.007 CRYSTALLIZATION OF *CRITHIDIA FASCICULATA* TRYPAREDOXIN. Magnus S. Alphey[1], Gordon A. Leonard[2], David G. Gourley[1], Emmanuel Tetaud[1], Alan H. Fairlamb[1] and William N. Hunter[1]. [1] Department of Biochemistry, Wellcome Trust Building, University of Dundee, Dundee, DD1 5EH, Scotland, UK. [2] Joint Structural Biology Group, ESRF, BP 220, F38043, Grenoble, CEDEX, France.

Recombinant tryparedoxin, a thioredoxin homologue from *Crithidia fasciculata* has been purified from an *Escherichia coli* expression system and used in crystallization trials. Orthorhombic needles in space group $P2_12_12_1$, with unit cell dimensions of a = 38.63, b = 51.47, and c = 73.41 Å have been obtained. The crystals present a monomer of approximate molecular mass 16 kDa in the asymmetric unit and diffract to high resolution using synchrotron radiation. Structure determination will further understanding of the role tryparedoxin plays in regulating oxidative stress in parasitic trypanosomatids.

P13.04.009 X-RAY STRUCTURAL STUDIES OF THE CYTOPLASMIC MOLYBDATE BINDING PROTEIN MODG L. Delarbre, C.E.M. Williams, D.J. White, L.A. Mitchenall, R.N. Pau and D.M. Lawson, Nitrogen Fixation Laboratory, John Innes Centre, Norwich NR4 7UH, UK.

A. vinelandii ModG belongs to a novel family of intracellular molybdate-binding proteins that also bind tungstate but not sulfate, and are described as molbindins [1]. They appear to be involved in intracellular molybdenum homeostasis, and in diazotrophs such as *A. vinelandii*, may have a role in nitrogenase cofactor biosynthesis. The simplest molbindin identified to date is the Mop protein from *H. influenzae*, which is a homotetramer of 7kDa subunits. ModG however, has a subunit molecular weight of 14kDa which is made up of a tandem repeat of Mop-like sequences [2]. We have solved the structure of the ligand-bound form of ModG at 2.2 Å resolution by MAD phasing on tungstate. Moreover, we anticipate that by a combination of MAD phasing on a gold derivative and Molecular Replacement using the ligand-bound structure, we will be able to solve the apo structure. ModG is comprised almost entirely of β-strands and makes use of positively charged amino acids to bind its ligand, in sharp contrast to the periplasmic receptor (ModA), which relies on local dipoles provided by α-helices to dissipate the negative charge [3]. Through site-directed mutagenesis, we aim to probe the specificity of these binding sites. Furthermore, through comparison with the apo form we will be able to characterise the conformational changes associated with ligand binding.

1. D.M. Lawson, C.E. Williams, D.J. White, A.P. Choay, L.A. Mitchenall & R.N. Pau (1997). J. Chem. Soc., Dalton Trans., 3981-3984.
2. N.J. Mouncey, L.A. Mitchenall & R.N. Pau (1996). Microbiol. 142, 1997-2004.
3. D.M. Lawson, C.E.M. Williams, L.A. Mitchenall & R.N. Pau (1998).Structure 6, 1529-1539.

P13.04.010 TOPOLOGICAL STRUCTURE OF ARTIFICIAL INHIBITORS DETERMINED BY X-RAY CRYSTALLOGRAPHY IN CYCLOHEXANE. Qichen Huang, Yanshi Zhu, Minxie Qian and Youqi Tang, Department of Chemistry, Peking University, Beijing 100871, P. R. China.

Two active trypsin inhibiting components, SPC1 and SPC2 with the same sequence of amino acid, were obtained during the synthesis of a 22-residue peptide of mimic mung bean inhibitor. The Ki values of SPC1 and SPC2 are 1.2×10^{-7} and 4.0×10^{-8} M respectively. In order to determine the difference between the structures of SPC1 and SPC2, X-ray diffraction studies were carried out on the complexes of SPC1 and SPC2 with bovine β-trypsin, only the binding loop (9 residues) of SPC1 resolved at 2.2Å resolution due to conformational flexibility of the other residues[1]. The amino acid sequence was re-determined and electrospray mass spectroscopy was also carried out to ensure that no deamidation occurred on SPC1 and the primary sequences of SPC1 and SPC2 are chemically identical. As has been proved proteins are more rigid in nonaqueous media [2,3], that is, some disordered regions may become more order when the protein crystal is transferred into organic solvents from water. So the complex of SPC1 was treated with cyclohexane for about 20 minutes and then subjected to X-ray diffraction analysis. The result showed that all the 22 residues of SPC1 were located in the electron density map perfectly. The crystal structure of SPC1 complex with bovine β-trypsin was refined to a final R value of 0.185 using data of 7.0-2.2Å resolution. So the topological structures of SPC1 and SPC2 have been determined which are responsible for the different inhibitory activity, suggesting that crystal treatment with cyclohexane may be used as a general method to determine disordered regions of proteins in the future.

1. Li, Y., Huang, Q., Zhang, S., Liu, S., Chi, C., and Tang, Y. (1994). J. Biochem. 116, 18-25.
2. Yennawar, N. H, Yennawar, H. P., and Farber, G. K. (1994). Biochemistry 33, 7326-7336.

P13.04.011 CRYSTAL STRUCTURE OF THE COMPLEX OF BOVINE β-TRYPSIN AND MCTI-A, A TRYPSIN INHIBITOR OF SQUASH FAMILY. Yanshi Zhu, Qichen Huang, Minxie Qian and Youqi Tang, Department of Chemistry, Peking University, Beijing 100871, P. R. China.

In our previous study of the crystal structure of the complex formed between porcine β-trypsin and MCTI-A, a trypsin inhibitor from Bitter Gourd seeds (*Momordica charantia*, Linn. *Cucurbitaceae*), five residues, including 1I, 2I at the N terminus, 11I, 19I at/near the site of contact with symmetry-related molecules, and 24I within a tight type turn, could not be identified clearly because of weak and irregular side chain electron density map[1]. MCTI-A complex with bovine β-trypsin was crystallized and its crystal structure was refined to a final R value of 0.176 using data of 7.0-1.8Å resolution. The primary sequence of the inhibitor was determined by recognizing the electron density map. These five residues mentioned above can be determined unambiguously in the electron density map. So its sequence is completely resolved as

RICPRIWMECKRDSDCMAECICVMGHCG.

The ionised electrospray mass spectroscopy was also carried out, showing that the molecular weight of MCTI-A is 3240.8±0.8, which is consistent with the sequence of MCTI-A. Compared with other squash family inhibitors, 13 amino acids of the total 28 residues of MCTI-A are conserved[2]. MCTI-A roughly exhibits the shape of a flat-iron with the base plate made up of the polypeptide chain from Met8I on, and the grip formed by the protruding reactive site loop containing the scissile peptide bond Arg5I C-Ile6I N[3]. The inhibitor has no regular secondary structures, except a type II tight turn at Met17I-Cys20I and t type I' turn at Met23I-His26I.

1. Huang, Q., Liu, S., Tang, Y., Zeng, F. and Qian, R. (1992). FEBS Letters 297, 143-146.
2. Hara, S., Makino, J. and Ikenaka, T. (1989). J. Biochem(Tokyo). 105, 88-92.
3. Bode, W., Greyling, H. J., Huber, R., Otlewski, J. and Wilusz, T. (1989). FEBS Letters, 242, 285-292.

P13.04.012 LIGAND RECOGNITION BY SERUM AMYLOID P COMPONENT A.P. Purvis, D. Thompson, A.R. Coker and S.P. Wood [1], V. Pye [2], M.B. Pepys [3], [1]School of Biological Sciences, University of Southampton, Southampton SO16 7PX, UK, [2]Birkbeck College, Malet Street, London WC1E 7HX, UK, [3]Immunology Medicine Unit, ICSM, Hammersmith Hospital, Du Cane Road, London W12 0NN, U.K.

Serum amyloid P component is a normal plasma glycoprotein composed of 5 identical subunits, each of 23.5 kDa, known to bind amyloid deposits, DNA, a range of different proteins and various low molecular weight ligands in a calcium dependent interaction. The structure of this pentameric protein has been reported previously (1) and shows a double calcium site on each subunit as the site of ligand binding. Each subunit is made up of a flattened ß-jellyroll fold, extremely similar to that of the legume lectins. We will report a range of structures for different ligand/protein complexes that aim to map the properties of the binding site and illustrate the key residues involved in ligand recognition.

1) Emsley, J. et al (1994) Structure of pentameric human serum amyloid P component. Nature 367, 338-345.

P13.04.014 STRUCTURE DETERMINATION OF HALOALKANE DEHALOGENASE LINB FROM *SPHINGOMONAS PAUCIMOBILIS* UT26. I. Smatanová and J. Marek, Laboratory of Biomolecular Structure and Dynamics, Faculty of Science, Masaryk University, Kotlářská 2, CZ 611 37 Brno, Czech Republic, Y. Nagata and M. Takagi, Department of Biotechnology, The University of Tokyo, Yayoi, Bunkyo-ku, Tokio 113, Japan, and L. Anders Svensson, Department of Molecular Bophysics, Center for Chemistry and Chemical Engineering, Lund University, S-221 00 Lund, Sweden.

Haloalkane dehalogenase LinB from *Sphingomonas paucimobilis* UT26 is an enzyme releasing chlorine or bromine from *n*-halogenated alkanes with a broad range of substrate specificity catalyses.

The enzyme was crystallized by using the hanging-drop vapor-diffusion method. The best crystals were obtaining by micro-seeding with a precipitant containing 18-20 % (w/v) PEG6000, 0.2M $CaAc_2$ and 0.1M TRIS-HCl (pH 8.9). The crystals diffract to at least 1.60 using synchrotron X-ray at cryogenic (100 K) conditions. They belong to the orthorhombic space group $P2_12_12$ with unit-cell parameters a=50.49, b=71.97, c=73.03 Å, the asymmetric unit contains one molecule of the enzyme.

Initial trials to solve the phase problem by isomorphous replacement had no success. That is why we were used isomorphous replacement method. We found two useful heavy atom derivatives: potassium tetra chloroplatinate(II), $K_2[PtCl_4]$, and potassium dicyanoaurate, $K[Au(CN)_2]$. We collected both derivative data to 2.5 Å, interpreted difference Patterson map and built MIRAS electron density map.

The poster will present our recent progress towards a crystallographic structure determination of this protein.

JM thanks Svenska Institutet for his scholarship. This work was supported in part by a grant-in-aid from the Ministry of Education, Science, and Culture of Japan (to YN and MT) and by grant VS96095 from Department of Education of the Czech Republic (to IS and JM).

P13.04.016 CRYSTALLOGRAPHIC STUDIES OF HUMAN C-REACTIVE PROTEIN/LIGAND COMPLEXES D.Thompson and S.P. Wood, Department of Biochemistry, School of Biological Sciences, University of Southampton, Southampton SO16 7PX, UK and M.B. Pepys, Immunological Medicine Unit, ICSM, Hammersmith Hospital, Du Cane Road, London W12 0NN, UK.

Human C-reactive protein (CRP) is a normal plasma protein, the circulating concentration of which rises dramatically in a cytokine-mediated response to most forms of tissue injury, infection and inflammation, and serum CRP values are widely measured in clinical practice as an objective index of disease activity. Complexed or aggregated CRP is also known to bind to the complement protein C1q and activate the complement cascade.

Several CRP-ligand complex structures have been solved with the aim of understanding the nature of interaction between this protein and its physiological ligands and also to determine the possible role played by CRP after tissue injury. Here we propose how multipoint attachment of one planar face of the CRP molecule to a cell membrane would leave possible recognition sites for C1q exposed.

P13.04.017 CRYSTAL STRUCTURE OF AN IκBα/NF-κB COMPLEX. De-Bin Huang, Tom Huxford, Shiva Malek, and Gourisankar Ghosh, Department of Chemistry and Biochemistry, University of California, San Diego, 9500 Gilman Drive, La Jolla, CA 92093-0359, USA

The crystal structure of the IκBα/NF-κB complex has been solved by a combination of multiple isomorphous replacement and molecular replacement phases and refined to an R value 0.22 and R-free 0.27 at 2.3 Å resolution.

Nuclear factor kappa B(NF-κB) is a dimeric transcription factor that regulates the expression of many cellular genes in response to a variety of signals. The classical NF-κB dimer is comprised of two subunits, p50 and p65. In resting cells, NF-κB is sequestered in the cytoplasm as complexes with inhibitor IκB proteins. Various NF-κB activating signals such as cytokines, growth factors, bacterial products, viruses, and uv light trigger a reaction cascade that ultimately phosphorylates IκB of NF-κB/IκB complexes. Phospho-IκB proteins are then ubiquitinated and degraded by the proteosome. Free NF-κB enters the nucleus to modulate transcription. Among other genes, NF-κB also induce the expression of IκBα, one of the IκB proteins. Newly synthesized IκBα, in the absence of any cytoplasmic NF-κB migrates to the nucleus and blocks transcriptional activity of NF-κB by dissociating NF-κB/DNA complexes.

The structure explains how IκBα inhibits NF-κB's function both in the cytoplasm and in the nucleus. The presence of IκBα allows large en bloc movement of the NF-κB p65 subunit amino-terminal domain. This conformational change induces allosteric inhibition of NF-κB DNA-binding. Amino acid residues immediately preceding the nuclear localization signals of both NF-κB p50 and p65 subunits are tethered to the IκBα amino-terminal ankyrin repeats impeding NF-κB from nuclear import machinery recognition.

P13.04.018 A NEW MECHANISM OF ANTIBIOTIC RESISTANCE: CRYSTAL STRUCTURE OF CHLORAMPHENICOL PHOSPHOTRANSFERASE. Tina Izard & Jacqueline Ellis Department of Biochemistry, University of Leicester, LE1 7RH, UK.

Chloramphenicol (Cm) is a broad-spectrum antibiotic produced by Streptomyces venezuelae that binds to the peptidyltransferase centre of 50S prokaryotic ribosomes thereby inhibiting protein biosynthesis. The internal mycelial resistance/tolerance mechanism of the producing organism was recently discovered to be due to a novel Cm-inactivating enzyme, chloramphenicol phosphotransferase (CPT). CPT inactivates Cm by modification of the primary hydroxyl, in this case by phosphoryl transfer between ATP and Cm. The product, 3-phospho-Cm, has little or no demonstrable antibiotic activity.

CPT from Streptomyces venezuelae has been overexpressed, purified and crystallised. The CPT-Cm crystals belong to the cubic space group I4(1)32 with unit cell dimensions a = 200 Å. Here we describe the three-dimensional structure and some insights into its mechanism of reaction.

P13.04.019 THE STRUCTURE OF THE MOLYBDATE-DEPENDENT TRANSCRIPTIONAL REGULATOR (ModE) FROM *ESCHERICHIA COLI*. David R. Hall, David G. Gourley, Lisa A. Anderson, David H. Boxer, William N. Hunter, Department of Biochemistry, University of Dundee, Dundee, DD1 5EH, United Kingdom, Gordon A. Leonard, Joint Structural Biology Group, ESRF, BP 220, F38043 Grenoble CEDEX, France, and Elizabeth M. H. Duke, CCLRC-DL, Daresbury Laboratory, Warrington, Cheshire, WA4 4AD, United Kingdom.

The molybdate-dependent transcriptional regulator (ModE) from *Escherichia coli* functions both as a sensor of intracellular molybdate concentration and a regulator for transcription of several operons involved in the uptake and utilisation of the essential element, molybdenum. The high-

resolution crystal structure of ModE was determined using multi-wavelength anomalous dispersion methods targeting a selenomethionine derivatised protein. The selenomethionyl protein and native ModE have been refined to 1.75 and 2.1Å respectively. The models describe the architecture and structural detail of a complete transcriptional regulator. ModE is functional as a homodimer and the subunits comprise distinct N-terminal and C-terminal domains. The N-terminal domain carries a winged helix-turn-helix motif for binding to DNA and is primarily responsible for dimerisation of ModE. The C-terminal domain contains the molybdate-binding site and residues implicated in binding the oxyanion are identified. This domain can be divided into sub-domains *a* and *b* which have similar folds although the organisation of secondary structure elements varies. The sub-domain fold is related to the oligomer binding-fold and is similar to that observed for the subunits of several toxins which are involved in extensive protein-protein interactions. This suggests a role for the C-terminal domain of ModE in the formation of ModE-protein-DNA complexes necessary for the regulation of transcription. Modelling of ModE interacting with DNA suggests that a large scale distortion of DNA may not be required for complex formation.

P13.04.023 MAD STRUCTURE OF THE REGULATORY SUBUNIT OF HUMAN PROTEIN KINASE CK2. L. Chantalat[1], D. Leroy[2], O. Filhol[2], A. Nuedo[2], M. J. Benitez[2], C. Cochet[2], O. Dideberg[1]. [1]LCM, Institut de Biologie Structurale Jean-Pierre Ebel, CNRS/CEA. [2] LBRCE, Unité INSERM 244, Département de Biologie Moléculaire et Structurale CEA, Grenoble, FRANCE.

Protein kinase CK2 is a heterotetramer Ser/Thr protein kinase made by the association of two α catalytic subunits (CK2α) and two β regulatory subunits (CK2β). Although its exact physiological role is not clear, CK2 is essential for the viability of *Saccharomyces. cerevisiae*. Several studies support its implication in cell division and transformation. The β subunit is important for the regulation of the enzyme and the specificity of the interaction of CK2 with substrates and inhibitors.

The crystal structure of CK2β has been solved to 1.74 Å resolution, using multi-wavelength anomalous dispersion (MAD) phasing methods. The data were collected at the ESRF, beamline BM14, on a perfectly aligned crystal. The selenium positions found with SOLVE were used to calculate experimental phases to 2Å resolution with an overall figure of merit of 0.65, yielding a map of excellent quality. An initial model was built with the program wARP. The final structure has been refined to an R_{work} = 19.3% (R_{free}= 21.8%) to 1.74 Å resolution. The model contains two CK2β subunits and 321 water molecules. The structure shows a crescent-shaped dimer with a two-fold symmetry. Two striking structural features are unique to this new structure. Firstly, a zinc finger motifs mediate the interaction between the two monomers. Secondly, the two ends of the crescent bear a highly acidic region. In this region a deep groove can easily accommodate a spermine molecule that is an activator of CK2. The CK2β structure helps in understanding the formation of the heterotetramer

P13.04.027 CRYSTAL STRUCTURE OF HUMAN ERYTHROPOIETIN COMPLEXED TO ITS RECEPTOR AT 1.9Å. Rashid Syed, Cuiwei Li, Janet Cheetham, Kenneth Aoki, Timothy Osslund, Arthur Chirino, Jiandong Zhang, Steven Elliott, Karen Sitney, John Wendoloski, Joan Egrie [1], Scott Reid, Beishan Liu, Hangjun Zhan, Bradley Katz, David Matthews [2]. Janet Finer-Moore, Robert Stroud [3]. [1] Amgen Inc., Thousand Oaks, CA 91320, [2] Axys Pharmaceuticals Inc., S. San Francisco, CA 94080, [3] University of California at San Francisco, San Francisco, CA 94143.

Human erythropoietin (EPO) is a hematopoietic cytokine required for the differentiation and proliferation of precursor cells into red blood cells. It activates by binding and orienting two cell surface receptors (EPOR) that trigger an intracellular phosphorylation cascade. The crystal structure of EPO complexed to the extracellular ligand binding domains of the EPO receptor (EPObp), determined at 1.9 Å and from two crystal forms, reveals a tri-molecular complex of one EPO and two EPObp molecules. EPO belongs to the four helical bundle cytokine family with an up-up-down-down topology. The receptor molecules are dimerized through extensive interactions at two distinct sites on EPO. The structure shows that EPO imposes a unique 120° angular relationship and orientation that may be responsible for optimal signaling through intracellular kinase pathways.

P13.04.028 ANTIBODY VERSUS ENZYME CATALYSIS: STRUCTURAL STUDIES OF ALDOLASES. A. Heine, E.A. Stura, J.G. Luz, C.F. Barbas III, C.H. Wong, R.A. Lerner and I.A. Wilson; The Scripps Research Institute, 10550 N. Torrey Pines Rd., La Jolla, CA 92037

The diversity of the immune system can be exploited to generate catalytic antibodies, which catalyze a wide variety of reactions similar to enzymes. A comparison of antibody mechanisms with those of the corresponding enzymes can illuminate the reasons for the differential rate enhancements and specificity. The natural class I aldolase enzyme has a lysine residue in the active site that forms a Schiff base during catalysis. A similar mechanism is proposed for the catalytic antibody 33F12 and indeed, was expected due to the mode of selection of the antibody by a process of reactive immunization. The structure of antibody Fab 33F12 at 2.15 Å resolution shows a lysine is buried at the bottom of the active site in a hydrophobic environment that can severely perturb its pKa. The X-ray structure determination of a corresponding enzyme, DERA, is in progress. The Se-Met substituted enzyme was used for a MAD experiment, collecting four data sets at different wavelength to 1.8 Å resolution. Crystals of the native enzyme diffract to better than 1.05 Å resolution and a complete data set to 1.07 Å has been obtained. After the molecule has been traced, the high resolution data refinement should reveal detailed insight into the mechanism of enzyme catalysis and will allow for comparison with the antibody.

P13.04.029 CRYSTAL STRUCTURE OF RAT HBP23, A NOVEL ANTIOXIDANT PROTEIN. S. Hirotsu, K. Okada, Y. Fuji, M. Kato, Y. Abe[1], N.Nagahara[1], H. Hori[1], T. Nishino[1], Y. Maru[2], and T. Hakoshima, Dept. of Molecular Biology, Nara Inst of Sci. and Tech, 8916-5 Takayama, Ikoma, Nara 630-0101, JP. and [1]Dept. Biochem. and Mol. Biol., Nippon Medical School, 1-1-5 Sendagi, Bunkyoku, Tokyo 113-8602, JP. and [2]Inst.for Medical Science, Univ. of Tokyo, 4-6-1 Shiroganedai, Minatoku, Tokyo 108-8639, JP.

HBP23 (heme binding protein 23kDa) was originally identified from rat liver cytosol with a high binding affinity with heme. Sequence analysis revealed that it belongs to a novel family of antioxidant proteins, referred to as peroxiredoxin (Prx), which has a peroxidase activity[1] . Most of Prx proteins, including HBP23, contain two conserved cysteine residues that relate to peroxidase activity and rely on thioredoxin as a source of reducing equivalents for the reduction of hydrogen peroxide. Recently, a human homologue of HBP23, Pag, has been reported to bind to SH3 domain of a non-receptor-type tyrosine kinase c-Abl and to inhibit its tyrosine kinase activity in vivo[2]. In order to understand the molecular mechanism of HBP23, we analyzed the crystal structure of HBP23 at 2.6Å resolution

For structural determination, the conventional multiple isomorphous replacement was used for phase problem. After phase improvement with solvent flipping, we obtained an

interpretative MIR density map. Several cycles of the structure refinements resulted in the current structure with an *R*-value of 0.216 (R_{free} = 0.268). This model showed that the oxidized form of rat HBP23 exists as a dimer composed of identical subunits. Each subunit contains the typical structure motif of the thioredoxin fold that contains a cental β-sheet and flanking α-helices.The active residue Cys52 of one subunit of a dimer forms a disulfide bond with Cys173 of the other subunit. Based on this structure together with biochemical results, we will discuss the mechanisms how the protein control the peroxidase activity with two conserved Cys residues and will try to identify the binding sites to heme and c-Abl.

1. Iwahara, S., Satoh, H., Song, D., Webb, J., Burlingame, Nagae, Y., and Eberhard, U.M. (1995). Biochemistry 34, 13398-13406.
2. Web, S., and Van Etten, R.A. (1997). Genes & Development 11, 2456-2467.

P13.04.030 CRYSTAL STRUCTURE OF PROTEIN HISTIDINE PHOSPHATASE SIXA. K. Hamada, M. Kato, K. Ihara, T. Shimizu, T. Mizuno[1], and T. Hakoshima, Department of Molecular Biology, Nara Institute of Science and Technology (NAIST), 8916-5 Takayama, Ikoma, Nara 630-0101, JP. and [1]School of Agricultural Science, Nagoya University, Chikusa-ku, Nagoya 464-8601, JP.

SixA has been isolated from *Escherichia coli* as the first protein to exert a phospho-histidine phosphatase activity. Recent biochemical studies have shown that SixA is involved in the signal transduction of the His-Asp phosphorelay through the dephosphorylation of the HPt (histidine-containing phosphotransfer) domain of the anaerobic sensor kinase ArcB [1]. In order to understand the mechanism of action of novel protein phosphatase SixA, we have determined the crystal structure of SixA.

X-ray crystallographic analysis revealed that crystals of SixA belonged to space group $P2_12_12_1$ with unit-cell dimensions *a*=39.2, *b*=48.62, *c*=83.18Å, having one molecule in the crystallographic asymmetric unit [2]. We have determined the 2.06Å crystal structure of SixA by the multiple isomorphous replacement method (MIR) and refined the model to a crystallographic R-factor of 16.6 % and free R-factor of 22.9 %.

The structure of this protein is composed of a single α/β domain containing a central six-stranded mixed β-sheet, surrounded by five α -helices and two 310 helices on both sides. The active site contains basic residues, Arg7, Arg55 and His108, as well as the catalytic residue, His8. These positively charged residues interact with tungstate ion as a phosphate analog, suggesting that they are required for phosphate binding in the catalytic reaction.

SixA is structurally similar to the α/β domain of Phosphoglycerate Mutase, Fructose-2,6-bisphosphatase and Acid Phosphatase which catalyze the dephosphorylation of phospho-chemicals. These proteins have conserved catalytic residues, although SixA has low sequence similarity to these proteins. We have found that there is structural similarity between SixA and the low molecular weight tyrosine phosphatase from eukaryotic cells.

1. Ogino, T., Matsubara, M., Kato, N., Nakamura, Y., Mizuno, T. (1998). Molecular Microbiology **27**, 573-585.
2. Hamada, K., Kato, M., Mizuno, T., Hakoshima, T. (1999). Acta Crystallographica D**55**, 269-271.

P13.04.031 CRYSTAL STRUCTURE OF HUMAN ZN-α_2-GLYCOPROTEIN: A FAT-DEPLETING FACTOR RELATED TO MHC MOLECULES. Arthur J. Chirino[†], Luis M. Sánchez, and Pamela J. Bjorkman[†] ,Division of Biology 156-29 and [†]Howard Hughes Medical Institute, California Institute of Technology, Pasadena, CA 91125, U.S.A.

Zn-α_2-glycoprotein (ZAG) stimulates lipid degradation in adipocytes and causes the extensive fat losses associated with some advanced cancers [1]. ZAG is normally present in serum and other tissue but is overexpressed by carcinomas that induce fat loss and not by tumors that do not. This implies that ZAG normally functions in the degradation of lipids, which increases to a pathological extent in cancer-induced weight loss, or cachexia. ZAG is a soluble protein that shares 30-40% amino acid sequence identity with the extracellular portions of class I major histocompatibility complex (MHC) heavy chains. The 2.8 Å crystal structure of ZAG resembles a class I MHC heavy chain, but ZAG does not bind the class I light chain β_2-microglobulin (ß2m). Nonetheless, ZAG's thermal stability is comparable to MHC I and other ß2m-binding molecules. The overall shape of ZAG is similar to an inverted letter L, in which the long axis of the α_3 domain is roughly perpendicular to the flat side of the α_1-α_2 platform, whereas the comparable angle is acute in ß2m-binding proteins. ZAG's overall quaternary structure in the absence of ß2m is stabilized by both the presence of additional interdomain hydrogen bonds and increased buried surface area at the α_1-α_2 and α_3 interface relative to MHC I. Although ZAG does not associate with peptides, the helices in both the α_1 and α_2 domains are almost identically positioned to their counterparts in peptide binding class I MHC molecules. The ZAG counterpart of the MHC peptide binding groove contains electron density corresponding to a hydrophobic, non-peptidic compound that may be implicated in lipid catabolism under normal or pathological conditions. ZAG and MHC-related proteins such as the neonatal Fc receptor and HFE illustrate the versatility of the MHC fold and raise intriguing questions about the ancestral function and evolutionary relationships of MHC and MHC-related proteins.

1. P. T. Todorov, et al., *Cancer Res.* **58**, 2353 (1998)

P13.04.032 CRYSTAL STRUCTURES OF DNA MISMATCH REPAIR PROTEINS. W. Yang and C. Ban, Lab. Mol. Biol., NIDDK, NIH, Bethesda, MD 20892

The MutL DNA mismatch repair protein has recently been shown to be an ATPase and belong to an emerging ATPase superfamily that includes DNA topoisomerase II and Hsp90. We report here the crystal structures of a 40KDa ATPase fragment of *E. coli* MutL (LN40) complexed with a substrate analog, ADPnP, and with product ADP. LN40 undergoes extensive conformational changes and dimerizes upon binding to the ATP analog. More than sixty residues that are disordered in the apoprotein structure become ordered and contribute to both nucleotide binding and dimerization. The rate limiting step in ATP hydrolysis is dimerization of the LN40 fragment. Hydrolysis of ATP, signified by subsequent release of the γ-phosphate, unleashes two key loops and leads to dissociation of the LN40 dimer. The nucleotide-induced structural transformation thoroughly alters the MutL contact surface and allows it to coordinate DNA mismatch repair.

P13.04.033 THE STRUCTURE OF PTERIDINE REDUCTASE 1 FROM *LEISHMANIA*. David G. Gourley, William N. Hunter, Department of Biochemistry, University of Dundee, Dundee, DD1 5EH, United Kingdom, Gordon A. Leonard, Joint Structural Biology Group, ESRF, BP 220, F38043 Grenoble CEDEX, France, James Luba, Larry W. Hardy, Dept. of Pharmacology & Molecular Toxicology,University of Massachussetts Medical School, 373 Plantation St., Worcester MA 01605 USA; Stephen M. Beverley, Dept. of Molecular Microbiology, Washington University School of Medcine,760 McDonnell Science Building, 660 S. Euclid Avenue, St. Louis, MO 63110-1093 USA.

The enzyme Pteridine reductase 1 (PTR1) from the protozoan parasite *Leishmania* is a validated target for therapeutic intervention. PTR1 is responsible for the salvage of pteridines and folates and has the ability to catalyse the same overall reaction as dihydrofolate reductase and so can confer resistance to the antifolate drug methotrexate. Crystals of recombinant PTR1 have been grown that diffract to a resolution of 2.1 Å. The space group is $P2_12_12_1$ with unit cell dimensions of a = 96.22, b = 103.86, c = 134.74 Å. Structure determination is on going and will be presented at this meeting.

05. CRYSTALLOGRAPHY OF BIOLOGICAL SMALL MOLECULES

P07.05.001 ATTEMPTS TO DESIGN PEPTIDE HELICES HAVING PREFERED SCREW SENSE USING DEHYDRO AMINO ACIDS. U.A Ramagopal and S. Ramakumar, Dept. of Physics, Indian Institute of Science, Bangalore-560012, India. R.M Joshi, and V.S Chauhan, ICGEB, Aruna Asaf Ali Marg, New Delhi-110067, India.

Peptides containing α,β-dehydroamino acid residues are found to exhibit specific conformational preference and altered biological activity. They are found in many naturally occurring peptides and proteins of microbial and fungal origin. Among the dehydro amino acids, dehydro phenylalanine(ΔPhe) is one of the well studied and has become the most promising conformation restricting residue. In order to explore the preference for particular screw sense in the $(\Delta Phe)_n$ systems, we have carried out a crystallographic analysis of two peptides namely I and II. The peptide(I) has left handed 3_{10}-helical conformation, where as the peptide(II) crystallises with two conformers per asymmetric unit. One of the conformers is a slightly distorted right handed 3_{10}-helix(A) and the other is a left handed 3_{10}-helix(B). To our knowledge this is the first observation of dehydropeptide without preferred screw sense and having chiral coded amino acid both at N-terminus and at the centre of the molecule. The crystal packing in II is mostly through C−H···O hydrogen bonds between the helices of opposite screw sense (A and B) and solvent mediated C−H···O and N−H···O hydrogen bonds. The crystal structures of the two peptides will be discussed in comparison with other ΔPhe containing peptides as well as α,α-disubstituted amino acids, highlighting the utility of ΔPhe as a complementary 'designer residue'.

	Peptide Sequence	Conformation
I	Boc-LAla-$(\Delta Phe)_4$-NHMe	TL
II	Boc-LAla-$(\Delta Phe)_4$-LAla-$(\Delta Phe)_3$-Gly-OMe	TL/R

T: 3_{10}-helix, L: Left-handed, R: Right-handed.

P07.05.002 ANTIAMOEBIN, AN INTERMEDIATE-SIZED MEMBRANE-ACTIVE POLYPEPTIDE. B.A. Wallace, C.F. Snook, Department of Crystallography, Birkbeck College, University of London, London WC1H 0HA U.K.

The structure of antiamoebin (AAM), a 16 amino acid peptaibol that can form both ion channels and carriers in phospholipid membranes, was solved by molecular replacement techniques to 1.4 Å resolution in crystals grown from methanol. Despite the fact that AAM is monomeric in the crystals, and its membrane-active form must be multimeric (the channel form is apparently a hexamer), circular dichroism spectroscopic studies confirm that its secondary structure in the crystal is the same as in phospholipid vesicles. Coincident with our solving the structure in methanol [1], Karle et al [2] also solved its structure in crystals grown from octanol. Even though the solvents used were considerably different in their chemical properties, and the packing of the molecules in the two crystal forms was different, the two structures are virtually identical. They are helical molecules with a deep bend in the middle caused by the presence of three imino acids. Their polypeptide main chain atoms differ by only ~0.25 Å RMSD, and their bend angles by less than 3 degrees. The angle of the bend in AAM is much larger than it is in zervamcin, a highly homologous (44 % identical) molecule, and is likely an important reason for the difference in membrane activity profiles between these two molecules. AAM is unique, with respect to membrane-active peptides examined to date, in that it can act as either an ion carrier and an ion channel, depending on the type of lipids used to form the membrane [3]. Models for the two functional forms are proposed based on the crystal structure and functional studies.

1. C.F. Snook, G. Oliva, V. Pattabhi, S.P. Wood, T.L. Blundell, & B.A. Wallace (1998). Structure, 6, 783-792.
2. I.L. Karle, M.A. Perozzo, V.K. Mishra, & P. Balaram (1998). PNAS, 95, 5501-5504.
3. H. Duclohier, C.F. Snook, & B.A. Wallace (1998). BBA, 1415, 255-260.

P07.05.003 MOLECULAR PACKING FEATURES OF C-TERMINAL AMIDATED AMINO ACIDS AND DIPEPTIDES. Y. In, M. Fujii, S. Tani, K. Tomoo, T. Ishida, Department of Physical Chemistry, Osaka University of Pharmaceutical Sciences, 4-20-1 Nasahara, Takatsuki, Osaka 569-1094, Japan

Most of the biologically active peptides such as endomorphin-1, fulicin, dermorphin and calcitonin are amidated at the C-terminal, and the activities are disappeared when they are deamidated. We believe such drastic change could result from the change in the interaction mode of the peptide with the receptor, rather than the molecular conformation change. Especially, the hydrogen-bonding pattern at the binding pocket of receptor could be expected to be largely different between the C-terminal free and the amidated peptides. The three-dimensional information on the C-terminal amidated bioactive peptide–receptor complex is not available at present. So, we analysed the crystal structures of C-terminal amidated amino acids and dipeptides, and compared the respective intermolecular interactions with those of the corresponding free amino acid and dipeptides, in order to examine the role of C-terminal amidation for the intermolecular packing, because these information would be useful to consider the binding mode which is necessary for its bioactivity of the peptide in the active site of receptor.

A series of C-terminal amidated amino acids and peptides were dissolved in various solvents or their mixtures, and single crystals of C- terminal amidated Tyr, AcTyr, Cys(trt), Trp, Glu, Val, Asp, Ile, Thr, Tyr-Lys, Z-Gly-Phe and Asp-Phe were obtained from water, alcohol, water/alcohol mixture, or alcohol/ethyl acetate mixture by the slow evaporation at room temperature. The respective structure determination and refinement were carried out in the usual way. When the respective molecular conformations were compared with those of the corresponding free amino acids and dipeptides, the common conformational change by the amidation was not observed. Alternatively, the intermolecular interactions, including hydrogen bonding pattern, was very similar to one another, and was considerably different from those observed for the free amino acids and peptides The detailed analyses are now in progress.

P07.05.004 PEPTIDE DESIGN: A DISTORTED 3_{10} HELIX IN A DEHYDRO HEXAPEPTIDE Boc-Val-ΔPhe-Leu-Ala-ΔPhe-Ala-OMe. S. Ramakumar[1], Anil Kumar P.[1], V. S. Chauhan[2], [1]Department of Physics, Indian Institute of Science, Bangalore – 560 012, India. [2]International Centre for Genetic Engineering and Biotechnology, Aruna Asaf Ali Marg, New Delhi - 110 067, India.

α,β-Dehydro amino acid residues are found in several naturally occurring bioactive peptides as well as in some proteins. Their presence in peptide chain produces remarkable conformational consequences. As a part of our program on *de novo* design of protein secondary structure mimetics, we have determined the X-ray crystal structure to atomic resolution of a dehydro hexapeptide Boc-LVal[1]-ΔPhe[2]-LLeu[3]-LAla[4]-ΔPhe[5]-LAla[6]-OMe. Crystals grown in aqueous methanol solution by the slow

evaporation method belong to monoclinic space group $P2_1$, with cell dimensions *a*=10.90, *b*=10.07, *c*=20.00Å, β=94.4°, Z=2. The crystal structure was determined using direct methods and refined using least-squares technique to R-factor better than 5.3% for 3025 reflections having $|F_o| \geq 4\sigma |F_o|$. The peptide is stabilised by three consecutive and overlapping type III β-turns. The overall structure of the molecule is a right-handed, distorted 3_{10} helix with an average (ϕ, ψ) value of (-67.7°, -22.7°) and ranging from (-81.1°, -9.6°) for ΔPhe^5 to (-55.1°, -36.3°) for Leu^3. Comparison of the structure with those of other dehydro oligopeptides suggests that the helical conformation of the hexapeptide might have arisen due to the presence of a bulky Leu^3 residue in the two residue spacer segment between ΔPhe^2 and ΔPhe^5. The crystal packing is in the form of helical rods aligned along the crystallographic *a*-axis. The helical rods are connected in head to tail fashion with N-H···O hydrogen bonds with additional support from C-H···O hydrogen bonds. The overall crystal packing is mainly through hydrophobic interactions with adjacent helices being anti parallel to each other.

P07.05.005 SOLID STATE CONFORMATION OF SERINE^3-DPDPE. Judith. L. Flippen-Anderson,[1] Jeffrey R. Deschamps, [1] Clifford George, [1] Victor J. Hruby,[2] Mark Shenderovich,[2] Andrzej Lipkowski,[3] and Aleksandra Misicka[4] from [1]Laboratory for the Structure of Matter, Naval Research Laboratory, Washington, DC 20375 USA, [2]Dept of Chemistry, University of Arizona, Tucson, Arizona 85721 USA, [3]Medical Research Centre, Polish Academy of Sciences, Warsaw, Poland and [4]Dept of Chemistry, Warsaw University, Warsaw, Poland

Understanding the structural basis of receptor selectivity for opioid peptide – receptor interactions requires extensive study of the conformational (φ,ψ) and topographical (χ^1, χ^2) properties of the peptide ligand. The enkephalins themselves are not very useful in these studies because of their low selectivity and their high degree of conformational freedom. Early work on these ligands did identify the 2 aromatic rings, an amino group, and a lipophilic surface as key pharmacophoric elements. Systematic rational approaches to designing more potent and selective ligands have endeavored to preserve these key structural elements. One of the first successes of this approach was the development of the highly potent and δ opioid receptor-selective enkephalin analogue DPDPE (Tyr-cyclo(D-Pen-Gly-Phe-D-Pen)-OH). DPDPE is now the δ opioid receptor selectivity standard against which new derivatives are measured for specificity and potency. We have already reported on the solid state structure of DPDPE itself as well as a number of modified DPDPE compounds. This paper will describe the X-ray structure of Ser^3-DPDPE which has a lower affinity for the δ receptor site, but is possibly more selective [A. Misicka, et al, Peptides Chemistry and Biology, J. A. Smith and J. E. Rivier (Eds) ESCOM, Leiden, The Netherlands, 1992, p140-141]. Small crystals (0.05 x 0.1 x 0.25 mm) were grown by vapor diffusion and data were collected at –75°C on a 1K Bruker Smart CCD system using a 5 kW Cu rotating anode and Göbel mirror system. It crystallizes in the monoclinic space group $P2_1$ with 2 independent peptide molecules and several water molecules per asymmetric unit. The structure was solved and refined on F^2 values using SHELXTL-PLUS. Supported in part by ONR and NIDA.

P07.05.006 STRUCTURAL STUDIES ON COLLAGEN-MODEL PEPTIDES WITH (Pro-Pro-Gly) AND (Pro-Hyp-Gly) SEQUENCE REPEAT. V. Nagarajan, S. Kamitori and K. Okuyama, Faculty of Technology, Tokyo Univeristy of Agriculture and Technology, 2-24-16, Naka-cho, Koganei-shi, Tokyo 184-8588, Japan.

Even though the elucidation of the structure of collagen have been attempted for a very long time, the exact structure of collagen has not been known, till date. Several models for collagen have been proposed of which two have been generally accepted, one is the 10/3-helical model [1] while the other is the 7/2-helical model [2]. Due to difficulties in analyzing the detailed structure of collagen, those peptides which mimic the triple helical nature of collagen have been the targets of study. Two such collagen model peptides namely, $(Pro\text{-}Pro\text{-}Gly)_{10}$ and $(Pro\text{-}Hyp\text{-}Gly)_{10}$ have been analyzed. The average structures of these peptides, have revealed that, these triple helical peptides are essentially the same as the 7/2-helical model. Similarity in their molecular structure clearly shows that presence of hydroxyproline at the Y-position does not have any structural influence in the imino acid rich regions of collagen. The packing considerations of these peptides are different, implying that hydroxyproline does have an influence on the local environment of the triple helix. The number of water molecules identified in our study was considerably lower than that obtained by a different group [3,4] because of differences in the refinement procedure, while we took crystallographic free *R* into consideration, the other group did not. Identification of a considerably lower number of water molecules in hydroxyproline containing peptide seem to support a recent report [5] that the extra stability associated with the hydroxyproline containing peptides may not be due to the excess water bridges formed by the hydroxyl group of the hydroxyproline.

1. Rich, A., and Crick, F.H.C. (1961) *J. Mol. Biol.* **3**, 483
2. Okuyama, K., Okuyama, K., Arnott, S., Takayanagi, M. and Kakudo, M., (1981) *J. Mol. Biol.* **152**, 427
3. Kramer, R.Z., Vitagliano, L., Bella, J., Berisio, R., Mazzarella, L., Brodsky, B., Zagari, A. and Berman, H.M. (1998) *J. Mol. Biol.*, **280**, 623
4. Bella, J., Brodsky, B., and Berman, H.M.(1995) *Structure*, **3**, 893
5. Holmgren, S.K., Taylor, K.M., Bretscher, L.E. and Raines, R.T. (1998) *Nature* **392**, 666

P07.05.007 IS THE RICH AND CRICK MODEL FOR COLLAGEN REALLY TRUE? –EVIDENCES FROM MODEL PEPTIDES. K.Okuyama, V.Nagarajan, C.Hongo and S.Kamitori, Tokyo University of Agriculture and Technology, Koganei, Tokyo 184-8588, Japan.

Collagen molecule has a triple-helical structure due to the strict sequence constraints with glycine as every third residue and a high content of imino acids. After about fifty years since this triple-helical structure was proposed, the prevailing model is the Rich and Crick model in which three strands form a left-handed 10/3-helix with an axial repeat of 28.6Å [1]. However, there is one more model which can explain X-ray fiber diffraction patterns of native collagen. That is the Okuyama model in which three strands form a left-handed 7/2-helix with an axial repeat of 20Å[2]. This was deduced based on the structure of (Pro-Pro-Gly)10 single crystal by means of the linked-atom technique used for fiber diffraction analyses. Recently, we succeeded in obtaining single crystals of collagen model peptides, (Pro-Pro-Gly)n (n=9, 10, 11), (Pro-Hyp-Gly)10 and (Pro-Pro-Gly)4 -X-Y-Gly-(Pro-Pro-Gly) 4 with one of (X=Ala, Y=Pro), (X=Pro, Y=Ala) and (X=Y=Ala). Structure of (Pro-Pro-Gly)n (n=9, 10) and (Pro-Hyp-Gly)10 were analyzed by means of the recent technique. All the obtained structures in this study together with the results from other groups confirmed that these molecular structures were essentially the same as the Okuyama model. Furthermore, not only these three, all the X-ray diffraction data in this study showed the 7/2-helical symmetry and 20Å axial repeat (Okuyama model) from their cylindrical Patterson maps. On the other hand, the Rich and Crick model has no such supporting data other than fiber diffraction analysis of collagen.

Rich, A. & Crick, F.H.C., J. Mol. Biol., 3, 483 (1961).
Okuyama, K., et al. Polymer J., 9, 341 (1977) ;
Okuyama, K., et al. J. Mol. Biol., 152, 427 (1981).

P07.05.008 ELECTROSTATIC STABILIZATION OF BOUND OXYGEN IN MYOGLOBIN. R.R. Leininger, Y. Dou, G. N. Phillips, Jr., and J.S. Olson, Department of Biochemistry and Cell Biology, Rice University, Houston, TX.

The distal histidine, His64(E7),in myoglobin (Mb) has been shown to play an essential role in governing relative carbon monoxide and oxygen affinities, specifically by the polarity of its imidazole side chain. This residue promotes O_2 binding by preferential formation of a hydrogen bond with the Fe-O_2 complex and inhibition of CO binding by the requirement for water displacement from the distal pocket of deoxyMb. Double mutants have been constructed to test the general importance of favourable electrostatic interactions by replacing the distal histidine with an apolar leucine residue and then adding hydrogen bond donors at other positions adjacent to the bound ligand. The H64L/V68N double substitution causes an ~2-fold increase in O_2 affinity compared to wild-type Mb, whereas the H64L/V68Q replacements cause an ~100-fold decrease. Analyses of the x-ray crystal structures and IR spectra of these proteins show, in agreement with the work of Kryzwda et al. [1] on single mutants, that the amide side chain of Asn68 can form a strong hydrogen bond with bound O_2, whereas the side chain of Gln68 is too large causing the amide to point away from the active site.

Supported by: NIH grants GM08280AR (trainee RRL), 40252 (GNP), GM 35649 (JSO), HL 47020 (JSO); Grants C-1142 (GNP) and C-612 (JSO) from the Robert A. Welch Foundation;; and the W. M. Keck Foundation

1. Kryzwda et al. (1998). Biochemistry, **37**, 15896-15907.

P07.05.009 CRYSTALLOGRAPHIC STUDIES OF A LYTIC PEPTIDE WITH ANTI-BACTERIAL AND ANTI-TUMOR ACTIVITIES. Hidong Kim[1], Lance J. Stewart[1], Jesse M. Jaynes[2]. [1]Emerald BioStructures, Inc., 7869 NE Day Rd. W, Bainbridge Island, WA 98110, USA; [2]Demegen, Inc., 1051 Brinton Rd., Pittsburgh, PA 15221, USA.

Naturally occurring lytic peptides have innate immunological activities in various species. These peptides, such as the cecropins produced by the giant silk moth *Hyalophora cecropia* and the magainins found in the skin of the frog *Xenopus laevis*, show antimicrobial activity. Their natural functions may thus be to protect the host against bacterial infection. Although diverse in amino acid sequence, these lytic peptides of 20-40 residues exhibit a characteristically positively charged and amphipathic helical or sheet structure, indicating that overall physical properties may be more important than specific residues in their lytic functions. The mechanism of action of the naturally occurring lytic peptides is not fully understood, but lysis is thought to result from interactions of the peptide with the cell membrane itself, rather than via a specific peptide-receptor interaction.

Peptidyl membrane interactive molecules™ (MIMs) are synthetic peptides based on the properties of naturally occurring lytic peptides. These synthetic peptides show cytotoxic effects against both cancer cells and pathogenic bacteria. The LD_{50} of one 23-mer Peptidyl MIM™, D2A21, is 0.882 μM against a certain prostate cancer cell line. This compares well to the LD_{50} of the standard chemotherapeutic agent cisplatin, which ranges from 2-17 μM against the same cell line. D2A21 is also effective in killing pathogenic bacteria, with MICs of <1 μg/ml against *Pseudomonas aeruginosa*, and <10 μg/ml against methicillin-resistant *Staphylococcus aureus*. These findings indicate that Peptidyl MIMs™ may be effective as chemotherapeutic or antibiotic agents. Here, we present results of our X-ray crystallographic studies of D2A21.

P07.05.010 STRUCTURE OF SHORT CHAINS OF THE OLIGOPEPTIDE TYPE. J.Hasek, J.Duskova, Institute of Macromolecular Chemistry, Academy of Sciences of the Czech Republic, Heyrovskeho nam.2, 162 06 Praha 6

Several types of short peptide-like synthetic chains possessing a large scale of enzymatic stabilities and activity are studied for their applications as enzymatically degradable spacers for polymer drug carriers, enzymatically activated suicide inhibitors, substrate-like directed inhibitors.

The global hydrophobicity, conformational flexibility, position and orientation of hydrophobic and hydrogen-bond-forming monomers are decisive for enzymatic activity of oligomer. Therefore, the classification of substrate or inhibitor oligomers should be based on graphical representation of all these global and spatial properties.

The crystal structures and models based on empirical potentials of several peptide-like chains are discussed in detail. Special attention is devoted to Boc-Gly-L-Leu-Gly-p-nitro-phenyl, as a representative of enzymatically degradable spacer, (4S)-4-[1-(N-butoxycarbonylamino)-2-phenyl]-2,2-dibenzyl-4-butyrolactone and at last subnanomolar (K_i range 0.02-200 nMol) peptide-like inhibitors of HIV protease Boc-Phe-Ψ[(R/S)CHX CH_2 NH]-Phe-Glu/Gln/Ile-Phe-NH_2 , where X=H or OH /1/. Comparison with similar molecular structures compiled in CSD /2/ and IsoStar /3/ show some similar features of these distinct groups of compounds.

The project is supported by GACR 203/98/PO31, GAAV A4050811 and thanks to GA CR 203/99/0067 for providing the structural databases.

1 J.Konvalinka et al. (1997). Eur.J.Biochem. 250, 559-566.
2 F.H.Allen, O.Kennard (1993). Chem.Design Autom.News, 8, 31-37.
3 I.J.Bruno et al (1997). J.Comp.-Aided Molecular design, 11-6, 525-537.

P07.05.011 MEMBRANE ION TRANSPORT BY ANTIBIOTICS AND TOXINS. W.L. Duax[1], B.M. Burkhart[1], D. Ghosh[1,2] N. Li[1], [1]Hauptman-Woodward Institute, Buffalo, NY 14203, [2]Roswell Park Cancer Institute, Buffalo, NY 14263, and V. Pletnev[3], [3]Shemyakin Institute, Moscow, Russia.

Recent X-ray crystal structure determinations a Cs^+, K^+, and Rb^+ complexes of gramicidin D and an NH_4^+ complex of a virally encoded killer toxin, KP6a, reveal previously undetected modes of ion coordination that are ideally suited to facile movement of ions through membrane channels. Our isomorphous crystal structures of Cs^+, K^+, and Rb^+ gramicidin D revealed a right-handed anti-parallel double stranded double helix (DSDH5) that is consistent with a large body spectroscopic data. The DSDH5 structure has an ion channel with a single partially solvated Cs^+ ion distributed over three binding sites. The channel is relatively smooth and electrostatically negative on the interior as required for cation passage, while the exterior is electrostatically neutral, a requirement for membrane insertion. The "coordination" of the Cs^+ ion is achieved by interaction with the π orbitals of the carbonyls which do not point toward the ions. The K^+ binding sites, which are similar in position to Cs^+ binding sites, are shifted off center towards the wall of the channel. Our X-ray crystal structure determination of KP6a has revealed a trimer stabilized by salt bridges that forms a solvent filled funnel with charged residues on the inside. The funnel tapers to an opening which is lined by three phenyl rings. The 4.2Å diameter opening at the center of the phenyl rings has ideal dimensions to coordinate to NH_4^+ and K^+ ion via the π clouds of the phenyl rings. Electron density on the symmetry axis within the barrel of

the funnel surrounded by the phenyl rings is compatible with an NH_4^+ ion. The observed ion coordination is analogous to the arrangement of phenyl rings around NH_4^+ and K^+ ions in crystals of ammonium and potassium tetraphenylborate. This type of coordination for K^+ has been proposed to account for ion selectivity in insect and mammalian K^+ channels on the basis of ab initio calculations.

This work is supported by National Institutes of Health Grant No. GM32812.

P12.05.001 (3,3-DICHLORO-4-(P-METHOXY-PHENYL)-1-(P-CHLOROPHENYL)-2-AZETIDINONE). T. N. Durlu, K. Güven, M. Kabak, Department of Physics, Faculty of Art and Sciences, University of Kırıkkale, 71450 Yahşihan, Kırıkkale, Turkey, and V. Güner, Department of Chemistry, Faculty of Sciences, University of Hacettepe, 06532, Beytepe, Ankara, Turkey.

The crystal structure of the title compound, $C_{16}H_{11}Cl_3NO_2$, is monoclinic, $P2_1/n$, a=5.865(2), b=14.179(3), c=19.487(3) Å, ß=94.33(4)º, V= 1615.7(7) $Å^3$, Z=4, D_x=1.466 Mgr/cm^3, $\lambda_{MoK\alpha}$=0.71073 Å [1]. The Cl1-C8-Cl2 plane is nearly perpendicular to the four membered β-lactam group 89.6(2)º and the C-C bond distances on this lactam group are 1.550(8) and 1.568(7)Å, respectively. The most deviated atom from the N1-C7-C8-C9 plane is C7 atom with the 0.030(4) Å [1]. Chlorophenyl and methoxyphenyl rings are nearly perpendicular to each other (81.1(4)º). The antibacterial activity of the monocylic ß-lactam compounds could be explained by the non-planarity of the lactam ring [2 and references therein] and the ß-lactam compounds show important role in the antibacterial compounds [3, 4]. Besides, selectivity or activity can be decisively influenced by the substituents of the β-lactam ring [5, 6]. Quantum mechanical calculations were carried out to investigate the conformation analysis of the crystal structure according to the AM1 methods and compared with the previous studies.

Molecular Structure Corporation. (1997). teXsan for Windows version 1.03. Single Crystal Structure Analysis Software. Version 1.03. MSC, 3200 Research Forest Drive, The Woodlands, TX 77381, USA.
S.Pain, G. Biswas, A. Bose & A. Banerjee. (1992). Acta Cryst. C48, 666-669.
S.D Sharma & U. Mehra (1988). S. Scient. Ind. Res. 47, 451-458.
L.R. Verma & C.S. Narayanan (1991). Indian J. Chem. 30B, 676-679.
V. M. Duirne, O. Mazzoni, E. Piscopo & A. Bolognose (1992). Farmaco, 47, 239-241.
R. Kumar, S. Giri & J. Nizameddun (1993). Pestic. Sci. 18, 9-13.

P12.05.002 (3, 3-DICHLORO-1, 4-DIPHENYL-2-AZET-IDINONE). K. Güven, T.N.Durlu, M.Kabak, Department of Physics, Faculty of Art and Sciences, University of Kırıkkale, 71450 Yahşihan, Kırıkkale, Turkey, and V.Güner. Department of Chemistry, Faculty of Sciences, University of Hacettepe, 06532, Beytepe, Ankara, Turkey.

The crystal structure of title compound, $C_{15}H_{11}NOCl_2$, is monoclinic, C2/c, a=19.305(2), b=5.958(1), c=23.847(2) Å, β=91.9(8)°, V=2741.0(5)A^{-3}, Z=8, D_x= 1.416 Mgr/cm^3, $\lambda_{MoK\alpha}$=0.71073 Å. The Cl1-C8-Cl2 plane is nearly perpendicular to the four membered β-lactam group 89.0(2)º and the C-C bond distances on this group are 1.571(6) and 1.543(7) Å, respectively. The most deviated atom from the N1-C7-C8-C9 plane is C7 (-0.025(5) Å). Two phenyl rings are nearly perpendicular to each other 77.4(2)º. Developments in the field of β-lactams during the last decade have shown that the only essential feature for the antibacterial activity in these compounds is the presence of β-lactams ring (2-azetidinone) [1, 2, 3, 4]. Selectivity or activity can be decisively influenced by the substituents of the ring [5, 6]. It was reported that the biologically activity of the β-lactams by Chambers and Doedens, 1980 and the structural studies Ercan, Ülkü & Güner, 1996; Ülkü, Ercan & Güner, 1997. The four atoms of lactam ring are coplanar to within the experimental error in other β-lactams [10].

1. S.D. Sharma & U. Mehra (1988). S. Scient. Ind. Res. 47, 451-458.
2. L.R. Verma & C.S. Narayanan (1991). Indian J. Chem. 30B, 676-679.
3. E. Grochowski & K. Pupek (1991). Tetrahedron. 34, 1731-1733.
4. M.S. Manhas, D.R. Wagle, J. Ciang & A.K. Bose (1998). Heterocycles. 27, 1755-1758.
5. V.M. Duirno, O. Mazzoni, E. Piscopo and A. Bolognose (1992). Farmaco, 47,239-241.
6. R. Kumar, S. Giri & J. Nizameddun (1993). Pestic.Sci. 18, 9-13.
7. R. Chambers & R.J. Doedens (1980). Acta Cryst. B36, 1507-1510.
8. F. Ercan, D. Ülkü & V. Güner (1996). Acta Cryst. C52, 1779-1780.
9. D. Ülkü, F. Ercan & V. Güner. (1997). Acta Cryst. C53, 1945-1947.
10. E.F. Paulus, D. Kobelt & H. Jensen. (1969). Angew. Chem. In. Ed. Engl. 8, 990-991.

P12.05.003 STRUCTURE & CONFORMATION OF 2,10 -DICHLORO DIBENZO[D,G] [1,3,6,2] DIOXATHIA AND [1,3,2] DIOXA-PHOSPHOCIN-6-OXIDES. M. Krish-naiah, N. Jagadeesh Kumar, Department of Physics, Sri Venkateswara University, Tirupathi - 517 502. India.

Heterocycles with suitably substituted Phosphoryl unit exhibit significant Physiological activity. These compounds are often important interms of multiple applications as insecticides, bactericides, fungicides and also in polymer and oil industries as stabilizer and antioxidants. Some of these family were evaluated for toxicity in the insect P-americana. The structural investigations on the titled compounds have been studied to understand the conformation of heterocyclic rings & to identify the biological active phosphorus moieties. The present study is devoted on (I) 6-[bis(2-chloro-ethyl) amino] , (II) 6-tri-chloromethyl 2,10-dichloro dibenzo [d,g][1,3,6,2] dioxathiaphosphocin 6-oxides, (III) 1,2,4,8,10,11- hexachloro-6- trichloromethyl & (IV) 2,10 dichloro-6-[bis-(2-chloromethyl)amino] 12-trichloromethyl 12H-dibenzo-[d,g][1,3,2] dioxaphosphocin 6-oxides.

Crystal data: (I) $C_{16}H_{14}Cl_4NO_3PS$, Monoclinic $P2_1/c$ a=9.188(2), b=20.588(5), c=10.861(3)Å , β = 102.5 (2)°, Z=4, R=0.034 for 2932 reflections. (II.) $C_{13}H_6Cl_5O_3PS$, $P2_1/n$, a = 11.624(7), b=11.091(3), c=14.407(4)Å, β = 107.8(3)º, Z=4, R = 0.045 for 2525 reflections. (III) $C_{14}H_4Cl_9O_3$ P, $P2_1/c$ a = 9.235(4), b=23.155(3), c=9.301(3)Å, β= 98.9(3)°, Z=4, R=0.035 for 2733 reflections. (IV) $C_{18}H_{15}Cl_7O_3P$, orthorhombic $P2_12_12_1$ a = 11.566(3), b= 12.836(4) and c=15.312(4)Å, Z=4, R=0.041 for 2011 reflections. All the strucutres solved by direct methods and refined by full matrix least square methods using SHELXS-86 & SHELXL-93.

The conformation for the eight membered dioxathiophophocin ring is a boat-chair(B.C.) in I , twist boat (T.B) in II and for dioxaphosphocin ring it is a distorted boat (D.B) in III and IV. The orientation of the substitutents and their influence on the conformation and geometrical parameters are compared to the corresponding ones reported and discussed with respect to their biological activity.

P12.05.004 CRYSTAL AND MOLECULAR STRUCTURE OF CINCHONAN ALKALOID K.A. NIRMALA, P.KUMARADHA Dept. Of Physics, Bangalore University, Jnana Bharathi, Bangalore 560056, Karnataka, India

The crystal structure of the title compound ($C_{27}H_{29}ClN_2O_3.HCl$) has been studied due to their considerable interest as antimalarial drug. The crystals were grown from acetone. Crystal data: orthorhombic, $P2_12_12_1$, Z=4, a=11.745(3), b=12.353(6) c=17.253(6) A and V=2503(2) A^3. The structure has

been solved by Direct methods using SHELXS-86 and refined by least-squares method using SHELXL-93 to the final R value 0.062 for 2155 observed reflections The detailed molecular conformation of the structure and the effect of the substituents on the molecular geometry, that is, the conformation of the quinuclidine ring and chlorobenzoate group will be discussed.

P12.05.005 STRUCTURE AND CONFORMATION OF 4,4 DIETHOXY CARBONYL -3,5(4-METHYL PHENYL)-1-THIAN-1,1, DIOXIDE. S. Narasinga Rao, Department of Physics, University of Central Oklahoma, Edmond, OK, USA; M. Krishnaiah, N. Jagadeesh Kumar, Gan Srinivasa Rao, Department of Physics, Sri Venkateswara University, Tirupati 517502, India; D. Bhaskar Reddy, M. Muralidharan, Department of Chemistry, Sri Venkateswara University, Tirupati 517502, India; G. Aguirre-Hernandez, F. Ortega-Chocote, and Manuel Soriano-Garcia, Centro de Gradudos e Investigacion del Instituto Technologico de Tijuana, Mexico

Considerable interest has been shown in the crystal structural studies of heterocyclic compounds, particularly the ones containing sulfur in the ring at the 1-position, mainly because of their wide spectrum of physiological action. They find applications in pharmacology, bacterial and fungicidal studies.

The study of the present crystal has been undertaken to understand the effects of substituents on the conformation of the heterocyclic rings and its geometrical parameters.

The compound ($C_{25}H_{30}O_6S$) crystallizes in space group P-1. The cell parameters are a=8.9010(10), b=11.700(2), c=13.0260(10) Å, α=64.24°, β=88.97°, γ=78.97°, V=1195.9(3) Å^3. There are 2 molecules in the unit cell. The structure has been refined to a final R factor of 0.07.

In the structure, thian dioxide assumes a chair conformation as expected like in the cyclohexane moiety in its preferred rigid conformation. The two aryl groups at 3 and 5 adopt an equatorial position in cis-conformation. The structure is stabilized by H-bonds C-H...O and van der wall contacts.

P12.05.006 STRUCTURE AND CONFORMATION OF 4,4 DIMETHOXY CARBONYL -3,(4-CHLORYL PHENYL)-1-THIAN-1,1, DIOXIDE. M. Krishnaiah, N. Jagadeesh Kumar, Gan Srinivasa Rao, Department of Physics, Sri Venkateswara University, Tirupati 517502, India; D. Bhaskar Reddy, V. Padmavathi, Department of Chemistry, Sri Venkateswara University, Tirupati 517502, India; G. Aguirre-Hernandez, F. Ortega-Chocote, Manuel Soriano-Garcia, Centro de Gradudos e Investigacion del Instituto Technologico de Tijuana, Mexico; and S. Narasinga Rao, Department of Physics, University of Central Oklahoma, Edmond, OK, USA

Considerable interest has been shown in the crystal structural studies of heterocyclic compounds, particularly the ones containing sulfur in the ring at the 1-position, mainly because of their wide spectrum of physiological action. They find applications in pharmacology, bacterial and fungicidal studies.

The study of the present crystal has been undertaken to understand the effects of substituents on the conformation of the heterocyclic rings and its geometrical parameters.

The compound ($C_{22}H_{23}Cl O_6S$) crystallizes in space group P-1. The cell parameters are a=9.1980(10)Å, b=10.2320(10)Å, c=12.625(2)Å, α=74.653(9)°, β=72.459(9)°, and γ=78.827(9)°. V=1084.1(2) Å^3. There are 2 molecules in the unit cell. The structure has been refined to a final R factor of 0.07.

In the structure, thian dioxide assumes a chair conformation as expected like in the cyclohexane moiety in its preferred rigid conformation. The two aryl groups at 3 and 5 adopt an equatorial position in cis-conformation. The structure is stabilized by H-bonds C-H...O and van der wall contacts.

P12.05.007 STRUCTURAL INVESTIGATIONS ON PLEUROMUTILINS: A SERIES OF ANTIBIOTICS TO COUNTER BACTERIAL RESISTANCE. Royston C. B. Copley[1], Drake S. Eggleston[1], R. Curtis Haltiwanger[2] & Eric Hunt,[1] SmithKline Beecham Pharmaceuticals, Research and Development, [1] New Frontiers Science Park (North), Third Avenue, Harlow, Essex CM19 5AW, UK and [2] P.O. Box 1539, King of Prussia, Pennsylvania 19406, USA.

Bacterial resistance to existing antibiotics is an issue of international concern and has been the subject of much media attention. To combat this problem, the pharmaceutical industry is looking to identify drug molecules whose mode of action is distinct from those of established agents and which display activity against the resistant bacterial strains. Pleuromutilin is just such a compound and is a natural product that was first isolated from the basidiomycete *Pleurotus mutilus* in the early 1950s. Whilst semi-synthetic pleuromutilins were studied in the 1970s and 1980s by the Sandoz group, no drug was ever brought to the market for human use. Investigation of such under-exploited antibiotics represents a realistic approach to solving the problem of resistant bacterial strains.

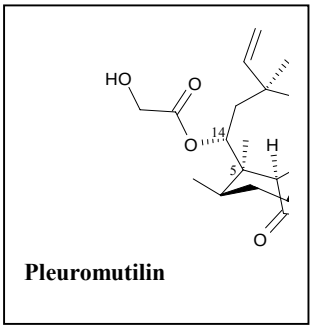

Pleuromutilin

We describe the single crystal X-ray structure of the natural product and of a number of semi-synthetic pleuromutilins derived from this. The tricyclic core represents a rigid moiety which generally remains unperturbed as substituents are varied as will be illustrated by a series of structures where there is interchange of the side chain at position 14. The conformational effects of opening the five and six-membered rings will be described, as will the effect of introducing functionality that dictates a dramatic conformational change.

P12.05.008 CRYSTALLISATION AND CHARACTER-ISATION OF PSEUDOPOLYMORPHS OF NOR-FLOXACIN. E. A. Wright, A. J. Florence and N. Shankland, Department of Pharmaceutical Science, University of Strathclyde, Glasgow G4 0NR, UK, and A. R. Kennedy, Department of Pure and Applied Chemistry, University of Strathclyde, Glasgow G1 1XL, UK, and P. J. Cox, School of Pharmacy, Robert Gordon University, Aberdeen AB10 1FR, UK

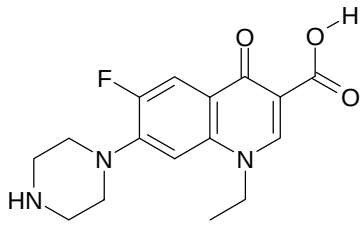

Norfloxacin ($C_{16}H_{18}FN_3O_3$) is a fluoroquinolone antibiotic that is active against a large variety of Gram-positive and Gram-negative bacteria.

Although two polymorphic forms of norfloxacin have been reported [1], no crystal structures are currently available in the literature. We have crystallised norfloxacin from a range of organic solvents at room temperature and screened for polymorphs using FT-IR and DSC. From these samples, two crystal structures have been determined, and are reported here for the first time. The first is a dihydrate (monoclinic $P2_1/c$, a = 8.265(3), b = 21.698(4), c = 9.525(17) Å, β = 110.79(2)°); the second is a disordered hydrate (monoclinic, $P2_1/a$, a = 8.573(17), b = 22.288(2), c = 8.837(2) Å, β = 106.93(2)°), in which the water molecules and the ethyl side chain are disordered. A comparison of these crystal structures is presented.

[1] B.Sustar,N. Bukovec,and P.Bukovec, J. Thermal Anal., 40 (1993), 475-481

P12.05.009 CRYSTAL STRUCTURE OF (23S, 25R)-3β-BROMO- 6β-ACETOXY-5α-SPIROSTAN-23-OL MONO-HYDRATE. O. Au-Alvarez, Dept. of Chemistry, Fac. of Sciences, University of Oriente, Santiago de Cuba 90500, Cuba, R. C. Peterson, Dept. of Geological Sciences, Queen's University, Kingston, Ontario K7L 3N6, Canada, M.A. Iglesias Arteaga, R. Pérez Gil and F. Coll Manchado, Lab. of Natural Products, Fac. of Chemistry, University of Havana, Havana, Cuba and R. Pomés Hernández, National Center for Scientific Research, P.O.Box 6990, Havana, Cuba.

During our study of bioactive steroids derived from sapogenins we synthesized the title compound (I), $C_{29}H_{47}BrO_6$. After the synthesis it was questioned whether it crystallized in anhydrous form or hydrated. In order to solved this question we undertook the determination of its crystal structure. The results obtained in this study clearly showed that (I) crystallizes with one molecule of water. This molecule is linked to the 23-hydroxil group of the spyrostan moiety via a hydrogen bond. The compound is monoclinic, space group $P2_1$ with a=16.404(5), b=7.135(5), c=12.536(5) Å, β=103.32(3)^o and Z=2. The Br atom bonded to C3 is equatorially oriented and does not disturb the chair conformation of ring A. Rings C, D and F also have chair conformation [1]. The A/B, B/C and C/D ring junctions are trans. The angle between the l.s. plane to ring A and that to B-C-D is 5.10^o. Ring D has a 15β-envelope conformation. The molecule is practically not twisted about the length of the molecule as is evident from the value of the C19-C10...C13-C18 pseudotorsion angle [2]. The carbonyl distance (1.198 Å) of the acetate group is smaller than expected. The angle between the l.s. plane to the four non-hydrogen atoms of the acetate group and the B l.s. plane is 75.9^o.

1. Pfieffer, D., Kushchabsky, L., Kretschmer, R.G., Collect, F. & Adam, G. (1985). Z. Chem. 25, 183-4.
2. Duax, W.L., Weeks, C.M. & Rohrer, C.D. (1976). Topics in Stereochemistry, Vol. 9, ed. E.L. Eliel & N. Allinger, New York, John Wiley.

P12.05.010 PSEUDOSYMMETRY AND DISORDER IN THE STRUCTURE OF CHOLESTEROL AT 37° C. Christer E. Nordman and Leh-Yeh Hsu, Department of Chemistry, University of Michigan, Ann Arbor, MI 48109, USA.

This structure, space group P1, Z = 16, is refined in a cell with *a* = 27.565, *b* = 38.624, *c* = 10.748, α = 93.49, β = 90.90, γ= 117.15, related to the "reduced" cell [1], by **a** = $\mathbf{a}_{red}$, **b** = $\mathbf{b}_{red}$ - $\mathbf{a}_{red}$, **c** = $\mathbf{c}_{red}$. This unit cell is related to the room temperature cell [2], similarly transformed, by an approximate doubling of the *a*-axis. The structure shows a remarkable 2-fold rotational and screw-rotational pseudosymmetry. The "pseudoasymmetric unit" is the 8-molecule cluster A1, B1, C1, D1, A2, B2, C2, D2 in the previously used notation [1], comprising half of the cell content. This cluster is related to the other half of the unit cell, E2, F2, G2, H2, E1, F1, G1, H1, by a "$2_{0.5,\ 1.5}$" screw axis nearly parallel to **c**, at *x*,*y* = 0, 0.5 and 0.5, 0.5, and having alternating translational components of Δ*z* = 0.25 and 0.75. Parallel with these are 2_1 screw axes at x, y = 0,0 and 0.5, 0, which relate, respectively, the A1, .., D2 cluster to the E2,..,H1 cluster in the cell translated by –**b** or to that in the cell translated by –**b**–**a**. Coaxial with these are 2-fold rotation axes which relate A1,..,D2 to E2,..,H1 in the cell translated by +**b**. These symmetries extend throughout the structure in the **a** and **b** directions. In the *z*-direction the pseudo-symmetry is less closely obeyed as these 2-fold axes are not exactly parallel with the **c**-axis, but make an angle of 1.4° with it. The side chains of all the cholesterol molecules suffer from high thermal motion or disorder. Despite this it is clear that many of the side chains obey the pseudosymmetry closely. In other cases the difficult-to-model disorder may show some violation.

1. Hsu, L.-Y. and Nordman, C. E. (1983) *Science* **220**, 604-606.
2. Hsieh, H. S., Hoard, L. G. and Nordman, C. E. (1977) *Nature* **267**, 287-289; (1981) *Acta Cryst.* **B37**, 1538-1543.

P12.05.011 STEROIDS AS CHIRAL LIGANDS: SYNTHESIS AND CRYSTAL STRUCTURES OF 1-ENAMINO-3-OXO COMPOUNDS AND AZOMETHINES FROM STEROIDAL AMINO ALCOHOLS. H. Görls, Institut für Anorganische und Analytische Chemie der Universität Jena, August-Bebel-Str. 2, 07743 Jena, Germany, M. Dubs, R. Krieg and B. Schönecker, Institut für Organische und Makromolekulare Chemie der Universität Jena, Humboldtstr. 10, 07743 Jena, Germany.

For stereochemical and biological investigations new steroids as chelating ligands have been synthesized. Condensation of the four 16-amino-17-hydroxy-3-methoxy-estra-1,3,5(10)-trienes with aliphatic 1,3-dioxo compounds (or derivatives), aromatic ortho-hydroxy aldehydes or heteroaromatic a-aldehydes gave 16-(1-enamino-3-oxo) compounds with a 17-hydroxy group (type I) or the corresponding 16-imines (type II and III), respectively. By reduction of compounds of the type II and III new N-substituted 16-amino-17-hydroxy compounds (type IV) are available.

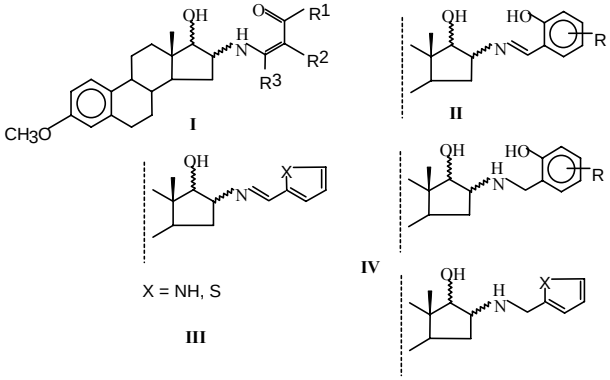

Two kinds of copper(II) complexes are described: steroid/copper(II) = 2 : 1 for 16,17-trans compounds, steroid/copper(II) = 1 : 1 for 16,17-cis compounds.

P12.05.012 A STUDY OF THE ACTIVE SITES OF STEROIDAL RECEPTORS: THE 17-SPIRO LACTIDE OF HYDROCORTISONE. A.J. Mora, B.M. Ramírez, G. Delgado [1] R. Little [2], [1] Laboratorio de Cristalografía, Departamento de Química, Facultad de Ciencias, Universidad de Los Andes, Mérida 5101, Venezuela, [2] Laboratorio de Fisicoquímica Orgánica, Departamento de Química, Facultad de Ciencias, Universidad de Los Andes, Mérida 5101, Venezuela.

In the process of developing new soft drugs based on hydrocotisone, which are used as topical anti-inflammatory agents, the cyclic 17-spiro lactide modification in which the R groups of the 17a, 17b diesters are joined into one alkyl group was prepared as a mixture of epimers. The epimer, which has the absolute configuration R at the 6' -position, was investigated using X-ray diffraction. The compound, (6'R)-6'-methyl-2',5'-dioxo-(17R)spiro [11b-hydroxy-androst-4-en-3-one-17,3'-[1,4]-dioxane], of chemical formula $C_{23}H_{30}O_6$, is orthorhombic, space group $P2_12_12_1$ with a = 25.869(8) Å, b = 12.494(4) Å, c = 6.198(2) Å, V = 2003(1) Å^3, Z = 4, d_x = 1.334 g/Å^3.

The conformation of the steroid ring system is similar to those found for other hydrocortisone derivatives. The spiro lactide ring is in the half chair conformation, with its 6'-methyl substituent oriented towards the steroid ring, and the two polar esther carbonyl groups directly opposing each other. These two factors have an apparent detrimental effect to binding globulin if compared with the 6´-S epimer.

The molecules are held together by a hydrogen bond, which forms a zigzag pattern of chains parallel to the (010) direction.

This work was supported by CONICIT, grant S1-97000821, for the establishment of the Laboratorio Nacional de Difracción de Rayos-X, and CDCHT-ULA.

P12.05.013 [SECALONIC ACID D]$_3$FE$_2$, A SIDEROPHORE? C.L. Barnes and R.K. Murmann, Department of Chemistry, University of Missouri, Columbia, MO 65211, USA, R. Ubillas, Phytera, 377 Plantation St., Worcester, MA 01605, USA, M.S. Tempesta, Pharmaprint, 846 San Carlos Ave., El Granada, CA 94018, USA.

Secalonic acids A through G are dimeric hydroxanthone derivatives produced by a number of fungi commonly isolated from stored grains and animal feeds. Secalonic acid D (**SAD**), produced by *Penicillium oxalicum*, and arguably the most studied of this family of mycotoxins, is teratogenic and has been shown to cause cleft palate and other physical and behavioral deficits in test animals [1,2].

While it was early noted that the secalonic acids gave a wine-red color reaction with Fe^{3+}, the resulting complex has not before been characterised. Our X-ray crystal structure of the iron complex of **SAD** reveals a helical arrangement in which three **SAD** molecules chelate two Fe^{3+} cations with octahedral arrays of six O atoms. The O atoms about each iron center include three deprotonated phenolic O atoms to yield a neutral complex.

Most fungi produce siderophores, small molecular weight iron-binding molecules, under conditions of low iron stress. Typical fungal siderophores bind iron with an octahedral array of six O atoms, reminiscent of the **SAD**$_3$Fe$_2$ complex. To meet the definition of a classical siderophore, the biosynthesis of secalonic acid must be under stringent control by iron. We will culture *P. oxalicum* on defined media to see if **SAD** meets this criterion.

1. C.S. Reddy, R.V. Reddy, A.W. Hayes & A. Ciegler (1981). J. Toxicology & Environmental Health, **7**, 445-455.
2. B. Bolon & V.E. St. Omer (1992). Neuroscience and Behavioral Reviews, **16**, 171-175.

P12.05.014 CINCHONA ALKALOID INTERACTIONS WITH METAL ATOMS. B. J. Oleksyn, P. Pytel and J. Œliwiñski, Faculty of Chemistry, Jagiellonian University, R. Ingardena 3, 30-060 Kraków, Poland.

Malaria parasites, *Plasmodium sp.*, which live in mammalian erythrocytes feeding on their hemoglobin amino acids, are able to polymerize heme, poisonous for them in its water-soluble monomolecular form. Cinchona alkaloids are believed to interact with heme iron and block the formation of polymeric hemozoine which is the product of *Plasmodium* life processes. In view of difficulties in obtaining crystalline heme-alkaloid complexes we have undertaken systematic studies of Cinchona alkaloid interactions with different metal atoms in various coordination surroundings.

In the crystalline cinchoninium salts with tetrachlorocadmium and tetra-chlorocopper anions, described by us previously, metal atoms interact with alkaloid *via* coordinated chlorines which are proton acceptors in the intermolecular hydrogen bonds with quinuclidine nitrogen, N1. In the complex (HQ)$CoCl_3$, obtained recently by us from alkohol solution of $CoCl_2{\cdot}6H_2O$ and quinine (Q), cobalt atom is directly linked to N13 atom of the quinoline moiety (N13-Co = 2.070(2) Å) and to three chlorines. Cl atoms are acceptors of protons bonded to N1 and O12 atoms of Q. The conformation of Q is similar to that of the free base.

Co-Q interaction which occurs in (HQ)$CoCl_3$ is different from those observed e.g. in ruthenium complex with cinchonine [1] and osmium complex with a derivative of dihydroquinidine [2]. In the first of them metal atom is coordinated by N1 and O12 of the alkaloid molecule, while in the second - only by N1.

Crystal data for (HQ)$CoCl_3$: M.F.: $C_{20}H_{25}N_2O_2CoCl_3$, FW = 490.721, CuK_α, $P2_12_12_1$, a = 7.6262(4), b = 11.4902(8), c = 24.6214(9) Å, Z = 4, D_m = 1.52(1) gcm^{-3}, D_x = 1.50 gcm^{-3}, R1 = 0.0416 for 4290 $F_o > 4\sigma(F_o)$, *w*R2 = 0.1029, S =1.036.

[1] Ch. Missling et al. (1996). Chem. Berichte, **129**, 331.
[2] J. S. Svendsen et al. (1989). J. Org. Chem., **54**, 2263.

P12.05.015 STRUCTURAL STUDIES OF BAICALEIN, A PLANT FLAVONOID WITH BIOLOGICAL ACTIVITY. Pamela Constantinou, Ryan Meyer, Miriam Rossi, Department of Chemistry, Vassar College, Poughkeepsie, NY 12604-0484, USA and Francesco Caruso, Istituto di Strutturistica Chimica, CNR, CP#10, 00016, Monterotondo Stazione (Rome) Italy.

Many flavonoids are biologically active compounds that are ubiquitous in plants. Baicalein (5,6,7-trihydroxyflavone), $C_{15}O_5H_{10}$, is the principal component of a traditional Asian drug, Sho-saiko-to. The crystal and molecular structure reveal that baicalein exists in an almost planar conformation, with an 8° torsion angle about the single bond connecting the phenyl and the pyrone rings. The disposition of the hydroxyl groups is to maximize intramolecular hydrogen bonding and each of the hydroxyl hydrogen atoms is involved in a three-center hydrogen bonding situation involving inter- and intramolecular interactions. Two baicalein molecules exist as hydrogen bonded dimers related by an inversion center. There are also stacking interactions among the almost planar hydrogen bonded dimers. The stacking of the molecules is roughly perpendicular to the *c* axis in the *ab* plane. Studies in trying to clarify how baicalein interacts with proteins and nucleic acids will be described. Baicalein crystallizes in $P2_1/n$ with *a* = 7.907(4) Å, *b* = 13.367(5) Å, *c* = 12.911(6) Å, β = 117.26(2)°.

P12.05.016 NEW DETAILS OF ANTIBACTERIAL QUINOLONES ACTION DERIVED FROM THEIR CRYSTAL STRUCTURES. Marek L. Glówka and D. Martynowski, Institute of General and Ecological Chemistry, Technical University of Lódz, ul. Zwirki 36, 90-924 Lódz

The crucial structural requirements for antibacterial activity of a quinolone is N1-substituted 4-oxo-1,4-dihydroquinoline with an acidic function in the C3 position. 3-Carboxylic acids with cyclic amines (preferably piperazine and pyrrolidine) at C7 and a fluorine at C6 are the most common agents (I). Two main models of quinolones actions have been proposed, one based on their interactions with gyrase-DNA complex (by hydrogen bonds with guanine) and the other on intercalation with DNA. As a detailed molecular mechanism of antibacterial quinolones action is not known, structural information from crystal structures of quinolones and their analogs is very valuable. Over 20 crystal structures of quinolones may be found in CSD, which combined with 10 of cinnoline analogs (II) determined in our laboratory, gives a sound base for our observation of some patterns relevant to quinolones action. Our most important findings are: (*i*) quinolones show good permeability through cell membranes by ”locking” acidic hydrogen in 3-carboxylic group into an intramolecular hydrogen bond with 4-oxo substituent, (*ii*) preference for specific stacking

in crystal structure of quinolones suggests that particular DNA sequence is a target for quinolones and (*iii*) analogs of quinolones, designed by us to interact with a base complementary to guanine (cytosine), showed antibacterial activity similar to that of nalidixic acid.

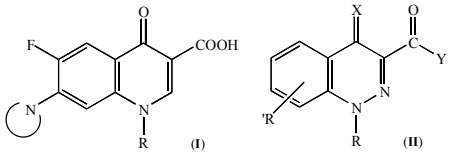

P12.05.017 X-RAY POWDER DIFFRACTION STUDY OF CHITIN AND CHITOSAN OBTAINED WITH ENZYME PROCESSES. A.D.Zuev and A.Ertel, X-Ray Lab, University of Applied Sciences, 23562 Luebeck, Germany.

A biopolymer chitin, poly-ß-(1→4) linked N-acetyl-D-glycosamine, and especially its derivative chitosan prepared from chitin by acetylation n-acetyl-glycosamine units in strong alkali have a wide field of applications [1]. The structure of the most distributed α-chitin were determined with single crystal structure analysis in [2]. It belongs to the orthorhombic space group $P2_12_12_1$ with unit cell dimensions a=4.74Å, b=18.86Å, c=10.32Å. The powder chitin and particularly chitosan show the low crystallinity. The one of the alternative to the traditional acid-alkali way of the manufacture chitin/chitosan from shellfish waste is enzyme proceeding [3]. For the control of its quality the comparison of the X-ray powder diffraction diagram of the chitin from the different sources were made. The simulations of the powder data carried out with PowderCell [4] and FullProf [5] show that with enzyme method proceeding chitin is identified as α-chitin. The preliminary refinement with the program FullProf were made. The measurement were carried out with thin film too. Depending on the preparation method the thin films show different grads of the crystallinity up to the amorph state.

1. Chitin, Chitosan, and Related Enzymes. Ed. By John P. Zikakis. 1984. Academic Press, Inc.
2. R. Minke and J. Blackwell. The structure of the α-chitin. J. Mol. Biol. (1978) 120, 167-181.
3. J.Fischer, U.Englisch. Personal communication, 1998.
4. W. Kraus and G.Nolze. PowderCell, version 2.0 beta.
5. Juan Rodríguez-Carvajal (Lab. Leon Brillouin, Saclay) FullProf, 3.1d

P12.05.018 STRUCTURAL STUDY OF NOVEL PYRIDONE DERIVATIVES: THREE POTENTIAL CARDIOVASCULAR AGENTS. M. Suárez[1], Y. Verdecia[1] , E. Ochoa[1], R. Pomes[2], J. Duque[2], H. Novoa[3], N. Blaton[4], O. M. Peeters[4]. [1]Laboratory of Organic Synthesis, Faculty. of Chemistry, Havana University, Cuba. [2]National Center for Scientific Research, Havana, Cuba. [3]Center of Pharmaceutical Chemistry. Havana, Cuba. [4]Katholieke Universiteit Leuven. Laboratorium voor Analytische Chemie en Medicinale Fysicochemie, Belgium.

In the aid of finding new cardiotonic agents, we developed the structural study of novel 2(1H)-pyridones derivatives of dihydropyridine-type.

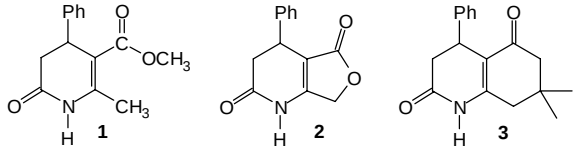

	a (Å)	b (Å)	c (Å)	β (°)	Sp. Group	Final R.(%)	S
1	8.983(2)	13.196(3)	21.125(4)	90.00 (0)	Pcab	4.99	1.165
2	11.297(1)	6.949(1)	13.732(2)	91.95 (0)	$P2_1/c$	5.43	1.162
3	9.2810(4)	22.498(2)	7.5278(7)	113.06(4)	$P2_1/c$	4.66	1.056

The X-ray structure of compounds 1, 2 and 3 shows a skew-boat conformation for the pyridone ring, with the phenyl ring occupying a pseudo-axial position and is orthogonal to the mean plane of the pyridone ring. The lactone ring fused to the pyridone ring in 2 is perfectly plane and the fused cyclohexanone ring in 3 has a conformation close to an envelope. The molecules are linked by N-H···O hydrogen bonds forming dimers. The hydrogen bond is formed between the N-H group and the oxygen atom of the pyridone exocyclic carbonyl group for each compound.

P12.05.019 STRUCTURAL DETERMINATION OF 1-(4-X-BENZOYL)-3,3-DIMETHYLTHIOUREA. R. Pomes[1*], G. Aguero[2], A. M. Plutín[2], H. Márquez[2] and Y. I. Rodríguez[2]. [1]National Centre for Scientific Research, P.O. Box: 6880, Havana, Cuba. [2]Laboratory of Organic Synthesis, Faculty of Chemistry, Havana University, P.O. Box 10400, Havana, Cuba.

1-(X-benzoyl)-3,3-dimethylthioureas (X= Br, Cl and CH_3) are well recognised compounds because of their known applications in medicine and as bio-active and anticorrosive agents.

Structural studies of a number of benzoyl thioureas have proved them to be in the thioamidic form and to possess an intra-molecular hydrogen bond between N-H and the benzoyl oxygen.

Crystal and molecular structure of 1-(4-X-benzoyl)-3,3-dimethylthioureas have been determined by means of spectroscopic techniques such as IR, NMR ^1H, ^{13}C and X-Ray Diffraction.

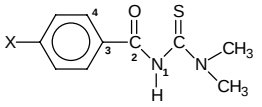

	a (Å)	b (Å)	c (Å)	β (°)	Sp. Group	Final R.(%)	No. of Reflec.
Cl	11.175(1)	5.454(1)	8.056(2)	92.22 (1)	$P2_1/c$	4.1	2511
Br	11.308 (5)	5.578(5)	18.322(5)	91.88 (1)	$P2_1/c$	5.1	2600
CH_3	12.703 (3)	5.577(2)	17.389(4)	103.93(1)	$P2_1/c$	7.1	771

In the structures are present intra-molecular hydrogen bond N-H···S. The torsion angles between atoms O-2-3-4 and 1-2-3-4 vary with the X substituent.

P12.05.020 ABSOLUTE CONFIGURATION OF SECOND GENERATION ANTIMALARIAL ARTEMISININ COMPOUNDS. Jean M. Karle, Ai J. Lin, and Apurba K. Bhattacharjee, Departments of Pharmacology and Medicinal Chemistry, Division of Experimental Therapeutics, Walter Reed Army Institute of Research, Washington, DC 20307, U.S.A.

The artemisinin family of compounds is very important for the treatment of malaria due to their potency against chloroquine-, mefloquine-, and multidrug-resistant parasites. Artemisinin, the parent compound, is a sesquiterpene endoperoxide, naturally occurring in the Chinese herb *Artemisia annua*. Artelinic acid, a water soluble synthetic derivative, is currently in preclinical development. Artelinic acid derivatives were synthesized in the hopes of being more efficacious, possessing a longer plasma half-life, keeping the compound water soluble, and preventing enzymatic conversion to dihydroartemisinin, a known toxic metabolite of artemisinin analogs in rats and dogs. Crystal structures of diastereomeric methyl 4-(*p*-chlorophenyl)-4(*R* or *S*)-[10(α or β)-dihydroartemisininoxy]butyrates were determined to assign the absolute configuration and to provide an experimentally determined conformation. The x-ray structures are consistent with their proton nmr spectra suggesting that the crystalline and solution structures are similar. The most abundant and

thermodynamically stable conformations of the acid analogs of the butyrates at the 3-21G* level also match the crystalline conformations of the methyl esters. Enhanced antimalarial activity was achieved. However, the acid form of the *R*(β)-diastereomer is not very soluble in water. Computed electrostatic potentials indicate that the acid form of the *R*(β)-diastereomer is more lipophilic than artelinic acid. Computations also indicate that protonation of the ether oxygen atom requires more energy for the *R*(β)-diastereomer than artelinic acid suggesting a slower conversion than artelinic acid to dihydroartemisinin.

S(α)-diastereomer: $C_{26}H_{35}O_7Cl$, $P2_12_12_1$, a = 10.292(2), b = 15.663(3), c = 16.277(4) Å, Z = 4, V = 2623.91 Å^3, Cu K(α), *R1* = 0.0713, *wR2* = 0.3316.

R(β)-diastereomer: $C_{26}H_{35}O_7Cl$, $P2_1$, a = 9.715(1), b = 10.532(1), c = 27.821(2) Å, β = 92.29(1)°, Z = 4, V = 2844.33 Å^3, Cu K(α), *R1* = 0.1241, /.*wR2* = 0.3420.

P12.05.021 WATER MEDIATED HYDROGEN BONDING NETWORK IN AN ACRIDINE CARBOXAMIDE DERIVATIVE. J.Jeyakanthan and D.Velmurugan, Department of Crystallography and Biophysics, University of Madras, Guindy Campus, Chennai 600 025, INDIA, and Thainash Muthu Josephrajan and V.T. Ramakrishnan, Department of Organic Chemistry, University of Madras, Guindy Campus, Chennai 600 025, INDIA.

Acridine derivatives have general use in medicine, especially as antitumor agents and anti bacterial agents for wound therapy. The biological activity of the acridines are mainely due to its ability to interact with DNA. Acridine orange and 9-amino acridine are widely studied towards understanding their intercalating behaviour. In these derivative central ring (Pyridine) is approximately planar and the outer two rings adopt distorted half-chair conformations. The molecules are stabilized by many hydrogen bonds. The inter molecular -OH (hydroxyl group)....-C = O(keto) oxygen hydrogen bond makes a molecular chain along c axis. The inter-chain interactions (running along b axis) by water molecules makes a three dimensional hydrogen bonding network. Crystal data: C_{20} H_{20} O_5 N_2, a = 11.142(4), b = 12.266(2) and c = 13.320(2)Å, β = 91.76(2)º and V = 1819.6(1)Å^3, F.W = 368.4, Monoclinic, $P2_1$/ c and Z = 4. The final R = 0.052 and R_w = 0.15 for 3430 reflections (CuKα, λ = 1.5418Å). Structure solution : SHELXS97, Refinement SHELXL97. All conformational features will be presented.

P12.05.022 HYDROGEN BONDING ANALYSIS AND MOLECULAR CONFORMATION OF MONONUCLEAR COPPER AND MANGANESE COMPLEXES S. Shanmuga Sundara Raj, X-ray Crystallography Unit, School of Physics, Universiti Sains Malaysia, Penang, 11800, Malaysia

The function and properties of the active sites are determined by the environment and coordination sites around the metal ion. The Cu,Zn,Mn and Fe complexes are better model compound for metalloenzymes and proteins as they mimic the active site. A stable, non-toxic, low molecular weight mononuclear copper(II) and manganese(II) complex possess clinical applications. The metal ions are in square planar environment; the O and N atoms being the dentating centres with same kind of coordination. The water molecule and the perchlorate ions play major role in the packing by involving in intra- and inter molecular hydrogen bonds. The reported structures are isostructural.

Crystal data: I: $[C_{28}H_{38}N_4O_4Cu.2(CLO_4).H_2O]$, a = 8.9654(3) , b =9.6447(3) and c = 20.0666(5)Å, α=78.475(1), β = 81.518(1), γ=83.786(1)º and V = 1675.99(9)Å^3, triclinic, P-1 and Z = 2. R = 0.068 and R_w = 0.16 for 7898 reflections. II: $[C_{28}H_{38}N_4O_4Mn.2(CLO_4).H_2O]$, a = 8.9162(1), b =9.6764(1) and c = 20.0766(1)Å, α=78.536(1), β = 81.520(1), γ=83.922(1) º and V = 1673.79(3) Å^3, triclinic, P-1 and Z = 2. R = 0.064 and R_w = 0.19 for 6440 reflections. The complete details of the structure and the modelling studies will be reported.

P12.05.023 N-H…S AND C-H…π HYDROGEN BONDING IN THIOUREA DERIVATIVES. S. Shanmuga Sundara Raj,[a] D.Velmurugan[b] and Hoong Kun Fun[a], [a]X-ray Crystallography Unit, School of Physics, Universiti Sains Malaysia, Penang, 11800, Malaysia and [b]Department of Crystallography and Biophysics, University of Madras, Guindy Campus, Chennai 600 025, INDIA

The thiourea derivatives are found useful as rubber accelerators, intermediate materials in dye preparation and very useful agrochemical intermediates. Recently they were found to possess non-linear optical properties. The C-S bond distances show that the double bond nature and this may be influenced by the nature of the substituent group and in particular its ability to participate in π-conjugation. The phenyl ring makes a trans-cis orientation with the central bridge which favours the dimer formation among the molecules through an almost linear N-H...S intermolecular hydrogen bonding. The molecules are packed in a centrosymmetric manner forming two dimensional layer. The C_{sp}^2-H atom participates in π-interaction with the centroid of the other ring and there is an attraction between the centroids of the same rings oriented in opposite direction.

Crystal data: I: $[C_{15}H_{14}N_2OS]$, a = 8.4551(2), b = 8.9044(2) and c = 10.7293(3)Å, α = 91.142(1), β = 107.437(1), γ=113.035(1)º and V = 700.50(3)Å^3, triclinic, P-1 and Z = 2. S=0.93, R = 0.041 and R_w = 0.095 for 3325 reflections. II: $[C_{16}H_{16}N_2OS]$, a = 5.4664(1), b =28.0208(4) and c = 9.8585(1)Å, β = 94.262(1) º and V = 1505.88(4) Å^3, monoclinic, $P2_1/c$ and Z = 4. S=1.06, R = 0.053 and R_w = 0.16 for 3688 reflections. The data were collected on Siemens SMART CCD area detector diffractometer and solved by SHELXTL package. The complete details of the conformation and the hydrogen bonding will be presented..

06. CRYSTALLOGRAPHY OF ORGANIC COMPOUNDS

P05.06.001 MODIFIED CLUSTER VARIATION METHOD FOR PHASE DIAGRAM CALCULATION IN BINARY CRYSTAL STRUCTURES R.V. Chepulskyy [1] Department of Solid State Theory, Institute for Metal Physics, National Academy of Sciences of Ukraine, 36 Acad. Vernadsky Blvd., UA-252680 Kyiv-142, Ukraine

By the use of the radius of interatomic correlations as a small parameter in the cluster expansion, a modified cluster variation method is developed. The proposed method is applied for calculation of the short-range and long-range orders as well as phase diagrams in a number of two-component crystal structures. The high accuracy and high convergence of the method is demonstrated on the basis of comparison with the results of the Monte Carlo simulation.

The proposed modified cluster variation method is successfully applied for development of the inverse methods of calculation the many-body (including non-pair) interatomic correlations and interactions through the data on the diffuse scattering intensity and Mossbauer spectra of two-component crystal structures.

The developed methods can be used under investigation of alloys, low-dimensional lattice systems, semiconductors and magnetics.

P05.06.002 SOLID-STATE PHOTODIMERIZATION CONTROLLED BY THE BUFFER ZONE. N.Hirayama [1], N.Marubayashi, T.Ogawa [2], [1] Department of Biological Science and Technology, Tokai University, 317 Nishino, Numazu, Shizuoka 410-0321,Japan, [2] Research Laboratories, Yoshitomi Pharmaceutical Industries Ltd., 955 Koiwai, Yoshitomi-cho, Chikujo-gun, Fukuoka 871, Japan

Solid-state photodimerization of olefins is one of the well-known topochemical photodimerizations. On the basis of Schmidt's rule [1], it seems that bulky olefins should not undergo solid-state photodimerization due to the significant steric hindrance. We discovered that bulky olefins can undergo solid-state photo-dimerization in spite of a highly steric hindrance. Detailed inspection of the crystal structures revealed that there is a certain space between reacting molecules in the crystal to allow initiation of photodimerization. The space which is not necessarily located near the reaction site buffers the steric hindrance from which the reacting molecules suffer when they approach each other. The space, designated as buffer zone[2], is essential for the crystalline-state reactions. The role of the buffer zone in the crystalline-state reactions will be discussed.

1. M.D.Cohen & G.M.Schmidt (1964).J.Chem.Soc.,1996.
2. N.Marubayashi, T.Ogawa, T.Hamasaki & N.Hirayama(1997). J. Chem.Soc.,Perkin Trans.2,1309.

P05.06.003 TAUTOMERISM OF A NITRO DERIVATIVE OF SALICYLIDENEANILINE IN CRYSTALS. T. Fujiwara and K. Ogawa, Department of Chemistry, Graduate School of Arts and Sciences, The University of Tokyo, Komaba, Meguro-ku, Tokyo, 153-8902 Japan

N-Salicylideneanilines belong to a class of the popular compounds which show thermo- or photochromism in crystals. Extensive studies have revealed that the chromisms are closely related to the tautomerism between the OH and NH forms and that most of *N*-salicylideneanilines including the parent compound (**1**) greatly favour the OH form in both crystals and solutions.[1] However, if a nitro group is introduced into the benzene ring of the salicylaldehyde part, the tautomeric behavior is changed significantly. For example, it was reported that *N*-(2-hydroxy-3-nitrobenzylidene)aniline (**2**) exists as the OH form in saturated-hydrocarbon solvents at room temperature but an aggregate at 77 K where the NH form is involved. The behaviour of **2** in crystals has, however, remained unknown. We report here the tautomerism of **2** in crystals on the basis of X-ray crystallography and electronic spectroscopy.

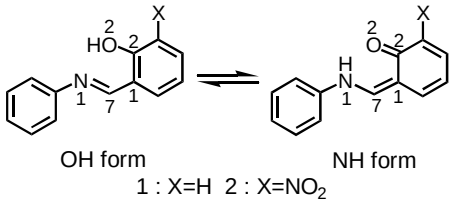

K Ogawa, Y. Kasahara, Y. Ohtani & J. Harada (1998). J. Am. Chem. Soc., 120, 7107.

P05.06.004 SOLID STATE PHOTOREACTION OF 2-PYRONE DERIVATIVES WITH MALEIMIDES. M. Kawaminami, Department of Physics, Faculty of Science, Kagoshima University, Korimoto, Kagashima 890-0065, Japan. T. Obata, T. Shimo and K. Somekawa, Department of Applied Chemistry and Chemical Engineering, Faculty of Engineering, Kagoshima University, Korimoto, Kagoshima 890-0065, Japan.

Photoreaction of a 1:1 complex crystal of 4-methoxy-6-methyl-2-pyrone (**1**) with maleimide (**2**) gave [2+2]cycloadduct (**3**) peri-, site- and stereospecifically. It was inferred to be effectively brought by two sets of the hydrogen bonding and CT stacking between **1** and **2**.

Solid state photoreaction, 1:1 Complex crystal, Photocycloadduct

Photochemical reactions in the solid state afford unusual and interesting results because molecules are disposed tightly and regularly in the environment[1]. In this paper the solid state photocycloaddition reaction of **1** with **2** is described.

Irradiation of a 1:1 complex crystal between **1** and **2**, which was prepared by recrysrtallization of the equimolar substrates from acetonitrile, with a 400W high-pressure mercury lamp under nitrogen at room temperature gave [2+2]cycloadduct **3** in 54% yield as a sole product. On the other hand, the two starting materials in solution photoreaction afforded two kinds of products containing the cycloadduct **3** as a minor product. The crystal and experimental data of the 1:1 complex crystal of **1** with **2** are as follows: chemical formula=$C_{11}H_{11}NO_5$, crystal system = monoclinic, space group= $P2_1/n$, Z=4, lattice constant a=6.678(2), b=11.354(2), c=15.105(4), b_= 94.44(2), volume of unitcell V=1141.84, R=0.075, R_w=0.095.

The photochemical behavior can be readily interpreted by X-ray structure analysis of the 1:1 complex crystal. The molecular **1** is connected to another molecule **2** in the hydrogen bonding. The intermolecular distances of two facing double bonds between **1** and **2** are within the normal photoreaction distance in the solid state. The existence of the hydrogen bonding is also found to be necessary to the [2+2]cycloaddition in addition to the CT stacking in this system.

V. Ramamurthy, K. Venkatesan, *Chem.. Rev.*, **87**, 433 (1987).

P05.06.006 COPOLYESTERS BY SOLID-STATE REACTION M. Siedler, M. Epple, Institute of Inorganic and Applied Chemistry, University of Hamburg, Martin-Luther-King-Platz 6, D-20146 Hamburg, Germany

Biodegradable polyesters like poly(hydroxyacetic acid) (polyglycolide) or poly(lactic acid) (polylactide) are of great importance in medicine and pharmaceutical technology. Especially in medicine, these polymers are employed as absorbable surgical sutures, devices for bone fracture internal fixation and as controlled drug-delivery systems. Fine-tuning of mechanical and biological properties is possible by chemical "mixing" of both polymers to copolymers. Conventionally, such polymers are produced by ring-opening polymerization of the corresponding cyclic diesters (dilactones).

Here we report on the formation of copolyesters of polyglycolide and polylactide in a solid-state reaction by simply heating mixed crystals of alkali halogenoacetates and alkali 2-halogenopropionates (e.g., sodium chloroacetate and sodium 2-chloropropionate). This reaction type is well known for the preparation of the pure polyesters: polyglycolide from halogenoacetates and polylactide from alkali 2-chloropropionate. During the reaction, an alkali halide (e.g., NaCl) is eliminated and the remainder of the molecule undergoes polymerization. Chemical composition, morphology and physical properties of a series of poly(lactide-co-glycolide) polymers were studied by X-ray powder diffraction, IR and NMR spectroscopy and viscosimetry.

P05.06.007 PREORGANIZATION EFFECTS IN SOLUTION AND SOLVENT FREE BISAMIDATION REACTION OF ALIPHATIC DIAMINOETHERS. Zofia Urbañczyk-Lipkowska, Institute of Organic Chemistry, Polish Academy of Sciences, 01-224 Warsaw, Poland

Preorganization between substrates and/or solvent molecules is leading factor in many organic reactions. Recently, it has been found that in some cases elimination of solvent allows for product formation with high yield and stereoselectivity [1]. The 1:1 reaction between aliphatic diaminoethers and active esters of aminoacids has been performed in protic (MeOH), polar aprotic (MeCN) and solvent free media. The composition of products (monoacylated diacylated and free amine) has been characterized and separation has been done using HPLC methodology. For comparison, reaction with various diamines was performed under the same conditions. Several products were characterized by X-ray structure analysis.

1. F. Toda (1993). Synlett, 5, 303.

P05.06.008 NORRISH TYPE II PHOTOCHEMISTRY OF SPIRO-ADAMANTYL KETONES IN THE CRYSTALLINE STATE. Eugene Cheung, Matthew Netherton, John R. Scheffer, and James Trotter, Department of Chemistry, 2036 Main Mall, University of British Columbia, Vancouver, B.C., British Columbia, Canada, V6T 1Z1.

The photochemistry of a homologous series of spiro-adamantyl ketones (**1**) shows a range of Norrish type II reactions in the solid state. By obtaining the crystal structures of the reactants and using the Crystal Structure-Solid State Reactivity Correlation Method to analyze the geometry of each of the materials, we were able to rationalize the formation of the photoproducts. Parameters for γ-hydrogen abstraction were calculated and used to identify which ketones would yield Norrish type II biradicals that cleave and/or cyclize to the corresponding cyclobutanols. Crystal structure analysis also allowed rationalization of *endo*- or *exo*-aryl stereochemistry of the photoproducts.

The structures of the strained polycyclic photoproducts were confirmed by X-ray crystallography. In particular, irradiation of the six-membered ring spiro-adamantyl ketone gave an unexpected photoproduct, which is likely the result of a thermal rearrangement of the initial Norrish-Yang cyclization photoproduct.

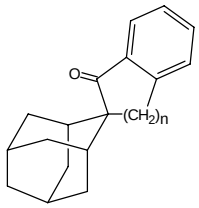

1 (n = 1 - 4)

P05.06.009 PHOTODIMERIZATION IN SINGLE CRYSTAL OF THYMINE DERIVATIVES HAVING LONG ALKYL CHAIN. N. Yasui[1], E. Mochizuki[1], N. Kanehisa[1], Y. Kai[1], N. Tohnai[2], Y. Inaki [2] and M. Miyata[2], [1]Department of Materials Chemistry, and [2]Department of Material & Life Science, Graduate School of Engineering, Osaka University, Suita, Osaka, 565-0871, Japan.

Thymine derivatives give photodimer upon irradiation with UV light near 280nm. The photodimer split to afford the original monomers very efficiently upon irradiation at a shorter wavelength (240 nm). In this study, the crystal structures of 1-octylthymine recrystallized from ethyl acetate and ethanol were determined by X-ray diffraction method. We report the relationship between the molecular orientation of thymine bases and the reactivity for photodimerization.

Crystal data for 1-octylthymine recrystallized from ethyl acetate (1): $C_{13}H_{22}N_2O_2$, monoclinic, space group $C2/c$, a=32.34(1), b=11.790(6), c=17.538(8)Å, β=112.65(2)°, V=6171(5)Å^3, Z=16 R=0.116. Crystal data for 1-octylthymine recrystallized from ethanol (2): $C_{13}H_{22}N_2O_2$, monoclinic, space group $P2_1/n$, a=15.11(1), b=12.115(4), c=16.471(5) Å, β=106.35(5)°, V=2894(2) Å^3, Z=8, R=0.083. The single crystal from ethyl acetate shows a very high photoreactivity, and gives only one stereo isomer (*trans-anti*) of the photodimer. But, the single crystal from ethanol does not give the photodimer. Both crystal structures are consisted of the hydrophilic layers of thymine bases and the hydrophobic layers of long alkyl groups. The thymine base of the crystal obtained from ethyl acetate faces another thymine base in the opposite plane with head-to-head, and the distance between two thymine bases is short to be able to photodimerize. In the crystal obtained from ethanol, however, the thymine bases are unsuitable orientation for the formation of the photodimer.

P05.06.010 PHASE SEQUENCE AND STRUCTURE ANALYSIS OF ß-CHLOROPIVALIC ACID C. Buhrmester and H. Fuess, Department of Materials Science, University of Technology Darmstadt, Petersenstr. 23, 64287 Darmstadt, Germany and S. Mason, Institut Laue-Langevin, Grenoble, France.

The existence of an ordered disordered phase or so called plastic phase has been established several decades ago. The ODIC phase for pivalic acid $(CH_3)_3COOH$ has been observed by Longueville et al. Extensive studies [1,2] indicated the temperature range between 308.5 K and 279.9 K for the ODIC phase. Further cooling does not lead to a complete ordered structure.

The substitution of one methyl group of pivalic acid leads to ß-chloropivalic acid $(CH_3)_2(CH_2Cl)COOH$. The influence of this substitution on the phase sequence and on the stability range of the plastic phase is at present under study.

Based on x-ray and neutron diffraction and thermal analysis four phases were detected. The phase range of phase I is only 4K (302K to 298K) and is isostructural to the plastic phase of pivalic acid; face centered cubic with Z=4 and a=8.84Å. Further cooling leads to phase II. The structure II is triclinic P-1 with Z=2, a=5.993(3)Å, b=6.042(4)Å, c=11.166(4)Å and α=98.49(4)°, ß=90.83(4), γ=115.71° at T=297K and reveals a disorder of the chlorine atoms establishing two conformers. At T=265K phase III is established. The phase transformation II↔III could only be seen by diffraction experiments and exists between 120K and 100K. Phases III and IV does not show significant structural differences. The structures are monoclinic $P2_1/m$ with Z=4 and a=6.332(2)Å, b=9.766(5)Å, c=10.931(6) Å and ß=97.94(2) at T=120K.

1. W. Longueville, H. Fontaine, F. Baert & G. Odou (1978) Acta Cryst.,A34, 188.
2. M. Bee, W. Longueville, J. Amoureux & R. Fouret (1986) J. Physique, 47, 305

P05.06.011 NEUTRON DIFFRACTION STUDY OF THE 3-1 PHOTOISOMERIZATION OF 3-CYANOPROPYL COBALOXIME COMPLEX. T. Ohhara, J. Harada and Y. Ohashi, Department of Chemistry and Materials Science, Tokyo Institute of Technology, Meguro-ku, Tokyo 152-8551, Japan, I. Tanaka, S. Kumazawa and N. Niimura, Advanced Science Research Center, JAERI, Tokai-mura, Ibaraki 319-1195, Japan.

It was found that the (3-cyanopropyl)[(*R*)-1-phenylethylamine] cobaloxime complex isomerized to the 1-cyanopropyl cobaloxime on exposure to visible light with retention of the single crystal form. In addition, the produced 1-cyanopropyl group in this isomerization revealed high enantio-selectivity.

The X-ray structure analyses before and after the isomerization made clear the reason why the produced 1-cyanopropyl group showed high selectivity. However, the mechanism of this 3-1 isomerization remains equivocal. It must be made clear the intermediate structure, and the relationship between the enantio-selectivity and the hydrogen transfer in the process of the isomerization. The complex of (3-cyanopropyl-d_2^{α})[(*R*)-1-phenylethylamine]cobaloxime was prepared. To reduce the background of neutron scattering, the hydrogen atoms of (*R*)-1-phenylethylamine and cobaloxime moieties were replaced with the deuterium atoms. A crystal with dimension 3.5 x 3.5 x 0.7 mm was irradiated with a xenon lamp for 7 days and the crystal structure was analyzed by neutron diffraction at JAERI.

The analyzed structure indicated that the conversion ratio of the 3-1 isomerization was about 90%, and the 2-cyanopropyl group must be produced as an intermediate structure in the process of the isomerization. In addition, the D-C*-H chiral methylene group at the β-position of produced 1-cyanopropyl group was racemic. Stereo-selectivity of this chiral methylene can be considered to correlate with the stereochemistry of intermediate 2-cyanopropyl group, and further study is now in progress.

P05.06.012 HITTING THE BREAK! A STUDY ON THE CONFORMATIONAL BEHAVIOUR OF N-O BONDS. I. Svoboda, H. Fuess, J. Hartung, and M. Heubes. Fachbereich Materialwissenschaft, Fachgebiet Struktur-forschung, Technische Universität Darmstadt, Petersenstraße 23, D-64287 Darmstadt, Germany, and Institut für Organische Chemie, Universität Würzburg, Am Hubland, D-97074 Würzburg, Germany.

Rotations about N-O bonds are highly dynamic processes which are generally associated with low energy barriers. Energetic minima and maxima arise from superposition of (i) steric congestions between substituents at nitrogen and at oxygen and (ii) repulsion between doubly occupied nonbonding orbitals.

In order to separate two dynamic effects at nitrogen - rotation about neighbouring bonds and inversion at the central atom - *N*-alkoxy substituted fully unsaturated and therefore planar heterocyclic compounds were selected for the present study. Thus, *N*-(alkoxy)-4-*p*-chlorophenylthiazole-2(3*H*)-thiones and *N*-alkoxypyridine-2(1*H*)-thiones were prepared and studied by X-ray diffraction (T = 298 K), by variable temperature NMR (T = 130 K - 298 K), and by NOE-experiments in solution [1]. All compounds showed highly dynamic behaviour in solution at T = 298 K. Majorly populated conformers quickly interconverted by rotation about N-O bonds. This movement was shown to slow down significantly on cooling. At T = 130 K two distinct rotamers were observed. The solid state geometries of these compounds which were derived from X-ray diffraction are remeniscent to snapshots of low temperature NMR-experiments. Thus, 1:1 ratios of each rotamer were observed in the unit cell of every heterocyle. A correlation between energetic and steric parameters will be given and discussed in the present work.

[1] J. Hartung, M. Hiller, M. Schwarz, I. Svoboda, H. Fuess, *Liebigs Ann.* **1996**, 2091-2097.

P05.06.013 HYDROGEN CYANIDE (HCN) AND DCN. Göran Svensson, Inorganic Chemistry, Chalmers University of Technology, SE-412 96 Göteborg, Sweden.

Two crystal structures of solid HCN are known with a phase transition at about -100°C. The structure transforms from the orthorhombic space group Imm2 to the tetragonal I4mm, according to ref 1. The structure of HCN has been studied by several groups using various theoretical methods. These calculations often results in a structure where the HCN are arranged in parallel chains [2]. Parallel chains was also suggested from an early single crystal structure determination[1]. The energy difference between the parallel and anti-parallel models are, however, only a few kcal. In order to experimentally clarify if the chains are parallel or not, data have been collected from powder samples using neutron and synchrotron radiation. Data for both phases of HCN have been collected and the phase transition have been studied by synchrotron radiation. Neutron diffraction data sets for HCN at 140 and 193 K and DCN at 10 and 193 K were collected at the neutron reactor at Studsvik, Sweden. Synchrotron data have been collected with a image plate system at NSLS at Brookhaven National Laboratory, USA, and with a INEL CPS120 detector at MAX 2 in Lund, Sweden.

Analysis of the neutron data sets did not give a clear answer if the structure contains parallel or anti-parallel chains. Both models could be fitted equally well to the data sets. These results as well as results from the synchrotron radiation experiments will be presented.

1. W. J. Dulmage & W. N. Lipscomb, Acta Cryst. 4 (1951) 330-334
2. I. Panas, Chem Phys Lett. 194 (1992) 239-246

P05.06.014 A NOVEL REARRANGEMENT IN THE SELECTIVE SUBSTITUTION OF SILYL-PROTECTED O-BROMOPHENYL ARYLSYDNONES, David A. Grossie, Douglas M. Krein, and Kenneth Turnbull, Department of Chemistry, Wright State University, Dayton, Ohio 45435.

Sydnones are, in most cases, extremely stable crystalline compounds that exhibit a distinct polarity. The five-membered heterocyclic ring is subject to electrophilic substitution at the C-4 position. Only with a strongly activating group present will the 3-aryl group compete effectively for the electrophile, due to the considerable partial positive change at the 3-position of the sydnone ring. Accordingly, it is of interest to explore other avenues to arylsubstituted sydnones. Herein, we report on attempts to react selectively at the ortho position, leading to an interesting 1,5 silyl shift, as shown below.

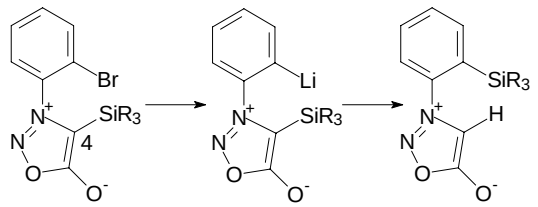

R = Me_3, *i*-Pr_3, *t*-$BuMe_2$, *t*-$BuPh_2$

The precursors and products involving different silyl protecting agents have been examined by single-crystal X-ray diffraction and molecular mechanics in an attempt to understand the mechanism behind this rearrangement.

P05.06.015 INTERMOLECULAR INTERACTIONS OF $(C_5H_4R)Re(CO)Br_2L$ AND SOLID STATE REACTIVITY. Leanne Cook, D.C.Levendis, J.C.A. Boeyens, N.J. Coville, L.Cheng. Centre for Molecular Design, Chemistry Department, University of the Witwatersrand, Wits,2050, South Africa. e-mail: leanne@hobbes.gh.wits.ac.za

It has been demonstrated that the isomerisation of substituted cyclopentadienyl metal-dicarbonyl-dibromo "piano-stool" compounds [1,2] $(C_5H_4R)Re(CO)Br_2L$, is strongly dependent on the molecular environment. For example[1] when R = Me and L = CO isomerisation from the *diag* to the *lat* form occurs in the solid state (at about 105^0C). The reverse isomerisation does not occur in the solid state. However, in solution, the same complex undergoes only the reverse *lat* to *diag* isomerisation. When R = ^{t}Bu and L = CO, no solid state isomerisation is observed (although the *lat-diag* reaction still occurs in solution).

In addition to DSC and optical results, the X-ray crystal structures of several of these complexes have now been completed. The crystal and molecular structures and crystal packing have been modeled using molecular mechanics computer models[3]. In this paper, a summary of some of the recent crystallographic findings related to "piano-stool" complexes will be outlined, as well as some preliminary results of molecular and crystal packing modeling calculations.

Cheng, L.; Coville, N.J. Organometallics, 1996, 15, 867.
Boeyens, J.C.A..,Cheng, L., Coville, N.J., Levendis, D.C. and McIntosh, K., Journal of Chemical Crystallography, 1998.
Programs used include HyperChem and MPA (by D.E.Williams).

P06.06.001 SCHIFF'S BASES OR *N*-GLYCOSIDES: OPEN-CHAIN AND CYCLIC DERIVATIVES OF D-MANNOSE. William H. Ojala, Chemistry Department, University of St. Thomas, St. Paul, Minnesota 55105 USA; Charles R. Ojala and Joanne M. Ostman, Chemistry Department, Normandale Community College, Bloomington, Minnesota 55431 USA; William B. Gleason, Department of Laboratory Medicine and Pathology, University of Minnesota, Minneapolis, Minnesota 55455 USA

Reaction with ammonia derivatives converts monosaccharides into open-chain Schiff's bases in some cases and into cyclic *N*-glycosides in others. We have found D-mannose to show striking variability in this reaction. Previous investigations have shown the solid-state structures of its phenylhydrazone [1] and *p*-bromophenylhydrazone [2] to be open chains. Here we describe the structures of the derivatives formed from the reaction of D-mannose with three different nitrogenous bases. Reaction with hydroxylamine yields a conventional, open-chain oxime (**I**, R = OH). Reactions with semicarbazide and with *p*-chloroaniline yield cyclic *N*-glycosides (**II**, R = NH-C(O)-NH_2 and **III**, R = C_6H_4Cl).

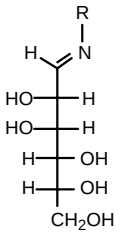

I

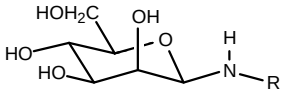

II , III

The hydroxyl group of the oxime is *trans* with respect to the fully extended carbon chain. The semicarbazide derivative crystallizes as a dihydrate, the carbonyl group being linked intramolecularly to the O6 hydroxyl by a hydrogen-bonded bridge consisting of two water molecules. In both *N*-glycosides the substituent at C1 is located in the equatorial position (beta anomer).

[1] Ojala, W. H. & Gleason, W. B. (1996) *Acta Cryst.* **C52**, 3188-3190.
[2] Furberg, S. & Solbakk, J. (1969) *Acta Chem. Scand.* **23**, 3248-3256.

P06.06.002 TWO DERIVATIVES OF TREHALOSE. S.M. Clow and P.J. Cox, School of Pharmacy, The Robert Gordon University, Schoolhill, Aberdeen, AB10 1FR, Scotland and J.L. Wardell, Department of Chemistry, Aberdeen University, Meston Walk, Old Aberdeen, AB24 3UE, Scotland.

Trehalose (α-D-Glucopyranosyl-α-D-glucopyranoside) - shown below - is a naturally occurring disaccharide found in plants, insects, bacteria, yeasts and fungi. It supports anhydrobiosis (life without water) and can be used to preserve the structural integrity of biological assemblies on dehydration (1). In order to investigate its mode of action we have prepared derivatives in which the number of hydroxy groups have been varied.

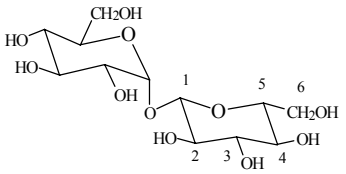

X-ray data collected on the first derivative (which contains no -OH groups) were very weak (crystal size 0.21x0.10x0.10 mm) with only approximately 12% of the data with $I > 2\sigma I$. Restraints were applied to the anisotropic displacement parameters to achieve a successful refinement. The derivative crystallised in the space group $P2_12_12_1$ as the monohydrate.

Data for the second derivative (which contains one -OH group) were normal (crystal size 0.55x0.20x0.20 mm). This derivative crystallised in space group $P2_1$.

1. C.L.A. Paiva and A.D. Panek, Biotechnology Annual Review, Vol. 2, M.R. El-Gewely (editor), Elsevier, Amsterdam, 1996. pp 293-314.

P06.06.003 STRUCTURAL ANALOGY BETWEEN β' TRIACYLGLYCEROLS AND *N*-ALKANES TOWARDS THE CRYSTAL STRUCTURE OF β'-2 P.P+2.P TRIACYLGLYCEROLS. Jacco van de Streek,[1,2] Paul Verwer,[1] René de Gelder[3] and Frank Hollander.[2] [1] CAOS/CAMM Center, [2] Department of Solid State Chemistry, [3] Crystallography Laboratory, University of Nijmegen, Toernooiveld 1, 6525 ED Nijmegen, The Netherlands.

Based on the analogy with *n*-alkane structures, a crystal structure for β'-2 1,3-dicaproyl-2-lauroylglycerol is proposed. The structural elements of the β'-2 polymorph of 1,3-dilauroyl-2-

myristoylglycerol as found by Birker *et al*. were also observed in the crystal structures of other long chain compounds. This analogy led to the assembly of a β'-2 structure at atomic level from known crystallographic data. The structure was optimized by molecular mechanics and was consistent with experimental data, including satisfactory reproduction of the X-ray powder pattern. To the best of our knowledge, this is the first β' structure with a 1,2 configuration and an intramolecular orthorhombic subcell which was fully optimized by molecular mechanics to date. It shows all structural elements found earlier by Birker *et al*.

Birker, P.J.M.W.L., De Jong, S., Roijers, E.C. & Van Soest, T.C. (1991). *J. Am. Oil Chem. Soc.* **68**, 895-906.

P06.06.004 CRYSTAL STRUCTURE OF CHOLESTERYL HEMISUCCINATE. Young-Ja Park, Department of Chemistry, Sook Myung Women's University, Seoul 140-742, KOREA

Crystals of cholesteryl hemisuccinate($C_{31}H_{50}O_4$) are orthorhombic, space group $P2_12_12_1$, with *a*=9.371(5), *b*=24.434(12), *c*=50.491(20), having four molecules in an asymmetric unit. The crystal structure has been determined by the direct method using SnB program and refined by Fourier and full matrix least-squares methods. The R facor is 0.13 for 7815 observed reflections collected on a Nonius CAD-4 diffractometer with Mo-Kα radiation to a maximum 2θ value of 44.

Cholesteryl hemisuccinate belongs to the layer type crystal structure as in cholesteryl hexanoate, hexyl carbonate, octanoate, oleate and linolelaidate. At the center of the layer there is an interlocking arrangement of cholesteryl groups. The molecular long axes of all 4 symmetrically independent molecules are parallel to the *c*-axis and these molecules stack along 2_1 screw axes. The crystal has the liquid crystalline phase. The cholesteric phases are formed at 186.8 and melts at 194.3 to form an isotropic liquid.

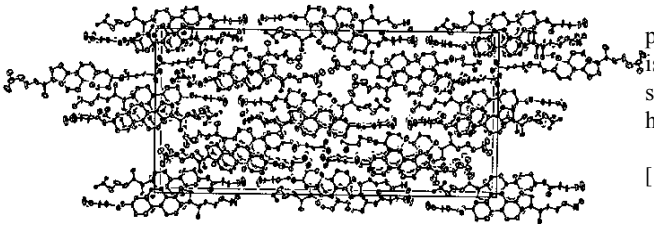

P06.06.005 CRYSTAL STRUCTURES OF GLYCOLIPIDS. Yutaka Abe[1], Takamitsu Tamura,[1] Masami Fujiwara,[1] Kazuo Ohbu,[1] and Kazuaki Harata,[2] 1:Material Science Research Center, Lion Corp., 7-13-12 Hirai Edogawa-ku Tokyo, Japan, 2:National Institute of Bioscience and Human-Technology, 1-1Higashi Tsukuba Ibaraki, Japan.

Crystal structures of model glycolipids, methyl 6-O-acylglycosides were investigated. An glycolipid including a sugar moiety as a hydrophilic group is important as a type of material in cell membrane and as a surfactant for dissolving and crystallizing of membrane proteins. Physico-chemical properties of the amphiphiles are affected by types of the sugar moieties. The crystal structures of glycolipids are known for acylglycoamides, glyconic amides and alkyl glycosides. Hydrophobic and hydrophilic layers like a cell membrane are formed by these crystals. The crystals are characterized by the hydrogen bonding systems between sugar moieties. The thermal stability of a crystal is significantly affected by the type of sugar moiety. Since the difficulty of crystallization of those amphiphiles, there is no systematic study to relate between the crystal structures and physico-chemical properties. We have investigated the crystal structures of methyl 6-O-acylglycosides having types of sugar moieties, methyl α and β-glucosides and α and β-galactosides, respectively with various length of alkyl chains. Each crystal with a type of sugar moiety has a crystal packing with a hydrogen bonding system. The hydrogen bonding system significantly affects to the crystal stability. The crystals of the α-galacotosides have infinite hydrogen bonding linkage in contrast of the finite linkage in those of β-glucosides. The crystals of α-glucosides have a disorder structure of the sugar moieties. The importance of the hydrogen bonding system to the thermal stability was shown by evaluation of packing energy of the crystals with molecular mechanics.

P06.06.006 A NOVEL DOMINO REACTION: STRUCTURAL X-RAYS STUDIES. E. García-Rodríguez and S. García-Granda, Physical and Analytical Chemistry Department, University of Oviedo, E-33071 Oviedo, Spain and L.J. Álvarez-García; I. Llorente; J.M. González; G.P. Romanelli, J. Barluenga, Instituto Universitario de Química Organometálica "Enrique Moles", Unidad asociada al CSIC, University of Oviedo, E-33071 Oviedo, Spain.

It has been recently shown [1] that terminal alkynes modified by a phenylsulfide substituent can be coupled, either intra- or intermolecularly, to yield condensed thiin structures upon reaction with IPy_2BF_4. X-ray analysis was used to ultimately determine the structure of some of the resulting heterocycles, as for instance:

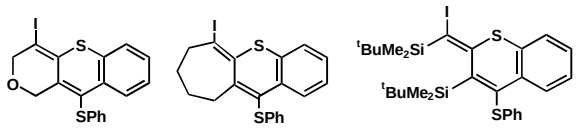

(1) (2) (3)

The structural analysis, including intermolecular and packing interactions, will be discussed. Interestingly compound 3 is severely distorted from planarity as revealed by its molecular structure from X ray data, thus presenting an unexpected source of helical chirality [2].

[1] J. Barluenga; G.P. Romanelli; L.J. Álvarez-García; I. Llorente; J.M. González; E. García-Rodríguez; S. García-Granda. *Angew. Chem. Int. Ed.* **1998**, *37*, No. 22, pp. 3136-3139.

[2] B.L. Feringa, N.P.M. Huck, A.M. Schoevaars; *Adv. Mater.* **1996**, 8, pp. 681-684

P06.06.007 THE CRYSTAL AND MOLECULAR STRUCTURE OF 2,2', 4,4', 6,6'-HEXAMETHYL-BIS 4,4'-(4H)-PYRANE, $C_{16}H_{22}O_2$. S. A. Chawdhury, The University of Asia Pacific

The title compound results from the action of strong organic reducing agents on the 2,4, 6 - trimethy1 pyrylium cation (Conrow and Radlick, 1961). The substance is very non-polar and the two bipyran rings are linked by a single bond. NMR and spectroscopic measurements failed to prove unambiguously the exact nature of the molecule.

The molecule lies on the centre of symmetry. Moreover, the molecule has its own symmetry, 2/m with two fold axis nearly parallel to [122] direction. R. M. S. deviation of atomic positions from the 2/m symmetry is about 0.01 Å. The pyrane ring is planar, the maximum displacement being about 0.04 Å for 0 atom from the best plane passing through all the other atoms of the ring.

P06.06.009 CRYSTAL STRUCTURE OF 5-AMINO-4-(4-METHOXYPHENYL)-2-PHENYL-7-(PYRROLIDIN-1-YL)-1,6-NAPHTHYRIDINE-8-CARBONITRILE.
R.Sankaranarayanan and D.Velmurugan, Department of Crystallography and Biophysics, Univesity of Madras, Guindy Campus, Chennai-600 025, INDIA, S.S.S.Raj and H.K.Fun, School of Physics, Universiti Sains Malaysia, 11800 USM, Penang, MALAYSIA and V.Raghukumar and V.T.Ramakrishnan, Department of Organic Chemistry, University of Madras, Guindy Campus, Chennai - 600 025, INDIA.

The naphthyridine derivatives are known to exhibit wide range of biological activities such as bactericidal, fungicidal, anti-inflammatory, anti-convulsant and insecticidal activities. They are also known to possess lasing action. In the title compound studied, interestingly, there are two molecules in an asymmetric unit. The naphthyridine moiety in both the molecules are folded. The pyrrolidine rings adopt half-chair conformation. The molecular packing is stabilised by C-H...N type hydrogen bonds. Crystal data : $C_{26}N_5OH_{23}$, Triclinic, P-1, λ=0.71703Å, a=9.6808(1)Å, b=11.4468(2)Å, c=19.8557(1)Å, α = 100.047(1)° , β = 95.804(1)°, γ = 90.318(1)°, Z=4, F(000)=888, R [I>2σ(I)] = 0.062, R_w = 0.13, Observed reflections = 6085, Structure solution program:SHELXS97, Refinement program: SHELXL97. The conformational features will be presented in detail.

P06.06.010 COMBINATION OF ENERGY MINIMIZ-ATION AND VECTOR SEARCH METHODS USING DIRDIF PROCEDURES: STRUCTURE SOLUTION OF BENZOPYRANS. L.Vijayalakshmi and V. Parthasarathi, Department of Physics, Bharathidasan University, Tiruchirapalli, India.

The connectivity scheme of the compound was generated and its geometry was optimized by energy minimization using MOPAC 6.0 program. This molecule was used as the input to the orient option of the DIRDIF(Beurskens et al., 1996) program which uses the Nordman vector search rotation functions to orient the molecule to give maximum consistency with the Patterson function. The resulting set of atomic parameters is used for the translation function in DIRDIF fourier space. The resulting shift vector, if any, is applied to the atomic parameters and the correctly positioned molecule is used to phase a weighted Fourier synthesis. The procedure was adopted to solve the compounds namely, 4-(2'-(4''-methyl thiophenyl)ethenyl)-3-cyano-2H-1-benzopyran-2-one; 4-(2'-(1"-naphthyl)ethenyl)-3-cyano-2H-1-benzopyran-2-one and 6-methyl-4-(2'-(1''-naphthyl)ethenyl)-3-cyano-2H-1-benzopyran-2-one. Thereafter the structures were refined by SHELXL-97 program successfully to a final value of 0.05, 0.03 and 0.06 respectively.

Thailambal, V. G. and Vasantha Pattabhi (1986). Acta Cryst. C42, 1017-1019.
Beurskens, P. T. , Gezina Beurskens., Bosman, W. P., Rene de Gelder., Garcia Granda, S., Gould, R. O., Israel, R. and Smits, J. M. M. (1996). DIRDIF-96. Direct Methods Applied to Difference Structure factors, 1-665.

P06.06.011 THE CRYSTAL STRUCTURE ANALYSIS OF 2,7DIOXA[3,4BENZO(5,6COUMARINO)]DECALIN. R. Krishna[a] D.Velmurugan[a] S.Sanmuga Sundara Raj[b] and H.K. Fun [b] a Department of Crystallography and Biophysics, University ofMadras, Guindy campus, Chennai -25, India. b X-ray Crystallographic unit, School of Physics, Universiti sainsMalaysia, 11800 USM Penang, Malaysia.

Coumarin derivatives occuring in plants have differentbiological activities. Some synthetic modifications of natural coumarinslike acsculamin, folescutol are of pharmacological importance. Coumarin and its derivatives are used in oral anticoagulation therapy. The crystal structure of 2, 7 dioxa [3,4-benzo-(5,6-coumarino)]decalin has been determined by X-ray analysis. The cell parameters are: a = 12.225(1) Å b = 16.335(1) Å c = 15.340(2) Å , β = 109.21(1) °. The system is monoclinic with space group $P2_1/c$ and the final R-factor = 0.046. The structure consists of a coumarin moiety and three six membered rings. The coumarinmoiety is in planar conformation. The structure is completelystabilized by C-H...O type intermolecular interactions. Other geomentrical features will be presented in theposter.

P06.06.012 CRYSTAL STRUCTURE AND MO CALCULATIONS OF CONDENSED BENZENIC 1,2,5-THIADIAZOLE DERIVATIVES. E.E. Castellano, Inst. Física de São Carlos, Univ. de São Paulo, C.P. 369, 13560 São Carlos (SP), Brazil, and O.E. Piro, Dept. Física, Ftad. C. Exactas (FCE), Univ. Nacional de La Plata (UNLP), C.C. 67, 1900 La Plata, Argentina, and J.A. Caram, M.V. Mirífico and E.J. Vasini, INIFTA (CONICET), UNLP, C.C. 16, 1900 La Plata, Argentina and M.D. Glossman, CEQUINOR (CONICET), Dept. Química, FCE, UNLP, C.C. 962, 1900 La Plata, Argentina.

The 1,2,5-thiadiazoles have been broadly applied in pharmaceutical, agricultural, industrial and polymer chemistry. The potential pharmacologic applications include antibiotics, histamine H_2-receptor antagonists and β-adrenergic blocking agents. A number of other thiadiazoles have been found that are active as fungicides, bactericides, herbicides, plant-growth regulators and insecticides. Furthermore, the 1,2,5-thiadiazole ring has been incorporated into the backbone of a number of polymers with desirable chemical and thermal stability. As part of physical chemistry studies on several 3,4 substituted 1,1-dioxide derivatives of 1,2,5-thiadiazole, we report here a single crystal X-ray diffraction study on the molecular structure of the following derivatives: phenantro[9,10-c]-1,2,5-thiadiazole 1,1-dioxide (I) and acetonaphto[1,2-c] 1,2,5-thiadiazole 1,1-dioxide (II). We shall also report *ab initio* HF/6-31G** Hartree-Fock-LCAO molecular orbital (MO) calculations on the electronic structure, conformation and reactivity of compounds I and II, as well as results of a charge sensitivity analysis performed by resorting to several concepts derived from density functional theory.

P06.06.013 EXPERIMENTAL AND HEORETICAL DETERMINATION OF THE STRUCTURE OF 2 ,7 - NAPHTHALENE – DIOL. N.A. Ahmed, E. El-Kholy, S.M. El-Derby, R.H. El-Oraini, Physics Department, National Research Center, Dokki, Cairo, Egypt.

The crystal and molecular structures of 2,7 -naphthalene diol were determined experimentally by x-ray diffraction. Three-dimensional data obtained from equi-inclination Weissenberg photographs was obtained using Cu k_α radiation. The structure was solved by the direct method using the program Shelxs-86 and refined by the method of least squares using the full matrix program Shelxl-93 up to a value of R1=0.0563**.** The molecule is planar and the oxygen atoms are out of the molecular plane by 0.01 Aº on opposite sides of the plane.

The theoretical structure was calculated by the method of atom-atom potentials. Minimization of the lattice energy gave lowest value of minimum energy for the completely planar molecule. The atomic coordinates are comparable with those obtained experimentally.

P06.06.014 CRYSTAL STRUCTURE OF 3-CHLORO-2(N-(4-CHLORO-2-METHYL) PHENYL)FORMIMIDOYL INDOLE. D. Velmurugan and R.Krishna, Department of Crystallography and Biophysics, University of Madras, Chennai - 25, India

Indoles show interesting chemical and biological activities. They act as anti-inflammatory, anti-bacterial, and analgesic agents. They also intercalate with DNA. The crystal structure of the title compound has been determined. The compound crystallizes in monoclinic system with space group $P2_1$. The cell dimensions are : a =4.670(1) Å, b=9.930(2) Å, c= 15.360(3) Å and $\beta = 97.8(1)°$. The structure was solved by direct methods and refined by full matrix least squares to a final R-value of 0.053 with 1370 unique reflections. The angle between the mean planes of the indole moiety and the phenyl ring is 20.6(1)°. Amino(or) amide N-H...π (aromatic) interaction has recently been theoretically postulated in model system and experimentally described in globular proteins. It has also been suggested that such interactions may provide stability, contribute to the folding process, and (or) have a functional role in proteins. N-H..π hydrogen bond is uncommon because it occurs only in acceptor-poor systems. Such non conventional aromatic hydrogen bonds are currently under intense investigation in structural biology. The above structure has a weak N-H...π intermolecular hydrogen bond. The other conformational details and a comparison of this structure with two related indole compounds will be described in the poster.

P06.06.015 CRYSTAL STRUCTURE OF N-CYCLOHEXYL-2-BENZOYL 4,5-DIPHENYL PYRROLIDINO SPIRO-[3-3']-H'-CHROMANONE. S.Thinagar and D.Velmurugan, Department of Crystallography and Biophysics, University of Madras, Guindy campus, Chennai 600 025, India.

3-phenyl chromanone is the skeleton for Isoflavonoids which are found in the plants of sub-family papilionoidae of Leguminosae. They are known to possess antifungal and antibacterial properties. Crystal data of the title compound : Monoclinic, Space group - $P2_1/c$, a = 14.021(3) Å, b = 18.682(4) Å, c= 11.362(2)Å, $\beta = 95.75(3)°$, R-value = 0.066. The two phenyl rings directly attached to the pyrrolidine ring are nearly perpendicular to it. The keto group containing the ring of the chromanone moiety adopts a half-chair conformation while the cyclohexane ring attached to the pyrrolidine ring adopts a chair conformation. The best plane passing through the chromanone moiety makes a dihedral angle of 82.2(3)° with pyrrolidine ring. The molecule is stabilized by one intra and two inter molecular C-H...O hydrogen bonds. The other structural features will be discussed in detail.

P06.06.016 CRYSTAL AND MOLECULAR STRUCTURES OF SOME ACRIDINONE DERIVATIVES. M.S.Kumar, D.Kumaran and M.N.Ponnuswamy Department of Crystallography and Biophysics, University of Madras, Guindy Campus, Chennai – 600 025, India.

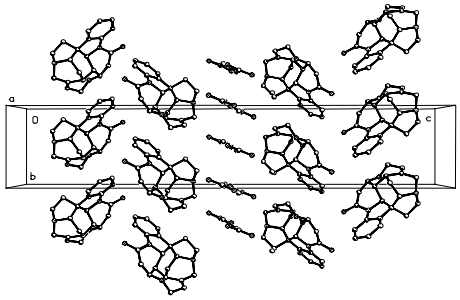

The biological activity of acridine derivatives is often manifest in their mutagenic properties. Interestingly these derivatives intercalate with DNA. The principle behind is the planar chromophore common to the acridines which involve in stacking interactions with the pyrimidine-purine base pairs. This objective has received support from a large body of physical and biological data. A series of acridinone derivatives have been synthesized by a novel method and the structures are determined by crystallographic methods. In halide derivatives, the study reveals the electronic effect of chloro and fluoro substitution on the acridinone ring system geometry and the stacking properties of the planar chromophores. The central ring of the acridinedione moiety deviates from planarity. The molecules are stabilized by weak C-H...O interactions in addition to the van der Waals forces.

P06.06.017 A NEW CRYSTAL MODIFICATION FOR DIPHENYLPICRYLHYDRAZINE. M. Gary Newton, Department of Chemistry, University of Georgia, Athens, GA; John P. Rose, B.-C. Wang, Zhi-Jie Liu, Georgia X-ray Crystallography Center, University of Georgia, Athens, GA; Róbert Tuba and Ferenc Ungváry, Department of Organic Chemistry, Univ. of Vesprém and Research Center for Petrochemistry of the Hungarian Academy of Sciences, Vesprém, Hungary.

The reaction of diphenylpicrylhydrazyl radical with dicobalt octacarbonyl produced a crystalline product, which has now been identified as diphenylpicrylhydrazine (DPPH) via single-crystal X-ray diffraction. The crystals were monoclinic with a=25.814(1), b=10.7440(4), c=26.6230(7) Å and β=106.98(2)°, Z=16. The space group was determined as C2/c from systematic absences and from the successful structure solution. Diffraction data were measured to Θ=65° on a Bruker 2x2K CCD detector system; data were processed using SMART and SAINT data analysis systems. The structure was solved and refined using the program suite in TEXSAN. R=5.7%, Rw=5.3%.

A search of the Cambridge database did not find any report of the current monoclinic modification of DPPH. There are four previous reports of structural investigations of DPPH; all but one contains an included molecule of solvent. No coordinates were determined for the solvent-free system, reported as space group R-3. The two DPPH structures for which coordinates exist belong to space group R-3 and contain a cylindrical cavity at special positions in the cell which are filled with disordered solvent molecules, specifically THF and CHCl3. [H. Wang et al., J. Inclusion Phnom. 10, 203, 1991]. An early report of preliminary Weissenberg data describes a crystal of DPPH·benzene solvate in space group $P2_1$ but no structural coordinates were provided. [Ellison and Holmberg, Acta Cryst., 13, 446, 1960]. Thus, the current monoclinic crystals of DPPH apparently represent a new crystal modification.

Many features of the previously reported structures are found in the current modification. Particularly notable is a strong H-bond between the hydrazine NH and an O of an ortho-nitro group; the other ortho-nitro group is rotated considerably out of the picryl group plane. The para-nitro group is co-planar with the picryl group. A comparison of packings and cavity sizes will be discussed as part of the presentation.

P06.06.018 PACKING MOTIFS IN STRYCHNINE SALTS. Robert O. Gould, Caroline Dick, Fokke J.J. Dijksma, Simon Parsons, Sonja Schwarzl, Paul Taylor and Malcolm D. Walkinshaw Department of Chemistry and Institute for Cell and Molecular Biology, The University of Edinburgh, Edinburgh EH9 3JJ, United Kingdom.

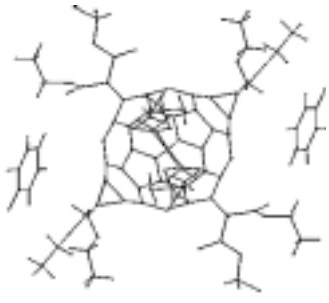

Strychnine alkaloids have long been used as resolving agents for chiral organic molecules. We have recently reported data on the commonest packing modes of brucine, dimethoxystrychnine, which is the alkaloid in this series most commonly employed [1]. Strychnine itself is less successful at chiral recognition, and we now report the packing motifs of strychnine with several simple organic anions. The puckered monolayers seen in most brucine structures are absent here, and the commonest motif appear to be the bilayer shown above in plan. The unit mesh of these bilayers is approximately 7.6 x 7.6 Å, and they pack such that the polar parts of the molecules are directed outward towards a layer containing counterions and water. The overall effect is a surface less flexible and less complex that that shown by brucine.

1. Dijksma, Gould, Parsons, Taylor and Walkinshaw, *Chem. Commun.***1998**, 745-746

P08.06.001 PSEUDOSYMMETRY IN FULLERENE COMPOUNDS V.V. Gritsenko and O.A. Dyachenko, Institute for Chemical Physics Research, Russian Academy of Sciences, Chernogolovka, Moscow Region, 142432 Russia

An X-ray diffraction analysis was used to examine the structures of the fullerene compounds: $(Ph_4P)_2C_{60}Hal$ (Hal = Br (1) and I (2)), $(Ph_4As)_2C_{60}Cl$ (3) [1],$(C_{70})_3(BNDY)_4(C_6H_6)_4$ (BNDY — binaphtho [1.6-d,e]-1,3-dithiin-2-ilidene) (4), $C_{60}2[(Ph)_3PAuCl]$ (5). The presence of pseudosymmetry in the crystal structures of 1—5 is their specific feature.

In the course of our work on the study of the fullerene compounds [1], we found that the pseudosymmetry was characteristic of the crystal structures of 1—5. The positions of $(Ph_4P)^+$ or $(Ph_4As)^+$ cations and Br^- or I^- anions in the salts 1—3 conformed to the tetragonal space group, *I4/m*, in which the *4/m* centers and C_{60} centers coincided, that conflicting with the inherent Ih symmetry of fullerene. The structure was determined in space group $C\bar{1}$ [1]. In complex 4, the positions of the BNDY molecules and C_6H_6 solvates corresponded to the $P4_2/nm$ space group, in which a part of the independent fullerenes should lie on the $\bar{4}$ axis. In this case, that should also disturb their own symmetry. The structure was solved in the $P4_2mc$ space group, in which C_{70} were localized on axes 4_2 and *2*. In complex 5, the positions of the fullerene atoms answered the $R\bar{3}m$ space group, while the positions of the $(Ph_3)PAuCl$ molecules corresponded only to *P3*. The structure was solved in the *P3* space group. We believe that the pseudosymmetry in the crystals of compounds C_{60} and C_{70} is the consequence of the high inherent symmetry of the fullerene molecules, as well as of the presence of some disordering in them in the structures. Neglecting the presence of the pseudosymmetry in the crystals based on C_{60} leads to the errors in structure determination [2,3].

1. V. V. Gritsenko, O. A. Dyachenko, G. V. Shilov, N. G. Spitsyna, E. B. Yagubskii, *Russian Chemical Bulletin*, 1997, 46, 1878.
2. A. Penicaud, A. Perez-Benitez, R. V. Gleason, E. P. Munoz, R. Escudero, *J. Am. Chem. Soc*., 1993, 115, 10392.
3. U. Bilow and M. Jansen, *J. Chem. Soc., Chem. Commun*., 1994, 403.

P08.06.002 STRUCTURE AND CHARGE DENSITY STUDIES OF A C_{60}-FULLERENE DERIVATIVE WITH DIFFERENT SOLVENTS. D.Zobel, M.Strumpel, P.Bombicz, M.Weber, R.Flaig & P.Luger, Institut fur Kristallographie, Freie Universitat Berlin, Takustr. 6, D-14195 Berlin

X-ray data of a hexa-cyclo substituted C_{60}-fullerene, co-crystallized with (a) 1,2 difluorobenzene and (b) with 1,2 dichlorobenzene, were collected with synchrotron radiation at 100 K and with conventional MoKα-radiation at 120 K respectively, using CCD area detectors (Bruker-AXS) in both cases. The molecules were compared to each other and to the same compound crystallized from bromobenzene by Hirsch et al.[1].The C_{60}-cage distortion data were compared to those listed in Zobel et al.[2].

Charge density maps could be generated from the synchrotron data set of (a) confirming the difference in bond electron density maxima between the 6-6 bonds with double bond character and the 5-6 bonds with single bond character within the C_{60}-cage. In addition typical "banana bent" bonds were observed on the bridging cyclopropane rings of the substituent moiety. Also *Ab initio* calculations were carried out on the C_{60}-cage and on the cage includingparts of the substituents with Gaussian 94.These results were compared to the experimental data. The picture shows the molecular structure of dodecakis-(ethoxycarbonyl)-[C60]-fullerene with 1,2 difluorobenzene (a).

We thank the Deutsche Forschungsgemeinschaft for financial support.

[1] I.Lamparth, C.Maichle-Mossmer, A.Hirsch, Angew. Chem. Int. Ed. Engl., 34, 1607, (1995).
[2] D.Zobel, M.Strumpel, P.Luger, M.Ramm, W.Duczek, H-J. Niclas, Zeitsch. f. Krist. (1999) in press.

P08.06.003 WHY FULLERENE STRUCTURES ARE BAD? NEW RESULTS OF X-RAY DIFFRACTION STUDIES. Y.L.Slovokhotov[*], I.S.Neretin[*], Y.V.Zubavichus[*], A.S.Batsanov[**], J.A.K.Howard[**], [*] Institute of Organoelement Compounds R.A.S., Moscow, Russia, [**] Department of Chemistry, University of Durham, Durham, UK

Molecular geometry and packing in $C_{60}\cdot 2PhX$ (I; X=Me,Br), $C_{70}\cdot 2(o\text{-xylene})$ (II), $C_{60}\cdot$tripticene (III), $C_{60}Ir(CO)(PPh_3)_2Cl\cdot solv$ (IV) $C_{60}\cdot$(4-benzoyl-3-Me-1-Ph-pyrazolone) (V), and $2C_{60}\cdot$(tetraphenylporphyrine)$\cdot(2.33+x)C_6H_6$ (VI), are discussed on the basis of single crystal X-ray data. Positions of solvent molecules and the rotational disorder of fullerene moieties are analysed. Hexagonal layers (I), double layers (II), honeycomb layers with $Ir(CO)(PPh_3)_2Cl$ fragment in between, and three-dimensional networks of fullerene molecules (III,V,VI) were found in these complexes, with donor and solvent molecules in the cavities.

Powder XRD data for I-III,V as well as for simple solvates $C_{60,70}\cdot 2o\text{-}C_6H_4X_2$ (X=Me,Cl) and $2C_{60}\cdot$arene (with mesitylene and $m\text{-}C_6H_4X_2$, X=Me,Cl), were collected. Due to a poor reflectivity of the samples, SR data were used for IV (Daresbury Laboratory) and several solvates (Siberian SR Centre). Powder patterns calculated from the atomic positions and simulated using single crystal *I(hkl)* datasets, are compared with the experimental ones.

The highly anisotropic mosaic spread of stacked crystal blocks in fullerene derivatives results in anisotropic extinction that distorts *both* the powder *and* the single-crystal diffraction intensities. The resulting biased statistics of *E*'s (rather than a dynamics on the molecular level) dictates a poor quality of many "fullerene" datasets and hinders a routine phase determination in direct methods. This problem is discussed on the examples of V and VI; some remedies are suggested.

P08.06.004 SUPRAMOLECULAR ARCHITECTURE OF CROWN ETHER STYRYL DYES FROM X-RAY CRYSTAL STRUCTURE ANALYSIS. G.G. Alexandrov, L.G. Kuz'mina, A.V. Churakov, Institute of General and Inorganic Chemistry, Russian Academy of Sciences, Leninskii pr. 31, Moscow 117907, Russia, and J.A.K. Howard, Chemistry Department, University of Durham, Durham DH1 3LE, UK

The crystal packing of aza- and benzocrown ether dyes of benzothiazolinium and quinolinium series is analyzed based on our X-ray structural results. All of the crystals contain stacks of

the conjugated dye molecules with a “head-to-tail” or “head-to-head” mutual arrangement. Very loosely packed channels and layers of crown ether moieties are also typical for these single crystals. In the head-to-tail stacks, the ethylene fragments of two adjacent, centrally symmetrically related dye molecules are closely spaced (the C...C distances are about 3.5 A). This arrangement is favorable for the photochemical [2+2] cycloaddition reaction characteristic of these compounds in solutions and films. The very flexible environment of these ethylene pairs in the crystal represented by crown ether channels makes it possible to suggest that the above-mentioned reaction can proceed in the single crystal at least in its separate regions.

We thank the Russian Foundation for Basic Research for funding this work (project number 98-03-33142).

P08.06.005 ENANTIOMERIC RECOGNITION OF (R)- AND (S)-ALPHA-(NAPHTHYL)-ETHYLAMINE BY CROWN ETHERS. T. Gérczei, Z. Böcskei [1], G. M. Keserû [2], P. Huszthy [3], [1] Department of Theoretical Chemistry, Eötvös University, H-1518 Budapest 112. POB 32., Hungary, [2] Department of Chemical Information Technologies, Technical University of Budapest, H-1512 Budapest, Gellért tér 4., Hungary, [3] Department of Organic Chemistry, Technical University of Budapest, H-1512 Budapest, Gellért tér 4., Hungary.

There has been much interest in designing certain information into macrocyclic hosts, which enables these molecules to recognize specific guests. In this design process determination of the crystal structures of pure hosts as well as those of the host - guest complexes provides information on the chemical, steric and electrostatic interactions between the interacting counterparts and facilitates the optimization of favorable interactions which may result in improved specificity of the recognition process.

Specific recognition of chiral compounds is of particular interest due to important industrial applications. Chiral crowns have been demonstrated to be selective chiral resolving agents in many instances. Our recent study is focused on the structure determination of a (R,R)-phenazyno-18-crown-6 in its uncomplexed form as well as in its complexes with both naphtyl-ethyl-ammonium perchlorate.

Differences in stability of the two diastereomeric compounds provide explanation for the specificity of the phenazyno-18-crown-6. The three structural factors responsible for stability of the complexes are: H-bond distances between naphtyl-NH3+ and crown heteroatoms, p-p interaction between the aromatic moiety of host and guest (attractive) and steric repulsion between host and guest hydrogens (repulsive). The examinations are also supported by molecular mechanical calculations. A comparison with similar studies based on a CSD search will also be presented.

1 Z. Böcskei, G. M. Keserû, D. Menyhárd, P. Huszthy, J. S. Bradshaw & R. M. Izatt (1996). Acta Cryst. C52, 463-466.

P08.06.006 INSECTS, SPIDERS, INCLUSIONS AND OTHER CURIOSITIES: *SEXI*PEDAL AND *OCTA*PEDAL HOST MOLECULES. Mátyás Czugler, David D. MacNicol and Derek R. Wilson, Chemistry Department, University of Glasgow, Glasgow G12 8QQ, Scotland

Cocrystallisation experiments of the hexahost[1] hexakis(p-hydroxyphenylthio)benzene (**1**) yielded to crystals and LT-X-ray structure determinations of the pure host **1** from *Hünigs base* and its unusual stoichiometry inclusions from 1,4-dioxane (**1a**, 1:4) and dimethylsulfoxide and water (**1b**, 1:4:2) as well. Respective guests in **1a** and **1b** are anchored through H-bonding and steric fit. The host molecule shows conformation change in its side wings orientations upon guest binding. Molecular graphics analyses revealed that host **1** conformation is changed such that on binding the host molecules assume a more open conformation. Rotations in the side wings accompany associate formation. One guest in inclusion **1a** is bound by steric fit and van der Waals interactions. In **1b** one of the DMSO guests is partly bound by the fit to the central aromatic ring of the host molecule and concurrent hydrogen bonding to the sulfoxide O atom.

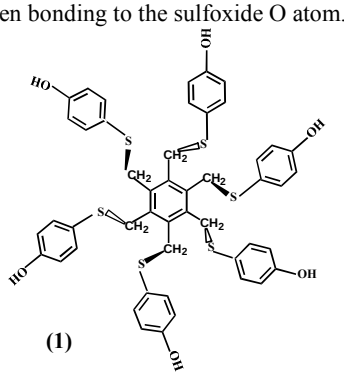

An octakisthio-naphtalene host has also been done. It is substituted with camphor groups in accord with earlier studies aiming at providing chirality in the host molecule.

[1] D. D. MacNicol, D. R. Wilson, *J. Chem. Soc., Chem. Commun.* **1976**, 494-495.

P08.06.007 CALIX[4]RESORCINARENES - SELF-ASSOCIATION AND CRYSTAL PACKING. A.T. Gubaidullin, A.E.Arbuzov Institute of Organic and Physical Chemistry, Kazan Scientific Centre of the Russian Academy of Sciences, Arbuzov str., 8, Kazan 420088 Russia

There is a general trend to consider the three-dimensional crystal packing of the calix[4]arene complexes as bilayered structures. But highly solvated structures can be considered as crystals built up of molecules strongly bound by their first solvation shells. Using X-ray single crystal, X-ray powder diffraction and small-angle X-ray scattering methods we investigate the supramolecular structure of a series of new calix[4]arene derivatives and their ionic metal (Zn, Pd, Cd, Co, Ni) chloride complexes, where calixarene residues exist in neutral, protonated and deprotonated forms. It was shown that the structure of the calixarene moiety and three dimensional arrangement of the complexes depend greatly on the ”guest” metal and inclusion of solvate molecules. Conformational modifications of the macrocycles induced by the process of complexation are discussed based on the comparative analysis of these data with data obtained for neutral “host” calixarene molecules. In compounds under investigation the hydrophobic and hydrophilic regions are strongly localised in crystals. As building units of the three dimensional packing a fragmentary structure, consisting of infinite one-dimensional stick, is chosen. This stick consists of hydrophobic calixarene residues, whereas polar substituents, inorganic ions and/or solvate molecules form hydrophilic shell around the sticks. Several types of superstructures which differ by the host: guest stoichiometry and the respective disposition of guest and host molecules is observed. The factors determining the process of complex formation are discussed. The results of kinetic investigation of crystal formation from self-associates in solution to single-crystal is presented. It was shown that the solid state structure of calixarenes and complexes is reorganized upon the solvent exclusion and temperature increasing. For these complexes the formation of molecular aggregation in solution is observed, the shape and parameters of aggregates is analysed. The influence of solvent and host-guest molecules on the supramolecular structure is discussed.

P08.06.008 STRUCTURES OF A *P-TERT*-BUTYL CALIX(4)ARENE DERIVATIVE AND ITS SODIUM COMPLEX. O.E. Piro, Dept. Física, Ftad. C. Exactas, Univ. Nacional de La Plata, C.C. 67, 1900 La Plata, Argentina, N.J. Al Rawi and A.F. Danil De Namor, Lab. of Thermochemistry, Univ. of Surrey, Guildford, Surrey, UK GU2 5XH and E.E. Castellano, Inst. Física de São Carlos, Univ. de São Paulo, C.P. 369, 13560 São Carlos (SP), Brazil

Recently, we reported the synthesis, ^{1}H NMR characterization and X-ray structure of 5,11,17,23-tetra-*tert*-butyl-[25,27-bis(2-pyridylethyl)oxy-26,28-bis(methylthiodiethyl)oxy] calix(4)arene, $C_{62}H_{78}N_2O_4S_2$[1]. The hydrophobic calix bounded by the four phenyl rings has the usual distorted cone conformation exhibited by a whole variety of *p-tert*-butylcalix(4)arene derivatives. The hydrophilic cavity is defined by alternating OCH_2Py and $O(CH_2)_2SCH_3$ pendant groups. The complex with the sodium ion crystallises in the tetragonal system with *a*=15.201(4), *c*=13.376(3) Å and Z=2. Preliminary results assuming P-4 space group show the complex sited on a twofold axis and large positional disorder of the pendant groups that conform the hydrophilic cavity. The Na^+ ion is found in this cavity coordinated by the four phenolic oxygens [average d(Na-O)=2.42 Å] as in the case of the sodium complex of the related derivative where all four pendant groups are OCH_2Py[2]. The structural studies confirm the key role played by the O-CH_2-(2-pyridyl) pendant group in the ability of *p-tert*-butylcalix(4)arene derivatives to complex and transport metal cations in solution.

1. N.J. Al Rawi, A.F. Danil de Namor, O.E. Piro and E.E. Castellano, Annual Meeting Royal Society of Chemistry Macrocyclic and Supramolecular Chemistry Group, January 1999, University of Surrey, UK.
2. A.F. Danil de Namor, E.E. Castellano, L.E. Pulcha Salazar, O.E. Piro & O. Jafou, Phys. Chem. Chem. Phys. 1, 285 (1999).

P08.06.009 STRUCTURAL STUDY OF DIBENZO-30-CROWN-10 COMPLEXES. Matijasic I.[1], Dapporto P.[2], Tusek-Bozic Lj.[3], [1] Laboratory of Organic Chemistry, Faculty of Science, Zagreb, Croatia, [2] Dipartimento di Energetica, Universita di Firenze, Firenze, Italy, [3] Department of Chemistry, Ruder Boskovic Institute, Zagreb, Croatia

Host-guest chemistry of macrocyclic polyethers has the considerably biological relevance as model substances of naturally occurring ionophores for the study of ion-transport processes in cell membranes and investigation of receptor-enzyme interactions.

The chemistry of metal-ion macrocyclic complexes and their crystal structures are influenced by a variety of factors, which include the size and ionic character of the cation respectively the flexibility and cavity size of the ring. All these factors must be taken into account when tailoring ligands to recognize particular metal ions. Much effort has centered on understanding the effects of altering the nature of metal or ligand on the stoichiometry and structure of the complexes formed.

In the continuation of our systematic investigation on the complexes with different crown ethers[1,2] we are focusing here on the crystal and molecular structure of potassium (**1**) and ammonium hexafluorophosphate complex (**2**) with dibenzo-30-crown-10. In both complexes the cation is completely encapsulated by this large crown molecule having a quite similar conformation.

P. Dapporto, P. Paoli, I. Matijasic, Lj. Tusek-Bozic, (1996) Inorg. Chim. Acta, 252, 383.
P. Dapporto, P. Paoli, I. Matijasic, Lj. Tusek-Bozic, (1998) Inorg. Chim. Acta, 282**,** 71.

P08.06.010 HOLES IN CRYSTALS? Mr. Peter Müller, Institut für Anorganische Chemie, Tammannstr. 4, Göttingen, Germany

In collaboration with the groups of Prof. Schlumlter (Institut für Organische Chemie, FU Berlin) and Prof. Saenger (Institut für Kristallographie,FU Berlin) we have determined the crystal structure of a cyclotetraicosaphenylene, an oligophenylene with 24 phenylene rings.[1] After some less sucessfull crystallization experiments, good looking crystals that diffract disappointingly weak but acceptably were obtained from chloroform. Highly redundant data were collected at 133 K on a rotating anode / multiwire proportional counter system up to 0.95 Å to a completeness of 99.9 %. In this context it should be emphasized that the quality of data is highly influenced by the redundancy. Although a higher redundancy tends to increase the merging R-value Rsym [2], it also improves the quality and I/sigma ratio for the averaged reflections. The structure was solved with conventional direct methods using SHELXS [3]. The packing of the cyclotetraicosaphenylene in the crystal shows large empty channels (diameter 18 Å ring;) through the whole crystal. The cocrystallized solvent molecules whose position could be determined are located outside this holes and between the *n*-hexyl chains. Presumably, the holes are filled with highly disordered and maybe even liquid chloroform.

1. V. Hensel, A. D. Schluml;ter, Chemistry, (1999) 421-428
2. K. Diederichs, A. Karplus, *nature structural biology*,4/4 (1997) 269-275.
3. G.M. Sheldrick, Acta Crystallogr. Sect A46 (1990) 467-473

P08.06.012 DNA BINDING STUDIES ON QUINOLONES BY SPECTROSCOPIC METHODS. L.Sudha and K.Subramanian, Department Of Physics, College Of Engineering, Anna University, Chennai 600 025, INDIA

This paper presents the evidence for the formation of the complexes between quinolones and ct-DNA. The quinolones represent a relatively new class of antibiotics with outstanding therapeutic potential, attributable to their broad spectrum of antimicrobial activity and favourable distribution. We have determined the structure of these compounds by X-ray methods.The interaction of three quinolones namely

(1) 5-Amino-8-methyl-2-quinolone monohydrate[quinolone I]
(2) 5-(Dimethylamino)-8-methyl -2- quinolone[quinolone II]
(3) 5-(Isopropylamino)-8-methyl -2- quinolone[quinolone III]

to DNA are studied by spectroscopic methods.

Spectrophotometric and Spectrofluorimetric methods were employed to study the interaction with calf thymus(ct) DNA. From the results of these studies various binding prameters were evaluated. Extensive hypochromism, broadening and red shifts in the absorption and fluorescence apectra were observed when quinolones bind to ct-DNA.In absorption spectra there is a maximum red shift of 3,5 and 5nm were observed at 279, 315 and 319nm for quinolone I, II and III. Binding of the quinolone probe to the ct-DNA helix was found to quench the probe fluorescence strongly. It essentially involves a maximum red shift of 9, 6 and 6nm for quinolones I, II and III. Scatchard plots constructed from these data are used to calculate the binding constants. Stern-Volmer quenching constants were obtained from the linear quenching plots. Strong hypochroism, strong quenching of the probe fluorescence and red shifted absorption and fluorescent spectra strongly support the binding of the quinolone chromophore.

P08.06.013 CONFORMATIONAL ANALYSIS OF NAPHTHOYLENE-IMIDES-MODEL COMPOUNDS OF RIGID-CHAIN HETERO-CYCLIC POLYMERS. A.Yu. Kovalevsky, I.A. Ronova, I.I. Ponomarev, A.N. Nesmeyanov Institute of Organoelement Compounds, Russian Academy of Sciences, 28 Vavilov st., Moscow 117813, Russia, and O.V. Shishkin, SRD Alkali Halide Crystals, STC «Institute for Single Crystals», National Academy of Sciences of the Ukraine, 60 Lenin ave., Kharkov 310001, Ukraine.

Using X-ray structural analysis and calculations by semi-empirical quantum-chemical method AM1, molecular structure and conformational flexibility of series of naphthoyleneimide derivatives have been studied.

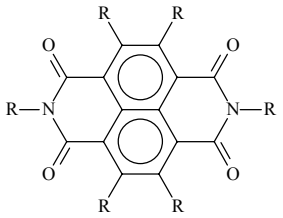

R=H, Me, Ph, *tert*-Bu, o-COOH-C_6H_4, m-OMe-C_6H_4, p-OMe-C_6H_4, p-NO_2-C_6H_4,

The six-membered partly hydrogenated imide cycle in naphthoyleneimide possesses high conformational flexibility, The transition from a planar equilibrium conformation to a sofa with the C(Ar)-C(=O)-NH-C(=O) torsion angle ±20° results in energy increase only about 2.5 kcal/mol. Equilibrium conformation of mono (Me, Ph, t-Bu), di and tetra (Me, Ph) substituted molecules is planar. But imide cycle in di and tetra t-Bu subsituted molecules has a distorted boat conformation. Steric repulsion between atoms of the substituents and adjacent carbonyl groups causes appreciable increase of conformational flexibility of imide ring. The latter grows as substituent volume enlarges in the row of Me, Ph, t-Bu.

Using Monte-Carlo method, the values of Kuhn segment of polymers contained in their structural unit naphthoyleneimide moiety have been calculated. Polymer conformational rigidity depends on the conformational flexibility of imide cycle. The calculation showed that the rigidity of polynaphthoylenimided encreases on going from unsustituted to mono, di and tetra substituted monomeric units.

P08.06.014 CRYSTAL STRUCTURE STUDIES ON FLUORINATED BENZYLIDENE ANILINES. K.V.Arjuna Gowda, M.K.Kokila, Puttaraja, Department of Physics, Jnana.Bharathi. Campus, Bangalore University, Bangalore-560 056 M.V.Kulkarni, Department of Chemistry, Karnataka University, Dharwad 580 003 and N.C.Shivaprakash, Department of Instrumentation, Indian Institute of Science, Bangalore-560 012, INDIA.

Benzylidine anilines(I) have been found to be non-planar compared to the Azobenzenes(II). Further studies on the crystal structure of (I) with substituents like-chloro,-nitro and methoxy at different positions in the rings A and B give rise to interesting solid state confirmations with the angle of twist around CN bond up to 45^0.

We have studied a variety of benzylidine anilines (I) which have 4-Fluoro 3-Chloro substitution in ring A where as ring B has 4-Chloro, 4-dimethylamino, 3,4,5-methoxy and other groups. These compounds have been studied for their densities, molecular packing and their solid state geometries. The results obtained during this investigation indicate the presence intermolecular C-H…F bonds as the forces of stabilisation. The molecules adopt E-configuration and a non-planar arrangement across CN bond.

The structures have been solved by direct methods using SHELXS-86 and refined by a full-matrix least-squares method using SHELXL-93 program.

P08.06.015 STRUCTURE AND MECHANISM OF PHOTOCHEMICAL AND PHOTOPHYSICAL TRANSFORMATION OF NEW SPIROOXAZINES AND 2R-CHROMENES. S.M.Aldoshin and I.I.Chuev, Institute for Chemical Physics Research, Russian Academy of Sciences, Chernogolovka, 142432, Moscow Region, Russia

New photochromic substituted spiro[indoline-2,3'-[3H]-naphtho[2,1-b] [1,4] oxazines (**SO**) with substituents of different types, R_1, R_2-chromenes (**CH**) (CH_3, CH_3; CH_3, Ph; Ph, Ph) and fluorenechromenes have been synthesized. Influence of their specific structural features on photochemical properties (photocolorability, kinetics of dark bleaching) has been studied by using X-ray analysis and quantum chemistry methods. The C-O bond being broken upon photoexcitation was shown to be elongated in the ground state, like in indoline spiropyrans (**SP**). Based on *ab initio* quantum-chemical calculations (3-21G basis), influence of the **SO** molecule geometry on efficiency of anomeric interaction of the lone electron pair of the nitrogen atom with antibonding orbital of the Cspiro – O bond has been studied. The decisive role of this interaction for the elongation of the Cspiro –O bond in the ground and electron-excited states has been shown.

Electron and spatial influence of substituents on the structure, photocolorability and dark bleaching of **SO** and **CH** has been studied. Correlation of photocolorability and the energy of steric strain of the pyran (oxazine) ring has been found for a series of similar **SO** and **CH**.

By purposeful modifying of the **CH** molecular structure, Ph,Ph-chromenes with phenyl rings linked by bridges of different length and nature have been synthesized and studied. Arrangement of the Ph-rings with respect to the C – O bond being broken was shown to influence essentially the photocolorability.

Using the semi-empirical quantum-chemical method (PM3 (MOPAC93)), coordinates of the reaction of cycles disclosure in the ground and the first singlet-excited state have been studied for molecules **SO**, **SP** and R_1, R_2-**CH**.

The ways for structural modification of **SO**, **SP** and **CH** to improve their photochromic properties have been formulated and realized.

P08.06.016 INFLUENCE OF HYDROGEN BONDING ON CONFORMATION OF PHOSPHORYL COMPOUNDS IN SOLUTION AND SOLID STATE. Susan A Bourne, Department of Chemistry, University of Cape Town, Rondebosch 7701, South Africa and Tomasz A Modro, Centre for Heteroatom Chemistry, Department of Chemistry, University of Pretoria, Pretoria 0002, South Africa.

In recent years we have studied a series of compounds containing the phosphoryl moiety. These have yielded interesting correlations between their reactivity and structural features. Of particular interest is the connection between the hydrogen bonding (which often persists in solution) and reactivity.

Compounds **1** and **2** form strong intermolecular hydrogen bonds between N-H and P=O groups of adjacent molecules in the crystalline state. The intramolecular O-P-N-H torsion angle is close to zero in **2** and *ca.* 120° in **1**. These conformations have also been shown to exist in solution and have a profound impact on the use of these compounds as hydrogen bonding reagents in resolution crystallisation.

Compound **3** displays weak (sp^3)C-H...O=P hydrogen bonding that is strong enough to persist even in polar organic solvents. This type of interaction may have relevance to the

structure and reactivity of biomolecules containing organophosphorus functions.

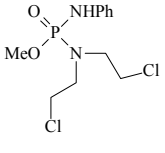

1

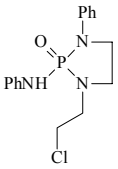

2

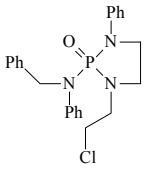

3

P08.06.018 LOCAL ARRANGEMENTS OF ESTER LINKAGES IN CRYSTALS. K. Hori and N. Seo Graduate School of Humanities and Sciences, Ochanomizu University, Bunkyo-ku, Tokyo 112-8610, Japan

Biphenyl ester is a typical mesogenic unit, which produces various mesophases according to the substituents. Relationships between molecular structures and packing modes of molecules are essential to understand the mesophase behavior. We have carried out systematic crystal structure analysis for biphenyl esters with the general formura, R1-C6H4-C6H4-COO-C6H4-R2. Two types of local arrangements of ester linkages were found for compounds, where R1 or R2 is chiral [1]. For componds with chiral R1, an antiparallel arrangement of ester linkages is found, while for those with normal alkoxy chain as R1, a closely arranged ester and ether linkages of the alkoxy chain is found. The latter mode has been found also in many antiferroelectric mesogens. Crystal structure analysis has been extended to biphenyl esters with normal alkyl and/or alkoxy chains for both R1 and R2. Different arrangements of ester linkages are observed in these crystals. They are two kinds of one-dimensional chains of close arrangements of ester linkages; C=O...C=O...C=O with O...C distances of 3.2-3.6 A and O-C=O...O-C=O with rather long O...O distances of 3.8-3.9 A. The former is found mainly for compounds with a normal alkoxy chain as R1. The latter is found for those with a normal alkyl chain as R1, regardless of the type of R2 (chiral or normal).

1. K. Hori and Y. Ohashi (1991). Mol. Cryst. Liq. Cryst. 203, 171.

P08.06.019 MOLECULAR MODELLING, CRYSTAL AND MOLECULAR STRUCTURES OF SOME N-ACYLISOXAZOL-5(2H)-ONES. Max R. Taylor, Mei Fong, Rolf H. Prager and Kia S. Wallwork, Chemistry Department, The Flinders University of South Australia, GPO Box 2100, Adelaide, Australia 5001.

We have reported that N-acylisoxazol-5(2H)-ones, **1**, undergo loss of CO_2 when irradiated at 300 nm, or when subjected to flash vacuum pyrolysis, to give oxazoles[1] (Scheme 1). Theoretical calculations suggest a number of steps are involved in attaining the ideal geometry for cyclisation of the carbene intermediate. In an attempt to predict the reactivity of variously substituted isoxazolones we have carried out *ab initio* calculations at the RHF/16-31G* level of theory to predict the geometry of C3-N2-C2'-O in **1** substituted with groups with varying electronic and steric characteristics, and have confirmed the usefulness of this approach by single crystal X-ray structure elucidation. Considerable deviations from planarity, both at the N and CO group were predicted and confirmed.

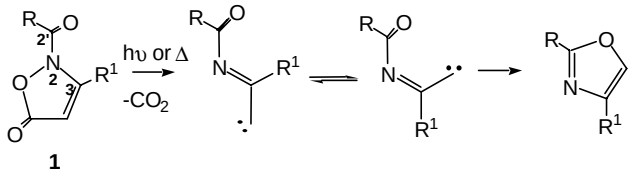

1

Scheme 1

The crystal and molecular structures of five different substituted isoxazolones will be presented and inferences drawn between the computational and experimental evidence. Relationships between conformations found in the crystalline environment, the gas phase and reactivity will be explored.

1. R.H. Prager, J.A. Smith, B. Weber & C.M. Williams (1997). *J. Chem. Soc. Perkin Trans*., 2665.

P08.06.020 CRYSTAL STRUCTURES OF 6-CHLORO-4-HYDRAZINE-2-PHENYL-3-PYRIDAZINONE. Anna Katrusiak and S. Baloniak [1], Andrzej Katrusiak [2], [1] Department of Organic Chemistry, School of Medicine, Grunwaldzka 6, 60-780 Poznan, [2] Department of Crystal Chemistry, Adam Mickiewicz University, Grunwaldzka 6, 60-780 Poznan, Poland

The molecules of 6-chloro-4-(N,N-dimethyl-aminemethylidenohydrazine)-2- phenyl-3(2H)-pyridazinone are hydrogen-bonded by a pair of N(3)H--O= bonds into centrosymmetric dimers. The crystal structures of this compound and of its inclusion compound with water were determined by X-rays [1]. Presently we report the N(3)-methyl derivative of this compound, where the H-donor is blocked and no hydrogen bonds can be formed. We were mainly interested in the modifications of the pharmaceutical activity of this substance, in the changes of its solubility, stability and other physical and chemical characteristics, however we have also investigated by X-ray diffraction the changes induced into the molecular conformation by the methyl substitute, and also in the changes in the intermolecular interactions of the molecules in the crystal structure. In order to elucidate the binding sites of these molecules in living tissues, a quantitative analysis of the changes in their molecular aggregation will be presented.

1. A. Katrusiak and A. Katrusiak, J. Mol. Struct. 374 (1996) 251.

P08.06.021 CRYSTAL STRUCTURE OF A MESOGENIC COMPOUND : P-BUTOXYPHENYL TRANS-4-PROPYL CYCLOHEXANE CARBOXYLATE. S. Ghosh, S. K. Giri, P. K. Mandal, S. Paul [1], T. Manisekaran [2], [1] Department of Physics, University of North Bengal, Siliguri, Darjeeling-734 430, W.B., India, [2] Indian Institute of Technology, Chennai-600 036, India

The studies of the physical properties like the density, refractive index, magnetic susceptibility anisotropy, bend & splay elastic constants and also the X-ray diffraction on p-butoxyphenyl trans-4-propyl cyclohexane carboxylate (BPPCC in short) in its mesophases are carried out by N. K. Pradhan et al.[1]. The molecular arrangement in the crystalline structure is one of the factors which in most cases predetermines the occurrence of thermal mesomorphism in organic compounds and in this context we have undertaken the crystal structure determination. The crystal and molecular structure of the above compound is solved by direct method. The crystal belongs to the monoclinic system with space group P21/a, a =11.2483, b=20.2968, c=17.6311, beta = 100.3425 and eight molecules per unit cell. The structure refined to an R value of 0.07 by full matrix least squares for 5434 observed reflections. Some of the bond-length and temperature parameter values are found to be very large. It means the structure

is highly disordered. Acknowledgement : S. Ghosh and S. K. Giri are thankful to DST, India for providing Research Fellowships. The authors would like to acknowledge Prof. R. Dabrowski for kindly donating the sample used in this work.

[1] N. K. Pradhan, PhD Thesis submitted to University of North Bengal (1998).

P08.06.022 MOLECULAR STRUCTURE OF 2-(4'-*N,N*-DIETHYL-AMINOPHENYLAZO)PYRIDINE. Kanidtha Hansongnern and S. Onganusorn, Department of Chemistry, Faculty of Science, Prince of Songkla University, Hat-Yai, Songkla 90112; Kenneth J. Haller, School of Chemistry, Suranaree University of Technology, Nakhon Ratchasima 30000, Thailand.

The red colored title compound was synthesized and the structure characterized. It is a derivative of 2-(phenylazo)pyridine (azpy) which acts as an excellent ligand to stabilize ruthenium(II) in complexes (S. Goswami, A.R. Chakravarty, A. Chakravorty, *Inorg. Chem.* 22 (1983) 602-9). Its use as a potential ligand to ruthenium is currently under investigation.

The structure shows the phenyl and pyridine rings to be trans and essentially coplanar with the azo linkage; the C5-N2-N3-C6 torsional angle is -179.2 (2)º and the azo bond length, N2=N3, is 1.215 (3) Å. The angle between the planes of the phenyl and pyridine rings is 2.5 (2)º, largely due to rotation relative to the long axis of the molecule.

Bonding in the linkage between the phenyl and pyridine is altered compared to complexes containing azpy as ligands. The azo distance is significantly shorter than that in complexes, *eg.* Ru(azpy)$(N_3)_2$, N=N = 1.289(9) & 1.291(9) Å, (K. Krause, R.A. Krause, S. Larsen, B. Rasmussen, *Acta Chem. Scand.* A39 (1985) 375-88); and the azo-phenyl distance is significantly longer, C-N = 1.371(10) & 1.370(10) Å, compared to N2-C5 = 1.487(3) Å in the title compound, while the azo N=N-phenyl C angle, C-N-N = 111.8(6) & 112.1(6), in the complex, is nearly tetrahedral, C5-N2-N3 = 109.2(2), in the title compound.

Recrystallized from ethanol solution as thick red plate crystals. *Crystal Data:* $C_{15}H_{18}N_4$, *MW*=254.34, *MP*=105-6 ºC, orthorhombic $P2_12_12_1$ (No. 19), *a*=7.483 (1), *b*=9.096 (1), *c*=21.019 (3) Å, *V*=1430.7 (4) Å^3, *T*=297±2 K, *z*=4, d_{calc}=1.181 Mg m^{-3}, μ=0.073 mm^{-1}, MoKα radiation, *F(000)*=544., $sin\theta/\lambda_{max}$=0.615 Å^{-1}, R_{int}=0.043, 2738 unique data, 1788 $F_o>4\sigma(F_o)$, R_1=0.043, wR_2=0.115, gof=1.01.

P08.06.023 MOLECULAR STRUCTURE OF THE ZWITTERIONIC 4-HYDROXY-*N*-METHYL-L-PROLINE. Kenneth J. Haller, School of Chemistry, Suranaree University of Technology, Nakhon Ratchasima 30000, Amorn Petsom, Sophon Roengsumran, Dep Shiengthong, Weeraya Lertwanitch, Prapapan Techasauvapak, Waraporn Rungruangkanokkul, Department of Chemistry, Faculty of Science, Chulalongkorn University, Bangkok, 10330, Thailand

The title compound was isolated from the ground dried flowers of *Aglaia odorata* Lour, and identified by its physical and chemical properties (Shiengthong, Lertwanitch, Techasauvapak, Rungruangkanokkul, Roengsumran, Petsom, Haller, *18th Congress on Science and Technology in Thailand*, (1992) Abstract A-52); representing the first report of the compound in *Aglaia* species.

The carboxylic acid proton has transferred to the nitrogen atom giving a zwitterion in the solid state. The C-N distances are unremarkable, C_α-N=1.494(2), C_δ-N=1.504(2), and C_{Me}-N=1.486(2) Å. The anionic carboxylate exhibits essentially equal C-O bonds, 1.244(2) and 1.249(2) Å and a somewhat opened O-C-O angle, 127.4(2)º as normal. The remaining ring distances are: C_α-C_β=1.524(3), C_β-C_γ=1.524(3), C_γ-C_δ=1.533(2), Å, and the distances for the carboxylate carbon-Cα and the hydroxy O-Cγ bonds are 1.529(2) and 1.417(2) respectively.

Recrystallized from methanol solution as large clear colorless rod shaped crystals. *Crystal Data:* $C_6H_{11}NO_3$, *MW*=145.16, *MP*=236-38 ºC, monoclinic $P2_1$ (No. 4), *a*=6.7396 (6), *b*=5.8417 (8), *c*=8.8800 (9) Å, β=100.836 (6)º, *V*=343.38 (8) Å^3, *T*=297±2 K, *z*=2, d_{calc}=1.404 Mg m^{-3}, μ=0.011 mm^{-1}, MoKα radiation, *F(000)*=156., $sin\theta/\lambda_{max}$=0.595 Å^{-1}, R_{int}=0.0102 (from 215 pairs), 1007 unique data, 792 $F_o>4\sigma(F_o)$, R_1=0.0258, wR_2=0.0727, gof=1.113.

P09.06.001 A VOLUMETRIC MEASURE OF ISO-STRUCTURALITY. László Fábián and Alajos Kálmán, Institute of Chemistry, Chemical Research Center, Hungarian Academy of Sciences, P.O.Box 17, H-1525 Budapest, Hungary.

The study of isostructurality is a useful tool in the understanding of related crystal structures. A detailed analysis requires numerical descriptors as well. However, the application of the isostructurality index introduced by Kálmán *et al.* [1] is limited to cases where a straightforward atom-atom correspondence can be established between the structures under investigation.

Hence a new measure of isostructurality based on the overlap of molecular volumes is suggested:

$$I_v = \frac{2V_\cap}{V_1 + V_2} 100\%$$

where $V_\cap$ is the overlap of the two molecular volumes V_1 and V_2. A numerical algorithm has been developed for the calculation of I_v and the method has been extended to treat disordered structures as well.

The results of I_v calculations on selected literature examples will be presented. They provide additional insight into the close packing of both homomolecular crystals and inclusion compounds. The examples illustrate the tolerance of crystal structures to molecular alternations, the stiffness or looseness of different structural units and the relative strength of host-guest interactions.

1. A. Kálmán, Gy. Argay, L. Párkányi (1993). *Acta Cryst.* B**49**, 1039-1049.

P09.06.002 SOLID STATE INVESTIGATION ON THE POLYMORPHIC SYSTEM OF APROBARBITAL- 5-ALLYL-5-ISOPROPYLBARBITURIC ACID Navon O.[1.], Bernstein J.[1] [1.]Department of Chemistry, Ben-Gurion University of the Negev, Beer Sheva 84105 Israel.

Barbiturates are a class of drugs which exhibit widespread polymorphism. Barbiturates have diverse actions in biological systems. In addition to their widely known sedative effects, they are also regarded as general metabolic depressants because they inhibit a large number of enzyme systems. They have well defined hydrogen bonding networks. In the course of investigating of a number of molecules in this family we worked on the molecule 5-ally - 5-isopropylbarbituric acid.

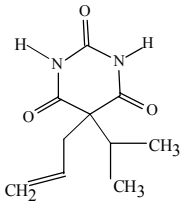

There is only one known structure in the Cambridge Crystallographic Database [1], although Kuhnert - Brandstätter [2] reported the existence of six polymorphs. We can report here of three new forms. We will present the solid state characterization

of the different forms, using: single crystal X-ray structure analysis, X-ray powder diffraction, solid state NMR thermal analysis, graph set analysis, and lattice energy calculations, in an effort to understand and to control the structure and polymorphic form.

1. A.D.Rae, Cryst.Struct.Commun.189,4,457,1975.
2. Kuhnert-Brandstatter, M., "Thermomicroscopy in the Analysis of Pharmaceuticals., International Series of Monographs in Analytical Chemistry, Pergamon Press, New York, vol 45, 1972.

P09.06.003 PHASE TRANSITIONS IN $H_2T(4\text{-}OC_{12}H_{25})PP$ BY SINGLE-CRYSTAL X-RAY DIFFRACTOMETRY. J. Slowikowska[a], G.L. Perlovich[b], J. Lipkowski[a], W. Zielenkiewicz[a]; [a]Institute of Physical Chemistry, Polish Academy of Sciences, ul. Kasprzaka 44/52, 01-224 Warsaw, Poland; [b]Institute of Solution Chemistry, Russian Academy of Sciences, Academicheskaya Str., Ivanovo, 153045, Russia.

Polymorphism and phase transitions are the two phenomena which have gained an increasing attention in the recent years as crucial in such key areas of chemistry as pharmaceutical industry and rapidly developing crystal engineering. Various applications of porphyrin derivatives, starting from anti-cancer agents to building blocks in design of programmed crystal architectures, place this class of compounds at the intersection of these two domains making them particularly interesting for thorough studies of their structural changes.

The phase behaviour of $H_2T(4\text{-}OC_{12}H_{25})PP$ porphyrin (**1**) has been investigated by single-crystal X-ray diffraction at temperatures ranging from 100K to 362K. The changes in the unit cell dimensions, volume and intensities of individual reflections were monitored, giving a total of 15 unit cell determinations. At least six discrete reversible phase transitions were observed within 240-355K by DSC measurements. It is worth to note that the single crystal is preserved during all these phase transformations. Intensity data collection were done at 120K, 295K, 345K, and 362K. The structure is well ordered at 120K, but at room temperature only the central part of the molecule could be localised. At higher temperatures poor intensity data do not allow a complete structural analysis. However, interesting structural behaviour was observed in the form of superstructure (in a very narrow temperature range at about 350K) resulting in a doubling of the unit cell *a* constant and a decrease in β angle. It is concluded that the phase transformations in **1** are ascribed mostly to order-disorder type transitions in long alkyl chains of the phenyl rings.

Crystal data for **1** at 120K: ($P2_1/c$, a = 19.432(3)Å, b = 19.213(3)Å, c = 10.552(2)Å, β = 93.71(1)º).

P09.06.004 $Ba_2Cu(HCOO)_6$, THERMAL BEHAVIOR AND CRYSTAL STRUCTURE OF THE ROOM TEMPERATURE PHASE. P.K. de Perazzo, D. Vega, G. Polla, A.G. Leyva, H. Lanza, , R. Baggio, M.A.R. de Benyacar, .U. A. Fisica, CNEA, Avda del Libertador 8250, 1429 Cap. Fed., Argentina, J. Ellena, Depto de Fisica, Facultad de Ciencias Exactas, Universidad Nacional de La Plata, La Plata, Argentina, and H.Tolentino and M do Carmo Martins Alves, Laboratorio Nacional Luz Sincrotron, Campinas, San Pablo, Brasil.

$Ba_2Cu(HCOO)_6$ grown at room temperature crystallises in space group $P2_1$; a = 11.092 Å, b = 7.079 Å, c = 17.391 Å, β = 91.64^0; V = 1365 Å^3, Z = 4, D_c = 2.96gr/cm^3. On heating the following changes are observed : 1) a reversible, hysteretic, first order phase transition at about 60-90^o C; 2) partial decomposition at 190^o C and 3) an irreversible change at 230^o C related to decomposition. We have assigned to a new γ-$Ba(HCOO)_2$ metastable phase one of the main components found in $Ba_2Cu(HCOO)_6$ samples quenched from 190^o C.

A room temperature model structure of $Ba_2Cu(HCOO)_6$ is given. The copper atoms are surrounded by 7 oxygen atoms: 5 of them defining an almost perfect square pyramid, and the remaining two, opposite to the apex, at hemicoordination distances of ca. 2.85Å. Even though the two nearest neighbours contributions accounted fairly well for many of the details of the EXAFS absorption curve, only the inclusion of the oxygens at 2.85 Å made the match nearly perfect.

The barium atoms display irregular, ninefold coordination polyhedra arranged as corrugated planes which share two faces with the copper coordination polyhedra. This crystal structure is different from those reported for the copper-dicalcium and the copper-strontium anhydrous double formates.

P09.06.005 MOLECULAR PACKING AND POLYMORPHISM IN INORGANIC FLUORIDES. Arkady Ellern. Ben-Gurion University of the Negev, Chemistry Department, P.O.B. 653, Beer-Sheva, Israel.*

If the substance in solid state forms molecular crystals, two reasons for a polymorphism can be found in principle. The first one is the different molecular structure of the molecule. In this case the origin blocks for a building of the crystal (the molecule) in different polymorphs are chemically equivalent, but have different geometrical parameters. The majority of the cases of the polymorphism in organic chemistry belong to this type, because the organic molecule can be rather flexible. Even a small change of the conformations of substituent (as Et, Bu etc) can be responsible for the crystallization in different crystal packing mode. The second type of polymorphism includes the cases when the molecules have absolutely the same geometrical parameters in both modifications and the reason for polymorphism is a different kind of intermolecular interaction or a small distortion of the crystal lattice.

The molecular structure can be qualitatively predicted for most of the binary fluorides, because usually they can adopt the only molecular geometry. The obtained phase diagram of the system BrF_3-BF_3 shows the existence of polymorphism of the second type even for such simple fluorides as BF_3 and ClF_3. The results of precise low-temperature X-ray analysis of all compounds in this system will be presented in this contribution.

The X-ray data for the variety of the derivatives of halogen fluorides and xenon fluorides show that the surprising packing mode of ClF is not the only exception from the “F-bridging” model, which is typical for inorganic fluorides.

The work was supported in part by Alexander von Humboldt Foundation.

P09.06.006 AN IN-DEPTH STUDY OF GROWTH SPIRALS ON CdI_2 CRYSTALS IN RELATION TO THE FORMATION OF POLYTYPES. Rajendra Singh and G.C. Trigunayat, Department of Physics and Astrophysics, University of Delhi, Delhi-110007, India and S.B. Samanta and A.V. Narlikar, National Physical Laboratory, K.S. Krishnan Marg, New Delhi-110012, India.

A collective sequential study of growth spirals on the basal surfaces of the richly polytypic cadmium iodide crystals has been carried out by optical microscopy, scanning electron microscopy and scanning tunneling microscopy, which has yielded some novel results. The STM enables an unambiguous and accurate measurement of the step heights. When the large height growth steps viewed through optical microscopy are further examined by SEM, a large number of additional steps of smaller height are discovered to exist between any two originally seen adjacent growth steps. When next viewed through STM, which provides still higher resolution of images, numerous unit substeps are found to exist between two consecutive additional steps. The height of each substep equals the unit cell height of the underlying

polytype (hence termed as "unit" substep) and the height of the larger aforesaid additional step is found to be an integral multiple of the unit cell height. The results have important bearing on understanding the creation of polytypes. Besides, the spacing between two successive growth steps turns out to be an integral multiple of the lattice parameter a. The interspacing of the growth steps of same step height is found to vary at different positions on the same crystal face. Additionally, the STM pictures clearly reveal the value of unit cell a (=b) dimension to be equal to 0.428 nm and the value of the interaxial angle γ to be equal to 120°, in exact conformity with the known structural data.

P09.06.007 POLYMORPHS OF DIMETHYLSULFIDE-DINITRATOPALLADIUM (II). M. Johansson and A. Oskarsson, Inorganic Chemistry 1, Chemical Centre, University of Lund, P.O. Box 124, S-221 00 Lund, Sweden.

There exists at least two polymorphs, denoted A and B, of the title compound. Both crystallize in the monoclinic space group $P2_1/n$, but with Z=4 and 8 for A and B, respectively.

Polymorph A was found in a batch prepared from $Pd(OAc)_2$ + dms + HNO_3 while B was in a batch prepared from $PdCl_2(dms)_2$ + aq + $AgNO_3$. It is reasonable to assume that both polymorps are present in both batches and this point is under investigation.

The volume per complex is 305.2(1) and 298.4(1) A^3 at room temperature while at 150 K the corresponding values are 289.3(1) and 288.8(1) A^3. Thus there is a significant difference in packing efficiency at room temperature but not at 150 K.

The donor atoms in polymorph A are disordered both at room temperature and at 150 K, while for polymorph B the donor atoms of one of the complexes are disordered at room temperature but not at 150 K. However, different crystals were used at room temperature and at 150 K and the disorder of different crystal individuals may be different.

The following aspects will be discussed on the poster

Do the synthetic procedure have effects on the relative amounts of the polymorps formed?

Is it possible to observe a temperature dependent phase transformation by studying the structures at different temperatures.

The packing in the different polymorphs will be discussed as well as the influence of intermolecular forces on intramolecular bond distances, bond angles and torsion angles.

P09.06.008 THERMALLY INDUCED TRANSFORMATIONS IN META-NITROANILINE CRYSTAL. G.Wójcik, J.Holband, M. M. Szostak, Institute of Physical and Theoretical Chemistry, Wroclaw University of Technology, Wyb. Wyspiañskiego 27, 50-370 Wroclaw, Poland.

Molecular packing changes in m-nitroaniline crystal on heating above room temperature were observed by direct dilatometry and near IR spectroscopy, suggesting possibility of a second order phase transition at 330 K [1]. Dielectric relaxation studies evidenced increasing molecular dynamics coupled with growing electric conductivity from above room temperature. An anomaly on the real part of permittivity dependence on temperature occured at 365 K. It was depicted in terms of a rotative phase - plastic phase transition. Also calorimetry (DSC) revealed a very weak anomaly at about 365 K and, additionnally, a glassy-type transition at about 160 K [2]. Structural investigations on a 4-circle automatic KUMA diffractometer with a CCD detector, equipped with an Oxford Cryosystem Unit were performed in a wide range of temperatures with the aim to verify the occurence of the transitions and to find m-nitroaniline crystal structures above the high temperature transition point and below the low-temperature one. Thermal expansion was measured in several crystallographic directions. Molecular dynamics was monitored by the evolution of mean square atomic displacements on temperature. The low temperature transition is depicted in terms of reorientations of supra-molecular strands. The role of weak hydrogen bondings is discussed.

1. M. M. Szostak, B. Jakubowski, M. Komorowska, Mol. Cryst. Liq. Cryst. (1993) **229**, 7.
2. M. M. Szostak, G. Wójcik, J. Gallier, M. Berteault, P. Freundlich, H. A. Kolodziej, Chem. Phys. (1998) **229**, 275.

P09.06.010 ANALYSIS OF PROBABILITY OF FORMATION OF INTRAMOLECULAR HYDROGEN-BONDED RINGS. C. Bilton, J.A.K. Howard, Department of Chemistry, University of Durham, Durham, UK. F.H. Allen, G.P.Shields, W.D.S. Motherwell. Cambridge Crystallographic Data Centre, Cambridge, UK.

Using a modified version (1) of the Cambridge Structural Database (CSD) (2) software, the April 1998 release of the database was used to analyse the probability of formation of intramolecular hydrogen-bonded rings. All intramolecular ring motifs containing between 4 and 10 atoms, formed via O-H --- O, O-H --- N, N-H --- O or N-H --- N hydrogen bonds in organic structures were recorded. The motifs were then ranked in order of their probability of formation .The results were then taken and investigated in further detail. The effect of formation of the ring on the localised geometry of the molecule and also on the potential for both the donor and acceptor to form additional hydrogen bonds will be discussed.

G.P.Shields, 1998, private communication.
F.H. Allen and O.Kennard, *Chem. Des. Autom. News*, 1993, **8**, 1;31.

P09.06.011 DEHYDRATION PROCESS OF COPPER OXINATE DIHYDRATE - GENERATION OF TWINNING. T. Nemoto, S. Terada, S.Isoda and T. Kobayashi, Institute for Chemical Research, Kyoto University, Uji, Kyoto 611-0011, Japan.

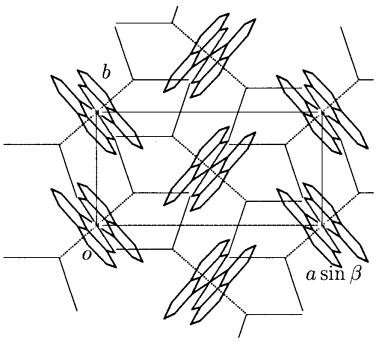

The copper oxinate complex crystal has various polymorphs depending on its formation process [1]. One of the polymorphs, β-form, undergoes dehydration at high temperature in air or under vacuum. This dehydration process was analyzed by X-ray and electron diffraction.

The β-form crystal was obtained from aqueous acetic acid solution of copper oxinate dihydrate. It is a hexagonal plate-like crystal and belongs to the space group $P2_1/a$, Z=2 The structure determined from X-ray diffraction intensities is almost the same as that of zinc oxinate dihydrate. This result consists with that reported previously from the consideration on cell dimensions[2].

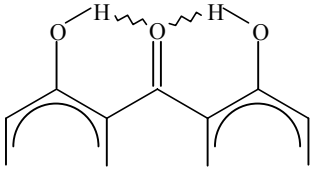

Hydrogen bond network in β-form

The two dimensional hydrogen bond network layer exists perpendicular to the c axis, and the crystal grows along this layer.

After dehydration under vacuum in TEM, the, electron diffraction photograph shows twinning[1].

The angle between the *b1** and *b2** axes of the two twin domains was 30°. The direction of c axis is common before and after dehydration. Such angle is explained from the crystal structure of the β -form.

[1] Suito, B., *et al.* (1966). *Kolloid-Z. Z. Polym., 212*, 155-
[2] Kruh, R., *et al.* (1954). *J. Am. Chem. Soc., 77,* 806-

P09.06.012 CRYSTAL STRUCTURE OF A NOVEL DIMESOGEN. J. Shashidhara Prasad and M.A Sridhar, Department of Studies in Physics, University of Mysore, Mysore 570006, INDIA and V. Surendranath, Department of Physics, Kent State University, Kent OH 44242, USA.

The title compound, 4-(cholestroxycarbonyl)pentyloxy-4′-heptyloxycarbonylbiphenyl ($C_{53}H_{78}O_5$), is a novel dimesogen which comprises of two mesogenic units dissimilar in nature. It crystallizes in the orthorhombic space group $P2_12_12_1$ with the cell parameters a = 6.241(3)Å, b = 17.943(5)Å, c = 43.13(5)Å, Z = 4. The structure was solved using SHELXS [1] and refined using SHELXL [1]. The final residual was R = 0.0803 for 1769 reflections with $I > 2\sigma(I)$. The molecule is linear and the terminal groups show stretching with higher bond distances. The packing of the molecules shows imbrication, herringbone and stacking along the *a*, *b* and *c* axes respectively. The structure also exhbits an intermolecular hydrogen bond of the type CH…O. The structure indicates the requirement to exhibit incommensurate smectic phase.

1. G.M. Sheldrick, University of Göttingen, Germany (1997).

P09.06.013 STATISTICAL ASPECTS OF THE OCCURRENCE OF CRYSTAL FORMS AMONG ORGANIC DRUG SUBSTANCES. U. J. Griesser and A. Burger, Institute of Pharmacognosy, University of Innsbruck, Innrain 52, 6020 Innsbruck, Austria.

The occurrence of polymorphic modifications, hydrates and solvates with organic solvents of more than 550, chemically well defined organic drug compounds (European Pharmacopoeia 97) has been examined. This set of substances represents a random selection of generally well characterized compounds from a variety of chemical classes, which makes this set particularly attractive for a statistical analysis.

More than 55% of these substances are known to exist in more than one crystal form, 35% form polymorphic modifications, 30% hydrates and 10% solvates. These numbers represent the accessible, present knowledge but are certainly too low. However, neither the Cambridge Structural Database, nor the Beilstein database or the Merck Index provide comparable information. Here we roughly estimated 20%, 1% and 7% respectively for entries with hints to polymorphism or solvate/hydrate formation.

Generally, the different crystal species can be found in all compound classes but certain accumulations can be established. So, non-salts with low relative molecular masses (< 350) show the highest tendency to form polymorphs (> 50%). On the other hand, this group reveals the lowest amount of hydrate forming compounds (< 20%). Salt formation doubtless favors the hydrate formation but decreases the tendency to form solvates with organic solvents – besides, both the occurrence of hydrates and solvates increases with increasing size of the molecules. Thus, the highest amount of solvates (> 20%) can be recognized among non-salts with molecular masses greater than 350.

The analysis also reveals that particularly badly soluble compounds tend to occur in different polymorphic forms or as solvates. This result, as well as the fact that the occurrence of these phenomena among compounds with known bioavailability problems is above the average, indicates the importance to know and characterize any crystal form of drug substances.

P09.06.014 STRUCTURE OF α-FORM QUINACRIDONE BY ELECTRON CRYSTALLOGRAPHY. T.Ogawa, C.Furukawa, S.Moriguchi,T.Nemoto, S.Isoda and T.Kobayashi, Institute for Chemical Research, Kyoto University, Uji, Kyoto 611-0011, Japan.

For linear *trans*-quinacridone, only the structure of γ-form has been reported, even though it shows many polymorphs like α, β, γ, δ and γ'. Recently the α-form has been tried to be analysed by Lincke *et al.* [1]. They have proposed the structure from the analogical consideration on the known γ-form structure. In the present study, we tried to analyse the α-form of the quinacridone by electron crystallography with imaging plate.

The purified sample was vacuum-deposited on alkali-halide single crystalline substrate (KCl, KBr, KI or NaCl). The epitaxial orientations were different depending on the substrate used, but the electron diffraction patterns could be assigned to be the same α-form from comparison with the reported lattice spacings [2] for all substrates. By tilting the specimen films in a TEM, three-dimensional reciprocal lattice dimensions were examined. As a result, we obtained monoclinic unit cell of a=1.45nm, b=0.42nm, c=0.637nm and β=103° with Z=1, which means the density is about 1.38g/cm^3. These lattice dimensions are different from those by Linke *et al*.

In order to determine the molecular packing, the a*c*-net pattern from the epitaxial film is recorded on an imaging plate to measure the diffraction intensities as reported previously [3]. From a Patterson map and a high resolution image, rough estimation of molecular packing was firstly done, and detailed packing was determined so as for the orientation of molecule to fit the measured intensities. In the analysed structure, a quinacridone exhibits hydrogen bonding with the neighbouring molecule.

1 G.Lincke, *et al*. (1996). Cryst.Res.Technol., **31**, 441.
2 S.S.Labana, *et al*. (1967). Chem.Rev., **67**, 1.
3 T.Ogawa, *et al*. (1993). Polymer, **35**, 1132.

P09.06.015 POLYMORPHISM AND ITS EFFECTS ON THE SOLID STATE PHOTODIMERIZATION OF A LTB4 ANTAGONIST DRUG CANDIDATE. R. Curtis Haltiwanger*, Robert A. Daines+ and Drake S. Eggleston*, Departments of Physical and Structural Chemistry* and Medicinal Chemistry+, SmithKline Beecham Pharmaceuticals, P.O. Box 1569, King of Prussia, Pennsylvania 19406, USA.

(E)-3-[6-[[(2,6-Dichlorophenyl)thio]methyl]-3-(2-phenylethoxy)-2-pyridinyl]-2-propenoic acid, **1**, is a Leukotriene B_4 receptor antagonist representative of a class of drug molecules with the potential to treat psoriasis and other inflammatory diseases. Since exposure to sunlight is an accepted psoriasis treatment, the light-stability of this compound is of considerable interest.

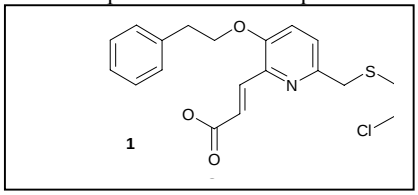

There are two known Polymorphs of **1**. Form I, in the solid state, degrades nearly completely to a cyclobutane dimer after 4 hours of exposure to xenon light. Under the same conditions Form II shows approximately 4% degradation to polymeric products with no evidence of the cycloadditon product. The crystal structures of Forms I and II and of the Form I degradation product provide a clear explanation for the differences in stability between the two forms. In the crystal lattice of Form I the acrylate double bonds in adjacent molecules are nicely aligned to facilitate the light

catalyzed cycloaddition reaction. In Form 2 these double bonds are well separated and cycloaddition is not favored.

Form I - aligned double bonds

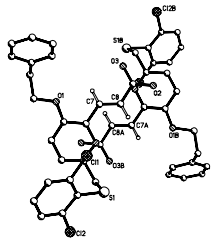

	Form I	Form II	Dimer
Sp Grp	C2/c	P1	P1bar
a	28.630(6)Å	10.639(4)Å	8.325(6)Å
b	9.07(2)Å	14.612(5)Å	12.473(4)Å
c	17.599(4)Å	15.273(5)Å	13.212(5)Å
α	90°	78.36(3)°	76.68(3)°
β	109.24(3)°	70.96(3)°	85.27(4)°
γ	90°	79.56(3)°	81,54(4)°
Vol	4428(2)Å^3	2181(1)Å^3	1318(1)Å^3
Z	8	4	1
Refl(uniq)	3525	8121	4199
(obs),I>2σI	3093	6955	3388
R1(obs)	0.055	0.042	0.056
wR2(all)	0.154	0.112	0.162

P09.06.016 THE ROLE OF H-BONDS IN THE ANISOTROPY OF STRUCTURAL DISTORTION OF PARACETAMOL AT HIGH PRESSURE. T.P. Shakhtshneider and E.V. Boldyreva, Institute of Solid State Chemistry and Mechanochemistry SB RAS, Kutateladze, 18, Novosibirsk, 128, 630128 Russia, email elena@solid.nsk.su, and H. Ahsbahs, Institute of Mineralogy of Marburg University, Hans-Meerwein Strasse, 35043 Germany.

The anisotropy of structural distortion of paracetamol (p-hydroxy-acetanilide) at hydrostatic pressures up to 4.0 GPa was followed by single-crystal X-ray diffraction in the diamond anvil cell. The crystal structure was refined anisotropically to R=0.02-0.03 at 1.0 GPa, 2.0 GPa, 3.0 GPa, 4.0 GPa. The changes in the intra- and intermolecular distances and angles were followed. The compressibility of NH...O and OH...O hydrogen bonds was measured. The role of these hydrogen bonds in the anisotropy of pressure-induced structural distortion is discussed. The diffraction data are correlated with the results of high-pressure IR-spectroscopy.

P09.06.017 NEW MEMBERS IN THE FAMILY OF NON-CLASSICAL HETEROPHANES. C. Alvarez-Rúa and S. García-Granda, Departamento de Química Física y Analítica, Universidad de Oviedo, Spain, and E. Alcalde, L. Pérez-García and N. Mesquida, Facultad de Farmacia, Universidad de Barcelona, Spain.

A great variety of molecular architectures can be found among the macrocyclic systems. Cyclophanes, phanes and heterophanes can be synthesised from different types of building blocks, which determine the physical and structural characteristics of the macrocyclic compounds. The ring components present in heterophanes are normally uncharged heteroatomic moieties, and, in the few cases in which they bear a charge, this is normally negative.

The crystal structures of some dicationic [1_4] heterophanes have been studied [1]. This kind of compounds exhibit the ability of forming specific complexes with some anions via non-covalent interactions. Crystals of these compounds are quite unstable, since a complex network of hydrogen bonding interactions appears within the crystalline lattice.

Progress in the study of the conformational analysis and non-covalent interactions of these heterophanes will be discussed.

1. E. Alcalde et al. (1999). *J. Chem. Soc., Chem. Commun.* (submitted).

P09.06.018 UNUSUAL C-H…π HYDROGEN BONDING. C.K.Broder, M.G.Davidson, J.A.K.Howard, University of Durham, Durham, DH1 3LE.

It has been firmly established through structural, structure correlation, and theoretical studies[1] that attractive C-H…X interactions can play a decisive role in the supramolecular structure of solids in much the same way as the stronger O-H…X and N-H…X hydrogen bonds.

We have been studying a series of novel double C-H…π bonded systems where a guest C-H donor sits in the cleft of a bis-phenol LH_2 or L^{2-} molecule. Previously, such non-classical hydrogen bonds have been seen to aid the formation of related host-guest complexes[2,3].

The compounds studied in detail here are the adduct of triphenylmethylphosphonium and L^{2-}, and the adduct of 1,3-dimethyl-2-imidazolidinone (DMI) and LH_2.

Both compounds have been studied using x-ray and neutron diffraction and the results will be discussed here.

Compound A:

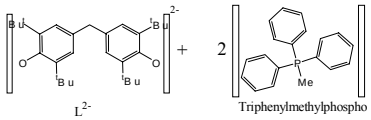

Compound B:

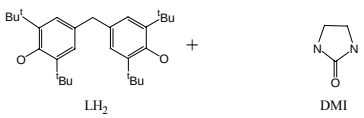

1) G.R.Desiraju. *Acc. Chem. Res*. 1996 **29** 441, and ref therein; D.R.Armstrong, M.G.Davidson, D.Moncrieff. *Angew. Chem. Int. Ed Engl.* 1995 **34** 478. M.G.Davidson. *Chem Commun.* 1995 919.
2) R.J.Blanch, M.Williams, G.D.Fallon, M.G.Gardiner, R.Kaddour, C.L.Raston. *Angew. Chem.Int.Ed.Engl.* 1997 **36** 504.
3) A.L.Balch, V.J.Calalano, J.W.Lee, M.M.Olmstead. J.Am. Chem. Soc. 1992 **114** 5455

P09.06.019 RACEMIC COMPOUND FORMATION VS. CONGLOMERATE FORMATION AMONG THE ACIDIC SALTS OF α-PHENYLETHYLAMINE WITH ACHIRAL DICARBOXYLIC ACIDS. D. Kozma[1], Z. Kovári[2], Z. Böcskei[2] and E. Fogassy[1]. [1]Department of Organic Chemical Technology, Technical University of Budapest, [2]Department of Theoretical Chemistry, Eötvös University of Budapest, Hungary

The crystal structures of a number of acidic salts of achiral dicarboxylic acids with α-phenylethylamine were investigated in order to find structural grounds for the conglomerate forming ability. Out of the eight examined dicarboxylic acids only two formed conglomerates (ithaconic and succinic acids)[1]. The others (malonic, maleinic, fumaric, glutaric, adipic and phtalic acids) form molecular compounds. We attempted the crystallization of all 14 possible racemic and optically pure salts, but succeeded only in five cases. It was found that conglomerate formation takes place when the protonated and deprotonated carboxylic groups form hydrogen bonded chains rather than cyclic intramolecular hydrogen bonds. Two of the racemate forming structures (ortho-phatlic and malonic acid salts) have the protonated dicarboxylic acids with intramolecular hydrogenbonds. In these structures the donors and acceptors are prealigned for these interactions to occur. In the P1 structure containing the optically pure form of the racemate forming adipic acid salt two crystallographycally

independent "ion pairs" are found. Interestingly in one of them the adipic acid has both of its carboxylates in the protonated form, while the other moiety is a totally deprotonated adipic acid.

All of the structures are donor deficient and therefore all donor hydrogens are involved in hydrogen bonds. A detailed qualitative and quantitative analysis of the hydrogen bond interactions and a correlation with the conglomerate forming ability will be presented.

1. Z. Böcskei, Cs. Kassai, K. Simon, E. Fogassy & D. Kozma (1996). J. Chem. Soc. Perkin Trans. 2, 1511.

P09.06.020 UNDERSTANDING NITROANILINES USING NEUTRON DIFFRACTION. A.E. Goeta and J.A.K. Howard, Chemistry Department, Durham University, Durham DH1 3LE, UK, J. Ellena, Instituto de Física de Saõ Carlos, USP, Saõ Carlos, SP, Brasil, G. Punte, LANADI y PROFIMO, Depto. de Física, UNLP, CC 67, (1900) La Plata, Argentina, J.C. Autino, LADECOM, Depto. de Química, UNLP, Argentina and C.C. Wilson, ISIS Facility, CLRC Rutherford Appleton Laboratory, Chilton, Didcot, Oxon OX11 0QX, UK.

Much effort has been devoted in the last decade to the study, design and understanding of the aggregation of organic molecules. The considerable interest in the field has been based on the fact that crystal engineering, the ability to predict and/or direct the three-dimensional arrangement, can be used to tailor materials of biological or technological importance. Intermolecular hydrogen bonds are an effective tool for organising molecules, and in the case of non-linear optical compounds this is very well typified by nitroaniline compounds, which associate via intermolecular H-bonds between the amino and nitro groups. Nitroanilines have received special attention due to their recognized second harmonic generation capability and their large microscopic hyperpolarizabilities. In addition, aniline planarity has been backed by most organic text book assumptions and even by surveys of the geometry of unsubstituted and substituted aromatic amines. We will present here results from single crystal neutron diffraction experiments on 2-methyl-5-nitroaniline and *m*-nitroaniline performed on the SXD instrument at ISIS. The aim of these studies has been to establish the degree of planarity of the amino group and to add to the understanding of the role of the hydrogen bonds in the molecular organization of nitroanilines.

P09.06.021 HYDROGEN BONDED ADDUCTS BETWEEN TRIPHENYLSILANOL AND AROMATIC AMINES S.E. Lawrence, A. O'Dowd and T.R. Spalding Chemistry Department, University College Cork, Cork, Ireland.

Attention is currently focussed on the interaction between silanols and amines, spanning areas of interest from environmental silicon chemistry to siloxane polymers. Surprising, there have been few accounts concerning the hydrogen bonded adducts of tertiary silanols with amines, e.g. only adducts involving *N,N,N',N'*-tetramethylethylenediamine (TMEDA) and tris(2-aminoethyl)amine [1] have been discussed.

In this study we present crystal structures of the adducts formed between triphenylsilanol (Ph_3SiOH) and aromatic amines, such as 4,4'-bipyridyl and 4-phenylpyridine. Different structures are seen, depending on the silanol:amine ratio and the nature of the aromatic amine used, and these will be discussed.

[1] I. Baxter, L.D. Cother, C.Dupuy, P.D. Lickiss, A.J.P.White and D.J. Williams, http://www.ch.ic.ac.uk/ectoc/ectoc-3/pub/010/index.htm 1997.

P09.06.022 LOCALIZATION OF HYDROGEN AND H-BONDING IN CLUSTER CHALCOCYANIDE HYDRATES N.G. Naumov, N.K. Moroz, V.E.Fedorov, Institute of Inorganic Chemistry SB RAS, Novosibirsk, Russia.

Recently a new class of inorganic cyanides, namely, octahedral cluster rhenium chalcocyanides based on cluster anions $\{[Re_6Q_8](CN)_6\}^{4-}$ where Q=S, Se, Te was discovered. Several interesting compounds with intrigue compositions and structures were synthesized and characterized structurally. In much of them especially in the compounds containing large quantity of water molecules, for example, $(H_3O)_2Mn_3[Re_6Se_8(CN)_6]_2*23.5H_2O$, $(H_3O)_2Mn_3[Re_6Se_8(CN)_6]_2*14.5H_2O$, $Ba_2[Re_6Te_8(CN)_6]*12H_2O$, H-bonding is of crucial importance in stability and transformation of their structures. However, attempts to locate hydrogen atoms in such structures were unsuccessful.

We developed a new approach for this propose based on combination of X-ray data of heavy atom positions with 1Н solid state NMR as well as structure modelling. This allows us to determine hydrogen position in structure with accuracy typical for neutron diffraction method. We demonstrate here this approach on example of new cluster chalcocyanide hydrate $Ba_2Re_6Te_8(CN)_6*12H_2O$. The compound is crystallised with triclinic symmetry. In the structure barium atoms are co-ordinated by six water molecules bonded by two bridged water molecules in dimer $\{[Ba*5H_2O]_2\}^{4+}$; uncoordinated water is located in canals of structure which is running in [001] direction. A peculiarity of this structure implies that only half of protons is involved in H-bonding with characteristic distances about 2.78-2.86 A (O-H...O) and 2.92-3.13 A (O-H...N). The system of hydrogen bonds undergoes subsequent transformation with phase transitions at crystal heating. The approach developed seems very fruitful for complex crystalline hydrates.

This work was supported by Russian Foundation for Basic Research.

P09.06.023 TWO ASPECTS OF CHIRALITY IN ORGANIC CRYSTALS RESULTING FROM OPTICAL ACTIVITY. K. Stadnicka, Faculty of Chemistry, Jagiellonian University, Ingardena 3, 30-060 Kraków, Poland.

Following the rules derived from the inspection of simple inorganic ionic structures [1] a relation between structure and optical rotation for several organic crystals, for which both the absolute structure and the gyration tensor are known, is traced. The discussion will concentrate on such structures as those of dirubidium (+) tartrate - $P3_221$, ammonium Rochelle salt - $P2_12_12$, L-glutamic acid (β-form) - $P2_12_12_1$, D-mannitol - $P2_12_12_1$, and L(+)-tartaric acid - $P2_1$, all of which are built of chiral molecules and are able to display optical activity when dissolved. In the presented examples, according to our earlier conclusions [2], there is a need to distinguish (in an analogy to polar crystals and polar directions) two meanings of chirality: the chirality of a finite object (like molecules or crystals - in the sense of their shape and habit) - invariable under the point group symmetry of proper rotations, and the chirality of specified directions in the crystal structure related to helical intermolecular arrangements of polarizable atoms. This approach seems to be in agreement with the extended definition of chirality by Whyte [3]. A comment will be made on the contribution of a single molecule to the gyration tensor of a given crystal [4] and on mutual relation between the orientation of the gyration surface and the optical idicatrix when these orientations are not fixed by symmetry.

1. A.M. Glazer, K. Stadnicka, (1986). J. Appl. Cryst. 19, 108.
2. A.M. Glazer, K. Stadnicka, (1989). Acta. Cryst. A45, 234.
3. L.L. Whyte, (1958). Nature 182, 198.
4. R.W. Munn, (1994). J. Chem. Phys. 100, 6203.

P09.06.024 STRUCTURES AND SHORT HYDROGEN BONDS OF ACID SALTS OF GLUTACONIC ACID. S. Kashino [1], J. Taka [2], H. Ishida [1], [1]Department of Chemistry, Okayama University, Okayama 700-8530, Japan, [2]Institute for Protein Research, Osaka University, Suita 565-0871, Japan

Patterns of short O-H…O hydrogen bonds were studied for acid salts potassium hydrogen glutaconate monohydrate (1), sodium hydrogen glutaconate (2) and ammonium hydrogen glutaconate (3). Two O-H…O hydrogen bonds in (1) are centrosymmetric and short. The hydrogen bonds in (2) and (3) are non-symmetric. The second order phase transition was observed for (1) around 265 K by the difference scanning calorimetry, while the transition was not observed for (2) and (3) in the temperature range of 173 to 323 K. The distances of hydrogen bonds and those of coordination involving the water molecule in (1) were significantly shorter at 40 K than 295 K. No other structural change including that of the short hydrogen bonds was significant for (1) between the two temperatures. The difference electron density maps around the short hydrogen bonds in (1) suggested that the O-H…O hydrogen bonds have single-minimum potential wells.

P09.06.025 STRUCTURE OF 2'-CHLOROAZO-BENZENE - 2 - SULPHENYL BROMIDES. Karmakar [1], A. N. Talukdar [2], P. Barman and S. Bhattacharjee [3], [1] University Science Instrumentation Centre (USIC), Gauhati University, Guwahati - 781 014. India, [2] Department of Physics, Gauhati University, Guwahati - 781 014. India, [3] Department of Chemistry, Gauhati University, Guwahati - 781 014. India

The title compound belongs to the marcaptoazo group which has biological activities to some plant pathogenic fungi. The compound has been undertaken in order to study the effect of ionisation of the Br atom on the azo group and to investigate the intermolecular hydrogen bond of the molecule. The compound crystallises in orthorhombic space group P $2_12_12_1$ with a=7.421(6); b =15.763 (2); c = 21.018(5)Å; V= 2458.63Å^3; Z = 8; λ =1.5418 A; D_0 = 1.77 ; D_x =1.76 gm /cm3 ; m =7.95 mm-1 ; F(000) = 1296; T=293 K ; R = .0620 for 2411 observed reflections. The two phenyl rings make angles of 0.87^0 and 45.82^0 with the central five membered ring. The Br -ion and the N7 atom makes H- bonding with symmetrically related C - H atoms of the adjacent molecule. The Cl 3 atom is in the plane passing through the phenyl ring to which it is attached.

P09.06.026 HYDROGEN BONDING IN BIS(2-PYRIDYL)-PYRAZINE-DICARBOXYLIC ACIDS. H. Stoeckli-Evans, M. Alfonso & Y. Wang, Institut de Chimie, Université de Neuchâtel, Av. de Bellevaux 51, CH-2000 Neuchâtel, Switzerland.

The ligands, 2,5-bis(2-pyridyl)-pyrazine-3,6-dicarboxylic acid (**1**) and 2,3-bis(2-pyridyl)-pyrazine-5,6-dicarboxylic acid (**2**) have been synthesized to study the formation of coordination polymers with first row transition metals. They both exhibit considerable diversity in their coordination modes. A prominent characteristic of these compounds is their amphoteric property. They have been shown to exist as inner salt zwitterions and as different charged species.

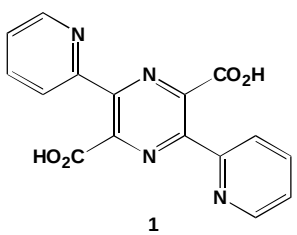

1

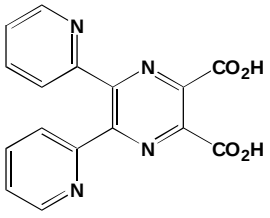

2

For compound **1** three forms have been isolated. The inner salt zwitterion, **1a**, a charged form **1b**, with both pyridine nitrogen atoms protonated, and, the neutral form, **1c**. For compound **2** three forms have also been prepared. The inner salt zwitterion **2a**, a charged form **2b**, with both pyridine nitrogen atoms protonated and one carboxylate group, and **2c,** a seconded charges species obtained as isomorphous ClO_4^- or PF_6^- salts.

The two inner salt zwitterions, **1a** and **2a**, both form hydrogen bonded polymers. **1a** is a double stranded cross-linked polymer while **2a** exhibits a channel type structure with hydrophobic walls and an hydrophyllic external base. The hydrogen bonding in all six compounds will be discussed.

P09.06.027 HYDROGEN BONDING IN THE STRUCTURE OF TRIS-(HYDROXY-DIMETHYLARSINE OXIDE) HYDROGEN TRI-IODIDE. *Y. Iimura, *K. Yamanaka and *M. Hoshino, *The Institute of Physical and Chemical Research (RIKEN), 2-1 Horosawa, Wako-shi, Saitama, 351-0198 Japan and *Nihon University College of Pharmacy, Funabashi, Chiba, Japan.

We have studied the photochemistry of dimethylarsine iodide $(CH_3)_2AsI$, in aerated toluene containing 4.4 X10^{-3}M water. The toluene solution was irradiated for 5 hrs. The photochemical product form $(CH_3)_2AsI$ was recrystallized from chloroform solutions.The photoproduct was found to have the molecular structure with a unique hydrogen bond.

The crystal and molecular structure of the product has been determined by single-crystal X-ray analysis(Enraf-Nonius CAD4,MoK,omega-scan)

Crystal Data: $C_6H_{22}As_3I_3O_6$, Orthorhombic, Pbcn, a=5.6046(5), b=21.936(1), c=17.1464(8)Å, V=2108.0(2)Å^3, Z=4, R=0.035, Rw=0.063.

Structure analysis confirmed the molecule is as follows.

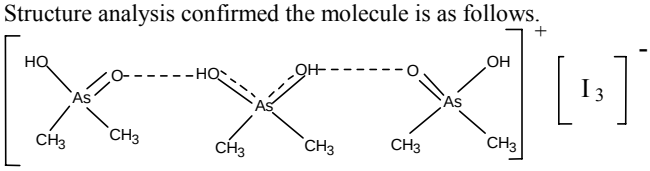

Intermolecular hydrogen bonds make a two dimensional network along a and c axis directions.

These result indicates that $(CH_3)_2AsI$ undergoes photodissociation of the As-I bond to yield $(CH_3)As$, which further reacts with oxygen and water resulting in the formation of $[(CH_3)_2AsO_2H]_3[HI_3]$.

P09.06.028 DISAPPEARING AND REAPPEARING POLYMORPHS J. Bernstein and A. Ellern, Department of Chemistry Ben-Gurion Universi-ty of the Negev, P.O. Box 653, Beer Sheva 84105, Israel, and J.-O. Henck, Institut für Pharmakognosie, Josef-Moeller-Haus, Universität Innsbruck Innrain 52, A-6020 Innsbruck, Austria

Polymorphism is a frequently observed phenomenon in molecular com-pounds. Since a particular polymorph may have desirable properties com-pared to its congeners, it may be required to develop a robust method to obtain that polymorphic modification consistently and reproducibly. Difficulties in obtaining crystals of a particular known modification or in re-producing results from another laboratory (or even one`s own) have had serious practical or economic consequences. We recently documented a number of representative cases in which it was difficult to obtain a given polymorphic form even though previously it had often been obtained routinely over long periods of time - so-called ‘disappearing poly-morphs’.[1] One of the

challenges to those dealing with the preparation of solids for any purpose is to be able to rationally develop the conditions to control the polymorphic form obtained - in many instances to recover a disappeared polymorph.

In the work reported here we employed methods of chemical and thermal microscopy along with thermal analysis to identify polymorphic forms and to provide guidelines for finding the conditions for the selective and controlled preparation of particular polymorphic forms of materials. The crystals so obtained were used to determine and compare the crystal structures of the various polymorphs.

1. J.D. Dunitz & J. Bernstein (1995) *Acc. Chem. Res*. 28, 193-200.

P09.06.029 PHARMACEUTICAL APPLICATION OF HIGH TEMPERATURE XRD UNDER CONTROLLED RELATIVE HUMIDITY Suneel Rastogi and Raj Suryanarayanan, College of Pharmacy, University of Minnesota, Minneapolis, MN 55455, U.S.A. Marek Zakrzewski, Philips Analytical X-Ray, Almelo, The Netherlands (present address: Rhone-Poulenc Rorer, Collegeville, PA 19426, U.S.A.).

Solid-state reactions and phase transitions induced during pharmaceutical processing and storage can profoundly influence the performance of dosage forms. The objective of this study was to investigate the effects of temperature *and* water vapor pressure on the kinetics of complex decomposition reactions in solid pharmaceuticals. Thermoanalytical techniques have been widely used for the investigation of these reactions. High temperature XRD under controlled relative humidity is an excellent compliment to thermoanalytical techniques and provides critical information about the reaction mechanism. The studies were carried out in a θ-θ powder X-Ray diffractometer (Philips X-Pert MPD system) with a position-sensitive detector (Raytech®). The instrument was equipped with a high temperature attachment (TTK, Anton Paar) which was specially modified so that in addition to maintaining the sample at the chosen temperature, the atmosphere above the sample could be maintained at the desired relative humidity. The decomposition of aminophylline monohydrate (**I**) was studied at several temperatures (in the range of 60 and 115°C) over a range of RH values (0 to 80%). Aminophylline monohydrate (**I**) decomposes to anhydrous theophylline (**III**) either directly or through an intermediate phase (anhydrous aminophylline, **II**). The XRD patterns revealed that the lines with d-spacings of 8.26, 7.82 and 7.02 Å were unique to **I**, **II** and **III** respectively. By measuring the integrated intensities of these lines, it was possible to simultaneously quantify the three phases during the entire reaction. In the absence of water vapor (i.e. at 0 % RH), all the reaction steps followed first-order kinetics. The activation energies for the three reaction steps were determined from Arrhenius plots. The next step was to study the influence of water vapor pressure on the reaction kinetics and mechanism. The desired water vapor pressure in the sample chamber was rapidly attained using a prototype humidity generator. In the presence of water vapor, the intermediate phase was not detected suggesting that a direct transition from **I** to **III** is the major decomposition pathway. Under isothermal conditions, an increase in water vapor pressure resulted in an overall increase in the reaction rate.

P09.06.030 DISORDERED STRUCTURE OF A MIXTURE OF THE N-O^{-} RADICAL AND THE N-OH DERIVATIVE OF 6,6-BIS-(p-TOLYL)-5,6-DIHYDRO-PHENANTHRIDIN-N-OXYL. F. Iwasaki, M. Suzuki, D. Hashizume and M. Yasui, Dept. of Applied Physics and Chemistry, The Univ. of Electro-Communications, Chofu, Tokyo 182-8585, Japan.

In the course of studies on the structures of organic radical crystals showing magnetic interactions, an unusually long radical N-O bond (1.334 Å; normal radical N-O bonds = 1.28~9 Å) and a short intermolecular O···O contact (2.769 Å) were observed in the crystals from the batch I of 6,6'-bis-(p-tolyl)-5,6-dihydrophenanthridin-N-oxyl. Significant positive peaks were observed on the O···O line in the D-maps. Then we tried the intensity measurement again using a crystal obtained from a new batch (II). In this case, a normal N-O distance (1.282 Å) and an O···O van der Waals contact (2.979 Å) were observed at 140K. No peaks were observed on the O···O line in the D-maps. Detailed examinations showed that dimensions of the crystal lattice were slightly different between I and II.

	T/K	a/Å	b/Å	c/Å	β/Þ	V/Å^3	meas.	obs.	R
I	293	10.976(2)	13.112(2)	14.142(2)	105.00(1)	1966.0(5)	4512	2118	0.050
	150	10.905(2)	12.942(2)	14.099(2)	104.97(1)	1922.3(4)			
	100	10.876(3)	12.875(3)	14.095(2)	104.89(2)	1907.5(8)	4377	2471	0.046
II	300	10.938(3)	13.130(3)	14.173(2)	104.25(2)	1972.9(7)			
	140	10.852(4)	13.089(3)	14.023(2)	104.63(2)	1927.3(7)	4407	3366	0.041

These facts suggests that the first crystals (I) are constructed by the mixture of N-O radicals and their deactivated substances. A disordered structure, which contained radical N-O and N-O-H bonds with occupancy factors of 0.5, was refined using data at 100K. After an assignment of the peak on the O···O line of the D-map to the H atom attached to the non-radical O atom, the structure converged to the R value of 0.046. In the crystals of I, disoreded intermolecular hydrogen-bonds, N-O-H···O-N and N-O···H-O-N are formed. The geometry of the hydrogen-bond is: 2.755, 1.06, 1.76 Å and 154° for O···O, O-H, H···O and O-H···O, respectively. The disordered form is considered to be crystallized from the solution with trace water or inadequate activation during the synthesis. It is very interesting that the structure of the pure radical crystals is isomorphous with that being constructed by the hydrogen-bonding.

P09.06.031 A STUDY OF THE N(H…H(B HYDROGEN BOND INCLUDING THE CRYSTAL STRUCTURE OF BORANE-AMINE, BH3NH3, BY NEUTRON DIFFRACTION. T.F. Koetzle and W. T. Klooster, Chemistry Department, Brookhaven National Laboratory, P.O. Box 5000, Upton, NY 11973-5000, USA, and P.E.M. Siegbahn, Department of Physics, Stockholm University, Box 7630, S-113 85 Stockholm, Sweden, and T.B. Richardson and R.H. Crabtree, Chemistry Department, Yale University, New Haven, CT 06520-8107, USA.

Borane-amines tend to have close H···H contacts as a result of the intermolecular interaction of the NH proton with the BH bond. The strength of this type of interaction, which is sometimes called a *dihydrogen bond*, has been suggested to be 4-6 kcal/mol - a value comparable to that for a classical hydrogen bond.

A CSD search provides characteristic metric data for the N-H···H-B interaction: The H-H distance is in the range 1.7-2.2 Å, and the N-H···H group tends to be linear (150°), while B···H-H tends to be bent (95°-115°). The structure of BH_3NH_3 reported in the literature seemed to be a singular exception in having bent N-H···H and linear B···H-H. Our neutron diffraction study of BH_3NH_3 now reveals the source of the problem: B and N have been interchanged in the published x-ray structure. With the correct assignment we obtain angles of N-H···H 156(3)° and B···H-H 106(1)° in the close (d_{HH} 2.02(3) Å) intermolecular N-H···H-B interaction, as expected.

This work was supported by the US DOE Office of Basic Energy Sciences, under contract DE-AC02-98CH10886, and by the US NSF.

P13.06.001 INCLUSION COMPOUNDS OF AN ACETYLENIC ALCOHOL HOST A.Jacobs, M.R.Caira, L.R.Nassimbeni, Department of Chemistry, University of Cape Town, Rondebosch 7701, South Africa

The inclusion behaviour of the host compound 1,1,6,6-tetraphenyl-hexa-2,4-diyne-1,6-diol was studied. Host-guest complexation was observed between the above host and the guests: carbon-tetrachloride, acetonitrile, pyridine and 3-picolene. The crystal structures of these inclusion compounds were elucidated using single crystal X-ray diffraction. Hydrogen bonding between the host and the guest was observed for those guests that had functional groups suitable for hydrogen bonding. ie. acetonitrile, pyridine and 3-picolene. Intermolecular hydrogen bonding between the hydroxy moieties of the host molecules was observed in the inclusion compound formed with carbon-tetrachloride. Thermogravimetric analysis (TGA) was used to determine the stoichiometry of the inclusion compounds. Thermal changes in the complexes were monitored using differential scanning calorimetry (DSC). Kinetics of desolvation of these compounds were studied and the activation energies were interpreted in terms of the host-guest packing.

P13.06.002 CHIRAL RECOGNITION AND CRYSTAL STRUCTURES OF DCA INCLUSION COMPOUND WITH LIMONENE. M.I. Mohamed Tahir and C.K. Prout, Chemical Crystallography Laboratory, 9 Parks Road, Oxford OX1 3PD,UK, S. Mahey and S.J. Heyes, Inorganic Chemistry Laboratory, South Parks Road, Oxford OX1 3QR,UK.

Chiral recognition of guests by host lattices of inclusion compounds is an important property and yet to be fully understood. Deoxycholic acid (DCA) as host studied, provides tunnels or channels which are chiral in the lattices. The channels are hydrophobic and resides between adjacent bilayers of DCA molecules connected through hydrogen bonding. Due to the hydrophobic nature of the channels most of the guests that have been studied are organic compounds.

The inclusion compounds of the 2:1 complex between DCA and R,S,RS-limonene (DCRLIM, DCSLIM, DCRSLIM) have been examined by CP/MAS ^{13}C NMR. At ambient temperature the NMR spectrum shows that each inclusion compound contains two DCA molecules in the asymmetric unit and that the spectrum of the DCRSLIM is the sum of the spectra DCRLIM and DCSLIM. This suggests that the DCRSLIM compounds consists of separate crystallites of DCSLIM and DCRLIM complexes. The VT CP/MAS ^{13}C NMR suggests a phase change above room temperature to a form with only one DCA molecule in the asymmetric unit.

We are examining the crystals structures of these compounds crystallographically. Preliminary results indicate the compounds to be monoclinic at ambient temperature similar to the low temperature form of DCA with d-camphor (DCRLIM: $P2_1$, a=7.27, b=13.82, c=26.63 Å, γ=90.10º, DCSLIM: $P2_1$, a=7.29, b=13.89, c=26.40 Å, γ=90.21º). However, for the limonene complex the unique axis is c whereas for d-camphor the unique axis is b.

P13.06.003 CONTROL OF MOLECULAR CAVITIES BY SIDE CHAIN LENGTH OF CHOLIC ACID M. Sugahara, K. Sada, and M. Miyata, Material and Life Science, Graduate School of Engineering, Osaka University, Yamadaoka, Suita, Osaka 565-0871, Japan.

Molecular design of organic crystalline materials that have nanocavities with controlled size, shape, chirality and chemical environment, is of great interest in organic solid state chemistry [1]. However, fine-tuning of nanocavities is in its infancy. For example, it is difficult to design relatively large cavities without changing 3D framework against chemical modification. We present here a novel strategy for controlling nanocavities due to different side chain length of cholic acid (CA). CA with one or two more methylene units is called homocholic acid or bishomocholic acid (BHCA), respectively.

Their inclusion crystals have been obtained by re-crystallisation from various organic compounds. It was found that BHCA included organic compounds, such as naphthalene derivatives, with a 1:1 molar ratio. X-ray diffraction studies made clear that BHCA forms a similar bilayered structure [2] to CA, indicating that both the hosts form the robust motif. Detailed comparison indicates that BHCA with 1-methylnaphthalene forms larger interlayered channels than CA with benzene. Such a difference might be explained by similar conformations of the side chains. The terminal carboxy groups have similar direction, and the substantial length of the chains are different.

1. K. Sada, N. Shiomi, and M. Miyata (1998). *J. Am. Chem. Soc*., **120**, 10543.
2. M. Miyata and K. Sada (1996). in *Comprehensive Supramolecular Chemistry*, edited by J. M. Lehn (Pergamon, Oxford), Vol. 6, 147.

P13.06.004 SYNTHESIS AND CRYSTAL STRUCTURE OF SODIUM 1,1,1-TRIMETHYLOLPROPANE BORATE TRIHYDRATE. I.Zviedre and J.Schwartz, Institute of Inorganic Chemistry of the Riga Technical University, Riga, Latvia, and V.Belsky, L.Karpov Institute of Physical Chemistry, Moscow, 103064, Russia.

In the interaction of boric acid with polyhydroxy compounds the spiran-tipe 1:2 and 1:1 complexes containing bidentatic ligands are formed. When ligand possess more than two hydroxyl groups, the possibility to form the cage complexes containing tridentatic ligand appears. The latter complexes are synthesized from cyclitols, e.g. from scyllo-inositol, and the crystal structure of $Na_2(C_6H_8B_2O_8)\cdot 10H_2O$ has been determined [1]. Boric acid with β,β^1- triols can form complexes containing bidentatically as well as tridentatically coordinated ligands. Data on the structure of the tridentatic cage complexes 1:1 are indirect. The monocrystals of $Na[C_2H_5C(CH_2O)_3BOH]\cdot 3H_2O$ were obtained using the modified synthesis method [2].

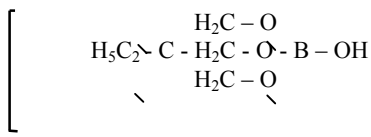

In the complex anion (Fig.) the boron atom is bonded to ligand via three O atoms, (the B-O bond lengths being 1.475 ÷ 1.501Å) and to OH (1.401 Å). The O-C distances are of 1.407 ÷ 1.414 Å. Four O-B-O bond angles are of 108.2^0 in average, the two other (exocyclic) are 112.8^0 and 113.4^0; angles C-O-B and C-C-C amounting to 110.9^0 and 106.7^0 in average, respectively. Three six-membered heterocycles -C-C$^{/}$-C-O-B-O- are inflected along the C$^{/}$-B axis with which they are mutually conjugated. Each Na^+ ion is octahedrally coordinated with O atoms of five water molecules (Na...O distances 2.318 ÷ 2.513 Å) and one hydroxyl group (2.365 Å). In the crystals the anions form with NaO_6 octahedra bilayer parallel to the *ab* plane. Lattice parameters: a=6.9310(10) Å; b=6.2680(10) Å; c=27.053(5) Å; β=93.37(3)°, V=1173.2(3) Å^3; Z=4; ρ_c=1.336 g/cm^3; sp.gr. $P2_1/c$; R=0.0527; R_w=0.1198.

1. C.T.Grainger (1981). Acta Cryst. B37, 563-568.
2. A.Terauda,J.Schwartz, A.Ievins(1973). Zh.Org. Khim. (Russia) XLIII, 2277.

P13.06.005 PHASE TRANSITIONS IN THE THIOUREA CYCLOOCTANE INCLUSION COMPOUND. T. Maris, M.J. Henson and C.K. Prout, Chemical Crystallography Laboratory, 9 Parks Road, Oxford, OX1 3PD, UK, and S.J. Heyes, Inorganic Chemistry Laboratory, South Parks Road, Oxford, OX1 3QR, UK.

Thiourea is known to form inclusion compounds with a host lattice made of channels with an approximate diameter of 6.1 Å. These channels can accommodate large guest molecules such as long branched hydrocarbons and cycloalkanes. In general, the room temperature crystal structure of the adducts is rhombohedral and the guest molecule is usually found in a substantially disordered state.

Variable temperature single X-ray experiments have been performed on the thiourea cyclooctane adduct and show three different phases. In addition to the classical rhombohedral room temperature form and the monoclinic low temperature phase, which usually exists in several cycloalkanes-thiourea clathrate, a supplementary monoclinic phase having a doubled b axis can be observed at lower temperature.

A single X-ray crystallographic characterisation has been performed for each of these three phases. As expected in the rhombohedral room temperature form (a = 16.223(2) Å, c = 12.493(4) Å), the cyclooctane guest molecule is highly disordered. In the intermediate monoclinic phase, (T = 210 K, $P2_1/c$, a = 12.468(4), b = 15.551(7) Å, c = 10.397(3) Å, β = 114.01(2)°) the cyclooctane seems to be disordered between two main conformations. In the lower temperature phase (T = 150 K, $P2_1/c$, a = 12.416(1), b = 30.918(2) Å, c = 10.371(1) Å, β = 113.85(1)°), the structure shows two cyclooctane rings having the same conformation but different orientations within the channels. These results are completed by solid state NMR experiment for probing the conformational dynamics of the guest molecules.

P13.06.006 GUEST-DEPENDENT VERSATILITY IN CRYSTALS OF A BULKY, CYCLOPROPANE-BASED DICARBOXYLIC ACID HOST Petra Bombicz[a], Ingeborg Csöregh[b], Mátyás Czugler[a], Alajos Kálmán[a]. [a]Institute of Chemistry, Chemical Research Center, Hungarian Academy of Sciences, Budapest POB 17, H-1525 Hungary. [b]Structural Chemistry, Stockholm University, S-106 91 Stockholm, Sweden

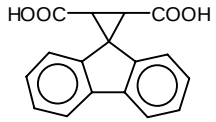

H

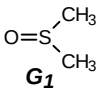

G1

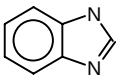

G2

H : G1 = 1 : 2

H : G2 = 1 : 1

Wide variation of the host-host and host-guest interactions depending on the guest character has been observed in the crystalline heteromolecular complexes to be presented. Bulky cyclopropane-based hosts (*cf.* scheme) proved to be efficient in inclusion formation with aprotic and polar guests. The recognition of the DMSO guest (***G1***) involves strong *(CO)O-H...O=S* bonds and *(-CH2)-H...O=C* type interactions. One of the solvent molecules is enclathrated in a cage formed by four host molecules (***H***) *via C-H...π* interactions, while the other one is in a separate layer and shows partial disorder. Following the dissolution of the ***H:G1*** clathrate crystals in a benzimidazole containing ethanol solution, the benzimidazole guest (***G2***) has displaced the DMSO molecules, thus forming ***H:G2*** co-crystals with fundamentally altered host-host and host-guest interactions, hence with completely different packing arrangement. The host forms an infinite chain *via* strong *O-H...O* interactions of the carboxyl groups perpendicular to the fluorenes' plane. Fluorene and benzimidazole aromatic rings are parallel and have *π...π* intermolecular interactions. In the host molecule the rigidly maintained, ideal bisecting conformation of the aromatic moiety with the cyclopropyl ring makes electronic effects possible. This leads to lengthened vicinal bonds and to a shortened distal bond in the cyclopropane moiety. This bisecting conformation is also stabilised by an intramolecular *C-H...O* interaction.

P13.06.007 ORGANOALKALI METAL COMPLEXES FOR ORGANIC SYNTHESIS P. Williard, P. Williard, C. Sun, M. Jacobson, D. Walther, Department of Chemistry, Brown University, Providence, Rhode Island, 02912 USA & Department of Pure and Applied Chemistry, 295 Cathedral Street, Strathclyde University, Glasgow G1 1XL, United Kingdom

Several examples of organo alkali metal complexes containing different alkali metal cations, e.g. Li, Na and/or K, and some extremely widely used carbanions such as enolate anions and amide bases will be presented. Complexes of n-butyl lithium, the most commonly utilized alkyl lithium reagent throughout the world, with chiral amide ligands will be presented. We will describe the structures of some new complexes of amide bases and carbanions that are used in enantioselective reactions. An overall scheme which incorporates this aggregated structures into a reaction pathway will be presented. Some solution phase NMR data will serve to correlate the solid state structures with the corresponding species that exist in solution.

P13.06.008 CONTROL OF THE CRYSTALLINE-STATE PHOTORACEMIZATION BY FORMING THE HOST-GUEST COMPLEXES A. Sekine, N. Sugimoto, H. Aoki, T. Suzuki, H. Uekusa, Y. Ohashi, Department of Chemistry, Tokyo Institute of Technology, Tokyo 152-8551, Japan

It has found that the chiral 1-cyanoethyl group in cobaloxime complexes is racemized on the exposure to visible light with reteintion of the single crystal form. A serises of the cobaloxime complexes have been examined so far.

In order to control the reactivity we tried to make the host-guest complex using the chiral 1-cyanoethyl cobaloxmie crystals as a guest. The two host-guest crystals were obtained using dicyclohexylamine(1) and cyclohexylheptylamine(2) as host molecules. The chiral 1-cyanoethyl groups in the two host-guest complexes as well as the pure guest complex(3) were racemized with retaining the single crystal form on exposure to a xenon lamp. The crystal structures were analysed before and after the irradiation. The racemization rates of the crystals were estimated from the change of the HPLC peaks. The rate constants obtained assuming first-order kinetics are significantly different from each other. The analyzed structures indicate that the different reaction rates have a quantitative correlation with the volumes of the reaction cavities for the 1-cyanoethyl groups in the crystals. The reaction rate can be controlled by the host-guest complexes and/or changing the host molecules.

P13.06.009 SELECTIVE COMPLEXATION OF CEPHALOSPORIN ANTIBIOTICS R. de Gelder, G.J. Kemperman, F.J. Dommerholt, A.J.H. Klunder, B. Zwanenburg [1] [1] NSR Centre for Molecular Structure, Design and Synthesis, University of Nijmegen, Toernooiveld, 6525 ED Nijmegen, The Netherlands

The Cephalosporin derivatives Cephalexin, Cephradine, Cefaclor and Cefadroxil are widely used life-saving antibiotics. Isolation and purification of these compounds by means of selective complexation, e.g. using beta-naphtol [1], is a powerful

method, however, despite its industrial relevance, the mechanism and the structural details of the resulting complexes are unknown.

We have studied the complexation behaviour of the cephalosporins for a large variety of naphthalene derivatives and investigated the structures using X-ray diffraction. The complexes formed appeared to be inclusion compounds of the clathrate type in which the antibiotic molecules form a host lattice and the complexing agents play the role of guest.

A remarkable isomorphism is found for three of the cephalosporins. The different behaviour and selectivity of the fourth one, Cefadroxil, is explained on the basis of the crystal structures of the complexes.

1. U.S. Patent no. 4003896 (NOVO Nordisk), 1992.

P13.06.010 INCLUSION COMPOUNDS BETWEEN APOCHO-LIC ACID AND POLYETHERS. K. Suehiro, R. Kishikawa, K. Matsushita, and M. Kuramori, Department of Chemistry and Applied Chemistry, Faculty of Science and Engineering, Saga University, Saga 840-8502, Japan

A large number of inclusion compounds of deoxycholic acid (DCA), apocholic acid (ACA), and cholic acid (CA) with small organic molecules have been prepared and characterized [1-3]. Unlike DCA, CA does not form inclusion compounds with polyethers. In the present study, the preparation of inclusion complexes of ACA with aliphatic polyethers was examined.

ACA was prepared by dehydration of CA in the presence of ZnCl2 in acetone solution. Complexation was attempted by slow evaporation of solvent from ethanolic solutions of ACA and polyethers.

Crystalline inclusion compounds were obtained for polyethers such as poly(propylene glycol), polytetrahydrofuran, poly(ethylene glycol) mono-stearate. These crystals belong to the orthorhombic space group $P212121$. The cell dimensions are: a = 25.15, b = 13.95, c = 7.42; a = 25.00, b = 13.78, c = 7.49 Å for the poly(propylene glycol) and polytetrahydrofuran complexes, respectively. Four ACA molecules are contained in the unit cell and two polymer chains pass through it in parallel with the c axis. The structure of these crystals is analogous to that of the orthorhombic inclusion compounds of DCA [2, 4].

ACA crystal that contains no guest molecules is also orthorhombic and has the same space group. The cell dimensions determined from powder X-ray diffraction patterns are: a = 21.97, b = 14.21, and c = 7.54 Å . The a axis is approximately 12% shorter than that of the inclusion crystals, due to the absence of the guest molecules, whereas the b and c axes are only a few percent longer. The ACA molecules are thought to form a bilayer; however no channels were observed.

1. W. C. Herndon, *J. Chem. Educ*., **44**, 724 (1967).
2. E. Giglio, *Inclusion Compounds*, Vol. 2, ed. J. L. Atwood et al., Academic, London, 1984, Ch. 7, pp. 207-229.
3. M. Miyata et al., *Chem Lett*., 605 (1987).
4. K. Suehiro and M. Kuramori, *J. Macromol. Sci.-Phys*., **B33**, 1 (1994).

P13.06.011 POLYMORPHISM IN CLATHRATE STRUCTURES. T.H. Brehmer, W. Seichter, S. Nitsche, T. Hens & E. Weber, Organic Chemistry, TU Freiberg, D-09596 Freiberg, Germany and F.H. Cano, Crystalografía, Rocasolano (CSIC), E-28006 Madrid, Spain.

It is a well known fact that the solvent of crystallization may determine the packing arrangement in crystal structures and lead to polymorphism. In particular this is true in inclusion crystals, where host molecules are capable to change their conformation or association mode to fit a guest compound into the host lattice. Host molecule **1** based on the characteristic 9,10-diethy-nylanthracene[1] subunit and appended 9-fluorenol clathratogenic groups has been synthesized and studied with regard to their crystalline inclusions involving acetone, DMSO and N,N´-DMF as guest molecules. All three crystal structures show a host guest ratio of 1:2 and crystallize with two molecules per asymmetric unit. However the conformation of **1** differs and thus also the crystallographic symmetry. This change is caused by the different solvent polarities, while the molecular geometry of the guests is rather similar. In the monoclinic clathrate structure **1**•acetone [$P2_1/c$; a=8.475(3), b=8.237(3), c=27.974(3)Å, β=90.746(3)°; V=1952.7(1)Å^3] the terminal 9-fluorenol groups point at opposite directions making the host molecule to adopt an *anti*-conformation with a centre of symmetry in the anthracene unit. On the other hand, the host molecule shows an identical *syn*-conformation, in the two triclinic clathrate structures, **1**•DMSO [P-1; a=15.4476(9), b=11.6576(6), c=11.2357(6) Å, α=105.702(4), β=82.360(4), γ=98.378(5)°; V=1917.7(2) Å3] and **1**•DMF [P-1; a=15.9748(2), b=11.5648(3), c=11.1881(2) Å, α=105.67(2), β=85.04(3), γ=97.00(4)°; V=1972.19(3) Å^3]. The two triclinic structures are isostructural, including the same type of dimer motif between two guest molecules [graph set $R_2^2(8)$] linking two host molecules by means of O-H...O hydrogen bonding. The structures will be discussed in terms of conformation-polymorphism, pseudo-polymorphism and guest-dependent polymorphism.

1. P.P. Korkas, E. Weber, M. Czugler, G. Naray-Szabo (1995) J. Chem. Soc., Chem. Commun., 2229.

P13.06.013 CRYSTAL STRUCTURE OF FURAN CLATHRATE HYDRATE FROM NEUTRON POWDER DIFFRACTION DATA. T. H. Plumridge and R. D. Waigh, Department of Pharmaceutical Sciences, University of Strathclyde, Glasgow G4 0NR, UK, G. Steele, Astra Charnwood, Bakewell Rd, Loughborough LE11 5RH, UK, and K. S. Knight, ISIS Facility, CLRC Rutherford Appleton Laboratory, Chilton, Didcot, Oxon, OX11 0QX, UK.

Hydrate inclusion compounds are solid crystalline complexes in which various types of guest molecule are accommodated inside regular cage structures formed by hydrogen-bonded water molecules. Clathrate hydrates are the simplest of these, and although these compounds were first prepared in the 1950s, only a handful of crystal structures have ever been investigated[e.g.1,2]. Here we report a structural investigation of furan clathrate hydrate. The hydrate was prepared by mixing deuterated furan and deuterated water in a ratio (C_4D_4O .17D_2O) corresponding to the stoichiometry of a previous crystallographic study of tetrahydrofuran clathrate[2] and cooling to 6.9^{O}C. DSC scans of the resulting crystals showed the sample to contain some, but not much, ice Because of the extensive hydrogen-bonding in clathrate systems, neutron diffraction is the preferred method for structural analysis. The structure of the furan clathrate at 4.2, 100, and 200K was refined using data collected from a deuterated sample on HRPD, the high resolution powder diffractometer at the *ISIS* facility of the Rutherford Appleton Laboratory, and is presented here.

1. O. Yamamuro, T. Matsuo, H. Suga, W. I. F. David, R. M. Ibberson, A. J. Leadbetter (1995) Physica B 213&214, 405
2. T.C.W. Mak and R. K. McMullan (1965) J.Chem.Phys. 42, 2732.

P13.06.014 INTERACTIONS GUEST-HOST AND HOST-GUEST IN SELECTED ORGANIC ZEOLITE NETWORKS. J.Pielaszek(1), A.Yu.Manakov(2) and J.Lipkowski(1), (1)-Institute of Physical Chemistry, Polish Academy of Sciences, Warszawa, Poland, (2)-Institute of Inorganic Chemistry, Siberian Branch of Russian Academy of Sciences, Novosibirsk, Russia.

Analysis of changes in the structure of host lattice of eleven β-[$Ni(NCS)_2$(4- methylpyridine)$_4$] clathrates (known to have the organic zeolite type structure) on inclusion of different guest molecules was performed.

In-situ XRD patterns were recorded for a series of the clathrates subjected to saturation by different guest molecules at different temperatures: 150, 175, 200 and 300 K. The patterns were interpreted in terms of clathrate lattice expansion-contraction on absorption-desorption of the guest component. EENY [1] program was used for calculations of the intermolecular energy (the Empirical Force Field approach) and CRYSRULER [2] and XP [3] for calculations of the bond angles, torsion angles, interatomic distances and for the analysis of the molecular structures whereas an original algorithm was used for calculations of volume and linear sizes of the „free space" within a clathrate lattice.

Generalization of the obtained data allowed to put forward a model of the changes of the host-host interactions in the studied compounds as a function of the amount of absorbed guest.

1. S.Motherwell: EENY June 1974, Potential Energy Program, University Chemical Laboratory, Cambridge (UK),
2. C.Rizzoli, V.Sangermano, D.Calestani & G.D.Andretti: CRYSRULER, ver.2.0, Universita Degli Studi di Parma (1989),
3. G.M.Sheldrick: SHELXTL PC ver. 4.1., Siemens Analytical X-Ray Instruments, Inc., Madisom Wisc. (USA).

P13.06.015 INCLUSION COMPOUNDS OF ALKALINE-EARTH METAL O,O'-DIBENZOYL TARTRATES. Luigi R Nassimbeni, Hong Su, Department of Chemistry, University of Cape Town, Rondebosch 7701, South Africa

Mg, Ca and Sr salts of (2R,3R)-(-)-O,O'-dibenzoyltartaric acid with methoxyethanol, ethanol and water have been synthesized and characterized by X-ray, thermal and spectroscopic methods: 1: Mg . DBT . ME. E. 3H2O 2: Ca . DBT . 2(ME) . H2O ME = Methoxyethanol; E = Ethanol 3: Sr . DBT . 2(ME) . H2O The crystal structures of the three compounds have been elucidated and their thermal stabilities have been measured using Thermal Gravimetry (TG) and Differential Scanning Calorimetry (DSC). In particular, compound 2 exhibits two distinct mass loss steps (TG) the first of which is endothermic and the second is exothermic (DSC). In order to fully characterize the thermal decomposition of this compound we caried out Evolved Gas Analysis (EGA). The IR spectra recorded during the mass loss steps identified methoxyethanol as the first compound to desolvate, followed by carbon dioxide in the second step.

P13.06.016 ALKALI METAL ION RECOGNITION BY FLUORESCENT SIGNALLING CROWN ETHERS. J.F. Malone, A.P. de Silva, D.G. MacKerracher and T.S. Moody, School of Chemistry, The Queen's University of Belfast, Belfast BT9 5AG, Northern Ireland, UK.

Complex life processes often depend on a few simple cations, *e.g.* protons in bioenergetics, sodium and potassium in membrane potential generation and calcium ions in intracellular signalling. Therefore the development of cation sensors is important for pure biological studies and finds wide application in the medical and biotechnological fields. The field of fluorescent sensors has developed to the point where a range of inorganic cations can be targeted successfully [1].

Many Group I and II metal sensors and switches rely on photo-induced electron transfer (PET) for sensing purposes, *e.g.* by the 'off-on' switching of fluorescence. N-(9-anthryl-methyl)monoaza-18-crown-6 and the 15-crown-5 analogue are very weakly fluorescent in methanol solution in the presence of proton scavengers. Addition of sodium or potassium, but not lithium, ions results in an enhancement of the fluorescence. The anthracene fluorescence, which is quenched by PET from the lone pair of the nitrogen in the metal free receptor, is recovered upon encapsulation of Na^+/K^+ into the monoaza crown ether, with flourescence enhancement (FE) of up to 47 [2].

A number of crystal structures of both metal-free and metal-bound azacrowns have been determined. Structures presented will include metal free N-(9-anthryl-methyl)diethanolamine, N-(9-anthryl-methyl)monoaza-15-crown-5 and N-(9-anthryl-methyl)monoaza-18-crown-6, and the same azacrowns bound to metal ions.

1. B. Valeur, E. Bardez (1995), *Chem. Brit.,* **31,** 216.
2. A.P. de Silva, H.Q.N Gunaratne, T. Gunnlaugsson, A.J.M Huxley, C.P. McCoy, J.T. Rademacher, T.E. Rice (1997), *Chem. Rev.,* **97,** 1515.

07. CRYSTALLOGRAPHY OF ORGANOMETALLIC, CO-ORDINATION, MAIN GROUP COMPOUNDS

P06.07.001 STRUCTURAL CHARACTERIZATION OF SYNTHETIC Mo-COFACTOR OF SULFITE OXIDASE. Nirmalya Prasun Nayak & Alok Kumar Mukherjee, Department of Physics, Jadavpur University, Calcutta 700 032, INDIA.

X-ray crystallographic study of coordination of the Mo-cofactor (MoCo) in chicken liver sulfite oxidase provides vital informations regarding the early failures to isolate pure Moco from its apoprotien and to synthesize a structural analogue of Moco. During our study on synthetic analogues of Mo-Cofactor oxidised sulfite oxidase we have isolated $[Bu_4N]_2[\{Mo^VO(S_2$-dithiolene) $(SPh)\}_2\mu(O)]$ **(1)** and its bromo analogue $[Bu_4N]_2[\{Mo^VO(S_2$-dithiolene) $(Br)\}_2\mu(O)]$ **(2)**. X-structure determinations of **(1)** and **(2)** revealed that the anions contained a linear Mo - O- Mo bridging unit with crystallographically imposed center of symmetry and the terminal oxo-group being Trans to each other. The bridging oxygen atom was located at the inversion center and the asymmetric units of **(1)** and **(2)** comprised of half of the anions and one $[Bu_4N]^+$ cation respectively . Each crystallographic independent Mo atom in **(1)** and **(2)** is penta coordinated in a distorted square pyramidal arrangement with the terminal oxo-group occupying the axial positions. In **(1)** the equatorial positions were occupied by two dithiolene sulfurs, one thiolate sulfur and one oxo bridged ligation while in **(2)** thiolate sulfur being replaced by a Bromine atom. The structural features of both the complexes are identical to the reported structure of Moco of native sulfite oxidase in respect to Mo coordinate sphere. The final crystallographic R-values for complex (1) and (2) were 0.0538 and 0.0578 respectively.

P06.07.002 LANTHANIDE COMPLEXES OF CARBOXYETHYL DOTA – DISPARITY BETWEEN STRUCTURE IN SOLID AND SOLUTION. Janet M. Moloney, Mark Woods, Judith A.K. Howard and David Parker. Department of Chemistry, University of Durham, Durham, DH1 3LE, U.K.

The co-ordination chemistry of the lanthanide ions with octadentate ligands derived from 1,4,7,10-tetraazacyclododecane has been documented comprehensively. The archetypal ligand for lanthanide elements, 'dota', forms kinetically robust complexes *in vivo*, and when tetra-*N*-substituted with phosphinate or carboxamide yields complexes with applications in MRI and targeted radiotherapy.

This poster will report on the structures of a new series of lanthanide complexes of 'dota' derivatives, namely the tetra(carboxyethyl) derivatives. In these complexes, there are two independent elements of chirality defined by the N-C-C-N and N-C-C-O torsion angles. The predominant isomer in solution epimerises and the minor isomer crystallises preferentially. The structures of the europium [1], gadolinium and terbium complexes exhibit remarkable structural similarity binding to the faces of a square antiprism and binding one additional water molecule whereas preliminary results suggest that the smaller ytterbium complex remains eight co-ordinate.

J.A.K. Howard, A.M. Kenwright, J.M. Moloney, D. Parker, M. Port, M. Navet, O. Rousseau and M. Woods. *J. Chem. Soc. Chem. Commun.,* 1998, 1381.

P06.07.003 SYNTHESIS AND CRYSTAL STRUCTURE OF Ni(II) COMPLEX WITH TRITHIOCYANURIC ACID. Z. Trávníček and P. Kopel, Dept. of Inorganic and Physical Chemistry, Palacký University, 771 47 Olomouc, CZ, and J. Marek, X-Ray Laboratory of Dept. of Inorganic Chemistry & Laboratory of Biomolecular Structure and Dynamics, Masaryk University, 611 37 Brno, CZ.

We are engaged in the synthesis and structures of nickel(II) complexes with trithiocyanuric acid and various nitrogen-donor ligands [1,2]. The [Ni(ttcH)(pmdien)] complex has been isolated in form of green crystals *via* reaction of $NiCl_2.6H_2O$ and *pmdien* (N,N,N′,N′,N″ -pentamethyldiethylene-triamine) in ethanol with water solution of *ttcNa*$_3$ (trisodium salt of trithiocyanuric acid) and 0.1M HCl. The structure was determined by X-ray diffraction and it was found that nickel atom is five coordinated in distorted trigonal bipyramidal arrangement. X-ray structural parameters we want to confront with quantum chemistry *semi-empirical* and *ab initio* calculations.

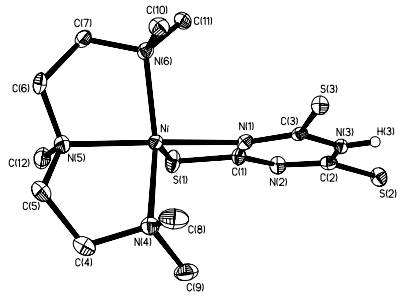

Crystal data and structure refinement: $C_{12}H_{24}N_6NiS_3$, monoclinic crystal system, $P2_1/n$, a = 12.496(7) Å, b = 9.226(2) Å, c = 16.385(4) Å, β = 111.46(4)°, V = 1758.0(11) Å^3, Z = 4, M_r = 407.26, T = 150 K, d_x = 1.539 g/cm^3, λ = 0.71073 Å, μ = 1.464 mm^{-1}, *F(000)* = 856, reflection collected / unique 3115 / 2974, [R(int) = 0.0401], R indices [I > 2σ(I)], *R1* = 0.0526, *wR2* = 0.1518, and the largest diff. peak and hole 1.230 e.Å^{-3} [0.99 Å from Ni] and –0.790 e.Å^{-3} [1.01 Ĺ from S1].

We thank the Grant Agency of the Czech Republic (203/98/P220) and MŠMT (VS 96095) for financial support.

P. Kopel, Z. Trávníček, R. Panchártková, Z. Šindelář & J. Marek (1998). *J. Coord. Chem*. 44, 205.
P. Kopel, Trávníček, R. Panchártková, M. Biler & J. Marek (1998). *Transition Met. Chem*, in press.

P06.07.004 STRUCTURAL DETAILS OF MAMMALIAN BONE MINERAL REVEALED BY RIETVELD ANALYSIS. P. Zioupos and K.D.Rogers, Department of Materials & Medical Sciences, Cranfield University, Shrivenham, Swindon, Wiltshire SN6 8LA, U.K.

Bone is a composite, multifunctional material that possesses both chemical and mechanical properties that are critically dependent upon its mineral component structure. However, the minerals' natural form (e.g. its small crystallite size, non-stoichiometry and inhomogeneity) has continued to provide difficulties for crystallographic, diffraction interpretation.

Using a combination of laboratory and synchrotron powder X-ray diffraction, we have applied Rietveld analysis to data produced from specimens of human femur, bovine femur, tympanic bulla of a blue whale and the rostrum of Mesoplodon densirostris. This particular species of whale has been shown previously to possess the greatest density of bone available in

nature and we have utilised it to model the effects of hypermineralisation. The mineral has been examined in situ and in a homogenised form. Microstructural features such as preferred orientation and average crystallite morphology have been determined. Rietveld analysis has also enabled us compare distortions in the atomic structures due to heteroionic substitutions such as carbonate. The findings are further supported by FTIR characterisation.

We have found that the rostrum is an extreme biological mineral, both in terms of its crystallite morphology and texture. Further, we believe that we have identified 2 populations of rostrum crystallites which may be distinguished by their degree of texture and heteroionic substitution. In contrast, the mineral of the bulla and femur, possess significantly lower degrees of preferred orientation and smaller crystallites. Optical microscopy of the rostrum also revealed signs of accelerated 'ageing' and an extensive degree of secondary remodelling with compacted osteons of a very atypical unidirectional nature.

P06.07.005 DIFFERENT CRYSTAL STRUCTURES OF THE Ln(DOTA) COMPLEXES. G. Bombieri, Istituto di Chimica Farmaceutica, Università di Milano, I and F. Benetollo, ICTIMA - CNR, Padova, I and S. Aime and M. Botta, Dipartimento di Chimica, Università di Torino, I and L. Calabi, Bracco Spa, Milano, I.

Ln(III) complexes with the octadentate ligand DOTA (H_4DOTA = 1,4,7,10 tetraazacyclododecane-N,N',N'',N'''-tetraacetic acid) are having a great deal of interest in view of their use in diagnostic techniques. An isostructural series of complexes $Na[M(DOTA)(H_2O)]\cdot 4H_2O$ (M= Y^1, $Eu^{2a,b}$ Gd^3, Ho^{2b} and Lu^4) is known, as well a new polymeric structure $Na[La(DOTA)La(HDOTA)]\cdot 10H_2O$[5]. Continuing our investigations we have obtained crystals of Ce, Pr, Nd, Dy and Tm of formula $Na[Ce(DOTA)(H_2O)]NaHCO_3\cdot 7H_2O$, $Na[Ln(DOTA).(H_2O)]\cdot 4H_2O$ (Ln = Pr, Nd), $Na[Dy(DOTA)(H_2O)]NaOH\cdot 7H_2O$ and $K[Tm(DOTA)]\cdot 6H_2O$ respectively. The structural results will be presented and discussed in the context of the different isomeric forms found in solution.

1) Parker, D.; Pulukkody, K.; Smith, F.C.; Batsanov, A.; Howard, J.A.K. *J. Chem. Soc., Dalton Trans*. 1994, 689.
2) (a) Spirlet, M.R.; Rebizant, J.; Desreux, J.F.; Loncin, M. F. *Inorg. Chem.* 1984, *23*, 359. (b) Benetollo. F.; Bombieri. G.; Aime. S.; Botta, M. *Acta Cryst. C*. 1999, (in the press).
3) (a) Dubost, J.P.; Leger, M.; Langlois, M.I.; Meyer, D.; Schaefer, M.C.R. *Sci. Paris Ser*. 2 1991, *312*, 349. (b) Chang, C. A.; Francesconi, I.C.; Malley, M.F.; Kumar, K.; Gougoutas, J.Z.; Tweedle, M.F.; Lee, D.W.; Wilson, L. *Inorg. Chem*. 1993, *32*, 3501.
4) Aime, S.; Barge, A.; Botta, M.; Fasano, M.; Ayala, J.D.; Bombieri, G. *Inorg. Chim. Acta* 1996, *246*, 423.
5) Aime, S.; Barge, A.; Benetollo, F.; Bombieri, G.; Botta, M. and Uggeri F.; *Inorg. Chem* 1997, *36*, 4287.

P07.07.001 CRYSTALLOCHEMICAL INVESTIGATION OF THE COORDINATION COMPOUND OF SCHIFF-BASE WITH CHROMIUM(III) CHLORIDE. G.Y.S.K. Swamy and K. Ravikumar, Laboratory of Crystallography, Indian Institute of Chemical Technology, Hyderabad 500 007, INDIA.

This communication discusses the problem into two ways.

1). Synthesis and structure elucidation of the title molecule through X-ray single crystal method.

2). Further confirmation of the structure through other spectroscopic techniques like UV, IR etc.

The complex crystallizes in the space group $P2_1/n$, with cell parameters a=10.017(2)Å, b=25.136(4)Å, c=10.582(2)Å , β=115.4(2)°, Z=4 and Mr=2055.8. The structure has been solved by patterson and subsequent Fourier synthesis led to an R = 0.045. The structure consists of discrete [bis(N-salicylidene-N'-(2-hydroxyethyl) ethylenediamine)Cr(III)] units together with uncoordinated chloride ions. The asymmetric unit contains two crystallographically independent but geometrically similar SalNEdien molecules attached together to the Cr(III) ion. The Cr atom has six nearest neighbors and the coordinate geometry may be described as slightly distorted octahedron. The two tridentate SalNEdien ligands forming almost perpendicular planes at the metal atom (a dihedral angle of 93.4°). The five membered ring equires envelope conformation with asymmetric parameter ΔCs[C9]=8.98° in one molecule, while in another molecule it has half-chair conformation with asymmetric parameter ΔC2[Cr,N1]=8.88°. The uncoordinated chloride ion is involved in an intra and intermolecular hydrogen bonding. In this attempt, it is forming pseudo five membered rings. Additional features of the structure will be presented.

P07.07.002 CRYSTAL AND MOLECULAR STRUCTURE DETERMINATION OF THE BIS(4-METHYL-1-PIPERAZINEGLYOXIMATO) DI PYRIDINATO COBALT(III). CHLORO DINITRATE THREE HYDRATE. S. Öztürk, Department of Physics, Faculty of Arts and Sciences, Erciyes University, Kayseri-38039, TURKEY, and Ş. Işık, Department of Physics, Faculty of Arts and Sciences, Ondokuz Mayıs University, Kurupelit, Samsun-55139, TURKEY, and M. Macit, Department of Chemistry, Faculty of Arts and Sciences, Ondokuz Mayıs University, Kurupelit, Samsun-55139, TURKEY, and H. K. Fun, X-ray Crystallography Unit, School of Physics, Universiti Sains Malaysia, 11800 USM, MALAYSIA.

Recently, since the increasing use of coordination compound in analytical, bio, pigment and medical chemistry, many investigators have studied these topics. Especially vic-dioximes have been widely investigated as analytical reagents 1,2 and models for biological systems 3,4, such as vitamin B1,2 [1-2]. The possibly chelating ligand oxamid-oxime(diaminoglyoxime) recently received new interest when the X-ray structure determinations of them [3-5]. The Co(III) ion in this complexe is a octahedral geometry and the dipyridine rings are in planar and piperazine rings assume chair conformation. In the solid state, the unit of $CoC_{24}H_{36}N_{10}O_4$ with the (NO_3) and Cl ions are linked to form infinite "zigzag" chains along the c-axis. The crystal structure is stabilised by van der Waals interaction also. Crystal Data: $C_{24}H_{36}CoN_{10}O_4.2(NO_3).3(H_2O).Cl$, M_r=801.06, Monoc., Cc (No. 9), a=17.6920(4), b=11.8163(2), c=16.4752(4)Å, γ=91.679(1)°, V= 3442.7(1) $Å^3$, Z=4, T=293(2)K, R=0.0458 for 5254 observed data with $I > 2\sigma I$.

1. Serin S., Gök Y., Karabücek S. & Gültekin N. (1994). Analyst.,119, 1629-1632.
2. Chakrovorty A. (1974). Coord. Chim. Rev., 13,1-5.
3. Bekaroğlu, Ö.,Saribasan, S., Koray, A.R. & Ziegler, M. L. (1977). Z. Naturforsch. Teil. B32, 387-392.
4. Endres, H. (1978). Acta Cryst. B34, 2306-2309.
5. Bekaroğlu, Ö.,Saribasan, S., Koray, A.R., Nuber, B.Weidenhammer, K.,Weiss, J.& Ziegler, M. L. (1978). Acta Cryst. B34, 3591-3593.

P07.07.003 CONFACIAL BIOCTAHEDRAL DITUNGSTEN III THIOETHER METALLOLIGANDS. Masood Parvez, Vivian J. Mozol & P. Michael Boorman. Department of Chemistry, University of Calgary, Calgary, Alberta, Canada T2N 1N4.

C-S bond cleavage of a μ-thioether in $Cl_3W(\mu\text{-}L)_3WCl_3$ (L = cyclic thioether) leads to species having pendant arms possessing a variety of donor atoms. Successful complexation of these pendant arms to a secondary metal center, could establish a

use for C-S bond cleavage in the construction of site specific metalloligands. As such, the complexes $[PPh_4][Cl_3W(\mu\text{-}L)_2(\mu\text{-}CH_2)_2E(CH_2)_2SC_6H_4(o\text{-}PPh_2)WCl_3]$ (L = tetrahydrothiophene = tht, E = no atoms; L = 1,4-thioxane, E = O; L = pentamethylene sulfide = pms, E = CH_2) were reacted with one equivalent of $AgBF_4$, which resulted in the formation of (1), (2) and (3). The results of the X-ray crystallographic analyses of (1), (2) and (3) will be presented.

(1) Crystal data: $C_{30}H_{38}Cl_6PS_4AgW_2.0.5C_3H_6O.0.5C_4H_{10}O$, FW = 1312.23, orthorhombic, $P2_12_12$, a = 17.150(5) Å, b = 30.28(1) Å, c = 9.012(9) Å, V = 4681(4) Å^3, Z = 4, D_x = 1.86 Mg m^{-3}, λ (Mo Kα) = 0.71069 Å, μ = 5.903 mm^{-1}, T = 200 K, θ_{max} = 25.0°, measured reflections = 4679, observed data [I > 3σ(I)] = 1499, R = 0.053, wR = 0.051.

(2) Crystal data: $C_{30}H_{38}Cl_6O_3PS_4AgW_2.0.5CH_2Cl_2$, FW = 1336.59, monoclinic, $P2_1/c$, a = 9.125(1) Å, b = 18.743(2) Å, c = 25.389(3) Å, β = 99.24(1)°, V = 4285.9(8) Å^3, Z = 4, D_x = 2.07 Mg m^{-3}, λ (Mo Kα) = 0.71069 Å, μ = 6.511 mm^{-1}, T = 170 K, θ_{max} = 27.5°, measured reflections = 7254, observed data [I > 3σ(I)] = 4250, R = 0.092, wR = 0.096.

(3) Crystal data: $C_{33}H_{44}Cl_6PS_4AgW_2.3CHCl_3$, FW = 1646.34, monoclinic, $P2_1/c$, a = 13.553(3) Å, b = 27.799(4) Å, c = 15.931(3) Å, β = 112.10(1)°, V = 5561(2) Å^3, Z = 4, D_x = 1.97 Mg m^{-3}, λ (Mo Kα) = 0.71069 Å, μ = 5.405 mm^{-1}, T = 170 K, θ_{max} = 27.5°, measured reflections = 13670, observed data [I > 3σ(I)] = 5709, R = 0.081, wR = 0.093.

P07.07.004 SYNTHESIS AND CRYSTAL STRUCTURE OF ALKOXO- AND PHENOXO- BRIDGED DINUCLEAR FE(III) COMPLEXES. Tian-Huey Lu,[a] K. Panneerselvam,[a] H. Aneetha[b] and Chung-Sun Chung[b], [a]Department of Physics, [b]Department of Chemistry, National Tsing Hua University, Hsinchu, Taiwan 300, R.O.C.

Synthesis and study of dinuclear complexes with metal ions in close proximity has attracted considerable attention, since homo or heterodinuclear metal centers form the active sites in many enzymes. These bridged complexes are also studied because of their interesting spectral, magnetic and redox properties. The presence of oxo-bridged dinuclear iron centers in several nonheme proteins has resulted in synthesis of several dinuclear Fe(II) and Fe(III) complexes in an effort to model such active sites. These complexes exhibit strong magnetic interactions and extent of magnetic exchange parameter *J* dependence on Fe-O-Fe bridge angle and the geometry at the metal ion. In course of our investigations, we have isolated alkoxy bridged and phenoxy bridged dinuclear Fe(III) complexes. Complex **1**, $[FeL^1]_2$ (L^1=N,N'-bissalicylidene-1,3-diaminopropan-2-ol) crystallizes in P1bar with a=13.880(3), b=15.151(2), c=19.557(2)A, α=94.36(1), β=108.59(1), γ=113.87(1)^o, Z=4, R=0.087, wR^2=0.283 for 8319 reflections with I>2σ(I). There are two molecules in the asymmetric unit. Each molecule consists of two iron(III) centers, which are bridged by two phenolate oxygen atoms. The phenolate oxygen atom bridge is somewhat asymmetrically disposed in molecule A while in molecule B it is highly symmetric. The geometry at the metal ions is distorted octahedral, the other four positions being occupied by two terminal phenolate oxygen atoms and two nitrogen atoms of the ligand. Complex **2**, $[FeL^2]_2$ (L^2=2,6-bis(salicyl ideneaminomethyl)-4-methylphenol) crystallizes in P1bar with a=10.0188(1), b=13.3004(2) c=15.9861(2)A, α=84.622(1), β=82.602(1), γ=80.938(1)^o, Z=2, R=0.072, wR^2=0.214 for 5353 reflections with I>2σ(I). The asymmetric center has two metal ions bridged by two phenoxy oxygen atoms. The geometry at the metal ion is distorted octahedral coordinated by four oxygen atoms in equatorial position and two nitrogen atoms of the Schiff base ligand in axial position.

We thank the National Science Council, R.O.C., for support under the grants NSC88-2112-M007-013 and NSC88-2811-M007-0004.

P07.07.005 STRUCTURAL STUDY OF ORGANO-PALLADIUM COMPLEXES. C. Thompson and G.J. Kruger, Dept. of Chemistry and Biochemistry, Rand Afrikaans University, P.O.Box 524, Auckland Park, 2006, SA. and H.G.Raubenheimer, Dept. of Chemistry, Private Bag X1, University of Stellenbosch, Matieland, 7602, SA.

Palladium complexes have been long been known for their catalytic activities (1). An important development in the understanding of catalysts came with the definition by Rauchfuss (2) of the concept of hemilability. This phenomenon involves a monodentate ligand coordinating to the central metal through a second atom to become bidentate, and then disassociating again. The present study furnishes conclusive proof of the hemilability of a series of S^O and Se^O ligands of Pd complexes. These complexes exhibited the following equilibrium in solution:

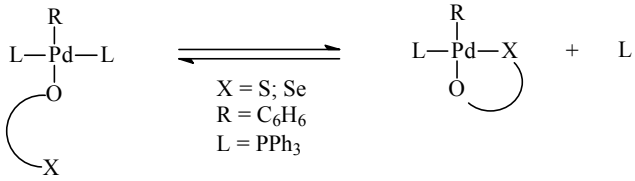

Crystallisation of these solutions yielded two different crystal morphologies. Characterisation by single crystal x-ray diffraction proved that these crystals showed two different types of molecular structure corresponding to the monodentate and bidentate cases respectively.

1. A. Bader, E. Lindner (1991) *Coord. Chem. Rev.*, 108, 27-110.
2. T.B. Rauchfuss, F.T. Patino, D.M. Roundhill (1975) *Inorg. Chem.*, 14, 652.

P07.07.006 SYNTHESIS AND CRYSTAL STRUCTURE OF CU(II) COMPLEXES OF DI-N-CYANOETHYLATED TETRAAZA MACROCYCLE. K. Panneerselvam,[a] Tian-Huey Lu,[a] H. Aneetha[b] and Chung-Sun Chung[b], [a]Department of Physics, [a]Department of Chemistry, National Tsing Hua University, Hsinchu, Taiwan 300, R.O.C.

The coordination chemistry of polyaza macrocyles has been a topic of research interest and more recently N-alkylated polyaza macrocycles have attracted considerable attention since complexes of these ligands exhibit properties that are distinctly different from their unsubstituted parent macrocyclic complexes. For example, Cu(II) complex of 1, 4, 8, 11-tetrakis (2-hydroxyethyl) - 1, 4, 8, 11 - tetraazacyclotetradecane shows increased lability in dissociation reactions, whereas Cu(II) complex of 1, 4, 8, 11-tetraazacyclotetradecane is extremely stable. Most of the studies involved complexes of completely N-alkylated tetraaza macrocycles with very few reports on complexes of partially N-alkylated macrocycles. In continuation to our work on synthesis and kinetics of the macrocyclic complexes, here, we report crystal stuctures of partially N-alkylated Cu(II) complexes of C-*rac*- (**1**) and C-*meso*- (**2**) isomers of 1, 8-bis (2-cyanoethyl) 5, 5, 7, 12, 12, 14 - hexamethyl - 1, 4, 8, 11 - tetraazacyclotetradecane. (**1**) violet and (**2**) orange crystals were obtained by slow evaporation of aqueous solution. Crystal data for (**1**): Orthorhombic, Fdd2 with lattice parameters a = 22.1089(9), b = 30.5304(12), c = 8.7632(4)A, Z = 8. The refinement on F^2 converged at R = 0.049, wR^2 = 0.120, S = 1.03 for 2761 reflections with I > 2σ(I). Crystal data for (**2**): Monoclinic, $P2_1/n$

with lattice parameters a = 11.1755(3), b = 10.9103(2), c = 13.1061(2)A, β = 92.961(1)°, Z = 2, R = 0.053, wR^2 = 0.160, S = 1.07 for 2747 reflections with I > 2σ(I).The macrocyclic ligand in complex **1** adapts unstable *trans*-I stereochemistry while in complex **2** it is in stable *trans* –III sterochemistry. In both the complexes the geometry around the metal ion is square planar with maximum distortions in complex **1**. For the conformation of both complexes, the two six-membered rings are in chair and the two five-membered rings are in gauche forms.

We thank the National Science Council, R.O.C., for support under the grants NSC88-2811-M007-0004 and NSC88-2112-M007-013

P07.07.007 I/BR DISORDER IN THE STRUCTURE OF A NOVEL CU/PB MIXED-ANION COMPLEX AT LOW TEMPERATURE. L.A. Kovbasyuk, O.Yu. Vassilyeva, V.N. Kokozay, Dpt of Chemistry, Kyiv Shevchenko University, Volodimirska St. 64, Kyiv 252033, Ukraine, and Paul Raithby, Dpt of Chemistry, Lensfield Road, Cambridge CB2 1EW, U.K.

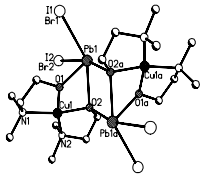

As part of our continuing research in the rational design of new mixed metal Cu/M (M - Pb, Co, Ni, Mn) compounds by employing zerovalent copper and metal salt as starting materials,[1] a novel Cu/Pb mixed-anion (Br/I) complex containing dimethylaminoethanol (HL) has been prepared. Its exact composition was established from the X-ray crystallographic study at 180(2) K. The compound appeared to be isomorphous with the Cu/Pb iodide $[CuPbI_2L_2]_2$,[2] but possessed substantially shorter Pb - halogen distances (3.153(2) and 3.189(1) for the Br/I compound against 3.1966(9) and 3.2381(8) Å for the pure iodide). The model on which the refinement was based assumed that halide ligands could be treated as 60% I + 40% Br for the first halogen site and 60% Br + 40% I for the second. The refinement converged at R = 0.0480 and wR2 = 0.1172 for 2017 observed ($I > 2\sigma(I)$) reflections, justified this assumption. $[CuPbBrIL_2]_2$ crystallizes in the monoclinic space group $P2_1/c$, with a = 12.316(5), b = 8.380(2), c = 15.312(2) Å, β = 93.94(3) °.

L.A. Kovbasyuk, O.Yu. Vassilyeva, V.N. Kokozay, W. Linert, J. Reedijk, B.W. Skelton and A.G. Oliver. *J. Chem. Soc.*, *Dalton Trans*., 1998, 2735.
O.Yu.Vassilyeva, L.A. Kovbasyuk, V.N. Kokozay, B.W. Skelton and W. Linert. *Polyhedron* 1998, **17**, N1, 85.

P07.07.008 A SEVEN COORDINATE MOLYBDENUM(II)-DICARBONYL COMPLEX SHOWING A CAPPED OCTAHEDRON GEOMETRY. J. Borge and S. García-Granda, Departamento de Química Física y Analítica, Facultad de Química, Universidad de Oviedo. C/ Julián Clavería, 8. 33006 Oviedo. Spain.

It is well established that molybdenum(II) complexes are typical examples of the seven coordination geometry. Many carbonyl complexes of the type $[MoX_2(CO)_3(L\text{-}L)]$, $[MoX_2(CO)(L\text{-}L)_2]$ and $[MoX_2(CO)_2(L\text{-}L)(\eta^1\text{-}L\text{-}L)]$ (X = halide; L-L = bidentate ligand) have been described and their solid state molecular structures studied by X-ray crystallography. In contrast, cationic complexes of the type $[MoX(CO)_2(L\text{-}L)_2]^+$ are much less known and to the best of our knowledge only the following examples have been described and structurally characterized: $[MoCl(CO)_2(dmpe)_2]^+$ (dmpe = 1,2-bis(dimethylphosphino)ethane), $[MoCl(CO)_2(diars)_2]^+$ (diars = *o*-phenylenebis(dimethylarsine)), $[MI(CO)_2(dmpe)_2]^+$ (M = Mo, W). The coordination chemistry of the bidentate ligand bis(diphenylphosphine) methane (ddpm) has been extensively studied.

In order to study the conformational preference of seven coordinate cationic Mo(II) complexes containing chelating ligands to adopt capped octahedron (C.O.), pentagonal bipyramid (P.B.) or capped trigonal prismatic (C.T.P.) geometries, the synthesis of bromodicarbonyl [bis(diphenylphosphino) methane-κ^2P] molybdenum(II) hexafluorophosphate complex ($C_{52}H_{44}BrF_6MoO_2P_5{\cdot}2CH_2Cl_2$) is described. The complex has been characterized by IR and $^{31}P\{^1H\}$-NMR spectroscopy. The structure has been determined by X-ray diffraction methods. It crystallizes in the monoclinic space group C2/c, Z = 8, a = 42.71(1) Å, b = 11.47(1) Å, c = 26.72(1), and β = 118.58(1)º. The structure determination shows a capped octahedron geometry around the molybdenum atom.

P07.07.009 CRYSTAL STRUCTURE OF $[Cu(NCS)_2(HL)]_2$ (HL=3,5-DIMETHYL-1-CARBOXAMIDE-PYRAZOLE). Z.K. Jacimovic, Faculty of Metallurgy and Technology, University of Montenegro, Yugoslavia, and G.A. Bogdanovic, Institute of Nuclear Sciences "Vinca", Yugoslavia, and A. Spasojevic-de Bire, Ecole Centrale Paris, France, and V.M. Leovac, and E.Z. Iveges Institute of Chemistry, Faculty of Sciences, University of Novi Sad, Yugoslavia.

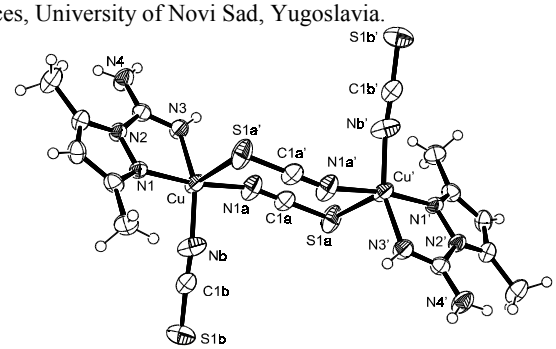

Hot ethanolic solution of the 3,5-dimethyl-1-carboxamidepyrazolium nitrate ($HL{\cdot}HNO_3$) and $Cu(NO_3)_2$ in mole ratio 2:1, in the presence of NH_4SCN excess forms complex of the formula $[Cu(NCS)_2(HL)]_2$.

Crystal data: triclinic, space group P-1, a=7.181(6)Å, b=8.749(2)Å, c=11.366(3)Å, α=70.30(2)°, β=85.86(5)°, γ=66.98(2)°, V=617.3(6)Å^3, Z=1, μ=2.097 mm^{-1}, Dc=1.713 g/cm^3, CAD-4, MoK$_\alpha$=0,71073,theta-max=27.01.

The structure was solved by direct methods and refined by full matrix least-squares using SHELXL 93 program to a final R=0.046 for 2099 reflections with I>2σI. The complex has a dimeric pentacoordinated structure which is, in addition to the endo-bidentate(N,N)coordination of the pyrazole ligand, formed by both non-bridging(N) and bridging(NS) coordination of the NCS-group. The center of the 8-membered Cu2(NCS)2 ring coincides with a crystallographic inversion center.

P07.07.010 CRYSTAL STRUCTURES OF CIS-$(Et_3NH)[MoCl_4L_2]$ AND TRANS-$(LH)[MoBr_4L_2]$ (L = 4-Ethylpyridine). J.V.Brenčič and B.Modec, Faculty of Chemistry and Chemical Technology, Aškerčeva 5, P.O.B. 537, 1001 Ljubljana, SLOVENIA.

Coordination compounds containing 4-Ethylpyridine ligand are rare. The products of reaction between $(NH_4)_2[MoX_5.H_2O]$(X=Cl,Br) with diluted solutions of 4-Ethylpyridine in organic solvents are several. At room temperature, depending on experimental conditions, ionic compounds containing cis and/or trans-$[MoX_4L_2]^-$(X=Cl,Br;L=4-

Ethylpyridine) were isolated. Single crystals were grown by concentrating acetonitrile solutions of the crude products.

Cis-$(Et_3NH)[MoCl_4L_2]$ is orthorhombic ($Pca2_1$) with a=13.703(1), b=7.766(2) and c=16.793(1)Å. The structure was solved by direct methods and refined to R_1 = 0.029 and wR_2 = 0.0638. Average Mo - Cl and Mo - N (4-Ethylpyridine) bonds are 2.43(1) and 2.20(1)Å. Weak hydrogen bonds exist between the cation and the chlorine atoms of the anion.

Trans- $(LH)[MoBr_4L_2]$ is monoclinic ($P2_1/n$) with a=11.764(2), b=29.059(5), c=15.755(1)Å and β=96.36(1)^0. The structure was solved by direct methods and refined to R_1 = 0.0409 and wR_2 = 0.0918. Mo - Br bonds are from 2.554(1) to 2.602(1)Å, average Mo - N(4-Ethylpyridine) bond is 2.22(1)Å. Trans 4-Ethylpyridine ligands are in eclipsed conformation. Hydrogen bonds between the cation and the bromine atoms of the anion are present.

Mo - halogen and Mo - nitrogen bonds are in the same range as found before in the structures of $(PyH)_2[MoCl_5Py]$ and trans,trans - $[MoX_2Py_4].[MoX_4Py_2]$ (Py = pyridine, C_5H_5N; X = Cl,Br) [1,2]

1 B.Modec, R.Papoular & J.V.Brenčič (1998).Acta cryst.,C54,736.
2. J.V.Brenčič, L.Golič, I.Leban, R.Rotar & J.Sieler (1996). Z.anorg.allg.Chem.,622,2124.

P07.07.011 SOME EIGHT-COORDINATE COMPLEXES OF EUROPIUM AND GADOLINIUM. T.A. Hamor, C.J. Jones, K. Paxton and R.G. Lawrence, School of Chemistry, University of Birmingham, Birmingham B15 2TT, UK.

We have synthesised a number of complexes [Ln(Tp)X], Ln = trivalent lanthanide, Tp = hydrotris(pyrazol-1-yl)borate, X = diketonate or benzoate, and containing either one or two Tp ligands. The crystal structures of complexes with Ln = Eu or Gd, and X = acetylacetonate, benzoylacetonate, benzene-1,4-dicarboxylate and benzoate have been determined. In every case these were found to be 8-coordinate. Dimeric compounds are formed when X = benzoate. Analysis of interfacial angles [M.G.B. Drew, Coord. Chem. Rev., 1977, 24, 179 - 275] shows that the coordination polyhedra approximate to a greater or lesser extent to standard 8-coordinate dodecahedral (DOD), square antiprismatic (SAP) or bicapped trigonal prismatic (BCTP) geometry. Deviation from ideal geometries, however, is inevitable due to the presence of the rigid tripodal Tp ligand. Results for the structures listed below will be presented, and will be compared with analogous structures, also containing the Tp ligand, determined previously [C. J. Jones et al., J. Chem. Soc. Dalton Trans., 1989, 1393; 1990, 581; 1996, 501; D.L. Reger et al., Inorg. Chem., 1990, 29, 416].

Compound	Coordination Geometry
(1) (benzoylacetonato)bis(Tp)Eu	SAP
(2) (acetylacetonato)bis(Tp)Eu	BCTP
(3) bis[bis(benzoato)(Tp)Eu]	BCTP / DOD *
(4) bis(Tp)Gd(OOCPhCOO)bis(Tp)Gd	SAP
(5) bis[(benzoato)bis(Tp)Eu]	DOD / DOD

* Compound (3) crystallises with two independent dimeric centrosymmetric molecules in the unit cell.

P07.07.012 STRUCTURAL STUDIES OF NOVEL MIXED RUBIDIUM LITHIUM ALKOXIDE CAGES LINKED BY BRIDGING LIGANDS. S. T. Liddle and W. Clegg, Department of Chemistry, University of Newcastle upon Tyne, Newcastle upon Tyne, UK, NE1 7RU, and R. E. Mulvey and A.M. Drummond, Department of Pure and Applied Chemistry, University of Strathclyde, Glasgow, UK, G1 1XL.

Recent times have seen a revival of interest in hetero-alkali metal complexes,[1] and metal alkoxides for use via sol gel processing in electronic and ceramic industries.[2]

Such complexes are principally known for their role in difficult and selective proton abstraction reactions, often succeeding where more conventional alkyl lithium reagents fail.[3]

Two mixed rubidium lithium alkoxide cages are presented and discussed. Modified synthesis generated two alkoxide cages. Both are unprecedented. Indeed the dearth of organorubidium structures was highlighted in a recent review.[4] Bridging tetramethylethylenediamine, an unusual, but not unheard of occurrence, is present in both solid state structures.

Single crystal X-ray crystallography has proved invaluable in structurally characterising these two complexes at 160K. For a sneak preview see *Chem. Commun*., 2391, 1998.

1) R. E. Mulvey, *Chemical Society Reviews*, 27, 339,1998
2) D. C. Bradley, *Chem. Rev*., 89, 1317, 1989
3) V. Snieckus, *JAI Press*, London, 1, 1, 1992
4) Snaith, *Specialist Periodical Reports, Organometallic Chemistry*, The Royal Society of Chemistry, Cambridge, 26, 1, 1998

P07.07.013 STRUCTURAL INVESTIGATIONS ON HEXA-AZA-MACROCYCLE PRECURSORS. J.Costamagna, F.Caruso(*), J.Canales and J.Ramirez. Faculty of Chemistry and Biology, Universidad de Santiago, Santiago-33, Chile; (*) : Istituto de Strutturistica Chimica, CNR, Monterotondo Stz., Rome, Italy.

Compounds **I** and **II** has been employed as electro- and photo-catalysts in the synthesis of fuels from the reduction of carbon dioxide[1]. Diamino-phenanthroline (**DAPHE)**, and diamino-bipyridine (**DABP**), are precursors in the synthesis of **I** and **II ,** respectively. Structure determination by single crystal X-ray diffraction has been performed for [Co(**DAPHE**)$(CH_3COO)_2$] and [M(**DABP**)$(CH_3COO)_2$] (M = Ni, Cu).

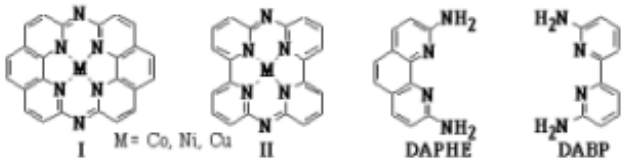

Crystal data are summarized next.

[Co(**DAPHE**)$(CH_3COO)_2$]: monoclinic, C2/c, a=12.813(6), b=10.218(6), c=13.811(5)Å,β=118.17(2)º, Z=4. R=0.046, wR=0.078, for 1787 reflections.

[Ni(**DABP**)$(CH_3COO)_2$]: monoclinic, $P2_1/n$, a=8.124(5), b=10.343(6), c=18.723(12)Å,β=98.35(2)º, Z=4, R=0.069, wR=0.095, for 2537 reflections.

[Cu(**DABP**)$(CH_3COO)_2$]: triclinic, P-1, a=10.099(5), b=10.257(5), c=8.015(4)Å, α=112.97(2), β=93.13(2), γ=92.96(2)º, Z=2, R==0.076, R=0.098, for 2603 reflections

Distortions from regular octahedron, coordination of acetate and comparison between these structures will be presented and discussed. This work was supported by a grant (Nº 1970354) from Fondecyt.

[1] J.Costamagna, J.Canales, J.Vargas, G.Ferraudi, "Carbon DioxideActivation by Aza-macrocyclic Complexes", *Coord.Chem.Rev.,* 148(1996) 221-248.

P07.07.014 CHALCOGENIDE CYANIDE CLUSTERS OF TRANSITION METALS: FROM MOLECULAR COMPLEXES TO EXTENDED SOLID-STATE STRUCTURES. A.V.Virovets, Institute of Inorganic Chemistry SB RAS, Novosibirsk 630090, Russia

Transition metal cyanides form Hoffman clathrates, Prussian Blue type compounds and demonstrate unique properties, structures and chemical reactivity. Recently we have prepared and systematically investigated salts of cyanide cluster anions $[M_4Q_4(CN)_{12}]^{q-}$ (tetrahedral core, M=Mo, W, Re, Q=S, Se, Te, q=4-7) [1] and $[Re_6Q_8(CN)_6]^{4-}$ (octahedral core, Q=S, Se) [2,3].

The tetrahedral anions were found to have the similar structure in the solid state, M-M bond distances of cluster cores being dependent on average oxidation state of M (+4 for Re, +3, +3.25, +3.5 for Mo, W).

Polymeric compounds with a common formula $Cat_xM'_y[Re_6Q_8(CN)_6]_z{*}mH_2O$ ($Cat=H_3O^+$, Cs^+, $(C_nH_{2n+1})_4N^+$, $M'=Mn^{2+}$, Fe^{2+}, Co^{2+}, Ni^{2+}, Cu^{2+}) were prepared for the first time [3]. The structural study has shown that M' atoms are coordinated to N atoms of CN ligands forming polymeric C-N-M'-N-C-Re_6Q_8-C-N-M'... crystal structures. The dimension of polymeric framework depends on the nature of Q and size of Cat^+: 3D polymers for Q=S or Se, $Cat^+=H_3O^+$, Cs^+, Me_4N^+, Et_4N^+, layered structure for Q=S, $Cat=Cs^+$, chains for Q=S, $Cat=Pr_4N^+$. The 3D frameworks contain large cavities filled by Cat^+ and H_2O molecules.

This work was supported by INTAS (Grant No. 96-1256) and RFBR (Grants No. 96-03-32955, 96-03-33018).

1. V.P.Fedin, et al. *Chem.Commun.* (1998) 237
2. Yu.V.Mironov, et al. *Angew.Chem. Int.Ed.* 37 (1998), 2507.
3. N.G.Naumov, et al. *Angew. Chem. Int. Ed*. 37 (1998), 1943.

P07.07.015 CRYSTAL STRUCTURE OF THE ORGANOMETALLIC COMPLEX $RuCl_2$(TRIPOD-N)·2.5$CHCl_3$·H_2O. G. Delgado, G. Díaz de Delgado [1], A. Anzellotti, B. Fontal [2], [1] Laboratorio de Cristalografía, Departamento de Química, Facultad de Ciencias, Universidad de Los Andes, Mérida 5101, Venezuela, [2] Laboratorio de Organometálicos, Departamento de Química, Facultad de Ciencias, Universidad de Los Andes, Mérida 5101, Venezuela.

This work presents the crystal X-ray structure determination of the complex cis-dichloro[tris-(diphenylphosphinoethyl)amine] ruthenium(II) chloroform solvate monohydrate.

The compound, of formula $RuCl_2$(TRIPOD-N)·2.5$CHCl_3$·H_2O or ($C_{44.5}H_{44}Cl_{9.5}NOP_3Ru$), was prepared by reaction of $RuCl_2(DMSO)_4$ and TRIPOD-N ligand in toluene solution. Crystals of the complex were obtained by slow evaporation of a chloroform solution of the complex.

The crystal structure is monoclinic, space group P21/c, a= 17.541(3), b= 12.112(1), c= 24.950(3)Å, β= 109.26(1)°, V= 5004.2Å^3, Z= 4, R(F^2)= 0.076, Rw(F^2)= 0.183.

The structure consists of discrete molecules of the complex and solvents held together by normal van der Waals forces. The ruthenium atom is coordinated by two chlorine atoms and one tris-(diphenylphosphinoethyl) amine (TRIPOD-N) ligand, which ocuppies four coordination positions in a facial arrangement. The arrangement around Ru is a distorted octahedron, with P(1)-Ru-P(3)= 95.4(1)°, P(1)-Ru-Cl(2)= 98.8(1)° and P(1)-Ru-Cl(2)= 81.0(1)°. The two chloro atoms are in a cis conformation, as in the parent compound $RuCl_2(DMSO)_4$. The bond distances Ru-Cl(1) and Ru-Cl(2) are 2.488(2) and 2.464(2)Å, larger than 2.413(2) and 2.432(2)Å in $RuCl(DMSO)_4$. Three $CHCl_3$ molecules and one H_2O molecule are included as solvent of crystallization. One of the $CHCl_3$ molecules is disordered.

This work was supported by CONICIT, Grant LAB-97000821, for the establishment of the Laboratorio Nacional de Difracción de Rayos-X.

P07.07.016 STRUCTURE OF Ni(II) COMPLEX WITH MORPHOLINEDITHIO-CARBAMATE AND 1,1´-BIS(DIPHENYLPHOSPHINO) FERROCENE. J. Kameníček and R. Pastorek, Dept. of Inorganic and Physical Chemistry, Faculty of Science, Palacký University, 771 47 Olomouc, Czech Republic.

The new compound of composition [Ni(morphdtc)(dppf)]-ClO_4.C_2H_5OH (morph = C_4H_8O, dtc = S_2CN^-, dppf = 1,1´-bis(diphenylphosphino)ferrocene was prepared by reaction of Ni(morphdtc)$_2$, Ni(ClO_4)$_2$ .6H_2O and dppf in boiled ethanol.

Results of X-ray structure analysis: Basic crystallographic data – space group $P2_1/c$, Z = 4; a = 13.108(3), b = 10.280(2), c = 29.839(6) Ĺ, β = 99.34(3)°. The central atom of nickel is coordinated in approximately square planar arrangement (see Fig.) with S_2P_2 chromophore atoms (the deviations from ideal NiS_2P_2-plane are less then 0.05 Ĺ).

Figure. Molecule of [Ni(morphdtc)(dppf)]ClO_4 (solvent and H-atoms are omitted)

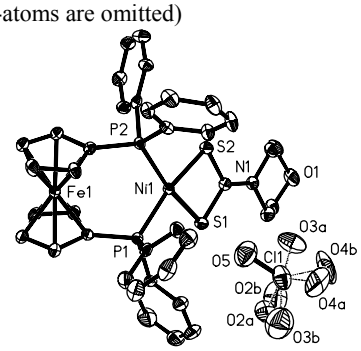

The best convergence was reached by assumption of two possible orientation of ClO_4^- group with occupancy factors of three O-atoms equal to 0.5 (R_1 = 0.0376). The details will be discussed at poster.

P07.07.017 STRUCTURE AND STABILITY OF FIVE-COORDINATE ORGANOALUMINUM COMPLEXES. Roman Luboradzki[a], Janusz Lipkowski[a], Janusz Lewinski[b], Piotr Gos[b]; a)Institute of Physical Chemistry, Polish Academy of Sciences, Kasprzaka 44/52, 01-224 Warsaw, Poland b)Department of Chemistry, Warsaw University of Technology, Noakowskiego 3, 00-664 Warsaw, Poland

It has been extensively demonstrated recently that pentacoordination plays a significant role in selective organic transformation mediated by organoaluminum compounds, however, the nature of intermediates are elusive. Structurally characterized five-coordinate aluminum alkyls are dominated by derivatives of macrocyclic or multidentate open-chain ligands, and the fully characterized mononuclear compounds with mono- or bi-dentate ligands, which could serve as a useful structural model, are very scarce. It is apparent from our study that electrophilicity of the metal center and the trans influence of axial substituents are overriding factors determining the structure and stability of five-coordinate aluminum complexes. The respective correlation data will be presented in addition to two novel complexes investigated by using X-ray diffraction method: $Me_2Al(hacet)$*py-Me (**1**) and $MeAl(hacet)_2$ (**2**) (where hacet = deprotonated 2'-hydroxyacetophenone, py-Me = γ-picoline). Compound **1** is the first structurally characterized five-coordinate adduct of dialkylaluminum chelate complex with monodentate Lewis base.

Crystal data of **1:** space group $P2_1/n$; a = 8.615(2), b = 7.499(1), c = 23.746(5) Å, β = 93.12(3)º, V = 1531.8(5) Å^3, Z = 4.

Crystal data of **2:** space group C2/c, a = 12.365(2), b = 10.856(2), c = 11.709(5) Å, β = 95.98(2)º, V = 1563.2(5) Å^3, Z = 4.

P07.07.018 TRITHIOPHOSPHITES – CONFORMATIONAL FLEXIBILITY AND COORDINATION PROPERTIES. O.N. Kataeva, A.T. Gubaidullin, D.B.Krivolapov, I.A. Litvinov, A.E. Arbuzov Institute of Organic and Physical Chemistry, Russian Academy of Sciences, A.E.Arbuzov str., 8, Kazan 420088, RUSSIA

A series of trithiophosphites, as well as their complexes with transition metals has been studied by X-ray single crystal diffraction: $CuHal{\cdot}P(SR)_3$, $CuHal{\cdot}P(SR)_3{\cdot}NCMe$, $CuBr{\cdot}P(SR)_2NRt_2$, $CuSCN{\cdot}P(SR)_3$, $CpMn(CO)_2{\cdot}P(SR)_3$, $MesCr(CO)_2{\cdot}P(SR)_3$ with Hal = Cl, Br, I and R = Me, Et, Pr, i-Pr, Bu, Ph. Depending on the metal center, substituents R at sulfur, the conditions of reactions and crystal growth, different coordination modes have been observed: “classical” monodentate binding via phosphorus, unusual bidentate mode with participation of both P and S donor atoms of the ambident P - S system, as well as both monodentate and bidentate modes in one complex. The metal -phosphorus bond was found to be much stronger and correspondingly shorter than metal - sulfur bond in all complexes. Coordination properties of trithiophosphites were found to be different from those of analogous oxygen and nitrogen containing ligands, phosphites and amidophosphites, which usually exhibit monodentate coordination. The factors determining coordination properties of thiophosphites are considered.

The diversity of coordination modes manifested by trithiophosphites is to a great extent determined by their conformational flexibility due to internal rotation around the P-S bonds. Trithiophosphites retain their flexibility upon complexation. The elongation of the alkyl chain at sulfur results in the increase of the flexibility of thiophosphites and in their conformational inhomogeneity in crystals. The structure of free thiophosphites, including new potential ligands, $P(SR)_3$ with ferrocenyl and cymantrenyl substituents at sulfur, was studied and compared with their structure in coordination compounds. The reasons of conformational changes observed in trithiophosphites after the formation of the coordination bonds are considered.

This research was supported by Russian Foundation for Basic Research, grant 98-03-32777.

P07.07.019 CRYSTAL STRUCTURE OF A NOVEL BINUCLEAR COPPER COMPLEX WITH DIACETYLDIOXIME, $Cu_2(C_4H_7N_2O_2)_3(H_2O)(ClO_4)$. S. Lin and S.-X. Liu*, Dept. of Chem., Fuzhou University, Fuzhou 350002, China.

A novel binuclear copper complex with diacetyldioxime, $Cu_2(C_4H_7N_2O_2)_3(H_2O)(ClO_4)$, was prepared and characterized. Deep blue crystals of $Cu_2(C_4H_7N_2O_2)_3(H_2O)(ClO_4)$ are monoclinic, space group P $2_1/n$, a=10.404, b=20.785, c=10.816 Å, β=112.19°, V=2166 Å^3, Z=4.

The structure has some interesting features. The two copper atoms in the title complex molecule have a distorted square pyramidal geometry with the CuN_3O_2 and CuN_2O_3 coordination types, respectively. In the Cu(1) square pyramid, the equatorial plane is defined by the three nitrogen atoms (N(1), N(3), N(4)) and one oxygen atom (O(2)) from the two diacetyldioxime ligands, while the perchlorate oxygen atom being the apical position. However, in the Cu(2) square pyramid, the two oxygen atoms and two nitrogen atoms of the three diacetyldioxime ligands build the base plane, the axial site being occupied by a water molecule. The two copper atoms are bridged in pairs by a oxygen atom and a deprotonated oxime NO group.

It is worth noting that the three diacetyldioxime ligands have different coordination ways in the title complex molecule. The first diacetyldioxime is a bridging bidentate ligand, one oxime is coordinated to two copper atoms (Cu(1) and Cu(2)) through its oxygen atom (O(2)), while the other oxime is coordinated to one copper atom(Cu(1)) through its nitrogen atom(N(1)). The second diacetyldioxime is a bridging tridentate ligand, the nitrogen atom (N(4)) and oxygen atom(O(4)) in one oxime are joined to Cu(1) and Cu(2) atoms, when the nitrogen atom(N(3)) is coordinated to Cu(1) atom. The two oxime nitrogen atoms in the third diacetyldioxime are coordinated to Cu(2) atom. Therefore, the third diacetyldioxime is a chelating ligand.

The authors thank the financial support of the Natural Science Foundation of China. Mrs. S. Lin is leave on from Dept. of Chem., Fujian Teachers' University.

P07.07.020 N-H...O AND C-H...O HYDROGEN BONDS IN4,4'-DIMETHY-6,6'-BIS(MORPHOLINOMETHYL)-2,2'-ETHYLINEDINITRILODIMETHYLIDYNE)MANGANESE(II)DIPERCHLORATE MONOHYDRATE. R. Thirumurugan[a], S. Shanmuga Sundara Raj[b], G. Shanmugam[a] , H . K. Fun. (a) Department of Crystallography andBiophysics, University of Madras, Guindy Campus, Chennai - 600 025, India.(b) X-ray Crystallography Unit, School of Physics, Universiti SainsMalaysia, 11800 USM, Penang, Malaysia.

The main function of defence in mammalian organisms for controlling extracellular and intracellular superoxide radical anions are the Cu , Zn, Mn and Fe containing superoxide dismutase enzymes. A stable non-toxic, low molecular weight mononuclear manganese(II) or (III) complex that catalyses the dismutase in clinical applications with the desirable qualities of low cost, cell permeability and non-immunogenicity. We have attempted to develop manganese based mononuclear complex, because it is a better model compound for metalloenzymes. Many of the manganese(II) and (III) are known to exhibit superoxide dismutase-type activity. In the title compound crystallizes in the triclinic system with space group P-1. The cell parameters: a = 8.9162(1) Å, b = 9.6764(1) Å, c =20.0766(1) Å, α = 78.536(1) °, β = 81.520(1) °, γ = 83.922(1)° , Z = 2. The geometry around the Mn ion is slightly distorted from square planar system. The dihedral angle between the coordination planes [N-Mn-N and O-Mn-O] is 10°. The molecules are stabilized by N-H...O and C-H...O of hydrogen bonds. The structural details will be presented in the poster.

P07.07.021 SHORT HYDROGEN BOND IN ZINC AND POTASSIUM SALTS OF 1,2,4,5-BENZENETETRACARBOXYLIC ACID. R. Diniz, N. G. Fernandes, M. T. C. Sansiviero, Department of Chemistry, Federal University of Minas Gerais, Belo Horizonte, Brazil.

Structures of (I) zinc dihydrogen-1,2,4,5-benzenetetracarboxylate hexahydrate, $C_{10}H_{16}O_{14}Zn$, and (II) potassium trihydrogen-1,2,4,5-benzenetetracarboxylate trihydrate, $C_{10}H_{11}O_{11}K$ have been determinated. Compound(I): Monoclinic, C2/c, Z = 4, μ = 0.86 mm^{-1}, λ(MoKa) = 0.71073 Å, a = 21.948(1) Å, b = 9.760(1) Å, c = 7.291(1) Å, b = 105.51(1)º, V = 1503.7(1) Å^3, R(F^2) = 0.048, wR = 0.108, S = 1.210, 2019 independent observed reflections. Compound(II): Monoclinic, $P2_1/c$, Z = 4, μ = 0.46 mm^{-1}, λ (MoKa) = 0.71073 Å, a = 7.561(1) Å, b = 19.514(1) Å, c = 9.731(1) Å, b = 111.11(1)º, V = 1339.4(2) Å^3, R(F^2) = 0.081, wR = 0.120, S = 2.297, 3085 independent observed reflections. Crystallographic studies show the existence of short hydrogen bond in both compounds. The O...O distances are respectively 2.410(3) Å and 2.389(3)Å. Zinc atom is coordinate to six water molecules. Eight oxygen atoms form the coordination around potassium atom, three from water molecules and five from trihydrogen-1,2,4,5-benzenetetracarboxylate group.

The presence of strong hydrogen bond also was observed in the infrared absorption spectra proper broad envelopes from 1800 to 900 cm^{-1} and band in 795 cm^{-1} observed in acid which

disappear in compound(I) and less relative intensity in compound(II). Raman spectra have broad band of weak intensity in 858 cm^{-1} in compound(I) and 897 cm^{-1} in compound(II) will bee associate short hydrogen bond vibrations. In Raman spectra the region of 1700 to 1400 cm-1 has bands characteristics of a carboxylate group which show difference in the compounds. Compound(I) the separation between symmetric and antisymmetric carboxylate stretching (D) is 142 cm^{-1} which to agree with to ionic compounds. Compound(II) D is 181 cm^{-1}. This D value is intermediate between monodentate and bridging bidentate coordination which to agree to crystallographic data.

P07.07.022 A NOVEL ISOMERISM IN COPPER(I) IODIDE: ETHYLENETHIOUREA (1:2). Chaveng Pakawatchai and Yupa Thanyasirikul, Department of Chemistry, Prince of Songkla University, Hat-Yai, Songkla 90112, Thailand and Brian W. Skelton and Allan H. White, Department of Chemistry, University of Western Australia, Nedlands, WA 6907, Australia.

The 1:2 complex, formed between copper(I) iodide and 'ethylenethiourea', 'etu', $(CH_2NH)_2CS$, has been isolated in two distinct crystalline forms, each corresponding to a distinct isomer. Monomeric $[(etu)_2CuI]$ is monoclinic, $P2_1/m$, a = 7.469(4), b = 14.669(5), c = 11.726(4) Å, β = 101.73(3)°, V = 1258 $Å^3$, Z = 4; final R on $|F|$ for 1353 'observed' (= N_o) (I>3σ(I)) reflections was 0.044. Two independent molecules are found, one half of each comprising the asymmetric unit of the structure, each having a trigonal planar S_2CuI core with crystallographic mirror planes normal to the coordination planes and containing the Cu-I bonds. Cu-I, S are 2.551(2), 2.234(2) (x2)(mol.1); 2.554(2), 2.236(3) Å (x2)(mol.2), with S-Cu-S, I being 116.3(1), 121.82(6) (x2)(mol.1); 117.3(1), 121.27(7)° (x2)(mol.2). Trimeric $[(etu)_2CuI]_3$, monoclinic, $P2_1/n$, a = 12.580(5), b = 16.925(9), c = 17.025(8) Å, β = 96.56(4)°, V = 3601 $Å^3$, Z = 4 trimers; R = 0.059 for N_o = 3278, has one trimer in the asymmetric unit, the three four-coordinate copper atoms being linked into a six-membered Cu_3S_3 ring by alternating bridging etu sulfur atoms, I and the other *S*-etu being terminal ligands. Cu-I,S (terminal) are 2.614(3)-2.637(2), 2.296(5)-2.317(5), with Cu-S (bridging) 2.322(5)-2.384(5) Å. Within the ring, angles at the copper and sulfur atoms are 94.7(2)-107.3(2), 124.8(3)-143.1(2)°.

P07.07.023 THE STRUCTURE OF NOVEL METALLO-PORPHYRINS DETERMINED USING SYNCHROTRON X-RAY RADIATION. N. Feeder, P.R. Raithby, J.K.M. Sanders and S. L. Darling, Department of Chemistry, University of Cambridge, Lensfield Road, Cambridge, CB2 1EW, UK.

The study of Metallo-porphyrins is an exciting and rapidly developing area of chemistry. A knowledge of the structures of these complex molecules is vital to the understanding of their synthesis and catalytic activity. Crystals of these materials, however, are weakly diffracting and contain disordered solvent molecules. Attempts to collect data on these systems using conventional lab sources and diffractometers has failed.

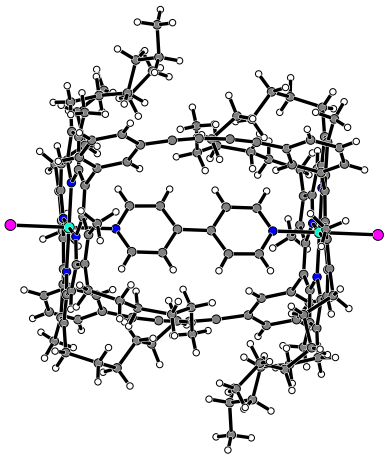

The high intensity X-ray source at the CLRC Daresbury Laboratory has made successful data collections possible using the dedicated Bruker SMART diffractometer. We present the structures of a series of these key molecules.

P07.07.024 STRUCTURAL SYSTEMATICS OF 1:1 COPPER(I) HALIDE BIS(DIPHENYLPHOSPHINO)-ALKANE COMPLEXES. Neil Somers, Brian W. Skelton & Allan H. White, Department of Chemistry, The University of Western Australia, Nedlands, 6907, Australia.

Room temperature single crystal x-ray studies of a number of adducts of the copper(I) halide, CuX, (X=Cl, Br, I), with bis(diphenylphosphino)alkane ligands L='dppx', $Ph_2P(CH_2)_nPPh_2$, of intrinsic 1:1 stoichiometry, has been undertaken.

With n=3, (dppp), a μμ'-dihalo bridged dimer, $[LCu(\mu\text{-}X)_2CuL]$, is formed. Each phosphine ligand chelates one copper atom and structures for all X are isomorphous, (Monoclinic, $P2_1/n$, a~10.2, b~18.5, c~13.5Å, β=104.5°).

For n=5, (dpppn) and X=I, the form is also binuclear, but the length of the $(CH_2)_n$ link in each ligand now allows them to bridge both copper atoms. Comparison of the P_2CuI_2 geometry's for n=3 cf. n=5, show Cu-P to be essentially constant, (ca 2.27Å). However, P-Cu-P is enlarged in the n=5 adduct, (ca 118, cf. 103.6°), with I-Cu-I diminished, (ca 97, cf. 109°).

By contrast, for n=1, (dppm) and X=Cl, the familiar array $[Cu_3X_3(dppm)_3]X^-$ with a cation of quasi-3 symmetry is found. The bromide and iodide adducts so far isolated have the linear, non-coordinated $[XCuX]^-$ counterion instead of the simple X^-. Both chloride and bromide adducts are solvated in the lattice with acetonitrile.

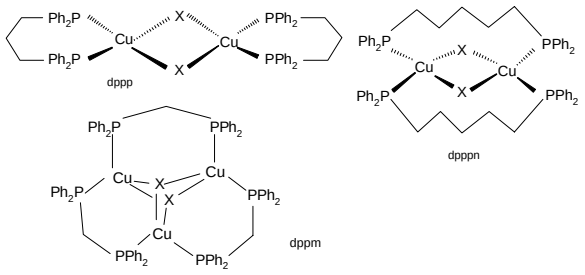

P07.07.025 PECULIARITIES OF STRUCTURE OF In(III) AND Sb(III) INTERNAL COMPLEXES WITH 8-HYDROXY-, 8-MERCAPTO- AND 8-HYDROSELENOQUINOLINE. E.Silina, Yu.Bankovsky, L.Pech and J.Ashaks, Institute of Inorganic Chemistry of the Riga Technical University, Latvia, and V.Belsky and A.Stash, L.Karpov Institute of Physical Chemistry, Moscow, 103064, Russia.

Comparison of crystal structures of the III, V and VIII group trivalent metal 8-mercaptoquinolinates [1] has revealed the different regularities of their structure.

In the present work the effect of substitution of the donor atom (O, S, Se) in the ligand on the nature of valence bonds, geometry of the metal atom coordination polyhedron and on conformation of the metal-containing rings has been evaluated on the basis of investigation of crystal structures of $In(C_9H_6NO)_3.C_2H_5OH$ (I), $In(C_9H_6NS)_3.CHCl_3$ (II), $In(C_9H_6NSe)_3$ (III), $Sb(C_9H_6NO)_3$ (IV), $Sb(C_9H_6NS)_3$ (V), $Sb(C_9H_6NSe)_3$ (VI). The significance of the unshared electron pair in the studied antimony complexes has been discussed.

In the investigated complexes, the bidentatic function is characteristic for ligands, and the coordination number of the central atom equals to 6 [3O(S,Se)+3N]. Coordination polyhedra: distorted octahedron (asymmetric isomer in I - III, symmetrical one - in V, VI), strongly distorted pentagonal pyramid - in IV.

Crystal structures of 8-hydroxyquinolinates are characterized by shortening of bonds M – O in the coordination polyhedra of indium and antimony atoms in comparison with the sum of covalent radii. M – N bonds in all studied compounds are weak coordination bonds. In the 8-hydroselenoquinolinate complexes the noticeable inflections of the metal-containing rings are characteristic.

1. E.J.Silina, L.J.Pech, Yu.A.Bankovsky (1998). E.C.M. Abstracts, 18, 1998.

P07.07.026 STRUCTURAL STUDIES OF THE $[M(C_9H_6NSe)_2]$ [M=Pt(II), Cd(II)] COMPLEXES. L.Pech, Yu..Bankovsky, E.Silina and J.Ashaks, Institute of Inorganic Chemistry of the Riga Technical University, Latvia, and V.Belsky and A.Stash, L.Karpov Institute of Physical Chemistry, Moscow, 103064, Russia.

Two new compounds : 8-selenolquinolinates of platinum (I) and cadmium (II) have been synthesised for first time and their full X-ray structural investigation has been carried out. Lattice parameters for: I- a=7.2220(10), b=8.027(2), c=7.876(2)Å, α=79.13(3), β=89.92(3), γ=117.21(3)^o, sp.gr. P-1, Z=1, for II- a=4.0270(10), b=15.663(2), c=12.820(2)Å, β=91.940(10)^o, sp.gr. $P2_1/c$, Z=2.

Complexes I and II have been compared with the previously studied platinum-8-mercaptoquinolinate, 2-methyl-, 2,7-dimethyl-, 2-isopropyl-, 7-methyl-8-mercaptoquinolinate and 2-methyl-5-methylthio-8-hydroxy-quinolinate (III-VIII) and cadmium-2-methyl- and cadmium-2-phenyl-8-mercaptoquinolinate (IX-X). In this paper we repert the structure of complexes of 8-selenol-,8-mercapto- and 8-hydroxyquinoline and their derivatives in order to study dependence of direct donor-acceptor (DA) π -bond formation strength and electron mechanism on the nature of the central (Pt, Cd) and ligand (O,S,Se) atoms [1]. The obtained results of X-ray structure analysis, show that in molecules of square-planar 8-mercaptoquinolinates DA π - bond strength increases in succession Ni<<Pt<Pd . Transition metal ability to form direct DA π -bond increases in the succession of ligand atoms O<<Se<S. Along with increase of direct DA π - bond strength mentioned series the coordination number of central atoms decreases and solubility of chelate compounds in inert organic solvents increases.

1. Yu.A.Bankovsky, Ya.E.Lejejs, L.J.Pech, Ya.V.Ashaks, I.R.Berzina, D.E.Zaruma, E.J.Silina, M.A.Cirule, A.P.Sturis (1998) Mendelejev Congress on General Applied Chemistry, Abstracts, 16, 1998.

P07.07.028 SYNTHESIS AND CRYSTAL STRUCTURES OF $[Me_4N]_2N[CU_2(CS_4)_2]N$ (I) AND $[Me_4N]_4[Cu_4(CS_4)_4]$ (II). Xianglin Jin, Kaluo Tang,Yaoling Long,Youqi Tang, Institute of Physical Chemistry, Peking University, Beijing 100871, P.R. China

The solutions of tetranuclear copper cluster anionic complexes $[Me_4N]_2[Cu_4(SePh)_6]$ or$[Me_4N]_2[Cu_4(SPh)_6]$ in DMF or CH_3CN reacted with CS_2 in the presence of a small amount of S. From the resulting solutions brown block-shaped crystals (I) or orange block-shaped crystals (II) were formed, respectively. Crystal data: (I) Orthorhombic, space group Pbca, a=11.385(4), b=16.683(4), c=10.921(2)Å, V=2074.2(9)Å^3. μ=2.846mm^{-1}, F(000)=1136e, D_c=1.777g/cm^3, for Z=8, R=0.0544 for 1821 observed reflections. (II) Tetragonal, space group P-42(1)c, a=13.952(2), b=13.952(2), c=11.350(2)Å, V=2209.4(6)Å^3. μ=2.677mm^{-1}, F(000)=1136e, Dc=1.671/cm^3, for Z=8, R=0.0645 for 1114 observed reflections. The X-ray crystal structure determination indicated that the molecule of the complex (I) consists of a polymeric anion $[Cu_2(CS_4)_2]_{n-2}$ and cations $[Me_4N]^+$. In the polymeric anion, the repeated unit is a dinuclear copper complex $[Cu_2(CS_4)_2]$-2, which linked to four surrounding aggregations through sulfur bridges to form a two-dimensional layer structure. The Cu-Cu distance is 2.844(2)Å. In the ligand CS_4, the C-S distances average 1.710Å, S-S is 2.049Å. The cations $[Me_4N]^+$ locate between the layers. The molecule of complex (II) consists of a tetranuclear copper cluster anion with four perthiocarbonate ligands $[Cu_4(CS_4)_4]$-4 and four cations $[Me_4N]^+$. The four copper atoms form a tetrahedron, in which Cu-Cu distances average 2.883Å. One of the sulfur atoms in each CS_4 ligand forms the sulfur bridge with Cu atoms while the other is coordinated to only one copper. The C-S distances average 1.706Å, S-S is 2.065Å.

P07.07.029 STRUCTURAL CHRACTERIZATION OF A SERIES OF POLYMERIC AND CHAIN-LIKE Mo(W) CLUSTER COMPOUNDS. Shaofang Lu, Rongmin Yu, Yuchang Liang, Fuxia Sun, Qiangjin Wu, Xiaoying Huang, Jianquan Huang, State Key Laboratory of Structural Chemistry, Fujian Institute of Research on the Structure of Matter, Chinese Academy of Sciences, Fuzhou, Fujian 350002, China

Polymeric and chain-like cluster compounds are expected to exhibit many novel and peculiar electric, magnetic and optical properties on account of their bonding configurations including simullaneous metal-metal and metal-ligand interactions, thus forming a unique electronic structure. Obviously, they are most important potential structure type in the development of new technical materials and therefore have strickingly been attached. Meanwhile, the design of synthetic pathways in terms of the solution reaction remains to be in the ascendant for the structural chemists.

In this paper, the crystal structures of twelve new cluster compounds are systematically described, Their molecular formulas are as follows: (1) $[(WS_4Ag)\cdot Li(DMF)_4]_\infty$ (2). $Mo_2S_4[S_2CN(CH_2CH_2OH)_2]_2$ (3). $W_2S_4[S_2CN(CH_2CH_2OH)_2]_2$ (4). $Mo_2S_2O_2[S_2CN(CH_2CH_2OH)_2]_2$ (5). $[Mo_2S_4(i\text{-}mnt)_2](Et_4N)_2$ (6). $[Mo_2S_4(i\text{-}mnt)_2]_2K(Et_4N)_3$ (7). $[Mo_3S_4(\mu\text{-}SO_3C_6H_4CH_3)(dtp)_3\cdot H_2O]$ (8). $[Mo_3OS_3(HOC_6H_4COO)(dtp)_3\cdot DMF]$ (9). $\{Mo_3[Pb(dtp)_2]OS_3(\mu\text{-}OAc)_2(py)_3(\mu\text{-}O)\}_2$ (10). $\{Mo_3[BiI_3]OS_3(\mu\text{-}OAc)_2(py)_3(\mu\text{-}O)\}_2\cdot 2H_2O$ (11) $[Mo_3(PbI_3)S_4(dtp)_3(C_3H_4N_2)_3][(CH_3)_2CO]]_2$ (12)$[Mo_6(\mu_3\text{-}S)_3(\mu\text{-}S)_3(\mu\text{-}S_2)_3(\mu\text{-}OAc)(dtp)_5]$

All these clusters have a dimeric, polymeric or chain-like packing structures linked by (μ-S), (μ-O), the bridging ligands,

S···S supermolecular interaction or the intermolecular hydrogen bonds. The measurement of the temperature-change specific conductivity reveals that these clusters belong to some kinds of semiconducting crystals. The bond structures of these clusters have also be given in this investigation.

P07.07.030 Cu(II) COMPLEXES OF BIS(PYRIDYL)-PYRAZINE Jorunn Sletten and Hilde Grove, Department of Chemistry, University of Bergen, Allégaten 41, N-5007, Bergen, Norway.

As part of our program of structural and magnetic investigations of di- and polynuclear pyrazine-bridged complexes we have prepared and structurally characterised three new Cu(II) complexes bridged by 2,3-bis(2-pyridyl)pyr-azine; the dinuclear $[Cu_2(dpp)(H_2O)(dmso)Cl_4]\cdot dmso$ (1), and the chain com-pounds $[Cu(dpp)(H_2O)_2]_x(NO_3)_{2x}$ (2) and $[Cu(dpp)(H_2O)_2]_x(BF_4)_{2x}\cdot 2xH_2O$ (3). In 1 one Cu ion is square pyramidal while the other Cu has approximately trigonal bipyramidal environment, the pyrazine nitrogen atoms coordinating equatorially to both metal ions. In 2 the linear chain is extended along a threefold screw axis, Cu has elongated octahedral coordination with pyra-zine nitrogen in the axial positions. In 3 the chain is zig-zag-shaped, the Cu ion has a compressed octahedral coordination geometry, an inverted Jahn-Teller distortion, with pyrazine nitrogen atoms in equatorial positions. Three other dpp-bridged Cu(II) complexes have previously been characterized.[1,2] but only in the present dinuclear complex is the bridging and coordination geometry such that significant magnetic interaction may be expected.

Complex **1**

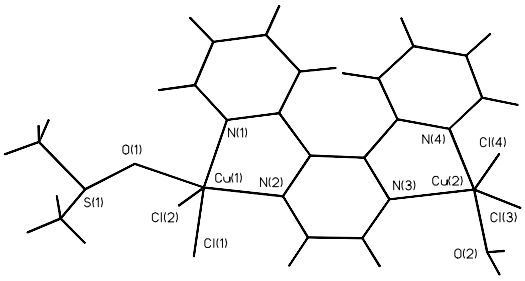

1. J. Sletten, and O. Bjørsvik, *Acta Chem.Scand. 52* (1998) 770.
2. L. W. Morgan *et al., Inorg Chim. Acta 177* (1992) 1103.

P07.07.031 $RE(HCO_2)_3(HNO_2)(H_2CO_2)$ (RE = Y, Tb, Dy, Ho, Er): SYNTHESIS AND CHARACTERIZATIONS.* J.T. Zhao, G.M. He, Y.T. Xu, B.R. Zeng, S.Y. Mao, J.X. Mi, College of Chemistry and Chemical Engineering,, Xiamen University, Xiamen 361005, China

There are few rare earth based non-linear optical materials. Rare earth formates group show NLO properties [1]. The new title compounds with potential NLO properties were synthesized by solution methods at mild temperature and structures characterized by X-ray methods [2]. Unit cell parameters: Y : 6.664(4), 18.36(2), 8.439(5)Å, 1032.7(9)$Å^3$; Tb : 6.686(2), 18.488(9), 8.472(4)Å, 1047.3(5)$Å^3$; Dy : 6.649(9), 18.43(3), 8.451(9)Å, 1036(2)$Å^3$; Ho : 6.666(2), 18.403(9), 8.446(3)Å, 1036.2(4)$Å^3$; Er : 6.641(2), 18.32(1), 8.427(3)Å, 1025.2(6)$Å^3$. The orthorhombic structure was shown to be a new type with a non-centrosymmetric space group $C222_1$ by single crystal structure determinations. It is characterized by networks of rare earth centered square anti-prisms formed by eight oxygen atoms through bridging carbon and nitrogen atoms. The guest formic acid molecules H_2CO_2 are distributed inside the open tunnels along the crystallographic a-axis and bounded to the network through weak hydrogen bonds. The DTA-TGA measurements show the compounds are stable below 170?g(for Y). The magnetic susceptibility ~ temperature variations show the Curie-Weiss type for the heavy rare earth compounds and the calculated number of Bohr magnetons are 9.6, 11.0, 10.6 and 9.8 for Tb, Dy, Ho and Er respectively and they are consistent with the RE^{3+} ions (9.72, 10.63, 10.60 and 9.59 for Tb, Dy, Ho and Er respectively)[3]. The yttrium compound shows very weak temperature independent paramagnetism.

*Project supported by Found for the Returned Overseas Scholars from the Education Comission of China

1. V.A.Trunov, et al. Solid State Communications, (1986), 59,95.
2. J.T.Zhao, et al. J. Rare Earths, (1999), in press.
3. C.Kittel. Introduction to Solid State Physics. sixth edition, New York, USA: John Wiley & Sons, (1986), p405.

P07.07.032 DINUCLEAR Cu(II) COMPLEXES WITH 4,7-PHENANTHROLINO-5,6:5',6'-PYRAZINE AS BRIDGING LIGAND Hilde Grove and Jorunn Sletten, Department of Chemistry, University of Bergen, N-5007 Bergen, Norway

The first X-ray crystallographic structure determinations of metal complexes of 4,7-phenanthrolino-5,6:5',6'-pyrazine (pap) are hereby reported; the dinuclear pap-bridged Cu(II) complexes $[Cu_2(pap)(ox)_2]\cdot 5H_2O$ (1), $[Cu_2(pap)(H_2O)_7(SO_4)]SO_4\cdot 3H_2O$ (2) and $[Cu_2(pap)(H_2O)_3(NO_3)_3]NO_3$ (3). Crystal data: 1 C2/m, a = 18.369(1) Å, b = 17.6964(7) Å, c = 7.0048(4) Å, β = 102.902(2)º; 2 P-1, a = 7.3457(2) Å, b=13.2214(4) Å, c = 14.5128(3) Å, α = 114.229(1)º, β = 99.134(1)º, γ = 90.252(1)º; 3 $P2_1/n$, a = 8.7376(7) Å, b= 9.0449(8) Å, c = 27.740(2) Å, β = 97.547(1)º. In 1 the copper coordination is square planar; in 2 elongated octahedral, the pap ligand in both com-pounds being essentially parallel to the copper equatorial planes. In 3 the coordination geometry of one copper is square pyramidal while the other is intermediate between square pyramidal and trigonal bipyramidal. Bridging ligands related to pap, like bipyrimidine and pyrazine, have been shown to propagate magnetic interaction between metal centres. The coordination geometries found in the present complexes are favourable for magnetic exchange. Magnetic studies of the compounds will be undertaken.

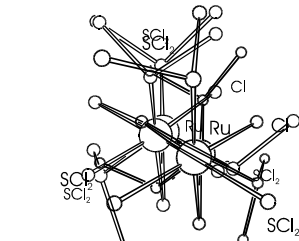

Complex 1

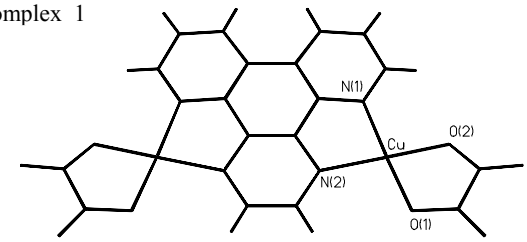

P07.07.033 CONFORMATIONAL POLYMORPHISM OF DICHLORO [(E)-2-CHLORO-1-VINYLCYCLO-HEXANOL](4-METHOXY PHENYL) Te(IV). J. Zukerman-Schpector, R. L. Camillo and I. Caracelli, Laboratório de Cristalografia, Estereodinâmica e Modelagem Molecular, DQ-UFSCar, C. P. 676, 13565-905, São Carlos, SP Brazil and J.V. Comasseto, H. A. Stefani and A. Chieffi, Instituto de Química, Universidade de São Paulo, SP, Brazil

The reaction of aryltellurium halides to acetylenes leading to vinylic tellurides has been reported [1]. After several attempts to get crystals of the title compound, varying the solvent, two different shaped were obtained and the very first determination showed that both unit cells were monoclinic, $P2_1$ /c, having the same volume but different parameters. In both structures the Te^{IV} atom displays a primary disphenoidal geometry, with the chlorine atoms in the apical positions and the C-atoms and the Te lone pair in the equatorial positions.

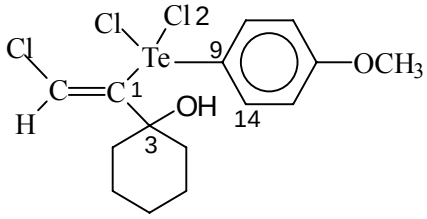

The main differences between the polymorphs are the torsion angles, given for (I) and (II) respectively: C1-Te-C9-C14: 133.0(6) and -126.0(6)^o , and C1-C3-O-H(O): -118 and 176^o. Regarding the packing the molecules are linked through O-H...Cl interactions, but in (I) a secondary interaction, which inexists in (II), was found, Te...Cl2' 3.837(2) Å, approximately *trans* to C1 [Cl2'...Te-C1 = 160.45(13)^o], giving rise to a distorted octahedral arrangement about Te, with the sixth position vacant.

Acknowledgments: FAPESP, CNPq, CAPES.

1. J.V. Comasseto, H.A. Stefani, A. Chieffi & J. Zukerman-Schpector (1991). Organometallics, 10, 845-846.

P07.07.034 MIXED-METAL MACROCYCLES ACTING AS "INVERSE CROWN ETHERS". A.R. Kennedy, R.E. Mulvey and R.B. Rowlings, Department of Pure & Applied Chemistry, University of Strathclyde, Glasgow G1 1XL, UK.

Our interest in modifying the behaviour of *s*-block metal amides by synthesis of heterometallic species containing both group 1 and group 2 metals has led us to a remarkable new structural type [1, 2]. We discovered that rather than being archetypal moisture and oxygen-sensitive compounds these systems react controllably with dry oxygen to form eight membered $[Mg_2M_2N_4]^{2+}$ rings (M = Li or Na, N = hexamethyldisilazane or tetramethylpiperidine) with O^{2-} or O_2^{2-} as guests at the core. These mixed-metal macrocycles are " inverse crown ethers" in a dual sense - the rings are largely metal-based not oxygen-based and the species in the cavities are anions not metal cations.

Recently we have extended these reactions to form larger twelve membered rings $[Mg_2Na_4N_6]^{2+}$ that dideprotonate arene solvents to host $(C_6H_3Me)^{2-}$ and $(C_6H_4)^{2-}$ fragments [3]. A further extension to potassium gives the polymeric species $[Mg_2K_2(O_2)(HMDS)_4]_\infty$ constructed via relatively short K...Me($SiMe_2$) interactions [4].

1. A.R. Kennedy, R.E. Mulvey & R.B. Rowlings. J. Amer. Chem. Soc. (1998), 120, 7816.
2. A.R. Kennedy, R.E. Mulvey & R.B. Rowlings. Angew. Chem. Int. Ed. Engl. (1998), 37, 3180.
3. D.R. Armstrong, A.R. Kennedy, R.E. Mulvey & R.B. Rowlings. Angew. Chem. Int. Ed. Engl. (1999), 38, 131.
4. A.R. Kennedy, R.E. Mulvey, C.L. Raston, B.A. Roberts & R.B. Rowlings. J. Chem. Soc. Chem. Commun. (1999) in press.

P07.07.035 A NOVEL HOMOLEPTIC NICKEL THIOLATE WITH A HEXAGONAL–PRISMATIC SULFUR FRAMEWORK. A. H. Mahmoudkhani, Department of Inorganic Chemistry, Göteborg University, SE–412 96 Göteborg, Sweden, and V. Langer, Department of Environmental Inorganic Chemistry, Chalmers University of Technology, SE–412 96 Göteborg, Sweden.

Metal thiolates, including nickel thiolates, are of interest not only due to their rich chemistry and structural diversity, but also as synthetic models, both for the active sites in some biological systems and for metal sulfide catalysis. So far, several polynuclear complexes of nickel thiolates have been synthesized and characterized. In these complexes involving bridged thiolates and approximately planar, rectangular NiS_4 units, there is a strong tendency to form cyclic tetramers, pentamers, hexamers and even higher polynuclear complexes, as well as folded one–dimensional chain fragments. It has been suggested (Henkel & Chen, 1993) that an electronic modification of the thiolate–S atom might be of significant influence on the magnitude of the Ni—S—Ni angle and therefore on the structure of cyclic polynuclear complex. A theoretical study (Alemany & Hoffmann, 1993) on the structure and bonding also revealed that the structural features of nickel thiolates are dominated by Ni—S bonding, while Ni…Ni interactions may destabilize the structure and S…S interactions have minor importance. As a part of our ongoing efforts to elucidate the structural chemistry of these complexes, we have prepared hexakis[di–μ–(trimethylsilylethanethiolato) nickel] and characterized it by single crystal X-ray diffraction analysis. The main building block of this complex, NiS_4 unit, is significantly apart from planar geometry in comparison to other known hexanuclear thiolates. The steric effect of the bulky groups at β-position in thiolate ligands is suggested to be responsible for a tetrahedral distortion of the NiS_4 units in clusters with large rings.

Henkel, G. & Chen, C. (1993). *Inorg. Chem*., **32**, 1064-1065.
Alemany, P. & Hoffmann, R. (1993). *J. Am. Chem. Soc*., **115**, 8290-8297.

P07.07.036 RUTHENIUM(II)-HALOGENOCOMPLEX-ES STABILIZED BY SCl_2. Ch.Wagner and G.Thiele, Institut für Anorganische Chemie, Universität Freiburg, Alberstr.21a, 79104 Freiburg, Germany

By reaction with sulfur and chlorine Ru-metal forms complexes $RuCl_n(SCl_2)_m$ with SCl_2 ligands [1,2]. In spite of the presence of the strong oxidation agents Cl_2 and SCl_2 Ru(II) complexes as RuS_4Cl_{12} = $[RuCl_3(SCl_2)_3]^-[SCl_3]^+$ or $Ru_2S_6Cl_{16}$ = $[(SCl_2)_2Cl_2Ru(\mu\text{-}Cl)_2Ru(SCl_2)_2Cl_2]$ prevail. SCl_2 is a voluminous ligand with one stereochemical active electrone pair. In consequence the SCl_2-ligands show an interesting stereochemical behaviour , as proofed by structure determination of several SCl_2-complexes. $Ru_2Cl_5(SCl_2)_4$ is a mixed valence binuclear complex $[(SCl_2)_3Ru(\mu\text{-}Cl)_3Ru(SCl_2)Cl_2]$. Its crystal structure contains two different molecules of the same constitution but of different orientation of the SCl_2-ligands (rotamers). This is the first time that in a single crystal structure polymorphic molecules have been found.

Forms of $Ru_2S_4Cl_{13}$ = $[(SCl_2)_3Ru(\mu\text{-}Cl)_3Ru(SCl_2)Cl_2]$ in

two modifications

[1] M.Paulus, G.Thiele, *Z.Naturforsch.* **47b** (1992), 253
[2] Ch.Wagner, F.Herzog, J.Knaudt, G.Thiele, *Z.Naturforsch*., in press

P07.07.037 ON FORMATION OF MERCURY POLYATOMIC CATIONS. L.M. Volkova, Institute of Chemistry, FE Branch of RAS, Vladivostok 690022, Russia, and S.A. Magarill, Institute of Inorganic Chemistry, Sib Branch of RAS, Novosibirsk 630090, Russia

A distinguishing crystallochemical feature of mercury is the ability to form polyatomic Hg_n cations. A large body of research has not yet recognised all factors contributing to the formation of the Hg_n cations. This work analysed a relationship between the formation of polyatomic cations Hg_n and a change in the number of the Hg atoms, Hg-Hg bond values as well as a dependence of the cation structure on increasing the number of electrons on 6s orbitals of Hg ions. The 5d AO expansion magnitude that increases with the number of 6s electrons and due to relativistic effects was shown to be crucial importance in the formation of Hg_n cations, a regular chance in the number of Hg atoms and Hg-Hg bond values, and the structure of these cations. From the fulfilment of the virial theorem in Hg_n containing compounds we can assumed that with the number of electrons on 6s AO of Hg ions greater then 1, twice decrease in electron kinetic energy will progressively be ahead of the rise in potential gravitation energy of electrons to the nucleus ($2T_e < -V_{Ne}$) owing to relativistic increase in the expansion of 5d AO. It was shown that to fulfil the conditions for state of equilibrium of a system according to the virial theorem, potential energy of the system (compound) may increase as required only through the formation of polyatomic Hg_n cations. The magnitude of the interaction potential energy between mercury ions in the Hg_n cations is determined by the number of the Hg ions, the Hg-Hg bond, and geometry of the cation. A deviation of the Hg_3^{4+} structure from general regularity and a transformation of the close-packed Hg_n layers into the linear chains on heating have been explained on the base of the virial theorem. A steric influence of 5d AO pronounced in elongation of the Hg-Hg bond with the expansion of 5d AO in response to increase in 6s orbital occupation is discussed. It is shown that in the Hg_n cations the Hg-Hg bond elongate with decreasing the possible overflow of 6s electron density from Hg to the ligand at identical average formal charge on the mercury atom.

This work is financially supported by RFBR (Grant 98-05-65223).

P07.07.038 VALENCE TRAPPING PROCESSES IN UNSOL-VATED MIXED VALENCE TRINUCLEAR IRON COMPLEXES. Finn K. Larsen, Claire Wilson, Bo B. Iversen, Marianne L. Hansen, Department of Chemistry, University of Aarhus, DK-8000 Århus C, Denmark, Sergiu P. Palii, Grigore A. Timco, Nicolae V. Gerbeleu, Institute of Chemistry, Academy of Sciences of the Republic Moldova, Acadamei Str. 3, Chisinau, MD-2028, Moldova, Guang Wu, Department of Chemistry, State University of New York, Buffalo, New York 14260-3000, USA.

Intramolecular electron transfer processes in trinuclear mixed-valence compounds of the type $[M_3O(O_2CR)_6L_3]S$ have been the subject of many studies [1]. In particular work has been carried out on trinuclear mixed-valence iron systems, $[Fe^{III}_2Fe^{II}O(O_2CR)_6L_3]\cdot S$, which allow the use of Mössbauer spectroscopy. A number of systems show temperature dependent Mössbauer spectra, changing from a trapped to a detrapped system on raising the temperature. Hendrickson and co-workers have shown that solvate molecules in the crystal can affect the rate of intramolecular electron transfer [2]. Phase transitions have been observed in many systems and it has been suggested that the valence trapping process occurs as an order-disorder phase transition involving the solvate molecules or bulky ligands. However, unsolvated systems undergoing valence trapping have also been reported. It is therefore not always clear that the phase transitions are directly connected to the electron transfer process.

We have measured multi-temperature crystallographic data on two nonsolvated mixed valence complexes $[Fe_3O(O_2CC(CH_3)_3)_6(C_5H_5N)_3]$ and $[Fe_3O(O_2CC(CH_3)_3)_6(C_5H_{10}N)_3]$. Since the complexes differ slightly only in one type of ligand, they provide suitable systems for probing what factors affect the potential energy surface of the Fe_3O core. In both complexes electron transfer mainly takes place between two of the iron sites, while the third site appears trapped at all temperatures. The dynamic behaviour of the systems leads to temperature dependent apparent bond length changes. Presumed Boltzmann distribution over three potential minima allows to estimate potential differences from the bond length distribution.

[1] Cannon, R. D.; White, R.P. *Prog. Inorg. Chem*. 1988, 36, 195-297.
[2] Wu, C. C.; Hunt, S. A.; Gantzel, P. K.; Gutlich, P.; Hendrickson, D. N. *Inorg. Chem*. 1997, 36, 4717-4733.

P07.07.039 Z-SHAPED METALLOMACROCYCLE ISOMER BROUGHT TO LIGHT. Georgina Rosair, James Cameron and Duncan P. Nicol, Department of Chemistry, Heriot-Watt University, Edinburgh, EH14 4AS

The expected saddle conformation for [16] membered Jager-type metallomacrocycles contains a cavity suitable for the binding of small molecules such as dioxygen to the metal centre. The efficacy of such reactions is dependant on cavity geometry and the interactions with the surrounding structure.

Unexpectedly, another isomer was found [1], possessing a previously unseen Z-type conformation. This isomer appears alongside the well-established saddle species in the reaction mixture.

Several by-products were structurally characterised to trace the origin of the Z isomer, one, a tris-bidentate nickel complex has three chemically distinct ligands and another, a polymer, consists of Ni centres linked by diaminopropane ligands.

Conformational and other geometric differences between the saddle and Z isomers were explored, particularly the saturated chelate ring conformation. Using the Cambridge Structural Database, conformations of related rings in [16] membered macrocycles were examined by Principal Component Analysis.

1. J. H. Cameron, D. P. Nicol and G. M. Rosair, J. Chem. Soc., Chem. Commun., 1998, 1595 - 1596.

P07.07.040 CRYSTAL STRUCTURE OF SODIUM TETRAHEXANOATOZINCATE. Primož Šegedin, Nina Lah, Gregor Rep, Ljubo Golič and Ivan Leban, Faculty of Chemistry and Chemical Technology, University of Ljubljana, Aškerčeva 5, P.O.B. 537, 1000 Ljubljana, Slovenia.

Thin plate colourless crystals of the title compound were isolated from equimolar solution of zinc hexanoate and sodium hexanoate in 96% ethanol. Each zinc atom is tetrahedrally coordinated by four O atoms from different hexanoate ligands [1.954(2), 1.964(2) Å]. Two crystallographically different sodium ions are six coordinated. Zinc bonded carboxylate oxygen atoms are coordinated to only one sodium ion, whilst the remaining oxygens are coordinated to two sodium ions. Two sets of significantly different C-O bond lengths were observed [1.279(4), 1.233(4) and 1.291(3), 1.235(4) Å].

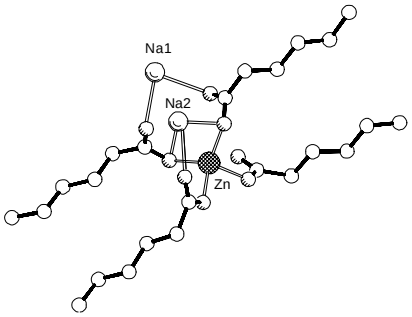

Crystal data: $C_{24}H_{44}Na_2Zn$, M_r= 571.98, monoclinic, C2/c, $\lambda_{MoK\alpha}$ = 0.71073 Å, Enraf-Nonius CAD-4 diffractometer; a = 37.605(7), b=7.7797(6), c = 10.347(2) Å, ß = 90.82(2)°, V = 3027(1) Å^3, Z = 4, D_{calc}=1.255 g/mL; R_1=0.054 for 2340 observed reflections (I>2σI), wR_2=0.147 for all 3653 reflections, refinement on F^2, 162 parameters (SHELX 97).

P07.07.041 CRYSTAL STRUCTURE OF MOLYBDENUM - RHODIUM SULFIDO CLUSTER CONTAINING $Mo_3Rh(\mu_3\text{-}S)_4$ CUBE. Haruo Akashi,[1] Akiko Nakao,[2] Takashi Shibahara,[3] [1]Research Institute of Natural Sciences, Okayama University of Science, Ridai-cho Okayama, 700-0005 Japan. [2] MAC Science Co., Ltd., Shin-yokohama Kouhoku-ku, Yokohama, 222-0033 Japan. [3] Chemistry Department, Okayama University of Science, Ridai - cho Okayama, 700-0005 Japan.

A novel sulfur bridged molybdenum – rhodium cluster $[Mo_3(\mu_3\text{-}S)_4Cp^*Rh(H_2O)_7(\mu_2\text{-}O)]_4(pts)_{16}\bullet 33H_2O$ (**1**), where Hpts = *p*-toluensulfonic acid, was synthesized by a metal incorporation reaction of $Mo_3S_4^{4+}$(aq) with pentamethylcyclopentadienyl – rhodium (III) chloride dimer $[Cp^*Rh(\mu_2\text{-}Cl)Cl]_2$.

A black crystal of **1** having approximate dimensions 0.4 x 0.35 x 0.3 mm was mounted in a glass capillary. All measurements were performed on MAC Science MXC18 (at 20°C) and DIP 2020 (at –150°C) with graphite monochromated Mo – Kα radiation. Crystal Data: **1** (at 20°C): monoclinic C2/c, a=34.111(8)Å, b=14.539(2)Å, c=25.832(4)Å, β=101.12(2)°, V=12570(3)Å^3, Z=2, R=0.055, R_w=0.065. **1** (at –150°C): triclinic P-1, a=18.3470(3)Å, b=25.772(1)Å, c=27.735(1)Å, α=99.082(1)°, β=105.111(2)°, γ=77.914(2)°, V=12305.8(7)Å^3, Z=2, R=0.051, R_w=0.1457. The structure was solved by and expanded using SHELXS-97 (Sheldrick, 1997). All calculations were performed using the maXus software package of MAC Science Corporation.

The crystal structure of **1** shows a temperature dependence, that is, the crystal system of **1** changes from monoclinic (20°C) to triclinic (–150°C). The structural disorder of pts anions at 20°C disappeared at –150°C.

P07.07.042 CRYSTALLINE COMPLEX $CUL_2(NO_3)_2$ (L=N,N'-DIETHYLETHYLENEDIAMINE) AS A VAPOCHROMIC HOST FOR WATER AND AMMONIA VAPOURS. Beena Narayanan, Discipline of Silicate and Catalysis, Central Salt and Marine Chemicals Research Institute, Bhavnagar 364 002, INDIA Mohan M. Bhadbhade, Physical Chemistry Division, National Chemical Laboratory, Pune 411 008, INDIA

There are increasing research efforts in designing sensor materials for volatile organic compounds and toxic gases. In the course of our studies on thermochromic complexes of Cu(II) and Ni(II) with the ligand N,N-Diethylethylenediamine, red copper complex $CuL_2(NO_3)_2$ which exhibits thermochromic phase transition (red ⇔ blue, 150 ° C) also showed another reversible colour change; the complex changes to blue when exposed to the open atmosphere and comes back to red when heated to 50 °C. This transition was considered as a vapochromic behaviour of the complex due to the adsorption / desorption of water molecules from the atmosphere. Several smaller gaseous entities were tried for the diffusion experiments with the red complex, but only vapours of ammonia changed the color from red to greenish-blue; which upon heating to 65°C gave back the original red complex. The diffusion into the crystalline host system and the reversible binding of these entities forming the fifth coordination with the metal center was established from the single crystal X-ray structures of complexes $[CuL_2(H_2O)](NO_3)_2$ and $[CuL_2(NH_3)](NO_3)_2$. Packing of the molecules in the parent red complex shows sufficient voids for the diffusion to take place. The square planar CuN_4 coordination geometry upon the fifth coordination from water (ammonia) changes to the distorted trigonal bipyramidal environment in both the complexes. Rotation of the ethyl groups and the orientaional changes in the nitrate anions are suggested as a mechanism for the 'vapochromic' transition due to the incoming coordinating species. It is noteworthy that one of the cell axes perpendicular to the chelate rings is constant (~ 8.3 Å) in all the three complexes. As sensing of moisture and ammonia are relevant in the industrial atmosphere, a case study with a simple transition metal complex provides some insight in designing vapochromic host systems.

P07.07.043 NEW COMPLEXES OF RUTHENIUM WITH o-BENZOQUINONEDIIMINE. Venegas-Yazigi D.[$], Mirza H.[b] , Lever A.B.P.[b#], Costamagna J[c]., Latorre R.O., Universidad de Chile, Facultad de Ciencias, Dept. Química, Casilla 653, Santiago, Chile. [$]E-mail: diego@uchile.cl, [b]York University, Dept. of Chemistry, Faculty of Pure and Applied Sciences, 4700 Keele St., Toronto, Ontario, Canada M3J 1P3. [#]E-mail: blever@yorku.ca, [c]Faculty of Chemistry and Bilogy, Universidad de Santiago, Santiago-33, Chile

Questions have been raised with respect to the evaluation of ligand electrochemical parameters [1], when the ligands concerned are themselves redox active, so called "non-innocent" ligands. In order to gain additional information, we have synthesised new complexes of ruthenium with o-benzoquinonediimine (BQDI) and various spectator innocent ligands. In this work, we show the crystal structure and some spectroscopic-structural correlations for the complexes,- $Ru(BQDI)(PPh_3)_2(Cl)_2$, $[Ru(BQDI)(PPh_3)_2(Cl)(MeCN)][PF_6]$, $[Ru(BQDI)(PPh_3)_2(MeCN)_2][PF_6]_2$.

The authors would like to thank Dr. Alan Lough of University of Toronto for X-ray assistance. We would like to thank to FONDECYT Projects 2980026 and 1970354.

[1] Lever A.B.P., *Inorg. Chem*. 1990, *29*, 1271

P07.07.044 THIOCYANATOMETALLATES OF COPPER(I) AND SILVER(I). R.Hehl, G.Thiele, Institut für Anorganische Chemie und Materialforschungszentrum FMF der Albert-Ludwigs-Universität, Freiburg. Albertstr. 21, 79104 Freiburg, Germany

In solid state structures of Halogenocuprates(I) and Halogenoargentates(I) a very large number of different polyanionic complexes can be found, due to the co-ordination flexibilty of these d^{10} cations [1]. Especially iodometallates of Ag(I) and Cu(I) exhibit an enormous diversity of their anionic structures as shown by H.Hartl et al. [2].

The application of pseudohalide ligands instead of halides in this context opens up new variation possibilities. Namely the use of the unsymmetrical SCN^- brings in the following options: function as a donor ligand with the "soft" S end

function as a donor ligand with the "hard" N end (together with the convenience of an easy distinction between the two by X-ray analysis)or function as a bridging ligand in various ways.

In the course of our investigations of the synthesis and structure of polynuclear pseudo-halogenocomplexes of d^{10}-metals we have been examining thiocyanato complexes of Ag^+ and Cu^+ [3]. Through variation of the counter ions a wide range of structural motives could be found, showing many different combinations of the possibilities of the co-ordination behaviour of SCN^-.

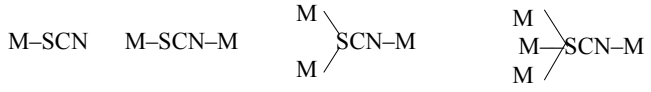

Structures with large counter ions (e.g. PPN^+) yield isolated thiocyanatometallat complexes where as smaller ones lead to one or two dimensional polymeric structures (e.g. $CsCu(SCN)_2$ and $N(CH_3)Cu(SCN)_2$ resp.). $Ph_4PCu(SCN)_2$ is an example of a compound that exists in both an isolated and a polymeric modification [3,4]. Also three-dimensional polymeric thiocyanatometallates have been synthesised.

[1] S.Jagner, G.Helgesson. *Adv. Inorg. Chem.* 37, 1991, 1.
[2] H.Hartl, F.Mahdjour-Hassan-Adabi. *Z. Anorg. Allg. Chem.* 106, 1996, 1929, and ref. therein.
[3] G.Thiele, R.Hehl. *Z. Anorg. Allg. Chem.* 624, 1998, 1736.
[4] A.Wilk, W.Massa, C.Friebel, D.Reinen. *Z. Anorg. Allg. Chem.* 608, 1992, 88.

P07.07.045 STRUCTURE OF TWO POLYMERIZABLE CHELATORS DESIGNED FOR REMEDIATION OF HEAVY METALS. Jeffrey R. Deschamps, Judith L. Flippen-Anderson and Clifford George, Naval Research Laboratory, Code 6030, Washington, DC, 20375, USA, Alok Singh, Qin Lu*, and Eddie L. Chang Naval Research Laboratory, Code 6930, Washington, DC, 20375, USA (* GeoCenters, Inc).

Remediation of heavy metals from wastewater requires the selective removal of heavy-metal ions from the waste stream. We are investigating the utilization of metal-ion templating to make ligand-bound polymers that have increased selectivity for the target metal ions. The approach is to create a polymerizable chelator monomer that can be pre-organized by templating with a target metal ion. Templating is followed by reaction with cross-linking agents to lock in the pre-organized chelation coordination. The resulting macroporous polymer is treated before use to remove the metal ions. In this study we examine how the attachment of a linker group to the chelator affects the coordination of the target metal ion with the chelator.

The structures of two polymerizable copper chelates were determined by x-ray diffraction. Data were collected with a SMART-1000 CCD. The coordination geometry of the complexes and the distance between the copper and its ligands were the key features to be studied. Compound 1 (a diamine) crystallized as plates in the space group $P2_1/c$. This compound has a coordination number of 6 (octahedral geometry with a tetragonal distortion). Compound 2 (a triamine) crystallized as rods in the space group $P2_1/n$. This compound has a coordination number of 5 (square pyramidal geometry).

This research was support in part by the Office of Naval Research.

P07.07.046 A NOVEL OXO-BRIDGED DINUCLEAR HEPTA-COORDINATED IRON(III) COMPLEX. A. Bacchi and G. Pelizzi, Dipartimento di Chimica Generale ed Inorganica, Chimica Analitica, Chimica Fisica, University of Parma, Italy , and I. Ivanovic-Burmazovic and K. Andjelkovic, Faculty of Chemistry, University of Belgrade, Yugoslavia

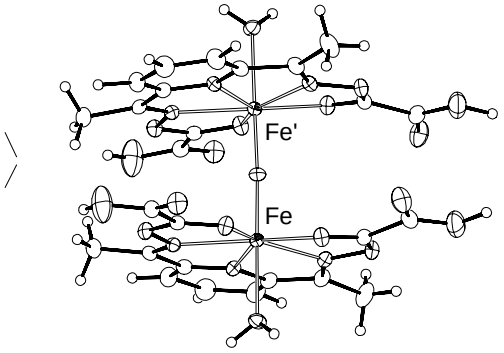

$[Fe(dapoamh)(H_2O)]_2O$

By hydrolysis of paramagnetic $[Fe(Hdapsox)Cl_2]$ [1] (H_2dapsox=2,6-diacetylpyridine bis (oxamic acid hydrazone)), the dinuclear dimeric diamagnetic complex $[Fe(dapoxl)(H_2O)]_2O{\cdot}3H_2O$ [H_2dapoamh=2,6-diacetylpyridine bis (oxalic acid monohydrazone)] is obtained. Complexes of this type may serve as synthons for methemerythrin core models. The ligand coordinates one Fe(III) by a N_3O_2 planar pentadentate system. The metal hepta-coordination geometry is completed to pentagonal bipyramid by one water molecule and one O^{2-} ion. The latter bridges two metals, giving a dinuclear dimeric neutral molecule. In the solid-state the oxo bridge sits on a crystallographic two-fold axis, and, in the dimeric complex, the two symmetry related ligands are on parallel planes and staggered by a rotation of about 140° around the Fe···Fe' direction. The angle Fe-O-Fe' is 177°. The crystal packing is based on strong hydrogen bonds involving the complex and the crystallization waters. Until now only two structures of seven-coordinated dinuclear iron(III) complexes[2] have been observed; one containing a macrocyclic ligand and the other bidentate ligands.

1. I.Ivanovic-Burmazovic, A.Bacchi, G.Pelizzi, V.M.Leovac and K.Andjelkovic, Polyhedron (1998) in press
2. H. Matsushima, K.Iwasawa, K.Ide, Md.Y.Reza, M.Kaikawa and T.Tokii, Inorg. Chim. Acta, 274 (1998) 224-228

P07.07.047 STRUCTURE OF LUMINESCENT $[AgL(PPh_3)_2NO_3]$ AND $[AgL(PPh_3)_2]NO_3$ (L=THIOUREA DERIVATIVES) COMPOUNDS. G. Pelosi, E. Cavalli, P. Tarasconi and A. Trucco, Department of General and Inorganic Chemistry, Analytical Chemistry, Physical Chemistry, Parco Area delle Scienze, Università di Parma, 43100 Parma, Italy.

The growing interest in molecule-based technologies necessitates the developments of novel materials. Among these, luminescent substances are candidates for photochemical molecular devices, as photosensitizers in electron transfer processes, as luminescent probes for biological applications and for lasers. In this context we have synthesised three ligands (Pptu, Pmptu, Pftu) having a common N-phenylthiourea moiety and different aromatic substituents on nitrogen N'.

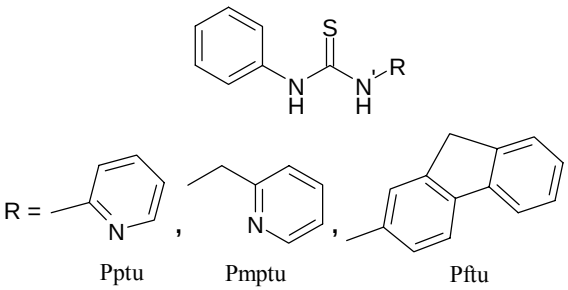

Pptu Pmptu Pftu

These compounds were stoichiometrically reacted with $[Ag(PPh_3)_2NO_3]$ in acetone/acetonitrile(1:1 V/V). The crystals obtained, $[Ag(Pptu)(PPh_3)_2NO_3]$, $[Ag(Pmptu)(PPh_3)_2]NO_3$, $[Ag(Pftu)(PPh_3)_2]NO_3$ were characterised by single crystal X-ray diffraction. The three adducts present different geometries that are related to the donor potentiality of the ligand and to the bulk of the thiourea aromatic substituent. Successively luminescence properties of these compounds were investigated and compared with the analogous Cu(I) complexes both at room temperature and at 10 K.

P07.07.048 A NOVEL METHYLOXOTIN(IV) CLUSTER CONTAINING COCARBOXYLASE. Carmen Taboada, José Sordo, María D. Couce, Agustín Sánchez and José S. Casas, Departamento de Química Inorgánica, Universidad de Santiago de Compostela, 15706 Santiago de Compostela, Spain, E.E. Castellano, Instituto de Física de São Carlos, Universidade de São Paulo, 13560 São Carlos, Brazil and Michael Ruf, Bruker AXS GmbH, P.O. Box D-76181 Karlsruhe, Germany.

The coordination chemistry of vitamin B1 (thiamine, TCl) has been extensively studied during the last twenty years, showing that this vitamin is a very versatile ligand. In spite of that, the interaction of metal ions with cocarboxylase (thiamine diphosphate, H_3CoTCl, the catalytic form of thiamine) is almost unexplored, even though a metal ion participates in the catalytic process in which cocarboxylase is involved. In order to increase the knowledge in this field, and as a part of our work on mixed diorganotin(IV) compounds, we reacted methylphenyltin(IV) dichloride with cocarboxylase in water at pH = 6. The reaction, after elimination of a phenyl group, afforded crystals of the compound {[MeSn(OH)(HCoT)]$_3$O} (OH) . 21 H_20, as was shown by a three-dimensional X-ray analysis. The structure crystallizes in the space group R $\bar{3}$, with a = b = 24.485(3) and c = 27.103(3). Data were collected using a Siemens SMART system equipped with a CCD detector; the model refined to R(F)=0.056 for 3283 reflections with I>2*sigma(I). The trimer displays crystallographic three-fold symmetry; an oxygen atom coordinated to the three Sn cations and an OH anion, both sited on a three-fold symmetry axis, contribute three electrons to the overall balance of charge.

P07.07.049 FACILE TRANSFORMATION FROM ISOLATED FRAGMENTS TO INFINITE CHAINS IN RHENIUM CHALCOCYANIDE CLUSTERS. S.B.Artemkina, N.G.Naumov, A.V.Virovets, V.E.Fedorov, Institute of Inorganic Chemistry SB RAS, Novosibirsk 630090, Russia

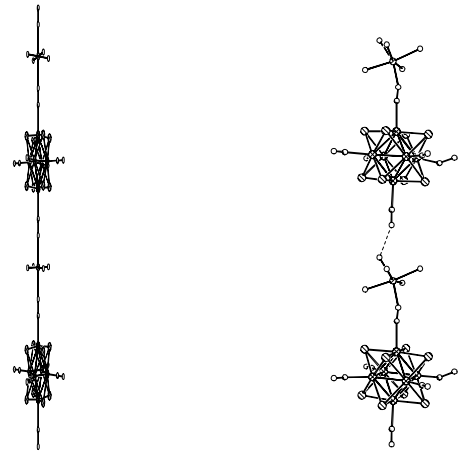

Interaction of aqueous solutions of $(n\text{-}Pr_4N)_4[Re_6S_8(CN)_6]$ and manganese nitrate results in formation of crystallohydrates of two structural types. Compound $(Pr_4N)_2Mn[Re_6S_8(CN)_6]\cdot 6H_2O$ (**1**) crystallises in space group $\boldsymbol{P2_12_12_1}$ with cell parameters a=18.286(2), b=18.345(2), c=16.568(2) □, Z=4, and consists fragments $\{Mn(H_2O)_5Re_6S_8(CN)_6\}^{2-}$ linked by hydrogen bonds (left). Compound $(Pr_4N)_2Mn[Re_6S_8(CN)_6]\cdot 4H_2O$ (**2**) crystallises in space group ***I4/m*** with cell parameters a=13.255(2), c=14.432(3) □, Z=2, and consists infinite chains $\{Mn(H_2O)_4Re_6X_8(CN)_6\}^{2-}$ formed by covalent Mn-NC-Re interactions along c axis (right). Structure of **1** may be considered as superstructure of **2**, $\boldsymbol{a_2=a_1+b_1}$, $\boldsymbol{b_2=a_1-b_1}$, $\boldsymbol{c_2=c_1}$. In both structures the cluster anions form face-centred packing motif. In the case of **2** it corresponds with the packing of whole structure in ***I4/m*** space group. But in **1** the arrangement of cations and water is less symmetrical.

Dehydratation of **1** under mild conditions results in loss of two water molecules and formation of **2**, outlining close relationships of structures. This work was supported by RFBR and Program for Support of Young Scientists of Siberian Branch of RAS.

P07.07.050 SUPRAMOLECULAR ASSEMBLY IN THE CHIRAL CRYSTAL STRUCTURE OF THE CYANINE DECAHYDRO-DECABORATE. T.M. Polyanskaya, Institute of Inorganic Chemistry SB RAS, Novosibirsk, 630090 Russia.

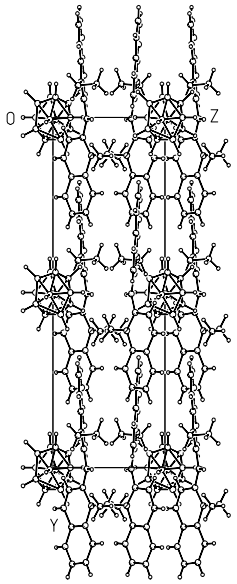

Non-centrosymmetric cyanine borates are considerably of interest owing to their potential use as nonlinear optical materials. We have carried out single crystal X-ray analysis of the title compound, $(C_{23}H_{23}N_2)^{+}{}_2\ (B_{10}H_{10})^{2-}$ (1) whose chiral structure is shown below. It is the first example of a supramolecular assembly

with participation of the ions above. The 1,1'-diethyl-2,2'-cyanine dye cation adopts a skewed conformation with approximate symmetry 2 (C_2); the dihedral angle between the roughly planar quinoline rings is 45.8°. The cations are stacked face-to-face by each quinoline ring along [001]. The molecular long axis is elongated along [010]. The overlapping of the quinoline rings is incomplete. In the columns the plane separations are greater than the usual graphite separation of about 3.4 Å because the H atoms of the ethyl groups prevent a closer mutual approach of the quinoline rings. The anions are packed in the gaps between the dye cation columns and are connected by them through close B-H...H-C contacts. The crystal data: the system is monoclinic, space group *C*2, *a*=12.293(1), *b*=22.466(3), *c*=8.1110(6) Å, β=109.35(1)°, *Z*=2, R_I=0.037. The author is grateful to Prof. V.V. Volkov for the disposable single crystals of 1.

P07.07.051 DOES AMMONIUM HEXAFLUORO-NIOBATE (V) EXIST? Frank R. Fronczek, Pamela L. Bryant, Katherine Wu, Youngil Lee, Ae Ja Kim, and Leslie G. Butler, Department of Chemistry, Louisiana State University, Baton Rouge, LA 70803-1804, USA.

Evidence for the existence of the title compound is anecdotal. We obtained samples purported to be "(NH_4) NbF_6" from a prominent commercial supplier, to be used as a tuning standard for MAS and frequency-swept ^{93}Nb solid-state NMR experiments. This compound was expected to contain octahedral Nb, and thus yield simple spectra, but its intriguing NMR behaviour led to additional NMR experiments and variable temperature X-ray crystallography. Crystal structure determinations at 100K and 333K demonstrate that this compound is actually $[NH_4]_5[NbF_4O][NbF_7]_2$, isomorphous with the previously reported Rb salt, $Rb_5[NbF_4O][NbF_7]_2$. The structure is tetragonal, I4cm, and contains both 6-coordinate NbF_4O^- (site symmetry 4) and 7-coordinate NbF_7^{2-} (site symmetry m). The NbF_4O^- moieties have axial Nb...O interactions (2.12(1) Å), forming chains in the **c** direction. Displacement parameters for F atoms of the NbF_7^{2-} moiety are large at 333K, particularly for one F lying on the mirror, which is resolved into off-mirror sites separated by 0.76(2) Å at 100K. Current solid-state NMR interest in the compound lies in its utility as a test sample for experiments designed to observe "invisible" aluminum in zeolites. Here, the NbF_4O^- is easily observed, and serves as an internal reference. The NbF_7^{2-} site is difficult to observe at 303 K, but easy at 333 K. At 100K: a=15.346(3), c=7.800(2) Å, R=0.035; at 333K: a=15.564(1), c=7.8056(4) Å, R=0.026.

P07.07.052 STRUCTURE ANALYSES OF POLYOXO-TUNGSTATES AT SPRING-8 AND BY A NEW IMAGING PLATE DIFFRACTOMETER. Tomoji Ozeki and Yuji Ohashi, Department of Chemistry and Materials Science, Tokyo Institute of Technology, 2-12-1, O-okayama, Meguro-ku, Tokyo 152-8551, Japan

The absorption effect is one of the most severe difficulties in the precise X-ray structure analyses of the crystals containing heavy elements. High energy X-rays from the third generation synchrotrons, *e.g.*, SPring-8, suffer much less absorption and are expected to provide data of high quality. To evaluate this effect, the crystal structure of sodium paradodecatungstate, $Na_{10}[H_2W_{12}O_{42}]\cdot 26H_2O$, was analyzed at the BL02B1 beamline of SPring-8 using monochromatized X-rays with 30.748keV (λ=0.3937Å). The absorption coefficient of the title compound for λ=0.3937Å is 5.25mm^{-1}, while it is 23.2mm^{-1} for the MoK_α radiation. Diffraction data up to $(\sin\theta/\lambda)_{max}$=0.90Å^{-1} were collected by a prototypic cylindrical vacuum camera attached to a Huber 7-axis goniometer. Currently no correction was applied for the absorption effect. However, the structure was refined to the $R(F)$ factor of 0.042 for 14592 reflections with $F_o>4\sigma(F_o)$, which demonstrates the effect of employing high energy X-rays.

To bring our project into the second stage, we designed a new diffractometer, named *DIP LABO*, furnished with an automated imaging-plate reader in cooperation with MAC Science Co., Ltd. The prototypic one used above required manual loading of the imaging plates. *DIP LABO* has a cylindrical imaging plate with the size of 240mm×420mm, covering the 2θ range from –60 to 140º and the ν range of ±45º. It has a κ-type 3-axis goniometer to enable versatile crystal orientation. The automatic data collection procedure utilizes the goniometer to measure all of the independent reciprocal space and invokes the *DENZO* program suite for the data integration and the scaling. It showed satisfactory performance in the preliminary experiments with the sealed tube MoK_α radiation. Now we are planing to place this diffractometer in SPring-8 to enable the automatic rapid data collection with the high energy and high brilliance X-rays.

P07.07.053 STRUCTURES OF METAL DERIVATIVES OF CIS-4-CYCLOHEXENE-1,2-DICARBOXYLIC ACID. B. M. Ramírez, G. Díaz de Delgado and J.E. Contreras, Laboratorio de Cristalografía, and W.O. Velásquez, Laboratorio de Fisicoquímica Orgánica, Departamento de Química, Facultad de Ciencias, Universidad de los Andes, Mérida 5101, Venezuela.

A series of metal complexes of *cis*-4-cyclohexene-1,2-dicarboxylic acid have been prepared in aqueous solutions by mixing stoequiometric quantities of the acid and the corresponding metal carbonate. Crystals were grown by controlled evaporation of the solvent. The complexes were characterized by FTIR and Thermal Analysis (TGA an DSC), and by single crystal X-ray diffraction at 297 K. The coordination of the metal atom, the packing arrangement, and the hydrogen bonding patterns will be presented and discussed in detail. Among the materials studied are: (1) $[Ba(C_8H_8O_4)(OH_2)]\cdot H_2O$: aqua(*cis*-4-cyclohexene-1,2-dicarboxylate) Barium(II), monoclinic, $P2_1/c$, a=12.698(1), b=8.0945(7), c=9.8361(9)Å, β=94.382(2)º, V=1008.03(15)Å^3, Z=4, Dc=2.250gcm^{-3}, R1=0.0345, wR^2=0.0934, S=0.936 for 1445 reflexions I>2σ(I (2) $[Cd(C_8H_9O_4)_2(OH_2)_3]$: triaaquabis(hydrogen *cis*-4-cyclohexene-1,2-dicarboxylate) Cadmium(II), orthorhombic, Pnma, a=12.268(4), b=27.897(8), c=5.513(3)Å, V=1886.8(13)Å^3, Z=4, Dc=1.777 g cm^{-3}, R1=0.0310, wR2=0.0816, S=1.102, for 2207 reflexions with I>2σ(I).

This work was supported by CONICIT, grants S1-95000938 and Lab-97000821, for the establishment of the Laboratorio Nacional de Difracción de Rayos-X, and by CDCHT-ULA, C-727-95-08-A. Part of this work made use of the MRL-UCSB Central Facilities supported by the National Science Foundation under Award No. DMR96-32716.

P07.07.054 CRYSTAL STRUCTURE DETERMINAT-ION OF HEXANEDIAMMONIUM FERRIC TETRACHL-ORIDE, $[C_6H_{12}(NH_3)_2Fe_{(III)}Cl_4]$. I.S.Ahmed Farag, National Research Centre, Physics Dept., Cairo, Egypt, and V.B. Rybakov, Moscow State University, Faculty of Chemistry, Moscow, Russia.

The title compound was prepared by adding $FeCl_2.4H_2O$ solution to an excess hexanediammonium chloride, dissolved in an acidified ethanol water, and then heating for one hour followed by very slow cooling. Prismatic yellowish-brown crystals were obtained with crystallographic data : a = 19.214(4) , b = 19.214(4), c = 14,458(3) Å; V = 5338(2) Å^3 ; the number of formula units = 8 ; the calculated density 1.345 g/cm^3 ; space group I 4_1/ a ; R = 0.0476 , R_w = 0.0541. The intensity data were collected on an Enraf-Nonius CAD-4 computer controlled diffractometer using Mo kα-radiation. The structure was solved by Patterson heavy-atom method and refined by full matrix least-squares using anisotropic temperature factor for all atoms, except

for hydrogen ones, which were treated isotropically. A full discussion was given to describe the structure, which consists of tetra- and hexa-coordinated Fe atoms distributed in layers. These layers are bounded to each other by the organic molecules through three dimensional network of hydrogen bonds and Van der Waals forces. $\alpha\alpha\alpha$ $\alpha\alpha\beta_{\alpha\alpha}$.

P07.07.055 IRON(0) ISOCYANIDE DERIVATIVES. J.F. Gallagher, Dublin City University, Dublin 9, Ireland, N.L. Cromhout, A.R. Manning, University College Dublin, Dublin 4, Ireland, A.J. Lough, University of Toronto, Ont., Canada, M5S 3H6.

We are studying isocyanide derivatives of iron(0) carbonyl phosphite complexes and several will be presented including the following:

(**1**) $Fe(CO)_2\{P(OPh)_3\}_2$(CN-phenyl), monoclinic, $P2_1/n$, a = 20.7273(5), b = 19.9376(6), c = 21.7240(6) Å, β = 116.863(12)°, V = 8008.7(4) Å^3, Z = 8, T = 150 K, D_x = 1.386 Mg.m^{-3}, R = 0.045 for 8753 reflections > 2σ(I). Compound (**1**) crystallises with two molecules in the asymmetric unit, **A** which is not disordered and a highly disordered molecule **B**.

(**2**) $Fe(CO)_2\{P(OPh)_3\}_2$(CN-*p*-tolyl), monoclinic, *C2/c*, a = 17.6897(10), b = 12.9983(10), c = 17.6460(15) Å, β = 96.079(6)°, V = 4034.6(5) Å^3, Z = 4, D_x = 1.399 Mg.m^{-3}, R = 0.037 for 3760 reflections > 2σ(I). Compound **2** resides about a two-fold axis which contains the iron atom and the tolyl isocyanide ligand.

(**3**) $Fe(CO)_2\{P(OPh)_3\}_2$(CN-mesityl), monoclinic, *C2/c*, a = 19.277(3), b = 13.0802(10), c = 18.251(4) Å, β = 109.697(14)°, V = 4332.6(11) Å^3, Z = 4, D_x = 1.345 Mg.m^{-3}, R = 0.041 for 4972 reflections > 2σ(I). Compound **3** resides about a two-fold axis which contains the iron atom and the mesityl isocyanide ligand.

P07.07.056 CRYSTALLOGRAPHIC STUDY OF DIMETHYL SULFOXIDE COMPLEXES OF ZIRCONIUM SULPHATE. G.J. Kruger, Department of Chemistry and Biochemistry, Rand Afrikaans University, P O Box 524, Auckland Park, Johannesburg 2006, South Africa and H-J. de Jager, Institute of Applied Materials, University of Pretoria, Pretoria 0002, South Africa.

Some of the products which are formed when the oxides of Ti, Zr and Hf are reacted with ammonium sulphate, are soluble in water and can be purified by filtration and recrystallization from various solvents. The preparation and structures of these products are currently under investigation. The complex tetra(dimethyl sulfoxide)zirconium sulphate is one of the adducts that resulted during an attempt to grow single crystals by recrystallization from mixtures of water and dimethyl sulfoxide. The structure of $Zr(SO_4)_2(dmso)_4$ is shown in the figure.

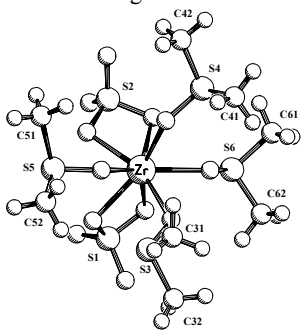

The complex contains a pseudo two-fold axis. It crystallises in the space group Cc with four formula units per monoclinic cell with dimensions a=16.1956(18)Å, b=9.7844(14)Å, c=14.6308(18)Å and beta=104.243(9) degrees.

P07.07.057 REACTION OF [IrCl(diphosphine)]$_2$ WITH NEUTRAL LIGANDS AND THE STRUCTURE OF IrCl(binap)PPh$_3$. T. Yamagata, K. Nakajima, A. Iseki and K. Tani. Department of Chemistry, Graduate School of Engineering Science, Osaka University, Toyonaka, Osaka 560-8531, Japan.

In recent years we have reported the isolation and the structure of the extremely air-sensitive dinuclear complex, $[IrCl\{(R)\text{-binap}\}]_2$[1] (BINAP = 2,2'-bis(diphenylphosphino)-1,1'-binaphthyl) and its unique reactivity toward in methanol and water.[2] In addition, the complex $[IrCl(binap)]_2$ served as an efficient catalyst precursor for asymmetric hydrogenation of prochiral imines.[3] Thus, we have taken a great interest in the reactivity of complexes, $[IrCl(diphosphine)]_2$ (**1**) (diphosphine = BINAP, diphosphine = BPBP: 2,2'-bis(diphenylphosphino)-1,1'-biphenyl) and examined the reaction of **1** with monodentate neutral ligands.

The complex **1** easily reacted with two equivalents of several neutral ligands, L (L = PPh_3, $P(OPh)_3$, etc) at ambient temperature to give the corresponding mononuclear complexes, [IrCl(diphosphine)(L)], in good yield fairly air-stable crystals. The structure of $IrCl\{(R)\text{-binap}\}PPh_3$ (**2**) has been determined by X-ray crystallography.

Crystal Data for **2**: a = 18.579(5), b = 18.579, c = 13.368(6) Å, γ= 120.0º, V = 3996(2) Å^3, trigonal, $P3_1$, Z = 3, μ = 2.684 mm^{-1}, F(000) = 1674, refinement on F^2, R1 = 0.0467, wR2 = 0.1323 for 9687 reflections ($I > 2\sigma(I)$), R1 = 0.0751, wR2 = 0.1470 for 12250 reflections (all data).

T. Yamagata, A. Iseki & K. Tani (1997). Chem. Lett, 1215-1216.
K. Tani, A. Iseki & T. Yamagata (1998). Angew. Chem. Int. Ed., **37**, 3381-3383.
K. Tani, J-I. Onouchi, T. Yamagata & Y. Kataoka (1995). Chem. Lett, 955-956.

P07.07.058 COORDINATION, PACKING ARRANGEMENTS, AND HYDROGEN BONDING PATTERNS IN METAL CITRACONATES AND MESACONATES. G. Díaz de Delgado, A. Briceño, and T. González. Laboratorio de Cristalografía, Departamento de Química, Facultad de Ciencias, Universidad de Los Andes, Mérida, 5101, Venezuela.

The results presented in this contribution are part of a systematic study of the structures of metal derivatives of citraconic (methylmaleic) and mesaconic (methylfumaric) acid. The interest in this type of materials arise from previous observations of dimerization, polymerization, and isomerization reactions in related metal derivatives of unsaturated mono- and dicarboxylic acids.

The metal citraconates and mesaconates studied tend to crystallize as two-dimensional coordination polymers. In some cases, the layers are connected through hydrogen bonds, as in the case of Ba-mesaconate. The two-dimensional nature of the structure of these materials favors a parallel disposition of the potentially reactive double bonds, which could make them reactive in the solid state. For example, in Ba-mesaconate there is an infinite chain of contacts of 4.168 Å between double bonds of neighboring molecules related by translation.

The geometric disposition of the potentially reactive double bonds, the coordination environment of the metal atoms and the carboxylate groups, as well as the hydrogen bond patterns will be presented and discussed in detail.

This work was supported by CONICIT, grants S1-95000938 and LAB-97000821 which established the Laboratorio Nacional de Difracción de Rayos-X and by CDCHT-ULA, grant

C-727-95-08-A. Part of this work made use of the MRL-UCSB Central Facilities, supported by the National Science Foundation under Award No. DMR96-32716.

P07.07.059 THE CRYSTAL STRUCTURE OF $[Co(H_2biim)_3][NO_3]_3$. S. Borg, D. Karlsson and L. Öhrström, Department of Inorganic Chemistry, Chalmers University of Technology, SE-412 96 Göteborg, Sweden

The preparation of structures with predefined properties by assembling discrete molecular units is a fast developing area in synthetic chemistry. 1-, 2- and 3-dimensional networks can be created by using transition metal complexes with bis-chelating ligands or ligands that can form hydrogen bonds. These building blocks can be joined by other metal ions, organic molecules or other complex ions.

$[Co(H_2biim)_3][NO_3]_3$ (H_2biim = 2,2′-biimidazole) is an example of a transition metal complex with capacity for both metal coordination and hydrogen bonding. The structure of racemic $[Co(H_2biim)_3][NO_3]_3$ has been determined by single crystal X-ray diffraction. It consists of Co(III) centers hexacoordinated by three H_2biim ligands in an octahedral arrangement. Each H_2biim ligand is hydrogen bonded to one nitrate ion. It is worthwhile noting that in most crystal structure determinations with biimidazole ligands it is the mono- or di-deprotonated form that is present.

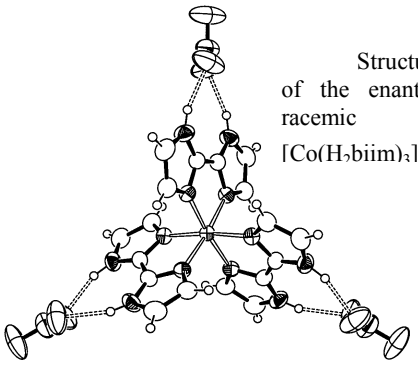

Structure of one of the enantiomers of racemic $[Co(H_2biim)_3][NO_3]_3$.

P07.07.060 COORDINATION CHEMISTRY: BIS-BIDENTATE NiN_2X_2 COMPLEXES, H-BONDING IN V(V) COMPLEXES, & Li- AND H-BONDING TO $-CF_3$. Oren P. Anderson, Sean S. Amin, Thomas Barbarich, Agnete la Cour, Debbie C. Crans, Subodh K. Dutta, Anastasios D. Keramidas, Mohammad Mahroof-Tahir, Susie M. Miller, & Steven H. Strauss, Department of Chemistry, Colorado State University, Fort Collins, Colorado 80523, USA; Alan Hazell, Department of Chemistry, Aarhus University, Århus, Denmark; Lothar Hennig, Department of Chemistry, Leipzig University, Leipzig, Germany.

We have investigated the spin state in non-coordinating solvent of similarly substituted bis-bidentate four-coordinate nickel(II)N_2X_2 complexes and of their Lewis acidity in coordinating solvent by ^1H NMR and electronic spectroscopy. The N_2S_2 aza complexes are low-spin in solution, the N_2S_2 Schiff-base and the N_2O_2 aza complexes are in spin equilibrium, and the N_2O_2 Schiff-base complexes are high spin. We present here the crystal structures of selected ligands and of their corresponding four-coordinate (X = S) or six-coordinate (X = O) nickel(II) complexes.

Hydrogen bonding patterns between oxovanadium(V) complexes were investigated in an attempt to discover a hydrogen-bonded dimeric mode of binding for LV(O)(OH) that would be analogous to the dimeric hydrogen bonding commonly found for carboxylic acids RC(O)OH. Among the diverse intercomplex hydrogen bonding patterns studied, the closest example of this analogous dimeric hydrogen bonding was found for the complexes [VO(Hhnbide)(OR)] (R = Me, Et).

Lithium salts of fluoroalkoxo-aluminate anions of the types $Li^+Al(OCR(CF_3)_2)_4^-$, $Li^+AlR(OCR(CF_3)_2)_3^-$, and $Li^+AlF(OCR(CF_3)_2)_3^-$ (R = alkyl, fluoroalkyl, aryl, or fluoroaryl) containing 3–6 Li–F(C) bonds were studied. Significant lengthening of C–F(Li) bonds and significant shortening of the other C–F bonds in a CF_3 group interacting with Li^+ ion was observed. In highly fluorinated alcohols of the type $HO(Ar_f)(CF_3)_2$, O–H···F–C hydrogen bonding can be linear and can slow the rotation of the CF_3 group so that separate ^{19}F NMR resonances are observed.

P07.07.061 STRUCTURAL AND MAGNETIC PROPERTIES OF NEW ORGANOMETALLIC VANADIUM COMPOUNDS. Ramos Silva, M., Paixão, J. A., Matos Beja, A. Alte da Veiga, L. Departamento de Física, Universidade de Coimbra, 3000 COIMBRA, Portugal

The aim of this study was to prepare compounds where there was formation of magnetic entities or isolated magnetic chains. Two hexafluoro-vanadium compounds have been prepared and their structural and magnetic properties investigated. One of these, diphenylguanidinium hexafluorovanadate, crystallizes in a monoclinic structure with space group C2/c. The vanadium atoms lie in a special position of –1 symmetry. The conformation of the cation ($C_{13}N_3H_{14}$) is such that the two phenyl rings are both oriented *anti* to the unsubstituted N atom (other conformations of this ion have been reported [1], [2]). An hydrogen bonding system stabilizes the structure linking each diphenylguanidinium ion with two different VF_6 ions.

The other compound, argininium hexafluorovanadate, crystallizes in a monoclinic structure with $P2_1$ space group . In the assymetric unit cell there are three argininium ions, one hexafluorovanadium ion, and three water molecules. Two of the argininium ions ($C_6H_{14}N_4O_2$) have closely similar conformations while the other is slightly disordered. The crystal packing is stabilized by an extensive three-dimensional network of hydrogen bonds.

Magnetization measurements results will be presented.

1. "N-N'-Diphenylguanidinium hydrogenselenite monohydrate", J. A. Paixão, A. Matos Beja, M. Ramos Silva, E. de Matos Gomes, J. Martín-Gil, F. Javier Martín-Gil, Acta Cryst. C53(1997) 1113-1115.
2. "Crystal structure of N,N′-diphenylguanidinium perchlorate", J. A. Paixão, P. S. Pereira Silva, A. Matos Beja, M. Ramos Silva, L. Alte da Veiga, Z. Kristallogr. 213 (1998) 419-420.

P07.07.062 CHALCOGENIDE CLUSTERS $H_2Fe_3X(CO)_9$ (X = Se, Te) AND THEIR HETERONUCLEAR DERIVATIVES: SOME STRUCTURAL FEATURES. S.N. Konchenko, A.V.Virovets and N.V.Podberezskaya, Institute of Inorganic Chemistry SB RAS, Novosibirsk 630090, Russia.

It has been shown that the chalcogenide carbonyl clusters $H_2Fe_3X(CO)_9$ (X = Se, Te) are the useful starting reagents for the synthesis of heteronuclear derivatives through the addition of another vertex to the cluster core or through the isolobal substitution of organometallic fragments. The number of the Co, Mo, W-substituted compounds and the compounds containing both 16 and 15 groups elements have been obtained by these methods. The examples of the structures determined are represented in the figures:

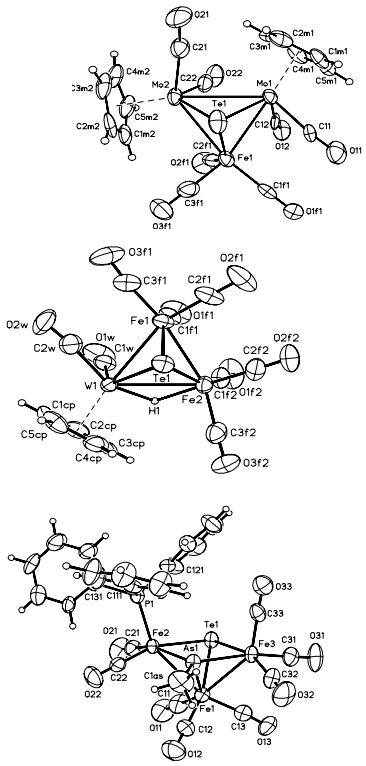

Some interesting structural features have been found: all the molecule are non-symmetric in the crystalline state; the structures of all telluride compounds significantly differ from their selenide analogs; the coordination number of Te in $FeMo_2Te(CO)_7Cp_2$ is 7 due to the short contacts with C and O atoms of carbonyl ligands, etc. (see [1,2] and literature cited therein).

This work was supported by RFBR.

1. S.N. Konchenko, et al. *Polyhedron.* (1997) **16**, 1689.
2. S.N. Konchenko, et al. *Zhurn. Strukt. Khim.* (1998) **39**, 894 (in Russian).

P07.07.063 STRUCTURE OF POLYNUCLEAR HYDROXOCOMPLEXES OF PALLADIUM (II). E.M.Moroz, S.Yu.Troitskii, S.V.Bogdanov, V.A.Likholobov. Boreskov Institute of catalysis, 630090, Novosibirsk, Russia

We have studied how the polynuclear hydroxokomplexes of palladium(II) (PHC) absorb on carbon materials. We have found that PHC do not change their chemical composition when sorb from their aqueous solutions.

The X-ray RED (radial electronic density distribution) method shows that initial PHC consists of clusters (<10 Å), where metal-metal distances are typical for the chain fragments of PdO structure. As PHC adsorb on carbon materials at room temperature or as the PHC suspension is dried in air at 400 ^{0}C, the bulk particles of PdO structure start to form. The size of PdO particles obtained via adsorption is 15 Å, while that of the particles obtained via drying without carbon support is 25 Å.

We have also obtained the atomic resolution TEM images of sorbed PHC. Simulating the images and using the crystal structure models we have shown that the final product of sorbed PHC drying represents PdO particles containing 100 Pd atoms each. At the high degrees of support surface coverage the PHC particles can grow as complexes of low nuclearity migrate over the surface.

P07.07.064 NITROSYL COMPLEXES OF RHENIUM. T.J. Bartczak and W. Czurak, X-Ray Crystallography Laboratory, Institute of Ecological and General Chemistry, Technical University of Lodz, 90-924 Lodz, Poland, and J.O. Dziegielewski[†], A. Jankowska[†], B. Machura,[†], J. Kusz[‡] and J. Warczewski[‡], Department of Inorganic and Radiation Chemistry[†], Institute of Physics[‡], Silesian University, 40-006 Katowice, Poland.

More than ten new rhenium nitrosyl, six-coordinate complexes of general formula $[ReX_3(NO)(L_2)]$ (where X = Cl or Br, L = PPh_3 or $OPPh_3$) have been prepared via new synthetic routes and characterised by X-ray crystallo-graphy, IR, UV-Vis, ^{31}P NMR and magnetochemical measurements. All complexes can be considered as derived formally from $[ReCl_4(PPh_3)_2]$ [1] by substitution of Cl for Br and NO group and PPh_3 for $OPPh_3$ in some cases. The $[ReBr_3(NO)(PPh_3)]$ complex (I) crystallises in the monoclinic space group C2/c, with Z = 4 and a = 24.621(2), b = 9.570(1), c = 16.005(1) Å, β = 116.96(1)^o; the $ReBr_3(NO)(OPPh_3)]$ complex (II) crystallises also in C2/c, with Z = 4 and a = 14.087(1), b = 13.232(1), c = 19.739(2) Å, β = 96.04(1)^o. The complexes (I) and (II) are isostructural with their chloride counterparts: $[ReCl_3(NO)(PPh_3)_2]$ (III) [2] and $[ReCl_3(NO)(OPPh_3)_2]$ (IV) [3]. The $[ReCl_2(CO)(NO)(PPh_3)_2]$ (V) [2] is also isostructural with (I) and (III).This complex has been prepared by simpler two-stage synthesis:

- $[ReOCl_3(PPh_3)_2] \rightarrow [ReCl_3(NO)(OPPh_3)(PPh_3)]$
  $\rightarrow [ReCl_2(CO)(NO)(PPh_3)]$

instead of a five-stage process described before. The metal coordination is distorted octahedral in all complexes with a linear Re—N—O system.

This work was financially supported by the Polish State Committee for Scientific Research (contract N^o PB 1218/T09/97/12).

1. J.O. Dziegielewski, T.J. Bartczak & B. Machura (1996). Polyhedron, 15, 2813.
2. T.J. Bartczak, W. Czurak, J.O. Dziegielewski, B. Machura, A. Jankowska, J. Kusz & J. Warczewski (1999). Submitted to Polyhedron.
3. J.O. Dziegielewski, B. Machura, T. Kupka, T.J. Bartczak, W. Czurak, J. Warczewski & J. Kusz. J. Coord. Chem. (1999). In press.

P07.07.065 STRUCTURAL PROPERTIES OF NEUTRAL AND CATIONIC (η^2DIARYLKETONE)-(HYDRIDO)ZIRCONOCENE COMPLEXES. R. Fröhlich, U. Blaschke, and G. Erker, Organisch-Chemisches Institut der Universität Münster, Corrensstraße 40, D-48149 Münster, Germany , and M. Nissinen, and E. Wegelius, University Jyväskylä, Department of Chemistry, P.O.Box 35, FIN-40351 Jyväskylä, Finland.

The (η^2-diarylketone) zirconocene $[Cp_2Zr(OCAryl_2)]_2$ dimers react with group 4 metallocene dihyride complexes $^RCp_2MH_2$ yielding dimetallic compounds [1]. Main structural feature of this dimetallabicyclic framework is the bridging of the two metal centers by the η^2-diarylketone ligand oxygen atom and a μ-hydride ligand. The remaining hydride ligand ist trans-oriented to the μ-H moiety of the $^RCp_2M$ unit. Variations of the metal (Zr, Hf), the aryl part (phenyl, p-tolyl), and ^RCp ligands (Cp, MeCp) lead to several compounds, three of them were characterized by X-ray diffraction. In most cases the hydrogen atoms could be located from Difference Fourier maps.

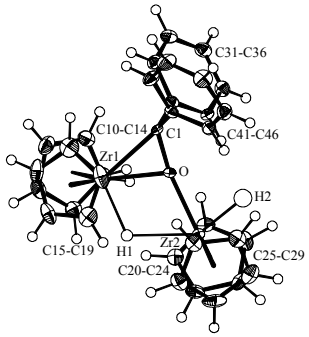

Treatment of this complexes with $B(C_6F_5)_3$ lead to selective abstraction of the terminal hydride atom and the formation of the corresponding cationic compounds, again a dimetallabicyclic framework with the same bridging of the metals.

Details of the analyses and a comparison of the structures will be presented.

1. U. Blaschke, G. Erker, M.. Nissinen, E. Wegelius & R. Fröhlich, (1999), *Organometallics* **18**, in press.

P07.07.066 CRYSTAL STRUCTURE OF $(Ph)_2NCH_2P(Ph)_2$ AND $[(Ph)_2NCH_2P(Ph)_2]_2AgCl$. Ju-Chun Wang, J. Y. Chen and Tai-Chiun Keng, Department of Chemistry, Soochow University, Taipei, Taiwan, 111, ROC.

Compound $(Ph)_2NCH_2P(Ph)_2$ (1) abbreviated as PCN, crystallized in a P1 chiral space group. Four phenyl-rings on the molecule are the major contribution to the crystal packing. Thus, three central atoms P,C and N, are packed disordered. The site occupancy factor for these three atoms is 60% for P1C1N1 and 40% for P2C2N2. Due to this disorder, the P-C (central C-atom) and N-C (central C-atom) distances are constrained to 1.80(2)Å and 1.540(1)Å, respectively. Compound $[(Ph)_2NCH_2P(Ph)_2]_2AgCl$ (2) is formed by the reaction of PCN with AgCl in a two to one mole ratio. Both two PCN ligands use their P-atom to coordinate to the Ag metal ion and leave their N-atom free. The coordination geometry about Ag is close to a trigonal planar with the Ag-P distances of 2.419(1) and 2.448(1)Å and the Ag-Cl distance of 2.507(1)Å. The largest deviation from the plane formed by Ag-Cl-P1-P2 is 0.01Å. Due to the large steric effect of the organic ligand, the P-Cu-P angle is 135.36(3)° that is about 15° larger than the normal 120°.
Crystal data: (1), a=5.7290(6), b=8.8486(10), c=10.3876(12)Å, α=73.601(2) β=81.788(2), γ=89.312(2)°, V=499.76(10)Å^3, triclinic, P1, R1=0.0512; (2), a=17.946(2), b=11.451(2), c=22.036(2)Å, β=106.780(7)°, V=4335.6(9)Å^3, monoclinic, $P2_1/c$, R1=0.0383.

P07.07.067 PRECURSOR OF A POTENTIAL X-RAY CONTRAST AGENT, $C_{39}H_{51}BiO_9$. M.S.Løiten, H. Stener, B. Fjærtoft, School of Pharmacy, Department of Medicinal Chemistry, University of Oslo, Norway

As the main contrast parameter in X-ray imaging is electron density, heavy atoms are essential in potential contrast agents. Soft tissue gives low contrast effect relative to the surrounding organs and a contrast agent is often nessesary to improve the images to give the correct diagnosis.

As a part of our work on pharmaceuticals for medial imaging and precursors thereof, we here present one such compound.

The structure of tris-[2-(2,2-dimethyl-1,3-dioxolane-4-(methoxymethyl)-phenyl]bismuth, $C_{39}H_{51}BiO_9$, Mw = 872.78 g mol-1 has been determined by single crystal X-ray diffraction at 150 K. The compound crystallizes in a trigonal space group, no. 148, Z = 6. R = 0.0432 for 7616 unique reflections.

The compound has three chiral carbon atoms. The crystal structure has a trigonal symmetry, with one third of the molecule (i.e. one of the three 1,3-dioxolane substituted side chains and the phenyl ring) in the asymmetic unit and bismuth in a special position. The aromatic rings from two molecules are inclined at 90°, the shortest distance being 3.5 Å between the rings. Hydrophilic parts in the molecules pack against each other. The five-membered 1,3-dioxolane ring has an envelope conformation. Bi is surrounded by 3 + 3 oxygen atoms at 2.276(2) Å and 2.998(2) Å.

P07.07.068 STRUCTURE CHARACTERISTICS OF SIX ORGANOMETALLIC COMPOUNDS CONTAINING SI AND FE. Yao Xinkan and Wang Honggen, Central Laboratory, Nankai University, Tianjin, 300071, China, and Zhou Xiuzhong, Chemistry Department, Nankai University, Tianjin, 300071, China.

The crystal and molecular structures of six compounds containing both of dimethylsilyl(dimethylgermyl) and dicarbonyliron were determined. The skeleton structure formula of these compounds follows (Cp = tert.-butylcyclopentadienyl or tetramethylcyclopentadinyl or indenyl or tetrahydroindenyl)

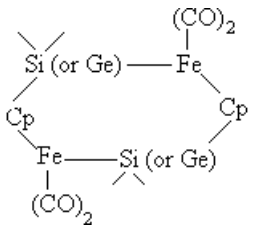

The distances between Fe atom and five C atoms of the cyclopentadinyl of Cp for these six compounds are in the range of 2.106~2.125 Å. So it can be seen that the π-bonding formed by Fe and five C atoms of the cyclopentadinyl of the Cp is the rigid part of the whole molecule, no matter that the Fe is bonded to Si or to Ge, and no matter what the Cp is.

Some of the least-squares planes formed by two Fe atoms and two Si (or Ge) atoms are the crystallographic planes, and some of them are not (the deviations from the plane are in the range of 0.1~0.4Å), even if the same molecules exist in one crystal. The dihedral angles between this plane and the five-member ring plane included in Cp is various, from 45.9° until 118.5° .It seems that the different Cp has an important influence on conformations of this kind of molecules, and yet any regularity was not been found out.

As long as the Cp was the same, the dihedral angle value between two five-member ring planes included in one molecule was the same, no matter that the molecule was composed of Fe-Si or Fe-Ge.

When Cp was different, the bond lengths of Fe-Si were not changed obviously, but the bond lengths of Fe-Ge were changed quite obviously.

All the non-bond distances Fe-Si, Fe-Ge, Fe-Fe, Si-Si, and Ge-Ge in molecules were changed obviously owing to the different Cp, thus the flexibility of this kind of compounds emerged.

P07.07.069 $(C_8H_{12}N)_2CuCl_4$: FIRST EXAMPLE OF A PLANAR $CuCl_4^{2-}$ ION IN THE ABSENCE OF STRONG HYDROGEN BONDING. Marcus R. Bond and Michael L. Rodgers, Department of Chemistry, Southeast Missouri State University, Cape Girardeau, MO 63701; Carl J. Carrano, Department of Chemistry, Southeast Missouri State University, San Marcos, TX 78666.

$CuCl_4^{2-}$ exhibits coordination geometries, ranging from distorted tetrahedral to square planar, that are matched by a corresponding range of colors, from orange to dark green. Tetrahedral geometry generally occurs in the presence of weak

hydrogen-bonding cations (such as quaternary ammonium ions); square planar geometry has, until now, been found only in the presence of strong hydrogen-bonding cations.

The title compound crystallizes by slow evaporation as large emerald green blocks from concentrated HCl solution containing stoichiometric amounts of 1,2,3-trimethylpyridinium chloride and copper(II) chloride dihydrate. A crystal structure determination with complementary spectroscopic measurements confirms the presence of square planar $CuCl_4^{2-}$ that was first indicated by the color. This geometry is achieved, surprisingly enough, in the presence of a quaternary pyridinium cation that should be incapable of strong hydrogen-bonding. The square planar geometry in this case appears to provide optimal packing of the anionic metal complex with the planar cation and suggests that packing forces must also play a major role in determining $CuCl_4^{2-}$ geometry.

Crystal data: Monoclinic C2/c, a=13.380(5)Å, b=9.285(2)Å, c=8.769(2)Å, β=116.83(3)°, V=972.1(6)Å^3, *Z*=2, 716 reflections collected (553 unique, observed), least-squares refinement of 89 parameters to *R*=0.0431 and *wR*=0.0518.

P07.07.070 A TRINUCLEAR RUTHENIUM(II) COMPLEX WITH RARE S,O-BRIDGING SULFOXIDE LIGANDS. P.H. van Rooyen, S. F. Lessing, S. Lotz and H.M. Roos. Department of Chemistry, University of Pretoria, Pretroia 0002, South Africa.

The trimetallic compound $[Ru_3(\mu\text{-}mpso\text{-}S,O)_2(\mu\text{-}Cl)_4(mpso\text{-}S)_4Cl_2]$ (*mpso* = C_7H_8OS, methyl phenyl sulfoxide) **1**, was prepared from hydrated $RuCl_3$ and methyl phenyl sulfoxide. A crystal structure determination of **1** revealed a linearly arranged molecule with three ruthenium atoms in distorted octahedral configurations with bridging chloro and S,O-*mpso* ligands. This is the first example of S,O-bridging sulfoxide ligands other than *dmso,* and where two such bridges are found between two Ru-atoms . For the Ru metals with triply bridged chloro ligands, the Ru - Cl - Ru angles are 81.8(4), 82.7(1) and 83.2(1)°, and the Ru...Ru non-bonded distance is 3.218A. In contrast, the Ru - Cl - Ru angle on the bridging *mpso* part of the molecule is 100.7 (1)°, and the Ru...Ru non-bonded distance is 3.686A. The configuration at sulfur on S2, S3, S4 and S5 is opposite to that at S1 and S6. In solution, the methyl resonances in the ^1H and ^{13}C NMR spectra of **1** are found in the δ-ranges of 3.81 - 2.70 and 49.7-44.9 ppm, respectively. The methyl resonances of the S,O-bridging *mpso* ligands are shifted upfield in the ^1H NMR spectrum, but furthest downfield in the ^{13}C NMR spectrum.

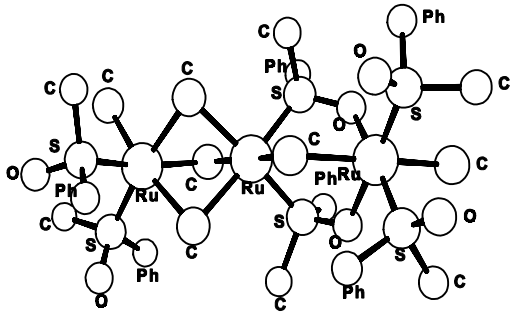

Ph = phenyl

P07.07.071 SPECTRAL SIMILARITY BETWEEN TETRACYANOPYRROLI-ZINATO METAL COMPLEXES AND PHTHALOCYANINES. V. Fares, A.Flamini, and A. Pifferi, ICMAT / ISC, Area della Ricerca del CNR, Roma, Italy.

The metal(II) complexes ML_2 of a tetracyanoethylene derivative, the ligand 1,2,6,7- tetracyano - 3,5 - dihydro -3,5-diimino-pyrrolizinide (L), show optical spectra, due to the π - π * transition, closely similar, specially in the low-energy region (Q band), to those of metal phthalocyanines MPc's, so that they could be used as spectroscopic models for better understanding the electronic structure of porphyrinic systems. In this context, by using polarized specular reflectance measurements on single crystals, the optical spectrum of FeL_2 was assigned in D_{2h} [1]. It was found that the Q band in this system is originated from four different electronic transitions ($Q_{(x)}$, $Q'_{(y)}$, $R_{(x)}$, $R'_{(y)}$). By analogy the same band in the MPc's (D_{4h}) should be composed of two electronic transitions ($Q_{(x,y)}$, $R_{(x,y)}$), in contrast with the widely accepted assignment, according to which the Q band in MPc's is due to a single electronic transition plus a vibronic component.

Recently we found that the acetylacetonide ligand (Acac) may coexist with L in coordinating the same metal center, and that the monopyrrolizinato ML(Acac) derivatives too have optical spectra stictly similar to the corresponding MPc's.

On these grounds, we synthesized and characterized a series of homologous monopyrrolizinates in order to compare their optical spectra with those of ML_2 and MPc's, with the aim of providing further experimental data for a rationalization of the observed spectra based on molecular orbital calculations.

Furthermore, the nickel complex NiL(DPM) (DPM = 2,4-t-butyl acac) shows an exceptional solvatochromism in solution by varying the coordination properties of the solvent.

The X-ray analysis of NiL(DPM) (1) and the corresponding pyridine solvate $NiL(DPM)(Pyr)_2.2Pyr$ (2) was undertaken. Given the micro-dimensions of its crystals, intensity data of compound 1 were collected on the synchrotron Hard X-ray Diffraction beam-line of ELETTRA (Trieste) and processed by DENZO and CCP4 programs. The structural results suggest that the observed solvatochromism is due to a large variation of the Q band in both energy and intensity related to a significant variation (0.19 □) of the Ni-N bond distances in the molecular plane.

1. Hoffman, C.B.; Fares, V.; Flamini, A.; Musselman, R.L. *Inorg. Chem*., in press

P07.07.072 A NEW TRINUCLEAR COPPER(II) COMPLEX INVOLVING A PYRAMIDAL Cu_3 O(H) CORE. M. Liu-Gonzalez*and F. Sanz-Ruiz, Department of Termology, Faculty of Physics, University of Valencia, 46100 Burjassot, Valencia , Spain and S. Ferrer and Y. Bertomeu, Department of Inorganic Chemistry, Faculty of pharmacy, University of Valencia, 46100 Burjassot, Valencia , Spain.

The reaction of the ligand Haaat (Haaat =3-Acetylamino-5-amino-1,2,4-triazol (3mmol) with copper nitrate (3 mmol) in presence of ethylendiamine (1 drop) in water has allowed us to isolate single crystals of $[Cu_3(aaat)_3(\mu_3\text{-}OH)(H_2O)_3)(NO_3)_2.(H_2O)$ (1), As far as we know, this is the first structure described of a compound of (H)aaat. The complex contains a triangular Cu_3 skeleton in which the copper atoms are held together by two bridging systems:(i) the oxygen atom of the tridentate OH group, and (ii) the *N1,N2*-diazinic groups from the triazole rings of three pseudo symmetry-related aaat ligands.

Crystal Data: $Cu_3O_{14}N_{27}C_{12}H_{27}$, Mr = 824.13, Triclinic, space group P-1, a =8.8518(12) Å, b = 11.491 (3) Å, c = 15.404 (3) Å, α = 70.43(3)º, β = 75.11(2)º, γ = 88.43 (3)º, V= 1423.8 (5) A^3 , Z = 2, D_X = 1.922 Mg/m^3, Mo Kα radiation (graphite crystal Monochromator, λ = 0.7173 Å), μ =2.315 mm^{-1}, F(000) = 834, T = 293 K., Final conventional R = 0.0828, and wR2 = 0.2326 for 3432 'observed' reflections and 460 variables. Throughout the experiments Mo Kα was used with a graphite crystal monochromator on a Enraf-Nonius CAD4 Single Crystal Diffractometer (λ= 0.71073 Å).

P07.07.073 SYNTHESIS AND CRYSTAL STRUCTURE OF N-2-PYRIDYL-METHYLIDENE-1-PHENYLETHYL-AMINE-PDCL$_2$ COMPLEXES. E. Lukevics, I. Iovel, A. Mishnev. Latvian Institute of Organic Synthesis, 21 Aizkraukles St., LV-1006 Riga, Latvia

The complexes of transition metals with optically active ligands, including Schiff bases, are used as the chiral inductors in a large number of the asymmetric catalytic processes. The complexes of $PdCl_2$ with imines have been derived from 2-pyridinealdehyde and (*R*)- and (*S*)-1-phenylethylamine (complexes **I** and **II** respectively). The palladium complex **I** ($C_{14}H_{14}N_2PdCl_2 \cdot 1/2$ 1,4-dioxane) crystallizes in $P2_1/c$ space group while complex **II** ($3\cdot C_{14}H_{14}N_2PdCl_2$) in $P2_1$.

The X-ray study of **I** and **II** confirmed the *cis* chelate co-ordination of the ligand and almost square-planar co-ordination geometry. In structure **I**

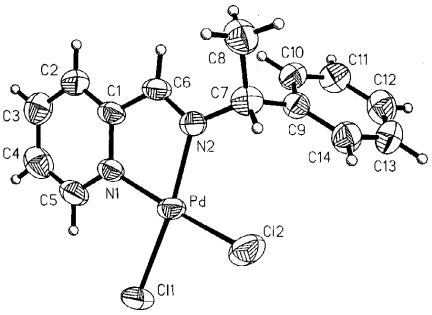

the Pd - Cl1, Pd - Cl2, Pd - N1 and Pd - N2 distances are 2.286(2), 2.270(2), 2.014(5) and 2.032(4)Å, respectively. The smallest bond angle at Pd atom is N1 - Pd – N2 = 80.7(2)°. Pyridine plane forms a dihedral angle of 6.1° with co-ordination plane. The phenyl ring is turned out from the co-ordination plane by dihedral angle of 74.8°. In crystal molecular fragments of the complex **I** form stacks with Pd...Pd intermolecular distances of 4.376 Å. Channels between the stacks are filled with 1,4-dioxane molecules. In structure **II** there are three independent molecules in the asymmetric unit cell. The molecules differ mainly by the orientation of the phenyl rings. The torsion angle N2-C7-C9-C10 assumes the values of 173, -125 and 143°, respectively. The values of bond lengths and angles averaged over the three molecules are nearly the same as their values in structure **I**.

P07.07.074 THE X-RAY CRYSTAL STRUCTURES OF THE $[Mo_2(V)O_2S(OCOCH(S)CH_3)_3]_2^-$ AND $[Mo_2(V)O_2S_2(OCOCH(S)CH_3)_2]_2^-$. M.Liu-Gonzalez*, F. Sanz-Ruiz [1], V. Sanz-Persiva, P. Palanca-Alandes [2], Esther García Rodriguez [3], S. García-Granda [3], [1] Departamento de Termología, Facultat de Física, Universitat de València, Spain. [2] Departamento de Química Orgánica, Facultat de Química, Universitat de València, Spain. [3] Departamento de Química Física, Universidad de Oviedo, Spain.

The reaction of $(NBu_4)_2[Mo_2(VI)O_2(OCOCH(S)CH_3)_2]$ with an excess of ac. 2-mercaptopropanoic in methanol yields the binuclear oxomolybdenum (V) complexes $(NBu_4)_2[Mo_2(V)O_2S(OCOCH(S)CH_3)_3]$ H_2O (1) and $(NBu_4)_2[Mo_2(V)O_2S_2(OCOCH(S)CH_3)_2]$ (2). The complex (1) exhibits the confacial bioctahedral geometry characteristic of this class of complexes in contrast with the tetrahedric geometry present in the complex (2). Crystal data. Complex 1: Triclinic space group P -1, a= 10.498(2) Å, b= 14.555(2) Å, c= 18.546(2) Å, α = 96.61(3)°, β = 101.64(3)°, γ = 97.86(3)°, V=2716.6(7)Å^3, Z= 2, D_x= 1.308 mg/m^3; structure solution and refinement based on 9571 'observed' reflections and 559 variables, R= 0.0666 and wR_2=0.1342. Complex (2): Triclinic space group P -1, a = 11.366(9) Å, b =11.429(8) Å, c = 20.450(12) Å, α = 96.42(4)°, β = 99.87(5)°, γ =101.56(10)°, V = 2535(3) Å^3, Z = 2, D_x = 1.286 mg/m^3; structure solution and refinement based on 9571 'observed' reflections and 559 variables, R=0.0666 and wR_2= 0.1342. Throughout the experiments Mo Kα was used with a graphite crystal monochromator on a Enraf-Nonius CAD4 single crystal diffractometer (λ = 0.71073 Å).

1. L. Ma, S. Liu, H. Zhu, J. Zubieta (1989). Polyhedron, 8, 669.
2. A. Cervilla, E. Llopis, J. A. Ramirez, A. Doménech, P. Palanca, M. T. Picher, C. A. Ghilardi, A. Orlandini (1994). J. Chem. Soc. Dalton Trans, 175.

P07.07.075 ISOMER DISCRIMINATION OF $[Co(dien)_2]^{3+}$ ON FORMATION OF HALOGENOLEAD(II) SALTS. H. Miyamae, M. Iwaoka, M. Terakawa, G. Hihara, Department of Chemistry, Josai University, Keyakidai 1-1, Sakado-shi, Saitama 350-0295, Japan

Halogenolead(II) anion is a family of polymeric anion whose composition and structure show a dependence to the charge, size and shape of the counter cation in the salt.[1)] Here, we are going to depict new members formed with title cation.

When $[Co(dien)_2]X_3$ (dien=diethylenetriamine; X=Cl, Br or I) was mixed with PbX_2 in solution, two of three isomers of $[Co(dien)_2]^{3+}$ were discriminated forming *sym-fac*-$[Co(dien)_2](Pb_2Cl_7)$ (**1**), *mer*-$[Co(dien)_2]_2$- $[PbBr_6]Br_2$ (**2**), *sym-fac*-$[Co(dien)_2](Pb_3I_9)\cdot 2DMF$ (**3**), and *mer*-$[Co(dien)_2]$-$(Pb_4I_{11})\cdot 3DMF$ (**4**).

Except **2**, distorted octahedral 6-coordinated Pb atoms form 1D or 2D network in the crystal, while the cations are scattered in the cavity formed by the network. In **2**, it is very interesting that the highly negative charged $[PbBr_6]^{4-}$ ion is isolated between the *mer*-isomer of the cationic complex.

Crystal data: (**1**) Orange plate, Mr. 927.84, triclinic, P-1, a=8.833(4), b=9.764(3), c=7.611(3) Å, α=101.07(3), β=110.80(3), γ=96.73(3)°, V=589.8(4) Å^3, Z=1, Dx=2.611 g cm^{-3}, μ(Mo Kα)=15.38 mm^{-1}.

(**2**) Orange prism, Mr. 1376.97, monoclinic, $P2_1/n$, a=9.129(14), b=14.043(10), c=15.379(10) Å, β=101.29(8)°, V=1933(3) Å^3, Z=2, Dx=2.364 g cm^{-3}, μ(Mo Kα)=13.44 mm^{-1}.

(**3**) Yellow prism, Mr 2175.2, triclinic, P-1, a=10.624(5), b=12.145(8), c=9.401(63) Å, α=105.50(5), β=93.81(5), γ=111.78(4)°, V=10678(14) Å^3, Z=1, Dx=3.385 g cm^{-3}, μ(Mo Kα)=18.75 mm^{-1}.

(**4**) Orange prism, Mr. 2709.3, monoclinic, $P2_1/n$, a=12.067(7), b=27.958(21), c=17.063(180) Å, β=111.539(7)°, V=53553(8) Å^3, Z=4, Dx=3.359 g cm^{-3}, μ(Mo Kα)=19.24 mm^{-1}.

1) A.F.Wells, "Structural Inorganic Chemistry" 5th ed., 118(1986).

P07.07.076 DINUCLEAR COPPER(II) COMPLEXES WITH SIMPLE PYRAZOLATE BRIDGES. E. Spodine, A. M. Atria, J. Valenzuela, Facultad de Ciencias Químicas y Farmacéuticas, Universidad de Chile. Casilla 233 Santiago, Chile, and J. Manzur, A. M. García, M. T. Garland, Facultad de Ciencias Físicas y Matemáticas, Universidad de Chile. Casilla 2777 Santiago, Chile.

Three new copper(II) dimeric complexes with simple pyrazolate bridges have been prepared: $[Cu_2(pz)_2(dpa)_2(Cl)(H_2O)]Cl\cdot H_2O$ 1, $[Cu_2(pz)_2(phen)_2Cl_2]\cdot 2C_2H_5OH$ 2 and $[Cu_2(pz)(phen)_2Cl_3]\cdot 2H_2O$ 3. (pzH: pyrazole, dpa: di(2-pyridyl)amine, phen:1,10-phenanthroline).

The crystal and molecular structures of complexes 1, 2 and 3 are reported. Complex 1 crystallizes in the orthorhombic system, space group $P2_12_12_1$; a = 13.892(2), b = 13.975(2) and c = 15.156(2) Å. Complexes 2 and 3 crystallize in the monoclinic system, space group C2/c; a = 25.753(2), b = 9.706(2), c = 16.627(5) Å, β = 125.86(2)° and a = 17.824(4), b = 11.612(2), c

= 13.647(3) Å, β = 106.01(2)º respectively. The copper centres in the binuclear cation in 1 have a square pyramidal geometry at Cu1 and a distorted octahedral geometry at Cu2. The neutral complexes 2 and 3 have the copper atoms in a distorted square pyramidal geometry. Complexes 1 and 2 are bibridged by pyrazolate bridges, while 3 is monobridged by this same ligand.

The crystal packing of complex 1 presents molecules in four different orientations. They are stabilized in infinite chains by hydrogen-bridged water and chlorine molecules. The packing of complex 2 is stabilized by ethanol molecules occupying the interstitial holes, which are hydrogen bridged to the terminal chlorine ions (Cl···O distance 3.256(5) Å). The crystal packing of compound 3 shows linear chains of complex molecules, joined by hydrogen bonded water molecules.

This research was supported in part by Fundación Andes and FONDECYT (projects 1980896-7980050). We are also grateful to the ECOS (France)-CONICYT (Chile) collaboration program (project C97E01).

P07.07.077 INTERPRETATION MODEL OF THE STRUCTURAL X-RAY RESULTS BASED ON HYPERCONJUGATIVE INTERACTIONS. I.A.Litvinov, A.T.Gubaidullin, O.N.Kataeva, A.E. Arbuzov Institute of Organic and Physical Chemistry, Russian Academy of Sciences, A.E.Arbuzov str., 8, Kazan 420088, RUSSIA.

The interpretation model of the molecular geometry derived from X-ray diffraction data, which gives good results in the structures of symmetric medium size 1,3,2-dioxa- and 1,3,2-diazaphosphacyclanes (from 5- to 8-membered), is extended on the new classes of non-symmetric sterically hindered structures of 1,3,2-oxaheterophosphorinanes, 5,6-benzo-1,2-oxaphospho-rines, 6,7-benzo-1,3,2- and 1,4,2-dioxa- and oxaza-phosphepines. It is shown, that steric ineractions may invert the anomeric effect of substituents. The observed changes of bond lengths are explained by electron density transfer as a result of hyperconjugative electronic interactions. This model is suitable not only to describe the bond length changes observed depending on the electron density transfer but also the difference of chemically equivalent bonds. The inversion of the anomeric interaction has been observed due to steric hindrance leading to the opposite distribution of the geometrical parameters The interpretation model is supported by the results of analysis of more than 30 structures.

On asymmetric 1,3,2-oxaheterophosphorinanes, asymmetrical 6- and 7-membered unsaturated cycles we can conclude the model of hyperconjugative stereoelectronic interactions satisfactorily describes the position of substituents at phosphorus. This model is also applicable to explain geometrical changes in the absence of strong intermolecular interactions — hydrogen bonds or anion-cation interactions.

This research was supported by Russian Foundation for Basic Research, grant 98-03-33266.

P07.07.078 STRUCTURE OF HEXAPHENYLGERM-OLE. John Ricci and Henry Tracy, Department of Chemistry, University of Southern Maine, Portland, ME 04104, USA and Wim Klooster, Chemistry Department, Brookhaven National Laboratory, Upton, NY 11973, USA.

We have undertaken the X-ray analysis of a phenyl-substituted Group14 metallacyclopentadiene, hexaphenylgermole (GePh), to determine the origin of the dramatic difference in luminescence between this compound and the methyl-substituted analog.

The structural features of the germanium methyl-substituted derivative have been described (1). The luminescence emission of the germanium phenyl compound (excitation at 350 ± 10 nm) exhibits a significant bathochromic shift from its methyl analog; emission is at 480 nm for GePh and 388 nm or GeMe.

We find the geometry of the heterocyclic ring carbon fragment in GePh to be identical to those in the previously published structures. Thus, it is proposed that the difference in luminescence properties must be electronic rather than structural in nature.

Crystallographic data: spacegroup P-1, Z = 2, a= 10.280(1), b=16.520(3), c = 9.641(2) α =100.20(2), β= 108.29(1), γ= 77.06(1) 5489 refls., $R(F^2)$ = 0.066, $R_w(F^2)$ = 0.111, S = 1.92.

Work at BNL was carried out under contract DE-AC02-98CH10886 with the U.S. Department of Energy, Office of Basic Energy Sciences

1. Meier-Brocks, F.; Weiss, E. J.Organomet. Chem. 1993,453

P07.07.079 STRUCTURE OF SILYL AND GERMYL SUBSTITUTED THIOPHENE-1,1-DIOXIDES AND DIRECTION OF CYCLOADDITION. S.Belyakov, P.Arsenyan, O.Pudova, and E.Lukevics, Latvian Institute of Organic Synthesis, 21 Aizkraukles, Riga, LV-1006, Latvia.

The [2+3] dipolar cycloaddition of nitrile oxides to the double bond of thiophene-1,1-dioxides **1** has been investigated. It was shown that the reaction pathway strongly depends on the substituents M and M' in the heterocycle and the method of nitrile oxide generation. Cycloaddition proceeds with high regioselectivity. It should be noted that only one double C=C bond of **1** is involved into the interaction. The direction of cycloaddition was confirmed by X-ray structure analysis of fused isoxazoline **2** (M = C).

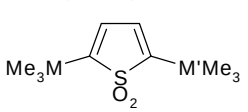

1

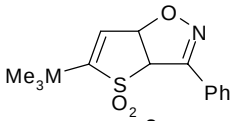

2

M, M' = C, Si, Ge

The crystallographic data for the studied compounds are:

	1 M= C, M'=Si	**1** M=Si , M'=Ge	**1** M= M'=Ge	**2** M =C
S p. gr.	C 2/c	P nmm	P nmm	P 1
Z	4	4	4	2
a [Å]	11. 257(1)	6.513 (1)	6.5 25(1)	6 .373(1)
b [Å]	6.4 391(7)	15.40 6(3)	15. 505(3)	1 0.794(3)
c [Å]	19. 735(2)	15.55 6(4)	15. 600(4)	1 2.007(3)
α [º]	90	90	90	1 11.36(2)
β [º]	92.6 8(1)	90	90	9 7.92(2)
γ [º]	90	90	90	9 5.08(2)

P07.07.080 SYNTHESIS AND STRUCTURE OF BIS(ARYLTELLURO)ETHYNES, ArTeC≡CTeAr. M.V. Capparelli[a,b], J. Farran[a], A. Alva-rez-Larena[a], J.F. Piniella[a] and L.Torres-Castellanos[c]. [a]Univ. Autónoma de Barcelona, Bellaterra, Spain; [b]Univ. Central de Venezuela, Caracas, Venezuela; [c]Univ. Nacional de Colombia, Bogotá, Colombia.

Although many telluroethynes (RTeC≡CR´) are known, only a few bis(alkyl-telluro)ethynes (AkTeC≡CTeAk) were described, and only one bis(aryltelluro)ethyne (ArTeC≡CTeAr) has been reported so far [1]. Within our program of synthetic and structural studies of organotellurium compounds [2] we prepared 12 new bis(aryltelluro)ethynes [Ar: C_6H_5(**1**), *p*-MeC_6H_4(**2**), *p*-MeO-C_6H_4(**3**), *p*-$Me_2NC_6H_4$(**4**), *p*-FC_6H_4(**5**), *p*-ClC_6H_4(**6**), *p*-BrC_6H_4 (**7**), *p*-IC_6H_4 (**8**), *p*-PhC_6H_4(**9**), *p*-$PhOC_6H_4$(**10**), α-$C_{10}H_7$(**11**), β-$C_{10}H_7$(**12**)] by reacting BrMgC≡CMgBr with the corresponding ArTeBr formed *in situ.* The X-ray crystal structures of **1**, **2**, **4**, **8** and **10** were determined.

All compounds display approximate linear Te-C≡C-Te moieties, in which deviations from the least-squares lines are small [0.0093(6)-0.067(7)Å]. Co-ordination at the Te atoms is angular, with C-Te-C angles [94.2(3)-97.2(2)°] substantially smaller than the tetrahedral value. As expected, the Te-C(sp^2) distances [2.103(5)-2.142(6)Å] are significantly longer than the Te-C(sp^1) bond lengths [2.021(6)-2.058(6)Å]. In all compounds the Te atoms are approximately coplanar with the bonded phenyl rings [max. dev.: 0.1503(4) Å]. The C(sp^2)-Te···Te-C(sp^2) torsion angles vary widely, due to the unhindered rotation about the Te-C(sp^1) bonds. This feature is the only important difference between the solid-state molecular geometries.

Although Te(IV) compounds show a tendency to form secondary bonds [2], this is not frequent in Te(II) compounds. Packing in **1**, **2**, **4**, **8** and **10** is mainly due to van der Waals interactions; non-bonded contacts shorter than the sum of van der Waals radii are only marginally so.

1. M. de Matheus, L. Torres, C. Cabiativa, A. Fuertes & C. Miravitlles (1991), *Acta Cryst*., **C47**, 977.
2. J. Farran, A. Alvarez-Larena, M.V. Capparelli, J.F. Piniella, G. Germain & L. Torres-Castellanos (1998), *Acta Cryst*., **C54**, 995, and refs. therein.

P07.07.081 MOLECULAR STRUCTURES OF THREE UNUSUAL TELLURIUM COMPLEXES. S. Husebye and K. W. Törnroos, Department of Chemistry, University of Bergen, 5007 Bergen, Norway, J. Novosad and M. Necas, Department of Inorganic Chemistry, Masaryk University, 611 37 Brno, Czech Republic and A. M. Z. Slawin and J. D. Woollins, Department of Chemistry, Loughborough University, Loughborough LE11 3TU, UK.

The three compounds, [Te_2(μ-Cl)$_2${$Ph_2P(S)NP(S)Ph_2$}$_2$], **1**, [(4-$MeOC_6H_4TeCl_3$)$_2$ {μ-$Ph_2P(S)(CH_2)_2P(S)Ph_2$}], **2**, and [Te_2(μ-Ph_2PS_2)$_2$], **3**, have been synthesized and their structures solved by means of conventional X-ray crystallographic methods. Complex **1** is a dinuclear, centrosymmetric, square planar Te(II) complex where each Te atom is coordinated to the two S atoms of the bidentate dithiolate ligand and the two bridging Cl^- ligands. In **2**, the dithio ligand is neutral and adds a 4-$MeOPhTeCl_3$ molecule at each S atom, thus bridging the two Te(IV) atoms. The coordination of both Te atoms is ψ-octahedral with the anisyl group and a lone pair of electrons in axial positions. Complex **3** is a binuclear Te(I) complex, mainly held together by a Te-Te bond. Both anisobidentate $Ph_2PS_2^-$ ligands bridge the two Te atoms. The resulting coordination around each Te atom is best described as T-shaped, with the Te-Te bond along the stem. The molecules are connected into zigzag chains by weak intermolecular Te---S contacts. The average Te-S bond length is 2.502 Å in **1,** compared to 2.797 Å in **2**. This difference is related to the difference in basicity of the ligands. Average Te-S bond lengths in **3** are 2.491 Å for the two strong bonds and 2.990Å for the two weaker ones. The Te-Te bond length in **3** is 2.730(1)Å while the Te-Cl bond lengths in **1** have an average value of 2.915Å and in **2** range from 2.425 to 2.534Å, those *trans* to S being shortest.

P07.07.082 CHEMICAL REACTION IN THE COORDINATION SPHERE OF Cu(II) ATOM AS A RESOURCE OF NEW ANIONIC CHELATE LIGANDS. M. Dunaj-Jurèo, D.Mikloš, Department of Inorganic Chemistry, Slovak Technical University, SK-812 37 Bratislava, Slovak Republic, and I.Potoèòák, Department of Inorganic Chemistry, P. J. Šafárik University, SK- 041 54 Košice, Slovak Republic

The non-linear pseudohalide anions $ONC(CN)_2^-$, $N(CN)_2^-$ and $C(CN)_3^-$ are known to have good coordination ability. For the first two of them nucleophilic addition reactions have been observed which lead to formation of new chelate anionic ligands in the coordination sphere of the Cu(II) atom. Crystal structures of [Cu(bipy)(mcoe)(NCO)] [1], [Cu(bipy)(mcoe) ($ONC(CN)_2$] [2], [Cu(bipy)(mcoe)($N(CN)_2$] [3] and [Cu(bipy)(coe)] [1] are presented, and supplemented by [Cu(mcoe)$_2$ (H_2O)$_2$] [4] [Cu(ecoe)$_2$ (H_2O)$_2$] [5], and [Cu(mici)$_2$] [6], where *bipy* = 2,2'-bipyridine, *mcoe*, *ecoe*, *coe* and *mici* are the anionic chelate ligands *m*ethyl(2-*c*yano-2-imido*x*y *e*thaneimidate), [(ON)(NC)C-C(NH)(OCH_3)]$^{1-}$, *e*thyl(2-*c*yano-2-imido*x*y *e*thaneimidate), [(ON)(NC)C-C(NH)(O-CH_2 -CH_3)]$^{1-}$, 2-*c*yano-2-imido*x*y *e*thaneimidate, [(ON)(NC)C-C(NH)(O)]$^{2-}$ and di*m*ethyl*i*midodi*c*arbon- *i*midate, [(HN)(CH_3O)C-N-C(OCH_3)(NH)]$^{1-}$, formed by nucleophilic addition of methanol, ethanol and hydroxide ion to the coordinatively activated β-carbon of the nitrosodicyanomethanide (*mcoe*,*ecoe*,*coe*) or methanol to the dicyanamide (*mici*) anions. Formation of the hydroxide ion from water in the reaction mixture can be explained by protonation of the $C(CN)_3^-$ anion.

[1] M. Dunaj-Jurèo, I. Potoèòák, D. Mikloš & R. Klement, Collect. Czech. Chem. Commun., submitted.
[2] M. Dunaj-Jurèo, D. Mikloš & I. Potoèòák (1998). Acta Cryst., C54, 1763.
[3] M. Dunaj-Jurèo, D. Mikloš, I. Potoèòák & L. Jäger (1996). Acta Cryst., C52, 2409.
[4] J.W. Buchler, M. Hvastijová, J. Kohout & J. Kožíšek (1998). Transition Met. Chem., 23, 215.
[5] C. Tretner, L. Jäger, C. Wagner & K. Merzweiler. Z.Anorg.Allg.Chem., submitted.
[6] R.Boèa, M.Hvastijová, J.Kožíšek & M.Valko (1996). Inorg.Chem., 35, 4794.

P07.07.083 ACTIVE LONE-PAIR INFLUENCE ON THE COORDINATION BETWEEN LEAD(II) AND OXYDIACETIC ACID. S. Norberg, G. Svensson, S. Olson and J. Albertsson, Department of Inorganic Chemistry, Chalmers University of Technology, SE-412 96 Göteborg, Sweden. E-mail: stn@inoc.chalmers.se

Lone-pair electron activity in two different lead(II) oxydiacetic acid complexes is described. The complexes are, $Pb(C_4H_4O_5)(H_2O)$ [1] and $Pb_4(C_4H_4O_5)_3(NO_3)_2(H_2O)$ [2].

The oxydiacetate ligand $[O_2C—CH_2—O—CH_2—CO_2]^{2-}$ can be mono-, bi- or tridentate and may form bridges between metal atoms. By using a multi-dentate ligand the $6s^2$ lone-pair electrons in Pb(II) are likely to actively affect the coordination polyhedron around the Pb atom.

In $Pb(C_4H_4O_5)(H_2O)$ a distorted square antiprism is formed and the lone-pair $6s^2$ electrons show stereochemical activity. The Pb—O distances are in the range 2.49(3)-2.909(17)Å. The shortest distances are found on the opposite side of the lone-pair, which is in accordance with the VSEPR theory. $Pb_4(C_4H_4O_5)_3(NO_3)_2(H_2O)$ comprises of three crystallographically independent Pb atoms , with coordination numbers seven, eight and nine. At least the seven- and eight-coordinate Pb atoms are influenced by a stereochemically active lone-pair.

[1] Norberg, S., Svensson, G. & Albertsson, J., (1999). *Acta Cryst C***55**. In press.
[2] Svensson, G., Olson, S. & Albertsson, J., (1998). *Acta Chem. Scand.* **52**, 868-872.

P07.07.084 STRUCTURAL STUDIES OF THE NOVEL Hg(II) COMPLEXES WITH 3,4,5,6-TETRAHYDRO-2-PYRIMIDINETHIOL. D. Matković-Čalogović, Z. Popović, G. Pavlović and Ž. Soldin, Chemistry Department, Faculty of Science, University of Zagreb, Ul. kralja Zvonimira 8, 10000 Zagreb, Croatia

Toxicity of mercury(II) and methylmercury(II) cations in biological systems derives from the affinity of these ions for cysteinyl sulphur residues. Heterocyclic thiols can be used to mimic bio-relevant mercury(II)-sulphur interactions. A series of complexes HgX_2L_2 and HgX_2L (X = Cl^-, Br^-, I^-, CN^-, SCN^-; L = H_4pymtH, 3,4,5,6-tetrahydro-2-pyrimidinethiol) has been prepared and characterized by elemental chemical analysis, NMR and IR spectroscopy and thermal analysis (TGA and DSC). X-ray powder data showed that the complexes are not isostructural. Crystal structures of $HgCl_2(H_4pymtH)$ (1), $Hg(SCN)_2(H_4pymtH)_2$ (2) and $HgBr_2(H_4pymtH)_2$ (3) have been determined by single crystal X-ray diffraction. *Crystal data*: (1) $C_{16}H_{32}Hg_4Cl_8N_8S_4$, *Mr*=1550.74, triclinic, *P* $\bar{1}$, *a*=10.045(2), *b*=13.530(2), *c*=14.162(2) Å, α=103.01(1), β= 92.00(2), γ=90.34(2)°, *Z*=2, $D_{calc.}$=2.748 gcm^{-3}, μ=17.2 mm^{-1}, *R*=0.062, R_w=0.085 for 4900 reflections with $I \geq 2\sigma(I)$. (2) $C_{10}H_{16}HgN_6S_4$, *Mr*=549.10, triclinic, *P* $\bar{1}$, *a*=7.6508(7), *b*=8.4976(7), *c*=14.1751(22)Å, α=105.97(1), β= 89.94(1), γ=92.00(1)°, *Z*=2, $D_{calc.}$=2.060 gcm^{-3}, μ=9.14 mm^{-1}, *R*=0.057, R_w=0.070 for 2964 reflections with $I \geq 2\sigma(I)$. (3) $C_8H_{14}HgBr_2N_4S_4$, *Mr*=592.76, monoclinic, $P2_1/c$, *a*=7.870(1), *b*=15.644(2), *c*=12.882(2)Å, β=98.79(2)°, *Z*=4, $D_{calc.}$=2.512 gcm^{-3}, μ=15.1mm^{-1}, *R*=0.040, R_w=0.049 for 1828 reflections with $I \geq 2\sigma I$.

Complex 1 is tetrameric with two tetrahedral $HgCl_4$ moieties and two Hg atoms with short Hg-S (from H_4pymtH) bonds and longer Hg···Cl interactions in a 2+2 coordination sphere. In the structures of 2 and 3 there are discrete molecules with tetrahedrally coordinated mercury. In 2 the coordination sphere is built up of four S atoms, two from the tiocyanate and two from the zwitterionic thionate ligand. In 3 two Br atoms and two S atoms from the thionate ligand complete the coordination sphere.

P07.07.085 CRYSTAL CHEMISTRY OF HETEROCOMPLEX COMPOUNDS OF LEAD AND COPPER BIS- β-DIKETONATES. V.V. Krisyuk, P.A. Stabnikov, I.A. Baidina, I.K. Igumenov, Institute of Inorganic Chemistry SB RAS, Novosibirsk, Russia, 630090, Lavrentiev Avenue 3.

The coordination unsaturation of lead atom in beta-diketonate complexes has allowed to assume an opportunity of saturation of coordination sphere of central atom by additional ligands at formation of crystals from investigated lead complexes and beta-diketonates of other metals. For experiment lead bis-hexafluroacetylacetonate - Pb(hfa)2 and complexes of copper(II) were chosen. At crystallization from organic solvent the heterocomplex compounds were obtained with composition $Pb(hfa)_2$*$Cu(hfa)_2$, $Pb(hfa)_2$*$Cu(aa)_2$, $Pb(hfa)_2$*$Cu(zis)_2$, where aa = acetylacetonate, zis = 2-methoxy-2,6,6-trimethylheptane-3,5-dionate.

X-ray diffraction and crystal analysis have confirmed the single phase and shown that irrespective of composition of initial solution only 1:1 heterocomplexes have been separated. Carried out crystal structure investigation of new compounds has allowed to establish features of packing of molecules and coordination behavior of metal atoms.

P07.07.086 CRYSTAL STRUCTURES OF THE NEW ALKALI METAL BORATOBORATES $Rb_8B_{12}(BSe_3)_6$, $Rb_4Hg_2B_{12}(BSe_3)_6$ AND $Cs_4Hg_2B_{12}(BSe_3)_6$. Arno Lindemann, Joachim Kuchinke, Christian Köster and Bernt Krebs, Anorganisch-Chemisches Institut der Universität Münster, D-48149 Münster, Germany

The three new alkali and alkali-mercury selenoboratoborates were synthesized by reaction of stoichiometric amounts of the metal selenides, amorphous boron and selenium in carbon coated, evacuated silica tubes at higher temperature. The novel chalcogenoborates contain B_{12} icosahedra completely saturated with selenium ligands. Six trigonal-planar selenoborate entities functioning as bidentate ligands complete the B_{12} icosahedron to form a persubstituted closo-dodecaborate ion. Besides $Cs_8B_{12}(BSe_3)_6$ [1,2] which we have described recently, these compounds are further examples of the new class of boron clusters yielded from solid state reactions. $Rb_8B_{12}(BSe_3)_6$ crystallizes in the triclinic space group P-1 with a = 10.542(5) Å, b = 10.450(3) Å, c = 10.946(4) Å, α = 104.53(3)°, β = 91.16(4)°, γ = 109.11(3)° and Z = 1. The complex $[B_{12}(BSe_3)_6]^{8-}$-anions are interconnected via eight rubidium cations. These are eight- and ninefold coordinated by selenium atoms, respectively.

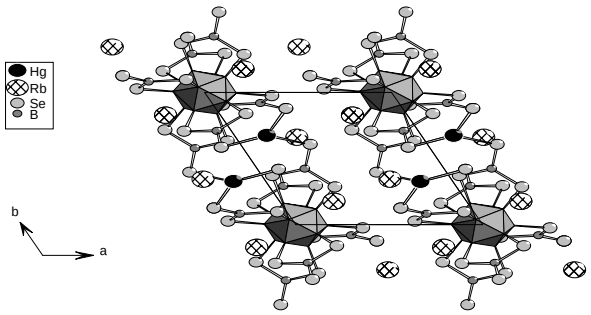

Fig. 1: Projection of $Rb_4Hg_2B_{12}(BSe_3)_6$ along the c-axis

The compounds $Rb_4Hg_2B_{12}(BSe_3)_6$ (A) and $Cs_4Hg_2B_{12}(BSe_3)_6$ (B) contain the same type of anions. Substitution of four monovalent cations by two bivalent Hg-cations results in a new layered structure of space group P-1. The crystal data for the selenoborates are given below.

A: a = 9.560(2) Å, b = 10.418(2) Å,c = 11.104(2) Å,
α = 99.27(3)°, β = 91.08(3)°, γ = 116.33(3)° (at T = 213 K);
B: a = 9.838(2) Å, b = 10.716(2) Å, c = 11.081(2) Å,
α = 99.82(3)°, β = 90.80(3)°, γ = 116.08(3)° (at T = 293 K).

[1] O. Conrad, C. Jansen, B. Krebs, *Angew. Chem. Int. Ed.* **37** (1998) 3208
[2] J. Küper, O. Conrad, B. Krebs, *Angew. Chem. Int. Ed. Engl.* **36** (1997) 1903

P07.07.087 STRUCTURAL STUDIES OF SYNTHETIC PB AND CA APATITES. J.Y. Kim, B.J. Kennedy and R.R. Fenton, School of Chemistry, University of Sydney, N.S.W., 2006, Australia, and B.A. Hunter, ANSTO, PMB 1 Menai, N.S.W., 2234, Australia.

Hydroxyapatite, $Ca_{10}(PO_4)_6(OH)_2$, is a major mineral component of calcified tissues, including bones and teeth. It is a

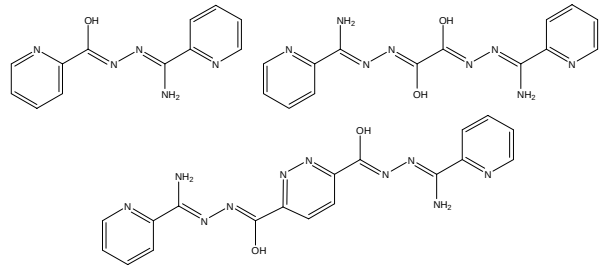

good model system for natural apatites, having a structure which can easily accommodate a great variety of anionic and cationic substitutions. It acts as a natural sink for heavy metals, especially Pb and Cd, in biological systems. The hydroxyl ion can be partially replaced by other anions and one aim of the present work is to establish how such substitutions influence the ability of apatites to sequest and immobilise heavy metals. We have used a combination of synchrotron X-ray diffraction and high resolution powder neutron methods for our structural studies, of some substituted apatites.

We have refined the structures of eight apatites $M_{10}(PO_4)_6X_2$, M = Pb, Ca and X = OH, F, Cl, Br, using the Rietveld method. In these there are two cation sites, a channel of M-I atoms and a triangle of M-II atoms. The anion interacts most strongly with the M-II atoms at (., ,. ,¼). For the Ca compounds, the F ion sits within the triangles at (0, 0, 0), while the larger OH and Cl anions are disordered above and below the M-II triangles. The Br is at (0, 0, ½). Despite the larger size of the isostructural Pb compounds, no anions are found in the triangles. The F, Cl and Br ions are at (0, 0, ½) and the OH ion is disordered at (0, 0, *z*). This difference in behaviour is possibly related to the stereochemical activity of the Pb 6s electrons.

While synchrotron X-ray methods have been important in determining the positional parameters of the heavy elements (Pb, Ca *etc*.), neutron scattering methods have been essential in determining the positional parameters of the lighter elements (H, F, O *etc*.) in the presence of the heavy Pb atom. In this paper we present both the experimental results and discuss the possible reasons for the observed differences.

P07.07.088 THERMAL BEHAVIOUR OF STRUVITE-CONTAINING URINARY STONE. T.A. Korneva, T.N.Grigor'eva, and N.A. Palchik. United Institute of Geology, Geophysics and Mineralogy, Siberian Branch of Russian Academy of Science, Novosibirsk 630090, Russia.

A human urinary stone weighing as much as 105g was composed of different colour concentric layers. Three specimens separated from the urinary stone were distinguished by their colour (white, brown, and yellow). X-ray showed that all three specimens consisted mainly of struvite $MgNH_4PO_4{\cdot}6H_2O$ with cell parameter *a* ranging from 6.901 to 6.988 Å for different samples and with lattice constants *b*=11.19 Å and *c*=6.15Å. The spectrum analysis of struvite has revealed the significant content of Ca and Na and trace of Cu, Mn, and Sr. DTA along with TGA indicated the removal of the major amount of water of crystallization and NH_3 up to temperature of about 220°C. X-ray of the specimen heated at that temperature showed the presence of nearly X-ray amorphous struvite with only two broadened (200) and (040) reflections. After exothermic effect on the DTA curve at 360° connected with removal of organic matter (about 1.0%) no changes was observed by thermal and X-ray analyses up to 660°C. The practically amorphous anhydrite product was recrystallized exothermically at ≈660°C When the specimen was heated at 670°C, X-ray pattern showed the phase corresponding to sufficiently crystallized Mg -pyrophosphate and whitlockite. The trace of the crystalline phase with apatite structure was observed likewise. After the second exothermic reaction, the further crystallization proceeded during glass transition. The specimen heated at 1000°C constituted a hardened glass-like substance. X-ray pattern of the substance exhibited well crystallized Mg-pyrophosphate $Mg_2P_2O_7$, whitlockite, $Mg_3(PO_4)_2$, and trace of oxyapatite. The total weight loss of the specimen in the temperature interval from 20 to 1000°C was 41.8% whereas the theoretical content of volatile in struvite is 51,42%. It follows that the urinary stone investigated was not completely consisted of struvite, but contained X-ray amorphous Ca-rich phase. The work is supported by RFFI grant N 97-05-65305.

P07.07.089 UNUSUAL CRYSTAL MORPHOLOGY OF TWO BIOMINERALS: BARIUM SULFATE AND STRONTIUM SULFATE B. Hasse, M. Epple, Institute of Inorganic and Applied Chemistry, University of Hamburg, Martin-Luther-King-Platz 6, D-20146 Hamburg, Germany

Barium sulfate (baryte) and strontium sulfate (coelestine) are found in the living nature as biominerals: BaSO4 is used as gravity sensor and SrSO4 serves as skeleton for a class of deep-sea single-cell organisms (acantharia). Nature has developed ways to grow such highly insoluble materials in desired shape and morphology. Conventional crystallization in a chemist's laboratory by adding solutions of cations and anions usually results in rapid crystallization of unstructured, micrometer-sized crystals due to fast nucleation. In order to mimic natural processes, it is imperative to slow down the nucleation and crystal growth process.

We have crystallized both earth alkaline sulfates in and on a porous polymer matrix containing micrometer-sized pores. Barium sulfate aggregates were found either as platelets or as highly ordered aggregates of small spheres. Strontium sulfate crystallized in rhombohedrical crystals that showed other different crystallographic faces compared to natural coelestine. In early stages of strontium sulfate crystallization, porous crystals were found.

Mixed crystals of BaSO4 and SrSO4 of different composition were also precipitated. The morphology changed from spherical to rhombohedrical crystals with increasing strontium content. These results may help to understand biological crystallization of earth alkaline sulfates.

P07.07.090 BIOMIMETIC GROWTH OF CALCIUM PHOSPHATES IN AND ON POROUS POLYMERS M. Epple, F. Peters, K. Schwarz, Institute of Inorganic and Applied Chemistry, University of Hamburg, Martin-Luther-King-Platz 6, D-20146 Hamburg, Germany

Among the most important inorganic materials used by nature as building block in the living world are calcium phosphates, namely, apatite phases. The parent compound is hydroxyapatite $Ca_{10}(PO_4)_6(OH)_2$ that occurs in mammalian bone as nanometer-sized crystals that are crystallized in a matrix of collagen. The ability of hydroxyapatite to incorporate other cations (e.g., Mg^{2+}) and anions (e.g., CO_3^{2-}, F^-, Cl^-) makes it a very flexible material whose biological and mechanical properties can be adjusted in a wide range.

Control of the crystallization process is necessary to prepare larger crystals of apatite. We have slowed down the nucleation process by employing a double-diffusion technique where two solutions containing Ca^{2+} and PO_4^{3-} were separated by a porous polymer matrix with pores in the sub-micrometer range. Under these conditions, the crystallization time was of the order of weeks. Unusual growth morphologies were observed inside the polymer matrix: elongated hexagonal prisms with fractal growth for fluoroapatite $Ca_{10}(PO_4)_6F_2$ and oriented flat hexagonal platelets for hydroxyapatite. Other experiments involved the controlled crystallization of hydroxyapatite on porous polymers where nucleation took place on the polymer surface. The results are compared to structural investigations on natural bone samples with various methods (diffraction, EXAFS, thermal analysis).

P07.07.091 LOW TEMPERATURE STRUCTURAL STUDIES OF MAGNETICALLY INTERESTING CLUSTER COMPLEXES. R. S. Hampshire[$], C. Wilson[$], L. K. Thompson[#], J. A. K. Howard[$]. $ - Dept. of Chemistry, University of Durham, Durham DH1 3LE, UK. # - Dept. of Chemistry, Memorial University of Newfoundland, St. John's, Newfoundland A1B 3X7, Canada.

Currently[1,2] there is much interest in polynuclear transition metal cluster complexes that exhibit interesting magnetic properties. One series of compounds that we are studying includes polynuclear transition metal complexes of a group of substituted diazine ligands (Fig. 1).

Fig. 1 Diagrams of the ligands PHAAP, PTTP and PPDP respectively.

Clusters derived from these ligands show a wide variety of structural arrangements, e.g. Chains, Squares, Spirals, Trigonal Bi-Pyramids and Tetrahedra, although we believe that not all possible conformations have as yet been determined for this particular series of compounds.

Structural results on several structural types will be presented at the meeting.

L.K.Thompson, Z.Xu, A.E.Goeta, J.A.K.Howard, H.J.Chase, D.O.Miller *Inorg. Chem.* **1998**, 37, 3217- 3229.
F.Letard, P.Guionneau, L.Rabardel, J.A.K.Howard, A.E.Goeta, D.Chasseau, O, Kahn. *Inorg. Chem.* **1998,** 37, 4432-4441.

P07.07.092 TWO SPIN ISOMERS IN THE SAME CRYSTAL. Alan Hazell, Chemistry Dept. Aarhus University, DK-8000 Århus. C, Denmark, and Benoit Chansou and Hans Toftlund. Chemistry Dept. Odense University, DK-5230 Odense.M, Denmark.

Fe(II) forms octahedral complexes with a d ^{6} electron confguration and can exist either as low spin (t_{2g}^6) or high spin ($t_{2g}^4 e_g^2$) species. We have studied several polypyridyl Fe(ii) complexes: [Fe(tpa)$(NCS)_2$)] incorporating various solvate molecules and [Fe(btpa)]$(PF_6)_2$, and find that three of these crystallize with two complexes in the asymmetric unit with one complex low-spin while the other is high-spin. On cooling the tpa complexes there is a spin cross-over so that both Fe atoms are essentially low spin, this process is reversible.

The average Fe-N distances, in Å, are:

	2 95K	1 20K	1 00K
[Fe(tpa)$(NCS)_2$.CH_3CN	2 .057 2.152	1 .960 1.964	1 .958 1.963
[Fe(tpa)$(NCS)_2$.C$_2$H$_5$OH	2 .092 2.145	1 .959 1.964	
[Fe(tpa)$(NCS)_2$.C$_5$H$_5$N	2 .168	crystal splits on cooling	
[Fe(btpa)]$(PF_6)_2$	1 .989 2.230	1 .993 2.243	

The structures of two Fe doped [Zn(tpa)$(NCS)_2$)] complexes will also be presented.

(tpa = tris(2-pyridylmethyl)amine; **btpa** = 6,6'-bis[bis(2-pyridylmethyl)aminomethyl]-2,2'-bipyridine)

P07.07.093 ANALYSIS OF THE CHEMICAL BONDING IN HOMOGENEOUS SETS OF STRUCTURES CREATED WITH CAMBRIDGE DATABASE. Carlo Mealli, ISSECC-CNR, Via J. Nardi 39, 50132 Firenze, Italy.

Mononuclear and polynuclear transition metal compounds, expected to be similar on the basis of simple chemical rules are, can show remarkably different structures. This occurs for compounds having the same metal-ligand framework and a consistent number of valence electrons: a change of the metal (within the same triad) or of the ligand donor strength (also related to the substituents steric hindrance) can have dramatic effects. On the other hand, the addition or removal of electrons within a given framework (electron tuning) causes alternative structural rearrangements.

The author has explored whole categories of compounds by searching exhaustively within the Cambridge Database. The screened structures are tabulated in terms of significant stereochemical parameters, total electron count, nature of metals, number and type of the ligands, etc. Among others the following species have been analyzed in detail: *i)* octahedral M_6 Clusters [1] *ii)* dimers containing coniugate chelates with N_2, P_2 or S_2, donors riding L3M-ML3 sawhorses [2] *iii)* dimers with the inner core M_2X_2 (X= naked chalcogenide atom) which is present in many molecules with biological and catalytic relevance [3]. *iv)* species with the $M_3(\mu\text{-}PR_2)_2$ framework [4] *v)* Pd_2 or Pt_2 dimers with a single phosphido bridge [4].

The interpretional tool of the chemical bonding is the MO theory, both *ab-initio* and qualitative. The latter approach, facilitated by the graphic interface offered by the package CACAO [6], still allows to draw important correlations between the structural prototypes and is rich of chemical hints.

1). Mealli C., Lopéz J.A., Yan S., Calhorda M.J. *Inorg.Chim.Acta*, *213* (1993) 199.
2) Mealli C., Ienco A., Anillo A., Garcia-Granda, Obeso-Rosete R. *Inorg.Chem., 36*, (1997) 3724.
3) Mealli C., Orlandini A. in *Metal Clusters in Chemistry,* Eds P. Braunstein, L. Oro, P. Raithby, *Wiley-VCH, Weinheim* 1999.
4) Wang W., Carty A.J., Sappa E. Gervasio G. Mealli C., Ienco A.Perez-Carreño E. *submitted.*
5) Mealli C., Ienco A., Galindo A., Perez-Carreño E. *submitted.*
6) Mealli, C.; Proserpio, D. M. *J. Chem. Educ. 67* (1990) 399. Mealli, C.; Ienco, A.; Proserpio, D. M. *Abstracts of the XXXIII ICCC*, Florence, 1998.

P07.07.094 NONCOVALENT BONDING INTERACTIONS ASSISTED WITH OFURAN IN MG AND CA FURANCARBOXYLATES. B. Paluchowska, Jan K. Maurin, Institute of Atomic Energy, 05-400 Swierk-Otwock, Poland.

Molecular modeling studies of 2- and 3-furancarboxylic acids (2-FA and 3-FA) and their complexes with magnesium and calcium had been carried out to elucidate electrondonor properties of the furan ring oxygen atom. Ab initio studies of 3-FA packing forces indicates the importance of O-H···Ofuran and O-H···Ofuran bonding interactions. Subsequently, semiempirical calculations on Mg 2-FA, Mg 3-FA, Ca 2-FA and Ca 3-FA models, which had been constructed taking into account gained knowledge about ligand binding preferences, shows some general features of ligand-metal interactions.

X-ray single crystal data for Ca 2-FA confirmed, that the furan ring oxygen is involved in chelating calcium cations, leading to the formation of five-membered rings (Ca-Ofuran-Cring-Ccarboxyl-Ocarboxyl). In the case of Ca 3-FA real crystal the packing arrangement of the molecules is maintained by C-H···Ofuran hydrogen bonds. In studying Mg 3- and 3-furancarboxylate complexes the Ofuran activity is observed in second coordination sphere, most probably due to the rigidity of Mg surrounding octahedron.

P07.07.095 TWO NOVEL MANGANESE CARBENE COMPLEXES. D.G. Billing, Department of Chemistry and Biochemistry, Rand Afrikaans University, Johannesburg, 2006 South Africa and A;. Neveling; H.G. Raubenheimer; S. Cronje. Department of Chemistry, University of Stellenbosch, Stellenbosch 7600, South Africa.

We recently synthesized cationic carbene complexes (compounds **I** and **II**) by alkylation and protonation of the pentacarbonyl complexes, using the common reagents CF_3SO_3Me and CF_3SO_3H. Crystals suitable for crystallographic study were grown from dichlorormethane. The complexes were also characterized by MS, IR-, ^{1}H-NMR- and ^{13}C-NMR spectroscopy. A search through the Cambridge database revealed that although many manganese pentacarbonyls of the type $RMn(CO)_5$ (R = alkyl and aryl) have been synthesised and characterized, no manganese carbenes are known.

I : R = H

II : R = Me

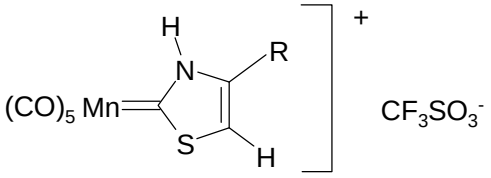

The crystal structures of **I** and **II** represent the first complete characterization of this bonding type, with an average Mn-C(carbene) bond length of 2.03 Å.

P07.07.096 STRUCTURE *VS.* REACTIVITY: RHODIUM(I) CENTRE ACCESSIBILITY BY INTERCHANGING TERTIARY PHOSPHINES WITH ARSINES AND STIBINES. A. Roodt, S. Otto, and S.N. Mzamane, Department of Chemistry, University of the Free State, P.O. Box 339, Bloemfontein, 9300, South Africa.

Solid state and solution investigations were done on the effect of tertiary **arsine** and **stibine** and variations of phospine ligands in Rh(I) models to Vaska's complex, *trans*-$[Ir(CO)(Cl)(PPh_3)_2]$ (widely recognized for different catalytic reactions).

Upon introduction of $SbPh_3$, the novel five-coordinate trigonal bypyrimidal tris-tertiary stibine complex of Rh(I), *trans*-$[Rh(CO)(Cl)(SbPh_3)_3]$, is formed, which will be presented. The structures of the isomorphous $[Rh(CO)(Cl)\{Y(p\text{Tol})_3\}]$ (Y = P, As) were also done [1] and the reactivity with regard to iodomethane oxidative addition rate showed direct correlation with the 'cavity' available at the Rh(I) centre in an associative process.

Next, an example of how a range of these complexes were used to quantify the electronic effect of a tertiary phosphine, PPh_2Fc (ferrocenyldiphenylphosphine) is illustrated. This include correlations between IR, ^{31}P NMR and structural effects vs. kinetic data.

NMR and crystallographic investigations were also done to extend the series and include a range of tertiary arsine and stibine complexes – a field very limitedly exploited to date.

[1] S. Otto, S.N. Mzamane & A. Roodt. (1999). Acta. Cryst. **C55**, 67, and refs within.

P07.07.097 MOLECULAR STRUCTURE OF HYDROGEN-CARBONATO-BRIDGED DINUCLEAR COPPER(II) COMPLEX: $[Cu_2(L)(HCO_3)](ClO_4)_2$. N. Kanehisa and Y. Kai, Department of Materials Chemistry, Graduated School of Engineering, Osaka University, Suita Osaka 565-0871, JAPAN and Y. Nishida, A. Yatani and Y. Nakao, Chemical Laboratory, Faculty of Education, Okayama University, Okayama 700-8530, JAPAN.

The increase of CO_2 concentration in atmosphere is coming a serious problem because of the rise of atmospheric temperature. A study on CO_2 fixation is now one of the most attractive current topics.

Recently, Nakao et al. reported the first X-ray structure analysis of hydrogencarbonato-bridged dinuclear copper(II) complex $[Cu_2(L)(HCO_3)]$- $(BF_4)_2.5H_2O$ (**1**) [1] obtained by leaving the solution containing a copper(II) complex $[Cu_2(L)(OH)](BF_4)_2.6H_2O$, where HL is *N,N,N',N'*-tetrakis[(1-methyl-2-benzimidazoyl)methyl]-2-hydroxy-1,3-diamino-propane. Bridged HCO_3^- moiety is considered to come from the atmospheric CO_2. Recently, we prepared and isolated a new copper(II) complex **2** having ClO_4 instead of BF_4 of complex **1** from $Cu(ClO_4)_2.6H_2O$, HL and $NaHCO_3$. We took the X-ray structure analysis of complex **2** to consider CO_2 fixation mechanism by the dinuclear copper(II) complex.

It is found that the complex **2** is isomorphous with **1**. Therefore, it may be considered that the complex **2** is also hydrogencarbonato-bridged dinuclear copper(II) complex although the hydrogen atom of bridged HCO_3^-moiety could not be located. It may also be considered that there is a possibility of obtaining complex **2** by adopting CO_2 in atmosphere through the synthetic process.

1. Y. Nishida, A. Yatani, Y. Nakao, J. Taka, S. Kashino, W. Mori and S. Suzuki, *Chem. Lett*., (1999) 135

P07.07.098 ELECTRON DELOCALIZATION IN -N=C-C=N- BRIDGED COBALT CHELATE. M. Klinga, T.V. Laine and M. Leskelä, Laboratory of Inorganic Chemistry, University of Helsinki, Box 55, 00014 Helsinki, Finland.

In our study of late transition metal based catalyst precursors for ethene polymerization we have determined the crystal structure of a cobalt(II) complex with a symmetric bidentate ligand in which diimine bridge connects two bulky aromatic groups. Complexation leads to aromatization of the bridge itself with bond lengths N=C, C-C and C=N are 1.340(12), 1.33(2) and 1.340(12) Å, respectively. The angles N=C-C and C-C=N are both for symmetry reasons 119.6(5)°. In the pure ligand the bond distances in -N=C-C=N- bridge are typical for this kind of conjugated double bond system, namely 1.266(3), 1.467(5) and 1.266(3) Å.

There are only few examples in the CSD where the bond lengths and angles resemble our situation even if the estimated standard deviations are taken in account. Also found in the CSD are examples in which a transition metal chelate and the corresponding ligand have crystallized in the same structure and there is no indication of delocalization in the bridge due to chelatization.

$[CoBr_2(C_{26}H_{36}N_2)]$

Space group C2/c (#15), M=595.32, T=193 K, Z=4, MoKα, a=20.864(6), b=6.882(4), c=19.890(6) Å, β=106.77(4)° V=2735(2) Å^3, R_1=0.0793.

$[C_{26}H_{36}N_2]$

Space group $P2_1/c$ (#14), M=376.57, T=193 K, Z=2, MoKα, a=8.624(2), b=12.710(3), c=10.868(2) Å, β=92.89(3)° V=1189.7(5) Å^3, R_1=0.0613.

1. F.H.Allen, O.Kennard & R.Taylor (1983). Cambridge Data Base, Acc. Chem. Res. 16, 146-153.

P08.07.001 ADAMANTANE-LIKE CAGE TERTIARY PHOSPHINE LIGANDS: MOLECULAR MECHANICS AND CRYSTALLOGRAPHY STUDIES. Hirihattaya Phetmung and A. Guy Orpen, School of Chemistry, University of Bristol, Cantock's Close, Bristol, BS8 1TS, UK.

Adamantane-like tertiary phosphine complexes *trans*-$PdCl_2L_2$, **I**, and *trans*-$RhCl(CO)L_2$, **II**, (L = $PhP(CH_2)_2O_3(CCF_3)_2(CMe)_2$) have been studied by molecular mechanics (MM2 and UFF force fields)[1,2] and X-ray crystallographic methods. Both are four-coordinate d^8 metal complexes with square planar geometries. The structures show large variation of ligand-metal-ligand and intra-ligand bond angles from ideal values. The sterically demanding nature of the cage ligand is shown by its cone angle of 166.5° of **I** (*cf.* 145° for PPh_3)[3]. The X-ray determined geometries are in good agreement with those from molecular mechanics.

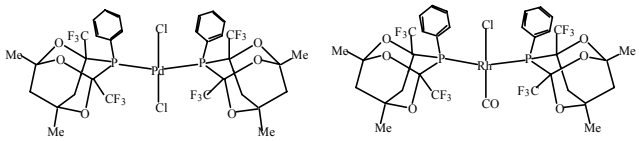

I **II**

1. U. Burkert and N.L. Allinger, *Molecular Mechanics*, ACS Monograph 177, American Chemical Society, Washington D.C., 1982.
2. A.K. Rappe', K.S. Colwell and C.J. Casewit, *Inorg. Chem.*, 1993, **32**, 3438.
3. C.A. Tolman, *Chem. Rev.*, 1977, **77**, 313.

P08.07.002 ANION AND GUEST MOLECULE SITES WITHIN THE TUNNELS AND CAVITIES OF "CHINESE LANTERN" CRYSTALS. Wendy I Cross, Department of Chemistry, University of Manchester Institute of Science and Technology, PO Box 88, Manchester, M60 1QD, UK.

The molecular structure of the transition metal complex $[Mn_2(\mu\text{-}dppO_2)_4(NCS)_2](NCS)_2$, 1 [$dppO_2$ = $Ph_2P(O)(CH_2)_3P(O)Ph_2$] was structurally characterized by X-ray crystallography(1) and was dubbed the "Chinese Lantern" owing to its unusual shape (Fig1).

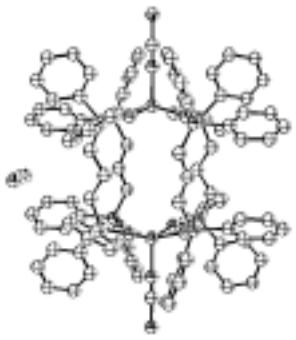

Fig1. The Chinese Lantern structure, 1

Furthermore, it was found to reversibly adsorb sulfur dioxide thus making it a potentially useful compound for the removal of sulfur dioxide from flue gas emissions.

The complexes $[Mn_2(\mu\text{-}dppO_2)_4(X)_2]X_2$, X = Cl, Br, I have been synthesized and structurally characterized by single crystal X-ray diffraction. The complexes all crystallize in the same space group (Tetragonal, I4/m) and superficially appear similar to complex 1. However, by varying the size of the anion, fundamental changes in the molecular structure are observed. The crystal packing of all the complexes reveals the presence of tunnels and cavities running through the structure in which anions and guest molecules such as sulfur dioxide may be found.

(1) C.A. McAuliffe, B. Beagley, G. Dyer, P.P. MacRory, R.G. Pritchard. *Journal of the Chemical Society, Chem. Commun*. (1991) pp 965-966.

P08.07.003 CRYSTAL STRUCTURES OF NOVEL CARBORANE COMPLEXES. Dianne Ellis*, A. Franken, P. A. Jelliss, J. M. Malget and F. G. A. Stone, Department of Chemistry, Baylor University, Waco, TX 76798 U.S.A.

Co-workers in this laboratory have prepared a series of complexes using $[\eta^5\text{-}nido\text{-}7\text{-}CB_{10}H_{11}]^{3-}$ and $[\eta^5\text{-}nido\text{-}7,8\text{-}C_2B_9H_{11}]^{2-}$ ligands exhibiting a variety of co-ordination modes for the cage systems.

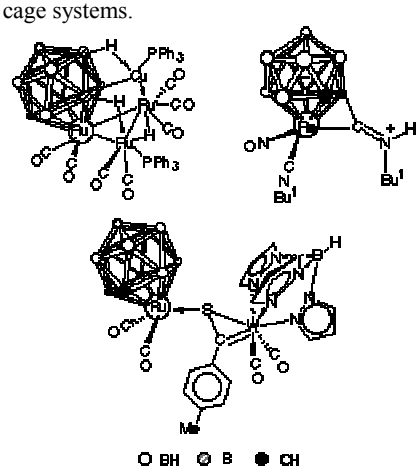

The formation of *closo*-metallacarboranes from reactions of these 11-vertex *nido*-carboranes with low valent metals, has shown that the cages can adopt a non-spectator role utilising bonding to exopolyhedral groups as well as the traditional pentahapto ligation modes. This poster will illustrate a number of these molecules whose structures have been established using X-ray diffraction.

P13.07.001 HYDROTHERMAL SYNTHESIS AND CRYST STRUCT OF 1 OR 2D POLYOXOANION CLUSTERS BRIDGED BY INORGANIC LIGAND Wei-Ming Bu, Ling Ye, Yu-Guo Fan [1], Guo-Yu Yang, Ji-Qing Xu [2], [1] Fan, Key Lab of Superomolecular Structure and Spectroscopy, Jilin University, Changchun 130023,P.R.China, [2] Department of Chemistry, Jilin University, Changchun 130023,P.R.China

The hundreds of known examples of polyoxoanions comprise a class of inorganic complexes of unrivaled versatility and structural variation, and have application in many fields of scinece.(1)There are indications that the synthesis of polyoxometalate clusters by rational design remains elusive.(2). Utilizing molecular building blocks,the polyoxoanion family can be linked through organic or inorganic tethers to form extended structures. Zubieta et al. found that transition metal coordination compounds may function as charge compensating templates which influence the structure of the metal oxide network.(3)These observations suggested transion metal coordination compounds could act as inorganic bridging ligands. The essential element as a general method of synthesis proved to be the use of hydrothermal techniques.

The title complexes 1-3 were prepared hydrothermally employing conditions reported before. Crystal

data:$[Co(en)_3][\{Co(en)_2\}_2\ As_6V_{15}O_{42}].8H_2O$ (1): Monoclinic P2(1)/n, a=18.9133(3)A, b=19.7213(3)A, c=20.0968(4)A, beta=98.676(3) ,V=7410.23(12), z=2, R=0.0459, wR=0.0883;$[Ni(en)_2]_2\ [Ni(en)_2Mo_6V_{10}O_{40}(PO_4)].4H_2O$ (2): Monoclinc C2/c, a=26.065(2)A, b=19.730(3), c=13.485(2), beta=106.04(7), V=6664.18(10), Z=2, R=0.066; $[Cu(H_2O)_4][Cu(en)_2][\{Cu(en)(H_2O)_2Cu(en)_2\}_{0.5}\{Mo_8V_8O_{40}(MoO_4)\}].13H_2O$ (3): Orthorhombic P2(1)2(1)2, a=26.8124(4)A, b=13.6684(2)A,c=19.6058(4)A, V=7185.19(20),Z=2,R=0.048.

The compound 1 consists of infinite chains of As-V-O clusters $[As_8V_{14}O_{42}]^{6-}$ covalently linked through $[Co(en)_2]^{2+}$ groups,with isolated $[Co(en)_2]^{2+}$ cations occupying the interchain regions and providing charge compensation. The bridging Co(II) sites exhibit strong covalent interactions to the two adjacent clusters with Co-O distances of 2.091A.

The compound 2 is a Mo-V-O cluster $[Mo_6V_{10}O_{40}(PO_4)]^{4-}$ of one dimensional extended network linked through inorganic bridging ligands $[Ni(en)_2]^{2+}$. Each $[Mo_6V_{10}O_{40}(PO_4)]^{4-}$ forms strong covalent interactions to two $[Co(en)_2]^{2+}$ with Co-O distances of 2.091A.In contrast,the Ni sites of a $[Ni(en)_2Mo_6V_{10}O_{40}(PO_4)]$ cluster exhibit only weak interactions with neighboring clusters,with axial Ni...O distances of 2.98A.

The structure of 3 consists of $[Mo_8V_8O_{40}(MoO_4)]$ clusters linked by $[Cu(en)_2]$ and $Cu(en)(H_2O)_2$ groups into a two-dimensional network. Each $[Mo_8V_8O_{40}(MoO_4)]$ cluster forms strong covalent interactions to two different bridge $(Cu(en)_2]$ and $Cu(en)(H_2O)_2)$ groups with Cu-O distances of 1.901-2.025A. It is noteworthy that the structure of 1-3 exhibit hydrogen-bonding interactions between the nitrogen atoms and water molecules or terminal oxo groups of the clusters.

The title compounds 1-3 provide an intermediate prototype between polyoxoanions with surface-bound inorganic moieties and true extended polyoxoanion coordination compound assembies.Furthermore,the title compounds demonstrate that the vast class of polyoxoanion clusters may be used as building blocks in the design of solid state materials.

1. M.T.Pope,Encyclopedia of Inorganic Chemistry; (Ed.:R.B.King),Wiley, Chrichester,1994,pp.3361-3371;
2. F.J.DiSalvo,Science,247(1990)649;
3. Jeffrey R.D.DeBord,Robert C.Haushalter et.al,Inorganica Chimica Acta, 256(1997)165-168.

P13.07.002 NOVEL COORDINATION POLYMERIC NETWORKS OF COBALT(II) CENTRES WITH N,N' BIDENTATE SPACERS AND THEIR INCLUSION PROPERTIES. Mohan M. Bhadbhade, Physical Chemistry Division, National Chemical Laboratory, Pune 411 008, INDIA and E. Suresh and R. V. Jasra, Discipline of Silicate and Catalysis, Central Salt and Marine Chemicals Research Institute, Bhavnagar 364 002, INDIA

The coordination polymers, in which metal centers are linked by the organic molecules offer an enormous potential in designing new microporous materials to be used for separation, selective adsorption and catalysis as there is a wide choice of metal ions and spacers. In this paper, we report four X-ray structures having novel coordination polymeric frameworks of Co(II) with the ligands 4,4'-bipyridyl(**1, 2**) and 1,2-bis(4-pyridyl)ethane (**3**, **4**). Although the anions are different, complexes **1** and **2** are isostructural showing a novel two-dimensional network essentially governed by π…π interactions between the bpy moieties. Intertwined linear chains of $\{Co(H_2O)_2(4,4'\text{-bpy})_2$ - 4,4'-bpy$\}_n$ create micro channels of dimensions ~ 7 x 12 Å filled with molecules of 4,4'-bpy and disordered anions and waters.

Interestingly, complex **3** with a flexible linker also generates a two-dimensional architecture showing π…π interactions that creates micro channels of similar dimensions in which spacer molecules and anions are included. The flexibility of the ligand is manifested in a layered structure **4** devoid of any micro channels; the layer of Co(II) ions doubly bridged by two spacer molecules is alternated with the anionic layer. The possibility of utilizing the micro channels as in **1**(**2**) and **3** for shape selectivity of aromatic guests and for suitable catalytic reactions is being explored.

P13.07.003 X-RAY STUDY OF COMPOUNDS OF HYPERVALENT SILICON. E.A.Zelbst and A.A.Kashaev, Pedagogical University,Physic Faculty,N. Naberegnaya st.,6, Irkutsk,Russia; M.P.Demidov and M.G.Voronkov, Institute of Chemistry of Academ Nauk of Russia, Favorskogo st.,1, Irkutsk, Russia.

Winnowed full X-ray study of number of silicon-organic compounds with the total formula $X\text{-}C_6H_4C(O)YCH_2SiF_3$ (X=4-F,-Cl,-Br,2-Cl with Y=O; Y=O,S,NCH_3 with X=H) and their analogues. Discovered particularities of the crystall structure (aroiloximethyl)threefluorsilanes allow to refer these compound to the new class of representatives hypervalent silicon.

(Aroiloximethyl)threefluorsilanes exist in stable intracoordinate form, containing fivemember cycle, closed intramolekular coordination bond O-Si. Fivecoordination atom silicon in their molecules inheres in the centre an trygonal bipyramid with axyal by the location an atom of the fluorine and oxygen.

Stated that length of the communication O-Si in these molecules is changed within 1.91-2.08 A. This existance is stipulated high elektrofilates of the atom silicon, connected with three atoms of the fluorine.

Of the Molecule (aroiloximethyl)threefluorsilanes and their analogues are bound in the crystal by power van-der-vaals. However in number of events between they exist an abbreviated intermolecular contacts.

Continuing studies of compounds of hypervalent silicon , we have defined crystall structure parameters of new compounds of this type (β-phenyl-propionyloximethyl) threefluorsilanes: $(C_6H_5CH_2CH_2COOCH_2SiF_3)$ a=7.71(1), b=6.85(2), c=10.35(2) A, β=99.78, sp.gr. $P2_1$. Expected that in this molecule is kept coordinate communication O-Si, however interfacing between five-member cycle and benzol ring, probably, lowered.

P13.07.004 MOLECULAR METALWIRES. Yih-Lih Jang, Wen-Ju Lee, Chih-Chieh Wang, Gene-Hsiang Lee, Man-kit Leung, Shie-Ming Peng, Department of Chemistry, National Taiwan University, Taipei, Taiwan

The metal string complexes with different metal ions and various lengths have been successfully synthesized and structurally characterized.[1-6]

M^{II} = Cr, Co, Ni
n = 0, 1, 2, 3

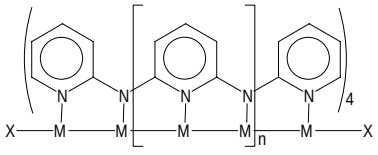

The crystal and molecular structure of nonanickel complex $[Ni_9(\mu_9\text{-}(peptea)_4Cl_2]$ which is the longest metal string at this moment will be reported. Crystal data for $[Ni_9(\mu_9\text{-}(peptea)_4Cl_2]\cdot(C_2H_4Cl_2)_{10}$: Space group, monoclinic C 2/c, a = 27.395(4), b = 42.476(9), c = 37.743(8) Å, β = 108.74(2)°, V = 41,590(13) $Å^3$, Z = 12, R_F = 8 % for the observed reflections ($I > 2\sigma(I)$).

The band structure calculation of infinite one-dimensional metal chains of Ni^{II} and Cr^{II} based on the structure of nanonickel complex will be presented. Finally, the metal string complexes $[M^{II}{}_nL_4X_2]$ will be chemsorbed on the Ag or Au surface and the potential application of these complexes as a molecular metal wire will be demonstrated.

Sheu, J. T.; Liu, C. C.; Chao, I.; Wang, C. C.; Peng, S. M. *Chem. Commun.* 1996, 315.
Shieh, S. J.; Chou, C. C.; Lee, G. H.; Wang, C. C.; Peng, S. M. *Angew. Chem. Int. Ed. Engl.,* 1997, *36*, 56.
Yang, M. H.; Lin, T. W.; Chou, C. C.; Lee, H. C.; Chang, H. C.; Lee, G. H.; Leung, M. K.; Peng, S. M. Chem. Commun. *1997, 2279.*
Wang, C. C.; Lo, W. C.; Chou, C. C.; Lee, G. H.; Chen, J. M.; Peng, S. M. *Inorg. Chem.* 1998, *37*, 4059.
Lai, S. Y.; Lin, Z. W.; Chen, Y. H.; Wang, C. C.; Lee, G. H.; Yang, M. H.; Leung, M.-k.; Peng, S. M. *J. Am Chem. Soc.* 1999, *121*, 250.

P13.07.005 THE STRUCTURAL CHARACTERISATION OF METAL ION ACTIVATED SUPRAMOLECULAR RECEPTOR MOLECULES. Kia S. Wallwork, Christopher B. Smith, Max R. Taylor and Kevin P. Wainwright, Department of Chemistry, The Flinders University of South Australia, GPO Box 2100, Adelaide, Australia 5001.

Complexation of pendant donor macrocycles derived from cyclen (1,4,7,10-tetraazacyclododecane) with eight coordinate metal ions such as Cd^{2+} or Pb^{2+}, has been shown to give rise to binary complexes where all four pendant arms project in the same direction. The ligand, *S*-thphpc12 (1,4,7,10-tetrakis((*S*)-2-hydroxy-3-phenoxypropyl)-1,4,7,10-tetraazacyclododecane), **1**, has recently been synthesised and its coordination and host-guest chemistry is being studied. Ligands such as this are of interest for their ability to preferentially uptake cationic, anionic or neutral substrates. The subsequent system can then be used in a variety of applications, including, the transportation of radioactive isotopes to cancerous tissue.[1]

Early X-ray crystallography studies of the perchlorate salt of **1** show that the aromatic moieties delineate a molecular basket similar to that of calixarenes. Upon reaction with species such as sodium *p*-toluenesulfonate and sodium *p*-aminobenzoate, sodium perchlorate is eliminated and inclusion complexes containing *p*-toluenesulfonate or *p*-aminobenzoate can be formed.

The ternary complexes containing *p*-toluenesulfonate and *p*-aminobenzoate have been characterised. Both systems crystallise in the non-centrosymmetric space group P1, with Z=1. The guest anion is held within the host cavity via hydrogen bonding. There does not appear to be any non-bonding interaction between the ligand and the guest, in the molecular structure, but there is within the crystal structure. The characteristics, including the non-bonded inter- and intra-molecular interactions, of four of these ternary complexes will be presented and inferences will be drawn between the related compounds.

1. D. Parker (1990). *Chem. Br.* **26**, 942.

P13.07.006 SUPRAMOLECULAR ARCHITECTURE OF $Mo_3S_7dtc_4$ (dtc = DIETHYLDITHIOCARBAMATE). E.A. Il'inchik, T.M. Polyanskaya and K.G. Myakishev, Institute of Inorganic Chemistry SB RAS, Novosibirsk, 630090 Russia.

We have carried out single crystal X-ray analysis of the title compound whose structure fragment is shown below. The structure parameters of the cation core itself are closely related to those of other complexes containing the $[Mo_3S_7dtc_3]^+$ moiety. The dtc^- anion is located in such a way that its sulfur atoms have the contacts to the axial sulfur atoms of the cation μ_2S_2 ligands which are shorter than the sum of the corresponding van der Waals radii. Besides, one anion S atom has the short contact with the S atom of the next cation ligand dtc. The geometry of the anion NCS_2 fragment is distorted. The cation ligand dtc next to the anion is not planar. According to XPS, the binding energy of 2p electrons of the anion sulfur atoms, E(S2p)=161.7 eV, coincides with that for Na^+dtc^-. The sulfur atoms of the $[Mo_3S_7dtc_3]^+$ cation have E(S2p)=163.0 eV. So, all sulfur atoms of the compound have a negative charge and the short contacts take place between the same charged sulfur atoms. The Mo atoms have a positive charge that reflected by E($Mo3d_{5/2}$)=229.7 eV. The crystal data: the system is triclinic, space group $P\bar{1}$, a=10.786(2), b=11.155(1), c=16.710(3) Å, α=93.59(1), β=90.66(1), γ=100.25(1)°, Z=2, R_F=0.023.

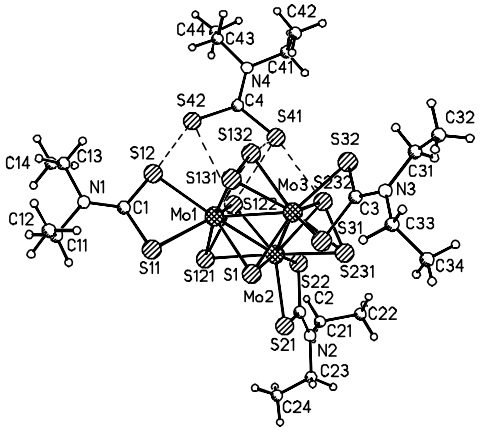

P13.07.007 SUPRAMOLECULAR ISOMERISM IN INORGANIC COORDINATION POLYMERS. A.J. Blake, N.R. Brooks, N.R. Champness, M. Crew, D.H. Gregory, P. Hubberstey and M. Schr`der, School of Chemistry, University of Nottingham, University Park, Nottingham, NG7 2RD, UK, A.M. Deveson and D. Fenske, Institut fur Anorganische Chemie, Universitat Karlsruhe, Engesserstr. Geb-Nr. 30.45, 76128 Karlsruhe, Germany, and L.R. Hanton, Department of Chemistry, University of Otago, P.O. Box 56, Dunedin, New Zealand

The field of crystal engineering using bridging bidentate ligands with late transition metals to form co-ordination polymers, has received growing attention, with much of this work using the 4,4=-bipyridine (4,4=-bipy) ligand and its analogues. We are currently investigating the factors that affect the formation of these coordination networks. One aspect of this work is our studies into the arrays formed by CuX (X = Cl, Br, I, SCN) and bridging bipyridyl ligands. Our research into the extended polymers constructed from CuI and the bowed bipyridyl ligand bis-(4-pyridyl)disulfide (bpds) has generated a pair of supramolecular isomers. This unusual phenomenon has been seen for the polymers $[(CuI)_2(bpds)]_4$ which have a tubular structure when crystals are grown from $MeCN/CH_2Cl_2$ but a necklace motif is observed when $EtCN/CH_2Cl_2$ are used as crystallisation solvents. The different connectivities of these two compounds represents an extremely rare example of supramolecular isomerism.

P13.07.008 MOLECULAR PACKING ANALYSIS FOR MIXED CRYSTALS OF A COBALT COMPLEX. R. Wang and U. Englert, Institute of Inorganic Chemistry, RWTH Aachen, Prof.-Pirlet-Str. 1, 52074 Aachen, Germany

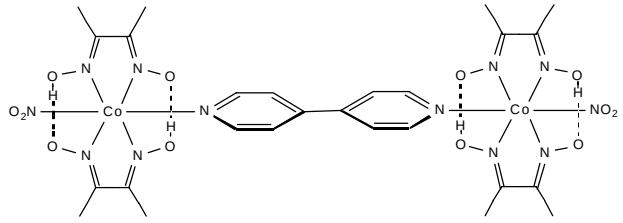

Complex [{Co(III)(dmgH)2(NO2)}2(4,4'-bipy)] (s. Fig.) crystallizes with a variety of small guest molecules f. e. H_2O, CH_2Cl_2, CH_3NO_2, C_6H_6, THF and so on

Different packing arrangements and the geometry of the Cobalt complex component in seven crystal structures are studied.

Lattice-energy calculation have been carried out with program PCK83[1] basing on the Atom-Atom Potential Method[2,3] for the seven crystal structures. In all seven cases the local minima from the experimental crystal structures are reproducible.

Structure:

1: Co-Complex·2 CH_2Cl_2·2C_6H_6

2: Co-Complex·2 CH_2Cl_2·2H_2O

3: Co-Complex·0.5H_2O

4: Co-Complex·2.5 CH_2Cl_2

5: Co-Complex·2 CH_3NO_2· H_2O

6: Co-Complex· CH_2Cl_2·THF

7: Co-Complex·CH_2Cl_2·CH_3COOEt

[1] Williams, D. E. "PCK83, a crystal molecular packing analysis program" Quantum Chemistry Programs Exchange, 1983.
[2] A. J. Pertsin, A. I. Kitaigorodsky *The Atom-Atom Potential Method*; Springer Verlag, Berlin-Heidelberg-New York, 1987.
[3] Schmidt, M. U.; Englert, U. *J. Chem. Soc. Dalton Trans.* (1996) 2077.

P13.07.009 β-CYCLODEXTRIN AND BUTYL/ CYCLOHEXYL (AQUA) COBALOXIME INCLUSION COMPLEXS. H.K. Fun and K.Chinnakali, X-ray Crystallography Unit, School of Physics, Universiti Sains Malaysia,11800USM, Penang, Malaysia, and Y.Chen, L.Luo and H.Chen, Coordination Chemistry Institute, State Key Laboratory of Coordination Chemistry,Nanjing University, Nanjing, 210093, P. R. China.

Cyclodextrins are a class of cyclic oligosaccharides consisting of six (α), seven (β) or eight (γ) α-1,4 linked D-glucopyranose units, with a toroidal hydrophobic cavity capable of including a variety of inorganic and organic guest species. They have been proposed to act as artificial enzymes due to their ability to form inclusion complexes and to show regiospecificity and stereospecificity with respect to the substrate and product during catalytic processing. Recently, our group synthesised a series of alkylcobaloxime/CD inclusion complexes[1,2], in which guest and host associate through non-covalent interaction, such as hydrophobic and van der Waals interactions. Here we report the crystal and molecular structures of butyl(aqua) cobaloxime (I) and its inclusion complex with β-CD (II), as well as cyclohexyl(aqua)cobaloxime (III) and its β-CD inclusion complex (IV). In (II) and (IV) , the β-cyclodextrin molecule is in the shape of a truncated heptagonal cone. In (II), the butyl group is inserted into the cyclodextrin's cavity from its wider opening such that the chain is lying below the mean plane composed of O atoms associated with the fourteen secondary OH groups. In (IV), the cyclohexyl ring is encapsulated by cyclodextrin cavity from secondary hydroxyl side and the terminal C atom lies at 2.860(5)Å below the mean plane of the secondary OH groups. The present investigations show that there are some structural and conformational changes of *n*-$C_4H_9Co(DH)_2H_2O$ after the insertion of butyl group into the β-CD cavity. That is (a) the obvious lengthening of Co-O bond and (b) the slight displacement of cobalt atom from the mean plane of four nitrogen atoms.

1. L.B.Luo, H.L.Chen, W.X.Tang, Z.Y.Zhang & T.C.W. Mak (1996). *J. Chem. Soc., Dalton Trans.*, 4425.
2. L.B.Luo, Y.Chen, H.L.Chen, W.X.Tang (1996). *Spectrosc. Lett.*, *29*, 449.

P13.07.010 THE SOLID-STATE STRUCTURE OF A SERIES OF DITHIINS AND RELATED SELENIUM DERIVATIVES. François Brisse, Mohamed Atfani, Jean-Yves Bergeron and Michel Armand Département de chimie, Université de Montréal, C.P. 6128, Succursale Centre-ville, Montréal, QC, H3C 3J7, Canada

Charge transfer complexes and radical cation salts derived from 1,4-dithiins and derivatives exhibit high electrical conductivity. 1,4-dithiins normally adopt the boat conformation in which the sulfur atoms are tilted towards one another. However, various molecular orbital calculations have indicated that the energy barrier between the planar and the boat conformations is very small. Thus we have investigated the structure of 1,4-dithiintetracarboxylic N,N' dimethyldiimide (1) and that of the related selenium derivative (2). The structure of 1,4-dithiintetracarboxylic N,N' di tert-butyldiimide (3) was also established. Both (1) and (2) crystallize in the monoclinic system, space group P21/n with Z=2, are isostructural. The refinements converged to R=0.038 (1) and R=0.030 (2). The tert-butyl derivative forms very thin hair-like crystals. They belong to the triclinic system. However, it seems that all the crystals that we examined are twinned, the structure was solved and R converged to 0.068 (3). It is found that all three compounds are planar. Most bond distances and angles are normal with the exception of the X-C(sp2)-C(sp2)-O distances which are significantly and systematically longer than the usual C(sp2)-C(sp2) bond distance. This observation may be attributed to the electronic repulsion between the lone pair of the heteroatom, X, and that of the the oxygen atom. The crystals are very colorful, in solution or in the solid-state. Their physical properties will be discussed in terms of packing. The crystal structures of other members of the series, where the methyl group is replaced by hexyl, decyl or phenyl groups, will be presented.

08. CRYSTAL ENGINEERING

P11.08.001 THE USE OF KETO CARBOXYLIC ACIDS AS A MODEL SYSTEM FOR CRYSTAL STRUCTURE PREDICTION. A. P. J. Brunskill, R. A. Lalancette and H. W. Thompson. Rutgers University, Department of Chemistry, 73 Warren St., Newark, NJ 07102, USA.

The dominance of hydrogen bonding in directing molecular association in crystals has long been recognized. The carboxylic acid dimer in particular has been viewed as a robust "molecular synthon". However as other hydrogen bond acceptors are added to a molecule it has been found that other H-bonding motifs are often preferred. Organic keto carboxylic acids provide a useful model system to study factors that cause variation in hydrogen bonding patterns when competing H-bond acceptors have similar electronegativities. We have synthesized and determined the solid state structures of over 50 keto carboxylic acids of varying topology, size and chirality. Many others have been found in a survey of the CSD. To date 5 distinct hydrogen bonding patterns have been found: acid-to-acid dimers, acid-to-ketone catemers (infinite chains), internal H bonds, acid-to-acid catemers and acid-to-ketone dimers. Observation of the characteristics for molecules falling into each hydrogen bonding category suggest definite methods to direct H bonding, such as control of handedness, structural rigidity and shape. By employing these design methods we have been able to produce molecules in which we have successfully directed H-bonding.

Knowledge of probable H-bonding association, combined with strict symmetry constraints and the high probability of close packing reduces considerably the number of structures that need to be considered as potential crystal structures. In effect, large parts of the energy hypersurface can be neglected, considerably reducing the computational complexity of ab initio crystal structures prediction.

Results of our experimental work and crystal structure prediction methodology will be presented.

P11.08.002 INTRAMOLECULAR NON-BONDING INTERACTIONS BETWEEN HALOGEN AND OXYGEN. G. Punte and G. Echeverría, LANADI-PROFIMO, Departamento de Física, Facultad de Ciencias Exactas, Universidad Nacional de La Plata, C.C. 67 (1900) La Plata, Argentina, A. E. Goeta, Chemistry Department, Durham University, Durham DH1 3LE, UK and J. Ellena, Instituto de Física de Saõ Carlos, USP, Saõ Carlos, SP, Brasil, A. Rubert, Departamento de Química, Facultad de Ciencias Exactas, UNLP, calles 47 y 115 (1900) La Plata, Argentina, G. P. Romanelli and J. C. Autino, LADECOR, Departamento de Química, Facultad de Ciencias Exactas, UNLP, calles 47 y 115 (1900) La Plata, Argentina

The role and nature of weak non-bonded interactions in the conformation and aggregation of organic molecules is the subject of numerous experimental investigations, extensive data base searches and quantum mechanical calculations. This is due to its importance in material engineering. From the analysis, performed on several compounds presenting differently substituted halogen-C-C-oxygen moiety/ies located in dissimilar molecular environments, we have found a tendency in these fragments to establish intramolecular halogen···oxygen short contacts. Moreover, we have shown that a short Br···O intramolecular interaction allows explaining the very good reaction yields in a novel synthesis of substituted 3-aryloxypropionitriles [1]. In this paper we go deeper in the examination of those interactions by means of different experimental techniques complemented with theoretical calculations.

1. J. Ellena, G. Punte, J. C. Autino, G. P. Romanelli & A. E. Goeta (1998). Cryst. Res. Technol., 33, 145-151.

P11.08.003 SUPRAMOLECULAR ASSEMBLY OF HYDROPHOBIC DIPEPTIDES INTO MOLECULAR HONEYCOMB PATTERNS Gorbitz, C. H. Department of Chemistry, University of Oslo, N-0315 Oslo, Norway

Dipeptides with two hydrophobic residues (hydrophobic dipeptides) can form layered structures in which the hydroxyl group of cocrystallized alcohol molecules constitute an integrate part of the hydrogen bond pattern.[1] Some of these dipeptides, however, form honeycomb patterns by hydrogen bonding of six molecules around hexagonal crystallographic axes in the P65 space group. The hydrogen bonding pattern is invariant, but the diameter of the resulting empty central channel is inversely related to the size of the amino acid side chains lining the hydrophobic inner surface. Accordingly, the types of molecules which can be accommodated as guests vary with the dipeptide composition. Previously the structure of L-Val-L-Ala has been presented.[2] We now report the crystal structures of L-Val-L-Val and L-Ile-L-Ala together with preliminary theoretical and experimental results for several other compounds.The aim of this study is to design structures which will absorb only one or a few types of guest molecules with high specificity.

1. Gorbitz, C. H. and Torgersen, E. (1999). Acta Cryst. B55, in print.
2. Gorbitz, C. H. and Gundersen, E. (1996). Acta Cryst. C52, 1764-1767.

P11.08.004 EXTENDED MULTIDECKER SANDWICH ARCHITEC-TURE OF THE Cs^+ - 18-CROWN-6 COMPLEXES. J.A. Rusanova, K.V. Domasevitch, O.Yu. Vassilyeva, V.N. Kokozay, Chemistry Dpt., Kiev Shevchenko University, Volodimirska St. 64, Kiev 252033,Ukraine, J. Sieler, WB Anorganische Chemie, Universität Leipzig, Deutschland;P.J. Squattrito, Chemistry Dpt., Central Michigan University, Mt. Pleasant, USA ; P. Raithby, Chemistry Dpt., Cambrige, UK

An approach to synthesis of the triple-decker club sandwiches, in particular $Cs_2(18c6)_3^{2+}$, can be based on the observation that the large cations tend to be stabilized by large anions and *vice versa*. The suitable systems in this context are iodocuprates(I), the typical feature of which is the formation of high-nuclearity low-nucleophilicity $Cu_nI_m^{(m-n)-}$ anionic clusters. We have isolated three different iodocuprate(I) species employing zerovalent copper, 18c6, CsI and NH_4I as starting materials. $Cs(18c6)_2Cu_5I_6{\cdot}2MeCN$ (1) is a unique example for such a large

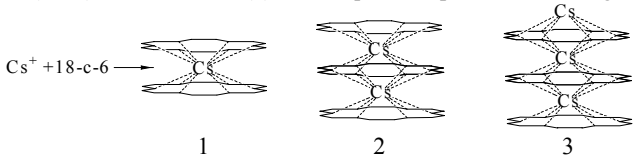

1 2 3

multidecker club sandwich, free from disorder or extremely high anisotropy in the thermal motion of the atoms. $Cs_2(18c6)_3Cu_8I_{10}{\cdot}2MeCN$ (2) is built up from the novel finite iodocuprate(I) $[Cu_8I_{10}(MeCN)_2]^{2-}$ and cations $Cs_2(18c6)_3^{2+}$, while $Cs_9(18c6)_9Cu_{24}I_{33}$ (3) includes iodocuprate(I) clusters $[Cu_4I_7]^{3-}$, $[Cu_7I_{10}]^{3-}$, $[Cu_{13}I_{14}]^{-}$, iodide anions and the 3:3 club sandwich $Cs_3(18c6)_3^{3+}$. The novel unit $[Cu_{13}I_{14}]^{-}$ is the largest finite iodocuprate(I), it has a perfect nearly spherical structure, in which 12 copper atoms are arranged in a truncated tetrahedron centered by the 13th copper atom (Cu-I 2.53(2)-3.098(6) Å). Thus in the light of the present work and our report [1], formation of the club sandwiches $Cs_n(18c6)_3^{n+}$ should be considered as a general feature of a 18-crown-6 chemistry.

K.V. Domasevitch, et al., J. Chem. Soc., Dalton Trans., 1997, 1177.

P11.08.005 INTER-MOLECULAR INTERACTIONS IN P-BLOCK CHEMISTRY: TOWARDS CRYSTAL ENGINEERING BASED ON SECONDARY BONDING. Jonathan Starbuck and A. Guy Orpen, School of Chemistry, University of Bristol, Cantock's Close, Bristol, BS8 1TS, UK.

'Crystal engineering' – the design and synthesis of the crystalline phase of molecular solids – is a field that is attracting the attention of chemists from a broad range of fields. In this work, individual molecular species have been synthesised and the broad range of structures present in the Cambridge Structural Database (CSD)[1] have been surveyed to determine the way in which popular inter-molecular interactions build into structure-forming packing motifs.

The initial systems chosen for study were those containing the bismuth (Bi) or antimony (Sb) halide moiety. The electronegativity difference that exists between Bi/Sb and halides results in polar covalent bonds leading to a tendency to form bridging interactions in the solid state. The E:::X inter-molecular interaction was originally defined by Alcock[2] as a 'secondary bond'. These interactions have been observed to play a vital role in the aggregation of molecular species centred on the heavier p-block elements.

The topology of hydrogen bonding networks has been described using 'graph-set analysis', a technique principally developed by Etter, Bernstein, Davis and co-workers.[3] These techniques have been applied to inorganic systems in an attempt to describe the topology of the interactions in a systematic and informative way.

[1] F.H. Allen *et al*, *J. Chem. Inf. Comput. Sci.*, 1987, **31**, 187.
[2] N.W. Alcock, *Adv. Inorg. Chem. Radiochem.*, 1972, **15**, 1.
[3] J. Bernstein, R.E. Davis, L. Shimoni and N.L. Chang, *Angew. Chem. Int. Ed. Engl.*, 1995, **34**, 1555.

P11.08.006 POLYIODIDE NETWORKS IN CRYSTALS. Ian Dance, Louise Berben, Basem Ali, Marcia Scudder and Don Craig, School of Chemistry, University of New South Wales, Sydney 2052, Australia.

A series of crystals containing polyiodide anions with $[Fe(phen)3]^{2+}$ cations will be presented. A significant result is the variety of polyiodide networks which can be formed with the same cation. The crystal supramolecularity of this class of compounds will be presented, and the reasons for the diversity of structure type investigated. The four types of intermolecular motif recognised in these crystals are the the multiple aryl embraces which provide attraction between $[Fe(phen)_3]^{2+}$ cations, I•••I attractions, η^6-C•••I, and C–H•••I hydrogen bonds. The polyiodide networks are one-, two- and three-dimensional. Intermolecular energies have been calculated. Polyiodide chains fit well between and around the aryl rings of the embracing cations. The ability to predict and control the structures of crystals containing polyiodide anions with cations of this type will be considered, together with the implications for crystal engineering.

P11.08.007 PHENYL EMBRACES IN THE CRYSTAL SUPRAMOLECULARITY OF COMPOUNDS CONTAING PHS–, PH4P+, XPH3 AND SN . Basem F. Ali, Ian G. Dance, Marcia L. Scudder and Don C. Craig [1] [1] Department of Inorganic and Nuclear Chemistry, University of New South Wales, Sydney 2052, Australia

The crystal supramolecularity of two classes of compounds containing sulfur are reported: Ph3X(S)nXPh3 (X = C, Si, Ge; n = 1–6) and the dimorphs of (Ph4P)2[Cd2(SPh)6] (Ph = phenyl). In both classes of crystal there are multiple phenyl embraces1 involving the phenyl rings on the periphery of the molecules and ions. The supramolecularity of each compounds is investigated through analysis of the crystal packing and the calculation of intermolecular energies. The crystal packing of the set of compounds Ph3X(S)nXPh3 is dominated by the attractive sixfold phenyl embraces between the XPh3 groups at the ends of the chain, while S•••S and S•••Ph interactions are lesser influences. The crystal packing in the dimorphs of (Ph4P)2[Cd2(SPh)6] involves attractive multiple phenyl embraces between Ph4P+ cations and between Ph4P+ and [Cd2(SPh)6]2– complexes. Similar intermolecular energies are calculated for the two crystals.

1 Dance, I. G. and Scudder, M. L., Chem. Eur. J., 1996, 2, 481.

P11.08.008 STOICHIOMETRIC COEFFICIENTS, MULTIPLICITIES AND POSITIONS. N.L. Smirnova, Department of Geology, Moscow State University, Moscow 119899, Russia.

A.V. Shubnicov suggested to use multiplicities as stoichiometric coefficients (indices) in chemical formulas in 1922. I found all 385 possible sets of different multiplicities (*Md*) in 1989. Since each atom can occupy *x* positions with a given multiplicity each index has to be multiplied by *x*. *Different* multipliers *x* in formula form set - positional formula (*Pd*). The number of positions with the same multiplicity in all (230) *G*3 is 1 to 9 and .12 (digit number). The set 0, 1, 2, 12 is denoted by letter *K* and 0, 1 by *M*. All 91 *Pd* in *G*3 are given below: 1, 2, 12, (*K*)**3**, **[***K*, (*K*)3**]4**, {*K*, (*K*)3, [*K*, (*K*)3]4, [*K*, (*M*)4]6, [*M*, (*M*)4]7, [*M*, (*M*)4]8**}5**, {*K*, (*K*)3, (*M*)4, [*K*, (*M*)4]7, (*M*)8, (*M*).12, [(*M*)8].12**}6**, {*K*, (*M*)4, (*M*)8}7, {*M*, (*M*)3, [*M*, (*M*)3]4, (*M*)9, (*M*).12**}8**, (*M*)**9**, (*M*).**12**. In A_mB_n *Pd* for A+B are given without asteriscs, for A or B with asteriscs, for A - by plus sign, for B - in *italic*: *+1*, *+2*, *+12*, **(***+0*, *+1*, *+2*, *+12***)3**, **[***+0*, *+1*, *+2*, *+12*, (*+0*, *+1*, *2*, 12)3**]4**, {*+0*, *+1*, *+2*, *+12*, (*0*, *1*, 2, 12)3, [*+0**, 1, *2*, 12, (1, 2, 12)3]4, (*0*, 123)6, (*0*, 1)8, (0, *1**, 123, 14, 6)9, (1, *12*, 123).10, (*0**, 24, .10).11, .14, .15, 2.21**}5**, {*+0*,*+1*,*+2*, *12*, (*0*, 1, *2*)3, [0, *2*, (1, 2)3]4, (0, 1, 12)7, (0, 2)8, 9, .10, (0, *2**, 24).11, .12, (2, 3).13, 1.14, .16, .18, .31, .33**}6**, {*+0*, *1*, *2**, 12, (*0*, 1, 2)3, (*0*, 1, 2)4, (+0, *1*, .16)8, *.16**}7, {*+0*, *+1**, *+2*, (*+0*, *2*)4, (0, 12)9, (0, *4*).12, .14, .15, 2.17, 2.10.18, .20, 1.23, .88**}8**, {*+0**, *+1**, *+2*, (0, *2*)3, (0, *1**, *2*, 12)4, (12, 14).10, .11, 2.13, .16, 2.18, 1.24**}9**, {*+0**, *+1**, *2**, *12*, (*0*, *1*, 12, 13)4, (0, 1).12, *.18*, .21**}.10**, {*0**, *+1**, *2**, 3, 4, 12.12**}.11**, {*+0*, +1*, *2**, 3, 4, 12.14, .18, .24**}.12**, {*0**,*+2**, *3**, 14, 12.34**}.13**, {*+0**, *+1**, *2**, 4, .20, 12.34**}.14**, {*0**, +1*, 12.16**}.15**, {*0**, *2***}.16**, ***.17****, {*+0**, .33**}.18**, {*+0**, .26**}.20**, {*0**, *2***}.21**, {*1**, +2*, 2.26**}.23**, {*+0**, *1**, .36, .44**}.24**, {*0**, *2***}.26**, ***.31****, {+0*, .62**}.32**, ***.33****, *2.**34****, ***.36****, ***.44****, ***.62****, ***.88****. These sets of indices are found for thousands of compounds. The number of symbols in *Pd* is drastically reduced at the arity equal to 5. If the symbol in *Pd* is 5 or higher then the number of these symbols can be 1, 2 and very rarely 3, i.e. the parsimony law is observed.

P11.08.009 CATION DISTRIBUTIONS AND PROPERTIES OF SOME WHITLOCKITE-LIKE COMPOUNDS. A.A. Belik, B.I. Lazoryak, V.A. Morozov, and N. Khan, Department of Chemistry, Moscow State University, 119899 Moscow, Russia, and S.S. Khasanov, Institute of Solid State Physics, 142452 Chernogolovka, Russia.

Using crystal chemistry information about the structure of β-$Ca_3(PO_4)_2$ (S.G. *R*3*c*) over 130 new isotypic compounds were modeled [1] and then synthesized by solid state method: $Ca_9R(XO_4)_7$ (*R* = rare earth, Y, Bi; *X* = P, V), $Ca_8MgR(PO_4)_7$ (*R* = rare earth, Y, Bi), $Ca_{10}M(PO_4)_7$ (*M* = Li, Na, K, Cu), $Ca_9MeM(PO_4)_7$, $Ca_{9.5}Me(PO_4)_7$ (*M* = Li, Na, K; *Me* = Mg, Mn, Co, Ni, Fe, Cu, Zn), $Ca_9R(PO_4)_7$ (*R* = Fe, Cr, Ga, In, Sc, Al, Co), $Ca_9MR_{2/3}(PO_4)_7$ (*M* = Li, Na; R = rare earth), $Sr_9R(PO_4)_7$ (*R* = Fe, Cr, Ga, In, Sc), $Sr_{18}Me_3(PO_4)_{14}$ (*Me* = Cu, Co, Ni), $Sr_9MeM(PO_4)_7$

(*M*= Na. K; *Me* = Cu, Co, Ni). Crystal structures of these compounds were studied by Rietveld method. Regularities of cation distributions over five independent cation sites were found depending on cation size and charge, and total composition of whitlockite-like phase. The cation with r>0.9A occupy the $M(1)O_8$, $M(2)O_8$, and $M(3)O_8$ polyhedra, while the cation with r<0.9A occupy the $M(5)O_6$ polyhedron. Alkali cations occupy different sites along the threefold axis into the $M(4)O_{15}$ cavity. Correlation between cation distribution and unit cell parameters are made. The influence of composition on properties were studied for 1) redox reactions in $Me_9Fe(PO_4)_7$ (*Me* = Ca, Sr) and $Ca_{19}Cu_2(PO_4)_{14}$ and $Sr_{18}Cu_3(PO_4)_{14}$; 2) luminescence properties of $Ca_9MR_{2/3}(PO_4)_7$ (*M* = Li, Na; R = rare earth) and β-$Ca_3(PO_4)_2$:Eu, $Ca_9MeM(PO_4)_7$:Eu (*M* = Li, Na, K; *Me* = Ca, Mg); 3) phase transition in $Me'_9MeM(PO_4)_7$ (*Me'* = Ca, Sr; *Me* = Cu, Fe, Ni, Co, Mg; *M* = alkali cation) associated with displacement of alkali cations into the $M(4)O_{15}$ cavity of the structure.

Lazoryak B.I. Rus. Chem. Reviews (1996), **65(4)**, 287-305.

P11.08.010 UNEXPECTED POTASSIUM DISORDER IN CRYSTAL STRUCTURES OF RHENIUM (III) THIOCHALIDE CLUSTER COMPOUNDS

S.F.Solodovnikov, S.S.Yarovoi, A.V.Virovets, V.E.Fedorov [1]
[1] Institute of Inorganic Chemistry, Russian Academy of Sciences, Novosibirsk, 630090, Russia

The single crystals of titled rhenium (III) cluster compounds (I) and (II) were prepared and their structures were studied. The both compounds are monoclinic: (I) a=9.932, b=13.528, c=12.413Å, β= 110.21°, Z=2, Sp.gr. P21/c, R=0.034; (II) a=10.614, b=17.268, c=10.448Å, b=110.75°, Z=2, Sp.gr. C2/m, R=0.042. The selected interatomic distances in (I) and (II) are Re-Re 2.586-2.597 (I) and 2.581-2.590Å (II), Re-Hal 2.550-2.574 (I) and 2.424-2.431Å (II). The separations Re-S 2.411-2.462Å in I are slightly greater compared with Re-S 2.401-2.411Å in II due to the presence of Br atoms along with sulphurs in the cluster core [Re6(S7Br)] of I. The anions [Re6S7Br7]3- and [Re6S8Cl6]4- in both structures have an layer-by-layer arrays parallel to (100) in I and (001) in II with the opposite vertices of m(3)-L8-cubes approximately perpendicular to the layer.

The most striking feature of I and II is a substantial disorder of potassium distribution over atomic positions. The K occupancies are 0.17-0.34 (I) and 0.01-0.26 (II) that being in direct dependence on the site coordination (CN =5-9 and 2-7 for I and II respectively). In I the potassium positions aggregate to form isolated tetrahedral and angle clusters whereas in II both discrete cyclic clusters (4- and 6-membered) and winding chains from vertex- and edge-linked tetrahedral clusters of K sites running along a axis are observed. The shortest distances between K positions in 'clusters' are 1.31-1.54 (I) and 0.66-1.65Å (II). Perhaps the disorder of potassium atoms results from their insufficient size to adopt large cavities between the cluster anions that makes cations to be shifted from the cavity centres and occupy 'unstable' positions. A high disorder of potassium ions in I and II make us to suggest their significant ionic conductivity (especially for II).

P11.08.011 STRUCTURAL CHANGE IN CUBIC BORON NITRIDE / DIAMOND ALLOY.

I.Ya. Nikiforov, T.P. Zhdanova, V.V. Ylyasov, Yu.V. Ilyasov. Department of Physics, Don Technical University, Gagarin Sq.1, Rostov-on-Don, 344010, Russia

The effective search of new materials with special physical properties requires the deep understanding of the laws of formation of electron structure in these materials. That is why the researches, concerning various crystalline network inhomogenities influence on the electron structure of $B_xN_yC_z$, might be of considerable interest now. Different physical properties of compounds are essentially affected by crystalline network defects. The calculations were performed for the systems $BN_{1-x}C_x$ and $B_{1-x}NC_x$ (x=0.25); with zink-blend lattice, where the C atoms substituted the B(N) atoms in a regular way (Fig.1).

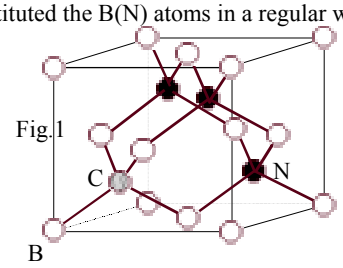

Fig.1

The crystalline potential was constructed as standard muffin-tin, including Coulomb, exchange (Slater's version) and Madelung contributions involving 15 coordination spheres[1]. Each type of chemical elements represented in the lattice corresponded to a muffin-tin sphere of its own type, using which the calculations of the energy-dependent single-site matrces $t_l(E)$ were undertaken. The lattice parameters of the solid solutions were determined according to Vegard's rule. Fig.2 demonstrates the total densities of states (TDOS) in 3-component systems $BN_{1-x}C_x$ ($B_{1-x}NC_x$), x=0.25; TDOS of binary c-BN is shown for comparison as well. The increase of the valence band top width in studied compounds is probably caused by a high degree of *s-p*-hybridization of B, N and C, the electronic states delocalization (the most evident on D-peaks) accompanied by the band displacement towards the higher energies. The displacement is maximal for $B_{0.75}NC_{0.25}$ and reaches 0.2Ry. It is interesting to notice that the peaks in the case of N-C substitution and those in the case of N-O substitution are displaced to the same side comparatively to the corresponding peaks of pure N [2]. In our opinion, it means the displacement to depend on the modulus of the difference between the electron numbers in substituted and binar compounds. So, if the element is substituted by that of the group situated to the left from its own, we suppose scattering on the "hole", otherwise - scattering on the electron.

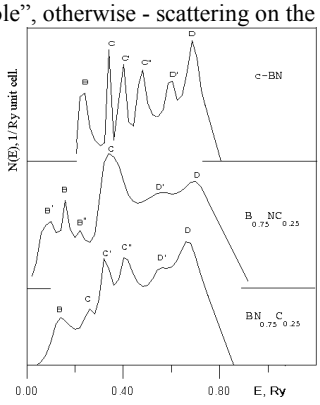

Figure 2

The estimated valence partial electron numbers following conclussions about the properties of the electron structure:

To the cubic boron nitride / diamond having a place the different types of admixture influence on the electronic distribution. In the case, when boron is substituted the energy gap decreases, evidently, owing to the covalent directed bonds per atom decrease, that leads to the lower chemical cohesive energy comparitively to binar *c*-BN. In the case of the nitrogen substitution the energy gap increases.

For the system $B_{1-x}NC_x$ (x = 0.25) electronic change transfer (0.19) from nitrogen to boron takes place. The carbon plays the role of the donor for the electronic configurations of B and N.

1. I.Ya.Nikiforov, V.V.Ilyasov, N.Yu.Safontseva, J. Phys: C. **7** (1995), 6035.
2. T.P. Zhdanova, V.V. Ilyasov, I.Ya. Nikiforov, Zh.Structur. Khim.. (in press)

P11.08.012 π–STACKED COORDINATION FRAME-WORKS FORMED FROM ASSEMBLY OF BINUCLEAR METAL SQUARATE INFINITE CHAINS. Kuan-Jiuh Lin, Institute of Chemistry, Academia Sinica, Nankang, Taipei, Taiwan, ROC

Crystalline inorganic materials such as aluminosilicates (zeolites), aluminophsphates, pillared clays, and other layers are widely used in catalyst and in separation applications. Recently, crystal engineering of coordination polymers and organic networks sustained by coordinate covalent bonds and directional noncovalent interactions has become a rapidly expanding field. However, a major challenge in the relational design of highly porous organic or coordination materials is their fragility. Unlike zeolites held together with rugged covalent bonds, their solid molecules are glued with relatively weak intermolecular forces. Encouraged by our success in using squarate ligand as a robust, rigid tether for the construction of extended solids under hydrothermal conditions [1], we have turned our attention to introduce noncovalent π-π interactions in the metal squarate phases to generate new classes of coordination zeolites with hydrophilic and hydrophobic characteristics. In this report, we describe our exploratory synthesis using hydrothermal methods and structures of two novel coordination polymer, $[(FeCl)_2(C_4O_4)(phen)_2]_n$ **1** and $[(VO)_2(OH)_2(C_4O_4)(phen)_2{\cdot}H_2O]_n$ **2,** where engineering is achieved both by changes in the length of various coordination modes of squarate and by the use of highly directional π-π interactions of phen rings.

1. Lin, K. J.; Lii, K. H. *Angew. Chem. Int. Ed. Engl.* **1997**, *36*, 2076 ─ 2077

P11.08.013 ROLES OF GUEST MOLECULES IN DECAVANADATE CRYSTALS. S. Nakamura, T. Ozeki, Department of Chemistry and Materials Science, Tokyo Institute of Technology, Ookayama 2-12-1, Meguro-ku, Tokyo, Japan

Decavanadate anions, [HnV10O28]n-6, are the stable oxovanadate(V) species in acidic aqueous solution. In their tetraalkylammonium salts, we observed various molecular interactions, such as hydrogen-bonded oligomerization of protonated anions. It is a noticeable feature that the degree of protonation increases systematically as the size of the cation becomes larger. Tetra-n-propyl- and tetra-n-butylammonium cations give the closest packings. The smaller or larger cations give looser packings, leaving room for guest molecules to be included.

Our objective in this study is to investigate the roles of guest molecules in the decavanadate crystals. The term guest molecule used here refers to the solvent molecules of crystallization as well as the neutral compound like urea. This is the first step to control the molecular aggregation and crystal structure. We carried out X-ray analyses of the crystals containing urea, its alkylderivatives, and various organic solvents, each of which can function as a hydrogen bond acceptor, a hydrogen bond donor, or a dipole. Protophilic guest molecules stabilize di- or tetraprotonated monomers by hydrogen bonds. Both hydrogen bond acceptor and donor groups in the guest molecules connect to the adjacent protonated anions, to form a hydrogen-bonded chain or layer structure. Polar protophobic solvents prefer the hydrogen-bonded dimeric structures of the triprotonated anions, in the crystal of which the solvent molecules align their dipoles parallel to the electric field formed between the cations and anions. These results indicate that the electric properties of guest compounds primarily determine the aggregation patterns of the protonated decavanadate anions.

P11.08.014 VERDET CONSTANT OF TELLURIUM DIOXIDE ACOUSTO-OPTIC SINGLE CRYSTALS. A.I.Kolesnikov, R.M.Grechishkin, V.Ya.Molchanov and Yu.M.Smirnov. Tver State University, Zheliabova Str., 33, 170000 Tver, Russia

The optical activity of transparent crystals, besides being of phenomenological interest, is important to the design of acousto-optical devices because there are configurations which exploit its effect on Bragg diffracted light [1]. In the visible and in the near infrared tellurium dioxide, which is one of the most important acousto-optic crystals, is characterized by a large *natural* optical rotatory power ranging from ≈ 24 to 270 deg/mm in the interval of wavelengths from 3.4 to 0.44 μm [1]. However there is, to our knowledge, no information on the *induced* optical activity of this material which may be caused by external magnetic fields. In the present work we report the first measurements of the magnetic field effect on the Faraday rotation in tellurium dioxide single crystals of optical quality.

Large (up to 5 cm-in diameter) single crystals of optical quality were grown from the melt by Czochralsky method. Measurement of the Faraday rotation was performed for a cubic sample (10×10×10 mm) cut parallel to the crystallographic planes (001), (110) and $(1\bar{1}0)$ with optically flat (001) faces perpendicular to the laser beam to minimize the birefringence effect. Rather large values of Verdet constants (0.21 min/A at the wavelength 530 nm, 0.13 min/A at 632 nm) were measured. The dispersion of the Faraday effect is dependent upon the optical absorption bands of the material under study. The observed magnetooptic activity of paratellurite may find its use in narrow-band acousto-optical tunable filters for magnetic trimming of the spectral transmission function.

1. L.N.Magdich and V.Ya.Molchanov (1989). *Acoustooptic Devices and Their Applications* (Gordon and Breach Sci. Publ.).
2. K.A. McCarthy et al (1987). *Optical rotatory power in crystals of the mercurous halides and tellurium dioxide.* Optics Communications, v.64(2), pp.157-159.

P11.08.015 CATION DISTRIBUTION OF $MgAl_2O_4$-$MgFe_2O_4$ SPINEL SOLID-SOLUTION Nakatsuka, H. Ueno, N. Nakayama and T. Mizota Department of Advanced Materials Science and Engineering, Yamaguchi University, Ube, Yamaguchi 755-8611, Japan

Single crystals of $MgAl_2O_4$-$MgFe_2O_4$ spinel solid-solution were synthesized using PbF_2 flux. Powder X-ray diffraction patterns of the synthesized single crystals show that the miscibility gap exists in the intermediate compositional range of this spinel solid-solution. Cation distribution of this solid-solution in the single phase region was investigated using single crystal X-ray diffraction method; the result shows that Al^{3+} occupies B-site (six-coordinated site) more preferentially than A-site (four-coordinated site). This cation distribution cannot be explained from the viewpoints of cation size ($r_{Al} < r_{Fe} < r_{Mg}$; Shannon [1]), because the smallest ion (Al^{3+}) preferentially occupies the larger site (B-site). On the basis of the results obtained from the structural refinements, the causes of this peculiar cation distribution and the miscibility gap will be discussed from the viewpoints of crystal chemistry.

[1] Shannon, R.D. (1976). *Acta Cryst.* A32, 751-767.

P11.08.016 THE STRUCTURES OF METAL COMPLEXES OF THE SCHIFF BASE LIGAND DERIVED FROM 2-(2-AMINOETHYLAMINO)-ETHANOL. Ray J. Butcher and William Townes, Department of Chemistry, Howard University, Washington DC 20059

The condensation of 2-(2-aminoethylamino)ethanol with various hydroxyaldehydes and hydroxyketones results in a tetradentate ligand (X-HL, where X is the substituent on the phenyl ring and H is the phenolic proton), with an N_2O_2 donor set. Reaction of these ligands with the perchlorate salts of zinc (II), copper(II), nickel(II), and manganese(II) results in a series of complexes in which the structural requirements of the ligand and the electronic requirements of the metal are expressed in different ways. In the case of Mn(II), in the resulting complex the preformed ligand has hydrolyzed forming $[Mn(5\text{-}NO_2\text{-}salen)(CH_3OH)(H_2O)](ClO_4)$ with the manganese oxidized to Mn(III). In the case of nickel the resulting compound has Ni(II) in both 4- and 5-coordinate geometries, $[Ni(5\text{-}ClL)]^+[\ Ni(5\text{-}ClL)(CH_3OH)]^+(ClO_4)_{\ 2}$. Complimentary hydrogen bonding interactions between the deprotonated phenolic oxygen and the alcoholic proton of an adjoining complex link the 4- and 5-coordinate moieties into a ribbon. An isostructural Cu(II) complex is formed with the same ligand. With the ligand derived from 5-nitrosalicylaldehyde, on the other hand, the resulting copper complex has the stoichiometry $[Cu(5\text{-}NO_2\text{-}L)(H_2O)](ClO_4)$. The reaction of zinc with this latter ligand results in an unusual dimeric complex where the two Zn(II) ions are linked by an unprecedented five coordinate trigonal bipyramidal (angles very close to 90 and 120 degrees) $(CH_3)_2PO_3^{2-}$ moiety through oxygen. These structures will be compared and contrasted and related to both the nature of the ligand and the requirements of the metal.

P11.08.017 TRIGONAL PRISMATIC AND OCTAHEDRAL HEXAKIS(METHYLBENZENETHIO-LATO) ZIRCONATE COMPLEXES. Kristin Kirschbaum, Dean M. Giolando,* Carsten Cornelissen, Jan Friese, Han Vinh Huynh; Department of Chemistry, University of Toledo, Toledo, OH 43606 USA

Recently, the interplay of energetics between octahedral and trigonal prismatic geometry of six-coordinate complexes of transition metal has become a topic of considerable experimental and theoretical interest. Twisting of the MS_6 geometry between these two geometric limits has been attributed to several factors. While experimental and theoretical work suggests electronic factors are primarily responsible for observed coordination geometry it is difficult to deconvolute contributions made by electrostatic factors. Our studies on six-coordinate thiolate complexes began with a set of titanium complexes containing thiolate ligands exhibiting large twists away from the octahedral limit. To further explore this phenomena we synthesized monometallic complexes containing unidentate thiolates by treating $[Zr(CH_3)_6]^{2-}$ with aryl thiols. The resultant $[Zr(SC_6H_4\text{-}x\text{-}CH_3)_6]^{2-}$

($\mathbf{1}^{2-}$) complexes (x = 2{$\mathbf{1o}^{2-}$}, 3{$\mathbf{1m}^{2-}$} and 4{$\mathbf{1p}^{2-}$}) contain a nearly trigonal prismatic ZrS_6 core for x = 2 and 4, while for x = 3 the core is octahedral. In terms of electronic donating factors the 2- and the 4-position exert similar influences, which are usually distinctly different from that of the 3-position. Hence it is expected that complexes would exhibit a different coordination geometry dependent on the position of the aryl substitute. However, in the case of $SC_6H_4\text{-}x\text{-}CH_3$ the pKa values for the thiols are very similar, which suggests that the level of charge on the sulfur atoms is about the same in all three thiolates. This observation suggests that electrostatic or VSEPR contributions to the coordination geometry are not significant and that electronic factors are the principle governing influence.

P11.08.018 GENERALIZED VEGARD´S LAW. R. R. Mijangos (1), A. Cordero-Borboa (2), V. M. Castaño (2), (1) Centro de Investigación en Física, Universidad de Sonora, A. P. 5-88, 83190, Hermosillo Sonora, Mexico, (2) Instituto de Física, UNAM, A. P. 20-364, Mexico, D. F. 01000, Mexico.

We found as valid a Vegard´s law generalization. The original law gives the value for the lattice constant of a mixed alkali halide crystal with two miscible components, this law gets the form: a=a1(1-X)+a2X, being a1 and a2 the lattice constants of these components and X its molar fraction, Its validity is confirmed by X ray analysis, in crystals such as KCl(1-x):KBrx. We finding miscibility in crystals of three and four components, the generalization is carried out based in the measuring of the lattice constant by X rays diffraction of a ternary crystal KCl:KBr:RbCl (three components) with similar molar fraction (0.33:0.33:0.33)(1) and a quaternary crystal KCl:KBr:RbCl:RbBr with molar fraction (0.3:0.3:0.3:0.1); both crystals shown a single phase. The average value given by a generalized Vegard´s law of the lattice constant is encountered as valid in these crystals. The Raman spectra of the ternary crystal reveals crystallographic texture.

(1) R. R. Mijangos, A. Cordero-Borboa, E. Camarillo, H. Riveros, V. M. Castaño, PHYSYCS LETTERS A 245 (1998) 123-126

P11.08.020 CRYSTAL ENGINEERING OF IRON SPIN-TRANSITIONS. V. McKee and C. Brennan, Chemistry Department, Queen's University, Belfast BT9 5AG, Northern Ireland.

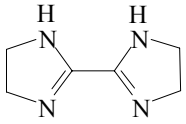

BI

Spin-transition complexes have potential application as thermal or optical switching devices [1, 2]. This requires that the transition occurs about the temperature of interest and shows hysteresis over a wide temperature range. In general terms, the presence of hysteresis can be related to the strength of interactions between individual iron centres in the lattice.

Some iron(II) and iron(III) complexes of ligand 2,2'-bi-2-imidazoline (*BI*) show spin-crossover behaviour ($^5T_2 \leftrightarrow {}^1A_1$ and $^6A1 \leftrightarrow {}^2T_2$ transitions for Fe(II) and Fe(III), respectively) [3]. The temperature and sharpness of the spin transitions are dependent on the anion present. As the anion is not directly coordinated to the iron, it is probable that the properties of the transition are controlled by H-bonding between the non-coordinated amines of BI and the anions. Consequently, the spin-transition parameters might be engineered by rational design of the lattice H-bonding.

The iron complexes are difficult to crystallise so we have combined single-crystal studies on some iron complexes of *BI* with those on other transition metal complexes and with powder diffraction methods to establish the lattice packing in a range of complexes. There is extensive isomorphism of, for example, $[M(BI)_3](X)_2$ systems provided the anions (X) have similar size and geometry (e.g. ClO_4^- and BF_4^-). The magnetic and Mössbauer properties of the iron complexes are also being studied and related to the structural data.

1. P. Gutlich, A. Hauser and H. Spiering, Angew. Chem. Int. Ed. Engl., 1994, **33**, 2024.
2. O. Kahn and C.J. Martinez, Science, 1998, **279**, 44.
3. M.G. Burnett, V. McKee and S.M. Nelson, J. Chem. Soc., DaltonTrans., 1981, 1492.

P11.08.021 MULTIANIONIC PHOSPHAZENATES. Gavin T. Lawson, Alexander Steiner, Department of Chemistry, University of Liverpool, Crown Street, Liverpool L69 7ZD, UK

Recently we have discovered the multianionic ligand system $[P_3N_3(NR)_6]^{6-}$, which is isoelectronic to the trimeric metasilicate ion $[Si_3O_9]^{6-}$, but in addition contains organic groups.[1] $[P_3N_3(NR)_6]^{6-}$ is derived from the amino substituted phosphazene $P_3N_3\{N(H)R\}_6$,which reacts as a hexaprotic acid in the presence of strong organometallic bases, such as butyllithium. Due to their multiple charge we called these systems phosphazenates.

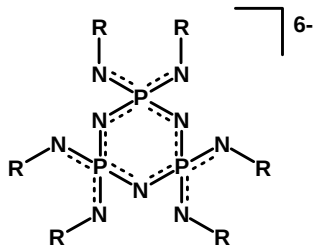

The striking difference of phosphazenates to isoelectronic silicates is the extensive organic surface, which covers the central metal phosphazenate cores. This provides good solubility in aprotic organic solvents and facilitates organometallic chemsitry on the multiple charged system. Another distinguishing feature is the high kinetic stability of the flexible P-N-backbone, preventing ring cleavage reactions in the presence of strong nucleophiles, such as organometallic bases. In the solid state phosphazenates exist as molecular arrangements rather than showing extended polymeric lattice of silicates. On our poster we describe crystal structures of organometallic derivatives of phosphazenates.

[1] A. Steiner, D.S. Wright, *Angew. Chem. Int. Ed. Engl.* 35 (1996) 636.

P11.08.022 THE MELTING POINT ALTERNATION IN α,ω-ALKANE DIOLS AND α,ω-ALKANE DIAMINES. Venkat R. Thalladi, Hans-Christoph Weiss and Roland Boese,* Institut für Anorganische Chemie, Universität-GH Essen, Universitätsstraße 5-7, D-45117 Essen, Germany.

It is known for a long time that *n*-alkanes show an alternation in their melting points with the even members exhibiting systematically higher melting points compared to the odd members. A logical explanation for such an alternation has been given very recently on the basis of thorough crystal structural analysis [1]. The alternation of melting points and other physical properties is also observed in several α-substituted and α,ω-disubstituted *n*-alkanes. In this connection we have determined the crystal structures of α,ω-alkane diols and α,ω-alkane diamines at low temperature.

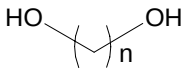

n = 2-9

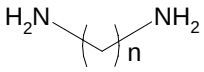

n = 2-8

The analysis of the crystal structures has revealed the interplay between hydrogen bonding and hydrophobic interactions. The rationale for the remarkable structural similarities within the series of even or odd members and the distinct differences between even and odd series is presented.

R. Boese, H.C. Weiss, D. Bläser (1999). Angew. Chem. Int. Ed. Engl. **38**, in press.

P11.08.023 CRYSTAL STRUCTURE OF THE 1-D COMPOUND $[Cu(NCS)_2bpk]_n$ (bpk=bis-2-pyridiylketone). R. Cortés[a], Z. E. Serna[b], M. K. Urtiaga[c], M. G. Barandika[a], L. Lezama[b], T. Rojo[b]. Departamentos de Química Inorgánica[a,b] y Mineralogía-Petrología[c], Facultad de Farmacia[a] y Facultad de Ciencias[b,c], Universidad del País Vasco, Apdo. 450, Vitoria-01080 SPAIN, Apdo. 644, Bilbao-48080, Spain.

High-dimensional magnetic-molecular systems can be obtained by promoting a number of vacant sites around the metal coordination sphere which can be filled by the appropriate bridging ligands. This can be carried out by combining the use of pseudohalide ions with one unit of a bidentate organic ligand. In this work, the thiocyanate and bpk ligands have been selected for the preparation of an extended system of general formula $[Cu(NCS)_2bpk]_n$.

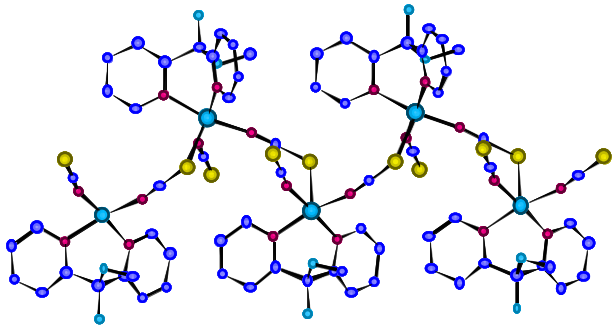

Figure 1

X-Ray single-crystal diffraction analysis revealed that the structure consists of μ-(1,3)-NCS-bridged Cu(II)-chains in which the bidentate bpk ligands and terminal NCS groups complete the copper coordination sphere (figure 1). The compound is monoclinic, $P2_1/n$, a=9.080(1) Å, b=8.942(2) Å, c=20.523(4) Å, ß=101.94(2)°, Z=4.

P11.08.024 INFLUENCE OF THE GUEST ON THE PACKING OF DIMERIC α-CYCLODEXTRIN COMPLEXES. I. M. Mavridis and S. Makedonopoulou, Institute of Physical Chemistry, N.C.S.R. "Demokritos" Aghia Paraskevi 153 10, Athens, Greece.

Packing pattern of host:guest complexes of β-cyclodextrin (βCD) are discussed. In most of βCD inclusion complexes two βCD molecules self-assemble and form a dimer which encloses one or more molecules of guest. The whole is a supermolecule held together by intermolecular non-bonding interactions. The dimer has the shape of a cylinder whose dimensions and external surface remain unchanged irrespective of the guest. The latter influences only the top and bottom faces of the cylinder where some parts of it are exposed. As a result of this influence four packing modes are encountered [1].

The study of the molecular packing of the βCD complexes in conjunction with the nature of the guest is a means towards a better understanding of the association of the supermolecular units and the way that molecules are recognized. Conversely, if we understand molecular recognition we can select appropriate building blocks that interact according to specific rules and organize into pre-designed systems that will lead to the design of crystal structures with specific characteristics.

1. D. Mentzafos, I. M. Mavridis, G. Le Bas, G. Tsoucaris (1991) *Acta Crystallogr. B47*, 746-757.

P11.08.025 MICROSCOPIC STUDIES ON CRYSTALS OF INSULIN MUTATED AT CRYSTAL CONTACT SURFACES. U. Schell and R. Hilgenfeld, Institute of Molecular Biotechnology, Department of Structural Biology & Crystallography, Beutenbergstr. 11, 07745 Jena, Germany.

Insulins mutated at crystal contact surfaces are excellent objects to study the effects of the alterations on crystallisation conditions, crystal contacts, crystal quality and stability. The mutant DesPheB1 of porcine insulin was crystallised in the presence of Zn^{2+} and phenol, which is often added as preservative in pharmaceutical insulin preparations. It has been shown previously that phenolic compounds bind to specific sites on the insulin hexamer and act as allosteric effectors, inducing a transformation of the T_6 hexamer (in rhombohedral spacegroup R3) to the R_6 hexamer (mostly in monoclinic spacegroup $P2_1$) [1]. However, mutant DesPheB1, in the presence of phenol, exclusively crystallised in the rhombohedral spacegroup R3. This indicates that residue B1 is obviously essential for interhexameric contacts in monoclinic crystal forms. The structure of this mutant is presently under investigation. We will present preliminary results on the visualization of the crystal faces by atomic force microscopy which has been used only recently to detect packing defects at near molecular resolution [2]. A novel high-magnification stereo-microscope constructed in our department is used to follow crystal growth.

[1] U. Derewenda et al., Nature, 338 (1989) 594.
[2] C. M. Yip et al., Biophys. J., 74 (1998) 2199.

P11.08.026 ATTRACTIVE INTERACTIONS IN TWO NOVEL PERI-NAPHTHALENE DERIVATIVES. Jane O'Leary, Wolfgang Skranc and John Wallis, Centre for Materials Research, School of Physical Sciences, University of Kent, Canterbury, England.

Phenylisocyanate reacts with 8-lithio-1-dimethylaminonaphthalene to give a novel 2:1 product along with the expected 1:1 anilide. The former contains a H-bonded six-membered cyclic system, not represented in the current CSD, the (N-)H---O distance being 1.86 Å with a NHO angle of 141°. In both structures the dimethylamino group has pyramidal geometry and the nitrogen atom's lone pair of electrons is directed towards the carbonyl carbon of the second substituent. Both structures contain peri N----C=O interactions, with N----C distances of 2.619(2)Å and 2.647(2)Å and small pyramidalisation (+0.053(1)Å and +0.046(2)Å) at the carbonyl groups, similar to those represented in other systems [1].

1. W. B. Schweizer, G. Procter, M. Kaftory and J. D. Dunitz, Helv. Chim. Acta, 61, 2783 (1978).

P11.08.027 C-H...O HYDROGEN BONDS OBSERVED BY X-RAY DIFRACTION IN BISIMINE SELF MOLECULAR ASSEMBLY. A. Reyes-A., J. Nájera-M., H. Salgado-Z. and J. Tamariz-M. Departamento de Química Orgánica. Escuela Nacional de Ciencias Biológicas, IPN. Carpio y Plan de Ayala S/N. Colonia Santo Tomás. 11340 México D. F.

Intermolecular C-H...O contacts [1] in the self-molecular assembly of bis(4-nitrobenzylidene)ethylenediamine have been observed by X-ray crystallographic studies.

The non-formation of a supramolecule between the above mentioned bisimine with either hydroquinone or meso-1,2-diphenyl-1,2-ethanediol (meso-hydrobenzoin) suggests that these unique C-H...O non-bonding interactions should be of considerable strenght to favour the self-assembly process.

The poor solubility of the compound in most organic solvents might be explained in similar terms.

1. G. R. Desiraju (1991). Acc. Chem. Res., 24, 10, 290-296.

P11.08.029 STRUCTURES OF TWO NEW NICKEL 42-OXO- DODECATUNGSTATES. Z.Žák and J.Taraba, Department of Inorganic Chemistry, Masaryk University, Brno, Czech Republic.

The chemistry of polynuclear oxometalate anions, polyoxometalates, have attracted much attention recently[1]. There have been many polytungstates of alkaline metals synthetized and their structures determined [2] but only very few containing transition metal cations are known. Recently, we have published syntheses and structure determinations of two cobalt 42-oxododecatungstates, one of them being one of the very few containing only a transition metal cation [3]. Now, we have succeeded in the synthesis and structure determination of another example of transition metal paratungtates, $[Ni_5(H_2O)_{22}][H_2W_{12}O_{42}].16H_2O$ (NIWOL) and $[Ni_3Na(H_2O)_{16}][H_3(H_2W_{12}O_{42})].18H_2O$ (NIWL). The structures are built from $H_2W_{12}O_{42}^{10-}$ anions joined by cations into three-dimensional networks. The $H_2W_{12}O_{42}^{10-}$ cage in NIWL is situated on a symmetry center, while that of NIWOL lies in a general position. The figure depicts "molecules" of both compounds in a polyhedral representation including symmetry related Ni-O_6 (crossed) and Na-O_6 (blank) octahedra.

Grant GACR no. 203/98/0676 is gratefully acknowledged.

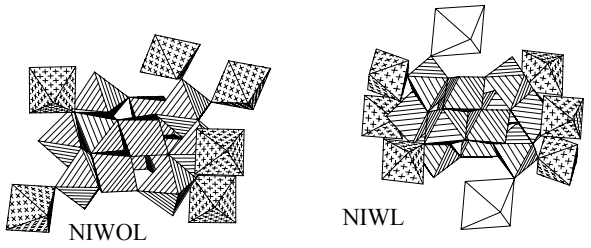

NIWOL NIWL

1. C.L.Hill (1998). Chem.Rev., **98**, 1
2. Inorganic Crystal Structure Database (1998). FIZ Karlsruhe, Germany
3. Z.Žák, J.Perùtka, J.Havel, I..Císaøová, G Giester (1998). J. Alloys and Comp., **281**,169

P11.08.030 STRUCTURAL ANALYSIS OF THE 2-D COMPOUND $[Mn(N_3)_2bpa]_n$ (bpa=1,2-bis(4-pyridiyl)ethane). M. G. Barandika[a], M. L. Hernández-Pino[b], M. K. Urtiaga[c], R. Cortés[a], L. Lezama[b], M. Arriortua[c]. Departamentos de Química Inorgánica[a,b] y Mineralogía-Petrología[c], Facultad de Farmacia[a] y Facultad de Ciencias[b,c], Universidad del País Vasco, Apdo. 450, Vitoria-01080 SPAIN, Apdo. 644, Bilbao-48080, Spain.

High-magnetic-ordering systems based on transition-metal supramolecular arrays can be obtained by enhancing the linking of smaller structural units. This can be carried out by combining the use of pseudohalide ligands with N,N' bidentated organic spacers. In this work, the azide and bpa (bpa=1,2-bis(4-pyridyl)ethane) ligands have been selected for the preparation of an extended system of general formula $[Mn(N_3)_2bpa]_n$.

X-Ray single-crystal diffrac-tion analysis revealed that the structure consists of di-μ-(1,3)-N3-bridged Mn(II)-chains which are linked by bpa ligands resulting in a 2D arrangement (figure 1). The compound is monoclinic, C2/c, a = 9.991(3) Å, b = 13.883(2) Å, c = 10.482(3) Å, ß=103.15(2)°, Z=4).

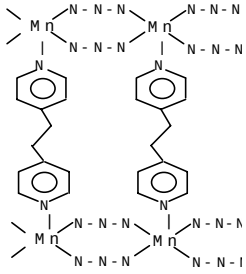

Figure 1

09. INORGANIC CRYSTALLOGRAPHY AND GEOPHYSICS

P05.09.001 LONSDALITE MONOCRYSTAL - THE SOLID PART OF THE EARTH KERNEL. R.V.Galiulin, Institute of Crystallography Russian Academy of Scieces, Moscow 117333 Leninsky Prospect 59

They say that Kathleen Lonsdale was very sorry that the big crystals of lonsdalite was not found. Apparently unique place for this crystals is the Earth Kernel (the temperature is 3000 grad., the preasure is 3500 kilobars) where it can grow from a carbon solution in a ferric melt as a dendrite crystal. In Mantle this crystals continue to grow as a diamond. Some of it branches burns out (heating the Earth) and through volcanoes will be rejected on a surface of the Earth where they using solar energy catching by the plants and turn into the coal. The last one turns to graphite (nets of which are two dimensional Euclidean diamond crystals [1]). Graphite turns in- to the diamond and last one reaching The Mantle turns into the lonsdalite. In this process take part all crystal modifications of carbon - soot (zerodimensional diamond - orbifold, and one-dimensional spherical diamonds), fulerenes (two-dimensional spherical diamonds), quasicrystals of carbon with fivefold and seven-fold symmetry (hyperbolic's diamonds). Some other elements take part in trans- porting solar heat to the Kernel too [2]. It is possible because of nonlinearity of the laws of motions of atoms [3] the attractor of which are solid part of the Earth Kernel.

1. R.V.Galiulin. A Geometric Theory of Crystal Formation. Crystallography Reports, 1998, N 2, pp. 332-340
2. N.V.Belov. Geochemical accumulators. Proc. of Institute of Crystallography, 1952, 7, pp.73-80
3. R.V.Galiulin. Axiomatics of Geology. Experiment in Geoscience, 1998, vol.7, No.2, p.57

P05.09.002 ICE TEMPERATURE EFFECT ON PROTON-ORDERED ARRANGEMENT IN ANTARCTIC ICE. Hiroshi Fukazawa, Shinji Mae, Department of Applied Physics, Faculty of Engineering, Hokkaido University, N13 W8, Sapporo 060-8628, Japan. Susumu Ikeda, Institute of Materials Structure Science, High Energy Accelerator Research Organization (KEK), Oho 1-1, Tsukuba, Ibaraki 305, Japan

Analysis of the Raman spectra of Antarctic ice showed that a second-order phase transition from the proton-disordered phase to a proton-ordered phase takes place at T_i = 237 K (T_i; ice temperature in the ice sheet) in the Antarctic ice sheet [1]. We measured the neutron scattering of ice recovered from Antarctic ice sheet. From the scattering spectra, we calculated the T_i dependence of the order parameter (the ratio of ordered protons in ice), which is consistent with the theory of the order-disorder phase-transition from proton arrangements in ordinary ice to proton-ordered arrangements at T_i = 237 K. The results indicate that Antarctic ice in which $T_i \leq 237$ K (about one third of the Antarctic ice mass) contains proton-ordered arrangements.

1. H. Fukazawa, S. Mae, S. Ikeda and O. Watanabe (1998), Chem. Phys. Lett., **294**, 554-558.

P05.09.003 CRYSTAL STRUCTURE OF $NaLiMnP_2O_7$ G.S. Gopalakrishna, Department of Studies in Geology, University of Mysore, Mysore 570006, INDIA and M.A. Sridhar and J. Shashidhara Prasad, Department of Studies in Physics, University of Mysore, Mysore 570006, INDIA

The study of Sodium Superionic Conductors has become popular particularly, after the development of NASICON groups of fast ionic conductors. Manifold variations by suitable substitutions to these compounds have led to the development of many new solid electrolytes. These fast ionic conductors still pose challenges to material scientists in growth and characterization because of their polycrystallinity, non-stoichiometric composition and complex conduction mechanism. NASICON or its analogues always have only the triorthophosphate end members and their structures were directly related to $Na_3Sc_2P_3O_{12}$. The title compound is a new phosphate compound which is a prospective fast ionic conductor. $(Na_2LiMnP_2O_7)_2$ crystals were synthesised by hydrothermal technique at relatively low temperature and pressure. The title compound, a nasicon analogue, crystallises in the triclinic space group $P\bar{1}$ with a = 6.657(3)Å, b = 6.714(6)Å, c = 6.518(4)Å, α = 112.31(6)°, β = 92.14(4)°, γ = 83.89(5)° and Z = 2. The structure was solved using SIR92 [1] and refined using teXsan [2]. The final residual is R = 0.064 for 923 reflections with $I > 3\sigma(I)$. The refinement was carried out by treating all oxygen atoms as isotropic and the rest as anisotropic. The procedure is similar to structure solution of similar compounds reported earlier [3,4].

1. A. Altomare, M. Cascarano, C. Giacovazzo and A. Guagliardi, (1993), J. Appl. Cryst., 26, 343.
2. Molecular Structure Corporation. (1995). teXsan. Single Crystal Structure Analysis Software. Version 1.7. MSC, 3200 Research Forest Drive, The Woodlands, TX 77381, USA.
3. Salvador Gali, K. Byrappa and G.S. Gopalakrishna, (1989), Acta Crystallogr., **C45** 1667
4. Salvador Gali, A. Carddenas, K. Byrappa and G.S. Gopalakrishna, (1992), Acta Crystallogr., **C48** 1650

P05.09.004 A NOVEL FAMILY OF LAYERED BISMUTH COMPOUNDS. D.O.Charkin, P.S.Berdonosov, and V.A.Dolgikh, Dept. of Chemistry, Moscow State University, Moscow 119899 Russia; P.Lightfoot, School of Chemistry, University of St.Andrews, St.Andrews, FIFE, United Kingdom

Multinary Bi, Ln (An) oxides, oxide halogenides, chalcogenides, etc. constitute a large family of compounds which exhibit unusual crystal structures and prospective physical properties. Many of them possess layered structures with fluorite-related positively charged layers separated by negatively charged ones derived from different structural types. Some of the compounds are known as ionic conductors, ferroelectrics, HT superconductors, etc. In particular, oxide halogenides are interesting as possible ferroelectrics and oxidation catalysts. In their structures, fluorite-related layers are separated by either halogenide ion sheets, or NaCl-type layers. There is hitherto a unique intergrowth structure, where CsCl-related anionic layers also can be met together with single $[Cl^-]$ anion sheets [1].

We have modelled and synthesized a series of 20 novel multinary Bi oxyhalides. In their crystal structure, fluorite-related layers are separated either only by CsCl-related layers (type A), or alternatively by CsCl-type layers and double $[Cl^-]$ sheets (type B). The crystal structure of $Pb_{0.3}Cs_{0.3}Bi_{0.7}OCl$ (type A) was solved from powder data ($I4/mmm$, Z=4, R_p=0.063, R_{wp}=0.081), while the structure of $Pb_{0.15}Cs_{0.15}Bi_{0.85}OCl$ (type B) was solved from single crystal data ($I4/mmm$, Z=8, R=0.08, R_w=0.11). In the fluorite-related layers, Bi^{3+} ions can be substituted, besides Ca^{2+}, by Pb^{2+}, Na^+, Sr^{2+}, and Ba^{2+}, similar to that in the so-called Sillén phases. The CsCl-related layers can contain also Rb^+ and Br^-; the a cell parameters are almost insensitive to replacement of Cs^+ by Rb^+ in the cubic voids. Differences and similarities in crystal chemistry of the novel compounds and related ones containing the same fluorite-type layers are analyzed. A general classification of crystal structures with the fluorite-like and anti-fluorite-like layers is given.

1. K.Harris, W.Ueda, *et al. Angew.Chem.(Int.Ed.)* **27** (1998), 1364.

P05.09.005 ON PENTAIODIDES. K.-F. Tebbe and I. Pantenburg, Institut für Anorganische Chemie der Universität zu Köln. Greinstraße 6, D-50939 Köln, Germany.

A special property of polyiodides is the variability regarding their composition and structure [1]. Addition rules for one (I^-) and two (I_2) units lead to the formula I_x^- with x = 1 + 2i + 2k/l describing all possible definite compositions. The structures of polyiodide units in crystalline solids are characterized by fluctuation of distances and angles, connectivity (coordination number) and dimensionality. Distances range from the value for the iodine molecule (≈270 pm) to the van der Waals contact (≈ 430 pm) with pronounced accumulations for essential structural motifs, e.g. elongated iodine molecules I_2 (≈ 275 pm), symmetric (≈ 292 pm) and asymmetrical triiodide ions I_3^- (280 to 315 pm), close contacts between iodine molecules I_2 and iodide ions I^- or triiodide ions I_3^- (≈ 320 pm), between two iodine molecules (≈ 340 pm) or between two triiodide ions (≈ 360 pm) and short van der Waals type contacts (> 370 pm). Most angles are distributed around 90 ^{o} and 180 ^{o} even for the longer distances. The connectivity may range from 1 to 6, the dimensionality from 0 to 3. The preference of the angles leads to the concept of orthogonal lattices $^n_\infty(I^-nI_2)$ and their fragments [2]. Pentaiodides I_5^- are suitable to demonstrate such concepts because they separate compounds I_x^- with lower (x < 5) from those with higher (x > 5) iodine contents [3]. Fourfold connected nets $^n_\infty[I^-4(I_2)_{1/2}]$ with iodide ions I^- in the knots and iodine molecules I_2 on the connecting lines have the composition of pentaiodides. In particular the infinite planar checkered (4,4)-net fulfills in addition the condition of orthogonality. This may be riped up (by the cations) into chains of different kind and at least into the isolated V-shaped anion. Most of the observed structures (≈ 50) have been classified within such a scheme. One example may be derived from the diamond net.

1. K.-F. Tebbe (1996). Z. Kristallogr. Suppl. 11, 52.
2. M. El Essawi, I. Dombrowski, Th. Gilles, A. Kavoosian & K.-F. Tebbe (1998). Z. Kristallogr. Suppl. 15, 61.
3. K.-F. Tebbe & I. Pantenburg (1999). Z. Naturforsch. 54b, in preparation.

P05.09.006 A PAIR OF BISMUTH TANTALALUM OXIDES WITH 'BLOCK-DISLOCATION' MODULATED FLUORITE-TYPE STRUCTURES. C.D. Ling, J.G. Thompson, R.L. Withers and S. Schmid, Research School of Chemistry, Australian National University, Canberra, ACT 0200, Australia.

The high-temperature phase of bismuth oxide (δ-Bi_2O_3) is one of the best oxygen ion conductor known. It cannot, however, be quenched to room temperature. Bismuth-rich phases in ternary oxide systems involving certain transition metal oxides appear to approximately preserve both the fluorite-type structure and ionic conduction properties. $Bi_7Ta_3O_{18}$ and $Bi_4Ta_2O_{11}$ were previously described in this context as superstructures of fluorite-type [1].

During an extensive reinvestigation [2] we found the unit cells reported for $Bi_7Ta_3O_{18}$ and $Bi_4Ta_2O_{11}$, based on superstructures of fluorite-type, to be incorrect. Using the correct cell we were able to solve the *P*1 (pseudo-*C*2/*m*) structure of $Bi_7Ta_3O_{18}$ using single-crystal synchrotron X-ray data [3]. By comparing unit cells, compositions and symmetries, an unambiguous $P\bar{1}$ model for the structure of $Bi_4Ta_2O_{11}$ could be derived from that of $Bi_7Ta_3O_{18}$. This model was successfully Rietveld-refined using synchrotron XRD and powder neutron diffraction data [4]. Both structures are fully ordered, with columns of TaO_6 octahedra and variously coordinated Bi^{3+} ions. The metal atom arrays approximate fluorite-type with regular 'block-dislocation' defects perpendicular to $[1\,1\,1]_f$. This structural motif is responsible for confusing electron diffraction and XRD patterns, on the basis of which they were originally mis-indexed as simple superstructures of fluorite-type.

1. W. Zhou (1992). J. Solid State Chem. **101**, 1-17.
2. C.D. Ling, R.L. Withers, S. Schmid & J.G. Thompson (1998). J. Solid State Chem. **137**, 42-61.
3. C.D. Ling, S. Schmid, R.L. Withers, J.G. Thompson, N. Ishizawa & S. Kishimoto (1998). Acta Cryst. B, In press.
4. C.D. Ling, J.G. Thompson, R.L. Withers & S. Schmid (1998). J. Solid State Chem. **141**, In press.

P05.09.007 QUANTITATIVE WIDE ANGLE CBED APPLIED TO NON-STOICHIOMETRIC RARE-EARTH ZIRCONATE PYROCHLORES. Y. Tabira and R. L. Withers, Research School of Chemistry, Australian National University, Canberra,A.C.T.0200

The crystal structure of a wide range non-stoichiometric samarium zirconate pyrochlore has been investigated as a function of composition using a Wide-Angle Convergent Beam Electron Diffraction (WACBED) technique. Systematic changes in the one unknown oxygen atom fractional co-ordinate are found as a function of composition.

Solid solutions $Ln_yZr_{1-y}O_{2-y/2}$ have the pyrochlore structure for rare earths from *Ln* = La to Gd. In the ideal pyrochlore structure (corresponding to y = 0.5), there is only one unknown oxygen atom fractional co-ordinate. No structural models for off-stoichiometric composition have to date been reported. The exact extent of the various solid solutions as a function of rare earth ion has yet to be determined.

Cell dimensions as a function of chemical composition show a very narrow (less than 2 mole % in full width) solid solution (ss) field for the $LaO_{1.5}$-ZrO_2 pyrochlore system which increases systematically to 18 mole % in full width for the $SmO_{1.5}$-ZrO_2 pyrochlore system (from 37.5 mole % $SmO_{1.5}$ to 55 mole % $SmO_{1.5}$). The dependence of the width of the pyrochlore solid solution field upon the rare earth ion is attributed to the ionic size difference between Ln^{3+} and Zr^{4+}.

The WACBED technique can be applied to small irradiated areas and is quite sensitive to the position of light atom species (such as oxygen atoms in heavy metal oxides)[1-2]. The unknown oxygen atom fractional co-ordinate x is found to be about 0.352 in the case of the 40 mole % $SmO_{1.5}$ specimen which is significantly larger than that (x = 0.343) found for the stoichiometric 50 mole % $SmO_{1.5}$ specimen. The increased x value is consistent with a systematic shift towards the defect fluorite structure, which appears on both sides of the relevant ss field.

1. Y. Tabira & R.L.Withers (1998), Phil. Mag. A, *in press*.
2. Y. Tabira & R.L.Withers, Phys. Chem. Min. *submitted*.

P05.09.008 STRUCTURAL SERIES IN COMPLEX CUPRATES. V.Maltsev[1], L.Leonyuk[1], G.-J.Babonas[2] [1] Department of Geology, Moscow State University, Moscow 119899, Russia [2] Semiconductor Physics Institute, Vilnius LT-2600, Lithuania

The series of compounds in the family of complex cuprates were distinguished in order to reveal the generic relationship [1] between the structures and to emphasise the characteristic structural features. In the fragment approximation various combinations of different blocks can be distinguished in the compounds which are grouped into the *plesiotypic, merotypic, polytypic or polysomatic* series of structures [2, 3]. The terms characterise the relationship between the structures which constitute a particular series. In a great variety of cuprate structures various groups of compounds are expected to form the series of a different type. The structures of several cuprate groups are considered. The polysomatic and other type series are distinguished in order to reveal the general regularities in the structures of complex cuprates.

Layered cuprates with CuO_2-planes : The compounds in the Ba-Ca-Cu-O system can be considered as *polytypic* series, into

which Y(Ca)$Ba_2Cu_3O_x$ can be included taking into account a possible substitution Y↔Ca. The Bi-2212-type compound can be regarded as the polysome *AB* of the chemical composition $(Bi_2O_{3-x})(Sr_2CaCu_2O_6)$ in the *polysomatic* series with the end-members $(Sr,Ca)_2(Sr,Ca)Cu_2O_6$ (*A*) and Bi_2O_3 (*B*) or in another polysomatic series with the end members $CaCuO_2$ (infinite layer structure) and $Sr_{1+x}Bi_{1-x}O_3$ (perovskite with monoclinic distortion).

Layered cuprates with Cu_2O_3-planes (ladder-type structures) : The $[M_2Cu_2O_3]_m[CuO_2]_n$-type phase (M=Sr, Ca, Bi) of incommensurate structure can be considered in the polysomatic approach as the polysome $[MCu_2O_3]_m[M_{m/n}CuO_2]_n$ (AB) [4].

Polysomatic series in the structures of doped Ca, Sr-cuprates : The general scheme of polysomatic series in the structures of earth alkaline cuprates is proposed. The scheme allows one to predict the formation of new structural types in the group of doped Ca, Sr-cuprates.

[1] Leonyuk, L.I., Babonas, G.-J., Pushcharovskii, D.Yu. & Maltsev, V.V. (1998a). Crystallography Reports **43**, 256-270.
[2] Veblen, D.R. (1991). Am. Mineral. **76**, 801-826.
[3] Makovicky, E. (1997). EMU Notes in Mineralogy, V.1, Chapter 5, pp. 315-343.
[4] Leonyuk, L., Babonas, G.-J., Maltsev, V., Shvanskaya, L. & Dapkus, L. (1998b). J. Cryst. Growth **187**, 65-71.

P05.09.009 CRYSTAL STRUCTURE OF THE SOLID SOLUTION $Li_xMg_{(17-x)}Al_{12}$ (x = 3.64). G.S. Dmytriv, V.V. Pavlyuk and O.I.Bodak, Inorganic Chemistry Department, Ivan Franko Lviv State University, Kyryla I Mefodia str. 6, 290005 Lviv, Ukraine, and R.Cerny and K.Yvon, Laboratoire de Cristallographie, Universite de Geneve, 24, quai Ernest-Ansermet, CH-1211 Geneva 4, Switzerland.

Existence of a solid solution with wide homogeneity range based on the $Mg_{17}Al_{12}$ binary compound (superstructure to the α-Mn type) was confirmed [1] in the Li-Mg-Al system at 470 K. We have investigated this solid solution using X-ray diffraction methods (single crystal and powder). The single crystal was obtained from a three-phases alloy with the nominal composition $LiMgAl_2$. Structure was refined in the $I\bar{4}3m$ space group, a=1.0266(5) nm, Stoe Stadi4 diffractometer, MoK_α radiation with graphite monochromator, ω/2θ scan mode, 189 unique reflections, Xtal3.2 program, R=0.054, wR=0.026, GoF=1.344. Atomic positional, equivalent isotropic displacement and site occupation parameters are given below:

Atom	Site	x/a	y/b	z/c	U	PP
Al(1)	24(*g*)	0.0926(3)		0.2799(3)	0.0200(8)	
Mg(1)	2(*a*)	0		0	0.023(7)	0.80(7)
Li(1)	2(*a*)	0		0	0.023(7)	0.20(7)
Mg(2)	8(*c*)	0.3213(4)		x	0.030(4)	0.74(4)
Li(2)	8(*c*)	0.3213(4)		x	0.030(4)	0.26(4)
Mg(3)	24(*g*)	0.3581(4)		0.0382(4)	0.020(1)	0.80(2)
Li(3)	24(*g*)	0.3581(4)		0.0382(4)	0.020(1)	0.20(2)

The same results were obtained also by the powder Rietveld refinement. The Li atoms substitute only the Mg atoms because of the similar atomic radii.

1 N.C.Goel & J.R.Cahoon (1990). *Bulletin of Alloy Phase Diagrams*,**11**,528.

P05.09.010 $DyCu_{5-x}$ - A NEW SUPERSTRUCTURE DERIVED FROM CUBIC $AuBe_5$-TYPE. L. Guénée, R. Cerny and K. Yvon, Laboratoire de Cristallographie, University of Geneva, 24, quai Ernest-Ansermet, CH-1211 Geneva 4, Switzerland.

A compound $DyCu_{5-x}$ crystallises with monoclinic symmetry. Its structure is derived from the cubic $AuBe_5$-type structure. The analysis of precession photographs lead us to determine the 3x3x2.5 supercell having the cell parameters a^s = 21.48 Å, b^s = 21.38 Å, c^s = 17.90 Å, β = 93.5°.

This structure is compared to that of $YbCu_{4.5}$, which crystallises also in structure derived from $AuBe_5$-type however in a supercell of the multiplicity 7x7x6.5 [1]. In this compound, the ordering of planar defects parallel to {hhh} is responsible for the superstructure.

Based on the investigations of $YbCu_{4.5}$, a model to explain the supercell multiplicity of $DyCu_{5-x}$ is proposed, which leads to a prediction of new series of compounds in the RE-Cu systems.

[1] R.Cerny, M.François, K.Yvon, D.Jaccard, E.Walker, V.Petricek, I.Cisarova, H-U.Nissen and R.Wessicken, *J. Phys.: Condens. Matter*,**8**, (1996),4485-4493.

P05.09.011 VARIABLE TEMPERATURE X-RAY DIFFRACTION STUDY OF $BiMg_2VO_6$. I. Radosavljevic, A.W. Sleight, Department of Chemistry, Oregon State University, Corvallis, OR. 97331, U.S.A.

Bismuth magnesium vanadate, $BiMg_2VO_6$, belongs to the BiM_2AO_6 (M=divalent cation, A=pentavalent cation) family of compounds. The structures of these phases can be described as consisting of three common structural elements: one-dimensional BiO_2 chains, AO_4 tetrahedra and interspersed M cations [1,2].

The room temperature structure of $BiMg_2VO_6$, solved from single crystal X-ray diffraction data, was reported in 1992 [3]. The compound was reported as centred orthorhombic, space group Amma. Despite a very good agreement factor obtained for the refinement, the thermal ellipsoid on one of the oxygen atoms was of problematic size and shape.

A variable temperature X-ray diffraction experiment was carried out in order to gain an understanding of this situation. Six data collections were performed in the range from 100 K to 350 K. Refinements of the data sets indicated that the low temperature structure is in fact primitive orthorhombic and that the compound undergoes a centring phase transition above room temperature. The transition is a low energy one and it involves mainly the rotation of the VO4 tetrahedra.

1. I. Radosavljevic, J.S.O. Evans and A.W. Sleight, J. Solid State Chem., 137, 1, (1998)
2. I. Radosavljevic, J.S.O. Evans and A.W. Sleight, J. Solid State Chem., 141, 1, (1998)
3. J. Huang and A.W. Sleight, J. Solid State Chem., 100, 170 (1992)

P05.09.012 THE ORDERED PHASES OF THE W_2C CARBIDE AND PHASE EQUILIBRIA IN THE W-C SYSTEM. T.Ya. Velikanova and V.Z.Kubliy, I.N.Frantsevich Institute for Problems of Materials Science, National Academy of Science of Ukraine, Kiev, Ukraine.

In the handbooks [1-3] published recently there are contradictions. They deal with the quantity, sequence of the change and type of the ordering of the W_2C modifications.

The W-C alloys containing W_2C carbide were melted in an arc melting furnace and then annealed at subsolidus temperature about 1.5 hour. After that the alloys were subjected either annealing at 1450-2650°C and following quenching or long-time (hundreds of hours) annealing lower 1200°C.

The single-crystal X-ray method was applied for crystal grains extracted from the alloys. The method is more informative in comparison with powder diffraction (X-ray and neutron) even at investigation of ordering in carbides of such "heavy" metals as Mo and W [4,5].

In first we obtained the sufficiently total sets of extra reflections appearing due to ordering carbon atoms. The W_2C carbide was shown to exist in two hexagonal modifications, the ordering phase of ε-Fe_2N type and disordering L'3 one. At 1250°C and lower the carbide undergoes to decomposition (W_2C ∀ W +

WC) and to form the metastable ordering orthorhombic modification of ζ-Fe_2N type.

On the bases of obtained results we represent the reviewed the W-C phase diagram.

[1] T.B.Massalski, Binary Alloy Phase Diagrams ASM, Metals Park, OH, 2nd, (1990).
[2] O.M.Barabash and Yu N. Koval The crystal structure of the metals and alloys, Kiev, Naukova dumka. (1986), 596 p. Ceram. Soc., 50, 5 (1967), p. 272-273.
[3] The phase Diagrams of the binary Metal Systems. Handbook in 3 Bd. ed. by N.P.Lyakishev, Moskow, Mashinostroenie, 1996, 992 P.
[4] B.V.Khayenko, T.Ya.Velikanova and V.Z. Kubliy, Dopovidi AN USSR, A, (1986), 10, P. 78-82.
[5] B.V.Khayenko, T.Ya.Velikanova, V.Z.Kubliy and S.I.Makhovitskaya, Phasoviye ravnovesiya stabilnost phas I metastabilniye sostoyaniya v metall. sistemach Institut Problem materialovedeniya, Kyiv (1993), s. 119-124.

P05.09.013 NEW PHASE $Cr_4(P_2S_6)_3$: ROOM TEMPERATURE SYNTHESIS AND CHARACTER-IZATION*. Z.L. Huang, J.T. Zhao, J.X. Mi, S.Y. Mao, L.S. Zheng, Department of Chemistry, Xiamen University, 361005-Xiamen, People Republic of China and S.Vilminot, Groupe des Materiaux Inorganiques de l'IPCMS, EHICS, 1, rue Blaise Pascal, B.P.296, 67008 Strasbourg Cedex, France.

In the last two decades, considerable interest has been focused on the first row transition metal hexathiodiphosphate $M_2P_2S_6$[1] (M=Mn, Fe, Co, Ni, Zn) . It is reasonable to expect metal deficient compounds of the $M_2P_2S_6$ type with a M^{3+} cation, many efforts were made to obtain $Cr_{4/3}[\ ]_{2/3}P_2S_6$ phase by the traditional high temperature method but failed. Here we report the synthesis and characterization of this new phase by solid state reaction between $Na_4P_2S_6{\cdot}6H_2O$ and $CrCl_3{\cdot}6H_2O$ at room temperature rather than by the ceramic method. The process of reaction by grinding and the heat treatment of reaction products were monitored by XRD, implying the following reaction route.

$$4CrCl_3{\cdot}6H_2O + 3Na_4P_2S_6{\cdot}6H_2O \rightarrow Cr_4(P_2S_6)_3 + 12NaCl + 44H_2O$$

The final product was characterized by means of XRD, Raman spectroscopy and magnetic measurements. XRD shows that the compound, isostructural with $Ga_4(P_2S_6)_3$[2], crystallizes in the monoclinic system with a=0.8692(5)nm, b=0.7562(6)nm, c=0.8344(6)nm, β=91.97(7)°. The most intense peak at 381cm^{-1} of the Raman spectrum bearing the characteristics for the $P_2S_6^{4-}$ anion group is attributed to the mixed symmetric P-P and P-S stretching modes. Magnetic susceptibility measurements showed the Curie-Weiss type with number of Bohr magnetons 3.62μ_B/Cr, revealing the existence of a d^3 Cr^{3+} cation. These results correspond to the charge balance $Cr^{3+}{}_4(P^{4+}{}_2S^{2-}{}_6)_3$.

*The Project is Sponsored by Scientific Research Foundation for Returned Overseas Chinese Scholars, State Education Commission of China.

1. R.Brec, Solid State Ionics, 22,3(1986).
2. D.S.Kyriakos, A.N.Anagnostopoulos, P.Christidis and V.Gountsidou, J.Crystal Growth, 76, 6(1986).

P05.09.014 $RECu_{1+x}Sb_2$ (RE = La, Ce, Pr, Nd, Sm, Gd, Tb, Dy, Ho and Y) WITH DEFECT $CaBe_2Ge_2$ - TYPE*. S.K.Zhou, J.T.Zhao, M.H.Song, J.X.Mi, Z.L.Huang, S.Y.Mao, College of Chemistry and Chemical Engineering, Xiamen University, Xiamen 361005, P.R.China

Non-stoichiometry seems to be a characteristic feature for many ternary AT_2X_2 (A = rare earth metals and actinoides, T = late transition metals and X = p-block elements) compounds which adopt the primitive tetragonal $CaBe_2Ge_2$ structure [1]. In the RE-Cu-Sb systems $CeCu_2Sb_2$ was the only phase reported [2] with the $CaBe_2Ge_2$ type but no detailed information on the Cu deficiency was given. The ten title compounds are synthesized by arcmelting methods and their crystal structures refined using X-ray powder Rietveld method and DBWS-9006PC package [3]. For the light rare earth (RE = La, Ce, Pr, Nd, Sm) compounds, one of the copper sites is partially occupied (reaches the maximum for $LaCu_{1.39}Sb_2$), while the occupancies of the same site are almost negligible for the compounds with rare earth metals heavier than Gd including Y metal leading to 1:1:2 stoichiometry. The unit cell parameters show lanthanide contraction. The three dimensional structure is characterized by intergrowth of two distinct layers along c-axis. One layer is quite rigid and formed by connected covalent bonded Cu-Sb tetrahedra. While another layer is quite flexible which consist of bonded Sb square net and the disordered Cu atoms. The ability of accommodating disordered Cu atoms in the voids decrease with lanthanide contraction.

*Project supported by the NNSF of China and Fund for excellent young teachers from the Education Comission of China

1. B. Eisenmman et al., Z. Naturforsch., 27B, 1155, 1972.
2. P.Villars & L.D. Calvert, Pearson's Handbook of Crystallographic Data for Intermetallic Phases, Vol.2,3,4, Metals Park, Ohio (USA): American Society for Metals, 1991.
3. A. Sakthivel & R.A. Young, User's Guide to Programs DBWS-9006 and DBWS-9006PC for Rietveld Analysis of X-Ray and Neutron Powder Diffraction Patterns, 1991.

P05.09.015 METALLIC ZINTL PHASES $RE_3Cu_3Sb_4$ (RE = Nd, Sm, Tb, Dy, Ho): SYNTHESIS AND CHARACTERIZATION*. M.H. Song, J.T.Zhao, S.H.Zhou, Z.L.Huang, J.X.Mi, S.Y.Mao, College of Chemistry and Chemical Engineering, Xiamen University, Xiamen 361005, P.R.China

The idea of "Metallic Zintl Phase" has provided us with new viewpoints of deeper and wider understandings of intermetallic compounds with transitional bonding features in a large category of which the structures follow the Zintl Rule down playing their weak metallic conductivity properties [1]. The title compounds were synthesized by arcmelting method and their crystal structures were characterized by powder X-ray Rietveld methods and DBWS-9006PC package[2]. Crystallographic data: cubic system, $Y_3Au_3Sb_4$-typecI40, space group I-43d, Z=4. Unit cell parameters$Nd_3Cu_3Sb_4$: a = 9.6749(1)Å, V = 905.61(3)$Å^3$;

P08.09.004 STRUCTURAL RELATIONSHIP BET-WEEN CATHO-DOLUMINESCENCE AND DISLOCATION ROZETTES BY MICROINDENTATION. Daria Z. Grabco, Institute of Applied Physics, Academy of Sciences, Academy str.5. MD-2028, Chisinau, Moldova

Microstructure and specific deformation of KCl, LiF and MgO ionic crystals are investigated by (001) plane microindentation in large tempera- ture interval ($T_{def.}$=77-800K).

On the MgO single crystals it is shown that the good correlation be- tween the dislocation arrangement in crystals volume near indentations and cathodoluminescence image is observed in temperature interval T_{def}=0.03- 0.15$T_{melt.}$

Relationship of principal deformation regularities by microindentation with thermal properties of investigated crystals, in particular, with De- bye temperature (θ_D) is established; it is revealed that temperature about θ_D corresponds to border that separates the temperature region between frail and plastic deformation mechanisms by formation of indentations.

It is shown that cathodoluminescence rosettes equal in size to dislocation ones appear aroud the indentations by deformation temperature T_{def}<0.5 θ_D. With temperature growth the dimension of cathodoluminescence rosettes decreases unlike the dislocation structures, and by $T_{def.} \approx 1.0\ \theta_D$ the luminescence occupies the area hardly bigger then indentation size. The rest of dislocation rosette is dark.

Obtained results indicate that various temperature stages of crystals deformation exist by microindentation in large temperature interval.

P08.09.005 A DISORDERED PHASE OF MANGANOUS FLUOSILICATE HEXAHYDRATE AT HIGH TEMPERATURE. Golam Mostafa and Siddhartha Ray, Department of Solid State Physics, Indian Association for the Cultivation of Science, Calcutta 700032, India.

Room temperature structure of $MnSiF_6.6H_2O$ crystals consists of domains of periodic orientational antiphase. An individual domain has symmetry $P\bar{3}$ but existence of mirror-related domains in equal quantity augments the symmetry to $P\bar{3}m$. Below -50^{0}C the crystal has an ordered monoclinic structure. Antiphase being generally an intermediate state between an ordered and a disordered phase, a disordered phase of the crystal at high temperature was expected.

A DSC curve showed a peak at 57^{0}C. Weissenberg photographs of the crystal maintained at 66^{0}C showed that the spots with $-h+k+l=3n\pm1$ were absent. The symmetry was found to have become $R\bar{3}m$. This indicates that in the high temperature phase, while Mn and Si are situated on the 3-fold axes, O and F are randomly distributed in equal numbers among mirror-related general positions, giving rise to disorder.

It was also observed that in first layer Weissenberg photographs about *c*-axis, taken at intervals of 10^{0}C from room temperature to the transition temperature, intensity of the spots with $-h+k+l=3n\pm1$ diminished gradually. This indicates that the process of randomisation of O and F positions starts with raising of temperature and at the transition temperature, the process is accelerated and takes place *en masse.*

P08.09.006 DESTRUCTION MODELS OF SOME LAYER MINERALS. Arkhipenko D.K., Moroz T.N., Grigorieva T.N. United Institute of Geology, Geophysics and Mineraloqy, Siberian Branch RAS, 630090 Novosibirsk, Russia.

Infrared spectroscopy and X-ray powder diffraction methods were used to study structural transformation and destruction of some layer minerals, namely, natural hydrotalcite, hydrotalcite-serpentine, chlorite, flogopite after temperature, pressure, T+P treatment. X-ray diffraction patterns show the dynamic of change of CO32+-H2O interlayer space of hydrotalcite-serpentine up to 260oC after T-treatment and up to 300oC after p+T treatment. Reflections d 003, d 006 decrease from 7.71A, 3.84 A to 6.60, 3.64 A and increase after pressure influence in autoclave (T=300oC, 24h) to 8.6, 4.31A, respectively. We observed 6.6 and 5.52A reflections for natural hydrotalcite samples after heating at 250 o C, 5h, the latter being absent in hydrotalcite-serpentine sample. 300-600oC temperature interval both hydrotalcite and hydrotalcite-serpentine are X-ray amorphous. In this temperature interval we can determine the transformation of the structure by means of IR spectroscopy. The pattern of the two different dehydroxilated phases: forsterite (olivine) and enstatite, are observed in 1000oC thermal decomposition of hydrotalcite-serpentine, chlorite, (flogopite) in different composition. The structure and composition of resulting product are shown to depend on regime of heating (dynamical, isoteral, heating in stone skin, in atmosphere or in aqueous solution), joint T+P influence or separately.

As consequence, for minerals with important industrial properties it is possible to choose such regime of T,P influence which may give the necessary products, to offer an explanation for anomalous combination of minerals in natural conditions and to model different geological process.

This work was supported in part by RFBR Foundation No 98-05-65204a.

P08.09.007 PHASE RELATIONS OF ZRO2 UNDER HIGH PRESSURE AND TEMPERATURE. O. Ohtaka, H. Fukui, T. Fujisawa [1], K. Funakoshi [2], W. Utsumi [3], T. Irifune [4], [1] Earth and Space Science, Osaka University, Toyonaka, Osaka 560-0043, Japan, [2] JASRI, Spring-8, Sayo-gun, Hyogo 679-5198, Japan, [3] JAERI, Spring-8, Sayo-gun, Hyogo 679-5198, Japan, [4] Earth Sciences, Ehime University, Matsuyama, 790-8577, Japan

In order to reveal the phase relation and the crystal structures of high pressure and temperature ZrO_2 phases, we have attempted a series of in situ observations by means of the double stage multi-anvil type high pressure apparatus, SPEED 1500 system, installed at SPring-8. Using this system, it has become possible to perform x-ray in situ experiments in energy dispersive mode up to 25GPa and 2000°;.

We found that cotunnite-type ZrO_2, orthoII, is stable up to 1800°; at pressures ranging from 14 to 21 GPa and determined the phase boundary between orthoII and fluorite-type ZrO_2.

The present results are remarkably different from those of previous works mainly done by synthesis experiments. Obtained orthoII-orthoI phase boundary is located at a lower pressure region and its slope is much more steep comparing with previous results. OrthoII is stable at as high as 1800°;. By quench experiments, a boundary between orthoII and its high temperature phase (hexagonal phase?) was determined; orthoII is quenchable below 1100°; while samples heated above 1100°; reverted to monoclinic on releasing pressure, which suggests the existence of another unquenchable phase. Combining DAC and laser heating, thermally quenched ZrO_2 under pressure was found to have a hexagonal symmetry. The hexagonal phase, however, has not been observed in the present experiments. The hexagonal phase may be an artifact produced by uniaxial compression in DAC and laser heating accompanying large thermal gradient. In our present study, when orthoII formed at 1400°; at 20 GPa is quenched under pressure and decompressed at room temperature, it shows a reverse transition to monoclinic phase. This mystery about the quenchability of orthoII is still left to be solved.

P08.09.008 $Ca_3TiSi_2(Al_2Si_{0.5}Ti_{0.5})O_{14}$, A NEW HIGH-PRESSURE PHASE IN A PETROLOGIC RELEVANT SYSTEM. P. Scheuermann, A. Kutoglu, M. Schosnig and E. Hoffer, Department of Earth Sciences, Philipps University Marburg, D-35032 Marburg, Germany.

In the course of systematic studies to investigate the dependencies of element partitioning on pressure, temperature and compositional variations in the system $CaO-Al_2O_3-TiO_2-SiO_2$ (CATS) a new alumo-titanium-silicate phase with the idealized formula $Ca_3TiSi_2(Al_2Si_{0.5}Ti_{0.5})O_{14}$ was identified.

The new phase is present in all experimental run products at pressures above 1.2 GPa and temperatures of 1375°C and is part of the equilibrium paragenesis with anorthite, titanite, perovskite, and liquid in the pseudoternary section anorthite-titanite-perovskite of the CATS system. The experiments have been performed from atmospheric conditions up to 1.5 GPa at 1300° - 1500°C using double ellipsoid mirror furnace and piston cylinder apparatus. All phases have been checked for homogeneity with electron microprobe and by SEM element mappings.

The structure of $Ca_3TiSi_2(Al_2Si_{0.5}Ti_{0.5})O_{14}$ has been determined with X-ray diffraction data on a single crystal (dimension 0.8 x 0.3 x 0.2 mm) with a conventional four circle diffractometer whereby the space group P321 with a=7.943(1)Å and c=4.930(1)Å was found. The diffraction data indicate that the new compound consists of two different layers parallel (001), in which sheets of corner linked pure SiO_4 and statistically distributed (Al, Si, Ti)O_4 tetrahedra centered at z=1/2 alternate

with those sheets occupied by six fold coordinated Ti^{4+} and eight fold coordinated Ca^{2+} at z=0.

The identified type of structure with the general formula $A_x^{[8]}B_y^{[6]}T_z^{[4]}O_{14}$ is also known for some synthetic germanates [1] and another high-pressure silicate $Na_{1.8}Ca_{1.1}Si_6O_{14}$ [2].

[1] Belokoneva, E.L. and Belov, N.V. (1981) Doklady Akademii Nauk SSSR, 260, 1363-1366
[2] Gasparik, T., Parise, J.B., Eiben, B. and Hriljac, J.A. (1995) Amer. Mineral., 80, 1269-1276

P08.09.009 STRUCTURAL CHANGES OF $ZnFe_2O_4$ AT HIGH PRESSURE. D. Levy and M. Hanfland, ESRF, BP 220 F-38043 Grenoble Cedex, France and A. Pavese, Dip. di Scienze della Terra, Università di Milano, V. Botticelli 23, 20133 Milano, Italy

Franklinite ($ZnFe_2O_4$) is an oxide-mineral with spinel-like structure (Fd3m, Z=8). The studied sample was synthetic and was structurally and chemically characterised by X-ray powder diffraction and X-ray fluorescence. The chemical formula was found to be $Zn_{0.97}Fe_{2.02}O_4$ (0.1 vacancies p.f.u.) and spinel structure can be described as 'normal' (4-fold co-ordinated Zn^{2+} and 6-fold co-ordinated Fe^{3+}). The high-pressure experiment was performed with a Diamond Anvil Cell (DAC) at ID9 (ESRF, Grenoble, France). Powder diffraction patterns were collected with the angle dispersion technique, by means of an image plate, in the pressure range 1.8-36.2 GPa and sequentially analysed with the Rietveld method. The only structural degree of freedom in spinel-like structure is the co-ordinate of oxygen that shifts along [111]: this co-ordinate was refined to study the distortion of cation sites. The cell volume exhibits a smooth trend up to 25 GPa, and it can be fitted by the Birch-Murnaghan equation of state [1]. The following elastic properties were obtained: B_0=166.4 GPa, B'_0=9.3. Above 24.4 GPa, a new phase along with spinel was observed and was attributed to a $CaTi_2O_4$-like structure ($Bb2_1m$, Z=4). In this phase, Zn^{2+} changes co-ordination number from 4 to 8 (tetrahedron→two-cap trigonal prism), while Fe^{3+} is still co-ordinated 6-fold (octahedron). The cell-edge and the structure of the high-pressure phase were refined to analyse its compression behaviour, but not enough points have been collected to extrapolate the equation of state.

[1] F.Birch, J. Geophys. Res., 91, 4949 (1986)

P08.09.010 HIGH-PRESSURE PHASE TRANSITION IN SPODUMENE $LiAlSi_2O_6$. Thilo Arlt and Ross Angel, Bayerisches Geoinstitut, University of Bayreuth, D-95440 Bayreuth

The single-chain silicates of the pyroxene group, generally $M2M1Si_2O_6$ are known to exhibit a complicated polymorphism with pressure and temperature. Clinopyroxenes with low Ca- or Na-contents, e.g. enstatite-ferrosilite, pigeonite and kanoite, undergo displacive phase transitions at high-pressure in which the symmetry increases from space group $P2_1/c$ to HP $C2/c$. In enstatite that phase transition causes a weak seismic dicontinuity in the Earths upper mantle. In this study we found a symmetry change from $C2/c$ to $P2_1/c$ which is opposite to the transformation reported in other pyroxenes with increasing pressure.

The high-pressure behavior of natural spodumene $LiAlSi_2O_6$, space group $C2/c$ was studied by single-crystal X-ray diffraction in a diamond-anvil cell. Nonlinearities of cell parameters and birefringence showed a displacive phase transition at about 3.2 GPa. The transformation is rapid, reversible, non-quenchable and first order in character. The cell dimension b increases while a, c and the angle β decrease strongly resulting in a total volume decrease of about 1.3 % at the transition. The h + k = odd reflections, characteristic of a primitive lattice, appear suddenly at the phase transition. The space group $P2_1/c$ of high-pressure spodumene was confirmed by structure refinement from single-crystal X-ray intensity data collected in a diamond-anvil cell at 3.3 GPa. At ambient conditions both chains are S-rotated (O3-O3´-O3´´= 170.5°) but they become distinct in the high pressure form which decreases the symmetry to $P2_1/c$. While the A-chain remains S-rotated with an O3-O3´-O3´´ angle of 157.0(4)°, the B-chain rotates about 37° during the phase transition to an O-rotated chain angle of 152.4(5)°.

High-pressure phase transitions from $C2/c$ to $P2_1/c$ were also observed in the clinopyroxenes $LiScSi_2O_6$ at about 0.6 GPa and $ZnSiO_3$ at 1.9 GPa. To explain that observation, the C-centered forms at ambient conditions are considered to be isotypic to the high-temperature (HT) $C2/c$ polymorphs of, e.g. $MgSiO_3$ and $FeSiO_3$. Consequently, the high-pressure polymorphs of Li-pyroxenes are equivalents to the low-$P2_1/c$ clinopyroxenes. In LiSc-Cpx the nonlinearities in cell parameters are significant, but much weaker than those found in spodumene and those reported in temperature dependent $P2_1/c$-HT $C2/c$ phase transitions (best studied in pigeonite). The continous and linear increase of h+k = odd reflections indicate a second order transformation mechanism for $LiScSi_2O_6$. In $ZnSiO_3$ the intermediar $P2_1/c$ phase further transforms to the HP-$C2/c$ form at about 5.1 GPa which confirms that HT $C2/c$ and HP $C2/c$ clinopyroxenes have distinct stability fields in the P/T space.

P08.09.011 STRUCTURAL CHANGES IN TlF WITH TEMPERATURE AND PRESSURE. S. Hull, ISIS Facility, CLRC Rutherford Appleton Laboratory, Chilton, Didcot, Oxon OX11 0QX, UK and P. Berastegui, Inorganic Chemistry, Arrhenius Laboratory, Stockholm University, S-10691 Stockholm, Sweden.

The phase diagram of thallium(I) fluoride indicates the existence of three polymorphs [1]. The ambient (TlF-I) and high (TlF-II) temperature phases have been proposed to adopt distorted NaCl-type structures, probably due to the stereochemistry of the distorted Tl s^2 lone pair [1,2]. The existence of a third polymorph at high pressures (TlF-III) has been proposed from the calculation of very small volume changes by differential thermal analysis.

In this work, the structural behaviour of TlF with temperature and pressure has been studied using neutron powder diffraction measurements. In contrast to previous studies using single crystals (where the presence of weak reflections resulted in uncertainty in the space group determination), the ambient temperature structure has been unambiguously assigned to space group $Pbcm$ (No. 57) with a= 6.09556(8), b= 5.48860(7) and c= 5.18300(7) Å, Z=4. The structure can be fully described with Tl and F at 4d (x, y, ¼) sites, with the former near the ideal position but in a highly irregular fluoride ion co-ordination with four short Tl-F bond lengths (2.43-2.71 Å) and two longer at 3.12 and 3.70 Å. The high temperature structure was investigated at 90°C and refined in space group $P4/nmm$ (No. 129) with a= 3.78283(2) and c= 6.12312(5) Å, Z=2. The two ions can be located at 2c (¼, ¼, z) sites, with Tl near the ideal position at z= 0.7461(2) and F at z= 0.1426(2). This results in a more regular octahedron with Tl-F bond lengths of 2.43, 2.76 (×4) and 3.69 Å. TlF was also studied at pressures up to 4 GPa but no structural transition was observed. There are no significant changes in the atomic positions, though the a-axis is found to be somewhat more compressible than the other two axes.

1. C.W.F.T. Pistorius and J.B. Clarke, Physical Review **173** (1968) 692.
2. N.W. Alcock and H.D.B. Jenkins, J.C.S. Dalton **17** (1974) 1907.

P08.09.012 HIGH TEMPERATURE SUPERIONIC PHASES IN THE $(PBF_2)_{1-X}$-$(MF)_X$, SYSTEMS WITH M= K, RB AND CS. P. Berastegui, Inorganic Chemistry, Arrhenius Laboratory, Stockholm University, S-10691 Stockholm, Sweden and S. Hull, ISIS Facility, CLRC Rutherford Appleton Laboratory, Chilton, Didcot, Oxon OX11 0QX, UK.

The crystal structure and ionic conductivity of polycrystalline samples of PbF_2 doped with KF, RbF and CsF have been investigated at temperatures up to ~700K using neutron diffraction and complex impedance measurements. The maximum solubility of KF in β-PbF_2 was found to be about 1 %, while the creation of charge compensating anion vacancies induced an increase in the ionic conductivity at ambient temperature by a factor 5.6×10^3. At higher KF contents of $0.333 \leq x \leq 0.68$, a high temperature superionic phase with a body centred cubic cation sublattice was observed above a transition temperature of T_c ~ 520-590 K, with a related abrupt increase in the ionic conductivity. Within this high temperature modification, the anions are predominantly disordered over the tetrahedral interstices, and its structure can thus be described as an *anti* α-AgI type. In the case of $(PbF_2)_{1-x}$-$(RbF)_x$, an increased tendency towards ordering of the two cation species over the 0,0,0 and ½,½,½ sites was observed as the dopant content increased within the stability range $0.333 \leq x \leq 0.5$. This is accompanied by a change in the preferred anion location towards the octahedral positions as the mean structure tends towards a partially ordered perovskite-type arrangement. A fully ordered perovskite-type structure was observed in the $(PbF_2)_{1-x}$-$(CsF)_x$ system where only a single line phase at x = 0.5 can be observed. This phase shows no evidence of superionic behaviour at elevated temperatures.

P08.09.013 HIGH TEMPERATURE STRUCTURE TRANSITIONS OF $SrHFO_3$. S.L. Cuffini [1], J.A. Guevara, Y.P. Mascarenhas [2], A.N. Fitch[3]. [1] INFIQC, Fac. Ciencias Quimicas. U.N.C. Agencia 4, CP. 61 - Córdoba. Argentina. [2] IFSC-USP, C.P. 369-15690-970. Sao Carlos. Brazil. [3] ESRF, BP 220, F-38043 Grenoble Cedex, France.

Strontium hafniate (SH) is a refractory compound melting at 2730 C, which belongs to the perovskite family. Although this compound has been known for well over 50 years, the crystal structures at high temperature, where phase transitions have been reported, have not been examined thoroughly (1).The purpose of this work is to report the crystal structures of this compound not only at room temperature but also at high temperature in order to determine the nature of the structural phase transitions. The x-ray diffraction patterns collected at beam line BM16 at ESRF were refined using Rietveld Method and the temperature range studied was from room temperature up to 1000C. At room temperature, the structure showed a small deviation from the pattern of a cubic perovskite, however the small superlattice reflections could be refined in space group Pnma with lattice parameters, a=5.7889(2)A, b=8.1716(3)A and c=5.7772(2)A. At higher temperatures, SH showed a phase transition from Pnma to I4/mcm at around 500C and from I4/mcm to Pm-3m around 900C. This behaviour is comparable with other perovskite like SrRuO3 and SrZrO3 which exhibit similar transitions in this temperature range.

(1) V.P. Red'ko, A.V. Shevchenko and L.M. Lopato, Inorganicheskie Materialy, 24, 2027 (1988)

P08.09.015 HIGH PRESSURE STUDIES ON CHALGOGENIDE MISFIT LAYER STRUCTURES, AND THEIR COMPONENT STRUCTURES. Wulf Depmeier, Karsten Knorr and Lars Ehm, Institut für Geowissenschaften, Mineralogie / Kristallographie, Universität Kiel, Olshausenstr. 40, D 24098 Kiel, Germany

In the context of an interdisciplinary research project, comprising theoretical and experimental physicists, inorganic chemists and crystallographers, we have started an investigation into the high pressure behaviour of misfit compounds with the idealised formula $(MX)_{1+x}(TX_2)_m$ with M = Sn, Pb, Bi, Rare Earth; T = Ti, V, Cr, Nb, Ta and X = S, Se. The ultimate goal of the project is to gain a thorough understanding of the detailed geometrical and electronic structure of the compounds, and their associated properties.

The focus is on the interfaces between MX and TX_2 layers, and the van-der-Waals gaps between adjacent TX_2 layers. In order to facilitate the understanding of the complex and usually aperiodic misfit compounds [1], we decided to start high pressure work on the much simpler component structures, such as PbS, 1T-TiS_2, and 2H-NbS_2. Despite their simplicity, very little is known about the high pressure behaviour of these compounds. Experiments use x-ray powder diffraction in diamond anvil cells up to 100 kbars. The high pressure studies on misfit compounds and their component structures are interesting, because the topology of the structures, the electronic configuration of the constituents, and the band structures of the crystals promise to present a rich phenomenology [2]. The experiments are accompanied by theoretical studies on the ab initio level, performed in parallel in our group.

[1] Rouxel, J., Meerschaut, A. & Wiegers, G.A.: Chalcogenide misfit layer compounds. J. Alloys and Compounds 229, 144 - 157 (1995).
[2] Wiegers, G.A.: Charge transfer between layers in misfit layer compounds. J. Alloys and Compounds 219, 152 - 156 (1995).

P08.09.016 COMPLEX OXIDES WITH OCTAHEDRAL FRAMEWORKS: LEWISITE AND LOPARITE. N. V. Zubkova, D. Yu. Pushcharovsky, Geology Department, Moscow State University, 119899 Moscow, Russia, Arakcheeva A. V., Institute of Metallurgy RAN, Leninsky av., 49, 117334 Moscow, Russia, D. Atencio, University of Sao Paolo, Sao Paolo, Brasil

Pyrochlore - like structure of lewisite (general formula - $A_{2-m}B_2[O_6(OH)]$ from Tripui, Ouro Preto, Minas Gerais, Brazil was refined up to R_{hkl} = 0.022 in space group *Fd3m*, a = 10.311(6)Å, V = 1096.23Å^3. The averaged results of the EDS chemical analyses corresponded to the chemical formula: $(Ca_{0.91},Na_{0.12},Fe_{0.22},Al_{0.13},Sb^{3+}_{0.32})(Sb^{5+}_{1.27},Ti_{0.72})O_6(OH)$.

Similarly to pyrochlore [1], the structure of lewisite is based on a defect simple cubic packing of (OH) - groups and O atoms, with A - and B - atoms occupying 1/2 of cubic voids. Large A - cations have cubic coordination and B - atoms - 6 coordination due to the vacancies.

Crystal structure of loparite, $(Ti,Nb)(Na,Ce,Ca,Sr)O_3$ from Lovozero alkaline massive, was refined up to R_{hkl} = 0.041 in space group *Pn3m* with double perovskite parameters of the cubic unit cell a = 7.767(1)A [2]. The lattice dimensions of loparite are doubled because of the ordering of A - and B - cations. Thus loparite can be characterized by general formula $A'A''_3B'_2B''_2O_{12}$.

Both structures comprise the octahedral frameworks. In loparite the voids are filled by ordered Ca,REE and Na,REE cations. In lewisite the voids are filled by (OH) - group surrounded by 4 (Ca,Sb) - cations.

1. Lima-de-Faria, J. (1994), Structural Mineralogy, Kluwer A. P., Dordrecht,1994.
2. Zubkova, N.V., Arakcheeva, A. V., Pushcharovsky, D.Yu., (1998) ECM-18 Abstracts, 1998.

P09.09.001 CHEMICAL PROPERTIES OF TRANSITION METAL CATIONS IN ION EXCHANGED ZEOLITES. AN AB INITIO STUDY. Judit E. Šponer, J. Heyrovský Institute of Physical Chemistry, Academy of Sciences of the Czech Republic, Dolejškova 3, Prague 8, Czech Republic

This study is intended to provide a generalised view on the basic chemical properties of Fe^{2+}/Fe^{3+}, Cu^{+}/Cu^{2+}, Co^{2+}, and Ni^{2+} containing zeolites. Siting of transition metal cations in a number of zeolites of various structural types has already been investigated employing both spectroscopic (UV-VIS, IR, EPR) and diffraction (EXAFS) techniques.

Simple models have been optimised at DFT/Becke3LYP level of theory. Different aluminium distribution in high and low silica zeolites has also been taken into consideration. Charge density distributions have been analysed to interpret the influence of the zeolite matrix on the redox properties of the various transition metal cations.

It has been found that metal cations possessing two stable oxidation states (such as Fe^{2+}/Fe^{3+} and Cu^{+}/Cu^{2+}) tend to adopt the more stable one. Thus, in presence of one framework aluminium a considerable charge transfer has been found from Fe^{2+} to the aluminosilicate skeleton, the Fe^{3+} form with a d^5 electronic configuration being more stable than the less symmetrical Fe^{2+} form (d^6). On the contrary, copper is trying to adopt the more stable d^{10} electronic configuration by a charge transfer from the skeleton to Cu^{2+} resulting in formation of Cu^{+} ions (d^{10} closed shell electronic configuration). In presence of water the charge transfer between the aluminosilicate skeleton and the metal cation is weaker because of the negative charge donated by the water ligand. Weak Lewis base molecules, such as CO have a much weaker impact on the charge distribution between the metal and the zeolite.

P09.09.002 IDENTIFICATION AND ENRICHMENT OF INDONESIAN ZEOLITE USING CATION FLOATATION METHOD. Muhammad Hikam, Department of Physics, Faculty of Mathematics and Sciences, University of Indonesia, Depok 16424 Indonesia, Endang Asijati and Dian Ratnasari, Department of Chemistry, University of Indonesia, Depok 16424 Indonesia.

Most of natural zeolite in Indonesia contains mordenite type A, $[Na_2CaK_2]$ $Al_2Si_{10}O_{24}.7H_2O$. This material has many valuable applications in agriculture, environment and energy; it could be used as adsorbent and ion exchange, however the purity of this natural product is too low for direct use. We have employed cation floatation method to enrich the A-modernite fraction by observing the change of the mixture density, pH, type and concentration of collector and concentration of HF as function of the floated quantity of this A-mordernite.

X-ray diffraction analysis using Shimadzu XD-D1 was conducted to examine the specimens for several variations and settings. The d-spacing identifications were done by comparing the experimental data with the ICDD database and then quantitative analyses were performed. Before the treatment, the existence of A-mordenite in this natural product was confirmed, it has space group Fd3m with lattice parameters a = (24.46 ± 0.96) Å. The average weight concentration before the treatment was 41,02%. The remaining mineral identified as epistilbite $Ca_3Si_9Al_3O_{24}.8H_2O$, clinoptilolite $[KNa_2K_2]$ $Al_2Si_{10}O_{24}7H_2O$ and B-mordernite $[CaNa_2K_2]Al_2Si_{10}O_{24}.7H_2O$.

After the treatment, higher concentration of A-mordenite was obtained by setting higher collector concentration, lower HF activator and pH value to the value 5.0. The highest concentration of A-mordenite achieved by the setting was 66.45%. The crystallographic structure remained the same since there was neither violence chemical reactions nor heating in all the processes.

P09.09.003 MINERALS AND SYNTHETIC COMPOUNDS WITH OPEN FRAMEWORK STRUCTURES: NEW DATA. O.V.Yakubovich, Moscow Lomonosov State University, Department of Geology, Vorob'evy Gory, 119899 Moscow, Russia and W.Massa, Philipps-University, Department of Chemistry, D-35032 Marburg, Germany.

The results of X-ray crystal structure investigations of two natural molecular sieves - a pure alkali variety of merlinoite and a K-variety of chabazite, the new zeolite-like mineral bakhchisaraitsevite and a synthetic microporous Mn-phosphate, are presented.

cryst.	merlinoite	chabazite	bakhchisarai-tsevite	Mn-phosphate
form-ula	$Na_5K_7(H_2O)_{24}$ $[Al_{12}Si_{20}O_{64}]$	$K_6Na_4Ca(H_2O)_{27}$ $[Al_{12}Si_{24}O_{72}]$	$Na_2\{(Mg_{4.5}Fe_{0.4}$ $Mn_{0.1})[PO_4]_4$ $(H_2O)_6\}H_2O$	$Mn_3[PO_4]_2$ $0.5H_2O$
unit cell	a 13.840(3)	13.840(7)	8.3086(8)	9.310(7)
	b 14.104(2)		12.906(1)	17.414(9)
	c 10.040(3)	15.100(9)	17.486(1)	8.161(3)
, (°)	β		102.01(1)	92.58(5)
sp.gr.	*I m m m*	*R* $\bar{3}$ *m*	*P* $2_1/c$	*C c*
Z	1	1	4	2
T	120 K	300 K	193 K	300 K
R	0.043	0.054	0.033	0.033

The structure refinements of merlinoite, chabazite and $Mn_3[PO_4]_20.5H_2O$ had to be done with the supposition of twinning of the crystals. The disorder of the tetrahedral framework has been found in chabazite. The interdependence between the degree of orthorhombic distortion in the merlinoite structure and the way of interstitial component distribution is discussed. The positions of all hydrogen atoms have been found and refined in the cases of the new mineral bakhchisaraitsevite and synthetic Mn-phosphate hemihydrate.

P09.09.004 A STUDY OF THE NEW ION EXCHANGED DERIVATIVES OF HIGHLY CRYSTALLINE LOW-SILICA MAP. Jose Geraldo Nery [1], Yvonne P. Mascarenhas [1], Anthony K. Cheetham [2], [1] Instituto de Fisica de Sao Carlos-USP, Cx. Postal 369,CEP 13560-970, Sao Carlos, SP, Brazil, [2] Materials Research Laboratory, University of California, Santa Barbara, CA 93106.

This is an extensive study of the Cd-MAP, Mn-MAP, Ba-MAP, Sr-MAP and Pb-MAP, the new ion exchanged derivatives of highly crystalline low-silica NaP with an Si/Al ratio of 1.0. All the structures were refined from conventional X-Ray data in the monoclinic crystal system and all the structures have the GIS framework topology. The extra-framework sites for Cd, Mn, Ba, Sr, Pb and water molecules were located. The incorporation of Cd, Mn, Ba, Sr and Pb cations produces distortions in the GIS framework due to its high flexibility. Besides the distortions induced by the cations incorporation, the Si NMR data and the Si-O and Al-O bonds show that all the structure present a strict ordering scheme of Si and Al. The number water molecules per unit cell differs between the title compounds, as does their dehydration behaviour. Dehydration of Cd-MAP and Mn-MAP induces the formation of new phases, however under rehydration conditions these new phases are restored to the original ones. On the other hand, dehydration of Sr-MAP and Pb-MAP induces the formation of new phases which are irreversible under rehydration conditions. Dehydration of Ba-MAP at 140-180C induces the formation of a new phase which is restored to the original one under the rehydration conditions. However, above this temperature range the new phases formed are irreversible.

P09.09.005 A $^{69/71}$GA AND ^{29}SI MAS NMR STUDY OF ZEOLITE-ANALOGUE GALLOALUMOSILICATES WITH CANCRINITE STRUCTURE. F. Stief, M. Fechtelkord, J.-Chr. Buhl, Institut für Mineralogie der Universität Hannover, Welfengarten 1, D-30167 Hannover, Germany.

Isomorphous substitution of aluminium by gallium on framework positions of zeolites has a large influence on the

catalytic and sorption properties. A well known application is the so-called Cyclar process, where short-chain paraffin molecules are converted to aromatics by using a gallium-loaded zeolite catalyst [1]. The most appropriate method to distinguish framework and extra-framework gallium is $^{69/71}$Ga NMR. Both nuclei have different quadrupolar properties which allow the determination of the individual coupling constant by observing both isotopes at the same static magnetic field. Most $^{69/71}$Ga MAS NMR spectra are accumulated with single pulse experiments but signal broadening and the occurrence of spinning sidebands require Hahn echo spectra with stepped offset (variable offset cumulative spectrum VOCS) [2]. Samples with different initial Al/Ga ratios have been synthesised at mild conditions to investigate the influence of framework gallium on the structure and properties on nitrate cancrinite. All specimens are highly crystalline with crystal sizes up to 20 μm. ^{29}Si MAS NMR spectra show different Q^4(nAl, (4-n)Ga) signals due to changes in the second coordination sphere of Si. The Al/Ga ratios deduced from these spectra are lower than the value of the initial materials of syntheses. The ^{29}Si MAS NMR resonance of the sample with Al/Ga = 0 is shifted to lower field compared with its alumosilicate analogue due to increased bond angles and the different electronegativity of gallium related to aluminium.

1. J.M. Thomas, X.S. Liu. J. Phys. Chem. 90 (1986) 4843.
2. D. Massiot, I. Farnan, N. Gautier, Trumeau, A. Trokiner, J.P. Coutures. Solid State Nuclear Magnetic Resonance 4 (1995) 241.

P09.09.006 STRUCTURE REFINEMENT OF AS-SYNTHESIZED VPI-5 AT 295 AND 90 K. C.L. Lengauer, T. Brehmer and E. Tillmanns, Institut für Mineralogie und Kristallographie, Universität Wien – Geozentrum, A-1090 Vienna, Austria, and J. de Onate, Laboratorium für Kristallographie, ETH, CH-8092 Zurich, Switzerland.

Common to some aluminophosphate molecular sieves is a channel type pore opening within the tetrahedrally coordinated framework, which is characterized by an alternate occupation of Al^{3+} and P^{5+} over the crystallographic T-sites. This atomic arrangement of the cations enables polar framework sym-metries, which are the basis for interesting physical properties in inorganic crystalline materials. In the case of VPI-5 with the VFI topology and a nominal composition of $Al_{18}P_{18}O_{72}\cdot 42H_2O$, the symmetry of the polar framework is further reduced from $P6_3cm$ to space group $P6_3$ due to a triple-helix like arrangement of the water molecules within the channels [1]. It is known from X-ray powder refinements at 385 K [2], that the framework of VPI-5 exhibits a strong anisotropic thermal behaviour. This is caused by a temperature induced disordering of the water molecules within the channels, which allows the re-establishing of the higher framework symmetry. The refinement of the structure of VPI-5 at 295 K with a = 19.985(3) Å and c = 8.119(2) Å confirmed for the framework geometry the results of a former single crystal investigation [3], however, there is a clear difference in the occurrence of two new sites for water molecules. Concerning the previously described water positions [1] the two water sites OW5 and OW7 were not occupied in this single crystal material, thus preventing the establishing of the triple-helix. The unit cell of the low temperature form of VPI-5 with a = 19.978(3) Å and c = 8.052(2) Å shows a pronounced shortening along [001], which is in accordance to the trend of the partially dehydrated form [2]. This shrinkage increases the deviation from the ideal symmetry, which at 90 K is mainly caused by the framework and minor by the water molecules.

1. L.B. McCusker et al. (1991) Zeolites, vol.11, 308.;
2. J. de Onate et al. (1998) Microp.Mesop.Materials, vol.22, 127;
3. G. Cheetham and M.M. Harding (1996) Zeolites, vol.16, 245.

P09.09.007 A SPECTROSCOPIC STUDY ON STRUCTURE CONTROLLING PARAMETERS IN ORGANOTHERMAL SYNTHESES OF CANCRINITE. B. Posnatzki, M. Fechtelkord and J.-Chr. Buhl, Institut für Mineralogie, Universität Hannover, Welfengarten 1, D - 30167 Hannover, Germany

The zeolite-like mineral cancrinite $Na_8[AlSiO_4]_6X^{2-}\ nH_2O$ is a promising material for future technical applications. Its characteristic structural feature is a single 12-ring channel parallel to the c-axis [1]. This one-dimensional channel system with a diameter of about 6.8 Å is a perfect matrix for the enclathration of orientated molecules [2, 3]. The insertion of organic macromolecules as reactive compounds for later catalytic reactions is possible, as well as the incorporation of small organic molecules that can be removed by heating.

In conventional syntheses cancrinite is prepared under hydrothermal conditions in systems consisting of Na_2O-SiO_2-Al_2O_3-H_2O in the presence of a large variety of salts [4]. These cancrinites contain inorganic anions that are blocking the pores and prevent a technical utilisation as defined by a zeolite.

During synthesis in non-aqueous solvents the nature of Al-, Si-source, solvent, base and the temperature has a large influence on the formation of the desired product. Investigations of these structure controlling parameters and of the calcination process were made by various methods of analyses, like NMR- and IR-spectroscopy, as well as X-ray powder diffraction and thermal analysis. Different Al_2O_3 - SiO_2 - sources were employed. Best results were received by application of sol-gels of various compositions; 1,3- and 1,4-butane-diol are the solvents used. The calcination process plays an important part in improving the sorption capacity of the material. Therefore several calcination methods were checked like thermal and chemical treatment.

1 O. Jarchow, *Z. Krist*., **122**, (1965), 407;
2. G.G. Lindner et al, *J. Solid. State Chem*., **126**, (1996);
3. Y.A. Barnakov et al., *Inorg. Mater*., **31**, (1995), 748;
4. R.M. Barrer et al., *J. Chem. Soc. A*, (1990), 1523

P09.09.008 TETRATHIAFULVALENE AND TETRA-CYANO-P-QUINODI-METHANE IN FAUJASITE. C. Baehtz, H. Fuess, Materials Science, Darmstadt University of Technology, Petersenstr. 23, D-64287 Darmstadt, Germany

The last few years have seen an increasing interest in host-guest-systems with zeolites because their chemical and physical properties [1]. We are focusing on the systems Tetrathiafulvalene (TTF) in Faujasite NaY, Tetracyano-p-quinodimethane (TCNQ) in NaY and the charge-transfer-complexe TTF and TCNQ in NaY, which have been investigated by powder-diffraction, DRIFT-,UVVIS- and EPR-spectroscopy.

The guest molecules are incorporated in the host lattice by adsorption from the liquid-phase. The solvent is removed by heating under high vacuum. Powder diffraction pattern with synchrotron radiation with λ=1.16Å at 10 K and CuKα1-radiation at 293K exhibit considerable differences of intensities as compared to the unloaded host. The localisation of the guest is performed through a determination of the rest electrondensity by Fourier analysis and subsequent Rietveld refinement. The TCNQ molecule is in the center of the 12-ring window while the CN-groups mount into the two neighbouring supercages and are coordinated by the SII* sodium ions. DRIFT measurements of TCNQ in NaY show a CN-signal shifted to higher wavenumbers as in the pure TCNQ spectra. In the case of the charge-transfer-complexe in NaY, this signal is split into two peak at lower wavenumbers. Due to the arrangement of TCNQ in the host and the coordination of the functional groups to the sodium ions, strong interactions between the lattice and the guest molecules result. This explains the strong and broad EPR-signal and the shifted UVVIS-absorption bands.

This work is financially supported by the Deutsche Forschungs-gemeinschaft.

[1] K. B. Yoon, J. K. Kochi, J. Phys. Chem. **99** (1995) 7042

P09.09.009 POWDER NEUTRON DIFFRACTION AND ^{13}C MAS NMR STUDIES OF NAY ZEOLITES WITH CHEMISORBED METHYL GROUPS. S. Vratislav, M. Dlouhá, Faculty of Nuclear Sciences and Physical Engineering, Břehová 7, 115 19 Prague 1, Czech Republic, and V. Bosáček, Heyrovský Institute of Physical Chemistry, Dolejškova 3, 182 23 Prague 8, Czech Republic.

Zeolites exhibit regular structure which can be easily modified and therefore are important candidates for effective catalysts [1].

The crystal structure of NaY zeolite with chemisorbed methylium ion have been investigated by powder neutron diffraction on the KSN-2 diffractometer which is placed at the LVR-15 research reactor in Řez near Prague. Structural parameters were determined by Rietveld analysis of powder neutron patterns (collected at 7 K) using the GSAS package. Difference Fourier maps were calculated to localize the nonframework cations and the CD_3 groups. Experimental evidence of the created chemisorbed methyl groups after reaction of methyliodide with Na+ cations of the zeolite was obtained from ^{13}C MAS NMR spectra [2].

Our studies of chemisorbed NaY zeolites show that chemisorbed CD_3^+ groups are preferentially located in alfa cages at O(l) oxygen sites. A complete set of the structural parameters in the frame of Fd3m space group for unperturbed NaY and for NaY after the formation of surface methoxy groups (a = 2.4897(8) nm, R_{wp} = 0.0712, R_p = 0.0568) were given and an influence of chemisorbed species on the distribution of Na^+ cations in the lattice was detected by neutron diffraction [3]. While the occupation of S_{II} in NaY without adsorbate was 32 Na^+ per unit cell (i.e. 100%), after the chemisorption of CD_3I was found 21.4 (67%).

[1] H.Gies in " Studies in Surface Sci. & Catal." Vol. 85, Elsevier 1994, p. 295.
[2] V. Bosáček : J. Phys. Chem. (1993) , **93,** 10732
[3] S.Vratislav, M. Dlouhá, V.Bosáček, Physica B 241 - 243 (1998) 400 - 402

P09.09.010 LOCATION OF BRØNSTED SITES IN D-MORDENITES BY NEUTRON POWDER DIFFRACTION. G. Cruciani and A. Martucci, Istituto di Mineralogia, University of Ferrara, Ferrara, Italy

Neutron Rietveld refinements of one natural mordenite (Si/Al=5.4) and two synthetic mordenites (Si/Al=5.6 and 10.0) in their deuterium form were performed in the *Cmcm* space group.

From the structure refinements four Brønsted acid sites were recognized. The first, D1, was on framework oxygen O10 and headed towards the center of the 12-ring; the second, D2, was on the framework oxygen O6 and headed towards the side pocket; the third, D3, was on O5 and, as D1, headed towards, the center of the 12-ring; the last, D4, was on O9 and headed toward the center of the 8-ring. The T-O distances involving the Brønsted sites were always among the largest T-O distances of the tetrahedra, thus confirming the correct location of OD groups. The deuterium sites had occupancies varying in the range 7-24%, with the O6-D2 group always showing the highest occupancy. All the OD groups show regular site geometry, and about half of the theoretical value of Brønsted sites (calculated on the basis of the aluminum content) has been localized. This result can be explained considering that, in the case of elevated Al content, the concentration of Brønsted sites is remarkably lower than would be expected on the basis of the aluminum content [1,2,3]. On the whole about half of the acid sites vibrate in the 12-ring channel, and half in the smaller channels. Few other extraframework sites, with low occupancy and at large distances from the framework oxygens, have been attributed to residual ND_4 groups.

Sonnemans, M.H.W., den Heejer, C., and Crocker, M. (1993) *J. Phys. Chem*., **97**, 440.
Bankos, I., Valyon, J., Kapustin, G.I., Kallo, D., Klyachko, A.L. and Brueva, T.R. (1988) *Zeolites*, **8**, 189.
Karge, H.G. and Dondur, V.J. (1990) *J. Phys. Chem*., **94**, 765.

P09.09.011 STRUCTURE REFINEMENTS OF CO-FERRIERITES. M. C. Dalconi and G. Cruciani, Istituto di Mineralogia, University of Ferrara, Italy.

The catalytic reduction of nitrogen oxides (NO_x) in the presence of excess oxygen is now one of the most important subjects from the viewpoint of environmental protection. Li and Armor (1) recently showed that Co^{2+}-exchanged ferrierite is a particularly active catalyst for the reduction of NO_x with methane in the presence of excess oxygen.

This study is devoted to clarifying the structural modifications undergone by ferrierite when loaded with increasing amounts of Co cations.

Room temperature synchrotron X-ray diffraction data were collected on three samples of Co-ferrierite ion-exchanged with different amounts of Co. Rietveld structure refinements were performed by the GSAS package. Assuming the framework composition of the as-synthesised zeolite (Engelhard), we found that the Co^{2+}, Na^+ and K^+ cations in the Co-Fer.1S sample were not enough to counterbalance the framework charge.

The remainder of the charge is probably compensated by the presence of Brønsted acid sites produced during thermal decomposition of the residual NH_4^+ cations (2), and/or by residual NH_4^+ cations themselves (as indicated by IR analysis). In the case of the Co-Fer.3S sample the ion-exchange appear to be complete. The over-loaded Co-Fer.7S was completely ion-exchanged, and the excess of cobalt is probably located in an unidentified second phase outside the framework. The structure refinements of the three samples were performed using the space group *Immm*; there was no evidence for a lowering of symmetry to $P2_1/n$. The restoration of the apparent topological symmetry *Immm* was attributed to the presence of the $Co(H_2O)_6^{2+}$ octahedron in the large ferrierite cage. In all three samples Co^{2+} was seen to be coordinated to six water molecules in a regular octahedral configuration at the centre of the ferrierite cage.

1) Li, Y., Armor, J. N., Applied Catalysis B, 3 (1993).
2) Attfield, M. P., Weigel, S. J., Cheetham, A. K., J of Catal., 172, 274 (1997).

10. CRYSTALLOGRAPHY IN MATERIAL SCIENCE

P05.10.001 SUPERIONIC TRANSITIONS IN THE $KTiOPO_4$:Nb CRYSTALS. T.Yu.Losevskaya, V.I.Voronkova, and V.K.Yanovskii, Department of Physics, Moscow State University, Moscow 119899, Russia.

The $KTiOPO_4$ (KTP) and other crystals of this family are well known as excellent active elements for non-linear optical applications. At the same time they are of great scientific interest as representatives of a new specific variety of solid state materials, namely, ferroelectrics - superionics in which phenomena of electrical ordering combine with anomalous high ionic conductivity. The latter is attributed to the presence of movable alkaline or thallium cations in the wide channels along c-axis of the KTP-type structure and can be changed by way of heterovalent substitutions. On the other hand from previous investigations it follows that the conductivity of KTP crystals has a monotonous temperature dependence without any pronounced anomalies characteristic of many ordinary superionic crystals. The present study shows for the first time that large jumps of conductivity may be observed in the KTP crystals doped with niobium.

The crystals studied were grown with the use of flux method from the melts with the substitutions of 3-60 at.% of Ti by Nb with the slow cooling within temperature interval of 900 to 750ºC. As a rule the crystals had dimensions of order of several mm and week brown coloration which can be eliminated by heating in air atmosphere at 800-900ºC. The samples for conductivity studies were cut in the form of plates perpendicular to crystallographic axes and were supplied with silver electrodes. Measurements were made at the frequency of 1 Mc with the bridge Tesla BM 431E.

The conductivity jumps which are typical of superionic transitions were observed along c-axis in the crystals grown from the melts with 6-8 at.% Nb. Their value ranges up to 3 orders of magnitude depending on the crystal composition and thermal history. Temperature of such the jumps lies in the region from 20 to 400ºC and can vary up to several tens of degrees from one measurement to another for the same specimen. No noticeable changes were found in the crystal structure at these transitions so they seem to have a pure electronic nature.

P05.10.002 PHASE TRANSITIONS AND PHYSICAL PROPERTIES OF THE $K_3Nb_3B_2O_{12}$ CRYSTALS AND THEIR SOLID SOLUTIONS. E.P.Haritonova, V.I.Voronkova and V.K.Yanovskii. Department of Physics, Moscow State University, Moscow 119899, Russia.

$K_3Nb_3B_2O_{12}$ (KNB) crystals attract attention as new interesting solid state materials with the unusual combination of ferroelectric, antiferroelectric, ferroelastic and superionic properties. The main aim of the present work were growth of the KNB single crystals, pure and doped with Na and Ta, and the study of their phase transitions and physical properties.

Because of incongruent melting the KNB crystals with the sizes up to 2 cm were obtained by way of flux growth from the melts in the systems $K_2O(Na_2O)$-B_2O_3-$Nb_2O_5(Ta_2O_5)$. They had the appearance of colorless transparent hexagonal prisms with the well developed faces of prisms of the first and second type, hexagonal pyramid and pinacoids.

As follows from the x-ray analysis and investigations of optical and electrophysical properties the KNB crystals exhibit a complex sequence of phase transformations at 470, 400, 110, -85 and -97ºC. The diffuse transition at 470ºC with the large anomaly of dielectric permeability seems to be antiferroelectric with the appearance of antipolarization along the c-axis and multiplication of elementary cell, whereas the transition at 110ºC has ferroelectric nature. Other transitions are manifested in the formation of domain structure with the domain walls along $\{10\bar{1}0\}$ and $\{11\bar{2}0\}$ planes and in the changes of optical axes orientation and interference colors. At the room temperature the crystals show ferroelastic properties.

Partial substitution of K by Na increases the temperature of ferroelectric transition and decreases that of antiferroelectric transition. In the Ta doped crystals all the transitions became more diffuse and their temperature decreases. So, the temperature of ferroelectric transition in the crystals with 30 at.% Ta lies below 20ºC.

Electrical conductivity of the KNB crystals is found to be mainly ionic and has the value of order of 10^{-5} $Ohm^{-1}cm^{-1}$ at the room temperature. Phase transformations at 400 and especially 470ºC are followed by the conductivity jumps typical of superionic transitions.

P05.10.003 OPTICAL ROTATION IN THE LOW TEMPERATURE PHASE OF K_2ZnCl_4. D.-Y. Kim and W. Kaminsky, Clarendon Laboratory, University of Oxford, Parks Road, Oxford OX1 3PU, UK.

The recently developed 'tilter' method [1] was successfully utilized to measure the optical rotation and linear birefringence of K_2ZnCl_4 (KZC) in the temperature range between 50 K and 290 K. KZC exhibits a ferroelectric - ferroelastic phase transition from SG $P2_1cn$ to $C1c1$ at T_c = 145K [2]. In the room-temperature phase only the optical rotation component ρ_{12} is allowed by symmetry (The physical reference system is $\mathbf{x} // \mathbf{a}_3$, $\mathbf{y} // \mathbf{a}_2$, $\mathbf{z} // -\mathbf{a}_1$). Below T_c, a second component ρ_{23} arises as a result of the monoclinic symmetry.

Because there is a chiral lock-in modulation along ca. [110] in KZC due to the low-temperature super-structure [3] (this is along the diagonal between the y- and z-axis), we expected to observe an increase in optical rotation in the component ρ_{23}. Calculations with the dipole-dipole model [4] resulted in a jump of optical rotatory power of about 3 degrees/mm at 100K. Significantly increased optical rotation below T_c was indeed experimentally detected in ρ_{23}. The observed rotation showed a discontinuity of about ±2 degrees/mm at T_c and exchanged signs between different temperature runs as a result of domain formation. ρ_{12} seems to be less affected by the transition. The absolute values of birefringence measured as well, confirming an earlier observation which showed only the relative changes [5].

W.Kaminsky, A.M.Glazer (1996). Ferroelectrics **183** 133.
K.Gesi (1978). J. Phys. Soc. Jpn. **45** 1431.
M.Quilichini, G.Heger, P.Schweiss (1988). Ferroelectrics **79** 117.
V.Devarajan, A.M. Glazer (1986) Acta Crystallogr. **B44** 356.
S.V.Mel'nikova, I.N.Stolovitskaya, T.N.Davydova, A.T.Anistratov (1985). Fiz. Tverd. Tela **27** 2992.

P05.10.004 REAL STRUCTURE OF WO_3 CRYSTALS. O. Goncharova, K. Abdulvakhidov, M. Kupriyanov, Rostov State University, 5 Zorge, Rostov-on-Don, 344090, Russia.

Comprehensive structural characterization of ferroelectric single crystals performed by different x-ray diffraction methods seems to be a powerful method of testing possible microscopic mechanisms responsible for the changes in their physical properties under various external conditions.

In this work we studied the changes of real structure of antiferroelectric WO_3 crystals under constant electric fields.

The structural studies of the plate – like crystals by x-ray diffraction (HZG-4B diffractometer, CuKα radiation) included an investigation of domain and block structures and the peculiarities of the structural changes under electric fields. We studied twinning effects determined the lattice parameters and diffraction

effects affected by surface layers of crystals by measuring the x-ray scattering intensity distributions $Y(2\theta,\omega)$ near Bragg reflections and the changes of such distributions under electric fields by using a special device with electrodes transparent to x-rays.

Some new results obtained for WO_3 structure changes under different regimes of electric field application (field heating , field cooling) will be presented.

P05.10.005 CHANGES AT ATOMIC LEVEL IN DKDP UPON APPLICATION OF AN ELECTRIC FIELD. S.J. van Reeuwijk and H. Graafsma, European Synchrotron Radiation Facility, Avenue des Martyrs, 38043 Grenoble, France, P.H. Zwart, Laboratory of Crystallography, University of Amsterdam, The Netherlands.

The piezoelectric crystal DKDP, the 98% deuterated isomorph of KDP, potassium dihydrogen phosphate, undergoes structural changes upon application of an external electric field. The structural changes manifest themselves as 1) changes in unit cell parameters, giving rise to a shift of the reflection in direct space, and 2) changes in the electron density (atomic positions and polarisations), giving rise to a change in the diffracted intensity.

At the newly developed set-up at ID15C at the ESRF, a 0.3 mm thick, plate like and c-cut DKDP crystal was mounted on a 4-circle diffractometer. The faces of the crystal were covered with Al electrodes. Electric fields up to $1.3\cdot10^6$ V/m were applied parallel to the crystallographic c-axis.

From the relationship between the shift of the reflection due to the applied electric field and $\tan\Theta$ the d_{36} piezoelectric constant at room temperature was determined to be 52(2) pC/N, which is close to values reported in literature [1].

Due to the applied electric field the space group changes from I_{-42d} to F_{dd2}. Reflections *hkl* and *khl*, symmetry equivalents in space group I_{-42d}, are not related by symmetry in space group F_{dd2}.

The relative change in integrated intensity, $\Delta I/I$, was measured for 35 reflections. Merging the reflections, where R_{merge} = 23.09%, resulted in 11 unique reflections. The broken symmetry is clearly present in the data: $\Delta I/I$ for *hkl* differs significantly from $\Delta I/I$ for *khl*. The data are currently used to determine the changes in the atomic positions upon application of an electric field. The results of this refinement will be presented.

1. Landolt-Börnstein (1993), New Series III/29B, 151.

P05.10.006 TENSOR DISTINCTION OF DOMAIN STATES. V. Kopský, Institute of Physics AV CR, Na Slovance 2, 182 21 Praha 8, Czech Republic.

The phenomenon of the splitting of a material which undergoes a ferroic phase transition into domains is well know. Domains are distinct regions in the ferroic phase which are completely identical up to their orientation in space. The point symmetry of each domain is one of the set of conjugate subgroups F_i and its tensor properties are different with reference to the same co-ordinate system. The distinction between these properties is the first step in the consideration of boundary effects at interfaces of domain pairs. The numbers of independent tensor components in which domain states of pairs differ are available in the recent literature up to fourth rank tensors. We shall demonstrate tables from which explicit tensor components can be found which are either common to the pair or in which the pair differs. The solution is seen immediately in cases of the completely transposable domain pairs where the differing components have an opposite sign; other cases need further elaboration of the provided results. The tables will constitute a part of a software which is to be released as an appendix to *Vol. D: "Physical Properties of Crystals"* of the *International Tables for Crystallography* series. The components of the following tensors characterised by Jahn symbols are considered: enantiomorphism (chirality) ε, spontaneous polarization V and deformation (or permittivity) $[V]^2$, optical activity (gyrotropy) $\varepsilon[V]^2$, piezoelectricity (electro-optics) $V[V]^2$, electrogyration $\varepsilon V[V]^2$, linear elasticity $[[V^2]^2]$, and piezo-optics (electrostriction) $[V^2]^2$. Tables include also the explicit form of the electric and elastic switching interactions. The scheme is at the moment developed for the ordinary point groups but the extension to the magnetic point groups where domain pairs will be distinguished also by tensors which reflect magnetic effects is a matter of routine application of the same methods. The software is also a first step of a project of Group Informatics the aim of which is the standardisation and computerisation of group theoretical procedures.

P05.10.007 STRUCTURAL STUDY OF THE FERROELECTRIC AND PARAELECTRIC PHASES OF $PbNb_2O_6$. W.F. Reeve, Department of Physics. Clarendon Laboratory, University of Oxford, Parks Road, Oxford OX1 3PU, UK.

The structure of lead niobate ($PbNb_2O_6$) has been investigated using both synchrotron X-ray single crystal diffraction and neutron powder diffraction data.

Lead niobate is an industrially important ferroelectric that possesses a tetragonal tungsten bronze type structure. Previous structural studies had been limited to that of Labbé et al. [1] who deduced the prototype structure. For this study the single crystals have been grown by the flux method. The X-ray experiments have been carried out on the single crystal diffraction station at the Daresbury laboratory synchrotron light source in the U.K. This station is equipped with an area detector, which combined with the intense radiation from the synchrotron has allowed diffuse scattering from $PbNb_2O_6$ crystals to be observed.

Data collections at room temperature and above the Curie temperature of 840K have been undertaken. The room temperature phase is orthorhombic with lattice parameters a=35.292(3)Å, b=17.948(2)Å, c=7.736(1)Å, space group $Bb2_1m$. Both occupational and displacement disorder of the Pb atoms are present in the structure and from the study of the diffuse scattering patterns, short-range ordering models are presented. The high temperature phase is tetragonal with lattice parameters a=b=12.696(2)Å, c=3.880(1)Å, space group P4/mbm.

This work, coupled with powder neutron diffraction experiments at the ILL, France, has allowed accurate structural models for this material to be refined.

1. Labbé, O., Frey, M., Allais, G., *Acta Cryst.*, **B29**, 2204, (1973)

P05.10.008 STRUCTURE REFINEMENT OF AN AURIVILLIUS PHASE $Bi_5Ti_3FeO_{15}$ USING NEUTRON POWDER DIFFRACTION. T. Ko, Department of Ceramic Engineering, Inha University, 253 Yonghyun-dong, Nam-gu, Incheon, Republic of Korea and J. Lee, Korea Atomic Energy Research Institute, 150 Dukjin-dong, Yusong-gu, Taejon, Republic of Korea.

$Bi_5Ti_3FeO_{15}$ is a compound which has commensurate displacive modulations of constituent atoms in Bi_2O_2 layers and perovskite structural units. The room temperature structure[1] of this compound has been reported to have a space group of *F2mm*. However, our neutron powder diffraction revealed that some weak reflections would violate *F*-centering. Since the former study[1] was carried out using X-ray diffraction, it might not be possible to observe such weak scattering essentially from oxygen atoms. In this study, a diffraction measurement of $Bi_5Ti_3FeO_{15}$ was measured at HRPD of HANARO, which is a newly constructed research reactor in the Republic of Korea, with a constant wavelength of 1.8339 Å and a step scan of 0.05 deg using 32 multi-dectectors covering 0 ~ 160 deg. A Rietveld refinement

with a space group of $A2_1am$ was converged at R_p = 5.69%, R_{wp}= 7.36% and S = 1.715 for an isotropic temperature model with 59 variables. In contrast, with the space group of *F2mm*, the refinement was not successful. We observed that with the space group of $A2_1am$, the octahedra of transition metal atoms become tilted in a modulation mode of *Amam,* which is a soft mode related to the rotation of the octahedra about a polar *a* axis. This may create a rather coherent distribution of Bi-O distances in the perovskite units, compared to those of *F2mm*. Besides, a Fourier map shows that electron density is completely absent at Ti and Fe atom sites, suggesting that their atoms are disordered. For Bi atoms of the Bi_2O_2 layers, Bi –O distances of the layers are much shorter than the distances of the Bi atoms to the nearest apical oxygen atoms of the octahedra of the perovskite units. These Bi environments are highly asymmetric showing the effect of a lone pair of electrons.

F. Kubel & H. Schmid (1992). Ferroelectrics, 129, 101.

P05.10.009 CHANGE OF SURFACE MORPHOLOGY WITH THE STRUCTURAL PHASE TRANSITION IN $BaTiO_3$ SINGLE CRYSTAL. S.Doi and I.Takahashi, Advanced Research Center of Science (ARCS), School of Science, Kwansei Gakuin University, Sanda 669-1337, Japan

The emergence of self-organized structures on surfaces, triggered by the phase transition or generated in the crystal growth process, is a very surprising phenomenon we often encounter. These intriguing structures are commonly characterized by the spatial and temporal *pattern formation*.

Dielectric substances, which generally turn into a complex polydomain structure at the structural phase transition, could be analogous to the above systems. In the dielectric crystal, since the average size of domains is small, say, in '*mesoscopic*' length scale in the vicinity of transition temperature T_c, the domain configuration is subject to thermal excitation, external electric field or stress, and fluctuations of order parameter. In the case of perovskite-type crystals which exhibit a variety of phase transitions such as ferroelectric or ferroelastic transition, a typical '*a-c*' 90°domain structure arises and the occurrence and temperature evolution of this domain arrangement affect directly on the surface morphology. Therefore, a unique pattern of surface morphology and a surface critical behavior with the phase transition induced by various fluctuations could be observed with varying temperature.

We investigated the morphology of $BaTiO_3$ (001) surface through the cubic-tetragonal phase transition by using the X-ray reflectivity (XR) technique, which is sensitive to surface structure at wide spatial length scale. We obtained information on the domain structure of crystal surface from XR peak profiles, like as the change of Bragg diffraction pattern due to the domains in bulk. We will report in detail about novel aspects of the surface behavior as compared with the bulk.

P05.10.010 STRUCTURES OF DEUTERATED FERROELECTRIC TRICHLOROACETAMIDE AS STUDIED BY NEUTRON POWDER DIFFRACTION. M. Hashimoto, S. Matsumoto, M. Ozawa, Department of Chemistry, Faculty of Science, Kobe University, Nadaku Kobe 657-8501, Japan Y. Kamishina, Faculty of Education, Shimane University, Matsue 690-8504, Japan,T. Kamiyama, Institute of Materials Science, University of Ttsukuba, Tsukuba, Ibaraki 305-8573, Japan, and F. Izumi, National Institute for Research in Inorganic Materials, Ibaraki 305-0044, Japan

Phase III of trichloroacetamide (Cl_3CCONH_2, TCAA) undergoes a ferroelectric transition at 354.6 K (ca.353K for Cl_3CCOND_2, TCAA-d) to give phase II, which is transformed into phase I at 356.9K[1]. At the high temperatures the X-ray work was difficult owing to vigorous sublimation of the compound. In the present work the crystal structures of TCAA-d at 90, 300, 343 K (phase III) and that at 370 K (phase I) were investigated by neutron powder diffraction method. The crystal data at 300 K [those at 370 K]: monoclinic [monoclinic], space group $P2_1$ [$P2_1$], a=1041.13(4) [1046.48(7)], b=578.41(2) [581.87(3)], c=1017.30 [1021.77(8)] pm, β=107.616(3) [107.611(2)] degrees. The structural changes due to the phase transitions were found to be quite subtle. A small angle reorientation of the CCl_3 group in one of the two independent TCAA-d molecules is likely to be accompanied by the phase transition(s). One of the four N-D...O hydrogen bonds in phase III seems to include a weak N-D...Cl interaction.

1. Y. Kamishina, Y. Akishige & M. Hashimoto (1991) J. Phys. Soc. Jpn., 60, 2147.

P05.10.011 EVEN AND ODD EFFECT IN STRUCTURE OF $C_nH_{2n+1}NH_3H_2PO_4$ CRYSTALS. H.Kasatani, Department of Materials Science, Shizuoka Institute of Science & Technology, 2200-2 Toyosawa, Fukuroi, Shizuoka 437-8555, JAPAN, and H.Terauchi, Advanced Research Center of Science & School of Science, Kwansei-Gakuin University, Sanda, Hyogo 669-1337, JAPAN, and M.Iwata and Y.Ishibashi, Department of Applied Physics, School oh Engineering, Nagoya University, Chikusa-ku, Nagoya 464-8601, JAPAN.

The title new compounds of *n*-alkyl ammonium dihydrogen phosphate, ($C_nH_{2n+1}NH_3H_2PO_4$, abbreviated as C_nADP), with 1-9 and 12 have unique properties; such as ferroelasticity, successive phase transitions and even and odd effect[1]. The x-ray single crystal structure analyses of C_nADP with n=2-6 were carried out at room temperature in order to clarify the even and odd effect[2,3]. The crystal system of these compounds was monoclinic system and the space group was $P2_1/n$(Z=8). The characteristics of these crystal structures were that the anti-parallel planner organic chains ($C_nH_{2n+1}NH_3$) were along *b*-axis, and the inorganic PO_4 tetrahedra were bonded by ordered H-atoms in *b*-plane. On the other hand, two different points for these crystal structures were observed. One was the difference of the molecular kind on 2_1-screw axis. Another was the difference of the packing pattern of the methyl group of the end parts in the anti-parallel planner organic chains. It is thought that these differences on crystal structure were related to the even and odd effect.

[1] J.Kroupa & A.Fuith (1993). Phys. Rev., **B48**, 4119.
[2] H.Kasatani, M.Iwata, Y.Ishibashi & H.Terauchi (1998). J. Korean Phys. Soc., **32**, S1807.
[3] H.Kasatani, M.Iwata, H.Terauchi & Y.Ishibashi (to be published in proceedings of AMF-2).

P05.10.012 A STUDY OF THE FREQUENCY DEPENDENCE OF THE DIELECTRIC MAXIMUM IN PMN-PT CERAMIC. V. K. Wadhawan, Gurvinderjit Singh and V. S. Tiwari, Laser Materials Laboratory, Centre for Advanced Technology, Indore 452 013, India

We have synthesized (by the coulombite route) the relaxor-ferroelectric ceramic PMN-PT ($PbMg_{0.3}Nb_{0.6}Ti_{0.1}O_3$). Processing conditions were optimized to achieve 95% of the theoretical density for the ceramic. The material was investigated for its dielectric behavior at various temperatures and frequencies. The maximum relative dielectric constant obtained by us is 18000 at 1 kHz. Polarization hysteresis behavior was also studied in a wide temperature range, as also the electric-field-induced strain. As expected for a relaxor ferroelectric, the real part of the dielectric constant showed a maximum (ε_m) at a characteristic temperature T_m, and ε was found to obey the equation $1/\varepsilon = 1/\varepsilon_m [1+(T-T_m)^{\gamma}/2\delta^2]$. The parameters γ and δ exhibit a parabolic dependence on the probing frequency (for the range 100 Hz to

100 kHz). The observed dielectric relaxation times were found to be best explained by the equation $\tau = (\omega_0)^{-1} \exp[T_0/(T_m-T_f)]^p$. The `best-fit' parameters are: $\omega_0 = 3.6 \times 10^8$ Hz, $T_0 = 172$ K, $T_f = 179$ K, and $p = 12.76$. The introduction and use of this equation by us [which is a modification of the equation used by Cheng et al. (*J. Appl. Phys*., **79**, 8615 (1996))], is an improvement, in the sense that we do not assume that $T_f = 0$; only for a Debye solid can T_f (the freezing temperature) be zero.

P05.10.013 SEPARATING LEAD(II) FROM BISMUTH(III) IN METAL OXIDES BY ANOMALOUS DISPERSION METHODS. Brendan J. Kennedy, School of Chemistry, The University of Sydney, Sydney, NSW 2006, Australia.

Lead(II) and bismuth(III) are isoelectronic and contain 6s electrons that can exhibit sterochemical activity. The similarity of the structural requirements of Pb(II) and Bi(III) leads to the possibility of disorder of these cations over available sites, which can be difficult to detect using "chemical knowledge". PbBi2Nb2O9 is an important ferroelectric oxide that adopts a two-layer Aurivillius structure, where the Pb is in the perovskite type blocks that are separated by (Bi2O2) layers. Thermal treatment of this oxide alters the ferroelectric properties of this material and the cell volume and these observations offer indirect evidence for site disorder, where some of the Pb is located in the (Bi2O2) layers. Powder neutron studies apparently confirm the presence of such disorder however since Pb and Bi have similar neutron scattering lengths the results were less definitive than anticipated.

In the present presentation we describe the use of anomalous dispersion methods to quantify the Pb/Bi site disorder in PbBi2Nb2O9. High quality powder diffraction data was collected, using synchrotron radiation, above and below both the Pb and Bi L(III) edges. The structure was then refined using these data, together with powder neutron diffraction data, by the Rietveld method. Attempts to chemically control the extent of disorder through doping of the oxides with Sr or Ba will also be presented.

P05.10.014 PHASE DIAGRAMS AND CORRES-PONDING PROPERTIES OF ISOMORPHOUS CRYSTALS $CH_3NH_3\ Bi_2X_{11}$, X = Cl Br. E.S.Larin and Yu.M.Gufan, North Caucacian Scientific Centre,344006 Rostov on Don, Russia, and K.Gesi, Department of Material Science , Ivaki, Fokushima, 970-8551, Japan .

Two members of a rich family of alkilammonium halogenobismuthate crystals suffer successive phase transitions (PT) with the same changing of symmetry D_{2h}^{15} - C_{2v}^5 - C_{2v}^5 - C_2^1. Both compounds crystallized in the form of pseudohexagonal prism. It suggests the idea that theirs parent phase (PPh) is characterized by the hexagonal symmetry. The (PPh) approximation (PPhA) represents the first step of perturbation theory in the framework of Landau Theory (LT) of PT . The actual one-component order parameter (OP) describing PT C_{2v} – C_2 in the PPhA becomes two- component (e_1 e_2) ferroelastic OP , which insert the third order invariant in the Landau potential. According the theory, basing on Landau Potential, $F = A_1P_z^2 + A_2P_z^4 + a_1I_1 + a_2I_1^2 + a_3I_1^3 + b_1I_2 + b_2I_2^2 + +c_{12}\,I_1\,I_2$ (Here $I_1 = c_1^2 + c_2^2$, $I_2 = e_1^3 + 3e_1e_2^2$) the isostructural PT C_{2v}^5 - C_{2v}^5 exists as a natural consequence of the third – order invariant in the Landau potential. On the basis of the LT with two interacting OP's (ferroelastic two-components) and ferroelectric (Pz) we constructed the phase diagram and defined the thermodynamic paths , which are proper for $(CH_3NH_3)_5Bi_2X_{11}$ (X=Cl (MAPCB) or Br (MAPBB)). The MAPBB's path crosses the line of IPT and path of (MAPCB) crosses the trace continuing IPT after critical endpoint. The corresponding differences in dielectric and elastic modulus anomalies for these two compounds, originate from the differences of theirs thermodynamic paths. In this research the complete set of dielectric susceptibilities, elastic modulus and lattice constants dependencies on the temperature are estimated in the framework of LT basing on the PPhA. We are grateful to Russian Fund of Basic Researches for financial support .

P05.10.015 EFFECT OF LAYER BISMUTH COMPOUNDS IN RELATION TO THE STRUCTURAL MODIFICATION OF FERROELECTRIC $BaTiO_3$. Sujata Mazumdar, Central Glass & Ceramic Research Institute, 196 Raja S.C.Mullick Road, Calcutta- 700032, INDIA

Ferroelectric $BaTiO_3$ with certain structural modification is considered for special application in electronic industry [1]. Modifiers chosen for present study are primarily perovskite like layered bismuth componds [2] with general formula $(Bi_2O_2)^{2+}$ $(A_{m-1}B_mO_{3m+1})^{2-}$ where A is a combination of ions adequate for twelve coordinated interstices, B is a combination of ions adequate for octahedrally coordinated sites and m is an integer between 1 & 7. The crystallo-chemical study for the choice of metal ions in A and B of the original lattice have been done. The stability of the structure is lost by dimensional mismatch between perovskite layer and bismuth oxide layer. Based on the theory that site potentials of oxygen ions in an oxide perovskites are more or less same, combination of $BaTiO_3$ as well as modifier perovskites can easily produce either a chemical homogenity or controlled chemical heterogenity within the structure under suitable experimental condition. The results of the x-ray analysis on the determination of structures of modified $BaTiO_3$ has been discussed in order to establish the structure-dielectric property correlation.

1. Electronic Ceramics, Properties,Devices and Applications, ch. IV ,pp 197-200, edited by Lionel M. Levinson,U.S.A Marcel Dekker,inc.
2. E.C.Subbarao, A Family of ferroelectric Bismuth Compounds, J.Phys.Chem.Solids. , 23 , pp 665-675(1962).

P05.10.016 STRUCTURAL AND MAGNETIC PROPERTIES OF $(Fe_{1-x}Mn_x)_3P$ COMPOUNDS. Hui-ping Liu,[1] Y.Andersson,[1] P.James,[2] O.Eriksson[2] B.Kalska[2], L.Häggstöm[2], A.Broddefalk,[3] P.Granberg,[3] and P.Nordblad[3], [1]Dept. of Inorg. Chem., Box 538, S-751 21, Uppsala University, Sweden, [2]Dept. of Physics, Box 530, S-751 21, Uppsala University, Sweden, [3]Dept.of Materials Science, Box 534, S-751 21, Uppsala University, Sweden

In $(Fe_{1-x}Mn_x)_3P$ system, the tetragonal Fe_3P-type structure [1] predominate. The substitution range of Mn for Fe on the Fe-rich side was found to be $x < 0.25$, which is less than the previous reported 0.3 [2], while on the Mn-rich side, it was found to be $x > 0.65$.

The structural and magnetic properties of $(Fe_{1-x}Mn_x)_3P$ compounds have been investigated by means of X-ray and neutron powder diffraction experiments, magnetisation measurements, Mössbauer Spectrum and first principles calculations. The substitution of Fe with Mn leads to an enlargement of the crystal unit cell, since the radius of Mn is larger than that of Fe. The occupancies and magnetic moments on the three non-equivalent metal sites are determined. Results show that Mn preferentially substitutes Fe on two of the metal sites. The magnetization measurements on the Fe-rich side indicate that the compounds order ferromagnetically below the Curie temperature. Both the saturation magnetisation and T_c decrease with increasing Mn content. But on the Mn-rich side, antiferromagnetic ordering lowers the magnetic moments significantly. Both the moments and T_N drop with the Mn concentration. Pure Mn_3P posses a very small net magnetic moment, the T_N was found around 35 K which is not consistent with the previous reported $M_{Mn} = 1.68\mu_B$, $T_N = 115$ K [3].

S.Rundqvist, Acta Chem. Scand. 16, 1-19(1962).
M.Goto et al. Jpn. J. Appl. Phys.16 (1977) 2175.
R.J.Gambino et al., Journal of Applied Physics.Vol.38, No.3 (1967)1253.

P05.10.017 CRYSTAL STRUCTURE AND DIELECTRIC RELAXATION STUDIES IN $[N(CH_3)_3H]_3Sb_{2(1-x)}Bi_{2x}Cl_9$ (TMACAB). J. Zaleski and G. Bator Institute of Chemistry, University of Opole, Oleska 48, 45-951 Opole, Poland Faculty of Chemistry, University of Wrocław, Joliot-Curie 1450-383 Wrocław, Poland

$[N(CH_3)_3H]_3Sb_2Cl_9$ (TMACA), ferroelectric at room temperature, belongs to the family of alkylammonium halogenoantimonates(III) of the general formula $R_aSb_bX_{(3b+a)}$ (R - alkylammonium cation, X - chlorine, bromine or iodine) [1].

The crystal structure of TMACA is characterised by the two-dimensional layer structure of polyanions [2]. In the ferroelectric phase there are three non-equivalent $NH(CH_3)_3^+$ cations in the crystal structure . Two of them, placed between the layers, are ordered while the third one, located inside a voids of the anionic sublattice is disordered.

The dielectric response in TMACA around $T_c = 364$ K exhibits features typical of a para-ferroelectric phase transition. The macroscopic dielectric relaxation time in the paraelectric phase in TMACA shows "critical slowing down" close to T_c.

It is well known, that the physical properties of the crystals may be modified by the exchange of the metal atoms (Sb→Bi) in the crystal lattice. A strong influence on the value of ε (a drastic reduction) at the phase transition and a shift of T_c toward higher temperature, with the increase of the Sb contents was found e.g. in the $[CH_3NH_3]_3Bi_{2(1-x)}Sb_{2x}Cl_{11}$ [3].

In the present contribution we present results of the investigation of the influence of the metal atom replacement on the structure and dielectric properties of the mixed $[N(CH_3)_3H]_3Sb_{2(1-x)}Bi_{2x}Cl_9$ (TMACAB) crystals. The determination of the phase diagram, for TMACAB is interesting from the point of view of possible technical applications and particularly, the recognition of the influence of the concentration of impurities on the dynamical properties of these crystals.

1. L. Sobczyk, R. Jakubas and J. Zaleski, Polish J. Chem., **71** (1997) 265.
2. A. Kallel and J.W. Bats, Acta Cryst., C41 (1985) 1022
3. R. Jakubas, G. Bator, J. Zaleski, A. Pietraszko and R. Decressain, J. Phys.: Condens. Matter, **8** (1996) 367.

P05.10.018 PHASE TRANSITION AND STRUCTURE OF $K_2Fe(SO_4)\cdot 2.2H_2O$. H. Ishigami, M. Sumita [1], S. Sato [2], T. Hikita [3], [1] Faculty of Engineering, Shibaura Institute of Technology, [2] X-ray Research Laboratory, Rigaku Corporation, [3] School of Engineering, Tohoku University

$K_2Fe(SO_4)\cdot 2.2H_2O$ shows anomalies of specific heat and electric susceptibility at 364 K [1]; structural details were not reported so far. Very recently we have determined the crystal structure of the compound at 297 K and 373 K.

The crystal structure of triclinic $K_2Fe(SO_4)\cdot 2.2H_2O$ at 297 K was determined by use of an automatic four circle X-ray diffractometer in space group P1, a=7.308(1), b=10.816(2), c=6.531(1)Å, α=109.03(1), β=110.50(2), γ=94.53(1)º, V=446.1(2)A^3, Z=2.

The cell dimension at 373 K are; a=7.296(2)A, b = 5.377(2)A, c=6.567(2)A, α=107.99(2), β=110.13(2), γ=94.59(2)º, V=446.1(2)A^3, Z=1. The space group was P-1. This crystal undergoes a phase transition at 364 K.

The phase is transformed to the same triclinic structure, but the space group is different P1-P-1. The structure successfully converged: R=0.025, R_w=0.045 and S=1.94 for the low temperature phase, and R= 0.034, R_w=0.069 and S=2.21 for the high temperature phase.

H. Ishigami and M. Sumita (1998). Ferroelectrics 217, 201.

P06.10.001 MODULATED CRYSTAL STRUCTURE OF $Sr_6Rh_5O_{15}$. C. Schinzer, Institut de Chimie de la Matière Condensée de Bordeaux (I.C.M.C.B.–CNRS UPR 9048), Av. Dr. A. Schweitzer, F-33608 Pessac cedex, France.

The compound $Sr_6Rh_5O_{15}$ has been synthesized by standard solid state techniques starting from $Sr(NO_3)_2$ and $Rh_2O_3 \cdot 5\ H_2O$.

A structural model has been proposed previously by Claridge and zur Loye [1] on the basis of x-ray powder data. The structure is described as a variant of the $Sr_6Co_5O_{15}$ type which is a n = 1 member of the so-called Darriet-Subramanian-phases [2] with general formula $A_{3+3n}A'_nB_{1+3n}O_{9+6n}$ (A = Sr; A', B = Rh). Claridge and zur Loye have been able to refine their product in a superstructure of the ideal $Sr_6Co_5O_{15}$ type doubling the hexagonal lattice parameter a with good reliability.

However, electron microscopy studies of our product indicate an incommensurately modulated structure. The modulation vector was determined on the basis of the ED pattern, which was indexedusing four Miller indices [3]. The modulation is one-dimensional obeying the value

u* = (0 0 0.608).

A subsequent translation of these results into the setup of the unit cell of $Sr_6Co_5O_{15}$ allowed to perform Rietveld refinements of the modulated structure on synchrotron powder patterns using the SIMREF 2.5 software [4].

Possible descriptions of the structure of $Sr_6Rh_5O_{15}$ comprise compositionally or displacively modulated as well as composite models with 3D subcells for the Sr- and the Rh-O networks.

The results of Rietveld refinements and of several chemical substitutions (series Sr_xRhO_3; $Sr_6ARh_4O_{15}$, A = Ca, Mg, Zn) will be presented.

[1] J. B. Claridge & H.-C. zur Loye (1998). J. Mater. Chem. xx, xxx, 1998.
[2] J. Darriet & M. Subramanian (1993). J. Mater. Chem. 83, 287, 1993.
[3] F. Weill & C. Schinzer (1998). unpublished results.
[4] H. Ritter, K. Maichle, W. Prandl & J. Ihringer (19xx). SIMREF 2.5 – a software for simultaneous refinement of powder diffraction data. http://www.uni-tuebingen.de/pki/simref

P06.10.002 DEBYE-WALLER FACTORS IN A QUASICRYSTAL. R. Colella, Y. Zhang, J. P. Sutter, S. N. Ehrlich, Purdue University, Dept. of Physics, West Lafayette, IN 47907-1396, U.S.A. and S. W. Kycia, CHESS, Cornell University, Ithaca, NY 14853-8001, U.S.A.

The mean square vibrational amplitude $< U^2 >$ for five reflections located on a two-fold axis of an icosahedral quasicrystal $Al_{71.0}Pd_{20.5}Mn_{8.5}$ have been determined between room temperature (RT) and below 20 K by x-ray diffraction. Their Q-vectors ($Q = 2\sin\theta/\lambda$) range from 1.278 $Å^{-1}$ to 2.556 $Å^{-1}$. For four reflections, the logarithm of the integrated intensity is linear, proportional to temperature, near and below RT, and tends to saturate to a constant value at low temperatures (LT), an effect of the zero point energy. It is assumed that $< U^2 >$ is contributed mostly by low frequency acoustic modes, for which the atoms of Al, Pd and Mn vibrate together. All plots for these four reflections are indeed linear at RT and below, and saturate at LT to values that are different from those predicted by Debye theory. This behaviour is reminiscent of that of layered crystals[1] such as graphite or TaS_2, in which the anomaly could be explained by considering the effect of reduced dimensionality and anisotropy,

none of which can be applied to icosahedral quasicrystals. Furthermore, the Debye temperatures obtained from the linear regions of the four plots are substantially different, for different Q's. The fifth reflection (Q = 2.252 $Å^{-1}$) displays a temperature dependence that does not lead to a single mean square vibrational amplitude. In other words, the logarithm of the integrated intensity is not linear with temperature in the high temperature region (T ≥ 100 K). Since the fifth reflection is very weak, it is possible that a strong negative interference between different atoms is taking place. In this situation it is no longer permissible to talk about a single ``global" Debye-Waller factor, corresponding to a single vibrating mass.

Work is in progress to understand the physical origin of non-Debye behaviour in a quasicrystal.

1 S. M. Hsieh and R. Colella, Solid State Commun. **63**, 47 (1987).

P06.10.003 A (3+1+1) MISFIT LAYER OXIDE COMPOUND: $Bi_{1.85}Sr_2Co_{1.85}O_{8-\delta}$. D. Grebille, H. Leligny, O. Pérez, A. C. Masset, M. Hervieu and B. Raveau, Lab. CRISMAT (UMR CNRS 6508), ISMRA, 6 Bd du Maréchal Juin, 14050 Caen cedex France.

The system Bi-Sr-Co-O is rich of a lot of modulation phases, closely related to the family of high T_c superconducting oxides. A new compound $Bi_{1.85}Sr_2Co_{1.85}O_{8-\delta}$ was synthetized and present original features. Its structure was refined using X-ray single crystal diffraction data.

The electron and X-ray diffraction patterns clearly show a composite structure with two subsystems of monoclinic symmetry, sharing **a** and **c** cell parameters but with irrationnaly related **b** parameters (**a** = 4.905 Å, $\mathbf{b}_I$ = 5.112 Å, $\mathbf{b}_{II}$ = 2.808 Å,**c** = 29.857 Å, β = 93.45°). Moreover, the first subsystem is also characterized by an intrinsic incommensurate modulation with a wave vector $\mathbf{q}^*_{11}$ = 0.293(2) $\mathbf{a}^*_{11}$ +0.915(2) $\mathbf{a}^*_{13}$ in the common monoclinic plane. Structure refinement was achieved using the 5D superspace formalism (superspace group I2/a (α 0 γ, 0 μ 0) pmm or I2/a (α 0 γ, 1 μ 0) pmm) leading to very satisfactory agreement factor (R_G=0.0405, R^I_0=0.0335, R^I_1=0.0427, R^I_2=0.1090, $R^{I,II}$=0.0319, R^{II}_0=0.0817).

Subsystem I appears to be very similar to the usual modulated [$BiSrO_2$] layers of the so called 2201 type structure with regards to the longitudinal modulated displacements. Subsystem II is consistent with the coexistence in the same crystal of two variants with different centering conditions, built from the stacking of [CoO_2] layers. The interaction between the two subsystems appears to be very weak and could not be measured.

This structure can be compared with equivalent sulphur compounds, but is quite original in oxide systems.

P06.10.004 SURFACE STRUCTURE OF $Sr_2Nb_2O_7$ (010) STUDIED BY X-RAY DIFFRACTION. R.Suetoshi[1], S.Doi[1], I.Takahashi[1], and K.Ohi[2], [1]Advanced Research Center of Science(ARCS), Kwansei Gakuin University, Sanda 669-1337, Japan, [2]School of Science and Engineering, Waseda University, Tokyo 169-0072, Japan

Many dielectric substances are known to possess incommensurate (IC) phases between the disordered (paraelectric) and the ordered (ferroelectric or ferroelastic) phases. Although such an interesting phase transition should be ascribed to some competing interactions, we do not know how a crystal acquires the long-period which often exceeds hundreds Angstrom. A breakthrough, which should be brought by a novel experiment, is surely longing. On the other hand, effects of the bulk IC structures on the surface structures have been scarcely dealt with as yet. We started to investigate the surface structure of IC dielectrics on a microscopic standpoint, since this problem is thought to gives us a key to reveal the origin of the bulk IC phase transitions. In the present study, we investigate the (010) surface of strontium niobate ($Sr_2Nb_2O_7$), which has the IC structure at room temperature. $Sr_2Nb_2O_7$, which is composed of slabs with distorted perovskite type octahedra stacked along the [010] axis, has the strong cleavage parallel to the b-plane. Since the (0k0) CTR (Crystal Truncation Rod) scattering from the cleaved (010) surface was observed clearly, we found that the surface was flat in atomic level. After least-squares procedures, the probability of finding the Sr atom at the top of the surface, which occupies on the right site, is about 50%. This fact leads us to consider that half of the Sr atoms were lost or arranged disorderly when the crystal was cleaved. Moreover, the diffuse scattering emanating from satellite reflections almost perpendicular to the (010) surface such as connecting each satellite was observed. The diffuse scattering had been observed by electron microscopy and regarded as the effect of the irregularity of modulation wave due to phase shift in some perovskite-type slabs[1]. Temperature dependence of these scatterings is now in progress, we would like to present the quantitative evaluation of the IC structure at the surface and in bulk.

[1] Yamamoto, N. (1983). *Acta Cryst.* B **39**, 210-216.

P06.10.005 THE LARGEST RATIONAL APPROXIMANT TO THE DECAGONAL PHASE IN THE SYSTEM Al-Co-Ni Katja Lemster[1], Michael E. Estermann[1], Walter Steurer[1] & Benjamin Grushko[2] [1]Laboratory of Crystallography, Swiss Federal Institute of Technology, CH-8092 Zurich, Switzerland [2]IFF, Research Center Julich, D-52425 Julich, Germany

A novel decagonal approximant with the largest unit cell of all known intermetallic compounds was found in the system Al-Co-Ni. This approximant is a link of the transition between quasicrystal and crystal. The structure of the approximant with nominal composition $Al_{71}Co_{14.5}Ni_{14.5}$ was solved with single-crystal X-ray diffraction techniques.

Although the unit cell shows almost orthorhombic symmetry, with unit cell parameters of a = 8.17(5)Å, b = 75.05(5)Å, c = 78.90(5)Å, α = 90.02(5)°, β = 89.99(5)°, γ = 89.98(5) °, the diffraction symmetry is monoclinic with space group $P2_1/n$ (unique axis **c**).

The intensity distribution of Bragg peaks shows strong tenfold pseudosymmetry. The monoclinic axis **c** is perpendicular and not parallel to the pseudosymmetric tenfold direction, which runs along **a**. A columnar cluster (*monopteros*) with an average fivefold symmetry is found as a structural building unit [1].

The structure was solved with “image seeking” Patterson methods [2].

In our contribution we want to show the process from the data collection to the refinement of the structural model. With respect to the size of the unit cell, the pseudosymmetry, and the numerous diffraction data we shall demonstrate useful methods and techniques for this kind of problem.

Steurer, W., Haibach, T., Zhang, B., Kek, S. & Lück, R.: The structure of decagonal $Al_{70}Co_{15}Ni_{15}$, Acta Cryst. B**49** (1993), 661-675.
Estermann, M. A.: Solving Crystal Structures with the Symmetry Minimum Function, Nuclear Instruments and Methods in Physics Research, Section A **354** (1995), 126-133.

P06.10.006 APERIODIC CRYSTAL STRUCTURE AND CONDUCTIVITY OF DENTAL ENAMELS AND A SPECIAL PORCELAIN ENAMEL. Nguyen Van Tri, Institute of Engineering Physics, Hanoi University of Technology, Hanoi, Vietnam.

From the experimental results on the temperature variation of electrical resistivity of dental enamels and of a special porcelain

enamel, a special conduction effect of these enamel films was revealed : At normal room temperatures these enamels are highly insulative and with rising temperature they experience a very strong increase in conductivity. Especially, once the temperature falls to below the room one these enamels transform suddenly into good conductors. This particular property of the enamels is similar to that for the typical stable quasicrystal material recently discovered, basically made of seventy atomic percent of Aluminium and of transition metals[1].

On the other hand, the careful ESR studies on these non-crystalline enamel films suggest that the films show a very outstanding angular dependence effect being exactly the same as of a single crystal sample with a typical highfold axial symmetry. The symmetry axis is perpendicular to the enamel surface. The ESR results also suggest detailedly this quasicrystal effect is closely connected with the fivefold symmetry combination clusters distributed in the enamel film, whose planes are parallel to enamel surface. Every this fivefold structure unit is combined by fivefold (2F-2A) rhombs of four spin centers super-exchange-interacting and creating two diagonal spin couple pairs : the pair A (Antiferromagnetic) on the long diagonal with a high population density of the singlet electron state at lower temperatures and the pair F (Ferromagnetic) on the short diagonal with a high population density of the singlet electron state at higher temperatures. Evidently, the particular properties of the enamel are in close internal connection with this electronic dynamics of its quasicrystal structure.

Wonderly, the fivefold combination clusters in the mentioned enamels are also observed directly to the first time by the respective AFM recordings.

1. J.M. Dubois, Supplement to Acta Crystallographica Vol. 52, IUCr XVII Seattle Washington USA 1996, C-3.

P06.10.007 MAXIMUM ENTROPY ATOMIC SURFACES RECONSTRUCTION: THE *nD* STRUCTU- RE OF DECAGONAL AlOsPd. A.Cervellino, T.Haibach and W.Steurer, Laboratorium für Kristallographie, ETHZ, CH-8092 Zürich, Switzerland.

The power of the Maximum Entropy method to reconstruct the electron density[1] has been effectively combined with the simplicity of the *nD* embedding model[2] to describe a decagonal phase[3]. AlOsPd is the largest existing decagonal ($P10_5/mmc$) quasicrystal. Its z-period is 16.750(3)Å, comprising eight layers. The electron density peaks in the Maximum Entropy-reconstructed asymmetric unit have first been localized in very good agreement ($\sim 10^{-2}$Å) with the corresponding βZ module-inferred coordinates. The electron density peaks have then been integrated and lifted on the corresponding atomic surfaces. Two important indications are hence obtained: the chemical partition of the atomic surfaces and the estimate of the z-displacements from the average layers located at the eighths of the z-period.

1. Haibach,T., Cervellino,A., & Steurer,W. (1998), Z. für Krist. Suppl., **15**, 140.
2. Cervellino,A., Haibach,T., & Steurer,W., (1998), Phys. Rev. B, **57**, 11223.
3. Haibach,T., Cervellino,A., & Steurer,W., (1999), in preparation.

P06.10.008 TWO FLUORITE-RELATED PHASES AND THEIR MODULATED STRUCTURES IN Bi_2O_3-Ta_2O_5 OXIDES. R. Miida and T. Saito, SUT, Suwa College, Toyohira 5000-1, Chino, Nagano 391-0292, Japan, and M. Tanaka, RISM, Tohoku University, Sendai 980-8577, Japan

In the oxides $(Bi_2O_3)_{1-x}(Ta_2O_5)_x$, a fluorite-related phase has been reported to exist in the compositional range from x=0.21 to 0.25 [1]. In addition to that, another fluorite-related phase was recently found at compositions between x=0.05 and 0.08, and these two phases were called as FI for $0.21<x<0.25$ and FII for $0.05<x<0.08$ [2]. In the present study, we examined these phases by means of electron diffraction and microscopy.

The diffraction pattern of FI showed satellite spots at $n\boldsymbol{q}\boldsymbol{G}_{111}$ (n=1, 2, . . ,) and equivalent positions with them together with the fundamental Bragg spots, where $\boldsymbol{G}_{111}$ denotes the 111 reciprocal lattice vector. The value of q varies from 0.373 to 0.380 with increasing x in the FI zone. The diffraction pattern is quite similar to that of Bi_2O_3-Nb_2O_5 reported already. [3].

The diffraction pattern of FII showed a pair of diffuse spots at $(\frac{1}{2}\pm\pm)\boldsymbol{G}_{111}$ and equivalent positions with them, where q varies from 0.125 to 0.135 with increasing x in the uniform zone. The pair of diffuse spots can be regarded as the reflections split from the $\frac{1}{2}\frac{1}{2}\frac{1}{2}$ superlattice reflection due to the introduction of pseudo-periodic anti-phase boundaries (APBs) parallel to the (111) planes. The structural model for q=0.125 contains APBs at intervals of $4d_{(111)}$ ($d_{(111)}$=spacing of (111) planes) in the displacement type ordered structure with the period of $2d_{(111)}$. The introduction of APBs modifies the sequence of local periods in the [111] direction as . 123212321232 in $d_{(111)}$ unit. A sinusoidal modulation with the period of $8d_{(111)}$ is imposed on the atomic displacements. The model roughly reproduces the intensity distribution in the electron diffraction pattern.

1. T. Takahashi, et al. (1977). J. Electrochem. Soc. **124** 1563.
2. T. Saito and R. Miida. to be published.
3. R. Miida and M. Tanaka (1990). Jpn. J. Appl. Phys. **29** 1132.

P06.10.009 PARTICLE SIZE DISTRIBUTIONS AND STRUCTURE INVESTIGATIONS IN SYSTEMS OF COLLAPSED GELS. E.V.Shtykova, D.I.Svergun and A.T.Dembo, Institute of Crystallography, Russian Academy of Sciences, Leninsky pr., 59, 117333 Moscow, Russia, L.M.Bronstein and P.M.Veletsky, Nesmeyanov Institute of Organoelement Compounds, Rassian Academy of Sciences, Vavilov st., 28, 117813 Moscow, Russia and A.R.Khokhlov, Physical Department, Moscow State University, Russia.

Small-angle X-ray scattering is used to study collapsed gel structures and size distributions of metal nanoparticles embedded in polyelectrolyte hydrogels with oppositely charged surfactants. A procedure is proposed to subtract matrix scattering and to extract pure scattering due to the nanoparticles allowing to evaluate their size distribution functions by means of a regularization technique.The main results of the study are the following: metall compounds in the gels form small clusters transforming into pure metal particles after reduction;collapsed gel/surfactant complexes stabilize the nanoparticles produced;the ordering in the collapsed gels structure is preserved upon reduction if the gel charge coincides with that of the metal ions;fast reduction yields much smaller particles than the slow one;metal ion charge and geometry influence considerably the particle size distributions;the use of the collapsed gels permits to produce metal nanoparticles with desired size distributions.The obtained results illustrate the potential of the small-angle X-ray scattering method allowing a systematic selection of the materials and reducing agents for the preparation of new compounds with desired properties.

P06.10.010 RESIDUAL STRESS MEASUREMENTS IN MICRON REGIONS BY MEANS OF THE KOSSEL TECHNIQUE. J. Brechbühl, J. Bauch, H.-J. Ullrich, Institute of Materials Science, Dresden University of Technology, 01062 Dresden, Germany.

Most of the conventional X-ray diffraction methods, e. g. the $\sin^2\Psi$ - method, are intended to obtain residual stresses from the surface of multicrystalline materials. Thus, by the procedure of measurement, these methods only provide average stress values of

many grains in areas of several square millimeters. Local deviations from the measured mean values of the stress components, especially within a single grain, cannot be identified. Hence, for the last twenty years new methods for diffractometer measurements in single grains have been developed and applied successfully. But even in the case of coarse-grained materials, when the diameter of the primary X-ray beam may be enlarged to hit still a single crystal, the measuring time is several hours up to several days. Therefore, we have been looking for nonconventional methods to shorten the high measuring time as well as to improve the local resolution.

In the submitted contribution, a new method for fast measurements of residual stresses in micron regions based on the Kossel diffraction is represented. Recently, we performed the first measurements of residual stresses by using synchrotron excited Kossel diffraction (at the HASYLAB, Hamburg). Our new findings as well as the principle of the determination procedure for obtaining residual stresses from Kossel lines are presented. The Kossel technique is a very suitable method for fast measurements (a few seconds / minutes) of local residual stresses in micron regions (spot diameter of the beam: electron excitation: 1-10 μm, excitation by synchrotron radiation: 10-200 μm). Because of the high lateral resolution even residual stresses of third order (inhomogeneities of the stress state within a grain) can be proved and calculated. It is shown that both the measuring time and the measuring errors could be minimized extremely because of the simultaneous registration of differently orientated net planes in one Kossel pattern. There is no necessity to tilt and twist sample and detector during the measurement.

P06.10.011 X-RAY POWDER DIFFRACTION MEASUREMENTS OF THE RESIDUAL STRAINS IN $MgAl_2O_4$-ZrO_2 CERAMIC COMPOSITES. O.Masson, ESRF, BP 220, F-38043 Grenoble Cedex, France, R.Guinebretiere, Z.Oudjedi and A.Dauger, SPCTS, 47 avenue A. Thomas, 87065 Limoges Cedex, France.

The introduction of tetragonal ZrO_2 particles into a ceramic matrix can result in significant increases of fracture toughness and strength. This reinforcement largely depends on the strain field in the matrix and particles.

Because neutrons have a penetration power much higher than X-rays, neutron diffraction is generally preferred for the measurement of bulk residual strains[1]. However, X-ray diffraction is well suited to measure the small line broadening and peak shift induced by inclusions and thus enable valuable strain information to be obtained on the near-surface of the sample.

We present some results concerning X-ray powder diffraction measurements of the residual strains in $MgAl_2O_4$-ZrO_2 composites containing 3 and 12 vol% ZrO_2. The diffraction data were analysed by pattern decomposition. The average lattice strains were determined thanks to the diffraction peak shifts observed in several crystallographic directions. The analysis shows that for all samples the zirconia particles are in tension and the matrix is in compression. Moreover, these lattice strains vary with inclusion content and are anisotropic within the ZrO_2 particles.

Line broadening analysis by the Voigt function method[2] was used to determine the local mean-squared strain. For both phases, microstrains were found to increase with the inclusion content. Finally, the W.A. method[3] was applied to obtain more information on the strain field distribution. Fourier coefficients were beforehand computed by using a regularisation method in order to avoid spurious oscillations caused by the instrumental broadening correction. We then show that the strain field gradient induced by inclusions within the matrix is small.

[1] A. Riessen & B. O'Connor (1993). J. Am. Ceram. Soc., 76[8], 2133.
[2] J.I. Langford (1992). NIST Spec. Publ., **846**, 110-126.
[3] B.E. Warren & B.L. Averbach (1952). J. Appl. Phys., **23**[4], 497.

P06.10.012 STRAIN IMAGING BY NEUTRON TRANSMISSION. P. Withers [1], L. Edwards [2], M. Johnson, M. Daymond [3], A. Steuwer [4], [1] Manchester Materials Science Centre, UMIST, Grosvenor Street, Manchester M1 7HS, [2] Materials Discipline, The Open University, Walton Hall, Milton Keynes, [3] ISIS Facility, Rutherford Appleton Laboratory, Chilton, Didcot, Oxon OX11 0QX, [4] Department of Materials Science & Metallurgy, University of Cambridge, Pembroke Street, Cambridge CB2 3QZ

In the time-of-flight method, the intensity of neutrons transmitted through a polycrystalline sample exhibits sudden, well-defined increases when the neutron wavelength exceeds the Bragg condition for coherent scattering by lattice planes. The shape and position of these edges reflect the crystalline state of the material, and information about residual stress, texture and phases present in the material can be extracted from the spectrum. The transmission method has two key advantages over conventional neutron diffraction. The use of pixellated 1D or 2D detectors enables simultaneous spatial imaging of stress fields and, at the same time, allows for the determination of the unstressed lattice spacing by taking a set of images at different sample inclinations. In this paper we present analysis and preliminary results to show how neutron transmission can be used for accurate strain measurements in materials, based on single-edge and Rietveld-type multiple-edge refinement.

P07.10.001 A SYNCHROTRON DIFFRACTION STUDY OF AMORPHOUS $BaSi_2O_5$. H. Schlenz, R. Grabinski and A. Kirfel, Mineralogisch-Petrologisches Institut, Universität Bonn, D-53115 Bonn, Germany, schlenz@uni-bonn.de

The structure of a synthetic Ba-silicate glass of composition $BaSi_2O_5$ has been studied by high energy synchrotron diffraction (150 keV) at the wiggler synchrotron beam-line BW5 at HASYLAB/DESY (Germany), and at three different energies (35.5, 36.8 and 37.3 keV) near the Ba K-absorption edge, at the synchrotron beam-line F1 (HASYLAB/DESY). Hard X-rays (150 keV) were used, because a higher resolution in direct space desired for disordered materials can be achieved, and the required corrections are smaller, particularly that for absorption. Due to smaller scattering angles, even the polarization correction is almost negligible [1]. All experiments were carried out in Debye-Scherrer geometry illuminating a capillary with 3 mm and 1mm diameter respectively (Sample holder: pure silica glass capillary, 0.01mm wall thickness). At 150 keV the sample was placed into a vacuum chamber (P = 0.001 mbar), in order to reduce air scattering at low values of Q (= $4\pi\sin\Theta/\lambda$). The experiments at lower energies were performed at normal conditions. Data were recorded in a range of Q between 0.8 and 38.7 $Å^{-1}$. In order to employ experimental anomalous dispersion correction terms, f ' (E) and f " (E), in the course of data processing, the Ba K-edge was studied by EXAFS-scans. Effective absorption coefficients μ (E) were determined from sample transmission measurements at all energies. The data were evaluated conventionally, and the differential anomalous scattering method (DAS) was applied [2], in order to obtain interatomic distances of next nearest neighbours, i.e. the Ba-Ba distances from the partial Ba-Ba structure factor.

[1] Poulsen, H.F., Neuefeind, J., Neumann, H.-B., Schneider, J.R., Zeidler, M.D.: J. of Non-Crystalline Solids 188 (1995), 63-74.
[2] Raoux, D., In: Resonant Anomalous X-Ray Scattering, G. Materlik, C.J. Sparks, K. Fischer (Eds.), 1994, Elsevier Science B.V..

P07.10.002 STRUCTURE AND PHASE TRANSITION IN Ti-Ni ALLOYS DUE TO CRYSTALLIZATION AMORPHOUS ALLOYS. I. Doonichev and A. Kosilov, Department of Physical of Metals, Voronezh State Technical University, 394026 Voronezh, Russia, Yu. Barmin and S. Lebedinsky, Department of Solid State Phisics, Voronezh State Technical University, 394026 Voronezh, Russia.

Amorphous alloys $Ti_{1-x}Ni_x$ ($0{,}16 \le x \le 0{,}74$) were prepared by sputter-deposition as substrateless films 10-15 μm thickness. Compositions of alloys were measured by electrone probe microanalysis. Investigations of alloys structure in initial state and after annealing were study by X-ray diffraction. The survey was conducted in the Bragg-Brentano geometry with application of a graphite monochromator in a diffracted beam and scintillation counter detector arranged to eliminate $\lambda/2$ contributions.

Amorphous alloys were annealed at two various temperature. The degree of vacuum prior to starting annealing was nearly $1 \cdot 10^{-6}$ Pa. The amorphous specimens for fist annealing were heated few higher the crystallization temperature for 5 min. Ti-Ni alloys for second annealing were heated for 1 h at 1000 K. Structure in initial state and after annealing were study in this work The short-range order of the crystallite phases is analysed in connection with the structures of amorphous alloys.

P07.10.003 ATOMIC STRUCTURE AND PHASE TRANSFORMATION OF AMORPHOUS ALLOYS $Re_{100-X}Hf_X$ (X=4 - 91 AT.%). E.V. Lebedinskaya, S.A. Lebedinskiy and Yu.V. Barmin, Dept. of Solid State Physics, Voronezh State Technical University, 394026 Voronezh, Russia.

Amorphous alloys $Re_{100-x}Hf_x$ (x = 4 – 91 at. %) were prepared by vapour quenching (high rate sputter deposition) of composite target as a substrateless foils 10 - 15 μm. The composition of alloys was determined by electron-probe microanalysis method with 0,5 at. % accuracy.

The atomic structure of initial structure and phase transformation of amorphous alloys Re-Hf during to heating was studied by X-ray diffraction. As a result of X-ray experiment using $Mo_{k\alpha}$ radiation calculations the radial distribution functions and the structure factors for all amorphous alloys in all concentration range $4 \le x \le 91$ were obtained.

In order to study the phase transformation during heating the special treatment was carried out with heating rate 10 K/min.

The short range order parameters (interatomic distances R_i and coordination number Z_1) were determined. The values of R_i/R_1 and Z_1 are constant in all compositional range. Crystallization only to α-Hf, Laves phase, Re_2Hf, and Re but not to equilibrium σ- or χ-phases was established.

P07.10.004 XRD, XANES AND EXAFS STUDY OF NiO XEROGELS. H. Fischer and A.F. Craievich, Instituto de Física, CP 66318,05315-970, USP, São Paulo, SP, Brasil and P.K. Sharma, Materials Center, SUNY, Binghamton, USA.

Porous *NiO*-based xerogels were prepared using the sol-gel procedure. The precursor sol is composed of nickel chloride and different amount of water (1 and 9 mol), in the presence of 0.1 mol of acetic acid, dissolved in butanol. The liquid solutions were refluxed and the resulting sols dried and held during one hour at temperatures ranging from 150 up to 900°C. The structure of *NiO* xerogels, treated at different temperatures, was studied by X-ray diffraction (XRD), XANES and EXAFS techniques [1]. XRD spectra corresponding to low temperatures (150 to 300°C) exhibit diffraction lines of $NiCl_2\ xH_2O$ (x=2, 4 and 6) crystals. For samples treated at higher temperatures, the intensity of these peaks progressively decreases and others corresponding to the cubic *NiO* phase appear. XANES spectra of low temperature xerogels, corresponding to *Ni* atoms surrounded by *Cl*, smoothly approach, as temperature grows, that of *NiO* standard. The same type of transformation is apparent in the variation of the area of the *Ni-Ni* peak of EXAFS results. We propose that this variation is produced by the progressive formation of crystalline *NiO* volume domains, in which *Ni-Ni* distances are equivalent to those of the *NiO* standard. In order to determine the volume fraction of transformed *NiO* phase, *c(T)*, XANES spectra corresponding to intermediate temperatures were modeled as linear combinations of the reference spectra of the two standards ($NiCl_2$ and *NiO*). *c(T)* was independently determined using EXAFS results. A sigmoidal function was fitted to the experimental values *c(T)* yielding an average transformation temperature T_t=476°C and a transformation range width ΔT=52°C for 1 mol H_2O. When water content is increased, the phase transformation shifts slightly toward lower temperatures and the extent of the transformation range is reduced (T_t=460°C and ΔT=42°C for 9 mol H_2O).

XANES and EXAFS experiments were performed at the National Synchrotron Light Laboratory, Campinas, Brazil.

P07.10.005 SHORT RANGE ORDER AND PHASE TRANSFORMATIONS OF Re-Si AMORPHOUS ALLOYS. I.V.Babkina, Yu.V.Barmin, V.G.Samoilov Department of Solid State Physics, Voronezh State Technical University, Moskovskii Prospekt 14, 394026 Voronezh, Russia.

The atomic structure of $Re_{100-x}Si_x$ (x=0, 4, 11, 20, 31, 47, 54, 70, 82, 88, 100) amorphous alloys (AA) was studied by X-ray diffraction. Amorphous alloys were prepared by high-rate sputter deposition. The compositional range formation of the amorphous state in Re-Si system (10-100 at.% Si) was determined.

In as-quenched alloys two amorphous phase were observed: the AI-phase - 10-90 at.% Si and the AII-phase - 45-100 at.% Si, especially that in the composition range 45-90 at.% Si is the coexistence of two phase AI and AII. The values of interatomic distance R_1=2,63-2,71 A and total coordination number Z_1=9,6-9,9 have been determined for the one-phase region.

The interrelation between the topological short-range order parameters, the thermal stability (crystallization temperature T_x) and the structure of crystallized metastable phases (MS) of Re-Si AA have been investigated. After the crystallization the basic phases are Re_5Si_3 and $ReSi_2$, with the extended of the compound $ReSi_2$ existence area, while the ReSi-phase is not identified among the crystallization products. The linear dependence of T_x upon the composition is found for AA crystallized into Re_5Si_3 and $ReSi_2$ compounds that is conditioned by the similarity of their topological short range order structure. The decreasing of T_x with the alloy composition changing from the stoichiometry of Re_5Si_3 and $ReSi_2$ is the cause of the changing of the composition short range order of these compounds and corresponding AA.

As a conclusion - the short-range order of AI-phase and coordination polyhedrones of Re_5Si_3 and $ReSi_2$ compounds is similar. The structure of AII-phase is the same as a-Si.

P07.10.006 NEUTRON POWDER DIFFRACTION STUDIES OF ETTRINGITE. R. Pisula, Department of Crystallography, Birkbeck College, Malet Street, London WC1E 7HX.

Ettringite ($Ca_6[Al(OH)_6]_2.(SO_4)_3.26H_2O$) is an important product in the hydration of Portland cement, where its early formation is critical for set regulation and rheology. The subsequent 'to and fro' conversion of ettringite and calcium monosulphate aluminate ($[Ca_2Al(OH)_6.xH_2O]$, a solid solution series), that occurs in older cements is critical for the long term strength of the cement matrix.

In this study we are investigating the effect of temperature and crystallite modification on this transformation reaction. Our

interest is to relate the kinetics of this conversion to the structure and composition of the mono- sulphate phases. We have also prepared high-purity crystalline ettringite in a deuterated form for a complementary neutron diffraction study to monitor water content during the transformation. The data analysis shows the decomposition process clearly and the emergence and subsequent disappearance of the important fragment mono-sulphate. Based on these results we discuss the nature of the transformation, and the water content of each phase during decomposition.

P07.10.007 SYNCHROTRON E.D. DIFFRACTION TOMOGRAPHY STUDIES ON PORTLAND CEMENT TREATED WITH SUPERCRITICAL CO_2. Shane Morgan, Birkbeck College.

Cement studies continue to yield new processes of modifying cement to improve and diversify its properties for various applications. A recent novel area of research is into a way of hardening Ordinary Portland Cement (OPC), using supercritical carbon dioxide ($SCCO_2$). Strengthening of cement does occur naturally due to carbonation, where calcium compounds in the cement react with carbon dioxide in the atmosphere to form calcium carbonate (Limestone)and water, over long periods of time. We can mimic the conditions of exposure to carbon dioxide, but over very short periods of time by bathing the OPC in $SCCO_2$. This diffuses easily while under pressure through the cement altering the cement chemistry as it progresses. In this work we are interested in mapping the progress of this cement/$SCCO_2$ interaction using Synchrotron Energy Dispersive Diffraction (SEDD). We have produced cement samples with varying levels of carbonation and water content and observed these using Energy-dispersive x-ray diffraction tomography at Daresbury Laboratories on station 16.4. We have mapped the composition of crystalline material in the cement, along a path from interior to exterior of the sample. Analysis shows clearly the changes in the cement chemistry i.e the formation of calcium carbonate and disappearance calcium hydroxide as we move into the sample and the appearance of unexpected phases. Using SEDD we have shown non-destructively the main alterations that give improved strengths to the cements and correlated these to various $SCCO_2$ treatments.

P07.10.008 COMPOSITION EFFECTS ON THE CRYSTALLININTY OF BERYLLIUM-RICH COATINGS. A. Jankowski, Chemistry and Materials Science, Lawrence Livermore National Laboratory, Livermore, California, USA

The material properties of sputter deposited coatings are sensitive to the growth morphology and microstructure of the deposit. For example, the application of an applied bias to the substrate can densify the columnar microstructure of a crystalline coating through ion bombardment thereby minimizing porosity and increasing the mechanical strength of the coating. We are developing a process to sputter deposit Be-rich, thick coatings that must be homogeneous, isotropic, mechanically strong, smooth and serve as a membrane across which gas permeation is controllable. The refinement of grain size to the nanoscale is preferable for each of these attributes.

It is widely known from prior studies of evaporation and sputter deposition that the grain size of nominally pure beryllium, that is beryllium with greater than 99.8 atomic percent purity, can be dramatically refined through the incorporation of specific metal impurities like iron. Additionally, the use of boron doping may serve as a potential glassy phase former in the composition range greater than at the depressed eutectic seen in the binary alloy phase diagram. We report on the changes in crystallinity and growth morphology found in these Be-rich coatings. The effects of dopant additions are characterized with electron diffraction and microscopies.

This work was performed under the auspices of the US Department of Energy by Lawrence Livermore National Laboratory under Contract No. W-7405-ENG-48.

P07.10.009 OXIDE PHASES IN SYSTEMS xR_2O_3-$(1-x)Fe_2O_3$, R=RARE EARTH. S. Popovic, Physics Department, Faculty of Science, POB. 162; and M. Ristic and S. Music, Rudjer Boskovic Institute, POB. 1016; 10001 Zagreb, Croatia

Rare earth ferrites find wide-scope applications in telecommunication and electronic devices, due to their specific physical properties. For that reason a systematic study of the influence of the preparation procedure on the formation of particular oxides and their properties has been undertaken. The main characterization techniques have been XRD, FT-IR, Mössbauer and Raman spectroscopy.

R=Eu,Gd: Samples were prepared by chemical coprecipitation of corresponding hydroxides. For $x \approx 0.4$ and 0.5 the garnet-type ferrite and orthoferrite, respectively, were dominant in samples heated at 900°C, while samples heated up to 600°C were of poor crystallinity. There was no evidence for formation of solid solutions, even at ends of the concentration range. The distribution of observed oxides was determined as a function of x. For samples prepared by ceramic sintering a temperature of 1200°C was necessary for formation of the garnet-type ferrite and orthoferrite at $x = 3/8$ and $x = 0.5$, respectively.

R=Nd: In samples prepared by chemical coprecipitation and heated up to 900°C the highest fraction of orthoferrite was obtained for $x = 0.5$.

R=Sm: Samples were prepared by solid-state reaction. For x=0.5 orthoferrite was detected as one of oxide phases after heating up to 800°C, and as a single phase above 1000°C. For $x = 3/8$ garnet-type ferrite was a single phase in samples heated at 1300°C.

R=Er: Samples were prepared by chemical coprecipitation. For $x = 3/8$ samples heated up to 650°C were amorphous, heated up to 800°C showed the garnet-type ferrite and orthoferrite, while heated up to 1300°C contained the garnet-type ferrite as a single phase.The present study shows strong relationships between the preparation procedure, nature of metal cations and structural and chemical properties of the formed oxides.

P07.10.010 STRUCTURAL STUDY OF BORON CARBIDE MODIFIED BY INDUCTION PLASMA TREATMENT. T. Tanaka, Technical Research Laboratories, Nisshin Flour Milling Co., Ltd., 5-3-1, Tsurugaoka, Oi, Saitama 356-8511, Japan, and X. Fan and T. Ishigaki, National Institute for Research in Inorganic Materials, 1-1, Namiki, Tsukuba, Ibaraki 305-0044, Japan.

Transmission electron microscopic and powder X-ray diffraction studies revealed that the structural modification in boron carbide was induced by an in-flight R.F. induction plasma treatment, which is characterized by its high enthalpy and the presence of chemically active species. Boron carbide (B_xC), which has a rhombohedral cell with space group $R\bar{3}m$, was known one of non-metallic hard materials and expected to the coating material in spray plasma coating process. In this study, B_xC powders were modified by the Ar-H_2, Ar-N_2 and Ar-H_2-NH_3 R.F. induction plasma treatment, and the changes of their stoichiometry and crystal structure were investigated by transmission electron microscopic and powder X-ray diffraction technique. In transmission electron microscopic study, a lot of crystallites with stacking faults were observed in the thinned cross section of Ar-H_2 treated B_xC particles. It was considered that these particles were melted completely during plasma treatment. On the other hand, the formation of boron, which has a doubled a length in

comparison with B_xC unit cell, and remarkable change in profile intensity of B_xC was observed in powder X-ray diffraction study of each plasma-treated powder. The Rietveld analysis revealed that the unit cell volume of each plasma-treated B_xC increased with the increases in the occupancy of 1*b* site (0,0,1/2) of space group $R\bar{3}m$. In addition, the unit cell volumes of Ar-N_2 or Ar-H_2-NH_3 plasma-treated B_xC were slightly bigger than those of Ar-H_2 treated one. It was suggested the oxygen or nitrogen atoms took the place of boron atom at 1*b* site through the plasma treatment, considering the atomic radii of each atom. The change of chemical composition in plasma-treated boron carbide agreed with the above results of Rietveld analysis.

P07.10.011 HIGH TEMPERATURE NEUTRON STRUCTURE ANALYSIS OF 3:2 MULLITE. G.Brunauer, H. Boysen and F. Frey [1], T. Hansen [2], W. Kriven [3], [1] Institut für Kristallographie, LMU, 80333 München, Germany, [2] ILL, 38042 Grenoble, France, [3] Department of Material Science, University of Illinois, Urbana, USA

Hydrothermally grown powder of mullite with stoichiometry Al4.5Si1.5O9.75 was prepared by Kriven et al. [1] using the hotpressing method. By neutron diffraction, the temperature behaviour of the mullite sample was examined up to 1923 K. The measurements have been performed at the neutron diffractometers MAN-I (FRM Garching) and D2B (ILL), and have been evaluated with the Rietveld programs FullProf and RTB. During the first heating cycle an anomaly occured including an irreversible change of the expansion coefficient and a change of the sample colour at about 1400 K. This is correlated with a decrease of the occupation of the so called O(3) oxygen site and an increase of the occupation of the so called O(*) site.

First results of the structure refinement are: The atomic displacement parameters show larger values along z, the direction of the tetrahedral and octahedral chains in the structure of mullite, as compared to the directions of x or y. In addition, discontinuities of the lattice expansion could be observed in the temperature regimes between 800 and 1000 K, and 1700 and 1900 K, which might be of importance for applications of mullite based ceramics.

This work is supplied by funds of the DFG under FR747/15-1.

[1] W. M. Kriven et al., J. Eur. Ceramic Soc. (in press)

P07.10.012 THE REAL STRUCTURE OF γ-ALUMINA. D.O.Klenov, G.N.Kryukova, S.V.Tsybulya, Boreskov Institute of Catalysis, Novosibirsk, pr. Lavrentieva 5, Russia

Using simulation of high resolution electron microscopic images and X-ray powder diffraction patterns the crystal structure of γ-Al_2O_3 prepared by thermal decomposition of boehmite and pseudoboehmite at different temperatures has been refined. It was found that difference between two forms is caused by the peculiarities of vacancy distribution over cation sublattice in the structure: samples of γ-Al_2O_3 synthesized from pseudoboehmite are characterized by statistical distribution of vacancies over cation positions whereas in the samples of boehmite series vacancies are concentrated on the defect planes formed by the shift along (110) and (111) that leads to the appearance of the specific closed pseudohexagonal loops.

The relationship between the atomic arrangement and microstructure of γ-Al_2O_3 has been established. In the samples of pseudoboehmite series the cubic spinel structure preserves in the volume of isolated micrograin of 2-3nm in size from those the big (over 100 nm) polycrystalline aggregates are formed. In the samples of boehmite series the structural coherence is still the same in the volume of every isolated particles being in the form of thin monocrystalline platelet of 100 nm in size, but symmetry lowering of the unit cell to tetragonal one is observed. This tetragonal cell is oriented in a definite way with respect to the plane of defects.

This work was made possible by Grant N97-03-33497 from the RFBR

P07.10.013 THE "IN SITU" INVESTIGATION OF THE NIWO4 SYNTHETHIS BY SR-DIFFRACTION AND XAFS. M.R.Sharafutdinov, B.P.Tolochko, N.Z.Lyakhov [1], S.G.Nikitenko [2], [1] Institute of Solid State Chemistry, Novosibirsk, 630128, Russia, [2] Institute of Catalysis, Novosibirsk, 630090, Russia .

The "in situ" information about NiWO4 solid state synthesis was received by synchrotron radiation time resolved diffraction and XAFS methods. At initial stage of the reaction, NiWO4 was formed with deformed structure, which is different from equilibrium one (lattice parameter is greater, structure is nonstoichiometric). During the reaction the structure of already formed NiWO4 changed. It's possible to suggest, that mechanisms of nucleation of NiWO4 are different for initial and following stages of reaction. At initial stage there are formation of nucleus directly on the NiO and WO3 interfaces, then appears particles, contacting with product and one of the components. Thus, the properties of nucleus is different for different time. The nucleus of different size were formed at different temperatures (310 A at 720 C, 280 A at 680). During the reaction the particles size were growing by exponential low , from 310 A to 530 at 720 C (for ~1600 s) , from 280 A to 400 A at 640 C (for ~5000 s). Integral intensity of the NiWO4 peaks growth described by Avrami-Erofeev model at the initial stage of reaction. After formation of the product layer (alpha > 0.2) kinetics were described by Gistling-Brounstein model. At the temperature about 700 C the constant (k) of reaction was the same for all time of reaction, whereas at 640 one was changed about alpha ~0.5. Considering that at 720 C lattice parameter of WO3 is constant and decrease by 0.1 % at 640 we can suggest that formation of solid solution (NiO)WO3 take a place.

P07.10.014 CRYSTALLOGRAPHIC STUDIES OF NEW PHASES IN THE LA2O3-LI2O-TIO2 SYSTEM. C.A. Kirk, A.R. West, J.M.S. Skakle and S.M. Blake, Department of Chemistry, University of Aberdeen, Meston Walk, Old Aberdeen, AB24 3UE

A study of the compound formation and crystal structure in the system La_2O_3-Li_2O-TiO_2 has shown the existence of five phases, two of which are new. The crystal structure of three of these phases, (B $La_{32}Li_{20}Ti_4O_{66}$, C $La_{14}Li_{20}Ti_3O_{37}$ and D $Li_{0.333}LaTi_{0.667}O_3$) have been studied using a combination of XRD, ND and SAED. Phase B is cubic with a = 12.2163Å and space group Im-3m. Phase C is tetragonal with a = 13.24Å and c = 7.46Å and space group P4/mbm. Phase D is perovskite related and tetragonal with a = 7.87 and c = 7.86 and space group P4/nbm.

P07.10.015 THEORY OF THE CERAMIC FORMATION UNDER THE PRESSURE. A.Yu.Gufan and E.N.Klimova , Applied Mathematical Department, Rostov State University, 5 Zorge st., 344090 Rostov on Don, Russia, and S.O.Kramarov Rostov State Pedagojical University, 33 B.Sadovaya st., 344082 Rostov on Don, Russia.

The process of the ceramic formation under the pressure we have roughly divided on three stages. At the first stage a covities between the grains disappear, defining the compressibility of almost powder specimens. Hardness intergrain contacts restrict the total changing of the volume at the duration of this stage. The second stage is characterized by the grain deformation and

disappearing of interfaces between the grains. The hardness of material becomes almost the hardness of grains. The third stage is characterized by the rising cracks inside of the grain, skeleton suffers distraction and some part of specimen becomes powder as initial one. These stages may be imaged as a mesoscopic first order phase transitions between the phases of materials. The simplest model of this transformations may be characterized by the density of potential energy $w = w/v = (1-c)(k_1 z_1^2)/2 + c(k_2(z_2 - z_0)/2 + w) - pl$ (1) . Where v- samples volume, p-pressure acting on ceramic pill, $l=cz_2 + (1-c)z_1$ – total deformation of the pill, c- is concentration of prepared ceramic, k_1 and k_2 are rigidities of the first and the second stage of ceramic formation which may be defined by dilatometrir measurements, z_1 and z_2 are the corresponding changing of pills height. The theory predicts the critical pressure $p_0 = k_1 k_2 z_0 / (k_2 - k_1)$, defining the interval of the second stage of ceramic formations $p_1<p<p_2$, where $p_{2,1} = p_0[1 +-(1-w_0/w_c)^{1/2}]$ and $w_c = k_1 k_2 z_0^2/2(k_2-k_1)$, p_2 define in the beginning of cracks growing.The relation between the total deformation and the volume sprouting by skeleton of rigid intergrain contacts $[(1-c_1)/v]$ and p_1 is defined by equation: $c_1 = (1-p_1/k_1) / [(p_1/k_2 - p_1/k_1) + z_0]$. The volume of cracked part of ceramic specimen $[(1-c_2)/v]$ is defined by equation $c_2=(1-p_2/k_2) / [(p_2/k_2 - p_2/k_1) + z_0]$. The temperature influence on the ceramic formation in the framework of model (1) will be carefully presented in poster. We are thankful to RFBR for financial support.

P07.10.016 PHASE TRANSITIONS ON THE SCALE OF GRAINS IN THE COURSE OF HARD PILLS MOULDING. V.M.Il'in Rostov Devision Academy of Service, 125 Varfolomeev str. 344018 Rostov ob Don, Russia and A.Yu.Gufan Appl.Math.Department of Rostov State Univ. 5Zorge st., 344090, Rostov on Don, Russia.

Dependence of the powder pills height versus, pressure in a course of solid pills preparation at low temperature displays two jumps corresponding to physical nature of compressibility substitutions. At the beginning, the samples are friable with the vacant holes between the grains. These states rigidity is defined by the holes filling. The second state is characterized by the tightly contacts between the grain surfaces and disappearing of intergrain boundaries. The compressibility in this state is equal to proper compressibility of compounds. Next state, forming under highest pressure is characterized by the creation of new cracks. The pills in this state are crumbly. The successive replacing one state by another may be imaged as a first order phase transition, characterized by the jump of volume at T=0: $v_2 - v_1 = v_2 - v_3 = v_0(1-w_0 w_c^{-1})^{1/2}$. Here $v_i = l_i s$(i=1,2,3), volume at the transition pressure p_1 and p_2; $w_c = k_1 k_2 z_0^2/2(k_2-k_1)$. All other notation are clear from the view of free energies $f = w-TS = w - T[clnc +(1-c)ln(1-c) + ln [(V_{in} - ls)/V_{in}]$. Two first items in rectangular brackets represent configuration entropy (c-the quota of grains with tight integration contacts), third term is the entropy of free volume. The internal energy $w = (1-c)k_1 z_1^2/2 + ck_2(z_2 - z_0)^2/2 + cw_0$, where z_2 is the averaging height of the grains with rigid contacts . The slope of the curve represents dependence of total volume per one grain ($v=sl=s[cz_1 + (1-c)z_2]$) versus pressure permits to define 5 stable phases of pills: 1),5) c=0, powder phases $l=z_1$, $p = k_1 l + T(v_{in} - ls)^{-1}$; 2)4) 0<c<1(intermediate phases), $z_1 = [p-T(v_{in} - ls)^{-1}] / k_1$; $z_2 = z_0+[p-T(v_{in} - ls)^{-1}]/k_2$ $p = p_{1,2}+T(v_{in} - ls)^{-1}(dp/dl = T/(v_{in}^2)$; 3) c=1 (solid phase) , $l =z_2$, $p=k_2(l-z_0) + T(v_{in} - ls)^{-1}$ .The jumps of compressibility,heat capacity and coefficient of thermal expansion satisfy the Erenfest equation. It means that rising the temperature in a course of pills formation makes them more strength even at pressure overcoming the limit p_2, defining the cracks .

P07.10.017 MOLECULAR MODELING OF THE MESOMORPHIC POLYSILOXANES E. Boda, T.V. Timofeeva, N.N.Makarova [1] E.V. Matuhkina [2] [1] Institute of Organoelement Compounds, RAS, 28 Vavilov St.,Moscow, 117813, Russia, [2]Moscow State Pedagogical University, 1 Malaya Pirogovskaya St., Moscow, 119882 Russia

Molecular models of mesomorphic cyclochain organosilicon compounds are presented in our work. These compounds are capable of forming thermotropic mesophases without traditional mesogenic groups [1]. Also, these materials are the only organo silicon compounds which form multilayer LB films [2].To clarify the chain confor mation and mesophase structure the atom-atom potential method [3] was used. The simulations showed that the conformation of the tetrasiloxane cycle depends on t he bulk of the organic substituents. Molecular packing simulations of mesophases of polycyclotetrasiloxane with Me, Et and Pr substituents, based on the X-ray data, reveal structure which resembles columnar liquid crystals.

1. Godovsky Yu.K., Makarova N.N., Petrova I.M., Zhdanov A.A. Makromol. Chem., Rapid Commun. 1984. v.5. 3 p. 427.
2. Fang J., Dennin M., Knobler C.M., Godovsky Yu.K., Makarova N.N., Yokoyama H. J Phys. Chem., B, 1997, v.101, P. 3147-3154.
3. Pertsin A.J., Kitaigorodsky A.I., The Atom-atom potential method, Springer-Verlag, 1987.

P07.10.018 MODULATED STRUCTURES IN AN SPATIAL ORDERING OF IMPURITIES WITHIN THE LAYER MESOMORPHIC MEDIUM V. A. Tatarenko and V. Yu. Reshetnyak Dept. of Solid State Theory, Inst. of Metal Physics, 36 Academician Vernadsky Blvd., UA-252680 Kyyiv-142, Ukraine.

Anisotropic phases of the macroscopically homogeneous mesomorphic medium should manifest themselves by specific responses to an external perturbance. Some macroscopical displays are considered in this paper.

The necessary conditions for the origin of a modulated lamellar superstructure in the framework of positional distribution of rigid-sphere-like impurity macroparticles (e.g. macromolecules of very large relative molecular mass or aggregates of small molecules), intruded into a mesomorphic host medium, are analysed within the continuum model of a mesomorphic dispersion-medium phase with nematic-analogous elastic properties, and also by means of both static-fluctulation-wave methods and mean self-consistent-field approximations in statistical-thermodynamic theory of ordering or decomposition reactions for a quasi-lattice-gas model.

Such a partly "ordered" state of an impurity subsystem (e.g. in the early stage of its spinodal decomposition) within a dispersion medium, somewhat similar to the mesomorphic phase called smectic A packing with a spatial periodicity and with a long-range orientational order in mutual arrangement of its elongated ("nonspherical") molecules, is thus typified, with respect to the disordered mutual distribution of impurity macroparticles throughout the nematic host-medium bulk, by a sole breaking of translational symmetry along the direction of the "preferential" orientation of host-medium molecules.

A specific indirect interaction of impurity macroparticies with each other, resulting from interference of static director-field curvatures produced by different impurity macroparticles in a host-medium texture, serves as a co-operative mechanism of structural transformations in a disperse system even for relatively small amounts of impurities (due to the long-range character of this interaction).

Variations in external thermodynamic parameters (temperature etc.) should result in variations of the host-medium-elasticity parameters as well as the Fourier components of the energies of "bending-induced" interactions between impurity macroparticles embedded in the mesomorphic host medium and

thus shift the wave vectors generating the periodic modulations of quasi-stable intermediate superstructures.

These modulated suprastructures within a mesomorphic dispersion medium may be proposed in particular as the objects for further experimental exploration, both in view of the potential for their applications and for their fundamental interest concerning the behviour of dispersed particles in a restricted mesomorphic environment. Gaining information about them is the first necessary step in understanding physical-chemical properties of a mesomorphic disperse system which are associated with its medium-range structure.

The necessary thermodynamic conditions for the appearance of an impurity layer superstructure based on a mesomorphic dispersion medium with smectic-analogous elastic properties are discussed in conclusion allowing for additional long-range indirect, i.e. "strain-induced", interaction between impurity macro-particles as well as the usual direct, for instance Van-der-Waals-type, one. The representative value of energy of the first of these interactions may be considerably changeable with increasing temperature.

P07.10.019 CRYSTALLIZATION AND CRYSTALLOGRAPHY OF SOME LIQUID CRYSTALLINE MATERIALS. Rajnikant and V.K.Gupta, X-ray Laboratory, Post Graduate Department of Physics, University of Jammu, Jammu Tawi - 180 006, India.

An exhaustive literature survey has revealed that very less work has been reported on the single crystalline growth and three-dimensional structural aspects of liquid crystalline materials. Therefore, a variety of liquid crystalline compounds, spread over to three series, were under-taken for the growth of X-ray diffraction quality crystals from slow evaporation technique by using various non-aqueous organic solvent systems. The chance of success for the growth of single crystals, in the present investigation, is not more than 35%. Crystal structures of the materials which could crystallize well have been determined by direct methods. The growth data we have recorded has some interesting features. Growth and the crystallographic data would be presented.

P07.10.020 CRYSTAL STRUCTURE OF LONG CHAIN COMPOUND, 1,10-DECANEDIOL. N.Nakamura and T.Sato, Department of Chemistry, Ritsumeikan University, Kusatsu, Shiga 525-8577, Japan

The crystal structure of 1,10-decanediol was analyzed as one of the model compounds of liquid crystals, because crystal structure of normal long chain compounds is very similar to that of liquid crystals. For example, normal paraffin shows smectic A or smectic C like structure. And some of them exhibit high temperature phase in which molecules rotate around its long axes. A selected crystal of the title compound having approximate dimensions of 0.10 x 0.10 x 0.10 mm was used. The intensity data from a single crystal were collected by RIGAKU AFC5R diffractometer with graphite monochromatized CuKα radiation. The data were collected at a room temperature of 296 ± 1K using θ-2θ scan technique to a maximum 2θ value of 140.0°. The intensities of three representative reflections were measured after every 150 reflections. An empirical adsorption correction based on azimuthal scans of several reflections was applied. The structure was solved by direct methods with SAPI91 and expanded using Fourier with DIRDIF94. The final cycle of full-matrix least-squares refinement was based on observed reflections [I>2.0σ(I)] and 55 variable parameters, $[w(|Fo-Fc|)]^2$ minimized, R=0.040, Rw=0.062. Crystal data obtained are as follows, $C_{10}H_{22}O_2$=174.28, a=21.148(2), b=5.160(2), c=4.9140(4)Å, β=96.69(1)°, $P2_1/a$, Z=2. The structure is very similar to that of homologues with an even number of carbon atoms [1,2].

1. N.Nakamura & T.Yamamoto (1994). *Acta Cryst.* C50, 946-948.
2. N.Nakamura & S.Setodoi (1997). *Acta Cryst.* C53, 1883-1885.

P07.10.021 STRUCTURE OF A LIQUID CRYSTALLINE COMPOUND WITH NLO PROPERTIES. Vedavati G. Puranik, Physical Chemistry Division, National Chemical Laboratory, Pune 411 008, INDIA, Satya V. N. Raju, S. Ponrathnam, Polymer Science and Engineering Division, National Chemical Laboratory, Pune 411 008, INDIA

There has been a lot of interest in designing new organic molecules with NLO properties in view of their numerous applications. It has been found that, if NLO chromophore and nematic, smectic A / C character is incorporated into a molecular structure, a five fold increase in NLO response could be achieved. In this respect π - conjugated systems capped on both ends with electron donor and electron acceptor have been studied. A liquid crystal 2(4 -cyano benzylidine)-6-(4-hydroxy benzylidine) cyclohexanone, nematic in character has been studied by single crystal X-ray diffraction. Compound belongs to monoclinic space group $P2_1/n$ with a=14.545 (3), b=7.796 (2), c=15.324 (2) Å, β=105.69 (2) °, Z=4 and has been refined to R=0.061. The centrosymmetric dimers are formed by hydrogen bonds through keto group and water molecules. Further these hydrogen bonded dimers are

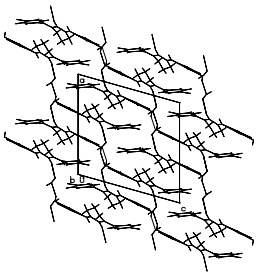

linked via water molecules to form a supramolecular organization. The π - π interaction has been observed between the aromatic benzylidine rings. This donor-acceptor π conjugated aromatic chain greatly stabilizes the NLO property mainly due to the hyper polarizability. When this chromophore is extended at the donor end through a polymethylene spacer and grafted on to an atactic polymeric backbone, NLO effects have been observed after poling.

P07.10.022 PHASE TRANSITIONS AND WATER DYNAMICS IN $[Mn(H_2O)_6](ClO_4)_2$, STUDY BY NEUTRON SCATTERING METHODS. I Natkaniec, Frank Laboratory of Neutron Physics, JINR, 141980 Dubna, Russia, and H. Niewodniczanski Institute of Nuclear Physics, 31-342 Krakow, Poland, E. Mikuli and A. Migdal-Mikuli, Department of Chemical Physics, Jagiellonian University, 30-060 Krakow, Poland.

The hexaaquametal(II) chlorates(VII) form at room temperature body centered orthorhombic-pseudohexagonal structures (***Pmn2***$_1$ - C^7_{2v}) with two metal ions per unit cell [1]. Phase transitions in these compounds have been detected by many methods, however exist considerable disagreement concerning the transition temperatures and even the number of phases, especially with Me=Mn, Fe and Co [2]. Following transition temperatures were detected for $[Mn(H_2O)_6](ClO_4)_2$ by: calorimetry - 323, 247 and 135K, NMR - 160 and 89K, magnetic susceptibility - 120K, IR and RS - 341, 248 and 161K. We have study this compound by neutron powder diffraction (NPD) and inelastic incoherent neutron scattering (IINS) in the temperature range of 290 - 20K. The NDP and IINS spectra were measured simultaneously by time-of-flight method on the NERA spectrometer [3] at the high

flux pulsed reactor IBR-2 at Dubna. At the room temperature water molecules perform fast stochastic reorientations at the rate of THz phonon frequencies. Disorder characteristic for the room temperature can be easily overcooled and frozen. Even relatively slow cooling of ca. 40K/hour from 290 to 100K, freeze an metastable orientational (protonic) glass phase below ca. 160K. Below ca. 90K structural phase transition was observed by the NDP, however the IINS spectra indicate the pure ordered low temperature phase only after annealing the sample a few hours at 100K. At heating structural phase transition take place at ca. 120K, and at ca. 200K water molecules starts fast reorientations in crystalline structure of the room temperature phase.

M. Ghosh and S. Ray. *Z. Kristall*., **145**, 146 (1977).
E. Mikuli, A. Migdal-Mikuli, J. Mayer. *Mol. Materials,* **8**, 273 (1997).
I. Natkaniec, S.I. Bragin, J. Brankowski, J. Mayer. *in Proceedings of the ICANS XII Meeting, Abingdon 1993*, *RAL Report* 94-025, Vol. I., p. 89-96 (1994).

P08.10.001 $LiMn_2O_4$, $LiMxMn_{2-x}O_4$ CATHODE MATERIALS: SYNTHESIS OF BULK MATERIALS BY SOL-GEL AND FABRICATION OF THIN FILMS BY ELECTRON BEAM, THERMAL EVAPORATIONS AND SPRAY PYROLYSIS. Tran Dai Lam, Department of General and Inorganic Chemistry, Hanoi University of Technology, 1 Dai Co Viet, Hanoi, Vietnam. Ngo Quoc Quyen, Laboratory of Applied Electrochemistry, Institute of Chemistry, National Centre for Natural Sciences and Technology, Nghiado, Caugiay, Hanoi, Vietnam.

The spinel $LiMn_2O_4$ has been studied extensively as a positive material for lithium ion batteries. In the paper, we report sol-gel citrate procedure for synthesising the bulk $LiMn_2O_4$ and $LiM_xMn_{2-x}O_4$ (M= Co,Ni, Cu) (x£ 0,5) , based on polymerisation reaction of citric acid and via carbonyl groups in metal acetates (without Ethylene Glycol, used in Pechini process). TA data (SHIMADZU TA-50) indicates that the violent combustion of organic groups in xerogels seem to set up the spinel formation at much lower firing temperature than that of solid state reaction. The xerogel structure has been explored by IR spectroscopy (IMPACT FTIR-410) and TEM (magnification 100000 times). The excellent phase purity and 3d substution of materials has been verified by X-Ray Diffraction (SIEMENS D-5000). This substution is believed to enhance the structural stability of electrode during insertion/extraction lithium ions, maintaining the cubic symmetry (Fd3m).

Thin film fabrication is a good solution to improve the electrochemical performance of electrode. Therefore, electron beam, thermal evaporations and electric spray pyrolysis are applied for this purpose. In the electron beam evaporation, the starting bulk $LiMn_2O_4$ is used. The substrate is ITO, the oxygen pressure is 5.10-4Torr. Two-source thermal evaporation, each of these sources is used for Mn acetate and Li carbonate (taken in proper mole ratio). Spray pyrolysis from the acetate solution of Mn, Li and doped 3d metals at 300-4000C is also successfully adapted. All thin films obtained by these methods have been compared structurally with the bulk materia by using XRD and SEM and investigated electrochemically by Cyclic voltamettry (CV) and Impedance Spectroscopy (EIS).

1. Ngo Quoc Quyen, Tran Dai Lam et al, Proceedings of ScientificReports of NCNS&T, Hanoi, 1997.
2. Tran Dai Lam et al, Proceedings of Scientific Reports, HanoiNational University, Hanoi, 1998.
3. M. Thackeray, J. Electrochem. Soc., 144, 100 (1997).
4. R. Dahn et al, ibid., 145, 851 (1998).
5. Amine et al, ibid., 143, 1607 (1996).
6. E. Eli et al, ibid., 145, 1238 (1998).
7. Liu et al, ibid., 143, 879 (1996).

P08.10.002 POLYMERS OF SINGLE WALL NANOTUBES: GEOMETRY AND DIFFRACTION PATTERN MODELING. L.A. Chernozatonskii, Institute of Biochemical Physics, 117977 Moscow, RUSSIA, N.R. Serebryanaya, Center of Superhard Materials, 142092 Troitsk, RUSSIA

Modelling of polymerized carbon single-wall nanotubes (SWNT), which are possible to prepare under high pressures and temperatures, are represented.

We have considered the following polymers and restructured figures of (n,0) and (n,n) nanotubes and their X-ray diffraction patterns:

Chain structures of polymerized identical SWNT's with 2+2 and Osawa's rectangle bonds (changing of tube geometry from cycle to oval; X-ray diffraction patterns of a chain polymerized SWNT crystal, and graphite-like needle, transformed from SWNT rope via NT chain polymerization);

SWNT zeolites in which NT polymerization occurs by bonding of 6 sp^3 atomic pairs in each NT unit cell with similar atomic pairs located on 6 neighbouring tubes alike 2+2 cycladditions in rhombic C_{60} polymer layer (geometry optimization, and X-ray diffraction patterns).

This work was supported by Russian Fund for Fundamental Research.

P08.10.003 A NEW FORM OF CRYSTALLINE LAYERERD CARBON: CHARACTERISATION, STABILITY AND ELECTRONIC PROPERTIES. M. Terrones[a,b], J-C. Charlier[c], N. Grobert[a], P. M. Ajayan[d] and H. Terrones[b], [a] School of Chemistry, Physics and Environmental Science, University of Sussex, Brighton, BN1 9 QJ, United Kingdom, [b] Instituto de Física, UNAM, Apartado Postal 20-364, 01000 México, [c] UniversitÈ Catholique de Louvain, Unite PCPM, Place Croix du Sud 1, 1348 Louvain-la-Neuve, Belgium, [d] Department of Materials Science & Engineering, Rensselaer Polytechnic Institute, Troy, NY 12180-3590, U.S.A.

Soon after Carbon nanotubes were identified by Transmission Electron Micorscopy (TEM), their electronic and mechanical properties were thought to be remarkable. In this context, early theoretical calculations predicted that these rolled graphene sheets could behave as metals or semiconductors depending upon diameter and the hexagonal pattern along the direction of the tube axis (helicity). Recent local density of states measurements on different single-walled carbon nanotubes revealed that they can indeed be either metals or semiconductors depending on small variations in the chiral angle or diameter. Furthermore, Young´s moduli studies show that the single and multi-walled carbon nanotubes are much stronger than steel and conventional carbon fibres and are extraordinarily flexible when subjected to large strain.

In this account, We propose novel crystals consisting of layered sp^2-like carbon, containing periodic arrangements of pentagons, heptagons and hexagons. The proposed layered crystals exhibit stable hexagonal, orthorhobic (Fig. 1a) and monoclinic structures. In addition, these sheets are rolled so as to generate carbon nanotubes (Fig. 1b) with intriguing electronic properties. Local density of states (LDOS) calculations of all crystals and tubes revealed an intrinsic metallic behaviour, independent of orientation, tube diameter and chirality. Interestingly, all nanotubes exhibit Van Hove singularities as a signature of 1D systems. Particularly, an unusual high intensity LDOS peak at the Fermi level is noticed for the hexagonal crystal and its respective nanotubes, thus suggesting the possible existence of superconductivity. For all capped nanotubes, localized states appear close to the Fermi energy when approaching the nanotube end, thus implying an enhancement of the field emission current. X-ray and electron diffraction simulations of the proposed nanostructures are also studied, and

possible synthetic routes to this new family of covalently bonded layered materials are discussed.

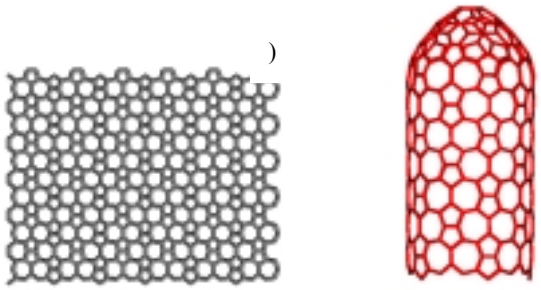

Fig 1. (a) Carbon layer of the orthorhombic crystal consisting of pentagons and heptagons only. It is noteworthy the periodicity of the carbon rings; (b) a nanotube generated by rolling up the carbon layer depicted in a, the cap contains additional pentagons for closure. Tight binding calculations show that both structures are metallic.

P08.10.004 STRUCTURAL STUDIES ON SOME IONIC AND MIXED CONDUCTORS BASED ON Li_4GeO_4. R.P. Gunawardane, M.A.K.L. Dissanayake and H.H. Sumathipala Faculty of Science, University of Peradeniya, Peradeniya, Sri Lanka

Three new types of Li_4GeO_4 based solid solution with γ-LISICON structure have been found. In the Li_4GeO_4- Li_3CrO_4 binary system[1], an extensive range of solid solutions $Li_{3+x}Cr_{1-x}Ge_xO_4$ with γ-LISICON structure has been found with probable solid solution mechanism $Cr^{5+} \rightarrow Li^{+} + Ge^{4+}$. These solid solutions are unusual in that it contains Cr^{5+}. X-ray powder diffraction data for the γ solid solution can be indexed on an orthorhombic unit cell, Pmnb. It is very similar to other γ-phases such as γ -Li_3PO_4 and LISICON. Li^{+}ion conductivity increases with x; at x=0.90,(bulk), $1.4x10^{-5}$ S cm^{-1} at 27^0C rising to 0.044 S cm^{-1} at 300^0C. These ionic conductivities are among the highest found for solid Li^{+}ion conductors in the LISICON/γ family.

In the Li_4GeO_4-Li_2CoGeO_4 system, a new LISICON type γ-solid solution range with formula $Li_{4-2x}Co_xGeO_4$ has been found for $0.15<x<0.8$. Powder X-ray diffraction data for the γ-solid solution can be indexed on an orthorhomsic unit cell, Pmnb, similar to γ-Li_3PO_4 structure. The highest net conductivity, $8.4x10^{-6}$ Scm^{-1}, was observed for x=0.25 at 27^0C, charge/discharge polarization measurements and low frequency a.c. impedance measurements show the occurrence of mixed Li^{+} ion and electronic conductivity in the material.

In the Li_4GeO_4-Li_2SO_4 binary system, a new LISICON type γ solid solution range with formula $Li_{4-2x}Ge_{1-x}S_xO_4$ has been found for $0.08<x<0.42$. The γ-solid solutions are structurally related to orthorhombic γ-Li_3PO_4 and contain interstitial Li^{+}ions.

1. M.A.K.L. Dissanayake, R.P. Gunawardane, H.H. Sumathipala and A.R. West, (1995), Solid State Ionics 76, 215.

P08.10.005 DEFECT STRUCTURE AND LATTICE HEAT CAPACITY OF ZIRCONIA. T. Atake and T. Tojo, Materials and Structures Laboratory, Tokyo Institute of Technology, Yokohama, 226-8503 JAPAN, and T. Mori, National Institute for Research in Inorganic Materials, Tsukuba, 305-0044 JAPAN, and H. Yamamura, Faculty of Engineering, Kanagawa University, Yokohama, 221-8686 JAPAN, and O. Yamamoto, Faculty of Engineering, Mie University, Tsu, 514-8507 JAPAN.

The heat capacities of zirconia (ZrO_2) have been measured for the three polymorphs of monoclinic, tetragonal and cubic structures between 13 and 300 K using a high precision adiabatic calorimeter [1,2]. The latter two polymorphs, which are the high temperature forms of zirconia, are stabilized down to room temperature by yttria- or scandia-doping, while pure zirconia undergoes phase transition and the structure is of monoclinic at room temperature. Several samples of various doping at most 11 mol % of yttria or scandia were used for the present study. Highly doped samples are of cubic and lower doped samples are of tetragonal. It has been found that the doped samples have excess heat capacity at low temperatures compared with pure zirconia. The excess heat capacity decreases with increasing doping. However, the detailed mechanism in the stabilized zirconia has not been clarified yet. In the present study, molecular dynamics simulation has been performed and the calculated phonon density of states are successfully compared with the measured heat capacities.

T. Tojo, T. Atake, T. Mori & H. Yamamura, J. Therm. Anal. & Calorimetry (in press).
T. Tojo, T. Atake, T. Mori & H. Yamamura, J. Chem. Thermodyn. (in press).

P08.10.006 *IN SITU* XRD STUDIES OF GRAPHITE ELECTRODES IN THE Li-ION BATTERY. Kristina Edström, Inorganic Chemistry, Ångström Laboratory, Uppsala University, Box 538, SE-751 21 Uppsala, Sweden

Diffraction techniques are valuable for studying structural change in battery electrode materials at an atomic level. There are many examples of the use of X-ray diffraction in determining cell parameters, for phase identification and for assessing crystallinity connected to battery research. Several non-standard methods can be exploited, however, to provide a more detailed understanding of atomic-level processes in Li-ion or Li-polymer batteries. This will be illustrated here with examples taken from potential anode materials. A number of features will be addressed: phase analysis; structural changes on lithium insertion; temperature dependence of structural changes; lithium insertion mechanisms; structural kinetics. The *in situ* X-ray diffraction methods demonstrated are all performed in transmission mode using a STOE position-sensitive detector (PSD) powder diffractometer.

The Li-ion battery comprises a transition-metal oxide cathode, an anode material which serves as lithium-ion host, and a mechanical separator soaked in some lithium salt solution as electrolyte. The anode currently used in commercial Li-ion batteries is a carboneous material, typically graphite. In this work, graphite is studied at low voltage against a Li counter-electrode.

Some results will be presented from structural studies which will illustrate the performance of the graphite electrode at both ambient and elevated temperatures and under conditions of pulsed charging/discharging, as occurs in mobile-phone applications.

P08.10.007 STRUCTURE OF CATHODE AND ITS RELATION TO CAPACITY FADE IN LI-SPINEL BATTERY. T. Kamiyama, I. Nakai[a], Y. Terada[a], S. Gotoh, K. Oikawa[b], Y. Shiraishi[a], F. Nishikawa[c] and F. Izumi[d], Institute of Materials Science, University of Tsukuba, Tsukuba, Ibaraki 305-8573, Japan, [a]Department of Applied Chemistry, Science University of Tokyo, Kagurazaka, Tokyo 162-0825, Japan, [b]Advanced Science Research Center, JAERI, Tokai, Ibaraki 319-1195, Japan, [c]Asahi Chemical Industry Co. Ltd., Kawasaki, Kanagawa 210, Japan, [d]National Institute for Research in Inorganic Materials, Tsukuba, Ibaraki 305-0044, Japan.

Although $LiCoO_2$ is widely used for cathodes in commercial Li-ion batteries, a spinel-type oxide, $LiMn_2O_4$, is now intensively studied commercially because it is preferable in terms of the large abundance and safety, i.e., cheap and non toxic. However, inferior charge/discharge properties should be overcome before application.

The relation among crystal structures, microstructures and cycling performance of batteries will be revealed through in situ neutron diffraction. However, in situ neutron diffraction is not easy because a battery cell consists of various components which prevent precise structure determination. Choice and arrangement of those components is important to clarify what occurs in the structure and which is harmful for the cycling performance.

With the Li-spinel cell developed for neutron diffraction experiments, unwanted Bragg reflections were minimized. After 50% charging, the occupancy of a Li site decreases with little change in the rest of the structure. However, after deep charging, phase separation occurred and two phases with different Li content emerged. In the phase of lower Li content, Li ions are most likely to occupy at 16c site in addition to original one. We speculated that the second phase is unstable in the electrolyte. This is consistent with the fact that deep charging degrades the cycling performance.

P08.10.009 FLUORITE RELATED SUPERSTRUCTURE OF A NEW OXYPHOSPHATE OF LEAD AND BISMUTH : $Pb_4Bi_{19}P_4O_{42.5}$. Sophie Giraud[1,2], Jean-Pierre Wignacourt[1], Michel Drache[1], Pierre Conflant[1], Hugo Steinfink[2], [1]Laboratoire de Cristallochimie et Physicochimie du Solide, URA CNRS 452, ENSCL, BP 108, 59652 Villeneuve d'Ascq Cedex, France ; [2]Texas Materials Institute, Department of Chemical Engineering, University of Texas, Austin, Texas 78712, USA.

The structure of a new oxyphosphate with high bismuth content, $Pb_4Bi_{19}P_4O_{42.5}$, can be derived from the cubic δ-Bi_2O_3 [1] structure, which itself is a CaF_2 (fluorite) structure derivative. The initial F centered cubic cell of δ-Bi_2O_3 (a = 5.648 Å) can be transformed to a smaller tetragonal I centered cell, a, b = 3.9 Å and c = 5.5 Å . Weissenberg photographs and the X-ray data collected on a single crystal of $Pb_4Bi_{19}P_4O_{42.5}$ show weak superstructure reflections leading to a pseudo orthorhombic cell with parameters a = 11.885(2) Å, b = 11.540(2) Å, c = 15.636(3) Å and β = 90.23(3)°. The cell is I centered. The oxyphosphate can be described by a 3 x 3 x 3 superstructure derived from the fluorite "small cell". The structure was solved in the monoclinic system, superstructure cell space group I2, using X-ray synchrotron data, λ = 0.1602 Å, which avoids an absorption correction. The structure refinement converged to R<0.05. The atomic positions of the heavy atoms adopt an orthorhombic symmetry, but the oxygen atoms reduce the symmetry to monoclinic. The details of the structure will be presented.

We thank Dr. Richard Harlow for the synchrotron data collection.

[1] Laura E. Depero and Luigi Sangaletti, J. Solid State Chem., **122**, 439-443 (1996).

P08.10.010 THE CHALLENGE OF X-RAY DIFFRACTION RESIDUAL STRESS MEASUREMENTS ON HELICAL COMPRESSION SPRINGS. C. K. Lowe-Ma, A. R. Drews, and A. R. Krause, Ford Research Laboratories, Ford Motor Company, Dearborn, MI 48121, USA.

Helical compression springs used for suspension in automobiles must meet specific requirements for loading, operating stress range, fatigue life, mass and space constraints, and geometrical tolerance under various temperature and corrosion conditions. Compression springs that are produced by the cold coil method have an advantage in surface quality over those produced by hot coiling that translates to a smaller diameter wire for equivalent operating stresses. However, in the production of cold-coiled springs, several manufacturing steps affect the final fatigue performance of the spring. The variables in these processing steps must be optimized and remain constant to attain the specified fatigue life. The residual stress profile in compression springs is an excellent gauge of the processing parameters and of any changes occurring during production runs. X-ray diffraction can be used to measure the residual stresses, but, in reality, conducting X-ray diffraction-based residual stress measurements on a spring (without destroying the spring!) present a challenge. Fundamental issues and selected results from laboratory and production plant measurements of X-ray diffraction-based residual stress will be presented and discussed in the context of process monitoring.

P09.10.000 THE CALCULATION OF ANHARMONIC MOTION AND DISORDERING OF CATIONS IN THE STRUCTURE OF $K_{1-X}Tl_XTiOPO_4$ CRYSTALS. D.Y.Lee, Department of electrical materials, Korea Electrotechnology Research Institute

Precise X-ray structural analysis of $KTiOPO_4$(KTP) type single crystals often meets the difficulties in analysis of electron density distribution around the positions of one valance cations, which locate in the channels between hard frames of TiO_6 octahedron chains and PO_4 tetrahedron. In these positions significant residual peaks are found on the difference Fourier map of electron density after anisotropic refinement of crystal structure in some crystals of this type. This means that further refinement is necessary for more exact decision of these structures. In this case, in order to solve this problem, two models can be suggested: 1. dynamic model of anharmonic motion of atoms and 2. static model of disordering of atoms in these positions.

In this study, these two models were applied for solving the problems of residual peaks around the positions of (K, Tl) cations on the difference Fourier map of electron density in the structural of $K_{1-x}Tl_xTiOPO_4$ crystals, in which x = 0.18, 0.41 and 1.

Anharmonic refinement of thermal parameters of (K, Tl) atoms were calculated to 6^{th} rank tensor by Gram-Charlier and Edgeworth expansions, using program PROMETHEUS. [1]

Structural analysis of disordering has difficulties, connected to strong correlation between some parameters of atoms in seperated positions, including coordinates, occupancies and thermal parameters. These difficulties were solved by step-by-step scanning method.[2]

U.H.Zucker, & H.Schulz (1982) Acta Cryst. A.38, 563-568
L.A.Muradiyn, S.F.Radayev, & V.I.Simonov (1989) Method of structural analysis. (Hauka) 5-20

P09.10.001 STRUCTURAL CHARACTERISTICS OF FLUX GROWN CRYSTALS OF THE $NdAl_3(BO_3)_4$-$GdAl_3(BO_3)_4$ SYSTEM. G.Bocelli and L.Righi, CSSD-CNR, University of Parma, Parma-43100, Italy, N.I.Leonyuk and E.V.Koporulina, Moscow State University, Moscow-119899, Russia.

The solid solutions based on the system $NdAl_3(BO_3)_4$-$GdAl_3(BO_3)_4$ (NAB-GAB) belong to the famous family of polyfunctional orthoborates with device potential [1]. Of these materials, the non-centrosymmetric Nd_xGd_{1-x} $Al_3(BO_3)_4$ (NGAB) crystals are promising materials for non-linear optics and self-frequency-doubling lasers [2]. Low-temperature forms of the end members of these solid solutions belong to the non-centrosymmetric huntite *R32* space group, but the high forms of NAB and GAB crystals have the centrosymmetric monoclinic space groups *C2/c* and *C2* respectively. The purpose of this work was to find a correlation between the growth conditions, compositions, and structural characteristics of these solid solutions.

The crystals of NAB, GAB and GYAB were grown by both TSSG and spontaneous nucleation using a $K_2Mo_3O_{10}$ based flux. The Nd, Gd and Mo concentrations in the crystals obtained

were measured by microprobe analysis. The neodymium distribution coefficient K is usually close to 1, but it slightly depends on the crystal growth conditions. The structures of NAB, $Nd_{0.17}Gd_{0.83}Al_3(BO_3)_4$ and GAB crystals obtained under different growth conditions were refined. As a result, a correlation between the crystal structure, growth conditions and compositions of the grown crystals will be discussed.

[1] N.I.Leonyuk & L.I.Leonyuk (1995) *Prog. Crystal. Growth and Charact.* Vol. 31, pp.179-278.
[2] T. Chaoyang, L.Zundu, G.Chen & G.Wang (1994) *Cryst. Res. Technol*. Vol.29, No 3, K 47-50.

P09.10.002 CRYSTALLISATION AND STRUCTURAL CHARACTERISATION OF La,Nd BOROSILICATES. E.P.Shvanskii, N.I.Leonyuk, E.L.Belokoneva, Department of Crystallography, Moscow State University, Moscow 119899, Russia, and G. Bocelli, L. Righi, Centro di Studio per la Strutturistica Diffrattometrica CNR, Viale delle Scienze, Parma 43100, Italy

The $LaBSiO_5$ crystals with the stillwellite type structure belong to the new ferroelectric family, and at the same time, they possess non-linear optical (NLO) and piezoelectric properties [1]. Neodymium doped stillwellite crystals can be considered as a new laser materials.

Crystals of stillwellite-like La and La,Nd borosilicate were obtained from high temperature solutions. Also, new La borosilicate, $La_3BSi_2O_{10}$ was obtained by this method. The choice of fluxes was based on the potassium trimolybdate with an excess of lithium and potassium fluoride. The composition of grown crystals was studied by electron microprobe analysis, and powder diffraction patterns were determined for all the crystals. Results of detailed structural study will be presented for all the crystals.

Some aspects of the synthesis of new La and La,Nd borosilicates with controlled and desirable composition, structure and properties will be discussed.

1. S.Yu Stefanovich, V.N.Sigaev, A.V.Dechev, A.V. Mosunov, V.R.Samygina and P.D.Sarkisov (1995). Izv. RAN, Ser. Neorgan. Mater., 31, 819.

P09.10.003 $(Y,Gd)Al_3(BO_3)_4$ AND $(Y,Nd)Al_3(BO_3)_4$ SOLID SOLUTIONS WITH DEVICE POTENTIAL: CRYSTAL GROWTH, COMPOSITION AND STRUCTURE E.V.Koporulina and N.I.Leonyuk, Geological Faculty, Moscow State University, Moscow 119899, Russia, and A.V.Mokhov, Institute of Ore Deposits Geology, Petrography, Mineralogy and Geochemistry RAS, Staromonetny 35, Moscow 109017, Russia.

Non-centrosymmetric solid solutions based on the $(Nd_xY_{1-x})Al_3(BO_3)_4$ (NYAB) system are excellent materials for self-frequency-doubling lasers, and $(Gd_xY_{1-x})Al_3(BO_3)_4$ (GYAB) crystals have considerable potential for the application of high frequency acoustic wave devices in the 8-9 GHz range [1]. However, there are problems to obtain these solid solutions with desirable structure and homogeneity because the YAB belongs to the R32 sp. gr., but each of other end members exists, at least, in two polymorphic modifications: R32 and C2/c sp. gr. (NAB), R32 and C2 sp. gr. (GAB). In this work, the structures, composition and homogeneity of these solid solutions have been studied depending on the growth conditions.

The crystals of NYAB (x=0.05, 0.1, 0.6, 0.75) and GYAB (x=0.1, 0.2, 0.3, 0.4, 0.6, 0.65, 0.7 and 0.75) were grown by both spontaneous nucleation and TSSG from a $K_2Mo_3O_{10}$-containing fluxed melts in the temperature ranges 1060-990°C and 1050-1010°C respectively. The structures of the NYAB (x=0.75) and GYAB (x= 0.65, 0.7 and 0.75) crystals have been studied.

The temperatures and concentration ranges of phase transitions are determined using X-ray technique, EMPA, optical and electron microscopies.

[1] N.I.Leonyuk and L.I.Leonyuk. Prog. Crystal. Growth and Charact. 31 (1995) 179-278.

P09.10.004 NEUTRON AND X-RAY DIFFRACTION STUDY OF YTTRIUM-ALUMINIUM BORATE. E. Sváb, Gy. Mészáros, E. Beregi, Research Institute for Solid State Physics and Optics, H-1525 Budapest, POB 49 and M. Tóth, Hungarian Academy of Sciences Laboratory for Geochemical Research, H-1112 Budapest, Budaőrsi str. 45, Hungary

Yttrium-aluminium borate – $YAl_3(BO_3)_4$ (YAB) single crystals have excellent non-linear optical properties, and the doped YAB crystals are important for building microchip lasers. Pure and doped (Cr, Ga) YAB single crystals were grown by top-seeded high temperature solution (flux) method. The single crystals were powdered into fine grains to obtain good powder spectrum suitable for Rietveld refinement. The measurements were performed using the PSD neutron diffractometer (λ=1.0577 Å) at the 10 MW Budapest research reactor and a Philips X-ray diffractometer with monochromatic $CuK_{\alpha 1}$ (1.5406 Å) radiation. The starting parameters for data treatment were taken from [1]. The space group is hexagonal R32 (No.155) with trigonal symmetry. The results for pure YAB are summarised in Table 1. Refined crystallographic parameters will be presented for doped YAB crystals as well.

Table 1. Crystallographic data for $YAl_3(BO_3)_4$.
Lattice parameters: a=9.275(6) Å and c=7.223(9) Å

Atom (position)	x	y	z
Y (3a)	0	0	0
Al (9d)	0.553(4)	0	0
B(1) (3b)	0	0	0.5
B(2) (9e)	0.444(8)	0	0.5
O(1) (9e)	0.850(5)	0	0.5
O(2) (9e)	0.587(6)	0	0.5
O(3) (18f)	0.448(9)	0.154(4)	0.515(2)

1. E.L. Belokoneva, A.V. Azizov, N.I. Leonyuk, M.A. Simonov & N.V. Belov (1981). Zhurnal Structurnoi Khimii, **22**, 196.

P09.10.005 LINEAR AND NONLINEAR OPTICAL PROPERTIES OFBiB_3O_6 (BIBO) H. Hellwig, J. Liebertz, L. Bohatý, University of Cologne, Institute of Crystallography, Zülpicher Str. 49 b, D-50674 Köln, Germany

Finding new materials for nonlinear optics is still a current topic because of the increasing variety of applications. Borates are a large reservoir of non-centrosymmetric crystals with the nonlinear optically efficient $[BO_3]$ group.We determined the linear and nonlinear optical properties of the monoclinic bismuth borate BiB_3O_6, abbreviated as BIBO [1]. BIBO crystallizes monoclinic in the polar space group C2. Its structure consists of distorted $[BO_3]$ triangles and $[BO_4]$ tetrahedra in ratio 2:1 which form sheets, linked by six-coordinated bismuth cations [2]. The lone pair of the bismuth atom seems to play an important role for the stability of the crystal structure and its properties. Single crystals were first grown by Liebertz. Becker improved the growth method and grows large single crystals of optical quality with dimensions of several centimeters [3].The linear optical properties allow a wide range of phase matching processes. Due to the symmetry (one 2-fold axis only), there are 8 independent nonlinear optical coefficients d^{SHG}_{ijk} which describe second harmonic generation. We used the *Maker* fringe technique and special software for data evaluation to determine all of the 8 coefficients and their relative signs. With these data we are able to calculate most of the

nonlinear optical processes in a quantitative manner.We will present the results of this measurements and will demonstrate solutions for problems arising, if *Maker* fringe curves are to be analyzed. With our methods we are able to recalculate the measured curves with hardly any systematic discrepancy considering of multiple reflections and *Fabry-Perot* interferences [4].

[1] H. Hellwig, J. Liebertz, L. Bohatý: Solid State Comm. **109** (1999) 249
[2] R. Fröhlich, L. Bohatý, J. Liebertz: Acta Cryst. **C 40** (1984) 343
[3] P. Becker, J. Liebertz, L. Bohatý: subm. to J. Cryst. Growth (1999)
[4] H. Hellwig, L. Bohatý: accepted by Opt. Comm. (1999)

P09.10.006 CRYSTAL GROWTH AND SPECTROSCOPIC PROPERTIES OF RE : BiB_3O_6 (RE = Pr, Gd, Eu, Er). *P. Becker and **C. Wickleder, University of Cologne, *Institute of Crystallography, Zülpicher Str. 49 b, 50674 Köln, Germany; **Institute of Inorganic Chemistry, Greinstr. 6, 50939 Köln, Germany.

During the last 15 years, compounds of the borate group turned out to be interesting materials for nonlinear optical applications. They are superior in UV-applications to other commonly used NLO materials like KH_2PO_4 or $LiNbO_3$ because of their high UV-transmittance combined with a high damage threshold. Bismuth triborate, BiB_3O_6, is a new, very promising material for nonlinear optics with a d_{eff}^{SHG} which is higher than that for most other materials being in use for applications, like $KTiOPO_4$, β-BaB_2O_4 or LiB_3O_5 [1]. It crystallizes in the monoclinic, polar space group C2; the structure consists of borate layers built by [BO_4] tetrahedra and [BO_3] triangles in a ratio of 1:2, alternating with layers of 6-fold coordinated Bi atoms [2].

Crystals of BiB_3O_6 were doped with the rare earth elements Pr, Gd, Eu and Er in order to combine its high frequency conversion capability with the host for potentially luminescent ions in one crystal. Large single crystals of doped BiB_3O_6 were grown from highly viscous melts with concentrations of 0.5 mole% RE_2O_3 (RE = Pr, Gd, Eu, Er), respectively. Crystals of good quality with sizes up to 12 x 12 x 18 mm^3 were obtained by using the top seeding technique and with growth parameters similar to those used for undoped BiB_3O_6 [3].

To characterise the crystal field levels of the rare earth ions in the host lattice, we present absorption spectra in the wavelength range from 200 nm to 2000 nm, measured with an absorption spectrometer (Varian, Cary 5E). For the knowledge of the phonon energies, IR- and Raman spectra were recorded (Bruker, IFS 66V/S and FRA 106/S).

[1] H. Hellwig, J. Liebertz, L. Bohatý: Solid State Comm. **109** (1999), 249.
[2] R. Fröhlich, L. Bohatý, J. Liebertz: Acta Cryst. **C 40** (1984), 343.
[3] P. Becker, J. Liebertz, L. Bohatý: J. Cryst. Growth (1999), submitted.

P09.10.007 STRUCTURE AND PROPERTIES OF THE CRYSTALS IN THE $RbTiOPO_4$-$CsTiPO_5$ SYSTEM. Liu Wen, V.I.Voronkova, and V.K.Yanovskii, Department of Physics, Moscow State University, Moscow 119899, Russia, and N.I.Sorokina, I.A.Verin and V.I.Simonov, Institute of Crystallography RAS, Moscow 117333, Russia.

Potassium titanyl phosphate $KTiOPO_4$ and other crystals of this family are of great interest as nonlinear optical materials, ferroelectrics and superionic conductors. The present paper deals with the precise X-ray analysis and some physical properties of the mixed composition crystals in the system $RbTiOPO_4$ (RTP)-$CsTiPO_5$ (CTP) with the main attention paid to solid solutions on the base of RTP.

The investigations of the RTP-CTP system in the subsolidus region shows that it is pseudobinary one with the limited solid solutions $Rb_{1-x}Cs_xTiOPO_4$ of the KTP-type structure and $Cs_{1-x}Rb_xTiPO_5$ of pyrochlore-type. The width of the former solution area is $0<x<0.2$ at 700°C and diminishes as the temperature increases. At higher temperatures and higher Cs concentrations the pyrochlore-type structure is more stabile. The unit cell parameters of RTP:Cs and CTP:Rb solutions obey well the Vegard law.

Single crystals of $Rb_{1-x}Cs_xTiOPO_4$ with x=0.00, x=0.05 and x=0.11 were grown with the use of flux method from melts of Rb_2O-Cs_2O-TiO_2-P_2O_5 system and their atomic structures were refined by means of precise X-ray analysis. The partial substitution of Rb by Cs leads to the increase of the unit cell parameters *a* and *b* and to more loose crystal structure with incomplete occupation of Ti, P and O positions. Cs atoms show tendency to occupy mainly one of two possible positions having more large coordination with oxygen. The distortion of TiO_6 octahedra, responsible partially for the appearance of spontaneous polarization at the ferroelectric transition, decreases with this substitution.

Temperature dependencies of the dielectric permeability ε_{33} and electrical conductivity σ_{33} of the $RbTiOPO_4$ and $Rb_{0.95}Cs_{0.05}TiOPO_4$ single crystals are studied. A small substitution of Rb by Cs results in the lowering of ferroelectric transition point by 20°C and to increasing of ionic conductivity by about one order of magnitude.

P09.10.008 THE CRYSTAL STRUCTURES OF TWO EXTENDED π-BRIDGED OPTICALLY NONLINEAR CHROMOPHORES. G.J. Gainsford and A.D. Woolhouse, Industrial Research Limited, Gracefield Road, Lower Hutt, New Zealand and R.A. Myers and T.H. Barnes, Department of Physics, University of Auckland, Private Bag 92019, Auckland, New Zealand.

As part of our research effort to make usable $\chi^{(2)}$ polymers from tetherable equivalents of a number of accessible high β chromophores, we were able to produce crystals of representatives of two extended π-bridge systems: 6-[4-N,N-Bis(2-hydroxyethyl)amino]phenylene-4-(dicyano)methylidene-2-methyl-4*H*-pyran (I) and 5-{3-[4-N,N-Bis(2-hydroxyethyl)amino]-phenylene-5,5-dimethyl-2-cyclohexen-1-ylidene}-1,3-dimethyl-1,3-dihydro-2-thioxo-1*H*,5*H*-pyrimidine-4,6-dione (II). Both are characterized by the presence of *hetero*aromatisable acceptors that should, in principle proffer energetic compensation for the loss of aromatic stabilization in the donor moiety.

(I) Crystallizes in P-1, *a*=7.3398(3), *b*=10.4970(5) ,*c*= 7.3398(3) Å, α 79.705(2), β 80.925(2), γ 81.989(2) deg, V 941.06(7) Å^3, Z=2. It contains discrete molecules of $C_{21}H_{21}N_3O_3$ hydrogen bonded via the hydroxyl hydrogen atoms to adjacent oxygen and cyano-nitrogen atoms (s).

(II) $C_{28}H_{32}N_3O_4S$ crystallizes in P 2_1/c, *a*=19.0643(12), *b*=9.2783(6), *c*= 16.9017(11) Å, β=90.462(1)°, with an ethanol molecule of crystallization (Z=4, V=2980.6(3) Å^3). The two molecules form an hydrogen-bonded infinite two-dimensional network.

Bond length alternation values (*bla*) [A] and the results of other measurements will be presented.

A. Shu, C.F., Shu, Y-C., Gong, Z., Peng, S-M., Lee,G-H. & Jen, A.K.Y., Chem. Mater. (1998),10, 3284-3286 and references therein.

P09.10.009 $LiNBO_3$ REVISITED. B. Etschmann, N. Ishizawa, Y. Matsushima & K. Suda-Saito, Materials and Structures Laboratory, Tokyo Institute of Technology, 4256 Nagatsuta, Midori-ku, Yokohama 226, Japan

$LiNbO_3$ is a ferroelectric material which has been studied extensively due to its wide range of applicability in linear and non-linear optical and acoustic devices. Optimal use of lithium niobate in such devices depends on the Li:Nb ratio, as this critically affects many physical properties of the sample. This has resulted in numerous types of investigations, including single-crystal diffraction experiments, to determine the Li:Nb ratio. However, previous single crystal studies suffered severely from extinction [e.g. 1-2], and corrections for extinction and anharmonic thermal vibrations may affect the calculation of the Li:Nb ratio [3].

Extinction effects may be reduced by using a smaller crystal, thus diffraction data was collected on an eight micron lithium niobate crystal at BL14A, Photon Factory, in Tsukuba, Japan. Preliminary refinements indicate that the extinction is virtually negligible (y_{min} = 0.97), with an R-factor around 1%. The atoms vibrate anisotropically, however, no pronounced anharmonicity has been detected. Electron density maps have similar features to maps published previously, such as an accumulation of electrons around Li, but the features are much less pronounced.

[1] S. C. Abrahams & P. Marsh, (1986). Acta Cryst. B42, 61.
[2] R. Hsu, E. N. Maslen, D. Du Boulay & N. Ishizawa, (1997). Acta Cryst. B53, 420.
[3] N. Iyi, K. Kitamura, F. Izumi, J. K. Yamamoto, T. Hayashi, H. Asano & S. Kimura (1992), J. Solid. State. Chem., 101, 340.

P09.10.010 NEUTRON DIFFRACTION STUDIES ON MIXED CRYSTALS OF $RbTiOAsO_4$ AND $CsTiOAsO_4$. Jörgen Albertsson, Jenni Almgren and Göran Svensson, Department of Inorganic Chemistry, Chalmers University of Technology, SE - 412 96 Göteborg, Sweden (jean@inoc.chalmers.se).

The $KTiOPO_4$ isomorhpic family consists of $MTiOXO_4$ compounds where M, among others is K, Rb, or Cs and X is P or As. These materials are known for their non-linear optical properties. In IR generating laser experiments the arsenates are needed as these have higher transmission than phosphate analogues. It is very difficult to get large CTA crystals of optical quality and we are therefore growing mixed crystals of RTA and CTA. Spontaneously grown crystals measure up to $3 \times 3 \times 3$ mm and even larger pieces of optical quality can be cut from top seeded grown crystals.

RTA and CTA have network structures of AsO_4 tetrahedra and TiO_6 octahedra with chains of - AsO_4 - TiO_6 - AsO_4 - TiO_6 - along the *a*, *b* and *ac* directions. The Ti atoms in the octahedra are displaced, giving long and short Ti - O bonds that are partially responsible for the optical non-linearity. The network has open channels along the *c* axis with two different sites for the cation. Powder data has been collected for three different mixtures of RTA and CTA together with the pure compounds. This is done to study the coordination sites and to determine the Rb/Cs occupancies in different mixtures.

Single crystal X-ray diffraction studies show odd displacement parameters, which are probably due to the high absorption of the heavy atoms causing problems with the absorption correction. An improved structure model is needed for precision electron density studies [1], and for this purpose 1466 reflections has been collected at 295 K using neutron single crystal diffraction. The RTA sample used in this experiment was cut to the size $5 \times 3 \times 2$ mm^3 in *a*, *b* and *c* directions.

1. Almgren, J., Streltsov, V. A., Sobolev, A. N. & Albertsson, J., *Acta Cryst* B, submitted.

P09.10.011 CRYSTAL STRUCTURE AND PIEZO-ELECTRIC PROPERTIES OF La-, Pr- AND Nd-LANGASITE. [1]H. Ohsato, [2]H. Morikoshi, [1]D. Sakakibara, [1]K. Suito, [2]J. Sato, [2]K. Kawasaki and [1]K. Tanaka, [1]Nagoya Institute of Technology, Gokiso-cho, Showa-ku, Nagoya 466-8555, Japan, [2]Materials Research Center, TDK Co., Matugashita 570-4, Minamihatori, Narita 286-0805, Japan.

Recently, one of promising piezoelectric materials for high-bit rates digital communication is $R_3GaGa_3(Ga,Si)O_{14}$ (*R*= rare earth) designated as langasite, which has larger electromechanical coupling factor than quartz and also has nearly the same temperature stability as quartz. The piezoelectric constant increases with the ionic radius of *R* [1]. In this study, the mechanism of the piezoelectricity was clarified based on the crystal structure.

The intensity data of langasite crystals grown by the Czochralski method were measured by the four circle X-ray diffractometer with rotating anode.

Crystal data of typical La-langasite are as follows; Sphere r=0.11mm, Trigonal, $P321$ (No.150), a=8.1539(3), c=5.0904(4) Å, Z=1, D_x=5.766Mgm^{-3}, λ=0.71073 Å, μ=228.44, 2θ<95°, final R=3.26%, wR=3.63%.

The atomic coordination of La- and Pr-langasite as follows:

Atoms:site	*x*: L/PGS	*y*: L/PGS	*z*: L/PGS
A:La/Pr:3e	.41872/.41793(4)	0	0
B:Ga,:1a	0	0	0
C:Ga2:3f	.76527/.76469(8)	0	1/2
D:Ga, Si:2d	1/3	2/3	.46780/.4654(3)
O:2d	1/3	2/3	.805/.802(2)
O:6g	.4649/.4693(6)	.3105/.3173(6)	.6833/.6885(9)
O:6g	.2229/.2250(7)	.0815/.0787(7)	.2356/.2381(9)

The initial atomic parmeters were quated from Mill *et al*.[2]. Those of Nd-langasite will also presented at the conference.

The piezoelectric constant of La-langasite was improved by the magunitude of the polarity of *R* ions in the *A*-site of $A_3BC_3D_2O_{14}$ general formula, which was produced by the size difference of the polyhedra of *R* ion.

1. J.Sato *et al*., J. Crystal Growth, **191**(1998)746-53. 2. Mill *et al*., Dokl. Akad. Nauk SSR, **264** (1982) 1385-89.

P09.10.012 ELECTRON DENSITY IN $Rb(Cs)TiOAsO_4$ FROM SYNCHROTRON RADIATION DATA. J. Almgren[a], V.A. Streltsov[b] and J. Albertsson[a], [a]Department of Inorganic Chemistry, Chalmers University of Technology, Sweden, [b]Crystallography Centre, University of Western Australia, Australia (jean@inoc.chalmers.se).

High-flux synchrotron X-radiation has been used to study the electron density distribution in $MTiOAsO_4$ (M = Rb (RTA), Cs (CTA)) at room temperature and 100 K, respectively. The electron density maps for RTA resemble those obtained at 9.6 K [1]. However, the electron density near the Rb atoms is significantly diffuse and there are indications of splitting of the Rb positions at room temperature.

RTA and CTA belong to the $KTiOPO_4$ isomorphic family of compounds with strong non-linear optical properties. X-ray diffraction data at 9.6 K has shown significant shifts of the alkali atoms from their room temperature positions and dipole-like deformations of the electron density near the Ti atoms along the polar *c* axis. This indicates that these atoms contribute to the spontaneous polarization of the studied compounds. The electron density accumulates near the exceptionally short Ti - O bonds, which can be partly responsible for the non-linear optical properties.

The data were collected at BL14A, KEK Photon Factory, Tskuba, Japan. The RTA data set was measured at 295 K with λ = 0.75 Å. The total number of reflections were 47232 (44053 > $2\sigma(I)$), for a full sphere of data up to 2θ = 120°. A second data set

of half a sphere up to 2θ = 110° was collected at 100 K for a mixed RTA – CTA crystal, grown from a self-flux containing 60 % Rb and 40 % Cs. The structural results are similar to those reported in [2].

1. Almgren, J., Streltsov, V.A., Sobolev, A.N. & Albertsson, J., *Acta Cryst.* B, submitted.
2. Womersley, M.N., Thomas, P.A. & Corker, D.L., *Acta Cryst.,* B**54** (1998) 635- 644.

P09.10.013 $Na_4Co_3H_2(PO_4)_4{\cdot}8H_2O$ WITH A NEW STRUCTURE TYPE*. S.Y.Mao, Y.X.Huang, Z.B.Wei, J.X.Mi, Z.L.Huang and J.T.Zhao, College of Chemistry and Chemical Engineering, Xiamen University, Xiamen 361005, P.R. China

The recent work of Stucky et al.[1] concerning three-dimensional microporous alkali metal cobalt phosphates prompts us to report our new results. The title compound was synthesized by mild hydrothermal method in glass tubes under autogenous pressure and the crystal structure characterized by single crystal X-ray method. The structure was solved and refined using the SDP program package [2]. It possess a new type: monoclinic, mP106, $P2_1/c$, a = 7.3547(9)Å, b = 9.222(1)Å, c = 15.186(2)Å, β = 95.18(1), V = 1025.9(3)Å^3, Z = 2. It is characterized by stacked layers of corner sharing CoO_6 octahedra and CoO_5 trigonal bipyramids with PO_4 tetrahedra sandwiched by sodium cations and water molecules through hydrogen bonds. The tetrahedron around one of the P atoms is rather regular with average P-O distance of 1.539Å and angle of 109.5 but the other has some deformation caused by the OH group. Two Co atoms have different oxygen coordination : a regular octahedron (average distance of 2.094Å) and a deformed trigonal-bipyramid (to one of the epical O : 2.397Å; and to other O : range from 1.994 to 2.026Å) with the Co shifted out off the basil plane. Two Na atoms are octahedrally coordinated by oxygen atoms. The temperature dependence of the magnetic susceptibility follows the Curie-Weiss law and the effective magnetic moment per Co calculated is 4.69μ_B falling in the range of the expected values of 4.30 to 5.20 for the octahedrally coordinated high spin Co^{2+} ion [3].

This study was supported by the NNSF of China.

1. P.Feng, X.Xu & G.D.Stucky, Nature, **388**, 735, 1997.
2. B.A. Frenz and Associates, Inc., "SDP User's Guide", College Station, Texas 77840 and Enraf-Nonius, Delft, Holland, 1985.
3. L.Carlin, Magnetochemistry, Springer-Verlag, Berlin Heiderberg, p.53-65, 1986.

P09.10.014 STRUCTURE AND DEFECT STRUCTURE OF TEMPLATED SUBSTITUTED ALPO-5 R.B. Neder and K. Hradil, Institut f. Mineralogie, Am Hubland, 97074 Würzburg, Germany and A.N. Christensen, Department of Inorganic Chemistry, Aarhus University, 8000-Aarhus C, Denmark

We observed diffuse scattering by templated Mn substituded aluminum phosphate #5 micro-crystals. The sample displays diffuse streaks parallel to [001]* through Bragg reflections. Several broad bands of diffuse scattering are observed that are normal to [001]*. Near the hk0 plane broad bands roughly parallel to [001]* are observed. A unique feature, not known from any other sample, is two thin layers of diffuse intensity approximately normal to [001]*. The shape of these layers is roughly sinusoidal and the two layers intersect. The diffuse scattering is interpreted in terms of disorder of the templating molecule, triethylamine, which can assume different positions within the 1-D channels of the host structure.

Different space groups are reported for templated and calcined ALPO-5. We collected data for as grown Mn, Co and Zn substituted ALPO-5 micro-crystals (~ 110 x 20 x 20 μm) templated by triethylamine. The diffraction pattern of the Zn compound revealed split Bragg reflections, indicating orthorhombic symmetry. The Co and Mn compounds showed no indication of lower symmetry. Details of the structure refinement in space groups P6cc and Ccc2 will be reported. The refinements indicate hexagonal symmetry and an ordered Al and P distribution. Refined bond lengths and bond angles agree well with theoretical calculations.

P09.10.015 EXTENDED FRAMEWORKS STRUCTURES ENCAPSULATING FACIAL {MoO_3} CORE. Sue-Lein Wang, Kuei-Fang Hsu, Department of Chemistry, National Tsing Hua University, Hsinchu, Taiwan 300 ROC

Three new alkaline-earth metal molybdenum(VI) arsenates, $Ba_3(MoO_3)_3(H_2O)(AsO_4)_2$ (1), $SrMoO_3HAsO_4.H_2O$ (2) and $Sr(MoO_2AsO_4)_2$ (3), have been prepared and structurally characterized by single-crystal X-ray diffraction and thermogravimetric analysis. Crystal data: 1, monoclinic, $P2_1/c$, a = 10.1814(2) Å, b = 17.5553(1) Å, c = 17.0799(1) Å, β = 90.349(1)°, V = 3052.75(7) Å^3, and Z = 8; 2, monoclinic, C2/c, a = 15.1927(11) Å, b = 10.2590(8) Å, c = 9.6550(7) Å, β = 121.877(1)°, V = 1277.9(3) Å^3, and Z = 8; 3, monoclinic, $P2_1/c$, a = 6.5904(3) Å, b = 6.8592(3) Å, c = 10.4472(5) Å, β = 92.106(2)°, V = 471.94(6) Å^3, and Z = 2. Crystal 1 adopts a novel open-framework structure which is composed of isolated MoO_6 and $Mo(H_2O)O_5$ octahedra linked by AsO_4 tetrahedra, resulting in intersecting tunnels where Ba^{2+} cations reside. Crystal 2 has a layer structure in which MoO_6 octahedra are corner-shared with $HAsO_4$ tetrahedra forming infinite sheets parallel to the (100) planes. The Sr^{2+} cations and water molecules are between the layers. Crystal 3 adopts a tunnel structure which is isotypic with the phosphates $A(MoO_2PO_4)_2$ (A = Ba, Pb). As a common feature, all of the MoO_6 octahedra possess three terminal O^{2-} ions in 1 and 2. They are the first extended structures encapsulating fac {MoO_3} units. Thermal analysis and powder X-ray diffraction studies revealed these units in 2 will progressively dissociate into cis {MoO_2} groups under heating, resulting in the structural transformation into 3. In this paper, the syntheses, crystal structures, thermogravimetric studies, and structural relationship are presented.

P09.10.016 SYNTHESIS AND CHARACTERIZATION OF NOVEL GALLIUM PHOSPHATES: $[Ga_4(C_{10}H_9N_2)_2(PO_4)(H_{0.5}PO_4)_2(HPO_4)_2(H_2PO_4)_2(H_2O)_2]$ AND $[Ga_5(OH)_2(C_{10}H_9N_2)(C_2O_4)(PO_4)_4]$. Kwang-Hwa Lii, Ching-Yeh Chen, Department of Chemistry, National Central University, Chungli, Taiwan ROC

The hydrothermal reactions of $Ga(NO_3)$, $4H_2O$, 4,4'-bypiridine, H_3PO_4, H_2O and butanol, and Ga_2O_3, 2-methylpiperazine, 4,4'-bipiridine, oxalic acid, H_3PO_4 and H_2O yield light brown crystals of $[Ga_4(C_{10}H_9N_2)_2(PO_4)(H_{0.5}PO_4)_2(HPO_4)_2(H_2PO_4)_2(H_2O)_2].?H_2O$ (1) and pale yellow crystals of $[Ga_5(OH)_2(C_{10}H_9N_2)(C_2O_4)(PO_4)_4].?2H2O$ (2), respectively, which have been characterized by single-crystal X-ray diffraction and solid state NMR spectroscopy. 1 crystallizes in the monoclinic space group C2/c with a = 26.4161(6), b = 8.0416(1), c = 20.3515(4) Å, b = 111.194(1)°, V = 4030.8(1) Å^3 and Z = 8. The compound has a 2-D layered structure in which the coordination environments around gallium are tetrahedral and octahedral; 4,4'-bipyridine is directly connected to the 6-coordinated Ga. This compound is unique in such a way that it is the first example in which four different types of phosphates, PO_4, $H_{0.5}PO_4$, HPO_4, and H_2PO_4 are present. 2 crystallizes in the monoclinic space group C2/c with a = 18.3430(2), b = 15.9372(4), c = 9.1019(2) Å, b = 90.867(1)°, V = 2660.5(1) Å^3 and Z = 4. The structure consists of GaO_4 tetrahedra and GaO_6 octahedra linked by phosphate and oxalate groups to form two dimensional sheets between which are the GaO_4N square pyramids, generating

tunnels in which the monoprotonated 4,4'-bipyridinium cations reside. 71Ga NMR shows a good correspondence between the fitted NMR parameters and the crystallographic data.

P09.10.017 THE ANTAGONISTIC THERMAL EXPANSION EFFECT IN ZEOLITES: A SINGLE CRYSTAL STUDY ON THE GUEST/HOST INTERACTIONS OF ZEOLITE NaX. J. Felsche and S. Riemann, Dept. Chemistry, University of Konstanz, Postfach M729, D-78457 Konstanz

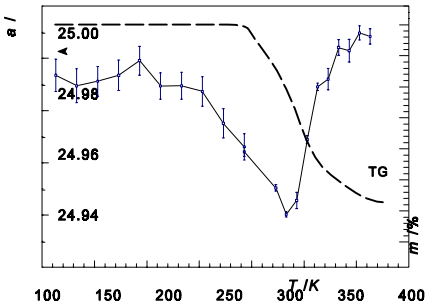

The single crystal diffraction study and supplementary IR- and MAS-NMR spectroscopy at temperatures of 110-800 K confirm the antagonistic effect of thermal expansion in alumosilicate zeolites which have the sodalite cage in the 4,2-network structures in common [1]. The closing and subsequent opening feature around the inversion temperature of 340 K in zeolite NaX occurs during the continuous thermally induced desorption of H_2O molecules.The positions of the sodium atoms - detected by the diffraction methods - correspond to the minishing H_2O molecules in the super cage by moving into the center position of the sixfold rings at a critical H_2O-concentration. The positions of most of the guest atoms were not detectable by diffraction methods because of the dynamics in the nature of the hydrogen and the oxygen atoms, which show hoping frequences of 10^5 - 10^{15} cps at the interface to the tetrahedral host structure. The special key/lock mechanism between the sodium ions and the oxygen atoms of the 4,2-network shows an antagonistic character which is not well understood by the models sofar given for the thermal expansion in tetrahedral 3D-network structures. The big challenge to modern crystallography will be the deeper understanding of atoms in the 3D-space to time structure, which can only be ensured by using manifold analytical methods beyond diffraction.

[1] Felsche, Luger; *Thermochim. Acta* 1987 118 35; S.Riemann; PhDThesis, University of Konstanz 1998; [2] Baur; *J. Solid State Chem.* 1992 97 243.

P11.10.001 EFFECT OF Al DOPING ON STRUCTURAL CHARACTERISTICS AND SUPER-CONDUCTIVITY OF RE-123-TYPE SINGLE CRYSTALS. A.Zhilyaeva, L.Leonyuk, N.I.Leonyuk, Moscow State University, 119899 Moscow, Russia Bocelli Gabriele, Righi Lara Centro di Studio per la Strutturistica Diffrattometrica CNR, I-43100 Parma, Italy G.-J.Babonas, A.Reza Semiconductor Physics Institute, 2600 Vilnius, Lithuania R.Szymczak, H.Szymczak, M.Baran Institute of Physics, 02-668 Warsaw, Poland B.Sherriff University of Manitoba, Winnipeg, Canada

The series of RE-123-type (RE are rare earth elements) single crystals with the various Al-content has been grown by a self-flux method. The structural features were investigated directly by the XRD and NMR methods as well as by the analysis of Raman and optical spectra. The superconducting (SC) properties estimated by the measurements of magnetic susceptibility were correlated to the particular structure of the single crystals under consideration. The structural data for all compounds were analyzed in the space group *P4/mmm*.

	Composition	*a* (Å)	*c* (Å)	T_c (K)
1	$Sm(Ba_{1.8}Sm_{0.2})Cu_{2.63}Al_{0.37}O_{6.94}$	3.897(1)	11.580(2)	Nsc
2	$GdBa_2Cu_{2.70}Al_{0.30}O_{6.88}$	3.894(1)	11.702(3)	25
3	$Dy(Ba_{1.92}Dy_{0.08})Cu_{2.80}Al_{0.20}O_{6.49}$	3.877(1)	11.754(2)	50
4	$Gd(Ba_{1.98}Na_{0.02})Cu_{2.68}Al_{0.17}Na_{0.15}O_{6.55}$	3.887(1)	11.660(3)	35
5	$Sm(Ba_{1.86}Sm_{0.14})Cu_{2.64}Al_{0.36}O_{7.1}$	3.900(1)	11.638(3)	40

Taking into account the data obtained from NMR, Raman and optical spectroscopy, the structural model was proposed for the sample 1 which represents the tetragonal supercell with the Al and oxygen amount corresponding to these determined by XRD. According to the NMR data, Al is in a four-fold coordination in sample 1. The sample 5 contains the same Al-amount but in octahedral coordination and a slightly higher oxygen concentration. The sample 3 was assumed to possess the structure ortho-II. The occurrence of tweed structure is highly probable in the sample 2. The formation of a superstructure along the *c*-axis due to the ordered distribution of Al and Na cations in the alternating layers can be proposed for the sample 4.

The present studies have shown that the physical properties of the RE-123-type crystals are strongly dependent on the concentration and distribution of the Al-atoms.

P11.10.002 STRUCTURAL FEATURES OF SUPERCONDUCTING AND NON-SUPERCONDUCTING $[M_2Cu_2O_3]_5[CuO_2]_7$-TYPE (M=Sr, Ca, Bi) PHASES. L.Shvanskaya[1], L.Leonyuk[1], G.-J.Babonas[2], V.Maltsev[1], A.Reza[2] [1]Moscow State University, 119899 Moscow, Russia [2]Semiconductor Physics Institute, 2600 Vilnius, Lithuania

Superconducting (SC) and non-superconducting (NSC) single crystals of the $[M_2Cu_2O_3]_5[CuO_2]_7$-type (M=Sr, Ca, Bi) phases were grown from the solution in the melt Bi_2O_3-CuO [1].

	Composition	*a* (Å)	*b* (Å)	*c* (Å)
	$(Sr_{4.02}Ca_{5.84}Bi_{0.14})Cu_{15.84}O_{29.00}$	11.351(2)	12.809(3)	19.52(1)
I	$(Sr_{3.1}Ca_{5.9}Pb_{03}Bi_{0.4}Y_{0.3})Cu_{16.7}O_{29..0}$	11.316(2)	12.763(3)	19.49(1)
II	$(Sr_{4.42}Ca_{4.86}Bi_{0.05})Cu_{17.00}O_{29.00}$	11.349(7)	12.896(5)	19.49(3)
V	$(Sr_{6.07}Ca_{3.38}Pb_{0.07}Bi_{0.08}Y_{0.39})Cu_{16.73}O_{28.39}$	11.346(3)	12.996(3)	19.586(9)

The structural refinement was performed in the space group *F222* for SC phases I-III [1,2] and NSC phase IV. The most significant structural difference between SC and NSC phases was indicated in the local environment of Cu-atoms in the ladder-plane $M_2Cu_2O_3$. In the ladder plane the Cu-O squares were more distorted and the Cu-O distances were larger in the NSC crystals than in SC phases. However, the Cu-O distance for "apical" oxygen in NSC phase (2.57-2.79 Å) was significantly shorter than in SC phase (2.85-3.14 Å). Therefore the Cu in the ladder plane of NSC phase can be assumed to be in the pyramidal environment.

The present studies have shown the correlation between the structural and superconducting properties for the $[M_2Cu_2O_3]_5[CuO_2]_7$-type crystals similar to that [3] noted for Y-123-type compounds: an approach of apical oxygen to Cu atom in the ladder-type $M_2Cu_2O_3$ or ordinary CuO_2 plane leads to a suppression of superconductivity.

The difference between the optical spectra of SC and NSC $[M_2Cu_2O_3]_5[CuO_2]_7$-type compounds was also indicated and interpreted by the corresponding changes in the structure of two sublattices.

[1] L.Leonyuk, G. -J.Babonas, R.Szymczak, H.Szymczak, M.Baran, A.Reza, V.Maltsev, L.Shvanskaya, V. Rybakov, Superconductivity in two-leg spin ladders $[A_2Cu_2O_3]_5[CuO_2]_7$ (A=Sr, Ca, Bi, Y, Pb), Europhys. Lett. (accepted)
[2] L.Leonyuk, G.-J.Babonas, V.Rybakov, E.Sokolova, R.Szymczak, V.Maltsev, L.Shvanskaya, J. Phys. Chem. Solids **59**, 9 (1998) 1591-1595
[3] O.A.Usov, N.F.Kartenko, S.I.Goloshchapov, S.G.Konnikov, JETP Lett. **20** (1994) 21-25

P11.10.003 ISOMORPHISM AND SUPERCONDUCTIVITY IN COMPLEX CUPRATES. L.Leonyuk[1], G.-J.Babonas[2], R.Szymczak[3], V.Maltsev[1] [1]Moscow State University, 119899 Moscow, Russia [2]Semiconductor Physics Institute, 2600 Vilnius, Lithuania [3]Institute of Physics, 02-668 Warsaw, Poland

A knowledge of stability region for solid solutions plays a dominant role in a search of new superconductors. In the present work recent data of isomorphic substitutions in complex cuprates are summarized and analyzed in order to estimate the possibility of the manifestation of superconductivity. At the substitution of basic elements in cuprates three main cases were considered

1. Complete isomorphism. A typical example is the substitution of Y by rare earth elements (RE) from the Y-group in the structural type Y-123 at which the superconductivity is maintained. As the superconductivity is related to the metastability of the structure [1], this case occurs quite rarely.

2. Absence of isomorphism: the substitution of basic elements leads to the formation of a new structural type. For example, the substitution of Y^{3+}+Ba^{2+} and Bi^{3+}+$(Ca,Sr)^{2+}$ for La^{3+}+Sr^{2+} in $(La,Sr)_2CuO_4$ resulted in the formation of Y-123 and Bi-2212-type compounds, respectively.

3. Limited isomorphism: *the structure as well as the superconducting properties *change at a substitution of basic elements.

3.1. The structural distortions occur at the substitutions as, e.g., in Y-123-type compounds doped by RE of the Ce-group and Al, Ca, Sr.

3.2. Formation of intergrowths due to narrow temperature-concentration crystallization regions of metastable superconducting phases (Bi-2212 at the substitution of Pb and RE for Bi and Ca, respectively [2].

3.3. Formation of inclusions of secondary phases due to the local ordering of cations (indication of T_c=110 K in the infinite-layer structure [3] and T_c=82 K in $(Sr,Ca)CuO_2$ [4]).

The formation of intergrowths and inclusions correlates with an increase of the T_c-values in superconducting compounds and occurrence of superconductivity in non-superconducting phases. It is reasonable to assume that the intergrowths and inclusions *illustrate* the metastability of the main phase**.

[1] B.T.Matthias. Physica **69** (1973) 54-56
[2] G.-J.Babonas, L.Leonyuk, V.Maltsev. Acta Phys. Polonica A **92** (1997) 251-254.
[3] M.Azuma, Z.Hiroi, M.Takano, Y.Bando, Y.Takeda. Nature **356** (1992) 775-776.
[4] L.Leonyuk, G.-J.Babonas, V.Rybakov, E.Sokolova, R.Szymczak, V.Maltsev, L.Shvanskaya. J.Phys.Chem.Solids **59** (1998) 1591-1595.

P11.10.004 STUDIES OF MOLYBDENUM DOPED POTASSIUM AND CESIUM HEXAGONAL TUNGSTEN BRONZE. A. Hussain , A. U. Monir, A. N. M. M. Rahman, Department of Chemistry, University of Dhaka, Dhaka - 1000, Bangladesh

Although it is more than a century since tungsten bronze, M_xWO_3, was first reported and even today these compounds have attracted much attention because of their interesting physical and chemical properties (1) .Recently, the effect of substitution of W atoms by other pentavalent or hexavalent transition metal atoms (2,3) and synthesis of mixed metal tungsten bronzes (4) have created interest among scientists.

Molybdenum doped potassium and cesium hexagonal tungsten bronzes, $M_{0.30}Mo_y W_{(1-y)} O_3$, where M = K and Cs and y = 0.05 -0.25 were prepared from homogeneous mixture of oxides in vacuum at 800°C . The products were then characterized by x-ray powder diffraction method. X-ray powder patterns of the samples were indexed as pure hexagonal tungsten bronze, HTB, type phase. The cell parameters of these Mo doped HTB were refined.

The cell parameters a and c in $K_{0.30}Mo_yW_{(1-y)}O_3$ decrease with increasing molybdenum content whereas the cell parameter a decreases while c increases with increasing molybdenum content in $Cs_{0.30}$ Mo_y $W_{(1-y)}$ O_3.

1. Ph.Labbe(1992). Key Engineering Materials, 68, 293, 1992.
2. R.Sharma (1985). Chem.Commun.Univ.Stockholm, 3, 1985.
3. A.Hussain & A.U.Monir (1998). AsCA abstracts, 15P29,1998.
4. A.Hussain & L.Kihlborg (1987). Acta Chem. Scand, A41,18,1987.

P11.10.005 CRYSTAL STRUCTURE AND LATTICE DYNAMICS OF RARE-EARTH HEXABORIDES. D. Yu. Chernyshov and V.A. Trounov, Condensed Matter Department of Petersburg Nuclear Physics Institute, Gatchina, 188360, RUSSIA, and M.B. Smirnov, Institute for Silicate Chemistry, St.-Petersburg, 199034, RUSSIA.

The structure properties of the series or rare-earth hexaborides (ReB_6, Re=La,Ce,Pr,Nd,Sm,Eu,Yb) have been studied by means of high-resolution neutron powder and single crystal x-ray diffraction methods. The established dependencies of structural parameters as well as the changes in the electronic structure and lattice dynamics of these compounds are discussed. The different dynamical properties (phonon frequencies, elastic constants and Debay-Waller factors) have been jointly treated in the lattice dynamics modeling. The important role of internal tension in dynamics of hexaborides has been proclaimed. This valence force field concept enables to explain the difference in dynamical properties of hexaborides with different rare-earth ion valences.

P11.10.007 ANOMALOUS COMPOSITION AND TEMPERATURE DEPENDENCE OF THE STRUCTURAL PARAMETERS FOR THE $NdBa_{2-x}Nd_xCu_3O_{7-\delta}$ SOLID SOLUTIONS. V.S. Mel'nikov, Institute of Geochemistry and Mineralogy, National Academy of Sciences of Ukraine, Kiev, Ukraine, Nedilko S.A. and Drozd V.A., Kiev Taras Shevchenko University, Ukraine.

$NdBa_2Cu_3O_7$ (Nd123) is a rare-earth analogue of high-T_c superconductor $YBa_2Cu_3O_7$ (Y123) but it has higher critical temperature of 93-97K. A difference between ionic radii of Ba^{2+} and Nd^{3+} is about 10% that leads to the $NdBa_{2-x}Nd_xCu_3O_{7\pm\delta}$ solid solutions formation at high temperature and to the phase separation at low temperature.

The samples $NdBa_{2-x}Nd_xCu_3O_{7-\delta}$ with x = 0-0.9 (x incrementation 0.05) have been synthesized by the citrate precursor method. To achieve the maximum oxygen saturation the samples on the final stage of the synthesis have been slowly cooling in the O_2-flow from 950 to 400°C. Single phase region in the $NdBa_{2-x}Nd_xCu_3O_{7-\delta}$ solid solutions was found to be x=0-0.9.

Temperature and composition dependencies of the structural parameters on the Nd/Ba ratio show some features which are not common for the Y123 phase. Tetragonal phase is formed at the 600-650°C for the stoichiometric samples (x = 0), but it is stable at room temperature if $x \geq 0.1$. In the temperature range of 400-1050°C there is a monotonous increase of c parameter with temperature ($dc/dT \approx 1.05 \cdot 10^{-4}$ Å/°C) for the

stoichiometric composition ($x = 0$), but if $x > 0.1$ the slope of $c(x)$ curve tends zero ($dc/dT \rightarrow 0$). For the compositions with $x > 0.15$ the parameter c does not depend on T.

Composition (x) dependence of the crystal lattice parameters show anomaly caused by the heterogenization of the solid solutions. Linear decrease a and c parameters with x growth is changed by "plateau" region ($da,c/dT \approx 0$) at $0.3 \leq x \leq 0.5$. Results of XRD study is in a good agreement with thin lamella, coherent conjugate structure formation during solid solutions decomposition.

Superexcess oxygen content in the $NdBa_{2-x}Nd_xCu_3O_{7+\delta}$, type of it distribution through the crystal structure and the features of heterogeneous structure have strong affect on the critical parameters (T_c, J_c) of the superconducting materials on the bases of Y123.

P11.10.008 NEW GADOLINIUM POLYSULFIDE CELL: 12-FOLD PbFCl-TYPE SUPERSTRUCTURE. I.A. Matveenko and G.M. Kuz'micheva, Department of Solid State Physics and Chemistry, Lomonosov State Academy of Fine Chemical Technology, Vernadsky pr. 86, Moscow 117571, Russia, and V.B. Rybakov, M. V. Lomonosov State University, Vorobyevy gory, Moscow 119899, Russia and I.G. Vasil'eva, RAS Insitute of Inorganic Chemistry, Acad. Lavrent'ev prosp. 3, Novosibirsk 90, Russia.

PbFCl structure type is basal for all the rare-earth (RE) polychalcogenides with general composition $[Ln^{3+}X^{2-}](X^{2-}_2)_{(x-0.5v)}(X)_{0.5-x}[\ ]_v\in_y$ ($0<x\leq0.5$, $y=0.5-x$) ([ ]-vacancy, $\in$ - missing position compared with PbFCl structure). Depending on Ln sort and deficiency rate anion vacancies can order in different directions (<100><110><210>, etc.) to form PbFCl (a_0, c_0) superstructures. Structural investigation of $GdS_{1.85}$ single crystal synthesised by solution-in-melt technique has been carried out. The crystal had a plate-like form and dark-red colour. Cell parameters found are unusually long for an inorganic substance: a = 46.651 (13), b = 46.651 (13), c = 15.825 (5)Å. It led us to suggest 12-fold a and b lattice parameters (m=n=12) and 2-fold c parameter (p=2) enlargement compare with PbFCl unit cell. This kind of subcells stacking should result in body-centred I-cell. Considering systematic extinction among reflections obtained and as a result of structural modelling we suggested I 4/mmm or I $\bar{4}$m2 space group with 96 Gd and 672 S atoms in unit cell. The structural features of this phase are under further investigation and discussion.

P11.10.009 LATTICE DISTORTION IN HIGH-T_c SUPECONDUCTOR $La_{2-x}Sr_xCuO_4$, H. Yamada, Y. Soejima, A. Okazaki, Department of Physics, Kyushu University, Fukuoka 812-8581, Japan, I Tanaka and H. Kojima, Institute of Inorganic Synthesis, Yamanashi University, Kofu 400-0021, Japan

High-resolution X-ray diffraction measurements of the lattice constants of $La_{2-x}Sr_xCuO_4$ (x=0.143) have been made at temperatures down to 17 K. Below the structural phase transition at 185 K, the lattice distortion of the orthorhombic cell indicates the condensation of not only the buckling mode but also the scissors mode of phonons. At temperatures below the superconducting transition at 35 K, it is found that the lattice distortion is frozen so that the thermal expansion coefficients of the lattice constants a and b are almost temperature independent. On the other hand, the sign of the thermal expansion coefficient of c changes, on cooling, from positive to negative at the transition. In the recent neutron diffraction experiments made by the present authors, the intensity, though extremely weak, has been observed at the X point in Brillouin zone in both the normal and superconducting phases. The intensity is about one tenth of that at the M point corresponding to the condensation of the buckling. The results suggest that a reinvestigation of the lattice distortion in both the low-temperature orthorhombic phase and the superconducting phase is necessary.

P11.10.010 SECONDARY CHEMICAL BONDS AS CONDUCTION PATH OF PHOTO-SEMICONDUCTING ELECTRONS: A CASE STUDY. F. Liebau, Institut für Geowissenschaften der Universität Kiel, D-24098 Kiel, Deutschland

To derive an insight into the conduction mechanism of a semiconductor, it is common practice to calculate its electronic band structure. Here it is shown that, under favourable conditions, the conduction paths of electrons can be deduced from the crystal structure with the help of careful bond-valence calculations. – At present eight cetineite-type phases of composition

$\mathbf{A}_6[Sb(2,3)_{12}O_{18}][Sb(1)\mathbf{X}_3]_2[\mathbf{D}_x(H_2O, OH, O)_{6-y}]$ with **A** = Na, K, Rb, Sr, Ba; **X** = S^{2-}, Se^{2-}; **D** = Na, Sb^{3+}, C are known [1] and their crystal structures have been refined. Four of these phases were found to be photo-semiconducting. Their optical band gaps were measured and their band structures were calculated [2]. Strong covalent bonds between trivalent Sb(2, 3) and oxygen atoms produce electroneutral $[Sb_{12}O_{18}]$ tubes which are held together by strong ionic bonds between the **A** cations within the tubes and the $\mathbf{X}^{2-}$ ions of the $[Sb(1)\mathbf{X}_3]$ groups. Results of bond-valence calculations indicate that:

bond-valence sums, ^{eff}V, of Sb(1) vary strongly (3.27-3.99 v.u.) and are considerably larger than the formal valence of antimony,+3;

the ^{eff}V-values of Sb(2) and Sb(3) vary only between 3.00 and 3.31 v.u.;

in addition to the strong primary bonds Sb(1)–**X**, Sb(2)–O, **A**–O, and **A**–**X**, each Sb(3) atom has two weak secondary bonds Sb(3)–**X** of up to 0.23 v.u., which form chains spiraling along [001]. Calculated band gaps are correlated with the sums of the valences of these secondary bonds.

Conclusions: 1) The strongly stereoactive Sb(1) atoms provide the electrons which then use the weak secondary Sb(3)—**X** bonds as conduction paths.

With necessary carefulness, conclusions about conduction mechanisms of semicoductors can be drawn from crystal structure with the aid of bond-valence calculations.

[1] W. Wang & F. Liebau (1998). Eur. J. Solid State Inorg. Chem. **35**, 27.
[2] F. Starrost et al. (1998). Phys. Rev. Lett. **80**, 3316.

P11.10.011 NEUTRON POWDER DIFFRACTION STUDY OF $Tb_{2-x}Ba_{2+x}Ti_2Cu_{2+y}O_{11}$. J.-E. Jørgensen, Department of Chemistry, University of Århus, DK-8000 Århus C, Denmark.

The $Ln_2Ba_2Cu_2Ti_2O_{11}$ compounds are structurally related to many of the high temperature superconducting cuprates but they have no yet been made superconducting. Structurally they are quadrupled perovskite containing a CuO_2-Ln-CuO_2 sandwich similar to what is found in many high T_c compounds. The $Ln_2Ba_2Cu_2Ti_2O_{11}$ compounds have been prepared for Ln= Nd, Sm, Eu and Tb. We have prepared samples of composition : $Tb_{1.8}Ba_{2.2}Ti_2Cu_2O_{11}$, $Tb_{1.8}Ba_{2.2}Ti_2Cu_{2.1}O_{11}$ and $Tb_{1.8}Ba_{2.2}Ti_2Cu_{2.1}O_{11}$ and neutron powder diffraction data were collected at room temperature and Rietveld refinements were performed with the GSAS program package. The $Tb_2Ba_2Ti_2Cu_2O_{11}$ compounds are tetragonal with space group P4/mmm (a ≈ 3.89 and c ≈ 15.70 Å) and the atomic positions in the fully ordered structure are:

Tb(1) 1c (1/2 1/2 0), Tb(2) 1d (1/2 1/2 1/2), Ba 2h (1/2 1/2 z_{Ba}), Cu 2g (0 0 z_{Cu}), Ti 2g (0 0 z_{Ti}), O(1) 1b (0 0 1/2), O(2) 4i (0 1/2 z_2), O(3) 2g (0 0 z_2), O(4) 4i (0 1/2 z_4)

In addition to the positional parameters site occupation factors for the cations were refined and it was found that cation disorder is present in all three samples. Cu and Ti were found to be distributed over the 2g sites while Tb and Ba are distributed over the 1d and 2h sites. The 1c site, which is located between the CuO_2 layers, was found to contain Tb only. Our study also shows that the excess Cu in $Tb_{1.8}Ba_{2.2}Ti_2Cu_{2.1}O_{11}$ ensures that the Cu site in the CuO_2 layers are 100% occupied by Cu. Excess copper is therefore presumably a necessity for making these compounds superconducting although the studied samples were non-superconducting. The results for the $Tb_{2-x}Ba_{2+x}Ti_2Cu_{2+y}O_{11}$ compounds will be compared with our earlier study of the the $Nd_{2-x}Ba_{2+x}Ti_2Cu_{2+y}O_{11}$ compounds. [1]

1. A. Markvardsen, J.-E. Jørgensen, A. Wannberg and R. G. Delaplane Physica C300 (1998) 110-114.

P11.10.012 STRUCTURAL CHANGE IN $YBa_2Cu_3O_x$ CRYSTALS BY H_2O ABSORPTION. S. Edo, Department of Mechanical System Technology, Hokkaido Polytechnic College, Zenibako 3-190, Otaru 047-02, Japan and T. Takama, Department of Applied Physics, Faculty of Engineering, Hokkaido University, Kita-ku, Sapporo 060, Japan.

Structural change induced by absorption of H_2O molecules of the high-T_c superconductor $YBa_2Cu_3O_x$ has been investigated by X-ray diffraction measurement. The single crystals were prepared by the self-flux method using a mixture of $BaCO_3$ and CuO powders as a flux. They showed a shape of rectangular prism. They were annealed at 725 °C in air and subsequently quenched into liquid nitrogen to obtain oxygen content x of ~6.4. The diffraction profiles were measured along given directions in the reciprocal space at room temperature using a full-circle goniometer and Cu Kα radiatoin. The profile measured along c* indicated that the lattice parameter c increased to 13.61 Å. This means that the crystal is elongated by ~16% along the c-axis owing to H2O absorption. Superlattice reflections were clearly observed at the positions of (l+l/2)c*. In contrast to the c-axis, changes in a and b were relatively small (a=3.87 Å and b=3.88 Å). Setting angles of the goniometer suggested that a, b, and c are perpendicular to each other. From the experimental facts, it is revealed that the compound transformed to tetragonal-like structure with a superlattice along the c-axis by the absorption. The profile along c* showed broad peaks, while the profiles along a* and b* showed relatively sharp peaks. It is thought that inhomogeneous strain was introduced into the sample by the large elongation along the c-axis and broadened the profiles along c*. The structural change will be discussed in comparison with that observed in the polycrystals.

P11.10.013 STRUCTURAL INVESTIGATION OF SnO_2 DOPED WITH ANTIMONY. E. Tkalcec and C. Goebbert, Institut für Neue Materialien, 66123 Saarbrücken, Germany and B. Grzeta, Rudjer Boskovic Institute, POB 1016, 10001 Zagreb, Croatia.

Tin oxide, SnO_2, has been widely used as a conductor in electronic devices. Dopands, such as antimony, incorporated into SnO_2 thin films cause the change in resistivity of such films. The resistivity decreases for lightly-doped SnO_2, and increases for heavily-doped SnO_2 [1]. The mechanism of this phenomenon is not well understood yet. The aim of the present work is to examine the influence of Sb dopand on the structure of SnO_2. A series of Sb-doped SnO_2 samples, with doping level of 0, 2.9, 5.9 and 12.3 at% Sb, was hydrothermally prepared and characterized by X-ray powder diffraction. The samples were tetragonal, space group $P4_2/mnm$ and isostructural with TiO_2(rutile). Both *a* and *c* unit-cell parameters increased as the Sb doping content increased, but the ratio *c*/*a* remained constant at the value characteristic for SnO_2. Diffraction lines were broadened, indicating nanosized crystallites in the samples. The lines of pure SnO_2 showed the greatest broadening. As the amount of dopand increased the broadening decreased. Also, the lines *hk*0 were systematically broader than the lines *hk*1, *hk*2 and *hk*3 for all samples as a consequence of elongation of the crystallites along the *c*-axis. The structure of samples containing 5.9 and 12.3 at% Sb was refined by the Rietveld method [2]. Crystal structure results indicated that both Sn^{3+} and Sb^{5+} were substituted for Sn^{4+} in the non-stoichiometric rutile-type phase with oxygen deficiency.

1. A. Rohatgi, T. R. Viverito & L. H. Slack (1974). J. Am. Ceram. Soc., **57**, 278-279.
2. H. M. Rietveld (1969). J. Appl. Cryst., **2**, 65-71.

P11.10.014 MAGNETIC ORDER AND STRUCTURE INVESTIGATIONS OF RB2C2 RARE EARTH BOROCARBIDES. J. van Duijn, J.P. Attfield [1], K. Suzuki [2], [1] Dept. of Chemistry, University of Cambridge, Lensfield Road, Cambridge CB2 1EW, England, [2] Graduate school of Enginering, Yokohama National University, 79-5 Tokiwadai, Hodogaya-ku, Yokohama 240-8501, Japan

The rare earth diborodicarbides (RB_2C_2) have been known for some years, but until now their low temperature properties have not been explored. They have a simple tetragonal structure consisting of extended planar boron-carbon sheets of linked four- and eight-membered rings with the R atoms between the eight membered rings of successive layers. Previous room temperature X-ray studies indicate that the eight-membered rings consist of alternating B_2 and C_2 pairs [1,2], although band structure calculations indicate that the alternation of individual B and C atoms is more stable [3]. Magnetisation measurements show that the RB_2C_2 compounds order antiferromagnetically, perhaps helimagnetically in some cases, with ordering temperatures ranging from 6.5 K for CeB_2C_2 to 23.5 K for TbB_2C_2. Neutron powder diffraction data have been collected from several ofthese compounds using diffractometer D2B at ILL, Grenoble. The samples were enriched with boron-11 to reduce absorption, enabling crystal and magnetic structures to be determined.

1. J. Bauer & O. Bars, Acta Cryst., B36, 1540 (1980).
2. J. Bauer, J. Less Common Metals, 87, 45 (1982).
3. J.K. Burdett, E. Canadell & T. Hughbanks, J. Am. Chem. Soc., 108,3971 (1986).

P11.10.015 CRYSTAL STRUCTURE SOLUTION OF COMPOUND SEMICONDUCTOR $Cu_3In_7Se_{12}$ FROM COMBINED CONVERGENT BEAM ELECTRON DIFFRACTION, X-RAY POWDER DIFFRACTION, AND X-RAY ABSORPTION FINE STRUCTURE DATA. C.-H. Chang and T.J. Anderson, Department of Chemical Engineering, University of Florida, Gainesville, FL 32611, E. Fodran, Department of Materials Science and Engineering, University of Florida, Gainesville, FL 32611, E.A. Payzant, High Temperature Materials Laboratory, Oak Ridge National Laboratory, Oak Ridge, TN 37831-6064, R. DURAN, Department of Chemistry, University of Florida, Gainesville, FL 32611

Great efforts are being devoted to the development of polycrystalline thin film solar cells based on chalcopyrite $CuInSe_2$ and related compounds. The observed junction between $CuInSe_2$ and the In-rich compounds (*e.g.* $Cu_2In_4Se_7$, $Cu_3In_7Se_{12}$, and $CuIn_3Se_5$) appears to play an important role in the photovoltaic process. In general the structure of these compounds belong to

defect tetrahedral structures. They can be described as normal tetrahedral structures with a certain fixed number of unoccupied structure sites. In spite of many efforts have been devoted to investigate the structure for these compounds. There remain many inconsistencies in the reported structure solutions. The reasons for these inconsistencies are associated with the difficulty in assigning the space group based on X-ray diffraction data, and disordering in the cation sublattice.

Convergent Beam Electron Diffraction was carried out to obtain the symmetry information for compound semiconductor $Cu_3In_7Se_{12}$. The resulted space group and unit cell parameters were used in the analysis of X-ray diffraction powder data. The local structure data, which were derived from X-ray Absorption Fine Structure measurements on Cu_K and Se_K edge, were used as building blocks for assigning atomic positions. Rietveld refinement was performed to obtain the final structure solution.

P11.10.016 VARIATION OF Cu IN Bi-BASED HIGH-T_C SUPERCONDUCTORS. Muhammad Anis-Ur-Rehman Thermal Physics Laboratory, Department Of Physics, Quaid-I-Azam University, Islamabad, Pakistan.

Samples with nominal composition $Bi_{1.6}Pb_{0.4}Sr_2Ca_2Cu_{2+X}O_Y$ and $Bi_{1.6}Pb_{0.2+X}Sr_2Ca_2Cu_4O_Y$ were prepared by the solid state reaction method. Resistivity, ac magnetic susceptibility and X-ray diffraction studies were done. Sample with X=2.0 in the first composition showed T_c at 127 but the recipe was often not reproducible. Increase in Cu ratio (i.e. x=2.5) did not show any dramatically high Tc. So the role of Pb was studied. Increase in Pb ratio showed the adverse effects. Decreasing Pb improved the results. Samples with nominal composition $Bi_{1.6}Pb_{0.4}Sr_2Ca_2Cu_{2+X}O_Y$ (x=2.5) and $Bi_{1.6}Pb_{0.2+X}Sr_2Ca_2Cu_4O_Y$ (x=0.0) showed somewhat similar behaviour. It means that the compositions are not only sensitive to ratio of Cu but also to that of Pb.

Properties of the samples also depend on the thermal process. Step sintering was found to be more favourable towards magnetic properties of the samples. Prolonged sintering makes the systems more metallic like and smooth variation in resistivity with temperature, is observed. After final sintering XRD patterns were obtained. The superconducting phase identified by XRD analysis is the high-Tc phase in all the four samples, similar results of resistivity and susceptibility measurements were observed.

P11.10.017 STRUCTURAL RELATIONSHIPS PRESENT IN THE $CuFeX_2$ (X=S, Se, and Te) FAMILY OF SEMICONDUCTORS. J.M. Delgado, R.A. Guevara, E. Roque-Infante, Laboratorio Nacional de Difracción de Rayos-X, Facultad de Ciencias, Universidad de Los Andes, Mérida 5101, Venezuela.

It would be expected that the three ABX_2 copper iron chalcogenides would exhibit the chalcopyrite type of structure that is typical of the I III VI_2 semiconducting compounds. But, it is surprising that only one of them, $CuFeS_2$, displays such a structure which, coincidentally, was named after the mineral with this particular chemical composition.

In this contribution, a comparison of the characteristic features of the structure of $CuFeS_2$ and $CuFeSe_2$ as well as the structural aspects of the disordered structure recently reported for $CuFeTe_2$ will be examined [space group *P4/nmm* with *a*=3.989(1) and *c*=6.094(3)Å]. It must be mentioned that no report of its eventual ordered structure has been found in the literature. Several attempts to prepare X-ray quality single crystals of this material have failed to produce the expected results so far. However, good single crystals of Cu_3FeTe_3, a previously unknown material have been obtained in the batchs intended to produce $CuFeTe_2$. During this investigation it has been determined that Cu_3FeTe_3 crystallizes in space group *Cmma* with *a*=5.656(1), *b*=17.478(4), and *c*=6.073(2)Å and represents an ordered superstructure derived from the disordered structure reported for $CuFeTe_2$. The relation between the orthorhombic unit cell obtained for Cu_3FeTe_3 and the tetragonal unit cell reported for $CuFeTe_2$ is given by $[\mathbf{a},\mathbf{b},\mathbf{c}]_O = [1,-1,0/3,3,0/0,0,1][\mathbf{a}_1,\mathbf{a}_2,\mathbf{c}]_T$.

This work was supported by CONICIT, grant LAB-97000821 which established the Laboratorio Nacional de Difracción de Rayos-X and by CDCHT-ULA, grant C-727-95-08-A in Venezuela. Part of this work made use of the MRL-UCSB Central Facilities, supported by the National Science Foundation under Award No. DMR96-32716 in the USA.

P11.10.018 ROLLING AND RECRYSTALLIZATION TEXTURES IN PURE SILVER SHEET. J. Palacios-Gómez, H. Mendoza-León and J. G. Cabañas-Moreno, H. A. Calderón, Instituto Politécnico Nacional, Apdo. Postal 75-373, 07300 México, D.F., México, and A. de Ita, Universidad Autónoma Metropolitana, México D.F., and C. Falcony-Guajardo, CINVESTAV-IPN, México, D.F.

One of the forms in which high temperature superconductors are intended to be of practical use is as films on strongly textured metal substrates [1]. Silver represents one of a handful of metals possessing attractive features as a metal substrate for this purpose [1]. In particular, there exists a very good match between the (100) atomic arrangements in silver and the corresponding arrangements on the basal plane of some ceramic superconductors, like the ytrium-base and thallium-base ceramic oxides [1].

A preferred orientation of (100) planes parallel to the rolling plane in some fcc metals is found in the so-called cubic recrystallization texture, namely, the (100)<001>texture. This texture is usually developed by the recrystallization of material originally having a strong copper-type rolling texture, which in turn makes necessary the application of large rolling reductions. Pure silver requires rolling at temperatures higher than 150-200°C to develop the copper-type texture; this, however, also promotes dynamic and/or static recrystallization of silver, which prevents the generation of a strong rolling texture.

Experimente to determine the effects of temperature of deformation, as well as time and temperature of annealing on the resulting textures of nominally 99.9 and 99.99% silver sheet have been performed. X-ray diffraction studies were used to characterize the textures produced by the different rolling-annealing treatments.

As expected, heavy rolling of silver at room temperature produced the brass-type rolling texture, namely, (110)<1-12>. The changes resulting from annealing the cold-rolled material at temperatures between 400 and 900°C were quite complex; in general terms, a significant cube component appeared at the lower annealing temperatures - coexisting with a brass-type component, but the former was found to diminish in intensity as the annealing temperature was increased. Basically, random crystallite orientations were obtained with annealing temperatures of 800°C (and higher). Additional results concerning texture formation will also be presented.

1. A. Goyal et al., J. Mater. Res., 12(1997), 2924

P11.10.019 HRTEM ANALYSIS OF NEW OXYCARBONATE SUPERCONDUCTORS DOPED WITH NITROGEN. Y. Matsui[1], Y. Ishida[1,2], Y. Anan[1,2], J. Hatano[2], N. D.Zhigadlo[1], A. T.Matveev[1], E. Takayama-Muromachi[1], [1] National Institute for Research in Inorganic Materials, 1-1 Namiki, Tsukuba, Ibaraki 305-0044, Japan, [2] Faculty of Industrial Science and Technology, Science University of Tokyo, 2641 Yamazaki, Noda, Chiba 278-8510, Japan

Plenty of new oxide superconductors have successfully been prepared by high-pressure synthesis technique, and their crystal

structures have been analyzed by high-resolution transmission electron microscopy (HRTEM). Especially, some of new oxycarbonate superconductors, containing CO_3 groups, are revealed to have unique superstructures due to ordered arrangements of CO_3 groups in the charge-reservoir blocks[1]. In the present study, we performed HRTEM investigation on the structural features of a new series of nitrogen-doped oxycarbonate superconductors, prepared in a Sr-Ca-Cu-N-C-O system under high-pressure.

Series of homologous compounds with nominal compositions of $(Cu,N,C)Sr_2Ca_{n-1}Cu_nO_y$ were synthesized by solid state reactions of CuO (99.9%), $Sr(NO_3)_2$ (99.9%), $SrCuO_2$, SrO_2, Ca_2CuO_3, $SrCuO_3$ (99.9%) and $CaCuO_3$ (99.9%), under high-pressure of 5-6GPa at 1200-1375 C, for 1-6 hours. TEM specimens were prepared by the crushing method and then examined by Hitachi H-1500 type HRTEM which is developed at NIRIM[2]. In this study, all of the HRTEM observations were made by 800kV acceleration voltage.

Four compounds, with n-values from 3 to 6, were obtained as stable phases in the present system. All the four phases showed superconductivity, with the highest T_c=113K for $(Cu,N,C)Sr_2Ca_3Cu_4O_y$ (n=4). Possibilities of superstructures due to ordered arrangements of Cu and (CO_3 + NO_3) are examined by electron diffraction and HRTEM method. Ordered arrangements of Cu and (CO_3 + NO_3) are observed in both n=3 and n=4 phases. Superstructure with 4-times periodicity a_S=4a, due to -Cu-X-X-X-Cu-X-X-X-Cu- (X=CO_3 or NO_3) in the charge-reservoir blocks, are observed only in both n=3 phase. While the superstructure with twice periodicity a_S=2a due to -Cu-X-Cu-X-Cu- (X=CO_3 or NO_3) sequence was observed in both n=3 and n=4 phases. On the other hand, no evidence of superstructures have been detected in both n=5 and n=6 phases, and it is considered that Cu and CO_3 (or NO_3) are almost randomly distributed in the charge-reservoir blocks.

1) Y.Matsui: J.Electron Microsc. 46(2) (1997) 135-150.
2) Y.Matsui et. al.: Ultramicroscopy 39 (1991) 8-20.

P11.10.020 STRUCTURE INVESTIGATIONS OF DOPED Hg-CONTAINING SUPERCONDUCTING OXIDES. I. Bryntse and M. Valldor, Dept. of Inorganic Chemistry, Arrhenius Laboratory, Stockholm University, S-10691 Stockholm, Sweden.

The structures of the superconducting cuprates $HgBa_2CaCu_2O_{6+\delta}$ "1212" and $(Hg,Tl)_2Ba_2Ca_1Cu_2O_{8+\delta}$ "2212" possess a larger Ba-site where Ba^{2+} is co-ordinating approximately 9 oxygen atoms and a smaller Ca^{2+}-site surrounded by 8 nearest oxygens. We have investigated how the unit cell, structure details and superconducting properties are affected by dopants or replacements at these positions in particular.

At first, the Ba-site was attempted to be completely replaced by the smaller isovalent Sr^{2+} in the 2212 type phase. It was found by single crystal analysis that Sr and Ca were mixed at both the sites described above, with an excess of Sr at the larger site. Structural data of the phases with starting compositions $(Hg,Tl)_2Sr_2CaCu_2O_{8+\delta}$ and $(Hg,Tl)_2(BaSr)_2(CaSr)Cu_2O_{8+\delta}$, will be presented and compared to the structure of $(Hg,Tl)_2Ba_2Ca_1Cu_2O_{8+\delta}$. Superconducting transitions were determined by magnetic susceptibility to 45-100 K, depending upon the degree of Sr substitution.

Then, Ba was replaced by the trivalent cation La^{3+} in the 1212 type phase. 20% of lanthanum at the Ba-site was found to almost completely destroy the superconductivity. The unit cell parameters were refined to *a*=3.899(2) Å and *c*=12.423(9) Å, indicating that the metal-oxygen distances in the *ab*-plane increase slightly and the apical distances shrink significantly compared to undoped Hg-1212, which usually has the cellparameters *a*≈3.864 Å and *c*≈12.71 Å. Structural data obtained from a Rietveld refinement will be presented as well as an electron microscopy study.

At last, the synthesis problems and hopefully results of substituting a mono-valent cation for Ba will be discussed.

P11.10.021 STUDY OF ATOMIC DISTRIBUTION FUNCTIONS IN PEROVSKITE CRYSTALS. D.A. Kovtun, A.P. Kovtun and M.F. Kupriyanov, Department of Physics, Rostov State University, 5 Zorge Str., 344090 Rostov-on-Don, Russia.

In the work we investigated the atomic distribution functions with the X-ray structure amplitudes from single-crystal of $SrTiO_3$ at various temperatures. We considered two atomic distributions: conventional Gauss distribution and S-distribution that implies the uniform disorder of the atom over a sphere. The structure was refined by least-squares refinement procedure using derived analytical expression of the scattering form-factors.

We obtained that the atomic distribution function of titanium atom was principally of S-type. The radius of the sphere was observed to be practically independent of the temperature.

The work presents the theory that explains the atomic distributions observed in perovskite crystals. Moreover, we show the explanations of the results published earlier in a great deal of papers, according to which the heavy atoms have the larger temperature parameters than those of the light atoms in the structure.

P11.10.022 EFFECTS OF SHORT - ORDERING IN PMN CRYSTALS. Alla R. Lebedinskaya, Faculty of Physics and Chemistry, Azov - BlackSea State Agro Engeniheering Academy, Zernograd, Rostov Region, 347720, Russia, Mikhail F. Kupriyanov, Faculty of Physics, Rostov State University, Rostov on Don, 344090, Russia

The crystal of complex compound $PbMg_{1/3}Nb_{2/3}O_3$ at room temperature has a cubic perovskite structure with the lattice constant a=4.034 Å. and exhibits the properties of ferroelectric - relaxors in a broad interval of temperatures.The microscopic mechanism of the structural transformations in relaxor ferroelectrics is not clear yet. Earlier is established, that for low temperatures and for applying the electric constant field the PMN has a rhombohedral phase. It was found that the lead ions are shifted from the special position (0,0,0) at the temperatures low then average Curie temperature 230 K.

At the same time, on data of the electrongraphic analysis the effect of ordering of atoms of a different grade in the same sublattice of a type 1:1 is established, that will be poorly agreed with chemical PMN structure : Mg/Nb = 1:2.

With the purpose of clearing up of a real of these effects by us are analysed the results of a X-ray diffraction of monocrystal $PbMg_{1/3}Nb_{2/3}O_3$ for temperatures 103K, 183K and 293 K and proposed the model of PMN behaviour at two low temperatures.

From the analysis of reflections is obvious, that the reflexes with nonzero significance L (type 00L) hardly are overestimated on a comparison with reflexes for zero significance L. It was determined the factors of Debay - Waller of atoms for temperatures of 103, 183 and 293 K. It was determined, that for these temperatures B (Pb) > B (O) > B (Mg/Nb). In our opinion, the biggest Debay - Waller factor for atom of lead is explained by not only the thermal displacements from an ideal item of this atoms in PMN crystals.

The obtained maps of distribution of electronic densities allow to assume the disordered character of displacements from an ideal item of atoms of lead mainly in a plane {ZX} and the ordering of Mg/Nb ions in that plane . The order of a Pb displacement does not exceed 0.28 Å. In the present work we determined also the shifts of O^{2-} ions at this temperatures . We supposed that this shifts depend from the behaviour of the lead ions and from effect of Mg/Nb ordering.

P11.10.023 INFLUENCE OF COMPOSITION RELATION MG:NB IN PMN ON ITS PROPERTIES. Alla R. Lebedinskaya, Faculty of Physics and Chemistry, Azov - BlackSea State Agro Engenireering Academy, Zernograd, Rostov Region, 347720, Russia, Mikhail F. Kupriyanov, Faculty of Physics, Rostov State University, Rostov on Don, 344090, Russia, Richard Skulskiy, Silesian University, Katowice, Poland

The purpose of this work is the clearing of a reality of ordering effects in a pseudo-binary system of solid solutions (1-x)$PbMg_{1/3}Nb_{2/3}O_3$ -(x)$PbMg_{1/2}Nb_{1/2}O_{2.75}$.

The compositions with x = 0; 0.1; 0.2;..1.0 were prepared on usual technology of the solid - phase reactions.

The Debey- Waller factors of atoms are determined with the using of integrated intensities of diffractional reflections from these system on diffractometer CAD-4 (MoK_α - the radiation, $Sin\theta/\lambda < 1.01$ Å^{-1}).

First, the crystal of complex compound $PbMg_{1/3}Nb_{2/3}O_3$ at room temperature has a cubic disodered perovskite structure with the lattice constant a=4.034 Å. Then, for the system of (1-x) *$PbMg_{1/3}Nb_{2/3}O_3$-(x) *$PbMg_{1/2}Nb_{1/2}O_{2.75}$ lattice constants, dielectric constants, spontaneous polarization and thermal expansion were measured as a function of temperature for varying x.

It is established, that in the given system the continuous solid solutions will be depended on a character of modifications of parameters of a lattice. Dielectric measurements of ceramic have shown , that relaxor properties are definited a diffusion of ferroelectric phase transition, depending from the structure of a solid solution, i.e. parameter x.

The correlations beween structure evolution and dielectric properties in lead magnoniobate are discussed.

P11.10.024 NEW PHASES IN La-Cu-O AND (La,Ba)-Cu-O SYSTEMS: SYNTHESIS, COMPOSITION, STRUCTURES, PECULIARITIES. V.V. Luparev and G.M. Kuz'micheva, Department of Solid State Physics and Chemistry, Lomonosov State Academy of Fine Chemical Technology, Vernadsky pr. 86, Moscow 117571, Russia, and E.P. Khlybov, L.F. Vereschagin Institute for High Pressure RAS, Troitsk, Russia, and A.V. Mitin, P.L. Kapitsa Institute for Physical Problems RAS, Kosygina ul. 2, Moscow 117973, Russia.

We applied high pressure-high temperature technique to synthesise cubic perovskite and prepared phases with rhombohedral lattice, which represent a small distortion of the perovskite cubic cell: a_R≈3.8612Å, α_R≈90.69° (I, Sp.gr. R $\bar{3}$m, p=3.5 GPa, t=1000°C, τ=10 min) and a_R≈3.8597Å, α_R≈90.63°(II, p=4 GPa, t=1250°C, τ=10 min), moreover we revealed such type of distortion for the first time. We carried out the Rietveld refinement of crystal structures by DBWS-9411 program with x-ray powder diffraction data. It was found that the most probable compositions are $La_{0.99(1)}CuO_{3.00(3)}$ (I, Formal valence FV Cu~3.00) and $La_{0.98(1)}CuO_{2.94(6)}$ (II, FV Cu~2.94). Phase with tetragonal perovskite-like structure $La_{0.99(1)}CuO_{2.90(2)}$ (a=3.8183(1), c=3.9782(1)Å) was formed from rhombohedral one (I) under annealing in Ar atmosphere (t=280°C, τ=40 min). From initial composition $(La_{1-x}Ba_x)CuO_{3-\delta}$ we prepared samples, which distinguish in contents of cubic and superstructure ($a \approx a_0$, $c \approx 3a_0$) phases depending on conditions of synthesis (p=5-7 GPa, t=800-1100°C or without high-pressure under t=920-1000°C) and x values (x=0.25-0.67). The more temperature or pressure, the more content of cubic phase. Optimum initial composition for cubic phase synthesis was found to be x=0.3. From analysis of dependencies (between cubic subcell parameter of $(La_{0.5}Ba_{0.5})CuO_{3-\delta}$ phases and δ value; T_c and FV Cu), which were built on literature and own experimental data we state that for the first time superconducting cubic phase $(La_{0.5}Ba_{0.5})CuO_{2.45(5)}$ (T_c=21K, FV Cu=2.40, Sp.gr. Pm $\bar{3}$m, a=3.9064(8)Å) was synthesised.

P11.10.025 STRUCTURE DETERMINATION OF LEAD INDONIOBATE AND LEAD FERRONIOBATE CRYSTALS. O.Lavrova, R.Kolesova, M.Kupriyanov, Department of Physics and V.Kolesov, Department of Mechanics and Mathematics, Rostov State University, 5 Zorge str., 344090, Rostov-on-Don, Russia.

An x-ray diffraction study of $PbIn_{0.5}Nb_{0.5}O_3$ (PIN) and $PbFe_{0.5}Nb_{0.5}O_3$ (PFN) single crystals was made with MoK_α radiation at room temperature for PIN and at 160°C for PFN. Under an assumption the ideal perovskite structure (the space group O^1_h) are unusually large values of Debye-Waller factors (DWFs) of Pb atoms: B(Pb)=4.80 Å², B(In/Nb)=0.91 Å², B(O)=4.62 Å² and R=0.0923 for PIN; B(Pb)=4.40 Å² , B(Fe/Nb)=0.80 Å², B(O)=1.40 Å² and R=0.0600 for PFN.

An assumption that atoms dynamically or statistically occupy a position 48: (n) of the group O^1_h permits to lower R-factors to 0.0383 for PIN, to 0.0181 for PFN and DWFs: B(Pb)=1.30 Å², B(O)=2.27 Å² for PIN; B(Pb)=1.36 Å², B(O)=0.82 Å² for PFN. A difference synthesis of electron density calculated for the model of ideal perovskite structure shows there are 2 sets of positional parameters with probabilities P_i and (1 - P_i) for PFN.

Disordered displacements of Pb atoms from the 1: (a) position of the group O^1_h in PIN and PFN can be considered as an indication of the formation of metastable polarization regions which are typical for the ferroelectric-relaxors.

P11.10.026 COMPUTATIONAL SIMULATIONS OF NOVEL A-SITE SUBSTITUTED PEROVSKITES. V. Jennings, P.A. Thomas, Department of Physics, University of Warwick, Coventry, CV4 7AL, UK.

The Perovskites (generic formula ABO_3) show many useful properties, such as ferroelectricity, piezoelectricity and high dielectric constant. They are important not only for these properties, but also because their relatively simple basic structure facilitates the study and understanding of the relationship between these properties and the structure.

The structure, minimal energy configurations and possible phases of novel A-site substituted perovskite compounds (as opposed to solid solutions) based on $Na_{(0.5)}Bi_{(0.5)}TiO_{(3)}$ have been investigated for varying dopants on the A-site using computational methods. The methods used were density functinoal theory (FLAPW method implemented using the WIEN97 [1] code) and the Mott-Littleton method (GULP [2] code). Preliminary results of modelling studies on this class of compounds will be presented.

1. P.Blaha, K.Schwarz and J.Luitz, WIEN97, Vienna University of Technology, Vienna 1997, Updated version of P.Blaha, K.Schwarz, P.Sorantin, and S.B.Trickey. Comp.Phys,Commun 59, 399, 1990.
2. General Utility Lattice Program, Julian Gale, Imperial College, London, U.K. (1993).

P11.10.027 INVESTIGATION OF THE STRUCTURE AND PHASE TRANSITIONS IN THE FERROELECTRIC CRYSTAL $Na_{0.5}Bi_{0.5}TiO_3$. G.O. Jones, P.A. Thomas, Department of Physics, University of Warwick, Coventry, CV4 7AL, UK.

Sodium-Bismuth Titanate, Na0.5Bi0.5TiO3 (NBT), has the perovskite structure, with general formula ABO3. This is one of a handful of perovskites compounds with substitution at the A-cation site, whereas the majority of the perovoskite compounds substitute on the B-site. NBT was first described by Smolensky and co-workers [1], and to date many of its characteristics have

been investigated[2-4]. However, there is considerable controversy within the published literature about the ferroic nature of the different phases and the temperature range over which they exist.

The results of neutron powder profile refinement at room temperature has revealed a rhombohedral phase (space group R3c), exhibiting an antiphase oxygen octahedra tilt system, giving rise to a doubled unit cell. Cation displacements and octahedral distortions for this temperature are reported. On thermal-cycling an observed pattern change consistent with the loss of the room temperature rhombohedral distortion giving a high temperature cubic phase is seen.

Single-crystal data has been collected using a Bruker SMART system at room temperature and 120K. The results hence far support the neutron diffraction data but suggest either twinning or disorder in the single crystal. The results of refinement of twinning/disordered models are presented and discussed.

[1] Smolensky, G. A., Isupov, V. A., Agranovskaya, A. I. & Krainik, N. N. (1961). Sov. Phys.-Solid State, 2, 2428-2432.
[2] Suchanicz, J. & Ptak, W. (1990). Ferroelectrics Letters 12, 71-78.
[3] Suchanicz, J.& Kwapulinski, J. (1988). Ferroelectrics 165, 247-253.
[4] Tu, C. S., Siny, I G. & Schmidt, V H. (1994). Phys. Rev. B 49, 11550-11559.

P11.10.029 INTERATOMIC BOND STRAINS EFFECT ON FERROELECTRIC PROPERTIES OF $NaNbO_3$-BASED SOLID SOLUTIONS. G.A.Geguzina, N.V. Nastas'ina and L.A.Reznitchenko. Institute of Physics at Rostov State University, 194 Stachki Ave., Rostov-on-Don, 344090. Russia.

Two groups of both synthesised first [1] and famous binary systems of solid solutions (SS) on the basis of perovskite $NaNbO_3$ (NN) with the second components (SC): ANb_2O_6 (1) and $ATiO_3$ (2) (where A=Ni, Cu, Co, Mg, Zn, Mn, Cd, Ca, Sr, Pb, Ba, $(NaBi)_{0.5}$, $(AgBi)_{0.5}$ and $(KBi)_{0.5}$) are considered. Most of these SC are nonisostructured to NN. They have various structure types: columbite, ilmenite, KW-bronze or pyrochlore. Only the Cd,Ca,Sr,Pb,Ba, $(NaBi)_{0.5}$, $(KBi)_{0.5}$ titanates are isostructured to NN. Nevertheless they all form restricted at least SS series on the NN basis. The partial Na atoms substitution with A atom occurs in all of systems, but also Nb atoms are substituted by Ti atoms in (2) systems.

Several regularities of electrophysical properties variation depending on substituting atoms characteristics and interatomic A-O bond strains have been found. The last ones are determined as $\delta_{AO} = (L_{AO}-L^o_{AO})/ L^o_{AO}$ where L_{AO} is strained (real) interatomic A-O bond length in the complex compound or SS and L^o_{AO} is the unstrained (free) one. As the calculations have shown, the high tensile relative strain of Na-O bond and significant compressive relative strain of Nb-O bond are observed in SS. The sharp decrease of A-O bond tension and the sharp increase of Nb-O and Ti-O bonds compression are observed in SS when varying A atoms. The graphic and analytic (by the use of statistical analysis) correlations between Curie temperature, dielectric permittivity, piezoelectric constants, electromechanical coupling factor at one hand and interatomic bond strains, $\delta_{AO,}$ at other hand have been constructed. Given analytic correlations between SS properties and the interatomic bond A-O strains allow to predict SS ferroelectric properties when the computed a'priori interatomic bond strains change in NN-based SS systems.

1. L.A.Reznitchenko, et al. Ferroelectrics, (1998), **214,** 241-253.

P11.10.031 STRUCTURAL RELATIONSHIPS OF TRIIODOMETALLATES OF GERMANIUM (II), TIN (II) AND LEAD (II) WITH METHYLAMMONIUM IONS. G. Wittenburg, B. Serr, G. Heckert, H. W. Rotter, G. Thiele*, Institut für Anorganische und Analytische Chemie der Albert-Ludwigs-Universität, Albertstraße 21, 79104 Freiburg i. Br., Germany

Structural investigations show that most of the trihalogenometallates of germanium(II), tin(II) and lead(II) crystallize in distorted structures of the cubic perovskite or in the NH_4CdCl_3-type and undergo temperature and pressure induced phase transitions[1]. In this context the influence of the non-bonding electron pair („lone pair") has been a topic of intensive and actual research.

The triiodometallates AMX_3 with methyl ammonium ions $A=[(CH_3)_{4-x}NH_x]^+$ though form structures related to the hexagonal perovskite (aristotype: $CsNiCl_3$, space group: $P6_3/mmc$). These structures are characterized by linear chains of face-sharing $[MI_{6/2}]$-octahedra. Structural distortions of the simple and highly symmetrical topology of the $CsNiCl_3$-type are induced by the orientation of the counterions and the formation of hydrogen bonds.

Good examples are the compounds $(CH_3)_2NH_2MI_3$, with M=Ge(II), Sn(II), Pb(II), which crystallize orthorhombic (space group: P n a 2_1, Ge: a = 8.911 Å, b = 14.268 Å, c = 7.973 Å; Sn: a = 8.789 Å, b = 14.659 Å, c = 8.294 Å; Pb: a = 8.750 Å, b = 15.155 Å, c = 8.179 Å) and show a characteristic deformation of the I_{12}-anticuboctahedra surrounding the dimethyl ammonium ions and differences in the coordination of the metal cations. The germanium ions are shifted to one of the triangular faces and adopt approximately a [3 + 3]-distorted octahedral coordination. The tin and lead ions show a [2 + 2 + 2]-distorted coordination, where the common octahedral faces are tilted against each other. The different kind of distortion found, may be caused by a stronger lone pair character of the non-bonding electron pair in the germanium compound. This effect is markedly smaller in the tin and lead compounds. In this cases the distortion must be ascribed to the dominance of the spacefilling properties of the dimethyl ammonium counterion and the formation of hydrogen bonds. Close structural relationships between the described dimethyl ammonium compounds and the other triiodometallates with tri- or tetramethyl ammonium ions[2] will be discussed.

Additional information about the dynamical behavior and the deviations from the regular octahedra geometry have been received by vibrational spectroscopy. The results of FTIR- and Raman spectroscopy are in good agreement with the results of single crystal x-ray investigations.

[1] D.K. Seo, N.-H. Whangbo, H. Hillebrecht, G. Thiele, *Inorg. Chem. 37*, 1998, S. 407-411.
[2] J.G. Contreras, G.V. Seguel, B. Ungerer, *J. Mol. Struc. 102*, 1983, S. 295-304.

P11.10.032 STRUCTURAL AND DYNAMICAL STUDIES OF THE ORTHORHOMBIC $NaZnF_3$ PEROVSKITE AT LOW TEMPERATURES. A. Ratuszna and J. Rybczynski, Institute of Physics, University of Silesia, Katowice (Poland) Ph. Daniel and J.Y. Gesland Faculté des Sciences, Lab. PEC – UPRES A CNRS n°6087, Université du Maine, Le Mans (France).

$NaZnF_3$, similar to another perovskite as $NaMgF_3$ [1], $NaMnF_3$ [2] possesses an orthorhombic symmetry at and below room temperature. This symmetry is a result of the fluorine octahedra rotation associated to the $a^-b^+a^-$ tilt system [3], as well as the shifting of the Na cations and distortion of these octahedra. Such mechanism leads to stabilise the crystal symmetry without any additional phase change down to the lowest temperatures [4]. Type and value of the tilting angles has been estimated from the splitting of the main diffracted lines on the x-ray powder diffraction pattern. The observed superstructure lines allows to confirm the origin of the tilts around the pseudo-cubic axes. From Rietveld profile refinement the proposed model has been confirmed and additionally from the coordinates of atoms the distortion of ZnF_6 octahedra and displacement of Na cations have been fully determined.

The discussion relative to this distorted perovskite, the bond distances between cations, cation-fluorine, and possible shifting of Na^+ has been enlarged with a Raman study, which has been performed from room temperature down to 40K. In spite of the polydomain character of these samples, Raman spectra of $NaZnF_3$ could be assigned in the orthorhombic Pnma space group thanks to previous group theory analysis and with comparison to the single crystal $NaMnF_3$ [5]. In this framework, 15 Raman lines were then indexed compared to the 24 modes predicted. This work constitutes the first step of a more extensive study devoted to the non well-known antiferrodistortive high temperature phase transition ($T_c \approx 680°C$) occurring in this compound [6].

1. Y. Zhao, D. Weidner, J. Parise & D.Cox (1993) Phys. Earth Planet. Interiors 76, 1-34
2. A. Ratuszna, K. Majewska & T. Lis (1993), Acta Cryst. C45, 548-551
3. A. M. Glazer (1972), Acta Cryst. B28, 3384-3392
4. P. M. Woodward (1997) Acta Cryst. B53, 32-66
5. Ph. Daniel, A. Ratuszna et al, Phys. Rev. B 51(18), 12337-12346 (1995)
6. O. Schmitz-Dupont et al, Z. Anorg. Allg. Chem. 287, 120-137 (1956)

P11.10.034 CRYSTALLOGRAPHIC STUDY OF THE HIGH- AND LOW-TEMPERATURE FORMS OF $Bi_2(Sr,Ca)_4O_x$. W. Wong-Ng, Q. Huang, R.S. Roth, Materials Science and Engineering Laboratory, NIST, Gaithersburg, MD 20899, USA; J. Kaduk, BP Amoco PLC Research Center, Naperville, IL 60566, USA; and T. Siegrist, Inorganic Chemistry, Lund University, Sweden.

$Bi_2(Sr,Ca)_4O_x$ is an important phase because it is in equilibrium with all three superconductors found in the Bi-Pb-Sr-Ca-Cu-O (BSCCO) system. During processing, $Bi_2(Sr,Ca)_4O_x$ frequently appears as an impurity, therefore crystal chemistry and structural characterization of this phase is deemed important for the study of the BSCCO high-temperature superconductors.

$Bi_2(Sr,Ca)_4O_x$ exists in both high- and low-temperature oxidized forms. The high-temperature form of the composition $Bi_{34.0}Sr_{49.5}Ca_{16.5}O_x$ (prepared at 860°C, yellow) shows a complicated x-ray diffraction pattern as compared to that of the the low-temperature one, which was obtained by annealing the high-temperature sample in oxygen at 620°C (black).

Combined Rietveld refinements of the low-temperature oxidized form $Bi_{34.0}Sr_{49.5}Ca_{16.5}O_x$ using both neutron and x-ray diffraction showed it to be indexable on a distorted ABO_3 perovskite lattice. The structure was found to have a monoclinic space group $P2_1/n$, with lattice parameters a= 8.38917(7)Å, b=5.99436(5) Å, c=5.89592(5) Å and β=89.965(3)°. There are two independent B sites , one of which is mostly populated by Bi^{5+}, and the other about equally by Bi^{5+} and Ca^{2+}. The A site appears to be populated solely by Sr^{2+}. All bismuth atoms adopt distorted octahedral environment. The high-temperature reduced form was found to be also monoclinc with a space group Pc, and a=11.0896 (15) Å, b=5.9734(5) Å, c=19.8216(26) Å, and β=101.504(11)°. Single crystal x-ray study showed the structure consist of two types of Bi atoms. The first type has distorted octahedral coordination while the other one only coordinate to three oxygens. The latter Bi atoms are located around broad channels with lone-pair electrons concentrated in these channels.

P11.10.035 NEUTRON DIFFRACTION STUDIES OF OXYGEN-DEFICIENCY IN HEXAGONAL BARIUM TITANATE. J. M. S. Skakle and D. C. Sinclair, Department of Chemistry, University of Aberdeen, Meston Walk, Aberdeen AB24 3UE, UK, and T. P. Beales, Centre for Superconducting and Electronic Materials, University of Wollongong, NSW 2522, Australia.

Rietveld refinement using neutron diffraction data has been used to determine the crystal structure and oxygen content of a series of reduced, oxygen-deficient barium titanate powders. These were found to crystallise in a 6H-hexagonal perovskite structure, with (O1) oxygen vacancies in the h-BaO_3 layers which separate pairs of face-sharing Ti-O octahedra. No evidence was found for formation of vacancies in the (O2) sites, associated with corner-sharing octahedra. The oxygen deficiency is accompanied by a partial reduction of Ti^{IV} to Ti^{III}, to give general formula $BaTi^{+IV}_{1-x}Ti^{III}_xO_{3-x/2}$; for x=0.3, the material is a band-gap semiconductor at 300K. As the temperature decreases, the material undergoes a change in the conduction mechanism over the range 240-160K, below which the resistivity increases by several orders of magnitude. Low temperature neutron diffraction data showed no evidence for a structural phase transistion: the change in conduction is attributed to variable range hopping of electrons.

P11.10.036 X-RAY DIFFUSE SCATTERING STUDY ON ATOMIC-DISORDERING EFFECTS IN RELAXOR LEAD SCANDIUM NIOBATE. N. Takesue and Y. Fujii, Neutron Scattering Lab., ISSP, U. of Tokyo, Tokai, Naka, Ibaraki 319-1106, Japan, M. Ichihara, Materials Design and Characterization Lab., ISSP, U. of Tokyo, 7-22-1 Roppongi, Minato-ku, Tokyo 106-8666, Japan, H. Chen, Dept. of Materials Science and Engineering, Univ. of Illinois, 1304 W. Green St., Urbana, IL 61801, USA.

Effects of atomic disordering in $Pb(Sc_{1/2}Nb_{1/2})O_3$ (PSN), a type of simple-perovskite relaxor ferroelectrics, were investigated using an x-ray diffuse scattering technique [1,2]. The measurements were performed on two kinds of the single crystals; one has a high degree of ordering of Sc^{3+} and Nb^{5+}, located in the oxigen octahedrons, and the other has the disordered arrangements. Since disordering of the two ions generates size-effect lattice distortions, an unusual behavior of the transition is expected to appear. Results of the ordered crystal indicate lattice instabilities at the Γ and M points in one temperature region, and the freezing behaviors are of a type of normal soft-phonon modes. On the other hand, results of the disordered crystal reveal the diffuse transition behaviors at the two points. An origin of the diffuse feature is suggested to be the lattice relaxation through two-mode partitioning of thermal energy. The distortions are self-accomodated in atomic displacement patterns at the Γ and M points, and are ordered as forms of ferroelectric and antiferroelectric regions. Their frustration may give a sort of dipole-glass states, and is thought to be a cause of dielectric behaviors of PSN.

[1] N. Takesue, Y. Fujii, M. Ichihara, H. Chen, submitted to Phys. Lett. A.
[2] N. Takesue, Y. Fujii, M. Ichihara, H. Chen, submitted to Phys. Rev. Lett.

P11.10.037 REAL STRUCTURE OF FERRO-ELECTRIC LEAD PEROVSKITES. G. Baldinozzi, J.M. Kiat and G. Calvarin, SPMS, CNRS-Ecole Centrale Paris, Grande Voie des Vignes, F-92295 Châtenay-Malabry Cedex, FRANCE

Translational periodicity results in a considerable reduction of the amount of information necessary to model the structure of solids. Any deviation from this ideal description appears as large thermal displacement parameters when this is handled within the Debye-Waller approximation. The two basical hypothesis of this approximation (periodicity and harmonic lattice vibrations) are not well satisfied for ferroelectric compounds [1,2]. In particular, the atoms in ferroelectric solids present random local off-site displacements (multi-well potentials ...) and are generally modeled with very large Debye-Waller factors.

The object of this work is to go beyond the *average* structure approximation usually obtained in conventional Rietveld refinements and to compare different approaches to better model these local structural displacements (real space approach, anharmonic treatments ...).

In order to clarify the structural features of various perovskite compounds ($PbMg_{1/3}Nb_{2/3}O_3$, Pb_2MgWO_6, Pb_2YbNbO_6, ...) presenting compositional and displacive disorder, we have spanned a very large portion of the Ewald sphere up to a **Q** momentum transfer of about 15 $Å^{-1}$ using synchrotron radiation at ESRF. Diffraction patterns at different temperatures (90-900 K) are investigated to study the thermal evolution of disorder in the cubic and low temperature phases.

The knowledge of these deviations from the ideal structure at different temperatures are the necessary basis for the understanding of the relationships between structural modifications and physical properties.

1. T. Egami, H. D. Rosenfeld and R. Hu (1992). Ferroelectrics, 136, 15-25.
2. H. D. Rosenfeld and T. Egami (1994). Ferroelectrics, 158, 351-356.

P11.10.038 X-RAY AND MAGNETIZATION STUDY OF Sn DOPED $LaMnO_y$ PEROVSKITE. L. Morales, D. Vega, A. Serquis, G. Alejandro, R. Sánchez, and A. Caneiro, Centro Atómico Bariloche – Instituto Balseiro, Av. E. Bustillo, km 9.500 (8400), Rio Negro, Argentina.

The discovery of "colossal magnetoresistance" (CMR) near the Curie temperature in perovskite-based $La_{1-x}A_xMnO_3$ (A = Ca, Sr, Ba) has generated renewed interest in their magnetic, structural, and electronic properties.

Most of the studied systems correspond to the substitution of La^{3+} by divalent atoms. The effect of substitution of divalent, trivalent and tetravalent cations in the Mn site on the magnetic and transport properties has also been reported in many papers. However, controversial results have been reported on the Sn occupancy site and its effect on the magnetic properties of the LaMnOy perovskite.

In order to investigate the influence of the Sn doping on the physical properties of $LaMnO_3$ manganites, we prepared, characterised and measured the magnetic response of two families of samples with nominal compositions $(La_{1-x}Sn_x)MnO_y$ and $LaSn_xMn_{1-x}O_y$ (x = 0.00, 0.02, 0.05, 0.10, and 0.15). The powder X-ray diffraction data of samples prepared by chemical methods were refined by the Rietveld method and their magnetic susceptibility measured with a SQUID magnetometer. Electron Paramagnetic Resonance (EPR) results are also discussed.

The Mn-O-Mn angle and the Mn-O average distance obtained by Rietveld refinement strongly suggest that Sn replace Mn in the perovskite structure. The defect structure for both families of samples is analysed and its effect on the magnetic response is discussed.

P11.10.039 THE CRYSTAL STRUCTURE OF THE COMPOUND $CS_3MG_2Cl_7$. H.Homeida [1], A.A.Al-Aql, Z.H.Dughaish, A.Al-Jufali, K.M. Al-Sheibani, A. Flimban [2], [1] The Academy of Medical Sciences & Technology, Khartoum, Sudan, [2] King Saud University, Riyadh, Saudi Arabia

The crystal structure of the compound $Cs_3Mg_2Cl_7$ is studied and found to consist of layers of distinct double pervoskite type formed parallel to the plane (001) and the following layers are displaced by $a/\sqrt{2}$ in the direction [110].

The compound is tetragonal of the space group 14/mmm and the lattice parameters are: a =0.505(1)nm, c =2.630(5)nm
The experimental density, D_m = 3.40 g cm^{-3} and the theoretical density D_x=3.45 g cm-3. The number of molecules per unit cell Z=2 and the reliability factor R_w=5.8%.

The Mg^{++},Cs^+(1) and Cs^+ (2),Z=0.1899 (6) for Cs^+ (1) and Z=0.4021 (8) for Mg^{++}. The Mg^{++} is surrounded approximately octahedrally by six chlorine ions, while Cs^+(1) by nine chloride ions, and Cs^+(2) by twelve chlorine ions.

P11.10.040 CONFIGURATION OF A1 AND A2 SITES ON THE MICROWAVE DIELECTRIC $Ba_{6-3x}Sm_{8+2x}Ti_{18}O_{54}$ SOLID SOLUTIONS. H. Sakashita, H. Ohsato, A. Komura and T. Okuda, Nagoya Institute of Technology, Gokiso-cho, Showa-ku, Nagoya 466-8555, Japan

Recently, $Ba_{6-3x}Sm_{8+2x}Ti_{18}O_{54}$ solid solutions have been used for ceramic resonator in microwave telecommunication. The dielectric ceramics have high quality dielectric properties, that is high dielectric constant (ε>80), high quality factor (Q>10000) and low temperature coefficient. The solid solutions have the tungsten bronze type structure with perovskite blocks (A1-site), pentagonal columns (A2-site) and trigonal columns (C-site). In this work, we describe the polyhedral coordination numbers based on the configuration of rhombic A1-sites and pentagonal A2-sites of the solid solutions with x=0.5 as representative composition. The crystal data of $Ba_{4.5}Sm_9Ti_{18}O_{54}$ (x=0.5) with super structure have been obtained by X–ray crystal structural analysis. The crystal data are; Orthorhombic system; Pbnm (No.62); a=12.16(4), b=22.363(8), c=7.662(2) Å, V=2083.7 $Å^3$, Z=2; D_x=5.897g/cm^3; R=4.49%, wR=4.99%. Although the coordination number of the A1-sites of perovskite is usually twelve, in this solid solutions, the sites are distorted to rhombic. We decided that A1-sites became 8 coordination number due to the bond-length and configuration of rhombic sites. Coordination numbers of the A2-sites have been also derived from the bond length and the configuration of pentagonal sites to be 10.

1. H. Ohsato et al., Jpn. J. Appl. Phys. , 37(9B), 5357–5359 (1998).
2. H. Okudera et al. , J. Solid State Chem. , in press (1999)

P11.10.041 PHASE TRANSITIONS IN SODIUM NIOBATE. C.N.W. Darlington [1], K.S.Knight [2], [1] School of Physics, University of Birmingham, Birmingham, B15 2TT, [2] ISIS Facility, CLRC Rutherford Appleton Laboratory, Chilton, Didcot, Oxon OX11 OQX

The phases exhibited by Sodium Niobate at room temperature and above have been re-examined using the high-resolution diffractometer, HRPD, at the neutron spallation source, Rutherford Appleton Laboratory. We have found that the symmetry of the phase stable at room temperature, phase P, is monoclinic rather than orthorhombic, and that the multiplicities of the next two phases, R and S, are 2 x 4 x 6, and not 2 x 2 x 6 and 2 x 2 x 2 as reported in the literature. We confirm that the structures of the phases stable above 793K are as reported in the literature, and present details of the evolution of their stuctures with change in temperature. The octahedra at high temperature are tilted and deformed, with the deformation proportional to the square of the tilt angle.

P11.10.042 STRUCTURE CHANGE AND PHASE TRANSITION OF PEROVSKITE-TYPE ABO_3 DUE TO THE IONIC SUBSTITUTION. H.Horiuchi, Department of Natural Science, Faculty of Education, Hirosaki University, Hirosaki 036-8560, Japan, T.Shishido and A.Yoshikawa, Institute for Materials Research, Tohoku University, Sendai 980-8577, Japan, A.Saitow and M.Tanaka, Photon Factory, Tsukuba 305-0810, Japan, and S.Hosoya, Engineering Department, Yamanashi University, Kofu 400-8511, Japan.

Structural change and phase transition of perovskite-type ABO_3 were investigated based upon X-ray powder diffraction data

measured mainly by a laboratory shield tube X-ray source (40kV, 30mA, CuKα) by pyrolitic graphite monochromator and partially by SR for the samples synthesized by a systematic combination of A and/or B with appropriate size of ions[1]. Phases studied in this investigation are RAlO$_3$, RGaO$_3$, BaRO$_3$ etc., where, R is one of a series of rare earth ions of La^{3+}~Lu^{3+} for aluminates and garates, and is Ce^{4+}, Pr^{4+} or Tb^{4+} for BaRO$_3$, in addition, the structures of solid solutions of $(Nd_x,Sm_{1-x})AlO_3$ and $Ba(Pr_{1-x},Tb_x)O_3$ were also investigated in detail on the relationship among their average ionic radius of R, the deformation from ideal cubic lattice and phase transition temperature T_c. Lattice parameters were precisely determined using about 50 reflections which were carefully analyzed by a profile decomposition program[2] for the most of samples. The change from orthorhombic to rhombohedral structure is observed in the phase of $(Nd_x,Sm_{1-x})AlO_3$. The phase transition at room temperature (T_c=22ºC) occurs in the phase with x = 0.73, and the T_c decreases about 35ºC by 1% increase of the amount of substitution of Nd for Sm. All structures of $BaCeO_3$, $BaPrO_3$ and $BaTbO_3$ were confirmed to be orthorhombic with space group of *Pbnm* or *Pbn2$_1$* in this study, although it is reported for $BaTbO_3$ to be rhombohedral in some literature [3]. As a result, no structural changes like (Nd,Sm)AlO$_3$ were observed in the solid solution of Ba(Pr,Tb)O$_3$ at room temperature. Lattice deformation from the ideal cubic is not linearly correlated with the amount of substitution of Pr for Tb in Ba(Pr,Tb)O$_3$. The structures closer to pure compositions with no substitution show a smaller deformation than those with a larger amount of substitution of one ion for another. The structures of $SrCeO_3$ and $BaCeO_3$ were also studied and reconfirmed to be orthorhombic with *Pbnm* or *Pbn2$_1$*. The lattice deformation of $SrCeO_3$ from ideal cubic is much large as compares with that of $BaCeO_3$ which is relatively close to ideal cubic lattice.

1. Shannon R.D. and Prewitt C.T.(1969), Acta Crystallogr.,**B25**, 925-946.
2. Toraya, H.(1986), Jour. Appl. Crystallogr.,**19**, 440-447.
3. Tofield,B.C, *et al*.(1972), Solid State Chem.,**5**, 2887-2895.

P11.10.043 THERMOELECTRIC CLATHRATES. B.C. Chakoumakos, B.C. Sales, D.G. Mandrus [1], J.W. Sharp, G.S. Nolas [2], [1] Solid State Division, Oak Ridge National Laboratory, Oak Ridge, TN 37831 USA, [2] Research and Development Division, Marlow Industries, Dallas, TX 75238 USA

New directions in the research of thermoelectric materials are focusing on clathrate compounds, which exploits the "phonon glass - electron crystal" concept. Atomic displacement parameters (ADP) and thermal conductivity measured as a function of temperature for several promising thermoelectric compounds show that in each case one of the atoms is weakly bound and "rattles" within its atomic cage, resulting in low lattice thermal conductivity. Low lattice thermal conductivity is essential for the design of thermoelectric materials with improved efficiencies. For many clathrate-like compounds, ADP values can be used to estimate the Debye temperature, velocity of sound, heat capacity, mean free path of phonons, lattice thermal conductivity, and Einstein frequency of the "rattler."

Using neutron powder diffraction, the ADP values have been measured for a variety of clathrate and clathrate-like compounds: filled skutterudite-type antimonides ($R_xCo_yFe_ySb_{12}$, where R = La, Ce or Tl), Tl_2SnTe_5, Tl_2GeTe_5, and X_8E_{46}-type germanides ($X_8Ga_{16}Ge_{30}$, X = Sr, Ba). The neutron diffraction data were collected at the High Flux Isotope Reactor at Oak Ridge.

Oak Ridge National Laboratory is supported by the Division of Materials Sciences, U.S. D.O.E. (contract DE-AC05-96OR22464 with Lockheed Martin Energy Research Corporation).

P12.10.001 STUDY OF CRYSTALLOGRAPHIC STRUCTURE OF THE COLOSSAL MAGNETO-RESISTANCE COMPOUND $La_{0.75}Ca_{0.25}MnO_3$. G.Iannone[(1)], C. Meneghini[(2)], S-W. Cheong[(3)], D.D. Sarma[(4)] and P.G. Radaelli[(5)], (1) ILL, avenue des Martyrs BP 156 38042 Grenoble Cedex France, (2) ESRF, avenue des Martyrs BP 220 38043 Grenoble Cedex France, AT&T Bell Lab, (3)Murray Hill, New Jersey 07974, (4) SSCU IISc Bangalore 560 012 India, (5) ISIS Facility Rutherford App. Lab., Chilton, Didcot, Oxon. OX11 OQX United Kingdom.

Manganese oxides with perovskite structure and formula unit $A_{1-x}A'_xMnO_3$ (x<0.30, A= La, Pr,..., A'=Ca, Sr,...) undergo a transition from an insulating to a metallic state near the ferromagnetic order temperature of Mn spins (Tc). A weak magnetic field inhibits this phenomenon so these systems show colossal magnetoresistance (CMR) at Tc. Several experimental works have been performed in order to investigate the crystallographic structure against the atomic species on A/A' site (1) and several theories have pointed out the role of the structural changes that take place at Tc(2). We investigated the crystallographic structure of the compound $La_{0.75}Ca_{0.25}MnO_3$ against temperature (20-800K), applied pressure (0-5Kbar) and magnetic field (0-3Tesla) by means of neutron powder diffraction. All measurements were performed at the Institut Laue Langevin on high-resolution diffractometer D2B.

We observed that the structure is very sensitive to the external condition: in particular a structural phase transition from an orthorhombic Pnma to a trigonal R3c phase takes place in the compound at T = 650K (without magnetic field and at ambient pressure). We observed also that the coupled magnetic and metal insulator transition is induced at constant temperature by the applied pressure or by the applied magnetic field.

(1) P.G. Radaelli, G. Iannone, M.Marezio, H.Y. Hwang, S.W. Cheong, J.D. Jorgesen, and D.N. Argyriou, Phys. Rev. B 56, 8265 (1997)
(2) A.J. Millis, Boris I.Shraiman and R. Mueller, Phys.Rev.Lett. 77, 175, (1995)

P12.10.002 STRUCTURAL STUDY OF EXCIMER LASER TREATED Ag/Co MULTILAYERS EXHIBITING GMR EFFECT. M. Jergel, A. Anopcenko, E. Majková, M. Spasova, and Š. Luby, Institute of Physics of the Slovak Academy of Sciences, Dúbravská cesta 9, 842 28 Bratislava, Slovakia, V. Holý, Laboratory of Thin Films and Nanostructures, Masaryk University, Kotlárská 2, 611 37 Brno, Czech Republic, M. Brunel, Laboratoire de Cristallographie du CNRS, B.P.166, 38042 Grenoble Cedex 09, France, and A.Luches and M.Martino, I.N.F.M. and University of Lecce, Department of Physics, 73100 Lecce, Italy

The work is devoted to a study of interplay between the structure and giant magnetoresistance (GMR) evolution in Ag/Co multilayers exposed to excimer XeCl laser pulses with the fluences of (0.1-0.25) Jcm^{-2} for (1-200) times. Three as-deposited samples, labeled according to layer thickness ratio as Ag_2Co_1, Ag_4Co_1, and Ag_6Co_1, exhibit polycrystalline fcc structure of Ag layers, as revealed by XRD measured both in grazing incidence and Bragg-Brentano modes. The satellites around Ag 111 reflection in the latter mode hint at a superlattice-like character of Ag_4Co_1 multilayer while in other two, the layers are not structurally coherent. Consequently, the grain boundary diffusion of Ag into Co layers occurs due to laser treatment in Ag_6Co_1 leading to the formation of a discontinuous multilayer which enhances the GMR ratio more than twice. In Ag_2Co_1, the temperature window for diffusion is too narrow to improve systematically the GMR ratio as rather thin Ag layers start melting at low fluences. A strong texture in Ag_4Co_1 stabilizes the multilayer structure in the irradiation regime without melting and

the GMR varies non-systematically in a rather narrow interval around the original value. When the Ag melting threshold is reached, rapid solidification produces a granular-like monolayer structure irrespective of the structural character of the original multilayer and the GMR value changes unpredictably in a broad interval. These conclusions are supported by the hard X-ray reflectivity and diffuse scattering measurements at grazing incidence evaluated by the Fresnel algorithm and within the distorted-wave Born approximation, respectively. Transmission electron microscopy and magnetization measurements up to 4.2 K complete the investigation.

P12.10.003 MODELS OF THE CRYSTAL STRUCTURES OF PHASES IN DOPED LANTHANUM MANGANITES. T.V.Novoselova and V.E.Naish, Institute for Metal Physics, Ural Division of Russian Academy of Science, Ekaterinburg, GSP-170, Russia

The crystal structures of all phases typical of phase diagrams for $La_{1x}A_xMnO_3$ manganites have been found by a systematic exhaustion of all possible tilting and Yahn-Tellers modes combinations. The symmetric analysis of any such a combination allows the models of all crystal structures for these manganites to be obtained unambiguously. The particular qualitative differences between two orthorhombic phases so called O' and O" observed by experiment have been brought to light. Their quantitative description has been done and the nature of the distortion modes that form the phase structures has been finally established.

In spite of the fact that a lot of works [1-3] discussed the fascinating structural properties of manganese perovskites does exist yet, we pretend to clarify and systematise the set of phases on the phase diagram in lanthanum manganites.

By an identification of several X-ray diffraction patterns obtained anew the satisfaction agreement of proposed models and experimental data has been achieved. Our conclusions are strongly supported by wellknown results from [1] also.

1. H.Kawano, R.Kajimoto, M.Kuboto, H.Yoshizawa (1996). Phys.Rev., **53B**, 22, 14709.
2. Y.Yamada, O.Hino, S.Kanao, T.Inami, S.Katano. (1996). Phys.Rew.Letters, **77**, 5, 904.
3. J.L.Garcia-Munoz, M.Suaaidi, J.Fontcuberta, J.Rodriguez-Carvajal (1997) Phys.Rev., **55B**, 1, 34

P12.10.004 X-RAY STUDY ON DIFFUSE SCATTERING IN $(Nd_{0.125}Sm_{0.875})_{0.52}Sr_{0.48}MnO_3$. S. Shimomura, K. Tajima and N. Wakabayashi, Dept. of Phys., Faculty of Sci. and Tech., Keio Univ., 3-14-1 Hiyoshi, Kohoku-ku, Yokohama 223-8522, Japan, H. Kuwahara, Dept. of Phys., Sophia Univ., Tokyo 102-8554, Japan, and Y. Tokura, JRCAT, Tsukuba 305-0046, and Dept. of Applied Phys., Univ. of Tokyo, Tokyo 113-0033, Japan.

A group of compounds, hole-doped manganese oxides with a distorted perovskite structure, $A_{1-x}B_xMnO_3$, has been subjects of great interest because of their colossal magnetoresistance. The compounds with finely controlled ionic radii of the *A* sites, $(Nd_{1-y}Sm_y)_{0.5}Sr_{0.5}MnO_3$ (y=0.875), show a drop in resistivity of more than three orders of magnitude at theferromagnetic transition temperature (T_C), accompanied by discontinuous changes in the lattice parameters. The large resistivity above T_C has been attributed to the presence of polarons.

X-ray scattering study of $(Nd_{0.125}Sm_{0.875})_{0.52}Sr_{0.48}MnO_3$ has revealed that the existence of the diffuse scattering around Bragg peaks in the paramagnetic and insulating phase. The diffuse scattering shows characteristic distribution of its intensity depending on coordinates of reciprocal lattice points. With decreasing temperature from 300K, the intensity of the diffuse scattering increases but seems to vanish abruptly at T_C = 133K. This diffuse scattering can be interpreted as due to a result of the local lattice distortion produced by the localized carriers on the Mn sites (polaron). The number of the polarons presumably increases with decreasing temperature, and below T_C the delocalization of the carriers results in relaxing the local lattice distortion. We have calculated the intensity distributions on the basis of randomly distributed Jahn-Teller polarons. The results of the calculation qualitatively agree with the observations.

P12.10.005 ORDERING PHENOMENA AND ELECTRONIC PROPERTIES OF $Ln_{1-x}Ca_xMnO_3$ PEROVSKITES (Ln =Pr, Sm, Y). Z. Jirak and J. Hejtmanek, Institute of Physics, Prague, Czech Republic, and C. Martin, M. Hervieu, A. Maignan, F. Damay and B. Raveau, Laboratoire CRISMAT, Caen, France.

Behavior of e_g electrons in mixed-valent manganites has been investigated in numerous systems of parent Pnma symmetry with medium and low Mn^{3+} content. With the help of the high-resolution neutron diffraction data, electron microscopy, electrical transport data and magnetic measurements, several low-temperature phases were distinguished and their structure refined. As to the occurrence of charge and/or orbital ordering, magnetic and transport properties, the phase diagram shows three distinct compositional regions. The first region, $0.3<x\leq 0.75$, is characterized by an additional pseudotetragonal compression of the perovskite lattice, which occurs below a critical temperature T_{CO} due to concomitant Mn^{3+}/Mn^{4+} charge and orbital order. This is accompanied with a sudden electronic localization. The magnetic groundstate is of the CE type and, in dependence of the size of interpolated cation, the antiferromagnetic transition takes place at temperatures well below T_{CO}. The samples in the second region, $0.75<x<0.85$, show no charge order. Instead, they undergo a structural transition due to orbital ordering (polarization) of e_g orbitals, which is most readily manifested by a tetragonal elongation of MnO_6 octahedra along the [101] direction with respect to the Pnma lattice. The structure thus acquires a characteristic monoclinic distortion. This transition is followed with a carrier localization, the electrical resistivity is, however, several orders of magnitude lower compared to the charge ordered samples. The antiferromagnetic ordering is of the C type. Finally, the samples with $x\geq 0.85$ preserve pseudocubic metrics down to lowest temperatures. They exhibit the G type antiferromagnetism below T_N~115 K. In addition, ferromagnetic clusters are always present in this regime and are responsible for giant magnetoresistance in x~0.85 samples. The ferromagnetic component achieves maximum for x~0.9 and the compounds (metallic in paramagnetic state) preserve then their high electrical conductivity even below T_N.

P12.10.006 THE $La_{1-X}Sr_XMnO_{3-\delta}$ SYSTEM: A NEUTRON POWDER DIFFRACTION AND INELASTIC LIGHT SCATTERING STUDY. S.- G. Eriksson[1], S. Ivanov[2], J. Eriksen[3], R. McGreevy[3], H. Rundlöf[4], P. Berastegui[5], P. Björnsson[6], M. Rubhausen[6], J. Bäckström[6], M. Käll[6] and L. Börjesson[6], [1]Dept. of Inorganic Chemistry, GU, SE-412 96 Göteborg & NFL, Studsvik, SE-611 82 Nyköping, Sweden, [2]Karpov Institute of Physical Chemistry, RU-103064 K-64 Moscow, Russia, [3]NFL, Studsvik, SE-611 82 Nyköping, Sweden, [4]Inorganic Chemistry, Ångström Laboratory, SE- 751 21 Uppsala, Sweden, [5]Dept. of Inorganic Chemistry, SU, SE-10691 Stockholm, Sweden, [6]Condensed Matter Physics, CTH, SE-412 96, Sweden

The atomic and magnetic structure of $La_{1-X}Sr_XMnO_{3-\delta}$ ($0< x< 0.2$) is controlled by cation composition as well as by oxygen

content. The atomic order and thus the lattice symmetry, is also affected by the temperature.

The samples were prepared from the constituent oxides or carbonates. The total sintering time were more than 2 weeks at temperatures from 1223 K to 1623 K. Neutron powder diffraction data were collected at the R2 reactor, Studsvik, Sweden, and data analysed with the Rietveld program FULLPROF. The light scattering measurements have been performed in backscattering geometry on a Dilor XY800 micro-Raman, and a SPEX Triplemate macro-Raman setup.

We have investigated a series of powdered materials at temperatures between 10 K and 300 K. Most samples, as prepared in air, were single phase, either showing rhombohedral or orthorhombic lattice symmetry. They crystallise in space group R-3c (a= 5.52 Å and c= 13.34 Å: hexagonal setting) and Pnma (a= 5.50 Å, b= 7.78 Å, and c= 5.53 Å), respectively. The change of magnetic structure with temperature and doping was also investigated. The inelastic light scattering data do confirm the change in lattice symmetry, and do also indicate the importance of a coupling of lattice and electronic degrees of freedom for the magnetic phase transition.

In order to obtain a more detailed understanding for the La-Sr-Mn-O system we intend to perform complementary studies on samples prepared under controlled oxygen partial pressure, i.e. on samples with different oxygen content, and also investigate samples under an external magnetic field.

P12.10.007 PHASE SEPARATION AND SPIN/ CHARGE ORDERING IN $La_{1-x}Ca_xMnO_3$ (x=047, 0.5, and 0.53). Q. Huang, J. W. Lynn, R. W. Erwin, D. C. Dender, A. Santoro, NIST Center for Neutron Research, NIST, Gaithersburg, MD 20899, USA; V. N. Smolyaninova, K. Ghosh, and R. L. Greene, University of Maryland, College Park, MD 20742, USA.

$La_{1-X}Ca_XMnO_3$, with x near 0.5 has been the subject of renewed interest due to the competition between ferromagnetic double exchange coupling and charge/orbital ordering. Neutron powder diffraction has been used to study the crystal structure, bonding, magnetic ordering, and the phase relationships and the properties of the system near the metal-insulator transition at x=0.5, as a function of temperature and magnetic field. The high temperature phase (HTP) has the P*nma* symmetry and is ordered ferromagnetically below ~270 K. The low temperature phase (LTP) develops at ~230 K and is ordered antiferromagnetically below 160 K. As the temperature decreases from 230 K to 100 K, the fraction of the LTP increases to 42, 78, and 90% for x=0.47, 0.50, and 0.53, respectively, and remains almost constant on further cooling. The temperature depen-dence of the broadening of the $(031)_{LTP}$ reflection peak indicates that the LTP phase develops in three steps: phase formation with very small crystallite size (from 230 to 200 K); increase of crystallite size (from 200 to 160 K); and increase of the relative proportion in the sample (from 160 to 100 K).

The development of the LTP is inhibited when a magnetic field is applied. For example, for x=0.5, the amount of the LTP is 68% when the sample is cooled in zero field and a magnetic field of 8.5 T is applied at 5 K. On the other hand, only 24% and 58% of this phase is formed when the sample is cooled in magnetic fields of 8.5 and 5 T, respectively. The curves of the magnetic moment, LTP phase fraction, lattice parameters, and Mn-O distances, as a function of temperature, show a change of slope between 230 and 160 K only on cooling, while smooth curves are observed on warming.

P12.10.008 TUNING OF Tc BY CO-DOPING IN LANTHANUM MANGANITE SINGLE CRYSTALS. Suja Elizabeth, Amlan Biswas, S. Brahadeeswaran and H.L. Bhat [1], A.K. Raychaudhuri [2], [1] Department of Physics, Indian Institute of Science, Bangalore-560012, India, [2] National Physical Laboratory, New Delhi-110012, India

Many rare-earth manganites exhibit colossal magnetoresistance in which the magnetoresistance peaks in the vicinity of magnetic and metal-insulator transition. It is relevant to tune the transition temperature (Tc) of these materials closer to room temperature for practical applications. In these perovskites, Tc is known to vary with the average radius <rA> of A-site cation: hence smaller ionic radius, along with divalent lead, in trivalent lanthanum site. Single crystals of co-doped $[La_{(1-y)}Nd_y]_{(1-x)}Pb_xMnO_3$ have been grown by flux technique. Growth temperature and cooling program are optimized and crystals of typical dimensions 3.5x3x2 mm^3 are obtained. Temperature variation of resistivity and susceptibility measurements conducted on these crystals confirm that ferromagnetic transition occurs in the close vicinity of insulator-metal transition. In particular, $La_{0.36}Nd_{0.37}Pb_{0.27}MnO_3$ crystals exhibit transitions at 275K. In addition, a peak magnetoresistance of 65% is realized in these crystals near this temperature at a relatively low magnetic field of 3 Tesla. Tuning of Tc without compromising important properties like MR is a significant achievement of this study.

1. A. Biswas, Suja Elizabeth, A.K. Raychaudhuri and H.L. Bhat (1999). Phys. Rev. B.(in press).

11. SURFACES, INTERFACES, LIQUIDS AND THIN FILMS

P06.11.001 STRUCTURE OF SINGLE CRYSTALS Fe-Ni ALLOYS AFTER NITRIDING. V.E. Danil'chenko, Institute for Metal Physics, Academy of Sciences of Ukraine, 36 Vernadsky Blvd., 252680 Kiev, Ukraine

X-ray method of single crystals are used to investigate structure state of Fe-Ni alloys after nitriding. The nitriding was performed in the mixture of ammonia and 10-25 % hydrogen at 400-850 °C of $0.5 \cdot 10^{-4}$ min. The sample, quenched in cold water immediately after nitriding, were austenitic at room temperature.

It is found first stages of forming nitrous austenite. Parameter of nitrous austenite lattice deduced during nitriding to five minute and remained practically unchanged later on. The γ′-nitride Fe_4N with fcc lattice is formed in diffusion layer of alloy with 30 wt. %N. He appear after achievement limit equilibrium concentration of nitrogen in γ-solid solution. Diffusive strips, uniting the reflection of γ′-nitride and nitrous austenite with initial austenite, explained by coherence of lattice of these phases.

During nitriding by electric heating are formed fcc γ-nitride and hcp ε-nitride. The γ′- and ε-nitrides are formed as polycrystalline component in the initial single crystalline matrix. In alloy with 30 wt. %N and 5 wt. %Ti γ′-nitride is of single crystalline nature.

The solubility limit of nitrogen is increasing in alloy, contenting 5 wt. %Ti. The γ′-nitride in diffusional layer of alloy with 30 wt. %Ni had ordered structure and correspond composition Fe_3NiN, in alloy with 30 wt. %Ni and 5 wt. %Ti - $Fe_3(Ni, Ti)N$.

P06.11.002 EFFECT OF THE LASER TREATMENT ON RECRYSTALIZATION OF SINGLE CRYSTAL α-IRON. V. I. Bondar, V.E. Danil'chenko, B. Polchuk, Institute for Metal Physics, Academy of Sciences of Ukraine, 36 Vernadsky Blvd., 252680 Kiev, Ukraine.

Laser pulse heating of α-iron single crystals with a beam energy density from 5 to 20 J/mm^2 visually did not change the above-mentioned parameter. A further increase in the energy of the laser beam led to no changes in the diffraction pattern. However, heating in the regime of visually observed surface melting resulted in significant changes in the diffraction pattern and, consequently, in the structural state of the initial a-iron single crystal. The rapid cooling of the liquid surface layer led to the formation of polycrystalline α-iron with the bcc lattice whose parameter coincided with the lattice parameter of the initial specimen. This is evidenced by the formation of continuous Debye reflections of α-iron passing through all the reflections of an initial single crystal.

When the energy density reached 22 J/mm^2 qualitative changes in diffraction patterns were observed. In this case, in addition to the α-phase, the γ-phase was identified as isolated reflections from single-crystal grains. No polycrystalline component of the γ-phase was observed. In different experiments, the number of orientations of the γ-phase lattice with respect to the initial single-crystal a-phase varied from two to four.

When the energy densities were high (higher than 26 J/mm^2). laser remelting did not lead to γ-phase formation. Consequently, γ-phase formation upon laser treatment was observed only in a specific range of energy densities (18-22 J/mm^2).

P06.11.003 THREE-WAVE GRAZING INCIDENT X-RAY DIFFRACTION: DIRECT PHASE DETERMINATION OF SURFACE REFLECTION. Y.S. Huang, S.L. Chang, and C.H. Chao, Department of Physics, National Tsing Hua University, Hsinchu, Taiwan, R.O.C. M.T. Tang, Synchrotron Radiation Research Center, Hsinchu, Taiwan, R.O.C., and Y.u.P. Stetsko, Department of Physics, National Tsing Hua University, Hsinchu, Taiwan, R.O.C. and Chernovtsy State University, Chernovtsy, Ukraine.

Three-wave grazing incidence x-ray diffraction is realized by tuning the x-ray photon energy to match the incident wavevector with the coplanar momentum transfers of crystal surface in-plane reflections. Near the resonance energy, the observed specularly diffracted intensities decreasing at lower energies and increasing at higher energies or vice versa reveal the effects of reflection phases due to the coherent interaction of x-ray surface waves. This experiment thus provides a new way of direct phase determination for surface in-plane reflections. This phasing technique has been applied to overlayered systems and the corresponding interface structures will be reported and discussed.

P06.11.004 A RECIPROCAL LATTICE SIMULATION TO EPITAXIAL THIN FILMS IN THE FOUR-CIRCLE DIFFRACTOMETER GEOMETRY. Ryouichi Yokoyama and Jimpei Harada, X-Ray Research Laboratory, Rigaku, Tokyo, Japan

A new method has been developed which simulates reciprocal lattices in thin crystalline films. In characterizing of epitaxial thin films on some substrate crystal, it is essential to know the crystallographic relationships between those thin crystals. Since such an X-ray measurement is usually based on the four-circle diffractometer geometry, a technique to determine the crystal orientation matrix which has been utilized in the single crystal structure analysis was applied to the thin film study. The complicated mutual relationships between several thin films and a substrate crystal were found to be determined within the accuracy of less than 0.01 degrees in omega angle by the crystal orientation matrix determined. The present simulation is also designed so as to visualize the mutually related reciprocal lattices of thin crystals, the limiting sphere and the Ewald sphere with an intuitive way. Thus it is very easy to find out scattering condition of any symmetrical and asymmetrical settings, with grazing incidence. Furthermore, as the movement of the reciprocal lattices in CRT was connected with the motor drivers for four circle goniometer, any measurements of X-ray scattering from thin films were fully automated by this guide.

P06.11.005 GROWTH OF GE AND PB ON GE(113) SURFACES STUDIED BY X-RAY DIFFRACTION AND LEED. M. Albrecht, A. Hirnet, A. Iglesias, M. Gierer, W. Moritz D. Wolf and H. Schulz, Institute of Crystallography and Applied Mineralogy, University of Munich, 80333 Munich, Fed. Rep. of Germany

The (113) surfaces of Ge and Si are very stable and exhibit a surface energy nearly as low as that found for the (100) surfaces [1] but do not exhibit two rotational domains. The (113) surfaces are therefore possible candidates for growth of Si-Ge multilayers. The clean surfaces are stabilised by subsurface interstitial atoms which form a (3x1) superstructure at room temperature [2,3]. At low temperatures the interstitial sites order and a (3x2) structure is formed. We have studied the homoepitaxy of Ge on Ge(113) and the influence of Pb on the growth process. The measurements have been performed using synchrotron radiation at HASYLAB with a new UHV x-ray diffractometer which allows to study the

growth process in situ. The results show that at a temperature of 450 K and at submololayer coverages Ge on Ge(113) forms islands. The surface becomes rough with increasing coverage. At 800 K the surface remains well ordered and Ge grows in a step flow modus. The roughness and the island size as a function of substrate temperature has been investigated with SPA-LEED measurements.

Pb grows on Ge(113) in the Stranski-Krastanov mode. Two ordered phases exist with one and two Pb atoms per (1x1) unit cell. At submonolayer coverages Pb removes the (3x1) reconstruction and terminates the Ge(113) surface by substitutional sites. At a coverage above 1 monolayer Pb forms islands. Pb does not intermix with Ge and is a possible surfactant for the growth of Ge on Ge or Si. Our results show little influence on the homoepitaxy of Ge on Ge(113) probably because the low desorption temperature of about 600 K.

[1] W.Ranke. Phys. Rev. B 41, 5243 (1990)
[2] J.Dabrowski, H.-J.Müssig, and G.Wolff, Phys. Rev.Lett.73, 1660 (1994)
[3] H.Vogler,A.Iglesias, W.Moritz, and H.Over, Phys. Rev. B57 (1998)2315

P06.11.006 HIGH RESOLUTION X-RAY MULTI-BEAM DIFFRACTION STUDIES OF THIN FILM AND INTERFACES. M.V.Kovalchuk, L.Samoilova, A.Kreines, I.Orlov Institute of Crystallography RAS, Leninsky pr. 59, 117333 Moscow, Russia

X-ray multiple diffraction (XMD) is known as an effective tool to solve the phase problem in X-ray crystallography. If one of diffracted beam is weak (i.e. on the "tail" of rocking curve) it can be considered by analogy to optical holography as a reference one and its intensity is determined by phase ratio between amplitudes of incident beam and other (strong) diffracted one. Similar effects in Renninger scheme can be used to study thin surface layer structure of nearly perfect crystals, heterostructures [1] and interface characterization of thin films [2] and buried ?-layers. In this work we have studied theoretically and experimentally the three-beam diffraction from InGaP(0.8mkm)/GaAs(111), InGaP(0.5mkm)/GaAs(111) and Ga As(5.5nm)/GaInAs(2nm)/ GaAs(111) heterostructures. The modulation of the intensity of the secondary, weak reflection in the vicinity of the Bragg condition of the primary, strong reflection allows to determine the film thickness, lattice mismatch, tetragonal distortions and, for thin film, the bond length at the interface.

[1] M.V.Kovalchuk, A.Kreines, L.Samoilova, NIM (1998) A405, 445
[2] M.V.Kovalchuk, A.Kreines, L.Samoilova, A.Mel'nikov, J.Synchrotron Radiation (1997), V.4, p.180

P06.11.007 THE FORMATION OF MARTENSITE AND ITS ORIENTATIONS IN SURFACE LAYER OF LASER IRRADIATED Fe-Al-C ALLOYS SAMPLES. E.N.Dzevin, V.A.Andryushchenko. G.V.Kurdyumov Institute for Metal Physics NAS Ukraine, 252142 Kiev-142, Vernadsky blvd. 36, Ukraine.

The structure of martensite which forms in nearsurface layer of pulse laser irradiated quenched Fe-Al-C alloys samples have been investigated by X-ray technique. After cooling down of the austenite Fe-4%Al-2%C single crystals to the liquid nitrogen temperature, undergone to multiple pulse laser irradiation along the [001] axis of the f.c.c. austenite crystalline lattice with surface melting off, the martensit transformation occurs. The martensite which was formed has a various tetragonality degree and various orientation concerning to austenite on different depth from melted surface. On the stereografic projections the martensite poles (001) and (10.0) asymmetrically situated around austenite (100) and (110) poles, as against this fixes after usually quenching (Greninger-Trojano oriental rates, 48 variants). The quantity of the martensite poles decreases on some depths and the halfwidth of martensite $(002)_\alpha$ difraction spots less nearly two times than another one of high degree tetragonality martensite. This fact has been explained by disturbance of coherency between phase components in these layers.

In single crystals of Fe-8%Al-2,5%C alloy laser irradiated along $[111]_\gamma$ direction, the picture after cooling down to the liquid nitrogen was complicated by presence an α-martensite which was oriented concerning to austenite by Nishijama oriental rates in initial (after quenching) state. The analysis of α-martensite elementary crystal lattice sell changes and its variants of orientations let us to do an assumption that surface layer consist of some streaks. The structure of these streaks have been defined.

P06.11.008 RECONSTRUCTION OF TRANSITION METAL OXIDE SURFACES, T. Gloege, H. Zajonz, F. Wendler, H.L. Meyerheim, W. Moritz and H. Schulz, Institut of Crystallography and Applied Mineralogy, University of Munich, Fed. Rep. of Germany

The structure of oxide surfaces has been far less frequently studied than metal and semiconductor surfaces in spite of their technical importance in various fields such as heterogeneous catalysis and thin film technology. The reconstruction of these surfaces and the role of defects in their chemical and physical properties are not well understood. This is due to the complexity of the first principles structure calculation of these structures and because of sparse experimental data. In many cases the transition metals occur in different oxidation states so that the surface composition cannot be predicted by the simple requirement of an electrostatically neutral surface. We have studied the reconstruction of the clean surfaces $TiO_2(100)$, $Fe_3O_4(100)$ and $Cr_2O_3(0001)$ and one adsorbate structure of K on TiO2(100) by surface x-ray diffraction. The preparation of the clean single crystal surfaces in UHV followed standard methods. In all three clean surfaces we found that defects play an important role. The (100) surface of rutile, TiO2, exhibits a (1x3) reconstruction which can be described by microfacetting due to the formation of (110) planes and a partially populated interstitial site. The surface is terminated by a Ti^{3+}[2]. The Fe_3O_4 surface exhibits a c(2x2) reconstruction which is characterised by a half occupied Fe layer and additional occupation of interstitial sites in subsurface layers. The $Cr_2O_3(0001)$ exhibits no ordered superstructure at room temperature. The surface is terminated by a disordered Cr^{3+}-layer in which 2/3 of the sites are occupied and 1/3 of interstital sites below the top oxygen layer is occupied by Cr leaving an electrostatically neutral termination. The only adsorption system studied so far is K on $TiO_2(100)$ which forms a c(2x2) structure. This surface is characterised by a half occupied Ti-layer oxygen defects and strong relaxation over several subsurface layers.

[1] G. Renaud, Surface Science Reports 32 (1998) 1-90.
[2] H.Zajonz, H.L.Meyerheim, T. Gloege, W. Moritz, D. Wolf, Surf. Sci. 398 (1998) 369-378.

P06.11.009 NEUTRON STANDING WAVES UNDER THE TWO BEAM DYNAMICAL DIFFRACTION. V. Nosik, M. Kovalchuk, S. Zheludeva; A.V. Shubnikov, Institute of Crystallography, Russian Academy of Sciences

The well known X-ray Standing Wave (XSW) method is based on the registration of angular variation of the yield of secondary process excited by dynamical X-ray wave field, (see e.g. [1]). The first experimental evidences of variation of secondary process (gamma quanta emitted due to neutron capture) under the neutron dynamical diffraction were obtained during the search of neutron's Borrmann effect [2] and as far as we know for more then 30 years these effects were out of the scope. It is

surprising but neutron standing waves were discovered in 1956, i.e. BEFORE the X-ray ones.

The principle of this experiment is well known. Coherent superposition of diffracted and transmitted waves inside the crystal forms the neutron standing wave with antinodes changing its position relatively the atoms in diffracting plane with the variation of the incident angle of primary radiation. The period of NSW (as well as XSW) is equal to interplanar distance for given reflection (1-10Å) and can be varied by choosing the proper reflex. In neutron diffraction experiment the modulation of absorption due to NSW is revealed through the "lack" of intensity from the side of low angles of rocking curve, in secondary process yield the formation of NSW can be seen through the variation of angular dependence [2] .

The developed theory explains the angular modulation of secondary process yield (products of nuclear reaction: gamma quanta emitted due to the neutron capture, alpha-, beta- particles and conversion electrons) due to the formation of neutron standing waves (NSW) under the condition of Bragg and Laue diffraction of thermal neutrons in crystal. Due to the small absorption the neutron diffraction provides us with a perfect nuclear yardstick with the period about 1-10Å and the tick distance about nuclear size (10^{-15} m). The variety of the secondary process and magnetic scattering of neutrons opens new possibility for structure characterization. This theory was successfully applied for the explanation of the data obtained in [2].

1. M.V.Kovalchuk and V.G. Kohn *Uspekhi Fiz. Nauk* **149**, 69 (1986).
2. J.W. Knowles. *Acta Cryst.* **9**, 61 (1956).

P06.11.010 DYNAMIC THEORY OF X-RAY DIFFUSE SCATTERING IN MULTILAYERS WITH VERY ROUGH INTERFACES. A.V.Andreev, I.R.Prudnikov, Physics Department, Moscow State University, Moscow 119899, Russia

Grazing incidence X-ray diffuse scattering is now widely used for investigations of interface roughness in multilayered structures and obtaining information on roughness parameters. Up to now, the theoretical approach based on Distorted Wave Born Approximation have been commonly used for the theoretical description of diffuse scattering. It is well known that the area of this method application is restricted to the roughness of the small root-mean square (rms) height [1]. In our paper we have used the dynamic scattering theory which is valid in the case of arbitrary rms height of roughness [2]. The roughness profiles at different interfaces were modeled by harmonic functions, i.e., sine or cosine, with different amplitudes and phases. This model enables us to simulate the different correlation properties of the interface roughness. The variation of the sine amplitudes with the depth makes it possible to study the influence of the of the vertical correlation onto the angular spectra of scattering. The variation in the phases of the successive layers enables to model the different degree of roughness replication from substrate to upper layer. The variation in the lateral correlation length can be modeled by beating of amplitude of the two sine functions with the close but different periods. In the case of the harmonic relief of interfaces the Bragg sheet is really a sequence of the maxima. The variation in the correlation properties of interfaces results in the variation of the Bragg sheet envelope as well as in the position and angular width of the successive maxima. The results of the computer simulations show that the relation between the intensities of the adjacent peaks depends significantly on the vertical correlation length. The equidistant phase shift for the successive layers results in the tilt of the Bragg sheets.

1. S.K.Sinha et al. (1988). Phys.Rev. B**38,** 2297.
2. A.V.Andreev (1996). Physics Letters A **219** , 349.

P06.11.011 RAPID ANALYSIS OF THE SURFACE ROUGHNESS OF GLASS SUBSTRATES. I.Pape, B.K.Tanner, Department of Physics, University of Durham, South Road, Durham, DH1 3LE, UK. M. Wormington, Bede Scientific Inc., 14 Inverness Drive East, Suite - G104, Englewood, Colorado 80112, USA.

The control of surface roughness is extremely important in the production of float glass, as high roughness values increase the amount of diffusely scattered light. Grazing incidence x-ray scattering is an extremely sensitive technique for the study of surface roughness. Through simulations of the diffusely scattered x-rays, roughness values in the range 1 - 30Å can easily be obtained. An unfortunate drawback of this method is the time taken in producing accurate simulations limits the throughput of samples which can be achieved in a quality control environment.

Savage *et al*. [1] proposed a method for deducing the surface roughness, σ, from the diffuse scatter without the need for simulations. This method works well, but underestimates the true roughness values as some of the diffuse scatter is cut-off by the shadow of the specimen edges. We have extended this technique by correcting the roughness values using a look-up table based on the Distorted Wave Born Approximation. To test this approach, grazing incidence x-ray scattering measurements were performed on a series of glass specimens produced by Corning Glass. Simulations of the specular and diffuse scatter were performed for several x-ray optical conditions, leading to a high degree of confidence in the surface roughness values obtained. For all samples, agreement within experimental error was found between the roughness obtained from full DWBA simulations and that deduced from the above method. We suggest that this method is advantageous in a production line environment, where large numbers of similar samples are encountered.

[1] Savage, D.E., J. Appl. Phys. 69 (3), 1411 - 1424, 1991

P06.11.012 CHARACTERIZATION BY X-RAY DIFFRACTION OF YBACUO THIN FILMS ON Si SUBSTRATE WITH BUFFER LAYER. S D. Boschetto [1], F. Schimdt [2], [1] Institute of Optic and Quantum Electronics, F. Schiller University of Jena, Jena, Germany, [2] Institute of Solid State Physics, F. Schiller University of Jena, Jena, Germany.

It is already known that the YBaCuO thin film deposited on SiTiO3 as substrate gives really good superconduction properties. The combination of high temperature YBaCuO superconductor and semiconductor technology makes interesting the use of silicon as a substrate because it is economical and it is between the most useful element to made the electronic circuits. The incorporation of buffer thin films is essential for the refinement of YBaCuO thin films deposited on such a substrate. One possibility is to use CeO_2 and $Y:ZrO_2$ as a buffer. The YBaCuO thin films as well as the buffer interfaces are made by laser ablation and sputter deposition at different substrate temperatures. X-ray diffraction methods permit to point out the crystalline perfection of the grown YBaCuO thin films concerning the crystallite orientation, crystallite size and inherent lattice tension and makes possible the correlation to the superconductor properties. So it is possible to compare the results of the well-known YBaCuO thin films on $SiTiO_3$ as substrate with YBaCuO thin films on silicon as substrate.

P06.11.013 THE STRUCTURE OF Cu-V MULTILAYER FILMS. V.P.Ampilogov, V.M.Ievlev, E.K.Belonogov, Department of Physics, Voronezh State Technical University, Moskovskii Prospekt 14, 394026 Voronezh, Russia.

The multilayer Cu-V films were received by electron-beam evaporation. The structure and orientation of Cu and V

layers were investigation by the methods of X-ray diffraction and transmission electron microscopy in depending on the number of bilayers. There was a good agreement between the experimental and calculated X-ray spectra in the absence of transition regions between the metal layers. The multipositional epitaxial nucleation of V on Cu takes place with the orientational relationships allowed by (011)[21$\bar{1}$] V ‖ (100)[011] Cu (*), which leads to the formation of oriented polycrystal structures of high dispersity. The effect of bilayers is in the increase of metal film dispersity, the increase in deviation from the exact azimuthal orientations (*), and, in the long run, in the formation of axial texture.

P06.11.014 X-RAY DIFFRACTION ANALYSIS OF THIN ALUMINA FILMS. O.A. Yakovleva, Mathematics Department, Petrozavodsk State University, Petrozavodsk 185640, Russia, A.N. Yakovlev, Physics Department, Petrozavodsk State University, Petrozavodsk 185640, Russia and N.M. Yakovleva, Physics and Mathematics Department, Karelian State Pedagogical University, Petrozavodsk 185680, Russia.

Widespread use of thin oxide films of aluminium makes it necessary to investigate their electrical and structural behaviour. Many workers have carried out intensive studies of the electrical properties of alumina as dielectric. However, in the case of amorphous oxides only little attention has been paid to the problem of short-range order (SRO) as well as if and how exposure to temperatures close to the transition into crystalline state can alter SRO and hence can lead to the changes of electrical properties of oxides. The information on previous investigations concerning the SRO of amorphous oxides is limited. But only the application of pair functions method (PFM) made possible the construction of distribution of electron density of amorphous materials resulted from the experimental x-ray scattering intensities to obtain the complete structural data i.e. the radii of the co-ordination spheres and their blurring, the co-ordination numbers.

In the present work x-ray diffraction analysis and direct observations by scanning electron microscopy of amorphous oxide films of aluminium have been made. Aluminas were prepared by the method of anodisation of aluminium foil in different electrolytes. The SRO-parameters for four co-ordination spheres have been calculated by the PFM, and SRO identification has been made. Special attention is given to explanation of the possible mechanism of SRO formation under such conditions. Series of experiments (also including high temperature x-ray diffraction) have been initiated to study the effect of the thermal treatment on amorphous oxides in pre-crystallisation temperature region. The SRO structural changes are first analysed. Crystalline phase growth dynamics due to thermal treatment will be also discussed beginning with the budding of crystalline phase and ending with complete crystallisation.

P06.11.015 SURFACE ROUGHNESS IN LANGMUIR-BLODGETT MULTILAYER FILMS STUDIED BY AFM AND X-RAY DIFFRACTION. T. Pusztai [1], N. Rozlosnik, G. Antal [2], [1] Research Institute for Solid State Physics and Optics, H-1525 Budapest, P O Box 49, Hungary, [2] Eötvös University, Department of Atomic Physics, H-1518 Budapest, P O Box 32, Hungary.

Langmuir-Blodgett multilayer films consisting of up to 100 layers of cadmium substituted arachidic acid on silicon wafer have been studied. The samples were deposited from water subphase containing Cd2+ ions using an alternate layer LB trough under computer control. Long range orientational order was observed by AFM on the surface of films with a small number of layers. The X-ray reflectivity curves shows regularly spaced Bragg peaks arising from multilayer structure. The periodicity of the LB film is in agreement with twice the estimated molecular length, which confirms that the multilayer structure has a bilayer (Y) configuration. We demonstrate that the growth process of the LB films must have been stochastic. Our results are in good agreement with the Eden model of growing.

P06.11.016 INFLUENCES OF DOPED-MATERIALS ON THE CREATION OF CLUSTERS IN THE SN(Y)OX-THIN FILMS. Vo Vong [1], Nguyen Thi Huong [2], [1] Laboratory of Electron Microscopy , National Centre for Natural Science and Technology , Nghiado Caugiay - Hanoi, Vietnam, [2] Department of Physics , National University of Hanoi, Nguyen Trai str. Dong Da District - Hanoi, Vietnam.

In the paper we report the new results, which we received recently by study the Sn(Y)Ox - thin films. Y in the formular is a doped material. The films made by evaporating method. Tin (Sn) and antimony (Sb) or noble metals such as silver (Ag), platinum (Pt), which are doped material, were evaporated from a molybdenum boat in high vacuum of 2.10^{-6}Torr.

Tin and the doped material - one of the Sb , Ag or Pt - which have mass - rate from of 6 : 1 to 10 : 1 pure 99,999%, were put on two differential boats. And then both boats were simultaneously heated to evaporate materials on it.

The films of two mixed metals (Sn and Sb , Ag or Pt) were deposited on substract (110)-NaCl monocrystal. In following, the films were annealed in atmosphere, which is rich oxygen at the temperatures: 300, 400 and 500 ^{o}C in 120 minutes.

The creation of clusters in each temperatural step was studied by X-ray diffraction (D-5000) and transmission electron microscope EM-125K. Through the electron microscopy imagers and X-ray diffraction patterns, the influences of doped materials on the creation of clusters were discussed.

The optical and electrical properties of the Sn(Y)Ox thin films were investigated in the work too.

Vo Vong , Nguyen An , Nguyen Thi Huong , Proceedings of the 2nd International Workshop on Materials Science (IWOM'95). Part 1 p. 232 – 235.

P06.11.017 SOFT X-RAY MAGNETIC DICHROISM IN $R_{1-x}M_x$ AMORPHOUS FILMS (R= RARE-EARTH, M= Co, Fe). O. Zaharko, H. Grimmer, PSI, Villigen, Switzerland, H.-Ch. Mertins, F. Schäfers, BESSY, Berlin, Germany.

Rare-earth (R)/transition metal (M) amorphous films are widely used as high-density recording media [1] due to a number of useful properties concerning magnetization, Curie temperature, compensation temperature, uniaxial anisotropy, coercivity and Kerr rotation.

R/M amorphous films show considerable X-ray magnetic circular (MCD) and linear (MLD) dichroism [2] at the $M_{4,5}$-edges of R- and the $L_{2,3}$-edges of M-elements. These effects are governed by the interplay of various effects: exchange and spin-orbit coupling, presence of a crystal field.

We propose to make use of these properties and to employ R/M amorphous films in a new tunable polarimeter for the characterization of a synchrotron beam's polarization state in the 700 - 1400 eV range.

Characterization of the sputtered R/M films and the first results on the MCD effects in Ho/M films measured by the transmission method at beamline PM4 at BESSY using the soft X-ray polarimeter [3] are presented.

1. P. Hansen 'Magnetic amorphous alloys' in 'Handbook of magnetic materials' ed. K. H. J. Buschow 6 (1991), 289.
2. J. Vogel et al. JMMM 150 (1995) 293.
3. H.- Ch. Mertins et al. SRN 11, No. 4 (1998) 42.

P06.11.018 NEW TYPE OF INTERFERENCE FRINGES IN BRAGG-CASE SECTION TOPOGRAPHY OF IMPLANTATED $A^{III}B^{V}$ CRYSTALS. K. Wieteska[1], W. K. Wierzchowski[2], A. Turos[2], W. Graeff[3], G. Gawlik[2] and R. Grötzschel[4]: [1]Institute of Atomic Energy, Świerk-Otwock, Poland, [2]Institute of Electronic Materials Technology, Warsaw, Poland, [3]HASYLAB at DESY, Hamburg, Germany, [4]Rossendorf Research Centre, Germany. 11.11 16.03

A new type of interference fringes was obtained in synchrotron patterns exposed using synchrotron white beam limited by 5 μm slit in the implanted GaAs and $Al_xGa_{1-x}As$ layers. The implantations were performed with 170 keV protons, 1.5 MeV Se and 1.0 MeV Si ions with the depth range of induced effect not exceeding 1.5 μm, as it was evaluated with a number of characterisation methods. Some implantations performed at channeling condition were also studied. A relatively large film-to crystal and small glancing angle of 4° were used to enhance the deformation effect revealed by the white beam topograph.

The new intense interference fringes were observed only in the cases when the strain profiles was expected to produce a maximum situated under the distinct shot-through layer. That was mostly in the case of the proton implantation and in the case of selenium implantation at channeling condition. On this reason they provide a new possibility of the present method of very effective identification of the presence of the shot-through layer. The fringes appeared in the area between more distinct stripes corresponding to the maximum from the shot through layer and the maximum of the mostly deformed layer. It was also found that the fringes are revealed along the directions corresponding to the change of diffraction vector corresponding to the tetragonal deformation differently from the fringes observed in the case of Bragg-case section and pin-hole patterns in bent crystals.

The possible mechanism of the fringes is the interference of the radiation diffracted at the same angle by the two lamella on both sides of the mostly deformed layer with the same tetragonal deformation. This model provides an easy way of the approximate simulation of the fringes based on the kinematical theory of diffraction.

P06.11.019 THE DETERMINATION OF THE IMPLANTATION INDUCED STRAIN PROFILES IN GaAs AND $Al_xGa_{1-x}As$. W.K. Wierzchowski[1], K. Wieteska[2], A. Turos[1], W. Graeff[3], G. Gawlik[1] and R. Grötzschel[4]: [1]Institute of Electronic Materials Technology, Warsaw, POLAND, [2]Institute of Atomic Energy, Świerk-Otwock, POLAND, [3]HASYLAB at DESY, Hamburg, GERMANY, [4]Rossendorf Research Centre, GERMANY. 11.11 16.03

The MOCVD grown $Al_xGa_{1-x}As$ with $x=0.45$ and GaAs with initial dislocation density smaller than $10^3/cm^2$ were implanted with different doses of 1.5 MeV Se and 1.0 MeV Si ions and 170 keV protons at room and liquid nitrogen temperatures. The energies of ion were chosen to produce the similar expected range of ions, close to 0.7 μm while the range of doses were chosen to exceed distinctly the expected amorphisation level. Part of the samples were thermally annealed at 300°.

The samples were studied with a number of complementary X-ray methods realised both with synchrotron and conventional sources of X-rays. The most important method of characterisation was recording of rocking curves using highly monochromatized synchrotron beam of very small size and the white beam Bragg-case synchrotron topography. The synchrotron rocking curves and plane-wave topographs reproduced many details of interference maxima and were used for strain profile analysis based on fiting of the simulated rocking curves obtained by numerical integration of the Takagi -Taupin equations.

It was found that the amorphisation of $Al_xGa_{1-x}As$ took place only when the implantation was performed at liquid nitrogen temperature. Differently the increasing of the dose at room temperature causing the saturation of the implantation induced lattice parameter change. Together with that we observed the flattening of the strain profile close to the surface and the increase of the thicness of the layer with introduced lattice parameter change. The last was 1.5-2×greater than the expected ion range and we found a number of evidence that it is not caused by the channelling.

The distinct shot through layer with lattice parameter smaller than deeper mostly deformed layer was stated only in the case of the lowest Se and Si ion doses, but it was mostly visible in case of proton implantation and Se and Si implantation at channeling condition. The shot-through layer often caused some additional interference features in the rocking curves but the distinct evidences were obtained from the Bragg-case section topographs.

It was also proved that thermal annealing at 300° decreased the value of the implantation induced strain at its whole depth range, proportional to the annealing time.

P06.11.020 ATOMIC STRUCTURE OF THE THERMAL OXIDE LAYERS ON Si(001), (111) AND (110) WAFERS. T.Shimura, and M.Umeno, Department of Material & Life Science, Osaka University, 2-1 Yamadaoka, Suita, Osaka 565-0871, JAPAN.

In the X-ray diffraction patterns from the thermal oxide layers on Si(001), vicinal (111), and (110) substrates, the extra diffraction peaks with the Laue-function-like intensity profile were observed, of which period corresponds to the inverse of the film thickness. This result means that the oxide layers do not have simple amorphous structure, but have ordered structure not only close to the interface, but also in the whole part of the oxide layer. Furthermore, the ordered structures are distinct from each other, because the extra peaks from the oxide layers with the different substrate were observed at their respective positions in reciprocal space.

The pseudo-cristobalite structure has been proposed for the oxide layers on Si(001) substrates, which can explain the diffraction pattern very well [1]. Therefore, the pseudo-cristobalite structure was extended for the oxide layers on Si(111) and (110) substrates, in which the oxygen atoms were located between the Si atoms and the lattice spacings perpendicular to the interface were approximately twice as that of the each substrate, while the lateral lattice spacings were exactly the same as that of the substrate. These structures have some problems from the crystallographic view point, because they might contain different bond lengths and angles. However, it was found that the extra peaks from the oxide layers were reproduced in the simulated diffraction patterns by Fourier transform of the models at the same positions as were observed in the X-ray diffraction experiments.

I.Takahashi, T.Shimura, and J.Harada (1993), J. Phys.: Condens. Matter 5, 6525.

P06.11.021 X-RAY SCATTERING FROM THE CRYSTALLINE SiO_2 IN BURIED OXIDE LAYERS OF SIMOX WAFERS. Takuji Hosoi, Takayoshi Shimura and Masataka Umeno, Department of Material & Life Science, Graduate School of Osaka University, 2-1 Yamadaoka, Suita, 565-0871, JAPAN.

We have investigated the existence of crystalline SiO_2 in buried oxide (BOX) layers of SIMOX wafers by the x-ray diffraction technique. The extra diffraction streaks perpendicular to the interfaces were found at the middle of reciprocal lattice points of Si, such as 0.5 0.5 L and 1.5 0.5 L. This means that there exists an ordered structure in SIMOX wafers, having epitaxial relationship with the Si substrates. In order to investigate the position and distribution of the ordered structure, several samples

with different thicknesses of the BOX layers were prepared by HF etching. The peak intensity of the extra diffraction streak at the position of 0.5 0.5 L in reciprocal space decreased with the reduction of the BOX thicknesses. The streak disappeared when the BOX layer was completely removed. This indicates that the streak originates from the crystalline SiO_2 in the BOX layer, and the crystalline SiO_2 exists not only close to the interfaces but distributes also in the whole part of the BOX layer. The structure factors for the β-cristobalite model [1] and the tridymite model [2] were calculated, which have been proposed for the crystalline transition layer at the interface between thermal oxide and Si substrate. The extinction rule for the β-cristobalite model completely disagreed with the present measurements, while the structure factors for the tridymite model partially agreed.

M.Hane, Y.Miyamoto & A.Oshiyama (1990). Phys. Rev. B**41**, 12637.
A.Ourmazd, D.W.Taylor & J.A.Rentshler (1987). Phys. Rev. Lett., **59**, 213.

P06.11.022 STRUCTURAL CHANGES DURING A TYPE CONVERSION ANNEAL OF CDS-CDTE HETEROJUNCTION SOLAR CELLS. K.D.Rogers and D.W.Lane and J.D.Painter and D.A.Wood, Department of Materials & Medical Sciences, Cranfield University, Shrivenham, Swindon, Wilts. SN6 8LA U.K.

Second generation, thin film solar cells based upon CdS-CdTe heterojunctions are becoming a viable alternative to silicon based technologies. Cell efficiencies depend upon the nature of structures formed during deposition and any subsequent processing, e.g. an essential type conversion anneal.

We have undertaken an extensive examination of the as-deposited CdS-CdTe structures and their response to heat treatments. Principally, a combination of X-ray diffraction and Rutherford backscattering spectrometry has been applied to samples consisting of electrodeposited and PVD CdTe (~2.0 μm) supported upon CdS (<0.1μm). We have developed novel methods of depth profiling using a chemical bevel process that has enabled us to determine structural characteristics through the films.

The results show that the annealing causes the formation of intermixed regions consisting of $CdTe_{(1-x)}S_x$ and $CdS_{(1-y)}Te_y$ which modify the spectral response of the final device. Using synchrotron techniques, the formation process is mapped dynamically to reveal details of a recrystallisation process that occurs in association with the interdiffusion. Further, we demonstrate that the extent of the intermixed region is mediated by the initial, as-deposited structures rather than system thermodynamics. Implications for the control of the extent of this non-stoichiometric region through changes to fabrication parameters are discussed.

P06.11.023 IN-SITU RADICAL BEAM OXIDATION OF MBE-Si GROWN ON A HYDROGEN TERMINATED Si(111). M. Umeno, Y. Yoshioka, T. Muta, K. Mizobata and T. Shimura, Department of Material & Life Science, Osaka University, Suita, JAPAN.

Thermal oxidation is a significant key process of the Si LSI technology and the vast amount of researches on Si-SiO_2 systems have been done. Recently, existences of some crystalline oxide phases in the thermal oxide layer on Si wafers have been ascertained [1]. It is found that the structure of the crystalline phase depends on the orientation of the substrate wafer and that their amount seems to closely relate to the electrical properties of the oxide film. The fact that the oxide films with the higher C-mode break down ratios contain the more crystalline phase might indicate that the understanding of the crystalline SiO_2 phase is useful to develop new oxidation processes.

We performed an oxidation experiment with the extremely ideal atomically flat Si surfaces prepared by the molecular beam epitaxy (MBE) method, in which we adopted the hydrogen termination by dipping into the NH_4F solution for the surface cleaning as well as to obtain atomically flat Si(111) surface. When the specimen was heated in UHV, the (111) surface structure changed from the initial 1×1 at room temperature to the $\sqrt{3}\times\sqrt{3}\,R30°$ at about 600°C and then to the 7×7 at 700°C. The epitaxial silicon layers were easily formed on the 7×7 surface at 750°C keeping the same surface. The monitoring of the surface structures and the film thickness were done with an ellipsometor as well as with the RHEED method. It was found that the polarizing parameters Δ and ψ in ellipsometry showed oscillations during the MBE growth. The oscillation periods were not the same as that of the RHEED oscillation, indicating the measurement of different information of the surface irregularities at the same time. The oxidation of the MBE silicon was performed in the chamber connected to the main MBE chamber without exposing to any environments before the oxidation process at relatively lower temperatures than usual case using a radical O_2 beam or with an O_2 atmosphere.

[1] T. Shimura, et al., J. Crystal Growth, 166 (1996) 786, and refs. therein.

P06.11.024 THE HRXRD INVESTIGATION OF THE LATERAL CHEMICAL COMPOSITION DISTRIBUTION IN SUPERLATTICE CRYSTALS. Jarek Gaca, Marek Wojcik, Institute of Electronic Materials Technology, Warsaw, Poland.

The most distinctive feature of the superlattice crystal (SL) is that the periodic variation of its chemical composition occurs only in the growth direction. The homogeneity of the composition in the lateral directions is achieved by placing the substrate crystal on a stage that is rotated during the deposition process. However if the rotation speed is too slow or the flow of the gases is not properly controlled then there may appear additional variation of the composition (lateral composition gradient - LCG). In this case it is not possible to characterise the chemical composition profile in the whole volume of the crystal by one composition modulation wave.

In order to describe the SL crystal in which there exists a composition gradient it is assumed that this crystal can be divided into domains. Each domain is considered to be an ideal SL crystal, fully characterised by a one composition modulation wave. Neighbouring domains differ in that they are characterised by different chemical composition modulation wave. In order to fully characterise the SL crystal with LCG, it is necessary to apply so many independent waves as there are domains. The introduced division is an approximation to the real structure of the SL crystal and is quite arbitrary. It serves only to facilitate the calculation of the diffraction profile from the SL crystal with LCG. So the sizes of the domains can be chosen so that they make a system of weights providing the probability that the domain characterised by a given composition modulation wave appears in the crystal.

In case of single domain the knowledge of the chemical composition of each atomic plane makes it possible to calculate the planar scattering abilities and due to Vegard law the separation between the atomic planes. Hence using the kinematical diffraction theory the scattering amplitude can be calculated. The scattered intensity from the SL crystal with LCG is calculated assuming that the incident beam is diffracted independently by each domain. The error made by this assumption is in most cases negligible.

To investigate the influence of the LCG on the diffraction pattern two InGaAs/InP SL samples were grown by MOCVD technique on the 001 InP substrate. One sample was rotated during the growth process to ensure its homogeneity, the other one

was not rotated in order to introduce the intentional LCG. The samples were measured by applying the θ/2θ scan mode with the diffraction vector parallel to 001 growth direction.

It was shown that the X-ray diffraction profile from SL crystal with a LCG is modified in comparison to that from an ideal SL crystal. The satellite reflections show characteristic broadening related to the variation of the modulation period. Computer simulation of the diffraction profile based on the domain model allows to determine the profile of the LCG in the SL crystal. It was shown that the LCG causes the variation of the modulation period, which may be brought about by the variation of the number of atomic planes and/or by the changes in their chemical composition.

P06.11.025 MICROSTRUCTURE, CHEMICAL COMPOSITION, AND ELECTRICAL CHARACTERISTICS OF ZnO THIN FILMS. J.H. Choi, and B.J. Kim, Dept. of Materials Sci. and Engineering, Inha University, Inchon, Korea

402-ZnO and Al-doped ZnO thin films were prepared by rf magnetron sputter techniques. The effect of substrate temperature, sputter gas, surface sputter, and post-deposition heat-treatment on the microstructure, surface morphology, chemical composition, and electrical characteristics of the films were investigated with sputter gas of pure argon as well as at room temperature with sputter gas of a mixture of argon and oxygen exhibit a strong tendency of 002 preferred orientation. The thin films with 002 preferred orientation has a chemical stoichiometry of Zn/O=1.01, a band gap of 3.3 eV, and a packing density of 98%, respectively. When a particular content of Al is doped, the crystallinity, surface flatness, and electrical conductivity of the films increased significantly. The films, which were annealed at various atmosphers, exhibit sheet resistance ranging from a few charge carrier concentrations of and optical band gap of 3.2 to 3.6 eV. When the surface of the film was sputtered at particular conditions, the surface area was increased, making the films more sensitive to heat-treatments at particular atmospheres

P06.11.026 STRUCTURAL PROPERTIES OF NANOCOMPOSITE THIN FILMS CONTAINING MAGNETIC NANOPARTICLES. O.Nittono, A.G.Roy, M.Azumi, M.Wakamori, Y.Haga and Y.Nakamura, Department of Metallurgy, Tokyo Institute of Technology, Meguro-ku, Tokyo, Japan

In this study nanocomposite films such as carbon and aluminum nitride(AlN)thin films contaning transition metals and carbides were prepared by a codeposition technique of metal and carbon, and also by a reactive sputtering deposition using composite targets such as Al-Fe, Al-Co and Al-Fe-Co, and nitrogen gas as sputtering gas. Magnetic and electrical properties of such films were investigated with respect to microstructures of the films subjected to various annealing conditions. Microstructures as well as phase stability including phase decomposition and cystallization in the films were evaluated by X-ray diffraction and by electron diffraction- transmission electron microscopy. Main results are as follows:(I)Carbon films: Transition metal carbides such as Ni3C, Co2C and Co3C were found to be formed easily under special deposition conditions where kinematical reactions are thought to take place easily. Microstructures of as-deposited films were strongly dependent on the gas flow of carbon. The films were composed of metal and/or carbide nanoparticles, amorphous carbon and graphite. Such nanoparticles were embeded in the matrix film. The films showed positive or negative thermal coefficients of resistivity depending on the distribution state of nanoparticles in the composite films. Decomposition processes of these metal carbides were found to be well interpreted based on the equilibrium phase diagrams taking account of decarbonization out of the film. Graphite particles were seen to grow through the metal mediated crystallization process for these carbides. (II) AlN films: As-deposited films appeared amorphous-like depending on the content of metal, and after annealing metal nanoparticles such as Co and Fe precipitated from the matrix film which is supersaturated with metals, and then decomposed, although the crystal lattice of AlN was not recovered completely even after annealing at 800K. No cobaltnitride was formed, but ironnitrides were easily formed at the initial stage of sputtering, then decomposed into iron particles at higher temperatures. When the content of iron increased, FeAl alloys were formed, which did not show ferromagnetism. Magnetic properties were invesigated in terms of microstructures during annealing process. Finally we summarized common features of structural properties for such nanocomposite films.

P06.11.027 STRUCTURAL CHARACTERIZATION OF VACUUM EVAPORATED THIN FILMS OF ZnSe. Pradip Kr. Kalita,B.K.Sarma, H.L.Das Department of Physics, Gauhati University, Guwahati-781014, Assam, India

X-ray diffraction pattern of thin films of ZnSe deposited by vacuum evaporation at substrate temprature within the range 303K to 623K have been recorded for the study.All ZnSe thin films were found to be of pollycrystalline nature have f.c.c cubic zincblende structure irrespective of substrate temperature (Ts) and thickness .The grain size, microstrain,average stress, dislocation density and degree of orientation have been estimated. It is observed that grainsize increases with Ts whereas average stress, microstrain,dislocation density decreases with Ts . Attempt is made to correlate the structural variations with photosensitivity of the films.

P06.11.028 CRYSTALLINE PROPERTIES OF Al\\Al_2O_3 MULTILAYERS. C. Malibert, C. Le Paven-Thivet, Ph. Houdy, LMN, Université d'Evry Val d'Essonne, bd F. Mitterrand, 91025 Evry Cedex, France.

Materials based on multilayers have became of great interest in recent years, due to the improvement of physical properties of such systems compared to single layers or bulk materials. Interesting physical properties can be achieved by the complementarity of the two materials [1]. Enhancement of wear-resistance mechanical properties can be achieved in different composites systems, like Ti/TiN [2] and Al/Al_2O_3 [3,4] multilayers.

In this work, crystalline properties of these nanoscale Al/Al_2O_3 system have been studied by X-ray diffraction and reflectivity. They have been correlated to morphological and chemical properties (characterized by MEB and SIMS), as well as mechanical properties.

Al/Al_2O_3 multilayers have been deposited by reactive rf-sputtering onto (100) sicilon wafers, for substrate temperature T_S ranging from –90°C to 600°C, and also with different period thickness. Polycrystallised aluminium films exhibit a rough surface, with grain size increasing with substrate temperature whereas alumina films are amorphous, with smooth surface. Although multilayers present a granular surface, X-ray reflectivity patterns show Bragg peaks, typical of multilayers character. This character depends on T_S temperature, on the roughness of aluminium layers and the existence of interfaces.

[1] S.L.Lehoczky, *Phys. Rev. Lett.*, 41 (1978) 1814
[2] S.Labdi,P.Houdy,P.Psyllaki,M.Jeandin,*Thin Solid Films*, 275 (1995) 213
[3] Y.Ding, Z.Farhat, D.O.Northwood, A.T.Alpas, *Sur. Coat. Tech*, 68 (1994) 459
[4] C.Le Paven-Thivet, C.Malibert, Ph.Houdy, to appeared in *Thin Solid Films* (1999)

P06.11.029 DEPTH-RESOLVED DETERMINATION OF SHORT-RANGE ORDER OF IRON IN FE/AL MULTILAYERS. D.C.Meyer [1], P.Gawlitza [2], T.Holz[2], K.Richter [1], P.Paufler [1]. [1] Institut f.Kristallographie u. Festkoerperphysik der TU,D-01062 Dresden, Germany. [2] Fraunhofer-Institut f.Werkstoff- u. Strahltechnik Dresden, D-01277 Dresden, Germany

A multilayer consisting of 4.6nm AlOx , 1x 12.3nm Al, 6 x (4.3nm Fe + 10.4nm Al) as obtained by Pulsed Laser Deposition has been investigated using a combi- nation of X-ray absorption fine structure , X-ray reflectometry and X-ray standing wave techniques at the HASYLAB Hamburg. According to this the average Fe atoms were found to be surrounded by 8.1 Al atoms and 5.9 Fe atoms (nearest plus next-nearest neighbours),respectively, while the structure retained of the tungsten type. Formation of a CsCl type phase could be excluded. For the Al/Fe interface an Al content lower than 47% Al has been evaluated, whereas the corresponding figures near the Fe/Al interface came up to 6.6 Al and 7.4 Fe. The difference is obviously due to a kinetic intermixing effect.

P06.11.030 POLYIMIDE LANGMUIR-BLODGETT FILMS BASED ON THE DIFFERENT PREPOLYMERS V.V.Klechkovskaya, N.D.Stepina, I.A.Fedorinin and L.A.Feigin [1], V.P.Sklizkova and V.V.Kudriavtsev [2], [1] Electron Diffraction and Small Angle Diffraction Laboratories, Institute of Crystallography, Russian Acad.Sci., Moscow 117333, Russia, [2] Laboratory of Polyimides, Institute of Macromolecular Compounds, Russian Acad.Sci., St.-Petersburg 199004, Russia

Mono- and multilayer Langmuir-Blodgett (LB) films of rigid-chains polyimide prepolymers (the amphyphylic derivatives of polyamide acid PAA) have been studied. Among those are: 1) hexadecyl ester of PAA based on the 4,4`-diaminodiphenyl ether and pyromellite dianhydride, 2) alkyl-ammonium salt of PAA based on the dianhydride of 3,3`,4,4`-diphenyltetracarboxylic acid and o-tolidine (PAA-C16). The influence of solvent composition on the structure of LB-films has been investigated. The dependence of structure ordering on the preparation technique (casting on glass or Langmuir-Blodgett method) has been revealed.

Diluted solutions of PAA-C16 in a mixed solvent consisting of N,N`-dimethylacetamide and benzene in a ratio 50:50 were studied. The formation of associates of fluctuative origin was observed. The associates possessed a microanisotropic structure. The formation of perfect and homogeneous films occured only in a freshly prepared solution of PAA-C16 salts. The optimal solution concentration for the ordered packing of intramolecular fragments in monolayer was determined.

This work was financially supported by Russian Foundation for Basic Research, Grant No 98-03-33427a.

P06.11.031 X-RAY STRUCTURE OF SIGE/SI SUPERLATTICE INTERFACES GROWN ON VICINAL SI(111) SUBSTRATES Y. Yamaguchi and H. Hashizume [1], J.H. Li [2], [1] Material. and Structural. Lab., Tokyo Inst. Tech., Yokohama 226-8503, Japan, [2] Inst. of Phys., Chinese Acad. Sci., Beijing 100080, PRC

Si(1-x)Ge(x)/Si superlattices grown on vicinal Si substrates show low-angle x-ray diffuse scattering arising from random and periodic interface roughness. The periodic component is due to the arrayed atomic steps at the SiGe/Si interfaces, replicated from the substrate surface, of which terrace width and step height distribute around the mean values. The mean structure gives rise to Bragg-like peaks near the specular peak. To simulate complicated diffuse pattern in 2D reciprocal space, we developed a formulation using the distorted-wave Born approximation, which allows us to determine the height-height correlation functions for the random and periodic roughness simultaneously. The formulation explains well the very different x-ray diffuse patterns observed from two samples with 0.1 and 0.3 for x, grown on 0.6 degrees offset Si(111) substrates with other multilayer parameters quite similar. We will present the interface structures of these two samples revealed by applying our formulation, with discussion on the role of lattice strain on the different interface structures.

P06.11.032 TECHNOLOGICAL PECULIARITIES OF FORMATION AND QUALITIES OF THIN FILM COATINGS ON THE BASIS OF FLUORINE-CONTAINING POLYMERS AND OLIGOMERS. Yu.S. Boiko, V.A. Struk, Physis & Ingineering Departament of Grodno State Uneversity, Ozheshko st. 22, Grodno 230023, Belarus.

The subject of study is thin films on the basis of polytetrafluorinethylene and fluorine-containing oligomers. The aim of the prezent paper is the investigation of physical and chemical aspects and technological peculiarities of the formation of thin coatings on the basic of fluorine-containing polymers and oligomers on the friction surfaces and their influence on the operational parameters of metal-polymers tribosistems. In the terms of relaxation diflysion theory of interphase processes the phenomenological model was developed for the formation of thin film coatings from the active phase on the solid surfaces of various nature. Analytical expressions of active fragments distribution in coatings' depending from the structure of metal-polymer systems and technological factors of formations were acquired. The influence of technological factors (temperature, medium, energy influens doses, solutions concentration) on the structure and properties of fluorine-containing polymer and oligomer films on the metals and non-metals was established. The technological regimes of formation of films with the given adhesive and cohesive durability were defined. The complex investigations of operational, including tribotechnical, properties of oligomer films in metal-polymers systems were ander taken. The peculiarities of providing ofhydrophobic, anti-oxidant and anti-wear effect of thin films on non-metallic substances depending on their structure and formation technology were established. The experimental industrial testing of the effeciency of application of thin film coatings from fluorine-containing polymers and oligomers in tribotechnical and tennoregulated systems structures was carried out. The economical effect from the application of the working out of the problem was considerable.

P06.11.033 3-D STRUCTURE OF MIXED $Sr(Ca)CuO_2$ and $BaCuO_2$ SUPERLATTICES EPITAXIALLY GROWN ON $SrTiO_3$. S. Harkema, G.J. van Hummel, G. Koster, A.J.H.M. Rijnders, D.H.A. Blank and H.Rogalla, Low Temperature Division, Dept. of Applied Physics, University of Twente, P.O.Box 217, 7500AE Enschede, the Netherlands.

In our laboratory a method has been developed to prepare singly terminated $SrTiO_3$ surfaces of high quality [1]. The $SrTiO_3$ surfaces prepared this way are ideally suited for the layer by layer growth of epitaxial layers. A number of layers consisting of alternating blocks of different size of composition $(Sr(Ca)CuO_2)_n$ $(BaCuO_2)_m$ has been prepared by Pulsed Laser Deposition.

The quality of the layers (thickness 50nm) is such that single crystal like methods can be used to determine their structure. Results for the 3-dimensional structures of these layer systems will be presented.

[1] G. Koster, B.L. Kropman, G.J.H.M. Rijnders, D.H.A. Blank & H.Rogalla Appl. Physics Lett. **73**, (1998), 2920

P06.11.034 MAGNETIC PROPERTIES OF V OVERLAYERS ON THE (100) AND (110)W SURFACES. S. V. Man'kovsky G. V. Kurdyumov Inst. for Metal Physics of N.A.S.U, 36 Acad. Vernadsky Blvd., UA-252680 Kiev-142, Ukraine

The magnetic properties of V overlayers on the (100) and (110)W were studied using full-potential LAPW method. The features of electronic structures for different crystallografic planes and the effects of surface relaxation are studied. The total energy calculation for one V monolayer on the (100) W surface predicts the nonmagnetic ground state of this system. However, there was found ferromagnetic ordering in V overlaers for the 2V/ W (100). The role of hybridisation of V d-states with W d-states in ground state formation is analysed.

P06.11.036 GALVANO-MAGNETIC PROPERTIES OF AMORPHOUS THIN FILMS OF TRANSITION METALS. S.A. Lebedinskiy, O.A. Kordin and Yu.V. Barmin, Dept. of Solid State Physics, Voronezh State Technical University, 394026 Voronezh, Russia.

Amorphous Re - T_{3d} alloys were prepared by high rate sputter deposition of composite target as a substrateless foils 10 - 15 μm. The composition of alloys was determined by electron-probe microanalysis method with 0,5 at. % accuracy.

The temperature dependence (4,2 - 300 K) of the Hall coefficient $R_H(T)$ in amorphous Re - T_{3d} alloys have been measured. The anomaly (deep minimum) of $R_H(T)$ dependence in Re-Cr alloys have been observed, with the absence of it in the case of Re-Nb. The temperature of this anomaly is increased with increasing the concentration of Cr atoms.

To reveal the nature of this effect the complex of low-temperature measurements of galvano-magnetic properties have been done: magnetoresistance ρ(H), electrical resistivity ρ(T), ac susceptibility χ(T) and dc magnetization M (T).

P06.11.037 MAGNETIC STRUCTURES OF METAL MULTILAYERS BY RESONANT X-RAY MAGNETIC SCATTERING. H. Hashizume, N. Ishimatsu, S. Miya, Y. Yamaguchi [1], N. Hosoito [2], G. Srajer, C. Venkataraman, J. Lang, C. Nelson [3], [1] Materi. and Struc. Lab., Tokyo Inst. Tech., Yokohama 226-8503, Japan, [2] Inst. for Chem. Res., Kyoto Univ., Uji 611-0011, Japan, [3] APS, Argonne Nat. Lab, IL 60439, USA

We report the magnetization structures of a few metal multilayers determined by measuring resonant x-ray magnetic specular reflections with circular polarized probing x-rays at synchrotron sources. The technique is element specific and allows us to determine the depth-dependent strengths and spatial orientations of local magnetic moments with respect to the applied in-plane field at few Angstroms resolutions. In case of a [Fe(3.5nm)/Gd(5.4nm)]15 multilayers, we have confirmed for the first time the phase change in the Gd layers between the aligned and twisted states. The Gd layers nearly fully magnetize at the Fe/Gd interfaces even at RT, whereas the central sublayers show spontaneous magnetizations below 240 K, suggesting a Curie temperature much lower than that for bulk Gd. The twist angles of local Gd moments show interesting behaviors as a function of temperature. Results for Fe/Dy, Fe/Cr multilayers and NiFe/SmCo bilayers will also be reported. Furthermore, magnetic roughness at the Fe/Gd interface will be discussed in reference to magnetic diffuse scattering measurements made on the Fe/Gd sample.

P07.11.001 X-RAY STUDY OF ELLIPTICINE INTERACTION WITH MODEL MEMBRANES. I.L. Torriani and L.P. Cavalcanti, Instituto de Física, Universidade Estadual de Campinas, C.P.6165, 13083 Campinas, SP, Brazil and C.R. Zacharias, UNESP, Guaratingueta, SP, Brazil.

For almost two decades, ellipticine (5,11-dimethyl-[6H]-pyrido[4,3-b]-carbazole) (ELPT) and some of its derivatives have been known to posses cytotoxic effects and have been tested as antitumor agents in human cancer cells. Ionic and hydrophobic interaction of ELPT molecules with natural and model membranes has been investigated in experiments with phospholipid multilayered vesicles, suggesting that the interaction was stronger in the case of negatively charged lipids [1]. These molecules have a quasi planar structure and a highly hydrophobic nature, so they are expected to occupy some position in the membrane hydrophobic region. For most of our experiments single component or mixed multilayered liposomes of Dipalmitoyl Phosphatidyl Choline (DPPC) and Cardiolipin (CL) were used as a host for ELPT intercalation. The samples were prepared in several molar ratios to obtain a single phase and stable lipid bilayer structure, producing low angle X-ray diffraction patterns with up to eight lamelar reflections. ELPT was added to DPPC and mixed DPPC:CL samples in gradually increasing ratios, until X-ray reflections from the crystalline form of ELPT were detected. This was a way of monitoring incorporation of the drug in the membrane and the perturbation produced in its structure. Several pH values for the aqueous media were also used, to test incorporation of the protonated form of ELPT. Changes in the host bilayer structure can be observed in the electron density profile maps calculated for the DPPC:ELPT and DPPC:CL:ELPT multilayer systems. Since encapsulation of ELPT reduces its toxicity [2], these results are relevant for the design of an adequate drug carrier.

[1] F.Terce, J-F Tocanne, & G.Laneelle (1982) Eur.JBiochem.125, 203-207.
[2] A.M. Sautereau, S.Cros & J-F Tocanne (1985) Biopharm.Drug. Disp. 7, 357-371.

P07.11.003 THE USE OF MULTIPLE SCATTERING TO ENHANCE SANS EXPERIMENTS. T M Sabine and W K Bertram, Materials Division, Australian Nuclear Science and Technology Organisation, Menai, NSW 2234, Australia

Multiple scattering of neutrons by the inhomogeneities responsible for small angle scattering during the passage of the beam through the specimen can be used to provide valuable information about the shape of the objects, and the absolute value of the contrast between the scattering particles and the matrix.

The neutrons that emerge from the specimen are classified according to the number of times, n, they have been scattered during their passage through the specimen. The values of n range from zero to infinity. The remnant of the incident beam is that component for which n = 0. Depletion of the incident beam during its passage through the specimen is taken into account.

Each group contributes separately to the scattering profile. The cross-section for scattering into the small angle region is independent of the neutron wavelength only for n = 1. Thus collection of data as a function of specimen thickness, and of neutron wavelength will provide a number of different diffraction profiles describing the same physical situation.

It is shown that SANS patterns from specimens which are of different thicknesses, but are otherwise identical, not only provide information on the shape and size of the scattering entity but also provide absolute values of the scattering contrast between the particles responsible for SANS and the matrix. No separate calibration of the incident beam is required.

This method of analysis is applied to SANS data on hydrated cement paste. The data was collected on the Ultra High

Resolution SANS Diffractometer at Oak Ridge National Laboratory, USA.

P07.11.004 NEUTRON DIFFRACTION AND SANS IN HIGH-NITROGEN Fe-19Cr-19Mn-0.9N AUSTENITE. V. M. Nadutov [1], V. M. Garamus [2], A.Ch. Islamov [3], [1] G. V. Kurdyumov Institute for Metal Physics of the Academy of Sciences of Ukraine, Kiev, Ukraine, [2] Frank Laboratory of Neutron Physics, Joint Institute for Nuclear Research, Dubna, Russia & GKSS Research Centre, Max Plank Strasse, Geesthacht 21502, Germany, [3] Frank Laboratory of Neutron Physics, Joint Institute for Nuclear Research, Dubna, Russia

The purpose of the present work is to examine a structure and a solid solution state of nitrogen-containing Fe-19%Cr-19%Mn-0.9%N (wt %) austenite after solution treatment at 1125oC and water quenched and then ageing treatment at 250-350oC. The high-nitrogen steel was studied by means of neutron diffraction and small-angle neutron scattering (SANS). The neutron diffraction experiment was carried out on the DN-2 time-of-flight instrument and the measurements of SANS were performed using 'MURN' time-of-flight small-angle neutron scattering spectrometer at the IBR-2 pulsed reactor at the Frank Laboratory of Neutron Physics, Joint Institute for Nuclear Research, Dubna, Russia.

The neutron diffraction measurements show a single-phase austenitic state after annealing of the steel. A change of the diffraction peak position and line width is not observed after ageing treatment.

SANS is observed both in as-quenched and age-treated samples. The analysis within Guinier and Porod approximation has shown that SANS is attributed to inhomogeneities. They are characterized by non-spherical shape. The estimated average size of the inhomogeneities is approximately 200 Å. The contrast of the inhomogeneities decreases under ageing that we attribute to atomic redistribution in austenite.

P07.11.005 SMALL ANGLE X-RAY SCATTERING REVEALS CONFORMATIONAL AND OLIGOMERIZATION FORM CHANGES IN PIG S100A12. M.C.Nonato, W.P.Jesus, S.A.Sculaccio, R.C. Garratt, G.Oliva [1], C. Barberato [2], C. Schleicher, J. A. Santomé [3], [1] Laboratório de Cristalografia de Proteínas e Biologia Estrutural, Instituto de Física de São Carlos, São Carlos, Brazil, [2] Departamento de Informática, Faculdades Associadas de São Paulo (FASP), São Paulo, Brazil, [3] Instituto de Química y Fisicoquímica Biológicas, Universidad de Buenos Aires, Argentina.

The S100 family consists of small acidic proteins, belonging to the EF-hand class of calcium-binding proteins. They are primarily regulatory proteins, involved in cell growth, cell structure regulation and signal transduction. p-S100A12 is a member of the S100 family extracted from pig granulocytes, which has been shown to bind not only calcium but also zinc ions, as already observed for other members of the same family. Small Angle X-ray Scattering experiments were performed for p-S100A12 solutions in four different metal binding conditions: the apo, Ca^{2+}, Zn^{2+} and $Ca^{2+}Zn^{2+}$ forms. The differences in the scattering curves show that p-S100A12 undergoes conformational changes in the presence of calcium ions and increases its oligomerisation state upon addition of zinc ions. The results corroborate the suggestion that Ca^{2+} and Zn^{2+} ions bind to different sites. We propose here that p-S100A12 may have two different functions in the immune system according to the ion binding, as an intracellular regulatory Ca^{2+}-binding protein and as part of an anti-microbial host defence system via Zn^{2+} binding dependent.

Dell'Angelica, E.C., Schleicher, C.H. and Santomé J.A.(1994) J. Biol. Chem., 269, 28929-28936.
Nonato, M.C., Garratt, R.C., Schleicher, C.H., Samtomé, J. and Oliva G.(1997) Acta Cryst.D, 53, 200-202.

P07.11.006 EFFECT OF X-RAY ANOMALOUS DISPERSION ON SMALL ANGLE SCATTERING OF Cu IONIZED NIPA-GEL. S. Kuwajima, Y. Soejima, M. Sugiyama, Department of Physics, Kyushu University, Fukuoka 812-8581, Japan, K. Hara, Faculty of Engineering, Kyushu University, Fukuoka 812-8581, Japan, A. Nakamura, N. Hiramatsu, Faculty of Science, Fukuoka University, Fukuoka 814-0133, Japan, and A. Suzuki, Faculty of Engineering, Yokohama National University, Yokohama 240-0067, Japan

The relation between the size of gel molecules and that of adsorbed metal ions of N-isopropyleacryleamide (NIPA) gel containing Cu ions has been investigated. The intensity of small angle scattering as a function of incident X-ray energy around Cu K absorption edge has been measured at PF, Tsukuba. The intensity variation due to the anomalous dispersion of Cu ion is observed only in the momentum region around 0.30 nm^{-1}, where the scattering peak corresponding to the formation of gel molecule clusters is observed. The results show that the size of the clusters of adsorbed Cu ions is of the same order of magnitude as that of the cluster of gel molecules. This supports, at the same time, the idea that the metal ions are adsorbed into the cluster structure of the gel molecule. It is confirmed that there is no other momentum regions where the intensity varies as a function of incident energy, and, consequently, that the cluster of metal ions is formed only in this size. Moreover, measurements have been made of the gel without Cu ions; the intensity peak is observed at 0.23 nm^{-1}. The results indicate that the size of the cluster of gel molecule is larger than that in the case of gel containing Cu ions.

P07.11.007 SMALL-ANGLE NEUTRON SCATTERING STUDY OF *BOMBYX MORI* CYTOPLASMIC POLYHEDROSIS VIRUS. M. Sato, Graduate School of Integrated Science, Yokohama City University, 22-2 Seto, Kanazawa-ku, Yokohama, Japan and T. Hasegawa, Institute for Protein Research, Osaka University, 3-2 Yamada-oka, Suita, Osaka, Japan and M. Nagao, Neutron Scattering Laboratory, Institute for Solid State Physics, University of Tokyo, 106-1 Shirakata, Tokai, Naka, Ibaraki, Japan and M. Tomita, Department of Chemistry for Materials, Mie University, 1515 Kamihama, Tsu, Japan

Silkworm *Bombyx mori* Cytoplasmic Polyhedrosis Virus (BmCPV), a genus of the Reoviridae, consists of ten dsRNA segments and polyhedrin that forms occlusion bodies, and forms a very large particle of a biological supramolecular complex with a molar mass of about 10^8. The overall and internal structures of BmCPV was investigated by small-angle neutron scattering (SANS) using the contrast variation method.

The SANS experiments were carried out by SANS-U, installed at C1-2 beam port of the JRR-3M reactor of JAERI at Tokai, Japan. SANS data were collected in aqueous buffer solutions containing 0%, 50%, 75%, and 100% D_2O in the q range of 0.002 to 0.0774 A^{-1} at 5 C. The radius of gyration at infinite contrast was estimated to be 336 A. The contrast matching point of the virus was determined to correspond to about 50% D_2O level, evidence that the virus is composed of protein and nucleic acid.

The virus particle was basically spherical and had a diameter of about 700 A. The main feature of the virus structure is the clustering of protein into two concentric shells separated by about 100 A. Most of the RNA moieties are located in the central core and between these two protein shells. However, the distance distribution function, P(r) showed the minor distribution beyond a distance of r = 700Å, resulting in 1350Å as the maximum particle

distance of the virus. This is indicative of the further existence of the external structure region, with very low scattering density, other than the basic spherical structure. This external region is thought to correspond to twelve pyramidal protruding spikes shown by electron microscopic studies.

P08.11.001 X-RAY REFLECTIVITY CHARACTERIZATION OF ARCHITECTURAL COATINGS ON GLASS. M. Eber and S.T. Misture, New York State College of Ceramics at Alfred University Alfred, NY 14802, USA.

Commercial thin film optical coatings on flat architectural glasses were characterized using specular and diffuse x-ray reflectivity. Low-emissivity coatings for thermal control containing up to five discrete thin films were investigated.

X-ray reflectivity was used to determine thickness, density, and interface roughness, while diffuse scattering was used to corroborate surface roughness. Secondary ion mass spectroscopy was used to confirm the chemical compositions of the optical thin films.

The surface of the glass itself, which is produced using the tin float technique, contains a Sn-rich layer with a low-density surface. Successful models required accurate descriptions of the surface of the float glass.

Multilayer coatings consisting of noble metals and oxides of zinc, titanium, and bismuth were characterized and correlated with the optical properties of coated glasses. Specifically, the normal-incidence optical reflectance could be calculated using the physical models determined from the x-ray measurements. Modifications of optical models for the materials were made which account for interface roughness, which is useful in designing film deposition strategies.

P08.11.002 CONSTRUCTION OF AN X-RAY REFLECTION SYSTEM FOR LIQUID-VAPOR INTERFACES USING AN IMAGING PLATE. Yohko F. Yano and Takao Iijima, Department of Chemistry, Gakushuin University, Toshima-ku, Tokyo, 171-8588, Japan

X-ray reflectivity measurements are now widely used mainly in the investigation of solid surfaces. Only a few groups have applied this technique to the study of liquid surfaces [1]. Most of those studies were performed using synchrotron radiation sources.

We have constructed an x-ray reflection apparatus for liquid-vapor interfaces using a conventional x-ray tube. The main features of our apparatus are as follows. Highly collimated and monochromated x-ray beams are generated using an asymmetrically cut Ge(111) crystal monochromater. An imaging plate, which has a high detective quantum efficiency, a low quantization noise and a wide dynamic range [2] is used as an area detector. The sample position is slowly elevated to compensate for evaporation during measurements. A device for surface tension measurement by the ring method is combined so that *in situ* measurements may be possible.

By measuring specular reflectivity, the vertical structural information such as the width of the liquid-vapor interface, namely, the root-mean square roughness can be obtained. From the nonspecular reflectivity (diffuse scattering), the horizontal structural information can be obtained as was formulated by Sinha *et al* [3]. In the case of liquid surfaces, the diffuse scattering can be represented by the height-height correlation function related to the surface tension [4].

By using an imaging plate, both of the specular and nonspecular reflection can be measured easily and simultaneously.

1. P. S. Pershan, *Physica* A **200** 50 (1993).
2. Y. Amemiya *et al*., *Nucl. Instr. and Meth*. A **266** 645 (1988).
3. S. K. Sinha *et al*., *Phys. Rev*. B **38** 2297 (1988).
4. M. K. Sanyal *et al*., *Phys. Rev. Lett*., **66**, 628 (1991).

P08.11.003 DRASTIC DEFORMATION OF EPITAXIAL MICRO-CRYSTALS IN THERMALLY OXIDIZED LAYER ON ULTRA-THIN SI(001). I. Takahashi, S. Doi, R. Suetoshi, K. Ueda, T. Kada [1], N. Awaji, Y. Sugita, S. Komiya [2], [1]Advanced Research Center of Science(ARCS) Kwansei Gakuin University, Sanda 669-1337, Japan, [2]Fujitsu Laboratories Ltd., Atsugi 243-0197, Japan

Structure of oxidized Si layers on Si(001) wafers has remained the objects of intensive studies the past few years, because of their potential ability for VLSI technology in the 21st century. We have investigated the structure of various oxide/Si(001) interfaces by a complementary use of X-ray crystal truncation rod scattering and X-ray reflectivity. Throughout these researches, we have established the coherent micro-crystals distributed in the amorphous oxide. Subsequent studies revealed that the interfacial strain played an important role for stabilizing the micro-crystals. In the present work, we prepared thermal oxide layers grown on very thin Si films ranging from 100 to 2000 Angstrom so as to see the effect of the substrate on the micro-crystals, since part of the interfacial strain can be controlled by the thickness of the oxide and that of the substrate. Quantitative analyses of the diffraction data have successfully been performed. We will discuss in detail the existence of the novel critical thickness of the substrate which affects the relaxation process of the micro-crystals: if the thickness of the Si film is smaller than the critical value, novel relaxation process emerges where the micro-crystals can affect the local structure of the substrate. The process is also characterized by a drastic shrinkage of the crystal parameter of the micro-crystals along the surface normal direction; it shows a sharp contrast with the usual relaxation process where the micro-crystals always relax by expanding their dimensions.

P08.11.004 SCHILLER LAYERS IN β-FERRIC OXY-HYDROXIDE SOL AS AN ORDER-DISORDER PHASE SEPARATING SYSTEM. Yoshiko Maeda and Hideatsu Maeda*, University of Tsukuba, 1-1 Tennodai, Tsukuba, Ibaraki, 305 Japan, and *National Institute of Bioscience and Human-Technology, 1-1 Higashi, Tsukuba, Ibaraki, 305-8566 Japan

The structure and properties of Schiller layers in β-ferric oxyhydroxide (β-FeOOH) sol are studied by microscopic observation. The structure is determined to be smectic. Rod-like particles of β-FeOOH sol gather to form mat-like assemblies, in each of which the rods are packed with their axes nearly perpendicular to mat face. The mats are superimposed one on the other, to make up the whole structure. Two spatial periodicities in this structure would be the cause of the iridescence. This ordered structure coexisted in equilibrium with disordered suspension of the same sol. The Schiller layer systems usually have very low pH values (~ 2) and in these cases attractive interaction or the effect of the secondary minimum is eminent. However, at moderately low pH(~ 4), the interaction between the particles became repulsive, and, in spite of this, Schiller layers are formed when the sol is condensed to a certain extent. Formation of Schiller layers is a phase separation in monodisperse sol.

P08.11.005 GROWTH OF HIGHLY CRYSTALLINE SILICATE FILMS AT THE AIR WATER INTERFACE. J.W. White and A.S. Brown, S.A. Holt, P.A. Reynolds and J.L. Ruggles, Research School of Chemistry, Australian National University, ACT 0200, Australia.

The application of constrained refinement fitting to x-ray and neutron reflectometry data collected on self-assembled mesoporous silicate films growing at the air/liquid interface has been very successful [1,2]. The complementary nature of this method has enabled us able to follow the structure development from a simple surfactant surface excess through to a highly

crystalline mesoporous film thousands of layers thick. Recently we have begun work on the study of in-plane interface structure in these systems [3]. This presentation will give an outline of the background work and present data demonstrating the high degree of order in these self assembled systems.

1. A.S. Brown, S.A. Holt, M. Trau, Thien Dam & J.W. White. *Langmuir*, **13 (24)**, pp 6363 - 6365, 1997.
2. A.S. Brown, S.A. Holt, P.A. Reynolds, J. Penfold & J.W. White. *Langmuir*, **14 (19)**, pp 5532 - 5538, 1998.
3. S.A. Holt, G.J. Foran & J.W. White. La*ngmuir*. Accepted for Publication (1999).

P08.11.006 AN ATOMIC FORCE MICROSCOPY STUDY FOR ORDERED ASSEMBLIES OF ROD-LIKE MOLECULES FORMED ON GLASS SUBSTRATES.
Hideatsu Maeda, National Institute of Bioscience and Human-Technology, 1-1 Higashi, Tsukuba, Ibaraki, 305-8566 Japan

In highly concentrated systems of rod-like molecules, the onset of various ordered phases (dependent on molecular concentration and ratio of the molecular length to diameter) has been theoretically suggested and experimentally investigated by many workers.

We formed ordered assembly structures of tobacco mosaic virus (TMV) particles (300nm length and 15nm diameter) and monodisperse rod-like crystals of b-FeOOH (typically 350nm and 60nm diameter, although variable) on glass substrates, and examined their structures using atomic force microscope (AFM) and electron microscope.

For TMV suspensions with a concentration of 50 mg/ml, several characteristic ordered regions appeared, e.g., highly oriented regions in which the particles were uniaxially oriented, intermeshing side-by-side and interconnecting end-to-end. The critical bending angle of the individual TMV particles was also determined to be approximately 60 degrees.

12. FIBRE DIFFRACTION

P06.12.001 COMPARATIVE STUDY OF NORMAL AND ACID TREATED POLYESTER FIBRE BY SAXS , XRD, SEM AND INSTRON. T. Patel, S. Bal and B. Mallick, Department of Physics, R. E. College, Rourkela-769008 (Orissa), INDIA.

Physical and Macromolecular properties of draw texturised fibre (DTF) of Polyester have been investigated applying Small Angle Scattering (SAXS) technique using the theories of Vonk[1] and Ruland [2] treating the fibre as an non-ideal two-phase system. Intensity data have been collected using compact kratky camera having counter device. The parameters obtained for normal and acid treated fibre are tabulated below where the symbols used in the table carry usual meaning.

Para-eters	ℓ_1 (Å)	ℓ_2 (Å)	r (Å)	c (Å)	e	E_v/D (%)	S/V	φ_1	φ_2
Original	40	8	3	28	.76	3	.006	.85	.15
Acid Treated	97	5	0	24	.77	2	.007	.84	.16

Crystallinity indices of the original and the treated sample have been calculated to be 25% and 23% respectively from their x-ray diffractogram. These samples contain crystallities of different sizes having orientations 1.45^0, 4.3^0, 3.875^0 and 1.6^0, 3.55^0, 4.35^0 with respect to their fibre axes. The fibre diameters estimated from SEM are 2100 Å and 2500 Å respectively. The percent elongation calculated from Instron vary between 10-20 % for original sample and 30-40 % for acid treated sample having corresponding Young's moduli $(31\text{-}52)\times10^8$ and $(19\text{-}20)\times 10^8$ N/m^2. The analysis of all the above parameters leads us to conclude that even strong acid (H_2SO_4) of pH 1 does not have much effect on the fibre at ambient temperature. Further analysis is in progress.

Vonk; C. G(1973,75,76,78), J. Appl. Cryst. 6:81, 8:340, 9:433, 11:541
Ruland; W. (1971), J. Appl. Cryst. 4:70

P06.12.002 NEUTRON STRUCTURE ANALYSIS AND STRUCTURAL DISORDER OF POLY(P-PHENYLENE BENZOBISOXAZOLE). Y. Takahashi, Department of Macromolecular Science, Faculty of Science, Osaka University, Toyonaka, Osaka 560, Japan.

On the X-ray fibre diagram of poly(p-phenylene benzobisoxazole) (PBO), the diffuse streak scatterings are observed along the first and third layer lines, while Laue spots can be observed on the second and fourth layer lines. This shows that the molecular heights of PBO are disordered by a half of the fiber period. Therefore, the cell parameter c reduced to a half of the fiber period, 12.05 ü. All the observed reflections can be indexed by the one-chain unit cell with parameters, a = 5.651Å, b = 3.570Å, c = 6.03Å, and $\gamma = 101.4°$ (at 295K) and the space group Pm.

Neutron diffraction has the several advantages in comparison with X-ray diffraction. The scattering length of hydrogen atom by neutron is larger than by X-ray diffraction and furthermore, the scattering lengths are independent of the scattering angle. Absorption of neutron by most elements is small in comparison with X-ray diffraction. Accordingly, the detailed crystal structure analyses of crystalline polymers can be carried out at low temperatures. Neutron diffraction measurements were made on the equator at 17K, 100K, 200K, and 295K, and the structure analyses were carried out. The half-widths of the reflections do not depend on the temperature. This shows that the crystallite size and lattice distortion are independent of the temperature. The R-factors converged to 9.9, 9.5, 13.1,and 12.1 % for the intensity data at 17K, 100K, 200K, and 295K, respectively. The azimuthal angle of the benzobisoxazole plane with respect to the a-axis is estimated to be 161.2° at 295K. The angle between the benzobisoxazole and the phenyl rings is 25.7° at 295K. The temperature dependences of the unit cell dimensions, molecular orientation, and temperature parameter are small in comparison with those of polyethylene, one of the flexible polymers. This may reflect the rigidity of the PBO molecule.

P06.12.003 AXIAL MOLECULAR PACKING OF FIBRILLAR TYPE I COLLAGEN. A HIGH RESOLUTION STUDY. J.P.R.O. Orgel, T.J. Wess, and I. Alberts, DBS, University of Stirling, Stirling. FK9 4LA, U.K. A. Miller, Principal's office, University of Stirling, Stirling, FK9 4LA, U.K. A. P. Hammersley, ESRF, BP 220 F-38043 Grenoble, Cedex, France.

The meridional Bragg reflections within the collagen type I diffraction pattern contain detailed information about the axial projection of collagen microfibrils. An unambiguous solution of the phase components of the structure factors combined with the measured amplitudes at high-resolution enables an accurate interpretation of the axial packing arrangement of fibrillar type I collagen.

Diffraction data has been recorded for the native protein and three highly isomorphus derivatives, using synchrotron radiation sources. The phase component of the structure factors has been calculated for 124 orders of diffraction through multiple isomorphus addition calculations to produce a high-resolution definition of the projected axial structure of collagen. This provides detailed information about the conformation of the non-helical telopeptides, the relative ratio of the gap/overlap period, and the axial alignment of the collagen molecules within the microfibril. The majority of previous studies of collagen structure have been negatively biased by their largely model dependent nature. Since in this study the phase components have not been calculated via a modeling approach, the results presented here should be seen as the most accurate to date.

T.J. Wess, A.P. Hammersley, L. Wess, A. Miller (1998). J. Mol. Biol. 275, 255-267.
J.P. Bradshaw, A. Miller, and T.J. Wess (1989). J. Mol. Biol. 205, 685-694.
D.J.S. Hulmes, A. Miller, S.W. White, B. Brodsky Doyle. (1977). 110, 643-666.

P06.12.004 NEW STRUCTURAL MARKERS OF BREAST CANCER MEASURED USING SAXS. R.A. Lewis, CLRC, Daresbury Laboratory, Warrington, Cheshire, WA4 4AD, U.K., and K.D. Rogers, Department of Materials & Medical Sciences, Cranfield University, Swindon, Wilts. SN6 8LA, U.K. and C. Hall and E. Towns-Andrews and S. Slawson, CLRC, Daresbury Laboratory, and A. Evans and S. Pinder and I. Ellis Departments of Radiology & Histopathology, City Hospital, Nottingham, U.K. and C.R. Boggis' Manchester Breast Screening, Withington Hospital, Manchester, U.K. and A. Hufton Department of Medical Physics,Christie Hospital, Manchester, U.K.

Characterising the natural history of breast cancer is important for understanding associated biological mechanisms and for diagnosis. However, there have been few studies of the collagen structure associated with human breast tissue and, in particular, that of breast tumours. We report the findings of a study of breast tissue collagen that has investigated structural changes due to tumour genesis.

Small angle, synchrotron X-ray scattering data was collected on station 16.1 at the SRS, Daresbury using a camera length of 6.6m. Typical, 'core cut' biopsy specimens were provided both from patients and excised from reduction mammoplasty tissues. No specimen preparation was required. Radial integration of the 2-dimensional diffraction data enabled us to examine Bragg reflections and Bessel function peaks simultaneously.

We have found that, although both tumour and normal breast tissue collagens are of similar type (type I & III mix, D=64nm) their diffraction data is remarkably and consistently different. We demonstrate that there are significant structural differences between tumour and normal breast tissues with respect to supramolecular collagen architecture ; fibril ordering within the tumour tissues is almost absent. The data is supported by histopathological analyses that confirms the preponderance of collagen within all the specimens. The implications of these findings in the context of using molecular structure characteristics as new and novel markers of disease progression are discussed.

P06.12.005 WOOD FIBRE DIFFRACTION USING CCD DETECTORS IN FOREST PLANTING PROGRAMS. Renuka Kadirvelraj, Greg Smith and Ward T. Robinson, Department of Chemistry, and Ian D. Cave, Wood Technology Research Centre, University of Canterbury, Christchurch, New Zealand and Altaf Hussain, Department of Chemistry, Dhaka University, Dhaka, Bangladesh.

Strategies used to improve the mechanical properties of timber require a knowledge of the orientation of the constituent cellulose microfibrils present in the wood cell walls. Many methods like polarising, fluorescence and electron microscopy and iodine staining have been used to estimate the mean microfibril angle, which is the winding angle the cellulose microfibrils make with the cell wall. These methods are tedious and time consuming since the variability of biological material requires a large number of measurements in order to give meaningful average values. X-ray diffraction, using an area detector, produces a mean diffraction pattern from several thousand filaments in a single exposure and fast observation time. A diffraction pattern from wood recorded on an on-axis flat plate device such as an X-ray sensitive film or a CCD area detector consists of interrupted arcs on a set of concentric rings. These rings can be indexed as corresponding to the spacing of crystalline planes within the cellulose crystalline microfibrils. Analysis of the intensity distribution around these diffraction rings can give the mean microfibril angle (*mfa*) which is used as the predictor of stiffness of the wood sample. As the *mfa* decreases gradually from around 40 degrees in the pith to around 10 degrees in the cambium, the stiffness of the wood cell wall increases enormously. Thus *mfa* has important potential use in forestry planting and breeding programmes. There are many advantages in using wide angle X-ray diffraction techniques sensitive to the preferred *mfa* orientation and the speed of the area detectors in data collection makes large scale surveying of *mfa* possible.

P06.12.006 STRUCTURAL STUDY ON CHITOSAN/INORGANIC ACID COMPLEX. K. Noguchi, M. Kanenari, and K. Okuyama, Faculty of Technology, Tokyo University of Agriculture and Technology, 2-24-16 Naka-cho, Koganei, Tokyo 184-8588, Japan and K. Ogawa, Research Institute for Advanced Science and Technology, Osaka Prefecture University, 1-2 Gakuen-cho, Sakai, Osaka 593, Japan.

Chitosan, the N-deacetylated chitin, has received much attention as a functional biopolymer for its industrial and medical use. Since chitosan has a free amino group on each residue, it exhibits a remarkable ability to form specific complexes with a number of ions, inorganic and organic acids when immersed in their aqueous solution [1,2]. We have already analysed the crystal structures of the anhydrous [3] and the hydrated form [4] of tendon chitosan. Although several structural studies of the chitosan complexes have been attempted so far, none of the crystal structures have been analysed because of their complexity. Recently, we have found that certain chitosan/inorganic acid complexes can be obtained not only by immersing chitosan specimen in aqueous inorganic acid solutions, but also by exposing chitosan to their vapour. Among them, the X-ray diffraction pattern from the chitosan/HNO_3 complex obtained by the latter method (39 observed reflections) shows a better orientation and crystallinity compared with that obtained by the former method (22 observed reflections). All the observed reflections could be indexed in terms of an orthorhombic unit cell with dimensions of a = 9.63, b = 17.54, and c(chain axis) = 10.34 . The polymer chains take a 2-fold helical conformation and the unit cell contains four chains and eight HNO_3 molecules. The packing of molecules in this complex crystal is similar to that of hydrated chitosan [4]. Polysaccharide chains make a sheet structure parallel to the *bc*-plane. These sheets stack along the *a*-axis. HNO_3 molecules form columns between these sheets. Details of their molecular interactions will be discussed.

1. K. Ogawa, K. Oka, & T. Yui (1993), *Chem. Mater*., 5, 726-728.
2. K. Ogawa & S. Inukai (1987), *Carbohydr. Res*., 160, 425-433.
3. K. Okuyama, Y. Hanafusa, K. Osawa, K. Noguchi & K. Ogawa (1999). *Int. J. Biol. Macromol*., in press.
4. K. Okuyama, K. Noguchi, T. Miyazawa, T. Yui & K. Ogawa (1997), *Macromolecules*, 27, 7601-7605.

P06.12.007 FIBRILLIN: DIFFRACTION STUDIES OF AN ELASTIC PROTEIN. T.J.Wess [1], P.P. Purslow [2], C.M.Kielty [3]. [1] DBS University of Stirling FK9 4LA. [2] Meat science division KVL Copenhagen. [3] Department of Biological Science University of Manchester M13 9PT

Microfibrils are ubiquitous fibrillin-rich polymers which are thought to provide long-range elasticity to extracellular matrices, including the zonular filaments of mammalian eyes. The microfibrils appear in electron microscopy as beaded structures several hundred nm in length with a fundamental bead periodicity of around 56nm. The possible basis for elasticity of the tissue is based on the reversible changes in the beaded periodicity. X-ray diffraction of hydrated bovine zonular filaments (at the Daresbury Synchrotron) demonstrated meridional diffraction peaks indexing on a fundamental periodicity of ~56nm[1]. The effect of stretching the tissue up to 50% of the rest length had little effect on the position of meridional Bragg reflections, indicating a static population of bead lengths. The effect of extension up to 100% causes a deterioration of the diffraction signal and a weak fundamental peak can be observed at 84nm[2]. A Ca2+ induced reversible change in the intensities of the meridional Bragg peaks indicated that supramolecular rearrangements occurred in response to altered concentrations of free Ca2+. In the presence of Ca2+, the dominant diffracting subspecies were microfibrils aligned in an axial 0.33 D stagger. The removal of Ca2+ caused an overall enhanced regularity in molecular spacing, and the contribution from microfibrils not involved in staggered arrays became more dominant[3]. Simulated diffraction profiles and analyses of the staggered arrays of isolated microfibrils formed in vitro in the presence of Ca2+ were used to interpret the effects of Ca2+. These observations indicate how Ca2+ could modulate the organisation of individual microfibrils and three-dimensional arrays in vivo. This data allows a mechanism for elasticity at the molecular level to be related to the macroscopic tissue elasticity. Under the usual conditions of extension in the eye, bead periodicty changes in a discrete population along fibrils to facilitate elasticity. Molecular junctions of specifically staggered microfibrils maintain the integrity of the tissue and serve as anchors connecting the stretched microfibrils and allows the stored force to be transmitted through the tissue. The removal of Ca2+ enhances the regularity of the bead regions where stretching occurs and also allows the diffraction from unstaggered

beads to be observed.

[1] Wess T.J. Purslow P.P and Kielty C.M. (1997) Fibrillin rich microfibrils: an X-ray diffraction study of the fundamental axial periodicity. FEBS Lett. 413 424-428.
[2] Wess T.J. Kielty C.M. Purslow P.P. (1998) Calcium determines the supramolecular organisation of fibrillin rich microfibrils. J.Cell .Biol. 141 829-837.
[3] Wess T.J. Purslow P.P. and Kielty C.M. (1998) Fibrillin elasticity an X-ray diffraction study. J.Struct.Biol. 122 123-127

P06.12.008 NONLINEAR ATOMIC PACKING AND THE THREE PHASE MODEL OF FIBROUS POLYMERS. Anuradha Mukhopadhyay, Department of Physics, Jadavpur University, Calcutta 700032, India and G.B.Mitra, Department of C.S.S., Indian Association for the Cultivation of Science, Calcutta 700032, India.

The simultaneous presence of three phases, viz the crystalline, the paracrystalline and the amorphous in fibrous polymers must be attributed to the long chain of atoms and the folding of these chains. Because of these folds, the atomic conglommerates tend to become crowded in parts and sparsely distributed in other parts. The sparsity of distribution is of varying magnitude. The atoms appear to be arranged on cylinders or conglommerates of coaxial cylinders. Along the axes of the cylinders, there will be equal slabs of atoms arranged equiangularly on concentric circles. The crystallinity is due to the equally spaced slabs along the axes of the cylinders. The paracrystallinity will be due to the circularly arranged atoms normal to the cylinder. The amorphosity is due to the random arrangement of atomic conglommerates in the matrix. In some variants, the circles may be replaced by ellipses while the axis of the cylinder may be slightly curved. These variants give rise to the diversity of the diffraction pattern. In the present work a mathematical analysis of these aspects has been developed.

P06.12.009 X-RAY STUDY OF STRUCTURE OF WOOD CELLULOSE IN NATIVE CONDITION AND AFTER VARIOUS PROCESSING. L.A.Lugovskaya, L.A.Aleshina, V.V.Petrova, M.V.Podoinikova S.V.Glazkova, A.D.Fofanov. Department of Solid State Physics, Petrozavodsk State University, pr. Lenina 33, 185640 Petrozavodsk, Russia.

An X-ray researches of structure has been performed and the data on the structural characteristics of samples of natural cellulose (bark, bast, early and late pine wood, raised in various ecological conditions and semifinished products received at first three work cycle stages of manufacturing of a paper) has been obtained. The samples were studies by an X-ray difractometer DRON-4 using Mo- Cu- and Fe-K_α radiations. The calculations of the experimental short-range order characteristics were carried out for amorphous components of cellulose by the Finbak method.

The sizes of the ordered areas and degree of crystallinity of samples for various orientations of a sample relatively of falling beams were determined. It is shown, that for a number of samples from native cellulose and samples received on the first production stages of a paper, is characteristic anisotropy of x-ray pattern. Besides in a matrix with the average size of coherence areas, equal 30-40 A, in natural samples and samples of semifinished products present in tens time larger ordered crystallites.

Largest diffuse of X-ray pattern of natural cellulose complicates the problem solving of indexing of the X-ray patterns and, as a consequence, correct estimation of the crystal lattice periods from diffraction data. In the given work the attempt was made to decide this problem by construction of model X-ray pattern, being based on the information on the atomic structure of unit cells of various polymorphic types of cellulose.

13. CHARGE, SPIN AND MOMENTUM DENSITY

P06.13.001 ELECTRON DENSITY DISTRIBUTION IN MEI-SENHEIMER COMPLEXES OF AROMATIC NITRO COMPOUNDS. O.Ya. Borbulevych, K.A. Lyssenko, M.Yu. Antipin, X-ray structural center, Institute of Organoelement Compounds, Russian Academy of Sciences, 28 Vavilov str., Moscow 117813, Russia, and O.V. Shishkin. SRD Alkali Halide Crystals, STC «Institute for Single Crystals», National Academy of Sciences of the Ukraine, 60 Lenina ave., Khar'kov 310001, Ukraine

An electron density distribution in the crystal of Meisenheimer complex — derivatives of 2,4,6-trinitrobenzole and 5,7-dinitro-quinoline **1-4** were studied using precision X-ray diffraction method at 153K.

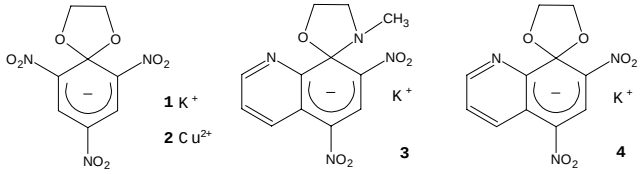

Features of electron density distribution in organic anions (non-equivalent character of nitro groups and the C-C bonds within partially hydrogenated rings) have been revealed using Bader's topological theory. Molecular structure of various complexes of anions **1,3,4** — K^+ with different coordination of the cation to oxygen atoms has been calculated by high level *ab initio* methods.

Comparison of experimental and theoretical data have demonstrated that topological characteristics (e.g. bonds ellipticity) of electron density function within six-membered ring and nitro groups strongly depends on position of cation.

P06.13.002 BOND CHARACTERIZATION OF Cr–L MULTIPLE BONDS, L = C. N. O. Chih-Chieh Wang and Yu Wang, Department of Chemistry, National Taiwan University, Taipei, Taiwan, ROC.

Four chromium complexes with Cr–L (L = O, N, C) multiple bonds, are studied using ab-initio/DFT calculations based on the geometry obtained from single crystal X-ray diffraction data. They are $[Cr^{(I)}(CPh)(CO)_4(Cl)]$ **1**; $[Cr^{(V)}(N)(bpb)]$ **2**, [bpb^{2-} = (1,2-bis(pyridine-2-carboxamido)benzene)]; $[Cr^{(V)}$(N-*t*-Bu)(bpb)(Cl)] **3** and [(TPPOMe)$Cr^{(IV)}$O] **4**, [TPPOMe = (5,10,15,20-para-methoxyphenyl)porphyrin)]. Detailed descriptions of Cr–O_{oxo}, Cr–$N_{nitrido}$, Cr–N_{imido}, Cr–$C_{carbyne}$ bonds based the natural bonding orbital (NBO) analyses are presented. The bonding feature among these multiple bonds is essentially a triple bond character consisting of one σ and two π bonds. Bond characterisation will be shown in terms of Laplacian of electron density, Fermi-Hole function, electron localization function (ELF) where all the bonding information is embedded. The topological properties associated with the bond critical point (B.C.P.) of these four compounds will be compared. The relationship between bond order and the density (ρ_c) at BCP for various types of Cr–L bonds are well correlated based on theoretical comparison. The triple bond feature of Cr–$C_{carbyne}$, Cr–$N_{nitrido}$, Cr–N_{imido}, and Cr–O_{oxo} is displayed nicely by Fermi-Hole function. A comparison of such density distribution and topological properties between experiment and theory will be presented for compound **1** and **2**. The agreement between experiment and theory is encouraging.

P06.13.003 TOPOLOGICAL ANALYSIS AND CHARGE DENSITY STUDY OF OCTAAZA MACROCYCLIC Co(II) AND Ni(II) COMPLEX. Jey-Jau Lee and Yu Wang, Department of Chemistry, National Taiwan University, Taipei, Taiwan.

Accurate single crystal diffraction data are measured on $[Co(C_{12}H_{20}N_8)(H_2O)_2][ClO_4]_2$ crystal using MoKα radiation at 125K. It crystallises in the space group of P bca at 125 K. The final agreement index R is 0.033 and Rw is 0.037 based on 5547 observed reflections; the site symmetry of cobalt is at –1. Co(II) ion is co-ordinated in a square bipyramidal fashion with four immino-N at the equatorial plane and two water molecules at the axial positions. There are H-bonding between the cations and anions. Deformation density distribution based on the multipole model obtained experimentally is compared with those based on the HF and DFT calculations obtained theoretically. The agreement between experiment and theory is generally good. From NBO analysis, The bond between Co(II) ion and immino N is a dative bond and nitrogen atom is sp^2 hybridisation. Negative Laplacian around Co nucleus gives symmetric local density accumulation along x- and y- directions, which are at the bisection of N-Co-N angles. The C-C, C-N and N-N bonds of the ligand are all in covalent character and essentially a delocalised π-bond character. The theoretical electron density distribution and Topological analysis is also performed on the Ni(II) complex of the similar ligand, but the Ni(II) complex is in a four-co-ordinated square planar geometry. The orbital energies of Co d-orbitals in this complex is such that $E_{xz} \approx E_{yz} \approx E_{x^2-y^2} < E_z^2 < E_{xy}$. The Co(II) ion is in a low spin state with the singly occupied d_{z^2} orbital whereas the Ni(II) ion is doubly occupied on d_{z^2} orbital.

P06.13.004 THE OCCURRENCE OF NON-NUCLEAR MAXIMA OF THE ELECTRON DENSITY. V. Luaña, A. Martín Pendás, P. Mori-Sánchez, A. Costales, and M. A. Blanco, Departamento de Química Física y Analítica, Universidad de Oviedo, 33007-Oviedo, Spain.

Simple arguments and high quality quantum mechanical calculations are used to analyze the occurrence of non-nuclear maxima (nnm) [1] in the electron density of molecules and crystals. Rather than being a rarity, nnm are shown to be a normal step in the chemical bonding of homonuclear systems ... if analyzed in the appropriate range of internuclear distances. For most elements, however, this range occurs far away from the stable geometry under normal thermodynamical conditions. Heteronuclear combinations, on the other hand, behave quite differently, and nnm should only appear under exceptional circumstances. This discussion should contribute to the recent controversy over the experimental existence of nnm [2,3,4,5].

[1] R. F. W. Bader, *Atoms in Molecules - A Quantum Theory*, (Oxford U.P., Oxford, 1990).
[2] B. B. Iversen, F. K. Larsen, M. Souhassou, and M. Takata, Acta Cryst. A **51** (1995) 580-591.
[3] R. Y. de Vries, W. J. Briels and D. Feil, Phys. Rev. Lett. **77** (1996) 1719-1722.
[4] B. B. Iversen, J. L. Jensen, and J. Danielsen, Acta Cryst. A **53** (1997) 376-387.
[5] D. Jayatilaka, Phys. Rev. Lett. **80** (1998) 798-801.

P06.13.005 PHOSPHONIUM YLIDE: THE CHARGE DENSITY STUDY AND *AIM* ANALYSIS. D.S.Yufit, J.A.K.Howard, M.G.Davidson, Department of Chemistry, University of Durham, Durham, UK DH1 3LE

The results of experimental determination of charge density distribution in molecule of phosphonium ylide Ph3P=CH-Ph (1) will be presented. For the best of our knowledge this is the first example of topological analysis of the experimental electron distribution in ylides. The data were collected at 100K on the Siemens SMART CCD 1K diffractometer and multipole refinement was carried out using XD [1] program package. Our experience of using CCD for charge density studies (data collection and processing) will be discussed. The bonding in (1) as well as intermolecular interactions in structure (1) is analyzed in terms of *AIM* [2] theory. Special attention is paid to parameters of C-H...C interactions that allegedly determine the packing of the molecules (1) in crystal.

1. T.Koritsanszky, S.T.Howard, P.R.Mallinson, Z.Su, T.Richter, N.Hansen. Berlin (1995).
2. R.F.W.Bader, *Atoms in Molecules - a Quantum Theory* (Oxford 1990)

P06.13.006 ANALYSIS OF XYLITOLS CRYSTAL CHARGE DENSITY. Anders Østergaard Madsen, Henning Osholm Sørensen and Sine Larsen, Centre for Crystallographic Studies, University of Copenhagen, Chemistry Laboratory IV, Universitetsparken 5, 2100 KøbenhavnØ, Denmark.

The crystal strucure of xylitol, $C_5H_{12}O_5$, in its stable orthorohombic form (space group $P2_1\,2_1\,2_1$) has been investigated earlier. It showed that the meso-pentitol xylitol in common with its diastereomer ribitol, has a non-planar conformation of the carbon chain, and that its five hydroxo groups are engaged in a complex pattern of hydrogen bonds. In order to elucidate the different intermolecular interactions of xylitol a new lowtemperature (122K) data collection was performed using MoKα radiation. The data extends to $(\sin\theta)/\lambda = 1.1 Å^{-1}$, R_{int} = 0.0219.

The multipole formalism for modeling of experimental electron densities is a well established method for the analysis of centrosymmetric structures, but has not been employed to the same extent to acentric space groups due to the latters lack of general phase restrictions. We report here our results from the multipole refinements for xylitol carried out using XD[2] and VALRAY[3]. The subsequent topological analysis of the experimental charge density is used to characterise the different intermolecular interactions found in xylitol.

H.S Kim and G.A. Jeffrey, Acta Cryst. (1969). B25, 2607.
T. Koritsánszky, P. Mallinson, Z. Su, T. Richter & N. Hansen (1996); *XD, A Computer Program Package for Multipole Refinement and Analysis of Electron Densities from Diffraction Data, 1.2 edn.*
R. F. Stewart, M. A. Spackman & C. Flensburg (July 1998); *VALRAY98 Users manual*.

P06.13.007 COMPARISON OF THE EXPERIMENTAL AND THEORETICAL CHARGE DENSITY OF *p*-FLUOROMANDELIC ACID. Henning Osholm Sørensen, Claus Flensburg and Sine Larsen, Centre for Crystallographic Studies, Chemistry Laboratory IV, University of Copenhagen, Universitetsparken 5, 2100 Copenhagen Ø, Denmark

Structural and physico-chemical studies of racemic and optically active monofluoro-substituted mandelic acids have revealed a number of interesting intermolecular interactions in addition to the expected O-H…O hydrogen bonds, e.g. C-F contacts and C-H…O hydrogen bonds[1,2]. A topological analysis of the theoretical (periodic Hartree-Fock) charge density for optically active *p*-fluoromandelic acid showed (3,-1) critical points between carbon atoms from adjacent phenyl groups. In order to analyse the intermolecular interactions further we have collected a data set to high resolution ($\sin\theta_{max}/\lambda = 1.12$ Å^{-1}) and of high quality (R_{int}=0.0172) for optically active *p*-fluoromandelic acid. The compound crystallises in space group C2 and we are aware that the subsequent analysis could be hampered both by the lack of phase restrictions in non-centrosymmetric space groups and the lack of accurate (neutron) parameters for the hydrogen atoms. Different approaches have been employed to investigate how this lack of information influences the experimental charge density. This includes a comparison of the results obtained using different multipole refinement programs, XD[4] and VALRAY[5], and a comparison with the theoretical charge density.

1. S. Larsen and K. Marthi. *Acta Crystallogr.*, B**50**:373-381, 1994.
2. S. Larsen and K. Marthi. *Acta Crystallogr.*, B**53**:280-292, 1997.
3. H. S. Bengaard. Cand. scient. thesis, University of Copenhagen, February 1998.
4. T. Koritsánszky *et al. XD: A Computer Program Package for Multipole Refinement and Analysis of Electron Densities from Diffraction Data*, 1996.
5. R. F. Stewart, M. A. Spackman, and C. Flensburg. *VALRAY98 Users Manual*, July 1998.

P06.13.008 A CHARGE DENSITY STUDY OF THE EFFECT OF IRRADIATION α-FORM OF π-NITRO-PHENOL. P. Kumaradhas, R. Srinivasa Gopalan, G. U. Kulkarni, Chemistry and Physics of Materials Unit, Jawaharlal Nehru Centre for Advanced Scientific Research, Jakkur, Bangalore – 560 064, India

A careful investigation of the structure and charge density of the α polymorph of *p*-nitrophenol has been carried out following prolonged irradiation by visible light. Though the change in color from yellow to red is remarkable, the molecular geometry and the intermolecular hydrogen contacts exhibit only minor changes. However, a charge density analysis in comparison with the pristine α and the β polymorphs has brought out significant differences in the charge distribution in the intra- and intermolecular bonding regions. The deformation density map of the α form reveals many differences in the bonding regions of the molecule before and after irradiation. Charge migration from the nitro and the hydroxyl groups to the phenyl ring of the molecule occurs on irradiation, resembling more like the charge distribution in the light stable β form. The molecular dipole moment in the irradiated crystal has been compared to that before irradiation. Relief maps of the negative Laplacian in the hydrogen bond region show less polarization of the oxygen lone-pairs compared to before irradiation.

P06.13.009 ELECTROSTATIC PROPERTIES OF NITROANILINES. J. Ellena, Instituto de Física de Saõ Carlos, USP, C.P. 369, 13560, Saõ Carlos, SP, Brasil, A.E. Goeta and J.A.K. Howard, Chemistry Department, Durham University, Durham DH1 3LE, UK, and G. Punte, LANADI y PROFIMO, Depto de Física, UNLP, CC 67, (1900) La Plata, Argentina.

The needs of the telecommunications industry have stimulated the research and develop of organic materials presenting non-linear optical responses. In this context, nitroaniline derivatives have been widely studied in the literature. However, some of the results coming from the currently available new techniques have renewed the interest in them, showing the need for a revision of both the existing knowledge on these compounds and the models which have been used to analyze them. In order to contribute to the understanding of these systems, the electron charge distribution of 2-methyl-5-nitroaniline was determined from high-resolution X-ray diffraction and neutron diffraction data, and compared with the one obtained from *ab-initio* calculations. The present work would indicate that the N-H...O interactions that generate the nitroaniline polar chains are two-centres interactions. The redistribution of the molecular

charge density, induced by molecular aggregation, explains the observed Car-H...O interactions, that help to stabilize 2-methyl-4-nitroaniline and other related compounds, with chains build from similar N-H...O synthons and assembled head-to-head. It has also been established that the in-crystal molecular electric dipolar moment is higher than that of the free molecule, the latter coincident with the one in solution. This finding along with the topological analysis of the electron charge density and the comparison of the experimental and theoretical determined electrostatic potentials seem to indicate the existence of cooperative effects.

P06.13.010 ELECTROSTATIC ENERGIES AND X-RAY DATA REFINEMENT. N.J. O'Toole and V.A. Streltsov, Crystallography Centre, The University of Western Australia, Nedlands, WA 6907, Australia.

The electrostatic self-electronic energy (E_{es}) has been computed from a variety of accurate X-ray data sets. It is demonstrated that by consideration of this property during data refinement, the obscuration of important features in experimental $\Delta\rho$ distributions due to biasing of parameters such as the structure factor scale can be avoided.

E_{es} is a relatively simple functional of the ground-state charge density in a crystal. The conventional representation of crystalline electron density ρ as the sum of the "pro-crystal" density ρ_{pro} and the deformation density $\Delta\rho$ leads to the expression of E_{es} as $E_{pro} + \Delta E$, these terms being the energy of the pro-crystal and deformation density respectively. It has been shown that E_{pro} is a rather good first approximation to the experimental cohesive energy for a wide range of materials [1]. The remaining (presumably small by comparison to E_{pro}) contributions to the cohesive energy are from charge transfer and polarization effects (i.e. ΔE) and the exchange/correlation energy.

Calculations of ΔE using the highly accurate experimental and theoretical data sets for the Group IV elements illustrate an extreme sensitivity of ΔE to the structure factor scale. Minute variations in the scale yield ΔE values with an unphysical magnitude. This sensitivity has been exploited during the refinement of synchrotron X-ray data sets for the rutile-type structures CoF_2 and ZnF_2, collected at the "Photon Factory" (Tsukuba, Japan); the scale and extinction parameters were constrained to produce $\Delta\rho$ distributions with physically reasonable energies. Much useful qualitative information in these $\Delta\rho$ maps is obscured without inclusion of this technique.

M. G. Trefry, E. N. Maslen & M. A. Spackman (1987). *J. Phys.* C20, 19-28.

P06.13.011 CONTRIBUTION TO THE CHARGE DENSITY STUDIES OF Cu^{II}-COMPLEXES. J. Kozisek, Department of Inorganic Chemistry, Slovak University of Technology, SK-81237 Bratislava, Slovakia, H. Fuess, Material Science, Darmstadt University of Technology, D-64287 Darmstadt, Germany and N.K. Hansen, Laboratoire de Cristallographie et Modélisation des Matériaux Minéraux et Biologiques, Université Henri Poincaré, BP 239, 54506 Nancy CEDEX, France.

More than 8800 crystal structures of co-ordination compounds with Cu^{II} central atom in Cambridge Structural Database is an evidence of big variety of compounds with this element. Our recent study revealed the changing of reactivity of the ligand due to his co-ordination to the central atom. A nucleophilic addition of small molecules (methanol, water) to non-linear pseudohalides (like dicyanamide and nitrosodicyanomethanide), in the co-ordination sphere of *3d*-elements [mainly Cu(II), Ni(II) and Co(II)] leads to the formation of new anionic ligand [1,2]. Reactions in the co-ordination sphere of central atoms are of big importance not only for co-ordination chemistry. The systematic study of *d*-electron distribution in different co-ordination polyhedra of Cu^{II} could throw a new light on understanding the essentially properties of co-ordination bond. In order to examine the redistribution of valence electron density in different co-ordination environment charge density studies on some chosen compounds was done.

Experimental diffraction data were obtained with a Stoe Stadi 4 dif-fractometer at 120(1)K using the Oxford cryosystems low temperature attachment. A typical strategy for the data collection was to measure low angle reflections ($0 < \theta < 30°$), and the high angle reflections ($30 < \theta < 45°$). For the absorption correction the crystal habitus was measured and a Gaussian quadrature method employed.

The results of the multipole refinement will be discussed.

1. Hvastijová M., Kohout J., Buchler J.W., Boca R., Kozisek J. & Jäger L.; *Coord. Chem. Rev.,* **175** , 17-42 (1998).
2. R. Boca, M. Hvastijová, J. Kozisek, and M. Valko; *Inorg. Chem.*, **35** 4794-4797 (1996).

P06.13.012 CHARGE DENSITY STUDY OF AN ANTITHROMBOTIC DRUG - NEW ASPECTS IN DRUG DESIGN. R. Flaig and P. Luger, Institut für Kristallographie, Freie Universität Berlin, Takustr. 6, 14195 Berlin, Germany, and R. Soyka, Boehringer Ingelheim Pharma KG, Biberach, Germany, and T. Koritsánszky, Department of Chemistry, University of the Witwatersrand, Private Bag 3, WITS 2050, Johannesburg, South Africa

It has recently been shown [1] that the short data acquisition time using CCD area detection makes it possible to collect high quality X-ray diffraction data suitable for charge density determination. Such advances allow the method [2] to be applied for large systems of biological and pharmacological importance and open new perspectives for molecular modelling, recognition and drug design. We present a diffraction experiment, leading to a high resolution data set ($\sin\theta/\lambda_{max} = 1.24$ Å^{-1}, MoKα) of approximately 220000 reflections collected at 100 K with a CCD area detector, and the corresponding electron density of an antithrombotic drug containing more than 50 atoms. The multipole refinement and the topological analysis [3] of the static electron density was carried out with the program package XD [4]. All atom-atom interactions were characterized based on the topology of the density. In addition, different electronic properties of the crystalline state (dipole moment and electrostatic potential) were derived from the data and compared with those obtained from the wave function at the Hartree-Fock level of theory for the isolated molecule.

1. T. Koritsánszky, R. Flaig, D. Zobel, H.-G. Krane, W. Morgenroth, P. Luger, Science 279, 356 (1998)
2. P. Coppens, ``X-ray charge densities and chemical bonding", Oxford Science Publications, (1997).
3. R.F.W. Bader, ``Atoms in Molecules", Monograph, Clarendon Press, Oxford, (1990).
4. T. Koritsánszky, S. Howard, R.P. Mallinson, Z.W. Su, T. Richter, N.K. Hansen: XD, A Computer Program Package for Multipole Refinement and Analysis of Charge Densities from X-ray Diffraction Data. Freie Universität Berlin. User Manual (1995).

P06.13.013 CHARGE DENSITY STUDY ON THREE PENICILLIN DERIVATIVES. A. Wagner, P. Bombicz, R. Flaig, P. Luger, Institut für Kristallographie, Freie Universität Berlin, Takustr. 6, 14195 Berlin, Germany, and T. Koritsänszky, Department of Chemistry, University of the Witwatersrand, Private Bag 3, WITS 2050, Johannesburg, South Africa

Due to recent theoretical and experimental developments in charge density determination it is now possible to examine

large molecules of pharmaceutical interest. With the combination of the highly intensive synchrotron radiation and a CCD area detector one can collect high resolution data sets in a few days [1]. Penicillins, although being in therapeutical use for several decades, still provide the most widely used antibacterial drugs. An enormous amount of chemical derivatives have been synthesized and tested. The penicillin ring skeleton is formed by L-cysteine and D-valine and therefore it contains the D-alanyl-D-alanine moiety.

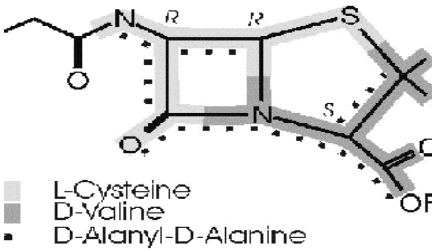

Based on the work on several amino acids we started to investigate the charge density of penamecillin, its corresponding biological inactive 1-β-sulfoxide and free phenoxymethylpenicillin. Intensity data of 73961, 80595 and 54463 reflections were collected at the beamlines F1 and D3 (HASYLAB/DESY, λ~0.5Å) with a Bruker SMART CCD area detector at 100 K up to a resolution of $\sin\theta/\lambda$ = 1.08, 1.26 and 1.24. A multipole refinement (program package XD) and a subsequent topological analysis was performed. In addition theoretical charge densities based on HF/6-311++G(d,p) wave functions were generated. A comparison of molecular topological properties of the three penicillin derivatives is presented.

[1] T. Koritsänszky, R. Flaig, D. Zobel, H.-G. Krane, W. Morgenroth, P. Luger, Science 279, 356 (1998)

P06.13.014 FROM AMINO ACIDS TO DIPEPTIDES - AN EXPERIMENTAL CHARGE DENSITY STUDY. B. Dittrich, P. Luger, R. Flaig, Institut für Kristallographie, Freie Universität Berlin, Takustr. 6, 14195 Berlin, Germany, and T. Koritsánszky, Department of Chemistry, University of the Witwatersrand, Private Bag 3, WITS 2050, Johannesburg, South Africa.

The topological analysis of the total electron density leads to the real-space definition of density units associated with atoms or functional groups [1]. The tranferability of different electronic properties of these subsystems is essential to the theoretical building of macromolecules from monomers [2]. Such applications might be limited to the extent to which the topology of the density is affected by the molecular conformation and intermolecular interactions. The study of experimental densities being characteristic to the crystalline rather than to an isolated state are well suited to elucidate these effects. Here we examine the transferability of simple topological properties of the electron densities extracted from X-ray diffraction data and compare the results obtained for a dipeptide with those of the building amino acids. The analyses are performed by the computer package XD [3] and based on synchrotron CCD data (HASYLAB/DESY) for the former and conventional (AgKα) data collected at around 20K for the latter structures.

We thank the BMBF (project 05 SM8 KEA 0) and the Fonds der Chemischen Industrie for financial support

1. R.F.W. Bader, ``Atoms in Molecules", Monograph, Clarendon Press, Oxford, (1990).
2. P.L.A. Popelier, R.F.W. Bader, J. Phys. Chem. 98, (1994), 4473.
3. T. Koritsánszky, S. Howard, R.P. Mallinson, Z.W. Su, T. Richter, N.K. Hansen: XD, A Computer Program Package for Multipole Refinement and Analysis of Charge Densities from X-ray Diffraction Data. Freie Universität Berlin. User Manual (1995)

P06.13.015 THE CHARGE DENSITY AND THE DIPOLE MOMENT OF PHOSPHANGULENE, A MOLECULAR PYROELECTRIC MATERIAL. Georg K. H. Madsen, Finn K. Larsen, Department of chemistry, University of Aarhus, DK-8000 Århus C, Denmark. Frederik C. Krebs, Macromolecular Chemistry Group, Department of Solid State Physics, Risø national laboratory, DK-4000 Roskilde, Denmark.

The charge density of the molecular pyroelectric material phosphangulene has been studied by multipolar modelling of very low-temperature (10 K) AgKα X-ray diffraction data, and the solid state dipole moment is evaluated. Due to the stacking arrangement of the molecules in the polar space group and consequent electric field over the crystal, the dipole moment in the solid state is enhanced compared to the value measured in chloroform and that calculated by *ab initio* methods for a gas phase molecule.

A polar space group is a prerequisite for a material to exhibit pyroelectric properties. Phosphangulene belongs to the space-group R3m.[1] Two main factors contribute uncertainty to the derivation of a reliable solid state dipole moment, namely the non-centrosymmetry of the spacegroup and the precision and accuracy of the hydrogen atom parameters. The influence of the non-centrosymmetry on the accuracy of the extracted electron density[2,3] is evaluated by modelling a set of theoretically calculated structure factors. The second main factor influencing the accuracy of the evaluated dipole moment is the modelling of the hydrogen pseudo-atoms. The high-symmetry space-group and the relatively small trigonal unit cell (a=b=16.654(1) Å, c= 4.166(1) Å) allows the determination of the hydrogen positions by neutron powder diffraction. An improved value for the pyroelectric coefficient of phosphagulene is estimated on the basis of the derived solid state dipole moment.

[1] Krebs, F. C.; Larsen, P. S.; Larsen, J.; Jacobsen, C. S.; Boutton, C.; Thorup, N. *J. Am. Chem. Soc* **1997**, 119, 1208-1216.
[2] El Haouzi, A.; Hansen, N. K.; Le Hénaff, C.; Protas, J. *Acta Cryst* **1996**, A52, 291-301.
[3] Spackman, M. A.; Byrom, P. G. *Acta Cryst* **1997**, B53, 553-564.

P06.13.016 THE MOLECULAR POLARIZABILITY OF NON LINEAR OPTICAL COMPOUND FROM X-RAY DIFFRACTION STUDY. F. Hamzaoui, N. Bettahar, A. Addou [1], F. Baert [2], [1] I.C.I. Université de Mostaganem. BP. 188 Mostaganem 27000 Algeria, [2] L.D.S.M.M. Université de Lille1. 59655 Villeneuve d'Ascq France

The ambition underlying this work, in addition to the electronic density determination is to revisit the earlier Robinson model which proposed to derived the non linear optical properties of a molecule from its ground state charge distribution.[1] The Robinson model has been applied to the 3-Methyl 4-Nitropyridine N-Oxide (POM) a prototypical nonlinear organic crystal, whereby relations between polarizabilities and multipolar moments of the electronic charge distribution have been evidenced. The experimental electronic density analysis has been carried out by use of the aspherical model of Hansen and Coppens. The electrostatic moments were then estimated by direct integration methods using both discret and fuzzy boundary space partitioning. Atomic net charges and dipolar moments derived therefrom clearly evidence the donor-acceptor character of substituents attached to the pyridine transmitter. The dipolar molecular

moment obtained by several methods have similar values, of the order of 1 Debye, in agreement with the small to vanishing dipole feature purposely engineered in POM.[2] The obtained results mimic very closely those published recently by Fkyerat et al. on the N-(4-nitrophenyl)-(L) Prolinol (NPP) another very efficient nonlinear optical compound.[3] The average value of linear polarizability is in agreement with the corresponding one inferred from the Finite Field Method. However, It seems difficult to infer from the Unsöld approximation a faithful description of the molecular optical properties, whereas an estimation of the first order hyperpolarizability components seems out of reach.

[1] F. N. H. Robinson. Bell System Technical Journal, 913-956 (1967).
[2] F.Hamzaoui, F.Baert & J.Zyss. J. Mat. Chem. 6(7), 1123-1130(1996)
[3] A.Fkyerat, A.Guelzim & F. Baert. Phys. Rev. B53 16236-16246 (1996)

P06.13.017 DIPOLE MOMENT DETERMINED BY QUANTUM THEORY OF ATOMS IN MOLECULES. C. Flensburg, and S. Larsen, Centre for Crystallographic Studies, University of Copenhagen, Denmark.

The dipole moment is one of the properties, that can be derived from a charge density, which has been subject to considerable attention. The literature contains several examples of the determination of the dipole moment of molecular entities in crystals based on diffraction data that rely on different schemes of space partitioning[1].

The dipole moment of the water molecules has been determined employing the *Quantum Theory of Atoms in Molecules*[2] on the experimental charge distribution of methylammonium hydrogen succinate[3] and oxalic acid dihydrate[4]. The determination of the zero-flux surfaces was performed with the program VALRAY98 [5]. The dipole moments derived from the experimental data compare well with the equivalent quantities determined from the theoretical charge distributions obtained by the *ab initio* method as implemented in the programs CRYSTAL95 [6] and TOPOND97 [7]. The differences between the dipole moment of the water molecule in the two structures can be related to differences in their crystalline environments.

The dipole moments determined by application of QTAM are compared with the results derived from the conventional methods of obtaining the dipole moment from experimental charge distributions.

1. Spackman, M. (1992). *Chemical Reviews*. *92*, 1769-1797.
2. Bader, R. F. W. (1990). *Atoms in Molecules*, Oxford University Press, Oxford.
3. Flensburg, C., Larsen, S., and Stewart, R. F. (1995). *J. Phys. Chem.*. *99*, 10130-10141.
4. Dam, J.,*et al.* (1984). *Acta Crystallogr. A*. *40*, 184-195.
5. VALRAY98. (1998). *Users Manual*. Stewart, R. F., Spackman, M. A., and Flensburg, C. University of Pittsburgh and University of Copenhagen.
6. CRYSTAL95. (1995). *Users Manual*, Dovesi, R., *et al.* University of Turin and Daresbury Laboratory.
7. TOPOND97. (1997). *Users Manual*. Gatti, C. CSRSRC - CNR, Milano.

P06.13.018 EXPERIMENTAL CHARGE DENSITY STUDY OF THE MN-MN BOND IN $Mn_2(CO)_{10}$. Paul R. Mallinson, Louis J. Farrugia, and Dmitrii S. Yufit, Chemistry Department, University of Glasgow, Glasgow G12 8QQ, UK.

Complexes with direct bonds between transition metals have been of interest for some time, especially in the context of the Cluster-Surface analogy. A number of charge density studies on relatively simple examples of such compounds have been carried out in the past, in order to understand the nature of the metal-metal bond. These have almost exclusively been X-X or X-N studies on the deformation density.

One interesting example is $Mn_2(CO)_{10}$ which is a fundamental example of a compound containing an unsupported metal-metal bond. The suggestion of Bader [1] which identifies a bond path as a universal indicator of a bonding interaction has led us to re-examine the charge density in $Mn_2(CO)_{10}$ using this methodology. During the course of these investigations, another such study was also reported by Italian workers [2]. The package XD [3] was used in a multipole refinement with X-ray diffraction data, to obtain bond path and critical point (CP) analyses. The distribution of atomic charges is consistent with some occupancy of the valence π^* orbitals of the CO ligands *via* back bonding from the manganese. (3,-1) CPs are situated on cross-interaction lines linking the Mn atoms with two equatorial carbon atoms of a C_2-related $Mn(CO)_5$ unit. In the region earlier supposed to be the site of metal-metal bonding, where there is only a small density accumulation, the topological feature is found to be a ring CP, rather than a bond CP.

[1] R.F.W. Bader. *J. Phys. Chem.* (1998), 102, 7314-7323.
[2] R. Bianchi, G. Gervasio and D. Marabello. *J. Chem. Soc. Chem. Commun.* (1998), 1535-1536.
[3] T. Koritsanszky, S.T. Howard, T. Richter, P.R. Mallinson, Z. Su, and N.K. Hansen. *XD, a computer program package for multipole refinement and analysis of charge densities from X-ray diffraction data*, 1995.

P06.13.019 MOMENTUM DENSITY OF K_XC_{60}. Ch. Bellin, M. Marangolo, G. Loupias, LMCP, Université Paris VI, case 115, 4 place Jussieu, 75252 Paris cedex 05, France, J. Moscovici, LPMD, Université Paris XII, UFR Sciences, 61 Av. du Général de Gaulle, 94010 Créteil, France, S. Erwin, Complex Systems Theory Branch, Naval Research Laboratory, Washington DC 20375, USA, S. Rabii, Dept. of Electrical Engineering, University of Pennsylvania, Philadelphia, PA 19104, USA

Compton scattering measurements have been demonstrated to provide an accurate check of conduction and valence electron densities of solids, in the electronic ground-state. Since the scattering is incoherent, this technique, which is a bulk probe, is insensitive to crystal defects.

Compton profiles, i.e. energy-loss spectra of scattered photons were measured on powder samples, using 16keV monochromatic beam provided by the french synchrotron facility. All the K_XC_{60} samples (x=3,4, and 6) were intercalated and kept under controlled atmosphere all the time. For comparison, C_{60} powder was measured in same experimental conditions. Theoretical Compton profiles were calculated from the *ab initio* SCF ground-state wavefunctions. These calculations were carried out within the local-density-approximation (LDA) by the LCAO technique and using all electron potentials. The directional profiles were then averaged for comparison with the measurement on powder samples.

In order to describe the electronic structures, differences between K_XC_{60} and C_{60} measured Compton profiles are compared with theoretical profile differences. Since Compton scattering is particularly sensitive to the hybridization between carbon and alkali orbitals as it was demonstrated in the case of graphite intercalation compounds, the distorsion of C_{60} molecule is discussed as a function of x. In addition, "charge transfer" between the intercalate and the C_{60} molecules as well as magnitude of e^--e^- correlations (essential to understand the superconductivity) are studied in this set of materials.

P06.13.020 THE EXPERIMENTAL CHARGE DENSITY DISTRIBUTION IN 4-STYRYL-7-FLUOROCOUMARIN: FIRST SHORT F...F INTERACTION. Tayur N. Guru Row[a], Paul R. Mallinson[b], Marahanakuli D. Prasanna[a], and Simon J. Teat[c], [a]Indian Institute of Science, Bangalore 560012, India. [b]Chemistry Department, University of Glasgow, Glasgow G12 8QQ, UK. [c]CCLRC Daresbury Laboratory, Daresbury, Warrington WA4 4AD, UK.

Fluoro substituted styryl coumarins have been studied recently to understand the principles of photodimerization in engineering such molecules in the crystal lattice [1]. The title compound is an unique exception in not generating the crystal packing favourable for the photo reaction. The presence of a short F...F contact across the centre of symmetry appears to be dominant in the crystal packing. Recent charge density studies [2] have clearly brought out the features of weak interactions and the present study aims at mapping the electron density distributions in a short F...F contact for the first time.

The data were collected at the CCLRC Daresbury CCD facility at 100K using radiation of wavelength 0.4855 Å. Multipole refinement using the XD [3] package preceded an analysis of critical point (CP) properties. The CP and bond paths clearly establish the features and properties of the F...F intermolecular interaction.

[1] K. Vishnumurthy, T.N. Guru Row and K. Venkatesan. *J. Chem. Soc. Perkin Trans. 2* (1997), 615-619.
[2] P.R. Mallinson, K. Wo\'zniak, G.T. Smith, K.L. McCormack. *J. Amer. Chem. Soc.* (1997), 119, 11502-11509.
[3] T. Koritsanszky, S.T. Howard, T. Richter, P.R. Mallinson, Z. Su, and N.K. Hansen. *XD, a computer program package for multipole refinement and analysis of charge densities from X-ray diffraction data*, 1995.

P06.13.021 MAGNETIC STRUCTURE DETERMINATIONS AND PHASE TRANSITIONS IN $(Mn_{1-x}Fe_x)Sn_2$. B. Lebech, Condensed Matter Physics and Chemistry Department, Risø National Laboratory, Denmark, and A. Menshikov and A. Vokhmyanin, Institute of Metal Physics RAS, Ural Division, Ekaterinburg, Russia, and H. Shiraishi Shibaura Institute of Technology, Oomiya, Soitama 330, Japan

With the aim to determine the magnetic phase diagram of the $(Mn_{1-x}Fe_x)Sn_2$ system we have collected neutron powder diffraction data for x = 0, 0.1, 0.2, 0.4, 0.6, 0.7, 0.85 and 0.9. The diffraction diagrams have been measured at various temperatures in the temperature range from 5 to 300 K and they were analysed by means of profile structure refinement in order to map out the magnetic phase diagram. The intermetallic compounds $MnSn_2$ and $FeSn_2$ crystallise in the *bct* C16 crystal structure. $MnSn_2$ orders magnetically below T_N = 325 K to a collinear antiferromagnet with alternating spins in the [1 1 0] layers (+ – + –), *i.e.* to a spin structure with wave vector $\boldsymbol{k}$ = (½ ½ 0). At T_2 ~ 74 K, this spin structure changes to a double layered structure (+ + – –). Below T_N =380 K, $FeSn_2$ orders to a collinear magnetic structure with wave vector $\boldsymbol{k}$ = (1 0 0). At T_2 ~ 93 K, this structure becomes non-collinear.

A major part of our efforts have been concentrated on understanding the concentration dependence of the antiferromagnetic phase transition close to x_c ~ 0.8 in the $(Mn_{1-x}Fe_x)Sn_2$ system. In this concentration region, the antiferromagnetic order with wave vector $\boldsymbol{k}_1$ = (½ ½ 0) changes to another magnetic structure with wave vector $\boldsymbol{k}_2$ = (1 0 0). The neutron diffraction data show that non-collinear magnetic structures exist in the transition region. These may be described by two co-existing orthogonal wave vectors $\boldsymbol{k}_1$ = (½ ½ 0) and $\boldsymbol{k}_2$ = (1 0 0). However, so far it has been difficult to explain the change of the paramagnetic Curie temperature from positive to negative with concentration and we expect that the present detailed neutron diffraction study of the $(Mn_{1-x}Fe_x)Sn_2$ alloy system can help us to overcome this problem.

P06.13.022 KOHN-SHAM ONE MATRICES FROM X-RAY DIFFRACTION DATA. Garry T. Smith and Vedene H. Smith Jr., Department of Chemistry, Queen's University, Kingston, Ontario, Canada, K7L 3N6.

Least-squares analysis of experimental structure factor data for extraction of the one-particle electron density requires a suitable model to be used in the fit. The multipole models currently in use provide a good fit to the data and chemically informative electron densities and related properties. However the electron density so obtained does not meet the fundamental requirements of quantum chemistry, *i.e* the N-representability criteria. For example there is no requirement for a strictly positive density built into the model.

An alternative model of the charge density is as an expansion of basis function products leading to a one-particle density matrix which reproduces the experimental density. Additionally, this matrix may be tested for N-representability by examination of its eigenvalues. Unfortunately the mapping between density and density matrix is, in the general case, non-unique. However by minimising the kinetic energy within the constrained search formulation of density functional theory, one obtains the wavefunction of the non-interacting system. This is a single Slater Determinant, composed of the Kohn-Sham orbitals which are the eigenvalues of the fitted density matrix up to a unitary transformation.

Several fitted Kohn-Sham one matrices for the experimental structure factors from formamide in the Gaussian basis sets STO-6G, 6-31G* and 6-311G** are analysed for both local and non-local properties, especially the non-interacting kinetic energy $T_s[\rho]$ and the "exact" exchange energy.

P06.13.023 CHARACTERIZATION OF A Li···H-C AGOSTIC INTERACTION BY A TOPOLOGICAL CHARGE DENSITY ANALYSIS. M. Grosche, W. Scherer, M. Gardener, W. A. Herrmann, Anorganisch-chemisches Institut, Technische Universität München, Lichtenbergstr. 4, D-85747 Garching, Germany

Alkyllithium complexes are of fundamental importance in organic synthesis and as anion transfer reagents in organometallic synthesis. Their crystal structures display a remarkable range of bonding modes. Complexes featuring a *lithium coordination number of only 2* - as in the investigated compound $[\{2\text{-}(Me_3Si)_2ClicC_5H_4N\}_2]$ **1** - have been observed in a rare number of cases. Little is known about the details of interactions which compensate for the electron deficiencies of the metal centres in their reduced coordination state, and include, (i) close Li···Li contacts and (ii), close *"agostic" type Li···H-C interactions.*

Agostic interactions as displayed by **1** are also of particular interest in organometallic chemistry in view of their potential relevance to important processes like C-H activation in catalytic reactions. Reliable ways of pinning down these interactions are still at a premium, notwithstanding the numerous examples reported on the basis of structural or spectroscopic measurements or of theoretical studies [1].

The nature of Li···H-C agostic interactions has been investigated by topological analysis of experimental charge densities in **1**. Strong agostic Li···H-C interaction are signalled by short Li···H distances [2] (of around 2.20 Å which are ca. 0.7 Å less than the sum of the Van der Waals radii of the lithium and hydrogen atoms).

Preliminary charge density studies based on high resolution X-ray data ($\sin\theta/\lambda_{max}$ = 1.17 @ 100K) lead to reasonable topological parameters for all bond critical points.

1 W. Scherer, W. Hieringer, M. Spiegler, P. Sirsch, G. S. McGrady, A. J. Downs, A. Haaland and B. Pedersen, *J. Chem. Soc., Chem. Commun*., **1998**, 2471.
2 R. I. Papasergio, C. L. Raston and A. H. White, *J. Chem. Soc., Chem. Commun*., **1983**, 1419.

P09.13.001 THE ENDOHEDRAL STRUCTURES OF SCANDIUM METALLO-FULLERENES. E. Nishibori, M. Sakata, Department of Applied Physics, Nagoya University, Nagoya, Japan and M. Takata, Department of Material Science, Shimane University, Matsue, Japan and H. Shinohara, Department of Chemistry, Nagoya University, Nagoya, Japan.

The endohedral structures of scandium fullerenes, $Sc@C_{82}$ and $Sc_2@C_{84}$, are determined by the maximum entropy method (MEM) using synchrotron radiation powder data. The obtained MEM charge densities show a clear distinction of the endohedral natures of the mono- and di-metallofullerene.

From the MEM charge density of $Sc@C_{82}$, the cage structure of this molecule is determined to have C_{2V} symmetry. Inside the carbon cage, the Sc atom is located at an off-center position adjacent to a carbon six-membered ring. The nearest Sc-C distance determined from the MEM charge density is 2.53(8)Å. The charge transfer from Sc to fullerene is estimated as 2.2e.The Sc charge density has a saucer-like feature along the six-membered ring of the carbon cage.

The MEM charge density of $Sc_2@C_{84}$ clearly shows the D_{2d} symmetry cage structure. Inside the carbon cage, the Sc atoms are located in nearly symmetric positions with respect to the center of the cage. The encapsulated Sc-Sc distance and the nearest Sc-C distance are 3.9(1) Å and 2.4(1) Å. respectively. The positive charge of the Sc atom from the MEM charge density is determined as 2.2e. The charge transfer from Sc ions to fullerene is estimated to be 4.4e. The Sc charge density has tear drop feature as if the two Sc atoms are in a stretching vibration within the C_{84} cage.

The MEM charge density of $Sc@C_{82}$ molecule shows a strong contrast with that of $Sc_2@C_{84}$. The five and six-membered ring networks of $Sc_2@C_{84}$ can be seen more clearly than that of $Sc@C_{82}$.

P09.13.002 ELECTRON DENSITY DISTRIBUTION IN FAYALITE DETERMINED WITH SYNCHROTRON DATA. F.Marumo, Y.Tabira and M.Okui, Deptartment of Geosystem Sciences, Nihon University, Sakurajosui 3-25-40, Tokyo 156-8550, Japan, and N.Ishizawa, Materials and Structures Laboratory, Tokyo Institute of Technology, Nagatsuta 4259, Yokohama 226-8503, Japan, and O.Tamada,Graduate School of Human and Environmental Studies, Kyoto University, Kyoto 606-8316, Japan, and H.Takei, Faculty of Science, Osaka University, Toyonaka 560-0043, Japan.

Electron density distribution in a fayalite crystal (Fe_2SiO_4) has been re-examined by collecting diffraction data with 0.750Å synchrotron radiations. The specimen was shaped into a sphere with the diameter of 0.040 mm. The minimum and maximum transmission factors are 0.7235 and 0.7328 for the 200 and 74,11 reflections. The structure refinement with the free ion model converged to give the R and Rw values of 0.020 and 0.022 for 2047 independent reflections. In the difference Fourier map synthesized after the refinement, positive residual densities with 1.5 e $Å^{-3}$ heights are observed at positions about 0.5 Å apart from Fe(2) along the a-axis on either side of the atom. In addition, positive residual densities of about 0.5 e $Å^{-3}$ and 0.3 e $Å^{-3}$ heights are observed around Fe(2) at distances of 0.5Å along b. The map is much flatter around Fe(1) than around Fe(2). The highest peaks around Fe(1) have heights 0.5 e $Å^{-3}$, locating at 0.5 Å apart from Fe(1) approximately in the direction parallel to a. An ab-initio calculation of the electronic state was carried out by the DV-Xa method. Differences between the theoretical and promolecular electron densities were evaluated and compared with the experimental results. Features of the theoretical residual densities are qualitatively in an agreement with those of the experimental ones around Fe(2), whereas no good agreement was obtained around Fe(1). The estimated net charge of Fe(2) is larger than that of Fe(1) in conformity with the crystal chemical evidence

P09.13.003 BOND CHARACTERS OF MnS_2 BY SYNCHROTRON X-RAY DIFFRACTION AND MOLECULAR ORBITAL CALCULATIONS. S. Kuze, N. Ishizawa and M. Ueki, Materials and Structures Laboratory, Tokyo Institute of Technology, 4259, Nagatuta, Midori-ku, Yokohama 226-8503, Japan

MnS_2 is a paramagnetic semiconductor with a pyrite-type structure. Mn has a $3d^5$ electron configuration with the *d* electrons in the high-spin states. The electron density distribution of MnS_2 was investigated by single crystal X-ray diffraction with a horizontal-type four-circle diffractometer at KEK BL14A using synchrotron radiation with the wavelength of 0.75Å [1]. The least-squares refinement, employing atomic scattering factors of neutral atoms, yielded a final R/Rw value of 0.0119/0.0122 for 539 independent reflections in the range $2\theta<138°$. In the difference Fourier maps, an accumulation of electron density was found slightly off from the line connecting Mn and the first neighbour S.

To clarify the contribution of atomic orbitals to the bonding between Mn and S, DV-Xα molecular orbital calculations were carried out using the SCAT program package [2]. The result suggested that the 3*d* atomic orbitals of the Mn atoms and the 3*p* orbitals of the first and second neighbour S atoms were mixed together to form molecular orbitals which are responsible for the observed charge density topography between the Mn atom and S_2^{2-} molecule.

[1] M. Ueki, N. Ishizawa and F. Marumo, Presented at the second AsCA Meeting, Bangkok, Thailand (1995)
[2] H. Adachi, M. Tsukada, and C. Satoko, J. Phys. Soc. Jpn., 45, 875(1978)

P09.13.004 MAXIMUM ENTROPY ELECTRON DENSITY ANALYSIS OF CHEMICAL INTERACTIONS IN ANHYDROUS SODALITES. Bo Brummerstedt Iversen, Department of Chemistry, University of Aarhus, DK-8000 Århus C, DenmarK, Susan Latturner, Galen Stucky, Department of Chemistry, University of California, Santa Barbara, CA 93106, USA

We have carried out combined Rietveld and maximum entropy method (MEM) analysis on synchrotron X-ray powder diffraction data of a series of anhydrous sodalites, $M_6(AlSiO_4)_6$, M = Na, Ag, Tl. Analysis of the MEM electron densities reveals the nature of the interactions in the structures. The sodium atoms are bonded to the framework with predominantly electrostatic closed shell interactions, whereas the heavy metal ions form partly covalent bonds to the framework oxygens. At the same time the heavy metal atoms are close to being neutral, while the sodiums, as expected, are positively charged. The differences in the atomic charges and in the chemical interaction between the guest atoms and the framework can explain the varying dynamical behaviour of the guest atoms. While the alkali system exhibit a phase transition due to dipole-dipole interactions creating an ordering of the metal atoms, the heavy metal systems remain pseudocubic with a locked in static disorder. The guest-host interactions have pronounced effects on the framework atoms with Al, especially, showing reduced density. The removal of electron density from the framework bonds upon formation of covalent guest-host bonds

is the cause of the abnormal chemical shifts and quadrupole coupling constants found in NMR for the heavy metal compounds.

The thallium compound is of particular interest due to the presence of a completely regular array of quantum confined Tl clusters. The electron density does not show evidence of stereoactive lone pairs, which are often postulated to be present in low valent Tl-compounds. It is furthermore found that the Tl cluster has weak covalent bonding interactions between every pair of Tl atoms in the cluster. This is somewhat at variance with *ab initio* calculations on simple RTl-TlR model dimers, and may be a result of the ability of porous frameworks to alter the electronic structure, and thereby the chemical reactivity, of suspended guest species. The fact that experimental electron densities can be derived from powder diffraction data gives great promise for increasing the understanding of the chemical and physical properties of a wide range of technologically important materials.

P09.13.005 ELECTRON AND NUCLEAR DENSITIES OF HYDROGEN IN KDP AND ADP BY MAXIMUM ENTROPY METHOD. Shigefumi Yamamura and Yoko Sugawara, Department of Physics, School of Science, Kitasato University, Sagamihara 228-8555, Japan and Masaki Takata, Department of Material Science, Interdisciplinary Faculty of Science and Engineering, Shimane University, Matsue 690-8504, Japan and Makoto Sakata, Department of Applied Physics, Graduate School of Engineering, Nagoya University, Nagoya 464-8603, Japan.

In order to investigate the nature of the hydrogen bond, the electron and nuclear density distributions of KDP (KH_2PO_4) and ADP ($NH_4H_2PO_4$) were obtained by the maximum entropy method (MEM) using X-ray and neutron powder diffraction data. In this study, no single crystals and no deuterated samples were used, although single crystal analysis is believed to provide accurate structural information compared with powder one and deuterated specimens are often used for neutron diffraction experiments with hydrogen compounds to reduce the large incoherent scattering from protons.

KDP and ADP is hydrogen-bonded ferro- and antiferroelectrics, respectively. In both compounds, hydrogen atoms are considered to play an important role in phase transition and the phase transition temperature is increased by about 100 K when hydrogen atoms are substituted by deuterium atoms. In order to explain such a large isotope effect, it is necessary to understand the behavior of hydrogen as well as that of deuteron. In this study, it is demonstrated that the nature of the hydrogen bond in KDP and ADP can be described by MEM using only powder data. It is not an easy task to detect the precise electron and nuclear density distributions of hydrogen bond, because the scattering power of hydrogen for X-ray is markedly lower than that of other elements and the large incoherent scattering from protons cannot be avoided in neutron diffraction experiment.

The data sets used in the analyses were collected at the Photon Factory, Tsukuba for X-ray data and at Japan Atomic Energy Research Institute, Tokai for neutron ones. The powder data were analyzed by a sophisticated method which is the combination of Rietveld method and MEM.[1] From the MEM electron density maps in O-H-O hydrogen bond at room temperature, hydrogen shows no local maxima but contour lines link two O atoms. This feature is consistent with corresponding nuclear density maps in which proton shows double maxima in the two O atoms. Furthermore, it could be detected that the electron density distribution of N-H-O, another hydrogen bond in ADP, shows rather ionic nature, which is different from that of O-H-O.

[1] M. Takata *et al.*, Nature (London), **377** (1995) 46.

P09.13.006 MULTI-POLE ANALYSIS OF HEXA-METHYLENETETRAMINE IN REAL SPACE USING MEM ELECTRON DENSITIES. T.Ikeda and M.Sakata, Department of Applied Physics, Nagoya University, Nagoya, Japan and M.Takata, Department of Material Science, Shimane University, Matue, Japan

In conventional multi-pole analysis, the least squares calculations are executed in reciprocal space by using multi-pole structure factors, although a multi-pole electron density model is constructed in real space. Multi-pole structure factors are, of course, the Fourier transformation of multipole electron density model. This process may cause unnecessary complexities and severe co-relations between multi-pole parameters. By using the Maximum Entropy Method (MEM), it is now possible to derive an electron density distribution, which is consistent with the observed structure factors. This brings a new possibility to perform a multi-pole analysis in real space. In this study, we tried a real space multi-pole analysis that is to fit the multipole density model to the MEM in the case hexamethylenetetramine ($C_6H_{12}N_4$).

X-ray diffraction data is collected by powder method using Synchrotron Radiation at KEK PF BL-6A$_2$. Electron densities are obtained by the combined analysis of MEM and Rietveld method. Multipole refinement is executed in real space by using Stewart model. Multi-pole densities are agreed with MEM densities except core regions. From the obtained multipole deformation map, the strong C-N and the weak C-H covalent bond electrons are clearly shown. It should be noted that the real space multi-pole analysis does not suffer severe co-relation of parameters and that MEM charge densities helps to construct multi-pole model.

P09.13.007 CHARGE DENSITY DATA SETS FROM 1 AND 2 K CCD DETECTORS, MO AND AG RADIATION, N_2 AND He COOLING. A.A. Pinkerton, P. Burckel, Y.-S. Chen, K. Kirschbaum, A. Martin and D. Parrish, Department of Chemistry, University of Toledo, Toledo, OH 43606, USA.

A series of charge density studies have been carried out on a number of small organic molecules. All data were collected with SMART platform diffractometers. Some used a 1 k CCD detector, others a 2 k CCD detector. Some were measured using liquid nitrogen cooling (90 K), others were cooled with liquid helium (20 K). Some were measured using Mo-Kα radiation, others using Ag-Kα radiation.

The differences in the data collection protocols using the various experimental conditions will be presented. The quality of the data thus obtained will be statistically analyzed. Selected deformation maps will be presented for comparison purposes.

P09.13.008 EXPERIMENTAL ELECTRON DENSITY ON COBALT BISHYDROGENMALEATE TETRA-HYDRATE. N. G. Fernandes, M. D. D. Costa, Department of Chemistry, Federal University of Minas Gerais, CP 702, 31270-901, Belo Horizonte, Br

Metal hydrogenmaleate, M(C4H3O4)2(H2O), M = Mn, Fe, Co, Ni, Zn are known be isomorphic with ligand and water molecules forming a infinite network of H-bonds and a short intramolecular hydrogen bond. The present work reports a deformation refinement for cobalt compound.

X-ray data were collected on a SIEMENS four-circle diffractometer at 100K, using MoKα radiation up to $\sin\theta/\lambda$ = 1.20Å^{-1}. For a P space group, 9529 reflections were measured, 8089 unique reflections. In the final refinement, R(F^2) = 0.0487, wR = 0.0513.

The short hydrogen bond has a O---O distance of 2.415(1)Å, it is a quasi-linear intramolecular hydrogen bond. The

cobalt atom is surrounded by six oxygen atoms in a octahedral arrangement .

Static deformation density maps show Co atom in a pseudo 4/mmm site symmetry. In the water molecules two distinct maxima of ~0.50 e/Å^3 and lower broad peak of ~0.20 e/Å^3 in the lone pair region. For the short hydrogen bond, O---H---O, there are two maxima of 0.20 e/Å^3 between O---H bonds. Deformation maps also show that there are two types of C-C in the ligand.

P09.13.009 A CHARGE DENSITY STUDY ON THE INTER-METALLIC COMPOUNDS $MgZn_2$ AND $MgCu_2$ BY THE MAXIMUM ENTROPY METHOD. Yoshiki Kubota, Masaki Takata[1], Makoto Sakata[2], Takuya Ohba[3], Kouichi Kifune and Tsugio Tadaki, Department of Natural Science, Osaka Women's University, Sakai, Osaka 590-0035, Japan, [1]Department of Material Science, Shimane University, Matsue 690-8504, Japan, [2]Department of Applied Physics, Nagoya University, Nagoya 464-8603, Japan, [3]Department of Materials Science and Engineering, Teikyo University, Utsunomiya 320-8551, Japan.

The charge density distributions of the intermetallic compounds $MgZn_2$ and $MgCu_2$ were obtained by the maximum entropy method (MEM). In the MEM charge density map of $MgCu_2$, the overlapped electron densities were seen between the Cu atoms. It is probably due to the hybridization of atomic orbitals to form Cu-Cu covalent bond. There are practically no overlaps of electron densities between Mg atom and Cu atom. It was found that the Cu-Cu covalent bond is forming a tetrahedral kagome network. By the geometrical consideration, such a feature of bonding with six lobes can be interpreted as p^3d^3 hybridization. In addition to the Cu-Cu bond, the shift of bonding electron from the line connecting the Cu atoms toward the Mg atom was found. The valence of Mg atom was estimated to be about +2. This shows that there are an ionic interaction between the Mg atom and the hybridized orbitals.

As for the $MgZn_2$, the fundamental features of the charge density, which are the covalent bond between the Zn atoms, the shift of bonding, were essentially the same as $MgCu_2$. But the MEM map of $MgZn_2$ shows the less covalency within the kagome net plane. By the geometrical consideration, the bonding due to the p^3d^3 hybrid orbitals has a slight distortion by the hexagonal zigzag stacking sequence in $MgZn_2$, while the tetrahedra with sharing corners by the ABCABC stacking sequence in $MgCu_2$ does not distort p^3d^3 hybrid orbitals. It may be interpreted that the distortions of the p^3d^3 hybrid orbitals cause a decrease of bonding electrons of the kagome net plane in $MgZn_2$. The analysis for $MgNi_2$ is now in progress.

P09.13.010 SOME CHARACTERISTICS OF MEM CHARGE DENSITIES OBTAINED FROM UNIFORM PRIOR DENSITIES IN COLLINS' FORMALISM. M.Sakata, S. Morishita, T.Ikeda and E.Nishibori, Department of Applied Physics, Nagoya University, Nagoya 464-8601, Japan and M.Takata, Department of Material Science, Shimane University, Mtasue 690-8504, Japan

Collins (1982) developed a simple method to solve the Maximum Entropy (ME) equation. In his method, the prior density($\mathbf{r}$) at pixel $\mathbf{r}$ are replaced at each iteration by newly obtained density($\mathbf{r}$). It enables us to solve ME equation either from uniform or non-uniform prior density distribution. It is not well established what kind of prior densities to be used. The answer of such a question may not be just one but can be dependent what for ME used. The purpose of this study is to describe some characteristics of MEM charge density distribution to provide more materials to have the better answer for the question.

In a simple structure such as Be or CeO_2, so called artifact exists. When it appear, the artifact appears always at high symmetry position in a unit cell. In complicated structures, it does not appear. In the case of CeO_2, it disappears as the number of reflections is increased. Such an artifact is also found in difference Fourier map in CeO_2. In Be case, the appearance of the artifact is related what kind of error bar, □ is used. It is extremely difficult to conclude whether so called artifact in Be is purely artifact or just exaggerated.

It must be pointed out that it is not possible to derive 'true' or 'exact' electron density distribution from limited number of structure factors with ambiguities. This is why 'Entropy'; the measure of uncertainties, is introduced to analyze the experimental data which are limited and have some ambiguities. It must be advisable in many cases to use uniform prior knowing such characteristics of MEM charge densities rather than trying to find out the 'exact' densities by using non-uniform prior or some other method since the number of data experimentally available is always limited. It seems the ME method is based on the idea that the truth will never out.

1. D. M. Collins (1982) *Nature,* **298**, 49-51.

P09.13.011 AN ELECTRON DENSITY STUDY OF UREA-PHOSPHORIC ACID ADDUCT AT 100K. B. L. Rodrigues, N. G. Fernandes [1], R. Tellgren [2], [1] Department of Chemistry, Federal University of Minas Gerais, CP 702, 31270-901 - Belo Horizonte, Brazil, [2] Institute of Chemistry, University of Uppsala, Box 531, S-751 21 - Uppsala, Sweden.

The experimental electron density of the adduct compound $H_3PO_4.CO(NH_2)_2$ is reported. Phosphoric acid and urea are linked by a N-H---O bond and a very short O---H---O bond [d(O-O)=2.415(1)Å]. Data was interpreted using the Hirshfeld formalism. In the final model, 216 parameters were refined, R(F2)=0.0455 and wR(F2)=0.0529 for 7257 independent reflections.

Deformation density maps show maxima of 0.40e/Å^3 between phosphorus and hydroxyl oxygens, while two remaining P-O bonds have peak maxima of 0.50 e/Å^3. The electron density distribution in Urea region is similar to previous study on urea crystal [1].

The N-H---O bond has of electron density excess of 0.20e/Å^3 in the O---H line near oxygen. It is also observed in this line a depletion of 0.30e/Å^3 close to hydrogen atom. All other long hydrogen bonds in this compound have similar electron distribution. On the other hand, in the short O---H---O bond, there are two maxima peak heights of 0.40 and 0.60e/Å^3 approximately equidistant of O and H atoms.

1. Swaminathan, S.; Craven, B. M.; Spackman, M. A & Stewart, R. F. (1984) Acta Cryst, B40, 398 - 404.

P09.13.012 THE CHARGE DENSITY ANALYSIS OF 1,4,8,11-TETRATHIACYCLOTETRADECANE USING CCD DATA. Michael D. Carducci and John H. Enemark, Department of Chemistry, University of Arizona, Tucson, Arizona 85721

Recent advances in X-ray detector technology and data analysis software have greatly improved the results which can be obtained from charge density analysis of high quality, low temperature X-ray diffraction data sets. The remarkable increase in speed with which CCD area detectors allow data sets to be collected eliminate or greatly reduce error due to long term icing problems, X-ray beam stability(or availability) and crystal decay. Coverage of reciprocal space is more complete, has a higher redundancy, and is of higher accuracy, especially for weak reflections, when an area detector is utilized. At the same time, the software available for analyzing that data has matured from simply modeling the observed density to include determining molecular

properties and displaying results in color and multiple dimensions with the latest computer graphics techniques.

1,4,8,11-Tetrathiacyclotetradecane (TTCD) was previously examined in this laboratory [1] utilizing a serial diffractometer and the refinement program Molly [2]. Those results, which suffered from time dependent errors during two months of data collection, will be compared with a new data set determined with a CCD area detector diffractometer and refined with the XD package [3].

1. Carducci, M.D. and Enemark, J.H. ACA Annual Meeting Albuquerque NM, May 24,1993 Abstract:PG04.
2. Hansen, N.K. and Coppens, P. Acta Crystallogr. A**34**,909 (1978)
3. Koritsanszky, T., Howard, S., Mallison, P.R., Su, Z., Richter, T. & Hansen, N.K. XD. A Computer Program Package for Multipole Refinement and Analysis of Electron Densities from Diffraction Data. User's Manual. Free University of Berlin, Germany. (1995).

P09.13.013 DETERMINATION OF CHARGE TRANSFER AND IONICITY BY ELECTRON DIFFRACTION. J. Tafto [1], Lijun Wu, Yimei Zhu [2], [1] Department of Physics, University of Oslo, PO Box 1048, Blindern, N-0316 Oslo, Norway, [2] Materials Science Division, Department of Applied Science, Brookhaven National Laboratory, Upton, NY 11973, USA

In electron diffraction, the structure factors of reflections at low scattering angles are strongly influenced by the distribution of the valence electron distribution in the crystal. This makes electron diffraction an excellent technique to study charge transfer, in particular in crystals with large unit cells and thus reflections at very short reciprocal distances. We use convergent beam electron diffraction and focus the electron probe above a thin wedge-shaped area. By this procedure we acquire shadow images and thickness fringes of many reflections simultaneously [1].

We have used this approach to study the spatial distribution of divalent and trivalent iron in the crystal unit cell of magnetite, and to determine the electron hole distribution in high temperature superconductors. Our results are consistent with the hole distribution reported by other investigators based on electronic structure calculations, and the distribution which is inferred from bond valence calculations using accurate atomic positions from neutron diffraction data.

1. J. Tafto, Yimei Zhu & Lijun Wu (1998) Acta Cryst. A54, 532

P09.13.014 ELECTRON DENSITY IN VANADIUM PENTOXYDE. Jean-Michel Savariault, Centre D'elaboration De Materiaux Et D'etudes Structurales - CNRS, 29 Rue Jeanne Marvig - BP 4347, 31055 Toulouse Cedex 4, France.

The vanadium oxide bronzes appear more and mode interesting as material electrode in lithium batteries and more recently as compounds with highly correlated electrons (spin chained, spin ladder, spin frustration...). The interpretation of such behaviours assumes that the starting material is well known. The divanadium pentoxide with a formula similar to the diniobium pentoxide exhibit a different structure. In order to understand these structural variation and such behaviours, the determination of the electron density in the divanadium pentoxide was undertaken by X ray diffraction. The measurement was performed at 135K with molybdenum radiation on a CAD4. The X-X technique was used and the cut-off was chosen at $0.8\ \text{Å}^{-1}$. The electron density around the vanadium atom appears as a dz^2 function oriented towards the O vanadyl, an accumulation of density along the axis and a deficiency in the plane of the layer perpendicular to the axis. The different sections show that each vanadium oxygen bonds exhibit different electron density distribution. The shape of each density around atoms will be discussed in term of bond type. A multipole treatment allows to extract information's about the charges on the atoms and the d orbital population around vanadium.

P09.13.015 CRYSTAL ORIENTATION DETERMINATION IN VCIP METHOD FOR ACCURATE MEASUREMENTS. K.Tanaka, E. Zhurova, [1] Y.Takenaka [2]. [1]Dept. Mat. Sci. & Eng., Nagoya Inst. Tech., Gokiso-cho, Showa-ku, Nagoya, 466-8555 [2}Hokkaido Univ. Education at Hakodate, Hachiman 1-2, Hakodate, 040, Hokkaido.

Vacuum camera (VC) is an evacuated cylinder with an imaging plate (IP) on the inside wall and allows for data collection by oscillation method. It enables to measure intensities without air-scattering. VC's are installed at our lab. and BL02B1 of SPring-8. It gave us Bragg peaks clearly at high angles. We call this method as VCIP (Vacuum Camera Imaging Plate) method. In spite of the advantage, refinement of intensity data of KNiF3 measured with VCIP gave almost the same results as those measured with four-circle diffractometer. The reason for it is quite clear. We could not get crystal orientation accurate enough to correct for systematic errors.

Since in our present VCIP method VC is removed from the diffractometer after each measurement and IP is also removed from VC for intensity readout, camera and detector parameters, and crystal orientations need be determined from the measured peak positions on IP. The correlations among them were analyzed and they were refined with the least-squares method. The camera parameters are;film radius, inclination of VC and displacement of the camera center from the crystal position. The film parameters are; incident beam position and IP rotation in the readout system. And each element of the orientation matrix of the crystal is refined. Finally observed and calculated peak positions of KNiF3 agreed within a pixel of 0.05x0.05mm2.

P09.13.018 STRUCTURAL PROPERTIES AND ELECTRON DENSITY DISTRIBUTION OF LUNI$_2$B$_2$C. U. Jaenicke-Roessler, P. Paufler and G. Zahn, Institut für Kristallographie und Festkörperphysik, Technische Universität Dresden, D-01062 Dresden, Germany.

Superconducting materials of the RT_2B_2C type (R=rare earth metal, T=transition metal) are of much interest concerning their physical and structural properties because of their relatively high superconducting transition temperatures T_C and because of the interesting interaction between superconductivity and magnetic ordering phenomena that they exhibit.

Single crystalline samples of $LuNi_2B_2C$ (a=3.46084 Å, c=10.63406 Å, space group (139) I4/mmm-edba, tI 12, T_C=16.6K [1]) were examined by monochromatized MoK_α radiation on a STOE Stadi4 four-circle-diffractometer at 15 different temperatures from T_1=360 K down to T_{15}=90 K. Precise lattice parameters were determined by a profile-fitting method utilising α_1-α_2-splitting of reflections at higher 2ϑ angles, refined over all reflections of the data collection with a certain I/σ_I-ratio. Data collection was carried out over a 2ϑ range from 3° to 120°, measuring a half sphere with Friedel pairs at -2ϑ, accounting to a total of 4242 reflections, thus reaching a resolution of 0.4103 Å. Agreement factors R of the least square refinements lie at about 2.4 % for all data.

Expansion coefficients α_a vary between $1.23\cdot10^{-5}$ K^{-1} and $0.422\cdot10^{-5}$ K^{-1}, α_c between $0.0918\cdot10^{-6}$ K^{-1} and $-3.38\cdot10^{-6}$ K^{-1} and bulk expansion β between $2.57\cdot10^{-5}$ K^{-1} and $1.06\cdot10^{-5}$ K^{-1}, at T_1 or T_{15}, respectively. They are smaller than for other RNi_2B_2C compounds we examined. α_c reverts sign as it does for other RNi_2B_2C compounds, too, but at a much lower temperature (at about 140 K).

The free structure parameter z_B (0.1392(4)) and the tetrahedral angle B-Ni-B' α (108.4(1)°) were examined with regard to temperature, but no significant dependence was found

taking the errors into consideration. Anisotropic temperature factors have been determined, confirming the general tendency for these compounds, that U_{ij} parallel to the c direction have the highest values.

Electron density distribution was refined for the first time starting from our measured intensities and contours were drawn [2]. These results were compared to theoretical considerations according to [3].

Our thanks are due to H. von Lips for supplying the specimens.

References

[1] T. Siegrist, H.W. Zandbergen, R.J. Cava, J.J. Krajewski, and W.F. Peck, Jr., Nature (London) **367**, 254 (1994).

[2] T. Koritsanszky, S.T Howard, Z. Su, P.R. Mallinson, T. Richter and N.K. Hansen: XD: Computer Program Package for Multipole Refinement and Analysis of Electron Densities from Diffraction Data (4.95).

[3] P. Ravindran, B. Johansson, O. Eriksson: Electronic structure, chemical bonding, phase stability, and ground state properties of $YNi_{2-x}(Co/Cu)_xB_2C$. Phys. Rev. B **58**, 3381 (1998).

P09.13.019 X-RAY STRUCTURE BIAS DUE TO WAVELENGTH DISPERSION. A.T.H. Lenstra, B. Rousseau, Dep. Of Chemistry, University of Antwerp (UIA), Belgium.

While the phenomenon of dispersion is well known, its impact on the x-ray structure determination is seldom realized. We studied the various aspects with a standard CAD4-diffractometer in combination with an x-ray tube. This setup is representative for the usual situation in structure analysis.

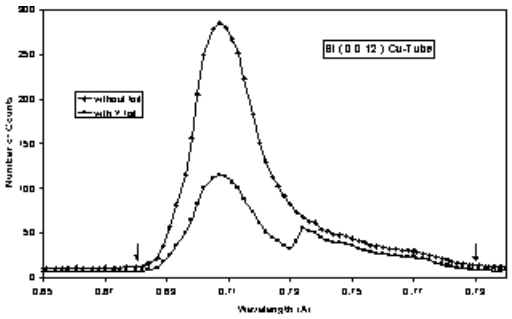

The spectral distribution in a monochromated x-ray beam with λ = 0.71Å was analyzed via a Si (0 0 12) reflection. The beam spectrum – here in the absence of the characteristic Mo-K_α intensity – is shown in Figure 1. We observe a wavelength dispersion $\Delta\lambda/\lambda$ of 0.15 with λ_{min} = 0.68Å and λ_{max} = 0.79Å.

During data collection intensity measurements are made using a scan angle given by (a + b tg θ)° with b = $\Delta\lambda/\lambda$ 360/2π. With $\Delta\lambda/\lambda$ = 0.15 this scan angle becomes larger than the separation between individual Bragg spots along, say, C*. In our analysis of $NiSO_4.6H_2O$ (space group $P4_12_12$; a=6.782Å, c=18.274Å) we used a scan angle of (1.3 + 0.4 tg θ)°. This scan range is tailored to $\Delta\lambda/\lambda$ of 0.007 only. Therefore the practical scan underestimates the real reflection intensity due to spectral truncation. The truncation error increases with θ. Since B is the only model parameter linking I to θ, the spectral truncation leads to biased ADP-values with $B_{model} > B_{true}$.

The size of the truncation error is maximal in the absence of characteristic radiation. When the $\Delta\lambda$-window includes K_α emission lines the truncation error is minimal at the highest tube voltage.

Atom	Cu λ=0.71 Å	Mo-25kV λ=0.71 Å	Mo-50kV λ=0.71 Å	Synchrotron λ=0.64 Å
Ni	1.57(2)	1.285(5)	1.120(4)	1.020(8)
S	1.88(4)	1.466(7)	1.300(5)	1.215(12)
O1	2.90(10)	2.64(3)	2.46(2)	2.42(6)
O2	2.68(6)	2.36(2)	2.18(2)	2.11(5)
OW1	2.90(10)	2.47(3)	2.29(2)	2.22(5)
OW2	2.40(10)	1.89(2)	1.76(1)	1.64(4)
OW3	2.32(9)	1.80(2)	1.66(1)	1.57(4)

The impact of the truncation errors on the ADP's in $NiSO_4$ is shown in the table above, which includes a synchrotron model measured at Brookhaven with λ = 0.643Å. These ADP's are free from truncation-error because $\Delta\lambda/\lambda \approx 0.0002$. ΔB's between different measuring schemes appear to be temp. independent.

14. DIFFRACTION PHYSICS AND OPTICS

P06.14.002 THEORETICAL ANALYSIS OF SURFACE CONTRIBUTION TO TDS OF X-RAYS S.A.Grigoryan, I.A. Vartanyants, M.V.Kovalchuk. A.V. Shubnikov Institute of Crystallography, Leninsky pr. 59, 111395 Moscow, Russia.

Third generation synchrotron radiation facilities gives unique possibility for the study of inelastic X-ray scattering processes. One of such inelastic decay channels is Thermal Diffuse Scattering (TDS) of X-rays on thermal phonons. In the previous papers it was assumed, that the main contribution to the yield of the TDS is coming from inelastic scattering of X-rays on the volume acoustic modes of thermal vibrations. In this paper theoretical analysis is made for the contribution of the surface excitations to this process. The most effective way to take into account this processes is to express correlation function of atomic displacements through the corresponding Green functions of the elasticity theory. It will be shown that in the long wavelength limit of acoustic modes the contribution of the surface excitations to the TDS near the surface is becoming comparable and can even exceed the volume one. Peculiarities of the process while the dynamical scattering of X-rays, when in the crystal due to coherent superposition of the incident and diffracted wave exist the X-ray standing wave will be also discussed.

P06.14.003 BRAGG DIFFRACTION FOCUSING TECHNIQUES FOR NEUTRON SCATTERING INSTRUMENTATION. P. Mikula and M. Vrana, Nuclear Physics Institute, 250 68 Rez near Prague, Czech Republic, and M. Ono, Kyoto University Reactor Research Institute, Kumatori, Japan, and V. Wagner, Physikalisch Technische Bundesanstalt, 38116 Braunschweig, Germany.

By a simple implementation of the bent-perfect-crystal (BPC) elements on conventional scattering devices one can considerably benefit from real or/and momentum space focusing, especially for small slit-like samples. Working with open beams without Soller collimators [1-3] and with position sensitive detectors (PSD) such devices can be dramatically superior to the conventional ones equipped with flat mosaic crystals and multidetectors. A double crystal diffractometer equipped with the BPC elements can be effectivelly used for a high resolution SANS. In single crystal diffraction the nondispersive arrangement can be adjusted even in case of the different lattice constants d of the monochromator and the sample. In powder diffraction, contrary to the conventional case (a minimum Δd-resolution takes place for $2\tan\theta_S = \tan\theta_M$), by setting a proper monochromator radius $R_M = 2\,L_{MS}/[\sin\theta_M(2 - \tan\theta_M/\tan\theta_S)]$, where L_{MS} is the monochromator-sample distance and $2\theta_M$ is the monochromator take-off angle, the minimum of the Δd-resolution can be shifted to higher scattering angles $2\theta_S$. Then, combined with super-mirror guides and PSD focusing devices may represent a new generation of thermal neutron-scattering instruments which make optimal use of the available neutron flux and achieve high intensities and excellent resolution. Examples of the powerful use of the Bragg diffraction optics for routine neutron scattering experiments in diffractometers of NPI Øež, KURRI Kumatori and PTB Braunschweig will be demonstrated.

1. P. Mikula, V. Wagner & R. Scherm, PTB-Report, PTB-N-17, Braunschweig, June 1994, p. 1-32.
2. M. Popovici & W.B. Yelon, J. Neutron Research, 3 (1995) 1-25.
3. P. Mikula, J. Kulda, P. Lukas, P. Strunz, J. Saroun, M. Vrana & V. Wagner, PTB-Report, PTB-N-29, Braunschweig, November 1997, p. 1-53.

P06.14.004 NONCOMMUTATION OF PAULI SPIN OPERATORS DUE TO BALANCED GEOMETRICDAL AND DYNAMICAL PHASES. Y. Hasegawa* and G. Badurek, Institute of Nuclear Physics, Vienna University of Technology, Stadionallee 2, A-1020 Wien, Austria.

Neutron spin polarimetry, which is essentially grounded on the application of Pauli spin operators, has turned out as a powerful tool to clearly demonstrate or even to verify some of the foundations of quantum mechanics. We performed a neutron polarimetric experiment to demonstrate the noncommutation properties of the Pauli spin operators. The polarization of the transmitted neutron beam depends upon the sequential order of two successive spin flip devices with mutually inclined precession axes. It is shown that the phase shift caused by the two successive spin rotations carries specific information about the intermediate state and finally results in the well-known commutation relation of Pauli spin operators. Furthermore, an interpretation of the observed results is presented in terms of an intrinsic phase shift between two interfering mutually orthogonal spin states, which in a sequence of two successive spinor transformations stores particular information about the intermediate state. We discuss this phase shift with respect to its geometrical and dynamical components and its formal connection with the non-commuting properties of Pauli spin operators is explicitly shown.

Y. Hasegawa, S. Menhart, R. Meixner, and G. Badurek, Phys. Lett. A 234 (1997) 322-328.

P12.14.001 PERFORMANCE EVALUATION FOR MULTILAYER OPTICS USING RAY TRACING METHOD. Boris Verman, Karsten Dan Joenson, and Licai Jiang, Osmic, Inc., 1788 Northwood, Troy, Michigan, USA.

A novel multilayer beam conditioning optic, called Confocal Max-Flux® (CMF) Optics, was proposed and tested for hard x-rays in the last two years [1]. These new optics have been applied to a variety of applications such as x-ray diffraction and small angle x-ray scattering. Experimental evidence has shown that flux and many other system parameters are significantly improved by using CMF optics. This paper will discuss the performance evaluation of CMF optics by means of ray tracing compared against experimental results.

The performance of the optical systems studied depends on many factors including the optical layout, multilayer characteristics, x-ray source characteristics and specific applications. In this paper, the source model is described first, then the performance of some standard ideal CMF optics are discussed. Special attention is paid to obtaining parameters relevant for various applications: beam width, flux, divergence etc. The effect of optical imperfections such as curvature and d-spacing errors are discussed, and related to present state-of-the-art capability. Finally the authors will discuss possible improvements to current optics and propose new optics for different applications.

[1] Confocal graded d-spacing multilayer beam conditioning optics. Boris Verman, Licai Jiang, Bonglea Kim, Rick Smith, and Nick Grupido, Advances in X-ray Analysis, 1998.

P12.14.002 LOWERING TAILS OF DIFFRACTION PROFILES. Go Fujinawa, X-ray Research Laboratory, Rigaku Corporation, H. Toraya, Ceramics Research Laboratory, Nagoya Institute of Technology, and J. L. Staudenmann, Physics Department, National Institute of Standards and Technology.

Parallel-slit analyzer (PSA) was developed for lowering tails of profiles in powder and thin-film diffraction. Four kinds of foil materials, sintered and hot-pressed tungsten (W), cold worked

stainless steel (SUS) and Be-bronze ($Cu_{4\ 98}Be_{4\ 2}$), and chemically surface-processed Be-bronze (CuO_x) were used for constructing PSA's. They were tested in a parallel-beam geometry using CuKα radiation collimated with a graded *d*-spacing parabolic multi-layer. The W- and CuO_x-PSA's gave the pseudo-Voigt profiles of ~80% Gaussian for direct beam. Rough surfaces of sintered and hot-pressed W and chemically surface-processed CuO_x foils are considered to be effective for depressing the total reflection on the surfaces of foil materials, and consequently for lowering the tails of diffraction peaks.

P12.14.003 MONOCRYSTAL X- RAY OPTIC ELEMENTS. N.Yu.Strelnikova, V.V.Lider, M.V.Kovalchuk [1], N.V.Zhavoronkov [2], [1] Institute of Crystallography RAS, Leninsky pr. 59, 117333 Moscow, Russia, [2] Research Institute of Material Science and Technology, 103460 Moscow

Crystal monochromators and analyzers are widely used for structural characterization of solid matter utilizing X- ray tubes or synchrotron radiation (SR). Institute of Crystallography RAS and Research Institute of Material Science and Technology had gained great experience in parameter calculations of separate optical elements and their assembles [1], their manufacture and characterization. This monocrystal X- ray optic elements are [2]: flat symmetric and asymmetric monochromators for X- ray beam of desired angle- and spectral divergence formation; monolithic grooved monochromators for X- ray beam formation without changing the direction of primary beam and (or) for forming the beam with homogeneous angle intensity distribution; flat triangle monochromators for X- rays focusing; monochromators of complicated configurations for sagittal focusing; water- cooled monochromators of different configurations [3] for effective SR beam thermoloading elimination.

1. V.V.Lider (1991) Nucl. Instrum. and Methods, A308, 407.
2. V.V.Lider, M.V.Kovalchuk, N.V.Zhavoronkov, S.I.Mazurenko (1997) Collection of papers of National Conference on using X-rays, SR, neutrons and electrons for Material Investigations, Dubna, Vol.2,289.
3. R.G.Silfhout (1998) Synchrotron Radiation News, 11, 11.

P12.14.004 DOUBLE CRYSTAL MONOCHROM-ATORS FOR SYNCHROTRON RADIATION. Yu.N.Shilin, V.A.Shishkov, M.V.Kovalchuk, V.V.Lider, S.I.Zheludeva Institute of Crystallography RAS, Leninsky pr. 59, 117333 Moscow, Russia

Double crystal monochromator for synchrotron radiation (SR) was designed to provide smooth change of X- ray beam energy in wide range without exit beam position changing, and higher harmonics suppretion [1]. Three modifications of monochromator are proposed: Model 1. X- ray beam energy change is realized by translation of Bragg axis of second crystal-monochromator along horizontal guide in the SR beam direction. Model 2. Horizontal translation of both crystal - monochromators is provided. This design permits to enlarge the changeable exit beam energy region (see Table). Model 3. As the model 1, has only one movable Bragg axis, but is more compact at the cost of the soft X- ray spectrum region (less required than the hard one). All modifications are remote- controlled and supplied with vacuum chambers; modules of second crystal- monochromator are high- precision torsion goniometers with piezodriver; there are possibilities of water- cooling of the first- and sagittal curvature of the second crystal-monochromator.

	Model 1	Model 2	Model 3
Region of Bragg angle	5 - 80°	3 - 87°	5 - 25°
Region of exit Si(111)	2.01 - 23	1 .98 - 38	4 .7 - 23
Beam energy (keV) Si(311)	3.85 - 44	3.79 - 72	9.0 - 44
Region of translation (mm)			
1-st crystal	0	715	0
2-nd crystal	640	715	365
Max. dimensions of crystals	60x80x10 mm3		

1. V.V.Lider, M.V.Kovalchuk, S.I.Zheludeva, A.Ja.Krejnes (1998) Poverchnost , 8 - 9, 21.

P12.14.005 DIAMOND MONOCHROMATOR-SPLITTER FOR SYNCHROTRON RADIATION WITH IMPROVED REFLECTIVITY. V.V.Lider, L.V.Samoilova, M.V.Kovalchuk, S.I.Zheludeva. A.V.Shubnikov Institute of Crystallography RAS, Leninsky pr. 59, 117333 Moscow, Russia.

The thermoelastic tolerance and transparency for X- rays of diamond crystals are the main reason to use them as powerful synchrotron radiation (SR) beam monochromators and splitters [1,2]. One of their disadvantages is low scattering capacity. Studying results [3] to avoid this drawback it is proposed to use diamond crystalline plate with thin damaged layer as a monochromator. Layer is formed on the entrance surface by mechanical grinding and polishing. Applying symmetrical Laue reflection (422) and $Mo_{K\alpha}$ radiation the experimental value of integral intensity of X- ray beam, diffracted on diamond plate 0.9mm thick was 2.5 times larger, than the theoretical one. At the same time the intrinsic FWHM of the rocking curve was 1.3 sec.of arc. This value shows that energy resolution of this optical element is still good enough ($\Delta E/E = 1.1x10^{-5}$).

X- ray diffractometry applying several Bragg reflections with different asymmetry showed, that thickness and mosaic spread of the damaged layer are equal to 3μm and 19 sec of arc.

Apparently it is worth while to design damaged layer with optimal parameters for getting maximum integral intensity of diffracted beam. The low value of energy resolution in some cases (f.e., X- rays focusing [2]) should not be considered as limiting factor.

L.E.Berman, J.B.Hastings, D.P.Siddons, M.Koike, V.Stojanoff, M.Hart (1993) Nucl. Instrum. and Methods, A329, 555.
M.Sanchez del Rio, G.Gribel, J.Als- Nielsen, M.Nielsen (1995) Rev. Sci. Instrum., 66, 5148.
S.M.A.Gani, B.K.Tanner, T.G.McKenney, H.T.Hingle, D.K.Bowen (1984) J.Appl. Cryst., 17, 111.

P12.14.006 A VERSATILE FOCUSING MONOCHROMATOR FOR THE D8 ADVANCE. Lange, J., Menges, G. and Kern, A., Bruker Analytical X-Ray Systems GmbH, Östliche Rheinbrückenstraße 50, 76187 Karlsruhe, Germany

The D8 ADVANCE goniometer allows the easy component exchange and precise movement of X-ray optics, X-ray tube and detectors along high precision dovetail tracks. Following this concept a versatile focussing primary monochromator was developed to make measurements possible in different diffraction geometries. By sliding the tube monochromator unit along the primary dovetail track you can change from transmission over capillary to reflection mode. So you have the flexibility to meet any analytical challenge by optimum signal-to-background ratio, maximum stability, high resolution and best performance and a minimum of alignment.

This concept and instrument features will be presented. Furthermore measurements in different diffraction geometries and typical applications will be presented and discussed.

P12.14.007 A MONOLITHIC MONOCROMATOR-COLLIMATOR FOR X-RAYS. C. Ferrari, C.N.R. Maspec Institute, Area Parco delle Scienze 37/A, 43010 Fontanini, Parma, Italy, and D. Korytar, Institute for Electrical Engineering S.A.S., Vrbovska cesta 102, 92191 Piestany, Slovakia .

A new design for a monolithic monochromator-collimator based on Germanium or Silicon defect free single crystals is presented. On the same crystal block four coplanar diffractions take place obtaining an exit X-ray beam in the direction of the incident beam. By using a conventional copper X-ray tube as a source a wavelength dispersion $\Delta\lambda/\lambda$ lower than 10^{-4} and a final divergence of 10 seconds of arc can be achieved. With respect to existing high resolution monochromators, based on multiple diffractions from two distinct channel cut crystals, the present device offers the advantage of a more compact design and of an easier alignment with comparable intensity of the exit X-ray beam.

The use as an accurate tool for X-ray optics with synchrotron radiation is proposed.

P12.14.008 THE APPLICATION OF GRADED MULTILAYER OPTICS IN THE DIFFRACTED X-RAY BEAM D. Bahr, L. Brügemann and R. Stömmer Bruker-AXS GmbH, 76181 Karlsruhe, Germany

Since years now the Göbel mirror is a well known optical component for X-ray diffraction investigations. The mirror provides a parallel and pseudo monochromatic X-ray beam incident on the sample. The optimum benefit of these parallel beam conditions is achieved by using the same kind of optics in the diffracted beam, too.

We will point out the principles of the diffracted beam Göbel mirror and will describe the advantages of this optical component in comparison to classic parallel beam optics. Several measurement examples from various applications presented will explain which method of investigation benefits from the diffracted beam Göbel mirror.

P13.14.000 THE ATS SCATTERING OF IRON PYRITE AND MAGNETITE. K. Ishida, M.Kanazawa, K.Hagiwara, K. Horie, J. Kokubun, Department of Physics, Faculty of Science and Technology, Science University of Tokyo, Noda, Chiba 278-8510, Japan.

Near an absorption edge, anisotropic effect of tensorial atomic scattering factor becomes so large that reflections forbidden by screw or/and glide rule can be observed (ATS reflections)[1]. ATS reflections were observed in some crystals with synchrotron radiations[2-5]. We measured energy dependence of ATS reflection intensity of pyrite (FeS2) and magnetite (Fe3O4) near the Fe K-absorption edge.

For a pyrite crystal, the observed energy spectra are quite different from that of the absorption measurement. In the region above the edge, the ATS intensities for (001), (003) and (011) reflections showed the same energy dependence, two sharp and one broad peaks. To study nature of the scattering, we measured polarisation property and azimuthal dependence of the reflections. The result can be understood on the basis of electric dipole transition. But below the edge, the energy spectra of the ATS intensity depend on the reflection plane. The azimuthal dependence of the intensity cannot be explained by the calculation based on only the dipole transition. Quadrupole transition may contribute to the scattering. While, for a magnetite crystal, there are two peaks above and below the edge, which are also different from the absorption experiment. The azimuthal dependence of the peaks can be explained by dipole transition. The energy spectrum of the scattering measured at 80K was almost the same as that at room temperature except for an additional intensity enhancement due to the structural transition.

1. V.E. Dmitrienko (1983). Acta Cryst. A39, 29.; (1984). A40, 89.
2. D.H. Templeton and L.K. Templeton (1986). Acta Cryst. A42, 478.
3. A. Petcov, A. Kirfel and K. Fischer (1990). Acta Cryst. A46, 754.; (1991). A47, 180.
4. T. Nagano et al. (1996). J. Phys. Soc. Jpn. 65, 3060.
5. J. Kokubun et al. (1998) J.Phys. Soc. Jpn. 67, 3114.

P13.14.001 INVERSION OF DYNAMICAL FAST ELECTRON ELASTIC SCATTERING FROM CRYSTALS. A.E.C. Spargo , L.J. Allen, School of Physics, University of Melbourne, Parkville 3052, Australia and H. Leeb, Institut fur Kernphysik, Technische Universtat Wien, Vienna, Austria.

The retrieval of a unique crystal potential from the scattering matrix in high energy transmission electron scattering has been achieved, at least in principle. It is shown that data recorded at a single crystal orientation are, in general, not sufficient to determine all the elements of the matrix. Additional measurements with defined tiled beam are required for the determination of the entire matrix. Extraction of the crystal potential from the scattering matrix can be achieved using equations of constraint defined by the principal orientation and/or a set of linear equations that reflect the symmetry of the fundamental (Bethe) matrix when written in an appropriate form.

P13.14.002 FORBIDDEN REFLECTION NEAR EDGE DIFFRACTION OF INCOMMENSURATELY MODULATED STRUCTURE Rb_2ZnCl_4. K. Matsuoka, S. Kuwajima, S. Nagao and Y. Soejima, Department of Physics, Kyushu University, Fukuoka 812-8581, Japan

Intensity distribution in reciprocal space of forbidden reflection near edge diffraction (FRED) due to the anisotropy of tensor of susceptibility (ATS) has been determined for Rb_2ZnCl_4. The measurements are made as a function of incident X-ray energy around the Rb K absorption edge, and also as a function of temperature through the normal/incommensurate and incommensurate/commensurate phase transitions. It is found that, on the 041 forbidden reflection of the incommensurate structure, the FRED intensity appears at two slightly separate positions in reciprocal space, and at two incident energies. It is observed that one of the two FRED intensities disappears in the normal phase, and the other one does in the commensurate phase. The results indicate that the anisotropy of electron distribution in Rb atom is different in the normal and commensurate phases, and that the two kinds of anisotropy coexist in the incommensurate phase. Accordingly, we conclude that the FRED intensity is strongly related to the structure, and the intensity distribution is affected by the incommensuration. A theoretical study on the X-ray resonant scattering in the incommensurately modulated structure has been reported by Ovchinnikova & Dmitrienko (to be published in Acta Cryst.). It is to be hoped that theoretical explanation of the present experimental results will be given.

P13.14.003 RESONANT X-RAY DIFFRACTION BY MODULATED CRYSTALS. E.N.Ovchinnikova, Physical Department of Moscow State University, Moscow 119899, Russia and V.E.Dmitrienko, Institute of Crystallography, 59 Leninski pr., 117333, Moscow, Russia

We consider conditions for the appearence of additional ("forbidden") reflections owing to the anisotropy of anomalous X-ray scattering by modulated crystals. These reflections are forbidden in the diffraction pattern far from the absorption edges and can be observed only with the synchrotron radiation. It is shown that the modulation (displacive or occupational) can change the local symmetry of atomic environments and hence becomes a source of additional anisotropy for each resonant scatterer inducing the modulated behaviour of susceptibility

tensor. The modulation can change both the resonant spectra and the tensorial properties of susceptibility. The four-dimensional approach is used to calculate the set of possible reflections near the absorption edges in the case of incommensurate modulation [1]. This approach allows to show that no additional reflections can appear owing to the variation of the resonant spectra in the resonant X-ray diffraction by incommensutately modulated crystal in opposite to the case of commensurate modulation. The additional reflections can appear owing to the modulation of the angular part of the susceptibility. It is found, that both a system of forbidden main reflections and forbidden satellites can occur even in those cases when the resonant atoms in fundamental structure are located in position with cubic local symmetry. These reflections correspond to glide planes, screw axes and centering translations in four-dimensional space. Symmetry restrictions on the intensities and polarization properties of forbidden main reflections and satellites are found for incommensurately modulated crystals. It was shown that the properties (such as azimuthal and polarization dependencies) of main forbidden reflections can differ >from those of forbidden satellites and they depend on the modulation type in a crystal. The comparison of the azimuthal dependences of main forbidden reflections and satellites would allow to calculate the correction to the susceptibility, which appear due to the modulation. The crystal structures in which the listed effects can be observed are presented, for example the additional reflections near the K-edge of Ni in diffraction pattern of La_2NiO_{4+x}.

1. E.N.Ovchinnikova & V.E.Dmitrienko (1999). Acta Cryst., A**55**, 20-29.

P13.14.004 X-RAY DOUBLE AND QUADRUPLE PHASE RETARDER SYSTEMS COMPENSATING SPHERICAL AND CHROMATIC ABERRATIONS. K. Okitsu, University of Tokyo, 2-11-16 Yayoi, Bunkyo, Tokyo 113-8656 Japan, Y. Ueji, The Graduate University for Advanced Studies, 1-1 Oho, Tsukuba, Ibaraki 305-0801 Japan, K. Sato and Y. Amemiya, University of Tokyo, 7-3-1 Hongo, Bunkyo, Tokyo 113-8656 Japan.

The transmission x-ray phase retarder [1] developed by Hirano, Ishikawa and Kikuta is widely used as a decisive x-ray optical device for controlling polarized states of x ray beam. However, it has a problem of phase-shift aberration due to angular and energy spread of incident x rays when a high degree of pure polarization state is required.

In order to overcome this problem, we have developed an x-ray double phase retarder system which can compensate the spherical aberration. The system is composed of two phase retarders which are set so as to give Bragg reflections in the opposite directions. We could obtain a vertical linear polarization with a 99 % of P_l ($=I_v$-I_h/I_v+I_h) from horizontally polarized x rays with this system. This value favourably compares with 85 % which was obtained by a single phase retarder with the same total thickness. The double phase retarder system has been used for the switching of the helicity of circular-polarized x-rays, with which the x-ray natural circular dichroism (XNCD) has been successfully measured in the vicinity of Ni *K* absorption edge. (see Ueji *et al.* at the present congress).

Furthermore, we have developed an x-ray quadruple phase retarder system which can compensate both spherical and chromatic aberrations. This system consists of four transmission phase retarders whose scattering planes are inclined by α, α +90, α +180, α +270 degrees from the polarization plane of the incident linearly polarized x rays.

[1] K. Hirano, T. Ishikawa & S. Kikuta : Rev. Sci. Instrum. 66, 1604 (1995).

P13.14.005 DARWIN'S METHOD IN THE THEORY OF X-RAY DYNAMICAL DIFFRACTION IN DISTORTED CRYSTALS AND IMPERFECT CRYSTALLINE MULTILAYERED STRUCTURES. I.R.Prudnikov, Physics Department, M.V.Lomonosov Moscow State University, Moscow 119899, Russia.

At present, the approach based on the recursion equations for the amplitude reflection and transmission coefficients of individual layers is widely used in theoretical studies and computer simulation of X-ray diffraction in layered crystals and multilayered materials. The recursion equations were first obtained by Darwin [1] for solving the problem of dynamical diffraction by perfect crystals. In the paper Darwin's method is extended to the case of X-ray dynamical diffraction in distorted crystals and imperfect multilayered structures where the deformation field and the polarizability are functions of three coordinates (x, y, z) of the point inside the sample. We have derived the recursion equations describing three-dimensional dynamical diffraction in these crystals and structures. We have considered both Bragg-case diffraction [2] and Laue-case diffraction. On the basis of the obtained recursion equations we have developed algorithms for computer simulation of X-ray dynamical diffraction in structures with a spatial modulation of crystal lattice parameter and/or the polarizability (e.g., multilayered structures with lateral periodicity, a crystal under surface acoustic wave excitation, porous materials). The above results make it possible to map the angular distribution of diffraction intensity near reciprocal-lattice points. In the paper we give numerical examples of calculated reciprocal space maps. Advantages and limitations of the above approach in comparison with the well-known approaches of the dynamical diffraction theory are discussed.

1. C.G. Darwin (1914). Philos. Mag., **27**, 675.
2. I.R. Prudnikov (1998). Acta Cryst., A54, 1034.

P13.14.006 INTERFERENCE PATTERNS FROM SEMI-INFINITE AND FINITE CRYSTALS. H.B. Larsen and G. Thorkildsen, Department of Mathematics and Natural Science, Stavanger College, Ullandhaug, 4004 Stavanger, Norway.

A theoretical investigation of X-ray interference patterns from semi-infinite and finite perfect crystals has been undertaken. By using the boundary value Green function technique along with the Takagi-Taupin equations [1], expressions for the diffracted intensity pattern at the exit surfaces of a *t* ×*l* crystal have been derived. The formalism is general and enables the study of different types of waves (plane, spherical and point source) impinging the crystal. In addition, the effect of varying the width of the incoming beam by slits is modelled. Anomalous absorption is taken into account using complex expansion parameters. In the corners of a semi-infinite crystal the standard Borrmann-Lehmann interference pattern [2,3] is retrieved. The present approach includes the possibility of non-symmetrical reflections and utilizes the full Bessel-function representation for the fields. Simulations for a variety of $t \times l$ crystal geometries have been performed using diamond as a model system. The results are described by assessing the contributions from the various geometrical scattering regions formed within the crystal. For a crystal of finite size this may lead to a more complex pattern owing to the possibility of an increased number of such regions. Both reflection and transmission modes are addressed. The simulated interference patterns are significantly influenced by minor changes of the input parameters, thus reflection asymmetry, positioning of source point and slit size *etc.* play crucial roles when interpreting such patterns.

1. G. Thorkildsen and H.B. Larsen (1998) *Acta Cryst.* A**54**, 416-429.
2. K. Lehmann and G. Borrmann (1967) *Z. Krist.* 125, 234-248.
3. A.R. Lang, G. Kowalski and A.P.W. Makepeace (1990) *Acta Cryst.* A**46**, 215-227.

P13.14.007 APPLICATION OF STATISTICAL DYNAMICAL THEORY TO X-RAY DIFFRACTION PROFILE BY DOUBLE-CRYSTAL METHOD. T. Takama and M. Miyazawa, Faculty of Engineering, Hokkaido University, Kita-ku, Sapporo 060-8628, Japan.

Kato constructed the statistical theory of dynamical diffraction [1] based upon the equations of Takagi-Taupin. It describes an X-ray wave-field and an integrated intensity in a distorted crystal with defects statistically distributed over the volume. The theory was further developed to explain the angular distribution of the diffracted intensity by Bushuev [2]. In the present study, the latter theory is applied to analyze the X-ray profiles measured for Si with micro-defects. The micro-defects of SiO_2 distributed over the volume were introduced into Cz-Si wafers by annealing in Ar gas at 1223K for 25 to 260 hr. The angular distribution of the diffracted intensity on the symmetrical Laue case was measured by double-crystal method using Mo Kα. The measurements were performed for the (400) reflection. The width of the profile increased with an increase in the heating time. A shoulder in the intensity was observed at higher side of the Bragg angle for longer time annealing. In the analysis we assumed that the crystal consists of mosaic blocks disoriented with an angular distribution function W. In addition, the correlation length of wave-fields was assumed to be ten percent of the correlation length of the phase factor. We utilized the values of the static Debye-Waller factor measured for the same samples by the Pendellosung fringes method [3]. The calculated profiles were compared with the experiments. The results showed that the model describes fairly well the measured angular profiles including the shoulder in intensity, when the function W has the form of exp(-a/δ)/2δ. For example, the value of δ was 2.1 sec in arc for 260 hr annealing. When the Gaussian distributiopn was employed for W, the theory did not explain the profiles.

1. N. Kato (1980). Acta Cryst., A36, 763.
2. V. A. Bushuev (1989). Sov. Phys. Crystallogr., 34, 163.
3. T. Takama et al. (1994). Acta Cryst., A50, 239.

P13.14.008 ON THE FEASIBILITY OF TRIPLET PHASE DETERMINATION FROM NON-PERFECT CRYSTALS. J. Zellner, E. Weckert, R. Müller, Institut für Kristallographie, Universität Karlsruhe (TH), D-76128 Karlsruhe, Germany and M. Drakopoulos, A. Snigirev, ESRF, F-38043 Grenoble, France.

Three-beam interference experiments have been carried out successfully with crystals of a number of different compounds ranging from small molecule structures to quasicrystals and protein crystals [1]. The invariant triplet phase $\phi_T = \phi(\mathbf{g})+\phi(\mathbf{h}-\mathbf{g})-\phi(\mathbf{h})$ can be determined by the three-beam interference which forms a characteristic intensity modulation. The methods main drawback, however, is the requirement of crystals with very low mosaicity.

To overcome this problem, two methods have been investigated: **1.** In case of mosaic crystals showing well separated blocks the very parallel synchrotron beam can be used to select only a single block for the three-beam interference experiment. This technique requires the exact knowledge of the mosaic distribution which can be determined by the characterization of the mosaic structure using *reciprocal space tomography*. **2.** In addition to this 'reciprocal space' separation of single mosaic blocks the availability of high resolution CCD cameras [2] enables a real space separation of crystal blocks by on-line topography like techniques.

Experiments were carried out on samples of the semi-conductor material silicon carbide SiC and a non-perfect decagonal quasicrystal $Al_{70}Ni_{15}Co_{15}$.

1. E. Weckert & K. Hümmer (1997) *Acta Cryst.* A**53**, 108-143
2. A. Koch, C. Raven, P. Spanne. A. Snigirev, JOSA (1998) **A**15, 1940.

P13.14.009 SECONDARY EXTINCTION IN CYLINDRICAL AND SPHERICAL CRYSTALS FOR X-RAY AND NEUTRON DIFFRACTION. Hua-Chen Hu, China Institute of Atomic Energy, Graduate School of Nuclear Industry, P. O. Box 275(18), Beijing 102413, People's Republic of China.

Based on the study of extinction in plane crystals (Hu,1997), a systematic investigation of secondary extinction and integrated intensity for absorbing cylindrical and spherical crystals has been carried out by more accurate numerical calculation for all Bragg angle θ_B range (0°-90°) and samples with reduced radius $\Sigma_s R$ from 0-20 and absorption to scattering cross section ratio μ/Σ_s from 0-8. Many new and hitherto unsuspected effects are obtained, particularly for large extinction. We find that: 1. A minimum appears in the extinction factor Y *versus* $\Sigma_s R$ curves for $\mu/\Sigma_s > 0$ when $\theta_B > 0^\circ$. The dip is more pronounced for μ/Σ_s between 0.5 and 1.0 and $\theta_B < 45^\circ$. 2. The shape of the Y *versus* θ_B curve changes considerably with $\Sigma_s R$ or μ/Σ_s. Thus a dramatic increase of the extinction factor with increasing θ_B from 0°-20° appears when $\Sigma_s R > 5$ and $\mu/\Sigma_s > 0.5$. 3. When the extinction factor of a sphere is compared with that of a cylinder of the same radius, the Y value for the sphere is usually larger than that of the cylinder, and conversely when $\mu/\Sigma_s > 1$ and $\Sigma_s R > 5$. These behaviors originate in a complex combination of Laue and Bragg geometries and the rather sensitive dependence of the extinction on θ_B and μ/Σ_s for a large crystal. We believe that none of them would be found if absorption and scattering were treated separately. The intensity distribution of the exit beam from a cylinder for both multiple and single reflection is also evaluated for the first time. The later being directly related to the mean path length T_μ in conventional extinction theory. One can estimate from these curves that for the same μ and R the mean path length in the multiple reflection case is shorter than that of single reflection case and the difference is more pronounced for small μ/Σ_s and large R. The effect on Y for different shapes of mosaic distribution will also be discussed.

P13.14.010 QUANTITATIVE DETERMINATION OF TRIPLET PHASE INVARIANTS: UNIVERSALITY OF THREE-WAVE PEAK PROFILES. C.H. Chao and S.L. Chang, Department of Physics, National Tsing Hua University, Hsinchu,Taiwan 30043, ROC and Synchrotron Radiation Research Center, Hsinchu, Taiwan 30077, ROC. and Yu.P. Stetsko, Department of Physics, National Tsing Hua University, Hsinchu, Taiwan 30043, ROC and Chernovtsy State University, Chernovtsy 274012, Ukraine.

The procedure for quantitative determination of the triplet phase invariants is proposed, based on the comparison of the peak intensities of two symmetry-related three-wave X-rays diffractions. The procedure maps the three-wave peak profiles into a set of the dimensionless universal curves. The geometrical interpretation of the value of triplet phase invariant is given. A method for the determination of the zero point and the width of the measured three-wave peak profile is also proposed. The approbation of the procedure on the dynamically calculated peak profiles with the specified values of phase invariants as well as on the experimentally measured peak profiles for several organic and macromolecular crystals with known values of phase invariants is

carried out. The determined values of the triplet phase invariants are in good agreement with the above mentioned values.

P13.14.011 INELASTIC NEUTRON SCATTERING BY ULTRA -SOUND IN CRYSTALS. EXTINCTION EFFECTS. E.Iolin, E.Raitman, L.Rusevich, Institute of Physical Energetics, Riga, LV-1006, Latvia and B.Farago, Institute Laue-Langevin, BP-156, F-38042 Grenoble Cedex 9, France and F.Mezei, Hahn-Meitner Institute, 14091 Berlin, Germany.

We have observed, for the first time, inelastic neutron scattering (INS) from phonons (AW) externally excited in single crystals. We have used ultrasonic transducers (f_S=30 - 200 MHz) for exciting and Neutron Spin Echo (NSE) spectroscopy for the observation AW. It allowed us to trace the evolution of the elastic Bragg intensity I(0) and of the phonon harmonics Ih(n) up to n=7 as a function of the excitation power P in perfect and deformed Si. In deformed Si I(0) strongly decreases at low P. These results are in agreement with dynamical theory calculations. At the highest power we observed a cross-over to a chaotic phonon behavior. Rapid decay of NSE signal was described here by means of model of quasi mosaic crystal. For the case of classical mosaic crystal KBr we found new secondary extinction effect. Mosaic block is vibrated as a whole in the AW (we suppose that $\lambda_S >> L$, L is linear block dimension). The exchange of small energy ~ 0.6 μeV between AW and cold neutron (λ≈0.54 -0.57 nm) leads to the deviation of neutron impulse from the Bragg position at the value $\delta k_i = 2\pi f_S /(v \sin(2\Theta_B))$ (v -neutron velocity). If $\delta k_i L \geq \pi$ elastic and one-phonon scattering are realized in the different parts of the impulse space in the *one* mosaic block. Therefore secondary extinction for the elastic and inelastic scattering should be considered separately and ultrasound leads to the increasing of the *total* intensity of scattering Iht in the crystal with moderate (several μm) size of mosaic blocks. Results of secondary extinction calculations are in a good agreement with the results of our NSE experiment with KBr (f_S=111 MHz). We clearly observed INS in the strongly excited pyrolitic graphite (λ_S ≈60μm). However the effect of the AW at Iht was absent. Condition $\delta k_i L \geq \pi$ wasn't fulfilled due to the bad structure of PG. It seems that similar experiments could be applied for the estimate of the size of the mosaic blocks even without application of NSE technique.

P13.14.012 THICKNESS DEPENDENCE OF X-RAY INTEGRATED INTENSITY FROM SILICON CRYSTALS WITH DISLOCATIONS. D. Sakaki and T. Takama. Faculty of Engineering, Hokkaido University, Kita-ku, Sapporo 060-8628, Japan.

One of the urgent problems in the diffraction crystallography is to establish the accurate method for extinction correction applicable to distorted crystals with arbitrary imperfection. The answer was given by Kato as the statistical dynamical theory [1]. It has been revised and developed by many investigators. The theory was tested experimentally by comparing the observed integrated intensities with the theory [2], [3]. The tests showed that the correlation length of the amplitude G is much shorter than the Kato proposal that G is equal to L/E (L: extinction distance). These experimental tests were performed only for crystals with relatively high perfection with the static Debye-Waller factor E close to 1. In the present study, crystals with dislocations are selected for test sample and the measured intensities are compared with the theory.

The parallel-sided Si single crystals with dislocation densities of 600 and 10^6/cm^2 were prepared. The X-ray integrated intensities of the (220), (400) and (440) reflections were measured by a four-circle diffractometer using Mo Kα as a function of crystal thickness by changing the effective thickness using the φ inclination method. The thickness fringe disappeared for the crystals. The measured intensities were compared with the theory and the values of E, G and the correlation length of the phase factor τ were determined for each sample by the least-squares method. The values of E ranges from 0.1 to 0.52 depending on the reflection plane and the dislocation density. On the other hand, τ has the length with the same order as the previous result [3]. The value of G, however, had length with the same order as the extinction distance. This indicates that the detail study for G is needed to apply the theory for the extinction correction and characterization of crystal.

1. N. Kato (1980). Acta Cryst., A36, 763.
2. J. R. Schneider et al. (1992). Acta Cryst., A48, 804.
3. T. Takama et al. (1994). Acta Cryst., A50, 239.

P13.14.014 SPECIMEN ABSORPTION CORRECTION FOR DIFFRACTION EXPERIMENTS WITH AREA DETECTOR SYSTEMS. S. Scheidegger, M.A. Estermann and W. Steurer, Laboratorium fur Kristallographie, Eidgenoessische Technische Hochschule, ETH-Zentrum, CH-8092 Zurich, Switzerland.

Methods, dedicated to two-dimensional area detector systems and broad diffuse scattering phenomena, for correcting specimen absorption in X-ray diffraction experiments are implemented and tested. The respective transmission factors, in relation to the crystal or specimen shape, are applied to the intensity of every pixel of the two-dimensional detector. This is in contrast to routine data reduction where the transmission factors are applied to the integrated Bragg intensities only. Single-crystals and amorphous specimen are treated the same way. This allows for a fully quantitative treatment of continuous diffraction information, such as diffuse scattering or amorphous scattering, which is collected with a two-dimensional detector system. Furthermore, it is possible to assign different linear attenuation coefficients to the paths of the incident and scattered beam, as is desirable, for instance, in the case of X-ray holography with an internal resonant scatterer. To test the pixel-wise approach, the continuous scattering from an amorphous lead-glass specimen of defined shape is utilised. Synchrotron radiation was used to study in detail the influence of experimental parameters onto the accuracy of the pixel-wise absorption correction, and we will present the results of numerical calculations.

1. Busing, W. R., Levy, H. A. (1957). Acta Cryst. 10, 180-182.
2. Blanc, E., Schwarzenbach, D. & Flack, H. D. (1991) Acta Cryst. 24, 1035-1041..
3. Meulenaer, J. & Tompa, H. (1965). Acta Cryst. 19, 1014-1018.
4. Schwarzenbach, D. & Flack, H. D. (1989). J. Appl. Cryst. 22, 601-605.
5. Tegze, M. & Faigl, G. (1996). Nature 380, 49-51.

P13.14.015 THREE-WAVE X-RAY DIFFRACTION: POLARIZATION ASPECTS OF PHASE SENSITIVITY. Yu.P. Stetsko, Department of Physics, National Tsing Hua University, Hsinchu, Taiwan 30043, R.O.C. and Chernovtsy State University, Chernovtsy 274012, Ukraine. S.L. Chang and Y.S. Huang, Department of Physics, National Tsing Hua University, Hsinchu,Taiwan 30043, R.O.C. and Synchrotron Radiation Research Center, Hsinchu, Taiwan 30077, R.O.C.

A model of analyzing the phase sensitivity of the reflection coefficients of diffracted waves in the case of three-wave X-ray diffraction is proposed. This model considers three-wave diffraction as the interference of the directly and the "Umweg" - excited diffracted waves and seems to properly account for the phase sensitivity, as well as the behavior of an involved diffracted wave as a function of the triplet phase invariant, the polarization state of the incident wave, and the

diffraction geometry. Dependence of the three-wave peak profiles of the diffracted wave on the polarization of the incident and diffracted waves is investigated. General conditions of change of the peak profile asymmetry as well as conditions of high phase sensitivity of peak profiles are obtained. Good agreement between theoretical and experimental results is shown. Consideration on practical issues for phase determination is also given.

P13.14.016 X-RAY STANDING WAVE METHOD UNDER MULTI-BEAM DIFFRACTION CONDITION. M.V.Kovalchuk, L.Samoilova, A.Kreines, A.Zozulja Institute of Crystallography RAS, Leninsky pr. 59, 117333 Moscow, Russia

Full crystallographic characterization of the thin film structure and buried layers in single crystals requires two-dimensional determination of atom position. This can be achieved by combining of the X-ray standing wave (XSW) method with multi-beam diffraction [1,2]. In this presentation formation and behavior of X-ray wavefields in crystal are studied under condition of three-beam diffraction in Bragg geometry experimentally and theoretically. Numerical simulation based on multi- beam dynamical theory was used to determine principal scattering parameters and X-ray wavefield attenuation with depth and study its modulation in the directions of diffraction vectors. In XSW technique X-ray fluorescence and photoelectrons are often used as secondary process. Photoelectron escape depth is less than X-rays penetration depth under dynamical diffraction condition (so-called extinction length) and probability of photoelectron yield is proportional to XSW field intensity at atomic position. So photoelectrons can play a role of very sensitive probe to observe the two-dimension XSW intensity distribution in thin subsurface layer. One of the advantages of multiple diffraction is its phase sensitivity. So XSW method under multiple diffraction condition can be realized without measuring of any secondary radiation [3]. The experimental XSW studies of semiconductor single crystals under multi-beam diffraction condition will be presented in detail.

[1] N. Greizer, G.Materlik, Z.Phys.B: Condens.Matter, (1987) 66, p.83
[2] A. Kazimirov, M.V.Kovalchuk, V.G.Kohn, I.Kharitonov, L.Samoilova, T.Ishikawa, S.Kikuta, K.Hirano Phys.Stat.Sol. (1993) A135, p.507
[3]. M.V.Kovalchuk, A.Kazimirov, V.Kohn, A.Kreines, L.Samoilova Physica B (1996) 221, p.445

P13.14.017 PHASE SENSITIVE DIFFRACTION FOR ONE DIMENSIONALLY DISTORTED CRYSTALS. Klaus Schroer[a,b], Kerstin Hölzer[a,b], Edgar Weckert[b], and Kurt Hümmer[b], [a]Biology Department, Brookhaven National Laboratory, Upton, New York 11973, USA, [b]Institut für Kristallographie, Universität Karlsruhe (TH), D-76128 Karlsruhe, Germany.

For ideal single crystals only the integrated intensities of discrete reciprocal lattice points must be collected in order to solve the atomic structure. In contrary for layered samples and surface structures intensity profiles have to be measured as a continues function of the position in reciprocal space around and between the reciprocal lattice points respectively.

It was shown for single crystals that three-beam interference experiments can be used to get phase information by determining the triplet phase of the contributing reflections [1]. The application of this technique to layered samples consisting of semiconductor materials has been investigated [2]. An algorithm based on the Takagi equations has been developed to simulate the resulting interference profiles. The influence of different system parameters (layer thickness, lattice strain) on the form of the interference profiles was determined in theoretical calculations.

Experiments were carried out on SiGe and SiC layers of different thickness grown on Si. The intensity change for different positions on the rocking curve of a primary reflection due to the interference with a substrate reflection was recorded for several three-beam cases. When moving to different positions on the rocking curve of one of the contributing reflections, in the interference profiles one can see clearly a shift of the "triplet phase", which shows that it can be described as a continues function of the reciprocal lattice coordinates. Using the Takagi algorithm the measured interference profiles were simulated and showed a good agreement between the measurements and the theoretical predictions.

[1] Weckert E. and Hümmer K. (1997) Acta Cryst. **A**53, 108-143.
[2] Schroer K. (1998) Ph.D. Thesis, Universität Karlsruhe (TH), Germany

P13.14.018 SYNCHROTRON RADIATION X-RAY MULTIPLE DIFFRACTION APPLIED TO THE STUDY OF ELECTRIC FIELD INDUCED STRAIN IN MBANP ORGANIC NONLINEAR OPTICAL CRYSTALS. L. H. Avanci[1], L. P. Cardoso[1], S. E. Girdwood[2], D. Pugh[2], J. N. Sherwood[2], J. M. Sasaki[3,4], K. J. Roberts[3]. [1]IFGW/Universidade Estadual de Campinas, 13083-970, Campinas, SP, Brazil; [2]Pure and Applied Chemistry Department, Strathclyde University, Glasgow, G1 1XL, UK; and [3]CMIE/DMCE, Heriot-Watt University, E14 4AS, Edinburgh, UK, [4]Departamento de Física/Universidade Federal do Ceará, 60455-760, Fortaleza, CE, Brazil

In this work, distortions produced in the unit cell of a MBANP [(-)-2-(α-metilbenzilamina)-5-nitropiridina] nonlinear organic crystal under the influence of an applied electric field, E, are investigated by using synchrotron radiation x-ray multiple diffraction (XRMD). The method is based in the inherent sensitivity of this technique to determine small changes in the crystal lattice which provide peak position changes in the XRMD pattern (Renninger scan). A typical Renninger scan shows numerous secondary peaks, each one carrying information on one particular direction within the crystal. The ($hk\ell$) peak position in the pattern, for a fixed wavelength, is basically a function of the unit cell lattice parameters. Thus, small changes in any parameter due to a strain produced by E give rise to a corresponding variation in the ($hk\ell$) peak position and the observed strain is related to the piezoelectric coefficients. The advantage of this method is the possibility of determining more than one piezoelectric coefficient from a single Renninger scan measurement [1]. The method has been applied to the MBANP (monoclinic, point group 2) crystal and we were able to determine four piezoelectric coefficients: $|d_{21}| = 0{,}2(1) \times 10^{-11}$ Vm^{-1}, $|d_{22}| = 24{,}8(3) \times 10^{-11}$ Vm^{-1}, $|d_{23}| = 1{,}3(1) \times 10^{-11}$ Vm^{-1} and $|d_{25}| = 5{,}9(1) \times 10^{-11}$ Vm^{-1}. The measurements have been carried out at the SRS, stations 7.6 and 16.3, Daresbury Laboratory, Warrington, UK.

Support from EPSRC-UK and CNPq, FAPESP, FAEP-UNICAMP (Brazil).

[1] L. H. Avanci, L. P. Cardoso, S. E. Girdwood, D. Pugh, J. N. Sherwood and K. J. Roberts. *Physical Review Letters* 81(24), 5426-5429 (1998).

P13.14.019 OBSERVATION OF HYSTERESIS- LIKE BEHAVIOUR IN mNA ORGANIC CRYSTALS USING X-RAY DIFFRACTION. L. H. Avanci[1], R. S. Braga[1], L. P. Cardoso[1], D. S. Galvão[1] and J. N. Sherwood[2]. [1]IFGW/Universidade Estadual de Campinas, 13083-970, Campinas, SP, Brazil; [2]Pure and Applied Chemistry Department, Strathclyde University, Glasgow, G1 1XL, UK

Recently [1], geometrical distortions produced in the unit cell of a meta-nitroaniline (mNA) under the influence of an applied electric field were investigated and the piezoelectric coefficients determined. This investigation was carried out using synchrotron x-ray multiple diffraction. In the present work we

report first time experimentally observed hysteresys-like behaviour in mNA organic crystals using X-ray diffraction techniques. The mNA crystallises in the orthorhombic system with point group mm2, has 4 molecules per unit cell and lattice parameters a = 6.501 Å, b = 19.330 Å and c = 5.082 Å. The molecule is essentially planar with dipole moment directed from N_1 in the amino towards N_2 in the nitro group and the polar axis of the material is $\boldsymbol{c} \equiv [001]$. From a theoretical point of view we investigated the hysteresis-like behaviour analysing the geometrical distortions of mNA molecules under the influence of an external applied electrical field that can be varied. The calculations were carried out using the well known semi-empirical method AM1 (Austin Method One) with a modified code to explicitly include an external field into the Hamiltonian [2]. The unit cell distortions were detected through the peak shifts in two-beam diffraction case (rocking curves) measured for each field strength. Our results have shown that the experimental data can be explained in terms of changes in the acceptor-donor properties of mNA molecules.

Support from CNPq, FAPESP, FAEP-UNICAMP (Brazil).

[1] L. H. Avanci, L. P. Cardoso, S. E. Girdwood, D. Pugh, J. N. Sherwood and K. J. Roberts. *Physical Review Letters* **81**(24), 5426-5429 (1998).
[2] S. O. Dantas, M. C. Santos and D. S. Galvao, *Chemical Physics Letters* **256**, 207 (1996).

P13.14.020 THE DETERMINATION OF THE ABSOLUTE STRUCTURE OF LOW Z <= 7 COMPOUNDS BY THREE-BEAM DIFFRACTION. K.Hummer, T. Jouffre, R. Muller, E. Weckert and J. Zellner, Institut fur Kristallographie, Universitat Karlsruhe, D-76128 Karlsruhe, Germany

The determination of the absolute structure of compounds containing nitrogen as the heaviest element can hardly be accomplished by standard methods exploiting anomalous dispersion effects. This problem, however, can easily be solved by the experimental determination of triplet phases by means of three-beam interference experiments [1], since this method does not require the presence of anomalous dispersion effects.

Three-beam interferences lead to characteristic intensity changes from which the triplet phases can be deduced [2]. Most suitable for the determination of the absolute structure are triplet phases close to 90 or -90 °.

The results of a number of C-N-H compounds such as $C_{28}N_2H_{20}$ or $C_{23}N_2H_{25}$ as well as O-N-C-H compounds with very low oxygen content will be presented.

1. K. Hummer, E. Weckert (1995) Acta Cryst. A 51, 431-459.
2. E. Weckert, K. Hummer (1997) Acta Cryst. A 53, 108-143.

P13.14.021 MANY-BEAM X-RAY DIFFRACTION FROM SILICON AT EXACT BACKSCATTERING. J.P. Sutter , Purdue University and Argonne National Laboratory; E.E. Alp, G. Bortel, M.Y. Hu, P. Lee, W. Sturhahn, and T.S. Toellner, Advanced Photon Source, Argonne National Laboratory, Argonne, IL 60439, USA; R. Colella, Department of Physics, Purdue University, West Lafayette, IN 47907, USA; H. Sinn, Fachbereich Physik, University of Rostock, 18051 Rostock, Germany.

We have examined the (12 4 0) reflection in silicon at exact backscattering. It can be shown that for a cubic lattice, if a reflection (HKL) is set to backscattering, all reflections (hkl) for which $h^2+k^2+l^2= hH+kK+lL$ are excited also. As a result, (12 4 0) backscattering in silicon is found to occur with 22 secondary reflections, of which 10 are in the Bragg geometry. An inspection of the backscattering case has been difficult in the past due to the lack of sufficiently monochromatic and tunable X-rays. However, the use of a monochromator of bandwidth 2.3 meV (less than the (12 4 0) backscattering bandpass of 6.2 meV) has made such an inspection possible with a synchrotron X- ray source. We have scanned the backscattered intensity versus the incident angles at the exact backscattering energy (14.438 keV) and at 30 meV above this energy. At certain incident angles, deviations of this intensity from the normally expected values are observed; each of these can be ascribed to the simultaneous excitation of a specific set of secondary reflections. The polarization dependence of these secondary excitations is also studied. Finally, we used a calibrated image plate to gather intensity data on the 10 Bragg-geometry secondary beams. We will compare these data with the predictions made by many-beam dynamical diffraction theory [1] and discuss the implications for backscattering applications.

This work was supported by the U.S. Department of Energy, Basic Energy Sciences, Office of Energy Research, under Contract W-31-10- ENG-38

1. R. Colella, Acta Cryst. , (1974), A30 , 413-423.

P13.14.022 NEW PRECISION MEASUREMENTS OF ATOMIC FORM FACTORS USING SYNCHROTRON RADIATION: SILICON, COPPER, SILVER AND GOLD. Z. Barnea, C.Q. Tran, C.T. Chantler, D. Paterson, D.X. Balaic, D.J. Cookson†, School of Physics, University of Melbourne, Parkville, Victoria 3052, Australia. † Chem-Mat-CARS ,Argonne National Laboratory, 9700 S. Cass Avenue, Argonne, IL 60439

Complex X-ray form factors are used in many fields including crystallography, material science, medical diagnosis and XAFS studies. Discrepancies between theories and between experiments of 10% or more over central X-ray energies prevent investigations of new physics and new structural determinations. Until recently, few references claimed experimental accuracies of 1%, and many experts believed that accuracies and precisions below 1% were not possible. We present new experimental measurements with accuracies below 0.3%, and precision of order 0.01%, for attenuation coefficients of Silicon (5keV to 20keV) and of Copper (8.84keV to 20keV), and the latest results from recent experiments at the APS (Chicago). Many sources of error neglected in previous experiments have been carefully investigated. Major discrepancies are systematically addressed with this data and approach.

P13.14.023 NEW THEORY RESOLVING DISCREPANCIES OF ATOMIC FORM FACTORS AND ATTENUATION COEFFICIENTS FOR NEAR-EDGE SOFT X-RAYS. C. T. Chantler, School of Physics, University of Melbourne, Parkville, Victoria 3052, Australia.

Reliable knowledge of the complex X-ray form factor and the photoelectric attenuation coefficient is required for crystallography, medical diagnosis, radiation safety and XAFS studies. Discrepancies between currently used theoretical approaches of 200% exist for numerous elements from 1 keV to 3 keV X-ray energies. This work addresses key discrepancies and derives new theoretical results in near-edge soft X-ray regions [1].

The current result improves upon the theoretical uncertainty in these difficult regions to σ = 20% - 30% and appears to reduce the error of this method to less than one standard deviation. Related work has recently confirmed the importance of theoretical computations of form factors for many experiments in general X-ray regions, with accuracy approaching 1%. This is achieved by this formalism [2].

[1] C. T. Chantler, Rad. Phys. Chem. 55 (1999) 231-237.
[2] C. T. Chantler, Z. Barnea, J. Phys. Condensed Matter 11 (1999) 4087-4091.

15. CRYSTAL GROWTH – TECHNIQUES, INSTRUMENTATION/APPLICATIONS

P06.15.001 PHASE EQUILIBRIUM AND EPITAXIAL GROWTH IN Bi-Al-Ga-As SYSTEM. Oskomova N.V., Antoschenko V.S., Taurbaev T.I. Optoelectronics Laboratory, Kazakh State University.

LPE of solid solutions in Bi-Al-Ga-As system at $X_{Ga}= X_{Al}$ has not been carried out before. It is explained by the fact that system becomes unstable in case of using pure Bi as a solvent. This leads to heterogeneous dissolution of the substrate and makes epitaxial growth impossible. In the present work the reasons of interphase instability are considered and epitaxial films of AlGaAs grown from Bi-Al solvent are obtained.

Calculations of phase diagrams revealed that the main factor of solid solution/substrate interface instability is abnormally high distribution coefficient of Al in the considered system. This leads to transition of most part of Al to solid phase while approaching the equilibrium and to additional dissolution of the substrate. Analysis of liquidus isotherms showed considerable divergence between experimental and calculated data at $X_{Ga}= X_{Al}$ within narrow interval of concentration of Al. For X_{Ga} exceeding 2 at.% experimental and calculated data are in good agreement (See Fig.). Applying the original techniques of epitaxial growth at this region of composition, it became possible to obtain monocrystalline films AlGaAs of 1-20 mcm of thickness and of good quality separated from the initial substrate by a layer of metal Bi. Crystallisation on the substrate directly took place when it was more than 2 at. % of Ga, added to the liquid phase. It was found that the main condition determining the mechanism of interface relaxation is the intersection of the liquidus isotherm $X_{Ga}= X_{Al}$ with other 'isogallium isotherms'. Phenomenological simulation has been suggested.

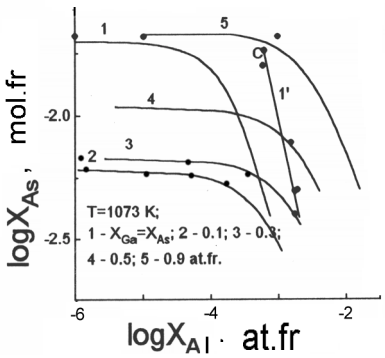

P06.15.002 HIGH RESOLUTION X-RAY CHARACTERISATION OF STRAINED SiGe/Si MULTILAYER DEVICE STRUCTURES WITH HIGH Ge FRACTION. J.C. Jones, A.M. Keir, W.Y. Leong, R.T. Carline, G.M. Williams, D.J. Wallis. Defence Evaluation and Research Agency, DERA, St Andrews Road, Malvern, Worcestershire WR14 3PS.

Pseudomorphic $Si/Si_{1-x}Ge_x$ single photon avalanche detectors (SPAD's) are being grown with x>0.3. The high Ge fraction gives increased absorption for the detection of light of wavelength ≥1.3μm. The high strain sensitivity and non destructive nature of high resolution X-ray diffraction (HRXRD) means that it is a powerful technique for the characterisation of these structures.

In this paper a range of low-pressure vapour phase epitaxial grown SiGe/Si multi-quantum well (MQW) heterostructures have been characterised by HRXRD and modelled using dynamical simulation software. A number of important parameters can be fitted using this technique. For example the technique is especially sensitive to the MQW period, and is able to detect <1% period variation in a 25-period stack, although many samples show much greater variation than this. Deviation from the idealised abrupt well shape can also be modelled. Non-uniformity in both period and well shape across the wafer have been investigated and can be related to growth conditions such as substrate temperature. Thickness measurements from transmission electron microscopy are also used for comparison.

P06.15.003 THE STRUCTURAL MECHANISM OF IMPURITY INFLUENCE ON CRYSTAL GROWTH. V.A. Kuznetsov, T.A. Eremina, T.M. Okhrimenko, N.G. Furmanova, and E.P. Efremova, Institute of Crystallography, Leninsky pr. 59, Moscow 117333, Russia, and N.N. Eremin, Moscow State University, Moscow 117234, Russia.

New aspect of the impurity influence mechanism on crystal growth is considered. The experiments revealed the difference of influence of the M^{3+} and M^{2+} metal ions on growth kinetics and the quality of KDP and KAP crystals, which could not be explained by modern crystal growth theory. The growth promoting effect of M^{3+} ions was typical phenomenon (but at higher supersaturation only), while M^{2+} ions decreased the growth rates deteriorating simultaneously the crystal quality. The computer modelling of the structure of KDP crystals doped by M^{3+} and M^{2+} ionsrevealed the different structures of defect centres formed by these ions: M^{3+} formed isolated centres, while the impurity claster centres were typical for M^{2+} ions. The latter generated more lattice strain.The defect formation energies, structure deformations in defect regions, and generated lattice strain were estimated.The general mechanism of impurity influence taking account of both surface impurity adsorption and the structure deformations is proposed. From the standpoint of this mechanism the difference of the distribution coefficients of M^{3+} and M^{2+} ions, the different influence of them on growth kinetics and quality of crystals were explained.

P07.15.001 ON THE ANOMALOUS PHENOMENA IN CRYSTAL GROWTH OF HIGH QUALITY PINACOIDS OF DIMOLYBDENUM(II,II) TETRACARBOXYLATES. Boris Udovic, Faculty of Chemistry and Chemical Technology, University of Ljubljana, P.O. Box 537, 1001 Ljubljana, Slovenia.

The protonated dimolybdenum(II,II) 3,5-diaminobenzoate tetracarboxylate units $Mo_2(O_2CC_6H_3(NH_3^+)_2)_4$ crystallize in the form of bright pinacoids from concentrated solutions of Cl^-, Br^- or I^- counterions in highly acidic water solutions. The presence of bromide anions offers the easiest way to obtain a solid hydrate compound. On the other hand, the iodide solutions persist in the viscous liquid state also at −22 °C although the stoichiometric ratio of the solvated component remains unchanged. Some observed particularities confirm that the iodide anion is very nearly unhydrated. The electrolytic concentration like temperature effects break up the hydrogen bonds to some extent and water become more close-packed with increase in the percentage of bonds broken. In the highly structured liquid matrix, the larger ions increase the dielectric relaxation effects and generate fault sites, which propagate over large distances. The reduced dielectric saturation causes electrostriction phenomena on shared water molecules of solvent-separated ion-pairs to decrease. Only one proton of water molecule can be directed toward an anion, a lower surface charge density of I^- in comparison to Cl^- reduce the orientation effects on solvent molecules and exert more influence on the effective dielectric constant in its neighbourhood. The hydrogen bonded ionic species $H_3O^+(H_2O)_3$ or $H_9O_4^+$ molecular clusters with rather open structure are indeed broken and the solid phase growth from the acidic solution matrix is hindered also at lower temperatures. The remarkable differences between known negative changes in the self-diffusion activation energy $\Delta E_i^{\neq}$/*Kcal*

mol^{-1} –0.35(NH_4^+), –0.21(Cl^-), –0.39(Br^-) and –0.24(I^-) for water exchange between the first hydration shell and the bulk water at 25 °C give some indications also on the 'structural temperature' effects. The water structure breaking properties of the charged components promote the exceptional solubility of the $Mo_2(O_2CC_6H_3(NH_3^+)_2)_4$ tetracarboxylate.

Crystals of highly protonated 3,5-diaminobenzoic acid in the form of bis(hydrogen chloride) hemihydrate $(H_2N)_2C_6H_3CO_2H\cdot 2HCl\cdot 1/2H_2O$ were grown from a highly electrostricted ionic matrix of water " structure breaking " and " structure making" ions. These were the precursor components in the chaotropic synthesis of in a viscous acceptor microphase of interlattice H_2O and declustered Cl^- counterions. I.R. spectroscopic manifestations of N–H antisymm. and symm. stretch. at 3593 and 3494 cm^{-1} were detected accordingly to the longest C– NH_3^+ bond length 1.471(5) Å in the solved structure of the reference hemihydrate, but appreciably shorter C–N bond lengths 1.444(7) Å and 1.458(6) Å or 1.476(5) Å and 1.475(5) Å are given within equatorial ligands of the $Mo_2(O_2CC_6H_3(NH_2)_2)_4\cdot 8HCl\cdot 16H_2O$ compound with N–H antisymm. and symm. stretch. broadened and shifted to 3356 cm^{-1}. Proton jumps between $-NH_3^+$ and Cl^- in the neighbour water microphase lead to a small amount of double-bond character in the averaged length of C–N bonds, the prospected impulsive +I effects on the aromatic rings promote substantial donic (p–d)π interactions from the equatorial carboxylate groups to the attractive center on the axially tightened dimolybdenum(II,II) core. The shorter equatorial Mo—O_i mean distance 2.109(3) Å in comparison to 2.111(5) Å and 2.119(4) Å in tetrapivalate and tetraacetate compounds confirms the enhanced shielding effect of oxygen atoms on Mo atoms with a slight lengthening of the dimolybdenum quadruply bond 2.1063(8) Å in comparison to 2.088(1) Å, 2.0934(8) Å, 2.096(1) Å bond lengths in tetrapivalate, tetraacetate and tetrabenzoate complexes.

P07.15.003 GROWTH OF DOPED TRIGLYCINE SULFATE CRYSTAL BY SOLUTION METHOD K. Meera, S. Aravazhi and P. Ramasamy [1], [1] Crystal Growth Centre, Anna University, Chennai - 600 025, India

Triglycine Sulfate (TGS) is a ferroelectric material which finds application as room temperature IR detector. This material is synthesised by taking analar grade glycine and sulfuric acid in the molar ratio 3:1. TGS crystals are grown from aqueous solution by slow cooling technique. L-Cystine doped TGS crystals were grown for different mol% of L-Cystine. This dopant is added to the TGS solution in order to bring the crystal to the single domain state. Powder XRD and single crystal XRD has been carried out to identify the lattice parameters and also to demonstrate the crystallinity. Morphological changes has been observed and the results are discussed. Also the presence of dopants has been confirmed by the FTIR analysis taken in the wavelength range 400cm^{-1} to 4000 cm^{-1}. The ICP studies has been carried out to find the composition of sulfur in the crystal. Microhardness has been carried out in the (010) plane. The hardness is found to be decreased when compared with the pure TGS crystal. The results are presented in detail.

P07.15.004 GROWTH AND CHARACTERIZATION OF Cs_XRb_{1-X} $LiSO_4$ SINGLE CRYSTALS BY X-RAY POWDER DIFFRACTION AND RAMAN SPECTROSCOPY MEASUREMENTS. R.J.C. Lima, J.M. Sasaki, P.T.C. Freire, J.M. Filho, F.E.A., Melo, Departamento de Física/Universidade Federal do Ceará, 60455-760, Fortaleza, Ce, Brazil

Good perfect single crystal of mixed $Cs_xRb_{1-x}LiSO_4$ were grown from aqueous solutions by evaporation method at various temperature for nominal Cs concentration within the range of $0 \leq x \leq 1$. This set of crystals were studied by x-ray powder diffraction and Raman spectroscopy. Two distinct phases were observed by x-ray powder diffraction patterns in the range of concentration: monoclinic (for $0.5 > x \geq 0$) and orthorhombic (for $0.6 < x \leq 1$). The volume of the unit cell was determined using Rietveld method (DBWS9411) [1] applied to the x-ray powder diffraction patterns, and this result led to a good indication that the Cs element is getting into the unit cell. By Raman scattering data, we have found an evidence that the rotation mode of the SO_4 ions is more free in $RbLiSO_4$ than in $CsLiSO_4$ crystal. This result is in accordance with both the theoretical results of Katkanant [2] on increasing potential barrier of SO_4 ions as well as the results of Hasebe and Asahi [3] using single crystal x-ray diffraction data for low concentration of Cs. A new crystal was obtained for the nominal concentration of x=0.5 and x=0.6 at 40^{o}C. The attempt to refine the lattice parameter for these crystal with the same space group ($P2_1/c$ – ab2cβ) as proposed by Pietraszko [4] failed. A new symmetry for this crystal was obtained using the DICVOL [5] and ITO [6] programs yielding a good FOM. Both programs gave us an orthorhombic symmetry with lattice parameter: a=15.978Å, b=5.184Å, c=5.042Å. Also, the group theoretical analysis and the Raman results were used to aid the identification of the point group symmetry C_{2v}^4(Pma2) of the new material.

This work is supported by Brazilian Agencies CNPq, FINEP and FUNCAP/FCPC/UFC

[1] R.A. Young, A. Sakthivel, T.S. Moss, C.O. Paiva-Santos, User's Guide to Program DBWS-9411 (1995)
[2] V. Katkanant, Phys. Rev.B51, 146 (1995)
[3] K. Hasebe and T. Asahi, Ferroelectrics, 96, 63-66 (1989)
[4] A. Pietraszko, Acta Cryst. A37, 1981, C109
[5] D. Louer & M. Louer, J. Appl. Cryst. 5, 271-275 (1972)
[6] de Wolff and Visser, J. Appl. Cryst., 2, 89 (1969)

P07.15.007 PRECRYSTALLIZATION CLUSTERS (QUATARONS) AND CRYSTAL GROWTH. A.M.Askhabov, Institute of Geology of the Komi Science Centre, Uralian Division of RAS, Syktyvkar, Russia.

There are two alternative concepts developing in the theory of crystal growth. According to the first, the building blocks for crystals are atoms (ions) or molecules (atomic growth). The second concept suggests that crystals grow by joining ready crystalline blocks (microblock growth). We have put forward a new model of crystal growth suggesting that peculiar atom or molecular associations (clusters of a transient "hidden" phase) arise in crystal-forming media. These clusters were named "quatarons" according to the characteristic ball-like shape ("quatara" means "a ball" in the native tongue of the author). Quatarons have a number of properties which distinguish them from ordinary clusters and crystal nuclei described in the classical theory of crystal growth. In particular, quatarons have the limiting size. The limiting size quatarons act as potential crystallisation centres. They display neither crystalline structure nor translational symmetry. The quataron mechanism of crystal growth is extremely simple. A quataron adsorbed on crystal surface grows in size at the expense of atoms from the crystal lattice. A situation when one part of atoms is arranged into a lattice and the other is in a dynamic state cannot long exist in such "effective" quatarons. Crystallisation of quatarons becomes unavoidable and occurs at far smaller supersaturations than the limiting one. Thus, quatarons resolve the fundamental problem of the origin of stages during crystal growth by layers and account for continuous crystal growth in weakly supersaturated media and in the absence of dislocations. The only exception from the rule is precipitation of rigid fullerene-like quatarons with fully closed bonds on a base. This case accounts for formation of solid noncrystalline materials - quatarites.

The work was supported by RFFI, grant No.99-05-64883.

P07.15.010 GROWTH AND CHARACTERISATION OF BISMUTH THIO CHLORIDE. D. Arivuoli and G. Kanchana Department of Physics, Anna University, Chennai-25, India.

Bismuth sulfo chloride belongs to SbSI type compounds showing interesting physical properties like ferroelectric and semiconducting. Single crystals of bismuth thiochloride were grown from sodium meta silicate gel at room temperature. Bismuth chloride and thiourea were used as the outer and inner reactants with various concentrations. The crystals were also grown in acidic medium at room temperature. The gel grown crystals exhibited interesting dendritic, platelet and hopper morphology depending upon the concentration of the inner and outer reactant. The dendrites grew within days when the inner and outer concentration exceeded 2M. The arms of the dendrites were not well pronounced with the primary arm orienting along (001) direction and in most of the dendrites secondary arms were observed only on one side of the primary arm. Some of the platelets showed dendritic patterns at the edges of the faces. Larger size single crystals of 16mm x 12mm x 8mm were obtained for the gel density of 1.05 with 1M bismuth chloride and thiourea. On increasing the concentration of the bismuth chloride, more crystals were found to be twinned. SEM pictures of hopper crystals showed step like structures and the hopper was found to be more pronounced along [100] direction than the other faces. Some of the solution grown crystals showed twinning. Thermal characteristics were determined using TGA and DSC. EDAX analysis showed the presence of stoichiometric composition of the elements. FTIR and X-ray analysis were also carried out to identify the compounds.

P07.15.011 GROWTH OF CUSO4×5H2O CRYSTALS IN SLIGHTLY CROSS-LINKED POLY(VINYL-CAPROLACTAM) GELS. Nasimova I.R., Evlanova N.F., Makhaeva E.E., Khokhlov A.R. Physics Department, Moscow State University, Moscow, 117234, Russia.

The present work is devoted to the study of the application of slightly cross-linked poly(vinylcaprolactam) (PVCa) gels as a medium for growth of CuSO4×5H2O crystals. PVCa is known to be a good absorbent for different substances. The efficient absorption of CuSO4 by the PVCa gels from aqueous solution was observed. The absorption was being accompanied with the gel shrinking. The further immersion of the gels containing CuSO4 into ethanol leads to the growth of CuSO4 crystals inside the PVCa gel. The growth of crystals was a result of the saturation of CuSO4 solution inside the gel due to diffusion of ethanol molecules into the gel and back diffusion of water molecules into external solution. The experiments were made for the gels with different polymer content (4% and 7% PVCa). In the both cases the growth of dendrite crystals was observed. It was shown that the crystals habit depends on the density of polymer network. A pattern of crystals growth in the gel differs from that in solution with the same water/ethanol ratio. This fact is explained by the absence of convection flows in gels. Therefore the results obtained show that slightly cross-linked PVCa gel is promising as a medium for growth of crystals.

P07.15.012 SINGLE CRYSTAL GROWTH OF POLYMORPHIC ER2SI2O7 CERAMICS. Asghari Maqsood Thermal Physics Laboratory, Department of Physics, Quaid-i-Azam University, Islamabad, Pakistan.

Optically clear single crystals of the polymorphic Er2Si2O7 have been produced by the flux method. X-ray diffraction studies show that Er2Si2O7 exists in three modifications - a triclinic low temperature phase(type B), a monoclinic modification (type C) and a high temperature monoclinic modification (type D). Starting compositions and experimental conditions for crystal growth are discussed at length. The lattice constants along with the space groups are also reported.

P07.15.013 MORPHOLOGY OF CARBON DIOXIDE CLATHRATE HYDRATE CRYSTAL. Tomoko Ikeda and Shinji Mae, Department of Applied Physics, Faculty of Engineering, Hokkaido University, N13 W8, Sapporo 060-8628, Japan.

In-situ study on crystal growth of carbon dioxide clathrate hydrate in aqueous solutions has been performed. Using a high-pressure cell on an optical microscope stage, we observed the formation and growth processes of CO_2 clathrate hydrate in temperature range of 275-283 K, and pressure range of 3.7-4.5 MPa. From observation of the growth rate and morphology of the crystal, we found that the orientation of the surface of the crystal as it growth is dominated by supercooled temperature DT. The crystal with the <110> axis perpendicular to the surface grows at DT < 3.5 K. We measured Raman spectra of the crystal in order to investigate the effect of motion of the guest molecules (i.e., CO_2) on the orientation of the crystal growth. It was found that the CO_2 molecule inside the tetrakaidecahedral cage rotates about the symmetry axis of the cage as proposed by the previous studies [1]. Using neutron powder diffraction, Ikeda et al.[2] showed that the surrounding hydrogen atoms are temporally attracted and released by the oxygen atoms of the rotating CO_2. Thus, the interaction between the CO_2 molecule and the hydrogen atoms of the lattice is thought to be strong. We conclude that the crystal growth of clathrate hydrate is influenced by the anisotropic rotation of the guest molecules.

1 T. Ikeda, S. Mae & T. Uchida (1998), J. Chem. Phys., 108, 1352.
2 T. Ikeda, O. Yamamuro, T. Matsuo, K. Mori, S. Torii, T. Kamiyama, F. Izumi, S. Ikea & S. Mae, J. Phys. Chem. Solids (in press)

P07.15.014 CONTROL OF POLYMORPHIC CRYSTALLIZATIONS BASED ON AN ENERGY-TEMPERATURE DIAGRAM. Joseph G. Stowell, Xiaorong He, Ulrich J. Griesser, and Stephen R. Byrn. Department of Industrial and Physical Pharmacy, Purdue University, West Lafayette, IN USA 47907-1336.

Four polychromic forms of 5-methyl-2-[(4-methyl-2-nitrophenyl)amino]-3-cyanothiophenecarbonitrile (4'-Me) were studied in order to develop laboratory-scale crystallization conditions that would control the polymorph obtained. The polymorphs were characterized by DCS, XRPD, FTIR, and hot-stage microscopy, as well as solubility and slurry-convertions studies. Based on these results, an energy-temperature diagram was constructed. Batch crystallizations of 4'-Me were performed at various supersaturations and various cooling rates in anhydrous ethanol.

The temperatures at which the four energetically similar, enantiotrop-ically related polymorphs [red (R), dark red (DR), light red (LR), and orange (O)] interconvert were predicted by the solubility and slurry-conversion studies. The results followed the density rule. The thermodynamically most stable form above 60 °C is R. The O, LR, and DR polymorphs transform to R upon heating to 100 °C in anhydrous ethanol. At 25–60 °C, O is the thermodynamically most stable form. Below –30 °C, LR is the themo-dynamically most stable form. Throughout the entire temperature range studied, DR is metastable.

Batch crystallization above 60 °C gave R preferentially without seeding. Similarly, LR was obtained at temperatures between 10 °C and 50 °C without seeding. Seeding supersaturated solutions with DR crystals (0.5% w/w) afforded DR when the crystals were harvested immediately after

crystallization. Prolonged slurrying of R, LR, or DR at temperatures between 25 °C and 60 °C yield O. Thus, the formation of a particular polymorph can be predicted by understanding the complex thermodynamic relationships between the four polychromic polymorphs of 4'-Me.

P07.15.015 STUDY OF SURFACE FEATURES AND POLYTYPISM IN DENTRITIC SINGLE CRYSTALS OF CdI_2. Binay Kumar & G. C. Trigunayat, Department of Physics & Astrophysics, University of Delhi, Delhi-110007.

Dendritic single crystals of cadmium iodide are grown by vapour method. The basal surfaces of the as-grown crystals are examined by optical and electron microscopy and then they are etched by water vapour for different time intervals and at different temperatures. The etch pits are examined by microscopic methods. Next, CdI_2 crystals are grown with doping of isostructural compound PbI_2 and subsequently subjected to similar studies. The crystal polytypes are identified by x-ray diffraction for both doped and undoped crystals. The x-ray photographs are found to display arcing and streaking of the reflections, too. A wide variety of growth features are observed on the crystal surfaces, viz. growth steps and their bunching, overgrowths, slip lines and slip bands, apart from usual dendritic features. The etching produces hexagonal pits in the case of undoped crystals while both hexagonal and triangular pits are observed in the case of doped crystals. The density, shape and size of etch pits differ for two cases. Regarding polytype composition, the undoped crystals are mostly found to consist of the common four layered hexagonal polytype, 4H. On the other hand, the doped crystals are found to contain twelve layered rhombohedral polytype, 12R, too. The occurrence of polytypes, arcing and streaking of the reflections are explained on the basis of defects created during the growth of crystals. The bearing of these defects on the surface features are also analysed.

P07.15.016 POLYMORPHISM AND NONLINEAR OPTICAL ACTIVITY IN SODIUM P-NITROPHENOLATE. S. Brahadeeswaran and H.L. Bhat, Department of Physics, Indian Institute of Science, Bangalore- 560012, INDIA.

In recent years extensive research has been done on polymorphism in organic nonlinear optical (NLO) materials. Prior knowledge of polymorphism is essential for crystal growers, particularly working in the field of organic NLO materials, since polymorphs may exist due to varying solvents, changing crystallisation conditions, etc. In this paper we report our results on the studies performed on sodium p-nitrophenolate (NPNa). Two solvents, viz. methanol and water were used to grow the crystals of NPNa. While the methanol solution gave transparent and stable crystals of NPNa dihydrate [1] the water solution gave two polymorphs which were very distinguishable from their colours (yellowish and reddish brown). One of the water grown forms (yellowish) lost its transparency on exposure to atmosphere whereas the other form (reddish brown) was quite stable. These two forms were also distinguishable by other characterisation studies such as thermal analyses, powder x-ray diffraction (XRD) and powder SHG employing Kurtz technique. Subsequently, we have solved the structures of these two forms by the single crystal XRD technique. Of these two forms, the yellowish crystal was identified as NPNa tetrahydrate and the reddish brown as NPNa monohydrate. While the former exhibited a centrosymmetric ($P2_1/C$) space group with lattice parameters a = 11.944 Å, b = 6.968 Å, c = 26.002 Å, β = 101.36° and Z = 8, the latter had a noncentrosymmetric (C2) structure with lattice parameters a = 21.193 Å, b = 3.669 Å, c = 10.358 Å, β = 117.22° and Z = 4, and exhibited NLO activity. The coordination and hydrogen bondings of these structures will be discussed in detail and compared with that of NPNa dihydrate.

S. Brahadeeswaran, V. Venkataramanan, J.N. Sherwood and H.L. Bhat (1998). J. Mater. Chem, 8, 613.

P07.15.017 THREE DIMENSIONAL INSTABILITY AND TEMPERATURE OSCILLATIONS, INDUCED BY GRAVITY-DRIVEN AND ROTATIONAL FLOWS IN CZOCHRALSKI SYSTEM. MICROGRAVITY ALTERNATIVES. V.I. Polezhaev ,V.G. Kosushkin, S.A.Nikitin, N.V.Nikitin, Institut Of Problems In Mechanics Ras, Vernadskogo Pr. ,101, Moscow 117526, Russia

Temperature oscillations of gravity-driven fluid flow with rotation and nonlinear interaction in Czochralski system are studied using direct computer simulation and stability analysis on the basis of unsteady Navier- Stokes equations (Boussinesque approach) for axisymmetry and three- dimensional approaches. A focus of the paper is concentrated on the results of parametrical analysis of nonlinear coupling fluid flows using new mathematical modelling technique, comparison with experimental data and analysis of the microgravity alternatives to avoid instability and temperature oscilations in the melt.

Analysis with the use of the parameters of international benchmark (the case with prescribed temperatures on the seed and crucible wall, and isolation of the crucible bottom and linear temperature distribution on the melt surface) are done in a first part of the paper. Oscillations nature and damping of oscillations using adiabatic melt surface is discussed.

Second part of the paper is related to the parametrical analysis of ground-based regime of GaAs crystal growth with counterrotation. Oscillation's mechanism for the case of zero rotation and for the coupling nonlinear case are presented in axisymmetrical and three dimensial approaches. Two types of gravity - driven convection - Rayleigh - Bernard type due to cooling above of the disk and side heating of crucible are shown. Validation of computational solutions is discussed using comparison with experimental data of temperature oscillation.

Computer simulation and video visualization of the unsteady convective processes are done on the basis of special version of PC-based system "COMGA".

The work is supported by the joint NASA-RSA program (project N TM-11)

P07.15.018 VAPOR TRANSPORT GROWTH OF ORGANIC CRYSTALS: MORPHOLOGY VERSUS GRAVITY. M. Ittu Zugrav, Consortium for Materials Development in Space, University of Alabama in Huntsville, Huntsville, Alabama 35899, USA, F. C. Wessling, Department of Mechanical and Aerospace Engineering, University of Alabama in Huntsville, Huntsville, Alabama 35899, USA and W. E. Carswell, Alliance for Microgravity Materials Science and Applications, University of Alabama in Huntsville, Huntsville, Alabama 35899, USA.

Effusive ampoule physical vapor transport (EAPVT) has been used to grow crystals of N,N–dimethyl–p–(2,2 dicyanovinyl) aniline (DCVA). A series of multi-parameter experiments have been conducted both in microgravity on board the Space Shuttle Endeavour and in the laboratory as ground controls using the Moderate Temperature Facility (MTF). MTF uses very little power for materials processing and is capable of operating on several different microgravity experiment carriers, including the Space Transportation System (STS) and the International Space Station (ISS). Special design considerations allow the facility to operate at a 130°C interior temperature with a power consumption of 2.4 W in a 20°C environment. This thermal efficiency is achieved by minimizing radiative, conductive, and convective heat losses. The facility has flown on four Space missions so far and is planned to fly on the ISS. The EAPVT hardware consists of six

ovens and each oven contains two separate growth cells which allow the independent processing of two samples simultaneously. During Earth-based processing by EAPVT, DCVA forms exclusively bulk crystals. The space grown samples, however, showed a completely different growth form than did the ground samples. Instead of the bulk crystals, all of the space samples were thin film deposits. Oriented and ordered DCVA thin films were reproducibly grown in microgravity during two flights (STS-59; CONCAP IV-2 and STS-69; CONCAP IV-3). The experiments have demonstrated that the morphology of DCVA crystals is highly dependent upon gravity. The premise is that the bonds are weak in nature (Van der Waals) and are significantly impacted by gravity. Ground-based research have intensified to determine the validity of this theory, that is, if the impact of gravitational forces can be overcome by other process parameters. This result will add considerable insight into the "Van der Waals" nature of the epitaxial growth process for DCVA and will have influential impact in the field. To date, the STS-59 and STS-69 results obtained for the growth of DCVA in microgravity, have not been duplicated in a normal gravity environment. The results are discussed with reference to the growth parameters.

P07.15.019 MACROMOLECULAR CRYSTAL GROWTH EXPERIMENTS IN MICROGRAVITY. Karen Moore, Marianna Long and Lawrence DeLucas, Center for Macromolecular Crystallography, University of Alabama at Birmingham, 288 MCLM, 1918 University Boulevard, UAB Station, Birmingham, Alabama, USA.

Vapor diffusion crystallization experiments have been conducted in a microgravity environment since 1984, using a variety of launch vehicles including the US Space Shuttle and the MIR Station. Results from these experiments have shown that minimization of gravity-induced convective flows can be beneficial for macromolecular crystal growth. Crystals grown in microgravity frequently have improved optical and crystallographic quality relative to those grown in conventional 1-g experiments [1-3].

Vapor diffusion and temperature-induced crystallization experiments have been conducted by the Center for Macromolecular Crystallography aboard thirty seven missions of the US Space Shuttle. These experiments included an extensive selection of macromolecular compounds flown in collaboration with crystallographers throughout the world. Experiments conducted on three recent Shuttle flights, STS-94, STS-86 and STS-95, have produced outstanding results. Twenty eight different macromolecular compounds were involved in the vapor diffusion experiments conducted on STS-94 and STS-95, and the temperature-induced crystallization experiments conducted on STS-85 involved several formulations of the same protein.

A review of the development of space-flight hardware for vapor diffusion and temperature-induced crystallization experiments will be presented along with a discussion of experimental techniques developed for the microgravity environment. An overview of microgravity experiments conducted on STS the recent shuttle missions will be presented and the results of the crystallographic studies of crystals grown in these will discussed relative to results from earth-grown crystals.

[1] DeLucas, L. J., et al. (1993). Journal of Physics D: Applied Physics, 26:B100-103.
[2] DeLucas, L. J., et al (1994). Journal of Crystal Growth, 135:183-195.
[3] Weber, W., Betzel, C., Moore, K. M., DeLucas, L. D., and Bugg, C. E., (1994) Microgravity Science and Technology, 7:242-5.

P07.15.024 PACKING PATTERN AND CONFORMATION OF LOW-MELTING-POINT COMPOUNDS IN CRYSTALLINE STATE. Y. Yokoyama, Synthesis Technology Laboratory, Chugai Pharmaceutical Co., Ltd., Ukima, Kita-ku, Tokyo and Y. Ohashi, Department of Chemistry, Tokyo Institute of Technology, Ookayama, Meguro-ku, Tokyo

The crystal structure of the compounds that are liquid at room temperature and atmospheric pressure were studied with in situ crystallization technique and X-ray diffraction analysis. The systematic crystal structure analyses of the simple molecules revealed some intermolecular interactions in the crystalline state. Some of these interactions were responsible to the preference conformations that the conformation in the crystalline state is not in agreement of the stable one in the gaseous state or on the basis of the ab initio molecular orbital calculation.

The compounds, which have the CN group, tend to form the hydrogen bonds to H2C-CN. This tendency is emphasized in the compounds S-CN, thiocyanate ester. Therefore the substitution of the methyl group in ethylthiocyanate by chloro leads to isomorphism. In the compounds, which have C-O or C-S bonds, the dimer-like pairs through the C-H...O or C-H...S hydrogen bonds are observed and form the four-, six- and eight-membered ring. Two molecules are coupled by two antiparallel C-H...O or C-H...S hydrogen bonds to form a four-membered ring. Such a dimer-like pair may be strengthened by the intermolecular interaction between the C-O or C-S bond moments in the four-membered ring. The six-membered ring may be related to the stabilization of the gauche conformation in the crystalline state, when the trans conformation is preferred in the gaseous state or stable on the basis of the ab initio molecular orbital calculation. The intermolecular interaction such as the anomeric effect in the six-membered ring leads to the gauche conformation. In addition, the CN...halogen interaction seems to stabilize the gauche conformation.

P07.15.025 DEVELOPMENT OF A CRYSTALL-ISATION SCREEN FOR ORGANIC COMPOUNDS. C. Keats, K. Prout, D. Watkin, Chemical Crystallography Laboratory, 9 Parks Road, Oxford, OX1 3PD, UK and G. Tranter, Glaxowellcome Medicines Research Centre, Gunnelswood Road, Stevenage, Hertfordshire, SG1 2NY, UK.

Molecular structure determination by X-ray diffraction has the potential to become a routine analytical tool. Single crystal analysis has been revolutionised by CCD diffractometers, which can collect analytical quality data in a few hours, and powder diffraction is gaining importance through new methods of ab-initio structure solution. Eventually, both techniques will be limited by the availability of suitable crystalline material. For single crystal work, a sample size of a few tenths of a mm is adequate. Well-crystallised material is needed even for powder diffraction. It has been shown that usually sample quality rather than instrument capability is the factor limiting the diffraction data resolution.

The growth of crystals for either technique is not well characterised, and though some systems have been intensely studied, there are no generally applicable rules or guidelines. Solution crystallisation is the easiest technique to implement into a screening process; the modifying factors are the properties of the solvent of evaporation and the interaction of the crystallisation molecule with the solvent molecules. Cluster analysis of many organic solvent properties, such as dielectric constant, hydrogen bonding and dipole moment has produced a subset of 60 solvents, which cover the widest range of properties and thus comprise a useful screen. A search of the CSD revealed very few small organic molecules that have more than 3 reported polymorphs. A group of 10 compounds exhibiting polymorphism have been selected that are or have been of pharmaceutical interest, and are

being systematically crystallised using the screening method. Analysis of the polymorphs is done by single crystal X-ray diffraction.

Information generated from the screen can be used to assess which conditions produce good quality crystals for a variety of systems and which polymorphs or solvates can be formed. Utilisation of information concerning the behaviour of a compound could dramatically limit the screen.

P09.15.001 STRUCTURAL PECULIARITIES OF $LIGAO_2$. G.M.Kuz'micheva, M.V.Lomonosov State Academy of Fine Chemical Technology, Vernadsky prosp. 86, Moscow 117571, A.V. Gaister and E.V. Zharikov, D. I. Mendeleev University of Chemical Technology, Miusskaya sq. 9, Moscow 125047, and V. B. Rybakov, M. V. Lomonosov State University, Vorobyevy gory, Moscow 119899, Russia.

The enantiomorphism is an ability of crystal to exist in two mirror equal forms ("right" and "left"). There is not symmetry centre, symmetry plane and inversion axis in the point symmetry of these crystals (1, 2, 3, 4, 6, 222, 32, 422, 622, 23, 432). Earlier it was theoretically suggested to exhibit enantiomorphism for point groups -4, -42m, m, mm2. Crystal structure of $LiGaO_2$ (space group $Pna2_1$, point group mm2) is derivative of wurzite structure. Li^{1+} and Ga^{3+}- ions occupy tetrahedrally-coordinated sites, shared with each other by oxygen ions. An analysis of experimental x-ray results indicated that the "milky" single crystal $LiGaO_2$ (LGII) is twinned one, that consists of the crystals with corrected (C) and inverted (I) structures in the ratio 60:40(%), whereas the "transparent" single crystals $LiGaO_2$ (LGI) is completely C-type. Samples LG(I) (C) and LG(II) (C) differ from each other by lithium contents (in LG(II) less than in LG(I)) and value of Z-position (in LG(II) much less than in LG(I)) and the longest interatomic distance (cation-anion) associated with it. The observed behavior of these parameters probably can be related with tendency toward cation transition from present tetrahedral sites (C-structure) into another ones (I-structure). According to results of structure refinement of $LiGaO_2$:Li,V (LG(V)), $LiGaO_2$:Li,Al,Cr (LG(Al,Cr)) and $LiGaO_2$:Li,Sc,Cr (LG(Sc,Cr)) obtained by the Czochralski technique, I and C structures realize for LG(V) ($r_v<r_{Ga}$), LG(Al,Cr) ($r_{Al}<r_{Ga}$) and LG(Sc,Cr) ($r_{Sc}>r_{Ga}$) respectively. It was concluded that the changes in the structure depend on the radius (r,A) of the cation and the kind of point defects.

P09.15.002 ELECTRIC FIELD AS INSTRUMENT FOR OBTAINING AS-GROWN PERIODIC POLED LITHIUM NIOBATE CRYSTALS. E.P.Kokanyan, Institute for Physical Research National Academy of Sciences of Armenia, Ashtarak, Armenia.

The increasing interest in ferroelectric crystals with a periodic poled domain structure requires search of new technological methods of their obtaining.

In the present work lithium niobate crystals with a periodic poled domain structure (PPLN) have been grown by the Czochralski technique using an electric field applied to the crystal-melt system during the growth process. The change of the polarity of applied electric field and the density of electric current passing through the crystal-melt system lead to change of effective distribution coefficient of impurities and main components of the system caused by electrochemical processes arising in the crystal melt-system [1]. These instantaneous changes along the growth direction give a possibility of PPLN crystals with controlled period growing. The PPLN structure with a period of 3-60mkm obtained in this way was studied using selective chemical etching and electron microscope.

R.N.Balasanyan, V.T.Gabrielyan, E.P.Kokanyan, I.Foldvari (1990). Sov. Kristallografiya, 35, 1540.

P09.15.003 PERIODICALLY POLED CZOCHRALSKI GROWN LITHIUM NIOBATE SINGLE CRYSTAL. T.O.Chaplina, I.I.Naumova, N.F.Evlanova, S.A.Blokhin, S.V.Lavrishchev[1], Physical Dep. Moscow State University, Moscow 119899, [1]General Physical Institute RAS, Moscow 117924, Russia

Bulk periodically poled $LiNbO_3$ single crystal is a promising material for nonlinear optical devices using quasi-phase-matching (QPM). The domain structure of crystals and the distribution of impurities depend on the crystallographic orientation of seed. Earlier we investigated periodically poled Nd:Mg:$LiNbO_3$ crystals grown by the Czochralski method along the normal to the $(01\bar{1}2)$ face[1,2]. The face on the growth front favored of formation of flat and regularly spaced ferroelectric domain boundaries. Using selective chemical etching, scanning electron microscope (SEM) and wave dispersive X-ray microanalysis we showed that the ferroelectric domain walls coincide with the maxima and minima Nd-impurity modulation[2]. Along this growth direction the concentration of Nd and Mg impurities are in antiphase.

Y: $LiNbO_3$ and Y:Mg: $LiNbO_3$ crystals were grown by the Czochralski method along $[2\bar{1}\bar{1}0]$ (X-axis). This growth direction is a good practice for using the highest nonlinear coefficient d_{33} in the QPM nonlinear-optical conversions. The regular domain structure with a period 7-60 mkm was studied with selective chemical etching and metallographic microscope. In a system of the regular domains corresponding to the usual rotation striations we observed additional domains associated with the concetration phenomena on the growth front.

The modulation of Y- and Mg- impurities along the growth directions was measured with wave dispersive X-ray microanalysis in the SEM. In the Nd:Mg:$LiNbO_3$ crystal grown along X-axis we showed earlier [1] that Nd-modulation in the periodically poled region had larger gradient of the concentration than in the nearest single domain region of this crystal In the present work we discuss the peculiarities of the domain structure and impurity concentration distribution associated with the used crystallographic growth direction.

[1] I.I.Naumova, N.F.Evlanova, O.A.Gliko, S.V.Lavrishchev, Journal of Crystal Growth, 181 (1997) 160-164.
[2] I.I.Naumova, N.F.Evlanova, S.A.Blokhin, S.V.Lavrishchev, Journal of Crystal Growth, 187 (1998) 102-106.

P09.15.004 GROWTH AND OPTICAL PROPERTIES OF Nd-DOPED $Bi_4Ge_3O_{12}$ SINGLE CRYSTALS. C.M. Whang, Dept. of Ceramic Engineering, Inha University, Inchon 402-751, Republic of Korea and I.K. Bae, Division of Geology, Korean Institute of Geology, Mining and Materials, Daejon 305-350, Republic of Korea.

Single crystals of $Bi_4Ge_3O_{12}$ (BGO) doped with rare earth elements such as Nd is of practical interest because of its potential use as laser materials. The Nd-doped BGO has a broader absorption band at about 800nm compared with Nd:YAG, so it can absorb the pump light of a diode laser more efficiently.

In this work, the Nd-doped BGO crystals were grown in the auto-diameter control system equipped with frequency weighing sensor by the Czochralski method. The Nd doping level was varied from 1 to 3 at.%. The optimum growth conditions, under O_2 atmosphere, of the single crystals were as follows: Pulling rate; 1mm/hr: rotation rate; 34rpm: temperature gradient; 100 deg/cm. Transparent and light purple colored crystals grown have typical size of approximately 25mm in diameter and 50mm

in length. The preferred growth direction was confirmed to be <110>. The dislocation density was estimated to be $10^3/cm^2$.

Growth parameter, morphology and chemical composition of the grown single crystal were studied. Although Nd^{3+} needs no charge compensation as it substitutes for Bi^{3+} ions, its ionic radius is little larger than that of Bi^{3+}. The crystallochemical behavior of the Bi^{3+} ion is more closely related to the larger trivalent rare earth ions such as Nd^{3+} than to the smaller ones, just as Kaminskii [1] suggested. The effective distribution coefficient $K_{eff}(X_{crystal}/X_{melt})$ of Nd^{+3} ion obtained by chemical analysis was 0.93 which is in good agreement with the result of Kaminskii. Distribution of Nd ion concentration of Nd-doped BGO was investigated by PIXE analyzer and found to be uniform. Also, we report optical properties of the crystals obtained by IR, Raman and Luminescence spectra.

A.A. Kaminskii, D. Schultze & B. Hermoneit (1976). Phys. Status Solidi A, 33, 737.

P09.15.005 X-RAY IMAGING OF ALLOY SOLIDIFICATION PROCESSES. R. H. Mathiesen[a], L. Arnberg[a], F. Mo[a], T. Weitkamp[b] & A. Snigirev[b]. [a] Norges Teknisk Naturvitenskapelige Universitet, NTNU, Trondheim, Norway. [b] ESRF, Grenoble, France.

In situ experimental studies of dendritic alloy solidification processes have been carried out for the first time. $Sn_{0.9}Pb_{0.1}$ enclosed in a glass cuvette of dimensions $30\times20\times0.15mm^3$ was melted and introduced rapidly into a directional temperature gradient field varied in the range $dT/dx \in$ [1,20 K/mm]. 23.89 keV monochromatic X-rays were used to make images of a 1×1 mm^2 cross section with resolution down to 2 μm during the solidification. Exposure times down to 0.1 s with a read-out time of the same magnitude was obtained using a Fast REad-Out Low Noise (FRELON I) CCD camera giving a 0.2 s time-elapse between consecutive frames. This time and spatial resolution was adequate to provide quantitative and qualitative information for dendritic growth rates as high as 2.5 mm/s. The dendritic growth of the $Sn_{0.9}Pb_{0.1}$ alloys showed the predicted relationship between dendritic tip radius, temperature gradient and growth rate. A balance between two effects was decisive for the growth process: Under-cooling of the melt at the solidification front with heat conducted through a crystalline solid and an effective diffusion field for the alloying elements at the solidus/liquidus interface. The latter effect has not been observed previously.

P09.15.006 GAS-BUBBLE ENTRAPMENT IN TeO_2 SINGLE CRYSTALS. R.M.Grechishkin, A.I.Kolesnikov and S.S.Soshin, Tver State University, Zheliabova Str., 33, 170000 Tver, Russia

Gas bubbles are inadmissible defects which restrict the use of paratellurite (TeO_2) single crystals in acoustooptical devices [1]. In the present work we study the gas bubble distribution by size and location inside the Czochralsky-grown paratellurite crystals by optical methods including polarized anisotropic dark field observation (PADO). Large single crystals produced under varying conditions of growth were examined. The bubbles were found to locate mainly in the central parts of the crystal corresponding to the crystallization front convex downwards. The measured bubble radii fall into the range of 1.5 to 25 μm and exhibit either one maximum at 8-10 μm or (unexpectedly) two maxima at 3-4 and 14-18 μm, respectively. In the latter case bubble radii in the range of 6-12 μm are completely absent.

To explain this phenomenon and to find the conditions for bubble-free Czochralsky growth of paratellurite we have calculated the bubble diffusion growth rates and the forces on the bubble near the ctystallization front. It was found that in the case of high axial temperature gradients in the melt and low pulling rates a complete push off of the bubbles is possible by the following mechanism. Bubbles having sizes below a critical value are dissolved in itself in the melt. The bubbles with a radius slightly above the critical value grow rapidly and are dragged downwards by the thermocapillar forces and so they are not captured by the growing crystal. These bubbles, when they become large enough during further growth, tend to float again to the crystallization front under the action of Archimedean force, but are carried out from under the crystal to the free surface of the melt by the horizontal flux component forced by the crystal rotation.

The results of the study were used in the refinement of the technology of producing bubble-free paratellurite single crystals of optical quality with a diameter up to 80 mm.

1. I.Foldvari, R.Voszka and A.Peter. Comments on the gas-bubble entrapment in TeO_2 single crystals. J.Cryst. Growth 59 (1982) 651-653.

P09.15.007 COMPOSITIONAL DEISTRIBUTION AND DEFECTS OF HGCDTE CRYSTAL GROWING IN MAGENTIC FIELD. R. D. Xia [1], M. Lan, S. Ye, Y. Mei, S. Zhou [2], [1] Electrical and Electronic Engineering, University of Nottingham, University Park, Nottingham, NG7 2RD, UK, [2] Harbin Institute of Technology, Box328, 150001, P. R. China

The Cadmium Mercury Telluride (Hg1-xCdxTe) single crystal with homogeneous composition in large area is a potential material for infrared focal plane detector. However, the composition uniformity demanded for device fabrication can not be satisfied due to the large margin existing between solid and liquid lines on its phase diagram [1]. In this work, the compositional distribution and defects in Hg1-xCdxTe grown by means of Bridgman method are investigated. The result shows that the crystal quality can be improved by the suppression of magnetise field on convection, mass transportation and heat conduction.

The results of composition study indicate that the transverse magnetic field applied during the growth of Hg1-xCdxTe crystal can convert the axisymmetrical radial compositional distribution into eccentric distribution, which lead to a significant decrease on the deviation of the radial compositional distribution. The corrosion analyses on sub-boundaries and dislocations show that the average density of dislocation exhibits an axisymmetrical distribution with a maximum density at centre in the samples without magnetic field applied but a homogeneous distribution in those with magnetic field applied.

[1] J. L. Schmit and C. Speerschneider, Phase Diagram of Hg1-xCdxTe, J. Infrared Phys. 1968, 8, 427

P09.15.008 GROWTH OF HIGH MOBILITY INSB CRYSTALS BY VERTICAL BRIDGMAN METHOD. Premila Mohan [1], N. Senguttuvan [2], S. Moorthy Babu [1] and P. Ramasamy [1], [1] Crystal Growth Centre, Anna University, Chennai - 600 025, India, [2] Shonan Institute of Technology, Fujisawa, Japan

Indium antimonide (InSb) is a technologically important III-V semiconducting material which finds application as a mid-wave infrared detector and infrared filter. Its relatively low melting point, direct small energy gap and large carrier mobility makes it suitable for such devices. The responsivity and detectivity of the detectors are directly related to the internal parameters of the semiconductor including electron and hole concentrations and mobilities. In the present work InSb crystals were grown from 6N pure In and 6N pure Sb by vertical Bridgman technique. An indigenously developed vertical Bridgman setup

consisting of a two zone resistive heating furnace controlled by two separate Eurotherm controllers and an electronic ampoule lowering assembly was used for the purpose. Series of experiments were carried out to optimise the growth conditions such as the axial temperature gradient and ampoule lowering rate. The ampoule geometry was also found to play a dominant role in the quality of the crystals. The grown crystals were characterised by various techniques such as powder x-ray diffraction, energy dispersive X-ray analysis and electron probe microanalysis. The electrical properties of the grown crystals were studied using the Vander Pauw technique. The variation of the carrier concentration along the length of the crystal was also studied. The mobility of the crystal was found to be nearly 60000cm^2/Vs.

P09.15.009 GROWTH RATE AND MORPHOLOGY OF WATER-SOLUBLE IONIC CRYSTALS: MODELING WITH COULOMB-ONLY POTENTIALS. L.J. Soltzberg, G.S. Defoe, Z. Khan, E. Madden, and D.L. Marr, Department of Chemistry, Simmons College, Boston, MA 02115.

We have recorded the crystal morphologies of ten water-soluble univalent ionic compounds grown over a wide range of supersaturation. These crystals represent a variety of space groups and structure types, including two with extensive hydrogen bonding. Growth rates range from very slow growth giving mature, "late-growth" crystals; through faster growth characteristic of the early stages of crystallization, giving "early-growth" morphology; to very rapid crystallization producing dendritic morphology. We have modelled the morphologies of each of these crystals using attachment energies computed with the MARVIN code [1]. The predicted morphologies generally give very good agreement with observed late-growth morphologies. Further, the early-growth morphologies can be modeled by artificially reducing the relative attachment energies of one or, occasionally, two growth directions as shown below. Directions of needle crystal growth marking the onset of dendritic crystallization correspond to high attachment energies and correspondingly rapid growth. It is noteworthy that we can model these morphologies using only Coulomb potentials, presumably because electrostatic interaction dominates the lattice energy in these ionic systems.

$NaIO_4 \cdot 3H_2O$

observed
late-growth morphology

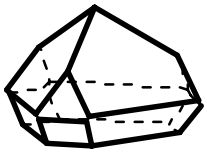

observed
early-growth morphology

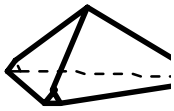

computed
AE morphology

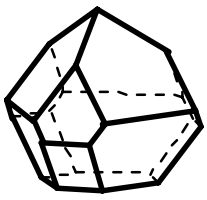

$AE_{00\text{-}1}$
reduced

1. D.H. Gay and A.L. Rohl (1995). *J. Chem. Soc. Faraday Trans*. 91, 925-936.

P09.15.010 NUMERICAL SIMULATION AND OBSERVATION OF THE GROWTH DIFFERENCE ALONG THE POLAR AXIS OF LiB_3O_5. J. H. Jung, H. M. Park* and S. J. Chung, School of Materials Science and Engineering, Seoul National University, Seoul 151-742, Korea. *Materials Evaluation Center, KRISS, Taejon 305-600, Korea.

The single crystals of lithium triborate (abbr.; LBO) were grown by top-seeded solution growth using <010> seed normal to the polar axis and the difference of growth rate between the opposite ends of polar direction was observed during the growth process.

In the beginning stage of cooling range down to 3º during the growth process, the growth rate in one of the polar direction is much higher than that of in the opposite direction. After cooling down to 3º the difference of growth rate is reduced gradually.

The growth rates and the lengths of grown crystal along the polar axis were numerically simulated with some known data related to LBO crystal and the solution. The assumptions that the spontaneous polarization of LBO crystal form an electric field only near the interface between the crystal and the conductive solution and this spontaneous polarization due to the asymmetric arrangement of structural building units results in the repulsive or attractive forces to the charged growth units and the difference of mass transfer between both ends of the polar axis were introduced in the simulation.

The calculated results were compared with the experimental observations and they fit well together. The polar direction of the grown crystals were detected by the observations of etch pits and the measurements of pyroelectric coefficient which was even much smaller then that of the other pyroelectric crystals.

P09.15.011 IDENTIFICATION OF CLEAVAGE PLANES IN SALTS USING MOLECULAR MODELLING. J.C. Osborn and P. York, Drug Delivery Group, School of Pharmacy, University of Bradford, Bradford BD7 1DP, UK, and R.C. Rowe and R.J. Roberts, Zeneca Pharmaceuticals, Alderley Park, Macclesfield Cheshire SK10 2NA, UK.

The cleavage properties of crystalline pharmaceutical materials are important in the processing of tablets. Previously molecular modelling has been employed to predict morphology and slip planes in molecular materials. However many drugs are formulated as salts so that an extension of these techniques to molecular salts is required.

The surface attachment energy which is calculated in models of crystal growth may be utilised to identify cleavage planes by postulating that the most weakly attached plane has the least resistance to slip. Attachment energy calculations for salts require allowance for the long-range electrostatic interactions. Calculations have been performed using the Cerius[2] molecular modelling package (Molecular Simulations, Inc.) and the MARVIN surface modelling program [1].

Results for several salts will be presented. Determination of the preferred slip planes is important in the study of powder processing, as milling enhances the exposure of the cleavage planes, thus modifying the sorption properties of the powder. A study of the effect of milling on the surface properties of the drug dl-propranolol hydrochloride, using inverse gas chromatography [2], has yielded results consistent with the slip plane predicted by molecular modelling.

1 D.H. Gay and A.L. Rohl (1995). J. Chem. Soc. Faraday Trans. **91**, 925.
2 P. York, M.D. Ticehurst, J.C. Osborn, R.J. Roberts and R.C. Rowe (1998). Int. J. Pharm. **174**, 179.

P09.15.012 FACET FORMATION OF Ag_2S SMALL CRYSTALS EQUILIBRATED WITH SOLID Ag. T. Ohachi Department of Electrical Engineering, Doshisha University, Kyotanabe, Kyoto 610-0321 Japan

Self ordering of nano meter size crystals is currently studied extensively for application of quantum dots electronics devices. The understanding of equilibrium form (EF) needs the understanding of surface free energy density. The surface free energy density, which gives EF, is determined not only by the properties of bulk crystal but also the surface condition such as adsorption or contact substance at the interface. Facet formation of EF with sulfur vapor was determined only by vapor pressure and temperature. Facet formation, however, equilibrated with solid state silver is determined by temperature and the orientation difference between Ag2S and Ag. This paper reports experimental results obtained from the experiment mentioned the title of this abstract. Equilibrium crystals were prepared by annealing of single crystals of Ag2S grown by quenching from liquid Ag2S droplets within liquid silver. The high temperature phase of Ag2S, which is an ionic and electronic mixed conductor, has two crystal phases bcc and fcc and is easy to equilibrate even mm size.[1][2] Liquid droplets of Ag2S, which were nucleated in liquid silver, solidified after liquid silver solidification. The grain size of the matrix silver became large during annealing experiment. After the formation of the large grain size of the matrix silver, the Ag2S crystals, which were in the matrix silver, were melted and crystallized again to much the orientation of the matrix silver and equilibrated. Crystal shape was observed by scanning electron microscape at a scanning room temprature after removing the matrix silber. Above 700 deg C {111} facet of fcc Ag2S was obtained when 3 axis(2 axis) crystal orientations of the matrix Ag and fcc Ag2S were coincide. Only one axis coincidence formed circle disk of two facets. On nealing below 700 deg C rounded EF with {110} facets a belonging to bcc Ag2S were obtained.

[1] T.Ohachi and I,Taniguchi, J,Crystal Growth 65(1983)84.
[2] T.Ohachi and I.Taniguchi, in Morphology and Growth Unit of Crystals ed.by I.Sunagawa(TERRA Sci.Pub.TOKYO) pp 185-199(1989).

P12.15.001 THE TWINS FORMATION DURING LEC GROWTH OF GaAs AND InAs CRYSTALS. V.G. Kossoushkin , Institute of Technics and Technologies, Kaluga, Russia, 248001, p/b 323, Kaluga, Russia.

One of the difficulties in the growth of GaAs and InAs single crystals is the strong tendency to twin. The twin formation during crystal growth has been correlated to many growth factors. The probability of twinning can be suppressed to a lower value by optimizing of the growth factors but the mechanism involved for the twin formation is not well understood at present.

The GaAs and InAs single crystals were grown by the LEC method with careful control of growth conditions. We used new method of temperature measurement in subcrystalline region during all crystal growth process. More than sixty crystals, some with twins and some twin-free were cut into {110} wafers. The {110} wafers were parallel to the growth direction and perpendicular to the twin boundary. The striations, facets and twin boundaries on the surface revealed by diluted Sirtl-like solution under light illumination (DSL solution) were observed by optical microscopy.

From chemical etching study it can be concluded that the growth conditions, which result in the generation of large irregular facets, also favor the formation of twins. However, the facets are not necessarily the nucleation sites of twins. Our results suggest that the 60^0 rotation twin has lower energy that the inversion twin.

In some crystals twinning begin at the facets and were found to depend on the peripheral interface shape, independent of the shape of the central parts. Twinning occurs during shoulder growth when facets extend deeply into the crystal and temperature fluctuations cause frequent meltbacks. The use of 1MHz ultrasonic vibrations was found to prevent twinning by stabilizing the growth conditions near crystal -melt interface. This results confirm that control of the growth interface shape is the key in the technology of crystal growth. The twinning can be reduce by the special low energetic influences.

P12.15.002 ON THE NATURE OF TWINNING. Robert A. Sparks, Bruker-AXS, Inc., 6300 Enterprise Lane, Madison WI, 53719, USA and Victor G. Young Jr., Department of Chemistry, University of Minnesota, 207 Pleasant St. S. E. Minneapolis, MN 55455, USA

Using the Bruker SMART CCD diffractometer it is almost always possible to solve and refine the crystal structures of twinned samples. It is also often possible to determine the type of twinning present and the molecular nature of the interface between the twin components.

With special twin software, TWINDX and TWUTIL, it is possible to determine the indices for each observed reflection for each twin component. With the lattice parameter least square procedure in the program, SMART, it is sometimes possible to measure the crystal center for each twin component. With the program, TWROT, it is possible to determine the twin axis and the angle of rotation about this twin axis. With the integration program, SAINT, the reflection intensities are obtained for all reflections for each twin component. With the program, TWHKL, the reflection intensities are merged into an HKLF5 file that the program SHELXTL can use to refine the atomic parameters of the twinned crystal structure. It is usually possible to solve and refine the crystal structure of most twinned samples with a precision almost as good as that obtained for single crystals.

By viewing the packing diagram from many different directions it is often possible to determine the nature of the bonding across the twin interface.

Examples are given of the use of these procedures. From the results of crystal structure determinations of many twinned samples conclusions concerning the nature of twinning are presented.

16. CHARACTERISATION OF DEFECTS, MICROSTRUCTURES AND TEXTURES

P05.16.000 SUBSTITUTION IN Ta_3O_7F AND ITS EFFECTS ON TWINNING. L. Jahnberg, and M. Sundberg, Department of Inorganic Chemistry, Arrhenius laboratory, Stockholm University, S-10691 Stockholm, Sweden.

The low-temperature form of Ta_3O_7F [1], as well as the high-pressure form of Nb_3O_7F [2], has a structure related to U_3O_8. It can be described as consisting of pentagonal bipyramids and octahedra, sharing edges and corners in the (001) plane. The polyhedra are repeated in the [001] direction by corner sharing. The ratio octahedra to bipyramids is 1:2.

In this structure the metal atoms can to some extent be replaced by titanium or zirconium. Since titanium occurs six-coordinated, the composition $TiTa_2O_6F_2$ was expected to be possible. It was synthesised from $TiO_2{\cdot}2TaO_2F$ in Pt-tubes. The obtained unit cell dimensions, a=6.394, b=10.487 and c = 3.888 Å, are somewhat shorter than those given in ref. 1.

EDS analysis using a JEOL 2000 FX II / LINK OX-200 microscope showed the Ti content to be approximately 28 atom% e.g. slightly less than 1/3, which agrees well with a small weight loss in the preparation.

A Rietveld refinement on powder diffractometer data and with 85% titanium in the octahedral position gave the R_F-value 0.089. This agreement was reasonable considering the problematic peak shapes from the sample which probably was due to extensive twinning and defects. Since the orthorhombic structure has a pseudohexagonal symmetry it has a tendency to grow as twins. This tendency seems to increase with titanium in the octahedra.

HRTEM images show alternating strings of two twins with the (110) plane as twin plane. This growing has a similarity to the periodicity in low-Ta_2O_5. Also substitution with zirconium has been performed and found to have a stabilizing effect on this modification of Ta_3O_7F and Nb_3O_7F.

1. M. Vlasse, C. Morilière, J.-P. Chaminade and M. Pouchard, Bull. Soc. fr. Minéral. Cristallogr. 98 (1975) 325.
2. L. Jahnberg, Chem. Comm. Stockholm Univ. (1971) no 13.

P05.16.001 SIMULATION OF X-RAY DIFFRACTION PATTERNS OF A ONE-DIMENSIONAL DELTA-CRYSTAL. I.A. Kasatkin, Dept. of Crystallography St. Petersburg State University, Universitetskaya nab. 7/9, 199034, Saint-Petersburg, Russia.

Mixed crystals grown under non-stationary conditions are always inhomogeneous and can show a gradient of composition along a direction of growth resulting in a gradient of lattice spacing. Such crystals display some specific features of diffraction patterns if the change in lattice constant is about 1 % per cm. If properly cut and bent, they can serve as active elements of focusing monochromators, lenses, and other X-ray optic devices [1]. It is desirable to have a method for testing the value of gradient in as-grown delta-crystals.

A model has been designed [2] that allows to predict the distribution of the intensity of X-rays diffracted by a single crystal along a given direction in reciprocal space that is parallel to the direction of gradient. The intensity of the beam scattered by the crystal under a given Bragg angle is calculated as a sum of the intensities scattered by different "homogeneous" regions, each of which consists of a number of coherent domains with their sizes distributed according to a certain law. A region is characterised by a mean lattice constant that changes stepwise with the position (depth from the surface) according to the value of gradient. The absorption of X-rays by a crystal, the variability of the lattice constant gradient and the shape of instrumental function of diffractometer are taken into account in the model.

The profiles of 0k0 reflections from the delta-crystal of $(K_xRb_{1-x})C_8H_5O_4$ (x changes from 0 at the seed to 0.25 at the surface) [3] have been simulated with considerable precision. The values of gradient obtained were found to be close to those measured directly. The work was supported by RFBR.

1. H. Bradaczek et al. Coll. Abstr. XVI Congr of IUCr, Beijing, 1993, p.374.
2. I.A. Kasatkin & T.I. Ivanova, Cryst. Rep. (1998) 43 (6) 1074-1077.
3. S.V. Moshkin et al., J. Cryst. Growth 172 (1997) 226-230.

P05.16.002 STRAIN-INDUCED INTERACTIONS OF β-STABILISING SUBSTITUTIONAL IMPURITY ATOMS IN H.C.P.-TITANIUM MATRIX. S.V. Shevchenko, V. A. Tatarenko, N.S. Kosenko, and C.L. Tsynman. Institute for Metal Physics, National Academy of Sciences of the Ukraine, 252142, 36 Vernadsky blvd. Kiev, Ukraine.

An instability with respect to the phase transformations in h.c.p.-Ti alloys with isomorphous (Mo, Ta, Nb) and eutectoid (Fe, Cr) β-stabilising elements is studied by analysis of the strain-induced and «electrochemical» interatomic interactions of substitutional impurity atoms, as well as related microstructural features of the martensite in binary titanium alloys.

The method of static concentration waves is used to describe impurity subsystem distribution. Dependencies of the «mixing»-energies Fourier-components' matrix eigenvalues along 12 main directions within the Brillouin zone are obtained. Analysis of these dependencies had shown that the alloys under consideration are unstable, and an atomic ordering with formation of antiphase isostructure domains is expected; besides, bulk modulations in substitutional atom distribution for these systems must occur within the basal plane, but along the corresponding directions. It has been found that the strain-induced contribution to the impurity—impurity interaction energy in α-Ti has a remarkable value and is about ~0.2-0.6 eV/atom in magnitude.

If the strain-induced interaction is considered only (which would be acceptable for the latest stages of decomposition), the h.c.p. solution should be unstable too, and the character of the phase transformations should be distinct. Isomorphous systems would be tend to spinodal decomposition, and layered atomic ordering along the hexagonal axis would occur in eutectoid systems.

P05.16.003 MICROINDENTATION STUDIES OF THE CHALCO HALIDES OF ANTIMONY AND BISMUTH. G. Kanchana and D.Arivuoli, Department of Physics, Anna University, Chennai-600 025, India.

Group Vb chalcohalides show interesting properties like ferro-elecity, semi-conducting and photo-conductivity and some of the crystals also piezoelectric and pyro-electric properties. The mechanical properties of these compounds have not been studied in detail due to the difficulty in growing larger size crystals. The compounds show needle morphology due to inherent chain type structure along the c-axis and hence higher growth rate along c direction than the other directions. The mechanical properties of the larger size single crystals, grown both by using vapour phase technique and gel growth technique, were studied using pyramidal vicker's indentation technique. The indentations were carried out along the (110) axis for all the crystals. The micro-hardness increased with increase of load and exhibited a constant value after a particular load. The hardness was found to decrease on annealing the compounds at different temperatures but below the dissociation temperature of the volatile compounds. The dislocation density was also found to decrease slightly with

annealing temperature. The surface of the indented regions at various loads was studied using SEM and also etching the crystals after indentation. In some of the crystals crack was found to propagate on increasing the load and hence the other related mechanical properties as brittleness index and fracture toughness were also deduced. An empirical correlation of the hardness with inter-planar spacing cell volume and bond energy were found for the compounds exhibiting the same crystallographic structure.

P05.16.004 RIETVELD REFINEMENT WITH WAVELET COMPRESSED DATA SETS. Lubo Smrčok, Institute of Inorganic Chemistry, SAS, SK-842 36 Bratislava, Slovak Republic

Recording of experimental data is one of the crucial steps in Rietveld refinement. The most widely accepted procedure prescribes to scan a pattern using an arbitrarily chosen, but a constant step, typically equal to hundredths of 2Θ. Such a simple strategy leads to oversampling, which is mostly ignored. The aim of this study was to explore how wavelet compressed data sets mimic the original ones in Rietveld refinement.

Crystal structures of triclinic kaolinite, cubic HMT and a part of the structure of a monoclinic rare sugar were refined using wavelet compressed sets of intensities. Wavelets are a family of basis functions which can be used to approximate measured signals either in one, or in multiple dimensions. Compression of intensities sets was accomplished by a discrete wavelet transform (DWT) [1] using Daubechies4 [2] wavelet. The original sets consisting of 4096 intensities were step-by-step compressed to 2048, 1024, 512 and 256 intensities, which were the inputs to refinements. It was found that accuracy of refined positional parameters did not change significantly even f the compression ratio reached 8:1, or 16:1. Similarly, quantitative phase analysis of a three-components mixture done by Rietveld method provided very close estimates of phase composition for compression ratios 2:1 and 4:1.

Application of DWT compressed data reduced the time needed for a refinement to 50-60% without significant loss of information [3]. This procedure may accelerate molecular modelling based on powder data, or speed up introductory steps of Rietveld refinements with extensive data/parameters sets.

[1] Chui, C.K. Introduction to wavelets. Academic Press, Boston, 1991
[2] Daubechies, I. Comm. Pure Appl. Mathematics 41 (1988) 909
[3] Smrčok, Ľ. Z.Kristallogr. (1998) Submitted.

P05.16.005 GRAIN BOUNDARY MAPS FROM EPIFLUORESCENCE SIGNALS OF EUROPIUM IONS INTO ALKALINE HALIDE CRYSTALS. A.E. Cordero-Borboa, Instituto de Física, UNAM, A.P. 20-364, D.A. Obregón, México D.F. 01000, México, and L.F. Jiménez-García, Facultad de Ciencias, UNAM, Cd. Universitaria, México D.F., México.

A simple method to make visible the three dimensional array of grain boundaries in transparent crystals has been developed and applied to the study of the architecture of grain boundaries in NaCl, KCl, RbCl and mixed alkaline halide crystals grown by the Czrochalski technique. In this method the grain boundaries are visible under an epifluorescence microscope by exciting the emission spectra of europium ions previously added as impurities to the melts from the which the crystals are going to grow. The as-grown crystals are heated and quenched to assure an hazardous distribution of the europium ions into the crystal matrices. Then the crystals are long annealed to allow the europium ions to gently move and found each other into the crystal lattices up to form europium chloride aggregates of microscopic size. These aggregates grow preferently at the grain boundaries of the alkaline halide crystals due to the mechanical relaxation of the stress in these boundaries. Three dimensional grain boundary maps for NaCl, KCl, RbCl and a mixed crystal particles are presented. These maps are accompanied by and X-ray diffraction study by using Weissenberg and Buerger-precession photographs.

P05.16.006 MEASUREMENTS OF BIREFRINGENCE IN NONHOMOGENOUS SAMPLES. M.A. Geday, W. Kaminsky and A.M. Glazer Department of Physics, Clarendon Laboratory, University of Oxford, Parks Road, Oxford OX1 3PU, UK.

A previously presented optical imaging system [1] has been revised and a Windows application has been written to derive and analyse birefringence data. Birefringence (= difference between refractive indices n2-n1 as a result of the anisotropy of the medium) is described by extinction angles and a phase difference (delta = (n2-n1)*L*2pi/lambda, where L is the thickness of the sample and lambda is the wavelength of the light).

The system is capable of determining the birefringence, its orientation and the absorption for each pixel within an image. The data are presented as colour coded images.

The system comprising a rotating polariser and a circular analyser was fitted to an optical microscope. Images of any transparent object are generated using a CCD-camera connected to a PC.

The new code has been extended to correct for polarising imperfections in the light path, and thus provides data of a higher quality needed to calculate the phase difference beyond the first order. This is done by a new algorithm based on comparisons between data generated at different wavelengths.

As examples conoscopic and orthoscopic images of mineral samples, crystals and biological specimens will be shown.

For example images see:
http://xtal.physics.ox.ac.uk/Research.html#Current

1: A.M. Glazer, J.G. Lewis and W. Kaminsky (1996). Proc. R. Soc. Lond. A 452, 2751-2765.

P05.16.007 THREE-FOLD TWINNED PARTICLES IN FE ION IMPLANTED GaAs. K. Sun, Structural Chemistry, Stockholm University, S-106 91 Stockholm, Sweden; Beijing Laboratory of Electron Microscopy, Chinese Academy of Sciences, 100080 Beijing, China.

In the study of iron ions implanted single crystal (100) GaAs wafers, submicron three-fold twinned particles were found in the ion implanted layers. These twins have been confirmed by dark-field electron microscopy and high resolution electron microscopy. The morphologies of these particles are mostly hexagonal cylinders, consisting of three pairs of large twins. Stacking faults were observed inside each part of the twins. The GaAs wafers were implanted with Fe ions with a total dose of 5´1017 Fe+/cm2 at an energy of 100 KeV. They were sealed in evacuated silica tubes and then furnace annealed at 600 °C for ten hours. The compositions of these particles were measured by energy dispersive X-ray analysis with ~97 at.% Ga, ~ 3 at.% Fe and ~ 2 at.% As (Ga-rich phase). Selected area electron diffraction and zone axis microdiffraction analysis indicated this Ga-rich phase is primitive orthorhombic. Its lattice parameters are about a = 0.46 nm , b = 0.89 nm, and c = 0.79 nm.

The Ga-rich phase is stable under the electron beam irradiation. But it is different from those usually found in Ga-As-Fe bulk materials [1] or in Fe ions implanted and rapidly thermal annealed layers of single crystal GaAs wafers [2]. In both two cases, only two different Fe-rich hexagonal Fe_3GaAs phases (H1: $P6_3/mmc$, a = 0.4006 nm, c = 0.5040 nm and H2: $P6_3/mmc$, a = 0.8012 nm and c = 0.5040 nm) had been found.

1. O.M. Elena & M. El-Boragy (1986). J. Appl. Crystallogr. 19, 80; E. Devlin, N.A. Smith, I.R. Harris, B. Cockayne & W.R. MacEwan (1990). J. Less-common Metals 157, 315.
2. J.C.P. Chang, N. Otsuka, E.S. Harmon, M.R. Melloch & J.M. Woodall (1994). Appl. Phys. Lett. 65, 2801.

P05.16.008 PHASE INTERGROWTH WITHIN OH-BEARING INCLUSIONS IN EXPERIMENTALLY OXIDIZED OLIVINE: NANOMETER-SCALE INVESTIGATION. N.R.Khisina, Institute of Geochemistry and Analytical Chemistry of Russian Academy of Sciences, Moscow117975, Russia; R.Wirth, GeoForschungsZentrum Potsdam, Potsdam D-14473, Germany.

Olivine grain of natural origin annealed in a laboratory at 700 C in air was investigated by TEM including HRTEM, AEM, EELS SAED and CBED technique. Inclusions up to several hundred nanometers in size were observed in ion-thinned (100) section of the grain. The inclusions were of hexagon-like shape with the coherent inclusion/matrix interfaces parallel to (010), +/-(01-1), +/-(011) of the olivine matrix and exhibitted a chemical separation by Mg and Fe with a Fe-rich Mg-poor silicate core and a rim close by composition to the olivine matrix. Sharp coherent core/rim boundaries were observed parallel to (001), (010), +/-(021), +/-(021-) of olivine matrix with a strong moire patterns in the core. EELS spectroscopy data indicated a presence of water and/or Fe3+ in a core. SAED and CBED patterns were obtained with the electron beam parallel to [100], [2-11] and [31-1-] directions of the olivine matrix and a superposition of reflections from several phases was observed: olivine matrix (m); SiO2 beta-crystobalite (cr) and FeOOH feroxihite (f) in the core of inclusions; a secondary olivine (ol) in the rim of inclusions; with (100)m // (001)f // (111)cr // (100)ol; [010]m // [11-0]f // [110]cr // [010]ol. Inside the core the f and cr layers were found to be alternated along [100]ol. Such a complex microstructure of the inclusions is interpreted as a solid state transformation of inclusions created by a precursor phase like a hydrous Mg-silicate (HMS). The transformation of HMS under experimental annealing is assumed to involve the processes of oxidation and partial dehydratation of the precursor phase accompanied by a phase separation inside inclusions and Mg-Fe exchange between the Fe-free HMS inclusions and Fe-bearing olivine matrix.

P05.16.009 STRUCTURAL STUDIES OF QUANTUM DOTS BY TEM. W. Neumann, H. Kirmse, R. Schneider, Institute of Physics, Chair of Crystallography, Humboldt University of Berlin, Invalidenstrasse 110, D-10115 Berlin, Germany, and K. Scheerschmidt, D. Conrad, Max Planck Institute of Microstructure Physics, Weinberg 2, D-06120 Halle, Germany.

The optoelectronic properties of quantum dot (QD) test and device structures are essentially controlled by the structural perfection of the individual QDs, including their size, shape, and arrangement, as well as by their chemical composition. Owing to typical QD's dimensions of some nanometres transmission electron microscope (TEM) techniques have to be applied to elucidate the above-mentioned peculiarities.

Various II-VI compound semiconductor QD samples were investigated in detail by diffraction-contrast and high-resolution TEM imaging, where information on the size distribution, arrangement, and orientation relationship with respect to the wetting layer was particularly gained in plan view, and on the nanocrystal morphology in cross-section [1]. Since the image contrast visible in the QD regions is strongly influenced by the strain field arising from the lattice mismatch image interpretation was performed by means of image processing and computer simulation. Several crystallographic structure models, i.e. complete and truncated pyramids with different facets and different orientations to the underlying layer, were taken into account. The whole supercell used to describe the complex materials system (substrate, wetting layer with quantum dot, capping layer) was energetically relaxed by molecular dynamics calculations [2]. Simulated diffraction-contrast and high-resolution images are compared with the experimental findings.

[1] H. Kirmse, R. Schneider, M. Rabe, W. Neumann, F. Henneberger, Appl. Phys. Lett. **72** (1998), 1329
[2] W. Neumann, H. Kirmse, R. Schneider, K. Scheerschmidt, D. Conrad, M. Rabe, F. Henneberger, Proc. 14th Int. Cong. Electr. Microsc., Eds. H.A.C. Benavides, M.J. Yacaman, IOP Publishing, Bristol and Philadelphia, 1998, 367

P05.16.010 MICRODOMAIN STRUCTURE IN Fe_2O_3-DOPED ZnO AND THE FORMATION OF SPINEL. F. Wolf and W. Mader, Institut für Anorganische Chemie der Universität Bonn, Römerstr. 164, 53117 Bonn, Germany

Modulated structures in doped ZnO ceramics have been discussed in the literature [1-4]. However, the nature of the defect microstructure has not yet been clarified. In the present study zinc oxide crystals were prepared at 1200 C via conventional solid state route from powder mixtures of ZnO with 1 mol% and 12.5 mol% Fe_2O_3, respectively. The crystals were investigated by means of transmission electron microscopy. Elemental maps were calculated from energy-specific images obtained with a post-column electron energy imaging filter (GIF).

Typical are planar faults of two types: (i) faults parallel to the basal plane, {0001}, and (ii) faults parallel to pyramidal planes, $\{2\bar{1}\bar{1}5\}$. All these defects were identified as inversion domain boundaries (IDBs) resulting in an inversion domain microstructure. This was proved by dark field imaging using the {0002} reflections and by microdiffraction analysis from single domains. The elemental maps reveal the additive to be preferentially incorporated into the inversion domain boundaries.

The higher concentration (12.5 mol% Fe_2O_3) leads to a microstructure with alternating ZnO and spinel layers, where the ZnO layers still contain micro-domains. The crystallographic orientation relationship is: $(0001)_{ZnO} \parallel (111)_{ZnFe2O4}$ and $[2\bar{1}\bar{1}0]_{ZnO} \parallel [1\bar{1}0]_{ZnFe2O4}$. Hence, the close- packed planes and thus also the directions of the oxygen sublattices in both crystals are parallel.

The crystals with low additive concentration (1 mol% Fe_2O_3) cause diffraction streaks and diffuse lines which can be interpreted to be caused by lattice mismatch between ZnO and $ZnFe_2O_4$. Hence, the defects may be considered as nucleation sites of spinel.

[1] N. Uchida, Y. Bando, M. Nakamura, N. Kimizuka, Proc. ICEM-13 Vol. 2b, 891 (1994) Paris
[2] E. Olsson, G. Svensson, T. Hörlin, Proc. EUREM-11 Vol. 1, 208 (1996) Dublin
[3] A. Loewe, W. Mader, Proc. ICEM-14 Vol. 3, 309 (1998) Cancun
[4] C. Li, Y. Bando, M. Nakamura, N. Kimizuka, J. Solid State Chem. 142, 174 (1999)

P05.16.011 IN SITU INVESTIGATION OF DEFORMED ALUMINIUM TOPOGRAPHY. Afanasyev V. [1], Semukhin B., Zuev L [2], [1] Applied Mathematics and Cybernetic Faculty,Tomsk State University, [2] Department of Strenght Physics,Institute of Strength Physics and Material Science Siberian Branch of Russian Academy of Sciences, [3] Department of Strenght Physics,Institute of Strength Physics and Material Science Siberian Branch of Russian Academy of Sciences

Using a modified technique of the Fujiwara X-ray topography, the evolution of 200 and 311 images of coarse-grained aluminium specimens under deformation has been examined. A study has been made of the initial stage of deformation during which no marked changes occur in the

structure or substructure of the material investigated. The study was made on an Instron-1185 test machine with one immovable clamp using aluminium specimens having grain size of 1 - 3 cm. By specimen deformation, the position of the Lauer spot was defined for a large-sized grain of the working portion of the polycrystalline specimen and the rate of ultrasound propagation was measured simultaneously at the same point, the latter quantity being a structure-sensitive one. A microfocus tube having a 40 mm focus and a copper anode was used as an X-ray source.

As a result of the study it has been found that at the initial stage of plastic deformation, the material's substructure undergoes a change, which is manifested in rotations of individual grain volumes.With increasing level of deformation, the rate of ultrasound propagation also grows, which might be attributed to greater crystallite perfection due to grain volumes rotation. As the level of deformation, e, approaches 0.5 %, the local rotations become readily detectable.

Analysis of the electron density distribution over the grain area allows the microvolume sizes involved in the process of deformation to be evaluated; they are found to be a few hundreds of microns. Thus, using a modified technique of the Fujiwara X-ray topography, in situ investigations of plastic deformation can be carried out to yield scale parameters of the process that give an insight into the physical laws governing deformation of solids.

P05.16.012 FORMATION OF A RADIATION POINT DEFECTS ENSEMBLE IN THIN SI^+-DOPED GAAS LAYERS. K.D. Chtcherbatchev, V.T. Bublik, Yu.N. Parkhomenko, Moscow State Institute of Steel and Alloys, Leninskii pr.,4, 117936 Moscow, Russian Federation.

The formation of a radiation point defects ensemble in SI-GaAs (001) wafers that were implanted by Si^+ ions at 50 keV and various doses ($1\cdot10^{15}$ and $1\cdot10^{14}$ cm^{-2}) and annealed during 10 min at 850°C in arsine air was studied by high-resolution X-ray diffraction (HRXRD). Distribution of the implanted dopant was monitored by the secondary ion mass spectrometry (SIMS) method. Distribution of radiation point defects causes the distribution of strain in the distorted subsurface layer. Thus, an analysis of the strain depth profiles was used for an explanation of the behaviour of point defects in as-implanted and annealed samples. The Frenkel type defect is assumed to be a major one in irradiated samples. To reconstruct the strain depth profiles the diffraction patterns were fitted using the simulation software based on the theory of a dynamical diffraction. The strain depth profiles were found out to be extremely close in as implanted samples for both doses despite the tenfold difference in doses. Nevertheless, the analysis of an X-ray diffuse scattering showed that the total concentration of radiation point defects must be greater for the sample implanted by the highest dose. It can be explained by running of two processes that plays an essential role in the formation of defect layer during implantation. The first one is an annihilation that reduces the concentration of radiation point defects. Another one is the sink of the most mobile interstitials to the surface. It leads to the disbalance of interstitial and vacancy components of Frenkel's pairs and formation of the thin subsurface layer enriched by vacancy type point defects. The thickness of the layer increases after annealing. This layer is stable that can be caused by small mobility of vacancies. This layer is shown influence on redistribution of implanted impurity and stimulates diffusion of the impurity to the surface.

P05.16.013 CHEMICAL AND CRYSTALLOGRAPHIC CHARACTERIZATION OF SYNTHETIC CORUNDUM (Al_2O_3). C.Rinaudo and P.Orione, Dipartimento Scienze Mineralogiche e Petrologiche- Università di Torino, Via Valperga Caluso 35-10125 TORINO-Italy

Synthetic corundum samples, synthesized by Verneuil and Czochralski methods, have been studied as regards the chemical and crystallographic aspects.

The samples were "boules", colourless or red, cut in slices (about 1 mm in thickness) normal or parallel to the elongation axis. The different slices have been studied by optical microscopy, EDS, X-ray topography using white beam of the synchrotron radiation at LURE (Orsay-Paris). Analyses by Raman spectroscopy with a source in the NIR were also performed.

For all the examined samples, independently from the growth method, the slices obtained from the first-grown parts of the boule resulted single crystals, but the X ray topography revealed disorientation in different regions of a given slice. Studying the slices from the middle part and from the top of the boule, the samples were no longer single crystals but a trend to crack into subparallel domains were evidentiated.

Raman spectroscopy was applied on the slices with different orientation with respect to the laser source and the obtained results have been related to the crystallographic characteristics of the slices in the different orientations.

All the observed phenomena will be discussed taking into account the different stages of the growth process and a practical application on cut gem stones used for gemmmological applications will be shown.

P05.16.014 BRAGG-CASE SECTION IMAGES OF STACKING FAULTS IN DIAMOND. Moreton Moore and W.K. Wierzchowski[1], Royal Holloway University of London, Egham, Surrey, TW20 0EX, U.K., [1]Permanent address: Institute of Electronic Materials Technology, Warsaw, POLAND.

Bragg-case section images of stacking faults were obtained at experimental Station 7.6 at the synchrotron source of the CCLRC Daresbury Laboratory. The sample was a $4 \times 4 \times 0.7$ mm^3 slab prepared from a large truncated octahedral synthetic diamond grown by De Beers, which was used by us previously for studying plane-wave images of stacking faults in Bragg-case [1]. The sample was cut using a laser saw and polished along the (001) crystallographic planes.

Bragg-case section topographs of stacking faults were obtained using a well-collimated white synchrotron beam using the 400 symmetrical reflection of wavelength 1.26 Å (with a very small amount of higher harmonics). The images of the stacking faults may be classified as corresponding to the Bragg-Laue case, *i.e.* the wavefields decomposed by the stacking fault next undergo diffraction in the transmission case. The obtained images contained a series of distinct fringes appearing behind the direct image of the intersection of the stacking fault with the incident beam.

The experimental images of the stacking faults were compared with simulated theoretical images obtained by numerical integration of the Takagi-Taupin equations, where the stacking fault was approximated by a suitable step change of phase in the Fourier coefficient of dielectric susceptibility. Good agreement between the theory and the experiments was obtained. The formation of different parts of the image was also analyzed by visualisation of the distribution of $|D_o|^2$ and $|D_g|^2$ intensities in the plane of diffraction. The latter allowed us to find some analogies with the better known formation of images of stacking faults in transmission, avoiding difficulties associated with the validity of the plane-wave approximation.

[1] W. Wierzchowski, M. Moore: Acta Cryst. A51 (1995) 831-840.

P05.16.015 A HIGH RESOLUTION DIFFRACTION STUDY OF THE 222 'FORBIDDEN' REFLECTION OF DIAMOND. John S. Reid, School of Physics, University of Aberdeen, Aberdeen AB24 3UE, Scotland, Moreton Moore and Mina Golshan, Physics Department, Royal Holloway, University of London, Egham TW20 0EX, UK, Grzegorz Kowalski, Institute of Experimental Physics, University of Warsaw, Warsaw 00-681, Poland, Steve Collins and Bridget Murphy, CLRC Daresbury Laboratory, Daresbury, Warrington WA4 4AD, UK.

Recent theoretical calculations [1] of forbidden reflections suggest that such reflections are not actually forbidden but have high intensities and extremely narrow angular widths. We report here experimental evidence that supports the general predictions of this theory, using high-resolution reciprocal space mapping with 1 Å synchrotron X-rays at the Daresbury station 16.3. The specimens were (1) a type Ia natural diamond, (2) a single crystal of synthetic diamond grown under conditions of high pressure and high temperature by the reconstitution technique. In addition we took measurements on a 'perfect' single crystal of Si. All maps obtained from three different specimens confirm the existence of the forbidden 222 reflection in the diamond structure. A narrow sharp peak characteristic of this reflection has been displayed in each of the maps. However, it is noticeable that in the case of silicon the peak was smaller than that of both natural and synthetic diamonds, where the intensity of the reflection was increased by strain associated with defects. We believe that the forbidden reflection structure in diamond could be a sensitive measure of strain induced by cluster impurities and other defects.

1. Ignatovich, V.K., Masahiko Utsuro & Ignatovich, Ph.V., (1997), Forbidden reflections in Laue geometry, *Phys. Rev. B*, **55,** 14039.

P05.16.016 IN-SITU DOUBLE CRYSTAL X-RAY TOPOGRAPHIC IMAGING OF AS-GROWING CRYSTAL SURFACES. R. M. Vrcelj, P. J. Halfpenny, D. B. Sheen, J. N. Sherwood, Department of Pure and Applied Chemistry, University of Strathclyde, Thomas Graham Building, 295 Cathedral Street, Glasgow, G1 1XL

The (111) face of potassium aluminium sulphate dodecahydrate (potash alum) has been studied growing from an aqueous solution in-situ by both reflection and double crystal topographic methods utilising synchrotron sources. Comparison of these two methods shows that although the experimental layout and geometrical configuration for a simple reflection experiment are easier to maintain, the quality of results of the double crystal experiments exceed those from simple reflection.

The double crystal images show that it is possible to follow the growth processes of a crystal whether it has a well preserved or damaged surface, as long as the growth conditions are suitable for slow growth of the crystal surface. Much useful information, such as areas where refeacetting occur, the sites of emergent defects and areas of high perfection of the crystal can be clearly seen.

The ability to capture such images is a combination of a variety of factors, high photon flux from a synchrotron source, the design of an optimised cell and the availability of a choice of suitable reflections are among those of importance.

P05.16.017 OBSERVATION OF X-RAY ANOMALOUS TRANSMISSION EFFECT IN TUNGSTEN CRYSTALS. I.K.Bdikin, S.I.Bozhko and V.N.Semenov, Institute of Solid State Physicists, Chernogolovka, Moscow distr.,142432, Russia.

Dynamic diffraction effects are realize in perfect crystals only. At present there is limited number of crystals, technology of growth that, allows to reach to be required for the dynamic diffraction density of defects, not more $10^6 sm^{-2}$. Single crystals in which high melting temperature are grow with certain difficulty. This is connected with the small energy of arising the defects of lattice and with technical difficulties of getting the small temperature gradients when growing the crystals. Modern methods of preparing single crystals of tungsten allow get samples with density of defects less $10^4 sm^{-2}$ [1]. In given work are present results on observing dynamic diffraction on such crystals.

Crystals of tungsten by mechanical and electro polished were prepare plates by size $20x10x0.3mm^3$. Their broad grain oriented with the plane (110). X-rays anomalous transmission effect (Borrmann effect) in crystal tungsten realizes in scheme on transmission on copper and molybdenum radiation. Calculation on kinematics theory shows that for copper radiation at thickness of sample 0.3 mm ($\mu t \sim 98$) absorption is 10^{-43}. Under available X-ray sources to get intensity on the transmission impossible, however in dynamical perfect crystals of tungsten we easily realize topography in transmission geometry in copper radiation on (110) reflection. For molybdenum radiation exact measurements of factor of absorbing diffraction radiation $\mu_i t$=7.3. Design value of factor of line absorption tungsten by thickness 0.3mm on molybdenum radiation μt= 53.4 (μ/μ_i =7.3). Evident excess a relations μ/μ_i units be a direct effect of anomalous transmission of X-rays. However width of crocking curve determined in this case is ~50".

The interest presents using and development of theory the effects dynamic diffraction of X-ray for tungsten because it has Im3m simplest structure with two atoms in the unit cell and high X-ray absorption.

1. V.G.Glebovsky,V.N.Semenov,V.V.Lomteyko, J. Crystal Growth 87, 142, 1988.

P05.16.018 X-RAY TOPOGRAPHY and SEM OBSERVATIONS OF $LnBa_2Cu_3O_{6+x}$ (Ln=Tm, Lu) SINGLE CRYSTALS. G.M.Rilov, Institute of Mineralogy and Petrology SB RAS, Novosibirsk 630090, Russia, and M.Yu.Kameneva, L.P.Kozeeva and A.N.Lavrov, Institute of Inorganic Chemistry SB RAS, University of Novosibirsk, Novosibirsk 630090, Russia

Using X-ray topography (XRT) and scanning electron microscopy (SEM) the microstructural features of high-temperature superconductors, $LnBa_2Cu_3O_{6+x}$ (123-Ln) with Ln=Tm, Lu single crystals, were studied. The crystals were grown by spontaneous crystallization from the flux and had an orthorhombic structure. For determination of the defects within the volume of the crystal XRT experiments were carried out by the transmission techniques with Mo K_α-radiation. The surface images were received by "reflection" techniques with Cu K_α-radiation. Diffraction reflection curve method on the set of reflections 200, 020 and 006 was used too. High linear (1-2μm) and angular (several sec.) resolution in diffraction contrast images was achievable using microfocus source in combination with linear collimator.

The defects in the form of large blocks and twin domains elongated in <110> directions were revealed. The domains misorientation (1 degree for large lamels and 10-30 min for smaller ones) was obtained. Along [001] direction the crystals constituted 2-3 subparallel layers (misorientation about 30 min.) with different defect images. No contrast directly attributable to growth screw dislocations on the (001) faces was detectable on XRT. To determine such defects the etching method was used. Besides the pyramidal etch pits associated with growth spirals numerous flat etch pits bounded by {100}/{010} walls were observed by SEM. Demonstrating the similar patterns the topographs of 006-type reflections gave evidence of their tilting.

Data obtained for crystals growing in different conditions was vital for conclusion about mechanism and optimization of the growth process.

The work is partially supported by grants of Federal directed Program K0042, “Superconductivity” Program № 98009 and “Russia Universities” № 1785.

P05.16.019 DISORDERED STRUCTURES BY HIGH RESOLUTION POWDER DIFFRACTION. R.E. Dinnebier, Laboratory of Crystallography, University of Bayreuth, D-95440 Bayreuth, Germany

According to a text book definition, the perfect crystal is a container in which the fundamental component (structural motif) is replicated in the 3-dimensions of space by a combination of symmetry operations and translations. On contrary, the real crystal has a number of defects and exhibits all kinds of disorder, where disorder means the distortion of translation symmetry. Disorder can be divided into two categories: static and dynamic disorder. Examples for static disorder are mosaic spread, surface defects (e.g. grain boundaries), substitution, point defects (e.g. Frenkel or Schottky type), planar defects (e.g. stacking faults), dislocations, impurities, lattice strain etc. Examples for dynamic disorder are reorientational jumps, thermal motion (translation + vibration), rotation of molecules, (continuous, stepwise, around axis, spherical) etc. With single crystal diffraction, it is often possible to detect certain types of disorder directly and to refine disordered crystal structures. In the case of powder data, the reduced content of information renders it quite complicated to model disorder. Nevertheless, in some cases, the occurrence and the type of disorder can be extracted from a high resolution powder pattern by analyzing diffuse scattering, additional lines inconsistent with space group symmetry, 'strange' line shapes, anisotropic peak broadening and reflection intensities. Examples of disordered structures will be given which have been solved from powder data by applying different methods like anomalous dispersion, the split atom model, Rigid Body Rietveld refinement, the maximum entropy method, energy minimization, spherical shell form factors, anisotropical FWHM distribution, pattern simulation, investigation of anisotropic temperature factors etc.

P05.16.020 THE ATOMIC-FORCE MICROSCOPY INVESTIGATION OF DYNAMICS VARIATIONS OF THE NEW FORMED CRYSTAL SURFACES. V.A. Liopo, A.F. Sen'ko, Physics & Ingineering Department of Grodno State University, Ozheshko st. 22, Grodno 230023, Belarus, and A.U. Sheleg, A.V. Kartavtzev, Institute of Solid State and Semiconductor Physics National Academy of Sciences of Belarus, P.Brovka st. 17, Minsk 220072, Belarus.

The most important and perspective direction of the applying atomic-force microscopy (AFM) as a variety of scaning probe microscopy is the using for investigation dynamics of changes (DC) of new formed surfaces (NFS). The DC of surfaces activity was analysed in the same points. We investigated NFS of monocrystals with perfect cleavage. For our analysis we took the di-and trioctahedral mica crystals. The new formed surfaces of these natural crystals are constructed by silicon-oxigen tetrahedron faces with random interlayer cations distributions. Besides we researched the isostructural semiconductors $TlGaSe_2$ and TlInSSe crystals. $TlGaSe_2$ crystalls have the trilayers structure from Se tetrahedron with Ga atom in its center. Tetrahedrons form the layers parallel (001)…. Point group of mica and analysed by us semiconductors is $C2/_m$. The NFS are obtained by means splitting along cleavage plane of the crystals directly before AFM-investigation. We revealed the surfaces active islands with sizes from 1,2 μm to 580 nm. The high of surface adsorbtion production are about 20-50 nm. Besides these processes we discovered the going out of some part of matter from inner bulk crystal regions as usually near the surfaces defects. Together with these processes the degree of surface roughness changings take place. All processes on the juvenile crystals surfaces may go on about tens minutes. The surface changing processes are the most appreciable for new formed surfaces constructed by tetrahedron structural layers. The processes are less noticeable for nontetrahedral crystal surfaces and practically absent for juvenile surface of different glasses.

P05.16.021 CLUSTERIC STATES OF METALLIC MATERIALS INDUCED BY ION IRRADIATION. V.S. Khmelevskaya and V.G. Malynkin, Institute of Nuclear Power Engineering, Studgorodok 1, 249020, Obninsk, Kaluga region, Russia

The new states of metallic materials including solid solutions and pure metals (Fe-Ni, Fe-Cr-Ni, Ni-Cr, Cu-Ni, Fe-Cr, V-Ti-Cr, Zr, Ti) have been found after ion irradiation within a narrow range of radiation parameters, namely, doses, irradiation temperatures and flux intensities. The main their features are following: significant changes of X-ray diffraction patterns (splitting of X-ray peaks or characteristic changes of X-ray line forms) indicating an appearance of heterogeneity in a formerly homogeneous and equilibrium systems; accompanied changes of material properties including increase several times of microhardness; unusual morphology, in particular, an appearance of little (30-40 A) clusters in a initial matrix. Adding to this phenomena of a spatial self-organization are observed on different scale levels (registered by both optical and electron microscopical methods) [1]. The model is proposed based on consideration of local restructuring of a crystal lattice in a vicinity of a point defects (vacancies). In FCC crystal lattice coordinational polyhedron (cuboctahedron) transforms into an atom group with icosahedral symmetry, then little clusters of changed symmetry appear in a matrix. In BCC crystal lattice deformation along <111> axis leads to the formation of the Frank-Kasper polyhedron [2]. As computer experiments show it is possible to explain experimental results described by such crystal lattice transformation. The formation of these states is apparently universal phenomenon since it observed in various materials with FCC, BCC and HCP crystal lattices and after different types of irradiation, namely, in an accelerator (Ar+, 20-50 keV; Ni+, V+, 30-50 keV; Ar+, 1 MeV), by impulse or stationary plasma (Ar+).

[1] V.S.Khmelevskaya and V.G.Malynkin, Phase Transitions, 1997, **60**, 59-65.
[2] V.S.Khmelevskaya, V.S.Kraposhin and V.G.Malynkin, Int.Journ.of Non-Equilibrium Processing, 1998, **10**, 323-331.

P05.16.022 THE EFFECTS OF TEMPERATURE AND NACL CONCENTRATION ON THE CRYSTAL GROWTH OF TETRAGONAL LYSOZYME USI. L. Rong and T. Yamane [1], N. Niimura [2], [1] Department of Biotechnology, Graduate School of Engineering, Nagoya University, Chikusa-ku, Nagoya 464-8601, Japan, [2] Neutron in Biology, Advanced Science Research Center, Japan Atomic Energy Research Institute, Tokai-mura, Naka-gun, Ibaraki 319-1195, Japan

It is known that the Atomic force microscope (AFM), a relatively new and rapidly advancing technique, could be applied to obtain useful information for the crystallization of macromolecules. In 1992, Durbin and Carlson first demonstrated that the AFM could be used to observe growth steps on the surface of lysozyme crystals in mother liquor [1]. However, for most experiments to date, since the sample solution is not tightly sealed in avessel, evaporation of solvent water was a problem because slight changes in solution concentration could occur during a measurement. It is, therefore, difficult not only to investigate the crystal growth of a protein quantitatively, but also to carry out measurement of the crystal growth for a long period using an AFM. In order to solve this problem, sealed AFM vessel was developed, and quantitative and long-time measurements of crystal growth step rate of hen egg-white lysozyme (HEWL), were

carried out under several supersaturated conditions [2]. Furthermore, the effects of temperature and NaCl concentration on the crystal growth are determined with the sealed vessel.

Crystals were grown on a round cover glass with sitting drop method and 0.5-1.0mm crystals were selected for use in the AFM measurement (SPI 3800, Seiko Instruments Inc., Japan). The cover glass was fixed to the bottom of the sealed vessel with teflon screws. It was found that bunching of growth steps were often observed at higher temperature (more than 25 deg.C) and that bunching of growth steps do not occur by changing NaCl concentration or lysozyme concentration. This phenomenon has not been explained yet at present time. However, at least this implies that the effect of temperature is different from that of NaCl or lysozyme concentration on the aggregates of protein in solution. The aggregates of protein in solution might be an indicator relevant to the crystal growth mechanism of protein.

1. S. D. Durbin and W. E. Carlson (1992), J. Crystal Growth, 122, 71-79.
2. L. Rong, T. Yamane and N. Niimura, AsCA' 98, 14P28, 1998.

P05.16.023 PARAMETERS FOR ANALYSIS OF SURFACE ROUGHNESS AND MICRORELIEF MATERIALS BY AFM. A.L.Tolstikhina, Institute of Crystallography, Moscow 117333, Russia, and P.A. Arutyunov and V.N. Demidov, Moscow State Institute of Electronics and Mathematics, Moscow 109028, Russia.

The system of parameters for analysis of the roughness and microrelief of thin film surfaces and crystals by means of Atomic force microscopy is developed. The parameters are determined in the terms of classical statistics, spectral analysis and fractal geometry. We classify two groups of parameters: metric parameters (amplitude, functional and 3-dimensional parameters) and fractal ones. Amplitude parameters are the following: peak-to-peak value, average roughness, root-mean-square roughness, ten point height, surface skewness, surface kurtosis, function of kurtosis, autocorrelation function, power spectral density, coherence function, roughness correlation function, roughness hierarchy function, mean summit curvature, root mean square slope. Functional parameters are the following: mean summit curvature, root mean square slope, surface area ratio, surface bearing index, core fluid retention index, valley fluid retention index, reduced peak height, core roughness depth, reduced valley height, density of summits. Many of them are governed by international standards. The functional parameters unlike amplitude parameters classified microrelief and properties of a smooth surface. The 3-dimensional parameters are the radial wavelength index, texture direction, texture direction index, radial wavelength. This group allows to determine the surface anisotropy and structural periodicity. In the latter group, the numerical data of surface image are used after the discrete Fourier transformation. The atomic force microscopy images of various material surfaces and calculated dependencies of roughness parameters are presented.

P05.16.024 RECIPROCAL SPACE MAPPING OF MACROMOLECULAR CRYSTALS IN THE HOME LABORATORY. Edward H. Snell [1], Paul F. Fewster [2], Norman Andrew [2], Titus J. Boggon [3], Russell A. Judge [1], Marc L. Pusey [1], [1] NASA, Code ES 76, Bldg. 4464, Marshall Space Flight Center, Huntsville, AL 35812, [2] Philips Research Laboratories, Redhill, Surrey, RH1 5HA, England, [3] Chemistry Department, University of Manchester, Manchester, M13 9PL, England

Reciprocal space mapping techniques are used widely by the materials science community to provide physical information about their crystal samples. We have used similar methods at synchrotron sources to look at the quality of macromolecular crystals produced both on the ground and under microgravity conditions. The limited nature of synchrotron time s to explore the use of a high resolution materials research diffractometer to perform similar measurements in the home laboratory. Although the available intensity is much reduced due to the beam conditioning necessary for high reciprocal space resolution, lower resolution data can be collected in the same detail as the synchrotron source. Experiments can be optimized at home to make most benefit from synchrotron time available. Preliminary results including information on the mosaicity and internal strains from reciprocal space maps will be presented.

P05.16.025 SYNCHROTRON X-RAY RECIPROCAL SPACE MAPPING AND TOPOGRAPHY OF MACROMOLECULAR CRYSTAL QUALITY. Titus J. Boggon [1], John R. Helliwell, David Moorcroft [2], Russell A. Judge, Edward H. Snell [3], D. Peter Siddons [4], Vivian Stojanoff [5], [1] Department of Physiology and Biophysics, Mount Sinai School of Medicine, 1425 Madison Avenue, New York, NY 10029, USA, [2] Department of Chemistry, University of Manchester, Oxford Road, Manchester, M13 9PL, UK, [3] NASA Laboratory for Structural Biology, Code ES76, MSFC, Huntsville, AL 35812, USA, [4] NSLS, Brookhaven National Laboratory, Upton, New York, USA, [5] ESRF, BP220, Grenoble Cedex, France.

A comprehensive study of microgravity and ground grown chicken egg white lysozyme crystals is presented using synchrotron X-ray reciprocal space mapping and topography techniques. Microgravity crystals displayed, on average, reduced intrinsic mosaicities but increased delta d-star over their earth grown counterparts. Topographic analysis revealed that in the microgravity case the majority of the crystal was contributing to the peak of the reflection at the appropriate Bragg angle. In the earth case at the diffraction peak only a small volume of the crystal contributed to the intensity.

The techniques prove to be highly complementary with the reciprocal space mapping providing a quantitative measure of the crystal mosaicity and stress (or variation in lattice spacing) and the topography providing a qualitative overall assessment of the crystal in terms of its X-ray diffraction properties. Structural data collection was also carried out both at the synchrotron and in the laboratory.

P05.16.026 PREPARATION OF STM/AFM PROBES OF SPECIAL SHAPE WITH DIAMOND TIPS. A.N.Stepanova, E.I.Givargizov, and L.N.Obolenskaya, Institute of Crystallography, Russian Academy of Sciences, Moscow 117333, E.S.Mashkova and V.A.Molchanov, Moscow State University, Moscow 119899, M.E.Givargizov, Crystals and Technology, Ltd., Moscow 117333, Russia, and I.W.Rangelow, University of Kassel, Kassel 34132, Germany.

For investigations of submicron grooves with vertical walls, typical for microelectronic technologies, and of objects with coarse surfaces such as biological macromolecules special STM/AFM probes with small-diameter cylindrical or prismatic upper part of probes are necessary. Such probes have been prepared by growing of special-geometry single-crystalline silicon whiskers on (111)-oriented substrates by the vapour-liquid-solid mechanism. In order to prepare (111)-oriented cantilevers for AFM probes, special technologies have been used. From the whiskers grown, ultrasharp tips with curvature radii as small as several nanometers were prepared. The tips were coated by crystalline diamond by hot-filament chemical vapour deposition. The diamond coating was then sharpened by ion-beam bombardment. Curvature radii of diamond tips as small as 100 nanometers were obtained.

P05.16.027 PERIODICAL SYSTEM OF CRYSTALLOGRAPHIC INDEXES AS BASIS FOR TEXTURE OF GRAINS AND BOUNDARIES. V.I.Slavov, O.M.Naoumova and T.P.Jakovleva. Severstal JSC, Russia

The main topic presented here is a theoretical approach to orientational factors on basis of Periodical System of Crystallographic Indexes (PSCI). A crystallographic indexes may be represented in form of PSCI, which consists of 8 groups (G) in accordance with the laws of square indexes sum. The components of axial or planar texture are subdivided on 7 types (N) with a different positions of lattice direction <uvw> or lattice plane (hkl) of unit cell relatively to the main external axes. Any crystallographic orientation can be expressed by group's symmetry orientation (GSO) as four numbers ($NG_1G_2G_3$) in the three-dimensional pattern. Lots of GSO are exactly coincident with the 230 number of well-know space groups of crystals.

If the stress field acts on polycrystalline material, physical sense of crystallographic orientation consists in a resulting symmetry of the interaction between a crystallite and stress field. Lots of stress fields may be described by 14 symmetry groups of second-order tensors. On the basis of the superposition principle for crystalline body and stress field it may predict the grain orientation in terms of GSO.

A great number of Σ for special boundaries of cubic polycrystals with different misorientation axes was calculated using PSCI.

In the present paper we have shown that it is possibly to calculate different CSL at any values Σ, to classify CSL on definite groups and to represent crystalline materials under a new point of view PSCI.

P05.16.028 GROWTH AND CHARACTERISATION OF NEARLY PERFECT BISMUTH GERMANATE CRYSTALS. Krishan Lal[a], R.V.Anantha Murthy[a], M.Ravikumar[a], A.Choubey[a], G. Bhagavannarayana[a], Lyudmila Kharachenko[b], V. Shleguel[b], V. Guerasimov[b] and Yu. Shubin[b], [a]National Physical Laboratory, Dr. K. S. Krishnan Road, New Delhi 110012, India, [b]Institute of Inorganic Chemistry, SB RAS, Novosibirsk, Russia.

Bismuth Germanium Oxide (BGO) $Bi_3Ge_4O_{12}$ are grown from melt to meet the stringent requirements as scintillators for X-rays and γ-rays. Till recently, Bridgman method had been employed to grow BGO crystals with good degree of perfection. Recent efforts have shown that nearly perfect BGO single crystals can be grown by Low Thermal Gradient (LTG) Czochralski method with Automatic Weight Control Process [Murthy et al, J. Crystal Growth 1999]. For structural characterization, high-resolution X-ray diffractometry and topography methods were employed. Point defects and their clusters have been investigated by diffuse X-ray scattering measurements. The crystal growth system has been developed at IIC, Novosibirsk and the multi-crystal X-ray diffractometers employed in this study were developed at NPL. The crucible weighing system has an accuracy of 10 mg in 1 kg range and 50 mg in 25 kg range. The diameter control is effected through crucible weight control. The temperature gradient above the crystal – melt interface is negligible in a zone of ~4 cm. Platinum crucible was used to melt the charge, which was heated at a rate of 250^o C/h. Nearly perfect crystals were grown under following growth conditions: pulling rate - 2.5 mm/h, seed rotation rate - 38 rpm, growth rate - 30 g/h and post growth cooling rate - 150^o C/h. Crystal dimensions were ~ 80 mm long and ~ 40 mm in diameter [weighing ~ 800g]. Diffraction curves were quite sharp with typical half width values of ~9 arc sec in the central region. Some regions at the periphery had *very* low angle grain boundaries with angular tilts of only ~33 arc sec. Thermal annealing at elevated temperatures reduced the tilt angles and improvements in crystalline perfection were observed. Diffuse X-ray scattering measurements showed significant differences in defect structure with direction of growth. Variations in trace impurities in starting materials, which apparently led to different tinges, did not produce appreciable effect on the point defect clusters.

P05.16.029 DIFFUSE X-RAY SCATTERING STUDY OF POINT DEFECT CLUSTERS IN BISMUTH GERMANATE SINGLE CRYSTALS. G. Bhagavannarayana[1], A. Choubey[1], Yu. Shubin[2] and Krishan Lal[1], [1]National Physical Laboratory, Dr. K.S. Krishnan Road, New Delhi –12 . [2] Institute of Inorganic Chemistry, SB RAS, Novosibirsk, Russia.

Recently, it has been shown that nearly perfect crystals of bismuth germanate (BGO) can be grown by the newly developed low thermal gradient Czochralski technique [Murthy et al, J. Crystal Growth, in press]. It has been observed that BGO crystals are generally colourless (Type A), but a yellow tinge is often observed in some crystals (Type B) due to different impurities in the raw material. Fairly large volumes of specimens are free from boundaries and dislocations in both types of specimens. However, these crystals contain point defect clusters. Crystals grown along both [111] and [112] directions have been chosen as specimens. A multicrystal X-ray diffractometer set in (+,-,-,+) configuration with a well collimated and highly monochromated $MoK_{\alpha 1}$ beam as exploring beam and a high resolution diffuse X-ray scattering (DXS) measurement technique developed at NPL have been employed. DXS measurements were made in symmetrical Bragg geometry around 444 and 224 reciprocal lattice points (RLPs), respectively for the samples grown along [111] and [112] directions. Diffraction curves were recorded before DXS experiments. Both types of crystals gave quite narrow curves with half widths ~7 arc sec for 444 RLP and ~9 arc sec for 224 RLP [theoretical values for perfect BGO crystals = 1.3 arc sec (444 RLP) and 3.4 arc sec (224 RLP)]. Experimental data of DXS intensity could be analyzed by using a phenomenological model for small concentration of dislocation loops wherein the point defects are loosely clustered with weak interactions among them. From the analysis, cluster radius R_{cl}, cluster volume A_{cl} and the number of point defects within a cluster N_{cl} have been determined. There was no significant difference in the values of R_{cl}, A_{cl}, and N_{cl} for type A and type B crystals. However, growth direction had appreciable effect. Typical values of R_{cl}, A_{cl} and N_{cl} were respectively 7.4×10^{-5} cm, 8.3×10^{-17} cm^3, 2.86×10^4 (grown along [111]) and 3.6×10^{-5} cm, 2.78×10^{17} cm^3, 9.6×10^4 (grown along [112]).

P05.16.030 STRUCTURAL CHARACTERIZATION OF III-V HETEROSTRUCTURES BY HIGH-RESOLUTION X-RAY DIFFRACTION TECHNIQUES. Niranjana Goswami and Krishan Lal, National Physical Laboratory, New Delhi-110012, India, A. Vogt and H. L. Hartnagel, Institut fuer Hochfrequenztechnik, Technische Hochschule Darmstadt, D-64283 Darmstadt, Federal Republic of Germany.

GaSb/GaAs, GaAs/InAs/GaAs and GaAs/AlGaAs/GaAs structures for resonant tunnelling diodes and high frequency applications have been characterized by using high resolution X-ray diffractometry and topography. These heteroepitaxial films were grown by molecular beam epitaxy (MBE) on (100) semi-insulating GaAs substrates. The film thicknesses were in the range: ~ 4 nm – 5 μm. A five crystal X-ray diffractometer, developed at NPL was employed in (+, –, +) configuration with $MoK\alpha_1$ exploring beam and (400) diffracting planes in symmetrical Bragg geometry. The diffraction curves consisted of film and substrate peaks separated by a large angle of more than a degree in some cases. Half widths of diffraction curves of GaAs substrates were in the range: 14 – 22 arc sec, showing good crystalline quality of the starting wafer. Broad diffraction curves but single peaks were observed from the interface and film regions. Half widths of film diffraction curves were found to be in

the range: 164 – 527 arc sec, showing considerable stress at the interface. The stress could be relaxed through the introduction of buffer layers as revealed by the decrease of diffraction curve half widths. The observed angular separation between the substrate and film peaks were found to be not only due to lattice mismatch but also due to large angles between the lattice planes of the substrate and films. A methodology was developed for quantitative determination of these two mismatches. Two azimuthal orientations of the specimen were selected at which the direction of the diffraction vector was in the plane of diffraction. From the observed angular separations at the two azimuthal orientations, the lattice mismatch was determined quantitatively. These experiments lead to determine correct values of the composition of films. In multilayered structures, different layers are found to have different physical misorientations. In GaAs/InAs/GaAs structures, the lattice planes of the GaAs film and GaAs substrate had substantial tilt with respect to each other.

P05.16.031 HIGH RESOLUTION X-RAY DIFFRACTOMETRIC AND TOPOGRAPHIC STUDIES OF AS GROWN AND ANNEALED BGO CRYSTALS. A. Choubey[1], Yu. Shubin[2], G. Bhagavannarayana[1] and Krishan Lal[1], [1]National Physical Laboratory, Dr. K.S. Krishnan Road, New Delhi –12 . [2] Institute of Inorganic Chemistry, SB RAS, Novosibirsk, Russia.

Crystalline perfection of bismuth germanate (BGO) single crystals grown by the recently developed low thermal gradient (LTG) Czochralski technique has been investigated by double crystal X-ray diffractometry and topography techniques. A variation in the degree of perfection of crystals grown under different conditions was observed. Good number of the specimens were nearly perfect. Half widths of their diffraction curves were in the range 6.5-8.8 arc sec for (444) planes, 9-10 arc sec for (422) planes and 9-11 arc sec for (400) planes. These values are close to the theoretical values [1.3, 3.4 and 3.8 arc sec respectively for (444), (224) and (400) planes obtained from the plane wave dynamical theory of X-ray diffraction]. Some of the specimens contained *very* low angle boundaries. Diffraction curves showed two or more peaks with tilt angles in the range: 20-140 arc sec. To improve the perfection of these specimens, these were annealed at ~1000 ^{o}C. Duration of annealing was increased step wise from 8 hrs to 80 hrs. Traverse topographs and diffraction curves were recorded after each annealing step. A considerable improvement in crystalline perfection of the specimens was observed even after first 8 hrs of annealing. Some low angle boundaries were removed and angular separation between the boundaries decreased from 58 to 41 arc sec in a typical case. After 32 hrs of annealing, the degree of perfection of individual grains is slightly improved and the angular separation further decreased upto 39 arc sec. Further increase in annealing time did not improve any degree of perfection. Higher annealing temperature would be necessary to remove these boundaries.

P05.16.033 CHARACTERIZATION OF FERROELECTRIC DOMAIN WALLS BY WEAK BEAM AND HRTEM ELECTRON MICROSCOPY. P.A. Buffat, A. Sfera, M. Foeth and P. Stadelmann, Centre Interdépartemental de Microscopie Electronique, Ecole Polytechnique Fédérale de Lausanne, 1015 Lausanne, Switzerland

New means for quantitative interpretation of Weak Beam and High Resolution Transmission Electron Microscopy images have been developed to study extended interfaces. They are applied here to the thickness determination of ferroelectric domain walls in $PbTiO_3$ at room temperature and their broadening close to the ferroelectric to paraelectric transition temperature.

HRTEM is in principle a straightforward method to observe the position of atom rows in crystals. However most often black or white dots do not correspond to the precise atoms position. Image simulation based on models of the structure and of the microscope is required for interpretation. The atom position shift remains small and this very detailed information requires some mathematical approach to be summarised into a few numerical values. This technique is limited to the cases where interfaces can be oriented parallel to the electron beam while remaining on a suitable zone axis with respect to the resolving power of the microscope and the low thickness of the sample may introduce relaxation effects.

The observation of thickness fringes at inclined boundaries under weak beam conditions is much less stringent (lower resolving power, sample thickness and orientation…). The interpretation of the fringe profiles is performed here using a fitting procedure. Although several parameters are required to model the interface, the material and the experimental conditions, only rough estimates of the parameters are required to lead to a fast convergence of the algorithm and all of them can be more accurately deduced this way. A check for consistency is easily performed by repeating the analysis on different thickness areas or orientations.

The relative merits and drawbacks of both techniques will be discussed with reference to recent results obtained on PbTiO3 ferroelectric domain walls at room temperature and to observations under way at high temperature.

17. ELECTRON MICROSCOPY

P06.17.001 CAPSID STRUCTURE OF A GEMINIVIRUS, AS DETERMINED BY CRYO-ELECTRON MICROSCOPY. Lee Faulkner [1], Wei Zhang [2], Norm Olson [2], Timothy S. Baker [2], Margaret Boulton [3], Jeffrey Davies [3], Mavis Agbandje-McKenna [1] and Robert McKenna [1], [1] Department of Biological Sciences, University of Warwick, Gibbett Hill Road, Coventry CV4 7AL, UK, [2] Department of Biological Sciences, Purdue University, West Lafayette, Indiana 47907-1392, USA, [3] Department of Virus Research, John Innes Centre, Norwich Research Park, Colney, Norwich, Norfolk NR4 7UH, UK

We have used cryo-electron microscopy (cryo-EM) and three-dimensional image reconstruction methods to determine the structure of maize streak virus (MSV). The first structure of a geminate virus to be obtained. Using an amino acid sequence comparison alignment of the capsid proteins (CP) of satellite tobacco necrosis virus (STNV) (1) to that of MSV, made possible, the fitting of an atomic model of the MSV CP into the cryo-EM density map, to build a complete geminate capsid. The twinned quasi-isometric geminate particle is made up of 110 CP subunits (~28kD) arranged in 22 capsomeres and has a dimension of approximately 20-30nm. The CP has the usual viral jelly-roll made up of eight stranded b-barrels. The corners of the b-barrel strands have inserted residues compared to the STNV structure and this can explain the increase in size of the MSV capsid to that of STNV. The five CP subunits closest to the interface of the two particles have their helical N-terminal domains “flipped out” such that they form a-bridges between the two particles. The helical region of the CP has been identified as the DNA binding site (2).

1. T.A.Jones and L Liljas (1984). J Mol Biol 177 735-767
2. L.Haunting, M.Boulton and J.Davies (1997). J of Gen Vir 78 1265-1270

P06.17.002 CRYO-ELECTRON MICROSCOPY OF GDP-TUBULIN RINGS. W.V. Nicholson [1], M. Lee [1], K.H. Downing [2], E. Nogales [1, 2], [1] MCB, UC at Berkeley, Berkeley, CA 94720, USA, [2] Life Sciences, LBNL, Berkeley, CA 94720, USA

Rings of GDP-tubulin formed in the presence of divalent cations have been studied using cryo-electron microscopy. The structure of such rings resembles that of depolymerizing microtubule ends and corresponds to an unconstrained conformation of tubulin in its GDP state. The use of cryo-techniques has allowed us to image the ring polymers free from dehydration and flattening artifacts. Preparations of frozen-hydrated GDP-tubulin rings are generally heterogeneous and contain a mixture of double, triple and incomplete rings, as well as spirals and some rare single rings. Images of different polymer types can be identified and classified into groups that are then amenable for averaging and single particle reconstruction methods. Identifying the differences in tubulin structure between straight and curve protofilaments will be important to understand the molecular basis of dynamic instability in microtubules. A 3D reconstruction obtained from cryo-EM of tubulin double rings will be described.

P06.17.003 THE 3-D STRUCTURE OF ALEUTIAN MINK DISEASE PARVOVIRUS: IMPLICATIONS FOR DISEASE PATHOGENICITY. Robert McKenna [1], Norman H. Olson, Paul R. Chipman, Timothy S. Baker [2], Tim .F. Booth [3], Jesper Christensen, Bent Aasted [4], James M. Fox, Marshall E. Bloom, James B. Wolfinbarger [5], Mavis Agbandje-McKenna [1], [1] Department of Biological Sciences, University of Warwick, Coventry CV4 7AL, UK, [2] Department of Biological Sciences, Purdue University, West Lafayette, Indiana 47907-1392, USA, [3] NERC Institute of Virology and Environmental Microbiology, Oxford, UK, [4] Lab. of Virology and Immunology, Dept. of Veterinary Microbiology, The Royal Veterinary and Agricultural University, Copenhagen, DK, [5] Lab. of Persistent Viral Diseases, NIAID, Hamilton, MT, USA

The three-dimensional structure of expressed VP2 capsids of Aleutian mink disease parvovirus, strain G (ADVG-VP2), has been determined to 22Å resolution with cryo-electron microscopy and image reconstruction techniques. A structure-based sequence alignment of the VP2 capsid protein of canine parvovirus (CPV) provided a means to construct an atomic model of the ADVG-VP2 capsid. The ADVG-VP2 reconstruction reveals a capsid structure of mean external radius of 128Å with several surface features similar to those found in human parvovirus B19 (B19), CPV, feline panleukopenia virus (FPV), and minute virus of mice (MVM). Dimple-like depressions occur at the icosahedral two-fold axes, canyon-like regions encircle the five-fold axes, and spike-like protrusions decorate the three-fold axes. These spikes are not present in B19, and they are more prominent in ADV compared to the other parvoviruses owing to the presence of loop insertions which create 'mounds' near the three-fold axes.

Cylindrical channels along the five-fold axes of CPV, FPV and MVM, which are surrounded by five, symmetry-related b-ribbons, are closed in ADVG-VP2 and B19. Immunoreactive peptides made from segments of the ADVG-VP2 capsid protein map to residues in the mound structures. In vitro tissue tropism and in vivo pathogenic properties of ADV map to residues at the three-fold axes and to the wall of the dimples.

P06.17.004 EFFECT OF MICROSTRUCTURAL EVOLUTION ON IMPACT FATIGUE OF COMPRESSOR VALVE STEEL Ping Liu, Guocai Chai and Sören Olsson, R & D Centre, AB Sandvik Steel, 811 81 Sandviken, Sweden

Conventional stainless steel used for compressor valve with a composition of 0.37 C-0.39Si-0.60 Mn-13.5 Cr-1.0 Mo-0.20 P-0.002 S (wt%) consists of martensites (α') and Cr-enriched $M_{23}C_6$ carbites as shown in Fig.1. A modification of the structure resulted in an improvement of the impact and bending fatigue. These were partly attributed to the increase of retained austenite from 2 to 10 vol %(1). For the improved steel the number of $M_{23}C_6$ (Fm3m; a=10.6 Å) particles is dramatically reduced as shown in Fig. 2. As a result the carbon activity in the matrix increased and the precipitation of small particles (<100nm) of Fe_3C (Pnma; a=5.0915 Å, b=6.7446 Å and c=4.5276 Å) took place as indicated in Fig.3 and Fig.4. It is well known that large particles reduce the fatigue life by both facilitating crack nucleation by slip band/particle interaction and increasing crack growth rates by interface decohesion and voiding within the plastic zone at the crack tip. Small particles, on the other hand, can have beneficial effects by homogenising the slip pattern and delaying fatigue-crack nucleation. Thus, the precipitation of small carbide particles may also contribute to the improvement of impact fatigue of the studied steel.

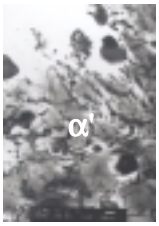

Fig.1 $M_{23}C_6$

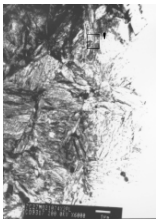

Fig.2 $M_{23}C_6$

Fig.3 Fe_3C

Fig.4 Fe_3C

1) M. Nyström, P. Liu, T. Larsson, S. Olsson and G. Svensk, ”Impac fatigue of compressor valve steel, Compressor Technology”, USA, 1996.

$<100>_{\alpha'}//<110>_{Fe_3C}$

18. ELECTRON DIFFRACTION

P05.18.001 KIKUCHI ELECTRON DOUBLE DIFFRACTION. R.K. Karakhanyan and S.E. Bezirganyan, Department of Physics, Yere-van State University, #1, A. Manoogian St., Yerevan 375025, Armenia.

The purpose of the present work is to extend the phenomenon of the Electron Double Diffraction (EDD) to include the Kikuchi patterns. Kikuchi EDD means that once and twice diffracted electron beams as well as the primary electron beam can become sources of Kikuchi patterns, i.e. these diffracted beams are exposed to inelastic scattering process, which takes place for the primary electron beam [1]. The resulting Kikuchi pattern is a superposition of the primary pattern with the source in the incident beam and of secondary patterns with sources in once and twice diffracted beams. The single crystalline silicon films were used as specimens for investigations. Silicon Kikuchi transmission patterns were obtained when the incident beam is approximately parallel to [112], [110], [210], [310] and [111] axes.

Formation of forbidden and unindexed Kikuchi lines, enhancement of excess forbidden Kikuchi lines near spot reflexes with the same indices, mutual reversal contrast of excess and defect Kikuchi lines under passing of excess line near strong spot reflex with other indices, enhancement of excess line near spot reflex with other indices under passing of correspondent defect line near strong spot reflex are the direct consequence of Kikuchi EDD. It is shown [2,3], that under decrease of diffracted beams' intensity by means of crystal thickness, temperature, orientation variation and electron energy change all above mentioned manifestations of Kikuchi EDD grow weak, which confirms correctness of mechanism of their appearance proposed in present work.

1. R.K. Karakhanyan, P.A. Aleksanyan & J.K. Manucharova (1990).Phys.Stat.Sol.(a), 121, K1.
2. R.K. Karakhanyan, P.A. Aleksanyan (1991). Kristallografiya, 36, 1289.
3. R.K. Karakhanyan (1997). Kristallografiya, 42, 927.

P05.18.002 SIMULATION OF DIFFUSE SCATTERING FROM SHORT-RANGE-ORDERED Cu_3Au TYPE FACE-CENTRED CUBIC STRUCTURE. X. J. Jiang, J. K. Bording and J. Tafto, Centre for Materials Science/Department of Physics, University of Oslo, Gaustadalleen 21, N-0371 Oslo, Norway.

It is well known that in some binary alloys, such as Cu_3Au, small domains of the ordered structure are present, separated by antiphase domain boundaries. The antiphase domains give rise to characteristic short-range-order diffuse scattering in the diffraction patterns. Several antiphase configurations and corresponding diffuse scattering have been proposed in the literature [1,2].

We have performed computer simulation using Cu_3Au as an example. In a wider perspective we intend to approach the more complex system Al-Zn-Mg that exhibits similar diffuse scattering. The atomic arrangement and resulting short-range-order scattering of Cu_3Au were simulated for different cooling rates. Special attention was focused on the antiphase domain boundary types and the accompanying diffuse scattering. The results of the simulation are in good agreement with the experimental observations of split spots presented in the literature.

S. H. Rahman, Acta Cryst., 1993, A49:68.
J. Zhu and J. M. Cowley, Acta Cryst., 1982, A38:718.

P05.18.003 STRUCTURE DETERMINATION OF METAL-RICH COMPOUNDS FROM SELECTED AREA ELECTRON DIFFRACTION. Th. E. Weirich, Mat. Science, Darmstadt Univ. of Technology, 64287 Darmstadt, Germany, X.D. Zou, S. Hovmöller, Structural Chemistry, Stockholm Univ., 10691 Stockholm, Sweden, A. Simon, Max-Planck-Inst. f. Festkörperforschung, 70506 Stuttgart, Germany, G. Cascarano, C. Giacovazzo, CNR-IRMEC Dip. Geomineralogico, Campus Univ. Via Orabona 4, 70125 Bari, Italy

Electron diffraction (ED) is due to the strong interaction of electrons with matter an excellent tool for studying the interior structure of small crystalline samples down to few nanometers in size. On the other hand the strong interaction gives rise to dynamical diffraction (multiple scattering) effects which often leads to diffracted intensities far away from the predicted by the kinematic theory. Although ED without any dynamical contribution can hardly be realised in practice, it is possible to find experimental conditions under which the dynamical effects can be kept at a low level. Such data can be treated in the first approximation as pseudo-kinematic, *i.e.* traditional strategies for solving crystal structures are expected to work. Here we show that quantified ED patterns can be used for solving crystal structures of non-light element compounds to high accuracy. Several known metal-rich structures M_xX_y (M = Ti, Zr; X = S, Se; $x > y$) were investigated in a 300 kV Philips CM30ST microscope. Selected area ED patterns were recorded from prominent zone axis - in this series always along a short 3.5 Å crystal axis - and processed by ELD [1] for extracting integrated intensities. These 2D data sets were fed into SIR97 [2] modified with electron scattering factors and the most probable E-maps were calculated. The trial structures proposed by SIR97 revealed in all cases the complete structures. The projected atom positions agreed on average within 0.2 Å with those from the X-ray determination on single crystals. The obtained results show that dynamical effects can be controlled in a standard ED experiment so that direct methods can be applied for solving crystal structures in a quasi-automatic manner.

[1] X.D. Zou *et al*. (1993) Ultramicroscopy, **52**, 436.
[2] SIR97: http://www.ba.cnr.it/IRMEC/SirWare.html

P05.18.004 NEW METHOD OF ANALYSING ELECTRON DIFFRACTION DATA. U. Wilke and W. Mader Institut für Anorganische Chemie der Universität Bonn, Römerstrasse 164, 53117 Bonn, Germany

Structure determination of small and defected crystals is the domain of electron diffraction. We present an application of a microdiffraction technique to inorganic crystal structure refinement. Our method is based on the program package ELSTRU by Jansen et al. [1]. We use convergent beam diffraction patterns taken with a spot size of $\approx$ 8 nm. Intensities for various beam directions are given by the corresponding position within the diffraction discs. This allows to obtain up to nine data sets for one specimen thickness. The discs obtained should not overlap because the background intensity around each diffraction disc needs to be substracted which is perfomed by extrapolation. The intensities serve as input data for the program package ELSTRU. The method was tested on simulated [2] and on experimental diffraction patterns of corundum (α-Al_2O_3). The results calculated from different data sets of diffraction pattern (simulated as well as experimental) reproduced the same thickness and the known structural parameters. The different data sets corresponding to different directions of the incident beam yield shifts of the centers of Laue circles as expected. Experimental intensities are recorded on a 2k×2k CCD camera (Gatan Megascan) attached to a Philips CM300 UT FEG electron microscope.

[1] J. Jansen, D. Tang, H.W. Zandbergen, H. Schenk, Acta Cryst. (1998) A54, 91
[2] P. Stadelmann, Ultramicroscopy 21, (1987), 131

19. NON-AMBIENT CONDITIONS

P08.19.003 PRESSURE INDUCED T_C AND STRUCTURAL VARIATIONS OF $PrBa_2Cu_3O_x$ SUPERCONDUCTOR. J. Ye and A. Matsushita, National Research Institute for Metals, 1-2-1 Sengen, Tsukuba, Ibaraki, Japan, and Z. Zou, Electrotechnical Laboratory, 1-1-4 Umezono, Tsukuba, Ibaraki 305, Japan

T_C and structural parameters of $PrBa_2Cu_3O_X$ were investigated as a function of pressure up to 10 GPa. The compound has been considered as an exceptional material to be non-superconductive among the $RBa_2Cu_3O_X$ (R = rare earth) compounds, since the discovery of the oxide high-T_C superconductors in 1986. Recently, however, superconducting $PrBa_2Cu_3O_X$ has been grown by travelling-solvent floating-zone method [1]. In order to clarify the origin of the superconductivity, we have studied pressure dependence of T_c of the compound by electrical resistance measurements using a cubic anvil apparatus under hydrostatic pressure up to 10 GPa [2]. A large positive pressure coefficient of T_C, dT_C/dP, with a maximum of 7.4 K/GPa, was observed. The results showed an opposite behaviour with those expected from the widely accepted "hybridization model", which was proposed to explain the non-superconductivity of $PrBa_2Cu_3O_X$. We have further carried out X-ray diffraction under pressure using a diamond anvil cell. The *a*-, *b*-, and *c*-lattice parameters were found to compressed linearly as a function of pressure. The linear compressibilities, -dln*a*/dP, -dln*b*/dP, and -dln*c*/dP, were evaluated to be $2.07x10^{-3}$, $1.71x10^{-3}$, and $3.76x10^{-3}$ GPa^{-1}, respectively. The details of the experiment and Rietveld structural refinement to the high pressure diffraction patterns will be reported. The distribution of carriers in $PrBa_2Cu_3O_X$ under high pressure will also be discussed.

1. Z. Zou, J. Ye, K. Oka, Y. Nishihara (1998). Phys. Rev. Lett. **80**, 1074.
2. J. Ye, Z. Zou, A. Matsushita, K. Oka, Y. Nishihara, and M. Matsumoto (1998). Phys. Rev. **B 58**, R619.

P08.19.004 HIGH PRESSURE STUDIES OF VANADIUM DOPED Bi 2212 SYSTEM. Ravhi S Kumar, A.Sekar, N.Victor Jaya and S.Natarajan, Department of Physics , Anna University , Chennai 600 025 , INDIA.

The Bi based 2212 superconductors exhibit metal insulator transition when a rare earth is doped at the calcium site [1- 4]. By keeping the rare earth concentration at the calcium site invariant, doping of Pb at the Bi site also drives the system to exhibit the phenomena [5]. We have synthesised ($Bi_{1-x}V_x)_2 Sr_2 Ca_{0.7} Y_{0.3} Cu_2 0_{8+y}$ samples with nominal V concentrations (0.025, 0.05 and 0.1) as successful V doping has been reported in Bi 2212 [6] . High pressure resistivity and high pressure X ray diffraction studies were performed up to 15GPa employing a diamond anvil cell on the system for V concentration 0.025 for possible structural phase transitions. The results will be discussed in comparison with the high pressure reports available for other systems.

[1] A.Q.Pham, N.Merrien, A.Maignan, F.Studer, C.Michel and B.Raveau, *Physica C* **210**, 1993, 350.
[2] B.Jayaram, P.C.Lanchester and M.T.Weller, *Phys.Rev.B.***43**, 1991,5444.
[3] P.Mandal, A.Poddar, B.Ghosh and P.Choudhury, *Phys.Rev.B.* **43**, 1991, 13102.
[4] C.Quitmann, B.Beschoten, R.J.Kelly, G.Guntherodt and M.Onellion, *Phys.Rev.B.***51**, 1995, 11647.
[5] Noburu Fukushima and Mashiko Yoshiki , *Phys.Rev.B*, **50**, 1994, 2696. [6] P.C.W.Fung, Z.C.Lin, Z.M.Liu, Ying Xin, Z.Z.Sheng, F.T.Chan, K.W.Wong,Yong-NianXu,W.Y.Ching, *Solid State Commun.,***75**,1990,211.

P08.19.005 HIGH-PRESSURE STRUCTURAL STUDIES OF STRONTIUM. T.Bovornratanaraks, D.R. Allan, R.J. Nelmes, M.I. McMahon and S.A. Belmonte Department of Physics and Astronomy, University of Edinburgh, JCMB, Kings' Building, Mayfield Road, Edinburgh, U.K. EH9 3JZ.

The alkali-earth metals Ca, Sr and Ba have a rich variety of high-pressure crystal structure and have stimulated a substantial number of experimental and theoretical studies of their transition mechanisms. In previous high-pressure energy dispersive powder diffraction studies of Sr[1,2], the following sequence has been reported: face-centred cubic to body-centred cubic at 3.5 GPa; to Sr-III with the orthorhombic structure *Imma* structure at 26 GPa; to a more complex Sr-IV at 35 GPa; and to the Sr-V phase at 40 GPa. We have embarked on a re-examination of the high-pressure structures and transitions using angle-dispersive powder diffraction techniques with the image-plate area detector on station 9.1 at SRS Daresbury Laboratory. We find the same sequence as has been previously reported up to Sr-III, but the two-dimensional data obtained from the image plate clearly shows that Sr-III has the tetragonal β-tin structure[3], and not an orthorhombic *Imma* structure as previously thought [2]. We have now obtained extensive data through the transition to Sr-IV and in the Sr-IV phase. The transition appears to involve an intermediate structure that has yet to be understood, but the structure of Sr-IV has been solved as a quite complex monoclinic structure. Pseudopotential calculations are now also in progress using the CASTEP code. The lastest results of both the diffraction studies and the calculations will be presented.

[1] H. Olijnyk, W.B. Holzapfel, *Physics Letters.* A 100, 191 (1984).
[2] M. Winzenick, W. Holzapfel, *Phys. Rev. B.* 53, 2151 (1996).
[3] D.R. Allan, R.J. Nelmes, M.I. McMahon, S.A. Belmonte, T. Bovornratanaraks, *Rev. High Pressure Sci Technol.*, Vol 7 , 236 (1998)

P08.19.006 ACCURATE STRUCTURE ANALYSES OF Cs HIGH PRESSURE PHASES USING SR UNDULATOR BEAM AT SPring-8. Y.Ohishi and O.Shimomura, SPring-8, Hyogo 679-5198, Japan, M.Takata, Dept. of Material Science, Shimane University, Matsue 690-8504, Japan, and E.Nishibori and M.Sakata, Dept. of Applied Physics, Nagoya University, Nagoya 464-8601, Japan

In the last two decades, the progress of accurate structure analyses using an advanced synchrotron radiation x-ray source can provide the electronic level structural studies in the field of high-pressure science. Cesium shows bcc-fcc(I)-fcc(II) phase transitions through 0~5 GPa. The theoretical study has suggested that the charge transfer causes these transitions from *s*- to *d*-orbital under high-pressure (*s*-*d* transition). Although the lattice constant change at bcc-fcc(I)-fcc(II) transition is clearly observed, the direct structural evidence of the *s*-*d* transition has never been experimentally obtained. If the *s*-*d* transition really exists, the electronic level structure analysis should enable one to observe

deformation of electron density due to *s-d* transition. The purpose of the this study is 1) to establish such an electronic level structure analysis under high pressure utilizing third generation undulator beam and 2) to examine the phase transitions of Cs by the established method.

In order to observe an electronic level structure, the essential importance is to collect an accurate x-ray diffraction data. In the present study, synchrotron powder data of Cs under high pressure is measured using the Diamond Anvil Cell (DAC) with a high energy, high brilliance and high efficiency beam emanating from the undulator at BL10XU in SPring-8. The charge density analysis is performed by the Maximum Entropy Method (MEM).

P08.19.009 MAGNETIC AND CRYST. STRUCT. OF THE LAVES HYDRIDES. INFLUENCE OF CHEMICAL SUBSTITUTION AND APPLIED PRESSURE. O.L. Makarova [1], I.N.Goncharenko [2], I.Mirebeau [3], A.V.Irodova [1], [1] RRC "Kurchatov Institute", [2] RRC "Kurchatov Institute", Laboratoire Leon Brillouin, CEA-CNRS CEA/Saclay, [3] Laboratoire Leon Brillouin, CEA-CNRS CEA/Saclay.

RMn_2 compounds (R=Y, rare earth) show very interesting features, namely frustration in the Mn magnetic sublattice and instability of the Mn magnetic moments. Mn magnetism, being close to limit of instability between localized and delocalised state, is very sensitive to the change of the interatomic distances. Hydrogen doping increases the lattice parameter (acting as "negative pressure") and stabilizes Mn magnetism. At the same time, we found a very unusual coupling between structural and magnetic properties in the hydrides. The magnetic R, Mn and structural H sublattices order simultaneously through a first order magneto-structural transition. We present a neutron diffraction study of the magnetic and crystal structures of the Laves hydrides $RMn_2D_{4.3}$ and $(R_xY_{1-x})Mn_2D_{4.3}$ (R= Tb, Dy, Ho) at ambient pressure and pressures up to 12 GPa. The combination of chemical substitution and applied pressure allow us to separate the effects of interatomic distances, hydrogen order, and dilutions in the magnetic sublattices.

The compounds $(R_xY_{1-x})Mn_2D_{4.3}$ (R=Er, Tm, Lu) and $(Ho_xSc_{1-x})Mn_2D_{4.3}$ show another interesting example of coupling between magnetic and structural properties. In this case, chemical substitution leads to a change in the crystal structure from the cubic C15 to the hexagonal C14. We have studied the intermediate defect structures with stacking faults. We got a very unusual result: the defect phases, having no long range structural order, show a long range magnetic order.

P08.19.010 HIGH PRESSURE STRUCTURAL STUDIES OF ICES AND ICE MIXTURES. J.S.Loveday, R.J.Nelmes and M.Guthrie, Department of Physics and Astronomy, The University of Edinburgh, Edinburgh EH9 3 JZ, United Kingdom, S.Klotz, J.M.Besson and G.Hamel, Université P et M Curie, Paris 75252, France, D.J.Francis, Rutherford Appleton Laboratory, Chilton, OX11 0QX, United Kingdom.

The high-pressure behaviour of ices (for example H_2O, NH_3 ,CH_4, H_2S) and ice mixtures provides fundamental information on the density dependence of interatomic potentials. In addition, since ices are the major component of the outer planets and their satellites, high-pressure properties underpin modelling of these bodies. Accurate structural information at high-pressure is vital to the understanding of high-pressure behaviour, and the development of the Paris-Edinburgh cell for neutron diffraction has made it possible to obtain accurate structural information over a wide range of pressures on H-containing systems.

Studies of the high-pressure structures of deuterium sulphide (D_2S) suggest increasing orientational order of the molecules and the onset of significant hydrogen bonding at high pressure. A detailed comparison of the structures of ices VII and VIII to 20 GPa has explored the pressure dependence of both the dynamics and the multi-site disordering of the oxygen sublattice in ice VII. Neutron diffraction studies of ammonia monohydrate - the first neutron study of a molecular mixture above 0.5 GPa - reveal an unexpectedly rich phase diagram and suggest remarkable structural complexity at high pressure. Similar structural complexity is also observed in the high-pressure phases of methane. Complexity is emerging as a common feature of the high-pressure structures of ices, in contrast to previous expectations of a general trend towards structural simplicity under increasing pressure.

P08.19.011 THE CRYSTAL STRUCTURES OF TWO HIGH-PRESSURE POLYMORPHS OF Ta_2O_5. M. Sundberg[1], I.P. Zibrov[2], V.P. Filonenko[3] and P.-E. Werner[1], [1]Department of Inorganic and Structural Chemistry, Arrhenius laboratory, Stockholm University, S-106 91 Stockholm, Sweden, and [2]Institute of Crystallography, Russian Academy of Sciences, 117333 Moscow, Russia, [3] Institute for High Pressure Physics, Russian Academy of Sciences, Troitsk, 142092 Moscow Region, Russia

The crystal structures of two high-pressure forms of Ta_2O_5, B-Ta_2O_5 and Z-Ta_2O_5, prepared at *P*=80 kbar, have been solved from X-ray powder diffraction data. The X-ray powder pattern taken from the Ta_2O_5 sample was very similar to the one recently taken from a two phase mixture of B-Nb_2O_5 and Z-Nb_2O_5 (1). The X-ray data thus indicated that the Ta_2O_5 phases were isostructural with the niobium oxides.

The unit cell dimensions are: *a*=12.785, *b*=4.853, *c*=5.527 Å and β=104.26° (B-Ta_2O_5) and *a*=5.225, *b*=4.699, *c*=5.853 and β=108.20° (Z-Ta_2O_5).

The final R-values from the Rietveld refinement of the two-phase sample are 0.026 (B-Ta_2O_5) and 0.032 (Z-Ta_2O_5). The tantalum atoms are six-coordinated in B-Ta_2O_5 and seven coordinated in Z-Ta_2O_5. A similar kind of seven-coordination as found for Z-Ta_2O_5 has been observed in the mineral baddeleyite ZrO_2 (2). B-Ta_2O_5 has previously been prepared by hydrothermal methods (3), while Z-Ta_2O_5 represents a new polymorph of Ta_2O_5.

High-resolution electron microscopy studies of the sample showed defects and intergrowth of the two phases. Structure models have been deduced. It is interesting to note that the electron microscopy results showed that due to the similarities in structures, it would not have been possible to deduce the unknown crystal structure of Z-Ta_2O_5 from the HREM images only.

1 I.P. Zibrov, V.P. Filonenko, P.-E. Werner, B.-O. Marinder and Sundberg, J. Solid State Chem. 141 (1998) 205.
2. J.D. McCullough and K.N. Trueblood, Acta Cryst. 12 (1959)507.
3. Fujio Izumi and Hiroshi Komada, J. Less-Common metals, 63(1979)305.

P08.19.012 COMPRESSIBILITY, PHASE TRANSITION AND STRUCTURE OF NOSEAN AT HIGH PRESSURE. H. Schulz, S. Werner, J. Wittlinger, Institut für Kristallographie und Angewandte Mineralogie, Universität München, Theresienstr. 41, D-80333 München, Germany.

The mineral nosean ($Na_8[Si_6Al_6O_{24}]SO_4$) crystallizes in the space group P23. The topology of the aluminosilicate framework is that of sodalite [1].

At a pressure of 2.8(4) GPa, nosean shows a phase transition as concluded from a discontinuity in the pressure dependence of the unit cell volume (Fig.).

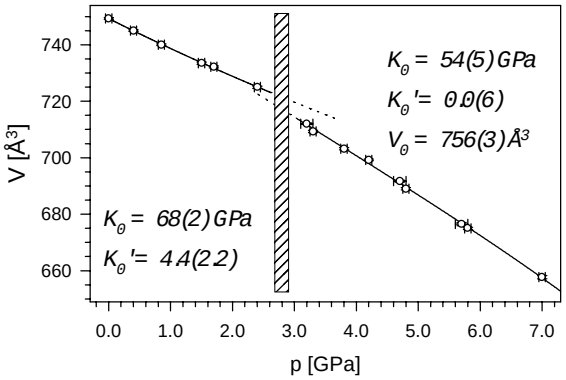

Structure determinations at 0, 1.70(5) and 3.2(1) GPa revealed, that every second cage within the aluminosilicate framework is empty. Whereas the sulphate ion is disordered in the phase stable at ambient conditions, it adopts an ordered arrangement within the high pressure phase (space group R3). The symmetry reduction from cubic to trigonal allows separate compression mechanisms for the empty and filled cages.

At 7.6(1) GPa, a pressure induced amorphisation was observed.

[1] Pauling, L.: The structure of sodalite and helvite. *Z. Kristallogr.* **74** (1930) 213-225.

P08.19.013 STRUCTURE ANALYSIS OF NON-MOLECULAR PHASE OF SnI_4 USING ANOMALOUS X-RAY SCATTERING AT HIGH PRESSURE. K. Sato and N. Hamaya, Graduate School of Humanities and Sciences, Ochanomizu University, Tokyo 112, Japan.

Molecular crystal SnI_4 exhibits novel phenomena such as metallization, amorphization, and molecular dissociation at high pressure. Our previous work demonstrated that SnI_4 showed the high-pressure structure sequence, first crystalline phase (CP-I ; insulator) - second crystalline phase (CP-II ; metallic) - amorphous state - third crystalline phase (CP-III). Diffraction patterns of CP-III measured above 61 GPa can be explained by the fcc lattice. A very small value of the nearest interatomic distance in CP-III is almost the same as that of non-molecular solid iodine, which indicates the dissociation of SnI_4 molecules. Three crystal structures can account for the observed fcc pattern; (1) phase separation into I_2 and amorphous Sn or amorphous SnI_2, (2) full disorder structure in which both iodine and tin ions are randomly located at the fcc sites, (3) partial disorder structure in which iodine ions are located at the ideal fcc sites and tin ions randomly occupy the interstitial sites. The purpose of this work is to clarify the atomic arrangement in CP-III of SnI_4 using x-ray anomalous dispersion effect near the K absorption edge of Sn.

We have carried out high-pressure powder x-ray diffraction measurements using synchrotron radiation at the SPring-8 (BL10XU). The radiation was monochromatized to an energy between 28.796 keV and 29.186 keV. The incident beam intensity was monitored continuously by a pin photodiode placed in front of a diamond anvil cell set at 63 GPa. Absorption coefficient of the sample was measured using another pin photodiode. Obtained intensities of reflections were found to decrease at energies very close to the absorption edge. Such an intensity variation is consistent with that expected from the full disorder structure model.

P08.19.014 STRUCTURES AND TRANSITIONS IN BARIUM ABOVE 12GPA: A SOLUTION FOR Ba-IV. R.J. Nelmes, M.I. McMahon, S.A. Belmonte and D.R. Allan, Department of Physics and Astronomy, The University of Edinburgh, Edinburgh EH9 3JZ, UK.

Barium is known to transform at 12.6GPa from an hcp phase to phase IV. The structure of this phase has eluded several attempts at solution [1]. The powder patterns are strongly textured and the structure is evidently quite complex [1]. We have collected image-plate diffraction data on station 9.1 at SRS Daresbury. These show that a gradual increase in pressure through the transition region over several hours leads to the formation of quite large crystallites, and 2-d patterns displaying strong diffuse scattering. In some cases, it has proved possible to obtain a small number of crystallites – just one in one case – which has allowed the collection of single-crystal data, both with the image plate and on a laboratory-source 4-circle diffractometer. It appears that there is an intermediate phase and that the structures of it and phase IV are of an unusual and complex kind, including a disordered component. These structures have been determined and refined from both the powder and the single-crystal data. Full details will be presented.

1. See K. Takemura, Phys. Rev. B**50**, 16238 (1994).

P08.19.015 HIGH-PRESSURE STRUCTURE VARIATION OF SPIN-PEIERLS CRYSTAL $CuGeO_3$. T.Yamanaka, A. Yoshiasa, T. Nagai, G. Yagyu Dept. Earth and Space Sci. Graduate School of Sci. Osaka Univ. 1-1 Machikaneyama Toyonaka Osaka 560-0043 Japan

$CuGeO_3$ characterized by spin-Peierls transition has several polymorphic transitions under the conditions of different hydrostaticity. Pressure-induced phase transition of $CuGeO_3$ has been elucidated using diamond anvil together with synchrotron radiation in order to comprehend the magnetic spin-lattice interaction under the condition of compression. Structure change of Phase I with pressure Phase I stable at ambient condition (Pbmm a=0.481nm, b=0.847nm, c=0.294nm) has an einer tetrahedral chain structure of GeO_4. CuO_6 octahedra link each other by shared edge in the direction of parallel to c axis. The octahedra is deformed by Jahn-Teller effect. Single crystal structure analyses at 2.93GPa, 3.90GPa and 5.3GPa reveal the rotation of octahedra and more deformation of octahedron to produced a dimarization. Jahn-Teller effect on Cu-O bond becomes less obvious with pressure. Volume of CuO6 is noticably compressed, while GeO_4 tetrahedron little changes. Hydrostaticity of compression brings different bulk modulus (Ko) of 47.1GPa under hydrostatic and 85GPa under nonhydrostatic condition. Structure determination of Phase IIUnder hydrostatic compression Phase I is reversibly transformed to a high pressure form (Phase II) at 6.3GPa. Despite the noticeable shrinkage of b axis and a little elongation of a axis of Phase I, this first-order transition is reversible. Consequetty in situ intensity measurement is required for the structure analysis. The structure of Phase II ($P2_1/c$ a=0.4935(57)nm, b=0.6754(7)nm, c=0.6208(11)nm β = 92.668(29)° has been clarified by single crystal structure analysis. Diffraction intensities were collected at 6.4GPa by using DAC with hydrostatic pressure media of methanol-ethanol mixture. Striking features are (1) germanium ion changes its coordination number to 5-fold (GeO_5), (2) copper ion occupies a position of 7-folded sites (CuO_7) and (3) these changes are caused by the martensic transition. Phase III and Phase IV under nonhydrostatic pressure Nonhydrostatic compression without pressure media brings Phase III (blue) at 7.5GPa and furthermore to Phase IV (green) at 9.5GPa. These structure transitions are brought about by the stress. At decompression, Phase Ireversibly changes to Phase III at 5GPa and the latter remains its structure at room pressure (Jayaraman et al., 1995). Phase III has an irreversible and then it is quenchable. The crystal structures of the both high pressure forms are still unknown. The nonhydrostatic stress produces various phases which are mostly irreversible and some indicate a monotropic path.

P08.19.016 HIGH PRESSURE STUDIES OF NbO_2F. S. Carlson, ESRF, B.P. 220, F-38043 Grenoble Cedex, France, and A.-K. Larsson and F. Rohrer, Inorganic Chemistry Dept., Stockholm University, S-10941 Stockholm, Sweden.

High pressure *X*-ray powder diffraction studies of NbO_2F, in the pressure range from ambient to 31 GPa, have been performed at the high pressure beamline ID30, ESRF.

The investigations were made with a membrane driven diamond anvil cell (diamond tip diameter 0.3 mm, and gasket hole diameter 0.125 mm). Pressure medium was silicon oil, and the pressure was monitored with the ruby fluorescence method. The *X*-ray radiation (0.4246 Å) from two phased undulators, reduced down to a beam spot size of 0.09x0.09 mm^2, was used.

Preliminary results show that the cubic ReO_3-type structure (space group: *Pm*-3*m*) of NbO_2F undergoes several pressure induced phase transitions in the investigated pressure range. At 9.2 GPa, the structure has transformed to the hexagonal symmetry, and Rietveld refinements indicate that it is of the VF_3-type (space group: *R*-3*c*). Over ~20 GPa, the diffraction patterns indicate that NbO_2F transforms back to cubic symmetry, but display also marked signs of amorphization with the disappearance of diffraction peaks at higher angles.

P08.19.018 IN-SITU HIGH PRESSURE X-RAY DIFFRACTION STUDY ON $CuGeO_3$. S. R. Shieh, H. K. Mao, R. J. Hemley, A. Jayaraman, Geophysical Lab and Center for High Pressure Research, Carnegie Institution of Washington

The discovery of spin-Peierls transition on $CuGeO_3$ at 14 K and ambient pressure has attracted lots of attention. Recently Raman spectroscopy and energy dispersive X-ray studies show that $CuGeO_3$ has encountered a phase transition near 7 GPa when pressure medium is strictly hydrostatic. However, the new high pressure phase has been assigned as either monoclinic (Adams et al. 1991) or orthorhombic (Jayaraman et al. 1997 and Ming et al. 1998). An attemp has been made to use the high resolution angular dispersive X-ray diffraction method to determine the high pressure structure of $CuGeO_3$ at pressure above 7 GPa.

In this study, the ungrinded $CuGeO_3$ powder was loaded in a Mao-Bell type diamond anvil cell with either He or 4:1 mixture of methanol/ethanol as pressure medium. Pressure was determined by the ruby fluorescence method. The sample was examined in angular dispersive X-ray diffraction using synchrotron radiation source with wavelength l =0.4956 angstron at Cornell High Energy Synchrotron Source (CHESS). Two phase transitions were observed when pressure was compressed up to 26 GPa. The first phase transition takes place at about 7 GPa, the other phase transition occurs at about 18 GPa. The detail structural information will be provided in this paper.

P08.19.019 ON THE PRESSURE-INDUCED CRYST-ALLINE-TO-AMORPHOUS TRANSITION IN BISMUTH OXIDE. S. Desgreniers S. Pilod, and C. Chouinard. Department of Physics and Ottawa-Carleton Institute of Physics, University of Ottawa, 150 Louis Pasteur, Ottawa, Ontario, Canada. K1N 6N5.

A crystalline-to-amorphous transition has been observed in pressure-densified bismuth oxide, starting the monoclinic α-phase. The onset of the transition to the amorphous state is at around 15 GPa and the disordered state is retained as the pressure is released from above 25 GPa to room pressure. From the X-ray structure factors, obtained by energy-dispersive and angle-dispersive X-ray diffraction and corrected for incoherent scattering, the average radial pair distribution function of the amorphous phase are extracted as a function of pressure. It is found that the Bi-Bi nearest neighbors distance in the disordered state changes by 7 % following a compression to 25 GPa. We also report on the Raman spectroscopic evidence for the crystalline-to-amorphous transition.

P08.19.020 MODELLING TRANSFORMATIONS OF HYDROGEN-BONDED STRUCTURES AT HIGH PRESSURES. Andrzej Katrusiak, Department of Crystal Chemistry, Adam Mickiewicz University, Grunwaldzka 6, 60-780 Poznan, Poland

Hydrogen bonds have much lower energy than covalent bonds binding atoms into molecules, or than electrostatic interactions in ionic crystals. Thus, like van der Waals interactions, the hydrogen bonds are prone to transformations when a substance changes its thermodynamic conditions. At the same time, because the hydrogen bonds are relatively weak, their transformations are often blurred by other effects in a transforming structure. Therefore it is important to understand and to be able to model the response of the hydrogen bonds to elevated pressures. Such models would be helpful for predicting the properties of hydrogen-bonded structures in the function of temperature and pressure, for example of pressure-preserved food, of high-pressure polymorphs of ices, or of hydrogen-bonded ferroelectric crystals. Of the immense variety of types of hydrogen bonds we chose bonds OH- -O, NH- -N and NH- -O for our initial studies. They are relatively strong and most abandoned in Nature. A simple model of the OH- -O bond transformations affords a straightforward explanation of the coupling between atomic displacements and H-disordering, of the occurrence of tricritical points in ferroelectric crystals, anomalies in thermal expansion, and gives the quantitative temperature function of their phase-transition temperatures [1-3]. Most recently we investigated the stability of protons in NH- -N bonds [4], and found a new group of NH- -N bonded ferroelectrics [5].

1. A. Katrusiak. Phys. Rev. B48 (1993) 2992; B51 (1995) 589.
2. A. Katrusiak, Ferroelectrics 188 (1996) 5.
3. A. Katrusiak, Phys. Rev. Lett. 77 (1997) 4366.
4. A. Katrusiak, J. Mol. Struct. 474 (1999) 125.
5. A. Katrusiak and M. Szafranski, Phys. Rev. Lett. 82 (1999) 576.

P08.19.021 ON THE ORIGIN OF 'DEBYE-SCHERRER ELLIPSES' FROM 3-D FULLERENE POLYMERS. L.Marques, Dept. Física, Universidade de Aveiro, 3800 Aveiro, Portugal. M.Mezouar, E. S. R. F., 38041 Grenoble, France. J-L.Hodeau, Laboratoire de Cristallographie, C.N.R.S., BP166 Cedex 09, 38000 Grenoble, France. M.Núñez-Regueiro, C.R.T.B.T., C.N.R.S., BP166 Cedex 09, 38000 Grenoble, France. N.R.Serebryanaya and V.A.Ivdenko, Inst. of Spectrosc. RAS, Troitsk Moscow Region, 142092 Russia. and V.D.Blank and G.A.Dubitsky, Res. Cent. Superhard Materials, 7-a Centralnaya Str., Troisk Moscow Region 142092 Russia.

High pressure studies have up to now determined the existence of 1-D and 2-D polymer fullerene structures. Synchrotron radiation powder diffraction measurements using a 2D fast scan detector were performed on C_{60} samples quenched from 13GPa and 820K. The analysis of all the reciprocal spectra indicates that the sample is a 3-D polymerized fullerite. For the same bulk sample, the observed elliptical shape of the Debye-Scherrer rings varies, depending on the orientation of the sample with respect to the incident beam, and can reach nearly perfect circles. These fullerene samples have been produced under uniaxial compression conditions and therefore we must conclude that the stress gradient, under which they were made, remain recorded in the quenched samples via a lattice deformation. This observed permanent anisotropic deformation is due to an irreversible change in the intermolecular bonding during the phase transformation. Structural models for the 3D C_{60} polymer will be presented.

P08.19.022 EXPERIMENTAL AND COMPUTATIONAL STUDIES OF InSb-IV. M.I. McMahon, G.J. Ackland and R.J. Nelmes, Department of Physics and Astronomy. The University of Edinburgh, Edinburgh EH9 3JZ, UK.

The high-pressure structures and phase diagram of InSb continue to attract considerable attention. Recent room-temperature imaging-plate studies [1], and high-temperature energy-dispersive studies [2], have revealed a phase diagram very different from that constructed in the 1960's. Below 8GPa and 300°C, the dominant form of InSb is InSb-IV, or the P4 phase, the structure of which is a surprisingly complex superstructure of that proposed initially in 1978 [1,3]. Although the P4 structure does have the same spacegroup (Cmcm) as the high-pressure phase of several other III-V and II-VI semiconductors, the superstructure nature of P4 remains, as yet, unique to InSb.

In this paper we review the most recent phase diagram of InSb, and present results from ab-initio pseudo-potential calculations aimed at understanding the reasons for the structural complexity of InSb-IV. The calculations confirm the superstructure to have a lower energy than the simpler Cmcm structure observed in other III-V and II-VI systems, and verify the nature of the atomic ordering.

1. M.I. McMahon and R.J Nelmes, Phys. Rev. Lett. **74**, 106 (1995).
2. M. Mezouar *et al.*, Phys. Stat. Sol. (b) **198**, 403 (1996).
3. S.C Yu *et al.*, J. Appl. Phys. **49**, 4741 (1978).

P08.19.023 X-RAY DIFFRACTION STUDY OF DILUTE MAGNETIC SEMICONDUCTORS (DMS) UNDER HIGH PRESSURE PART I: $Zn_xCo_{1-x}S$. D. Gómez, Grupo de Cristalografía Dpto de Química, Facultad de Ciencias. Universidad de Los Andes Mérida, Venezuela. T. Tinoco, S. A. López. Lab. de Física Aplicada, Dpto de Física, Facultad de Ciencias, Universidad de Los Andes,Mérida, Venezuela. A. Polian and J.P. Itié. Physique des Milieux Condensés, Université Pierre et Marie Curie, B 77, 4, Place Jussieu, Paris-France.

Dilute magnetic semiconductors (DMS) constitute a class of semiconducting materials formed by randomly substituting a fraction of cations (in the II-VI or III-V compounds) by magnetic ions X(X= V, Cr, Mn, Co or Ni). These alloys exhibit a variety of novel magneto-optical properties coming from the exchange interaction between the magnetic ions and the conduction or valence electrons (s-p exchange interaction). This interaction is increased at high pressure and may induce phase transitions. In this work, $Zn_{0.9}Co_{0.1}S$ has been studied under high pressure up to 28 GPa. At high pressure the most intense peaks of the blende phase have been observed up to 17 GPa, but new peaks appear above 12,7 GPa. The new peaks have been indexed in a disordered rock-salt phase. This phase is stable at least up to 28 Gpa (maximum pressure reached in this experiment) The unit cell volume has been fitted with a firstorder Murnaghan equation of state. This deduced bulk moduli are B = (84 2) GPa in the zinc blende phase and B = (119 16) GPa in the NaCl phase, with B' = 4 in both cases. The recovered phase is identical to the initial phase at 0 GPa.

The samples used were prepared by chemical transport with nominal cobalt concentration x=0.1 The present experiments were conducted in a diamond anvil cell. Stainless-steel gaskets were used to confine the samples. The pressure-transmitting medium was silicon oil and the pressure was measured using the linear ruby fluorescence scale. EDX experiments were performed at the DW11 station on the wiggler line of the LURE synchrotron facility (Orsay, France) using the DCI storage ring.

P08.19.024 PHASE TRANSITION IN $CaCuGe_2O_6$. M. Tovar and W. Eysel, Mineralogisches Institut, University of Heidelberg, Germany

The compound $CaCuGe_2O_6$ [1] exhibits at room temperature a distorted pyroxen structure ($P2_1/c$) [2]. With increasing temperatures a sluggish phase transition between two monoclinic pyroxen-like forms $P2_1/c \rightarrow P2_1/n$ occurs [3]. High temperature X-ray powder investigations were performed by means of a Siemens powder diffractometer D500 (Ge primary monochroma-tor, $CuK\alpha_1$) with a high temperature device Buehler HDK 2.3 (platinum strip as sample holder and heater).

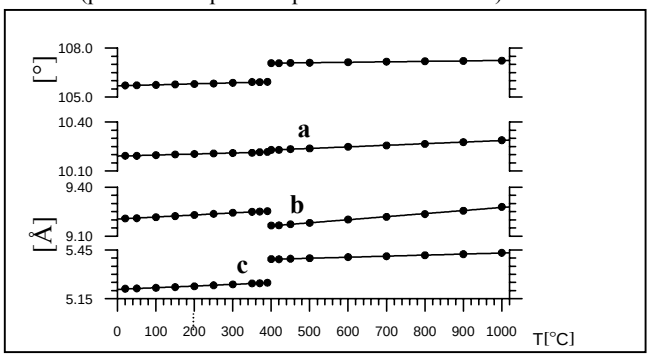

Fig. 1: Lattice parameters of $CaCuGe_2O_6$ from 20° to 1000°C

Applying whole powder pattern fitting the lattice parameters were determined from room temperature up to 1000°C in varying temperature intervals (Fig. 1). These measurements reveal the phase transition at 400°C. In both phases the lattice parameters change linearly. Together with previous DTA results the jump in the lattice parameters indicates a first order transition. High temperature Rietveld refinements are in progress.

[1] PDF No. 34-274
[2] Behruzi, M., Breuer, K.H., Eysel, W., Z.Krist. 176 (1986), 205-217
[3] Breuer, K.H., W. Eysel, Behruzi, M., Z.Krist. 176 (1986), 219-232

P09.19.001 X-RAY DIFFRACTION UNDER NON-HYDROSTATIC CONDITIONS. L. Dubrovinsky, N. Dubrovinskaia, S. Saxena Department of Earth Sciences, Uppsala University

The stress state in a solid specimen compressed between two flat and parallel anvil faces (in a diamond anvil cell (DAC), for example) is nonhydrostatic. The resulting lattice strains measured by X-ray diffraction exhibit certain features which are absent if truly hydrostatic conditions prevails. We analysed the influence of deviotoric stresses on the behaviour of the samples in DAC from a point of view of nonhydrostatic thermodynamics. Such phenomena as recrystallization and preferred orientation, changing the pressure and temperature parameters of phase transitions and chemical reactions under stress could be quantitatively described. Application of the theory is demonstrated on an example of a study of wustite FeO at pressure up to 16 GPa. We found that pressure of phase transition is proportional to the uniaxial stress component and rises from 10.1 GPa for compression without pressure medium to the 15.4 GPa in Ar pressure medium. Extrapolation to zero stress conditions gives the value 16.8 GPa. This value is in good agreement with data by Fei (1996) (powder diffraction data, compression in He pressure medium, Ptr= 17(1) GPa) and Shu et al. (1998) (single crystal diffraction data, compression in He pressure medium, Ptr= 18(1) GPa).

Recently, a method to estimate single-crystal elastic moduli from polycrystalline X-ray diffraction of non-hydrostatically compressed material has been introduced (Singh, 1993; Singh and Balasingh, 1994; Singh et al., 1998). The method of analysis of lattice strain in non-hydrostatic stress states (NSS) is

based on transformation of the stress axis into crystal axis and further on calculations of the strain for given direction (diffracting plane normal) from elastic moduli (Singh, 1993; Singh and Balasingh, 1994; Uchida et al., 1996; Singh et al., 1998). It was assumed that the stresses for all crystallites with common direction of diffracted plane normal, could be averaged out (if crystallites are randomly oriented) (Singh, 1993; Singh and Balasingh, 1994; Uchida et al., 1996; Singh et al., 1998). But if the load direction is fixed, stresses transformed to crystal axis, depend on the orientation of the crystal and produce different strains. We propose the algorithm for calculating the shape of the diffraction lines from the non-hydrostatically compressed solid and apply it to study CsI and Pt at high pressures and temperatures.

P09.19.002 MICRO: A NEUTRON DIFFRACTOMETER, SPECIALIZED FOR HIGH PRESSURE MAGNETIC STUDIES. Goncharenko I.N. [1], Mirebeau I. [2], Gabriel A. [3], Molina P. [4], Böni P. [5], [1] Laboratoire Leon Brillouin, CEA Saclay, 91191 Gif-sur-Yvette, France and Russian Research Center "Kurchatov Institute", [2] Laboratoire Leon Brillouin, CEA Saclay, 91191 Gif-sur-Yvette, France, [3] European Molecular Biological Laboratory, 38043, Grenoble, France, [4] Ecole Centrale de Nantes, 1 rue de la Noé, 44000 Nantes, France, [5] Laboratoire for Neutron Scattering ETH&PSI, CH-5232 Villigen PSI, Switzerland

Starting from 1992, a project for neutron diffraction under very high pressures (up to 40- 50 GPa) is under development in the Laboratoire Léon Brillouin (Saclay), in collaboration with Kurchatov Institute (Moscow). The important part of the project is a new powder diffractometer MICRO (modified version of the spectrometer G6.1), specialized for high pressure studies of small samples in diamond or sapphire anvil cells. The diffractometer is located on a cold neutron guide of the ORPHEE reactor and operates with a long wavelength, very suitable for studies of magnetic or medium-scale structures. Focusing systems (made from Ni-Ti supermirrors) allow us to increase the flux at the sample place by one order of magnitude, whereas special environments reduce background down to a very low level (a few counts/per channel/ per hour). The allowed temperature range is from 1.5 to 300 K, the pressure range could vary from 0 - 8 GPa to 0 - 50 GPa depending on the values of magnetic moments and the complexity of crystal and magnetic structures.

The diffractometer is operating in the high pressure mode for about 150 days per year and is open for research proposals from external groups. This year we expect a new important step in the development of the MICRO diffractometer. A new multidetector, based on the delay line technique, is now under construction in the European Molecular Biological Laboratory (Grenoble). The multidetector, covering a higher solid angle, is expected to increase luminosity by another factor of 5.

P09.19.003 TEXTURE AS AN AID TO INDEXING AND STRUCTURE SOLUTION IN POWDER DIFFRACTION. Scott A. Belmonte and Richard J. Nelmes, Department of Physics and Astronomy, The University of Edinburgh, Mayfield Road, Edinburgh, EH9 3JZ, U.K.

The presence of texture in a sample is generally regarded as a hindrance when trying to determine a crystal structure from powder diffraction data. However, if handled correctly, there is potentially a wealth of additional information available from a textured sample, over a non-textured sample, which can possibly **aid** the structure determination process.

In a textured powder sample, the relative intensities of the diffraction peaks depend not only on the arrangement of atoms in the unit-cell, but also on the orientation of the sample with respect to the incident beam. The manner in which the intensities vary as the sample orientation is changed depends on the orientation distribution of the crystallites in the sample **and** the magnitude and direction - with respect to the unit-cell axes - of the reciprocal lattice vectors that contribute to each reflection. By collecting diffraction patterns from a textured sample in many different orientations and fitting the observed changes in intensity it is possible, in principle, to use the (hkl)-dependence of the variations to obtain reciprocal lattice vectors and thus index the powder pattern.

A description of texture and how it can be used to index a powder pattern will be given. It will also be shown how, once the correct unit-cell is known, texture can make it possible to extract relative intensities from exactly overlapping reflections thus helping structure solution. Examples of the successful application of these techniques to actual data collected from highly textured samples will be presented.

P09.19.004 CORRECTION OF DIFFRACTION OPTICS AND P-V-T DATA USING MULTIPLE THERMOELASTIC EQUATIONS OF STATE. Yusheng Zhao, Robert B. Von Dreele [1], Donald J. Weidner [2], [1] LANSCE, Los Alamos National Laboratory, Los Alamos, NM 87545, U.S.A, [2] CHiPR and Mineral Physics Institute, University at Stony Brook, NY 11794, U.S.A

The necessity of P-V-T data correction is vital in case of misalignment in diffraction optics and/or failure of thermocouple. This paper discusses how to correct the observed P-V-T data and diffraction optics from a diffraction spectrum using thermoelastic equations of state (EOS) of multiple phases. The unit cell volumes of multiple phases (derived from the same diffraction pattern) can be used to derive the experimental P-T conditions when the thermoelastic EOS of the multiple phases are well established and sufficiently different. The large intersection angle of isochoric lines of these phases in P-T space ensures the determination of P-T with satisfactory precision. Apparently, this method is very helpful when thermocouples fail in the experiment. On the other hand, severe “strain-shift” problem can be caused by the displacement of diffraction center as pressure and/or temperature changes. The strain-shift is calculated to be: $\delta(d/d) = \delta(2\Theta) \times \cot(\Theta)$, where $\delta(2\Theta) = (\text{dis.}/L)$, and dis. is the displacement of the diffraction center along the incident beam (Θ=180) direction and L is the distance of the diffraction center to detector. For the high P-T neutron diffraction experiment, such strain-shift problem becomes very serious when using a ceramic gasket for simultaneous high pressure and temperature experiment, where the hydraulic ram movement (roughly about twice of the dis.) is significant, especially at the initial compression stage. The consequence of the strain-shift is an apparent over-compression of the unit cell dimension and thus an overestimate of the pressure. This problem can be solved simply by monitoring the movement of the diffraction center and mechanically adjust of the press so as to restore the correct diffraction optics as calibrated at ambient conditions. As an intellectual exercise and also for the practical necessity, we have worked out a method to correct the strain-shift using the known thermoelastic equations of state of multiple phases. This approach assumes that all the multiple phases in the sample mixture experience the same pressure and temperature in the diffraction volume. The analytical solution of pressure, temperature, and volume can be derived by simple algebra. In real practice, the iso_(P,T) condition can be achieved readily via numerical computation by step-iteration of the strain-shift. The uncertainty of the P-V-T determination is inversely correlated to the precision of the diffraction refinement as well as to the contrast of thermoelastic parameters of the pressure standards. The experimental uncertainties of the P-V-T data related to the sample mixture method of the multiple phases are also discussed.

P11.19.001 THE ANISOTROPY OF STRUCTURAL DISTORTION OF Co^{III}-NITROAMMINES AT HIGH PRESSURE. E.V. Boldyreva and D.Y. Naumov, Institute of Solid State Chemistry and Mechanochemistry SB RAS, Kutateladze, 18, Novosibirsk, 128, 630128 Russia, email elena@solid.nsk.su, and H. Ahsbahs, Institute of Mineralogy of Marburg University, Hans-Meerwein Strasse, 35043 Germany.

Hydrogen bonds were shown to play a major role in the anisotropy of structural distortion of Co^{III}-nitropentaammine coordination compounds on cooling [1]. In the present contribution we report on the role of hydrogen bonds in the anisotropy of structural distortion of the same compounds induced by another isotropic action - hydrostatic high pressure - which was shown to be qualitatively different from that on cooling [2]. Single-crystal X-ray diffraction in the diamond anvil cell was used to follow the changes in lattice parameters with increasing pressure up to 5.0 GPa and to refine crystal structures at several pressures. The changes in the intra- and intermolecular distances and angles were followed. The compressibility of NH...O and NH...Cl hydrogen bonds was measured. The role of these hydrogen bonds in the anisotropy of pressure-induced structural distortion is discussed. It is compared with the role of hydrogen bonds in the distortion of the same structures on cooling and during homogeneous linkage isomerization [3]. The data from diffraction experiments are correlated with the results of high-pressure IR-spectroscopy [4].

E.V.Boldyreva, J.Kivikoski, J.A.K.Howard (1997) Acta Cryst. B53, 394-404, 405-414.
E.V.Boldyreva, D.Naumov, H.Ahsbahs (1998) Acta Cryst. B54, 798-808.
E.V.Boldyreva (1996), in: V.V.Boldyrev (Ed.), Reactivity of Solids, Past, Present, Future, IUPAC Series Chemistry for the 21st Century, Blackwells: Oxford, 141-184.
E.V.Boldyreva, E.B.Burgina, V.P.Baltakhinov, H.Ahsbahs et al (1992), Ber. Bunsenges. Phys. Chem., 96(7), 931-937.

P11.19.004 THE INFLUENCE OF TEMPERATURE AND PRESSURE ON ACETONE. S. Parsons and C.R. Pulham, Department of Chemistry, The University of Edinburgh, Edinburgh, EH9 3JJ, D.R. Allan, Department of Physics and Astronomy, The University of Edinburgh, Edinburgh, EH9 3JZ, S.J. Clark, Department of Physics, The University of Durham, Durham, DH1 3LE, R.M. Ibberson, ISIS Facility, Rutherford Appleton Laboratory, Chilton, Didcot, OX11 OQX and L. Sawyer, Institute of Cell and Molecular Biology, The University of Edinburgh, EH9 3JR.

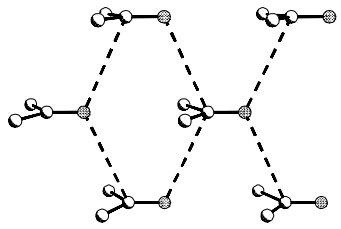

At high pressure (15 kBar) acetone forms layers in which each molecule is involved in four C..O contacts formed in a sheared-parallel motif. Although this structure is metastable at low temperature (165 K), the preferred structure at low temperature consists of layers in which pairs of acetone molecules interact in an antiparallel fashion, with each pair forming C..O contacts perpendicular to the planes of the molecules forming neighbouring pairs. Frozen acetone exhibits an unusual change in its heat capacity at around 130 K, although the nature of this transition has remained a mystery since it was first identified in 1929. Neutron powder-diffraction measure-ments at 5 K and a variable temperature X-ray diffraction study enable us to suggest that this is ascribable to strengthened C..O and CH..O contacts.

P11.19.007 HIGH-TEMPERATURE X-RAY DIFFRACTION STUDY OF Al-Ni-Cr INTERMETALLIC COMPOUND ALLOYED WITH VANADIUM AND TITANIUM. S.A.Petrova, R.G.Zakarov, V.L.Zyazev, and N.A.Vatolin, Institute of Metallurgy, Urals' Division, Russian Academy of Science, Ekatherinburg, 620 016, Russia.

Ternary Al-Ni-Cr intermetallic compound alloyed with vanadium and titanium were investigated using an automated diffractometer DRON-UM1 ($Cu_{K\alpha}$-radiation, pyrographite monochromator). Crystal structure of the main phase (85%) was defined to be of Al_3Ni_2 structural type, P-3m1 space group (PSC: hP5). X-ray phase analysis of the samples after DTA revealed an oxidation of the non-alloyed compound (a = 4.044(1) Å, c = 4.897(1) Å, F20 = 79 (.012, 21)); no oxidation of the compound alloyed with vanadium (a = 4.048(1) Å, c = 4.900(1) Å, F20 = 65 (.013, 24)) and titanium(a = 4.047(1) Å, c = 4.899(1) Å, F20 = 95 (.008, 26)) was observed by X-rays. With the use of the UVD-2000 attachment a high-temperature X-ray investigation of the above-mentioned alloys was carried out in the temperature range of 25-1350°C *in situ* in helium atmosphere. According to the results obtained temperature dependencies of crystal lattice parameters for phases available and coefficients of thermal expansion along *a* and *c* axes have been detected. It was found a structural transition of the initial phase with Al_3Ni_2 structure to the phase with AlNi-type structure (PSC: cP2) nearby 1000°C.

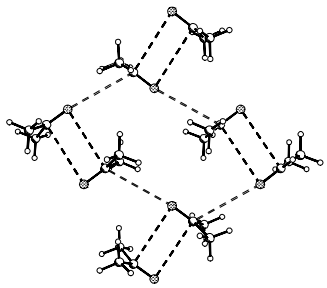

This work is supported by the Russian Foundation for Fundamental Research (grand N 98-03-32655).

P11.19.009 LOW TEMPERATURE CRYSTAL GROWTH & MULTIPLE TEMPERATURE STRUCTURAL STUDY OF $Cu(H_2PO_2)_2$ & ITS COMPLEXES. D.Y. Naumov and E.V. Boldyreva, Institute of Solid State Chemistry and Mechanochemistry SB RAS, Kutateladze, 18, Novosibirsk, 128, 630128 Russia, email d.y.naumov@iname.com, and D.S. Yufit and J.A.K. Howard, Chemistry Department, University of Durham, Durham DH1 3LE, UK.

Copper hypophosphite $Cu(H_2PO_2)_2$ and its complexes find important applications in the advanced technologies. Solid-state decomposition of these compounds gives at the initial stages latent copper centers with unusual chemical properties and increased catalytic activity, and can therefore be used as the basis of a number of new cheaper and cleaner technologies, including recording and storing information using non-silver photographic materials, metallization of dielectrics, manufacturing of printed forms in polygraphy [1].

Although they were needed for understanding the mechanism of the decomposition and for optimizing the technologies, molecular and crystal structures of these compounds remained unknown, since the compounds are highly unstable, low temperatures are required for crystal growth, low temperatures and rapid data collection - for a structural study.

The present contribution describes the results obtained with a Oxford Cryosystems Cryostream cooling device applied both for crystal growth and for data collection. Three polymorphs of copper hypophosphite and its urea complex were grown and studied with a Siemens SMART CCD area detector (down to 100K) and a Huber 4-circle diffractometer with a Siemens rotating anode generator with a Displex LT-unit (15K). The variable temperature data collection made it possible to study hydrogen bonds in the crystals and to discuss their possible role in solid-state reactivity.

1. O.I.Lomovsky, V.V.Boldyrev (1994), J. Mater. Synthes. Proces., 2(4), 199-206.

P11.19.010 STRUCTURAL CHANGES OF TITANIUM UNDER ELECTRO THERMAL TREATMENT IN LIQUID NITROGEN ENVIRONMENT. I.S.Braude, F.F.Lavrentev, V.N.Nikiforenko, O.P.Salita, B.Verkin Institute for Low temperature Physics and Engineering, Ukraine Nat. Acad. of Sci., Kharkov 310164, Ukraine

Effect of electrical heating by current of $5x10^5$ A/cm^2 density in liquid nitrogen on titanium structure has been studied. The research is carried out on commercial Ti (BT-1.0) with initial grain size 6 mkm. The applied experimental methods are X-ray, resistometric and metallographic technics. The rolled specimens put into the bath with liquid nitrogen and current in impulse regime passed through them. X-ray phase determination has revealed the formation of new phase rutile TiO_2 simultaneously with grain size increase (by factor of about 3). The latter observation was supported by metallographic measurements. The rutile formation was explained by activation of oxygen diffusion from liquid nitrogen under heating by current. The grain size increased with collective recrystallization. Resistometric measurements favored with the view that electro thermal treatment facilitated higher mobility of oxygen and the role of the latter in the structure changes was a basic one. The role of the other defects of titanium crystal in the structure evolution after electro thermal treatment is discussed.

P11.19.011 A SCHEME FOR UNIQUELY LABELING POLYMORPHIC PHASES. Reuben Rudman, Chemistry Department, Adelphi University, Garden City, NY 11530, USA.

The nomenclature used for identifying polymorphic crystalline phases is inconsistent. Roman numerals, Greek letters, and, occasionally, Arabic numerals have all been used; the sequence of symbols may follow the historical order of the discovery of the phases, or it may start with the room-temperature phase or the phase formed from the melt or the low-temperature phase. Usually once a particular phase has been labeled and referred to in the literature, any new phases that are discovered subsequently are given their own unique labels. The reason for this is obvious. If the same symbol is used for different phases, unique identification of the phase in the literature will be difficult and retrieval from subsequent databases will be impaired. Unfortunately, in some cases the authors have relabeled all the phases, so that the literature now contains two different phases with the same label. This is singularly unfortunate, especially, in cases where the purported new phase is later shown not to exist. Other authors have commented on this problem too. For example, van Eijck et al. [Acta Cryst. (1998) B**54**, 291], in discussing the pressure-induced polymorphs of benzene, state: We deplore the practice of renaming known modifications, which is bound to lead to confusion sooner or later.

It is proposed here to uniquely identify a crystalline phase of a pure material by incorporating into its label the following information: (i) phase identifier, (ii) temperature of formation, (iii) pressure of formation, (iv) whether it forms as the temperature (or pressure) is being raised or lowered, and (v) the phase identifier of the immediately preceding phase.

Examples of the application of this phase-labeling nomenclature will be presented, along with a comparison of this system with that proposed by the IUCr Working Group on Phase Transition Nomenclature [Acta Cryst. (1998) A**54**, 1028]. Hysteresis effects, solid solutions, and label compactness are some of the topics the Working Group did not fully address.

P11.19.012 PHASE TRANSFORMATIONS IN TITANIUM OXYCARBIDE. M.Yu.Tashmetov, V.T.Em [1], B.N.Savenko, G.Batdemberel [2], [1] Institute Nuclear of Physics Uzbekistan Academy of Sciences, Uzbekistan, [2] Joint Institute Nuclear of Research, Russia.

According to theory, the ordering in interstitial phases is principially caused by the deformation interaction between the interstitial solutes. It is known that in interstitial phases interaction between the interstitial solutes determines crystall structure and its properties. In this work X-ray and neutron diffraction methods used to investigate phase transformations in titanium oxycarbide.

The titanium oxycarbide were found to have cubic (sp.gr.Fd3m) and trigonal (sp.gr.P3121) ordered structures. In the space group Fd3m,the Ti atoms occupy the 32(e) positions whereas the carbon and oxygen atoms occupy the 16(c) and 16(d) octahedral interstitial positions. In the trigonal structure, the titanium atoms occupy position 6(c), while the carbon and oxygen atoms occupy positions 3(a) and 3(b). In both ordered structures the metal atoms are shifted from vacancies toward the nonmetal atoms, also positions 16(c) and 3(b) are partially occupied by nonmetal atoms. The cubic ordered structure (sp.gr.Fd3m) is low temperature phase and high temperature phase is trigonal. At 1020K trigonal ordered phase decomposes into two phases. Phase transformations takes place according to the following scheme:
Cubic (Fd3m)→Trigon(P3121)→Ti+Trigon(P3121) →Ti+Cubic(Fm3m)

P11.19.013 X-RAY DIFFRACTION AND CALOR-IMETRIC STUDIES ON PHASE TRANSITION IN $CsPbCl_3$. Y.Yoshimura, Y.Kawase, C.Kimura, H.Iwasaki [1], A.Kojima [2], K.Tozaki [3], [1] Faculty of Science and Engineering, Ritsumeikan University, Kusatsu, Shiga 525-8577, Japan, [2] Department of Materials Science, The University of Shiga Prefecture, Hikone, Shiga 522-8533, Japan, [3] Department of Physics,Faculty of Education, Chiba University, Inage, Chiba 263-8522, Japan

A "hyperfine multistage transition" within 0.1 K was first observed at the 320 K transition in $CsPbCl_3$. Besides this transition, the crystal undergoes phase transitions at 315 and 310 K, explained by the condensation of a soft phonon mode. Another phase change was also reported to exist at 200 K. Hence, X-ray photographic and calorimetric studies were performed over the wide temperature range 340 - 90 K, to make clear the whole transition mechanism. On cooling from room temperature, at approximate 260 K, an abrupt increase of intensity was observed at R- and X-point superlattice reflections appeared at 315 and 310 K transition, respectively. No increase was, however, observed at the temperature concerning M-point appeared at 320 K transition. Corresponding to the X-ray data, a little change of the baseline was observed by means of heat flow measurements. These results suggest there is a new structural phase transition at 260 K and also heterogeneous structural change takes place from the 320 K.

P11.19.014 THE CRYSTAL STRUCTURE OF SPINEL-TYPE $CuIr_2S_4$ AT LOW TEMPERATURE. H. Ishibashi, T. Sakai and K. Nakahigashi, College of Integrated Arts and Sciences, Osaka Prefecture University, Gakuen-cho 1-1, Sakai, Osaka 599-8531, Japan, and R. Oshima, Research Institute for Advanced Science and Technology, Osaka Prefecture University, Gakuen-cho 1-2, Sakai, Osaka 599-8570, Japan.

We have studied the crystal structure of a spinel-type compound $CuIr_2S_4$ at low temperature by using powder X-ray and electron diffraction. $CuIr_2S_4$ is known to show a metal-insulator transition at T_t = 230 K with a structural transition from cubic phase to tetragonally distorted one[1]. However some weak reflections cannot be explained by the assumed structure, therefore, the crystal structure below T_t has not been determined completely.

The high resolution powder X-ray diffraction experiments at 50 K were performed by using synchrotron radiation at Photon Factory in Tsukuba. The powder pattern shows that 400 and 440 reflections split into three and six peaks, respectively, where the basis vectors are corresponding to the cubic axis in the high temperature phase, therefore the crystal structure of the low temperature phase has a triclinic symmetry. Furthermore, there appear many superlattice reflections which are indexed by h, k, l = (all half integer) such as 1/2 1/2 1/2 and (all integer). Consequently, all reflections including superlattice ones can be indexed by assuming a triclinic structure with the cell parameters of a = 19.3787 Å, b = 11.9480 Å, c = 6.9841 Å, α = 91.02°, β = 90.04°, γ= 144.27°. The new unit cell vectors $\boldsymbol{a}$, $\boldsymbol{b}$ and $\boldsymbol{c}$ are given by $\boldsymbol{a} = 2\boldsymbol{a}'$, $\boldsymbol{b} = (-2\boldsymbol{a}' + \boldsymbol{b}' + \boldsymbol{c}')/2$ and $\boldsymbol{c} = (-\boldsymbol{b}' + \boldsymbol{c}')/2$, where $\boldsymbol{a}'$, $\boldsymbol{b}'$ and $\boldsymbol{c}'$ are lattice vectors corresponding to the cubic axis. This structural model also can explain the results of electron diffraction pattern. The detail of the atomic displacements of each atom will be discussed in the conference.

Furubayashi, T., Matsumoto, T., Hagino, T. & Nagata, S. (1994). *J. Phys. Soc. Jpn.*, **63**, 3333-3339.

P11.19.015 ^{7}LI AND ^{23}NA SPIN-LATTICE-RELAXATION IN $LINASO_4$. H.-C. Freiheit, A. Fischer, H. Kroll, A. Putnis, Institut für Mineralogie, Muenster, Germany

$LiNaSO_4$ is a plastic crystalline at high temperatures, where Na atoms become highly mobile. The phase transition relating from the trigonal LT-phase (*P31c*) to the superionic conducting phase (*Im3m*) occurs at T_{tr}=788K. It has a pronounced first order character. Anomalies in the heat capacity C_p, the cell volume V and the isotropic displacement parameters of the oxygen atoms $B(O)$ observed at T>500-600K indicate a continuous increase of the orientational disorder of the SO_4-groups well below T_{tr} [1]. The phase transition may thus be triggered by the rotation of SO_4-groups in the low temperature form. In addition coupling between the rotation of the SO_4-groups and the cationic motion is to be expected. In order to verify the supposed transition model we have carried out T_1-spin-lattice-relaxation measurements for ^{7}Li at 155.5 MHz and16 MHz using a (n·90°-τ-90°)-acquisition – and ^{23}Na at 105.8MHz and 16 MHz using a (180°-τ-90°)-acquisition. A mono-exponential recovery of the magnetization at all temperatures is observed for the Li nucleus at both Larmor frequencies and for the Na nucleus at 16MHz. At 105.8MHz the Na nucleus shows a bi-exponential behaviour below 550K resulting in two relaxation times T_{1a} and T_{1b} due to quadrupole interactions [2]. At low temperatures the relaxation is slow for both nuclei with a slight temperature dependence ($\propto T^2$) due to phonons. Above 550K the relaxation rates follow a BPP-behaviour ($T_1 \propto \omega^2$). The change from phonon-induced relaxation to BPP-behaviour at 550K, i. e., the onset of "successful" jumps, indicates a coupling of the cationic motion and the SO_4-rotation according to the trigger-model.

[1] Freiheit, H.-C., Kroll, H., Putnis, A.: The trigonal-to-cubic phase transition in $LiNaSO_4$: A X-ray and calorimetric study. Z. Kristallogr. **213** (1998), 575-584
[2] Hubbard, P. S.: Nonexponential Nuclear Magnetic Relaxation by Quadrupole Interactions. J. Chem. Phys. **53** (1970), 985-987

P11.19.016 ELASTIC SCATTERING FROM INTERMEDIATE STATE IN AUCD ALLOYS. T. Ohba [1], K. Sato [1] and K. Otsuka [2]. [1] Dept. of Materials Science and Engineering, Teikyo University, 1-1, Toyosatodai, Utsunomiya, 320-8551, Japan. [2] Institute of Materials Science, University of Tsukuba, Tsukuba, 305-8573, Japan.

Martensitic transformation is understood to be a diffusionless and displacive transformation. It has been utilized a steel hardening and it is an origin of shape memory effect of alloys. Despite of many industrial applications of martensitic transformation, fundamental research of martensitic transformation has not completed yet. 'Phenomenological theory of martensitic transformation' was proposed in 1950's and successive researches revealed that macroscopic feature such as habit plane, twin plane of martensite were described well by the theory. However, mechanism of transformation from microscopic point of view was not solved completely. AuCd alloy is one of typical alloys which shows martensitic transformation. It has distinct martensite called gamma2' and zeta2' close to equi-atomic composition. gamma2' phase appears close to Au-47.5at%Cd and zeta2' phase appears close to Au-50at%Cd. Crystal structure of gamma2' martensite is produced by alternative motion of (110) plane and that of zeta2' is produced by motion of every three planes of (110). Phonon softening, which correspond to the above and is attractive picture of transformation, were observed for both composition alloys. X-ray measurements were performed around 1/3 and 1/2 reflections at parent phase. Considering crystal structure of gamma2' martensite, 1/2 reflections were expected in composition of Au-47.5at%Cd. However no extra reflection was observed at 1/2 position in Au-47.5at%Cd. Diffuse scattering were observed at 1/3 position for both composition and different feature was observed for each composition. When temperature was lowered below transformation temperature, the diffuse scattering was split into two reflections corresponding to martensite phase. This means that diffuse scattering observed at parent phase did not come form martensite and that intermediate state exists prior to the transformation.

P11.19.017 THE ELASTIC SOFTENING UNDER THE COMMENSURATE - INCOMMENSURATE PHASE TRANSITION. V.K.Yatsenko[1], I.N.Mochtchenko[2], A.N.Sadkov[1], V.I.Snejkov[2], [1]Institute of Physics, Stachki 194, Rostov-on-Don, 344090, Russia, [2]North Caucasus Scientific Center, Pushkinskaia 140, Rostov-on-Don, 344006, Russia.

The monocrystal of $Na_{4.5}FeP_2O_8$ (NFP) superionic (presented by H.B.Bolotina, B.A.Maximov, Crystallography Institute of RAS) was investigated by acoustic methods in the 20° - 550° C region. The elastic anomaly under the commensurate – incommensurate phase transition (about 440° C) was observed. The elastic modulus C_{33} is decrease under the increasing of temperature. However the inverse dependence is observed for range 440° - 550° C with sharp minimum at 440° C and slow maximum at about 550° C. In this temperature region the intensities of the main reflections are decrease and of the satellite ones are increase [1]. Two variants of the structure may cause such behavior. The first is the mixture of the phases. The second is the intermediate state with the superlattice formed by the commensurate phase modulated by the incommensurate one. In the framework of the phenomenological theory of the phase transition the temperature dependencies of the elastic moduluses were calculated for both cases. The theoretical results correspond

to the experimental ones for the second variant and it show that softening of phason mode inducing the modulation in the intermediate phase causes the elastic anomaly. Hence in the NFP superionic under the heating occur two phase transitions: commensurate – intermediate states and intermediate - incommensurate states. The measuring and theoretical calculation of the temperature dependencies of the conductivity confirmed this and showed that the superionic properties arise only in the last phase and that the superlattice of the intermediate state was modulated along one direction.

This work was supported by RFBR, grant N 97-03-32139a

1. N.E.Klokova and all, Ferroelectrics, 1990, Vol.107, pp. 259-264

P11.19.018 COMPLEX INVESTIGATION OF THE SUPERIONIC COMPOUNDS. A.N.Sadkov[1], I.N. Mochtchenko[2], V.K.Yatsenko[1], [1]Institute of Physics, Stachki 194, Rostov-on-Don, 344090, Russia, [2]North Caucasus Scientific Center, Pushkinskaia 140, Rostov-on-Don, 344006, Russia.

In 20° C - 550° C temperature region the x-ray, acoustic and electrophysics measurements were performed for superionic compound consisting from the CuI matrix and Al_2O_3 addendum (0-25 mol.%). The x-ray structure investigations showed that the γ-β phase transition temperature is decreased when the Al_2O_3 concentration is increased. The acoustic measurements confirmed this result. For example, the temperature dependence of the longitudinal sound velocity for different Al_2O_3 concentrations (0-0%, 1-5%, 2-10%, 3-15%, 4-20%, 5-25%) is presented in figure.

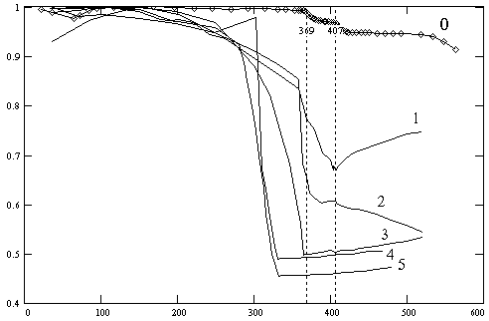

The γ-β phase transition is clear indicated by the sharp full of the velocity. It was also obtained that at the temperature above 200° C the Al_2O_3 addendum in CuI lead to the softening of the elastic moduluses. These results show that the intermediate interphase boundary layer occupies macroscopic region and forms all physical properties of superionic compound.

This work was supported by RFBR, grant N 97-03-32139a.

P11.19.019 NONEQUILIBRIUM STATES IN SOLIDS AS STUDIED USING THE MOST POWERFUL NEUTRON SOURCE IBR-2. G.M.Mironova, Frank Laboratory of Neutron Physics, JINR, 141980 Dubna, Moscow reg., Russia

The unique experimental tool – angle-resolved TOF neutron transmission and scattering method developed at the most powerful neutron source IBR-2 has been applied to investigations of nonequilibrium state of matter in real time. Thermal shock (sample heating-cooling) acts as a kind of a pump and induces a response in the sample consisting in after-bleaching or after-absorbing in the small angle scattering region. The strength of the effect depends on the material, point of temperature reverse and prehistory of the sample. The details of the responses are very similar to those occurring at the phase transition temperatures. General mechanism of these phenomena is proposed.

P11.19.020 METHOD OF DETERMINATION OF MULTI-k STRUCTURES. A.V.Yeremenko, Department of Magnetism, Institute for Low Temperature Physics and Engineering, Kharkov, 310164 Ukraine, and Yu.G.Pashkevich, Donetsk Phystech Institute, Donetsk, 340114 Ukraine.

A new method of determination of the multiple spin-density wave states (multi-**k** structures) in crystals is proposed. By historical tradition the most part of neutronograms has been interpreted *a priori* as the domains of collinear magnetism. However, the latter one (1**k**-structure) has no advantages and, therefore, is a particular case of the multi-**k** structures. Besides, despite of the essential progress of the magnetic neutronography methods, the problem of determination of the multi-**k** structures is still very difficult to solve either for homogeneous magnets, or for inhomogeneous structures.

An alternative method of determination of the multi-**k** structures is based on the symmetry analysis of the spin-dependent first order (one-phonon) infrared absorption in crystal exhibiting crystallographic cell replication at the Neel temperature. This phenomenon has been theoretically predicted and experimentally found in the exchange-noncollinear, but coplanar magnet Nd_2CuO_4 [1]. In the present report we discuss different effective mechanisms of infrared absorption in non-coplanar structures like UO_2 with the special emphasis on the related problem of crystal structure distortions, and also in magnetic spiral structures. The proposed method has to stimulated experimental and theoretical reinvestigation of the a wide set of magnetic crystals.

This research is supported in part by INTAS (grant 96-0410).

1. Yu.G.Pashkevich, V.V.Pishko, V.V.Tsapenko, and A.V.Yeremenko (1995) Low Temp. Phys. **21**, 587.

P11.19.021 ON THE GROUND STATE OF NaV_2O_5. Tapan Chatterji, Institut Laue-Langevin, B.P. 156X, 38042 Grenoble Cedex, France, and Max-Planck-Institut für Physik Komplexer Systeme, Dresden, Germany, G.J. McIntyre, Institut Laue-Langevin, B.P. 156X, 38042 Grenoble Cedex, France, and A. Revcolevschi, Laboratoire de Chemie des Solides, Université Paris XI, F-91405 Orsay, France

The recent discovery of a spin-Peierls-like ground state in the inorganic system α′-NaV_2O_5 has induced many investigations. Magnetic susceptibility measurements on both polycrystalline samples and single crystals have shown that a spin gap opens below $T_{SP} \approx 34$ K, and X-ray diffraction measurements showed superstructure reflections corresponding to the propagation vector [(*k*)\vec] = $^1/_2,^1/_2,0$) below T_{SP}. We have performed X-ray and neutron diffraction measurements on single crystals of α′-NaV_2O_5. Least-squares refinements of the structure models against the X-ray and neutron diffraction data at room temperature were performed in both the centrosymmetric (*Pmmn*) and the non-centrosymmetric ($P2_1mn$) space groups. A comparison of these two refinements led us to conclude that the space group of α′-NaV_2O_5 is the centrosymmetric *Pmmn* and not the non-centrosymmetric $P2_1mn$ as claimed previously. There is therefore only one symmetry independent V atom in the unit cell and to describe the structure as having magnetic V^{4+} chains separated by non-magnetic V^{5+}-chains along the b axis is not correct, at least not at room temperature. Instead one should consider zig-zag chains of crystallographically indistinguishable V ions with an average valence of 4.5. We detected superlattice reflections below $T_{SP} \approx 34$ K corresponding to the cell doubling along a and b and quadrupling along c both by X-ray and neutron diffraction. We measured the intensities of several main and superlattice reflections at 5 K by using a neutron wavelength of 1.26 Å. The superlattice reflections are very weak being of the order of about 10^{-4} of the main reflections. We have also measured the intensities of the main and the superstructure reflections by synchrotron X-

ray diffraction at T = 15 K. Joint refinement of the X-ray and neutron diffraction data has led us to a possible model of the low-temperature structure of α'-NaV_2O_5.

P11.19.022 AVERAGED STRUCTURE RESPONSE TO SUPERCONDUCTIVITY. V.N.Molchanov and V.I.Simonov Institute of Crystallography RAS, Leninsky prospect 59, 117333, Moscow, Russia

The behaviour of the crystal structure during the phase transition to the superconducting state is one of the most important problems concerning superconductivity phenomena. Detailed comparison of our precision X-ray diffraction studies of $Tl_2Ba_2CaCu_2O_8$ and $YBa_2Cu_4O_8$ single crystals with some published results on other high-T_c superconducting samples provides the following insights into averaged structure response to charge (hole) redistribution upon the phase transition to the superconducting state.

The most significant changes in the interatomic distances involve oxygen atoms in the CuO_5 pyramid with short in-plane Cu-O bonds and a longer bond to apical oxygen. The Cu-O(apical) distance is minimal exactly in the vicinity of T_c, thus reflecting charge redistribution between the 'reservoir layer' and the 'superconducting slab' *via* the bridging oxygen atom. It should be noted that longer Cu-O apical bonds, such as in Tl-based superconductors, decrease more readily than shorter bonds in yttrium compounds. This effect is accompanied by a small jump-like decrease of Cu-O and/or O-O distances in CuO_2 plane. Both effects clearly indicate an increasing of formal positive charge of Cu atom, thus reflecting transfer of a small portion of holes from reservoir layer to CuO_2 planes. It seems to be the common structural feature for hole-doped high-T_c superconductors.

Anomalous changes of atomic displacement parameters of in-plane oxygen atoms could be interpreted in terms of the strengthening of Cu-O bonds, decreasing or increasing of rotational instability of CuO_5 pyramids and hardening of thermal vibration along *c*-axis. Also, these effects must be closely related to the changes in the character of locally correlated dynamic displacements of atoms above and below T_c.

This work was financially supported by the Russian Scientific Council on High Temperature Superconductivity, Project No 96077.

P11.19.023 MARTENSITIC TRASFORMATION AND MAGNETIC TRANSITION OF HEUSLER-TYPE Ni_2MnGa-BASED COMPOUNDS. Kazuko Inoue, Kazuyuki Enami [1], Yasuo Yamaguchi, Kenji Ohoyama [2], [1] Fac. Sci. & Tech., Ryukoku Univ., Otsu, 520-2194, Japan, [2] IMR, Tohoku Univ., Sendai, 980-8577, Japan

We replaced some atoms of Heusler-type Ni_2MnGa compounds with the other kind of atoms, in order to bring the martensitic transformation temperature (about 200K) and the Curie temperature of mother Heusler alloy (about 370K) close to the room temperature. Then we can control the martensitic transformation using the external magnetic field at room temperature and the shape memory effect originated from the transformation. In the case of $Ni_2(Pd_{0.16}Mn_{0.84})Ga$, we have been able to bring the two transformation temperatures near to the room temperature. We have made the magnetization measurements and the powder neutron diffraction of this material and investigated the phenomena occurring around the transformation region. From magnetization measurements, the martensitic transformation temperature is near 280K and the Curie temperature is near 310K. Rietveld analysis of the powder neutron diffraction pattern of cubic paramagnetic phase at 400K shows that the best fitting is obtained when Pd atoms exist on Ga sites and the eliminated Ga atoms go to Mn sites. At low temperatures, two structures coexist, those are, an orthorhombic structure distorted from the cubic structure and a monoclinic structure with the periodic shuffling of 6 layers of (220) planes of this orthorhombic one. Between 280K and 350K, three structures coexist and the mass fraction of the cubic structure increases gradually with increasing temperature.

P11.19.024 DIRECT OBSERVATION OF CHARGE-ORDERED STATE IN NaV_2O_5. H. Nakao, K. Ohwada, N. Takesue, Y. Fujii, M. Isobe, Y. Ueda , ISSP, University of Tokyo, 7-22-1 Roppongi, Tokyo 106-8666,Japan, M. v. Zimmermann, J. Hill, D. Gibbs, J. Woicik, BNL, Upton, NY 11973-5000, USA, I. Koyama, and Y. Murakami, Photon Factory, KEK, Tsukuba, Ibaraki 305-0801, Japan.

A mixed valent compound NaV_2O_5 [1] undergoes an exotic phase transition associated with its spin, charge and lattice systems at T_C = 35 K. Recent X-ray[2], NMR[3], and theoretical[4,5] works imply that all V-sites are equivalent as a mixed valent state of V^{4+} and V^{5+}, namely an average valence of $V^{4.5+}$ (*disorder model*), above T_C. The crystal structure and charge ordering pattern below T_C, however, are still open question. The charge-ordered state is theoretically predicted as either *chain model* [4] or *zigzag model* [5]. In order to experimentally analyze the charge ordered state of V atoms above and below T_C, we have carried out X-ray anomalous scattering experiments at PF (KEK) and NSLS (BNL). By this method using the *K*-absorption edge, we can obtain an exclusive information on V atoms. The absorption energies of V^{4+} and V^{5+}, moreover, are different by about 1.8 eV; therefore, one can distinguish between V^{4+} and V^{5+}.

We have succeeded in observation of the anomalous energy dependence of superlattice peaks such as ([15/ 2],$^1/_2$,$^1/_4$) and ([17/ 2],$^1/_2$,$^1/_4$) indicating charge ordering. These anomaly can be successfully explained only by the *zigzag model*, while the *chain model* is ruled out. Moreover, the order parameter of the charge-ordered state, i.e. the charge disproportionation, was found to continuously develop below T_C.

[1] M. Isobe and Y. Ueda, J. Phys. Soc. Jpn. **65** (1996) 1178; Y. Fujii *et al.*, J. Phys. Soc. Jpn. **66** (1997) 326.
[2] H. Smolinski *et al.*, Phys. Rev. Lett. **80** (1998) 5164; H. G. von Schnering *et al.*, Z. Kristallogr. **213** (1998) 246; A. Meetsma *et al.*, cond-mat/9806081.
[3] T. Ohama *et al.*, Phys. Rev. **B** (1999).
[4] P. Thalmeier and P. Fulde, cond-mat/9805230.
[5] H. Seo and H. Fukuyama, J. Phys. Soc. Jpn. **67** (1998) 2602; M. V. Mostovoy and D. I. Khomskii, cond-mat/9806215.

P11.19.025 STUDY OF THE METASTABLE EXCITED STATE MS1 OF $Na_2[Ru(NO_2)_4NOOH]2H_2O$ BY SYNCHROTRON RADIATION. A. Puig-Molina, H. Müller, H. Graafsma, Å. Kvick, European Synchrotron Radiation Facility, 38043 Grenoble, France.

$Na_2[Ru(NO_2)_4NOOH]2H_2O$ is a photochromic material suitable for information storage on the basis of long-living metastable excited states [1]. The study of its metastable excited state MS1 by synchrotron X-ray diffraction and IR spectroscopy is presented. A phase transition was detected at 240K by differential scanning calorimetry. The structure at 298K exhibits the C2/m monoclinic space group. The low temperature structure exhibits the P21/n monoclinic space group. The study of the low temperature phase by synchrotron X-rays diffraction is also presented.

The IR spectroscopy was carried out at 80K on laser light-excited sample. It showed the appearance of a new band at 1792 cm^{-1} corresponding to the ν(NO) stretching mode. The band disappeared above 210K.

Synchrotron X-rays diffraction data was collected on laser-irradiated $Na_2[Ru(NO_2)_4NOOH]2H_2O$ monocrystals at ID11 at the ESRF using the Brucker Smart CCD at 110K and 50.2KeV. In the analysis of the excited data different models were used for the geometry of the MS1 taking in account the IR results and considering excitation percentages from 0 upto 50%. The best

results were obtained with a rigid body model for the ground state and MS1 molecules with freedom to refine the Ru-N-O geometry of the MS1 molecules considering 20-30% of the molecules in the excited state MS1. An agreement factor R of 7.86% for 1732 and 52 parameters (isotropic refinement) was obtained with this model. The excited state shows an increase in the N-O distance by 0.19(5) Å as well as a decrease in the Ru-N-O bond angle by 6(2)º relative to the ground state geometry.

1. Th. Woike, W. Kirchner, G. Schetter, Th. Barthel, Kim Hyung-sang, S. Haussühl (1994) Optics Communications 106, 6-10.

20. SYMMETRY AND ITS GENERALISATIONS

P13.20.002 ALGORITHMS FOR DERIVING CRYST-ALLOGRAPHIC SPACE-GROUP INFORMATION. R.W. Grosse-Kunstleve Yale University, New Haven, Connecticut 06520-8114, U.S.A.

Algorithms are presented for 3-dimensional crystallographic space groups, handling tasks such as the generation of symmetry operations, the characterization of symmetry operations (determination of rotation-part type, axis direction, sense of rotation, screw or glide part and location part), the determination of space-group type (identified by the space group number in the International Tables for Crystallography) and the generation of structure-seminvariant vectors and moduli. The latter are an algebraic description of allowed origin shifts, which are important in crystal structure determination methods or for comparing crystal structures.

The space-group type determination produces a change-of-basis matrix which transforms a given space-group representation to the standard one according to the International Tables. This change-of-basis matrix can be used to transform symmetry related information which is difficult to generate from first principles, but easily tabulated for the standard space-group representations, for example asymmetric units and Euclidean normalizers.

The algorithms were implemented and tested using the SgInfo library, which is written in the programming language ANSI C. The source code can be obtained free of charge for non-commercial applications.

P13.20.003 ANTISYMMETRY OF PLASTIC DEFORMATION M.Sh.Akchurin, R.V.Galiulin [1] [1] Shubnicov Institute of Crystallography, Russian Academy of Sciences, Moscow, Russia

We suggest the experimental results of the motion of point defects in fields of mechanical stress in a (Y, Al)-garnet crystal in which the center of inversion is replace by an anticenter. It connect the directions of motion of interstitial atoms with the directions of motion of vacancies. In such way, a crystal acquires the ability to remove the stress arising under the action of various mechanical factors. This experiment show, the motion of interstitial atoms and vacancies is not necessarily associated with dislocation. The absence of the center of inversion in these crystals was checked by morphological methods. The discrepancy between the symmetries determined by the X-ray and the morphological methods was noticed earlier. We believe that the well-known controversy between A.V.Shubnikov and N.V.Belov about which method is more appropriate for determining the crystal structure - morphology or the X-ray structure analysis - can be solved based on the consideration of antisymmetry. In the light of the above consideration, we can state that the reduction of the symmetry group indicated by the morphological methods is associated with the change of the center of symmetry to the anticenter, which can hardly be recorded by the X-ray diffraction method.

M.Sh.Akchurin and R.V.Galiulin. Antisymmetry in Plastic Deformation. Crystallography Reports, Vol.43, N 3, 1998, pp. 493-495

P13.20.004 A MODEL WITH P1 SYMMETRY, SHOWING CUBIC SYMMETRY M3M IN DIFFRACTION. Takeo Matsumoto and Sinichi Hashimoto, Dept.Earth Sciences, Faculty of Science, Kanazawa University, Kakumamachi, Kanazawa, 920-1192, Japan.

Enhancement of diffraction symmetry, which means the appearance of a higher Laue symmetry than normally expected, has been reported by several authors. This is caused by special relations among the symmetry operations in the unit cell, and has been theoretically studied mainly in Japan.

Sadanaga and Ohsumi (1979) have shown that the symmetry of diffraction equals to the point group symmetry of the corresponding vector set and arrived the conclusion that an enhanced vector symmetry necessarily leads to a structure built up according to self-homometry or a certain space groupoid. Many examples and models with enhancement of diffraction symmetry have been reported, however, the structure model of triclinic symmetry, showing the cubic symmetry in diffraction, has not been reported.

Here we show such a model. The structure is composed of the same 7x7x7 atoms. The lattice is metrically cubic, and three homometric mates on three axes (Patterson,1944). The atomic parameters as follows;

A:1/16{0,1,2,3,6,11,15},B:1/16{0,1,2,3,5,6,10},
C:1/16{0,1,2,3,6,7,14}.

One plane configuration denoted A*B has been derived by modified convolution of A with B, where B is homometric with A. In this case, the A*B configuration corresponds to the intersections of xj in A and yk in B, where 1ÅÖj,kÅÖ7. Although this plane model is triclinic (plane group:p1, point group:1), its vector symmetry (diffraction symmetry) is not triclinic but tetragonal,4mm. The B*C and C*A configurations are the same situation.

Moreover, a model denoted A*B*C, is obtained in the same way by convolution of A*B with C. The space group of this model is P1, point group 1, however, the diffraction symmetry (vector symmetry) is m3m. Then this structure should show the enhancement of diffraction symmetry, if anomalous dispersion can be ignored. There are special phase relations, in addition to Friedel's law, among 48 reflections (corresponding to equivalent reflections in m3m), such as αhkl+αlhk+αklh = αlkh+αkhl+αhlk.

This model shows the highest enhancement of diffraction symmetry (from 1 to m3m).

A.L.Patterson (1944), Phys.Rev.,65,195-201.
R.Sadanaga and K.Ohsumi (1979), Acta Cryst.,A35,115-122.
T.Matsumoto and S.Hashimoto (1998), AsCA 98 Abstracts,13P02.

P13.20.005 SYMMETRY OF SURFACE. Yu.M. Smirnov, Tver State University, Zheliabova Str., 33, 170000 Tver, Russia

According to Gyarmati [1] the tensor of pressure for moving liquids and gases has the form $\vec{\vec{P}} = (p + p^v)\vec{\vec{\delta}} + \vec{\vec{P}}^{vs} + \overset{\circ}{P}{}^{va}$, where p is the equilibrium pressure, p^v is the viscous pressure, $\vec{\vec{\delta}}$ is the unit tensor, and $\vec{\vec{P}}^{vs}$ and $\overset{\circ}{P}{}^{va}$ are the symmetrical and antisymmetrical parts of the viscous pressure tensor, respectively.

For p (p^v), $\vec{\vec{P}}^{vs}$ and $\overset{\circ}{P}{}^{va}$ the most general Curie groups will be $\infty/\infty m$, ∞/mmm and ∞/m, respectively. Drawing an analogy, one may express in a similar form the surface characteristics of systems – free energy, tension and stress. The surface free energy (scalar quantity) will be described by the Curie group $\infty/\infty m$, while the Curie group ∞/mmm will be associated with the surface tension (polar tensor of the second rank). Then it follows that the surface tension is an axial vector described by the Curie group ∞/m. The axial vector is dualistic to an antisymmetrical tensor of the second rank [2]. All components of pressures and stresses have a common element in their symmetry groups – inversion, and, from this point of view, they are even tensor quantities [2].

In expressions for energy and work the thermodynamical forces (stresses) are directly connected to the surface change of a system. As an example one may consider a simple equation $dW = \sigma dA$, where A is the surface (area). It follows that the surface should be considered as an even tensor quantity, whose symmetry is described by one of the subordinated Curie groups $\infty/\infty m$, ∞/mmm and ∞/m.

D. Gyarmati. *Non-Equilibrium Thermodynamics* (Springer-Verlag, B.-H.-N.Y., 1970)
Yu.M.Smirnov. *Symmetry of Transport Processes in Crystal Growth from the Melt, in* XII Europ. Crystallogr. Meeting, Vol.1, p.76 (1989)

P13.20.006 LINEAR CONTINUOUS INHOMOGENEOUS STRAINS IN QUASICRYSTALS. Serguei Rochal, Igor Lebedyuk Physical Faculty, Rostov State University, 5 Zorge St., Rostov-on-Don, 344090 Russia

Together with the well-known linear phasons, a quasicrystalline symmetry permits the existence of the linear continuous inhomogeneous strains (LCISs) related to the "freezing" of certain vibrational degrees of freedom of the QC lattice [1]. At such strains, the magnitudes of position displacements are proportional to the strain value and the flip-flaps of positions are absent. Under a certain LCIS value, the QC lattice transforms into the appropriate defect average periodic lattice. Manifestations of the LCIS in a reciprocal space lead to a redistribution of intensities of the reflections without changing their positions. In a quasicrystalline structure, LCISs may arise spontaneously with variation of the environmental conditions, e.g., with the decrease of temperature, and forcedly - in the case of application of external fields, e.g., under the action of the linear homogeneous field of stresses. As the phason strains, LCISs contribute to the free energy of the quasicrystal (QC) state of a substance. The spontaneous LCIS may be used as an intrinsic order parameter for describing phase transitions from the QC to the low-symmetry aperiodic structure, whose reflections are indexed by the reciprocal-space basis vectors of the ideal QC. LCISs can be also the non-intrinsic order parameters at different phase transitions from the QC phase, for instance, at the QC-to-crystal transformation [2].

1. S.B. Rochal, I.V. Lebedyuk, Physics Letters A 250, 152 (1999).
2. S.B. Rochal, Physics Letters A (1999), to be published.

21. APERIODIC AND INCOMMENSURATE STRUCTURES

P13.21.001 STRUCTURE ANALYSIS OF $Bi_2Sr_2PrCu_2O_{8+\delta}$ AND $(Bi_{1-X}Pb_x)_2$ $Sr_2CaCu_2O_{8+\delta}$ SINGLE CRYSTALS USING WEISSENBERG METHOD. Tsong-Jen Lee, Chien-Fon Wan, Chin-Chiang Teo, Ting-I Hsu, Yuping Sun, Huan-Chiu Ku, Yu Huang and Kow-Wei Yeh, Dept. of Physics and Material Science Center, National Tsing Hua University, Hsinchu 300,Taiwan –China.

The difference in the modulated structure for high quality $Bi_2Sr_2PrCu_2O_{8+\delta}$ and $(Bi_{1-x}Pbx)_2Sr_2CaCu_2O_{8+\delta}$ single crystal samples was investigated, using Weissenberg images taken with high intensity synchrotron hard X-ray (λ = 1 Å) in Photon Factory. The two kinds of crystals were prepared by the traveling solvent floating zone and self-flux melting methods, respectively. The crystal symmetry of $Bi_2Sr_2PrCu_2O_{8+\delta}$ belongs to orthorhombic Amaa with lattice parameters: a = 5.490(1), b = 5.525(1), c = 30.425(3) Å. The crystal have a structural modulation along the b-axis with q* = 0.247b* + c*. The effect of Pr substitution for Ca and Pb doping in Bi site on structural modulation of Bi-2212 system is discussed.

P13.21.002 TREATING INCOMMENSURATES AS QUASI-COMMENSURATE. L.Häming, M.Ruf, C.Campana, Application Laboratory, Bruker Analytical X-ray Systems, Karlsruhe, Germany

Incommensurate structures often lead to problems when standard diffractometers equipped with szitillation detectors are used. Either the satellite reflections are not found, or the super-cell will increase the data acquisition time enormously. The first will lead to a data set with reasonable intensity statistics and systematic absences, but finally the structure can not be solved or refined properly. Due to the much bigger number of reciprocal lattice points the later case will keep the instrument busy for weeks.

Modern CCD area detectors like the Bruker SMART can scan the complete reciprocal space. The full three circle goniometer does not miss a single satellite reflection. The short readout time of about one second allows to scan the crystal very time efficient. Once the reciprocal space has been stored these digital information can be interpreted with different unit cell definitions.

Incommensurate problem structures may be treated as quasi-commensurate. The seven fold incommensurate structure of a carbaborane will be presented. The point detector system did give a 7x10x16 Å unit cell. The structure could not be solved nor refined. Therefor the crystals were left on the shelf for many years. Whereas the SMART detector did immediately find the satellite reflections to index on the 49x10x16 Å super-cell. More than 112.000 reflections were collected in a single day on a standard SMART lab system. All hydrogen positions of the seven carbaborane molecules could be found in the difference fourier map. In addition the final model did show two rotational disordered carbaboranes.

Scanning complete reciprocal space with the SMART CCD detector offers an easy and fast way to work on problem structures like modulated structures. Without additional software tools incommensurate structures can be treated as quasi-commensurate.

P13.21.003 FIFTY EIGHT NEW SILICON CARBIDE POLYTYPES. Chang-lin Guo, X-Ray Crystallography Laboratory, Shanghai Institute of Ceramics, Chinese Academy of Sciences, 1295 Dingxi Road, Shanghai, 200050, P.R.China

Silicon carbide is a most typical substance of polytypism. Up to present more than 160 polytypes of SiC are discovered, in which we have discovered 84 new polytypes. In this paper, 58 new silicon carbide polytypes which have been found by using the analytical method of the relationship between lattice points in reciprocal lattice are described. More than 1000 industrial silicon carbide single crystals have been studied by X-ray modified Laue method. 10% of the crystals contained higher-layers polytypes other than basic-types 6H, 15R, 21R, 4H and 8H. High resolution X-ray special Laue photographs were taken for the crystals containing higher-layer polytypes by using the large-diameter (ϕ 153mm) cylindrical camera with very narrow -incident slit[1]. Since the coaxial coalescence of high-layer polytypes with the basic type in silicon carbide is a very general phenomenon, the point relation method [1] based on the analysis of relationships between lattice points of polytypes and the basic type may be considered as the most effective method on the investigation on SiC polytypism. 58 new SiC polytypes we have found as following: 234H, 136H, 133H, 126H, 117H, 114H, 113H, 102H, 87H, 70H, 67H, 30H, 1116R, 1026R, 891R, 879R, 759R, 714R, 585R, 582R, 570R, 543R, 528R, 525R, 519R, 438R, 432R, 423R, 402R, 399R, 396R, 390R, 375R, 372R, $357R_{(a)}$, $357R_{(b)}$, 327R, 324R, 315R, 312R, 309R, 297R, 291R, $267R_{(b)}$, 258R, 255R, 225R, 219R, 204R, $201R_{(b)}$, 198R, 186R, 177R, 144R, 138R, $75R_{(b)}$, 63R and 54R.

The crystal structures of several new polytypes were determined by a special Laue method [2,3]. The crystal structure of $357R_{(a)}$ is $[(33)_{19}32]_3$, $357R_{(b)}$ is $[(23)_{23}22]_3$, $267R_{(b)}$ is $[(33)_{14}32]_3$, $201R_{(b)}$ is $[(33)_{10}34]_3$ and $75R_{(b)}$ is $[(33)_334]_3$.

Chang-lin Guo (Chang-lin Kuo), Scientia Sinica (Science in China), 13(1964),1605; 1773; Chinese Science Bulletin, 41(1996),1666.
C.L.Kuo (Chang-lin Guo), J.Zhou, H.Q. Ye and K.H.Kuo, J. Appl. Cryst., 15(1982),199.
Chang-lin Guo (Chang-lin Kuo), Acta Physica Sinica, 31(1982),1369; Chines Physics, 3(1983),54.

P13.21.004 INCOMMENSURATE CRYSTAL STRUCTURE OF LAZURITE. N.B. Bolotina, V.I. Simonov, Institute of Crystallography RAS, 117333 Moscow, Russia

Lazurite, a sodalite-group mineral, ideally $Na_6Ca_2(Al_6Si_6O_{24})$ $(SO_4,S)_2$, is known in cubic, orthorhombic, monoclinic and triclinic modifications [1,2], where three last ones are superstructures with linear parameters a, $a\sqrt{2}$, $na\sqrt{2}$ (n - integer) in reference to the cubic cell with parameter a. Given crystal sample from Baikal region corresponds to the case of incommensurate modulation of basic cubic cell, a = 9.07 Å. Satellites are located on six plane diagonals, so that up to 12 satellites could be located at $\pm 0.218a^*\sqrt{2}$ around each main reflection. Average cubic structure corresponds to sp. gr. $P\bar{4}3n$ [1].

To explain observed diffraction pattern and describe the symmetry of modulated structure, different models of modulation are calculated.

(1) There is 3D modulation with wave vectors $q_1 = (\gamma, 0, 0)$, $q_2 = (0, \gamma, 0)$, $q_3 = (0, 0, \gamma)$, $\gamma \cong 0.218$ in the basis of given cubic cell. All satellites are described as the second order ones of the *hkl110* type, whereas the first order satellites of the *hkl100* type are not observed. This fact should be taken into account with extinction rule $m+n+p = 2N$ for *hklmnp* reflections, so that for symmetry description (3+3)D group P23:P23 with additional translation (0, 0, 0, 1/2, 1/2, 1/2) should be chosen. The group P23 is selected instead of $P\bar{4}3n$ on view of intensities of symmetry - equivalent satellites.

(2) There is 3D modulation with wave vectors $q_1 = (\gamma, \gamma, 0)$, $q_2 = (\gamma, 0, \gamma)$, $q_3 = (0, \gamma, \gamma)$, $\gamma \cong 0.218$ in the basis of the same cubic cell. All satellites are separated into two types: the first order satellites

along q_1, q_2, q_3 directions and the second order satellites along three other plane diagonals.
(3) The sample is twin formed by six parts. For a cell of each part, its $a_o b_o$ plane (cell parameters $a_o = b_o = a\sqrt{2}$, $c_o = a$) is coinsident with a side of twinning cubic cell and rotated on 45°, whereas the symmetry of each part is orthorhombic one, its structure is modulated on *x* and *y* directions.

1. I. Hassan, R.C. Peterson & H.D. Grundy (1985) Acta Cryst. C41, 827.
2. V.G. Evsjunin et al. (1998) Kristallographiya, Vol. 43, No 6, 1057.

P13.21.005 THE MODULATED STRUCTURE OF QUININIUM (R)-MANDELATE - AN INCOMMENSURATE DESCRIPTION IN SUPERSPACE. A. Schönleber and G. Chapuis, Institut de Cristallographie, Université de Lausanne, BSP Dorigny,1015 Lausanne, Switzerland

In addition to main reflections the diffraction pattern of quininium(R)-mandelate, $C_{20}H_{25}N_2O_2^+ \cdot C_8H_7O_3^-$, exhibits satellites up to very high order. A commensurate structure model in a 15-fold supercell was presented by [1].

In agreement with [1] single crystal diffraction measurements at room temperature and at T = 120 K show no changes in the cell parameters or in the $\vec{q}$ -vector components. The main reflections can be indexed in a $P2_1$ basic cell with one formula unit per asymmetric unit and a =6.57 Å, b = 18.46 Å, c = 10.26 Å and β =107.23°. With respect to this cell, the $\vec{q}$ -vector is $\vec{q} = 0.33\,\vec{a}^{\,*} + 0.27\,\vec{c}^{\,*}$ (T = 120K).

The structure was solved within a commensurate approximation in a 3X5 supercell in $P2_1$ with 15 formula units per asymmetric unit and a = 19.71 Å, b = 18.46 Å, c = 50.27 Å and β =77.29° (T = 120 K).

The results of the refinements of the incommensurate structure with MSR [2] and JANA'98[3] will be presented. The temperature dependence of the satellite intensities in respect to the main reflections will be investigated.

1. A. B. Gjerløv et al. (1995) Abstract ACA'95
2. W. A. Paciorek (1995) MSR - The program system for 1-dimensional incommensurate structure refinement.
3. V. Petrícek and M. Dusek. (1998) JANA'98 - Crystallographic Computing System.

P13.21.006 NEUTRON DIFFRACTION STUDIES OF INCOMMENSURATE MAGNETIC ORDER IN TRANSITION METAL OXOSALTS. J P Wright, J P Attfield [1], J B Forsyth, W I F David, D Martin y Marero [2], [1] Department of Chemistry, Cambridge University, Lensfield Road, Cambridge CB2 1EW, [2] Rutherford Appleton Laboratory, Chilton, Didcot, Oxon OX11 0QX

The use of cold neutrons for long d-spacing powder diffraction at the spallation source ISIS allows very high resolution data to be obtained for the solution and Rietveld refinement of complex magnetic structures. We have used the IRIS and OSIRIS diffractometers to study incommensurate magnetic order in monoclinic $FeAsO_4$ [1] and the isostructural doped compounds $Fe_{(1-x)}Ga_{(x)}AsO_4$ for x=0-8% and $FeAs_{(1-x)}P_{(x)}O_4$ for x=0-16%. The propagation vector of (0.04994(3), 0, -0.24725(2)) indexes the helimagnetic structure in $FeAsO_4$ where the spins of 4.01(2) Bohr magnetons rotate in a plane containing b* and making an angle of 34.1(7) degrees to [001] in beta-obtuse. All of the doped compounds exhibit an analogous magnetic structure to that of $FeAsO_4$, although the propagation vector varies in the ac plane proportionally to the degree of substitution. We have also studied the $CrP_{(1-x)}V_{(x)}O_4$ system (x=0-8%) using the HRPD diffractometer. The cycloidal spiral magnetic structure is incommensurate with the crystal structure, having a propagation vector of (0.3305(2),0,0) for x = 0 and which increases with x. This indicates that any single ion anisotropic effects are too weak to lock this structure into a commensurate configuration, and that the near-commensurate structure arises through a coincidental balance of exchange interactions.

[1] JB Forsyth, JP Wright, MD Marcos, JP Attfield and C Wilkinson. J Phys Condensed Matter (1999) 11, 1473-1478.

P13.21.007 ON THE DIFFUSE LAYERS IN DECAGONAL AlCoNi QUASICRYSTALS. F.Frey and E.Weidner, Institut für Kristallographie, LMU, 80333 München, Germany, K.Hradil, Institut für Mineralogie, Universität, 97074 Würzburg, M.deBoissieu, LTPCM/ENSEEG, 38042 St.Martin d'Heres, France, and R.Currat, ILL, 38042 Grenoble, France

Diffraction patterns of many decagonal phases exhibit diffuse layers perpendicular to the "periodic" axis c (1(. The layer line distance corresponds to a period 2c in most cases, a period 4c was observed in Al71.5Co16.5Ni11. The layers consist of a homogeneous diffuse background and superimposed short range order maxima (2(. Their widths and positions depend on the exact stoichiometry as well as on the prior thermal history of the sample. A diffuse background exists also beneath the Bragg layers. The layers vanish at high temperatures (3(. The temperature behavior differs from that of other diffuse phenomena within the quasiperiodic planes. From the characteristics in reciprocal space a column-like order along c is concluded. Lateral short range correlations between the columns are responsible for the sro maxima. Co/Ni superorder along c can be excluded due to the results of a neutron diffraction experiment on Al71.5Co16.5Ni12, binary decagonal phases exhibit diffuse layers as well (4(. A chemical superorder can be ruled out due to absent sharp reflections at positions (0000n/2) (n=1,2,..). A displacive disorder along c is most conclusive. A quantitative analysis is performed which is based on a 1D (domain) model consisting of columns of icosahedral clusters. Due to molecular dynamical calculations (5(icosahedral clusters are formed by Al atoms which have left the decagonal layers. As the diffuse layers remain sharp up to high Q-values - shown by neutron diffraction - a long range order of the 1D superstructure exists along c.

Work supported by funds of the German DFG under Fr 747/13-1

(1) K.Hiraga et al. (1991). Mat.Trans.JIM, 32, 308
(2) F.Frey & W.Steurer (1993). J.Non-Cryst.Sol., 153/154, 600
(3) K.Hradil et al. (1995). Phil. Mag. B71, 955
(4) A.P.Tsai et al. (1995). Phil.Mag.Lett. 71, 151
(5) J.Stadler & H.-R.Trebin (1998). J.Non-Cryst.Sol., 223, 152

P13.21.008 STRUCTURE OF DECAGONAL QUIASICRYSTALS AND THEIR APPROXIMANTS WITH FIVEFOLD ATOM CLUSTERS. K. Saitoh, T. Yokosawa, M. Tanaka [1], A. P. Tsai [2], [1] Research Insitute for Scientific Measurements, Tohoku University, Sendai 980-8577, JAPAN, [2] National Research Institute for Metals, Tsukuba, 305-0047, JAPAN

High-angle annular dark-field (HAADF) images of a melt-quenched $Al_{70}Ni_{15}Fe_{15}$ decagonal quasicrystal and a monoclinic tau2-$Al_{13}Co_4$ approximant have been taken using a scanning electron microscope. We have found that both alloys are composed of 2-nm diameter atom-clusters with fivefold symmetry. Structural models of both alloys have been constructed on the basis of the HAADF images and a structure of the monoclinic $Al_{13}Fe_4$ approximant. Furthermore, we have been constructed, on the basis of the observation of high-resolution electron microscope images, a model of a structural transformation from

the tau2-monoclinic $Al_{13}Co_4$ approximant to the Al-Co decagonal quasicrystal which has the same structure as $Al_{70}Ni_{15}Fe_{15}$.

P13.21.009 SYMMETRY ANALYSIS OF MAGNETIC ORDERING IN RFe_4Al_8 (R=La, Ce, Y, Lu, AND Tb) COMPOUNDS. W.Sikora, Faculty of Physics and Nuclear Techniques, UMM, al.Mickiewicza 30, 30-059 Krakow, Poland, P.Schobinger-Papamantellos, Laboratorium fur Kristallographie, ETHZ, CH-8092 Zurich, Switzerland, K.H.J.Buschow, Van der Waals-Zeeman Institute, University of Amsterdam, 1018 XE Amsterdam, The Netherlands

Representation analysis [1] [2] of the neutron diffraction data of RFe_4Al_8 (R= La, Ce, Y, Lu, and Tb) tetragonal compounds (I4/mmm), for the wave vectors $\mathbf{q}_1=(00q_z)$, and $\mathbf{q}_2=(q_xq_x0)$ [3] leads to various modulated structures. The R atoms at 2(a) positions remain in one orbit in relation to the G_k group for both **q** vectors. The calculations lead to the following models: sin-wave, simple spirals or cycloid spirals . For $\mathbf{q}_2$ the Fe atoms at (8f) positions split into two distinct sets (orbits), which may order independently as sine wave, simple spiral or cycloid spiral structures. The spirals of the two Fe orbits may have different chiralities and even different planes of rotation. For a given model, within each orbit the relation between magnetic moments is fixed by symmetry. This leads to considerable parameter reduction. The phase shift between various orbits, not fixed by symmetry relations, has to be found by data analysis. For $\mathbf{q}_1$, the Fe atoms at 8(f) positions remain in one orbit and there is a large number of sine wave structures described by one irreducible representation of I4/mmm group, with different directions and fixed couplings. All models with components in (001) plane comprise two groups of atoms, the magnetic moments of these groups are either confined to mutually perpendicular planes or are shifted by the phase $\pi/2$. Representation analysis provides a) the full information concerning the free parameters needed for the refinements, b) the order parameters describing the phase transition and their dimension, and c) enables a systematic classification of the used models in the neutron data analysis.

1 Yu.A.Izyumov, V.E.Naish, R.P Ozerov Neutron diffraction of magnetic materials, Consultans Bureau,NewYork, 1991
2 W.Sikora, Proceedins of SSPCM, Zajaczkowo,Poland, (1994) p.484
3 P.Schobinger-Papamantellos, K.H.J.Buschow and C.Ritter, J.Magn.Magn.Mat. **186** (1998) 21

P13.21.010 COMMENSURATE AND INCOMMENSURATE Li^+-ORDERING IN ε- AND ε′-$Li_xV_2O_5$ AS A FUNCTION OF TEMPERATURE. H. Katzke and M. Czank, Institute of Geosciences, Olshausenstr. 40, 24098 Kiel, Germany.

ε- and ε′-$Li_xV_2O_5$ belong to a group of intercalation compounds which are formed during the topotactic intercalation reaction of lithium ions into the host structure V_2O_5. With means of electron diffraction the possibility of superstructure formations, due to Li^+ ordering processes, was studied as a function of temperature. In the course of these investigations a series of thermally induced structural phase transitions was detected, which can be mostly attributed to order/disorder transitions of the intercalated lithium ions. The structural diversity comprises phases with dynamical disorder, incommensurately modulated structures and commensurate phases with statical disorder. In the temperature range 550 K - 110 K two reversible phase transitions can be detected for ε- ($0.32 \le x \le 0.52$) and ε′-$Li_xV_2O_5$ ($0.52 \le x \le 0.80$). The high-temperature phase crystallizes in both cases in the orthorhombic space group *Pmmn* with probably dynamically disordered Li^+ ions. On decreasing temperature, the Li^+ ions order, resulting in incommensurately modulated structures at room-temperature [1,2], and commensurate structures with probably statical disorder at low-temperatures [3,4]. Structural models on the basis of competing interactions of attractive guest/host- and repulsive guest/guest-interactions are proposed for the different states of Li^+-ordering.

[1] H. Katzke, M. Czank, W. Depmeier, S. van Smaalen (1997). Phil. Mag. **B 75**, 757-767.
[2] H. Katzke, M. Czank, W. Depmeier, S. van Smaalen (1997). J. of Phys. Condens. Matter **9**, 6231-6239.
[3] H. Katzke, W. Depmeier (1994). Adv. Mat. Res. **1-2**, 129-135.
[4] H. Katzke, W. Depmeier (1996). Phase Transitions **59**, 94-104.

P13.21.011 DISTORTIONS OF SECOND ORDER IN THE INCOMMENSURATE CDW STATE OF $NITA_2SE_7$. S. van Smaalen, J. Lüdecke, M. Schneider, Laboratory of Crystallography, University of Bayreuth, D-95440 Bayreuth, Germany

The incommensurately modulated low temperature structure of $NiTa_2Se_7$ has been studied in detail using synchrotron radiation. The modulated low temperature phase is a charge density wave (CDW) state caused by chains of transition metal atoms along the crystallographic b-axis [1]. To determine the modulated structure, satellite reflections up to second order have been measured at a temperature of 15 K. The structure was refined with two harmonics of the modulation functions. Modulation with the first harmonic was found on the Ni atoms and the surrounding Se atoms, which is in good agreement with an earlier investigation [2]. As a surprising result, the modulation with the second harmonic appeared on completely different atoms. One of the Ta chains was modulated longitudinally. The distortions of first and second harmonic on different parts of the structure clearly rules out the latter to be a second-order effect. This result is in agreement with the temperature dependence of the q and the 2q critical scattering observed by electron diffraction above T_{CDW}. It indicated different origins of both distortions. A complete understanding of the observed distortions has not been achieved yet.

1. R.M.Fleming et al., Phys.Rev.B **42**, 4954 (1990)
2. A.Spijkerman et al., Phys.Rev.B **52**, 3892 (1995)

P13.21.012 WEAK BRAGG SCATTERING IN ICOSAHEDRAL Mg-Y-Zn. M.A. Estermann, T. Haibach, A. Cervellino and W. Steurer, Laboratorium für Kristallographie, Eidgenössische Technische Hochschule, ETH-Zentrum, CH-8092 Zürich, Switzerland.

At present, Mg-Y-Zn is the best ordered quasicrystalline material available, and with crystal sizes suitable for neutron diffraction experiments. No disorder diffuse scattering was observed in our sample which had the composition $Mg_{29}Y_9Zn_{62}$. Therefore it is possible to address the nature of perfect quasiperiodic ordering directly, without the need to include short-range structural disorder in the analysis of the perfect long-range order. The obvious question is whether the present Mg-Y-Zn phase is an ideally perfect crystal in accordance with the mathematical framework of higher-dimensional crystallography [1]. Of particular interest are the weak intensities of the Bragg peaks with high perpendicular component of the scattering vector, and the study of possible structural models. To clarify this question experimentally, two diffraction experiments were performed. One experiment was performed at the HASYLAB synchrotron radiation source with a fixed wavelength rotation geometry set-up and a marresearch imaging plate detector system. Software was developed to index the data automatically and to produce arbitrary slices through reciprocal space [2]. The other experiment was performed at the ISIS time-of-flight neutron spallation source with the SXD Laue diffractometer. The results of this two complementary studies will be presented.

1. Janssen, T. (1986). *Acta Cryst*. **A42**, 261.
2. Estermann, M.A. and Steurer, W. (1998). *Phase Transitions.*

P13.21.013 THE QUASICRYSTAL MODELS WITH THE DISCRETE SPECTRUM. E.V.Olchanskaia, I.N.Mochtchenko, A.M.Mojaev, North Caucasus Scientific Center, Pushkinskaia 140, Rostov-on-Don, 344006, Russia.

The quasicrystal models characterised discrete Fourier images are presented. The models were constructed by using the quasilattice algorithm early elaborated. The spectrums of these models were investigated by analytical methods and the methods of quantity analysis including the theory of approximation of the integral functions. The structures with discrete spectrum were selected. The examples of such models are the quasilattices with the knots determined by the maximum of the next functions:

$Z=\max(\cos k_i r)$, $k_i=(\cos(2\pi i/5); \sin(2\pi i/5))$, $i=0\ldots4$; (1)

$Z=\Sigma(\cos(k_i r))$, $k_i=(\cos(2\pi i/5); \sin(2\pi i/5))$, $i=0\ldots4$; (2)

Then spectrums were numerical calculated using regularisation methods. The elaborated models and their spectrums are the base elements for the determination of the quasicrystal structures from diffraction data. For example, using the model (1) we approximated the experimental data and calculated the quasicrystal structure as a Fourier image of the model. The result is presented in figure (left), where the high-resolution electron micrography is also presented (right) for comparison.

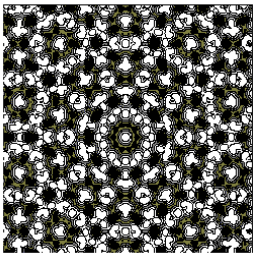

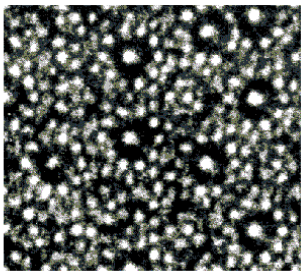

This work was supported by RFBR, grant N 97-02-17024.

22. CRYSTALLOGRAPHIC TOPOLOGY

P13.22.001 ENUMERATION OF CRYSTAL-STRUCTURE TYPES USING A FINITE SUPERGROUP OF ALL THE BRAVAIS LATTICES. Masahiko Hosoya Dept. of Physics, University of the Ryukyus, Senbaru 1, Nishihara, Okinawa 903-0213, Japan

A finite group was found which derives all the Bravais lattices as its subgroup. The analysis of its structure enables us to enumerate many crystallographic objects such as the point groups automatically. Especially this method is useful when it is applied to the enumeration of crystal-structure types. Every crystal-structure type is regarded as a Bravais lattice type in the higher-dimensional space.

P13.22.002 SELF-INTERSECTING MINIMAL SURFACES: SPATIAL SUBUNITS AND LABYRINTH GRAPHS. Elke Koch, Institute for Mineralogy, University of Marburg, D-35032 Marburg, Germany.

Three-periodic minimal surfaces with self-intersections along straight lines subdivide R^3 either into a finite number of three-periodic spatial subunits (labyrinths) or into infinitely many two-periodic, one-periodic or finite spatial subunits (flat labyrinths, tubes or polyhedra, respectively).

So far, 78 different families of such self-intersecting minimal surfaces have been derived with the aid of skew polygons formed by the even-fold rotation axes of some space group [1, 2], and their geometrical and topological properties have been analysed. Their Euler characteristics χ vary between −3 and −20. Most of these surfaces (68 families) are non-orientable.

The minimal surfaces of 47 families subdivide R^3 into a finite number of congruent, three-periodic labyrinths with Euler characteristics χ_{lab} between −4 and −24. Two labyrinths occur 42 times, four labyrinths 3 times and eight labyrinths 2 times [3].

Congruent flat labyrinths are generated by the minimal surfaces of 14 families [4]. In most cases (11 families) all flat labyrinths run parallel. The flat labyrinths of 3 families, however, are subdivided into two sets which run perpendicular to each other.

8 families of minimal surfaces subdivide R^3 into congruent tubes, 1 family into two sets of non-congruent tubes, 3 families into tubes and polyhedra, 1 family into congruent polyhedra, and 4 families into two kinds of polyhedra [5].

1. W. Fischer & E. Koch (1996). Philos. Trans. R. Soc. London Ser. A, **354**, 2105-2142.
2. E. Koch W. Fischer (1999). Acta Cryst. A**55**, 58-64.
3. E. Koch (1999). Acta Cryst. A**55**, submitted.
4. E. Koch (1999). Acta Cryst. A, in preparation.
5. E. Koch (1999). Acta Cryst. A, in preparation.

P13.22.003 TILINGS ON HYPERBOLIC SURFACES AS REPRESENTATIVES OF CHEMICAL NETWORKS. S. Leoni, R. Nesper, Laboratory of Inorganic Chemistry, ETH Zurich, Universitätstrasse 6, CH-8092 Zurich, CH

The great benefits of using a structure-enveloping continuous function in the description of chemical structures have been exemplified many times [1-3]. The strategy of calculation takes advantage of the topological information contained in the most fundamental structure factors, as was proposed by Nesper and von Schnering [1]. The result is a family of continuous, orientable, 3-periodic surfaces, which resume the symmetry information of a space group. The surface, which corresponds to the roots of the generating function, is called PNS [1]. The consequence of the application of such shapes to periodic structures is the understanding of their organisation. The two-dimensional character of iso-surfaces of such three-dimensional functions reveals a hierarchical organisation of the forces involved in the structures. Further deepening of the relation between symmetry and covalent networks can be gained if a new method is implemented, which allows to design hyperbolic networks directly on the curved shape of a PNS. Two different iso-surfaces are allowed to overlap [3]. The result is a complete covering of the hyperbolic surface by hyperbolic tiles. With this method it is an easy task to redesign the network of well-known zeolites, other networks like the one those of clathrates, but also some hypothetical graphitic-like networks, like those already proposed [4] and finally some completely new networks [3]. This method allows for an easy generation of new networks, but also for an enumeration of all the networks which are compatible with a given curved shape, permitting to grasp the correlation between growing complexity, organisation and hierarchy of the forces.

[1] H.G. v.Schnering, R. Nesper, Z.Phys. B83, 407(1991)
[2] H.G. v.Schnering, R. Nesper, Angew. Chem. Int. Ed. Engl. 26, 1059(1987)
[3] S.Leoni, PhD Thesis Nr. 12783, ETH Zürich (1998)
[4] H. Terrones, A.L. Mackay, Prog. Crystal Growth and Character, 34 (1997), 25-36

P13.22.005 AlPdMn QUASICRYSTALS REVISITED. L. Loreto, R. Farinato [1], C. Janot [1,2], [1] Dipartimento di Scienze della Terra, Universita' di Roma 'La Sapienza', P.zzale A. Moro 5, 00185 Roma, Italy, [2] Laboratoire de Cristallographie, CNRS, BP 166 38042 Grenoble Cedex 9, France

The structure of icosahedral quasicrystals of the AlPdMn has been previously investigated using X-ray and neutron diffraction [1]. The result is a periodic image in a six-dimensional space from which it is possible to deduce a physical three-dimensional arrangement of the atoms. This structure is essentially based on atomic clusters whose geometry is close to that of a Mackay icosahedron and that have been termed Pseudo-Mackay icosahedron (PMI). The whole structure can be described as a dense covering of space by overlapping PMI. Two PMI, when overlapping, have in common a double hexagonal-like flat pyramid whose axis is along a two-fold direction. The PMI overlap around vacancy-like sites (t^3 times smaller than a PMI, t=1.618033 the golden number) which are distributed at the vertices of big dodecahedra and icosahedra. Space scans around these vacancy sites show that they are the empty center of pseudo-Bergman clusters (PBC). Indeed, one find two shells of atoms surrounding these vacancies, one icosahedron and one dodecahedron respectively. Further atomic shells are triacontahedra and truncated icosahedra (soccer-ball like). The interesting point is that PBC show up here as a mere consequence of the PMI. If the geometry of the PMI is rather well defined within the whole structure, there is quite a large distribution in their chemical composition and in details of their shapes. Central atoms of the PMI are basically Mn, sometime Pd. The internal shells, or cores, contain an average of 7 atoms that can fluctuate from 5 to 14. The external shell is well defined and is made of 30 sites of an icosidodecahedron plus 12 sites of an icosahedron. The chemical composition of the external shell fluctuates around two main contributions of about 70% and 30% respectively (30Al + 6 to 9Mn + 3 to 6Pd on the one hand; 20 to 23Al + 22 to 19Pd on the other hand). The 66% of the cores are pentagons of Al, with various orientations. Other cores have complex polyhedral shapes with 10 to 14 atoms, mainly Al with occasional Pd. Cluster geometry and composition along with their association rules are basic ingredients that can be used for modelling the structure of real quasicrystals.

1. Boudard M. et al.(1992). J. Phys.: condens. Matter, 4, 10149.

P13.22.006 THE GROWTH OF QUASICRYSTALS D. Joseph [1], V. Elser [2], [1] Max-Planck-Insitute for Physics of Complex Systems Noethnitzer Str. 38, 01187 Dresden, Germany, [2] Laboratory of Atomic ans Solid State Physics, Clark Hall, Ithaca NY 14853-2501, USA

The growth of quasicrystals is one of the unsolved problems in condensed matter theory. Although the problem was attacked right at the beginning there is no complete picture at hand. For the class of entropically stabilized quasicrystals we recently proposed a model that circumvents some major concerns. So it is possible to grow macroscopic big samples without violating the limits set by experiment. In this contribution we present the model and discuss its properties in 2 and 3 dimensions.

P13.22.007 ICOSAHEDRAL ORDER AND DISORDER IN Si AND Ge. V.E. Dmitrienko, Institute of Crystallography, 59 Leninski pr., Moscow, 117333, Russia and M. Kléman, Laboratoire de Minéralogie-Cristallographie, Universités Paris VI et Paris VII, 4, place Jussieu, Paris Cedex 05, 75252, France.

Hidden icosahedral symmetry of interatomic bonds is found in four-coordinated phases of silicon and germanium. For example, in the BC8-*Ia* $\bar{3}$ phase, three bonds of each atom are directed almost exactly along *fivefold* icosahedral axes and the fourth bond is directed along a threefold axis. It is shown that this phase may be considered as a 1/0 crystalline approximant of a hypothetical icosahedral quasicrystal with a *body-centred* six-dimensional lattice and that all the atomic positions in BC8 crystals may be obtained as projections from that six-dimensional lattice. The diffraction pattern of the BC8 phase has hierarchical organisation typical of both approximants and quasicrystals.

A specific type of topological disorder, related with phason flips, is suggested. Those phason flips are quite unusual because they lead to 90° rotation of icosahedral directions. The experimentally observed BC8-R8 phase transition can be regarded as resulting from coherent phason flips of this type. The positions of atoms in the perpendicular space and the perpendicular projections of the phason flips are analyzed. It shown that the phason flips may result in many other structures, ordered and disordered, without dangling bonds. The X-ray scattering in the phason-disordered structure is shown to be similar to the scattering in the amorphous Si. A new *scenario* for crystalline-to-amorphous transformation is proposed.

A dual relationship with approximants of conventional quasicrystals is used to construct a 1/1 approximant with *Ia* $\bar{3}$ symmetry (64 atoms per unit cell). In this approximant, the phason flips provide a mechanism of annihilation of dangling bonds. Construction of higher order approximants is discussed.

P13.22.008 TEMPERATURE BEHAVIOUR OF THE DISORDER SCATTERING IN DECAGONAL ALNICO INVESTIGATED BY SYNCHROTRON RADIATION. K. Hradil and R.B. Neder, Universität Würzburg, Institut für Mineralogie, Am Hubland, D-97074 Würzburg, Germany, E. Weidner and F. Frey, LMU München, Institut für Kristallographie und Angew. Mineralogie, Theresienstr. 41, D-80333 München, Germany.

Decagonal phases are two-dimensional quasicrystals (qc) exhibiting translational order along the unique 5- or 10-fold axis and quasiperiodic order perpendicular to it. Diffraction patterns of thermodynamically stable decagonal phases in the Al-Ni-Co systems exhibit, beside very sharp Bragg reflections corresponding to a long-range ordered average structure, disorder diffuse and superorder scattering in the qc layers and along the periodic direction [see e.g. 1]. In this work we focus on the temperature dependence of the disorder and superorder scattering within the qc Bragglayers of a decagonal sample with nominal composition Al:Ni:Co=72.5:11:16.5.

The in-situ temperature measurement was carried out around two Bragg reflections up to 1100 K in reducing atmosphere at the 4-circle-diffractometer at beamline D3, DESY/HASYLAB, Hamburg using a mirror furnace [2]. Both the intensities of the Bragg reflection and the surrounding satellite reflections were collected in **Q**-scan mode with a resolution of 1.5×10^{-4} Å^{-1}.

As evident from two-dimensional **Q**-scans around the $(100\bar{1}0)$ and (10000) Bragg reflections the sample was in a decagonal state at room temperature. A complex temperature behaviour of the disorder diffuse and superorder scattering around these Bragg reflections is observed within the temperature range up to 1100 K. Between 870 K and 990 K a significant intensity decrease of the satellite scattering (30%) can be found. Heating up to 1100 K a remarkable intensity increase is observed. This is accompanied by a broadening of the satellite profiles.

1 F. Frey (1997), Z. Kristallogr. **212**, 257.
2 Th. Proffen, F. Frey, H. Ploeckl & H.G. Krane, J. Syn. Rad., **2**, 229.

P13.22.009 STRUCTURAL ANALYSIS OF AN $Al_{72}Ni_{20}Co_8$ DECAGONAL QUASICRYSTAL. Hiroyuki Takakura[1,2], Akiji Yamamoto [3], Steffen Weber [3], An Pang Tsai[1], [1] Natonal Research Institute for Metals, Tsukuba 305-0047, Japan.[2]CREST, Japan Science and Technology Corporation, Kawaguchi, Saitama, Japan.[3]National Institute for Research in Inorganic Materials, Tsukuba 305-0044, Japan.

The structure of a water quenched $Al_{72}Ni_{20}Co_8$ ($P10_5/mmc$, c=4.11Å) decagonal quasicrystal has been analyzed using the single crystal X-ray data for the first time by higher dimensional structure analysis. Newly developed softwares for imaging plate Weissenberg camera were used to obtain 607 independent integrated intensities. The $Al_{72}Ni_{20}Co_8$ is belonging to a simple decagonal phase, which shows neither superlattice reflections nor diffuse streaks by electron diffraction [1,2]. Recent structural study based on an electron diffraction has shown that there are small fundamental structure units having a 4Å radius instead of symmetrical 20Å cluster [3]. We confirmed that there is no diffuse scattering even in a sub-millimeter size sample suitable for X-ray scatteirng study. The large occupation domains are located at A:(1,1,1,1,1.25)/5, B:(2,2,2,2,1.25)/5, which are subdivided by more smaller parts. In the analysis, shift from an ideal atom position is introduced. The occupation domain A is similar to that of corresponding one proposed recently in terms of shape and distribution of TM (Transition metals)[4]. This reveals a symmetry breaking of 20 Å decagonal cluster. On the other hand, the distribution of TM in the occupation domain B is somewhat different from that proposed. The $Al_{72}Ni_{20}Co_8$ is only stable as a high temperature phase. It is thus expected that many disorder sites exist in the structure. Indeed, our results suggest that disorder sites exist in real structure.

[1] S.Ritsch, C.Beeli, H.-U.Nissen, T.Gödecke, M.Scheffer and R.Luck, Phil. Mag. A71} (1996) 99.
[2] A.P.Tsai, A.Fujiwara, A.Inoue & T.Masumoto, Phil. Mag. Lett. 74 (1996) 233.
[3] K.Saitoh, K.Tsuda, M.Tanaka, K.Kaneko & A.P.Tsai, Jpn. J. Appl. Phys. 36} (1997) L1400.
[4] K.Saitoh, K.Tsuda & M.Tanaka, J. Phys. Soc. Jpn., 67 (1998) 2578.

P13.22.011 NEW GEOMETRIES FOR NEW MATERIALS. Alan L. Mackay, Dept. of Crystallography, Birkbeck College (University of London), Malet Street, London WC1E 7HX, Eric A. Lord, Dept. of Metallurgy, Indian Institute of Science, Bangalore 560012, India and Jacek Klinowski, Dept. of Physical Chemistry, University of Cambridge, Cambridge CB2 1EW.

Modern computational software has facilitated the generation and exploration of a very wide range of intriguing new geometrical structures which may be realisable at any scale between those of mega-engineering and of nanotechnology. Some of these structures are solutions to partial differential equations, corresponding to physical conditions such as minimum area or minimum splay energy, with various imposed symmetries or boundary conditions. Minimisation of energies of aggregates of atoms correspond to levels of organisation above that of individual atoms and molecules. Many of these structures are absolutes, like the Platonic solids, without parameters.

The geometry derives from extensions of classical crystallography following the lead of Delone, Voronoi, Engel and Dress, turning it inside out and working out from the connectivity of the asymmetric unit rather than inwards from the picture-frames of the symmetry elements in the 230 space groups. Elements of surface or of tubes, rather than the isolated atoms of crystal structure, are placed in the various asymmetric domains and connected up. The key advance is in devising notations which can be handled by computer. This approach permits a seamless transition to quasi-periodic and hierarchic structures which arise naturally and which are now beginning to be recognised experimentally as X-ray crystal structure analysis passes to electron microscopy as the dominant method of observation.

The numerous periodic minimal surfaces and the enumeration of periodic networks are recent prominent examples. Stereo-pairs or material models are necessary for the proper apprehension of their topologies.

P13.22.012 CRYSTALLIZATION OF GaMgZn ALLOY NEAR THE QUASICRYSTAL PHASE EXISTENCE REGION. Marian Surowiec and Piotr Jelen, Institute of Physics and Chemistry of Metals, University of Silesia, 40 007 Katowice, Bankowa 12, Poland.

Quasicrystal icosahedral phase is formed in the vicinity of Frank and Kasper intermetallic phases. In the case of GaMgZn alloy corresponding Frank and Kasper phase was determined [1] and it is known as the Bergman cubic phase $Ga_{16}Mg_{32}Zn_{52}$. On the other hand icosahedral quasicrystal phase was found [2] and equilibrium icosahedral single quasicrystal forms with pentagonal dodecaedral growth morphology were observed in shrinkage cavity of GaMgZn ingot [3]. The aim of our investigation was to elaborate process of technology enabling crystallization of the GaMgZn alloy under superpressure and mixed gas atmosphere (nitrogen plus helium) and to perform investigations of phase composition of the alloy. During crystallization process mechanical mixing of alloy was applied in order to improve uniform distribution of elements in the sample. X-ray powder diffraction (INEL diffractometer), selected area electron diffraction, X-ray microprobe and differential thermal analysis were employed during investigation. Our experimental work had three aspects. The main task was concerned on the phase composition investigations. We have confirmed existence of the cubic phase however aperiodic phase was not found. The crystallized material had porous character and inside pours faceted crystal forms were observed. The polygonal single crystals appeared to be Mg crystals. In addition we have found composite character of the alloy. Inside of the parent phase growth of colonies of Zn faceted whiskers took place. The whiskers appeared when parent phase was dissolved and removed. Zn whiskers had hexagonal cross section and [0001] growth direction. They exhibited high degree of perfection.

1. W. Ohashi, Ph.D. Thesis, Harvard Univ., 1989.
2. H.S. Chen and A. Inuoe, Scripta Metalurg. 1987, **21,** 527.
3. W. Ohashi and F. Speapen, Nature, 1987, **330,** 555.

23. DATA BASES

P07.23.001 FURTHER DEVELOPMENTS OF THE BILBAO CRYSTALLOGRAPHIC SERVER. E. Kroumova, J.M. Pérez-Mato, S. Ivantchev, G. Madariaga, Departamentos de Física de la Materia Condensada y Física Aplicada II, Universidad del País Vasco, Apdo. 644, 48080 Bilbao, Spain, and M.I. Aroyo, A.K. Kirov, Condensed Matter Physics Dept, Sofia University, 1164 Sofia, Bulgaria, and H. Wondratschek, Institut für Kristallographie der Universität Karlsruhe, D-76128 Karlsruhe, Germany

The Bilbao Crystallographic Server (**http://www.cryst.ehu.es**) has already been under use for more than a year [1]. The aim of this contribution is to report on the recent advances in the development of the server.

The main kernel contains a set of databases which include: (i) data from the space-group tables of *International Tables for Crystallography*, vol. A, (ii) data from the subgroup tables of *International Tables for Crystallography*, vol. A1. Recently, we have added a database of incommensurate structures with an interface which permits simple queries and input of new structures. In addition to the programs already reported [1], we have included a pseudosymmetry check program which detects for a given crystal structure any kind of crystallographic pseudosymmetry within a chosen tolerance factor [2]. We have also started the development of the shell on tools using representation theory of space groups. The server now offers access to (i) the program KAREP for constructing little-group and full-group representations of space groups, and (ii) the program CORREL for investigating the correlations between irreducible representations of group-subgroup related space groups.

[1] E.Kroumova, J.M. Pérez-Mato, M.I. Aroyo, S. Ivantchev, G.Madariaga, H.Wondratschek, *Materials structure - ECM-18 abstracts*, **A** (1998); E. Kroumova, M.I.Aroyo, J.M. Pérez-Mato, *J. Appl. Cryst.* **31** (1998), 646

[2] Igartua J. M., Aroyo M.I. and Pérez-Mato J.M., *Phys. Rev.*, **B 54** (1996), 12744

P07.23.002 INTERACTIVE MOLECULAR STRUCTURE DATABASE ON INTRANET. Fusen Han, Structure, Analytical and Medicinal Chemistry, Pharmacia & Upjohn Inc., 301 Henrietta Street, Kalamazoo, MI 49007, USA

With simple *.html and *.pdb files, crystal structures can be displayed via the "Chime[1]" plug-in software on a internet home page. However, the functions of Chime are limited. The new Script Technology, especially the new released VBScript[2] plus Internet Explorer[2] 4.0, makes it possible to develop more sophisticated molecule displaying software on the internet without the limit of a plug-in.

We have set up our internal small molecule structure database on our company Intranet. It is the most efficient method to deliver our crystal structure results to our research community worldwide. Two versions of this database are being tested: one uses Chime only and the other one uses VBScript plus Chime. The second version has more functions and is much more flexible to manipulate with VBScript. The current VBScript version contains most of the ActiveX[2] Controls used in Visual Basic[2] 5.0. In addition, FileSystemObject[2] is necessary for manipulating data files. With these tools, accessing data files and creating graphic user interfaces on the internet becomes very simple and user friendly.

In this poster, the database components, user interfaces, control elements, script code and sample molecule structures are presented and discussed.

It is also possible to protect the script source code by encoding the script file using Microsoft Script Encoder[2].

1. Software product of MDL Information Systems, Inc..
2. Software products of Microsoft Corporation.

P07.23.003 CRYSTMET: AN INTEGRATED STRUCTURE AND POWDER DATABASE FOR INTERMETALLICS. Peter S. White, Department of Chemistry, University of North Carolina at Chapel Hill, NC, USA, John R. Rodgers, Toth Information Systems Inc, 2045 Quincy Avenue, Gloucester, ON, Canada and Yvon Le Page, National Research Council of Canada, Ottawa, ON, Canada.

The intermetallics database, *CRYSTMET*, is supported and being actively developed by Toth Information Systems Inc. The database was originally developed by the National Research Council of Canada as part of the CISTI numerical databases. This paper will describe the contents of the database, its transfer to a relational database structure, its extension to support X-ray and neutron powder pattern matching, and the software currently being developed for searching and analyzing results.

The *CRYSTMET* database consists of a number of records, which contain bibliographic, structural and limited physical property information about each entry. About 50% of the current entries include atomic coordinates. Within the relational database the data is stored in a set of tables designed to optimize search and retrieval operations.

The search program provides the user with a simple, intuitive graphical interface to develop queries. A variety of query types are available, including chemical composition, symmetry and structure type, and unit cell dimensions In addition, entries with coordinates can be searched using tables of computed powder patterns. Entries which do not include atomic coordinates are optionally searched on tables of valid d-spacings.

The results of such queries are stored as sets of entries that can be edited or logically combined with other result sets. A single entry can be listed in detail and functions are available to generate a structural diagram, generate and display a powder pattern, and compute various geometrical quantities. Facilities are also provided to graphically examine the distribution of a property over an entire set of entries.

The database and search software is currently available from Toth for use on PCs running Windows 95, 98 or NT.

P07.23.004 A NEW SEARCH/MATCH SYSTEM-NK-7. Yong Bing Peng [1], Lian Hu Wei, Ron Chen Yuan, Yuan Qiao, Shao Fan Lin [2], Yu Hu Xu [3], [1] Institute of Elemento-organic Chemistry, NanKai University, TianJin, 300071(China), [2] Central Laboratory, NanKai University, TianJin, 300071(China), [3] Guangdong Part Time University of Science and Technology Guangzhou 510090 P.R.China

In this article, a new method for identifying components in crystalline mixtures from their X-ray powder diffraction data is presented. It can be run in Windows-95 and Windows-98. The database comes from the powder diffraction files (PDF) provided by the JCPDS-International Centre for Diffraction Data.

It has been demonstrated that the method can give the definite phase compositions of the unknown multiphase mixtures rapidly and correctly. This method uses the weight factor for each diffraction peak as a criterion, and can not only give a list possible phases but also the definite components of the unknown sample by a simulation process. Actual samples included organic samples have been tested with high performance. The key points in this system are:

1. The TMIP (three most intensive peaks) filtering: Compare the sample PDF data with each standard pattern in the database to see if its TMIP exist in the sample pattern. If yes, then keep this phase as a candidate.

2. Element filtering by comparing the elemental composition (EC) of each candidate with the sample of the Elements existed in candidate include in sample. If yes then it was conceded as possible phase existed in sample (Selected Phases).

3. Calculation the value FOP (Factor Of Possibly) of Selected Phases: The value FOP of each Selected Phases is then calculated and a list is printed according to the descending order of the FOP. The phases with higher FOP have more possibility existed in the experimental pattern.

Similar with these first three steps, all the existing methods can give an ordered list of 10 to 50 phases which may be present in the sample but we have not found any previous method which can give a definite answer. Our program tries to get the definite answer after following steps.

4. Pattern Simulation: The program uses those Selected Phases as the basic units to simulate the sample pattern with various combinations. If all the components of the sample are within the Selected Phases, then there must be a case in the complete combinations is the real components of sample.

5. Evaluation of the simulated patterns:

To evaluate each simulated pattern, the program calculates the value FOS (Factor of similarity) according to: A. The EC of the simulated pattern should be the same as that of the sample. Otherwise the value of FEC (Factor of EC) should be reduced. B. Compare the peaks and the intensities between simulated pattern and sample pattern to calculate the value SPI (Similarity of Peaks and Intensities) C. Calculate the FOS according to the value FEC and SPI. The components of the simulated pattern, which has highest value FOS, would be the components of sample.

P07.23.006 STATISTICAL ANALYSIS OF DISTRIBUTION OF CSD STRUCTURES BY SPACE GROUPS AND BY STRUCTURAL CLASSES. Oleynikov P.N., Zorky P.M. Chemistry Department, MSU, Russia

A statistical analysis of the distribution of ~ 163000 crystal structures by space groups (SG) and by structural classes (SC) has been carried out. These structures correspond to 181309 entries contained in Cambridge Structural Database (April 1998). It has been discovered that this distribution is substantially different for diverse classes of chemical substances. Typical features of the studied distributions emerge when the set of CSD structures is subdivided into *crystal chemistry classes*.

As crystal chemistry classes the number of representatives in CSD of which is sufficient for revealing statistical regularities we considered: 1) homomolecular crystals consisting of chemically identical molecules (n = 1), 2) heteromolecular crystals containing molecules (particles) of two kinds (n = 2), among the latter we particularly distinguished salts, molecular complexes, solvates and hydrates. For all the named groups of substances we separately studied: 1) organic substances, which contain only organogenic elements, 2) other CSD structures (we call them non-organic).

Two types of SG distributions have been revealed for organic substances: the first is characteristic of homomolecular substances and salts, the second, of molecular complexes and solvates. The presence of these two types is not so pronounced among non-organic substances, the considerable decrease of the contribution of chiral groups ($P2_12_12_1$, $P2_1$ etc.) as compared with organic crystals being found in all crystal chemistry classes.

The distinction between crystal chemistry classes manifests itself even more vividly in SC distributions (SC is SG plus a list of the orbits occupied by particles). The most impressive regularity is the sharp distinction between some SC popularities for organic and non-organic crystals.

P07.23.007 STRUCTURAL SYSTEMATICS – A STUDY OF CARBONYL MIGRATION ON M_2 and M_3 UNITS. Amy L. Gillon and A. Guy Orpen, School of Chemistry, University of Bristol, Cantock's Close, Bristol, BS8 1TS, UK.

Data were retrieved from the Cambridge Structural Database from crystal structures containing suitable geometric data for complexes containing the metal-metal bonded fragments $M_2(CO)$ and $M_3(CO)$ (where M = Fe, Ru, Os, Co, Rh, Ir).

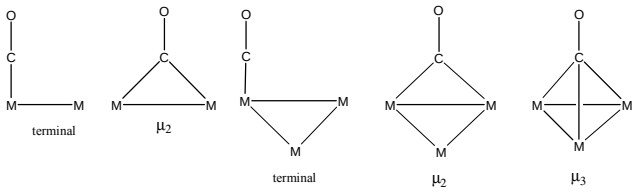

These data were analysed, using the structure correlation method[1], to examine the locations of the carbonyl ligands in all positions from terminal to bridging, to triply bridging (in the case of $M_3(CO)$ fragments). The dimetal case shows a clear continuum of points through the two dimensional plot of metal carbon distances, in agreement with previous studies[2,3]. The distribution of points may be taken to indicate the reaction pathway for bridge-terminal exchange in polynuclear metal carbonyls. Similarly the data obtained for the trimetal case allows the examination of the distribution of carbonyl geometries across the triangular metal array. The distribution of points shows pathways linking the terminal μ_2 and μ_3 carbonyl geometries and may indicate preferred pathways for the movement of a carbonyl across a close packed metal array.

H.B.Bürgi and J.D.Dunitz, *Acc.Chem.Res.,* 1983, **16**, 153
R.H.Crabtree and M.Lavin, *Inorg. Chem.,* 1986, **25**, 805
A.G.Orpen, *Chem. Soc. Rev.,* 1993, 191

P07.23.008 CHLORIDE, ORGANOCHLORINE, AND METAL CHLORIDE HYDROGEN BOND ACCEPTORS. Owen D. Hayward and A. Guy Orpen, School of Chemistry, University of Bristol, Cantock's Close, Bristol. BS8 1TS. UK.

The design and synthesis of specific structural aggregates in the solid state often relies on a knowledge of robust hydrogen bonding interactions that can be used to "bind" together individual molecular building blocks[1]. Hydrogen bonding is one of the most significant forces in crystal packing with even C-H hydrogen bonds playing an important role in the patterns formed by molecules in the crystalline state. The chloride acceptor has been found to play an important role in crystal packing, and in recent years metal chlorides have also been identified as having a potentially significant effect on the packing of many structures.

Recent advances in the 3D searching capabilities of the Cambridge Structural Database (CSD)[2] have led to a large number of geometrical studies of various hydrogen bonding donors and acceptors. However there has been relatively little analysis of the donor co-ordination numbers of acceptors.

The co-ordination of the hydrogen bonding acceptors chloride (Cl^-), metal chloride (M-Cl) and organic chlorine (C-Cl) will be discussed and data on the relative frequency of hydrogen bonding occurring will be presented. O-H, N-H and C-H will be considered as potential donor systems. Unique examples will be highlighted and the more robust interactions will be portrayed as potential sythons for crystal engineering.

1 See for example C.B. Aakeröy, *Acta Cryst*., 1997, **B53**, 569
2 F.H. Allen and O. Kennard, *Chemical Design Automation News*, 1993, 8(1), 1 & 31

P07.23.009 PSEUDOSYMMETRICAL ORTHOGONAL LAYERS IN TRICLINIC ORGANIC CRYSTALS Muydinov R.Yu., Zorky P.M., Department of Chemistry, Moscow State University, Leninskie Gory, Moscow 119899, Russia

In most organic homomolecular crystals molecules occupy only one orbit (k = 1), i.e. an asymmetric part of the cell contains only one molecule. However, in ~10% of such crystals k>1 (k = 2 in ~7% of them). If crystals with k = 1 are considered to be normal, the formation of a structure with k>1 requires an interpretation: in each case it is necessary to explain why it is just this structure that arises.

The formation of polysystem (k>1) structures is certainly caused by different reasons. In the study of structures belonging to class $P\bar{1}$, Z=4 (1^2) we have found one of the mechanisms leading to the arising of polysystem structures: it is the formation of pseudosymmetrical orthogonal layers the superposition of which causes the disturbance of the potential function and a triclinic crystal is formed. Examples are crystals of MNPPRB and MBSIND (see CSD). In the former one can see clearly defined chains with local pseudosymmetry P_c c, in the latter, $P_c 2_1$. The chains are superimposed with inversion centers; and in both cases layers $P_l 2_1/c$ arise. A superposition of such layers commonly leads to class $P_l 2_1/c$, Z=4 (1). In the considered cases, however, the layers appear to be too rigid (unadaptable). As a result there arise a triclinic bisystem crystal in which the given symmetry of layers is present as local pseudosymmetry.

In CSD we have found 1246 organic homomolecular crystals of class $P\bar{1}$, Z=4 (1^2). In 299 of them (24%) there are orthogonal two-dimensional sublattices, which seems to indicate the presence of pseudosymmetrical orthogonal layers.

P07.23.010 INVESTIGATION OF INTER CONVERSION PATHWAYS BETWEEN METAL COORDINATION SPHERE GEOMETRY FROM CRYSTALLOGRAPHIC DATA. Jing Wen Yao and Judith A. K. Howard, Department of Chemistry, University of Durham, Durham, DH1 3LE, UK and Frank H. Allen, CCDC, 12 Union Road, Cambridge, CB2 1EZ, UK.

A useful method to solve the problem and complexity in detecting geometrical preference of metal 7-coordiantion sphere by using the CSD data has been given[1]. A calculated Euclidean dissimilarity between the idealized metal-ligand valence angles and observed angles provides a numerical measurement, from which geometrical deviation of an observed structure from the standard polyhedra can be obtained.

This method can be also used generally in lower coordination numbers (n = 3-6). The scatterplots of the two specified discrepancy indices [$R_c(x)$] reveal not only geometry preference to the representative polyhedra in these coordination species but also interconversion pathways between the reference geometries.

A preliminary work has been carried out to investigate a possible reaction pathway from 6+1 to 7 coordination from the structural data. An extra ligand is supposed to attack to the central metal atom in a 6-coordination octahedral sphere and form a 7-coordination sphere[2]. The preferential direction of the attacking ligand has been observed and compared with 7-coordination species. It can be seen that all attacks are either from a triangular face of octahedron to form COC/CTP or from an edge of the square plane of octahedron to form a PBP. All the observed points fall into the range between these two extreme cases. This means that it is possible to use these data to further explore the relationships from 6+1 coordination leading to 7-coordination by geometrical similarity.

1. Howard, J. A. K, Copley, R. C. B., Yao, J. W. and Allen, F. H., *Chem. Commun.*, 2175, (1998).
2. Drew, M. G. B., *Prog. in Inorg. Chem.* 23, 1, (1977).

P07.23.011 THE AGGREGATION OF METAL COMPLEXES BY M-μ–Cl INTERACTIONS. Kirsty M. Anderson and A. Guy Orpen, School of Chemistry, University of Bristol, Cantock's Close, Bristol, BS8 1TS. UK.

A large number of solid state structures are known in which metal bound chloride forms secondary interactions though hydrogen bonding or by lone pair donation to another metal. These interactions play an important role in the aggregation of metal complexes with the characterisation and understanding of the interactions being an important aspect of the developing field of crystal engineering.

The interactions between the metal bound chloride and its surrounding atoms can be described using a variety of structural parameters. Using the Cambridge Structural Database (CSD) bond lengths and angles for the following system were extracted and analysed.

Where M = Group 10 & 11 metal
A = M, H-D, Tr
and D = N or O

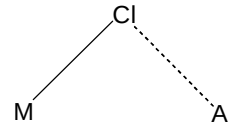

The dependence of these parameters on the nature of M and A (eg. d-electron count, formal oxidation state, the number of bridging interactions formed per M and A) are discussed and interesting examples highlighted.

The use of bridging chlorides, to provide solutions to crystal engineering problems involving these elements, and also as robust synthons for crystal engineering will be discussed.

1. F.H. Allen and O. Kennard, *Chemical Design Automation News*, 1993, **8(1)**, 1 &31

P07.23.012 GRAPH SET HYDROGEN BONDING ANALYSIS AND CRYSTAL STRUCTURE PREDICTION OF OXIMES. L.C. Kerr, P.R. Raithby [1], W.D.S. Motherwell, G.P. Shields [2], [1] Department of Chemistry, University of Cambridge, Cambridge CB2 1EW, [2] Cambridge Crystallographic Data Centre, 12 Union Road, Cambridge CB2 1EZ.

A graph set analysis[1] of the hydrogen bonding of oximes in the Cambridge Structural Database has been performed, showing that when there is only one oxime group in each molecule, they hydrogen bond preferentially in a dimeric structure. In certain cases, however, chain-type structures have been found. This difference is thought to be due to steric factors. In order to verify this, a new crystal structure prediction program, Rancel[2], was used to predict the packing for some of the oximes. The results tend to predict the packing with some success and also to confirm the potential of the Rancel program in structure prediction.

1. M.C. Etter, Acc. Chem. Res., 1990, 23, 120-126.
2. Rancel, program written by W.D.S. Motherwell, CCDC, 12 Union Road, Cambridge CB2 1EZ.

P07.23.014 PACKSTAR: A CRYSTAL STRUCTURE PREDICTION PROGRAM. J.P.M. Lommerse W.D.S. Motherwell Cambridge Crystallographic Data Centre, 12 Union Road, Cambridge CB2 1EZ, United Kingdom

An ab initio method is presented to predict crystal structures of small organic molecules. In contrast to most methods

in this field, the program is not based on calculation of energies, but uses data from the Cambridge Structural Database (CSD) [1]. Stochastic methods (Genetic Algorithms (GA) and Simulated Annealing (SA)) are applied to search for minima in a given spacegroup. The cost function for the GA/SA is calculated from a composite crystal field environment. This field is built up from small functional groups that are constituents of the molecule of interest. From the CSD distributions of one group around another can be extracted, transformed into density maps and combined to form a crystal field environment around a molecule [2]. Information about directionality, such as a hydroxyl group pointing toward an acceptor, is preserved. In the calculated crystal structure, the fit of all functional groups in the crystal field environment determines the cost for the GA/SA. It is assumed that the experimental structure has lowest cost, which should represent the best fit with the CSD. The accuracy of the method largely depends on the quantity of data available in the CSD. A grid is used to store values of the density maps around the molecule. The grid size typically is 0.5-0.8 Angstrom. This determines the accuracy of the method, in terms of cell dimensions and orientation and position of the molecules in the cell. Therefore, a subsequent minimisation using empirical energy functions is applied to obtain the final crystal structure [3].

1. F.H. Allen, J.E. Galloy, O.J. Johnson, et al. (1991). J. Chem. Inf. Comput. Sci. 31, 187-204.
2. M.L. Verdonk, J.C. Cole and R. Taylor (1999) J. Mol. Biol., submitted for publication.
3. A. Gavezzotti (1994). Acc. Chem. Res. 27,309-314.

P07.23.015 CRYSTAL STRUCTURE PREDICTION USING ATOM CONTACT DISTRIBUTIONS FROM THE CAMBRIDGE STRUCTURAL DATABASE. Sam Motherwell Cambridge Crystallographic Data Centre, 12 Union Rd., Cambridge CB2 1EZ

A methodology has been developed for calculation of probable crystal structures based on the intermolecular atom-atom distances in the Cambridge Structural Database (CSD). GA methods have been used to find calculated crystal structures using rigid molecular models in common space groups. A fitness function is calculated which is a minimum when the calculated distance frequency distribution agrees best with the CSD for each atom-type in the molecule. All contacts are counted to each atom, giving a frequency distribution for a normalised distance D = Rij - Rv, where Rij is the distance between atoms i and j, and Rv is the sum of the van der Waals radii. The method makes no assumptions about energy, but seeks to reproduce the CSD frequencies characteristic of a selected set of similar molecules in the CSD. Extra fitting information can be given for patterns of close contact D < Rv, where a sample of chemically similar CSD molecules shows a good probability of occurrence, H-bonds being a typical example. These expectation values can be set even though we have no theoretical explanation of such patterns, and may often have kinetic reasons for formation [1]. It is interesting that the method is often successful even though the fitness criteria are essentially non-directional, but based only on atom pair distributions. The results of a program, RANCEL [2], are given showing successes and failures of the method to a variety of chemical species.

1. A. Gavezzotti, Acc. Chem. Res. (1994) 27, 309-314.
2. W.D.S. Motherwell, Nova Acta Leopoldina, (1999) NF79, 89-98.

P07.23.016 THE GEOMETRY OF THE TETRAETHYLAMMONIUM CATION. Joan Halfpenny, Department of Chemistry and Physics, Nottingham Trent University, Clifton Lane, Nottingham, NG11 8NS, UK.

The structure of the ionic compound bis(tetraethylammonium) dichlorodiisothiocyanatodimethylstannate(IV) determined by the author contains two crystallographically non-equivalent tetraethylammonium groups of differing geometries. When viewed along the four-fold inversion axis of symmetry it is apparent that one tetraethylammonium cation has the ethyl groups arranged 'linearly' and the other in a 'propeller' shape around the tetrahedrally-substituted nitrogen. The latter geometry is slightly more efficient at space filling. There are no unexpected intermolecular contacts, inter- or intra-molecular interactions affecting one cation more than the other and therefore the fact that both species coexist in this particular structure is of considerable interest. The results of energy minimisation calculations on the relative stabilities of the 'linear' and 'propeller' tetrahedral geometries will be presented, together with statistics derived from a survey of more than 1500 compounds containing the tetraethylammonium cation in the Cambridge Crystallographic Database. Approximately half of these compound formulae contain two or more tetraethylammonium cations although in many structures the groups are crystallographically equivalent. The relative incidence of each type of geometry and its relation to the coordination environment of the cation will be discussed.

Crystal data. $[(C_2H_5)N^+]_2$ $[SnCl_2(CH_3)_2(NCS)_2]^{2-}$, monoclinic, $P2_1/c$, Z = 4, a = 13.750(10), b = 17.86(2), c = 13.420(10) Å, β = 113.90(10)°, V = 3013(5) Å^3, μ = 1.177 mm^{-1}, D_x = 1.315 Mg m^{-3}, R = 0.0527, *w*R = 0.1446 for 3800 unique reflections recorded on a STOE Stadi-2 2-circle diffractometer with MoK_α radiation, λ = 0.7107 Å, room temperature. N-C bond lengths in tetraethylammonium ions: 'linear' arrangement 1.498(8), 1.513(8), 1.516(8), 1.533(8) Å, 'propeller' arrangement 1.505(8), 1.512(8), 1.518(7), 1.525(8) Å.

P07.23.017 STRUCTURAL STUDIES OF DIRUTHENIUM COMPLEXES-A LOCAL DATABASE STUDY. J.P.H. Charmant, S.A.R. Knox and A.G. Orpen, School of Chemistry, University of Bristol, Cantock's Close, Bristol BS8 1TS, UK.

Recent advances in X-ray diffraction instrumentation have led to a substantial increase in the speed of a typical single crystal structure determination. This inevitably leads to the publication of only those results considered to be of particular importance.

In Bristol, a large number of diruthenium cyclopentadienyl complexes have been characterised by single-crystal X-ray diffraction studies. Many of these results have been published1 but many more have not. We have recently started building a local database of unpublished structural information using diruthenium cyclopentadienyl complexes as a starting point. The database has been built using PreQUEST software supplied as part of the Cambridge Structural Database (CSD) System.

We wish to use this local database to study metal-carbon interactions that are fundamental to many organometallic processes. Our initial work is an investigation of carbon monoxide bonding modes at diruthenium centres. We have compared the results obtained from our local database of unpublished structure determination data with studies carried out on published data contained in the CSD. Conclusions are drawn about carbonyl migration pathways at a dimetal centre and the reliability of local data sets compared to the more substantial data set of the CSD.

1. see, for example, R.E. Colborn, A.F. Dyke, B.P. Gracey, S.A.R. Knox, K.A. Macpherson, K.A. Mead and A.G. Orpen, J. Chem. Soc., Dalton Trans., 1990, 761 and references therein.

P07.23.021 APPLICATION OF NEW METHODS FOR CRYSTALLOGRAPHIC DATA QUALITY CONTROL. Y. Kotliarov, Institute of Inorganic Chemistry, SB RAS, Novosibirsk 630090, Russia, and S. Iwata, Research into Artifacts, Center for Engineering, the University of Tokyo, Tokyo 153, Japan.

Two methods for crystallographic data quality control have been developed and applied for use with Inorganic Crystal Structure Database. Those methods can detect data where individual atoms or structural fragments are located too far from each other, forming impossibly large gaps.

The first method separates atoms in a unit cell into sets of atoms lying in planar parallel **layers**, perpendicular to some direction: for example, one of the main coordinate axes. If a distance between adjacent layers longer than some critical distance is found, one can conclude that there is no connection between those layers, and the structure can be said to be disconnected.

The layer method is fast and easy to apply. It is especially reliable for actually layered structures. However, it is only a rough evaluation of gaps in structure, because interlayer distances are most commonly shorter than interatomic distances and do not reflect the real connectivity between atoms. The second method--with application of **graph theory**--does not have those disadvantages.

The crystal structure can be described as a graph with atoms as vertices and bonds as edges. To make the graph finite, only atoms inside the unit cell are included in it. Although such a graph loses the space arrangement of atoms and symmetry elements, it can mathematically describe the relationship between atoms in terms of their connections. Two atoms are considered as connected if the distance between them is shorter than some critical distance, and the connectivity matrix can be constructed. Then the connectivity test on a structure graph (whether the structure graph is connected or not) can help to reveal disconnected structures.

Both methods have been applied to data from ICSD and have helped to detect several erroneous disconnected structures, which the conventional test has failed to do.

P07.23.022 ICSD-FOR-WWW, A DEMONSTRATION OF THE LATEST FEATURES, INCLUDING BOND VALENCE. Alan Hewat, Institut Laue-Langevin, BP 156X, Grenoble 38042, FRANCE.

A demonstration of ICSD-for-WWW will show how easy it is to access the almost 50,000 structures in the Inorganic Crystal Structure Database via the WWW, or at least a local server (eg see http://barns.ill.fr/dif/icsd/). The latest features include automatic calculation of bond-valence sums as a check on the structure during preparations for visualisation using VRML.

The WWW interface looks the same on any computer, Windows-PC, Macintosh or Unix workstation. A selection of structures is obtained by entering the usual search criteria, then the search can be narrowed with additional criteria. The resulting entries can be printed out in standard reference format for cut-and-paste into manuscripts, or in EndNote bibliographic format. They can be ordered according to date, formula, author, space group or mineral name for further processing.

Individual entries can be compared, listed in full, and used to generate X-ray or neutron powder diffraction patterns, with peaks automatically indexed. Finally the 3D structure can be drawn, zoomed and rotated, with the usual space-filling, ball-and-stick or co-ordination polyhedrae models available.

The latest features include automatic calculation of Brown-Shannon valence sums to check the chemical validity of the structure, the illustration of sites of different valence state with different colours, the drawing of mixed-atom polyhedrae such as in oxy-chlorides etc.

ICSD-for-WWW servers have already been set up in France, Germany, the UK, USA and Japan, the software is distributed free of charge for a limited demonstration data-set, and also with the licence for the full ICSD data-set from FIZ Karlsruhe.

P07.23.024 STOCHASTIC MODELING OF THE EVOLUTION OF PROTEIN SEQUENCE LENGTH IN GENOMES: PREFERRED DOMAIN SIZES. R. Jain and S. Ramakumar, Physics Department, Indian Institute of Science, Bangalore 560012, India, and Bioinformatics Centre, Indian Institute of Science, Bangalore 560012, India.

We have proposed for the first time a stochastic model, which explains the protein sequence length distribution in all the fully sequenced microbial genomes. The stochastic model is universal since it has been possible to explain the overall features of the length distribution of all the genomes in terms of it. Analysis of protein sequence length distribution for 17 organisms (12 bacteria, 4 archaea and 1 eukaryote) yields a log-normal distribution. According to the stochastic model, mutation can be considered to be a random multiplicative process that takes place in discrete steps. Then, the length of the protein S_t at time t, is related to its length $S_{t+\Delta t}$ at time $t+\Delta t$ by: $S_{t+\Delta t} = \varepsilon_t S_t$. Here ε_t is a random number slightly different from one. $\varepsilon_t < 1$ corresponds to a decrease in the protein length due to deletion of amino acids, $\varepsilon_t > 1$ corresponds to increase in length due to addition of amino acids, and $\varepsilon_t = 1$ corresponds to no change or to point mutation. Thus the length S_N at the Nth level of mutation is given by the product of N random variables: $S_N = S_0 \prod \varepsilon j$ where the product is over j from 0 to N-1. Hence, according to Central Limit Theorem, the logarithm of the protein length distribution is a Gaussian. Therefore the distribution is a log-normal. Peaks due to the clustering of proteins characterize the fine structure of the distributions. These peak regions probably contain genome specific proteins, which could therefore be potential targets for structure determination for purpose of identification of novel folds as in structural genomics project. Fourier analysis of the distributions reveals an underlying periodicity. The periodicity in the protein length distribution implies domain size preference for that organism. The preferred domain size is found to be genome specific. This work is important as it offers opportunities to identify preferred domain size and provides a model to mimic evolution.

R. Jain thanks CSIR (India) for a scholarship.

P07.23.025 SBDBASE: A DATABASE OF COMPUTER GENERATED STRUCTURE MODELS OF TARGET PROTEINS. M. Prabhakaran, S. E. Mylvaganam, G. Raghunathan, M. D. Shenderovich, C. L. Fisher and K. Ramnarayan. Structural Bioinformatics Inc., Dept. of Structural Sciences, 10929 Technology Place, San Diego, CA 92127 USA.

Using existing structural and sequence information, we have developed the Structural Bioinformatics dataBase (SBdBase) of computer-generated protein structure models directly from sequence. Our computational approach in protein modelling from sequence relies on the concept that proteins within a superfamily of similar sequences share common three-dimensional folds and functions. At Structural Bioinformatics Inc. our focus is to obtain three-dimensional representations of proteins for which structures are unavailable but which have sequence similarities with existing NMR and X-ray crystal structures. Additional computer schemes are also applied to define the proteins' detailed structural features, such as active sites, surface chemistry and topology. In the absence of precise three-dimensional structures, the SBdBase provides structural information for a number of human sequences and other protein targets that are potential candidates for drug design and protein engineering.

P09.23.001 JOINT REFINEMENT OF A PROTEIN STRUCTURE AGAINST NMR AND X-RAY DATA. M.L. Raves[1], J.F. Doreleijers[1], H. Vis[1], C.E. Vorgias[2], Z. Dauter[3], K.S. Wilson[4] and R. Kaptein[1], [1] Bijvoet Center for Biomolecular Research, Utrecht University, The Netherlands, [2] EMBL, Hamburg, Germany, [3] Brookhaven National Lab., USA, [4] Protein Structure Group, York University, UK.

Joint refinement, *i.e.* the simultaneous refinement of a structure agains NMR and X-ray data [1], was done in order to investigate the compatibility of the two data sets. Wherever a conflict was found, attempts have been made to determine whether it arose from misinterpretation of the experimental data or from real differences of the protein conformation in solution *vs.* that in the crystal.

The DNA-binding protein HU was taken as a test-case. Its structure consists of a rigid core and two flexible 'arms' and was solved independently by NMR [2] and by X-ray crystallogaphy [3]. The joint refinement procedure started with an unbiased random structure, which was folded using the NMR restraints and then placed in the crystallographic unit cell by molecular replacement. Important differences in main-chain conformations and secondary structure were identified and investigated.

[1] B. Shaanan *et al.* (1992) *Science* **257**, 961-964
[2] H. Vis *et al.* (1995) *J. Mol. Biol.* **254**, 692-703
[3] Z. Dauter and K.S. Wilson, manuscript in preparation

24. INDUSTRIAL CRYSTALLOGRAPHY

P05.24.001 DETERMINATION OF RETAINED AUSTENITE IN AUSTEMPERED VERMICULAR IRON BY RIETVELD ANALYSIS. R.L. Mannheim and J.L. Garin, Department of Metallurgical Engineering, Universidad de Santiago de Chile, Casilla 10233, Santiago, Chile.

Austempered vermicular iron (AVI) alloys have received much attention because of their interesting mechanical properties and applications in the automotive and mining industries.

During heat treatment of AVI alloys variable amounts of austenite are retained in the ferritic matrix, giving place to the so-called ausferritic microstructure. Since the formation of the austenitic phase strongly affects the mechanical properties of the material, a complete characterization of a given alloy must include the relative amount of austenite in the matrix.

Owing to the fact that the heat treatments of this kind of alloys yield nearly complete resolution of the (110) and (111) reflections of the alpha and gamma phases respectively, a Rietveld analysis was conveniently carried out on the material to determine the content of retained austenite. A series of samples was prepared by austenizing at 900 °C and austempering in the range of 280 - 410 °C to yield various amounts of austenite from 4 to 40%. The room temperature data collection for each specimen was carried out over the range of 20 - 90° (2θ), with 3500 step intensities, using Cu Kα radiation and grapite monochromator. The X-ray analysis was performed assuming asymmetric Pearson VII profiles for all reflections. The refinement cycles were based upon the variation of isotropic thermal parameters, scale factors, preferred orientation coefficients, surface roughness, background polynomial coefficients, sample transparency and displacement and so on.

The described procedure based upon using of the Rietveld software proved to be very reliable, mainly when the effects of preferred orientations on the intensities have to be corrected for.

P05.24.002 SYNTHESIS AND CHARACTERIZATION OF NANOCRYSTALLINE Ni_3Al BY CHEMICAL ROUTE. S.K. Pradhan [1], A. Datta [2], M. Pal [3], P. Bose [1], D. Chakravorty [3], [1] Department of Physics, The University of Burdwan, Golapbag, Burdwan -713104, [2] Institute of Atomic and Molecular Science, Academia Sinica, P.O. Box 23-166, Taipei, Taiwan 106, [3] Indian Association for the Cultivation of Science, Jadavpur, Calcutta 700 032, India.

Both ordered and disordered alloys of Ni_3Al in the nanocrystalline form were synthesized by a sol-gel technique followed by hot pressing at temperatures in the range 873 to 1173 K. The crystallite size, r.m.s. strain and the dislocation density were determined by a modified Rietveld method and Warren-Averbach's peak broadening analysis. For most of the specimens the particle size and r.m.s. strain were found to be anisotropic in nature. The average diameters varied from 10 to 30 nm depending on the hot pressing conditions.

P05.24.003 SMALL ANGLE NEUTRON SCATTERING AS A POWERFUL TOOL TO INVESTIGATE PRECIPITATES IN SUPER-ALLOYS. R. Gilles[1], P. Strunz[2], D. Mukherji[3], A. Wiedenmann[2] and H. Fuess[1]. [1] University of Technology Darmstadt, Petersenstr. 23, 64287 Darmstadt, Germany, [2] Hahn-Meitner-Institut, Glienicker Str. 100, 14109 Berlin and [3] University of Technology Braunschweig, Langer Kamp 8, 38106 Braunschweig, Germany.

Single-crystal nickel-base superalloys, recently developed for blade applications in land-based gas turbines, were characterized using the Small Angle Neutron Scattering (SANS) instrument V4 in HMI Berlin. Superalloys are strengthened by the γ′ precipitates ($L1_2$ structure), which are coherently embedded in a single-crystal γ matrix of nickel solid-solution (fcc). It is well known that the precipitate morphology, their distribution in the matrix and their volume fraction strongly influence the strength of the alloys.

Specimens heat treated to produce a homogeneous distribution of γ′ precipitates of different sizes were investigated by detecting 2D scattering patterns as a function of orientation of the specimen. Analysis of the data resulted in values of size, interparticle distance, volume fraction and orientation distribution of precipitates. These parameters describe well the morphology of the precipitates. To determine the individual microstructural characteristics, a comparison of iso-intensity profiles of measured and simulated 2D curves was performed on the basis of a microstructural model of the superalloy. Supplementary measurements with TEM, SEM and XRD completed and confirmed our SANS results.

1. R. Gilles, D. Mukherji, P. Strunz, A. Wiedenmann, R.P. Wahi, Scripta Materialia. Vol. 38, 5, 803, 1998.
2. R. Gilles, D. Mukherji, P. Strunz, A. Wiedenmann, R.P. Wahi, Physica B 241-243, 347, 1998.

P05.24.004 STRAIN DISTRIBUTION IN NANOCRYSTALLINE TITANIUM. Partha Chatterjee , S. P. Sen Gupta, Department of Materials Science, IACS, Jadavpur, Calcutta-700032, India

An X-ray line broadening study of ball-milled Titanium metal is presented. A profile fitting methodology with a Pseudo-voigt profile shape function is adopted. Fourier line shape study for both the fault-affected and fault-unaffected reflections are carried out. It is found that ball-milling results in the formation of nanocrystalline Ti phase. The values of the crystallite size range from 11-13 nm for different crystallographic direction. The values of rms microstrains are of the order of 0.2-0.3 %. The variation of the rms microstrain with coherence lengths in terms of local strain and its derivatives indicate that the strains are non-uniform for small column lengths and this is indicative of strongly localized strain fields in the crystallite interfaces. The present analysis could not bring out the presence of stacking faults in the nanocrystalline region.

P05.24.005 CRYSTAL STRUCTURE OF DISORDERED MAGNESIUM TITANATES IN CONCENTRATION, TEMPERATURE AND TIME DIMENSIONS. G. Kimmel,[1] J. Zabicky,[1] and P. Arigur.[2] Ben-Gurion University of the Negev, POB 653, Beer-Sheva 84105, Israel;[1] and Western Michigan University, Kalamazoo, MI 49008, USA.[2]

Three equilibrium crystalline phases are known for the MgO-TiO_2 system: Mg_2TiO_4 (qandilite), $MgTiO_3$ (geikielite) and $MgTi_2O_5$ (karrooite), that are isomorphous with inverse spinel, ilmenite and disordered brookites, respectively. Qandilite and karrooite are high temperature phases which can retain the H.T. structure at room temperature on rapid cooling. After prolongued thermal annealing, a cubic to tetragonal phase transformation of qandilite and modifications of the unit cell parameters of geikielite and karrooite have been reported.

In this work all the precursors were prepared by the sol-gel method. Most samples were studied by XRPD, but some of them were also investigated by neutron diffraction. The following results were obtained by various experimental procedures: (a) Energetic milling of separately prepared precursors of MgO and TiO_2 for long periods (up to 24 h) was insufficient to produce a

unique nanocrystalline magnesium titanate phase, corresponding to the Mg:Ti ratio of the precursors; instead, mixtures of geikielite, qandilite, and periclase pointed to incomplete thermal annealig and states far from equilibrium. (b) Coprecipitated precursors with a wide range of Mg:Ti atomic ratios (x:y), yielded nanocrystalline powders of composition $xMgO.yTiO_2$, after a short (2-4 h) primary heat treatment at 600°C. The diffractgrams of nonstoichiometric qandilite were severely broadened, but the cell parameters were left unchanged. Atomic disordering of the inverse spinel nanophase took place for Mg:Ti atomic ratios from 2:1 to about 1.3:1. Deviation from stoichiometry of karrooite (from 1:2 to about1:1.5) caused modification of the unit cell parameters. (c) The products of item (b) are metastable. Secondary heating at 800°C returns the system into equilibrium within several hours. (d) The precursors of item (b) were rapidly heated to a constant temperature in the 550 to 1300°C range, for a real-time kinetical study by HTXRD.

P05.24.006 CHARACTERISATION OF PMA COATED NANO-CRYSTALLINE γ-Fe_2O_3. M. Hagelstein, E. Pellegrin, S. Doyle, H. O. Moser, Forschungszentrum Karlsruhe, PEA, P. O. Box 3640, D-76021 Karlsruhe, Germany, and J. Fuchs, D. Vollath, D. V. Szabó, Forschungszentrum Karlsruhe, IMF-III, P. O. Box 3640, D-76021 Karlsruhe, Germany, and C. Ferrero, A. Fitch, European Synchrotron Radiation Facility, B. P. 220, F–38043 Grenoble Cedex, France

A new type of magnetic nanocomposites made of coated nanoparticles for applications has been synthesised using the microwave plasma process [1]. Due to their small size, PMA coated nanoparticles of γ-Fe_2O_3 show superparamagnetism. Transmission electron diffraction and Mößbauer-spectroscopy indicate structural disorder. This might explain the small saturation magnetisation found in this material. Sophisticated analytical techniques using synchrotron radiation, like x-ray powder diffraction, x-ray absorption spectroscopy and soft x-ray magnetic circular dichroism have been applied for additional characterisation of the chemical, structural and magnetic properties of the material.

A lower particle size limit of 4 nm was determined by X-ray powder diffraction. The experimental powder pattern was Rietveld refined using the magnetite structure, although it was complicated due to the presence of two crystalline phases. The Fe-O and Fe-Fe distances and co-ordination numbers have been derived from x-ray absorption fine structure spectra at the Fe K edge. Four shells from 0.189 nm to 0.340 nm have been refined successfully indicating a reduced occupation of octahedral Fe sites.

D. Vollath, D. V. Szabo, R. D. Taylor, J. O. Willis, J. Mater. Res., Vol. 12, No. 8 (1997) 2175-2182

P05.24.007 SYNTHESES AND STRUCTURAL CHARACTERIZATIONS OF TWO NEW NANOPOROUS MANGANESE-GALLIUM PHOSPHATES. K. F. Hsu, S. L. Wang Department of Chemistry, University of Tsing Hua, Hsinchu 300, Taiwan

Hydrothermal syntheses of gallium phosphates characterized with nanoporous structures and catalytic properties have been investigated. By employing various organic cations as structure-directing reagents, piperazine and 4, 4'-trimethylenedipiperidine, two novel manganese-substituted gallium phosphates, $(C_4N_2H_{12})_2Ga_6(H_2O)Mn(PO_4)_8$ (1) and $Ga_4Mn_3(H_2O)_6(PO_4)_6$ (2), were obtained respectively. Phase 1 adopts a 3D open framework, which consists of GaO_6 octahedra, GaO_5 bipyramid and GaO_4, MnO_4 and PO_4 tetrahedra. These polyhedra are interconnected via a corner-sharing manner to give a zeolitic framework in which 8-, 6- and 4-membered straight channels are formed inside the structure. The piperazinium cations are residing in the tunnels and staggering along the direction of 8-membered channels. In search for larger channels inside the framework, we replace piperazine with 4, 4'-trimethylenedipiperidine under the same hydrothermal condition. A new 3D framework of 2 was then formed. The framework is built up of MnO_6 octahedra, GaO_5 bipyramid and PO_4 tetrahedra in which three MnO_6 octahedra and one PO4 tetrahedra are linked by the edge-sharing forming a tetrameric unit. The tetrameric units were extended into a 3D framework by the corner-sharing with GaO_5 bipyramid and PO_4 tetrahedra. The oxidation states of Mn atoms in both structures are determined to be "+2". In this paper, hydrothermal syntheses, crystal structures, and thermal properties of the title compounds will be presented in detail.

P06.24.001 NEUTRON DIFFRACTION STUDY OF THE STRUCTURAL CHANGES, INDUCED IN NICKEL FOILS BY PULSED ELECTRON BEAM IRRADIATION. V.V.Sikolenko, G.D.Bokuchava, S.A.Korenev, A.V.Kalmykov Joint Institute for Nuclear Research, Dubna, Russia

Here we present the results of the high resolution neutron diffraction study of the structure changes of nickel foils, irradiated by the high-current pulsed electron beam with different fluxes.

The experiments on foil irradiation were carried out at the ELIONA experimental setup intended to produce electron and ion beams. We used an explosive emission vacuum diode with an Arcadyev-Marx pulse voltage generator. The beam current is exceed 1000 A with a pulse duration equals to 300 ns. The neutron diffraction experiments were carried out at the high resolution Fourier diffractometer HRFD at the IBR-2 pulsed nuclear reactor. Unirradiated, and irradiated for 10 and 20 minutes nickel foils were investigated. As a result of high temperature gradient, an elastic deformation wave arises in the irradiated foil. We demonstrate linear enhancement of the lattice parameter with an increase of flux as a result of the action of the deformation shock wave. The recrystallisation from the melted condition takes place in the period between electron beam pulses. This process can be accompanied by partial amorphisation. But the analysis of the main diffraction peaks width dependence on their positions for samples irradiated by different fluxes, shows the absence of amorphisation.

P06.24.002 ON-LINE X-RAY ANALYSIS SOFTWARE OF THE TITANIUM AND IRON ALLOYS. A.R.Gokhman X-Ray Laboratory, Department of Physics, SU Pedagogical University, Staroportofrankovskaya 26, 270020-Odessa, Ukraine

Correlation formulas between X-ray Analysis data and mechanical properties of the Ti and Fe alloys are found under working out of the On-line X-ray analysis software. Young modulus, shear modulus, yield stress, strength and plasticity coefficient are considered as the mechanical characteristics.

Integral texture parameters (ITP), residual stress of the first and second kind, X-ray residual strain, X-ray elastic moduli (XEM) and average size of crystallites are determined from X-ray investigations. Elastic moduli are measured by dynamic method. Other mechanical characteristics are measured on the testing machine “INSTRON”.

Average size of crystallites and residual stress of the second kind are found from the physical broadening. X-ray residual strain is measured from the angle position of the set of X-ray lines. ITP are calculated by probabilistic method from the two experimental inverse pole figures of some directions in the titanium or iron alloys. Due to the extrapolation procedure complete pole figure (PF) (222) is found from incomplete PF and then ITP of the iron alloys are calculated by method that uses the elastic isotropy of the (222) crystallographic plane of the cubic crystals. ITP of the hexagonal titanium alloys are determined by the likely way from incomplete PF (0002).

XEM are calculated from PF(222) and (0002) in accordance with choice of the X-ray line for measuring of the residual strain. Residual stress are found from the residual strain and XEM by a Hook's law. Correlation formulas for software of the On-line X-ray Analysis are determined for Fe and Ti alloys after rolling as well as after thermal and mechanical-thermal treatment.

P06.24.003 ON-LINE X-RAY ANALYSIS SOFTWARE OF THE PBS PHOTODETECTORS. A.R.Gokhman. A.Ye. Kiv, X-Ray Laboratory, Department of Physics, SU Pedagogical University,Staroportofrankovskaya 26, 270020-Odessa, Ukraine

Polycrystalline PbS-layers are advanced materials for obtaining of high-sensitive photoresistors in the IR field. Dark resistance and noise voltage are the important characteristics of PbS resistors. The problem to predict these parameters on the base of X-ray data is the problem of our presentation.

The films photoelectical properties-average grain size extreme dependence has been found. The properties of PbS films are symmetrical with respect to the axis normal to them surface plane. It allows consideration of the crystallographic texture as axial and to describe it by inverse pole figures but not ODF. The values of texture parameters defining the films optimum characteristics are found. The most preferable texture component is the axial component <200> with percentage in 37-38% interval. The high level of PbS-resistors flicker-noise-to- so-called X-ray elastic constants correlations is revealed also. A minimum noise level and maximum value of the dark resistance of the PbS films corresponded to residual strain 0.0006 and residual strain – 7.8MPa. It is based the following conclusion: under applying of the Pbs physical layers the main problem is not to take off fully the mechanical strain and stress but to to lead theirs to the given optimum values.

On-line X-ray analysis software of the dark resistance and noise voltage of PbS photodetectors is worked out.

P07.24.001 Ni PARTICLES ON SILICA STUDIED BY ANOMALOUS SMALL ANGLE SCATTERING. F. Berg Rasmussen, A. M. Molenbroek, B. S. Clausen, Haldor Topsøe Research Laboratories, Lyngby, Denmark and R. Feidenhans'l, Condensed Matter Physics and Chemistry Dept. Risø National Laboratory, Roskilde, Denmark.

Nano-dispersed Ni particles on silica and alumina supports play an important role in catalysis. Ni is used as a catalyst for e.g. steam reforming but also as a promoter in e.g. Mo-based catalysts for hydrotreating.

This contribution concerns ASAXS investigations of Ni particles on silica performed at the JUSIFA beamline in HASYLAB, Hamburg. The extracted small angle scattering of the Ni-particles is characterised by two regimes. At low q-values the intensity is proportional to q^{-D} with $D \approx 3$ indicating scattering from compact aggregates. At high q-values $I \propto q^{-D}$ ($D \approx 4$) known as the Porod region.

From the cross-over between the two regions an estimated size of the scattering particles of 90 Å is obtained in reasonable agreement with a mean Ni particle size estimated from the broadening of x-ray powder diffraction lines. We interpret the extracted scattering curve in terms of a hard-sphere model and extract a particles size distribution of the Ni particles.

P08.24.001 CHARACTERISATION OF THE MICRO-STRUCTURES OF ISOTHERMALLY TRANSFORMED MARTENSITE AT LOW TEMPERATURE IN Fe-23Ni-3.6Mn ALLOY BY RIETVELD'S METHOD. A.Chanda, H.Pal, and M.De, Department of Materials science, Indian Association For the Cultivation of Science, Jadavpur, Calcutta-700 032, India.

The present study reports x-ray characterisation of the microstructures of the martensites of Fe-23Ni-3.6Mn alloy, transformed isothermally at low temperature, both in the austenite powder and bulk forms of the material. The analysis is done adopting Rietveld's whole X-ray profile fitting method incorporating preferred orientation of the crystallites. Martensitic transformation for annealed powders of grain size~50μm of this alloy done at 150K revealed the highest degree of transformation showing about 8 volume percentage of martensites. This value is about 81% for cold-worked powders (at R.T) and 69% for bulk transformed at 170K, each showing the highest degree of transformation. The results of the x-ray profile study also revealed the state of the microstructure of both the austenite (fcc) phase and the martensitic (bcc) phase in terms of various x-ray line profile-related defect parameters viz. stacking faults, compound fault probabilities, crystallite (domain) sizes, r.m.s. strains, dislocation density etc. On comparing the results it is found that the martensitic phase has smaller crystallite size, larger r.m.s. strain, higher dislocation density compared to those of the austenite. The value of microhardness for the bulk martensite is considerably higher compared to that of the bulk austenite.

P08.24.002 X-RAY STUDIES ON THE KINETICS OF MICROSTRUCTURAL EVOLUTION OF Ni_3Al SYNTHESIZED BY BALL-MILLED ELEMENTAL POWDERS. M.De, S.K.Shee, Department of Materials Science, Indian Association for the Culltivation of Science, Jadavpur, Calcutta-700 032, India, S.K.Pradhan, Department of Physics, University of Burdwan, West Bengal, India.

The study reports the x-ray characterization of microstructures as evoluted in course of ball-milling of elemental blends of Ni and Al mixed in the nominal composition of Ni_3Al. The kinetics of evolution of the products at various intermediate stages of milling, starting from the initial to final, have been studied through the evaluation of X-ray profile-related defect parameters viz. stacking faults, crystallite sizes, r.m.s.strains, dislocation densities, percentage of different phases formed as a function of milling time. The method of analysis used involves Rietveld's whole profile fitting technique. The results reveal formation of increased NiAl solid solution at the early stages of milling, transforming gradually to fully disordered intermetallic Ni_3Al at about 57 hrs of milling .The final milling product possessed high propensity of faulting with high r.m.s.strain and dislocation density ($\sim 10^{12} cm^{-2}$). The crystallite sizes assumed nano-order dimension.

P08.24.003 A FEW COMMENTS ON PSEUDOVOIGT PROFILES. Prabal Dasgupta, Department of C.S.S., Indian Association for the Cultivation of Science, Jadavpur, Calcutta 700 032, India.

The analytical expression of pseudovoigt function used by most of the crystallographers is written as

$$I_p(x) = I_p[\eta\, C(x) + (1-\eta)\, G(x)]$$

Where $C(x) = (1+x^2)^{-1}$ and $G(x) = \exp[-(\ln 2)x^2]$ with $x = (2\theta - 2\theta_0)/ w$; $w = ½$ FWHM and η = Cauchy content, $2\theta_0$ is the position of the peak maxima. This work reveals that for above form of Pseudovoigt function Cauchy content η must be greater

than 0.328, otherwise no meaningful result in terms of crystallite size can be extracted from it. η values published by three authors viz Benedetti et al (1988) J. Appl. Cryst. 21 543-549, Sanchez-Bajo et al (1997) J. Appl. Cryst. 30 427-436 and Le Bail et al (1997) J. Appl. Cryst 30 265-271, agree with the present theory.

An expression for $\langle D \rangle_v$ / $\langle D \rangle_a$ in terms of η alone has also been worked out. Efficacy of this expression has been tested with η and $\langle D \rangle_v$ and $\langle D \rangle_a$ values published by Bendetti et al (1988) J. Appl. Cryst 21 543-549.

P08.24.004 MICROSTRUCTURE AND GROWTH KINETICS OF NANOSCALE CRYSTALLITES OBTAINED FROM HYDRATED CERIUM OXIDES. D. Louër, N. Audebrand and J.-P. Auffrédic, Laboratoire de Chimie du Solide et Inorganique Moléculaire, Université de Rennes I, 35042 Rennes, France.

Previous X-ray diffraction line broadening studies of nanoscale CeO_2, prepared from the thermal decomposition of mixed cerium nitrates, have revealed spherical crystallite shapes and the presence of microstrains [1]. In the present study, two hydrated oxides, $CeO_2.xH_2O$, have been obtained from hydrolysis by ammonia of $Ce(SO_4)_2.4H_2O$ and $(NH_4)_2Ce(NO_3)_6$ solutions. Due to a severe diffraction line broadening, the microstructure has been characterised by pattern modelling, using a trial-and-error procedure based on the Rietveld method. In the case of the ex-sulphate phase, crystallites are isotropic with a diameter of 19 Å. The nanoscale cerium oxides, named *sul*-CeO_2 and *am*-CeO_2, have been prepared by dehydration of the hydrated phases, in both isothermal and dynamical régimes. Powder diffraction data have been collected with a high-resolution diffractometer (isothermal mode) and with temperature-dependent X-ray diffractometry (dynamical mode). Crystallite size and shape have been determined from sixteen diffraction lines with the Fourier analysis (software *Prof*FOU [2] based on the output data from *PROFILE*/Socabim) and, also, with the Langford method for samples prepared isothermally, while a simplified procedure was applied to the resolved diffraction line 111 in the dynamical diffraction study. It has been shown that the crystallites are, on average, spherical and that *am*-CeO_2 contains a small amount of microstrains decreasing with temperature, whereas *sul*-CeO_2 is strain-free whatever the preparation temperature. Crystallite growth has been studied in the temperature range ~300-800 °C showing an increase of the diameters D from ~50 Å to ~1000 Å. The crystallite growth kinetics follow the general law $D = Kt^n$. It is shown that strain-free CeO_2 with controlled crystallite size and shape can be easily prepared and that *sul*-CeO_2 appears as a candidate for a reference material in terms of crystallite sizes.

1. N. Guillou, J. P. Auffrédic & D. Louër (1994). *J. Solid State Chem.* 112, 45.
2. D. Louër & N. Audebrand (1998). *Adv. X-ray Anal.* Vol. 41, in press.

P08.24.005 ON THE RELIABILITY AND APPLICABILITY OF PROFILE FITTING METHOD: A CASE STUDY. S. P. Sen Gupta, Partha Chatterjee, Department of Materials Science, IACS, Jadavpur, Calcutta-700032, India

A critical analysis of the Powder Profile Fitting method in connection with line broadening studies on Warren-Averbach method of Fourier analysis is presented. It is observed that for narrow and asymmetric profiles the correspondence of the Fourier coefficients is good only in the small n or column length region. For broad and symmetric profiles the Profile fitting method yields good results. Moreover, the hook effect is minimized indicating that a good powder profile analysis based on single reflection is possible. This is illustrated with recent experimental data.

P08.24.006 IN-SITU HIGH TEMPERATURE X-RAY ANALYSIS OF MgO-CaO-RICH BASIC REFRACTORIES UP TO 1600°C IN AIR. A. Preisinger and L. Petrás, Institute of Mineralogy, Crystallography and Structural Chemistry, Techn. University of Vienna, Getreidemarkt 9,A-1060 Vienna, Austria and M. Fuehrer, Institute of Mineral Processing and Refractories, University of Leoben, Leoben, Austria and K. Riepl, Veitsch-Radex AG, Research Institute Leoben, Leoben, Austria.

Basic refractory samples in the compositional range of 60-80%wt. MgO, 15-30%wt. CaO and <5%wt. Fe_2O_3, <1%wt. SiO_2 and <1%wt. Al_2O_3 as well as samples in the range of 50-60%wt. CaO, 20-30%wt. MgO, ~15%wt. Fe_2O_3, 7%wt. SiO_2 and 0,3%wt. Al_2O_3, respectively have been investigated in a high temperature PMP 1600 type [1] powder diffraction chamber in combination with Philips X´Pert MPD in Θ-Θ geometry using Cu-Kα radiation. The starting samples have been chemically analysed by means of XFA. Quantitative phase compositions have been determined using RIETVELD refinement at room temperature and "in situ" in the temperature range between 800°C and 1600°C.

In the low SiO_2 containing samples between 900°C and 1000°C Periclase, Lime and Brownmillerite have been found. At higher temperatures of 1300°C to 1400°C a partial melting process occurs which causes Brownmillerite lines to vanish. The high SiO_2 containing samples showed additionally reaction between Dicalciumsilicate and Lime giving Tricalciumsilicate at about 1300°C. Comparison of the RIETVELD refinement derived thermal expansion values with literature data [2] allows the determination of trace element content in MgO and CaO at different temperatures. Phase transitions and reactions are given in detail.

[1] L.Petrás, A.Preisinger, K.Mereiter: Materials Science Forum, Vol.278-281, (1998) p.396
[2] D.Taylor: Thermal Expansion Data I. British Ceram. Trans. Journal, Vol.83, (1984), p.5-9

P08.24.008 ABSOLUTE CONFIGURATION OF RAMIPRIL INTERMEDIATE. K. Vyas, J. Moses Babu, S. Raju, P. Rajender Kumar, M. R. Sarma, G. Om Reddy, Dr. Reddy's Research Foundation, Bollaram Road, Miyapur, Hyderabad - 500 050.

The title compound, [S,S,S] azobicyclo [3,3,0] octane-3-carboxylic acid benzyl ester hydrochloride, is an important intermediate in the synthesis of the anti-hypertensive drug, Ramipril. The compound is crystallized from n-propanol and methanol mixture. It crystallizes in the orthorhombic space group $P2_12_12_1$ with a = 9.869(1), b = 19.483(3), c = 7.451(1) Å, V = 1432.7(3) Å^3, Z=4. The intensity data were collected on a Rigaku AFC7S diffractometer with Cu Kα radiation. The structure is solved by direct methods (SIR92) and refined by least square methods. The present R factor is 4.4%. It is interesting to note that the ring junction between A & B is "cis" and two rings are like an open book. These two rings subtend an angle of 59°. There is hydrogen bonding interaction between chloride ion and nitrogen. Absolute configuration of the molecule has been determined to be SSS by means of anomalous dispersion measurements.

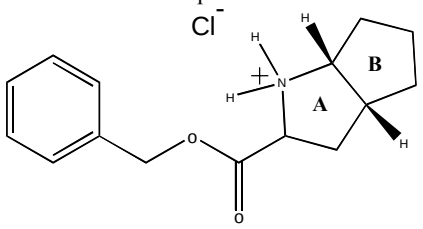

* DRF Publication No.: 90

P08.24.009 CRYSTAL STRUCTURE OF PEROXETINE INTERMEDIATE. A. Sivalakshmidevi, K. Vyas, P. Rajender Kumar, T. Suresh, M. R. Sarma and G. Om Reddy, Dr. Reddy's Research Foundation, Bollaram Road, Miyapur, Hyderabad - 500 050.

The compound 3-ethoxycarbonyl-4- (4-fluorophenyl) -1-methyl -2,6-piperidinedione is an intermediate of Peroxetine. The compound is crystallized from ethyl acetate. It crystallizes in the triclinic space group P-1 with a = 11.976(2), b = 12.232(2), c = 10.667(2) Å, α = 106.13(1), β = 94.75(1), γ = 72.16(1), V = 1428.8 (4) Å^3, Z=4. The intensity data were collected on a Rigaku AFC7S diffractometer with Cu Kα radiation. The structure is solved by direct methods (SIR92) and refined by least square methods. There are two independent molecules in the unit cell. The piperidinedione ring assumes sofa conformation as evidenced by endocyclic torsion angles. The molecules are stabilized in the lattice by vander Waals interactions. The R factor is 6.9% for 3189 observed reflections.

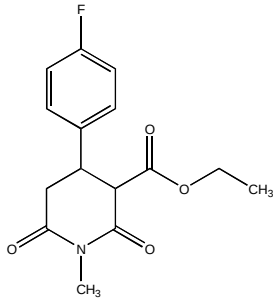

* DRF Publication No.: 89

P08.24.010 CRYSTAL STRUCTURE OF QUINAZOLINONE DERIVATIVE. K. Shashi Rekha, R. Vasu Dev, J. Moses Babu, K. Vyas, M. Ravikanth Reddy, C. Prabhakar, M. R. Sarma and G. Om Reddy, Dr. Reddy's Research Foundation, Bollaram Road, Miyapur, Hyderabad - 500 050.

A new quinazolinone derivative was prepared as an intermediate during our research on discovery of anti-diabetic drugs. The mass spectrum displayed a molecular ion at m/z = 280 corresponding to the molecular formula $C_{16}H_{12}O_3N_2$. Steady state 1D-nOe experiment by saturation of the methyl singlet at δ 2.12 gave dipolar contact to the ortho aromatic proton at δ 7.60, fixing the site of the phenyl group on the quinazolinone moiety. Interestingly the compound (1) exhibits polymorphism. Crystal structure of one of the polymorphs has been solved by single crystal X-ray diffraction technique.The X-ray structure provides unambiguous proof for the structure elucidated from spectral data.

The compound is crystallized from methanol. It crystallizes in the orthorhombic space group Pbca with a = 18.375(5), b = 20.094(2), c = 7.214(2) Å, V = 2663.5 (5) Å^3, Z = 8. The intensity data were collected on a Rigaku AFC7S diffractometer with Mo Kα radiation. The structure is solved by direct methods (SIR92) and refined by least square methods. The final R = 0.067, R_w = 0.038 for 1529 observed reflections.

The dihedral angle between the two aromatic rings is 92°. The molecules are stabilized by inter molecular hydrogen bonding between hydroxyl group and the nitrogen (N1) of quinazolinone.

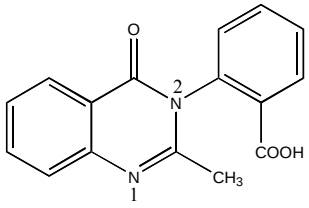

* DRF Publication No.: 91

P08.24.011 CRYSTAL STRUCTURES OF RIZATRIPTAN BENZOATE AND SOME ANALOGUES. Nancy N. Tsou and Richard G. Ball, Merck Research Laboratories, P.O. Box 2000, Rahway, New Jersey, 07065-0900, USA.

A large amount of recent work[1-3] has greatly expanded our knowledge of the diversity of serotonin (5-HT) (**1**) receptors. These receptors are implicated in a broad range of neurotransmission dysfunctions and the search for receptor subtype-specific ligands for use as pharmacological tools and therapies has lead to some interesting results.

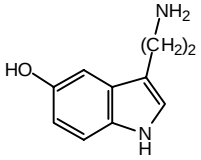

1

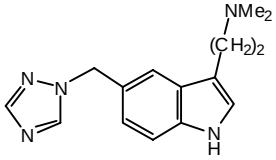

2

The 5-HT$_1$ family of receptors appears to comprise at least five subtypes and agonist ligands specific to the 5-HT$_{1D}$ receptor appear to be effective in the treatment of migraine. To date, agonists with high specificity for the 5-HT$_{1D}$ receptor are all based[4] on a 3,5-disubstituted indole framework in which the 3 substituent is a short alkyl chain carrying an aminic nitrogen and the 5 substituent (OH in serotonin itself) can range through a variety of hydrogen-bond acceptor groups. Since the structural literature contains no examples of this class of compounds we are reporting herein the structures of Rizatriptan (**2**) and three related indoles. They are discussed in terms of their biological activity as well as their solid-state conformations.

(1) Brancheck, T., *Curr. Biol.*, **1993**, *3*, 315-317.
(2) Beer, M.S.; Middlemiss, D.N.; McAllister, G., *Trends Pharmacol. Sci.*, **1993**, *14*, 228-231.
(3) Monsma, F.J.; Shen, Y.; Ward, R,P.; Hamblin, M.W.; Sibley, D.R., *Mol. Pharmacol.*, **1993**, *43*, 320-327.
(4) Street, L.J.; *et al.*, *J. Med. Chem.*, **1995**, *38*, 1799-1810.

P08.24.012 CONFORMATIONAL FEATURES OF SOME DIAZAPINE MOLECULES. M. Suresh Kumar, D.Kumaran, and M.N.Ponnuswamy, Department of Crystallography and Biophysics, University of Madras, Guindy Campus, Chennai – 600 025, India and K.Chinnakali and H.K.Fun, School of Physics, Universiti Sains Malaysia, Penang, Malaysia.

Many derivatives of the benzodiazapine family display pharmacological properties such as tranquilizing, muscle relaxant, anticonvulsant and sedative effects. Benzodiazapines are in general not depressants of the CNS but they affect only discrete areas of the brain. The crystallographic studies of some diazapine derivatives have been done to understand the Structure Activity Relationships (SAR).

The structures were solved by direct methods and refined by full-matrix least-squares procedures. The diazapine ring in all the molecules adopt distorted boat conformation. The structures are stabilized by C-H...O and C-H...N type of interactions in addition to van der Waals forces. A comparative study on these compounds reveals many interesting results and will be presented.

P08.24.013 CONFORMATIONAL ASPECTS OF SOME PIPERIDIN-4-ONES. M.N.Ponnuswamy, M.Suresh Kumar and D.Kumaran, Department of Crystallography and Biophysics, University of Madras, Guindy Campus, Chennai – 600 025, India.

The piperidine derivatives are found to be pharmacologically important but their N-nitroso derivatives are found to be carcinogens in nature. Though the unsubstituted N-nitrosopiperidines are potential carcinogens, the alkyl/aryl derivatives are found to be non-carcinogens. It appears that blocking of the (-positions to the ring nitrogen atom by methyl groups in cyclic nitrosamines is responsible for reducing the carcinogenic acitiviy. Bulkiness of the substituents at different positions of piperidine ring reduces the carcinogenicity. To correlate the structure with activity, a series of piperidinone derivatives have been studied by crystallographic methods. In N-alkyl and N-free piperidine derivatives, the piperidine ring adopts chair conformation but in N-electron withdrawing piperidine derivatives, it adopts boat conformation. The detailed conformational aspects including the energy concepts are to be presented.

P08.24.014 STRUCTURE AND CONFORMATION OF SOME AZA BICYCLIC RING COMPOUNDS. D.Kumaran, and M.N.Ponnuswamy, Department of Crystallography and Biophysics, University of Madras, Guindy Campus, Chennai –600 025, India.

Several 3-azabicyclononanes have been synthesized and studied widely in view of their conformational flexibilities and intermolecular interactions. These compounds also possess medicinal and pharmacological properties. The substituent effects on the conformation of the bicyclic ring systems are analysed and presented. The crystallographic studies on 2,4-diaryl azabicyclononanes show that the bicyclic ring sytems adopt chair-chair conformation. When electron withdrawing groups such as acetyl, nitroso and ester groups are substituted at the nitrogen atom, the piperidine ring gets distorted. The detailed conformational analysis on the diazabicyclo [5.3.0] decanone derivatives indicate that the bicyclic ring system adopts chair-envelope conformation with slight distortion. The conformational restriction is imposed due to the presence of two torsional constraints in the seven membered ring, namely, the planar rigid lactam group (N-C-O) and the fusion to a five membered ring. The energy calculations have also been carried out and presented.

P08.24.015 CRYSTAL STRUCTURE OF 9-DEOXO-9-[2"-OXOPROPYL] PODOPHYLLOTOXIN. Y. Ravindra Kumar, A. Sivalakshmidevi, K. Vyas, G. Om Reddy, B. Renuka and D. Subrahmanyam, Dr. Reddy's Research Foundation, Bollaram Road, Miyapur, Hyderabad - 500 050.

The title compound is semi-synthetic derivative of Podophyllotoxin with in vitro cytotoxic activity. The compound is crystallized from methanol and dichloromethane mixture. It crystallizes in the orthorhombic space group $P2_12_12_1$, with a = 13.221(10), b = 28.806(9), c = 12.526(9) Å, V = 4766.8 (4.2) Å ^{3}, Z=8. The intensity data were collected on a Rigaku AFC7S diffractometer with Mo Kα radiation. The structure is solved by direct methods (SIR92) and refined by least square methods. The present R factor is 7.1%.

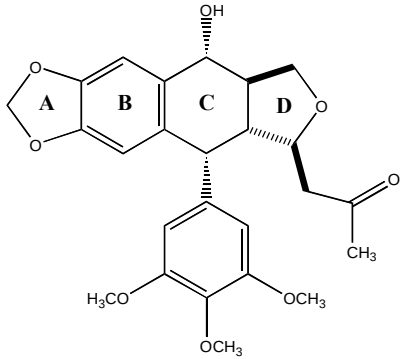

There are two independent molecules in the unit cell. In both the molecules the confirmation of the rings A and D is envelope whereas the rings C assume half chair confirmation. There is an intermolecular hydrogen bonding between the hydroxyl oxygen atoms of the independent molecules.

P08.24.016 STRUCTURES OF A HYDROXAMIC ACID INHIBITOR COMPLEXED WITH MMP1, MMP3, AND MMP13 F. Gu, C.M. Dunaway, L. Chen, T. Rydel, M.G. Natchus, G.E. Mieling, B.L. Barnett Structural Biology, Discovery Research, Procter & Gamble Pharmaceuticals, Mason Ohio, 45040, USA

MMP inhibitors are potential therapeutic agents for various diseases including cancer and osteoarthritis. Recent data from clinical trials with MMP inhibitors indicate that there is a great need for selective inhibitors. X-ray crystallography has been used as a tool to help understand specific binding interactions of inhibitors to various MMPs. We report in this study several structures of a hydroxamic acid inhibitor complexed to MMP1, MMP3, and MMP13 catalytic domains. The inhibitor was soaked into the MMP3 crystals or co-crystallized with the enzyme. Large conformational changes at the active site have been noted when comparing the structures of the active MMP3 catalytic domain and the one inhibited. The same inhibitor has also been co-crystallized with MMP1 and MMP13. Comparisons of the structures of three inhibited enzymes, MMP1, 3, and 13 show that MMP3 and 13 are extremely similar. There are major differences in the binding pockets, especially in the S1' pocket between MMP1 and MMP3/13. These studies can help design more selective inhibitors.

P09.24.001 HYDROTHERMAL SYNTHESIS & CHARACTERIZATION OF U-POROUS ZINC-GALLIUM PHOSPHATE $[N_2C_6H_{16}][Ga_2Zn_2P_4O_{16}]$. Chia-Heir Lin [1], Sue-Lein Wang [2]. [1] Department of Chemistry, National Tsing Hua University, Hsinchu, Taiwan 300. [2] Department of Chemistry, National Tsing Hua University, Hsinchu, Taiwan 300

A novel compound of $[N_2C_6H_{16}][Ga_2Zn_2P_4O_{16}]$ (1) has been prepared under mild hydrothermal conditions and structurally characterized by single-crystal X-ray diffraction and thermal analysis. Crystal data for compound 1 is as follows: a = 14.3196(7) Å, b = 16.2550(8) Å, c = 8.8552(4) Å, β = 90.134(1)°, V = 2061.18(4) Å^3, Z = 4, R = 0.0407 for 3703 observed reflections with I>3σ(I). Compound 1 adopts a 3D open framework structure which contains three types of tetrahedra: GaO_4, ZnO_4, and PO_4. These tetrahedra are interconnected via a corner-sharing manner to give a zeolitic framework in which large channels are formed. The protonated 1,2-diaminocyclohexane cations are residing in the tunnels. The hydrothermal synthesis, crystal structure, and thermal properties of the title compound will present in detail.

25. CRYSTALLOGRAPHIC TEACHING

P12.25.001 TRAINING IN RESEARCH INSTITUTIONS AS AN EFFECTIVE TOOL OF TEACHING CRYSTAL GROWTH FOR CRYSTALLOGRAPHERS. N.I.Leonyuk, Dept. of Crystallography and Crystallochemistry, Geological Faculty, Moscow State University, Moscow 119899, Russia; V.I.Lyutin, E.V.Polianski, P.P.Chvanski, A.A.Mar'in, S.A.Smirnova, S.Yu.Stepanov and N.G.Sanzharlinski, VNIISIMS, Aleksandrov 601600, Vladimir Distr., Russia

Crystal growth is being taught in many universities, and the course scope specifically depends on the profile of interests of the department and/or college. Our crystal growth course has evolved as a self-consistent curriculum for students-crystallographers of Moscow State University (MSU) in collaboration with other universities, academic institutions and industry. There are three stages of this long-term crystal growth teaching: (1) general course of lectures and seminars for all students; (2) training and laboratory courses for all students; (3) research work for students-crystal grower. This paper concerns of the research training of the MSU students in laboratories of the All-Russian Research Institute for the Synthesis of Minerals (VNIISIMS) for nearly three decades. This four-week training is offered for students after the 3rd academic year and covered topics: (a) Hydrothermal growth of piezo-quartz; (b) Hydrothermal growth of optical calcite; (c) Hydrothermal growth of zincite; (d) Czochralski growth of bismuth orthogermanate crystals; (e) Growth of rare earth aluminate crystals by zone melting; (f) Synthesis of diamond. At the end of this training, all the students should complete and defend publicly their research projects. The research training provides a helpful practical experience, many important details for the course and can help with making some models of crystal growth more concrete. It also allows students to take knowledge and practical experience concerned with obtaining crystalline materials required for their own experimental programs. Strong interaction and integration between the University Education Program, Research Institutions, and Industry seems to be one of the keys to developing effective researchers and engineers for the future.

P12.25.002 SOFTWARE FOR CALCULATING DIRICHLET DOMAINS. N.E.Kashcheeva and D.Y. Naumov, Novosibirsk State University and Institute of Solid State Chemistry and Mechanochemistry SB RAS, Kutateladze, 18, Novosibirsk, 128, 630128 Russia.

A computing program NADI for calculating and visualizing the Dirichlet domains in crystal structures is described [1,2]. NADI allows one to calculate DD choosing optionally the types of atoms to be considered, the atomic / ionic radii, and the method of dividing the distances between the atoms by planes. This flexibility makes it possible to choose between the application of various published methods and, if necessary, to compare the results they give for the same system. The program can operate both with points (of one or several types) and with spheres (of the same or of different radii). It is possible to operate also with centroids of molecules or molecular fragments, or with any other selected points.

NADI calculates the volumes of DD, the number and the areas of faces, the solid angles corresponding to the faces, the distances from the central atom to the atoms that give rise to the faces, the distance to the nearest face and to the furthest vertex of DD. Symmetry codes and the coordinates of points in the structure corresponding to the faces of DD are also given. The calculated data are prepared as an output file, and can be also (optionally) viewed on the screen in various projections and rotated quickly or slowly. The DD can be shown with respect to crystallographic axes of the structure and also with respect to the atoms of the crystal structure (either all or selected). NADI can generate plots in HPGL format.

1. D.Y.Naumov, E.V. Boldyreva (1999). Russ. J. Struct. Chem. (Zh. Strukt. Khim. Russ. Ed.), **40,** 102-10.
2. N. E. Kashcheeva, D. Yu. Naumov, E. V. Boldyreva, accepted to Z.Krist.

P12.25.003 TITAN: A PROGRAM TO AID STRUCTURE SOLUTION AND REFINEMENT WITH THE SHELX SUITE OF PROGRAMS. Jim Simpson and Keith A. Hunter, Department of Chemistry, University of Otago, P.O. Box 56, Dunedin, NEW ZEALAND.

TITAN is a Windows based molecular graphics program designed to be used exclusively in conjunction with the SHELX-97[1] suite of programs. The program facilitates the on-screen assignment of peaks from the direct methods E-map or Patterson map, generated by SHELXS-97, to individual atom designations. Once these designations are completed, a file is written that can be input directly to the SHELXL-97 refinement program without modification. *TITAN* can also be used in the location of additional atoms in series of least-squares and difference Fourier cycles and as an aid to the inclusion of hydrogen atoms into the refinement using the HFIX and/or AFIX commands.

TITAN is a 32-bit program and runs in the Windows-95/98 or Windows NT environment It also serves as a shell from which to launch the SHELXL refinement program so that the complete refinement of a structure can be completed within the program. Hard-copy plots can be obtained using any Windows compatible printer. A demonstration of the operation of the *TITAN* program will be given as part of this poster presentation.

1. Sheldrick, G.M. (1997) SHELXS-97 'Programs for the solution and refinement of crystal structures from diffraction data.' University of Gottingen, Federal Republic of Germany

27. OTHER TOPICS

P07.27.001 NEW DEVELOPMENTS IN HARD X-RAY HOLOGRAPHY. G. Faigel, M. Tegze, Research Institute for Solid State Physics and Optics, H-1525 Budapest, POB 49, Hungary, S. Marchesini, M. Belakhovsky, Service de Physique des Matériaux et Microstructures, Département de Recherche Fondamentale sur la Matière Condensée, CEA Grenoble, 17 rue des Martyrs, F-38054 Grenoble, France

In the last few years a new technique, the hard x-ray holography is emerging for the study of 3D atomic arrangements in solids [1,2]. Two types of this method have been developed: one in which the atoms of the sample serve as inside sources of x-radiation, this is called "normal holography", and the other "" in which the atoms are used as detectors of the interference field originating from the incident and scattered waves this is called " inverse holography". Though the first steps in this field looked very promising, only very few experiments have been done so far. The cause of this is manifold : there are experimental and evaluation related problems. In the experimental side one of the most important point to solve is the acquisition of reliable and evaluable data at synchrotron sources. In the evaluation side a reconstruction algorithm has to be developed which gives isotropic real space resolution and suppresses the twin images and spurious oscillations. In this poster we discuss these problems and show the solutions for many of them. The results are demonstrated by experimental examples.

1. M. Tegze, G. Faigel, Nature 380, 49, (1996)
2. T. Gog et al. Phys. Rev. Lett. 76, 3132, (1996)

P05.00.000 DON'T TRY THIS AT HOME: HANDLING ABSTRACT SUBMISSION FOR IUCR 1999. C.C. Wilson, K. Shankland and T. Csoka, Rutherford Appleton Laboratory, Chilton, Didcot, Oxon. OX11 0QX, U.K.

The abstract submission procedure for IUCr 1999 was intended to be 100% electronic. This has been realised, indicating that we have truly entered a paperless age for crystallography conference abstract submission.

A key step in the process has been the use of a database system (based upon mySQL) which stores all information as it is received and allocates abstract numbers automatically. This, coupled with a WWW interface to the database has allowed abstracts to be received efficiently and corrections made with relatively little effort on the part of the Abstracts Team. On the other hand, e-mailed submissions have required a significantly higher level of manual intervention, as one has no control over the format of the incoming messages.

The hardware and software implementation of the abstracts server will be presented, together with the pros and cons of attempting to do everything not only electronically, but automatically.

OPEN COMMISSION MEETINGS

TB INTERNATIONAL TABLES

C06.TB.001 STATUS OF VOLUME A: SPACE-GROUP SYMMETRY. Theo Hahn, Institut für Kristallographie, RWTH Aachen, D-52056 Aachen, Germany.

The Fourth, revised edition of Volume A of *International Tables of Crystallography* appeared in 1995. Due to great demand two corrected reprints became necessary; they were published in 1996 and 1998. Presently, the Fifth, revised edition is in preparation; the scheduled publication date is spring 2000.

The Fifth edition will contain corrections of all errors and flaws known so far. The new glide-plane symbol '*e*', introduced in the Fourth edition, will be systematically incorporated in all tables, diagrams and text sections. A new Section 9.4, *Some further properties of lattices*, will be contributed by B. Gruber, Prague.

From the Fifth edition onwards, Vol. A, large parts of which were originally type-set 'by hand', will be printed from a computer-based file as follows:

the space-group tables (Sections 6 and 7) will be transferred to Latex files by Mois Aroyo and his colleagues in Sofia, Bulgaria. These files will be the basis for the printing;

the text sections will be re-keyed in Chester and printed from SGML files.

The space-group program was completed at the end of 1998; the re-keying and proofreading of the text will be done in the summer and fall of 1999. For the future, an electronic version of Vol. A is contemplated.

The Fourth, revised and enlarged edition of the *Brief Teaching Edition of Volume A* was published in 1996.

C06.TB.002 STATUS OF VOLUME B: RECIPROCAL SPACE. Uri Shmueli School of Chemistry, Tel Aviv University, 69 978 Tel Aviv, Israel.

The first edition of Volume B was published in 1993, its first corrected reprint appeared in 1996 and the work on the second edition was in an advanced stage during the 1996 IUCr Congress in Seattle.The editorial work on the second edition, now completed, consisted of (i) major revisions and/or corrections of several chapters and sections of Volume B, and (ii) incorpora- tion of the following new contributions in the second edition of the Volume:

B.1.5. Crystallographic viewpoints in the classification of space-group representations (by M.I. Aroyo and H. Wondratschek)

B.2.5.6. Direct methods in electron crystallography (by D.L. Dorset)

B.4.5. Polymer crystallography (by D.L. Dorset and R.P. Millane)

B.4.6. Reciprocal-space images of aperiodic crystals (by W. Steurer and T. Haibach)

B.5.3. Dynamical theory of neutron diffraction (by M. Schlenker and J.-P. Guigay)

An annotated Table of Contents of the second edition of Volume B will be presented and discussed in the Open Meeting. This edition of Volume B is expected to be published in the spring of 2000.

The somewhat late expected date of publication is due to the translation of Volume B to SGML (Standardized Generalized Markup Language) and the production of an electronic version of the Volume. However, this will result in great time savings in the production of future editions.

C06.TB.003 STATUS OF VOLUME C: MATHEMATICAL, PHYSICAL, AND CHEMICAL TABLES. E. Prince, NIST Center for Neutron Research, National Institute of Standards and Technology, 100 Bureau Drive, Stop 8562, Gaithersburg, Maryland 20899-8562, USA.

A revised and expanded edition of Volume C was published in the spring of 1999. Its ten parts contain 228 sections in 56 chapters, all of them written by acknowledged experts in their specialties. Two chapters, one on neutron topography and one on neutron reflectometry, are completely new. The first edition, because of a need to publish without further delay when chapters on some desired topics were still outstanding, contained several chapters that were carried over with minor editorial changes from the earlier series of *International Tables*. Of these only one remains, and that one, a chapter on the determination of refractive indices, was judged to be still sufficiently authoritative that no revision was necessary.

When work began on the first edition in 1983 and 1984, computer-based word processing systems were just beginning to appear, and authors were invited to submit machine-readable files in addition to their manuscripts. Many of them did, in a wide variety of formats, but efforts to utilize these files in the production process were almost totally unsuccessful. At the time of A. J. C. Wilson's death in 1995 the process of collecting material for the second edition was well along, but production had not yet begun. Most new text was then available on diskette, and this was successfully imported into the software used by commercial typesetters, but chapters that had received only minor revision had to be typeset again by hand. The entire text of Volume C now exists on machine-readable files, and future revisions will be much easier and cheaper.

The timely publication of this volume was made possible by the cooperation of many authors and the expert and diligent efforts of the staff in Chester. The entire crystallographic community is in their debt.

C06.TB.004 VOLUME D, PHYSICAL PROPERTIES OF CRYSTALS. Andre Authier, LMCP, Universite P.et M. Curie, Case115, 4, Place Jussieu, 75252 Paris CEDEX 05, France.

Volume D will consist of three parts: (i) Tensorial Aspects of Physical Properties, (ii) Symmetry Aspects of Excitations, (iii) Symmetry Aspects of Structural Phase Transitions, Twinning and Domain Structures. It will be accompanied by a Compact Disk with two softwares**:**

The first one, dealing with tensors and irreducible representations, calculates representations of finite 3-dimensional point groups and the components of invariant tensors in arbitrary dimension, of arbitrary rank and with arbitrary permutation symmetry of the indices under the action of a 3-dimensional crystallographic point group.

The second one, dealing with phase transitions will give tables for equitranslational phase transitions, and for tensor properties at any group-subgroup phase transition: spontaneous tensor components, up the rank 4, that appear in the distorted phase and non-zero tensor components that are the same in both phases.

It is expected that all manuscripts will have been received by the time of the XVIIIth IUCr Congress and that the volume can be printed in the 2000.

C06.TB.005 STATUS OF VOLUME E: SUBPERIODIC GROUPS - A PROGRESS REPORT. V. Kopsky and D.B. Litvin.

Abstract not available.

C06.TB.006 STATUS OF VOLUME F: MACROMOLECULAR CRYSTALLOGRAPHY - A PROGRESS REPORT. M.G. Rossman and E.A. Arnold

Abstract not available.

C06.TB.007 STATUS OF VOLUME G: CRYSTALLOGRAPHIC INFORMATION. S. R. Hall, Crystallography Centre, University of Western Australia, Nedlands 6907, Australia, and B. McMahon, International Union of Crystallography, 5 Abbey Square, Chester CH1 2HU, England.

Volume G will contain a complete specification of the crystallographic information exchange mechanism sponsored and supported by the IUCr. It is intended as a working handbook for structural crystallographers needing to exchange or archive crystallographic data and will provide up-to-date information on data definitions and CIF compliant applications. An accompanying CD-ROM will contain the dictionaries in machine-readable form and a collection of libraries and utility programs.

The volume will include the latest versions of all CIF dictionaries approved by the IUCr Committee for the Maintenance of the CIF Standard (COMCIFS), and in particular version 2.1 of the CIF Core Dictionary (originally published in *Acta Cryst.* (1991), A**47**, 655-685), together with new dictionaries for use in powder and macromolecular structure determination work.

Full documentation on the file structure of CIF and STAR Files will be provided, as well as detailed commentary on the way that the CIF data definitions are specified, and on the use of the file in data archival and publishing. Documentation of software libraries will be included for the use of software developers.

C06.TB.008 PROPOSAL, INTERN. TABLES VOL. A2: RELATIONS BETWEEN WYCKOFF POSITIONS IN GROUP-SUBGROUP RELATIONS Ulrich Müller, Fachbereich Biologie/Chemie, Universität Gh Kassel, D-34109 Kassel, Germany

The importance of crystallographic group-subgroup relations in crystal chemistry, crystal physics, and mathematical crystallography has become widely accepted. Important applications such as the derivation of structural relationships between crystal structures or the consideration of structural changes taking place during phase transitions require the knowledge of the relations among the atomic positions (Wyckoff positions) in a space group and in its subgroups. These relations have been compiled completely and will be a valuable tool for the practical work of crystal chemists and physicists.

The new tables, suggested to become volume A2 of the *International Tables for Crystallography*, contain:

1. An introductory text pointing out some applications, treating topics referred to the relations, citing the group-theoretical background, and giving instructions.

2. For every space group, a complete listing of its maximal subgroups, including the infinity of all isomorphic subgroups.

3. If needed, formulae for the transformations of the base vectors, site coordinates, and origin shifts.

4. For all Wyckoff positions of the space group, the relations to the Wyckoff positions of all of its maximal subgroups.

There is a complete one-to-one correspondence with the listings of the forthcoming volume A1, albeit with very different contents. Sample pages have been presented on two conferences [1].

1. U. Müller, Z. Kristallogr. suppl. **5** (1992) 172 and suppl. **8** (1994) 203.

ID INNOVATIVE USES OF THE INORGANIC CRYSTAL STRUCTURE DATABASES

C07.ID.001 ICSD: NEW DEVELOPMENTS. H. Behrens FIZ Karlsruhe, 76012 Karlsruhe, Germany.

In the paper the new developments for the Inorganic Crystal Structure Database (ICSD) will be described. These are i) creation of a new PC software for retrieval and visualisation, ii) the establishment of a new software system for the production of the database, iii) offer of the database via WWW, and iv) systematic corrections of a number of data. These points will be illustrated and discussed in detail.

C07.ID.002 MATERIALS DATABASES FOR THE NEXT DECADE: THE PAULING'S FILE (LPF). M.Berndt and K.Brandenburg, CRYSTAL IMPACT GbR, Postfach 1251, D-53002 Bonn, Germany, K.Cenzual, Departement de Chimie Minerale, Analytique et Appliquee, University of Geneva, Switzerland, and S.Iwata, University of Tokyo, Japan, and T.Atago, JST, Tokyo, Japan, and P.Villars, MPDS, Vitznau, Switzerland.

A new materials phases database system called "Pauling's File" is introduced to demonstrate concepts and techniques for building up a new structural database. This contribution should be taken as a case study to learn how to meet the needs for the next decade.

Pauling's File is based on a relational database system consisting of: a) Structural data such as cell, space group, atomic coordinates, etc., b) measured and calculated powder diffraction patterns, c) phase diagrams (stored as vector plots), and d) over 50 different physical properties.

The value of a scientific database depends on how much it meets the criteria of completeness and accuracy. Like other databases LPF reflects the published literature. Until today about 130,000 publications have been scanned. Accuracy is ensured by using modern scanning and OCR techniques completed by a multiple-step validation process to uncover "wrong" structures.

A comprehensive database like LPF needs flexible software tools to extract the informations. Beside a foolproof visual retrieval system and a flexible statistics program Pauling's File also includes:

a powerful 2D and 3D visualization system for crystal structures and diffraction diagrams, based on the well known DIAMOND technology. This tool can also identify structures from measured powder patterns using modelling techniques, Rietveld refinement, and search match techniques.

an innovative, semi-empiric tool to correlate atomic property expressions of its constituent chemical elements and its compound/system properties. This software was designed to discover systematically hidden patterns and should help to predict (and design) compound properties.

Further software developments are intended and proposals for collaborations are always welcome. Some examples and illustrations will be shown for the techniques and components mentioned above.

C07.ID.003 ICSD-FOR-WWW, A DEMONSTRATION OF THE LATEST FEATURES, INCLUDING BOND VALENCE. Alan Hewat, Institut Laue-Langevin, BP 156X, Grenoble 38042, FRANCE.

A demonstration of ICSD-for-WWW will show how easy it is to access the almost 50,000 structures in the Inorganic Crystal Structure Database via the WWW, or at least a local server (eg see http://barns.ill.fr/dif/icsd/). The latest features include automatic calculation of bond-valence sums as a check on the structure during preparations for visualisation using VRML.

The WWW interface looks the same on any computer, Windows-PC, Macintosh or Unix workstation. A selection of structures is obtained by entering the usual search criteria, then the search can be narrowed with additional criteria. The resulting entries can be printed out in standard reference format for cut-and-paste into manuscripts, or in EndNote bibliographic format. They can be ordered according to date, formula, author, space group or mineral name for further processing.

Individual entries can be compared, listed in full, and used to generate X-ray or neutron powder diffraction patterns, with peaks automatically indexed. Finally the 3D structure can be drawn, zoomed and rotated, with the usual space-filling, ball-and-stick or co-ordination polyhedrae models available.

The latest features include automatic calculation of Brown-Shannon valence sums to check the chemical validity of the structure, the illustration of sites of different valence state with different colours, the drawing of mixed-atom polyhedrae such as in oxy-chlorides etc.

ICSD-for-WWW servers have already been set up in France, Germany, the UK, USA and Japan, the software is distributed free of charge for a limited demonstration data-set, and also with the licence for the full ICSD data-set from FIZ Karlsruhe.

C07.ID.004 THE ICSD AS A SOURCE OF NOVEL MATERIALS. S. C. Abrahams, Physics Department, Southern Oregon University, Ashland, OR 97520, USA.

Determination of relationships between given crystal structures and their intrinsic properties, if applicable also to a wide range of structures, offers the possibility of major advances. The principal crystallographic databases provide well-organised access to published structural studies and hence allow opportunities for predicting desirable properties in series of materials that previously may have been studied for totally unconnected reasons. Systematic analysis of atomic co-ordinates in the ICSD has identified numerous materials with novel properties by virtue of relationships that depend upon the magnitudes of atomic displacement between the listed polar structure, at a given temperature and pressure, and derivative structures either in a supergroup of that listed or with a discontinuity in characteristic tensor property. Magnitudes that satisfy related structural criteria are predicted to be ferroelectric, the property that follows from this relationship. A resulting series of newly-predicted ferroelectrics has now been experimentally verified, including $Ba_6CoNb_9O_{30}$, Sr_2SbMnO_6, fresnoite, $K_2(NbO)_2Si_4O_{12}$, $YInO_3$ and $CN_4H_8ZrF_6$ among others. Analysis of all entries in five higher-symmetry polar point groups listed in ICSD has resulted in over 200 such predictions. Since many are to families with multiple members, this analysis is enough to double the present number of known single-phase ferroelectrics if all predictions prove to be verifiable. In a field of technological importance, these results demonstrate the database to be a highly effective source of materials with novel properties. Several improvements in the CD-ROM DOS version that would substantially enhance its efficacy may, however, be identified. These include upgrading it to a Windows environment and providing greater search flexibility, as available already in the WWW version. Others to be discussed include updating the nomenclature, listing all references within ICSD to a given material in each entry, improving the present structure visualisation program and providing direct access to such other visualisation programs as xtal-3d and DRAWxtl in the Virtual Reality Modelling Language format.

C07.ID.005 FROM ICSD TO SICS: A TOOL FOR ANALYZING STRUCTURAL RELATIONSHIPS. G. Bergerhoff, M.Berndt and K.Brandenburg, Institute for Inorganic Chemistry, University of Bonn, Germany.

Structural relationships between inorganic structures can be detected automatically by a fingertip in a database if

a) data are presented in an appropriate manner,

b) the interesting relationships are well defined so that they can be transformed to a program.

To fulfill the first condition data stored in ICSD from the literature have been standardized following Gelato and Parthé (J.Appl.Cryst. 20 (1987) 139-143), reduced to the ´best´ representative of each phase, and provided with the difference **Δ** between each pair of structures within an isopointal set. The details of the so-formed new database SICS (**S**tandardized **I**norganic **C**rystal **S**tructures) are described in Bergerhoff et al., Acta Cryst. B55 (1999) Issue 4.

Relationships between inorganic structures can be described in different terms: Isopointal structures, Isotypism, Antitypes, Interstitial types, Group-subgroup relations, etc. Because of the large amount of structures the full information on relationships hided in SICS can only be found by means of the new database SICS itself. It is available from the authors for subscribers of the ICSD. Here we want to demonstrate the effectivity with new examples showing the relationships between structures with octahedral coordination of one cation and of the general formula types **ABX6** (A2X6), **AB2X6** (ABCX6, A3X6=AX2), **AB3X6** (ABCDX6, ABC2X6, A4X6=A2X3), **AB4X6** (ABCS2X6, ABC3X6, AB2C2X6, A5X6), **AB5X6** (AB2C3X6, ABC4X6, ABC2D2X6, A6X6=AX), **AB6X6** (AB2C4X6), **AB7X6** (ABC6X6, AB3C4X6), **AB8X6** (AB2C6X6), **AB9X6** (AB3C6X6).

C07.ID.006 BLASTING THE *CRYSTMET* MINE: POWDER DATA, 3-D PLOTS, BEYOND THE TYPE, PROPERTIES, VIRTUAL MATERIALS. John R. Rodgers, Toth Information Systems, Inc., 2045, Quincy Avenue, Glouceter, ON, Canada, Yvon Le Page, National Research Council Canada, Ottawa, ON, Canada, Peter S. White, University of North Carolina at Chapel Hill, NC, USA, John Harris, Institut fuer Festkoerperforschung, Forschungszentrum Juelich, GmbH, D-52425 Juelich, Germany and Paul Saxe, SciCo Inc., 5031 Palermo Drive, Oceanside, CA, USA

Rapid progress in computational methods and power, combined with developments in visualization, data mining strategies and experimentation techniques (combinatorial chemistry), is creating new design opportunities in materials science. This presentation will highlight a number of developments used for mining *CRYSTMET*, currently a database of intermetallic crystal structures with corresponding calculated powder data, and integrated structure plotting software for 3-D viewing of intermetallic and inorganic structures.

Emphasis for expansion of *CRYSTMET* will be on tools for calculating structure and physical properties to complement published data. Results of first-principles density functional methods, producing accurate structural and powder information from rough structure-type data will be presented. Such quantum modelling can also be used for the calculation of electrical, optical, thermal and mechanical properties of materials in structure databases. The use of these computational methods is greatly improving the data integrity, value and usefulness of *CRYSTMET* and it is providing information which would be costly

and/or difficult to measure, especially for virtual compounds modelled after existing ones.
New concepts for the direct manipulation of *CRYSTMET*, using dynamic queries, which allow users to formulate queries with graphical widgets, such as rangesliders, toggles and alphasliders, and visualize the results as 2-D or 3-D plots will be illustrated. Such visual representation of the results of database queries is a powerful means to access information on trends, clusters, gaps and outliers, and give the user tools for data exploration.

C07.ID.007 DATA MINING USING THE ICDD POWDER DIFFRACTION FILE, RELEASE 1999: THE BENEFITS OF EXPLOITING POWDER DATA FROM THE PDF AND ICSD. J. Faber, R. Jenkins and R.L. Snyder

Abstract not available.

JR IUCr JOURNALS

C08.JR.001 OVERVIEW OF IUCR'S JOURNALS. John R Helliwell [1], Peter Strickland [2], [1] Editor-in-Chief of Acta Crystallographica and Chairman of the IUCr's Commission on Journals, Department of Chemistry, University of Manchester, M13 9PL, UK, [2] Managing Editor, IUCr, 5 Abbey Square, Chester, CH1 2HU, UK.

In the last triennium we highlight a number of developments for the IUCr Journals. Details of each Journal however can be found in the accompanying abstracts for this Journals' Open Commission session. Authors' choice within the IUCr Journals is broad, encompassing all aspects of crystallography and its cognate subjects across the sciences. The further expansion into the synchrotron field has been greatly facilitated by the Journal of Synchrotron Radiation, and which has now published the major proceedings from SRI'97 held in Japan and also the XAFS X Conference held in Chicago in 1998. The biological community expands apace and Acta Cryst D is now published monthly. Publication of the very popular 'Daresbury CCP4 Conference Proceedings' series commenced as a supplement to Acta Cryst D in 1998. Chemical crystallography capability has also greatly expanded and to handle this all crystal structure data for publication in Acta Cryst C, and Acta Cryst B, are now all submitted electronically via cif. The IUCr www coverage of the Journals, including the services to authors and Coeditors for manuscript tracking, is now extensive. A 50 year searchable index is now available, and which is a powerful tool for accessing the vast archive of IUCr publications. In the last triennium the 50th Anniversary of Acta Cryst and the IUCr occurred, as did the 30th Anniversary of J Appl Cryst. A special 50th Anniversary Issue of Acta Cryst was published in section A in November 1998, comprising especially commissioned articles. This special issue was distributed to all subscribers of IUCr Journals free of charge and is available for purchase at a very competitive price in book form. The upcoming triennium includes an expansion of electronic access for subscribers to the IUCr's Journals and a greater emphasis on the marketing of the Journal titles to the crystallographic community, as well as to structural science communities in biology, chemistry, materials science and physics. Highlighting via mini-reviews of IUCr Journal articles within the IUCr Newsletter, whose collaboration we gratefully acknowledge, also opens a channel to 15,000 readers and is clearly an exciting promotional strategy.

C08.JR.002 CRYSTALLOGRAPHIC PUBLISHING IN THE ELECTRONIC ERA. B. McMahon and P.R. Strickland, IUCr, 5 Abbey Square, Chester CH1 2HU, England, H. D. Flack, Lab. de Cristallographie, 24 quai Ernest-Ansermet, CH-1211 Genève 4, Switzerland, Y. Epelboin, Lab. de Mineralogie-Cristallographie, Tour 16, Univ. P. et M. Curie, 4 place Jussieu, 75252 Paris Cedex 05, France, and L. M. D. Cranswick, CCP14, Daresbury Laboratory, Warrington, WA4 4AD, England. (IUCr Committee on Electronic Publishing, Dissemination and Storage of Information.)

For the last half century, the IUCr has published the results of crystallographic research in its flagship journal *Acta Crystallographica*. As the new century beckons, the Union is involved in publishing a wide and growing range of journals, reference books, directories and educational materials. Increasingly, the medium of publication is electronic, on both magnetic or magneto-optic media, and the global Internet. In the last triennium the Union's Electronic Publishing Committee has been reconstituted as a technical working group with a remit to advise on and coordinate the Union's publication programme.

The Committee works closely with the Commission on Journals in the electronification of the journals described elsewhere in this session. It acts as the General Editorial Board for the web services maintained through the Chester server and at a number of mirror sites. Chester is a hub for the web-based information network, collecting material from the Crystallography World Wide and SinCris sites and from various Commissions, and supplying regular updates to the mirrors. The result is a rich information resource, conveying both topical information on subjects such as meetings, jobs and software releases, and more durable information such as journals contents, supplementary data and the records of the Union's activities. Other projects include: revision of the *World Database of Crystallographers* to expand its content and improve access; provision and management of discussion lists on specialised topics for the Union's Commissions and Committees; and investigations into suitable CD-ROM publications, including collaboration on the abstracts CD-ROM for this Congress.

C08.JR.003 ELECTRONIFICATION OF THE IUCr EDITORIAL OFFICE. P.R. Strickland and B. McMahon, International Union of Crystallography, 5 Abbey Square, Chester CH1 2HU, England.

The key concern of the IUCr Editorial Office, which is based in Chester, UK, is the rapid, accurate and high-quality publication of the Union's journals, *Acta Crystallographica*, *Journal of Applied Crystallography* and *Journal of Synchrotron Radiation*. "Electronification" of the Editorial Office has been under way for several years and has a number of aims; these include increasing the speed of publication, improving the efficiency of review, technical editing and printing processes, and the provision of electronic versions of the journals.

The main steps in the electronification process have been the introduction of the use of CIF for the production of *Acta Crystallographica Section C* in 1991 and the adoption, in 1997, of new production methods based on SGML (standard generalized mark-up language), the publishing industry standard for electronic publishing.

Most stages of the publication process have already, or will shortly, become electronified. Submission of electronic manuscripts will be joined by electronic review procedures and electronic proofs. Transmission of papers to our printers is already an electronic process, and electronic versions of the journals will become available shortly. Other publications produced by the Editorial Office, *e.g. International Tables for Crystallography*, will also be electronified.

These developments will be described and the experience gained from them will be discussed.

C08.JR.004 ACTA CRYSTALLOGRAPHICA, SECTION A, FOUNDATIONS OF CRYSTALLOGRAPHY. Andre Authier, LMCP, Universite P.et M. Curie, Case115, 4, Place Jussieu, 75252 Paris CEDEX 05, France.

In the triennium 1996-1998, Section A has published 18 bimonthly issues and a special issue dedicated to the 50th Anniversary of Acta Crystallographica and of the IUCr. The total number of pages was 2922, corresponding to 227 Research Papers, 3 Lead Articles, 2 Topical Reviews, 26 papers in the special issue, and 32 Short Communications. The number of pages and of papers published in 1997 was low, but picked up again in 1998. Many efforts have been devoted successfully at every stage to reduce the processing and printing time and these efforts will continue as this is a crucial issue.

The Guest Editor for the Special Issue was Professor Henk Schenk. The Special Issue starts with a paper about the history of the IUCr and spans all aspects of crystallography, symmetrical, structural, physical, chemical and biological, with papers devoted to the most important landmarks in the development of crystallography over the past 50 years. It was also reprinted as a book, under the title, "Crystallography across the sciences". This special issue is undoubtedly a success and more are planned. More Lead Articles and Topical Reviews are also in the pipeline.

The format of Section A seems well adapted to its purpose and no suggestions to modify it have been received in the past, but any suggestion for modification and improvement will be welcome.

C08.JR.005 ACTA CRYSTALLOGRAPHICA, SECTION B Frank H.Allen, CCDC, 12 Union Road, Cambridge CB2 1EZ, England.

Section B of Acta began publication with the section title "Structural Science" in 1983. From the outset its remit was to publish original research papers and short communications in which 'structure' was the central theme of each article. During the '90s, this remit has extended to the publication of limited review material as Lead Articles or Topical Reviews. Originally, Section B was concerned with the chemical, physical and biological implications of novel structure determinations, or of systematic analyses of existing structural information retrieved from databases. The loss of the biological component to the newly created Section D of Acta in 1993 led to some initial reduction in Section B submissions.

Section B now publishes papers in structural chemistry and physics across a broad spectrum from inorganics and minerals, through metal-organics to purely organic compounds. Within that spectrum, experiments at non-standard temperatures and pressures, and studies of the physical properties of novel materials, phase transitions, charge densities, intermolecular interactions, supramolecular structural organisation, database applications, and structure determination from powder data, reflect current leading-edge developments in the subject area.

In the triennium 1996-1998, Section B has published 18 bimonthly issues (3066 pages) containing 335 full papers, 16 short communications and 3 topical reviews (with more in the pipeline). On the basis of citation statistics, Section B has an impact factor of 1.612 and is ranked 4th of 17 crystallographic journals, the top three also being IUCr publications. Machine-readable submissions to Section B have become a reality during the triennium.

Comments on the future development of Section B will be welcomed. Issues for discussion might include (a) complementarity between Section B and Section C, (b) the diversity of content of Section B and its competitiveness with non-IUCr journals, particularly in the the chemical arena, and (c) the commissioning and inclusion of more high-quality review material.

C08.JR.006 RECENT SECTION C INITIATIVES: AUTOMATIC DATA VALIDATION AND ELECTRONIC PUBLICATION. S.R.Hall Crystallography Centre, University of Western Australia, Nedlands 6907, Australia

The Acta Crystallographic Section C board has instituted a number of initiatives in the past triennium intended to make publishing structural studies more efficient both in terms of author submissions and journal production. These include: the introduction of a CIF-access submission mode as a fast minimum-text option to publishing new structure determinations (introduced in 1997); the explicit specification of data standards for published structural material (with the 1997 Notes for Authors); a briefer full paper publication format (e.g. the removal of coordinate tables); improved access to the Acta published material with increased web services and add-on CIF facilities (in 1997- 8); and, recently, automatic validation and checking of manuscripts, which includes the facility for author submitted validation responses.

The effectiveness of these changes will be discussed in terms of their short and long term objectives. In particular, the reasons for shifting the responsibility for CIF validation from the Acta office to the author will be explained, as well as the overall implications for papers reporting challenging (i.e. difficult!) structural studies. Future expected editorial and publication initiatives will be summarised.

C08.JR.007 ACTA CRYSTALLOGRAPHICA D: CURRENT STATUS AND FUTURE PLANS Jenny P. Glusker The Institute for Cancer Research, The Fox Chase Cancer Center, 7701 Burholme Avenue, Philadelphia, PA 19111 USA

Acta Crystallographica D, devoted to biological crystallography, is now appearing monthly. Its sections include articles on methods of structure determination, crystal characterization and descriptions of structures. We thank the contributors, the co-editors and reviewers who have made this new journal, as of January 1993, a viable publication, and John Helliwell, the Editor-in-Chief, for his continued support and advice. The coeditors and reviewers have worked hard to maintain high standards for this IUCr journal and contributors have been good-humored in responding to requests for revisions. The staff at Chester, particularly Louise Clark-Jones, have then ensured that there is care in the processing of manuscripts and the appearance of the final publication. The handling of manuscripts has been accelerated by the addition of Simon Glynn to the Acta D staff at Chester, so that the time between acceptance and publication is now greatly reduced. Figures in color are provided free of charge, but only when the color adds to the scientific content of the article. In addition, all authors are asked to sign a form attesting to the fact that they have seen the final manuscript; this is done to obviate some problems we have had in the past. Authors of structural papers are required to deposit atomic coordinates and structure factors in the Protein Data Bank. Delay in the release of these data to the scientific community is currently possible, but this is under review by the IUCr Executive Committee. We hope to receive mmCIF files, which contain information on the diffraction experiments and the structure determination, from authors.

Future plans include the solicitation of more reviews and general introductory articles. If you wish to contribute such an article please contact a member of the editorial staff. We have considered whether or not to publish crystallization reports; some scientists applaud their inclusion and others feel that the data should appear in more biological journals or merely in the final structural publication. Our current conclusion has been that they provide important information for the crystallographic community. Your remarks and criticisms are welcome and play an important role in improving this journal.

C08.JR.008 JOURNAL OF APPLIED CRYSTALLOGRAPHY. A.M. Glazer, Clarendon Laboratory, Parks Rd., Oxford, OX1 3PU, United Kingdom.

The Journal of Applied Crystallography is now over 30 years old. The developments in the journal over this time will be briefly reviewed, and a description given of the sections at present offered, including Research Papers, Fast Communications, Cryocrystallography Notes, Laboratory Notes, Computer Programs and Abstracts, Short Communications, Lead Articles, Software Reviews and New Products. In addition from time to time J. Appl. Cryst. publishes Special Issues, and this is an area that I hope will grow. Some statistics relating to production matters will also be presented, which will illustrate the general health of the journal. As retiring Editor of J.Appl. Cryst., I shall point to some of the highlights published, including the seminal work of Rietveld, which has made an enormous impact on the field of powder diffraction, and suggest some ideas for the future development of the journal. Comments and suggestions from the audience will be particularly welcome, especially since a new Editor will be taking over during the IUCr Congress.

C08.JR.009 JOURNAL OF SYNCHROTRON RADIATION : CURRENT STATUS. S Samar Hasnain[1], John R Helliwell[2] and Hiromichi Kamitsubo[3] [1]Synchrotron Radiation Department, CCLRC Daresbury Laboratory, Warrington WA4 4AD, UK, [2]Department of Chemistry, Manchester University, Manchester M13 9PL, UK, [3]SPring-8, JAERI-RIKEN, Kamigori-cho, Hyogo-ken 678-12, Japan

It is now four years since the Journal of Synchrotron Radiation was launched. In this time we have published approximately 500 research articles in over 2500 pages providing a focus for the whole of the synchrotron radiation community.The number of papers published in JSR over the last few years have steadily beeen increasing. For the journal, the main achievement of 1998 was the successful publication of the SRI'97 Proceedings. The papers for this issue were refereed to the usual JSR standards, rather than at the meeting, and we believe that this effort is reflected in the improved quality of the Proceedings which formed the May 1998 issue. Many of the lessons learnt with SRI'97 have been applied to the Proceedings of the XAFS X Meeting, held in Chicago in August 1998, which is to be published in May 1999. This is again fully refereed but is produced as camera ready. We have recently entered into the citation ranking tables and are already ranked third out of thirty seven Journals covering instruments and instrumentation with Rev Scintific Instruments placed FIFTH, NIMS B placed sixth and NIMS A placed 8TH. The review and production times for the journal continue to be rapid. Centralised submission, introduced in 1997, is being used to further improve review times and our current strategy is to cut production times by increasing electronification of the journal. We are currently putting together a SR-structural biology issue (July 1998) to celebrate Dr. John Walkers Nobel prize, which is indeed the first SR related Nobel prize.In 2001, we expect to cover SRI-2000 (Berlin) & XAFS XI (Ako, Japan). We see these special Issues as an important part of increasing the Impact of the Journal, its distribution, readership and thus increasing its subscriptions by the widest possible scientific community.

CC COMPUTING: IMPROVED DATA ACCURACY AND VALIDATION THROUGH SOFTWARE

C09.CC.001 GOODNESS OF FIT-FACT OR FICTION. Peter S. White, University of North Carolina at Chapel Hill, NC, USA, Eric J. Gabe and Gary D. Enright, Steacie Institute for Molecular Sciences, National Research Council of Canada, Ottawa, ON, Canada.

In the last year or so it has become apparent that a number of Acta referees, and editors, have adopted a rather inflexible approach to the application of several criteria for the acceptance of structure papers. This has prompted an examination of some of these quantities in order to clarify our feelings on what constitutes an acceptable structure and whether unbiased quality indicators can be developed. The following comments are based on actual experiences.

1. Goodness-of Fit Values

Ideally, GoF values from correctly weighted least-squares processes approach 1.0. This rarely happens with structure refinement and for good reason. Statistical weights and scattering factors are not perfect, the model uses an inadequate thermal expression and neglects bonding electron effects. Refinement with good data, on well-behaved structures, using F_{obs} or F_{obs}^2, and conventional models yields GoF values in the range 1.5 to 3.0. Adjusting the weights to bring GoF close to 1.0, is more cosmetic than scientific, possibly leads to optimistic esd values and invalidates GoF as a quality control index.

2. An inflexible cutoff for the Nobs/Npar ratio (Rop).

Least-squares is so successful for structure refinement because it is so over-determined. How over-determined is enough? The answer is not a rigid 'If Rop < X, the refinement is no good.'. Papers with Rop > 7 have been rejected, which is unreasonable. More scientific discretion is needed.

3. Insistence on F_{obs}^2 refinement.

Similar remarks apply. Using F_{obs}^2, rather than F_{obs}, is mathematically more correct, but for most structures it makes no significant difference.

Reliance on computer generated 'Alerts' is very tempting, especially to journals with less crystallographic expertise. Acta should ensure that its rules are reasonable and make clear that those rules must be tempered by the informed judgement of referees and editors. At the moment it is unfortunately true that many potential authors are 'voting with their feet'.

C09.CC.002 DATA VALIDATION AT THE PDB. Helen M. Berman, Kyle Burkhardt, Zukang Feng, Shri Jain, Rachel Kramer, Bohdan Schneider, and John Westbrook. Research Collaboratory for Structural Bioinformatics. Rutgers University, 610 Taylor Road, Piscataway, NJ 08854-8087 USA

The new Protein Data Bank (PDB) has created a single integrated system for data deposition, processing, annotation, database management, and archiving. The Auto Dep Input Tool (ADIT, 1), is used for all aspects of structural and experimental validation. For each structure, the following checks are made: nomenclature and numbering, valence geometry, stereochemistry, nonbonded contacts, torsion angle distributions, and structure factors. The ADIT results are sent to the author in a summary letter. These reports, in addition to the output files from NUCheck [2], PROCHECK [3], and SFCheck [4], are provided to the author on a Web page.

These validation reports can also be created without the intervention of the PDB staff. The ADIT Validation server (http://pdb.rutgers.edu/validate/) accepts coordinate and structure factor data to produce the validation reports independent of structure deposition.

The validation features of this system will be discussed.

The PDB is supported by the NSF, DOE, and NIH (NIGMS and NLM)

1. J.Westbrook, Z.Feng, and H.M.Berman. (1998). ADIT, Rutgers University, RCSB-99.
2. Z.Feng, J.Westbrook, and H.M.Berman. (1998). NUCheck, Rutgers University, New Brunswick, NJ. NDB-407.
3. R.A.Laskowski, M.W.McArthur, D.S.Moss, J.M.Thornton. (1993). J.Appl.Cryst. 26, 283-291.
4. A.A. Vaguine, J. Richelle, and S.J. Wodak (1999). Acta Cryst. D55, 191-205.

C09.CC.003 COMPUTING PROGRAMS IN LATTICE DYNAMICS COMPATIBLE WITH USUAL CRYSTALLOGRAPHIC PRACTICE. Carlo M.Gramaccioli, Earth Science Department, University of Milano, Via Botticelli 23, I-20133 Milano, Italy.

Notwithstanding its close relationships to their own discipline, too many crystallographers do not seem to consider lattice dynamics to be an argument of basic importance. Such an importance becomes particularly evident whenever the links between crystallography and solid state physics, or even with arguments of physical chemistry, such as vibrational spectroscopy and thermodynamics, are considered.

Moreover, there has been a growing interest in some results of accurate crystal structure refinement, such as for instance ADPs or “thermal parameters”, as they are still improperly called too often. The neglection of such data is due to their comparatively low accuracy, which at least in part and in most cases depends on their strong correlation with TDS, or with the interpretation of diffraction profiles and the difficulty of distinguishing a peak from its background; there is also notable correlation with other refinable parameters, such as the electron density distribution, scale factors, population parameters, etc.etc.: all these points might lead to some wonder whether ADP’s, just like atomic form factors, rather than from crystal structure refinement, could be derived instead “a priori”, at least in many cases. On the other hand, from the theoretical side there are the difficulty of interpreting the vibrational spectra of crystals, and the insufficient availability of adequate computer programs starting from “usual” crystallographic information: an illustrative point in this respect is the problem of routinely deriving spectroscopic symmetry and Brillouin-zone information from space group operations.

In these respects, computing programs which can be easily used by crystallographers are needed; the feasibilty of the procedure can be illustrated

In practice by a series of examples dealing with molecular and non-molecular crystals, and showing new and interesting possibilities in interpreting thermal motion.

C09.CC.004 *ACTA CRYST. C* DATA VALIDATION AND QUALITY ASSESSMENT: RATIONALE FOR THE CURRENT CRITERIA. J. Albertsson, Department of Inorganic Chemistry, Chalmers University of Technology, S-412 96 Göteborg, Sweden, G. Ferguson, Department of Chemistry and Biochemistry, University of Guelph, Guelph, Ontario, Canada N1G 2W1, S.R. Hall, Crystallography Centre, University of Western Australia, Nedlands 6907, Australia, and A.L. Spek, Department of Crystal and Structural Chemistry, Bijvoet Center for Biomedical Research, Utrecht University, Padualaan 8, 3584 CH Utrecht, The Netherlands.

The rapid growth in the number of crystal structure determinations with the advent of area detectors, coupled with changes in the scientific journal industry in the past decade, are the main reasons for a number of new publication initiatives for *Section C* of *Acta Crystallographica* These include the electronic submission of manuscripts (text and data), faster review and editorial handling procedures, the provision of an electronic publishing mode (CIF-access) and expanded facilities for the online access to the archived published material. Recently, automatic data validation software has been installed so that authors can check their manuscripts prior to submission.

These automated facilities provide not only for comprehensive checking of the completeness and internal consistency of submitted data but also a consistent approach to assessing the quality of the studies accepted for *Section C*. To this end the *Commission on Journals* has set criteria requiring the results of structural studies to meet basic quality and reliability standards. These tests are part of the *CHECKCIF* e-mail or web facilities and they are now a required part of a submission to the journal. The *CHECKCIF* facility applies a complete suite of validation tests and reports to authors any data requirements or standards not met as diagnostic warnings and alerts of varying severity.

This presentation will discuss the reasons for the criteria used to test data standards in *Section C*, as determined by the Commission on Journals and published at

http://www.iucr.org/iucr-top/journals/acta/dv.html.

C09.CC.005 *ACTA CRYST. C* DATA VALIDATION AND QUALITY ASSESSMENT: IMPLEMENTATION AND HANDLING PROCEDURES. M. A. Hoyland and B. McMahon, IUCr, 5 Abbey Square, Chester CH1 2HU, England, A. Linden, Institute of Organic Chemistry, University of Zürich, Winterthurerstrasse 190, CH-8057 Zürich, Switzerland, and S. R. Hall and D. J. du Boulay, Crystallography Centre, University of Western Australia, Nedlands 6907, Australia.

The data validation criteria published for *Acta Crystallographica Section C* (**`http://www.iucr.org/iucr-top/journals/acta/dv.html`**) are applied through the IUCr *checkcif* software suite and the *PLATON* program (A. L. Spek; **`http://www.cryst.chem.uu.nl/platon/`**). Several program authors have made their software available over several years in the development of structure checking for *Acta Crystallographica*, and are gratefully thanked.

Prospective authors are required to assess their structures via *checkcif*, by emailing a CIF to **`checkcif@iucr.org`**, or by web upload *via* the URL **`http://www.iucr.org/iucr-top/journals/acta/c/services/checkcif.html`**. A summary report is returned, listing missing or incorrectly formatted data items, and indicating numerical values that lie outside expected norms. Such outliers are assigned an appropriate level of severity, and the report draws the attention of authors to the need to take action to correct or explain the values, preferably by ensuring details are included in the experimental text. An author unable to eliminate the cause of the outlier, but who believes there is a scientific explanation for the deviation, may write an explanation, using the validation response form supplied with the *checkcif* report, and insert it into the CIF. Such submissions are scrutinised by a 'Validation Coeditor' from the journal editorial board before the normal editorial process begins. The presentation will include a report by the current Validation Coeditor, A. Linden, on how authors react to and benefit from this system.

The IUCr offers different configurations of *checkcif* as a service to other journal publishers and structural database managers.

TC TEACHING: BASIC PHYSICAL CHEMICAL KNOWLEDGE FOR EVALUATING CRYSTALLOGRAPHIC DATA

C11.TC.001 CHEMISTRY AND SYMMETRY IN THE EVALUATION OF INORGANIC STRUCTURES. I.D. Brown, Brockhouse Institute for Materials Research, McMaster University, Hamilton, Ontario, Canada L8S 4M1

The Principle of Maximum Symmetry states that a crystal structure will adopt the highest symmetry possible consistent with the constraints acting in the system. These constraints include the strict requirements of 3-dimensional space as expressed by space group theory and the less strict requirements of chemistry, usually expressed by empirical rules describing the bonding geometry. Because the refined structure does not necessarily satisfy the chemical constraints, the geometry should be checked against the empirical rules of bonding geometry.

The space group may be chosen with too high a symmetry as a result of a failure to recognise the presence of a symmetry-breaking constraint, or it may be chosen with too low a symmetry as a result of failure to recognise a higher symmetry in the bonding topology. These failures can be avoided by an analysis of the bonding topology and geometry.

In inorganic compounds one should always check that the bond topology does not have a symmetry that can be accommodated in a space group of higher symmetry. Further, experimental bond valences determined from bond lengths should match the theoretical bond valences determined from the bonding topology. Differences are expected around cations with anisotropic electron distributions and around cations that are in cavities that are too large, but otherwise such differences, if not arising from an incorrect interpretation of the structure, are evidence of bond strain. The structure should be examined to pinpoint the origin of the strain. If the strain is excessive, the structure may have been refined in a space group with too high a symmetry. In a correctly determined crystal structure all deviations between the experimental and theoretical bond valences should be accounted for.

C11.TC.002 WEB-MODULES FOR THE INTER-ACTIVE TEACHING OF CRYSTALLOGRAPHY. Chapuis G. [1], Hardaker W. [2], [1] Institut de cristallographie, Université de Lausanne, 1015 Lausanne, Switzerland, [2] Information Technology, University of California at Davis, Davis CA 95616, U.S.A.

The teaching of crystallography is greatly facilitated by the use of computers. They open new dimensions in terms of structure visualizations and simulations of diffraction phenomena. Many excellent commercial and freely available software packages exist that the teacher can use to help illustrate his course. The system and hardware requirements imposed by the software, or perhaps by the licensing restrictions, will unfortunately limit the choice or even discourage the use of the software.

The new possibilities offered by the ubiquitous web can avoid this serious drawback. The Java programming language allows platform-independent development of applications that can be directly accessed from web browsers. Present web browsers are all able to handle "java applets", which consist of small Java applications that can be used to illustrate specific aspects in a lecture or a conference. From a computer laboratory or from home, the student can have access to the same software demonstrations as the teacher and thus can complete his training and formation according to his own schedule.

We have developed a series of Java applications with the aim of illustrating some basic concepts of crystallography: point group symmetry, space group symmetry and the elements of crystal diffraction.

Currently, a few websites dispersed all over the world offer already a selection of applets illustrating additional aspects of crystallography. It is thus very easy to include pointers referring to these sites in order to extend the possibilities of training offered to the students.

C11.TC.003 CRYSTALLOGRAPHIC TOOLS FOR CHEMISTS. R. Cooper, K. Prout, D. Watkin, Chemical Crystallography Laboratory, 9 Parks Road, Oxford, OX1 3PD, UK, and F. Allen, S. Motherwell, CCDC, 12 Union Road, Cambridge, CB2 1EZ, UK.

Modern diffractometers allow users to collect 1 to 3 data sets per day and routine structures can be solved and refined by even relatively inexperienced crystallographers. To ensure that analyses are optimal, techniques have been devised to detect problems with the structure and to assist the user in correcting or understanding the problems.

Signalling problems with an analysis at the publication stage is inefficient and ineffective. To ensure optimal results, problems should be detected and corrected as the analysis proceeds. Using the Crystals program, features of the structure can be verified with observations derived from the Cambridge Structural Database, or against a chemist's idea of the two-dimensional structure. Values that are going to cause failure or require explanation when submitting the structure to journals or databases can be checked.

Tools are provided to enable the user to resolve problems during analysis:

A 3D model of the structure is available at all times following structure solution. The model can be used to inspect, edit and analyse the structure, to display graphical information such as existing restraints and deviating bond lengths, and to initiate atom or fragment based commands.

Disorder can be investigated using generalised Fourier sections through the volume of interest, and can be modelled by constraining or restraining physical quantities such as occupancies, and thermal parameters. The program will detect if any axis of a thermal ellipsoid has become too large and tools can be used to split the elliptical atom into two new atoms at the foci of the original ellipse. For more complicated disorder a diffuse electron density can be modelled over non-atomic shapes.

Adding restraints to the refinement is often necessary when there is insufficient data to refine the model. Tools are available to quickly restrain any distances or angles in the structure, and values and weights for the restraints can be suggested from the information obtained from the CSD.

C11.TC.004 THE IMPACT OF TEACHING SCHOOLS ON THE DEVELOPMENTS OF CRYSTALLOGRAPHY IN THE THIRD WORLD COUNTRIES. Karimat El-Sayed, Physics Department, Faculty of Science, Ain Shams University, Cairo, Egypt.

The post-graduate students and even the University Lecturers of the developing countries are not usually in a good scientific atmosphere. This is mainly due to the lack of; equipments, scientific books, Journals, research grants, attending conferences and lastly having contacts with International Scientists and Experts. Crystallography is the most affected subject in this unhealthy scientific climate because it is considered by the policy makers not to be a real subject. Teaching Schools and Workshops are the only methodologies which could counteracts all these mentioned difficulties present in the Third World Countries. They are the only means by which international outstanding lecturers can come to teach the most developed techniques and advanced topics to researchers. They allow the

students to discuss topics at the frontiers of research and to know the most recent applications of crystallography in material science, chemistry, biology, etc. They allow the researchers to have the school and Workshops proceedings which counteract the books deficiency. Several Schools and Workshops were held in Egypt, the programs of each Schools were designed in accordance with the need of the researchers and the goal which will be achieved in each stage. These items will be discussed in details in the given paper.

C11.TC.005 TEACHING STRUCTURAL CRYSTALLOGRAPHY: SOME SIMPLE CONCEPTS USED IN TEACHING COMMISSION SCHOOLS. Jenny P. Glusker, The Institute for Cancer Research, The Fox Chase Cancer Center, 7701 Burholme Avenue, Philadelphia, PA 19111, USA

Some tips on methods of teaching crystallography will be provided for those giving courses on the solid state and the structures of ions, molecules and crystals. The results of X-ray diffraction studies of crystalline materials are simple to comprehend if three-dimensional models are built. The methods used to arrive at the results that enabled such models to be built are, however, complex; the teacher needs to pay careful attention to the individual conceptual needs of the students when describing them. One of the most difficult areas for a teacher of structural crystallography to describe and explain is the connection between the intensities in the X-ray diffraction pattern and the electron density map that results, that is, the Fourier transform, what it is and why it is applicable for this transformation. Some students readily understand the mathematical equations used, while others do better with descriptions of waves and optical analogies. Some examples of methods used to teach molecular structure determination at IUCr Teaching Commission Schools will be provided. In this I have been helped by Professors Ken Trueblood, Joel Sussmann, Miriam Rossi, Mitchell Lewis, and the text "X-ray Analysis of Crystals" by J. M. Bijvoet, N. H. Kolkmeyer and C. H. McGillavry.

Some of the concepts to be addressed are the Patterson function (including convolutions), the Fourier transform, precision versus accuracy, and the term "resolution." Their significance in small-molecule and macromolecular structure determinations will be addressed with some examples of structures and intermolecular interactions.

This work was supported by a grant CA-10925 from the National Institutes of Health, US Public Health Service.

C11.TC.006 THE IMPORTANCE OF ADEQUATE KNOWLEDGE OF PHYSICAL CHEMICAL ARGUMENTS IN CRYSTALLOGRAPHY. Carlo M. Gramaccioli, Earth Science Department, University of Milano, Via Botticelli 23, I-20133 Milano, Italy.

Active participation together with other groups of specialists in other disciplines is of utmost importance for crystallographers, in order not to be considered as mere technicians. Such a participation especially concerns either a careful planning of the experiments to be carried out on a selected group of substances, or also the interpretation of the data as they have been obtained from the solution and refinement of crystal structures.

In such a respect, in spite of the qualification of crystallography as a discipline with a sophisticated mathematical and physical background, in too many crystallographic papers only a superficial knowledge of physical chemical arguments can be noticed frequently. Such a lack of detailed basic general knowledge in particular concerns spectroscopy, thermodynamics, or also quantum mechanics.

For instance, there has been too little emphasis on the relationships of symmetry as it is used by spectroscopists with the corresponding concepts in crystallography: this point has often been one of the major drawbacks concerning a correct interpretation of vibrational spectra of crystals; at the same time, crystal structure modelling would be dramatically improved if not only the “static” crystal structure data are satisfactorily interpreted and reproduced, but thermodynamic properties could be reproduced as well at different temperatures.

Unfortunately, too many models currently used by crystallographers contain fundamental errors, such as the interpretation of ionic inorganic structures using molecular models, or the neglection of zero-point effects in considering the vibrational energy and the amplitude of atomic motion, or even the interpretation of the amplitude of vibration of certain groups or molecules more or less exclusively based on Raman- or infrared spectra.

For these reasons, the organization of adequate schools for crystallographers dealing with these subjects would be strongly recommended, as an argument of primary importance.

C11.TC.007 THE IMPORTANCE OF X-RAY DIFFRACTION IN THE REAL WORLD OF REAL PEOPLE. Michael Laing School of Chemistry, University of Natal, Durban 4041, Republic of South Africa

For many science students, X-ray crystallography is the tough course to be avoided. For most chemists, it is the mysterious source of information about molecular structure and bond lengths. It is the task of the teacher to show the average science student the enormous value of X-ray crystallography and its power to supply information that will help the scientists to solve problems. In particular, the student needs to learn how the identity of the crystalline phases in a solid can be used together with chemical knowledge to explain chemical phenomena that would otherwise be intractable problems.

For example, X-ray diffraction can help build better roads (by identifying mineral species in the soil); help urologists to heal their patients who suffer from calculi (by identifying the crystalline components of the calculi and therefore their cause); help improve efficiency in a platinum metal refinery (by identifying the intractable solid phases and thus indicating changes in processes to dissolve the solids); characterise fossils of ancient hominids (by determining the components in the bone and surrounding breccia); play a vital forensic role for the police (anything from identifying paint samples to determining the temperature of a fire).

The data required in each of these examples is easily collected but to evaluate it requires a sound understanding of the chemistry relevant to the problem. Teaching this step is the challenge to the chemical crystallographer.

C11.TC.008 THE USE OF THE MOLECULAR GRAPHICS PROGRAM TITAN IN TEACHING X-RAY CRYSTALLOGRAPHY. Jim Simpson and Keith A Hunter, Department of Chemistry, University of Otago, P.O. Box 56, Dunedin 9001, New Zealand.

The TITAN molecular graphics program was developed as a readily accessible graphical tool to allow classes of undergraduate students to experience the solution and refinement of a small molecule crystal structures, using the widely available SHELX programs. Over the past several years the program has evolved to give an easy to use and reasonably intuitive tool for the display and manipulation of molecular structures from the output of the SHELXS and SHELXL programs. Input from students using the program has been important in this development.

This presentation will highlight some features of the program, from a teaching perspective, and the experience of the presenting author in using the program in an undergraduate teaching situation.

C11.TC.009 TEACHING THEORETICAL AND PHYSICAL CRYSTAL CHEMISTRY FOR CRYSTALLOGRAPHERS OF MOSCOW UNIVERSITY. Vadim S.Urusov, Department of Crystallography and Crystal Chemistry, Geological Faculty, Moscow University, 119899 Moscow, Russia

Teaching in theoretical and physical crystal chemistry for the students which are specialized in crystallography of minerals is divided into two stages. First of them is a familiarity with foundations of theoretical crystal chemistry for all students of geochemical division during the first two years of education. It involves an introduction in the theory of chemical bonding in crystals, characterization of crystal chemical properties of atoms, principles and rules of a structure type stability, structural homology, polymorphism and polytypism, isomorphous substitutions in crystals.

The second stage is training in the methods of theoretical and physical crystal chemistry for students-crystallographers of the last two years of education. This consists of two parts: 1)a general introduction to symmetry and crystal chemical constraints on the structures of inorganic solids, 2)a closer inspection of the methods and approachs to prediction of probable structures of minerals and inorganic crystals. The latter involves both the prediction of bonding topology and refinement the topological description by modern methods of the least squares fitting to the expected geometry and lattice energy minimization with semi-empirical and ab-initio potentials. The course of lectures is supplemented with the practical training in using the crystal structure databases and programm packages.

HP HIGH PRESSURE

C12.HP.001 HIGH-PRESSURE, ANGLE-DISPERSIVE, X-RAY POWDER DIFFRACTION USING A LABORATORY SOURCE. J. Haines and J. M. Léger, Laboratoire de Physico-Chimie des Matériaux, C.N.R.S., 1, place Aristide Briand 92195 Meudon cedex, France.

A laboratory-based, high-pressure, angle-dispersive, x-ray powder diffraction experiment will be described. The equipment consists of an 800 W molybdenum microfocus tube, x-ray capillary optics and imaging plates. Two high-pressure experiments using diamond anvil cells can be performed simultaneously using the two point foci of the tube. The use of x-ray capillary optics results in a five-fold increase in flux with respect to traditional collimation. The diffraction profiles obtained upon integrating the 2D images can be routinely used for Rietveld refinement. Comparison will be made between refinements performed using data from this source and synchrotron data. The need to minimize deviatoric stress through the use of hydrostatic, pressure-transmitting media and annealing at high temperature will be emphasized. A large number of high-pressure, x-ray diffraction experiments can be performed in the laboratory and some examples concerning oxides, oxynitrides and semiconductors will be presented.

C12.HP.002 X-RAY IN SITU STUDIES OF SOME EARTH'S MATERIALS AT HIGH P-T CONDITIONS WITH IN-HOUSE FACILITIES. L. S. Dubrovinsky, N. A. Dubrovinskaia, S. K. Saxena Theoretical Geochemistry Program, Department of Earth Sciences, Uppsala University, Villavägen 16, 752 36 Uppsala, Sweden

Experimental studies of geophysically important materials at high pressures require in situ x-ray diffraction. It is practically the only method which provides direct information on phase relations and structures. We developed in-house X-ray facility which allows us to collect diffraction patterns in megabar pressure range at temperature to 1000 C. We obtain powder X-ray diffraction data with a Siemens X-ray system consisting of a Smart CCD Area Detector and a direct-drive rotating anode as X-ray generator. With the capillary optic installed, a high-intensity focus of X-rays is produced at the sample position, and its width is controlled by the choice of field aperture. This system allows us to obtain X-ray beam from 85 mu FWHM with 95% of initial intensity (intensity after shutter) to 35 mu FWHM with 25% of initial intensity. Small size of the X-ray beam and high sensitivity of CCD area detector open the way to study phase transitions and elastic volumetric properties of solids up to 100 GPa at room temperature using different types of high-pressure cells (Mao-Bell, Merril-Basset etc.) and thermal expansion, phase transitions and chemical reactions of solids up to 3600 K in inert atmosphere at ambient pressure. In-house x-ray facilities were used to study, for example, the phase transition in iron and interaction between iron and MgO. Using our in-house facilities we obtained new X-ray in situ data on thermal expansion of refractory metals (Cr, Ta, W) and oxides (MgO, HfO2, Y2O3) and thermal expansion, phase relations and compressibility of alloys and compounds in Mg-Si-O, Fe-Al-C, Co-Ti-C , and Co-W-C systems.

C12.HP.003 THE LIMITS OF ACCURATE HIGH-PRESSURE SINGLE-CRYSTAL X-RAY DIFF. STUDIES ON A LAB SEALED-TUBE SOURCE. D.R. Allan Department of Physics and Astronomy, University of Edinburgh, Edinburgh, UK

Single-crystal x-ray diffraction is the longest established technique for obtaining truly accurate crystallographic information from samples held at high pressure, and it still provides the best structural data for a whole range of contrasting systems - despite some recent advances in powder-diffraction techniques using synchrotron and neutron radiation. Here, as well as outlining basic high-pressure single-crystal techniques, examples will be given of work on weakly scattering systems (such as boron and small organic molecules) at the very limit of what can be achieved successfully on a laboratory-based sealed-tube source. The results of some of this work will be compared with parallel studies conducted on station 9.8 at the Synchrotron Radiation Source, Daresbury.

C12.HP.004 OPTIMIZING MEASUREMENTS OF EQUATIONS OF STATE WITH IN-HOUSE SINGLE-CRYSTAL X-RAY DIFFRACTION. R.J. Angel, Bayerisches Geoinstitut, Universität Bayreuth, D95440 Bayreuth, Germany.

Equations of state can be determined by static compression of crystals in a diamond anvil cell, with the lattice parameters (and hence volume) determined by diffraction.

With special precautions, the current achievable precision in unit-cell parameters is about 1 part in 30-60,000, corresponding to a precision in unit-cell volumes of 1 part in 10-20,000. With this precision, pressure can be determined from an internal diffraction standard, such as quartz to better than 0.01 GPa over the pressure range 0-10 GPa. At this level of measurement precision, the resulting precision in the equation of state parameters of the sample crystal depends upon the ratio of its bulk modulus to the pressure range over which the data are collected, and only weakly upon the number of data points.

The precision of in-house X-ray diffraction experiments are therefore limited by a number of factors. Temperature in the X-ray enclosure must be controlled to better than 1 K in order for thermal expansion not to contribute significantly to data scatter. This sensitivity to temperature is also the reason for using an internal diffraction standard to measure pressure. The wavelengths and relative intensities of the components of the incident X-ray beam must remain constant; wavelengths to much better than 1 part in 50,000. This argues against the use of monochromators, or synchrotron sources. The ultimate limit to the precision to be

achieved in the future is the maximum pressure to which single-crystals can be compressed hydrostatically in a diamond-anvil pressure cell; with current techniques 10 GPa is routine, but higher pressures require exotic pressure media of uncertain properties.

C12.HP.005 EQUATION OF STATE MEASUREMENTS BY BRILLOUIN SCATTERING AT HIGH P AND T AND TEMPERATURES. Jay D Bass, Stanislav V Sinogeikin, Department of Geology, University of Illinois, 1301 W. Green St., Urbana, Illinios 61801 USA

Brillouin scattering provides information on the P-V equation of state. It is an inelastic light scattering technique, similar in many ways to Raman scattering, but the quantities which are measured in a Brillouin experiment are the compressional and shear elastic wave velocities (known in the Earth sciences as P and S waves). The elastic wave (sound wave) velocities are in turn related to the bulk modulus, which by definition gives the P-V relation at a given P and T. The experiment can be performed on single crystals (the most common application), or in favorable instances on polycrystals. The sound velocities for single crystals are generally a strong function of crystallographic direction. That is, they are anisotropic. By measuring the directional dependence of sound velocity, the single-crystal elastic moduli are determined. It is critical to know the crystallographic orientation of a sample throughout the experiment and this is determined using single crystal x-ray methods. Brillouin scattering experiments are being performed at high P and T using diamond anvil cells and high temperature furnaces. Diamond cells are well suited for this type of work, because all that is required for a Brillouin experiment is to be able to see the sample. We will discuss the special considerations needed for high P and T Brillouin experiments, and we will describe a high temperature furnace we designed that is suitable for many types of high temperature scattering experiments with single crystals, including x-ray scattering.

C12.HP.006 POSSIBILITIES AND LIMITATIONS OF THE APPLICATION OF THE HIGH-PRESSURE MÖSSBAUER EFFECT TECHNIQUE. M Abd-Elmeguid , II. Physikalisches Institut, Universität zu Köln, Zülpicher Straße 77, 50937 Köln, Germany.

The high pressure Mössbauer effect technique is a powerful tool which allows the determination of pressure-induced changes of electronic and magnetic properties of systems containing Mössbauer isotopes. In this contribution I will give a brief review on possibilities, limitation and the experimental problems of using these technique.

C12.HP.007 SEVERAL ASPECTS OF EXPERIMENTAL TECHNIQUES AT MBAR REGION K.Amaya Graduate School of Engineering Science, Osaka University, 1-3 Machikaneyama, Toyonaka, Osaka, Japan.

Techniques to produce ultra-high pressure exceeding 200GPa and to measure electrical resistance and magnetization of the sample confined in the pressure cell (DAC) are reviewed. Varieties of pressure-induced superconductivity observed in our laboratory are also reviewed. Experimental difficulties and possibilities toward higher pressure are discussed.

JMR THE MONTEATH-ROBERTSON SYMPOSIUM

JMR.07.001 FROM AROMATIC HYDROCARBONS TO VIRUS STRUCTURE. Michael G. Rossmann, Department of Biological Sciences, Purdue University, West Lafayette, IN 47907-1392, USA

A short history will be given of the technical changes that have occurred in structural crystallography between 1953 (when I entered J.M. Robertson's laboratory) and today. In the 50's, the Robertson Sorting Board and Beevers Lipson Strips were being used for structure determinations that had short cell axes, thus permitting the resolution of atoms when viewed in projection. Compounds suitable for crystallographic studies were usually limited to those with less than about 30 or 40 non-hydrogen atoms. Electronic computers, introduced in the late 50's, made possible routine three-dimensional analyses. The first low resolution protein structures were solved in Cambridge using home-built computers. Model building was dependent on hand-drawn electron density sections. The Richard's optical comparator ("Fred's Folly") was a tremendous advance in model building. This was the basis for the subsequent electronic "Richard boxes" - computer graphics. The techniques for solving the phase problem increased in parallel with the ever-increasing power of computers. Synchrotron X-ray sources improved both the quality and speed of data collection. The rate of protein structure determinations has increased exponentially in the 80's and 90's. The first spherical virus structures were solved in the late 70's. Now there exist numerous structures of viruses and their complexes with receptors and neutralizing antibodies. The power of electron microscopy has also been increasing to allow a gradual merging with crystallographic results. Some recent structural investigations of viruses will be discussed. In some instances, viruses with over 50 million Daltons molecular weight have been investigated to atomic resolution.

JMR.07.002 FROM MOLECULES TO PHYSICAL PROPERTIES. S. C. Abrahams, Physics Department, Southern Oregon University, Ashland, OR 97520, USA.

Selection of Glasgow as the venue for the second IUCr Congress organised in the UK is a measure of the high esteem in which J. Monteath Robertson, founder of the Glasgow school of crystallography, is held. This presentation will sketch a series of interactions at several levels with JM, as he was known to his students, through a variety of interconnected themes. The first starts with an association that began in 1942 when he came to Glasgow as a newly appointed Professor and the writer arrived nearly simultaneously as a first year undergraduate student. A separate motif traces the evolution of interests that originated in the X-ray diffraction study of organic molecules under JM’s guidance and the course of their development under the early application of digital computers to diffraction results. The availability of neutrons from a graphite reactor led first to a need for automating the manual diffraction measurements that were normal at that time and then to an associated requirement for improved understanding of the uncertainties in the resulting quantities. The related question whether structure determination is better regarded as an end or a means subsequently initiated investigations into the relationships between crystal structure and material physical properties implied by the present title. A further theme considers the influence that several early developments in our field have had both on methods in use today and on new materials, including the discovery of some materials with physical properties of potentially high technological value. Another introduces additional founders of our branch of science and their connections to JM in addition to outlining some links between him and the IUCr. The remaining theme relates JM’s influence on his graduate students to the range of crystallography they

subsequently came to encompass. Among the results anticipated from this evening discourse are both the evocation of a personality and an enhanced appreciation of particular physical properties.

JMR.07.003 CHEMICAL CRYSTALLOGRAPHY: FROM THEN TILL NOW. Jack D. Dunitz, Organic Chemistry Laboratory, Swiss Federal Institute of Technology, ETH-Zentrum, CH-8092 Zurich, Switzerland.

In those days we knew practically every crystal structure that had ever been determined, who had done it, how had it been solved. Today no one can keep pace with the world wide output of crystallographic data, nor would anyone want to. In JMR's time, to be a chemical crystallographer, you needed a good memory, today you need the Cambridge Structural Database (CSD) and the Protein Data Bank (PDB). Robertson's Glasgow school cannot completely disclaim responsibility for this transition. Its graduates spread out over the world. Some of the ways in which crystallography influenced the development of chemistry will be briefly sketched.

JMR.07.004 PROTEIN CRYSTALLOGRAPHY IN GLASGOW. N.W. Isaacs, Department of Chemistry, University of Glasgow, Glasgow G12 8QQ, UK.

Since the appointment in 1942 of J. M. Robertson to the Gardner Chair in the Chemistry Department, the University of Glasgow has been a centre of excellence in crystallography. A roll call of the academic and research staff and students who have passed through the department shows a large number of outstanding crystallographers. George Sim, Robertson's successor, was instrumental in bringing protein crystallography to Glasgow with the appointment of Ian Swan to a lectureship in 1975. Ian's untimely death a few years later interrupted this initiative and it was not until 1989, that a protein crystallographic laboratory was re-established. The Robertson Protein Crystallography Laboratory has flourished in the past ten years, with the structures of human chorionic gonadotropin and the integral membrane light-harvesting complex among its notable achievements. With strong links to research in the biological sciences in the University, the programme of work in the laboratory covers broad range of problems. This presentation will describe some of this ongoing work.

LATE ABSTRACTS

The following abstracts were received or processed after the Abstract Book went to print.

M08.AA.005 PROTEIN FOLDS, FUNCTIONS AND EVOLUTION. J.M. Thornton, A. Kasuya, R. A. Laskowski, D. Milburn, C. A. Orengo, and C. Porter, Department of Biochemistry and Molecular Biology, University College London, Gower Street, London, WC1E 6BT, England, UK

As more gene sequences are determined, the demand for better methods to predict protein function from sequence grows. Currently the only reliable approach is to predict function by recognising sequence and/or structural homology to a related protein, whose function is known. Recognising close relatives is easy using standard algorithms, but recognition of more distant homologues becomes more difficult as sequences and structures diverge. Recent methods have improved recognition by using family information and iterative scanning to build up a 'sequence profile'. Our interest lies in the relationship between protein sequence, structure and function. An overview will be presented of our current knowledge of the universe of protein structures, and how sequences, structures and functions evolve. In particular, we will consider the relationship between fold and function using our classification scheme of protein structures called CATH (1). Every structure includes much information on detailed interactions, involved in biological function, yet very little of this information is used in genome analysis. We have therefore developed some software tools which seek to improve the annotation of sequences by the structural and functional information, especially regarding inter- and intra-molecular interactions. This resource is available on the web at http://www.biochem.ucl.ac.uk/bsm. Various methods to extract and classify functional information from structural work will also be discussed (3, 4).

1. Orengo, C.A. et al. CATH - A Hierarchic Classification of Protein Domain Structures. Structure, 5, 1093-1108 (1997).
2. Milburn, D., R. A. Laskowski and J. M. Thornton. SAS: Sequences Annotated by Structure: a Tool to Facilitate the Use of Structural Information in Sequence Analysis. Protein Engineering, 11, 855-859.
3. Wallace, A.C., Borkakoti, N. & Thornton, J.M., (1997). TESS: A Geometric Hashing Algorithm for Deriving 3D Coordinate Templates for Searching Structural Databases. Application to Enzyme Active Sites. Protein Science, 6, 2308-2323.
4. Kasuya, A. & Thornton, J.M., (1999). Three-dimensional Structure Analysis of PROSITE Patterns. Journal of Molecular Biology, 286, 5, 1673-1691.

P12.04.018 CRYSTAL STRUCTURE OF SIMIAN IMMUNODEFICIENCY VIRUS INTEGRASE CONTAINING THE CORE AND C-TERMINAL DOMAIN (RESIDUES 50-293) – AN INITIAL GLANCE OF THE VIRAL DNA BINDING PLATFORM. Zhongguo Chen, Youwei Yan, Sanjeev Munshi, Ying Li, Joan Zugay-Murphy, Bei Xu, Marc Witmer, Peter Felock, Abigail Wolfe, Vinod Sardana, Daria Hazuda, Emilio A. Emini, and Lawrence C. Kuo. Department of Antiviral Research, Merck Research Laboratories, West Point, Pennsylvania 19486-0004.

The crystal structure of simian immunodeficiency virus integrase that contains in a single polypeptide the core and the C-terminal deoxyoligonucleotide binding domain (DBD) has been determined at 3Å resolution. The cell constants of the crystal obtained at pH 5.5 are *a* =79.57Å, *b*=100.0Å, *c* =150.5Å and $\alpha=\beta=\gamma=90°$ in the space group $P2_12_12_1$ with Z=4. Four integrase core domains and one DBD are found to be well defined in the asymmetric unit. The other three DBD domains are disordered and cannot be located. The final R-factor is 0.232.

The four core domains are grouped in the asymmetric unit as two dimers related by a 90° rotation about and a 23Å translation along the *c*-axis. Each has the same overall fold and inter-domain interactions as seen for the human immunodeficiency virus-1 (HIV-1) integrase dimer [1]. The C_α tracing of the DBD domain is also similar to the reported DBD structure from HIV-1 integrase [2]. However, the dimeric form seen in the NMR structure cannot exist as related by the non-crystallographic symmetry in the SIV integrase crystal.

In the 2-domain crystal structure, the segment encompassing residues 114-121 assumes the same position as seen in the integrase core domain of avian sacoma virus and HIV-1 crystallized in the absence of sodium cacodylate [3, 4]. The flexible loop in the active site, composed of residues 142-153, remains incompletely defined, but the location of Glu152 is clearly defined; its side-chain points toward Asp64 and Asp116 to form a triad. The residues from 210-218 that link the core and DBD domains can be traced as an extension of α6 helix from the core with a short gap at residues 216-218. The two flexible loops of the DBD, residues 228-236 and residues 244-249, are much better fixed in the crystal structure with the former in the immediate vicinity of the flexible loop of the core domain. The interface between the two domains encompasses a surface area of ~1,500Å^2. Residues from both domains purportedly involved in DNA binding are narrowly distributed on the same face of the molecule. They include Asp64, Asp116, Glu157 and Lys159 from the core and Arg231, Leu234, Arg262, Arg263 and Lys264 from the DBD. A model for DNA binding is proposed to show that the DNA bridges the two domains by tethering the 228-236 loop of the DBD and the disordered loop of the core.

[1] Dyde, et al, (1995) Science 266,1981-1986.
[2] Eijkelenboom, et at, (1995) Nature Struct. Biol 2, 807-810.
[3] Bujacz, et al, (1996) Structure 4, 89-96
[4] Goldgur, et al, (1998) Proc. Natl. Acad. Sci. 95, 9105-9154.

P07.FF.008 AN UNEXPECTED DISCREPANCY IN THE ASYMMETRIC UNIT OF ISOCYANATO-(VINYL-IMIDAZOLE)-COBALOXIME. T. Wagner, Department of Pharmacology, University of Virginia, Charlottesville, USA. N. Knur and U. Englert, Institut für Anorganische Chemie, RWTH Aachen, Germany.

Bis(dimethylglyoximato)isocyanato(3-vinyl-imidazole) cobalt(III) crystallizes in the monoclinic space group $P2_1/c$ with two molecules in the asymmetric unit. As one would expect, the molecules are very similar with respect to their bond lengths and angles. There is, however, a striking difference in the orientation of the planar axial base. In one case the plane through the five ring atoms of the imidazole is almost parallel to the midpoints of the carbon-carbon bonds in the glyoximato moieties while in the other it is approximately perpendicular. This indicates that the conformation of the base in this type of compounds is a soft degree of freedom which may easily be adjusted to assure packing efficiency during crystallization. A survey of the literature suggests a rather electronic nature for this feature. If the aromatic ligand is a pyridine derivative, the arrangement is close to perpendicular in all cases whereas it is almost parallel for ligands such as imidazole [1].

Our presentation will address three different aspects of this unusual crystal structure:

We are currently analyzing if the more than 70 cobaloximes with an aromatic base in at least one of the axial positions found in the Cambridge Structural Database exhibit the preferences described more than a decade ago for a much smaller number of compounds [1].

A minimization of both molecules with semiempirical methods should verify our hypothesis that one of them is indeed an energetic minimum, but the difference to the other conformation is small enough to be overcome even by weak forces like those exerted by the crystal surroundings.

A comparison of the lattice energies of our experimental and a hypothetical structure with both molecules in the same conformation reveals that the packing of identical molecules is less favorable in terms of energy as well as space filling.

1. C. Lopez, S. Alvarez, X. Solans & M. Font-Alba (1986). Inorg. Chem., **25**, 2962-2969.

P05.04.015 STRUCTURAL ASPECTS OF AGONISM AND ANTAGONISM IN OESTROGEN RECEPTOR ISOFORMS. A.C.W. Pike, A.M. Brzozowski, J. Walton, and R.E. Hubbard, Structural Biology Laboratory, Chemistry Department, University of York, York YO10 5DD, U.K., T. Bonn and M. Carlquist, Karo Bio AB, NOVUM, S-14157 Huddinge, Sweden and J-Å. Gustafsson, Karolinska Institute, NOVUM, S-14186 Huddinge, Sweden.

The oestrogen receptor (ER) is a ligand-activated transcription factor. The recent unexpected discovery of a second ER, termed ERβ, has provoked extreme interest in the respective roles of the two ER isoforms in oestrogen action. ERα (classical ER) and ERβ share modest overall sequence identity but differ substantially in tissue distribution, ligand binding and in transactivation properties.

We have determined the crystal structures of the ligand-binding domain of ERβ (ERβ-LBD) in complex with the phytoestrogen genistein and the anti-osteoporosis agent, raloxifene at resolutions of 1.8Å and 2.3Å respectively. Comparison of these structures with liganded ERα-LBD [1] give a unique insight into the structural principles that underlie ligand recognition and selectivity, cavity plasticity and recruitment of coactivators by the respective receptor isoforms. Each ligand interacts with a unique set of residues within the hormone binding cavity. As in ERα, the bulky sidechain of the antagonist raloxifene protrudes from the cavity and physically prevents the alignment of the activation helix (H12) over the bound ligand. In contrast, genistein is completely buried within the protein and binds in a manner similar to that observed for the natural hormone, 17β-oestradiol. However, in the ERβ-genistein complex H12 does not adopt the distinctive agonist position. Such a sub-optimal alignment is consistent with genistein's partial agonist character in ERβ and demonstrates how ER's transcriptional response to certain bound ligands is attenuated.

1. Brzozowski, A.M., Pike, A.C.W., Dauter, Z., *et al*. (1997) *Nature* **389**, 753-758.

P13.22.004 FORMATION OF QUASICRYSTALLINE D-AL-NI-CO BY SOLID STATE REACTIONS OF MULTILAYERS PREPARED BY PLD. S. Braun [1], D. Meyer, P. Paufler [2], [1] Fraunhofer Institute Material and Beam Technology Dresden, Germany, [2] Institute of Crystallography and Solid State Physics, Technical University Dresden, Germany

Thin layers of the decagonal phase of the Al-Ni-Co system were synthesized by Pulsed Laser Deposition (PLD). The short range order of these layers was characterized by Extended X-Ray Absorption Fine Structure (EXAFS) measurements. It is shown that single-phased decagonal structures can be formed by solid state reactions of PLD prepared multilayers. A 10-period Co/Al/Ni multilayer has been fabricated under UHV conditions (low 1.0e-8mbar), using the first harmonic of a Nd:YAG pulsed laser (tau=10ns, lambda=1064nm). After determination of deposition rates of each material, the element composition of the layer stack can be adjusted very exactly, because of the high precision of the PLD process. Finally, the formation of the decagonal phase was reached by post-annealing of the multilayer at 700°C for 5 hours. The five-fold symmetry of the structure is shown in a TEM micrograph cross-section. Specular X-ray diffraction investigations indicate that the periodic direction of the decagonal structure is aligned perpendicularly to the substrate surface. This is in correspondence with known results of the isotypic structure of decagonal Al-Cu-Co. The comparison of the EXAFS measurements of the quasicrystalline thin layers with a quasicrystalline reference sample shows a very high level of similarity. Therefore both the short range order and the long range order (responsible for the x-ray diffraction pattern) of the produced quasicrystalline samples were found to be equivalent to the short and long range order in a quasicrystalline reference sample.

P13.OA.005 CRYSTAL STRUCTURE OF THE PROTEIN DISULFIDE BOND ISOMERASE, DSBC, FROM *ESCHERICHIA COLI*. A. A. McCarthy, P. Haebel, E. N. Baker, and P. Metcalf, University of Auckland

Protein disulfide isomerases are essential for the correct pairing of disulfide bonds during the folding of proteins with multiple disulfide bonds *in vivo*. The best characterised *E. coli.* disulfide bond isomerase, DsbC, is one of seven gene products (DsbA-G), essential for disulfide bond formation in the periplasm. The crystal structure of DsbC, determined by MAD phasing and refined to 1.9Å also contains a thioredoxin fold. The thioredoxin sub-domain contains the redox-active disulfide bond at the N-terminus of the first helix and a *cis*-proline abutting the active site disulfide bond, similar to other thiol/disulfide oxidoreductases. Arg125 observed near the active site is ideally positioned to stabilise a negatively charged thiolate form through both a direct charge stabilisation and an enhancement of a helical dipole stabilisation effect. An acidic/basic motif comprised of Arg125 and Asp95 was observed in the vicinity of the more N-terminal and solvent exposed active site Cys and may participate in the catalytic mechanism of DsbC. Prominent clefts or grooves observed near the active site are notably absent in DsbC. DsbC appears to have evolved from a simple thioredoxin fold into a two-domain structure to facilitate the complex conformational changes necessary for protein disulfide isomerisation.

P06.11.035 X-RAY DIFFRACTION STUDIES OF CdF_2/CaF_2 SUPERLATTICES ON Si(111). R.N.Kyutt, N.S.Sokolov, S.M.Suturin, Ioffe Physico-Technical Institute, St.Petersburg 194021, Russia, J.Harada, K.Inaba, X-ray Research Laboratory, Rigaku Co, Tokyo 196-8666, Japan

Structural parameters of CdF_2/CaF_2 superlattices (SLs) grown on Si (111) substrates by MBE -method with various periods (from 2 to 40 nm) and total thickness from 100 to 350 nm are studied by double and triple crystal X-ray diffractometry. The measurements have been carried out in a wide range of the diffraction conditions including Bragg and Laue diffraction as well as in-plane geometry. By using the semikinematical approach, simulation of rocking curves has been performed and main parameters of the SLs have been determined.

The data obtained in different geometries allowed estimation of the contribution of three periodic distributions (out-

of-plane, in-plane interplanar spacing and scattering ability) to the resulting diffraction curves. Well-pronounced superstructure reflections (up to 5th order) and thickness fringes indicated high periodicity of the SLs and flatness both surface and SL/Si(111) interface. For short period SLs (d<10-20nm) narrow ω-curves (~10 arc.sec) showed their very high structural perfection.

However for the SLs with longer periods, triple crystal mapping and ω-scan cross sections showed noticeable distortion of the diffraction patterns. Atomic force microscopy measurements revealed multilayer columns on the surface of these structures. Depending on the SL period, the columns covered 10-20% of the surface. Coherency of the columns with the silicon substrate and their possible origin are discussed.

P09.06.032 FATS CHALLENGE CRYSTALLOGRAPHY. H. Schenk, R. Peschar, A.J. van Langevelde and K.F. van Malssen, Laboratory for Crystallography, University of Amsterdam, Nieuwe Achtergracht 166, 1018 WV Amsterdam, The Netherlands.

Triacylglycerols (TAGs) are long-chain hydro-carbon compounds with specific difficulties for crystallographers. The typical polymorphism (six different polymorphs are known) and the domination of diffraction by the chains make structure determination extremely difficult. The growth characteristics is the first problem to be overcome, secondly the measurements hare handicapped by the three very different crystal axes and finally the structure remains a problem in itself. As a result there were 3 crystal structures known only. The current research project took the challenge and tackled part of these difficulties. Controlled solidification resulted in single crystals of various TAGs. Crystals of tripalmitin appeared good enough for accurate data collection, resulting in the crystal structure of the largest TAG so far. Extreme difficulties in growing single crystals in other phases than the ß phase, or from other TAGs than mono-acid even-numbered TAGs, made the help of High Resolution Powder Diffraction at BM16 of the ESRF necessary. Using the combined information of series of TAGs, molecular modeling revealed information about the crystal structure of the ß' phase. Finally, the polymorphic behavior, being of large practical importance in food industry, has been studied with time-resolved powder diffraction (tr-XRD). In contrast to commonly used methods like Differential Scanning Calorimetry, tr-XRD can provide information about the polymorphs as well. Since synchrotron radiation is too expensive for exhaustive time-resolved experiments, a special designed tr-XRD equipment has been used to study the phase behavior of cocoa butter and milk fat, bringing more insight in phenomena like the memory effect.

P05.04.018 DEATH BY LETHAL INJECTION: STRUCTURE OF A NOVEL PHOSPHOTYROSINE BINDING DOMAIN. Craig L. Smith, James B. Bliska*, and Mark A. Saper, Biophysics Research Division and Department of Biological Chemistry, University of Michigan, Ann Arbor MI 48109, *Department of Molecular Genetics and Microbiology, SUNY Stony Brook, Stony Brook, NY 11794

YopH is a modular protein that is secreted and translocated into host macrophages by the contact dependent type III "injectosome" of the Yersinia sp.. YopH inibits phagocytosis supressing primary host defenses through dephosphorylation of host proteins p130Cas, paxillin, and focal adhesion kinase (FAK) by its C-terminal tyrosine phosphatase domain. Motifs responsible for the secretion and translocation of YopH are located in the first 71 residues of the N-terminal domain. This domain also binds to p130Cas and paxillin in a phosphotyrosine dependent manner. Although N-terminal domain of YopH binds phosphotyrosine peptides like SH2 and PTB domains, it lacks significant homology to these domains and may represent a novel protein-protein interaction module.

Our lab previously solved the crystal structure of the catalytic domain (163-468) to 2.5 Å resolution. We have now crystallized and solved the structure of the N-terminal domain of YopH (1-130) to 2.2 Å resolution. The protein crystallizes in the orthorhombic space group C2221 with unit cell parameters a=47.9 Å, b=120.7 Å, c=48.8 Å. A 2.8 Å MIR map using phases from three heavy atom derivatives (FOM=0.49 to 2.2 Å) produced high quality electron density allowing for tracing of over 80% main chain and 70% of the sidechain. After several cycles of refinement and phase combination, we currently have a model that includes 125 of the 130 residues with an R_{work}=0.29 and an R_{free}=0.37. The fold is unlike that of other phosphotyrosine binding proteins such as SH2 and PTB. Further refinement and co-crystallization with phosphotyrosine peptides is in progress.

M05.OF.005 FORMATION OF REGULAR SUBMICRON SURFACE PATTERN BY MEANS OF BLOCK COPOLYMERS. Martin Möller, Laboratory of Organic and Macromolecular Chemistry, University of Ulm, Germany.

Highly branched polymer structures, like dendrimers, cylindrical polymer brushes, and block copolymer micelles do not interpenetrate each other in concentrated solution or the melt to the same extent as linear macromolecules. While the latter form random coil conformations which can overlap with each other and interact via many molecular segments, highly branched or brush type structures interact via a more or less well defined molecular surface. This inability to undergo extensive interpenetration has also the consequence that dissolved, i.e., solvent swollen molecules undergo a collapse to form compact particles upon decreasing solvent quality or upon drying a solution. A simple, nevertheless intriguing consequence of the particulate character of highly branched polymer structures is the ability to form spontaneously very well defined monofilms if a solution is cast on a flat substrate. Long range lateral interactions in connection with capillary forces enforce the formation of a closed film, similarly like it is observed in the film formation of latices.

In the case blockcopolymer micelles such a formation of regular monofilms can be used to prepare quasi regular arrays of nanometer sized metal and metal oxide clusters on flat substrates. In the first place polymers micelles with a polar core were generated by dissolution of poly(styrene)-block-poly(2-vinylpyridine) and poly(styrene)-block-poly(ethyleneoxide) in toluene. These micelles were used as nanocompartments which were loaded with a defined amount of a metal salt. Then a suitable substrate was coated by a monolayer of the micelles. Exposure to an oxygen plasma allowed to remove the polymer completely leaving back the naked metal particles firmly attached to the substrate in the same quasi-hexagonal order as in the film. The height of the clusters could be varied between 1 nm and 15 nm depending on the concentration of the metal salt. The interparticle distance could be varied between 30 nm and 170 nm. Such lattices of Au particles have been used to bind other molecules like streptavidine proteines in an ordered array and for patterned SAMs. The approach has been extended to other noble metals but also to magnetic Co and Ni particles, in the latter case by by using a reductive plasma.

M09.OA.001 STRUCTURES OF THE N-TERMINAL AND HEXAMERIZATION DOMAINS OF N-ETHYLMALEIMIDE-SENSITIVE FUSION PROTEIN. W.I. Weis, A.P. May, K.M.S. Misura, C.U. Lenzen, S.W. Whiteheart*, Dept. of Structural Biology, Stanford University School of Medicine, Stanford, CA 94305 USA and *Dept. of Biochemistry, Chandler Medical Center, University of Kentucky College of Medicine, Lexington, KY 40536 USA

The cytosolic ATPase NSF disassembles complexes of membrane-bound proteins known as SNAREs, an activity essential for vesicular trafficking. The amino-terminal domain of NSF (NSF-N) is required for the interaction of NSF with the SNARE complex through the adaptor protein α-SNAP. NSF-N is followed by two homologous ATP-binding cassettes, designated D1 and D2, that possess essential ATPase and hexamerization activities, respectively. The crystal structures of NSF-N and D2 and their implications for NSF mechanism will be described.

P07.07.027 (N, N -DIMETHYLPIPERIDINIUM)$_4$ CU_5CL_{14}: A RARE EXAMPLE OF AN IRREGULAR CU(II) CHLORIDE CHAIN STRUCTURE. Allison Talley and Marcus R.Bond, Department of Chemistry, Southeast Missouri State University, Cape Girardeau, MO 63701; Carl J. Carrano, Department of Chemistry, Southeast Missouri State University, San Marcos, TX 78666.

This compound is the third known example of a rare class of $A_{n-1}Cu_nCl_{3n-1}$ compounds that are found only for a narrow range of A cation size. These compounds contain irregular, linear copper(II) chloride chains where tri(μ-chloro) bridging occurs between copper (II) ions within a pentanuclear oligomeric repeat unit and these repeat units are linked together by di(μ-chloro) bridges. The coordination geometries of the Cu(II) ions within the oligomeric unit differ dramatically, ranging from elongated octahedral to distorted square pyramidal. The title compound contains the largest known A cation in this class, yet still crystallizes with a chain structure similar to that found for the smallest A cation The oligomeric unit is, however, noticeably stretched as a result of including the larger cation. The title compound crystallizes in a crystal class (triclinic) that differs from both examples known already (monoclinic and orthorhombic). This provides a range of structural data that enables us to make the first attempt at describing the crystal chemistry of these unusual compounds.

Crystal data: triclinic P $\overline{1}$, a = 9.066(2) Å, b = 11.859(3) Å, c =13.046(4) Å, α = 87.22(3)° β = 71.81(3)°, γ = 67.62(2)° V =1228.3(5)Å^3, *Z* = 1, 3433 reflections collected (2505 unique, observed), least-squares refinement of 260 parameters to *R* = 0.0408 and *wR* =0.0556.

P05.04.008 CRYSTAL STRUCTURE OF THE INTEGRIN α2β1 INSERTED DOMAIN IN COMPLEX WITH A COLLAGEN LIKE PEPTIDE. [*]J. Emsley, [¥]C.G. Knight, [¥]R.W. Farndale, [¥]M.J. Barnes, [*]R.C. Liddington, [*]Department Of Biochemistry, Leicester University, Leicester, Le17rh, [¥]Department Of Biochemistry, Cambridge University, Tennis Court Road, Cambridge Cb2 2pt.

Integrin α2β1 is a collagen receptor that plays an essential role in the adhesion of platelets during primary haemostasis. α2β1 binding to collagen is magnesium dependant and is mediated through the 200 residue inserted 'I' domain of the alpha subunit (α2-I). The triple-helical structure of collagen is required for α2-I domain recognition and several groups have reported similar binding affinities in the range 50-500 nanomolar. We have previously reported the crystal structure of the α2-I domain determined to high resolution [1]. The α2-I domain structure adopts the dinucleotide binding fold, and contains a metal ion dependent adhesion site (MIDAS) motif with bound Mg^{2+} at the top of the beta-sheet. This structure revealed a new helix (the C-helix) protruding from the MIDAS site face which creates a groove centred on the magnesium ion. Recently the specific collagen sequences recognised by the a2-I domain have been identified as a 6 residue segment GFPGER (P=hyroxyproline) using overlapping synthetic peptides derived from a bovine collagen type I fragment. The ER residues of this segment have been shown to play an essential role in binding. By mixing together the collagen like peptide and the integrin α2-I domain in the presence of a divalent cation small crystals of the complex could be grown from sitting drop crystallisation experiments. The structure was solved to 2.5Å resolution and revealed the collagen triple helix bound at the MIDAS site with a glutamate sidechain from the GER motif coordinating to the metal ion on the I domain.

[1] Emsley, J., King, S.L., Bergelson, J.M., Liddington, R.C. *J. Biol. Chem.* (1997) **272**, 28512-28517.

P06.04.077 HIGH RESOLUTION CRYSTAL STRUCTURE OF THE DNA-BINDING DOMAIN OF MOUSE C-MYB. T.H. Tahirov, M. Sasaki [1,2], K. Sato [1,3], H. Morii, S. Ishii [4], S. Adachi [5], K. Ogata [1,2], [1] Kanagawa Academy of Science and Technology, [2] Department of Structural Biology, [3] Department of Biochemistry, Yokohama City University School of Medicine, 3-9 Fukuura, Kanazawa-ku, Yokohama 236-0004, Japan, [4] Protein Folding Group, National Institute of Bioscience and Human Technology, 1-1 Higashi, Tsukuba, Ibaraki 305-0074, Japan [5] RIKEN Harima Institute, 323-3, Mihara, Mikazuki, Sayo, Hyogo 679-5143, Japan

c-Myb is a transcription regulatory protein. It contains three functional domains responsible for DNA binding (homologous repeats R1, R2 and R3), transcriptional activation, and negative regulation of DNA binding. The Myb DNA-binding domain is highly conserved and involved in recognition of regulatory proteins such as C/EBP family members and Cyp-40. Thin needle like crystals of R2R3, a minimal DNA-binding fragment, were obtained by vapour diffusion method. Transformation of crystals to low-humidity form allowed high resolution data collection at BL44B2. Structure was solved by molecular replacement method and refined at 1.6 Å resolution. Overall fold of the core of each repeat is similar to "myb fold" determined by NMR, however, the relative orientation of repeats and the structure of the linker region in free state are different compare to DNA-bound state. A sodium/potassium binding site was found in each repeat and one of them mediates the interaction between the R2 and R3 repeats. Surface properties and possible interaction sites of R2R3 fragment will be discussed in detail.

P05.24.008 CHARACTERISATION OF MANGANESE OXIDES OBTAINED BY SOL-GEL TECHNOLOGY. C. Vázquez Vázquez & M.A. López Quintela Facultade de Química. Departamento de Química Física Universidade de Santiago de Compostela. Avenida das Ciencias, s/n E-15706 Santiago de Compostela (Spain)

We have synthesized nanoparticles of manganese oxides by the sol-gel method. Urea was used as gelificant agent because of the slow decomposition of urea in hot aqueous solutions, releasing hydroxide ions. The gel was decomposed at 250 ºC and the resulting powders were calcined at temperatures up to 1000 ºC. The nanoparticles were structurally characterized by X-ray diffraction and the Rietveld method was used in order to extract structural and microstructural parameters.

At low temperatures, the main phases are Mn_5O_8 and bixbyite-O, α-Mn_2O_3 (orthorhombic). Increasing temperature, above 400 ºC, bixbyite-O remains as unique stable phase. At 900 ºC it is observed the starting transformation between bixbyite-O to haussmanite, Mn_3O_4. Crystallite size of bixbyite-O ranges from 22 to 70 nm as calcination temperature increases.

The above phase transitions are well observed by thermogravimetry: the transformation of bixbyite-O to haussmanite is complete due to the flowing nitrogen atmosphere, free of oxygen.

P08.09.002 ANALYSIS OF QUALITATIVE CATIONIC COMPOSITION OF SILICATES. O.E.Gorchakova and N.L.Smirnova, Department of Chemistry, All-Russian Inst. of Scientific and Technical Information, Moscow, Russia.

A mineral systematics variant based on qualitative *sfdp*-formulae is suggested, where *s* is alkali and earth-alkali elements including H (14 elements); *f*-lanthanoids and actinides (28); there are 30 *d*-elements from Sc to Hg and 30 *p*-elements from B to Rn. Only ideal qualitative formulae consisting of main (species forming) elements without isomorphic admixtures, coefficients and atomic charges are considered. Silicates containing one cation are considered, these are 294 mineral species and, consequently, 294 cationic formulae. A mineral species corresponds to every cation, so the cationic composition systematics represent that of mineral species. It was found 193 (66%) *s*-cations, 6 (2%) *f*-cations, 72 (24%) *d*-cations and 23 (8%) *p*-cations among 294 cations. Eight (57%) of 14 *s*-elements are present in ordinary silicates: Li (1,1%), Be (1,1%), Na (23,3%), Mg (28%), K (8,2%), Ca (33,2%) Sr (1,1%), Ba (4,0%). Ca, Mg, Na (84,5%) are leaders among *s*-cations. Elements *f* are represented only by 5 (18%) of 28: Ce (16,7%), Yb (16,7%), Th (33,2%), U (16,7%), TR (16,7%). Only 9 (32%) of *d*- elements were found in the ordinary silicates: Sc (1,4%), Mn (23,6%), Fe(43,0%), Ni(12,5%), Cu(2,8%), Zn(9,7%), Y(4,3%),Hf(1,4%). Leaders are Fe, Mn (66,6%) among *d*-cations. The silicates considered contain only 4 (13%) of 30 *p*-elements: N (13%), Al (74%), Pb (8,7%), Bi (4,3%). Al (74%) is a leader among *p*-elements. There are 26 various cations in the ordinary silicates and only 4 (15,5%) are leaders: Ca, Mg, Na, Fe. Mean frequency of K, Mn, Al (11,5%) is the same as of Ba, Zn, Ni (11,5%), and it is low for the rest 16 (61,5%) cations. The frequency for these four groups of cations is different if to consider all 294 mineral species. Leaders are Ca, Mg, Na, Fe (66%), cations K, Mn, Al (17%) have a middle frequency, Ba, Zn, Ni (8,2%) are met rarely; the rest 16 cations will be the rarest ones (8,8%). Thus, study of silicates with one cation revealed a sharp preference of these minerals to 4 cation-leaders: Ca, Mg, Na, Fe. Analysis of the qualitative composition of minerals can be an important characteristic for an economic geology prognosis.

P06.06.019 X-RAY DIFFRACTION STUDIES OF PHASE TRANSITIONS IN OLEIC ACID. P. Tandon, R. Neubert [1], G. Föster [2], S. Wartewig [3], [1] Department of Pharmacy, Martin-Luther-Universität Halle-Wittenberg, D-06120 Halle(Saale), Germany, [2] Department of Chemistry, Martin-Luther-Universität Halle-Wittenberg, D-06099 Halle(Saale), Germany, [3] Institute of Applied Dermatopharmacy, Martin-Luther-Universität Halle-Wittenberg, D-06120 Halle(Saale), Germany

Oleic acid (OA) is an unsaturated lipid and plays an important role in many biological systems. The solid-solid gamma to alpha transition has been investigated using X-ray diffraction, FT-Raman spectroscopy and DSC. The X-ray diffraction and the molecular simulation studies using CERIUS2 program indicate that the gamma phase of OA crystallized from melt has a monoclinic unit cell with beta = 91° and the other unit cell parameters are the same as given by Abrahamsson and Ryderstedt-Nahringbauer [1]. Both X-ray diffraction and FT-Raman studies indicate that the conformation of the olefin group changes due to the gamma to alpha transition. In the alpha phase, the olefin group is in the skew-cis-trans conformation. This change in the conformation of the olefin group results in a changed orientation of the methyl-sided chains, whereas the orientation of the carboxyl-sided chains remains the same. In the gamma phase, the methylene chains at both sides of the C=C group form the O'parallel subcell. Simulation studies demonstrate that during the gamma to alpha transition only the subcell of methyl-sided chains transforms to the O perpendicular one, while the carboxyl-terminal chains keep the O'parallel subcell. The unit cell parameter for these two phases are not very different, only the cross sectional area of the unit cell and the long spacing show an ordinary thermal expansion caused by the gamma to alpha transition. The FT-Raman studies indicate that the number of gauche conformers in the methyl-terminal alkyl chains drastically increases in the course of the gamma to alpha transition, but the end of the methyl-sided chain remains mostly in the ordered tt conformation in the alpha phase, too. However, the carboxyl-sided alkyl chains exist in the ordered conformation in both the alpha and gamma phases. Financial assistance to P.T. from the Alexander von Humboldt Foundation is gratefully acknowledged.

[1] S. Abrahamsson & I. Ryderstedt-Nahringbauer (1962) Acta Cryst.,15, 1261-1268.

P07.07.99 CYANO-BRIDGED BIMETALLIC COMPLEXES WITH NITROPRUSSIDE OR HEXACYANO-FERRATE(II). Z. Smékal and Z. Trávníček, Dept. of Inorganic and Physical Chemistry, Palacký University, 771 47 Olomouc, CZ, and J. Marek, X-Ray Laboratory of Dept. Inorg. Chemistry & Laboratory of Biomolecular Strukture and Dynamics, Masaryk University, 611 37 Brno, CZ.

We are concerned in the synthesis and physico-chemical study of μ-cyano copper(II) and nickel(II) complexes [1]. The complexes of composition $[Cu(1,2\text{-pn})_2Fe(CN)_5NO].H_2O$ (1,2-pn = 1,2-diaminopropane), $[Cu(L)Fe(CN)_5NO].xH_2O$ (L = N,N,N',N'-tetramethyl-ethylenediamine, x = 0.5; L = N,N,N'-trimethylethylenediamine, x = 1; L = diethylenetriamine, x = 0; L = 3,3'-diamino-N-methyl-dipropylamine, x = 2) and $[Cu(ept)]_3[Fe(CN)_6](ClO_4)_2.5H_2O$ (ept = N-(2-aminoethyl)-1,3-diamino-propane) have been prepared. The structures of $[Cu(1,2\text{-pn})_2Fe(CN)_5NO].H_2O$ (Fig. 1) and $[Cu(ept)]_3[Fe(CN)_6](ClO_4)_2.6H_2O$ (Fig. 2) were determined by single crystal X-ray analysis. The compound (1) is binuclear with one bridged cyano group between copper and iron atoms. Polymeric complex (2) exhibits 2D sheet structure (all cyano groups form bridges).

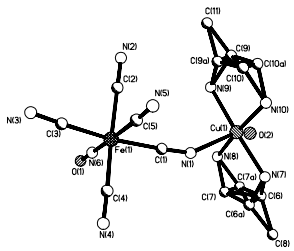

*Fig. **1***

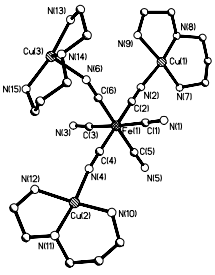

*Fig. **2***

We thank the Grant Agency of the Czech Republic (203/98/P221) and MŠMT (VS 96095) for financial support.

Z. Smékal, F. Březina, Z. Šindelář, R. Klička, D. Krausová & M. Nádvorník (1996). *Synth. React. Inorg. Met. – Org. Chem.* 26, 1537.

A

B

C

D

H

I

L

M

N

O

P

Q

R

S

T

U

V

W

X